Title 40 CFR Part 191
Subparts B and C
Compliance Recertification Application 2014
for the
Waste Isolation Pilot Plant

Structure of the CRA-2014

United States Department of Energy
Waste Isolation Pilot Plant

Carlsbad Field Office
Carlsbad, New Mexico

Compliance Recertification Application 2014
Structure of the CRA-2014

Table of Contents

List of Figures

This page intentionally left blank.

Acronyms and Abbreviations

CCA	Compliance Certification Application
CFR	Code of Federal Regulations
CRA	Compliance Recertification Application
DOE	U.S. Department of Energy
EPA	U.S. Environmental Protection Agency
WIPP	Waste Isolation Pilot Plant

This page intentionally left blank.

Structure of the CRA-2014

The format of the 2014 Compliance Recertification Application (CRA-2014) is the same as that used in the CRA-2009. The CRA-2014 follows the structure and organization of the sections of 40 CFR Part 194. This format aligns with the format used in the U.S. Environmental Protection Agency's (EPA's) Compliance Application Review Documents and is intended to facilitate the EPA and stakeholder reviews of the application. This format is expected to allow a direct evaluation of any changed information with respect to previous applications.

In each section of the CRA-2014, information that is "new" since the CRA-2009 is located in Section 7 through Section 9. In most cases, "old" text is unchanged except where it contained errors or omissions, to reflect changes in references/citations, and to change verb tense in text describing future events that have now taken place. The CBFO Quality Assurance Program Document is now included as a reference instead of as an appendix.

CRA-2014 Section 23 and Section 34 retain the format that was used in CRA-2009 and differ slightly from the format described below. In Section 23 and Section 34, the information contained under "Background," "1998 Certification Decision," "Changes in the CRA-2004," etc., is provided for each first and second level paragraph of the CFR (194.23(c)(1), 194.23(c)(2), etc.). In the remainder of the document, information contained under "Background," "1998 Certification Decision," "Changes in the CRA-2004," etc., is provided at the section level (e.g., 194.15).

Each section includes the following components:

1. **Requirements**: The text of the regulation.

2. **Background**: The historical context of how the U.S. Department of Energy (DOE) and the Waste Isolation Pilot Plant (WIPP) have complied with the regulation.

3. **1998 Certification Decision**: A summary of the Compliance Certification Application (CCA) and the EPA's evaluation of compliance to the regulation.

4. **Changes in the CRA-2004**: An identification and summary of changes from the CCA to the CRA-2004 directly related to the regulation.

5. **EPA's Evaluation of Compliance for the 2004 Recertification**: A summary of the EPA's evaluation of the CRA-2004.

6. **Changes or New Information Between the CRA-2004 and the CRA-2009 (Previously: Changes or New Information Since the 2004 Recertification)**: The changes that resulted from continuing scientific investigations and operations at the WIPP during the time period between the submittal of the CRA-2004 and the appropriate data cut-off date of the CRA-2009.

7. **EPA's Evaluation of Compliance for the 2009 Recertification**: A summary of the EPA's evaluation of the CRA-2009.

8. **Changes or New Information Since the CRA-2009:** The changes that resulted from continuing scientific investigations and operations at the WIPP during the time period between January 1, 2008, and the CRA-2014 data cut-off date of December 31, 2012.

9. **References:** References cited in the CRA-2014 documentation. References that were not submitted in any previous CRA are followed by an asterisk. At the request of the EPA, an electronic version of the CRA-2014 is included in this application. The electronic version includes hyperlinks to all references cited in the text, except for copyrighted references.

Sections, appendices, and attachments included in this application are listed below.

CRA-2014 Sections (Corresponding to 40 CFR 194 Sections)	CRA-2014 Appendices	CRA-2014 Attachments
• Structure of the CRA-2014 • Executive Summary • 8: Approval Process for Waste Shipment from Waste Generator Sites for Disposal at the WIPP • 15: Content of Compliance Recertification Application(s) • 21: Inspections • 22: Quality Assurance • 23: Models and Computer Codes • 24: Waste Characterization • 25: Future State Assumptions • 26: Expert Judgment • 27: Peer Review • 31: Application of Release Limits • 32: Scope of Performance Assessments • 33: Consideration of Drilling Events in Performance Assessments • 34: Results of Performance Assessments • 41: Active Institutional Controls • 42: Monitoring • 43: Passive Institutional Controls • 44: Engineered Barriers • 45: Consideration of the Presence of Resources • 46: Removal of Waste • 51-52: Consideration of Protected Individual and Exposure Pathways • 53: Consideration of Underground Sources of Drinking Water • 54: Scope of Compliance Assessments • 55: Results of Compliance Assessments	• Appendix AUD: Audits and Surveillances • Appendix DATA: Monitoring Data and Reports • Appendix HYDRO: Hydrologic Investigations • Appendix IGP: Individual and Groundwater Protection Requirements • Appendix MASS: Performance Assessment Modeling Assumptions • Appendix MgO: Magnesium Oxide as an Engineered Barrier • Appendix MON: WIPP Monitoring Programs • Appendix PA: Performance Assessment • Appendix PORSURF: Porosity Surface • Appendix SCR: Feature, Event, and Process Screening for Performance Assessment • Appendix SOTERM: Actinide Chemistry Source Team • Appendix TFIELD: Transmissivity Fields	• Attachment A: TFIELD Visualization

There are many cases where an appendix contains technical information similar to that covered in a section. In these cases, the section is a summary of the information provided in the appendix.

Figure STRUCT-1 maps all 23 sections and 13 appendices and the relationship of each appendix to specific sections in the CRA-2014.

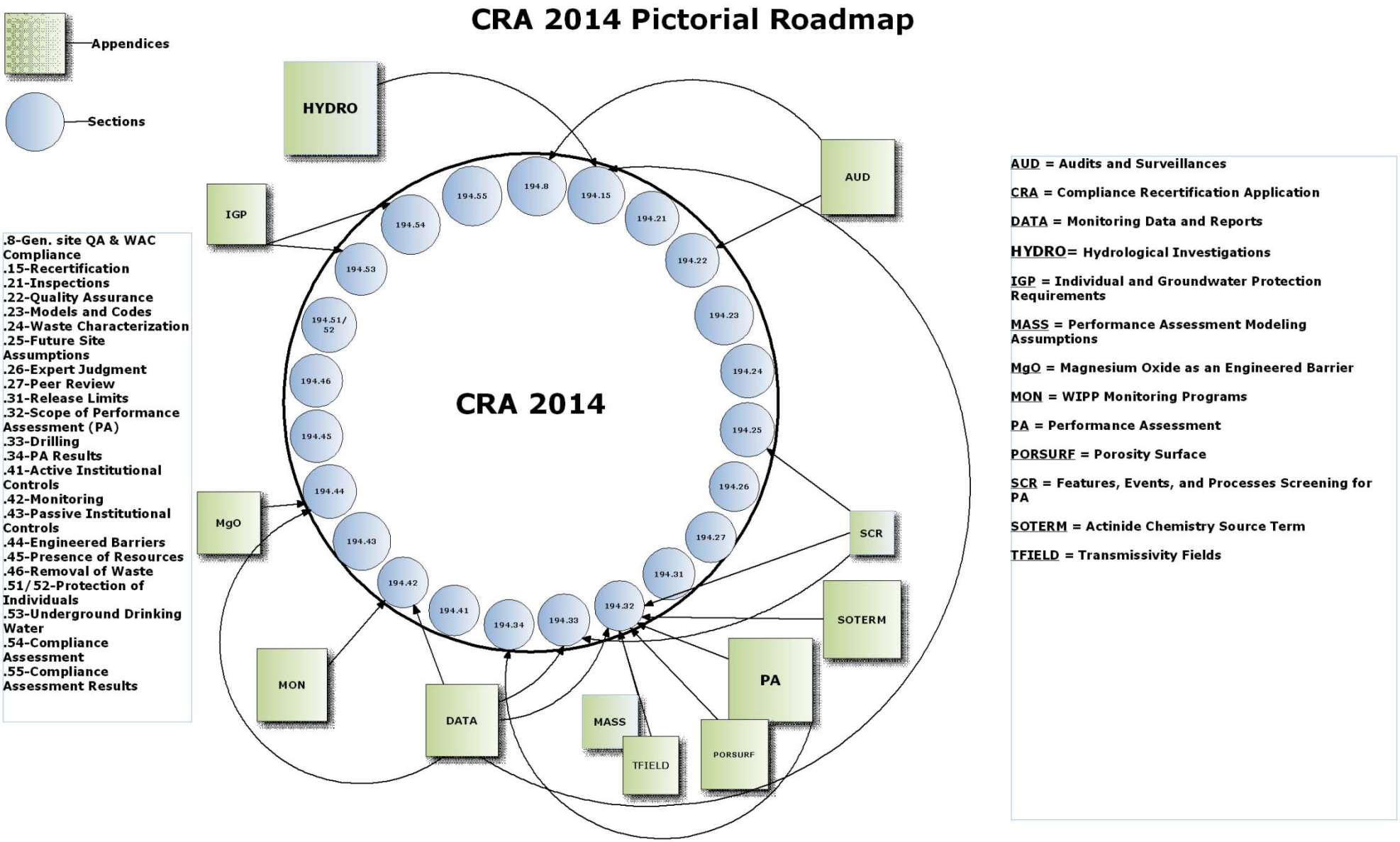

Figure STRUCT-1. CRA-2014 Pictorial Roadmap

Title 40 CFR Part 191
Subparts B and C
Compliance Recertification Application 2014
for the
Waste Isolation Pilot Plant

Executive Summary

United States Department of Energy
Waste Isolation Pilot Plant

Carlsbad Field Office
Carlsbad, New Mexico

Compliance Recertification Application 2014
Executive Summary

Table of Contents

List of Figures

List of Tables

This page intentionally left blank.

Acronyms and Abbreviations

CCA	Compliance Certification Application
CCDF	complementary cumulative distribution functions
CFR	Code of Federal Regulations
CH	contact-handled
CRA	Compliance Recertification Application
DOE	U.S. Department of Energy
EPA	U.S. Environmental Protection Agency
FEPs	features, events, and processes
LWA	Land Withdrawal Act
MgO	magnesium oxide
PA	performance assessment
PABC	Performance Assessment Baseline Calculation
PCN	planned change notice
PCR	planned change request
PCS	Panel Closure System
RH	remote-handled
SDI	Salt Disposal Investigations
TRU	transuranic
ROMPCS	Run-of-Mine Panel Closure System
WIPP	Waste Isolation Pilot Plant

This page intentionally left blank.

EXECUTIVE SUMMARY

EXECSUM-1.0 Overview

The Waste Isolation Pilot Plant (WIPP), located near Carlsbad, New Mexico, is a deep geologic repository for the disposal of defense-related transuranic (TRU) waste. The WIPP Land Withdrawal Act (LWA) (Pub. L. 102-579, 106 stat. 4777, as amended by Pub. L. 104-201, 110 stat. 2422) requires the U.S. Environmental Protection Agency (EPA) to certify the WIPP's compliance with the disposal regulations of Title 40 CFR Part 191 Subparts B and C prior to the commencement of disposal operations. To meet this requirement, the U.S. Department of Energy (DOE) submitted the Compliance Certification Application (CCA) in October 1996, demonstrating compliance with the disposal standards and the criteria established in Title 40 CFR Part 194. The CCA demonstrated that the geological, hydrological, physical, chemical, and environmental characteristics of the site, along with engineered features of the facility, would safely contain radioactive waste for the 10,000-year regulatory time period. After a thorough review of the CCA, the EPA certified the WIPP's compliance with these regulations in May 1998, paving the way for waste disposal operations which began on March 26, 1999.

The WIPP LWA requires the DOE to submit documentation of the WIPP's continued compliance with the disposal regulations to the EPA not later than five years after initial receipt of TRU waste for disposal at the repository, and every five years thereafter until the decommissioning of the facility is completed. This periodic documentation of continued compliance is referred to as "recertification." The DOE has completed two recertification cycles. The first Compliance Recertification Application (CRA-2004) was received by the EPA on March 26, 2004. After a thorough review, the EPA recertified the WIPP's compliance on March 29, 2006. The second Compliance Recertification Application (CRA-2009) was received by the EPA on March 26, 2009, and the EPA recertified the WIPP's compliance on November 18, 2010. The third five-year recertification cycle begins on March 26, 2014. The CRA-2014 is being submitted to the EPA in accordance with the provisions of the LWA, and is the DOE's documentation of the WIPP's continued compliance with the applicable radioactive waste disposal standards and WIPP Compliance Criteria.

According to the WIPP Compliance Criteria in 40 CFR § 194.15, recertification applications must include any information that is new or different from information contained in the most recent compliance application. Therefore, the DOE must review any new information that relates to the WIPP's certification basis and include the new information in each CRA. The CRA-2014 includes several changes that resulted from continuing scientific investigations and operations at the WIPP during the time period between January 1, 2008, and the CRA-2014 data cut-off date of December 31, 2012. These changes include planned repository changes, performance assessment (PA) parameter updates based on new WIPP-specific data, and PA implementation refinements. Other non-significant changes, such as procedure revisions and PA software and hardware changes, are summarized in the Annual Change Reports submitted to the EPA as required by 40 CFR § 194.4(b)(4). None of the changes compromise compliance with the radioactive waste disposal standards. The PA results in this recertification application show that the repository will not adversely impact public health or the environment during the 10,000-

year regulatory compliance time period. The CRA-2014 demonstrates that the WIPP remains in compliance with EPA requirements.

EXECSUM-1.1 Contents of the CRA-2014

The CRA-2014 has been developed in accordance with the EPA's Certification Criteria found in Part 194. This document addresses all topics relevant to the certification process. Topics addressed in the CRA-2014 include, but are not limited to, the following:

- Natural and engineered features of the disposal system, including geology, geophysics, and hydrogeology of the repository and its environs, as well as the geochemistry and actinide chemistry of interactions between the disposal system and the emplaced TRU wastes.

- Information concerning the inventories of TRU waste emplaced in the repository, waste stored at DOE sites, and waste expected to be generated at those sites and shipped to the WIPP in the future.

- WIPP-relevant features, events, and processes (FEPs), updated based on data and information acquired since the CRA-2009.

- Assessments of the disposal system's long-term performance, including the input parameters and models used in those assessments.

- Demonstration that the WIPP meets or exceeds individual and groundwater protection standards and will continue to do so.

- Assurance requirements, including active and passive institutional controls, monitoring, engineered barriers and the effects of natural resource extraction.

EXECSUM-1.2 Programmatic Changes Since the CRA-2009

This application incorporates information about changes that have taken place since the CRA-2009. These changes have been proposed by the DOE and approved by the EPA, requested by the EPA, or driven by the availability of new data, and include:

- Inventory: The inventory used in the CRA-2014 is updated from that used in the CRA-2009 Performance Assessment Baseline Calculation (PABC). Section 24 of this application contains a summary of the CRA-2014 waste inventory.

- CRA-2009 PABC Parameters: Changes to the CRA-2009 PA were made during the recertification process as part of the CRA-2009 PABC. The CRA-2009 PABC included updated information on transmissivity fields found in the Culebra Dolomite Member and updated Culebra matrix partition coefficients. These changes are brought forward to the CRA-2014 PA.

- Planned Repository Changes:

Shielded Containers - On November 15, 2007, the DOE submitted a planned change request (PCR) to the EPA for the use of shielded containers for the disposal of a portion of the remote-handled (RH) waste inventory in the rooms of the WIPP. The walls of the shielded container include a layer of lead, making it more effective than previously authorized containers in maintaining a low dose rate at its external surface. Shielded containers could be managed and disposed of as contact-handled (CH) waste based on the external surface dose rate. Even though the RH-TRU waste in shielded containers will be handled as if it were CH-TRU waste, these containers will still be recorded as RH-TRU waste in the WIPP Waste Data System, and the volume of the waste will be counted against the limit of 250,000 cubic feet (7,080 cubic meters) of RH-TRU waste, as set by the Consultation and Cooperation Agreement between the DOE and the State of New Mexico. This PCR was described in detail in the CRA-2009. On August 8, 2011, the EPA granted the DOE conditional approval to dispose of shielded containers pending the demonstration of a consistent complex-wide procedure to ensure the surface dose rate limit is not greater than 200 millirems per hour.

Neutron Shielded Canister - On May 21, 2010, the DOE submitted to the EPA a planned change notice (PCN) to employ a polyethylene liner inside some standard RH-TRU waste canisters to shield neutron-emitting waste destined for disposal at the WIPP.

Salt Disposal Investigations (SDI) - The DOE submitted a PCN to the EPA on August 11, 2011, that presented plans to carry out additional excavation to the WIPP experimental area for the SDI research project and showed that there will be no impact on operations or post-closure performance. A PA was performed to determine the impact of the additional SDI excavation on long-term WIPP performance. Total normalized releases calculated with the additional excavation were indistinguishable from those obtained in the CRA-2009 PABC, and remained below regulatory release limits. After reviewing the DOE proposal and written responses to questions related to the effects of increasing the mined area, the EPA found that the mining phase of the SDI activities will not adversely impact the WIPP's waste handling activities, air monitoring, disposal operations, or long-term repository performance. The CRA-2014 PA includes this additional excavated volume in the WIPP experimental area. The implementation of the additional volume is described in Appendix PA-2014, Section PA-1.1.2 and the references therein. Subsequent to the EPA's November 17, 2011, response, the EPA was further notified of planned changes to the testing in this volume related to ventilation (May 18, 2012) and reduction of thermal loads (June 13, 2012).

Repository Reconfiguration - On August 30, 2011, the DOE submitted to the EPA a PCR for the reconfiguration of Panels 9 and 10 within the WIPP repository footprint. The proposed change replaces the use of the north-south access drifts as future Panels 9 and 10 with two new panels mined to the south of Panels 4 and 5. This proposed change continues to be important to the DOE, even though it is only mentioned briefly in a few sections.

Panel Closure System - The 1998 rulemaking that certified the WIPP to receive TRU waste required the DOE to implement the "Option D" Panel Closure System (PCS). The DOE has reassessed the engineering of the panel closure and has proposed a revised design which is simpler, more cost effective and easier to construct. The DOE submitted a PCR to the EPA on September 28, 2011, requesting that the EPA modify Condition 1 of the Final Certification Rulemaking for 40 CFR Part 194 for the WIPP, and that a revised PCS design be approved for use in the repository. The revised PCS design, denoted as the Run-of-Mine Panel Closure System (ROMPCS), is comprised of 100 feet of run-of-mine salt (i.e., unaltered, mined WIPP salt) with barriers to restrict personnel access and control ventilation at each end. Regulatory compliance impacts associated with the implementation of the ROMPCS in the WIPP were assessed in a PA titled PCS-2012. Total normalized releases calculated in the PCS-2012 PA remained below the regulatory limits. Long-term WIPP performance with the ROMPCS design is similar to that seen with Option D, and the WIPP remains in compliance with the containment requirements of 40 CFR Part 191 with the new panel closure. Details regarding the ROMPCS and its modeling can be found in Appendix PA-2014, Section PA-4.2.8. The ROMPCS is implemented in the CRA-2014 PA.

Placement of Magnesium Oxide (MgO) - On February 14, 2012, the DOE submitted a PCN, based on operating experience and historical data, to inform the EPA that a process was being instituted to emplace MgO on every other row of waste containers, in contrast to emplacing MgO on every waste stack. Historical data showed the MgO excess factor on a per room basis ranged from 1.22 to 2.85 when MgO was placed on every stack of waste. These values were higher than the excess factor of 1.2 mandated by the EPA's letter dated February 11, 2008. The PCN also described the process that requires the Waste Handling Engineer to continue to calculate the excess factor at the end of each shift and to direct the placement of additional MgO if the excess factor dropped below 1.2. Details regarding this change can be found in Appendix MgO, Section MgO-2.1.4.

- CRA-2014 PA Updates: Changes to PA since the CRA-2009 PABC include parameter updates and WIPP PA implementation refinements. Parameters were updated based on new data and include drilling rate and corresponding plugging pattern parameters, radionuclide solubilities and their uncertainties, colloid enhancement factors, the probability of encountering pressurized brine during a hypothetical drilling intrusion, the corrosion rate of steel, and the effective shear strength of WIPP waste. These parameter changes are made to accommodate new data. The repository water balance implementation is refined in the CRA-2014 PA in order to include major gas and brine producing and consuming reactions. Radionuclide concentrations in brine are more closely linked to repository brine volume in the CRA-2014 PA through the use of a variable volume, eliminating a mass imbalance for ligands in the PA calculations. These updates are discussed in Appendix PA-2014, Section PA-1.1.

EXECSUM-1.3 PA Results

Performance of the WIPP disposal system is evaluated by means of the WIPP PA, which gives rise to a methodology for quantifying the probabilistic distribution of possible radionuclide releases from the WIPP repository over the next 10,000 years and characterizing the uncertainty

in the distribution. The WIPP PA results are required to be expressed as complementary cumulative distribution functions (CCDFs). A CCDF represents the probability of exceeding various levels of cumulative release. Compliance analyses performed on the undisturbed repository result in no releases from the repository to the accessible boundary. As a result, all total normalized releases in the CRA-2014 PA correspond to the disturbed repository. The CRA-2014 compliance analysis demonstrates that the overall mean releases have decreased since the CRA-2009 and that the WIPP continues to comply with the individual and groundwater protection standards in Part 191 Subparts B and C. The mean CCDFs for total normalized release from the CRA-2009 PABC and the CRA-2014 PA are shown in Figure EXECSUM-1. The mean CCDF for the CRA-2014 is further to the left of the mean CCDF for the CRA-2009 PABC, indicating lower normalized releases for the CRA-2014 PA at most probabilities, and the WIPP remains in compliance. In addition, there is a greater than 95% level-of-confidence that the mean of the population of CCDFs is in compliance with the containment requirements of 40 CFR § 191.13. The 95% level-of-confidence limits are not shown in Figure EXECSUM-1 (see Appendix PA-2014, Section PA-9.5, Figure PA-81).

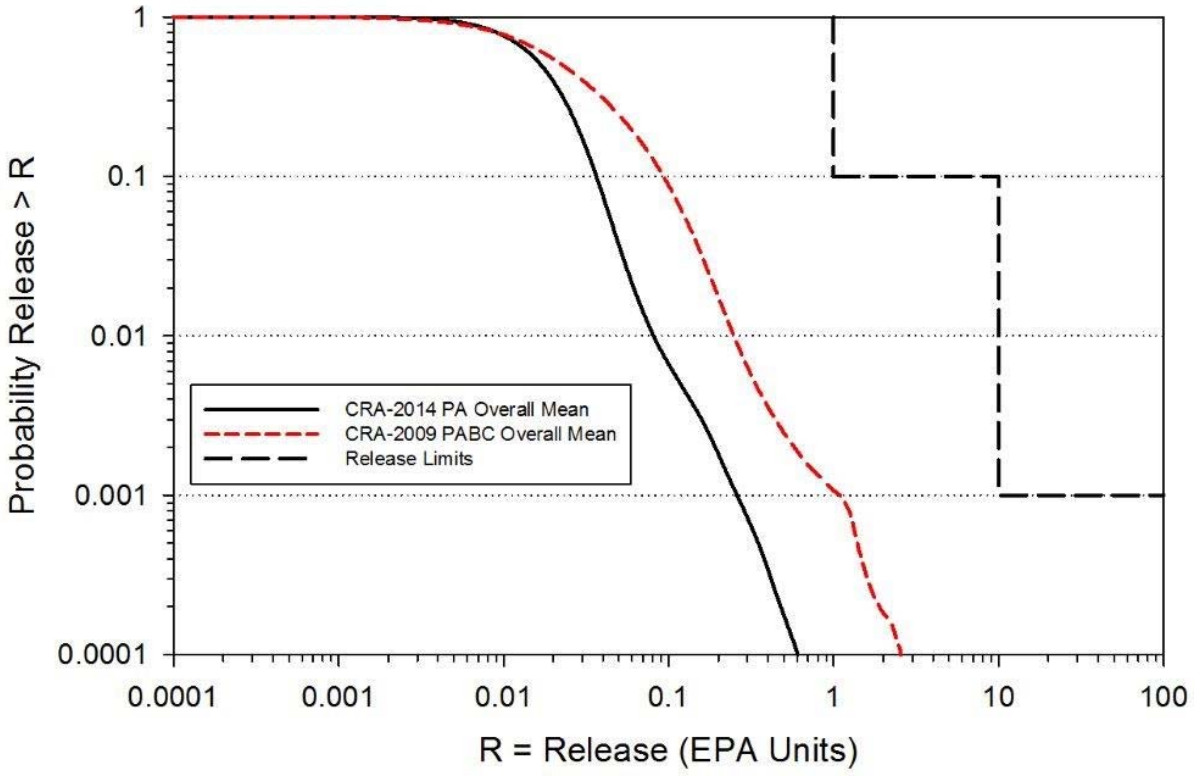

Figure EXECSUM-1. CRA-2014 PA and CRA-2009 PABC Overall Mean CCDFs for Total Normalized Releases

The waste shear strength is the maximum shear stress at which erosion of the waste can occur. Cavings release volumes comprise the solid waste material eroded from the walls of an intrusion borehole by shear stresses from the circulating drill fluid. The impact of the CRA-2014 PA waste shear strength refinement is to reduce cavings release volumes. The combined impact of changes included in the CRA-2014 PA is an overall net reduction to normalized direct brine

releases and spallings releases as compared to the CRA-2009 PABC. Radionuclide transport releases to the Culebra are most likely to occur during hypothetical drilling intrusions that encounter pressurized brine in the Castile Formation. The refinement to the probability that a drilling intrusion results in a pressurized brine pocket intersection results in increased Culebra transport releases for some futures and decreases in others. The net effect is a reduction in normalized Culebra transport releases in the CRA-2014 PA as compared to the CRA-2009 PABC. Total normalized releases decrease from the CRA-2009 PABC to the CRA-2014 PA as each contributing component is reduced in the CRA-2014 PA.

EXECSUM-1.4 Summary of Changes to the Application

Table EXECSUM-1 and Table EXECSUM-2 present a high-level summary of changes made to each section, appendix and attachment of the CRA-2014.

Table EXECSUM-1. CRA-2014 Sections, Appendices and Attachments with Non-Significant to No Changes Since the CRA-2009

CRA-2014 Sections and Appendices with Editorial or No Change Since the CRA-2009	CRA-2014 Sections, Appendices and Attachments with Changes Incorporating Updated Data Since the CRA-2009*
Section 26: Expert Judgment	Section 8: Approval Process for Waste Shipment From Waste Generator Sites for Disposal at the WIPP
Section 31: Application of Release Limits	Section 21: Inspections
Section 41: Active Institutional Controls	Section 22: Quality Assurance
Section 42: Monitoring	Section 25: Future States Assumptions
Section 43: Passive Institutional Controls	Section 33: Consideration of Drilling Events in Performance Assessments
Section 45: Consideration of the Presence of Resources	Section 51-52: Consideration of Protected Individual and Exposure Pathways
Section 46: Removal of Waste	Section 53: Consideration of Underground Sources of Drinking Water
Section 54: Scope of Compliance Assessments	Appendix AUD: Audits and Surveillances
Section 55: Results of Compliance Assessments	Appendix DATA: Monitoring Data and Reports
Appendix MON: WIPP Monitoring Programs	Appendix HYDRO: Hydrological Investigations
Appendix PORSURF: Porosity Surface	Appendix IGP: Individual and Groundwater Protection Requirements
	Appendix MASS: Performance Assessment Modeling Assumptions
	Appendix MgO: Magnesium Oxide as an Engineered Barrier
	Appendix TFIELD: Transmissivity Fields
	Attachment A: TFIELD Visualization

*Changes are routine data updates since the CRA-2009.

Table EXECSUM-2. CRA-2014 Sections and Appendices with Moderate Changes Since the CRA-2009

CRA-2014 Section or Appendix	Summary of Change
Section 15: Content of Compliance Recertification Application(s)	• Updated geologic, geophysical, geochemical, hydrologic, and meteorological information • New waste shear strength and iron and lead corrosion experiments • Status of mining and waste emplacement • PCN and PCR submittals
Section 23: Models and Computer Codes	• Repository planned changes (i.e., additional excavated area in the northern experimental area) • Parameter updates • Refinements to PA implementation • Two new codes, EQ3/6 and JAS3D, were added
Section 24: Waste Characterization	Changes in projected waste streams that directly affect the contact-handled and remote-handled waste scaling factors
Section 27: Peer Review	Added one peer review, the Savannah River Site Historical Radiochemistry Data Peer Review
Section 32: Scope of Performance Assessments	Updated the FEPs baseline for the CRA-2014 to account for planned changes, new information, or new data
Section 34: Results of Performance Assessments	Repository planned changes, parameter updates, and refinements to PA implementation
Section 44: Engineered Barriers	• The EPA accepted the DOE's PCN to emplace MgO supersacks on every other row unless additional sacks are needed to meet the 1.2 excess factor • The standard MgO supersack weight was changed to 3,000 pounds • MgO hydration studies have been completed and refinements were made to the water balance used in PA, which now includes the impact of MgO hydration/carbonation
Appendix PA: Performance Assessment	Updated to reflect repository planned changes, parameter refinements, and PA implementation changes occurring since the CRA-2009 PA
Appendix SCR: Feature, Event, and Process Screening for PA	Updated the FEPs baseline for the CRA-2014 to account for planned changes, new information, or new data
Appendix SOTERM: Actinide Chemistry Source Term	• New project-specific data in the areas of metal corrosion, microbial ecology, actinide/analog solubility in brine, and colloid enhancement parameters were added • Model parameters were modified in PA in two areas: 1) gas generation rates due to metal corrosion and 2) colloid enhancement parameters for mineral, intrinsic and microbial colloids • Geochemical modeling is now based on the EQ3/6 geochemical code and implements a variable brine volume approach to more realistically predict actinide concentrations

Title 40 CFR Part 191
Subparts B and C
Compliance Recertification Application 2014
for the
Waste Isolation Pilot Plant

Approval Process for Waste Shipment From Waste Generator Sites for Disposal at the WIPP
(40 CFR § 194.8)

United States Department of Energy
Waste Isolation Pilot Plant

Carlsbad Field Office
Carlsbad, New Mexico

Compliance Recertification Application 2014 Approval Process for Waste Shipment From Waste Generator Sites for Disposal at the WIPP
(40 CFR § 194.8)

Table of Contents

List of Tables

This page intentionally left blank.

Acronyms and Abbreviations

AMWTP	Advanced Mixed Waste Treatment Project
ACL	Analytical Chemistry Laboratory
AERHDM	Argonne East Remote Handled Debris Mix
ANL	Argonne National Laboratory
BAPL	Bettis Atomic Power Laboratory
BCL	Battelle Columbus Laboratory
CARD	Compliance Application Review Document
CCP	Central Characterization Project
CFR	Code of Federal Regulations
CH-TRU	contact-handled transuranic
CRA	Compliance Recertification Application
DOE	U.S. Department of Energy
EPA	U.S. Environmental Protection Agency
FEW	Fuel Examination Waste
FY	fiscal year
GEVNC	General Electric Vallecitos Nuclear Center
HENC	High Efficiency Neutron Counter
INL	Idaho National Laboratory
LANL	Los Alamos National Laboratory
LLNL	Lawrence Livermore National Laboratory
NABC	Nondestructive Assay Box Counter
NTS	Nevada Test Site
ORNL	Oak Ridge National Laboratory
QA	quality assurance
RFETS	Rocky Flats Environmental Technology Site
RH-TRU	remote-handled transuranic
RL	Hanford-Richland
SuperHENC	Super High Efficiency Neutron Counter
SRS	Savannah River Site
TRU	transuranic
VE	visual examination

WIPP	Waste Isolation Pilot Plant
WWIS	WIPP Waste Information System

This page intentionally left blank.

8.0 Approval Process for Waste Shipment From Waste Generator Sites for Disposal at the WIPP (40 CFR § 194.8)

8.1 Requirements

§ 194.8 Approval Process for Waste Shipment From Waste Generator Sites for Disposal at the WIPP

(a) *Quality Assurance Programs at Waste Generator Sites.* The Agency will determine compliance with requirements for site-specific quality assurance programs as set forth below:

(1) Upon submission by the Department of a site-specific quality assurance program plan the Agency will evaluate the plan to determine whether it establishes the applicable Nuclear Quality Assurance (NQA) requirements of § 194.22(a)(1) for the items and activities of §§ 194.22(a)(2)(i), 194.24(c)(3) and 194.24(c)(5). The program plan and other documentation submitted by the Department will be placed in the dockets described in § 194.67.

(2) The Agency will conduct a quality assurance audit or an inspection of a Department quality assurance audit at the relevant site for the purpose of verifying proper execution of the site specific quality assurance program plan. The Agency will publish a notice in the Federal Register announcing a scheduled inspection or audit. In that or another notice, the Agency will also solicit public comment on the quality assurance program plan and appropriate Department documentation described in paragraph (a)(1) of this section. A public comment period of at least 30 days will be allowed.

(3) The Agency's written decision regarding compliance with the requisite quality assurance requirements at a waste generator site will be conveyed in a letter from the Administrator's authorized representative to the Department. No such compliance determination shall be granted until after the end of the public comment period described in paragraph (a)(2) of this section. A copy of the Agency's compliance determination letter will be placed in the public dockets in accordance with § 194.67. The results of any inspections or audits conducted by the Agency to evaluate the quality assurance programs described in paragraph (a)(1) of this section will also be placed in the dockets described in § 194.67.

(4) Subsequent to any positive determination of compliance as described in paragraph (a)(3) of this section, the Agency intends to conduct inspections, in accordance with §§194.21 and 194.22(e), to confirm the continued compliance of the programs approved under paragraphs (a)(2) and (a)(3) of this section. The results of such inspections will be made available to the public through the Agency's public dockets, as described in § 194.67.

(b) *Waste characterization programs at transuranic waste sites.* The Agency will establish compliance with Condition 3 of the certification using the following process:

(1) DOE will implement waste characterization programs and processes in accordance with § 194.24(c)(4) to confirm that the total amount of each waste component that will be emplaced in the disposal system will not exceed the upper limiting value or fall below the lower limiting value described in the introductory text of § 194.24(c). Waste characterization processes will include the collection and use of acceptable knowledge; destructive and/or nondestructive techniques for identifying and measuring waste components; and the validation, control, and transmittal to the WIPP Waste Information System database of waste characterization data, in accordance with § 194.24(c)(4).

(2) The Agency will verify the compliance of waste characterization programs and processes identified in paragraph (b)(1) of this section at sites without EPA approval prior to October 14, 2004, using the following process:

(i) DOE will notify EPA by letter that a transuranic waste site is prepared to ship waste to the WIPP and has established adequate waste characterization processes and programs. DOE also will provide the relevant waste characterization program plans and documentation. EPA may request additional information from DOE.

(ii) EPA will conduct a baseline compliance inspection at the site to verify that adequate waste characterization program plans and technical procedures have been established, and that those plans and procedures are effectively implemented. The inspection will include a demonstration or test by the site of the waste characterization processes identified in paragraph (b)(1) of this section. If an inspection does not lead to approval, we will send an inspection report to DOE identifying deficiencies and place the report in the public docket described in § 194.67. More than one inspection may be necessary to resolve compliance issues.

(iii) The Agency will announce in the Federal Register a proposed Baseline Compliance Decision to accept the site's compliance with § 194.24(c)(4). We will place the inspection report(s) and any supporting documentation in the public docket described in § 194.67. The site inspection report supporting the proposal will describe any limitations on approved waste streams or waste characterization processes. It will also identify (through tier

designations in accordance with paragraph (b)(4) of this section) what changes to the approved waste characterization processes must be reported to and approved by EPA before they can be implemented. In the notice, we will solicit public comment (for a minimum of 45 days) on the proposed Baseline Compliance Decision, including any limitations and the tier designations for future changes or expansions to the site's waste characterization program.

(iv) Our written decision regarding compliance with the requirements for waste characterization programs and processes described in paragraph (b)(1) of this section will be conveyed in a letter from the Administrator's authorized representative to DOE. EPA will not issue a compliance decision until after the end of the public comment period described in paragraph (b)(2)(iii) of this section. EPA's compliance decision will respond to significant and timely-received comments. A copy of our compliance decision will be placed in the public docket described in § 194.67. DOE will comply with any requirements identified in the compliance decision and the accompanying inspection report.

(3) Subsequent to any positive determination of compliance as described in paragraph (b)(2)(iv) of this section, the Agency intends to conduct inspections, in accordance with § 194.24(h), to confirm the continued compliance of approved waste characterization programs and processes at transuranic waste sites. EPA will make the results of these inspections available to the public in the dockets described in § 194.67.

(4) Subsequent to any positive determination of compliance as described in paragraph (b)(2)(iv) of this section, the Department must report changes or expansions to the approved waste characterization program at a site in accordance with the tier designations established in the Baseline Compliance Decision.

(i) For changes or expansions to the waste characterization program designated as ''Tier 1,'' the Department shall provide written notification to the Agency. The Department shall not ship for disposal at WIPP any waste that has been characterized using the new or revised processes, equipment, or waste streams until EPA has provided written approval of such new or revised systems.

(ii) For changes or expansions to the waste characterization program designated as ''Tier 2,'' the Department shall provide written notification to the Agency. Waste characterized using the new or revised processes, equipment, or waste streams may be disposed at WIPP without written EPA approval.

(iii) EPA may conduct inspections in accordance with § 194.24(h) to evaluate the implementation of Tier 1 and Tier 2 changes or expansions to the waste characterization program at a site.

(iv) Waste characterization program changes or expansions that are not identified as either "Tier 1" or "Tier 2" will not require written notification by the Department to the Agency before implementation or before shipping waste for disposal at WIPP.

(5) Subsequent to any positive determination of compliance as described in paragraph (b)(2)(iii) of this section, EPA may revise the tier designations for approving changes or expansions to the waste characterization program at a site using the following process:

(i) The Agency shall announce the proposed tier changes in a letter to the Department. The letter will describe the Agency's reasons for the proposed change in tier designation(s). The letter and any supporting inspection report(s) or other documentation will be placed in the dockets described in § 194.67.

(ii) If the revised designation entails more stringent notification and approval requirements (*e.g.*, from Tier 2 to Tier 1, or from undesignated to Tier 2), the change shall become effective immediately and the site shall operate under the more stringent requirements without delay.

(iii) If the revised designated entails less stringent notification and approval requirements, (*e.g.*, from Tier 1 to Tier 2, or from Tier 2 to undesignated), EPA will solicit comments from the public for a minimum of 30 days. The site will continue to operate under the more stringent approval requirements until the public comment period is closed and EPA notifies DOE in writing of the Agency's final decision.

(6) A waste generator site that EPA approved for characterizing and disposing transuranic waste at the WIPP under this section prior to October 14, 2004, may continue characterizing and disposing such waste at the WIPP under paragraph (c) of this section until EPA has conducted a baseline compliance inspection and provided a Baseline Compliance Decision under paragraph (b)(2) of this section.

(i) Until EPA provides a Baseline Compliance Decision for such a site, EPA may approve additional transuranic waste streams for disposal at WIPP under the provisions of paragraph (c) of this section. Prior to the effective date of EPA's Baseline Compliance Decision for such a site, EPA will continue to conduct inspections of the site in accordance with § 194.24(c).

(ii) EPA shall conduct a baseline compliance inspection and issue a Baseline Compliance Decision for such previously approved sites in accordance with the provisions of paragraph (b) of this section, except that the site shall not be required to provide written notification of readiness as described in paragraph (b)(2)(i) of this section.

(c) *Waste characterization programs at waste generator sites with prior approval.* For a waste generator site that EPA approved for characterizing and disposing transuranic waste at the WIPP under this section prior to October 14, 2004, the Agency will determine compliance with the requirements for use of process knowledge and a system of controls at waste generator sites as set in this paragraph (c). Approvals for a site to characterize and dispose of transuranic waste at WIPP will proceed according to this section only until EPA has conducted a baseline compliance inspection and provided a Baseline Compliance Decision for a site under paragraph (b)(2) of this section.

(1) For each waste stream or group of waste streams at a site, the Department must:

(i) Provide information on how process knowledge will be used for waste characterization of the waste stream(s) proposed for disposal at the WIPP; and

(ii) Implement a system of controls at the site, in accordance with § 194.24(c)(4), to confirm that the total amount of each waste component that will be emplaced in the disposal system will not exceed the upper limiting value or fall below the lower limiting value described in the introductory text of § 194.24(c). The implementation of such a system of controls shall include a demonstration that the site has procedures in place for adding data to the WIPP Waste Information System ("WWIS"), and that such information can be transmitted from that site to the WWIS database; and a demonstration that measurement techniques and control methods can be implemented in accordance with § 194.24(c)(4) for the waste stream(s) proposed for disposal at the WIPP.

(2) The Agency will conduct an audit or an inspection of a Department audit for the purpose of evaluating the use of process knowledge and the implementation of a system of controls for each waste stream or group of waste streams at a waste generator site. The Agency will announce a scheduled inspection or audit by the Agency with a notice in the Federal Register. In that or another notice, the Agency will also solicit public comment on the relevant waste characterization program plans and Department documentation, which will be placed in the dockets described in § 194.67. A public comment period of at least 30 days will be allowed.

(3) The Agency's written decision regarding compliance with the requirements for waste characterization programs described in paragraph (b)(1) of this section for one or more waste streams from a waste generator site will be conveyed in a letter from the Administrator's authorized representative to the Department. No such compliance determination shall be granted until after the end of the public comment period described in paragraph (b)(2) of this section. A copy of the Agency's compliance determination letter will be placed in the public dockets in accordance with § 194.67. The results of any inspections or audits conducted by the Agency to evaluate the plans described in paragraph (b)(1) of this section will also be placed in the dockets described in § 194.67.

(4) Subsequent to any positive determination of compliance as described in paragraph (b)(3) of this section, the Agency intends to conduct inspections, in accordance with §§194.21 and 194.24(h), to confirm the continued compliance of the programs approved under paragraphs (b)(2) and (b)(3) of this section. The results of such inspections will be made available to the public through the Agency's public dockets, as described in § 194.67.

[63 FR 27404, May 18, 1998, as amended at 69 FR 42581, July 16, 2004]

8.2 Background

The requirements of 40 CFR § 194.8 (U.S. EPA 2004a) apply to the process used by the U.S. Environmental Protection Agency (EPA) to approve the shipment of transuranic (TRU) waste from U.S. Department of Energy (DOE) waste generator sites to the Waste Isolation Pilot Plant (WIPP) facility for disposal.

The requirements were established at the time of the EPA's 1998 Certification Decision to address compliance of site-specific quality assurance (QA) programs and a system of waste characterization and controls at waste generator sites.

8.3 1998 Certification Decision

In order to clarify its original intent for the compliance criteria regarding approval of site-specific activities, the EPA amended the compliance criteria at 40 CFR Part 194 to include the site-

specific approval process (U.S. EPA 1998, pp. 27404–406). Appendix A of the EPA's Certification Decision contains the requirements for the approval process and four certification-related conditions. Two of the four conditions included in this appendix are related to QA and waste characterization. Condition 2 specifies that no waste generator site other than the Los Alamos National Laboratory (LANL) shall be allowed to ship waste for disposal at the WIPP until the EPA determines that the site has established and executed a QA program in accordance with 40 CFR §§ 194.22(a)(2)(i) (U.S. EPA 1996), 194.14(c)(3) (U.S. EPA 1996), and 194.24(c)(5) (U.S. EPA 2004a) for waste characterization activities and assumptions. Condition 3 specifies that no waste from any additional LANL waste streams (other than the ones already certified) or from any waste generator site other than LANL shall be shipped for disposal at the WIPP until the EPA has approved the process for characterizing those waste streams for shipment using the process set forth in section 194.8. The approval process includes an opportunity for public comment and an inspection (of a DOE audit) or audit of the waste generator site by the EPA. The procedures for demonstrating compliance with Conditions 2 and 3 of the EPA's 1998 Certification Decision were incorporated in the final rule as a new section to section 194.8, "Approval Process for Waste Shipment from Waste Generator Sites for Disposal at the WIPP."

For both QA and waste characterization programs, the approval process includes placement in the docket of site-specific documentation submitted by the DOE, publication of a *Federal Register* notice by the EPA announcing a scheduled inspection or audit, a period of at least 30 days for the public to comment on information placed in the docket, and the EPA's written decision regarding the approval of these programs in the form of a letter from the EPA to the DOE. The EPA proposed to approve QA programs on a site-wide basis and to approve waste characterization measures and controls on the basis of waste streams or, where multiple waste streams may be characterized by the same waste characterization processes and techniques, groups of waste streams.

8.4 Changes in the CRA-2004

A discussion of the requirements for section 194.8 was added to the Compliance Recertification Application of 2004 (CRA-2004) (U.S. DOE 2004, Chapter 4.0). The CRA-2004 notes, "based on EPA acceptance of the site-specific TRU waste characterization and QA program, the Carlsbad Field Office Manager is responsible for granting and revoking the program certification that allows the TRU waste site to characterize and to ship waste to WIPP," but also adds, "consistent with the provisions of section 194.8, EPA also has a role in the approval process. The EPA determines compliance with requirements for site-specific QA programs."

In addition to determining QA compliance, the EPA also approves relevant portions of the waste characterization programs at generator sites to ensure that the system of controls required to track important components is technically adequate.

The CRA-2004 noted that as of September 30, 2002, the following five sites had approved QA and waste characterization programs under section 194.8 requirements: Hanford-Richland (RL), the Idaho National Engineering and Environmental Laboratory (now called the Idaho National Laboratory [INL]), LANL, the Rocky Flats Environmental Technology Site (RFETS), and the Savannah River Site (SRS). Additionally, the DOE's Central Characterization Project (CCP)

had been approved to characterize and ship waste from SRS, Argonne National Laboratory (ANL), and the Nevada Test Site (NTS).

8.5 EPA's Evaluation of Compliance for the 2004 Recertification

The CRA-2004 did not identify instances where waste had been shipped to the WIPP facility from a generator site prior to approval of its waste characterization programs by the EPA before the CRA-2004 cutoff date of September 22, 2002. However, there were instances where waste was shipped before approval of instrumentation or techniques used to characterize that waste by the EPA Compliance Application Review Document (CARD) 8 (U.S. EPA 2006a). In these cases, the DOE discontinued shipment of the waste under investigation until the EPA completed its inspection and approval. The EPA received no public comments on the DOE's continued compliance with the approval process for waste shipment from waste generator sites for disposal at the WIPP facility.

Based on its review and evaluation of the CRA-2004, supplemental information provided by the DOE, and the EPA inspections and audits, the EPA determined that the DOE continued to comply at that time with the requirements of section 194.8 (U.S. EPA 2006b).

8.6 Changes or New Information Between the CRA-2004 and the CRA-2009 (Previously: Changes or New Information Since the 2004 Recertification)

The TRU waste sites approved by the EPA to ship CH-TRU waste to the WIPP facility in accordance with the requirements of section 194.8 were RL, INL/CCP, the Advanced Mixed Waste Treatment Project (AMWTP), SRS/CCP, Oak Ridge National Laboratory (ORNL)/CCP (EPA-ORNL-CCP-CH-11.07-8) (U.S. EPA 2008a), and LANL/CCP.

The TRU waste sites identified in the CRA-2004 that had shipped CH-TRU waste to the WIPP facility but were not currently active were Lawrence Livermore National Laboratory (LLNL), NTS, ANL, and RFETS.

RFETS had completed shipping its TRU waste. LLNL was certified after the CRA-2004 was submitted (EPA-LANL-CCP-5.04-8) (U.S. EPA 2004b). Since the CRA-2004, TRU waste characterization at LANL, SRS, and INL that had previously been performed using site resources was being performed by CCP resources.

On March 26, 2004, the EPA announced its final decision (Marcinowski 2004) to approve the DOE's Remote-Handled TRU Waste Characterization Program Implementation Plan (U.S. DOE 2003a) and (U.S. DOE 2003b). The EPA stated that on-site inspections and approval of site-specific, remote-handled transuranic (RH-TRU) waste characterization programs will be conducted under the authority at section 194.8 or 40 CFR § 194.24, as appropriate. Table 8-1 lists all EPA inspections and tier evaluations at generator sites for the period between the CRA-2004 and CRA-2009.

Table 8-1. EPA Activities Performed Between the CRA-2004 and CRA-2009 at TRU Waste Generator Sites

Site	Activity Performed	Date Performed	Results	References
LANL/CCP	Baseline Inspection	April 2004	Approval was granted in August 2004 for the CCP to characterize and ship CH-TRU waste from LANL	EPA-LANL-CCP-4.04.08 U.S. EPA 2004c
	Baseline Inspection	February 2008	In February 2008, the EPA approved the baseline for RH-TRU Waste Characterization for LANL/CCP	EPA-LANL-CCP-RH-05.07-8 U.S. EPA 2008d
INL/CCP	Baseline Inspection and QA Audit	May 2005	Approval was granted on November 1, 2005, for the CCP to characterize and ship CH-TRU waste from INL	EPA-INL-CCP-05.05-08 U.S. EPA 2004d
	Baseline Inspection	June 2006 and August 2006	Approval of the characterization program was granted on January 12, 2007. The baseline approval designated the initiation of the WWIS for RH-TRU waste as a Tier 1 change	EPA-INL-CCP-RH-6.06-8 U.S. EPA 2007a
	Tier 1 Change Evaluation	January 2008	The EPA approved the Tier 1 change to add K-Cell waste to the RH-TRU Waste Certification for INL/CCP	U.S. EPA 2008b
	Baseline Inspection and QA Audit	May 2005	Approval was granted on November 1, 2005, for the CCP to characterize and ship CH-TRU waste from the INL	EPA-INL-CCP-05.05-08 U.S. EPA 2004d
INL/CCP and ANL/CCP	Inspection	November 2006	The WWIS system was determined to be adequate for RH-TRU waste characterized	Reyes 2007
ANL/CCP	Baseline Inspection and QA Audit	September 2006	The QA program was approved on December 20, 2006, and the characterization program was approved on January 16, 2007. As with INL/CCP, the baseline approval designated the initiation of the WWIS for RH-TRU waste as a Tier 1 change.	EPA-ANL-CCP-RH-09.06-08 Reyes 2006 and U.S. EPA 2007b
	Tier 1 Change Evaluation	July 2008	The EPA approved the Tier 1 change to add newly packaged waste to the RH-TRU Waste Certification for ANL/CCP	U.S. EPA 2008c
SRS-Battelle	Baseline Inspection	July 2007	In August 2008, the EPA approved the baseline for RH-	EPA-SRS-CCP-

Site	Activity Performed	Date Performed	Results	References
Columbus Laboratory (BCL/CCP)			TRU Waste Characterization for BCL/CCP	RH-07.07-8 U.S. EPA 2008e
ORNL/CCP	Baseline Inspection	July 2008	On February 3, 2009, the EPA approved RH-TRU waste characterization for ORNL/CCP	EPA Docket No. A-98-49; II-A4-111

The EPA determined that the DOE continued to comply with the requirements of section 194.8 and there were no outstanding issues with the EPA related to section 194.8.

8.7 EPA's Evaluation of Compliance for the 2009 Recertification

Detailed technical evaluation of the CRA-2009 (U.S. DOE 2009), Section 8, was provided in CARD 8 (U.S. EPA 2010a). The CRA-2009 did not identify instances where waste had been shipped to the WIPP facility from a generator site prior to approval of its waste characterization programs by the EPA before the CRA-2009 cutoff date of December 31, 2007. However, AMWTP and LANL shipped uncertified waste containers to the WIPP facility for disposal during 2007 and 2009, respectively. The QA Specialists at these sites identified errant drums of waste that were mistakenly sent to the WIPP facility. The DOE stopped all TRU waste shipments from these sites to the WIPP facility for disposal until the EPA completed its inspection and concurred with the DOE's decision to resume shipments. The issues associated with errors were ultimately resolved and corrective actions were taken to avoid future occurrences.

The EPA received no public comments on the DOE's continued compliance with the approval process for waste shipment from waste generator sites for disposal at the WIPP facility. Based on a review and evaluation of the CRA-2009, supplemental information provided by the DOE, and EPA inspections and audits, the EPA determined that the DOE continued to comply with the requirements of section 194.8 (U.S. EPA 2010b).

8.8 Changes or New Information Since the CRA-2009

The TRU waste sites approved by the EPA to ship CH-TRU waste to the WIPP facility in accordance with the requirements of section 194.8 since the CRA-2009 are as follows: AMWTP, RL/CCP, INL/CCP, LANL/CCP, ORNL/CCP and SRS/CCP. Since the CRA-2009, suspension of CH-TRU waste characterization activities occurred at ORNL/CCP and RL/CCP

The TRU waste sites approved by the EPA to ship RH-TRU waste to the WIPP facility in accordance with the requirements of section 194.8 since the CRA-2009 are ANL/CCP, Bettis Atomic Power Laboratory (BAPL)/CCP, General Electric Vallecitos Nuclear Center (GEVNC)/CCP, INL/CCP, , ORNL/CCP, and SRS/CCP.Since the CRA-2009, suspension of RH-TRU waste characterization activities has occurred at BAPL/CCP, GEVNC/CCP, RL/CCP, and ORNL/CCP.

Table 8-2 summarizes the EPA waste characterization inspections and tier 1 evaluations at generator sites for the period since the CRA-2009.

Table 8-2. EPA Waste Characterization Inspections/Tier 1 Evaluations Conducted Since the CRA-2009 Application

Site	Inspection/Tier 1 Evaluation	Date Performed	Date Approved	EPA Docket
AMWTP	Tier 1 addition of BN-510 waste stream	March 2, 2010	June 10, 2010	EPA Docket No. A-98-49; II-14-127
	Continued Compliance Inspection	November 17-18, 2010	March 16, 2011	EPA Docket No. A-98-49; II-A4-143
	Continued Compliance Inspection	October 30 to November 1, 2012	Not yet received	Not yet received
ANL/CCP	Tier 1 RH Visual Examination (VE) newly packaged waste	May 28, 2008	July 10, 2008	EPA Docket No. A-98-49; II-A4-102
	Tier 1 addition of 30 containers to Argonne East Remote Handled Debris Mixed (AERHDM) waste stream	May 20-21, 2010	September 13, 2010	EPA Docket No. A-98-49; II-A4-132
	Tier 1 addition of 120 containers to AERHDM waste stream	June 29, 2010	September 28, 2010	EPA Docket No. A-98-49; II-A4-134
	Tier 1 addition of 30-gallon containers of fuel examination waste (FEW) to previously approved RH debris AERHDM waste stream	May 4 and 18, 2010	November 22, 2010	EPA Docket No. A-98-49; II-A4-140
	Tier 1 to add eight 55-gallon K-Wing FEW containers to RH debris waste stream AERHDM	September 2011	February13, 2012	EPA Docket No. A-98-49; II-A4-158
	Tier 1 to evaluate Radiation Characterization Approach of Solidified Liquid Waste from K-Wing, Building 205, 55-gallon	January 3, 2012	June 14, 2012	EPA Docket No. A-98-49; II-A4-162
	Tier 1 for debris from the Reduced Enrichment for Research and Test Reactors program and the second batch of FEW packaged in 30-gallon containers	February – June, 2012	October 4, 2012	EPA Docket No. A-98-49; II-A4-140
	Tier 1 of the Analytical Chemistry Lab (ACL)	July 31-August 1, 2012	September 4, 2012	EPA Docket No. A-98-49; II-A4-165

Site	Inspection/Tier 1 Evaluation	Date Performed	Date Approved	EPA Docket
BAPL/CCP	Baseline Inspection	August 30, 2010, September 23, 2010, December 8, 2010, and April 12-13, 2011	July 28, 2011	EPA Docket No. A-98-49; II-A4-151
GEVNC/CCP	RH Initial Certification	December 2-4, 2008	August 26, 2009	EPA Docket No. A-98-49; II-A4-115
RL/CCP	CH Baseline Inspection	April 27-29, 2010	December 21, 2010	EPA Docket No. A-98-49; II-A4-138
INL/CCP	Tier 1 Waste Area Groups density range extension	June 9, 2008	October 7, 2008	EPA Docket No. A-98-49; II-A4-107
	Tier 1 addition of VE CH S5000 retrievably stored waste stream	December 9-11, 2008	March 4, 2009	EPA Docket No. A-98-49; II-A4-110
	Tier 1 addition of ID-HFEF-S5400-RH Lot 1A and ID-ANLE-S5000 waste streams	December 9-11, 2008	February 1, 2010	EPA Docket No. A-98-49; II-A4-122
	Tier 1 addition of ID-MFC-S5400-RH waste stream	April-May 2010	June 11, 2010	EPA Docket No. A-98-49; II-A4-126
	Tier 1 addition of ID-INTEC-RH waste stream	December 8-9, 2009, January 12-13, 2010, and February 17, 2010	August 17, 2010	EPA Docket No. A-98-49; II-A4-130
	Tier 1 addition of Osprey and ID-HFEF-S5400-RH Lot 1B waste streams	July 13, 2009, to June 2010	August 23, 2010	EPA Docket No. A-98-49; II-A4-131
	Tier 1 High Efficiency Neutron Counter (HENC) operating range extension	July 1, 2009	September 22, 2010	EPA Docket No. A-98-49; II-A4-119
	Tier 1 addition of ID-RTC-S3000 waste stream	September 22, 2009	November 1, 2010	EPA Docket No. A-98-49; II-A4-137
	Tier 1 addition of IN-ID-NRF-153 waste stream	August 9-10, 2010	November 1, 2010	EPA Docket No. A-98-49; II-A4-135
	Continued Compliance Inspection	November 16-17, 2010	March 16, 2011	EPA Docket No. A-98-49; II-A4-142
	Tier 1 to include RH waste stream IN-ID-NRF-SPC	October 4-5, 2011	March 12, 2012	EPA Docket No. A-98-49; II-A4-159
	Tier 1 to include Lot 2 waste ID-ANLE-S5000	May 8-9, 2012	July 25, 2012	EPA Docket No. A-98-49; II-A4-163
LANL/CCP	Initial RH Certification	May 8-10, 2007	February 19, 2008	EPA Docket No. A-98-49; II-A4-96
	Tier 1 HENC2 Report (Non-Approval)	May 25-26, 2010	November 8, 2010	EPA Docket No. A-98-49; II-A4-139
	LANL/CCP CH TRU	May 25-26, 2010	February 9, 2011	EPA Docket No. A-

Site	Inspection/Tier 1 Evaluation	Date Performed	Date Approved	EPA Docket
	Continued Compliance Inspection			98-49; II-A4-141
	CH Tier 1 request expanding the calibration range to the HENC2 to accommodate CH lead-lined 55-gallon drums	April 28, 2010	April 30, 2012	EPA docket No. A-98-49; II-A4-139
	CH Tier 1 request for calibration range extension for the Super High Efficiency Neutron Counter (SuperHENC) and the extendability for the HENC unit 1 to assay lead-lined 55-gallon drums containing solidified materials	June 20-21, 2012	August 14, 2012	EPA Docket No. A-98-49; II-A4-164
	Tier 1 approval to add Summary Category Group S4000	September – November, 2012	December 31, 2012	EPA Docket No. A-98-49; II-A4-168
ORNL/CCP	CH Baseline Inspection	November 2007	August 25, 2008	EPA Docket No. A-98-49; II-A4-103
	Tier 1 CH Calibration Extension for segmented gamma scanner	Unknown	October 8, 2008	EPA Docket No. A-98-49; II-A4-108
	Tier 1 CH Calibration Extension for Drum Waste Assay System Imaging Passive Active Neutron	November 17, 2008	January 8, 2009	EPA Docket No. A-98-49; II-A4-109
	RH Baseline Inspection	June 30-July 2, 2008	February 3, 2009	EPA Docket No. A-98-49; II-A4-111
	Tier 1 OR-REDC-RH-HET to include Solvent Extraction Test Facility Time Period (November 1978-November 1991) waste	May 6, 2009	November 30, 2009	EPA Docket No. A-98-49; II-A4-120
	Tier 1 addition of CH Summary Category Group S4000 waste	August 11-12, 2009	October 7, 2009	EPA Docket No. A-98-49; II-A4-117
	Tier 1 addition of CH VE and adding the IQ3	February 23-24, 2010	March 30, 2010	EPA Docket No. A-98-49; II-A4-125
	Tier 1 addition of RH Solvent Extraction Test Facility Pre-79 waste stream	February-March, 2010	April 21, 2010	EPA Docket No. A-98-49; II-A4-124
SNL/CCP	Tier 1 to include RH containers generated from waste groups PKE00027/54 and PKE00047 in existing waste stream SNL-HCF-S5400-RH	December 2011 to January 2012	March 28, 2012	EPA Docket No. A-98-49; II-A4-160
SRS/CCP	Tier 1 addition of SRS Battelle Columbus Laboratory waste stream SR-RL-BCLDP.001	July 17-19, 2007, July 31-August 2, 2007, and December 4-5,	August 25, 2008	EPA Docket No. A-98-49; II-A4-104

Site	Inspection/Tier 1 Evaluation	Date Performed	Date Approved	EPA Docket
		2007		
	Tier 1 addition of Nondestructive Assay Box Counter (NABC)	March 24-26, 2009	August 4, 2009	EPA Docket No. A-98-49; II-A4-114
	Tier 1 addition of CH S3000 waste	September 30, 2010	March 23, 2010	EPA Docket No. A-98-49; II-A4-123
	Tier 1 addition of SR-BCLDP.001.001, SR-BCLDP.001.002, SR-BCLDP.002, SR-BCLDP.003, SR-BCLDP.004.002, SR-BCLDP.004.003 waste streams	November 2009 – March 2010	September 13, 2010	EPA Docket No. A-98-49; II-A4-129
	Tier 1 extension of calibration to the NABC	March 24-26, 2009	September 14, 2010	EPA Docket No. A-98-49; II-A4-133
	Tier 1 allowing use of American Society for Testing and Materials standard efficiency calibration method for NABC	May 12, 2011 timeframe	May 31, 2011	EPA Docket No. A-98-49; II-A4-148
	RH Baseline Inspection	July 26, 2011	April 18, 2012	EPA Docket No. A-98-49; II-A4-161
	Tier 1 request for using 5-foot setback configuration for the NABC	August 14-15, 2012	September 11, 2012	EPA Docket No. A-98-49; II-A4-166

Other EPA approvals, including Tier 1 and 2 changes, and other decisions since the CRA-2009 are summarized in Table 8-3.

Table 8-3. Other EPA Approvals and Decisions Since the CRA-2009 Application

Site	Implementing Document or Changed Activity	Description of Change (Approval Not Required for Tier 2)	Date Approved	EPA Docket
ANL/CCP	Tier 1 Request	Approval of request for the addition of the K-Wing solidified liquid waste to the RH waste stream AERHDM at ANL	June 14, 2012	EPA Docket No. A-98-49; II-A4-162
	Tier 1 Request	Approval of the RH AERHDM K-Wing FEW waste	February 13, 2012	EPA Docket No. A-98-49; II-A4-158
	Evaluation	Evaluation of the ACL located at ANL resulted in numerous technical deficiencies identified, and the EPA informed the DOE that no data generated by the ACL after July 31, 2012, can be used by ANL/CCP to characterize WIPP-destined TRU waste until deficiencies are addressed and ACL receives EPA approval	September 4, 2012	EPA Docket No. A-98-49; II-A4-165
	Tier 1 Request	Approval to add two RH debris types to the AERHDM waste stream	October 4, 2012	EPA Docket No. A-98-49; II-A4-167
RL/CCP	Tier 1 Request	Approval of waste stream RLCCPPUNIT	November 10, 2011	EPA Docket No. A-98-49; II-A4-154
INL/CCP		Confirmation that INL/CCP characterization of Small Quantity Site waste from Nuclear Radiation Development is consistent with the conditions and limitations set forth in the EPA's baseline approval and subsequent Tier 1 changes	January 4, 2012	EPA Docket No. A-98-49; II-A4-157
	Tier 1 Request	Approval for disposal at the WIPP of the "RH TRU" waste stream IN-ID-NRF-SPC	March 12, 2012	EPA Docket No. A-98-49; II-A4-159
	Tier 1 Request	Approval of Tier 1 request to add Lot 2 waste to the "RH TRU" waste stream ID-ANLE-S5000	July 25, 2012	EPA Docket No. A-98-49; II-A4-163
LANL/CCP	Tier 1 Request	Approval of two Tier 1 requests: (1) extension of the gamma density range of the HENC No. 1 non-	August 14, 2012	EPA Docket No. A-98-49; II-A4-164

Site	Implementing Document or Changed Activity	Description of Change (Approval Not Required for Tier 2)	Date Approved	EPA Docket
		destructive analysis, and (2) extension of the gamma density range of the SuperHENC		
	Tier 1 Request	Approval of the addition of Summary Category Group S4000 to the baseline approval of LANL/CCP	December 31, 2012	EPA Docket No. A-98-49; II-A4-168
SNL/CCP	Baseline Inspection	Determination that the RH debris waste stream SNL-HCF-S5400-RH waste characterization program was adequate for: (1) the Acceptable Knowledge process for 19 containers of group PKE00044, and (2) the radiological characterization process in CCP-AK-SNL-501, revision 1	November 23, 2011	EPA Docket No. A-98-49; II-A4-155
	Baseline Inspection	Approval to add containers generated from waste groups PKE00027/54 and PKE00047 to waste stream SNL-HCF-S5400-RH	March 28, 2012	EPA Docket No. A-98-49; II-A4-160
SRS/CCP	Tier 1 Request	Approval of request for a 5-foot setback configuration (55-gallon drums only) for the NABC	September 11, 2012	EPA Docket No. A-98-49; II-A4-166
AMWTP and CCP activities at ANL, RL, INL, LANL, ORNL and SRS	Fiscal Year (FY) 11 Quarterly Tier 2 reports, second quarter	Concurrence of FY11 second quarter Tier 2 changes at AMWTP and CCP	July 5, 2011	N/A
	FY11 Quarterly Tier 2 reports, third quarter	The EPA did not object to any of the Tier 2 changes for the third quarter of FY11	November 9, 2011	N/A
	FY12 Quarterly Tier 2 reports, first quarter	The EPA did not object to any of the Tier 2 changes for AMWTP and CCP reported for the first quarter of FY12	March 28, 2012	N/A
	FY12 Quarterly Tier 2 reports, second quarter	The EPA did not object to any of the Tier 2 changes reported for the second quarter of FY12	June 4, 2012	N/A
WIPP	Annual WIPP Inspection	Determination that WIPP activities related to emissions monitoring	November 23, 2011	EPA Docket No. A-98-49; II-B3-116

Site	Implementing Document or Changed Activity	Description of Change (Approval Not Required for Tier 2)	Date Approved	EPA Docket
		during waste management and storage, monitoring of the ten parameters for long-term containment and waste emplacement were adequate and compliant with 40 CFR Part 191, Subpart A and the 1998 Certification Decision		
WIPP	Planned Change Request, Planned Change Notice	Conditional approval of the shielded container planned change request for "RH TRU" waste inventory disposal	August 8, 2011	EPA Docket No. A-98-49, II-B3-117
CBFO	Quality Assurance Audit	EPA audits determined that the Carlsbad Field Office QA Program continues to be properly executed and did not find any nonconformance with NQA-1-1989	April 9, 2012	EPA Docket No. A-98-49; II-A1-110
CBFO	RH TRU Waste Characterization Program Implementation Plan	Approval of the "RH-TRU" Waste Characterization Program Implementation Plan, DOE/WIPP-02-3214, Revision 3, Draft E, with exceptions	September 4, 2012	Peak 2012

The DOE continues to comply with the requirements of section 194.8 and there are no outstanding issues with the EPA related to section 194.8.

8.9 References

(*Indicates a reference that has not been previously submitted.)

Marcinowski, F. 2004. Letter (with attachments) to R. Paul Detwiler. 26 March 2004. Washington, DC: U.S. Environmental Protection Agency, Office of Air and Radiation.

Peak, T. 2012. Letter to Jose R. Franco, Manager. 4 September 2012. Washington, DC: U.S. Environmental Protection Agency, Office of Air and Radiation.*

Reyes, J. 2006. Memorandum to Dr. David Moody, Manager. 20 December 2006. Washington, DC: U.S. Environmental Protection Agency, Office of Air and Radiation.

Reyes, J. 2007. Memorandum to David Moody, Ph.D., Manager. 17 January 2007. Washington, DC: U.S. Environmental Protection Agency, Office of Air and Radiation.

U.S. Department of Energy (DOE). 2003a. *Remote-Handled TRU Waste Characterization Program Implementation Plan* (Revision 0D, October 30). DOE/WIPP 02-3214. Carlsbad, NM: Carlsbad Field Office.

U.S. Department of Energy (DOE). 2003b. *Notification of Planned Change to the EPA 40 CFR Part 194 Certification of the Waste Isolation Pilot Plant: Remote-Handled TRU Waste Characterization Plan* (April 30). Carlsbad, NM: Carlsbad Field Office.

U.S. Department of Energy (DOE). 2004. *Title 40 CFR Part 191 Compliance Recertification Application for the Waste Isolation Pilot Plant* (March). 10 vols. DOE/WIPP 2004-3231. Carlsbad, NM: Carlsbad Field Office.

U.S. Department of Energy (DOE). 2009. *Title 40 CFR Part 191 Compliance Recertification Application for Waste Isolation Pilot Plant* (March). DOE/WIPP 2009-3423, Carlsbad, NM: Carlsbad Field Office.*

U.S. Environmental Protection Agency (EPA). 1996. "40 CFR Part 194: Criteria for the Certification and Recertification of the Waste Isolation Pilot Plant's Compliance with the 40 CFR Part 191 Disposal Regulations; Final Rule." *Federal Register*, vol. 61 (February 9, 1996): 52234–45.

U.S. Environmental Protection Agency (EPA). 1998. "40 CFR Part 194: Criteria for the Certification and Recertification of the Waste Isolation Pilot Plant's Compliance with the Disposal Regulations: Certification Decision; Final Rule." *Federal Register*, vol. 63 (May 18, 1998): 27353–406.

U.S. Environmental Protection Agency (EPA). 2004a. "40 CFR Part 194: Criteria for the Certification and Recertification of the Waste Isolation Pilot Plant's Compliance with the Disposal Regulations; Alternative Provisions" (Final Rule). *Federal Register*, vol. 69 (July 16, 2004): 42571–583.

U.S. Environmental Protection Agency (EPA). 2004b. *Waste Characterization Inspection Report: EPA Inspection No. EPA-LLNL-CCP-05.04-8 of the Central Characterization Project (CCP) as Implemented at the Lawrence Livermore National Laboratory (LLNL) Site May 4–7, 2004* (August). Washington, DC: Office of Radiation and Indoor Air.

U.S. Environmental Protection Agency (EPA). 2004c. *EPA Inspection No. EPA-LANL-CCP-4.04-08 of the Central Characterization Project (CCP) as Implemented at the Los Alamos National Laboratory, April 26–April 30, 2004* (August). Waste Characterization Inspection Report. Washington, DC: Office of Radiation and Indoor Air.

U.S. Environmental Protection Agency (EPA). 2004d. *EPA Inspection No. EPA-INL-CCP-05.05-08 of the Central Characterization Project (CCP) as Implemented at the Idaho National Laboratory, May 3 – 5, 2005.* Washington, DC: Office of Radiation and Indoor Air.

U.S. Environmental Protection Agency (EPA). 2006a. "Recertification CARD No. 8: Approval Process for Waste Shipment from Waste Generator Sites for Disposal at the WIPP." *Compliance Application Review Documents for the Criteria for the Certification and Recertification of the Waste Isolation Pilot Plant's Compliance with the 40 CFR Part 191 Disposal Regulations: Final Recertification Decision* (March) (pp. 8-1 through 8-10). Washington, DC: Office of Radiation and Indoor Air.

U.S. Environmental Protection Agency (EPA). 2006b. "40 CFR Part 194: Criteria for the Certification and Recertification of the Waste Isolation Pilot Plant's Compliance with the Disposal Regulations: Recertification Decision" (Final Notice). *Federal Register*, vol. 71 (April 10, 2006): 18010–021.

U.S. Environmental Protection Agency (EPA). 2007a. *Waste Characterization Inspection Report: EPA Baseline Inspection No. EPA-INLl-CCP-RH-6.06-8 of the Central Characterization Project Remote-Handled Transuranic Waste Characterization Program at the Idaho National Laboratory June 12–16, and August 9 and 29, 2006* (January). Washington, DC: Office of Radiation and Indoor Air.

U.S. Environmental Protection Agency (EPA). 2007b. *Waste Characterization Inspection Report EPA Baseline Inspection No. EPA-ANL-CCP-RH-9.06-8 of the Central Characterization Project Remote-Handled Transuranic Waste Characterization Program at the Argonne National Laboratory September 12–14, 2006* (January). Washington, DC: Office of Radiation and Indoor Air.

U.S. Environmental Protection Agency (EPA). 2008a. *Waste Characterization Inspection Report and Approval: EPA Baseline Inspection No. EPA-ORNL-CCP-CH-11.07-8 of the Central Characterization Project Waste Characterization Program at the Oak Ridge National Laboratory November 13–15, 2007* (August). Washington, DC: Office of Radiation and Indoor Air.

U.S. Environmental Protection Agency (EPA). 2008b. *Waste Characterization Report: Tier 1 Change: Evaluation of the Modification of the Central Characterization's Remote Handled TRU Waste Characterization Program at the Idaho National Laboratory to Add Containers of K-Cell Waste to Waste Stream ID-ANLE-S5000* (January). Washington, DC: Office of Radiation and Indoor Air.

U.S. Environmental Protection Agency (EPA). 2008c. *Waste Characterization Report: Tier 1 Change Evaluation: New Process for Visual Examination for Newly-Packaged Waste at the Central Characterization Program's Remote-Handled TRU Waste at Argonne National Laboratory May 28, 2008* (June). Washington, DC: Office of Radiation and Indoor Air.

U.S. Environmental Protection Agency (EPA). 2008d. *EPA Baseline Inspection No. EPA-LANL-CCP-RH-5.07-8 of the Central Characterization Project: Remote-Handled Transuranic Waste Characterization Program at the Los Alamos National Laboratory, May 8–10, 2007* (February). Waste Characterization Inspection Report. Washington, DC: Office of Radiation and Indoor Air.

U.S. Environmental Protection Agency (EPA). 2008e. *Waste Characterization Inspection Report: EPA Baseline Inspection No. EPA-SRS-CCP-RH-7.07-8 of the Central Characterization Project Remote-Handled Transuranic Waste Characterization Program for Battelle Columbus Laboratories Decommissioning Project Wastes Stored at the Savannah River Site July–December 2007* (August). Washington, DC: Office of Radiation and Indoor Air.

U.S. Environmental Protection Agency (EPA). 2010a. "2009 Compliance Recertification Application (CRA-2009) Compliance Application Review Document (CARD) No. 8, "Approval Process for Waste Shipment From Waste Generator Sites for Disposal at the WIPP." EPA Docket FDMS Docket ID No. EPA-HQ-OAR-2009-0330-0031. Washington, DC: Office of Radiation and Indoor Air.*

U.S. Environmental Protection Agency (EPA). 2010b. "40 CFR Part 194: Criteria for the Certification and Recertification of the Waste Isolation Pilot Plant's Compliance with the Disposal Regulations: Recertification Decision; Final Rule." *Federal Register*, vol. 75 (November 18, 2010): 70584-595.*

Title 40 CFR Part 191
Subparts B and C
Compliance Recertification Application 2014
for the
Waste Isolation Pilot Plant

Content of Compliance
Recertification Application(s)
(40 CFR § 194.15)

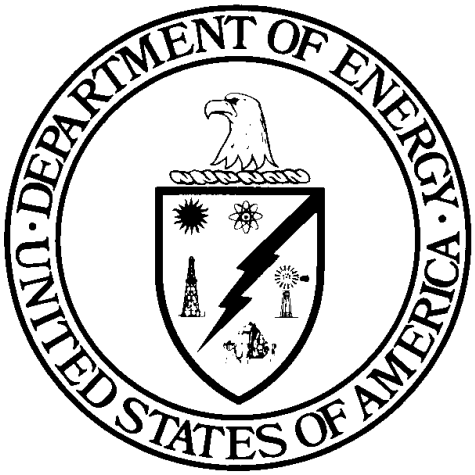

United States Department of Energy
Waste Isolation Pilot Plant

Carlsbad Field Office
Carlsbad, New Mexico

Compliance Recertification Application 2014
Content of Compliance Recertification Application(s) (40 CFR § 194.15)

Table of Contents

List of Figures

List of Tables

Acronyms and Abbreviations

ASER	Annual Site Environmental Report
ATWIR	Annual Transuranic Waste Inventory Report
CARD	Compliance Application Review Document
CCA	Compliance Certification Application
CFR	Code of Federal Regulations
CH	contact-handled
COMP	compliance monitoring parameter
CRA	Compliance Recertification Application
DM	dark matter
DOE	U.S. Department of Energy
EPA	U.S. Environmental Protection Agency
EXO	Enriched Xenon Observatory
ft	foot/feet
km	kilometer
LBRE	Low Background Radiation Experiment
LWA	Land Withdrawal Act
m	meter(s)
MEGA	Multiple Element Germanium Array
mi	mile
PA	performance assessment
PCN	Planned Change Notice
PCR	Planned Change Request
RH	remote-handled
SEGA	Segmented Enriched Germanium Assembly
SDDI	Salt Defense Disposal Investigations
SDI	Salt Disposal Investigations
TPC	Time Projection Chamber
TRU	transuranic
WIPP	Waste Isolation Pilot Plant

Elements and Chemical Compounds

Am	americium
MgO	magnesium oxide
Nd	neodymium
Pu	plutonium
U	uranium

15.0 Content of Compliance Recertification Application(s) (40 CFR § 194.15)

15.1 Requirements

§ 194.15 Content of Compliance Recertification Application(s)

(a) In submitting documentation of continued compliance pursuant to section 8(f) of the WIPP LWA, the previous compliance application shall be updated to provide sufficient information for the Administrator to determine whether or not the WIPP continues to be in compliance with the disposal regulations. Updated documentation shall include:

(1) All additional geologic, geophysical, geochemical, hydrologic, and meteorological information;

(2) All additional monitoring data, analyses and results;

(3) All additional analyses and results of laboratory experiments conducted by the Department or its contractors as part of the WIPP program;

(4) An identification of any activities or assumptions that deviate from the most recent compliance application;

(5) A description of all waste emplaced in the disposal systems since the most recent compliance certification or re-certification application. Such description shall consist of a description of the waste characteristics and waste components identified in § 194.24(b)(1) and § 194.24(b)(2);

(6) Any significant information not previously included in a compliance certification or re-certification application related to whether the disposal system continues to be in compliance with the disposal regulations; and

(7) Any additional information requested by the Administrator or the Administrator's authorized representative.

(b) To the extent that information required for a re-certification of compliance remains valid and has been submitted in previous certification or re-certification applications(s), such information need not be duplicated in subsequent applications; such information may be summarized and referenced.

15.2 Background

Information documented in each Compliance Recertification Application (CRA) is prescribed in 40 CFR § 194.15 (U.S. EPA 1996). These documentation requirements parallel the requirements of 40 CFR § 194.14 (U.S. EPA 1996), which apply to the original application, the Compliance Certification Application (CCA) (U.S. DOE 1996). The focus of section 194.15 is to ensure that each CRA includes documentation regarding any changes to the disposal system that may have occurred since the previous certification or recertification. Updated information regarding relevant aspects of the waste and the disposal system is documented. However, in cases where information and assumptions have not changed, no new information needs to be documented; a CRA may reference or summarize such unchanged information.

Each CRA must identify relevant systems and program changes implemented during the preceding five-year period. Any activity or assumption that deviates from what was described in the most recent recertification application would be considered a change. Each CRA also documents changes reviewed and approved by the U.S. Environmental Protection Agency (EPA) in the preceding five-year period (through modification of the certification or other processes). Each CRA documents instances where new baseline program elements were established as a result of changes.

15.3 1998 Certification Decision

The CCA, Chapters 2.0 and 3.0 and Appendices GCR, HYDRO, and MASS, include general information about the Waste Isolation Pilot Plant (WIPP) site and disposal system design and specifically support section 194.14. Other site characteristics, design, location, and construction information is primarily provided in the CCA, Chapter 7.0 and Appendices BACK, DEL, PCS, and SEAL, which also specifically support section 194.14. All other chapters and appendices of the CCA are not specifically relevant to section 194.14. After its review, the EPA concluded that the U.S. Department of Energy (DOE) adequately addressed the geology, geophysics, hydrogeology, hydrology, meteorology, climatology, and effects of waste and geochemistry of the disposal system and its vicinity, and how these conditions are expected to change and interact over the regulatory time frame (Compliance Application Review Document [CARD] 14, U.S. EPA 1998a). The EPA reviewed the DOE's CCA and additional information submitted by the DOE and determined that the DOE complied with each of the criteria of section 194.14. A complete description of the EPA's 1998 Certification Decision for section 194.14 can be found in U.S. EPA 1998b, as well as CARD 14 (U.S. EPA 1998a).

15.4 Changes in the CRA-2004

Baseline documentation for section 194.14 was established at the time of the original EPA certification. Information on changes to section 194.14 topics that occurred since the original certification is required to be documented by section 194.15. Changes that occurred during the five-year period following the original certification are documented in the CRA-2004 (U.S. DOE 2004), which was submitted by the DOE and reviewed by the EPA under the requirements of section 194.15.

During public review of the CRA-2004, the EPA received comments regarding karst features, vertical fracturing, and transport through the Magenta Dolomite Member. The EPA assessed these comments and concluded that the DOE has demonstrated continued compliance. The EPA responses to comments on the CRA-2004 are documented in CARD 14/15, Appendix 15-A (U.S. EPA 2006a).

15.5 EPA's Evaluation of Compliance for the 2004 Recertification

Based on a review and evaluation of the CRA-2004 and supplemental information provided by the DOE (available for review in EPA Docket A-98-49), the EPA determined that the DOE continued to comply with the disposal standards (U.S. EPA 2006b).

15.6 Changes or New Information Between the CRA-2004 and the CRA-2009 (Previously: Changes or New Information Since the 2004 Recertification)

Baseline documentation for section 194.14 was established at the time of the original EPA certification. Information on changes to section 194.14 topics that occurred since the CCA was documented in the CRA-2004 (U.S. DOE 2004). Changes that occurred during the five-year period following the CRA-2004 were documented in Section 15 of the CRA-2009 (U.S. DOE

2009a), which was submitted by the DOE and reviewed by the EPA under the requirements of 40 CFR 194.15.

The EPA provided opportunities for public comment throughout the recertification process. Public comments received during the CRA-2009 public comment period, along with the EPA's responses, are documented in CARD 14/15, Appendix 15-C (U.S. EPA 2010a). The EPA responses to hydrologic comments are documented in CARD 14/15, Appendix 15-B (U.S. EPA 2010a).

15.7 EPA's Evaluation of Compliance for the 2009 Recertification

Based on a review and evaluation of the CRA-2009 and supplemental information provided by the DOE (available for review in Federal Document Management System Docket ID No EPA-HQ-OAR-2009-0330, Air Docket A-98-49) the EPA determined that the DOE continued to comply with the disposal standards (U.S. EPA 2010b). The EPA assessed all of the public comments received and concluded that the DOE demonstrated continued compliance.

15.8 Changes or New Information Since the CRA-2009

To document that the WIPP continues to comply with the disposal standards in each five-year recertification cycle, changes and new information and their impacts on compliance since the previous recertification must be described. Changes and new information since the CRA-2009 related to 40 CFR 194.15 are either described below, or references are provided to other sections or appendices of the CRA-2014 that provide the necessary information.

Much of the information provided in this section was obtained from routinely published reports. Table 15-1 lists these reports and summarizes the type of information contained in each report. The specific reports referenced in Table 15-1 are the latest annual or biennial versions submitted to the EPA or published for the EPA's review before this CRA's cutoff date of December 31, 2012.

Table 15-1. Routine Reports

Description	Summary	Frequency	Reference[a]
WIPP Annual Site Environmental Report (ASER)	Describes compliance status with applicable environmental laws and regulations and environmental monitoring performed during the year at the WIPP. Highlights any significant monitoring results or findings.	Annual	U.S. DOE 2012a
Geotechnical Analysis Report	Reports data related to the geotechnical performance of the various underground facility components, including the shafts, shaft stations, access drifts, and waste disposal areas. Volume 1 describes the overall program; Volume 2 provides a compilation of the collected data.	Annual	U.S. DOE 2012b
Annual Change Report	Provides information each year on any change in conditions or activities related to the disposal system, as required by 40 CFR § 194.4(b)(4)[b]. The majority of the items reported are inspections, reports, and modifications to written plans and procedures. In addition, the Annual Change Report provides updates on waste volumes of several parameters and radionuclides upon which the EPA imposes limits.	Annual	U.S. DOE 2012c
Delaware Basin Monitoring Annual Report	Lists changes in drilling including rates for shallow and deep drilling; pipeline activity; borehole plugging; injection wells; potash, sulfur, and solution mining; and any other new activity related primarily to human intrusion. This report generates data needed to demonstrate compliance with 40 CFR 194.33.	Annual	U.S. DOE 2012d
Compliance Monitoring Parameter (COMP) Assessment	The DOE uses Performance Assessment (PA) to simulate the expected long-term performance of the WIPP. COMPs are used to indicate conditions that are not within expected PA data ranges or conceptual model assumptions, and to alert the project to unexpected conditions. These assessments, in part, demonstrate compliance with 40 CFR 194.42 monitoring requirements. Examples of COMPs include waste activity, changes in groundwater conditions, and creep closure rate.	Annual	Sandia National Laboratories 2012
WIPP Subsidence Monument Leveling Survey	Includes determination of the elevation of each of the existing subsidence monuments and the WIPP baseline survey, and of the National Geodetic Survey's vertical control points.	Annual	U.S. DOE 2012e
Annual Transuranic Waste Inventory Report (ATWIR)	Documents the total inventory (stored and projected) of transuranic (TRU) waste as defined by the TRU waste sites to provide current TRU waste inventory information.	Annual	U.S. DOE 2012f
WIPP Biennial Environmental Compliance Report	As required by the WIPP Land Withdrawal Act (LWA), this document reports the status of the project's compliance with a variety of environmental protection laws and regulations.	Biennial	U.S. DOE 2012g

[a]The entry in this column is the most recent report available.
[b]U.S. EPA 1996

1

15.8.1 40 CFR § 194.15(a)(1)

40 CFR § 194.15(a)(1) requires the submittal of "all additional geologic, geophysical, geochemical, hydrologic, and meteorological information." Information related to this requirement is provided in Sections 15.8.1.1 through 15.8.1.5.

15.8.1.1 Geologic Information

Since the preparation of the CRA-2009, no new geologic mapping has been reported and no new WIPP monitoring wells have been drilled at new locations. Existing WIPP monitoring wells in deteriorated condition have been replaced and/or plugged and abandoned, as discussed in Appendix HYDRO-2014. The information collected during drilling of replacement wells did not provide new geologic information. In 2011, two exploratory potash boreholes were drilled by The Mosaic Company in township 22S range 31E sections 9 and 10 immediately north of the WIPP Land Withdrawal Boundary. The cuttings and geophysical logs collected from these boreholes (MOS-20 and MOS-21) confirmed the stratigraphy of the geologic units above the Salado Formation, as observed in nearby monitoring wells.

15.8.1.2 Geophysical Information

As described in Appendix SCR-2014, the DOE continues to screen out the impacts of all tectonic-, magmatic-, and structural-related geophysical processes on the basis of probability and/or consequence. Tectonic activity was used as the siting criterion and for the purposes of determining seismic design parameters for the facility. The intent was to avoid tectonic conditions such as faulting and igneous activity that would jeopardize waste isolation over the long term and to avoid areas where earthquake size and frequency could impact facility design and operations.

The purpose of continued monitoring of seismic activity is to maintain a database from which to trend ground motions that the WIPP repository may be subjected to in the near and distant future. The concern about seismic effects in the near future, i.e., during the operational period, pertains mainly to the design requirements for surface and underground structures for providing containment during seismic events. The concern about effects occurring over the long term, after the repository has been decommissioned and sealed, pertains more to relative motions (faulting) within the repository and possible effects of faulting on the integrity of the salt beds and/or shaft seals.

During the CRA-2014 monitoring period (October 2007 through December 2012) there were 543 seismic events recorded within approximately 300 kilometers (km) (187 miles (mi)) of the WIPP site. One notable seismic event occurred on March 18, 2012, with a magnitude of 2.4, as recorded by the WIPP's seismic array. This seismic event was associated with a potash mine roof fall that caused cracks and subsidence on the surface. This seismic event occurred 14 km (9 mi) from the WIPP site, and caused no observable damage at the WIPP.

The Delaware Basin Drilling Surveillance Program collects seismic information on areas within and outside of the Delaware Basin (defined in 40 CFR 194.2). However, only the Delaware Basin is used as the defining area for data collection and input into PAs. Recorded events that

have occurred within the Delaware Basin between 1971 and December 2012 are listed in Table 15-2, Seismic Events in the Delaware Basin.

Earthquake catalogs are usually divided into categories according to the magnitude registered for each event. Most catalogs have a section detailing seismic events with a magnitude greater than 3.0 because this is the point at which most seismic events can be felt. Below the magnitude of 3.0, most events are very seldom or barely felt. Only 62 seismic events have been reported with a magnitude greater than 3.0 within 300 km (187 mi) of the WIPP site. Of these 62 events, only four have occurred in the Delaware Basin. The closest seismic event with a magnitude of 3.2 occurred on October 19, 1997, 14 km (9 mi) from the WIPP site, and was the result of a roof fall in one of the local potash mines.

Table 15-2. Seismic Events in the Delaware Basin*

County	No. of Events	Earliest Event	Latest Event	Smallest Magnitude	Largest Magnitude
Culberson	15	10/27/1992	06/28/2007	1.1	2.4
Eddy	19	11/28/1975	03/18/2012	-1.3	3.7
Lea	1	06/23/1993	06/23/1993	2.1	2.1
Loving	3	02/04/1976	04/28/1997	1.1	1.6
Pecos	19	01/30/1975	03/10/2010	1.0	2.6
Reeves	21	02/19/1976	10/09/2012	0.6	2.4
Ward	50	09/03/1976	07/01/2009	0.3	2.8
Winkler	9	09/24/1971	10/19/2007	0.0	3.0

Key:
Magnitude
Less than 2 Very seldom felt
2.0 to 3.4 Barely felt
3.5 to 4.2 Felt as a rumble
4.3 to 4.9 Shakes furniture; objects may fall and break
5.0 to 5.9 Dislodges heavy objects; cracks walls
6.0 to 6.9 Considerable damage to buildings
7.0 to 7.3 Major damage to buildings; breaks underground pipes
7.4 to 7.9 Great damage; destroys masonry and frame buildings
Above 8.0 Complete destruction; ground moves in waves
*Source: seismic events for calendar years 1990 through 2012 compiled from (U.S. DOE 2008a; U.S. DOE 2009b; U.S. DOE 2010a; U.S. DOE 2011a; U.S. DOE 2012d).

15.8.1.3 Geochemical Information

New hydrogeochemical information has been collected and summarized since the CRA-2009. This new information is described in detail by Domski et al. (Domski et al.2011) and in Appendix HYDRO-2014. Groundwater sampling for the geochemical evaluation has been performed in replacement wells and selected older wells. The last major geochemical evaluation of the Culebra Dolomite Member groundwater was performed by Domski and Beauheim (Domski and Beauheim 2008) based on samples from 59 wells. The more recent Culebra analyses in Domski et al. (Domski et al.2011) are an update of Domski and Beauheim (Domski and Beauheim 2008). Domski et al. (Domski et al.2011) provides some updated Culebra

information, confirming the distribution of Culebra geochemical facies, and primarily contains geochemical analysis for the other hydrologic units above the Salado Formation present near the WIPP site. The spatial distribution of these facies is consistent with the locations of the Rustler Formation halite margins, the distribution of transmissivity in the Culebra, and the areas of known or suspected recharge to the Culebra.

15.8.1.4 Hydrologic Information

No new monitoring well locations have been added to the WIPP monitoring network since the CRA-2009, but several old monitoring wells have either been plugged and abandoned or plugged, abandoned and replaced. Updated hydrologic data and well construction and replacement information are provided in Appendix HYDRO-2014. Appendix HYDRO-2014 describes the new information collected since 2007; a brief summary is provided below.

The Culebra monitoring network optimization study was revised (Kuhlman 2010) to identify locations where new Culebra monitoring wells would be of greatest value and to identify wells that could be removed from the network with little loss of information. Details are provided in Appendix HYDRO-2014, Section 9.0.

The WIPP groundwater monitoring program has continued monthly water-level measurements with continuous (nominally hourly) fluid-pressure measurements using downhole pressure gauges in all Culebra wells except for the Water Quality Sampling Program wells. Continuous monitoring now also includes Magenta, Bell Canyon Formation, and Santa Rosa Formation/Dewey Lake Redbeds Formation wells. The high-frequency monitoring network continues to provide information about the temporal fluctuations of water levels in the Culebra, due to both natural and human-caused events. Details regarding the WIPP groundwater monitoring activities are described in Appendix HYDRO-2014, Section 7.0.

15.8.1.5 Meteorological Information

The Meteorological Monitoring Program measures atmospheric data for the WIPP site. This section provides a brief description of the program and updated meteorological data covering the years 2007 through 2011. No anomalous weather events or changes in climatic conditions occurred during that time period. Information related to recent meteorological conditions is provided below.

The annual average, maximum, and minimum temperatures from 1990 through 2011 are listed in Table 15-3.

1 **Table 15-3. Annual Average, Maximum, and Minimum Temperatures***

Year	Annual Average Temperature		Maximum Temperature		Minimum Temperature	
	(ºC)	(ºF)	(ºC)	(ºF)	(ºC)	(ºF)
1990	17.8	64.0	46.1	115.0	-13.9	7.0
1991	17.2	63.0	42.8	109.0	-7.8	18.0
1992	17.2	63.0	42.8	109.0	-10.0	14.0
1993	17.8	64.0	42.8	109.0	-18.9	-2.0
1994	17.8	64.0	50.0	122.0	-14.4	6.0
1995	17.0	63.0	42.0	107.0	-7.0	19.0
1996	17.0	63.0	41.0	106.0	-7.0	19.0
1997	16.3	61.4	38.6	101.5	-11.4	11.4
1998	18.3	64.9	41.6	106.9	-10.8	12.6
1999	18.1	64.6	40.9	105.6	-7.9	17.8
2000	17.4	63.3	40.2	104.4	-6.8	19.7
2001	17.5	63.5	39.5	103.2	-7.8	18.0
2002	17.2	62.3	40.8	105.5	-10.4	13.3
2003	18.1	64.6	39.2	102.7	-9.1	15.6
2004	16.8	62.2	38.6	101.5	-12.0	10.4
2005	16.8	62.2	39.8	103.6	-13.0	8.6
2006	18.3	65.0	39.6	103.3	-6.0	21.1
2007	17.0	62.7	38.8	101.9	-6.9	19.6
2008	17.7	63.8	40.6	105.0	-8.6	16.6
2009	17.7	63.8	38.1	100.6	-6.1	21.1
2010	17.3	63.2	41.3	106.3	-8.0	17.7
2011	18.9	66.0	41.7	107.0	-16.6	2.1
Average	17.5	63.5	41.2	106.2	-10.0	13.9

*Source: monthly average based on meteorological data in the WIPP Met database from the WIPP Meteorological Station, 10 meters above the ground.

2

Monthly average, maximum, and minimum precipitation data recorded at the WIPP site from 1990 through 2011 are provided in Figure 15-1. Data are from the WIPP ASERs.

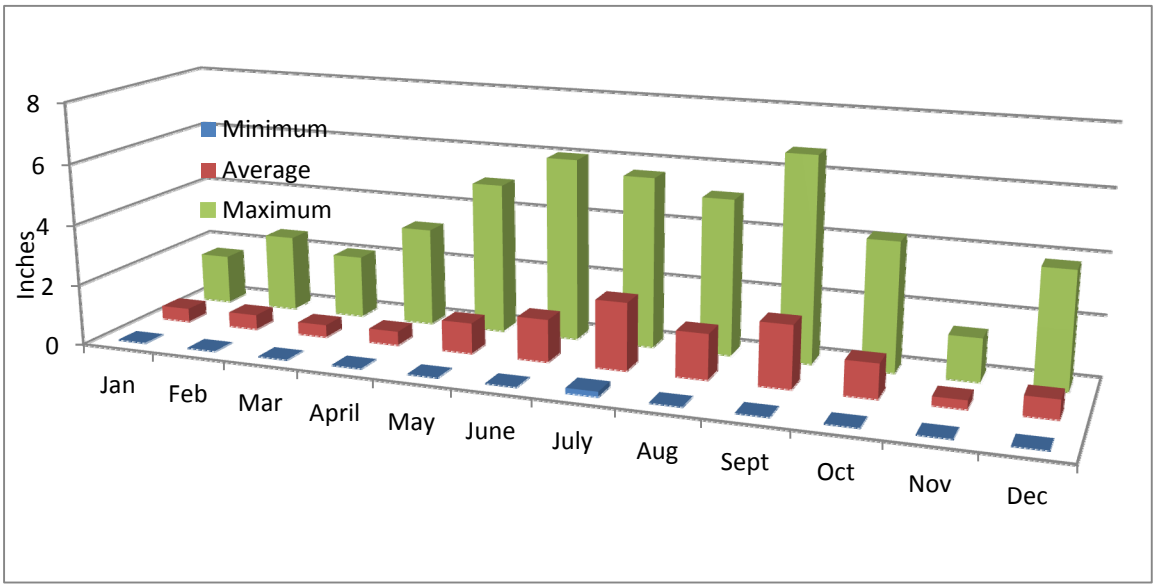

Figure 15-1. Monthly Average, Maximum, and Minimum Precipitation for the WIPP Site, 1990-2011*

*Source: precipitation data for calendar years 1990 through 2011 compiled from (U.S. DOE 2008b; U.S. DOE 2009c; U.S. DOE 2010b; U.S. DOE 2011b; U.S. DOE 2012a).

Wind rose plots at 10 meters (m) (33 feet [ft]) indicating the frequency of wind speeds and directions at the WIPP site from 2007 through 2011 are provided as Figure 15-2, Figure 15-3, Figure 15-4, Figure 15-5 and Figure 15-6. Data are from the WIPP ASERs.

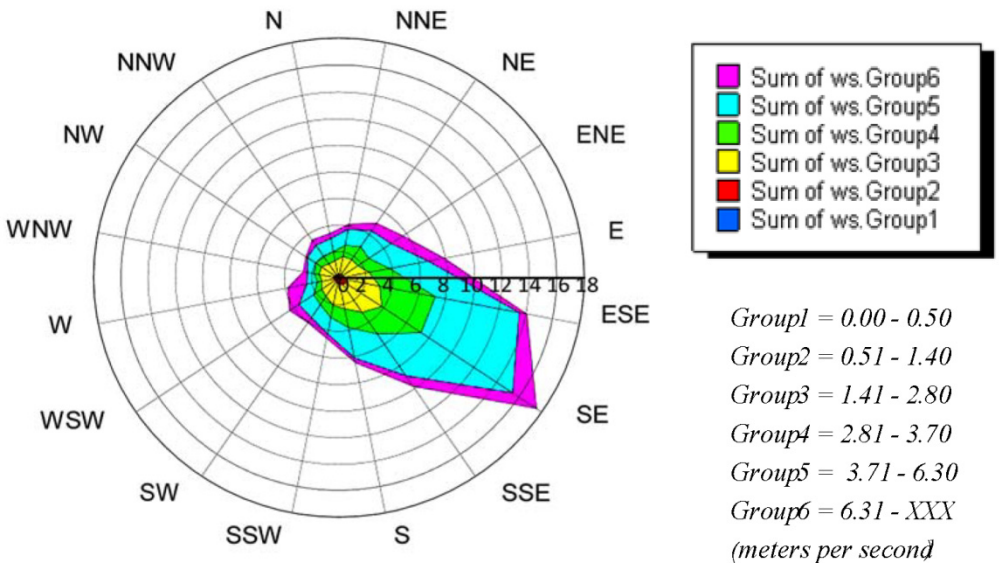

Figure 15-2. 2007 Annual Wind Rose at 10-m (33-ft) Height at the WIPP Site*

*Source: U.S. DOE 2008b

1

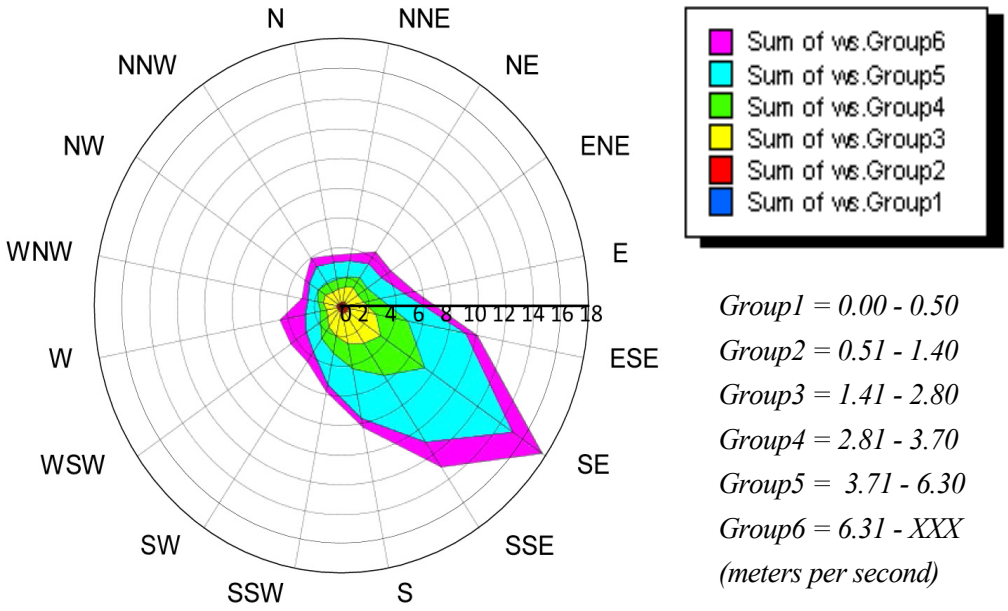

Figure 15-3. 2008 Annual Wind Rose at 10-m (33-ft) Height at the WIPP Site*

*Source: U.S. DOE 2009c

2

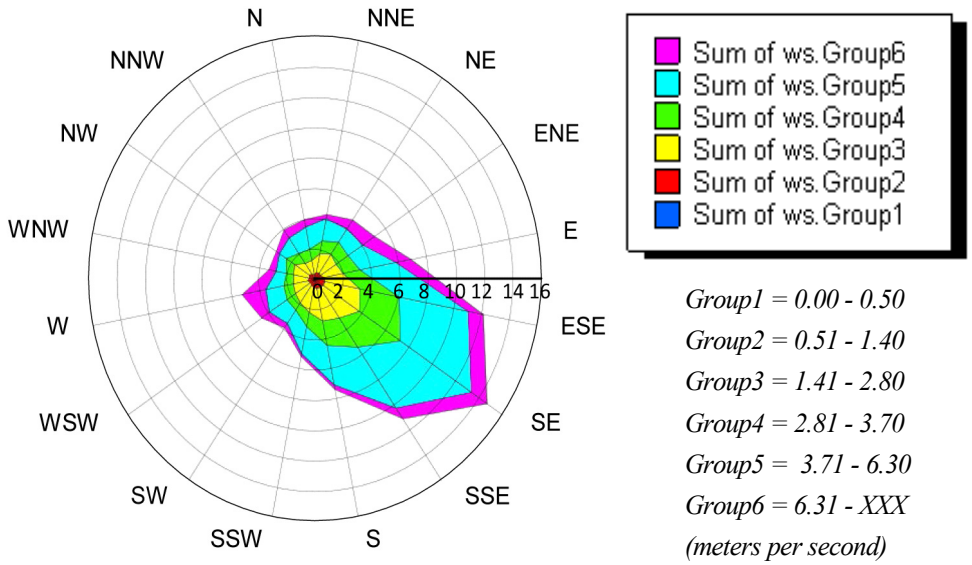

Figure 15-4. 2009 Annual Wind Rose at 10-m (33-ft) Height at the WIPP Site*

*Source: U.S. DOE 2010b

1

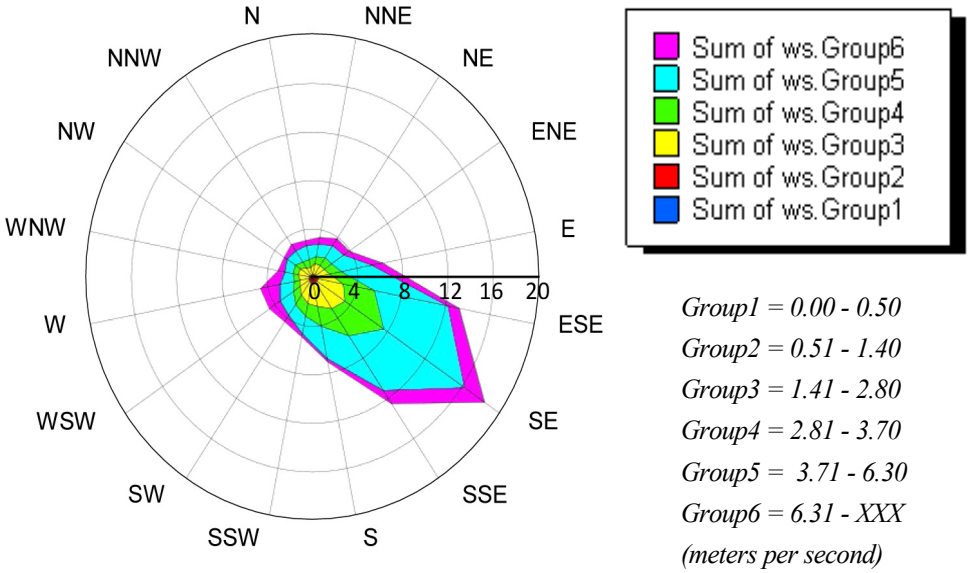

Figure 15-5. 2010 Annual Wind Rose at 10-m (33-ft) Height at the WIPP Site*

*Source: U.S. DOE 2011b

2

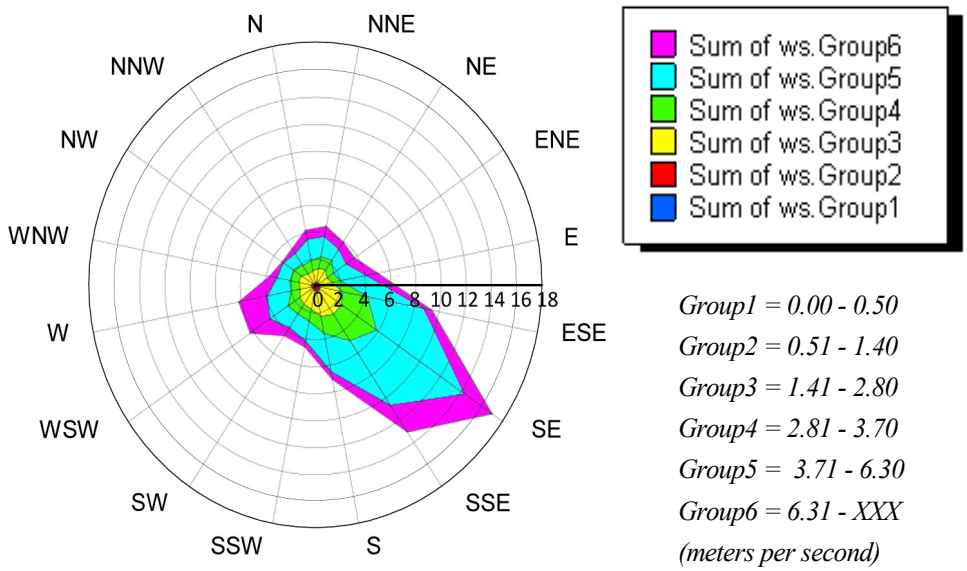

Figure 15-6. 2011 Annual Wind Rose at 10-m (33-ft) Height at the WIPP Site*

*Source: U.S. DOE 2012a

15.8.2 40 CFR § 194.15(a)(2)

40 CFR § 194.15(a)(2) requires the submittal of "all additional monitoring data, analyses, and results." Information related to this requirement is provided below.

The DOE has implemented and/or continued several experimental activities designed to address specific issues and needs of the WIPP repository. In addition, other investigations were initiated to examine the impacts of planned changes.

Environmental monitoring programs and references to relevant reports are included in Appendix MON-2014 and Appendix DATA-2014. Data on parameters required for pre-closure and post-closure monitoring, including programs for geotechnical and geoscience monitoring, are described in Appendix MON-2014, which focuses on parameters that may be relevant to the long-term performance of the repository. Appendix DATA-2014, Sections DATA-2.0 and DATA-3.0, describe the data collection procedures and reference the reports related to parameters in the Delaware Basin, including drilling rates, oil and gas production activities, and subsidence monitoring. Appendix DATA-2014, Attachment A, WIPP Borehole Update, provides an updated list of boreholes in the vicinity of the WIPP.

15.8.3 40 CFR § 194.15(a)(3)

40 CFR § 194.15(a)(3) requires the submittal of "all additional analyses and results of laboratory experiments conducted by the Department or its contractors as part of the WIPP program." Sections 15.8.3.1 through 15.8.3.5 describe experimental work conducted since the CRA-2009 in

the areas of WIPP repository conditions and parameters, waste shear strength experiments, magnesium oxide (MgO) characterization and chemistry, actinide studies, and iron and lead corrosion experiments.

15.8.3.1 WIPP Repository Conditions, Chemistry, and Processes

There were no significant changes in the WIPP repository conditions, chemistry assumptions, or subsurface processes used in PA to establish compliance since the CRA-2009. Appendix DATA-2014, Section DATA-9.0 provides references that describe waste shear strength experiments, actinide chemistry experiments, and iron and lead corrosion experiments and their results with respect to the impact on PA that occurred after the CRA-2009. A detailed description of the current conditions and assumptions used in PA is provided in Appendix MASS-2014.

15.8.3.2 Waste Shear Strength Experiments

The limits of the range of values for the hydrodynamic waste shear strength have been debated since the Cuttings model was introduced in 1992 (Berglund 1992). Since the Performance Assessment Verification Test, the lower limit has been based on a literature review and the upper limit based on a waste particle size analysis, both being chosen based on a lack of experimental results on a suitable surrogate waste material. (Hansen et al. 1997) developed a surrogate material believed to represent an extreme state of degradation, far weaker than any possible future state of the waste, and used this material to develop the material parameter values used in the Spallings model. The DOE again used this material for a series of tests in a vertical flume to assess the lower limit of the waste shear strength. Based on experimental results that realistically simulate the effect of a drilling intrusion using an accepted surrogate waste material, the DOE proposed that the waste shear strength parameter values have a range of 2.22 – 77.0 Pascals and a uniform distribution (Herrick et al. 2012; Herrick and Kirchner 2013). This range and distribution type is used in CRA-2014.

15.8.3.3 MgO Studies and Characterization

On July 10, 2007, the DOE submitted a letter in response to the EPA's questions pertaining to the efficacy of the MgO supplied to the WIPP (Patterson 2007). The letter included documents which demonstrate the stability of the MgO product in terms of both the stability of the feedstock and of the statistical data on the composition of the product. On February 11, 2008, the EPA approved the DOE's Planned Change Request (PCR) to reduce the safety factor from 1.67 to 1.2 with two conditions: 1) the DOE must continue to calculate and track both the carbon disposed and the required MgO needed on a room-by-room basis; and 2) the DOE must annually verify the reactivity of MgO and ensure that it is maintained at 94% or greater as assumed in supporting documentation (Reyes 2008).

On March 16, 2009, the DOE submitted a notification to the EPA of implementation of the 1.2 excess factor for MgO emplacement and verification of 94% or greater reactivity (Patterson 2009). A description of the change in MgO emplacement is given in CRA-2014, Engineered Barriers, Section 44.8.1. The DOE continues to implement the 1.2 excess factor of MgO on a

room-by-room basis and to ensure the MgO emplaced in the WIPP has a minimum reactivity of 94%.

15.8.3.4 Actinide Investigations

Experimental investigations to establish the speciation and solubility of actinides under WIPP-related conditions were reinitiated after the CRA-2004 and have continued through the CRA-2014. These investigations initially focused on three areas: (1) the solubility of neodymium, Nd (III), as an analogue for the plutonium, Pu (III), and americium, Am (III), oxidation states, in simulated WIPP brine; (2) the reduction of higher valent Pu (V/VI) by iron to form lower-solubility Pu (III/IV) phases; and (3) the solubility of uranium, U (VI), in carbonate-free WIPP brine. Since the CRA-2009, this has expanded to include various aspects of actinide-relevant brine chemistry, microbial effects, and actinide colloid studies. The details of these experimental studies are given in Appendix SOTERM-2014, Sections SOTERM-2 and SOTERM-3. All results reported in these studies support the existing PA assumptions for geochemistry and did not lead to conceptual model changes in the CRA-2014 PA, although a number of parameters were updated.

15.8.3.5 Iron and Lead Corrosion Experiments

Since the CRA-2009, a new series of steel and lead corrosion experiments has been conducted (Roselle 2009; Roselle 2010; Roselle 2011a; Roselle 2011b; Roselle 2013). The purpose of these experiments has been to determine steel and lead corrosion rates under more WIPP-relevant conditions. The results of these experiments have led to a revised iron corrosion rate parameter (Roselle 2013). No other changes have been made as a result of these experiments. Appendix MgO-2014, Section MgO-5.3.2.1 provides a description of the effects of MgO on gas generation from anoxic corrosion of steels and other iron-based alloys, while Appendix SOTERM-2014, Section SOTERM-2.3.4 describes the iron chemistry and corrosion assumptions that are implemented in the CRA-2014 PA.

15.8.4 40 CFR § 194.15(a)(4)

40 CFR § 194.15(a)(4) requires that the DOE "identify any activities or assumptions that deviate from the most recent compliance application." Information related to this requirement is provided in Sections 15.8.4.1 through 15.8.4.6.

15.8.4.1 Status of Underground Excavation

The status of mining in the WIPP underground repository is shown in Figure 15-7. As of December 31, 2012, Panels 1 through 7 had been mined completely and Panels 1, 2, 3, 4 and 5 were completely filled with waste. Waste was being emplaced in Panel 6 and mining of Panel 7 was completed on December 28, 2012.

The geotechnical analysis reports from 2008 through 2012 show that no major ground control problems or events have occurred since the CRA-2009 (U.S. DOE 2008c ; U.S. DOE 2009d; U.S. DOE 2010c; U.S. DOE 2011c; U.S. DOE 2012b). As expected, slow deterioration of ground conditions has occurred in the WIPP underground repository as a result of aging, but this

has been mitigated by routine maintenance and the implementation of engineered systems, as needed.

15.8.4.2 Remote-Handled Transuranic Waste Emplacement

The original plans for waste emplacement included the placement of remote-handled TRU (RH-TRU) waste in horizontal boreholes in the walls of waste-emplacement rooms, followed by the emplacement of contact-handled TRU (CH-TRU) waste in containers on the floor of each room. This configuration was planned to be used in all panels in the underground repository. Because CH-TRU waste disposal was approved about six years before RH-TRU waste approval, RH-TRU waste was emplaced in Panels 4, 5, and 6, but not in Panels 1, 2, and 3 (see Figure 15-7).

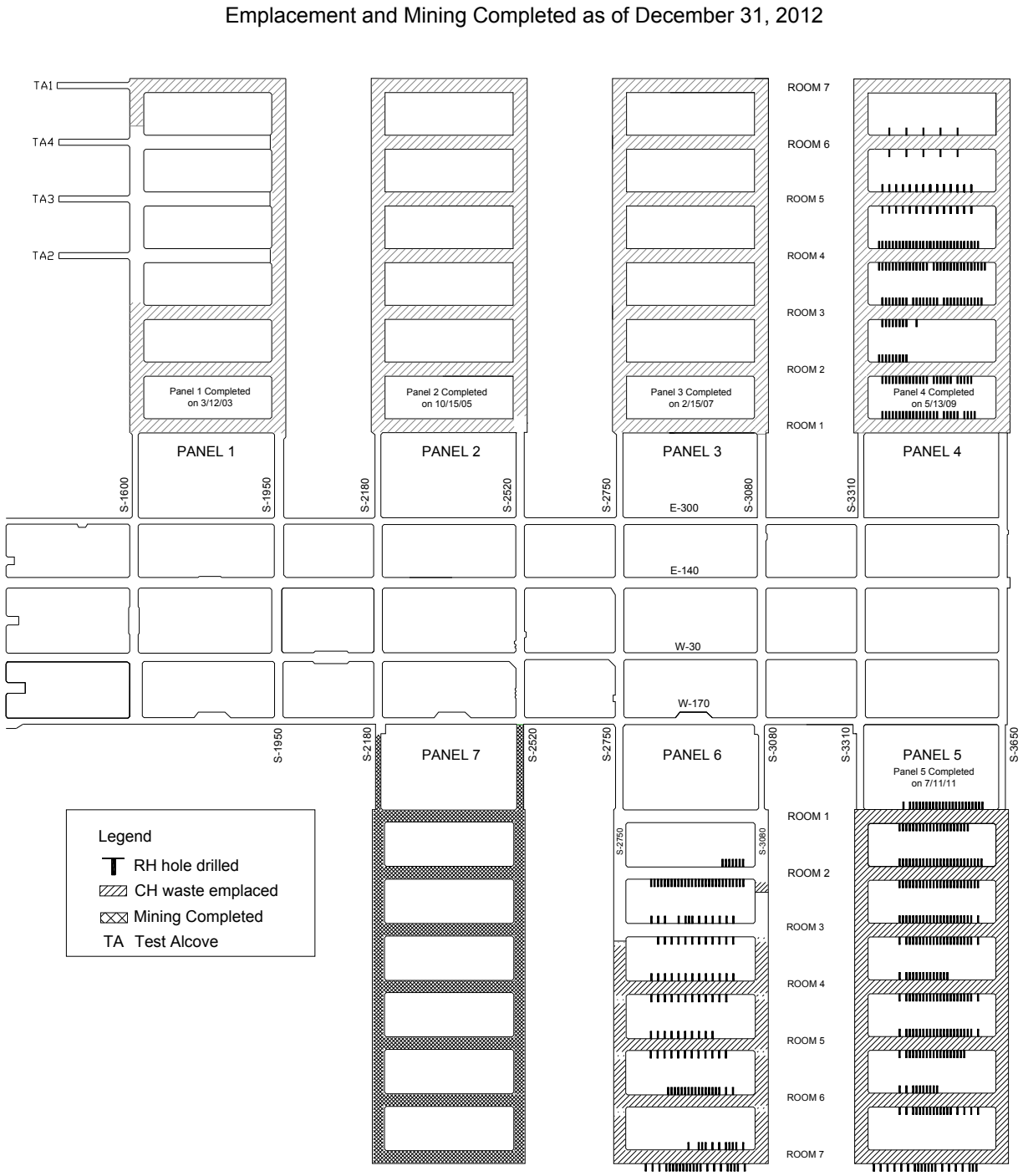

Figure 15-7. Status of Mining and Waste Emplacement as of December 31, 2012

15.8.4.3 Proposed RH-TRU Waste Container Modifications

On November 15, 2007, the DOE submitted a PCR to the EPA for approval to emplace a portion of the RH-TRU waste in shielded containers in the WIPP (Moody 2007). The shielded container has approximately the same exterior dimensions as a 55-gallon drum. It has 1-inch thick lead shielding placed between a double-walled steel shell. The external steel wall is 1/8-inch thick, and the internal steel wall is 3/16-inch thick. The lid and the bottom of the containers are made of carbon steel and are 3 inches thick. The containers are designed to hold a 30-gallon container filled with RH-TRU waste, and would be shipped to the WIPP in HalfPACT transportation containers. The shielded container would be handled and emplaced like CH-TRU waste containers because the surface dose rate for a shielded container would be no higher than 200 millirem/hour. Even though the RH-TRU waste in shielded containers will be handled as if it were CH-TRU waste, these containers will still be recorded as RH-TRU waste in the WIPP Waste Data System, and the volume of the waste will be counted against the limit of 250,000 cubic feet (7,080 cubic meters) of RH-TRU waste, as set by the Consultation and Cooperation Agreement between the DOE and the State of New Mexico.

On December 7, 2007, the EPA sent the DOE its first letter with the results of a preliminary review and comments on the shielded container PCR and requested additional documentation (Reyes 2007). The DOE submitted supplemental information on April 30, 2008, and October 29, 2008, in response to the EPA's request (Moody 2008a and Moody 2008b).

On March 25, 2011, the EPA determined that the DOE had fulfilled all documentation requirements set forth by the EPA and had demonstrated that the use of shielded containers in the repository would not affect facility compliance with either 40 CFR Part 191or 40 CFR Part 194 (Edwards 2011a). The EPA proposed the approval of the shielded container assembly for use at the WIPP, pending the solicitation and resolution of public comments.

The EPA opened an informal 60-day comment period, which was later extended to 90 days at the request of the stakeholders and closed on June 24, 2011. The EPA considered all comments submitted and found that no new technical issues had been raised.

On August 8, 2011, the EPA issued its technical approval of the DOE's PCR for the emplacement of RH-TRU waste in shielded containers with one condition (Edwards 2011b): prior to shipping shielded containers to the WIPP, the DOE will demonstrate a consistent complex-wide procedure to ensure that shielded containers containing RH-TRU waste remain below the WIPP LWA surface dose rate limit for CH-TRU waste of 200 millirem per hour.

15.8.4.4 Neutrino Experiments in the WIPP Underground Repository

Several new research projects have been initiated at the WIPP. Although these projects are not related to the expected performance of the repository, they are described here because they are being performed in the WIPP underground facility. The WIPP underground repository is a desirable location for these experiments because it provides an environment shielded from cosmic radiation that would otherwise interfere with the experiments. Equipment used during these experiments will be removed before closure of the repository.

The Segmented Enriched Germanium Assembly (SEGA) and the Multiple Element Germanium Array (MEGA) projects are being performed to investigate double-beta decay, a rare type of nuclear decay that provides information on the mass of the neutrino. The SEGA and MEGA projects are being performed by a collaboration of several universities, with Stanford University serving as the lead. The SEGA and MEGA experiments have been ongoing since 2008.

Los Alamos National Laboratory is leading the Enriched Xenon Observatory (EXO) project, also in the WIPP underground repository. This project is investigating neutrinoless double-beta decay. The first two clean room modules for the EXO project were successfully placed in the WIPP underground in 2007. The detector for the EXO project, called the Time Projection Chamber (TPC), was installed in January 2010. Data-taking mode began when the EXO detector was filled with xenon containing 80% xenon-136. Construction of the EXO is approximately 90% complete. Experimental modules continue to be assembled, outfitted, tested and emplaced in the WIPP underground.

On May 28, 2009, the DOE submitted to the EPA the notification of intent to emplace the Dark Matter (DM) TPC in the northern part of the North Experimental Area in the WIPP underground (Moody 2009a). The EPA approved the DM-TPC on July 23, 2009 (Edwards 2009a). The experiment was assembled in the WIPP underground in 2010. The DM-TPC continues to operate safely and reliably.

On January 8, 2009, the DOE submitted to the EPA the notification of intent to begin the Low Background Radiation Experiment (LBRE) (Moody 2009b). The LBRE is designed to examine the effects of very low background radiation on bacteria. The EPA approved the intent to begin the LBRE on January 28, 2009 (Edwards 2009b). Experimental protocols were developed and incubators were emplaced above ground and underground. Experiments have been ongoing in the WIPP underground since 2009.

15.8.4.5 Planned Change Notice Submittals

A Planned Change Notice (PCN) is a formal submittal of information to the EPA that describes minor, insignificant changes to activities and conditions at the WIPP that are different from those described in the compliance baseline. A summary of the PCNs submitted since the CRA-2009 is provided below.

Planned Change Notice for Salt Disposal Investigations

On August 11, 2011, the DOE submitted to the EPA a PCN to initiate mining activities for the Salt Disposal Investigations (SDI) project in the WIPP underground (Ziemianski 2011a). The objective of the SDI experiment is to investigate thermal and hydro-geochemical responses to temperature sources in excess of 160º Celsius located in bedded salt.

On November 17, 2011, the EPA agreed that the DOE may conduct the initial preparatory phase of the SDI program and found that the mining phase of the SDI activities will not adversely impact the WIPP's waste handling activities, air monitoring, disposal operations, or long-term repository performance (Edwards 2011c). The initial preparatory phase of the mining project began on December 1, 2011.

On June 20, 2012, the DOE notified the EPA (Franco 2012a) that an additional component, and possible alternative to the SDI project, had been developed entitled the Salt Defense Disposal Investigations (SDDI). The SDDI project would test an in-drift emplacement concept with thermal loads more closely aligned with the DOE defense high-level waste canisters.

Planned Change Notice for RH-72B Neutron Shielded Canister

On May 21, 2010, the DOE submitted to the EPA a PCN to employ a polyethylene liner inside some standard RH-TRU waste canisters to shield neutron-emitting waste destined for disposal at the WIPP (Moody 2010).

Planned Change Notice for Placement of Magnesium Oxide

On February 14, 2012, the DOE submitted a PCN, based on operating experience and historical data, to inform the EPA that a process was being instituted to emplace MgO on every other row of waste containers, in contrast to emplacing MgO on every waste stack (Franco 2012b). Historical data showed the MgO excess factor on a per room basis to range from 1.22 to 2.85 when MgO was placed on every stack of waste. These values were higher than the excess factor of 1.2 mandated by the EPA's letter dated February 11, 2008 (Reyes 2008). The PCN also described the process that requires the Waste Handling Engineer to continue to calculate the excess factor at the end of each shift and to direct the placement of additional MgO if the excess factor dropped below 1.2. The EPA agreed to this operational change in an email from Peake to Franco dated July 13, 2012. Details regarding this change can be found in Appendix MgO, Section MgO-2.1.4.

15.8.4.6 Planned Change Request Submittals

A PCR is a formal submittal of information to the EPA that describes and requests approval for the implementation of more complex changes to activities and conditions at the WIPP that are different from those described in the compliance baseline. A summary of the PCRs submitted since the CRA-2009 is provided below.

Planned Change Request for Repository Reconfiguration

On August 30, 2011, the DOE submitted a Repository Reconfiguration PCR to the EPA to relocate Panels 9 and 10 from the main north-south access drift to south of the existing Panels 4 and 5 (Ziemianski 2011b). The DOE stated that relocating Panels 9 and 10 to south of the existing Panels 4 and 5 will enhance worker safety and reduce maintenance requirements by providing a more stable geotechnical environment for the two new waste emplacement panels in the repository.

Planned Change Request for Panel Closure Redesign

On September 28, 2011, the DOE submitted to the EPA a PCR for panel closure redesign (Ziemianski 2011c). The DOE has requested that the EPA modify Condition 1 of the Final Certification Decision for 40 CFR Part 194 by replacing the current approved panel closure design, “Option D,” with the proposed design, Run-of-Mine Panel Closure.

Condition 1 of the Final Certification Decision for 40 CFR Part 194 specifies that the panel closure system to be used in the WIPP repository be "Option D," as specified in the CCA (U.S. DOE 1996). "Option D" specified that certain components be constructed using Salado Mass Concrete. In 2007, the DOE initiated hydrogen and methane monitoring to gather data to determine more realistic accumulation rates for these gases in filled panels. More realistic accumulation rates for hydrogen and methane could be used to establish a panel closure design that would be less complex than the Option D design.

On December 22, 2011, the EPA provided a set of initial questions and comments to the DOE focusing on the justification for Run-of-Mine Panel Closure representation and its parameters in the reconfiguration PCR PA that were different from those in the 2009 Performance Assessment Baseline Calculation (Perrin 2011).

On April 17, 2012, the DOE replied to the initial set of review questions and comments related to the PCR for replacing the current "Option D" panel closure system (Franco 2012c).

In 2012, the DOE submitted a PA, Panel Closure System-2012, for the proposed panel closure redesign. The results of the PA demonstrated that the WIPP will remain in compliance with the containment requirements found in 40 CFR §191.13.

15.8.5 40 CFR § 194.15(a)(5)

40 CFR § 194.15(a)(5) requires that the CRA-2014 include "a description of all waste emplaced in the disposal system since the most recent compliance certification or recertification application. Such description shall consist of a description of the waste characteristics and waste components identified in § 194.24(b)(1) and § 194.24(b)(2)." Information related to these requirements is provided in Sections 15.8.5.1 and 15.8.5.2.

15.8.5.1 Status of Waste Emplacement

The status of waste emplacement in the WIPP underground repository is illustrated in Figure 15-7. Additional detail is provided in Section 24, Waste Characterization.

15.8.5.2 Waste Characteristics and Components Important to Demonstration of Compliance

Section 24 provides an updated waste inventory of waste anticipated to be emplaced in the WIPP and waste that has already been emplaced since the CRA-2009. Section 24 also reports an analysis of the impacts of waste inventory on the performance of the WIPP disposal system. Information about the limits imposed by the DOE on significant components or characteristics of the waste to ensure that they are consistent with assumptions made for the CRA-2014 PA is also provided in Section 24.

There have been five inventory updates (ATWIR-2008, ATWIR-2009, ATWIR-2010, ATWIR-2011 and ATWIR-2012) since the CRA-2009. The DOE used the ATWIR-2012 data for the CRA-2014 inventory, after it was scaled for PA. The scaled inventory was documented in the Performance Assessment Inventory Report - 2012 (Van Soest 2012).

15.8.6 40 CFR § 194.15(a)(6)

40 CFR § 194.15(a)(6) requires the submittal of "any significant information not previously included in a compliance certification or recertification application related to whether the disposal system continues to be in compliance with the disposal regulations."

The information required by this section of the certification criteria is provided in the sections and appendices of the CRA-2014. The DOE believes that this information demonstrates that the WIPP continues to comply with the disposal regulations.

15.8.7 40 CFR § 194.15(a)(7)

40 CFR § 194.15(a)(7) requires the submittal of "any additional information requested by the Administrator or the Administrator's authorized representative."

There currently are no outstanding requests from the EPA for additional information. As such, the DOE is in compliance with this certification criterion.

15.8.8 40 CFR § 194.15(b)

40 CFR § 194.15(b) states, "To the extent that information required for a re-certification of compliance remains valid and has been submitted in previous certification or re-certification applications(s), such information need not be duplicated in subsequent applications; such information may be summarized and referenced."

The DOE has followed this direction in the preparation of this recertification application. To the extent appropriate, information from the CCA, the CRA-2004, and the CRA-2009 that remains valid and unchanged is not repeated in this recertification application; instead, it is summarized and incorporated by reference.

15.8.9 Status of Compliance with 40 CFR § 194.15

The information in this section and in the other sections and appendices of the CRA-2014 establishes that the DOE continues to demonstrate compliance with the requirements of section 194.15.

15.9 References

(*Indicates a reference that has not been previously submitted.)

Berglund, J.W. 1992. Mechanisms Governing the Direct Removal of Wastes from the Waste Isolation Pilot Plant Repository Caused by Exploratory Drilling. SAND92-7295. Sandia National Laboratories, Albuquerque, NM.

Domski, P.S., and R.L. Beauheim. 2008. *Evaluation of Culebra Brine Chemistry*. AP-125. ERMS 549336. Sandia National Laboratories, Carlsbad, NM.*

Domski, P.S., Beauheim, R.L., and Johnson, P.B. 2011. "AP-147 Analysis Report: Evaluation of WIPP Groundwater Compositions." ERMS 556581. Sandia National Laboratories, Carlsbad, NM.*

Edwards, J. 2009a. Letter to D. Moody (Subject: *EPA's approval of DOE's Dark Matter-Time Projection Chamber (DM-TPC) experiment*). 23 July 2009. U.S. Environmental Protection Agency, Office of Radiation and Indoor Air, Washington, DC.*

Edwards, J. 2009b. Letter to D. Moody (Subject: *U.S. EPA's approval of the DOE's Low Background Radiation Experiment in the WIPP*). 28 January 2009. U.S. Environmental Protection Agency, Office of Radiation and Indoor Air, Washington, DC.*

Edwards, J. 2011a. Letter to E. Ziemianski (Subject: *EPA's proposed decision to approve the DOE's Planned Change Request to emplace a portion of the RH-TRU waste inventory in specially designed shielded containers at the WIPP)*. 25 March 2011. U.S. Environmental Protection Agency, Office of Radiation and Indoor Air, Washington, DC.*

Edwards, J. 2011b. Letter to E. Ziemianski (Subject: *U.S. EPA's technical approval of the DOE's Shielded Container Planned Change Request*). 8 August 2011. U.S. Environmental Protection Agency, Office of Radiation and Indoor Air, Washington, DC.*

Edwards, J. 2011c. Letter to E. Ziemianski (Subject: *U.S. EPA's review of DOE's Salt Disposal Investigations Proposal*). 17 November 2011. U.S. Environmental Protection Agency, Office of Radiation and Indoor Air, Washington, DC.*

Franco, J.R. 2012a. Letter to J. Edwards (Subject: *Notification of Revisions to the Salt Disposal Investigations Testing Concepts*). 20 June 2012. U.S. Department of Energy, Carlsbad Field Office, Carlsbad, NM.*

Franco, J.R. 2012b. Letter to A. Perrin (Subject: *Planned Change Notice for Placement of Magnesium Oxide Supersacks*). 14 February 2012. U.S. Department of Energy, Carlsbad Field Office, Carlsbad, NM.*

Franco, J.R. 2012c. Letter to J. Edwards (Subject: *Response to EPA Letter Dated December 22, 2011*). 17 April 2012. U.S. Department of Energy, Carlsbad Field Office, Carlsbad, NM.*

Hansen, F.D., M. K. Knowles, T. W. Thompson, M. Gross, J. D. McLennan, and J. F. Schatz. 1997. Description and Evaluation of a Mechanistically Based Conceptual Model for Spall. SAND97–1369. Sandia National Laboratories, Albuquerque, NM.

Herrick, C.G., M.D. Schuhen, D.M. Chapin, and D.C. Kicker. 2012. Determining the Hydrodynamic Shear Strength of Surrogate Degraded TRU Waste Materials as an Estimate for the Lower Limit of the Performance Assessment Parameter TAUFAIL. ERMS 558479. Sandia National Laboratories, Carlsbad, NM.*

Herrick, C.G. and T. Kirchner. 2013. Follow-up to questions concerning TAUFAIL flume testing raised during the November 14-15, 2012 technical exchange between the DOE and EPA.*

Kuhlman, K.L. 2010. "Analysis Report AP-111 Revision 1, Culebra Water Level Monitoring Network Design." ERMS 554054, Sandia National Laboratories, Carlsbad, NM.*

Moody, D.C. 2007. Letter to J. Reyes (Subject: T*ransmittal of Planned Change Request for Shielded Containers*). 15 November 2007. U.S. Department of Energy, Carlsbad Field Office, Carlsbad, NM.*

Moody, D.C. 2008a. Letter to J. Reyes (7 Attachments). 30 April 2008. U.S. Department of Energy, Carlsbad Field Office, Carlsbad, NM.*

Moody, D.C. 2008b. Letter to J. Reyes (8 Attachments). 29 October 2008. U.S. Department of Energy, Carlsbad Field Office, Carlsbad, NM.*

Moody, D.C. 2009a. Letter to J. Edwards (Subject: *Notification of Intent to Begin the Dark Matter Time Projection Chamber Experiment*). 28 May 2009. U.S. Department of Energy, Carlsbad Field Office, Carlsbad, NM.*

Moody, D.C. 2009b. Letter to J. Edwards (Subject: *Notification of Intent to Begin Low Background Radiation Experiment)*. 8 January 2009. U.S. Department of Energy, Carlsbad Field Office, Carlsbad, NM.*

Moody, D.C. 2010. Letter to J. Edwards (Subject: *Planned Change Notice for the RH-72B Neutron Shielded Canister*). 21 May 2010. U.S. Department of Energy, Carlsbad Field Office, Carlsbad, NM.*

Patterson, R.L. 2007. Letter to J. Reyes (Chemical Analysis of the MagChem 10 WTS 60 as supplied to the Waste Isolation Pilot Plant). 10 July 2007. U.S. Department of Energy, Carlsbad Field Office, Carlsbad, NM.

Patterson, R.L. 2009. Letter to J. Edward (Subject: *Notification of Implementation of the Excess Factor for Magnesium Oxide Emplacement at the Waste Isolation Pilot Plant*). 16 March 2009. U.S. Department of Energy, Carlsbad Field Office, Carlsbad, NM.*

Perrin, A.D. 2011. Letter to E. Ziemianski (Subject: Additional Questions and Comments to DOE related to the PCS and the Repository Reconfiguration). 22 December 2011. U.S. Environmental Protection Agency, Office of Radiation and Indoor Air, Washington, DC.*

Reyes, J. 2007. Letter to D. Moody (Subject: *Preliminary review and comments on the Shielded Container Planned Change Request*). 7 December 2007. U.S. Environmental Protection Agency, Office of Radiation and Indoor Air, Washington, DC.

Reyes, J. 2008. Letter to D. Moody (5 Enclosures). 11 February 2008. U.S. Environmental Protection Agency, Office of Radiation and Indoor Air, Washington, DC.*

Roselle, G.T. 2009. *Iron and Lead Corrosion in WIPP-Relevant Conditions: Six Month Results.* Milestone report. October 7, 2009. ERMS 552218. Sandia National Laboratories, Carlsbad, NM.*

Roselle, G.T. 2010. *Iron and Lead Corrosion in WIPP-Relevant Conditions: 12 Month Results*. Milestone report. October 14, 2010. ERMS 554383. Sandia National Laboratories, Carlsbad, NM.*

Roselle, G.T. 2011a. *Iron and Lead Corrosion in WIPP-Relevant Conditions: 18 Month Results*. Milestone report. January 5, 2011. ERMS 554715. Sandia National Laboratories, Carlsbad, NM.*

Roselle, G.T. 2011b. *Iron and Lead Corrosion in WIPP-Relevant Conditions: 24 Month Results*. Milestone report. May 3, 2011. ERMS 555426. Sandia National Laboratories, Carlsbad, NM.*

Roselle, G.T. 2013. *Determination of Corrosion Rates from Iron/Lead Corrosion Experiments to be Used for Gas Generation Calculations*, Rev. 1. Analysis report. January 23, 2013. ERMS 559077. Sandia National Laboratories, Carlsbad, NM.*

Sandia National Laboratories. 2012. *Sandia National Laboratories Compliance Monitoring Parameter Assessment for 2012, WBS 1.3.1, November 2012*. Sandia National Laboratories, Carlsbad, NM.*

U.S. Department of Energy (DOE). 1996. *Title 40 CFR Part 191 Compliance Certification Application for the Waste Isolation Pilot Plant* (October). 21 vols. DOE/CAO 1996-2184. Carlsbad Field Office, Carlsbad, NM.

U.S. Department of Energy (DOE). 2004. *Title 40 CFR Part 191 Compliance Recertification Application for the Waste Isolation Pilot Plant* (March). 10 vols. DOE/WIPP 2004-3231. Carlsbad Field Office, Carlsbad, NM.

U.S. Department of Energy (DOE). 2008a. *Delaware Basin Monitoring Annual Report* (September). DOE/WIPP 08-2308. Carlsbad Field Office, Carlsbad, NM.*

U.S. Department of Energy (DOE). 2008b. *Waste Isolation Pilot Plant Annual Site Environmental Report for 2007* (September). DOE/WIPP 08-2225. Carlsbad Field Office, Carlsbad, NM.*

U.S. Department of Energy (DOE). 2008c. *Geotechnical Analysis Report for July 2006–June 2007*. DOE/WIPP 08-3177. Carlsbad Field Office, Carlsbad, NM.*

U.S. Department of Energy (DOE). 2009a. *Title 40 CFR Part 191 Compliance Recertification Application for the Waste Isolation Pilot Plant* (March). DOE/WIPP 2009-3424. Carlsbad Field Office, Carlsbad, NM.*

U.S. Department of Energy (DOE). 2009b. *Delaware Basin Monitoring Annual Report* (September). DOE/WIPP 09-2308. Carlsbad Field Office, Carlsbad, NM.*

U.S. Department of Energy (DOE). 2009c. *Waste Isolation Pilot Plant Annual Site Environmental Report for 2008* (September). DOE/WIPP 09-2225. Carlsbad Field Office, Carlsbad, NM.*

U.S. Department of Energy (DOE). 2009d. *Geotechnical Analysis Report for July 2007–June 2008*. DOE/WIPP 09-3177. Carlsbad Field Office, Carlsbad, NM.*

U.S. Department of Energy (DOE). 2010a. *Delaware Basin Monitoring Annual Report* (September). DOE/WIPP 10-2308. Carlsbad Field Office, Carlsbad, NM.*

U.S. Department of Energy (DOE). 2010b. *Waste Isolation Pilot Plant Annual Site Environmental Report for 2009* (September). DOE/WIPP 10-2225. Carlsbad Field Office, Carlsbad, NM.*

U.S. Department of Energy (DOE). 2010c. *Geotechnical Analysis Report for July 2008–June 2009*. DOE/WIPP 10-3177. Carlsbad Field Office, Carlsbad, NM.*

U.S. Department of Energy (DOE). 2011a. *Delaware Basin Monitoring Annual Report* (September). DOE/WIPP 11-2308. Carlsbad Field Office, Carlsbad, NM.*

U.S. Department of Energy (DOE). 2011b. *Waste Isolation Pilot Plant Annual Site Environmental Report for 2010* (September). DOE/WIPP 11-2225. Carlsbad Field Office, Carlsbad, NM.*

U.S. Department of Energy (DOE). 2011c. *Geotechnical Analysis Report for July 2009–June 2010*. DOE/WIPP 11-3177. Carlsbad Field Office, Carlsbad, NM.*

U.S. Department of Energy (DOE). 2012a. *Waste Isolation Pilot Plant Annual Site Environmental Report for 2011* (September). DOE/WIPP 12-3489. Carlsbad Field Office, Carlsbad, NM.*

U.S. Department of Energy (DOE). 2012b. *Geotechnical Analysis Report for July 2010–June 2011*. DOE/WIPP 12-3484. Carlsbad Field Office, Carlsbad, NM.*

U.S. Department of Energy (DOE). 2012c. *Annual Change Report 2011/2012: From July 1, 2011, to June 30, 2012* (October). DOE/WIPP 12-3496. Carlsbad Field Office, Carlsbad, NM.*

U.S. Department of Energy (DOE). 2012d. *Delaware Basin Monitoring Annual Report* (September). DOE/WIPP 12-2308. Carlsbad Field Office, Carlsbad, NM.*

U.S. Department of Energy (DOE). 2012e. *WIPP Subsidence Monument Leveling Survey 2012* (December 2012). DOE/WIPP 12-3497. Carlsbad Field Office, Carlsbad, NM.*

U.S. Department of Energy (DOE). 2012f. *Annual Transuranic Waste Inventory Report – 2012*. DOE/TRU-12-3425, Revision 0. Carlsbad Field Office, Carlsbad, NM.*

U.S. Department of Energy (DOE). 2012g. *Waste Isolation Pilot Plant Biennial Environmental Compliance Report*. DOE/WIPP 12-3487, Revision 0. Carlsbad Field Office, Carlsbad, NM.*

U.S. Environmental Protection Agency (EPA). 1996. "40 CFR Part 194: Criteria for the Certification and Recertification of the Waste Isolation Pilot Plant's Compliance with the 40 CFR Part 191 Disposal Regulations; Final Rule." *Federal Register*, vol. 61 (February 9, 1996): 5223–45.

U.S. Environmental Protection Agency (EPA). 1998a. "CARD No. 14: Content of Compliance Certification Application." *Compliance Application Review Documents for the Criteria for the Certification and Recertification of the Waste Isolation Pilot Plant's Compliance with the 40 CFR Part 191 Disposal Regulations: Final Certification Decision* (May) (pp. 14-1 through 14-86). Office of Radiation and Indoor Air, Washington, DC.

U.S. Environmental Protection Agency (EPA). 1998b. "40 CFR Part 194: Criteria for the Certification and Recertification of the Waste Isolation Pilot Plant's Compliance with the Disposal Regulations: Certification Decision; Final Rule." *Federal Register*, vol. 63 (May 18, 1998): 27353–406.

U.S. Environmental Protection Agency (EPA). 2006a. "Recertification CARD Nos. 14/15: Content of Compliance Certification Application and Compliance Recertification Application(s)." *Compliance Application Review Documents for the Criteria for the Certification and Recertification of the Waste Isolation Pilot Plant's Compliance with the 40 CFR Part 191 Disposal Regulations: Final Recertification Decision* (March) (pp. 14/15-1 through 14/15-34, pp. 14-A-1 through 14-A-3, and pp. 15-A-1 through 15-A-17). Office of Radiation and Indoor Air, Washington, DC.

U.S. Environmental Protection Agency (EPA). 2006b. "40 CFR Part 194: Criteria for the Certification and Recertification of the Waste Isolation Pilot Plant's Compliance with the Disposal Regulations: Recertification Decision" (Final Notice). *Federal Register*, vol. 71 (April 10, 2006): 18010–021.

U.S. Environmental Protection Agency (EPA). 2010a. "2009 Compliance Recertification Application (2009 CRA) Compliance Application Review Documents (CARD) 194.14 and 194.15: Content of Compliance Certification Application; Content of Compliance Recertification Application(s)." EPA Docket FDMS Docket ID No. EPA-HQ-OAR-2009-0330. Office of Radiation and Indoor Air, Washington, DC.*

U.S. Environmental Protection Agency (EPA). 2010b. "40 CFR Part 194 Criteria for the Certification and Recertification of the Waste Isolation Pilot Plant's Compliance with the Disposal Regulations: Recertification Decision; Final Notice." Federal Register, vol. 75. (November 18, 2010).*

Van Soest, G.D. 2012. *Performance Assessment Inventory Report – 2012,* INV-PA-12, Revision 0. Los Alamos National Laboratory-Carlsbad Operations, Carlsbad, NM.*

Ziemianski, E. 2011a. Letter to J. Edwards (Subject: *Notification of Intent to Begin the Salt Disposal Investigations*). 11 August 2011. U.S. Department of Energy, Carlsbad Field Office, Carlsbad, NM.*

Ziemianski, E. 2011b. Letter to J. Edwards (Subject: *Transmittal of Planned Change Request for Repository Reconfiguration*). 30 August 2011. U.S. Department of Energy, Carlsbad Field Office, Carlsbad, NM.*

Ziemianski, E. 2011c. Letter to J. Edwards (Subject: *Transmittal of Planned Change Request for Panel Closure Redesign*). 28 September 2011. U.S. Department of Energy, Carlsbad Field Office, Carlsbad, NM.*

Title 40 CFR Part 191
Subparts B and C
Compliance Recertification Application 2014
for the
Waste Isolation Pilot Plant

Inspections
(40 CFR § 194.21)

United States Department of Energy
Waste Isolation Pilot Plant

Carlsbad Field Office
Carlsbad, New Mexico

Compliance Recertification Application 2014
Inspections
(40 CFR § 194.21)

Table of Contents

List of Tables

This page intentionally left blank.

Acronyms and Abbreviations

AMWTF	Advanced Mixed Waste Treatment Facility
CCA	Compliance Certification Application
CARD	Compliance Application Review Document
CCP	Central Characterization Project
CFR	Code of Federal Regulations
CH-TRU	contact-handled transuranic
CRA	Compliance Recertification Application
DOE	U.S. Department of Energy
EPA	U.S. Environmental Protection Agency
INL	Idaho National Laboratory
LANL	Los Alamos National Laboratory
NRD	Naval Reactor Division
ORNL	Oak Ridge National Laboratory
QA	quality assurance
RH-TRU	remote-handled transuranic
TRU	transuranic
WIPP	Waste Isolation Pilot Plant
WWIS	WIPP Waste Information System

Elements and Chemical Compounds

MgO	magnesium oxide

This page intentionally left blank.

21.0 Inspections (40 CFR § 194.21)

21.1 Requirements

§ 194.21 Inspections

(a) The Administrator or the Administrator's authorized representative(s) shall, at any time:

(1) Be afforded unfettered and unannounced access to inspect any area of the WIPP, and any locations performing activities that provide information relevant to compliance application(s), to which the Department has rights of access. Such access shall be equivalent to access afforded Department employees upon presentation of credentials and other required documents.

(2) Be allowed to obtain samples, including split samples, and to monitor and measure aspects of the disposal system and the waste proposed for disposal in the disposal system.

(b) Records (including data and other information in any form) kept by the Department pertaining to the WIPP shall be made available to the Administrator or the Administrator's authorized representative upon request. If requested records are not immediately available, they shall be delivered within 30 calendar days of the request.

(c) The Department shall, upon request by the Administrator or the Administrator's authorized representative, provide permanent, private office space that is accessible to the disposal system. The office space shall be for the exclusive use of the Administrator or the Administrator's authorized representative(s).

(d) The Administrator or the Administrator's authorized representative(s) shall comply with applicable access control measures for security, radiological protection, and personal safety when conducting activities pursuant to this section.

21.2 Background

40 CFR § 194.21 (U.S. EPA 1996) provides the U.S. Environmental Protection Agency (EPA) with the authority to inspect all activities at the Waste Isolation Pilot Plant (WIPP) and all activities located off-site that provide information relevant to any compliance applications.

21.3 1998 Certification Decision

The EPA conducted no inspection under the authority of section 194.21 prior to the 1998 Certification Decision. With the issuance of its 1998 Certification Decision (U.S. EPA 1998), the EPA identified inspections that may be performed under the authority at section 194.21. These include the following:

- The inspection of the panel closure system on waste panels that have been filled and are being sealed to confirm compliance with Condition 1 of the EPA's 1998 Certification Decision (U.S. EPA 1998)

- The verification that specific actions identified by the U.S. Department of Energy (DOE) in the Certification and supplementary information (and in any additional documentation submitted in accordance with Condition 4) are being taken to test and implement passive institutional controls

- Announced and unannounced inspections of activities at the WIPP and at all off-site facilities that provide information included in certification applications

- The inspection of the DOE's implementation of the monitoring plans that the DOE has set forth to demonstrate compliance with 40 CFR § 194.42

- The inspection of any records relevant to the Certification kept by the DOE, including those records required to be generated in accordance with the compliance criteria

- The inspections of approved quality assurance (QA) programs at the WIPP and at waste generator sites to ensure the programs are being adequately maintained and documented

After the 1998 Certification Decision, the EPA began using the authority given by section 194.21 to conduct inspections at the WIPP. Inspections include magnesium oxide (MgO) backfill, waste emplacement, the monitoring programs established to collect data for each of the monitored parameters identified in Table 21-1, and the examination of documentation (records) to verify compliance at the WIPP.

Table 21-1. Monitored Parameters

Monitored Parameters	
Geomechanical Parameters • Creep closure • Extent of deformation • Initiation of brittle deformation • Displacement of deformation features Hydrological Parameters • Culebra groundwater composition • Change in Culebra groundwater flow direction	Waste Activity Parameters • Waste activity subsidence parameter • Subsidence measurements Drilling-Related Parameters • Drilling rate • The probability of encountering a Castile brine reservoir

The monitoring inspection activities included an examination of monitoring and sampling equipment both on- and off-site and underground. The EPA also reviewed sampling procedures and measurement techniques and verified implementation of an effective QA program for monitoring activities.

This provision of the EPA's Compliance Criteria was not applied prior to the 1998 Certification Decision. After 1998, the EPA used the authority given by section 194.21 to inspect the WIPP monitoring programs, MgO backfill, and waste emplacement requirements.

21.4 Changes in the CRA-2004

The 2004 Compliance Recertification Application (CRA-2004) (U.S. DOE 2004) did not address the EPA's inspection activities under section 194.21. However, the EPA inspection activities were addressed in Compliance Application Review Document (CARD) 21 (U.S. EPA 2006a). CARD 21 identified monitoring inspections and waste emplacement inspections that were conducted from March 23, 1999, through July 12, 2005. This information is duplicated in Table 21-2.

Table 21-2. CRA-2004 Monitoring and Waste Emplacement Inspection Results (1999–2005)

Date of Inspection	Inspection Type	Inspection Results	Reference
March 24–25, 1999	Monitoring	The EPA had no findings or concerns during this inspection.	(U.S. EPA 1999a)
September 8, 1999	Waste Emplacement	The EPA had no findings. The EPA had one minor concern that two procedures did not specify the form that records must take. This concern did not require a response from the DOE.	(U.S. EPA 2000a)
June 21–22, 2000	Monitoring	The EPA had no findings or concerns during this inspection.	(U.S. EPA 2000a)
June 20–22, 2000	Waste Emplacement	The EPA had no findings or concerns during this inspection.	(U.S. EPA 2000b)
June 20–21, 2001	Monitoring	The EPA had one finding and no concerns. The finding noted that the subsidence monitoring program at the WIPP did not have an adequate written procedure to implement an effective QA program. In response to the EPA's finding, the DOE developed a new subsidence procedure. The EPA evaluated the procedure and found it to be adequate.	(U.S. EPA 2001a)
June 21, 2001	Waste Emplacement	The EPA had no findings and one concern. The concern noted that the DOE did not appear to have a procedure that required proper documentation of off-normal events. This concern did not require a response from the DOE because the DOE provided all documentation requested.	(U.S. EPA 2001b)
June 26–28, 2002	Monitoring	The EPA had no findings or concerns during this inspection.	(U.S. EPA 2002a)
June 24–27, 2002	Waste Emplacement	The EPA had no findings or concerns during this inspection.	U.S. EPA 2002b)
June 18–19, 2003	Monitoring	The EPA had no findings or concerns during this inspection.	(U.S. EPA 2003a)
June 17–19, 2003	Waste Emplacement	The EPA had one finding and no concerns during this inspection. The EPA was unable to determine that waste was being emplaced in a random manner. This finding was resolved in the CRA-2004.	(U.S. EPA 2003b)

Table 21-2. CRA-2004 Monitoring and Waste Emplacement Inspection Results (1999–2005) (continued)

Date of Inspection	Inspection Type	Inspection Results	Reference
June 28 through July 1, 2004	Monitoring	The EPA had no findings or concerns during this inspection.	(U.S. EPA 2004a)
June 28 through July 1, 2004	Waste Emplacement	The EPA had no findings and one concern during this inspection. The EPA found that the DOE did not appear to have a real-time system to track and calculate the actual MgO placed with waste at disposal. This concern was resolved by using the WIPP Waste Information System (WWIS) to track the quantities of MgO.	(U.S. EPA 2004b)
July 12–15, 2005	Monitoring	The EPA had no findings or concerns during this inspection.	(U.S. EPA 2005a)
May 17–19, 2005	Waste Emplacement	The EPA had no findings and one concern during this inspection. The EPA found that the DOE needed to develop a formal procedure that guides the MgO emplacement decision-making process rather than using training materials, and that the WWIS needed to be back-populated with the quantity of emplaced MgO. In response to this concern, the WWIS was back-populated.	(U.S. EPA 2005b)

21.5 EPA's Evaluation of Compliance for the 2004 Recertification

During each of the inspections listed in Table 21-3, the DOE provided the EPA with unfettered access to facilities, lists of records, access to these records as requested, and access to private office space. Additionally, the DOE actively supported the EPA's inspection activities. Based on the EPA's review and evaluation of the CRA-2004, the EPA determined that the DOE continued to comply with the requirements for section 194.21 (U.S. EPA 2006a).

21.6 Changes or New Information Between the CRA-2004 and the CRA-2009 (Previously: Changes or New Information Since the 2004 Recertification)

Table 21-3 lists the seven inspections conducted by the EPA under the authority of section 194.21 since the inspections reported in CARD 21 (U.S. EPA 2006a).

During each of the inspections listed in Table 21-3, the DOE met all the requirements of section 194.21, providing the EPA with unfettered access to facilities, lists of records, access to the

records requested, and access to private office space. Additionally, the DOE actively supported the EPA's inspection activities as required by section 194.21.

Table 21-3. Post-CRA-2004 Monitoring and Waste Emplacement Inspection Results (2006–2007)

Date of Inspection	Inspection Type	Inspection Results	Reference
June 20–22, 2006	Monitoring	The EPA had no findings or concerns during this inspection.	(U.S. EPA(2006b)
June 20–22, 2006	Waste Emplacement	The EPA had no findings or concerns during this inspection.	(U.S. EPA 2006c)
July 10–12, 2007	Monitoring	The EPA had no findings or concerns during this inspection.	(U.S. EPA 2007a)
July 10-12, 2007	Waste Emplacement	The EPA had no findings or concerns during this inspection.	(U.S. EPA 2007b)
January 9–11, 2007	Remote-handled Transuranic (RH-TRU) Emplacement Plan	The EPA had no findings or concerns during this inspection. The EPA verified that RH-TRU waste could be emplaced in the WIPP repository according to the RH-TRU Emplacement Plan.	(U.S. EPA 2007c)
October 7, 2007	Unannounced inspection at the Advanced Mixed Waste Treatment Facility (AMWTF) and the Accelerated Retrieval Project at the Idaho National Laboratory (INL)	The EPA had no findings or concerns during the inspections. However, the EPA requested information on the process used for regrouping four pre-1970 buried waste streams. EPA also requested information for estimating transuranic (TRU), mixed TRU, and low-level waste volumes. On December 28, 2007, the DOE provided the EPA with the requested information. Letter from the EPA to the DOE (March 18, 2008) acknowledging receipt of additional information requested that adequately addressed the EPA concerns.	(U.S. EPA 2007d) (U.S. EPA 2008a)
November 21–28, 2007	DOE document development and review process	The EPA made five process improvement recommendations.	(Reyes 2008)

21.7 EPA's Evaluation of Compliance for the 2009 Recertification

The inspections section of the compliance criteria, 40 CFR 194.21, lists specific requirements related to the EPA's ability to perform inspections involving the WIPP. These requirements include unfettered and unannounced access equivalent to that of DOE employees, availability of records for review, and private office access if needed to perform inspections. The EPA

evaluated the DOE implementation of these requirements at each of the inspections documented in Table 21-3, and found that the DOE actively supported EPA inspection activities.

Based on a review and evaluation of the CRA-2009 (U.S. DOE 2009) and supplemental information provided by the DOE (Federal Document Management System Docket ID No. EPA-HQ-OAR-2009-0330, Air Docket A-98-49), the EPA determined that the DOE continued to comply with the requirements of section 194.21 (U.S. EPA 2010b) since those reported in the CRA-2009.

21.8 Changes or New Information Since the CRA-2009

Table 21-4 lists the inspections conducted by the EPA under the authority of section 194.21 since the ones reported in the CRA-2009.

During each of the inspections listed in Table 21-4, the DOE met all the requirements of section 194.21, providing the EPA with unfettered access to facilities, lists of records, access to the records requested, and access to private office space. Additionally, the DOE actively supported the EPA's inspection activities as required by section 194.21.

Table 21-4. Post-CRA--2009 40 CFR 194.21 Inspection Results (2007–2012)

Date of Inspection	Inspection Type	Inspection Results	Reference
June 25, 2008, and July 29, 2008	Other - Inspection at Los Alamos National Laboratory (LANL) concerning the disposal of TRU waste drum # LAS817174 at the WIPP. Follow-up inspection at LANL regarding drum # LAS817174 to verify adequacy of corrective actions.	At the end of the EPA's June 25, 2008, inspection, the DOE committed to wait to resume waste shipments from LANL until the EPA complete its investigation concerning a nonconformance report on TRU waste drum # LAS817174. On July 29, 2008, the EPA performed a follow-up inspection to review corrective actions taken and concurred with CBFO's decision to resume shipment of waste from LANL except for most containers from the MIN-03 and CIN-02 waste streams. On August 21, 2008, the EPA concurred with full resumption of shipments from LANL.	(U.S. EPA 2008b) (U.S. EPA 2008c) (U.S. EPA 2008d)
July 22–24, 2008	Inspections at the WIPP to examine the DOE's ability to monitor the 10 parameters listed in the Compliance Certification Application (CCA) section 7.0 Table 7.7, and to verify the proper emplacement of waste and MgO	The EPA found that the DOE effectively monitored the required 10 parameters identified in Table 7-7 of the CCA, and confirmed that the results of the monitoring programs were reported annually. The EPA also concluded that waste emplacement activities were adequate and	(U.S. EPA 2008e)

Table 21-4. Post-CRA--2009 40 CFR 194.21 Inspection Results (2007–2012)

Date of Inspection	Inspection Type	Inspection Results	Reference
	in the WIPP repository.	MgO was calculated and emplaced properly. The EPA had no findings or concerns during the inspection. However, the EPA recommended the DOE maintain a permanent photographic record of the RH canister number as it is removed from the transportation cask.	
June 24–25, 2009	Other – Unannounced Inspection at Oak Ridge National Laboratory (ORNL) of the Central Characterization Project (CCP) waste characterization program for contact-handled transuranic (CH-TRU) and RH-TRU waste focusing on radiological characterization and visual examination of RH-TRU wastes, and real-time radiography of CH-TRU waste. Chain-of-custody practices for CH and RH-TRU wastes were also reviewed.	The EPA had no findings or concerns during this inspection.	(U.S. EPA 2009b)
July 14–16, 2009	Inspections at the WIPP to examine the DOE's ability to monitor the 10 parameters listed in the CCA section 7.0 Table 7.7, and to verify the proper emplacement of waste and MgO in the WIPP repository.	The EPA found that the DOE effectively monitored the required 10 parameters identified in Table 7-7 of the CCA, and confirmed that the results of the monitoring programs were reported annually. The EPA also concluded that waste emplacement activities were adequate and MgO was calculated and emplaced properly. The EPA had no findings or concerns during the inspection. However, the EPA recommended that procedure documentation errors be corrected, as noted in the emplacement inspection report. A new procedure, WP 05-WH.02, Revision 1, *WIPP Waste Handling Operations WDS User's Manual*, corrected this issue.	(U.S. EPA 2009a) (WP05-WH.02)
June 29–July 1, 2010	Inspections at the WIPP to examine the DOE's ability to monitor the 10 parameters listed in the CCA section 7.0 Table 7.7, and to verify the proper emplacement of waste and MgO in the WIPP repository.	The EPA found that the DOE effectively monitored the required 10 parameters identified in Table 7-7 of the CCA, and confirmed that the results of the monitoring programs were reported annually. The EPA also concluded that waste emplacement activities were adequate and MgO was calculated and emplaced properly. The EPA had no findings or concerns during the inspection.	(U.S. EPA 2010a)
May 10–12, 2011	Inspections at the WIPP to examine the DOE's ability to monitor the 10 parameters listed in	The EPA found that the DOE effectively monitored the required 10 parameters identified in Table 7-7 of the CCA, and	(U.S. EPA 2011)

Table 21-4. Post-CRA--2009 40 CFR 194.21 Inspection Results (2007–2012)

Date of Inspection	Inspection Type	Inspection Results	Reference
	the CCA section 7.0 Table 7.7, and to verify the proper emplacement of waste and MgO in the WIPP repository.	confirmed that the results of the monitoring programs were reported annually. The EPA also concluded that waste emplacement activities were adequate and MgO was calculated and emplaced properly. The EPA had no findings or concerns during the inspection.	
September 19–20, 2011	Other – Unannounced inspections at INL and the CBFO for CCP waste characterization program activities for CH-TRU.	The EPA confirmed that INL-CCP characterization of small quantity site waste from the Naval Reactor Division (NRD) is consistent with the conditions and limitations set forth in the EPA's baseline approval and subsequent Tier 1 changes.	(U.S. EPA 2012)
July 17–19, 2012	Inspections at the WIPP to examine the DOE's ability to monitor the 10 parameters listed in the CCA section 7.0 Table 7.7, and to verify the proper emplacement of waste and MgO in the WIPP repository.	Inspection results were not received by the data cutoff date of December 31, 2012.	None

The DOE continues to comply with section 194.21, and there are no outstanding issues with the EPA regarding section 194.21.

21.9 References

(*Indicates a reference that has not been previously submitted.)

Reyes, J. 2008. Letter to D. Moody. 21 February 2008. U.S. EPA, Office of Air and Radiation, Washington, DC.

U.S. Department of Energy (DOE). 2004. Title 40 CFR Part 191 Compliance Recertification Application for the Waste Isolation Pilot Plant (March). 10 vols. DOE/WIPP 2004-3231. Carlsbad, NM: Carlsbad Field Office.

U.S. Department of Energy (DOE). 2009. Title 40 CFR Part 191 Compliance Recertification Application for the Waste Isolation Pilot Plant (March). DOE/WIPP-09-3424. Carlsbad, NM: Carlsbad Field Office.*

U.S. Environmental Protection Agency (EPA). 1996. "40 CFR Part 194: Criteria for the Certification and Recertification of the Waste Isolation Pilot Plant's Compliance with the 40 CFR Part 191 Disposal Regulations:" 61 Federal Register, 5235 (February 9, 1996).

U.S. Environmental Protection Agency (EPA). 1998. "40 CFR Part 194: Criteria for the Certification and Recertification of the Waste Isolation Pilot Plant's Compliance with the Disposal Regulations: Certification Decision; Final Rule" *Federal Register*, vol.5235 63 (May 18, 1998): 27353–406.

U.S. Environmental Protection Agency (EPA). 1999a. Monitoring Inspection Report (40 CFR 194.42) of the Waste Isolation Pilot Plant, *March 24–25, 1999*. Washington, DC: Office of Radiation and Indoor Air.

U.S. Environmental Protection Agency (EPA). 1999b. Report*: EPA Inspection No. EPA-WIPP-9.99-21 of the Waste Isolation Pilot Plant, September 8, 1999* (October). Washington, DC: Office of Radiation and Indoor Air.

U.S. Environmental Protection Agency (EPA). 2000a. *Inspection No. EPA-WIPP-6.00-21 (Monitoring) of the Waste Isolation Pilot Plant, June 21–22, 2000* (August). Inspection Report. Washington, DC: Office of Radiation and Indoor Air.

U.S. Environmental Protection Agency (EPA). 2000b. Inspection *No. EPA-WIPP-6.00-21A (Waste Emplacement) of the Waste Isolation Pilot Plant, June 20–22, 2000* (August). Inspection Report. Washington, DC: Office of Radiation and Indoor Air.

U.S. Environmental Protection Agency (EPA). 2001a. *Inspection No. EPA-WIPP-6.01-21c of the Waste Isolation Pilot Plant, June 20–21, 2001* (September). Monitoring Inspection Report. Washington, DC: Office of Radiation and Indoor Air.

U.S. Environmental Protection Agency (EPA). 2001b. *Inspection No. EPA-WIPP-6.01-21b of the Waste Isolation Pilot Plant, June 21, 2001* (September). Emplacement Inspection Report. Washington, DC: Office of Radiation and Indoor Air.

U.S. Environmental Protection Agency (EPA). 2002a. *Inspection No. EPA-WIPP-6.02-21c of the Waste Isolation Pilot Plant, June 26–28, 2002* (November). Parameter Monitoring Inspection Report. Washington, DC: Office of Radiation and Indoor Air.

U.S. Environmental Protection Agency (EPA). 2002b. *EPA Inspection No. EPA-WIPP-6.02-21b of the Waste Isolation Pilot Plant, June 24–27, 2002* (November). Waste Emplacement Inspection Report. Washington, DC: Office of Radiation and Indoor Air.

U.S. Environmental Protection Agency (EPA). 2003a. *Inspection Number EPA-WIPP-6.03-18c of the Waste Isolation Pilot Plant, June 18–19, 2003* (October). Monitoring Inspection Report. Washington, DC: Office of Radiation and Indoor Air.

U.S. Environmental Protection Agency (EPA). 2003b. *EPA Inspection Number EPA-WIPP-6.03-17b of the Waste Isolation Pilot Plant, June 17–19, 2003* (October). Emplacement Inspection Report. Washington, DC: Office of Radiation and Indoor Air.

U.S. Environmental Protection Agency (EPA). 2004a. *Inspection No. EPA-WIPP-6.04-28c of the Waste Isolation Pilot Plant, June 28 to July 1, 2004* (August). Monitoring Inspection Report. Washington, DC: Office of Radiation and Indoor Air.

U.S. Environmental Protection Agency (EPA). 2004b. *EPA Inspection Number EPA-WIPP-6.04-28b of the Waste Isolation Pilot Plant, June 28–July 1, 2004* (August). Emplacement Inspection Report. Washington, DC: Office of Radiation and Indoor Air.

U.S. Environmental Protection Agency (EPA). 2005a. *Inspection No. EPA-WIPP-7.05-12b of the Waste Isolation Pilot Plant, July 12 to July 15, 2005* (August). Monitoring Inspection Report. Washington, DC: Office of Radiation and Indoor Air.

U.S. Environmental Protection Agency (EPA). 2005b. *EPA Inspection No. EPA-WIPP-05021 of the Waste Isolation Pilot Plant, May 17–19, 2005* (June). Emplacement Inspection Report. Washington, DC: Office of Radiation and Indoor Air.

U.S. Environmental Protection Agency (EPA). 2006a. "Recertification CARD No. 21: Inspections." *Compliance Application Review Documents for the Criteria for the Certification and Recertification of the Waste Isolation Pilot Plant's Compliance with the 40 CFR Part 191 Disposal Regulations: Final Recertification Decision* (March) (pp. 21-1 through 21-5). Washington, DC: Office of Radiation and Indoor Air.

U.S. Environmental Protection Agency (EPA). 2006b. *Inspection No. EPA-WIPP-6.06-20b of the Waste Isolation Pilot Plant, June 20 to June 22, 2006* (September). Monitoring Inspection Report. Washington, DC: Office of Radiation and Indoor Air.

U.S. Environmental Protection Agency (EPA). 2006c. *EPA Inspection Number EPA-WIPP-6.06-20c of the Waste Isolation Pilot Plant, June 20–22, 2006* (September). Emplacement Inspection Report. Washington, DC: Office of Radiation and Indoor Air.

U.S. Environmental Protection Agency (EPA). 2007a. *Inspection Number EPA-WIPP-7.07-10b of the Waste Isolation Pilot Plant, July 10 to 12, 2007* (August). Monitoring Inspection Report. Washington, DC: Office of Radiation and Indoor Air.

U.S. Environmental Protection Agency (EPA). 2007b. *EPA Inspection Number EPA-WIPP-7.07-10c of the Waste Isolation Pilot Plant, July 10–12, 2007* (September). Emplacement Inspection Report. Washington, DC: Office of Radiation and Indoor Air.

U.S. Environmental Protection Agency (EPA). 2007c. Emplacement Inspection for First Receipt of RH Waste: EPA Inspection of the Waste Isolation Pilot Plant, January 9–11, 2007. Washington, DC: Office of Radiation and Indoor Air.

U.S. Environmental Protection Agency (EPA). 2007d. Unannounced EPA Inspection at AMWTP, October 7, 2007. Washington, DC: Office of Radiation and Indoor Air.

U.S. Environmental Protection Agency (EPA). 2008a. Letter From Juan Reyes, Director ,Radiation Protection Division, EPA, to Dr. Dave Moody, Manager, Carlsbad Field Office, March 18, 2008, Unannounced Inspection at the Idaho National Laboratory.*

U.S. Environmental Protection Agency (EPA). 2008b. Letter From Jonathan Edwards, Director, Radiation Protection Division, EPA, to Dr. Dave Moody, Manager, Carlsbad Field Office, July 14, 2008.*

U.S. Environmental Protection Agency (EPA). 2008c. Letter From Jonathan Edwards, Director, Radiation Protection Division, EPA, to Dr. Dave Moody, Manager, Carlsbad Field Office, July 30, 2008.*

U.S. Environmental Protection Agency (EPA). 2008d. Letter From Jonathan Edwards, Director, Radiation Protection Division, EPA, to Dr. Dave Moody, Manager, Carlsbad Field Office, August 21, 2008.*

U.S. Environmental Protection Agency (EPA). 2008e. Letter From Jonathan Edwards, Director, Radiation Protection Division, EPA, to Dr. Dave Moody, Manager, Carlsbad Field Office, October 6, 2008, EPA Inspection Number *EPA-WIPP-7.08-22a, b and c* of the Waste Isolation Pilot Plant, Monitoring and Waste Emplacement, July 10–12, 2007.*

U.S. Environmental Protection Agency (EPA). 2009a. Letter From Jonathan Edwards, Director, Radiation Protection Division, EPA, to Dr. Dave Moody, Manager, Carlsbad Field Office, October 7, 2009, EPA Inspection Number *EPA-WIPP-7.09-14a, b and c* of the Waste Isolation Pilot Plant, Monitoring and Waste Emplacement, July 14–16, 2009.*

U.S. Environmental Protection Agency (EPA). 2009b. Letter From Tom Peake, Director, Center for Waste Management and Regulations, EPA, to J. R. Stroble, Acting Manager, National TRU Program, November 23, 2009, Unannounced Continued Compliance Inspection, *EPA-ORNL-CCP-CH-RH-UA-06.09-24.**

U.S. Environmental Protection Agency (EPA). 2010a. Letter From Jonathan Edwards, Director, Radiation Protection Division, EPA, to Dr. Dave Moody, Manager, Carlsbad Field Office, October.22, 2010, EPA Inspection Number *EPA-WIPP-6.10-29a, b and c* of the Waste Isolation Pilot Plant, Monitoring and Waste Emplacement, June 29–July 1, 2010.*

U.S. Environmental Protection Agency (EPA). 2010b. "Recertification CARD No. 21: Inspections." 2009 Compliance Recertification Application (2009 CRA) Compliance Application Review Document (CARD) No. 21; Inspections (November 18, 2010). Washington, DC: Office of Radiation and Indoor Air.*

U.S. Environmental Protection Agency (EPA). 2011. Letter From Jonathan Edwards, Director, Radiation Protection Division, EPA, to Ed Ziemianski, Carlsbad Field Office, U.S. Department of Energy, November 23, 2011, EPA Inspection Number *EPA-WIPP-5.11-10a, b and c* of the Waste Isolation Pilot Plant, Monitoring and Waste Emplacement, May 10–12, 2010.*

U.S. Environmental Protection Agency (EPA). 2012. Letter From Tom Peake, Director, Center for Waste Management and Regulations, EPA, to J. R. Stroble, Acting Manager, National TRU Program, January 4, 2012, Unannounced Inspection, EPA-NRD-CH-UA-09.11-24, September 19-20, 2011.*

Washington TRU Solutions. WP 05-WH.02, Rev.1 WIPP Waste Handling Operations WDS User's Manual.*

Title 40 CFR Part 191
Subparts B and C
Compliance Recertification Application 2014
for the
Waste Isolation Pilot Plant

Quality Assurance
(40 CFR § 194.22)

United States Department of Energy
Waste Isolation Pilot Plant

Carlsbad Field Office
Carlsbad, New Mexico

Compliance Recertification Application 2014
Quality Assurance
(40 CFR § 194.22)

Table of Contents

This page intentionally left blank.

Acronyms and Abbreviations

ANL	Argonne National Laboratory
ASME	American Society of Mechanical Engineers
BAPL	Bettis Atomic Power Laboratory
CARD	Compliance Application Review Document
CBFO	Carlsbad Field Office
CCA	Compliance Certification Application
CCP	Central Characterization Project
CFR	Code of Federal Regulation
CRA	Compliance Recertification Application
DOE	U.S. Department of Energy
EPA	U.S. Environmental Protection Agency
GEVNC	General Electric Vallecitos Nuclear Center
INL	Idaho National Laboratory
LANL	Los Alamos National Laboratory
MP	management procedure
NQA	Nuclear Quality Assurance
ORNL	Oak Ridge National Laboratory
QA	quality assurance
QAPD	Quality Assurance Program Document
RL	Hanford-Richland
RH-TRU	remote-handled transuranic
SRS	Savannah River Site
TP	team procedure
TRU	transuranic
WIPP	Waste Isolation Pilot Plant

This page intentionally left blank.

22.0 Quality Assurance (40 CFR § 194.22)

22.1 Requirements

§ 194.22 Quality Assurance

(a)(1) As soon as practicable after April 9, 1996, the Department shall adhere to a quality assurance program that implements the requirements of ASME NQA–1–1989 edition, ASME NQA– 2a-1990 addenda, part 2.7, to ASME NQA–2–1989 edition, and ASME NQA–3– 1989 edition (excluding Section 2.1 (b) and (c), and Section 17.1). (Incorporation by reference as specified in § 194.5.)

(2) Any compliance application shall include information which demonstrates that the quality assurance program required pursuant to paragraph (a)(1) of this section has been established and executed for:

(i) Waste characterization activities and assumptions;

(ii) Environmental monitoring, monitoring of the performance of the disposal system, and sampling and analysis activities;

(iii) Field measurements of geologic factors, ground water, meteorologic, and topographic characteristics;

(iv) Computations, computer codes, models and methods used to demonstrate compliance with the disposal regulations in accordance with the provisions of this part;

(v) Procedures for implementation of expert judgment elicitation used to support applications for certification or re-certification of compliance;

(vi) Design of the disposal system and actions taken to ensure compliance with design specifications;

(vii) The collection of data and information used to support compliance application(s); and

(viii) Other systems, structures, components, and activities important to the containment of waste in the disposal system.

(b) Any compliance application shall include information which demonstrates that data and information collected prior to the implementation of the quality assurance program required pursuant to paragraph (a)(1) of this section have been qualified in accordance with an alternate methodology, approved by the Administrator or the Administrator's authorized representative, that employs one or more of the following methods: Peer review, conducted in a manner that is compatible with NUREG–1297, ''Peer Review for High-Level Nuclear Waste Repositories,'' published February 1988 (incorporation by reference as specified in § 194.5); corroborating data; confirmatory testing; or a quality assurance program that is equivalent in effect to ASME NQA–1–1989 edition, ASME NQA– 2a–1990 addenda, part 2.7, to ASME NQA–2–1989 edition, and ASME NQA–3– 1989 edition (excluding Section 2.1 (b) and (c) and Section 17.1). (Incorporation by reference as specified in § 194.5.)

(c) Any compliance application shall provide, to the extent practicable, information which describes how all data used to support the compliance application have been assessed for their quality characteristics, including:

(1) Data accuracy, i.e., the degree to which data agree with an accepted reference or true value;

(2) Data precision, i.e., a measure of the mutual agreement between comparable data gathered or developed under similar conditions expressed in terms of a standard deviation;

(3) Data representativeness, i.e., the degree to which data accurately and precisely represent a characteristic of a population, a parameter, variations at a sampling point, or environmental conditions;

(4) Data completeness, i.e., a measure of the amount of valid data obtained compared to the amount that was expected; and

(5) Data comparability, i.e., a measure of the confidence with which one data set can be compared to another.

(d) Any compliance application shall provide information which demonstrates how all data are qualified for use in the demonstration of compliance.

(e) The Administrator will verify appropriate execution of quality assurance programs through inspections, record reviews and record keeping requirements, which may include, but may not be limited to, surveillance, audits and management systems reviews.

22.2 Background

40 CFR § 194.22 (U.S. EPA 1996) establishes quality assurance (QA) requirements for the Waste Isolation Pilot Plant (WIPP). The QA process enhances the reliability of technical data

and analyses used for the U.S. Department of Energy's (DOE's) Compliance Certification Application (CCA) (U.S. DOE 1996), and subsequent Compliance Recertification Applications (CRAs) (U.S. DOE 2004 and 2009a) and this CRA, which demonstrate compliance with U.S. Environmental Protection Agency (EPA) disposal standards. Section 194.22 requires the DOE to (1) establish and execute a QA program for all items and activities important to the containment of waste in the disposal system, (2) qualify data that are collected prior to implementation of the required QA program, (3) assess data for their quality characteristics, to the extent practicable, (4) demonstrate how data are qualified for use, and (5) allow verification of the above measures through EPA inspections and audits. The DOE's QA program is required to adhere to specific Nuclear Quality Assurance (NQA) standards issued by the American Society of Mechanical Engineers (ASME) NQA-1-1989, NQA-2a-1990 addenda part 2.7, and NQA-3-1989 (ASME 1989; ASME 1990a; ASME 1990b).

22.3 1998 Certification Decision

The EPA's Certification Decision was provided in *Federal Register* vol. 63 (U.S. EPA 1998), pp. 27353–406, "40 CFR Part 194 Criteria for the Certification and Recertification of the Waste Isolation Pilot Plant's Compliance with the Disposal Regulations: Certification Decision; Final Rule." A complete description of the EPA's 1998 Certification Decision for section 194.22 is contained in Docket A-93-02, Items V-A-1 and V-B-2 (U.S. EPA 1998).

The EPA performed three types of assessments during review of the CCA to determine compliance with section 194.22:

1. Determine if the DOE correctly established and implemented QA programs for items and activities important to the long-term isolation of transuranic (TRU) waste in the disposal system (40 CFR § 194.22(a))

2. Determine if the DOE qualified all data, including existing data collected prior to the implementation of QA programs (40 CFR §§ 194.22(b) and (d))

3. Determine if the DOE assessed the CCA data for their quality characteristics (40 CFR § 194.22(c))

The EPA took two general steps to perform each of the three assessments listed above. First, the EPA reviewed the CCA and associated references to determine if the DOE provided a satisfactory description of compliance with the QA requirements. During this stage, the EPA requested and reviewed additional information.

In the second step, the EPA conducted formal audits at WIPP-related facilities to verify compliance with the requirements of section 194.22. These audits were conducted under the authority of 40 CFR § 194.22(e) and were essential to verifying implementation of the QA requirements. Each WIPP-related facility generated much activity and documentation, and it was not practical to visit each facility to witness proper implementation of QA programs. Neither was it considered adequate to assess proper QA program implementation at each facility based solely on documents provided by the DOE. Therefore, the EPA auditors went to four DOE facilities to witness the proper implementation of the QA requirements of section 194.22.

As a result of the audits, the EPA approved the WIPP's QA programs at the DOE Carlsbad Field Office (CBFO), the WIPP site (managed by Washington TRU Solutions, LLC), Sandia National Laboratories, and Los Alamos National Laboratory (LANL). These four WIPP-related facilities are all located in New Mexico.

At that time (1996–1998), other WIPP-related facilities located outside of New Mexico were not approved by the EPA. 40 CFR § 194.22(a)(2)(i) requires the DOE to apply QA programs for waste characterization activities prior to certification. The criteria in 40 CFR § 194.24(c)(3) and 40 CFR § 194.24(c)(5) cross-reference the QA requirements set forth in section 194.22(a)(2)(i). The CCA indicated that waste generator sites outside New Mexico would not begin waste characterization until after 1997 and that it was not reasonable to implement QA programs at that time for future waste characterization. The EPA applied a condition to the approval of the CCA that sites without approved QA programs could not dispose of TRU waste at the WIPP. After the approval of the CCA, each unapproved site would have to be audited to verify compliance prior to shipping waste.

The EPA examined the application of QA for waste characterization at one waste generator site as part of the CCA review. After the DOE informed the EPA that LANL was ready for an audit, the EPA auditors reviewed the LANL QA Plan to verify establishment of QA requirements, and later to verify proper implementation of the QA Plan. Based on the audit samples taken, the EPA determined that LANL had properly established and implemented a QA program for its waste characterization. The other waste generator sites required EPA audits of their individual QA programs before the EPA could allow them to send waste to the WIPP.

After the EPA approved the CCA, the agency conducted periodic audits at the four approved facilities to verify continued compliance. The EPA also began to audit other facilities that had not been ready to perform work at the time of the CCA.

22.4 Changes in the CRA-2004

The 2004 Compliance Recertification Application (CRA-2004) (U.S. DOE 2004a), Chapter 5.0, like the CCA, Chapter 5.0, discussed the QA programs for the WIPP. The DOE extensively revised the CRA-2004, Chapter 5.0 to make it clearly match the structure of the NQA standards and to update information. Changes to the QA portions of the CRA-2004 reflected a maturing and expansion of the CBFO QA program since the CCA. The QA programs that were new at the time of the CCA had increased their effectiveness over time. Between 1998 and 2004, new waste generator sites were added, thus adding more QA programs.

The QA document that establishes the NQA standards for the WIPP is the CBFO *Quality Assurance Program Documen*t (QAPD). As in the CCA, Appendix QAPD-2004 contained the current QAPD at the time. The DOE revised the QAPD between the CCA and the CRA-2004 to more clearly establish each of the applicable NQA elements and to update the DOE organizational structure. Appendices PEER-2004 and AUD-2004 were also updated to include peer reviews and audits performed since the CCA.

22.5 EPA's Evaluation of Compliance for the 2004 Recertification

The EPA's Recertification Decision was published in *Federal Register* vol. 71 (2006), pp. 18010–021 (U.S. EPA 2006a), "40 CFR Part 194 [EPA–HQ–OAR–2004–0025; FRL–8055–1] Criteria for the Certification and Recertification of the Waste Isolation Pilot Plant's Compliance with the Disposal Regulations: Recertification Decision." Detailed technical evaluation of the CRA-2004, Chapter 5.0, Quality Assurance, was provided in Compliance Application Review Document (CARD) 22 (U.S. EPA 2006b). The following is a summary of the EPA's evaluation of compliance with section 194.22 (CRA-2004, Chapter 5.0, and Appendices PEER-2004 and AUD-2004), as contained in the EPA documents mentioned above.

22.5.1 NQA Standards

The CRA-2004 provided information on the DOE's implementation of the NQA standards. ASME NQA-1-1989 (ASME 1989) requirements were addressed in the CRA-2004, Chapter 5.0, Sections 5.3.1 through 5.3.19. ASME NQA-2a-1990 addenda part 2.7 (ASME 1990a) was addressed in the CRA-2004, Chapter 5.0, Section 5.3.20. ASME NQA-3-1989 (ASME 1990b) was addressed in the CRA-2004, Chapter 5.0, Sections 5.3.21, 5.3.22, and 5.3.23 (Docket A-93-02 Items V-A-1 and V-B-2).

The CBFO QA document that implemented the NQA standards, the QAPD, was provided in Appendix QAPD-2004. Since the CCA, the EPA periodically audited the QAPD to verify the continued proper establishment of the NQA standards.

The EPA found that the CBFO QAPD (Appendix QAPD-2004) properly established the applicable elements of the NQA standards invoked under section 194.22 for items and activities important to the long-term isolation of TRU waste.

22.5.2 Audits of QA Plan Implementation

The CRA-2004 provided information on internal and external auditing of the implementation of the CBFO QAPD in the CRA-2004, Chapter 5.0, Sections 5.3.19 and 5.7. The CRA-2004, Chapter 5.0, Section 5.7 described the CBFO audit process that covered internal and external audits, audit schedules, and audit team leader qualification requirements. Appendix AUD-2004, Table AUD-10, provided a summary of audits conducted on the CBFO QAPD.

The EPA determined that the CRA-2004 provided references to general and auditable information regarding internal and external audits to verify proper implementation of the CBFO QAPD. Further, the EPA conducted periodic audits since the CCA to verify the proper implementation of the CBFO QAPD.

22.5.3 Audits of QA Programs at Lower-Tier Organizations

The CRA-2004, Chapter 5.0, Section 5.3.19 addressed internal and external auditing of the CBFO QAPD as a requirement of NQA-1-1989, and the CRA-2004, Chapter 5.0, Section 5.7 described the CBFO audit process that covers internal and external audits, audit schedules, and audit team leader qualification requirements. An audit history of assessments of TRU waste

generator sites and suppliers performing quality-affecting work between 1999 and 2003 is located in Appendix AUD-2004, Tables AUD-1 through AUD-11. All audits were assigned an audit number, which allowed traceability.

Audited suppliers included the CBFO Technical Assistance Contractor, Argonne National Laboratory (ANL) – East, Battelle Columbus Laboratories, Mobile Characterization Services, LLC, and the Carlsbad Environmental Monitoring and Research Center.

The EPA found that the CRA-2004 contained general and auditable information describing an active CBFO auditing program of lower-tier and supplier organizations. Further, the EPA had conducted periodic audits since the CCA to verify the proper execution of QA programs at the lower-tier organizations.

22.5.4 NUREG-1297 for Peer Reviews

U. S. Nuclear Regulatory Commission NUREG-1297 (NRC 1988) provides guidance on the definitions of peer reviews, the area for which peer review is appropriate, the acceptability of peers, and the conduct and documentation of peer reviews. The CBFO peer review process was outlined in the CRA-2004, Chapter 9.0, Section 9.2, which is broken into Sections 9.2.1 through 9.2.8 that generally mirror the topics in NUREG-1297 (NRC 1988. The remainder of the CRA-2004, Chapter 9.0 discussed the results of peer reviews conducted prior to 2004.

CBFO Management Procedure (MP) 10.5 defines the process for conducting peer reviews for compliance with the requirements of NUREG-1297(NRC 1988. The EPA evaluated MP 10.5 and its description in the CRA-2004, Chapter 9.0, Sections 9.2.1 through 9.2.8, and found it to be acceptable.

22.5.5 Assessments of Data Quality Characteristics

The CRA-2004 provided information that described how all data used to support the compliance application were assessed for accuracy, precision, representativeness, completeness, and comparability.

The DOE applied the data quality characteristics to tasks involving the quantification of specific constituents in an environmental medium through sampling and analysis, and applied these data quality characteristics to activities such as the determination of the presence or absence of constituents within TRU waste streams. In these cases, the performance measurement is the concentration of the constituent of interest. Data quality measures are found in the CRA-2004, Chapter 5.0, Section 5.3.22.

The EPA found that the CRA-2004 provided information that describes how all data used to support the compliance application were assessed for their quality characteristics.

22.5.6 Data Qualifications

The CRA-2004, Chapter 5.0, Section 5.3.23 provided information on how all data were qualified for use in the demonstration of compliance by applying one or more of five methods. Audits

were conducted to verify that data not qualified by one of these methods were not used for demonstrating compliance. The EPA found that the CRA-2004 provided information describing how all data used to support the compliance application were qualified.

Based on a review and evaluation of the CRA-2004 and supplemental information provided by the DOE, the EPA determined that the DOE continued to comply with the requirements of section 194.22.

22.6 Changes or New Information Between the CRA-2004 and the CRA-2009 (Previously: Changes or New Information Since the 2004 Recertification)

Changes between the CRA-2004 and CRA-2009 (U.S. DOE 2009a) reflected maturation and expansion of the CBFO QA program since the CCA. The QA programs that were new at the time of the CCA had increased their effectiveness over time. As was the case between the CCA and CRA-2004, new waste generator sites were added between the CRA-2004 and CRA-2009, thus adding more QA programs.

The QA document that establishes the NQA standards for the WIPP is the QAPD. Appendix QAPD-2009, as in the CRA-2004, contained the current QAPD at the time. The DOE revised the QAPD between the CRA-2004 and the CRA-2009 to more clearly establish each of the applicable NQA elements and to update the DOE organizational structure. Appendix AUD-2009 was updated to identify the audits performed since the CRA-2004.

22.6.1 Changes to the QAPD

Changes to the QAPD between CRA-2004 and CRA-2009, as noted in the revision histories, are summarized below. Document citations were added to include remote-handled transuranic (RH-TRU) waste packaging. The detailed changes were incorporated within the document.

In October 2004, Revision 6 of the QAPD (U.S. DOE 2004b) implemented the restructured CBFO organization.

In July 2005, changes implemented in Revision 7 of the QAPD (U.S. DOE 2005) were the direct result of DOE Headquarters (DOE EM 3-2) comments relative to compliance with DOE Order 414.1B.

The changes implemented in Revision 8 of the QAPD (U.S. DOE 2006), effective November 2006, were made to address 13 minor findings and 1 concern from an EPA inspection of the CBFO QA program. Document citations were added to include RH-TRU waste packaging. The exemption of National Environmental Policy Act–related software from the requirements of the QAPD was deleted. The applicability of software QA to safety software was clarified. Editorial changes related to the June 26, 2006, reorganization of the CBFO were also incorporated.

In December 2007, Revision 9 of the QAPD (U.S. DOE 2007) clarified that reliance on administrative controls alone is not sufficient for differentiating between waste that is acceptable for shipment to the WIPP and waste that does not meet the WIPP waste acceptance criteria. The classification of conditions adverse to quality related to the Hazardous Waste Facility Permit was

also clarified. The language regarding reporting nonconformances was revised to comply with the November 16, 2006, Permit Modification. The requirements for records disposition were revised to comply with the Class 1 Permit Modification that took effect on September 13, 2007.

22.6.2 Changes to CBFO/DOE Procedures

The following CBFO procedures were revised between the CRA-2004 and CRA-2009:

- MP 1.2, *Selection of Quality Levels*
- MP 3.1, *Corrective Action Reports*
- MP 4.1, *Preparation and Maintenance of CBFO Procedures*
- MP 4.2, *Document Review*
- MP 4.4, *Document Preparation and Control*
- MP 4.10, *Processing of TRU Waste Site Documents*
- MP 5.2, *TRU Waste Site Certification/Recertification*
- MP 7.1, *QA Requirements for Procurement of Services*
- MP 9.1, *Management Assessments*
- Team Procedure (TP) 10.1, *Qualification of Audit Personnel and Certification of Lead Auditors*
- MP 10.2, *Surveillances*
- MP 10.3, *Audits*
- MP 10.5, *Peer Review*
- TP 10.7, *Operational Assessments*

The following CBFO procedures were added between the CRA-2004 and CRA-2009:

- MP 3.2, *Trend Identification and Reporting* (changed from a TP to an MP)
- MP 3.4, *CBFO Manager Actions upon Notification of Potential Noncompliant Waste Identified During the Waste Confirmation Process*
- TP 3.3, *Protocol for CBFO Observers at Baseline Inspections*
- MP 4.11, *Safety Basis Review Procedure*

- MP 4.12, *National Environmental Policy Act Compliance*
- MP 4.14, *Review of Acceptable Knowledge Sufficiency Determination Requests*
- MP 5.4, *Orders Compliance Program Implementation*

The following procedure was inactivated:

- MP 2.1, *Personnel Qualification and Training*

22.6.3 Updated List of Waste Generator Sites Certified under the QA Program

The contact-handled TRU waste generator sites certified between the CRA-2004 and CRA-2009 under the QA program included:

- LANL Central Characterization Project (LANL/CCP)
- Hanford-Richland (RL/CCP)
- Idaho National Laboratory (INL/CCP)
- Savannah River Site (SRS/CCP)
- Advanced Mixed Waste Treatment Project (AMWTP)
- Oak Ridge National Laboratory (ORNL/CCP)

Between the CRA-2004 and the CRA-2009, two RH-TRU waste generator sites, INL/CCP and ANL/CCP, were certified (see CRA-2009, Section 8, Approval Process of Waste Shipment from Waste Generator Sites for Disposal at the WIPP).Four peer reviews were conducted between the CRA-2004 and the CRA-2009 (see Section 27, Peer Review). A listing of audits and surveillances performed by CBFO can be found in Appendix AUD-2009.

The changes identified to the QAPD and its implementing procedures represented normal evolution and improvement in the CBFO QA program. The CBFO QA program was effectively managed and maintained as demonstrated through CBFO audits and surveillances (see Appendix AUD-2009), and met the provisions of section 194.22.

22.7 EPA's Evaluation of Compliance for the 2009 Recertification

The EPA's Recertification Decision was published in *Federal Register* vol. 75 (2010), pp. 70584–595 (U.S. EPA 2010a), as "40 CFR Part 194 [EPA–HQ–OAR–2009–0330; FRL–9227–4], Criteria for the Certification and Recertification of the Waste Isolation Pilot Plant's Compliance with the Disposal Regulations: Recertification Decision." Detailed technical evaluation of the CRA-2009, Section 22, Quality Assurance, was provided in CARD 22 (U.S. EPA 2010b). The following is a summary of the EPA's evaluation of compliance with section

194.22 (CRA-2009, Section 22, and Appendices AUD-2009 and QAPD-2009) as contained in the EPA documents mentioned above.

22.7.1 NQA Standards

The CRA-2009 provided information on the DOE's implementation of the NQA standards. ASME NQA-1-1989 (ASME 1989), ASME NQA-2a-1990 addenda part 2 (ASME 1990a), and ASME NQA-3-1989 (ASME 1990b) requirements were addressed in Appendix QAPD-2009.

The DOE QA document that implemented the NQA standards, the QAPD, was provided in Appendix QAPD-2009. Since the CCA, the EPA periodically audited the QAPD to verify the continued proper establishment of the NQA standards.

The EPA found that the CBFO QAPD (Appendix QAPD-2009) properly established the applicable elements of the NQA standards invoked under section 194.22 for items and activities important to the long-term isolation of TRU waste.

22.7.2 Audits of QA Plan Implementation

The CRA-2009 provided information on internal and external auditing of the implementation of the CBFO QAPD in Appendix AUD-2009. Appendix QAPD-2009, Section QAPD-4.2.2 described the CBFO audit process that covered internal and external audits, audit schedules, and audit team leader requirements. Appendix AUD-2009 provided a summary of audits conducted on the CBFO QAPD. The EPA determined that the CRA-2009 provided references to general and auditable information regarding internal and external audits to verify proper implementation of the CBFO QAPD. Further, the EPA conducted periodic audits since the CRA-2004 to verify the proper implementation of the CBFO QAPD.

22.7.3 Audits of QA Programs at Lower-Tier Organizations

Appendix QAPD-2009, Section QAPD-4.2.2 addressed internal and external auditing of the CBFO QAPD as a requirement of NQA-1-1989, and described the CBFO audit process. An audit history of assessments of TRU waste generator sites and suppliers performing quality-affecting work between 2003 and 2008 were located in Appendix AUD-2009. All audits were assigned an audit number, which allowed traceability.

Audited suppliers included the Carlsbad Environmental Monitoring and Research Center, Environmental Resource Associates, L&M Technologies (project records services), and Portage Environmental, Inc.

The EPA found that the CRA-2009 contained general and auditable information describing an active auditing program by the CBFO of lower-tier and supplier organizations. Further, the EPA conducted periodic audits since the CRA-2004 to verify the proper execution of QA programs at the lower-tier organizations.

22.7.4 NUREG-1297 for Peer Reviews

U. S. Nuclear Regulatory Commission NUREG-1297 (NRC 1988) provides guidance on the definitions of peer reviews, the area for which peer review is appropriate, the acceptability of peers, and the conduct and documentation of peer reviews. The CBFO peer review process was outlined in the CRA-2009, Section 27.0, which also documented the results of peer reviews conducted since the CRA-2004.

CBFO MP 10.5 defines the process for conducting peer reviews for compliance with the requirements of NUREG-1297 (NRC 1988. The EPA evaluated MP 10.5 and its description in the CRA-2009, Section 27.0, and found it to be acceptable.

22.7.5 Assessments of Data Quality Characteristics

The CRA-2009 provided information that described how all data used to support the compliance application were assessed for accuracy, precision, representativeness, completeness, and comparability.

The DOE applied the data quality characteristics to tasks involving the quantification of specific constituents in an environmental medium through sampling and analysis. The DOE also applied these data quality characteristics to activities such as the determination of the presence or absence of constituents within TRU waste streams. In these cases, the performance measurement is the concentration of the constituent of interest. Data quality measures were found in Appendix QAPD-2009, Section QAPD-6.3.

The EPA found that the CRA-2009 provided information that described how all data used to support the compliance application were assessed for their quality characteristics.

22.7.6 Data Qualifications

Appendix QAPD-2009, Section QAPD-6.3 provided information on how all data were qualified for use in the demonstration of compliance by applying one or more of five methods. Audits were conducted to verify that data not qualified by one of these methods were not used for demonstrating compliance. The EPA found that the CRA-2009 provided information describing how all data used to support the compliance application have been qualified.

Based on a review and evaluation of the CRA-2009, the EPA determined that the DOE continued to comply with the requirements of section 194.22 (U.S. EPA 2010a; U.S. EPA 2010b).

22.8 Changes or New Information Since the CRA-2009

Changes to the QAPD since the CRA-2009, additions and changes to the CBFO implementing procedures, and an updated list of waste generator sites certified as of the CRA-2009 under the QA program are described in this section.

22.8.1 Changes to QAPD

Two revisions to the QAPD occurred since the CRA-2009, as summarized below.

In April 2009, Revision 10 of the QAPD (U.S. DOE 2009b) addressed the following:

- CBFO Corrective Action Report 08-026 regarding the adequacy of the test control requirements as stated in Revision 9 of the QAPD
- Requirements for the use of administrative controls to differentiate waste that is acceptable for shipment to the WIPP to address "as low as reasonably achievable" considerations for remote-handled waste
- Editorial revisions to the reference document sections to address changes to documents since the last revision of the QAPD
- Minor clarifications in response to comments during CBFO internal review and to address a recent reorganization of CBFO

In May 2010, Revision 11 of the QAPD (U.S. DOE 2011) addressed the April 1, 2010, WIPP Hazardous Waste Facility Permit modification for the time allowed for reporting nonconformances to data quality objectives first identified at the Site Project Manager level.

22.8.2 Changes to DOE/CBFO Procedures

The following CBFO procedures were added since the CRA-2009:

- MP 2.2, *Lessons Learned*
- MP 5.5, *CBFO Telework Requirements*
- MP 5.6, *Subcontract Consent Reviews*
- MP 5.7, *CBFO Injury/Illness Reporting*
- TP 9.2, *CBFO Work Control Oversight*
- MP 10.7, *CBFO Oversight Evaluation*

The following CBFO procedures were revised since the CRA-2009:

- MP 1.2, *Selection of Quality Levels*
- MP 3.1, *Corrective Action Reports*
- MP 3.4, *CBFO Manager Actions Upon Notification of Potential Noncompliant Waste Identified During The Waste Confirmation Process*

- MP 4.1, *Preparation and Maintenance of CBFO Procedures*
- MP 4.2, *Document Review*
- MP 4.4, *Document Preparation and Control*
- MP 4.5, *Generating, Receiving, Storing, and Controlling Active CBFO Program Records*
- MP 4.6, *Records Filing, Inventorying, Scheduling, and Dispositioning*
- MP 4.7, *Disposal of Nonpermanent Records*
- MP 4.8, *Records Transfer and Retrieval*
- MP 4.9, *Quality Assurance Records*
- MP 4.11, *Safety Basis Review Procedure*
- MP 4.12, *National Environmental Policy Act Compliance*
- MP 4.14, *CBFO Review of Acceptable Knowledge Sufficiency Determination Requests*
- MP 5.1, *Approval of Contractor-Generated Confirmation Data Packages*
- MP 5.2, *TRU Waste Site Certification/Recertification*
- MP 5.4, *Directives Compliance Program*
- MP 9.1, *Management Assessments*
- MP 10.3, *Audits*

The following procedures have been cancelled since the CRA-2009:

- OP 10.3, *Operational Evaluations*
- TP 10.7, *Operational Evaluations*

22.8.3 Updated List of Waste Generator Sites Certified under the QA Program

The TRU waste sites approved by the EPA to ship contact-handled TRU waste to the WIPP in accordance with the requirements of section 194.8 since CRA-2009 are as follows: Advanced Mixed Waste Treatment Project, RL/CCP, INL/CCP, LANL/CCP, ORNL/CCP and SRS/CCP. Since the CRA-2009, suspension of CH waste characterization activities occurred at ORNL/CCP and RL/CCP.

The TRU waste sites approved by the EPA to ship RH-TRU waste to the WIPP in accordance with the requirements of section 194.8 since CRA-2009 are as follows: ANL/CCP, Bettis Atomic Power Laboratory (BAPL/CCP), General Electric Vallecitos Nuclear Center (GEVNC)/CCP, INL/CCP, ORNL/CCP and SRS/CCP. Since the CRA-2009, suspension of RH waste characterization activities occurred at the following sites: BAPL/CCP, GEVNC/CCP, RL/CCP, and ORNL/CCP.

A listing of audits and surveillances performed by CBFO can be found in Appendix AUD-2014.

The results of audits and surveillances performed by CBFO concluded that the DOE continues to comply with all the requirements of section 194.22.

The changes identified to the QAPD and its implementing procedures represent normal evolution and improvement in the CBFO QA program. The current CBFO QA program is effectively managed and maintained as demonstrated by the CBFO audit and surveillance program (see Appendix AUD-2014), and meets the provisions of section 194.22.

22.9 References

(*Indicates a reference that has not been previously submitted.)

U.S. Department of Energy (DOE). 1996. *Title 40 CFR Part 191 Compliance Certification Application for the Waste Isolation Pilot Plant* (October). 21 vols. DOE/CAO 1996-2184. Carlsbad, NM: Carlsbad Area Office.

U.S. Department of Energy (DOE). 2004a. *Title 40 CFR Part 191 Compliance Recertification Application for the Waste Isolation Pilot Plant* (March). 10 vols. DOE/WIPP 2004-3231. Carlsbad, NM: Carlsbad Field Office.

U.S. Department of Energy (DOE). 2004b. Carlsbad Field Office, Quality Assurance Program Document, DOE/CBFO-94-1012, Revision 6.

U.S. Department of Energy (DOE). 2005. Carlsbad Field Office, Quality Assurance Program Document, DOE/CBFO-94-1012, Revision 7.

U.S. Department of Energy (DOE). 2006. Carlsbad Field Office, Quality Assurance Program Document, DOE/CBFO-94-1012, Revision 8.

U.S. Department of Energy (DOE). 2007. Carlsbad Field Office, Quality Assurance Program Document, DOE/CBFO-94-1012, Revision 9.

U.S. Department of Energy (DOE). 2009a. *Title 40 CFR Part 191 Compliance Recertification Application for Waste Isolation Pilot Plant* (March). DOE/WIPP 2009-3423, Carlsbad, NM: Carlsbad Field Office.*

U.S. Department of Energy (DOE). 2009b. Carlsbad Field Office, Quality Assurance Program Document, DOE/CBFO-94-1012, Revision 10.*

U.S. Department of Energy (DOE). 2011. Carlsbad Field Office, Quality Assurance Program Document, DOE/CBFO-94-1012, Revision 11.*

U.S. Environmental Protection Agency (EPA). 1996. "40 CFR Part 194: Criteria for the Certification and Recertification of the Waste Isolation Pilot Plant's Compliance With the 40 CFR Part 191 Disposal Regulations; Final Rule." *Federal Register*, vol. 61 (February 9, 1996): 5223-45.

U.S. Environmental Protection Agency (EPA). 1998. "40 CFR Part 194: Criteria for the Certification and Recertification of the Waste Isolation Pilot Plant's Compliance with the Disposal Regulations: Certification Decision; Final Rule." *Federal Register*, vol. 63 (May 18, 1998): 27353–406.

U.S. Environmental Protection Agency (EPA). 2006a. "40 CFR Part 194: Criteria for the Certification and Recertification of the Waste Isolation Pilot Plant's Compliance with the Disposal Regulations: Recertification Decision" (Final Notice). *Federal Register*, vol. 71 (April 10, 2006): 18010–021.

U.S. Environmental Protection Agency (EPA). 2006b. "Recertification CARD No. 22: Quality Assurance." *Compliance Application Review Documents for the Criteria for the Certification and Recertification of the Waste Isolation Pilot Plant's Compliance with the 40 CFR Part 191 Disposal Regulations: Final Recertification Decision* (March) (pp. 22-1 through 22-17). Washington, DC: Office of Radiation and Indoor Air.

U.S. Nuclear Regulatory Commission (NRC). 1988. *Peer Review for High-Level Nuclear Waste Repositories*: *Generic Technical Position.* NUREG-1297. Washington, DC: U.S. Nuclear Regulatory Commission.

U.S. Environmental Protection Agency (EPA). 2010a. "40 CFR Part 194: Criteria for the Certification and Recertification of the Waste Isolation Pilot Plant's Compliance with the Disposal Regulations: Recertification Decision; Final Rule." *Federal Register*, vol. 75 (November 18, 2010): 70584-595.*

U.S. Environmental Protection Agency (EPA). 2010b. "2009 Compliance Recertification Application (CRA-2009) Compliance Application Review Document (CARD) No. 22, Quality Assurance." EPA Docket FDMS Docket ID No. EPA-HQ-OAR-2009-0330. Washington, DC: Office of Radiation and Indoor Air.*

The American Society of Mechanical Engineers (ASME). 1989. Quality Assurance Program Requirements for Nuclear Facilities. ASME/NQA-1, 1989 Edition.*

The American Society of Mechanical Engineers (ASME). 1990a. Quality Assurance Requirements of Computer Software for Nuclear Facility Applications. ASME/NQA-2a-1990 Addenda, Part 2.7.

The American Society of Mechanical Engineers (ASME). 1990b. Quality Assurance Program Requirements for the collection of Scientific and Technical Information for Site Characterization of High-Level Nuclear Waste Repositories. ASME/NQA-3-1989.

Title 40 CFR Part 191
Subparts B and C
Compliance Recertification Application-2014
for the
Waste Isolation Pilot Plant

Models and Computer Codes
(40 CFR § 194.23)

United States Department of Energy
Waste Isolation Pilot Plant

Carlsbad Field Office
Carlsbad, New Mexico

Compliance Recertification Application 2014
Models and Computer Codes
(40 CFR § 194.23)

Table of Contents

List of Tables

This page intentionally left blank.

Acronyms and Abbreviations

AP	Analysis Package
ASME	American Society of Mechanical Engineers
CARD	Compliance Application Review Document
CBFO	Carlsbad Field Office
CCA	Compliance Certification Application
CFR	Code of Federal Regulations
CRA	Compliance Recertification Application
DD	Design Document
DOE	U.S. Department of Energy
DRP	Data Records Packages
DRZ	Disturbed Rock Zone
EPA	U.S. Environmental Protection Agency
FDMS	Federal Document Management System
FEPs	Features, events, and processes
F/T	Flow and Transport
ID	Implementation Document
LHS	Latin Hypercube Sampling
NQA	Nuclear Quality Assurance
PA	Performance assessment
PABC	Performance Assessment Baseline Calculation
PEF	Parameter Entry Form
PIRP	Principal Investigator Records Package
QA	Quality assurance
QAP	Quality Assurance Procedure
QAPD	Quality Assurance Program Document
RD	Requirements Document
ROMPCS	Run-of-Mine Panel Closure System
SNL	Sandia National Laboratories
T-field	Transmissivity field
UM	User's Manual
VD	Validation Document

VVP	Verification and Validation Plan
WIPP	Waste Isolation Pilot Plant

This page intentionally left blank.

23.0 Models and Computer Codes (40 CFR § 194.23)

23.1 Requirements

§ 194.23 Models and Computer Codes

(a) Any compliance application shall include:

(1) A description of the conceptual models and scenario construction used to support any compliance application.

(2) A description of plausible, alternative conceptual model(s) seriously considered but not used to support such application, and an explanation of the reason(s) why such model(s) was not deemed to accurately portray performance of the disposal system.

(3) Documentation that:

(i) Conceptual models and scenarios reasonably represent possible future states of the disposal system.

(ii) Mathematical models incorporate equations and boundary conditions which reasonably represent the mathematical formulation of the conceptual models.

(iii) Numerical models provide numerical schemes which enable the mathematical models to obtain stable solutions.

(iv) Computer models accurately implement the numerical models; i.e., computer codes are free of coding errors and produce stable solutions.

(v) Conceptual models have undergone peer review according to §194.27.

(b) Computer codes used to support any compliance application shall be documented in a manner that complies with the requirements of ASME NQA-2a-1990 addenda, part 2.7, to ASME NQA-2-1989 edition.

(c) Documentation of all models and computer codes included as part of a compliance application performance assessment calculation shall be provided. Such documentation shall include, but shall not be limited to:

(1) Descriptions of the theoretical backgrounds of each model and the method of analysis or assessment.

(2) General descriptions of the models; discussions of the limits of applicability of each model; detailed instructions for executing the computer codes, including hardware and software requirements, input and output formats with explanations of each input and output variable and parameter (e.g., parameter name and units); listing of input and output files from a sample computer run; and reports on code verification, bench marking, validation, and quality assurance procedures.

(3) Detailed descriptions of the structure of the computer codes and complete listings of the source codes.

(4) Detailed descriptions of data collection procedures, data reduction and analysis, and code input parameter development.

(5) Any necessary licenses;

(6) An explanation of the manner in which models and computer codes incorporate the effects of parameter correlation.

(d) The Administrator or the Administrator's authorized representative may verify the results of computer simulations used to support any compliance application by performing independent simulations. Data files, source codes, executable versions of computer software for each model, other material or information needed to permit the Administrator or the Administrator's authorized representative to perform independent simulations, and to access necessary hardware to perform such simulations, shall be provided within 30 calendar days of a request by the Administrator or the Administrator's authorized representative.

23.2 40 CFR § 194.23(a)(1)

23.2.1 Background

The criteria in 40 CFR § 194.23(a)(1) (U.S. EPA 1996) requires descriptions of the conceptual models and scenario construction used to demonstrate compliance.

23.2.2 1998 Certification Decision

To meet the requirements for section 194.23(a)(1), the U.S. Environmental Protection Agency (EPA) expected the U.S. Department of Energy (DOE) to include a complete, clear, and logical description of each conceptual model used to demonstrate compliance in the application. Documentation of the conceptual models was expected to describe site characteristics and processes active at the site (e.g., gas generation or creep closure of the Salado Formation salt). The conceptual models were to consider both natural and engineered barriers. The DOE developed 24 conceptual models to describe the Waste Isolation Pilot Plant (WIPP) disposal system.

For the Compliance Certification Application (CCA) (U.S. DOE 1996), the EPA reviewed each of the 24 conceptual models included in the CCA (see Table 23-1) using information contained in the CCA, supplementary peer review panel reports, and supplementary information provided to the EPA by the DOE in response to specific EPA comments. Upon the conclusion of the conceptual model peer review, the panel stated, "With the exception of the Spallings Model presented in the CCA (U.S. DOE 1996), which the Panel continues to find inadequate, all remaining conceptual models have been determined to be adequate and all significant issues regarding their adequacy have been resolved." The peer review panel also stated, "Although further refinement in understanding and predictive capability for spallings events would be desirable as part of a new conceptual model, the Panel has determined that the additional information presented by the DOE is sufficiently complete at this time to support a conclusion that the spallings volumes used in the CCA are reasonable, and may actually overestimate the actual waste volumes that would be expected to be released by the spallings process at the WIPP" (Appendix PEER-2004, Section PEER-2004 1.1.5 and Section 4.0) (U.S. DOE 2004). The EPA agreed with the peer review panel that all models, with the exception of spallings, were considered adequate to represent future states of the repository. In the case of the spallings model, the EPA considered the results adequate because the DOE showed in its additional spallings modeling that the release of solid waste predicted by the performance assessment (PA) spallings model overestimated releases by a factor of 10 or more (Sandia National Laboratories and Carlsbad Area Office Technical Assistance Contractor 1997).

The EPA determined that the CCA and supporting documentation contained a complete and accurate description of each conceptual model and the scenario construction methods used in PA. The scenario construction descriptions included sufficient detail to explain the basis for selecting some scenarios and rejecting others, and were adequate for use in the CCA PA calculations (U.S. DOE 1996). The EPA found the DOE to be in compliance with the requirements of section 194.23(a)(1) (Compliance Application Review Document [CARD] 23, Section 1.4) (U.S. EPA 1998a).

A complete description of the EPA's 1998 Certification Decision for section 194.23(a)(1) can be obtained from CARD 23, Section 1.4 (U.S. EPA 1998a).

Table 23-1. WIPP Conceptual Models

Conceptual Model	Component
1 Disposal System Geometry[a]	**Salado Flow and Transport (F/T)**
2 Culebra Hydrogeology[b]	Non-Salado F/T
3 Repository Fluid Flow	**Salado F/T**
4 Salado	Salado F/T
5 Impure Halite	Salado F/T
6 Salado Interbeds	Salado F/T
7 Disturbed Rock Zone (DRZ)	**Salado F/T**
8 Actinide Transport in the Salado	Salado F/T
9 Units Above the Salado	Non-Salado F/T
10 Transport of Dissolved Actinides in the Culebra	Non-Salado F/T
11 Transport of Colloidal Actinides in the Culebra	Non-Salado F/T
12 Exploration Boreholes	Human Intrusion
13 Cuttings and Cavings	Human Intrusion
14 Spallings	**Human Intrusion**
15 Direct Brine Release	Human Intrusion
16 Castile Formation and Brine Reservoir	Human Intrusion
17 Multiple Intrusions	Human Intrusion
18 Climate Change	Non-Salado F/T
19 Creep Closure	Salado F/T
20 Shafts and Shaft Seals	Salado F/T
21 Gas Generation	Salado F/T
22 Chemical Conditions	Salado F/T
23 Dissolved Actinide Source Term	Salado F/T
24 Colloidal Actinide Source Term	Salado F/T

[a] Entries in bold were modified and peer reviewed for the CRA-2004 PA.
[b] Culebra Hydrogeology Model was peer reviewed in the CRA-2009 PABC (U.S. DOE 2009).

23.2.3 Changes in the CRA-2004

For the 2004 Compliance Recertification Application (CRA-2004), the DOE undertook an extensive screening process to determine which features, events, and processes (FEPs) were still applicable to the disposal system and which changes were appropriate. The DOE's scenario construction methods had not changed since the CCA. The DOE constructed two basic scenarios, undisturbed performance and disturbed performance, which included drilling and mining events (U.S. DOE 2004).

Although minor changes were made to the FEPs, the results of the reassessment did not impact the original conceptual models or scenarios (Appendix PA-2004, Attachment SCR, and Chapter 6.0, Section 6.2.6) (U.S. DOE 2004). Hence, the 24 original conceptual models were maintained

in the CRA-2004 PA to describe the WIPP disposal systems. The DOE did, however, modify three conceptual models related to the Salado Formation modeling: Disposal System Geometry, Repository Fluid Flow, and the Disturbed Rock Zone (DRZ) (U.S. DOE 2004). Furthermore, the DOE developed a new spallings model for the CRA-2004 (U.S. DOE 2004). The 24 conceptual models that were included in the CCA and the CRA-2004 are listed in Table 23-1. The four conceptual models that were changed are noted in bold type.

23.2.4 EPA's Evaluation of Compliance for the 2004 Recertification

The EPA's review of the CRA-2004 for compliance with section 194.23(a)(1) focused on changes to FEPs, conceptual models, scenarios, or models since the 1998 Certification Decision (U.S. EPA 1998b). The CCA and CRA-2004 scenario construction process had not changed and was based on screening decisions using a comprehensive list of FEPs developed for the Swedish Nuclear Power Inspectorate (also known as SKI), and other WIPP-specific FEPs developed by the DOE (CRA-2004, Chapter 6.0, Section 6.2.1, and the CCA, Chapter 6.0) (U.S. DOE 2004). The DOE's methods for addressing conceptual model development and scenario construction had not changed since the CCA, and consisted primarily of identifying and screening processes and events and combining them into scenarios. The EPA reviewed each of the steps used in this process during its evaluation and review of changes since the CCA. The EPA reviewed the DOE's FEPs reevaluation and found the documentation to be adequate and the reasons for changes to the FEPs reasonable (U.S. EPA 2006a).

During the CRA-2004 evaluation, the EPA paid particular attention to any FEP changes concerning human intrusion scenarios related to mining and oil and gas drilling, such as fluid injection and air drilling (U.S. EPA 2006b). As noted in U.S. EPA (2006b), some parameters, such as drilling rate and other drilling-related values, had been updated since the CCA as a result of continued activities in the Delaware Basin. The parameter changes did not have a detrimental impact on the compliance determination, as exhibited by the results of the subsequent PA, the CRA-2004 Performance Assessment Baseline Calculation (PABC) (U.S. EPA 2006c, Section 11.3). Drilling practices (such as injection techniques and air drilling) and mining activities have not significantly changed since the CCA. Therefore, the EPA did not believe that the original conclusions during the CCA needed to be modified for the CRA-2004.

In the EPA's August 2002 Guidance Letter (Marcinowski 2002), the EPA instructed the DOE to develop a new spallings model for the CRA-2004 PA. The new spallings model (Appendix PA-2004, Attachment MASS-2004, Section 16.1.3) (U.S. DOE 2004) included three major elements: consideration of multiphase flow processes in the intrusion borehole, consideration of fluidization and transport of waste particulates from the intact waste mass to the intrusion borehole, and a numerical solution for the coupled mechanical and hydrological response of the waste as a porous medium. The new spallings model was peer reviewed in 2003 and found to be adequate (CRA-2004, Chapter 9.0, Section 9.3.1.3.5, and Appendix PEER-2004, Section PEER-2004 3.0) (U.S. DOE 2004). The EPA found the spallings model peer review to be adequate ((U.S. EPA 2006d), Section 5.0) and the new spallings model to be appropriate for use in the CRA-2004 PA ((U.S. EPA 2006c), Section 10.3.1).

The DOE modified the Disposal System Geometry, Repository Fluid Flow, and DRZ conceptual models to reflect new information on the Salado and to incorporate the EPA-mandated Option D

panel closure design requirements. The DOE modified the BRAGFLO computational grid and the computational grid for the direct brine release calculations to include the Option D panel closure design requirements. The DOE also simplified the shaft in the BRAGFLO grid and refined the BRAGFLO grid. These modified conceptual models were peer reviewed during 2002 and 2003 and found to be adequate (CRA-2004, Chapter 9.0, Section 9.3.1.3.4, and Appendix PEER-2004, Section PEER-2004 2.0) (U.S. DOE 2004). The EPA found the changes to the Salado Flow Conceptual Models to be adequate ((U.S. EPA 2006e), Section 5.0). The EPA determined that while these new models better reflected the knowledge of the disposal system, the changes had little impact on the results of the PA ((U.S. EPA 2006c), Section 12.0).

The EPA's review found that the CRA-2004 and supplementary information contained a complete and accurate description of each conceptual model that changed, and that documentation of all conceptual models continued to adequately discuss site characteristics and processes at the site. The EPA determined that the conceptual models continued to adequately represent those characteristics, processes, and attributes of the WIPP disposal system affecting its performance, and that the conceptual models considered both natural and engineered barriers. The EPA found that the DOE considered conceptual models that continued to adequately describe the future characteristics of the disposal system. The conceptual models continued to reasonably describe the expected performance of the disposal system and incorporate reasonable simplifying assumptions of the disposal system's behavior. The EPA found that the modifications to four of the conceptual models were reasonable and the related CRA-2004 documentation was complete (CARD 23, Section Recertification Decision 194.23(a)(1)) (U.S. EPA 2006f).

Based on a review and evaluation of the CRA-2004 and supplemental information provided by the DOE, the EPA determined that the DOE continued to comply with the requirements for section 194.23(a)(1) (CARD 23, Section Recertification Decision 194.23(a)(1)) (U.S. EPA 2006f).

23.2.5 Changes or New Information Between the CRA-2004 and the CRA-2009 (Previously: Changes or New Information Since the 2004 Recertification)

A reassessment of the FEPs was conducted for the CRA-2009 and the results are documented in Appendix SCR-2009, Section SCR-1.0 (U.S. DOE 2009). Of the 235 FEPs considered for the CRA-2004, 188 did not change, 35 were updated with new information, 10 were split into 20 similar but more descriptive FEPs, one screening argument was changed to correct errors discovered during review, and one FEPs screening decision was changed (Appendix SCR-2009, Table SCR-2) (U.S. DOE 2009).

No changes in the 24 conceptual models or scenario construction methodology resulted from the FEPs reevaluation. However, because of new information, the Culebra Hydrogeology conceptual model was modified, peer reviewed (U.S. EPA 2010b; Burgess et al. 2008), and used in the CRA-2009 PABC (Kuhlman 2010).

23.2.6 EPA's Evaluation of Compliance for the 2009 Recertification

The EPA verified that no changes in the 24 conceptual models or scenario construction methodology resulted from the CRA-2009 FEPs reevaluation (U.S. EPA 2010b). The DOE's scenario construction methodology had not changed since the CRA-2004 PA. The 24 conceptual models included in the CCA and the CRA-2004 had not changed for the CRA-2009 (U.S. DOE 2009). These conceptual models are described in Section 23.1.2 and listed in Table 23-1.

One model was changed for the CRA-2009 PABC by incorporating new information derived from new monitoring wells and well testing activities. The DOE modified the Culebra Hydrogeology Conceptual Model by making the transmissivity fields (T-fields) more geology-based. The EPA concluded that the DOE's computational approach was basically the same as in the CRA-2004, but the parameterization and some assumptions were changed and refined based on new well and well testing data (Appendix TFIELD-2009, Section TFIELD-1.0; (Kuhlman 2010), Sections 2.0 and 3.0) (U.S. DOE 2009).

The EPA examined the DOE's conceptual model peer review (Burgess et al. 2008) and model implementation changes in developing the T-fields (Section 3.0(Kuhlman 2010)). The DOE conducted new studies of Culebra hydrogeology, the results of which were summarized in Beauheim (Beauheim 2008) and peer-reviewed by Burgess et al. (Burgess 2008). These results were implemented in the generation of a new set of T-fields (Kuhlman 2010) that integrated geologic, hydrologic, and geochemical data. The resulting implementation of the Culebra conceptual model related the flow properties of the Culebra to geologic factors that can be mapped with varying degrees of certainty over the model domain. The model provided a statistical/stochastic basis for estimating hydrologic properties over the area of interest. Geochemical observations were shown to be consistent with the conceptual model. The revised Culebra Hydrology Conceptual Model was used in the CRA-2009 PABC.

The EPA's review of the technical work leading to the model revisions is described in CARD 15, Sections 15.2.4 and 15.2.5 (U.S. EPA 2010b). The EPA's oversight of the Culebra Hydrogeology Conceptual Model Peer review is discussed in CARD 27, Peer Review, Section 27.4.1 (U.S. EPA 2010b).

The EPA approved of the Culebra Hydrology Conceptual model revisions and concluded that the CRA-2009 contained an adequate description of conceptual models and scenario construction methods, and that conceptual model and scenario construction descriptions included sufficient detail to explain the basis for selecting some scenarios and rejecting others (U.S. EPA 2010b). Thus, the EPA determined that the DOE continued to demonstrate compliance with the provisions of section 194.23(a)(1) (CARD 23, Section 23.1.7) (U.S. EPA 2010b).

23.2.7 Changes or New Information Since the CRA-2009

The DOE conducted an extensive FEPs reassessment for the CRA-2014 to determine which FEPs were still applicable to the disposal system and which changes were appropriate. This reassessment and the results are documented in Appendix SCR-2014, Section SCR-1.0 and Section 32 (U.S. DOE 2014).

No changes in the 24 conceptual models or scenario construction methodology resulted from the FEPs reevaluation. However, several changes in the implementation of certain FEPs in PA have occurred since the CRA-2009 and are included in the CRA-2014. These include the repository planned changes (i.e., additional excavated area in the northern experimental area), parameter updates (i.e., PBRINE, TAUFAIL, iron corrosion rate, and other parameters updates detailed in Camphouse (Camphouse 2013b)), and refinements to PA implementation. The specific changes since the CRA-2009 that are included in the CRA-2014, none of which constitute or result in conceptual model changes, are detailed in Camphouse (Camphouse 2013a) and in Appendix PA-2014 (U.S. DOE 2014).

Given that no changes or new information in description of conceptual models or scenario construction methodology resulted from the FEPs reassessment or from the changes since the CRA-2009, the DOE continues to demonstrate compliance with the provisions of section 194.23(a)(1).

23.3 40 CFR § 194.23(a)(2)

23.3.1 Background

40 CFR § 194.23(a)(2) requires a description of those conceptual models that were identified or developed while preparing the compliance application, but were determined not to be appropriate for portraying disposal system performance. It also requires that the reasons for not using these models be explained.

23.3.2 1998 Certification Decision

To meet the requirements of section 194.23(a)(2), the DOE described in the CCA the plausible alternative conceptual models considered but not used and explained why these models were not used (CCA Chapters 2.0, 9.0, and Appendix MASS) (U.S DOE 1996). Descriptions of the rejected alternative models did not need to be as detailed as descriptions of the models actually used in the CCA. The DOE also explained why these alternative models were not used to describe the performance of the repository. The descriptions of the alternative models and justifications for the conceptual model selections were summarized in Dials (Dials 1997), Table 1. The EPA reviewed the material on alternative conceptual models and the comments made by the Conceptual Models Peer Review Panel on alternative models. The panel identified no substantive issues regarding alternative models. The EPA found the DOE to be in compliance with the requirements of section 194.23(a)(2) (CARD 23, Section 2.4) (U.S. EPA 1998a).

A complete description of the EPA's 1998 Certification Decision for section 194.23(a)(2) can be obtained from CARD 23, Section 2.4 (U.S. EPA 1998a).

23.3.3 Changes in the CRA-2004

As stated at the time of the CCA, the DOE's position is that the basic elements of the conceptual models used in the CCA have been developed over a number of years, as a result of continuing analysis of alternatives and elimination of those alternative conceptual models found to be unacceptable or inappropriate.

In the CRA-2004, Chapter 2.0, Chapter 6.0, Section 6.4, and Chapter 9.0, Section 9.3.1, the DOE described the conceptual models used to evaluate the WIPP's performance. Since the CCA, the DOE changed four conceptual models, developed a new spallings model for the CRA-2004, and made minor changes to three other conceptual models (Disposal System Geometry, Repository Fluid Flow, and DRZ). All of these models were peer reviewed as required by section 194.27. The Spallings and Salado Flow Conceptual Models Peer Review Panels' consideration of alternative conceptual models for the four changed conceptual models is described in Appendix PEER-2004, Sections PEER-2004 2.0 and PEER-2004 3.0 (U.S. DOE 2004).

23.3.4 EPA's Evaluation of Compliance for the 2004 Recertification

The EPA reviewed the CRA-2004 documentation listed above and reevaluated the CCA documentation. The EPA reviewed all aspects of the DOE's work related to alternative conceptual models to confirm that the DOE continued to comply with the requirements of section 194.23(a)(2) (CARD 23, Section Evaluation of Compliance for Recertification 194.23(a)(2)) (U.S. EPA 2006f).

As part of its alternative model review, the EPA examined the CRA-2004 documentation to determine if any other models had changed or if any new alternative models had been developed since the CCA. The EPA also reexamined the CCA for alternative conceptual models seriously considered in the CCA, as summarized in Dials (Dials 1997), Table 1, to determine if any of the DOE's original approach or justification had changed since the original certification. Based on this review, the EPA determined that all alternative models had been appropriately considered by the DOE and that the DOE continued to be in compliance with the requirements of section 194.23(a)(2) (CARD 23, Section Recertification Decision 194.23(a)(2)) (U.S. EPA 2006f).

Members of the public suggested that karst formation and processes may be a possible alternative conceptual model for flow in the Rustler Formation. Karst may be defined as voids in near-surface or subsurface rock created by water flowing when rock is dissolved. Public comments included statements that karst could develop interconnected "underground rivers" that may enhance the release of radioactive materials from the WIPP. Because of this comment, the EPA required the DOE to perform a thorough reexamination of all historical data, information, and reports by the DOE and others, to determine if karst features or development had been missed during previous work done at the WIPP. The DOE's findings are summarized in Lorenz (Lorenz 2006a;Lorenz 2006b). The EPA also conducted a thorough reevaluation of karst and of the work done during the CCA (U.S. EPA 2006g). The EPA's reevaluation of historical evidence and recent work by the DOE did not show even the remotest possibility of an "underground river" near the WIPP, nor did it change the CCA conclusions. Therefore, the EPA believed karst was not a viable alternative model at the WIPP. For a more complete discussion of the reevaluation of karst, see CARD 14/15 (U.S. EPA 2006h) and Lorenz (Lorenz 2006a;Lorenz 2006b).

Based on a review and evaluation of the CRA-2004 and supplemental information provided by the DOE, the EPA determined that the DOE continued to comply with the requirements of section 194.23(a)(2) (CARD 23, Section Recertification Decision 194.23(a)(2)) (U.S. EPA 2006f).

23.3.5 Changes or New Information Between the CRA-2004 and the CRA-2009 (Previously: Changes or New Information Since the 2004 Recertification)

The implementation and parameterization of one of the 24 conceptual models was changed after the CRA-2004 decision in March 2006. The computational implementation and parameterization of the Culebra Hydrogeology Conceptual Model was changed between the CRA-2004 and CRA-2009. No other alternative conceptual models were implemented for the CRA-2009 PA calculations.

23.3.6 EPA's Evaluation of Compliance for the 2009 Recertification

The EPA reviewed the DOE's documentation for CRA-2009, namely Appendices PA-2009, SCR-2009, and MASS-2009 (U.S. DOE 2009), and verified that only one of the 24 conceptual models had been changed since CRA-2004, and that no new alternative conceptual models had been considered in the CRA-2009. In 2007, as part of its continuous evaluation of alternative conceptual models, the DOE proposed modifications that would affect two of the existing conceptual models, Cuttings and Cavings and DRZ (Vugrin and Nemer 2007). It was determined that since these proposed modifications would impact the conceptual models, an independent technical peer review on the adequacy of the proposed changes to the approved conceptual models should be performed in accordance with the requirements of section 194.27. In October 2007, before the peer review was completed, the DOE decided to postpone the consideration of the proposed modifications (see Section 27.7.3). The EPA verified that these potential alternative conceptual models were never implemented in the CRA-2009 PA calculations.

The Culebra Hydrogeology Conceptual Model Peer Review was performed in 2008 (Burgess et al. 2008). This peer review evaluated changes to the computational implementation and parameterization of the Culebra Hydrogeology Conceptual Model. The EPA examined the peer review plan and the final peer review report for this model and found them to adequately fulfill the requirements of section 194.27 and the U.S. Nuclear Regulatory Commission (U.S. NRC 1988). The EPA also observed the selection of the panel, the interaction of the peer review panel with the DOE and Sandia National Laboratories (SNL), the actual performance of the peer review panel members, and the documents produced during and as a result of the peer review process (S. Cohen and Associates 2008). The EPA found the process to comply with requirements of section 194.27 and the guidance in U.S. NRC (U. S. NRC 1988).

Once again, public comments suggested that karst processes may be an alternative model (see U.S. EPA 2010b, Section 15.2.4 for the EPA's review). Karst was considered and rejected as an alternate conceptual model by the Culebra Hydrogeology Peer Review Panel (Burgess et al. 2008). The EPA likewise thoroughly reviewed all available data and determined that karst processes are not active at the WIPP site and should not be included in the WIPP conceptual models.

Based on a thorough review and evaluation of the CRA-2009 and supplemental information provided by the DOE (Federal Document Management System (FDMS) Docket ID No. U.S. EPA-HQ-OAR-2009-0330, Air Docket A-98-49), the EPA determined that the DOE continues to

demonstrate compliance with the requirements of section 194.23(a)(2) (CARD 23, Section 23.2.7) (U.S. EPA 2010b).

23.3.7 Changes or New Information Since the CRA-2009

The 24 conceptual models have not changed since the CRA-2009 recertification decision following the changes to the Culebra Hydrogeology Conceptual Model implemented in the CRA-2009 PABC. No new, plausible alternative conceptual models have been implemented or considered by the DOE since the CRA-2009 and the CRA-2009 PABC (U.S. DOE 2009). The implementation of the conceptual models has been modified to incorporate new parameters and changes in parameter values as discussed here in Section 23.2.7. Hence, the DOE continues to demonstrate compliance with the requirements for section 194.23(a)(2).

23.4 40 CFR § 194.23(a)(3)

23.4.1 Background

40 CFR § 194.23(a)(3) includes provisions to ensure documentation of the basis for conceptual models used in compliance applications. Specific requirements are for documentation that:

i. Conceptual models and scenarios reasonably represent possible future states of the disposal system.

ii. The equations and boundary conditions in a model reasonably represent the mathematical basis of the conceptual model.

iii. Numerical schemes enable the mathematical models to obtain stable solutions.

iv. Computer models implement the numerical models, have no coding errors, and produce stable solutions.

v. Peer review according to section 194.27 has been conducted on the conceptual models.

23.4.2 1998 Certification Decision

For the CCA, the DOE convened a Conceptual Models Peer Review Panel to review the 24 conceptual models used in PA (see Section 23.2.2). The EPA concurred with the panel's findings and found the DOE in compliance with the requirements of sections 194.23(a)(3)(i) and 194.23(a)(3)(v).

During the CCA, the EPA performed an independent review of the computer codes, focusing on (1) whether mathematical models incorporated equations and boundary conditions that reasonably represented the mathematical formulation of the conceptual models reviewed under section 194.23(a)(1); (2) whether the numerical models provided numerical schemes that enabled the mathematical models to obtain stable solutions; and (3) whether the computer codes were properly implemented.

The EPA independently reviewed the mathematical models and boundary conditions for the following codes: CUTTINGS_S, SECOFL2D, SECOTP2D, CCDFGF, PANEL, BRAGFLO, NUTS, FMT, SANTOS, and GRASP-INV. The codes that used numerical solvers included CUTTINGS_S, SECOFL2D, SECOTP2D, PANEL, BRAGFLO, NUTS, and SANTOS. The EPA concluded that the mathematical models incorporated equations that reasonably represented the conceptual models.

A complete description of the EPA's 1998 Certification Decision for section 194.23(a)(3) can be obtained from CARD 23, Sections 4.4, 5.4, 6.4, and 7.4 (U.S. EPA 1998a).

23.4.3 Changes in the CRA-2004

23.4.3.1 Documentation

A description of the code documentation is given here for completeness and to aid in further discussion.

- User's Manual (UM)—describes the code's purpose and function, mathematical governing equations, model assumptions, the user's interaction with the code, and the models and methods employed by the code. The UM includes:

  – The numerical solution strategy and computational sequence, including program flowcharts and block diagrams.

  – The relationship between the numerical strategy and the mathematical strategy (e.g., how boundary or initial conditions are introduced).

  – A clear explanation of model derivation. The derivation starts from generally accepted principles and scientifically proven theories. The UM justifies each step in the derivation and notes the introduction of assumptions and limitations. For empirical and semi-empirical models, the documentation describes how experimental data are used to arrive at the final form of the models. The UM clearly states the final mathematical form of the model and its application in the computer code.

  – Descriptions of any numerical method used in the model that go beyond simple algebra (e.g., finite-difference, Simpson's rule, cubic splines, Newton-Raphson Methods, and Jacobian Methods). The UM explains the implementation of these methods in the computer code in sufficient detail that an independent reviewer can understand them.

  – The derivation of the numerical procedure from the mathematical component model. The UM gives references for all numerical methods. It explains the final form of the numerical model and its algorithms. If the numerical model produces only an intermediate result, such as terms in a large set of linear equations that are later solved by another numerical model, then the UM explains how the model uses intermediate results. The documentation also indicates those variables that are input to and output from the component model.

- Analysis Packages (APs)—contain detailed information on how the computer codes were used in the PA, including code implementation approaches and justification of parameters used. The DOE required each code to supply the following information relevant to section 194.23(c)(1) in its APs:

  – Description of the overall nature and purpose of the general analysis performed by the model. The APs describe the specific aspects of the analysis for which the model is used. The APs discuss the input and output parameters for each model.

  – The modeling information describing the components (e.g., unsaturated vs. saturated) and their role in the overall modeling effort. The APs identify the contribution of each component model to the complete solution of the problem and the linkages between the component models. The documentation uses flowcharts and block diagrams to describe the mathematical solution strategy for the PA.

The DOE continued to use five additional documents as secondary references for the CRA-2004:

- Requirements Document (RD)—identifies the computational requirements of the code (e.g., MODFLOW must be able to simulate groundwater flow under steady-state conditions).

- Verification and Validation Plan (VVP)—identifies tests and associated acceptance criteria for the code and validation that all aspects of the code work properly together.

- Design Document (DD)—describes the major features of the software design: the theoretical basis; the embodied mathematical model; control flow; control logic; data structures; functionalities and interfaces of objects; components, functions, and subroutines used in the software; and the allowed or prescribed ranges for data inputs and outputs in a manner that can be implemented.

- Implementation Document (ID)—provides the information necessary to recreate the code used in the PAs. Using this information, the computer user can reconstruct the code or install it on an identical platform to that used in the PAs. The document includes the source code listing, subroutine-call hierarchy, and code compilation information.

- Validation Document (VD)—summarizes the results of the testing activities prescribed in the RD/VVP documents for the individual codes and provides evaluations based on those results. The VD contains listings of sample input and output files from computer runs of each model. The VD also contains reports on code verification, benchmarking, and validation, and documents the results of the quality assurance procedures (QAPs).

23.4.3.2 Conceptual Models

Analogous to the original certification, all modified conceptual models used in the CRA-2004 PA were reviewed by conceptual model peer review panels. The peer review panels considered whether a conceptual model represents possible future states of the disposal system. For each of the four changed conceptual models in the CRA-2004 PA (see Section 23.2.3), the peer review

panels approved the conceptual models considered (see Appendix PEER-2004, Sections PEER-2004 2.0 and PEER-2004 3.0) (U.S. DOE 2004).

23.4.3.3 Mathematical Models

In the CRA-2004, the DOE consolidated computer code documentation of mathematical models and initial and boundary conditions, primarily in the Appendix PA-2004, Section PA-4.0 (U.S. DOE 2004). The DOE also discussed specific topics in Appendix PA-2004, and Attachments PORSURF-2004, MASS-2004, SOTERM-2004, and TFIELD-2004 (U.S. DOE 2004). The DOE documented each code's characteristics in the UM and the other documents listed in Section 23.4.3.1.

The mathematical models or initial or boundary conditions for the following codes did not change after the CCA: SANTOS, BRAGFLO, FMT, NUTS, PANEL, and SECOTP2D. The cuttings and cavings mathematical models in CUTTINGS_S were not changed, but the spallings mathematical models were replaced by the new DRSPALL code. Three new codes were included in the EPA's review for the CRA-2004: MODFLOW, PEST, and DRSPALL. See U.S. EPA (2006i and 2006j) for more information on the code review conducted for the CRA-2004.

23.4.3.4 Numerical Models

Information used to evaluate the stability of the numerical schemes was provided in the VDs and APs that the DOE prepared for each of the CRA-2004 PA computer codes. The DOE's evaluation of numerical schemes to ensure the stability of the numerical solutions included an evaluation of the impact on previous analyses and any appropriate corrective actions to either the computer code or the earlier analyses. Errors that qualified as conditions adverse to quality, such as computer code stability problems, were controlled and resolved as described in the CRA-2004 Chapter 5.0, Section 5.3.20 (U.S. DOE 2004).

The DOE maintains a record of whether any of the codes experienced stability problems during the PA calculations. This record is documented in the output for each code and notes the convergence criteria and the number of numerical iterations required to reach convergence. Convergence criteria, and the maximum number of iterations allowed to achieve convergence, are set within various subroutines in the computer codes, where appropriate. The codes generate messages if the mathematical solution algorithm does not converge within the user-specified criteria (see the UM for each computer code). Problems are documented in the AP for each code.

23.4.3.5 Computer Codes

As in the CCA, to ensure that the DOE computer codes accurately implement the numerical models and are free of coding errors, a number of QAPs were adopted (see the CRA-2004, Chapter 5.0) (U.S. DOE 2004). The QAPs specify quality assurance (QA) requirements for each step of the software development process (see CARD 22 (U.S. EPA 2006k) for a discussion of the EPA's review of the DOE QA program). This process involved four primary development phases: (1) requirements, (2) design, (3) implementation, and (4) verification and validation (CRA-2004, Chapter 5.0, Section 5.3.20, and Appendix QAPD-2004, Section 6.0) (U.S. DOE 2004). The objective of each phase is discussed below.

The requirements phase consists of defining and documenting both the functional requirements that the software must meet and the verification and validation activities that must be performed to demonstrate that the computational requirements for the software are met. Two documents are produced during this phase: the RD and the VVP, which, when combined, are called RD/VVP. The RD contains the functional requirements that the proposed software must satisfy, with specific requirements relating to the aspects of the system to be simulated with a particular computer code. For example, groundwater flow through the Culebra Dolomite Member of the Rustler (hereafter referred to as Culebra) is assumed to be steady through time. Therefore, MODFLOW was required to demonstrate that the flow equation provided accurate solutions over time under steady-state conditions. The VVP identifies tests and associated acceptance criteria to ensure verification of each software development phase (i.e., that the portion of the code being tested matches known solutions) and validation of the entire software baseline the first time the computer code is placed under QA control (i.e., that all aspects of the code work together properly). The RD documents what the PA computer codes do by listing the functional requirements of each code. The VVP explains the various tests needed to show that the computer code properly performed the functional requirements listed in the RD.

The design phase consists of developing and documenting the overall structure of the software and the reduction of the overall software structure into descriptions of how the code works. During this phase, the software structural design may necessitate modifying the RD and VVP. The DD describes the theoretical model, the mathematical model, and the major components of the software.

The implementation phase consists of developing source code using a programming language (e.g., FORTRAN) or other form suitable for compilation or translation into executable computer software. The design, as described in the DD, is used as the basis for the software development, and it may need to be modified to reflect changes identified in the implementation phase. Two documents are produced during this phase: the ID and the UM. The ID provides the source code listing and describes the process performed to generate executable software, and the UM provides information that assists the user in understanding and using the code.

The verification and validation phase consists of executing the functional test cases identified in the VVP to demonstrate that the developed software meets the requirements defined for it in the VVP. The tests demonstrate the capability of the software to produce valid results for problems encompassing the range of permitted usage as defined by the UM. One document, the VD, is produced during this phase. The VD documents the test case input and output files and evaluates the results against the acceptance criteria in the VVP.

In the CCA, the DOE used these procedures and documents to show that the PA computer codes calculated numerical models properly, were free of coding errors, and produced stable results. The DOE used the same process and requirements for the CRA-2004 PA computer codes.

23.4.3.6 Peer Review

The DOE performed two peer reviews to support the CRA-2004 PA calculations. These peer reviews evaluated the new spallings model and the minor changes made to the Disposal System Geometry, Repository Fluid Flow, and DRZ conceptual models.

The Spallings Conceptual Model Peer Review Report was performed from July 2003 to October 2003; the final report was published in October 2003 (Appendix PEER-2004, Section PEER-2004-3.1.2) (U.S. DOE 2004). The new spallings model includes three major elements: consideration of multiphase flow processes in the intrusion borehole, consideration of fluidization and transport of waste particulates from the intact waste mass to the borehole, and a numerical solution for the coupled mechanical and hydrological response of the waste as a porous medium. The DOE developed a new numerical code, DRSPALL, to implement the new spallings conceptual model that calculates the volume of WIPP solid waste that may undergo material failure and be transported to the surface as a result of a drilling intrusion.

The Salado Flow Conceptual Models Peer Review was performed from April 2002 to March 2003; the final report was published in May 2003 (Appendix PEER-2004, Section PEER-2004-2.1.3) (U.S. DOE 2004). This peer review evaluated changes made to three conceptual models (Disposal System Geometry, Repository Fluid Flow, and DRZ) as a result of (1) new information acquired after the original certification decision; or (2) changes to conceptual model assumptions mandated by the EPA in the final CCA decision, such as the Option D panel closure condition. The changes included: (1) modification of the computational grid to accommodate the new panel closure requirement, (2) shaft simplification, and (3) refinement to the BRAGFLO grid.

The results of these peer reviews are discussed in Section 23.4.4.5.

23.4.4 EPA's Evaluation of Compliance for the 2004 Recertification

23.4.4.1 Conceptual Models

As in the CCA, all conceptual models used in the CRA-2004 were approved by conceptual model peer reviews that considered whether or not conceptual models represented possible futures of the disposal system (see Section 23.2.4 for more discussion of the results of the CCA conceptual model peer review). The EPA agreed with the peer review panels and therefore found that the DOE continued to be in compliance with section 194.23(a)(3)(i) (CARD 23, Section Recertification Decision 194.23(a)(3)) (U.S. EPA 2006f).

23.4.4.2 Mathematical Models

In the evaluation for recertification, the EPA evaluated each of the mathematical models for the computer codes used in the CRA-2004 PA to determine if the governing equations (e.g., flow and transport governing equations), process-related equations (e.g., the anhydrite fracture model), and boundary conditions (e.g., no-flow boundary assumptions) included in each mathematical model provided a reasonable representation of each conceptual model used in the CRA-2004 PA. Appendix PA-2004, Section PA-4.0 (U.S. DOE 2004) and UMs and APs for each code were the primary sources of information on the mathematical models employed in PA. In general, mathematical formulations were adequately explained and reasonable. The DOE adequately documented and described simplifications of conceptual models in the CRA-2004 PA. The EPA found that the DOE provided an adequate technical basis to support the mathematical formulations (CARD 23, Section Recertification Decision 194.23(a)(3)) (U.S. EPA 2006f).

The EPA also reevaluated the functional tests described in the VD for each computer code to ensure that the DOE's tests of the computer codes demonstrated that they performed as specified in the RD. The EPA reviewed the testing of each code to verify that the DOE adequately tested functional requirements listed for each computer code. This analysis and testing indicated that equations and boundary conditions were properly incorporated into the mathematical models and those boundary conditions were reasonable representations of how the conceptual models should be implemented. The EPA found that the DOE continued to comply with section 194.23(a)(3)(ii) (U.S. EPA 2006c), Section 12.0, (U.S. EPA 2006j), Section 6.0, and (U.S. EPA 2006i), Section 6.0) and CARD 23, Section Recertification Decision 194.23(a)(3) (U.S. EPA 2006f).

23.4.4.3 Numerical Models

For the CRA-2004, the EPA reviewed all relevant documentation on numerical models solution schemes, which was primarily contained in the Appendix PA-2004 (U.S. DOE 2004), APs, and supplementary information (e.g., UMs, VDs). The EPA also reviewed each code's QA documentation package for completeness and technical adequacy.

For the CRA-2004, the EPA reviewed the testing used to qualify each code for use in the CRA-2004 PA. The EPA found that the DOE had adequately set the range of functional tests for each code to verify that the code would perform as expected and provide reasonable results (see each code's VD for details of this testing). The EPA found that the DOE continued to comply with the requirements of section 194.23(a)(3)(iii) (U.S. EPA 2006c), Section 12.0, (U.S. EPA 2006j), Section 6.0 and (U.S. EPA2006i), Section 6.0) and CARD 23, Section Recertification Decision 194.23(a)(3) (U.S. EPA 2006f).

23.4.4.4 Computer Codes

The EPA reviewed all of the relevant documentation (UM, DD, RD, VVP, and VD) pertaining to each of the major codes described above, as well as Appendix PA-2004 and associated attachments (U.S. DOE 2004). Since the CCA, the EPA also periodically performed an independent review of the DOE's testing of each code to verify that results appeared accurate and free of coding error (U.S. EPA 2006c;U.S. EPA 2006i;U.S.EPA 2006j). The EPA ultimately found that each PA computer code produced results that showed continued compliance with this requirement.

During its review, the EPA questioned whether SANTOS produced results that were an accurate implementation of the numerical models and were free of coding errors (Cotsworth 2004). Specifically, the EPA questioned whether SANTOS was properly tested for accuracy and whether the average stress of less than 5 megapascals that SANTOS predicted for waste was reasonable. In the DOE's response (Detwiler 2004a), the DOE showed that a full functionality test of SANTOS was performed as part of the code qualification and that the results of SANTOS calculations were compared to the results of another computer code called SPECTROM-32. These activities showed that SANTOS produced results that were adequate for the development of porosity surfaces used in the CRA-2004 PA and was therefore accepted by the EPA ((U.S. EPA 2006l), Section 6.0).

The DOE replaced the SECOFL2D flow code used in the CCA with the MODFLOW flow code. The primary reasons given for the change are (1) that MODFLOW is well supported by a large user base and is continuing to be developed, while SECOFL2D is not; (2) MODFLOW is designed to operate on multiple computer platforms, while SECOFL2D was designed to work on only the VAX/Alpha platforms; and (3) the new pilot point estimation code, PEST, was designed to use only MODFLOW (Detwiler 2004b). The EPA determined that MODFLOW is a reasonable replacement to SECOFL2D and that the MODFLOW/PEST T-field estimate combination is a significant improvement over the SECOFL2D/GRASP-INV combination used in the CCA (U.S. EPA 2006c).

The EPA was able to determine that the CRA-2004 PA computer codes continued to comply with section 194.23(a)(3)(iv) (CARD 23, Section Recertification Decision 194.23(a)(3)) (U.S. EPA 2006f).

23.4.4.5 Peer Review

The DOE performed two peer reviews to support the CRA-2004 PA calculations. The DOE developed a new spallings model and made minor changes to the Disposal System Geometry, Repository Fluid Flow, and DRZ models.

The EPA examined the peer review plan and the final peer review report for the Spallings Conceptual Model Peer Review and found that they adequately fulfilled the requirements of section 194.27 and U.S. NRC (U.S. NRC 1988). The EPA also observed the actual performance of the peer review panel, the selection of the panel members, the interaction of the panel with the DOE, and the documents produced during and as a result of the peer review. The EPA found the process satisfied the requirements of section 194.27 and the guidance in U.S. NRC (U.S. NRC 1988) (U.S. EPA 2006d, Section 5.0).

The EPA examined the peer review plan and the final peer review report for the Salado Flow Conceptual Models Peer Review and found that they adequately fulfilled the requirements of section 194.27 and U.S. NRC (U.S. NRC 1988). The EPA also observed the actual performance of the peer review panel members, the selection of the panel, the interaction of the peer review panel with the DOE, and the documents produced during and as a result of the peer review. The EPA found the process compatible with the requirements of section 194.27 and the guidance in U.S. NRC (U.S. NRC 1988) ((U.S. EPA 2006e), Section 5.0).

Based on a review and evaluation of the CRA-2004 and supplemental information provided by the DOE, the EPA determined that the DOE continued to comply with the requirements of section 194.23(a)(3)(v) (CARD 23, Section Recertification Decision 194.23(a)(3)) (U.S. EPA 2006f).

23.4.5 Changes or New Information Between the CRA-2004 and the CRA-2009 (Previously: Changes or New Information Since the 2004 Recertification)

23.4.5.1 Conceptual Models

All conceptual models used in the CRA-2009 PA were previously peer reviewed. No modifications were made to the conceptual models from the 2006 recertification decision to the CRA-2009. Thus, there was no new information provided in the CRA-2009, and the DOE continued to demonstrate compliance with the provisions of section 194.23(a)(3)(i).

23.4.5.2 Mathematical Models

No changes were made in the methodology used to document mathematical models and initial and boundary conditions from the CRA-2004. Discussion of the mathematical models and initial and boundary conditions are found in Appendices PA-2009, PORSURF-2009, SOTERM-2009, and TFIELD-2009 (U.S. DOE 2009). UMs and APs are also used to document mathematical models and the initial and boundary conditions for the CRA-2009. Table 23-2 lists the APs for the CRA-2009 PA.

Table 23-2. APs for the CRA-2009 PA

AP	Reference
Parameters	Kirchner 2008a; Fox 2008
Cuttings & Cavings	Ismail 2008
Spallings	Vugrin 2005; Ismail 2008
Direct Brine Release	Clayton 2008
Actinide Mobilization	Garner and Leigh 2005
Salado Flow	Nemer and Clayton 2008
Salado Transport	Ismail and Garner 2008
Culebra Flow	Lowry and Kanney 2005
Culebra Transport	Lowry and Kanney 2005
Normalized Release	Dunagan 2008
Sensitivity Study	Kirchner 2008b
Summary	Clayton et al. 2008

No new codes were added to the WIPP PA since the CRA-2004 PABC. Two codes, BRAGFLO and NUTS, were modified for the CRA-2009 PA. BRAGFLO was modified from version 5.0 to version 6.0 to incorporate additional capabilities and flexibility (Nemer 2006). The UM (Nemer 2007a), RD/VVP (Nemer 2007b), ID (Nemer 2007c), and VD (Nemer 2007d) were generated for BRAGFLO version 6.0. NUTS version 2.05a had a time and date incompatibility with the upgraded operating system (Gilkey 2006), and was modified to version 2.05c. The only difference between version 2.05a and 2.05c is the change made to correct the time and date

incompatibility. As this was a minor code change, only the ID (Gilkey 2006) was updated and no changes were made to the UM, RD/VVP, or VD.

The DOE continued to provide documentation that mathematical models incorporate equations and boundary conditions that reasonably represent the mathematical formulation of the conceptual models, and thus continued to demonstrate compliance with the provisions of section 194.23(a)(3)(ii).

23.4.5.3 Numerical Models

As in the CRA-2004, the information used to evaluate the stability of the numerical schemes was provided in the VDs and APs that the DOE prepared for each of the CRA-2009 PA computer codes. The DOE's approach has not changed since the CRA-2004. Therefore, the DOE continued to provide documentation that numerical models provide numerical schemes that enable the mathematical models to obtain stable solutions and thus continued to demonstrate compliance with the provisions of section 194.23(a)(3)(iii).

23.4.5.4 Computer Codes

As in the CRA-2004, the information used to show that the PA computer codes calculated numerical models properly, were free of coding errors, and produced stable results was provided in the RD/VVP and VD prepared for each of the CRA-2009 PA computer codes. Therefore, the DOE continued to provide documentation that computer models accurately implement the numerical models and thus, continued to demonstrate compliance with the provisions of section 194.23(a)(3)(iv).

23.4.5.5 Peer Review

No additional peer review results since the 2006 recertification decision were included in the CRA-2009 PA calculations. Thus, there was no new information to provide in the CRA-2009, and the DOE continued to demonstrate compliance with the provisions of section 194.23(a)(3)(v).

23.4.6 EPA's Evaluation of Compliance for the 2009 Recertification

Based on a review and evaluation of CRA-2009 and supplemental information provided by the DOE (FDMS Docket ID No. U.S. EPA-HQ-OAR-2009-0330, Air Docket A-98-49), the EPA determined that the DOE continues to demonstrate compliance with the provisions of section 194.23(a)(3) (CARD 23, Section 23.3.7) (U.S. EPA 2010b). The following sections discuss the EPA's evaluation of compliance to each of the four provisions of section 194.23(a)(3).

23.4.6.1 Conceptual Models

As in the original CCA and CRA-2004, all conceptual models were approved by conceptual model peer reviews that considered whether conceptual models reasonably represent possible futures of the disposal system. The EPA agreed with the peer review results and determined that

the DOE was in compliance with the provisions of section 194.23(a)(3)(i) (CARD 23, Section 23.3.6) (U.S. EPA 2010b).

23.4.6.2 Mathematical Models

The EPA evaluated each of the mathematical models for the computer codes used in the CRA-2009 PA to determine if the governing equations, process-related equations, and boundary conditions included in each mathematical model provided a reasonable representation of each conceptual model (U.S. EPA 2010). After thorough evaluation of the information in Appendix PA-2009 (U.S. DOE 2009) and the BRAGFLO User's Manual (Nemer 2007a), the EPA determined that the mathematical formulations were adequately documented and explained, and were reasonable (U.S. EPA 2010b). Thus, the EPA determined that the DOE continues to adequately document and describe simplifications of conceptual models in the CRA-2009 PA, and continues to provide an adequate technical basis to support the mathematical formulations (U.S. EPA 2010b).

The EPA also reevaluated the functional tests for the CRA-2009 PA computer codes, described in the VD for each computer code, to ensure that the codes had not been changed and that the DOE's tests of the computer codes demonstrate that the codes continue to perform as specified in the respective RDs. The EPA reviewed the testing of each code to verify that the DOE adequately tested functional requirements listed for each computer code. This analysis and testing indicated that equations and boundary conditions were properly incorporated into the mathematical models and that boundary conditions were reasonable representations of how the conceptual models should be implemented. The EPA determined that the DOE continued to demonstrate compliance with the provisions of section 194.23(a)(3)(ii) (CARD 23, Section 23.3.6) (U.S. EPA 2010b).

23.4.6.3 Numerical Models

The EPA reviewed all relevant documentation on numerical model solution schemes, which were primarily contained in Appendix PA-2009 (U.S. DOE 2009), APs, and supplementary information (e.g., UMs, VDs). The EPA also reviewed the QA documentation packages for each code for completeness and technical adequacy (U.S. EPA 2010a).

The EPA reviewed the testing used to qualify each code for use in the CRA-2009 PA calculations. The EPA determined that the DOE continues to (1) adequately set the range of functional tests for each code to verify that the code will perform as expected and provide reasonable results, and (2) provide documentation that numerical models provide numerical schemes that enable the mathematical models to obtain stable solutions (U.S. EPA 2010b). The EPA determined that the DOE continued to demonstrate compliance with the provisions of section 194.23(a)(3)(iii) (CARD 23, Section 23.3.6) (U.S. EPA 2010b).

23.4.6.4 Computer Codes

The EPA reviewed all of the relevant documentation pertaining to each of the major codes used in the CRA-2009 PA calculations (i.e., DD, RD, VVP and VD) and Appendix PA-2009 (U.S. EPA 2010a). The EPA found that each performance assessment code produced results that show

that the DOE continues to demonstrate compliance with the provisions of section 194.23(a)(3)(iv) (CARD 23, Section 23.3.6) (U.S. EPA 2010b).

23.4.6.5 Peer Review

There was no new peer review process information to provide in the CRA-2009. The EPA determined that the DOE continued to demonstrate compliance with the provisions of section 194.23(a)(3)(v) (CARD 23, Section 23.3.6) (U.S. EPA 2010b).

23.4.7 Changes or New Information Since the CRA-2009

23.4.7.1 Conceptual Models

After the DOE submitted the CRA-2009 documentation (U.S. DOE 2009), the DOE revised the Culebra Hydrogeology Conceptual Model by changing its implementation, and submitted the results of the CRA-2009 PABC calculations. The process used to calculate Culebra transmissivity fields used in the flow calculations was changed. The original CCA peer review panel had determined that the Culebra Hydrogeology Conceptual Model did not establish a strong correlation between the conceptual model and the numerical model used in PA calculations (SCA 2008). The objective of the new implementation of the conceptual model for the CRA-2009 PABC was to develop transmissivity fields for the Culebra that are: (a) geologically based, (b) consistent with observed groundwater heads, (c) consistent with groundwater responses in the Culebra pumping tests, and (d) consistent with water chemistry data.

The changes to the process for deriving the transmissivity fields did not change the underlying flow conceptual model or the mathematical formulations incorporated into the computer codes. The inclusion of more pumping test data, additional pilot points, and geologic effects, represents an implementation change, not a conceptual model change (Kuhlman 2010). The new Culebra Hydrogeology Conceptual Model was peer reviewed and approved for use in PA calculations (Burgess et al. 2008). Thus, the DOE continues to demonstrate compliance with the provisions of section 194.23(a)(3)(i).

23.4.7.2 Mathematical Models

No changes were made in the methodology used to document mathematical models and initial and boundary conditions from the CRA-2009. The only changes were updates to parameters and the implementation of mathematical models using the new transmissivity field development process (Burgess et al. 2008; Kuhlman 2010). Discussion of the mathematical models using the new transmissivity field development process can be found in Appendix TFIELD-2014. Discussion of the other models can be found in Appendices PA-2014, PORSURF-2014, and SOTERM-2014. UMs and APs are also used to document mathematical models and the initial and boundary conditions for the CRA-2014. The DOE continues to demonstrate compliance with the provisions of section 194.23(a)(3)(ii).

23.4.7.3 Numerical Models

As in the CRA-2004 and CRA-2009 PA calculations, the information used to evaluate the stability of numerical schemes continues to be provided in the VDs and APs that the DOE prepared for each of the CRA-2014 PA computer codes. The DOE's approach has not changed since the CRA-2004. Thus, the DOE remained in compliance with the provisions of section 194.23(a)(3)(iii).

23.4.7.4 Computer Codes

To show that the PA computer codes continued to be free of coding errors, produce stable results, and implement the numerical models correctly, the DOE used the same computer code development process and requirements for the CRA-2014 PA computer codes as was used in the CRA-2004 and CRA-2009 PA calculations, which consisted of four primary development phases: (1) requirements phase; (2) design phase; (3) implementation phase; and (4) software verification and validation. This information is contained in the RD/VVP and VD prepared for each of the codes used in the CRA-2014 PA calculations. On this basis, the DOE continued to demonstrate compliance with the provisions of section 194.23(a)(3)(iv).

23.4.7.5 Peer Review

After the CRA-2009 PA, the DOE completed one peer review to support the CRA-2009 PABC calculations. The DOE developed a new implementation and parameterization of the Culebra Hydrogeology Conceptual Model that was included in the CRA-2009 PABC calculations.

The Culebra Hydrogeology Conceptual Model Peer Review was completed in 2008 (Burgess et al. 2008). The peer review panel evaluated changes to the implementation and parameterization of the Culebra Hydrogeology Conceptual Model. The EPA examined the peer review plan and the final peer review report and found the process to adequately fulfill the requirements of section 194.27 and U.S. NRC (U.S. NRC 1988) (U.S. EPA 2010b). The EPA also observed the selection of the panel, the interaction of the panel with the DOE and SNL, the actual performance of the peer review panel members, and the resulting documents. The EPA found the peer review process to fulfill the requirements of section 194.27 and the guidance in U.S. NRC (U.S. NRC 1988) (SCA 2008). Thus, the DOE continued to demonstrate compliance with the provisions of section 194.23(a)(3)(v) (U.S. EPA 2010b).

23.5 40 CFR § 194.23(b)

23.5.1 Background

40 CFR § 194.23(b) requires that computer codes be documented in accordance with an appropriate quality assurance standard.

23.5.2 1998 Certification Decision

In the CCA, to meet the requirements of section 194.23(b), the DOE provided documentation of compliance with quality assurance requirements of American Society of Mechanical Engineers

(ASME) Nuclear Quality Assurance (NQA)-2a-1990 addenda, Part 2.7, to ASME NQA-2-1989 edition. This documentation included plans for QA software, software requirements documentation, software design and implementation documentation, software verification and validation documentation, and user documentation. Based on EPA audits and the CCA review, the EPA found the DOE in compliance with the requirements of section 194.23(b).

A complete description of the EPA's 1998 Certification Decision for section 194.23(b) can be found in CARD 23, Section 8.4 (U.S. EPA 1998a).

23.5.3 Changes in the CRA-2004

The DOE QA program is described in U.S. DOE (2004), Chapter 5.0. Software QA is described in U.S. DOE (2004), Chapter 5.0, Section 5.3.20. The DOE Carlsbad Field Office (CBFO) Quality Assurance Program Document (QAPD), dated May 2003, is contained in Appendix QAPD-2004 (U.S. DOE 2004). Section 6 of the QAPD incorporated the requirements of ASME NQA-2a-1990 addenda, Part 2.7, to ASME NQA-2-1989 edition. See CARD 22 for further discussion of the EPA's review of the DOE's approach to the QA requirements for computer codes and models (U.S. EPA 2006k).

23.5.4 EPA's Evaluation of Compliance for the 2004 Recertification

The EPA verified compliance with the requirements of section 194.22(a)(2)(iv) by reviewing Section 6.0 of the CBFO QAPD and conducting periodic inspections of the SNL and Washington TRU Solutions QA programs since the CCA decision. The DOE documentation included plan(s) for software QA, software requirements documentation, software design and implementation documentation, software verification and validation documentation, and user documentation. The EPA found that the DOE's QA requirements for computer codes used in the PA and compliance assessment continued to be in agreement with those specified in section 194.22, and that their code documentation was adequate. See CARD 22, Section Evaluation of Compliance for Recertification (U.S. EPA 2006k), for further discussion of the EPA's review.

Based on a review and evaluation of the CRA-2004 and supplemental information provided by the DOE, the EPA determined that the DOE continued to comply with the requirements for section 194.23(b) (CARD 23, Section Recertification Decision 194.23(b)) (U.S. EPA 2006f).

23.5.5 Changes or New Information Between the CRA-2004 and the CRA-2009 (Previously: Changes or New Information Since the 2004 Recertification)

The DOE QA program and documentation standards for the computer codes used in PA calculations did not change between the CRA-2004 and CRA-2009 decisions. Thus, no new information on the DOE's QA program was included in the CRA-2009. The DOE QA program, as applied to the CRA-2009, was contained in Appendix QAPD-2009 (U.S. DOE 2009). The DOE continued to demonstrate compliance with the provisions of section 194.23(b).

23.5.6 EPA's Evaluation of Compliance for the 2009 Recertification

The EPA verified that the DOE continued to comply with the requirements of section 194.22(a)(2)(iv) by reviewing Section 7.0 of the CBFO QAPD and conducting periodic inspections of SNL and the Management and Operating Contractor QA programs since the CRA-2004 CCA decision. The DOE's documentation included plan(s) for software quality assurance, software requirements documentation, software design and implementation documentation, software verification and validation documentation, and user manual documentation. The EPA determined that the DOE QA requirements for computer codes used in the CRA-2009 PA and CRA-2009 PABC calculations and compliance assessment continued to be in agreement with those specified in section 194.22, and that DOE code documentation is adequate (U.S. EPA 2010b). Thus, the EPA determined that the DOE continued to demonstrate compliance with the provisions of section 194.23(b) (CARD 23, Section 23.4.8) (U.S. EPA 2010b).

23.5.7 Changes or New Information Since the CRA-2009

The documentation standards of the computer codes have not changed since the CRA-2004 and CRA-2009 decisions. Thus, there is no new information on the DOE QA program to provide in the CRA-2014. The DOE's quality assurance program, as applied to the CRA-2014, is contained in Appendix QAPD-2014. The DOE continues to demonstrate compliance with the provisions of section 194.23(b).

23.6 40 CFR § 194.23(c)(1)

23.6.1 Background

40 CFR § 194.23(c)(1) requires documentation of all models and computer codes, including descriptions of the theoretical backgrounds and the method of analysis for each model.

23.6.2 1998 Certification Decision

In the CCA, the DOE provided documentation of all models and computer codes, including descriptions of the theoretical backgrounds and the method of analysis for each model. The EPA's evaluation found that the CCA and supplementary information provided an adequate description of the theoretical backgrounds and method of analysis for each model used in the calculations. The DOE's documentation of conceptual models, alternative conceptual models, and the Conceptual Models Peer Review Panel is discussed in CARD 23, Sections 1.4, 2.4, and 7.4, respectively (U.S. EPA 1998a).

A complete description of the EPA's 1998 Certification Decision for section 194.23(c)(1) can be obtained from CARD 23, Section 9.4 (U.S. EPA 1998a).

23.6.3 Changes in the CRA-2004

Most of the major codes used for modeling the PA in the CRA-2004 had not changed since the CCA. Codes added to the CRA-2004 PA since the CCA were MODFLOW, PEST, and DRSPALL. Each of the CRA-2004 PA codes is documented in its own UM, AP, RD, VVP, DD,

ID, and VD (see Section 23.4.3.1 for a summary of each document). The DOE used these documents as the primary vehicles to describe the conceptual models, mathematical models, and numerical methods that provided the basis for the theory and the assumptions underlying the computer codes. The DOE included additional documentation in various appendices to the CRA-2004 (e.g., Appendix PA-2004, Attachment MASS-2004, and Attachment SOTERM-2004). The DOE's documentation also contained justification for the use of the models, conceptual model derivation, mathematical derivations, and solution methods used in the codes (see the CRA-2004 Chapter 6.0 and Appendix PA-2004) (U.S. DOE 2004).

23.6.4 EPA's Evaluation of Compliance for the 2004 Recertification

The primary codes that the EPA reviewed include: CUTTINGS_S, MODFLOW, SECOTP2D, SUMMARIZE, PRECCDFGF, CCDFGF, LHS, DRSPALL, PANEL, BRAGFLO, NUTS, FMT, PEST, SANTOS, and ALGEBRA. The EPA found the DOE's description of the theoretical background of each code, provided primarily in the UM and AP, to be adequate. With respect to the documentation pertaining to the method of analysis, the EPA found the descriptions in the AP for each code to be sufficiently complete.

For the CRA-2004, the EPA reevaluated all available documentation on each of the computer codes for completeness, clarity, and logical development of the theoretical bases for the conceptual models used in each computer code. Documentation was considered complete if it contained sufficient information from which to judge whether the codes were (1) formulated on a sound theoretical foundation, and (2) used properly in the PA analysis.

The EPA reviewed all of the relevant documentation pertaining to the theoretical development and application of the models. For further discussion of the EPA's review of documentation for conceptual models, alternative conceptual models, and the peer review panels, see Section 23.2, Section 23.3, and Section 23.4. The majority of the information was located in the UM and AP for each code. For the CRA-2004, the DOE's theoretical background for almost all of the codes had not changed since the CCA decision. Since the CCA, the DOE continued to test the PA codes to verify that they still perform as they did during the CCA. The EPA periodically reviewed and inspected these activities to verify that the PA codes continued to produce adequate results (U.S. EPA 2006i;U.S. EPA 2006j). Appendix PA-2004 (U.S. DOE 2004) included the theoretical background, mathematical development, and numerical development of the main PA codes and their use in the CRA-2004 PA analyses.

After the execution of the original CRA-2004 PA, the DOE discovered problems with the method of analysis for a number of input files and computer code errors related to the SUMMARIZE, PRECCDFGF, and CCDFGF sequence of calculations. The EPA requested that the DOE verify these errors had been corrected and that the codes passed the correct information to assure the analysis methods and assessments achieved correct results (Cotsworth 2005). The DOE modified the codes, corrected the analysis process, and retested to confirm that the errors had been corrected. The DOE also reran parts of the original CRA-2004 PA to assess the impact of these corrections. The EPA found that the DOE had corrected the errors and verified that the codes obtained the correct data to perform the CRA-2004 PABC (U.S. EPA 2006c, Section 12.0). The EPA found that the DOE's level of documentation continued to be consistent with the adequate level of documentation produced during the CCA review, and that the DOE continued

to be in compliance with section 194.23(c)(1) (CARD 23, Section Recertification Decision 194.23(c)) (U.S. EPA 2006f).

23.6.5 Changes or New Information Between the CRA-2004 and the CRA-2009 (Previously: Changes or New Information Since the 2004 Recertification)

No changes were made to the documentation procedure of PA computer codes used in the CRA-2009. The information reviewed by the EPA for the CRA-2009 was primarily contained in UMs, VDs, IDs, and RD/VVPs for each code. The primary codes that EPA reviewed for the CRA-2009 included: CUTTINGS_S, MODFLOW, SECOTP2D, SUMMARIZE, PRECCDFGF, CCDFGF, LHS, DRSPALL, PANEL, BRAGFLO, BRAGFLO as used for direct brine releases (BRAGFLO_DBR), NUTS, FMT, PEST, SANTOS, ORIGEN2, and ALGEBRA (U.S. EPA 2010). The major codes used in the CRA-2009 PA calculations had not changed since the CRA-2004 PA (Appendix PA-2009, Section PA-6.0) (U.S. EPA 2009). The DOE included additional documentation in various appendices to the CRA-2009 (e.g., Appendix PA-2009, Appendix MASS-2009, and Appendix SOTERM-2009). The DOE's documentation also contained justification for the use of the models, the conceptual model derivation, the mathematical derivations, and the solution methods used in the codes (Appendix PA-2009). Given that there was no new information provided as part of the CRA-2009, the DOE continued to demonstrate compliance with the provisions of section 194.23(c)(1).

23.6.6 EPA's Evaluation of Compliance for the 2009 Recertification

In its CRA-2009 review, after reviewing the CRA-2009 PABC, the EPA found the DOE's description of the theoretical background of each code to be adequately documented in each of the UMs and the various APs (U.S. EPA 2010b). With respect to the documentation pertaining to the method of analysis, the EPA found the descriptions in the APs (U.S. DOE (2009), Table 23-4) for each code to be sufficiently complete (CARD 23, Section 23.5.8.1) (U.S. EPA 2010b).

The EPA reevaluated all the documentation for each of the computer codes for completeness, clarity, and logical development of the theoretical bases of the conceptual models used in each computer code. The documentation was determined to continue to be complete if it contained sufficient information from which to judge whether the codes continued to be both formulated on a sound theoretical foundation and used properly in the CRA-2009 PA analyses (U.S. EPA 2010b).

The EPA reviewed all of the relevant CRA-2009 documentation pertaining to the theoretical development and application of the models. The majority of the information was located in the UMs and APs for each code. For the CRA-2009 PA calculations, the DOE's theoretical background for the codes did not change from that used in CRA-2004. It was determined that the DOE continued to test the PA codes to verify that the codes continued to perform as they did previously (U.S. EPA 2010b).

The EPA determined that the DOE's level of documentation continued to be adequate and consistent with the level of documentation produced previously (CARD 23, Section 23.5.8.1)

(U.S. EPA 2010b). Thus, the DOE continued to demonstrate compliance with the provisions of section 194.23(c)(1).

23.6.7 Changes or New Information Since the CRA-2009

No changes were made to the documentation procedure of PA computer codes used in the CRA-2014. Thus, there is no new information provided as part of the CRA-2014. Information regarding whether the computer codes continue to satisfy the requirements of section 194.23(c)(1) is contained in Appendix PA-2014, Section PA-6.0. The information for the CRA-2014 continues to be primarily contained in UMs, VDs, IDs, and RD/VVPs for each code. The primary codes used in the CRA-2014 included: CUTTINGS_S, MODFLOW, SECOTP2D, SUMMARIZE, PRECCDFGF, CCDFGF, LHS, DRSPALL, PANEL, BRAGFLO, BRAGFLO_DBR, NUTS, EQ3/6, PEST, SANTOS, JAS3D, and ALGEBRA.

The DOE has included supplemental documentation in various appendices to the CRA-2014 (e.g., Appendix PA-2014, Appendix MASS-2014, and Appendix SOTERM-2014). The DOE's documentation also contains justification for the use of the models, the conceptual model derivation, the mathematical derivations, and the solution methods used in the codes (Appendix PA-2009). Thus, the DOE continues to demonstrate compliance with the provisions of section 194.23(c)(1).

23.7 40 CFR § 194.23(c)(2)

23.7.1 Background

40 CFR § 194.23(c)(2) requires (1) general descriptions of the models; (2) discussions on the limits of applicability of each model; (3) detailed instructions for executing the computer codes, including hardware and software requirements; (4) input and output formats with explanations of each input and output variable and parameter (e.g., parameter name and units); (5) listings of input and output files from a sample computer run; and (6) reports on code verification, benchmarking, validation, and QAPs.

23.7.2 1998 Certification Decision

In the CCA, the DOE provided documentation of all models and computer codes; detailed descriptions of data collection, data reduction and analysis, and parameters developed from source data; detailed descriptions of the structure of the computer codes; and a complete listing of computer source codes. The EPA's evaluation found that the CCA and supplementary information included (1) an adequate description of each model used in the calculations; (2) a description of limits of applicability of each model; (3) detailed instructions for executing the computer codes; (4) hardware and software requirements to run these codes; (5) input and output formats with explanations of each input and output variable and parameter; (6) listings of input and output files from sample computer runs; and (7) reports of code verification, benchmarking, validation, and QAPs.

A complete description of the EPA's 1998 Certification Decision for section 194.23(c)(2) can be obtained from CARD 23, Section 10.4 (U.S. EPA 1998a).

23.7.3 Changes in the CRA-2004

As in the CCA, documentation for the CRA-2004 regarding the DOE's compliance with section 194.23(c)(2) is primarily contained in the UM, AP, VD, ID, DD, RD, and VVP for each code. Table 23-3 lists the requirements of section 194.23(c)(2) and where these requirements are addressed in the DOE documents.

Table 23-3. Location of Documentation for Models and Computer Codes Used in PA

Requirement in Compliance Application Guidance	Document Containing Information						
	UM	AP	VD	ID	DD	RD/VVP	SNL QA Procedures[a]
General descriptions of the models	X	X	—	—	X	—	—
Discussions of the limits of applicability of each model	X	X	—	—	X	—	X
Detailed instructions for executing the computer codes	—	X	—	X	X	—	X
Hardware requirements for executing the computer codes	X	X	—	X	—	—	X
Software requirements for executing the computer codes	X	X	—	—	—	—	X
Input and output formats with explanations of each input and output variable and parameter	X	X	—	—	X	—	—
Listings of input and output files from a sample computer run	X	X	—	—	—	—	X
Reports on code verification	—	X	X	—	—	X	X
Reports on benchmarking	—	X	X	—	—	X	X
Reports on validation	—	X	X	—	—	X	X
Reports on QAPs	—	X	—	—	—	—	X

X = Information meeting the requirement is found in this document.

[a] See Appendix QAPD-2004, Section 6.0 (U.S. DOE 2004).

23.7.4 EPA's Evaluation of Compliance for the 2004 Recertification

The EPA reviewed all of the relevant documentation pertaining to requirements specified in section 194.23(c)(2) for the following codes: CUTTINGS_S, MODFLOW, SECOTP2D, CCDFGF, LHS, PANEL, BRAGFLO, NUTS, FMT, PEST, DRSPALL, SANTOS, and ALGEBRA (U.S. EPA 2006c;(U.S. EPA 2006i;U.S. EPA 2006j). The DOE's code documentation provided enough information for the EPA to understand and execute the models, determine the possible impact of any assumptions, and verify that the codes were tested and quality assured.

The EPA determined that the DOE continued to demonstrate compliance with section 194.23(c)(2) (CARD 23, Section Evaluation of Compliance for Recertification 194.23(c)) (U.S. EPA 2006f).

23.7.5 Changes or New Information Between the CRA 2004 and the CRA 2009 (Previously: Changes or New Information Since the 2004 Recertification)

No changes were made to the documentation procedure of PA computer codes between the CRA-2004 and the CRA-2009. Hence, the requirements listed in Table 23-3 also applied to the computer codes used in the CRA-2009. The documentation for the CRA-2009 regarding DOE's compliance with section 194.23(c)(2) was primarily contained in UM, AP, VD, ID, and RD/VVP for each code. The codes used in the CRA-2009 include CUTTINGS_S, MODFLOW, SECOTP2D, SUMMARIZE, PRECCDFGF, CCDFGF, LHS, PANEL, NUTS, BRAGFLO, BRAGFLO_DBR, PEST, FMT, DRSPALL, SANTOS, ORIGEN2, and ALGEBRA. Given that there was no new information provided in the CRA-2009, the DOE continued to demonstrate compliance with the provisions of section 194.23(c)(2).

23.7.6 EPA's Evaluation of Compliance for the 2009 Recertification

The EPA reviewed all of the relevant documentation pertaining to the requirements specified in section 194.23(c)(2) for the following codes: CUTTINGS_S, MODFLOW, SECOTP2D, CCDFGF, LHS, PANEL, BRAGFLO, BRAGFLO_DBR, NUTS, FMT, PEST, DRSPALL, SANTOS, ORIGEN2, and ALGEBRA (U.S. EPA 2010a). The DOE's CRA-2009 code documentation provided sufficient information to allow the EPA to understand and execute the models, to determine the possible impact of any assumptions, and to verify that the codes were tested and underwent quality assurance review. The EPA determined that the DOE continued to demonstrate compliance with the provisions of section 194.23(c)(2) (CARD 23, Section 23.5.8.1) (U.S. EPA 2010b).

23.7.7 Changes or New Information Since the 2009 Recertification

No changes have been made to the documentation procedure of PA computer codes used in the CRA-2014. Hence, the requirements listed in Table 23-3 also apply to the computer codes used in the CRA-2014. The documentation for the CRA-2014 regarding DOE's compliance with section 194.23(c)(2) is contained in UM, AP, VD, ID, and RD/VVP for each code. The codes used in the CRA-2014 include CUTTINGS_S, MODFLOW, SECOTP2D, SUMMARIZE, PRECCDFGF, CCDFGF, LHS, PANEL, BRAGFLO, BRAGFLO_DBR, NUTS, EQ3/6, PEST, DRSPALL, SANTOS, JAS3D, and ALGEBRA. There is no new information for documentation procedures to provide in the CRA-2014. The documentation for the new codes EQ3/6 and JAS3D may be found in their respective UM, AP, VD, ID, and RD/VVP. The DOE continues to demonstrate compliance with the provisions of section 194.23(c)(2).

23.8 40 CFR § 194.23(c)(3)

23.8.1 Background

40 CFR § 194.23(c)(3) requires detailed descriptions of the computer code structures and a complete listing of computer source codes.

23.8.2 1998 Certification Decision

In the CCA, the DOE provided detailed descriptions of the computer code structure and a complete listing of computer source codes. The EPA's evaluation found that the CCA and supplementary information adequately provided a detailed description of the computer code structures and supplied a complete listing of the computer source code in supplementary documentation to the CCA. The documentation of computer codes described the structure of computer codes with sufficient detail to allow the EPA to understand how software subroutines are interrelated. The code structure documentation shows how the codes operate to provide accurate solutions of the conceptual models.

A complete description of the EPA's 1998 Certification Decision for section 194.23(c)(3) is contained in CARD 23, Section 11.4 (U.S. EPA 1998a).

23.8.3 Changes in the CRA-2004

The ID for each modeling code contained the information relevant to compliance with section 194.23(c)(3). The ID provided the information necessary for the recreation of the code as used in the CRA-2004 PA calculation. With this information, the user could compile the source code and install it on a computer system identical to that used in the CRA-2004 PA. The ID also included the source code listing and code compilation information.

23.8.4 EPA's Evaluation of Compliance for the 2004 Recertification

The EPA reviewed all of the relevant documentation, and in particular the ID for each computer code pertaining to the requirements specified in section 194.23(c)(3) for the following codes: CUTTINGS_S, MODFLOW, SECOTP2D, CCDFGF, LHS, PANEL, BRAGFLO, NUTS, FMT, PEST, SANTOS, DRSPALL, SUMMARIZE, and ALGEBRA. The EPA found that the DOE submitted all of the source code listings. The EPA identified no problems with the detailed descriptions of the structure of the computer codes. The CRA-2004 documentation of computer codes continued to adequately describe the structure of computer codes with sufficient detail to allow the EPA to understand how software subroutines were linked and how to execute the PA. The EPA determined that the DOE continued to demonstrate compliance with section 194.23(c)(3) (CARD 23, Section Recertification Decision 194.23(c)) (U.S. EPA 2006f).

23.8.5 Changes or New Information Between the CRA 2004 and the CRA 2009 (Previously: Changes or New Information Since the 2004 Recertification)

No changes were made to the documentation procedure of PA computer codes used in the CRA-2009. The primary documentation of model compliance with section 194.23(c)(3) was contained in the ID for each modeling code. These code IDs provided the information necessary for compiling the codes used in the CRA-2009 PA calculations, which allowed the user to compile the source code and install it on a computer system identical to that used in the CRA-2009 PA. The IDs included the source-code listings, the subroutine-call hierarchies, and code compilation information. Thus, the DOE continued to demonstrate compliance with the provisions of section 194.23(c)(3).

23.8.6 EPA's Evaluation of Compliance for the 2009 Recertification

During its CRA-2009 review, the EPA examined all of the relevant documentation, in particular the ID for each computer code pertaining to the requirements specified in section 194.23(c)(3), for the following codes: CUTTINGS_S, MODFLOW, SECOTP2D, CCDFGF, LHS, PANEL, BRAGFLO, BRAGFLO_DBR, NUTS, FMT, PEST, SANTOS, ORIGEN2, DRSPALL, SUMMARIZE, and ALGEBRA. The EPA found that the DOE submitted all of the source code listings. The EPA continued to find the detailed descriptions of the structure of the computer codes to be adequate (U.S. EPA 2010b). The CRA-2009 documentation of computer codes continued to adequately describe the structure of computer codes with sufficient detail to allow the EPA to understand how software subroutines were linked and how to execute the CRA-2009 PAs (U.S. EPA 2010b). The DOE continued to demonstrate compliance with the provisions of section 194.23(c)(3) (CARD 23, Section 23.5.8.3) (U.S. EPA 2010b).

23.8.7 Changes or New Information Since the CRA-2009

No changes have been made to the documentation procedure of PA computer codes used in the CRA-2014. As in the CRA-2004 and CRA-2009, the primary documentation of model compliance with section 194.23(c)(3) is contained in the ID for each modeling code. These code IDs provide the information necessary for the compiling of the codes as used in the CRA-2014 PA calculations. This information allows the user to compile the source code and install the code on a computer system identical or similar to that used in the CRA-2009 PA. The IDs include the source-code listings, the subroutine-call hierarchies, and code compilation information. The DOE continues to demonstrate compliance with the provisions of section 194.23(c)(3).

23.9 40 CFR § 194.23(c)(4)

23.9.1 Background

40 CFR § 194.23(c)(4) requires detailed descriptions of data collection, data reduction and analysis, and code input parameters development.

23.9.2 1998 Certification Decision

In the CCA, the DOE provided detailed descriptions of data collection, data reduction and analysis, and code input parameter development. The EPA's evaluation found that the CCA and supplementary information adequately (1) provided a detailed listing of the code input parameters; (2) listed sampled input parameters; (3) provided a description of parameters and the codes in which they are used; (4) discussed parameters important to releases; (5) described data collection procedures, sources of data, data reduction and analysis; and (6) described code input parameter development, including an explanation of QA activities.

A complete description of the EPA's 1998 Certification Decision for section 194.23(c)(4) can be obtained from CARD 23, Section 12.4 (U.S. EPA 1998a).

23.9.3 Changes in the CRA-2004

The primary sources of CRA-2004 parameter information are the CRA-2004 Chapter 6.0 (especially Tables 6-10 to 6-30), Appendix PA-2004, Attachment PAR-2004, and other appendices describing specific computer codes and parameter records (U.S. DOE 2004). Records of parameters for the CRA-2004 included the following:

- SNL Form NP 9-2-1 WIPP Parameter Entry Form (PEF): All PA parameters are defined using this form, which contains the numerical values and distributions of parameters used as input to PA codes, identifies the code the parameter is used in, and includes information to trace the development of each parameter. The PEF replaced Form 464 used in the CCA PA.

- Requestor Documents or Forms: Requestor documentation describes parameters that involve considerable data reduction and analysis by the SNL Principal Investigator or other technical personnel. Requestor documentation is the second step of PA parameter development. Data reduction and analysis are usually explained in this step. Requestor documentation replaced the Principal Investigator Records Packages (PIRPs) used during the CCA PA.

- Data Records Packages (DRPs): These documents are typically generated for parameters derived from empirical testing as a result of laboratory or field measurements (for example, actinide solubility experiments or brine inflow rate measurements in the WIPP underground repository). These packages are generally the first step that links the development of a parameter from the measured data to the values used in the PA.

- APs: These are supplementary documents that generally describe all parameters used by a particular code in the PA calculations.

The main source for parameter documentation is the PEF. The need for further documentation in the other three types of documents depends upon the nature of the parameter, such as whether it is a widely accepted chemical constant (e.g., atomic weight of an isotope) or a value requiring experimental data for verification. Table 23-4 describes the types of information found in each of these four documents and possible paths in documenting parameter record information.

The CCA contained approximately 1,600 parameters and the CRA-2004 contained approximately 1,700 parameters consisting of numerical values or ranges of numerical values that describe different physical and chemical aspects of the repository, the geology and geometry of the area surrounding the WIPP, and possible scenarios for human intrusion. Some parameters are well-established chemical constants, such as Avogadro's number or the universal gas constant. Other parameters describe attributes unique to the WIPP, such as the solubility and mobility of specific actinides in brines in the WIPP. An example of a parameter related to the geology of the WIPP is the permeability of the rock in the Culebra above the WIPP. The DOE also assigned parameters to consider the effects of human intrusion, such as the diameter of a drill bit used to drill a borehole that might penetrate the repository.

In the documents listed above, the DOE described the methods that develop and support the approximately 1,700 parameters used in the CRA-2004. All of the documents listed are used to explain the full development of parameter values used as inputs to the PA calculations. Table 23-4 indicates the documents that contain information required under section 194.23(c)(4).

Table 23-4. Location of Required Information on Parameters Used in Codes for CRA-2004 PA

Requirement in Compliance Application Guidance	Document Containing Information							
	PEF	Requestor Documents[d]	DRP	AP	CRA-2004[a]	Att. PAR[b]	App. QAPD[c]	Parameter Database
Detailed listings of code input parameters	—	—	—	—	—	—	—	X
Detailed listings of the sampled parameters	—	—	—	—	—	X	—	X
Codes in which the parameters were used	X	—	—	X	—	—	—	X
Computer code names of the sampled parameters	X	—	—	X	—	—	—	X
Descriptions of the data sources	X	X	X	X	—	—	—	X
Descriptions of the parameters	—	—	—	X	X	X	—	X
Descriptions of the data collection procedures	—	X	X	—	—	—	—	—
Descriptions of the data reduction and analysis	—	X	X	X	—	—	—	—
Descriptions of code input parameter development	—	—	X	—	—	—	—	—
Discussions of the linkage between input parameter information and data used to develop the input information	—	X	X	X	—	—	—	X
Discussions of the importance of the sampled parameters relative to final releases	—	—	—	X	—	—	—	—
Discussions of correlations among sampled parameters and how these are addressed in PA	—	—	—	—	—	X	—	—
Listing of the data sources used to establish parameters (e.g., experimentally derived, standard textbook values)	X	X	X	X	—	—	—	X
Data reduction methodologies used for PA parameters	—	X	X	X	—	—	—	—
Explanation of QA activities	—	—	—	—	X	—	X	—

X = Information meeting the requirement is found in this document.

[a] See CRA-2004, Chapter 6.0 for parameter descriptions, and CRA-2004, Chapter 5.0 for an explanation of QA activities (U.S. DOE 2004).

[b] Appendix PA-2004, Attachment PAR-2004 (U.S. DOE 2004).

[c] Appendix QAPD-2004 (U.S. DOE 2004).

[d] Formerly PIRPs.

23.9.4 EPA's Evaluation of Compliance for the 2004 Recertification

As for the CCA, the EPA performed a thorough review of the parameters and parameter development process for the CRA-2004. For the CRA-2004 parameter review, the EPA focused its review on parameters that had changed or were new since the CCA. The EPA's review of the parameters and parameter development is described in detail (U.S. EPA 2006m;U.S. EPA 2006n). The EPA reviewed parameter packages for a sample of approximately 1,700 parameters used in the CRA-2004 PA calculations. The parameter records include WIPP PEFs (NP 9-2-1), requestor documents or forms, DRPs requestor documents or forms, and APs.

The EPA's review of PA parameters took place in three phases. In 2003, the EPA reviewed the transfer of parameters from the CCA database to a new database system (U.S. EPA 2006n). Next, the EPA reviewed the parameters changed as a result of the parameter transfer to the CRA-2004 PA calculations (U.S. EPA 2006n). The EPA found 128 new parameters and 203 changes to existing parameters. Many of the parameter changes were due to revisions of the waste inventory values in the PA calculations and new parameter values used in the new spallings code, DRSPALL. The EPA was able to verify that the new and changed parameters were adequately recorded in the WIPP parameter database and that most of these parameters were justified and traceable to adequate supporting documentation. Finally, the EPA reviewed the parameter changes and documentation for values changed for the CRA-2004 PABC calculations required by the EPA to confirm the impact of code errors and parameter changes on the PA compliance results (U.S. EPA 2006m).

The EPA found minor concerns at each phase of the review, including that some CRA-2004 PA parameters were not recorded in the WIPP parameter database as expected. Parameters used in codes executed on other computer platforms, such as MODFLOW, PEST, and SANTOS, were not stored in the WIPP parameter database. EPA recommended placing all parameters used in the PA calculations in the PA parameter database or a centralized WIPP database as a more efficient means of identifying and reviewing parameters, thus facilitating traceability reviews. Ultimately, the DOE corrected each concern, and the EPA verified that parameters used in the CRA-2004 were adequately developed, documented, and traceable. The EPA determined that the DOE continued to comply with section 194.23(c)(4) (CARD 23, Section Recertification Decision 194.23(c)) (U.S. EPA 2006f).

During the EPA's completeness review, stakeholders commented on the drilling rate used in the CRA-2004 PA calculations. During meetings with stakeholders in July 2004, comments arose regarding the drilling rate used in the CRA-2004 and it was suggested that a number twice the existing rate should be used in PA calculations. In a December 3, 2004, email, the EPA informed the DOE that it was required to evaluate the impact of doubling the CRA-2004 PA drilling rate. The analysis was conducted and the DOE documented the results (Kanney and Kirchner 2004). The EPA reviewed the DOE's response and noted that while doubling the drilling rate increases predicted releases, the results are still well within regulatory release limits.

Ultimately, the EPA was able to determine that the DOE continued to be in compliance with section 194.23(c)(4) (CARD 23, Section Recertification Decision 194.23(c)) (U.S. EPA 2006f).

23.9.5 Changes or New Information Between the CRA 2004 and the CRA 2009 (Previously: Changes or New Information Since the 2004 Recertification)

For the CRA-2009, there were 90 new parameters and 15 modified parameters (Fox 2008, Table 6). The 15 modified parameters and 10 of the 90 new parameters were a result of corrections and parameter updates. The remaining 80 new parameters arose from capability improvements added to the BRAGFLO computer code. More discussion of the CRA-2009 parameters is found in Fox (Fox 2008).

As in the CRA-2004, the information used to show detailed descriptions of data collection procedures, data reduction and analysis, and code input parameter development was provided in the PEFs that the DOE prepared for each of the CRA-2009 PA parameters (see Fox (Fox 2008)). Therefore, the DOE continues to provide documentation of the parameter development and thus, continues to demonstrate compliance with the provisions of section 194.23(c)(4).

23.9.6 EPA's Evaluation of Compliance for the 2009 Recertification

The EPA performed a thorough review of the parameters and parameter development process for the CRA-2009 PA calculations, which are documented in CRA-2009, Section 23, (Fox 2008; Kirchner 2008a), and parameter records in the SNL WIPP Records Center. The parameter records in the SNL WIPP Records Center reviewed by the EPA included WIPP PEFs (NP 9-2-1), DRPs, and APs. The EPA reviewed parameter documentation and record packages for a sample of the approximately 1,700 parameters used in the CRA-2009 PA calculations.

The EPA found one minor concern related to the hand-coding of parameters that are not included in the parameter database but are instead input manually. The EPA recommended that these parameters need to be included in the parameter database to improve traceability. The DOE corrected this concern and the EPA verified that parameters used in the CRA-2009 PA calculations were adequately developed, documented, and traceable (U.S. EPA 2010b). The EPA determined that the DOE continued to demonstrate compliance with the provisions of section 194.23(c)(4) (CARD 23, Section 23.5.8.4) (U.S. EPA 2010b).

23.9.7 Changes or New Information Since the CRA-2009

For the CRA-2014, there are 20 new parameters and 15 modified parameters for use in the BRAGFLO computer code (Clayton 2013). Of the 15 modified parameters, 5 involved changes to their descriptions, 2 involved changes to their descriptions and values, 2 involved modifications of the parameter values, 3 were standard error adjustment factors for the uncertainties for each brine type used in magnesium oxide hydration modeling, and the remaining 3 were updates to the magnesium oxide hydration rate parameters. The 20 new parameters arose from the introduction of a refined water balance model in the BRAGFLO computer code. A complete discussion of the chemistry parameters for use in Salado flow modeling using the computer code BRAGFLO for the CRA-2014 can be found in Clayton (Clayton 2013), Kicker and Herrick (Kicker and Herrick 2013), and Appendix PA-2014. Additionally, a query of the parameter database indicated that there are 13 BRAGFLO parameters sampled with new distributions for the CRA-2014, primarily due to inventory

updates, implementation of the Run-of-Mine Panel Closure System (ROMPCS) and refinement of the water balance. A complete listing of all parameter changes for all the computer codes from CRA-2009 to CRA-2014 can be found in Kicker and Herrick (Kicker and Herrick 2013).

As in the CRA-2004 and CRA-2009, the information used to show detailed descriptions of data collection procedures, data reduction and analysis, and code input parameter development is contained in the PEFs that the DOE prepared for each of the CRA-2014 PA parameters (Kicker and Herrick 2013). The DOE continues to provide documentation of the parameter development and thus, continues to demonstrate compliance with the provisions of section 194.23(c)(4).

23.10 40 CFR § 194.23(c)(5)

23.10.1 Background

40 CFR § 194.23(c)(5) requires documentation of any necessary licenses for all models and computer codes.

23.10.2 1998 Certification Decision

The DOE did not use any software that requires a license, so the EPA found that the DOE demonstrated compliance with section 194.23(c)(5).

A complete description of the EPA's 1998 Certification Decision for section 194.23(c)(5) can be obtained from CARD 23, Section 13.1 (U.S. EPA 1998a).

23.10.3 Changes in the CRA-2004

As in the CCA, no licenses from software vendors were required to operate the codes essential for the CRA-2004 PA. Most of the computer codes for the CRA-2004 PA were developed and programmed by the DOE or its contractors as custom software, and require no license to execute or use the computer codes documented in the CCA and supplementary materials. MODFLOW and PEST are public domain codes and are readily accessible.

23.10.4 EPA's Evaluation of Compliance for the 2004 Recertification

As the DOE did not use any software that requires a license, the EPA determined that the DOE continued to comply with section 194.23(c)(5) (CARD 23, Section Recertification Decision 194.23(c)) (U.S. EPA 2006f).

23.10.5 Changes or New Information Between the CRA-2004 and the CRA-2009 (Previously: Changes or New Information Since the 2004 Recertification)

No new codes were added for the CRA-2009 PA and no software requiring a license was used. Thus, there was no new information provided in the CRA-2009, and the DOE continued to demonstrate compliance with the provisions of section 194.23(c)(5).

23.10.6 EPA's Evaluation of Compliance for the 2009 Recertification

The EPA verified that no licenses from software vendors are required to operate the codes essential for the CRA-2009 PA. The EPA also verified that most computer codes for the CRA-2009 PA were developed by and programmed by SNL or its contractors as custom software and required no license. The EPA confirmed that MODFLOW and PEST continue to be public domain codes and are readily accessible (U.S. EPA 2010b). Thus, the EPA determined that the DOE continued to demonstrate compliance with the provisions of section 194.23(c)(5) (CARD 23, Section 23.5.8.5) (U.S. EPA 2010b).

23.10.7 Changes or New Information Since the CRA-2009

Two new codes were added for CRA-2014, namely, EQ3/6 and JAS3D. No licenses are required for these codes. Thus, there is no new information to provide in the CRA-2014. The DOE continues to demonstrate compliance with the provisions of section 194.23(c)(5).

23.11 40 CFR § 194.23(c)(6)

23.11.1 Background

40 CFR § 194.23(c)(6) requires an explanation of the manner in which models and computer codes incorporate the effects of parameter correlation.

23.11.2 1998 Certification Decision

In the CCA, the DOE provided an explanation of the manner in which models and computer codes incorporate the effects of parameter correlation. The EPA's evaluation found that the CCA and supplementary information adequately discussed how the effects of parameter correlation are incorporated, explained the mathematical functions that describe these relationships, and described the potential impacts on the sampling of uncertain parameters. The CCA also adequately documented the effects of parameter correlation for both conceptual models and the formulation of computer codes, and appropriately incorporated these correlations in the PA.

A complete description of the EPA's 1998 Certification Decision for section 194.23(c)(6) is contained in CARD 23, Section 14.4 (U.S. EPA 1998a).

23.11.3 Changes in the CRA-2004

User-specified parameter correlations for sampled parameters were introduced into the CRA-2004 PA calculations using the Latin Hypercube Sampling (LHS) computer program. The DOE used two types of parameter correlations: user-specified and induced. User-specified (explicit) parameter correlations are input to the LHS computer code using a correlation matrix (see Kirchner (Kirchner 2005) for the complete list of parameters sampled in this manner).

When values sampled using the LHS computer code are used to calculate other values in the PA calculations, an induced correlation parameter relationship is created. This is the prevalent

method of parameter correlation in the CRA-2004 PA. CRA-2004 parameter correlations are described in Appendix PA-2004, Attachment PAR-2004, Section 4.0 (U.S. DOE 2004).

23.11.4 EPA's Evaluation of Compliance for the 2004 Recertification

The EPA determined that parameter correlations were adequately explained in the Appendix PA-2004, Attachment PAR-2004, Section PAR-4.0, and were adequately incorporated. The EPA also found that the CRA-2004 presented an adequate explanation of the manner in which models and computer codes incorporated the effects of parameter correlations. The EPA determined that the DOE continued to comply with section 194.23(c)(6) (CARD 23, Section Recertification Decision 194.23(c)) (U.S. EPA 2006f).

23.11.5 Changes or New Information Between the CRA-2004 and the CRA-2009 (Previously: Changes or New Information Since the 2004 Recertification)

The description of the parameter correlations used in the CRA-2009 PA can be found in Fox (Fox 2008), Section 4.0. No changes were made in the parameter correlations since the CRA-2004 PABC, except that the conditional relationship between the inundated and humid microbial cellulose degradation rates was modified from the CRA-2004 PABC methodology. For the CRA-2004 PABC, the conditional relationship was enforced in the preprocessing step for the BRAGFLO calculations by setting the humid rate equal to the inundated rate if the sampled humid rate was higher than the inundated rate for a single vector. Changing these values this way introduced a small error into the sensitivity analysis because the regression analysis was based on the sampled value rather than the conditional values.

For the CRA-2009 PA, a conditional relationship was applied so that the sampled inundated rate is used as the maximum in the sampling for the humid rate. This conditional relationship results in a correlation of 0.74 between the humid and inundated cellulose degradation rates (Kirchner 2008a). The conditional relationship was applied during the LHS process. The LHSEDIT utility was developed to account for this conditional relationship. The implementation and verification of the LHSEDIT utility is discussed in Kirchner (Kirchner 2008a).

The DOE continued to provide an explanation of the manner in which models and computer codes incorporate the effects of parameter correlation and thus demonstrate compliance with the provisions of section 194.23(c)(6).

23.11.6 EPA's Evaluation of Compliance for the 2009 Recertification

The EPA verified that the CRA-2009 documentation contained a complete discussion of how parameter correlations were incorporated into the PA, as well as an adequate explanation of the mathematical functions used to describe the correlation implementation in the CRA-2009 PA calculations (CRA-2009, Section 23.11.5 and Appendix PA-2009, Table PA-21 (U.S. DOE 2009); Fox (Fox 2008), Section 4.0; Clayton (Clayton 2010), Section 4.0). The EPA analyzed the computational aspects of the LHS computer program and functionality tests that implement the correlation check.

No changes were made in the parameter correlations since CRA-2004 PABC, except the modification of the conditional relationship between the inundated and humid microbial cellulose degradation rates. A conditional relationship was applied so that the sampled inundated rate is used as the maximum in the sampling for the humid rate, which improved the correlation (Kirchner 2008a).

The EPA determined that parameter correlations are adequately explained in CRA-2009 documents and are adequately incorporated in the CRA-2009 PA calculations (U.S. EPA 2010b). The EPA also found that the CRA-2009 presented an adequate explanation of the manner in which models and computer codes incorporated the effects of parameter correlations (U.S. EPA 2010b). The EPA determined that the DOE continued to demonstrate compliance with the provisions of section 194.23(c)(6) (CARD 23, Section 23.5.8.6) (U.S. EPA 2010b).

23.11.7 Changes or New Information Since the CRA-2009

The description of the parameter correlations used in the CRA-2014 PA can be found in Kirchner (2013). No changes were made in the parameter correlations since the CRA-2009 PABC, except for the conditional relationship between ROMPCS parameters for the different post-closure time periods modeled in Salado flow BRAGFLO computations. For the CRA-2014, the conditional relationship is enforced in the BRAGFLO calculations for the porosity values in the initial, secondary, and tertiary post-closure time periods (i.e., T1: 0-100 years, T2: 100-200 years, and T3: 200-10,000 years), and between humid and inundated biodegradation rate for cellulose (Camphouse 2013a); (Camphouse 2013b). Those conditional relationships are enforced by modifying values in the LHS transfer file, thus making the conditioned values available for use in the sensitivity analysis (Kirchner 2013).

As in the CRA-2009 PA, for the CRA-2014 PA, the cellulose biodegradation conditional relationship was applied so that the sampled inundated rate is used as the maximum in the sampling for the humid rate. This conditional relationship results in a correlation of 0.74 between the humid and inundated rates (Kirchner 2013).

The DOE continues to provide an explanation of the manner in which models and computer codes incorporate the effects of parameter correlation and thus demonstrate compliance with the provisions of section 194.23(c)(6).

23.12 40 CFR § 194.23(d)

23.12.1 Background

The DOE must provide the EPA free access to PA models and computer codes.

23.12.2 1998 Certification Decision

During the review of the CCA, the DOE provided the EPA with ready access to computer hardware required to perform independent computer simulations. Therefore, the EPA found the DOE in compliance with the requirements of 40 CFR § 194.23(d).

A complete description of the EPA's 1998 Certification Decision for section 194.23(d) can be obtained from CARD 23, Section 15.4 (U.S. EPA 1998a).

23.12.3 Changes in the CRA-2004

No specific changes were made to the CRA-2004 to demonstrate compliance with section 194.23(d). The DOE provided access for the EPA during the CRA-2004 to PA models and computer codes.

23.12.4 EPA's Evaluation of Compliance for the 2004 Recertification

The EPA expected the DOE to identify points of contact to facilitate the process for the EPA to perform independent simulations, provide ready access to the hardware and software needed to perform simulations related to the CRA-2004 evaluation, and assist EPA personnel in using the DOE computer codes.

The DOE provided contacts to assist the EPA in operating the hardware needed to perform the independent computer simulations necessary to verify the simulations related to the CRA-2004. The DOE provided the EPA and authorized personnel with unrestricted access to this computer hardware and software.

Based on adequate support and access to PA computer codes, input files, and PA-related documentation, the EPA determined that the DOE continued to comply with the requirements for section 194.23(d) (CARD 23, Section Recertification Decision 194.23(d)) (U.S. EPA 2006f).

23.12.5 Changes or New Information Between the CRA-2004 and the CRA-2009 (Previously: Changes or New Information Since the 2004 Recertification)

No specific changes were made to the CRA-2009 to demonstrate compliance with section 194.23(d). Thus, the DOE continued to provide the EPA with unrestricted access to the computer hardware and software and continued to demonstrate compliance with the provisions of section 194.23(d).

23.12.6 EPA's Evaluation of Compliance for the 2009 Recertification

The DOE continued to identify points of contact to facilitate the process for EPA to perform independent simulations, provide ready access to the hardware and software needed to perform simulations related to evaluation of the CRA-2009, and assist EPA personnel in using DOE computer codes as needed.

The DOE provided contacts at SNL and the Los Alamos National Laboratory to assist the EPA and EPA contractor personnel in operating the hardware needed to perform independent computer simulations necessary to verify the simulations related to the CRA-2009. Use of a special configuration management system on the Alpha cluster of VAX computers, and use of the Linux Concurrent Versions System file management systems, which contains all the codes and parameter data needed to run the PA, continued at SNL. These two systems archive all the

input files, output files, source code, and executable files of the modeling codes used by the DOE in the PA calculations. The DOE provided the EPA and authorized personnel with unrestricted access to this computer hardware and software.

The EPA did not receive any public comments on the DOE's continued compliance with the models and computer code requirements of section 194.23(d). Based on a review and evaluation of the CRA-2009 and supplemental information provided by the DOE (FDMS Docket ID No. U.S. EPA-HQ-OAR-2009-0330, Air Docket A-98-49), and adequate support and access to the CRA-2009 PA computer codes, input files, and PA-related documentation, the EPA determined that the DOE continued to demonstrate compliance with the requirements of section 194.23(d) (CARD 23, Section 23.6.8) (U.S. EPA 2010b).

23.12.7 Changes or New Information Since the CRA-2009

No specific changes were made to the CRA-2014 to demonstrate compliance with section 194.23(d). The DOE will continue to provide the EPA with unrestricted access to the computer hardware and software. Thus, the DOE continues to demonstrate compliance with the provisions of section 194.23(d).

23.13 References

(*Indicates a reference that has not been previously submitted.)

Beauheim, R.L. 2008. Summary of Conceptual Model and Supporting Field Evidence, Presentation for the Culebra Hydrogeology Conceptual Model Peer Review. August, 2008. ERMS 550002. Carlsbad NM: Sandia National Laboratories.

Burgess, A., T. Doe and T. Lowentrein. 2008. Culebra Hydrogeology Conceptual Model Peer Review, Final Report, September 24, 2008. Report for the Carlsbad Field Office Technical Assistance Contractor of the Department of Energy.

Camphouse, R.C. 2013a. Analysis Plan for the 2014 WIPP Compliance Recertification Application Performance Assessment. ERMS 559198. Carlsbad, NM: Sandia National Laboratories.

Camphouse, R.C. 2013b. Analysis Package for Salado Flow Modeling done in the 2014 Compliance Recertification Application Performance Assessment (CRA-2014 PA). ERMS 559980. Carlsbad, NM: Sandia National Laboratories.

Clayton, D.J. 2013. *Justification of Chemistry Parameters for Use in BRAGFLO for AP-164.* ERMS 559466. Albuquerque, NM: Sandia National Laboratories.*

Clayton, D.J. 2010. Parameter Summary Report: CRA-2009 PABC. ERMS 552889. Carlsbad, NM: Sandia National Laboratories.*

Clayton, D.J. 2008. *Analysis Package for Direct Brine Releases: Compliance Recertification Application–2009*. ERMS 548571. Carlsbad, NM: Sandia National Laboratories.

Clayton, D.J., S. Dunagan, J.W. Garner, A.E. Ismail, T.B. Kirchner, G.R. Kirkes, and M.B. Nemer. 2008. *Summary Report of the 2009 Compliance Recertification Application Performance Assessment.* ERMS 548862. Carlsbad, NM: Sandia National Laboratories.

Cotsworth, E. 2004. Letter to R.P. Detwiler (1 Enclosure). 20 May 2004. ERMS 535554. Washington, DC: U.S. Environmental Protection Agency, Office of Air and Radiation.

Cotsworth, E. 2005. Letter to U.S. Department of Energy (1 Enclosure). March 4, 2005. ERMS 538858. Washington, DC: U.S. Environmental Protection Agency, Office of Air and Radiation.

Detwiler, R.P. 2004a. Letter to E. Cotsworth. 29 September 2004. Carlsbad, NM: U.S. Department of Energy, Carlsbad Field Office.

Detwiler, R.P. 2004b. Letter to E. Cotsworth (Subject: Partial Response to U.S. EPA May 20, 2004, Letter on CRA; 1 Enclosure). 15 July 2004. Carlsbad, NM: U.S. Department of Energy, Carlsbad Field Office.

Dials, G.E. 1997. Letter to R. Trovato. 7 February 1997. Carlsbad, NM: U.S. Department of Energy, Carlsbad Field Office.

Dunagan, S. 2008. *Analysis Package for CCDFGF: 2009 Compliance Recertification Application*. ERMS 548776. Carlsbad, NM: Sandia National Laboratories.

Fox, B. 2008. *Parameter Report for the CRA-2009 PA* (Revision 0). ERMS 549747. Carlsbad, NM: Sandia National Laboratories.

Garner, J., and C. Leigh. 2005. *Analysis Package for PANEL, CRA-2004 Performance Assessment Baseline Calculation* (Revision 0). ERMS 540572. Carlsbad, NM: Sandia National Laboratories.

Gilkey, A.P. 2006. *Implementation Document for NUTS, Version 2.05c*. ERMS 543407. Carlsbad, NM: Sandia National Laboratories.

Ismail, A.E. 2008. *Analysis Package for CUTTINGS_S: Compliance Recertification Application 2009* (Revision 1). ERMS 548618. Carlsbad, NM: Sandia National Laboratories.

Ismail, A.E., and J.W. Garner. 2008. *Analysis Package for Salado Transport Calculations: Compliance Recertification Application 2009*. ERMS 548845. Carlsbad, NM: Sandia National Laboratories.

Kanney, J.F., and T.B. Kirchner. 2004. *Impact of Potential Drilling Rate Increases on WIPP Repository Performance*. ERMS 538262. Carlsbad, NM: Sandia National Laboratories.

Kicker, D.C. and Herrick, C. 2013. *Parameter Summary Report for the 2014 Compliance Recertification Application* (Revision 0). ERMS 560298. Carlsbad, NM: Sandia National Laboratories.*

Kirchner, T. 2013. *Generation of the LHS Samples for the CRA-2014 (AP-164) Revision 0 PA Calculations*. ERMS 559950. Carlsbad, NM: Sandia National Laboratories.*

Kirchner, T. 2008a. *Generation of the LHS Samples for the AP-137 Revision 0 (CRA09) PA Calculations*. ERMS 547971. Carlsbad, NM: Sandia National Laboratories.

Kirchner, T. 2008b. *Sensitivity of the CRA-2009 Performance Assessment Calculation Releases to Parameters*. ERMS 548788. Carlsbad, NM: Sandia National Laboratories.

Kirchner, T. 2005. *Generation of the LHS Samples for the CRA-2004 PA Baseline Calculations*. ERMS 540279. Carlsbad, NM: Sandia National Laboratories.*

Kuhlman, K.L. 2010. *Development of Culebra T Fields for CRA 2009 PABC*. ERMS 553276. Carlsbad, NM: Sandia National Laboratories.*

Lorenz, J.C. 2006a. Assessment of the Potential for Karst in the Rustler Formation at the WIPP Site. SAND2005-7303. Albuquerque, NM: Sandia National Laboratories.*

Lorenz, J.C. 2006b. "Assessment of the Geological Evidence for Karst in the Rustler Formation at the WIPP Site." Caves and Karst of Southeastern New Mexico (pp. 243–52). L. Land, V.W.*

Lowry, T.S., and J. Kanney. 2005. *Analysis Report for the CRA-2004 PABC Culebra Flow and Transport Calculations*. ERMS 541508. Carlsbad, NM: Sandia National Laboratories.

Marcinowski, F. 2002. Letter to I. Triay. 6 August 2002. ERMS 533337. Washington, DC: U.S. Environmental Protection Agency , Office of Air and Radiation.

Nemer, M.B. 2006. *Change Control for BRAGFLO, Version 5.0 (Proposed 6.0)*. ERMS 544904. Carlsbad, NM: Sandia National Laboratories.

Nemer, M.B. 2007a. *User's Manual for BRAGFLO, Version 6.0*. ERMS 545016. Carlsbad, NM: Sandia National Laboratories.

Nemer, M.B. 2007b. *Requirements Document and Validation and Verification Plan for BRAGFLO, Version 6.0*. ERMS 545014. Carlsbad, NM: Sandia National Laboratories.

Nemer, M.B. 2007c. *Implementation Document for BRAGFLO, Version 6.0*. ERMS 545017. Carlsbad, NM: Sandia National Laboratories.

Nemer, M.B. 2007d. *Validation Document for BRAGFLO, Version 6.0*. ERMS 545018. Carlsbad, NM: Sandia National Laboratories.

Nemer, M.B., and D.J. Clayton. 2008. *Analysis Package for Salado Flow Modeling, 2009 Compliance Recertification Application Calculation*. ERMS 548607. Carlsbad, NM: Sandia National Laboratories.

S. Cohen and Associates. 2008. Concerns and Comments on the Culebra Hydrology Conceptual Model and Peer Review-Waste Isolation Pilot Plant. SCA. November 2008. Vienna, Virginia.

Sandia National Laboratories and Carlsbad Area Office Technical Assistance Contractor. 1997. *Spallings Release Positions Paper: Description and Evaluation of a Mechanistically Based Conceptual Model for Spall*. ERMS 414916. Carlsbad, NM: Sandia National Laboratories.

U.S. Department of Energy (DOE). 1996. *Title 40 CFR Part 191 Compliance Certification Application for the Waste Isolation Pilot Plant* (October). 21 vols. U.S. DOE/CAO 1996-2184. Carlsbad, NM: Carlsbad Area Office.*

U.S. Department of Energy (DOE). 2004. *Title 40 CFR Part 191 Compliance Recertification Application for the Waste Isolation Pilot Plant* (March). 10 vols. U.S. DOE/WIPP 2004-3231. Carlsbad, NM: Carlsbad Field Office.

U.S. Department of Energy (DOE). 2009. *Title 40 CFR Part 191 Compliance Recertification Application for the Waste Isolation Pilot Plant*. DOE/WIPP 09-3424. Carlsbad, NM: U.S. Department of Energy, Carlsbad Field Office.*

U.S. Environmental Protection Agency (EPA). 1996. "40 CFR Part 194: Criteria for the Certification and Recertification of the Waste Isolation Pilot Plant's Compliance with the 40 CFR Part 191 Disposal Regulations; Final Rule." *Federal Register*, vol. 61 (February 9, 1996): 5223–45.

U.S. Environmental Protection Agency (EPA). 1998a. "CARD No. 23: Models and Computer Codes." *Compliance Application Review Documents for the Criteria for the Certification and Recertification of the Waste Isolation Pilot Plant's Compliance with the 40 CFR 191 Disposal Regulations: Final Certification Decision* (May) (pp. 23-1 through 23-93). Washington, DC: Office of Radiation and Indoor Air.

U.S. Environmental Protection Agency (EPA). 1998b. "40 CFR Part 194: Criteria for the Certification and Recertification of the Waste Isolation Pilot Plant's Compliance with the Disposal Regulations: Certification Decision; Final Rule." *Federal Register*, vol. 63 (May 18, 1998): 27353–406.

U.S. Environmental Protection Agency (EPA). 2006a. *Technical Support Document for Sections 194.25, 194.32 and 33: Compliance Recertification Application Review of Features, Events and Processes* (March). Washington, DC: Office of Radiation and Indoor Air.

U.S. Environmental Protection Agency (EPA). 2006b. *Technical Support Document for Sections 194.32 and 33: Compliance Recertification Application Re-Evaluation of Select Human Intrusion Activities*. Washington, DC: Office of Radiation and Indoor Air.

U.S. Environmental Protection Agency (EPA). 2006c. *Technical Support Document for Section 194.23: Review of the 2004 Compliance Recertification Performance Assessment Baseline Calculation* (March). Washington, DC: Office of Radiation and Indoor Air.

U.S. Environmental Protection Agency (EPA). 2006d. *Technical Support Document for Section 194.27: Spallings Conceptual Models Peer Review*. Washington, DC: Office of Radiation and Indoor Air.

U.S. Environmental Protection Agency (EPA). 2006e. *Technical Support Document for Section 194.27: Salado Flow Conceptual Models Peer Review*. Washington, DC: Office of Radiation and Indoor Air.

U.S. Environmental Protection Agency (EPA). 2006f. "Recertification CARD No. 23: Models and Computer Codes." *Compliance Application Review Documents for the Criteria for the Certification and Recertification of the Waste Isolation Pilot Plant's Compliance with the 40 CFR 191 Disposal Regulations: Final Recertification Decision* (March) (pp. 23-1 through 23-37). Washington, DC: Office of Radiation and Indoor Air.

U.S. Environmental Protection Agency (EPA). 2006g. *Technical Support Document for Section 194.14/15: Evaluation of Karst at the WIPP Site* (March). Washington, DC: Office of Radiation and Indoor Air.

U.S. Environmental Protection Agency (EPA). 2006h. "Recertification CARD No. 14/15: Content of Certification Application and Compliance Recertification Application(s)." *Compliance Application Review Documents for the Criteria for the Certification and Recertification of the Waste Isolation Pilot Plant's Compliance with the 40 CFR 191 Disposal Regulations: Final Recertification Decision* (March) (pp. 14/15-1 through 14/15-34, pp. 14-A-1 through 14-A-3, and pp. 15-A-1 through 15-A-17). Washington, DC: Office of Radiation and Indoor Air.

U.S. Environmental Protection Agency (EPA). 2006i. *Technical Support Document for Section 194.23: Models and Computer Codes* (March). PABC Codes Changes Review. Washington, DC: Office of Radiation and Indoor Air.

U.S. Environmental Protection Agency (EPA). 2006j. *Technical Support Document for Section 194.23: Review of WIPP Recertification Performance Assessment Computer Codes* (March). CRA Code Review. Washington, DC: Office of Radiation and Indoor Air.

U.S. Environmental Protection Agency (EPA). 2006k. "Recertification CARD No. 22: Quality Assurance." *Compliance Application Review Documents for the Criteria for the Certification and Recertification of the Waste Isolation Pilot Plant's Compliance with 40 CFR Part 191 Disposal Regulations: Final Recertification Decision* (March) (pp. 22-1 through 22-17). Washington, DC: Office of Radiation and Indoor Air.

U.S. Environmental Protection Agency (EPA). 2006l. *Technical Support Document for Section 194.27: SANTOS Computer Code in WIPP Performance Assessment*. Washington, DC: Office of Radiation and Indoor Air.

U.S. Environmental Protection Agency (EPA). 2006m. *Technical Support Document for Section 194.23: Review of Changes to the WIPP Performance Assessment Parameters from the Compliance Recertification Application to Performance Assessment Baseline Calculation* (March). PABC Parameter Review. Washington, DC: Office of Radiation and Indoor Air.

U.S. Environmental Protection Agency (EPA). 2006n. *Technical Support Document for Section 194.23: Review of Changes to the WIPP Performance Assessment Parameters Since the Database Migration: CRA Parameter Review*. Washington, DC: Office of Radiation and Indoor Air.

U.S. Environmental Protection Agency (EPA). 2010a. Technical Support Document for Section 194.23: Review of WIPP Performance Assessment Computer Code Migration Activities. Docket A-98-49, II-B1-22. Washington, DC: Office of Radiation and Indoor Air.*

U.S. Environmental Protection Agency (EPA). 2010b. 2009 Compliance Application Review Documents (2009 CARDs). Docket A-98-49, Item V-B2-2. Washington, DC: Office of Radiation and Indoor Air.*

U.S. Nuclear Regulatory Commission (NRC). 1988. *Peer Review for High-Level Nuclear Waste Repositories.* NUREG-1297. Washington, DC.

Vugrin, E.D. 2005. *Analysis Package for DRSPALL, CRA 2004 Performance Assessment Baseline Calculation*. ERMS 540415. Carlsbad, NM: Sandia National Laboratories.

Vugrin, E.D., and M.B. Nemer. 2007. *Analysis Plan for the 2009 Compliance Recertification Application Performance Assessment* (Revision 0). AP-132. ERMS 545496. Carlsbad, NM: Sandia National Laboratories.

Title 40 CFR Part 191
Subparts B and C
Compliance Recertification Application 2014
for the
Waste Isolation Pilot Plant

Waste Characterization
(40 CFR § 194.24)

United States Department of Energy
Waste Isolation Pilot Plant

Carlsbad Field Office
Carlsbad, New Mexico

Compliance Recertification Application 2014
Waste Characterization
(40 CFR § 194.24)

Table of Contents

List of Tables

This page intentionally left blank.

Acronyms and Abbreviations

AK	acceptable knowledge
AMWTF	Advanced Mixed Waste Treatment Facility
ATWIR	Annual Transuranic Waste Inventory Report
CAO	Carlsbad Area Office
CARD	Compliance Application Review Document
CBFO	Carlsbad Field Office
CCA	Compliance Certification Application
CFR	Code of Federal Regulations
CH	contact-handled
Ci	curie
CID	Comprehensive Inventory Database
CPR	cellulose, plastic and rubber
CRA	Compliance Recertification Application
DBR	direct brine release
DOE	U.S. Department of Energy
EPA	U.S. Environmental Protection Agency
FMT	Fracture-Matrix Transport
GWB	generic weep brine
HSG	headspace gas
ICP	Idaho Cleanup Project
INL	Idaho National Laboratory
kg	kilogram
LANL	Los Alamos National Laboratory
LWA	Land Withdrawal Act
m^3	cubic meters
NDA	nondestructive assay
NDE	nondestructive examination
PA	performance assessment
PABC	Performance Assessment Baseline Calculation
PAIR	Performance Assessment Inventory Report
PAVT	Performance Assessment Verification Test
PCR	Planned Change Request
PDP	performance demonstration program

QA	quality assurance
QAO	quality assurance objective
QAPD	Quality Assurance Program Document
QAPP	Quality Assurance Program Plan
rem	roentgen equivalent man
RFETS	Rocky Flats Environmental Technology Site
RH	remote-handled
RTR	real-time radiography
SRS	Savannah River Site
TRU	transuranic
TWBID	Transuranic Waste Baseline Inventory Database
TWBIR	Transuranic Waste Baseline Inventory Report
VE	visual examination
WAC	Waste Acceptance Criteria
WAP	Waste Analysis Plan
WCPIP	Waste Characterization Program Implementation Plan
WDS	Waste Data System
WIPP	Waste Isolation Pilot Plant
WTWBIR	WIPP Transuranic Waste Baseline Inventory Report
WUF	waste unit factor
WWIS	WIPP Waste Information System
yr	year

Elements and Chemical Compounds

Am	americium
An	actinide
An(III)	general actinide in the +3 oxidation state
An(IV)	general actinide in the +4 oxidation state
An(V)	general actinide in the +5 oxidation state
CH_4	methane
Cm	curium
CO_2	carbon dioxide
Cs	cesium
EDTA	ethylenediaminetetraacetic acid

$f(CO_2)$	fugacity of carbon dioxide
$Mg_5(CO_3)_4(OH)_2 \cdot 4H_2O$	hydromagnesite
Mg	magnesium
$Mg(OH)_2$	brucite
MgO	magnesium oxide
Np	neptunium
pH	the negative, common logarithm of the activity of H^+
Pu	plutonium
Sr	strontium
Th	thorium
$Th(OH)_4$	thorium hydrate
U	uranium

This page intentionally left blank.

24.0 Waste Characterization (40 CFR § 194.24)

24.1 Requirements

§ 194.24 Waste Characterization

(a) Any compliance application shall describe the chemical, radiological and physical composition of all existing waste proposed for disposal in the disposal system. To the extent practicable, any compliance application shall also describe the chemical, radiological and physical composition of to-be-generated waste proposed for disposal in the disposal system. These descriptions shall include a list of the waste components and their approximate quantities in the waste. This list may be derived from process knowledge, current non-destructive examination/assay, or other information and methods.

(b) The Department shall submit in the compliance certification application the results of an analysis which substantiates:

(1) That all waste characteristics influencing containment of waste in the disposal system have been identified and assessed for their impact on disposal system performance. The characteristics to be analyzed shall include, but shall not be limited to: solubility; formation of colloidal suspensions containing radionuclides; production of gas from the waste; shear strength; compactability; and other waste-related inputs into the computer models that are used in the performance assessment.

(2) That all waste components influencing the waste characteristics identified in paragraph (b)(1) of this section have been identified and assessed for their impact on disposal system performance. The components to be analyzed shall include, but shall not be limited to: metals; cellulosics; chelating agents; water and other liquids; and activity in curies of each isotope of the radionuclides present.

(3) Any decision to exclude consideration of any waste characteristic or waste component because such characteristic or component is not expected to significantly influence the containment of the waste in the disposal system.

(c) For each waste component identified and assessed pursuant to paragraph (b) of this section, the Department shall specify the limiting value (expressed as an upper or lower limit of mass, volume, curies, concentration, etc.), and the associated uncertainty (i.e., margin of error) for each limiting value, of the total inventory of such waste proposed for disposal in the disposal system. Any compliance application shall:

(1) Demonstrate that, for the total inventory of waste proposed for disposal in the disposal system, WIPP complies with the numeric requirements of §194.34 and §194.55 for the upper or lower limits (including the associated uncertainties), as appropriate, for each waste component identified in paragraph (b)(2) of this section, and for the plausible combinations of upper and lower limits of such waste components that would result in the greatest estimated release.

(2) Identify and describe the method(s) used to quantify the limits of waste components identified in paragraph (b)(2) of this section.

(3) Provide information which demonstrates that the use of process knowledge to quantify components in waste for disposal conforms with the quality assurance requirements found in Section 194.22.

(4) Provide information which demonstrates that a system of controls has been and will continue to be implemented to confirm that the total amount of each waste component that will be emplaced in the disposal system will not exceed the upper limiting value or fall below the lower limiting value described in the introductory text paragraph (c) of this section. The system of controls shall include, but shall not be limited to: Measurement; sampling; chain of custody records; record keeping systems; waste loading schemes used; and other documentation.

(5) Identify and describe such controls delineated in paragraph (c)(4) of this section and confirm that they are applied in accordance with the quality assurance requirements found in Section 194.22.

(d) The Department shall include a waste loading scheme in any compliance application, or else performance assessments conducted pursuant to § 194.32 and compliance assessments conducted pursuant to § 194.54 shall assume random placement of waste in the disposal system.

(e) Waste may be emplaced in the disposal system only if the emplaced components of such waste will not cause:

(1) The total quantity of waste in the disposal system to exceed the upper limiting value, including the associated uncertainty, described in the introductory text to paragraph (c) of this section; or

(2) The total quantity of waste that will have been emplaced in the disposal system, prior to closure, to fall below the lower limiting value, including the associated uncertainty, described in the introductory text to paragraph (c) of this section.

(f) Waste emplacement shall conform to the assumed waste loading conditions, if any, used in performance assessments conducted pursuant to §194.32 and compliance assessments conducted pursuant to §194.54.

(g) The Department shall demonstrate in any compliance application that the total inventory of waste emplaced in the disposal system complies with the limitations on transuranic waste disposal described in the WIPP LWA.

(h) The administrator will use inspections and records, such as audits, to verify compliance with this section.

24.2 Background

The U.S. Department of Energy (DOE) first demonstrated and documented compliance with the U.S. Environmental Protection Agency (EPA) radioactive waste disposal requirements found in 40 CFR Part 191 (U.S. EPA 1993) in its Compliance Certification Application (CCA) (U.S. DOE 1996a). The EPA reviewed the CCA against its Certification Criteria, found in 40 CFR Part 194 (U.S. EPA 1996), and certified that the DOE Waste Isolation Pilot Plant (WIPP) complies with the radioactive waste disposal regulations set forth in 40 CFR Part 191 Subparts B and C (Environmental Standards for the Management and Disposal of Spent Nuclear Fuel, High-Level and Transuranic Radioactive Waste) (U.S. EPA 1998a). In its demonstration of compliance, the DOE developed a computational modeling system to predict the future performance of the repository for 10,000 years (yrs) after closure. The system, called the WIPP Performance Assessment (PA), must consider both natural and man-made processes and events that affect the disposal system. The PA system is used to demonstrate compliance with the containment requirements of 40 CFR 191.13 (U.S. EPA 1993) and to provide input values to the compliance assessments. Compliance assessments may be regarded as a subset of PA, as defined in Section 54.

The WIPP PA requires many input parameters to represent the complex coupled processes that are expected to occur throughout the 10,000-yr regulatory time period. Some of these parameters relate directly to the transuranic (TRU) waste inventory. The TRU waste inventory includes information about materials in the waste (wood, metal, soil, etc.), materials used to package waste (steel drums, plastic liners, etc.), emplacement materials (cellulose, plastic, and rubber [CPR]), radionuclides in the waste, and key chemicals in the waste that are expected to impact or have a role in the performance of the repository. The TRU waste information needed as input to the WIPP PA is waste volumes, waste materials, packaging materials, emplacement materials, radionuclide activities, complexing agents (ethylenediaminetetraacetic acid [EDTA], acetate, citrate, oxalate, acetic acid, citric acid, and oxalic acid), and oxyanions (sulfate, nitrate, and phosphate).

TRU waste inventory has been reported by the DOE since 1994. The first inventory was reported as the *Waste Isolation Pilot Plant Transuranic Waste Baseline Inventory Report* (WTWBIR) (U.S. DOE 1994). This initial report was followed by WTWBIR Revision 1 (U.S. DOE 1995a), and two additional baseline reports, *Transuranic Waste Baseline Inventory Report* (TWBIR) Revisions 2 and 3 (U.S. DOE 1995b and U.S. DOE 1996b, respectively).

The TWBIR Revisions 2 and 3, included in the CCA, Appendix BIR, reported the TRU waste inventory basis for the CCA WIPP PA and the Performance Assessment Verification Test (PAVT) (U.S. DOE 1997). Following the receipt of the CCA PAVT analysis, the EPA ruled in May 1998 that the WIPP met the requirements for permanent disposal of TRU waste (U.S. EPA 1998a).

The first shipment of radioactive TRU waste from the nation's nuclear weapons complex arrived at the WIPP site in late March 1999. This marked the time for subsequent recertification of the WIPP every five years after initial waste receipt, as required by the Land Withdrawal Act (LWA) (U. S. Congress 1996). Thus, the first Compliance Recertification Application (CRA), CRA-2004 (U.S. DOE 2004), was submitted to the EPA by the DOE in March 2004. In the CRA-

2004, the DOE prepared a TRU waste inventory that was published in Appendix DATA, Attachment F and associated annexes.

During its review of the PA submitted in the CRA-2004, the EPA directed the DOE to conduct the CRA-2004 Performance Assessment Baseline Calculation (PABC) (Cotsworth 2005). Leigh, Trone, and Fox (Leigh, Trone, and Fox 2005) defined the inventory for the CRA-2004 PABC (Leigh et al. 2005). This inventory information was later published in the Transuranic Baseline Inventory Report-2004 (U.S. DOE 2006).

Following the receipt of the CRA-2004 PABC analysis, the EPA ruled on March 29, 2006, that the DOE demonstrated continued compliance with the requirements of 40 CFR § 194.24, and the repository was recertified for the first time (U.S. EPA 2006a).

After the CRA-2004, the DOE began to update the inventory on an annual basis. The inventory for the CRA-2009 PA (U.S. DOE 2009a and U.S. DOE 2009b) was the same inventory used for the CRA-2004 PABC (Leigh, Trone, and Fox 2005). The EPA reviewed the inventory updates, mainly the *Annual Transuranic Waste Inventory Report-2007* (ATWIR-2007) (DOE 2008a) and the ATWIR-2008 (DOE 2008b), and determined that a new performance assessment, the CRA-2009 PABC, needed to be conducted in order to include the increase in chemical components and other chemical properties. The EPA directed the DOE to perform the CRA-2009 PABC using the inventory contained in the ATWIR-2008 in its first completeness letter, dated May 21, 2009, items 1-G-3 and 1-23-1 (Cotsworth 2009a); thus, the *Performance Assessment Inventory Report-2008* (PAIR-2008) (Crawford et al. 2009) was produced for the CRA-2009 PABC.

Upon receipt and the determination of completeness (EPA 2010a) of the CRA-2009 PABC analysis, the EPA ruled on November 18, 2010, that the DOE demonstrated continued compliance with the requirements of 40 CFR § 194.24 and the repository was recertified for the second time (EPA 2010b).

The CRA-2014 inventory is presented in Section 24.8, Changes or New Information Since the CRA-2009 Recertification, and is based on the unscaled ATWIR-2012 (DOE 2012a) and the scaled (disposal) PAIR-2012 (Van Soest 2012), both with a data cut-off date of December 31, 2012.

24.3 1998 Certification Decision

24.3.1 40 CFR § 194.24(a)

In accordance with the requirements of 40 CFR § 194.24(a), the DOE provided in the CCA a description of existing TRU waste, a list of approximate quantities of waste components and, to the extent practicable, descriptions of TRU waste to be generated. This information was provided by the DOE in the form of waste profiles that were reviewed by the EPA. Upon completion of the review of these profiles, the EPA found the DOE in compliance with section 194.24(a) (Compliance Application Review Document [CARD] 24, Section 24.A.6, pp. 24-7 through 24-9) (U.S. EPA 1998b).

24.3.2 40 CFR § 194.24(b)(1)

In accordance with the requirements of 40 CFR § 194.24(b)(1), the DOE presented the results of its waste characteristics and components analyses in the CCA, Chapter 4.0 and Appendices MASS, WCA, SOTERM, and SA. The DOE indicated that the following characteristics were expected at the time of the CCA to have a significant effect on disposal system performance: radionuclide solubilities (including oxidation state distributions); formation of colloidal suspensions containing radionuclides; production of gas from the waste (hydrogen, and microbial substrate/nutrients for methane (CH_4) gas generation); shear strength, compactability (waste compressibility), and particle diameter; radioactivity in curies (Ci) for each isotope; and TRU radioactivity at closure.

These characteristics were included in the PA for the CCA. The EPA concluded that the DOE generally performed a thorough and well documented analysis, adequately identified all waste characteristics and, except for actinide (An) solubility and shear strength, appropriately assessed them as PA input parameters. The CCA PAVT was run using modified parameters, which satisfied the EPA's concerns (CARD 23, p. 23-10, and Section 12.4, pp. 23-42 through 23-68 (U.S. EPA 1998c), and CARD 24, Section 24.B.6, pp. 24-26 through 24-31 (U.S. EPA 1998b)).

24.3.3 40 CFR § 194.24(b)(2)

In accordance with the requirements of 40 CFR § 194.24(b)(2), the DOE identified a number of waste components and characteristics that would be important to performance. The EPA reviewed these components and characteristics and identified several issues with the DOE's treatment of them in the CCA PA. However, through independent analysis and changes made in the CCA PAVT, these issues were resolved and the EPA determined that the DOE complied with this section (CARD 24, Section 24.C.5, pp. 24-40 and 24-41) (U.S. EPA 1998b).

24.3.4 40 CFR § 194.24(b)(3)

In accordance with the requirements of 40 CFR § 194.24(b)(3), the DOE provided a list of those waste characteristics and components that were excluded from consideration in the PA for various reasons. The EPA had questions pertaining to assumptions and conclusions made by the DOE regarding organic ligands, but concluded that the DOE's treatment of organic ligands in the PA was adequate based on relevant literature and bounding assumptions using 1000 times the EDTA concentrations expected to be present in the repository (CARD 24, Section 24.D.5, pp. 24-43 and 24-44) (U.S. EPA 1998b).

24.3.5 40 CFR §§ 194.24(c)(1), (e)(1), (e)(2)

In accordance with the requirements of 40 CFR §§ 194.24(c)(1), (e)(1), and (e)(2), the DOE specified the limiting value of the following waste material components: ferrous metals (minimum 2×10^7 kilograms [kg]); CPR (maximum 2×10^7 kg); free water emplaced with the waste (maximum 1,684 cubic meters [m^3]); and nonferrous metals (metals not containing iron) (minimum 2×10^3 kg). In addition to these limits, the DOE provided plausible combinations of upper and lower limits and a rationale for these limits, the results of modeling code runs, the demonstration of numeric compliance, and the greatest release estimates. These limits, model

runs, maximum calculated releases, and release estimates were found to be adequately described according to the EPA (CARD 24, Section 24.F.5, pp. 24-58 through 24-65) (U.S. EPA 1998b).

The EPA also agreed that the PA appropriately accounted for the upper and lower limits because fixed values were used.

In a determination of compliance with sections 194.24(e)(1) and (e)(2), the EPA reviewed the DOE's description of system controls, chain-of-custody information, controls in place to track the WIPP TRU waste, waste record keeping and accountability systems, and the WIPP Waste Acceptance Criteria (WAC) requirements and controls. The EPA reviewed the CCA and determined that the DOE adequately referenced and summarized the WIPP WAC in the CCA (CARD 24, Section 24.H.5, pp. 24-80 through 24-84) (U.S. EPA 1998b).

24.3.6 40 CFR § 194.24(c)(2)

In accordance with 40 CFR § 194.24(c)(2), the DOE proposed using nondestructive examination (NDE). Real-time radiography (RTR) and visual examination (VE) were used to quantify the amounts of specific waste material components in TRU waste. The DOE described numerous nondestructive assay (NDA) instrument systems to determine radionuclides in the waste and described the equipment and instrumentation for NDA, RTR, and VE found in facilities. The DOE also provided information about performance demonstration programs (PDPs) intended to show that data obtained by each NDA method could meet data quality objectives established by the DOE including sensitivity, precision, and accuracy relative to limiting values.

The EPA found the methods described, when implemented appropriately, were adequate to characterize the important waste material components and radionuclides in TRU waste (CARD 24, Section 24.I.6, pp. 24-87 through 24-89) (U.S. EPA 1996 and U.S. EPA 1998b).

24.3.7 40 CFR § 194.24(c)(3)

In accordance with 40 CFR § 194.24(c)(3), the EPA determined that the DOE adequately described the use of acceptable knowledge (AK) only for legacy debris waste at the Los Alamos National Laboratory (LANL) (Dials 1997; U.S. EPA 1996; CARD 24; U.S. EPA 1998b).

24.3.8 40 CFR § 194.24(c)(4)

In accordance with the requirements of 40 CFR § 194.24(c)(4), the DOE described the system of documented controls used for waste characterization activities that described the management, operations, and quality assurance (QA) aspects of the program ensuring data completeness, accuracy, and discrepancy resolution prior to waste receipt at the WIPP. The DOE indicated that this system of controls would be monitored by the DOE/Carlsbad Field Office (CBFO) audit and surveillance program. In addition, the DOE provided descriptions of the documentation, data fields, and features of the WIPP Waste Information System (WWIS).

The EPA determined that the DOE provided an adequate description of the system controls and processes for maintaining centralized command and control over TRU waste characterization activities. This was inspected and verified by the EPA at LANL. Conditions 2 and 3 of the 1998

Certification Decision specified that the DOE was prohibited from shipping waste for disposal at the WIPP until the EPA approved site-specific waste characterization programs and controls (CARD 24, Section 24.H.5, pp. 24-80 through 24-84) (U.S. EPA 1998b).

24.3.9 40 CFR § 194.24(c)(5)

In accordance with the requirements of 40 CFR § 194.24(c)(5), the DOE described the PDP for NDA as required by the WIPP Quality Assurance Program Plan (QAPP). Under this CBFO program, the PDP standards address activity ranges relative to WAC limits, QAPP quality assurance objectives (QAOs), and NDA method detection limits. (See CARD 22 [U.S. EPA 1998d] for additional discussion of QA for waste characterization activities.) The EPA reviewed the updated PDP Plan for NDA and concluded that the DOE provided adequate information regarding the NDA PDP for LANL and the Rocky Flats Environmental Technology Site (RFETS) at the time of inspections. The EPA confirmed through inspections at LANL that the system of controls and the measurement techniques described and implemented at LANL were adequate to characterize waste and ensure compliance with the limits of waste components for disposal at the WIPP (CARD 22, Section 22.B-5, pp. 22-7 and 22-8) (U.S. EPA 1998d). The RFETS was later certified to ship waste to the WIPP.

24.3.10 40 CFR §§ 194.24(d) and (f)

In accordance with the requirements of 40 CFR §§ 194.24(d) and (f), the DOE had (1) assumed random waste loading and (2) evaluated the potential consequences resulting from the nonrandom loading of the highest-activity waste stream containing at least 810 drums in the WIPP. As a result of the evaluation, the DOE determined that a final waste loading plan was in fact unnecessary for the WIPP. The EPA therefore concluded that the DOE adequately cross-referenced the resultant waste distribution assumptions from the waste loading plan with the waste distribution assumptions used in the PA by random distribution of radioactive waste in the repository (CARD 24, Section 24.J.6, pp. 24-94 through 24-96) (U.S. EPA 1998b).

24.3.11 40 CFR § 194.24(g)

In accordance with the requirements of 40 CFR § 194.24(g), the DOE identified the following LWA limits to demonstrate compliance:

- Curie limits for remote-handled transuranic (RH-TRU) waste: 5.1 million Ci (approximately 1.89×10^{17} becquerels).

- Total capacity of RH-TRU and contact-handled transuranic (CH-TRU) waste that may be disposed: 6.2 million ft^3 (175,564 m^3).

- RH-TRU waste will not exceed 1,000 rem (roentgen equivalent man) per hour, no more than 5 percent (%) by volume of RH-TRU will exceed 100 rem per hour, and RH-TRU will not exceed 23 Ci per liter maximum activity level (averaged over the volume of the canister).

- In addition, the DOE provided numerous tables that presented the WIPP waste inventory in terms of activity (in Ci) and total volumes (in m^3). The EPA reviewed this information,

including the process the DOE outlined for controlling the waste and the use of the WWIS, and determined that the DOE had an adequate program for tracking and controlling the waste (CARD 24, Section 24.K.5, pp. 24-98 and 24-99) (U.S. EPA 1998b).

24.3.12 40 CFR § 194.24(h)

The EPA found the DOE in compliance with the provisions of 40 CFR § 194.24(h). Inspections, such as audits, and records are addressed by the EPA in CARD 22 (U.S. EPA 1998d).

24.4 Changes in the CRA-2004

24.4.1 40 CFR § 194.24(a)

To meet the requirements of section 194.24(a), the DOE described and categorized the TRU waste currently emplaced in the WIPP and the waste that existed or was expected to be generated at the DOE TRU waste sites in the CRA-2004 (U.S. DOE 2004). The DOE developed a descriptive methodology for collecting and grouping waste information obtained from each TRU waste site. The DOE also described and categorized the TRU waste that was currently emplaced in the WIPP and the waste that existed or was expected to be generated at the DOE TRU waste sites. The emplaced waste was tracked as reported in the WWIS and was included in the CRA-2004 inventory. The details of the CRA-2004 inventory are presented in the CRA-2004, Chapter 4.0, Appendix TRU WASTE-2004, and Appendix DATA-2004, Attachment F.

As a result of responses to questions from the EPA during its review of the CRA-2004 PA, the DOE was directed to conduct a new PA for recertification to incorporate inventory changes, as well as other technical changes (Cotsworth 2005). The new inventory components and radiological estimates were reported in TWBIR-2004 (U.S. DOE 2006) and subsequently summarized in the CRA-2004 PABC Inventory Report (Leigh, Trone, and Fox 2005).

24.4.1.1 Inventory Description

The CRA-2004 PABC Inventory Report, Table 4 (Leigh, Trone, and Fox 2005) lists the volumes of emplaced CH-TRU waste as of September 30, 2002 (the cutoff for inclusion in the CRA-2004 PA), and August 1, 2005 (the cutoff for inclusion in the CRA-2004 PABC). Table 5 of the same report lists the stored and projected CH-TRU waste estimates used for the CCA, the CRA-2004 PA, and the CRA-2004 PABC. The projected inventory information is derived from the updated waste stream profile forms and reflects each site's best determination of the waste expected to be generated. This inventory information is originally presented in the CRA-2004, Chapter 4.0, Section 4.1.3. Leigh, Trone, and Fox (Leigh, Trone, and Fox 2005), Tables 9 and 10, show the anticipated nonradioactive components of the TRU waste inventory.

For PA to model a full repository, the DOE used a scaling factor in the same manner used in the CCA. However, unlike in the CCA, the CRA-2004 also used this scaling methodology on RH-TRU waste. The techniques of inventory scaling are presented in TWBIR-2004 (U.S. DOE 2006).

24.4.1.2 Number of Curies

The radionuclide activity expected to be placed in the WIPP decreased from the CCA estimate of 3.44 million Ci to 2.32 million Ci in the CRA-2004 PABC Inventory Report (Leigh, Trone, and Fox 2005, Section 4.4, p. 36). Table 14 of the CRA-2004 PABC Inventory Report listed the activity by radionuclide for the CCA PA, the CRA-2004 PA, and the CRA-2004 PABC.

The new inventory items since 1998 that were included in the CRA-2004 PA and the CRA-2004 PABC inventory are listed below.

- Idaho National Laboratory (INL) Buried Waste—The DOE included the INL pre-1970 buried waste in the CRA-2004 PABC Inventory Report (Leigh, Trone, and Fox 2005) as a result of an April 2003 Federal District Court judgment against the DOE on the buried waste. The CRA-2004 PABC Inventory Report (Leigh, Trone, and Fox 2005) estimated 17,998 m^3 of TRU waste in five waste streams from the pre-1970 buried waste at INL.

- Supercompacted Waste—Supercompacted waste from INL's Advanced Mixed Waste Treatment Facility (AMWTF) was included in the CRA-2004 PABC TRU waste inventory estimate. After an extensive analysis of this waste (Marcinowski 2003), the EPA concluded that the supercompacted waste could be considered within the existing waste envelope and PA. The EPA approved the disposal of the supercompacted waste (Marcinowski 2004). Prior to shipping this waste, the EPA conducted a waste characterization inspection of the AMWTF (Gitlin 2005).

- Hanford Tank Waste—The DOE Office of River Protection determined that waste from 12 of the 177 tanks at the Hanford site was TRU waste or would be TRU waste after treatment. Descriptions of these tanks and their waste streams and generating processes are given in CARD 24, Table 24-1 (U.S. EPA 1998b). Patterson (Patterson 2005a and Patterson 2005b) presents the DOE's documentation for these TRU tanks.

- Hanford Waste from K-Basin—The DOE's CRA-2004 PABC TRU waste inventory also included two waste streams, RL-W445 and RL-W446, consisting of approximately 50 m^3 of waste, from the Hanford K-East and K-West Basins (Patterson 2005a and 2005b).

- Container Types—Container types new to the CRA-2004 PABC inventory included the ten-drum overpack, 5 × 5 × 8 boxes, 100-gallon drums, and pipe overpacks within drums. The container types were considered in the CRA-2004 PABC inventory development process since it was important to estimate the amount of CPR in the WIPP (Leigh, Trone, and Fox 2005, Section 4.2, p. 30).

- Organic Ligands—Four organic ligands were included in the Fracture-Matrix Transport (FMT) calculations of An solubilities: acetate, citrate, EDTA, and oxalate (Detwiler 2004a). Further discussion on organic ligands for the CCA can be found in the CCA, Appendix SOTERM, Section 5.0, and CARD 24, Section 24.C.5, pp. 24-40 and 24-41) (U.S. EPA 1998b). Organic ligands are further discussed in the CRA-2004 PA (Attachment SOTERM, Section 5.0, p. 42) and U.S. EPA (U.S. EPA 2006c).

Details of and changes occurring in the inventory processes and descriptions are discussed further in CARD 24 (U.S. EPA 2006d).

24.4.2 40 CFR § 194.24(b)(1)

There were no major changes to the waste characteristics between the CCA PAVT and the CRA-2004 PABC, but the DOE did change some of the waste components used in the PA. These changes are summarized in Table 24-2 of CARD 24 (U.S. EPA 2006d) and are presented here in Table 24-1.

Table 24-1. Significance and Changes in Components and Characteristics

Waste Component or Characteristic Used in PA	Increase or Decrease From CCA to CRA-2004 PABC	Significance
Radioactivity (Ci/m^3)	Decrease	Used in calculating releases
Solubility	Increase and decrease, depending on oxidation state	Higher solubility can lead to higher releases
Organic Ligands—complexing agents	Similar amounts	Increases solubility
Amount of Metals	Decrease	Maintains reducing environment, but also contributes to gas generation
Amount of CPRs	Increase	May increase gas generation from microbial processes
Oxyanions: nitrate, sulfate, and phosphate	Similar, but overall increase	Nutrients for microbes - affects gas generation
Cement	Decrease	Volume-related component
Shear Strength	No change	Affects mechanical releases during a drilling intrusion
Particle Diameter	The CRA-2004 PABC used the particle diameter determination from expert panel findings during the original certification	Used to calculate spallings releases
Formation of Colloidal Suspensions	No change in parameterization	Colloids can facilitate transport of radionuclides in groundwater

24.4.2.1 Assessment of Waste Characteristics and Waste Characteristic Input Parameters

In the CCA, the DOE identified several waste characteristics as being potentially important to the PA (the CCA, Appendix WCA, Section WCA.6, pp. WCA-42 and WCA-43) based on available information, including uncertainties and the WIPP system characterization. These analyses were summarized in the CCA, Appendices WCA, SOTERM, and MASS, and were augmented by the DOE's responses to the EPA comments (CARD 24, Sections 24.B.5 and 24.B.6, pp. 24-12 through 24-31) (U.S. EPA 1998b). The CRA-2004 identifies the same important characteristics, and also states that organic ligands could be important to solubility. The CRA-2004 PABC, therefore, includes the ligands in the solubility calculations (Brush and Xiong 2005).

24.4.2.2 Solubility

The DOE originally stated in the CCA that solubility of actinides was among the major characteristics of the radionuclides expected to affect disposal system performance (the CCA, Appendix WCA, Section WCA.4, pp. WCA-30 through WCA-34). The DOE assessed the solubility of thorium (Th), uranium (U), neptunium (Np), plutonium (Pu), and americium (Am) (Appendix SOTERM, U.S. DOE 1996a).

In addition, the DOE assumed that cesium (Cs) and strontium (Sr) were completely (100%) soluble; therefore, the concentrations of these two radionuclides were determined from the quantities listed in the inventory (the CCA, Appendix WCA, p. 30).

The DOE used the FMT geochemical modeling code and its associated database to calculate solubilities. No changes were made to the FMT code or conceptual models for the CRA-2004 PA or the CRA-2004 PABC. However, revisions were made to the input FMT database since the CCA PAVT. These changes included the addition of new aqueous An species to the database and revisions to existing species data because of the availability of new experimental data (see Appendix PA, Attachment SOTERM, U.S. DOE 2004). The DOE used the generic weep brine (GWB) Salado brine chemistry formulation instead of the Brine A formulation used in the CCA PA and PAVT. The most significant differences between the brine formulations were the lower magnesium concentration and higher sulfate concentration in GWB relative to Brine A. Comparison of geochemical modeling results using the two brine formulations indicated that GWB brines had slightly lower predicted An(III) solubilities and higher An(V) solubilities compared to Brine A.

24.4.2.3 Performance Assessment Parameters Related to Solubility

The solubility of actinides in the III, IV, V, and VI oxidation states for both the Castile and Salado brines were calculated by the DOE with the assumption that pH and the fugacity of carbon dioxide ($f(CO_2)$) were controlled by the brucite ($Mg(OH)_2$) –hydromagnesite ($Mg_5(CO_3)_4(OH)_2{\cdot}4H_2O$) buffer. The solubilities from the CCA and the CRA-2004 are listed in Table 24-3 of CARD 24 (U.S. EPA 2006d).

The uncertainty ranges for the actinides in the CRA-2004 PA were the same as those used in the CCA (Bynum 1996). The uncertainties in the An solubilities were used to define the range for Latin hypercube sampling of the An concentrations in the PA, assuming a log cumulative distribution (CARD 24, Section 24.B.5, pp. 24-15 and 25-16) (U.S. EPA 1998b).

24.4.2.4 Formation of Colloidal Suspensions Containing Radionuclides

Formation of colloidal suspensions was evaluated by the DOE as an important group of waste characteristics. Actinides can be mobilized in colloidal form as intrinsic colloids or absorbed on nonradioactive colloidal particles. In the CCA, the DOE determined that four types of colloids may be present in the WIPP repository: intrinsic colloids, mineral fragment colloids, humic colloids, and microbial colloids (the CCA, Appendix WCA, Section WCA.4.2, pp. WCA-34 through WCA-36). These colloids were modeled in the CRA-2004 PABC and were unchanged

from the CCA (see CARD 24, Sections 24.B.5 and 24.B.6, pp. 24-12 through 24-31 [U.S. EPA 1998b], and CCA Appendix SOTERM, Section 6.0 [U.S. DOE 1996a]).

The DOE implemented the colloidal An source term differently in the CRA-2004 PA than in the CCA. In the CCA, the DOE assumed all vectors would have a microbial colloid contribution to the An source term. For the CRA-2004 PA, the DOE assumed there would be microbial colloid transport only in vectors with microbial degradation. In the CRA-2004 PABC it was assumed that all vectors included microbial activity and thus included microbial colloid transport.

24.4.2.5 Production of Gas From the Waste (Including Microbial Substrate and Nutrients)

Gas generation included hydrogen gas generation as well as carbon dioxide (CO_2) and CH_4 generation by microbial degradation. Anoxic corrosion produces hydrogen gas and microbial action on microbial substrates such as CPR, as well as other microbial nutrients (nitrate, sulfate and phosphate), which produce CO_2 and CH_4.

The same conceptual model was used for microbial gas generation in the WIPP repository for both the CCA and the CRA-2004. Information about the models used for the CCA and the CRA-2004 can be found in the CCA, Appendix SOTERM, Section SOTERM-8.2.2, and Appendix PA-2004, Attachment SOTERM-2004, Section SOTERM-2.2.2, respectively.

Microbial gas generation rates used in the average stoichiometry model were based on experimental data from microbial consumption of papers (cellulose) under inundated and humid conditions (Wang and Brush 1996). A gas-generation rate is determined in BRAGFLO (fluid flow code) for the humid and inundated rates based on the effective liquid saturation (CRA-2004, Chapter 6.0, Section 6.4.3.3). These gas generation rates were calculated from the initial linear part of the experimental curve of CO_2 as a function of time (Appendix PA-2004, Attachment PAR-2004) (Wang and Brush 1996).

For the CRA-2004 PABC, the DOE requested a change to the gas generation rate PA parameters based on the DOE's review of additional experimental data collected over the last 10 years (Nemer and Stein 2005; Nemer, Stein, and Zelinski 2005). The gas generation experiments exhibited two rates: an initial higher rate, and a second lower rate. The DOE proposed to the EPA that the long-term rate be the gas generation rate used in the PA calculations, with the initial higher rate incorporated as an initial higher pressure.

The DOE used Latin hypercube sampling in the CRA-2004 PA for the following gas-generation-related parameters:

- Inundated steel corrosion rate
- Probability of microbial degradation of plastics and rubbers (in the event of microbial gas generation)
- Biodegradation rate of inundated and humic cellulosics
- Factor β for microbial reaction

24.4.2.6 Performance Assessment Parameters Related to Shear Strength, Compactability (Compressibility), and Particle Diameter

There were no changes in these parameters from the CCA PAVT through the CRA-2004 PABC.

24.4.2.7 Radioactivity in Curies

In the CCA (Sections 3.1 and 3.2, and Appendix WCA), the DOE indicated that the radioactivity of each isotope was important to the PA because it directly affected the waste unit factor (WUF) (number of million Ci of TRU isotopes in the WIPP inventory) (see the CCA, Appendix WCA, Table WCA-1). Since the same approach was used in the CRA-2004, the approach is summarized here.

At the time of the CCA, the following radionuclides were determined by the DOE to be important (the CCA, Appendix WCA, Figure WCA-4):

- Cuttings/cavings/spallings release: ^{238}Pu, ^{239}Pu, ^{240}Pu, ^{241}Pu, ^{241}Am, ^{233}U, ^{234}U, ^{90}Sr, ^{137}Cs, ^{244}Cm
- Direct brine release (DBR): ^{238}Pu, ^{239}Pu, ^{240}Pu, ^{241}Pu, ^{242}Pu, ^{241}Am, ^{243}Am, ^{233}U, ^{234}U, ^{235}U, ^{236}U, ^{238}U, ^{229}Th, ^{230}Th, ^{232}Th, ^{237}Np, ^{243}Cm, ^{244}Cm, ^{245}Cm
- Long-term groundwater release: ^{239}Pu, ^{240}Pu, ^{242}Pu, ^{241}Am, ^{233}U, ^{234}U, ^{229}Th, ^{230}Th

The DOE indicated that U and Th isotopes were required in DBR assessments because, although they comprise negligible fractions of the total EPA unit, they did influence the total quantity of dissolved radionuclides (the CCA, Appendix WCA, p. WCA-22). In addition, the DOE indicated that although EPA units for ^{90}Sr and ^{137}Cs at the time of WIPP closure were significant, they are not included in direct release of brine because they rapidly decay within the first few hundred years after closure and result in "negligible impact on the PA" (the CCA, Appendix WCA, p. WCA-26). In addition, the DOE indicated that if a DBR occurred early after closure, the total brine released would be minimal and the ^{90}Sr and ^{137}Cs would still, therefore, play a minor role in compliance (the CCA, Appendix WCA, p. WCA-26).

The DOE justified the radionuclide list for the long-term groundwater pathway (releases to the Culebra Dolomite Member of the Rustler Formation [hereafter referred to as Culebra]) in the CCA, Appendix WCA, Section WCA.3.2.3, pp. WCA-26 and WCA-27.

In the CRA-2004 PABC, the selection of isotopes for modeling transport in the disposal system using NUTS and PANEL was described in Appendix TRU WASTE-2004, Section TRU WASTE-2.0. PANEL runs included nearly all isotopes of the six actinides studied in the Actinide Source Term Program: Th, U, Np, Pu, Am, and curium (Cm). NUTS runs explicitly included five isotopes: ^{230}Th, ^{234}U, ^{238}Pu, ^{239}Pu, and ^{241}Am (Garner and Leigh 2005).

24.4.2.8 PA Parameters Related to Radioactivity in Curies of Each Isotope

The DOE used the information from the update of the CCA inventory to define the isotope inventory for the CRA-2004 PA (the CRA-2004, Chapter 4.0). The CRA-2004 PABC Inventory

Report (Leigh, Trone, and Fox 2005, Table 14, p. 37) provides the radioactivity in Ci of each isotope used in the CRA-2004 PABC.

24.4.2.9 TRU Radioactivity at Closure

The CRA-2004 PABC Inventory Report, Table 14 (Leigh, Trone, and Fox 2005) lists the DOE inventory at closure, based upon the September 2002 cutoff and the CRA-2004 PABC update as described in Section 24.4.1. The CRA-2004 PABC Inventory Report indicated that the inventory estimate was 2.32×10^6 Ci and the WUF was 2.32, with inventory activity decayed to the year 2033.

24.4.2.10 PA Parameters Related to TRU Radioactivity at Closure

The 2.32 WUF was the number of millions of curies of alpha-emitting TRU radionuclides with half-lives longer than 20 years used in the calculation of the EPA normalized unit. Overall, activity at 2033 for all TRU radionuclides has decreased from 2.55×10^6 Ci reported in the CCA, to 2.48×10^6 Ci in the CRA-2004 inventory estimate, to 2.32×10^6 Ci in the CRA-2004 PABC inventory estimate. The DOE discussed the WUF value in the CRA-2004 PABC Inventory Report (Leigh, Trone, and Fox 2005, p. 36).

24.4.3 40 CFR § 194.24(b)(2)

The DOE indicated that ferrous metals, cellulose, organic chelating agents, radioactivity in curies of each isotope, alpha-emitting TRU radionuclides with half-lives greater than 20 years, solid waste components (e.g., soils and cementitious materials), sulfates and nitrates were expected to have a significant effect on disposal system performance and so were used in the CCA PA, CRA-2004 PA, and the CRA-2004 PABC. Most of the inventory amounts of the listed components changed and were discussed in Appendix PA-2004, Attachment SOTERM-2004, Table SOTERM-4; Leigh, Trone, and Fox (Leigh, Trone, and Fox 2005); and U.S. EPA (U.S. EPA 2006e). The only significant change was the incorporation of organic ligands in the An solubility PA calculations. The DOE updated the FMT thermodynamic databases with information related to organics to account for the organic ligands' affect on An solubility (Appendix PA-2004, Attachment SOTERM-2004, Section SOTERM-5.0). Organic ligand inventories were recalculated for the CRA-2004 PABC (Brush and Xiong 2005).

Changes and details on the effects of components on disposal system performance are discussed further in CARD 24 (U.S. EPA 2006d).

24.4.4 40 CFR § 194.24(b)(3)

The DOE provided a list of waste characteristics and components that were excluded from consideration in the PA for various reasons, such as negligible impact (the CCA, Appendix WCA, Table WCA-4 and Appendix TRU WASTE-2004, Section TRU WASTE-6.0). The effect of organic ligands, however, is incorporated into the CRA-2004 PABC (Brush and Xiong 2005).

24.4.5 40 CFR §§ 194.24(c)(1), (e)(1), and (e)(2)

For the CRA-2004 PA, the DOE did not make any changes to the limits identified in the CCA or their implementation in the CRA-2004 PA. In reviewing the CRA-2004 PA, the EPA identified that the packaging materials for the INL supercompacted waste were omitted from the CPR total, but these packaging materials were included in the CRA-2004 PABC as part of the inventory estimate. See CARD 24 (U.S. EPA 2006d) for further discussion.

24.4.6 40 CFR § 194.24(c)(2)

As noted in 40 CFR § 194.24(b), the DOE did not modify the list of CCA components and characteristics requiring quantification. Therefore, the CRA-2004 did not identify any significant changes to the measurement techniques used in the waste characterization program (i.e., VE, RTR, AK, and NDA). In addition, the CRA-2004 did not propose changes to the current waste characterization program through use of different NDA and NDE characterization methodologies. The CRA-2004 indicated that the location of NDA and NDE methodology documentation and information regarding QAOs had changed since the CCA. There were also several minor changes to the characterization program. The changes the EPA identified are specified in CARD 24 (U.S. EPA 2006d).

24.4.7 40 CFR § 194.24(c)(3)

The CRA-2004 was revised to show that the AK process was presented in the CH-TRU WAC. The CH-TRU WAC was revised to include more discussion of AK with respect to radionuclides (U.S. DOE 2002). Modifications made to the CH-TRU WAC since the CCA that were pertinent to AK included the use of existing AK collected prior to the implementation of a QA program under 40 CFR § 194.22(a), methods for confirming isotopic ratios using AK, required and supplemental AK documentation, discrepancy resolution and data limitation identification, and AK-radioassay data measurement comparisons as a means to assess comparability. Existing AK collected prior to the implementation of a QA program under section 194.22(a) may be qualified by peer review, corroborating data, confirmatory testing, or collection of data under an equivalent QA program. See CARD 24 (U.S. EPA 2006d) for further discussion.

24.4.8 40 CFR § 194.24(c)(4)

The DOE uses the WWIS to track data for emplaced waste in the WIPP. For the CCA, the WWIS used Oracle Version 7, and for the CRA-2004, the WWIS used Oracle Version 9; there were no other changes. The CRA-2004 included the statement, “additional computing system upgrades may be implemented in the future.” See CARD 24 (U.S. EPA 2006d) for further discussion.

24.4.9 40 CFR § 194.24(c)(5)

The DOE described the changes to the PDP in the CRA-2004, Chapter 4.0, Section 4.3.3.1, PDP (p. 4-49). There were three significant changes in Section 4.3.3.1 relative to the CCA: (1) the QAPP is no longer referenced as the document defining the PDP QAO requirements, (2) the PDP Plan was removed as a reference and replaced by the statement, “the NDA PDP plans are revised

as required," and (3) the section no longer contains a detailed description of the isotopes to be analyzed and the configuration of the PDP tests. Other minor changes are addressed in CARD 24 (U.S. EPA 2006d).

The DOE also revised the quality document hierarchy for waste characterization activities by making the Carlsbad Area Office (CAO) Quality Assurance Program Document a higher-tier document and the QAPP of lesser importance. This new document hierarchy is shown in the CRA-2004, Chapter 4.0, Figure 4-3, which replaced the CCA, Chapter 4.0, Figure 4-6.

24.4.10 40 CFR §§ 194.24(d) and (f)

The DOE did not use a performance-based waste loading scheme for waste emplacement in the WIPP, and the DOE assumed random waste loading in its performance and compliance assessments. Prior to the CRA-2004, the EPA requested that the DOE analyze waste loading with respect to supercompacted waste, and the DOE identified that clustering of waste would not affect performance (Marcinowski 2003; Park and Hansen 2003; Marcinowski 2004). See CARD 24 (U.S. EPA 2006d) for further discussion.

24.4.11 40 CFR § 194.24(g)

The DOE uses the WWIS to track the limitations on TRU waste disposal described in the WIPP LWA. For the CCA, the WWIS used Oracle Version 7, and for the CRA-2004, the WWIS used Oracle Version 9; there were no other changes. The CRA-2004 included the statement, "additional computing system upgrades may be implemented in the future." See CARD 24 (U.S. EPA 2006d) for further discussion.

24.4.12 40 CFR § 194.24(h)

The EPA found the DOE in compliance with provisions of section 194.24(h). Inspections, such as audits, and records are addressed by the EPA in CARD 22 (U.S. EPA 2006b).

24.5 EPA's Evaluation of Compliance for the 2004 Recertification

24.5.1 40 CFR § 194.24(a)

The EPA reviewed the CRA-2004 and supplemental information to determine whether they provided sufficiently complete descriptions of the chemical, radiological, and physical composition of the emplaced, existing, and to-be-generated waste proposed for disposal in the WIPP. The EPA also reviewed the DOE's description of the approximate quantities of waste components (for both existing and to-be-generated waste). The EPA considered whether the DOE's waste descriptions were of sufficient detail to enable the EPA to conclude that the DOE did not overlook any component that is present in TRU waste and has significant potential to influence releases of radionuclides.

Based on the EPA's review and evaluation of this information and the consideration of public comments, the EPA determined that the DOE continued to comply with the requirements of section 194.24(a) (U.S. EPA 2005a, U.S. EPA 2006c, U.S. EPA 2006e, and U.S. EPA 2006f).

24.5.1.1 Chemical, Physical, and Radiological Description of Existing Waste

The EPA reviewed descriptions of the chemical, radiological, and physical components of the waste, which were documented in the CRA-2004 and supporting documents. This information was collected using methods similar to those used during the CCA, which were determined to be reasonable by the EPA.

The EPA concluded on the basis of this information that the CRA-2004 and supplemental information adequately described the chemical, radiological, and physical characteristics of each waste stream proposed for disposal at the WIPP. The EPA further concluded that the information presented by the DOE in the CRA-2004 provides adequate characterization of existing WIPP waste for use in PA.

The EPA concluded that the DOE's development of the disposal inventory was sufficient for PA purposes. The EPA agreed with the DOE that the use of projected waste inventory for scaling the CH-TRU WIPP inventory to meet the total WIPP capacity was appropriate. The DOE's use of the inventory scaling process was similar to that used in the CCA and was adequate for projecting inventory estimates.

24.5.1.2 Waste Forms and Packaging: Supercompacted Waste

The EPA approved the disposal of supercompacted waste from AMWTF at the WIPP (Marcinowski 2004). The CRA-2004 characterized, represented, and considered supercompacted waste from INL in the recertification inventory.

24.5.1.3 Waste Forms and Packaging: Container Types

The DOE's assortment of containers was expected to meet the metal limit regardless of container type, because they all are metal containers. The EPA found the container types used in the CRA-2004 PA to be reasonable.

24.5.1.4 Waste Forms and Packaging: Inclusion of Waste Packaging in Inventory

During the initial review of the recertification application, the EPA found that the DOE did not include emplacement materials in the CRA-2004 PA calculations (Cotsworth 2004a). These materials could contribute to gas generation. The DOE stated (Detwiler 2004b) that these materials accounted for only a 12.7% increase in CPR if they were included in the PA, and that they would have no effect on compliance. However, the DOE did include the additional emplacement material volume and mass in the CRA-2004 PABC (Leigh, Trone, and Fox 2005, Section 1.3.3, p. 11); therefore, the emplacement materials were reflected in the release estimates. The CRA-2004 PABC showed that the WIPP still complied with the new CPR amounts in the inventory. Thus, the use of increased CPR amounts was adequate, and the amount used in the CRA-2004 PABC established a new limit.

24.5.1.5 Number of Curies, Waste Streams, and Volume

The DOE estimated the activity in curies in the inventory on a site-by-site, waste-stream-by-waste-stream basis. The EPA required that the DOE produce a "list of the waste components and their approximate quantities." The EPA reviewed the estimate in the CRA-2004, Chapter 4.0, Appendix TRU WASTE-2004, and the TRU Waste Baseline Inventory Database (LANL 2005), and found sufficiently specific information on the species and quantities of individual radioisotopes in the waste.

24.5.1.6 Organic Ligands

The EPA requested that the DOE provide additional information regarding the possible effects of organic ligands concentrations on An solubilities in the WIPP repository (Cotsworth 2004b). In its response, the DOE described the results of a series of calculations designed to determine the sensitivity of An(III), An(IV), and An(V) solubilities to increases in organic ligand concentrations and the possible effects of microbially produced acetate and lactate. The EPA reviewed the updated calculations related to the effect of organic ligands on An solubility and determined that organic ligands are potentially important (U.S. EPA 2006c). The DOE included the effects of solubility of organic ligands in the CRA-2004 PABC and the CRA-2004 and supplemental information; therefore, the EPA found that the DOE appropriately included organic ligands in the CRA-2004 PABC (U.S. EPA 2006f).

24.5.1.7 Hanford Waste

In the CRA-2004, the DOE identified that it included waste from 12 tanks from Hanford – nine tanks of CH-TRU waste and three tanks of RH-TRU waste. The volume of the CH-TRU waste was estimated to be approximately 3,932 m^3 (2% of the total CH-TRU waste and 2% of the total inventory) and the RH-TRU waste was estimated at approximately 4,469 m^3 (63% of total RH-TRU waste and 2.5% of the total inventory). The DOE stated that these 12 tanks were considered TRU waste, although the tanks were managed as high-level waste. Furthermore, the DOE pointed out, if the waste was high-level waste, then by law it could not go to the WIPP. The DOE included waste from the 12 tanks in the CRA-2004 PA and the CRA-2004 PABC and began discussion about establishing a TRU waste determination process in the future.

The EPA allowed this waste to be included in the PA inventory for recertification and the DOE demonstrated that with the Hanford tank waste, the WIPP would continue to comply with the EPA's disposal regulations. However, it was noted that before any Hanford tank waste could be shipped to the WIPP, the DOE must demonstrate during characterization that the waste is, in fact, TRU waste that can legally go to the WIPP (CARD 24; U.S. EPA 2006d).

24.5.1.8 K-Basin Waste

The sludges from the K-Basin storage pools consist of debris, silt, sand, and material from operation of the pools at Hanford. The 50.4 m^3 of sludges contaminated with radionuclides associated with spent nuclear fuel that was exposed to water in the pools were included in the CRA-2004 PABC.

The EPA allowed this waste in the PA inventory because the waste form was similar to other waste going to the WIPP, was low in volume, and required processing and characterization before being shipped to the WIPP. In addition, the EPA stated the DOE must demonstrate that the waste meets technical and legal requirements prior to disposal.

24.5.1.9 INL Waste

The pre-1970 buried waste included in the CRA-2004 PABC (Leigh et al. 2005) is found in Appendix DATA-2004, Attachment F, Annex I, as waste stream IN-Z001. It was designated as non-WIPP TRU waste, but the DOE decided to include it in the CRA-2004 PABC because of a 2003 judgment against the DOE related to its removal at INL. This waste was not included in the CRA-2004 PA because the court judgment came after the September 30, 2002, cutoff date for inventory development (Leigh, Trone, and Fox 2005; Lott 2004). This waste appeared to be similar to other WIPP waste streams, but must still meet the WIPP WAC and remains subject to the EPA's inspection and approval process before being disposed of at the WIPP.

24.5.1.10 Other Issues

The DOE identified and corrected one error between the CRA-2004 PA and the CRA-2004 PABC concerning LANL CH-TRU waste stream LA-TA-55-48. This waste stream was a low-volume, high-radioactivity waste stream that skewed the results of the PA complimentary cumulative distribution functions upward. Upon further review, the DOE identified that this waste stream was mischaracterized; the Pu fissile gram equivalent mass was greater than shipping requirements allowed (Crawford 2004). The DOE reevaluated the waste stream, and modified the waste stream radioactivity and volume for the CRA-2004 PABC. Since this was an estimate and the waste will be characterized before going to the WIPP, the modification was found to be reasonable.

24.5.2 40 CFR § 194.24(b)(1)

For the CCA, the EPA reviewed information on waste characteristics and components in a number of technical documents. This review encompassed references, experimental programs, logical arguments, and modeling. The EPA determined all relevant waste characteristics and components were identified and evaluated. For the CRA-2004, the EPA focused on changes and new information that could affect the DOE's analyses and findings.

The EPA concluded that, with the combination of the CRA-2004, supplemental information, and the CRA-2004 PABC, the DOE continued to comply with the requirements for section 194.24(b)(1) (U.S. EPA 2006d).

24.5.2.1 Solubility

The EPA's review identified two areas in which the DOE did not adequately address solubility. First, the DOE did not update the U(VI) solubility to incorporate new data that became available since the certification decision. The data indicated that the U(VI) solubility should be higher than that used by the DOE in the CRA-2004 PA. Second, the DOE did not update the solubility uncertainty ranges used for An solubility oxidation states based on new data.

For the CRA-2004 PABC, the EPA stated that the solubility of U(VI) needed to be changed to a fixed value of 1×10^{-3} molar because of experimental data that became available after the CCA. In addition, the EPA required that new solubility uncertainty ranges, based on the FMT database and currently available experimental solubility data, be incorporated into the CRA-2004 PABC. The DOE made additional changes to the calculation of the An(III), An(IV), and An(V) solubilities based on revised thermodynamic data for the An(IV) actinides, a different Salado brine formulation, and revised concentrations of organic ligands. These changes were properly implemented as discussed in Section 7 of *Technical Support Document for* S*ection 194.24: Evaluation of the Compliance Recertification Actinide Source Term and Culebra Dolomite Distribution Coefficient Values* (U.S. EPA 2005b).

A summary of changes and improvements incorporated into the calculation of An solubilities for the CRA-2004 PABC that have been implemented since the CCA PAVT include the following:

- Organic ligand complexation data were incorporated into the FMT thermodynamic database so the effects of organic ligands on An(III), An(IV) and An(V) solubilities can be calculated directly. The organic ligand concentration changes, which in all cases but oxalate are defined by the inventory, were the result of corrections to the masses of organic ligands identified in the CRA-2004 PABC inventory (Leigh, Trone, and Fox 2005) and the minimum estimated brine volume required for a release from the repository.

- The TRU waste inventory data, including actinides, were updated.

- The FMT thermodynamic database for actinides was updated and used to calculate the An(III), An(IV), and An(V) solubilities. Most importantly, the free energy formation constant value for thorium hydrate ($Th(OH)_4$)(aq) was lowered, leading to better agreement between experimental and modeling results (Xiong 2005).

- Magnesium oxide (MgO)-reacted Salado GWB and Castile (ERDA-6) brines were used to calculate An solubilities. GWB, which has a lower magnesium (Mg) and higher sulfate content, replaces Brine A as the Salado brine formulation for An solubility calculations (Brush et al. 2006).

- Instantaneous equilibria among major GWB and ERDA-6 relevant minerals were assumed and the chemical environment was made more uniform due to the elimination of nonmicrobial vectors in PA.

- Correction of the minimum brine volume necessary for DBR (Stein 2005).

- Revision of the estimated U(VI) solubility to 0.001 molar accounts for the new data (U.S. EPA 2005b).

- Recalculation of An solubility uncertainties based on a much larger number of solubility measurements, with separate distributions developed for the An(III), An(IV), and An(V) solubilities (Xiong, Nowak, and Brush 2005).

24.5.2.2 Colloids

The CCA PAVT included microbial colloid transport of actinides for all vectors. The CRA-2004 PA included different assumptions about the colloidal source term concentrations for microbial and nonmicrobial vectors, with no microbial colloid transport of actinides assumed for nonmicrobial vectors. However, for the CRA-2004 PABC, it was assumed that all vectors included microbial activity. Therefore, the DOE included microbial colloid transport of actinides for all CRA-2004 PABC vectors (Brush 2005). This approach was, therefore, the same for the CCA PAVT and CRA-2004 PABC, and was consistent with the EPA's direction that all vectors include microbial activity.

24.5.2.3 Production of Gas from the Waste

Microbial degradation of CPR may influence the WIPP repository performance because of its effects on repository chemistry and gas generation. The EPA reviewed the approach and assumptions used by the DOE to model microbial degradation for the CRA-2004 PA. The EPA's comments to the DOE focused on the probability of significant microbial degradation, the nature of the microbial degradation reactions likely to occur in the repository, and microbial gas generation rates. As a result of the EPA's review and comments, the DOE changed the modeling of microbial degradation processes for the CRA-2004 PABC. Specifically, the EPA instructed the DOE to assume that microbial degradation of CPR would occur in all CRA-2004 PABC vectors.

During the review of the CRA-2004 PA, the DOE informed the EPA that the microbial gas generation experiments had continued and additional information related to microbial gas generation rates in the WIPP repository had become available since the CCA PA and the CCA PAVT. In the letter (Cotsworth 2005) directing the DOE to perform the CRA-2004 PABC, the EPA allowed the DOE to propose a new gas generation rate scheme based on the new experimental data.

At the EPA's direction, the DOE changed the probability of microbial degradation to account for new evidence regarding the presence and viability of microbes capable of degrading CPR in the WIPP repository. The revised probability parameters resulted in microbial degradation in all vectors for the CRA-2004 PABC. However, the DOE asserted that uncertainties remained regarding the viability of microbes in the repository because of different conditions in the repository compared to the conditions in the experiments. The DOE therefore introduced an additional sampled parameter, BIOGENFC. This parameter, which has a uniform distribution from 0 to 1, was multiplied by the microbial gas generation rates to effectively reduce the humid and inundated microbial gas generation rates from the experimentally determined long-term rates.

24.5.3 40 CFR §§ 194.24(b)(2) and (b)(3)

The concentrations of organic ligands were reevaluated for the CRA-2004 PABC An solubility calculations based on a revised estimate of the minimum amount of brine that could lead to a release from the repository. In addition, new data regarding the possible complexation of An(IV)

by EDTA were identified. These data were evaluated to determine the potential significance of EDTA to the An solubility calculations for the WIPP repository conditions.

During the EPA's review of the important waste components, the EPA identified that only organic ligands had been addressed differently than in the CCA. Organic ligands could increase An solubility, but the EPA determined that the DOE had adequately included their effects in the CRA-2004 PABC (U.S. EPA 2006d).

24.5.4 40 CFR §§ 194.24(c)(1), (e)(1), and (e)(2)

In the CCA, the EPA found that the DOE identified those waste components that required limits, and that the limits were reasonable and quantifiable. The EPA's main concern was that the waste components be kept to levels that ensure the repository remains in compliance with the disposal standards. The waste components of special concern were the amounts of CPR and their potential to generate gases that contribute to increased pressure in the repository.

As with the CCA, the DOE did not provide the associated uncertainty for the waste material component limits in the CRA-2004. The EPA identified two related issues regarding this claim of no uncertainty. The first was to ensure that the inventory remains within the waste component limits established by the DOE, and the second is that the performance of the repository was not compromised by the uncertainty in the inventory. This section required that the DOE identify the associated uncertainty for each limiting value. In the CRA-2004, as in the CCA, the DOE stated that the waste material component limits were fixed values with no associated uncertainties.

However, the EPA requested that the DOE review the issue of uncertainty. The DOE stated (Leigh 2006, p. 6) that the "sum of the weights of individual components in a container can at most differ from the total weight of the container by 5 percent." For the CCA, the EPA agreed with this approach, since the limiting value could be used to represent the "upper end" of an uncertainty value. However, the lack of information on the waste component inventory was of concern for the future, especially with the CPR materials, since they had the greatest potential to affect performance.

Since the inventory emplaced in the WIPP was at a fraction of the total inventory expected in the future, and since a significant fraction of the inventory was estimated and to be emplaced in the future, the EPA found that the use of point estimates was acceptable for the waste components and radionuclides for this recertification. In addition, the EPA found that since only a limited amount of waste has been emplaced, the inventory and its associated uncertainty was below the respective limiting values. However, the EPA suggested the DOE improve its knowledge of the measurement uncertainty for the next recertification and include these uncertainties into the PA process (U.S. EPA 2006d).

24.5.5 40 CFR § 194.24(c)(2)

Since the 1998 certification decision, the waste characterization program had been implemented at several DOE waste generator sites. This represented a change in activities since approval of the CCA, because only LANL was approved at that time. Since 1998, the EPA had approved

waste characterization at the larger generator sites, namely the AMWTF, Hanford, INL, RFETS, and the Savannah River Site (SRS). In addition, characterization was approved at the small generator sites Lawrence Livermore National Laboratory and the Nevada Test Site. These sites continued to characterize CH-TRU waste for disposal at the WIPP through the CRA-2004.

Based on the EPA's review of the CRA-2004, including the new information and references presented therein, the EPA agreed that the methods used to quantify the limits of waste components had not changed substantially since the 1998 certification decision. The EPA kept abreast of all the changes to the program, including information source document changes that transpired after the EPA's 1998 certification decision. Changes implemented up to the 2002 CH-TRU WAC and Waste Analysis Plan (WAP) referenced in the CCA had not affected the sites' abilities to adequately quantify waste components in individual containers. The DOE, therefore, continued to require each waste site to characterize radiological contents of every container of CH-TRU waste streams destined for WIPP disposal using the EPA-approved NDA systems. Similarly, each site continued to examine each TRU waste container to ensure the absence of prohibited items using the EPA-approved RTR and/or VE procedures (U.S. EPA 2006d).

24.5.6 40 CFR § 194.24(c)(3)

The EPA's WIPP regulations required the DOE to "provide information which demonstrates that the use of process knowledge to quantify components in waste for disposal conforms to the quality assurance requirements found in 40 CFR § 194.22" (U.S. EPA 1996, p. 5240).

The EPA found the information presented in the CRA-2004 adequate and that the adherence of TRU waste sites to the CRA-2004-based AK process will allow them to meet their regulatory obligations.

24.5.7 40 CFR § 194.24(c)(4)

The EPA determined that the general description of the WWIS in the CRA-2004 was adequate (CARD 24, pp. 24-44, U.S. EPA 2006d). Hardware modifications and software upgrades described in the CRA-2004 were necessary to maintain system reliability, security, and performance. The EPA reviewed the WWIS during its inspections of the WIPP and TRU waste generator sites and was aware of the changes to the WWIS since the CCA. The EPA determined that the WWIS adequately gathers, stores, and processes information pertaining to TRU waste destined for or disposed of at the WIPP (U.S. EPA 2006d).

The DOE stated that a majority of the 130 WWIS data fields were pertinent to demonstrate compliance with TRU waste transportation and disposal requirements. The EPA verified that the DOE adequately tracked more than these 130 data fields in the WWIS. The DOE had not changed its tracking methodology and in fact has added parameters to be tracked in the WWIS.

24.5.8 40 CFR § 194.24(c)(5)

The QAPP and the Methods Manual were replaced by the WAC and the New Mexico Environment Department WAP for the CRA-2004. The EPA was aware of these changes to the program requirements documents. The wording changes regarding the description of the PDP

test and the removal of the PDP plan did not affect the EPA's ability to ensure that the DOE has implemented a series of intercomparability tests for NDA equipment that develop similar results. The elimination of the PDP test description from the CRA-2004 required that the DOE make available to the EPA the PDP plans and test descriptions so the EPA could ensure that the program was indeed acting as a "true blind sample" program. The change in PDP certification from the facility to the equipment was acceptable.

The EPA continued to ensure, through audits and inspections, that the waste characterization program sufficiently met QA requirements. The inspection program was the primary method by which the EPA determined the implementation of QA controls to the waste characterization program.

The DOE's changes to the PDP program did not affect the EPA's ability to assess the implementation of quality controls to the waste characterization program. The wording changes allowed the DOE more flexibility in developing PDP tests. The changes to the QA document hierarchy do not lessen the implementation of quality controls to the waste characterization program.

Based on the EPA's review and evaluation of the CRA-2004 and supplemental information provided by the DOE, the EPA determined that the DOE continues to comply with the requirements for section 194.24(c)(5) (U.S. EPA 2006d).

24.5.9 40 CFR §§ 194.24(d) and (f)

In PAs, the DOE has assumed random waste emplacement. In the CCA, the EPA asked for additional analysis assuming clustering of waste. The DOE performed an analysis and showed that clustering waste streams would not significantly affect PA results. Indeed, RFETS waste was eventually clustered in the WIPP (Park and Hansen 2003). In addition, the EPA required the DOE to conduct another analysis assuming nonrandom waste emplacement as part of the review of supercompacted waste from INL. The results showed that nonrandom placement of waste was not significant (e.g., Appendix PA-2004, Attachment MASS-2004, Section MASS-21.0). Thus, no waste loading assumptions were necessary in PA calculations for CRA-2004.

Based on the EPA's review and evaluation of the CRA-2004 and supplemental information provided by the DOE, and because the DOE showed that waste loading assumptions were not necessary for use in PA, the EPA determined that the DOE continues to comply with the requirements for sections 194.24(d) and (f) (U.S. EPA 2006d).

24.5.10 40 CFR § 194.24(g)

The DOE has several years of experience with the WWIS and, through the EPA's inspections, the DOE has shown the WWIS to be effective in tracking and controlling waste disposed of at the WIPP. The DOE had not characterized or shipped any RH-TRU waste at the time of the CRA-2004.

Based on a review and evaluation of the CRA-2004 and supplemental information provided by the DOE, the EPA determined that the DOE continues to comply with the requirements for section 194.24(g) (U.S. EPA 2006d).

24.5.11 40 CFR § 194.24(h)

The EPA found the DOE in compliance with provisions of section 194.24(h). Discussion of inspections and records, such as audits, is addressed by the EPA in CARD 22 (U.S. EPA 2006b).

24.6 Changes or New Information Between the CRA-2004 and the CRA-2009 (Previously: Changes or New Information Since the 2004 Recertification)

24.6.1 40 CFR § 194.24(a)

To meet the section 194.24(a) requirements in the CRA-2004, the DOE described and categorized the TRU waste currently emplaced in the WIPP at that time and the waste that existed at various DOE facilities. The details of the inventory used for the CRA-2009 (U.S. DOE 2009a and U.S. DOE 2009b) were presented in the CRA-2004, Chapter 4.0 and Appendix TRU WASTE-2004, and the CRA-2004 PABC inventory (see Appendix BIR) was summarized in the CRA-2004 PABC Inventory Report (Leigh, Trone, and Fox 2005). The combination of the inventory presented in Appendix TRU WASTE-2004 and the CRA-2004 PABC Inventory Report was referred to as the CRA-2004 PABC Inventory Report. The inventory for the CRA-2009 PA was the same inventory used for the CRA-2004 PABC. Since the CRA-2004 PABC was completed, the *Annual Transuranic Waste Inventory Report–2007* (U.S. DOE 2008a) was published and provides updated inventory information. The DOE anticipated this inventory update would have only a small impact on normalized releases relative to the CRA-2009 PA, and was not significant for compliance. Therefore, the DOE was in compliance with section 194.24(a).

24.6.2 40 CFR § 194.24(b)(1)

There were no changes to the waste characteristics between the CRA-2004 PABC inventory and the CRA-2009 inventory, but the DOE did add inventory parameters used in the PA. Leigh, Trone, and Fox (Leigh, Trone, and Fox 2005) gave a comprehensive description of the projected inventory used for the CRA-2004 PABC. The CRA-2009 PA used the CRA-2004 PABC inventory with one set of modifications. The CRA-2004 PABC included CPR materials in the waste and container (packaging) materials that were also used in the CRA-2009 PA, but the CPR contents in emplacement materials were erroneously omitted from the CRA-2004 PABC (Nemer 2007). To correct this omission, six new parameters representing the density of CPR materials in emplacement materials were created and used in the CRA-2009 PA. Four additional parameters, which represent the density of cellulose and rubber materials in container (packaging) materials, were also created for the CRA-2009 PA (Nemer 2007).

Table 24-2 lists the names and descriptions of the CPR parameters used in the CRA-2009 PA, including the 10 additional parameters. The addition of the four container (packaging) CPR parameters was done solely for bookkeeping purposes, since container (packaging) materials do

not contain cellulose or rubber materials, as seen by the zero values in Table 24-2. The CRA-2009 PA used all the CPR parameters shown in Table 24-2.

There were no changes between the CRA-2004 PABC and CRA-2009 PA in the methodology and data used to calculate An solubilities or their colloidal concentration in the WIPP brine. The microbial assumptions and gas generation rates associated with this also remained unchanged in the CRA-2009 PA. Therefore, the DOE was in compliance with section 194.24(b)(1).

24.6.3 40 CFR § 194.24(b)(2)

The DOE determined that the components identified below were expected to have a significant effect on disposal system performance (see the CCA, Appendix WCA), and so were used in the CRA-2004 PABC.

- Ferrous metals
- Cellulose and chelating agents (i.e., organic ligands) as they pertain to enhanced An mobility
- Radioactivity in curies of each isotope
- alpha-emitting TRU radionuclides, $t_{1/2} > 20$ years ($t_{1/2}$ is the half-life)
- Radionuclides
- Solid waste components (e.g., soils and cementitious materials)
- Sulfates
- Nitrates

Table 24-2. CPR Parameters Used in the CRA-2009 PA

Name	Description	Value (kg/m^3)
WAS_AREA: DCELLCHW	Average density of cellulosics in CH-TRU waste materials	60.0
WAS_AREA: DCELLRHW	Average density of cellulosics in RH-TRU waste materials	9.3
WAS_AREA: DCELCCHW[a]	Average density of cellulosics in CH-TRU waste container (packaging) materials	0.0
WAS_AREA: DCELCRHW[a]	Average density of cellulosics in RH-TRU waste container (packaging) materials	0.0
WAS_AREA: DCELECHW[a]	Average density of cellulosics in CH-TRU waste emplacement materials	1.22
WAS_AREA: DCELERHW[a]	Average density of cellulosics in RH-TRU waste emplacement materials	0.0
WAS_AREA: DPLASCHW	Average density of plastic in CH-TRU waste materials	43.0
WAS_AREA: DPLASRHW	Average density of plastic in RH-TRU waste materials	8.0
WAS_AREA: DPLSCCHW	Average density of plastic in CH-TRU waste container (packaging) materials	17.0
WAS_AREA: DPLSCRHW	Average density of plastic in RH-TRU waste container (packaging) materials	3.1
WAS_AREA: DPLSECHW[a]	Average density of plastic in CH-TRU waste emplacement materials	8.76
WAS_AREA: DPLSERHW[a]	Average density of plastic in RH-TRU waste emplacement materials	0.0
WAS_AREA: DRUBBCHW	Average density of rubber in CH-TRU waste materials	13.0
WAS_AREA: DRUBBRHW	Average density of rubber in RH-TRU waste materials	6.7

Name	Description	Value (kg/m^3)
WAS_AREA: DRUBCCHW[a]	Average density of rubber in CH-TRU waste container (packaging) materials	0.0
WAS_AREA: DRUBCRHW[a]	Average density of rubber in RH-TRU waste container (packaging) materials	0.0
WAS_AREA: DRUBECHW[a]	Average density of rubber in CH-TRU waste emplacement materials	0.0
WAS_AREA: DRUBERHW[a]	Average density of rubber in RH-TRU waste emplacement materials	0.0

[a]Newly created for the CRA-2009 PA

These components in the CRA-2009 inventory were not changed from the CRA-2004 PABC inventory that was used for the CRA-2004 recertification decision. Therefore, the DOE was in compliance with section 194.24(b)(2).

24.6.4 40 CFR § 194.24(b)(3)

The DOE provided a list of those waste characteristics and components that were excluded from consideration in the PA for various reasons, such as negligible impact (Appendix TRU WASTE-2004, Section TRU WASTE-6.0, and Appendix PA-2009). There were no changes in the exclusion decisions for the important waste components and characteristics in the CRA-2009 PA since the CRA-2004 recertification decision. Therefore, the DOE was in compliance with section 194.24(b)(3).

24.6.5 40 CFR §§ 194.24(c)(1), (e)(1), and (e)(2)

The inventory used for the CRA-2009 PA was the same as the CRA-2004 PABC inventory. Therefore, the waste components and their associated uncertainties for the CRA-2009 were not changed since the CRA-2004 PABC. The only change from the CRA-2004 PABC was a change in the emplaced MgO.

In April 2006, the DOE submitted for EPA approval a Planned Change Request (PCR) to reduce the MgO excess factor from 1.67 to 1.2 (Moody 2006). To justify its request, the DOE used reasoned arguments regarding health-related transportation risks to the public, the cost of emplacing MgO, and the uncertainties inherent in predicting the extent of microbial consumption of CPR materials during the 10,000-yr WIPP regulatory period. The EPA responded that the "DOE needs to address the uncertainties related to MgO effectiveness, the size of the uncertainties, and the potential impact of the uncertainties on long-term performance" (Gitlin 2006).

The DOE carried out an uncertainty analysis (Vugrin, Nemer, and Wagner 2006) and several supporting analyses (Brush and Roselle 2006; Brush et al. 2006; Clayton and Nemer 2006; Deng et al. 2006; Kanney and Vugrin 2006; Kirchner and Vugrin 2006) in response to the EPA's request for additional information on the uncertainties related to MgO effectiveness. Appendix MgO-2009, Section MgO-6.2.4.4 (U.S. DOE 2009c) provided a complete description of the DOE uncertainty analyses. As part of this effort, Kirchner and Vugrin (Kirchner and Vugrin 2006) quantified the uncertainties in the estimates of the CPR material quantities emplaced in the WIPP disposal rooms. Their analysis was based on the differences between the masses of CPR

materials measured by RTR and VE, paired by waste container. They assumed that the VE measurements were the more accurate values and, because they observed no significant bias in the RTR measurements in a room, Kirchner and Vugrin (2006) then used Monte Carlo methods "to simulate potential errors in the RTR measurements and to construct a distribution representing the uncertainty in the CPR [materials] in a room," and concluded that "the uncertainty [standard deviation] on the total mass of CPR [materials] in a room would be less than 0.3%."

Based on these results, measurement uncertainty in the mass of CPR materials was not expected to significantly impact the expected mass of CPR materials in a room and consequently had little impact on repository performance. In addition, a limited amount of waste was emplaced relative to total capacity of the repository. It followed that the inventory and its associated uncertainty remained below the limiting value for the mass of CPR in the CRA-2009 PA, and the DOE remained in compliance with sections 194.24(c)(1), (e)(1), and (e)(2).

24.6.6 40 CFR § 194.24(c)(2)

As noted in section 194.24(b), the DOE did not modify the list of CRA-2004 components and characteristics requiring quantification. Therefore, the CRA-2009 did not identify any significant changes to the measurement techniques used in the waste characterization program (i.e., VE, RTR, AK, NDA).

Since the CRA-2004, the WIPP had received RH-TRU waste. RH-TRU waste normally contains more gamma-emitting radionuclides than CH-TRU waste (mostly ^{137}Cs), and the characterization method used to determine radionuclide activity is a Dose-to-Curie methodology as identified in the *Remote-Handled TRU Waste Characterization Program Implementation Plan*, Revision 0D (U.S. DOE 2003). RH-TRU waste normally contains more metal container material parameters because the preferred method for hot-cell operation is to place the waste into 30- or 55-gallon drums before placement into the RH-TRU canister. The addition of RH-TRU waste did not modify the list of components and characteristics requiring quantification. Therefore, the DOE was in compliance with section 194.24(c)(2).

24.6.7 40 CFR § 194.24(c)(3)

Since the CRA-2004, the AK process is now presented in the WIPP WAC, Revision 6.2 (U.S. DOE 2008c) for both the CH-TRU and RH-TRU waste. The WIPP WAC was revised to include more discussion of AK with respect to radionuclides (WAC, Appendix A). Modifications made to the WAC since the CRA-2004 that were pertinent to AK include the following:

- Use of existing AK collected prior to the implementation of a QA program under section 194.22(a) may be qualified in accordance with an alternative methodology and employs one or more of the following methods: peer review, corroborating data, confirmatory testing, and collection of data under an equivalent QA program for both the CH-TRU and RH-TRU waste.

- Methods for confirming isotopic ratios using AK (i.e., methods pertinent to sites generating weapons grade Pu vs. heat grade) for both the CH-TRU and RH-TRU waste.

- Required and supplemental AK documentation for both the CH-TRU and RH-TRU waste.
- Discrepancy resolution and data limitation identification for both the CH-TRU and RH-TRU waste.
- AK radioassay data measurement comparisons as a means to assess comparability for both the CH-TRU and RH-TRU waste.

These modifications effectively focused on the WIPP WAC to address specific allowances and requirements with respect to AK needs for radionuclide data on both the CH-TRU and RH-TRU waste. The revised WAP (New Mexico Environment Department 2008) retained AK requirements of data assembly, compilation, etc., included in the CRA-2004 and the CCA. Therefore, the DOE was in compliance with section 194.24(c)(3).

24.6.8 40 CFR § 194.24(c)(4)

The WWIS used the Oracle Version 9 database management system at the time of the CRA-2004 as described in CRA-2004, Chapter 4.0, Section 4.3.2. The computing system for CRA-2009 was Oracle Version 10g. Appendix TRU WASTE-2004, Section TRU WASTE-5.0, briefly described the WWIS as part of a system of controls that address sections 194.24(c)(4) and (c)(5), requirements for computer software for nuclear facility applications. Since the submittal of the CRA-2004, the WWIS had been updated to include data fields required for the disposal of RH-TRU waste. The WWIS was also modified by the addition of data fields to meet additional tracking and control requirements imposed on RH-TRU waste by the LWA. The WWIS was also updated since the CRA-2004 to track the amount of MgO emplaced in the repository. This addition was added to ensure the excess factor of 1.2 is met throughout the repository. The WWIS User's Manual, Appendix F (U.S. DOE 2008d), contained the WWIS Data Dictionary, which defines each data field for CH-TRU and RH-TRU waste. Therefore, the DOE was in compliance with section 194.24(c)(4).

24.6.9 40 CFR § 194.24(c)(5)

The DOE described the PDP program in the CRA-2004, Chapter 4.0, Section 4.3.3.1 PDP (p. 4-49). Since the CRA-2004, revisions were made to both the *Performance Demonstration Program Plan for Nondestructive Assay of Boxed Wastes for the TRU Waste Characterization Program*, Revision 1 (U.S. DOE 2008e), and the *Performance Demonstration Program Plan for Nondestructive Assay of Drummed Wastes for the TRU Waste Characterization Program*, Revision 1 (U.S. DOE 2005). The most important changes to these documents were implemented to better represent current practices, simplify and clarify the scoring section, clarify the explanation of the derivation of scoring criteria, and update the two NDA PDP Plans to be consistent with one another. The *Performance Demonstration Program Plan for Analysis of Simulated Headspace Gases*, Revision 6.1 (U.S. DOE 2007) was also revised since CRA-2004. The most important changes described the relationship between the Carlsbad Technical Assistance Contractor and the commercial suppliers of the headspace gas (HSG) PDP services, as well as the standard gases used to prepare the HSG PDP samples. Prior to this revision, the HSG PDP sample preparation contractor was a DOE national laboratory. Therefore, the DOE was in compliance with section 194.24(c)(5).

24.6.10 40 CFR §§ 194.24(d) and (f)

The CRA-2009 did not change in reference to provisions in sections 194.24(d) and (f) since the CRA-2004 decision. Therefore, the DOE was in compliance with sections 194.24(d) and (f).

24.6.11 40 CFR § 194.24(g)

The CRA-2009 inventory was unchanged from the CRA-2004 PABC inventory. Since the CRA-2004, the DOE had characterized and shipped RH-TRU waste. The WWIS was also modified by the addition of data fields to meet additional tracking and control requirements imposed on RH-TRU waste by the LWA. Therefore, the DOE was in compliance with section 194.24(g).

24.6.12 40 CFR § 194.24(h)

The DOE continued to comply with the inspection and records requirements. This is discussed in the CRA-2009, Section 22. Therefore, the DOE was in compliance with section 194.24(h).

24.7 EPA's Evaluation of Compliance for the 2009 Recertification

24.7.1 40 CFR § 194.24(a)

The EPA reviewed the CRA-2009 and supplemental information to determine whether it provided a complete description of the chemical, radiological and physical composition of the emplaced, existing, and to-be-generated waste proposed for disposal in the WIPP repository. The EPA also reviewed the DOE's description of the approximate quantities of waste components (for both existing and to-be-generated waste). The EPA considered whether the DOE waste descriptions were of sufficient detail to enable the EPA to conclude that the DOE did not overlook any component that was present in TRU waste and had significant potential to influence releases of radionuclides. The following information is a summary of the EPA's evaluation.

Chemical, Physical, and Radiological Description of Existing Waste

The CRA-2009 and supplemental information adequately described the chemical, radiological, and physical characteristics of each waste stream proposed for disposal at the WIPP facility.

The EPA noted the following changes in the waste: the DOE listed the to-be-generated (projected) waste in ATWIR-2008 (DOE 2008b). The projected waste was categorized similarly to existing waste (e.g., heterogeneous debris, filter material, soil). The amounts were ultimately expressed in density terms (kg/m^3) for PA purposes (U.S. EPA 2010c, Section 24.1.6).

The EPA concluded that the DOE's development of the disposal inventory was sufficient for PA purposes. The EPA continued to agree with the DOE that the use of projected waste inventory for scaling the WIPP CH-TRU and RH-TRU inventories to meet the total WIPP capacity was appropriate.

Waste Forms and Packaging

The only change for waste form and packaging since the CRA-2004 was that RH-TRU waste shipments had begun and the RH emplacement canisters were used for RH disposal operations. With their introduction, the metal in the repository increased. The DOE discovered that, "the CPR contents in emplacement materials were erroneously omitted from the CRA-2004 PABC" (Clayton et al. 2010). The DOE corrected this error in the CRA-2009 PA and the CRA-2009 PABC calculations (U.S. EPA 2010c, Section 24.1.6).

Number of Curies, Waste Streams and Volume

The DOE continued to estimate the number of curies in the inventory on a site-by-site, waste stream level using a reasonable process. The EPA required that the DOE produce a "list of the waste components and their approximate quantities." In addition to the radioisotope inventory information, the DOE also provided sufficient information on the chemical and physical waste components with descriptions in the ATWIR-2008 (DOE 2008b) and PAIR-2008 (Crawford et al. 2009) (U.S. EPA 2010c, Section 24.1.6).

Organic Ligands

The DOE properly included the impact of the increased organic ligands waste inventory in the CRA-2009 PABC calculations (U.S. EPA 2010c, Section 24.1.6).

Hanford Waste and K-Basin Waste

The original 12 tanks (9 tanks of CH waste and 3 tanks of RH waste) and the K-Basin knock-out pot sludge from Hanford that were included in the CRA-2004 PA were removed from the anticipated waste stream inventory and were not included in the CRA-2009 PABC calculations (U.S. EPA 2010c, Section 24.1.6).

Based on the review of the chemical, physical, and radiological descriptions of existing waste, waste forms, packaging, number of curies, waste streams, volumes, organic ligands, Hanford and K-basin waste and supplemental information, the EPA determined that the DOE continued to comply with the requirements of 194.24(a) (U.S. EPA 2010c, Section 24.1.7).

24.7.2 40 CFR § 194.24(b)(1)

In the CRA-2009, the EPA focused on changes and new information in the DOE analyses that could impact disposal system performance based on changes in waste characteristics, such as solubility, colloids, and gas generation. The EPA concluded that, with the combination of the CRA-2009, supplemental information, and the CRA-2009 PABC, the DOE performed an adequate update to the CCA and the 2004 recertification (U.S. EPA 2010c, Section 24.2.6).

The most recent 2008 inventory data on organic ligands (Crawford et al. 2009) showed that organic ligand quantities increased dramatically for acetic acid, citric acid, sodium citrate, and sodium EDTA. The EPA requested that the DOE consider the updated inventory of organic ligands and the extent to which ligands are likely to affect actinide solubilities. Moody (Moody 2009a and Moody 2009b) responded to the EPA's request and agreed to perform a new PA, the

CRA-2009 PABC, that included updated concentrations of EDTA, acetate, citrate, and oxalate concentrations, based on the information provided in Crawford et al. (Crawford et al. 2009), and provided documentation of the CRA-PABC to the EPA.

Other changes for the CRA-2009 PABC include changes to the MgO excess factor and MgO reactivity test procedure, and re-evaluation of the actinide distribution coefficients used in the CRA-2009 PABC to account for the effects of higher organic ligand concentrations (U.S. EPA 2010c, Section 24.2.6).

The uncertainty ranges for the actinides in the CRA-2009 were also changed for the CRA-2009 PABC and are listed in Table 24-3.

Table 24-3. Cumulative Distribution Function (CDF) Ranges Established by the Revised Actinide Solubility Uncertainty Analysis for the CRA-2009 PABC

Actinide Oxidation State	CDF Range
III	-4.20 to 2.70
IV	-2.25 to 3.30

Source: Xiong et al. 2009, Table 7 and Table 11

No changes were made to the colloidial actinide source term conceptual model or its implementation since the CCA PAVT. Data developed since the CCA PAVT indicated that the current model was likely to conservatively overestimate colloidal associated actinides in the source term.

The DOE was aware of experiments that the Argonne National Laboratory had performed on the structure of plutonium nanocolloids; however, the inclusion of intrinsic colloids in the PA conservatively takes into consideration the formation and transport of these colloids (U.S. EPA 2010c, Section 24.2.6).

The gas generation conceptual model and model implementation were not changed in the CRA-2009 PA (U.S. EPA 2010c, Section 24.2.6).

The EPA determined that the DOE continued to comply with the requirements for section 194.24(b)(1) (U.S. EPA 2010c, Section 24.2.7).

24.7.3 40 CFR §§ 194.24(b)(2) and (b)(3)

In section 194.24(b)(2), the DOE calculated new solubility values for the CRA-2009 PABC based on the ATWIR-2008 and the PAIR-2008 (U.S. EPA 2010c, Section 24.3.6). In section 194.24(b)(3), the EPA verified that excluded waste characteristics and components had not changed since the CRA-2004 (U.S. EPA 2010c, Section 24.4.6). The EPA determined that the DOE continued to comply with the requirements for section 194.24(b)(3) (U.S. EPA 2010c, Sections 24.3.7 and 24.4.7).

24.7.4 40 CFR §§ 194.24(c)(1), (e)(1), and (e)(2)

The EPA verified that the DOE continued to appropriately identify waste components that required limits, and the limits were reasonable. The EPA verified that the WWIS system was adequate for verifying waste emplaced in the WIPP repository. The DOE submitted a PCR to decrease the amount of MgO from 1.67 to 1.2 times the emplaced CPR waste components. The EPA directed the DOE to perform an uncertainty analysis to verify that a decreased amount of MgO would still ensure control of repository chemistry and safe operation of the WIPP for the long-term. The DOE analysis (DOE Appendix MgO 2009, Section 6.2.4.4) showed and verified that, even with the uncertainty considered, compliance with the release standards was demonstrated (U.S. EPA 2010c, Section 24.5.6).

The EPA found that the DOE continued to identify the limits of important waste components and that the PA implementation was adequate. Based on the review and evaluation of the CRA-2009, and supplemental information provided by the DOE, the EPA determined that the DOE continued to comply with the requirements for sections 194.24(c)(1) and 194.24(e)(1, 2) (U.S. EPA 2010c, Section 24.5.7).

24.7.5 40 CFR § 194.24(c)(2)

The EPA performed baseline inspections and Tier 1 evaluations of both CH- and RH-TRU waste characterization activities. CRA-2009 CARD 8 includes a summary of the EPA waste characterization inspections completed at different sites (U.S. EPA 2010d).

The RH waste characterization processes implemented by the Central Characterization Project and approved by the EPA were different than those discussed in the RH Waste Characterization Program Implementation Plan (WCPIP). The DOE agreed to revise the WCPIP and seek EPA concurrence before its implementation. The DOE requested one specific exception (baseline waste characterization at the Bettis Atomic Power Laboratory). The DOE could not characterize waste at any new RH-TRU site until these revisions were finalized. Using the revised processes, RH-TRU sites would quantify the radiological and physical contents of the waste to demonstrate compliance (U.S. EPA 2010c, Section 24.6.6).

Based on the review and evaluation of the CRA-2009 and supplemental information provided by the DOE, the EPA determined that the DOE continued to comply with the requirements for section 194.24(c)(2) (U.S. EPA 2010c, Section 24.6.7).

24.7.6 40 CFR § 194.24(c)(3)

The EPA required TRU waste generator sites to prepare a detailed AK Summary document containing all waste-specific information in one place, with properly cited references. The EPA suggested that information not necessarily needed by TRU waste generator site personnel in the AK summary documents could be included in appendices and adequately referenced (U.S. EPA 2010c, Section 24.7.7).

Based on the review and evaluation of the CRA-2009 and supplemental information provided by the DOE, the EPA determined that the DOE continued to comply with the requirements for section 194.24(c)(3) (U.S. EPA 2010c, Section 24.6.7).

24.7.7 40 CFR § 194.24(c)(4)

The EPA reviewed the WWIS modification to track RH waste content information from generators to the repository and found this change was acceptable (U.S. EPA 2010c, Section 24.8.6).

Based on the review and evaluation of the CRA-2009 and supplemental information provided by the DOE, the EPA determined that the DOE continued to comply with the waste data tracking requirements for section 194.24(c)(4) (U.S. EPA 2010c, Section 24.8.7).

24.7.8 40 CFR § 194.24(c)(5)

The changes made to the PDP since 2004 did not affect compliance with 40 CFR 194.24(c)(5) (U.S. EPA 2010c, Section 24.9.6). Based on the review and evaluation of the CRA-2009 and supplemental information provided by the DOE, the EPA determined that the DOE continued to comply with the requirements for section 194.24(c)(5) (U.S. EPA 2010c, Section 24.9.7).

24.7.9 40 CFR §§ 194.24(d) and (f)

In the CRA-2009, the EPA asked for additional analysis assuming clustering of waste. The DOE performed an analysis that showed nonrandom placement of waste was not significant and no waste loading assumptions were necessary in PA calculations. Based on the review and evaluation of the CRA-2009 and supplemental information provided by the DOE, and because the DOE had shown that waste loading assumptions were not necessary for use in PA, the EPA determined that the DOE continued to comply with the requirements for sections 194.24(d) and 194.24(f) for the 2009 recertification (U.S. EPA 2010c, Section 24.10.7).

24.7.10 40 CFR § 194.24(g)

The EPA verified that the DOE was using the WWIS to keep track of waste emplaced at the WIPP repository in its annual emplacement inspections. These annual inspections confirmed that the DOE continued to comply with section 194.24 (g) (U.S. EPA 2010c, Section 24.11.5).

Based on the review and evaluation of the CRA-2009 and supplemental information provided by the DOE, the EPA determined that the DOE continued to comply with the requirements for this section (U.S. EPA 2010c, Section 24.11.6).

24.8 Changes or New Information Since the CRA-2009 Recertification

24.8.1 40 CFR § 194.24(a)

To meet the requirements of section 194.24(a), the DOE described and categorized the TRU waste inventory emplaced in the WIPP repository and the waste that existed or was expected to

be generated at TRU waste sites since the CRA-2009, which was based on the inventory in the CRA-2004 PABC with an inventory cutoff date of September 30, 2002 (herein referred to as the CRA-2009) (U.S. DOE 2006; Leigh et al. 2005; Leigh, Trone, and Fox 2005). As a result of a full technical evaluation of CRA-2009 from the EPA during its completeness review, the DOE was directed to conduct a new PA for recertification to incorporate inventory changes as well as other technical changes (Cotsworth 2009a and Cotsworth 2009b). The new inventory components and chemical estimates were reported in the ATWIR-2008 (U.S. DOE 2008b) and the PAIR-2008 with an inventory cutoff date of December 31, 2007 (Crawford et al. 2009), and subsequently summarized in the CRA–2009 PABC (Clayton et al. 2010).

The TRU waste inventory used in the CRA-2014 is based on the unscaled ATWIR-2012 (U.S. DOE 2012a; data as of December 31, 2011, the cutoff for inclusion in the CRA-2014 PA), which is then scaled to a disposal inventory in the PAIR-2012 (Van Soest 2012) that supports PA calculations. The TRU waste inventory collection process and associated radiological and non-radiological components collected have remained the same since the CRA-2009 and CRA-2009 PABC.

The TRU waste inventory has been collected annually since 2007 and has changed from year to year (see Table 24-4). The emplaced waste was tracked as reported in the Waste Data System (WDS) (formerly the WWIS), and was included in the CRA–2009 and CRA–2009 PABC inventories, and currently in the CRA–2014. Table 24-4 provides a brief history of the inventory documents.

Table 24-4. Historical Inventory Documents

Title	Purpose
WTWBIR, Revision 0 (U.S. DOE 1994)	Initial inventory of the DOE complex to report all defense TRU waste at the waste-stream level.
WTWBIR, Revision 1 (U.S. DOE 1995a)	First update made to the original inventory data reported.
TWBIR, Revision 2 (U.S. DOE 1995b)	Used to show that the WIPP facility was in compliance with the disposal standards.
TWBIR, Revision 3 (U.S. DOE 1996b)	
Appendix DATA-2004, Attachment F of *Title 40 CFR 191, Subparts B and C, Compliance Recertification 2004* (U.S. DOE 2004)	Provided updated inventory information for the first recertification of the WIPP in 2004 (CRA-2004).
TWBIR–2004 (U.S. DOE 2006)	This was a revision of Appendix DATA, Attachment F. Provided updated inventory to support the PABC (CRA-2004 PABC) and was used for CRA-2009.
ATWIR–2007 (U.S. DOE 2008a)	The first annual inventory report that contained both scaled (calculations to represent a full repository) and unscaled data.
ATWIR–2008 (U.S. DOE 2008b)	First annual inventory report that reported only unscaled data.
PAIR–2008 (Crawford et al. 2009)	Provided data from ATWIR–2008 in the required format for CRA-2009 PA baseline calculations (CRA-2009 PABC).
ATWIR–2009 (U.S. DOE 2009d)	Provided updated annual inventory information.
ATWIR–2010 (U.S. DOE 2010a)	Provided updated annual inventory information.
ATWIR–2011(U.S. DOE 2011a)	Provided updated annual inventory information.
ATWIR–2012 (U.S. DOE 2012a)	Provides updated inventory information for this recertification application.
PAIR–2012 (Van Soest 2012)	Provides data from ATWIR–2012 in the required format for CRA–2014 PA (CRA-2014).

Volumes and characteristics (both physical and radiological) of waste that a TRU waste generator site may report as coming to the WIPP facility depend on factors that vary over time. Changes to the TRU waste inventory are attributed to:

- Availability and confidence in supplemental characterization information or process knowledge.
- Site estimates of projected TRU waste stream volumes. Changes in projected waste streams directly affect the CH and RH scaling factors that determine the disposal inventory for PA.
- Continuing waste emplacement at the WIPP facility.
- Regulations on the federal and state level.
- Waste program management decisions at the site, at the WIPP facility and on the national level.
- Site funding for waste management on sites.
- Inventory standardized collection methodologies and data check enhancements.

These are just a few of the interrelated factors that affect the estimates of waste stream volumes and associated characteristics.

24.8.1.1 Inventory Databases

The CRA–2009 TRU waste inventory data were captured in the Transuranic Waste Baseline Inventory Database (TWBID) Revision 2.1, Version 3.13, data version 4.16. The TWBID was subsequently superseded with the Comprehensive Inventory Database v.1.00 S.100 (CID1), which was released in December 2006. All relevant TWBID data and information were migrated into the CID1. The CID1 data version D.7.00 supported the issuance of the ATWIR-2008 and PAIR-2008. The TRU waste inventory information then was migrated from CID1 to CID, v.2.00 S.2.00 (CID2), released in August 2011. The CID2 subsequently underwent a minor software update to v.2.01 S.2.01 in March 2012. The CID2 data version D.11.00 supported the issuance of the ATWIR–2012 and the PAIR–2012, which provide input to the CRA–2014.

The CID1 and CID2 were qualified to the software quality assurance requirements of the *Quality Assurance Program Document* (QAPD) (U.S. DOE 2010b). Some of the major enhancements to CID2 include tracking waste and packaging materials and chemical components in mass units (kilograms [kg]), which were formerly tracked in density (kg/m^3) and weight percent (wt %), respectively, and tracking radionuclide activities (Ci), which were formerly tracked in activity concentrations (Ci/m^3). Additionally, CID2 added an Excel® import feature that increased data entry efficiency. The CID2 was also designed to facilitate automated execution and input/output processing for the radioactive decay and buildup calculations using the ORIGEN-S module of SCALE 6 (ORNL 2009). ORIGEN Version 2.2 (ORNL 2002) was used for the decay and buildup calculations for the previous compliance applications. ORIGEN-S is qualified to the software quality assurance requirements of the QAPD (U.S. DOE 2010b).

24.8.1.2 Inventory Description

For PA to model a full repository, the DOE used the same scaling methodology used in the CRA–2009 and CRA–2009 PABC. The method of inventory scaling is presented in TWBIR–2004 (U.S. DOE 2006), Leigh, Trone and Fox (Leigh, Trone, and Fox 2005), and the PAIR–2008 (Crawford et al. 2009). The CRA–2009, CRA–2009 PABC, and CRA–2014 are based on different inventories; therefore, they employ different waste scaling factors (Table 24-5).

Table 24-5. Inventory Scaling Factors (unitless)

Type	CRA–2009[1] (cutoff 9/30/2002)	CRA–2009 PABC[2] (cutoff 12/31/2007)	CRA–2014[3] (cutoff 12/31/2011)
CH-TRU	1.48	5.72	2.66
RH-TRU	0.861	4.87	3.67

[1]U.S. DOE 2006; [2]Crawford et al. 2009; [3]Van Soest 2012

The CH and RH scaling factors, when applied to their respective site-reported projected volumes, artificially increase the volumes such that the sum of the stored, projected, and emplaced volumes meet but do not exceed the legislated limit on total volume (6.2 million cubic feet [Land Withdrawal Act]) and permitted limit on RH volume (250,000 cubic feet [Hazardous Waste Facility Permit]).The scaling factors will continue to change due to the estimated volumes of CH and RH stored, emplaced, and projected waste for each recertification. To discuss changes in the inventories, the unscaled values are presented in the subsequent sections, as applicable, since scaled values do not provide a one-to-one comparison.

The data presented in Tables 24-6 through Table 24-10 are obtained from documents cited in the table footnotes, but in some cases the data were supplemented by database queries or reports so they could be presented in the appropriate units or totals.

24.8.1.3 TRU Waste Volume

For the CRA–2014, Table 3-1 and Table 3-2 of ATWIR–2012 list, by TRU waste site, the unscaled stored and projected volumes of CH-TRU and RH-TRU waste, respectively. Table 24-6 lists the total (sum of stored, projected, and emplaced) unscaled volumes by waste type for the CRA–2009, CRA–2009 PABC, and CRA–2014.

Table 24-6. Total CH and RH Waste Volumes (m^3)

	CRA–2009[1] (cutoff 9/30/2002)	CRA–2009 PABC[2] (cutoff 12/31/2007)	CRA–2014[3] (cutoff 12/31/2011)
CH	1.51×10^5	1.37×10^5	1.47×10^5
RH	7.40×10^3	2.91×10^3	3.84×10^3

[1]U.S. DOE 2006, LANL 2005 TWBID D.4.16; [2]U.S. DOE 2008b, LANL 2008 CID1 D.7.00; [3]U.S. DOE 2012a, LANL 2012 CID2 D.11.00

Between the CRA–2009 and the CRA–2009 PABC the major volume changes are due to: 1) resolution of legal issues with the State of Idaho. The 'Agreement to Implement', signed in July 2008, established requirements for retrieval of pre-1970 buried TRU waste. Prior to the 'Agreement to Implement', the Idaho Cleanup Project (ICP) had conservatively included additional volume to account for waste that could require disposal outside of Idaho, such as underburden soil, in addition to waste that was ultimately defined as 'targeted waste'. As a result of the 'Agreement to Implement', only "targeted waste" delineated in the Agreement was included in a revised ICP estimated CH volume. The revised estimate resulted in a decrease of approximately 10,500 cubic meters, and 2) the Hanford River Protection tank waste was removed from the WIPP-bound inventory, accounting for approximately 3,900 m^3 and 4,500 m^3 of the CH and RH volumes, respectively (U.S. DOE 2006 and U.S. DOE 2008a).

Between the CRA–2009 PABC and the CRA–2014, the inventory volume for both CH and RH waste has increased. The major increase in CH waste is attributed to the Hanford (Richland) site and INL, with a total increase between the two sites of approximately 7,000 m^3. The increase in RH waste volume is mainly attributed to Hanford, with an increase of about 1,300 m^3. For more details on the specific volume changes for the CRA–2009 PABC, refer to ATWIR–2008 (unscaled) and PAIR–2008 (scaled) (U.S. DOE 2008b; Crawford et al. 2009). For the CRA–2014, refer to the ATWIR–2012 (unscaled) and PAIR–2012 (scaled) (U.S. DOE 2012a; Van Soest 2012).

24.8.1.4 Number of Curies

Tables 3-10 and 3-11 of ATWIR–2012 (U.S. DOE 2012a) list the anticipated CH-TRU and RH-TRU radionuclide activities (decay and buildup corrected through 2011) by site and radionuclide, respectively. Table 24-7 lists the unscaled total (sum of stored, projected, and emplaced) CH and RH and activities for the CRA–2009, CRA–2009 PABC, and CRA–2014. These activities have different decay periods since, in the past, reporting period unscaled activities were not decayed to a common year, such as the closure year (2033).

Table 24-7. Total CH and RH Activity (Ci)

	CRA–2009[1] (cutoff 9/30/2002)	CRA–2009 PABC[2] (cutoff 12/31/2007)	CRA–2014[3] (cutoff 12/31/2011)
CH	4.30×10^6	3.56×10^6	3.48×10^6
RH	1.68×10^6	3.89×10^5	1.20×10^6

[1]U.S. DOE 2006, LANL 2005 TWBID D.4.16; [2]U.S. DOE 2008b, LANL 2008 CID1 D.7.00; [3]U.S. DOE 2012a, LANL 2012 CID2 D.11.00

Since the CRA–2009, the activity for CH waste has decreased consistently over the years. This is mainly due to more realistic estimates based on actual characterization data where the activity had previously been overestimated. Also contributing to the decrease, but to a much lesser extent, is the decay and buildup of radionuclide activities.

The ATWIR–2008 (U.S. DOE 2008b) began decaying unscaled activities to 2033 (WIPP facility closure) so that a comparison could be made with future collection years. The most significant decrease in activity since the CRA–2009 was due to the SRS, with a decrease of approximately 780,000 Ci due to two waste streams that were repackaged, characterized, and shipped. During the characterization of waste streams SR-W027-221H-HET and SR-MD-HET (formerly SR-W027-999-MD-HET), SRS realized that it had overestimated the activity of these two waste streams. Correction of the largest overestimate was for plutonium-238 (^{238}Pu), which caused this isotope to no longer be reported as the most predominant isotope in the CRA-2014, Section 31, Tables 31-4 and 31-5.

The re-evaluation of SRS activity is not the only reason that ^{238}Pu is not the dominate isotope for the CRA-2014 PA. Other contributing factors include the amount of projected waste SRS estimated for these two waste streams, and the effects of scaling the activity to a full repository. All of these factors contributed to the overall decrease in ^{238}Pu for the CRA–2014.

The RH activity increase between CRA–2009 PABC and the CRA–2014 is attributed to the Hanford (Richland) site. Hanford RH volume more than doubled, subsequently increasing the activity by approximately 530,000 Ci. For more details on these changes, refer to ATWIR–2008 (unscaled) and PAIR–2008 (scaled) for the CRA–2009 PABC, and ATWIR–2012 (unscaled) and PAIR–2012 (scaled) for the CRA–2014 (U.S. DOE 2008b; Crawford et al. 2009; U.S. DOE 2012a; Van Soest 2012).

24.8.1.5 Waste, Packaging, and Emplacement Materials

Table 3-4 of the ATWIR–2012 lists the unscaled stored and projected waste and packaging components of the CH-TRU and RH-TRU waste inventory. Table 24-8 lists the unscaled total (sum of CH and RH stored, projected, and emplaced) waste materials (iron, aluminum-based metal/alloys; other metal/alloys; other inorganic materials; cellulosic; rubber; plastics; cement; solidified inorganic and organic materials; soils; vitrified) and packaging materials (CPR, steel, lead) masses for the CRA–2009, CRA–2009 PABC, and CRA–2014.

Table 24-8. Total Waste and Packaging Materials (kg)

	CRA–2009[1] (cutoff 9/30/2002)	**CRA–2009 PABC[2]** (cutoff 12/31/2007)	**CRA–2014[3]** (cutoff 12/31/2011)
Waste Materials	9.45×10^7	5.34×10^7	4.57×10^7
Packaging Materials	3.51×10^6	3.03×10^7	3.39×10^7

[1]U.S. DOE 2006, LANL 2005 TWBID D.4.16; [2]U.S. DOE 2008b, LANL 2008 CID1 D.7.00; [3]U.S. DOE 2012a, LANL 2012 CID2 D.11.00

The waste materials have continuously decreased over the CRA time periods. This is mainly due to more realistic estimates based on actual characterization data where the masses of the packaging materials had previously been overestimated.

The largest single waste material decrease was related to the volume decrease for the ICP as reported in Section 24.8.1.3. Since ICP overestimated soil volume, this had a direct decrease in the soil mass for the waste material parameters. This accounted for approximately a 16 million kg decrease in soils between the CRA–2009 and the CRA–2009 PABC. The packaging materials have stayed fairly stable over the CRA reporting time frames, with the change in the total mass being related to the final container type stored and emplaced in the WIPP.

For more specific details on the waste and packaging material parameter changes refer to ATWIR–2008 (unscaled) and PAIR–2008 (scaled) for the CRA–2009 PABC, and ATWIR–2012 (unscaled) and PAIR–2012 (scaled) for the CRA–2014 (U.S. DOE 2008b; Crawford et al. 2009; U.S. DOE 2012a; Van Soest 2012).

Table 24-9 lists the total scaled emplacement material (cardboard slip sheets/stabilizer-cellulose; polypropylene supersacks, slip sheets, and stretch/shrink wrap-plastic) masses for the CRA–2009, CRA–2009 PABC, and CRA–2014.

Table 24-9. Total Scaled Emplacement Materials (kg)

CRA–2009[1] (cutoff 9/30/2002)	**CRA–2009 PABC**[2] (cutoff 12/31/2007)	**CRA–2014**[3] (cutoff 12/31/2011)
1.69×10^6	1.34×10^6	1.51×10^6

[1]U.S. DOE 2006; [2] Crawford et al. 2009; [3]Van Soest 2012

To determine the mass of emplacement materials when the WIPP repository is full, an analysis is performed for each CRA. The analysis uses scaled final form container data to determine the amount of emplacement materials required to emplace the total scaled number of final form containers in the WIPP repository. The emplacement material masses are only calculated using scaled container values; therefore, Table 24-9 only presents the scaled emplacement material masses.

Since scaled values are not comparable, some generalizations can be made as to why the values are different: 1) for each CRA, the scaling factors have changed, which has a direct change on the final values, 2) the emplacement materials will continue to change based on the actual containers that are emplaced in the WIPP repository, and 3) the analysis calculates what type of emplacement materials will be needed based on the estimated final containers reported by the sites. As these estimates change, so will the emplacement materials.

24.8.1.6 Organic Ligands and Oxyanions

Table 24-10 lists the total (sum of CH and RH stored, projected, and emplaced) scaled CH and RH organic ligands (acetate, acetic acid, citrate, citric acid, EDTA, oxalate, oxalic acid) and oxyanion (nitrate, phosphate, sulfate) masses for the CRA–2009, CRA–2009 PABC, and CRA–2014.

Table 24-10. Total Scaled Organic Ligands and Oxyanions (kg)

	CRA–2009[1] (cutoff 9/30/2002)	**CRA–2009 PABC[2]** (cutoff 12/31/2007)	**CRA–2014[3]** (cutoff 12/31/2011)
Organic Ligands	5.80×10^4	5.87×10^4	5.07×10^4
Oxyanions	3.22×10^6	2.52×10^6	2.38×10^6

[1]U.S. DOE 2006; [2]Crawford et al. 2009; [3]Van Soest 2012.

The data in Table 24-10 are presented as scaled data because the organic ligands and oxyanions are not tracked in the WDS; therefore, to account for their emplaced mass, an analysis is performed to account for all the organic ligands and oxyanions. This analysis is performed on the scaled data and is presented in the performance assessments inventory reports for the use in PA.

Since scaled values are not comparable for the organic ligands and oxyanions, the following generalizations are discerned: 1) for each CRA, the scaling factor has changed, which has a direct effect on the final values, 2) organic ligand and oxyanion masses have changed due to the development of additional AK documentation, and 3) the generator sites are reporting more accurate values for these components. For more specific details on organic ligand and oxyanion changes refer to ATWIR–2008 (unscaled) and PAIR–2008 (scaled) for the CRA–2009 PABC, and ATWIR–2012 (unscaled) and PAIR–2012 (scaled) for the CRA–2014 (U.S. DOE 2008b; Crawford et al. 2009; U.S. DOE 2012a; Van Soest 2012).

Based on the information presented in section 24.8.1, the DOE continues to demonstrate compliance with provisions of section 194.24(a).

24.8.2 40 CFR § 194.24(b)(1)

There were no major changes to the waste characteristics between the CRA–2009 PABC and the CRA–2014, but the DOE did update waste component information and add inventory parameters used in the WIPP PA. Additional parameters include the mass of waste and packaging materials, the solubilities calculated using multiples of the minimum brine volume necessary for a DBR to occur, and those to describe the additional biodegradation reactions implemented within the repository chemistry model. These changes are refinements to the implementation of the PA conceptual models; no changes were made to these models. Waste component changes are summarized in Table 24-11, and parameter value changes are discussed in the appropriate subsections below.

Based on the information presented in Section 24.8.2, the DOE continues to demonstrate compliance with provisions of section 194.24(b)(1).

Table 24-11. Significance and Changes in Components and Characteristics

Waste Component or Characteristic Used in PA	Increase or Decrease From CRA–2009 PABC to CRA–2014	Significance
Radioactivity (Ci/m^3)	Decrease	Used in calculating releases
Solubility	Increase and decrease, depending on oxidation state	Higher solubility can lead to higher releases
Organic Ligands—complexing agents	Decrease	Increases solubility
Amount of Metals	Decrease	Maintains reducing environment, but also contributes to gas generation
Amount of CPRs	Decrease	May increase gas generation from microbial processes
Oxyanions: nitrate, sulfate, and phosphate	Increase and decrease	Nutrients for microbes - affects gas generation
Cement	Decrease	Volume-related component
Shear Strength	Increase	Affects mechanical releases during a drilling intrusion
Particle Diameter	No change	Used to calculate spallings releases
Formation of Colloidal Suspensions	Increase and decrease	Colloids can facilitate transport of radionuclides in groundwater

24.8.2.1 Assessment of Waste Characteristics and Waste Characteristic Input Parameters

In the CCA, the DOE identified several waste characteristics as being potentially important to PA. The CRA–2014 identifies the same important characteristics as in the CCA. As was first done in the CRA–2004, the CRA–2014 continues to assert that organic ligands could be important to solubility and therefore organic ligands are included in the solubility calculations (Brush and Domski 2013a).

There were no changes to the conceptual models since the CRA–2009 PABC.

24.8.2.2 CRA–2014 Radioactivity in Curies

The DOE used the information from the PAIR–2012 (Van Soest 2012) as the basis for the PA isotope inventory for the CRA–2014. The CRA-2014 PA Radionuclide Inventory Screening Analysis (Kicker and Zeitler 2013) discusses the methodology used by the DOE to determine the WIPP repository radionuclide inventory information for use in CRA–2014 PA calculations. The parameters for the initial radionuclide inventory decayed to the WIPP facility closure date, and those calculated based on the initial radionuclide inventories such as the WUF, and the initial lumped radionuclide inventories were updated for use in the CRA–2014 (Kicker and Zeitler 2013).

24.8.2.3 CRA-2014 Solubility and Organic Ligands

The CRA–2014 includes new solubility values for Th(IV), Np(V) and Am(III) (Brush and Domski 2013a), and new solubility uncertainty factors (Brush and Domski 2013b). The DOE also implemented a new method for calculating the organic ligand concentrations for the minimum brine volumes necessary for a DBR by adding additional parameters (Camphouse 2013). The DOE utilized EQ3/6, Version 8.0, and the thermodynamic database DATA0.FMT.R2, also known as DATA0.FM1, for the analyses performed in support of the CRA–2014. The CRA–2014 continues to include the effects of organic ligands in the solubility calculations, as was first done in the CRA–2004.

More details are provided in Appendix SOTERM-2014, Sections SOTERM-3 and SOTERM-4 on the refinement of the baseline solubilities and solubility uncertainties and in Appendix MASS-2014, Section MASS-2.6.10 on the implementation of variable brine volume.

24.8.2.4 CRA-2014 Parameters Related to Metals, CPR and Oxyanions

The CRA–2014 used the inventory described in the PAIR–2012 (Van Soest 2012) to update the parameters related to metals, CPRs and oxyanions. Previous inventory reports included the densities of the waste and packaging materials, but the PAIR–2012 reports the masses of the waste and packaging materials. This change allows the reported values to be directly used in PA, and the conversion from densities to masses is no longer necessary. Twenty-two new parameters, shown in Table 24-12, were added to represent the new waste and packaging material mass values reported in the PAIR–2012 (Camphouse 2013).

Table 24-12. Waste and Packaging Material Parameters Added for the CRA–2014.

Material	Property	Description
WAS_AREA	CELCCHW	Mass of cellulosics in CH waste container materials
	CELCRHW	Mass of cellulosics in RH waste container materials
	CELECHW	Mass of cellulosics in CH waste emplacement materials
	CELERHW	Mass of cellulosics in RH waste emplacement materials
	CELLCHW	Mass of cellulosics in CH waste
	CELLRHW	Mass of cellulosics in RH waste
	IRNCCHW	Mass of iron containers, CH waste
	IRNCRHW	Mass of iron containers, RH waste
	IRONCHW	Mass of iron-based material in CH waste
	IRONRHW	Mass of iron-based material in RH waste
	PLASCHW	Mass of plastics in CH waste
	PLASRHW	Mass of plastics in RH waste
	PLSCCHW	Mass of plastic liners, CH waste
	PLSCRHW	Mass of plastic liners, RH waste
	PLSECHW	Mass of plastic in CH waste emplacement materials
	PLSERHW	Mass of plastic in RH waste emplacement materials
	RUBBCHW	Mass of rubber in CH waste
	RUBBRHW	Mass of rubber in RH waste
	RUBCCHW	Mass of rubber in CH waste container materials
	RUBCRHW	Mass of rubber in RH waste container materials
	RUBECHW	Mass of rubber in CH waste emplacement materials
	RUBERHW	Mass of rubber in RH waste emplacement materials

24.8.2.5 CRA-2014 Production of Gas from the Waste

Two changes related to the gas generation from the waste were implemented in the CRA–2014 PA: the refinement of the repository water balance and the update to the anoxic steel corrosion rate. Each is discussed below.

24.8.2.5.1 Repository Water Balance

As part of the CRA–2009, the EPA noted several issues for possible additional investigation, including the potential implementation of a more detailed repository water balance (U.S. EPA 2010c). The main objective of refining the repository water balance is to include the major gas- and brine-producing and consuming reactions in the existing conceptual model (Appendix PA-2014, Section PA-1.1.8). The CRA–2014 implements the same biodegradation pathways as implemented in the CRA–2009 PABC, but the generation of water is also considered. All reactions are further described in Camphouse (Camphouse 2012).

The CRA–2014 PA includes the following gas and brine reactions:

- Iron hydroxide with hydrogen sulfide, which consumes gas and produces water
- MgO hydration, which consumes water and produces brucite
- Carbonation of brucite to form Hydromagnesite
- Transformation of hydromagnesite to form magnesite, which produces water

BRAGFLO 6.02 was revised to include these additional reactions (see Appendix PA–2014, Section PA-4.2.5). As a result, several new parameters were added (see Table 24-13). Clayton (Clayton 2013) describes the justification of the chemistry parameter values used for the CRA-2014.

Table 24-13. Chemistry Parameters Added for the CRA-2014

Material	Property	Description
REFCON	DN_HYDRO	Hydromagnesite density
REFCON	MW_HYDRO	Hydromagnesite molecular weight
REFCON	STCO_*xy*	Stoichiometric coefficients for reaction *x*, species *y*
WAS_AREA	BRUCITEC, BRUCITES	MgO inundated hydration rate in Castile and Salado brines
WAS_AREA	BRUCITEH	Humid MgO hydration rate
WAS_AREA	HYMAGCON	Hydromagnesite conversion rate

24.8.2.5.2 Refinement of the Steel Corrosion Rate (STEEL:CORRMCO2)

In the WIPP PA, model gas generation is assumed to result from the microbial degradation of CPR materials and the anoxic corrosion of steel (see Appendix PA-2014, Sections PA-1.1.4 and

PA-4.2.5). The parameter STEEL:CORRMCO2 represents the anoxic steel corrosion rate for brine-inundated steel in the absence of microbially produced CO_2.

The DOE has updated both the distribution type and values for the parameter STEEL:CORRMCO2 for the CRA-2014 PA based on the experimental corrosion data reported by Roselle (Roselle 2013). Because the STEEL:CORRMCO2 parameter represents the corrosion rate as a constant in PA calculations, the best estimate of the corrosion rate is represented by the mean of the empirical data reported in Roselle (Roselle 2013). The uncertainty on the mean in this case is represented by a Student-t distribution. The DOE has updated both the distribution type and values for the parameter STEEL:CORRMCO2 for the CRA–2014 PA based on the experimental corrosion data reported by Roselle (Roselle 2013).

24.8.2.6 CRA-2014 Parameters Related to Waste Shear Strength

The parameter related to the waste shear strength was revised for the CRA-2014. Based on the recommendations of Herrick and Kirchner (Herrick and Kirchner 2013), the DOE included a refined distribution for the parameter BOREHOLE:TAUFAIL in the CRA–2014 PA calculations (Appendix PA-2014, Section PA-1.1.5). The DOE has updated the parameter for the CRA-2014 from a loguniform distribution with a range of 0.05 – 77.0 Pa, to a uniform distribution with a range of 2.22 – 77.0 Pa to best estimate the uncertainty range for parameter BOREHOLE:TAUFAIL.

24.8.2.7 CRA–2014 Formation of Colloidal Suspensions

The colloid enhancement parameters were re-examined for the CRA–2014 (Appendix PA-2014, Section PA-1.1.11). Based on the recommendations of Reed et al. (Reed et al. 2013), the DOE has updated the PA colloid parameters. Specifically, the PA parameter properties CONCINT, PROPMIC and CAPMIC were changed. More details are provided in SOTERM-2014, Section SOTERM-4.6.

24.8.3 40 CFR §§ 194.24(b)(2) and (b)(3)

The CRA–2014 identifies the same important waste characteristics as in the CCA, and also identifies organic ligands as being potentially important to PA. The CRA–2014 includes organic ligands in the solubility calculations (Brush and Domski 2013a). Most of the inventory amounts of the listed components have changed since the CRA–2009 PABC; these are described in the PAIR–2012 (Van Soest 2012).

The DOE provided a list of those waste characteristics and components that were excluded from consideration in the CCA PA for various reasons, such as negligible impact. There were no changes in the exclusion decisions for the important waste components and characteristics since the CRA–2009 PABC recertification decision. Therefore, the DOE continues to demonstrate compliance with provisions of section 194.24(b)(2) and (b)(3).

24.8.4 40 CFR §§ 194.24(c)(1), (e)(1), and (e)(2)

The rationale has changed for establishing or not establishing limits for the waste components identified as potentially significant in the CCA. The minimum emplacement limit for nonferrous metals has been eliminated. All other limits remain the same, and their implementation into the CRA-2014 PA has not changed.

The minimum emplacement value for nonferrous metals was established in the CCA as the minimum amount needed to bind to organic ligands, thereby reducing the impact of organic ligands on the solubility of radionuclides (the effects of organic ligands were not included in the CCA PA). Since the CRA-2004, the effect of organic ligands on actinide solubility has been included in the PA. The minimum emplacement limit is no longer necessary to eliminate the effect of organic ligands on the actinide solubility in the PA, however the mass of nonferrous metals will continue to be tracked as part of the DOE waste inventory.

In its evaluation of the CCA, the EPA concluded that while there is no limit for the radionuclide inventory, the EPA considers the radionuclide inventory used in the PA to be a *de facto* upper bound (U.S. EPA 2010c, Section 24.5.3). Therefore the inventory that is used in PA calculations to determine compliance with release standards resets the limits on radionuclide emplacement at the WIPP. Thus, the DOE is proposing a new upper bound for the radionuclide inventory by including the most recent DOE inventory data from the PAIR–2012 (Van Soest 2012) in the CRA–2014 PA.

Based on the information above, the DOE continues to demonstrate compliance with the provisions of section 194.24(c)(1), (e)(1), and (e)(2).

24.8.5 40 CFR § 194.24(c)(2)

As noted in Section 28.8.4 (40 CFR § 194.24(b)), the DOE did not modify the list of CRA–2009 components and characteristics requiring quantification. Therefore, the CRA–2014 does not identify any significant changes to the measurement techniques used in the waste characterization program (i.e., VE, RTR, AK, NDA).

Since the CRA–2009, the standard large box 2 has been added to handle oversized waste items, and the shielded container (see Appendix DATA-2014, DATA-B-1.3) has been conditionally approved by the EPA (Edwards 2011) to dispose of high gamma waste as CH, but will be accounted against the RH limits. The WIPP WAC (U.S. DOE 2008c) was revised to remove all references to limited VE (i.e., document all contents of a waste container) for CH waste. Revision 6.5 of the WAC (U.S. DOE 2010c) clarified the language regarding liquid prohibition and VE. The term "residual liquid" was replaced with "observable liquid." Observable liquid is liquid that can be seen by a trained radiography operator or by a trained operator performing VE of the waste. This terminology can be implemented consistently during characterization regardless of waste type. These changes, along with the addition of the standard large box 2, shielded containers, and the removal of all references to limited VE for CH waste, do not modify the list of components and characteristics requiring quantification. Therefore, the DOE is in compliance with section 194.24(c)(2).

24.8.6 40 CFR § 194.24(c)(3)

Since the CRA–2009, the AK process has not changed for CH and RH waste. The process is described in CRA-2009, Section 24.6.7. The DOE has added a gravimetric or dimensional analysis for RH unique waste streams where the activity on or within a waste stream is identified as discreet pieces of irradiated materials to estimate the activity content of the waste container or to confirm AK information for the same measurements. For the gravimetric method, the data are controlled under the formal measurement control program specified in the QAPD. The quality assurance objectives of 194.22(c) are specified for both methods (U.S. DOE 2011b). Therefore, the DOE is in compliance with section 194.24(c)(3).

24.8.7 40 CFR § 194.24(c)(4)

The WWIS used the Oracle Version 10g database management system at the time of the CRA–2009, as described in CRA–2009, Section 24.6.8. The WWIS was retired in December 2009, and replaced with the WDS to provide DOE with a modern approach to process controls and data sharing. The WDS uses Oracle DB 11g, and a web interface for user access. The EPA was provided with system access to the WDS in 2009. The WDS Data Dictionary (U.S. DOE 2013) is not included in the WDS User's Manual (U.S. DOE 2012b), but is included as a reference to this section for consistency with the CRA–2009. Appendix MON-2014, Section MON-3.6, briefly describes the WDS and its function for the monitoring program that was developed to meet commitments contained in the DOE's application to the EPA, which demonstrated compliance with radioactive waste disposal regulations 40 CFR Part 191 Subparts B and C and the certification criteria in 40 CFR Part 194. Therefore, the DOE is in compliance with section 194.24(c)(4).

24.8.8 40 CFR § 194.24(c)(5)

The DOE describes the PDP program in the CRA–2009, Section 24, Waste Characterization. Since the CRA–2009, both the *Performance Demonstration Program Plan for Nondestructive Assay of Boxed Wastes for the TRU Waste Characterization Program*, Revision 3 (U.S. DOE 2011c) and the *Performance Demonstration Program Plan for Nondestructive Assay of Drummed Wastes for the TRU Waste Characterization Program*, Revision 3 (U.S. DOE 2011d) have been revised. The most important changes to these documents were implemented to simplify sample preparation team requirements and instructions, better define the process to address failures of the tested NDA systems to meet NDA PDP criteria, single out the non-interfering matrix standard waste box and non-interfering matrix drum as distinct from other matrices tested and define their use for specialized circumstances, and to improve the descriptions of NDA PDP components and inventory of materials. The *Performance Demonstration Program Plan for Analysis of Simulated Headspace Gases*, Revision 7 (U.S. DOE 2010d) has also been revised since CRA–2009 to implement a change removing the compound *cis*-1,2-dichloroethylene from the target compound list. Therefore, the DOE is in compliance with section 194.24(c)(5).

24.8.9 40 CFR §§ 194.24(d) and (f)

For the CRA–2014 PA, the DOE did not make any changes to the waste loading scheme since the CRA–2009 PABC. The DOE did not use a performance-based waste loading scheme for waste emplacement in the WIPP repository, and the DOE assumed random placement of waste in its performance and compliance assessment. Therefore, the DOE continues to demonstrate compliance with provisions of section 194.24(d) and (f).

24.8.10 40 CFR § 194.24(g)

The CRA–2014 inventory has changed from the CRA–2009 PABC inventory and is described in Section 24.8.1 (40 CFR § 194.24(a)). The WDS tracks compliance with the limitations on CH-TRU and RH-TRU waste described in the WIPP LWA. Therefore, the DOE is in compliance with section 194.24(g).

24.8.11 40 CFR § 194.24(h)

The DOE continues to comply with the inspection and records requirements, as discussed in Section 22 of this application. Therefore, the DOE is in compliance with section 194.24(h).

24.9 References

(*Indicates a reference that has not been previously submitted.)

Brush, L.H. 2005. *Results of Calculations of Actinide Solubilities for the WIPP Performance Assessment Baseline Calculations* (May 18). ERMS 539800. Sandia National Laboratories, Carlsbad, NM.

Brush, L.H., and G.T. Roselle. 2006. Memorandum to E.D. Vugrin (Subject: *Geochemical Information for Calculation of the MgO Effective Excess Factor*). 17 November 2006. U.S. Department of Energy, Sandia National Laboratories, Carlsbad, NM.

Brush, L.H., and P.S. Domski. 2013a. *Prediction of Baseline Actinide Solubilities for the WIPP CRA-2014 PA*. Analysis report, January 21, 2013. ERMS 559138. Sandia National Laboratories, Carlsbad, NM.*

Brush, L.H., and P.S. Domski. 2013b. *Uncertainty Analysis of Actinide Solubilities for the WIPP CRA-2014 PA, Rev. 1 Supersedes ERMS 559278*. Analysis report, April, 2013. ERMS 559712. Sandia National Laboratories, Carlsbad, NM.*

Brush, L.H., and Y. Xiong. 2005. *Calculation of Organic-Ligand Concentrations for the WIPP Performance-Assessment Baseline Calculations* (May 4). ERMS 539635. Sandia National Laboratories, Carlsbad, NM.

Brush, L.H., Y. Xiong, J.W. Garner, A. Ismail, and G.T. Roselle. 2006. *Consumption of Carbon Dioxide by Precipitation of Carbonate Minerals Resulting from Dissolution of Sulfate Minerals in the Salado Formation In Response to Microbial Sulfate Reduction in the WIPP*. ERMS 544785. Sandia National Laboratories, Carlsbad, NM.

Bynum, R.V. 1996. *Analysis to Estimate the Uncertainty for Predicted Actinide Solubilities, WBS 1.1.10.1.1* (Revision 0, September 3). WPO41374. Sandia National Laboratories, Albuquerque, NM.

Camphouse, C. 2012. *User's Manual for BRAGFLO, Version 6.02*. ERMS 558663. Sandia National Laboratories, Carlsbad, NM.*

Camphouse, C. 2013. *Analysis Plan for the 2014 Compliance Recertification Application Performance Assessment*. January 31, 2013. ERMS 559198. Sandia National Laboratories, Carlsbad, NM.*

Clayton, D.J. 2013. Memorandum to Records Center (Subject: *Justification of Chemistry Parameters for Use in BRAGFLO for AP-164, Rev 1*). March 13, 2013. ERMS 559466. Sandia National Laboratories, Carlsbad, NM.*

Clayton, D.J., and M.B. Nemer. 2006. Memorandum to E.D. Vugrin (Subject: *Normalized Moles of Castile Sulfate Entering the Repository and Fraction of MgO Lost Due to Brine Flow Out of the Repository*). 9 October 2006. U.S. Department of Energy, Sandia National Laboratories, Carlsbad, NM.

Clayton, D.J., R.C. Camphouse, J.W. Garner, A.E. Ismail, T.B. Kirchner, K.L. Kuhlman, M.B. Nemer. 2010. *Summary Report of the CRA-2009 Performance Assessment Baseline Calculation*. ERMS 553039. Sandia National Laboratories, Carlsbad, NM.*

Cotsworth, E. 2004a. *Letter to R.P. Detwiler (1 Enclosure)*. 20 May 2004. ERMS 535554. U.S. Environmental Protection Agency, Office of Air and Radiation, Washington, DC.

Cotsworth, E. 2004b. *Letter to R.P. Detwiler, Acting Manager*. 12 July 2004. U.S. Environmental Protection Agency, Office of Air and Radiation, Washington DC.

Cotsworth, E. 2005. Letter to I. Triay (Subject: *EPA Letter on Conducting the Performance Assessment Baseline Change (PABC) Verification Test*). 4 March 2005. ERMS 538858. U.S. Environmental Protection Agency, Office of Air and Radiation, Washington, DC.

Cotsworth, E. 2009a. Letter to D. Moody (1 Enclosure). 21 May 2009. [*CRA-2009 First (1) Completeness Letter*]. U.S. Environmental Protection Agency, Office of Air and Radiation, Washington, DC.*

Cotsworth, E. 2009b. Letter to D. Moody (1 Enclosure). 16 July 2009. [*CRA-2009 Second (2) Completeness Letter*]. U.S. Environmental Protection Agency, Office of Air and Radiation, Washington, DC.*

Crawford, B. 2004. *Inventory Change/Addition Control Form* (November 12). SP9-6-3. ERMS 537921. Los Alamos National Laboratory, Carlsbad, NM.

Crawford, B., D. Guerin, S. Lott, B. McInroy, J. McTaggart, and G. Van Soest. 2009. *Performance Assessment Inventory Report-2008* (Revision 0, April). LA-UR-09-02260. Los Alamos National Laboratory, Carlsbad, NM.*

Deng, H., S.R. Johnsen, G.T. Roselle, and M.B. Nemer. 2006. *Analysis of Martin Marietta MagChem 10 WTS-60 MgO*. ERMS 544712. Sandia National Laboratories, Carlsbad, NM.

Detwiler, R.P. 2004a. Letter to E. Cotsworth (Subject: *Initial Response to Environmental Protection Agency (EPA) September 2, 2004, Letter on Compliance Recertification Application*; 6 Enclosures). 1 November 2004. U.S. Department of Energy, Carlsbad Field Office, Carlsbad, NM.

Detwiler, R.P. 2004b. Letter to Elizabeth Cotsworth, Director (Subject: *Partial Response to Environmental Protection Agency (EPA) May 20, 2004, Letter on CRA*; 1 Enclosure). 15 July 2004. U.S. Department of Energy, Carlsbad Field Office, Carlsbad, NM.

Dials, G.E. 1997. Memorandum (with attachments) to G. Thomas Todd, Area Manager, LAAO (Subject: *Site Certification of Los Alamos National Laboratory*). 12 September 1997. U.S. Department of Energy, Carlsbad Area Office, Carlsbad, NM.

Edwards, J. 2011. Letter to Mr. Edward Ziemianski (Acting CBFO Manager) (Subject: *Approval of DOE's PCR to emplace RH waste in shielded containers*). August 8, 2011. U.S. Environmental Protection Agency, Washington, DC.*

Garner, J., and C. Leigh. 2005. *Analysis Package for PANEL: CRA-2004 Performance Assessment Baseline Calculation* (Revision 0). ERMS 540572. Sandia National Laboratories Carlsbad, NM.

Gitlin, B.C. 2005. *Letter to I. Triay, Acting Manager*. 12 May 2005. U.S. Environmental Protection Agency, Office of Air and Radiation, Washington, DC.

Gitlin, B.C. 2006. Letter to D.C. Moody (Subject: *Response to Request to Reduce Excess MgO*). 28 April 2006. ERMS 543319. U.S. Environmental Protection Agency, Office of Air and Radiation, Washington, DC.

Herrick, C.G., and T. Kirchner. 2013. Memorandum to C. Camphouse (Subject: *Follow-up to Questions Concerning TAUFAIL Flume Testing Raised during the November 14-15, 2012 Technical Exchange Between the DOE and EPA*). 23 January 2013. ERMS 559081. Sandia National Laboratories, Carlsbad, NM.*

Kanney, J.F., and E.D. Vugrin. 2006. Memorandum to D.S. Kessel (Subject: *Updated Analysis of Characteristic Time and Length Scales for Mixing Processes in the WIPP Repository to Reflect the CRA-2004 PABC Technical Baseline and the Impact of Supercompacted Mixed Waste and Heterogeneous Waste Emplacement*). 31 August 2006. U.S. Department of Energy, Sandia National Laboratories, Carlsbad, NM.

Kicker, D.C., and T. Zeitler. 2013. *Radionuclide Inventory Screening Analysis for the 2014 Compliance Recertification Application Performance Assessment (CRA–2014 PA)*. ERMS 559257. Sandia National Laboratories, Carlsbad, NM.*

Kirchner, T.B., and E.D. Vugrin. 2006. Memorandum to D.S. Kessel (Subject: *Uncertainty in Cellulose, Plastic, and Rubber Measurements for the Waste Isolation Pilot Plant Inventory*). 12 June 2006. ERMS 543848. U.S. Department of Energy, Sandia National Laboratories, Carlsbad, NM.

Leigh, C. 2006. *Incorporation of Inventory Uncertainty in the CRA-2004 Performance Assessment Baseline Calculation*. ERMS 542308. Sandia National Laboratories, Carlsbad, NM.

Leigh, C., J. Kanney, L. Brush, J. Garner, G. Kirkes, T. Lowry, M. Nemer, J. Stein, E. Vugrin, S. Wagner, and T. Kirchner. 2005. *2004 Compliance Recertification Application Performance Assessment Baseline Calculation* (Revision 0). ERMS 541521. Sandia National Laboratories, Carlsbad, NM.

Leigh, C., J. Trone, and B. Fox. 2005. *TRU Waste Inventory for the 2004 Compliance Recertification Application Performance Assessment Baseline Calculation* (Revision 0). ERMS 541118. Sandia National Laboratories, Carlsbad, NM.

Los Alamos National Laboratory (LANL). 2005. *Transuranic Waste Baseline Inventory Database (TWBID),* Revision 2.1, Version 3.13, Data Version D.4.16. Los Alamos National Laboratory, Carlsbad, NM.

Los Alamos National Laboratory (LANL). 2008. *Comprehensive Inventory Database (CID),* software version v.1.00 S.1.00, data version D.7.00. Los Alamos National Laboratory, Carlsbad, NM.*

Los Alamos National Laboratory (LANL). 2012. *Comprehensive Inventory Database (CID),* software version v.2.01 S.2.01, data version D.11.00. Los Alamos National Laboratory, Carlsbad, NM.*

Lott, S. 2004. *Inventory Data Change/Addition Control Form* (November, Revision 2). SP9-6-3. ERMS 537966. Los Alamos National Laboratory, Carlsbad, NM.

Marcinowski, F. 2003. Letter to I. Triay, Manager (Subject: *Environmental Protection Agency (EPA) Preliminary Review of Information for the Advanced Mixed Waste Treatment Project (AMWTP)*). 21 March 2003. U.S. Environmental Protection Agency, Office of Indoor Air and Radiation, Washington, DC.

Marcinowski, F. 2004. *Letter to R.P. Detwiler (2 Enclosures).* 26 March 2004. U.S. Environmental Protection Agency, Office of Air and Radiation, Washington, DC.

Moody, D.C. 2006. Letter to E.A. Cotsworth (Subject: *Transmittal of Planned Change Request; 1 Enclosure*). 10 April 2006. ERMS 543262. U.S. Department of Energy, Carlsbad Field Office, Carlsbad, NM.

Moody, D.C. 2009a. Letter to Ms. Elizabeth Cotsworth (Subject: *Response to Environmental Protection Agency Letter Dated May 21, 2009 Regarding Compliance Recertification Application*). 24 August 2009. CBFO:ORC:RP:SES:09·0292:UFC 5486.00. U.S. Department of Energy, Carlsbad Field Office, Carlsbad, NM.*

Moody, D.C. 2009b. Letter to Ms. Elizabeth Cotsworth (Subject: *Response to Environmental Protection Agency May 21, 2009, and July 16, 2009, Letters on 2009 Compliance Recertification Application*; 1 Enclosure). 30 September 2009. CBFO:ORC:RP:GS:09-0319:UFC 5486.00. U.S. Department of Energy, Carlsbad Field Office, Carlsbad, NM.*

Nemer, M.B. 2007. Memorandum to WIPP SNL Records Center (Subject: *Effects of Not Including Emplacement Materials in CPR Inventory on Recent PA Results*). ERMS 545689. U.S. Department of Energy, Sandia National Laboratories, Carlsbad, NM.

Nemer, M.B., and J. Stein. 2005. *Analysis Package for BRAGFLO: 2004 Compliance Recertification Application Performance Assessment Baseline Calculation*. ERMS 540527. Sandia National Laboratories, Carlsbad NM.

Nemer, M.B., J. Stein, and W. Zelinski. 2005. *Analysis Report for BRAGFLO Preliminary Modeling Results With New Gas Generation Rates Based on Recent Experimental Results*. ERMS 539437. Sandia National Laboratories, Carlsbad, NM.

New Mexico Environment Department (NMED). 2008. *Waste Isolation Pilot Plant Hazardous Waste Permit, Attachment B, Waste Analysis Plan* (March 25). State of New Mexico, Santa Fe, NM.

Oak Ridge National Laboratory (ORNL). 2002. *RSICC Computer Code Collection: ORIGEN 2.2, Isotope Generation and Depletion Code Matrix Exponential Method, CCC-371*. Radiation Safety Information Computational Center at Oak Ridge National Laboratory, Oak Ridge, TN.*

Oak Ridge National Laboratory (ORNL). 2009. *SCALE: A Modular Code System for Performing Standardized Computer Analyses for Licensing Evaluation*. ORNL/TM-2005/39, Version 6, Vols. I–III, January 2009, Oak Ridge National Laboratory, Oak Ridge, TN. Available from Radiation Safety Information Computational Center (RSICC) at Oak Ridge National Laboratory as CCC-750.*

Park, B-Y, and F.D. Hansen. 2003. *Determination of Porosity Surfaces of the Disposal Room Containing Various Waste Inventories for WIPP PA* (Revision 0). ERMS 533216. Sandia National Laboratories, Carlsbad, NM.

Patterson, R. 2005a. Letter to Elizabeth Cotsworth (Subject: *Hanford Tank and K-Basin Wastes*). 8 March 2005. U.S. Department of Energy, Carlsbad Field Office, Carlsbad, NM.

Patterson, R. 2005b. Letter to Elizabeth Cotsworth (Subject: *Hanford Tank and K-Basin Wastes*). 11 May 2005. U.S. Department of Energy, Carlsbad Field Office, Carlsbad, NM.

Reed, D.J., J. Swanson, J.-F Lucchini, and M. Richman. 2013. *Intrinsic, Mineral and Microbial Colloid Enhancement Parameters for the WIPP Actinide Source Term*. ERMS 559200. LCO-ACP-18. Los Alamos National Laboratory, Carlsbad, NM.*

Roselle, G. 2013. *Determination of Corrosion Rates from Iron/Lead Corrosion Experiments to be used for Gas Generation Calculations* (Revision 1). ERMS 559077. Sandia National Laboratories, Carlsbad, NM.*

Stein, J.S. 2005. Memorandum to L.H. Brush (Subject: *Estimate of Volume of Brine in Repository That Leads to a Brine Release*). 13 April 2005. ERMS 539372. U.S. Department of Energy, Sandia National Laboratories, Albuquerque, NM.

U.S. Congress. 1996. Public Law 102-579. *Waste Isolation Pilot Plant Land Withdrawal Act of 1992*, as amended by Public Law 104-201, 1996.

U.S. Department of Energy (DOE). 1994. *Waste Isolation Pilot Plant Transuranic Waste Baseline Inventory Report* (Revision 0, June). 2 vols. CAO-94-1005. ERMS 503921. Carlsbad Area Office, Carlsbad, NM.

U.S. Department of Energy (DOE). 1995a. *Waste Isolation Pilot Plant Transuranic Waste Baseline Inventory Report* (Revision 1, February). DOE/CAO-94-1005. ERMS 243201. Carlsbad Area Office, Carlsbad, NM.

U.S. Department of Energy (DOE). 1995b. *Transuranic Waste Baseline Inventory Report* (Revision 2, December). DOE/CAO-95-1121. ERMS 531643. Carlsbad Area Office, Carlsbad, NM.

U.S. Department of Energy (DOE). 1996a. *Title 40 CFR Part 191 Compliance Certification Application for the Waste Isolation Pilot Plant* (October). 21 vols. DOE/CAO-1996-2184. Carlsbad Area Office, Carlsbad, NM.

U.S. Department of Energy (DOE). 1996b. *Transuranic Waste Baseline Inventory Report* (Revision 3, June). DOE/CAO-95-1121. ERMS 242330. Carlsbad Area Office, Carlsbad, NM.

U.S. Department of Energy (DOE). 1997. Supplemental Summary of EPA-Mandated Performance Assessment Verification Test (All Replicates) and Comparison with the Compliance Certification Application Calculations (August 8). WPO 46702. ERMS 414879. Carlsbad Area Office, Carlsbad, NM.

U.S. Department of Energy (DOE). 2002. *Contact-Handled Transuranic Waste Acceptance Criteria for the Waste Isolation Pilot Plant*. DOE/WIPP 02-3122. Carlsbad Area Office, Carlsbad, NM.

U.S. Department of Energy (DOE). 2003. *Remote-Handled TRU Waste Characterization Program Implementation Plan* (Revision 0D, October 30). DOE/WIPP 02-3214. Carlsbad Field Office, Carlsbad, NM.

U.S. Department of Energy (DOE). 2004. *Title 40 CFR Part 191 Compliance Recertification Application 2004* (March). 10 vols. DOE/WIPP 2004-3231. Carlsbad Field Office, Carlsbad, NM.

U.S. Department of Energy (DOE). 2005. *Performance Demonstration Program Plan for Nondestructive Assay of Drummed Wastes for the TRU Waste Characterization Program* (Revision 1, August). DOE/CBFO-01-1005. Carlsbad Field Office, Carlsbad, NM.

U.S. Department of Energy (DOE). 2006. *Transuranic Waste Baseline Inventory Report–2004* (September). DOE/TRU-2006-3344. Carlsbad Field Office, Carlsbad, NM.

U.S. Department of Energy (DOE). 2007. *Performance Demonstration Program Plan for Analysis of Simulated Headspace Gases* (Revision 6.1, November). DOE/CBFO-95-1076. Carlsbad Field Office, Carlsbad, NM.

U.S. Department of Energy (DOE). 2008a. *Annual Transuranic Waste Inventory Report–2007,* Revision 1 (April). DOE/TRU-2008-3379. Carlsbad Field Office, Carlsbad, NM.

U.S. Department of Energy (DOE). 2008b. *Annual Transuranic Waste Inventory Report–2008,* Revision 0 (December). DOE/TRU-2008-3425. Carlsbad Field Office, Carlsbad, NM.*

U.S. Department of Energy (DOE). 2008c. *Transuranic Waste Acceptance Criteria for the Waste Isolation Pilot Plant* (Revision 6.2, May 30). DOE/WIPP 02-3122. Carlsbad Field Office, Carlsbad, NM.

U.S. Department of Energy (DOE). 2008d. *WIPP Waste Information System User's Manual—WWIS Software Version 6.2* (May 15). DOE/CBFO-97-2273. Carlsbad Field Office, Carlsbad, NM.

U.S. Department of Energy (DOE). 2008e. *Performance Demonstration Program Plan for Nondestructive Assay of Boxed Wastes for the TRU Waste Characterization Program* (Revision 1, April). DOE/CBFO-01-1006. Carlsbad Field Office, Carlsbad, NM.

U.S. Department of Energy (DOE). 2009a. Appendix PA-2009 Section PA 4.2.5, Performance Assessment. *Title 40 CFR Part 191 Compliance Recertification Application 2009*. DOE/WIPP-2009-2225. Carlsbad Field Office, Carlsbad, NM.*

U.S. Department of Energy (DOE). 2009b. *Title 40 CFR Part 191 Compliance Recertification Application for the Waste Isolation Pilot Plant* (March). DOE/WIPP-09-3424. Carlsbad Field Office, Carlsbad, NM.*

U.S. Department of Energy (DOE). 2009c. Appendix MgO 2009, Section 6.2.4.4, Magnesium Oxide as an Engineered Barrier. *Title 40 CFR Part 191 Compliance Recertification Application 2009*. DOE/WIPP-2009-2225. Carlsbad Field Office, Carlsbad, NM.*

U.S. Department of Energy (DOE). 2009d. *Annual Transuranic Waste Inventory Report–2009,* Revision 0 (December). DOE/TRU-09-3425. Carlsbad Field Office, Carlsbad, NM.*

U.S. Department of Energy (DOE). 2010a. *Annual Transuranic Waste Inventory Report–2010,* Revision 0 (November). DOE/TRU-10-3425. Carlsbad Field Office, Carlsbad, NM.*

U.S. Department of Energy (DOE). 2010b. *Quality Assurance Program Document,* Revision 11 (June). DOE/CBFO-94-1012. Carlsbad Field Office, Carlsbad, NM.*

U.S. Department of Energy (DOE). 2010c. *Transuranic Waste Acceptance Criteria for the Waste Isolation Pilot Plant* (Revision 6.5, June 30). DOE/WIPP 02-3122. Carlsbad Field Office, Carlsbad, NM.*

U.S. Department of Energy (DOE). 2010d. *Performance Demonstration Program Plan for Analysis of Simulated Headspace Gases* (Revision 7, December). DOE/CBFO-95-1076. Carlsbad Field Office, Carlsbad, NM.*

U.S. Department of Energy (DOE). 2011a. *Annual Transuranic Waste Inventory Report–2011,* Revision 0 (November). DOE/TRU-11-3425. Carlsbad Field Office, Carlsbad, NM.*

U.S. Department of Energy (DOE). 2011b. *Remote-Handled TRU Waste Characterization Program Implementation Plan* (Revision 2, April 21). DOE/WIPP 02-3214. Carlsbad Field Office Carlsbad, NM.*

U.S. Department of Energy (DOE). 2011c. *Performance Demonstration Program Plan for Nondestructive Assay of Boxed Wastes for the TRU Waste Characterization Program* (Revision 3, May). DOE/CBFO-01-1006. Carlsbad Field Office, Carlsbad, NM.*

U.S. Department of Energy (DOE). 2011d. *Performance Demonstration Program Plan for Nondestructive Assay of Drummed Wastes for the TRU Waste Characterization Program* (Revision 3, June). DOE/CBFO-01-1005. Carlsbad Field Office, Carlsbad, NM.*

U.S. Department of Energy (DOE). 2012a. *Annual Transuranic Waste Inventory Report–2012,* Revision 0 (October). DOE/TRU-12-3425. Carlsbad Field Office, Carlsbad, NM.*

U.S. Department of Energy (DOE). 2012b. *Waste Data System User's Manual.* Revision 9 (July). DOE/WIPP-09-3427. Carlsbad Field Office, Carlsbad, NM.*

U.S. Department of Energy (DOE). 2013. *Waste Data System Data Dictionary* (March). Carlsbad Field Office, Carlsbad, NM.*

U.S. Environmental Protection Agency (EPA). 1993. "40 CFR Part 191: Environmental Radiation Protection Standards for the Management and Disposal of Spent Nuclear Fuel, High-Level and Transuranic Radioactive Wastes; Final Rule." *Federal Register,* vol. 58 (December 20, 1993): 66398–416.

U.S. Environmental Protection Agency (EPA). 1996. "40 CFR Part 194: Criteria for the Certification and Recertification of the Waste Isolation Pilot Plant's Compliance with the 40 CFR Part 191 Disposal Regulations; Final Rule." *Federal Register*, vol. 61 (February 9, 1996): 5223–45.

U.S. Environmental Protection Agency (EPA). 1998a. "40 CFR Part 194: Criteria for the Certification and Recertification of the Waste Isolation Pilot Plant's Compliance with the Disposal Regulations: Certification Decision; Final Rule." *Federal Register*, vol. 63 (May 18, 1998): 27353–406.

U.S. Environmental Protection Agency (EPA). 1998b. "CARD No. 24: Waste Characterization." *Compliance Application Review Documents for the Criteria for the Certification and Recertification of the Waste Isolation Pilot Plant's Compliance with the 40 CFR 191 Disposal Regulations: Final Certification Decision* (May) (pp. 24-1 through 24-102). Office of Radiation and Indoor Air, Washington, DC.

U.S. Environmental Protection Agency (EPA). 1998c. "CARD No. 23: Models and Computer Codes." *Compliance Application Review Documents for the Criteria for the Certification and Recertification of the Waste Isolation Pilot Plant's Compliance with the 40 CFR 191 Disposal Regulations: Final Certification Decision* (May) (pp. 23-1 through 23-93). Office of Radiation and Indoor Air, Washington, DC.

U.S. Environmental Protection Agency (EPA). 1998d. "CARD No. 22: Quality Assurance." *Compliance Application Review Documents for the Criteria for the Certification and Recertification of the Waste Isolation Pilot Plant's Compliance with the 40 CFR 191 Disposal Regulations: Final Certification Decision* (May) (pp. 22-1 through 22-32). Office of Radiation and Indoor Air, Washington, DC.

U.S. Environmental Protection Agency (EPA). 2005a. "40 CFR Part 194: Notification of Completeness of the Department of Energy's Compliance Recertification Application for the Waste Isolation Pilot Plant." *Federal Register*, vol. 70 (October 20, 2005): 61107–111.

U.S. Environmental Protection Agency (EPA). 2005b. Teleconference with U.S. Department of Energy (DOE), Sandia National Laboratories (SNL), and Los Alamos National Laboratory (LANL) (Subject: *Change in U(VI) Solubility Assumption to a Concentration to 1 M*). 2 March 2005.

U.S. Environmental Protection Agency (EPA). 2006a. "40 CFR Part 194: Criteria for the Certification and Recertification of the Waste Isolation Pilot Plant's Compliance with the Disposal Regulations: Recertification Decision" (Final Notice). *Federal Register*, vol. 71 (April 10, 2006): 18010–021.

U.S. Environmental Protection Agency (EPA). 2006b. "Recertification CARD No. 22: Quality Assurance." *Compliance Application Review Documents for the Criteria for the Certification and Recertification of the Waste Isolation Pilot Plant's Compliance with the 40 CFR 191 Disposal Regulations: Final Recertification Decision* (March) (pp. 22-1 through 22-17). Office of Radiation and Indoor Air, Washington, DC.

U.S. Environmental Protection Agency (EPA). 2006c. *Technical Support Document for Section 194.24: Evaluation of the Compliance Recertification Actinide Source Term and Culebra Dolomite Distribution Coefficient Values* (March). Office of Radiation and Indoor Air, Washington, DC.

U.S. Environmental Protection Agency (EPA). 2006d. "Recertification CARD No. 24: Waste Characterization." *Compliance Application Review Documents for the Criteria for the Certification and Recertification of the Waste Isolation Pilot Plant's Compliance with the 40 CFR 191 Disposal Regulations: Final Recertification Decision* (March) (pp. 24-1 through 24-50). Office of Air and Radiation, Washington, DC.

U.S. Environmental Protection Agency (EPA). 2006e. *Technical Support Document for Section 194.24: Review of the Baseline Inventory Used in the Compliance Recertification Application and the Performance Assessment Baseline Calculation* (March). Office of Air and Radiation, Washington, DC.

U.S. Environmental Protection Agency (EPA). 2006f. *Technical Support Document for Section 194.23: Review of the 2004 Compliance Recertification Performance Assessment Baseline Calculation* (March). Office of Air and Radiation, Washington, DC.

U.S. Environmental Protection Agency (EPA). 2010a. *Notification of Completeness of the Department of Energy's Compliance Recertification Application for the Waste Isolation Pilot*, Federal Register/Vol. 75, No. 136, pp. 41421 – 41424. Office of Air and Radiation, Washington, DC.*

U.S. Environmental Protection Agency (EPA). 2010b. "Criteria for the Certification and Recertification of the Waste Isolation Pilot Plant's Compliance with the Disposal Regulation: Recertification Decision," *Federal Register*,Vol. 75, No. 222, pp. 70548 – 70595 [EPA-HQ-OAR-2009-0330; FRL-9227-4]. Office of Air and Radiation, Washington, DC.*

U.S. Environmental Protection Agency (EPA). 2010c. *2009 Compliance Recertification Application (2009 CRA) Compliance Application Review Document (CARD) No. 24, Waste Characterization*. Office of Radiation and Indoor Air, Washington, DC.*

U.S. Environmental Protection Agency (EPA). 2010d. *2009 Compliance Recertification Application (2009 CRA) Compliance Application Review Document (CARD) No. 08: Approval Process for Waste Shipment from Waste Generator Sites for Disposal at WIPP*. Office of Radiation and Indoor Air, Washington, DC.*

Van Soest, G. 2012. *Performance Assessment Inventory Report–2012*. (Revision 0, November). INV-PA-12, LA-UR-12-26643, INV-1211-05-01-01. Los Alamos National Laboratory, Carlsbad, NM.*

Vugrin, E.D., M.B. Nemer, and S.W. Wagner. 2006. *Uncertainties Affecting MgO Effectiveness and Calculation of the MgO Effective Excess Factor* (Revision 0, November 17). Sandia National Laboratories, Carlsbad, NM.

Wang, Y., and L. Brush. 1996. Memorandum to M. Tierney (Subject: *Estimates of Gas-Generation Parameters for the Long-Term WIPP Performance Assessment*). 26 January 1996. ERMS 231943. U.S. Department of Energy, Sandia National Laboratories, Albuquerque, NM.

Xiong, Y. 2005. E-mail to J.F. Kanney and J.J. Long (Subject: *Release of FMT_050405.CHEMDAT*). 5 April 2005. ERMS 539304. U.S. Department of Energy, Sandia National Laboratories, Carlsbad, NM.

Xiong, Y., E.J. Nowak, and L.H. Brush. 2005. *Updated Uncertainty Analysis of Actinide Solubilities For the Response to EPA Comment C-23-16, Rev. 1* (April 28). ERMS 539595 (supersedes ERMS 538219). Sandia National Laboratories, Carlsbad, NM.

Xiong, Y., L.H. Brush, A.E. Ismail, and J.J. Long. 2009. *Uncertainty Analysis of Actinide Solubilities for the WIPP CRA-2009 PABC*. ERMS 552500. Sandia National Laboratories, Carlsbad, NM.*

Title 40 CFR Part 191
Subparts B and C
Compliance Recertification Application 2014
for the
Waste Isolation Pilot Plant

Future State Assumptions
(40 CFR § 194.25)

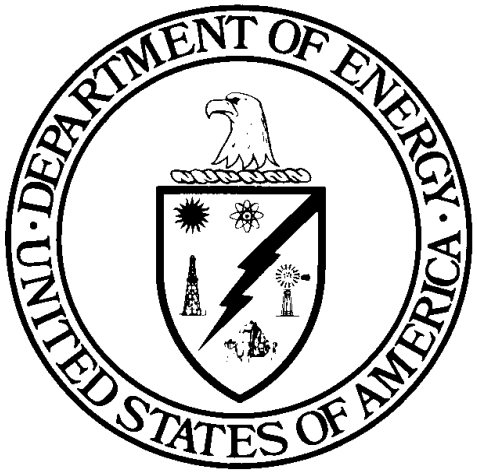

United States Department of Energy
Waste Isolation Pilot Plant

Carlsbad Field Office
Carlsbad, New Mexico

Compliance Recertification Application 2014
Future State Assumptions
(40 CFR § 194.25)

Table of Contents

List of Tables

This page intentionally left blank.

Acronyms and Abbreviations

CARD	Compliance Application Review Document
CCA	Compliance Certification Application
CFR	Code of Federal Regulations
CRA	Compliance Recertification Application
DOE	U.S. Department of Energy
DP	disturbed performance
EPA	U.S. Environmental Protection Agency
FEP	feature, event, and process
PA	performance assessment
T-field	transmissivity field
UP	undisturbed performance
WIPP	Waste Isolation Pilot Plant

This page intentionally left blank.

25.0 Future State Assumptions (40 CFR § 194.25)

25.1 Requirements

> § 194.25 Future State Assumptions
>
> (a) Unless otherwise specified in this part or in the disposal regulations, performance assessments and compliance assessments conducted pursuant to the provisions of this part to demonstrate compliance with § 191.13, § 191.15 and part 191, subpart C shall assume that characteristics of the future remain what they are at the time the compliance application is prepared, provided that such characteristics are not related to hydrogeologic, geologic or climatic conditions.
>
> (b) In considering future states pursuant to this section, the Department shall document in any compliance application, to the extent practicable, effects of potential future hydrogeologic, geologic and climatic conditions on the disposal system over the regulatory time frame. Such documentation shall be part of the activities undertaken pursuant to § 194.14, Content of compliance certification application; § 194.32, Scope of performance assessments; and § 194.54, Scope of compliance assessments.
>
> (1) In considering the effects of hydrogeologic conditions on the disposal system, the Department shall document in any compliance application, to the extent practicable, the effects of potential changes to hydrogeologic conditions.
>
> (2) In considering the effects of geologic conditions on the disposal system, the Department shall document in any compliance application, to the extent practicable, the effects of potential changes to geologic conditions, including, but not limited to: Dissolution; near surface geomorphic features and processes; and related subsidence in the geologic units of the disposal system.
>
> (3) In considering the effects of climatic conditions on the disposal system, the Department shall document in any compliance application, to the extent practicable, the effects of potential changes to future climate cycles of increased precipitation (as compared to the present conditions).

25.2 Background

The U.S. Environmental Protection Agency's (EPA's) purpose in issuing the Compliance Criteria at 40 CFR § 194.25 (U.S. EPA 1996) was to minimize the impact of inherently conjectural specifications of future states on the compliance application. The EPA has found no acceptable methodology to predict the future state of society, science, languages, or other characteristics of mankind. However, the EPA does believe that established scientific methods can make plausible predictions regarding the future state of geologic, hydrogeologic, and climatic conditions. Therefore, section 194.25 stipulates that the future state will resemble present conditions except for those relating to hydrogeologic, geologic, and climatic conditions. For example, the population density and land ownership patterns in the Waste Isolation Pilot Plant's (WIPP's) surrounding regions are assumed to remain consistent with today's conditions for the next 10,000 years. However, section 194.25 requires that performance and compliance assessments include dynamic analyses of changes in the geology, hydrology, and climatic conditions during the regulatory time frame.

25.3 1998 Certification Decision

Future state assumptions that are relevant to 40 CFR § 194.25(a) and may affect the containment of waste were identified by the U.S. Department of Energy (DOE) in the Compliance Certification Application (CCA), Chapter 6.0, Section 6.2 and Appendices SCR and MASS (U.S. DOE 1996). Many of these future state assumptions were derived from the development of

features, events, and processes (FEPs) that are potentially relevant to the performance of the waste disposal system, and can be found in the CCA, Appendix SCR (e.g., solution mining and anthropogenic climate changes). FEPs are screened using specific criteria to determine what phenomena and components of the disposal system can and should be dealt with in performance assessment (PA) calculations.

In its certification decision, the EPA first determined whether all FEPs and appropriate future state assumptions were identified and developed by the DOE. The EPA then evaluated the DOE's criteria to eliminate (screen out) inapplicable or irrelevant FEPs and associated assumptions. The EPA also analyzed whether there were potential variations in the DOE's assumed characteristics and determined whether the future state assumptions were in compliance with section 194.25(a).

The EPA's CCA review found no potentially significant omissions in the lists of FEPs, and no major inadequacies in the CCA's descriptions of FEPs and related future state assumptions. The EPA concluded that the DOE adequately described all the future state assumptions applicable under section 194.25(a) (U.S. EPA 1998a).

To comply with 40 CFR §§ 194.25(b)(1), (b)(2), and (b)(3), the DOE identified and described the hydrogeologic FEPs and related future state assumptions retained for further evaluation and inclusion in PA calculations in the CCA, Chapter 6.0, Section 6.3. The DOE described the effects of potential changes to hydrogeologic conditions on the disposal system in the CCA, Chapter 6.0, Sections 6.4.6 and 6.4.9 and Appendices SCR, TFIELD, and MASS. The DOE described the effects of potential changes to geologic conditions on the disposal system in the CCA, Chapter 6.0, Sections 6.2, 6.4.6, 6.5.4, and Appendices SCR and MASS. The DOE identified and described the effects of potential changes to future climate cycles of increased precipitation on the repository in the CCA, Chapter 6.0, Section 6.4.9.

The EPA concluded that the DOE adequately addressed the impacts of potential hydrogeologic, geologic, and climate changes to the disposal system (U.S. EPA 1998a). The EPA further stated that the CCA included all relevant elements of the PA and compliance assessments and was consistent with the requirements of section 194.25.

25.4 Changes in the CRA-2004

For the 2004 Compliance Recertification Application (CRA-2004), the DOE reevaluated all WIPP FEPs and made improvements and clarifications to several FEP descriptions, arguments, and screening decisions. The results of the FEPs reassessment were presented in Appendix PA-2004, Attachment SCR (U.S. DOE 2004). Table SCR-1 summarized these changes in the CRA-2004.

25.5 EPA's Evaluation of Compliance for the 2004 Recertification

To evaluate compliance with section 194.25 requirements, the EPA reviewed the CRA-2004 documentation, including Chapters 2.0, 6.0, 7.0, and 9.0; Appendix PA, Attachment SCR; Attachment TFIELD; and Attachment MASS. As in the 1998 Certification Decision (U.S. EPA 1998b), the EPA first determined whether all FEPs and appropriate future state assumptions were

identified and developed by the DOE. The EPA then evaluated the DOE's criteria to eliminate (screen out) inapplicable or irrelevant FEPs and associated assumptions. The EPA also analyzed whether there were potential variations in the DOE's assumed characteristics and determined whether the future state assumptions were in compliance with section 194.25(a).

25.5.1 40 CFR § 194.25(a)

The EPA verified that all appropriate FEPs were included in the list provided by the DOE for section 194.25(a). The EPA reviewed any changes in FEPs, including all screened-in and screened-out FEPs related to future states, to verify that their selections were made correctly. The EPA's FEPs review is documented in the CRA-2004 Technical Support Document for section 194.25, 40 CFR § 194.32, and 40 CFR § 194.33 (U.S. EPA 2006a).

25.5.2 40 CFR § 194.25(b)(1)

The EPA reexamined any hydrogeologic conditions that may have changed since the CCA review. The EPA determined that the DOE's review of FEPs related to hydrogeologic conditions and screening arguments was complete and that the conclusions drawn were appropriate. Changes in the hydrology at and around the WIPP site, such as water level changes in monitor wells and changes in potash mining, were appropriately included in PA modeling by updated changes in the Culebra Dolomite Member of the Rustler Formation (hereafter referred to as the Culebra) transmissivity fields (T-fields). See the CRA-2004 Compliance Application Review Document (CARD) 25 for more information (U.S. EPA 2006b).

25.5.3 40 CFR § 194.25(b)(2)

The EPA reexamined the DOE's characterization of future geologic conditions in the CRA-2004 documents (U.S. EPA 2006a). The EPA reexamined issues that were reviewed during the CCA, such as tectonics and deformation assumptions; fracture development and fault movement; ground shaking and seismic assumptions; volcanic and magmatic activity; metamorphic activity; shallow, lateral, and deep dissolution assumptions; and mineralization assumptions. The EPA also reviewed the CRA-2004 screening arguments related to geological screening decisions. The EPA determined that the DOE's geologic screening arguments were reasonable and adequate.

25.5.4 40 CFR § 194.25(b)(3)

As in the CCA, the EPA's review of climatic condition changes focused on applicable FEPs. The EPA found that new information since the CCA did not impact FEPs or screening decisions related to climate change (U.S. EPA 2006b).

25.5.5 EPA's Determination of Compliance for the 2004 Recertification

Based on a review and evaluation of the CRA-2004, Chapters 2.0, 6.0, 7.0, and 9.0; Appendix PA, Attachment SCR; Attachment TFIELD; Attachment MASS; and an assessment of changes since 1998, the EPA determined that the DOE continued to comply with the requirements of section 194.25 (U.S. EPA 2006c).

25.6 Changes or New Information Between the CRA-2004 and the CRA-2009 (Previously: Changes or New Information Since the 2004 Recertification)

25.6.1 40 CFR § 194.25(a)

The DOE reevaluated the basis of the WIPP FEPs for the CRA-2009 (U.S. DOE 2009). The results of this reevaluation are found in Appendix SCR-2009. Conclusions drawn from Appendix SCR-2009 were also summarized in Section 32 of the CRA-2009.

As described in Appendix SCR-2009, no screening decisions previously made using the future state assumption in section 194.25(a) were changed (although additional information may have been added to their descriptions); 16 FEPs were screened out based on this provision. Table 25-1 lists the 16 FEPs eliminated from PA calculations using the future state assumption.

Because there were no changes to the conditions and bases for FEPs screened out using the future state assumption, the DOE continued to be in compliance with the requirements of section 194.25(a).

25.6.2 40 CFR § 194.25(b)

40 CFR § 194.25(b) requires consideration of future hydrogeologic, geologic, and climate conditions during the regulatory time frame. Table 25-2 lists those FEPs that were screened into PA calculations according to the criteria in section 194.25(b). There were no changes to the screening decisions for those FEPs that represent the hydrogeologic, geologic, and climatic conditions in the future; they continued to be represented in performance calculations.

Section 1 of Clayton (Clayton 2008) lists the changes to the PA system used for the CRA-2009 calculations. None of the changes made for the CRA-2009 performance calculations affected the implementation of the FEPs screened in according to section 194.25(b).

In summary, no changes were made to screening decisions for those FEPs that represent the hydrologic, geologic, and climate-related conditions for the WIPP, and no changes were made to the representation of these elements within the PA system. Therefore, the DOE remained in compliance with the requirements of sections 194.25(b)(1), (b)(2), and (b)(3).

Table 25-1. FEPs Screened Out Using the 40 CFR § 194.25(a) Criterion[a]

EPA FEP I.D.	FEP Name	Change Summary
H6	Archeological investigations	None
H7	Drilling associated with thermal energy production	None
H10	Liquid waste disposal	None
H11	Hydrocarbon storage	None
H14	Mining for other resources (not potash)	None
H15	Excavation activities associated with tunneling	None
H16	Construction of underground facilities	None
H40	Changes in land use	None
H47	Anthropogenic climate change – Greenhouse gas effects	None
H48	Anthropogenic climate change – Acid rain	None
H49	Anthropogenic climate change – Damage to the ozone layer	None
H53	Changes in agricultural practices – Arable farming	None
H54	Changes in agricultural practices – Ranching	None
H55	Changes in agricultural practices – Fish farming	None
H56	Demographic change, urban developments, and technological developments	None
H58	Solution mining – Potash	None

[a] These screening classifications are consistent with current screening arguments and classifications as presented in Appendix SCR-2009.

Table 25-2. FEPs Screened In According to 40 CFR § 194.25(b)[a]

EPA FEP I.D.	FEP Name	Issue	Screening Classification	Method of Representation In PA
N1	***Stratigraphy***	Deposition and properties of geological formations in control of system performance.	Included in the Undisturbed Performance (UP) scenario	BRAGFLO grid incorporates relevant stratigraphic units.
N2	***Brine reservoirs***	Pressurized brine reservoirs may be present in the Castile Formation beneath the controlled area.	Included in the Disturbed Performance (DP) scenarios	The potential for brine pocket intrusion is represented by the parameter PBRINE in the E1 scenario.
N16	***Shallow Dissolution***	Percolation of groundwater and dissolution in the Rustler Formation may increase transmissivity.	UP	The effects of shallow dissolution, as in Nash Draw, on the transmissivity of the Culebra are represented in the Culebra T-field generation and calibration process.

[a] There have been no technical changes to this information since the CRA-2004, other than the correction of errors.

Table 25-2. FEPs Screened In According to 40 CFR § 194.25(b)[a] (Continued)

EPA FEP I.D.	FEP Name	Issue	Screening Classification	Method of Representation In PA
N23	***Saturated Groundwater Flow***	Groundwater flow beneath the water table is important to disposal system performance.	UP	Groundwater flow is represented by the Culebra T-fields.
N24	***Unsaturated Groundwater Flow***	The presence of air or other gas phases may influence groundwater flow.	UP	Unsaturated flow is a precursor to recharge to the Culebra, which is accounted for in the boundary conditions for the Culebra T=fields.
N25	***Fracture Flow***	Groundwater may flow along fractures as well as through interconnected pore space.	UP	Fracture flow is represented by the dual-porosity Culebra transport model.
N27	***Effects of Preferential Pathways***	Groundwater flow may not be uniform, and may occur along particular pathways.	UP	Preferential pathways are accounted for in the calibration of Culebra T-fields to transient hydraulic test responses.
N33	***Groundwater Geochemistry***	Groundwater geochemistry influences actinide retardation and colloid stability.	UP	Salado and Castile brine geochemistry are accounted for in actinide solubility values. Culebra brine geochemistry is accounted for in the retardation factors used in PA calculations of actinide transport.
N39	***Physiography***	The physiography of the area is a control on the surface water hydrology.	UP	Relevant aspects of the physiography are incorporated in the Culebra T-fields.
N53	***Groundwater Discharge***	The amount of water leaving the groundwater system to rivers, springs, and seeps affects the groundwater hydrology.	UP	Groundwater discharge is accounted for in the boundary conditions for the Culebra T-fields.
N54	***Groundwater Recharge***	The amount of water passing into the saturated zone affects the groundwater hydrology.	UP	Groundwater recharge is accounted for in the boundary conditions for the Culebra T-fields.
N55	***Infiltration***	The amount of water entering the unsaturated zone controls groundwater recharge.	UP	Infiltration is accounted for in the boundary conditions for the Culebra T-fields.

[a] There have been no technical changes to this information since the CRA-2004, other than the correction of errors.

Table 25-2. FEPs Screened In According to 40 CFR § 194.25(b)[a] (Continued)

EPA FEP I.D.	FEP Name	Issue	Screening Classification	Method of Representation In PA
N56	***Changes in Groundwater Recharge and Discharge***	Changes in climate and drainage pattern may affect the amount of water entering and leaving the groundwater system.	UP	Changes in groundwater recharge and discharge are accounted for in the Climate Index factor.
N59	***Precipitation (e.g., Rainfall)***	Rainfall is the source of water for infiltration and stream flow.	UP	Future variations in precipitation are accounted for in the Climate Index factor.
N60	***Temperature***	The temperature influences how much precipitation evaporates before it reaches streams or enters the ground.	UP	Future variations in temperature are accounted for in the Climate Index factor.
N61	***Climate Change***	Temperature and precipitation will vary as natural changes in the climate take place.	UP	Future climate change is accounted for in the Climate Index factor.

[a] There have been no technical changes to this information since the CRA-2004, other than the correction of errors.

25.7 EPA's Evaluation of Compliance for the 2009 Recertification

The EPA verified that all appropriate FEPs were included in the list provided by the DOE for section 194.25 (a): future states remained the same, none changed for the CRA-2009. The EPA reviewed any changes in FEPs, including all screened-in and screened-out FEPs related to future states to verify that their selection was made correctly. There were no changes in the hydrogeologic conditions for the CRA-2009. The EPA concluded that the DOE's review of FEPs related to the hydrogeologic conditions and their screening arguments was complete and accurate and found the DOE to be in compliance with section 194.25(b)(1). The EPA also reviewed the CRA-2009 screening arguments related to geological screening decisions. These arguments had not changed. The EPA determined that the DOE's geological screening arguments were reasonable and adequate and found them to be in compliance with section 194.25(b)(2). The EPA's review of climatic conditions focused on related FEPs, none of which changed for the CRA-2009. The EPA found that new information did not impact FEPs or screening decisions related to climate change, and that the DOE was in compliance with section 194.25(b)(3) (U.S. EPA 2010).

25.8 Changes or New Information Since the CRA-2009

25.8.1 40 CFR § 194.25(a)

The DOE reevaluated the basis of the WIPP FEPs for the CRA-2014 (Kirkes 2013) and presents the results of this reevaluation in Appendix SCR-2014. Updates to screening arguments and decisions are presented in Appendix SCR-2014 and are also summarized in Section 32.

As described in Appendix SCR-2014, no screening decisions previously made using the future state assumption in section 194.25(a) have changed (although additional information has been added to the discussion of FEP H58, "Solution Mining for Potash"). There continue to be 16 FEPs screened out based on the provision of 40 CFR 194.25(a), as shown in Table 25-3.

Table 25-3. FEPs Screened Out Using the 40 CFR § 194.25(a) Criterion[a]

EPA FEP I.D.	FEP Name	Change Summary
H6	Archeological investigations	None
H7	Drilling associated with thermal energy production	None
H10	Liquid waste disposal	None
H11	Hydrocarbon storage	None
H14	Mining for other resources (not potash)	None
H15	Excavation activities associated with tunneling	None
H16	Construction of underground facilities	None
H40	Changes in land use	None
H47	Anthropogenic climate change – Greenhouse gas effects	None
H48	Anthropogenic climate change – Acid rain	None
H49	Anthropogenic climate change – Damage to the ozone layer	None
H53	Changes in agricultural practices – Arable farming	None
H54	Changes in agricultural practices – Ranching	None
H55	Changes in agricultural practices – Fish farming	None
H56	Demographic change, urban developments, and technological developments	None
H58	Solution mining – Potash	Screening argument updated to describe solution mining project just outside Delaware Basin boundary.

[a] These screening classifications are consistent with current screening arguments and classifications as presented in Appendix SCR-2014.

25.8.2 40 CFR § 194.25(b)

There are no changes to the screening decisions for those FEPs that represent the hydrogeologic, geologic, and climatic conditions in the future; they continue to be represented in performance

calculations. The implementation of FEP N2, "Brine Reservoirs," has been changed by updating the probability distribution of intercepting pressurized brine beneath the repository, see (Camphouse 2013). However, as previously stated, this change does not impact the screening decision; FEP N2 remains screened in and is accounted for in PA calculations. Table 25-4 lists those FEPs that relate to the future state of the repository for hydrogeologic, geologic, and climatic conditions.

Table 25-4. FEPs Screened In According to 40 CFR § 194.25(b)

EPA FEP I.D.	FEP Name	Issue	Screening Classification	Method of Representation In PA
N1	***Stratigraphy***	Deposition and properties of geological formations in control of system performance.	Included in the UP scenario	BRAGFLO grid incorporates relevant stratigraphic units.
N2	***Brine reservoirs***	Pressurized brine reservoirs may be present in the Castile beneath the controlled area.	Included in the DP scenarios	The potential for brine pocket intrusion is represented by the parameter PBRINE in the E1 scenario.
N16	***Shallow Dissolution***	Percolation of groundwater and dissolution in the Rustler may increase transmissivity.	UP	The effects of shallow dissolution, as in Nash Draw, on the transmissivity of the Culebra are represented in the Culebra T-field generation and calibration process.
N23	***Saturated Groundwater Flow***	Groundwater flow beneath the water table is important to disposal system performance.	UP	Groundwater flow is represented by the Culebra T-fields.
N24	***Unsaturated Groundwater Flow***	The presence of air or other gas phases may influence groundwater flow.	UP	Unsaturated flow is a precursor to recharge to the Culebra, which is accounted for in the boundary conditions for the Culebra T-fields.
N25	***Fracture Flow***	Groundwater may flow along fractures as well as through interconnected pore space.	UP	Fracture flow is represented by the dual-porosity Culebra transport model.
N27	***Effects of Preferential Pathways***	Groundwater flow may not be uniform, and may occur along particular pathways.	UP	Preferential pathways are accounted for in the calibration of Culebra T-fields to transient hydraulic test responses.

Table 25-4. FEPs Screened In According to 40 CFR § 194.25(b)

EPA FEP I.D.	FEP Name	Issue	Screening Classification	Method of Representation In PA
N33	***Groundwater Geochemistry***	Groundwater geochemistry influences actinide retardation and colloid stability.	UP	Salado and Castile brine geochemistry are accounted for in actinide solubility values. Culebra brine geochemistry is accounted for in the retardation factors used in PA calculations of actinide transport.
N39	***Physiography***	The physiography of the area is a control on the surface water hydrology.	UP	Relevant aspects of the physiography are incorporated in the Culebra T-fields.
N53	***Groundwater Discharge***	The amount of water leaving the groundwater system to rivers, springs, and seeps affects the groundwater hydrology.	UP	Groundwater discharge is accounted for in the boundary conditions for the Culebra T-fields.
N54	***Groundwater Recharge***	The amount of water passing into the saturated zone affects the groundwater hydrology.	UP	Groundwater recharge is accounted for in the boundary conditions for the Culebra T-fields.
N55	***Infiltration***	The amount of water entering the unsaturated zone controls groundwater recharge.	UP	Infiltration is accounted for in the boundary conditions for the Culebra T-fields.
N56	***Changes in Groundwater Recharge and Discharge***	Changes in climate and drainage pattern may affect the amount of water entering and leaving the groundwater system.	UP	Changes in groundwater recharge and discharge are accounted for in the Climate Index factor.
N59	***Precipitation (e.g., Rainfall)***	Rainfall is the source of water for infiltration and stream flow.	UP	Future variations in precipitation are accounted for in the Climate Index factor.
N60	***Temperature***	The temperature influences how much precipitation evaporates before it reaches streams or enters the ground.	UP	Future variations in temperature are accounted for in the Climate Index factor.
N61	***Climate Change***	Temperature and precipitation will vary as natural changes in the climate take place.	UP	Future climate change is accounted for in the Climate Index factor.

1

In summary, no changes have been made to screening decisions for those FEPs that represent the hydrologic, geologic, and climate-related conditions for the WIPP. There are no changes made to the representation of these elements within the PA system for the CRA-2014 with respect to the requirements of 40 CFR 194.25(b). Therefore, the DOE remains in compliance with the requirements of sections 194.25(b)(1), (b)(2), and (b)(3).

25.9 References

(*Indicates a reference that has not been previously submitted.)

Camphouse, C. 2013. *Analysis Plan for the 2014 Compliance Recertification Application Performance Assessment.* (January 31, 2013). ERMS 559198. Carlsbad, NM: Sandia National Laboratories.*

Clayton, D.J. 2008. *Analysis Plan for the Performance Assessment for the 2009 Compliance Recertification Application* (Revision 1). AP-137. (January 22, 2008). ERMS 547905. Carlsbad, NM: Sandia National Laboratories.

Kirkes, G.R. 2013. *Features, Events and Processes Assessment for the Compliance Recertification Application—2014* (Revision 0). ERMS 560488. Carlsbad, NM: Sandia National Laboratories.

U.S. DOE. 1996. *Title 40 CFR Part 191 Compliance Certification Application for the Waste Isolation Pilot Plant* (October). 21 vols. DOE/CAO 1996-2184. Carlsbad, NM: Carlsbad Area Office.

U.S. DOE. 2004. *Title 40 CFR Part 191 Compliance Recertification Application for the Waste Isolation Pilot Plant* (March). 10 vols. DOE/WIPP 2004-3231. Carlsbad, NM: Carlsbad Field Office.

U.S. DOE. 2009. *Title 40 CFR Part 191 Compliance Recertification Application for the Waste Isolation Pilot Plant* (March). DOE/WIPP 2009-3424. Carlsbad, NM: Carlsbad Field Office.

U.S. EPA. 1996. "40 CFR Part 194: Criteria for the Certification and Recertification of the Waste Isolation Pilot Plant's Compliance with the 40 CFR Part 191 Disposal Regulations; Final Rule." *Federal Register*, vol. 61 (February 9, 1996): 5223–45.

U.S. EPA. 1998a. "CARD No. 25: Future State Assumptions." *Compliance Application Review Documents for the Criteria for the Certification and Recertification of the Waste Isolation Pilot Plant's Compliance with the 40 CFR Part 191 Disposal Regulations: Final Certification Decision* (May) (pp. 25-1 through 25-14). Washington, DC: Office of Radiation and Indoor Air.

U.S. EPA. 1998b. "40 CFR Part 194: Criteria for the Certification and Recertification of the Waste Isolation Pilot Plant's Compliance with the 40 CFR Part 191 Disposal Regulations: Certification Decision; Final Rule." *Federal Register*, vol. 63 (May 18, 1998): 27353–406.

U.S. EPA. 2006a. *Technical Support Documents for Sections 194.25, 194.32, and 194.33: Compliance Recertification Application Review of Features, Events, and Processes* (March). Washington, DC: Office of Radiation and Indoor Air.

U.S. EPA. 2006b. "Recertification CARD No. 25: Future State Assumptions." *Compliance Application Review Documents for the Criteria for the Certification and Recertification of the Waste Isolation Pilot Plant's Compliance with the 40 CFR 191 Disposal Regulations: Final Recertification Decision* (March) (pp. 25-1 through 25-5). Washington, DC: Office of Radiation and Indoor Air.

U.S. EPA. 2006c. "40 CFR Part 194: Criteria for the Certification and Recertification of the Waste Isolation Pilot Plant's Compliance with the 40 CFR Part 191 Disposal Regulations: Recertification Decision" (Final Notice). *Federal Register,* vol. 71 (April 10, 2006): 18010-021.

U.S. EPA. 2010 "2009 Compliance Recertification Application (2009 CRA) Compliance Application Review Document (CARD) No. 25, Future State Assumptions." EPA Docket FDMS Docket ID No. EPA-HQ-OAR-2009-0330. Washington, DC: Office of Radiation and Indoor Air. http://www.epa.gov/radiation/wipp/2010recertification.html.*

Title 40 CFR Part 191
Subparts B and C
Compliance Recertification Application 2014
for the
Waste Isolation Pilot Plant

Expert Judgment
(40 CFR § 194.26)

United States Department of Energy
Waste Isolation Pilot Plant

Carlsbad Field Office
Carlsbad, New Mexico

Compliance Recertification Application 2014
Expert Judgment
(40 CFR § 194.26)

Table of Contents

This page intentionally left blank.

Acronyms and Abbreviations

CARD	Compliance Application Review Document
CCA	Compliance Certification Application
CFR	Code of Federal Regulations
CRA	Compliance Recertification Application
DOE	U.S. Department of Energy
EPA	U.S. Environmental Protection Agency
PA	performance assessment
PIC	passive institutional control
WIPP	Waste Isolation Pilot Plant

This page intentionally left blank.

26.0 Expert Judgment (40 CFR § 194.26)

26.1 Requirements

§ 194.26 Expert Judgment

(a) Expert judgment, by an individual expert or panel of experts, may be used to support any compliance application, provided that expert judgment does not substitute for information that could reasonably be obtained through data collection or experimentation.

(b) Any compliance application shall:

(1) Identify any expert judgments used to support the application and shall identify experts (by name and employer) involved in any expert judgment elicitation processes used to support the application.

(2) Describe the process of eliciting expert judgment, and document the results of expert judgment elicitation processes and the reasoning behind those results. Documentation of interviews used to elicit judgments from experts, the questions or issues presented for elicitation of expert judgment, background information provided to experts, and deliberations and formal interactions among experts shall be provided. The opinions of all experts involved in each elicitation process shall be provided whether the opinions are used to support compliance applications or not.

(3) Provide documentation that the following restrictions and guidelines have been applied to any selection of individuals used to elicit expert judgments:

(i) Individuals who are members of the team of investigators requesting the judgment or the team of investigators who will use the judgment were not selected; and

(ii) Individuals who maintain, at any organizational level, a supervisory role or who are supervised by those who will utilize the judgment were not selected.

(4) Provide information which demonstrates that:

(i) The expertise of any individual involved in expert judgment elicitation comports with the level of knowledge required by the questions or issues presented to that individual; and

(ii) The expertise of any expert panel, as a whole, involved in expert judgment elicitation comports with the level and variety of knowledge required by the questions or issues presented to that panel.

(5) Explain the relationship among the information and issues presented to experts prior to the elicitation process, the elicited judgment of any expert panel or individual, and the purpose for which the expert judgment is being used in compliance applications(s) [*sic*].

(6) Provide documentation that the initial purpose for which expert judgment was intended, as presented to the expert panel, is consistent with the purpose for which this judgment was used in compliance application(s).

(7) Provide documentation that the following restrictions and guidelines have been applied in eliciting expert judgment:

(i) At least five individuals shall be used in any expert elicitation process, unless there is a lack or unavailability of experts and a documented rationale is provided that explains why fewer than five individuals were selected.

(ii) At least two-thirds of the experts involved in an elicitation shall consist of individuals who are not employed directly by the Department or by the Department's contractors, unless the Department can demonstrate and document that there is a lack or unavailability of qualified independent experts. If so demonstrated, at least one third of the experts involved in an elicitation shall consist of individuals who are not employed directly by the Department or by the Department's contractors.

(c) The public shall be afforded a reasonable opportunity to present its scientific and technical views to expert panels as input to any expert elicitation process.

26.2 Background

According to 40 CFR § 194.26 (U.S. EPA 1996), the expert judgment by an individual expert or panel of experts may be used to support any compliance application, provided that expert judgment does not substitute for information that could reasonably be obtained through data collection or experimentation.

The U.S. Environmental Protection Agency's (EPA's) Certification Decision (U.S. EPA 1998a) provides the following explanation of the use of the expert judgment process in demonstrating compliance with 40 CFR Part 194 (U.S. EPA 1996):

> The requirements of 40 CFR § 194.26 apply to expert judgment elicitation. Expert judgment is typically used to elicit two types of information: numerical values for parameters (variables) that are measurable only by experiments that cannot be conducted due to limitations of time, money, and physical situation; and essentially unknowable information, such as which features should be incorporated into passive institutional controls to deter human intrusion into the repository (61 FR 5228). Quality assurance (QA) requirements (specifically 40 CFR § 194.22(a)(2)(v)) must be applied to any expert judgment to verify that the procedures for conducting and documenting the expert elicitation have been followed.
>
> The requirements of 40 CFR Part 194 prohibit expert judgment from being used in place of experimental data, unless the Department of Energy (DOE) can justify that the necessary experiments cannot be conducted. Expert judgment may substitute for experimental data only in those instances in which limitations of time, resources, or physical setting preclude the successful or timely collection of data.

26.3 1998 Certification Decision

26.3.1 Expert Judgment for Performance Assessment Parameters

The Compliance Certification Application (CCA) (U.S. DOE 1996) does not identify any formal expert judgment activities related to the performance assessment (PA) parameters. During the EPA's review of the PA parameters, the EPA found inadequate explanation and information for 149 parameters that the U.S. Department of Energy (DOE) claimed had been derived using professional judgment. The compliance criteria do not provide for utilization of "professional judgment." Input parameters are to be derived from data collection, experimentation, or expert elicitation. The EPA requested that the DOE provide additional information on the derivation of the 149 parameters (Trovato 1997a;Trovato 1997b;Trovato 1997c).

The DOE responded to the EPA's request by adding information to and improving the quality of the records to enhance the traceability of parameter values. The EPA deemed the documentation provided by the DOE adequate to demonstrate proper derivation of all but one of the professional judgment parameters—the waste particle size distribution parameter. The EPA required the DOE to use the process of expert elicitation to develop the value for the waste particle size distribution parameter (Trovato 1997c).

The DOE conducted the expert judgment elicitation May 5-9, 1997. The results of the expert elicitation consisted of a model for predicting waste particle size distribution as a function of the processes occurring within the repository, as predicted by the PA. The DOE completed a final report entitled, *Expert Elicitation on WIPP Waste Particle Size Distributions(s) During the 10,000-Year Regulatory Post-Closure Period* (Carlsbad Area Office Technical Assistance Contractor (CTAC 1997). The particle size distribution derived from the expert elicitation was considered in the PA Verification Test parameterization.

The EPA's review of the DOE's compliance with the requirements of section 194.26 principally focused on the conduct of the elicitation process, since section 194.26 sets specific criteria for

the performance of an expert judgment elicitation. The EPA observed the DOE's elicitation process and conducted an audit of the documentation prepared in support of the DOE's compliance with section 194.26. The scope of the audit covered all aspects of the expert judgment elicitation process, including panel meetings, management and team procedures, curricula vitae of panel members, background documents, and presentation materials. The EPA also assessed compliance with the quality assurance requirements of 40 CFR § 194.22(a)(2)(v) (U.S. EPA 1996). The EPA found that the documentation was appropriate, that the panel members were appropriately qualified, and that the results of the elicitation were used consistently with the stated purpose; the EPA, therefore, found the DOE in compliance with section 194.26 (U.S. EPA 1998a).

Comments on the EPA's proposed decision for section 194.26 related to questions concerning two main issues: (1) DOE's statement that it did not conduct any expert judgment activities in developing the CCA, and (2) the use or role of professional judgment in the development of input parameters used in the CCA. In response, the EPA stated that the DOE's understanding of expert judgment was consistent with the EPA's use of the term "expert judgment" in the compliance criteria, namely a formal, highly structured elicitation of expert opinion. The EPA further stated that while the CCA initially did not contain adequate information to ascertain whether a large number of the input parameters had been properly derived, the DOE subsequently provided additional information that enabled the EPA to confirm that all but one of the parameters (i.e., particle size) was adequately supported (U.S. EPA 1998b).

Based on its review of documentation developed by the DOE and its contractors, the results of the EPA's audit, and consideration of public comments, the EPA concluded that the DOE complied with the requirements of section 194.26 in conducting the required expert elicitation. For further information on the EPA's evaluation of compliance with section 194.26 in the CCA, see Compliance Application Review Document (CARD) 26 (U.S. EPA 1998c).

26.3.2 Expert Judgment for Passive Institutional Control Credit

In the CCA, Appendix EPIC, the DOE proposed a 700-year credit for the passive institutional controls (PICs) to prevent human intrusion at the Waste Isolation Pilot Plant (WIPP) and argued that the PA for the WIPP need not consider human intrusion for the first 700 years due to the postulated effective active and passive institutional controls. Such credit is allowed by 40 CFR § 194.43(c) (U.S. EPA 1996).

In its discussion on the 1998 decision on the CCA, CARD 43, (U.S. EPA 1998d), the EPA did not allow the requested credit, based in part on the argument that the DOE did not conduct an expert judgment process in the manner prescribed by section 194.26 (Expert Judgment) to derive the PICs credit. EPA stated that instead of a formal expert judgment, the DOE prepared a credit proposal and submitted it to a peer review panel.

The EPA did not consider the peer review to be equivalent to an expert judgment elicitation, as prescribed in section 194.26. For instance, the EPA stated, the PIC peer review panel was composed of three members, whereas EPA's expert judgment requirements call for at least five members on a panel (40 CFR § 194.26(b)(7)(i)).

The EPA provided the following detailed discussion in CARD 43 for its decision:

> DOE undertook two expert judgment exercises related to PICs prior to the promulgation of the final compliance criteria. In one exercise, DOE asked groups of experts to predict the likelihood of various intrusion scenarios in the future. In another, DOE asked an expert panel to identify the elements of a marker system and to estimate the probability that such system would deter inadvertent intrusion. In neither case did DOE present the panel with the conceptual design for PICs that is in the CCA and ask the panel to derive a credit proposal based on that design. EPA therefore noted that the results of either exercise may not be viewed as directly relevant to DOE's credit proposal, and DOE has not requested that EPA consider them in this way.

26.4 Changes in the CRA-2004

No formal expert judgment elicitations were performed between the original certification decision (U.S. EPA 1998a) and the 2004 Compliance Recertification Application (CRA-2004) (U.S. DOE 2004).

26.5 EPA's Evaluation of Compliance for the 2004 Recertification

Because no activity relating to formal expert judgment had taken place after the original certification decision (U.S. EPA 1998a) and before submission of the CRA-2004, the EPA did not identify any issues relating to section 194.26 in the evaluation of compliance for the 2004 recertification. During its review of the CRA-2004, the EPA received no public comments on the DOE's continued compliance with the expert judgment requirements of section 194.26.

Based on its review of the material pertaining to the CRA-2004, the EPA concluded that the DOE demonstrated continued compliance with the requirements of section 194.26 (U.S. EPA 2006).

26.6 Changes or New Information Between the CRA-2004 and the CRA-2009 (Previously: Changes or New Information Since the 2004 Recertification)

No formal expert judgment elicitations were performed for the WIPP project between the CRA-2004 and the CRA-2009 (U.S. DOE 2009).

26.7 EPA's Evaluation of Compliance for the 2009 Recertification

Because no activity relating to formal expert judgment had taken place between the CRA-2004 and the CRA-2009, the EPA did not identify any issues relating to section 194.26 in the evaluation of compliance for the 2009 recertification. During its review of the CRA-2009, the EPA received no public comments on the DOE's continued compliance with the expert judgment requirements of section 194.26.

Based on its review of the material pertaining to the CRA-2009, the EPA concluded that the DOE demonstrated continued compliance with the requirements of section 194.26 (U.S. EPA 2010a;U.S. EPA 2010b).

26.8 Changes or New Information Since the CRA-2009

No formal expert judgment elicitations have been performed for the WIPP project since the CRA-2009 and EPA's second recertification decision (U.S. EPA 2010b). Information pertaining to expert judgment as provided for the CCA and the CRA-2004 remains unchanged. Therefore, the DOE believes it has demonstrated continued compliance with the provisions of section 194.26.

26.9 References

(*Indicates a reference that has not been previously submitted.)

Carlsbad Area Office Technical Assistance Contractor. 1997. Expert Elicitation on WIPP Waste Particle Size Distribution(s) During the 10,000-Year Regulatory Post-Closure Period (Final Report, June 3). ERMS 541365. Carlsbad, NM: Carlsbad Field Office.

Trovato, E.R. 1997a. Letter to A. Alm (6 Enclosures). 19 March 1997. ERMS 245835. U.S. Environmental Protection Agency, Washington, DC: Office of Air and Radiation.

Trovato, E.R. 1997b. Letter to G. Dials (2 Enclosures). 17 April 1997. ERMS 247196. U.S. Environmental Protection Agency, Washington, DC: Office of Air and Radiation.

Trovato, E.R. 1997c. Letter to G. Dials (2 Enclosures). 25 April 1997. ERMS 247206. U.S. Environmental Protection Agency, Washington, DC: Office of Air and Radiation.

U.S. Department of Energy (DOE). 1996. *Title 40 CFR Part 191 Compliance Certification Application for the Waste Isolation Pilot Plant* (October). 21 vols. DOE/CAO 1996-2184. Carlsbad, NM: Carlsbad Area Office.

U.S. Department of Energy (DOE). 2004. Title 40 CFR Part 191 Compliance Recertification Application for the Waste Isolation Pilot Plant (March). 10 vols. DOE/WIPP 2004-3231. Carlsbad, NM: Carlsbad Field Office.

U.S. Department of Energy (DOE). 2009. *Title 40 CFR Part 191 Compliance Recertification Application for the Waste Isolation Pilot Plant* (March). DOE/WIPP 2009-3424. Carlsbad, NM: Carlsbad Field Office.*

U.S. Environmental Protection Agency (EPA). 1996. "40 CFR Part 194: Criteria for the Certification and Recertification of the Waste Isolation Pilot Plant's Compliance with the 40 CFR 191 Disposal Regulations; Final Rule." *Federal Register*, vol. 61 (February 9, 1996): 5223–45.

U.S. Environmental Protection Agency (EPA). 1998a. "40 CFR Part 194: Criteria for the Certification and Recertification of the Waste Isolation Pilot Plant's Compliance with the Disposal Regulations: Certification Decision; Final Rule." *Federal Register*, vol. 63 (May 18, 1998): 27353–406.

U.S. Environmental Protection Agency (EPA). 1998b. Response to Comments: Criteria for the Certification and Recertification of the Waste Isolation Pilot Plant's Compliance with the 40 CFR Part 191 Disposal Regulations (May). Washington, DC: Office of Radiation and Indoor Air.

U.S. Environmental Protection Agency (EPA). 1998c. "CARD No. 26: Expert Judgment." *Compliance Application Review Documents for the Criteria for the Certification and Recertification of the Waste Isolation Pilot Plant's Compliance with the 40 CFR Part 191 Disposal Regulations: Final Certification Decision* (May) (pp. 26-1 through 26-9). Washington, DC: Office of Radiation and Indoor Air.

U.S. Environmental Protection Agency (EPA). 1998d. "CARD No. 43: Passive Institutional Controls." *Compliance Application Review Documents for the Criteria for the Certification and Recertification of the Waste Isolation Pilot Plant's Compliance with the 40 CFR Part 191 Disposal Regulations: Final Certification Decision* (May) (pp. 43-1 through 43-47). Washington, DC: Office of Radiation and Indoor Air.

U.S. Environmental Protection Agency (EPA). 2006. "40 CFR Part 194: Criteria for the Certification and Recertification of the Waste Isolation Pilot Plant's Compliance with the Disposal Regulations: Recertification Decision; Final Notice." *Federal Register*, vol. 71 (April 10, 2006): 18010–21.*

U.S. Environmental Protection Agency (EPA). 2010a. "2009 Compliance Recertification Application (CRA-2009) Compliance Application Review Document (CARD) No. 26, Expert Judgment." EPA Docket FDMS Docket ID No. EPA-HQ-OAR-2009-0330. Washington, DC: Office of Radiation and Indoor Air.*

U.S. Environmental Protection Agency (EPA). 2010b. "40 CFR Part 194 Criteria for the Certification and Recertification of the Waste Isolation Pilot Plant's Compliance with the Disposal Regulations: Recertification Decision; Final Notice." *Federal Register*, vol. 75. (November 18, 2010): 70584-95.*

Title 40 CFR Part 191
Subparts B and C
Compliance Recertification Application 2014
for the
Waste Isolation Pilot Plant

Peer Review
(40 CFR § 194.27)

United States Department of Energy
Waste Isolation Pilot Plant

Carlsbad Field Office
Carlsbad, New Mexico

Compliance Recertification Application 2014
Peer Review
(40 CFR § 194.27)

Table of Contents

This page intentionally left blank.

Acronyms and Abbreviations

BCLDP	Battelle Columbus Laboratory Decommissioning Project
CAO	Carlsbad Area Office
CARD	Compliance Application Review Document
CBFO	Carlsbad Field Office
CCA	Compliance Certification Application
CFR	Code of Federal Regulations
CRA	Compliance Recertification Application
CTAC	CBFO Technical Assistance Contractor
DOE	U.S. Department of Energy
DRZ	Disturbed Rock Zone
EEG	Environmental Evaluation Group
EPA	U.S. Environmental Protection Agency
IAEA	International Atomic Energy Agency
LANL	Los Alamos National Laboratory
MP	Management Procedure
NAS	National Academy of Sciences
NEA/OECD	Nuclear Energy Agency/Organization for Economic Cooperation and Development
QA	quality assurance
RCHCM	Revised Culebra Hydrology Conceptual Model
RHPIP	Remote-Handled TRU Waste Characterization Program Implementation Plan
RH	remote-handled
RSI	Institute for Regulatory Science
SNL	Sandia National Laboratories
SRS	Savannah River Site
T	transmissivity
TRU	transuranic
VE	visual examination
WAC	Waste Acceptance Criteria
WIPP	Waste Isolation Pilot Plant

Elements and Chemical Compounds

CO_2	carbon dioxide
MgO	magnesium oxide

This page intentionally left blank.

27.0 Peer Review (40 CFR § 194.27)

27.1 Requirements

§ 194.27 Peer Review

(a) Any compliance application shall include documentation of peer review that has been conducted, in a manner required by this section, for:

(1) Conceptual models selected and developed by the Department;

(2) Waste characterization analyses as required in § 194.24(b); and

(3) Engineered barrier evaluation as required in § 194.44.

(b) Peer review processes required in paragraph (a) of this section, and conducted subsequent to the promulgation of this part, shall be conducted in a manner that is compatible with NUREG–1297, ''Peer Review for High-Level Nuclear Waste Repositories,'' published February 1988. (Incorporation by reference as specified in § 194.5.)

(c) Any compliance application shall:

(1) Include information that demonstrates that peer review processes required in paragraph (a) of this section, and conducted prior to the implementation of the promulgation of this part, were conducted in accordance with an alternate process substantially equivalent in effect to NUREG–1297 and approved by the Administrator or the Administrator's authorized representative; and

(2) Document any peer review processes conducted in addition to those required pursuant to paragraph (a) of this section. Such documentation shall include formal requests, from the Department to outside review groups or individuals, to review or comment on any information used to support compliance applications, and the responses from such groups or individuals.

27.2 Background

According to 40 CFR § 194.27 (U.S. EPA 1996), the U.S. Department of Energy (DOE) is required to conduct peer review evaluations related to conceptual models, waste characterization analyses, and a comparative study of engineered barriers. A peer review involves an independent group of experts who perform an in-depth critique of assumptions, calculations, extrapolations, alternative interpretations, methodology and acceptance criteria employed, and conclusions drawn in the original work. Peer review confirms the adequacy of the work (NRC 1988). The required peer reviews must be performed in accordance with NUREG-1297, Peer Review for High-Level Nuclear Waste Repositories (NRC 1988), which establishes guidelines for the conduct of a peer review exercise. 40 CFR § 194.27(c)(2) also requires the DOE to document in the compliance application any additional peer reviews beyond those explicitly required. These additional peer reviews will be identified in this section as informal peer reviews.

For the formal peer reviews performed before submitting the Compliance Certification Application (CCA) (U.S. DOE 1996a), the DOE developed Carlsbad Area Office (CAO) Team Procedure 10.5, Peer Review (U.S. DOE 1996b), to guide all Waste Isolation Pilot Plant (WIPP) peer reviews and to show a process compatible with section 194.27 and NUREG-1297 requirements. For the 2004 Compliance Recertification Assessment (CRA-2004) (U.S. DOE 2004a), the DOE updated this procedure to Carlsbad Field Office (CBFO) Management Procedure (MP) 10.5, Peer Review (U.S. DOE 2002). MP 10.5 has been revised several times since 2002, and the latest version (Rev. 8, 2/16/10) (U.S. DOE 2010) provides the criteria for selecting the peer review panel, peer review process used, review plan development

requirements, peer review report preparation requirements, and many other aspects of the peer review process.

27.3 1998 Certification Decision

For the CCA, the DOE completed the required peer reviews and documented them in the CCA, Chapter 9.0 and Appendix PEER. The CCA, Chapter 9.0 and Appendix PEER, also contain documentation demonstrating that the DOE's procedures and plans for the required peer reviews are compatible with NUREG-1297. Peer reviews conducted after promulgation of 40 CFR Part 194 and intended to demonstrate compliance with section 194.27 were subject to the requirements of the pertinent procedures and plans. To assess the peer review process during the CCA, the U.S. Environmental Protection Agency (EPA) conducted an audit of the DOE's quality assurance (QA) records for peer review (U.S. EPA 1997). The audit consisted of an extensive review of the DOE's records and interviews of DOE staff and contractors responsible for managing the required peer reviews.

The EPA published the certification decision in 1998 (U.S. EPA 1998a). The EPA found the DOE in compliance with the requirements of section 194.27. The EPA's independent audit established that the DOE had conducted and documented the required peer reviews in a manner compatible with NUREG-1297. The EPA also determined that the DOE adequately documented additional peer reviews in the CCA (see Compliance Application Review Document [CARD] 27, U.S. EPA 1998b).

27.4 Changes in the CRA-2004

The DOE performed two conceptual model peer reviews between the CCA and the CRA-2004: the Salado Flow Conceptual Model Peer Review in March 2003 (see CRA-2004, Chapter 9.0, Section 9.3.1.3.4) and the Spallings Model Peer Review in September 2003 (see CRA-2004, Chapter 9.0, Section 9.3.1.3.5).

External informal peer reviews that fall under section 194.27(c)(2) requirements were also performed during this period. Reviews conducted by the National Academy of Sciences (NAS), the International Atomic Energy Agency (IAEA), the Nuclear Energy Agency of the Organization for Economic Cooperation and Development (NEA/OECD), the Institute for Regulatory Science (RSI), and the Environmental Evaluation Group (EEG) are described in the CRA-2004, Chapter 9.0, and the reports are included in Appendix PEER-2004.

27.5 EPA's Evaluation of Compliance for the 2004 Recertification

The EPA thoroughly reviewed MP 10.5, Rev. 5 (U.S. DOE 2003a) and determined that it was adequately comparable with section 194.27 requirements and NUREG-1297 guidance. The DOE followed MP 10.5, Rev. 5, for the Salado Flow Conceptual Model Peer Review (U.S. DOE 2003b) and the Spallings Model Peer Review (U.S. DOE 2003c).

The Salado Flow Conceptual Model Peer Review was performed from April 2002 to March 2003. The final peer review report was published in March 2003 (U.S. DOE 2003d). The EPA reviewed the peer review plan (U.S. DOE 2003b) and the final peer review report (U.S. DOE

2003d) for the Salado Flow Conceptual Model Peer Review. The EPA also observed the actual performance of the peer review, evaluated the process for the selection of the review panel, observed the interaction of the review panel with the DOE and Sandia National Laboratories (SNL), and reviewed the documents produced during and as a result of the peer review. The EPA determined that the peer review process and the implementation of MP 10.5 met the requirements of section 194.27 and the guidance in NUREG-1297 (U.S. EPA 2003a).

The Spallings Model Peer Review was performed from July 2003 to October 2003. The final report was published in October 2003 (U.S. DOE 2003e). The EPA reviewed the peer review plan (U.S. DOE 2003c) and the final peer review report (U.S. DOE 2003e ;U.S. DOE 2004b) and found them to adequately fulfill the requirements of section 194.27 and NUREG-1297. The EPA observed the actual performance of the peer review, evaluated the process for the selection of the panel, observed the interaction of the panel with the DOE and SNL, and reviewed the documents produced during and as a result of the peer review. The EPA determined the peer review process and the implementation of MP 10.5 met the requirements of section 194.27 and the guidance in NUREG-1297 (U.S. EPA 2003b).

The EPA conducted desktop evaluations of other reviews done since the CCA for compliance with section 194.27(c)(2). These included reviews done by the NAS, IAEA, NEA/OECD, RSI, and EEG from October 1996 to September 2003. The EPA found these reviews to be useful, reasonable, and helpful to the WIPP project, and determined that they reasonably fulfilled the requirements of section 194.27(c)(2).

The EPA did not receive any public comments on the DOE's continued compliance with the peer review requirements of section 194.27. Based on a review and evaluation of the CRA-2004 and supplemental information provided by the DOE (U.S. DOE 2004a), in Chapter 9.0 and Appendix PEER-2004, the EPA (U.S. EPA 2006a;U.S. EPA 2006b) determined that the DOE continued to comply with the requirements of section 194.27.

27.6 Changes or New Information Between the CRA-2004 and the CRA-2009 (Previously: Changes or New Information Since the 2004 Recertification)

The DOE initiated four, and completed three, peer reviews between the CRA-2004 and the CRA-2009 (U.S. DOE 2009a). Peer reviews of conceptual models included the WIPP Revised Disturbed Rock Zone (DRZ) and Cuttings and Cavings Sub-Models Peer Review (see CRA-2009, Section 27.6.3), and the Culebra Hydrogeology Conceptual Model Peer Review summarized below. The Culebra Hydrogeology Conceptual Model Peer Review was not described in the CRA-2009 since the DOE completed the peer review after the CRA-2009 Performance Assessment to support the 2009 Performance Assessment Baseline Calculation. Peer reviews of waste characterization analyses included the Los Alamos National Laboratory (LANL) Sealed Sources Peer Review (see CRA-2009, Section 27.6.1) and the LANL Remote-Handled (RH) Transuranic (TRU) Waste Visual Examination Data Verification Peer Review (see CRA-2009, Section 27.6.2). Additionally, the DOE conducted an external expert review of its Planned Change Request to reduce the magnesium oxide (MgO) excess factor from 1.67 to 1.2 (see CRA-2009, Section 27.6.4).

The Culebra Hydrogeology Conceptual Model Peer Review was conducted in Albuquerque, NM, from August 11 to 14, 2008. The Culebra Dolomite Member of the Rustler Formation is the most significant potential groundwater transport pathway for radionuclides released from the WIPP repository. The Culebra Hydrogeology Conceptual Model describes the overall hydrologic framework of the Culebra Dolomite Member of the Rustler Formation at the WIPP site, and provides the basis for the development of transmissivity (T) fields used in calculations of radionuclide transport. The original conceptual model developed for the CCA was found to be inadequate in the CCA's conceptual model peer review because a strong correlation was not established between the conceptual model and the numerical model used in performance assessment. Sandia National Laboratories proposed the Revised Culebra Hydrology Conceptual Model (RCHCM), incorporating information obtained and developed after the CCA, correlating measured hydrologic properties at well locations to geologic conditions in order to assign values to untested locations. The scope of the peer review was limited to Culebra flow modeling, and the Peer Review Report (Burgess, Doe, and Lowenstein 2008 (Burgess 2008)), issued September 24, 2008, concluded that the RCHCM demonstrated that the conceptual understanding of the Culebra is adequate to support the development of T-fields. The CBFO Office of Quality Assurance, with support from the CBFO Technical Assistance Contractor (CTAC), conducted the surveillance of the peer review process and found that it was satisfactorily performed and documented (Appendix AUD-2014, Table AUD-15, Surveillance S-08-17).

27.7 EPA's Evaluation of Compliance for the 2009 Recertification

The CBFO MP 10.5 was revised several times between the CRA-2004 and the CRA-2009. The latest version during this period was MP 10.5, Rev. 7 (U.S. DOE 2007). The EPA's review verified that the DOE's process used to perform these peer reviews continued to meet NUREG-1297 requirements.

In 2007, the DOE proposed to replace conservative estimates used in the DRZ Conceptual Model and Cuttings and Cavings Conceptual Model with experimental data. Since proposed modifications would impact 2 of the 24 conceptual models included in the Performance Assessment Baseline Calculation, an independent technical peer review on the adequacy of the proposed changes to the approved conceptual models was required under section 194.27. In October 2007, prior to the completion of the peer review, the DOE decided to indefinitely postpone consideration of the proposed modifications. On December 11, 2007, the peer review panel submitted a report (Time Solutions Corporation 2007b) documenting its interim findings.

The EPA examined the RCHCM peer review plan and the final peer review and found them to adequately fulfill the requirements of section 194.27 and NUREG-1297. The EPA observed the actual performance of the peer review, the selection of the panel, the interaction of the panel with the DOE and SNL, and the documents produced during and as a result of the peer review. The EPA determined the peer review process and the implementation of MP 10.5 met the requirements of section 194.27 and the guidance in NUREG-1297 (U.S. EPA 2010a).

The LANL Sealed Sources Peer Review was held October 27 to 31, 2003, at LANL. The purpose of the peer review was to determine whether actinide-containing sealed sources (those containing plutonium-238, plutonium-239, and americium-241) generated over the past 60 years

and recovered by the Off-Site Source Recovery Project could be adequately characterized for compliance with the WIPP Contact-Handled TRU Waste Acceptance Criteria using existing data from original production, transportation, or source control documents. The peer review panel published its report on December 5, 2003 (LANL 2003), concluding that these records, either uniquely or as a sum of several individual records, are adequate Acceptable Knowledge documentation for determining the radionuclide type, content, activity and either the date of manufacture or a more conservative date for decay correction.

Contrary to statements in the CRA-2009, Section 27.6.2 (U.S. DOE 2009a), the EPA was present to observe the actual performance of the peer review, and reviewed the documents produced during and as a result of the peer review. The EPA also conducted a waste characterization inspection of the LANL CCP in April 2005. The Waste Characterization Report, published by the EPA in June 2005 (U.S. EPA 2005), concluded that "[Acceptable Knowledge data] used to determine these values [radionuclide content for compliance with the WIPP waste acceptance criteria (WAC)] had undergone Peer Review in October 2003 in accordance with NUREG 1298." The EPA determined that the peer review process and the implementation of MP 10.5 met the requirements of section 194.27 and the guidance in NUREG-1297.

The LANL Remote-Handled TRU Waste Visual Examination Data Verification Peer Review was held from April 9 to 12, 2007, in Albuquerque, NM. The final report was published by Time Solutions Corporation on April 27, 2007 (Time Solutions Corporation 2007a). The panel was tasked with determining whether visual examination [VE] data recorded by LANL technicians from 1986 to 1992, prior to any WIPP-approved QA program, were technically robust enough to support decisions regarding the residual liquid content and physical form of wastes derived from the cleanup of hot cells located in Wing 9 of the Chemistry and Metallurgical Research Building. The panel determined that VE data may be used for the stated purposes.

The EPA examined the panel's report as part of its baseline inspection of the RH-TRU waste characterization program conducted at LANL May 8 to 10, 2007. The EPA's review found the results of the peer review process to be reasonable (U.S. EPA 2008, p. 44).

The RSI Expert Review of the DOE's use of MgO in the WIPP disposal rooms was conducted in 2005 at the request of the DOE. In its report (RSI 2006), the panel concluded that most of the MgO will be available for chemical reaction; only a small fraction of the cellulosic, plastic and rubber material is likely to be biodegraded to produce carbon dioxide (CO_2), and it is therefore likely that the EPA release standards would be met even if there is less MgO than the quantity required to consume all the CO_2 produced. The panel's findings were published in RSI 2006 (RSI 2006), and submitted to the EPA in 2006 in support of the DOE's Planned Change Request for reducing the MgO excess factor from 1.67 to 1.2. The EPA considered this review when evaluating the DOE Planned Change Request, and found it to reasonably fulfill the requirements of section 194.27(c)(2).

The EPA received one comment agreeing with its request for more information regarding revisions to the Culebra model, and suggesting that "Section 27 peer review is incomplete because it does not accurately reflect current information regarding the Disturbed Rock Zone

(DRZ) conceptual model EPA must have full information about deficiencies of the DRZ and cutting and caving sub-models, and how those limitations affect other aspects of the CRA." These models did not change since the CRA-2004, and the EPA has already approved them after considering their limitations and impacts (U.S. EPA 2010a, Section 27.4.1).

Based on a review and evaluation of the CRA-2009 and supplemental information provided by the DOE (Federal Document Management System Docket ID No. EPA-HQ-QAR-2009-0330, Air Docket A-98-49), the EPA determined that the DOE continued to comply with the requirements for section 194.27 (U.S. EPA 2010a, Section 27.4.2; U.S. EPA 2010b).

27.8 Changes or New Information Since the CRA-2009

The DOE performed one peer review since the CRA-2009, namely, the Savannah River Site (SRS) Historical Radiochemistry Data Peer Review. Two Battelle Columbus Laboratory Decommissioning Project (BCLDP) waste streams at SRS, SR-BCLDP-004.002 and SR-BCLDP-004.003, used radionuclide-specific scaling factors that had been developed based on radiometric and mass spectrometry analyses of samples collected from these waste streams. The CBFO Office of the National TRU Program chose the peer review process to qualify historical radiochemistry data analyzed by the Battelle Radioanalytical Laboratory, which was used to establish radiological properties for these two waste streams.

The SRS Historical Radiochemistry Data Peer Review was conducted in Albuquerque, NM, May 3 to 6, 2010. The peer review logistics, coordination, and project control support was performed by CTAC. The process and documents created during the peer review were subject to all of the protocols described in MP 10.5, Rev. 8 (U.S. DOE 2010). The CBFO Office of Quality Assurance, with support from CTAC, conducted the audit of the peer review process and found that it was satisfactorily performed and documented (Appendix AUD-2014, Table AUD-8; Audit A-10-22).

The two waste streams consist of RH composite filter debris waste that was packaged into 0.105-inch steel drum liners and placed into 55-gallon drums at the Battelle Memorial Institute, and then shipped to the SRS. The DOE directed that the peer review pertained only to the information used to establish radiological properties for waste streams SR-BCLDP-004.002 and SR-BCLDP-004.003, and that the peer review evaluated the applicable radiological analytical results related to the data quality objectives for radiological properties defined in DOE/WIPP-02-3214, Revision 1, *Remote-Handled TRU Waste Characterization Program Implementation Plan* (RHPIP) (U.S. DOE 2009b), specifically for TRU waste determination and activity determination.

The peer review also evaluated the radiological analytical results against the applicable quality assurance objectives for precision, accuracy, representativeness, completeness, and comparability identified in the RHPIP. After in-depth analysis and due consideration, the peer review panel concluded the following (Patera and Winkler 2010):

1. The documentation presented provides sufficient evidence that the data from the BCLDP radioanalysis were obtained under an industry-acceptable quality program.

2. The data from the radioanalysis are sufficient for use in addressing the data quality objectives and quality assurance objectives for the characterization of RH-TRU waste.

3. The data can be qualified under the requirements of the RHPIP.

The EPA also observed the actual performance of the peer review, evaluated the process for the selection of the review panel, observed the interaction of the review panel with the DOE, CTAC, and other attendees, and reviewed the documents produced during and as a result of the peer review. The EPA found that the peer review for waste streams SR-BCLDP-004.002 and SR-BCLDP-004.003 was acceptable (U.S. EPA 2010c). Based on this information, the DOE believes that continued compliance with the provisions of section 194.27 is demonstrated for the CRA-2014.

27.9 References

(*Indicates a reference that has not been previously submitted.)

Burgess, A., T. Doe, and T. Lowestein. 2008. *Conceptual Model Peer Review of Culebra Hydrology*, Final Report (September 24). Carlsbad, NM.*

Institute for Regulatory Science (RSI). 2006. *Application of Magnesium Oxide as an Engineered Barrier at Waste Isolation Pilot Plant*: *Report of the Expert Panel* (February 21). RSI-06-01. Alexandria, VA: Institute for Regulatory Science.

Los Alamos National Laboratory (LANL). 2003. Sealed Sources Peer Review Report (December 5). WSMS-LOS-03-0065. Los Alamos: LANL Off-Site Source Recovery (OSR) Project.

Patera Jr., E.S. and P.C. Winkler. 2010. *Savannah River Site Historical Radiochemistry Data Peer Review* (June 3). Carlsbad, NM.*

Time Solutions Corporation. 2007a. Los Alamos National Laboratory Remote Handled Waste Visual Examination Data Verification Peer Review Report (April). Albuquerque, NM.

Time Solutions Corporation. 2007b. Waste Isolation Pilot Plant Interim Report for the Revised DRZ and Cuttings & Cavings Sub-Models Peer Review (December). Albuquerque, NM.

U.S. Department of Energy (DOE). 1996a. Title 40 CFR Part 191 Compliance Certification Application for the Waste Isolation Pilot Plant (October). 21 vols. DOE/CAO 1996-2184. Carlsbad, NM: Carlsbad Area Office.

U.S. Department of Energy (DOE). 1996b. *CAO Team Procedure: Peer Review* (Revision 0). TP No. 10.5. Carlsbad, NM: Carlsbad Area Office.

U.S. Department of Energy (DOE). 2002. *CBFO Management Procedure: Peer Review* (Revision 4). MP No. 10.5. Carlsbad, NM: Carlsbad Field Office.

U.S. Department of Energy (DOE). 2003a. *CBFO Management Procedure: Peer Review* (Revision 5). MP No. 10.5. Carlsbad, NM: Carlsbad Field Office.

U.S. Department of Energy (DOE). 2003b. Salado Flow Peer Review Plan (Revision 1). Carlsbad, NM: Carlsbad Field Office.

U.S. Department of Energy (DOE). 2003c. Spallings Peer Review Plan (June 20). Carlsbad, NM: Carlsbad Field Office.

U.S. Department of Energy (DOE). 2003d. Salado Flow Conceptual Model Peer Final Review Report (March). Carlsbad, NM: Carlsbad Field Office.

U.S. Department of Energy (DOE). 2003e. Spallings Conceptual Model Peer Review Report (October). Carlsbad, NM: Carlsbad Field Office.

U.S. Department of Energy (DOE). 2004a. Title 40 CFR Part 191 Compliance Recertification Application for the Waste Isolation Pilot Plant (March). 10 vols. DOE/WIPP 2004-3231. Carlsbad, NM: Carlsbad Field Office.

U.S. Department of Energy (DOE). 2004b. Spallings Conceptual Model Peer Review Report: Errata (February 20). Carlsbad, NM: Carlsbad Field Office.

U.S. Department of Energy (DOE). 2007. CBFO Management Procedure 10.5, *Peer Review* (Rev. 7, Effective July 25, 2007 to July 25, 2009). Carlsbad, NM: Carlsbad Field Office.

U.S. Department of Energy (DOE). 2009a. *Title 40 CFR Part 191 Compliance Recertification Application for the Waste Isolation Pilot Plant* (March). DOE/WIPP 2009-3424. Carlsbad, NM: Carlsbad Field Office.*

U.S. Department of Energy (DOE). 2009b. Remote-Handled TRU Waste Characterization Program Implementation Plan (Revision 1, March 27). DOE/WIPP-02-3214. Carlsbad, NM: Carlsbad Field Office.*

U.S. Department of Energy (DOE). 2010. CBFO Management Procedure 10.5, *Peer Review* (Rev. 8, Effective February 16, 2010). Carlsbad, NM: Carlsbad Field Office.*

U.S. Environmental Protection Agency (EPA). 1996. "40 CFR Part 194: Criteria for the Certification and Recertification of the Waste Isolation Pilot Plant's Compliance with the 40 CFR Part 191 Disposal Regulations; Final Rule." *Federal Register*, vol. 61 (February 9, 1996): 5223–45.

U.S. Environmental Protection Agency (EPA). 1997. Audit of the Peer Review Process Conducted by the Department of Energy (Revision 0). Carlsbad, NM: Carlsbad Area Office.

U.S. Environmental Protection Agency (EPA). 1998a. "40 CFR Part 194: Criteria for the Certification and Recertification of the Waste Isolation Pilot Plant's Compliance with the Disposal Regulations: Certification Decision; Final Rule." *Federal Register*, vol. 63 (May 18, 1998): 27353–406.

U.S. Environmental Protection Agency (EPA). 1998b. "CARD No. 27: Peer Review." *Compliance Application Review Documents for the Criteria for the Certification and*

Recertification of the Waste Isolation Pilot Plant's Compliance with the 40 CFR Part 191 Disposal Regulations: Final Certification Decision (May) (pp. 27-1 through 27-11). EPA 402-R-97-013. Washington, DC: Office of Radiation and Indoor Air.

U.S. Environmental Protection Agency (EPA). 2003a. EPA Review of the U.S. Department of Energy Salado Flow Conceptual Model Peer Review (June). Washington, DC: Office of Radiation and Indoor Air.

U.S. Environmental Protection Agency (EPA). 2003b. EPA Review of the U.S. Department of Energy Spallings Conceptual Model Peer Review (December). Washington, DC: Office of Radiation and Indoor Air.

U.S. Environmental Protection Agency (EPA). 2005. *Waste Characterization Report: EPA Inspection No. EPA-LANL-CCP-OSRP-05.05-8 of the Offsite Source Recovery Program (OSRP) as Implemented by the Los Alamos National (LANL) Central Characterization Project (CCP). April 11-15, 2005* (June). Docket A-98-49, II-A4-55. Washington, DC: Office of Radiation and Indoor Air.*

U.S. Environmental Protection Agency (EPA). 2006a. "40 CFR Part 194: Criteria for the Certification and Recertification of the Waste Isolation Pilot Plant's Compliance with the Disposal Regulations: Recertification Decision" (Final Notice). *Federal Register*, vol. 71 (April 10, 2006): 18010–021.

U.S. Environmental Protection Agency (EPA). 2006b. "Recertification CARD No. 27: Peer Review." *Criteria for the Certification and Recertification of the Waste Isolation Pilot Plant's Compliance with the 40 CFR Part 191 Disposal Regulations: Final Recertification Decision* (March) (pp. 27-1 through 27-5). Washington, DC: Office of Radiation and Indoor Air.

U.S. Environmental Protection Agency (EPA). 2008. *EPA Baseline Inspection No. EPA-LANL-CCP-RH-5.07-8 of the Central Characterization Project: Remote-Handled Transuranic Waste Characterization Program at the Los Alamos National Laboratory, May 8–10, 2007* (February). Waste Characterization Inspection Report. Washington, DC: Office of Radiation and Indoor Air.

U.S. Environmental Protection Agency (EPA). 2010a. "2009 Compliance Recertification Application (CRA-2009) Compliance Application Review Document (CARD) No. 27, Peer Review." EPA Docket FDMS Docket ID No. EPA-HQ-OAR-2009-0330. Washington, DC: Office of Radiation and Indoor Air.*

U.S. Environmental Protection Agency (EPA). 2010b. "40 CFR Part 194 Criteria for the Certification and Recertification of the Waste Isolation Pilot Plant's Compliance with the Disposal Regulations: Recertification Decision; Final Notice." *Federal Register*, vol. 75. (November 18, 2010): 70584-95.*

U.S. Environmental Protection Agency (EPA). 2010c. *EPA Tier 1 Evaluation of the Central Characterization Project Remote-Handled Transuranic Waste Characterization Program Battelle Columbus Laboratories Decommissioning Project Wastes Stored at the Savannah River Site for Six Waste Streams: SR-BCLDP.001.001 – Homogenous Waste, SR-BCLDP.001.002 – Composite Filter Debris, SR-BCLDP.002 – Cemented Slugs, SR-BCLDP.003 – Hydraulic Sludge and Debris, SR-BCLDP.004.002 – Cartridge Water Filters, SR-BCLDP.004-003 – Tri-Nuc Vacuum Filters, November 2009 – March 2010*. Waste Characterization Report. Washington, DC: Office of Radiation and Indoor Air.*

U.S. Nuclear Regulatory Commission (NRC). 1988. Peer Review for High-Level Nuclear Waste Repositories: Generic Technical Position. NUREG-1297. Washington, DC.

Title 40 CFR Part 191
Subparts B and C
Compliance Recertification Application 2014
for the
Waste Isolation Pilot Plant

Application of Release Limits
(40 CFR § 194.31)

United States Department of Energy
Waste Isolation Pilot Plant

Carlsbad Field Office
Carlsbad, New Mexico

Compliance Recertification Application 2014
Application of Release Limits
(40 CFR § 194.31)

Table of Contents

List of Tables

This page intentionally left blank.

Acronyms and Abbreviations

ATWIR	Annual Transuranic Waste Inventory Report
CARD	Compliance Application Review Document
CCA	Compliance Certification Application
CH-TRU	contact-handled transuranic
Ci	curies
CRA	Compliance Recertification Application
DOE	U.S. Department of Energy
EPA	U.S. Environmental Protection Agency
m^3	cubic meters
MCi	million-curie
PA	performance assessment
PABC	Performance Assessment Baseline Calculation
PAIR	Performance Assessment Inventory Report
PAVT	Performance Assessment Verification Test
RH-TRU	remote-handled transuranic
WIPP	Waste Isolation Pilot Plant
WUF	waste unit factor

Elements and Chemical Compounds

Am	americium
Cs	cesium
Pu	plutonium
Sr	strontium
Y	yttrium
^{137m}Ba	metastable barium-137

This page intentionally left blank.

31.0 Application of Release Limits (40 CFR § 194.31)

31.1 Requirements

> § 194.31 Application of Release Limits
>
> The release limits shall be calculated according to part 191, appendix A of this chapter, using the total activity, in curies, that will exist in the disposal system at the time of disposal.

31.2 Background

The radioactive waste disposal regulations at 40 CFR Part 191 (U.S. EPA 1993) include requirements for the containment of radionuclides. The containment requirements specify that releases from a disposal system to the accessible environment must not exceed the release limits set forth in Part 191, Appendix A, Table 1. To calculate the applicable release limits for the Waste Isolation Pilot Plant (WIPP), information is needed on the expected total curie content in the repository. However, because the inventory estimates are updated as part of the recertification effort, and because the curie content of the waste inventory in the repository will change over time as a result of natural decay and in-growth of radionuclides, the U.S. Department of Energy (DOE) must establish an inventory for use in performance assessment (PA) and must determine a date for decay purposes to be used as a reference point for calculating the curie content of waste. 40 CFR § 194.31 (U.S. EPA 1996) specifies that release limits should be calculated based on the curie content at the time of disposal (that is, after the end of the operational period, when the shafts of the repository have been backfilled and sealed).

31.3 1998 Certification Decision

The U.S. Environmental Protection Agency (EPA) stated in Compliance Application Review Document (CARD) 31 (U.S. EPA 1998) that they expected the Compliance Certification Application (CCA) (U.S. DOE 1996) to estimate curies of each radionuclide in the disposal system at the time of disposal, and provide sample calculations of release limits, including the relative contribution of each radionuclide to the normalized releases. The EPA later determined as part of its compliance determination that the CCA PA and the EPA-mandated Performance Assessment Verification Test (PAVT) (U.S. DOE 1997) were calculated using release limits developed in accordance with 40 CFR Part 191, Appendix A.

A complete description of the EPA's 1998 Certification Decision for compliance with section 194.31 can be obtained from CARD 31 (U.S. EPA 1998).

31.4 Changes in the CRA-2004

In the 2004 Compliance Recertification Application (CRA-2004) (U.S. DOE 2004), the DOE used updated versions of the same computer codes as those used in the CCA and CCA PAVT to decay the radionuclide inventory and calculate EPA units per cubic meter of waste (Fox 2003). The only change of note was the CRA-2004 inventory, which is discussed in Appendix DATA-

2004, Attachment F, Appendix TRU WASTE-2004, and CARD 24 (U.S. EPA 2006a), and the CRA-2004 PABC inventory, as documented in U.S. DOE (2006).

Since the radioactivity in each waste stream is not measured at the same time, the waste stream activities were decay-corrected to December 31, 2001, using the computer code ORIGEN2 Version 2.2 (Oak Ridge National Laboratory 2002). The total radioactivity in the repository is based on contact-handled transuranic (CH-TRU) and remote-handled transuranic (RH-TRU) waste volumes of each radionuclide and then scaled to the WIPP's maximum allowable CH-TRU and RH-TRU volumes (168,485 cubic meters (m^3) and 7,079 m^3, respectively). The scaling factor for each type of waste is calculated by subtracting the stored and emplaced waste volumes from the disposal limit value (for disposal volumes of CH-TRU waste [168,485 m^3] and RH-TRU waste [7,079 m^3]) and dividing this value by the projected waste volume.

The total radioactivity associated with CH-TRU and RH-TRU wastes from the CCA PAVT, CRA-2004, and CRA-2004 Performance Assessment Baseline Calculation (PABC) are shown in Table 31-1. These RH-TRU waste values are substantially lower than the RH-TRU waste limit of 5.1 million curies (MCi) specified in the WIPP Land Withdrawal Act (U.S. Congress 1992).

Table 31-2 shows that the five radionuclides with the highest activity in the waste—americium-241 (^{241}Am), plutonium-238 (^{238}Pu), plutonium-239 (^{239}Pu), plutonium-240 (^{240}Pu), and plutonium-241 (^{241}Pu)—contribute 97% of the total CH-TRU waste activity in the CRA-2004 PABC, 97% in the CRA-2004, and 99% in the CCA PAVT.

Similar information on the five radionuclides with the highest activity in the RH-TRU waste—metastable barium-137 (^{137m}Ba), cesium-137 (^{137}Cs), ^{241}Pu, strontium-90 (^{90}Sr), and yttrium-90 (^{90}Y)—is presented in Table 31-3.

For use in the PA, these inventories are decayed using ORIGEN2 Version 2.2 to the year 2033, the assumed closure date for the WIPP, and to various dates up to 10,000 years after closure to obtain the radioactivity profiles as a function of time (e.g., see Appendix PA-2004, Attachment PAR, Table PAR-50).

Table 31-1. Total Radioactivity Associated with CH-TRU and RH-TRU Wastes

Analysis	CH-TRU Waste Total Activity (Ci)	RH-TRU Waste Total Activity (Ci)
CCA PAVT[a,c]	6.4×10^6	1.0×10^6
CRA-2004[b,c]	5.3×10^6	1.3×10^6
CRA-2004 PABC[b,d]	4.7×10^6	1.6×10^6

[a] Decayed through 1995
[b] Decayed through 2001
[c] Values from Appendix DATA-2004, Attachment F, Annex B, Table DATA-F-B-27
[d] Values from Transuranic Waste Baseline Inventory Report 2004, Table B.1-27 (U.S. DOE 2006)

Table 31-2. Radionuclides with Highest Activity in the CH-TRU Waste Inventory

Radionuclide	Radioactivity in CCA PAVT[a,c] (Ci)	Radioactivity in CRA-2004[b,c] (Ci)	Radioactivity in CRA-2004 PABC[b,d] (Ci)
^{241}Am	4.4×10^5	4.0×10^5	4.8×10^5
^{238}Pu	2.6×10^6	1.6×10^6	1.5×10^6
^{239}Pu	7.9×10^5	6.6×10^5	5.8×10^5
^{240}Pu	2.1×10^5	(1.1×10^5)[e]	9.4×10^4
^{241}Pu	2.3×10^6	(2.4×10^6)[f]	2.0×10^6
Fraction of Total Inventory	99%	97%	97%

[a] Decayed through 1995
[b] Decayed through 2001
[c] Values directly from Appendix DATA-2004, Attachment F, Annex B, Table DATA-F-B-27
[d] Values directly from Transuranic Waste Baseline Inventory Report 2004, Table B.1-27 (U.S. DOE 2006)
[e] Value incorrectly reported in CARD 31 as 2.40×10^6 (U.S. EPA 2006b)
[f] Value incorrectly reported in CARD 31 as 5.18×10^6 (U.S. EPA 2006b)

Table 31-3. Radionuclides with Highest Activity in the RH-TRU Waste Inventory

Radionuclide	Radioactivity in CCA PAVT[a,c] (Ci)	Radioactivity in CRA-2004[b,c] (Ci)	Radioactivity in CRA-2004 PABC[b,d] (Ci)
^{137m}Ba	2.0×10^5	3.4×10^5	3.9×10^5
^{137}Cs	2.2×10^5	3.7×10^5	4.3×10^5
^{241}Pu	1.4×10^5	1.1×10^5	1.3×10^5
^{90}Sr	2.1×10^5	2.5×10^5	3.2×10^5
^{90}Y	2.1×10^5	2.4×10^5	3.2×10^5
Fraction of Total Inventory	96%	98%	98%

[a] Decayed through 1995
[b] Decayed through 2001
[c] Values directly from Appendix DATA-2004, Attachment F, Annex B, Table DATA-F-B-28
[d] Values directly from Transuranic Waste Baseline Inventory Report 2004, Table B.1-28 (U.S. DOE 2006)

According to Part 191, Appendix A, Table 1 (Note 1e), release limits for the radionuclides specified in the rule are based on "an amount of TRU waste containing one million curies of alpha-emitting TRU radionuclides with half-lives greater than 20 years." To obtain release limits for use in the PA, the release limits per MCi specified in 40 CFR Part 191, Appendix A, Table 1 must be multiplied by a factor that defines the number of MCi of TRU radionuclides in the inventory. For PA purposes, this factor, defined as the waste unit factor (WUF), is expressed as

$$f_w = \frac{\sum W_f}{10^6 Ci} \tag{31.1}$$

where f_w is the WUF and W_f is the WIPP-scale inventory in curies of each alpha-emitting TRU radionuclide with a half-life of 20 years or more. The DOE identified a total of 138 radionuclides expected to be present in the waste based on the CRA-2004 PABC inventory. Of these, 17 meet the definition of TRU waste in Part 191, Appendix A, Table 1 for calculating the WUF. Table 2 of Leigh and Trone (Leigh and Trone 2005) identified these nuclides and

determined that they contribute 2.32×10^6 Ci at closure, resulting in a WUF of 2.32 in the CRA-2004 PABC. Appendix TRU WASTE-2004, and the CRA-2004 PABC Inventory Report (Leigh, Trone, and Fox 2005) discuss in detail the WUF calculations and the radionuclides important to the calculations.

31.5 EPA's Evaluation of Compliance for the 2004 Recertification

The CRA-2004 PABC Inventory Report (U.S. DOE 2006) was completed following the submittal of the CRA-2004 and was used in the CRA-2004 PABC calculations. Though this inventory was issued following the CRA-2004, it was included in the EPA's evaluation of the CRA-2004 (U.S. EPA 2004). The EPA reviewed the information collected by the DOE related to the waste inventory for the CRA-2004 PA and the CRA-2004 PABC, and conducted verification calculations on the data used by the DOE in the CRA-2004 PA (CARD 24, (U.S. EPA 2006a;U.S. EPA 2006c), Sections 3.4 and 4.4). The methodologies for calculating the WUF and release limits in the CRA-2004 PABC were unchanged from those used in the CCA and the CRA-2004, and the EPA determined that the approach used was appropriate and acceptable for the CRA-2004 PA (U.S. EPA 2006d).

To verify whether the ORIGEN2 Version 2.2 decay calculations were performed correctly, the EPA carried out independent calculations of the decay of the inventory. These calculations showed that, on a spot-check basis, the ORIGEN2 values derived by the DOE and used in EPAUNI[1] (Sandia National Laboratories 2003) were correct (CARD 31, U.S. EPA 2006b). During the CRA-2004 review, the EPA reviewed the codes and determined that they adequately performed the decay calculations. The EPA determined that the approach used by the DOE was appropriate and acceptable for the CRA-2004 PA (U.S. EPA 2006a).

31.6 Changes or New Information Between the CRA-2004 and the CRA-2009 (Previously: Changes or New Information Since the 2004 Recertification)

The CRA-2009 PA (Clayton et al. 2008) done in support of the CRA-2009 (U.S. DOE 2009) maintained the same inventory and WUF values that were used in the CRA-2004 PABC (Leigh, Trone, and Fox 2005) and previously accepted by the EPA. The CRA-2004 PABC inventory was the last published inventory (U.S. DOE 2006) at the time the PA calculation for the CRA-2009 commenced. After the CRA-2004 PABC was completed, the *Annual Transuranic Waste Inventory Report–2007* (U.S. DOE 2008a) was published and provided updated inventory information. The DOE anticipated this inventory update would only have a small impact on normalized releases for the CRA-2009, and would not be significant for compliance. The DOE's approach to demonstrating compliance with the application of release limits was not changed from that used in the CRA-2004 and CRA-2004 PABC, and therefore the DOE stated it continued to comply with section 194.31.

1 EPAUNI is a computer code that calculates the activity per m3 for each waste stream at a discrete set of times.

31.7 EPA's Evaluation of Compliance for the 2009 Recertification

Following receipt of results from the CRA-2009 PA, the EPA requested that an additional PA be performed that included updated inventory information (Cotsworth 2009). Consequently, the *Performance Assessment Inventory Report - 2008* (PAIR-2008) (Crawford et al. 2009) was generated using information contained in the *Annual Transuranic Waste Inventory Report-2008* (ATWIR-2008) (U.S. DOE 2008b). The ATWIR-2008 contained inventory information collected up to December 31, 2007. An additional PA calculation, referred to as the CRA-2009 PABC (Clayton et al. 2010), was executed to satisfy the EPA's request. The CRA-2009 PABC used inventory information contained in the PAIR-2008. The methodologies used for calculating the WUF and release limits in the CRA-2009 PABC were unchanged from those used in the CRA-2004 PABC, and were documented in Fox, Clayton, and Kirchner (Fox, Clayton, and Kirchner 2009). The value of the WUF used in the CRA-2009 PABC was 2.60 and was independently verified by the EPA (U.S. EPA 2010a).

The five radionuclides with the highest activity for the CH-TRU and the RH-TRU waste in the CRA-2009 PABC inventory, decayed through year 2033, are shown in Table 31-4. Values shown in the table are taken directly, or calculated from, Table 4-5 and Table A-1 of the PAIR-2008. As can be seen, five radionuclides—^{241}Am, ^{238}Pu, ^{239}Pu, ^{240}Pu, and ^{241}Pu—contributed 99.9% of the total CH-TRU waste activity in the CRA-2009 PABC. Radioisotopes ^{137}Cs, ^{137m}Ba, ^{90}Sr, ^{90}Y, and ^{238}Pu contributed 96.0% of the total RH-TRU waste activity in the CRA-2009 PABC.

Table 31-4. Radionuclides with Highest Activity in the CRA-2009 PABC Waste Inventory

Waste Type	Radionuclide	Radioactivity (Ci)	Fraction of Total Activity
Contact-handled TRU Total Activity 3.10×10^6 Ci	^{238}Pu	1.47×10^6	47.4%
	^{239}Pu	5.10×10^5	16.5%
	^{241}Pu	5.06×10^5	16.3%
	^{241}Am	4.68×10^5	15.1%
	^{240}Pu	1.44×10^5	4.6%
Remote-handled TRU Total Activity 3.50×10^5 Ci	^{137}Cs	8.89×10^4	25.4%
	^{137m}Ba	8.32×10^4	23.8%
	^{90}Sr	7.99×10^4	22.8%
	^{90}Y	7.89×10^4	22.5%
	^{238}Pu	5.11×10^3	1.5%

The EPA reviewed the information collected by the DOE related to the waste inventory for the CRA-2009 PA and the CRA-2009 PABC (CARD 31, (U.S. EPA 2010b)). The EPA also verified calculations on the data used by the DOE in the CRA-2009 PA and the CRA-2009 PABC (CARD 24, (U.S. EPA 2010;U.S. EPA 2010c)). In particular, the EPA verified that the ORIGEN2 Version 2.2 code was qualified appropriately and that decay calculations were

performed correctly. These decay calculations verified that the ORIGEN2 values derived by the DOE and used in EPAUNI were determined correctly.

The EPA's review of the CRA-2009 PA and the CRA-2009 PABC found that the DOE continued to comply with the application of release limits requirements of section 194.31.

31.8 Changes or New Information Since the CRA-2009

The inventory used in the CRA-2014 PA is updated from that used in the CRA-2009 PABC (Clayton et al. 2010). The *Annual Transuranic Waste Inventory Report-2012* (ATWIR-2012) (U.S. DOE 2012) contains an inventory of defense-related TRU waste information collected through December 31, 2011. The *Performance Assessment Inventory Report - 2012* (PAIR-2012) (Van Soest 2012) has been developed, and is based on the annual inventory collected from the TRU waste sites and documented in the ATWIR-2012. The CRA-2014 PA uses inventory information contained in the PAIR-2012. The methodologies used to calculate the WUF and release limits in the CRA-2014 PA are unchanged from those used in the CRA-2009 PABC, and are documented in Kicker and Zeitler (Kicker and Zeitler 2012). The value of the WUF used in the CRA-2014 PA is 2.06. The DOE anticipates this inventory update will have only a small impact on normalized releases relative to the CRA-2009 PABC, and will not be significant for compliance.

The five radionuclides with the highest activity for the CH-TRU and the RH-TRU waste in the CRA-2014 PA inventory, decayed through year 2033, are shown in Table 31-5. Values shown in that table are taken directly from, or calculated from, Table 5-3 and Table 5-4 of the PAIR-2012. As can be seen, five radionuclides—^{241}Am, ^{238}Pu, ^{239}Pu, ^{240}Pu, and ^{241}Pu—contribute 99% of the total CH-TRU waste activity in the CRA-2014 PA. Radioisotopes ^{137}Cs, ^{137m}Ba, ^{90}Sr, ^{90}Y, and ^{241}Pu contribute 94.2% of the total RH-TRU waste activity in the CRA-2014 PA.

Table 31-5. Radionuclides with Highest Activity in the CRA-2014 PA Waste Inventory

Waste Type	Radionuclide	Radioactivity (Ci)	Fraction of Total Activity
Contact-handled TRU Total Activity 2.70×10^6 Ci	^{241}Am	6.97×10^5	25.8%
	^{241}Pu	6.48×10^5	24.0%
	^{238}Pu	5.95×10^5	22.0%
	^{239}Pu	5.67×10^5	21.0%
	^{240}Pu	1.67×10^5	6.2%
Remote-handled TRU Total Activity 9.36×10^5 Ci	^{137}Cs	2.33×10^5	24.9%
	^{137m}Ba	2.20×10^5	23.5%
	^{90}Sr	2.07×10^5	22.1%
	^{90}Y	2.07×10^5	22.1%
	^{241}Pu	1.49×10^4	1.6%

The DOE's approach to demonstrating compliance with the application of release limits in the CRA-2014 PA has not changed from that used in the CRA-2009 PABC, and therefore continues to comply with section 194.31.

31.9 References

(*Indicates a reference than has not been previously submitted.)

Clayton, D., S. Dunagan, J. Garner, A. Ismail, T. Kirchner, R. Kirkes, and M. Nemer. 2008. *Summary Report of the 2009Compliance Recertification Application Performance Assessment.* ERMS 548862. Carlsbad, NM: Sandia National Laboratories.*

Clayton, D., R. Camphouse, J. Garner, A. Ismail, T. Kirchner, K. Kuhlman, and M. Nemer. 2010. *Summary Report of the CRA-2009 Performance Assessment Baseline Calculation.* ERMS 553039. Carlsbad, NM: Sandia National Laboratories.*

Cotsworth, E. 2009. *EPA Letter on CRA-2009 First Set of Completeness Comments*. ERMS 551444. U.S. EPA, Office of Radiation and Indoor Air, Washington DC.*

Crawford, B., D. Guerin, S. Lott, B. McInroy, J. McTaggart, G. Van Soest. 2009. *Performance Assessment Inventory Report – 2008*. LA-UR-09-02260. ERMS 551511. Carlsbad, NM: Los Alamos National Laboratory.*

Fox, B. 2003. *Analysis of EPA Unit Loading Calculation, Compliance Recertification Application* (Superceded ERMS 530304, Revision 1). ERMS 531582. Carlsbad, NM: Sandia National Laboratories.

Fox, B., D. Clayton, and T. Kirchner. 2009. *Radionuclide Inventory Screening Analysis Report for the PABC-2009*. ERMS 551679. Carlsbad, NM: Sandia National Laboratories.*

Kicker, D. and T. Zeitler. 2012. Radionuclide Inventory Screening Analysis for the 2014 Compliance Recertification Application Performance Assessment (CRA-2014 PA). ERMS 559257. Carlsbad, NM: Sandia National Laboratories.*

Leigh, C., and J. Trone. 2005. *Calculation of the Waste Unit Factor for the Performance Assessment Baseline Calculation* (Revision 0). ERMS 539613. Carlsbad, NM: Sandia National Laboratories.

Leigh, C., J. Trone, and B. Fox. 2005. TRU Waste Inventory for the 2004 Compliance Recertification Application Performance Assessment Baseline Calculation (Revision 0). ERMS 541118. Carlsbad, NM: Sandia National Laboratories.

Oak Ridge National Laboratory (ORNL). 2002. *RSICC Computer Code Collection ORIGEN 2.2* (June). CCC371 ORIGEN 2.2. ERMS 525791. Oak Ridge, TN: Radiation Safety Information Computational Center.

Sandia National Laboratories (SNL). 2003. *User's Manual for EPAUNI, Version 1.15A.* ERMS 530203. Carlsbad, NM: Sandia National Laboratories.

U.S. Congress. 1992. WIPP Land Withdrawal Act, Public Law 102-579, 106 Stat. 4777, 1992, as amended by Public Law 104-201, 110 Stat. 2422, 1996.

U.S. Department of Energy (DOE). 1996. *Title 40 CFR Part 191 Compliance Certification Application for the Waste Isolation Pilot Plant* (October). 21 vols. DOE/CAO 1996-2184. Carlsbad, NM: Carlsbad Area Office.

U.S. Department of Energy (DOE). 1997. Supplemental Summary of EPA-Mandated Performance Assessment Verification Test (All Replicates) and Comparison with the Compliance Certification Application Calculations (August 8). WPO 46702. ERMS 414879. Carlsbad, NM: Carlsbad Area Office.

U.S. Department of Energy (DOE). 2004. *Title 40 CFR Part 191 Compliance Recertification Application for the Waste Isolation Pilot Plant* (March). 10 vols. DOE/WIPP 2004-3231. Carlsbad, NM: Carlsbad Field Office.

U.S. Department of Energy (DOE). 2006. *Transuranic Waste Baseline Inventory Report–2004*. DOE/TRU 2006-3344. Carlsbad, NM: Carlsbad Field Office.

U.S. Department of Energy (DOE). 2008a. *Annual Transuranic Waste Inventory Report—2007* (Revision 1). DOE/TRU 2008-3379. Carlsbad, NM: Carlsbad Field Office.

U.S. Department of Energy (DOE). 2008b. *Annual Transuranic Waste Inventory Report—2008* (Revision 0). DOE/TRU 2008-3425. Carlsbad, NM: Carlsbad Field Office.*

U.S. Department of Energy (DOE). 2009. *Title 40 CFR Part 191 Compliance Recertification Application for the Waste Isolation Pilot Plant*. DOE/WIPP 09-3424. Carlsbad, NM: Carlsbad Field Office.

U.S. Department of Energy (DOE). 2012. *Annual Transuranic Waste Inventory Report—2012* (Revision 0). DOE/TRU 2012-3425. Carlsbad, NM: Carlsbad Field Office.*

U.S. Environmental Protection Agency (EPA). 1993. "40 CFR Part 191: Environmental Radiation Protection Standards for the Management and Disposal of Spent Nuclear Fuel, High-Level and Transuranic Radioactive Wastes; Final Rule." *Federal Register*, vol. 58 (December 20, 1993): 66398–416.

U.S. Environmental Protection Agency (EPA). 1996. "40 CFR Part 194: Criteria for the Certification and Recertification of the Waste Isolation Pilot Plant's Compliance with the 40 CFR Part 191 Disposal Regulations; Final Rule." *Federal Register*, vol. 61 (February 9, 1996): 5223–45.

U.S. Environmental Protection Agency (EPA). 1998. "CARD No. 31: Application of Release Limits." *Compliance Application Review Documents for the Criteria for the Certification and Recertification of the Waste Isolation Pilot Plant's Compliance with the 40 CFR 191 Disposal Regulations: Final Certification Decision* (May) (pp. 31-1 through 31-20). Washington, DC: Office of Radiation and Indoor Air.

U.S. Environmental Protection Agency (EPA). 2004. "40 CFR Part 194: Criteria for the Certification and Recertification of the Waste Isolation Pilot Plant's Compliance With the Disposal Regulations; Alternative Provisions" (Final Rule). *Federal Register*, vol. 69 (July 16, 2004): 42571–583.

U.S. Environmental Protection Agency (EPA). 2006a. "Recertification CARD No. 24: Waste Characterization." *Compliance Application Review Documents for the Criteria for the Certification and Recertification of the Waste Isolation Pilot Plant's Compliance with the 40 CFR Part 191 Disposal Regulations: Final Recertification Decision* (March) (pp. 24-1 through 24-50). Washington, DC: Office of Radiation and Indoor Air.

U.S. Environmental Protection Agency (EPA). 2006b. "Recertification CARD No. 31: Application of Release Limits." *Compliance Application Review Documents for the Criteria for the Certification and Recertification of the Waste Isolation Pilot Plant's Compliance with the 40 CFR Part 191 Disposal Regulations: Final Recertification Decision* (March) (pp. 31-1 through 31-4). Washington, DC: Office of Radiation and Indoor Air.

U.S. Environmental Protection Agency (EPA). 2006c. *Technical Support Document for Section 194.24: Review of the Baseline Inventory Used in the Compliance Recertification Application and the Performance Assessment Baseline Calculation* (March). Washington, DC: Office of Radiation and Indoor Air.

U.S. Environmental Protection Agency (EPA). 2006d. *Technical Support Document for Section 194.23: Review of WIPP Recertification Performance Assessment Computer Codes* (March). CRA Code Review. Washington, DC: Office of Radiation and Indoor Air.

U.S. Environmental Protection Agency (EPA). 2010a. Technical Support Document for Section 194.24: Review of the Baseline Inventory Used in the Compliance Recertification Application (CRA-2009) and the Performance Assessment Baseline Calculation. Washington, DC: Office of Radiation and Indoor Air.*

U.S. Environmental Protection Agency (EPA). 2010b. 2009 Compliance Recertification Application (2009 CRA) Compliance Application Review Document (CARD) No. 31: Application of Release Limits. Washington, DC: Office of Radiation and Indoor Air.*

U.S. Environmental Protection Agency (EPA). 2010c. 2009 Compliance Recertification Application (2009 CRA) Compliance Application Review Document (CARD) No. 24: Waste Characterization. Washington, DC: Office of Radiation and Indoor Air.*

Van Soest, G. 2012. *Performance Assessment Inventory Report – 2012*. LA-UR-12-26643. Carlsbad, NM: Los Alamos National Laboratory.*

Title 40 CFR Part 191
Subparts B and C
Compliance Recertification Application 2014
for the
Waste Isolation Pilot Plant
Scope of Performance Assessments
(40 CFR § 194.32)

United States Department of Energy
Waste Isolation Pilot Plant

Carlsbad Field Office
Carlsbad, New Mexico

Compliance Recertification Application 2014
Scope of Performance Assessments
(40 CFR § 194.32)

Table of Contents

List of Tables

This page intentionally left blank.

Acronyms and Abbreviations

CARD	Compliance Application Review Document
CCA	Compliance Certification Application
CFR	Code of Federal Regulations
CRA	Compliance Recertification Application
DOE	U.S. Department of Energy
DP	disturbed performance
EP	event and process
EPA	U.S. Environmental Protection Agency
FEP	feature, event, and process
HCN	historic, current, and near-future
PA	performance assessment
SO-C	screened out-consequence
SO-P	screened out-probability
SO-R	screened out-regulatory
SP	Specific Procedure
UP	undisturbed performance
WIPP	Waste Isolation Pilot Plant

This page intentionally left blank.

32.0 Scope of Performance Assessments (40 CFR § 194.32)

32.1 Requirements

§ 194.32 Scope of Performance Assessment

(a) "Performance assessments shall consider natural processes and events, mining, deep drilling, and shallow drilling that may affect the disposal system during the regulatory time frame."

(b) "Assessments of mining effects may be limited to changes in the hydraulic conductivity of the hydrogeologic units of the disposal system from excavation mining for natural resources. Mining shall be assumed to occur with a one in 100 probability in each century of the regulatory time frame. Performance assessments shall assume that mineral deposits of those resources, similar in quality and type to those resources currently extracted from the Delaware Basin, will be completely removed from the controlled area during the century in which such mining is randomly calculated to occur. Complete removal of such mineral resources shall be assumed to occur only once during the regulatory time frame."

(c) "Performance assessments shall include an analysis of the effects on the disposal system of any activities that occur in the vicinity of the disposal system prior to disposal and are expected to occur in the vicinity of the disposal system soon after disposal. Such activities shall include, but shall not be limited to, existing boreholes and the development of any existing leases that can be reasonably expected to be developed in the near future, including boreholes and leases that may be used for fluid injection activities."

(d) "Performance assessments need not consider processes and events that have less than one chance in 10,000 of occurring over 10,000 years."

(e) "Any compliance application(s) shall include information which:

(1) Identifies all potential processes, events or sequences and combinations of processes and events that may occur during the regulatory time frame and may affect the disposal system;

(2) Identifies the processes, events or sequences and combinations of processes and events included in performance assessments; and

(3) Documents why any processes, events or sequences and combinations of processes and events identified pursuant to paragraph (e)(1) of this section were not included in performance assessment results provided in any compliance application."

32.2 Background

Performance Assessment (PA) is a process that assesses the likelihood that the Waste Isolation Pilot Plant (WIPP) will meet the release limits specified by 40 CFR 191.13 for 10,000 years after disposal. The PA process must consider both natural and man-made processes and events which have an effect on this disposal system.

Section 194.32 (U.S. EPA 1996) requires that PAs consider the effects of excavation mining, drilling fluid injection, and future development of leases. In addition, the PA must also consider the effects of current activities such as secondary oil recovery methods (waterflooding), disposal of natural brine, and solution mining to extract brine in the vicinity of the repository. Section 194.32 requires identification of all features, events, and processes (FEPs), or sequences or combinations of processes and events that could occur during the regulatory time frame that may affect the repository, and documentation of why certain events or groups of events are not included, if so warranted.

Therefore, the PA methodology for the WIPP includes a process that compiles a comprehensive list of the FEPs that are relevant to disposal system performance. Those FEPs determined by screening analysis to have the potential to affect performance are represented in scenarios and

quantitative calculations using a system of linked computer models to describe the interaction of the repository with the natural system, both with and without human intrusion. For the Compliance Certification Application (CCA) (U.S. DOE 1996), the U.S. Department of Energy (DOE) first compiled a comprehensive list of FEPs which was then subjected to a screening process that eventually lead to the set of relevant FEPs used in PA to demonstrate the WIPP's compliance with the long-term disposal standards.

The screening criteria shown below were used to determine whether to include FEPs into conceptual models and performance scenarios:

- Screened Out-Regulation (SO-R): For example, future human-initiated events and processes (EPs) may be excluded from consideration for regulatory reasons (e.g., deliberate drilling intrusions). 40 CFR § 194.25(a) requires that characteristics of the future remain what they are at the time the compliance application is prepared, provided that such characteristics are not related to hydrogeologic, geologic, or climatic conditions.

- Screened Out-Probability (SO-P): 40 CFR § 194.32(d) states that PA need not consider processes and events that have less than 1 in 10,000 chance of occurring over 10,000 years.

- Screened Out-Consequence (SO-C): The DOE eliminated some FEPs based on their consequences according to the following two criteria:

    - Insignificant Consequences. The DOE eliminated FEPs where there was a reasonable expectation that the remaining probability distribution of cumulative releases would not be significantly changed by such omissions. These FEPs are designated SO-C.

    - Beneficial FEPs. FEPs that are potentially beneficial to disposal system or subsystem performance were eliminated to simplify the analysis. This argument may be used when there is uncertainty as to exactly how the FEP should be incorporated into assessment calculations, or when incorporation would incur unreasonable difficulties. This is considered a conservative decision. These FEPS are designated SO-C Beneficial (e.g., the accumulation of radioactive contaminants in soils).

The FEPs retained in the PA were accounted for under calculations of either the undisturbed performance (UP) or disturbed performance (DP) (see the CCA, Chapter 6.0, Sections 6.2.2.2 and 6.2.2.3).

- UP includes the predicted behavior of the disposal system assuming it is not disrupted by human intrusion or the occurrence of unlikely natural events.

- DP includes the predicted behavior of the disposal system assuming disruption by human intrusion or other actions, including future drilling and mining activities.

32.3 1998 Certification Decision

32.3.1 40 CFR § 194.32(a)

In the CCA, the DOE discussed the origin and development of the WIPP FEPs list, as well as well-defined screening criteria in the CCA, Appendix SCR. A list of the WIPP-relevant FEPs is also provided in the CCA, Chapter 6.0, Section 6.2. The DOE identified approximately 237 FEPs in three major categories: natural (N), waste- and repository-induced (W), and human-initiated (H). Of particular importance to the performance of the disposal system were those FEPs dealing with mining, deep drilling, and shallow drilling, because these FEPs have the greatest potential for disruption of the repository via inadvertent intrusion. The CCA and supporting documents illustrated the process used by the DOE to implement the FEPs in scenarios relevant to PA.

The U.S. Environmental Protection Agency (EPA) evaluated the adequacy of the natural FEPs appropriate to the disposal system and how these were considered in the PA. The EPA also evaluated the DOE's consideration of mining and drilling in the PA. The EPA performed a critical review of each step in the DOE FEP selection process for the CCA, including identification and listing of the potentially disruptive FEPs, screening of these FEPs, combination of FEPs to form scenarios, screening of scenarios, and the final formation of scenarios for use in the CCA PA.

The EPA concluded that the initial FEP list assembled by the DOE was sufficiently comprehensive. This list appropriately screened out EPs on the basis of probability, consequence, or regulatory requirements. The EPA concluded that the DOE considered and incorporated into PA numerous natural EPs, mining, and deep drilling. The EPA concluded that the DOE considered shallow drilling and appropriately screened it out on the basis of low consequence. The DOE also appropriately followed regulatory requirements when it did not consider future fluid injection activities (U.S. EPA 1998a).

32.3.2 40 CFR § 194.32(b)

The CCA described how mining is incorporated into the PA, including information on mining rates and probabilities, the application of institutional controls, hydraulic conductivity variations as a result of mining, and the extent of minable reserves (see the CCA, Chapter 6.0, Section 6.4.6.2.3). The DOE identified potash as the only natural resource currently being mined near the WIPP. The DOE used the EPA-specified frequency of mining and probability when considering changes in hydraulic conductivity up to 1,000 times the base hydraulic conductivity of the Culebra Dolomite Member of the Rustler Formation (hereafter referred to as Culebra). In its calculation of the potash area to be mined, the DOE considered minable reserves inside and outside the controlled area (the CCA, Appendix DEL, Section DEL.4.2.4).

In reviewing the DOE's compliance with 40 CFR § 194.32(b), the EPA considered whether the CCA included a detailed, accurate, and comprehensive analysis of mined resources in the WIPP area and sufficient information to demonstrate how mining probability was determined. Specifically, the EPA examined the validity of the DOE's potash reserve estimates, including the DOE's assumptions regarding potash reserve location, quality, and minable horizons. The EPA also examined the CCA to determine how hydraulic conductivity in the supra-Salado Formation

units was modified to address changes that could be caused by mining over the 10,000-year regulatory period (U.S. EPA 1998a).

The EPA's review of minable reserves found that the DOE identified current minable thicknesses and horizons near the WIPP. The DOE's estimate roughly corresponds to that identified in an EPA technical memorandum (Peake 1996). The EPA recognized that this is not necessarily representative of the entire Delaware Basin, and it is conceivable that additional reserves could be mined in the WIPP area. However, speculation of this nature would extend to other horizons or reserves, which is beyond the intent of section 194.32(b). The EPA therefore concurred with the DOE's approach.

The EPA also found that the DOE assumed mined resources will be completely removed from the controlled area within the century in which mining occurs, and complete removal of mineral resources was assumed to occur only once over the regulatory time frame, in accordance with section 194.32(b). The DOE assumed that mining will be done via room and pillar or other conventional methods, and solution mining of potash will not take place because of mineralogical and economic constraints.

Finally, the EPA determined that mining was properly incorporated in PA through the application of the 1 to 1,000 multiplier for hydraulic conductivity in the calculated transmissivity field for the Culebra. The CCA, Appendix TFIELD and related documentation include information pertinent to this application of the transmissivity multiplier.

32.3.3 40 CFR § 194.32(c)

In the CCA, the DOE identified appropriate events and analyses of their effects on the disposal system, as well as the effects of existing boreholes. The EPA considered how these events affected the disposal system and whether the DOE addressed the potential for slant drilling. The EPA also examined whether the DOE addressed potentially exploitable existing leases.

The DOE concluded that oil and gas exploration and exploitation and water and potash exploration are the only human-initiated activities that need to be considered for PA (see the CCA, Chapter 6.0, Section 6.3.2). The DOE divided human-initiated activities into two categories: (1) those that have been Historic, Current, and Near-Future (HCN), and (2) those that may happen in the future after disposal (Future). Human-initiated activities included three different drilling-related intrusion scenarios used in PA based on the screening analysis, designated by the DOE as E1, E2, and E1E2 (see the CCA, Chapter 6.0, Section 6.3.2). The E1 scenario assumed penetration of a panel by a borehole drilled through the repository, which then strikes a brine pocket present in the underlying Castile Formation. The E2 scenario included all future boreholes that penetrate a panel but do not strike an underlying brine pocket within the Castile. The E1E2 scenario was defined as the occurrence of multiple boreholes that intersect a single waste panel, with at least one of the events being an E1 occurrence.

The EPA evaluated the DOE's compliance with 40 CFR § 194.32(c) and determined that the DOE had used a reasonable approach to screen human-initiated activities that might impact the repository. The EPA concluded that, based on the discussion in the CCA, Appendix SCR, the DOE considered the appropriate issues, and the technical conclusions reached by the DOE

regarding screening of oil and gas exploration and extraction activities were valid (U.S. EPA 1998a).

32.3.4 40 CFR § 194.32(d)

The DOE listed FEPs eliminated from PA based on probability, and described why they were not included. The DOE used this requirement to screen out FEPs such as nuclear criticality, galvanic coupling, formation of new faults, glaciation, and impact of large meteorites.

The EPA examined the screening arguments and information in the CCA, Appendix SCR to assess the traceability of assumptions, approximations, and measures of uncertainties. The EPA examined the DOE's approach to determine whether it was well documented and adequately justified. The EPA examined assigned probabilities to determine whether they were appropriate, documented, and in accordance with EPA regulatory requirements, and examined the sufficiency of all data in terms of quantity and adequacy. In conclusion, the EPA concurred with the events and processes that were screened out by the DOE using the low-probability criterion (U.S EPA 1998a).

32.3.5 40 CFR § 194.32(e)

32.3.5.1 40 CFR § 194.32(e)(1)

40 CFR § 194.32(e)(1) specifies that all potential FEPs that may occur during the regulatory time period be identified and considered. In this criterion, a time frame of interest is applied to FEPs that may affect the disposal system. This criterion specifies "the regulatory time frame," which begins at repository closure and continues for 10,000 years in the future. This is in contrast to that specified in section 194.32(c), where the time period of interest is HCN.[1]

The CCA, Appendix SCR identified the processes and events, or sequences and combinations of processes and events, included in PA, including natural and human-initiated processes and events. The CCA, Appendix SCR provided a comprehensive analysis of all FEPs that may affect WIPP performance. In addition, the CCA, Appendix SCR and its attachments document the development of the WIPP FEPs list and describe its origin from over 1,200 FEPs identified through various international repository programs. The broad and comprehensive beginning of the WIPP FEPs list helps to assure that all potential WIPP-relevant FEPs can be properly identified. After refinement of the initial list, the DOE's FEP identification process resulted in approximately 237 FEPs that were retained for screening.

The EPA reviewed the DOE's initial FEPs list at each stage of development and review to determine whether it was comprehensive. In addition, the EPA examined information sources used by the DOE to compile the FEPs list for completeness and accuracy of technical information. The EPA concluded that the DOE identified those events and processes, and sequences or combinations of events and processes, that may occur during the regulatory time period and affect the repository. The EPA concluded that these FEPs represented those most critical in terms of affecting the disposal repository (U.S. EPA 1998a).

[1] Human-initiated FEPs are screened for both the HCN and Future time periods (i.e., 194.32(c) and 194.32(e)(1)).

32.3.5.2 40 CFR § 194.32(e)(2)

40 CFR § 194.32(e)(2) states that compliance applications must identify the processes, events or sequences and combinations of processes and events included in PA. To accomplish this, the DOE formulated conceptual models and scenarios that incorporated each of the FEPs screened in during the screening processes detailed in the CCA, Appendix SCR. The DOE developed scenarios to represent both undisturbed and disturbed system performance. FEPs were included into scenarios ranging from the effects of deep and shallow drilling and mining to undisturbed disposal system performance. In the CCA, Chapter 6.0, Section 6.2, Table 6-6, the DOE identified the specific locations in the CCA where information on the modeling of the individual FEP can be found.

The EPA reviewed the CCA to determine whether FEPs and subsequent scenarios were appropriately screened, adequately justified, and completely supported. In addition, the EPA examined combinations of FEPs and scenarios included in PA. The EPA concluded that the DOE used a process, the Statens Kärnkraftinspektion (SKI) list (modified to suit conditions at the WIPP site), that identified the processes, events, or sequences, or combinations of processes and events (Stenhouse, Chapman, and Sumerling 1993). As part of this process, the DOE adequately addressed and evaluated the effects of mining, deep drilling, and shallow drilling. The DOE evaluated the FEPs and sequences of FEPs through calculations, estimates of probability, and comparisons to regulatory requirements. The EPA concluded that the DOE appropriately identified, listed, and discussed the FEPs and the effects of the sequences and combinations of FEPs that result in modeled scenarios (U.S. EPA 1998a).

32.3.5.3 40 CFR § 194.32(e)(3)

40 CFR § 194.32(e)(3) requires that FEPs not included in PA calculations be adequately documented and justified. The DOE identified approximately 237 FEPs in the CCA, Appendix SCR, and the CCA, Chapter 6.0, Section 6.3. For each FEP, the DOE provided a description and a generalized rationale for screening classifications. Of the 237 FEPs analyzed, 154 were screened out on the basis of regulations (SO-R), low consequence (SO-C), or probability (SO-P). The CCA, Appendix SCR included the DOE's screening rationale for each of the 237 CCA FEPs.

To verify the DOE's compliance with this section, the EPA reviewed the information in the CCA, Appendix SCR and also conducted audits to verify the proper execution of quality assurance programs for all items and activities important to the containment of waste in the repository, including items and activities related to FEPs. As a result of these EPA audits, the EPA concluded that quality assurance programs were properly executed for FEP-related items and activities, and that the DOE had demonstrated compliance with the requirements of section 194.32 (U.S. EPA 1998a).

32.4 Changes in the CRA-2004

For the Compliance Recertification Application of 2004 (CRA-2004) (U.S. DOE 2004) and the subsequent Performance Assessment Baseline Calculation, the DOE reevaluated all WIPP FEPs to determine if any had changed or if new FEPs needed to be added. This reevaluation resulted in

only a few changes to the FEPs analysis. Wagner, Kirkes, and Martell (Wagner, Kirkes, and Martell 2003) concluded that of the original 237 FEPs included in the CCA, 106 did not change, 120 required updates to their FEP descriptions and/or screening arguments, and 7 of the original baseline FEPs screening decisions required a change from their original screening decision. Four of the original baseline FEPs were deleted or combined with other closely related FEPs, and two new FEPs were added to the baseline. These two FEPs were previously addressed in an existing FEP; they were separated for clarity. Therefore, for the CRA-2004, reevaluation resulted in a new FEPs baseline consisting of 235 FEPs, but did not change the CCA conceptual models or the scenarios developed for PA.

32.5 EPA's Evaluation of Compliance for the 2004 Recertification

For the CRA-2004, the DOE applied the same approach that was used for the CCA to develop and screen the list of FEPs that may have an effect on the disposal system. Since the WIPP FEPs were previously evaluated and approved in the initial certification process, the EPA focused its recertification review on the FEPs that had changed since the 1998 Certification Decision (U.S. EPA 1998b). The EPA verified that the DOE's FEP development and review process was fundamentally the same as the CCA process, and verified that the DOE's reevaluation properly considered changes since the original certification decision in 1998. The EPA verified that any changes to FEP screening arguments or FEP-related discussions were reasonable, appropriate, and complete.

The EPA received one public comment related to the scope of PA. Some stakeholders proposed that karst (FEP N20) should be included in the PA conceptual model development. The EPA reevaluated karst issues raised by stakeholders from the CCA, as well as new information made available since the original certification decision. The EPA's review is discussed in the Technical Support Document for Section 194.14: Evaluation of Karst at the WIPP Site (U.S. EPA 2006a). After a thorough review, the EPA determined that karst should not be screened into the PA process.

Based on a review and evaluation of the CRA-2004 and supplemental information provided by the DOE, the EPA determined that the DOE continued to comply with the requirements for section 194.32 (U.S. EPA 2006b and U.S. EPA 2006c).

32.6 Changes or New Information Between the CRA-2004 and the CRA-2009 (Previously: Changes or New Information Since the 2004 Recertification)

For the CRA-2009 (U.S. DOE 2009), the DOE identified all PA changes implemented since the CRA-2004 and determined their impacts to the FEPs baseline (Kirkes 2008). This assessment was very similar to the process used for the CRA-2004. The FEPs baseline was maintained according to Sandia National Laboratories Specific Procedure (SP) 9-4, *Performing FEPS Baseline Impact Assessments for Planned and Unplanned Changes* (Kirkes 2006). Any changes that affect the FEPs baseline were detailed in Appendix SCR-2009. As a result of the reevaluation, 35 FEPs were updated with new information, one screening argument was changed to correct errors discovered during review, and the screening decision for one FEP was changed from SO-R to SO-C. This latter change had no impact on PA calculations because the FEP continued to be excluded from PA, albeit via different screening rationale. Finally, there were 10

FEPs that were split into 20 similar but more specific FEPs. For the CRA-2009, there were 70 Natural FEPs, 61 Human-initiated EPs, and 114 Waste and Repository FEPs, resulting in 245 WIPP FEPs.

32.7 EPA's Evaluation of Compliance for the 2009 Recertification

For the CRA-2009, the EPA reviewed and verified the process that the DOE used to determine the set of FEPs that might have an effect on the disposal system. This process was essentially the same as used for the CCA and the CRA-2004, and resulted in 245 FEPs retained for evaluation in the CRA-2009. Since it had previously evaluated and approved this process, the EPA focused its 2009 recertification review on the FEPs that have changed since the 2004 Recertification Decision. The EPA verified that any changes to FEP screening arguments or FEP-related discussions were reasonable, appropriate and complete, and determined that the DOE was in compliance with the requirements of 40 CFR § 194.32. The EPA received one public comment stating that karst (FEP N20) should be included in PA conceptual models. The EPA concurred with the DOE's position that karst at the WIPP should not be included in performance calculations (U.S. EPA 2010). Based on a review and evaluation of the CRA-2009 and supplemental information provided by the DOE, the EPA determined that the DOE continued to comply with the requirements of section 194.32 (U.S. EPA 2010).

32.8 Changes or New Information since the CRA-2009

32.8.1 40 CFR § 194.32(a)

For the CRA-2014, changes to the WIPP baseline were identified and evaluated to determine their impact upon the WIPP FEPs baseline (Kirkes 2013a). The FEPs baseline continues to be maintained according to Sandia National Laboratories SP 9-4, *Performing FEPS Baseline Impact Assessments for Planned and Unplanned Changes* (Kirkes 2013b)[2]. This reevaluation process is the same process that was used for the CRA-2004 and CRA-2009 FEP assessments. For the CRA-2014, there are 70 Natural FEPs, 61 Human-initiated EPs, and 114 Waste and Repository FEPs, resulting in 245 WIPP FEPs. These are the same 245 FEPs retained for screening in the CRA-2009. There have been no additions or deletions. However, 61 of these FEPs have been updated in some way. The current FEPs baseline is presented in Appendix SCR-2014. Table 32-1 lists the CRA-2014 FEPs and their screening decisions, and summarizes any changes to related information since the CRA-2009.

[2] Note: Revision 3 of SP 9-4 was developed in response to EPA comments on the CRA-2009 Section 32, which identified inconsistencies in the documentation requirements as specified in SP 9-4 Revision 2.

Table 32-1. FEPs Summary for CRA-2014

EPA FEP I.D.[a,b,c, d]	FEP Name	Screening Argument Update?	Screening Decision Changed?	Screening Classification
N1	Stratigraphy	No change	No	UP
N2	Brine Reservoirs	Updated by new PA parameter GLOBAL:PBRINE	No	DP
N3	Changes in Regional Stress	No change	No	SO-C
N4	Regional Tectonics	No change	No	SO-C
N5	Regional Uplift and Subsidence	No change	No	SO-C
N6	Salt Deformation	No change	No	SO-P
N7	Diapirism	No change	No	SO-P
N8	Formation of Fractures	No change	No	SO-P UP (Repository)
N9	Changes in Fracture Properties	No change	No	SO-C UP (Near Repository)
N10	Formation of New Faults	No change	No	SO-P
N11	Fault Movement	No change	No	SO-P
N12	Seismic Activity	Updated with new seismic data	No	UP
N13	Volcanic Activity	No change	No	SO-P
N14	Magmatic Activity	No change	No	SO-C
N15	Metamorphic Activity	No change	No	SO-P
N16	Shallow Dissolution	No change	No	UP
N18	Deep Dissolution	No change	No	SO-P
N20	Breccia Pipes	No change	No	SO-P
N21	Collapse Breccias	No change	No	SO-P
N22	Fracture Infills	No change	No	SO-C - Beneficial
N23	Saturated Groundwater Flow	No change	No	UP
N24	Unsaturated Groundwater Flow	No change	No	UP
N25	Fracture Flow	No change	No	UP
N27	Effects of Preferential Pathways	No change	No	UP
N26	Density Effects on Groundwater Flow	No change	No	SO-C
N28	Thermal Effects on Groundwater Flow	No change	No	SO-C
N29	Saline Intrusion (Hydrogeological Effects)	No change	No	SO-P

Table 32-1. FEPs Summary for CRA-2014

EPA FEP I.D.[a,b,c, d]	FEP Name	Screening Argument Update?	Screening Decision Changed?	Screening Classification
N30	Freshwater Intrusion (Hydrogeological Effects)	No change	No	SO-P
N31	Hydrological Response to Earthquakes	No change	No	SO-C
N32	Natural Gas Intrusion	No change	No	SO-P
N33	Groundwater Geochemistry	No change	No	UP
N34	Saline Intrusion (Geochemical Effects)	No change	No	SO-C
N38	Effects of Dissolution	No change	No	SO-C
N35	Freshwater Intrusion (Geochemical Effects)	No change	No	SO-C
N36	Changes in Groundwater Eh	No change	No	SO-C
N37	Changes in Groundwater pH	No change	No	SO-C
N39	Physiography	No change	No	UP
N40	Impact of a Large Meteorite	No change	No	SO-P
N41	Mechanical Weathering	No change	No	SO-C
N42	Chemical Weathering	No change	No	SO-C
N43	Aeolian Erosion	No change	No	SO-C
N44	Fluvial Erosion	No change	No	SO-C
N45	Mass Wasting (Erosion)	No change	No	SO-C
N46	Aeolian Deposition	No change	No	SO-C
N47	Fluvial Deposition	No change	No	SO-C
N48	Lacustrine Deposition	No change	No	SO-C
N49	Mass Wasting (Deposition)	No change	No	SO-C
N50	Soil Development	No change	No	SO-C
N51	Stream and River Flow	No change	No	SO-C
N52	Surface Water Bodies	No change	No	SO-C
N53	Groundwater Discharge	No change	No	UP
N54	Groundwater Recharge	No change	No	UP
N55	Infiltration	No change	No	UP
N56	Changes in Groundwater Recharge and Discharge	No change	No	UP
N57	Lake Formation	No change	No	SO-C
N58	River Flooding	No change	No	SO-C
N59	Precipitation (e.g., Rainfall)	No change	No	UP
N60	Temperature	No change	No	UP
N61	Climate Change	No change	No	UP

Table 32-1. FEPs Summary for CRA-2014

EPA FEP I.D.[a,b,c, d]	FEP Name	Screening Argument Update?	Screening Decision Changed?	Screening Classification
N62	Glaciation	No change	No	SO-P
N63	Permafrost	No change	No	SO-P
N64	Seas and Oceans	No change	No	SO-C
N65	Estuaries	No change	No	SO-C
N66	Coastal Erosion	No change	No	SO-C
N67	Marine Sediment Transport and Deposition	No change	No	SO-C
N68	Sea Level Changes	No change	No	SO-C
N69	Plants	No change	No	SO-C
N70	Animals	No change	No	SO-C
N71	Microbes	No change	No	SO-C (UP - for colloidal effects and gas generation)
N72	Natural Ecological Development	No change	No	SO-C
H1	Oil and Gas Exploration	Updated with new drilling rate	No	SO-C (HCN) DP (Future)
H2	Potash Exploration	No change	No	SO-C (HCN) DP (Future)
H4	Oil and Gas Exploitation	Updated with new drilling rate	No	SO-C (HCN) DP (Future)
H8	Other Resources	No change	No	SO-C (HCN) DP (Future)
H9	Enhanced Oil and Gas Recovery	No change	No	SO-C (HCN) DP (Future)
H3	Water Resources Exploration	Updated with most recent monitoring information	No	SO-C (HCN) SO-C (Future)
H5	Groundwater Exploitation	Updated with most recent monitoring information	No	SO-C (HCN) SO-C (Future)
H6	Archaeological Investigations	No change	No	SO-R (HCN) SO-R (Future)
H7	Geothermal	No change	No	SO-R (HCN) SO-R (Future)
H10	Liquid Waste Disposal	No change	No	SO-R (HCN) SO-R (Future)
H11	Hydrocarbon Storage	No change	No	SO-R (HCN) SO-R (Future)

Table 32-1. FEPs Summary for CRA-2014

EPA FEP I.D.[a,b,c, d]	FEP Name	Screening Argument Update?	Screening Decision Changed?	Screening Classification
H12	Deliberate Drilling Intrusion	No change	No	SO-R (HCN) SO-R (Future)
H13	Conventional Underground Potash Mining	No change	No	UP (HCN) DP (Future)
H14	Other Resources (Mining For)	No change	No	SO-C (HCN) SO-R (Future)
H15	Tunneling	No change	No	SO-R (HCN) SO-R (Future)
H16	Construction of Underground Facilities (For Example, Storage, Disposal, Accommodation)	No change	No	SO-R (HCN) SO-R (Future)
H17	Archaeological Excavations	No change	No	SO-C (HCN) SO-R (Future)
H18	Deliberate Mining Intrusion	No change	No	SO-R (HCN) SO-R (Future)
H19	Explosions for Resource Recovery	No change	No	SO-C (HCN) SO-R (Future)
H20	Underground Nuclear Device Testing	No change	No	SO-C (HCN) SO-R (Future)
H21	Drilling Fluid Flow	No change	No	SO-C (HCN) DP (Future)
H22	Drilling Fluid Loss	No change	No	SO-C (HCN) DP (Future)
H23	Blowouts	Updated with new parameter GLOBAL:PBRINE	No	SO-C (HCN) DP (Future)
H24	Drilling-Induced Geochemical Changes	No change	No	UP (HCN) DP (Future)
H25	Oil and Gas Extraction	No change	No	SO-C (HCN) SO-R (Future)
H26	Groundwater Extraction	No change	No	SO-C (HCN) SO-R (Future)
H27	Liquid Waste Disposal–Outside Boundary (OB)	No change	No	SO-C (HCN) SO-C (Future)
H28	Enhanced Oil and Gas Production–OB	No change	No	SO-C (HCN) SO-C (Future)
H29	Hydrocarbon Storage–OB	No change	No	SO-C (HCN) SO-C (Future)
H60	Liquid Waste Disposal–Inside Boundary (IB)	No change	No	SO-R (HCN) SO-R (Future)

Table 32-1. FEPs Summary for CRA-2014

EPA FEP I.D.[a,b,c, d]	FEP Name	Screening Argument Update?	Screening Decision Changed?	Screening Classification
H61	Enhanced Oil and Gas Production–IB	No change	No	SO-R (HCN) SO-R (Future)
H62	Hydrocarbon Storage–IB	No change	No	SO-R (HCN) SO-R (Future)
H30	Fluid-Injection Induced Geochemical Changes	No change	No	UP (HCN) SO-R (Future)
H31	Natural Borehole Fluid Flow	Updated to reflect new plugging probabilities	No	SO-C (HCN) SO-C (Future, holes not penetrating waste panels) DP (Future, holes penetrating panels)
H32	Waste-Induced Borehole Flow	Updated to reflect new plugging probabilities	No	SO-R (HCN) DP (Future)
H34	Borehole-Induced Solution and Subsidence	No change	No	SO-C (HCN) SO-C (Future)
H35	Borehole-Induced Mineralization	No change	No	SO-C (HCN) SO-C (Future)
H36	Borehole-Induced Geochemical Changes	No change	No	UP (HCN) DP (Future) SO-C (for units other than the Culebra)
H37	Changes in Groundwater Flow Due to Mining	No change	No	UP (HCN) DP (Future)
H38	Changes in Geochemistry Due to Mining	No change	No	SO-C (HCN) SO-R (Future)
H39	Changes in Groundwater Flow Due to Explosions	No change	No	SO-C (HCN) SO-R (Future)
H40	Land Use Changes	No change	No	SO-R (HCN) SO-R (Future)
H41	Surface Disruptions	No change	No	UP (HCN) SO-C (Future)
H42	Damming of Streams or Rivers	No change	No	SO-C (HCN) SO-R (Future)
H43	Reservoirs	No change	No	SO-C (HCN) SO-R (Future)
H44	Irrigation	No change	No	SO-C (HCN) SO-R (Future)
H45	Lake Usage	No change	No	SO-R (HCN) SO-R (Future)

Table 32-1. FEPs Summary for CRA-2014

EPA FEP I.D.[a,b,c, d]	FEP Name	Screening Argument Update?	Screening Decision Changed?	Screening Classification
H46	Altered Soil or Surface Water Chemistry by Human Activities	No change	No	SO-C (HCN) SO-R (Future)
H47	Greenhouse Gas Effects	No change	No	SO-R (HCN) SO-R (Future)
H48	Acid Rain	No change	No	SO-R (HCN) SO-R (Future)
H49	Damage to the Ozone Layer	No change	No	SO-R (HCN) SO-R (Future)
H50	Coastal Water Use	No change	No	SO-R (HCN) SO-R (Future)
H51	Sea Water Use	No change	No	SO-R (HCN) SO-R (Future)
H52	Estuarine Water Use	No change	No	SO-R (HCN) SO-R (Future)
H53	Arable Farming	No change	No	SO-C (HCN) SO-R (Future)
H54	Ranching	No change	No	SO-C (HCN) SO-R (Future)
H55	Fish Farming	No change	No	SO-R (HCN) SO-R (Future)
H56	Demographic Change and Urban Development	No change	No	SO-R (HCN) SO-R (Future)
H57	Loss of Records	No change	No	NA (HCN) DP (Future)
H58	Solution Mining for Potash	Updated with information regarding solution mining activities in the region	No	SO-R (HCN) SO-R (Future)
H59	Solution Mining for Other Resources	Updated with new information regarding brine wells in the region	No	SO-C (HCN) SO-C (Future)
W1	Disposal Geometry	Updated with new information regarding additional mined area used for experiments	No	UP

Table 32-1. FEPs Summary for CRA-2014

EPA FEP I.D.[a,b,c, d]	FEP Name	Screening Argument Update?	Screening Decision Changed?	Screening Classification
W2	Waste Inventory	Updated to reflect the inventory data sources used for the CRA-2014 PA	No	UP
W3	Heterogeneity of Waste Forms	Updated to reflect the inventory data sources used for the CRA-2014 PA	No	DP
W4	Container Form	Updated to reflect the inventory data sources used for the CRA-2014 PA	No	SO-C – Beneficial
W5	Container Material Inventory	Updated to reflect the inventory data sources used for the CRA-2014 PA	No	UP
W6	Shaft Seal Geometry	No change	No	UP
W7	Shaft Seal Physical Properties	No change	No	UP
W109	Panel Closure Geometry	Updated with new information on panel closure design	No	UP
W110	Panel Closure Physical Properties	Updated with new information on panel closure design	No	UP
W8	Shaft Seal Chemical Composition	No change	No	SO-C Beneficial
W111	Panel Closure Chemical Composition	Updated with new information on panel closure design	No	SO-C Beneficial
W9	Backfill Physical Properties	No change	No	SO–C

Table 32-1. FEPs Summary for CRA-2014

EPA FEP I.D.[a,b,c, d]	FEP Name	Screening Argument Update?	Screening Decision Changed?	Screening Classification
W10	Backfill Chemical Composition	Updated to reflect implementation of water balance in PA	No	UP
W11	Post-Closure Monitoring	No change	No	SO-C
W12	Radionuclide Decay and In-Growth	No change	No	UP
W13	Heat from Radioactive Decay	Updated to reflect the inventory used for the CRA-2014 PA	No	SO-C
W14	Nuclear Criticality: Heat	Updated to reflect the inventory used for the CRA-2014 PA	No	SO-P
W15	Radiological Effects on Waste	Updated to reflect the inventory used for the CRA-2014 PA	No	SO-C
W16	Radiological Effects on Containers	Updated to reflect the inventory used for the CRA-2014 PA	No	SO-C
W17	Radiological Effects on Shaft Seals	Updated to reflect the inventory used for the CRA-2014 PA	No	SO-C
W112	Radionuclide Effects on Panel Closures	Updated to reflect the inventory used for the CRA-2014 PA	No	SO-C
W18	Disturbed Rock Zone (DRZ)	Updated to include new panel closure implementation	No	UP
W19	Excavation-Induced Changes in Stress	Updated to include new panel closure implementation	No	UP

Table 32-1. FEPs Summary for CRA-2014

EPA FEP I.D.[a,b,c, d]	FEP Name	Screening Argument Update?	Screening Decision Changed?	Screening Classification
W20	Salt Creep	Updated to include new panel closure implementation	No	UP
W21	Changes in the Stress Field	Updated to include new panel closure implementation	No	UP
W22	Roof Falls	No change	No	UP
W23	Subsidence	No change	No	SO-C
W24	Large Scale Rock Fracturing	No change	No	SO-P
W25	Disruption Due to Gas Effects	No change	No	UP
W26	Pressurization	Updated to reference new corrosion experiments and associated parameters	No	UP
W27	Gas Explosions	No change	No	UP
W28	Nuclear Explosions	Updated to reflect the inventory used for the CRA-2014 PA	No	SO-P
W29	Thermal Effects on Material Properties	Updated to reflect the inventory used for the CRA-2014 and planned thermal experiments	No	SO-C
W30	Thermally Induced Stress Changes	Updated to reflect the inventory used for the CRA-2014 and planned thermal experiments	No	SO-C

Table 32-1. FEPs Summary for CRA-2014

EPA FEP I.D.[a,b,c, d]	FEP Name	Screening Argument Update?	Screening Decision Changed?	Screening Classification
W31	Differing Thermal Expansion of Repository Components	Updated to reflect the inventory used for the CRA-2014 and planned thermal experiments	No	SO-C
W72	Exothermic Reactions	Updated to reflect the inventory used for the CRA-2014 and planned thermal experiments	No	SO-C
W73	Concrete Hydration	Updated to reflect the inventory used for the CRA-2014 and planned thermal experiments	No	SO-C
W32	Consolidation of Waste	No change	No	UP
W36	Consolidation of Shaft Seals	No change	No	UP
W37	Mechanical Degradation of Shaft Seals	No change	No	UP
W39	Underground Boreholes	No change	No	UP
W113	Consolidation of Panel Closures	Updated screening argument with new information regarding panel closure composition	No	UP
W114	Mechanical Degradation of Panel Closures	Updated screening argument with new information regarding panel closure composition	No	UP
W33	Movement of Containers	Updated to reference new inventory data	No	SO-C
W34	Container Integrity	No change	No	SO–C Beneficial

Table 32-1. FEPs Summary for CRA-2014

EPA FEP I.D.[a,b,c, d]	FEP Name	Screening Argument Update?	Screening Decision Changed?	Screening Classification
W35	Mechanical Effects of Backfill	No change	No	SO–C
W40	Brine Inflow	Updated to reflect water balance implementation in PA	No	UP
W41	Wicking	Updated to reflect water balance implementation in PA	No	UP
W42	Fluid Flow Due to Gas Production	Updated to reflect water balance implementation in PA and new steel corrosion rates	No	UP
W43	Convection	Updated to reflect planned thermal experiments	No	SO-C
W44	Degradation of Organic Material	Updated to reference new inventory data	No	UP
W45	Effects of Temperature on Microbial Gas Generation	Updated to reference new inventory data	No	UP
W48	Effects of Biofilms on Microbial Gas Generation	Updated to reference new inventory data	No	UP
W46	Effects of Pressure on Microbial Gas Generation	No change	No	SO-C
W47	Effects of Radiation on Microbial Gas Generation	Updated with new radionuclide inventory and information related to the EPA request for additional information on CRA-2009	No	SO-C

Table 32-1. FEPs Summary for CRA-2014

EPA FEP I.D.[a,b,c, d]	FEP Name	Screening Argument Update?	Screening Decision Changed?	Screening Classification
W49	Gases from Metal Corrosion	Updated to reference new corrosion experiments and inventory	No	UP
W51	Chemical Effects of Corrosion	Updated to reference new corrosion experiments and inventory	No	UP
W50	Galvanic Coupling (Within the Repository)	No change	No	SO-C
W52	Radiolysis of Brine	No change	No	SO-C
W53	Radiolysis of Cellulose	Screening argument updated with new radionuclide inventory	No	SO-C
W54	Helium Gas Production	Screening argument updated with new radionuclide inventory	No	SO-C
W55	Radioactive Gases	Updated to reference new inventory data	No	SO-C
W56	Speciation	Reference made to new solubility calculations based on new inventory components	No	UP in disposal rooms and Culebra. SO-C elsewhere, and SO-C Beneficial in cementitious seals
W57	Kinetics of Speciation	No change	No	SO-C
W58	Dissolution of Waste	No change	No	UP
W59	Precipitation of Secondary Minerals	No change	No	SO-C Beneficial
W60	Kinetics of Precipitation and Dissolution	No change	No	SO-C
W61	Actinide Sorption	No change	No	UP in the Culebra and Dewey Lake; SO-C—Beneficial in the disposal room, shaft seals, panel closures, and other geologic units.

Table 32-1. FEPs Summary for CRA-2014

EPA FEP I.D.[a,b,c, d]	FEP Name	Screening Argument Update?	Screening Decision Changed?	Screening Classification
W62	Kinetics of Sorption	No change	No	UP in the Culebra and Dewey Lake; SO-C—Beneficial in the disposal room, shaft seals, panel closures, and other geologic units.
W63	Changes in Sorptive Surfaces	No change	No	UP
W64	Effects of Metal Corrosion	No change	No	UP
W66	Reduction-Oxidation Kinetics	No change	No	UP
W65	Reduction-Oxidation Fronts	No change	No	SO-P
W67	Localized Reducing Zones	No change	No	SO-C
W68	Organic Complexation	Updated to reflect implementation of variable brine volume in PA	No	UP
W69	Organic Ligands	Updated to reflect implementation of variable brine volume, new inventory data	No	UP
W71	Kinetics of Organic Complexation	No change	No	SO-C
W70	Humic and Fulvic Acids	No change	No	UP
W74	Chemical Degradation of Shaft Seals	No change	No	UP
W76	Microbial Growth on Concrete	No change	No	UP
W115	Chemical Degradation of Panel Closures	Updated screening argument with new panel closure materials	Yes	SO-P
W75	Chemical Degradation of Backfill	No change	No	SO-C
W77	Solute Transport	No change	No	UP
W78	Colloid Transport	No change	No	UP
W79	Colloid Formation and Stability	No change	No	UP

Table 32-1. FEPs Summary for CRA-2014

EPA FEP I.D.[a,b,c, d]	FEP Name	Screening Argument Update?	Screening Decision Changed?	Screening Classification
W80	Colloid Filtration	No change	No	UP
W81	Colloid Sorption	No change	No	UP
W82	Suspensions of Particles	No change	No	DP
W83	Rinse	No change	No	SO-C
W84	Cuttings	No change	No	DP
W85	Cavings	Updated with new waste shear strength data	No	DP
W86	Spallings	Updated with new water balance implementation	No	DP
W87	Microbial Transport	No change	No	UP
W88	Biofilms	No change	No	SO-C Beneficial
W89	Transport of Radioactive Gases	Updated to reference CRA-2014 inventory data	No	SO-C
W90	Advection	No change	No	UP
W91	Diffusion	No change	No	UP
W92	Matrix Diffusion	No change	No	UP
W93	Soret Effect	Updated based on new inventory data	No	SO-C
W94	Electrochemical Effects	No change	No	SO-C
W95	Galvanic Coupling (Outside the Repository)	No change	No	SO-P
W96	Electrophoresis	No change	No	SO-C
W97	Chemical Gradients	No change	No	SO-C
W98	Osmotic Processes	No change	No	SO-C
W99	Alpha Recoil	No change	No	SO-C
W100	Enhanced Diffusion	No change	No	SO-C
W101	Plant Uptake	No change	No	SO-R (for section 191.13) SO-C (for section 191.15)
W102	Animal Uptake	No change	No	SO-R (for section 191.13) SO-C (for section 191.15)

Table 32-1. FEPs Summary for CRA-2014

EPA FEP I.D.[a,b,c,d]	FEP Name	Screening Argument Update?	Screening Decision Changed?	Screening Classification
W103	Accumulation in Soils	No change	No	SO-C Beneficial (for section 191.13) SO-C (for section 191.15)
W104	Ingestion	No change	No	SO-R SO-C (for section 191.15)
W105	Inhalation	No change	No	SO-R SO-C (for section 191.15)
W106	Irradiation	No change	No	SO-R SO-C (for section 191.15)
W107	Dermal Sorption	No change	No	SO-R SO-C (for section 191.15)
W108	Injection	No change	No	SO-R SO-C (for section 191.15)

[a] N = Natural FEP
[b] H = Human-induced event and process (EP)
[c] W = Waste- and Repository-induced FEP
[d] FEPs in this column that are not separated by rows represent FEPs that are similar in nature and are discussed and screened as a common group.

32.8.2 40 CFR § 194.32(b)

The requirements of section 194.32(b) specify assumptions regarding the implementation of mining in PA calculations. The PA modeling system used for the mining scenario is similar to that developed for the undisturbed repository scenario, but with a modified Culebra transmissivity field in the controlled area to account for the mining effects. Implementation of the mining scenario has not changed since the CRA-2009 Performance Assessment Baseline Calculation. Details regarding how mining processes are represented in PA models are described in Appendix PA-2014, Section PA-2.3.2.2.1, and Appendix MASS-2014, Section MASS-15.1. FEPs related to the presence of resources are described and considered in Appendix SCR-2014, Section SCR-5.0.

32.8.3 40 CFR § 194.32(c)

Section 194.32(c) provides specific time frames for the evaluation of activities that may affect the disposal system. This requirement focuses on activities that have occurred in the past, are occurring, or are expected to occur in the near future. The DOE classifies this time frame as HCN. Because section 194.32(e)(1) requires the evaluation of human-initiated EPs during the

regulatory time period, the DOE evaluates human-initiated FEPs for the period of time spanning from closure of the repository to 10,000 years into the future as well (Future) (see human-initiated EPs in Table 32-1). Human-initiated EPs are described and considered for both the HCN and Future time frames in Appendix SCR-2014, Section SCR-5.0. Therefore, the DOE is in compliance with the requirements of section 194.32(c).

32.8.4 40 CFR § 194.32(d)

Low-probability events can be excluded on the basis of the criterion provided in 40 CFR § 194.32(d), which states, "performance assessments need not consider processes and events that have less than one chance in 10,000 of occurring over 10,000 years." In practice, for most FEPs screened out on the basis of low probability of occurrence, it has not been possible to estimate a meaningful quantitative probability. In the absence of quantitative probability estimates, a qualitative argument was used. One FEP has been added to this screening classification since the CRA-2009. W115 Chemical Degradation of Panel Closures has been reclassified from UP to SO-P due to the newly designed panel closure system and its run-of-mine salt composition. Therefore, there are 22 FEPs screened using the SO-P criterion for the CRA-2014. FEPs screened out on the basis of low probability are listed in Table 32-2.

Table 32-2. FEPs Classified SO-P for the CRA-2014

FEP I.D.	FEP Name
N6	Salt Deformation
N7	Diapirism
N8	Formation of Fractures
N10	Formation of New Faults
N11	Fault Movement
N13	Volcanic Activity
N15	Metamorphic Activity
N18	Deep Dissolution
N20	Breccia Pipes
N21	Collapse Breccias
N29	Saline Intrusion (Hydrogeological Effects)
N30	Freshwater Intrusion (Hydrogeological Effects)
N32	Natural Gas Intrusion
N40	Impact of a Large Meteorite
N62	Glaciation
N63	Permafrost
W14	Nuclear Criticality: Heat
W24	Large Scale Rock Fracturing
W28	Nuclear Explosions
W65	Reduction-Oxidation Fronts
W95	Galvanic Coupling (Outside the Repository)
W115	Chemical Degradation of Panel Closures

32.8.5 40 CFR § 194.32(e)

The requirements in section 194.32(e) are met by the analyses of FEPs as documented in Appendix SCR-2014. Table 32-1 lists the CRA-2014 FEPs and summarizes any changes to screening decisions and arguments.

Section 194.32, "Scope of Performance Assessment," requires the identification, selection, screening, and incorporation of all significant processes and events into PA. The DOE has taken a comprehensive approach in meeting the requirements of the section as documented here and in Appendix SCR-2014. The process used is consistent with evaluations of WIPP FEPs in past compliance applications. Any new information that relates to WIPP FEPs is identified and incorporated into PA as appropriate.

In summary, based on the information in Section 32.8, the DOE continues to comply with all the requirements in section 194.32 for the CRA-2014.

32.9 References

(*Indicates a reference that has not been previously submitted.)

Kirkes, G.R. 2006. *Activity/Project Specific Procedure SP 9-4: Performing FEPs Baseline Impact Assessments for Planned or Unplanned Changes* (Revision 1, June 6). ERMS 543625. Carlsbad, NM: Sandia National Laboratories.

Kirkes, G.R. 2008. *Features, Events and Processes Assessment for the Compliance Recertification Application—2009* (Revision 0). ERMS 550489. Carlsbad, NM: Sandia National Laboratories.

Kirkes, G.R. 2013a. *Features, Events and Processes Assessment for the Compliance Recertification Application—2014* (Revision 0). ERMS 560488. Carlsbad, NM: Sandia National Laboratories.*

Kirkes, G.R. 2013b. *Activity/Project Specific Procedure SP 9-4: Performing FEPs Baseline Impact Assessments for Planned or Unplanned Changes* (Revision 3, June 19). ERMS 560371. Carlsbad, NM: Sandia National Laboratories.

Peake, Tom. 1996. Memorandum to Docket (Subject: *Examination of Mining and Hydraulic Conductivity*). 31 January 1996. Docket A-92-56, Item IV-B-7.

Stenhouse, M.J., N.A. Chapman, and T.J. Sumerling. 1993. *SITE-94 Scenario Development FEP Audit List Preparation: Methodology and Presentation, SKI Technical Report 93:27*. ERMS 241371. Swedish Nuclear Power Inspectorate, Stockholm. Available from NTIS as DE 94621513.

U.S. Department of Energy (DOE). 1996. *Title 40 CFR Part 191 Compliance Certification Application for the Waste Isolation Pilot Plant* (October). 21 vols. DOE/CAO 1996-2184. Carlsbad, NM: Carlsbad Area Office.

U.S. Department of Energy (DOE). 2004. *Title 40 CFR Part 191 Compliance Recertification Application for the Waste Isolation Pilot Plant* (March). 10 vols. DOE/WIPP 2004-3231. Carlsbad, NM: Carlsbad Field Office.

U.S. Department of Energy (DOE). 2009. *Title 40 CFR Part 191 Compliance Recertification Application for the Waste Isolation Pilot Plant* (March). DOE/WIPP 2009-3424. Carlsbad, NM: Carlsbad Field Office.

U.S. Environmental Protection Agency (EPA). 1996. "40 CFR Part 194: Criteria for the Certification and Recertification of the Waste Isolation Pilot Plant's Compliance with the 40 CFR Part 191 Disposal Regulations; Final Rule." *Federal Register*, vol. 61 (February 9, 1996): 5223–45.

U.S. Environmental Protection Agency (EPA). 1998a. "CARD No. 32: Scope of Performance Assessments." Compliance Application Review Documents for the Criteria for the Certification and Recertification of the Waste Isolation Pilot Plant's Compliance with the 40 CFR Part 191 Disposal Regulations: Final Certification Decision (May) (pp. 25-1 through 32-46). Washington, DC: Office of Radiation and Indoor Air.

U.S. Environmental Protection Agency (EPA). 1998b. "40 CFR Part 194: Criteria for the Certification and Recertification of the Waste Isolation Pilot Plant's Compliance with the 40 CFR Part 191 Disposal Regulations: Certification Decision; Final Rule." *Federal Register*, vol. 63 (May 18, 1998): 27353–406.

U.S. Environmental Protection Agency (EPA). 2006a. *Technical Support Document for Sections 194.14/15: Evaluation of Karst at the WIPP Site* (March). Washington, DC: Office of Radiation and Indoor Air.

U.S. Environmental Protection Agency (EPA). 2006b. "Recertification CARD No. 32: Scope of Performance Assessments." *Compliance Application Review Documents for the Criteria for the Certification and Recertification of the Waste Isolation Pilot Plant's Compliance with the 40 CFR 191 Disposal Regulations: Final Recertification Decision* (March) (pp. 32-1 through 32-10). Washington, DC: Office of Radiation and Indoor Air.

U.S. Environmental Protection Agency (EPA). 2006c. "40 CFR Part 194: Criteria for the Certification and Recertification of the Waste Isolation Pilot Plant's Compliance with the 40 CFR Part 191 Disposal Regulations: Recertification Decision" (Final Notice). *Federal Register*, vol. 71 (April 10, 2006): 18010-021.

U.S. Environmental Protection Agency (EPA). 2010. *2009 Compliance Recertification Application (2009 CRA) Compliance Application Review Document (CARD) No. 32, Scope of Performance Assessment*. EPA Docket FDMS Docket ID No. EPA-HQ-OAR-2009-0330. Washington, DC: Office of Radiation and Indoor Air.*

Wagner, S., R. Kirkes, and M.A. Martell. 2003. *Features, Events and Processes: Reassessment for Recertification Report*. ERMS 530184. Carlsbad, NM: Sandia National Laboratories, Carlsbad Programs Group.

Title 40 CFR Part 191
Subparts B and C
Compliance Recertification Application 2014
for the
Waste Isolation Pilot Plant

Consideration of Drilling Events in Performance Assessments (40 CFR § 194.33)

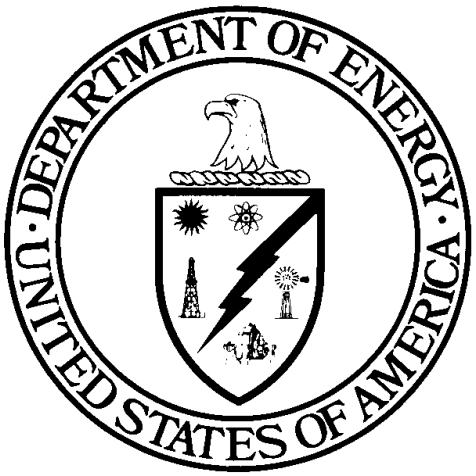

United States Department of Energy
Waste Isolation Pilot Plant

Carlsbad Field Office
Carlsbad, New Mexico

Compliance Recertification Application 2014
Consideration of Drilling Events in Performance Assessments
(40 CFR § 194.33)

Table of Contents

List of Tables

This page intentionally left blank.

Acronyms and Abbreviations

%	percent
AIC	active institutional control
BLM	U.S. Bureau of Land Management
CARD	Compliance Application Review Document
CCA	Compliance Certification Application
CFR	Code of Federal Regulations
CRA	Compliance Recertification Application
DBR	Direct Brine Release
DOE	U.S. Department of Energy
EPA	U.S. Environmental Protection Agency
EP	event and process
FEP	feature, event, and process
ft	feet
IB	inside boundary
in.	inch
km^2	square kilometer
m	meter
m^3	cubic meters
NMBMMR	New Mexico Bureau of Mines and Mineral Resources
NMOCD	New Mexico Oil Conservation Division
PA	performance assessment
PAVT	Performance Assessment Verification Test
PIC	passive institutional control
WIPP	Waste Isolation Pilot Plant
yrs	years

This page intentionally left blank.

33.0 Consideration of Drilling Events in Performance Assessments (40 CFR § 194.33)

33.1 Requirements

§ 194.33 Consideration of Drilling Events in Performance Assessments

(a) Performance assessments shall examine deep drilling and shallow drilling that may potentially affect the disposal system during the regulatory time frame.

(b) The following assumptions and process shall be used in assessing the likelihood and consequences of drilling events, and the results of such process shall be documented in any compliance application:

(1) Inadvertent and intermittent intrusion by drilling for resources (other than those resources provided by the waste in the disposal system or engineered barriers designed to isolate such waste) is the most severe human intrusion scenario.

(2) In performance assessments, drilling events shall be assumed to occur in the Delaware Basin at random intervals in time and space during the regulatory time frame.

(3) The frequency of deep drilling shall be calculated in the following manner:

(i) Identify deep drilling that has occurred for each resource in the Delaware Basin over the past 100 years prior to the time at which a compliance application is prepared

(ii) The total rate of deep drilling shall be the sum of the rates of deep drilling for each resource.

(4) The frequency of shallow drilling shall be calculated in the following manner:

(i) Identify shallow drilling that has occurred for each resource in the Delaware Basin over the past 100 years prior to the time at which a compliance application is prepared.

(ii) The total rate of shallow drilling shall be the sum of the rates of shallow drilling for each resource.

(iii) In considering the historical rate of all shallow drilling, the Department may, if justified, consider only the historical rate of shallow drilling for resources of similar type and quality to those in the controlled area.

(c) Performance assessments shall document that in analyzing the consequences of drilling events, the Department assumed that:

(1) Future drilling practices and technology will remain consistent with practices in the Delaware Basin at the time a compliance application is prepared. Such future drilling practices shall include, but shall not be limited to: the types and amounts of drilling fluids; borehole depths, diameters, and seals; and the fraction of such boreholes that are sealed by humans.

(2) Natural processes will degrade or otherwise affect the capability of boreholes to transmit fluids over the regulatory time frame.

(d) With respect to future drilling events, performance assessments need not analyze the effects of techniques used for resource recovery subsequent to the drilling of the borehole.

33.2 Background

40 CFR § 194.33 (U.S. EPA 1996) requires the U.S. Department of Energy (DOE) to make assumptions about future deep and shallow drilling in the Delaware Basin and the vicinity of the Waste Isolation Pilot Plant (WIPP). These assumptions pertain to the timing and duration of drilling, frequency of drilling, drilling practices and technology, and the effects of natural processes on boreholes.

Drilling in the near future within the Delaware Basin will most likely be for oil and gas exploration/exploitation, which constitutes a deep drilling event. Shallow drilling may occur for other resources (e.g., water), but has been screened out of this and past analyses due to lack of consequence on the disposal system (see the Compliance Certification Application [CCA], Chapter 6.0, Section 6.2.5.2 [U.S. DOE 1996], and the 2004 Compliance Recertification

Application [CRA-2004], Appendix PA, Attachment SCR; Appendix SCR-2009, and Appendix SCR-2014 [U.S. DOE 2004]). Drilling is incorporated in the performance assessment (PA) as a single event or combinations of events based upon different scenarios. Deep and shallow drilling rates and related activities directly affect the cumulative potential for radionuclide releases to the surface or to subsurface geologic units around the WIPP.

Deep drilling is defined by the U.S. Environmental Protection Agency (EPA) (U.S. EPA 1996) as events that terminate 655 meters (m) (2,150 feet [ft]) or more below ground surface, while shallow drilling events terminate no deeper than 655 m (2,150 ft) below ground surface. (Note that the repository level is 655 m (2,150 ft) below ground surface.)

33.3 1998 Certification Decision

33.3.1 40 CFR § 194.33(a) DOE Methodology and Conclusions

In the CCA (U.S. DOE 1996), Chapter 6.0, Section 6.2.5, the DOE identified oil and gas exploration/exploitation and water and potash exploration as the principal human activities that must be considered within the PA. The remaining human-initiated activities—such as exploration for geothermal energy, water supplies, and sulfur and brine extraction (solution mining)—were eliminated based upon low probability, low consequence, or for regulatory reasons.

33.3.1.1 Deep Drilling Methods

Descriptions of well drilling, plugging, and abandonment practices typically followed in the Delaware Basin were provided in the CCA, Appendix DEL, Section DEL.5, pp. DEL-26 through DEL-46. Chapter IX of the New Mexico Bureau of Mines and Mineral Resources (NMBMMR) Final Report (NMBMMR 1995),(pp. IX-1 through IX-69) includes a discussion of drilling targets and practices, with typical casing designs presented in the CCA, Appendix DEL, Figure DEL-13. The typical operation sequence for well installation was presented in Appendix DEL, Attachment 1 (Delaware Basin). Oil and gas exploration, exploitation, and production comprise 99% of the deep boreholes in the Delaware Basin, with the remainder being sulfur, potash, and stratigraphic test boreholes, as shown in Appendix DEL, Table DEL-4.

The CCA also provides extensive information pertaining to the deep drilling process, from acquisition of leases to well completion and abandonment (the CCA, Appendix DEL, Section DEL.6.1). In the area near the WIPP site, deep drilling typically terminates between approximately 1,524 to 4,695 m (5,000 to 15,400 ft) below ground surface. The DOE stated that mud rotary drilling is the typical drilling method used in the Delaware Basin. A summary of deep drilling activities is provided in the CCA, Appendix DEL, Section DEL.5.1.

33.3.1.2 Shallow Drilling Methods

The CCA discusses shallow drilling methods in Appendix DEL, Sections DEL.5.2 (Potash Coreholes) and DEL.5.3 (Water Wells). Although shallow drilling for hydrocarbons, sulfur, and brine extraction (solution mining) also occur, the CCA did not explicitly discuss drilling methods

for hydrocarbons and brine extraction (solution mining) because they are comparable to those for deep drilling, while drilling methods for sulfur are comparable to those for potash drilling.

33.3.1.3 Evaluation of Borehole Properties

Typical borehole sizes and depths were evaluated in the CCA, Appendix DEL, Section DEL.5, pp. DEL-26 through DEL-42. These borehole properties are described as having the potential to affect the disposal system through radionuclide migration and transport, as detailed below. The CCA, Chapter 6.0, Sections 6.5.3 and 6.5.5 provide the results of calculations showing that actinides expelled from the WIPP by these release mechanisms would not exceed EPA release limits. In addition, in Chapter 6.0, Section 6.4.7.2, pp. 6-156 through 6-161, the CCA showed that the properties and degradation history of borehole plugging material was very important to the containment capabilities of the WIPP.

33.3.1.4 Future Drilling Events Considered in the Performance Assessment

Future shallow drilling events were not considered in the PA because they were determined to be of low consequence to the PA calculations (CCA, Appendix SCR, Section SCR.3).

The CCA described three different combinations of drilling events considered in PA, E1, E2, and E1E2:

- The E1 Scenario: one or more boreholes penetrate a Castile brine reservoir and also intersect a repository panel (the CCA, Chapter 6.0, Figure 6-11)
- The E2 Scenario: one or more boreholes intersect a repository panel and do not penetrate a Castile brine reservoir (the CCA, Chapter 6.0, Figure 6-10)
- The E1E2 Scenario: multiple penetrations of the same waste panel where at least one penetration must be of the E1 type (the CCA, Chapter 6.0, Figure 6-12)

The following potential release mechanisms result from the intrusion scenarios listed above. Intrusions to the disposal system could affect radionuclide migration and transport via the following:

- Cuttings—material intersected by a rotary drilling bit
- Cavings—material eroded from a borehole wall during drilling
- Spallings—solid material carried into the borehole during rapid depressurization of the waste disposal region
- Direct Brine Releases (DBRs)—contaminated brine that may flow to the surface during drilling
- Long-Term Releases Following Drilling

Future drilling events are modeled through a random sampling procedure described in the CCA, Appendix CCDFGF, Sections 2 and 3. Uncertainty relative to the time and location of drilling is stochastic (i.e., derived from random processes, without knowledge about the future). Drilling is incorporated into the PA by repeatedly generating independent sequences of drilling-related events that could occur at the WIPP over the next 10,000 years (yrs). The defining parameters for the occurrence of future drilling events include not only the interval of time between drilling events and the location of drilling intrusions, but also the following four parameters:

- Activity of waste penetrated by each drilling intrusion (not related to deep or shallow drilling, but included for completeness)
- Plug configuration in the borehole
- Penetration of the Castile brine reservoir
- Occurrence of mining (not related to deep or shallow drilling, but included for completeness)

Random sampling from these distributions was used to calculate 10,000 different futures for the WIPP (the CCA, Chapter 6.0, Section 6.4.13.9).

33.3.2 40 CFR § 194.33(a) EPA Compliance Review

The EPA reviewed the information presented by the DOE in the CCA, Appendix DEL, Chapter DEL.6, Section 6.2, and Chapter IX of NMBMMR (NMBMMR 1995) to determine how extensively deep and shallow drilling was considered and whether the information provided was sufficiently comprehensive, accurate, and correctly calculated. The EPA examined the list of references presented in the CCA relative to drilling and conducted a literature search to evaluate the fluid injection study (U.S. EPA 1998a). The EPA determined that the DOE's scrutiny of resources to assess deep and shallow drilling practices and frequencies was comprehensive. The EPA also determined that the DOE's conclusions regarding representative drilling methods in the Delaware Basin are consistent with available data.

During the public comment period on the EPA's proposed certification, commenters raised the issue that both air and mud drilling might occur in the Delaware Basin and that releases from air drilling could be greater than from mud drilling, potentially causing the WIPP to fail the release limits of 40 CFR § 191.13 (U.S. EPA 1993). The DOE did not include air drilling in the CCA because it was not a technique commonly used in the area near the WIPP. In response to issues raised by stakeholders, the DOE provided several reports (Dials 1998) that examined both the likelihood and consequence of drilling with air at and near the WIPP. Likewise, the EPA examined the air drilling issue from several perspectives and documented its findings in the Technical Support Document *EPA's Analysis of Air Drilling at WIPP* (U.S. EPA 1998b), and in *Response to Comments*, Section 8 (U.S. EPA 1998c). The results of the EPA's analysis showed that air drilling is not common practice in the Delaware Basin. In addition, even if air drilling were to occur, the volume of spalled material released is within the range presented in the CCA.

The EPA evaluated the drilling-related information in the CCA to determine how both deep and shallow drilling affect the WIPP disposal system, including but not limited to, pressurization of the WIPP, brine/fluid removal, and circulation of brine within the panels. The EPA concluded that the DOE appropriately excluded shallow drilling from PA based upon low consequence. The EPA also concluded that the DOE appropriately simplified the intrusion scenarios to include the three types of drilling occurrences that, alone or in combination, are representative of potential future intrusion events in the WIPP.

33.3.3 40 CFR § 194.33(b) DOE Methodology and Conclusions

The CCA presents an analysis of all known wells, including hydrocarbon borehole exploratory and development wells in the Delaware Basin, and determines that inadvertent and intermittent drilling is the most severe human intrusion scenario. The CCA, Appendix DEL, Section DEL.7.3, and Appendix PA, Attachment SCR, Section SCR.3, include the DOE's analyses of drilling events in the WIPP area. The CCA, Chapter 6.0 identifies scenarios for human intrusion and calculated cumulative radionuclide releases assuming different intrusion events and combinations of events.

The CCA, Appendix DEL, Table DEL-3 presents a listing of the types and number of boreholes encountered within the Delaware Basin. The hydrocarbon borehole category is broken down into seven individual types, including oil, gas, oil/gas, dry, abandoned, injection, and service. Both exploratory wells (boreholes drilled to locate hydrocarbons) and developmental wells (boreholes drilled to exploit known reserves) are included within each category listed in the table. For example, if a well was drilled to explore for natural gas or with the intent to extract more gas by a secondary recovery method, both will be classified as gas wells.

By evaluating borehole types and standard well installation practices, the DOE determined that significant release of radionuclides from the disposal system can occur through only five drilling-related mechanisms for both exploratory and development wells (see CCA, Chapter 6.0, Section 6.0.2.3, p. 6-5).

33.3.4 40 CFR § 194.33(b)(1) EPA Compliance Review

The EPA evaluated resources considered by the DOE when developing human intrusion scenarios. The EPA examined resources identified by the DOE (the CCA, Chapter 2.0, Section 2.3.1, pp. 2-146 through 2-156, Appendix GCR, and Appendix DEL, Section DEL.4) and compared them with potential resources available in the area. The EPA reviewed the DOE's data pertaining to wells associated with the exploration and development related to these resources (the CCA, Appendix DEL, Section DEL.7) and concluded that the DOE considered the full spectrum of inadvertent and intermittent human intrusion scenarios possible in the Delaware Basin and incorporated them into the PA.

The EPA found that the DOE adequately demonstrated that it had considered inadvertent and intermittent drilling into or through the repository as the most severe human intrusion scenario (Compliance Application Review Document [CARD] 33, U.S. EPA 1998d). The EPA concluded that the DOE appropriately evaluated drilling in the Delaware Basin for inclusion in PA and adequately considered the drilling locations, depths, completion intervals, practices,

history, and occurrence of resources. Finally, the EPA concluded that exploratory and development wells were appropriately included in the DOE's analysis.

33.3.5 40 CFR § 194.33(b)(2) DOE Methodology and Conclusions

Based on the regulatory guidance and the historic rate of drilling in the Delaware Basin, the DOE calculated the rate of future drilling as 46.8 boreholes per square kilometer (km^2) per 10,000 yrs (the CCA, Chapter 6.0, Section 6.0.2.3, p. 6-5). In accordance with 40 CFR § 194.33(c)(1), the DOE assumed that current drilling practices will continue unchanged into the future.

The DOE discussed the drilling rate assumptions in the CCA, Chapter 6.0, Section 6.0.2.3, p. 6-5, and Appendix DEL, Section DEL.7, pp. 80–84. The DOE assumed random drilling events with respect to both location and time, allocated among three time periods:

- A period when institutional controls are active (0 to 100 yrs), during which no intrusions will occur
- A period when passive institutional controls (PICs) are effective (100 to 700 yrs), for which the drilling rate is two orders of magnitude lower than the rate experienced during the uncontrolled period
- An uncontrolled period (700 to 10,000 yrs)

In the CCA, Chapter 6.0, Section 6.4.12.2, pp. 182–83, the DOE outlined the process by which the random drilling rate assumptions were implemented. The number and time of intrusions were represented using a Poisson process to calculate the time period that elapsed between intrusions based on historical drilling activity and assuming a rate of 46.8 boreholes/km^2 (for the 700- to 10,000-year period), and 0.468 boreholes/km^2 for the period when PICs are effective (100 to 700 yrs). Specifically, the DOE stated in the CCA, Chapter 6.0, Section 6.4.12.2, p. 182, that both the number and time of intrusions are determined sequentially by sampling from a cumulative distribution function that describes the time elapsed between a given intrusion and the next intrusion. The potential time between intrusions varied from 0 to 9,900 yrs. Using this process, the DOE concluded that the most likely number of intrusions into a waste panel is 5, occurring with a probability of 0.1715. Zero intrusions occurred with a probability of 0.0041. The DOE found the largest number of intrusions that occurred is 14, with a probability of 0.0011 (the CCA, Chapter 6.0, Section 6.4.12.2, p. 183).

The DOE assigned drilling rates based on basin-wide borehole information. The drilling rate calculated for the basin was then applied to the area of the repository by the DOE randomly assigning intrusion borehole locations among 144 discrete regions in the repository. Each hypothetical intrusion was assumed to penetrate only 1 of the 144 blocks, and the probability of intersecting any given block was 1 in 144. Based on the ratio of excavated to undisturbed Salado Formation in each grid block, the DOE concluded that a borehole has a 20% probability of encountering excavated Salado (i.e., waste-filled repository or experimental regions) and an 80% chance of encountering unexcavated Salado (the CCA, Chapter 6.0, Section 6.4.12.3, p. 184).

The DOE did not consider boreholes relevant to the potential for release outside the boundaries of the repository, and therefore only calculated locations that could potentially intrude the repository. Specific well locations in the remainder of the Delaware Basin were not calculated. The CCA, Appendix CCDFGF presents details regarding how the probability of borehole intrusion scenarios was implemented in the construction of future realizations.

33.3.6 40 CFR § 194.33(b)(2) EPA Compliance Review

The EPA reviewed the DOE's implementation of drilling rate and location assumptions, and concluded that the DOE used appropriate methods to derive drilling rates and locations. The EPA determined (U.S. EPA 1998d) that the DOE adequately demonstrated that drilling events were assigned as occurring over random intervals of time and at random locations. The EPA also reviewed the DOE's implementation of drilling assumptions and determined that the method employed by the DOE in the calculations yields random drilling rate and location results. Use of Poisson distribution to project the time period that will elapse between intrusions was determined to be an acceptable approach. Division of the projected future into three distinct time periods was determined to be appropriately justified. The EPA disallowed PA credit for PICs. Nonetheless, the CCA Performance Assessment Verification Test (PAVT) calculations demonstrated that the effects of the proposed credits for active institutional controls (AICs) and PICs are insignificant, so that the PA results remain unaffected whether or not the credits are allowed (U.S. DOE 1997a).

33.3.7 40 CFR § 194.33(b)(3) DOE Methodology and Conclusions

In the CCA, Appendix DEL, Sections DEL.7.3 and DEL.7.4, the DOE identifies deep drilling that has occurred during the past 100 yrs for each resource known to occur in the Delaware Basin (hydrocarbons, potash, and sulfur), and calculates the total rate of deep drilling as the sum of the rates for each resource (the CCA, Appendix DEL, Section DEL.4.2). The DOE obtained information on deep drilling from two industry sources, Petroleum Information and the Midland Map Company, based on original records compiled by the New Mexico Oil Conservation Division (NMOCD) and the Railroad Commission of Texas Oil and Gas Division. Approximately 99% of the deep boreholes in the Delaware Basin were related to hydrocarbon exploration and exploitation. Industry database information regarding the number of deep drilling events/resource and information sources is presented in the CCA, Appendix DEL, Tables DEL-3, DEL-4, DEL-6, and DEL-7.

The DOE stated that drilling for deep resources near the boundary of the WIPP site since 1974 has demonstrated that profitable quantities of oil and gas resources are present near, and likely beneath, the WIPP site. The CCA, Appendix DEL, Figure DEL-6 shows oil and gas wells in the area surrounding the WIPP site (the CCA, Appendix DEL, Section DEL.4.2.2.4).

The DOE stated that three hydrocarbon exploration/exploitation deep wells have been drilled in the WIPP land withdrawal area (the CCA, Appendix DEL, Section DEL.4.2.3, p. DEL-20). Of these, two were drilled prior to 1982 and were later plugged and abandoned. The third well, drilled in 1982, is currently producing natural gas from a sandstone reservoir of Pennsylvanian Atokan age. Condemnation actions 77-071-B and 77-776-B by the United States currently withdraw all of Section 31, which is approximately 3.2 kilometers (2 miles) to the southwest of

the repository, from the surface to a depth of 1,829 m (6,000 ft) (the CCA, Appendix DEL, Section DEL.4.2.3). Leaseholders have mineral rights below 1,829 m (6,000 ft), which would be accessed by directional drilling from a surface location outside of Section 31.

The CCA, Appendix DEL, Section DEL.7.4, p. DEL-81, presents the DOE's calculated drilling rate in the Delaware Basin. The DOE calculated a rate of 46.8 deep holes per km^2 over 10,000 yrs and is shown below:

$$\text{Deep Drilling Rate} = \frac{(Total\ \#\ of\ deep\ boreholes) \times Regulatory\ Period}{Area\ of\ the\ Delaware\ Basin} \times \frac{1}{100\ yrs}$$

$$= \frac{(10{,}804) \times 10{,}000\ yrs}{23{,}102.1\ km^2} \times \frac{1}{100\ yrs}$$

$$= 46.765 \text{ deep boreholes per } km^2 \text{ per } 10{,}000 \text{ yrs}$$

The CCA contains tables that show the specific drilling rates for each type of well and for each type of resource (the CCA, Appendix DEL, pp. DEL-83 through DEL-84). The CCA, Chapter 6.0, Table 6-5 includes deep drilling events. The DOE used the drilling rates calculated from all available historical data as a basis for assigning future rates. These values and related calculation methods are shown in the CCA, Appendix DEL, Table DEL.6 and Table DEL.7. Reductions were made to these rates for AICs and PICs credit in the DOE analysis. As discussed in the CCA, Chapter 6.0, p. 6-181, AICs were credited for completely preventing inadvertent human intrusion for the first 100 yrs following repository closure. PICs were credited with reducing inadvertent intrusion to 1% of the calculated level for the period from 100 to 700 yrs after closure.

33.3.8 40 CFR § 194.33(b)(3) EPA Compliance Review

The EPA examined the CCA to determine the adequacy and accuracy of drilling rate calculations presented by the DOE, as well as supporting assumptions and determinations. The EPA examined the comprehensiveness and adequacy of deep drilling information and compared the DOE data to information on standard industry practice that had been collected for the Delaware Basin. The EPA checked the DOE's calculations regarding deep drilling frequency for accuracy and compared them with the EPA's calculations based upon an independently derived database (U.S. EPA 1998a).

The EPA's review determined that the DOE appropriately identified deep drilling that occurred in the Delaware Basin. The CCA identified resources for which deep drilling is used and estimated the number of drilling events that occurred over the past 100 yrs as 46.8 boreholes/km^2. The EPA found that the DOE's method was sufficiently explained and that the DOE adequately documented sources of supporting information. The EPA concluded that the DOE's results for the total rate of deep drilling are consistent with available data. The EPA disallowed credit for PICs. Therefore, the DOE did not take credit for PICs in the CCA PAVT calculations (U.S. DOE 1997a; U.S. DOE 1997b). The results of the PAVT were comparable to the original CCA results, in which PICs credit was employed; therefore, the EPA concluded that the PICs credit was not significant to the WIPP's compliance with the disposal standards.

The EPA found that the DOE's sources of information on deep drilling were reliable and that the DOE's confidence in the industry database was appropriate, based on the EPA's independent review of industry activity in the area (U.S. EPA 1998a). The DOE identified all resources relevant to deep drilling. Well databases are understood to contain all well types possible in the area, including both exploratory and development wells. Public comments on the proposed decision to certify the WIPP raised questions about the DOE's calculated deep drilling rate because commenters believed that the drilling rate used by the DOE was too low with respect to current drilling rates. The EPA concluded that the deep drilling rate used by the DOE was consistent with the requirements of 40 CFR Part 194.

33.3.9 40 CFR § 194.33(b)(4) DOE Methodology and Conclusions

The DOE examined the resources present within the Delaware Basin and determined that the shallow resources identified in the Delaware Basin are water, potash, sulfur, oil/gas, and brine wells (salt water "wells") (the CCA, Appendix DEL, Section DEL.4, Table DEL-5). Note: This table also presents stratigraphic and core test holes, but these apply to investigations associated with the five resources. The DOE examined these resources and determined that no shallow oil or gas is present in the controlled area or near the WIPP, and no minable sulfur reserves are present in the controlled area or near the WIPP (the CCA, Appendix DEL, p. DEL-81). The DOE also examined the possibility of brine extraction (solution mining) but excluded it from consideration in PA based upon low consequence.[1] The DOE concluded that water and potash are potential resources within the controlled area, but nevertheless included brine extraction (solution mining), and stratigraphic test holes (exclusive of those installed as part of the WIPP site characterization program) in its shallow drilling rate calculations.

The DOE identifies a total of 5,536 shallow boreholes that have been installed in the Delaware Basin, including those for sulfur coreholes (495 coreholes) but excluding those boreholes installed as part of the WIPP site characterization program (the CCA, Appendix DEL, Table DEL-5, p. DEL-83).

The DOE's method for calculating the shallow drilling rate was first to collect comprehensive information on shallow drilling in the Delaware Basin, including drilling for hydrocarbons, sulfur, potash, stratigraphic tests, water, and brine extraction (solution mining) wells (the CCA, Appendix DEL, Table DEL-5). The DOE stated that information regarding shallow drilling in the Delaware Basin was obtained from commercial and government sources. The DOE collected water well data from a commercial database developed by Whitestar Corporation of Englewood, Colorado; potash well data from Bureau of Land Management (BLM) records; and sulfur corehole data from a database developed jointly by Whitestar Corporation and Petroleum Information Corporation of Denver, Colorado (the CCA, Appendix DEL, Tables DEL-3, DEL-4, and DEL-7). Sources used to determine the type and quality of resources include those used to determine the drilling rate.

The DOE calculated the total rate of shallow drilling as the sum of the rates for shallow drilling of resources in the Delaware Basin of the type and quality similar to those in the WIPP-

[1] For the CCA, brine extraction was screened out based on low consequence. Subsequently, in the CRA-2004 and CRA-2009, this activity was screened out using the regulatory exclusion according to 40 CFR 194.25(a).

controlled area. The DOE excluded consideration of the 495 sulfur drill holes when calculating the drilling rate, since no economically extractible sulfur is located within the WIPP land withdrawal area (the CCA, Appendix DEL, pp. DEL-25 and DEL-81; NMBMMR 1995). Also, following EPA guidance, the DOE excluded consideration of shallow drill holes created as part of the WIPP site characterization efforts (the CCA, Appendix DEL, p. DEL-81). However, the DOE included drilling for oil/gas and brine solution mining in its rate calculations, even though the DOE indicated that it was not necessary to do so. The DOE calculated a shallow drilling rate over the past 100 yrs of 21.8 shallow holes per km^2 per 10,000 yrs (the CCA, Appendix DEL, Section DEL.7.4, p. DEL-81).

The DOE presents the shallow drilling rate for each resource in the CCA, Appendix DEL, Table DEL-5, p. DEL-83. The DOE indicated in a footnote to the CCA, Appendix DEL, Table DEL-5, p. DEL-83, that the number of shallow holes per km^2 is calculated as follows:

$$\text{Driling Rate} = \frac{(Total\ \#\ of\ boreholes - Sulfur\ coreholes) \times Regulatory\ Period}{Area\ of\ the\ Delaware\ Basin} \times \frac{1}{100\ yrs}$$

$$= \frac{(5536-495)\ 10{,}000\ yrs}{23{,}102.1\ km^2} \times \frac{1}{100\ yrs}$$

$$= 21.821 \text{ shallow holes per km}^2 \text{ per 10,000 yrs}$$

The DOE concluded in the CCA, Appendix SCR, that shallow drilling (Section SCR.3.2, Table SCR-3) could be screened from PA based on low consequence. As a result, the DOE did not include shallow drilling in its PA drilling rate calculations and did not include any reduction in shallow drilling rates during the AIC and PIC periods.

33.3.10 40 CFR § 194.33(b)(4) EPA Compliance Review

The EPA reviewed the CCA, Appendices DEL, SCR, GCR, FAC, HYDRO, and other references (e.g., NMBMMR) (NMBMMR 1995) and determined that the DOE appropriately identified shallow drilling resources and the number of drilling events for each resource over the past 100 yrs (U.S. EPA 1998d). The EPA concluded that the DOE's exclusion of sulfur coreholes from drilling was consistent with geologic data indicating that sulfur resources are not present in the area. In addition, the DOE's exclusion of site-investigation coreholes is consistent with EPA guidance. The DOE adequately discussed the basis for and calculation of the frequency of shallow drilling. The EPA concluded that the DOE properly calculated both the frequency of shallow drilling (using the historical rate of shallow drilling) and the sum of shallow drilling for all resources (whichever are used in the area, such as potash and water only).

The EPA reviewed information in the CCA, Chapter 6.0 and Appendix DEL, but did not collect an independent database for comparison with the DOE's data because the EPA concurred with the DOE's screening of shallow drilling from PA calculations (as presented in the CCA, Appendix SCR, Section SCR.3, and summarized in Table SCR-3). The DOE stated that since shallow boreholes would not penetrate the repository, the effects of boreholes on repository performance, including hydraulic effects of drilling-induced flow (e.g., the CCA, Appendix SCR, Section SCR.3.3.1.1.3, pp. SCR-113-14), could be excluded due to low consequence. This exclusion eliminated the need for a detailed evaluation of data used by the DOE to determine

shallow drilling rates, including whether the DOE's rates encompassed exploratory and development wells (although assessments included both). The DOE stated, "The effects of future shallow drilling within the controlled area have been eliminated from PA calculations on the basis of low consequence" (the CCA, Chapter 6.0, Section 6.2.5.2, p. 6-61). As such, the shallow drilling rate was not added to the deep drilling rate to obtain the total drilling rate used in the PA.

The EPA noted that the DOE took a combined approach relative to resources in the controlled area. That is, the DOE considered all the resources present in the area in shallow drilling rate calculations. Only drilling for potash and water wells fall in the shallow category (less than 655 m [2,150 ft] from the surface); thus, only these two resources were used in the calculation of shallow drilling rate for the controlled area. The EPA concluded that the DOE adequately discussed resources within the controlled area for those resources included, and justified the exclusion of other resources from consideration.

33.3.11 40 CFR § 194.33(c)(1) DOE Methodology and Conclusions

In the CCA, Appendix DEL, Section DEL.5.1, p. 26, the DOE stated that modern rotary drilling techniques, with a variety of mud systems, have been used for well completions in the vicinity of the WIPP. The DOE indicated that drilling depths range from 1,219 m (4,000 ft) to more than 4,267 m (14,000 ft), depending on the hydrocarbon-producing formation targeted. As stated in the CCA, Appendix DEL, Section DEL.4.2, the DOE took information regarding the depths of wells and probable resources primarily from Chapter IX of NMBMMR (NMBMMR 1995). The DOE stated that wells designed to penetrate the deeper Atokan natural gas plays (over 4,267 m [14,000 ft] below ground surface) tend to start at the surface with larger bits and conductor casings, and are completed with a long production string of 4½- to 5½-inches (in.) casing. In such wells, the larger casing string present through the lower salt sections tends to be 8 in., 9 in., or larger in diameter.

The DOE indicated that wells intended for completion in the relatively shallower (approximately 1,524 m to 2,438 m [5,000 to 8,000 ft] deep) Delaware Group are drilled with similar technology and mud systems through the salt sections. Long string casing present across the Bell Canyon varies from 4½ to 13 in. Completions may use 2- or 3-in. tubing strings. Standard completion technology for both the Delaware Group and Atokan wells includes perforation of the long string casing with a hydraulic fracture treatment using a variety of gelled fluids to emplace sand proppant into the fractures. The DOE indicates that acid treatments and acid fracture treatments are frequently used, especially for Brushy Canyon completions (the CCA, Appendix DEL, Section DEL.5.1.9, p. DEL-40).

The DOE assumed that all oil- and gas-related boreholes in the area will be plugged according to current applicable regulations. The DOE based this assumption on records for wells drilled on federal lands, for which the NMOCD data showed that all wells were either plugged or scheduled to be plugged in accordance with regulatory requirements. A DOE study, provided in the CCA, Appendix MASS, Attachment 16-1, indicated that 100% of wells drilled and abandoned since 1988 were, or are in the process of being plugged per applicable BLM or NMOCD regulatory standards pertaining to technical requirements.

33.3.12 40 CFR § 194.33(c)(1) EPA Compliance Review

Based on review of data presented in the CCA, Chapter 6.0, Section 6.4.7.2, and Appendices DEL and MASS, the EPA found that the DOE has assumed that future drilling practices and technology will remain consistent with current practices in the Delaware Basin. In addition, the EPA determined that the DOE performed appropriate assessments of future drilling practices and technologies—including the types/amounts of drilling fluids and borehole dimensions—and that the assessments were consistent with data presented in the above-referenced CCA appendices. The EPA's evaluation of state files, private database records, and independent industry practice information confirmed the DOE's assumptions regarding future drilling practices and technologies, including the types/amounts of drilling fluids, and borehole dimensions (U.S. EPA 1998a).

During the public comment period for the proposed certification decision, the EPA received comments that stated air drilling is current practice in the Delaware Basin. As a result of these comments, the EPA performed additional analyses of air drilling to determine whether it is common practice in the Delaware Basin. See the EPA's Analysis of Air Drilling at the WIPP (U.S. EPA 1998b) and Response to Comments, Section 8 (U.S. EPA 1998c). Based on this analysis, the EPA again determined that the use of mud as the drilling fluid is the current practice for drilling through the salt section (the Salado and Castile Formations) and that air drilling through the salt section is not consistent with current drilling practices in the Delaware Basin. Thus, the DOE properly excluded air drilling through the salt section from consideration in the WIPP PA.

The EPA informed the DOE in a letter dated December 19, 1996, that the DOE was required to provide detailed information about the large number (7,428) of unaccounted boreholes (the CCA, Appendix DEL, Table DEL-2) and about the inclusion of the effects of unplugged boreholes in the PA (Nichols 1996). The EPA required this information because the unplugged/abandoned borehole issue was not clearly presented in the CCA. The DOE's response to this comment was presented in three subparts (Dials 1997, Enclosure 2).

- The total number of boreholes listed in the CCA, Appendix DEL, Table DEL-2, is not consistent with the record keeping system of NMOCD (data source) because the categorization of data does not take into consideration the temporarily abandoned boreholes, service wells, injection wells, and dry wells. In addition, data came from different sources and different assumptions were made.

- The current regulatory process was designed, in part, to address the issue of unplugged boreholes. The EPA believed that the DOE appropriately identified that there are no unaccounted wells within the land withdrawal area. Wells in the land withdrawal area are either shallow or deep research boreholes drilled by the DOE, or several abandoned but plugged wells (see the CCA, Appendix DEL, Figure DEL-6). The DOE plans to follow State of New Mexico requirements in plugging boreholes drilled into the disposal system.

- The DOE stated that considering the degradation in plug properties to those of silty sand over time accounted for the issue of unplugged holes. The changes in properties were

included in PA. The EPA agrees that boreholes will degrade, but the EPA believed that the permeability range should be different than that selected by the DOE (see below).

The EPA found the DOE's discussion to be technically adequate because the boreholes in question are outside of the land withdrawal area and are not expected to affect the disposal system's capability to contain radionuclides. The EPA concluded that the DOE appropriately screened out abandoned boreholes drilled just meters away from the waste because of the limited communication through the low-permeability halite between the waste and the boreholes (U.S. EPA 1998e).

The DOE included in the PA boreholes drilled into the waste areas. The DOE assumed that abandoned boreholes would have the permeability of silty sand. The EPA agreed that the upper limit of permeability assumed by the DOE was appropriate. However, the EPA believed that it is possible for abandoned boreholes to have low permeability, similar to a recently plugged borehole (U.S. EPA 1998f). The EPA therefore required the DOE to include a larger range of long-term concrete plug permeability values in the CCA PAVT (Trovato 1997). This range in borehole permeability values is from 5×10^{-17} to 1×10^{-11} m^2, which the EPA believed covers the behavior of plugs in the Delaware Basin. The PAVT findings indicated that even with these changes in the borehole permeability, the releases did not violate the containment requirements.

33.3.13 40 CFR § 194.33(c)(2) DOE Methodology and Conclusions

The CCA, Appendix DEL, Attachment 7 (Inadvertent Intrusion Borehole Permeability) addressed borehole permeability variation. The CCA, Appendix DEL used published literature, plugging field tests, and oil and gas companies' experience to assess borehole permeability. The CCA, Appendix DEL also addressed wells that were plugged since 1988, when the State of New Mexico adopted new drilling and plugging regulations. Boreholes existing prior to 1988 are extremely limited in number within the WIPP land withdrawal area. The DOE accounted for the risk and uncertainties associated with boreholes drilled prior to 1988 in the PA by using various behaviors of plugs in the Delaware Basin. Borehole plug life for a two-plug configuration was considered in PA calculations to be 200 yrs; beyond that period, permeability was equivalent to marine silty sand and was held constant for the remainder of the regulatory period. The DOE assumed that processes that affect boreholes include steel casing corrosion and concrete plug alteration.

The DOE described different portions of the borehole over which degradation would act by first assigning plugging configurations for deep drilling in the Delaware Basin to one of three categories: a two-plug configuration, a three-plug configuration, and a continuous cement plug. The DOE evaluated the frequency of plug configurations based on those of 188 Delaware Basin wells installed since 1988. This provided an adequate database for analysis. Based on this study, the DOE assigned the following frequencies for each configuration (the CCA, Chapter 6.0, Section 6.4.12.7, p. 6-198):

- One continuous plug through the evaporite sequence: probability of 0.02.

- Two plugs—one in the Bell Canyon (below the potential brine reservoirs) and one in the Rustler Formation (between the Culebra Dolomite Member of the Rustler Formation (hereafter referred to as Culebra) aquifer and the repository): probability of 0.68.

- Three plugs—two as described for the two-plug form and a third plug in the Salado: probability of 0.30.

The DOE estimated that this plug system was expected to have an initial permeability of 5×10^{-17} m^2. The DOE assumed that casings would corrode due to the saline groundwater environment (the CCA, Appendix DEL, Attachment 7, Appendix B) and that concrete plugs would degrade when sufficient water entered a plug to cause matrix degradation (the CCA, Appendix DEL, Attachment 7, Appendix C). The DOE also assumed that shallower casing and cement plugs will degrade in 200 yrs, allowing for more potential fluid flow earlier in the regulatory period in shallower horizons compared to deeper casing, which was assumed to fail approximately 5000 yrs after installation. The DOE assumed that the "corroded casing and degraded plug will fill the hole with material with a permeability approximating that of silty sand (10^{-11} to 10^{-14} m^2), and over time any of this material below the repository will compress through creep closure of the borehole to a permeability about one order of magnitude lower" (the CCA, Appendix DEL, Attachment 7, p. 19). Plug configurations do not apply explicitly to shallow drilling, except that abandoned shallow boreholes typically are continuously cemented and "are expected to have no effect on the performance of the WIPP" (the CCA, Appendix DEL, Section DEL.5.2, p. DEL-41).

The DOE concluded in the CCA, Appendix DEL, Section DEL.7.4, that permeability for each of the three types of plug systems never exceeded that of silty sand (10^{-11} to 10^{-14} m^2) over the 10,000-year regulatory period. The DOE offered the following borehole permeability changes over time, with the higher permeabilities the result of natural borehole degradation that would also potentially allow for increased fluid flow:

- One plug: 5×10^{-17} m^2 for 10,000 yrs
- Two plugs:
  - Between the repository and the surface
    - 5×10^{-17} m^2 for 200 yrs
    - 10^{-14} to 10^{-11} m^2 after 200 yrs
  - Between the Castile and the repository
    - "very high" permeability to 200 yrs (10^{-9} m^2)
    - 10^{-14} to 10^{-11} m^2 up to 1,200 yrs
    - 10^{-15} to 10^{-12} m^2 after 1,200 yrs

- Three plugs:
  - Between the intermediate plug and the surface
    - 5×10^{-17} m^2 for 200 yrs
    - 10^{-14} to 10^{-11} m^2 after 200 yrs
  - Intermediate plug
    - 5×10^{-17} m^2 for a median time of 5,000 yrs
  - Borehole between the Castile and the repository
    - 10^{-14} to 10^{-11} m^2 for 1,000 years (after 5,000 yrs)
    - 10^{-15} to 10^{-12} m^2 after 6,000 yrs.

Dimensions of cement plugs for the scenarios above were assumed by the DOE to be

- One plug: 3,000 ft (900 m), 50 tons of concrete (20 cubic meters [m^3]), and
- Other plugs: 150 ft (45.73 m), 2.5 tons of concrete (1 m^3).

The DOE assumed that plug system permeability will change over time in 98% of the configurations and will not change in 2% of the configurations. The DOE assumed that permeability change with time behaved according to the following relationship (Thompson et al. 1996):

$$\Delta k = k_i \left(10^{7.39\Delta\eta - 1}\right)$$

where

Δk = change in permeability

k_i = initial hydraulic conductivity

$\Delta\eta$ = change in porosity from mineral alterations.

The DOE assumed that the permeability of plug systems is never greater than 10^{-11} m^2. Assumptions made by the DOE regarding borehole plug permeability and casing corrosion are presented in the CCA, Appendix DEL, Attachment 7.

33.3.14 40 CFR § 194.33(c)(2) EPA Compliance Review

The EPA reviewed the CCA, Appendices DEL and MASS, and determined that the DOE sufficiently identified natural borehole degradation mechanisms that will affect boreholes over time. The EPA also examined the plug configurations presented by the DOE and compared

these generalized configurations with those for oil/gas and potash resource boreholes in the WIPP vicinity, as evidenced by the resources targeted and necessary plugging techniques. The EPA determined that the DOE's plug configurations (which directly impact the portions of the borehole over which degradation processes are expected to act) and plug probabilities are adequate representations of the plugs in the WIPP area (U.S. EPA 1998d).

The EPA evaluated the effects that natural degradation of long-term borehole plugs would have on the plug system and the potential for increased transmissivity of abandoned well plugs due to such degradation. The EPA disagreed with the DOE's lower limit for borehole plug permeability. Although the DOE's permeabilities assigned for the various plug configurations were based on plausible data, the EPA believed the DOE assumed a low-end permeability that was too high. For further discussion of the EPA's analysis of borehole permeabilities, see the Parameter Justification Report (U.S. EPA 1998f).

If degraded boreholes are assumed to be filled with materials analogous to unconsolidated silt or silty sand, the permeabilities of 1×10^{-14} to 1×10^{-11} m^2 used by the DOE are not unreasonable estimates of values per industry standards (Freeze and Cherry 1979). (For purposes of comparison, the permeability range reported for shale and unweathered marine clay varies from 10^{-21} to 10^{-17} m^2. See the CCA, Appendix MASS, Attachment 16-3) (Thompson et al. 1996). However, as discussed below, the EPA investigated this assumption and found that permeability values could be lower than the DOE assumed. Lower values allow for greater gas pressurization of the WIPP and a subsequent increase in releases due to mechanisms such as spallings (U.S. EPA 1998d).

The EPA began by investigating the permeability of borehole materials and drilling fluids in the petroleum industry. Literature values for permeability of cement used in borehole applications can range from 9×10^{-21} to 1×10^{-16} m^2; these values are also cited in some of the publications referenced in the CCA. The EPA also investigated drilling muds. Filter cake and compacted clay-based drilling muds can yield permeabilities of less than 9.9×10^{-22} m^2 from field data for 11 pounds per gallon mud (U.S. EPA 1998d).

The EPA concluded that drilling mud circulated in Delaware Basin boreholes may not have the degree of clay-based solids loading typically experienced elsewhere (as discussed in the CCA, Appendix MASS, Attachment 16-3, Annex C); however, natural cuttings could contribute to lower borehole permeability than that postulated by the DOE. Lower initial permeabilities, more effective plug segments, mixed layers between plug components that would take time to degrade, and lower fluid velocities than the DOE assumed in its calculations could significantly retard plug degradation and could maintain the effective seal of the plug sequences for hundreds or thousands of yrs beyond that assumed by the DOE in the CCA, Appendix MASS, Attachment 16-3.

The DOE provided a variety of plausible mechanisms to increase plug permeability, and the EPA believed that this high range of permeability may be attained. However, the EPA also believed there is a limited probability that the lower borehole permeability (over several hundred vertical feet of borehole) would reach the relatively large permeabilities estimated by the DOE. Since permeability through any given borehole will actually be controlled by the permeabilities of all zones through which fluids must pass, the effective average permeability could be dominated by

small sections of remaining competent plug or other low permeability material. If complete degradation does not occur throughout a well, or if natural materials and mud provide additional layers with sealing properties, it is possible that the effective average permeability over several hundred feet of abandoned borehole could remain in the range of 9×10^{-21} to 1×10^{-16} m^2 over a period of hundreds, if not thousands, of yrs.

The EPA concluded that the borehole permeabilities assigned in the CCA (Appendix MASS, Attachment 16-3) were consistent with the broad range of available permeability data, but the DOE did not adequately consider the total range of permeability conditions that could exist in boreholes. Permeabilities assigned by the DOE may therefore overestimate the degree to which plugs would lose effectiveness. The EPA concluded that an alternative case could be made in which many of the plugs would retain a larger degree of effectiveness. As such, a lower maximum permeability value of approximately 1×10^{-17} m^2 (1×10^{-2} millidarcy) is quite possible (particularly for long-term conditions) and may have an impact on PA results. As a result, the EPA included both long- and short-term plug permeability changes in the CCA PAVT. The EPA required that PA simulations be conducted with lower permeabilities (concrete element of the borehole plug has a maximum of 10^{-19} m^2; silty sand element of the borehole plug has a maximum of 5×10^{-17} m^2) to account for possible cases in which complete degradation does not occur throughout a well, or natural materials and mud provide additional layers with sealing properties. Results of the CCA PAVT indicate that lower borehole permeability allows greater pressure buildup in the repository and, hence, greater release potential from mechanisms such as spallings. However, releases predicted by the CCA PAVT were still well below the EPA's release limits (U.S. DOE 1997a; U.S DOE 1997b).

In summary, the EPA agreed that the high permeabilities assumed by the DOE were generally appropriate; however, the EPA believed it is also possible for abandoned boreholes to have a lower permeability, similar to that of a recently plugged borehole. Therefore, the EPA required the DOE to include larger ranges of undegraded concrete plug and long-term borehole filling permeability values in the CCA PAVT (Trovato 1997). The range of 1×10^{-17} to 1×10^{-19} m^2 was used in the CCA PAVT for an undegraded concrete plug, and the range of 1×10^{-11} to 5×10^{-17} m^2 was used in the CCA PAVT for a degraded borehole filling. The EPA found that these ranges adequately cover the behavior of plugs in the Delaware Basin. The results of the CCA PAVT indicated that even with these changes in the range of permeabilities for degraded borehole plugs, releases did not violate the EPA's containment requirements (U.S. EPA 1998d).

The EPA believed that its detailed review of the DOE's borehole plugging assumptions provided an adequate basis for the EPA's conclusion that the DOE's assumptions were acceptable. Although the EPA originally questioned many of those assumptions, further investigations substantiated many of the DOE's assumptions, and the use of modified permeability ranges in the CCA PAVT did not cause releases to exceed regulatory limits.

33.3.15 40 CFR § 194.33(d) DOE Methodology and Conclusions

The DOE assumed that future drilling practices will be the same as current practice in terms of the type and rate of drilling, emplacement of casing in boreholes, and procedures for plugging and abandonment. The DOE did not include the impact of resource recovery subsequent to future drilling of boreholes on the basis of low consequence. The DOE did not include the

effects of resource recovery techniques in the PA analysis of future human intrusion. In addition, in the deep drilling disturbed performance scenario, the DOE examined three drilling-only scenarios, but these did not incorporate resource recovery techniques. The DOE stated in the CCA, Chapter 6.0, p. 6-60, that the PA did not analyze the effects of techniques used for resource recovery subsequent to the drilling of the borehole.

33.3.16 40 CFR § 194.33(d) EPA Compliance Review

The EPA determined that the DOE was in accordance with the provisions of 40 CFR § 194.33(d) as the PA did not analyze the effects of resource recovery techniques in future drilling events (U.S. EPA 1998d).

33.4 Changes in the CRA-2004

Table 33-1 presented changes in the CRA-2004 PA that relate to drilling for resources. This represented the migration of the PA baseline from the CCA to the CRA-2004. As noted below, most changes resulted from adopting the CCA PAVT parameters as directed by the EPA. Also, unless noted below, all other aspects of compliance with section 194.33 were consistent with those presented in the CCA, and did not represent changed or updated information.

Table 33-1. WIPP Project Changes and Cross References

WIPP Project Change	CRA-2004 Cross Reference
Incorporation of 1997 CCA PAVT Parameters	
Probability of Encountering a Brine Reservoir	6.0.2.3.8, 6.4.8, 6.4.12.6
Brine Reservoir Rock Compressibility	6.4.8
Brine Reservoir Porosity	6.4.8
Drill String Angular Velocity	Appendix PA, Attachment MASS (Section 16) and Attachment PAR
Long-term Borehole Permeability	6.4.7.2
Borehole Plug Permeability	6.4.7.2
Waste Shear Strength and Erodability	Appendix PA, Attachment MASS (Section 16)
Operational Changes	
Spallings Model	6.0.2.3.2; Appendix PA (Section 4.6) and Attachment MASS-16
Drilling Rate	6.0.2.3, 6.2.5.2; Appendix DATA (Section 2 and Attachment A)
Borehole Plugs Configuration Probability	6.4.7.2

33.5 EPA's Evaluation of Compliance for the 2004 Recertification

The EPA reviewed the DOE's CRA-2004 documentation of continuing compliance with section 194.33 and concurred that little had changed since the CCA for the consideration of drilling events. The DOE adopted the EPA's PAVT parameter values and updated a few parameters

based on the data collected from the Delaware Basin Monitoring Program. The EPA also concurred that the features, events, and processes (FEPs) had changed little for the CRA-2004. The EPA found the DOE adequately demonstrated that it had considered inadvertent and intermittent drilling into the repository as the most severe human intrusion scenario for the CRA-2004 PA. The EPA concluded that exploratory and development wells were appropriately included in the DOE's CRA-2004 analysis (CARD 23, U.S. EPA 2006).

Since the original CCA, the EPA has annually inspected the DOE's site monitoring program, in particular, the Delaware Basin drilling surveillance program. Each year, the EPA found the DOE's monitoring program to be adequate. The EPA found the DOE's compliance with the requirements of 40 CFR § 194.33(b)(4) related to shallow drilling to be adequate. The EPA found the DOE's documentation adequate to support its conclusion that drilling practices have not changed since the original CCA, and that the DOE's basin surveillance program is sufficient to evaluate and capture any changes in activities in the basin.

The EPA agreed that borehole plugging techniques assumed in the CCA and CRA-2004 PA calculations have not changed, and therefore the way these were incorporated into the PA calculations was appropriate. The EPA also agreed that the minor change in the occurrence probability of plug configurations was appropriate and of no consequence to PA results.

Public comments expressed concern that the drilling rate was underestimated in the CRA-2004 PA given the amount of drilling currently taking place throughout the Delaware Basin. Comments suggested that the drilling rate be doubled to demonstrate compliance. Although the EPA determined that the DOE appropriately calculated and implemented a drilling rate of 52.2 boreholes/km^2/year in compliance with 40 CFR § 194.33(b) for recertification, the EPA requested that the DOE calculate the impacts of doubling the current drilling rate to respond to stakeholder concerns.

The DOE performed the calculations for this analysis with the drilling rate increased to 105 boreholes/km^2/yr for 10,000 yrs. The results of computer modeling showed that doubling the drilling rate would increase releases from the repository. However, this increase is relatively small and still well below the EPA's regulatory release limits (CARD 23, U.S. EPA 2006).

33.6 Changes or New Information Between the CRA-2004 and the CRA-2009 (Previously: Changes or New Information Since the 2004 Recertfication)

There were two changes in the CRA-2009 (U.S. DOE 2009) that relate to the consideration of drilling in PA. First, the drilling rate was updated based on drilling activities in the Delaware Basin since the CRA-2004 in accordance with 40 CFR § 194.33(b)(3) (see Appendix PA-2009, Section PA-3.3). Second, the duration of DBR was modified to reflect current industry practice, in accordance with section 194.33(c)(1) (see Appendix PA-2009, Section PA-4.7.8). Furthermore, because recertification applications are expected to include any relevant updated activities and information since the most recent application, these changes were considered necessary to comply with the provisions of 40 CFR § 194.15(a)(4).

The following sections describe how these two changes related to the demonstration of compliance with the provisions of section 194.33. Unless noted below, all other aspects of

compliance with section 194.33 were consistent with that presented in the CRA-2004, and did not represent changed or updated information.

33.6.1 New Information Related to 40 CFR § 194.33(a) for CRA-2009

Potentially disruptive events and processes (EPs) that could affect the disposal system are identified, classified, and screened in Appendix PA-2004, Attachment SCR. EPs that were screened into PA calculations were then incorporated into the appropriate scenarios and conceptual models. For the CRA-2009, there were no changes in the EPs screened into PA, or the scenarios and conceptual models that represent them. Therefore, the DOE continued to comply with section 194.33(a).

33.6.2 New Information Related to 40 CFR § 194.33(b) for CRA-2009

There was no change in the implementation of the inadvertent human intrusion scenarios for the CRA-2009. PA continued to represent inadvertent and intermittent intrusion by drilling for resources as the most severe human intrusion scenario. Therefore, the DOE continued to comply with section 194.33(b)(1).

There was no change in the implementation of the location and timing of the intrusion borehole in the WIPP PA. Such events were assumed to occur randomly in space and time, as directed by the above criterion. These specific PA assumptions were implemented in the code CCDFGF, and described in the CCA, Chapter 6.0, Section 6.4.12. Additional details on the implementation of these assumptions were found in Appendix PA-2009, Section PA.3.2. Therefore, the DOE continued to comply with section 194.33(b)(2).

The method for determining the deep drilling rate for the WIPP PA was not changed. However, the drilling rate for the CRA-2009 was different from that used in the CRA-2004. This is due to the addition of recently drilled wells since the last recertification application. Derivation of the drilling rate used in PA is found in the Delaware Basin Monitoring Report for 2007 (U.S. DOE 2007). For the CRA-2009, the drilling rate is 58.5 boreholes/km^2. Therefore, the DOE continued to comply with section 194.33(b)(3).

The method for determining the shallow drilling rate for the WIPP did not change since the CRA-2004. The rate of shallow drilling was 22.87 boreholes/km^2 and was based on information provided by Hughes (Hughes 2008). The current shallow drilling rate was determined as follows:

$$\text{Drilling Rate} = \frac{Total\ shallow\ boreholes \times Regulatory\ Period}{Area\ of\ the\ Delaware\ Basin} \times \frac{1}{100\ yrs}$$

$$\text{Drilling Rate} = \frac{5{,}284 \times 10{,}000\ yrs}{23{,}102.1\ km^2} \times \frac{1}{100\ yrs}$$ [2]

$$= 22.87 \text{ shallow holes per km}^2 \text{ per } 10{,}000 \text{ yrs}$$

[2] The total shallow borehole count is derived by taking the total shallow count (6,179) as reported in U.S. DOE, Table 4 (2007), and removing sulfur holes (502), WIPP wells (199), and those holes currently being drilled or pending paperwork (194).

However, shallow drilling continued to be screened out of PA calculations for the CRA-2009 because of low consequence. Therefore, there were no changes with regard to compliance with this part of the compliance criteria, and the DOE continued to comply with section 194.33(b)(4).

33.6.3 New Information Related to 40 CFR § 194.33(c) for CRA-2009

The Delaware Basin Monitoring Annual Report for 2007 stated that drilling practices have not changed since previous reports (see U.S. DOE 2007, Section 4). However, one change was made to the WIPP PA system since the CRA-2004 that related to analyzing drilling-related events: the maximum time a DBR can occur was changed from 11 days to 4.5 days. The maximum DBR duration is represented in PA by the parameter MAXFLOW and used in the code BRAGFLO. (Kirkes 2007) documented that this change was in keeping with current drilling practices within the Delaware Basin and the previous assumption of 11 days was incorrect. (Kirkes and Clayton 2008) documented the impacts of reducing the maximum duration of DBR and showed that this change had a very minor impact upon performance predictions. Appendix PA-2009, Section PA.9.3 discussed the contribution of DBR to total releases for the CRA-2009 performance calculations. Therefore, the DOE continued to comply with section 194.33(c).

33.6.4 New Information Related to 40 CFR § 194.33(d) for CRA-2009

No changes occurred with respect to the WIPP's approach to compliance with this requirement. As in previous applications, certain EPs that relate to the extraction and production of resources can be screened out of PA calculations. Appendix SCR-2009 stated that the human-related FEPs H19, "Explosions for Resource Recovery," H25, "Oil and Gas Extraction," and H26, "Groundwater Extraction," were screened out according to the exclusion afforded by the provision of section 194.33(d), as these processes directly related to the recovery of resources subsequent to drilling. Three new FEPs for the CRA-2009 were also screened out according to the criteria of section 194.33(d): H60, "Liquid Waste Disposal–inside the WIPP boundary (IB)," H61, "Enhanced Oil and Gas Production–IB," and H62 "Hydrocarbon Storage–IB," were screened out for the future time frame using this regulatory provision. Therefore, the DOE continued to comply with section 194.33(d).

33.7 EPA's Evaluation of Compliance for the CRA-2009

The EPA verified that the DOE continues to consider the full spectrum of inadvertent and intermittent human intrusion scenarios as done in the CCA PA. The EPA found that the DOE adequately demonstrated that it had considered inadvertent and intermittent drilling into the repository as the most severe human intrusion scenario for the CRA-2009. The EPA continued to conclude that exploratory and development wells were appropriately included in the DOE's CRA-2009 analysis.

The EPA also concluded that borehole plugging techniques used in the CCA, CRA-2004, and CRA-2009 did not change and were appropriately incorporated into PA calculations. Based on its review and evaluation of this information, the EPA found that the DOE continued to comply with the requirements of section 194.33 (U.S. EPA 2010).

33.8 Changes or New Information Since the CRA-2009

There are three changes in the CRA-2014 that relate to the consideration of drilling in PA. First, the probability that a drilling intrusion into the repository will also intercept pressurized brine beneath the repository has been updated (see Section 33.8.1). Second, the drilling rate is updated based on drilling activities in the Delaware Basin since the CRA-2009 in accordance with section 194.33(b)(3) (see Section 33.8.2). Third, the plugging patterns employed in PA have been updated (see discussion in Section 33.8.3). Each of these changes is the result of incorporating newly gathered monitoring data into PA models and is considered necessary to comply with the provisions of section 194.15(a)(4).

The following sections describe how these three changes relate to the demonstration of compliance with the provisions of section 194.33.

33.8.1 New Information Related to 40 CFR § 194.33(a)

Potentially disruptive EPs that could affect the disposal system are identified, classified, and screened in the Appendix SCR-2014. EPs that are screened into PA calculations are then incorporated into the appropriate scenarios and conceptual models. For the CRA-2014, there were no changes in the EPs screened into PA, or the scenarios and conceptual models that represent them. However, there has been an update to the PA parameter that represents the probability that an inadvertent drilling intrusion will also intercept pressurized brine beneath the repository. The update to this parameter results from a re-examination of existing data while also including a greatly expanded set of drilling data for locations adjacent to the WIPP site that were not available for the development of the previous parameter distribution. (Kirchner et al. 2012) describes the update to this PA parameter. The DOE continues to comply with section 194.33(a).

33.8.2 New Information Related to 40 CFR § 194.33(b)

There is no change in the implementation of the inadvertent human intrusion scenarios for the CRA-2014. PA continues to represent inadvertent and intermittent intrusion by drilling for resources as the most severe human intrusion scenario. Therefore, the DOE continued to comply with section 194.33(b)(1).

There is no change in the implementation of the location and timing of the intrusion borehole in the WIPP PA. Such events are assumed to occur randomly in space and time, as directed by section 194.33(b)(2). These specific PA assumptions are implemented in the code CCDFGF. Additional details on the implementation of these assumptions are found in Appendix PA-2014, Section PA.3.2. Therefore, the DOE continues to comply with section 194.33(b)(2).

The method for determining the deep drilling rate for the WIPP PA has not changed for the CRA-2014. However, the drilling rate for the CRA-2014 has been updated. Derivation of the drilling rate used in PA is found in the Delaware Basin Monitoring Report for 2012 (U.S. DOE 2012). For the CRA-2014, the drilling rate is 67.3 boreholes/km^2, an increase from the previous value of 59.8 boreholes/km^2 for the CRA-2009 PABC. Therefore, the DOE continues to comply with section 194.33(b)(3).

The method for determining the shallow drilling rate for the WIPP has not changed since the CRA-2009. The rate of shallow drilling was 28.8 boreholes/km^2 and is based on information in (U.S. DOE 2012). However, shallow drilling continues to be screened out of PA calculations for the CRA-2014 because of low consequence. Therefore, there are no changes with regard to compliance with this part of the compliance criteria and the DOE continues to comply with section 194.33(b)(4).

33.8.3 New Information Related to 40 CFR § 194.33(c)

The U.S. DOE (2012) states that drilling practices have not changed since previous reports. Borehole diameters, depths, and plugging methods have not changed since the last recertification. However, the plug placement, types, and frequencies have changed slightly since the CRA-2009 due to what is considered a normal fluctuation in plugging and abandonment activities. Table 10 of U.S. DOE (2012) shows the historical changes in plug placement and types since the CCA. The plug types (i.e., number of plugs within the wellbore) are based on actual plugging data from the WIPP vicinity. The percentage of boreholes that are plugged through the entire salt section has increased to 4%, an increase of 1.8%. The percentage of boreholes with a plug between the repository and a hypothetical brine pocket is 36.6%, an increase from the previous value of 32.6%. The remaining plug configuration is now 59.4%, down from the previous value of 65.2%. Table 2-5 of Camphouse (Camphouse 2013) describes how these new plugging frequencies are incorporated into PA. Therefore, the DOE continues to comply with section 194.33(c).

33.8.4 New Information Related to 40 CFR § 194.33(d)

No changes occurred with respect to the WIPP's approach to compliance with this requirement. As in previous applications, certain EPs that relate to the extraction and production of resources can be screened out of PA calculations on the provisions of section 194.33(d). Appendix SCR-2014 states that the human-related FEPs H19, "Explosions for Resource Recovery," H25, "Oil and Gas Extraction," H26, "Groundwater Extraction," H60, "Liquid Waste Disposal–IB," H61, "Enhanced Oil and Gas Production–IB," and H62 "Hydrocarbon Storage–IB," are screened out according to the exclusion afforded by the provision of section 194.33(d), as these processes directly relate to the recovery of resources subsequent to drilling. Therefore, the DOE continues to comply with section 194.33(d).

33.9 References

(*Indicates a reference that has not been previously submitted.)

Camphouse, R.C. 2013. *Analysis Plan for the 2014 WIPP Compliance Recertification Application Performance Assessment.* ERMS 559198. Carlsbad, NM: Sandia National Laboratories.*

Dials, G. 1997. Letter to R. Trovato (Subject: Second Response Package Transmitting Supplemental Information for the Compliance Certification Application in Response to the December 19, 1996 EPA Request). 27 January 1997. Carlsbad, NM: U.S. Department of Energy, Carlsbad Area Office.

Dials, G. 1998. Letter to Mary Kruger (Subject: Regarding Certain Human Intrusion Scenarios). 26 January 1998. Carlsbad, NM: U.S. Department of Energy, Carlsbad Area Office.

Freeze, R.A., and J.A. Cherry. 1979. *Groundwater*. Englewood Cliffs, NJ: Prentice-Hall.

Hughes, D. 2008. *Shallow Drilling Rate for the Delaware Basin* (June). Carlsbad, NM: Washington Regulatory and Environmental Services.

Kirchner, T., T. Zeitler, and R. Kirkes. 2012. *Evaluating the Data in Order to Derive a Value for GLOBAL:PBRINE.* Memorandum to Sean Dunagan dated December 11, 2012. ERMS 558724. Carlsbad, NM: Sandia National Laboratories.

Kirkes, R. 2007. *Evaluation of the Duration of Direct Brine Release in WIPP Performance Assessment* (Revision 0). ERMS 545988. Carlsbad, NM: Sandia National Laboratories.

Kirkes, G.R., and D.J. Clayton. 2008. Impact Analysis of Decreased Duration of Directed Brine Release in WIPP Performance Assessment, Revision 0 (March 10). 2008. ERMS 548313. Carlsbad, NM: Sandia National Laboratories, Carlsbad Programs Group.

NMBMMR. (New Mexico Bureau of Mines and Mineral Resources) 1995. *Final Report: Evaluation of Mineral Resources at the Waste Isolation Pilot Plant (WIPP) Site* (March 31). 4 vols. ERMS 239149. Socorro, NM: New Mexico Bureau of Mines and Mineral Resources.

Nichols, M.D. 1996. Letter to A.L. Alm (1 Enclosure). 19 December 1996. Washington, DC: U.S. EPA, Office of Air and Radiation.

Thompson, T.W., W.E. Coons, J.L. Krumhansl, and F.D. Hansen, F.D. 1996. *Inadvertent Intrusion Borehole Permeability* (July). ERMS 241131. Albuquerque, NM: Sandia National Laboratories.

Trovato, E.R. 1997. Letter to G. Dials (2 Enclosures). 25 April 1997. ERMS 247206. Washington, DC: U.S. EPA, Office of Air and Radiation.

U.S. Department of Energy (DOE). 1996. *Title 40 CFR Part 191 Compliance Certification Application for the Waste Isolation Pilot Plant* (October). 21 vols. DOE/CAO 1996-2184. Carlsbad, NM: Carlsbad Area Office.

U.S. Department of Energy (DOE). 1997a. *Summary of EPA-Mandated Performance Assessment Verification Test (Replicate 1) and Comparison with the Compliance Certification Application Calculations.* WPO 46674. Carlsbad, NM: Carlsbad Area Office.

U.S. Department of Energy (DOE). 1997b. *Supplemental Summary of EPA-Mandated Performance Assessment Verification Test (All Replicates) and Comparison with the Compliance Certification Application Calculations* (August 8). WPO 46702. ERMS 414879. Carlsbad, NM: Carlsbad Area Office.

U.S. Department of Energy (DOE). 2004. *Title 40 CFR Part 191 Compliance Recertification Application for the Waste Isolation Pilot Plant* (March). 10 vols. DOE/WIPP 2004-3231. Carlsbad, NM: Carlsbad Field Office.

U.S. Department of Energy (DOE). 2007. *Delaware Basin Monitoring Annual Report* (September). DOE/WIPP-07-2308. Carlsbad, NM: Carlsbad Field Office.

U.S. Department of Energy (DOE). 2009. *Title 40 CFR Part 191 Compliance Recertification Application for the Waste Isolation Pilot Plant* (March). DOE/WIPP-09-3424. Carlsbad, NM: Carlsbad Field Office.*

U.S. Department of Energy (DOE). 2012. Delaware Basin Monitoring Annual Report. DOE/WIPP-12-2308. Carlsbad, NM: Carlsbad Field Office.*

U.S. Environmental Protection Agency (EPA). 1993. "40 CFR Part 191: Environmental Radiation Protection Standards for the Management and Disposal of Spent Nuclear Fuel, High-Level and Transuranic Radioactive Wastes; Final Rule." *Federal Register,* vol. 58 (December 20, 1993): 66398–416.

U.S. Environmental Protection Agency (EPA). 1996. "40 CFR Part 194: Criteria for the Certification and Recertification of the Waste Isolation Pilot Plant's Compliance with the 40 CFR Part 191 Disposal Regulations; Final Rule." *Federal Register,* vol. 61 (February 9, 1996). 5223–45.

U.S. Environmental Protection Agency (EPA). 1998a. *Technical Support Document for 194.32: Fluid Injection Analysis* (May). 3 vols. Washington, DC: Office of Radiation and Indoor Air.

U.S. Environmental Protection Agency (EPA). 1998b. *Technical Support Document: EPA's Analysis of Air Drilling at WIPP* (Rev. 1). Washington, DC: Office of Radiation and Indoor Air.

U.S. Environmental Protection Agency (EPA). 1998c. *Response to Comments: Criteria for the Certification and Recertification of the Waste Isolations Pilot Plant's Compliance with 40 CFR Part 191 Disposal Regulations* (May). Washington, DC: Office of Radiation and Indoor Air.

U.S. Environmental Protection Agency (EPA). 1998d. "CARD No. 33: Consideration of Drilling Events in Performance Assessments." *Compliance Application Review Documents for the Criteria for the Certification and Recertification of the Waste Isolation Pilot Plant's Compliance with the 40 CFR 191 Disposal Regulations: Final Certification Decision* (May) (pp. 33-1 through 33-31). Washington, DC: Office of Radiation and Indoor Air.

U.S. Environmental Protection Agency (EPA). 1998e. *Technical Support Document for Section 194.32: Scope of Performance Assessments* (May). Washington, DC: Office of Radiation and Indoor Air.

U.S. Environmental Protection Agency (EPA). 1998f. *Technical Support Document for Section 194.23: Parameter Justification Report* (May). Washington, DC: Office of Radiation and Indoor Air.

U.S. Environmental Protection Agency (EPA). 2006. "Recertification CARD No. 23: Models and Computer Codes." *Compliance Application Review Documents for the Criteria for the Certification and Recertification of the Waste Isolation Pilot Plant's Compliance with the 40 CFR 191 Disposal Regulations: Final Recertification Decision* (March) (pp. 23-1 through 23-37). Washington, DC: Office of Radiation and Indoor Air.

U.S. Environmental Protection Agency (EPA). 2010. "2009 Compliance Recertification Application (2009 CRA) Compliance Application Review Document (CARD) No. 33, Consideration of Drilling Events in Performance Assessments". EPA Docket FDMS Docket ID No. EPA-HQ-OAR-2009-0330. Washington, DC: Office of Radiation and Indoor Air. http://www.epa.gov/radiation/wipp/2010recertification.html.*

Title 40 CFR Part 191
Subparts B and C
Compliance Recertification Application 2014
for the
Waste Isolation Pilot Plant

Results of Performance Assessments
(40 CFR § 194.34)

United States Department of Energy
Waste Isolation Pilot Plant

Carlsbad Field Office
Carlsbad, New Mexico

Compliance Recertification Application 2014
Results of Performance Assessments
(40 CFR § 194.34)

Table of Contents

List of Figures

List of Tables

This page intentionally left blank.

Acronyms and Abbreviations

CARD	Compliance Application Review Document
CCA	Compliance Certification Application
CCDF	complementary cumulative distribution function
CFR	Code of Federal Regulations
CRA	Compliance Recertification Application
DBR	direct brine release
DOE	U.S. Department of Energy
EPA	U.S. Environmental Protection Agency
LHS	Latin hypercube sampling
PA	performance assessment
PABC	Performance Assessment Baseline Calculation
PAVT	Performance Assessment Verification Test
WIPP	Waste Isolation Pilot Plant

This page intentionally left blank.

34.0 Results of Performance Assessments (40 CFR § 194.34)

34.1 Requirements

§ 194.34 Results of Performance Assessments

(a) The results of performance assessments shall be assembled into complementary, cumulative distribution functions (CCDFs) that represent the probability of exceeding various levels of cumulative release caused by all significant processes and events.

(b) Probability distributions for uncertain disposal system parameter values used in performance assessments shall be developed and documented in any compliance application.

(c) Computational techniques, which draw random samples from across the entire range of the probability distributions developed pursuant to paragraph (b) of this section, shall be used in generating CCDFs and shall be documented in any compliance application.

(d) The number of CCDFs generated shall be large enough such that, at cumulative releases of 1 and 10, the maximum CCDF generated exceeds the 99th percentile of the population of CCDFs with at least a 0.95 probability. Values of cumulative release shall be calculated according to Note 6 of Table 1, Appendix A of Part 191 of this chapter.

(e) Any compliance application shall display the full range of CCDFs generated.

(f) Any compliance application shall provide information which demonstrates that there is at least a 95 percent level of statistical confidence that the mean of the population of CCDFs meets the containment requirements of 40 CFR 191.13.

34.2 40 CFR § 194.34(a)

34.2.1 Background

The radioactive waste disposal regulations of 40 CFR Part 191 Subparts B and C (U.S. EPA 1993) include containment requirements for radionuclides. The containment requirements of 40 CFR § 191.13 specify that releases from a disposal system to the accessible environment must not exceed the release limits set forth in Part 191 Appendix A, Table 1. Assessment of the likelihood that the Waste Isolation Pilot Plant (WIPP) will meet the release limits is conducted through a process known as a performance assessment (PA). The WIPP PA consists of a series of computer simulations that model the physical attributes of the repository (site, geology, waste forms and quantities, engineered features) in a manner that captures the expected behaviors and interactions among its various components over the 10,000-year regulatory time frame.

The PA must consider all significant processes and events that may affect the disposal system (see Section 32 of this application), and it must be structured and conducted in a way that (1) demonstrates an adequate understanding of the physical conditions at the disposal system and its surroundings, and (2) shows that the future performance of the system can be predicted with reasonable assurance. In addition, it must include simulations for both undisturbed conditions and human intrusion scenarios. The results of the PA are used to demonstrate compliance with the containment requirements of section 191.13.

The containment requirements place limits on the likelihood of radionuclide releases from a disposal system. A radionuclide release to the accessible environment is defined in terms of the location of the release and its magnitude. Any release of radionuclides to the ground surface, atmosphere, or surface water is considered a release to the accessible environment. In addition,

any subsurface transport of radionuclides beyond the boundary of the WIPP controlled area is also considered a release to the accessible environment.

The results of the WIPP PA are required to be expressed as complementary cumulative distribution functions (CCDFs). A CCDF indicates the probability of exceeding various levels of cumulative release. The CCDFs must be generated using random sampling techniques that draw upon the full range of values established for each uncertain parameter.

34.2.2 1998 Certification Decision

To meet the requirements of 40 CFR § 194.34(a) (U.S. EPA 1996), the U.S. Environmental Protection Agency (EPA) expected the U.S. Department of Energy (DOE) to demonstrate that:

1. The results of the PA were assembled into CCDFs.

2. The CCDFs represent the probability of exceeding various levels of cumulative release caused by all significant processes and events.

3. All significant processes and events that may affect the repository during the 10,000-year period after closure have been incorporated into the CCDFs presented.

The EPA reviewed the features, events, and processes for the WIPP disposal system and the construction of the CCDFs for the Compliance Certification Application (CCA) (U.S. DOE 1996). The EPA concluded that the DOE appropriately captured the significant processes and events that could occur during the regulatory period in the CCDFs and thus complied with the requirements of section 194.34(a).

A complete description of the EPA's 1998 Certification Decision for section 194.34(a) can be obtained from Compliance Application Review Document (CARD) 34, Section 34.A.6 (U.S. EPA 1998a).

34.2.3 Changes in the CRA-2004

The DOE developed CCDFs for the 2004 Compliance Recertification Application (CRA-2004) (U.S. DOE 2004) using the same methodology as used for the CCA and the CCA Performance Assessment Verification Test (PAVT) (U.S. EPA 1998b); the only changes were in the values of some parameters and modeling assumptions. See the CRA-2004, Chapter 6.0, Table 6-1.

The DOE used selected computer codes and input parameters to generate estimates of radionuclide releases for a large number of scenarios. A review of the CRA-2004 PA identified several errors, as discussed in Section 34.7.4, resulting in the development of the CRA-2004 Performance Assessment Baseline Calculation (PABC). In total, 300 CCDFs (100 for each of the 3 replicates) were constructed and presented in the PABC report (Leigh et al. 2005) for total normalized releases. Three hundred realizations were needed to satisfy the criteria of 40 CFR § 194.34(d). Normalized release results for 10,000 simulations of possible futures were used to calculate each of the 300 CCDF curves. In addition, the DOE provided CCDFs for individual pathways.

34.2.4 EPA's Evaluation of Compliance for the 2004 Recertification

The EPA's analysis concluded that the DOE adequately presented the PA results in CCDFs, which show the probability of exceeding various levels of cumulative releases (U.S. EPA 2006a, Section 12.0).

Based on a review and evaluation of the CRA-2004 and supplemental information provided by the DOE, the EPA determined that the DOE continued to comply with the requirements of section 194.34(a) (see Recertification CARD No. 34: Results of Performance Assessments [194.34(a)]) (U.S. EPA 2006b).

34.2.5 Changes or New Information Between the CRA-2004 and the CRA-2009 (Previously: Changes or New Information Since the 2004 Recertification)

There were changes in the CRA-2009 related to parameter updates, error corrections, and code improvements made since the CRA-2004 decision (see Appendix PA-2009, Section PA-2.1.1 for more details). The DOE developed CCDFs for the CRA-2009 using the same sampling process and CCDF computational technique as in the CCA and the CRA-2004 (see the CCA, Chapter 6.0, Section 6.1).

In total, 300 CCDFs (100 for each of the 3 replicates) for total normalized releases were constructed and presented in Appendix PA-2009 (Figure 34-1). Thus, the DOE continued to demonstrate compliance with the provisions of section 194.34(a).

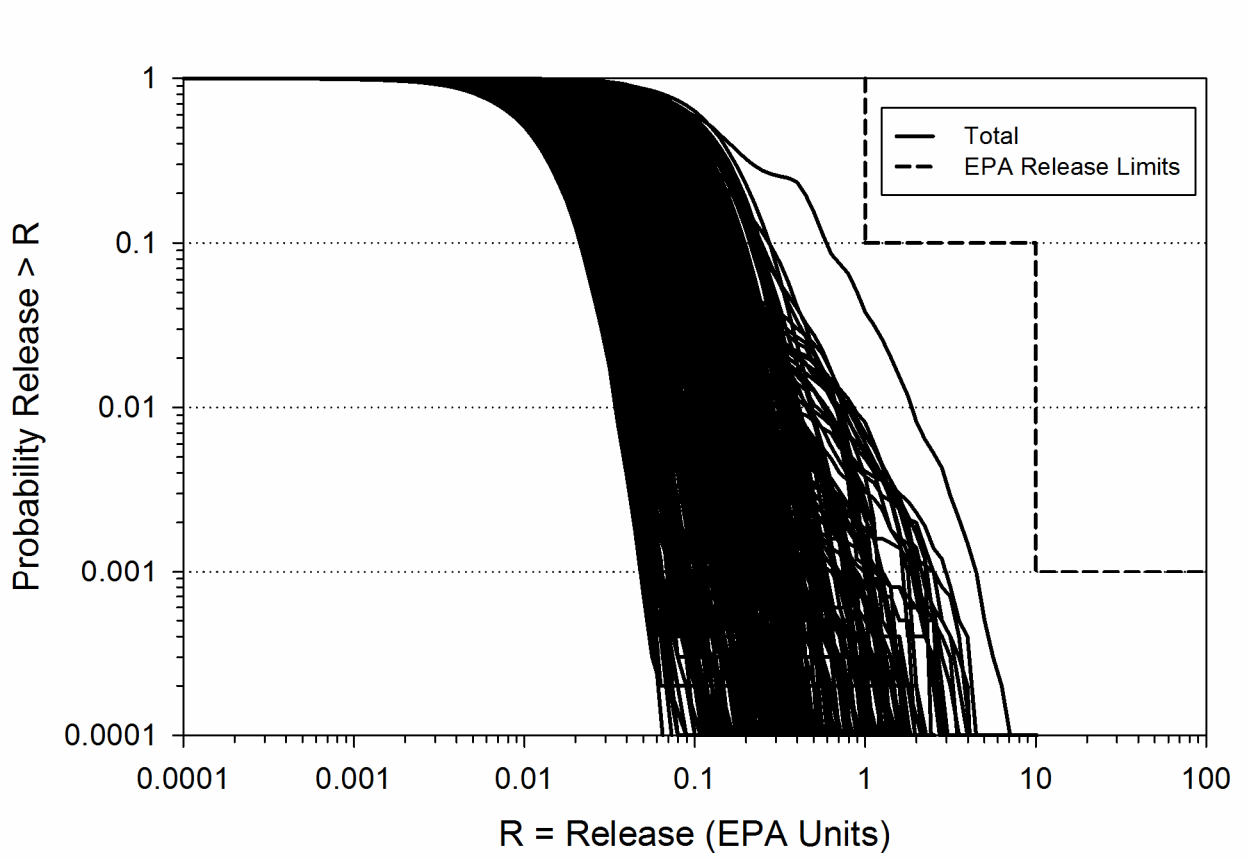

Figure 34-1. 300 CCDFs for Total Normalized Releases: CRA-2009 PA (from Figure 6-6 in Clayton et al. [2008], replotted with a maximum of 1 on the probability scale)

34.2.6 EPA's Evaluation of Compliance for the 2009 Recertification

In addition to the 300 CCDFs constructed for the CRA-2009 PA, 300 CCDFs were also constructed for total normalized releases for the CRA-2009 PABC (Figure 34-2) (Clayton et al. 2010; Camphouse 2010). Normalized release results for ten thousand future simulations were again used to calculate each of the 300 CCDF curves. In addition, the DOE provided CCDFs for individual pathways and by replicate. The EPA's analysis (U.S. EPA 2010a) concluded that the DOE adequately presented the PA results in CCDFs, which show the probability of exceeding various levels of cumulative releases.

Based on a review and evaluation of the CRA-2009 and supplemental information provided by the DOE, the EPA determined that the DOE continued to comply with the requirements of section 194.34(a) (see Recertification CARD No. 34: Results of Performance Assessments [194.34(a)]) (U.S. EPA 2010b).

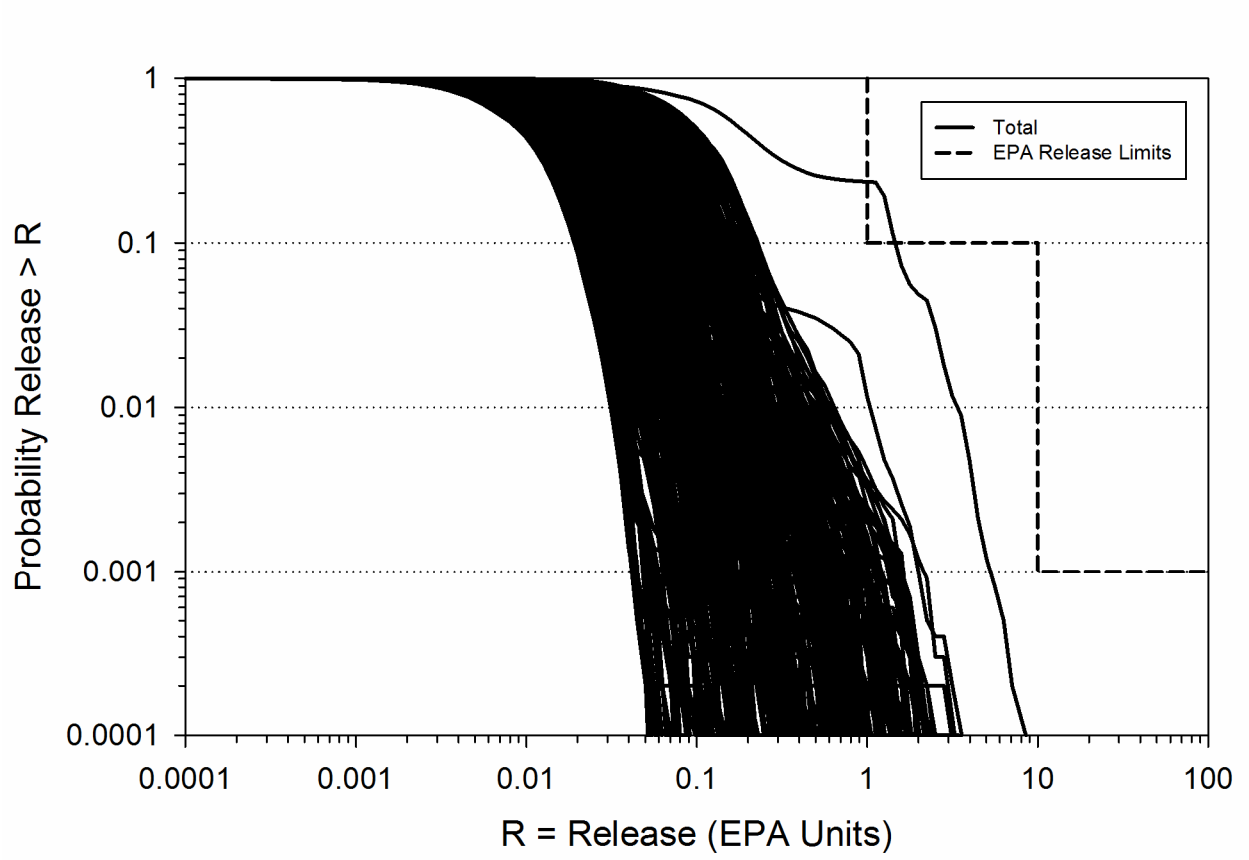

Figure 34-2. CRA-2009 PABC: Total Normalized Releases in EPA Units Replicates R1, R2, and R3 (Clayton et al. 2010, Figure 6-6, replotted with EPA release limits)

34.2.7 Changes or New Information Since the CRA-2009

There are changes in the CRA-2014 related to repository planned changes, parameter updates, and refinements to PA implementation made since the CRA-2009 decision (see Appendix PA-2014, Section PA-1.1 for more details). The DOE developed CCDFs for the CRA-2014 using the same sampling process and CCDF computational technique as in the CCA, CRA-2004, and CRA-2009 (see the CCA, Chapter 6.0, Section 6.1).

In total, 300 CCDFs (100 for each of the 3 replicates) for total normalized releases were constructed and presented in Camphouse et al. 2013 (Figure 34-3). Thus, the DOE continues to demonstrate compliance with the provisions of section 194.34(a).

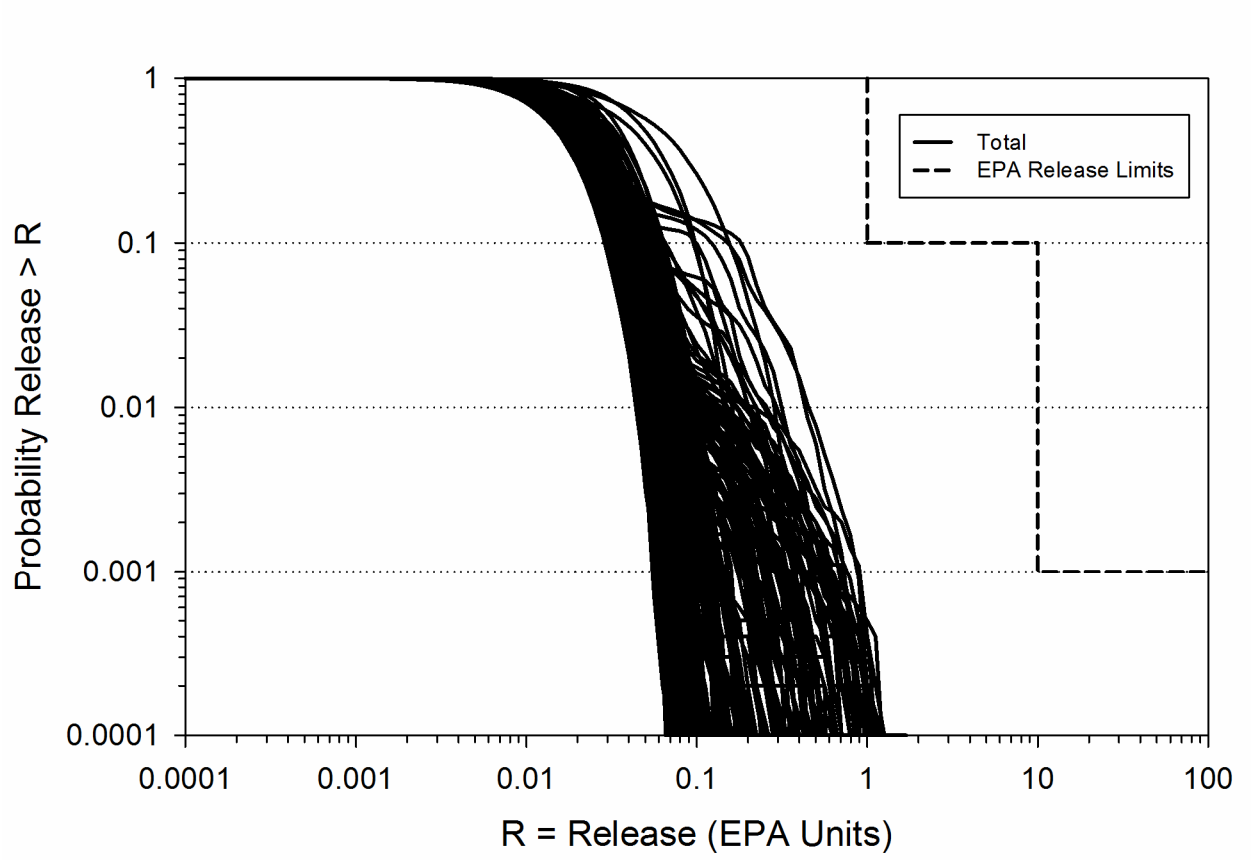

Figure 34-3. 300 CCDFs for Total Normalized Releases: CRA-2014 PA (Camphouse et al. 2013, Figure 6-51, replotted with EPA release limits)

34.3 40 CFR § 194.34(b)

34.3.1 Background

There is uncertainty associated with many of the parameters used in PA. 40 CFR § 194.34(b) addresses the need for the uncertain parameters to be sampled from a probability distribution (e.g., uniform, normal, etc.) that has been appropriately documented and justified.

34.3.2 1998 Certification Decision

To meet the criteria in section 194.34(b), the EPA expected the DOE to:

1. Discuss the sources used and the methods by which each of the probability distributions was developed (e.g., experimental data, field data, etc.)

2. Identify the functional form of the probability distributions (e.g., uniform, lognormal) used for the sampled parameters

3. Describe the statistics of each probability distribution, including the values for lower and upper ranges, mean (geometric mean when appropriate), and median

4. Demonstrate that the data used to develop the input parameter probability distribution were qualified and controlled in accordance with 40 CFR § 194.22

Upon reviewing the DOE's parameters, the EPA found that the DOE adequately documented the probability distributions in the CCA, Appendix PAR. In addition, the DOE discussed the data and method used to create the probability distribution of each of the 57 sampled variables. The DOE provided general information on probability distributions, data sources for parameter distribution, forms of distributions, bounds, and importance of parameters to releases. The EPA identified inconsistencies with some of the parameter values and probability distributions, but these were resolved for the CCA PAVT the EPA required the DOE to conduct (U.S. EPA 1998b, Section 5.0).

The EPA determined that the DOE complied with the requirements of section 194.34(b). A complete description of the EPA's 1998 Certification Decision for section 194.34(b) can be obtained from the CARD 34, Section 34.B.5 (U.S. EPA 1998a).

34.3.3 Changes in the CRA-2004

Some parameter values and probability distributions in the CRA-2004 PA changed from those in the CCA PAVT. Many of these changes are related to inventory changes, but some are related to modeling assumption changes (see Leigh et al. 2005, Section 2.0). However, the basic process the DOE used to develop the parameter information and sample the parameters did not change from the CCA methodology.

The DOE documented its selection of parameters and probability distributions for the key parameters in the CRA-2004, Chapter 6.0, Appendix PA-2004, Attachment PAR-2004, the CRA-2004 PABC report (Leigh et al. 2005), and associated references. The CRA-2004 PABC sampled 56 parameters whose values were obtained through random sampling in the PA (Kirchner 2005). There were changes to several of the parameters from the CRA-2004 PA for the CRA-2004 PABC (Leigh et al. 2005). The ultimate goal of parameter sampling was to capture uncertainties in the parameters and show their effects on the CCDFs, which the DOE discussed in the CRA-2004, Chapter 6.0, Sections 6.4 and 6.5, and in the CRA-2004 PABC report (see Leigh et al. 2005, Section 2.9).

34.3.4 EPA's Evaluation of Compliance for the 2004 Recertification

The EPA reviewed the DOE's parameter selection and probability distributions in several technical support documents related to computer codes (U.S. EPA 2006c and U.S. EPA 2006d), parameters (U.S. EPA 2006e, U.S. EPA 2006f, and U.S. EPA 2006g), and chemistry (U.S. EPA 2006a, U.S. EPA 2006f, and U.S. EPA 2006g). The EPA found that the DOE adequately documented the probability distributions. In addition, the DOE discussed the data and method used to create the probability distribution of each sampled variable.

Based on a review and evaluation of the CRA-2004 and PABC-2004 provided by the DOE, the EPA determined that the DOE continued to comply with the requirements of section 194.34(b) (see Recertification CARD No. 34: Results of Performance Assessments [194.34(b)]) (U.S. EPA 2006b).

34.3.5 Changes or New Information Between the CRA-2004 and the CRA-2009 (Previously: Changes or New Information Since the 2004 Recertification)

Although 15 parameters were modified and 90 were added (Fox 2008, Table 6), the process that the DOE used to develop the parameter information and sample the parameters did not change from the EPA-approved CCA methodology (see Fox 2008 for parameter sample distribution information). Thus, the DOE continued to demonstrate compliance with the provisions of section 194.34(b).

34.3.6 EPA's Evaluation of Compliance for the 2009 Recertification

The DOE documented its selection of parameters and probability distributions for the key parameters in Fox 2008 (Table 6), the Appendix PA-2009, the CRA-2009 PABC report (Clayton et al. 2010), and associated references. The CRA-2009 PABC also sampled 56 parameters; there were changes to several of the parameters for the CRA-2009 PABC (Clayton et al. 2010; Clayton 2010). The ultimate goal of parameter sampling continued to be to capture uncertainties in the parameters and show their effects on the CCDFs, which the DOE discussed in Fox (Fox 2008), Clayton et al. (Clayton et al. 2010), and Clayton (Clayton 2010).

The EPA reviewed the DOE's parameter selection and probability distributions in several Technical Support Documents related to computer codes (U.S. EPA 2010c), parameters (U.S. EPA 2010d), and chemistry (U.S. EPA 2010e). The EPA found that the DOE continued to adequately document the probability distributions and discussed the data from which, and the method by which, the probability distribution of each of the sampled variables was created.

Based on a review and evaluation of the CRA-2009 and supplemental information provided by the DOE, the EPA determined that the DOE continued to comply with the requirements of section 194.34(b) (see Recertification CARD No. 34: Results of Performance Assessments [194.34(b)) (U.S. EPA 2010b).

34.3.7 Changes or New Information Since the CRA-2009

Although 105 parameters were modified and 100 were added (Kicker and Herrick 2013, Table 3) since the CRA-2009 PABC, the process that the DOE used to develop the parameter information and sample the parameters did not change from the EPA-approved CCA methodology (see Kicker and Herrick (Kicker and Herrick 2013) for parameter sample distribution information). Thus, the DOE continues to demonstrate compliance with the provisions of section 194.34(b).

34.4 40 CFR § 194.34(c)

34.4.1 Background

The intent of 40 CFR § 194.34(c) is to ensure that the sampled parameters were appropriately selected for use in PA.

34.4.2 1998 Certification Decision

To demonstrate compliance with section 194.34(c), the EPA expected the DOE to do the following:

1. Discuss the computational techniques used for random sampling

2. Demonstrate that sampling occurred across the entire range of each parameter

The EPA agreed it was appropriate to use the Latin hypercube sampling (LHS) method for the 57 sampled parameters described in the CCA, Appendix PAR. The EPA concluded that the DOE adequately discussed the computational techniques and sampling ranges.

A complete description of the EPA's 1998 Certification Decision for section 194.34(c) can be obtained from CARD 34, Section 34.C.5 (U.S. EPA 1998a).

34.4.3 Changes in the CRA-2004

In the CRA-2004, the DOE used the same LHS methodology for sampling uncertain parameters as in the CCA. There was no change in the methodology.

34.4.4 EPA's Evaluation of Compliance for the 2004 Recertification

The EPA determined during the CCA review that the LHS method ensures parameter values will be selected from the entire range of the probability distributions because LHS stratifies the probability distributions into a number (100, in this case) of equal-probability regions and then samples one value from each region. The EPA noted that the LHS method is appropriate for generating random samples (CARD 34, Section 34.C.5) (U.S. EPA 1998a). The DOE used the same approach in the CRA-2004.

Based on a review and evaluation of the CRA-2004 and supplemental information provided by the DOE, the EPA determined that the DOE continued to comply with the criteria for section 194.34(c) (see Recertification CARD No. 34: Results of Performance Assessments [194.34(c)]) (U.S. EPA 2006b).

34.4.5 Changes or New Information Between the CRA-2004 and the CRA-2009 (Previously: Changes or New Information Since the 2004 Recertification)

In the CRA-2009, the DOE used the same LHS methodology for sampling uncertain parameters as in the CCA and CRA-2004. There was no change in the methodology. Thus, the DOE continued to demonstrate compliance with provisions of section 194.34(c).

34.4.6 EPA's Evaluation of Compliance for the 2009 Recertification

The EPA determined in the CCA and the CRA-2004 that the LHS sampling methodology ensures that parameter values will be selected from the entire range of the probability

distributions because LHS stratifies the probability distributions into a number (100, in this case) of equal-probability regions and then samples one value from each region. The EPA noted that the LHS sampling continued to be appropriate for generating random samples in the 2009 PAs.

Based on a review and evaluation of the CRA-2009 and supplemental information provided by the DOE, the EPA determined that the DOE continued to comply with the requirements of section 194.34(c) (see Recertification CARD No. 34: Results of Performance Assessments [194.34(c)]) (U.S. EPA 2010b).

34.4.7 Changes or New Information Since the CRA-2009

In the CRA-2014, the DOE uses the same LHS methodology for sampling uncertain parameters as in the CCA, CRA-2004, and CRA-2009 (Kirchner 2013). Thus, the DOE continues to demonstrate compliance with the provisions of section 194.34(c).

34.5 40 CFR § 194.34(d)

34.5.1 Background

The intent of 40 CFR § 194.34(d) is to ensure that PA modeling appropriately sampled uncertain parameters and that future scenarios were appropriately used in PA.

34.5.2 1998 Certification Decision

To demonstrate compliance with section 194.34(d), the EPA expected the DOE to do the following:

1. Identify the number of CCDFs generated

2. Discuss how the DOE determined the number of CCDFs to be generated

3. Demonstrate that the maximum CCDF generated, at cumulative normalized releases of 1 and 10, exceeds the 99th percentile with at least a 0.95 probability, including examples of calculations

The EPA found the analysis presented in the CCA, Chapter 8.0, sufficient to show that 298 CCDF curves would satisfy the statistical criterion. The EPA's independent analysis also verified that the 300 CCDF curves computed and presented in the CCA were sufficient (CARD 34, Section 34.D.5) (U.S. EPA 1998a). The DOE correctly interpreted the definition of the 99th percentile value, and applied standard mathematical expressions for deriving the probability of an outcome of multiple events (i.e., the generation of multiple CCDF curves). The probabilistic analysis was found to be appropriate for sampling with the LHS method, which achieves better coverage than nonstratified random sampling of parameter ranges.

A complete description of the EPA's 1998 Certification Decision for section 194.34(d) can be obtained from CARD 34, Section 34.D.5 (U.S. EPA 1998a).

34.5.3 Changes in the CRA-2004

In the CRA-2004, the DOE used the same methodology as in the CCA to generate 300 CCDFs in three sets (replicates) of 100. There was no change in the methodology.

34.5.4 EPA's Evaluation of Compliance for the 2004 Recertification

The EPA noted that the DOE generated 3 sets of 100 CCDFs each and discussed the statistical confidence levels based on the entire set of CCDFs. Based on the analysis in the CCA and the fact that the DOE used the same approach in the CRA-2004, the EPA concurred with the DOE's CRA-2004 analyses.

Based on a review and evaluation of the CRA-2004 and supplemental information provided by the DOE, the EPA determined that the DOE continued to comply with the requirements of section 194.34(d) (see Recertification CARD No. 34: Results of Performance Assessments [194.34(d)]) (U.S. EPA 2006b).

34.5.5 Changes or New Information Between the CRA-2004 and the CRA-2009 (Previously: Changes or New Information Since the 2004 Recertification)

In the CRA-2009, the DOE used the same methodology as in the CCA and CRA-2004 to generate 300 CCDFs in 3 sets (replicates) of 100. Thus, the DOE continued to demonstrate compliance with provisions of section 194.34(d).

34.5.6 EPA's Evaluation of Compliance for the 2009 Recertification

The DOE generated three sets of 100 CCDFs each and discussed the statistical confidence levels for the set of CCDFs (Clayton et al. 2010; Camphouse 2010). Based on the analysis in the CRA-2009 and the fact that the DOE used the same approach in the CRA-2009 as in the CCA and CRA-2004 PAs, the EPA concurred with the DOE's CRA analyses.

Based on a review and evaluation of the CRA-2009 and supplemental information provided by the DOE, the EPA determined that the DOE continued to comply with the requirements of section 194.34(d) (see Recertification CARD No. 34: Results of Performance Assessments [194.34(d)]) (U.S. EPA 2010b).

34.5.7 Changes or New Information Since the CRA-2009

In the CRA-2014, the DOE uses the same methodology as in the CCA, CRA-2004, and CRA-2009 to generate 300 CCDFs in 3 sets (replicates) of 100 (Zeitler 2013). Thus, the DOE continues to demonstrate compliance with provisions of section 194.34(d).

34.6 40 CFR § 194.34(e)

34.6.1 Background

The intent of 40 CFR § 194.34(e) is to show the full range of CCDFs in order to provide an indication of the nature of the releases.

34.6.2 1998 Certification Decision

To demonstrate compliance with section 194.34(e), the EPA expected the DOE to do the following:

1. Display the full range of CCDFs generated

2. Include descriptive statistics such as the range, mean, median, etc., for the estimated CCDFs at cumulative releases of 1 and 10

The DOE employed LHS to create 3 independent replicates of 100 realizations each, yielding 300 CCDF curves. The DOE concluded that the requirement of section 194.34(e) was met. The EPA concurred with this conclusion.

A complete description of the EPA's 1998 Certification Decision for section 194.34(e) can be obtained from CARD 34, Section 34.E.5 (U.S. EPA 1998a).

34.6.3 Changes in the CRA-2004

There were no changes to the approach used by the DOE with regard to section 194.34(e) in the CRA-2004. The DOE presented and discussed the results of the PA analysis in the CRA-2004, Chapter 6.0, and the CRA-2004 PABC report (Leigh et al. 2005, Chapter 6), which display the full range of CCDFs generated. Furthermore, appropriate information needed to confirm the analysis and descriptive statistics for the estimated CCDFs was provided.

34.6.4 EPA's Evaluation of Compliance for the 2004 Recertification

Based on a review and evaluation of the CRA-2004 and supplemental information provided by the DOE, the EPA determined that the DOE continued to comply with the requirements of section 194.34(e) (see Recertification CARD No. 34: Results of Performance Assessments [194.34(e)]) (U.S. EPA 2006b).

34.6.5 Changes or New Information Between the CRA-2004 and the CRA-2009 (Previously: Changes or New Information Since the 2004 Recertification)

There were no changes to the approach used by the DOE with regard to section 194.34(e) in the CRA-2009. The full range of CCDFs generated for the CRA-2009 PA is shown in Figure 34-1. Thus, the DOE continued to demonstrate compliance with the provisions of section 194.34(e).

34.6.6 EPA's Evaluation of Compliance for the 2009 Recertification

The DOE presented and discussed the results of the performance assessment analysis in the CRA-2009, Section 34 and the 2009 PABC report (Clayton et al. 2010). Figure 34-2 shows the 300 CCDFs (100 for each of the 3 replicates) for total normalized releases that were constructed and presented in the 2009 PABC (Clayton et al. 2010). It is discussed further in CARD 34, Section 34.29.1 (U.S. EPA 2010b).

Based on a review and evaluation of the CRA-2009 and supplemental information provided by the DOE and the fact that the DOE included the full range of CCDFs as required by this section, the EPA determined that the DOE continued to comply with the requirements of section 194.34(e) (see Recertification CARD No. 34: Results of Performance Assessments [194.34(e)]) (U.S. EPA 2010b).

34.6.7 Changes or New Information Since the CRA-2009

There are no changes to the approach used by the DOE with regard to section 194.34(e) in the CRA-2014 (Zeitler 2013). The full range of CCDFs generated for the CRA-2014 PA is shown in Figure 34-3. Thus, the DOE continues to demonstrate compliance with the provisions of section 194.34(e).

34.7 40 CFR § 194.34(f)

34.7.1 Background

Because of the unique nature of the WIPP disposal system, the EPA wanted to ensure that the PA results could be used to adequately support a certification decision. To this end, the EPA required the DOE to demonstrate compliance with a high statistical confidence. For 40 CFR § 194.34(f), the DOE must show, in effect, that the mean of its 300 CCDF curves, and the 95th percentile upper confidence limit of the population mean, meet the containment requirements of section 191.13 for the cumulative releases at 1 and 10 times the quantities in Part 191 Appendix A, Table 1.

34.7.2 1998 Certification Decision

To demonstrate compliance with section 194.34(f), the EPA expected the DOE to present appropriate information, including steps used to arrive at the result and the data used in the analysis, allowing the EPA to confirm that the mean of the CCDF population meets the containment requirements of section 191.13 with a 95% statistical confidence level.

Upon analysis of the CCA PA, the EPA identified inconsistencies with some of the parameter values and probability distributions, and so the EPA required the DOE to conduct the CCA PAVT, which resolved the issues (U.S. EPA 1998b, Section 5.0). The Certification Decision was based on the CCA PAVT results. The CCA PAVT results demonstrated that the mean of the CCDFs met the section 191.13 containment requirements and that the level of statistical confidence is significantly greater than 95%. Therefore, the EPA concluded that the final result of the CCA PAVT was in compliance with the containment requirements of section 191.13 and

that the results were presented in accordance with section 194.34(f) (see CARD 34, Section 34.F.5) (U.S. EPA 1998a).

34.7.3 Changes in the CRA-2004

In the CRA-2004, the DOE used the same general approach for calculating the statistical confidence for release limits as was used in the CCA. The DOE provided the CCDFs and uncertainty information in the CRA-2004 documentation.

34.7.4 EPA's Evaluation of Compliance for the 2004 Recertification

The EPA's and the DOE's review of the CRA-2004 identified several errors that may have affected the CRA-2004 PA's compliance with section 194.34(f) (Cotsworth 2005). Incorrect LHS transfer files were used as input to PRECCDFGF for Replicates 2 and 3; thus, some of the same parameter inputs were used multiple times instead of being appropriately sampled for each replicate. A spallings release calculation for the volume fraction of contact-handled transuranic waste was omitted from CCDFGF, and an error in the input control file for the computer code SUMMARIZE affected spallings results. Finally, only 50 vectors for DRSPALL calculations were run for the CRA-2004 PA, instead of a full set of 100 vectors for each of the three replicates, thus potentially reducing the range of spallings releases.

Because of these problems, the EPA required the DOE to run a full set of DRSPALL vectors and correct the problem with LHS transfer files in the CRA-2004 PABC. The results of the CRA-2004 PABC are provided in the DOE's CRA-2004 PABC report (Leigh et al. 2005). In its review of the CRA-2004 PABC, the EPA concurred that the errors were corrected (see Recertification CARD No. 34: Results of Performance Assessments [194.34(f)]) (U.S. EPA 2006b).

Based on a review and evaluation of the CRA-2004 and supplemental information provided by the DOE, the EPA determined that the DOE continued to comply with the requirements of section 194.34(f) (Recertification CARD No. 34: Results of Performance Assessments [194.34(f)]) (U.S. EPA 2006b).

34.7.5 Changes or New Information Between the CRA-2004 and the CRA-2009 (Previously: Changes or New Information Since the 2004 Recertification)

For the CRA-2009, the DOE used the same approach to calculate the statistical confidence for evaluation against the release limits as was used in the CCA and CRA-2004. The mean of the 300 CCDFs, along with the 95% confidence levels about the overall mean for the total normalized releases of the CRA-2009 PA, are shown in Figure 34-4. Table 34-1 lists the overall mean total normalized release CCDF values of the CRA-2009 PA at the compliance probabilities of 0.1 and 0.001, along with the values of the upper and lower 95% confidence limit CCDFs at the same probabilities. More details on the normalized release results of the CRA-2009 PA are discussed in Appendix PA-2009, Section PA-9.0. As seen in Figure 34-4 and Table 34-1, the results of the PA demonstrated a greater than 95% level of statistical confidence that the overall

mean of the population of CCDFs is in compliance with the containment requirements of section 191.13, and thus the DOE continued to comply with provisions of section 194.34(f).

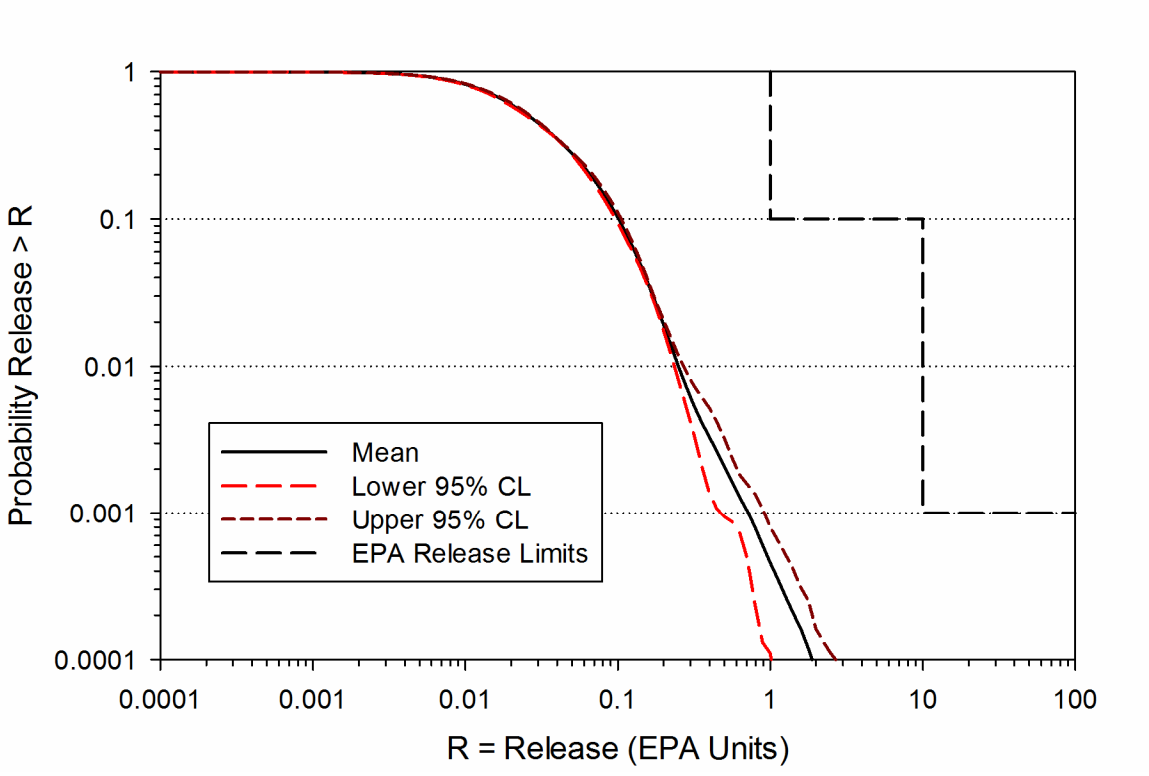

Figure 34-4. Mean and Confidence Interval CCDFs for Total Normalized Releases: CRA-2009 PA (from Figure 6-7 in Clayton et al. [2008])

Table 34-1. CRA-2009 PA Statistics on the Overall Mean for Total Normalized Releases at Probabilities of 0.1 and 0.001, All Replicates Pooled Compared with Release Limits (from Table 6-1 in Clayton et al. [2008])

Probability	Mean Total Release	Lower 95% Confidence Limit	Upper 95% Confidence Limit	Regulatory[a] Limit
0.1	0.10	0.10	0.11	1
0.001	0.72	0.48	0.92	10

[a] Releases divided by the release limits in Part 191 Appendix A, Table 1.

The DOE believed that the information presented in this section and additional information in Appendix PA-2009 demonstrated continued compliance with section 194.34.

34.7.6 EPA's Evaluation of Compliance for the 2009 Recertification

Figure 34-5 shows the overall mean of the total normalized releases for the 300 CCDFs, along with the 95% confidence levels about the overall mean, for the CRA-2009 PABC.

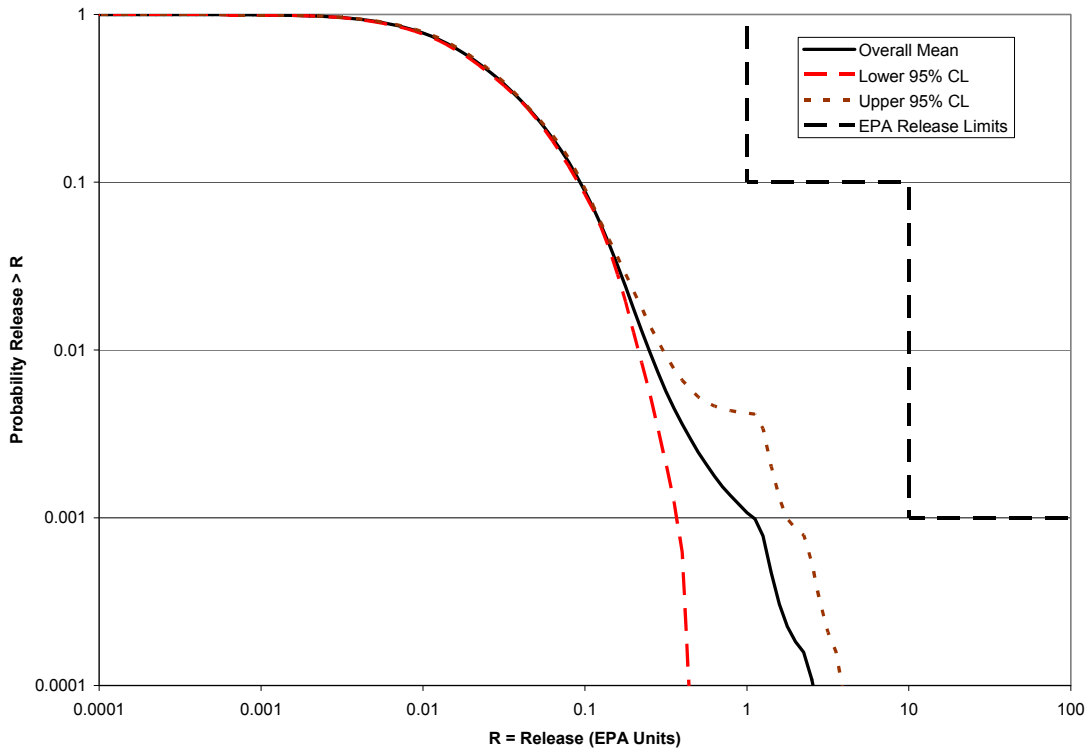

Figure 34-5. CRA-2009 PABC: Confidence Limits on Overall Mean for Total Normalized Releases (Camphouse 2010, Figure 3-33).

As seen in Figure 34-2, one CCDF differed considerably from the other 299, and exceeded the compliance release limit (1 EPA unit) at a probability of 0.1. The CCDF in question was dominated by direct brine releases (DBRs) (Clayton et al. 2010). Increases in radionuclide solubilities as a result of inventory changes in the CRA-2009 PABC led to greater amounts of mobilized radionuclides calculated by the PANEL code and available for DBR (Garner 2010). DBR releases were overestimated because the volume of brine used in PANEL to calculate mobilized radionuclides per brine volume did not limit the volume of brine available for DBR in CCDFGF. The EPA examined this CCDF and determined that it did not affect disposal system compliance, which is determined by the mean of the 300 vectors.

Table 34-2 shows the overall mean total normalized release CCDF values for the CRA-2009 PA and CRA-2009 PABC at the compliance probabilities of 0.1 and 0.001 and the upper and lower 95% confidence values. These are compared to the CCA and CRA-2004 PAs. The EPA examined the CRA-2009 Section 34, CRA-2009 Appendix PA-2009, and the CRA-2009 PABC report (Clayton et al. 2010) to verify that there is at least a 95% level of statistical confidence that the mean of the population of CCDFs meets the containment requirements of 40 CFR 191.13.

Table 34-2. For Various PAs: Statistics on the Overall Mean for Total Normalized Releases (in EPA Units) at Probabilities of 0.1 and 0.001, All Replicates Pooled (from Section Evaluation of Compliance for 2004 Recertification of U.S. EPA 2010b)

Probability	PA Analysis	Mean Total Release	90th Quantile Total Release	Lower 95% CL	Upper 95% CL	Release Limit
0.1	CCA PAVT	0.124	0.192	0.123	0.137	1
	CRA-2004	0.096	0.157	0.081	0.110	1
	PABC-2004	0.088	0.148	0.085	0.091	1
	CRA-2009	0.100	0.170	0.100	0.110	1
	PABC-2009	0.090	0.160	0.090	0.100	1
0.001	CCA PAVT	0.382	0.391	0.281	0.436	10
	CRA-2004	0.507	0.858	0.278	0.552	10
	PABC-2004	0.601	0.809	0.518	0.681	10
	CRA-2009	0.720	0.810	0.480	0.920	10
	PABC-2009	1.100	1.000	0.370	1.770	10

CL = Confidence Limit

Based on a review and evaluation of the CRA-2009 and supplemental information provided by the DOE, the EPA determined that the DOE continued to comply with the requirements of section 194.34(f) (see Recertification CARD No. 34: Results of Performance Assessments[194.34(f)]) (U.S. EPA 2010b).

34.7.7 Changes or New Information Since the CRA-2009

For the CRA-2014 PA, the DOE uses the same approach to calculate the statistical confidence for evaluation against the release limits as was used in the CCA, CRA-2004, and CRA-2009. The mean of the 300 CCDFs, along with the 95% confidence levels about the overall mean for the total normalized releases of the CRA-2014 PA, are shown in Figure 34-6. Table 34-3 lists the overall mean total normalized release CCDF values of the CRA-2014 PA at the compliance probabilities of 0.1 and 0.001, along with the values of the upper and lower 95% confidence limit CCDFs at the same probabilities. More details on the normalized release results of the CRA-2014 PA are discussed in Appendix PA-2014, Section PA-9.5. As seen in Figure 34-6 and Table 34-3, the results of the PA demonstrate a greater than 95% level of statistical confidence that the overall mean of the population of CCDFs is in compliance with the containment requirements of section 191.13, and thus the DOE continues to comply with provisions of section 194.34(f).

The overall mean CCDF is computed as the arithmetic mean of the three mean CCDFs from each replicate. Confidence limits are computed about the overall mean CCDF using the Student's t-distribution, the mean CCDFs from each replicate, and the standard error based on the three replicate means. Confidence limits, as they are implemented in PA, are defined vertically about the mean, rather than horizontally. An artifact of this convention is that lower confidence limits

can sometimes assume negative values, which cannot be plotted on a logarithmic scale. When this occurs, the resulting lower confidence curve appears incomplete (Zeitler 2013).

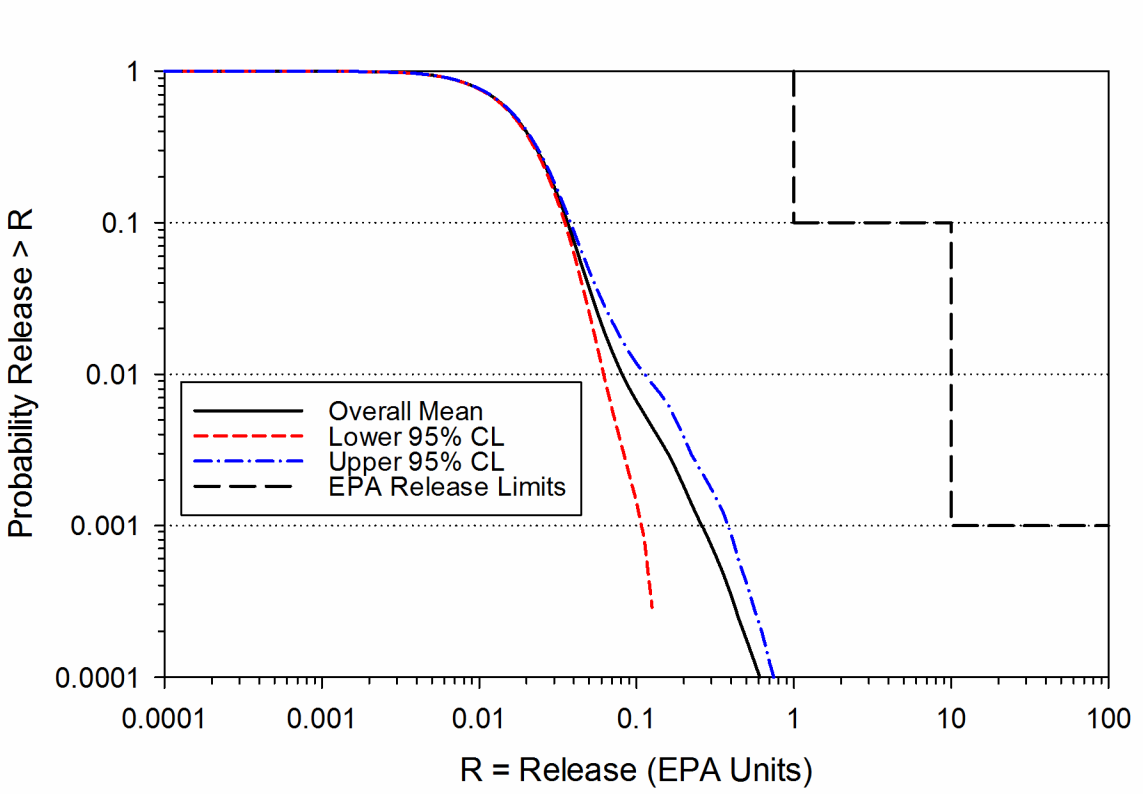

Figure 34-6. Mean and Confidence Interval CCDFs for Total Normalized Releases: CRA-2014 PA (from Figure 3-50 in Zeitler 2013)

Table 34-3. CRA-2014 PA Statistics on the Overall Mean for Total Normalized Releases at Probabilities of 0.1 and 0.001, All Replicates Pooled Compared with Release Limits (from Table 1 in Zeitler 2013)

Probability	Mean Total Release	Lower 95% Confidence Limit	Upper 95% Confidence Limit	Regulatory[a] Limit
0.1	0.0367	0.0352	0.0384	1
0.001	0.261	0.109	0.384	10

[a] Releases divided by the release limits in Part 191 Appendix A, Table 1.

34.8 References

(*Indicates a reference that has not been previously submitted.)

Camphouse, R.C. 2010. Analysis Package (AP) for CCDFGF: CRA-2009 Performance Assessment Baseline Calculation (PABC). ERMS 553027. Carlsbad, NM: Sandia National Laboratories.*

Camphouse, R.C., D.C. Kicker, S. Kim, T.B. Kirchner, J.J. Long, B.N. Malama, and T.R. Zeitler. 2013. *Summary Report of the 2014 Compliance Recertification Application Performance Assessment*. Carlsbad, NM: Sandia National Laboratories.*

Clayton, D.J., S. Dunagan, J.W. Garner, A.E. Ismail, T.B. Kirchner, G.R. Kirkes, and M.B. Nemer. 2008. *Summary Report of the 2009 Compliance Recertification Application Performance Assessment*. ERMS 548862. Carlsbad, NM: Sandia National Laboratories.

Clayton, D.J., R.C. Camphouse, J.W. Garner, A.E. Ismail, T.B. Kirchner, K.L. Kuhlman, and M.B. Nemer. 2010. *Summary Report of the CRA-2009 Performance Assessment Baseline Calculations*. ERMS 553039. Carlsbad, NM: Sandia National Laboratories.*

Clayton, D.J. 2010. *Parameter Summary Report: CRA-2009 PABC*. ERMS 552889. Carlsbad, NM: Sandia National Laboratories.*

Cotsworth, E. 2005. Letter to U.S. Department of Energy (1 Enclosure). March 4, 2005. ERMS 538858. Washington, DC: U.S. Environmental Protection Agency, Office of Air and Radiation.

Fox, B. 2008. *Parameter Report for the CRA-2009 PA* (Revision 0). ERMS 549747. Carlsbad, NM: Sandia National Laboratories.

Garner, J.W. 2010. *AP for PANEL: CRA-2009 PABC*. ERMS 553032. Carlsbad, NM: Sandia National Laboratories.*

Kicker, D.C. and C.G. Herrick. 2013. Parameter Summary Report for the 2014 Compliance Recertification Application. Carlsbad, NM: Sandia National Laboratories.*

Kirchner, T.B. 2005. *Generation of the LHS Samples for the CRA 2004 PA Baseline Calculations*. ERMS 540279. Carlsbad, NM: Sandia National Laboratories.

Kirchner, T. 2013. *Generation of the LHS Samples for the CRA-2014 (AP-164) PA Calculations, Revision 0*. ERMS 559950. Carlsbad, NM: Sandia National Laboratories.

Leigh, C., J. Kanney, L. Brush, J. Garner, G. Kirkes, T. Lowry, M. Nemer, J. Stein, E. Vugrin, S. Wagner, and T. Kirchner. 2005. *2004 Compliance Recertification Application Performance Assessment Baseline Calculation* (Revision 0). ERMS 541521. Carlsbad, NM: Sandia National Laboratories.

U.S. Department of Energy (DOE). 1996. *Title 40 CFR Part 191 Compliance Certification Application for the Waste Isolation Pilot Plant* (October). 21 vols. DOE/CAO 1996-2184. Carlsbad, NM: Carlsbad Area Office.

U.S. Department of Energy (DOE). 2004. *Title 40 CFR Part 191 Compliance Recertification Application for the Waste Isolation Pilot Plant* (March). 10 vols. DOE/WIPP 2004-3231. Carlsbad, NM: Carlsbad Field Office.

U.S. Environmental Protection Agency (EPA). 1993. "40 CFR Part 191: Environmental Radiation Protection Standards for the Management and Disposal of Spent Nuclear Fuel, High-Level and Transuranic Radioactive Wastes; Final Rule." *Federal Register,* vol. 58 (December 20, 1993): 66398–416.

U.S. Environmental Protection Agency (EPA). 1996. "40 CFR Part 194: Criteria for the Certification and Recertification of the Waste Isolation Pilot Plant's Compliance with the 40 CFR Part 191 Disposal Regulations; Final Rule." *Federal Register*, vol. 61 (February 9, 1996): 5223–45.

U.S. Environmental Protection Agency (EPA). 1998a. "CARD No. 34: Results of Performance Assessments." *Compliance Application Review Documents for the Criteria for the Certification and Recertification of the Waste Isolation Pilot Plant's Compliance with the 40 CFR Part 191 Disposal Regulations: Final Recertification Decision* (May) (pp. 34-1 through 34-29). Washington, DC: Office of Radiation and Indoor Air.

U.S. Environmental Protection Agency (EPA). 1998b. *Technical Support Document: Overview of Major Performance Assessment Issues* (May). Washington, DC: Office of Radiation and Indoor Air.

U.S. Environmental Protection Agency (EPA). 2006a. *Technical Support Document for Section 194.23: Review of the 2004 Compliance Recertification Performance Assessment Baseline Calculation* (March). Washington, DC: Office of Radiation and Indoor Air.

U.S. Environmental Protection Agency (EPA). 2006b. "Recertification CARD No. 34: Results of Performance Assessments." *Compliance Application Review Documents for the Criteria for the Certification and Recertification of the Waste Isolation Pilot Plant's Compliance with the 40 CFR Part 191 Disposal Regulations: Final Recertification Decision* (March) (pp. 34-1 through 34-12). Washington, DC: Office of Radiation and Indoor Air.

U.S. Environmental Protection Agency (EPA). 2006c. *Technical Support Document for Section 194.23: Models and Computer Codes* (March). PABC Code Changes Review. Washington, DC: Office of Radiation and Indoor Air.

U.S. Environmental Protection Agency (EPA). 2006d. *Technical Support Document for Section 194.23: Review of WIPP Recertification Performance Assessment Computer Codes* (March). CRA Code Review. Washington, DC: Office of Radiation and Indoor Air.

U.S. Environmental Protection Agency (EPA). 2006e. *Technical Support Document for Section 194.23: Review of Changes to the WIPP Performance Assessment Parameters from the Compliance Recertification Application to Performance Assessment Baseline Calculation* (March). PABC Parameter Review. Washington, DC: Office of Radiation and Indoor Air.

U.S. Environmental Protection Agency (EPA). 2006f. *Technical Support Document for Section 194.24: Evaluation of the Compliance Recertification Actinide Source Term and Culebra Dolomite Distribution Coefficient Values* (March). Washington, DC: Office of Radiation and Indoor Air.

U.S. Environmental Protection Agency (EPA). 2006g. *Technical Support Document for Section 194.24: Review of the Baseline Inventory Used in the Compliance Recertification Application and the Performance Assessment Baseline Calculation* (March). Washington, DC: Office of Radiation and Indoor Air.

U.S. Environmental Protection Agency (EPA). 2010a. *Technical Support Document for Section 194.23:* Review of the 2009 Compliance Recertification Performance Assessment Baseline Calculation (PABC-2009). Washington, DC: Office of Radiation and Indoor Air. Docket A-98-49, II-B2-23.*

U.S. Environmental Protection Agency (EPA). 2010b. "Results of Performance Assessments." *2009 Compliance Recertification Application (2009 CRA) Compliance Application Review Document (CARD) No. 34* (pp. 34-1 through 34-18). Washington, DC: Office of Radiation and Indoor Air.*

U.S. Environmental Protection Agency (EPA). 2010c. Technical Support Document for Sections 194.22 and 194.23: Review of WIPP Performance Assessment Computer Code Migration Activities. Docket A-98-48, II-B1-22. Washington, DC: Office of Radiation and Indoor Air.*

U.S. Environmental Protection Agency (EPA). 2010d. Technical Support Document for Section 194.23: Review of Changes to the WIPP Performance Assessment Parameters Since the 2004 PABC. Docket A-98-49, II-B1-21.* Washington, DC: Office of Radiation and Indoor Air.*

U.S. Environmental Protection Agency (EPA). 2010e. Technical Support Document for Section 194.24: Evaluation of the Compliance Recertification Actinide Source Term, Backfill Efficacy and Culebra Dolomite Distribution Coefficient Values. Docket A-98-49, II-B1-25. Washington, DC: Office of Radiation and Indoor Air.*

Zeitler, T.R. 2013. Analysis Package for CCDFGF: 2014 Compliance Recertification Application Performance Assessment (CRA-2014 PA). ERMS 560074. Carlsbad, NM: Sandia National Laboratories.*

Title 40 CFR Part 191
Subparts B and C
Compliance Recertification Application 2014
for the
Waste Isolation Pilot Plant

Active Institutional Controls
(40 CFR § 194.41)

United States Department of Energy
Waste Isolation Pilot Plant

Carlsbad Field Office
Carlsbad, New Mexico

Compliance Recertification Application 2014
Active Institutional Controls
(40 CFR § 194.41)

Table of Contents

This page intentionally left blank.

Acronyms and Abbreviations

AIC	active institutional control
CARD	Compliance Application Review Document
CCA	Compliance Certification Application
CFR	Code of Federal Regulations
CRA	Compliance Recertification Application
DOE	U.S. Department of Energy
EPA	U.S. Environmental Protection Agency
LMP	Land Management Plan
PA	performance assessment
WIPP	Waste Isolation Pilot Plant

This page intentionally left blank.

41.0 Active Institutional Controls (40 CFR § 194.41)

41.1 Requirements

> § 194.41 Active Institutional Controls
>
> (a) Any compliance application shall include detailed descriptions of proposed active institutional controls, the controls' location, and the period of time the controls are proposed to remain active. Assumptions pertaining to active institutional controls and their effectiveness in terms of preventing or reducing radionuclide releases shall be supported by such descriptions.
>
> (b) Performance assessments shall not consider any contributions from active institutional controls for more than 100 years after disposal.

41.2 Background

Assurance requirements are included in the disposal regulations to compensate in a qualitative manner for the inherent uncertainties in projecting the behavior of natural and engineered components of the Waste Isolation Pilot Plant (WIPP) for many thousands of years (U.S. EPA 1985, p. 38072, and Compliance Application Review Document [CARD] 41, U.S. EPA 1998a, Section 41.A.1). Section 194.41 is one of the compliance criteria. Active institutional controls (AICs) are defined in 40 CFR § 191.12 (U.S. EPA 1993) as "controlling access to a disposal site by any means other than passive institutional controls, performing maintenance operations or remedial actions at a site, controlling or cleaning up releases from a site, or monitoring parameters related to disposal system performance." Section 194.41 requires AICs to be maintained for as long a period of time as practicable after disposal; however, contributions from AICs for reducing the rate of human intrusion in the performance assessment (PA) may not be considered for more than 100 years after disposal.

41.3 1998 Certification Decision

To meet the requirements for section 194.41, the U.S. Environmental Protection Agency (EPA) expected the Compliance Certification Application (CCA) (U.S. DOE 1996) to describe in detail the proposed AICs and their location and function and to identify the period of time they are expected to remain active. The EPA also expected the U.S. Department of Energy (DOE) to provide detailed information regarding implementation of the controls, any assumptions pertaining to the effectiveness of active controls, a justification for any credit for the AICs used in the PA, and the method for determining the credit. The EPA specified that the PA could not assume that the AICs would be effective for a period longer than 100 years after disposal.

In the CCA, Chapter 7.0 and Appendix AIC, the DOE described its plan for the AICs, including constructing a fence and roadway around the surface footprint of the repository, posting warning signs, and performing routine patrols and surveillance. The DOE stated that the AICs will be maintained for 100 years after closure of the WIPP facility and would effectively prevent human intrusion during that time.

The EPA reviewed the DOE's proposed plans for the AICs in connection with the types of activities (U.S. EPA 1998a, Section 41.A.3) that may be expected to occur in the vicinity of the

WIPP site during the first 100 years after disposal (i.e., ranching, farming, hunting, scientific activities, utilities and transportation, groundwater pumping, surface excavation, potash exploration, construction, and hostile or illegal activities). The EPA also examined the assumptions made by the DOE to justify the assertion that the AICs will be completely effective for 100 years.

The EPA found that the DOE adequately described the proposed AICs and the bases for their assumed effectiveness and did not assume in the PA that the AICs would be effective for more than 100 years, and thus found the DOE to be in compliance with section 194.41.

A complete description of the EPA's 1998 Certification Decision for section 194.41 can be found in U.S. EPA (U.S. EPA 1998b).

41.4 Changes in the CRA-2004

The 2004 Compliance Recertification Application (CRA-2004) (U.S. DOE 2004), Chapter 7.0 contains the changes related to AICs since 1998. The DOE reported that the CCA, Appendix AIC was unchanged since 1998; however, the following changes were included in CRA-2004:

- A new timeline for implementation of AICs
- DOE's approach to maintaining and replacing AICs
- Minimum standards to apply during construction and maintenance of AICs

41.5 EPA's Evaluation of Compliance for the 2004 Recertification

Based on the EPA's review of the activities and conditions in and around the WIPP site, the EPA did not identify any significant changes in the planning and execution of the DOE's AICs plan since the 1998 Certification Decision (U.S. EPA 2006a, p. 41-2, paragraph 2 and paragraph 4).

The EPA concluded that the CRA-2004 adequately described, in detail, the proposed AICs and their location and function, and identified the basis for the DOE's assumed effectiveness. The EPA confirmed that the DOE's CRA-2004 Performance Assessment Baseline Calculations (Leigh et al. 2005) used the maximum allowable credit for the AICs against human intrusion (100 years). The EPA found reasonable the DOE's assertion that the AICs will completely prevent human intrusion for 100 years.

The EPA approved the removal of Appendix LMP (Land Management Plan) from recertification applications. The EPA found that information from Appendix LMP was not used as a basis for the EPA's 1998 Compliance Decision on section 194.41 (U.S. EPA 1998b). Because it does not directly support compliance demonstrations for the EPA's disposal regulations, its removal from the CRA-2004 was not significant, nor did it affect the EPA's evaluation of continued compliance.

During its review of the CRA-2004, the EPA received no public comments on the DOE's continued compliance with the AICs requirements of section 194.41. The EPA found (U.S. EPA 2006b) the DOE to be in continued compliance with the requirements of section 194.41.

41.6 Changes or New Information Between the CRA-2004 and the CRA-2009 (Previously: Changes or New Information Since the 2004 Recertification)

In the CRA-2009 (U.S. DOE 2009), the DOE did not propose any changes to the AICs program for the WIPP. Information pertaining to the program as provided in the CCA and the CRA-2004 remained unchanged. The DOE believed it had demonstrated continued compliance with the provisions of section 194.41.

41.7 EPA's Evaluation of Compliance for the 2009 Recertification

Based on a review and evaluation of the CRA-2009, CRA-2004, CCA Appendix AIC (U.S. DOE 1998a), and supplemental information provided by the DOE (Federal Document Management System Docket ID No. EPA-HQ-OAR-2009-0330, Air Docket A-98-49), the EPA determined that the DOE continued to comply with the requirements of section 194.41 (U.S. EPA 2010).

41.8 Changes or New Information Since the CRA-2009

In the CRA-2014, the DOE is not proposing any changes to the AICs program for the WIPP. Information pertaining to the program as provided in the CCA, CRA-2004 and CRA-2009 remains unchanged. The DOE believes it has demonstrated continued compliance with the provisions of section 194.41.

41.9 References

(*Indicates a reference that has not been previously submitted.)

Leigh, C., J. Kanney, L. Brush, J. Garner, G. Kirkes, T. Lowry, M. Nemer, J. Stein, E. Vugrin, S. Wagner, and T. Kirchner. 2005. *2004 Compliance Recertification Application Performance Assessment Baseline Calculation* (Revision 0). ERMS 541521. Carlsbad, NM: Sandia National Laboratories.*

U.S. Department of Energy (DOE). 1996. *Title 40 CFR Part 191 Compliance Certification Application for the Waste Isolation Pilot Plant* (October). 21 vols. DOE/CAO-1996-2184. Carlsbad, NM: Carlsbad Area Office.

U.S. Department of Energy (DOE). 2004. *Title 40 CFR Part 191 Compliance Recertification Application for the Waste Isolation Pilot Plant* (March). 10 vols. DOE/WIPP 2004-3231. Carlsbad, NM: Carlsbad Field Office.

U.S. Department of Energy (DOE). 2009. *Title 40 CFR Part 191 Compliance Recertification Application for the Waste Isolation Pilot Plant* (March). DOE/WIPP-09-3424. Carlsbad, NM: Carlsbad Field Office.*

U.S. Environmental Protection Agency (EPA). 1985. "40 CFR 191: Environmental Standards for the Management and Disposal of Spent Nuclear Fuel, High-Level and Transuranic Radioactive Wastes; Final Rule" *Federal Register*, vol. 50 (September 19, 1985): 38066–089.

U.S. Environmental Protection Agency (EPA). 1993. "40 CFR Part 191 Environmental Radiation Protection Standards for the Management and Disposal of Spent Nuclear Fuel, High-Level and Transuranic Radioactive Wastes; Final Rule." *Federal Register*, vol. 58 (December 20, 1993): 66398–416.

U.S. Environmental Protection Agency (EPA). 1998a. "CARD No. 41: Active Institutional Controls." *Compliance Application Review Documents for the Criteria for the Certification and Recertification of the Waste Isolation Pilot Plant's Compliance with the 40 CFR Part 191 Disposal Regulations: Final Certification Decision* (May) (pp. 41-1 through 41-6). Washington, DC: Office of Radiation and Indoor Air.

U.S. Environmental Protection Agency (EPA). 1998b. "40 CFR Part 194: Criteria for the Certification and Recertification of the Waste Isolation Pilot Plant's Compliance with the Disposal Regulations: Certification Decision; Final Rule." *Federal Register*, vol. 63 (May 18, 1998): 27353–406.

U.S. Environmental Protection Agency (EPA). 2006a. "Recertification CARD No. 41: Active Institutional Controls." *Compliance Application Review Documents for the Criteria for the Certification and Recertification of the Waste Isolation Pilot Plant's Compliance with the 40 CFR 191 Disposal Regulations: Final Recertification Decision* (pp. 41-1 through 41-3) (March). Washington, DC: Office of Radiation and Indoor Air.

U.S. Environmental Protection Agency (EPA). 2006b. "40 CFR Part 194: Criteria for the Certification and Recertification of the Waste Isolation Pilot Plant's Compliance with the Disposal Regulations: Recertification Decision" (Final Notice). *Federal Register*, vol. 71 (April 10, 2006): 18010–021.

U.S. Environmental Protection Agency (EPA). 2010 "Recertification CARD No. 41: Active Institutional Controls." 2009 Compliance Recertification Application (2009 CRA) *Compliance Application Review Document (CARD) No. 41; Active Institutional Controls* (November 16, 2010). Washington, DC: Office of Radiation and Indoor Air.*

Title 40 CFR Part 191
Subparts B and C
Compliance Recertification Application 2014
for the
Waste Isolation Pilot Plant

Monitoring
(40 CFR § 194.42)

United States Department of Energy
Waste Isolation Pilot Plant

Carlsbad Field Office
Carlsbad, New Mexico

Compliance Recertification Application 2014
Monitoring
(40 CFR § 194.42)

Table of Contents

This page intentionally left blank.

Acronyms and Abbreviations

CARD	Compliance Application Review Document
CCA	Compliance Certification Application
CFR	Code of Federal Regulations
CMP	Compliance Monitoring Program
COMP	Compliance Monitoring Parameter
CRA	Compliance Recertification Application
DOE	U.S. Department of Energy
EPA	U.S. Environmental Protection Agency
PA	performance assessment
PABC	Performance Assessment Baseline Calculation
WIPP	Waste Isolation Pilot Plant

This page intentionally left blank.

42.0 Monitoring (40 CFR § 194.42)

42.1 Requirements

§ 194.42 Monitoring

(a) The Department shall conduct an analysis of the effects of disposal system parameters on the containment of waste in the disposal system and shall include the results of such analysis in any compliance application. The results of the analysis shall be used in developing plans for pre-closure and post-closure monitoring required pursuant to paragraphs (c) and (d) of this section. The disposal system parameters analyzed shall include, at a minimum:

1. Properties of backfilled material, including porosity, permeability, and degree of compaction and reconsolidation;
2. Stresses and extent of deformation of the surrounding roof, walls, and floor of the waste disposal room;
3. Initiation or displacement of major brittle deformation features in the roof or surrounding rock;
4. Ground water flow and other effects of human intrusion in the vicinity of the disposal system;
5. Brine quantity, flux, composition, and spatial distribution;
6. Gas quantity and composition; and
7. Temperature distribution.

(b) For all disposal system parameters analyzed pursuant to paragraph (a) of this section, any compliance application shall document and substantiate the decision not to monitor a particular disposal system parameter because that parameter is considered to be insignificant to the containment of waste in the disposal system or to the verification of predictions about the future performance of the disposal system.

(c) Pre-closure monitoring. To the extent practicable, pre-closure monitoring shall be conducted of significant disposal system parameter(s) as identified by the analysis conducted pursuant to paragraph (a) of this section. A disposal system parameter shall be considered significant if it affects the system's ability to contain waste or the ability to verify predictions about the future performance of the disposal system. Such monitoring shall begin as soon as practicable; however, in no case shall waste be emplaced in the disposal system prior to the implementation of pre-closure monitoring. Pre-closure monitoring shall end at the time at which the shafts of the disposal system are backfilled and sealed.

(d) Post-closure monitoring. The disposal system shall, to the extent practicable, be monitored as soon as practicable after the shafts of the disposal system are backfilled and sealed to detect substantial and detrimental deviations from expected performance and shall end when the Department can demonstrate to the satisfaction of the Administrator that there are no significant concerns to be addressed by further monitoring. Post-closure monitoring shall be complementary to monitoring required pursuant to applicable federal hazardous waste regulations at parts 264, 265, 268, and 270 of this chapter and shall be conducted with techniques that do not jeopardize the containment of waste in the disposal system.

(e) Any compliance application shall include detailed pre-closure and post-closure monitoring plans for monitoring the performance of the disposal system. At a minimum, such plans shall:

(1) Identify the parameters that will be monitored and how baseline values will be determined;

(2) Indicate how each parameter will be used to evaluate any deviations from the expected performance of the disposal system; and

(3) Discuss the length of time over which each parameter will be monitored to detect deviations from expected performance.

42.2 Background

In 40 CFR §194.42 (U.S. EPA 1996), the U.S. Environmental Protection Agency (EPA) provides criteria to demonstrate compliance with the assurance requirement at 40 CFR §191.14(b) (U.S. EPA 1993) to monitor the disposal system. The purpose of this monitoring is “to detect substantial and detrimental deviations from expected performance,” with the expected performance predicted by performance assessment (PA). The criteria also require both a preclosure and postclosure monitoring program using techniques that do not jeopardize the

containment of waste in the disposal system. Ten monitoring parameters were identified in an analysis performed to fulfill the section 194.42 requirement during the original certification process. More detailed information describing the section 194.42 Compliance Monitoring Program (CMP) is located in the U.S. Department of Energy (DOE) Compliance Monitoring Implementation Plan (U.S. DOE 2005); the 2004 Compliance Recertification Application (CRA-2004) (U.S. DOE 2004), Chapter 7.0, Section 7.2; Appendix MON-2009 (U.S. DOE 2009); and Appendix Mon-2014.

The 10 parameters, their associated monitoring programs, the frequency of data collection and reporting, related PA parameters, and related screening decisions used to support the PA are listed in Appendix MON-2014, Table MON-1. These parameters are periodically evaluated to determine if there is an impact on the PA-related parameters, conceptual models, or features, events, and processes screening decisions (Wagner and Kuhlman 2010b; Wagner 2011; Wagner, Kuhlman, and Johnson 2012; Wagner 2013).

42.3 1998 Certification Decision

Based on information in the Compliance Certification Application (CCA) (U.S. DOE 1996) and supplemental monitoring-related information for the CCA submitted to the EPA in response to its request for additional information regarding the methodology of the MONPAR analysis, the EPA determined that the DOE was in compliance with the criteria of section 194.42 (U.S. EPA 1998a, Section VIII.D.2, Monitoring). Additional details of the EPA's evaluation of compliance can be found in the Compliance Application Review Document (CARD) 42, Monitoring (U.S. EPA 1998b).

42.4 Changes in the CRA-2004

Since 1998, the DOE has monitored and evaluated the 10 monitoring parameters listed in Appendix MON-2004, Table MON-1. For the CRA-2004, the DOE reassessed the CCA monitoring parameter analysis in light of changes in the monitoring program. This reassessment is documented in Kirkes and Wagner (Kirkes and Wagner 2003), and described in the CRA-2004, Chapter 7.0, Section 7.2. It was determined that the CCA, Appendix MON, Attachment MONPAR monitoring parameter analysis performed to comply with section 194.42 requirements was adequate and did not need to be redone for the CRA-2004. The 10 monitoring parameters identified in the CCA were still sufficient to be included in the Compliance Monitoring Program (CMP) to detect substantial deviations from performance expectations and to comply with the requirements of section 194.42. Supplemental information was submitted to the EPA in response to its request for compliance monitoring annual reports and monitoring data references (Response C-42-1 through C-42-4 [Detwiler 2004a]; Response C-42-5 and C-42-6 [Detwiler 2004b]). Since the CCA, the DOE found four monitoring parameters that either did not fall within the set trigger values or indicated a change from values used in the CCA. These parameters include:

- Changes in the Culebra Dolomite Member of the Rustler Formation (hereafter referred to as Culebra) water level that may impact Culebra groundwater flow direction and/or composition

- A change in the probability of encountering a Castile brine reservoir

- A change in the drilling rate because of continued oil and gas drilling in the Delaware Basin
- Changes in the waste activity caused by changes in the waste inventory

The impacts of these changes were considered in Appendix PA-2004 and the EPA-mandated CRA-2004 Performance Assessment Baseline Calculation (PABC) to assess their impact on compliance (see CARD 23, Models and Computer Codes [U.S. EPA 2006a]), which documented the EPA's review of these impacts and its determination of continued compliance with the disposal standards.

42.5 EPA's Evaluation of Compliance for the 2004 Recertification

In CARD 42, the EPA stated that through its annual monitoring and waste emplacement inspections it had determined that the DOE meets the requirements of section 194.42 (U.S. EPA 2006b). The results of these inspections are documented in CARD 21, Tables CARD 21-1 and 21-2 (U.S. EPA 2006c).

42.6 Changes or New Information Between the CRA-2004 and the CRA-2009 (Previously: Changes or New Information Since the 2004 Recertification)

The CMP outlined in Section 42.2 was developed to implement the requirements of section 194.42; the program continued to monitor the Waste Isolation Pilot Plant (WIPP) disposal system to detect substantial and detrimental deviations from expected performance. During this time, the program did not indicate such a condition. No changes were made to this program from that described in the CRA-2004, Chapter 7.0, Section 7.2, and Attachment MON-2004. New information that supplemented the information in the CRA-2004, Chapter 7.0, Section 7.2 included the following:

1. Results of the CMP since 2004 (Appendix DATA-2009) (U.S. DOE 2009)
2. Assessment of the impact of changes on the CMP (Wagner 2008)

The annual Compliance Monitoring Parameters (COMPs) report presented monitoring results and determined whether the results were within PA expectations, whether they impacted the assumptions or parameters used in PA, or whether they impacted the monitoring program. A review of the conclusions in the last four annual COMPs reports (Wagner 2008) showed the following:

- The results of the COMPs assessments concluded that there were no reportable conditions or events.
- Water levels in the Culebra continued to rise across the monitored region. The DOE continued its investigation of those events. Those investigations led to the inclusion of updated water-level information during the CRA-2004 PABC (see preface to Appendix TFIELD-2009). The CRA-2009 PA (U.S. DOE 2009) used the CRA-2004 PABC transmissivity fields.

- The CMP investigated sample collection and analytical laboratory techniques to reduce uncertainties in water chemistry results.

- No changes to the COMPs or CMP were recommended.

The results of the COMPs reports validated the need to monitor groundwater and demonstrated the importance of continued monitoring and the need to incorporate results into the PA (Sandia National Laboratories 2004).

The CCA, Appendix MON, Attachment MONPAR documented an analysis that was used to determine which monitoring parameters should be included in the CMP. A reassessment of this analysis, documented in Wagner (Wagner 2008), determined whether changes to elements of the WIPP program since the last certification affect the conclusions in the CCA, Appendix MON, Attachment MONPAR analysis. The reassessment first determined which changes should be considered, and then determined the impact of those changes on the conclusions drawn in the CCA, Appendix MON, Attachment MONPAR analysis. Changes to the following disposal system elements were evaluated:

1. Monitoring results

2. Experimental activities

3. PA changes: methodology, parameters, and implementation

4. WIPP operational changes

5. Proposed changes to activities and conditions approved by the EPA

Based on the review of operational activities, conditions, monitoring data, the PA, and experimental programs that occurred since the CRA-2004, the reassessment concluded, “the conclusions of the MONPAR analysis remain valid and its conclusions continue to be adequate for inclusion in the CRA-2009” (Wagner 2008).

The DOE believed the information presented in the CRA-2004, Chapter 7.0, Section 7.2; Appendix MON-2004; Appendix MON-2009; and the supplemental information provided in this section continued to demonstrate compliance with the provisions of section 194.42.

42.7 EPA’s Evaluation of Compliance for the 2009 Recertification

In the CRA-2009 CARD 42, the EPA outlined its review of information in the CRA-2009, supplemental information provided by the DOE and the results of the EPA’s annual inspections of the WIPP, and determined that the DOE continued to comply with the requirements of section 194.42 (U.S. EPA 2010a and U.S. EPA 2010b).

42.8 Changes or New Information Since the CRA-2009

The CMP in Section 42.2 implements the requirements of section 194.42, and the program continues to monitor the WIPP to detect substantial and detrimental deviations from expected performance. This program has not indicated such a condition. The DOE has continued to monitor and evaluate the 10 monitoring parameters. Minor changes have been made to the monitoring program from that described in the CRA-2009 or Appendix MON-2009 (U.S. DOE 2009). The DOE did not change its pre-closure or post-closure program plans or activities, so there are no changes to report for the requirements of 40 CFR 194.42(b), (c), (d), or (e). Due to a revision to the WIPP groundwater conceptual model during the CRA-2009 PABC, changes were needed to the related Culebra groundwater monitoring parameter derivation and trigger values. Other changes were made to parameter trigger values as part of the trigger value report revision (Wagner and Kuhlman 2010a).

Changes were also made to the Culebra Groundwater Monitoring Program regarding groundwater composition sampling frequency and the method for reporting the change in the groundwater flow parameter (Nuclear Waste Partnership LLC 2012). The DOE has changed from semi-annual sampling to an annual sampling schedule, based on 15 years of data showing little or no change in constituent concentrations. DOE also changed the method used to produce the annual water level map required by the WIPP Hazardous Waste Facility Permit (Permit). These changes to the Groundwater Monitoring Program Plan (Nuclear Waste Partnership LLC 2012) were necessary to align the 40 CFR 194.42 compliance monitoring program with related changes made to respond to a New Mexico Environment Department Class 2 Permit Modification request to revise the WIPP Groundwater Detection Monitoring Program Plan. This permit modification was approved January 31, 2012 (NMED 2012).

Minor changes to the 40 CFR 194.42 monitoring program have occurred over the last five-year recertification cycle. The trigger values for some of the monitoring parameters have been revised; however, no changes were made to the 10 monitoring parameters (Wagner and Kuhlman 2010a; Wagner Kuhlman and Johnson 2012). Changes were made to the process used to derive the Change in Culebra Groundwater Flow parameter and the sampling frequency has changed from biannually to annually for the Change in Groundwater Composition parameter (Wagner and Kuhlman 2010b, Section 2.3.2.2). The results of the CMP over this period have not identified any substantial and detrimental deviations from expected performance.

New monitoring information that supplements the information provided since the last recertification cycle includes the following:

1. Monitoring results for the 10 parameters since 2009 are contained in Appendix DATA-2014

2. Information included in the Trigger Value Derivation Report revision (Wagner and Kuhlman 2010a)

3. The reassessment of the parameters to determine if there is an impact on the PA-related parameters, conceptual models, or features, events, and processes screening decisions (Wagner 2013)

4. Changes to *Change in Culebra Composition*, and *Change in Culebra Groundwater Flow* parameters to align with the Permit (NMED 2012; Wagner and Kuhlman 2010b)

The DOE believes the information presented in this section, along with Appendix MON-2014 and Appendix DATA-2014, continues to demonstrate compliance with the provisions of section 194.42.

42.9 References

(*Indicates a reference that has not been previously submitted.)

Detwiler, R.P. 2004a. Letter to E. Cotsworth (Subject: *Partial Response to Environmental Protection Agency (EPA)* May 20, 2004, Letter on CRA; 4 Enclosures). 15 July 2004. U.S. Department of Energy, Carlsbad Field Office, Carlsbad, NM.

Detwiler, R.P. 2004b. Letter to E. Cotsworth (Subject: *Initial Response to Environmental Protection Agency (EPA)* September 2, 2004, Letter on Compliance Recertification Application; 6 Enclosures). 1 November 2004. U.S. Department of Energy, Carlsbad Field Office, Carlsbad, NM.

Kirkes, R., and S.W. Wagner. 2003. *MONPAR Reassessment*. ERMS 533098. Carlsbad, NM: Sandia National Laboratories.

New Mexico Environment Department (NMED). 2012. Letter to E. Ziemianski, and F. Sharif, (Subject: *Approval and partial denial of permit modification requests to update ventilation language, add a shielded container, and revise the WIPP Groundwater Detection Monitoring Program Plan, WIPP Hazardous Waste Facility Permit, EPA I.D. Number NM4890139088-TSDF*). 31, January 2012, New Mexico Environment Department, Santa Fe, NM

Nuclear Waste Partnership LLC. 2012. *WIPP Groundwater Monitoring Program Plan* (Rev. 12, November 30, 2012). WP 02-1. Carlsbad, NM: Carlsbad Field Office.

Sandia National Laboratories. 2004. *Sandia National Laboratories Annual Compliance Monitoring Parameter Assessment for 2003* (Revision 1, June). ERMS 535825. Carlsbad, NM: Sandia National Laboratories.

U.S. Department of Energy (DOE). 1996. *Title 40 CFR Part 191 Compliance Certification Application for the Waste Isolation Pilot Plant* (October). 21 vols. DOE/CAO 1996-2184. Carlsbad, NM: Carlsbad Area Office.

U.S. Department of Energy (DOE). 2004. *Title 40 CFR Part 191 Compliance Recertification Application for the Waste Isolation Pilot Plant* (March). 10 vols. DOE/WIPP 2004-3231. Carlsbad, NM: Carlsbad Field Office.

U.S. Department of Energy (DOE). 2005. *40 CFR Parts 191 and 194 Compliance Monitoring Implementation Plan* (April 06, 2005, Revision 4). DOE/WIPP 99-3119. Carlsbad, NM: Carlsbad Field Office.

U.S. Department of Energy (DOE). 2009. *Title 40 CFR Part 191 Compliance Recertification Application for the Waste Isolation Pilot Plant* (March). DOE/WIPP-09-3424. Carlsbad, NM: Carlsbad Field Office.*

U.S. Environmental Protection Agency (EPA). 1993. "40 CFR Part 191: Environmental Radiation Protection Standards for the Management and Disposal of Spent Nuclear Fuel, High-Level and Transuranic Radioactive Wastes; Final Rule." *Federal Register*, vol. 58 (December 20, 1993): 66398–416.

U.S. Environmental Protection Agency (EPA). 1996. "40 CFR Part 194: Criteria for the Certification and Re-Certification of the Waste Isolation Pilot Plant's Compliance with the 40 CFR Part 191 Disposal Regulations; Final Rule." *Federal Register*, vol. 61 (February 9, 1996): 5223–45.

U.S. Environmental Protection Agency (EPA). 1998a. "40 CFR Part 194: Criteria for the Certification and Recertification of the Waste Isolation Pilot Plant's Compliance with the Disposal Regulations: Certification Decision; Final Rule." *Federal Register*, vol. 63 (May 18, 1998): 27353–406.

U.S. Environmental Protection Agency (EPA). 1998b. "CARD No. 42: Monitoring." *Compliance Application Review Documents for the Criteria for the Certification and Recertification of the Waste Isolation Pilot Plant's Compliance with the 40 CFR 191 Disposal Regulations: Final Certification Decision* (May) (pp. 42-1 through 42-24). Washington, DC: Office of Radiation and Indoor Air.

U.S. Environmental Protection Agency (EPA). 2006a. "Recertification CARD No. 23: Models and Computer Codes." *Compliance Application Review Documents for the Criteria for the Certification and Recertification of the Waste Isolation Pilot Plant's Compliance with the 40 CFR 191 Disposal Regulations: Final Recertification Decision* (March) (pp. 23-1 through 23-37). Washington, DC: Office of Radiation and Indoor Air.

U.S. Environmental Protection Agency (EPA). 2006b. "Recertification CARD No. 42: Monitoring." *Compliance Application Review Documents for the Criteria for the Certification and Recertification of the Waste Isolation Pilot Plant's Compliance with the 40 CFR 191 Disposal Regulations: Final Recertification Decision* (March) (pp. 42-1 through 42-6). Washington, DC: Office of Radiation and Indoor Air.

U.S. Environmental Protection Agency (EPA). 2006c. "Recertification CARD No. 21: Inspections." *Compliance Application Review Documents for the Criteria for the Certification and Recertification of the Waste Isolation Pilot Plant's Compliance with the 40 CFR 191 Disposal Regulations: Final Recertification Decision* (March) (pp. 21-1 through 21-5). Washington, DC: Office of Radiation and Indoor Air.

U.S. Environmental Protection Agency (EPA). 2010a. "Recertification CARD No. 42: Monitoring." *2009 Compliance Recertification Application (2009 CRA) Compliance Application Review Document (CARD) No. 42; Monitoring* (November 18, 2010). Washington, DC: Office of Radiation and Indoor Air.*

U.S. Environmental Protection Agency (EPA). 2010b. "Recertification CARD No. 21: Monitoring." *2009 Compliance Recertification Application (2009 CRA) Compliance Application Review Document (CARD) No. 21; Inspections* (November 18, 2010). Washington, DC: Office of Radiation and Indoor Air.*

Wagner, S.W. 2008. *Reassessment of MONPAR Analysis for Use in the 2009 Compliance Recertification Application*. ERMS 548948. Carlsbad, NM: Sandia National Laboratories.*

Wagner, S.W. 2011. *Compliance Monitoring Parameter Assessment, and Recommendations*. ERMS 554957. Carlsbad, NM: Sandia National Laboratories.*

Wagner, S.W., and K.L. Kuhlman. 2010a. *Trigger Value Derivation Report*, Revision 2. ERMS 554605. Carlsbad, NM: Sandia National Laboratories.*

Wagner, S.W., and K.L. Kuhlman. 2010b. *Compliance Monitoring Parameter Assessment for 2010*. ERMS 554585. Carlsbad, NM: Sandia National Laboratories.*

Wagner, S.W., Kuhlman K.L., and P.B. Johnson. 2012. *Compliance Monitoring Parameter Assessment for 2012*. Revision 1. ERMS 558589. Carlsbad, NM: Sandia National Laboratories.*

Wagner, S.W. 2013. Reassessment of MONPAR Analysis for Use in the 2014 Compliance Recertification Application. ERMS 560164. Carlsbad, NM: Sandia National Laboratories.*

Title 40 CFR Part 191
Subparts B and C
Compliance Recertification Application 2014
for the
Waste Isolation Pilot Plant

Passive Institutional Controls
(40 CFR § 194.43)

United States Department of Energy
Waste Isolation Pilot Plant

Carlsbad Field Office
Carlsbad, New Mexico

Compliance Recertification Application 2014
Passive Institutional Controls
(40 CFR § 194.43)

Table of Contents

List of Tables

This page intentionally left blank.

Acronyms and Abbreviations

CCA	Compliance Certification Application
CFR	Code of Federal Regulations
CRA	Compliance Recertification Application
DOE	U.S. Department of Energy
EPA	Environmental Protection Agency
NEA	Nuclear Energy Agency
PIC	passive institutional control
RWMC	Radioactive Waste Management Committee
RK&M	Records, Knowledge and Memory
WIPP	Waste Isolation Pilot Plant

This page intentionally left blank.

43.0 Passive Institutional Controls (40 CFR § 194.43)

43.1 Requirements

§ 194.43 Passive Institutional Controls
(a) Any compliance application shall include detailed descriptions of the measures that will be employed to preserve knowledge about the location, design, and contents of the disposal system. Such measures shall include:
(1) Identification of the controlled area by markers that have been designed and will be fabricated and emplaced to be as permanent as practicable;
(2) Placement of records in the archives and land record systems of local, State, and Federal governments, and international archives, that would likely be consulted by individuals in search of unexploited resources. Such records shall identify:
(i) The location of the controlled area and the disposal system;
(ii) The design of the disposal system;
(iii) The nature and hazard of the waste;
(iv) Geologic, geochemical, hydrologic, and other site data pertinent to the containment of waste in the disposal system, or the location of such information; and
(v) The results of tests, experiments, and other analyses relating to backfill of excavated areas, shaft sealing, waste interaction with the disposal system, and other tests, experiments, or analyses pertinent to the containment of waste in the disposal system, or the location of such information.
(3) Other passive institutional controls practicable to indicate the dangers of the waste and its location.
(b) Any compliance application shall include the period of time passive institutional controls are expected to endure and be understood.
(c) The Administrator may allow the Department to assume passive institutional control credit, in the form of reduced likelihood of human intrusion, if the Department demonstrates in the compliance application that such credit is justified because the passive institutional controls are expected to endure and be understood by potential intruders for the time period approved by the Administrator. Such credit, or a smaller credit as determined by the Administrator, cannot be used for more than several hundred years and may decrease over time. In no case, however, shall passive institutional controls be assumed to eliminate the likelihood of human intrusion entirely.

43.2 Background

Regulations in 40 CFR Part 191 Subparts B and C (U.S. EPA 1993) state that disposal systems shall be designed and built such that they provide a reasonable expectation that for 10,000 years (1) the undisturbed performance of the system will not result in an annual committed effective dose to any member of the public in excess of 15 millirem, (2) the levels of radioactive contamination in groundwater will not exceed limits specified by the standard in 40 CFR § 191.24, and (3) the probability of releases from all significant processes and events acting on the disposal system will not exceed the specifications in 40 CFR § 191.13(a).

40 CFR Part 191 Appendix C states "that inadvertent and intermittent intrusion by exploratory drilling for resources can be the most severe intrusion scenario assumed by the DOE." Subsequent to Part 191 requirements, 40 CFR § 194.32 (U.S. EPA 1996) also requires that performance assessments include the effects of drilling. A goal of passive institutional controls (PICs) is to minimize the likelihood of inadvertent human activities that affect repository performance (U.S. DOE 1996, Compliance Certification Application [CCA], Appendix PIC).

43.3 1998 Certification Decision

To meet the requirements for 40 CFR § 194.43, the U.S. Environmental Protection Agency (EPA) expected the U.S. Department of Energy (DOE) to describe the markers that would be placed at the Waste Isolation Pilot Plant (WIPP) site to warn future generations about the disposal system's design and contents, including the presence and hazards of radioactive waste. The markers were to be as permanent as practicable using current technology. The DOE also needed to describe individual markers in detail, including information demonstrating that the markers were as permanent as practicable. Permanence refers to the markers' ability to withstand both natural and human-initiated forces that could reasonably be expected to occur at the site. Markers did not need to be designed to withstand catastrophic, low-probability events, such as nuclear war or a comet strike, since any attempt to do so would undoubtedly strain the practicability of the design. Practicability refers to the DOE's ability to emplace markers using currently available resources and technology.

In addition to describing markers that would be fabricated and emplaced, the DOE was also expected to provide a timeline for implementing the markers. Finally, the DOE was permitted to propose a credit for PICs in the performance assessment. A credit must be based on the proposed effectiveness of PICs over time, and would take the form of reduced likelihood in the performance assessment of human intrusion over several hundred years.

The CCA, Chapter 7.0, Section 7.3.3.1.1 and Section 7.3.3.3, and Appendices PIC and EPIC, and supplemental information requested by the EPA contain the information supporting the DOE's compliance with this requirement.

The EPA determined that the DOE complied with the requirements of section 194.43 because the measures proposed in the CCA are comprehensive, practicable, and likely to endure and be understood for long periods of time. The EPA denied the DOE's request for credit for a 99% reduction in the likelihood of human intrusion into the WIPP during the first 700 years after closure. The EPA denied the credit because the DOE did not use an expert judgment elicitation to derive the credit. The EPA also established as a condition of the 1998 Certification Decision (U.S. EPA 1998) that the DOE submit additional information concerning the schedule for completing PICs, fabrication of granite markers, and commitments by various recipients to accept WIPP records no later than the final recertification application.

A complete description of the EPA's 1998 Certification Decision for section 194.43 can be found in U.S. EPA 1998.

43.4 Changes in the CRA-2004

In the 2004 Compliance Recertification Application (CRA-2004) (U.S. DOE 2004), Chapter 7.0, Section 7.3.1 (Requirements for PICs), the DOE added language discussing Condition 4 of the EPA's 1998 Certification Decision. This condition requires the DOE to submit the following items prior to the final recertification application, which will be submitted before closure of the disposal system:

- A schedule for implementing PICs, which also describes the testing of all aspects of the conceptual design
- Documentation regarding the granite pieces for the proposed monuments
- Documentation regarding the archives and record centers maintaining the WIPP docket documents
- Documentation of a plan to ensure that the recipients of WIPP information continue to have access to docket documents and supplementary information

New information pertaining to the permanent markers portion of the PICs program and additional amendments to the planning process were also included in the CRA-2004, Chapter 7.0, Section 7.3.3 (Implementation of the PICs Program), which is documented in *Permanent Markers Testing Program Plan* (U.S. DOE 2000).

In the CRA-2004, Chapter 7.0, Section 7.3.3.1.1, the DOE assured the EPA that the permanent markers will be constructed of materials selected through an evaluation process; the berm design, including the materials of construction, will be refined; and the final design specifications will be provided to the EPA for approval prior to construction.

Examples of the types of files to be archived were added in the CRA-2004, Chapter 7.0, Section 7.3.3.1.2 (Records).

The CRA-2004, Chapter 7.0, Section 7.3.3.3 (PICs Timelines) discusses a new and revised schedule under which the DOE will implement its PICs program. The DOE referenced a letter sent to the EPA (Triay 2002) and the EPA's subsequent approval (Marcinowski 2002) of this revised timeline.

The DOE claimed no credit for the effectiveness of PICs for the 2004 Performance Assessment Baseline Calculation (U.S. EPA 2006a) (Leigh et al. 2005). As indicated previously by the EPA, the DOE has the right to claim such credit in future recertification applications.

43.5 EPA's Evaluation of Compliance for the 2004 Recertification

The EPA concluded that the DOE adequately described changes that had been made in the PICs program and continued to comply with the requirements of section 194.43 (U.S. EPA 2006b).

43.6 Changes or New Information Between the CRA-2004 and the CRA-2009 (Previously: Changes or New Information Since the 2004 Recertification)

In a letter dated January 11, 2007 (Moody 2007), the DOE requested an extension to start testing PICs 10 years before closure as identified in the DOE's letter of May 16, 2002 (Triay 2002), and agreed to in the EPA's letter of November 7, 2002 (Marcinowski 2002). This request for schedule extension by the DOE was to allow the maximum amount of time to determine the most updated design and materials technologies for implementation of PICs based upon projected

closure dates. The EPA responded to the DOE's schedule extension request in a letter dated March 7, 2008 (Reyes 2008). The EPA agreed to a modified schedule based on activities and current projections of the anticipated WIPP closure date. Table 43-1 is the revised list of approved schedule changes for PICs Testing.

Table 43-1. Approved Schedule Changes for PICs Testing[a]

Activity	Original Time Frame	November 2002 Time Frame	New (December 2007) Time Frame
Identify suitable source material	1999–2004	2007	2014, but with an annual progress report
Submit plans for test marker system to EPA	2003	2007	2016, but with an annual progress report
Construct berm and begin testing of berm and markers	2004–2009	2008	2018
Monitor performance of test berm and test markers	2007–2083	2009–closure	2019–closure
Develop final design of markers	2083–2090	2033 (anticipated)	2033 (anticipated)
Finalize messages	n/a	2033 (anticipated)	2033 (anticipated)

[a] Source: Reyes 2008.

In the CRA-2009 (U.S. DOE 2009), the DOE did not propose any changes to the PICs program for the WIPP. Information pertaining to the program provided for the CCA and the CRA-2004 remained unchanged, with the exception of the PICs testing schedule. The DOE believed it had demonstrated continued compliance with the provisions of section 194.43.

43.7 EPA's Evaluation of Compliance for the 2009 Recertification

The EPA concluded that the DOE adequately described changes that had been made in the PICs program and continued to comply with the requirements of section 194.43 (Federal Document Management System Docket ID No. EPA-HQ-OAR-2009-0330, Air Docket A-98-49) (U.S. EPA 2010).

43.8 Changes or New Information Since the CRA-2009

In this application, the DOE is not proposing any changes to the PICs program for the WIPP. Information pertaining to the program as provided by the CCA, CRA-2004 and CRA-2009 remains unchanged. The DOE has updated progress on PICs in the Annual Change Report provided to the EPA each year as requested in the Reyes 2008 letter (Reyes 2008).

In December 2009, the EPA requested that the DOE representatives from the WIPP become more involved with international efforts for nuclear waste disposal (December 2009 meeting in Washington, DC). As a result, the DOE became involved with the Nuclear Energy Agency

(NEA). The NEA's Radioactive Waste Management Committee (RWMC) issued and approved the Draft Vision Document for the Long-Term Preservation of Information and Memory project. This resulted in the establishment of the NEA's Records, Knowledge and Memory (RK&M) group of which the DOE is a member. The function of this group is to review and evaluate all current member country programs for PICs and propose a set of international guidelines for member countries to follow in developing PICs for geologic repositories at nuclear waste disposal sites.

As a result of its involvement with the RK&M, the DOE requested an extension of the EPA PIC's program schedule (Moody 2010).

The DOE believes it has demonstrated continued compliance with the provisions of section 194.43.

43.9 References

(*Indicates a reference that has not yet been previously submitted.)

Leigh, C., J. Kanney, L. Brush, J. Garner, G. Kirkes, T. Lowry, M. Nemer, J. Stein, E. Vugrin, S. Wagner, and T. Kirchner. 2005. *2004 Compliance Recertification Application Performance Assessment Baseline Calculation* (Revision 0). ERMS 541521. Sandia National Laboratories, Carlsbad, NM.*

Marcinowski, F. 2002. Letter to Dr. Inés Triay, Manager. 7 November 2002. U.S. Environmental Protection Agency, Office of Air and Radiation, Washington, DC.

Moody, D.C. 2007. Letter to Mr. Juan Reyes (Subject: Request for Extension). 11 January 2007. U.S. Department of Energy, Carlsbad Field Office, Carlsbad, NM.

Moody, D.C. 2010. Letter to Mr. Mike Flynn (Subject: Request for Extension in the Passive Institutional Controls Program Schedule). 28 July 2010. U.S. Department of Energy, Carlsbad Field Office, Carlsbad, NM.*

Reyes, J. 2008. Letter to Dave Moody, Ph.D., Manager. 7 March 2008. U.S. Environmental Protection Agency, Office of Air and Radiation, Washington, DC.

Triay, I.R. 2002. Letter to Mr. Frank Marcinowski. 16 May 2002. U.S. Department of Energy, Carlsbad Field Office, Carlsbad, NM.

U.S. Department of Energy (DOE). 1996. *Title 40 CFR Part 191 Compliance Certification Application for the Waste Isolation Pilot Plant* (October). 21 vols. DOE/CAO 1996-2184. Carlsbad Area Office, Carlsbad, NM.

U.S. Department of Energy (DOE). 2000. *Permanent Markers Testing Program Plan* (September 28). DOE/WIPP 00-3175. Carlsbad Area Office, Carlsbad, NM.

U.S. Department of Energy (DOE). 2004. *Title 40 CFR Part 191 Compliance Recertification Application for the Waste Isolation Pilot Plant* (March). 10 vols. DOE/WIPP 2004-3231. Carlsbad Field Office, Carlsbad, NM.

U.S. Department of Energy (DOE). 2009. *Title 40 CFR Part 191 Compliance Recertification Application for the Waste Isolation Pilot Plant* (March). DOE/WIPP-09-3424. Carlsbad Field Office, Carlsbad, NM.*

U.S. Environmental Protection Agency (EPA). 1993. "40 CFR Part 191: Environmental Radiation Protection Standards for the Management and Disposal of Spent Nuclear Fuel, High-Level and Transuranic Radioactive Wastes; Final Rule." *Federal Register,* vol. 58 (December 20, 1993): 66398–416.

U.S. Environmental Protection Agency (EPA). 1996. "40 CFR Part 194: Criteria for the Certification and Recertification of the Waste Isolation Pilot Plant's Compliance with the 40 CFR Part 191 Disposal Regulations; Final Rule." *Federal Register,* vol. 61 (February 9, 1996): 5223–45.

U.S. Environmental Protection Agency (EPA). 1998. "40 CFR Part 194: Criteria for the Certification and Recertification of the Waste Isolation Pilot Plant's Compliance with the Disposal Regulations: Certification Decision; Final Rule." *Federal Register,* vol. 63 (May 18, 1998): 27353–406.

U.S. Environmental Protection Agency (EPA). 2006a. Technical Support Document for Section 194.23: Review of the 2004 Compliance Recertification Performance Assessment Baseline Calculation (March). Office of Radiation and Indoor Air, Washington, DC.

U.S. Environmental Protection Agency (EPA). 2006b. "40 CFR Part 194: Criteria for the Certification and Recertification of the Waste Isolation Pilot Plant's Compliance with the Disposal Regulations: Recertification Decision" (Final Notice). *Federal Register*, vol. 71 (April 10, 2006): 18010–021.

U.S. Environmental Protection Agency (EPA). 2010. "2009 Compliance Recertification Application (2009 CRA) Compliance Application Review Document (CARD) No. 43 Passive Institutional Controls." Office of Radiation and Indoor Air, Washington, DC.*

Title 40 CFR Part 191
Subparts B and C
Compliance Recertification Application 2014
for the
Waste Isolation Pilot Plant

Engineered Barriers
(40 CFR § 194.44)

United States Department of Energy
Waste Isolation Pilot Plant

Carlsbad Field Office
Carlsbad, New Mexico

Compliance Recertification Application 2014
Engineered Barriers
(40 CFR § 194.44)

Table of Contents

List of Figures

List of Tables

This page intentionally left blank.

Acronyms and Abbreviations

CCA	Compliance Certification Application
CFR	Code of Federal Regulations
CH	contact-handled
CPR	cellulose, plastic, and rubber
CRA	Compliance Recertification Application
DOE	U.S. Department of Energy
EPA	U.S. Environmental Protection Agency
ft	feet
m	meter
PA	performance assessment
TRU	transuranic
WIPP	Waste Isolation Pilot Plant
WTS	Washington TRU Solutions, LLC

Elements and Chemical Compounds

MgO	magnesium oxide

This page intentionally left blank.

44.0 Engineered Barriers (40 CFR § 194.44)

44.1 Requirements

§ 194.44 Engineered Barriers

(a) Disposal systems shall incorporate engineered barrier(s) designed to prevent or substantially delay the movement of water or radionuclides toward the accessible environment.

(b) In selecting any engineered barrier(s) for the disposal system, DOE shall evaluate the benefit and detriment of engineered barrier alternatives, including but not limited to: cementation, shredding, supercompaction, incineration, vitrification, improved waste canisters, grout and bentonite backfill, melting of metals, alternative configurations of waste placements in the disposal system, and alternative disposal system dimensions. The results of this evaluation shall be included in any compliance application and shall be used to justify the selection and rejection of each engineered barrier evaluated.

(c)(1) In conducting the evaluation of engineered barrier alternatives, the following shall be considered, to the extent practicable:

(i) The ability of the engineered barrier to prevent or substantially delay the movement of water or waste toward the accessible environment;

(ii) The impact on worker exposure to radiation both during and after incorporation of engineered barriers;

(iii) The increased ease or difficulty of removing the waste from the disposal system;

(iv) The increased or reduced risk of transporting the waste to the disposal system;

(v) The increased or reduced uncertainty in compliance assessment;

(vi) Public comments requesting specific engineered barriers;

(vii) The increased or reduced total system costs;

(viii) The impact, if any, on other waste disposal programs from the incorporation of engineered barriers (e.g., the extent to which the incorporation of engineered barriers affects the volume of waste);

(ix) The effects on mitigating the consequences of human intrusion.

(2) If, after consideration of one or more of the factors in paragraph (c)(1) of this section, DOE concludes that an engineered barrier considered within the scope of the evaluation should be rejected without evaluating the remaining factors in paragraph (c)(1) of this section, then any compliance application shall provide a justification for this rejection explaining why the evaluation of the remaining factors would not alter the conclusion.

(d) In considering the ability of engineered barriers to prevent or substantially delay the movement of water or radionuclides toward the accessible environment, the benefit and detriment of engineered barriers for existing waste already packaged, existing waste not yet packaged, existing waste in need of repackaging, and to-be-generated waste shall be considered separately and described.

(e) The evaluation described in paragraphs (b), (c) and (d) of this section shall consider engineered barriers alone and in combination.

44.2 Background

Assurance requirements are included in the disposal standard to provide the confidence needed for long-term compliance with the requirements of 40 CFR § 191.13 (U.S. EPA 1993). 40 CFR § 194.44 (U.S. EPA 1996) is one of the six assurance requirements in the Compliance Criteria. Section 194.44 implements the assurance requirement of 40 CFR § 191.14(d) (U.S. EPA 1993) to incorporate one or more engineered barriers at radioactive waste disposal facilities. The disposal regulations at 40 CFR § 191.12(d) define a barrier as "any material or structure that prevents or substantially delays movement of water or radionuclides toward the accessible environment." Section 194.44 requires the U.S. Department of Energy (DOE) to conduct a study of available options for engineered barriers at the Waste Isolation Pilot Plant (WIPP) and submit this study and evidence of its use with the compliance application. Consistent with the containment requirement at section 191.13, the DOE analyzed the performance of the complete disposal system, including the engineered barrier(s).

44.3 1998 Certification Decision

The analysis of potential engineered barriers, including a comparison of the benefits and detriments of each, was documented in the DOE's Compliance Certification Application (CCA) (U.S. DOE 1996), Appendix EBS. In the CCA, the DOE proposed multiple barriers, including shaft seals, the panel closure system, magnesium oxide (MgO) backfill, and borehole plugs.

The U.S. Environmental Protection Agency (EPA) evaluated the information regarding engineered barriers provided by the DOE in the CCA, Chapter 3.0 (pp. 3-14 through 3-45), Chapter 6.0 (pp. 6-105 through 6-114), and Chapter 7.0 (pp. 7-89 through 7-96), as well as Appendices BACK, EBS, SEAL, PCS, SOTERM (Section SOTERM.2.2), and WCA (Section WCA.4.1). The DOE also provided supplemental information in the report "Implementation of Chemical Controls Through a Backfill System for the Waste Isolation Pilot Plant (WIPP)" (Sandia National Laboratories 1996).

The DOE specified the proposed method of incorporating the engineered barrier (MgO backfill) into the disposal system in the CCA, Chapter 3.0, Section 3.3.3, and Appendix BACK. The DOE identified MgO as an engineered barrier and provided the rationale for selecting the physical form of MgO to be used, the approximate grain size of the MgO to be emplaced, and the type and size of packages to be used to transport and emplace the MgO. The CCA also described how the MgO minisacks and supersacks would be arranged around waste containers in the disposal rooms and stated that the MgO backfill could be emplaced in the same manner and with the same equipment as the waste containers.

The EPA found that the DOE conducted the requisite analysis of engineered barriers and selected an engineered barrier designed to prevent or substantially delay the movement of water or radionuclides toward the accessible environment. In the 1998 Certification Decision (U.S. EPA 1998), the EPA specified that only the MgO backfill met the regulatory definition of an engineered barrier. The EPA determined that the DOE provided sufficient documentation to show that MgO can effectively reduce actinide solubility in the disposal system.

A complete description of the EPA's 1998 Certification Decision for section 194.44 can be found in U.S. EPA 1998.

44.4 Changes in the CRA-2004

In the 2004 Compliance Recertification Application (CRA-2004) (U.S. DOE 2004), the DOE did not report any significant changes to the information on which the EPA based the 1998 Certification Decision. The DOE submitted two planned change requests and one planned change notice after the original certification decision. The DOE's requests included a request to eliminate the MgO minisacks, the notification of a new MgO vendor, and a request to emplace compressed waste from Idaho National Laboratory (formerly Idaho National Engineering and Environmental Laboratory). These changes were approved by the EPA prior to the submission of the CRA-2004 (U.S. DOE 2004). These changes are also discussed in greater detail in Appendix MgO-2009 (see Section MgO-2.1.2 for the minisack elimination change, Section MgO-2.2 for the vendor change, and Section MgO-2.1.3 for the compressed waste change).

The DOE did not conduct a new analysis to evaluate the benefit and detriment of engineered alternatives (originally required by 40 CFR §§ 194.44(b) through (e)) because the DOE did not change the engineered barrier type, form or function. Therefore, there are no impacts to the conclusions of the original analysis. The CRA-2004 reflected the EPA's determination that only the MgO backfill met the EPA's requirements for an engineered barrier.

44.5 EPA's Evaluation of Compliance for the 2004 Recertification

The EPA did not identify any significant changes in the implementation of the requirement for engineered barriers based on its review of the activities and conditions in and around the WIPP site. The CRA-2004 did not reflect any changes to the analysis of engineered barriers documented in the CCA, Appendix EBS, and accurately reflected in the 1998 Certification Decision. The EPA concluded that the MgO backfill was the only engineered barrier that met its requirements for an engineered barrier (U.S. EPA 2006).

44.6 Changes or New Information Between the CRA-2004 and the CRA-2009 (Previously: Changes or New Information Since the 2004 Recertification)

There were no significant changes in the factors on which the EPA based the determination of compliance with section 194.44. The DOE did not change the engineered barrier type, form, or function and therefore did not conduct a new analysis to evaluate the benefit and detriment of engineered alternatives (originally required by sections 194.44(b) through (e)). The CRA-2009 followed the EPA's determination that only the MgO backfill met the EPA's requirements for an engineered barrier at section 191.14(d).

The DOE had proposed shaft seals, borehole plugs, and panel closures as engineered barriers in the CCA. Changes to the approved engineered barrier that have occurred between the CRA-2004 and the CRA-2009 and changes to other disposal system design features originally proposed as engineered barriers (termed disposal system barriers) are discussed in the following subsections for completeness.

44.6.1 Engineered Barrier

MgO is used in the WIPP to meet the requirements for multiple natural and engineered barriers. MgO acts as an engineered barrier by decreasing actinide solubilities through the consumption of essentially all carbon dioxide possibly produced by microbial activity. Since microbial activity is an uncertain process, the MgO engineered barrier reduces uncertainty in the repository chemical conditions by ensuring low carbon dioxide fugacity and by controlling pH (see Appendix MgO-2009, Section MgO-5.0, and Appendix SOTERM-2009, Section SOTERM-2.3).

The description of the supersacks and their placement in the disposal system is found in the CRA-2004, Chapter 3.0, Section 3.3.1. Minor emplacement changes were made as a result of an EPA-approved planned change for disposal of compressed waste (Marcinowski 2004). This change was approved prior to the submittal of the CRA-2004, but was not described in that application. This change is discussed in Section 44.6.1.2. The representation of the engineered barrier in performance assessment (PA) is described in the CRA-2004, Chapter 6.0, Section 6.4.6.4 (with minor editing in response to EPA Comment C-23-5 [Detwiler 2004]), Appendix PA-2009, Appendix MgO-2009, and Appendix SOTERM-2009. The editing corrects the stated MgO excess factor to the EPA-approved

1.67 value. A detailed history of the MgO engineered barrier is presented in Appendix MgO-2009 and describes the placement, function, and experimental activities associated with the barrier. Appendix MgO-2009 describes in greater detail the changes that occurred between the CRA-2004 and the CRA-2009.

The developments associated with the MgO engineered barrier that occurred between the EPA's 2004 Recertification Decision and the CRA-2009 include information from additional analyses and the DOE's planned change requests. These developments are:

1. A change in MgO vendor

2. The EPA's approval of the DOE's planned change request to dispose of compressed waste

3. The EPA's approval of the DOE's planned change request to change the MgO excess factor from 1.67 to 1.20

4. Results of ongoing MgO experimental investigations

Sections 44.6.1.1 through 44.6.1.4 describe each of these items in greater detail.

44.6.1.1 Change in MgO Vendors

National Magnesia Chemicals of Moss Landing, California, was the first vendor to provide MgO for the WIPP. National Magnesia supplied MgO from the opening of the WIPP in March 1999 (Panel 1, Room 7) through mid-April 2000, at which time National Magnesia stopped producing MgO. Based on cost and the results of a technical evaluation, the DOE selected Premier Chemicals of Gabbs, Nevada, as the MgO supplier (see Section 44.5). Premier Chemicals supplied MgO from mid-April 2000 (Panel 1, Room 7) through 2004 (Panel 2, Room 2). In 2004, Premier Chemicals informed WIPP Management and Operating Contractor Washington TRU Solutions, LLC (WTS) that it would soon be unable to provide MgO that met the requirement for the minimum concentration of MgO in the DOE's specification (WTS 2003). The DOE selected Martin Marietta Magnesia Specialties LLC, which has supplied the MgO emplaced since January 2005 (Panel 2, Room 2). The DOE selected Martin Marietta's MgO based on cost and a technical evaluation of its suitability by Wall (Wall 2005). The results of this study and additional characterization of Martin Marietta's MgO were described in detail in Appendix MgO-2009, Section MgO-4.3.

44.6.1.2 Change to Allow Compressed Waste from the Advanced Mixed Waste Treatment Project

In March 2004, the EPA approved the emplacement in the WIPP of compressed (supercompacted) waste from the Advanced Mixed Waste Treatment Project at the Idaho National Laboratory (Marcinowski 2004; Trinity Engineering Associates 2004; U.S. EPA 2004). However, the EPA specified that the DOE must maintain an MgO excess factor of 1.67 (see Section 44.5). The compressed waste contains concentrations of cellulose, plastic and rubber (CPR) materials that are higher than the average concentration of CPR materials in transuranic (TRU) waste, necessitating the emplacement of additional MgO. Therefore, in addition to the one supersack per stack configuration, the DOE has emplaced additional MgO supersacks on racks placed among the waste containers. These additional supersacks are emplaced as required to meet the excess factor. Each rack contains

five supersacks identical to those placed on top of the waste containers, and spans the same vertical distance normally occupied by three 7-packs of 208-liter (55-gallon) drums, 3 standard waste boxes, or various combinations of these and other waste containers. Thus, emplacement of additional MgO in the repository has used space normally occupied by contact-handled (CH) TRU waste.

44.6.1.3 Change in Excess Factor from 1.67 to 1.20

In April 2006, the DOE requested that the EPA approve a reduction in the MgO excess factor from 1.67 to 1.2 (Moody 2006a). To justify its request, the DOE used reasoned arguments regarding health-related transportation risks to the public, the cost of emplacing MgO, and the uncertainties inherent in predicting the extent of microbial consumption of CPR materials during the 10,000-year WIPP regulatory period. The EPA responded by requesting that the DOE address the uncertainties related to MgO effectiveness, the size of the uncertainties, and the potential impact of the uncertainties on long-term performance. In particular, the EPA instructed the DOE to (1) identify all uncertainties related to the calculation of the MgO excess factor, and (2) quantify these uncertainties, if possible (Gitlin 2006). The DOE responded to this request with a detailed uncertainty analysis (Moody 2006b). In February 2008, the EPA approved the reduction of the MgO excess factor to 1.2 (Reyes 2008; Langmuir 2007; Cohen and Associates 2008; U.S. EPA 2008).

44.6.1.4 MgO Investigations

MgO investigations include characterization of the vendor's (Martin Marietta) MgO, hydration and carbonation experimental updates, and independent reviews of the use of MgO as an engineered barrier at the WIPP. Deng et al. (Deng et al. 2006) and Deng, Xiong, and Nemer (Deng, Xiong, and Nemer 2007) investigated the characteristics and properties of a sample of MgO supplied by Martin Marietta that was identical to that emplaced in the WIPP. The analysis looked at the particle size and morphology; the weight percentage of magnesium, calcium, aluminum, iron, and silica of the sample; and the loss on ignition and gravimetric analysis of hydrated MgO. The investigation also included a qualitative analysis using scanning electron microscope imaging and the associated energy dispersive spectrum of the as-received MgO. The results of these investigations helped to confirm that the MgO backfill will perform as expected in the WIPP environment (see Appendix MgO-2009, Sections MgO-3.0 and MgO-4.0, for a summary of these investigations and their results).

44.6.2 Disposal System Barriers

The following sections discuss changes to three disposal system design features between the CRA-2004 and the CRA-2009 that were originally proposed as engineered barriers in the CCA: shaft seals, panel closures, and borehole plugs. While shaft seals, panel closures, and borehole plugs are not considered engineered barriers by the EPA, they are important physical elements of the WIPP disposal system. It is within this context that they are discussed below.

44.6.2.1 Shaft Seals

No changes were proposed by the DOE to the shaft seal information presented in the CRA-2004, Chapter 3.0, Section 3.3.2. Material specifications and construction techniques for the shaft seal system were given in the CRA-2004, Appendix BARRIERS, Section BARRIERS-3.2.2, and the CCA, Appendix SEAL, Sections 5.0 and 6.0. Appendix PA-2009, Section PA-4.2.7, summarized the

representation of the shafts in PA. Fox (Fox 2008, Table 19) provided parameter values used in the modeling of shaft seals.

44.6.2.2 Panel Closures

The baseline panel closure design, termed "Option D," was presented in the CRA-2004, Chapter 3.0, Section 3.3.3, and Appendix BARRIERS-2004, Section BARRIERS-3.2.1. The Option D design was not modified between the CRA-2004 and the CRA-2009. Representation of the panel closures in PA was described in Appendix PA-2009, Section PA-4.2.8; parameters relevant to the panel closures were provided in Fox (Fox 2008, Table 20).

The DOE submitted a planned change request to modify the panel closure design in 2002, prior to submittal of the CRA-2004 (Triay 2002). Because the EPA determined the change would require a rulemaking, EPA review was deferred until after the certification decision (Marcinowski 2002). In January 2007, the DOE renewed its request for EPA approval of the 2002 panel closure planned change request (Moody 2007a), with an additional request for a delay in permanent closure of panels to allow gas monitoring, through a substantial barrier, with the installation of the permanent closure depending on the results of the monitoring. The proposed monitoring was intended to develop an understanding of flammable gas generation rates in filled panels of waste in order to optimize the final panel closure design. The DOE also requested that the EPA modify Condition 1 of the original certification decision to acknowledge that the New Mexico Environment Department is responsible for regulating the design and construction of the panel closure system, provided that the DOE demonstrates there are no long-term impacts on performance. The DOE included a detailed justification for this request and stated that the closure is an operational period requirement (Moody 2007a). The purpose of the closure system is to control volatile organic compound emissions during operations and protect the health and safety of the workers. The EPA responded in a subsequent letter agreeing with the request to delay closure for gas monitoring, but denying the request to modify Condition 1 of the certification decision (Reyes 2007). The EPA stated that the panel closure design was a condition of the EPA's 1998 certification decision and that a change in the design is a significant departure from the most recent compliance application. The EPA also stated that under 40 CFR §194.65, the EPA is required to address changes to the panel closure design through a formal rulemaking process (Reyes 2007). Following a June 2007 panel closure meeting between the New Mexico Environment Department, the EPA, and the DOE, the DOE withdrew its request to modify the panel closure design pending results of the gas monitoring and development of a final closure design (Moody 2007b). Option D continued to be the WIPP baseline panel closure design at that time.

44.6.2.3 Borehole Plugs

Over the life of the WIPP project, many exploratory, monitoring, and characterization-related boreholes have been drilled by the DOE and its predecessors in the vicinity of the WIPP. In addition to the DOE-drilled wells, water wells have been drilled for livestock and homesteads, and wells have been drilled by oil, gas, and potash companies in their efforts to exploit resources in the Delaware Basin. Figure 44-1 identifies existing unplugged boreholes that lie within the WIPP site boundary. Of these boreholes, two are deep boreholes that exceed the depth of the repository (WIPP-13 and ERDA-9), and the remainder are shallow boreholes that do not reach the repository horizon. There were two additional boreholes deeper than the repository that have been plugged (DOE-1 and WIPP-12).

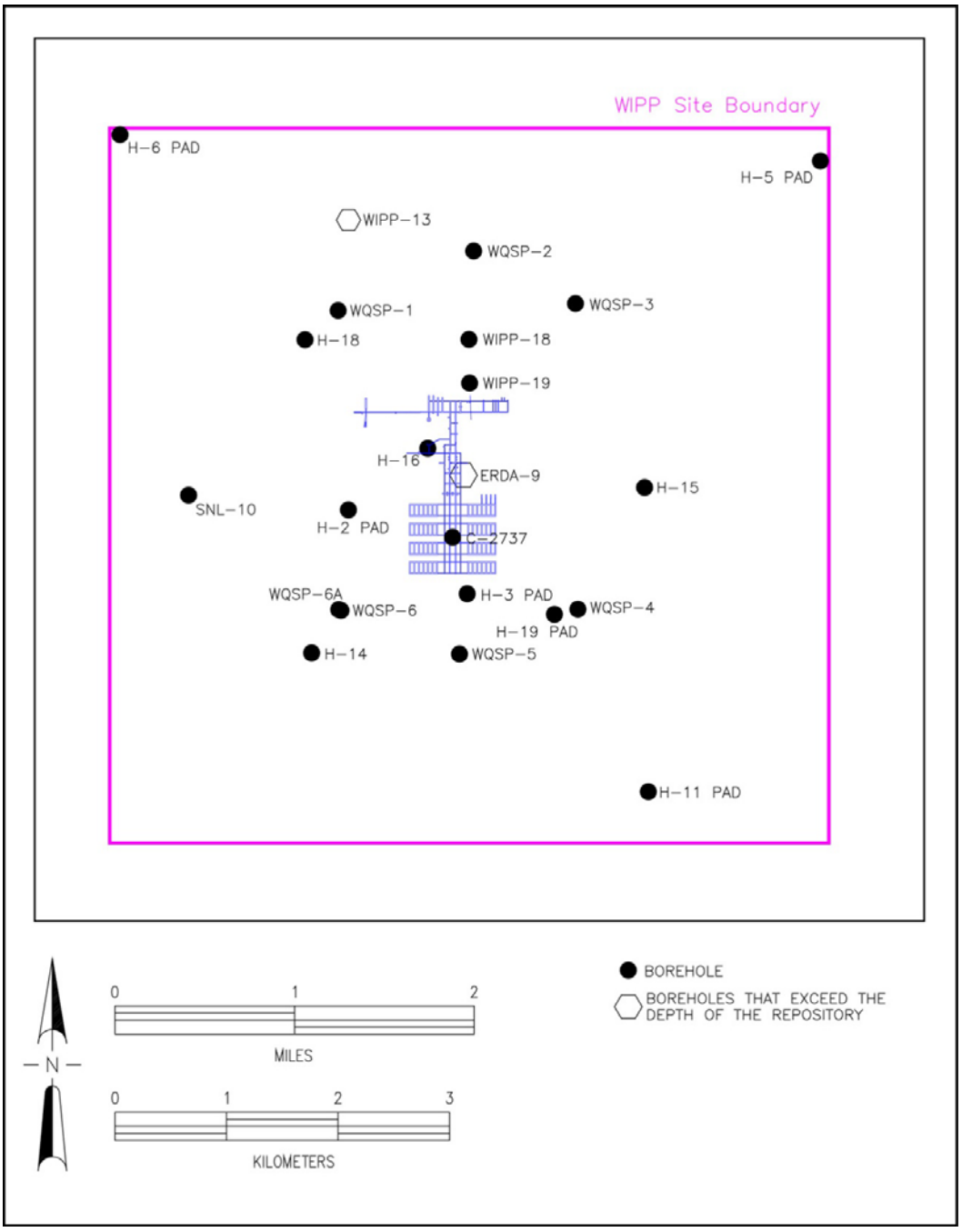

Figure 44-1. Approximate Locations of Unplugged Boreholes[1]

[1] Modified from the CRA-2004, Chapter 3.0, Figure 3-10.

To mitigate the potential for contaminants to migrate toward the accessible environment, the DOE uses established borehole plugging practices (Christensen and Peterson 1981) to limit the volume of water that could be introduced to the repository from the overlying water-bearing zones, and to limit the hypothetical volume of contaminated brine released from the repository to the accessible environment. The governing regulations for plugging and/or abandonment of boreholes are summarized in Table 44-1.

The CRA-2009 monitoring period was from 10/1/2002 through 9/30/2007. Appendix DATA-2009, Attachment A listed the operational monitoring wells within the WIPP vicinity. During the monitoring period, 19 new wells were drilled and put into service, 3 for the shallow water program and 16 for the groundwater program. The shallow water wells were all less than 23.5 meters (m) (77 feet [ft]) in depth. The groundwater-monitoring wells varied from 68.3 m to 414.5 m (224 ft to 1,360 ft) in depth. Sixteen groundwater-monitoring wells were plugged during the monitoring period; all were plugged solid with cement. During this monitoring period, two monitoring wells were plugged back, converted to water wells, and turned over to local ranchers for their use. In addition, one former potash borehole was converted to a groundwater-monitoring well. Appendix DATA-2009, Attachment A provides a description of the wells in the WIPP monitoring system at that time.

Four deep wells (greater than 655.3 m [2,150 ft] in depth), DOE 1, ERDA 9, WIPP 12, and WIPP 13, are required to be plugged in accordance with the State of New Mexico, Oil Conservation Division, Order No. R-111-P. The key provisions of Order No. R-111-P are as follows:

- A salt protection string of casing must be installed at least 30 m (100 ft) below and not more than 183 m (600 ft) below the base of the salt section. Cementing requirements for both shallow wells (above 1,524 m [5,000 ft]) and deep wells (below 1,524 m [5,000 ft]) above or below the Delaware Mountain Group are specified.

- All oil and gas wells drilled within the potash area must provide a solid cement plug through the salt section and any water-bearing horizon and prevent liquids or gases from entering the hole above or below the salt section.

- The fluid used to mix the (plugging) cement must be saturated with salts common to the salt section penetrated, but not more than 3% of calcium chloride by weight of cement wherever possible.

Table 44-1. Governing Regulations for Borehole Abandonment

Federal or State Land	Type of Well or Borehole	Governing Regulation	Summary of Requirements
Both	Groundwater Wells	Well Driller Licensing; Construction, Repair and Plugging of Wells (State of New Mexico 2005, Article 4-140)	Any specific plugging requirements and provisions made by the state engineer shall be set forth in the permit.
Federal	Oil and Gas Wells	Onshore Oil and Gas Operations (43 CFR 3160) (U.S. Department of the Interior 1983, p. 36583), Well Abandonment (43 CFR 3162.3-4) (U.S. Department of the Interior 1988a, p. 47765)	The operator shall promptly plug and abandon, in accordance with a plan first approved in writing or prescribed by the authorized officer.
Federal	Potash	Solid Minerals (Other than Coal) Exploration and Mining (43 CFR 3590) (U.S. Department of the Interior 1988b, p. 39461), Core or Test Hole Cores, Samples, Cuttings (43 CFR 3593.1) (U.S. Department of the Interior 1988c, p. 39461)	(b) Surface boreholes for development or holes for prospecting shall be abandoned to the satisfaction of the authorizing officer by cementing and/or casing or by other methods approved in advance by the authorized officer. The holes shall also be abandoned in a manner to protect the surface and not endanger any present or future underground operation, any deposit of oil, gas, or other mineral substances, or any aquifer.
State	Potash	Well Driller Licensing; Construction, Repair and Plugging of Wells (State of New Mexico 2005, Article 4-20.2)	In the event that the test or exploratory well is to be abandoned, the state engineer shall be notified. Such wells shall be plugged in accordance with Article 4-19.1 so that the fluids will be permanently confined to the specific strata in which they were originally encountered.
State	Oil and Gas Well Outside the Oil-Potash Area	Plugging and Permanent Abandonment (State of New Mexico 1996, Rule 202)	B. Plugging (1) Before an operator abandons a well, the operator shall plug the well in a manner that permanently confines all oil, gas and water in the separate strata in which they are originally found. The operator may accomplish this by using mud-laden fluid, cement and plugs singly or in combination as approved by the division on the notice of intention to plug.
			(2) The operator shall mark the exact location of plugged and abandoned wells with a steel marker not less than 10.2 centimeters (4 inches) in diameter set in cement and extending at least 1.2 m (4 ft) above mean ground level. The operator name, lease name and well number and location, including unit letter, section, township and range, shall be welded, stamped or otherwise permanently engraved into the marker's metal.

Table 44-1. Governing Regulations for Borehole Abandonment (Continued)

Federal or State Land	Type of Well or Borehole	Governing Regulation	Summary of Requirements
State	Oil and Gas Wells Inside the Oil-Potash Area	Order No. R-111-P (State of New Mexico 1988)	F. Plugging and Abandonment of Wells (1) All existing and future wells that are drilled within the potash area shall be plugged in accordance with the general rules established by the Division. A solid cement plug shall be provided through the salt section and any water-bearing horizon to prevent liquids or gases from entering the hole above or below the salt selection. It shall have suitable proportions—but no greater than three percent of calcium chloride by weight—of cement considered to be the desired mixture when possible.

Two of the four deep wells (WIPP-12 and DOE-1) were plugged and abandoned. The New Mexico Office of the State Engineer regulates the drilling, operation, and abandonment of groundwater wells. This agency has regulatory oversight of wells in the controlled area. Although WIPP-12 was plugged with standard cement slurry (no salt), the Office of the State Engineer subsequently agreed that the use of standard cement slurry was acceptable for this instance. DOE-1 was plugged using a salt-saturated cement through the salt section, and a standard cement slurry through the rest of the borehole.

The boreholes not used for monitoring will be plugged at decommissioning. See Appendix BARRIERS-2004, Section BARRIERS-3.2.3 for a detailed discussion of borehole plugs (excluding Section BARRIERS-3.2.3.2). Appendix PA-2009, Section PA-4.2.9 summarizes the representation of the borehole plugs in PA. Fox (Fox 2008, Tables 13 through 17) provided parameter values used in the PA modeling. A listing of all wells drilled in support of the WIPP and other boreholes located within the 16-section Land Withdrawal Area was first included as the CCA, Appendix BH. Appendix DATA-2004, Attachment G provides updates on all of the monitoring wells used in the CCA, Appendix BH, and the new monitoring wells drilled since the initial certification (U.S. DOE 2004) up to the CRA-2009 cutoff date. Appendix DATA-2009, Attachment A lists updates to the borehole information. A detailed discussion of the boreholes used in the groundwater monitoring at the WIPP was presented in Appendix HYDRO-2009, Section HYDRO-5.0.

44.6.3 Compliance Summary

The information provided in the CRA-2009 demonstrated continued compliance with the section 194.44 criteria.

44.7 EPA's Evaluation of Compliance for the CRA-2009

In its 2010 recertification decision (U.S. EPA 2010a) the EPA stated that the DOE did not report any significant changes to the information on which the EPA based its 1998 Certification and 2004 Recertification Decisions. The DOE did not conduct a new analysis to evaluate the benefit and detriment of engineered alternatives, as defined in 194.44 (b) through (e). The CRA-2009 continued to

reflect the EPA's determination that only MgO backfill meets the requirements for an engineered barrier. The EPA did not receive any public comments on the DOE's continued compliance with the requirements of section 194.44. As such, the EPA concluded that the DOE continued to comply with the requirements of 40 CFR 194.44 (U.S. EPA 2010b).

44.8 Changes or New Information Since the CRA-2009

There were no significant changes in the factors on which the EPA bases the determination of compliance with section 194.44. The DOE did not change the engineered barrier type, form, or function and therefore did not conduct a new analysis to evaluate the benefit and detriment of engineered alternatives (originally required by sections 194.44(b) through (e)). The CRA-2014 followed the EPA's determination that only the MgO backfill met the EPA's requirements for an engineered barrier at section 191.14(d).

The DOE had proposed shaft seals, borehole plugs, and panel closures as engineered barriers in the CCA. Changes to the approved engineered barrier that have occurred between the CRA-2009 and the CRA-2014 and changes to other disposal system design features originally proposed as engineered barriers (termed disposal system barriers) are discussed in the following subsections for completeness.

A detailed history of the MgO engineered barrier is presented in Appendix MgO-2009 and describes the placement, function, and experimental activities associated with the barrier since it was first proposed. Appendix MgO-2014 describes in greater detail the changes that occurred between the CRA-2009 and the CRA-2014.

44.8.1 Changes to the Approved Engineered Barrier

The following developments associated with the MgO engineered barrier that have occurred since the EPA's 2009 Recertification Decision include information from additional analyses and the DOE's planned change notice:

1. The EPA's approval of the DOE's planned change notice for placement of MgO supersacks, which includes:

    A. Emplacement of supersacks on every other row unless additional sacks are needed to meet the 1.2 excess factor.

    B. Standard supersacks weight of 3,000 pounds.

2. Completion of MgO hydration studies.

3. Refinement of water balance in PA to include the impact of MgO.

The following sections provide additional detail for these changes.

44.8.1.1 Planned Change Notice

In February 2012, the DOE submitted a planned change notice outlining an alternative placement scheme for MgO supersacks (Franco 2012). In July 2012, the EPA concurred with the emplacement approach in the DOE's change notice (Peake 2012).

The procedure for emplacement of MgO supersacks in the WIPP underground is WP 05-WH1025, titled CH Waste Downloading and Emplacement (WTS 2011). This procedure was changed to initially emplace a 3,000-pound supersack of MgO on every other waste stack or on each waste stack in every other row, rather than placing a supersack on every waste stack. The MgO excess factor is calculated at the end of each shift based on the amount of CPR emplaced during that shift. If the MgO excess factor for the room is less than 1.2, then additional MgO supersacks will be added as specified in the procedure. Additional information relating to this change is found in Appendix MgO-2014, Section MgO-2.1.4.

44.8.1.2 Hydration Studies

Hydration studies of MgO have been ongoing since 2000. A historical presentation of these studies is found in Appendix MgO-2009, Section MgO-4.0. Since the CRA-2009, Xiong (Xiong 2008), Deng et al. (Deng et al. 2009), and Xiong et al. (Xiong et al.2010) completed these hydration studies (as referenced). Appendix MgO-2014, Section MgO-4.1.1 discusses their results. The conclusion of these studies changed the way MgO is accounted for in actinide solubility calculations. A different MgO hydration phase is now used in solubility calculations for the two brines used in PA. The calculations now predict that the hydration of MgO in Generic Weep Brine will produce brucite and phase 5 instead of brucite and phase 3, and that hydration of MgO in ERDA-6 brine will produce only brucite. The implementation and impacts of this change are described in Appendix MgO-2014, Section MgO-5.0, and Appendix SOTERM-2014, Section SOTERM 2.3.

44.8.1.3 Refinement to Repository Water Balance

The repository water balance implementation was refined in the CRA-2014 PA to include brine and gas producing and consuming reactions in the existing conceptual model. The development of parameters used in the refined water budget implementation is described in Clayton (Clayton 2013). Parameters associated with the water balance refinement implemented in the CRA-2014 PA include those related to iron corrosion, MgO hydration and carbonation. A description of this change and a list of the specific parameters are found in Appendix PA, Section PA-7.1, and in Camphouse et al. (Camphouse et al. 2013), Section 2.10. The CRA-2014 PA sensitivity analysis concluded that the parameter changes related to MgO in the refined water balance analysis do not have a significant impact on potential releases from the repository (Kirchner 2013).

44.8.2 Changes to Other Disposal System Design Features Originally Proposed as Engineered Barriers

As stated earlier, the DOE had proposed MgO, shaft seals, borehole plugs, and panel closures as engineered barriers in the CCA. The EPA considered MgO backfill as the only feature that met their requirements for an engineered barrier at section 191.14(d). Since these other features are not recognized by the EPA as meeting the requirements for an engineered barrier under section 191.14(d),

they will no longer be discussed in this section. Information relating to borehole plugs can be found in Appendix DATA-2014, Attachment A, "WIPP Borehole Update." Information on the current representation of panel closures in PA can be found in Appendix PA-2014, Section PA-4.2.8, and in Camphouse et al. (Camphouse et al 2013), Section 2.1. There have been no changes to the representation of shaft seals in the CRA-2014 PA, nor is there new information to present (Appendix PA-2014, Section PA-4.2.7).

44.8.3 Compliance Summary

None of the changes relating to the WIPP engineered barrier impact activities and conditions that demonstrated compliance with section 194.44 criteria documented in prior recertification applications. The impacts of changes relating to the engineered barrier do not require modification of the CCA analysis that evaluated the benefit and detriment of engineered alternatives, as required by 194.44 (b) through (e). The DOE continues to demonstrate compliance with the requirements of section 194.44.

44.9 References

(*Indicates a reference that has not been previously submitted.)

Camphouse, R.C., D.C. Kicker, T.B. Kirchner, J.J. Long, B. Malama and T.R. Zeitler. 2013. Summary Report for the 2014 WIPP Compliance Recertification Application Performance Assessment, Rev. 0. ERMS 560252. Carlsbad, NM: Sandia National Laboratories.*

Clayton, D.J. 2013. Justification of Chemistry Parameters for Use in BRAGFLO for AP-164, Revision 1. Memorandum to SNL Records Center dated March 13, 2013. ERMS 559466. Carlsbad, NM: Sandia National Laboratories.*

Christensen, C.L., and E.W. Peterson. 1981. "Field-Test Programs of Borehole Plugs in Southeastern New Mexico." The Technology of High-Level Nuclear Waste Disposal Advantages in the Science and Engineering of the Management of High-Level Nuclear Wastes (vol. 1, pp. 354–69). P.L. Hofman and J.J. Breslin (eds.). SAND79-1634C. DOE/TIC-4621. Oak Ridge, TN: Technical Information Center of the U.S. Department of Energy.

Cohen and Associates. 2008. *Review of MgO-Related Uncertainties in the Waste Isolation Pilot Plant* (January 24). Vienna, VA: S. Cohen and Associates.

Deng, H., Y. Xiong, M. Nemer, and S. Johnsen. 2009. "Experimental Work Conducted on MgO Long-Term Hydration: 2008 Milestone Report." May 27, 2009. ERMS 551421. Carlsbad, NM: Sandia National Laboratories.*

Deng, H., Y. Xiong, and M. Nemer. 2007. *Experimental Work Conducted on MgO Characterization and Hydration, Milestone Report.* ERMS 546570. Carlsbad, NM: Sandia National Laboratories.

Deng, H., S. Johnsen, Y. Xiong, G.T. Roselle, and M. Nemer. 2006. *Analysis of Martin Marietta MagChem 10 WTS-60 MgO*. ERMS 544712. Carlsbad, NM: Sandia National Laboratories.

Detwiler, R.P. 2004. Letter to E. Cotsworth (Subject: Response to EPA May 20, 2004, Letter on CRA; 2 Enclosures). 29 September 2004. Carlsbad, NM: U.S. Department of Energy, Carlsbad Field Office.

Fox, B. 2008. *Parameter Summary Report for the CRA-2009 (Revision 0).* ERMS 549747. Carlsbad, NM: Sandia National Laboratories.

Franco, J.R. 2012. Letter to A. Perrin (Subject: *Planned Change Notice for Placement of MgO Supersacks," with enclosure (Analysis of an alternative placement scheme for MgO supersacks*). February 14, 2012. Carlsbad, NM: U.S. Department of Energy Carlsbad Field Office.*

Gitlin, B.C. 2006. Letter to D.C. Moody. 28 April 2006. ERMS 543319. Washington, DC: U.S. Environmental Protection Agency, Office of Radiation and Indoor Air.

Kirchner, T.B. 2013. Sensitivity of the CRA-2014 Performance Assessment Releases to Parameters, ERMS 560043. Carlsbad, NM: Sandia National Laboratories.*

Langmuir, D. 2007. Memorandum to S.L. Ostrow (Subject: *Letter Report Review of the SC&A Draft Report "Review of MgO-Related Uncertainties in the Waste Isolation Pilot Plant"*). November 4, 2007. Silverthorne, CO: Hydrochem Systems Corporation.

Marcinowski, F. 2002. Letter to I. Triay. 15 November 2002. Washington, DC: U.S. Environmental Protection Agency, Office of Air and Radiation.

Marcinowski, F. 2004. Letter to R.P. Detwiler (2 Enclosures). 26 March 2004. ERMS 534327. Washington, DC: U.S. Environmental Protection Agency, Office of Air and Radiation.

Moody, D.C. 2006a. Letter to E. Cotsworth (Subject: *Transmittal of Planned Change Request; 1 Enclosure*). 10 April 2006. ERMS 543262. Carlsbad, NM: U.S. Department of Energy, Carlsbad Field Office.

Moody, D.C. 2006b. Letter to J. Reyes (Subject: *Uncertainty Analysis for Planned Change Request on Magnesium Oxide (MgO) Emplacement; 4 Enclosures*). November 21, 2006. Carlsbad, NM: U.S. Department of Energy, Carlsbad Field Office.

Moody, D.C. 2007a. Letter to J. Reyes (Subject: Modification to Condition 1 of Certification Decision). 11 January 2007. ERMS 545491. Carlsbad, NM: U.S. Department of Energy, Carlsbad Field Office.

Moody, D.C. 2007b. Letter to J. Reyes (Subject: *Requesting Withdrawal of Panel Closure Change Request*). 9 October 2007. Carlsbad, NM: U.S. Department of Energy, Carlsbad Field Office.

Peake, T. 2012. Email to J.R. Franco (Subject; *"Magnesium Oxide Supersack Size Reduction and Alternative Emplacement Plan"*). July 13, 2012. Washington, DC: U.S. Environmental Protection Agency, Office of Radiation and Indoor Air.*

Reyes, J. 2007. Letter to D. Moody (Subject: *Response to DOE's letter dated January 11, 2007*). 22 February 2007. ERMS 545394. Washington, DC: U.S. Environmental Protection Agency, Office of Air and Radiation.

Reyes, J. 2008. Letter to D.C. Moody (5 Enclosures). 11 February 2008. Washington, DC: U.S. Environmental Protection Agency, Office of Air and Radiation.

Sandia National Laboratories (SNL). 1996. *Implementation of Chemical Controls Through a Backfill System for the Waste Isolation Pilot Plant (WIPP)*. SAND96-2656A. ERMS 242847. Albuquerque, NM: Sandia National Laboratories.

State of New Mexico. 1988. *Order R-111-P: Potash Areas of Eddy and Lea Counties, NM*. Case 9316, Revision to Order R-111-P. April 21, 1988. Oil Conservation Division, Energy, Minerals, and Natural Resources Department.

State of New Mexico. 1996. *Title 19, Chapter 15, Part 4, Rule 202, Plugging and Permanent Abandonment*. February 1, 1996. Oil Conservation Division, Energy, Minerals, and Natural Resources Department.

State of New Mexico. 2005. *19.27.4 NMAC: Well Driller Licensing; Construction, Repair and Plugging of Wells*. August 31, 2005. Oil Conservation Division, Energy, Minerals, and Natural Resources Department.

Triay, I. 2002. Letter to F. Marcinowski (Subject: *Request Planned Change to Panel Closure System*). 7 October 2002. Carlsbad, NM: U.S. Department of Energy, Carlsbad Field Office.

Trinity Engineering Associates (TEA). 2004. Review of Effects of Supercompacted Waste and Heterogeneous Waste Emplacement on WIPP Repository Performance (March 17). Cincinnati: Trinity Engineering Associates.

U.S. Department of Energy (DOE). 1996. *Title 40 CFR Part 191 Compliance Certification Application for the Waste Isolation Pilot Plant* (October). 21 vols. DOE/CAO-1996-2184. Carlsbad, NM: Carlsbad Area Office.

U.S. Department of Energy (DOE). 2004. *Title 40 CFR Part 191 Compliance Recertification Application for the Waste Isolation Pilot Plant* (March). 10 vols. DOE/WIPP 2004-3231. Carlsbad, NM: Carlsbad Field Office.

U.S. Environmental Protection Agency (EPA). 1993. "40 CFR Part 191 Environmental Radiation Protection Standards for the Management and Disposal of Spent Nuclear Fuel, High-Level and Transuranic Radioactive Wastes: Final Rule." *Federal Register*, vol. 58 (December 20, 1993): 66398–416.

U.S. Environmental Protection Agency (EPA). 1996. "40 CFR Part 194: Criteria for the Certification and Re-Certification of the Waste Isolation Pilot Plant's Compliance with the 40 CFR Part 191 Disposal Regulations; Final Rule." *Federal Register*, vol. 61 (February 9, 1996): 5224–45.

U.S. Environmental Protection Agency (EPA). 1998. "40 CFR Part 194 Criteria for the Certification and Recertification of the Waste Isolation Pilot Plant's Compliance with the Disposal Regulations: Certification Decision; Final Rule." *Federal Register*, vol. 63 (May 18, 1998): 27353–406.

U.S. Environmental Protection Agency (EPA). 2004. *Discussion of Major Issues Associated with EPA's Compressed Waste Review*. ERMS 534327. Washington, DC: Office of Air and Radiation.

U.S. Environmental Protection Agency (EPA). 2006. "40 CFR Part 194: Criteria for the Certification and Recertification of the Waste Isolation Pilot Plant's Compliance with the Disposal Regulations: Recertification Decision" (Final Notice). *Federal Register*, vol. 71 (April 10, 2006): 18010–021.*

U.S. Environmental Protection Agency (EPA). 2008. *Overview Summary of Planned Change Request Decision*. Washington, DC: Office of Radiation and Indoor Air.

U.S. Environmental Protection Agency (EPA). 2010a. "40 CFR Part 194 Criteria for the Certification and Recertification of the Waste Isolation Pilot Plant's Compliance with the Disposal Regulations: Recertification Decision; Final Notice." *Federal Register*, vol. 75 (November 18, 2010): 70584 - 595.*

U.S. Environmental Protection Agency (EPA). 2010b. "Recertification CARD Nos. 44: Engineered Barriers." *2009 Compliance Recertification Application (2009 CRA) Compliance Application Review Documents (CARD) Nos. 44.* EPA Docket FDMS Docket ID No. EPA-HQ-OAR-2009-0330 (November 18, 2010). Washington, DC: Office of Radiation and Indoor Air.*

Wall, N.A. 2005. *Preliminary Results for the Evaluation of Potential New MgO* (January 27). ERMS 538514. Carlsbad, NM: Sandia National Laboratories.

Washington TRU Solutions (WTS). 2003. *Specification for Prepackaged MgO Backfill* (Rev. 5). D-0101. Carlsbad, NM: Washington TRU Solutions.

Washington TRU Solutions (WTS). 2011. *CH Waste Downloading and Emplacement.* WP 05-WH1025, Carlsbad, NM: Nuclear Waste Partnership LLC.*

Xiong, Y.-L. 2008. "Thermodynamic Properties of Brucite Determined by Solubility Studies and Their Significance to Nuclear Waste Isolation." Aquatic Geochemistry. Vol. 14, no. 3, 223-238.*

Xiong, Y.-L., H.-R. Deng, M.B. Nemer, and S. Johnsen. 2010. "Experimental Determination of the Solubility Constant for Magnesium Chloride Hydroxide Hydrate ($Mg_3Cl(OH)_5 \cdot 4H_2O$, Phase 5) at Room Temperature, and Its Importance to Nuclear Waste Isolation in Geological Repositories in Salt Formations," Geochimica et Cosmochimica Acta. Vol. 74, no. 16, 4605– 4611.*

Title 40 CFR Part 191
Subparts B and C
Compliance Recertification Application 2014
for the
Waste Isolation Pilot Plant

Consideration of the Presence of Resources
(40 CFR § 194.45)

United States Department of Energy
Waste Isolation Pilot Plant

Carlsbad Field Office
Carlsbad, New Mexico

Compliance Recertification Application 2014
Consideration of the Presence of Resources
(40 CFR § 194.45)

Table of Contents

This page intentionally left blank.

Acronyms and Abbreviations

CCA	Compliance Certification Application
CFR	Code of Federal Regulations
CRA	Compliance Recertification Application
DOE	U.S. Department of Energy
EPA	U.S. Environmental Protection Agency
FEP	feature, event, and process
PA	performance assessment
PABC	performance assessment baseline calculation
WIPP	Waste Isolation Pilot Plant

This page intentionally left blank.

45.0 Consideration of the Presence of Resources (40 CFR § 194.45)

45.1 Requirements

> § 194.45 Consideration of the Presence of Resources
>
> Any compliance application shall include information that demonstrates that the favorable characteristics of the disposal system compensate for the presence of resources in the vicinity of the disposal system and the likelihood of the disposal system being disturbed as a result of the presence of those resources. If performance assessments predict that the disposal system meets the containment requirements of §191.13 of this chapter, then the Agency will assume that the requirements of this section and §191.14(e) of this chapter have been fulfilled.

45.2 Background

40 CFR § 194.45 (U.S. EPA 1996a) implements the assurance requirement that the disposal system be sited so that the benefits of the disposal system's natural barriers compensate for the increased probability of disruptions to the disposal system resulting from exploring and developing existing resources. In promulgating this requirement, the U.S. Environmental Protection Agency (EPA) determined that performance assessment (PA) provides a rigorous analytical methodology to determine whether the Waste Isolation Pilot Plant (WIPP) site has compensating features that outweigh the presence of resources (U.S. EPA 1996b). In accordance with the compliance criteria, the U.S. Department of Energy (DOE) must demonstrate that the PA has incorporated the potential effects of human activities near the WIPP prior to disposal, and of drilling and excavation mining over the regulatory time frame.

45.3 1998 Certification Decision

In the Compliance Certification Application (CCA) (U.S. DOE 1996), Chapter 7.0, Section 7.5, the DOE describes the measures taken to comply with the requirements of section 194.45. The CCA, Chapter 7.0, Section 7.5 states that the results of the PA, taking into account the potential for resource exploration, met the containment requirements of the EPA as dictated by the disposal regulations and compliance criteria. The CCA, Chapter 7.0, Section 7.5.2 states that the DOE concluded that the favorable characteristics of the WIPP compensate for any possible disturbance.

The EPA found that the information contained in the CCA, Chapter 7.0, Section 7.5, and portions of the CCA cross-referenced in Chapter 7.0, Section 7.5, demonstrates that the DOE accounted for potential resource exploration and met the EPA's requirements based on the results of the PA. Furthermore, the DOE's Final Environmental Impact Statement for the WIPP indicates that resource considerations were taken into account during the disposal system's site selection process (U.S. DOE 1980, Volume 1, Section 7.3.7). Based on these factors, the EPA concluded that the DOE complied with the requirements of section 194.45. A complete description of the EPA's 1998 Certification Decision for section 194.45 can be obtained from U.S. EPA 1998a and U.S. EPA 1998b.

45.4 Changes in the CRA-2004

The DOE did not report any significant changes to the information on which the EPA based the 1998 Certification Decision. The Compliance Recertification Application (CRA) of 2004 (CRA-2004) (U.S. DOE 2004), Chapter 7.0, Section 7.5, contains all the changes related to resource considerations since 1998. The DOE made some minor changes to the list of features, events, and processes (FEPs) considered in the CRA-2004, but the changes did not affect the outcome of the PA. (See the CRA-2004, Appendix SCR, Table SCR-1.)

In the CRA-2004, Chapter 7.0, Section 7.5, the DOE demonstrated that:

- The effects of mining and drilling over the regulatory time frame have been incorporated into the PA according to the requirements of sections 194.32, 194.33, and 194.43.

- The PA incorporates the effects on the disposal system of any activities that occur in the vicinity of the disposal system or are expected to occur in the vicinity of the disposal system during the 10,000-year regulatory period, according to the requirements of section 194.32.

- The results of the PA demonstrate compliance with the containment requirements of section 191.13 (U.S. EPA 1993).

The results of the recertification PA are documented in the CRA-2004, Chapter 6.0, Section 6.5, and in supplemental information on the CRA-2004 Performance Assessment Baseline Calculation (PABC) (Leigh et al. 2005). In addition, the impacts of resource development outside the controlled area were considered in the development of the WIPP's conceptual models, as well as in the site selection process.

45.5 EPA's Evaluation of Compliance for the 2004 Recertification

The EPA's review of the activities and conditions in and around the WIPP site did not identify any significant changes since the 1998 Certification Decision related to the presence of resources.

Based on a review and evaluation of the CRA-2004; supplemental information in the CCA, Appendices GCR, IRL, and DEL provided by the DOE in the CRA-2004; and an assessment of changes since 1998, the EPA determined that the DOE continued to comply with the requirements in section 194.45.

45.6 Changes or New Information Between the CRA-2004 and the CRA-2009 (Previously: Changes or New Information Since the 2004 Recertification)

Section 194.45 states, "If performance assessments predict that the disposal system meets the containment requirements of Section 191.13 of this chapter, then the Agency will assume that the requirements of this section and §191.14(e) of this chapter have been fulfilled." Therefore, provided that the PA appropriately incorporates processes relating to resource discovery and production, and predicts releases that are below limits established by the EPA, compliance with section 194.45 will have been demonstrated. This conditional logic relies heavily upon whether

or not the PA is structured to appropriately represent resource-related activities at the WIPP site. To accomplish this, the DOE used a structured methodology to identify and select FEPs that may have an impact on the disposal system. This process was documented in CRA-2009 (U.S. DOE 2009) Section 32, "Scope of Performance Assessment," and Appendix SCR-2009. There were no changes in screening decisions for resource-related FEPs for the CRA-2009.

While there were no screening changes for FEPs related to the presence of resources, there were two changes relating to the implementation of the presence of resources in PA models. These changes included a new drilling rate (LAMBDAD) (see Appendix DATA-2009 and Appendix PA-2009, Section PA-2.1.1) and a change in the duration of direct brine releases through the PA parameter MAXFLOW (see Appendix PA-2009, Section PA-2.1.1). These changes were not significant, but were made to incorporate the most recent information available relating to the exploitation of resources (see "Consideration of Drilling Events in Performance Assessment," Section 33). Besides these two drilling-related parameters, there were no planned changes adopted by the DOE since the CRA-2004 that impact the previous position and bases for demonstrating compliance with this section. The PA calculations responsive to section 191.13 showed predicted releases to be well within the regulated limits and demonstrated that the favorable characteristics and isolating capability of the WIPP outweigh the risks associated with the presence of resources at the site. Therefore, the requirements of section 194.45 were met.

45.7 EPA's Evaluation of Compliance for the 2009 Recertification

During the EPA's review of the activities and conditions in and around the WIPP site, no significant changes were identified that relate to the presence of resources since the 1998 Certification or 2004 Recertification decisions.

The EPA concluded that the PABC-2009 (Clayton et al. 2010) predicted releases within the regulatory limits; therefore, the favorable characteristics of the site continue to outweigh risks associated with the presence of resources. In addition, the impacts of resource development outside the controlled area were considered in the development of the WIPP's conceptual models, as well as in the site selection process. The EPA did not receive any public comments on the DOE's continued compliance with the Consideration of the Presence of Resources requirements of section 194.45 (U.S. EPA 2010a).

Therefore, based on a review and evaluation of the CRA-2009 and its supplemental information, the EPA determined that the DOE continued to comply with the requirements for section 194.45 (U.S. EPA 2010b).

45.8 Changes or New Information Since the CRA-2009

The DOE monitors resource-related activities within the WIPP vicinity, and updates parameters and/or models as appropriate to assure that current practices are accurately represented in the WIPP PA (U.S. DOE 2012). Since the last recertification application, the rate of drilling for petroleum resources has increased to 67.3 boreholes per square kilometer over 10,000 years. This is represented as PA parameter (LAMBDAD) (Kicker and Herrick 2013), and is an increase from the value of 59.8 boreholes per square kilometer used in the PABC-2009. Additionally, the representation of borehole plugs has changed slightly, based on minor changes in the number of

plugs emplaced per borehole in recently plugged and abandoned boreholes near the WIPP (U.S. DOE 2012). The WIPP PA parameter GLOBAL:PBRINE has been updated to reflect over 15 years of additional data in the immediate vicinity of the WIPP with regard to the occurrence of pressurized brine while drilling (Kirchner et al. 2012). Finally, the PA parameter BOREHOLE:TAUFAIL has also been updated based on the results of experiments conducted since the last certification application (Herrick et al. 2012). These parameter updates have a minimal impact upon PA results, which continue to show predicted releases well within the regulated limits established in section 191.13.

Conventional mining for potash is continuing within the vicinity of the WIPP. The effects of mining are accounted for in the WIPP PA as prescribed by section 194.32(b). The implementation of the mining scenario in the WIPP PA is described in Appendix PA-2014, Section PA-3.9.

A solution mining project operated by Intrepid Potash Corporation has begun just outside the Delaware Basin boundary since the CRA-2009. The initiation and operation of this activity does not affect the current representation of mining in the WIPP PA, and therefore no changes have been made to the WIPP models. The description, screening argument, and screening decision for this activity are presented in Appendix SCR-2014, Section SCR-5.2.2.3.

Because the WIPP PA results show that predicted releases are below the limits established by section 191.13, and because these calculations account for the exploitation of resources present, it has been demonstrated that the favorable characteristics and isolating capability of the WIPP outweigh the risks associated with the presence of resources at the site. Therefore, the requirements of section 194.45 are met.

45.9 References

(*Indicates a reference that has not been previously submitted.)

Clayton, D.J., C. Camphouse, J.W. Garner, A.E. Ismail, T.B. Kirchner, K.L. Kuhlman, and M.B. Nemer. 2010. Summary Report of the CRA-2009 Performance Assessment Baseline Calculation. ERMS 553039. February 11, 2010. Carlsbad, NM: Sandia National Laboratories.*

Herrick, C.G., M.D.Schuhen, D.M. Chapin, and D.C. Kicker. 2012. Determining the Hydrodynamic Shear Strength of Surrogate Degraded TRU Waste Materials as an Estimate for the Lower Limit of the Performance Assessment Parameter TAUFAIL. ERMS 558479. Carlsbad, NM: Sandia National Laboratories.*

Kicker, D.C. and C.G. Herrick. 2013. Parameter Summary Report for the 2014 Compliance Recertification Application (Revision 0). ERMS 560298. Carlsbad, NM: Sandia National Laboratories.*

Kirchner, T., T. Zeitler, and R. Kirkes. 2012. Evaluating the Data in Order to Derive a Value for GLOBAL:PBRINE. Memorandum to Sean Dunagan dated December 11, 2012. ERMS 558724. Carlsbad, NM: Sandia National Laboratories. *

Leigh, C., J. Kanney, L. Brush, J. Garner, R. Kirkes, T. Lowry, M. Nemer, J. Stein, E. Vugrin, S. Wagner, and T. Kirchner. 2005. *2004 Compliance Recertification Application Performance Assessment Baseline Calculation* (Revision 0). ERMS 541521. Carlsbad, NM: Sandia National Laboratories.

U.S. Department of Energy (DOE). 1980. (October). 2 vols. DOE/EIS-0026. ERMS 238835 and ERMS 238838. Washington, DC: U.S. Department of Energy.

U.S. Department of Energy (DOE). 1996. *Title 40 CFR Part 191 Compliance Certification Application for the Waste Isolation Pilot Plant* (October). 21 vols. DOE/CAO-1996-2184. Carlsbad, NM: Carlsbad Area Office.

U.S. Department of Energy (DOE). 2004. *Title 40 CFR Part 191 Compliance Recertification Application for the Waste Isolation Pilot Plant* (March). 10 vols. DOE/WIPP 2004-3231. Carlsbad, NM: Carlsbad Field Office.

U.S. Department of Energy (DOE). 2009. *Title 40 CFR Part 191 Compliance Recertification Application for the Waste Isolation Pilot Plant* (March). DOE/WIPP-09-3424. Carlsbad, NM: Carlsbad Field Office.*

U.S. Department of Energy (DOE). 2012. Delaware Basin Monitoring Annual Report. DOE/WIPP-12-2308. Carlsbad, NM: Carlsbad Field Office.*

U.S. Environmental Protection Agency (EPA). 1993. "40 CFR Part 191: Environmental Radiation Protection Standards for the Management and Disposal of Spent Nuclear Fuel, High-Level and Transuranic Radioactive Wastes; Final Rule." *Federal Register*, vol. 58 (December 20, 1993): 66398–416.

U.S. Environmental Protection Agency (EPA). 1996a. "40 CFR Part 194: Criteria for the Certification and Recertification of the Waste Isolation Pilot Plant's Compliance with the 40 CFR Part 191 Disposal Regulations; Final Rule." Federal Register, vol. 61 (February 9, 1996): 5223–45.

U.S. Environmental Protection Agency (EPA). 1996b. Response to Comments: 40 CFR Part 194: Criteria for the Certification and Recertification of the Waste Isolation Pilot Plant's Compliance with the 40 CFR Part 191 Disposal Regulations (January 31). EPA 402-R-96-001. Washington, DC: Office of Air and Radiation.

U.S. Environmental Protection Agency (EPA). 1998a. "40 CFR Part 194: Criteria for the Certification and Recertification of the Waste Isolation Pilot Plant's Compliance with the Disposal Regulations: Certification Decision; Final Rule." *Federal Register*, vol. 63 (May 18, 1998): 27353–406.

U.S. Environmental Protection Agency (EPA). 1998b. Compliance Application Review Documents for the Criteria for the Certification and Recertification of the Waste Isolation Pilot Plant's Compliance with the 40 CFR 191 Disposal Regulations: Final Recertification Decision (May). Washington, DC: Office of Radiation and Indoor Air.

U.S. Environmental Protection Agency (EPA). 2010a. "2009 Compliance Recertification Application (2009 CRA) Compliance Application Review Document (CARD) No. 45, Consideration of the Presence of Resources." EPA Docket FDMS Docket ID No. EPA-HQ-OAR-2009-0330. Washington, DC: Office of Radiation and Indoor Air. http://www.epa.gov/radiation/wipp/2010recertification.html.*

U.S. Environmental Protection Agency (EPA). 2010b. "40 CFR Part 194 Criteria for the Certification and Recertification of the Waste Isolation Pilot Plant's Compliance with the Disposal Regulations: Rectification Decision; Final Notice." *Federal Register,* vol. 75 (November 18, 2010): 70584 - 595. https://www.federalregister.gov/articles/2010/11/18/2010-28806/criteria-for-the-certification-and-recertification-of-the-waste-isolation-pilot-plants-compliancehttp://www.epa.gov/radiation/docs/wipp/recertification2/finaldecision_fr.pdf.*

Title 40 CFR Part 191
Subparts B and C
Compliance Recertification Application 2014
for the
Waste Isolation Pilot Plant

Removal of Waste
(40 CFR § 194.46)

United States Department of Energy
Waste Isolation Pilot Plant

Carlsbad Field Office
Carlsbad, New Mexico

Compliance Recertification Application 2014
Removal of Waste
(40 CFR § 194.46)

Table of Contents

This page intentionally left blank.

Acronyms and Abbreviations

CARD	Compliance Application Review Document
CCA	Compliance Certification Application
CFR	Code of Federal Regulations
CRA	Compliance Recertification Application
DOE	U.S. Department of Energy
EPA	U.S. Environmental Protection Agency
WIPP	Waste Isolation Pilot Plant

This page intentionally left blank.

46.0 Removal of Waste (40 CFR § 194.46)

46.1 Requirements

> § 194.46 Removal of Waste
> Any compliance application shall include documentation which demonstrates that removal of waste from the disposal system is feasible for a reasonable period of time after disposal. Such documentation shall include an analysis of the technological feasibility of mining the sealed disposal system, given technology levels at the time a compliance application is prepared.

46.2 Background

The U.S. Environmental Protection Agency's (EPA's) 40 CFR § 194.46, "Removal of Waste" (U.S. EPA 1996a), is one of the six assurance requirements in the Compliance Criteria. The EPA states in the preamble to the 1993 promulgation of the disposal standards of 40 CFR Part 191 (U.S. EPA 1993) that the assurance requirements were included in the disposal standards to compensate in a qualitative manner for the inherent uncertainties in projecting the behavior of natural and engineered components of the Waste Isolation Pilot Plant (WIPP) for many thousands of years.

46.3 1998 Certification Decision

To meet the criteria of section 194.46, the EPA states in its Compliance Application Guidance that compliance with the section 194.46 criteria is demonstrated by an analysis that includes (1) completeness of procedures for removal of waste after disposal, (2) descriptions of current technology that could be used in implementing these procedures, and (3) an estimate of when it will no longer be technologically feasible to remove the waste (U.S. EPA 1996b).

The U.S. Department of Energy's (DOE's) demonstration of compliance with section 194.46 was included in the Compliance Certification Application (CCA) (U.S. DOE 1996), Chapter 7.0 and Appendix WRAC. The DOE presented a five-phased approach to accomplish the removal of waste. This approach was supported by a discussion of techniques that could be used to remove the waste, given repository conditions at the time of removal. The EPA reviewed the material to assess the completeness of the strategy and the justification of the proposed technology for removing the waste. The EPA states in its 1998 Certification Decision (U.S. EPA 1998a) for section 194.46 that the DOE has demonstrated it is possible to remove waste from the repository for a reasonable period of time after disposal; therefore, the EPA found the DOE in compliance with section 194.46. A complete description of the EPA's decision can be found in U.S. EPA 1998a, Section VIII.D.6, and Compliance Application Review Document (CARD) 46 (U.S. EPA 1998b).

46.4 Changes in the CRA-2004

The DOE did not report any changes in the 2004 Compliance Recertification Application (CRA-2004) (U.S. DOE 2004) to the information on which the EPA based its 1998 Certification Decision (U.S. EPA 1998a). The DOE maintained its original position on waste removal after

closure, which was presented in the CCA, Chapter 7.0, Section 7.6. Only editorial changes were made to the original text in the CCA, Chapter 7.0, Section 7.6, pp. 7-90 and 7-91. The CRA-2004 included the CCA, Appendix WRAC by reference; no changes were made to Appendix WRAC.

46.5 EPA's Evaluation of Compliance for the 2004 Recertification

Based on the EPA's review of the activities and conditions in and around the WIPP site, the EPA did not identify any significant changes in the planning and execution of the DOE's strategy for removal of waste since the 1998 Certification Decision (U.S. EPA 1998a). The CRA-2004 provides documentation that the removal of waste from the disposal system is feasible for a reasonable period of time after disposal (see the CRA-2004, Chapter 7.0, Section 7.6.2).

The EPA did not receive any public comments on the DOE's continued compliance with the section 194.46 requirements for removal of waste presented in the CRA-2004.

Based on a review and evaluation of the CRA-2004 and the CCA, Appendix WRAC, the EPA determined that the DOE continued to comply with the requirements of section 194.46 (U.S. EPA 2006, Section V.E).

46.6 Changes or New Information Between the CRA-2004 and the CRA-2009 (Previously: Changes or New Information Since the 2004 Recertification)

The DOE did not change its position on waste removal presented in the CCA, Chapter 7.0, Section 7.6. There were no design changes or changes to the disposal system in waste emplacement within the disposal area between the CRA-2004 and the CRA-2009 (U.S. DOE 2009). There were no changes in the planning or execution of the DOE's strategy for removal of waste since the EPA's 1998 Certification Decision (U.S. EPA 1998a). Thus, there was no new information to be provided as part of the CRA-2009, and the information presented in the CRA-2004, Chapter 7.0, Section 7.6, pp. 7-90 and 7-91, and the CCA, Appendix WRAC, continued to demonstrate compliance with the provisions of section 194.46 at that time (see the CRA-2009, Section 46).

46.7 EPA's Evaluation of Compliance for the 2009 Recertification

Based on the EPA's review of the activities and conditions in and around the WIPP site, the EPA did not identify any significant changes in the planning and execution of the DOE's strategy for removal of waste since the 1998 Certification Decision (U.S. EPA 2010a).

The EPA did not receive any public comments on the DOE's continued compliance with the section 194.46 requirements for removal of waste presented in the CRA-2009.

Based on a review and evaluation of the CRA-2009 and the CCA, Appendix WRAC, the EPA determined that the DOE continued to comply with the requirements of section 194.46 (U.S. EPA 2010b, Section V.E.).

46.8 Changes or New Information Since the CRA-2009

The DOE has not changed its position on waste removal presented in the CCA, Chapter 7.0, Section 7.6. There have been no design changes or changes to the disposal system in waste emplacement within the disposal area since the CRA-2009. There have been no changes in the planning or execution of the DOE's strategy for removal of waste since the EPA's 1998 Certification Decision (U.S. EPA 1998a). Thus, there is no new information to be provided as part of the CRA-2014, and the information presented in the CRA-2004, Chapter 7.0, Section 7.6, pp. 7-90 and 7-91, and the CCA, Appendix WRAC, continues to demonstrate compliance with the provisions of section 194.46.

46.9 References

(*Indicates a reference that has not been previously submitted.)

U.S. Department of Energy (DOE). 1996. *Title 40 CFR Part 191 Compliance Certification Application for the Waste Isolation Pilot Plant* (October). 21 vols. DOE/CAO-1996-2184. Carlsbad, NM: Carlsbad Area Office.

U.S. Department of Energy (DOE). 2004. *Title 40 CFR Part 191 Compliance Recertification Application for the Waste Isolation Pilot Plant* (March). 10 vols. DOE/WIPP 2004-3231. Carlsbad, NM: Carlsbad Field Office.

U.S. Department of Energy (DOE). 2009. *Title 40 CFR Part 191 Compliance Recertification Application for the Waste Isolation Pilot Plant* (March). DOE 09-2434. Carlsbad, NM: Carlsbad Field Office.*

U.S. Environmental Protection Agency (EPA). 1993. "40 CFR Part 191: Environmental Radiation Protection Standards for the Management and Disposal of Spent Nuclear Fuel, High-Level and Transuranic Radioactive Wastes; Final Rule." *Federal Register*, vol. 58 (December 20, 1993): 66398–416.

U.S. Environmental Protection Agency (EPA). 1996a. "40 CFR Part 194: Criteria for the Certification and Recertification of the Waste Isolation Pilot Plant's Compliance with the 40 CFR Part 191 Disposal Regulations: Final Rule." *Federal Register*, vol. 61 (February 9, 1996): 52234–45.

U.S. Environmental Protection Agency (EPA). 1996b. *Compliance Application Guidance for 40 CFR 194* (March 29). EPA 402-R-95-014. Washington, DC: Office of Radiation and Indoor Air.

U.S. Environmental Protection Agency (EPA). 1998a. "40 CFR Part 194: Criteria for the Certification and Recertification of the Waste Isolation Pilot Plant's Compliance with the Disposal Regulations: Certification Decision; Final Rule." *Federal Register*, vol. 63 (May 18, 1998): 27353–406.

U.S. Environmental Protection Agency (EPA). 1998b. "CARD No. 46: Removal of Waste." *Compliance Application Review Documents for the Criteria for the Certification and Recertification of the Waste Isolation Pilot Plant's Compliance with the 40 CFR 191 Disposal Regulations: Final Certification Decision* (May) (pp. 46-1 through 46-4). Washington, DC: Office of Radiation and Indoor Air.

U.S. Environmental Protection Agency (EPA). 2006. "Recertification CARD No. 46: Removal of Waste." *Compliance Application Review Documents for the Criteria for the Certification and Recertification of the Waste Isolation Pilot Plant's Compliance with the 40 CFR 191 Disposal Regulations: Final Recertification Decision* (March) (pp. 46-1 through 46-2). Washington, DC: Office of Radiation and Indoor Air.

U.S. Environmental Protection Agency (EPA). 2010a. *2009 Compliance Recertification Application (CRA-2009) Compliance Application Review Document (CARD) No. 46, Removal of Waste*. EPA Docket FDMS Docket ID No. EPA-HQ-OAR-2009-0330. Washington, DC: Office of Radiation and Indoor Air.*

U.S. Environmental Protection Agency (EPA). 2010b. "40 CFR Part 194 Criteria for the Certification and Recertification of the Waste Isolation Pilot Plant's Compliance with the Disposal Regulations: Recertification Decision; Final Notice." *Federal Register*, vol. 75 (November 18, 2010): 70584 - 595.*

Title 40 CFR Part 191
Subparts B and C
Compliance Recertification Application 2014
for the
Waste Isolation Pilot Plant

Consideration of Protected Individual and Exposure Pathways (40 CFR §§ 194.51 and 194.52)

United States Department of Energy
Waste Isolation Pilot Plant

Carlsbad Field Office
Carlsbad, New Mexico

Compliance Recertification Application 2014
Consideration of Protected Individual and Exposure Pathways
(40 CFR §§ 194.51 and 194.52)

Table of Contents

This page intentionally left blank.

Acronyms and Abbreviations

CARD	Compliance Application Review Document
CCA	Compliance Certification Application
CFR	Code of Federal Regulations
CRA	Compliance Recertification Application
DOE	U.S. Department of Energy
EPA	U.S. Environmental Protection Agency
mrem	millirem
PA	performance assessment
pCi/L	picocuries per liter
USDW	underground source of drinking water
WIPP	Waste Isolation Pilot Plant

Elements and Chemical Compounds

Ra	radium

This page intentionally left blank.

51.0 Consideration of Protected Individual and Exposure Pathways (40 CFR §§ 194.51 and 194.52)

51.1 Requirements

> §194.51 Consideration of Protected Individual and Exposure Pathways
> Compliance assessments that analyze compliance with §191.15 of this chapter shall assume that an individual resides at the single geographic point on the surface of the accessible environment where that individual would be expected to receive the highest dose from radionuclide releases from the disposal system.
>
> §194.52 Consideration of Protected Individual and Exposure Pathways
> In compliance assessments that analyze compliance with §191.15 of this chapter, all potential exposure pathways from the disposal system to individuals shall be considered. Compliance assessments with part 191, subpart C and §191.15 of this chapter shall assume that individuals consume 2 liters per day of drinking water from any underground source of drinking water in the accessible environment.

51.2 Background

40 CFR §§ 194.51 and 194.52 (U.S. EPA 1996) of the Waste Isolation Pilot Plant (WIPP) certification criteria implement the individual protection requirements of 40 CFR § 191.15 and the groundwater protection standards of 40 CFR Part 191 Subpart C (U.S. EPA 1993). Section 194.51 requires the U.S. Department of Energy (DOE) to assume in its compliance assessments that an individual resides at the point where the dose from radionuclide releases from the WIPP would be greatest. Section 194.52 requires the DOE to consider in its compliance assessments all the potential exposure pathways for radioactive contaminants from the WIPP. Compliance with sections 194.51 and 194.52 is addressed in this single section because the criteria are closely related.

Assessment of the likelihood that the WIPP will meet the individual dose limits and radionuclide concentration limits for groundwater is conducted through a process known as compliance assessment. Compliance assessment uses methods similar to those of the performance assessment (PA) for the containment requirements, but is required to address only undisturbed performance of the disposal system. That is, compliance assessment does not include human intrusion scenarios (i.e., drilling or mining for resources). Compliance assessment can be considered a “subset” of PA.

The U.S. Environmental Protection Agency (EPA) incorporated requirements in 40 CFR Part 191 for the protection of individuals and 40 CFR 141 for the protection of groundwater. The individual protection requirements of Part 191 limit annual committed effective doses of radiation to members of the public to no more than 15 millirem (mrem). This requirement is concerned with human exposure to radionuclides from disposal systems for 10,000 years. These criteria address the definition of a protected individual, the consideration of exposure pathways, the consideration of underground sources of drinking water (USDWs), the scope of compliance assessments, and the basis for determining compliance with the Individual Protection Standards (U.S. EPA 1996).

51.3 1998 Certification Decision

To obtain the EPA's 1998 certification decision, the DOE was required to demonstrate a reasonable expectation that the potential releases from the undisturbed repository will result in radiation doses lower than the dose limit of 15 mrem per year, as established by section 191.15. This demonstration incorporated the provisions of sections 194.51 and 194.52, which require the DOE to identify the location of maximum potential exposure for an individual on the surface, consider all potential exposure pathways, and assume that drinking water from any contaminated underground source is consumed at the rate of two liters per day.

To demonstrate a reasonable expectation that the undisturbed performance of the WIPP will not exceed 15 mrem per year, the DOE showed that even a highly improbable, conservative case will meet the regulatory requirements, thereby suggesting that any more probable case must also be in compliance. The DOE referred to this approach as a "bounding" dose calculation because it identified an upper bound to possible exposures. The DOE's analysis is presented in the Compliance Certification Application (CCA) (U.S. DOE 1996), Chapter 8.0, Section 8.1.2.2. Supplemental analyses were also performed and are described in U.S. DOE 1997.

In the DOE's analysis, an individual receives the highest dose if one assumes that the individual consumes drinking water directly from a well in the Salado Formation located at the WIPP Land Withdrawal Boundary. The DOE assumed that an individual would receive the maximum estimated dose regardless of location on the surface and calculated the resultant doses accordingly. The EPA found this approach to be conservative and found the DOE in compliance with section 194.51.

To demonstrate compliance with section 194.52, the DOE had to assume that an individual consumes two liters per day of drinking water from any USDW from the Salado outside the WIPP controlled area. The DOE considered three ingestion pathways and one inhalation pathway:

- An individual consumes drinking water directly from the Salado.
- An individual ingests plants irrigated with contaminated water.
- An individual ingests milk and beef from cattle that consumed water from a stock pond that contained contaminated water from the Salado.
- An individual inhales dust from soil irrigated with contaminated water from the Salado.

Intended to result in the maximum dose, the DOE's assumption that water is ingested directly from the Salado is conservative, because Salado water is highly saline and would have to be greatly diluted to function as drinking or irrigation water.

The EPA determined that the DOE complied with section 194.52 because the DOE considered all potential exposure pathways and assumed that an individual consumes two liters of Salado water per day, following dilution to make the water usable (U.S. EPA 1998a).

A complete description of the EPA's 1998 Certification Decision for sections 194.51 and 194.52 is provided in the EPA's final certification decision (U.S. EPA 1998a) and in U.S. EPA Compliance Application Review Document (CARD) 51/52 (U.S. EPA 1998b).

51.4 Changes in the CRA-2004

In its 2004 Compliance Recertification Application (CRA-2004) (U.S. DOE 2004), the DOE did not report any significant changes to the information on which the EPA based its 1998 certification decision of compliance with the requirements of sections 194.51 and 194.52.

The compliance assessment combines the results of the PA (for the undisturbed case) with the dose calculation. The DOE did not modify the CCA dose-bounding calculations for the compliance assessment in the CRA-2004. Releases predicted by the CRA-2004 PAs are less than or similar to those predicted by the CCA PA results; therefore, the EPA concurred that the CCA dose bounding calculations did not need to be reexecuted for the CRA-2004 compliance assessment.

51.5 EPA's Evaluation of Compliance for the 2004 Recertification

Based on the EPA's review of the activities and conditions in and around the WIPP site, the EPA did not identify any significant changes in the consideration of the protected individual and exposure pathways (see the CRA-2004, Chapter 8.0). The EPA concluded that the CRA-2004 adequately describes the location of the protected individual and the potential exposure pathways (CARD 51/52, U.S. EPA 2006a).

During its review of the CRA-2004, the EPA received no public comments on the DOE's continued compliance with the certification criteria of sections 194.51 and 194.52.

Based on a review and evaluation of the CRA-2004 and supplemental information provided by the DOE, the EPA determined that the DOE continued to comply with the requirements of sections 194.51 and 194.52 (U.S. EPA 2006a and U.S. EPA 2006b).

51.6 Changes or New Information Between the CRA-2004 and the CRA-2009 (Previously: Changes or New Information Since the 2004 Recertification)

In support of the CRA-2009 (U.S. DOE 2009), the DOE reviewed and updated information provided in the CCA and the CRA-2004, Chapter 8.0, Individual and Groundwater Protection Requirements. The updated material was provided as Appendix IGP-2009. Changes or new information pertaining to the update are listed below.

1. The CRA-2009 evaluation showed that with undisturbed performance, only 1 of the 300 modeling system realizations resulted in radionuclide concentrations greater than zero reaching the accessible environment through the anhydrite interbeds in the Salado. The remaining 299 realizations showed no radionuclides reaching the accessible environment during the 10,000-year period (Appendix PA-2009, Section PA-7.2). In the case of the single realization showing releases to the accessible environment, the resulting calculated dose was an order of magnitude less than the value reported in the CCA (Appendix IGP-2009, Section

IGP-2.1). Accordingly, the CCA calculations bound the CRA-2009 results and demonstrated continued compliance with the 40 CFR § 191.15(a) individual protection standard (see Appendix IGP-2009, Section IGP-1.0).

2. To update the evaluation of the presence of any USDW at or near the WIPP, information pertaining to several new boreholes was presented in Appendix IGP-2009. Relevant data pertaining to total dissolved solids concentrations and water pumping rates were provided. An evaluation of the data from the new boreholes resulted in no new or changed conclusions regarding the presence of USDWs in the WIPP vicinity (see Appendix IGP-2009, Section IGP 3.2).

3. An updated evaluation of maximum potential radium-226 (^{226}Ra) and ^{228}Ra concentrations was provided in Appendix IGP-2009. The results of this evaluation indicated that the maximum concentration at the accessible environment boundary would be well below the 5-picocurie-per-liter (pCi/L) regulatory limit imposed by 40 CFR 141.66(b); therefore, continued compliance with the 40 CFR § 191 Subpart C groundwater protection standard was demonstrated (see Appendix IGP-2009, Section IGP-3.3.2).

4. For the CRA-2009 evaluation, the gross alpha particle activity, including ^{226}Ra and excluding radon and uranium at the boundary of the accessible environment, was expected to be essentially 0.07 pCi/L (equivalent to the concentration calculated for the CRA-2004). This compared with the standard imposed by 40 CFR 141.66(c) of 15 pCi/L. Continued compliance with the 40 CFR 191 Subpart C groundwater protection standard was demonstrated (see Appendix IGP-2009, Section IGP-3.3.3).

5. For the CRA-2009 evaluation, the maximum radionuclide concentration in the accessible environment was one order of magnitude less than the maximum bounding CCA value (Appendix IGP-2009, Section IGP-2.1). As such, resulting doses for the CRA-2009 case would be correspondingly lower and continued compliance with the 40 CFR § 191.15(a) annual dose equivalent standard was demonstrated (see Appendix IGP-2009, Section IGP-3.3.4).

6. The CCA compliance assessments assumed that an individual resides at the single geographic point on the surface of the accessible environment where that individual would be expected to receive the highest dose of radionuclide releases from the disposal system. Potential releases calculated for the CRA-2009 compliance assessment are less than those calculated for the CCA. Therefore the CCA dose calculation is bounding, and a new dose calculation was unnecessary for the CRA-2009 (see Appendix IGP-2009, Section IGP 4.0).

7. The CCA and CRA-2009 compliance assessments evaluated all potential exposure pathways from the disposal system to individuals. The assessments also included an assumption that individuals consume two liters per day of drinking water from any USDW in the accessible environment (see Appendix IGP-2009, Section IGP-2.2.2).

The DOE continued to comply with the provisions of sections 194.51 and 194.52 (see Appendix IGP-2009, Section IGP-4.0).

51.7 EPA's Evaluation of Compliance for the 2009 Recertification

Based on the EPA's review of the CRA-2009 and activities and conditions in and around the WIPP site, the EPA did not identify any significant changes in the consideration of the protected individual and exposure pathways. The EPA concluded that the CRA-2009 adequately describes the location of the protected individual and the potential exposure pathways (CARD 51/52, U.S. EPA 2010a).

During its review of the CRA-2009, the EPA received no public comments on the DOE's continued compliance with the certification criteria of sections 194.51 and 194.52.

Based on a review and evaluation of the CRA-2009 and supplemental information provided by the DOE, the EPA determined that the DOE continued to comply with the requirements of sections 194.51 and 195.52 (U.S. EPA 2010a and U.S. EPA 2010b).

51.8 Changes or New Information Since the CRA-2009

In support of the CRA-2014, the DOE reviewed and updated information provided in the CCA and previous CRA's sections relating to Individual and Groundwater Protection Requirements. The updated material is provided in Appendix IGP-2014. Changes or new information pertaining to the update are listed below.

1. The CRA-2014 evaluation showed that for the undisturbed performance scenario, none of the 300 modeling system realizations resulted in radionuclide concentrations greater than zero reaching the accessible environment through the anhydrite interbeds in the Salado Formation over the 10,000-year compliance period (Appendix PA-2014, Section PA-7.2). As with all previous CRAs, the CCA calculations bound the CRA-2014 results and are used to demonstrate continued compliance with the 40 CFR § 191.15(a) individual protection standard (see Appendix IGP-2014, Section IGP-1.0).

2. Because there were no realizations with concentrations greater than zero reaching the accessible environment, an updated evaluation of maximum potential ^{226}Ra and ^{228}Ra concentrations was unnecessary and was not provided in Appendix IGP-2014. Therefore, the PA results demonstrate continued compliance with the 40 CFR § 141.66(b) groundwater protection standard because they are below the 5-pCi/L regulatory limit (see Appendix IGP-2014, Section IGP-3.3.2).

3. For the CRA-2014 evaluation, the gross alpha particle activity, including ^{226}Ra and excluding radon and uranium at the boundary of the accessible environment, was zero. Continued compliance with the groundwater protection standard limit defined in 40 CFR § 141.66(c) of 15 pCi/L was demonstrated (see Appendix IGP-2014, Section IGP-3.3.3).

4. The bounding CCA compliance assessments assumed that an individual resides at the single geographic point on the surface of the accessible environment where that individual would be expected to receive the highest dose of radionuclide releases from the disposal system. Potential releases calculated for the CRA-2014 compliance assessment are zero and therefore less than those calculated for the CCA. As has been done for all previous CRAs, the CCA

dose calculation is used as the bounding case and a new dose calculation is unnecessary for the CRA-2014 (see Appendix IGP-2014, Section IGP 4.0).

5. The bounding CCA compliance assessments evaluate all potential exposure pathways from the disposal system to individuals. The assessments also included an assumption that individuals consume two liters per day of drinking water from any USDW in the accessible environment (see Appendix IGP-2009, Section IGP-2.2.2).

The DOE believes the information provided in this section demonstrates continued compliance with the requirements of 40 CFR 194.51 and 194.52 (see Appendix IGP-2014, Section IGP-4.0).

51.9 References

(*Indicates a reference that has not been previously submitted.)

U.S. Department of Energy (DOE). 1996. *Title 40 CFR Part 191 Compliance Certification Application for the Waste Isolation Pilot Plant* (October). 21 vols. DOE/CAO-1996-2184. Carlsbad, NM: Carlsbad Area Office.

U.S. Department of Energy (DOE). 1997. *Analysis Report for Estimating Dose from Cattle, Vegetable Consumption, and Inhalation Pathways Utilizing Contaminated Water from the Top of the Salado, Culebra, and Selected Marker Beds for an Undisturbed Case Supporting Review of the Compliance Certification Application (Version 1.01)*. ERMS 243298. Albuquerque, NM: Sandia National Laboratories.

U.S. Department of Energy (DOE). 2004. *Title 40 CFR Part 191 Compliance Recertification Application for the Waste Isolation Pilot Plant (March)*. 10 vols. DOE/WIPP 2004-3231. Carlsbad, NM: Carlsbad Field Office.

U.S. Department of Energy (DOE). 2009. *Title 40 CFR Part 191 Compliance Recertification Application for the Waste Isolation Pilot Plant* (March). DOE/WIPP 09-2434. Carlsbad, NM: Carlsbad Field Office.

U.S. Environmental Protection Agency (EPA). 1993. "40 CFR Part 191: Environmental Radiation Protection Standards for the Management and Disposal of Spent Nuclear Fuel, High-Level and Transuranic Radioactive Wastes; Final Rule." *Federal Register*, vol. 58 (December 20, 1993): 66398–416.

U.S. Environmental Protection Agency (EPA). 1996. "40 CFR Part 194: Criteria for the Certification and Determination of the Waste Isolation Pilot Plant's Compliance with Environmental Standards for the Management and Disposal of Spent Nuclear Fuel, High-Level and Transuranic Radioactive Wastes; Final Rule." *Federal Register*, vol. 61 (February 9, 1996): 5223–45.

U.S. Environmental Protection Agency (EPA). 1998a. "40 CFR Part 194: Criteria for the Certification and Recertification of the Waste Isolation Pilot Plant's Compliance with the Disposal Regulations: Certification Decision; Final Rule." *Federal Register*, vol. 63 (May 18, 1998): 27353–406.

U.S. Environmental Protection Agency (EPA). 1998b. "CARD No. 51/52: Consideration of Protected Individual/Exposure Pathways." *Compliance Application Review Documents for the Criteria for the Certification and Recertification of the Waste Isolation Pilot Plant's Compliance with the 40 CFR 191 Disposal Regulations: Final Certification Decision* (May) (pp. 51-1 through 51-11). Washington, DC: Office of Radiation and Indoor Air.

U.S. Environmental Protection Agency (EPA). 2006a. "Recertification CARD Nos. 51/52: Consideration of Protected Individual and Exposure Pathways." *Compliance Application Review Documents for the Criteria for the Certification and Recertification of the Waste Isolation Pilot Plant's Compliance with the 40 CFR 191 Disposal Regulations: Final Recertification Decision* (March) (pp. 51/52-1 through 51/52-3). Washington, DC: Office of Radiation and Indoor Air.

U.S. Environmental Protection Agency (EPA). 2006b. "40 CFR Part 194: Criteria for the Certification and Recertification of the Waste Isolation Pilot Plant's Compliance with the Disposal Regulations: Recertification Decision" (Final Notice). *Federal Register*, vol. 71 (April 10, 2006): 18010–021.

U.S. Environmental Protection Agency (EPA). 2010a. "Recertification CARD Nos. 51/52: Consideration of Protected Individual and Exposure Pathways." *2009 Compliance Recertification Application (2009 CRA) Compliance Application Review Documents (CARD) Nos. 51/52.* EPA Docket FDMS Docket ID No. EPA-HQ-OAR-2009-0330 (November 18, 2010). Washington, DC: Office of Radiation and Indoor Air.*

U.S. Environmental Protection Agency (EPA). 2010b. "40 CFR Part 194 Criteria for the Certification and Recertification of the Waste Isolation Pilot Plant's Compliance with the Disposal Regulations: Recertification Decision; Final Notice." *Federal Register*, vol. 75 (November 18, 2010): 70584 - 595.*

Title 40 CFR Part 191
Subparts B and C
Compliance Recertification Application 2014
for the
Waste Isolation Pilot Plant

Consideration of Underground Sources of Drinking Water (40 CFR § 194.53)

United States Department of Energy
Waste Isolation Pilot Plant

Carlsbad Field Office
Carlsbad, New Mexico

Compliance Recertification Application 2014
Consideration of Underground Sources of Drinking Water
(40 CFR § 194.53)

Table of Contents

This page intentionally left blank.

Acronyms and Abbreviations

CARD	Compliance Application Review Document
CCA	Compliance Certification Application
CFR	Code of Federal Regulations
CRA	Compliance Recertification Application
DOE	U.S. Department of Energy
EPA	U.S. Environmental Protection Agency
gpm	gallons per minute
L	liters
ppm	parts per million
TDS	total dissolved solids
USDW	Underground Source of Drinking Water
WIPP	Waste Isolation Pilot Plant

This page intentionally left blank.

53.0 Consideration of Underground Sources of Drinking Water (40 CFR § 194.53)

53.1 Requirements

> §194.53 Consideration of Underground Sources of Drinking Water
> In compliance assessments that analyze compliance with part 191, subpart C of this chapter, all underground sources of drinking water in the accessible environment that are expected to be affected by the disposal system over the regulatory time frame shall be considered. In determining whether underground sources of drinking water are expected to be affected by the disposal system, underground interconnections among bodies of surface water, groundwater, and underground sources of drinking water shall be considered.

53.2 Background

40 CFR § 194.53 (U.S. EPA 1996) requires the U.S. Department of Energy (DOE) to consider, in compliance assessments, underground sources of drinking water (USDWs) near the Waste Isolation Pilot Plant (WIPP) and their interconnections. A USDW is defined in 40 CFR §191.22 (U.S. EPA 1993) as "an aquifer or its portion which: (1) Supplies any public water system, or (2) Contains a sufficient quantity of ground water to supply a public water system; and (i) Currently supplies drinking water for human consumption; or (ii) Contains fewer than 10,000 milligrams of total dissolved solids per liter." The groundwater protection requirements limit releases to the maximum contamination level established in the Safe Drinking Water Act Regulations at 40 CFR Part 141 as they existed on January 19, 1994.

53.3 1998 Certification Decision

The Compliance Certification Application (CCA) (U.S. DOE 1996), Chapter 8.0, discusses the assumptions and approaches used to consider USDWs and the uncertainty associated with the analyses. The DOE provided detailed information on the location and nature of the USDWs, indicated the estimated concentrations of radionuclides in a hypothetical USDW in the accessible environment, and showed that the maximum contamination levels for radionuclides will not be exceeded during the regulatory time period.

In the CCA, the DOE presented an evaluation of the USDWs near the WIPP that could potentially be affected by the disposal system over the regulatory time frame. This information was included in the CCA, Chapter 8.0, Section 8.2, and Appendix USDW, Section USDW.3. Based on the definitions in section 191.22, the DOE identified three subcriteria to determine whether a water-bearing horizon located within the WIPP-controlled area would qualify as a USDW:

1. A minimum pumping rate of five gallons per minute (gpm)
2. A supply of water at a rate of five gpm for a 40-year period
3. A maximum of 10,000 milligrams per liter (10,000 parts per million [ppm]) of total dissolved solids (TDS)

These requirements characterize the capacity and quality of a public water system. A public water system is defined in section 191.22 as a system providing piped water for human consumption to 25 individuals, or one that has at least 15 service connections.

Applying these criteria, the DOE identified the Culebra Dolomite Member of the Rustler Formation (hereafter referred to as Culebra), the Dewey Lake Formation, and the Santa Rosa Formation as potential USDWs. The DOE conducted a bounding analysis of the contaminants' concentrations to assess compliance with 40 CFR Part 191, Subpart C. In this analysis, the DOE assumed 10,000 ppm TDS, which is much less than the observed concentration of brine derived from the Salado anhydrite marker beds. A USDW was also assumed to be present at and beyond the WIPP Land Withdrawal Boundary. The DOE indicated in the CCA, Chapter 8.0, Section 8.3, that the bounding analysis showed that the resulting radionuclide concentrations in the USDWs would be less than half the maximum limit specified in Part 141 (the U.S. Environmental Protection Agency's [EPA's] National Primary Drinking Water Standards), and the dose to a receptor drinking from the USDW would be a factor of 10 less than the individual protection standard.

The DOE believed the assumption that all contaminants reaching the accessible environment are directly available to the receptor is not realistic but conservative, because this results in overestimating potential doses to an individual. The DOE's findings indicated that even with this conservative approach, the estimated potential dose to an individual was below the Part 191 requirements. The CCA analysis also assumed that all contaminants reaching the accessible environment were directly available to the receptor so that the interconnections of surface, ground, and underground drinking water were all considered and treated as a single source.

The EPA examined the DOE's approach and assumptions associated with the USDW determination in the CCA. The EPA found the analyses to be well supported and accurate, including the uncertainty associated with these analyses. In addition, the EPA assessed all possible aquifers to determine how USDWs were identified and discussed in the CCA. The EPA also examined whether the flow rates and directions were included in the description. The modeling assumptions and specifications for the bounding analysis were examined to assess reliability and assurance of safety. The EPA reviewed the estimated concentrations of radionuclides to determine if they complied with the groundwater protection standard (see CCA Compliance Application Review Document [CARD] 53 (U.S EPA 1998) for details of the EPA's CCA review).

The EPA found that the DOE's determination of the USDWs was in accordance with definitions contained in section 191.22 and with the compliance criteria in section 194.53. The bounding analysis was performed with conservative assumptions for a hypothetical USDW to estimate contamination and potential doses to a receptor.

A complete description of the EPA's 1998 Certification Decision for section 194.53 is provided in CARD 53 (U.S. EPA 1998).

53.4 Changes in the CRA-2004

In the 2004 Compliance Recertification Application (CRA-2004) (U.S. DOE 2004), Chapter 8.0, the DOE updated some aspects of the USDW analysis. The DOE updated the data for groundwater quantity determination to define a USDW. In the CCA, the DOE used 1990 census data to determine the average water usage per person per day of 1067 liters (L) (282 gallons). (In the CRA-2004, the DOE used 2000 census data to determine that the average water usage per person per day had increased to 1155 L (305 gallons). The DOE did not believe it was necessary to change the subcriterion of a 5 gpm rate of production from a well to define a USDW (see the CRA-2004, Chapter 8.0, Section 8.2.1.1).

The DOE monitored and evaluated new wells drilled in the area since the completion of the CCA. A new well, C-2737, was drilled to replace H-1 in 2001. Water sampled from the Dewey Lake Formation showed 2,590 ppm TDS. Additional wells were drilled at the WIPP site to investigate the extent of groundwater at the contact of the Santa Rosa and Dewey Lake Formations. The groundwater samples indicated TDS at both below and above 10,000 ppm TDS. The DOE was unable to pump water from any one of these boreholes at a rate of 5 gpm or more.

The updates and changes made by the DOE in the CRA-2004 did not significantly impact the conclusions regarding USDWs in the CCA. In the CRA-2004, the DOE continued to identify the Culebra, Dewey Lake, and Santa Rosa as the only potential USDWs. The DOE stated that the conservative bounding analysis used for the 1998 Certification Decision compliance assessment was still applicable (see the CRA-2004, Chapter 8.0, Section 8.2.1.1).

53.5 EPA's Evaluation of Compliance for the 2004 Recertification

The EPA evaluated the information on the USDWs contained in the CRA-2004, Chapter 8.0 and examined data from the new wells drilled within the study area since the 1998 Certification Decision. The EPA determined that the DOE applied adequately conservative assumptions to the data for a hypothetical USDW to determine compliance with section 194.53.

Because of the lack of significant changes to the parameters for the protected individual, the potential exposure pathways, and the USDWs, the EPA agreed that the bounding analysis performed for the dose calculation in the CCA still applied. See CRA-2004 CARD 55 (U.S. EPA 2006) for more information on the results of the compliance assessment.

The EPA received no public comments on the DOE's continued compliance with the consideration of USDW requirements in section 194.53.

Based on a review and evaluation of the CRA-2004 and supplemental information provided by the DOE, the EPA determined that the DOE continued to comply with the requirements of section 194.53.

53.6 Changes or New Information Between the CRA-2004 and the CRA-2009 (Previously: Changes or New Information Since the 2004 Recertification)

In support of the CRA-2009 (U.S. DOE 2009), the DOE reviewed and updated information provided in the CCA and the CRA-2004, Chapter 8.0, Individual and Groundwater Protection Requirements. The updated material was provided as Appendix IGP-2009. Changes or new information pertaining to the update were as follows:

1. Updated information regarding average household water consumption in communities near the WIPP was obtained from the New Mexico Office of the State Engineer to assess the continued appropriateness of criteria for making USDW determinations. The updated information was included in Appendix IGP-2009, Section IGP-3.1.1. A review of these new data indicated that no change in the criteria for making USDW determinations was warranted.

2. Several new boreholes were drilled near the WIPP since the CRA-2004. These include wells to further characterize flow characteristics in the Culebra and to better understand shallow groundwater flow near the WIPP salt storage piles. Detail regarding these new wells was included in Appendix IGP-2009, Section IGP-3.2. Data from these wells indicated that no changes to the previous USDW determinations were warranted.

3. Based on the review of available data in support of the CRA-2009, the DOE concluded that no modification of the USDW determinations reported in the CCA, Chapter 8.0 and Appendix USDW was warranted (see Appendix IGP-2009, Section IGP-3.2). The DOE continued to conclude that USDWs are present in the Culebra, and potential USDWs are present in the Dewey Lake and the Santa Rosa. Based on this, the DOE concluded that all USDWs in the accessible environment expected to be affected by the disposal system over the regulatory time frame had been considered. In addition, the DOE approach ensured that underground interconnections among bodies of surface water, groundwater, and USDWs were considered.

Based on these considerations, the DOE believed that continued compliance with the provisions of section 194.53 was demonstrated for the CRA-2009.

53.7 EPA's Evaluation of Compliance for the 2009 Recertification

The EPA evaluated the information on USDWs contained in the CRA-2009, Section 53 and Appendix IGP-2009. The EPA examined the data from the new wells drilled within the study area since the 1998 Certification and the 2004 Recertification Decisions and determined that the DOE applied adequately conservative assumptions to determine compliance with 40 CFR 194.53.

The EPA concurred that there were no significant changes to the parameters for the protected individual, the potential exposure pathways, or the sources of underground drinking water. The EPA determined that the bounding analysis that was performed for the dose calculation in the CCA still applied. For the CRA-2009 evaluation (Appendix IGP-2009), the DOE noted that the maximum potential dose remained below the CCA value and continued compliance with the

individual protection standard was maintained. The EPA concurred that the potential concentrations of contaminants in the hypothetical USDW and the maximum potential dose to a receptor that drinks from the hypothetical USDW continued to be bounded by the CCA analysis results.

The EPA did not receive any public comments on the DOE's continued compliance with the consideration of underground sources of drinking water requirements of section 194.53.

Based on the EPA's review of the CRA-2009 and supplemental information provided by the DOE, the EPA determined that the DOE continued to comply with the requirements of section 194.53 (U.S. EPA 2010a and U.S. EPA 2010b).

53.8 Changes or New Information Since the CRA-2009

In support of the CRA-2014, the DOE reviewed and updated information provided in the CCA and previous CRA's individual and groundwater protection requirements. The updated material is provided as Appendix IGP-2014. Changes or new information pertaining to the update are as follows:

1. Updated information regarding average household water consumption in communities near the WIPP was obtained from the latest census to assess the continued appropriateness of criteria for making USDW determinations. The updated information is included in Appendix IGP-2014, Section IGP-3.1.1. A review of these new data indicated that no change in the criteria for making USDW determinations is warranted.

2. There were no new boreholes drilled at new locations since the CRA-2009. Five existing wells were plugged and replaced with new wells at the same locations. No new information relating to USDW was generated (see also Appendix HYDRO-2014, Section HYDRO-4.0).

3. No additional USDW investigations were performed as part of the CRA-2014 (see Appendix IGP-2014). Based on this review, no modification of the USDW determinations reported in the CCA, Appendix USDW is warranted. The DOE continues to conclude that there are no USDWs at the site boundary. In the vicinity of the WIPP, USDWs are present in the Culebra, and potential USDWs are present in the Dewey Lake and the Santa Rosa. Based on this, the DOE concludes that all USDWs in the accessible environment expected to be affected by the disposal system over the regulatory time frame have been considered. In addition, the DOE approach ensured that underground interconnections among bodies of surface water, groundwater, and USDWs were considered.

Based on these considerations, the DOE believes that continued compliance with the provisions of section 194.53 is demonstrated.

53.9 References

(*Indicates a reference that has not been previously submitted.)

U.S. Department of Energy (DOE). 1996. *Title 40 CFR Part 191 Compliance Certification Application for the Waste Isolation Pilot Plant* (October). 21 vols. DOE/CAO-1996-2184. Carlsbad, NM: Carlsbad Area Office.

U.S. Department of Energy (DOE). 2004. *Title 40 CFR Part 191 Compliance Recertification Application for the Waste Isolation Pilot Plant* (March). 10 vols. DOE/WIPP 2004-3231. Carlsbad, NM: Carlsbad Field Office.

U.S. Department of Energy (DOE). 2009. *Title 40 CFR Part 191 Compliance Recertification Application for the Waste Isolation Pilot Plant* (March). DOE/WIPP 09-2434. Carlsbad, NM: Carlsbad Field Office.

U.S. Environmental Protection Agency (EPA). 1993. "40 CFR Part 191 Environmental Radiation Protection Standards for the Management and Disposal of Spent Nuclear Fuel, High-Level and Transuranic Radioactive Wastes; Final Rule." *Federal Register*, vol. 58 (December 20, 1993): 66398–416.

U.S. Environmental Protection Agency (EPA). 1996. "40 CFR Part 194: Criteria for the Certification and Recertification of the Waste Isolation Pilot Plant's Compliance With the 40 CFR Part 191 Disposal Regulations; Final Rule." *Federal Register*, vol. 61 (February 9, 1996): 5223–45.

U.S. Environmental Protection Agency (EPA). 1998. "CARD No. 53: Consideration of Underground Sources of Drinking Water." *Compliance Application Review Documents for the Criteria for the Certification and Recertification of the Waste Isolation Pilot Plant's Compliance with the 40 CFR 191 Disposal Regulations: Final Certification Decision* (May) (pp. 53-1 through 53-6). Washington, DC: Office of Radiation and Indoor Air.

U.S. Environmental Protection Agency (EPA). 2006. "Recertification CARD No. 55: "Results of Compliance Assessments." *Compliance Application Review Documents for the Criteria for the Certification and Recertification of the Waste Isolation Pilot Plant's Compliance with the 40 CFR 191 Disposal Regulations: Final Recertification Decision* (March) (pp. 55-1 through 55-6). Washington, DC: Office of Radiation and Indoor Air.

U.S. Environmental Protection Agency (EPA). 2010a. "Recertification CARD Nos. 53: Consideration of Underground Sources of Drinking Water." *2009 Compliance Recertification Application (2009 CRA) Compliance Application Review Documents (CARD) Nos. 53.* EPA Docket FDMS Docket ID No. EPA-HQ-OAR-2009-0330 (November 18, 2010). Washington, DC: Office of Radiation and Indoor Air.*

U.S. Environmental Protection Agency (EPA). 2010b. "40 CFR Part 194 Criteria for the Certification and Recertification of the Waste Isolation Pilot Plant's Compliance with the Disposal Regulations: Recertification Decision; Final Notice." *Federal Register*, vol. 75 (November 18, 2010): 70584 - 595.*

Title 40 CFR Part 191
Subparts B and C
Compliance Recertification Application 2014
for the
Waste Isolation Pilot Plant

Scope of Compliance Assessments
(40 CFR § 194.54)

United States Department of Energy
Waste Isolation Pilot Plant

Carlsbad Field Office
Carlsbad, New Mexico

Compliance Recertification Application 2014
Scope of Compliance Assessments
(40 CFR § 194.54)

Table of Contents

This page intentionally left blank.

Acronyms and Abbreviations

CARD	Compliance Application Review Document
CCA	Compliance Certification Application
CFR	Code of Federal Regulation
CRA	Compliance Recertification Application
DOE	U.S. Department of Energy
EPA	U.S. Environmental Protection Agency
FEP	feature, event, and process
PA	performance assessment
WIPP	Waste Isolation Pilot Plant

This page intentionally left blank.

54.0 Scope of Compliance Assessments (40 CFR § 194.54)

54.1 Requirements

§ 194.54 Scope of Compliance Assessments

(a) Any compliance application shall contain compliance assessments required pursuant to this part. Compliance assessments shall include information which:

(1) Identifies potential processes, events, or sequences of processes and events that may occur over the regulatory time frame;

(2) Identifies the processes, events, or sequences of processes and events included in compliance assessment results provided in any compliance application; and

(3) Documents why any processes, events, or sequences of processes and events identified pursuant to paragraph (a)(1) of this section were not included in compliance assessment results provided in any compliance application.

(b) Compliance assessments of undisturbed performance shall include the effects on the disposal system of:

(1) Existing boreholes in the vicinity of the disposal system, with attention to the pathways they provide for migration of radionuclides from the site; and

(2) Any activities that occur in the vicinity of the disposal system prior to or soon after disposal. Such activities shall include, but shall not be limited to: Existing boreholes and the development of any existing leases that can be reasonably expected to be developed in the near future, including boreholes and leases that may be used for fluid injection activities.

54.2 Background

The individual and groundwater protection requirements (40 CFR § 191.15 and 40 CFR Part 191 Subpart C [U.S. EPA 1993]) place limitations on both the potential radiation exposure of individuals and the possible levels of radioactive contamination of groundwater resulting from disposal of waste in the Waste Isolation Pilot Plant (WIPP). The individual protection criteria of 40 CFR § 194.54 (U.S. EPA 1996) focuses on the annual radiation dose of a maximally exposed hypothetical person living on the surface just outside the boundary to the accessible environment.

In contrast to the containment requirements, the individual and groundwater protection requirements apply to the potential doses received by an individual over a human lifespan. Moreover, compliance assessments utilized to demonstrate compliance with the individual and groundwater protection requirements consider performance of the repository in the "undisturbed scenario," that is, without any human intrusion.

As with performance assessments (PAs), compliance assessments must consider features, events, and processes (FEPs) and the uncertainties associated with those FEPs. PAs are used to demonstrate compliance with the containment requirements of 40 CFR § 191.13 (U.S. EPA 1993). Compliance assessments may be regarded as a "subset" of PAs, inasmuch as the latter incorporate FEPs related to undisturbed conditions that are necessary for the compliance assessment. The results of the PAs are used as input values to the compliance assessments. Section 194.54 contains the criteria for assessments of the WIPP's compliance with the individual dose and groundwater protection requirements.

54.3 1998 Certification Decision

Per 40 CFR § 194.54(a), the U.S. Department of Energy (DOE) included in the Compliance Certification Application (CCA) (U.S. DOE 1996) a comprehensive list of FEPs evaluated through the compliance assessment. The U.S. Environmental Protection Agency (EPA) reviewed the DOE's initial FEP list to determine whether it was comprehensive in the CCA. The EPA examined information sources used by the DOE to compile FEP lists for technical accuracy. The EPA also examined FEP listings to determine whether the DOE's rationale for reducing the number of FEPs was appropriately documented and technically sufficient. The EPA concluded that the DOE adequately identified and considered any natural processes or events that may occur within the regulatory time frame in the WIPP area.

The EPA reviewed the CCA, Appendix SCR; numerous references; and FEP screening record packages. To evaluate compliance with 40 CFR § 194.54(b), the EPA reviewed the DOE's arguments concerning natural flow through abandoned boreholes within the Land Withdrawal Boundary, including natural fluid head conditions, abandonment techniques, and number and location of abandoned boreholes. The EPA concluded that the DOE's screening arguments and documentation were reasonable.

In accordance with section 194.54(b), the EPA's detailed review of the CCA indicated that the DOE appropriately screened the FEPs, although the limited justification of some FEPs required additional evaluation. The EPA ultimately concluded that the DOE appropriately identified and screened FEPs pertaining to undisturbed performance. The EPA concluded that criteria for screening FEPs were adequately described and implemented. Also, the EPA concluded that the DOE appropriately identified and discussed the effects of the sequences and combinations of FEPs that resulted in modeled scenarios.

In the CCA, the DOE screened out the possibility that oil and gas extraction would affect the WIPP based upon low consequence. The EPA concurred with the DOE's decision and concluded that the FEP screening appropriately considered the possibility of both subsidence and pressure gradients due to oil and gas extraction. The EPA concluded that the DOE considered the appropriate issues, and that the technical conclusions reached by the DOE regarding current and near-future screening of oil and gas extraction activities were valid. (See *Technical Support Document for* 40 CFR § *194.32: Fluid Injection Analysis*, U.S. EPA 1998a, for detailed results of the EPA's analysis. See Compliance Application Review Document [CARD] 32, U.S. EPA 1998b, for a discussion of the EPA's analysis of fluid injection.) A complete description of the EPA's 1998 Certification Decision for section 194.54 can be found in U.S. EPA 1998c.

Also in regard to section 194.54(b) for the CCA, the DOE screened out induced system changes due to hydrocarbon storage operations that have occurred thus far in the vicinity of the WIPP site, based on low consequence. The EPA concluded that this screening was appropriate. Although the DOE did not specify oil and gas field lifetimes in detail for each field near the WIPP in the CCA, Appendix DEL, the EPA found that it was possible to derive the expected active lifetimes of oil and gas fields from information presented in that appendix. The EPA agreed that the lease life estimation values presented in the CCA were reasonable, although the EPA asked the DOE to consider the effects of longer injection periods (Trovato 1997). In response, the DOE performed a second analysis applying more conservative assumptions,

including longer injection periods. The second analysis supported the conclusion of the earlier screening evaluations (Stoezel and Swift 1997).

54.4 Changes in the CRA-2004

The 2004 Compliance Recertification Application (CRA-2004) (U.S. DOE 2004) did not report significant changes related to the section 194.54 criteria. In the CCA, the DOE screened in 67 undisturbed performance FEPs. The DOE added three FEPs as a result of its CRA-2004 FEPs reevaluation (see Appendix PA-2004, Attachment SCR): Organic Complexation (W68), Organic Ligands (W69), and Surface Disruptions (H41). FEPs W68 and W69 were added because information acquired since the CCA indicates that organic ligands may increase actinide solubilities and should be included in assessments at the WIPP (see Appendix PA-2004, Attachment SCR, Section SCR-6.5.6.1.3). FEP H41 was added because surface activities may impact infiltration, requiring its inclusion in assessments (see Appendix PA-2004, Attachment SCR, Section SCR-5.3.1.2.3). All other undisturbed performance FEPs were unchanged in the CRA-2004; therefore, except for FEPs W68, W69, and H41, the DOE did not change the process, screening arguments, or final decisions related to 67 FEPs in the CCA.

The CRA-2004, Chapter 8.0, Section 8.1.1 documents that the DOE considered existing boreholes and potential boreholes as required by 40 CFR §§ 194.52(b)(1) and 194.52(b)(2) (U.S. EPA 1996). In the CRA-2004, the DOE confirmed that the most plausible undisturbed transport pathway is through the anhydrite marker beds as assumed in the CCA. Therefore, the DOE's approach had not changed since the CCA.

In the CRA-2004, the DOE did not change its dose calculation methodology. The DOE continued to assume an existing borehole (see the CRA-2004, Chapter 8.0, Section 8.1.2.1) and continued to use a bounding analysis (see the CRA-2004, Chapter 8.0, Section 8.1.2.2) if needed. The DOE determined that the maximum release concentrations predicted for undisturbed performance were lower than the CCA predictions; therefore, the new bounding dose calculations were not needed for the CRA-2004. The DOE reconsidered some parameters, such as average water use and its water quality determination, based on information acquired since the CCA (see the CRA-2004, Chapter 8.0, Sections 8.2.1 and 8.2.2). These parameter changes did not change the DOE's analysis.

54.5 EPA's Evaluation of Compliance for the 2004 Recertification

The EPA reviewed DOE compliance with the section 194.54 criteria (CARD 54, U.S. EPA 1998c). The EPA verified that the DOE's FEP development process had not changed since the CCA. The DOE reevaluated CCA FEPs in the CRA-2004, and the EPA found the CRA-2004 process to be reasonable and adequately documented. The EPA found that the DOE adequately identified FEPs that may occur over the regulatory time frame (see the CRA-2004, Chapter 6.0, Section 6.3.1), identified FEPs included in the compliance assessment (see the CRA-2004, Chapter 6.0, Section 6.3.1), and adequately documented why FEPs were not selected (see Appendix PA-2004, Attachment SCR). The EPA also found that the DOE adequately considered existing wells and activities that may occur in the vicinity of the WIPP (see the CRA-2004, Chapter 8.0, Section 8.1.1).

The EPA received no public comments on the DOE's continued compliance with the scope of compliance assessment requirements of section 194.54. After their review, the EPA found that the DOE continued to comply with the requirements of section 195.45 (U.S. EPA 2006).

54.6 Changes or New Information Between the CRA-2004 and the CRA-2009 (Previously: Changes or New Information Since the 2004 Recertification)

There were no significant changes related to the section 194.54 requirements between the CRA-2004 and the CRA-2009.

The screening decisions for the undisturbed performance FEPs did not change for the CRA-2009, but the justification for some screening decisions were changed as described in Appendix SCR-2009 (U.S. DOE 2009).

Appendix IGP-2009, Section IGP-2.1 demonstrated that the DOE continued to consider existing boreholes and potential boreholes as required by sections 194.54(b)(1) and (b)(2). The CRA-2009 PA analysis continued to confirm that the most plausible undisturbed transport pathway is through the anhydrite marker beds, as assumed in the CRA-2004 and the CCA (Appendix IGP-2009, Section IGP-2.2.1). The DOE's approach was not changed.

The DOE did not change its dose calculation methodology. The DOE continued to assume an existing borehole (Appendix IGP-2009, Section IGP-2.2.1) and still applied PA results in a bounding analysis (Appendix IGP-2009, Section IGP-2.2.2). The DOE continued to determine that the maximum release concentrations predicted for undisturbed performance were lower than the CCA predictions; therefore, new bounding dose calculations were not needed for the CRA-2009 (Appendix IGP-2009, Section IGP-2.3). The DOE also reconsidered some parameters, such as average water use and associated water-quantity determinations, based on acquired information since the CRA-2004 (Appendix IGP-2009, Sections IGP-3.1 and IGP-3.2). The new information provided by the DOE in the CRA-2009 did not warrant changes to the analyses.

Based on this information, the DOE believed continued compliance with the requirements of section 194.54 was demonstrated at that time.

54.7 EPA's Evaluation of Compliance for the 2009 Recertification

The EPA reviewed DOE compliance with the section 194.54 criteria (CARD 54, U.S. EPA 2010). The EPA verified that the DOE's FEP development process had not changed since the CCA. The DOE reevaluated FEPs in the CRA-2009, and the EPA found the CRA-2009 process to be reasonable and adequately documented. The EPA found that the DOE adequately identified FEPs that may occur over the regulatory time frame (see Appendix IGP-2009, Section IGP-2.1), identified FEPs included in the compliance assessment, and adequately documented why FEPs were not selected (see Appendix PA-2009 and Appendix SCR-2009). The EPA also found that the DOE adequately considered existing wells and activities that may occur in the vicinity of the WIPP.

The EPA received no public comments on the DOE's continued compliance with the scope of compliance assessment requirements of section 194.54. After its review, the EPA found that the DOE continued to comply with the requirements of section 195.54 (U.S. EPA 2010).

54.8 Changes or New Information Since the CRA-2009

There are no significant changes related to the section 194.54 requirements since the CRA-2009.

The screening decisions for the undisturbed performance FEPs have not changed for the CRA-2014, but the justification for some screening decisions has changed (Appendix SCR-2014).

Appendix IGP-2014, Section IGP-2.1 demonstrates that the DOE continues to consider existing boreholes and potential boreholes as required by sections 194.54(b)(1) and (b)(2). The CRA-2014 PA analysis continues to confirm that the most plausible undisturbed transport pathway is through the anhydrite marker beds, as assumed in previous CRAs and the CCA (Appendix IGP-2014, Section IGP-2.2.1). The DOE's approach to compliance assessments has not changed.

The DOE has not changed its dose calculation methodology. The DOE continues to assume an existing borehole (Appendix IGP-2014, Section IGP-2.2.1) and still applies PA results in a bounding analysis (Appendix IGP-2014, Section IGP-2.2.2). The DOE continues to determine that the maximum release concentrations predicted for undisturbed performance are lower than the CCA predictions; therefore, new bounding dose calculations were not needed for the CRA-2014 (Appendix IGP-2014, Section IGP-2.3). The DOE has also reconsidered some parameters, such as average household water use and associated water-quantity determinations, based on acquired information since the CRA-2009 (Appendix IGP-2014, Sections IGP-3.1 and IGP-3.2). The new information provided by the DOE in this document does not warrant changes to the original analyses.

Based on this information, the DOE believes continued compliance with the requirements of section 194.54 is demonstrated.

54.9 References

(*Indicates a reference that has not been previously submitted.)

Stoezel, D.M. and P.N. Swift. 1997. *Supplementary Analyses of the Effects of Salt Water Disposal and Waterflooding in the WIPP,* Revision 1.0. ERMS 244158. Albuquerque; Sandia National Laboratories.

Trovato, E.R. 1997. *Letter to A. Alm (6 Enclosures).* 19 March 1997. ERMS 245835. Washington, DC: U.S. Environmental Protection Agency, Office of Air and Radiation.

U.S. Department of Energy (DOE). 1996. *Title 40 CFR Part 191 Compliance Certification Application for the Waste Isolation Pilot Plant* (October). 21 vols. DOE/CAO 1996-2184. Carlsbad, NM: Carlsbad Area Office.

U.S. Department of Energy (DOE). 2004. *Title 40 CFR Part 191 Compliance Recertification Application for the Waste Isolation Pilot Plant* (March). 10 vols. DOE/WIPP 2004-3231. Carlsbad, NM: Carlsbad Field Office.

U.S. Department of Energy (DOE). 2009. *Title 40 CFR Part 191 Compliance Recertification Application for the Waste Isolation Pilot Plant* (March). DOE/WIPP-09-3424. Carlsbad, NM: Carlsbad Field Office.*

U.S. Environmental Protection Agency (EPA). 1993. "40 CFR Part 191: Environmental Radiation Protection Standards for the Management and Disposal of Spent Nuclear Fuel, High-Level and Transuranic Radioactive Wastes; Final Rule." *Federal Register*, vol. 58 (December 20, 1993): 66398–416.

U.S. Environmental Protection Agency (EPA). 1996. "40 CFR Part 194: Criteria for the Certification and Recertification of the Waste Isolation Pilot Plant's Compliance with the 40 CFR Part 191 Disposal Regulations; Final Rule." *Federal Register*, vol. 61 (February 9, 1996): 5223–45.

U.S. Environmental Protection Agency (EPA). 1998a. *Technical Support Document for Section 194.32: Fluid Injection Analysis* (May). 3 vols. Washington, DC: Office of Radiation and Indoor Air.

U.S. Environmental Protection Agency (EPA). 1998b. "CARD No. 32: Scope of Performance Assessments." *Compliance Application Review Documents for the Criteria for the Certification and Recertification of the Waste Isolation Pilot Plant's Compliance with the 40 CFR 191 Disposal Regulations: Final Certification Decision* (pp. 32-1 through 32-46) (May). Washington, DC: Office of Radiation and Indoor Air.

U.S. Environmental Protection Agency (EPA). 1998c. "CARD No. 54: Scope of Compliance Assessments." *Compliance Application Review Documents for the Criteria for the Certification and Recertification of the Waste Isolation Pilot Plant's Compliance with the 40 CFR 191 Disposal Regulations: Final Certification Decision* (pp. 54-1 through 54-17) (May). Washington, DC: Office of Radiation and Indoor Air.

U.S. Environmental Protection Agency (EPA). 2006. *Recertification CARD No. 54: Scope of Compliance Assessments* (April). Washington, DC: Office of Radiation and Indoor Air.*

U.S. Environmental Protection Agency (EPA). 2010. *2009 Compliance Recertification Application (2009 CRA) Compliance Application Review Document (CARD) No. 54, Scope of Compliance Assessments*. EPA Docket FDMS Docket ID No. EPA-HQ-OAR-2009-0330. Washington, DC: Office of Radiation and Indoor Air.*

Title 40 CFR Part 191
Subparts B and C
Compliance Recertification Application 2014
for the
Waste Isolation Pilot Plant

Results of Compliance Assessments
(40 CFR § 194.55)

United States Department of Energy
Waste Isolation Pilot Plant

Carlsbad Field Office
Carlsbad, New Mexico

Compliance Recertification Application 2014
Results of Compliance Assessments
(40 CFR § 194.55)

Table of Contents

This page intentionally left blank.

Acronyms and Abbreviations

CARD	Compliance Application Review Document
CCA	Compliance Certification Application
CFR	Code of Federal Regulations
CRA	Compliance Recertification Application
DOE	U.S. Department of Energy
EPA	U.S. Environmental Protection Agency
LHS	Latin hypercube sampling
mrem	millirem
PA	performance assessment
PAVT	Performance Assessment Verification Test
pCi/L	picocuries per liter
USDW	underground source of drinking water
WIPP	Waste Isolation Pilot Plant

Elements and Chemical Compounds

Am	americium
Pu	plutonium
Ra	radium
Rn	radon
Th	thorium
U	uranium

This page intentionally left blank.

55.0 Results of Compliance Assessments (40 CFR § 194.55)

55.1 Requirements

§ 194.55 Results of Compliance Assessments

(a) Compliance assessments shall consider and document uncertainty in the performance of the disposal system.

(b) Probability distributions for uncertain disposal system parameter values used in compliance assessments shall be developed and documented in any compliance application.

(c) Computational techniques which draw random samples from across the entire range of values of each probability distribution developed pursuant to paragraph (b) of this section shall be used to generate a range of:

(1) Estimated committed effective doses received from all pathways pursuant to § 194.51 and § 194.52;

(2) Estimated radionuclide concentrations in USDWs pursuant to § 194.53; and

(3) Estimated dose equivalent received from USDWs pursuant to § 194.52 and § 194.53.

(d) The number of estimates generated pursuant to paragraph (c) of this section shall be large enough such that the maximum estimates of doses and concentrations generated exceed the 99th percentile of the population of estimates with at least a 0.95 probability.

(e) Any compliance application shall display:

(1) The full range of estimated radiation doses; and

(2) The full range of estimated radionuclide concentrations.

(f) Any compliance application shall document that there is at least a 95 percent level of statistical confidence that the mean and the median of the range of estimated radiation doses and the range of estimated radionuclide concentrations meet the requirements of § 191.15 and part 191, subpart C of this chapter, respectively.

55.2 Background

The individual and groundwater protection requirements of 40 CFR § 191.15 and 40 CFR Part 191 Subpart C (U.S. EPA 1993) place limitations on both the potential radiation exposure of individuals and the possible levels of radioactive contamination of groundwater caused by disposal of waste in the Waste Isolation Pilot Plant (WIPP). The criteria for compliance are provided in 40 CFR §§ 194.51 through 194.55 (U.S. EPA 1996). The individual protection requirement focuses on the annual radiation dose of a maximally exposed person living on the surface just outside the Land Withdrawal Act boundary. In particular, section 191.15 requires that the WIPP be constructed in such a manner as to provide a reasonable expectation that, for 10,000 years after disposal, undisturbed performance of the disposal system will not cause the annual committed effective dose equivalent (hereafter called "dose") to exceed 15 millirems (mrem) (150 microsieverts) to any member of the public in the accessible environment. Part 191 Subpart C also requires that underground sources of drinking water (USDWs) be protected at least to the extent prescribed by the Safe Drinking Water Act regulations at 40 CFR Part 141 as they existed on January 19, 1994 (per 40 CFR § 191.24(a)(1)).

55.3 1998 Certification Decision

55.3.1 40 CFR § 194.55(a)

In the Compliance Certification Application (CCA) (U.S. DOE 1996), the U.S. Environmental Protection Agency (EPA) found that the U.S. Department of Energy (DOE) considered uncertainty in two ways: (1) by assigning probability distributions to 57 of the key parameters that describe the repository, and sampling from those distributions to carry out the performance

assessment (PA) (see the CCA, Chapter 6.0, pp. 6-21 to 6-23 and 6-173 to 6-199; and Appendix PAR), and (2) by translating from groundwater contaminant level to doses by means of the bounding analysis (see the CCA, Chapter 8.0, and Dials 1997).

The DOE's method of evaluation of uncertainty in the amounts of contaminants transported underground was essentially the same as that for the 300 scenarios involving human intrusion in the PA, as presented in the CCA, Chapter 6.0, Section 6.1.2, except that those uncertainties introduced by the borehole drilling process can be ignored. The EPA found this aspect of the treatment of uncertainties to be satisfactory.

The EPA reviewed the bounding calculation as presented in the CCA, Chapter 8.0 and supplementary information regarding models and computer codes, parameter values, dose calculations and related topics (Dials 1997) and reported the results of that evaluation in Compliance Application Review Document (CARD) 51/52 (U.S. EPA 1998a). The EPA determined that the DOE's conceptual model and the use of the GENII-A computer code to calculate radiation doses were appropriate. The EPA found this bounding calculation to be acceptable in lieu of further uncertainty analysis (CARD 55, U.S. EPA 1998b).

55.3.2 40 CFR § 194.55(b)

The probability distributions for uncertain disposal system parameter values used for demonstrating compliance with the individual dose and groundwater criteria of section 194.55 are identical to those used for the containment requirements in 40 CFR § 194.34 (U.S. EPA 1996). The EPA concluded that the DOE provided general information in the CCA on probability distributions, data sources for parameter distribution, forms of distributions, bounds, and importance of parameters to releases.

The EPA initially raised concerns about the completeness of the list of PA parameters in the CCA, the descriptions and justifications that support the development of some code input parameters, and the traceability of data reduction and analysis of parameter records. The DOE improved the documentation regarding the basis of parameters, and also developed better "roadmaps" that link parameter documentation and parameter development. Upon subsequent review of records, the EPA determined that the DOE adequately provided the required information for probability distributions of code input parameters (CARD 55, U.S. EPA 1998b).

55.3.3 40 CFR § 194.55(c)

The EPA examined the DOE's use of the Latin hypercube sampling (LHS) procedure and found that the LHS technique draws samples from the entire range of each sampled parameter, was appropriate for use in assessing the concentrations of radionuclides in groundwater, and was implemented correctly by the DOE.

The DOE's evaluation of individual doses and groundwater radionuclide contamination and assessment of USDWs were described in the CCA, Chapter 8.0. The EPA evaluated the conceptual model that the DOE used to estimate a maximum individual exposure in its bounding calculation. The EPA determined that the DOE's conceptual model and the use of the GENII-A computer code to calculate the radiation doses were appropriate (CARD 55, U.S. EPA 1998b).

55.3.4 40 CFR § 194.55(d)

Compliance with 40 CFR § 194.55(d) is described in detail in Appendix IGP-2009, Section IGP-2.4. A summary is provided here.

The number of estimates generated must be large enough that the probability is at least 0.95 that the maximum estimate exceeds the 99^{th} percentile of the population of estimates. If the 300 realizations were statistically independent, then the probability that the maximum estimate exceeded the 99^{th} percentile of the population of estimates would equal $1 - (0.99)^{300} = 0.951$, and the section 194.55(d) criterion would be satisfied. On that basis, the probability that the maximum estimate exceeds the 99^{th} percentile of the population of estimates exceeded 0.95, and the section 194.55(d) criterion was satisfied.

The determination of the groundwater concentration and individual dose was based on the PA analysis of releases to the Salado Formation interbeds. Therefore, the number of estimates of concentrations and doses caused by releases to the interbeds was the same as the number in the PA and was dependent on the same calculations. The EPA concluded that the assessment of 300 realizations of the modeling system meets the requirements of section 194.55(d) (CARD 55, U.S. EPA 1998b).

55.3.5 40 CFR § 194.55(e)

40 CFR § 194.55(e) requires the DOE to display the full ranges of estimated doses and concentrations. The EPA found that:

- The estimated doses caused by ingesting water from the USDW were reported in the CCA, Chapter 8.0, Table 8-2. The maximum estimated dose rate from the other relevant pathways (0.46 mrem per year) was reported in the DOE response document (Dials 1997). The all-pathway individual doses were obtained by adding 0.46 mrem per year to those values. The maximum annual dose obtained in this fashion was less than 1 mrem per year (0.93 mrem per year).

- The CCA, Chapter 8.0, Section 8.2.3, pp. 8-15 and 8-16, states that the maximum estimated radium (Ra) concentration across the nine nonzero realizations was 2.0 picocuries per liter (pCi/L).

- The CCA, Chapter 8.0, Table 8-1 contains the 300 estimated concentrations for the 5 radionuclides: americium-241(^{241}Am), plutonium-239 (^{239}Pu), plutonium-238 (^{238}Pu), uranium-234 (^{234}U), and thorium-230 (^{230}Th), of which only nine were above the selection criteria. The nine radium-226 (^{226}Ra) concentrations were not separately recorded, but the maximum gross alpha-particle concentration, including Ra and excluding radon (Rn) and uranium (U), was reported as 7.81 pCi/L. The confidence interval analysis described below under 40 CFR § 194.55(f) used a more conservative approach that added the total Ra concentration bound (2.0 pCi/L) to the total of the five radionuclide concentrations, including U.

- The USDW dose estimates were reported in the CCA, Chapter 8.0, Table 8-2.

The EPA found the DOE's calculations to be conservative and therefore acceptable (CARD 55, U.S. EPA 1998b).

55.3.6 40 CFR § 194.55(f)

As part of the CCA certification process, the EPA required the DOE to perform an additional PA termed the Performance Assessment Verification Test (PAVT; EPA 1998c) using modifications to the parameters and codes used in the CCA PA. Since WIPP compliance assessments are based on PA results, the DOE performed additional compliance assessment calculations of individual dose and radioactivity concentration as part of the CCA PAVT. The mean dose calculated in the CCA PAVT from all pathways was an order of magnitude below the limit of section 191.15. Because all radionuclides contributing to the dose were alpha-emitting, the CCA PAVT also demonstrated compliance with the annual dose equivalent to the total body or any internal organ from beta particle and photon radioactivity in USDWs. The mean radionuclide concentrations calculated in the CCA PAVT for alpha-emitting radionuclides (including Ra but excluding Rn and U) and for ^{226}Ra and ^{228}Ra were below the limits of 40 CFR Part 191 Subpart C (U.S. DOE 1997a).

The DOE was required to demonstrate that there was at least a 95% level of statistical confidence that the mean and the median of the range of estimated radiation doses were less than 15 mrem per year, and that the range of estimated radionuclide concentrations was compatible (after dilution, as discussed above) with the regulations developed under the Safe Drinking Water Act. The DOE's bounding analysis indirectly verified these requirements by showing that the maximum estimated dose or concentration was always lower than the maximum allowable value.

As with the CCA, the CCA PAVT involved groundwater modeling simulations for the undisturbed repository. The results of this modeling projected nonzero groundwater concentrations for 13 of the 300 modeling simulations (as opposed to 9 in the CCA, Appendix PA). The projected groundwater concentrations from the CCA PAVT are found in *Summary of EPA-Mandated Performance Assessment Verification Test (Replicate 1) and Comparison with the Compliance Certification Application Calculations* (U.S. DOE 1997b), and *Supplemental Summary of EPA-Mandated Performance Assessment Verification Test (All Replicates) and Comparison with the Compliance Certification Application Calculations* (U.S. DOE 1997c). The EPA found that the mean and median radionuclide concentrations in groundwater calculated in the CCA PAVT complied with the requirements of Part 191, Subpart C both for gross alpha particle radioactivity (including Ra but excluding Rn and U) and for radioactivity concentration for ^{226}Ra and ^{228}Ra (U.S. EPA 1998a).

Drinking-water and all-pathways doses corresponding to projected groundwater concentrations in the CCA PAVT were estimated using the modeling methodology established for the CCA. The DOE initially submitted results for the drinking-water pathway only, where the largest dose value was 3.2×10^{-2} mrem per year (U.S. DOE 1997a, Table 3). Later, in its *Summary of the EPA-Mandated Performance Assessment Verification Test Results for Individual Protection Requirements*, the DOE calculated 3.1×10^{-2} mrem per year for all other pathways combined (U.S. DOE 1997d, Table 5). This calculation again resulted in a value two orders of magnitude less than the 15 mrem per year requirement. The EPA's calculation of the total body dose from

the DOE's concentrations for the 13 nonzero realizations yielded a maximum value of 3.1×10^{-1} mrem per year (U.S. EPA 1998d).

The DOE's PAVT analysis of beta, electron, and photon doses to the whole body and to individual internal organs is shown in its *Summary of the EPA Mandated Performance Assessment Verification Test Results for Individual Protection Requirements* (U.S. DOE 1997d, Table 3). The DOE demonstrated that the largest organ dose is 2.9×10^{-4} mrem per year on the bone surface. The analysis also showed that the maximum effective dose from beta, electron, and photon emissions is 1.5×10^{-5} mrem per year.

Results of the CCA PAVT thus showed that the mean dose contributions from both alpha-emitting radionuclides and from photon- and beta-emitting radionuclides were below the limits in section 191.15 and Part 191 Subpart C.

Based on its review of the material provided by the DOE in the CCA and additional information from the CCA PAVT, the EPA concluded that the DOE demonstrated compliance with the requirements of section 194.55. A complete description of the EPA's 1998 Certification Decision for section 194.55 is found in U.S. EPA 1998e.

55.4 Changes in the CRA-2004

The DOE's methodology for demonstrating compliance with section 194.55 did not change since the CCA. The CRA-2004, Chapter 8.0 described the DOE's compliance with the individual and groundwater protection requirements (U.S. DOE 2004). The DOE considered and documented uncertainty as required by 40 CFR § 194.55(a), in the CRA-2004, Section 6.1.2. As noted in the CRA-2004, Chapter 8.0, Section 8.1.5, parameter uncertainty was discussed in Appendix PA-2004, Attachment PAR to verify compliance with 40 CFR § 194.55(b). The CRA-2004, Chapter 8.0 describes how the DOE calculated the effective dose and dose equivalent as required by section 194.55(c). The CRA-2004, Chapter 8.0, Section 8.1.4 also noted that the DOE's selection of more than 298 sampled vectors fulfilled the requirements of 40 CFR § 194.55(d). The DOE also noted in the CRA-2004, Chapter 8.0, Section 8.1.4 that their bounding analysis adequately fulfilled the requirements of section 194.55(f). The CRA-2004, Chapter 8.0, Section 8.1 showed how the DOE considered the full range of estimated radiation doses and radionuclide concentrations as required by section 194.55(e).

55.5 EPA's Evaluation of Compliance for the 2004 Recertification

The EPA reviewed the DOE's CRA-2004 documents, in particular Chapter 8.0. The EPA found that little had changed since the original certification decision. The EPA did not receive any public comments on the DOE's continued compliance with the compliance assessment requirements of section 194.55. The EPA concluded that the DOE continued to demonstrate compliance with the requirements of section 194.55 (CARD 55, U.S. EPA 2006).

55.6 Changes or New Information Between the CRA-2004 and the CRA-2009 (Previously: Changes or New Information Since the 2004 Recertification)

The DOE's methodology for demonstrating compliance with section 194.55 was not changed in the CRA-2009 from the methodology in the CRA-2004 or the CCA. Appendix IGP-2009 was an updated version of the CCA, Chapter 8.0 and the CRA-2004, Chapter 8.0. It documented the DOE's continued compliance with the individual and groundwater protection requirements. Compliance with the various subsections of section 194.55 was demonstrated in 2009 as follows:

- As indicated in Appendix IGP-2009, Section IGP-2.1, parameter uncertainty was discussed in Fox 2008, which demonstrated compliance with section 194.55(b).

- Appendix IGP-2009, Section IGP-2.2 described how the DOE calculated the effective dose and dose equivalent as required by 40 CFR § 194.55(c).

- Appendix IGP-2009, Section IGP-2.4 also explained that the DOE's selection of more than 298 sampled vectors fulfilled the requirements of section 194.55(d).

- Appendix IGP-2009, Sections IGP-2.1 and 2.2 demonstrated that the DOE considered the full range of estimated radionuclide concentrations and radiation doses as required by section 194.55(e).

- Appendix IGP-2009, Section IGP-2.4 demonstrated that the DOE's bounding analysis approach meet the requirements of section 194.55(f).

Based on this information, the DOE believed that continued compliance with the provisions of section 194.55 was demonstrated at that time.

55.7 EPA's Evaluation of Compliance for the 2009 Recertification

The EPA reviewed the DOE's CRA-2009 documents and found that little had changed since the original certification decision. The EPA did not receive any public comments on the DOE's continued compliance with the requirements of section 194.55. The EPA concluded that the DOE continued to demonstrate compliance with the requirements of section 194.55 (CARD 55, U.S. EPA 2010).

55.8 Changes or New Information Since the CRA-2009

The DOE's methodology for demonstrating compliance with section 194.55 has not changed since the CCA. Appendix IGP-2014 is an updated version of the CCA, Chapter 8.0 and the CRA-2004, Chapter 8.0. It documents the DOE's continued compliance with the individual and groundwater protection requirements. Compliance with the various subsections of section 194.55 is demonstrated as follows:

- As indicated in Appendix IGP-2014, Section IGP-2.1, parameter uncertainty is discussed in Kicker and Herrick 2013, which demonstrates compliance with section 194.55(b).

- Appendix IGP-2014, Section IGP-2.2 describes how the DOE calculates the effective dose and dose equivalent as required by 40 CFR § 194.55(c).

- Appendix IGP-2014, Section IGP-2.4 also explains that the DOE's selection of more than 298 sampled vectors fulfills the requirements of section 194.55(d).

- Appendix IGP-2014, Sections IGP-2.1 and 2.2 demonstrate that the DOE considered the full range of estimated radionuclide concentrations and radiation doses as required by section 194.55(e).

- Appendix IGP-2014, Section IGP-2.4 demonstrates that the DOE's bounding analysis approach meets the requirements of section 194.55(f).

Based on this information, the DOE believes that continued compliance with the provisions of section 194.55 is demonstrated.

55.9 References

(*Indicates a reference that has not been previously submitted.)

Dials, G. 1997. *Letter to R. Trovato (1 Enclosure)*. 26 February 1997. Carlsbad, NM: U.S. Department of Energy, Carlsbad Area Office.

Fox, B. 2008. *Parameter Summary Report for the CRA-2009* (Revision 0). ERMS 549747. Carlsbad, NM: Sandia National Laboratories.

Kicker, D.C., and C.G. Herrick. 2013. *Parameter Summary Report for the 2014 Compliance Recertification Application* (Revision 0). ERMS 560298. Carlsbad, NM: Sandia National Laboratories.*

U.S. Department of Energy (DOE). 1996. *Title 40 CFR Part 191 Compliance Certification Application for the Waste Isolation Pilot Plant* (October). 21 vols. DOE/CAO-1996-2184. Carlsbad, NM: Carlsbad Area Office.

U.S. Department of Energy (DOE). 1997a. *Summary of the EPA-Mandated Performance Assessment Verification Test Results for the Individual and Groundwater Protection Requirements* (September 12). WPO 47258. Carlsbad, NM: Carlsbad Field Office.

U.S. Department of Energy (DOE). 1997b. *Summary of EPA-Mandated Performance Assessment Verification Test (Replicate 1) and Comparison with the Compliance Certification Application Calculations*. WPO 46674. Carlsbad, NM: Carlsbad Area Office.

U.S. Department of Energy (DOE). 1997c. *Supplemental Summary of EPA-Mandated Performance Assessment Verification Test (All Replicates) and Comparison with the Compliance Certification Application Calculations* (August 8). WPO 46702. ERMS 414879. Carlsbad, NM: Carlsbad Area Office.

U.S. Department of Energy (DOE). 1997d. *Summary of the EPA-Mandated Performance Assessment Verification Test Results for Individual Protection Requirements: Estimated Doses to Internal Organs and Total Body from Groundwater Ingestion and to the Total Body from Beef Consumption, Vegetable Consumption and Inhalation of Soil* (September 22). WPO#47309. Carlsbad, NM: Carlsbad Field Office.

U.S. Department of Energy (DOE). 2004. *Title 40 CFR Part 191 Compliance Recertification Application for the Waste Isolation Pilot Plant* (March). 10 vols. DOE/WIPP 2004-3231. Carlsbad, NM: Carlsbad Field Office.

U.S. Department of Energy (DOE). 2009. *Title 40 CFR Part 191 Compliance Recertification Application for the Waste Isolation Pilot Plant* (March). DOE/WIPP-09-3424. Carlsbad, NM: Carlsbad Field Office.*

U.S. Environmental Protection Agency (EPA). 1993. "40 CFR Part 191 Environmental Radiation Protection Standards for the Management and Disposal of Spent Nuclear Fuel, High-Level and Transuranic Radioactive Wastes; Final Rule." *Federal Register,* vol. 58 (December 20, 1993): 66398–416.

U.S. Environmental Protection Agency (EPA). 1996. "40 CFR Part 194: Criteria for the Certification and Recertification of the Waste Isolation Pilot Plant's Compliance with the 40 CFR Part 191 Disposal Regulations; Final Rule." *Federal Register,* vol. 61 (February 9, 1996): 5223–45.

U.S. Environmental Protection Agency (EPA). 1998a. "CARD No. 51/52: Consideration of Protected Individual and Exposure Pathways." *Compliance Application Review Documents for the Criteria for the Certification of the Waste Isolation Pilot Plant's Compliance with the 40 CFR 191 Disposal Regulations: Final Certification Decision* (May) (pp. 51-1 through 51-11). Washington, DC: Office of Radiation and Indoor Air.

U.S. Environmental Protection Agency (EPA). 1998b. "CARD No. 55: Results of Compliance Assessments." *Compliance Application Review Documents for the Criteria for the Certification of the Waste Isolation Pilot Plant's Compliance with the 40 CFR 191 Disposal Regulations: Final Certification Decision* (May) (pp. 55-1 through 55-25). Washington, DC: Office of Radiation and Indoor Air.

U.S. Environmental Protection Agency (EPA). 1998c. *Technical Support Document: Overview of Major Performance Assessment Issues* (May). Washington, DC: Office of Radiation and Indoor Air.

U.S. Environmental Protection Agency (EPA). 1998d. *Technical Support Document for Sections 194.51, 19.52, and 194.55: Dose Verification Evaluation* (May). Washington, DC: Office of Radiation and Indoor Air.

U.S. Environmental Protection Agency (EPA). 1998e. "40 CFR Part 194: Criteria for the Certification and Recertification of the Waste Isolation Pilot Plant's Compliance with the Disposal Regulations: Certification Decision; Final Rule." *Federal Register,* vol. 63 (May 18, 1998): 27353–406.

U.S. Environmental Protection Agency (EPA). 2006. "Recertification CARD No. 55: Results of Compliance Assessments." *Compliance Application Review Documents for the Criteria for the Certification and Recertification of the Waste Isolation Pilot Plant's Compliance with the 40 CFR 191 Disposal Regulations: Final Recertification Decision* (March) (pp. 55-1 through 55-6). Washington, DC: Office of Radiation and Indoor Air.

U.S. Environmental Protection Agency (EPA). 2010. *2009 Compliance Recertification Application (2009 CRA) Compliance Application Review Document (CARD) No. 55, Results of Compliance Assessments*. EPA Docket FDMS Docket ID No. EPA-HQ-OAR-2009-0330. Washington, DC: Office of Radiation and Indoor Air.*

Title 40 CFR Part 191
Subparts B and C
Compliance Recertification Application 2014
for the
Waste Isolation Pilot Plant

Appendix AUD-2014
Audits and Surveillances

United States Department of Energy
Waste Isolation Pilot Plant

Carlsbad Field Office
Carlsbad, New Mexico

Compliance Recertification Application 2014

Appendix AUD

Table of Contents

List of Tables

This page intentionally left blank.

Acronyms and Abbreviations

ACL Analytical Chemistry Laboratory

AK acceptable knowledge

AMWTP Advanced Mixed Waste Treatment Project

ANL Argonne National Laboratory

ARP Accelerated Retrieval Project

BAPL Bettis Atomic Power Laboratory

BCL Battelle Columbus Laboratories

CAR corrective action report

CAST CAST Specialty Transportation, Inc.

CBFO Carlsbad Field Office

CCP Central Characterization Project

CEMRC Carlsbad Environmental Monitoring and Research Center

CFR Code of Federal Regulalions

CGI Commercial Grade Item

CH contact-handled

CMR Central Monitoring Room

CRA Compliance Recertification Application

DOE U.S. Department of Energy

DOT U.S. Department of Transportation

DSA Documented Safety Analyses

DTC dose-to-curie

ECL Environmental Chemistry Laboratory

FEW Fuel Examination Waste

GC/MS Gas Chromatograph/Mass Spectrometer

GEVNC General Electric Vallecitos Nuclear Center

GWAS Gamma Waste Assay System

HENC #1 High-Efficiency Neutron Counter #1

HERTR High-Energy Real-Time Radiography

HSG headspace gas

HSGS headspace gas sampling

HPLC-1 High Performance Liquid Chromatography

HWFP Hazardous Waste Facility Permit

I indeterminate

IDC Integrated Data Center

INL Idaho National Laboratory

INTEC Idaho Nuclear Technology and Engineering Center

IS&H Industrial Safety and Health

JHA Job Hazard Analysis

LANL Los Alamos National Laboratory

LANL-CO Los Alamos National Laboratory - Carlsbad Operations

LCNDE Large Container Non-Destructive Examination

LO/TO Lockout/Tagout

M marginal

M&O managment and operating

N/A not applicable

NABC Nondestructive Assay Box Counter

NDA nondestructive assay

NEPA National Environmental Policy Act

NESHAP National Emissions Standards for Hazardous Air Pollutants

NQA nuclear quality assurance

NTP National TRU Program

NWP Nuclear Waste Partnership LLC

ORNL Oak Ridge National Laboratory

OSO Office of Site Operations

PDP Performance Demonstration Program

PFP Plutonium Finishing Plant

PRS Project Records Services

QA quality assurance

QAP Quality Assurance Program

QAPD Quality Assurance Program Document

RADCON Radiological Control

RCRA Resource Conservation and Recovery Act

RH remote-handled

RHF Records Holding Facility

RH-TRU remote-handled transuranic

RL Hanford-Richland

RTR real-time radiography

RWMC Radioactive Waste Management Complex

S satisfactory; surveillance

SCG Summary Category Group

SDW Safe Drinking Water

SLB2s standard large box 2s

SNL Sandia National Laboratories

SNL/CPG Sandia National Laboratories/Carlsbad Program Group

SQA software quality assurance

SRS Savannah River Site

SSE salt storage evaporation

SWB standard waste box

TRANSCOM Transportation Tracking and Communication

TRU transuranic

TRUPACT-III Transuranic Package Transporter-III

TSR Technical Safety Requirements

U unsatisfactory

V&V verification and validation

VE visual examination

VET Visual Examination Technique

VOC volatile organic compound

WAC Waste Acceptance Criteria

WAP Waste Analysis Plan

WDS Waste Data System

WIPP Waste Isolation Pilot Plant

WRAP Waste Receiving and Processing

WRMS WIPP Records Management Services

WSCF Waste Sampling and Characterization Facility

WTS Washington TRU Solutions, LLC

WTS/RES Washington TRU Solutions Regulatory and Environmental Services

WTS/WRES Washington TRU Solutions Washington Regulatory and Environmental Services

WWIS WIPP Waste Information System

This page intentionally left blank.

AUD-1.0 Introduction

Tables AUD-1 through AUD-15 summarize assessments performed from December 31, 2007, through February 1, 2013. These assessments were performed to evaluate the adequacy and implementation of Waste Isolation Pilot Plant (WIPP) participant organizations' quality assurance (QA) programs, as well as compliance with DOE/CBFO-94-1012, CBFO *Quality Assurance Program Document* (QAPD) (U.S. DOE 2010) and the WIPP Hazardous Waste Facility Permit (HWFP).

This information supplements the information contained in the 2009 Compliance Recertification Application (CRA-2009) (U.S. DOE 2009). Some assessments were performed prior to the end of the Appendix AUD-2009 reporting period; however, the assessments were not considered complete until the final report was finished and associated regulatory approvals (if required) were obtained.

The following organizations were assessed: transuranic (TRU) waste generator sites; Sandia National Laboratories - Carlsbad Programs Group (SNL/CPG); Washington TRU Solutions, LLC (WTS); Nuclear Waste Partnership LLC (NWP); suppliers performing quality-affecting work; Los Alamos National Laboratory - Carlsbad Operations (LANL-CO), and the U.S. Department of Energy (DOE) Carlsbad Field Office (CBFO). Throughout this appendix, "CBFO" is used to include reference to the former Carlsbad Area Office, as appropriate.

Results of the assessment normally determine the adequacy, implementation, and effectiveness of an auditee's QA program. Adequacy addresses the migration of requirements from upper-tier program documents into implementing procedures. Implementation refers to the manner in which an organization applies the requirements of its QA program and of the QAPD to the activities performed. Effectiveness addresses whether the controls established in the implementing procedures produce the desired results or end products. All assessments were performed to the requirements in place at the time of the activity.

The summary tables identify the organization assessed, assessment number, assessment scope, and assessment results. Assessment results are expressed as "satisfactory" (S), "marginal" (M), "unsatisfactory" (U), "not applicable" (N/A), or "indeterminate" (I) for the three factors considered during an assessment (adequacy, implementation, and effectiveness). For assessments resulting in findings of M, U, and/or I, corrective actions are applied to address the concerns and issues identified until a satisfactory (S) result is achieved. Assessment findings of M, U, and I at TRU waste sites have been corrected or satisfactorily addressed and verified through subsequent audits, surveillances, corrective action reports (CARs), or other means prior to initial certification or continued certification for shipping waste to the WIPP.

Only those CBFO assessment activities directly related to 40 CFR Parts 191 (U.S. EPA 1993) and 194 (U.S. EPA 1996) are included in this appendix. Additional CBFO assessments are performed in other critical areas. In addition, each participant organization performs internal assessments of its own activities.

Table AUD-6 is entitled "Washington TRU Solutions/Nuclear Waste Partnership Assessments" to reflect the WIPP management and operating (M&O) contract award, which occurred on October 1, 2012. The "Organization Assessed" column identifies the M&O contractor as either WTS or NWP, as appropriate.

Table AUD-1. Idaho National Laboratory & INL Analytical Labs Assessments

Organization Assessed	Assessment Number	Assessment Dates	Scope of Assessments	Adequacy	Implementation	Effectiveness
INL	A-08-10	05/13 - 05/15/08	Evaluated continued adequacy, implementation and effectiveness of technical and QA elements as they relate to the WIPP Hazardous Waste Facility Permit (HWFP) for characterization and certification of Summary Category Group (SCG) S3000 homogeneous solids waste, S4000 soils/gravel waste, and S5000 debris waste.	S	S	S
				The defined QA program was satisfactorily implemented in accordance with the HWFP, CBFO Quality Assurance Program Document (QAPD), contract, and statement of work, as well as the Idaho National Laboratory (INL) implementing procedures. Technical areas evaluated were adequate, satisfactorily implemented, and effective.		
INL	A-08-11	01/29 - 01/30/08	Follow-up certification audit conducted to evaluate the adequacy, implementation, and effectiveness of the INL/Central Characterization Project (CCP) TRU waste characterization activities related to contact-handled (CH) SCG S4000 soils/gravel performed by the INL/CCP relative to the HWFP and upper-tier requirement documents	S	S	S
				The defined QA program was satisfactorily implemented in accordance with the CBFO QAPD, HWFP and the INL implementing procedures. Technical areas evaluated were adequate, satisfactorily implemented, and effective.		
INL Analytical Labs.	A-08-22	05/13 - 05/15/08	Evaluated continued adequacy, implementation and effectiveness of INL Analytical Labs TRU waste characterization activities performed under the CCP Program. Activities evaluated included headspace gas (HSG) analysis of SCG S5000 debris wastes; Analytical Laboratories Department analysis of S3000 homogeneous solids and S4000 soils/gravel; generation-level data verification and validation (V&V) of S3000 homogeneous solids, S4000 soils/gravel, and S5000 debris wastes; and SUMMA ®	S	S	S
				The defined QA program was satisfactorily implemented in accordance with the CBFO QAPD, and the INL Analytical Labs implementing procedures. Technical areas evaluated were adequate, satisfactorily implemented, and effective.		
INL	A-09-08	12/9 - 12/11/08	Limited preparation and certification of [illegible] for use by the generator sites.	S	S	S
				Based on the results of the corrective action verification for CBFO CARs 09-015 and 09-016, the audit team concluded that the VE process being performed by INL/CCP was adequate, satisfactorily implemented, and effective. Follow-up surveillance (S-09-21) was conducted in March, 2009 to verify effectiveness of actions completed for the two CARs.		
INL Analytical Labs.	A-09-13	05/5 - 05/07/09	Evaluated continued adequacy, implementation, and effectiveness of INL	S	S	S

Table AUD-1. Idaho National Laboratory & INL Analytical Labs Assessments

Organization Assessed	Assessment Number	Assessment Dates	Scope of Assessments	Adequacy	Implementation	Effectiveness
			Analytical Laboratories/CCP TRU waste characterization activities.	The defined QA program was satisfactorily implemented in accordance with the CBFO QAPD, and the INL Analytical Labs implementing procedures. Technical areas evaluated were adequate, satisfactorily implemented, and effective.		
INL	A-09-14	05/05 - 05/07/09	Evaluated continued adequacy, implementation, and effectiveness of technical and QA elements as they relate to the WIPP HWFP for characterization and certification of SCG S3000 homogeneous solids waste, S4000 soils/gravel waste, and S5000 debris waste.	S	S	S
				The defined QA program was satisfactorily implemented in accordance with the HWFP, CBFO QAPD, contract, and statement of work, as well as the INL implementing procedures. Technical areas evaluated were adequate, satisfactorily implemented, and effective.		
INL	A-10-03	10/06 - 10/07/09	Evaluated the adequacy, implementation, and effectiveness of the INL Visual Examination Technique (VET) waste characterization process including related technical and QA activities performed by the INL/CCP.	S	S	S
				The audit team concluded that the INL/CCP technical and QA programs, as applicable to the VET process, were adequate in addressing upper-tier requirements, satisfactorily implemented, and effective.		
INL	A-10-16	06/08 - 06/10/10	Evaluated continued adequacy, implementation and effectiveness of technical and QA elements as they relate to the WIPP HWFP for characterization and certification of SCG S3000 homogeneous solids waste, S4000 soils/gravel waste, and S5000 debris waste.	S	S	S
				The audit team concluded that the INL/CCP technical and QA program, with the exception of the dose-to-curie characterization discipline using the Osprey detector, continue to be adequate and satisfactorily implemented for characterizing SCG S3000, S4000 and S5000 waste. The dose-to-curie discipline was later evaluated during S-10-34 and determined to be adequate and satisfactorily implemented.		
INL Analytical Labs.	A-10-17	06/08 - 06/10/10	Evaluated continued adequacy, implementation and effectiveness of INL Analytical Laboratories/CCP TRU waste characterization activities.	S	S	S
				The defined QA program was satisfactorily implemented in accordance with the CBFO QAPD, and the INL Analytical Labs implementing procedures. Technical areas evaluated were adequate, satisfactorily implemented, and effective.		
INL Analytical Labs.	A-11-13	06/07 - 06/09/11	Evaluated continued adequacy, implementation and effectiveness of INL Analytical Laboratories/CCP TRU waste characterization activities.	S	S	S
				The defined QA program was satisfactorily implemented in accordance with the CBFO QAPD, and the INL Analytical Labs implementing procedures. Technical areas evaluated were adequate, satisfactorily implemented, and effective.		
INL	A-11-14	06/07 - 06/09/11	Evaluated continued adequacy, implementation, and effectiveness of INL TRU waste characterization activities performed for the INL by WTS/CCP. Activities were evaluated relative to the requirements of the WIPP HWFP, the CBFO QAPD and Waste Acceptance Criteria (WAC). Evaluated CH SCGs S3000 homogeneous solids waste, S4000 soils/gravel waste, and S5000 debris waste, and remote-handled (RH) SCGs S3000 homogeneous solids waste and S5000 debris waste, in addition to other technical elements, QA elements, and transportation activities.	S	S	S
				The defined QA program was satisfactorily implemented in accordance with the CBFO QAPD, and the INL implementing procedures. Technical areas evaluated were adequate, satisfactorily implemented, and effective.		
INL	A-12-13	06/11 - 06/14/12	Evaluated continued adequacy, implementation, and effectiveness of technical and QA elements as they relate to the WIPP HWFP for characterization and certification of SCG S3000 homogeneous solids waste, S4000 soils/gravel waste, and S5000 debris waste.	S	S	S
				The defined QA program was satisfactorily implemented in accordance with the CBFO QAPD, contract and statement of work, as well as the INL implementing procedures. Technical areas evaluated were adequate, satisfactorily implemented, and effective.		
INL Analytical Labs.	A-12-14	06/11 - 06/14/12	Evaluated continued adequacy, implementation and effectiveness of INL Analytical Laboratories/CCP TRU waste characterization activities. Activities evaluated included the Environmental Chemistry Laboratory (ECL) HSG analysis of SCG S5000 debris wastes; Analytical Chemistry Laboratory (ACL) solids analysis of SCGs S3000 homogeneous solids and S4000 soils/gravel wastes; generation-level data V&V; and SUMMA canister preparation and	S	S	S
				The defined QA program was satisfactorily implemented in accordance with the CBFO QAPD, and the INL Analytical Labs implementing procedures. Technical areas evaluated were adequate, satisfactorily implemented, and effective.		
INL	S-08-03	01/15 - 01/16/08	Evaluated the implementation and effectiveness of the policies, plans, and procedures related to the CCP shipment of RH TRU waste from the INL to the WIPP.	S	S	S
				Activities associated with operations necessary for the CCP's transportation of RH waste were appropriately proceduralized and effectively implemented.		
INL	S-08-07	01/15 - 01/18/08	Evaluated the implementation and effectiveness of policies, plans, and procedures related to the Accelerated Retrieval Project (ARP) VE process for	S	S	S

Table AUD-1. Idaho National Laboratory & INL Analytical Labs Assessments

Organization Assessed	Assessment Number	Assessment Dates	Scope of Assessments	Adequacy	Implementation	Effectiveness
			newly generated wastes performed at INL by the CCP.	The INL/CCP ARP VE activities were considered to be adequate, satisfactorily implemented, and effective.		
INL	S-08-16	08/05 - 08/15/08	Evaluated the adequacy, implementation, and effectiveness of the CCP technical and QA activities for remediation and repackaging of SCG S3000 waste, conducted at INL by the CCP. This included review of the Packaging Configuration Correction process described in Procedure CCP-TP-006, *CCP Visual Examination Technique for INL Newly Generated TRU Waste Remediated from Pits*	S	S	S
				Activities associated with remediation & repackaging of SCG S3000 were considered to be adequate, satisfactorily implemented, and effective.		
INL	S-09-08	12/16 - 12/17/08	Evaluated the adequacy, implementation, and effectiveness of the CCP technical and QA activities for remediation and repackaging of SCG S3000 homogeneous solid waste.	S	S	S
				The CCP technical and QA activities for remediation & repackaging of ARP S3000 waste were adequate, satisfactorily implemented, and effective.		
INL	S-09-21	03/25 - 03/26/09	Evaluated implementation of corrective actions associated with CBFO CARs 09-015 and 09-16 resulting from CBFO Audit A-09-08. CBFO Audit A-09-08 was performed December 09/11/2008, to evaluate the INL/CCP VE process.	S	S	S
				The surveillance team determined that corrective actions associated with CBFO CARs 09-015 and 09-16 were satisfactory, thus CBFO CARs 09-015 and 09-16 were closed. The surveillance team also verified the corrective actions were effective.		
INL	S-09-33	08/11/09	Evaluated the implementation and effectiveness of the VE process performed by the INL/CCP on RH SCG S5000 debris waste. Recertification Audit A-09-14 of INL/CCP did not include VE of RH waste.	S	S	S
				Surveillance team verified procedure compliance in performing VE on RH waste. Activities associated with VE on RH waste were adequate, satisfactorily implemented, and effective.		
INL	S-10-01	10/13 - 10/14/09	Evaluated the activities associated with the relocation of the Analytical Solids Laboratory from Building 602 at the Idaho Nuclear Technology and Engineering Center (INTEC) to a modular trailer facility at the INL Radioactive Waste Management Complex (RWMC) near Idaho Falls, ID.	S	S	S
				INL/CCP activities related to solids analysis were determined to be adequate, satisfactory, and effective at the new Analytical Solids Laboratory location.		
INL	S-10-20	02/23 - 02/24/10	Evaluated the documentation associated with INL/CCP RH waste sampling and analysis activities at the INL INTEC facility.	S	S	S
				INL/CCP activities related to RH sampling and analysis characterization operations were adequate, satisfactorily implemented, and effective.		
INL	S-10-22	03/03/10	Evaluated the implementation and effectiveness of the VE characterization process performed by the INL/CCP on RH SCG S3000 solids waste. Recertification Audit A-09-14 did not include VE of RH waste.	S	S	S
				The VE characterization process performed by the INL/CCP on RH SCG S3000 solids waste is adequately implemented and effective.		
INL	S-10-33	07/27/10	Evaluated VE of RH SCG S3000 solids waste. INL/CCP HSG sampling (HSGS) activities at the INL.	S	S	S
				This surveillance determined that the INL/CCP HSG sampling operations were adequate, satisfactorily implemented, and effective.		
INL	S-10-34	07/20 - 07/21/10	Evaluated the adequacy, procedure implementation, and effectiveness of project-level review of dose-to-curie (DTC) data measured using an Osprey detector. This surveillance was performed to address a determination of inadequacy of reporting due to the unavailability of final data packages for review at the time of CBFO Audit A-10-16.	S	S	S
				This surveillance satisfactorily closed out the radiological characterization (nondestructive assay [NDA] and RH/DTC) portion of Audit A-10-16. Activities were determined to be adequate, satisfactorily implemented, and effective.		
INL Analytical Labs.	S-11-31	9/21/11	Verified the operability, implementation, and effectiveness of two new instruments at the ECL, gas chromatography/mass spectrometry (GC/MS) instruments I and J (GC/MS-I and GC/MS-J), and their associated procedure, to confirm adequacy, implementation, and effectiveness of the characterization process for SCG S5000 debris waste relative to the requirements of the WIPP HWFP.	S	S	S
				The surveillance team concluded that the laboratory program's new instruments were adequate and the procedure is satisfactorily implemented and effective.		
INL	S-12-10	11/01/11	Verified the operability, implementation, and effectiveness of the High Performance Liquid Chromatography (HPLC-1) used for analysis of samples for hydrazine and formaldehyde, to confirm the adequacy, implementation and effectiveness of this process for SCG S3000 solids and S4000 soils/gravel waste relative to the requirements of the WIPP HWFP.	S	S	S
				The surveillance team concluded that formaldehyde and hydrazine HPLC-1 analyses at the INL/CCP ACL were acceptable, satisfactory, and effective.		
INL	S-12-20	05/07/12	Evaluated the operational capability of INL/CCP Real-Time Radiography (RTR) Unit #RTR-0659 at the INTEC for characterization of RH SCG S3000 solids waste. The surveillance team verified that the INTEC RTR unit (RTR-0659) was capable of	S	S	S

Table AUD-1. Idaho National Laboratory & INL Analytical Labs Assessments

Organization Assessed	Assessment Number	Assessment Dates	Scope of Assessments	Adequacy	Implementation	Effectiveness
			providing full penetration of the solid waste in waste stream IN-ID-BTO-030.	The surveillance team determined that the operational capability of RTR unit #RTR-0659 was acceptable, satisfactory and effective.		
INL	S-13-17	01/09 - 01/10/13	Evaluated the operability, implementation, and effectiveness of the Gas Chromatography Unit 7 instrument used for the dual-column gas chromatographic separation and detection of nonhalogenated volatile organic compounds (VOC) in extracts of solid samples.	S	S	S
				The surveillance team determined that the operational capability of the GC-7 instrument and procedures were acceptable, satisfactory, and effective.		
INL	S-13-19	01/24/13	Evaluated the VET process for characterizing retrievably stored CH SCG S3000 homogeneous solids waste at the RWMC ARP.	S	S	S
				The surveillance team concluded that VET operations for retrievably stored CH solids waste are adequate in meeting upper-tier requirements, and procedures are satisfactorily implemented and effective in achieving the desired results.		

Table AUD-2. Los Alamos National Laboratory Assessments

Organization Assessed	Assessment Number	Assessment Dates	Scope of Assessments	Adequacy	Implementation	Effectiveness
LANL	A-08-16	04/15 - 04/17/08	Evaluated the continued adequacy, implementation, and effectiveness of LANL TRU waste characterization and certification activities for CH SCG S3000 homogeneous solids and S5000 debris wastes, and RH S5000 debris waste performed for LANL by WTS/CCP relative to the requirements detailed in the WIPP HWFP, CBFO QAPD, and other upper-tier requirement documents.	S	S	S
				The defined QA program was satisfactorily implemented in accordance with the WIPP HWFP, CBFO QAPD, and requirement documents. Technical areas evaluated were adequate, satisfactorily implemented, and effective for compliance with the HWFP.		
LANL	A-09-12	04/07 - 04/09/09	Evaluated the continued adequacy, implementation, and effectiveness of LANL TRU waste characterization and certification activities for CH SCG S3000 homogeneous solids and S5000 debris wastes, and RH S5000 debris waste performed for LANL by WTS/CCP relative to the requirements detailed in the WIPP HWFP, CBFO QAPD, and other upper-tier requirement documents.	S	S	S
				The defined QA program was satisfactorily implemented in accordance with the WIPP HWFP, CBFO QAPD, and requirement documents. Technical areas evaluated were adequate, satisfactorily implemented, and effective for compliance with the HWFP.		
LANL	A-10-14	04/27 - 04/29/10	Evaluated the continued adequacy, implementation, and effectiveness of LANL TRU waste characterization and certification activities for CH SCG S3000 homogeneous solids and S5000 debris wastes, and RH S5000 debris waste performed for LANL by WTS/CCP relative to the requirements detailed in the WIPP HWFP, CBFO QAPD, and other upper-tier requirement documents, as well as VE in support of the Off-Site Recovery Program.	S	S	S
				The defined QA program was satisfactorily implemented in accordance with the WIPP HWFP, CBFO QAPD, and requirement documents. Technical areas evaluated were adequate, satisfactorily implemented, and effective for compliance with the HWFP. Four CARs were issued from this audit (10-025, 10-026, 10-027, and 10-028). Corrective actions plans were approved and actual actions verified. Follow-up surveillance S-10-31 was conducted to verify effectiveness of corrective actions for CAR 10-025.		
LANL	A-11-11	05/17 - 05/19/11	Evaluated the adequacy, implementation, and effectiveness of LANL TRU waste characterization activities performed for LANL by the WTS/CCP relative to the requirements detailed in the WIPP HWFP and CBFO QAPD. The audit team evaluated the characterization processes for CH SCG S3000 homogeneous solids waste and SCG S5000 debris waste.	S	S	S
				The defined QA program was satisfactorily implemented in accordance with the WIPP HWFP, CBFO QAPD, and requirement documents. Technical areas evaluated were adequate, satisfactorily implemented, and effective for compliance with the HWFP.		
LANL	A-12-12	07/24 - 07/26/12	Evaluated the adequacy, implementation, and effectiveness of LANL TRU waste characterization activities performed for LANL by WTS/CCP. The audit was conducted relative to the requirements detailed in the WIPP HWFP, the CBFO QAPD, and other upper-tier requirement documents. Evaluated the continuing characterization processes for CH SCG S3000 homogeneous solids and SCG S5000 debris wastes. The CBFO Office of the National TRU Program (NTP) requested that the audit team also evaluate the characterization process for CH SCG S4000 soils/gravel waste for initial certification. As part of the audit, the NTP requested a review of the extension of the calibration for the High-Efficiency Neutron Counter #1 (HENC #1) to include a population of lead-lined 55-gallon drums containing solidified materials, as well as a calibration extension of the high-resolution gamma spectrometry to 2.5 grams per cubic centimeter for the SuperHENC.	S for S3000/S500 I for S4000	S for S3000/S500 I for S4000	S for S3000/S500 I for S4000
				The audit team verified that the LANL/CCP technical and QA programs, including the NTP requested extensions, used for characterization and certification of CH SCG S3000 homogeneous solids and SCG S5000 debris waste were satisfactorily implemented and effective. The audit team was unable to determine the adequacy, implementation and effectiveness of the characterization of CH SCG S4000 soils/gravel waste because the team was not provided with any completed S4000 characterization packages. The team reviewed the preliminary Acceptable Knowledge (AK) documentation, reviewed the RTR and NDA characterization of S4000 soils/gravel waste, and reviewed a random selection memo for LANL S4000 waste. All were deemed to be adequate. No completed sampling batch data reports for LANL S4000 waste were provided to the team for evaluation, and therefore the audit team concluded that characterization activities of LANL/CCP for CH SCG S4000 soils/gravel waste were indeterminate. When additional documentation is available for review, it will be evaluated by surveillance.		
LANL	S-10-31	06/24/10		S	S	S

Table AUD-2. Los Alamos National Laboratory Assessments

Organization Assessed	Assessment Number	Assessment Dates	Scope of Assessments	Adequacy	Implementation	Effectiveness
			Evaluated the implementation and effectiveness of CCP corrective actions related to CBFO CAR 10-025 issued as a result of CBFO Audit A-10-14. The CAR identified issues related to the handling of raw data generated during VE activities.	Verified the corrective actions for CAR 10-025. Actions were implemented and determined to be adequate and effective.		
LANL	S-11-29	08/15/11	Evaluated and observed the Canberra NDA SuperHENC system and related process for the characterization of CH waste in standard waste boxes (SWBs), in support of an initial certification.	S	S	S
				LANL/CCP activities related to CH SCG S3000 and S5000 waste measurement in SWBs on the SuperHENC using the equipment and procedures examined and subject to the measurement controls in place were adequately established for compliance with upper-tier requirements, satisfactory in the implementation of these requirements, and effective in achieving the desired results.		
LANL	S-12-16	01/24 - 01/25/12	Evaluated the High Energy Real-Time Radiography (HERTR) unit for characterizing CH SCG S5000 debris waste and S3000 homogeneous solids waste. During LANL/CCP Recertification Audit A-11-11, performed May 17 - 19, 2011, the audit team was unable to complete the initial certification of the HERTR unit.	S	S	S
				LANL/CCP activities related to CH SCG S3000 and SCG S5000 wastes using the equipment and procedures examined were determined to be adequate, satisfactory in the implementation of those requirements, and effective in achieving the desired results.		
LANL	S-13-18	01/10/13	Evaluated the LANL/CCP solids sampling and analysis activities related to the characterization of CH SCG S4000 soils/gravel waste to provide a basis for initial approval	S	S	S
				The surveillance team reviewed the documentation supporting sampling and analysis activities, as well as final characterization of S4000 waste, and found them to be adequate, satisfactorily implemented and effective.		

Table AUD-3. Los Alamos National Laboratory - Carlsbad Operations Assessments

Organization Assessed	Assessment Number	Assessment Dates	Scope of Assessments	Adequacy	Implementation	Effectiveness
LANL-CO	A-08-13	02/26 - 02/28/08	Evaluated adequacy, effectiveness, and implementation of requirements in the LANL-CO/Carlsbad Environmental Monitoring and Research Center (CEMRC) Interface Document, LANL-CO Quality Assurance Plan (QAP), and LANL-CO implementing procedures.	S	S	S
				The defined QA program was satisfactorily implemented in accordance with the CBFO QAPD, and the LANL/CO - CEMRC implementing procedures. Technical areas evaluated were adequate, satisfactorily implemented, and effective.		
LANL-CO	A-09-09	02/03 - 02/05/09	Evaluated continued adequacy, effectiveness, and implementation of requirements in the LANL-CO/CEMRC Interface Document, LANL-CO QAP, and LANL-CO implementing procedures.	S	S	S
				The defined QA program was satisfactorily implemented in accordance with the CBFO QAPD, and the LANL/CO - CEMRC implementing procedures. Technical areas evaluated were adequate, satisfactorily implemented, and effective.		
LANL-CO	A-10-10	02/02 - 02/04/10	Evaluated continued adequacy, effectiveness, and implementation of requirements in the LANL-CO/CEMRC Interface Document, LANL-CO QAP, and LANL-CO implementing procedures.	S	S	S
				The defined QA program was satisfactorily implemented in accordance with the CBFO QAPD, and the LANL/CO - CEMRC implementing procedures. Technical areas evaluated were adequate, satisfactorily implemented, and effective.		
LANL-CO	A-11-05	04/26 - 04/28/11	Evaluated continued adequacy, effectiveness, and implementation of requirements in the LANL-CO/CEMRC Interface Document, LANL-CO QAP, and LANL-CO implementing procedures.	S	S	S
				The defined QA program was satisfactorily implemented in accordance with the CBFO QAPD, and the LANL/CO - CEMRC implementing procedures. Technical areas evaluated were adequate, satisfactorily implemented, and effective.		
LANL-CO	A-12-07	05/08 - 05/10/12	Evaluated continued adequacy, effectiveness, and implementation of requirements in the LANL-CO/CEMRC Interface Document, LANL-CO QAP, and LANL-CO implementing procedures.	S	S	S
				The defined QA program was satisfactorily implemented in accordance with the CBFO QAPD, and the LANL/CO - CEMRC implementing procedures. Technical areas evaluated were adequate, satisfactorily implemented, and effective.		

Table AUD-4. General Electric Vallecitos Nuclear Center Assessments

Organization Assessed	Assessment Number	Assessment Dates	Scope of Assessments	Adequacy	Implementation	Effectiveness
General Electric Vallecitos Nuclear Center (GEVNC)	A-09-05	12/02 - 12/04/08	Evaluated the adequacy, implementation, and effectiveness of (GEVNC) TRU waste characterization activities performed for RH SCG S5000 debris waste by WTS/CCP. Activities were evaluated relative to the requirements of the WIPP HWFP, the CBFO QAPD, and other upper-tier requirement documents.	S	S	S
				Technical and QA programs, as applicable to the audited activities, were adequate, satisfactorily implemented, and effective for compliance with applicable upper-tier requirements.		
GEVNC	A-10-04	01/26 - 01/28/10	Evaluated the continued adequacy, implementation, and effectiveness of GEVNC TRU waste characterization activities performed for RH SCG S5000 debris waste by WTS/CCP. Emphasis was placed on	S	S	S
				Technical and QA programs, as applicable to the audited activities, were adequate, satisfactorily implemented, and effective for compliance with applicable upper-tier requirements.		

Table AUD-4. General Electric Vallecitos Nuclear Center Assessments

Organization Assessed	Assessment Number	Assessment Dates	Scope of Assessments	Adequacy	Implementation	Effectiveness
			activities completed since the previous Audit A-09-05 and the process for project termination/closure activities due to the completion of the waste characterization campaign at GEVNC. All activities were evaluated to verify compliance with the applicable requirements of the WIPP HWFP, the CBFO QAPD, and other upper-tier requirement documents.			

Table AUD-5. Hanford-Richland Site Assessments

Organization Assessed	Assessment Number	Assessment Dates	Scope of Assessments	Adequacy	Implementation	Effectiveness
Richland (RL)	A-08-18	06/16 - 06/20/08	Evaluated the continued adequacy, implementation, and effectiveness of the Hanford QA Program and waste characterization and certification activities. Evaluated SCG S3000 homogeneous solids and S5000 debris waste characterized at the Waste Receiving and Processing (WRAP) facility, the Plutonium Finishing Plant (PFP), and the Waste Sampling and Characterization Facility (WSCF), as applicable. All activities were evaluated to verify compliance with the applicable requirements of the WIPP HWFP, the CBFO QAPD, and other upper-tier requirement documents.	S	S	S
				Technical and QA programs, as applicable to the audited activities, were adequate, satisfactorily implemented, and effective for compliance with applicable upper-tier requirements.		
RL	A-09-18	06/09 - 06/11/09	Evaluated the continued adequacy, implementation, and effectiveness of the Hanford QA Program and the Hanford Site TRU waste characterization and certification activities. Evaluated SCG S3000 and S5000 wastes characterized at the WRAP facility, the PFP, and the WSCF. Verified compliance with the applicable requirements of the WIPP HWFP, the CBFO QAPD, and other requirement documents. (In addition to the recertification of the Hanford TRU Program activities, consideration was given to the probability of retiring the Hanford TRU Program implementing procedures and the future implementation of the CCP as a viable option for Hanford's continued characterization and certification activities.)	S	S	S
				Technical and QA programs, as applicable to the audited activities, were adequate, satisfactorily implemented, and effective for compliance with applicable upper-tier requirements.		
RL	A-10-07	04/06 - 04/08/10	Evaluated the adequacy, implementation, and effectiveness of TRU waste characterization activities for SCG S5000 CH debris waste performed for the Hanford Site by WTS/CCP. Evaluated to verify compliance with the WIPP HWFP, the CBFO QAPD, and other upper-tier requirement documents. This was the initial certification for operations under the WTS/CCP Program.	S	S	S
				Technical and QA programs, as applicable to the audited activities, were adequate, satisfactorily implemented, and effective for compliance with applicable upper-tier requirements.		
RL	A-11-10	04/05 - 04/07/11	Evaluated continued adequacy, implementation, and effectiveness of the Hanford Site TRU waste characterization activities performed for CH SCGs S3000 homogeneous solids waste and S5000 debris waste WTS/CCP. Evaluated to verify compliance with the WIPP HWFP, the CBFO QAPD, and other requirement documents. (Also verified the initial certification activities related to the HERLR system for characterization of SWBs.	S	S	S
				Technical and QA programs, as applicable to the audited activities, were adequate, satisfactorily implemented, and effective for compliance with applicable upper-tier requirements.		
RL	A-12-11	05/15 - 05/16/12	Evaluated continued adequacy, implementation, and effectiveness of the Hanford Site TRU waste characterization activities performed for CH SCGs S3000 homogeneous solids waste and S5000 debris waste WTS/CCP. All activities were evaluated to verify compliance with the applicable requirements of the WIPP HWFP, the CBFO QAPD, and other requirement documents. Hanford/CCP suspended waste characterization activities at the end of September 2011, due to funding issues. No new containers of waste were introduced into the characterization process after September 2011; however, containers requiring the completion of generation-level data reviews and project-level data V&V activities to finalize the characterization process were managed for a short time thereafter.	S	I	I
				The audit team concluded that, for the documentation reviewed, the overall adequacy of the Hanford/CCP technical and QA programs was satisfactory in meeting upper-tier requirements as applicable to the audited activities. Since Hanford/CCP suspended waste characterization activities at the Hanford Site, the audit team was unable to evaluate HSG sampling, RTR, VE, and NDA characterization activities in the field to determine the implementation and effectiveness of characterization procedures, or to verify personnel and equipment were available to continue characterization activities. For this reason, these processes were deemed indeterminate.		
RL	S-08-11	04/28 - 04/29/08	Evaluated the implementation and effectiveness of the policies, plans, and procedures related to transportation activities at Hanford for the shipment of TRU waste to WIPP.	S	S	S
				The surveillance team determined that Hanford site procedures reviewed contained adequate flow-down of transportation requirements and the procedures were effectively implemented.		

Table AUD-5. Hanford-Richland Site Assessments

Organization Assessed	Assessment Number	Assessment Dates	Scope of Assessments	Adequacy	Implementation	Effectiveness
				N/A	S	S
				Implementation of the Hanford procedures for records closeout activities were evaluated and found to be effective.		
RL	S-10-19	03/30 - 03/31/10	Reviewed and evaluated the implementation and effectiveness of Hanford/CCP procedures related to transportation activities in accordance with CBFO and CCP procedure requirements.	S	S	S
				Implementation of the CCP procedures evaluated was effective for transportation of transuranic waste from Hanford to the WIPP. Hanford/CCP has satisfactorily and effectively implemented the requirements of CBFO and CCP procedures.		
RL	S-10-32	07/13/10	Evaluated the activities associated with Hanford/CCP HSG sampling activities at the Hanford Site facility.	S	S	S
				Activities related to HSG operations were adequate, satisfactorily implemented, and effective.		
RL	S-10-35	07/13/10	Evaluated the implementation and effectiveness of CCP corrective actions related to CAR 10-019 that resulted from audit A-10-07. The CAR identified issues related to the handling of raw data generated during VE activities.	S	S	S
				Corrective actions for CAR 10-019 were determined to be adequate, satisfactorily implemented, and effective.		

Table AUD-6. Washington TRU Solutions/Nuclear Waste Partnership Assessments

Organization Assessed	Assessment Number	Assessment Dates	Scope of Assessments	Adequacy	Implementation	Effectiveness
WTS	A-08-07	01/14 - 01/18/08	Evaluated the continued adequacy, implementation, and effectiveness of the WTS/CCP QAP, which was established for controlling quality-affecting activities associated with the characterization and certification of TRU waste by CCP destined for disposal WIPP repository.	S	S	S
				Activities related to the WTS/CCP QAP were adequate, satisfactorily implemented, and effective.		
WTS	A-08-14	02/12 - 02/14/08	Evaluated the adequacy, implementation, and effectiveness of the WTS WIPP Form Process, established for capturing, evaluating, and tracking the resolution of noted issues, deficiencies, and associated actions.	S	S	S
				Activities related to the WTS WIPP Form Process were adequate, satisfactorily implemented, and effective.		
WTS	A-08-15	03/24 - 03/27/08	Evaluated the continued adequacy and implementation of the WTS QA program related to the American Society of Mechanical Engineers Nuclear Quality Assurance (NQA) -1, 1989 Edition *Quality Assurance Program Requirements for Nuclear Facilities* Criteria 1-9.	S	S	S
				WTS QA program activities related to NQA-1 Criteria 1-9 were adequate and satisfactorily implemented relative to the flow-down of requirements from the upper-tier documents.		
WTS	A-08-17	04/08 - 04/11/08	Evaluated the adequacy, implementation, and effectiveness of QA and technical activities related to CH and RH waste handling operations at the WIPP. The activities were evaluated with respect to the requirements defined in the WIPP HWFP, CBFO QAPD, and other requirement documents	S	S	S
				Activities related to the WTS waste handling operations were adequate and satisfactorily implemented relative to the flow-down of requirements from the upper-tier documents.		
WTS	A-08-25	08/11 - 08/14/08	Evaluated the adequacy, implementation, and effectiveness of transportation activities performed under the CCP Program. The evaluation included CCP activities related to transportation activities performed by CCP at LANL, Savannah River Site (SRS), INL, and Oak Ridge National Laboratory (ORNL).	S	S	S
				Activities related to CCP transportation operations were adequate and satisfactorily implemented relative to the flow-down of requirements from the upper-tier documents.		
WTS	A-09-02	10/07 - 10/09/08	Evaluated WTS continued implementation of the QA program in relation to NQA-1, Criteria 10-18.	S	S	S
				WTS QA program activities related to NQA-1 Criteria 10-18 were adequate and satisfactorily implemented relative to the flow-down of requirements from the upper-tier documents.		
WTS	A-09-06	12/02 - 12/04/08	Evaluated the adequacy, implementation, and effectiveness of inter-site transportation activities performed under the WTS/CCP Program. The evaluation included CCP activities related to transportation activities performed by CCP at the Nevada Test Site.	S	S	S
				The audit team concluded that the CCP transportation activities evaluated were adequate, satisfactorily implemented, and effective.		
WTS	A-09-10	02/24 - 02/26/09	Evaluated the continued adequacy, implementation, and effectiveness of the WTS/CCP QAP which was established for controlling quality-affecting activities associated with the characterization and certification of TRU waste by CCP destined for disposal WIPP repository.	S	S	S
				Activities related to the WTS/CCP QAP were adequate, satisfactorily implemented, and effective.		
WTS	A-09-15	03/17 - 03/19/09	Evaluated the continued adequacy and implementation of the WTS QA Program related to NQA-1 Criteria 1-9.	S	S	S
				Activities related to the WTS QA Program were adequate, satisfactorily implemented, and effective.		
WTS	A-09-23	07/07 - 07/09/09	Evaluated the continued adequacy, implementation, and effectiveness of QA and technical activities related to CH and RH waste handling operations at the WIPP.	S	S	S
				Activities related to the WTS waste handling operations were adequate and satisfactorily implemented relative to the flow-down of requirements from the upper-tier documents.		

Table AUD-6. Washington TRU Solutions/Nuclear Waste Partnership Assessments

Organization Assessed	Assessment Number	Assessment Dates	Scope of Assessments	Adequacy	Implementation	Effectiveness
				S	S	S
				WTS compliance with DOE Order 226.1A adequately addressed applicable upper-tier requirements and was satisfactorily implemented and effective.		
WTS	A-09-27	09/29 - 10/01/09	Evaluated the adequacy, implementation, and effectiveness of transportation activities performed by CCP at LANL, SRS, INL, GEVNC, ORNL, and Argonne National Laboratory (ANL).	S	S	S
				Requirements associated with CCP technical and QA program activities related to transportation were satisfactorily implemented and effective relative to the CBFO QAPD and upper tier requirements.		
WTS	A-10-02	10/06 - 10/08/09	Evaluated WTS continued implementation of the QA program in relation to NQA-1 Criteria 10 - 18.	S	S	S
				Activities related to the WTS QA Program were adequate, satisfactorily implemented, and effective.		
WTS	A-10-05	06/22 - 06/24/10	Evaluated the adequacy, implementation, and effectiveness of inter-site transportation activities performed by the WTS/CCP. The evaluation included CCP transportation activities performed by CCP at the Lawrence Livermore National Laboratory.	S	S	S
				The audit team concluded that the CCP inter-site transportation activities evaluated were adequate, satisfactorily implemented, and effective.		
WTS	A-10-11	03/02 - 03/04/10	Continued adequacy, implementation, and effectiveness of the WTS/CCP QA Program, established for controlling quality-affecting activities associated with CCP characterization and certification of TRU waste destined for disposal at the WIPP.	S	S	S
				Activities related to the WTS/CCP QAP were adequate, satisfactorily implemented, and effective.		
WTS	A-10-18	09/14 - 09/16/10	Evaluated the continued adequacy, implementation, and effectiveness of QA and technical activities related to CH and RH waste handling operations at the WIPP.	S	S	S
				Activities related to the WTS waste handling operations were adequate and satisfactorily implemented relative to the flow-down of requirements from the upper-tier documents.		
WTS	A-10-20	05/10 - 05/13/10	Evaluated the continued adequacy and implementation of the WTS QA Program related to the WTS Monitoring Programs.	S	S	S
				Activities related to the WTS monitoring programs operations were adequate and satisfactorily implemented relative to the flow-down of requirements from the upper-tier documents.		
WTS	A-10-21	04/13 - 04/15/10	Evaluated the continued adequacy and implementation of the WTS QA Program as related to NQA-1 Criteria 1-9.	S	S	S
				Activities related to the WTS QA Program were adequate, satisfactorily implemented, and effective.		
WTS	A-10-25	09/21 - 09/23/10	Evaluated the adequacy, implementation, and effectiveness of transportation activities performed by CCP at LANL, SRS, INL, GEVNC, ORNL, Hanford, and ANL.	S	S	S
				Requirements associated with CCP technical and QA program activities related to transportation were satisfactorily implemented and effective relative to the CBFO QAPD and upper tier requirements.		
WTS	A-11-02	10/05 - 10/07/10	Evaluated WTS continued implementation of the QA program in relation to NQA-1 Criteria 10 - 18.	S	S	S
				Activities related to the WTS QA Program were adequate, satisfactorily implemented, and effective.		
WTS	A-11-06	03/01 - 03/03/11	Evaluated the continued adequacy, implementation, and effectiveness of the WTS/CCP QAP, which was established for controlling quality-affecting activities associated with the characterization and certification of TRU waste by CCP destined for disposal WIPP repository.	S	S	S
				Activities related to the WTS/CCP QAP were adequate, satisfactorily implemented, and effective.		
WTS	A-11-07	03/15 - 03/17/11	Evaluate the adequacy, implementation, and effectiveness of QA and technical activities related to records processes at the WIPP.	M	M	M
				The audit team concluded that overall, WTS records processes were marginally adequate in addressing applicable upper-tier requirements and marginally implemented and effective. Six CARs were issued. Follow-up surveillance (S-12-01) was conducted in October, 2011 to verify completion and adequacy of corrective actions.		
WTS	A-11-09	04/12 - 04/14/11	Evaluated the continued adequacy and implementation of the WTS QA Program as related to NQA-1 Criteria 1-9.	S	S	S
				Activities related to the WTS QA Program were adequate, satisfactorily implemented, and effective.		
WTS	A-11-16	08/30 - 09/01/11	Evaluated the continued adequacy, implementation, and effectiveness of QA and technical activities related to CH and RH waste handling operations at the WIPP.	S	S	S
				Activities related to the WTS waste handling operations were adequate and satisfactorily implemented relative to the flow-down of requirements from the upper-tier documents.		
WTS	A-11-17	05/10 - 05/12/11	Evaluated the continued adequacy and implementation of the WTS QA Program related to the WTS Monitoring Programs.	S	S	S
				Activities related to the WTS monitoring programs operations were adequate and satisfactorily implemented relative to the flow-down of requirements from the upper-tier documents.		
WTS	A-11-18	05/24 - 05/26/11	Evaluated the adequacy, implementation, and effectiveness of Transuranic Package	S	S	S

Table AUD-6. Washington TRU Solutions/Nuclear Waste Partnership Assessments

Organization Assessed	Assessment Number	Assessment Dates	Scope of Assessments	Adequacy	Implementation	Effectiveness
			Transporter-III (TRUPACT-III) activities related to shipping processes at the Mobile Loader Storage and Staging Site located in Carlsbad, NM.	The audit team concluded that overall, the TRUPACT -III activities evaluated were adequate in addressing applicable upper-tier requirements, satisfactorily implemented and effective.		
WTS	A-11-19	08/23 - 08/25/11	Evaluated the adequacy, implementation, and effectiveness of inter-site transportation activities performed by the WTS/CCP. The evaluation included documentation relating to waste shipped from various generator sites to the INL for characterization.	S	S	S
				The audit team concluded that the CCP inter-site transportation activities evaluated were adequate, satisfactorily implemented, and effective.		
WTS	A-11-24	09/20 - 09/22/11	Evaluated the adequacy, implementation, and effectiveness of transportation activities performed by CCP at LANL, SRS, INL GEVNC, ORNL, Hanford, and ANL.	S	S	S
				Requirements associated with CCP technical and QA program activities related to transportation were satisfactorily implemented and effective relative to the CBFO QAPD and upper tier requirements.		
WTS	A-12-01	10/04 - 10/06/11	Evaluated WTS continued implementation of the QA program in relation to NQA-1 Criteria 10 - 18.	S	S	S
				Activities related to the WTS QA Program were adequate, satisfactorily implemented, and effective.		
WTS	A-12-09	03/06 - 03/08/12	Evaluated the continued adequacy, implementation, and effectiveness of the WTS/CCP QAP, which was established for controlling quality-affecting activities associated with the characterization and certification of TRU waste by CCP destined for disposal WIPP repository.	S	S	S
				Activities related to the WTS/CCP QAP were adequate, satisfactorily implemented, and effective.		
WTS	A-12-17	04/03 - 04/05/12	Evaluate the adequacy, implementation, and effectiveness of QA and technical activities related to records processes at the WIPP.	S	S	S
				Activities related to the records processes were adequate, satisfactorily implemented, and effective.		
WTS	A-12-18	04/10 - 04/12/12	Evaluated the continued adequacy and implementation of the WTS QA Program related to NQA-1 Criteria 1-9.	S	S	S
				Activities related to the WTS QA Program were adequate, satisfactorily implemented, and effective.		
WTS	A-12-21	08/07 - 08/09/12	Evaluated the continued adequacy and implementation of the WTS QA Program related to the WTS Monitoring Programs.	S	S	S
				Activities related to the WTS monitoring programs operations were adequate and satisfactorily implemented relative to the flow-down of requirements from the upper-tier documents.		
WTS	A-12-22	06/26 - 06/28/12	Evaluated the adequacy, implementation, and effectiveness of inter-site transportation activities performed by the WTS/CCP. The evaluation included documentation relating to waste shipped from various generator sites to the INL for characterization.	S	S	S
				The audit team concluded that the CCP inter-site transportation activities evaluated were adequate, satisfactorily implemented, and effective.		
WTS	A-13-03	12/04 - 12/06/12	Evaluated the adequacy, implementation, and effectiveness of CCP plans and procedures related to waste transportation activities for shipment of TRU waste to the WIPP.	S	S	S
				The audit team concluded that the applicable CCP transportation activities were adequate, satisfactorily implemented, and effective for compliance with the upper-tier requirements documents.		
NWP	A-13-04	10/30 - 11/01/12	Evaluated NWP implementation of the QA program in relation to NQA-1 Criteria 10 - 18.	S	S	S
				Activities related to the NWP's QA Program were adequate, satisfactorily implemented, and effective.		
NWP	A-13-05	11/13 - 11/15/12	Evaluated the adequacy, implementation, and effectiveness of the NWP programs and related procedures for compliance with DOE Order 226.1 B, *Implementation of Department of Energy Oversight Policy*. The requirements prescribed in Attachment 1 of the Order, Contractor Requirements Document, were evaluated.	S	S	S
				The audit team determined that NWP programs adequately addressed the upper-tier requirements of the Order, were effectively implemented, and achieved the desired results.		
WTS	S-08-14	08/19 - 08/21/08	Evaluated the adequacy, implementation, and effectiveness of WTS National Emissions Standards for Hazardous Air Pollutants (NESHAP) activities.	S	S	S
				The WTS NESHAP processes and associated activities were satisfactorily implemented and effective.		
WTS	S-08-18	09/22 - 09/25/08	Evaluated the adequacy, implementation, and effectiveness of WTS Ground Control and Geotechnical Engineering processes.	S	S	S
				The surveillance team determined that the WTS Ground Control and Geotechnical Engineering processes and associated activities were satisfactorily implemented and effective.		
WTS	S-08-19	09/11/08 -10/02/08	Evaluated the implementation and effectiveness of the corrective actions taken by WTS/CCP, as a result of the CAR 08-025. CAR 08-025 was issued as a result of an NCR, not due to an independent audit.	S	S	S
				Activities observed during the surveillance were satisfactorily implemented and effective.		
WTS	S-09-01	10/14 - 10/16/08	Evaluated the degree of adequacy and implementation of the requirements established to support safe mine operations at the WIPP.	S	S	S
				The results of the surveillance concluded that the portions of the WTS program and procedures supporting safe mine operations were adequate for compliance with upper-tier requirements and effectively implemented.		

Table AUD-6. Washington TRU Solutions/Nuclear Waste Partnership Assessments

Organization Assessed	Assessment Number	Assessment Dates	Scope of Assessments	Adequacy	Implementation	Effectiveness
				S	S	S
				The WTS Engineering Fire Protection processes and associated activities were adequately documented, satisfactorily implemented, and effective.		
WTS	S-09-04	12/09 - 12/11/08	Evaluated the adequacy, implementation, and effectiveness of WTS Fire/Emergency Response at the WIPP.	S	S	S
				The WTS Fire/Emergency Response processes and associated activities were satisfactorily implemented and effective.		
WTS	S-09-07	12/16 - 12/18/08	Evaluated the adequacy, implementation, and effectiveness of the Subsidence Survey Data Acquisition process at the WIPP.	S	S	S
				The WTS Subsidence Survey Data Acquisition processes and associated activities were satisfactorily implemented, and effective.		
WTS	S-09-11	01/20 - 01/22/09	Evaluated the adequacy, implementation and effectiveness of the WTS WIPP Form process (Issues Management) for compliance with applicable requirements.	S	S	S
				The WTS WIPP Form process remains adequate for compliance with upper-tier requirements and is effectively implemented.		
WTS	S-09-12	02/17 - 02/19/09	Evaluated the adequacy, implementation, and effectiveness of the Washington TRU Solutions Washington Regulatory and Environmental Services (WTS/WRES) Waste Confirmation process.	S	S	S
				The WTS/WRES Waste Confirmation process and associated activities were adequately documented, satisfactorily implemented, and effective.		
WTS	S-09-13	08/25 - 08/27/09	Evaluated the adequacy, implementation, and effectiveness of WTS Engineering Documented Safety Analyses (DSA)/Technical Safety Requirements (TSR) processes.	S	S	S
				The surveillance team determined that the WTS Engineering DSA/TSR processes and associated activities were adequately documented, satisfactorily implemented, and effective.		
WTS	S-09-14	03/31 - 04/02/09	Evaluated the adequacy, implementation, and effectiveness of the WTS Maintenance Program, including calibration control processes.	S	S	S
				The WTS Maintenance Program, including calibration control processes and associated activities, was adequately documented, satisfactorily implemented, and effective.		
WTS	S-09-15	03/24 - 03/26/09	Evaluated the degree of adequacy and effective implementation of the WTS Groundwater Monitoring Program for compliance with applicable requirements.	S	S	S
				The WTS Groundwater Monitoring Program was adequately documented, satisfactorily implemented, and effective.		
WTS	S-09-18	03/10 - 03/12/09	Evaluated the WTS Centralized Procurement Program task of providing a standardized system of acquisition and distribution of common or critical TRU waste commodities for the CBFO.	S	S	S
				The WTS Centralized Procurement Program adequately incorporated upper-tier requirements into program plans and Procedures. The Program Plan and procedures are satisfactorily implemented and effective.		
WTS	S-09-19	04/04 - 04/06/09	Evaluated the adequacy, implementation, and effectiveness of WTS Seismic Monitoring Program at the WIPP.	U	U	U
				The WTS Seismic Monitoring Program processes and associated activities were inadequate, unsatisfactorily implemented, and not effective. A CAR (09-037) categorized as significant, was issued. A corrective action plan was submitted and approved. Corrective actions were verified. Monitoring Programs re-evaluated in S-10-28.		
WTS	S-09-20	03/24 - 03/25/09	Evaluated the changes to the WTS 10 CFR Part 71, Subpart H, QA Program, as applied to the Type "B" containers.	S	S	S
				The WTS 10 CFR Part 71, Subpart H, QA Program has been changed to adequately incorporate the Nuclear Regulatory Commission's changes made to their process. The WTS changes were satisfactorily implemented and effective.		
WTS	S-09-22	04/21 - 04/23/09	Evaluated the implementation and effectiveness of the policies, plans, and procedures related to the operation, inspection, and maintenance of the WTS mine ventilation system.	S	S	S
				Activities associated with the WTS mine ventilation system were adequate, satisfactory and effective.		
WTS	S-09-23	07/29 - 07/30/09	Evaluated the degree of adequacy and effective implementation of the WTS Meteorological Monitoring Program for compliance with applicable requirements.	S	S	S
				The WTS Meteorological Monitoring Program remains adequate for compliance with upper-tier requirements and is effectively implemented.		
WTS	S-09-24	07/21 - 07/23/09	Evaluated the implementation and effectiveness of selected requirements applicable to security services associated with the WIPP.	M	M	M
				Due to the limited scope and the number and nature of the concerns identified, the surveillance team concluded that implementation of the requirements governing security services was marginally effective. Three CARs were issued (09-052, 09-053, and 09-054). Corrective action plans were approved and resulting completed actions verified. Re-evaluated in S-13-16, after change in security contractor.		
WTS	S-09-26	06/02 - 06/03/09	Evaluated the degree of adequacy and effective implementation of the WTS Environmental Safe Drinking Water (SDW) Program for compliance with applicable requirements.	S	S	S

Table AUD-6. Washington TRU Solutions/Nuclear Waste Partnership Assessments

Organization Assessed	Assessment Number	Assessment Dates	Scope of Assessments	Adequacy	Implementation	Effectiveness
				The WTS Environmental SDW Program was adequate for compliance with upper-tier requirements and is effectively implemented.		
WTS	S-09-27	09/22 - 09/24/09	Evaluated the adequacy, implementation, and effectiveness of the WTS Graded Approach Program.	S	S	S
				The WTS Graded Approach Program was adequate, satisfactorily implemented, and effective.		
WTS	S-09-28	09/08 - 09/09/09	Evaluated the adequacy, implementation, and effectiveness of the WTS QA Program with respect to DP-831 procurement activities in accordance with CBFO documents. Verified the implementation and effectiveness of WTS engineering implementing processes for the new salt storage evaporation (SSE) pond.	S	S	S
				Activities associated with the procurement of materials for the DP-831 SSE pond were adequate, satisfactorily implemented, and effective.		
WTS	S-09-31	07/14 - 07/16/09	Evaluated the adequacy, implementation, and effectiveness of the WTS Radiological Control (RADCON) Program for site operations at the WIPP.	M	M	M
				The WTS RADCON Program was marginally adequate, marginally implemented, and marginally effective. Four CARs were issued (09-048, 09-049, 09-050, and 09-051). Corrective actions for all CARs were verified to be complete.		
WTS	S-09-34	09/08 - 09/10/09	Evaluated the adequacy, implementation, and effectiveness of WTS Confined Space Control, Fall Protection, and Hearing Protection.	S	S	S
				The WTS Confined Space, Fall, and Hearing Protection Program was adequate for compliance with upper-tier requirements and was effectively implemented.		
WTS	S-09-38	09/29 - 09/30/09	Evaluated the adequacy, implementation, and effectiveness of the WTS Central Monitoring Room (CMR) and Transportation Tracking and Communication (TRANSCOM) Operations at the WIPP.	S	S	S
				The WTS CMR and TRANSCOM Operations were adequate, satisfactorily implemented, and effective.		
WTS	S-10-02	11/17 - 11/19/09	Evaluated the implementation and effectiveness of the Type B Packaging Program, as performed by WTS on the CH and RH TRU waste.	S	S	S
				Activities associated with the Type B Packaging Program were adequate, satisfactorily implemented, and effective.		
WTS	S-10-03	11/03 - 11/05/09	Evaluated the degree of adequacy and effective implementation of the WTS Environmental Conduct of Operations Program for compliance with applicable requirements.	S	S	S
				The WTS Conduct of Operations Program was adequate, satisfactorily implemented, and effective.		
WTS	S-10-04	12/01 - 12/03/09	Evaluated the adequacy, implementation, and effectiveness of WTS Ground Control and Geotechnical Engineering programs.	S	S	S
				The WTS Ground Control and Geotechnical Engineering programs and associated activities were adequate, satisfactorily implemented, and effective.		
WTS	S-10-07	01/19 - 01/21/10	Evaluated the adequacy and implementation of the WIPP site fire/emergency response program.	S	S	S
				The WIPP site fire/emergency response program activities were adequate, satisfactorily implemented, and effective.		
WTS	S-10-08	01/05 - 01/07/10	Evaluated the adequacy and implementation of WP 12-3, *Dosimetry Program,* as applicable to activities at the WIPP.	S	S	S
				The WTS Dosimetry Program was determined to be adequate, satisfactorily implemented, and effective.		
WTS	S-10-11	10/20 - 10/21/09	Evaluated the implementation and effectiveness of the plans and procedures related to the Procurement and QA Oversight of the TRUPACT-III.	S	S	S
				The activities associated with Procurement and QA Oversight of the TRUPACT-III were adequate, satisfactorily implemented, and effective.		
WTS	S-10-12	12/17/09 01/27/10 02/10/10	Evaluated the adequacy and implementation of the WTS QA Program with respect to the new DP-831 storage pond. Surveillance was conducted over a period of time because of construction and weather delays. This surveillance also evaluated and verified the implementation and effectiveness of WTS engineering implementing processes for the new DP-831 SSE Pond.	S	S	S
				Activities associated with the DP-831 storage pond were adequate, satisfactorily implemented, and effective.		
WTS	S-10-13	11/10 - 11/12/09	Evaluated the adequacy, implementation, and effectiveness of software quality assurance (SQA) controls performed by WTS and Insei related to the development of the Waste Data System (WDS), a web-based software application that includes the current WIPP Waste Information System (WWIS) software application.	S	S	S
				WTS and Insei SQA procedures were adequate and satisfactorily implemented and documented, and implementation of the WTS/Insei SQA process effectively provides for control of WDS development and promotion of the WDS software to production.		
WTS	S-10-16	04/13 - 04/15/10	Evaluated the adequacy, implementation, and effectiveness of the WTS Maintenance Program, excluding calibration.	S	S	S
				The WTS Maintenance Program was adequately documented, satisfactorily implemented, and effective.		
WTS	S-10-24	05/04/10	Evaluated the adequacy, implementation, and effectiveness of the WTS activities that allow for the off-site shipment of Resource Conservation and Recovery Act (RCRA) hazardous waste to permitted disposal sites.	S	S	S
				The WTS off-site shipment activities were adequate, satisfactorily implemented, and effective.		
WTS	S-10-28			S	S	S

Table AUD-6. Washington TRU Solutions/Nuclear Waste Partnership Assessments

Organization Assessed	Assessment Number	Assessment Dates	Scope of Assessments	Adequacy	Implementation	Effectiveness
		06/22 - 06/24/10	Evaluated the adequacy, implementation, and effectiveness of the WTS Seismic Monitoring Program.	The WTS Seismic Monitoring activities are adequate, satisfactorily implemented, and effective.		
WTS	S-10-29	07/27 - 07/29/10	Evaluated the adequacy and implementation of selected portions of the WTS Industrial Safety and Health (IS&H) Program.	S	M	M
				Overall, the program elements evaluated were adequate in addressing applicable upper-tier requirements; however, due to the number of concerns identified, the associated requirements were determined to be marginally implemented and effective. Seven CARs were issued (10-040 throuh 10-047). Corrective action plans were approved and completed actions were verified.		
WTS	S-11-01	10/19 - 10/21/10	Evaluated the adequacy, implementation, and effectiveness of SQA controls performed by WTS related to the development of WDS, a web-based software application that incorporates elements of the WWIS software application.	S	S	S
				Activities associated with SQA controls performed by WTS were adequate, satisfactorily implemented, and effective.		
WTS	S-11-02	12/14 - 12/16/10	Evaluated the Job Hazard Analysis (JHA) Program, including generation, review, approval, and update of JHAs in both surface and underground operations.	S	S	S
				The JHA program elements were adequate in addressing applicable upper-tier requirements; satisfactorily implemented, and effective.		
WTS	S-11-03	12/07 - 12/09/10	Evaluated the implementation and effectiveness of the WTS policies, plans, and procedures related to the electrical safety programs being implemented at the WIPP. Special emphasis was placed on evaluation of Lockout/Tagout (LO/TO) practices being conducted during the current program outage.	S	S	S
				The WTS Electrical Safety Program and LO/TO processes were adequate, satisfactorily implemented, and effective.		
WTS	S-11-04	11/30 - 12/02/10	Evaluated the adequacy, implementation, and effectiveness of the WTS Ground Control program, as implemented during the annual maintenance outage.	S	S	S
				Activities related to the WTS Ground Control program were adequate, satisfactorily implemented, and effective.		
WTS	S-11-07	10/13/10	Evaluated the adequacy, implementation, and effectiveness of the WTS Action Request/Work Control Process.	S	S	S
				The WTS action request and work control process was adequate, satisfactorily implemented, and effective.		
WTS	S-11-09	01/20/11	Evaluated the adequacy and implementation of the WTS QA Program with respect to the new DP-831 SSE Pond in accordance with required documents and procedures.	S	S	S
				Activities associated with the DP-831 storage pond were adequate, satisfactorily implemented, and effective.		
WTS	S-11-17	03/01 -03/07/11	On February 12, 2011, during the processing of CH waste at the WIPP, Operations personnel noted twigs protruding from the corners of the lid/body joints of two SWBs being unloaded. The personnel notified the CMR and the CBFO site facility representative. The surveillance evaluated the WTS response and investigation of the incident as defined in WP 04-IM1000, Revision 8, *Issues Management Processing of WIPP Forms.*	S	S	S
				There were no deficiencies noted in WTS personnel handling of the identified issue. The conditions were identified immediately during unloading of the SWBs, documentation and proper notification were made in a timely manner, the issue was investigated in an acceptable and appropriate time frame, and the WIPP Form process was performed adequately to address the issue.		
WTS	S-11-19	07/26 - 07/28/11	Evaluated the implementation and effectiveness of selected WTS plans and procedures related to the WTS IS&H Program being implemented at the WIPP.	S	S	S
				The WTS IS&H Program activities evaluated were adequate, satisfactorily implemented, and effective.		
WTS	S-11-22	08/16/11	Evaluated the adequacy, implementation, and effectiveness of WTS NESHAP activities.	S	S	S
				WTS NESHAP activities evaluated were adequate, satisfactorily implemented, and effective.		
WTS	S-11-24	08/23 - 08/24/11	Evaluated the adequacy, implementation, and effectiveness of the WTS Commercial Grade Item (CGI) Dedication Program.	S	S	S
				WTS CGI Dedication activities evaluated were adequate, satisfactorily implemented, and effective.		
WTS	S-11-25	09/20 - 09/22/11	Conducted as a follow-up to CBFO CAR 11-043. identified during audit A-11-14, which identified that some of the required AK documents INL/CCP were missing in the CCP Records files. Team evaluated the adequacy, implementation, and effectiveness of the CCP collection and storage of the AK source documents and applicable forms.	S	S	S
				The CCP AK Records activities evaluated were adequate, satisfactorily implemented, and effective.		
WTS	S-11-26	09/06 - 09/08/11	Evaluated the WTS work control process for compliance with WTS Management Control Procedure WP 10-WC3011, *Work Control Process*.	S	S	S
				The WTS work control processes evaluated were adequate, satisfactorily implemented, and effective.		
WTS	S-12-01	10/04 - 10/06/11	Conducted as a follow-up to CARs 11-022 through 11-027 resulting from CBFO Audit A-11-07, which had identified numerous Conditions Adverse to Quality within the WTS Records Processes.	S	S	S
				The WTS Records Processes were determined to be adequate in addressing upper-tier requirements, satisfactory in implementation of these requirements, and effective in achieving the desired results.		
WTS	S-12-02	10/11 - 10/13/11		S	S	S

Table AUD-6. Washington TRU Solutions/Nuclear Waste Partnership Assessments

Organization Assessed	Assessment Number	Assessment Dates	Scope of Assessments	Adequacy	Implementation	Effectiveness
			Evaluated the degree of adequacy and implementation of the requirements established to support safe mine operations at the WIPP.	The surveillance team concluded that the WTS Mine Safety Program and applicable procedures are adequate for compliance with upper-tier requirements and effectively implemented.		
WTS	S-12-05	12/13 - 12/15/11	Evaluated the adequacy, implementation, and effectiveness of the WTS Ground Control Program, with respect to the associated implementing procedures and revised activities since the last surveillance.	S	S	S
				The surveillance team verified that the Ground Control Program meets the approved procedural requirements and is adequate, satisfactorily implemented, and effective.		
WTS	S-12-07	09/25 - 09/27/12	Reviewed and evaluated the adequacy, implementation, and effectiveness of WTS transuranic waste operations as related to TRUPACT-III unloading operations for compliance with requirements set forth in the *TRUPACT-III Operations Manual* and the *CBFO* QAPD.	S	S	S
				The surveillance team verified that TRUPACT-III unloading operations plans and procedures adequately address upper-tier requirements, are satisfactorily implemented, and are effective. The team determined that the TRUPACT-III processes and associated activities evaluated are satisfactorily implemented and effective.		
WTS	S-12-09	12/13 - 12/15/11	Evaluated the adequacy, implementation, and effectiveness of the Subsidence Survey Data Acquisition process at the WIPP.	S	S	S
				The surveillance team determined that the WTS Subsidence Monitoring Program was adequate, satisfactorily implemented, and effective.		
WTS	S-12-11	09/18 - 09/20/12	Reviewed documentation and records, interviewed responsible personnel, and witnessed activities relative to the WTS Hazardous Communication and Control of Hazardous Chemicals/Gases Programs at the WIPP to verify compliance with applicable requirements.	S	S	S
				The results of the surveillance confirm that the requirements applicable to WTS Hazard Communication (HazCom) and Control of Hazardous Chemicals/Gases are effectively implemented and the programs achieve the desired results.		
WTS	S-12-12	02/14 - 02/16/12	Verified the adequacy and implementation of Washington TRU Solutions Regulatory and Environmental Services (WTS/RES) Waste Confirmation activities in Carlsbad, NM, and Idaho Falls, ID.	S	S	S
				The results of the surveillance indicate that the WTS/RES Permittee Waste Confirmation activities are adequately established for compliance with upper-tier requirements, satisfactory in the implementation of those requirements, and effective in achieving the desired results.		
WTS	S-12-13	03/13 - 03/14/12	Evaluated the implementation and effectiveness of the policies, plans, and procedures related to the WTS Centralized Procurement Program for procurement of items and services utilized in the operation and maintenance of the WIPP.	S	S	S
				The team determined that the WTS Centralized Procurement Program was adequately established, satisfactorily implemented, and effective.		
WTS	S-12-15	04/03/12	Verified adequacy and WTS implementation of Title 10 Code of Federal Regulations (CFR) Part 71, Subpart H, Quality Assurance Program, as applied to Type B containers.	S	S	S
				The surveillance team determined that the WTS 10 CFR Part 71, Subpart H, Quality Assurance Program, is adequate. The WTS procedures reviewed were found to be satisfactorily implemented and effective.		
WTS	S-12-17	04/17 - 04/19/12	Evaluated the degree of adequacy and implementation of the requirements established to support mine ventilation operations at the WIPP.	S	S	S
				The results of the surveillance indicate that the WTS Mine Ventilation Program remains adequate for compliance with upper-tier requirements and is effectively implemented.		
WTS	S-12-18	07/10 - 07/11/12	Evaluated the degree of adequacy and effective implementation of requirements associated with the WIPP Meteorological Monitoring Program.	S	S	S
				Evidence assembled and evaluated during the course of this assessment suggests that WTS meteorological activities conducted prior to the surveillance were performed appropriately and the program was achieving the desired results.		
WTS	S-12-19	05/08/12	Evaluated the WTS Environmental SDW Program implementing procedures for compliance to applicable upper-tier requirements documents.	S	S	S
				The results of the surveillance indicate that the WTS Environmental SDW Program remains adequate for compliance with upper-tier requirements, satisfactorily implemented, and effective.		
WTS	S-12-25	09/18 - 09/20/12	Evaluated the effectiveness of requirements associated with the WTS Graded Approach Program.	S	S	S
				The requirements associated with the WTS Graded Approach Program were satisfactorily implemented and achieved the desired results.		
NWP	S-13-01	11/13 - 11/14/12	Evaluated the degree of adequacy and effective implementation of the NWP, LLC/CCP Integrated Data Center (IDC) On-Line Training System for compliance with applicable requirements.	S	S	S
				The results of the surveillance indicate that although the IDC On-line Training System is not fully implemented, it remains adequate for compliance with upper-tier requirements and all elements are implemented and captured either in the IDC system or in other off-line processes.		
NWP	S-13-02	11/13 - 11/15/12	Evaluated the adequacy, implementation, and effectiveness of the NWP CMR (CMR) and TRANSCOM Operations at the WIPP site.	S	S	S
				The surveillance team determined that the NWP CMR and TRANSCOM Operations were adequate, satisfactorily implemented, and effective.		
NWP	S-13-03			S	S	S

Table AUD-6. Washington TRU Solutions/Nuclear Waste Partnership Assessments

Organization Assessed	Assessment Number	Assessment Dates	Scope of Assessments	Adequacy	Implementation	Effectiveness
		12/04 - 12/06/12	Evaluated the effectiveness of requirements associated with the NWP IS&H Program.	The NWP IS&H Program at WIPP was found to be adequate, satisfactorily implemented, and effective in achieving the desired results.		
NWP	S-13-07	01/29 -01/31/13	Verified the adequacy and implementation of the NWP QA Program with respect to Type B packaging to be used at the WIPP.	S	S	S
				The surveillance team determined that the NWP 10 CFR Part 71, Subpart H, QA Program is adequate. The NWP procedures reviewed were found to be satisfactorily implemented and effective in achieving the desired results.		
NWP	S-13-11	10/10 - 10/11/12	Reviewed and evaluated the adequacy, implementation, and effectiveness of the NWP/CCP NDA waste characterization process using the Nondestructive Assay Box Counter (NABC) gamma modality with the Five Foot Setback Configuration for the purposes of characterizing and certifying CH SCGs S3000 homogeneous solids, S4000 soils/gravel, and S5000 debris wastes in 55-gallon drums.	S	S	S
				The team determined that the NABCs Five Foot Setback Configuration procedures adequately address upper-tier requirements, are satisfactorily implemented and are effective. The processes and associated activities evaluated are satisfactorily implemented and effective.		
NWP	S-13-16	01/15 - 01/17/13	Evaluated the implementation and effectiveness of selected portions of the WIPP security program established for compliance with security-related, upper-tier requirements and the CBFO QAPD.	S	S	S
				The surveillance team concluded the selected-scope of the WIPP Security Program is compliant with security-related, upper-tier requirements, and the program is adequate, satisfactorily implemented, and effective.		

Table AUD-7. Sandia National Laboratories/Carlsbad Program Group Assessments

Organization Assessed	Assessment Number	Assessment Dates	Scope of Assessments	Adequacy	Implementation	Effectiveness
SNL/CPG	A-09-04	11/04 - 11/05/08	Verified the continued adequacy, implementation, and effectiveness of the SNL/CPG WIPP QA program for WIPP activities in accordance with the CBFO QAPD.	S	S	S
				The SNL/CPG WIPP QA Program was found to be adequate, satisfactorily implemented, and effective in achieving the desired results.		
SNL/CPG	A-10-09	11/16 - 11/19/09	Verified the continued adequacy, implementation, and effectiveness of the SNL/CPG WIPP QA program for WIPP activities in accordance with the CBFO QAPD.	S	S	S
				The SNL/CPG WIPP QA Program was found to be adequate, satisfactorily implemented, and effective in achieving the desired results.		
SNL/CPG	A-11-03	11/16 - 11/23/10	Verified the continued adequacy, implementation, and effectiveness of the SNL/CPG WIPP QA program for WIPP activities in accordance with the CBFO QAPD.	S	S	S
				The SNL/CPG WIPP QA Program was found to be adequate, satisfactorily implemented, and effective in achieving the desired results.		
SNL/CPG	A-12-05	12/06 - 12/08/11	Verified the continued adequacy, implementation, and effectiveness of the SNL/CPG WIPP QA program for WIPP activities in accordance with the CBFO QAPD.	S	S	S
				The SNL/CPG WIPP QA Program was found to be adequate, satisfactorily implemented, and effective in achieving the desired results.		

Table AUD-8. Savannah River Site/CCP Assessments

Organization Assessed	Assessment Number	Assessment Dates	Scope of Assessments	Adequacy	Implementation	Effectiveness
SRS	A-09-01	10/28 - 10/30/08	Evaluated adequacy, implementation, and effectiveness of the SRS TRU waste characterization activities performed for SCGs S3000 homogeneous solids waste, S4000 soils/gravel waste, and S5000 debris waste, including RH S5000 debris waste, in addition to other technical and quality assurance elements.	S	S	S
				SRS technical and QA programs, as applicable to the audited activities, were adequate, satisfactorily implemented, and effective for compliance with applicable upper-tier requirements.		
SRS	A-09-16	06/23 - 06/24/09	Assessed the level of compliance of waste characterization and certification activities for SCG S5000 debris waste and SCG S4000 soils/gravel waste using RTR Unit 4.	S	S	S
				The audit team concluded that the applicable SRS/CCP TRU waste characterization activities, as described in the associated implementing procedures, are adequate, satisfactorily implemented, and effective.		
SRS	A-09-17	03/24 - 03/26/09	Evaluated the adequacy, implementation, and effectiveness of the SRS/CCP TRU waste characterization and certification activities using the NABC.	S	S	S
				The audit team concluded that the applicable SRS/CCP TRU waste characterization activities, as described in the associated implementing procedures, are adequate, satisfactorily implemented, and effective.		
SRS	A-10-01	10/27 - 10/29/09	Evaluated the continued adequacy, implementation, and effectiveness of the SRS/CCP TRU waste QA and technical areas and characterization and certification activities for SCG CH S4000 soils/gravel waste and CH S5000 debris waste, including RH S5000 debris waste for waste stream SR-RL-BCLDP.001. The audit team also evaluated for initial certification CH S3000 solids waste for compliance with the requirements of the HWFP.	S	S	S
				The audit team concluded that the applicable SRS/CCP TRU waste characterization and certification activities, as described in the associated SRS/CCP *Quality Assurance Project Plan* and implementing procedures, are adequate, satisfactorily implemented, and effective.		
SRS	A-10-22	05/04 - 06/02/10	Evaluated compliance with CBFO requirements for peer reviews. The peer review evaluated during this audit was performed to qualify historical radiochemistry data analyzed by Battelle Radioanalytical Laboratory. These data were used to establish radiological properties for two waste streams currently residing at SRS.	S	S	S
				The audit team concluded that the requirements governing the performance of this peer review were adequate, satisfactorily implemented, and effective.		
SRS	A-11-01	10/26 - 10/28/10	Evaluated the continued adequacy, implementation, and effectiveness of the SRS/CCP TRU waste characterization and certification activities as they relate to the WIPP HWFP for CH SCGs S3000 homogeneous solids waste, S4000 soils/gravel waste, and S5000 debris waste, and RH SCG S3000 homogeneous solids waste and S5000 debris waste. The audit team also evaluated for initial certification the RTR Unit 4 to characterize standard large box 2s (SLB2s)and the Large Container Non-Destructive Examination (LCNDE) system to characterize SWBs and SLB2s.	S	S	S
				The audit team concluded that overall, the SRS/CCP technical and QA programs, as applicable to audited activities, were adequately established for compliance with the applicable upper-tier requirements.		
SRS	A-12-02	11/14 - 11/17/11	The audit team evaluated the continued adequacy, implementation, and effectiveness of the SRS/CCP TRU waste characterization activities for CH SCGs S3000 homogeneous	S	S	S

Table AUD-8. Savannah River Site/CCP Assessments

Organization Assessed	Assessment Number	Assessment Dates	Scope of Assessments	Adequacy	Implementation	Effectiveness
			solids waste, S4000 soils/gravel waste, and 85000 debris waste. The initial Certification Audit, A-12-04, for RH SCG S5000 retrievably stored debris waste was conducted concurrently with this audit.	The audit team concluded that overall, the SRS/CCP technical and Waste Analysis Plan (WAP)-related QA and technical elements, as applicable to audited activities, were adequate in addressing upper-tier requirements and effective in achieving the desired results.		
SRS	A-12-04	11/14 - 11/17/11	Evaluated the adequacy, implementation, and effectiveness of the SRS/CCP TRU waste characterization and certification activities as they relate to the WIPP HWFP for RH SCG S5000 debris waste.	S	S	S
				The audit team concluded that overall, the SRS/CCP technical and QA programs, as applicable to audited activities, were adequately established for compliance with the applicable upper-tier requirements, satisfactorily implemented, and effective.		
SRS	S-08-04	12/04 - 12/06/07	Evaluated the implementation and effectiveness of the TRU waste Radiological Characterization DTC activities of the Battelle Columbus RH waste stream SR-RL-BCLDP.001, S5000 debris waste performed for SRS by WTS CCP. This surveillance was a follow-up and extension to CBFO Audit A-07-24 (Interim Report), performed July 31 through August 2, 2007. Corrective actions for CBFO CAR-07-016 were also assessed.	S	S	S
				The results of the surveillance were that, within the scope of the surveillance, the CCP procedures had been satisfactorily implemented and were effective.		
SRS	S-09-29	06/16 - 06/17/09	Evaluated the implementation and effectiveness of the policies, plans, and procedures related to the CCP shipment of remote-handled transuranic (RH-TRU) waste from the SRS to WIPP.	S	S	S
				The surveillance team determined that the activities associated with operations necessary for the CCP's transportation of RH waste are appropriately proceduralized and effectively implemented. Personnel have received the training appropriate to their assigned tasks.		
SRS	S-10-23	03/31/10 04/21/10	Verified the adequacy and implementation of the SRS/CCP process for VE of CH S5000 debris waste at the F Canyon facility. During the annual SRS/CCP Recertification Audit A-10-01, performed in October 2009, the SRS/CCP VE facility was not yet operational and the audit team was limited to procedural and training documentation reviews.	S	S	S
				The surveillance team determined that the SRS/CCP VE operations evaluated were adequate, satisfactorily implemented, and effective.		
SRS	S-11-10	11/30 - 12/01/10	Verified the adequacy, implementation, and effectiveness of the SRS/CCP LCNDE system used for characterizing CH and RH waste in SWBs and SLB2s.	S	S	S
				The surveillance team determined that the SRS/CCP LCNDE activities evaluated were adequate, satisfactorily implemented, and effective.		
SRS	S-11-18	04/18/11	Evaluated the TRU waste characterization processes for RH SCG S5000 debris waste from waste stream SR-Rl-BClDO.002, conducted by SRS/CCP for Batelle Columbus Laboratories (BCL) drum BC0148.	S	S	S
				The results of the surveillance indicate that the TRU waste characterization activities evaluated for BCL drum BC0148 were adequate, satisfactorily implemented, and effective.		
SRS	S-11-21	07/12 - 07/13/11	Verified the adequacy, implementation, and effectiveness of the SRS/CCP LCNDE System used for characterization of the SLB2.	S	S	S
				The surveillance team determined that the SRS/CCP LCNDE activities evaluated were adequate, satisfactorily implemented, and effective.		
SRS	S-11-23	08/22 - 08/25/11	Verified the adequacy, implementation, and effectiveness of TRUPACT-III Transportation operations activities.	S	S	S
				The surveillance team determined that the TRUPACT-III procedures reviewed were adequate and that processes and associated activities were satisfactorily implemented and effective.		

Table AUD-9. Carlsbad Field Office Assessments

Organization Assessed	Assessment Number	Assessment Dates	Scope of Assessments	Adequacy	Implementation	Effectiveness
CBFO	A-08-08	02/04 - 02/07/08	Evaluated the adequacy, implementation, and effectiveness of selected QA processes related to the CBFO QA Program. The audit included NQA-1-1989 Criteria 1-9.	S	S	S
				The audit team concluded that overall, the CBFO QAPD is adequate relative to the flow-down of requirements from the NQA-1-1989 edition, and the associated CBFO implementing procedures are adequate relative to the flow-down of requirements of the CBFO QAPD, and are satisfactorily implemented and effective.		
CBFO	A-08-20	05/06 - 05/07/08	Evaluated the adequacy, implementation, and effectiveness of technical and QA activities related to the Performance Demonstration Program (PDP).	S	S	S
				The audit team concluded that the PDP QA program was adequate for the work performed and was implemented in accordance with the required program documents. The technical areas evaluated were determined to be effective.		
CBFO	A-08-23	06/03 - 06/05/08	Evaluated the adequacy, implementation, and effectiveness (where applicable) of selected QA processes related to the CBFO QA Program. The audit included the NQA-1-1989 Criteria 10-18.	S	S	S
				The audit team concluded that overall, with the exception of the program element for the management of QA records, the CBFO QAPD is adequate relative to the flow-down of requirements from the NQA-1-1989 Edition, and the associated CBFO implementing procedures are adequate relative to the flow-down of requirements		

Table AUD-9. Carlsbad Field Office Assessments

Organization Assessed	Assessment Number	Assessment Dates	Scope of Assessments	Adequacy	Implementation	Effectiveness
				from the CBFO QAPD. The audit team also concluded the defined CBFO QA Program is satisfactorily implemented and effective.		
CBFO	A-09-11	02/10 - 02/12/09	Evaluated the adequacy, implementation, and effectiveness of selected QA processes related to the CBFO QA Program. The audit included NQA-1-1989 Criteria 1-9.	S	S	S
				The audit team concluded that overall, the CBFO QAPD is adequate relative to the flow-down of requirements from the NQA-1-1989 edition, and the associated CBFO implementing procedures are adequate relative to the flow-down of requirements of the CBFO QAPD, and are satisfactorily implemented and effective.		
CBFO	A-09-20	09/01 - 09/03/09	Evaluated the adequacy, implementation, and effectiveness (where applicable) of selected QA processes related to the CBFO QA Program. The audit included the NQA-1-1989 Criteria 10-18.	S	S	S
				The audit team concluded that overall, the CBFO QAPD is adequate relative to the flow-down of requirements from the NQA-1-1989 Edition, and the associated CBFO implementing procedures are adequate relative to the flow-down of requirements from the CBFO QAPD.		
CBFO	A-10-13	05/25 - 05/27/10	The scope of the audit included evaluations of CBFO processes governing oversight activities and associated records used to meet the requirements of DOE Order 226.1A. Compliance with the CBFO QA program was also included in the scope, as applicable to these activities.	S	S	S
				The audit team concluded that CBFO implementation of DOE Order 226.1A, both internal to CBFO and of external contractor organizations, was adequately documented, satisfactory, and effective.		
CBFO	A-10-15	05/04 - 05/06/10	Evaluated the adequacy, implementation, and effectiveness of QA processes related to the CBFO QA Program. The audit included NQA-1-1989 Criteria 1-18; NQA-2a-1990 addenda, Subpart 2.7, for software quality assurance; and CBFO National Environmental Policy Act (NEPA) Process	S	S	S
				The audit team concluded that overall the CBFO QAPD is adequate relative to the flow-down of requirements of NQA-1-1989 and NQA-2a-1990 addenda. Subpart 2.7, satisfactory, and effective. The associated CBFO implementing procedures are also adequate relative to the f1ow-down of requirements from the CBFO QAPD.		
CBFO	A-11-15	05/03 - 05/05/11	Evaluated the adequacy, implementation, and effectiveness of QA processes related to the CBFO QA Program. The audit included NQA-1-1989 Criteria 1-18; NQA-2a-1990 addenda, Subpart 2.7, for software quality assurance; and CBFO NEPA Process	S	S	S
				The audit team concluded that overall the defined CBFO QA Program is adequate, satisfactorily implemented, resulting in an effective QA Program.		
CBFO	A-11-22	09/19 - 09/22/11	Evaluated the adequacy, implementation, and effectiveness of technical and QA activities related to the PDP.	S	S	S
				The audit team concluded that the PDP QA program was adequate for the work performed and was implemented in accordance with the program documents. The technical areas evaluated were determined to be effective.		
CBFO	A-12-19	05/22 -05/31/12	Evaluated the adequacy, implementation, and effectiveness of QA processes related to the CBFO QA Program. The audit included NQA-1-1989 Criteria 1-18; NQA-2a-1990 addenda, Subpart 2.7, for software quality assurance; and CBFO NEPA Process	S	S	S
				The audit team concluded that overall, the CBFO QAPD is adequate relative to the flow-down of requirements of NQA-1-1989 and NQA-2a-1990 addenda, Subpart 2.7. The associated CBFO implementing procedures are also adequate, satisfactorily implemented and effective.		
CBFO	S-09-16	05/19 - 05/20/09	Evaluated the degree of adequacy, implementation, and effectiveness of the CBFO Office of Site Operations (OSO) operational assessment process defined in CBFO Team Procedure 10.7.	S	S	S
				The surveillance team determined that the OSO operational assessment activities were adequate with respect to the upper-tier requirements, and were satisfactorily implemented and effective.		
CBFO	S-09-37	09/15 -09/22/09	Evaluated the implementation and effectiveness of selected requirements within the CBFO NDA PDP as they apply to NDA source custodians and sample preparation team members at selected TRU waste generating sites.	S	S	S
				The results of the surveillance indicate that the NDA PDP is adequate and the requirements applicable to the activities of source custodians and sample preparation teams are satisfactorily implemented at the TRU waste sites visited during the surveillance.		

Table AUD-10. Oak Ridge National Laboratory Assessments

Organization Assessed	Assessment Number	Assessment Dates	Scope of Assessments	Adequacy	Implementation	Effectiveness
ORNL	A-08-12	06/30 - 07/02/08	Evaluated the adequacy, implementation, and effectiveness of the ORNL/CCP TRU waste characterization activities for SCG S5000 RH debris waste stream OR-REDC-RH-HET.	S	S	S
				The audit team concluded that the applicable ORNL/CCP TRU waste characterization activities, as described in the associated ORNL/CCP implementing procedures, are satisfactory in meeting the requirements of the HWFP resulting in an effective program.		
ORNL	A-09-07	01/13 - 01/15/09	Evaluated the continued adequacy, implementation, and effectiveness of the ORNL/CCP TRU waste characterization activities for SCG S5000 CH debris waste.	S	S	S
				The audit team concluded that the applicable ORNL/CCP TRU waste characterization activities, as described in the associated ORNL/CCP implementing procedures, are adequate, satisfactory in meeting the requirements of the HWFP resulting in an effective program.		

Table AUD-10. Oak Ridge National Laboratory Assessments

Organization Assessed	Assessment Number	Assessment Dates	Scope of Assessments	Adequacy	Implementation	Effectiveness
ORNL	A-09-22	06/23 - 06/25/09	Evaluated the continued adequacy, implementation, and effectiveness of the ORNL/CCP TRU waste characterization activities for SCG S5000 RH debris waste stream OR-REDC-RH-HET.	S	S	S
				The audit team concluded that overall, the applicable ORNL/CCP TRU waste characterization activities for RH SCG S5000 debris waste, as described in the implementing procedures, are adequate, satisfactorily implemented and effective.		
ORNL	A-09-24	07/28 - 07/30/09	Evaluated the adequacy, implementation, and effectiveness of the ORNL/CCP technical processes and related QA program elements of the TRU waste characterization and certification activities for CH S4000 soils/gravel waste.	S	S	S
				The audit team concluded that the applicable ORNL/CCP QA Program elements and TRU waste characterization activities, as described in the associated implementing procedures adequately meet the requirements of the CBFO QAPD and the HWFP. The audit team also concluded that the ORNL/CCP technical processes and related QA Program elements are adequate, satisfactorily implemented, and effective.		
ORNL	A-10-08	02/09 - 02/11/10	Evaluated the continued adequacy, implementation, and effectiveness of the ORNL/CCP TRU waste characterization activities for SCG S5000 RH and CH debris waste and SCG S4000 CH soils waste.	S	S	S
				The audit team concluded that overall, the applicable ORNL/CCP TRU waste characterization activities for RH and CH SCG S5000 debris waste and CH SCG S4000 soils waste, as described in the implementing procedures, are adequate, satisfactorily implemented, and effective.		
ORNL	A-11-08	02/08 - 02/10/11	Evaluated the continued adequacy, implementation, and effectiveness of the ORNL/CCP TRU waste characterization activities for SCG 55000 RH and CH debris waste and SCG S4000 CH soils/gravel waste.	S	S	S
				The audit team concluded that overall, the applicable ORNL/CCP TRU waste characterization activities for RH and CH SCG S5000 debris waste and CH SCG S4000 soils/gravel waste, as described in the implementing procedures, were adequate, satisfactorily implemented, and effective.		
ORNL	A-12-08	03/27 - 03/29/12	The audit team evaluated documentation to verify continued adequacy, implementation, and effectiveness of the ORNL/CCP TRU waste characterization activities for RH and CH SCG S5000 debris waste and CH SCG S4000 soil/gravel waste.	S	I	I
				The audit team concluded that for the documentation reviewed, the applicable activities as described in the implementing procedures were adequate, satisfactorily implemented, and effective.The audit team was unable to evaluate HSG sampling, RTR, VE, NDA, and DTC characterization activities in the field, or verify personnel and equipment were available to continue characterization activities due to the suspension of activities and funding at ORNL. For this reason, these processes were deemed indeterminate for continuing waste characterization activities at the ORNL. Once activities resume at ORNL an audit will be performed to recertify characterization activities at ORNL.		
ORNL	S-09-17	06/20 - 07/02/08	As a follow-up to Audit A-08-12, the surveillance team evaluated the documentation establishing that a QA program equivalent in effect to the NQA standards was applied to radiochemical measurements used to develop the isotopic scaling factors used by ORNL/CCP for characterization of RH waste.	S	S	S
				The surveillance team concluded that the radiochemical measurements were conducted in accordance with a QA program equivalent in effect to the NQA standards applicable to the WIPP. Upon issuance of Revision I, Draft J of CCP-AK-LANL-503 as a final document, the QA equivalency documentation for the radiochemical measurements performed by ORNL will be adequate, satisfactorily implemented, and effective. CCP-AK-LANL-503 was issued 7/21/06.		
ORNL	S-11-14	02/22/11	Observed and evaluated the RH SCG S5000 debris waste sampling and analysis processes being used at the ORNL/CCP in support of characterization of waste containers to be shipped to the WIPP.	S	S	S
				The results of the surveillance indicate that the ORNL/CCP activities related to RH Waste Sampling and Analysis operations are adequate, satisfactorily implemented, and effective.		
ORNL	S-11-16	03/29/11	Evaluated the ORNL/CCP transition from the obsolete Gamma Waste Assay System (GWAS) software for NDA 103 equipment to the new NDA 2000 software package and the implementation of and compliance to revised NDA 103 procedures.	S	S	S
				The results of the surveillance indicate that the ORNL/CCP transition to and implementation of the NDA 2000 software for the NDA 103 measurement system was adequate, satisfactorily implemented, and effective.		

Table AUD-11. Advanced Mixed Waste Treatment Project Assessments

Organization Assessed	Assessment Number	Assessment Dates	Scope of Assessments	Adequacy	Implementation	Effectiveness
AMWTP	A-08-09	06/24 - 06/25/08	Evaluated continued adequacy, implementation, and effectiveness of the Advanced Mixed Waste Treatment Project (AMWTP) QA program and the technical processes related to AMWTP characterization and certification activities for CH SCG S3000 homogeneous solids and CH SCG S5000 debris wastes	S	S	S
				The audit team concluded that the applicable AMWTP container-in-container solids sampling activities, as described in the associated AMWTP implementing procedure, are adequate, satisfactorily implemented, and effective in meeting the requirements of the HWFP.		
AMWTP	A-08-19	09/08 - 09/11/08	Evaluated continued adequacy, implementation, and effectiveness of the AMWTP QA program and the technical processes related to AMWTP characterization and certification activities for CH SCG S3000	S	S	S
				The audit team concluded that the applicable AMWTP waste characterization activities/QA and technical processes, as described in the associated implementing procedures, continue to adequately meet the requirements of the HWFP.		

Table AUD-11. Advanced Mixed Waste Treatment Project Assessments

Organization Assessed	Assessment Number	Assessment Dates	Scope of Assessments	Adequacy	Implementation	Effectiveness
			homogeneous solids and CH SCG S5000 debris wastes.			
AMWTP	A-09-19	08/18 - 08/20/09	Evaluated continued adequacy, implementation, and effectiveness of the AMWTP QA program and the technical processes related to AMWTP characterization and certification activities for CH SCG S3000 homogeneous solids and CH SCG S5000 debris wastes.	S	S	S
				The audit team concluded that the applicable AMWTP waste characterization activities/QA and technical processes, as described in the associated implementing procedures, continue to adequately meet the requirements of the HWFP.		
AMWTP	A-10-24	08/23 - 08/26/10	Evaluated continued adequacy, implementation, and effectiveness of the AMWTP QA program and the technical processes related to AMWTP characterization and certification activities for CH SCG S3000 homogeneous solids and CH SCG S5000 debris wastes.	S	S	S
				The audit team concluded that the applicable AMWTP waste characterization activities/QA and technical processes as described in the associated implementing procedures, continue to adequately meet the requirements of the HWFP.		
AMWTP	A-12-03	11/01 - 11/03/11	Evaluated continued adequacy, implementation, and effectiveness of the AMWTP QA program and the technical processes related to AMWTP characterization and certification activities for CH SCG S3000 homogeneous solids and CH SCG S5000 debris wastes.	S	S	S
				The audit team concluded that the applicable AMWTP waste characterization activities/ QA and technical processes, as described in the associated implementing procedures, continue to adequately meet the requirements of the HWFP.		
AMWTP	A-13-01	10/15 -10/18/12	Evaluated continued adequacy, implementation, and effectiveness of the AMWTP QA program and the technical processes related to AMWTP characterization and certification activities for CH SCG S3000 homogeneous solids and CH SCG S5000 debris wastes.	S	S	S
				The audit team concluded that the applicable AMWTP waste characterization activities/ QA and technical processes, as described in the associated implementing procedures, continue to adequately meet the requirements of the HWFP.		
AMWTP	S-11-30	08/30/11	Observed and evaluated the AMWTP VE operations performed at INL for characterizing SCG S3000 CH homogeneous solids waste.	S	S	S
				The results of the surveillance indicate that the AMWTP activities related to VE of CH SCG S3000 waste using the equipment and procedures examined and subject to the measurement controls in place are adequately established for compliance with upper-tier requirements, satisfactory in the implementation of the requirements, and effective in achieving the desired results.		

Table AUD-12. Argonne National Laboratory Assessments

Organization Assessed	Assessment Number	Assessment Dates	Scope of Assessments	Adequacy	Implementation	Effectiveness
ANL	A-08-03	05/28 - 05/29/08	Evaluated the adequacy, implementation, and effectiveness of the ANL/CCP RH SCG S5000 debris TRU waste characterization QA and technical activities.	S	S	S
				The audit team concluded that overall, the applicable ANL/CCP TRU waste characterization activities for RH SCG S5000 debris waste, as described in the implementing procedures, are adequate, satisfactorily implemented, and effective.		
ANL	A-08-24	08/05 - 08/07/08	Evaluated the continued adequacy, implementation, and effectiveness of the ANL/CCP RH SCG S5000 debris TRU waste characterization QA and technical activities.	S	S	S
				The audit team concluded that overall, the applicable ANL/CCP TRU waste characterization activities for RH SCG S5000 debris waste, as described in the implementing procedures, are adequate, satisfactorily implemented, and effective.		
ANL	A-09-21	08/04 - 08/06/09	Evaluated the continued adequacy, implementation, and effectiveness of the ANL/CCP RH SCG S5000 debris TRU waste characterization QA and technical activities.	S	S	S
				The audit team concluded that overall, the applicable ANL/CCP TRU waste characterization activities for RH SCG S5000 debris waste, as described in the implementing procedures, are adequate, satisfactorily implemented, and effective.		
ANL	A-10-23	08/03 - 08/05/10	Evaluated the continued adequacy, implementation, and effectiveness of the ANL/CCP RH SCG S5000 debris TRU waste characterization QA and technical activities.	S	S	S
				The audit team concluded that overall, the applicable ANL/CCP TRU waste characterization activities for RH SCG S5000 debris waste, as described in the implementing procedures, are adequate, satisfactorily implemented, and effective. *Note The gravimetric or dimensional measurement process was deemed indeterminate due to insufficient documentation. A surveillance will be performed for evaluation at a later date		
ANL	A-11-20	08/02 - 08/04/11	Evaluated the continued adequacy, implementation, and effectiveness of the ANL/CCP RH SCG S5000 debris TRU waste characterization QA and technical activities.	S	S	S
				The audit team concluded that overall, the applicable ANL/CCP TRU waste characterization activities for RH SCG S5000 debris waste, as described in the implementing procedures, are adequate, satisfactorily implemented, and effective.		
ANL	A-12-16	08/28 -08/30/12	Evaluated the continued adequacy, implementation, and effectiveness of the	S	S	S
				The audit team concluded that overall, the applicable ANL/CCP TRU waste characterization activities for ANL/CCP RH waste, as		

Table AUD-12. Argonne National Laboratory Assessments

Organization Assessed	Assessment Number	Assessment Dates	Scope of Assessments	Adequacy	Implementation	Effectiveness
			ANL/CCP RH SCG S5000 debris TRU waste characterization QA and technical activities.	described in the implementing procedures, are adequate, satisfactorily implemented, and effective.		
ANL	S-10-15	01/12 - 01/14/10	Evaluated the activities associated with RH waste sampling and VE at Building 205 - ANL site.	S	S	S
				The results of the surveillance indicate that the ANL/CCP activities related to RH sampling and VE characterization operations are adequate, satisfactory, and effective in the Building 205 location.		
ANL	S-11-06	03/08 - 03/09/11	Evaluated ANL/CCP's ability to perform gravimetric or dimensional measurement of RH debris waste SCG S5000 Fuel Examination Waste (FEW) material for certification and subsequent disposal at the WIPP	S	S	S
				The surveillance team deemed the gravimetric or dimensional measurement process to be adequate, satisfactorily implemented and effective.		

Table AUD-13. Bettis Atomic Power Laboratory Assessments

Organization Assessed	Assessment Number	Assessment Dates	Scope of Assessments	Adequacy	Implementation	Effectiveness
Bettis Atomic Power Laboratory (BAPL)	A-11-12	04/19 - 04/21/11	Evaluated the adequacy, implementation, and effectiveness of BAPL/CCP TRU waste characterization activities performed for RH SCG S5000 debris waste. Activities were evaluated relative to the WIPP HWFP and the CBFO QAPD.	S	S	S
				BAPL/CCP technical and QA programs, as applicable to the audited activities, were adequate, satisfactorily implemented, and effective for compliance with applicable upper-tier requirements.		
BAPL	A-12-10	4/24 - 04/26/12	Evaluated the adequacy, implementation, and effectiveness BAPL/CCP TRU waste characterization activities performed for RH SCG S5000 debris waste.	S	S	S
				BAPL/CCP technical and QA programs, as applicable to the audited activities, were adequate, satisfactorily implemented, and effective for compliance with applicable upper-tier requirements.		
BAPL	S-10-37	9/21 - 09/22/10	Observed and evaluated the VE and radiological sampling processes being used at the BAPL/CCP in support of characterization of waste containers to be shipped to the WIPP.	S	S	S
				The results of the surveillance indicate that the BAPL/CCP activities related to VE and radiological sampling operations are adequate, satisfactorily implemented, and effective		
BAPL	S-11-08	12/7 - 12/8/10	Observed and evaluated the HSGS and DTC processes being used at the BAPL/CCP in support of characterization of waste containers to be shipped to the WIPP.	S	S	S
				The results of the surveillance indicate that the BAPL/CCP characterization activities related to HSGS and DTC operations are adequate, satisfactorily implemented, and effective.		

Table AUD-14. Sandia National Laboratories/CCP Assessments

Organization Assessed	Assessment Number	Assessment Dates	Scope of Assessments	Adequacy	Implementation	Effectiveness
SNL/CCP	A-11-23	7/13 - 07/15/11	Evaluated the adequacy, implementation, and effectiveness of the QA and technical processes and requirements controlling SNL/CCP TRU waste characterization activities for RH SCG S5000 debris waste.	S	S	S
				The audit team concluded that with the exception of RH/DTC the SNL/CCP TRU waste characterization program is adequate, satisfactorily implemented, and effective for compliance with the requirements of the HWFP. A follow-up surveillance (S-12-04) was later conducted to evaluate RH/DTC.		
SNL/CCP	S-11-15	3/30 - 03/31/11	Observed and evaluated the VE and radiological sampling processes being used at the SNL/CCP in support of characterization of SCG S5000 RH debris waste containers to be shipped to WIPP.	S	S	S
				The results of the surveillance indicate that the SNL/CCP activities related to radiological sampling operations are adequate, satisfactorily implemented, and effective.		
SNL/CCP	S-11-20	5/16/11	Observed and evaluated the VE, HSGS, and DTC used at the SNL/CCP in support of characterization of RH SCG S5000 debris waste containers to be shipped to WIPP.	S	S	S
				The results of the surveillance indicate that the SNL/CCP activities related to VE, HSGS, and DTC operations are adequate, satisfactorily implemented, and effective.		
SNL/CCP	S-12-04	11/09/11	This surveillance was performed to close out the radiological characterization (RH/DTC) portion of Audit A-11-23.	S	S	S
				The surveillance team concluded that the radiological waste characterization components evaluated were adequate, satisfactorily implemented, and effective. This surveillance satisfactorily closed out the radiological characterization (RH/DTC) portion of Audit A-11-23.		

Table AUD-15. Supplier Assessments

Organization Assessed	Assessment Number	Assessment Dates	Scope of Assessments	Adequacy	Implementation	Effectiveness
CAST Specialty Transportation, Inc. (CAST)	S-09-02	12/09 - 12/10/08	Evaluated the implementation and effectiveness of CAST for compliance with the Department Of Energy (DOE) Contract and upper-tier requirement documents.	S	S	S
				The surveillance team concluded that CAST had satisfactorily implemented the requirements of the DOE Contract and Department of Transportation (DOT) regulatory requirements. Implementation of regulatory and contractual requirements was considered adequate and effective.		
CAST	S-10-06	12/15 -12/16/09	Evaluated the implementation and effectiveness of CAST for compliance with the DOE Contract and upper-tier requirement documents.	S	S	S
				The surveillance team concluded that CAST had satisfactorily implemented the requirements of the DOE Contract and DOT regulatory requirements. Implementation of regulatory and contractual requirements was considered adequate and effective.		
CAST	S-11-05	12/14/10	Evaluated the implementation and effectiveness of CAST for compliance with the DOE Contract and upper-tier requirement documents.	S	S	S
				The surveillance team concluded that CAST had satisfactorily implemented the requirements of the DOE Contract and DOT regulatory requirements. Implementation of regulatory and contractual requirements was considered adequate and effective.		
CAST	S-12-06	03/06/12	Evaluated the implementation and effectiveness of CAST for compliance with the DOE Contract and upper-tier requirement documents.	S	S	S
				The surveillance team concluded that CAST had satisfactorily implemented the requirements of the DOE Contract and DOT regulatory requirements. Implementation of regulatory and contractual requirements was considered adequate and effective.		
Culebra	S-08-17	08/11 - 08/14/08 and 9/30 - 9/31/08	Evaluated the adequacy, implementation, and effectiveness of associated requirements governing the performance of the peer review process. The peer review was conducted to evaluate the Culebra Hydrogeology Conceptual Model.	S	S	S
				This surveillance team concluded the performance of the Peer Review adequately incorporated upper-tier requirements and the requirements were satisfactorily implemented and effective.		
L&M Records Services	S-08-15	08/18 - 08/21/08	Evaluated the implementation and effectiveness of the Project Records Services (PRS) process performed by L&M Technologies.	S	S	S
				The surveillance team determined that PRS activities were adequately proceduralized, and the procedures were satisfactorily implemented and were effective.		
SM Stoller Records	S-09-36	08/25 - 08/27/09	Evaluated the implementation and effectiveness of the WIPP Records Management Services (WRMS) process performed by S. M. Stoller Corporation for WTS.	S	S	S
				The surveillance team determined that WRMS activities were satisfactorily implemented, adequate, and effective.		
SM Stoller Records	S-10-36	09/07 - 09/09/10	Evaluated the implementation and effectiveness of activities performed by the S. M. Stoller Corporation for WTS at the CBFO/WIPP Records Holding Facility (RHF) in Carlsbad, NM.	S	S	S
				Overall, the surveillance team determined that the applicable requirements for activities performed at the CBFO/WIPP RHF were satisfactorily implemented and effective.		
Visionary Solutions	S-08-06	01/29 - 01/30/08	Reviewed and evaluated the implementation and effectiveness of Visionary Solutions, LLC compliance with the DOE Contract and upper-tier requirement documents.	S	S	S
				The surveillance team concluded that Visionary Solutions has satisfactorily implemented the requirements of the DOE Contract and DOT regulatory requirements. Implementation of regulatory and contractual requirements was considered adequate and effective.		

Table AUD-15. Supplier Assessments

Organization Assessed	Assessment Number	Assessment Dates	Scope of Assessments	Adequacy	Implementation	Effectiveness
Visionary Solutions	S-09-10	02/03 - 02/04/09	Reviewed and evaluated the implementation and effectiveness of Visionary Solutions, LLC compliance with the DOE Contract and upper-tier requirement documents.	S	S	S
				The surveillance team concluded that Visionary Solutions has satisfactorily implemented the requirements of the DOE Contract and DOT regulatory requirements. Implementation of regulatory and contractual requirements was considered adequate and effective.		
Visionary Solutions	S-10-18	03/16 - 03/17/10	Reviewed and evaluated the implementation and effectiveness of Visionary Solutions, LLC, compliance with the DOE Contract and upper-tier requirement documents.	S	S	S
				The surveillance team concluded that Visionary Solutions has satisfactorily implemented the requirements of the DOE Contract and DOT regulatory requirements. Implementation of regulatory and contractual requirements was considered adequate and effective.		
Visionary Solutions	S-11-12	03/22 - 03/23/11	Reviewed and evaluated the implementation and effectiveness of Visionary Solutions, LLC, compliance with the DOE Contract and upper-tier requirement documents.	S	S	S
				The surveillance team concluded that Visionary Solutions has satisfactorily implemented the requirements of the DOE Contract and DOT regulatory requirements. Implementation of regulatory and contractual requirements was considered adequate and effective.		
Visionary Solutions	S-12-14	03/20/12	Reviewed and evaluated the implementation and effectiveness of Visionary Solutions, LLC compliance with the DOE Contract and upper-tier requirement documents.	S	S	S
				The surveillance team concluded that Visionary Solutions has satisfactorily implemented the requirements of the DOE Contract and DOT regulatory requirements. Implementation of regulatory and contractual requirements was considered adequate and effective.		

AUD-2.0 References

(*Indicates a reference that has not been previously submitted.)

U.S. Department of Energy (DOE). 2009. Title 40 CFR Part 191 Compliance Recertification Application for the Waste Isolation Pilot Plant (March). DOE/WIPP 2009-3424. Carlsbad, NM: Carlsbad Field Office.* [Author]

U.S. Department of Energy (DOE). 2010. Quality Assurance Program Document, Revision 11 (June). DOE/CBFO-94-1012. Carlsbad, NM: Carlsbad Field Office.* [PDF / Author]

U.S. Environmental Protection Agency (EPA). 1993. "40 CFR Part 191: Environmental Radiation Protection Standards for the Management and Disposal of Spent Nuclear Fuel, High Level and Transuranic Radioactive Wastes; Final Rule." Federal Register, vol. 58 (December 20, 1993): 66398-416. [PDF / Author]

U.S. Environmental Protection Agency (EPA). 1996. "40 CFR Part 194: Criteria for the Certification and Recertification of the Waste Isolation Pilot Plant's Compliance With the 40 CFR Part 191 Disposal Regulations; Final Rule." Federal Register, vol. 61 (February 9, 1996): 5223-45. [PDF / Author]

U.S. Environmental Protection Agency (EPA). 2010. "40 CFR Part 194: Criteria for the Certification and Recertification of the Waste Isolation Pilot Plant's Compliance with the Disposal Regulations: Recertification Decision; Final Rule." Federal Register, vol. 75 (November 18, 2010): 70584-595.* [PDF / Author]

Title 40 CFR Part 191
Subparts B and C
Compliance Recertification Application 2014
for the
Waste Isolation Pilot Plant

Appendix DATA-2014
Monitoring Data and Reports

United States Department of Energy
Waste Isolation Pilot Plant

Carlsbad Field Office
Carlsbad, New Mexico

Compliance Recertification Application 2014

Appendix DATA-2014

Table of Contents

Attachments

Attachment A: WIPP Borehole Update

Attachment B: WIPP Waste Containers and Emplacement

Acronyms and Abbreviations

CCA Compliance Certification Application

CFR Code of Federal Regulations

CH-TRU contact-handled transuranic

CMP Compliance Monitoring Program

COMP compliance monitoring parameter

CRA Compliance Recertification Application

DBDSP Delaware Basin Drilling Surveillance Program

DOE U.S. Department of Energy

EPA U.S. Environmental Protection Agency

ft foot

GMP Geotechnical Monitoring Program

GWMP Groundwater Monitoring Program

m meter

PA performance assessment

PABC performance assessment baseline calculation

RH-TRU remote-handled transuranic

SMP Subsidence Monitoring Program

WDS Waste Data System

WIPP Waste Isolation Pilot Plant

This page intentionally left blank.

DATA-1.0 Introduction

Appendix DATA-2014 provides references to the data used to develop the Compliance Recertification Application (CRA) of 2014 (CRA-2014). Interpretation and analysis of those data are provided in the appropriate sections of the CRA-2014.

Title 40 CFR § 194.15(a)(1), (2), (3), and (5) (U.S. EPA 1996), Content of Recertification Applications, require that the U.S. Department of Energy (DOE) provide information obtained since the Compliance Certification Application (CCA) (U.S. DOE 1996) related to site geology, hydrology, and meteorology. Additional monitoring results and the results of laboratory investigations completed after the CRA-2009 (U.S. DOE 2009a) must also be provided, as well as information regarding the waste emplaced in the disposal system.

The DOE uses various programs to capture and analyze relevant information. These programs and the resulting information are discussed in the appropriate sections of this appendix.

DATA-1.1 Reported Data

In the initial U.S. Environmental Protection Agency (EPA) certification of compliance for the Waste Isolation Pilot Plant (WIPP) (U.S. EPA 1998), the EPA agreed that 10 compliance monitoring parameters (COMPs) would be monitored during the operational period of the project. Monitoring is performed to detect substantial deviations from expected conditions in the WIPP performance assessment (PA). The locations of the data for the COMPs in this appendix are listed below:

COMP	Location in Appendix DATA-2014
Change in the Culebra groundwater flow	Section DATA-5.0, Section DATA-10.0, and Section DATA-11.0
Creep closure and stresses	Section DATA-4.0 and Section DATA-10.0
Culebra groundwater composition	Section DATA-5.0, Section DATA-10.0, and Section DATA-11.0
Displacement of deformation features	Section DATA-4.0 and Section DATA-10.0
Drilling rate	Section DATA-2.0 and Section DATA-10.0
Extent of brittle deformation	Section DATA-4.0, Section DATA-9.0, and Section DATA-10.0
Initiation of brittle deformation	Section DATA-4.0 and Section DATA-10.0
Probability of encountering a Castile brine reservoir	Section DATA-2.0 and Section DATA-10.0
Subsidence measurement	Section DATA-3.0 and Section DATA-10.0
Waste activity	Section DATA-7.0 and Section DATA-10.0

DATA-2.0 Delaware Basin Drilling Surveillance Program

The Delaware Basin Drilling Surveillance Program (DBDSP) monitors drilling activities in the Delaware Basin. This section provides a brief discussion of the program and identifies the relevant data reports.

DATA-2.1 Program Overview

The EPA requires the DOE to demonstrate the expected containment performance of the disposal system using a PA. The PAs documented in the CCA, CRA-2004 (U.S. DOE 2004), CRA-2009, and CRA-2014 demonstrated that the DOE complies with the EPA's containment standards for undisturbed and human intrusion scenarios.

The criteria in 40 CFR § 194.33 (U.S. EPA 1996) require the use of historic drilling information to derive the drilling rate for PA intrusion scenarios. The DBDSP continues to monitor drilling-related activities, providing data used to determine whether the assumptions and scenarios used in PA remain valid, and uses the monitoring data to determine the drilling rate. These monitoring activities will continue until the DOE and the EPA agree that no additional benefit can be gained by further monitoring.

DATA-2.2 Reported Data

The two COMP parameters monitored by the DBDSP are the drilling rate (67.3 boreholes per square kilometer) (U.S. DOE 2012a) and the probability of encountering a Castile brine reservoir (4.5%) (Callicoat 2013a), which are discussed in the annual reports for this program and also in the COMPs assessments described in Section DATA-10.0. Other information collected by this program include drilling-related data, mining information, and seismic information.

Relevant data generated through the Delaware Basin Monitoring Program are provided in the following reports published since the CRA-2009:

- Delaware Basin Monitoring Annual Report, DOE/WIPP-08-2308, September 2008 (U.S. DOE 2008a).
- Delaware Basin Monitoring Annual Report, DOE/WIPP-09-2308, September 2009 (U.S. DOE 2009b).
- Delaware Basin Monitoring Annual Report, DOE/WIPP-10-2308, September 2010 (U.S. DOE 2010a).
- Delaware Basin Monitoring Annual Report, DOE/WIPP-11-2308, September 2011 (U.S. DOE 2011a).
- Delaware Basin Monitoring Annual Report, DOE/WIPP-12-2308, September 2012 (U.S. DOE 2012a).
- Callicoat, J. 2013. "Castile Brine Encounters 2012." Memo to File, Regulatory Environmental Services, Carlsbad, NM; RES:13:106 (Callicoat 2013a).
- Callicoat, J. 2013. "Seismic Activity within the Delaware Basin 2012." Memo to File, Regulatory Environmental Services, Carlsbad, NM; RES:13:107 (Callicoat 2013b).

DATA-3.0 Subsidence Monitoring Program

Subsidence monitoring measures vertical movement of the land surface relative to a reference location. This section provides a brief discussion of the Subsidence Monitoring Program (SMP) and identifies the relevant data reports.

DATA-3.1 Program Overview

The SMP uses a leveling survey to measure the relative vertical height differences between benchmarks. A level survey consists of using one benchmark's elevation as a constant elevation and determining the elevation of all other benchmarks relative to it. Comparison between level surveys allows vertical movement patterns to be established over time. These comparative surveys allow substantial deviation of actual subsidence from expected subsidence to be detected.

DATA-3.2 Reported Data

Each year approximately 15 miles of leveling surveying is completed utilizing nine vertical control loops consisting of 48 subsidence monuments and 14 National Geodetic Survey vertical control

points. Subsidence rates are small and are approximately at the resolution level of the survey accuracy. The benchmarks with the highest rates are seen above the mined panels. All subsidence rates fall within the predicted values. Data generated through the SMP are provided in the following reports published since the CRA-2009. Each report includes previous years' data.

- WIPP Subsidence Monument Leveling Survey 2008, DOE/WIPP 09-2293, December 2008 (U.S. DOE 2008b).
- WIPP Subsidence Monument Leveling Survey 2009, DOE/WIPP 10-2293, December 2009 (U.S. DOE 2009c).
- WIPP Subsidence Monument Leveling Survey 2010, DOE/WIPP 11-2293, December 2010 (U.S. DOE 2010b).
- WIPP Subsidence Monument Leveling Survey 2011, DOE/WIPP 12-2293, December 2011 (U.S. DOE 2011b).
- WIPP Subsidence Monument Leveling Survey 2012, DOE/WIPP 12-3497, December 2012 (U.S. DOE 2012b).

DATA-4.0 Geotechnical Monitoring Program

The Geotechnical Monitoring Program (GMP) measures in situ geotechnical data in the WIPP repository. This section provides a brief discussion of the GMP and identifies the relevant data reports.

DATA-4.1 Program Overview

The GMP obtains in situ data to support the continuous assessment of underground facilities. A detailed description of the geotechnical programs and procedures is presented in WP 07-1, WIPP Geotechnical Engineering Program Plan (Nuclear Waste Partnership 2012). Specifically, the program provides for

- Early detection of conditions that could affect operational safety
- Guidance for design modifications and remedial actions
- Data for interpreting the behavior of underground openings compared to established design criteria

The GMP collects data through instrumentation and observation. These data are used to confirm the understanding of geomechanical characteristics and aid in assessing the stability and performance of the underground facility. Constituent programs, described below, include the Geosciences Program, the Geomechanical Monitoring Program, and the Rock Mechanics Program.

The Geosciences Program includes the collection of underground data used to assess the repository by documenting the existing geologic conditions and characteristics and monitoring excavation response. Activities associated with this program include geologic and fracture mapping of the excavation surface, core logging, and borehole observations.

The Geomechanical Monitoring Program includes monitoring the geomechanical response of the underground openings after mining using instrumentation installed in the shafts and drifts of the facility. Geotechnical instrumentation installed underground in the shafts and drifts includes tape extensometer points, convergence meters, borehole extensometers, piezometers, strain gauges, load cells, and crack meters. The instrumentation is sensitive enough to detect small changes in rock displacements and stresses.

To determine significant deviations from expected conditions, the Management and Operating Contractor uses the Rock Mechanics Program to assess the performance of the underground excavation for safety and stability during the operational phase. The results from these assessments allow the identification of potentially unstable areas and the application of remedial actions, if necessary. Field data are used to compare the actual mechanical performance of the excavations to expected results. Analytical methods, such as numerical modeling, determine the potential effects of mining new excavations, excavation sequence, and long-term behavior of the repository. Extensive experimental work and observations have established an understanding of time-dependent geomechanical properties of the salt that are used to predict its in situ mechanical performance. These assessments rely heavily on the in situ instrumentation data and field observations from the Geoscience and Geomechanical Monitoring Programs.

DATA-4.2 Reported Data

Data generated through the GMP are reported annually in the Geotechnical Analysis Report. References for reports prepared since the development of the CRA-2009 are provided below. Each report includes previous years' data. Four parameters, relating to information collected by the GMP, are required to be monitored by the DOE. These are creep closure, extent of deformation, initiation of brittle deformation, and displacement of deformation features. Creep closure and displacement of deformation features are quantitative. Extent of deformation and initiation of brittle deformation are qualitative. These four parameters are discussed and analyzed in the COMPs reports listed in Section DATA-10.2.

- Washington TRU Solutions, LLC, 2009, Geotechnical Analysis Report for July 2007-June 2008, DOE/WIPP 09-3177, Carlsbad, NM (U.S. DOE 2009d).

- Washington TRU Solutions, LLC, 2010, Geotechnical Analysis Report for July 2008-June 2009, DOE/WIPP 10-3177, Carlsbad, NM (U.S. DOE 2010c).

- Washington TRU Solutions, LLC, 2011, Geotechnical Analysis Report for July 2009-June 2010, DOE/WIPP 11-3177, Carlsbad, NM (U.S. DOE 2011c).

- Washington TRU Solutions, LLC, 2012, Geotechnical Analysis Report for July 2010-June 2011, DOE/WIPP 12-3484, Carlsbad, NM (U.S. DOE 2012c).

The Geotechnical Analysis Report for July 2011-June 2012 was issued after the February 2013 CRA-2014 publication cutoff date.

DATA-5.0 Groundwater Monitoring Program

The Groundwater Monitoring Program (GWMP) collects and analyzes data for various wells at or near the WIPP site. This section briefly describes the GWMP and identifies relevant reports.

DATA-5.1 Program Overview

One function of the GWMP is the collection of groundwater data from the Culebra Dolomite Member of the Rustler Formation (hereafter referred to as the Culebra), such as water levels and water quality, from numerous wells located at and near the facility. The Culebra was selected as the focus of the GWMP. It has been extensively studied during past hydrologic characterization programs and was found to be the most likely hydrologic pathway to the accessible environment for any potential human-intrusion-caused release scenario. Data obtained through this program are used to generate the Culebra groundwater composition and the Culebra groundwater flow COMPs. Details on how the program is implemented are provided in Appendix MON-2014.

DATA-5.2 Reported Data

The water quality data collected by the GWMP are discussed and analyzed in the reports listed below and also in the COMPs reports listed in Section DATA-10.2. This analysis provides validation of the various Culebra hydrological models for CRA-2014. Appendix HYDRO-2014 and the COMPs reports provide analyses of the water levels and the fluid density of the water columns in the various wells used in gathering data for the WIPP hydrological model. The following reports have been published since the CRA-2009:

- U.S. Department of Energy, 2008, Waste Isolation Pilot Plant Annual Site Environmental Report for 2007, DOE/WIPP 08-2225, Carlsbad, NM (U.S. DOE 2008c).

- U.S. Department of Energy, 2009, Waste Isolation Pilot Plant Annual Site Environmental Report for 2008, DOE/WIPP 09-2225, Carlsbad, NM (U.S. DOE 2009e).

- U.S. Department of Energy, 2010, Waste Isolation Pilot Plant Annual Site Environmental Report for 2009, DOE/WIPP 10-2225, Carlsbad, NM (U.S. DOE 2010d).

- U.S. Department of Energy, 2011, Waste Isolation Pilot Plant Annual Site Environmental Report for 2010, DOE/WIPP 11-2225, Carlsbad, NM (U.S. DOE 2011d).

- U.S. Department of Energy, 2012, Waste Isolation Pilot Plant Annual Site Environmental Report for 2011, DOE/WIPP 12-3489, Carlsbad, NM (U.S. DOE 2012d).

DATA-6.0 Meteorological Monitoring Program

The Meteorological Monitoring Program measures atmospheric data for the WIPP site. This section provides a brief description of the program and relevant reports.

DATA-6.1 Program Description

The primary WIPP meteorological station is located 600.5 meters (m) (1,970 feet (ft)) northeast of the Waste Handling Building. The main function of the station is to provide data for atmospheric modeling. The station measures and records wind speed, wind direction, and temperature at elevations

of 2, 10, and 50 m (6.5, 33, and 165 ft). The station records ground-level measurements of barometric pressure, relative humidity, precipitation, and solar radiation.

DATA-6.2 Reported Data

The annual site environmental reports listed in Section DATA-5.2 provide data relevant to the Meteorological Monitoring Program. The CCA, Appendix CLI provides information on past (long-term) climatic conditions and predicted future conditions at the WIPP site. A discussion of the wind, rainfall, and temperature variation can be found in CRA-2014, Section 15.

DATA-7.0 Waste Information

Two types of information related to waste characteristics are collected: (1) information regarding waste that has been emplaced in the WIPP underground repository, and (2) information regarding future inventory that will be emplaced in the WIPP underground repository during the entire lifetime of the project. This section provides a brief description of the programs and a list of relevant reports.

DATA-7.1 Program Overview

Information concerning waste that has been emplaced in the repository is tracked and recorded using the Waste Data System (WDS), formerly the WIPP Waste Information System. Information concerning future wastes to be emplaced in the WIPP is developed through periodic updates of the Annual Transuranic Waste Inventory Reports. The inventory for the CRA-2014 PA is from the Performance Assessment Inventory Report -2012 (Van Soest 2012) based on the *Annual Transuranic Waste Inventory Report-2012* (U.S. DOE 2012e), that provides updated inventory information. The DOE anticipates that these inventory updates will have only a small impact on normalized releases relative to the CRA-2014 PA, and therefore have no significant impact on compliance.

DATA-7.2 Reported Data

Summary information generated by the WDS on emplaced waste and radionuclides is provided in the following reports published since the CRA-2009. See page 21 of the Annual Change Report 2011/2012, DOE/WIPP-12-3496 (U.S. DOE 2012f) for a detailed listing of the emplaced waste in the repository.

- U.S. Department of Energy, Annual Change Report 2007/2008, DOE/WIPP 08-3317, November 15, 2008 (U.S. DOE 2008d).
- U.S. Department of Energy, Annual Change Report 2008/2009, DOE/WIPP 09-0335, November 13, 2009 (U.S. DOE 2009f).
- U.S. Department of Energy, Annual Change Report 2009/2010, DOE/WIPP 10-1660, November 15, 2010 (U.S. DOE 2010e).
- U.S. Department of Energy, Annual Change Report 2010/2011, DOE/WIPP 11-3479, August 30, 2011 (U.S. DOE 2011e).

- U.S. Department of Energy, Annual Change Report 2011/2012, DOE/WIPP 12-3496, October 2012 (U.S. DOE 2012f).

Information regarding current and future inventories stored at generator sites and in the WIPP is provided in the following reports published since the CRA-2009:

- U.S. Department of Energy, Annual Transuranic Waste Inventory Report-2008, DOE/TRU-08-3425, Revision 0 (U.S. DOE 2008e).
- U.S. Department of Energy, Annual Transuranic Waste Inventory Report-2009, DOE/TRU-09-3425, Revision 0 (U.S. DOE 2009g).
- U.S. Department of Energy, Annual Transuranic Waste Inventory Report-2010, DOE/TRU-10-3425, Revision 0 (U.S. DOE 2010f).
- U.S. Department of Energy, Annual Transuranic Waste Inventory Report-2011, DOE/TRU-11-3425, Revision 0 (U.S. DOE 2011f).
- U.S. Department of Energy, Annual Transuranic Waste Inventory Report-2012, DOE/TRU-12-3425, Revision 0 (U.S. DOE 2012e).

DATA-8.0 WIPP Boreholes

Information regarding WIPP monitoring wells is identified in this section, and relevant data are provided.

DATA-8.1 Program Overview

Information provided in this section was reported in DOE/WIPP 95-2092, Revision 1, Waste Isolation Pilot Plant Borehole Data Report (the CCA, Appendix BH). The CCA, Appendix BH serves as a central document providing data on boreholes. The report contains a comprehensive database of wells drilled in support of the WIPP Project and boreholes that were located within the 16-section land withdrawal area.

DATA-8.2 Reported Data

Attachment A to this appendix provides updates on all of the monitoring wells used in the CCA, Appendix BH, and the new monitoring wells drilled since the initial certification. The attachment also adds wells that were in use, but inadvertently omitted from the CCA, Appendix BH. There were 6 wells drilled and 7 wells plugged during the CRA-2014 monitoring period from October 1, 2007, through December 31, 2012.

DATA-9.0 Repository Investigations Program

The WIPP Repository Investigations Program conducts research activities to confirm assumptions, reduce uncertainty, and resolve issues regarding the conceptual models and parameters used in PA. The program is briefly described in this section and references to relevant reports are provided.

DATA-9.1 Program Overview

The DOE has implemented and/or continued several experimental activities designed to address specific issues and needs of the WIPP repository. In addition, other investigations have been initiated to examine impacts of planned changes. The general areas covered under these investigations include

- Geochemistry
- Actinide chemistry
- Engineered barriers
- Rock mechanics (Sandia National Laboratories)

DATA-9.2 Reported Data

Data acquired by the DOE from the repository investigations are available in the following reports, publications, and technical memoranda published since the CRA-2009. Abstracts, posters, presentations, test plans, and analysis plans are not included because they typically contain preliminary data.

Geochemistry

- "Proceedings of the International Workshops ABC-Salt (II) and HiTAC 2011" (Altmaier et al. 2012).
- "Numerical Values for Graphs Presented in Report LCO-ACP-17, Rev. 0, Entitled: "Solubility of An(UIV) in WIPP Brine: Thorium Analog Studies in WIPP Simulated Brine" (Borkowski 2012).
- "Actinide (III) Solubility in WIPP Brine: Data Summary and Recommendations" (Borkowski, Lucchini, Richmann, and Reed 2010).
- "Solubility of An(IV) in WIPP Brine: Thorium Analog Studies in WIPP Simulated Brine" (Borkowski, Richmann, and Lucchini 2012).
- "Complexation of Nd(III) with Tetraborate Ion and Its Effect on Actinide(III) Solubility in WIPP Brine" (Borkowski, Richmann, Reed, and Xiong 2010).
- "Predictions of the Compositions of Standard WIPP Brines as a Function of pcH for Laboratory Studies of the Speciation and Solubilities of Actinides" (Brush, Domski, and Xiong 2011).
- "Revised Predictions of WIPP Baseline Actinide Solubilities as a Function of the Volume of Standard Brines" (Brush, Domski, and Xiong 2012).
- "Predictions of Actinide Solubilities as a Function of the Volume of Standard WIPP Brines" (Brush, Domski, Xiong, and Long 2011).
- "Sensitivity of the Long-Term Performance of the WIPP to EDTA" (Brush, Xiong, Garner, Kirchner, and Long 2008).

- "Results of the Calculations of Actinide Solubilities for the CRA-2009 PABC" (Brush, Xiong, and Long 2009).
- "Solubility and Speciation of Cm(III) and Nd(III) in Borate Rich NaCl and $CaCl_2$ Solutions" (Hinz et al. 2012).
- Memorandum to Records Center (Subject: Derivation of Pitzer ion interaction parameters for the pair Na^+ and $FeEDTA^{2-}$) (Jang 2012a).
- Memorandum to Records Center (Subject: Derivation of the solubility product for ferrous iron oxalate dihydrate in NaCl solutions and related Pitzer ion interaction parameter) (Jang 2012b).
- "Iron, Lead, Sulfide, and EDTA Solubilities" (Jang, Xiong, Kim, and Nemer 2011).
- "Iron, Lead, Sulfide, and EDTA Solubilities" (Jang, Xiong, Kim, and Nemer 2012).
- "Uranium Solubility in Carbonate-Free ERDA-6 Brine" (Lucchini, Khaing, and Reed 2010).
- "Actinide (VI) Solubility in Carbonate-free WIPP Brine: Data Summary and Recommendations" (Lucchini, Khaing, Borkowski, Richmann, and Reed 2010).
- "WIPP Actinide-Relevant Brine Chemistry" (Lucchini et al. 2013).
- "Uranium(VI) Solubility in WIPP Brine" (Lucchini, Richmann, and Borkowski 2013).
- "Influence of Carbonate on Uranium Solubility in Brine" (Lucchini, Ballard, and Khaing 2012).
- "Solubility of $Fe_2(OH)_3Cl$ (pure-iron end-member of hibbingite) in NaCl and Na_2SO_4 brines" (Nemer, Xiong, Ismail, and Jang 2010).
- "Determination of ferrous and ferric iron in aqueous biological samples" (Pepper, Borkowski, Richmann, and Reed 2010).
- "Using Thermodynamic Models: Saline Systems" (Reed 2011).
- "Intrinsic, Mineral, and Microbial Colloid Enhancement Parameters for the WIPP Actinide Source Term" (Reed, Swanson, Lucchini, and Richmann 2013).
- "Redox-Controlling Processes for Multivalent Metals and Actinides in the WIPP" (Reed et al. 2012).
- "Subsurface Interactions of Actinide Species and Microorganisms" (Reed, Deo, and Rittmann 2010).
- "Comparison of the Calculated Thorium Solubility (Concentration) Using the Constants from the TMT_050405 Database with the Experimental Data Published in Altmaier, M., Neck, V., Muller, R. and Fanghanel, T. *Radiochimica Acta*, 93(2), 83-92 (2005)" (Richmann 2010).
- "Iron and Lead Corrosion in WIPP-Relevant Conditions: 12 Month Results" (Roselle 2010).
- "Determination of pC_{H+} Correction Factors in Brines" (Roselle 2011a).

- "Iron and Lead Corrosion in WIPP-Relevant Conditions: 18 Month Results" (Roselle 2011b).
- "Iron and Lead Corrosion in WIPP-Relevant Conditions: 24 Month Results" (Roselle 2011c).
- "Determination of Corrosion Rates from Iron/Lead Corrosion Experiments to be used for Gas Generation Calculations" (Roselle 2013).
- "Thermodynamic Modeling of Trivalent Am, Cm, and Eu-Citrate Complexation in Concentrated $NaClO_4$ Media" (Thakur, Xiong, Borkowski, and Choppin 2012).
- "Thermodynamic Properties of Brucite Determined by Solubility Studies and Their Significance to Nuclear Waste Isolation" (Xiong 2008a).
- "Experimental Determination of Solubility Constant of Hydromagnesite (5424) in NaCl Solutions up to 4.4 M at Room Temperature" (Xiong 2010a).
- Memorandum to Record Center (Subject: Calculations of Thermodynamic Parameters for Experimental Data Generated at Los Alamos National Laboratory Carlsbad Operation (LANL-CO)) (Xiong 2010b).
- Memorandum to Record Center (Subject: Summary Report for Migration of the WIPP Thermodynamic Code from FMT to EQ3/6 Version 8.0a) (Xiong 2010c).
- "Experimental Study of Thermodynamic Parameters of Borate in WIPP Relevant Brines at Sandia National Laboratories Carlsbad Facility" (Xiong 2011a).
- "Organic Species of Lanthanum in Natural Environments: Implications to Mobility of Rare Earth Elements in Low Temperature Environments" (Xiong 2011b).
- "WIPP Verification and Validation Plan/Validation Document for EQ3/6 Version 8.0a for Actinide Chemistry, Revision 1. Supersedes ERMS 550239" (Xiong 2011c).
- "Experimental Determination of Solubility Constant of Di-Calcium Ethylenediaminetetraacetic Acid (Ca_2EDTA), $Ca_2C_{10}H_{12}N_2O_8(S)$, in the NaCl-$H_2O$ System" (Xiong 2012a).
- "Thermodynamic Model for the Na-$B(OH)_3$-Cl-SO_4 System" (Xiong 2012b).
- "Thermodynamic Model for the Na-$B(OH)_3$-Cl-SO_4 System, Revision 1, Superseding ERMS 558111" (Xiong 2012c).
- "Experimental Investigations of the Reaction Path in the MgO-CO_2-H_2O System in Solutions with Various Ionic Strengths, and Their Applications to Nuclear Waste Isolation" (Xiong and Lord 2008).
- "Experimental determination of the solubility constant for magnesium chloride hydroxide hydrate ($Mg_3Cl(OH)_5$•$4H_2O$, Phase 5) at room temperature, and its importance to nuclear waste isolation in geological repositories in salt formations" (Xiong, Deng, Nemer, and Johnsen 2009a).

- Memorandum to Larry Brush (Subject: Thermodynamic Data for phase 5 ($Mg_3Cl(OH)_5 \cdot 4H_2O$) Determined from Solubility Experiments.) (Xiong, Deng, Nemer, and Johnsen 2009b).

- "Responses to Three EPA Comments Pertaining to Comparisons of Measured and Predicted Dissolved and Colloidal Th(IV) and Am(III) Concentrations" (Xiong, Brush, Garner, and Long 2010a).

- "Responses to Three EPA Comments Pertaining to Comparisons of Measured and Predicted Dissolved and Colloidal Th(IV) and Am(III) Concentrations, Revision 1. Supersedes ERMS 553409" (Xiong, Brush, Garner, and Long 2010b).

- "Uncertainty Analysis of Actinide Solubilities for the WIPP CRA-2009 PABC, Rev. 1, Supersedes ERMS 552500" (Xiong, Brush, Domski, and Long 2011).

- "Experimental Determination of Solubilities of Lead Oxalate (PbC_2O_4(cr)) in a NaCl Medium to High Ionic Strengths, and the Importance of Lead Oxalate in Low Temperature Environments" (Xiong, Kirkes, Westfall, Olivas, and Roselle 2011).

Microbiology

- "The Effect of High Ionic Strength on Neptunium (V) Adsorption to a Halophilic Bacterium" (Ams et al. 2013).

- "Update on Microbial Characterization of WIPP Groundwaters" (Swanson and Simmons 2013).

- "Degradation of Organic Complexing Agents by Halophilic Microorganisms in Brines" (Swanson, Norden, Khaing, and Reed 2012).

- "Status Report on the Microbial Characterization of Halite and Groundwater Samples from the WIPP" (Swanson, Reed, Ams, Norden, and Simmons 2012).

- "Biodegradation of Organic Complexing Agents by WIPP-indigenous Halophilic Microorganisms in Brines" (Swanson, Simmons, Norden, and Khaing 2013).

Performance Assessment

- "Calculation of Organic-Ligand Concentrations for the WIPP CRA-2014 PA" (Brush and Domski 2013a).

- "Prediction of Baseline Actinide Solubilities for the WIPP CRA-2014 PA" (Brush and Domski 2013b).

- "Uncertainty Analysis of Actinide Solubilities for the WIPP CRA-2014 PA" (Brush and Domski 2013c).

- "Calculation of Organic-Ligand Concentrations for the WIPP CRA-2009 PABC" (Brush and Xiong 2009).

- "Summary Report for the AP-151 (PC3R) Performance Assessment, Revision 1" (Camphouse, Clayton, Kicker, and Pasch 2011).
- Memorandum to WIPP Records Center (Subject: Recommendations and Justifications of Parameter Values for the Run-of-Mine Salt Panel Closure System Design Modeled in the PCS-2012 PA) (Camphouse, Gross, Herrick, Kicker, and Thompson 2012).
- "Summary Report and Run Control for the 2012 WIPP Panel Closure System Performance Assessment, Rev. 0" (Camphouse et al. 2012).
- Memorandum to the SNL WIPP Records Center Defense Waste Management Programs (Subject: Memo AP-154, Task 10 EQ3/6 Database Update) (Domski 2012).
- Memorandum to the WIPP Records Center (Subject: Calculations Performed in Support of Reconsolidation of Crushed Salt in Panel Closures) (Herrick 2012a).
- Memorandum to the WIPP Records Center (Subject: JAS3D Calculations Performed in Support of the PCS-2012 PA Parameters Selections) (Herrick 2012b).
- "Estimating the Extent of the Disturbed Rock Zone around a WIPP Disposal Room" (Herrick, Park, Lee, and Holcomb 2009).
- "Determining the Hydrodynamic Shear Strength of Surrogate Degraded TRU Waste Materials as an Estimate for the Lower Limit of the Performance Assessment Parameter TAUFAIL, Revision 0" (Herrick, Schuhen, Chapin, and Kicker 2012).
- Memorandum to Records (Subject: Verification of FMT database and conversion to EQ3/6 format) (Ismail, Deng, Jang, and Wolery 2009).
- Email to Tom Peake (Subject: Response to EPA Questions on Two-Phase Flow and ROM Permeability) (U.S. DOE 2012g).
- Letter to Mr. Jonathan Edwards (Subject: Response to EPA Letter Dated December 22, 2011) (U.S. DOE 2012h).
- "Verification and Validation Plan/Validation Document for EQ3/6 Version 8.0a for Actinide Chemistry, Document Version 8.10" (Wolery, Xiong, and Long 2010).
- Memorandum to Larry Brush (Subject: HMI-an EQ3/6 Database with Iron Species) (Xiong 2008b).
- Email to Jennifer Long (Subject: Release of FMT_090720.CHEMDAT) (Xiong 2009).
- Email to Jennifer Long (Subject: Release of EQ3/6 Database DATA0.FM1) (Xiong 2011d).
- "Experimental Study of Thermodynamic Parameters of Borate in WIPP Relevant Brines at Sandia National Laboratories Carlsbad Facility" (Xiong 2012d).

- Memorandum to The WIPP Record Center (Subject: Memo of Corrections for 'Second Milestone Report on Test Plan TP 08-02, "Iron, Lead, Sulfide, and EDTA Solubilities" (ERMS 557198)') (Xiong 2012e).

- "Establishment of Uncertainty Ranges and Probability Distributions of Actinide Solubilities for Performance Assessment in the Waste Isolation Pilot Plant" (Xiong, Nowak, Brush, Ismail, and Long 2010).

- "Uncertainty Analysis of Actinide Solubilities for the WIPP CRA-2009 PABC" (Xiong, Brush, Ismail, and Long 2009).

Engineered Barriers

- "Improvements in Our Understanding of How MgO Will Control pH in WIPP Disposal Rooms" (Brush 2008).

- "Experimental Work Conducted on MgO Long-Term Hydration" (Deng, Xiong, Nemer, and Johnsen 2009).

Rock Mechanics

- Memorandum to Chris Camphouse (Subject: Follow-up to questions concerning TAUFAIL flume testing raised during the November 14-15, 2012 technical exchange between the DOE and EPA) (Herrick and Kirchner 2013).

- "Data Report for Analysis Plan for Demonstration Test Process: Soil Flume Sixnet Data Acquisition System" (Schuhen 2011).

DATA-10.0 Compliance Monitoring Program

Annually, the Compliance Monitoring Program (CMP) extracts data from the repository investigations and five of the monitoring programs described above (DBDSP, SMP, GMP, GWMP, and WDS) to derive values for the 10 COMPs described in Section DATA-1.0 and to evaluate whether significant changes in the parameters have occurred. The CMP activities are briefly described in this section. Data generated under the CMP are also identified.

DATA-10.1 Program Overview

The objective of the CMP is to provide assurance that any deviations from the expected long-term performance of the repository are identified at the earliest possible time. The CMP is implemented in accordance with DOE/WIPP 99-3119, Compliance Monitoring Implementation Plan for 40 CFR §191.14(b), Assurance Requirement (U.S. DOE 2012i). Annual evaluations of the compliance parameters follow the requirements found in Sandia National Laboratories SP 9-8, Monitoring Parameter Assessment Per 40 CFR 194.42, Revision 1 (Wagner 2011).

DATA-10.2 Reported Data

The data and the results of the annual COMPs assessments performed in accordance with the requirements of the CMP are provided in the following reports published since the CRA-2009. There are no COMPs data or results that indicate a reportable event or condition adverse to predicted performance.

- Sandia National Laboratories, "Sandia National Laboratories Compliance Monitoring Parameter Assessment for 2008, WBS 1.3.1, January 2009," Carlsbad, NM (Sandia National Laboratories 2009).

- Sandia National Laboratories, "Sandia National Laboratories Compliance Monitoring Parameter Assessment for 2009, WBS 1.3.1, January 2010," Carlsbad, NM (Sandia National Laboratories 2010a).

- Sandia National Laboratories, "Sandia National Laboratories Compliance Monitoring Parameter Assessment for 2010, WBS 1.3.1, November 2010," Carlsbad, NM (Sandia National Laboratories 2010b).

- Sandia National Laboratories, "Sandia National Laboratories Compliance Monitoring Parameter Assessment for 2011, WBS 1.3.1, December 2011," Carlsbad, NM (Sandia National Laboratories 2011).

- Sandia National Laboratories, "Sandia National Laboratories Compliance Monitoring Parameter Assessment for 2012, WBS 1.3.1, November 2012," Carlsbad, NM (Sandia National Laboratories 2012).

A reassessment of the Trigger Values used to support the annual COMPs assessment is provided in "Sandia National Laboratories Trigger Value Derivation Report, Revision 2, WBS 1.3.1, December 2010," Carlsbad, NM (Sandia National Laboratories 2010c).

DATA-11.0 Hydrological Investigation

The Exhaust Shaft Hydraulic Assessment, now the Shallow Subsurface Water Investigation, was initiated in September 1996 to investigate the source and extent of water seepage into the exhaust shaft at the WIPP. An investigation of rising water levels in the Culebra was initiated in 1999. These hydrologic investigations are briefly described in this section. Sources of data generated from the investigations are also identified.

DATA-11.1 Program Overview

DATA-11.1.1 Shallow Subsurface Water Investigation

Investigations of water entering the exhaust shaft led to the observation of a shallow perched groundwater horizon in a saturated layer within the lower Santa Rosa Formation and the upper Dewey Lake Redbeds Formation, about 15 m (49 ft) below ground surface. During the original drilling and geological mapping of the shaft, no water was encountered at that horizon, indicating that the presence of water may be related to site activities subsequent to shaft drilling. Three wells and 12 piezometers were installed over an 80-acre area between September 1996 and July 1997 (INTERA 1997). In 2007, three more piezometers were installed. No new piezometers have been installed since

2007. Water-level and water-quality parameters continue to be monitored and reported on a regular basis.

DATA-11.1.2 Culebra Water-Level Rise Investigation

During the 1999 annual COMPs assessment, Culebra water levels in many of the WIPP monitoring wells exceeded the CCA ranges of uncertainty established for equilibrium freshwater heads to calibrate transmissivity fields needed for Culebra flow and transport calculations. Culebra water-level rises had also been observed at the time of the CCA submittal in 1996 but were attributed to natural recovery of water levels following years of hydraulic well testing at the WIPP site and grouting of the WIPP shafts. Subsequent to the 1999 COMPs assessment, Culebra water levels showed a continued rise even though water levels at the WIPP site were thought to have fully recovered from hydraulic testing and shaft grouting. In response to this observation, the DOE initiated an investigation into the cause of the water-level rise and the impact of the rise on the long-term performance of the WIPP, which is discussed in Appendix HYDRO-2009 and Appendix HYDRO-2014. Culebra water-level rises peaked around 2008 and have shown a continuing gradual decline since that time.

DATA-11.2 Reported Data

Data acquired from the two hydrologic investigations are provided in the reports cited below for the Shallow Subsurface Water Investigation and the Culebra water-level rise investigation.

DATA-11.2.1 Shallow Subsurface Water Investigation

The Geotechnical Analysis Reports listed in Section DATA-4.2 provide data relevant to the Shallow Subsurface Water Investigation. Additional detailed information on this subject is contained in "Hydrologic Assessment of Shallow Subsurface Water" (Daniel B. Stephens & Associates, Inc. 2008), and "Assessment of Lead in PZ-13 Near the Site and Preliminary Design Validation (SPDV) Pile at Waste Isolation Pilot Plant" (Daniel B. Stephens & Associates, Inc. 2010).

DATA-11.2.2 Culebra Water-Level Rise Investigation

The following reports are related to Culebra water-level investigations:

- Letter to Rick Beauheim (Subject: WIPP/SNL-6 (C)) (Hall Environmental Analysis Laboratory 2008a).
- Letter to Rick Beauheim (Subject: WIPP/H-15 (M)) (Hall Environmental Analysis Laboratory 2008b).
- Letter to Rick Beauheim (Subject: WIPP/LRL-7) (Hall Environmental Analysis Laboratory 2008c).
- Letter to Rick Beauheim (Subject: WIPP/USGS-4) (Hall Environmental Analysis Laboratory 2008d).
- Letter to Rick Beauheim (Subject: WIPP/USGS-8) (Hall Environmental Analysis Laboratory 2008e).
- Letter to Rick Beauheim (Subject: WIPP/H-6bR) (Hall Environmental Analysis Laboratory 2009a).

- Letter to Rick Beauheim (Subject: WIPP/H-15R) (Hall Environmental Analysis Laboratory 2009b).
- Letter to Rick Beauheim (Subject: WIPP/H-18 (M)) (Hall Environmental Analysis Laboratory 2009c).
- Letter to Rick Beauheim (Subject: WIPP/H-3b1 (M)) (Hall Environmental Analysis Laboratory 2009d).
- Letter to Rick Beauheim (Subject: WIPP/H-4bR) (Hall Environmental Analysis Laboratory 2009e).
- Letter to Rick Beauheim (Subject: WIPP/WIPP-18 (M)) (Hall Environmental Analysis Laboratory 2010a).
- Letter to Rick Beauheim (Subject: WIPP/H-6c (M)) (Hall Environmental Analysis Laboratory 2010b).
- Letter to Rick Beauheim (Subject: WIPP/H-8a (M)) (Hall Environmental Analysis Laboratory 2010c).
- Letter to Rick Beauheim (Subject: WIPP/H-2b1 (M)) (Hall Environmental Analysis Laboratory 2011a).
- Letter to Mike Schuhen (Subject: WIPP/H-4c (M)) (Hall Environmental Analysis Laboratory 2011b).
- Letter to Mike Schuhen (Subject: WIPP/H-9c (M)) (Hall Environmental Analysis Laboratory 2011c).
- Letter to Mike Schuhen (Subject: WIPP/H-9c (M)) (Hall Environmental Analysis Laboratory 2011d)
- Letter to Mike Schuhen (Subject: WIPP/H-9bR (C)) (Hall Environmental Analysis Laboratory 2011e).
- Letter to Mike Schuhen (Subject: WIPP/H-11b4R (C)) (Hall Environmental Analysis Laboratory 2012a).
- Letter to Mike Schuhen (Subject: WIPP/H-9bR (C)) (Hall Environmental Analysis Laboratory 2012b).
- Letter to Mike Schuhen (Subject: WIPP/H-9bR (C)) (Hall Environmental Analysis Laboratory 2012c).
- "2007 Calculated Densities for Use in Deriving Equivalent Freshwater Heads of the Culebra Dolomite Member of the Rustler Formation near the WIPP Site" (Johnson 2008).
- "2008 Calculated Densities for Use in Deriving Equivalent Freshwater Heads of the Culebra Dolomite Member of the Rustler Formation near the WIPP Site" (Johnson 2009).
- Memorandum to Records Center (Subject: 2009 Calculated Densities) (Johnson 2010).

- Memorandum to Records Center (Subject: Memo of Correction 2010 Calculated Densities) (Johnson 2011).
- Memorandum to Records Center (Subject: 2003 Calculated Densities) (Johnson 2012a).
- Memorandum to Records Center (Subject: 2004 Calculated Densities) (Johnson 2012b).
- Memorandum to Records Center (Subject: 2005 Calculated Densities) (Johnson 2012c).
- Memorandum to Records Center (Subject: 2006 Calculated Densities) (Johnson 2012d).
- Memorandum to Records Center (Subject: 2011 Calculated Densities) (Johnson 2012e).
- Memorandum to Records Center (Subject: 2012 Calculated Densities) (Johnson 2012f).
- "Culebra Water Level Monitoring Network Design" (Kuhlman 2010).

DATA-12.0 Waste Containers and Emplacement

Information regarding WIPP waste emplacement containers and underground waste emplacement layouts are provided in this section. Approved containers that are inside other containers, such as pipe overpacks, are not discussed.

DATA-12.1 Program Overview

Information provided in this section was compiled from several sources to serve as a central document describing both waste emplacement containers and waste emplacement layouts. Both contact-handled transuranic (CH-TRU) and remote-handled transuranic (RH-TRU) waste containers are described along with CH-TRU and RH-TRU waste emplacement layouts in a typical panel in the repository. Only containers approved for disposal in the repository are discussed.

DATA-12.2 Reported Data

Attachment B to this appendix provides detailed information on the various waste containers and their emplacement in the underground repository.

DATA-13.0 References

(*Indicates a reference that has not been previously submitted.)

Altmaier, M., C. Bube, B. Kienzler, V. Metz, and D.T. Reed (eds.). 2012. Proceedings of the International Workshops ABC-Salt (II) and HiTAC 2011. KIT Scientific Reports 7625. Karlsruhe, Germany.* [PDF / Author]

Ams, D.A., J.S. Swanson, J. Szymanowski, J.B. Fein, M. Richmann, and D.T. Reed. 2013. "The Effect of High Ionic Strength on Neptunium (V) Adsorption to a Halophilic Bacterium," Geochimica et Cosmochimica Acta, 110 (2013) 45057.* [PDF / Author]

Borkowski, M. 2012. Numerical Values for Graphs Presented in Report LCO-ACP-17, Rev. 0, Entitled: Solubility of An(UIV) in WIPP Brine: Thorium Analog Studies in WIPP Simulated Brine

and for Graphs Published in Borkowski, M., et al. Radiochimica Acta 98, (9-11) 577-582 (2010)." LA-UR 12-26640. Carlsbad, NM: Los Alamos National Laboratory.* [PDF / Author]

Borkowski, M. J-F. Lucchini, M.K. Richmann, and D.T. Reed. 2010. Actinide (III) Solubility in WIPP Brine: Data Summary and Recommendations. Report LA-14360. Los Alamos, NM: Los Alamos National Laboratory.* [PDF / Author]

Borkowski, M., M.K. Richmann, and J-F. Lucchini. 2012. Solubility of An(IV) in WIPP Brine: Thorium Analog Studies in WIPP Simulated Brine. Report LCO-ACP-17, LA-UR 12-24417. Carlsbad, NM: Los Alamos National Laboratory.* [PDF / Author]

Borkowski, M., M.K. Richmann, D.T. Reed, and Y.-L. Xiong. 2010. "Complexation of Nd(III) with Tetraborate Ion and Its Effect on Actinide(III) Solubility in WIPP Brine," Radiochimica Acta 98.9-11 (2010): 577-582.* [Author]

Brush, L.H. 2008. Improvements in Our Understanding of How MgO Will Control pH in WIPP Disposal Rooms. Write-up for inclusion in CRA-2009 Appendix SOTERM, April 9, 2008. ERMS 548629. Carlsbad, NM: Sandia National Laboratories.* [PDF / Author]

Brush, L.H., and P.S. Domski. 2013a. Calculation of Organic-Ligand Concentrations for the WIPP CRA-2014 PA. Analysis report, January 14, 2013. ERMS 559005. Carlsbad, NM: Sandia National Laboratories.* [PDF / Author]

Brush, L.H., and P.S. Domski. 2013b. Prediction of Baseline Actinide Solubilities for the WIPP CRA-2014 PA. Analysis report, January 21, 2013. ERMS 559138. Carlsbad, NM: Sandia National Laboratories.* [PDF / Author]

Brush, L.H., and P.S. Domski. 2013c. Uncertainty Analysis of Actinide Solubilities for the WIPP CRA-2014 PA. Analysis report, February 22, 2013. ERMS 559278. Carlsbad, NM: Sandia National Laboratories.* [PDF / Author]

Brush, L.H., and Y.-L. Xiong. 2009. Calculation of Organic-Ligand Concentrations for the WIPP CRA-2009 PABC. Analysis report, June 16, 2009. ERMS 551481. Carlsbad, NM: Sandia National Laboratories.* [PDF / Author]

Brush, L.H., P.S. Domski, and Y.-L. Xiong. 2011. Predictions of the Compositions of Standard WIPP Brines as a Function of pcH for Laboratory Studies of the Speciation and Solubilities of Actinides. Analysis report, June 24, 2011. ERMS 555727. Carlsbad, NM: Sandia National Laboratories.* [PDF / Author]

Brush, L.H., P.S. Domski, and Y.-L. Xiong. 2012. Revised Predictions of WIPP Baseline Actinide Solubilities as a Function of the Volume of Standard Brines. Analysis report, May 17, 2012. ERMS 557524. Carlsbad, NM: Sandia National Laboratories.* [PDF / Author]

Brush, L.H., P.S. Domski, Y.-L. Xiong, and J.J. Long. 2011. Predictions of Actinide Solubilities as a Function of the Volume of Standard WIPP Brines. Analysis Report, September 8, 2011. ERMS 556140. Carlsbad, NM: Sandia National Laboratories.* [PDF / Author]

Brush, L.H., Y.-L. Xiong, and J.J. Long. 2009. Results of the Calculations of Actinide Solubilities for the CRA-2009 PABC. Analysis Report, October 7, 2009. ERMS 552201. Carlsbad, NM: Sandia National Laboratories.* [PDF / Author]

Brush, L.H., Y.-L. Xiong, J.W. Garner, T.B Kirchner, and J.J. Long. 2008. Sensitivity of the Long-Term Performance of the WIPP to EDTA. Analysis report, March 20, 2008. ERMS 548398. Carlsbad, NM: Sandia National Laboratories.* [PDF / Author]

Callicoat, J. 2013a. Memorandum to File (Subject: Castile Brine Encounters 2012). February 12, 2013. RES:13:106. Carlsbad, NM: Regulatory Environmental Services.* [PDF / Author]

Callicoat, J. 2013b. Memorandum to File (Subject: Seismic Activity within the Delaware Basin 2012). February 13, 2013. RES:13:107. Carlsbad, NM: Regulatory Environmental Services.* [PDF / Author]

Camphouse, R.C., D.J. Clayton, D.C. Kicker, and J.J. Pasch. 2011. Summary Report for the AP-151 (PC3R) Performance Assessment, Revision 1. ERMS 555489. Carlsbad, NM: Sandia National Laboratories.* [PDF / Author]

Camphouse, R.C., M. Gross, C.G. Herrick, D.C. Kicker, and B. Thompson. 2012. Memorandum to WIPP Records Center (Subject: Recommendations and Justifications of Parameter Values for the Run-of-Mine Salt Panel Closure System Design Modeled in the PCS-2012 PA). May 3, 2012. ERMS 557396. Carlsbad, NM: Sandia National Laboratories.* [PDF / Author]

Camphouse, R.C., D.C. Kicker, T.B. Kirchner, J.J. Long, B. Malama, T.R. Zeitler. 2012. Summary Report and Run Control for the 2012 WIPP Panel Closure System Performance Assessment, Rev. 0. ERMS 558365. Carlsbad, NM: Sandia National Laboratories.* [PDF / Author]

Daniel B. Stephens & Associates, Inc. 2008. Hydrologic Assessment of Shallow Subsurface Water. December 18, 2008. Carlsbad, NM.* [PDF / Author]

Daniel B. Stephens & Associates, Inc. 2010. Assessment of Lead in PZ-13 Near the Site and Preliminary Design Validation (SPDV) Pile at Waste Isolation Pilot Plant. June 11, 2010. Carlsbad, NM.* [PDF / Author]

Deng, H., Y.-L. Xiong, M.B. Nemer, and S.R. Johnsen. 2009. Experimental Work Conducted on MgO Long-Term Hydration. 2008 Milestone Report. May 27, 2009. ERMS 551421. Carlsbad, NM: Sandia National Laboratories.* [PDF / Author]

Domski, P. 2012. Memorandum to the SNL WIPP Records Center Defense Waste Management Programs (Subject: Memo AP-154, Task 10 EQ3/6 Database Update). October 31, 2012. ERMS 558579. Carlsbad, NM: Sandia National Laboratories.* [PDF / Author]

Hall Environmental Analysis Laboratory. 2008a. Letter to Rick Beauheim (Subject: WIPP/SNL-6 (C)). February 5, 2008. Order No. 0801223.* [PDF / Author]

Hall Environmental Analysis Laboratory. 2008b. Letter to Rick Beauheim (Subject: WIPP/H-15 (M)). April 2, 2008. Order No. 0803246.* [PDF / Author]

Hall Environmental Analysis Laboratory. 2008c. Letter to Rick Beauheim (Subject: WIPP/LRL-7). August 26, 2008. Order No. 0807449.* [PDF / Author]

Hall Environmental Analysis Laboratory. 2008d. Letter to Rick Beauheim (Subject: WIPP/USGS-4). August 26, 2008. Order No. 0807447.* [PDF / Author]

Hall Environmental Analysis Laboratory. 2008e. Letter to Rick Beauheim (Subject: WIPP/USGS-8). August 26, 2008. Order No. 0807446.* [PDF / Author]

Hall Environmental Analysis Laboratory. 2009a. Letter to Rick Beauheim (Subject: WIPP/H-6bR). January 21, 2009. Order No. 0812250.* [PDF / Author]

Hall Environmental Analysis Laboratory. 2009b. Letter to Rick Beauheim (Subject: WIPP/H-15R). February 10, 2009. Order No. 0901317.* [PDF / Author]

Hall Environmental Analysis Laboratory. 2009c. Letter to Rick Beauheim (Subject: WIPP/H-18 (M)). May 20, 2009. Order No. 0904340.* [PDF / Author]

Hall Environmental Analysis Laboratory. 2009d. Letter to Rick Beauheim (Subject: WIPP/H-3b1 (M)). August 13, 2009. Order No. 0907569.* [PDF / Author]

Hall Environmental Analysis Laboratory. 2009e. Letter to Rick Beauheim (Subject: WIPP/H-4bR). August 25, 2009. Order No. 0908237.* [PDF / Author]

Hall Environmental Analysis Laboratory. 2010a. Letter to Rick Beauheim (Subject: WIPP/WIPP-18 (M)). April 6, 2010. Order No. 1003482.* [PDF / Author]

Hall Environmental Analysis Laboratory. 2010b. Letter to Rick Beauheim (Subject: WIPP/H-6c (M)). May 12, 2010. Order No. 1004666.* [PDF / Author]

Hall Environmental Analysis Laboratory. 2010c. Letter to Rick Beauheim (Subject: WIPP/H-8a (M)). May 26, 2010. Order No. 1004462.* [PDF / Author]

Hall Environmental Analysis Laboratory. 2011a. Letter to Rick Beauheim (Subject: WIPP/H-2b1 (M)). February 22, 2011. Order No. 1102238.* [PDF / Author]

Hall Environmental Analysis Laboratory. 2011b. Letter to Mike Schuhen (Subject: WIPP/H-4c (M)). March 16, 2011. Order No. 1103085.* [PDF / Author]

Hall Environmental Analysis Laboratory. 2011c. Letter to Mike Schuhen (Subject: WIPP/H-9c (M)). May 3, 2011. Order No. 1104715.* [PDF / Author]

Hall Environmental Analysis Laboratory. 2011d. Letter to Mike Schuhen (Subject: WIPP/H-9c (M)). May 3, 2011. Order No. 1104933.* [PDF / Author]

Hall Environmental Analysis Laboratory. 2011e. Letter to Mike Schuhen (Subject: WIPP/H-9bR (C)). February July 15, 2011. Order No. 1106C12.* [PDF / Author]

Hall Environmental Analysis Laboratory. 2012a. Letter to Mike Schuhen (Subject: WIPP/H-11b4R (C)). July 25, 2012. Order No. 1206571.* [PDF / Author]

Hall Environmental Analysis Laboratory. 2012b. Letter to Mike Schuhen (Subject: WIPP/H-9bR (C)). September 7, 2012. Order No. 1208942.* [PDF / Author]

Hall Environmental Analysis Laboratory. 2012c. Letter to Mike Schuhen (Subject: WIPP/H-9bR (C)). October 15, 2012. Order No. 1208471.* [PDF / Author]

Herrick, C.G. 2012a. Memorandum to the WIPP Records Center (Subject: Calculations Performed in Support of Reconsolidation of Crushed Salt in Panel Closures). March 29, 2012. ERMS 557150. Carlsbad, NM: Sandia National Laboratories.* [PDF / Author]

Herrick, C.G. 2012b. Memorandum to the WIPP Records Center (Subject: JAS3D Calculations Performed in Support of the PCS-2012 PA Parameters Selections). April 30, 2012. ERMS 557354. Carlsbad, NM: Sandia National Laboratories.* [PDF / Author]

Herrick, C.G. and T. Kirchner. 2013. Memorandum to Chris Camphouse (Subject: Follow-up to questions concerning TAUFAIL flume testing raised during the November 14-15, 2012 technical exchange between the DOE and EPA). January 24, 2013. ERMS 559081. Carlsbad, NM: Sandia National Laboratories.* [PDF / Author]

Herrick, C.G., B.Y Park, M.Y. Lee, and D.J. Holcomb. 2009. Estimating the Extent of the Disturbed Rock Zone around a WIPP Disposal Room. Paper ARMA 09-82 presented at 43th U.S. Rock Mechanics Symposium/4th U.S.-Canada Rock Mechanics Symposium. June 28-July 1. Asheville, NC.* [PDF / Author]

Herrick, C.G., M.D. Schuhen, D.M. Chapin, and D.C. Kicker. 2012. Determining the Hydrodynamic Shear Strength of Surrogate Degraded TRU Waste Materials as an Estimate for the Lower Limit of the Performance Assessment Parameter TAUFAIL, Revision 0. ERMS 558479. Carlsbad, NM: Sandia National Laboratories.* [PDF / Author]

Hinz, K., M. Altmaier, Th. Rabung, M.K. Richmann, M. Borkowski, D.T. Reed, and H. Geckeis. 2012. Solubility and Speciation of Cm(III) and Nd(III) in Borate Rich NaCl and CaCl2 Solutions. Poster (joint INE-LANL) presented at Plutonium Futures 2012, July 15-20. Cambridge, United Kingdom.* [PDF / Author]

INTERA. 1997. Exhaust Shaft Hydraulic Assessment Data Report. DOE/WIPP 97-2219. Carlsbad, NM: Waste Isolation Pilot Plant. [PDF / Author]

Ismail, A.E., H. Deng, J.-H. Jang, and T.J. Wolery. 2009. Memorandum to Records (Subject: Verification of FMT database and conversion to EQ3/6 format). ERMS 550689. Carlsbad, NM: Sandia National Laboratories.* [PDF / Author]

Jang, J.-H. 2012a. Memorandum to Records Center (Subject: Derivation of Pitzer ion interaction parameters for the pair Na+ and FeEDTA2-). October 31, 2012. ERMS 558578. Carlsbad, NM: Sandia National Laboratories.* [PDF / Author]

Jang, J.-H. 2012b. Memorandum to Records Center (Subject: Derivation of the solubility product for ferrous iron oxalate dihydrate in NaCl solutions and related Pitzer ion interaction parameter). ERMS 558084. Carlsbad, NM: Sandia National Laboratories.* [PDF / Author]

Jang, J.-H., Y.-L. Xiong, S. Kim, and M.B. Nemer. 2011. Iron, Lead, Sulfide, and EDTA Solubilities. Milestone Report on Test Plan TP 08-02. ERMS 555601. Carlsbad, NM: Sandia National Laboratories.* [PDF / Author]

Jang, J.-H., Y.-L. Xiong, S. Kim, and M.B. Nemer. 2012. Iron, Lead, Sulfide, and EDTA Solubilities. Second Milestone Report on Test Plan TP 08-02. ERMS 557198. Carlsbad, NM: Sandia National Laboratories.* [PDF / Author]

Johnson, P.B. 2008. 2007 Calculated Densities for Use in Deriving Equivalent Freshwater Heads of the Culebra Dolomite Member of the Rustler Formation near the WIPP Site. Routine Calculations Report in Support of Task 6 of AP-114, May 2007. ERMS 537208. Carlsbad, NM: Sandia National Laboratories.* [PDF / Author]

Johnson, P.B. 2009. 2008 Calculated Densities for Use in Deriving Equivalent Freshwater Heads of the Culebra Dolomite Member of the Rustler Formation near the WIPP Site. Routine Calculations Report in Support of Task 6 of AP-114, January 27, 2009. ERMS 537960. Carlsbad, NM: Sandia National Laboratories.* [PDF / Author]

Johnson, P.B. 2010. Memorandum to Records Center (Subject: 2009 Calculated Densities). January 13, 2010. ERMS 552839. Carlsbad, NM: Sandia National Laboratories.* [PDF / Author]

Johnson, P.B. 2011. Memorandum to Records Center (Subject: Memo of Correction 2010 Calculated Densities). ERMS 554805. Carlsbad, NM: Sandia National Laboratories.* [PDF / Author]

Johnson, P.B. 2012a. Memorandum to Records Center (Subject: 2003 Calculated Densities). ERMS 557402. Carlsbad, NM: Sandia National Laboratories.* [PDF / Author]

Johnson, P.B. 2012b. Memorandum to Records Center (Subject: 2004 Calculated Densities). ERMS 557405. Carlsbad, NM: Sandia National Laboratories.* [PDF / Author]

Johnson, P.B. 2012c. Memorandum to Records Center (Subject: 2005 Calculated Densities). ERMS 556883. Carlsbad, NM: Sandia National Laboratories.* [PDF / Author]

Johnson, P.B. 2012d. Memorandum to Records Center (Subject: 2006 Calculated Densities). ERMS 556887. Carlsbad, NM: Sandia National Laboratories.* [PDF / Author]

Johnson, P.B. 2012e. Memorandum to Records Center (Subject: 2011 Calculated Densities). ERMS 556866. Carlsbad, NM: Sandia National Laboratories.* [PDF / Author]

Johnson, P.B. 2012f. Memorandum to Records Center (Subject: 2012 Calculated Densities). ERMS 559277. Carlsbad, NM: Sandia National Laboratories.* [PDF / Author]

Kuhlman, K.L. 2010. Culebra Water Level Monitoring Network Design. Analysis Report, AP-111, Rev. 1. ERMS 554054. Carlsbad, NM: Sandia National Laboratories.* [PDF / Author]

Lucchini, J-F., H. Khaing, and D.T. Reed. 2010. Uranium Solubility in Carbonate-Free ERDA-6 Brine. Materials Research Society Symposium Proceedings, Vol. 1265, 21-26.* [PDF / Author]

Lucchini, J-F., H. Khaing, M. Borkowski, M.K. Richmann, and D.T. Reed. 2010. Actinide (VI) Solubility in Carbonate-free WIPP Brine: Data Summary and Recommendations. Report LCO-ACP-10, LA-UR 10-00497. Carlsbad, NM: Los Alamos National Laboratory. [PDF / Author]

Lucchini, J-F., M. Borkowski, H. Khaing, M.K. Richmann, J.S. Swanson, K.A. Simmons, and D.T. Reed. 2013. WIPP Actinide-Relevant Brine Chemistry. Report LCO-ACP-15, LA-UR 13-20620. Carlsbad, NM: Los Alamos National Laboratory.* [PDF / Author]

Lucchini, J-F., M.K. Richmann, and M. Borkowski. 2013. Uranium(VI) Solubility in WIPP Brine. Report LCO-ACP-14, LA-UR 13-20786. Carlsbad, NM: Los Alamos National Laboratory.* [PDF / Author]

Lucchini, J-F., S. Ballard, and H. Khaing. 2012. Influence of Carbonate on Uranium Solubility in Brine. Actinides and Nuclear Energy Materials, Material Research Society Symposium Proceedings, Vol. 1444, 217-222. LA-UR 12-20323.* [PDF / Author]

Nemer, M.B., Y.-L. Xiong, A.E. Ismail, and J.-H. Jang. 2010. "Solubility of Fe2(OH)3Cl (pure-iron end-member of hibbingite) in NaCl and Na2SO4 brines," Chemical Geology 280 (2010): 26-32. SAND 2010-6500J. ERMS 555524.* [PDF / Author]

Nuclear Waste Partnership LLC. 2012. WIPP Geotechnical Engineering Program Plan (Rev. 7, November 19, 2012). WP 07-1. Carlsbad, NM: Carlsbad Field Office.* [PDF / Author]

Pepper, S.E., M. Borkowski, M.K. Richmann, and D.T. Reed. 2010. "Determination of ferrous and ferric iron in aqueous biological samples." Analytica Chimica Acta 663 (2010) 172-177. [PDF / Author]

Reed, D.T. 2011. Using Thermodynamic Models: Saline Systems. From Thermodynamics to the Safety Case, TDB and Sorption projects Symposium Proceedings, Nuclear Energy Agency, pp. 41.* [PDF / Author]

Reed, D.T., J.S. Swanson, J-F. Lucchini, and M.K. Richmann. 2013. Intrinsic, Mineral, and Microbial Colloid Enhancement Parameters for the WIPP Actinide Source Term. Report LCO-ACP-18, LA-UR 13-20858. Carlsbad, NM: Los Alamos National Laboratory.* [PDF / Author]

Reed, D.T., M. Borkowski, J.S. Swanson, M.K. Richmann, H. Khaing, J-F. Lucchini, and D.A. Ams. 2012. Redox-Controlling Processes for Multivalent Metals and Actinides in the WIPP. 3rd Annual Workshop Proceedings of the Collaborative Project Redox Phenomena Controlling Systems, p. 251-263.* [PDF / Author]

Reed, D.T., R. Deo, and B.E. Rittmann. 2010. "Subsurface Interactions of Actinide Species and Microorganisms," In The Chemistry of the Actinide and Transactinide Elements by L.R. Morss, N.M. Edelstein and J. Fuger, eds., Chapter 33. Netherlands: Springer Press, 2010.* [PDF / Author]

Richmann, M.K. 2010. Comparison of the Calculated Thorium Solubility (Concentration) Using the Constants from the TMT_050405 Database with the Experimental Data Published in Altmaier, M., Neck, V., Muller, R. and Fanghanel, T. Radiochemistry Acta, 93(2), 83-92 (2005). LA-UR 10-01545. Carlsbad, NM: Los Alamos National Laboratory.* [PDF / Author]

Roselle, G.T. 2010. Iron and Lead Corrosion in WIPP-Relevant Conditions: 12 Month Results. Milestone report, October 14, 2010. ERMS 5548383. Carlsbad, NM: Sandia National Laboratories.* [PDF / Author]

Roselle, G.T. 2011a. Determination of pCH+ Correction Factors in Brines. Analysis report, AP-157, Rev. 0, December 1, 2011. ERMS 556699. Carlsbad, NM: Sandia National Laboratories.* [PDF / Author]

Roselle, G.T. 2011b. Iron and Lead Corrosion in WIPP-Relevant Conditions: 18 Month Results. Milestone report, January 5, 2011. ERMS 554715. Carlsbad, NM: Sandia National Laboratories.* [PDF / Author]

Roselle, G.T. 2011c. Iron and Lead Corrosion in WIPP-Relevant Conditions: 24 Month Results. Milestone report, May 3, 2011. ERMS 555426. Carlsbad, NM: Sandia National Laboratories.* [PDF / Author]

Roselle, G.T. 2013. Determination of Corrosion Rates from Iron/Lead Corrosion Experiments to be used for Gas Generation Calculations. Analysis report, AP-159, Rev. 1. ERMS 559077. Carlsbad, NM: Sandia National Laboratories.* [PDF / Author]

Sandia National Laboratories (SNL). 2009. Sandia National Laboratories Compliance Monitoring Parameter Assessment for 2008 (January 2009). ERMS 550744. Carlsbad, NM: Sandia National Laboratories.* [PDF / Author]

Sandia National Laboratories (SNL). 2010a. Sandia National Laboratories Compliance Monitoring Parameter Assessment for 2009 (January 2010). ERMS 552883. Carlsbad, NM: Sandia National Laboratories.* [PDF / Author]

Sandia National Laboratories (SNL). 2010b. Sandia National Laboratories Compliance Monitoring Parameter Assessment for 2010 (November 2010). ERMS 554585. Carlsbad, NM: Sandia National Laboratories.* [PDF / Author]

Sandia National Laboratories (SNL). 2010c. Sandia National Laboratories Trigger Value Derivation Report (Revision 2, December 2010). ERMS 554605. Carlsbad, NM: Sandia National Laboratories.* [PDF / Author]

Sandia National Laboratories (SNL). 2011. Sandia National Laboratories Compliance Monitoring Parameter Assessment for 2011 (December 2011). ERMS 556779. Carlsbad, NM: Sandia National Laboratories.* [PDF / Author]

Sandia National Laboratories (SNL). 2012. Sandia National Laboratories Compliance Monitoring Parameter Assessment for 2012 (November 2012). ERMS 558589. Carlsbad, NM: Sandia National Laboratories.* [PDF / Author]

Schuhen, M. 2011. Data Report for Analysis Plan for Demonstration Test Process: Soil Flume Sixnet Data Acquisition System. Analysis report, AP-148, Rev. 0. ERMS 555892. Carlsbad, NM: Sandia National Laboratories.* [PDF / Author]

Swanson, J.S., and K.A. Simmons. 2013. Update on Microbial Characterization of WIPP Groundwaters. Report LCO-ACP-20, LA-UR 13-20623. Carlsbad, NM: Los Alamos National Laboratory.* [PDF / Author]

Swanson, J.S., D.M. Norden, H. Khaing, and D.T. Reed. 2012. "Degradation of Organic Complexing Agents by Halophilic Microorganisms in Brines." GeoMicrobiology Journal, 30: 189-98.* [PDF / Author]

Swanson, J.S., D.T. Reed, D.A. Ams, D.M. Norden, and K.A. Simmons. 2012. Status Report on the Microbial Characterization of Halite and Groundwater Samples from the WIPP. Report LCO-ACP-12, LA-UR 12-22824. Carlsbad, NM: Los Alamos National Laboratory.* [PDF / Author]

Swanson, J.S., K.A. Simmons, D.M. Norden, and H. Khaing. 2013. Biodegradation of Organic Complexing Agents by WIPP-indigenous Halophilic Microorganisms in Brines. Report LCO-ACP-19, LA-UR 13-20616. Carlsbad, NM: Los Alamos National Laboratory.* [PDF / Author]

Thakur, P., Y.-L. Xiong, M. Borkowski, and G.R. Choppin. 2012. "Thermodynamic Modeling of Trivalent Am, Cm, and Eu-Citrate Complexation in Concentrated NaClO4 Media," Radiochimica Acta 100.3 (2012): 165-172.* [Author]

U.S. Department of Energy (DOE). 1996. Title 40 CFR Part 191 Compliance Certification Application for the Waste Isolation Pilot Plant (October). 21 vols. DOE/CAO 1996-2184. Carlsbad, NM: Carlsbad Area Office. [Author]

U.S. Department of Energy (DOE). 2004. Title 40 CFR Part 191 Compliance Recertification Application for the Waste Isolation Pilot Plant (March). 10 vols. DOE/WIPP 2004-3231. Carlsbad, NM: Carlsbad Field Office. [Author]

U.S. Department of Energy (DOE). 2008a. Delaware Basin Monitoring Annual Report (September 2008). DOE/WIPP-08-2308. Carlsbad, NM: Carlsbad Field Office.* [PDF / Author]

U.S. Department of Energy (DOE). 2008b. WIPP Subsidence Monument Leveling Survey 2008 (December 2008). DOE/WIPP 09-2293. Carlsbad, NM: Carlsbad Field Office.* [PDF / Author]

U.S. Department of Energy (DOE). 2008c. Waste Isolation Pilot Plant Annual Site Environmental Report for 2007 (September 2008). DOE/WIPP 08-2225. Carlsbad, NM: Carlsbad Field Office.* [PDF / Author]

U.S. Department of Energy (DOE). 2008d. Annual Change Report 2007/2008 (November 15, 2008). DOE/WIPP 08-3317. Carlsbad, NM: Carlsbad Field Office.* [PDF / Author]

U.S. Department of Energy (DOE). 2008e. Annual Transuranic Waste Inventory Report-2008 (Revision 0). DOE/TRU-08-3425. Carlsbad, NM: Carlsbad Field Office.* [PDF / Author]

U.S. Department of Energy (DOE). 2009a. Title 40 CFR Part 191 Compliance Recertification Application for the Waste Isolation Pilot Plant (March). DOE/WIPP 2009-3424. Carlsbad, NM: Carlsbad Field Office.* [Author]

U.S. Department of Energy (DOE). 2009b. Delaware Basin Monitoring Annual Report (September 2009). DOE/WIPP-09-2308. Carlsbad, NM: Carlsbad Field Office.* [PDF / Author]

U.S. Department of Energy (DOE). 2009c. WIPP Subsidence Monument Leveling Survey 2009 (December 2009). DOE/WIPP 10-2293. Carlsbad, NM: Carlsbad Field Office.* [PDF / Author]

U.S. Department of Energy (DOE). 2009d. Geotechnical Analysis Report for July 2007-June 2008 (March 2009). DOE/WIPP 09-3177. Carlsbad, NM: Carlsbad Field Office.* [PDF / Author]

U.S. Department of Energy (DOE). 2009e. Waste Isolation Pilot Plant Annual Site Environmental Report for 2008 (September 2009). DOE/WIPP 09-2225. Carlsbad, NM: Carlsbad Field Office.* [PDF / Author]

U.S. Department of Energy (DOE). 2009f. Annual Change Report 2008/2009 (November 13, 2009). DOE/WIPP 09-0335. Carlsbad, NM: Carlsbad Field Office.* [PDF / Author]

U.S. Department of Energy (DOE). 2009g. Annual Transuranic Waste Inventory Report-2009 (Revision 0). DOE/TRU-09-3425. Carlsbad, NM: Carlsbad Field Office.* [PDF / Author]

U.S. Department of Energy (DOE). 2010a. Delaware Basin Monitoring Annual Report (September 2010). DOE/WIPP-10-2308. Carlsbad, NM: Carlsbad Field Office.* [PDF / Author]

U.S. Department of Energy (DOE). 2010b. WIPP Subsidence Monument Leveling Survey 2010 (December 2010). DOE/WIPP 11-2293. Carlsbad, NM: Carlsbad Field Office.* [PDF / Author]

U.S. Department of Energy (DOE). 2010c. Geotechnical Analysis Report for July 2008-June 2009 (April 2010). DOE/WIPP 10-3177. Carlsbad, NM: Carlsbad Field Office.* [PDF / Author]

U.S. Department of Energy (DOE). 2010d. Waste Isolation Pilot Plant Annual Site Environmental Report for 2009 Errata (September 2010). DOE/WIPP 10-2225. Carlsbad, NM: Carlsbad Field Office.* [PDF / Author]

U.S. Department of Energy (DOE). 2010e. Annual Change Report 2009/2010 (November 15, 2010). DOE/WIPP 10-1660. Carlsbad, NM: Carlsbad Field Office.* [PDF / Author]

U.S. Department of Energy (DOE). 2010f. Annual Transuranic Waste Inventory Report-2010 (Revision 0, November 2010). DOE/TRU-10-3425. Carlsbad, NM: Carlsbad Field Office.* [PDF / Author]

U.S. Department of Energy (DOE). 2011a. Delaware Basin Monitoring Annual Report (September 2011). DOE/WIPP-11-2308. Carlsbad, NM: Carlsbad Field Office.* [PDF / Author]

U.S. Department of Energy (DOE). 2011b. WIPP Subsidence Monument Leveling Survey 2011 (December 2011). DOE/WIPP 12-2293. Carlsbad, NM: Carlsbad Field Office.* [PDF / Author]

U.S. Department of Energy (DOE). 2011c. Geotechnical Analysis Report for July 2009-June 2010 (March 2011). DOE/WIPP 11-3177. Carlsbad, NM: Carlsbad Field Office.* [PDF / Author]

U.S. Department of Energy (DOE). 2011d. Waste Isolation Pilot Plant Annual Site Environmental Report for 2010 (September 2011). DOE/WIPP 11-2225. Carlsbad, NM: Carlsbad Field Office.* [PDF / Author]

U.S. Department of Energy (DOE). 2011e. Annual Change Report 2010/2011 (August 30,2011). DOE/WIPP 11-3479. Carlsbad, NM: Carlsbad Field Office.* [PDF / Author]

U.S. Department of Energy (DOE). 2011f. Annual Transuranic Waste Inventory Report-2011 (Revision 0, November 2011). DOE/TRU-11-3425. Carlsbad, NM: Carlsbad Field Office.* [PDF / Author]

U.S. Department of Energy (DOE). 2012a. Delaware Basin Monitoring Annual Report (September 2012). DOE/WIPP-12-2308. Carlsbad, NM: Carlsbad Field Office.* [PDF / Author]

U.S. Department of Energy (DOE). 2012b. WIPP Subsidence Monument Leveling Survey 2012 (December 2012). DOE/WIPP 12-3497. Carlsbad, NM: Carlsbad Field Office.* [PDF / Author]

U.S. Department of Energy (DOE). 2012c. Geotechnical Analysis Report for July 2010-June 2011 (May 2012). DOE/WIPP 12-3484. Carlsbad, NM: Carlsbad Field Office.* [PDF / Author]

U.S. Department of Energy (DOE). 2012d. Waste Isolation Pilot Plant Annual Site Environmental Report for 2011 (Revision 0, September 2012). DOE/WIPP 12-3489. Carlsbad, NM: Carlsbad Field Office.* [PDF / Author]

U.S. Department of Energy (DOE). 2012e. Annual Transuranic Waste Inventory Report-2012 (Revision 0, October 2012). DOE/TRU-12-3425. Carlsbad, NM: Carlsbad Field Office.* [PDF / Author]

U.S. Department of Energy (DOE). 2012f. Annual Change Report 2011/2012 (October 2012). DOE/WIPP 12-3496. Carlsbad, NM: Carlsbad Field Office.* [PDF / Author]

U.S. Department of Energy (DOE). 2012g. Email to Tom Peake (Subject: Response to EPA Questions on Two-Phase Flow and ROM Permeability) June 15, 2012.* [PDF / Author]

U.S. Department of Energy (DOE). 2012h. Letter to Mr. Jonathan Edwards (Subject: Response to EPA Letter Dated December 22, 2011) April 17, 2012.* [PDF / Author]

U.S. Department of Energy (DOE). 2012i. Compliance Monitoring Implementation Plan for 40 CFR §191.14(b), Assurance Requirement, Revision 7. DOE/WIPP 99-3119. Carlsbad, NM: Carlsbad Field Office.* [PDF / Author]

U.S. Environmental Protection Agency (EPA). 1996. 40 CFR Part 194: Criteria for the Certification and Recertification of the Waste Isolation Pilot Plant's Compliance with the 40 CFR Part 191 Disposal Regulations; Final Rule. Federal Register, vol. 61 (February 9, 1996): 52234-45. [PDF / Author]

U.S. Environmental Protection Agency (EPA). 1998. 40 CFR Part 194: Criteria for the Certification and Recertification of the Waste Isolation Pilot Plant's Compliance with the Disposal Regulations: Certification Decision; Final Rule. Federal Register, vol. 63 (May 18, 1998): 27353-406. [PDF / Author]

Van Soest, G.D. 2012. Performance Assessment Inventory Report - 2012. Report INV-PA-12, Revision 0, INV-1211-05-01-01. Carlsbad, NM: Los Alamos National Laboratory.* [PDF / Author]

Wagner, S.W. 2011. Monitoring Parameter Assessment Per 40 CFR 194.42. SP 9-8, Rev. 1, May 26, 2011. Carlsbad, NM: Sandia National Laboratories.* [PDF / Author]

Wolery, T.J., Y.-L. Xiong, and J.J. Long. 2010. Verification and Validation Plan/Validation Document for EQ3/6 Version 8.0a for Actinide Chemistry, Document Version 8.10. ERMS 550239. Carlsbad, NM: Sandia National Laboratories.* [PDF / Author]

Xiong, Y.-L. 2008a. "Thermodynamic Properties of Brucite Determined by Solubility Studies and Their Significance to Nuclear Waste Isolation," Aquatic Geochemistry 14.3 (2008): 223-238. ERMS 546279. SAND2007-3373J.* [Author]

Xiong, Y.-L. 2008b. Memorandum to Larry Brush (Subject: HMI-an EQ3/6 Database with Iron Species.) April 14, 2008. ERMS 548633. Carlsbad, NM: Sandia National Laboratories.* [PDF / Author]

Xiong, Y.-L. 2009. Email to Jennifer Long (Subject: Release of FMT_090720.CHEMDAT.) July 22, 2009. ERMS 551706. Carlsbad, NM: Sandia National Laboratories.* [PDF / Author]

Xiong, Y.-L. 2010a. "Experimental Determination of Solubility Constant of Hydromagnesite (5424) in NaCl Solutions up to 4.4 M at Room Temperature," Chemical Geology 284.3-4 (2010): 262-269. October 12, 2010. ERMS 556406. SAND2010-7132J. Carlsbad, NM: Sandia National Laboratories.* [Author]

Xiong, Y.-L. 2010b. Memorandum to Record Center (Subject: Calculations of Thermodynamic Parameters for Experimental Data Generated at Los Alamos National Laboratory Carlsbad Operation (LANL-CO)). January 20, 2010. ERMS 552873. Carlsbad, NM: Sandia National Laboratories.* [PDF / Author]

Xiong, Y.-L. 2010c. Memorandum to Record Center (Subject: Summary Report for Migration of the WIPP Thermodynamic Code from FMT to EQ3/6 Version 8.0a.) December 9, 2010. ERMS 554632. Carlsbad, NM: Sandia National Laboratories.* [PDF / Author]

Xiong, Y.-L. 2011a. Experimental Study of Thermodynamic Parameters of Borate in WIPP Relevant Brines at Sandia National Laboratories Carlsbad Facility. Milestone Report on Test Plan TP 10-01. August 4, 2011. ERMS 556026. Carlsbad, NM: Sandia National Laboratories.* [PDF / Author]

Xiong, Y.-L. 2011b. "Organic Species of Lanthanum in Natural Environments: Implications to Mobility of Rare Earth Elements in Low Temperature Environments." Applied Geochemistry 26.7 (2011): 1130-1137.* [Author]

Xiong, Y.-L. 2011c. WIPP Verification and Validation Plan/Validation Document for EQ3/6 Version 8.0a for Actinide Chemistry, Revision 1. Supersedes ERMS 550239. May 12, 2011. ERMS 555358. Carlsbad, NM: Sandia National Laboratories.* [PDF / Author]

Xiong, Y.-L. 2011d. Email to Jennifer Long (Subject: Release of EQ3/6 Database DATA0.FM1) March 9, 2011. ERMS 555152. Carlsbad, NM: Sandia National Laboratories.* [PDF / Author]

Xiong, Y.-L. 2012a. Experimental Determination of Solubility Constant of Di-Calcium Ethylenediaminetetraacetic Acid (Ca2EDTA), Ca2C10H12N2O8(S), in the NaCl-H2O System. November 12, 2012. ERMS 558669. Carlsbad, NM: Sandia National Laboratories.* [PDF / Author]

Xiong, Y.-L. 2012b. Thermodynamic Model for the Na-B(OH)3-Cl-SO4 System. August 20, 2012. ERMS 558111. Carlsbad, NM: Sandia National Laboratories.* [PDF / Author]

Xiong, Y.-L. 2012c. Thermodynamic Model for the Na-B(OH)3-Cl-SO4 System, Revision 1, Superseding ERMS 558111. October 30, 2012. ERMS 558556. Carlsbad, NM: Sandia National Laboratories.* [PDF / Author]

Xiong, Y.-L. 2012d. Experimental Study of Thermodynamic Parameters of Borate in WIPP Relevant Brines at Sandia National Laboratories Carlsbad Facility. Second Milestone Report on Test Plan TP 10-01. April 23, 2012. ERMS 557333. Carlsbad, NM: Sandia National Laboratories.* [PDF / Author]

Xiong, Y.-L. 2012e. Memorandum to The WIPP Record Center (Subject: Memo of Corrections for 'Second Milestone Report on Test Plan TP 08-02, "Iron, Lead, Sulfide, and EDTA Solubilities" (ERMS 557198)'). October 30, 2012. ERMS 558553. Carlsbad, NM: Sandia National Laboratories.* [PDF / Author]

Xiong, Y.-L., and A.S. Lord. 2008. "Experimental Investigations of the Reaction Path in the MgO-CO2-H2O System in Solutions with Various Ionic Strengths, and Their Applications to Nuclear Waste Isolation," Applied Geochemistry 23.6 (2008): 1634-1659 ERMS 544728.* [Author]

Xiong, Y.-L., E.J. Nowak, L.H. Brush, A.E. Ismail, and J.J. Long. 2010. Establishment of Uncertainty Ranges and Probability Distributions of Actinide Solubilities for Performance Assessment in the Waste Isolation Pilot Plant. Materials Research Society Spring Meeting, April 5-9, 2010. San Francisco, CA. ERMS 555764. SAND2010-2013C.* [PDF / Author]

Xiong, Y.-L., H. Deng, M.B. Nemer, and S.R. Johnsen. 2009a. "Experimental determination of the solubility constant for magnesium chloride hydroxide hydrate (Mg3Cl(OH)5•4H2O, Phase 5) at room temperature, and its importance to nuclear waste isolation in geological repositories in salt formations," Geochimica et Cosmochimica Acta 74.16 (2009): 4605-4611. ERMS 552782. SAND2009-7912J. Carlsbad, NM: Sandia National Laboratories.* [Author]

Xiong, Y.-L., H. Deng, M.B. Nemer, and S.R. Johnsen. 2009b. Memorandum to Larry Brush (Subject: Thermodynamic Data for phase 5 (Mg3Cl(OH)5·4H2O) Determined from Solubility Experiments.) May 18, 2009. ERMS 551294. Carlsbad, NM: Sandia National Laboratories.* [PDF / Author]

Xiong, Y.-L., L.H. Brush, A.E. Ismail, and J.J. Long. 2009. Uncertainty Analysis of Actinide Solubilities for the WIPP CRA-2009 PABC. Analysis report, December 1, 2009. ERMS 552500. Carlsbad, NM: Sandia National Laboratories.* [PDF / Author]

Xiong, Y.-L., L.H. Brush, J.W. Garner, and J.J. Long. 2010a. Responses to Three EPA Comments Pertaining to Comparisons of Measured and Predicted Dissolved and Colloidal Th(IV) and Am(III) Concentrations. Analysis report, May 4, 2010. ERMS 553409. Carlsbad, NM: Sandia National Laboratories.* [PDF / Author]

Xiong, Y.-L., L.H. Brush, J.W. Garner, and J.J. Long. 2010b. Responses to Three EPA Comments Pertaining to Comparisons of Measured and Predicted Dissolved and Colloidal Th(IV) and Am(III) Concentrations, Revision 1. Supersedes ERMS 553409. Analysis report, May 19, 2010. ERMS 553595. Carlsbad, NM: Sandia National Laboratories.* [PDF / Author]

Xiong, Y.-L., L.H. Brush, P.S. Domski, and J.J. Long. 2011. Uncertainty Analysis of Actinide Solubilities for the WIPP CRA-2009 PABC, Rev. 1, Supersedes ERMS 552500. Analysis report, January 24, 2011. ERMS 554875. Carlsbad, NM: Sandia National Laboratories.* [PDF / Author]

Xiong, Y.-L., L. Kirkes, T. Westfall, T. Olivas, and R.A. Roselle. 2011. Experimental Determination of Solubilities of Lead Oxalate (PbC2O4(cr)) in a NaCl Medium to High Ionic Strengths, and the Importance of Lead Oxalate in Low Temperature Environments. ERMS 556753. SAND2011-9321J. Albuquerque, NM: Sandia National Laboratories.* [PDF / Author]

Title 40 CFR Part 191
Subparts B and C
Compliance Recertification Application 2014
for the
Waste Isolation Pilot Plant

Appendix DATA-2014
Attachment A: WIPP Borehole Update

United States Department of Energy
Waste Isolation Pilot Plant

Carlsbad Field Office
Carlsbad, New Mexico

Appendix DATA-2014
Attachment A: WIPP Borehole Update

Table of Contents

List of Tables

This page intentionally left blank.

Acronyms and Abbreviations

BLM Bureau of Land Management

CCA Compliance Certification Application

CRA Compliance Recertification Application

DOE Department of Energy

WIPP Waste Isolation Pilot Plant

This page intentionally left blank.

DATA-A-1.0 WIPP Boreholes

The U.S. Department of Energy (DOE) prepared DOE/WIPP 95-2092, Revision 1, Waste Isolation Pilot Plant (WIPP) Borehole Data Report (the Compliance Certification Application [CCA], Appendix BH) (U.S. DOE 1996) to serve as a central document, providing data on boreholes used in characterizing the site. The report contains a comprehensive database on wells drilled in support of the Waste Isolation Pilot Plant (WIPP) Project and boreholes located within the 16-section land withdrawal area.

The CCA, Appendix BH (U.S. DOE 1996) describes seven groups of boreholes: commercially drilled boreholes, DOE wells, geologic exploration boreholes, hydrologic test boreholes, potash boreholes, subsurface exploration boreholes, and Water Quality Sampling Program boreholes. There are 179 boreholes listed in the report. At the time of the CCA, 80 of those boreholes were being used as monitoring wells. The rest of the boreholes were plugged and abandoned after being drilled for their

specific purpose, i.e., potash information, hydrocarbon information, or WIPP site characterization information.

The Appendix DATA-2004, Attachment G, WIPP Borehole Update (U.S. DOE 2004), was provided to add the new monitoring wells drilled since the initial certification and wells that were in use but omitted from the CCA, Appendix BH. The Appendix DATA-2004, Attachment G provided information on 112 boreholes.

The Appendix DATA-2009, Attachment A, WIPP Borehole Update (U.S. DOE 2009), was provided to add the new monitoring wells. The Appendix DATA-2009, Attachment A provided information on 215 boreholes.

For the 2014 Compliance Recertification Application (CRA-2014), a thorough search was performed to define the number of boreholes associated with WIPP site characterization and monitoring. Currently, there are 221 boreholes that were either specifically drilled to support the WIPP site characterization process or obtained for monitoring purposes. This update provides the status for those boreholes.

Table DATA-A-1 provides the status of all 221 boreholes, including the name of the formation being monitored, whether the borehole is currently configured as a water or observation well, and whether it has been plugged and abandoned. A status of "N/A" means the borehole was not being used or had not yet been drilled at the time of the status report. "Observation" means the borehole was drilled for site characterization, but left unplugged for future monitoring purposes.

Table DATA-A- 1. Status of WIPP Boreholes December 2012 WIPP

Well Name	CCA Status	CRA-2004 Status	CRA-2009 Status	CRA-2014 Status	Original Depth	Year Drilled
AEC-7	Culebra	Culebra	Culebra	Culebra	4,734 ft	1974
AEC-8	Bell Canyon	Bell Canyon	Plugged	Plugged	4,922 ft	1974
B-1	Observation	Observation	Observation	Observation	58 ft	1978

Table DATA-A-1. Status of WIPP Boreholes December 2012 WIPP (Continued)

Well Name	CCA Status	CRA-2004 Status	CRA-2009 Status	CRA-2014 Status	Original Depth	Year Drilled
B-1A	Observation	Observation	Observation	Observation	13 ft	1978
B-2	Plugged	Plugged	Plugged	Plugged	34 ft	1978
B-3	Plugged	Plugged	Plugged	Plugged	29 ft	1978
B-4	Observation	Observation	Observation	Observation	39 ft	1978
B-4A	Observation	Observation	Observation	Observation	14 ft	1978
B-5	Plugged	Plugged	Plugged	Plugged	32 ft	1978
B-6	Plugged	Plugged	Plugged	Plugged	26 ft	1978
B-7	Plugged	Plugged	Plugged	Plugged	35 ft	1978
B-8	Plugged	Plugged	Plugged	Plugged	100 ft	1979
B-9	Plugged	Plugged	Plugged	Plugged	38 ft	1978
B-10	Plugged	Plugged	Plugged	Plugged	32 ft	1978
B-11	Plugged	Plugged	Plugged	Plugged	30 ft	1978

Table DATA-A-1. Status of WIPP Boreholes December 2012 WIPP (Continued)

Well Name	CCA Status	CRA-2004 Status	CRA-2009 Status	CRA-2014 Status	Original Depth	Year Drilled
B-12	Plugged	Plugged	Plugged	Plugged	41 ft	1978
B-13	Observation	Observation	Observation	Observation	28 ft	1978
B-14	Plugged	Plugged	Plugged	Plugged	25 ft	1978
B-15	Plugged	Plugged	Plugged	Plugged	57 ft	1978
B-16	Observation	Observation	Observation	Observation	31 ft	1978
B-17	Plugged	Plugged	Plugged	Plugged	26 ft	1978
B-18	Observation	Observation	Observation	Observation	33 ft	1978
B-19	Plugged	Plugged	Plugged	Plugged	39 ft	1978
B-20	Observation	Observation	Observation	Observation	14 ft	1978
B-20A	Observation	Observation	Observation	Observation	34 ft	1978
B-21	Plugged	Plugged	Plugged	Plugged	40 ft	1978
B-22	Plugged	Plugged	Plugged	Plugged	28 ft	1978
B-23	Plugged	Plugged	Plugged	Plugged	41 ft	1978
B-24	Plugged	Plugged	Plugged	Plugged	29 ft	1978
B-25	Plugged	Plugged	Plugged	Plugged	902 ft	1978
B-26	Plugged	Plugged	Plugged	Plugged	28 ft	1979
B-27	Plugged	Plugged	Plugged	Plugged	26 ft	1979
B-28	Plugged	Plugged	Plugged	Plugged	27 ft	1979
B-29	Plugged	Plugged	Plugged	Plugged	29 ft	1978
B-30	Plugged	Plugged	Plugged	Plugged	28 ft	1978
B-31	Plugged	Plugged	Plugged	Plugged	31 ft	1978
B-32	Plugged	Plugged	Plugged	Plugged	100 ft	1979
B-33	Plugged	Plugged	Plugged	Plugged	31 ft	1978
B-34	Plugged	Plugged	Plugged	Plugged	100 ft	1979
B-35	Plugged	Plugged	Plugged	Plugged	32 ft	1979
B-36	Plugged	Plugged	Plugged	Plugged	28 ft	1979
B-37	Plugged	Plugged	Plugged	Plugged	28 ft	1979
B-37A	Plugged	Plugged	Plugged	Plugged	22 ft	1979
B-38	Observation	Observation	Observation	Observation	50 ft	1979
B-39	Plugged	Plugged	Plugged	Plugged	28 ft	1979
B-40	Plugged	Plugged	Plugged	Plugged	28 ft	1979
B-41	Plugged	Plugged	Plugged	Plugged	100 ft	1979
B-42	Plugged	Plugged	Plugged	Plugged	100 ft	1979
B-43	Plugged	Plugged	Plugged	Plugged	100 ft	1979
B-44	Plugged	Plugged	Plugged	Plugged	100 ft	1979
B-45	Plugged	Plugged	Plugged	Plugged	100 ft	1979
B-46	Plugged	Plugged	Plugged	Plugged	100 ft	1979
B-47	Plugged	Plugged	Plugged	Plugged	18 ft	1979
B-48	Plugged	Plugged	Plugged	Plugged	16 ft	1979

Table DATA-A-1. Status of WIPP Boreholes December 2012 WIPP (Continued)

Well Name	CCA Status	CRA-2004 Status	CRA-2009 Status	CRA-2014 Status	Original Depth	Year Drilled
B-49	Plugged	Plugged	Plugged	Plugged	19 ft	1979
B-50	Plugged	Plugged	Plugged	Plugged	24 ft	1979
B-51	Plugged	Plugged	Plugged	Plugged	15 ft	1979
B-52	Plugged	Plugged	Plugged	Plugged	30 ft	1979
B-53	Plugged	Plugged	Plugged	Plugged	30 ft	1979
B-54	Observation	Observation	Observation	Observation	210 ft	1979
B-301	Plugged	Plugged	Plugged	Plugged	40 ft	1979
B-302	Plugged	Plugged	Plugged	Plugged	39 ft	1979
B-303	Plugged	Plugged	Plugged	Plugged	39 ft	1979
B-304	Plugged	Plugged	Plugged	Plugged	42 ft	1979
B-305	Plugged	Plugged	Plugged	Plugged	41 ft	1979
B-306	Plugged	Plugged	Plugged	Plugged	38 ft	1979
B-307	Plugged	Plugged	Plugged	Plugged	40 ft	1979
B-308	Plugged	Plugged	Plugged	Plugged	40 ft	1979
B-309	Plugged	Plugged	Plugged	Plugged	39 ft	1979
C-2505	N/A	Santa Rosa/Dewey Lake	Santa Rosa/Dewey Lake	Santa Rosa/Dewey Lake	97 ft	1996
C-2506	N/A	Santa Rosa/Dewey Lake	Santa Rosa/Dewey Lake	Santa Rosa/Dewey Lake	69 ft	1996
C-2507	N/A	Santa Rosa/Dewey Lake	Santa Rosa/Dewey Lake	Santa Rosa/Dewey Lake	73 ft	1996
C-2737	N/A	Culebra/Magenta	Culebra/Magenta	Culebra/Magenta	800 ft	2001
C-2811	N/A	Santa Rosa/Dewey Lake	Santa Rosa/Dewey Lake	Santa Rosa/Dewey Lake	80 ft	2001
CB-1	Culebra	Culebra/Bell Canyon	Bell Canyon	Culebra	4,299 ft	1974
D-268	Culebra	Rancher's Water Well	Rancher's Water Well	Rancher's Water Well	1,411 ft	1984
DOE-1	Culebra	Culebra	Plugged	Plugged	4,057 ft	1982
DOE-2	Culebra	Magenta	Bell Canyon	Magenta	4,325 ft	1984
ERDA-6	Plugged	Plugged	Plugged	Plugged	2,775 f	1975
ERDA-9	Culebra	Culebra	Culebra	Culebra	2,886 ft	1976
ERDA-10	Plugged	Plugged	Plugged	Plugged	4,430 ft	1977
ERDA-11	Plugged	Plugged	Plugged	Plugged	40 ft	1977
ES-001	N/A	Plugged	Plugged	Plugged	54 ft	1996
ES-002	N/A	Plugged	Plugged	Plugged	19 ft	1996
H-1	Culebra/Magenta	Plugged	Plugged	Plugged	856 ft	1976

Table DATA-A-1. Status of WIPP Boreholes December 2012 WIPP (Continued)

Well Name	CCA Status	CRA-2004 Status	CRA-2009 Status	CRA-2014 Status	Original Depth	Year Drilled
H-2A	Culebra	Culebra	Plugged	Plugged	672 ft	1977
H-2B1	Magenta	Magenta	Magenta	Magenta	661 ft	1977
H-2B2	Culebra	Culebra	Culebra	Culebra	660 ft	1983
H-2C	Magenta	Culebra	Plugged	Plugged	795 ft	1977
H-3B1	Magenta	Magenta	Magenta	Magenta	902 ft	1976
H-3B2	Culebra	Culebra	Culebra	Culebra	725 ft	1983
H-3B3	Magenta	Culebra	Plugged	Plugged	730 ft	1983
H-3D	Dewey Lake	Dewey Lake/Forty-niner	Santa Rosa/Dewey Lake	Santa Rosa/Dewey Lake	554 ft	1987
H-4A	N/A	Plugged	Plugged	Plugged	532 ft	1978
H-4B	Culebra	Culebra	Culebra	Plugged	529 ft	1978
H-4BR	N/A	N/A	N/A	Culebra	529 ft	2009
H-4C	Magenta	Magenta	Magenta	Magenta	661 ft	1978
H-5A	Culebra	Culebra	Plugged	Plugged	930 ft	1978
H-5B	Culebra	Culebra	Culebra	Culebra	925 ft	1978
H-5C	Magenta	Magenta	Not in Use	Magenta	1,076 ft	1978
H-6A	Culebra	Culebra	Plugged	Plugged	637 ft	1978
H-6B	Culebra	Culebra	Culebra	Plugged	640 ft	1978
H-6BR	N/A	N/A	N/A	Culebra	640 ft	2008
H-6C	Culebra	Culebra	Magenta	Magenta	741 ft	1978
H-7A	N/A	Plugged	Plugged	Plugged	154 ft	1979
H-7B1	Culebra	Culebra	Culebra	Culebra	286 ft	1979
H-7B2	Culebra	Culebra	Plugged	Plugged	295 ft	1983
H-7C	N/A	N/A	Rancher's Water Well	Rancher's Water Well	420 ft	1979
H-8A	Magenta	Magenta	Magenta	Magenta	505 ft	1979
H-8B	N/A	Rancher's Water Well	Rancher's Water Well	Rancher's Water Well	624 ft	1979
H-8C	Rustler	Rustler	Rancher's Water Well	Rancher's Water Well	808 ft	1979
H-9A	Culebra	Plugged	Plugged	Plugged	692 ft	1979
H-9B	Culebra	Culebra	Not in Use	Plugged	708 ft	1979
H-9BR	N/A	N/A	N/A	Culebra	686 ft	2010
H-9C	Culebra	Magenta	Culebra/Magenta	Magenta	816 ft	1979
H-10A	Magenta	Magenta	Magenta	Magenta	1,318 ft	1979
H-10B	Magenta	Plugged	Plugged	Plugged	1,398 ft	1979
H-10C	N/A	Culebra	Culebra	Culebra	1,550 ft	1979
H-11B1	Culebra	Culebra	Plugged	Plugged	785 ft	1983
H-11B2	Culebra	Magenta	Magenta	Magenta	776 ft	1983

Table DATA-A-1. Status of WIPP Boreholes December 2012 WIPP (Continued)

Well Name	CCA Status	CRA-2004 Status	CRA-2009 Status	CRA-2014 Status	Original Depth	Year Drilled
H-11B3	Culebra	Plugged	Plugged	Plugged	789 ft	1983
H-11B4	N/A	Culebra	Culebra	Plugged	765 ft	1988
H-11B4R	N/A	N/A	N/A	Culebra	755 ft	2011
H-11B4RA	N/A	N/A	N/A	Plugged	774 ft	2011
H-12	Culebra	Culebra	Culebra	Culebra	1,001 ft	1983
H-14	Culebra	Magenta	Magenta	Magenta	589 ft	1986
H-15	Culebra	Magenta	Culebra/Magenta	Magenta	900 ft	1986
H-15R	N/A	N/A	N/A	Culebra	924 ft	2009
H-16	Dewey Lake	N/A	Rustler	Rustler	851 ft	1987
H-17	Culebra	Culebra	Culebra	Culebra	880 ft	1987
H-18	Culebra	Magenta	Magenta	Magenta	840 ft	1987
H-19B	N/A	N/A	N/A	N/A	40 ft	1995
H-19B0	N/A	Culebra	Culebra	Culebra	779 ft	1995
H-19B1	N/A	Plugged	Plugged	Plugged	733 ft	1995
H-19B2	N/A	Culebra	Culebra	Culebra	785 ft	1995
H-19B3	N/A	Culebra	Culebra	Culebra	785 ft	1995
H-19B4	N/A	Culebra	Culebra	Culebra	782 ft	1995
H-19B5	N/A	Culebra	Culebra	Culebra	786 ft	1995
H-19B6	N/A	Culebra	Culebra	Culebra	788 ft	1995
H-19B7	N/A	Culebra	Culebra	Culebra	785 ft	1995
IMC-461	N/A	N/A	Culebra	Culebra	1,316 ft	2004
P-1	Plugged	Plugged	Plugged	Plugged	1,591 ft	1976
P-2	Plugged	Plugged	Plugged	Plugged	1,895 ft	1976
P-3	Plugged	Plugged	Plugged	Plugged	1,676 ft	1976
P-4	Plugged	Plugged	Plugged	Plugged	1,857 ft	1976
P-5	Plugged	Plugged	Plugged	Plugged	1,830 ft	1976
P-6	Plugged	Plugged	Plugged	Plugged	1,573 ft	1976
P-7	Plugged	Plugged	Plugged	Plugged	1,574 ft	1976
P-8	Plugged	Plugged	Plugged	Plugged	1,660 ft	1976
P-9	Plugged	Plugged	Plugged	Plugged	1,796 ft	1976
P-10	Plugged	Plugged	Plugged	Plugged	2,009 ft	1976
P-11	Plugged	Plugged	Plugged	Plugged	1,940 ft	1976
P-12	Plugged	Plugged	Plugged	Plugged	1,598 ft	1976
P-13	Plugged	Plugged	Plugged	Plugged	1,576 ft	1976
P-14	Culebra	Plugged	Plugged	Plugged	1,545 ft	1976
P-15	Culebra	Plugged	Plugged	Plugged	1,465 ft	1976
P-16	Plugged	Plugged	Plugged	Plugged	1,585 ft	1976
P-17	Culebra	Culebra	Plugged	Plugged	1,660 ft	1976
P-18	Culebra	Plugged	Plugged	Plugged	1,998 ft	1976

Table DATA-A-1. Status of WIPP Boreholes December 2012 WIPP (Continued)

Well Name	CCA Status	CRA-2004 Status	CRA-2009 Status	CRA-2014 Status	Original Depth	Year Drilled
P-19	Plugged	Plugged	Plugged	Plugged	2,000 ft	1976
P-20	Plugged	Plugged	Plugged	Plugged	1,995 ft	1976
P-21	Plugged	Plugged	Plugged	Plugged	1,915 ft	1976
PZ-1	N/A	Santa Rosa	Santa Rosa/Dewey Lake	Santa Rosa/Dewey Lake	68 ft	1997
PZ-2	N/A	Santa Rosa	Santa Rosa/Dewey Lake	Santa Rosa/Dewey Lake	65 ft	1997
PZ-3	N/A	Santa Rosa	Santa Rosa/Dewey Lake	Santa Rosa/Dewey Lake	71 ft	1997
PZ-4	N/A	Santa Rosa	Santa Rosa/Dewey Lake	Santa Rosa/Dewey Lake	65 ft	1997
PZ-5	N/A	Santa Rosa	Santa Rosa/Dewey Lake	Santa Rosa/Dewey Lake	72 ft	1997
PZ-6	N/A	Santa Rosa	Santa Rosa/Dewey Lake	Santa Rosa/Dewey Lake	66 ft	1997
PZ-7	N/A	Santa Rosa	Santa Rosa/Dewey Lake	Santa Rosa/Dewey Lake	72 ft	1997
PZ-8	N/A	Santa Rosa	Santa Rosa/Dewey Lake	Santa Rosa/Dewey Lake	68 ft	1997
PZ-9	N/A	Santa Rosa	Santa Rosa/Dewey Lake	Santa Rosa/Dewey Lake	82 ft	1997
PZ-10	N/A	Santa Rosa	Santa Rosa/Dewey Lake	Santa Rosa/Dewey Lake	57 ft	1997
PZ-11	N/A	Santa Rosa	Santa Rosa/Dewey Lake	Santa Rosa/Dewey Lake	82 ft	1997
PZ-12	N/A	Santa Rosa	Santa Rosa/Dewey Lake	Santa Rosa/Dewey Lake	72 ft	1997
PZ-13	N/A	N/A	Santa Rosa/Dewey Lake	Santa Rosa/Dewey Lake	77 ft	2007
PZ-14	N/A	N/A	Santa Rosa/Dewey Lake	Santa Rosa/Dewey Lake	73 ft	2007
PZ-15	N/A	N/A	Gatuña/Santa Rosa	Gatuña/Santa Rosa	56 ft	2007

Table DATA-A-1. Status of WIPP Boreholes December 2012 WIPP (Continued)

Well Name	CCA Status	CRA-2004 Status	CRA-2009 Status	CRA-2014 Status	Original Depth	Year Drilled
SNL-1	N/A	N/A	Culebra	Culebra	644 ft	2004
SNL-2	N/A	N/A	Culebra	Culebra	614 ft	2003
SNL-3	N/A	N/A	Culebra	Culebra	970 ft	2003
SNL-5	N/A	N/A	Culebra	Culebra	687 ft	2004
SNL-6	N/A	N/A	Culebra	Culebra	1,360 ft	2005
SNL-8	N/A	N/A	Culebra	Culebra	981 ft	2005
SNL-9	N/A	N/A	Culebra	Culebra	845 ft	2003
SNL-10	N/A	N/A	Culebra	Culebra	651 ft	2006
SNL-12	N/A	N/A	Culebra	Culebra	905 ft	2003
SNL-13	N/A	N/A	Culebra	Culebra	480 ft	2005
SNL-14	N/A	N/A	Culebra	Culebra	719 ft	2005
SNL-15	N/A	N/A	Culebra	Culebra	950 ft	2005
SNL-16	N/A	N/A	Culebra	Culebra	224 ft	2006
SNL-17A	N/A	N/A	Culebra	Culebra	375 ft	2006
SNL-17	N/A	N/A	Plugged	Plugged	365 ft	2006
SNL-18	N/A	N/A	Culebra	Culebra	566 ft	2006
SNL-19	N/A	N/A	Culebra	Culebra	381 ft	2006
WIPP-11	N/A	N/A	Culebra	Culebra	3,580 ft	1978
WIPP-12	Culebra	Culebra	Plugged	Plugged	3,928 ft	1978
WIPP-13	Culebra	Culebra	Culebra	Culebra	3,856 ft	1978
WIPP-14	Plugged	Plugged	Plugged	Plugged	1,000 ft	1981
WIPP-15	Water Well	Rancher's Water Well	Rancher's Water Well	Rancher's Water Well	810 ft	1978
WIPP-16	Plugged	Plugged	Plugged	Plugged	1,300 ft	1980
WIPP-18	Culebra	Magenta	Magenta	Magenta	1,060 ft	1978
WIPP-19	Culebra	Culebra	Culebra	Culebra	1,038 ft	1978
WIPP-21	Culebra	Culebra	Plugged	Plugged	1,045 ft	1978
WIPP-22	Culebra	Culebra	Plugged	Plugged	1,450 ft	1978
WIPP-25	Culebra/Magenta	Culebra/Magenta	Culebra/Magenta	Plugged	655 ft	1978
WIPP-26	Culebra	Culebra	Plugged	Plugged	503 ft	1978
WIPP-27	Culebra/Magenta	Culebra	Plugged	Plugged	592 ft	1978
WIPP-28	Rustler	Plugged	Plugged	Plugged	801 ft	1978
WIPP-29	Culebra	Culebra	Plugged	Plugged	377 ft	1978
WIPP-30	Culebra/Magenta	Culebra/Magenta	Culebra/Magenta	Plugged	912 ft	1978
WIPP-31	Plugged	Plugged	Plugged	Plugged	1,982 ft	1980
WIPP-32	Plugged	Plugged	Plugged	Plugged	390 ft	1979
WIPP-33	Plugged	Plugged	Plugged	Plugged	840 ft	1979
WIPP-34	Plugged	Plugged	Plugged	Plugged	1,820 ft	1979
WQSP-1	Culebra	Culebra	Culebra	Culebra	737 ft	1994

Table DATA-A-1. Status of WIPP Boreholes December 2012 WIPP (Continued)

Well Name	CCA Status	CRA-2004 Status	CRA-2009 Status	CRA-2014 Status	Original Depth	Year Drilled
WQSP-2	Culebra	Culebra	Culebra	Culebra	846 ft	1994
WQSP-3	Culebra	Culebra	Culebra	Culebra	879 ft	1994
WQSP-4	Culebra	Culebra	Culebra	Culebra	800 ft	1994
WQSP-5	Culebra	Culebra	Culebra	Culebra	681 ft	1994
WQSP-6	Culebra	Culebra	Culebra	Culebra	617 ft	1994
WQSP-6A	Dewey Lake	Dewey Lake	Dewey Lake	Dewey Lake	225 ft	1994

DATA-A-2.0 Individual Well Reports

This section provides basic data on the new wells drilled (6) and the wells plugged (7) during the CRA-2014 monitoring period (October 2007 through December 2012).

All WIPP monitoring wells have been drilled in New Mexico within the vicinity of the WIPP site. The Bureau of Land Management (BLM) controls the drilling, operation, and abandonment of hydrocarbon wells on federal land in New Mexico. The New Mexico Oil Conservation Division controls the drilling, operation, and abandonment of hydrocarbon wells on state and patented lands in New Mexico. The New Mexico Office of the State Engineer regulates the drilling, operation, and abandonment of groundwater wells (this includes mineral exploration, monitoring, and observation wells) in the State of New Mexico. This agency has regulatory oversight of wells in the WIPP land withdrawal area. All WIPP monitoring wells have been permitted through this agency and drilled according to the regulations in place at the time of drilling. Right-of-way permits have been acquired from the BLM when monitoring wells are located on federal lands outside the WIPP land withdrawal area.

DATA-A-2.1 New Wells Drilled Since the CRA-2009

H-4BR

Location: T22S-R31E-05 Year Drilled: 2009 Total Depth: 518 ft (158 m)

Status: Culebra Monitoring Well Elevation: 3332 ft (1016 m)

H-6BR

Location: T22S-R31E-18 Year Drilled: 2008 Total Depth: 640 ft (195 m)

Status: Culebra Monitoring Well Elevation: 3347 ft (1020 m)

H-9BR
Location: T24S-R31E-04 Year Drilled: 2010 Total Depth: 686 ft (209 m)
Status: Culebra Monitoring Well Elevation: 3405 ft (1038 m)

H-11B4R
Location: T22S-R31E-33 Year Drilled: 2011 Total Depth: 755 ft (230 m)
Status: Culebra Monitoring Well Elevation: 3409 ft (1039 m)

H-11B4RA
Location: T22S-R31E-33 Year Drilled: 2011 Total Depth: 774 ft (236 m)
Status: Culebra Monitoring Well Elevation: 3410 ft (1039 m)

H-15R
Location: T22S-R31E-28 Year Drilled: 2009 Total Depth: 924 ft (282 m)
Status: Culebra Monitoring Well Elevation: 3480 ft (1061 m)

DATA-A-2.2 Plugged Wells

H-4B
Location: T23S-R31E-05 Year Drilled: 1978 Total Depth: 529 ft (161 m)
Status: Plugged in 2009 Elevation: 3333 ft (1016 m)
Notes: The well was cemented to the surface using Class C neat cement.

H-6B
Location: T22S-R31E-18 Year Drilled: 1978 Total Depth: 640 ft (195 m)
Status: Plugged in 2008 Elevation: 3348 ft (1020 m)
Notes: The well was cemented to the surface using Class C neat cement.

H-9B
Location: T24S-R31E-04 Year Drilled: 1979 Total Depth: 708 ft (216 m)
Status: Plugged in 2010 Elevation: 3406 ft (1038 m)
Notes: In 2002, the open-hole portion of the well was inadvertently plugged during pressure grouting of well H-9A. The well was cemented to the surface using Class C neat cement.

H-11B4
Location: T22S-R31E-33 Year Drilled: 1988 Total Depth: 765 ft (233 m)
Status: Plugged in 2011 Elevation: 3409 ft (1039 m)
Notes: The well was cemented to the surface using Class C neat cement.

H-11B4RA
Location: T22S-R31E-15 Year Drilled: 2011 Total Depth: 774 ft (236 m)
Status: Plugged in 2011 Elevation: 3409 ft (1039 m)
Notes: Plugged due to improper screen depth by driller. The well was cemented to the surface using Class C neat cement.

WIPP-25
Location: T22S-R30E-15 Year Drilled: 1978 Total Depth: 655 ft (200 m)
Status: Plugged in 2009 Elevation: 3212 ft (979 m)
Notes: The well was cemented to the surface using Class C neat cement.

WIPP-30
Location: T21S-R31E-33 Year Drilled: 1978 Total Depth: 912 ft (278 m)
Status: Plugged in 2008 Elevation: 3428 ft (1045 m)
Notes: The well was cemented to the surface using Class C neat cement.

DATA-A-3.0 References

(*Indicates a reference that has not been previously submitted.)

U.S. Department of Energy (DOE). 1996. Title 40 CFR Part 191 Compliance Certification Application for the Waste Isolation Pilot Plant (October). 21 vols. DOE/CAO 1996-2184. Carlsbad, NM: Carlsbad Area Office. [Author]

U.S. Department of Energy (DOE). 2004. Title 40 CFR Part 191 Compliance Recertification Application for the Waste Isolation Pilot Plant (March). 10 vols. DOE/WIPP 2004-3231. Carlsbad, NM: Carlsbad Field Office. [Author]

U.S. Department of Energy (DOE). 2009. Title 40 CFR Part 191 Compliance Recertification Application for the Waste Isolation Pilot Plant (March). DOE/WIPP 2009-3424. Carlsbad, NM: Carlsbad Field Office.* [Author]

Title 40 CFR Part 191
Subparts B and C
Compliance Recertification Application 2014
for the
Waste Isolation Pilot Plant

Appendix DATA-2014
Attachment B: WIPP Waste Containers and Emplacement

United States Department of Energy
Waste Isolation Pilot Plant

Carlsbad Field Office
Carlsbad, New Mexico

Appendix DATA-2014 Attachment B: WIPP Waste Containers and Emplacement

Table of Contents

List of Figures

List of Tables

This page intentionally left blank.

Acronyms and Abbreviations

CH contact-handled

CH-TRU contact-handled transuranic

EPA U.S. Environmental Protection Agency

gal gallon

mm millimeter

RH remote-handled

RH-TRU remote-handled transuranic

SLB2 Standard Large Box 2

SWB Standard Waste Box

TDOP 10-Drum Overpack

TRU transuranic

This page intentionally left blank.

DATA-B-1.0 Authorized Waste Emplacement Containers

DATA-B-1.1 Container Descriptions

The following containers are identified as outer containment vessels for waste emplacement in the repository:

- 55-gallon (gal) Drum
- 85-gal Drum (Short)
- 85-gal Drum (Tall)
- 100-gal Drum
- Shielded Container
- Standard Large Box 2 (SLB2)
- Standard Waste Box (SWB)
- Ten-Drum Overpack (TDOP)
- Remote-handled transuranic (RH-TRU) 72B Canister (RH-TRU Waste Canister)

DATA-B-1.2 Dunnage Containers

Dunnage containers are empty containers used to complete a shipping configuration, such as the seven-pack, if too few containers that meet transportation requirements are available. Dunnage containers are clearly marked "Empty." The TDOP and the RH-TRU Waste Canister are not used as dunnage containers for shipping purposes. For emplacement purposes in the repository, the 55-, 85-, and 100-gal drums can be used as dunnage containers only if they arrive in a shrink-wrapped package assembly, such as the seven-pack, four-pack, or three-pack. To date, 55-gal drums and several SWBs have been emplaced in the repository as dunnage containers.

DATA-B-1.3 Payload Descriptions

This section gives a brief description of each payload container and its configuration for emplacement. This description also includes a figure and a table for each container.

The 55-gal drum is shipped in a seven-pack configuration and is normally emplaced in the repository in the same configuration but can be emplaced as an individual unit should the need arise. A single drum can be used for collecting and storing derived waste. An illustration of the 55-gal drum components and emplacement configuration is provided in Figure DATA-B-1. The drum specifications are provided in Table DATA-B-1.

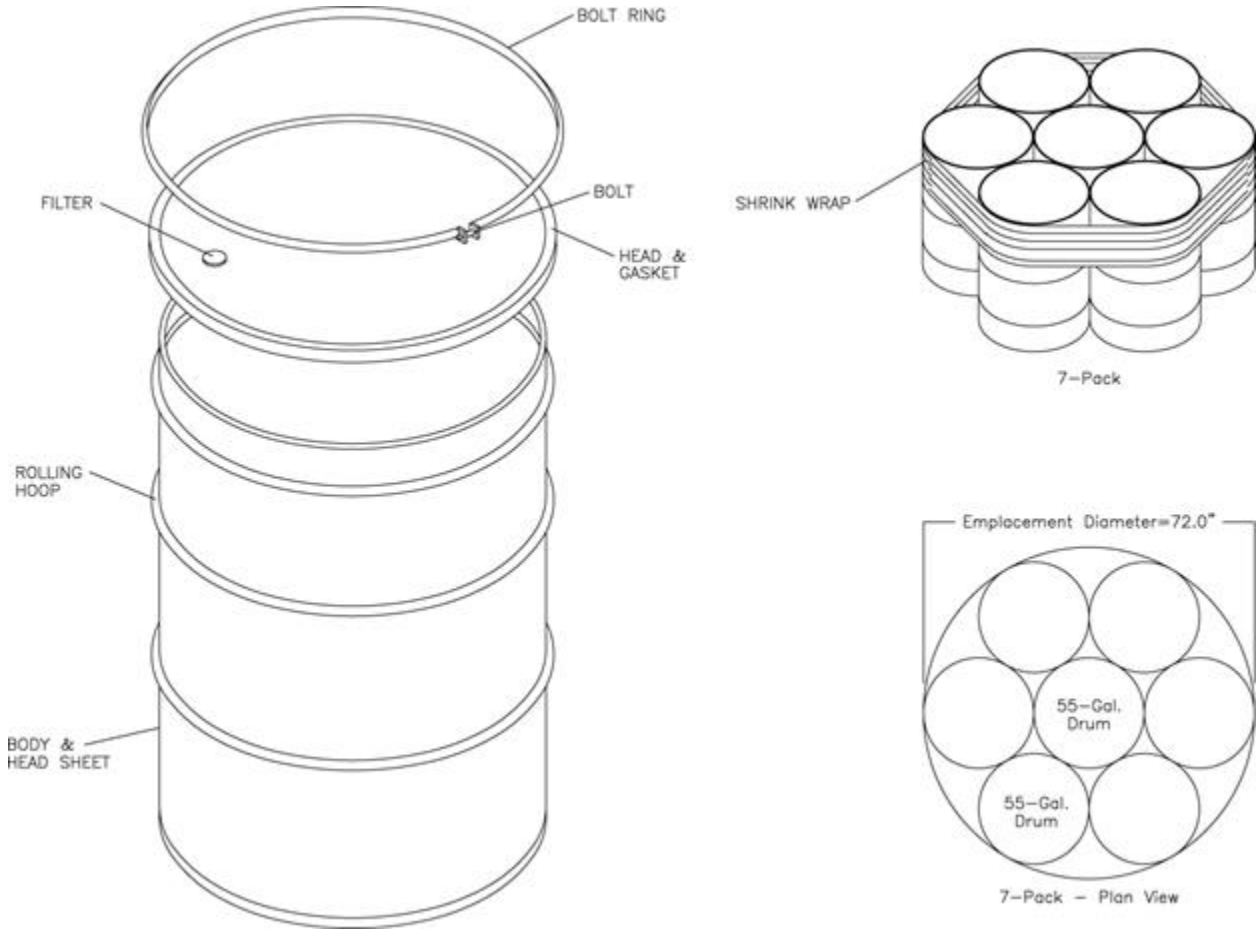

Figure DATA-B- 1. 55-gal Drum Components and Emplacement Configuration

Table DATA-B- 1. 55-gal Drum Specifications

Dimension	Approximate Measurement			
	Inside Dimension (inches)	Outside Dimension (inches)	Inside Dimension (mm)	Outside Dimension (mm)
Height	33 ¼	35	845	889
Diameter	22 ½	24	572	610

The 85-gal drum (short) is shipped in a four-pack configuration and will be emplaced in the repository in the same configuration but can be emplaced as an individual unit should the need arise. A single drum can be used for collecting and storing derived waste or for overpacking a 55-gal drum. An illustration of the 85-gal drum (short) components and emplacement configuration is provided in Figure DATA-B-2. The drum specifications are provided in Table DATA-B-2.

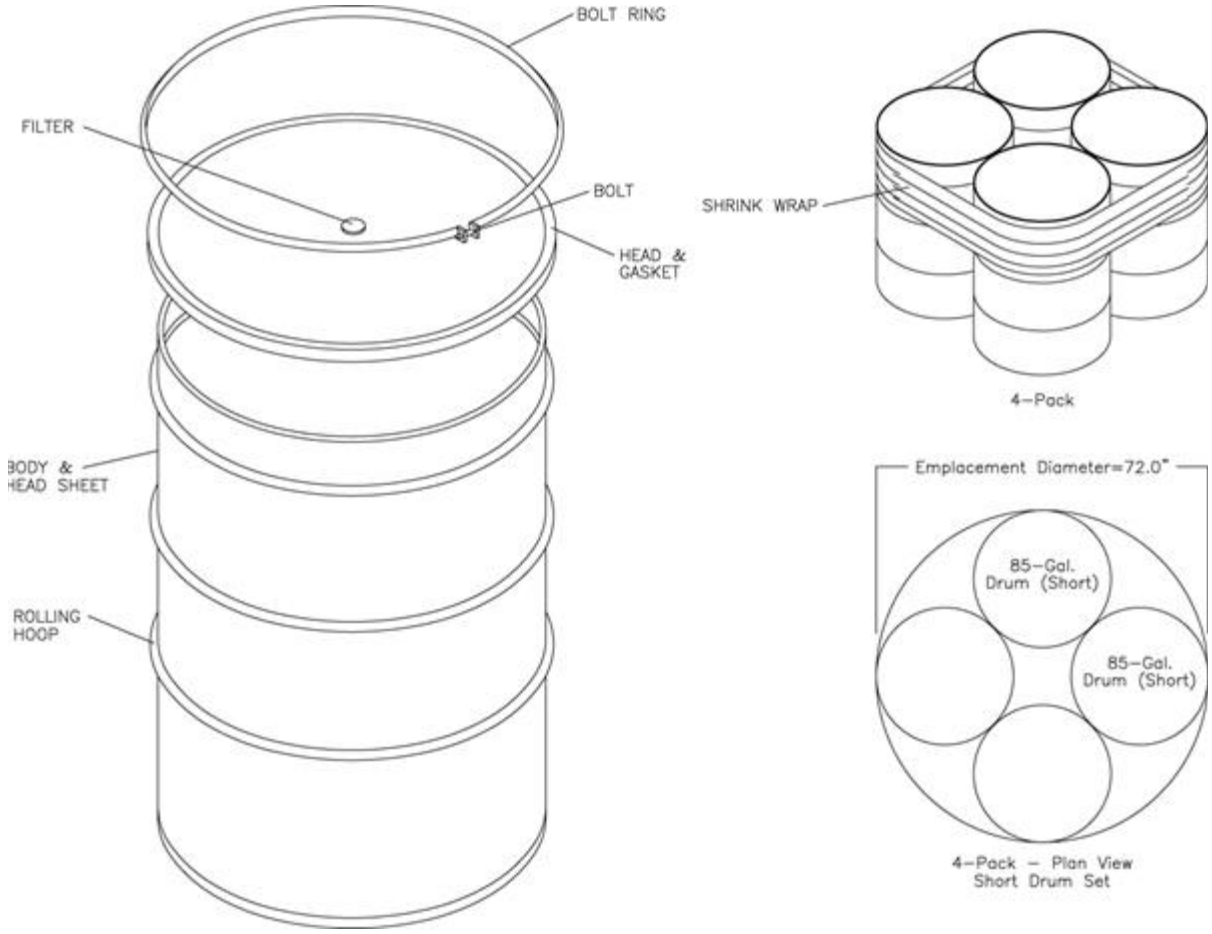

Figure DATA-B- 2. 85-gal Drum (Short) Components and Emplacement Configuration

Table DATA-B- 2. 85-gal Drum (Short) Specifications

Dimension	Approximate Measurement			
	Inside Dimension (inches)	Outside Dimension (inches)	Inside Dimension (mm)	Outside Dimension (mm)
Height	33 ¼	35	845	889
Diameter	27 ⅛	29 ¾	689	756

The 85-gal drum (tall) is shipped in a four-pack configuration and will be emplaced in the repository in the same configuration. It is also used for overpacking 55-gal drums that are individually emplaced in the repository. A single drum can be used for collecting and storing derived waste. An illustration of the 85-gal drum (tall) components and emplacement configuration is provided in Figure DATA-B-3. The drum specifications are provided in Table DATA-B-3.

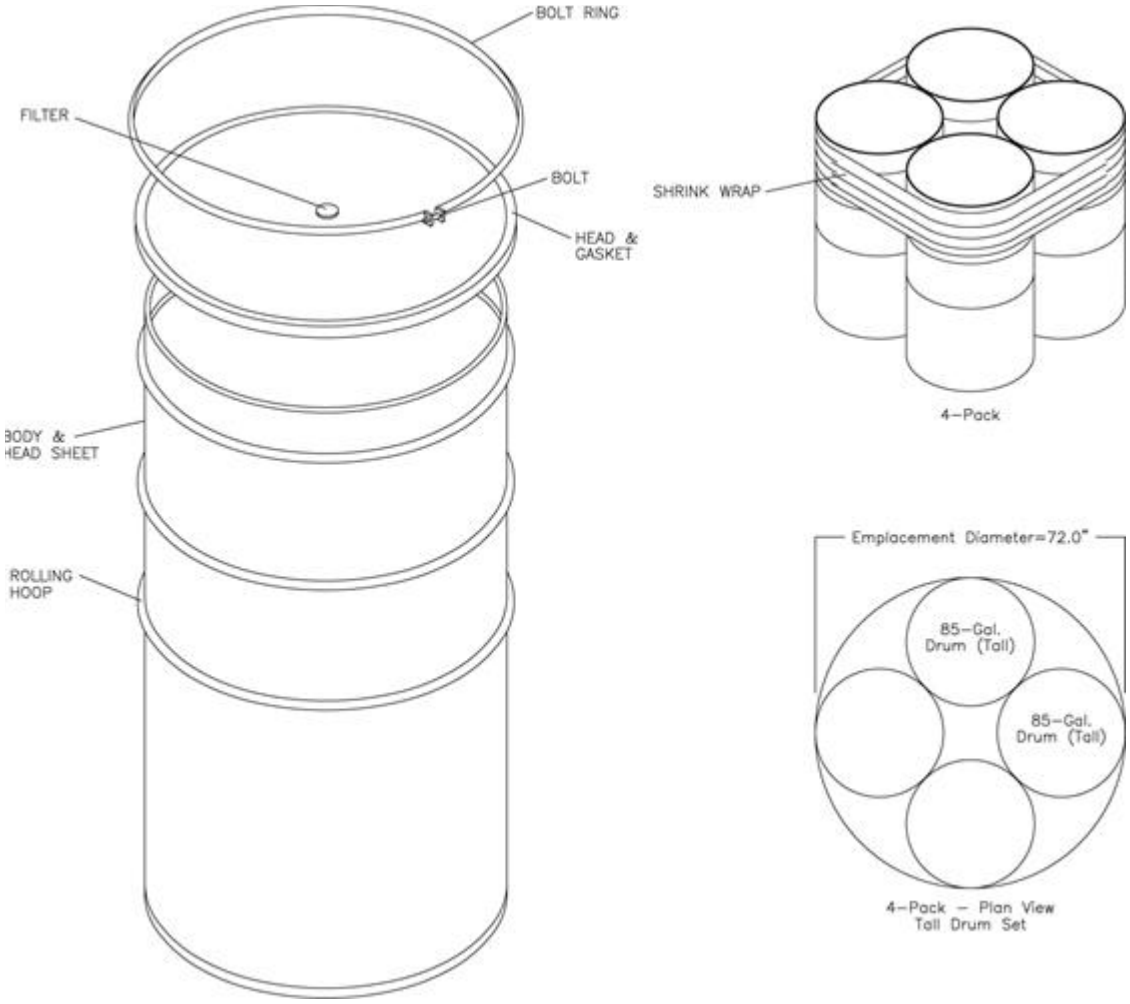

Figure DATA-B- 3. 85-gal Drum (Tall) Components and Emplacement Configuration

Table DATA-B- 3. 85-gal Drum (Tall) Specifications

Dimension	Approximate Measurement			
	Inside Dimension (inches)	Outside Dimension (inches)	Inside Dimension (mm)	Outside Dimension (mm)
Height	38 ¼	40 ¼	972	1,022
Diameter	26	28 ⅝	660	728

The 100-gal drum is shipped in a three-pack configuration and will be emplaced in the repository in the same configuration. The 100-gal drum can be emplaced as an individual unit should the need arise. An illustration of the 100-gal drum components and emplacement configuration is provided in Figure DATA-B-4. The drum specifications are provided in Table DATA-B-4.

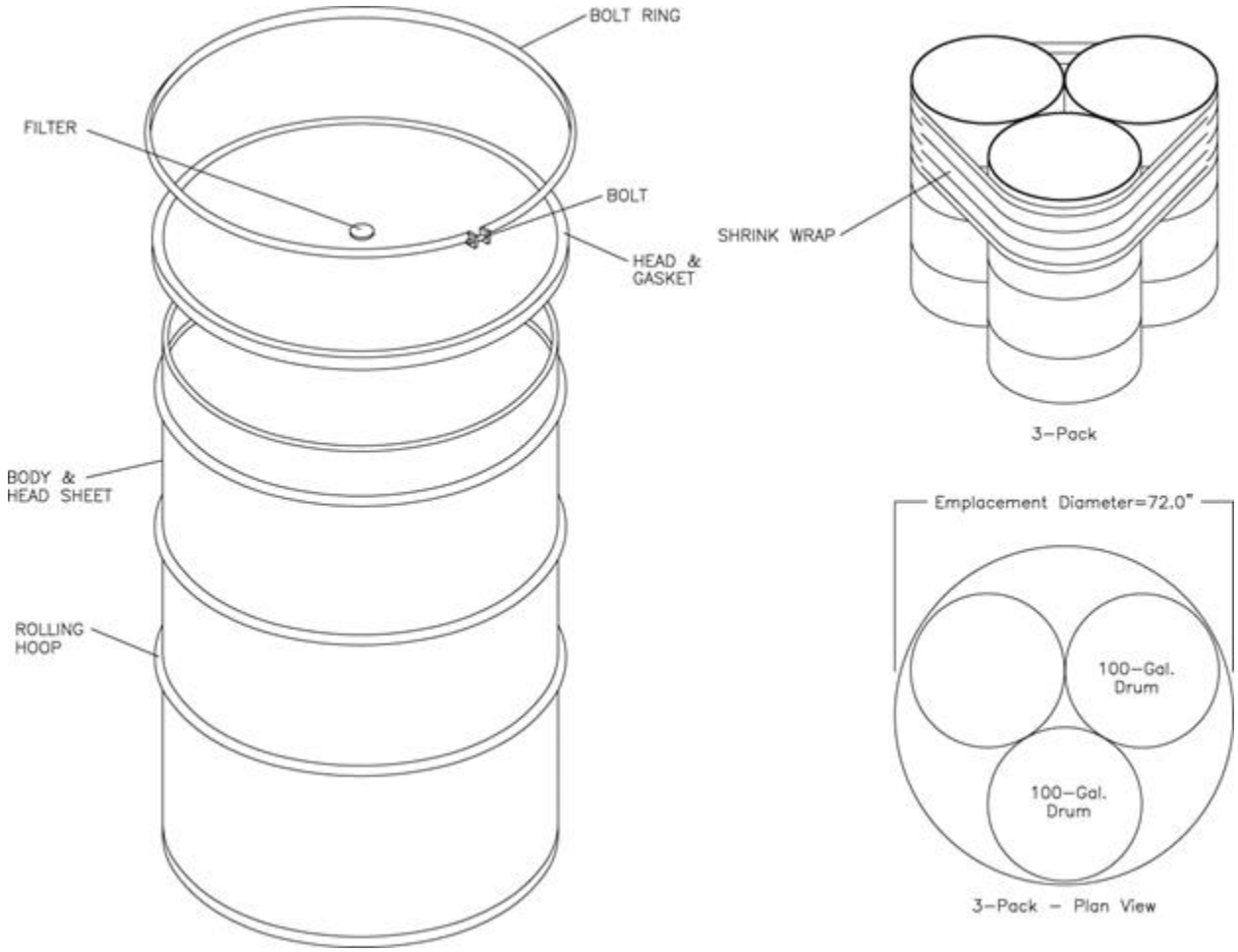

Figure DATA-B- 4. 100-gal Drum Components and Emplacement Configuration

Table DATA-B- 4. 100-gal Drum Specifications

Dimension	Approximate Measurement			
	Inside Dimension (inches)	Outside Dimension (inches)	Inside Dimension (mm)	Outside Dimension (mm)
Height	33	35	838	889
Diameter	30	32	762	813

The shielded container is shipped in a three-pack configuration and will be emplaced in the repository in the same configuration. The shielded container assemblies will be used to dispose of RH-TRU waste but will be managed and disposed of as contact-handled transuranic (CH-TRU) waste. An illustration of the shielded container components is provided in Figure DATA-B-5. The container specifications are provided in Table DATA-B-5.

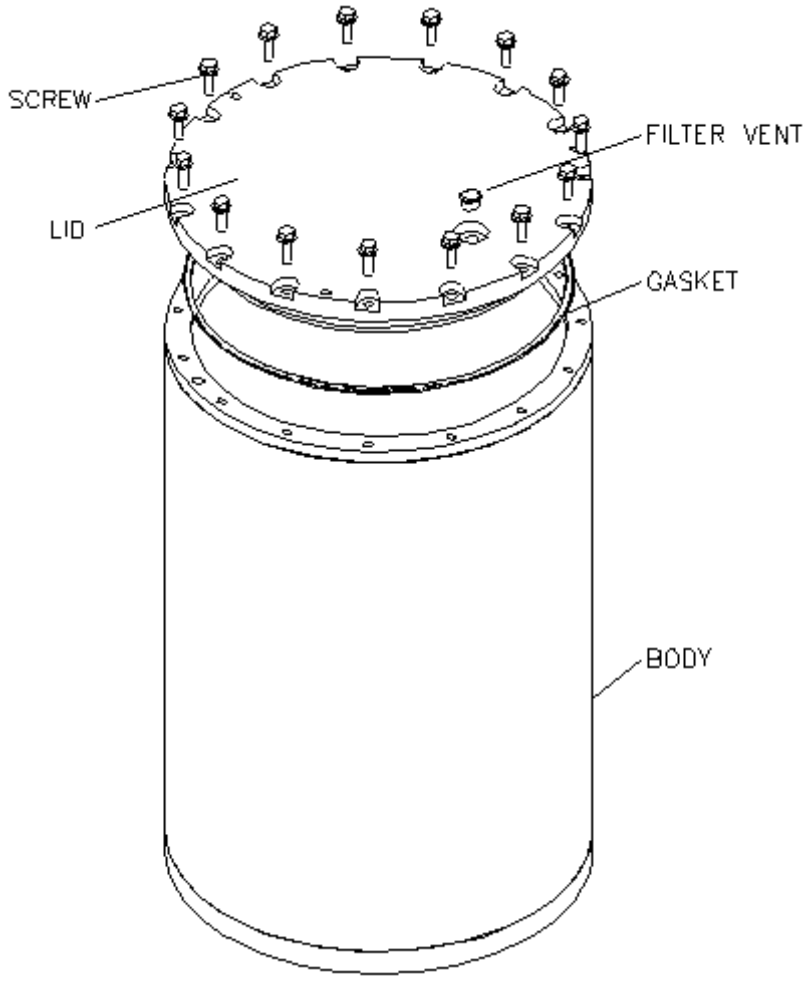

Figure DATA-B- 5. Illustration of a Shielded Container

Table DATA-B- 5. Shielded Container Specifications

Dimension	Approximate Measurement			
	Inside Dimension (inches)	Outside Dimension (inches)	Inside Dimension (mm)	Outside Dimension (mm)
Height	29 ¾	35 ¾	756	908
Diameter	20 3/8	23	518	584

The SLB2 is shipped and emplaced as an individual unit. An illustration of the SLB2 is provided in Figure DATA-B-6. The box specifications are provided in Table DATA-B-6.

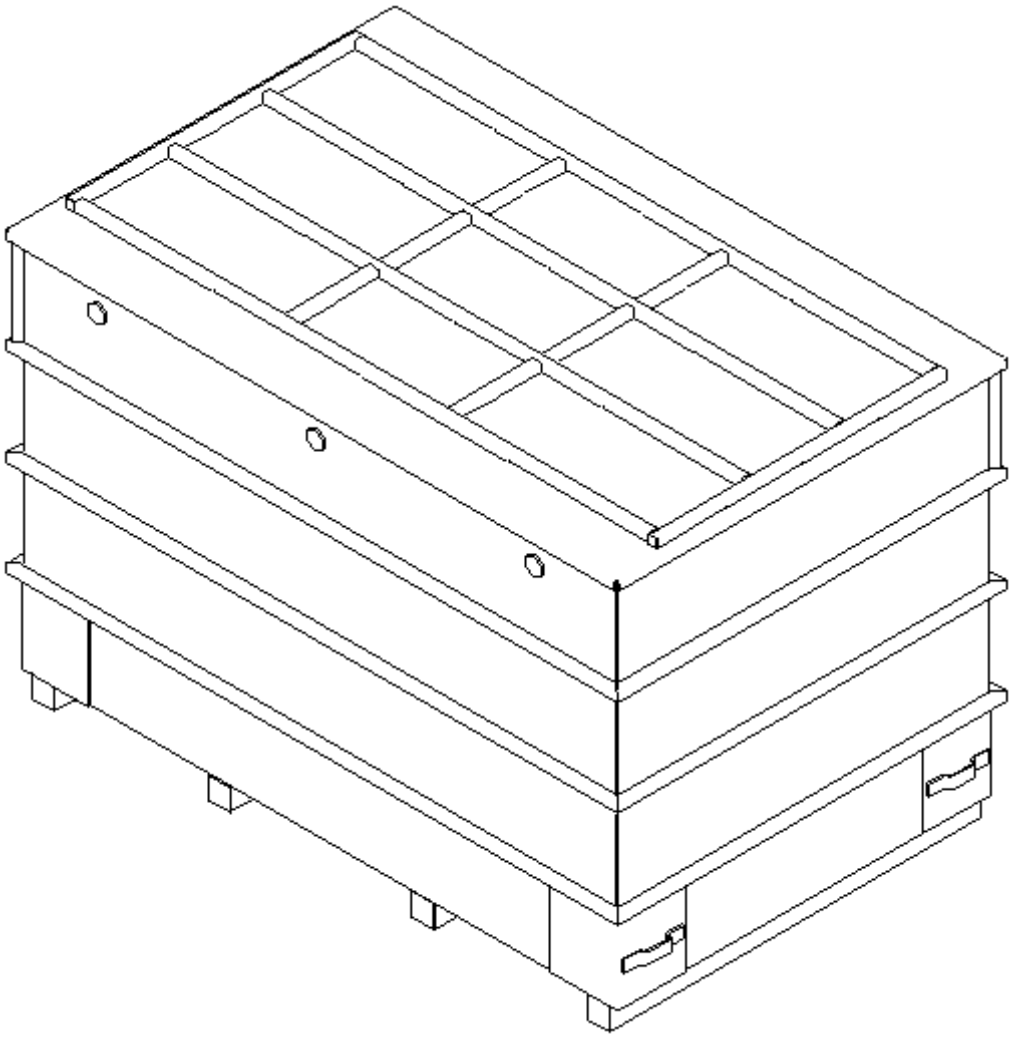

Figure DATA-B- 6. Illustration of a SLB2

Table DATA-B- 6. SLB2 Specifications

Dimension	Approximate Measurement			
	Inside Dimension (inches)	Outside Dimension (inches)	Inside Dimension (mm)	Outside Dimension (mm)
Height	66	73	1,676	1,854
Length	102	108	2,591	2,743
Width	63	69	1,600	1,753

The SWB is shipped and emplaced as an individual unit. An SWB can be used as an overpack or to collect derived waste in the Waste Handling Building CH Bay. An illustration of the SWB is provided in Figure DATA-B-7. The box specifications are provided in Table DATA-B-7.

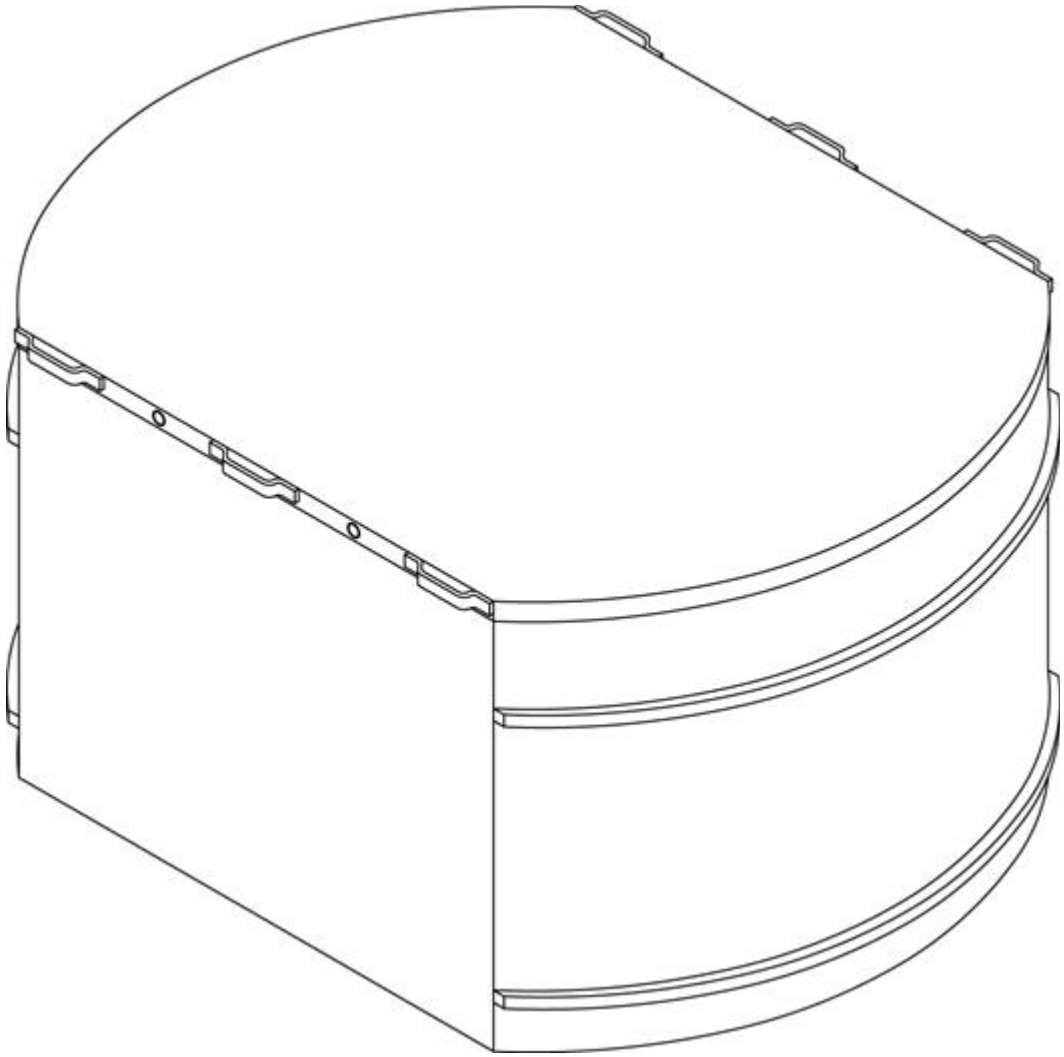

Figure DATA-B- 7. Illustration of a SWB

Table DATA-B- 7. SWB Specifications

Dimension	Approximate Measurement			
	Inside Dimension (inches)	Outside Dimension (inches)	Inside Dimension (mm)	Outside Dimension (mm)
Height	36 9/16	36 ⅞	929	937
Length	68 ¾	71	1,746	1,803
Width	52	54 ½	1,321	1,384

The TDOP is shipped as an individual unit and emplaced as an individual unit. An illustration of TDOP components is provided in Figure DATA-B-8. The TDOP specifications are provided in Table DATA-B-8.

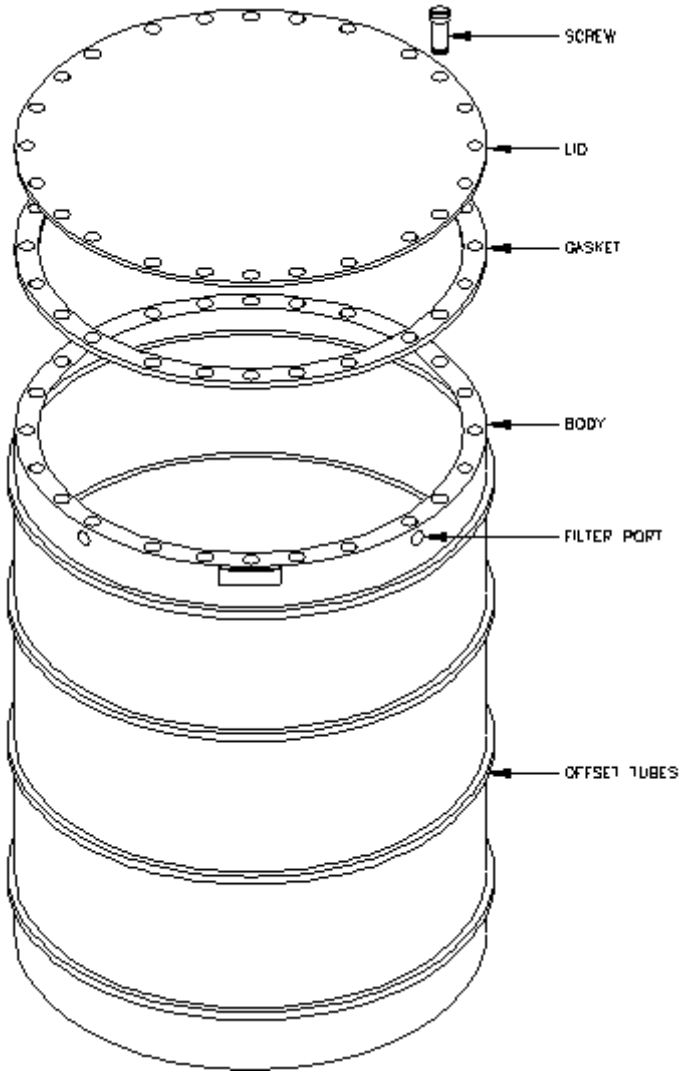

Figure DATA-B- 8. TDOP Components

Table DATA-B- 8. TDOP Specifications

Dimension	Approximate Measurement			
	Inside Dimension (inches)	Outside Dimension (inches)	Inside Dimension (mm)	Outside Dimension (mm)
Height	72 ⅝	73 ⅛	1,845	1,858
Diameter	68 ¾	71 ¼	1,746	1,810

The RH-TRU Waste Canister is shipped as a single unit and emplaced as a single unit. Illustrations of canister components are provided in Figure DATA-B-9. The canister specifications are provided in Table DATA-B-9.

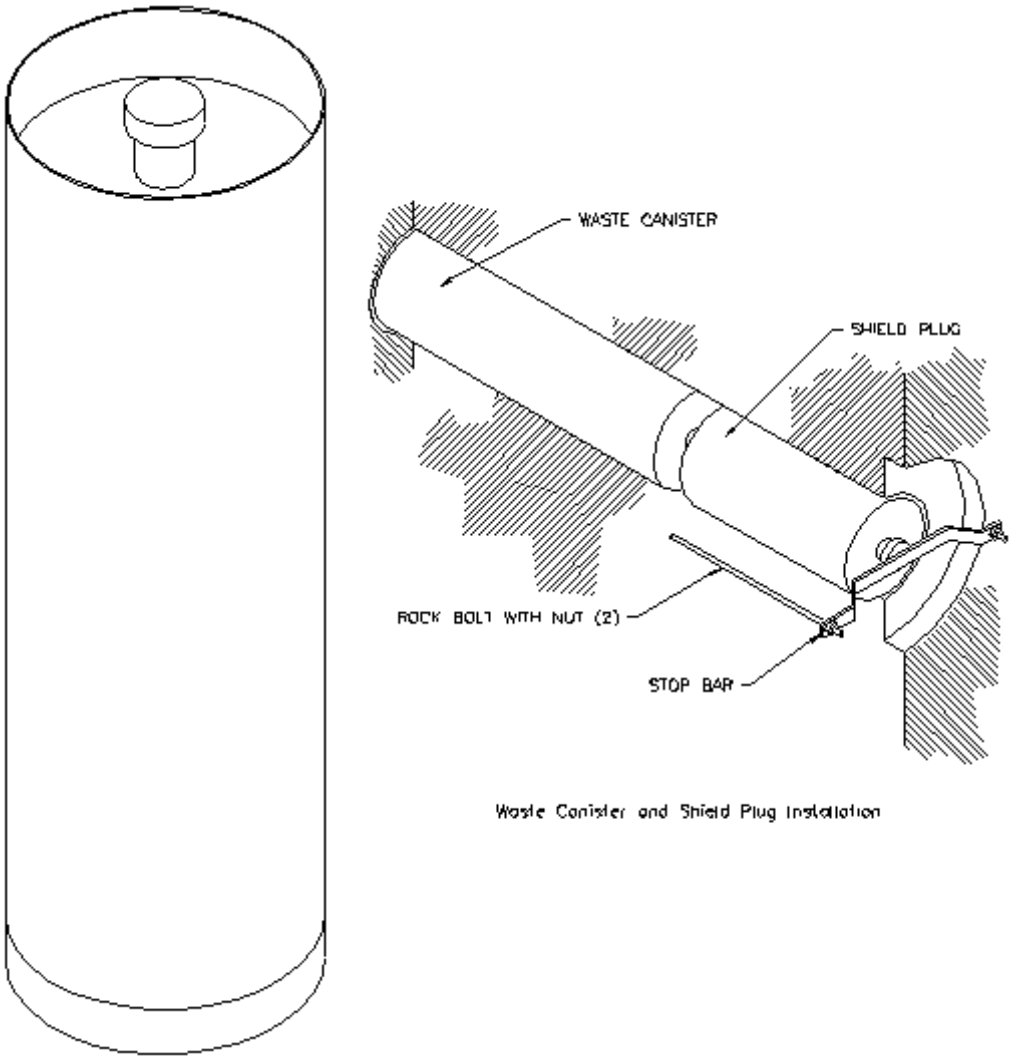

Figure DATA-B- 9. RH-TRU Waste Canister Components

Table DATA-B- 9. RH-TRU Waste Canister Specifications

Dimension	Approximate Measurement			
	Inside Dimension (inches)	Outside Dimension (inches)	Inside Dimension (mm)	Outside Dimension (mm)
Height	108	120 ½	2,743	3,061
Diameter	25 ½	26	648	660

DATA-B-1.4 Emplacement Configurations

Shown in Figure DATA-B-10 is the typical position for waste emplacement containers randomly emplaced in the room of a panel. TDOPs and SLB2s are only emplaced on the bottom position, with another assembly stacked on top. Most other assemblies can be stacked three high before the magnesium oxide (MgO) supersack is emplaced on the top of the stack, with the exception of shielded containers. The EPA has agreed with the DOE's recommendation to not place MgO supersacks on top of shielded container assemblies (Moody 2010). The CH-TRU waste emplacement within the

repository panels is shown in Figure DATA-B-11. The planned RH-TRU waste emplacement is shown in Figure DATA-B-12.

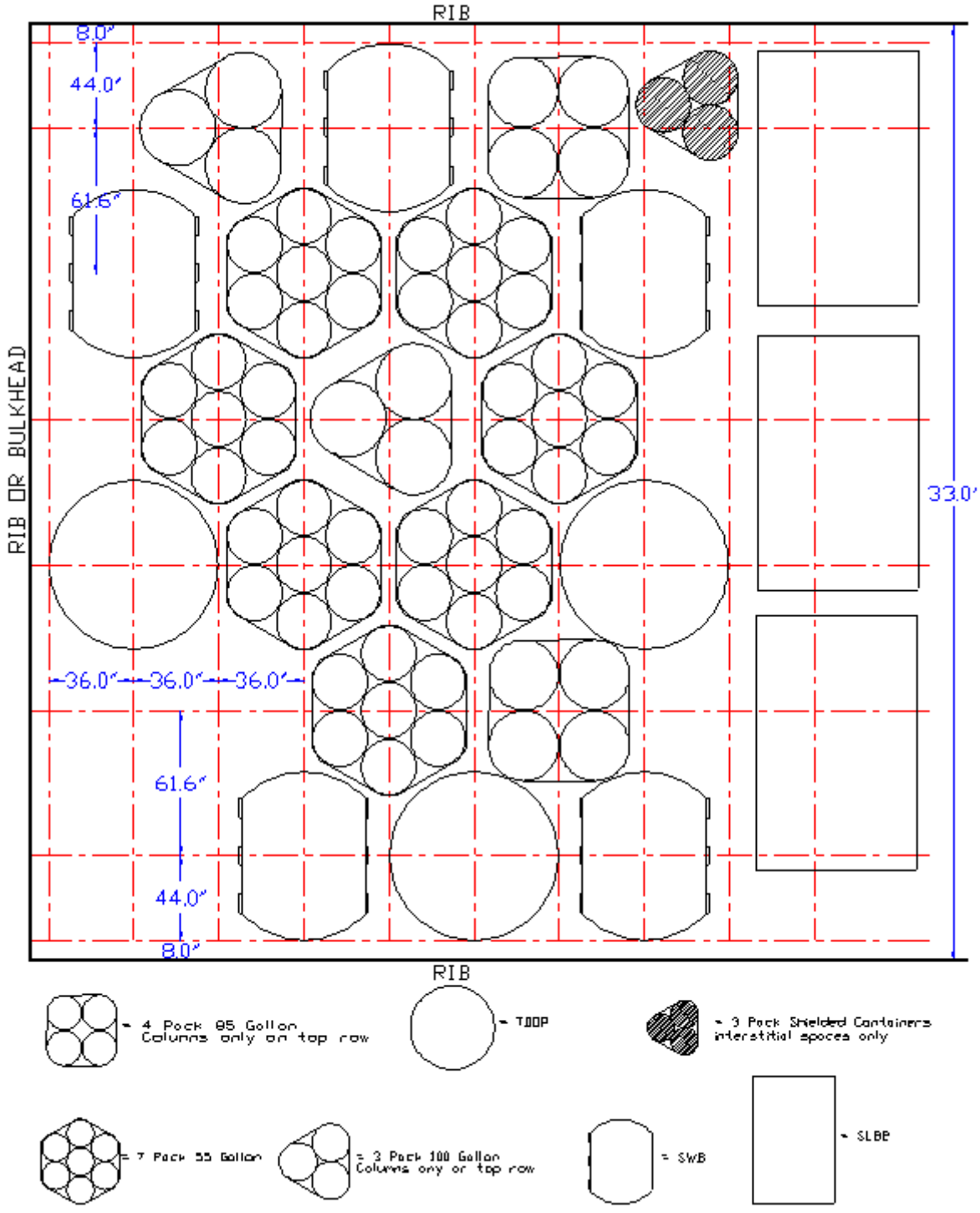

Figure DATA-B- 10. CH-TRU Waste Emplacement Layout

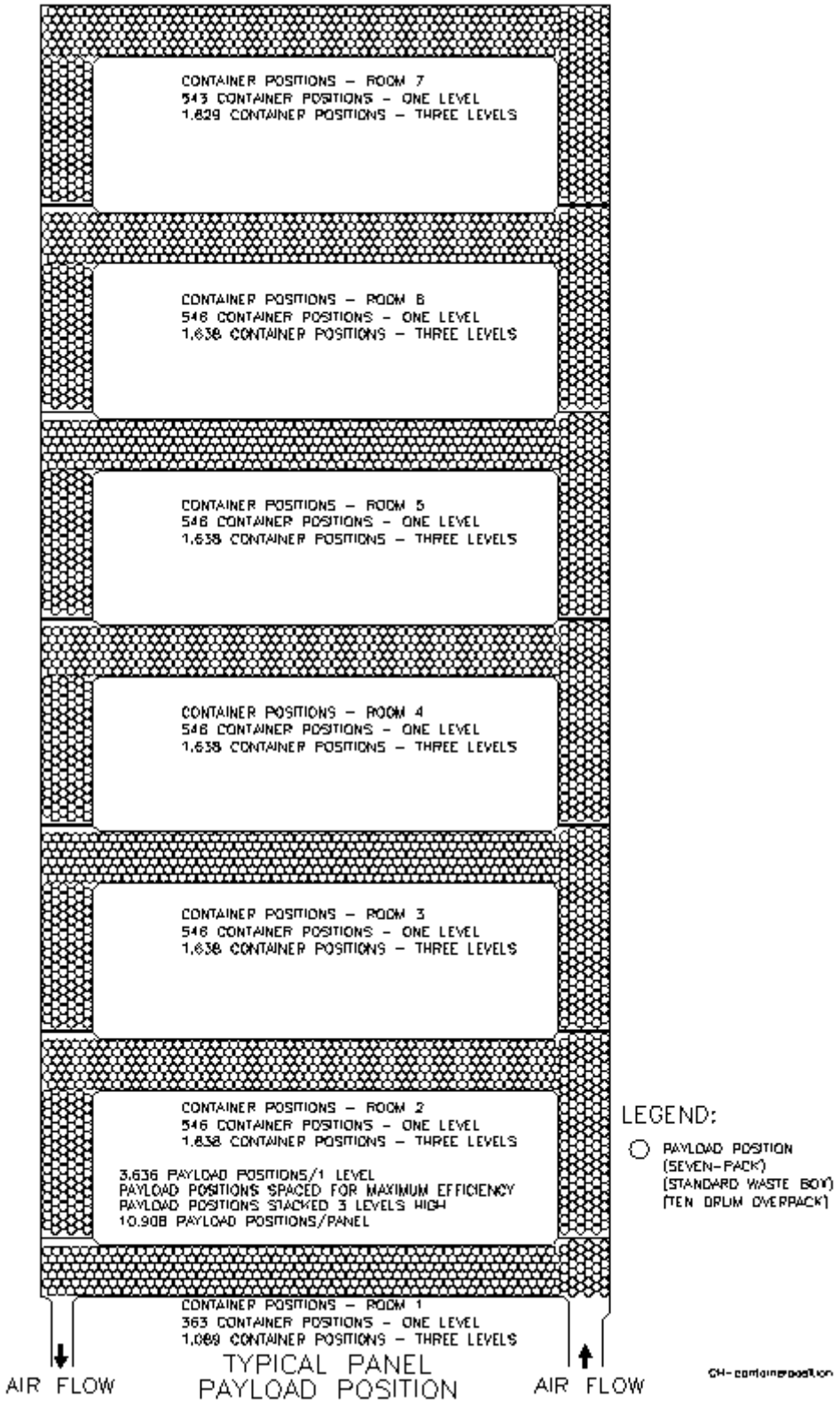

Figure DATA-B- 11. CH-TRU Waste Emplacement

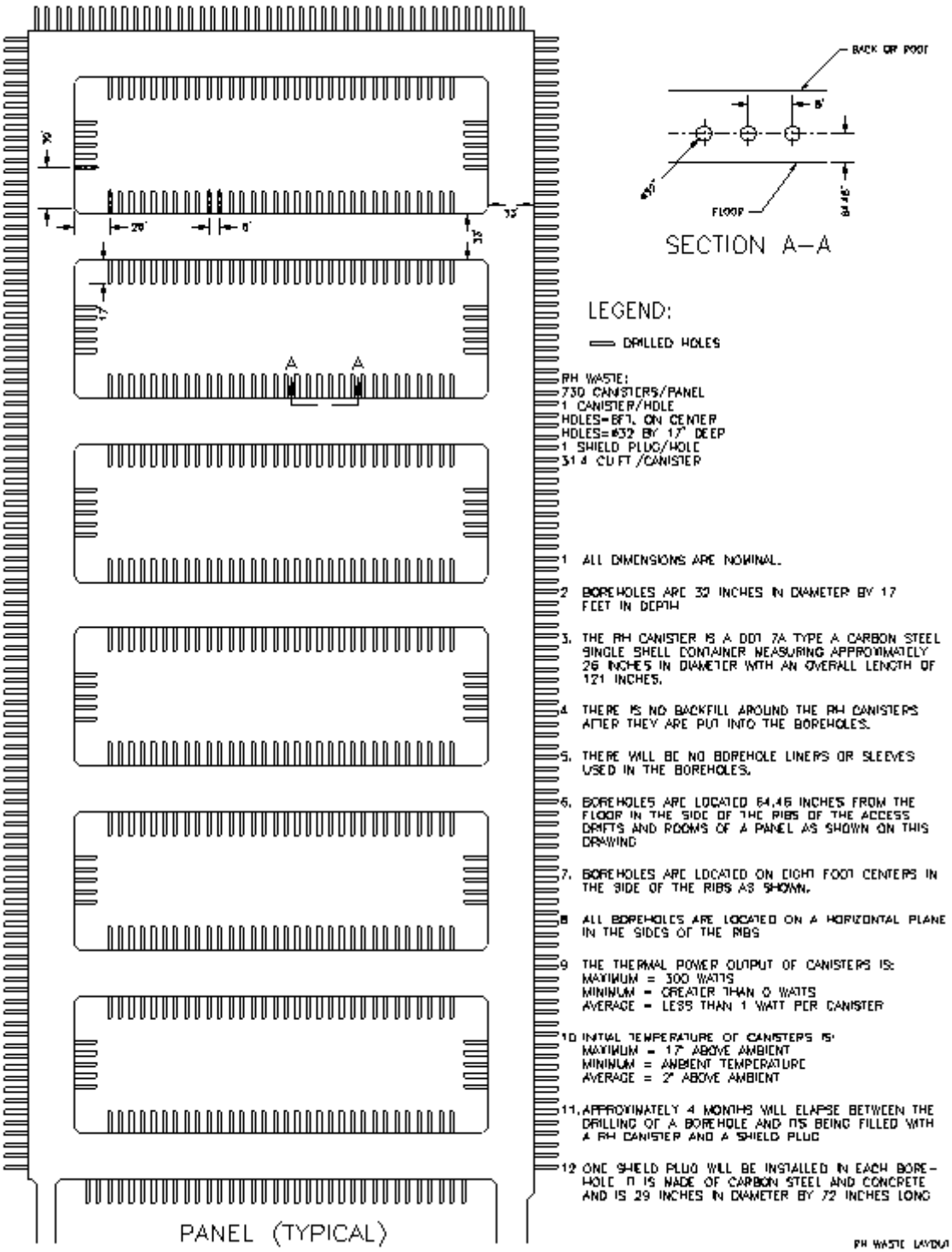

Figure DATA-B- 12. RH-TRU Waste Emplacement

DATA-B-2.0 References

(*Indicates a reference that has not been previously submitted.)

Moody, D.C. 2010. Letter to M. Flynn (Subject: Additional information regarding Shielded Containers). September 8, 2010. Carlsbad, NM: Carlsbad Field Office.* [PDF / Author]

Title 40 CFR Part 191
Subparts B and C
Compliance Recertification Application 2014
for the
Waste Isolation Pilot Plant

Appendix HYDRO-2014
Hydrological Investigations

United States Department of Energy
Waste Isolation Pilot Plant

Carlsbad Field Office
Carlsbad, New Mexico

Compliance Recertification Application 2014

Appendix HYDRO-2014

Table of Contents

List of Figures

List of Tables

Acronyms and Abbreviations

AMSL above mean sea level

AP analysis plan

ASER Annual Site Environmental Report

CB Cabin Baby

CFR Code of Federal Regulations

cm centimeter

CRA Compliance Recertification Application

DOE U.S. Department of Energy

EPA U.S. Environmental Protection Agency

LWB Land Withdrawal Boundary

m meter

m^2/s square meters per second

PA performance assessment

PABC Performance Assessment Baseline Calculation

P&A plugging and abandonment

S_c composite score

SNL Sandia National Laboratories

TP test plan

USGS U.S. Geological Survey

WIPP Waste Isolation Pilot Plant

WQSP Water Quality Sampling Program

HYDRO-1.0 Hydrological Studies

This appendix provides a summary of the new information on Waste Isolation Pilot Plant (WIPP) hydrology collected since 2008 (the data cutoff for the 2009 Compliance Recertification Application [CRA-2009]), in accordance with the requirements of 40 CFR § 194.15 (U.S. EPA 1996). Over that period, the U.S. Department of Energy (DOE) collected new information on WIPP hydrogeology as a result of ongoing monitoring programs.

Section HYDRO-2.0 describes an updated modeling study used to optimize the number and locations of wells in the Culebra monitoring network. Section HYDRO-3.0 describes a comprehensive geochemical study of the groundwater found in geologic units above the Salado Formation. Section HYDRO-4.0 lists wells replaced or plugged and abandoned since the CRA-2009. Section HYDRO-5.0 discusses geologic information collected since CRA-2009 in the WIPP monitoring network. Section HYDRO-6.0 lists hydraulic pumping and slug test analyses performed on wells in

the WIPP monitoring network. Section HYDRO-7.0 describes the water level monitoring performed since the CRA-2009 and the changes in water levels that have been observed. Section HYDRO-8.0 discusses the generation of piezometric surface maps using the Culebra groundwater model discussed in Appendix TFIELD-2014. Section HYDRO-9.0 provides an integration of all the new hydrological information collected since the CRA-2009.

For general reference, Figure HYDRO-1 provides a map showing the locations of all wells discussed in this appendix. Figure HYDRO-2 and Figure HYDRO-3 are stratigraphic columns showing the geologic units discussed below.

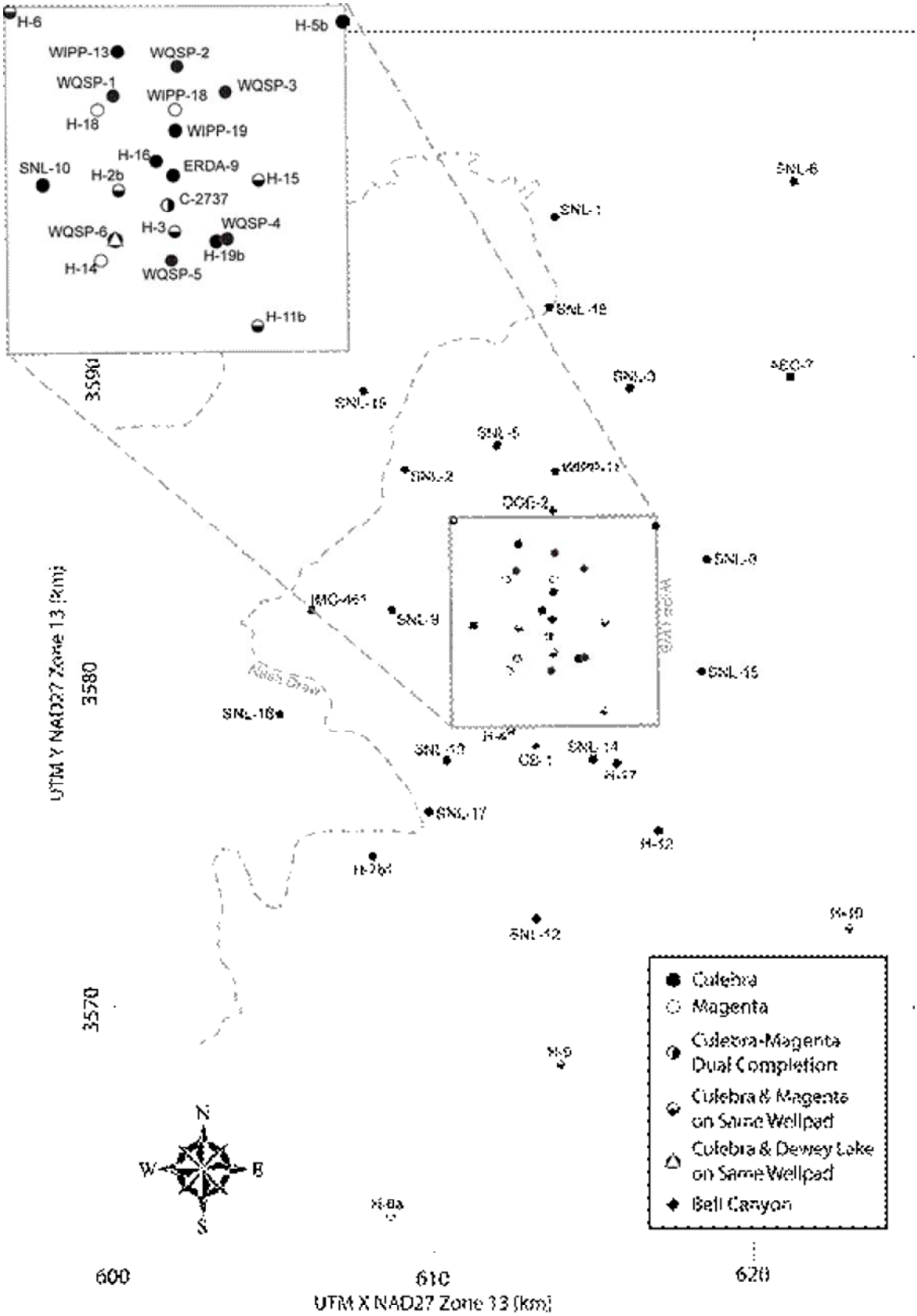

Figure HYDRO- 1. Locations of WIPP Wells and Wellpads

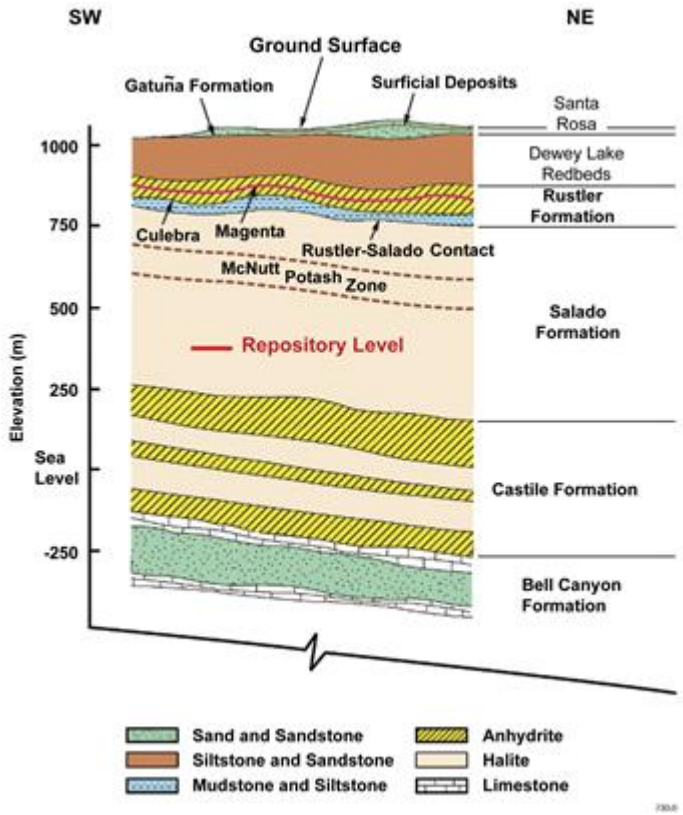

Figure HYDRO- 2. General Stratigraphic Column of Geologic Units at the WIPP Site

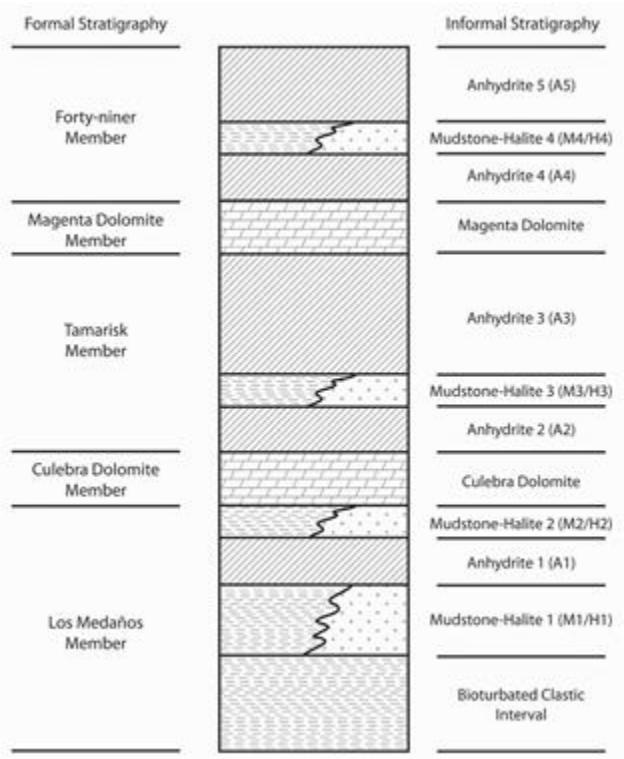

Figure HYDRO- 3. Detailed Rustler Formation Stratigraphy

HYDRO-2.0 Optimization of Culebra Monitoring Well Network

Kuhlman (Kuhlman 2010a) revised a well-network minimization and optimization study initially performed by McKenna (McKenna 2004) under analysis plan (AP) 111, *Analysis Plan for Optimization and Minimization of the Culebra Monitoring Network for the WIPP,* developed by Beauheim and McKenna (Beauheim and McKenna 2003). The results of this optimization study are used programmatically to provide a more quantitative measure of relative importance of steel-cased monitoring wells to the long-term Culebra monitoring network. This study used the 100 input parameter fields (i.e., transmissivity or *T* fields) developed for the CRA-2009 Performance Assessment Baseline Calculation (PABC) to identify the locations where head and transmissivity data from new wells might cause the greatest uncertainty reduction. Uncertainty changes are associated with calculating groundwater travel times in the Culebra Member of the Rustler Formation from a point above the center of the WIPP disposal panels to the WIPP Land Withdrawal Boundary (LWB). Kuhlman (Kuhlman 2010a) used three different methods to determine the value of an existing well or potential well location. The three metrics were combined to create maps showing the relative value of additional head data at points throughout the modeling domain. The three metrics used include:

1. reduction of freshwater head kriging variance,

2. optimization of the shape of triangles drawn between the wells for estimating head gradients (i.e., equilateral triangles are better than obtuse triangles), and

3. identification of areas where more head data in the model (i.e., from a new Culebra monitoring well) would likely have the largest positive impact on constraining model-predicted travel times.

These three different monitoring network assessment approaches are combined to rank:

1. possible locations for new wells, and

2. importance of replacement (rather than simple abandonment) for existing steel-cased well locations.

Figure HYDRO-4 (reproduced from Kuhlman 2010a) shows spatial distribution of the composite score (S_c), which is the sum of the three metrics (each ranging from -1 to 1). Orange areas are poor-quality locations for a new Culebra monitoring well, while dark blue areas are good potential locations for a new Culebra monitoring point. Areas between monitoring locations distant from the WIPP LWB (black square) have high rank (dark blue), because they reduce kriging variance between distal wells and they improve the aspect ratio of triangles made between observation locations (a typical way to estimate hydraulic head gradients - more uniform triangles are better than elongated triangles). Several areas roughly consisting of "spokes" radiating away from the WIPP LWB - along lines of monitoring wells - rank more poorly overall (yellow and orange). The areas within the WIPP LWB mostly have $S_c > 0$, because model-predicted heads at these locations are more highly correlated with model-predicted travel times within the WIPP LWB.

The same three metrics were used to rank locations of existing steel-cased wells, assuming fiberglass-cased wells will have a long life, since most steel-cased wells are currently near the end of their useful life. In Figure HYDRO-5 (reproduced from Kuhlman 2010a), symbol size is related to relative importance of each of the steel-cased wells, ranked via the three metrics. Many wells are important to one or two metrics and unimportant to another (e.g., closely spaced wells inside the WIPP LWB perform poorly in the kriging variance reduction, but might be in important areas for the model output correlation). Overall, wells H-12, H-11b4, and AEC-7 have relatively high ranks in all three metrics, while other wells distant from the WIPP LWB have relatively high ranks in at least two of the three

metrics (e.g., H-9c, H-10c, USGS-4). These wells are somewhat isolated and therefore are individually important in their contributions to the success of the overall monitoring network.

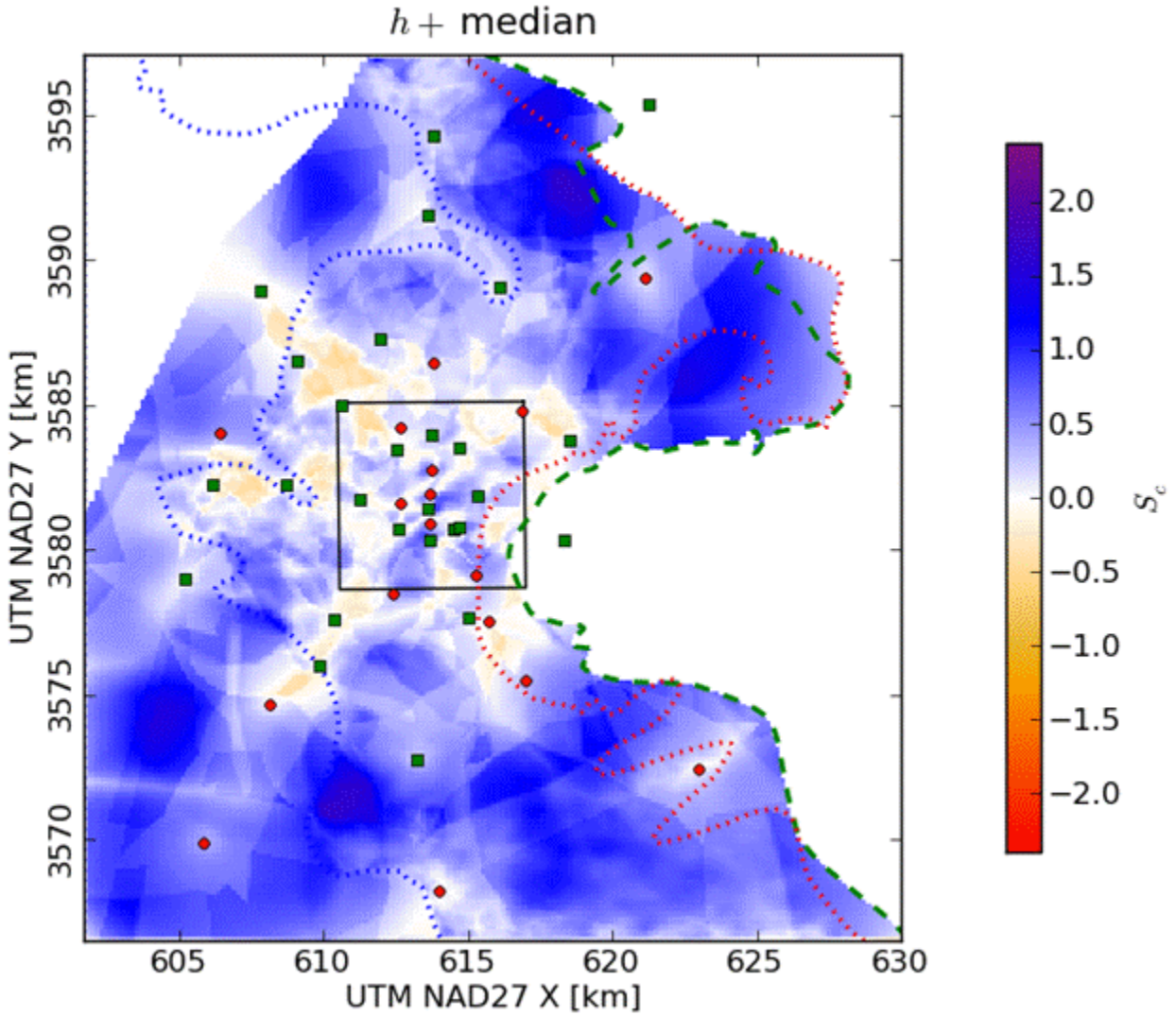

Figure HYDRO- 4. Combined Network Optimization Score for New Culebra Well Locations. Red dots are steel-cased wells and green squares are fiberglass-cased wells. Dashed lines represent Salado dissolution (blue), M3/H3 halite margin (red), and M2/H2 halite margin (green).

Since the Kuhlman (Kuhlman 2010a) report was prepared, WIPP-25 has been plugged and abandoned (without replacement), and wells H-9c, H-4b, and H-11b4 have been plugged and replaced with fiberglass-cased monitoring wells. The condition of individual steel wells, as observed with downhole video monitoring, is a significant factor in the selection of replacement wells; the results of this optimization study are considered as an additional source of information for decision making. Section HYDRO-4.0 includes more discussion about recent well drilling and plugging activities, including discussion of well recompletion activities occurring before the Kuhlman (Kuhlman 2010a) report, which are already incorporated into it (e.g., WIPP-30, H-6R and H-15R).

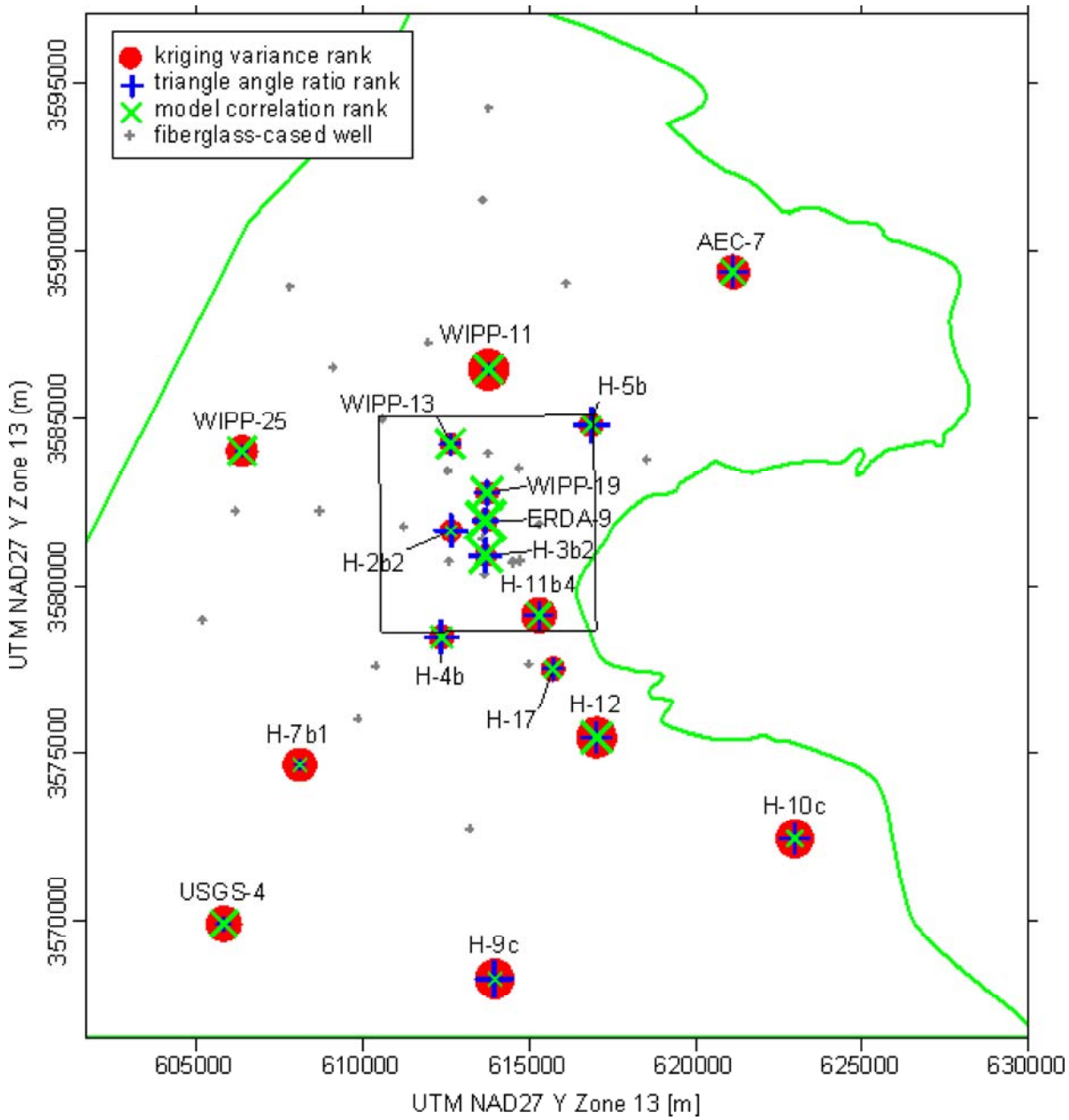

Figure HYDRO- 5. Ranking of Steel-cased Well Locations with Three Metrics. Each of the red, green and blue symbol sizes corresponds to the relative rank of the metric at that well. The green curve is the active portion of the CRA-2009 PABC Culebra groundwater flow model; the black square is the WIPP LWB.

HYDRO-3.0 Geochemical Analyses

Domski et al. (Domski et al. 2011) presented geochemical analysis of waters from WIPP wells completed above the Salado, focusing on groundwaters from the Rustler Formation, the Dewey Lake Redbeds Formation, and the Santa Rosa Formation. The study only included samples from the Culebra Dolomite Member of the Rustler Formation where new or historic samples were found, which were not included in the previous Culebra-specific geochemical study of Domski and Beauheim (Domski and Beauheim 2008).

Domski et al. (Domski et al. 2011) used similar methodology as Domski and Beauheim (Domski and Beauheim 2008), utilizing geochemical modeling and facies categorization based upon the chemical species observed in water quality samples. The spatial coverage of wells in these other formations is much less than well coverage in the Culebra, making it difficult to draw conclusions regarding the spatial distribution of geochemical facies, as was done for the Culebra in Domski and Beauheim (Domski and Beauheim 2008).

Samples from the Dewey Lake Formation generally had low ionic strength and had more significant sulfatic weathering components, related to the presence of gypsum-filled fractures in the Dewey Lake. Samples from Santa Rosa Formation wells were consistent with waters of meteoric origin, consistent with their relatively shallow occurrence.

Samples from the Magenta Member of the Rustler Formation generally were from the diagenetic facies in eastern wells near the Rustler mudstone-halite margins. Furthest to the west, Magenta wells belonged exclusively to the sulfatic weather facies. Wells centrally located within the WIPP site boundaries are likely the product of mixing between the sulfatic weathering composition to the west and the diagenetic waters in the east. Samples used in Domski et al. (Domski et al. 2011) from the Culebra Member of the Rustler were mostly from the southeastern arm of Nash Draw and in replacement wells drilled recently at the WIPP site. More recent and historic Culebra water quality analyses generally agreed with Domski and Beauhiem (Domski and Beauheim 2008), adding detail to the distribution of facies in the southeastern arm of Nash Draw. Samples from the Rustler-Salado contact are in general quite briney. East of Nash Draw, the formation contains magnesium-rich brines, which are believed to be diagenetic in origin, while wells in and closer to Nash Draw show effects of halite dissolution in the underlying Salado Formation.

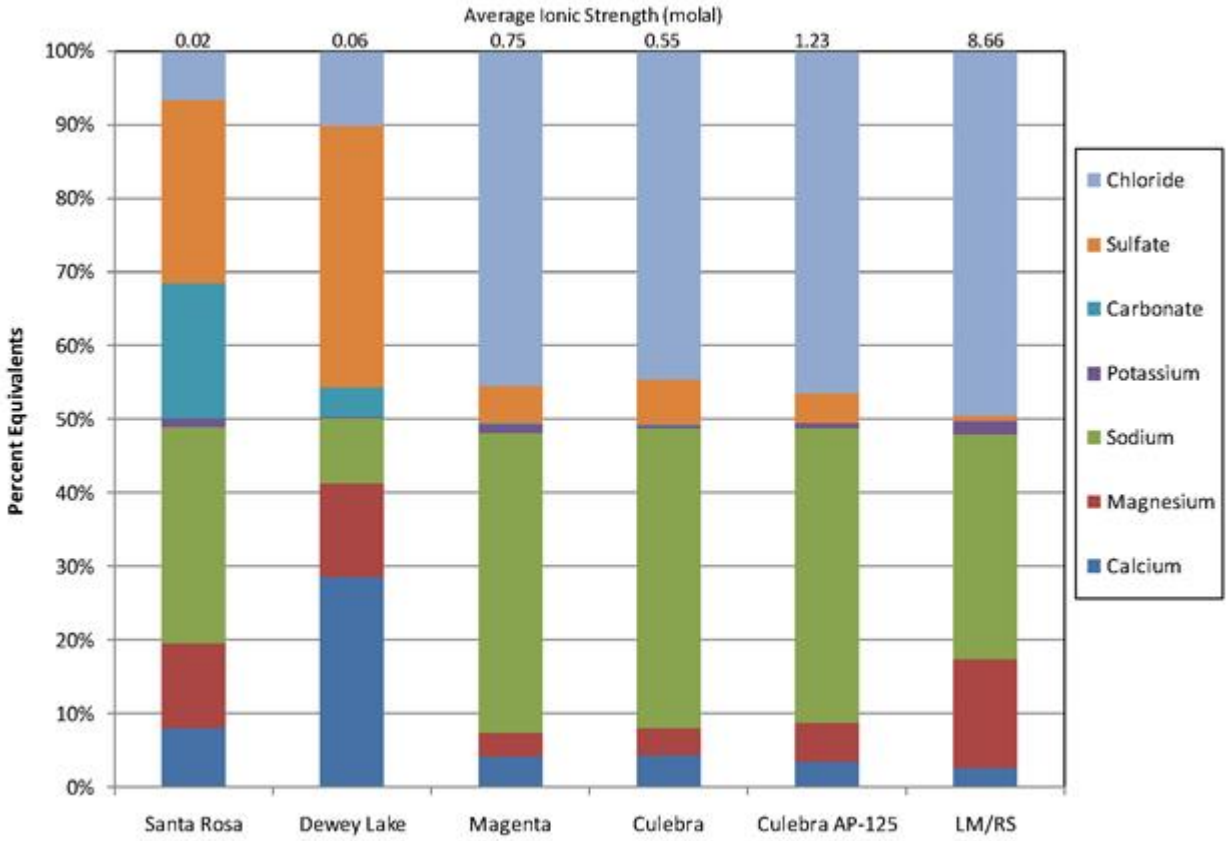

Figure HYDRO- 6. Average Water Composition and Ionic Strength for Water Quality Samples Taken From Geologic Units Above the Salado Formation. LM/RS indicates the Los Medaños or Rustler-Salado contact formation.

Figure HYDRO-6 (reproduced from Domski et al. 2011) shows the average composition of water quality samples collected above the Salado Formation. The "Culebra" bar is the average composition for the few Culebra samples in Domski et al. (Domski et al. 2011), while the "Culebra AP-125" bar represents the average of a much larger sample taken from Domski and Beauheim (Domski and Beauheim 2008). This figure clearly summarizes the difference in composition between samples collected from the Santa Rosa and Dewey Lake Formations, compared to samples from the Rustler Formation. Magenta compositions are very similar to Culebra compositions. Culebra average ionic strength is greater in the larger, more representative AP-125 dataset compared to the smaller dataset analyzed by Domski et al. (Domski et al. 2011).

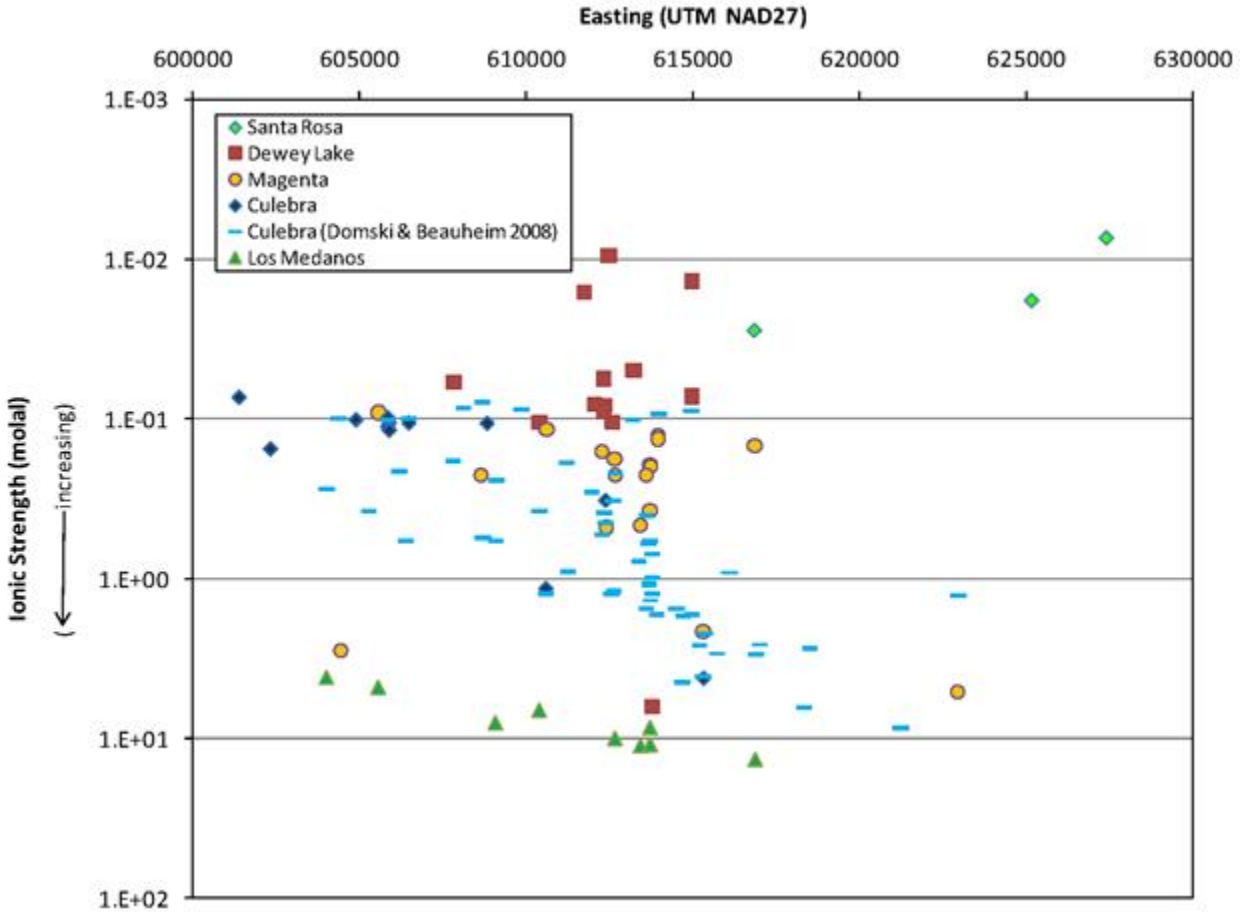

Figure HYDRO- 7. Ionic Strength Versus UTM Easting Coordinate for Water Quality Samples From All Wells Above the Salado Formation

Figure HYDRO-7 (reproduced from Domski et al. 2011) summarizes the relationship between ionic strength, geologic formation, and east-west location of wells completed above the Salado Formation at the WIPP. Ionic strength varies across more than three orders of magnitude between the Santa Rosa and the Los Medaños Member of the Rustler Formation. Regional groundwater chemistry undergoes radical changes over relatively short vertical distances, driven largely by proximity to the Salado Formation. In the Rustler Formation, waters tend to increase in ionic strength to the east, related to proximity to the mudstone-halite margins within the Rustler Formation (Domski and Beauheim

2008). Santa Rosa and Dewey Lake waters do not appear to follow a similar trend of increasing ionic strength to the east, likely related to their more direct vertical recharge path from precipitation (Domski et al. 2011). The sole Dewey Lake sample with high ionic strength is associated with potash mine tailings contamination (SNL-1), and is not representative of the Dewey Lake Formation in general.

Geochemical analysis of groundwater samples collected from formations above the Salado (Domski et al. 2011) agrees with previous analyses conducted on the Culebra (Domski and Beauheim 2008). These studies reveal how the geochemistry of the Culebra and Magenta fit into regional groundwater trends both vertically and horizontally. This information is supportive of the general conceptual model for groundwater recharge of shallow formations near the WIPP.

HYDRO-4.0 Steel-Cased Well Reconfiguration and Replacement

From the 1970s through 1994, all WIPP-constructed wells used steel well casing. Exposure to brine caused the steel casings to deteriorate, necessitating the plugging and abandonment (P&A) of many wells. During the peak of testing in the Culebra, many well pads had multiple Culebra wells within 50 meters (m) of one another. The cost to maintain such a density of monitoring locations is not justified based solely on the network's use for long-term monitoring. Previously, a large number of Culebra wells located on the same wellpad were plugged and abandoned. The current Culebra monitoring network is considered to have sufficient spatial coverage, and will be sustained for long-term Culebra monitoring. As the remaining steel-cased monitoring wells fail, they will be replaced with suitable fiberglass-reinforced, plastic-cased (or equivalent) wells.

Since 2008, two steel-cased wells have been plugged and abandoned without replacement (WIPP-25 and WIPP-30, see Table HYDRO-1). AEC-7 was reperforated across the Culebra in 2008 (U.S. DOE 2009a and U.S. DOE 2009c). Three multiple-completion wells have been permanently recompleted to monitor individual formations (H-15, H-16 and H-9c). H-9c was redrilled in 2010; its replacement is named H-9bR. Five replacement wells were drilled and completed with fiberglass-reinfored plastic casings (H-6bR, H-15R, H-4bR, H-9bR, and H-11b4R). In H-series wells up to H-11 (drilled by the U.S. Geological Survey in the 1970s), a, b, and c suffixes originally referred to Magenta, Culebra, and Rustler-Salado contact completions, respectively.

Table HYDRO- 1. Wells Plugged, Abandoned, and Reconfigured, 2008-2012

Well	Interval(s) Previously Monitored	Activity	Date of Activity	Current Interval Monitored
WIPP-30	Culebra and Magenta	Plugged and abandoned	February 2008	-
H-6b	Culebra	Plugged and abandoned, Culebra well replaced by H-6bR	February 2008	-
AEC-7	Culebra	Scraped and reperforated	March 2008	Culebra
H-15	Culebra and Magenta	Plugback and reconfigured, Cuelbra well replaced by H-15R	March 2008	Magenta
H-16	Forty-niner, Magenta, Tamarisk, Culebra, and Los Medaños	Reconfigured from multicompletion open-hole Rustler to screened Culebra	July 2008	Culebra

WIPP-25	Culebra and Magenta	Plugged and abandoned	June 2009	-
H-4b	Culebra	Plugged and abandoned, Culebra well replaced by H-4bR	July 2009	-
H-9c	Culebra and Magenta	Plugback, Culebra well replaced by H-9bR	September 2010	Magenta
H-11b4	Culebra	Plugged and abandoned, Culebra well replaced by H-11b4R	November 2011	-

HYDRO-5.0 Geological Information

In the previous five-year period (2003-2008), a significant number of new monitoring wells were drilled, greatly expanding and supporting the geologic understanding of the Rustler Formation. In the period 2008-2012, no new monitoring well locations were drilled to obtain new geologic information, but replacement wells were drilled on existing well pads (Table HYDRO-1). This type of activity does not typically produce new geologic information, but any cuttings and geophysical logs obtained do confirm our geologic conceptual model of the Rustler Formation.

From December 2010 to January 2011, two potash exploration boreholes (MOS-20 and MOS-21) were drilled to the McNutt Potash zone by Mosaic Potash in T22S R31E sections 9 and 10. Sandia National Laboratories (SNL) logged the cuttings of both wells through the Rustler Formation, and also geophysically logged borehole MOS-21 (Schuhen 2011). Both boreholes encountered the Gatuña Formation, but only the eastern MOS-21 borehole (in section 10) encountered a section of the Santa Rosa Formation, located stratigraphically between the Gatuña and Dewey Lake Formations.

These boreholes were plugged and abandoned after Mosaic collected their cores across the potash ore zones. The boreholes provided additional confirmatory information related to the geologic units above the Salado Formation.

HYDRO-6.0 Hydraulic Test Interpretation

Hydraulic testing at the WIPP is carried out under Test Plan (TP) 03-01 (Schuhen 2010a), while interpretation of hydraulic tests conducted at the WIPP is carried out under the Analysis Plan AP-070 (Beauheim 2009). Two summary interpretive reports on hydraulic property parameter estimates from hydraulic tests in Culebra and Magenta wells were recently issued. This section only discusses hydraulic tests recently analyzed; some of the Magenta tests were performed in the 1970s, but have been interpreted or re-interpreted recently.

Bowman and Roberts (Bowman and Roberts 2009) analyzed two Culebra slug tests (SNL-6 and IMC-461), a Magenta slug test (C-2737), and two low-flowrate Magenta pumping tests (H-11b2 and H-15). The slug and pumping tests were conducted between January 2005 and August 2008. The results of the analysis provided estimates of Culebra transmissivity (i.e., the product of formation hydraulic conductivity and formation thickness). The IMC-461 transmissivity estimate (1.92×10^{-4} square meters per second [m^2/s]) was used as supporting data in the calibration of the CRA-2009 PABC Culebra groundwater flow model, and the very low SNL-6 transmissivity value (8.72×10^{-12} m^2/s) was used in part to characterize the portion of the Culebra east of the H2/M2 and H3/M3 halite margins, where halite cements are present in the Culebra. The estimated Magenta transmissivity values were all

within an order of magnitude of each other: from a minimum of 1.11×10^{-7} m^2/s in the C-2737 injection test to a maximum of 9.50×10^{-7} m^2/s at H-15.

Bowman and Beauheim (Bowman and Beauheim 2010) interpreted transmissivity estimates for 15 pumping and slug tests conducted in the Magenta between 1978 and 2009. Slug injection and withdrawal tests were conducted in DOE-2, H-2a, H-3b1, H-4a, H-5a, H-6a, H-8a, H-9a, H-10a, H-14, H-16, WIPP-18, WIPP-27, and WIPP-30. A low-flowrate pumping test was conducted in H-18. The results included a very high far-field transmissivity value of 3.96×10^{-2} m^2/s at WIPP-27, in Nash Draw, where the Magenta is very shallow. Aside from this extremely high estimate, transmissivity values in the Magenta ranged across nearly three orders of magnitude, from a minimum of 1.80×10^{-9} m^2/s at DOE-2 to 9.70×10^{-7} m^2/s at H-9a.

HYDRO-7.0 Monitoring

Groundwater monitoring activities at the WIPP are carried out under the *Waste Isolation Pilot Plant Environmental Monitoring Plan* (U.S. DOE 2004) and under *Test Plan TP 06-01, Monitoring Water Levels in WIPP Wells, Revision 3* (Schuhen 2010b). The first monitoring program consists of monthly water-level measurements in all accessible wells, with results reported in the Annual Site Environmental Reports (ASERs) (U.S. DOE 2008, U.S. DOE 2009c, U.S. DOE 2010, U.S. DOE 2011 and U.S. DOE 2012). The second monitoring program involves both periodic water-level measurements and continuous measurement (typically at 1-hour intervals) of fluid pressure in wells instrumented with downhole pressure gauges.

Water-level monitoring provides a general picture of the changes in hydraulic head occurring in the formations being monitored. Water levels are currently being monitored in the Culebra and Magenta Members of the Rustler Formation, the Dewey Lake (Redbeds) Formation, and the Bell Canyon Formation. The monitored well locations are shown in Figure HYDRO-1. Reconfigured or plugged and abandoned wells are listed in Table HYDRO-1.

HYDRO-7.1 Culebra Monitoring

In addition to monitoring Culebra water levels, the DOE monitors the fluid pressure in many wells with downhole pressure transducers. The history of Culebra wells instrumented with downhole pressure transducers is given in Figure HYDRO-8. This figure shows the periods of time from January 2003 to the present during which pressure transducers were installed in Culebra wells. The continuous fluid-pressure measurements made using pressure transducers provide a clearer, more complete record of the changes in hydraulic head occurring in the wells than is provided by monthly water-level measurements alone. Currently, 38 Culebra wells are monitored with downhole pressure transducers. Of the wells that were monitored at one time, 7 wells had been monitored before having their Culebra completions plugged and abandoned (CB-1, DOE-1, P-17, WIPP-12, WIPP-25, WIPP-26, and WIPP-30), 5 wells shifted monitoring to a replacement well upon re-drilling (H-4b, H-6b, H-9c, H-11b4, and H-15), and 7 wells were only monitored on a temporary basis for testing purposes (H-8b, H-19b2, USGS-4, WQSP-1, WQSP-2, WQSP-3, and Engle - a privately owned windmill approximately 1 kilometer southeast of H-9).

Groundwater density calculations are carried out under Activity/Project Specific Procedure SP 9-11, *Calculation of Densities for Groundwater in WIPP Wells* (Johnson 2012a). Pressure transducers are

installed at midformation, which allows the combination of observed pressure, installation depth, and water level elevation measurements to yield an estimate of fluid density. Culebra groundwater density varies from nearly fresh in the southeastern arm of Nash Draw (e.g., H-7b1), to nearly saturated with respect to halite in wells SNL-6 and SNL-15. This procedure has been applied to both current years and historical data to produce estimates of fluid densities in wells from 2003 through 2012, although coverage was minimal in early years (Johnson 2010, Johnson 2011, Johnson 2012b, Johnson 2012c, Johnson 2012d, Johnson 2012e, and Johnson 2012f). This approach was also used to compute 2007 Culebra groundwater densities to estimate freshwater heads required for the calibration of the Culebra groundwater flow model for CRA-2009 PABC (Johnson 2008 and Johnson 2009).

The high-resolution pressure transducer data have shown that wells near Nash Draw respond rapidly to large rainfall events, with more muted and delayed responses to rainfall in wells further to the east of Nash Draw (Hillesheim et al. 2007). Thus, the Culebra appears to be unconfined in at least parts of Nash Draw, probably because of a combination of dissolution, collapse, and fracturing of the overlying units that act as confining beds under Livingston Ridge. This is not to say, however, that present-day rainfall actually enters the Culebra wherever a pressure response to rainfall is observed. Rather, the rainfall reaches a water table in a higher stratigraphic unit that is in sufficient hydraulic communication with the Culebra to transmit a *pressure* response rapidly. It takes a much longer time for water or dissolved constituents to move through the subsurface than it takes a pressure wave to propagate through a saturated porous medium.

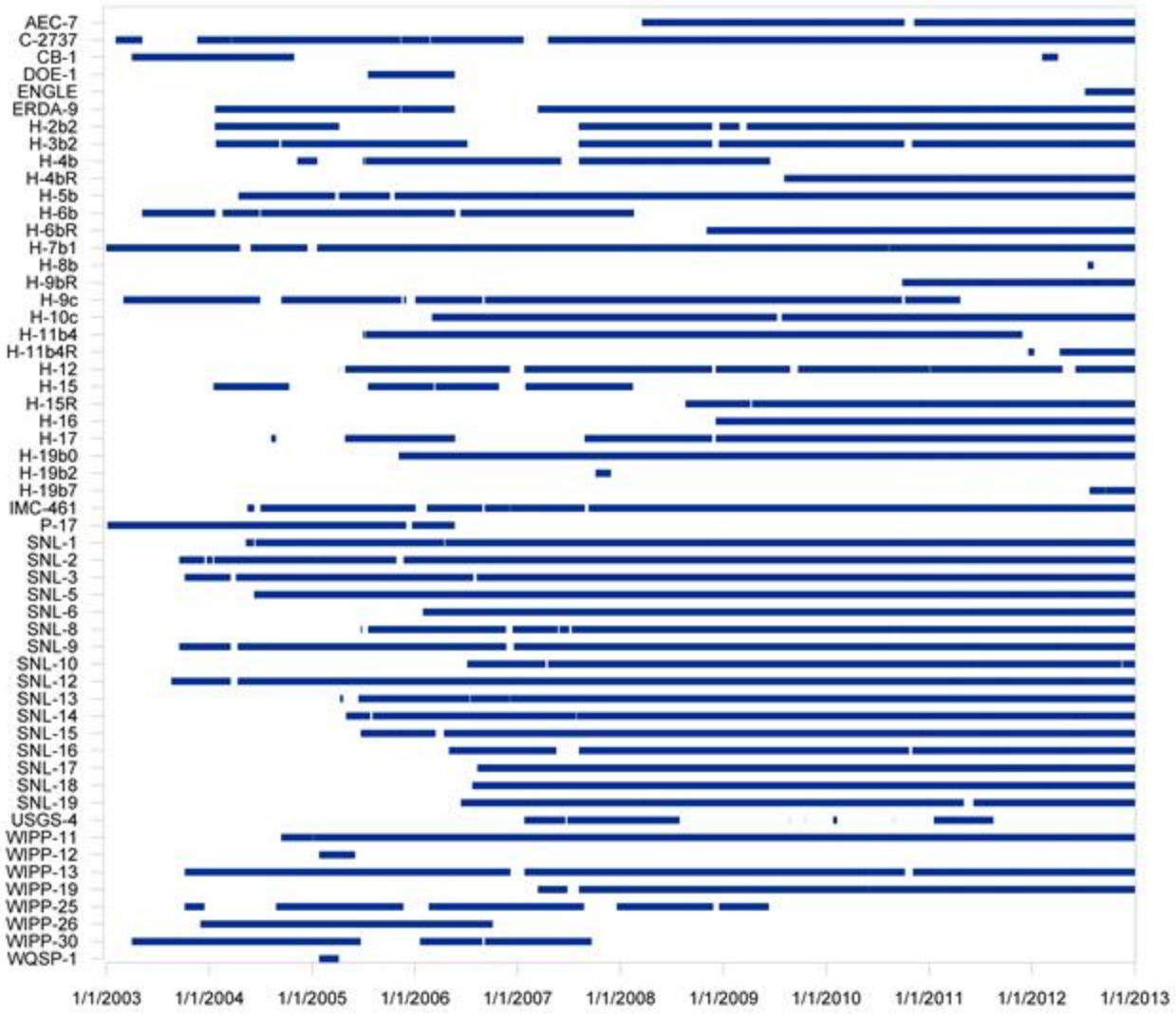

Figure HYDRO- 8. Culebra Well Downhole Pressure Transducer Data Coverage

Figure HYDRO-9 through Figure HYDRO-16 and Figure HYDRO-18 show manual water levels from almost all Culebra wells monitored by the WIPP for the period from 2006 through 2012. Refer to Figure HYDRO-1 for well locations. Wells are grouped together roughly by geographic locality, including consideration to keep together wells with similar temporal behavior or water level elevations. The reporting period for Culebra wells in this subsection was chosen to start in 2006 (rather than 2008) to clearly show the current stable or declining water levels in the context of the end of the long-term rise observed in most WIPP wells (which approximately ended in 2008).

Water levels observed in May 2007 were used along with observed responses to large-scale pumping tests as calibration targets for calibration of the Culebra groundwater flow models used in the WIPP Performance Assessment (PA) for the CRA-2009 PABC (see Appendix TFIELD-2014). May 2007 was near the peak of water levels observed to date at the WIPP site; water levels have remained relatively stable with slight declines observed since this time. Water levels in most Culebra wells roughly move up and down together. The water level "snapshot" chosen in 2007 as a steady-state calibration target for the Culebra PA model can be still considered representative of conditions at the WIPP.

Figure HYDRO-9 and Figure HYDRO-10 show water levels from wells north of the WIPP site and in the northern portion of the WIPP site. The water level trends from these 17 wells generally parallel one another. The seven wells in Figure HYDRO-9 generally respond together, with a peak water level elevation observed in late 2006 (SNL-2 and SNL-19) or late 2007 (SNL-5 and WIPP-11). After this peak, water levels in these seven wells have been declining slowly or leveling off, with a minor rise in 2010 followed by a more rapid decline in water levels, possibly related to low precipitation in 2011 (monthly precipitation data for the Carlsbad Airport from the National Oceanic and Atmospheric Administration National Climate Data Center, http://www.ncdc.noaa.gov/cdo-web/). Responses observed in SNL-2 and SNL-19 appear to precede those in other wells, in which responses tend to be delayed and comparatively muted.

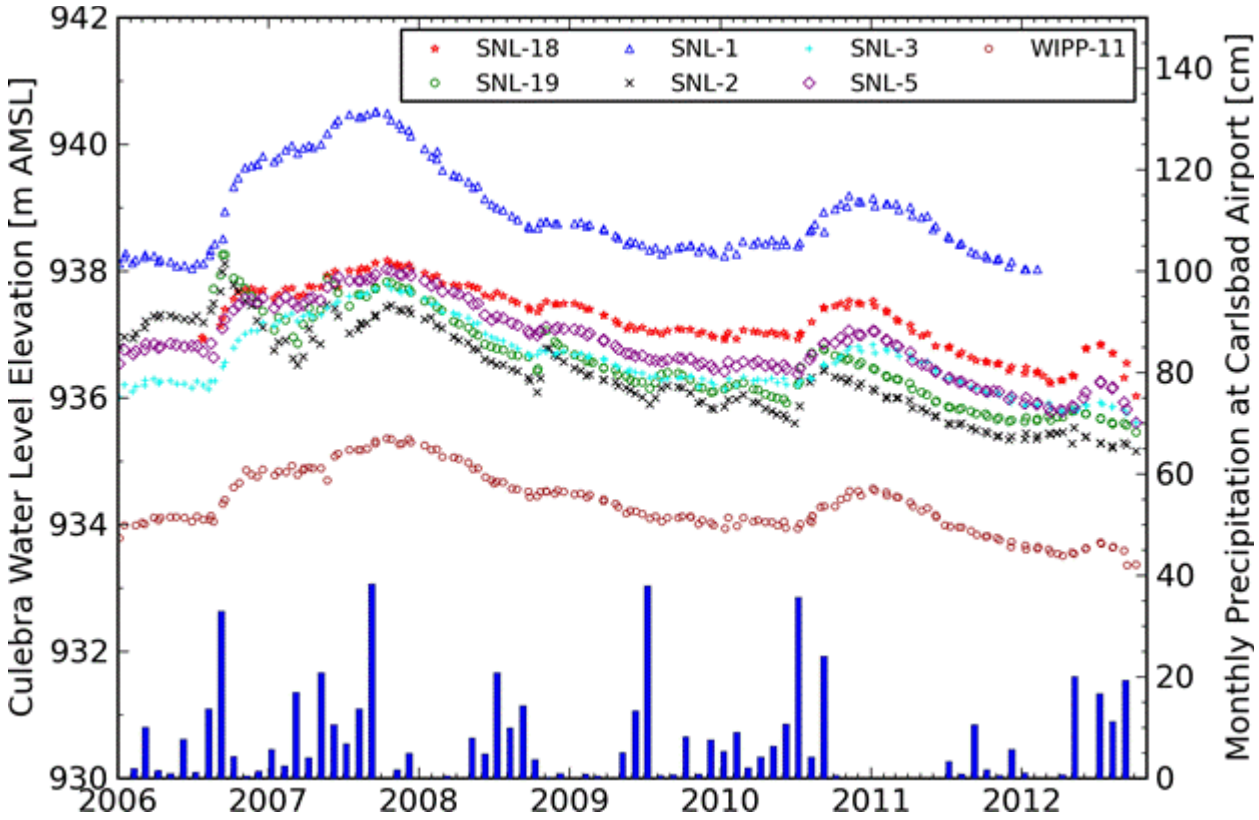

Figure HYDRO- 9. Water Levels In 7 Culebra Wells North of the WIPP Site

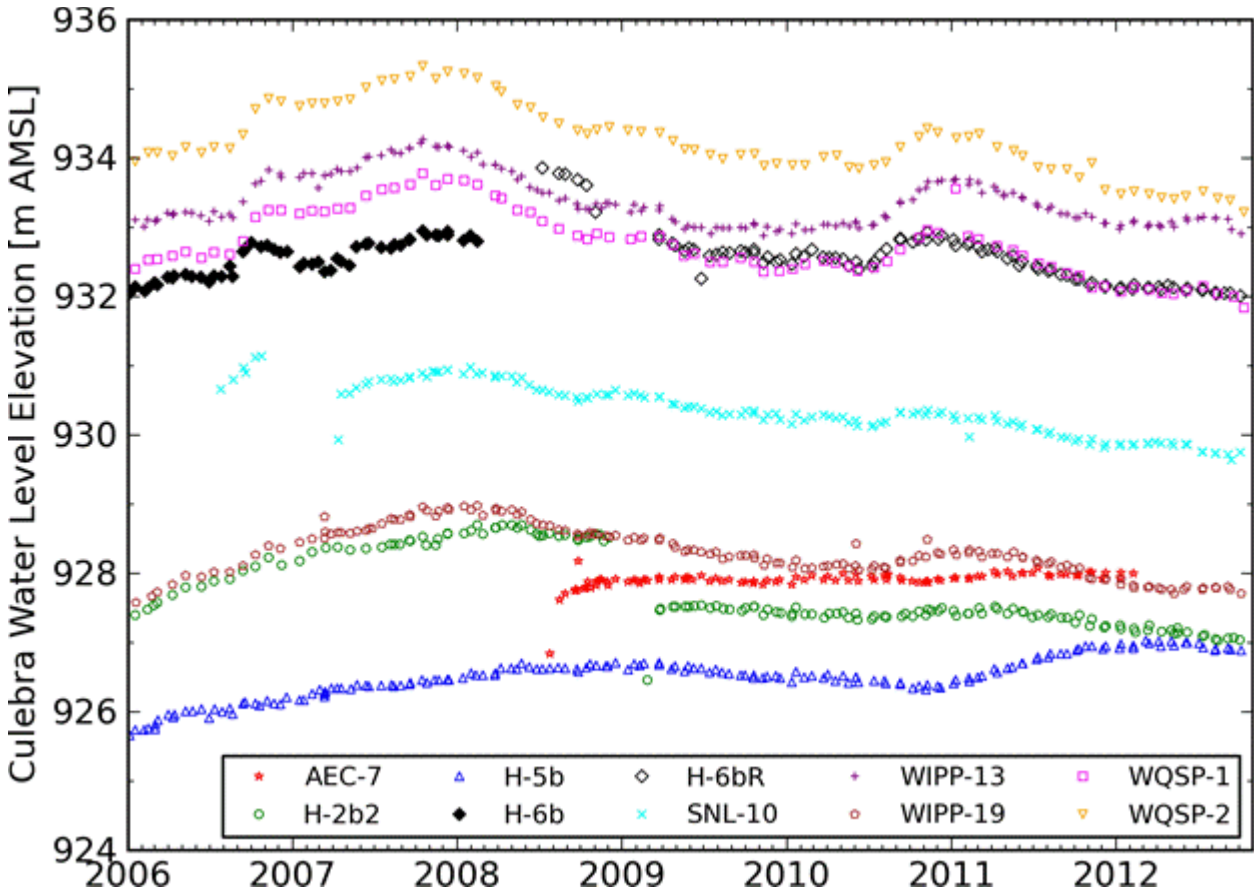

Figure HYDRO- 10. Water Levels In 10 Culebra Wells In the Northern Portion of the WIPP Site

The water level elevations plotted in Figure HYDRO-10 show similar, but more subdued trends to those in Figure HYDRO-9. Wells AEC-7 and H-5b do not noticeably fluctuate as do Culebra wells to their north and west. Well AEC-7 water levels before the reperforation event in early 2008 were not representative of the Culebra and are not plotted. Water levels were affected by water quality sampling performed in AEC-7 from March to June 2008 (U.S. DOE 2009c). The downward shift in H-2b2 water levels in early 2009 was the result of sampling activities, which removed fresh water present in the well since scraping and plugging and abandonment activities on the well pad in 2005 (U.S. DOE 2010). Well H-6b was replaced by H-6bR in 2008; Figure HYDRO-10 shows an open symbol for the replacement well, and a filled symbol for the historic well.

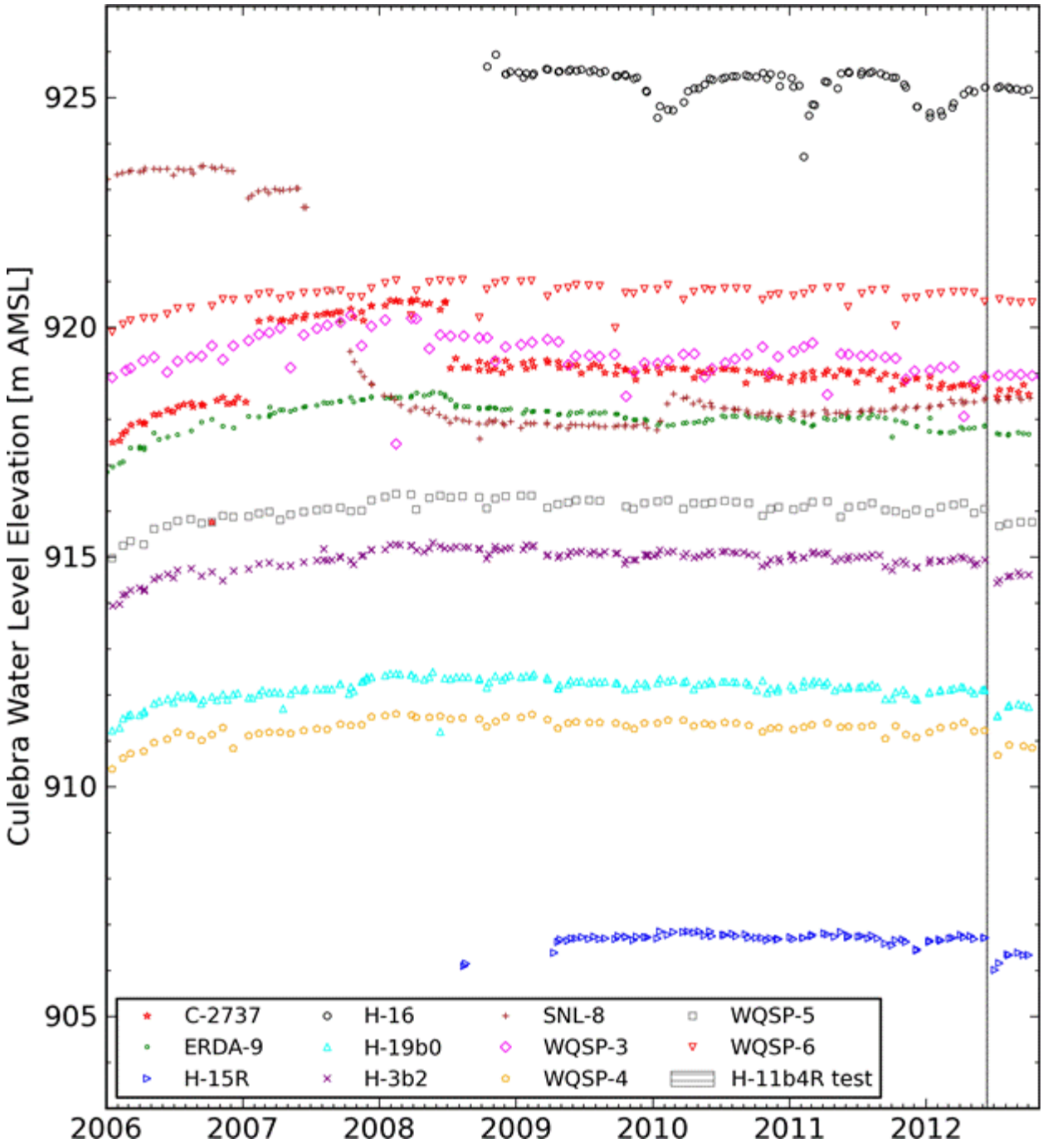

Figure HYDRO- 11. Water Levels In 11 Culebra Wells In the Central WIPP Site

Figure HYDRO-11 shows water levels from 11 Culebra wells in the central portion of the WIPP site. The water level trends in these wells mostly parallel one another, with the exception of SNL-8 and H-16. Water levels in SNL-8 changed significantly after pumping and sampling activities in 2007, which removed fresher water from the wellbore. Well SNL-8 is experiencing a slight increase in water levels since 2011; H-5b is also experiencing an increase during this period (Figure HYDRO-10). The step change in water levels in C-2737 from 2007 to 2008 was similarly due to density effects related to fresh water left in the packer, which was installed to allow simultaneous monitoring of the Culebra and Magenta (U.S. DOE 2008 and U.S. DOE 2009c). Since recompletion, H-16 has observed annual fluctuations, which are believed to be related to the well's proximity to the air intake shaft, less than 15 m away. Although the fluctuations appear to consistently occur during winter months, the

character of the drops is not consistent between years (Figure HYDRO-12), with the drop in 2011 being much more asymmetric than 2010 or 2012. Figure HYDRO-12 illustrates the usefulness of high-frequency pressure transducer data to confirm possible outliers in the water level data series (e.g., the low water level elevations measured in January 2010 or February 2011), and to catch transient extremes missed by monthly observations (e.g., the lowest pressure observed in December 2011).

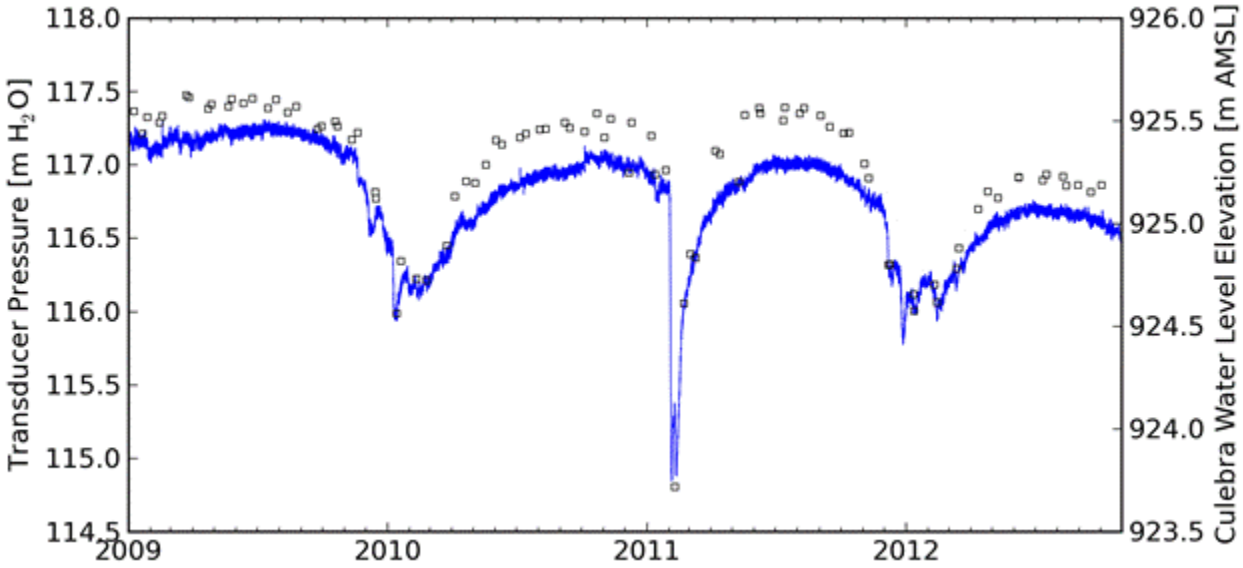

Figure HYDRO- 12. Water Levels (Symbols) and Pressure Transducer Data (Continuous Line) for Recompleted Culebra Well H-16 Near the WIPP Air Intake Shaft

Water level fluctuations observed in central wells were generally smaller than those observed in northern wells (i.e., wells in Figure HYDRO-9 and Figure HYDRO-10). Central wells also have maximum water levels in approximately mid-2008, followed by a very gradual decline in water level. Some wells respond to the semi-annual pumping in the WIPP Water Quality Sampling Program (WQSP) wells (e.g., H-19b0 and H-3b2). In 2012, the frequency of sampling has been reduced from semi-annual to annual. The effects of a 72-hour development pumping event in June 2012 were observed in some locations (the vertical line in Figure HYDRO-11 corresponds to the pumping duration at H-11b4R). Water levels from H-15R are plotted, but H-15 water levels are not plotted, as the latter are not believed to be representative of the Culebra. H-15 was a dual-completion well (Magenta and Culebra) that was disrupted by removing or replacing bridge plugs and production-injection packers for a variety of testing and water-quality sampling exercises.

Figure HYDRO-13 shows water levels in wells located south and southeast of the WIPP site. There are no large fluctuations in water levels in this area, aside from the large change in water levels at H-10c in July 2009. This change was related to removal of fresh water left over from well perforation activities in 2002 (U.S. DOE 2010). These wells only show a very slight rise and fall, similar in shape but lesser in magnitude to Culebra wells to the north, but they have been gradually declining since 2009 or 2010. Well H-4bR replaced H-4b in 2009 and H-11b4R replaced H-11b4 in 2011.

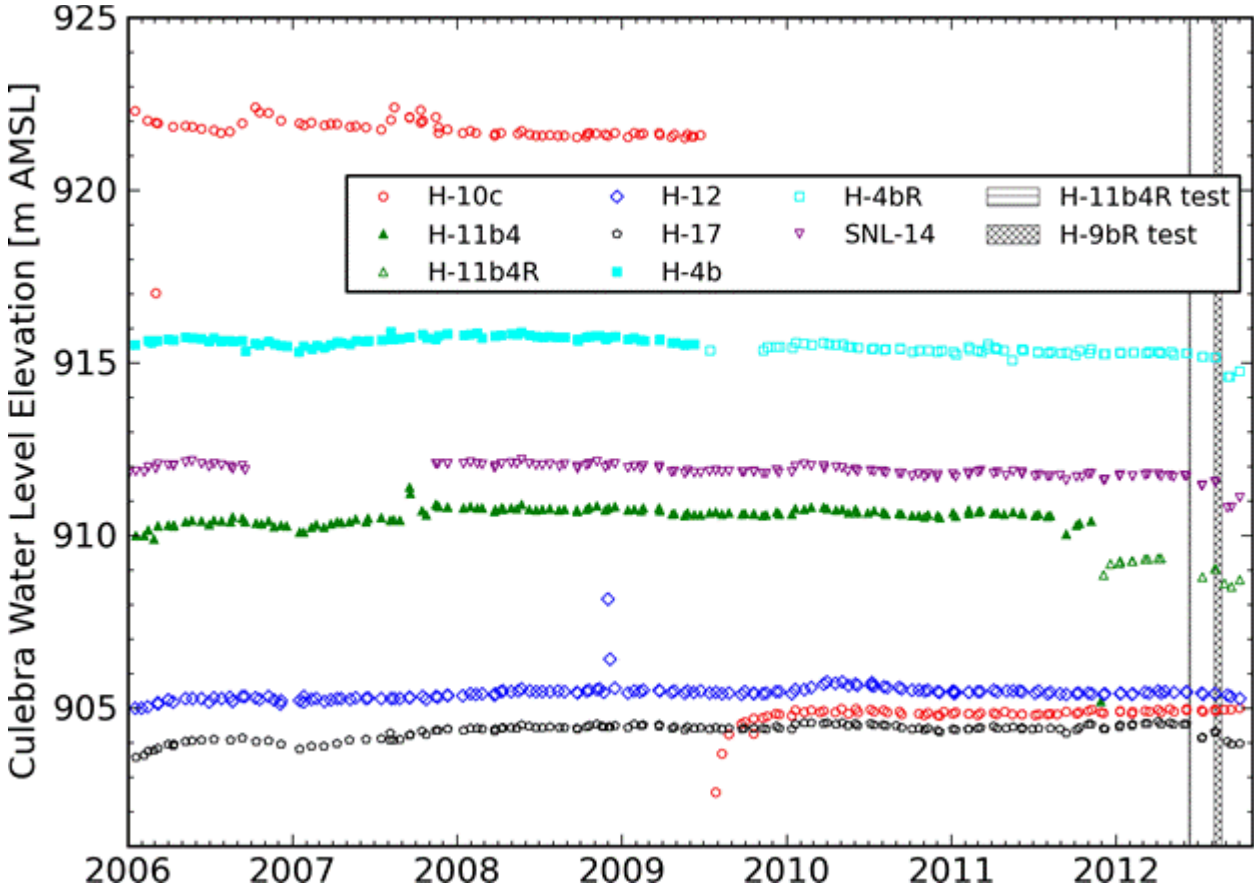

Figure HYDRO- 13. Water Levels In 8 Culebra Wells South of the WIPP Site

Figure HYDRO-14 shows water level time series in wells south and southwest of the WIPP site, near the southeastern arm of Nash Draw. The Culebra produces fresher water in this area, which is sometimes used for livestock watering. Some sustained pumping appears to have occurred near H-9c in the latter part of 2006, seen most clearly in the H-9c hydrograph but also recognizable in the hydrographs from SNL-12 (Figure HYDRO-14) and H-17, H-11b4, and H-4b (Figure HYDRO-13). This pumping may have been related to either livestock watering or oil and gas well drilling support activities. Most wells in the southeastern arm of Nash Draw have been gradually declining since 2008 or 2009. SNL-16 has a similar response to precipitation events as seen in Culebra wells north of the WIPP site.

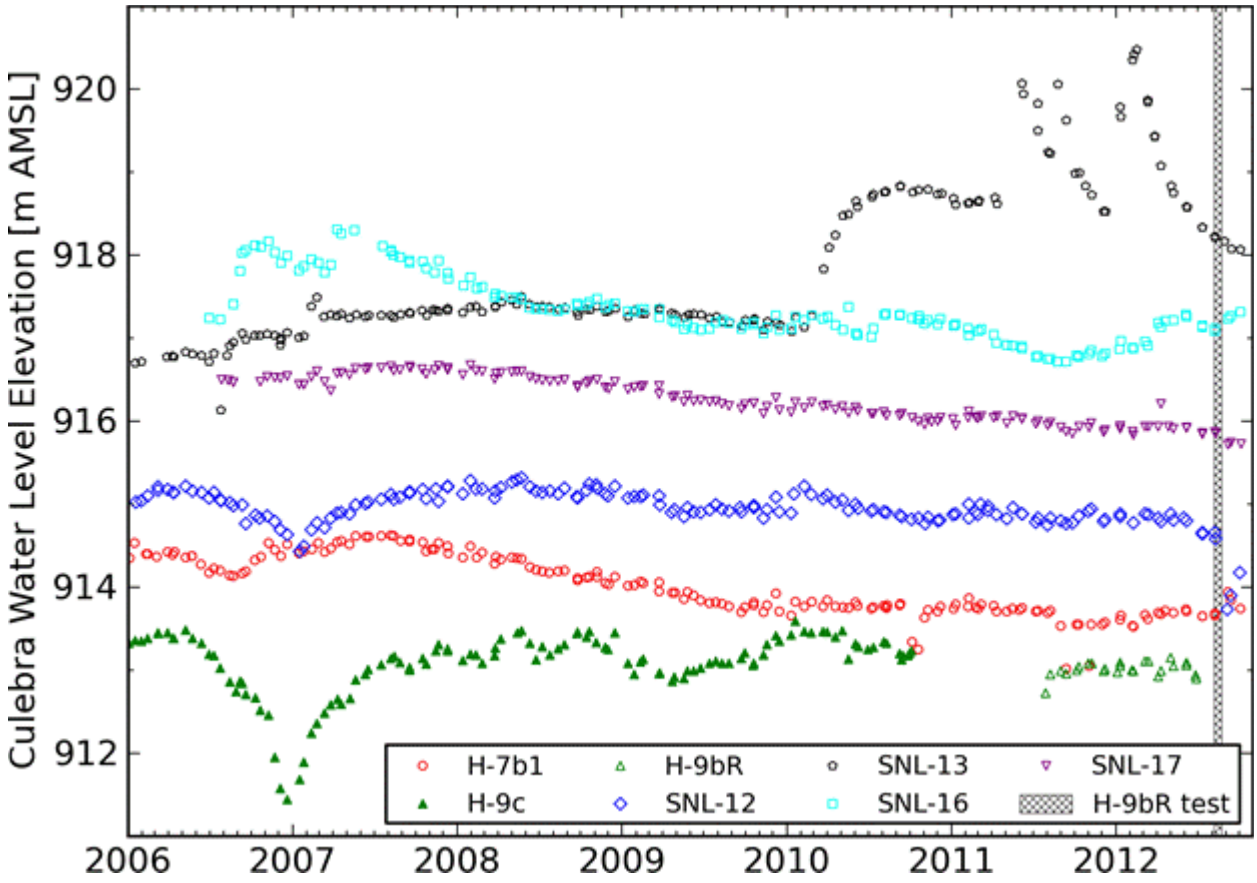

Figure HYDRO- 14. Water Levels In 7 Culebra Wells In and Near the Southeastern Arm of Nash Draw

SNL-13 has seen large fluctuations since a rise in 2010 attributed to oil and gas drilling in its vicinity. Figure HYDRO-15 shows both water levels and pressure transducer readings, along with spud dates obtained from the New Mexico Oil Conservation Division well search application (http://www.emnrd.state.nm.us/ocd/) for three sections surrounding SNL-13, T22S R30E Section 36, T23S R30E Section 1, and T23S R31E Section 6 (some wells in these sections did not have reported spud dates). In February 2012 an oilfield truck struck and became stuck on the SNL-13 surface casing, requiring the surface casing to be repaired (see the drop in pressure just after last peak in pressure transducer data shown in Figure HYDRO-15). The water levels and pressure transducer observations at SNL-13 appear to show effects of a longer-term slow rise and decay, beginning in early 2010, along with shorter-term rapid rises and decays through 2011 and 2012, some of which correspond closely to reported spud dates of nearby oil and gas wells. Neither the short- or long-term rises are observable in nearby Culebra wells SNL-17 (Figure HYDRO-14) or H-4bR (Figure HYDRO-13).

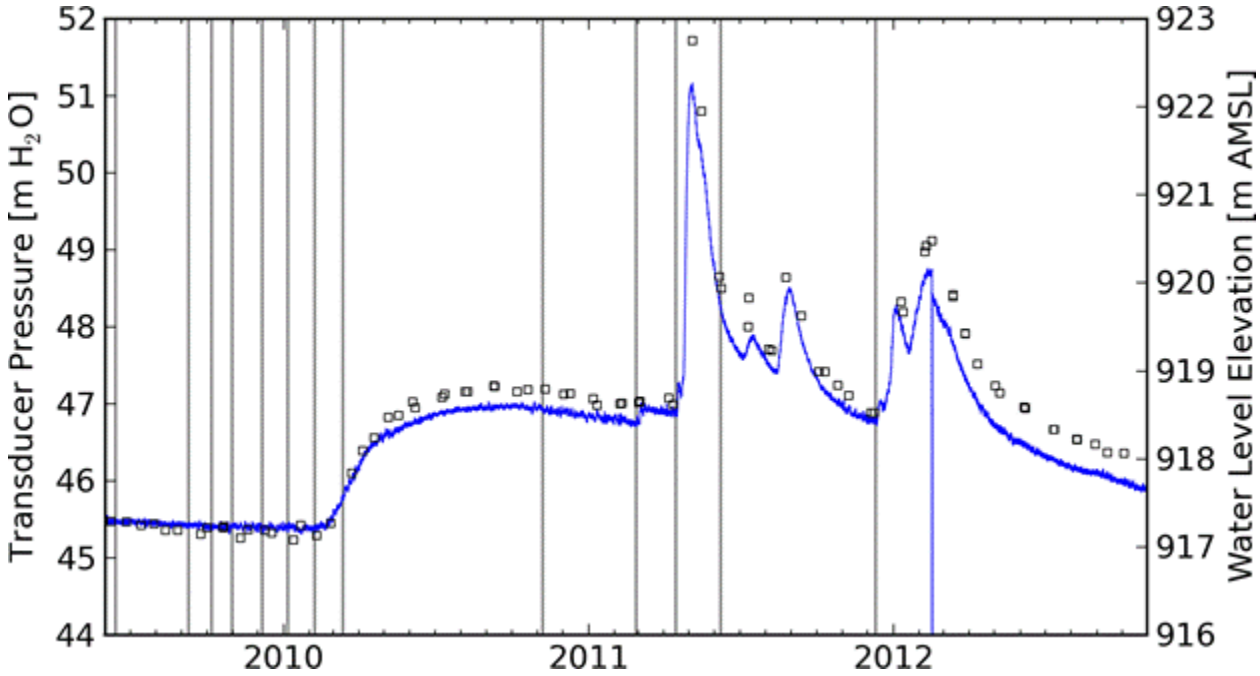

Figure HYDRO- 15. Water Levels (Symbols) and Pressure Transducer Data (Continuous Line) for Culebra Well SNL-13, with Spud Dates of Nearby Oil Wells (Vertical Lines).

Figure HYDRO-16 shows water level time series from Culebra wells SNL-9 and IMC-461 west of the WIPP site. The major upturns in water levels represent delayed responses to major rainfall events. Since peak water levels in 2006, water levels have generally been declining and following similar trends to wells north and west of the WIPP site (e.g., SNL-2 and SNL-19 in Figure HYDRO-9). Well IMC-461 had a significant shift in water level in March 2012 due to a collapse in a nearby potash mine.

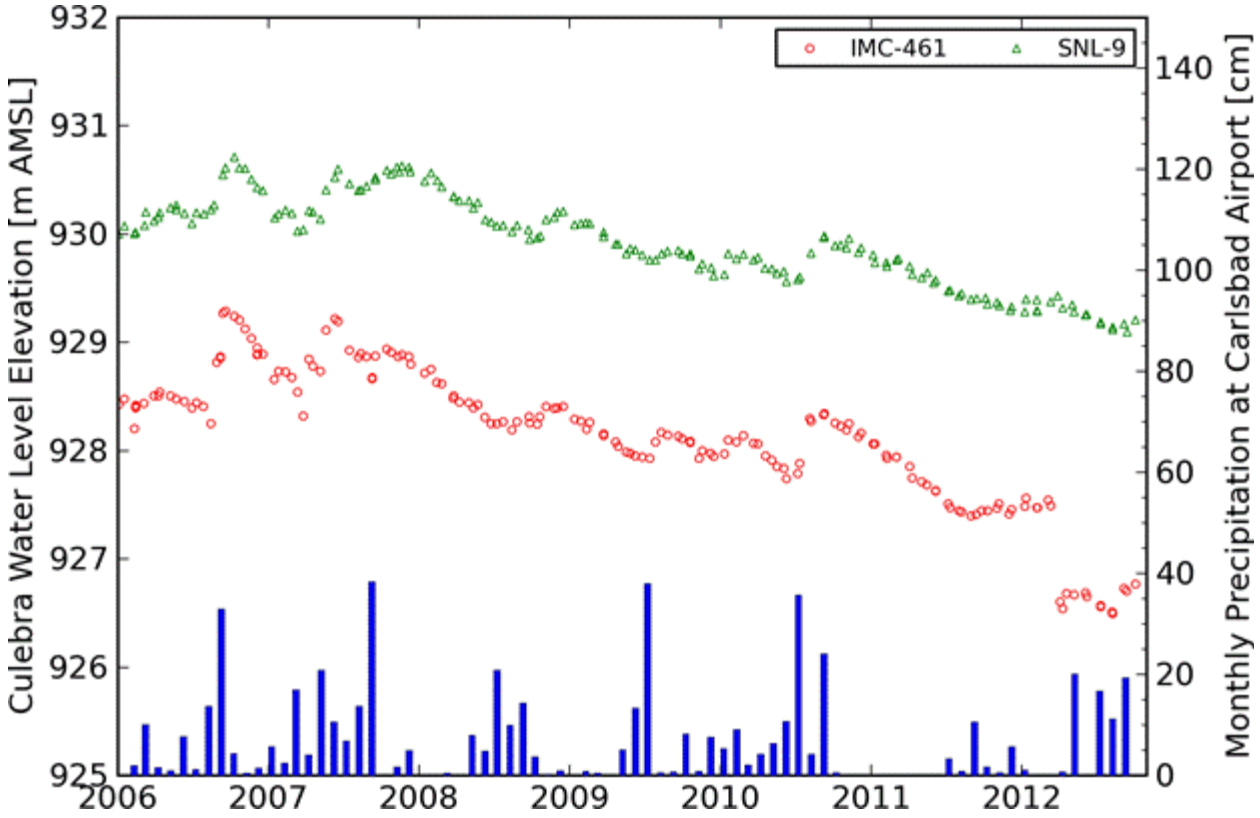

Figure HYDRO- 16. Water Levels In Culebra Wells IMC-461 and SNL-9 West of the WIPP Site

Figure HYDRO-17 shows the observed response of downhole pressure transducers in two Culebra wells to a significant roof collapse in a potash mine located in nearby Nash Draw. The collapse was registered in the U.S. Geological Survey (USGS) National Earthquake Information Center Database (http://earthquake.usgs.gov/regional/neic/) as a magnitude 3.1 event, occurring at 3:57:22 AM on March 18, 2012 (plotted as a vertical line in the closeup portion of Figure HYDRO-17). The upper plot in this figure shows the stability of the pressure observations both before and after the event, and clearly supports the observed shift in monthly water levels (see Figure HYDRO-14 and Figure HYDRO-16). Small-scale fluctuations in downhole pressure readings are due to effects of barometric pressure changes and Earth tides, which have a larger effect on IMC-461 than on SNL-16, possibly due to the different wellbore diameters. IMC-461 is completed using a 5.3-centimeter (cm) inner diameter schedule 80 polyvinyl chloride casing, while SNL-16 is completed using 12.3-cm inner diameter fiberglass-reinforced plastic casing (Powers 2009). The only transformation applied to the pressure data was a shift by the median pressure recorded over the 24-hour period before the event, to allow plotting of both wells on the same vertical pressure scale. Other Culebra or Magenta wells did not clearly respond immediately to the event, including nearby SNL-9.

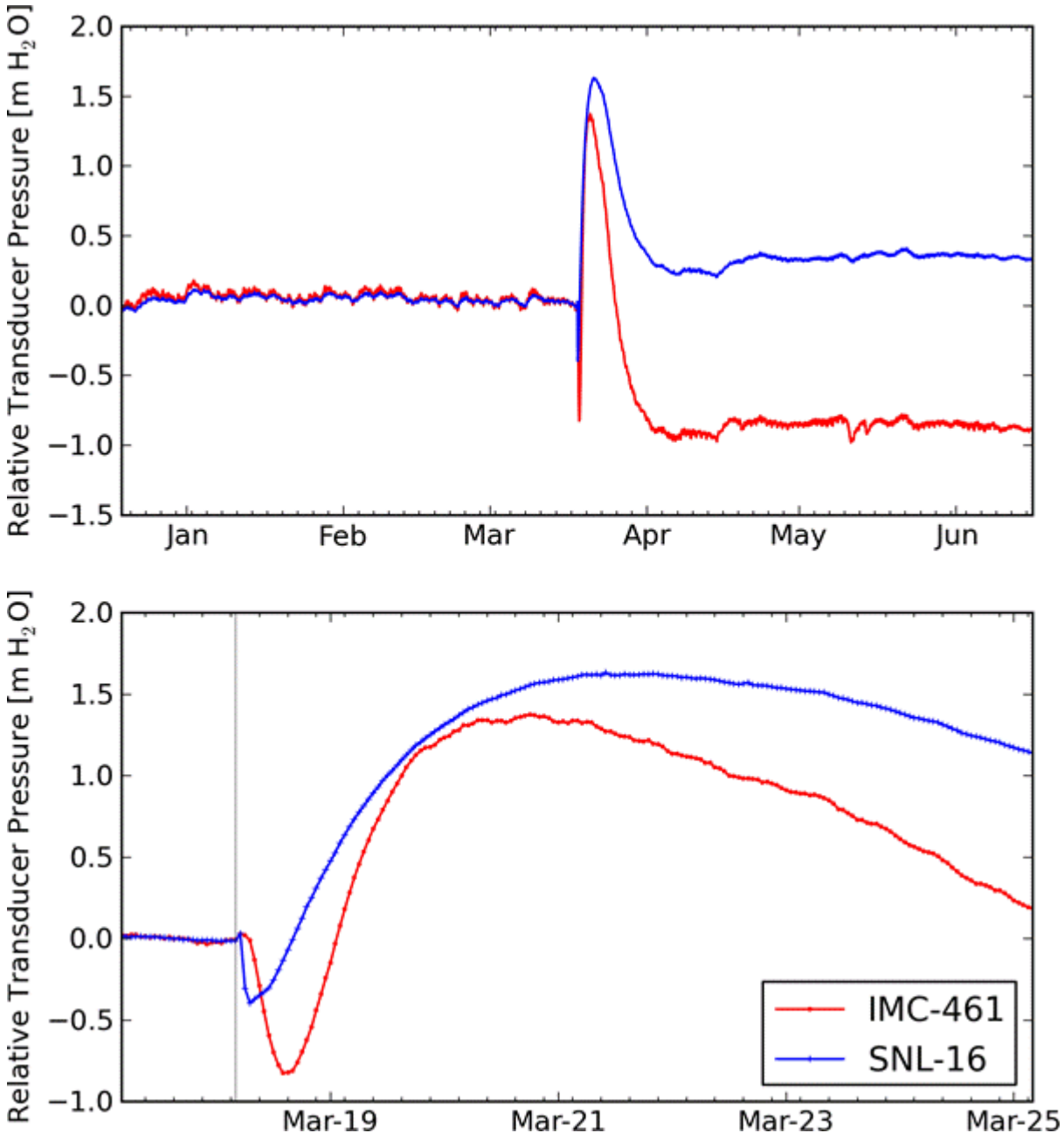

Figure HYDRO- 17. SNL-16 and IMC-461 Pressure Transducer Response to March 18, 2012 (3:57:22 AM MST) Potash Mine Roof Collapse

Figure HYDRO-18 shows water levels from Culebra wells SNL-6 and SNL-15. These wells were drilled in areas where the Culebra contains halite cements, and are recovering very slowly from well-development activities, including an April 2007 slug test in SNL-15 (U.S. DOE 2008), and January 2008 sampling in SNL-6 (U.S. DOE 2009c). Even at the rates these wells are recovering from minor pumping and sampling (e.g., an approximately 100 m rise in SNL-6 over 5 years), water levels will not be representative of undisturbed Culebra conditions for many years.

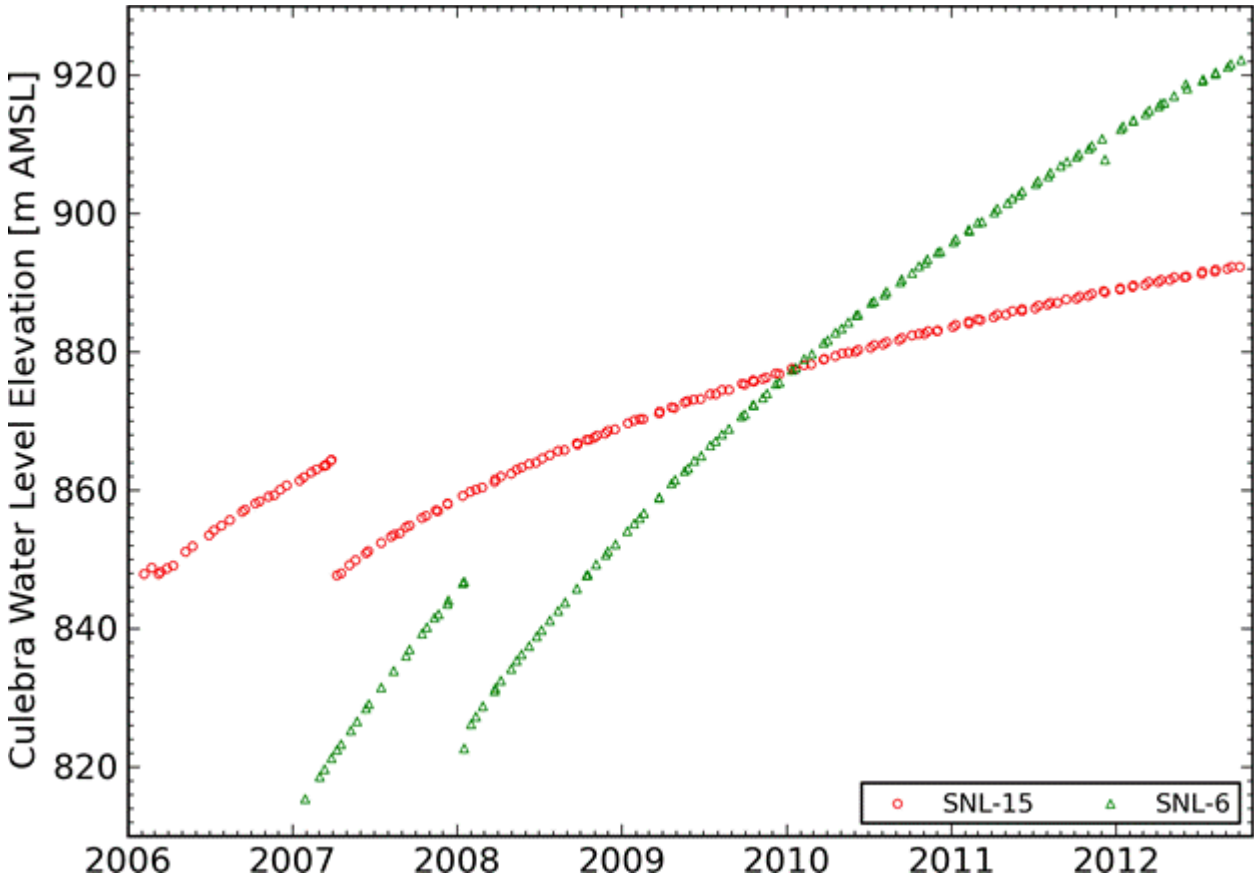

Figure HYDRO- 18. Water Levels In Culebra Wells SNL-6 and SNL-15 East of the H2/M2 Halite Margin

HYDRO-7.2 Magenta Monitoring

Magenta water levels were monitored in 13 wells during some or all of the period 2006 through 2012 (see Figure HYDRO-1 for locations). The wells being monitored through 2012 are shown in Figure HYDRO-19 through Figure HYDRO-21. Water levels in many Magenta wells were significantly disrupted by sampling, purging events, or hydraulic testing during the plotted 2006 through 2012 period.

Figure HYDRO-19 shows water levels from six Magenta wells, which indicate reasonably stable water levels, aside from recovery associated with pumping and purging events. Most wells show modest gradual increases in water level elevations over most of the 2006 through 2012 period. The gray dashed line in Figure HYDRO-19 illustrates a rise of 1 m over seven years (0.143 m/year), which appears to roughly parallel the trend in most of these wells and may be due to a slow recovery from pumping and sampling Magenta wells.

In C-2737, two water level drops in 2006 and 2007, along with a water level shift in 2008, are due to activities related to re-seating packers and swabbing foreign water from tubing (U.S. DOE 2009c). After increasing for several years, H-9c has shown a decrease since activities on the H-9 wellpad in late 2010 associated with plugback of H-9c to a Magenta-only well and drilling the H-9bR Culebra replacement well. Two observed perturbations in H-11b2 during 2011 are related to drilling replacement Culebra well H-11b4R, which involved drilling two separate boreholes. Water quality samples were obtained from H-11b2 from January through June 2008 (U.S. DOE 2009c). Well H-3b1

was pumped for water quality sampling from April through July 2009 and WIPP-18 was sampled from June through September and December 2009 (U.S. DOE 2010). H-4c was purged for water quality sampling in August 2010 (U.S. DOE 2011).

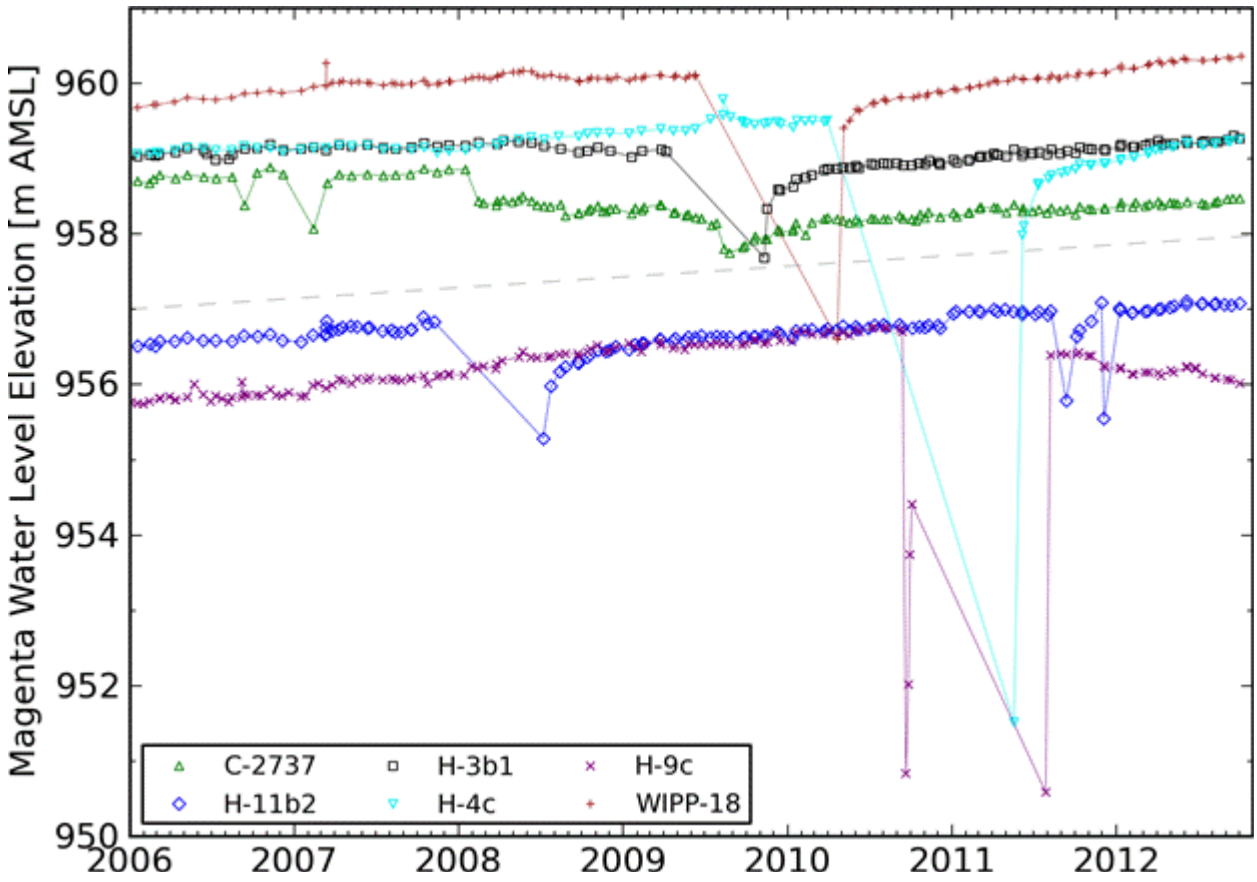

Figure HYDRO- 19. Water Levels In 6 Magenta Wells

Figure HYDRO-20 shows water levels in Magenta wells that experienced large-scale fluctuations. H-15 has been increasing steadily at a slope of approximately 1 m/year, with an unexplained meter-sized jump in 2010. H-15 was water-quality sampled in March 2008, after being completed as a Magenta-only well earlier in 2008 (U.S. DOE 2009c). H-18 has shown a steady rise from 2006 through 2012, but at a significantly steeper slope (approximately 0.43 m/year since 2010) than that observed in most wells in Figure HYDRO-19. Well H-18 was water-quality sampled in February through April 2009 (U.S. DOE 2010), and H-2b1 was sampled from April 2010 through February 2011 (U.S. DOE 2011; U.S. DOE 2012). Well H-10a was bailed in March 2010 to remove fresh water in the borehole (U.S. DOE 2011), causing a significant adjustment in water levels due to the change in density. Well H-14 recovered slowly from pumping activities in 2007 and a water-quality sampling purge event in February 2009 (U.S. DOE 2010).

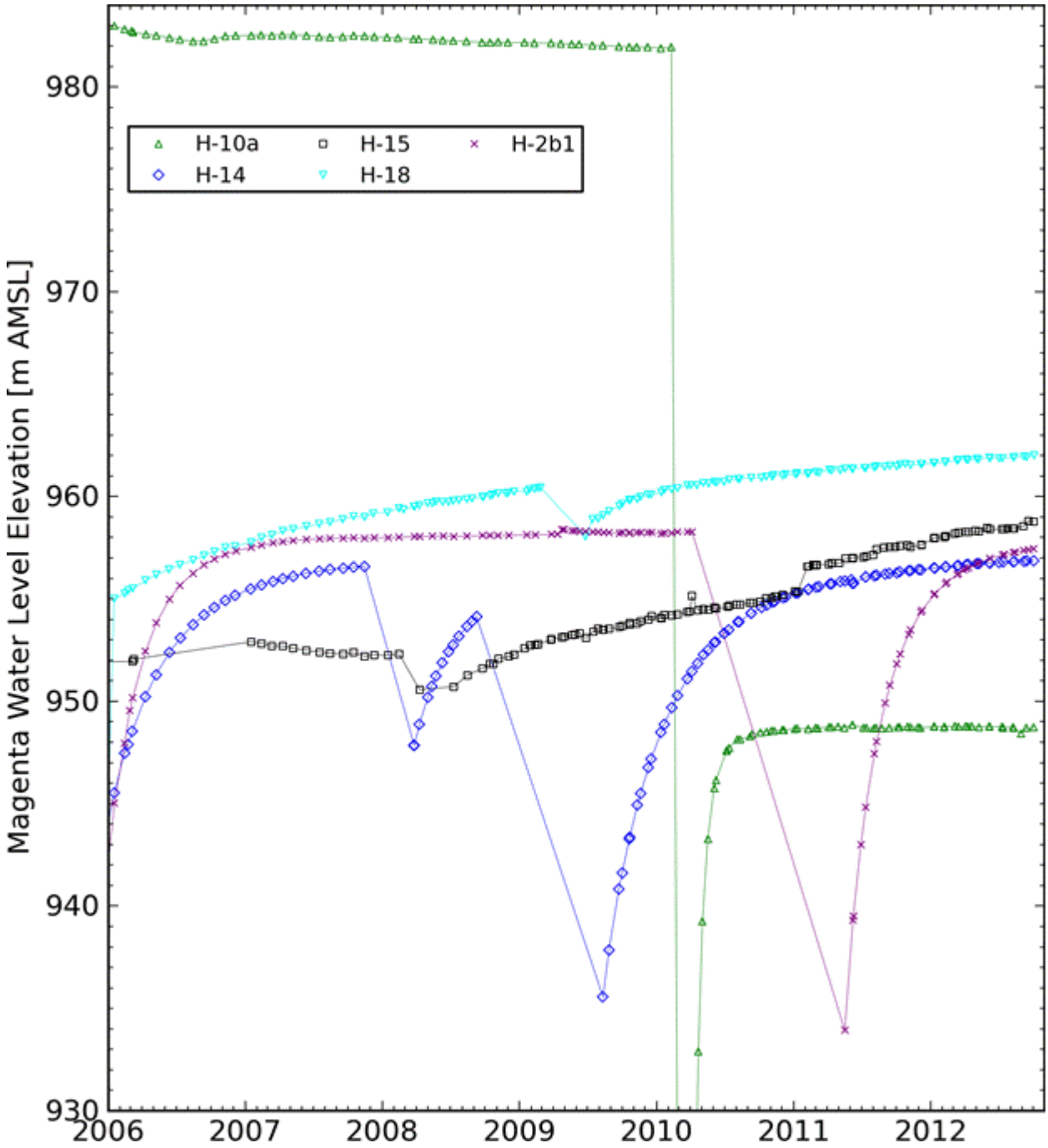

Figure HYDRO- 20. Water Levels In 5 Magenta Wells

Figure HYDRO-21 shows water levels in two Magenta wells (H-6c and H-8a) with lower water levels than other Magenta wells. Well H-6c shows a drop in 2008, associated with the plugging, abandonment, and re-drilling activities on the H-6 wellpad. A recent jump in H-6c water levels may be due to nearby oilfield activities, although no similar response was observed at H-6bR in the Culebra. Well H-8a was sampled in April 2010 (U.S. DOE 2011).

Downhole pressure transducers are currently monitoring 13 Magenta wells, while 2 previously monitored Magenta wells (WIPP-25 and WIPP-30) have been plugged and abandoned (Figure HYDRO-22). The pressure transducer data are consistent with the water-level measurements made in

those wells. The transducer data provide a more complete record of pumping, water-quality sampling, and other activities in the wells than the water-level data alone.

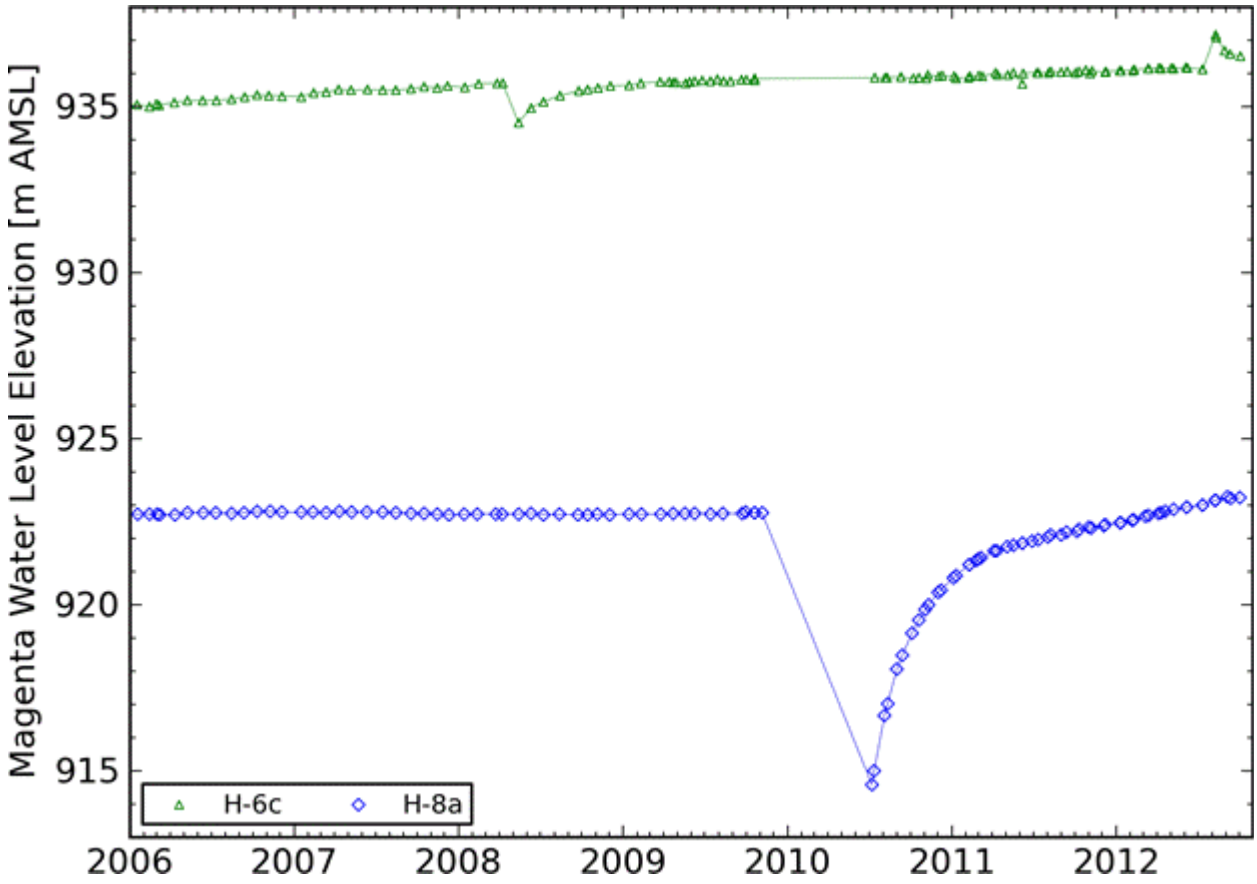

Figure HYDRO- 21. Water Levels In Magenta Wells H-6c and H-8a

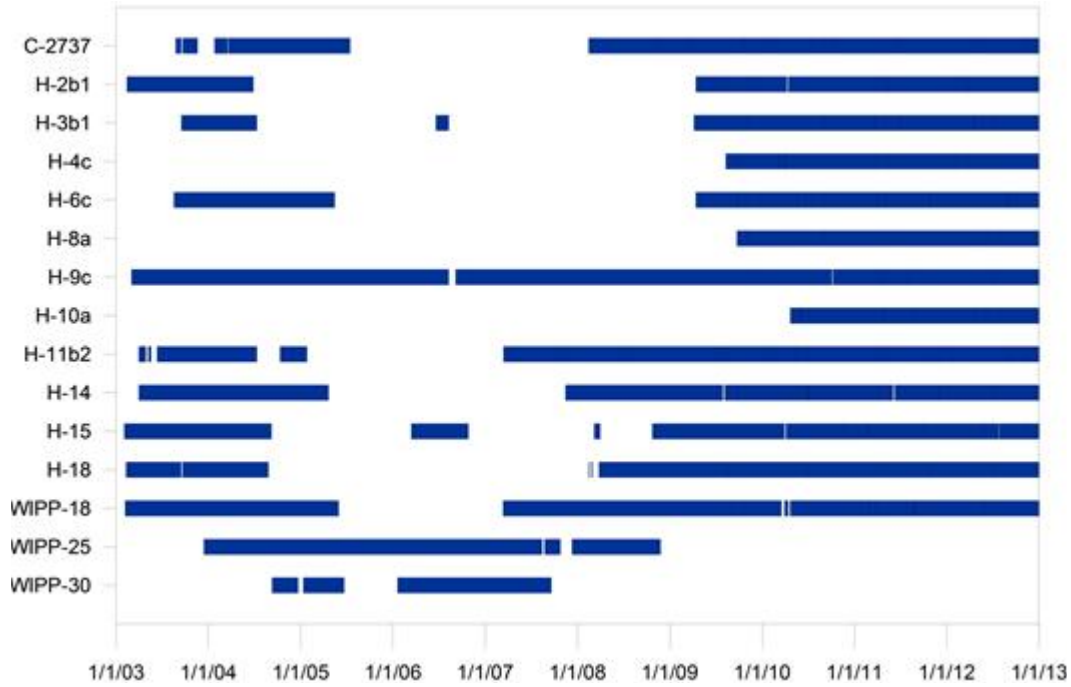

Figure HYDRO- 22. Magenta Well Downhole Pressure Transducer Data Coverage

HYDRO-7.3 Dewey Lake Monitoring

The DOE monitors Dewey Lake water levels in one well, WQSP-6A (see Figure HYDRO-1). Figure HYDRO-23 shows a time series of Dewey Lake water levels in WQSP-6A from 2006 through 2012. The hydrograph shows that water levels were stable within an approximately 50-cm band over that period, with a slightly increasing downward trend. Some of the observed water level fluctuations are probably related to the water-quality sampling performed in the well twice a year, which was stopped in 2012 (WQSP sampling will no longer include WQSP-6A).

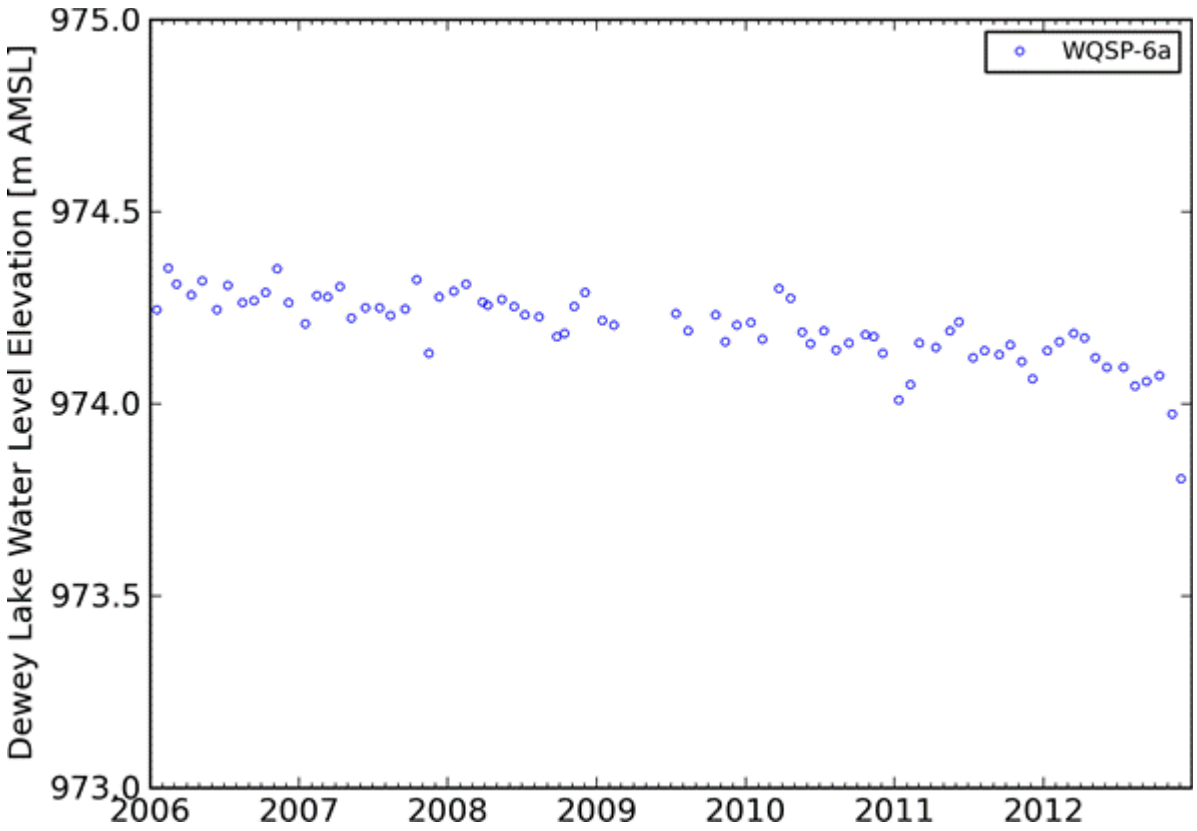

Figure HYDRO- 23. WQSP-6A Dewey Lake Water Levels

HYDRO-7.4 Bell Canyon Monitoring

Bell Canyon monitoring wells are situated at the northern (DOE-2) and southern (Cabin Baby [CB]-1) edges of the WIPP LWB (see Figure HYDRO-1 for well locations). The primary purpose of this monitoring is to determine if oil and gas activities in the Bell Canyon are affecting the hydraulic head of the Bell Canyon at the WIPP site. Water level elevations are plotted for the period 2003 through 2012 in Figure HYDRO-24. This time period was chosen to clearly show the effects of well recompletion in 2004 and bailing to remove brine-contaminated water from the tubing in 2008 (U.S. DOE 2009c). Since 2004, both wells are completed exclusively to the Bell Canyon Formation and since 2008 they both contain representative Bell Canyon water in their tubing. Water levels in DOE-2 have risen slowly, but have been nearly stable since bailing activities in 2008. Water levels in CB-1 have been rising since 2008 (approximately a 6-m rise over 4.5 years), with an increase in slope near the beginning of 2011.

Both CB-1 and DOE-2 are currently monitored with downhole pressure transducers, which have been collecting data since May 2011. Pressure transducer data agree with manual water-level trends and

also show clear effects of barometric fluctuations in both wells. Typically, barometric and Earth tide fluctuations are removed from pressure transducer observations using a least-squares barometric response function approach when analyzing pumping test data at the WIPP. See Toll and Rasmussen (2007) for the specific procedure and software used for this task.

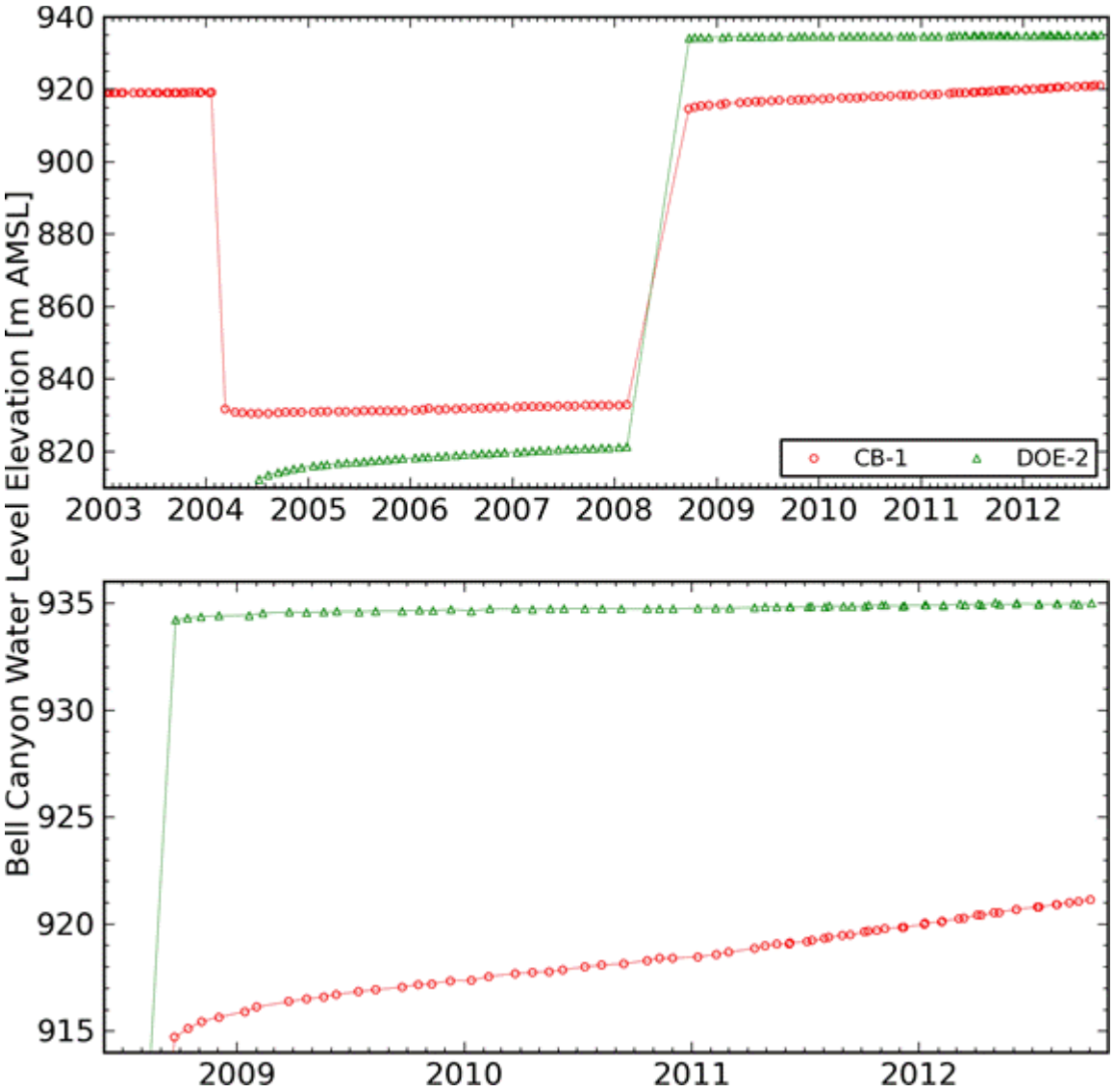

Figure HYDRO- 24. Bell Canyon Water Levels

HYDRO-7.5 Monitoring Summary

Water-level monitoring provides a general picture of the changes in hydraulic head occurring in the formations being monitored. Water levels are currently being monitored in the Culebra, Magenta, Dewey Lake, and Bell Canyon. Culebra water levels generally peaked in 2008, and fell gradually by 1 to 3 m between 2008 and 2012. Water levels fluctuated more in Nash Draw and north of the WIPP site than they did elsewhere. Water levels in most Magenta wells generally rose over the same period, by approximately 1 m (aside from a few wells rising at larger rates). The Dewey Lake water level (measured only in well WQSP-6A) was stable within a ~50-cm band over the last 5-year period. Bell Canyon water levels were stable in DOE-2 and rose steadily in CB-1 since being bailed in 2008.

In addition to monitoring water levels, fluid pressures in most Culebra, Magenta, and Bell Canyon wells are monitored on an hourly basis using downhole pressure transducers. The high-frequency fluid-pressure measurements provide a clearer, more complete record of the changes in hydraulic head occurring in the wells than that provided by monthly water-level measurements alone. The high-frequency pressure transducer data shows detailed fluctuations due to both natural (barometric, earth tides, and precipitation) and man-made (potash mine collapse and oil well drilling) stimuli.

HYDRO-8.0 Culebra Heads Contour Map Generation

The creation of model-generated contour maps of Culebra piezometric head follows Activity/Project Specific Procedure SP 9-9, *Preparation of Culebra Potentiometric Surface Contour Maps* (Kuhlman 2009a). Using an averaged form of the groundwater model discussed in Appendix TFIELD, boundary conditions of the model are adjusted to better match each year's observed equivalent freshwater heads (the equivalent height of freshwater in a well, which equals the pressure exerted by the actual column of brine). Procedure SP 9-9 has been used since 2009 (Kuhlman 2009b, Kuhlman 2010b, Kuhlman 2011, and Kuhlman 2012c) to generate annual Culebra contour maps for inclusion in the WIPP ASERs (U.S. DOE 2009c, U.S. DOE 2010, U.S. DOE 2011, and U.S. DOE 2012). Culebra contour maps were also recently generated for historic data going back to 2000, to present contour maps of heads in the Culebra in a consistent manner (Kuhlman 2012a and Kuhlman 2012b).

HYDRO-9.0 Summary and Conclusions

A Culebra monitoring-network optimization study was revised by Kuhlman (Kuhlman 2010a) to identify the locations where new Culebra monitoring wells would be of most value, and to identify wells that could be removed from the network with little loss of information. The WIPP Culebra monitoring network is now in a long-term monitoring configuration, rather than a configuration for testing. As steel-cased wells are aging and failing, they are being re-drilled and replaced with non-steel-cased wells designed for long-term stability in a saline environment.

Geochemical analysis of groundwater samples collected from formations above the Salado (Domski et al. 2011) reveals how the geochemistry of the Culebra and Magenta fit into regional groundwater trends both vertically and horizontally.

Several Culebra and Magenta slug and pumping tests were analyzed to interpret transmissivity parameter estimates at well locations. Some of the analyzed tests were conducted recently, but many of the Magenta tests were conducted historically. In the wells tested, the variability of the transmissivity of the Magenta Dolomite is less than that seen in the Culebra.

The WIPP groundwater-monitoring program has continued to augment monthly water-level measurements in wells with continuous (~hourly) fluid-pressure measurements using downhole programmable pressure gauges. Pressure transducer readings allow us to more clearly see effects of the Air Intake Shaft at H-16, nearby drilling of oil wells at SNL-13, and collapse of underlying potash mine workings (IMC-461 and SNL-16). A combination of pressure and depth-to-water measurements are used to estimate fluid density in Culebra wells at the WIPP. These densities are then used to compute equivalent freshwater heads, which are combined with an averaged version of the WIPP PA model to produce contour maps of piezometric head in the Culebra for inclusion in the WIPP ASER.

HYDRO-10.0 References

(*Indicates a reference that has not been previously submitted.)

Beauheim, R.L., and S.A. McKenna. 2003. Analysis Plan AP-111: Analysis Plan for Optimization and Minimization of the Culebra Monitoring Network for the WIPP. ERMS 533092. Carlsbad, NM: Sandia National Laboratories. [PDF / Author]

Beauheim, R.L. 2009. Analysis Plan AP-070: Analysis Plan for Hydraulic-Test Interpretations, Revision 2. ERMS 552209. Carlsbad, NM: Sandia National Laboratories.* [PDF / Author]

Bowman, D.O., and R.L. Beauheim. 2010. Analysis Report for AP-070: Analysis of Magenta Hydraulic Tests Performed Between December 1978 and June 2009. ERMS 554590. Carlsbad, NM: Sandia National Laboratories.* [PDF / Author]

Bowman, D.O., and R.M. Roberts. 2009. Analysis Report for AP-070: Analysis of Culebra and Magenta Hydraulic Tests Performed Between January 2005 and August 2008. ERMS 550906. Carlsbad, NM: Sandia National Laboratories.* [PDF / Author]

Domski, P.S., and R.L. Beauheim. 2008. Evaluation of Culebra Brine Chemistry. AP-125. ERMS 549336. Carlsbad, NM: Sandia National Laboratories. [PDF / Author]

Domski, P.S., R.L. Beauheim, and P.B. Johnson. 2011. AP-147 Analysis Report: Evaluation of WIPP Groundwater Compositions. ERMS 556581. Carlsbad, NM: Sandia National Laboratories.* [PDF / Author]

Hillesheim, M.B., L.A. Hillesheim, and N.J. Toll. 2007. "Mapping of Pressure-Head Responses of a Fractured Rock Aquifer to Rainfall Events." Proceedings of the 2007 U.S. EPA/NGWA Fractured Rock Conference (pp. 522-36). Westerville, OH: National Ground Water Association. [Author]

Johnson, P.B. 2008. Routine Calculations Report in Support of Task 6 of AP-114: 2007 Calculated Densities for Use in Deriving Equivalent Freshwater Heads of the Culebra Dolomite Member of the Rustler Formation near the WIPP Site, May 2007. ERMS 548127. Carlsbad, NM: Sandia National Laboratories. [PDF / Author]

Johnson, P.B. 2009. Routine Calculations Report in Support of Task 6 of AP-114: 2008 Calculated Densities for Use in Deriving Equivalent Freshwater Heads of the Culebra Dolomite Member of the Rustler Formation near the WIPP Site. ERMS 550755. Carlsbad, NM: Sandia National Laboratories.* [PDF / Author]

Johnson, P.B. 2010. Memo to Records Center (Subject: 2009 Calculated Densities). 13 January 2010. ERMS 552839. Carlsbad, NM: Sandia National Laboratories.* [PDF / Author]

Johnson, P.B. 2011. Memo to Records Center (Subject: Memo of Correction 2010 Calculated Densities). 19 January 2011. ERMS 554805. Carlsbad, NM: Sandia National Laboratories.* [PDF / Author]

Johnson, P.B. 2012a. Activity/Project Specific Procedure SP 9-11: Calculation of Densities for Groundwater in WIPP Wells, Revision 2. ERMS 558734. Carlsbad, NM: Sandia National Laboratories.* [PDF / Author]

Johnson, P.B. 2012b. Memo to Records Center (Subject: 2011 Calculated Densities). 13 January 2012. ERMS 556866. Carlsbad, NM: Sandia National Laboratories.* [PDF / Author]

Johnson, P.B. 2012c. Memo to Records Center (Subject: 2005 Calculated Densities). 23 January 2012. ERMS 556883. Carlsbad, NM: Sandia National Laboratories.* [PDF / Author]

Johnson, P.B. 2012d. Memo to Records Center (Subject: 2006 Calculated Densities). 30 January 2012. ERMS 556887. Carlsbad, NM: Sandia National Laboratories.* [PDF / Author]

Johnson, P.B. 2012e. Memo to Records Center (Subject: 2004 Calculated Densities). 9 May 2012. ERMS 557405. Carlsbad, NM: Sandia National Laboratories.* [PDF / Author]

Johnson, P.B. 2012f. Memo to Records Center (Subject: 2003 Calculated Densities). 9 May 2012. ERMS 557402. Carlsbad, NM: Sandia National Laboratories.* [PDF / Author]

Kuhlman, K.L. 2009a. Activity/Project Specific Procedure SP 9-9: Preparation of Culebra Potentiometric Surface Contour Maps. ERMS 552306. Carlsbad, NM: Sandia National Laboratories.* [PDF / Author]

Kuhlman, K.L. 2009b. Analysis Report for Preparation of 2008 Culebra Potentiometric Surface Contour Map. ERMS 552005. Carlsbad, NM: Sandia National Laboratories.* [PDF / Author]

Kuhlman, K.L. 2010a. Analysis Report AP-111 Revision 1, Culebra Water Level Monitoring Network Design. ERMS 554054. Carlsbad, NM: Sandia National Laboratories.* [PDF / Author]

Kuhlman, K.L. 2010b. Analysis Report for Preparation of 2009 Culebra Potentiometric Surface Contour Map. ERMS 553645. Carlsbad, NM: Sandia National Laboratories.* [PDF / Author]

Kuhlman, K.L. 2011. Analysis Report for Preparation of 2010 Culebra Potentiometric Surface Contour Map. ERMS 555318. Carlsbad, NM: Sandia National Laboratories.* [PDF / Author]

Kuhlman, K.L. 2012a. Analysis Report for Preparation of 2000-2004 Culebra Potentiometric Surface Contour Maps. ERMS 557660. Carlsbad, NM: Sandia National Laboratories.* [PDF / Author]

Kuhlman, K.L. 2012b. Analysis Report for Preparation of 2005-2007 Culebra Potentiometric Surface Contour Maps. ERMS 557494. Carlsbad, NM: Sandia National Laboratories.* [PDF / Author]

Kuhlman, K.L. 2012c. Analysis Report for Preparation of 2011 Culebra Potentiometric Surface Contour Map. ERMS 557633. Carlsbad, NM: Sandia National Laboratories.* [PDF / Author]

McKenna, S.A. 2004. Analysis Report: AP-111; Culebra Water Level Monitoring Network Design. AP-111. ERMS 540477. Carlsbad, NM: Sandia National Laboratories. [PDF / Author]

Powers, D.W. 2009. Basic Data Report for Drillhole SNL-16 (C-3220) (Waste Isolation Pilot Plant) (February). DOE/WIPP 07-3364. Carlsbad, NM: U.S. Department of Energy.* [PDF / Author]

Schuhen, M.D. 2010a. Test Plan TP 03-01: Test Plan for Testing of Wells at the WIPP Site, Revision 3. ERMS 553985. Carlsbad, NM: Sandia National Laboratories.* [PDF / Author]

Schuhen, M.D. 2010b. Test Plan TP 06-01: Monitoring Water Levels in WIPP Wells, Revision 3. ERMS 553993. Carlsbad, NM: Sandia National Laboratories.* [PDF / Author]

Schuhen, M.D. 2011. WIPP WGS-1 Laboratory Notebook, WIPP Geologic Samples. ERMS 555594. Carlsbad, NM: Sandia National Laboratories.* [PDF / Author]

Toll, N.J., and T.C. Rasmussen. 2007. "Removal of barometric pressure effects and earth tides from observed water levels," Ground Water, 45(1), 101-105. [Author]

U.S. Department of Energy (DOE). 2004. Waste Isolation Pilot Plant Environmental Monitoring Plan. DOE/WIPP 99-2194. Carlsbad, NM: U.S. Department of Energy. [Author]

U.S. Department of Energy (DOE). 2008. Waste Isolation Pilot Plant Annual Site Environmental Report for 2007. DOE/WIPP 08-2225. Carlsbad, NM: U.S. Department of Energy. [PDF / Author]

U.S. Department of Energy (DOE). 2009a. Basic Data Report for Well Plugging and Abandonment, Reconfiguration, and New Well Drilling Activities for Fiscal Year 2008. DOE/WIPP 08-3326. Carlsbad, NM: U.S. Department of Energy.* [PDF / Author]

U.S. Department of Energy (DOE). 2009b. Title 40 CFR Part 191 Subparts B and C Compliance Recertification Application for the Waste Isolation Pilot Plant. DOE/WIPP 2009-3424. Carlsbad, NM: US Department of Energy.* [Author]

U.S. Department of Energy (DOE). 2009c. Waste Isolation Pilot Plant Annual Site Environmental Report for 2008. DOE/WIPP 09-2225. Carlsbad, NM: U.S. Department of Energy.* [PDF / Author]

U.S. Department of Energy (DOE). 2010. Waste Isolation Pilot Plant Annual Site Environmental Report for 2009. DOE/WIPP 10-2225. Carlsbad, NM: U.S. Department of Energy.* [PDF / Author]

U.S. Department of Energy (DOE). 2011. Waste Isolation Pilot Plant Annual Site Environmental Report for 2010. DOE/WIPP 11-2225. Carlsbad, NM: U.S. Department of Energy.* [PDF / Author]

U.S. Department of Energy (DOE). 2012. Waste Isolation Pilot Plant Annual Site Environmental Report for 2011. DOE/WIPP 12-3489. Carlsbad, NM: U.S. Department of Energy.* [PDF / Author]

U.S. Environmental Protection Agency (EPA). 1996. "40 CFR Part 194: Criteria for the Certification and Recertification of the Waste Isolation Pilot Plant's Compliance with the 40 CFR Part 191 Disposal Regulations; Final Rule." Federal Register, vol. 61 (February 9, 1996): 5223-45. [PDF / Author]

Title 40 CFR Part 191
Subparts B and C
Compliance Recertification Application 2014
for the
Waste Isolation Pilot Plant

Appendix IGP-2014
Individual and Groundwater
Protection Requirements

United States Department of Energy
Waste Isolation Pilot Plant

Carlsbad Field Office
Carlsbad, New Mexico

Compliance Recertification Application 2014

Appendix IGP-2014
Individual and Groundwater Protection Requirements

Table of Contents

List of Figures

List of Tables

Acronyms and Abbreviations

% percent

CCA Compliance Certification Application

CFR Code of Federal Regulations

CH contact-handled

Ci curies

Ci/L curies per liter

CRA Compliance Recertification Application

DOE U.S. Department of Energy

EPA U.S. Environmental Protection Agency

FEPs features, events, and processes

gpm gallons per minute

kg kilogram

kg/m^3 kilogram per cubic meter

LWB Land Withdrawal Boundary

MB Marker Bed

mg/L milligrams per liter

mrem millirem

NUTS Nuclide Transport System

PA performance assessment

PAVT Performance Assessment Verification Test

pCi/L picocuries per liter

RH remote-handled

TDS total dissolved solids

TRU transuranic

UP undisturbed performance

USDW underground source of drinking water

WIPP Waste Isolation Pilot Plant

Elements and Chemical Compounds

Am americium

Pu plutonium

Ra radium

Rn radon

Th thorium

U uranium

IGP-1.0 Introduction

The quantitative release limits set forth in the containment requirements provisions of 40 CFR § 191.13 (U.S. EPA 1993) are one of three long-term numerical performance requirements contained in 40 CFR Part 191 Subparts B and C. The U.S. Department of Energy (DOE) must also comply with two other quantitative performance standards contained in the individual protection requirements (40 CFR § 191.15, U.S. EPA 1993) and groundwater protection requirements (Part 191 Subpart C). This appendix describes the DOE's demonstration of Waste Isolation Pilot Plant (WIPP) disposal system compliance with both the individual and groundwater protection requirements.

In performing the compliance assessment for the Compliance Certification Application (CCA) (U.S. DOE 1996), the CCA Performance Assessment Verification Test (PAVT) (Dials 1997a), and for subsequent Compliance Recertification Applications (CRAs), the DOE applied a bounding-analysis approach using conservative assumptions that overestimate potential doses and contaminant concentrations. To provide added assurance, the DOE assumed the presence of an underground source of drinking water (USDW) in close proximity to the WIPP Land Withdrawal Boundary (LWB), even though available data indicate that none exists near the boundary. Using this bounding-analysis approach, the maximum potential dose to an individual is 0.032 millirems (mrem) in the CCA PAVT

and 0.93 mrem for the CCA evaluation (as revised, consistent with U.S. Environmental Protection Agency (EPA) direction). Both values are well below the individual protection standard [40 CFR § 191.15(a)] of 15 mrem as an annual committed effective dose. In addition, the estimated potential maximum combined radium-226 (^{226}Ra) and ^{228}Ra concentration in groundwater is 0.49 picocuries per liter (pCi/L) in the CCA PAVT and 0.14 pCi/L in the CCA Performance Assessment (PA), both well below the acceptable standard of 5 pCi/L required by 40 CFR § 191.24(a)(1) (Dials 1997a).

This bounding-analysis approach also assumes that all contaminants reaching the accessible environment are directly available to a receptor. The analysis bounds potential impacts of underground interconnections among bodies of surface water, groundwater, and any potential USDW.

In support of its 2004 Compliance Recertification Application (CRA-2004) (U.S. DOE 2004) and the 2009 Compliance Recertification Application (CRA-2009)(U.S. DOE 2009), the DOE reexamined concentrations of radionuclides that could potentially reach the accessible environment under undisturbed conditions. The CRA-2004 and CRA-2009 evaluations showed that the maximum concentration of radionuclides reaching the boundary was projected to be at least an order of magnitude less than the maximum concentration projected in the CCA analyses. Based on this and additional, updated information presented in the CRA-2004, Chapter 8.0, and again in Appendix IGP-2009, the DOE concluded that the WIPP disposal system continued to comply with the individual and groundwater protection provisions of Part 191 Subparts B and C (U.S. DOE 2004 and 2009). The EPA reviewed the information presented by the DOE in 2004 and 2009 and determined that the DOE continued to demonstrate compliance for each recertification with the individual and groundwater protection requirements of 40 CFR 191 Subparts B and C (U.S. EPA 2006, U.S. EPA 2010a and U.S. EPA 2010b).

In support of the CRA-2014, the DOE has again reexamined concentrations of radionuclides that could potentially reach the accessible environment under undisturbed conditions. The CRA-2014 PA shows no releases to the accessible boundary for the undisturbed case. Therefore, there are no radionuclide concentrations within the USDW that is conservatively assumed to exist at the WIPP boundary. The additional data gathered for this CRA continue to show that there are no USDWs within or at the WIPP accessible boundary, although they do exist some distance away. The CRA-2014 analysis continues to show that the maximum concentration of radionuclides reaching the boundary (zero for this analysis) is projected to be less than the maximum concentration projected in the CCA, which has been used for each recertification as the bounding case for compliance assessment analyses. Based on this and additional information updated for the CRA-2014 evaluation in this appendix, the DOE concludes that the WIPP disposal system continues to comply with the individual and groundwater protection provisions of Part 191 Subparts B and C.

IGP-2.0 Individual Protection Requirements

The individual protection requirements are contained in section 191.15 of the long-term disposal regulations. Section 191.15(a) requires

> Disposal systems for waste and any associated radioactive material shall be designed to provide a reasonable expectation that, for 10,000 years after disposal, undisturbed performance of the disposal system shall not cause the annual committed effective dose, received through all potential pathways from the disposal system to any member of the public in the accessible environment, to exceed 15 mrems (150 microsieverts).

Undisturbed performance (UP) is defined in Part 191 Subpart B to mean "the predicted behavior of a disposal system, including consideration of the uncertainties in predicted behavior, if the disposal system is not disrupted by human intrusion or the occurrence of unlikely natural events" (40 CFR § 191.12, U.S. EPA 1993). The CCA and CRA-2004, Chapter 6.0, Section 6.3.1 provide a description of UP, the conceptual models associated with UP, and the screening of features, events, and processes (FEPs) that are important to UP.

The method used to evaluate compliance with the individual protection requirements is related to that developed for assessing compliance with the containment requirements. This method has not changed since the CCA. If the evaluation of the UP scenario considered for the containment requirements shows contaminants will reach the accessible environment, the resulting dose to exposed individuals must be calculated and compared to the 15 mrem annual committed effective dose specified in section 191.15.

Further guidance on the implementation of the individual protection requirements is found in 40 CFR Part 194. 40 CFR § 194.51 (U.S. EPA 1996) states,

> Compliance assessments that analyze compliance with § 191.15 of this chapter shall assume that an individual resides at the single geographic point on the surface of the accessible environment where that individual would be expected to receive the highest dose from radionuclide releases from the disposal system.

40 CFR § 194.52 (U.S. EPA 1996) states,

> In compliance assessments that analyze compliance with § 191.15 of this chapter, all potential exposure pathways from the disposal system to individuals shall be considered. Compliance assessments with part 191, subpart C and § 191.15 of this chapter shall assume that individuals consume 2 liters per day of drinking water from any underground sources of drinking water in the accessible environment.

In addition, 40 CFR § 194.25(a) (U.S. EPA 1996) provides criteria related to the assumptions that should be made when undertaking dose calculations:

> Unless otherwise specified in this part or in the disposal regulations, performance assessments and compliance assessments conducted pursuant to the provisions of this part to demonstrate compliance with § 191.13, § 191.15 and part 191, subpart C shall assume that characteristics of the future remain what they are at the time the compliance application is prepared, provided that such characteristics are not related to hydrogeologic, geologic or climatic conditions.

IGP-2.1 Compliance Assessment of Undisturbed Performance

Section 194.52 specifies that compliance assessments shall consider "all potential pathways from the disposal system to individuals." The DOE has considered the following potential pathways for groundwater flow and radionuclide transport:

- Existing boreholes, as required by 40 CFR § 194.55(b)(1) (U.S. EPA 1996)
- Potential boreholes, including those that may be used for fluid injection, as required by 40 CFR § 194.32(c) (U.S. EPA 1996) and 40 CFR § 194.54(b)(2) (U.S. EPA 1996)

After considering all of these pathways, the DOE found that contaminated brine may migrate away from the waste-disposal panels if pressure within the panels is elevated by gas generated from corrosion or microbial degradation. Two credible pathways by which radionuclides could reach the accessible environment have been identified.

1. Radionuclide transport may occur laterally, through the anhydrite interbeds toward the subsurface boundary of the accessible environment in the Salado Formation (hereafter referred to as the Salado).

2. Transport may occur through access drifts or anhydrite interbeds (primarily Marker Bed [MB] 139) to the base of the shafts. If the pressure in the panels is greater than the lithostatic pressure of the overlying strata, contaminated brine may migrate up the shafts. As a result, radionuclides may be transported directly to the ground surface or laterally away from the shafts, through permeable strata, such as the Culebra Dolomite Member of the Rustler Formation (hereafter referred to as Culebra), toward the subsurface boundary of the accessible environment.

These conceptual release pathways for UP are illustrated in Appendix PA-2014, Figure PA-8. The modeling system described in Appendix PA-2014, Section PA-2.3.1 does not preclude potential radionuclide transport along other pathways, such as migration through Salado halite. However, the natural properties of the undisturbed system make radionuclide transport to the accessible environment via these other pathways unlikely.

Although both pathways are possible, the PA modeling indicates that under undisturbed conditions, only the first is a potential pathway during the 10,000-year period of interest specified in the regulation (see Appendix PA-2014, Section PA-7.2).

The DOE has used the modeling system applied to the PA to make this determination. Scenario screening for the UP is described in Appendix SCR-2014. As specified by section 194.54(b)(2), Appendix SCR-2014 identifies activities that may occur in the vicinity of the disposal system prior to or soon after disposal, and documents which of these are included in the compliance assessment calculations. The CRA-2004, Chapter 6.0, Section 6.2, Table 6-8 identifies FEPs included in the UP modeling; these FEPs remain unchanged for the CRA-2014. Appendix SCR-2009also identifies new FEPs that were considered, but are not identified as UP. Therefore there are no new FEPs that were identified as UP in the CRA-2014.

As specified by 40 CFR § 194.55(a), uncertainty in the performance of the compliance assessment is documented in the CRA-2004, Chapter 6.0, Section 6.1.2. Probability distributions for uncertain disposal system parameter values used in the compliance assessment were developed and are documented in Kicker and Herrick (Kicker and Herrick 2013), which identifies sampled parameters used in the compliance assessment for the CRA-2014.

For the CCA compliance assessment and all CRAs, 300 realizations of the modeling system are generated to evaluate UP. These 300 realizations are composed of three sets of 100 realizations, each generated using the Latin hypercube sampling method. None ofthe 300 realizations show any radionuclides reaching the top of the Salado through the sealed shafts.

In the CCA evaluation, 9 of the 300 realizations show concentrations of radionuclides greater than 0 reaching the accessible environment through the anhydrite interbeds. None of the remaining 291 realizations show radionuclides reaching the accessible environment through the anhydrite interbeds during the 10,000-year period (a realization is considered to have a negligible release if it is less than 1×10^{-18} curies per liter [Ci/L]). The maximum concentrations of radionuclides calculated by the modeling evaluation as reaching the accessible environment in the nine nonzero CCA realizations are shown in Table IGP-1. The full range of estimated values for radionuclide concentrations in the CCA evaluation is from negligible (less than 1×10^{-18} Ci/L) to the values shown in Table IGP-1. The

maximum concentration values shown in Table IGP-1 occur 10,000 years aft er the time of decommissioning.

The maximum concentrations of radionuclides calculated by the CRA-2004, CRA-2009 and CRA-2014 evaluations that reach the accessible environment are also shown in Table IGP-1. In the CRA-2004 evaluation, only 1 of the 300 realizations shows concentrations of radionuclides greater than 0 reaching the accessible environment through the anhydrite interbeds (see Appendix PA-2004, Section PA-7.2). The remaining 299 realizations show no radionuclides reaching the accessible environment during the 10,000-year period. As with the CRA-2004 evaluation, the CRA-2009 evaluation shows that 1 of the 300 realizations results in concentrations of radionuclides greater than 0 reaching the accessible environment through the anhydrite interbeds (Ismail 2008). All of the remaining 299 realizations show no radionuclides reaching the accessible environment during the 10,000-year period. In the CRA-2014 evaluation, there were no realizations that required calculating a release concentration. Therefore all 300 realizations have no radionuclides (0 concentration) that reach the accessible environment (Kim and Camphouse 2013; see also Appendix PA-2014, Section PA-7.2).

As with all previous CRAs, the CCA dose calculations are bounding for the CRA-2014 evaluation. There were no vectors in the undisturbed scenario that passed the PA screening criteria such that all vectors had zero concentrations of actinides in the anhydrite interbeds at the accessible environment; no new dose calculations are necessary. The Nuclide Transport System (NUTS) PA computer code is used to determine releases to the WIPP boundary. It screens each vector based on a tracer concentration approach that assumes 1 kilogram (kg) of a radionuclide source is in the repository. If the calculated concentration of this radionuclide is above 1 x 10^{-7} kilograms per cubic meter (kg/m^3) at the boundary, it is screened in and a complete transport calculation is run for that vector with the actual radionuclide source information. None of the CRA-2014 vectors passed this screening.

It is important to understand that the magnitude of all the computed releases reported in Table IGP-1 is smaller than the effective numerical precision of the transport calculations. As explained in Lowry (Lowry 2005) and Ismail and Nemer (Ismail and Nemer 2008), the values for the single vector showing nonzero concentrations are believed to be the result of numerical dispersion inherent in the NUTS finite-difference solution method. The magnitude of the nonzero releases is indicative of numerical dispersion resulting from the coarse grid spacing between the repository and the LWB, rather than containment transport.

IGP-2.2 Dose Calculation

As quoted earlier, section 194.51 states that dose must be estimated for an individual who resides at the location in the accessible environment where that individual would be expected to receive the highest exposure to radionuclide releases from the disposal system. All potential pathways for exposure associated with the UP of the repository must be assessed (section 194.52).

Table IGP- 1 Maximum Concentrations of Radionuclides Within the Salado Interbeds at the Disposal System Boundary for the CCA and CRA Analyses

CCA Realization No.	Vector No.[a]	Maximum Concentrations (Ci/L)				
		^{241}Am	^{239}Pu	^{238}Pu	^{234}U	^{230}Th
1	Replicate 1 Vector 46	1.36×10^{-17}	4.33×10^{-12}	Negligible[b]	5.82×10^{-13}	2.10×10^{-14}
2		Negligible	5.13×10^{-14}	Negligible	6.77×10^{-15}	1.89×10^{-17}

	Replicate 2 Vector 16					
3	Replicate 2 Vector 25	Negligible	1.35×10^{-15}	Negligible	1.65×10^{-16}	7.00×10^{-18}
4	Replicate 2 Vector 33	1.32×10^{-17}	7.18×10^{-14}	Negligible	9.76×10^{-15}	9.36×10^{-16}
5	Replicate 2 Vector 81	Negligible	6.23×10^{-18}	Negligible	Negligible	Negligible
6	Replicate 2 Vector 90	Negligible	5.20×10^{-16}	Negligible	7.40×10^{-17}	Negligible
7	Replicate 3 Vector 3	3.50×10^{-18}	3.08×10^{-13}	Negligible	4.32×10^{-14}	1.07×10^{-16}
8	Replicate 3 Vector 60	5.98×10^{-17}	7.41×10^{-14}	Negligible	9.09×10^{-15}	2.30×10^{-15}
9	Replicate 3 Vector 64	5.42×10^{-17}	5.85×10^{-12}	Negligible	7.61×10^{-13}	4.68×10^{-15}
10-300	-	Negligible	Negligible	Negligible	Negligible	Negligible
CRA-2004 Realization No.	**Vector No.**	**Maximum Concentrations (Ci/L)**				
		^{241}Am	**^{239}Pu**	**^{238}Pu**	**^{234}U**	**^{230}Th**
1	Replicate 1 Vector 82	Negligible	2.53×10^{-18}	Negligible	Negligible	Negligible
2-300	-	Negligible	Negligible	Negligible	Negligible	Negligible
CRA-2009 Realization No.	**Vector No.**	**Maximum Concentrations (Ci/L)**				
		^{241}Am	**^{239}Pu**	**^{238}Pu**	**^{234}U**	**^{230}Th**
1	Replicate 1 Vector 53	1.71×10^{-18}	3.83×10^{-13}	Negligible	1.14×10^{-15}	1.83×10^{-16}
2-300	-	Negligible	Negligible	Negligible	Negligible	Negligible
CRA-2014 Realization No.	**Vector No.**	**Maximum Concentrations (Ci/L)**				
		^{241}Am	**^{239}Pu**	**^{238}Pu**	**^{234}U**	**^{230}Th**
NA	NA	0	0	0	0	0

[a] Parameter values applied to each vector may be found in the CCA, Appendix IRES, Table IRES-2 , Table IRES-3, and Table IRES-4.

[b] Values less than 10^{-18} Ci/L are considered negligible relative to the other values and are not reported.

IGP-2.2.1 Transport Pathway

To perform the required dose calculation for the CCA, it was necessary to select possible pathways for the transport of the contaminants from the anhydrite interbeds to a receptor. The chosen pathway is an abandoned, deep borehole that intersects the contaminant plume in the accessible environment. Consistent with assumptions described in the CRA-2004, Chapter 6.0, Section 6.4.7.2, and the information provided in the CCA, Appendix DEL, the hole is assumed to have the permeability of an uncased hole filled with silty sand after the degradation of a borehole plug in the Rustler Formation (hereafter referred to as the Rustler). A pressure gradient is assumed to exist because of the pressures in the anhydrite resulting from gas generation in the repository. The pressures are assumed to be greater than hydrostatic to force contaminants up the abandoned hole to the Culebra or the Dewey Lake Red Beds Formation (hereafter referred to as the Dewey Lake). The contaminants would then be available to a receptor through a well used to supply drinking water. This conceptual transport

pathway is shown in Figure IGP-1. This is the only credible pathway that the DOE has been able to identify. As specified in 40 CFR § 194.54(b), this pathway considers the presence of an existing borehole.

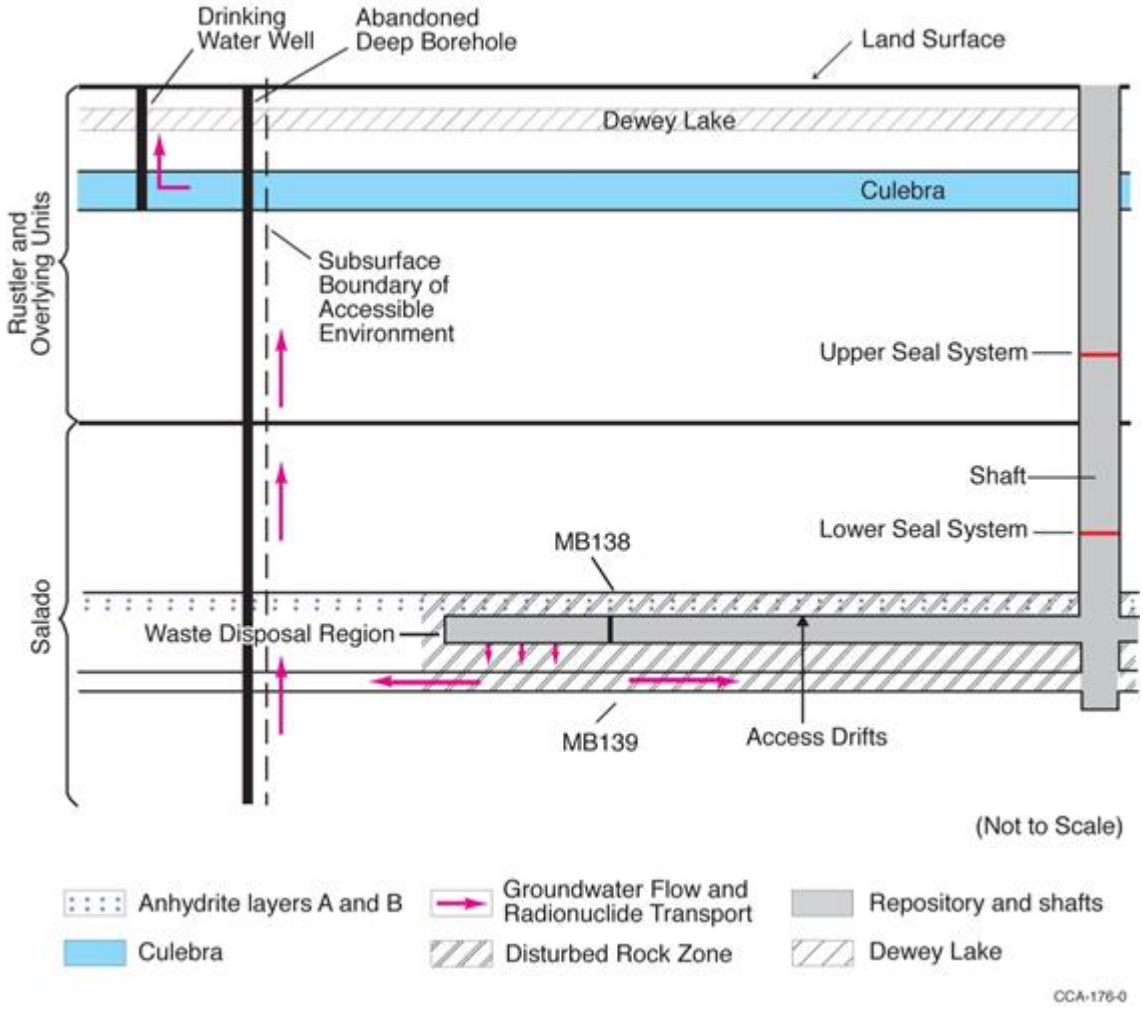

Figure IGP- 1. Conceptual Transport Pathway

IGP-2.2.2 Bounding Analysis

Uncertainty in calculating radionuclide concentrations in the anhydrite interbeds is described in the CRA-2004, Chapter 6.0, Section 6.1.2, and updated for the CRA-2014 by Kicker and Herrick (Kicker and Herrick 2013). Additional uncertainty is involved in the calculation of doses resulting from the specified exposure pathway. Given this uncertainty, the DOE elected for the CCA evaluation to perform a bounding analysis using assumptions that do not represent reality, but that would result in a bounding estimate much greater than any reasonably expected dose to a receptor. If this bounding analysis results in calculated doses to the receptor that are below the regulatory limit, compliance with the standard is demonstrated. If subsequent analyses, such as those performed to support this application, have lower initial concentrations than the bounding CCA analysis, recalculating the doses is unnecessary because the results of the original bounding analysis are below regulatory limits.

The bounding analysis used for the CCA assessment wasbased on the following factors and assumptions:

1. No specific transport mechanism was postulated. Instead, it was assumed that all contaminants reaching the accessible environment within the anhydrite interbeds during the year of maximum releases (that is, year 10,000) were available to a receptor.

2. Brine derived from the anhydrite interbeds had total dissolved solids (TDS) concentrations of about 324,000 parts per million; this represents a concentration that could not be consumed by humans. For the bounding analysis, the calculation includes the dilution of this brine by a factor of 32.4 to a TDS concentration of 10,000 parts per million.

3. The resulting annual committed effective dose was calculated based on a 50-year dose commitment. A 50-year dose commitment was selected because this period is specified in Part 191, Appendix B, and because it is the duration for which published external dose-rate conversion factors are readily available in the literature (U.S. DOE 1988).

4. The individual receptor was assumed to drink two liters of water each day (as specified in section 194.52) for one year (in accordance with the specification of an annual committed effective dose in Part 191, Appendix B).

Section 194.51 states that the DOE shall assume an individual resides at the single geographic point where that individual would receive the highest dose. With the bounding analysis, the DOE complies with the intent of this criterion, but the specific location of the receptor is not identified because all contaminants reaching the accessible environment within the anhydrite interbeds during the year of maximum releases are assumed to be directly available to the receptor, regardless of the receptor's location. The well from which the receptor drinks is assumed to be located where the contaminants reaching the anhydrite interbeds are delivered directly to the well.

The bounding analysis dose calculation was performed using the GENII-A code. The CCA, Appendix GENII describes the modeling method. GENII-A incorporates dose-calculation guidance provided in Part 191, Appendix B.

IGP-2.3 Dose Calculation Results

The maximum doses calculated from the CCA releases listed in Table IGP-1, after applying the factors and assumptions listed above, are shown in Table IGP-2. These doses are greater than any realistic doses that could be delivered to a receptor. The calculated doses are well below the regulatory standard, which is an annual committed effective dose of 15 mrem.

Table IGP- 2 Calculated Maximum Annual Committed Effective Doses for the CCA Evaluation

Realization No.	Vector No.[a]	Maximum Annual Committed Effective Dose (mrem)
1	Replicate 1 Vector 46	3.4×10^{-1}
2	Replicate 2 Vector 16	4.3×10^{-3}
3	Replicate 2 Vector 25	1.1×10^{-4}
4	Replicate 2 Vector 33	5.8×10^{-3}
5		5.1×10^{-7}

	Replicate 2 Vector 81	
6	Replicate 2 Vector 90	4.3×10^{-5}
7	Replicate 3 Vector 3	2.5×10^{-2}
8	Replicate 3 Vector 60	6.2×10^{-3}
9	Replicate 3 Vector 64	4.7×10^{-1}
10-300	-	Negligible[b]

[a] Parameter values applied to each vector may be found in the CCA, Appendix IRES, Table IRES-2 , Table IRES-3, and Table IRES-4.

[b] Doses derived from concentration values of less than 10^{-18} Ci/L are considered negligible and are not reported.

On February 26, 1997, the DOE submitted supplementary information to the EPA in response to an EPA request for additional information (Dials 1997b, Enclosure 2h). The supplementary information describes how the DOE extended its initial bounding analysis to account for exposure pathways other than direct ingestion of contaminated water by humans. Specifically, the analysis was expanded to include consumption of contaminated water by cattle (leading to the receptor's consumption of contaminated milk and beef), consumption of crops irrigated with contaminated water, and inhalation of airborne dust from soil contaminated by irrigation. The DOE found that the contribution of these pathways added 0.46 mrem per year to the calculated groundwater dose associated with the realization showing the highest concentration of radionuclides reaching the boundary of the accessible environment under undisturbed conditions of 0.47 mrem per year. Thus, the maximum total dose calculated from all pathways was 0.93 mrem per year, well below the 15-mrem-per-year standard.

Given that the maximum concentration of radionuclides shown to reach the accessible environment for the CRA-2014 analysis is zero, resulting potential doses to the receptor would be below the 15-mrem standard. For the CRA-2014, the dose would be zero. As such, the CCA dose calculation bounded any possible dose to a receptor for the CRA-2014 evaluation.

IGP-2.4 Statistical Assessment

40 CFR § 194.55(d) specifies that the "number of estimates generated pursuant to paragraph (c) of this section shall be large enough such that the maximum estimates of doses and concentrations generated exceed the 99th percentile of the population of estimates with at least a 0.95 probability." The probability that an individual estimate is below the 99th percentile is, by definition, 0.99. This means that only 1 in 100 estimates would have a value exceeding the 99th percentile, or conversely, 99 times out of 100 the estimate would have a value below the 99th percentile. It follows that for 2 independent estimates, the probability of both estimates having a value below the 99th percentile is equal to the product (0.99)(0.99), or $(0.99)^2$, and that for n estimates, the probability that all estimates have a value below the 99th percentile is equal to $(0.99)^n$. To ensure a value exceeds the 99th percentile with a specified probability, the complement $(1 - 0.99^n)$ is used to calculate the number of estimates required.

The probability specified by section 194.55(d) is 0.95, or 95% confidence, that the maximum estimates of doses and concentrations generated exceed the 99th percentile of the population of estimates. Therefore, the following equation can be solved for n, and the number of estimates required is

$1 - 0.99^{n} = 0.95$ or $(n)\log(0.99) = \log(0.05)$ (IGP.1)

which implies $n > 298$.

The solution requires n to be greater than 298 and was used to determine that 300 realizations of the modeling system is a sufficient number to meet the confidence level specified in section 194.55(d).

The 300 realizations of the modeling system (as described in Section IGP-2.1) report concentrations of radionuclides reaching the accessible environment within the Salado anhydrite interbeds and not doses to a receptor, as specified by section 194.55(d). Nevertheless, the maximum possible resulting annual dose to an individual for the CCA analysis is 0.93 mrem, the sum of 0.47 mrem (as reported in Table IGP-2) plus the additional value of 0.46 mrem determined to be contributed through additional dose pathways. All other calculated doses resulting from the 300 realizations of the modeling system for the CCA, and all subsequent CRA evaluations, are below this value.

40 CFR § 194.55(f) specifies that the DOE shall

> document that there is at least a 95 % level of statistical confidence that the mean and the median of the range of estimated radiation doses and the range of estimated radionuclide concentrations meet the requirements of § 191.15 and part 191, subpart C of this chapter, respectively.

The DOE has developed a bounding analysis that exceeds the mean and median doses, providing greater than 95% confidence that all potential doses will be below the 0.93 mrem value.

IGP-2.5 Parameter Values

Parameter values applied to the CCA modeling assessment for UP are described in the CCA, Appendix PAR and Chapter 8.0, Section 8.1.5. Parameters used in the PA and compliance assessment modeling program for the CRA-2014 are described in Kicker and Herrick (Kicker and Herrick 2013). As required by 40 CFR § 194.55(b), Kicker and Herrick (Kicker and Herrick 2013) also identify the probability distributions for these parameters, their units, the models and codes in which the parameters are used, the functional form of the probability distributions used for the sampled parameters, and associated input data.

IGP-2.6 Summary of Compliance with the Individual Protection Standard

In performing the compliance assessment, the DOE applied a bounding-analysis approach using conservative assumptions that overestimate potential doses and contaminant concentrations. This conservative approach assumes that all contaminants reaching the accessible environment are directly available to a receptor. Using this very conservative approach, the calculated maximum potential dose to an individual from the CCA evaluation would be about one-sixteenth of the individual protection standard. Given that modeled maximum radionuclide concentrations in the accessible environment for all CRA evaluations are well below those of the CCA evaluation, the CCA results are bounding and continued compliance with the individual protection standard is demonstrated.

IGP-3.0 Groundwater Protection Requirements

The groundwater protection requirements are contained in Part 191 Subpart C. In particular, 40 CFR § 191.24(a)(1) requires the following:

> *General.* Disposal systems for waste and any associated radioactive material shall be designed to provide a reasonable expectation that 10,000 years of undisturbed performance after disposal shall not cause the levels of radioactivity in any underground source of drinking water, in the accessible environment, to exceed the limits specified in 40 CFR Part 141 as they exist on January 19, 1994.

40 CFR Part 141 specifies the National Primary Drinking Water Standards. The limits for radioactivity and dose equivalent based on the January 19, 1994 National Primary Drinking Water Standards are:

1. Combined ^{226}Ra and ^{228}Ra (40 CFR § 141.15(a)): 5 pCi/L

2. Gross alpha particle activity, including ^{226}Ra but excluding radon (Rn) and uranium (U): 15 pCi/L

3. Annual dose equivalent to the total body or any internal organ from the average annual concentration of beta particle and photon radioactivity from man-made radionuclides: 4 mrem per year

In addition, 40 CFR § 194.53 (U.S. EPA 1996) applies to the DOE's consideration of USDWs. The criterion specifies

> In compliance assessments that analyze compliance with part 191, subpart C of this chapter, all underground sources of drinking water in the accessible environment that are expected to be affected by the disposal system over the regulatory time frame shall be considered. In determining whether underground sources of drinking water are expected to be affected by the disposal system, underground interconnections among bodies of surface water, groundwater, and underground sources of drinking water shall be considered.

To assess compliance with these provisions of the regulations, it is first necessary to identify if any USDWs are located near the WIPP disposal system. The DOE's evaluation of whether any USDW is located near the WIPP disposal system is provided in the CCA, Appendix USDW, and is summarized in the CCA, Chapter 8.0, Section 8.2.2. In developing the CRA-2004 and the CRA-2009, the DOE reevaluated the presence of USDWs near the WIPP disposal system and supplemented the information presented in the CCA, Appendix USDW. These reviews and associated supplemental information are provided in Appendix IGP-2009, Section IGP-3.1. For the CRA-2014, the DOE has again reevaluated the presence of USDWs near the WIPP disposal system. Supplemental information is provided in Section IGP-3.2. Based on this reevaluation, the DOE again concludes that no deviation from the CCA findings and conclusions is warranted.

IGP-3.1 Criteria for USDW Determination

In evaluating the presence of any USDW, it is necessary to establish criteria for water quality and quantity data from wells in the vicinity of the WIPP disposal system. The criteria must be based on the regulatory definition of a USDW, as provided in 40 CFR § 191.22 (U.S. EPA 1993). A USDW is defined in section 191.22 to mean an aquifer or its portion that

> (1) Supplies any public water system; or
> (2) Contains a sufficient quantity of groundwater to supply a public water system; and
> (i) Currently supplies drinking water for human consumption; or
> (ii) Contains fewer than 10,000 milligrams of total dissolved solids per liter.
> "Public water system" means a system for the provision to the public of piped water for human consumption, if such system has at least fifteen service connections or regularly serves at least twenty-five individuals. Such term includes:

(1) Any collection, treatment, storage, and distribution facilities under control of the operator of such system and used primarily in connection with such system; and

(2) Any collection or pretreatment storage facilities not under such control which are used primarily in connection with such system.

"Total dissolved solids" means the total dissolved (filterable) solids in water as determined by use of the method specified in 40 CFR Part 136.

Criteria based on these definitions were developed by the DOE and are used to assess the presence of any USDW near the WIPP disposal system. These criteria are defined in the sections that follow.

IGP-3.1.1 Groundwater Quantity

Since there are no public water systems in the WIPP vicinity, any possible USDW must meet the 40 CFR 191.22(2)(i) or (ii) requirements. Three subcriteria have been identified by the DOE and applied to these USDW requirements.

1. An aquifer or its portion must be capable of producing water at an adequate rate.

2. An aquifer or its portion must be capable of producing water for a sufficient duration.

3. An aquifer must contain fewer than 10,000 milligrams per liter (mg/L) of TDS.

Water-consumption information was evaluated by the DOE to define the first subcriterion (the ability to produce at an adequate rate). The value to be applied is determined by obtaining the following information:

1. The rate, over a 24-hour period, at which water is consumed by 15 service connections

2. The rate, over a 24-hour period, at which water is consumed by 25 individuals

To define a USDW, the lower of these two values is assigned by the DOE to the first subcriterion. Based on calculations presented in the CCA, Appendix USDW, a quantity of 5 gallons per minute (gpm) was assigned as the first subcriterion.

In updating these calculations for the CRA-2004 and CRA-2009, more current census data and water consumption data were obtained. The results of these calculations are found in Appendix IGP-2009, Section IGP-3.1.1. The results supported the continued use of the 5 gpm subcriteria rate. Data relating to the subcriteria rate were again reviewed for the CRA-2014 to ensure new information was consistent with the previous calculations. New census data were used; however, newer water consumption data were not available. The latest census data, the census data used in the CRA-2009, and the most current consumption data are shown in Table IGP-3.

Table IGP- 3 Per Person Household and Water Consumption Values Evaluated in the CRA-2014

Community	Persons Per Household, 2011[a] (CRA-2014)	Persons Per Household, 2001[b] (CRA-2009)	Gallons Per Capita Per Day[b]
Artesia	2.61	2.81	344
Carlsbad	2.51	2.56	271
Hobbs	2.72	2.82	257
Lovington	2.80	3.25	235

Roswell	2.58	2.58	256
Average	2.64	2.80	273

Sources: [a] U.S. Bureau of Census 2013; [b] CRA-2009, Appendix IGP, Table IGP-7

The rate derived based on 15 service connections is approximately twice the rate of that derived from 25 individuals (Appendix IGP-2009, Section IGP-3.1.1). This is because 15 service connections with 2.80 persons per household give a rate based on 42 individuals. Therefore, only the rate based on 25 individuals is necessary. Multiplying 273 gallons per capita per day times 25 people and converting to gallons per minute yields a rate of 4.74 gpm. Since the per capita data are the same as those used in the CRA-2009, this lower rate has not changed. Based on this information, it is concluded that applying the 5-gpm subcriterion is still valid for a bounding analysis. No change in this subcriterion is warranted as a result of applying the most current census data.

The definition of the second quantity subcriterion (the acceptable production duration of a well) is more subjective. Because the creation of a public water supply system involves considerable capital expense, it is reasonable to assume that such a water system would not be constructed unless the water source would continue to be available for some time, at least long enough to recover the capital expense. The Rural Utility Service of the U.S. Department of Agriculture provides loans to fund new rural water supply systems. The loan periods are generally 40 years in duration. Based on this, a duration of 40 years is applied by the DOE to the second quantity subcriterion. This is the same assumption that has been used since the CCA.

IGP-3.1.2 Groundwater Quality

A criterion of 10,000 mg/L of TDS is specified in section 191.22. Any aquifer or its water-producing portion with TDS concentrations below this level is determined to produce water that meets the quality criterion for a USDW. Any aquifer or its water-producing portion with TDS concentrations at or above this level is determined to produce water that does not meet the quality criterion and the regulatory definition of a USDW.

IGP-3.2 Comparison with USDW Determination Criteria

Previous analyses of water quality in the WIPP site characterization and groundwater investigation wells have determined that there are wells with groundwater TDSs below 10,000 mg/L in the WIPP vicinity. The WIPP vicinity is the area where these WIPP wells are located outside of the WIPP LWB. The WIPP LWB is the regulatory compliance point for individual and groundwater protection. Although for conservatism the DOE assumes there is a USDW at the WIPP boundary, analyses of available data concluded that no wells within the WIPP and at the boundary meet the criteria or definition of a USDW. These analyses are document in Appendix IGP-2009, Section IGP-3.2. There were no new wells drilled at new locations in the WIPP vicinity, only replacement wells (information on these wells are provided in Appendix HYDRO-2014, Section HYDRO-4.0). As such, there is no new information to assess for a USDW determination. No additional investigations were performed as part of the CRA-2014. Based on this review, no modification of the USDW determinations reported in the CCA, Appendix USDW is warranted. The DOE continues to conclude that there are no USDWs at the WIPP accessible boundary; however, in the vicinity of the WIPP disposal system, USDWs are present in the Culebra, and potential USDWs are present in the Dewey Lake and the Santa Rosa.

IGP-3.3 Comparison with the Limits Found in 40 CFR 141 as they Existed on January 19, 1994

To provide additional assurance of the safety of the WIPP disposal system, the DOE prepared a bounding assessment of the concentrations of contaminants that could occur in a nearby USDW. Bounding doses that could be received by drinking from the USDW are also calculated. As with the individual protection standard, the analysis is bounding; the results illustrate the maximum, yet unrealistic, concentrations of contaminants in a hypothetical USDW and the maximum, yet unrealistic, resulting doses. As with the dose calculations, maximum concentrations were summed to develop concentrations for comparison with the limits found in 40 CFR 141 as they existed on January 19, 1994. The conclusions of this work, provided below, illustrate that the consequences of the undisturbed repository are negligible, even when conservative assumptions are applied to the performance evaluation. Because a hypothetical USDW is assumed to exist at the site boundary in these analyses, the results of the bounding analysis support the position that additional characterization of groundwater near the WIPP disposal system to make a more definitive USDW determination is not warranted.

IGP-3.3.1 Transport Pathway

Section IGP-2.2.1 describes the transport pathway assumed for the bounding analysis performed to evaluate compliance with the individual protection standard. This same transport pathway is assessed to evaluate compliance with the groundwater protection standard.

This pathway assumes that a hypothetical USDW is located where the maximum possible concentration of radionuclides could be realized in the USDW and the maximum possible dose to an individual who drinks from the USDW could be delivered to the individual. As such, the analysis bounds the section 194.53 criterion specifying that the DOE must consider underground interconnections among bodies of surface water, groundwater, and USDWs.

IGP-3.3.2 Combined 226Ra and 228Ra

The modeling system employed to simulate the performance of the undisturbed repository tracks the transport of the most important radionuclides to releases in the accessible environment (see Appendix PA-2014, Section PA.2.1.3). These radionuclides, listed in Table IGP-1, are americium-241 (^{241}Am), plutonium-239 (^{239}Pu), ^{238}Pu, ^{234}U, and thorium-230 (^{230}Th). They do not include ^{226}Ra or ^{228}Ra because these radionuclides are not a prevalent component of the projected inventory (Kicker and Zeitler 2013). However, an analysis of ^{226}Ra and ^{228}Rais required to evaluate compliance with the groundwater protection standard.

To perform the bounding analysis for previous CRAs, the results of a NUTS code tracer exercise were used to scale the anticipated releases of ^{226}Ra and ^{228}Ra. The tracer exercise would screen in any vector with an initial 1 kg/m^3 concentration of radionuclides in the repository that resulted in a concentration at the accessible environment boundary with a concentration greater than 1.0×10^{-7} kg/m^3. By applying this scaling factor to the quantity of ^{226}Ra and ^{228}Ra projected to be emplaced in the repository, it was determined and reported in the CRA-2004 that the maximum concentration of these radionuclides in the accessible environment is 0.07 pCi/L (Wagner 2003), which is below 5 pCi/L.

This concentration was calculated by transporting the passive tracer in the flow field generated using the BRAGFLO code for Realization 1 (Replicate 1, Vector 82), shown in Table IGP-1. The calculation uses the mass and activity loads for ^{226}Ra and ^{228}Ra in the radionuclide inventory at closure and at 10,000 years. These values are provided in Table IGP-4. The ORIGEN 2.2 code was used to calculate the activity loads at 10,000 years; these loads are 51.43 curies (Ci) of ^{226}Ra in contact-handled transuranic (CH-TRU) and remote-handled transuranic (RH-TRU) waste and 7.95 Ci of ^{228}Ra in CH-TRU and RH-TRU waste. The calculated concentration is based on the volume of brine, 5,577 cubic meters (169,924 cubic feet), in the repository at time zero in the BRAGFLO calculation.

Table IGP- 4 Total Inventory and Mass Loading of ^{226}Ra and ^{228}Ra Reported in the CRA-2004

Radionuclide	Waste Type	Total Inventory at Closure (Ci)	Total Inventory at 10,000 Years (Ci)	Mass Loading (kg)
226Ra	CH	6.28 × 100	4.98 × 101	6.35 × 10-3
226Ra	RH	4.99 × 10-5	1.63 × 100	5.05 × 10-8
228Ra	CH	7.63 × 100	7.70 × 100	2.81 × 10-5
228Ra	RH	2.51 × 10-1	2.54 × 10-1	9.23 × 10-7

Source: (Fox 2003)

The total concentration (CH-TRU and RH-TRU) of either ^{226}Ra or ^{228}Ra at 10,000 years at the accessible environment boundary was calculated using the following steps:

1. Calculate the total mass load at 10,000 years by multiplying the total mass load at decommissioning by the ratio of activity loadings at 10,000 years and decommissioning, respectively.

2. Calculate the total mass concentration at the accessible environment boundary by dividing by the value of brine from the BRAGFLO simulation and multiplying by the NUTS scaling factor.

3. Convert to total concentration of activity at the accessible environment boundary by multiplying by the ratio of activity loading to mass loading at decommissioning.

4. Divide the concentration by the dilution factor 32.4 (see Section IGP-2.2.2).

The 0.07 pCi/L maximum concentration calculated for the CRA-2004 occurs in the anhydrite interbeds within the Salado and not in a zone that could realistically be a source of drinking water.

In the CCA, this value is reported as 2 pCi/L. During the PAVT (U.S. DOE 1997), it was determined that the CCA calculation used an inappropriate brine volume value and failed to account for the dilution factor. Accordingly, the PAVT analysis shows that the correct value that should have been reported in the CCA is 0.14 pCi/L (Dials 1997a).

For the CRA-2009, a new derivation concept was applied to demonstrate that the combined ^{226}Ra and ^{228}Ra concentrations were below the regulatory limit of 5 pCi/L over the 10,000-year performance period (Ismail and Nemer 2008). The new method better represented the actinide concentration at the LWB because it did not use the cumulative tracer scaling factor. Current PA calculations do not explicitly track Ra concentrations in the groundwater, so an alternate method was first used in the

CCA to derive conservative estimates of potential Ra concentrations at the LWB. This method was also used in the CRA-2004. The original method overestimated the potential Ra concentration because the estimates used a cumulative scaling factor. An alternate method was chosen that is more consistent with the methods used to calculate actinide concentrations in PA.

As described in Section IGP-2.1, Ismail (Ismail 2008) identifies only one vector in the CRA-2009 PA that had nonzero releases at the LWB. Replicate 1, Vector 53 showed a tracer concentration in the MB at the LWB of 1.24×10^{-4} kg/m^3 (Ismail 2008). The maximum concentrations of radionuclides at the LWB during the 10,000-year regulatory period are shown in Table IGP-1.

As stated above, the Ra concentration was not previously calculated in PA. However, a new analysis was performed using the current PA methods and including Ra. The analysis shows a maximum ^{226}Ra concentration of 1.7×10^{-5} pCi/L for the CRA-2009 PA and 6.5×10^{-7} for the CRA-2004 PABC. These concentrations of ^{226}Ra are more than five orders of magnitude below the regulatory limit of 5 pCi/L (Ismail 2008).

For the CRA-2014, no Ra concentration was calculated or predicted. No vectors passed the NUTS screening for the undisturbed scenario such that there were no radionuclide concentrations above zero at the accessible boundary (Kim and Camphouse 2013). Based on this information, continued compliance with the combined ^{226}Ra and ^{228}Ra standard is demonstrated.

IGP-3.3.3 Gross Alpha Particle Activity Including 226Ra but Excluding Rn and U

For the CCA evaluation, compliance with the groundwater protection standard was assessed by summing the maximum concentration values provided in Table IGP-1 for ^{241}Am, ^{239}Pu, ^{238}Pu, and ^{230}Th and adding the CCA value for ^{226}Ra obtained to perform the section IGP-3.3.2 assessment. The value obtained by this method is 7.81 pCi/L, which is below the section groundwater protection standard of 15 pCi/L. This concentration occurs in the anhydrite interbeds within the Salado and not in a zone that could realistically be a source of drinking water.

For the CRA-2004 evaluation, the only contributing radionuclide was ^{239}Pu, with a concentration of 2.53×10^{-6} pCi/L. This value, summed with the 0.07-pCi/L value derived for the section IGP-3.2.2 assessment, was essentially 0.07 pCi/L, well below the 15-pCi/L standard.

For the CRA-2009 evaluation, there were four contributing radionuclides with a total concentration of 3.84×10^{-1} pCi/L (Table IGP-1). As with the CRA-2004 analysis, this value, when summed with the 1.7×10^{-5} pCi/L value derived for the section IGP-3.2.2 assessment, remains essentially 3.84×10^{-1} pCi/L, well below the 15-pCi/L standard.

As described above, no contribution from ^{226}Ra is expected. The gross alpha particle activity including ^{226}Ra and excluding Rn and U is expected to be zero.

For the CRA-2014, no radionuclide concentrations are expected at the boundary over the regulatory time frame for the undisturbed scenario. As such, no additional analyses were performed. The gross alpha particle activity, including ^{226}Ra and excluding Rn and U, is again expected to be zero.

Continued compliance with the Gross Alpha Particle Activity Including ^{226}Ra But Excluding Rn and U standard is demonstrated.

IGP-3.3.4 Annual Dose Equivalent to the Total Body or Any Internal Organ from the Average Annual Concentration of Beta Particle and Photon Radioactivity from Man-made Radionuclides

To assess compliance with the total annual dose to the total body or any internal organ standard, an annual dose equivalent of 4 mrem per year, the transport of ^{239}Pu, ^{238}Pu, ^{234}U, and ^{230}Th was evaluated. The maximum annual committed effective dose calculated for the CCA evaluation from any of these radionuclides was 0.93 mrem, which is the value reported for transport through MB 139 and is well below the regulatory standard. The 0.93 mrem value includes alpha particle radioactivity, as well as beta particle and photon radioactivity. Thus, the value is very conservative, as the 4-mrem annual dose equivalent limit is only for beta particle and photon radioactivity.

By comparison, the maximum radionuclide concentration in the accessible environment calculated for the CRA-2004 evaluation was six orders of magnitude less than the maximum bounding value calculated for the CCA. Resulting doses for the CRA-2004 case would be correspondingly lower, as well.

For the CRA-2009 evaluation, the maximum radionuclide concentration in the accessible environment was one order of magnitude less than the maximum bounding CCA value. As such, resulting doses for the CRA-2009 case would be correspondingly lower, and continued compliance with the total annual dose to the total body or any internal organ standard is demonstrated.

The CRA-2014 calculations show that no radionuclides reach the accessible environment in the undisturbed scenario over the 10,000-year regulatory time period. As such, the CCA results continue to be bounding for the CRA-2014; continued compliance with the individual protection standard is demonstrated.

IGP-4.0 Compliance Summary

In performing the compliance assessment, the DOE applied a bounding-analysis approach using assumptions thatoverestimate potential doses and contaminant concentrations. To provide added assurance, the DOE assumed the presence of a USDW in close proximity to the WIPP LWB, even though available data indicate that none currently exists near the boundary. Using this bounding-analysis approach, the calculated maximum potential dose to an individual determined for the CCA evaluation would be about one-sixteenth of the individual protection standard.

For the CRA-2014 evaluation, the potential dose would be zero, which remains below the CCA value, and continued compliance with the individual protection standard is maintained. The potential concentrations of contaminants in the hypothetical USDW and the maximum potential dose to a receptor that drinks from the hypothetical USDW continue to be bounded by the CCA analysis.

This approach also conservatively assumes that all contaminants reaching the accessible environment are directly available to a receptor. The analysis bounds any potential impacts of underground interconnections among bodies of surface water, groundwater, and USDWs.

IGP-5.0 References

(*Indicates a reference that has not been previously submitted.)

Dials, G.E. 1997a. Letter to L. Weinstock (Subject: Summary of the EPA-Mandated Performance Assessment Verification Test Results for the Individual and Groundwater Protection Requirements). 15 September 1997. Carlsbad, NM: U.S. Department of Energy, Carlsbad Area Office. [PDF / Author]

Dials, G.E. 1997b. Letter to R. Trovato (1 Enclosure). 26 February 1997. Carlsbad, NM: U.S. Department of Energy, Carlsbad Area Office. [PDF / Author]

Fox, B. 2003. Calculation of Decayed Radionuclide Inventories for the Compliance Recertification Application (Revision 1, August 22). ERMS 530992. Carlsbad, NM: Sandia National Laboratories. [PDF / Author]

Ismail, A.E. 2008. Memorandum to the Records Center (Subject: Markerbed Concentrations for Undisturbed NUTS Scenarios in AP-132). Revision 1. ERMS 548515. Carlsbad, NM: Sandia National Laboratories. [PDF / Author]

Ismail, A.E., and M.B. Nemer. 2008. Radium-226 Concentrations in the CRA-2009 PA. ERMS 549387. Carlsbad, NM: Sandia National Laboratories. [PDF / Author]

Kicker, D.C., and C.G. Herrick. 2013. Parameter Summary Report for the 2014 Compliance Recertification Application. ERMS 560298. Carlsbad, NM: Sandia National Laboratories.* [PDF / Author]

Kicker, D.C., and T. Zeitler. 2013. Radionuclide Inventory Screening Analysis for the 2014 Compliance Recertification Application Performance Assessment (CRA-2014 PA). ERMS 559257. Carlsbad, NM: Sandia National Laboratories.* [PDF / Author]

Kim, S. and C.R. Camphouse. 2013. Marker Bed Concentrations and Radium-226 Concentrations for Undisturbed NUTS Scenario in AP-164. ERMS 559914. Carlsbad, NM: Sandia National Laboratories.* [PDF / Author]

Lowry, T.S. 2005. Analysis Package for Salado Transport Calculations: CRA-2004 PA Baseline Calculations (Revision 0). ERMS 541084. Carlsbad, NM: Sandia National Laboratories. [PDF / Author]

U.S. Bureau of the Census. 2013. 2007-2011 American Community Survey 5-Year Estimates. American FactFinder. Table GCT-1105. quickfacts.census.gov.* [PDF / Author]

U.S. Department of Energy (DOE). 1988. Internal Dose-Rate Conversion Factors for Calculation of Dose to the Public. DOE/EH-0071. Washington, DC: Office of Environmental Guidance and Compliance. [PDF / Author]

U.S. Department of Energy (DOE). 1996. Title 40 CFR Part 191 Compliance Certification Application for the Waste Isolation Pilot Plant (October). 21 vols. DOE/CAO 1996-2184. Carlsbad, NM: U.S. Department of Energy, Carlsbad Area Office. [Author]

U.S. Department of Energy (DOE). 1997. Summary of the EPA Mandated Performance Assessment Verification Test Results for Individual and Groundwater Protection Requirements (September 12). WPO 47258. Albuquerque, NM: Sandia National Laboratories. [PDF / Author]

U.S. Department of Energy (DOE). 2004. Title 40 CFR Part 191 Compliance Recertification Application for the Waste Isolation Pilot Plant (March). 10 vols. DOE/WIPP 2004-3231. Carlsbad, NM: Carlsbad Field Office. [Author]

U.S. Department of Energy (DOE). 2009. Title 40 CFR Part 191 Compliance Recertification Application for the Waste Isolation Pilot Plant (March). DOE/WIPP 09-2434. Carlsbad, NM: Carlsbad Field Office.* [Author]

U.S. Environmental Protection Agency (EPA). 1993. "40 CFR Part 191: Environmental Radiation Protection Standards for the Management and Disposal of Spent Nuclear Fuel, High-Level and Transuranic Radioactive Wastes; Final Rule." Federal Register, vol. 58 (December 20, 1993): 66398-416. [PDF / Author]

U.S. Environmental Protection Agency (EPA). 1996. "40 CFR Part 194: Criteria for the Certification and Recertification of the Waste Isolation Pilot Plant's Compliance with the 40 CFR Part 191 Disposal Regulations; Final Rule." Federal Register, vol. 61 (February 9, 1996): 5223-45. [PDF / Author]

U.S. Environmental Protection Agency (EPA). 2006. "40 CFR Part 194: Criteria for the Certification and Recertification of the Waste Isolation Pilot Plant's Compliance with the Disposal Regulations: Recertification Decision; Final Notice." Federal Register, vol. 71 (April 10, 2006): 18010-21.* [PDF / Author]

U.S. Environmental Protection Agency (EPA). 2010a. "Recertification CARD Nos. 51/52: Consideration of Protected Individual and Exposure Pathways." 2009 Compliance Recertification Application (2009 CRA) Compliance Application Review Documents (CARD) Nos. 51/52. EPA Docket FDMS Docket ID No. EPA-HQ-OAR-2009-0330 (November 18, 2010). Washington, DC: Office of Radiation and Indoor Air.* [PDF / Author]

U.S. Environmental Protection Agency (EPA). 2010b. "40 CFR Part 194 Criteria for the Certification and Recertification of the Waste Isolation Pilot Plant's Compliance with the Disposal Regulations: Recertification Decision; Final Notice." Federal Register, vol. 75 (November 18, 2010): 70584 - 595.* [PDF / Author]

Wagner, S.W. 2003. Memorandum to Cliff Hansen (Subject: Calculation of Combined 226Ra and 228Ra Concentrations at Boundary for Chapter 8 Compliance Assessment). 6 November 2003. ERMS 532804. Carlsbad, NM: Sandia National Laboratories. [PDF / Author]

Title 40 CFR Part 191
Subparts B and C

Compliance Recertification Application 2014

for the

Waste Isolation Pilot Plant

Appendix MASS-2014
Performance Assessment
Modeling Assumptions

United States Department of Energy
Waste Isolation Pilot Plant

Carlsbad Field Office
Carlsbad, New Mexico

Compliance Recertification Application 2014

Appendix MASS

Table of Contents

List of Figures

List of Tables

Table MASS-5. General Modeling Assumptions (Continued)
Table MASS-5. General Modeling Assumptions (Continued)
Table MASS-5. General Modeling Assumptions (Continued)
Table MASS-5. General Modeling Assumptions (Continued)
Table MASS-5. General Modeling Assumptions (Continued)

This page intentionally left blank.

Acronyms and Abbreviations

An actinide

CCA Compliance Certification Application

CCDF complementary cumulative distribution function

CFR Code of Federal Regulations

CH-TRU contact-handled transuranic

cm centimeters

CPR cellulosic, plastic, and rubber

CRA Compliance Recertification Application

DBR direct brine release

DOE U.S. Department of Energy

DRZ disturbed rock zone

EPA U.S. Environmental Protection Agency

FEP feature, event, and process

ft foot

in. inch

K_d Culebra matrix partition coefficient

km kilometer

lb pound

LHS Latin hypercube sample

m meter

MB marker bed

MPa megapascals

NIST National Institute of Standards and Technology

OS operating system

PA performance assessment

PABC Performance Assessment Baseline Calculation

PAIR Performance Assessment Inventory Report

PAVT Performance Assessment Verification Test

PC personal computer

PCS panel closure system

pH measure of the acidity or alkalinity of a solution

PR productivity ratio

QA quality assurance

RH-TRU remote-handled transuranic

ROM run-of-mine

ROMPCS Run-of-Mine Panel Closure System

RoR rest of repository

SMC Salado Mass Concrete

T field transmissivity field

TRU transuranic

WIPP Waste Isolation Pilot Plant

Elements and Chemical Compounds

Am americium

$CaCO_3$ calcite

CH_4 methane

Cm curium

CO_2 carbon dioxide

H_2 hydrogen

H_2S hydrogen sulfide

$Mg(OH)_2$ brucite, magnesium hydroxide

$Mg_5(CO_3)_4(OH)_2 \cdot 4H_2O$ hydromagnesite

MgO magnesium oxide

Np neptunium

Pu plutonium

Th thorium

U uranium

MASS-1.0 Introduction

This appendix presents supplementary information regarding the assumptions, simplifications, and approximations used in models that underlay the 2014 Compliance Recertification Application (CRA-2014) performance assessment (PA) of the Waste Isolation Pilot Plant (WIPP). The PA executed in support of the third WIPP recertification is denoted as the CRA-2014 PA. Within this appendix, relevant issues in the formulation or development of the various types of models (for example, conceptual, mathematical, numerical, or computer code) used for the topic under consideration in each section are discussed, and references to relevant historical information are included where appropriate. This appendix references the Compliance Certification Application (CCA) (U.S. DOE 1996), the 2004 Compliance Recertification Application (CRA-2004) (U.S. DOE 2004), and the 2009 Compliance Recertification Application (CRA-2009) (U.S. DOE 2009) when the information discussed has not changed from past demonstrations of compliance with the U.S. Environmental Protection Agency's (EPA's) disposal standards. Historical development of the WIPP conceptual models that led to the PA used in the CCA is documented in the CCA, Appendix MASS, Section MASS-2.0. Historical development of the modeling assumptions for the CRA-2004 PA is documented in Appendix PA-2004, Attachment MASS. Finally, historical development of modeling assumptions used in the CRA-2009 PA is documented in Appendix MASS-2009.

The technical baseline for the first WIPP recertification included modifications required by the EPA during its review of the CRA-2004 PA (Cotsworth 2005). These modifications resulted in a PA called the Performance Assessment Baseline Calculation (PABC), which was denoted as the CRA-2004 PABC. The PA executed in support of the second recertification, the CRA-2009 PA, included a number of technical changes and corrections, as well as updates to parameters and improvements to the PA computer codes (Clayton et al. 2008). To incorporate additional information received after the CRA-2009 PA was completed but before the submittal of the CRA-2009, the EPA requested an additional PA be undertaken, referred to as the CRA-2009 PABC (Clayton et al. 2010), which included updated information (Cotsworth 2009).

Several changes are incorporated in the CRA-2014 PA relative to the CRA-2009. The modifications included in the CRA-2014 PA include repository planned changes, parameter updates, and refinements to PA implementation. Section MASS-2.0 contains a summary of changes in PA since the CRA-2009. Section MASS-3.0 includes a discussion of general modeling assumptions applicable to the disposal system as a whole, including a table of assumptions made in PA models, with cross-references. The remainder of this appendix discusses assumptions specific to the conceptual models used in the CRA-2014 PA.

MASS-2.0 Summary of Changes in Performance Assessment

Since the CCA, there have been changes to a number of the conceptual models and processes important in assessing the performance of the WIPP. Changes for the second recertification were primarily discussed in Appendix PA-2009 and Appendix MASS-2009. Other recertification-related, EPA-mandated changes were documented in the CRA-2009 PABC (Clayton et al. 2010). The CRA-2009 PABC is the current technical baseline used to demonstrate compliance with regulatory disposal standards. Since the CRA-2009 PABC, ongoing confirmatory experiments, monitoring results, and operational practices have generated information relevant to the features, events, and processes (FEPs), modeling assumptions, and conceptual models for PA, and provided additional support to the conceptual basis of PA. Appendix MASS-2014 includes the PA implications of these ongoing investigations and results, which are incorporated in the CRA-2014 PA. Changes in this PA include the following:

1. Reassessment of FEPs

2. Results of compliance monitoring

3. Results of experimental activities

4. Assessment of model and systems changes and updates

5. Incorporation of changes included in the CRA-2009 PABC, such as

Changes to matrix partition coefficient parameters

Updated Culebra transmissivity fields (T fields)

6. Incorporation of CRA-2014 changes, including

A. Replacement of the "Option D" WIPP panel closure system (PCS) with a newly designed Run-of-Mine Panel Closure System (ROMPCS)

B. Inclusion of additional mined volume in the repository north end

C. An update to the probability that a drilling intrusion into a repository excavated region will result in a pressurized brine encounter

D. Refinement to the inundated corrosion rate of steel in the absence of carbon dioxide (CO_2)

E. Refinement to the effective shear strength of WIPP waste

F. Inventory updates

G. Updated drilling rate

H. Implementation of a more detailed repository water balance that includes magnesium oxide (MgO) hydration

I. Calculation of radionuclide concentration in brine as a function of the brine volume present in the waste panel

J. Updates to radionuclide solubilities and their associated uncertainties

K. Updated colloid enhancement parameters

7. Operational considerations

A summary of each change is presented in this section. References to appropriate sections of this appendix are provided for those changes that impact modeling assumptions. In addition, references are provided to other sections of the CRA-2014 where implementation of the changes is discussed.

MASS-2.1 FEPs Assessment

In the WIPP PA methodology (see Appendix PA-2014, Section PA-2.3), FEPs are elements used to develop the conceptual models and modeling assumptions represented in PA. The process used to develop and screen FEPs is outlined in Appendix SCR-2014, Section SCR-2.0. For the CRA-2014, a reassessment of the CRA-2009 baseline FEPs was conducted to determine whether changes in WIPP activities and conditions affected the current FEP descriptions, bases, or screening decisions. This assessment also determined whether additional or new FEPs should be included in the CRA baseline. The reassessment results are documented in Appendix SCR-2014, Section SCR-3.0 and Section 32 (Scope of Performance Assessment) of this application. Changes to the baseline FEPs include updating screening arguments with new information that has become available since the CRA-2009. No changes to PA implementation or modeling assumptions were made as a result of the FEPs reassessment. No FEPs that were previously screened out of PA calculations have been screened in for the CRA-2014 PA, and no FEPs that were previously screened in have been screened out.

MASS-2.2 Monitoring

Monitoring activities have continued since the certification of the WIPP. These activities are used to validate assumptions and PA parameters, and to detect substantial and detrimental deviation from expected repository performance. Monitoring, as discussed here, applies to the assurance requirement of 40 CFR § 191.14(b) (U.S. EPA 1993) and the monitoring criteria at 40 CFR § 194.42 (U.S. EPA 1996). Appendix MON-2014 details the monitoring program that meets these requirements. The monitoring program was assessed to determine if the results indicate that changes should be made to the monitoring program. The results did not indicate that changes were required in the context of WIPP PA (Wagner 2011). The monitoring program did, however, lead to a change in one monitored parameter used in PA: because of increased drilling in the Delaware Basin, the drilling rate parameter value used in the CRA-2014 PA has increased to comply with the requirements of 40 CFR § 194.33 (U.S. EPA 1996), as described in Section 33 of this application. No changes to modeling assumptions are necessary to account for this parameter change.

MASS-2.3 Experimental Activities

The EPA requires the recertification documentation to include an update of "additional analyses and results of laboratory experiments conducted by the Department or its contractors as part of the WIPP program" (40 CFR § 194.15(a)(3); see also 40 CFR § 194.15, U.S. EPA 1996). The following sections discuss analyses and experiments conducted to support compliance determinations. Only analyses with conclusions relevant to this recertification are discussed here.

MASS-2.3.1 Steel Corrosion Investigations

A series of steel and lead corrosion experiments has been conducted under Test Plan TP 06-02, *Iron and Lead Corrosion in WIPP-Relevant Conditions* (Wall and Enos 2006). The object of these experiments has been to determine steel and lead corrosion rates under WIPP-relevant conditions. A description of the experiments and the use of their results to determine a CRA-2014 PA update to the inundated corrosion rate of steel in the absence of CO_2 are presented in Roselle (Roselle 2013a).

MASS-2.3.2 Waste Shear Strength Investigations

WIPP PA includes scenarios in which human intrusion results in a borehole intersecting the repository. During the intrusion, drilling mud flowing up the borehole will apply a hydrodynamic shear stress on the borehole wall. Erosion of the wall material can occur if this stress is high enough, resulting in a release of radionuclides being carried up the borehole with the drilling mud. Experiments have been conducted to determine the erosive impact on surrogate waste materials that were developed to represent WIPP waste that is 50%, 75%, and 100% degraded by weight. A description of the experimental apparatus, the experiments conducted in it, and conclusions to be drawn from those experiments are discussed in Herrick et al. (Herrick et al. 2012). The use of the experimental results to determine an updated waste shear strength parameter in the CRA-2014 PA is discussed in Herrick (Herrick 2013).

MASS-2.3.3 Magnesium Oxide Investigations

Experiments have been performed to support the implementation of MgO as an engineered barrier. These experiments have characterized MgO and investigated the hydration and carbonation of MgO to confirm its ability to sequester CO_2, buffer brine pH (the measure of the acidity or alkalinity of a solution), and subsequently help establish low actinide solubilities in the repository. These activities are described in detail in Appendix MgO-2014. The CRA-2014 PA includes a more detailed repository water balance implementation that includes MgO hydration (Appendix PA-2014, Section PA-4.2.5).

MASS-2.3.4 Actinide Investigations

The U.S. Department of Energy (DOE) has continued to investigate actinide (An) speciation and solubilities since the certification of the WIPP. Since the CRA-2009, experiments to establish the microbial ecology, evaluate biodegradation of chelating agents, establish the solubility of thorium in WIPP brine, determine the effect of carbonate on uranium solubility, and assess the intrinsic, mineral, and microbial colloid enhancement parameters were completed. The current actinide experimental activities are described in Appendix SOTERM-2014, Section SOTERM-3.0. The CRA-2014 PA uses the same actinide assumptions as the CRA-2009 PABC.

MASS-2.4 Performance Assessment Models and Systems

The DOE has maintained the computational platforms used to execute the WIPP PA modeling codes. A small number of modeling tasks that feed into compliance calculations are performed on desktop personal computer (PC) workstations running the Microsoft Windows 7® operating system (OS), as well as PC-based workstations and clusters running the Red Hat Linux® OS. The WIPP PA parameter database is hosted on a Sun Microsystems Solaris® server running MySQL®. The vast majority of the WIPP PA modeling codes used directly in compliance calculations are run on the WIPP PA Alpha Cluster composed of Hewlett-Packard (formerly Compaq) AlphaServer™ systems. AlphaServers™ are built around the Alpha processor and run the OpenVMS™ OS. The current hardware and software versions used in the CRA-2014 PA calculations are shown in Table MASS-1 and Table MASS-2.

Changes have been made to the systems used to perform WIPP PA in the CRA-2014. The PA parameter database has been updated since the CRA-2009 PABC. This change was necessary to reduce dependence on aging hardware and to increase PA capabilities. Several of the codes used in WIPP PA have been updated in order to add new capabilities. Codes PREBRAG Version 8.00 and BRAGFLO Version 6.02 have been developed to incorporate the updated repository water balance implementation in the CRA-2014 PA that includes MgO hydration. Codes PRECCDFGF Version 2.0 and CCDFGF Version 6.0 have been developed to utilize radionuclide solubilities calculated over a range of brine volumes. All changes to systems used in WIPP PA are performed under the Carlsbad Field Office Quality Assurance (QA) Program implemented through the Quality Assurance Program Document (U.S. DOE 2010), and include testing, validation, and verification to ensure that there is no impact on PA implementation.

Outputs from previous certification PAs are again used in the CRA-2014 PA for those codes with unchanged input parameters. These outputs are identified in Long (Long 2013) and include the outputs of DRSPALL, MODFLOW, and SECOTP2D.

Table MASS- 1. CRA-2014 PA Codes

Code	Version	Executable	Build Date
ALGEBRACDB	2.35	ALGEBRACDB_PA96.EXE	31-01-96
BRAGFLO	6.0	BRAGFLO_QB0600.EXE	12-02-07
BRAGFLO	6.02	BRAGFLO_QB0602.EXE	11-29-12
CCDFGF	6.0	CCDFGF_QC0600.EXE	02-23-10
CUTTINGS_S	6.02	CUTTINGS_S_QA0602.EXE	09-06-05

EPAUNI	1.15A	EPAUNI_QA0115A.EXE	07-03-03
GENMESH	6.08	GM_PA96.EXE	31-01-96
ICSET	2.22	ICSET_PA96.EXE	01-02-96
LHS	2.42	LHS_QA0242.EXE	18-01-05
MATSET	9.20	MATSET_QA0920.EXE	04-01-12
NUTS	2.05C	NUTS_QA0205C.EXE	05-24-06
PANEL	4.03	PANEL_QA0403.EXE	04-25-05
PCCSRC	2.21	PCCSRC_PA96.EXE	05-23-96
POSTBRAG	4.00A	POSTBRAG_QA0400A.EXE	28-03-07
POSTLHS	4.07A	POSTLHS_QA0407A.EXE	25-04-05
PREBRAG	8.00	PREBRAG_QA0800.EXE	08-03-07
PREBRAG	8.02	PREBRAG_QA0802.EXE	11-29-12
PRECCDFGF	2.0	PRECCDFGF_QA0200.EXE	04-06-10
PRELHS	2.40	PRELHS_QA0240.EXE	04-01-12
RELATE	1.43	RELATE_PA96.EXE	06-03-96
STEPWISE	2.21	STEPWISE_PA96_2.EXE	02-12-96
SUMMARIZE	3.01	SUMMARIZE_QB0301.EXE	21-12-05

Table MASS- 2. CRA -2014 PA Hardware

Node	Hardware Type	CPU	Operating System
CCR	HP AlphaServer™ ES45	Alpha EV68	Open VMS 8.2
TDN	HP AlphaServer™ ES45	Alpha EV68	Open VMS 8.2
BTO	HP AlphaServer™ ES45	Alpha EV68	Open VMS 8.2
CSN	HP AlphaServer™ ES45	Alpha EV68	Open VMS 8.2
GNR	HP AlphaServer™ ES47	Alpha EV7	Open VMS 8.2
MC5	HP AlphaServer™ ES47	Alpha EV7	Open VMS 8.2
TRS	HP AlphaServer™ ES47	Alpha EV7	Open VMS 8.2
TBB	HP AlphaServer™ ES47	Alpha EV7	Open VMS 8.2

MASS-2.5 CRA-2009 PABC Changes

As part of its review of the CRA-2009, the EPA requested changes to the CRA-2009 PA (Cotsworth 2009). These changes included updates to the repository waste inventory, actinide solubilities, Culebra transmissivity fields, drilling parameters, and matrix partition coefficients. These changes were incorporated into the CRA-2009 PABC (Clayton et al. 2010). Repository performance with these requested changes was subsequently assessed by the EPA, and the WIPP was recertified in 2010 (U.S. EPA 2010a). The 2010 EPA recertification decision established the CRA-2009 PABC as the certified WIPP technical baseline. Changes included in the CRA-2009 PABC are shown in Table MASS-3.

Table MASS- 3. Changes Incorporated in the CRA-2009 PABC

Changes Included in the 2009 Performance Assessment Baseline Calculation		
EPA-Mandated Change	**Description of Change**	**Reference**
Inventory	Updated inventory parameters	CRA-2009 PABC Summary (Clayton et al. 2010, Section 2.1) CRA-2009 PABC Inventory Screening Analysis (Fox, Clayton, and Kirchner 2009)
Solubility Parameters	Updated baseline solubility limits for inventory actinides	CRA-2009 PABC Summary (Clayton et al. 2010, Section 2.2)
Solubility Uncertainty Ranges	Updated uncertainty ranges for actinide solubility limits	CRA-2009 PABC Summary (Clayton et al. 2010, Section 2.2)
Culebra Transmissivity Fields	Updated to include additional Culebra transmissivity data sets	CRA-2009 PABC Summary (Clayton et al. 2010, Section 2.3) Appendix HYDRO-2014, Attachment TFIELD
Drilling Parameters	Updated to include additional Delaware Basin drilling data	CRA-2009 PABC Analysis Plan (Clayton 2009a, Section 2.1.4)

Changes Included in the 2009 Performance Assessment Baseline Calculation		
EPA-Mandated Change	**Description of Change**	**Reference**
Matrix Partition Coefficients	Updated to account for higher organic ligand concentrations in the CRA-2009 PABC inventory	Justification of Updated K_d values (Clayton 2009b)

MASS-2.6 CRA-2014 PA Changes

A subset of the CRA-2009 PABC changes summarized in Table MASS-3 is also included in the CRA-2014 PA. The CRA-2014 PA uses the same Culebra transmissivity fields and matrix partition coefficients as were used in the CRA-2009 PABC. A number of additional changes are implemented in the CRA-2014 PA relative to the CRA-2009 PABC. These changes are discussed below and summarized in Table MASS-4.

MASS-2.6.1 Conceptual Model Changes

The CRA-2014 PA uses the same conceptual models as were used in the CRA-2009 PABC. No changes were made to the conceptual models used in the CRA-2009 PABC.

MASS-2.6.2 Replacement of Option D with the ROMPCS

The WIPP waste panel closures comprise a feature of the repository that has been represented in WIPP PA regulatory compliance demonstration since the CCA (U.S. DOE 1996). The 1998 rulemaking that certified the WIPP to receive transuranic (TRU) waste required the DOE to implement the Option D PCS at the WIPP. The DOE has submitted a planned change request to the EPA requesting that the EPA modify Condition 1 of the Final Certification Rulemaking for 40 CFR Part 194 (U.S. EPA 1998a) for the WIPP, and that a revised panel closure design be approved for use in all panels (U.S. DOE 2011a). The revised panel closure design, denoted as the ROMPCS, is comprised of 100 feet (ft) of run-of-mine (ROM) salt with barriers at each end. A PA was executed to quantify WIPP repository performance impacts associated with the replacement of the approved Option D PCS design with the ROMPCS (Camphouse et al. 2012). It was found that long-term WIPP performance with the ROMPCS design is similar to that seen with Option D. The ROMPCS design is implemented in the CRA-2014 PA.

MASS-2.6.3 Additional Mined Volume in the Repository North End

Following the recertification of the WIPP in November of 2010, the DOE submitted a planned change notice to the EPA that justified additional excavation to the WIPP experimental area (U.S. DOE 2011b). A performance assessment was undertaken to determine the impact of the additional excavation on the long-term performance of the facility (Camphouse et al. 2011). After reviewing the DOE proposal and written responses to questions related to the effects of increasing the mining area, the EPA found that the mining activities will not adversely impact WIPP waste handling activities, air monitoring, disposal operations, or long-term repository performance (U.S. EPA 2011). Additional excavation in the WIPP experimental area is included in the CRA-2014 PA.

MASS-2.6.4 Refinement to the Probability of Encountering Pressurized Brine

Penetration into a region of pressurized brine during a hypothetical WIPP drilling intrusion can have significant consequences with respect to releases. The WIPP PA parameter GLOBAL:PBRINE (hereafter called PBRINE) is used to specify the probability that a drilling intrusion into the excavated region of the repository encounters a region of pressurized brine below the repository. A framework that provides a quantitative argument for refinement of parameter PBRINE has been developed since the CRA-2009 PABC (Kirchner, Zeitler, and Kirkes 2012). The distribution for PBRINE that results from this framework is used in the CRA-2014 PA.

MASS-2.6.5 Refinement to the Corrosion Rate of Steel

The interaction of steel in the WIPP with repository brines results in the formation of hydrogen (H_2) gas due to anoxic corrosion of the metal. The rate of H_2 gas generation depends on the corrosion rate and the type of corrosion products formed. Experiments have been undertaken with the aim of determining steel and lead corrosion rates under WIPP-relevant conditions (see MASS-2.3.1). A description of the new experiments and the use of their results to determine an updated anoxic corrosion rate for brine-inundated steel in the absence of CO_2 are presented in Roselle (Roselle 2013a). This updated rate is used in the CRA-2014 PA.

MASS-2.6.6 Refinement to the Effective Shear Strength of WIPP Waste

WIPP PA includes scenarios in which a hypothetical human intrusion results in a borehole intersecting the repository. New experiments have been conducted to determine the erosive impact on surrogate waste materials that were developed to represent WIPP waste that is 50%, 75%, and 100% degraded by weight (see MASS-2.3.2). A description of the experimental configuration and conclusions made from the experimental results are given in Herrick et al. (Herrick et al. 2012). Based on the experimental results and analysis of existing data, Herrick (Herrick 2013) recommends a refinement to the waste shear strength parameter used in WIPP PA. The recommended refinement to this parameter is used in the CRA-2014 PA.

MASS-2.6.7 Waste Inventory Update

The waste information used in the CRA-2014 PA is updated from that used in the CRA-2009 PABC calculations. The Performance Assessment Inventory Report (PAIR) - 2012 (Van Soest 2012) was released on November 29, 2012. The PAIR - 2012 contains updated estimates to the radionuclide content and waste material parameters, scaled to a full repository, based on inventory information collected through December 31, 2011. The WIPP PA inventory parameters are updated in the CRA-2014 PA to account for this new information. Waste information in the CRA-2014 PA is discussed further in Kicker and Zeitler (Kicker and Zeitler 2013).

MASS-2.6.8 Updated Drilling Rate

The WIPP regulations require that current drilling practices be assumed when modeling hypothetical future drilling intrusions in WIPP PA. The DOE continues to survey drilling activity in the Delaware Basin in accordance with the criteria established in 40 CFR 194.33. Results for the year 2012 are documented in the 2012 Delaware Basin Monitoring Annual Report (U.S. DOE 2012). Drilling parameters are updated in the CRA-2014 PA to include information assembled through 2012 (see MASS-2.2).

MASS-2.6.9 Refinement to Repository Water Balance

The saturation and pressure history of the repository are used throughout PA. Along with flow in and out of the repository, the saturation and pressure are influenced by the reaction of materials placed in the repository with the surrounding environment. As part of the review of the CRA-2009, the EPA noted several issues for possible additional investigation, including the potential implementation of a more detailed repository water balance (U.S. EPA 2010b). The repository water balance implementation is refined in the CRA-2014 PA in order to include the major gas and brine producing and consuming reactions in the existing conceptual model and is discussed in Appendix PA-2014, Section PA-4.2.5.

MASS-2.6.10 Variable Brine Volume Implementation

To date, the minimum brine volume necessary for a direct brine release (DBR) has been used as an input to the radionuclide solubility calculation. The entire organic ligand inventory was assumed to be dissolved in the minimum necessary DBR brine volume, and the resulting organic ligand concentrations were then used in the calculation of baseline radionuclide solubilities. The trend toward increasing organic ligand content in the WIPP waste inventory has resulted in mass-balance issues when determining radionuclide solubilities from only the minimum brine volume necessary for a DBR. As a result, the calculation of baseline radionuclide solubilities is extended in the CRA-2014 so that they are dependent on the concentration of organic ligands which vary with the actual volume of brine present in the repository. Brine volumes of 1x, 2x, 3x, 4x, and 5x the minimum necessary DBR volume are used in the calculation of baseline radionuclide solubilities in the CRA-2014. The organic ligand waste inventory is assumed to be dissolved in each of these multiples of the minimum necessary brine volume. The resulting organic ligand concentrations, now dependent on a range of brine volumes, are then used to calculate baseline radionuclide solubilities corresponding to each brine volume. This approach keeps radionuclide mass constant over realized brine volumes, rather than keeping radionuclide concentration constant over realized brine volumes. Further discussion of this approach is given in Camphouse (Camphouse 2013).

MASS-2.6.11 Updated Radionuclide Solubilities and Uncertainty

The solubilities of actinide elements are influenced by the chemical components of the waste. With the release of the PAIR - 2012 (Van Soest 2012), updated information on the amount of various chemical components in the waste is available. To incorporate this updated information, parameters used to represent actinide solubilities are updated in the CRA-2014 PA. Solubilities are calculated in the CRA-2014 PA using multiples of the minimum brine volume necessary for a DBR to occur. Additional experimental results have been published in the literature since the CRA-2009 PABC, and this new information is used in the CRA-2014 PA to enhance the uncertainty ranges and probability distributions for actinide solubilities. More discussion of radionuclide solubilities and their associated uncertainties is given in Brush and Domski (Brush and Domski 2013a and Brush and Domski 2013b) and Appendix SOTERM 2014, Section SOTERM-5.0.

MASS-2.6.12 Updated Colloid Parameters

Colloid parameters are updated in the CRA-2014 PA to incorporate recently available data given in Reed et al. (Reed et al. 2013). Actinide colloid enhancement parameters were re-assessed and updated, as appropriate, to reflect recent literature and more extensive WIPP-specific data. The CRA-2014 PA contains no changes to the WIPP colloid model developed for the CCA.

MASS-2.6.13 Summary of CRA-2014 Changes

The CRA-2014 PA is updated based on new information since the CRA-2009 PABC. Information on the implementation of these changes is contained in Camphouse (Camphouse 2013), Section 2.1, and is summarized in Table MASS-4.

Table MASS- 4. Changes Incorporated in the CRA-2014

WIPP Project Change	Summary of Change and Cross-Reference
Panel Closure Design	The Option D PCS design is replaced with the ROMPCS design (Camphouse et al. 2012; Camphouse 2013).
Added Volume in the Repository Experimental Region	A volume of 60,335 cubic meters ($m^{3)}$ is added to the volume of the WIPP experimental region (Camphouse et al. 2011).
Probability of Encountering Pressurized Brine during a Drilling Intrusion	A revised distribution is used for WIPP PA parameter GLOBAL:PBRINE (Kirchner, Zeitler, and Kirkes 2012).
Refinement to Steel Corrosion Rate	A revised distribution is used for WIPP PA parameter STEEL:CORRMCO2 (Roselle 2013a).
Updated Waste Shear Strength	A revised distribution is used for WIPP PA parameter BOREHOLE:TAUFAIL (Herrick 2013).
Updated Waste Inventory Information	Inventory parameters in the CRA-2014 PA are updated to reflect information collected through December 31, 2011 (Van Soest 2012; Kicker and Zeitler 2013).
Drilling Rate	The drilling rate increased from 59.8 to 67.3 boreholes per square kilometer (km^2) over 10,000 years (Camphouse 2013).
Refined Water Balance Implementation	The repository water balance implementation is refined to include the major gas and brine producing and consuming reactions in the existing conceptual model (Camphouse 2013; Clayton 2013).
Variable Brine Volume	Radionuclide concentrations in brine are dependent on the volume of brine in the repository, rather than only the minimum brine volume of 17,400 m^3 necessary for a DBR (see MASS-2.6.10).
Radionuclide Solubilities and their Uncertainty	Radionuclide baseline solubilities are updated to reflect the organic ligand content in the CRA-2014 PA waste inventory, and are calculated using brine volumes that are multiples of 17,400 m^3. Solubility uncertainties are updated based on recently available results in published literature (Brush and Domski 2013a and Brush and Domski 2013b) and WIPP-specific data is included (SOTERM-2014, Sections SOTERM-3.0 and SOTERM-5.0).
Updated Colloid Parameters	Colloid parameters in the CRA-2014 are updated to reflect data presented in Reed et al. (Reed et al. 2013).

MASS-2.7 Operational Considerations

No operational changes that would impact modeling assumptions have been made at the WIPP since the second recertification decision. Operational changes for the emplacement of MgO in 3,000-pound (lb) or 4,200-lb supersacks on every other stack of waste were made since the CRA-2009. However, this change does not impact PA as enough MgO is always present to meet the required excess factor of 1.2. As a result, no changes were made to modeling assumptions for the CRA-2014 PA because of operational considerations.

MASS-3.0 General Assumptions in PA Models

A number of assumptions are applied generally to the disposal system through the conceptual and mathematical models implemented in the CRA-2014 PA.

Table MASS-5, which lists modeling assumptions used in the PA, is a guide to general modeling assumptions. Because many of the assumptions in that table have not changed since the CRA-2004, material submitted with the first recertification application is listed for reference. References to documents included in the CRA-2014 are also included where appropriate. Table MASS-5 provides guidance for integrating the assumptions with (1) the chapters, sections, or appendices in which they are discussed, and (2) the codes that implement them.

The FEPs discussed in Appendix SCR-2014 that are relevant to these assumptions are also indicated. The final column in the table indicates whether the DOE considers each assumption to be reasonable or conservative. The DOE has not attempted to bias the overall results of PA toward a conservative outcome. However, the DOE has chosen to use conservative assumptions where data or models are impractical to obtain, or where effects on performance are not expected to be significant enough to justify development of a more complicated model. In all other cases, best unbiased conceptual models and parameter values have been selected. The designator R (reasonable) in the final column indicates that the DOE considers the assumption to be reasonable based on WIPP-specific data or information, data or information considered analogous to the WIPP disposal system, expert judgment, or other reasoning. The designator C (conservative) indicates that the DOE considers the assumption may overestimate a process or effect that may contribute to releases to the accessible environment. The regulatory designator (Reg) indicates that the assumption is based on regulations in 40 CFR Part 191, criteria in 40 CFR Part 194, or other regulatory guidance.

Table MASS- 5. General Modeling Assumptions

Chapter or Section		Code	Modeling Assumption		

	Assumption Number			Related FEP in Appendix SCR-2014	Assumption Considered[a]
CRA-2014: MASS-3.0 General Assumptions in PA Models CRA-2014: MASS-3.1 Darcy's Law Applied for Fluid Flow calculated by BRAGFLO, MODFLOW-2000, and DRSPALL	1	BRAGFLO MODFLOW-2000	Flow is governed by mass conservation and Darcy's Law in porous media. Flow is laminar and fluids are Newtonian.	Saturated Groundwater Flow (N23) Unsaturated Groundwater Flow (N24) Brine Inflow (W40)	R
	2	BRAGFLO	Two-phase flow in the porous media is by simultaneous immiscible displacement.	Fluid Flow Due to Gas Production (W42)	R
	3	BRAGFLO	The Brooks-Corey or Van Genuchten/Parker equations represent interactions between brine and gas.	Fluid Flow Due to Gas Production (W42)	R
	4	BRAGFLO	The Klinkenberg effect is included for flow of gases at low pressures.	Fluid Flow Due to Gas Production (W42)	R
	5	BRAGFLO	Threshold displacement pressure for flow of gas into brine is constant.	Fluid Flow Due to Gas Production (W42)	R
	6	BRAGFLO MODFLOW-2000 SECOTP2D	Fluid composition and compressibility are constant.	Saturated Groundwater Flow (N23) Fluid Flow Due to Gas Production (W42)	R
CRA-2014: MASS-3.2 Hydrogen Gas as Surrogate for Waste-Generated Gas Physical Properties in BRAGFLO and DRSPALL	7	BRAGFLO DRSPALL	The gas phase is assigned the density and viscosity properties of hydrogen.	Fluid Flow Due to Gas Production (W42)	R
CRA-2014: MASS-3.3 Salado Brine as Surrogate for Liquid Phase Physical Properties in BRAGFLO	8	BRAGFLO	All liquid physical properties are assigned the properties of Salado brine.	Saturated Groundwater Flow (N23)	R

[a] R = Reasonable
C = Conservative
Reg. - Based on regulatory guidance
See above - Refers to assumptions 1 through 8 listed at the beginning of this table.

Table MASS-5. General Modeling Assumptions (Continued)

Chapter or Section	Code	Modeling Assumption	Related FEP in Appendix SCR-2014	Assumption Considered[a]
CRA-2004: 6.4.2 Model Geometries CRA-2004: 6.4.2.1 Disposal System Geometry CRA-2014: MASS-4.0 Model Geometries CRA-2014: MASS-4.1 Disposal System Geometry as Modeled in BRAGFLO	BRAGFLO	The disposal system is represented by a two-dimensional, north-south, vertical cross section.	Stratigraphy (N1) Physiography (N39)	R
	BRAGFLO	Flow in the disposal system is radially convergent or divergent centered on the repository, shaft, and borehole for disturbed performance.	Saturated Groundwater Flow (N23) Unsaturated Groundwater Flow (N24)	R
	BRAGFLO	Variable dip in the Salado is approximated by a 1 degree dip to the south.	Stratigraphy (N1)	R
	BRAGFLO	Stratigraphic layers are parallel.	Stratigraphy (N1)	R

Table MASS-5. General Modeling Assumptions (Continued)

Chapter or Section	Code	Modeling Assumption	Related FEP in Appendix SCR-2014	Assumption Considered[a]
	BRAGFLO	The stratigraphy consists of units above the Dewey Lake, the Forty-niner, the Magenta, the Tamarisk, the Culebra, the Los Medaños, and the Salado Formations (comprising impure halite, MB 138, anhydrites A and B [lumped together], and MB 139). The dimensions of these units are constant. A Castile brine reservoir is included in the BRAGFLO grid in all scenarios.	Stratigraphy (N1)	R
CRA-2004: 6.4.2.2 Culebra Geometry	MODFLOW-2000 SECOTP2D	The Culebra is represented by a two-dimensional, horizontal geometry for groundwater flow and radionuclide transport simulation.	Stratigraphy (N1)	R
	MODFLOW 2000 PEST	Transmissivity varies spatially. There is no vertical flow to or from the Culebra.	Groundwater Recharge (N54) Groundwater Discharge (N53)	R
	SECOTP2D	The regional flow field provides boundary conditions for local transport calculations (see CRA-2004, Chapter 6.0, Section 6.4.10.2).	Advection (W90)	R

[a] R = Reasonable
C = Conservative
Reg. - Based on regulatory guidance
See above - Refers to assumptions 1 through 8 listed at the beginning of this table.

Table MASS-5. General Modeling Assumptions (Continued)

Chapter or Section	Code	Modeling Assumption	Related FEP in Appendix SCR-2014	Assumption Considered[a]
CRA-2004: 6.4.3 The Repository CRA-2014: MASS-4.1 BRAGFLO Geometry of the Repository	BRAGFLO	The repository comprises five regions separated by panel closures: the waste panel, a north rest of repository (NRoR), a south RoR (SRoR) and the access drifts (separated by panel closures), the operations region, and the experimental region. A single shaft region is also modeled, and a borehole region is included for a borehole that intersects the separate waste panel. The dimensions of these regions are constant.	Disposal Geometry (W1)	R-C
	BRAGFLO	Long-term flow up plugged and abandoned boreholes modeled as if all intrusions occur into a downdip (southern) panel.	Disposal Geometry (W1)	C
	BRAGFLO	For each repository region, the model geometry preserves design volume.	Disposal Geometry (W1)	R
	BRAGFLO	Pillars, individual drifts, and rooms are not modeled for long-term performance, and containers provide no barrier to fluid flow.	Disposal Geometry (W1)	C

Table MASS-5. General Modeling Assumptions (Continued)

Chapter or Section	Code	Modeling Assumption	Related FEP in Appendix SCR-2014	Assumption Considered[a]
	BRAGFLO	Long-term flow is radial to and from the borehole that intersects the waste disposal panel during disturbed performance.	Waste-Induced Borehole Flow (H32)	R
	BRAGFLO	Disturbed rock zone (DRZ) provides a pathway to MBs.	-	R
	BRAGFLO	Grid and material properties are consistent with the ROMPCS panel closure design.	-	R

[a] R = Reasonable
C = Conservative
Reg. - Based on regulatory guidance
See above - Refers to assumptions 1 through 8 listed at the beginning of this table.

Table MASS-5. General Modeling Assumptions (Continued)

Chapter or Section	Code	Modeling Assumption	Related FEP in Appendix SCR-2014	Assumption Considered[a]
CRA-2004: 6.4.3.1 Creep Closure CRA-2014: MASS-5.0 Creep Closure CRA-2014: PORSURF	SANTOS	Creep closure is modeled using a two-dimensional model of a single room. Room interactions are insignificant.	Salt Creep (W20) Changes in the Stress Field (W21) Excavation-Induced Changes in Stress (W19)	R
	SANTOS	The amount of creep closure is a function of time, gas pressure, and waste-matrix strength.	Salt Creep (W20) Changes in the Stress Field (W21) Consolidation of Waste (W32) Pressurization (W26)	R
	BRAGFLO	Porosity of operations and experimental areas is fixed at a value representative of consolidated material.	Salt Creep (W20)	R
CRA-2004: 6.4.3.2 Repository Fluid Flow CRA-2014: MASS-6.0 Repository Fluid Flow	BRAGFLO	General assumptions 1 to 8.	-	See above
	BRAGFLO	The waste disposal region is assigned a constant permeability representative of average consolidated waste without backfill.	Saturated Groundwater Flow (N23) Unsaturated Groundwater Flow (N24)	R
CRA-2014: MASS-6.1 Flow Interactions with the Creep Closure Model	BRAGFLO	The experimental and operations regions are assigned a constant permeability representative of unconsolidated material and a constant porosity representative of consolidated material.	Saturated Groundwater Flow (N23) Unsaturated Groundwater Flow (N24) Salt Creep (N20)	C
CRA-2014: MASS-6.2 Flow Interactions with the Gas Generation Model	BRAGFLO	For gas generation calculations, the effects of wicking are accounted for by assuming that brine in the repository contacts waste to an extent greater than that calculated by the Darcy Flow model used.	Wicking (W41)	R

[a] R = Reasonable
C = Conservative
Reg. - Based on regulatory guidance
See above - Refers to assumptions 1 through 8 listed at the beginning of this table.

Table MASS-5. General Modeling Assumptions (Continued)

Chapter or Section	Code	Modeling Assumption	Related FEP in Appendix SCR-2014	Assumption Considered[a]
CRA-2004: 6.4.3.3 Gas Generation Appendix TRU WASTE-2004 CRA-2014: MASS-7.0 Gas Generation	BRAGFLO	Gas generation occurs by anoxic corrosion of steel containers and Fe and Fe-base alloys in the waste, giving H_2, and by microbial consumption of cellulosics and, possibly, plastics and rubbers, giving mainly CO_2 and hydrogen sulfide (H_2S). Radiolysis, oxic reactions, and other gas generation mechanisms are insignificant. Gas generation is calculated using the average-stoichiometry model, and is dependent on brine availability.	Container Material Inventory (W5) Waste Inventory (W2) Degradation of Organic Material (W44) Gases from Metal Corrosion (W49)	R
	BRAGFLO	The anoxic corrosion rate is dependent on liquid saturation. Anoxic corrosion of steel continues until all the steel is consumed. Steel corrosion will not be passivated by microbially generated gases (CO_2 or H_2S). The water in brine is consumed by the corrosion reaction.	Brine Inflow (W40) Gases from Metal Corrosion (W49) Degradation of Organic Material (W44)	R
	BRAGFLO	Laboratory-scale experimental measurements of gas generation rates at expected room temperatures are used to account for the effects of biofilms and chemical reactions.	Effects of Biofilms on Microbial Gas Generation (W48) Effects of Temperature on Microbial Gas Generation (W45) Chemical Effects of Corrosion (W51)	R

[a] R = Reasonable
C = Conservative
Reg. - Based on regulatory guidance
See above - Refers to assumptions 1 through 8 listed at the beginning of this table.

Table MASS-5. General Modeling Assumptions (Continued)

Chapter or Section	Code	Modeling Assumption	Related FEP in Appendix SCR-2014	Assumption Considered[a]
	BRAGFLO	The rate of microbial gas production is dependent on the amount of liquid present. Significant microbial activity occurs in all the simulations. In 75% of the simulations, microbes may consume all of the cellulosics but none of the plastics and rubbers. In the remaining 25% of the simulations, microbes may consume all of the cellulosics and all of the plastics and rubbers. Microbial production will continue until all biodegradable cellulosic, plastic, and rubber (CPR) materials are consumed if brine is present. The MgO backfill will react with all of the CO_2 and remove it from the gaseous phase.	Brine Inflow (W40) Degradation of Organic Material (W44) Waste Inventory (W2)	R
	BRAGFLO	Gas dissolution in brine is of negligible consequence.	Fluid Flow Due to Gas Production (W42)	R

Table MASS-5. General Modeling Assumptions (Continued)

Chapter or Section	Code	Modeling Assumption	Related FEP in Appendix SCR-2014	Assumption Considered[a]
	BRAGFLO	The gaseous phase is assigned the properties of hydrogen (General Assumption 7).	Fluid Flow Due to Gas Production (W42)	See above
CRA-2004: 6.4.3.4 Chemical Conditions in the Repository CRA-2014: SOTERM-2.0 Conceptual Framework of Chemical Conditions	NUTS PANEL	Chemical conditions in the repository will be constant. Chemical equilibrium is assumed for all reactions that occur between brine in the repository, waste, and abundant minerals, with the exceptions of gas generation and actinide redox reactions.	Speciation (W56) Reduction-Oxidation Kinetics (W66)	R
	NUTS PANEL	Brine and waste in the repository will contain a uniform mixture of dissolved and colloidal species. All actinides have instant access to all repository brine.	Heterogeneity of Waste Forms (W3) Speciation (W56)	C

[a] R = Reasonable
C = Conservative
Reg. - Based on regulatory guidance
See above - Refers to assumptions 1 through 8 listed at the beginning of this table.

Table MASS-5. General Modeling Assumptions (Continued)

Chapter or Section	Code	Modeling Assumption	Related FEP in Appendix SCR-2014	Assumption Considered[a]
	NUTS PANEL	No microenvironments that influence the overall chemical environment will persist.	Speciation (W56)	R
	NUTS PANEL	For the undisturbed performance and E2 scenarios, brine in the waste panels has the composition of Salado brine. For E1 and E1E2 (Appendix PA-2014, Section PA-2.3.2.2) scenarios, all brine in the waste panel intersected by the borehole has the composition of Castile brine.	Speciation (W56)	R
	NUTS PANEL	Chemical conditions in the waste panels will be reducing. However, a condition of redox disequilibrium will exist between the possible oxidation states of the An elements.	Reduction-Oxidation Kinetics (W66) Speciation (W56) Effects of Metal Corrosion (W64)	R
	NUTS PANEL	The pH and CO_2 fugacity in the waste panels will be controlled by the equilibrium between $Mg(OH)_2$ and $Mg_5(CO_3)_4(OH)_2 \cdot 4H_2O$. (A result of this assumption is low CO_2 fugacity and mildly basic conditions.)	Speciation (W56) Backfill Chemical Composition (W10)	R
CRA-2004: 6.4.3.5 Dissolved Actinide Source Term CRA-2014: SOTERM-3.3 The Fracture Matrix Transport Computer Code	NUTS PANEL	Radionuclide dissolution to solubility limits is instantaneous.	Dissolution of Waste (W58)	C

Table MASS-5. General Modeling Assumptions (Continued)

Chapter or Section	Code	Modeling Assumption	Related FEP in Appendix SCR-2014	Assumption Considered[a]
	NUTS PANEL	Six actinides (thorium (Th), uranium (U), neptunium (Np), plutonium (Pu), americium (Am), and curium (Cm)) are used in PANEL for calculations of radionuclide transport of brine (up a borehole). Four actinides (Th, U, Pu, and Am) are explicitly considered in NUTS for calculations of radionuclide transport in brine (porous materials) (Kicker and Zeitler 2013).	Waste Inventory (W2)	R

[a] R = Reasonable
C = Conservative
Reg. - Based on regulatory guidance
See above - Refers to assumptions 1 through 8 listed at the beginning of this table.

Table MASS-5. General Modeling Assumptions (Continued)

Chapter or Section	Code	Modeling Assumption	Related FEP in Appendix SCR-2014	Assumption Considered[a]
	NUTS PANEL	The reducing conditions in the repository will eliminate significant concentrations of Np(VI), Pu(V), Pu(VI), and Am(V) species. Am and Cm will exist predominantly in the III oxidation state; while Th will exist in the IV oxidation state. It is assumed that the solubilities and K_d values of U, Np, and Pu will be dominated by one of the remaining oxidation states: U(IV) or U (VI), Np(IV) or Np(V), and Pu (III) or Pu(IV) (See Appendix SOTERM-2014, Table SOTERM-15).	Speciation (W56) Reduction-Oxidation Kinetics (W66)	R
	NUTS PANEL	For a given oxidation state, the different actinides have similar solubilities.	Speciation (W56)	R
	NUTS PANEL	For undisturbed performance and for all aspects of disturbed performance, except for cuttings and cavings releases, radionuclides in the waste are distributed evenly throughout the disposal panel.	Waste Inventory (W2) Heterogeneity of Waste Forms (W3)	R
	NUTS PANEL	Mobilization of actinides in the gas phase is negligible.	Dissolution of Waste (W58)	R
	NUTS PANEL	An concentrations in the repository will be inventory limited when the mass of an An becomes depleted such that the predicted concentrations cannot be achieved.	Dissolution of Waste (W58)	R
CRA-2004: 6.4.3.6 Source Term for Colloidal Actinides	NUTS PANEL	Four types of colloids constitute the source term for colloidal actinides: intrinsic, mineral fragment, microbial, and humic.	Colloid Formation and Stability (W79) Humic and Fulvic Acids (W70)	R
	NUTS PANEL	Intrinsic colloids for all actinides are experimentally defined.	Colloid Formation and Stability (W79)	R

Table MASS-5. General Modeling Assumptions (Continued)

Chapter or Section	Code	Modeling Assumption	Related FEP in Appendix SCR-2014	Assumption Considered[a]

[a] R = Reasonable
C = Conservative
Reg. - Based on regulatory guidance
See above - Refers to assumptions 1 through 8 listed at the beginning of this table.

Table MASS-5. General Modeling Assumptions (Continued)

Chapter or Section	Code	Modeling Assumption	Related FEP in Appendix SCR-2014	Assumption Considered[a]
	NUTS PANEL	Concentrations of intrinsic colloids and mineral-fragment colloids are modeled as constants based on experimental observations. Humic and microbial colloidal An concentrations are modeled as proportional to dissolved An concentrations.	Colloid Formation and Stability (W79)	R
	NUTS PANEL	The maximum concentration of each An associated with each colloid type is constant.	Actinide Sorption (W61)	R
CRA-2004: 6.4.4 Shafts and Shaft Seals CRA-2014: MASS-11.0 Shafts and Shaft Seals	BRAGFLO	General Assumptions 1 to 8.	-	See above
	BRAGFLO	The four shafts connecting the repository to the surface are represented by a single shaft with a cross-section and volume equal to the total volume of the four real shafts and separated from the waste by less than the distance of the nearest real shaft.	Disposal Geometry (W1)	R
	BRAGFLO	The shaft seal system is represented by an upper and lower shaft region representing a composite of the actual materials in those regions.	Shaft Seal Geometry (W6) Shaft Seal Physical Properties (W7)	R
	BRAGFLO	The shaft is surrounded by a DRZ which heals with time. The DRZ is represented through the composite permeabilities of the shaft system itself, rather than as a discrete zone. The effective permeabilities of shaft materials are adjusted at 200 years after closure to reflect consolidation and possible degradation. Permeabilities are constant for the shaft seal materials through the Rustler formation.	Salt Creep (W20) Consolidation of Shaft Seals (W36) DRZ (W18) Microbial Growth on Concrete (W76) Chemical Degradation of Shaft Seals (W74) Mechanical Degradation of Shaft Seals (W37)	R

[a] R = Reasonable
C = Conservative
Reg. - Based on regulatory guidance
See above - Refers to assumptions 1 through 8 listed at the beginning of this table.

Table MASS-5. General Modeling Assumptions (Continued)

Chapter or Section	Code	Modeling Assumption	Related FEP in Appendix SCR-2014	Assumption Considered[a]
	NUTS	Radionuclides are not retarded by the seals.	Actinide Sorption (W61) Speciation (W56)	C

Table MASS-5. General Modeling Assumptions (Continued)

Chapter or Section	Code	Modeling Assumption	Related FEP in Appendix SCR-2014	Assumption Considered[a]
CRA-2004: 6.4.5 The Salado CRA-2014: MASS-12.0 Salado	BRAGFLO	General Assumptions 1 to 8.	-	See above
CRA-2004: 6.4.5.1 Impure Halite CRA-2014: MASS-12.1 High Threshold Pressure for Halite-Rich Salado Rock Units	BRAGFLO	Intact rock and hydrologic properties are constant.	Stratigraphy (N1)	R
CRA-2004: 6.4.5.2 Salado Interbeds CRA-2014: MASS-12.3 The Fracture Model	BRAGFLO	Interbeds have a fracture-initiation pressure above which local fracturing and changes in porosity and permeability occur in response to changes in pore pressure. A power function relates the permeability increase to the porosity increase. A pressure is specified above which porosity and permeability do not change.	Disruption Due to Gas Effects (W25)	R
	BRAGFLO	Interbeds have identical physical properties; they differ only in position, thickness, and some fracture parameters.	Saturated Groundwater Flow (N23)	R
CRA-2004: 6.4.5.3 Disturbed Rock Zone CRA-2014: MASS-12.4 Flow in the DRZ	BRAGFLO	The permeability of the DRZ is sampled with the low value similar to intact halite and the high value representing a fractured material. The DRZ porosity is equal to the porosity of Salado halite to plus 0.29%.	Disturbed Rock Zone (DRZ) (W18) Roof Falls (W22) Gas Explosions (W27) Seismic Activity (N12) Underground Boreholes (W39)	C-R
CRA-2004: 6.4.5.4 Actinide Transport in the Salado CRA-2014: MASS-12.5 Actinide Transport in the Salado	NUTS	Dissolved actinides and colloidal actinides are transported by advection in the Salado. Diffusion and dispersion are assumed negligible.	Advection (W90) Diffusion (W91) Matrix Diffusion (W92)	R

[a] R = Reasonable
C = Conservative
Reg. - Based on regulatory guidance
See above - Refers to assumptions 1 through 8 listed at the beginning of this table.

Table MASS-5. General Modeling Assumptions (Continued)

Chapter or Section	Code	Modeling Assumption	Related FEP in Appendix SCR-2014	Assumption Considered[a]

Table MASS-5. General Modeling Assumptions (Continued)

Chapter or Section	Code	Modeling Assumption	Related FEP in Appendix SCR-2014	Assumption Considered[a]
	NUTS	Sorption of actinides in the anhydrite interbeds, colloid retardation, colloid transport at higher than average velocities, coprecipitation of minerals containing actinides, channeled flow, and viscous fingering are not modeled.	Actinide Sorption (W61) Colloid Transport (W78) Colloid Filtration (W80) Colloid Sorption (W81) Fluid Flow Due to Gas Production (W42) Fracture Flow (N25)	R
	NUTS	Radionuclides having similar decay and transport properties have been grouped together for transport calculations as discussed in Kicker and Zeitler (Kicker and Zeitler 2013). See also assumptions for dissolved actinide source term.	Radionuclide Decay and Ingrowth (W12)	R
	NUTS	Sorption of actinides in the borehole is not modeled.	Actinide Sorption (W61)	C
CRA-2004: 6.4.6 Units Above the Salado CRA-2014: MASS-13.0 Geologic Units above the Salado	SECOTP2D	Above the Salado, lateral An transport to the accessible environment can occur only through the Culebra.	Saturated Groundwater Flow (N23) Unsaturated Groundwater Flow (N24) Solute Transport (W77)	R
CRA-2004: 6.4.6.1 Los Medaños	MODFLOW-2000 BRAGFLO	The Los Medaños member of the Rustler Formation, Tamarisk, and Forty-niner are assumed to be impermeable.	Saturated Groundwater Flow (N23)	C
CRA-2004: 6.4.6.2 The Culebra	MODFLOW-2000 SECOTP2D	General Assumptions 1, 6, and 8.	-	See above
CRA-2014: MASS-14.0 Flow through the Culebra	MODFLOW-2000	For fluid flow, the Culebra is modeled as a uniform (single-porosity) porous medium.	Saturated Groundwater flow (N23)	R
- CRA-2014: TFIELD				

[a] R = Reasonable
C = Conservative
Reg. - Based on regulatory guidance
See above - Refers to assumptions 1 through 8 listed at the beginning of this table.

Table MASS-5. General Modeling Assumptions (Continued)

Chapter or Section	Code	Modeling Assumption	Related FEP in Appendix SCR-2014	Assumption Considered[a]
	MODFLOW-2000	The Culebra flow field is determined from the observed hydraulic conditions and estimates of the effects of climate change and potash mining outside the controlled area, and does not change with time unless mining is predicted to occur in the disposal system in the future.	Saturated Groundwater Flow (N23) Climate Change (N61) Precipitation (e.g.,, Rainfall) (N59) Temperature (N60) Changes in Groundwater Flow Due to Mining (H37)	R

Table MASS-5. General Modeling Assumptions (Continued)

Chapter or Section	Code	Modeling Assumption	Related FEP in Appendix SCR-2014	Assumption Considered[a]
	BRAGFLO	The Culebra is assigned a single permeability to calculate brine flow into the unit from an intrusion borehole.	Natural Borehole Fluid Flow (H31) Waste-Induced Borehole Flow (H32)	R
	MODFLOW-2000	Gas flow in the Culebra is not modeled. Gas from the repository does not affect fluid flow in the Culebra.	Saturated Groundwater Flow (N23) Fluid Flow Due to Gas Production (W42)	R
	BRAGFLO MODFLOW-2000 SECOTP2D	Different thicknesses of the Culebra are assumed for BRAGFLO, MODFLOW-2000, and SECOTP2D calculations, although the transmissivities are consistent.	Effects of Preferential Pathways (N27)	R
	PEST	Uncertainty in the spatial variability of the Culebra transmissivity is accounted for by statistically generating 100 transmissivity fields for PA.	Saturated Groundwater Flow (N23) Fracture Flow (N25) Shallow Dissolution (N16)	R
	MODFLOW-2000 BRAGFLO	Potentiometric heads are set on the edges of the regional grid to represent flow in a portion of a much larger hydrologic system.	Groundwater Recharge (N54) Groundwater Discharge (N53) Changes in Groundwater Recharge and Discharge (N56) Infiltration (N55)	R

[a] R = Reasonable
C = Conservative
Reg. - Based on regulatory guidance
See above - Refers to assumptions 1 through 8 listed at the beginning of this table.

Table MASS-5. General Modeling Assumptions (Continued)

Chapter or Section	Code	Modeling Assumption	Related FEP in Appendix SCR-2014	Assumption Considered[a]
CRA-2004: 6.4.6.2.1 Transport of Dissolved Actinides in the Culebra CRA-2014: MASS-14.2 Dissolved Actinide Transport and Retardation in the Culebra	SECOTP2D	Dissolved actinides are transported by advection in high-permeability features and by diffusion in low-permeability features.	Solute Transport (W77) Advection (W90) Diffusion (W91) Matrix Diffusion (W92)	R
	SECOTP2D	Sorption occurs on dolomite in the matrix. Sorption on clays present in the Culebra is not modeled.	Actinide Sorption (W61) Changes in Sorptive Surfaces (W63)	C
	SECOTP2D	Sorption is represented using a linear isotherm model.	Actinide Sorption (W61) Kinetics of Sorption (W62)	R
	SECOTP2D	The possible effects on sorption of the injection of brines from the Castile and Salado into the Culebra are accounted for in the distribution of An K_d values.	Actinide Sorption (W61) Groundwater Geochemistry (N33) Changes in Groundwater Eh (N36) Changes in Groundwater pH (N37) Natural Borehole Fluid Flow (H31)	R

Table MASS-5. General Modeling Assumptions (Continued)

Chapter or Section	Code	Modeling Assumption	Related FEP in Appendix SCR-2014	Assumption Considered[a]
	SECOTP2D	Hydraulically significant fractures are assumed to be present everywhere in the Culebra.	Advection (W90)	C
CRA-2004: 6.4.6.2.2 Transport of Colloidal Actinides in the Culebra CRA-2014: MASS-14.3 Colloidal Actinide Transport and Retardation in the Culebra	SECOTP2D	An humic colloids are chemically retarded identically to dissolved actinides and are treated as dissolved actinides.	Advection (W90) Diffusion (W91) Colloid Transport (W78) Microbial Transport (W87)	R
	SECOTP2D	The concentration of intrinsic colloids is sufficiently low to justify elimination from PA transport calculations in the Culebra.	-	R

[a] R = Reasonable
C = Conservative
Reg. - Based on regulatory guidance
See above - Refers to assumptions 1 through 8 listed at the beginning of this table.

Table MASS-5. General Modeling Assumptions (Continued)

Chapter or Section	Code	Modeling Assumption	Related FEP in Appendix SCR-2014	Assumption Considered[a]
	SECOTP2D	Microbial colloids and mineral fragments are too large to undergo matrix diffusion. Filtration of these colloids, which is modeled using an exponential decay approach, occurs in high-permeability features. Attenuation is so effective that associated actinides are assumed to be retained within the disposal system and are not transported in SECOTP2D.	Microbial Transport (W87) Colloid Sorption (W81)	R
CRA-2004: 6.4.6.2.3 Subsidence Due to Potash Mining CRA-2014: MASS-14.4 Subsidence Caused by Potash Mining in the Culebra	MODFLOW-2000	The effect of potash mining is to increase the hydraulic conductivity in the Culebra by a factor between 1 and 1,000.	Conventional Underground Potash Mining (H13) Changes in Groundwater Flow Due to Mining (H37)	Reg.
CRA-2004: 6.4.6.3 The Tamarisk	MODFLOW-2000 BRAGFLO	The Tamarisk is assumed to be impermeable.	Saturated Groundwater Flow (N23)	R
CRA-2004: 6.4.6.4 The Magenta	BRAGFLO	General Assumptions 1 to 8.	-	See above
	BRAGFLO	The Magenta permeability is set to the lowest value measured near the center of the WIPP site. This increases the flow into the Culebra.	Saturated Groundwater Flow (N23)	R
	NUTS	No radionuclides entering the Magenta will reach the accessible environment. However, the volumes of brine and actinides entering and stored in the Magenta are modeled.	Solute Transport (W77)	R
CRA-2004: 6.4.6.5 The Forty-niner	BRAGFLO	The Forty-niner is assumed to be impermeable.	Saturated Groundwater Flow (N23)	R

[a] R = Reasonable
C = Conservative
Reg. - Based on regulatory guidance
See above - Refers to assumptions 1 through 8 listed at the beginning of this table.

Table MASS-5. General Modeling Assumptions (Continued)

Chapter or Section	Code	Modeling Assumption	Related FEP in Appendix SCR-2014	Assumption Considered[a]
CRA-2004: 6.4.6.6 Dewey Lake	BRAGFLO	General Assumptions 1 to 8.	-	See above
	NUTS	The sorptive capacity of the Dewey Lake is sufficiently large to prevent any release over 10,000 years.	Saturated Groundwater Flow (N23) Actinide Sorption (W61)	R
CRA-2004: 6.4.6.7 Supra-Dewey Lake Units	BRAGFLO	General Assumptions 1 to 8.	-	See above
	BRAGFLO	The units above the Dewey Lake are a single hydrostratigraphic unit.	Stratigraphy (N1)	R
	BRAGFLO	The units are thin and predominantly unsaturated.	Unsaturated Groundwater Flow (N24) Saturated Groundwater Flow (N23)	R
CRA-2004: 6.4.7 The Intrusion Borehole CRA-2004: 6.4.7.1 Releases during Drilling CRA-2014: MASS-15.0 Intrusion Borehole	CUTTINGS_S BRAGFLO DRSPALL	Any actinides that enter the borehole during drilling are assumed to reach the surface.	-	C
CRA-2014: MASS-15.1 Cuttings, Cavings, and Spall Releases during Drilling	BRAGFLO PANEL CUTTINGS_S DRSPALL	Future drilling practices will be the same as they are at present.	Oil and Gas Exploration (H1) Potash Exploration (H2) Oil and Gas Exploitation (H4) Other Resources (H8) Enhanced Oil and Gas Recovery (H9)	Reg.
	CUTTINGS_S DRSPALL	Releases of particulate waste material are modeled (cuttings, cavings, and spallings). Releases are corrected for radioactive decay until the time of intrusion.	Drilling Fluid Flow (H21) Suspension of Particles (W82) Cuttings (W84) Cavings (W85) Spallings (W86)	R
	CUTTINGS_S	Degraded waste properties are based on marine clays and surrogate materials.	Cavings (W85)	C

[a] R = Reasonable
C = Conservative
Reg. - Based on regulatory guidance
See above - Refers to assumptions 1 through 8 listed at the beginning of this table.

Table MASS-5. General Modeling Assumptions (Continued)

Chapter or Section	Code	Modeling Assumption	Related FEP in Appendix SCR-2014	Assumption Considered[a]
	DRSPALL	A hemispherical geometry with one-dimensional spherical symmetry defines the flow field and cavity in the waste.	Spallings (W86)	C
	DRSPALL	Tensile strength, based on completely degraded waste surrogates, is felt to represent extreme, low-end tensile strengths because it does not account for several strengthening mechanisms.	Spallings (W86)	C

Table MASS-5. General Modeling Assumptions (Continued)

Chapter or Section	Code	Modeling Assumption	Related FEP in Appendix SCR-2014	Assumption Considered[a]
	DRSPALL	Shape factor is 0.1, corresponding to particles that are easier to fluidize and entrain in the flow.	Spallings (W86)	C
CRA-2004: 6.4.7.1.1 Direct Brine Release During Drilling CRA-2014: MASS-15.2 Direct Brine Releases during Drilling	BRAGFLO PANEL	Brine containing actinides may flow to the surface during drilling. DBR will have negligible effect on the long-term pressure and saturation in the waste panel.	Blowouts (H23)	R
	BRAGFLO	A two-dimensional grid (one degree dip) on the scale of the waste disposal region is used for DBR calculations.	Blowouts (H23)	R
	BRAGFLO CCDFGF	Calculation of DBR from several different locations provides reference results for the variation in release associated with location.	Blowouts (H23)	R
CRA-2004: 6.4.7.2 Long-Term Releases Following Drilling CRA-2014: MASS-15.3 Long-Term Properties of the Abandoned Intrusion Borehole	BRAGFLO CCDFGF	Plugging and abandonment of future boreholes are assumed to be consistent with practices in the Delaware Basin.	Natural Borehole Fluid Flow (H31) Waste-Induced Borehole Flow (H32)	Reg.
CRA-2004: 6.4.7.2.1 Continuous Concrete Plug through the Salado and Castile (Plug type VI in U.S. DOE 2012)	BRAGFLO CCDFGF	A continuous concrete plug is assumed to exist throughout the Salado and Castile. Long-term releases through a continuous plug are analogous to releases through a sealed shaft.	Natural Borehole Fluid Flow (H31) Waste-Induced Borehole Flow (H32)	Reg.-R

[a] R = Reasonable
C = Conservative
Reg. - Based on regulatory guidance
See above - Refers to assumptions 1 through 8 listed at the beginning of this table.

Table MASS-5. General Modeling Assumptions (Continued)

Chapter or Section	Code	Modeling Assumption	Related FEP in Appendix SCR-2014	Assumption Considered[a]
CRA-2004: 6.4.7.2.2 The Two-Plug Configuration (Plug types I, III, and V in U.S. DOE 2012)	BRAGFLO	A lower plug is located between the Castile brine reservoir and underlying formations. A second plug is located immediately above the Salado. The brine reservoir and waste panel are in direct communication though an open cased hole.	Natural Borehole Fluid Flow (H31) Waste-Induced Borehole Flow (H32)	Reg.-R
	BRAGFLO	The casing and upper concrete plug are assumed to fail after 200 years, and the borehole is assumed to be filled with silty-sand-like material. At 1,200 years after abandonment, the permeability of the borehole below the waste panel is decreased by one order of magnitude as a result of salt creep.	Natural Borehole Fluid Flow (H31) Waste-Induced Borehole Flow (H32)	R

Table MASS-5. General Modeling Assumptions (Continued)

Chapter or Section	Code	Modeling Assumption	Related FEP in Appendix SCR-2014	Assumption Considered[a]
	BRAGFLO	In addition to the two-plug configuration, a third plug is placed within the Castile above the brine reservoir. The third plug is assumed not to fail over the regulatory time period.	Natural Borehole Fluid Flow (H31) Waste-Induced Borehole Flow (H32)	Reg.-R
CRA-2004: 6.4.8 Castile Brine Reservoir CRA-2014: MASS-17.0 Castile Brine Reservoir	BRAGFLO	The Castile region is assigned a low permeability, which inhibits fluid flow. Brine occurrences in the Castile are bounded systems. Brine reservoirs under the waste panels are assumed to have limited extent and interconnectivity, with effective radii on the order of several hundred meters (m).	Brine Reservoirs (N2)	R
CRA-2004: 6.4.9 Climate Change CRA-2014: MASS-16.0 Climate Change	SECOTP2D	Climate-related factors are treated through recharge. A parameter called the Climate Index is used to scale the Culebra flux field.	Climate Change (N61) Temperature (N60) Precipitation (e.g., Rainfall) (N59)	R

[a] R = Reasonable
C = Conservative
Reg. - Based on regulatory guidance
See above - Refers to assumptions 1 through 8 listed at the beginning of this table.

Table MASS-5. General Modeling Assumptions (Continued)

Chapter or Section	Code	Modeling Assumption	Related FEP in Appendix SCR-2014	Assumption Considered[a]
CRA-2004: 6.4.10 Initial and Boundary Conditions for Disposal System Modeling CRA-2004: 6.4.10.1 Disposal System Flow and Transport Modeling (BRAGFLO and NUTS)	BRAGFLO	There are no gradients for flow in the far-field of the Salado, and pressures are above hydrostatic but below lithostatic. Excavation and waste emplacement result in partial drainage of the DRZ.	Saturated Groundwater Flow (N23) Brine Inflow (W40)	R
	BRAGFLO	An initial water-table surface is set in the Dewey Lake at an elevation of 980 m (3,215 ft) above mean sea level. The initial pressures in the Salado are extrapolated from a sampled pressure in MB139 at the shaft and are in hydrostatic equilibrium. The excavated region is assigned an initial pressure of one atmosphere. The liquid saturation of the waste-disposal region is consistent with the liquid saturation of emplaced waste. Other excavated regions are assigned zero liquid saturation, except the shaft, which is fully saturated.	Saturated Groundwater Flow (N23)	R
	NUTS	Molecular transport boundary conditions are no diffusion or dispersion in the normal direction across far-field boundaries. Initial An concentrations are zero everywhere, except in the waste.	Radionuclide Decay and Ingrowth (W12) Solute Transport (W77)	R

Table MASS-5. General Modeling Assumptions (Continued)

Chapter or Section	Code	Modeling Assumption	Related FEP in Appendix SCR-2014	Assumption Considered[a]
	MODFLOW-2000	Constant head and no-flow boundary conditions are set on the far-field boundaries of the flow model.	Saturated Groundwater Flow (N23)	R
	MODFLOW-2000	Initial An concentrations in the Culebra are zero.	Solute Transport (W77)	R

[a] R = Reasonable
C = Conservative
Reg. - Based on regulatory guidance
See above - Refers to assumptions 1 through 8 listed at the beginning of this table.

Table MASS-5. General Modeling Assumptions (Continued)

Chapter or Section	Code	Modeling Assumption	Related FEP in Appendix SCR-2014	Assumption Considered[a]
CRA-2004: 6.4.10.3 Initial and Boundary Conditions for Other Computational Models	NUTS PANEL BRAGFLO (DBR) CUTTINGS_S	Initial and boundary conditions are interpolated from previously executed BRAGFLO calculations.	-	R
CRA-2004: 6.4.12 Sequences of Future Events	CCDFGF	Each 10,000-year future (random sequence of future events) is generated by randomly and repeatedly sampling (1) the time between drilling events, (2) the location of drilling events, (3) the activity level of the waste penetrated by each drilling intrusion, (4) the plug configuration of the borehole, and (5) the penetration of a Castile brine reservoir, and by randomly sampling the occurrence of mining in the disposal system.	Oil and Gas Exploration (H1) Potash Exploration (H2) Oil and Gas Exploitation (H4) Other Resources (H8) Enhanced Oil and Gas Recovery (H9) Natural Borehole Fluid Flow (N31) Waste-Induced Borehole Flow (H32)	Reg.-R
CRA-2004: 6.4.12.1 Active and Passive Institutional Controls in Performance Assessment	CCDFGF	Active institutional controls are effective for 100 years and completely eliminate the possibility of disruptive human activities (e.g., drilling and mining). No credit is taken for passive institutional controls.	-	Reg.-R
CRA-2004: 6.4.12.2 Number and Time of Drilling Intrusions	CCDFGF	Drilling may occur after 100 years according to a Poisson process.	Loss of Records (H57) Oil and Gas Exploration (H1) Potash Exploration (H2) Oil and Gas Exploitation (H4) Other Resources (H8)	Reg.-R
CRA-2004: 6.4.12.3 Location of Intrusion Boreholes	CCDFGF	The waste disposal region is discretized into 144 regions, each with an equal probability of being intersected. A borehole can penetrate only one region.	Disposal Geometry (W1)	R

[a] R = Reasonable
C = Conservative
Reg. - Based on regulatory guidance
See above - Refers to assumptions 1 through 8 listed at the beginning of this table.

Table MASS-5. General Modeling Assumptions (Continued)

Chapter or Section	Code	Modeling Assumption	Related FEP in Appendix SCR-2014	Assumption Considered[a]

Table MASS-5. General Modeling Assumptions (Continued)

Chapter or Section	Code	Modeling Assumption	Related FEP in Appendix SCR-2014	Assumption Considered[a]
CRA-2004: 6.4.12.4 Activity of the Intersected Waste Appendix TRU WASTE-2004	CCDFGF	Four-hundred fifty one waste streams are identified as contact-handled transuranic (CH-TRU). All 77 remote-handled transuranic (RH-TRU) waste streams were grouped (binned) together into one equivalent or average (WIPP-scale) RH-TRU waste stream.	Heterogeneity of Waste Forms (W3)	R
CRA-2004: 6.4.12.5 Diameter of the Intrusion Borehole	CUTTINGS_S	The diameter of the intrusion borehole is constant at 12.25 inches (in.) (31.12 centimeters [cm]).	-	Reg.-R
CRA-2004: 6.4.12.6 Probability of Intersecting a Brine Reservoir	CCDFGF	The probability that a deep borehole intersects the single brine reservoir below the waste panels is sampled from a normal distribution with a mean of 0.127 and a standard deviation equal to 0.0272 (see Kirchner, Zeitler, and Kirkes 2012).	Brine Reservoirs (N2)	R
CRA-2004: 6.4.12.7 Plug Configuration in the Abandoned Intrusion Borehole	CCDFGF	The two-plug configuration has a probability of 0.594. The three-plug configuration has a probability of 0.366. The continuous concrete plug has a probability of 0.04 (see Camphouse 2013).	-	Reg.-R
CRA-2004: 6.4.12.8 Probability of Mining Occurring in the Land Withdrawal Area	CCDFGF	Mining in the disposal system occurs a maximum of once in 10,000 years (a 10^{-4} probability per year).	-	Reg.-R
CRA-2004: 6.4.13 Construction of a Single Complementary Cumulative Distribution Function (CCDF)	CCDFGF	Deterministic calculations from BRAGFLO, NUTS, MODFLOW-2000, SECOTP2D, CUTTINGS_S, and PANEL are used to generate reference conditions that are used to estimate the consequences associated with random sequences of future events. These are, in turn, used to develop CCDFs.	-	R

[a] R = Reasonable
C = Conservative
Reg. - Based on regulatory guidance
See above - Refers to assumptions 1 through 8 listed at the beginning of this table.

Table MASS-5. General Modeling Assumptions (Continued)

Chapter or Section	Code	Modeling Assumption	Related FEP in Appendix SCR-2014	Assumption Considered[a]

Table MASS-5. General Modeling Assumptions (Continued)

Chapter or Section	Code	Modeling Assumption	Related FEP in Appendix SCR-2014	Assumption Considered[a]

Table MASS-5. General Modeling Assumptions (Continued)

Chapter or Section	Code	Modeling Assumption	Related FEP in Appendix SCR-2014	Assumption Considered[a]
	CCDFGF	Ten thousand random sequences of future events are generated for each CCDF plotted.	-	R
CRA-2004: 6.4.13.1 Constructing Consequences of the Undisturbed Performance Scenario	CCDFGF	A BRAGFLO and NUTS calculation with undisturbed conditions is sufficient for estimating the consequences of the undisturbed performance scenario.	-	R
CRA-2004: 6.4.13.2 Scaling Methodology for Disturbed Performance Scenarios	CCDFGF	Consequences for random sequences of future events are constructed by scaling the consequences associated with deterministic calculations (reference conditions) to other times, generally by interpolation, but sometimes by assuming either similarity or no consequence.	-	R
CRA-2004: 6.4.13.3 Estimating Long-Term Releases from the E1 Scenario	CCDFGF NUTS	Reference conditions are calculated or estimated for intrusions at 100, 350, 1,000, 3,000, 5,000, 7,000, and 9,000 years.	Waste-Induced Borehole Flow (H32)	R
CRA-2004: 6.4.13.4 Estimating Long-Term Releases from the E2 Scenario	CCDFGF NUTS SECOTP2D	The methodology is similar to the methodology for the E1 scenario. For multiple E1 intrusions into the same panel, the additional source term to the Culebra for the second and subsequent intrusions is assumed to be negligible.	Waste-Induced Borehole Flow (H32) Waste Inventory (W2)	R
CRA-2004: 6.4.13.5 Estimating Long-Term Releases from the E1E2 Scenario	CCDFGF PANEL	The concentration of actinides in liquid moving up the borehole assumes homogeneous mixing within the panel.	Waste-Induced Borehole Flow (H32)	C
	PANEL	Any actinides that enter the borehole for long-term flow calculations reach the Culebra.	Waste-Induced Borehole Flow (H32)	C

[a] R = Reasonable
C = Conservative
Reg. - Based on regulatory guidance
See above - Refers to assumptions 1 through 8 listed at the beginning of this table.

Table MASS-5. General Modeling Assumptions (Continued)

Chapter or Section	Code	Modeling Assumption	Related FEP in Appendix SCR-2014	Assumption Considered[a]
	CCDFGF PANEL	Reference conditions are calculated or estimated for intrusion at 100, 300, 1,000, 2,000, 4,000, 6,000 and 9,000 years.	Oil and Gas Exploration (H1)	-
CRA-2004: 6.4.13.6 Multiple Scenario Occurrences	CCDFGF PANEL	The panels are assumed not to be interconnected for long-term brine flow.	Saturated Groundwater Flow (N23) Unsaturated Groundwater Flow (N24)	R

Table MASS-5. General Modeling Assumptions (Continued)

Chapter or Section	Code	Modeling Assumption	Related FEP in Appendix SCR-2014	Assumption Considered[a]
CRA-2004: 6.4.13.7 Estimating Releases During Drilling for All Scenarios	CCDFGF PANEL NUTS	Repository conditions will be dominated by Castile brine if any borehole connects to a brine reservoir.	Brine Reservoirs (N2) Natural Borehole Fluid Flow (H31)	R
	CUTTINGS_S PANEL CCDFGF	Depletion of actinides in parts of the repository penetrated by boreholes is not accounted for in calculating the releases from subsequent intrusions at such locations.	Waste-Induced Borehole Flow (H32) Waste Inventory (W2)	C
CRA-2004: 6.4.13.8 Estimating Releases in the Culebra and the Impact of the Mining Scenario	CCDFGF	Releases from intrusions at random times in the future are scaled from releases calculated at 100 years with a unit source of radionuclides in the Culebra.	-	R
	CCDFGF	Actinides in transit in the Culebra when mining occurs are transported in the flow field used for the undisturbed case. Actinides introduced subsequent to mining are transported in the flow field used for the disturbed case (i.e., the mined case).	-	R

[a] R = Reasonable
C = Conservative
Reg. - Based on regulatory guidance
See above - Refers to assumptions 1 through 8 listed at the beginning of this table.

MASS-3.1 Darcy's Law Applied to Fluid Flow Calculated by BRAGFLO, MODFLOW-2000, and DRSPALL

A mathematical relationship expressing fluid flux as a function of hydraulic head gradients in a porous medium, commonly known as Darcy's Law, is applied to geologic media for all fluid-flow calculations. For details about the specific formulation of Darcy's Law used in these calculations, refer to Appendix PA-2014, Section PA-4.2 for the disposal system and Section PA-4.8 for the Culebra. Darcy's Law is not applied for flow up a borehole being drilled (see Section MASS-15.2; the CRA-2004, Chapter 6.0, Section 6.4.7.1.1; and Appendix PA-2014, Section PA-4.7 for more discussion of this topic).

Darcy's Law generally applies to flow models for which certain conditions are satisfied: (1) the flow occurs in a porous medium with interconnected porosity, (2) flow velocities are low enough that viscous forces dominate inertial forces, and (3) a threshold hydraulic gradient is exceeded. In the CCA, Appendix MASS, these conditions were shown to be valid for the WIPP PA.

Darcy's Law assumes laminar flow; that is, there is no motion of the fluid at the fluid/solid interface and velocity increases with distance from the fluid/solid interface. For liquids, it is reasonable to assume laminar flow under most conditions, including those found in and surrounding the WIPP repository. For gases at low pressure, however, gas molecules near the solid interface may not have intimate contact with the solid and may have finite velocity, not necessarily zero. This effect, which results in additional flux of gas above that predicted by application of Darcy's Law, is known as the slip phenomenon, or Klinkenberg effect (Bear 1972, p. 128). A correction to Darcy's Law for the Klinkenberg effect is incorporated into the BRAGFLO model (see Appendix PA-2014, Section PA-4.2).

Darcy flow for one and two phases implies that values for principal fluid and rock parameters must be specified. Fluid properties in the Darcy flow model used for the WIPP PA are density, viscosity, and compressibility, while rock properties are porosity, permeability, and compressibility (pore or bulk). In BRAGFLO, other parameters are required to describe the interactions or interference between the gas and brine phases present in the model because those phases can occupy the same pore space. In the WIPP application of Darcy flow models, compressibility of both the liquid and rock are related to porosity through a dependence on pressure. Fluid density, viscosity, and compressibility are functions of fluid composition, pressure, and temperature. It is assumed in BRAGFLO that fluid (both brine and gas) density and compressibility are pressure dependent, but fluid (both brine and gas) viscosity is constant. Fluid composition for the purposes of modeling flow and transport is assumed to be constant.

MASS-3.2 Hydrogen Gas as Surrogate for Waste-Generated Gas Physical Properties in BRAGFLO and DRSPALL

Hydrogen gas is produced as a result of the corrosion of steel in the repository by water or brine. As in the CCA, the gas phase in the BRAGFLO model is assigned the properties of hydrogen because hydrogen will, under most conditions reasonable for the WIPP, be the dominant component of the gas phase. The model for spallings, DRSPALL, also assigns the physical properties of hydrogen to the gas phase. As discussed in the following text, the effect of assuming flow of pure H_2 instead of a mixture of gases (including H_2,CO_2, H_2S, and methane (CH_4), can be shown to be minor relative to the permeability variations in the surrounding formations.

Other gases may be produced by processes occurring in the repository. If microbial degradation occurs, a significant amount of CO_2 and possibly CH_4 will be generated by microbial degradation of cellulosics and, possibly, plastics and rubbers in the waste. The CO_2 produced, however, will react with the magnesium-oxide (MgO) engineered barrier and cementitious materials to form brucite ($Mg(OH)_2$), hydromagnesite ($Mg_5(CO_3)_4(OH)_2 \cdot 4H_2O$), and calcite ($CaCO_3$), thus resulting in very low CO_2 fugacity in the repository. Although other gases exist in the disposal system, BRAGFLO calculations assume these gases are insignificant and they are not included in the model.

With the average stoichiometry gas generation model, the total number of moles of gas generated will be the same whether the gas is considered to be pure H_2 or a mixture of several gases, because the generation of other gases is accounted for by specifying the stoichiometric factor for microbial degradation of cellulose (see Appendix PA-2014, Section PA-4.2.5). Therefore, considering only the moles of gas generated, the pressure buildup in the repository will be approximately the same because the expected gases behave similarly to an ideal gas, even up to lithostatic pressures.

The effect of assuming pure H_2 instead of a mixture of gases (including H_2, CO_2, H_2S and CH_4) on flow behavior, and its resulting impact on the WIPP repository pressure, is as follows:

Radial flow in a fully saturated rock with nonideal gas is described by Darcy's Law, which, for the given problem, has a solution of the form (Amyx, Bass, and Whiting 1960, p. 78, Equation 2-33)

$$q_b = 1.988\times10^{-5}\left[\frac{T_b Z_b}{P_b}\frac{kh\left(P_e^2 - P_w^2\right)}{\mu_{avg} Z_{avg} \ln\left(\frac{r_e}{r_w}\right)}\right] \quad \text{(MASS.1)}$$

which can be rewritten as

$$P_e^2 - P_w^2 = \frac{q_b P_b}{1.988\times10^{-5} T_b Z_b} \times \frac{\mu_{avg} Z_{avg}}{kh} \ln\left(\frac{r_e}{r_w}\right) \quad \text{(MASS.2)}$$

where

q = gas flow rate (cubic ft per day at base (reference) conditions)

T = temperature (K)

P = pressure (pounds per square inch absolute)

k = permeability (millidarcys)

h = height (ft)

μ = viscosity (centipoises)

Z = gas compressibility factor (defined as the ratio of the actual molar volume of a gas to the corresponding ideal gas volume *RT/P* at the same temperature and pressure)

r = radius (consistent units)

R = ideal gas constant

e = denotes external boundary (repository)

w = denotes internal boundary (wellbore)

b = denotes base or reference conditions for gas (temperature, pressure, compressibility factor)

avg = denotes average properties between external and internal boundaries because u and z are functions of pressure, which change with time

This expression is useful for examining the effects of gas properties, specifically the viscosity (μ) and the compressibility (Z) and rock properties (namely k), on the flow rate (q) and the pressure (P).

To evaluate the effect of gas composition on q and P, SUPERTRAPP, a computer program developed by the National Institute of Standards and Technology (NIST), was used (National Institute of Standards and Technology 1992). SUPERTRAPP calculates gas properties for 116 pure fluids and mixtures of up to 20 components for temperatures to 1,000 K (726 °C, 1340 °F) and pressures to 300 megapascals (MPa). Because such small quantities of H_2S are anticipated at the WIPP, its impact is negligible.

Figure MASS-1 shows the relationship between gas viscosity and composition of H_2-CO_2 mixtures for various mole fractions of H_2 at pressures of 7 MPa and 15 MPa, as determined from SUPERTRAPP. The viscosity at 50% mole fraction H_2 is about 2.3 times greater than for 100% mole fraction H_2. As shown in Equation (MASS.1), viscosity has an inverse relationship to flow rate and, as shown in Equation (MASS.2), a direct relationship to the square of the repository pressure. Hence, viscosity differences that would result if gas properties other than those of hydrogen were incorporated would result in a decrease in flow rate and potentially higher pressures.

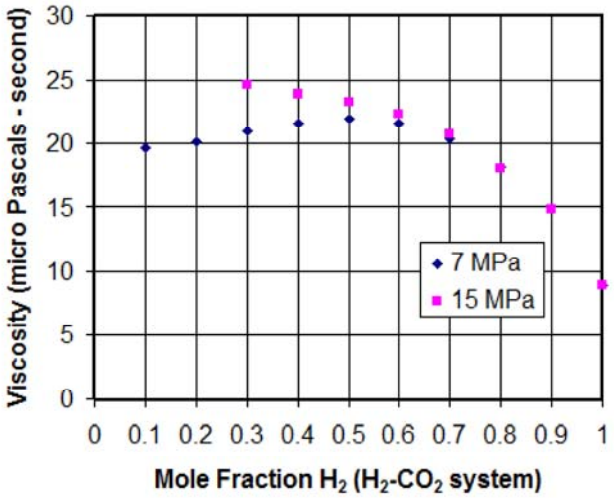

Figure MASS- 1. Gas Viscosity as a Function of Mole Fraction H_2 at 7 MPa and 15 MPa Pressure

As shown in Figure MASS-2, the gas compressibility at 50% mole fraction H_2 is about 0.9 times that of pure H_2. Like viscosity, the gas compressibility (actual volume/ideal volume) is inversely related to flow rate and directly related to the square of the repository pressure. Therefore, the impact of variation in gas compressibility caused by composition would be minor and it is not considered.

The viscosity and compressibility calculations described above for H_2-CO_2 mixtures were repeated for H_2-CH_4 mixtures for various mole fractions of H_2 at pressures of 7 MPa and 15 MPa (Kanney 2003). The variability of viscosity with the composition for the H_2-CH_4 mixtures is smaller than that observed for the H_2-CO_2 mixtures. For example, at 15 Mpa, the gas viscosity of H_2-CH_4 at 50% mole fraction is only 1.6 times greater than the viscosity at 100% mole fraction. The H_2-CH_4 mixtures are only slightly less compressible than the H_2-CO_2 mixtures. For example, at 15 MPa, the gas compressibility of the H_2-CH_4 at 50% mole fraction is approximately 0.94 times the compressibility at 100% mole fraction. Changing composition from 100% to 50% H_2 would result in a slight increase in flow rate and a decrease in pressure.

The permeability of each component of the formation plays a significant role in determining both flow rate and pressure. Because marker bed (MB) permeabilities and Salado impure halite permeabilities vary over three to four orders of magnitude (see Kicker and Herrick 2013), the permeabilities of these flow pathways will have a greater influence on pressure and flow rate determinations than either uncertainty in viscosity or gas compressibility effects.

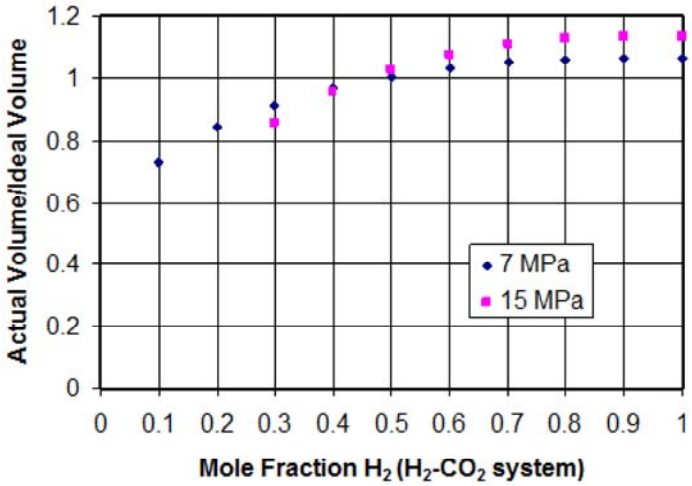

Figure MASS- 2. Gas Compressibility as a Function of Mole Fraction H_2

Note that the BRAGFLO code includes a pressure-induced fracture model that will limit pressure increases in the repository (Schreiber 1997). For example, at high repository pressures, the factor of 1.5 pressure increase calculated here using the simplified Darcy's Law model is unlikely to be seen in the BRAGFLO results, since fracturing will lead to increased permeability, effectively limiting pressure increases.

MASS-3.3 Salado Brine as Surrogate for Liquid-Phase Physical Properties in BRAGFLO

BRAGFLO uses Salado Formation brine properties as the physical properties for all liquids. However, liquid in the modeled region may consist of (1) brine originally in the Salado, (2) liquid introduced in the excavation during construction, maintenance, and ventilation during the operational phase, (3) a very small amount of liquid introduced as a component of the waste, (4) liquid from overlying units, and (5) liquid from the Castile brine reservoir. However, for BRAGFLO modeling, it is assumed that the properties of all of these liquids are similar enough to Salado brine properties that the effect of any variation in properties resulting from liquids mixing is negligible. The variations in chemical properties of brine are accounted for as discussed in Appendix SOTERM-2014, Section SOTERM-2.0 , Section SOTERM-2.3, and Section SOTERM-5.0.

MASS-4.0 Model Geometries

This section presents supplementary information on the disposal system geometry, and includes the representation of panel closures in that discussion. The principal process considered in defining the repository geometry is fluid flow.

MASS-4.1 Disposal System Geometry as Modeled in BRAGFLO

The geometry used to represent long-term fluid flow processes in the Salado, flow between a borehole and overlying units, and flow within the repository (where processes coupled to fluid flow such as creep closure and gas generation occur), is a vertical cross section through the repository on a north-south axis (see also Appendix PA-2014, Section PA-4.2.1). The dimension of this geometry in the direction perpendicular to the plane of the cross section varies so that spatial effects of repository processes can be represented. Using a two-dimensional geometry to represent the three-dimensional Salado flow is based on the assumption that brine and gas flow will converge upon and diverge from the repository horizon. Above and below the repository, it is assumed that any flow between the borehole or shaft (see CRA-2004, Chapter 6.0, Section 6.4.3) and surrounding materials will converge or diverge. Grid flaring is used in the BRAGFLO disposal system geometry, and flows are represented as divergent and convergent from the flaring center (see Section MASS-4.1.1.4). The impact of this implementation in a two-dimensional grid has been compared to a model that does not make the assumption of convergent and divergent flow (see Appendix PA-2004, Attachment MASS, Attachment 4-1 for additional information). The BRAGFLO representation of the Salado also includes the slight and variable dip of beds in the vicinity of the repository. Below the repository, the possible presence of a brine reservoir is considered to be important, so a hydrostratigraphic layer representing the Castile and a possible brine reservoir in it is included (see the CCA, Appendix MASS, Section MASS-4.2 for the disposal system geometry historical context prior to the CCA).

For modeling brine flow from the intruded panel to the borehole during drilling, the geometry represented in BRAGFLO is a two-dimensional, horizontal representation of the repository waste area as described in Section MASS-15.2.

Changes have been made to the disposal system geometry representation in BRAGFLO since that implemented in the CCA. The evolution of these changes is discussed in the following sections for the sake of completeness.

MASS-4.1.1 CCA to CRA-2004 Baseline Grid Changes

The baseline BRAGFLO grid used in the CCA PA and the CCA Performance Assessment Verification Test (PAVT) had 33 cells in the x direction and 31 cells in the y direction, and is shown in Figure MASS-3. Notably absent from the repository geometry are pillars, individual drifts, and rooms. These were, and still are, excluded for simplicity, as well as the assumption that they have either negligible impact on fluid-flow processes or, alternatively, that including them would be beneficial to long-term repository performance.

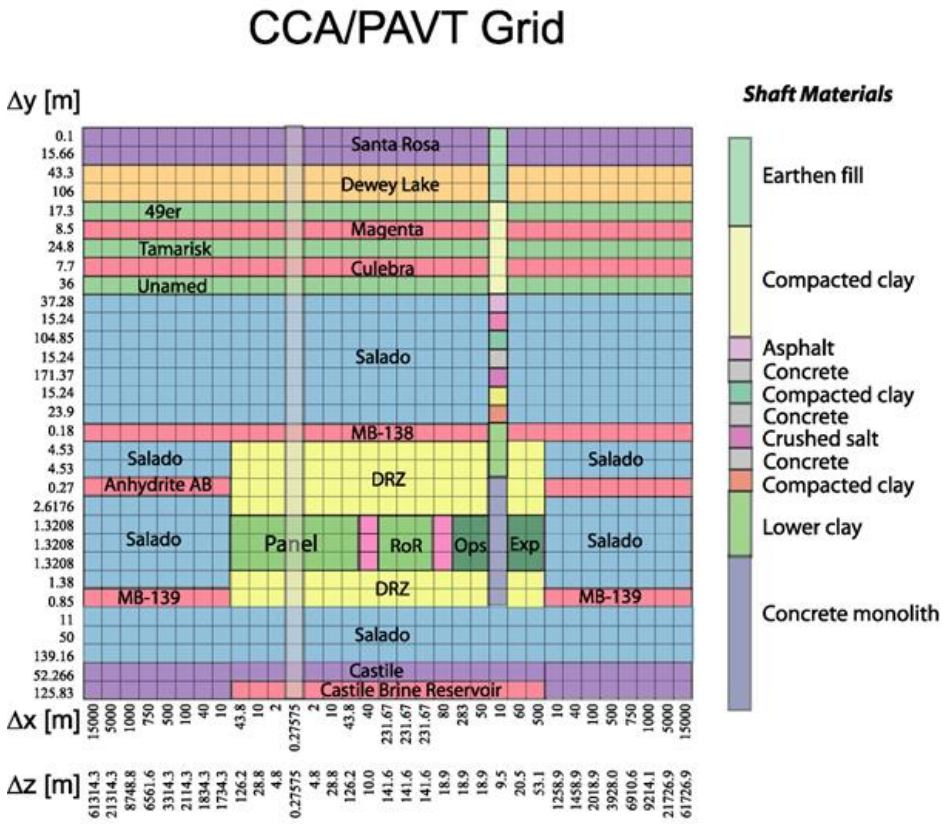

Figure MASS- 3. Logical Grid Used for the CCA PA BRAGFLO Calculations

Several changes were made to the CCA numerical grid as part of the CRA-2004. These changes consisted of the following:

1. A simplified shaft seal model
2. Implementation of Option D-type panel closures
3. Increased segmentation of repository waste regions
4. Refinement to the grid-flaring method
5. Refinement to the x-spacing of the grid beyond the repository to the north and south
6. Refinements to the y-spacing of the grid as allowed by the revised shaft seal model

These changes were substantial enough so as to be designated as modifications to existing conceptual models used in the CCA and the CCA PAVT. All conceptual model changes were approved by the Salado Flow Peer Review Panel in February 2003 (Caporuscio, Gibbons, and Oswald 2003). These changes were made and approved by the EPA in the 2004 recertification decision (U.S. EPA 2006).

MASS-4.1.1.1 CRA-2004 Simplified Shaft Seal Model

A shaft seal model was included in the CRA-2004 grid, and was implemented in a simpler fashion than that used for the CCA PA and the CCA PAVT. A comparison of the shaft seal representations used in the CCA and the CRA-2004 is shown in Figure MASS-4. A detailed description of the parameters used to define the simplified model is discussed in AP-094 (James and Stein 2002) and the resulting analysis report (James and Stein 2003). The simplified shaft model was tested in the AP-106 calculations (Stein and Zelinski 2003a and Stein and Zelinski 2003b). The results of this analysis demonstrated that brine flow through the simplified shaft

model was comparable to brine flows through the detailed shaft model in the CCA PAVT calculations (see the CRA-2004, Chapter 9.0, Section 9.1.3.4), and that shaft seals are very effective barriers to flow throughout the 10,000-year regulatory period.

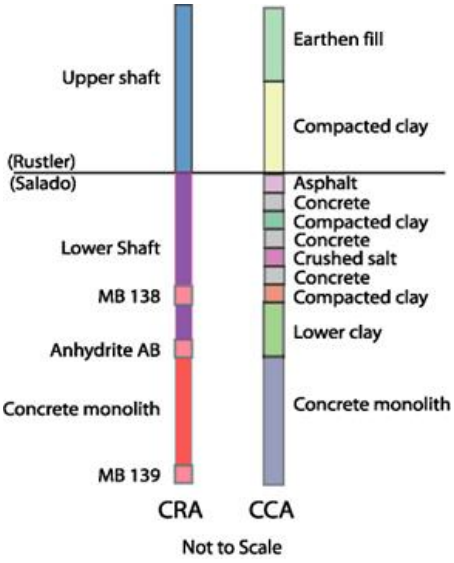

Figure MASS- 4. Comparison of the Simplified Shaft (CRA-2004) and the Detailed Shaft (CCA) Models

The shaft seal model used in the CRA-2004 PA is described by Stein and Zelinski (Stein and Zelinski 2003a and Stein and Zelinski 2003b), and was approved by the Salado Flow Peer Review Panel (Caporuscio, Gibbons, and Oswald 2003).

The CRA-2004 PA shaft representation was used in the CRA-2009 PA, and is also used in the CRA-2014 PA.

MASS-4.1.1.2 CRA-2004 Implementation of Option D-Type Panel Closure

The PA calculations that supported the CCA and the subsequent CCA PAVT calculations included generic panel closures in the BRAGFLO grid. The generic panel closures included in the CCA PA and the CCA PAVT calculations were relatively permeable and allowed gas to flow freely between panels. In the CCA PA and the CCA PAVT calculations, a drilling intrusion into a single panel generally caused pressures in the entire repository to decrease.

The DOE presented four panel closure design options (Options A through D) as part of the CCA. Upon reviewing the CCA, the EPA mandated the implementation of the Option D design. The Option D design consists of two components: a large monolith constructed of Salado Mass Concrete (SMC) that is keyed into the surrounding DRZ, and an explosion isolation wall constructed of concrete blocks, which is not keyed into the DRZ. For the CRA-2004, the true cross-sectional area of the Option D panel closure was represented in the flow model, and this implementation is described fully in Appendix PA-2004, Attachment MASS, Section MASS-4.2.4. Option D panel closures in the CRA-2004 were represented by the following four materials:

1. CONC_PCS: This material represents the concrete monolith, which has properties of SMC.

2. DRZ_PCS: This material represents the DRZ immediately above the concrete monolith that is expected to heal after the emplacement of the monolith.

3. DRF_PCS: This material represents the empty drift and explosion isolation wall portion of the panel closure. This material has the same properties as WAS_AREA (including creep closure).

4. MB materials S_ANH_AB and S_MB 139: These materials are the same as those used to represent the anhydrite MBs in other parts of the grid. MB materials were used because they have permeability ranges very close to the material CONC_PCS and in the case when pressures near the panel closures exceed the fracture initiation pressure of the MBs, fractures could extend around the concrete monolith out of the 2-D plane represented by the numerical grid. By using MB materials to represent the parts of the panel closures that intersect MBs, both the permeability of the closure and the potential fracture behavior of MB material near the closures are represented.

The logical grid representation of the Option D PCS implementation used in the CRA-2004 is shown in Figure MASS-5. The Option D PCS representation shown in that figure was also used in the CRA-2009 PA and CRA-2009 PABC. The Option D PCS is replaced by the ROMPCS in the CRA-2014 PA (see Section MASS-4.1.3).

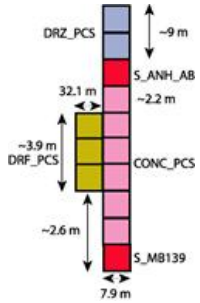

Figure MASS- 5. Logical Grid Representation of the Option D Panel Closures for the CRA-2004

MASS-4.1.1.3 Increased Segmentation of Waste Regions in Grid

The CCA PA and the CCA PAVT grid divided the waste region into a single panel in the southern end of the repository referred to as the Waste Panel, and a larger region containing the other nine panels referred to as the rest of repository (RoR). The Waste Panel was intersected by an intrusion borehole and was used to represent conditions in any panel intersected by a borehole. Preliminary tests of the Option D panel closure representation (Hansen et al. 2002) concluded that Option D panel closures were effective at impeding fluid flow between panels on the order of thousands of years, but that, given enough time, pressures slowly equilibrated. These results suggested that the effect of a single intrusion event on pressures in other panels depends on the number of panel closures that lie between the intruded panel and the other panels. Therefore, in the CRA-2004, the DOE divided the RoR region used in the CCA and PAVT into northern and southern blocks separated by a set of panel closures. The south RoR block represented conditions in a panel directly adjacent to an intruded panel. The north RoR block represented conditions in a nonadjacent panel far from the intruded panel (i.e., at least two panel closures are between it and the intruded panel). The panel closure between the north and south RoR represented a set of four panel closures located between the northern and southern internal extended panels. This representation assumed that the effects of drilling intrusions are damped in non-intruded panels, and the degree of damping depends on the proximity of the drilling intrusion and the number of panel closures separating the intruded panel from other regions of the repository. The CRA-2009 PA and CRA-2009 PABC used the same segmentation of the waste regions as in the CRA-2004 PA (see Appendix PA-2004, Attachment MASS, Section MASS-4.2.4 for a description of waste-region segmentation). The CRA-2014 PA also uses the waste region segmentation developed during the CRA-2004.

MASS-4.1.1.4 CRA-2004 Refinement to the Grid Flaring Method

Grid flaring is a method to represent three-dimensional volumes in a two-dimensional grid. Flaring is used when flows can be represented as divergent and convergent from the center of flaring. The CCA PA and CCA PAVT grids used flaring at two different scales: locally around the borehole and shaft, and regionally to the north and south of the excavated regions (around a point in the northern end of the RoR). For the CRA-2004 PA, the local flaring around the borehole was the same as in the CCA PA/CCA PAVT grid. The local flaring around the shaft was eliminated as it had been demonstrated to not be a release pathway. Likewise, the calculation of regional flaring was simplified. The CRA-2009 PA used the same grid flaring as in the CRA-2004 PA (see Appendix PA-2004, Attachment MASS, Section MASS-4.2.5 for a description of grid flaring). The same grid flaring method is used in the CRA-2014.

MASS-4.1.1.5 CRA-2004 Refinement of the X-Spacing Outside the Repository

The grid blocks to the north and south of the excavated region were refined in the x-direction during the CRA-2004. The x-dimension of grid cells immediately to the north and south of the repository were set to 2 m. Cell x-lengths were then increased by a factor of 1.45 toward the north and south.

Exceptions to this algorithm were made to ensure that the location of the Land Withdrawal Boundary and the total extent of the grid matched that of the CCA PA and CCA PAVT grids. This CRA-2004 PA refinement to the X-spacing of grid cells outside of the repository was chosen to reduce numerical dispersion caused by rapid increases in cell dimensions (Anderson and Woessner 1992; Wang and Anderson 1982). The CRA-2009 PA used this refinement, as does the CRA-2014 PA.

MASS-4.1.1.6 CRA-2004 Refinement of the Y-Spacing

During the CRA-2004 PA, grid spacing in the y direction for layers representing the Salado were changed from the CCA PA/CCA PAVT grid spacing. The Salado grid spacing used in the CCA PA was dictated by the thickness of different shaft seal materials. The simplification of the shaft seal representation used in the CRA-2004 allowed for uniform y-spacing in the Salado region of the grid. In addition, two layers were added immediately above and below MB 139 to refine the grid spacing and reduce numerical dispersion. These changes resulted in a total of 33 y divisions for the grid, and increased the numerical accuracy of flow and transport calculations.

The x- and y-direction refinements used in the CRA-2004 PA grid were included in the CRA-2009 PA, and are also included in the CRA-2014 PA.

MASS-4.1.1.7 CRA-2004 BRAGFLO Material Map and Numerical Grid

The combined changes to the BRAGFLO disposal system geometry developed during the CRA-2004 resulted in the BRAGFLO material map and numerical grid shown in Figure MASS-6. The grid shown in that figure has 68 grid cells in the x direction and 33 cells in the y direction.

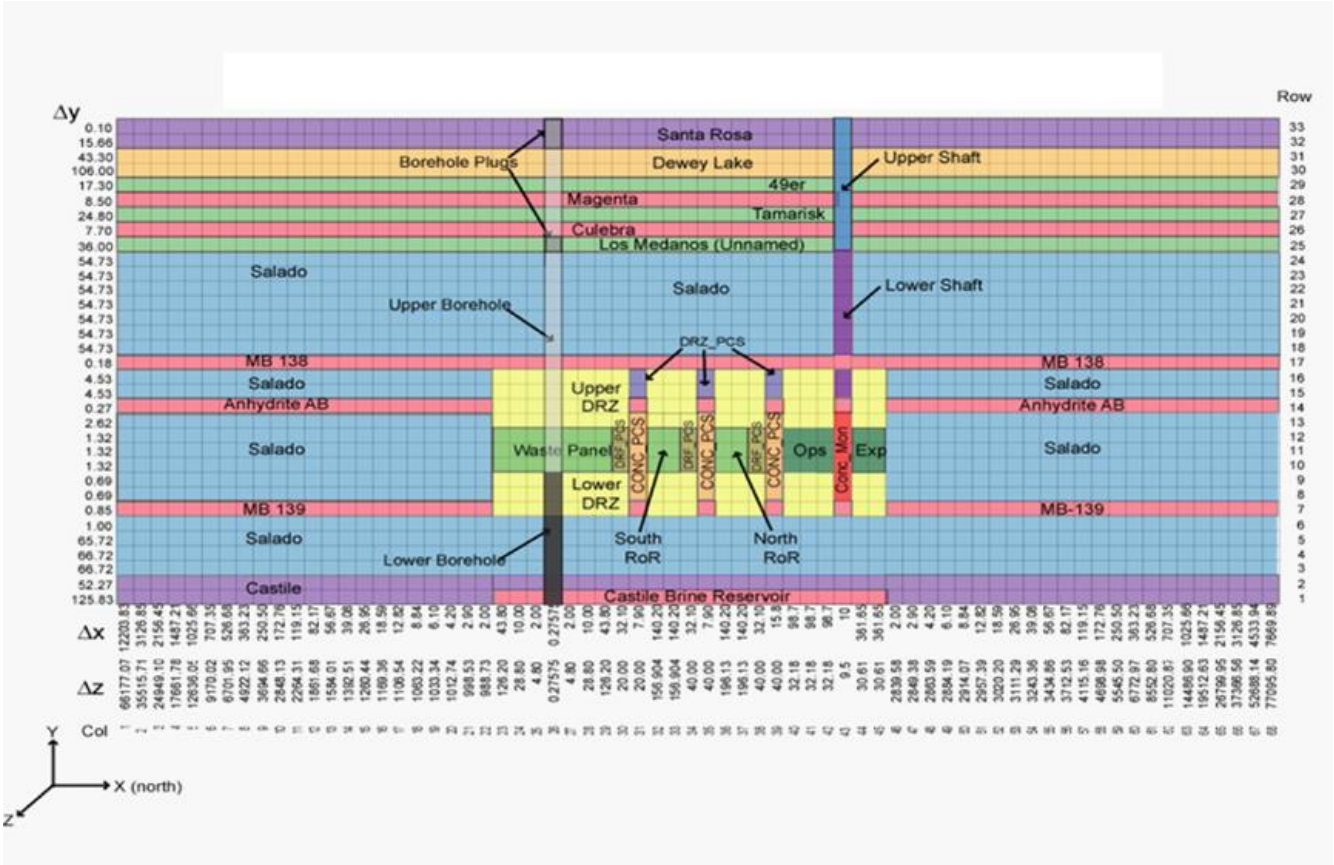

Figure MASS- 6. CRA-2004 BRAGFLO Grid and Material Map (Δx, Δy, and Δz dimensions in meters)

MASS-4.1.2 CRA-2004 to CRA-2009 Baseline Grid Changes

No changes were made to the BRAGFLO repository geometry developed during the CRA-2004 as part of the CRA-2009. The CRA-2009 PA used the BRAGFLO material map and numerical grid shown in Figure MASS-6.

MASS-4.1.3 CRA-2009 to CRA-2014 Baseline Grid Changes

The BRAGFLO material map and numerical grid used in the CRA-2014 PA is very similar to that developed during the CRA-2009. The primary change incorporated in the CRA-2014 BRAGFLO repository representation is the replacement of the Option D PCS with the ROMPCS. Added volume in the repository experimental area also slightly alters the BRAGFLO grid used in the CRA-2014 PA.

The WIPP waste panel closures comprise a feature of the repository that has been represented in WIPP PA regulatory compliance demonstration since the CCA. Following the selection of the Option D panel closure design in 1998, the DOE has reassessed the engineering of the panel closure and established a revised design which is simpler, easier to construct, and equally effective at performing its operational-period isolating function. The revised design is the ROMPCS, and is comprised of 100 ft of ROM salt with barriers at each end. The barriers consist of ventilation bulkheads, and are similar to those used in the panels as room closures. The ventilation bulkheads are designed to restrict air flows and prevent personnel access into waste-filled areas during the operational phase of the repository. The ventilation bulkheads are expected to have no significant impact on long-term performance of the panel closures and are therefore not included in the representation of the ROMPCS. Option D explosion isolation walls fabricated from concrete blocks have been emplaced in the entries of waste panels 1, 2, and 5, and replace the bulkheads on the waste side of the closure. It is expected that these walls will not be significant structures after the initial 100-year time period, due to the brittle, non-plastic behavior of concrete. The already emplaced explosion isolation walls are therefore expected to have no significant impact on

long-term panel closure performance, and so are also not included in the representation of the ROMPCS. Consequently, the ROMPCS is modeled as consisting of 100 ft of ROM salt in the CRA-2014 PA.

ROMPCS properties in the CRA-2014 PA are based on three time periods (see Camphouse et al. 2012). Consequently, the ROMPCS is represented by three materials, with each material representing the ROMPCS for a portion of the 10,000-year regulatory period. Material PCS_T1 represents the ROMPCS for the first 100 years after facility closure. Material PCS_T2 models the ROMPCS from 100 to 200 years. Finally, material PCS_T3 represents the ROMPCS from years 200 to 10,000. For the first 200 years post-closure, the DRZ above and below the ROMPCS maintains the same properties as specified to the DRZ surrounding the disposal rooms (PA material DRZ_1). After 200 years, the DRZ above and below the ROMPCS is modeled as having healed, and is represented by material DRZ_PCS. Materials DRZ_1 and DRZ_PCS have the same properties in the CRA-2014 PA as were assigned to them in the CRA-2009 PA. As previously discussed, segments of interbed material were included in the PA representation of the Option D panel closure, and are also included in the CRA-2014 PA representation of the ROMPCS.

The temporal evolution of the ROMPCS in BRAGFLO for the CRA-2014 PA is illustrated in Figure MASS-7 to Figure MASS-9. As seen in Figure MASS-7 and Figure MASS-8, the only change in the BRAGFLO grid and material map for time periods 0 to 100 years and 100 to 200 years is the material used to represent the panel closure. Material PCS_T1 is used to represent the ROMPCS for years 0 to 100, while material PCS_T2 represents the panel closure for years 100 to 200. As discussed above, the ROMPCS is modeled as having no impact on the DRZ above and below the closure for the first 200 years after emplacement. For the first 200 years, the DRZ material above and below the closure in the BRAGFLO material map is the same as the material above and below other repository regions. After 200 years, the material used to represent the ROMPCS changes to PCS_T3, and the regions of healed DRZ above and below the closure is modeled by material DRZ_PCS, as shown in Figure MASS-9. The repository representation shown in Figure MASS-9 is used for times between 200 years and the time of intrusion. The BRAGFLO grid and element maps corresponding to particular intrusion types are shown in Figure MASS-10 and Figure MASS-11.

The inclusion of the ROMPCS and additional mined volume in the repository north end slightly alters some of the element widths in the CRA-2014 BRAGFLO grid as compared to those used in the CRA-2004 and CRA-2009. The Option D panel closure implemented in the CRA-2004 and CRA-2009 is 40 m long, while the ROMPCS implemented in the CRA-2014 PA is 30.48 m (100 ft) long. Consequently, the panel closure length is reduced to a value of 30.48 m in the CRA-2014 PA, with panel closures represented by two elements in the x direction, each 15.24 m long. Similarly, elements corresponding to the repository experimental area are lengthened in the z direction to account for additional mined volume in that region. Two element lengths of 30.61 m in the z direction were used to represent the repository experimental area in the CRA-2009 PA. These two lengths are increased to 51.67 m and 51.68 m in the CRA-2014 PA to account for the additional mined volume in the experimental area.

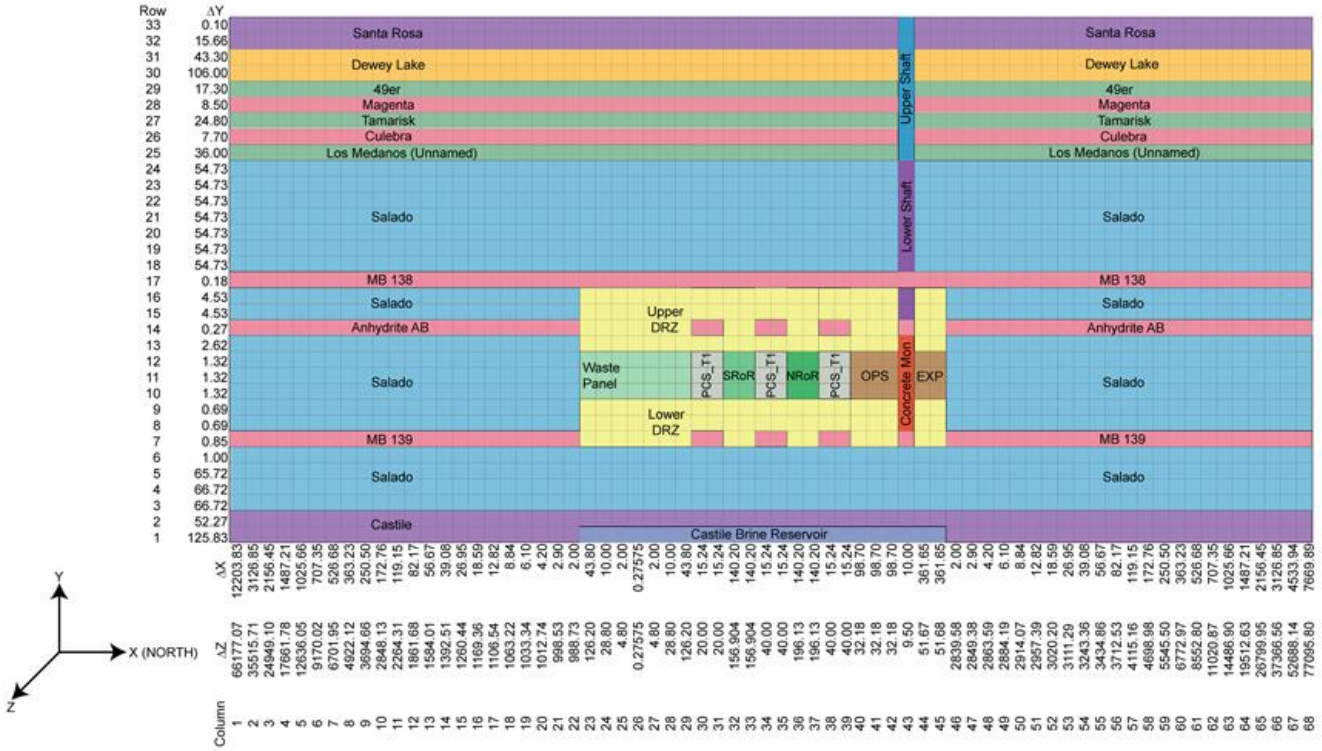

Figure MASS- 7. CRA-2014 PA BRAGFLO Grid and Material Map, Years 0 to 100

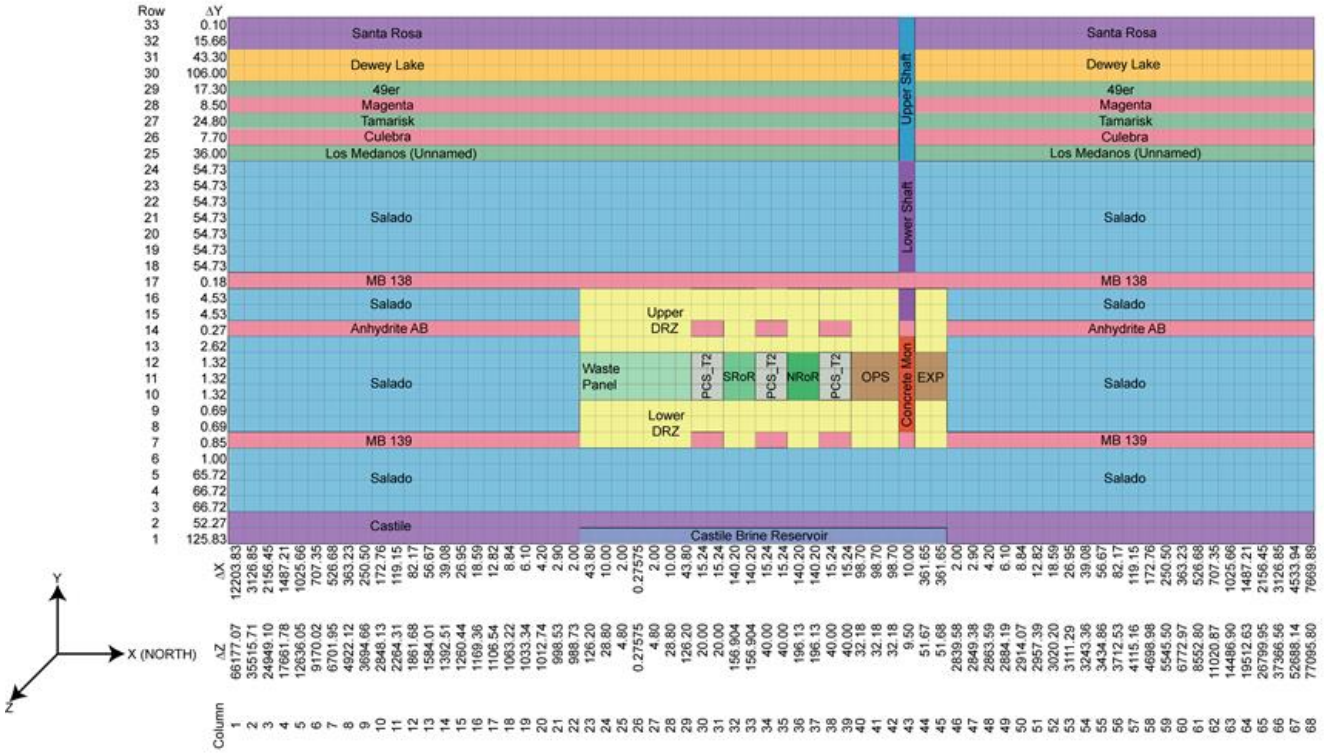

Figure MASS- 8. CRA-2014 PA BRAGFLO Grid and Material Map, Years 100 to 200

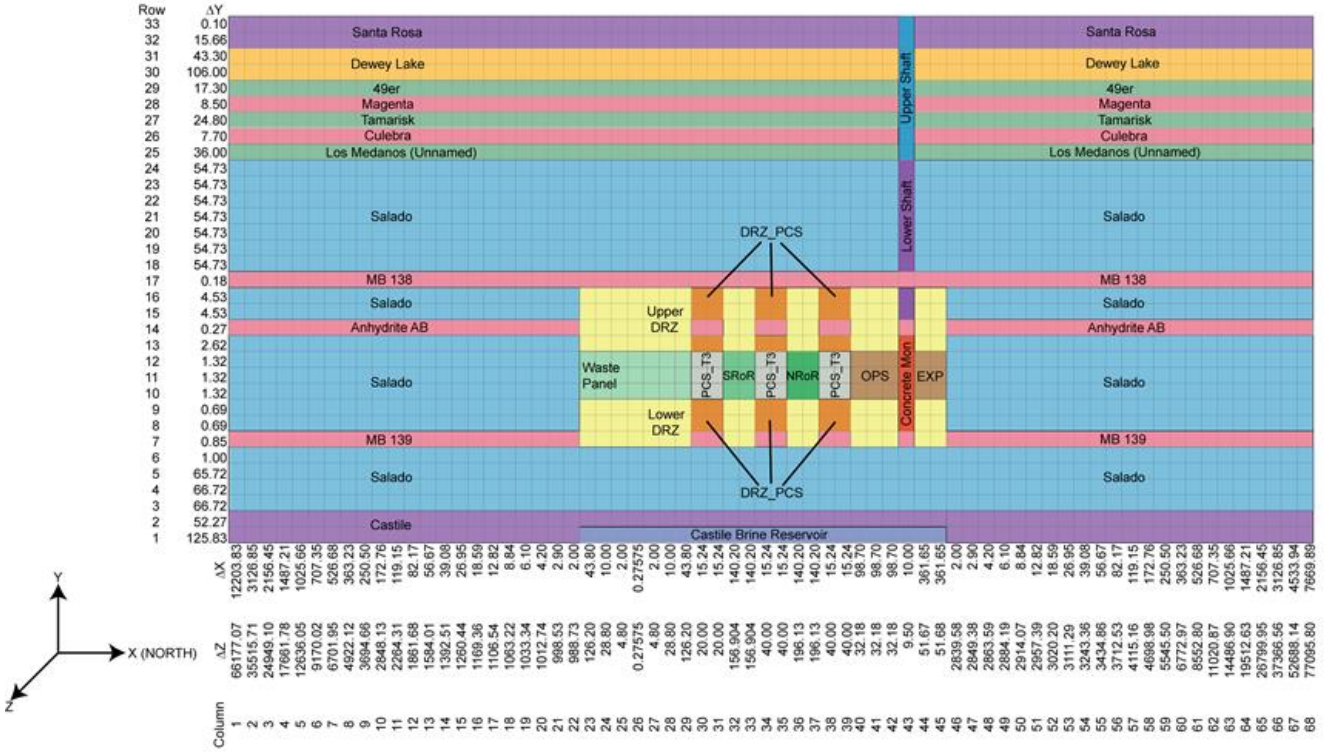

Figure MASS- 9. CRA-2014 PA BRAGFLO Grid and Material Map, Years 200 to Time of Intrusion

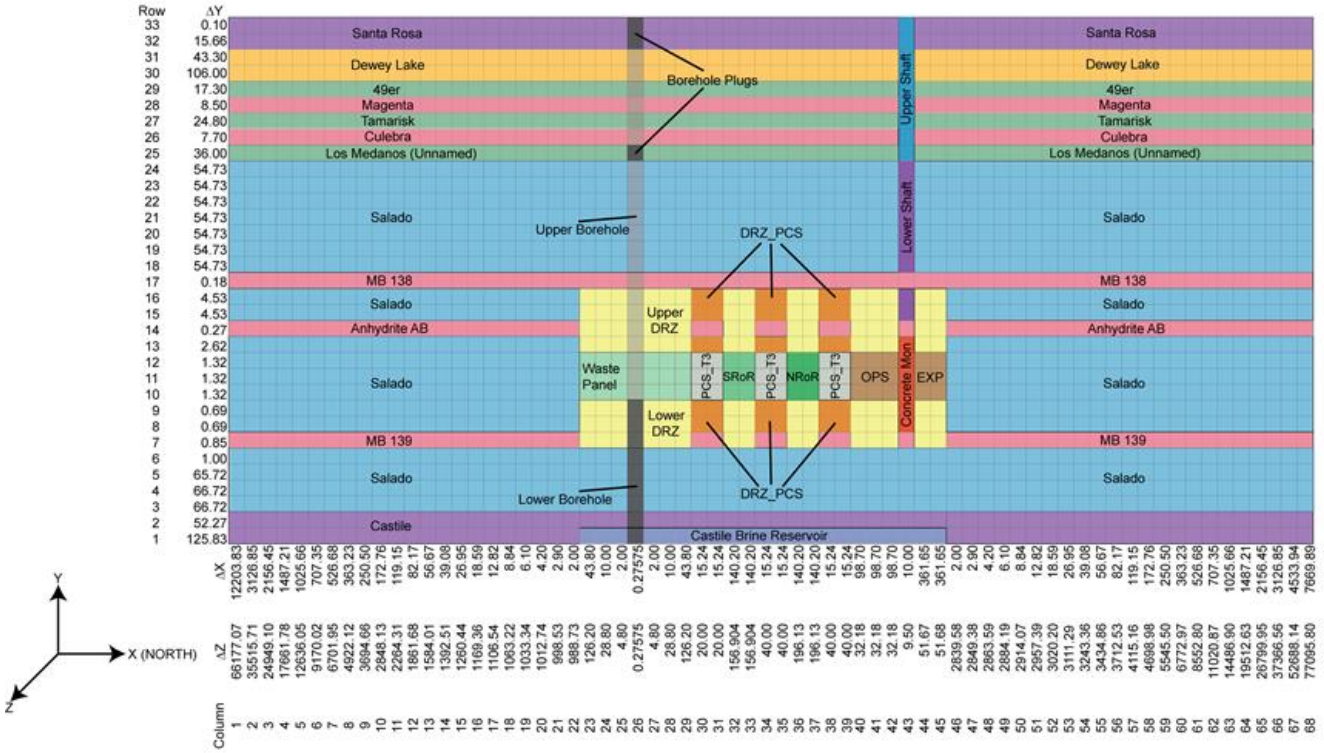

Figure MASS- 10. CRA-2014 PA BRAGFLO Grid and Material Map for an E1 Intrusion

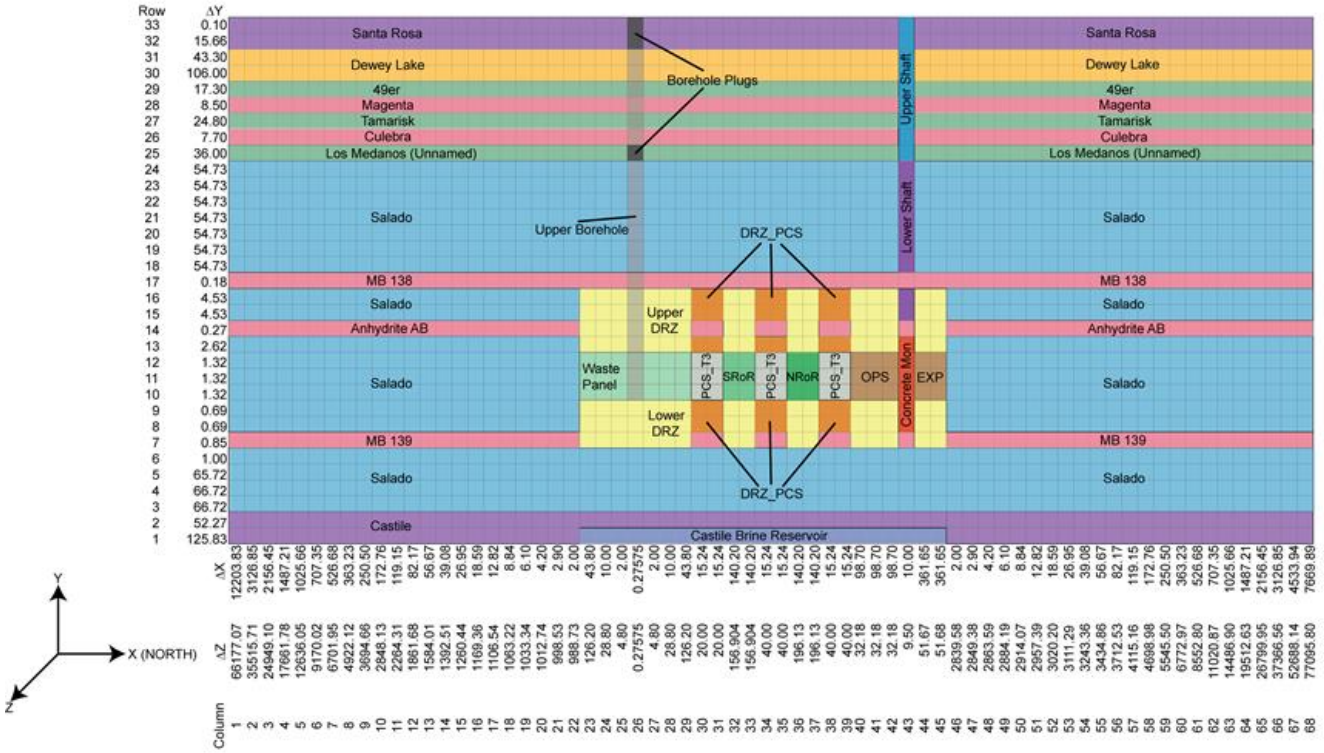

Figure MASS- 11. CRA-2014 PA BRAGFLO Grid and Material Map for an E2 Intrusion

MASS-5.0 Creep Closure

The creep closure model used in the CRA-2014 is the same as that used in the CRA-2009 and the CRA-2009 PABC. The model used for creep closure of the repository is discussed in Appendix PORSURF-2014. Historical information on creep closure modeling is also contained in Appendix PORSURF-2014.

MASS-6.0 Repository Fluid Flow

Most repository fluid flow assumptions have not changed from those used in the CRA-2009 PABC. Those that did not change are discussed in Section MASS-6.1 and Section MASS-6.2, while those that did change are discussed in Section MASS-6.3. The Repository Fluid Flow conceptual model represents the long-term flow behavior of liquid and gas in the repository and its interaction with other regions in which fluid flow may occur, such as the Salado, shafts, or an intrusion borehole. This model is not used to represent the interaction of fluids in the repository with a borehole during drilling. Historical information on alternative conceptual models for brine inflow to the repository is contained in the CCA, Appendix MASS, Section MASS-7.0.

The first principle in the conceptual model for fluid flow in the repository is that gas and brine can both be present and mobile (two-phase flow), governed by conservation of energy and mass and by Darcy's Law for their fluxes (see Appendix PA-2014, Section PA-4.2). Consistent with typical concepts of two-phase flow, the phases can affect each other by impeding flow caused by partial saturation (relative permeability effects) and by affecting pressure caused by capillary forces (capillary pressure effects).

The flow of brine and gas in the repository is assumed to behave as two-phase, immiscible, Darcy flow (see Appendix PA-2014, Section PA-4.2). BRAGFLO is used to simulate brine and gas flow in the repository and to incorporate the effects of disposal-room closure and gas generation. Fluid flow in the repository is affected by the following factors:

- The geometric association of pillars, rooms, and drifts; waste panel consolidation due to salt creep; and possible borehole locations
- The varied properties of the waste areas resulting from creep closure and heterogeneous contents
- Flow interactions with other parts of the disposal system
- Reactions that generate gas

The geometry of the panel around the intrusion borehole is consistent with the assumption that the fluid flow there will occur directly toward or directly away from the borehole. The geometry represents a semicircular volume north of the borehole and a semicircular volume south of the borehole (representing radial flow in a subregion of a two-dimensional representation of the repository).

Approximating convergent and divergent flow around the intrusion borehole creates a narrow neck in the otherwise fairly uniform numerical grid in the region representing the repository. In the undisturbed performance scenario, and under certain conditions in other scenarios, flow in the repository may pass laterally through this neck. In reality, this neck does not exist. Its presence in the model is expected to have a negligible or conservative impact on model predictions compared to predictions that would result from a more realistic model geometry. The time scale involved and the permeability contrast between the repository and surrounding rock are sufficient so that the lateral flow that may occur in the repository is restricted by the rate at which liquid gets into or out of the repository, rather than by the rate at which it flows through the repository.

Gas generation is affected by the quantity of liquid in contact with metal and CPR waste materials. However, the distribution of fluid in the repository can only be approximated. For example, capillary action can create wicking that would increase the overall region in which gas generation occurs, but modeling this at the necessary resolution to simulate these processes would greatly increase the time required to carry out the modeling (Appendix PA-2014, Section PA-4.2.6 , and CRA-2004, Section 6.4.3.3). Therefore, as a bounding measure for gas generation purposes, brine in the repository is distributed to an extent greater than estimated by the Darcy flow models or by the values of parameters chosen.

Modeling of flow within the repository is based on homogenizing the room contents into relatively large computational volumes. The approach ignores heterogeneities in disposal room contents that may influence gas and brine behavior by causing fluid flow among channels or creating preferential paths in the waste, bypassing entire regions. Isolated regions could exist for several reasons:

- They may be isolated by low-permeability regions of waste that serve as barriers.
- Connectivity with the interbeds may occur only at particular locations within the repository.
- The repository dip may promote preferential gas flow in the upper regions of the waste.

For the CCA, the adequacy of the repository homogeneity assumption was examined in screening analyses DR-1 (Webb 1995) and DR-6 (Vaughn, Lord, and MacKinnon 1995a). These analyses used an additional parameter in BRAGFLO to specify the minimum active (mobile) brine flow saturation (pseudoresidual brine saturation). Above this saturation, the normal descriptions of two-phase flow apply (i.e., either the Brooks and Corey or van Genuchten and Parker relative permeability models). Below this minimum, brine is immobile, although it is available for reaction and may still be consumed during gas-generation reactions. The assumption of a minimum saturation limit was justified based on the presumed heterogeneity of the waste and the slight dip in the repository. The

minimum active brine saturation was treated as an uncertain parameter and sampled uniformly between the values 0.1 and 0.8 during the analysis. This saturation limit was applied uniformly throughout the disposal room to bound the impact of heterogeneities on flow (Webb 1995; Vaughn, Lord, and MacKinnon 1995a). Results of this analysis showed that releases to the accessible environment in the baseline case (homogenization) are consistently higher.

The experimental and operations regions were represented in the CCA PA by a fixed porosity of 18.0% and a permeability of 10^{-11} m^2. The combination of low porosity and high permeability conservatively overestimated fluid flow through these regions and limited the capacity of these regions to store fluids, potentially overestimating releases to the environment. This conclusion was based on a screening analysis (Vaughn, Lord, and MacKinnon 1995b) that examined the importance of permeability varying with porosity in closure regions (waste disposal region, experimental region, and operations region). To perform this analysis, a model for estimating the change in permeability with porosity in the closure regions was implemented in BRAGFLO. A series of BRAGFLO simulations was performed to determine whether permeability varying with porosity in the closure regions could enhance contaminant migration to the accessible environment. Two basic scenarios were considered in the screening analysis: undisturbed performance and disturbed performance. To assess the sensitivity of system performance on dynamic permeability in the closure regions, CCDFs of normalized contaminated brine releases were constructed and compared with the corresponding baseline conditional CCDFs. The baseline model treated permeabilities in the closure regions as fixed values. Results of this analysis showed that the inclusion of dynamic closure of the waste disposal region, experimental region, and operations region in BRAGFLO resulted in computed releases to the accessible environment that are essentially equivalent to the baseline case.

A separate analysis (Park and Hansen 2003) examined the possible effects of heterogeneity in waste container and waste material strength on room closure. The analysis of room closure found that the room porosity may vary widely depending on the type of waste container and the emplacement of waste in the repository. However, analysis of a separate PA (Hansen et al. 2003) found that PA results are relatively insensitive to the uncertainty in room closure and room porosity. The conclusions of the separate PA are summarized in Section MASS-19.0 of this appendix.

MASS-6.1 Flow Interactions with the Creep Closure Model

The dynamic effect of halite creep and room consolidation on room porosity is modeled only in the waste disposal region. Other parts of the repository, such as the experimental region and the operations region, are modeled assuming fixed (invariant with time) properties. In these regions, the permeability is held at a fixed high value representative of unconsolidated material, while the porosity is maintained at relatively low values associated with highly consolidated material. This combination of low porosity and high permeability is assumed to conservatively overestimate flow through these regions and minimize the capacity of this material to store fluids, thus maximizing the release to the environment. To examine the acceptability of this assumption, a screening analysis (Vaughn, Lord, and MacKinnon 1995c) evaluated the effect of including closure of the experimental region and operations region. In this analysis, consolidation of the experimental region and operations region was implemented in BRAGFLO by relating pressure and time to porosity using a porosity-surface method. The porosity surface for the experimental region and operations region differs from the surface used for consolidation of the disposal room and is based on an empty excavation (see Appendix PORSURF-2014). The screening analysis showed that disregarding dynamic closure of the experimental region is acceptable because it is conservative: lower releases occur when closure of the experimental region and operations region is computed compared to simulations with time-invariant high permeability and low porosity.

MASS-6.2 Flow Interactions with the Gas Generation Model

Gas generation affects repository pressure, which in turn is an important parameter in other processes such as two-phase flow, creep closure, and fracturing of the interbeds and DRZ. Gas-generation processes considered in PA calculations include anoxic corrosion and microbial degradation. Radiolysis is excluded from PA calculations on the basis of laboratory experiments and a screening analysis (Vaughn et al. 1995) that concluded that radiolysis does not significantly affect repository performance.

In modeling gas generation, the effective liquid in a computational cell is the computed liquid in that cell plus an adjustment for the uncertainty associated with wicking by the waste (see Appendix PA-2014, Section PA-4.2.6). Capillary action (wicking) is the ability of a material to carry a fluid by capillary forces above the level it would normally seek in response to gravity. Because the current gas-generation model computes substantially different gas-generation rates depending on whether the waste is wet or merely surrounded by water vapor, the physical extent of wetting could be important. A screening analysis (Vaughn, Lord, and MacKinnon 1995d) examined wicking and concluded that it should be included in PA calculations.

The baseline gas-generation model in BRAGFLO accounts for corrosion of iron and microbial degradation of cellulose and possibly plastics and rubber. The net reaction rate of these processes depends directly on brine saturation: an increase in brine saturation will increase the net reaction rate by weighting the inundated portion more heavily and the slower humid portion less heavily. To simulate the effect of wicking on the net reaction rate, an effective brine saturation, which includes a wicking saturation contribution, is used to calculate reaction rates rather than the actual brine saturation (see Appendix PA-2014, Section PA-4.2.6).

MASS-6.3 Changes to Flow Interactions with the Gas-Generation Model in the CRA-2014

The CRA-2014 includes a refinement to the repository water balance implementation as compared to that used in the CRA-2009 PABC. The main objective of refining the repository water balance is to include the major gas and brine producing and consuming reactions in the existing conceptual model. As described in the Chemical Conditions Conceptual Model, the major reactions in the repository include the reactions of CPR, iron, and MgO with brine (U.S. DOE 2004, sections PEER-2004 1.1.3, PEER-2004 1.1.4 and PEER-2004 1.1.5). In the CRA-2014, the same biodegradation pathways are included as were implemented in the CRA-2009 PABC, but the generation of water in these pathways is also considered. The reaction of iron hydroxide with hydrogen sulfide, which consumes gas and produces water, is also included. It is assumed that the hydrogen sulfide preferentially reacts with the iron hydroxide versus metallic iron. MgO reactions are expanded in the CRA-2014 to include MgO hydration, which consumes water and produces brucite, and the carbonation of brucite, which is assumed to form hydromagnesite. It is assumed that the carbon dioxide preferentially reacts with the brucite versus the dry MgO. Since hydromagnesite is not thermodynamically stable under repository conditions, it is assumed to dehydrate to form magnesite. As a result, the reaction of hydromagnesite to form magnesite, which produces water, is also included in the CRA-2014. All chemical reactions and species are tracked on a cell-by-cell basis. There is a finite amount of each chemical species in each cell. Once any of them are used up, that particular reaction ceases. The WIPP PA codes PREBRAG v8.02 and BRAGFLO v6.02 have been developed and qualified for this refinement to the repository water balance, and are used in the CRA-2014 PA. The reactions that comprise the refinement to the repository water balance implementation are more fully discussed in Appendix PA-2014, Section PA-4.2.5.

MASS-7.0 Gas Generation

The gas generation model represents the possible generation of gas in the repository by corrosion of steel and microbial degradation of CPR materials. The CRA-2009 used the CRA-2004 PABC gas generation modeling assumptions, as does the CRA-2014. Additional discussion of this topic may be found in Appendix PA-2014, Section PA-4.2.5 and Appendix SCR-2014 (FEPs W44 through W48, W53, and N71) and the CRA-2004, Chapter 6.0, Section 6.4.3.3.

MASS-7.1 Historical Context of Gas Generation Modeling

See the CCA, Appendix MASS, Section MASS-8.1 for historical information on the development of the CCA gas-generation conceptual model.

MASS-8.0 Chemical Conditions

The modeling assumptions of chemical conditions used in the CRA-2014 are unchanged from those used in the CRA-2009 PABC. The implementation now includes the refined water budget discussed in MASS-6.3 and the variable brine volume discussed in MASS-2.6.10. The models used for chemical conditions in the repository are discussed in Appendix MgO-2014, Appendix SOTERM-2014, and Appendix PA-2014.

MASS-9.0 Dissolved Actinide Source Term

The dissolved actinide source term modeling assumptions used in the CRA-2009 were unchanged from those used in the CRA-2004 PABC, and remain unchanged in the CRA-2014. The models used for the dissolved actinide source term in the repository are discussed in Appendix SOTERM-2014, Section SOTERM-4.0 and Section SOTERM-5.0.

MASS-10.0 Colloidal Actinide Source Term

The colloidal actinide source term modeling assumptions used in the CRA-2009 were unchanged for the CRA-2014, but the model parameters are updated for the CRA-2014. The models used for the colloidal actinide source, and actinide source term updates included in the CRA-2014, are discussed in Appendix SOTERM-2014, Section SOTERM-5.0.

MASS-11.0 Shafts and Shaft Seals

The shafts and shaft seals modeling assumptions used in the CRA-2009 were unchanged from those used in the CRA-2004 PABC, and remain unchanged in the CRA-2014. The models used for shafts and shaft seals are discussed in Appendix PA-2004, Attachment MASS, Section MASS-12.0.

MASS-12.0 Salado

The far-field Salado modeling assumptions used in the CRA-2009 were unchanged from those used in the CRA-2004 PABC, and remain unchanged in the CRA-2014. The purpose of this model is to reasonably represent the effects of fluid flow in the Salado on long-term performance of the disposal system. The conceptual model is also discussed in the CRA-2004, Chapter 6.0, Section 6.4.5.

Fluid flow in the Salado is considered in the conceptual model of long-term disposal system performance for several reasons. First, some liquid could move from the Salado to the repository because of the considerable gradients that can form for liquid flow inward to the repository. This possibility is important because such fluid can affect creep closure, gas generation, actinide solubility, and other processes occurring in the repository. Second, gas generated in the repository is thought to be capable of fracturing the Salado

interbeds under certain conditions, creating increased permeability channels that could be pathways for lateral transport. The lateral transport pathway in intact Salado is also modeled, but it is considered unlikely to result in any significant radionuclide transport to the accessible environment boundary.

The fundamental principle in the conceptual model for fluid flow in the Salado is that it is a porous medium within which gas and brine can both be present and mobile (two-phase flow), governed by conservation of energy and mass and by Darcy's Law for their fluxes (see Appendix PA-2014, Sections PA-4.2). Consistent with typical concepts of two-phase flow, each phase can affect the other by impeding flow because of partial saturation (relative permeability effects) and by affecting pressure by capillary forces (capillary pressure effects). It was originally assumed that no waste-generated gas is present before repository closure. However, during the EPA completeness review of the CRA-2004, the representation of the gas-generation rate was changed for the CRA-2004 PABC (Cotsworth 2005). The repository was precharged after closure to represent the short-term, but initially faster, microbial gas-generation rate (see Leigh et al. 2005, Section 2.3). Future states are modeled as producing gas by corrosion and microbial activities. Should high pressure develop over the regulatory period, it is allowed to access MBs in the Salado.

Some variability in composition exists between different horizons of the Salado. The largest differences occur between the anhydrite-rich layers called interbeds and those dominated by halite. Within horizons dominated by halite, composition varies from nearly pure halite to halite plus several percent other minerals, in some instances including clay (see the CCA, Chapter 2.0, Section 2.1.3.4). The Salado is modeled as impure halite except for those interbeds that intersect the DRZ near the repository. This conceptual model and an alternative model that explicitly represented all stratigraphically distinct layers of the Salado near the repository (Christian-Frear and Webb 1996) produced similar results.

From other modeling and theoretical considerations, flow between the Salado and the repository is expected to occur primarily through interbeds that intersect the DRZ. Because of the large surface areas between the interbeds and surrounding halite, the interbeds serve as conduits for the flow of brine in two directions: from halite to interbeds to the repository or, for brine flowing out of the repository, from the repository into interbeds and then into halite. Because the repository is modeled as a relatively porous and permeable region, brine is considered most likely (but not constrained) to leave the repository through MB 139 below the repository because of the effect of gravity. If repository pressures become sufficiently high, gas is modeled to exit the repository via the MBs.

The effect of gravity may also be important in the Salado because of the slight and variable natural stratigraphic dip. For long-term performance modeling, the dip in the Salado within the domain is taken to be constant and 1 degree from north to south.

Fluid flow in the Salado is conceptualized as occurring either convergently into the repository or divergently from it, as discussed in detail in the CRA-2004, Chapter 6.0, Section 6.4.2.1. Because the repository is not conceptualized as homogeneous, implementing a geometry for the conceptual model of convergent or divergent flow in the Salado is somewhat complicated and is discussed in the CRA-2004, Chapter 6.0, Section 6.4.2.1.

The conceptual model for Salado fluid flow has primary interactions with three other conceptual models. The interbed fracture conceptual model allows porosity and permeability of the interbeds to increase as a function of pressure. The repository fluid flow model is directly coupled to the Salado fluid flow model by the governing equations of flow in BRAGFLO (in the governing equations of the mathematical model, they cannot be distinguished), and it differs only in the region modeled and the parameters assigned to materials. The Salado model for actinide transport is directly coupled to the conceptual model for flow in the Salado through the process of advection. Additional information on the treatment of the Salado in PA is found in Appendix PA-2014, Section PA-4.2.

MASS-12.1 High Threshold Pressure for Halite-Rich Salado Rock Units

An important parameter used to describe the effects of two-phase flow is threshold pressure, which helps to determine the ease with which gas can enter a liquid-saturated rock unit. For a brine-saturated rock, the threshold pressure is defined as "equal to the capillary pressure at which the relative permeability to the gas phase begins to rise from its zero value, corresponding to the incipient development of interconnected gas flow paths through the pore network" (Davies 1991, p. 9).

The threshold pressure, as well as other parameters used to describe two-phase characteristics, has not been measured for halite-rich rocks of the Salado. The Salado, however, is thought to be similar in pore structure to rocks for which threshold pressures have been measured (Davies 1991). Based on this observation, Davies (Davies 1991) postulated that the threshold pressure of the halite-rich rocks in the Salado could be estimated if an empirical correlation exists between rocks postulated to have similar pore structure.

Davies developed a correlation between threshold pressure and intrinsic permeability applicable to the Salado halites. A similar correlation was developed for Salado anhydrites; subsequent testing confirmed that the correlation predicted threshold pressures accurately. The correlation developed by Davies predicts threshold pressures in intact Salado halites on the order of 20 MPa or greater (Davies 1991). This threshold pressure predicted by correlation is much higher than that expected to persist in the repository, so that for all practical and predictive purposes, no gas will flow into intact Salado halites (see the CRA-2004, Chapter 6.0, Section 6.4.5.1).

Because threshold pressure helps control the flow of gas, and because the greatest volume of rock in the Salado is rich in halite, a high threshold pressure effectively limits the volume of gas that can be accommodated in the pore spaces of the intact host formation.

Thus, high threshold pressure is considered conservative, because if gas could flow into the pore spaces of intact Salado halite, repository pressures could be reduced dramatically.

MASS-12.2 Historical Context of the Salado Conceptual Model

See the CCA, Appendix MASS, Section MASS-13.2 for the historical information relating to the CCA Salado conceptual model. The Salado conceptual model is unchanged for the CRA-2014 PA.

MASS-12.3 The Fracture Model

The fracture model assumptions used in the CRA-2009 were unchanged from those used in the CRA-2004 PABC, and remain unchanged in the CRA-2014. The purpose of this model is to alter the porosity and permeability of the anhydrite interbeds and the DRZ if their pressure approaches lithostatic, simulating some of the hydraulic effects of fractures with the intent that unrealistically high pressures (in excess of lithostatic) do not occur in the repository or disposal system. The conceptual model is also discussed in the CRA-2004, Chapter 6.0, Section 6.4.5.2.

In the 1992 preliminary PA, repository pressures were shown to greatly exceed lithostatic pressure if a large quantity of gas was generated. Pressures within the waste repository and surrounding regions were predicted to be roughly 20 to 25 MPa. It is expected that fracturing within the anhydrite MBs would occur at pressures slightly above lithostatic pressure, and this fracturing is implemented through a pressure-dependent compressibility.

Two parametric behaviors must be quantified in the conceptual model. First, the change of porosity with pressure in the anhydrite MBs must be specified. This is done with a relatively simple equation, described in Appendix PA-2014, Section PA-4.2.4 , that relates porosity change to pressure change using an assumption that the fracturing can be thought of as increasing the compressibility of interbeds. Parameters in the model are treated as fitting parameters and have little relation to physical behavior except that they affect the porosity change. The second parametric behavior is the change of permeability with pressure, which is incorporated by a functional dependence on the porosity change. It is assumed that a power function is appropriate for relating the magnitude of permeability increase to the magnitude of porosity increase. The parameter in this power function, an exponent, is also treated as a fitting parameter and can be set so that the behavior of permeability increase with porosity increase fits the desired behavior.

The 1-degree dip modeled in BRAGFLO may affect fracture propagation direction; however, within the accuracy of the finite difference grid, a fracture will develop radially outward. This would not account for fracture fingering or a preferential fracturing direction; however, no existing evidence supports heterogeneous anhydrite properties that would contribute to preferential fracture propagation. This evidence is discussed in the CCA, Appendix MASS, Attachment 13-2.

The maximum enhanced fracture porosity controls the storativity within the fracture. The extent of the migration of the gas front into the MB is sensitive to this storativity. The additional storativity caused by porosity enhancement will mitigate gas migration within the MB. The enhancement of permeability by MB fracturing will make the gas more mobile and will contribute to longer gas-migration distances. Thus the effects of porosity enhancement at least partially counteract the effects of permeability enhancement in affecting the gas-migration distances.

Because intact anhydrite is partially fractured, the pressure at which porosity or permeability changes are initiated is close to the initial pressure within the anhydrite. The fracture treatment within the MBs will not contribute to early brine drainage from the MB because the pressures at these times are below the fracture initiation pressure.

The input data to the interbed fracture model (see Kicker and Herrick 2013) were chosen deterministically to produce the appropriate pressure and porosity response as predicted by a linear elastic fracture mechanics model, as discussed in Mendenhall and Gerstle (Mendenhall and Gerstle 1993).

MASS-12.4 Flow in the DRZ

The CRA-2009 modeling assumptions for flow in the salt DRZ were unchanged from those used in the CRA-2004 PABC, and remain unchanged in the CRA-2014. The conceptual model for the DRZ around the waste disposal, operations, and experimental regions has been chosen to provide a reasonably conservative estimate of fluid flow between the repository and the intact halite and anhydrite MBs. The conceptual model is also discussed in the CRA-2004, Chapter 6.0, Section 6.4.5.3.

The conceptual model implemented in the CCA PA used values for the permeability and porosity of the salt DRZ that did not vary with time. A screening analysis examined an alternative conceptual model for the DRZ in which permeability and porosity changed dynamically in response to changes in pressure (Vaughn, Lord, and MacKinnon 1995e). This analysis implemented a fracturing model in BRAGFLO for the salt DRZ. This fracturing model is used in the existing anhydrite interbed model. In this model, formation permeability and porosity depend on brine pressure, as described by Freeze, Larsen, and Davies (Freeze, Larsen, and Davies 1995, pp. 2-16 through 2-19) and Appendix PA-2014, Section PA-4.2.4. This model permits the representation of two important formation-alteration effects. First, pressure buildup caused by gas generation and creep closure within the waste will slightly increase porosity within the DRZ and offer additional fluid storage with lower pressures. Second, the accompanying increase in formation permeability will enhance fluid flow away from the DRZ. An increase in porosity tends to reduce outflow into the far

field. As a result, parameter values for this analysis were selected so that the DRZ alteration model greatly increases permeability while only modestly increasing porosity.

Two basic scenarios were considered in the screening analysis by Vaughn, Lord, and MacKinnon (Vaughn, Lord, and MacKinnon 1995e): undisturbed repository performance and disturbed repository performance. Both scenarios included a 1-degree formation dip downward to the south. Intrusion event E1 is considered in the disturbed scenario and consists of a borehole that penetrates the repository and pressurized brine in the underlying Castile. Two variations of intrusion event E1 were examined: E1 updip and E1 downdip. In the E1 updip event, the intruded panel region was located on the north end of the waste disposal region, whereas in the E1 downdip event, the intruded panel region was located on the south end of the disposal region. These two different geometries permitted evaluation of the possibility of increased brine flow into the panel region and the potential for subsequent impacts on contaminant migration. To incorporate the effects of uncertainty in each case (E1 updip, E1 downdip, and undisturbed), a Latin hypercube sample (LHS) size of 20 was used, for a total of 60 simulations. To assess the sensitivity of system performance on formation alteration of the DRZ, conditional CCDFs of normalized contaminated brine releases were constructed and compared with the corresponding baseline model conditional CCDFs that were computed with constant DRZ permeability and porosity values. Based on comparisons between conditional CCDFs, computed releases to the accessible environment were determined to be essentially equivalent between the two treatments. Since the two configurations were determined to have essentially equivalent impacts on releases, the intrusion borehole was assumed to intrude in the down-dip or south side of the repository where it is assumed brine would more readily accumulate (see Figure MASS-3).

Preliminary PAs considered alternative conceptual models that allowed for some lateral extent of the DRZ into the halite surrounding the waste disposal region and for the development of a transition zone between anhydrites A and B and MB 138 (WIPP Performance Assessment 1993, Volume 4, Figure 4.1-2 and Figure 5.1-2; Davies, Webb, and Gorham 1992; Gorham et al. 1992). The transition zone was envisioned as a region that had experienced some hydraulic depressurization and perhaps some elastic stress relief because of the excavation, but probably no irreversible rock damage and no large permeability changes. Modeling results indicated that including the lateral extent of the DRZ had no significant effect on fluid flow. Communication vertically to MB 138 was thought to be a potentially important process, however, and the model adopted for PA assumes that the DRZ extends upward to MB 138 and permeability is sampled over the same range used in the CCA PAVT. This representation continues to be used in the CRA-2014 PA.

MASS-12.5 Actinide Transport in the Salado

The actinide transport modeling assumptions used in the CRA-2009 were unchanged from those used in the CRA-2004 PABC, and remain unchanged in the CRA-2014. The purpose of this model, implemented in the code NUTS, is to represent the transport of actinides in the Salado. This model is also discussed in the CRA-2004, Chapter 6.0, Section 6.4.5.4, and Appendix PA-2014, Section PA-4.3.4.

Actinide transport in the Salado is conceptualized as occurring only by advection, or movement of material through the bulk flow of a fluid, through the porous medium described in the Salado hydrology conceptual model. Advection is a direct function of fluid flow, which is discussed in the conceptual model for Salado fluid flow. Other processes that might disperse actinides, such as diffusion, hydrodynamic dispersion, and channeling in discrete fractures, are not included in the conceptual model. Since these processes will reduce actinide transport, it is conservative to ignore these processes.

To model radionuclide transport in the Salado, NUTS takes as input BRAGFLO's velocity field, pressures, porosities, saturations, and other model parameters (including geometrical grid, residual saturation, material map, brine compressibility, and time step) averaged over a given number of time steps (20 for the CRA-2014 PA calculations). NUTS then models the transport of radionuclides within all the regions for which BRAGFLO computes brine and gas flow. The brine must pass through some part of the repository at some point during the 10,000-year regulatory period if it is to become contaminated. Radioactive constituents of the waste in the repository are assumed to dissolve into the brine while the brine is in the repository; the radionuclides are then transported by advection to other regions outside the repository. Consequently, the results of NUTS are subject to all the uncertainties associated with BRAGFLO's conceptual model and parameterization. Details of the source term, which specifies the types and amounts of radionuclides that are assumed to come into contact with the waste, are discussed in Appendix SOTERM-2014, Section SOTERM-3.0.

NUTS neglects molecular dispersion. For materials of interest in the WIPP repository system, molecular diffusion coefficients are, at most, on the order of 4×10^{-10} m^2 per second. Thus, the simplest scaling argument using a time scale of 10,000 years leads to a molecular diffusion (that is, mixing) length scale of approximately 10 m (33 ft), which is negligible compared to the lateral advection length scale of roughly 2,400 m (7,874 ft) (the lateral distance from the repository to the accessible environment).

NUTS also neglects mechanical dispersion (see the CRA-2004, Chapter 6.0, Section 6.4.5.4.2). Dispersion is quantified by dispersivities, which are empirical tensor factors proportional to flow velocity (to within geometrical factors related to flow direction). They account for both the downstream and cross-stream spreading of local extreme values in concentration of dissolved constituents. Physically, the spreading is caused by the fact that both the particle paths and velocity histories of once-neighboring particles can be vastly different because of material heterogeneities characterized by permeability variations. These variations arise from the irregular cross-sectional areas and tortuous inhomogeneous, anisotropic connectivity between pores. Because of its velocity dependence, the transverse component of mechanical dispersivity tends to transport dissolved constituents from regions of relatively rapid flow (where mechanical dispersion has a larger effect) to regions of slower flow (where mechanical dispersion has a smaller

effect). In the downstream direction, dispersivity merely spreads constituents in the flow direction. Conceptually, ignoring lateral spreading assures that dissolved constituents will remain in the rapid part of the flow field, which assures their transport toward the boundary. Similarly, ignoring longitudinal dispersivity ignores the elongation of a feature in the flow direction, which would delay the arrival of radionuclide constituents at the accessible environment. However, because the EPA release limits are time-integrated measures, the exact time of arrival is unimportant for constituents that arrive at the accessible environment, so long as arrival occurs within the assessment period (10,000 years).

NUTS conservatively disregards sorptive and other retarding effects throughout the entire flow region even though retardation must occur at some level within the repository, the MBs, and the anhydrite interbeds, and especially in zones with clay layers or clay as accessory minerals. Advection is, therefore, the only transport mechanism considered in NUTS. Because the Darcy flows are given by BRAGFLO to NUTS as input, the maximum solubility limits for combined dissolved and colloidal components are the most important NUTS parameters. These components are described in Appendix SOTERM-2014, Section SOTERM-5.0.

MASS-13.0 Geologic Units above the Salado

The modeling assumptions of the geologic units above the Salado used in the CRA-2009 were unchanged from those used in the CRA-2004 PABC, and remain unchanged in the CRA-2014. The model for geologic units above the Salado was developed to provide a reasonable and realistic basis for simulations of fluid flow within the disposal system and detailed simulations of groundwater flow and radionuclide transport in the Culebra. The conceptual model for these units is also discussed in the CRA-2004, Chapter 6.0, Section 6.4.6.

The conceptual model used in PA for the geologic units above the Salado is based on the overall concept of a groundwater basin, as introduced in the CRA-2004, Chapter 2.0, Section 2.2.1.1, and in the CCA, Appendix MASS, Section MASS-14.2. The computer code SECOFL3D was originally used to evaluate the effect on regional-scale fluid flow by recharge and rock properties in the groundwater basin above the Salado (see the CCA, Appendix MASS, Attachment 17-2). However, simpler models for this region are implemented in codes used in PA. For example, in the BRAGFLO model, layer thicknesses, important material properties including porosity and permeability, and hydrologic properties such as pressure and initial fluid saturation are specified, but the model geometry and boundary conditions are not suited to groundwater basin modeling (nor is the BRAGFLO model used to make inferences about groundwater flow in the units above the Salado). In PA, the Culebra is the only subsurface pathway modeled for radionuclide transport above the Salado, although the groundwater basin conceptual model includes other flow interactions. The Culebra model implemented in PA includes spatial variability in hydraulic conductivity and uncertainty and variability in physical and chemical transport processes. Thus, the geometries and properties of units in the different models applied to the units above the Salado by the DOE are chosen to be consistent with the purpose of the model.

The MODFLOW-2000 and SECOTP2D codes are used directly in PA to model fluid flow and transport in the Culebra. The assumptions made in these codes are discussed in the CRA-2004, Chapter 6.0, Section 6.4.6.2, and Appendix PA-2004, Attachment MASS, Section MASS-15.0.

With respect to the units above the Salado, the BRAGFLO model is used only for determination of fluid fluxes between the shaft or intrusion borehole and hydrostratigraphic units. For this purpose, it does not need to resolve regional or local flow characteristics.

The basic stratigraphy and hydrology of the units above the Salado are described in the CRA-2004, Chapter 2.0, Section 2.1.3.5, Section 2.1.3.6, Section 2.1.3.7, Section 2.1.3.8, Section 2.1.3.9, Section 2.1.3.10 and Section 2.2.1.4. Additional supporting information is contained in the CCA, Appendices GCR, HYDRO, and SUM. Details of the conceptual model for each unit are described in the CRA-2004, Chapter 6.0, Section 6.4.6.1, Section 6.4.6.2, Section 6.4.6.3, Section 6.4.6.4, Section 6.4.6.5, Section 6.4.6.6, and Section 6.4.6.7, and additional information on units above the Salado is found in Appendix HYDRO-2014.

The representation of units above the Salado in the CRA-2009 was unchanged from that used in the CRA-2004 PABC, and remains unchanged in the CRA-2014 PA.

MASS-13.1 Historical Context of the Units above the Salado Model

See the CCA, Appendix MASS, Section MASS-14.1 for historical information relating to the conceptual models for units above the Salado for the CCA. The conceptual models for the units above the Salado are unchanged for CRA-2014 PA.

MASS-13.2 Groundwater-Basin Conceptual Model

The groundwater-basin conceptual model and associated modeling assumptions used in the CRA-2009 were unchanged from those used in the CRA-2004 PABC, and remain unchanged in the CRA-2014. For a discussion on the groundwater-basin conceptual model, see the CCA, Appendix MASS, Section MASS-14.2.

MASS-14.0 Flow through the Culebra

The Culebra flow modeling assumptions used in the CRA-2009 were unchanged from those used in the CRA-2004 PABC, and remain unchanged in the CRA-2014. The conceptual model for groundwater flow in the Culebra (1) provides a reasonable and

realistic basis for simulating radionuclide transport in the Culebra, and (2) allows evaluation of the extent to which uncertainty about groundwater flow in the Culebra may contribute to uncertainty in the estimate of cumulative radionuclide releases from the disposal system. See the CRA-2004, Chapter 6.0, Section 6.4.6.2 for additional references to other relevant discussions on this conceptual model.

The conceptual model used in PA for groundwater flow in the Culebra treats the Culebra as a confined two-dimensional aquifer with constant thickness and spatially varying transmissivity (see the CCA, Appendix MASS, Attachment 15-7). Flow is modeled as single-phase (liquid) Darcy flow in a porous medium.

Basic stratigraphy and hydrology of the units above the Salado are described in the CRA-2004, Chapter 2.0, Section 2.1 and Section 2.2. Additional supporting information is contained in the CCA, Appendices GCR, HYDRO, and SUM.

The conceptual model for flow in the Culebra is discussed in the CRA-2004, Chapter 6.0, Section 6.4.6.2. Details of the calibration of the T fields, based on available field data, are given in Appendix TFIELD-2014. Initial and boundary conditions used in the model are given in the CRA-2004, Chapter 6.0, Section 6.4.10.2. A discussion of the adequacy of the two-dimensional assumption for PA calculations is included in the CCA, Appendix MASS, Attachment 15-7.

The principal parameter used in PA to characterize flow in the Culebra is an index parameter (the transmissivity index) used to select a single T field for each LHS element from a set of calibrated fields (see Kicker and Herrick 2013, Table 1), each of which is consistent with available data.

MASS-14.1 Historical Context of the Culebra Model

See Appendix PA-2004, Attachment MASS, Section MASS-15.1 for historical information relating to the Culebra conceptual model. The conceptual model for this unit is unchanged for the CRA-2014.

MASS-14.2 Dissolved Actinide Transport and Retardation in the Culebra

The purpose of this model is to represent the effects of advective transport and physical and chemical retardation on the movement of actinides in the Culebra. This conceptual model is also discussed in the CRA-2004, Chapter 6.0, Section 6.4.6.2.1. The same model is used in the CRA-2004 PABC and the CRA-2014 PA. For a historical presentation of this model, see Appendix PA-2004, Attachment MASS, Section MASS-15.2.

MASS-14.3 Colloidal Actinide Transport and Retardation in the Culebra

The purpose of this model is to represent the effects of colloidal actinide transport in the Culebra. This model is also discussed in the CRA-2004, Chapter 6.0, Section 6.4.6.2.2 and Appendix PA-2004, Attachment MASS, Attachments 15-2, 15-8, and 15-9. No changes have been made to this model since the CRA-2004. Additional information and historical information on colloidal actinide transport and retardation in the Culebra can be found in Appendix PA-2004, Attachment MASS, Section MASS-15.3.

MASS-14.4 Subsidence Caused by Potash Mining in the Culebra

The mining-related modeling assumptions used in the CRA-2009 were unchanged from those used in the CRA-2004 PABC, and remain unchanged in the CRA-2014. This model incorporates the effects of potash mining in the McNutt Potash Zone on disposal system performance (see Appendix SCR-2014, FEP H13, FEP H37, and FEP H38). Provisions in Part 194 provide a conceptual model and elements of a mathematical model for these effects. The DOE has implemented the EPA conceptual model (40 CFR § 194.32(b), U.S. EPA 1996) to be consistent with EPA criteria and guidance; this model is described in the CRA-2004, Chapter 6.0, Section 6.4.6.2.3. Additional information on the implementation of the mining subsidence model is available in Appendix TFIELD-2014; the CCA, Appendix MASS, Attachments 15-4 and 15-7; and Wallace (Wallace 1996).

The principal parameter in this model is the range assigned to a factor by which hydraulic conductivity in the Culebra is increased (see the CCA, Appendix MASS, Attachment 15-4). As allowed in supplementary information to Part 194, it is the only parameter changed to account for the effects of mining.

Mining has been included in scenario development for the WIPP since the earliest work on this topic (U.S. DOE 1980 [pp. 9-145 through 9-148]; Hunter 1989; Marietta et al. 1989; Guzowski 1990; Tierney 1991; WIPP Performance Assessment 1991). These early scenario developments considered both solution and room-and-pillar mining. The focus was generally on effects of mining outside the disposal system. In the CCA FEPs screening, solution mining was screened out during scenario development (see Appendix SCR-2014, FEP H58 and FEP H59). The two primary effects of mining considered were (1) changes in the hydraulic conductivity of the Culebra or other units, and (2) changes in recharge as a result of surface subsidence. These mining effects were not formally incorporated into quantitative assessment of repository performance in preliminary PAs.

The inclusion of mining in PA satisfies the requirements of section 194.32(b) to consider the effects of this activity on the disposal system.

MASS-15.0 Intrusion Borehole

The intrusion borehole modeling assumptions used in the CRA-2009 were unchanged from those used in the CRA-2004 PABC, and remain unchanged in the CRA-2014. The inclusion of intrusion boreholes in PA adds to the number of release pathways for radionuclides from the disposal system. Direct releases to the surface may occur during drilling as particulate material from cuttings, cavings, and spallings are carried to the surface. Also, dissolved actinides may be carried to the surface in brine during drilling. Once abandoned, the borehole presents a possible long-term pathway for fluid flow, such as might occur between a hypothetical Castile brine reservoir, the repository, and overlying units. This topic is also addressed in the CRA-2004, Chapter 6.0, Section 6.4.7, and Appendix SCR-2014 (FEP H1 and FEP H21).

MASS-15.1 Cuttings, Cavings, and Spallings Releases during Drilling

The cuttings, cavings, and spallings models estimate the quantity of actinides released as solids directly to the surface during drilling through the repository. The releases are caused by three mechanisms: the drill bit boring through the waste (cuttings); the drilling fluid eroding the walls of the borehole (cavings); and high repository gas pressure causing solid material failure and entrainment into the drilling fluid in the wellbore (spallings). See the CRA-2004, Chapter 6.0, Section 6.4.7.1, and references to other appendices cited in that section for additional information. Stochastic uncertainty in parameters relevant to these release mechanisms is addressed in the CRA-2004, Chapter 6.0, Section 6.4.12. The conceptual model for cuttings, cavings, and spallings is discussed in three parts because of the different processes that produce the three types of releases.

Cuttings are materials removed to the surface through drilling mud by the direct mechanical action of the drill bit. The volume of waste removed to the surface is a function of the repository height and the drill bit area. The principal parameter in the cuttings model is the diameter of the drill bit (see Attachment PAR-2014).

Cavings are materials introduced into the drilling mud by the erosive action of circulating drilling fluid on the waste in the walls of the borehole annulus. Erosion is driven solely by the shearing action of the drilling fluid (or mud) as it moves up the borehole annulus. Shearing may be caused by either laminar or turbulent flow. The principal parameters in the cavings model are the properties of the drilling mud, drilling rates, the drill string angular velocity, and the shear resistance of the waste (see MASS-15.1.2). (See Kicker and Herrick 2013 for details on the sampled parameters used in the cavings model, the drill string angular velocity, and the effective shear resistance to erosion.)

Spallings are solids introduced into the wellbore by the fluid pressure difference between the repository and the bottom of the wellbore. If the repository pressure is sufficiently high (more than about 12 MPa) relative to the well bottom hole pressure (about 8 MPa), the stress state in the repository may cause repository solids to fail in the vicinity of the wellbore. In turn, these solids may become entrained in the gas flowing toward the well, ultimately to be carried up to the land surface and constituting a release. The principal parameters in the spallings model are the gas pressure in the repository when it is penetrated and properties of the waste such as permeability, tensile strength, and particle diameter. Because the release associated with spalling is sensitive to gas pressure in the repository, it is strongly coupled to the BRAGFLO-calculated conditions in the repository at the time of penetration.

MASS-15.1.1 Historical Context of Cuttings, Cavings, and Spallings Models

Cuttings and cavings releases are straightforward. The analytical equations governing erosion (cavings) based on laminar and turbulent flow (Appendix PA-2014, Section PA-4.5) have been implemented in the code CUTTINGS_S. Using selected input based on assumed physical properties of the waste and other drilling parameters, this code calculates the final caved diameter of the borehole that intersects the waste.

The various approaches used for spallings up to the CCA PA are documented in the CCA, Appendix MASS, Section MASS-16.1.1. Since the CCA PA, the spallings model has been extensively revised and has changed fundamentally from an end-state erosional model to a mechanically based, coupled material failure and transport model (WIPP Performance Assessment 2003a). This model is implemented in the code DRSPALL. A discussion tracing the historical steps from the CCA erosional model to the current DRSPALL model can be found in Appendix PA-2004, Attachment MASS, Section MASS-16.1.1.

MASS-15.1.2 Waste Mechanistic Properties

Waste mechanical properties used in the CRA-2014 are updated from those used in the CRA-2009. For intrusion events considered in WIPP PA, drilling mud flowing up the borehole will apply a hydrodynamic shear stress on the borehole wall. Erosion of the wall material can occur if this stress is high enough, resulting in a release of radionuclides being carried up the borehole with the drilling mud. In this intrusion event, the drill bit would penetrate repository waste, and the drilling mud would flow up the borehole in a predominately vertical direction. In order to experimentally simulate these conditions, a flume was designed and constructed. In the flume experimental apparatus, eroding fluid enters a vertical channel from the bottom and flows past a specimen of surrogate WIPP waste. Experiments were conducted to determine the erosive impact on surrogate waste materials that were developed to represent WIPP waste that is 50%, 75%, and 100% degraded by weight. A description of the vertical flume, the experiments conducted in it, and conclusions to be drawn from those experiments are discussed in Herrick et al. (Herrick et al. 2012).

The WIPP PA uses the parameter BOREHOLE:TAUFAIL to represent the hydrodynamic shear strength of the waste in the numerical code CUTTINGS_S (see Appendix PA-2014, Section PA-4.5). It is officially called the "effective shear strength for erosion," but it is more commonly known as the "waste shear strength." Based on experimental results that realistically simulate the effect of a drilling intrusion on an accepted surrogate waste material, as well as analyses of existing data (see Herrick 2013), parameter BOREHOLE:TAUFAIL is updated in the CRA-2014 PA. Values specified for parameter BOREHOLE:TAUFAIL in the CRA-2014 PA are obtained by sampling a uniform distribution with a range of 2.22 Pa to 77 Pa.

MASS-15.1.3 Mechanistic Model for Spall

The CRA-2014 PA uses the same spallings model that was used in the CRA-2009 PABC and the CRA-2004 PABC. No changes were made to the model or implementation of the results in PA.

In the CRA-2004 PA, a new approach to modeling the WIPP spallings process was developed to address peer review concerns during the original certification process (see the CCA, Chapter 9.0, Section 9.3.1.2 and Appendix PEER-2004, Section PEER-2004 3.0). Instead of focusing on the end state after penetration, as was done in the original CCA erosional model, the new model sought to capture the system behavior from just before penetration through to the end state. In doing so, many more phenomena were included in the model. Considered in this new conceptual model was unsteady, convergent gas flow from the repository toward the wellbore that caused mechanical stress and potential failure of solids near the face of the wellbore. Pressure in the cavity at the point of penetration was balanced by the mud column in the wellbore and the repository pressure.

The new spall model, DRSPALL (WIPP Performance Assessment 2003a), is based on a predecessor code called GASOUT (Hansen et al. 1997, Appendix C). DRSPALL builds upon GASOUT by:

1. Adding a wellbore flow model that transports mud, repository gas, and waste solids from repository level to the land surface

2. Adding a fluidized bed model that evaluates the potential for failed particulate waste to fluidize and become entrained in the wellbore flow

The wellbore flow model in DRSPALL utilizes one-dimensional geometry with a compressible, viscous, isothermal, homogeneous mixture of mud, gas, and solids. Standard mass and momentum balance, friction loss, and slurry viscosity equations are used. Wellbore flow model results were successfully verified against those from an independent commercial code for several test problems (WIPP Performance Assessment 2003b).

DRSPALL applies the fluidized bed theory to determine the mobilization of failed material to the flow stream in the wellbore. If the escaping gas velocity exceeds the minimum fluidization velocity, failed material is fluidized and entrained for transport at the land surface. If gas velocity is too low to fluidize the bedded material, the cavity size is allowed to stabilize. The spall volumes predicted by DRSPALL are based on the following conservative assumptions for material properties and for the flow geometry within the repository:

- The particle size distribution for spallings is based on a detailed analysis (Wang 1997) of data from an expert elicitation (Carlsbad Area Office Technical Assistance Contractor [CTAC] 1997). This analysis considered several limiting cases in developing a conservative distribution for mean particle size ranging from 1 millimeter to 10 cm (Hansen, Pfeifle, and Lord 2003).

- The shape factor for fluidization of particles has a potential range from 0 to 1.0. Smaller values of the shape factor denote particles that are less spherical, and therefore more easily fluidized and transported in the flow. The shape factor is conservatively set to a value of 0.1 (Lord 2003).

- The tensile strength of the waste assigned for the spalling process is uncertain, ranging from 0.12 MPa to 0.17 MPa (Hansen, Pfeifle, and Lord 2003). Tensile strength data were measured in laboratory experiments on surrogate materials chosen to conservatively represent highly degraded residuals from typical wastes. The given range is felt to represent extreme, low-end tensile strengths because it does not account for several strengthening mechanisms, such as MgO hydration and halite precipitation/cementation (Hansen et al. 1997).

- DRSPALL uses a hemispherical geometry (one-dimensional spherical symmetry) for the flow field and cavity in the waste. This conceptual model is appropriate when the drill bit first penetrates the repository. But, as the drill bit passes completely through the compacted waste, the flow field transitions toward a cylindrically symmetric geometry. This transition is important because the largest spall release volumes are predicted to occur at late times, well after the drill bit has penetrated through the waste, and because the spall volumes predicted for a cylindrical geometry are less than for the hemispherical geometry (Lord, Rudeen, and Hansen 2003).

In summary, the conservative assumptions for waste properties, the waste flow geometry, and the driller's actions provide very conservative spalling release volumes (see also Appendix PA-2014, Section PA-4.6 for a description of the spallings model, and Appendix PEER-2004, Section PEER-2004 3.0 for the results of the spallings model peer review). As stated previously, the DRSPALL calculations from the CRA-2004 PABC were also used in the CRA-2014 PA (see Appendix PA-2014, Section PA-6.7.4 and Section PA-8.5.2).

MASS-15.1.4 Calculation of Cuttings, Cavings, and Spall Releases

The modeling assumptions relating to the calculations of cuttings, cavings and spallings releases have not changed since the CRA-2004. As detailed in Appendix PA-2014, Section PA-6.7.5 , cuttings and cavings releases for intrusions into CH-TRU waste are computed by multiplying the volume released (calculated by the code CUTTINGS_S) by the radioactivity in three independently selected waste streams, consistent with the conceptual assumption that waste streams are randomly emplaced in waste stacks that are three drums high. The effect of this assumption on PA results was examined in a separate PA (Hansen et al. 2003) in which cuttings and cavings releases were computed by assuming that each intrusion encounters only a single waste stream. The differences in repository performance (determined by comparing the mean CCDFs for releases) were determined to be minor. For more details on the analysis, see Appendix PA-2004, Attachment MASS, Section MASS-21.0.

Because spallings may release a relatively large volume of material (exceeding 4 m^3), spalling releases for intrusions into CH-TRU waste are computed by multiplying the volume of spalled material with the average concentration of radioactivity in the waste at the time of the intrusion. A separate PA (Hansen et al. 2003) compared spalling releases computed using the average concentration of radioactivity in the waste to spalling releases computed using the radioactivity of a single, randomly selected waste stream. The analysis determined that the assumption had only a minor effect on the mean CCDF for releases. For more details on the analysis, see Appendix PA-2004, Attachment MASS, Section MASS-21.0. During their completeness review of the CRA-2004, the EPA requested additional DRSPALL vectors be used in the CRA-2004 PABC. Minor changes were made to the implementation of spallings results that did not change the overall modeling assumptions. These implementation changes are outlined in Leigh et al. (Leigh et al. 2005, Section 7.8).

MASS-15.2 Direct Brine Releases during Drilling

The DBR modeling assumptions used in the CRA-2009 were unchanged from those used in the CRA-2004 PABC, and remain unchanged in the CRA-2014. This model provides a series of calculations to estimate the quantity of brine released directly to the surface during drilling. DBRs may occur when a driller penetrates the WIPP and unknowingly brings contaminated brine to the surface during drilling (these releases are not accounted for in the cuttings, cavings, and spallings calculations, which model only the solids removed during drilling). Appendix PA-2014, Section PA-4.7 , describes the DBR model used for the CRA-2014 PA. The CCA, Appendix MASS, Attachment 16-2 describes the DBR model used for the CCA PA. The conceptual model for DBRs is discussed in Appendix PA-2014, Section PA-4.7 , and the CRA-2004, Chapter 6.0, Section 6.4.7.1.1.

Uncertainty in the BRAGFLO DBR calculations is captured in the 10,000-year BRAGFLO calculations from which the initial and boundary conditions are derived. The model parameters that have the most influence on DBRs are repository pressure and brine saturation at the time of intrusion. Brine saturation is influenced by many factors, including Salado and MB permeability and gas-generation rates (for undisturbed scenario calculations). For E1 and E2 intrusion scenarios, Castile brine-reservoir pressure and volume, and abandoned borehole permeabilities influence conditions for the second and subsequent intrusions. The dip in the repository (hence the location of intrusions), two-phase flow parameters (residual brine and gas saturation), time of intrusion, and duration of flow have lesser impacts on brine releases.

The implementation of the DBR model is slightly adjusted in the CRA-2014 PA to incorporate the ROMPCS. The Option D panel closure modeled in the CRA-2009 PABC is 40 m long whereas the ROMPCS modeled in the CRA-2014 PA is 30.48 m (100 ft) long. As a result, grid cell lengths corresponding to panel closures are reduced to 30.48 m in the CRA-2014 PA. In addition, the ROMPCS, which is modeled as run-of-mine salt in the CRA-2014 PA, has no concrete component that is "keyed in" to the surrounding DRZ. As a result, material elements corresponding to equivalent DRZ/concrete in the CRA-2009 PABC are replaced by DRZ in the CRA-2014 PA. Figure MASS-12 shows the DBR grid and material map used in the CRA-2014 PA. (Note that the color scheme in Figure MASS-12 is chosen to match the color scheme of the CRA-2014 BRAGFLO grid and material maps shown in Figure MASS-7 to Figure MASS-11.) Figure MASS-8 of Appendix MASS-2009 shows the DBR grid and material map used in the CRA-2009 PA and PABC.

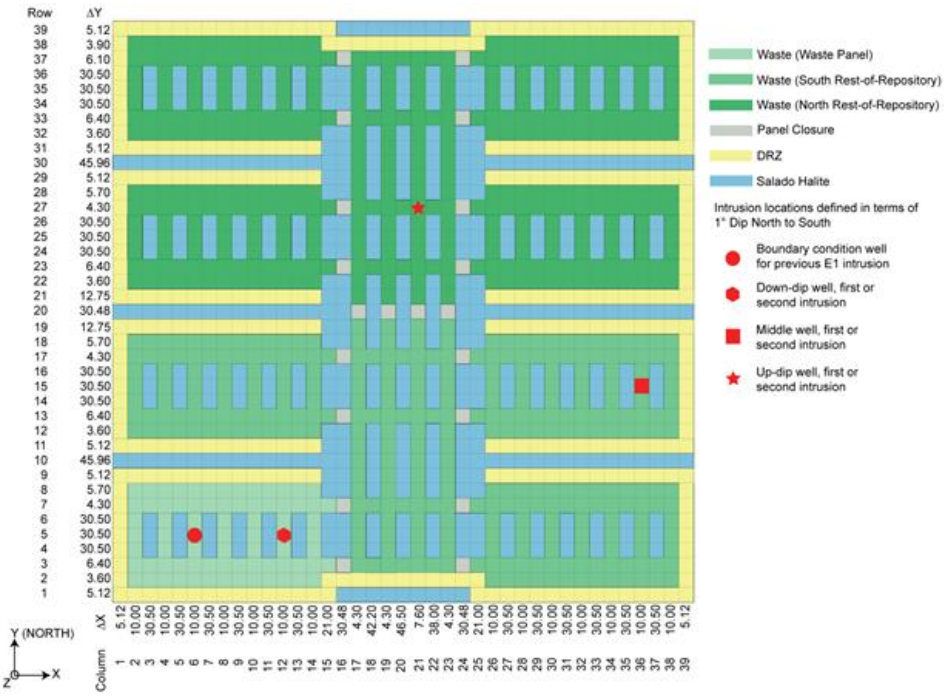

Figure MASS- 12. Repository-Scale Horizontal BRAGFLO Mesh Used for DBR Calculations

The CRA-2009 PA used a DBR maximum duration of 4.5 days, based on current drilling practices (see Kirkes 2007 and Appendix PA-2014, Section PA-4.7.8). This value is also used in the CRA-2014 PA.

MASS-15.3 Long-Term Properties of the Abandoned Intrusion Borehole

The long-term treatment and assumptions used to represent boreholes in the CRA-2009 PA were unchanged from those used in the CRA-2004 PABC, and remain unchanged in the CRA-2014. See Appendix PA-2004, Attachment MASS, Section MASS-16.3 , and CRA-2014, Section 33 , for the borehole modeling assumptions used in the CRA-2014 PA.

MASS-16.0 Climate Change

The purpose of this model is to allow quantitative consideration of the extent to which uncertainty about future climate may contribute to uncertainty in estimates of cumulative radionuclide releases from the disposal system. This model has not changed since the CCA and is used in the CRA-2014 PA. Consideration is limited to conditions that could result from reasonably possible natural climatic changes. The model is not intended to provide a quantitative prediction of future climate, nor is it intended to address uncertainty in system properties other than estimated cumulative radionuclide releases that may be affected by climate change. See Appendix PA-2004, Attachment MASS, Section MASS-17.0 , and Section MASS-17.1 for current and historical information on the climate change model. The implementation of this model in PA is also discussed in the CRA-2004, Chapter 6.0, Section 6.4.9 and Appendix PA-2004, Section PA-2.1.4.6. See also the CCA, Appendix CLI for information on expected climate variability over the 10,000-year regulatory time period.

MASS-17.0 Castile Brine Reservoir

The conceptual model for the hypothetical brine reservoir is included in PA to estimate the extent to which uncertainty about the existence of a brine reservoir under the waste disposal region may contribute to uncertainty in the estimate of cumulative radionuclide releases from the disposal system. The conceptual model is not intended to provide a realistic approximation of an actual brine reservoir under the waste disposal region. Data are insufficient to determine whether such a brine reservoir exists.

The representation of the Castile brine reservoir in BRAGFLO in the CRA-2014 PA has not changed from the CRA-2004 PA. However, this model is not the same as the one used in the original CCA PA. The following describes the changes to the model since the 1996 CCA PA.

The Castile Formation is treated as an impermeable unit in PA and plays no role in the analysis except to separate the Salado from the modeled brine reservoir in the BRAGFLO grid. In human-intrusion scenarios, the hypothetical brine reservoir can be penetrated by an intrusion borehole connecting it to the repository. The amount of brine that can enter the repository from the brine reservoir is

important to PA because brine is required for gas-generation reactions and can transport radionuclides in solution, contributing to potential releases.

The properties of the hypothetical brine reservoir defined for PA include permeability, porosity, pore volume, initial pressure, and various two-phase flow parameters. Values assigned for these properties were chosen to either be consistent with the available data from and analyses of borehole penetrations of brine reservoirs in the region, or provide a reasonable response in the BRAGFLO model.

The treatment of the brine reservoir for the CRA-2004 PA was different than that used in the CCA PA. The major changes to the brine reservoir representation were made by the EPA in the CCA PAVT (U.S. EPA 1998b). For the CCA PAVT, the EPA defined new parameter ranges for bulk compressibility and total pore volume. The range of bulk compressibility was based on a reevaluation of field test data from the WIPP-12 borehole following the CCA (Beauheim 1997). Since the total volume of the grid cells used to represent the brine reservoir in BRAGFLO is fixed, the range of total pore volume was set by defining a range of "effective" porosity (pore volume = grid volume × effective porosity). This range of porosity values is not representative of the actual host rock. It was chosen to produce a reasonable response in the BRAGFLO model by providing a predefined range of total pore volumes based on the field tests at WIPP-12.

For the CRA-2004 PA, the DOE implemented this approach by assuming that the productivity ratio (PR) remains constant (2.0051×10^{-3} m^3/Pa). The PR is defined as:

$$PR = V\frac{C_r}{\phi},$$

where V is the grid volume of the brine reservoir (18,462,514 m^3), C_r is the bulk compressibility (2×10^{-11} to 1×10^{-10} Pa^{-1}), and ϕ is the effective porosity (0.1842 to 0.9208). To maintain a constant pore volume in the brine reservoir, the porosity range used in the CRA-2004 PA is slightly modified from that used in the CCA PAVT because the fixed-grid volume increased slightly in the CRA-2004 BRAGFLO grid from the volume assumed in the CCA BRAGFLO grid. In this approach, bulk compressibility and effective porosity are directly proportional (Stein 2003). See Appendix PA-2014, Section PA-4.2.10 for the details on the implementation in PA.

Basic geologic information about the Castile is given in the CRA-2004, Chapter 2.0, Section 2.1.3.3. The hydrology of the known brine reservoirs is discussed in the CRA-2004, Chapter 2.0, Section 2.2.1.2.2. The treatment of the hypothetical brine reservoir in PA is discussed in the CRA-2004, Chapter 6.0, Section 6.4.8.

MASS-17.1 Historical Context of the Castile Brine Reservoir Model

See the CCA, Appendix MASS, Attachment 18.1 for historical information on the Castile brine reservoir model.

MASS-18.0 Summary of Clay Seam G Modeling Assumptions

One of the changes to the repository design since the CCA is the raising of the repository horizon in the southern half of the waste panels. Specifically, Panels 3, 4, 5, and 6, have been excavated at an elevation approximately 2.4 m above the level of Panels 1, 2, 7, and the operations and experimental areas. This change in horizon has brought the roof of the raised rooms to the level of the Clay Seam G. The change has improved roof conditions and enhanced operations and mine safety. The DOE submitted a planned change request to the EPA describing the change and argued that it would have minimal impact on long-term repository performance (Triay 2000). The EPA responded to the change request in a letter (Marcinowski 2000) in which it agreed with the DOE that the effects on long-term performance would be minimal. The modeling assumptions used to represent this change are described in Appendix PA-2004, Attachment MASS, Section MASS-20.0. No changes were made to these assumptions since the CRA-2004 PA. These assumptions have also been used in the CRA-2014 PA.

MASS-19.0 Evaluation of Waste Structural Impacts, Emplacement and Homogeneity

During the development of the CCA PA, the DOE chose to assume random placement of TRU waste in the WIPP, and developed conceptual and numerical models accordingly. The EPA reviewed these models and their results and determined that the DOE had adequately modeled random placement of waste in the disposal system. The CCA PA also assumed that all waste could be modeled as if the waste was emplaced in 55-gallon drums. In accordance with the requirements of 40 CFR § 194.24(d) (U.S. EPA 2004), all PAs have assumed that waste is emplaced in a random or homogeneous manner. The PAs executed in support of compliance applications have not specifically accounted for heterogeneity in waste materials or in waste containers.

Additional information about the waste and its emplacement has emerged since the CCA. Waste has been emplaced using several different types of waste containers, including standard waste boxes and pipe overpacks. Waste types, such as supercompacted waste, have been emplaced that were not considered in the CCA inventory (U.S. DOE 2002). At the Idaho National Laboratory, for

instance, debris waste is volume-reduced by supercompaction, resulting in a very dense waste form containing a high concentration of CPR material. In addition, the plutonium residues from the Rocky Flats Environmental Technology Site were packaged in pipe overpacks, which are more rigid than the typical 55-gallon drum assumed in the CCA. Actual waste emplacement is determined by the availability of waste at generator sites and the shipping schedules. Pipe overpacks occupy about 43% of the containers emplaced in Panel 1, suggesting that actual emplacement will not be statistically random. As a result of this information, the DOE performed analyses (Hansen et al. 2003) to determine if the waste emplacement assumptions used in PA adequately represent the waste. The analysis, reported in Hansen et al. (Hansen et al. 2003), focused on potential effects of supercompacted waste and waste in pipe overpacks on repository performance. Both waste types are structurally stiffer than the generic waste model used in the CCA PA, and the supercompacted waste in particular has high concentrations of CPR materials. The analysis began with a systematic reevaluation of the baseline FEPs to identify specific components of PA that could be affected by supercompacted waste. The reassessment concluded that the FEPs "screened in" were adequate to represent the variety of waste types and containers, and that none of the "screened out" FEPs should be reconsidered for implementation. The FEP assessment concluded that the following could be affected by heterogeneities in the waste materials and waste containers:

- creep closure of the repository
- chemical conditions of the waste
- gas generation models
- waste mechanical properties

Analysis of creep closure of waste-filled rooms, accounting for several types of waste materials and packaging, indicated that a wider range of long-term porosities could occur than that established in the CCA, given the uncertainties about the structural integrity of waste packages and their spatial arrangement in the repository (Park and Hansen 2003). For this reason, the analysis in Hansen et al. (Hansen et al. 2003) treated creep closure as an uncertain variable. Sensitivity analysis showed that this additional uncertainty did not significantly affect the results of PA.

Chemical conditions were also reexamined under a range of possible waste arrangements. The assessment found that, regardless of actual waste emplacement, the MgO would still be sufficient to maintain desired chemical conditions if distributed appropriately with the current excess factor. Moreover, the constituents of supercompacted waste would not alter the reactions that determine chemical equilibrium and, consequently, no changes to actinide solubilities or to the gas-generation models were warranted to account for waste heterogeneity. This topic was also addressed during the first recertification in response to comment G-12, in which the EPA requested that the DOE address potential effects of heterogeneous waste loading based on the assumption of homogeneous chemical conditions. The DOE's response indicated that the chemical conditions assumptions adequately addressed nonrandom waste loading (Piper 2004). This was again addressed during the evaluation of the MgO excess factor change from 1.67 to 1.20 (Reyes 2008). No changes were made to the chemical conditions model as a result of these investigations.

Supercompacted waste contains elevated amounts of CPR materials relative to other waste streams, and these materials generate gas when they comingle with brine and undergo microbial degradation. The future arrangement of supercompacted waste in the WIPP repository is uncertain. Sensitivity analysis has demonstrated that uncertainty in the spatial distribution and quantity of CPR materials has little effect on PA results. This was shown in an analysis performed during the 2004 recertification while responding to an EPA request for additional information (Response to Comment G-12, Dunagan, Hansen, and Zelinski 2004).

DBRs as a consequence of a drilling intrusion are calculated with the assumption of random waste emplacement in the repository. In addition, releases by spallings, DBR, and long-term radionuclide transport assume that radionuclides are homogeneously distributed throughout the waste. A sensitivity analysis determined that PA results are not greatly affected by the assumption of random waste emplacement or by the assumption that radionuclides are homogeneously distributed (Hansen et al. 2003). The representation of the waste properties was also considered; however, it was determined that no changes to permeability, shear strength, or tensile strength were warranted.

Based on the analysis reported in Hansen et al. (Hansen et al. 2003), the DOE concluded that:

1. Explicit representation of the specific features of supercompacted waste and of waste in pipe overpacks, such as structural rigidity, was not warranted in modeling, since PA results were primarily insensitive to the effects of such features.

2. PA results were not affected significantly by the assumption of nonrandom waste emplacement and the representation of these waste types as a homogeneous material.

Homogeneity issues were also addressed in response to another EPA comment during the CRA-2004 completeness review. The EPA questioned in comment C-23-10 whether neglecting container-scale variability was a valid assumption for spallings calculations (Cotsworth 2004). In the CRA-2004 PA, spallings releases were calculated using the average radioactivity in all CH-TRU waste streams. An analysis in Vugrin (Vugrin 2004) compared spallings results using three randomly sampled waste streams against results using the average radioactivity over all CH-TRU waste streams. The analysis concluded that the calculation of spallings releases is not significantly affected by waste-scale variability.

The DOE continues to assume in PA that waste is randomly emplaced in the WIPP repository. The CRA-2014 PA continues to use the same waste-related modeling approaches as were used in the CRA-2009 and the CRA-2004 PABC.

MASS-20.0 References

(*Indicates a reference that has not been previously submitted.)

Amyx, J.W., D.M. Bass, Jr., and R.L. Whiting. 1960. Petroleum Reservoir Engineering, Physical Properties. New York: McGraw. [Author]

Anderson, M.P., and W.W. Woessner. 1992. Applied Groundwater Modeling: Simulation of Flow and Advective Transport. New York: Academic Press. [Author]

Bear, J. 1972. Dynamics of Fluid in Porous Media. New York: Elsevier. [Author]

Beauheim, R.L. 1997. Memorandum to Palmer Vaughn (Subject: Revisions to Castile Brine Reservoir Parameter Packages). 16 January 1997. ERMS 244699. Albuquerque, NM: Sandia National Laboratories. [PDF / Author]

Brush, L., and P. Domski. 2013a. Th(IV), Np(V), and Am(III) Baseline Solubilities and Th(IV) and Am(III) Solubility Uncertainties for the CRA-2014 PA. ERMS 559279. Carlsbad, NM: Sandia National Laboratories.* [PDF / Author]

Brush, L., and P. Domski. 2013b. Uncertainty Analysis of Actinide Solubilities for the WIPP CRA-2014 PA, Rev. 1. ERMS 559712. Carlsbad, NM: Sandia National Laboratories.* [PDF / Author]

Camphouse, R.C. 2012. User's Manual for BRAGFLO, Version 6.02. ERMS 558663. Carlsbad, NM: Sandia National Laboratories.* [PDF / Author]

Camphouse, R.C. 2013. Analysis Plan for the 2014 WIPP Compliance Recertification Application Performance Assessment. ERMS 559198. Carlsbad, NM: Sandia National Laboratories.* [PDF / Author]

Camphouse, R.C., D.C. Kicker, T.B. Kirchner, J.J. Long, and J.J. Pasch. 2011. Impact Assessment of SDI Excavation on Long-Term WIPP Performance. ERMS 555824. Carlsbad, NM: Sandia National Laboratories.* [PDF / Author]

Camphouse, R.C., D.C. Kicker, T.B. Kirchner, J.J. Long, B. Malama, and T.R. Zeitler. 2012. Summary Report and Run Control for the 2012 WIPP Panel Closure System Performance Assessment. ERMS 558365. Carlsbad, NM: Sandia National Laboratories.* [PDF / Author]

Caporuscio, F., J. Gibbons, C. Li, and E. Oswald. 2003. Salado Flow Conceptual Models Final Peer Review Report (March). ERMS 526879. Carlsbad, NM: Carlsbad Area Office. [PDF / Author]

Carlsbad Area Office Technical Assistance Contractor (CTAC). 1997. Expert Elicitation on WIPP Waste Particle Diameter Size Distribution(s) During the 10,000-Year Regulatory Post-Closure Period (Final Report, June 3). ERMS 541365. Carlsbad, NM: U.S. Department of Energy. [PDF / Author]

Christian-Frear, T.L., and S.W. Webb. 1996. The Effect of Explicit Representation of the Stratigraphy on Brine and Gas Flow at the Waste Isolation Pilot Plant. SAND94-3173. WPO 37240. Albuquerque, NM: Sandia National Laboratories. [PDF / Author]

Clayton, D.J. 2009a. Analysis Plan for the CRA-2009 Performance Assessment Baseline Calculation. ERMS 551603. Carlsbad, NM: Sandia National Laboratories.* [PDF / Author]

Clayton, D.J. 2009b. Update to Kd Values for the PABC-2009. ERMS 552395. Carlsbad, NM: Sandia National Laboratories.* [PDF / Author]

Clayton, D.J. 2013. Justification of Chemistry Parameters for Use in BRAGFLO for AP-164, Revision 1. ERMS 559466. Carlsbad, NM: Sandia National Laboratories.* [PDF / Author]

Clayton, D.J., S. Dunagan, J.W. Garner, A.E. Ismail, T.B. Kirchner, G.R. Kirkes, M.B. Nemer. 2008. ERMS 548862. Summary Report of the 2009 Compliance Recertification Application Performance Assessment. ERMS 548862. Carlsbad, NM: Sandia National Laboratories.* [PDF / Author]

Clayton, D.J., R.C. Camphouse, J.W. Garner, A.E. Ismail, T.B. Kirchner, K.L. Kuhlman, M.B. Nemer. 2010. Summary Report of the CRA-2009 Performance Assessment Baseline Calculation. ERMS 553039. Carlsbad, NM: Sandia National Laboratories.* [PDF / Author]

Cotsworth, E. 2004. Letter to R.P. Detwiler (1 Enclosure). 20 May 2004. ERMS 535554. Washington, DC: U.S. Environmental Protection Agency, Office of Air and Radiation. [PDF / Author]

Cotsworth, E. 2005. Letter to I. Triay (1 Enclosure). 4 March 2005. ERMS 538858. Washington, DC: U.S. Environmental Protection Agency, Office of Air and Radiation. [PDF / Author]

Cotsworth, E. 2009. Letter to D. Moody (Subject: EPA CRA-2009 First Set of Completeness Comments). 21 May 2009. ERMS 551444. Washington, DC: U.S. Environmental Protection Agency, Office of Air and Radiation.* [PDF / Author]

Davies, P.B. 1991. Evaluation of the Role of Threshold Pressure in Controlling Flow of Waste-Generated Gas into Bedded Salt at the Waste Isolation Pilot Plant. SAND90-3246. WPO 26169. Albuquerque, NM: Sandia National Laboratories. [PDF / Author]

Davies, P.B., S.W. Webb, and E.D. Gorham. 1992. Memorandum to B.M. Butcher, J. Schreiber, and P. Vaughn (Subject: Feedback on "PA Modeling Using BRAGFLO -- 1992" 7-8-92 memo by J. Schreiber; 4 Attachments). 14 July 1992. Albuquerque, NM: Sandia National Laboratories. [PDF / Author]

Dunagan, S., C. Hansen, and W. Zelinski. 2004. Effects of Increasing Cellulosics, Plastics and Rubbers on WIPP Performance Assessment. ERMS 535941. Carlsbad, NM: Sandia National Laboratories. [PDF / Author]

Fox, B., D.J. Clayton, T.B. Kirchner. 2009. Radionuclide Inventory Screening Analysis Report for the PABC-2009. ERMS 551679. Carlsbad, NM: Sandia National Laboratories.* [PDF / Author]

Fox, B. 2008. Parameter Summary Report for CRA-2009 (Revision 0). ERMS 549747. Carlsbad, NM: Sandia National Laboratories. [PDF / Author]

Freeze, G.A., K.W. Larson, and P.B. Davies. 1995. Coupled Multiphase Flow and Closure Analysis of Repository Response to Waste-Generated Gas at the Waste Isolation Pilot Plant (WIPP). SAND93-1986. ERMS 229557. Albuquerque, NM: Sandia National Laboratories. [PDF / Author]

Gorham, E., R. Beauheim, P. Davies, S. Howarth, and S. Webb. 1992. "Recommendations to PA on Salado Formation Intrinsic Permeability and Pore Pressure for 40 CFR 191 Subpart B Calculations, June 15, 1992." Preliminary Performance Assessment for the Waste Isolation Pilot Plant, December 1993 (pp. A-49 through A-65). Volume 3, Model Parameters. SAND92-0700/3. Albuquerque, NM: Sandia National Laboratories. [PDF / Author]

Guzowski, R.V. 1990. Preliminary Identification of Scenarios for the Waste Isolation Pilot Plant, Southeastern New Mexico. SAND90-7090. WPO 25771. Albuquerque, NM: Sandia National Laboratories. [PDF / Author]

Hansen, F.D., M.K. Knowles, T.W. Thompson, M. Gross, J.D. McLennan and J.F. Schatz. 1997. Description and Evaluation of a Mechanically Based Conceptual Model for Spall. SAND97-1369. Albuquerque, NM: Sandia National Laboratories. [PDF / Author]

Hansen, C.W., C. Leigh, D. Lord, and J. Stein. 2002. BRAGFLO Results for the Technical Baseline Migration. ERMS 523209. Carlsbad, NM: Sandia National Laboratories. [PDF / Author]

Hansen, C.W., L.H. Brush, M.B. Gross, F.D. Hansen, B. Park, J.S. Stein, and T.W. Thompson. 2003. Effects of Supercompacted Waste and Heterogeneous Waste Emplacement on Repository Performance (Revision 1). ERMS 532475. Carlsbad, NM: Sandia National Laboratories. [PDF / Author]

Hansen, F.D., T.W. Pfeifle, and D.L. Lord. 2003. Parameter Justification Report for DRSPALL (Revision 0). SAND2003-2930. Carlsbad, NM: Sandia National Laboratories. [PDF / Author]

Herrick, C.G., M.D. Schuhen, D.M. Chapin, and D.C. Kicker. 2012. Determining the Hydrodynamic Shear Strength of Surrogate Degraded TRU Waste Materials as an Estimate for the Lower Limit of the Performance Assessment Parameter TAUFAIL. ERMS 558479. Carlsbad, NM: Sandia National Laboratories.* [PDF / Author]

Herrick, C.G. 2013. Memorandum to C Camphouse (Subject: Follow-up to Questions Concerning TAUFAIL Flume Testing Raised during the November 14-15, 2012 Technical Exchange Between the DOE and EPA). 23 January 2013. ERMS 559081. Carlsbad, NM: Sandia National Laboratories.* [PDF / Author]

Hunter, R.L. 1989. Events and Processes for Constructing Scenarios for the Release of Transuranic Waste from the Waste Isolation Pilot Plant, Southeastern New Mexico. SAND89-2546. WPO 27731. Albuquerque, NM: Sandia National Laboratories. [PDF / Author]

James, S.J., and J. Stein. 2002. Analysis Plan for the Development of a Simplified Shaft Seal Model for the WIPP Performance Assessment. AP-094. ERMS 524958. Carlsbad, NM: Sandia National Laboratories. [PDF / Author]

James, S.J., and J. Stein. 2003. Analysis Report for Development of a Simplified Shaft Seal Model for the WIPP Performance Assessment (Rev. 1). ERMS 525203. Carlsbad, NM: Sandia National Laboratories. [PDF / Author]

Kanney, J.F. 2003. Hydrogen Gas as a Surrogate for Waste-Generated Gas Physical Properties in BRAGFLO. Technical Memorandum. ERMS 532900. Carlsbad, NM: Sandia National Laboratories. [PDF / Author]

Kicker, D.C., and T. Zeitler. 2013. Radionuclide Inventory Screening Analysis Report for the 2014 Compliance Recertification Application Performance Assessment. ERMS 559257. Carlsbad, NM: Sandia National Laboratories.* [PDF / Author]

Kicker, D.C., and C. Herrick. 2013. Parameter Summary Report for the 2014 Compliance Recertification Application. Carlsbad, NM: Sandia National Laboratories.* [PDF / Author]

Kirchner, T., T. Zeitler, and R. Kirkes. 2012. Memorandum to S. Dunagan (Subject: Evaluating the Data in Order to Derive a Value for GLOBAL:PBRINE). 11 December 2012. ERMS 558724. Carlsbad, NM: Sandia National Laboratories.* [PDF / Author]

Kirkes, R. 2007. Evaluation of the Duration of Direct Brine Release in WIPP Performance Assessment (Revision 0). ERMS 545988. Carlsbad, NM: Sandia National Laboratories. [PDF / Author]

Leigh, C., J. Kanney, L. Brush, J. Garner, G. Kirkes, T. Lowery, M. Nemer, J. Stein, E. Vugrin, S. Wagner, and T. Kirchner. 2005. 2004 Compliance Recertification Application Baseline Performance Assessment Calculation (Revision 0). ERMS 541521. Carlsbad, NM: Sandia National Laboratories. [PDF / Author]

Long, J.J. 2013. Execution of Performance Assessment Codes for the CRA-2014 Performance Assessment. Carlsbad, NM: Sandia National Laboratories.* [PDF / Author]

Lord, D.L. 2003. Justification for Particle Diameter and Shape Factor used in DRSPALL. ERMS 531477. Carlsbad, NM: Sandia National Laboratories. [PDF / Author]

Lord, D., D. Rudeen, and C. Hansen. 2003. Analysis Package for DRSPALL: Compliance Recertification Application. Part I-Calculation of Spall Volumes. ERMS 532766. Carlsbad, NM: Sandia National Laboratories. [PDF / Author]

Marcinowski, F. 2000. Letter to Dr. I. Triay, Manager (Subject: Summary of EPA Review of Clay Seam & Mining Plan). 11 August 2000. Washington, DC: U.S. Environmental Protection Agency, Office of Air and Radiation. [PDF / Author]

Marietta, M.G., S.G. Bertram-Howery, D.R. Anderson, K.F. Brinster, R.V. Guzowski, H. Iuzzolino, and R.P. Rechard. 1989. Performance Assessment Methodology Demonstration: Methodology Development for Evaluating Compliance with EPA 40 CFR 191, Subpart B, for the Waste Isolation Pilot Plant. SAND89-2027. WPO 25952. Albuquerque, NM: Sandia National Laboratories. [PDF / Author]

Mendenhall, F.T., and W. Gerstle. 1993. Memorandum to Distribution (Subject: WIPP Anhydrite Fracture Modeling). 6 December 1993. SWCF-A: W.B.S. 1.1.7.1. WPO 39830. Albuquerque, NM: Sandia National Laboratories. [PDF / Author]

National Institute of Standards and Technology (NIST). 1992. NIST Thermophysical Properties of Hydrogen Mixtures Database (SUPERTRAPP) User's Guide (Version 1.0). Gaithersburg, MD: U.S. Department of Commerce, National Institute of Standards and Technology, Standard Reference Data Program. [Author]

Park, B., and F.D. Hansen. 2003. Analysis Report for Determination of the Porosity Surfaces of the Disposal Room Containing Various Waste Inventories for WIPP PA (Revision 0). ERMS 533216. Albuquerque, NM: Sandia National Laboratories. [PDF / Author]

Piper, L.L. 2004. Letter to U.S. Environmental Protection Agency (Subject: Partial Response to Environmental Protection Agency (EPA) September 2, 2004, Letter on Compliance Recertification Application, 6th Response Package, Comment G-12). 23 December 2004. Carlsbad, NM: Carlsbad Field Office. [PDF / Author]

Reed, D.J., J. Swanson, J.-F. Lucchini, and M. Richman. 2013. Intrinsic, Mineral and Microbial Colloid Enhancement Parameters for the WIPP Actinide Source Term. ERMS 559200. LCO-ACP-18. Carlsbad, NM: Los Alamos National Laboratory.* [PDF / Author]

Reyes, J. 2008. Letter to D.C. Moody (Subject: EPA 1.67 to 1.20 Excess Factor Change Approval Letter). 11 February 2008. Washington, DC: U.S. Environmental Protection Agency, Office of Air and Radiation. [PDF / Author]

Roselle, G.T. 2013a. Determination of Corrosion Rates from Iron/Lead Corrosion Experiments to be used for Gas Generation Calculations. ERMS 559077. Carlsbad, NM: Sandia National Laboratories.* [PDF / Author]

Roselle, G.T. 2013b. Summary of Colloid Parameters to be Implemented in the CRA-2014 PA. ERMS 559205. Carlsbad, NM: Sandia National Laboratories.* [PDF / Author]

Schreiber, J.D. 1997. WIPP PA User's Manual for BRAGFLO (Version 4.10, May). ERMS 245238. Carlsbad, NM: Sandia National Laboratories. [PDF / Author]

Stein, J.S. 2003. Memorandum to D. Kessel (Subject: Correlation Between Bulk Compressibility and Porosity in the Castile Brine Pocket as Modeled in BRAGFLO). April 2003. ERMS 527293. Carlsbad, NM: Sandia National Laboratories. [PDF / Author]

Stein, J.S., and W. Zelinski. 2003a. Analysis Plan for the Testing of a Proposed BRAGFLO Grid to be Used for the Compliance Recertification Application Performance Assessment Calculations. AP-106. ERMS 525236. Carlsbad, NM: Sandia National Laboratories. [PDF / Author]

Stein, J.S., and W. Zelinski. 2003b. Analysis Report for: Testing of a Proposed BRAGFLO Grid to be used for the Compliance Recertification Application Performance Assessment Calculations. ERMS 526868. Carlsbad, NM: Sandia National Laboratories. [PDF / Author]

Tierney, M.S. 1991. Combining Scenarios in a Calculation of the Overall Probability Distribution of Cumulative Releases of Radioactivity From the Waste Isolation Pilot Plant, Southeastern New Mexico. SAND90-0838. WPO 26030. Albuquerque, NM: Sandia National Laboratories. [PDF / Author]

Triay, I. 2000. Letter to Mr. F. Marcinowski, Director (Subject: Plans to Raise the Repository Horizon). June 26, 2000. Carlsbad, NM: U.S. Department of Energy, Carlsbad Field Office. [PDF / Author]

U.S. Department of Energy (DOE). 1980. Final Environmental Impact Statement, Waste Isolation Pilot Plant (October). 2 vols. DOE/EIS-0026. ERMS 238835 (vol. 1) and ERMS 238838 (vol. 2). Washington, DC: U.S. Department of Energy. [PDF / Author]

U.S. Department of Energy (DOE). 1996. Title 40 CFR Part 191 Compliance Certification Application for the Waste Isolation Pilot Plant (October). 21 vols. DOE/CAO 1996-2184. Carlsbad, NM: Carlsbad Area Office. [Author]

U.S. Department of Energy (DOE). 2002. Assessment Of Impacts On Long-Term Performance From Supercompacted Wastes Produced By The Advanced Mixed Waste Treatment Project (December 6). Carlsbad, NM: Carlsbad Area Office. [PDF / Author]

U.S. Department of Energy (DOE). 2004. Title 40 CFR Part 191 Compliance Recertification Application for the Waste Isolation Pilot Plant (March). 10 vols. DOE/WIPP 2004-3231. Carlsbad, NM: Carlsbad Field Office. [Author]

U.S. Department of Energy (DOE). 2009. Title 40 CFR Part 191 Compliance Recertification Application for the Waste Isolation Pilot Plant. DOE/WIPP 09-3424. Carlsbad, NM: Carlsbad Field Office.* [Author]

U.S. Department of Energy (DOE). 2010. Quality Assurance Program Document. DOE/CBFO-94-1012. Carlsbad, NM: Carlsbad Field Office.* [PDF / Author]

U.S. Department of Energy (DOE). 2011a. Panel Closure System Design, Planned Change Request to the EPA 40 CFR Part 194 Certification of the Waste Isolation Pilot Plant. DOE/CBFO-11-3479. Carlsbad, NM: Carlsbad Field Office.* [PDF / Author]

U.S. Department of Energy (DOE). 2011b. Letter to J. Edwards, Director (Subject: Notification of Intent to Begin the Salt Disposal Investigations). 11 August 2011. Carlsbad, NM: Carlsbad Field Office.* [PDF / Author]

U.S. Department of Energy (DOE). 2012. Delaware Basin Monitoring Annual Report (September 2012). DOE/WIPP-12-2308. Carlsbad, NM: Carlsbad Field Office.* [PDF / Author]

U.S. Environmental Protection Agency (EPA). 1993. "40 CFR Part 191: Environmental Radiation Protection Standards for the Management and Disposal of Spent Nuclear Fuel, High-Level and Transuranic Radioactive Wastes; Final Rule." Federal Register, vol. 58 (December 20, 1993): 66398-416. [PDF / Author]

U.S. Environmental Protection Agency (EPA). 1996. "40 CFR Part 194: Criteria for the Certification and Recertification of the Waste Isolation Pilot Plant's Compliance with the 40 CFR Part 191 Disposal Regulations; Final Rule." Federal Register, vol. 61 (February 9, 1996): 5223-45. [PDF / Author]

U.S. Environmental Protection Agency (EPA). 1998a. "40 CFR Part 194: Criteria for the Certification and Recertification of the Waste Isolation Pilot Plant's Compliance with the 40 CFR Part 191 Disposal Regulations: Certification Decision; Final Rule." Federal Register, vol. 63 (May 18, 1998): 27353-406. [PDF / Author]

U.S. Environmental Protection Agency (EPA). 1998b. Technical Support Document for 194.23: Parameter Justification Report (May). Washington DC: Office of Radiation and Indoor Air. [PDF / Author]

U.S. Environmental Protection Agency (EPA). 2004. "40 CFR Part 194: Criteria for the Certification and Recertification of the Waste Isolation Pilot Plant's Compliance with the Disposal Regulations; Alternative Provisions" (Final Rule). Federal Register, vol. 69 (July 16, 2004): 42571-83. [PDF / Author]

U.S. Environmental Protection Agency (EPA). 2006. "40 CFR Part 194: Criteria for the Certification and Recertification of the Waste Isolation Pilot Plant's Compliance with the Disposal Regulations: Recertification Decision" (Final Notice). Federal Register, vol. 71 (April 10, 2006): 18010-021. [PDF / Author]

U.S. Environmental Protection Agency (EPA). 2010a. "40 CFR Part 194 Criteria for the Certification and Recertification of the Waste Isolation Pilot Plant's Compliance With the Disposal Regulations: Recertification Decision." Federal Register, No. 222, Vol. 75, pp. 70584-70595, November 18, 2010.* [PDF / Author]

U.S. Environmental Protection Agency (EPA). 2010b. Technical Support Document for Section 194.24, Evaluation of the Compliance Recertification Actinide Source Term, Backfill Efficacy and Culebra Dolomite Distribution Coefficient Values (Revision 1), November 2010.* [PDF / Author]

U.S. Environmental Protection Agency (EPA). 2011. Letter from Jonathan Edwards to Ed Ziemianski dated November 17, 2011.* [PDF / Author]

Van Soest, G.D. 2012. Performance Assessment Inventory Report - 2012. LA-UR-12-26643. Carlsbad, NM: Los Alamos National Laboratory.* [PDF / Author]

Vaughn, P., M. Lord, and R. MacKinnon. 1995a. Memorandum to D.R. Anderson (Subject: DR-6: Brine Puddling in the Repository due to Heterogeneities). 21 December 1995. SWCF-A:1.1.6.3. WPO 30795. Albuquerque, NM: Sandia National Laboratories. [PDF / Author]

Vaughn, P., M. Lord, and R. MacKinnon. 1995b. Memorandum to D.R. Anderson (Subject: DR-7: Permeability Varying with Porosity in Closure Regions). 21 December 1995. SWCF-A:1.1.6.3. WPO 30796. Albuquerque, NM: Sandia National Laboratories. [PDF / Author]

Vaughn, P., M. Lord, and R. MacKinnon. 1995c. Memorandum to D. R. Anderson (Subject: DR3: Dynamic Closure of the North End and Hallways). 28 September 1995. SWCF-A:1.1.6.3. WPO 30798. Albuquerque, NM: Sandia National Laboratories. [PDF / Author]

Vaughn, P., M. Lord, and R. MacKinnon. 1995d. Memorandum to D.R. Anderson (Subject: DR-2: Capillary Action [Wicking] within the Waste Materials). 21 December 1995. SWCF-A:1.1.6.3. WPO 30793. Albuquerque, NM: Sandia National Laboratories. [PDF / Author]

Vaughn, P., M. Lord, and R. MacKinnon. 1995e. Memorandum to D.R. Anderson (Subject: S-6: Dynamic Alteration of the DRZ/Transition Zone). 28 September 1995. WPO 30798. Albuquerque, NM: Sandia National Laboratories. [PDF / Author]

Vaughn, P., M. Lord, J. Garner, and R. MacKinnon. 1995. Memorandum to D.R. Anderson (Subject: FEP Screening Issue GG-1). 10 October 1995. ERMS 230791. Albuquerque, NM: Sandia National Laboratories. [PDF / Author]

Vugrin, E.D. 2004. Memorandum to David Kessel (Subject: Container-Scale Variability and DRSPALL in response to C-23-10, Rev 1). 15 November 2004. ERMS 537870. Carlsbad, NM: Sandia National Laboratories. [PDF / Author]

Wagner, S.W. 2008. Reassessment of MONPAR Analysis for Use in the 2009 Compliance Recertification Application. ERMS 548948. Carlsbad, NM: Sandia National Laboratories. [PDF / Author]

Wagner, S.W. 2011. Compliance Monitoring Parameter Assessment, and Recommendations. ERMS 554957. Carlsbad, NM: Sandia National Laboratories.* [PDF / Author]

Wall, N.A., and D. Enos. 2006. Iron and Lead Corrosion in WIPP-Relevant Conditions, TP 06-02, Rev 1. ERMS 543238. Carlsbad, NM: Sandia National Laboratories.* [PDF / Author]

Wallace, M. 1996. "Summary Memo of Record for NS-11: Subsidence Associated with Mining Inside or Outside the Controlled Area." Records Package for Screening Effort NS-11: Subsidence Associated with Mining Inside or Outside the Controlled Area (November 21) (pp. 1-28). ERMS 412918. Albuquerque, NM: Sandia National Laboratories. [PDF / Author]

Wang, H.F., and M.P. Anderson. 1982. Introduction to Groundwater Modeling: Finite Difference and Finite Element Methods. New York: Academic Press. [Author]

Wang, Y. 1997. Memorandum to Margaret Chu (Subject: Estimate WIPP Waste Particle Sizes on Expert Elicitation Results: Revision 1). 5 August 1997. ERMS 246936. Albuquerque, NM: Sandia National Laboratories. [PDF / Author]

Webb, S. 1995. Memorandum to D.R. Anderson (Subject: DR-1:3D Room Flow Model with Dip). 30 May 1995. SWCF-A:1.1.6.3. WPO 22494. Albuquerque, NM: Sandia National Laboratories. [PDF / Author]

WIPP Performance Assessment. 1991. Preliminary Comparison with 40 CFR Part 191, Subpart B, for the Waste Isolation Pilot Plant, December 1991. 4 vol. SAND91-0893/1-4. Albuquerque, NM: Sandia National Laboratories. [PDF / Author]

WIPP Performance Assessment. 1993. Preliminary Performance Assessment for the Waste Isolation Pilot Plant, December 1992. Volume 4: Uncertainty and Sensitivity Analyses for 40 CFR 191, Subpart B. SAND92-0700/4. ERMS 223528. Albuquerque, NM: Sandia National Laboratories. [PDF / Author]

WIPP Performance Assessment. 2003a. Design Document for DRSPALL Version 1.00 (Version 1.10, September). ERMS 529878. Carlsbad, NM: Sandia National Laboratories. [PDF / Author]

WIPP Performance Assessment. 2003b. Verification and Validation Plan and Validation Document for DRSPALL Version 1.00 (Version 1.00, September). ERMS 524782. Carlsbad, NM: Sandia National Laboratories. [PDF / Author]

Title 40 CFR Part 191
Subparts B and C
Compliance Recertification Application 2014
for the
Waste Isolation Pilot Plant

Appendix MgO-2014
Magnesium Oxide as an Engineered Barrier

United States Department of Energy
Waste Isolation Pilot Plant

Carlsbad Field Office
Carlsbad, New Mexico

Compliance Recertification Application 2014

Appendix MgO-2014

Table of Contents

List of Figures

List of Tables

This page intentionally left blank.

Acronyms and Abbreviations

% percent

µm micrometer

AMWTP Advanced Mixed Waste Treatment Program

aq aqueous

atm atmosphere(s)

BRAGFLO Brine and Gas Flow

C Celsius

CCA Compliance Certification Application

CFR Code of Federal Regulations

CH-TRU contact-handled transuranic

CPR cellulosic, plastic, and rubber

CRA Compliance Recertification Application

DOE U.S. Department of Energy

ECO Engineering Change Order

EPA U.S. Environmental Protection Agency

ERDA Energy Research and Development Administration

FMT Fracture-Matrix Transport

g gaseous or gram

GWB Generic Weep Brine

HDPE high-density polyethylene

K_d matrix distribution coefficient

kg kilogram

L liter

lb pound

M molar

m^3 cubic meters

mL milliliter

mm millimeter

mol mole

PA performance assessment

PABC Performance Assessment Baseline Calculations

PAVT Performance Assessment Verification Test

ppm parts per million

RH relative humidity

RH-TRU remote-handled transuranic

s second(s) or solid

SPC Salado Primary Constituents

TIC total inorganic carbon

TRU transuranic

WDS Waste Data System

WIPP Waste Isolation Pilot Plant

WTS Washington TRU Solutions, LLC

XRD X-ray diffraction

Elements and Chemical Compounds

Am americium

An actinide

Br bromine

C carbon

Ca calcium

CaO calcium oxide or lime

$CaSO_4$ anhydrite

CH_4 methane

Cl^- chloride ion

Cl chlorine

CO_2 carbon dioxide

CO_3^{2-} carbonate ion

f_{co_2} fugacity of CO_2

Fe iron

H^+ hydrogen ion

H_2O water

H_2S hydrogen sulfide

Mg magnesium

$Mg(OH)_2$ brucite

$Mg_2(OH)_3Cl{\cdot}4H_2O$ phase 3

$Mg_3(OH)_5Cl{\cdot}4H_2O$ phase 5

$Mg_4(CO_3)_3(OH)_2 \cdot 3H_2O$ hydromagnesite (4323)

$Mg_5(CO_3)_4(OH)_2 \cdot 4H_2O$ hydromagnesite (5424)

$MgCO_3$ magnesite

$MgCO_3 \cdot 3H_2O$ nesquehonite

MgO magnesium oxide

N_2 nitrogen

Na sodium

$Na_2Ca(SO_4)_2$ glauberite

NaCl sodium chloride or halite

Np neptunium

O_2 oxygen

Pb lead

pH the negative, common logarithm of the activity of H^+

Pu plutonium

SO_4 sulfate

Th thorium

U uranium

This page intentionally left blank.

MgO-1.0 Introduction

The U.S. Department of Energy (DOE) is emplacing magnesium oxide (MgO) in the Waste Isolation Pilot Plant (WIPP) repository to provide an engineered barrier that decreases the solubilities of the actinide (An) elements in transuranic (TRU) waste in any brine present in the postclosure repository (Compliance Certification Application (CCA), Appendix BACK and Appendix SOTERM (U.S. DOE 1996); the 2004 Compliance Recertification Application (CRA-2004) Appendix BARRIERS-2004, Appendix PA-2004, and Attachment SOTERM-2004 (U.S. DOE 2004); and the CRA-2009 Appendix MgO-2009 and Appendix SOTERM-2009 (U.S. DOE 2009)). Because it will decrease An solubilities, MgO helps meet the U.S. Environmental Protection Agency (EPA) requirement for multiple natural and engineered barriers, one of the assurance requirements for radioactive waste repositories in 40 CFR § 191.14(d) (U.S. EPA 1993).

In 40 CFR § 191.12 (U.S. EPA 1993), the EPA defined barriers as "any material or structure that prevents or substantially delays movement of water or radionuclides toward the accessible environment. For example, a barrier may be a geologic structure, a canister, a waste form…or a material placed over and around waste provided that the material or structure substantially delays movement of water or radionuclides."

The DOE proposed four engineered barriers in the WIPP CCA, submitted to the EPA in October 1996 (U.S. DOE 1996). The barriers proposed were MgO, panel closures, shaft seals, and borehole plugs. The EPA specified MgO as the only engineered barrier in the WIPP disposal system that meets the assurance requirement in its May 1998 certification rulemaking (U.S. EPA 1998a and U.S. EPA 1998b) because it considered panel closures, shaft seals, and borehole plugs to be part of the disposal-system design.

As used in the WIPP, MgO will decrease An solubilities by consuming essentially all of the carbon dioxide (CO_2) that would be produced should microbial activity consume all of the cellulosic, plastic, and rubber (CPR) materials in the TRU waste, waste containers, and waste-emplacement materials in the repository. Although MgO will consume essentially all the CO_2, minute quantities (relative to the quantity that would be produced by microbial consumption of all of the CPR materials) will persist in the aqueous (aq) and gaseous (g) phases. The residual quantities would be so small relative to the initial quantity that the term "essentially" is hereafter omitted in this appendix.

Consumption of CO_2 will decrease An solubilities by (1) buffering the fugacity of CO_2 (f_{CO2}) at a value or within a range of values favorable from the standpoint of the speciation and solubilities of the An elements (the fugacity of a gaseous species, f_i, is similar to the partial pressure of that species, p_i); (2) controlling the pH at a value favorable from the standpoint of An solubilities; and (3) preventing the production of carbonate ion (CO_3^{2-}) in significant quantities. The effect of this residual CO_3^{2-} on the solubilities of An elements is described in Appendix SOTERM-2014, Section SOTERM-3.2.1 and Section SOTERM-3.3.1.3.

The effects of MgO carbonation (consumption of CO_2) have been included in WIPP performance assessment (PA) calculations by assuming that there will be no CO_2 in the repository. This assumption has been implemented in PA by (1) removing CO_2 from the gaseous phase in the Brine and Gas Flow (BRAGFLO) calculations, thereby somewhat reducing the predicted pressurization of

the repository; and (2) using the values of f_{CO2} and pH predicted for reactions among MgO, brine, and aqueous or gaseous CO_2 to calculate An solubilities. The assumption that there will be no CO_2 has been implemented in all compliance-related WIPP PA calculations. These include (1) the CCA PA calculations (Appendix SOTERM) (Novak, Moore, and Bynum 1996; U.S. DOE 1994); (2) the CCA Performance Assessment Verification Test (PAVT) (Novak 1997; U.S. EPA 1998c, U.S. EPA 1998d, and U.S. EPA 1998e); (3) the PA calculations for the CRA-2004 (Appendix PA and Attachment SOTERM) (Brush and Xiong 2003a, Brush and Xiong 2003b, Brush and Xiong 2003c, and Brush and Xiong 2003d; U.S. DOE 2004); (4) the CRA-2004 Performance Assessment Baseline Calculations (PABC) (Brush and Xiong 2005a and Brush and Xiong 2005b; Brush 2005; Leigh et al. 2005); (5) the PA calculations for the CRA-2009 (Appendix SOTERM-2009) (U.S. DOE 2009); (6) the CRA-2009 PABC calculations (Brush and Xiong 2009a and Brush and Xiong 2009b; Brush, Xiong, and Long 2009; U.S. DOE 2009); and (7) the CRA-2014 PA calculations (Appendix SOTERM-2014) (Brush, Domski, and Xiong 2012; Brush and Domski 2013a and Brush and Domski 2013b).

In this appendix, "MgO" refers to the bulk, granular material being emplaced in the WIPP to serve as the engineered barrier. MgO comprises periclase (pure, crystalline MgO-the main, reactive constituent of the WIPP engineered barrier) and various impurities described in Appendix MgO-2009, Section MgO-3.0 (U.S. DOE 2009). Pure, crystalline MgO is always referred to as periclase in this Appendix. The term periclase, and other mineral names used herein are, strictly speaking, restricted to naturally occurring forms of the materials that meet all the other requirements of the definition of a mineral (see, for example, Bates and Jackson 1984). However, mineral names are used in this report for convenience.

MgO-2.0 Description of the Engineered Barrier System

This section describes the emplacement of MgO in the WIPP disposal rooms (Section MgO-2.2) and the vendors that provided or are providing MgO to the WIPP (Section MgO-2.2).

Washington TRU Solutions, LLC (WTS) (WTS 2009b) provided the current specifications for the prepackaged MgO emplaced in the WIPP.

MgO-2.1 Emplacement of MgO

Sections 2.1.1 through 2.1.4 provide a history of the changes related to emplacement of MgO in the WIPP.

MgO-2.1.1 Supersacks

The DOE originally emplaced MgO in polypropylene supersacks atop each stack of waste containers. According to the original WTS specifications, each supersack contained 1905 ± 23 kilograms (kg) (4200 ± 50 pounds ([lb]) of MgO (WTS 2009b). (Section MgO-2.1.4 describes changes since the CRA-2009 in the placement of the supersacks on every other waste stack instead of every waste stack, and the weight of some of the supersacks.) Forklifts are used to place the supersacks on top of the waste stacks. Figure MgO-1 shows supersacks of MgO emplaced on top of the waste stacks.

Figure MgO- 1. Supersacks of MgO Emplaced on Top of the Waste Stacks

The use of supersacks facilitates handling and emplacement of the MgO, minimizes potential worker exposure to dust, and minimizes the exposure of periclase to atmospheric CO_2 and water (H_2O) during handling and emplacement, and prior to panel closure. WTS (WTS 2009b) provides the most current, detailed specifications for the supersacks. In particular, WTS (WTS 2009b) specifies that the supersacks "shall provide a barrier to atmospheric moisture and carbon dioxide (CO_2) … equivalent to or better than that provided by a standard commercial cement bag," and "must be able to retain [their] contents for a period of two years after emplacement without rupturing from [their] own weight." The specifications also require a certificate of compliance with all requirements of WTS (WTS 2009b) for every shipment of MgO (see Section MgO-3.1), and a certified chemical analysis for each new lot of MgO. The supersacks are subject to random receipt inspection at the WIPP to ensure compliance with the dimensions and labeling specified by WTS (WTS 2009b), and to identify any damage incurred during shipping.

The supersacks contain dry, granular MgO, of which less than 0.5% can exceed 9.5 millimeters (mm) (3/8 inch) in diameter (WTS 2009b). Emplacement of granular MgO instead of powder reduces the likelihood of dust formation and release in the event of premature supersack rupture, and ensures that the permeability of the material is high enough to promote complete reaction with aqueous or gaseous CO_2.

Creep closure of WIPP disposal rooms will rupture the supersacks and disperse the MgO among and within the ruptured waste containers. This will, in turn, expose the MgO to the room's atmosphere, to any CO_2 produced by the microbial consumption of CPR materials, and to H_2O vapor and any brine present.

MgO-2.1.2 Minisacks

From the first receipt of TRU waste at the WIPP in March 1999 until January 2001, the DOE emplaced MgO in both supersacks and 11-kg (25-lb) minisacks. During this period, the minisacks were emplaced among the waste containers and between the waste containers and the ribs (sides) of the disposal rooms. The MgO supersacks and minisacks constituted about 85% and 15%, respectively, of the total quantity of MgO emplaced in the repository.

In 2000, the DOE requested EPA approval to eliminate the minisacks (Triay 2000; U.S. DOE 2000); the EPA approved this request in 2001 (Marcinowski 2001; U.S. EPA 2001). Appendix MgO-2009, Section MgO-2.1.2 provides details on the DOE's request and the EPA's approval of this request.

MgO-2.1.3 Use of Racks to Emplace Additional MgO

In March 2004, the EPA approved the emplacement in the WIPP of compressed (supercompacted) waste from the Advanced Mixed Waste Treatment Project (AMWTP) at the Idaho National Engineering and Environmental Laboratory (Marcinowski 2004; Trinity Engineering Associates 2004; U.S. EPA 2004). However, the EPA required that the DOE maintain an MgO excess factor (Section MgO-6.0) of 1.67 on a room-by-room basis. Some of the AMWTP waste contains concentrations of CPR materials that are high relative to the average concentration of CPR materials in TRU waste, thereby necessitating the emplacement of additional MgO in the repository. To account for this, the DOE has emplaced additional MgO supersacks on racks among the waste containers. Each rack contains five supersacks identical to those placed on top of the waste containers, and spans the same vertical distance normally occupied by the waste stack and the supersack emplaced atop the waste stack. Thus, emplacing additional MgO in the repository uses space normally occupied by contact-handled transuranic (CH-TRU) waste. Figure MgO-2 shows a rack used to emplace additional MgO in the WIPP.

In February 2008, the EPA approved the DOE's request for a reduction of the MgO excess factor from 1.67 to 1.2 (see Appendix MgO-2009, Section MgO-6.2.4.6) (U.S. DOE 2009).

Figure MgO- 2. Racks Used to Emplace Additional MgO

MgO-2.1.4 Changes since the CRA-2009

In February 2012, the DOE submitted a planned change notice with an alternative placement scheme for MgO supersacks (Franco 2012). This scheme consists of emplacing the MgO supersacks on every

other row of waste stacks, and adjusting this frequency if necessary to accommodate high-CPR waste streams. The DOE proposed this new process because the data it had obtained by tracking the amounts of CPR materials and MgO emplaced in the repository for the last four years demonstrated that the MgO excess factor had exceeded the value of 1.2 approved by the EPA in February 2008 (see Appendix MgO-2009, Section MgO-6.2.4.6) (U.S. DOE 2009). The DOE stated that its new emplacement scheme would: (1) continue to calculate the excess factor at the end of each shift when waste-emplacement data are uploaded to the WIPP Waste Data System (WDS), (2) continue to allow designated personnel to direct that additional MgO be emplaced during the next shift if necessary, and (3) result in a more efficient distribution of MgO based on the CPR contents of the emplaced waste containers. The DOE's change notice included an analysis based on Kanney and Vugrin (Kanney and Vugrin 2006) that showed that molecular diffusion of microbially produced CO_2 through brine following a human intrusion into the repository would be sufficient to transport CO_2 from the waste to the MgO supersacks placed on every other row of waste stacks.

In July 2012, the EPA concurred with the DOE's change notice to emplace MgO supersacks on every other row of waste stacks and adjust this frequency if necessary for high-CPR waste streams (Peake 2012).

The DOE continues to emplace waste in several types of containers (Appendix DATA-2014, Attachment B), and is now emplacing MgO in 3000- and 4200-lb supersacks. WTS specified the addition of 1361 ± 23 kg (3000 ± 50 lb) supersacks in Engineering Change Order (ECO) 12137 (WTS 2009a). WTS added the 3000-lb supersacks after calculations using past MgO emplacement data and an MgO excess factor of 1.2 instead of 1.67 established that using both 3000- and 4200-lb supersacks would be more economical than using only 4200-lb supersacks. Furthermore, the WDS calculations showed that using both sizes would decrease the number of racks required (see Appendix MgO-2014, Section 2.1.3). Waste Handling Operations is now using the WDS to calculate which sizes of supersacks to emplace on every other row of waste stacks in order to maintain an MgO excess factor of 1.2 and to minimize the use of racks. ECO 12137 (WTS 2009a) also specified the addition of the reactivity test for periclase and lime (Appendix MgO-2014, Section 2.3.1) that was required by the EPA when it approved the DOE's request for a reduction of the MgO excess factor from 1.67 to 1.2 (Appendix MgO-2009, Section MgO-6.2.4.6) (U.S. DOE 2009). ECO 12137 necessitated the replacement of the previous specifications for prepackaged MgO emplaced in the WIPP (WTS 2005) with the current specifications (WTS 2009b). The first 3000-lb supersack was emplaced on August 25, 2009, in Panel 5 of Room 6. The DOE informed the EPA of this change during the EPA's annual inspection of the WIPP site on June 28, 2010 (U.S. EPA 2010a).

As of December 31, 2012, the DOE had emplaced 84,892.57 cubic meters (m^3) of CH-TRU waste in 17,108 stacks, and 309.68 m^3 of remote-handled transuranic (RH-TRU) waste in 620 boreholes in the repository. As of the same date, the DOE had emplaced 12,550 25-lb minisacks, 3,807 3,000-lb sacks, 71 4,100-lb supersacks, and 13,776 4,200-lb supersacks, and 142 racks. The overall MgO excess factor (see MgO-6.0) as of December 31, 2012, was 1.810 (Kouba 2013).

MgO-2.2 MgO Vendors

National Magnesia Chemicals in Moss Landing, CA, was the first vendor to provide MgO for the WIPP. National Magnesia supplied MgO from the opening of the WIPP in March 1999 through mid-April 2000; during this period, waste was emplaced only in Panel 1, Room 7. This vendor was sometimes referred to as National Refractory Materials (e.g., Papenguth 1999). Note that in every

seven-room WIPP panel, waste is first emplaced in Room 7, at the back of the panel, and is last emplaced in Room 1, at the front of the panel.

After National Magnesia stopped producing MgO, WTS considered Martin Marietta Magnesia Specialties LLC, currently headquartered in Baltimore, MD, and Premier Chemicals of Gabbs, NV, as potential vendors. At the request of the DOE Carlsbad Area Office, Papenguth (Papenguth 1999) carried out a technical evaluation of MgO from both Martin Marietta and Premier to support the selection of a new vendor. The criteria used for this evaluation included density, particle size, purity, and reactivity, quantified using a test developed by Krumhansl (Krumhansl et al. 1997). Based on cost and the results of the technical evaluation, WTS selected Premier Chemicals. Appendix MgO-2009, Section MgO-3.2 (U.S. DOE 2009) provides the results of the characterization of Premier MgO. This vendor supplied MgO from mid-April 2000 (Panel 1, Room 7) through January 2005 (Panel 2, Room 2).

Premier Chemicals informed WTS in 2004 that it would soon be unable to provide MgO that met the requirement for the minimum concentration of MgO specified by WTS (WTS 2003): "The sum of MgO plus calcium oxide (CaO) shall be a minimum of 95%, with MgO being no less than 90%."

Martin Marietta Magnesia Specialties, LLC, was selected and has supplied MgO to the WIPP since January 2005 (Panel 2, Room 2). The company was selected based on cost and a technical evaluation of suitability (Wall 2005). Appendix MgO-2009, Section MgO-3.3.2 (U.S. DOE 2009) contained the results of the evaluation and a detailed characterization of Martin Marietta MgO.

Martin Marietta is still providing MgO to the WIPP.

MgO-3.0 Characteristics of MgO

The CRA-2009, Appendix MgO-2009, Section MgO-3.0 (U.S. DOE 2009) described the characteristics of the MgO provided to the WIPP by National Magnesia Chemicals (Section MgO-3.1), Premier Chemicals (Section MgO-3.2), and Martin Marietta Magnesia Specialties, LLC (the current vendor). There is no new information since the CRA-2009 regarding the characteristics of these vendors and materials provided.

MgO-3.1 Changes since the CRA-2009

A new test to determine the concentration of the reactive constituents of the MgO (periclase and lime, or CaO) was developed by Sandia National Laboratories to satisfy one of the EPA's requirements that it specified when it approved the DOE's request for a reduction of the MgO excess factor from 1.67 to 1.2 (see Appendix MgO-2009, Section MgO-6.2.4.6) (U.S. DOE 2009). WTS specified the use of this test, entitled "Reactivity (mole % Periclase + Lime) Acceptance Test," in ECO 12137 (WTS 2009a), and it was incorporated in the current specifications for prepackaged MgO emplaced in the WIPP (WTS 2009b). An independent outside laboratory carries out the reactivity test to ensure that the MgO fulfills the EPA's requirement that the MgO contain a minimum of 96 mole (mol) % of reactive constituents. Since the implementation of the reactivity test in April 2009 through December 31, 2012, Waste Handling Operations purchased 37 shipments containing 250 tons of MgO. A total of 370 samples from these shipments were analyzed; the average reactivity of these samples was 97.4 mol % (Chavez 2013). These results are archived in the WIPP WDS.

MgO-4.0 Hydration and Carbonation of MgO

This section provides the results of the DOE studies of the hydration and carbonation of MgO (Section MgO-4.1 and Section MgO-4.2, respectively).

MgO-4.1 Hydration of MgO

The CRA-2009, Appendix MgO-2009, Section MgO-4.1 (U.S. DOE 2009) described the hydration of MgO provided by Premier Chemicals (the previous MgO vendor) and Martin Marietta Magnesia Specialties, LLC (the current vendor). There is no new information since the CRA-2009 regarding the hydration of Premier or Martin Marietta MgO (see Appendix MgO-2009 for discussions of the hydration of these products). However, some of the previous text is retained herein to provide background information for new results on the relative stabilities of two of the MgO hydration products expected in the WIPP.

Based on previous experiments (Appendix MgO-2009, Sections 4.1.1 and 4.1.2), the most important hydration reaction expected in the WIPP is

$$MgO(s) + H_2O(aq \text{ or } g) \rightleftharpoons Mg(OH)_2(s). \quad (MgO.1)$$

Reaction (MgO.1) was the only hydration reaction observed in the humid experiments. Reaction (MgO.1) was also the only hydration reaction observed in the inundated runs with ERDA-6 brine (Snider 2003b). ERDA-6 brine is a synthetic brine representative of fluids in brine reservoirs in the Castile Formation (Popielak et al. 1983). In inundated experiments with Generic Weep Brine (GWB), however, hydration produced both brucite and a crystalline Mg-OH-Cl-H_2O phase (Snider 2003a). GWB is the average composition of intergranular fluids collected from the Salado Formation at the original stratigraphic horizon of the repository (Krumhansl, Kimball, and Stein 1991; Snider 2003b). X-ray diffraction (XRD) analysis identified this phase as $Mg_3(OH)_5Cl{\cdot}4H_2O$, referred to herein as "phase 5" because its OH/Cl ratio (the molar ratio of OH to Cl) is five (Snider et al. 2003a). On the other hand, the thermodynamic speciation and solubility code Fracture-Matrix Transport (FMT) (Babb and Novak 1997 and addenda; Wang 1998), which was used at the time to predict near-field chemical conditions and An solubilities in the WIPP, predicted that both brucite and a similar Mg-OH-Cl-H_2O phase, $Mg_2(OH)_3Cl{\cdot}4H_2O$ (phase 3), would be present in GWB and Salado Primary Constituents (SPC) brine after these brines equilibrate with the solids in WIPP disposal rooms (Section MgO-5.1). SPC brine (Novak 1997) is similar to Brine A, another synthetic fluid that was used to represent intergranular Salado brines (see Section MgO-5.1.1.2 and Molecke 1983). The FMT thermodynamic database contained phase 3, but not phase 5, at the time. If phase 5 had been in the database, FMT would have predicted that phase 5 would be present in GWB instead of phase 3 (Section MgO-5.1). The hydration reaction that produces phase 5 is:

$$3Mg(OH)_2 + 3H_2O + H^+ + Cl^- \rightleftharpoons Mg_3(OH)_5Cl{\cdot}4H_2O \quad (MgO.2)$$

It should be noted that Freyer (Freyer 2012) concluded that phase 3 is stable with respect to phase 5 under the conditions expected in a German domal salt repository (see Section MgO-4.1.1).

MgO-4.1.1 Results since the CRA-2009

Deng et al. (Deng et al. 2009) conducted long-term hydration experiments with Martin Marietta MgO primarily to obtain information on the solid phases produced by the hydration of Martin Marietta MagChem 10 WTS MgO. This MagChem 10 WTS MgO is apparently identical to the Martin Marietta MagChem WTS-60 MgO, used by Deng, Xiong and Nemer (Deng, Xiong and Nemer 2007,

Section 5) in their accelerated hydration experiments (see Appendix MgO-2009, Section MgO-4.1.2) (U.S. DOE 2009), because the particle-size distributions reported by Deng, Xiong, and Nemer (Deng, Xiong, and Nemer 2007, Section 5) and Deng et al. (Deng et al. 2009) are identical. Deng et al. (Deng et al. 2009) used MgO with three particle sizes (as-received, < 75 μm, and 1.0-2.0 mm), three brines (GWB, "simplified GWB" (1 M $MgCl_2$ + 3.6 M NaCl), and ERDA-6), and two MgO/brine ratios (0.0403 and 0.273 grams per milliliter (g/mL)). They hydrated the MgO in 30 mL high-density polyethylene (HDPE) centrifuge tubes or 125 mL HDPE serum bottles at 28 °C for periods of up to about 16 months. Deng et al. (Deng et al. 2009) used a fractional factorial matrix similar to that used by Deng, Xiong and Nemer (Deng, Xiong and Nemer 2007, Section 5) in their accelerated hydration experiments (see above). Deng et al. (Deng et al. 2009) performed XRD and scanning electron microscopy analyses that confirmed that brucite and phase 5 (but not phase 3) form in GWB and simplified GWB, but that only brucite forms in ERDA-6 brine.

Because the results of numerous laboratory studies of MgO hydration showed that phase 5 forms in GWB instead of phase 3 (Wang and Bryan 2000; Wang, Bryan, and Wall 2001; Snider and Xiong 2002a and Snider and Xiong 2002b; Snider, Xiong, and Wall 2004; Deng et al. 2009), Xiong et al. (Xiong et al. 2009 and Xiong et al. 2010) determined the solubility of phase 5 and added its solubility product to the DATA0.FM1 database that was qualified for An-solubility calculations along with the EQ3/6 geochemical software package (Wolery 2008; Wolery et al. 2010; Xiong 2011a and Xiong 2011b). Therefore, EQ3/6 now predicts that the hydration of MgO in GWB will produce brucite and phase 5 instead of brucite and phase 3, and that hydration of MgO in ERDA-6 brine will produce only brucite. Therefore, both experimental and modeling studies now agree that phase 5 is stable with respect to phase 3 under conditions expected in WIPP disposal rooms.

Freyer (Freyer 2012), however, concluded that phase 3 is stable with respect to phase 5 under the conditions expected in a German domal salt repository. It is possible that phase 5 is stable under expected WIPP conditions but that phase 3 is stable in German domal salt repositories because the conditions expected in the WIPP differ from those in German repositories (e.g., different brine compositions, elevated temperatures in German repositories but not in the WIPP, etc.). Brush, Xiong, and Long (Brush, Xiong, and Long 2009) demonstrated that whether phase 3 or phase 5 is stable in GWB has very little effect on the predicted composition of this brine, including An solubilities. (Neither phase 3 nor phase 5 ever forms in ERDA-6 brine, so which of these phases is stable is irrelevant in the case of PA calculations using An solubilities predicted for this brine.)

MgO-4.2 Carbonation of MgO

The CRA-2009, Appendix MgO-2009, Section 4.2 (U.S. DOE 2009) discussed the carbonation of MgO, the formation of hydromagnesite and (perhaps) magnesite in the WIPP, and the possible passivation of MgO.

MgO-4.2.1 Results since the CRA-2009

Since the CRA-2009, Xiong determined the solubility constant of hydromagnesite (5424) ($Mg_5(CO_3)_4(OH)_2\ 4H_2O$) in NaCl solutions up to 4.4 M (Xiong 2011c).

MgO-5.0 Effects of MgO on the WIPP Disposal System

This section reviews the effects of MgO on (1) brine composition, f_{CO2}, pH, and An solubilities, including changes since the CRA-2009 (Section MgO-5.1); (2) colloidal An concentrations (Section

MgO-5.2); (3) other near-field processes and conditions, including repository H_2O content, gas generation, and room closure (Section MgO-5.3); and (4) far-field An transport (Section MgO-5.4).

MgO-5.1 Effects of MgO on Brine Composition, fCO2, pH, and An Solubilities

The DOE is emplacing MgO in the WIPP to decrease the solubilities of the An elements in TRU waste by consuming all the CO_2 that would be produced by microbial activity should all the CPR materials in the repository be consumed. Consumption of CO_2 will decrease An solubilities by (1) buffering f_{CO_2} at a low value or within a low range of values, (2) maintaining a mildly basic pH, and (3) preventing the production of significant carbonate ion (CO_3^{2-}) quantities.

The effects of MgO carbonation have been included in WIPP PA by removing CO_2 from the gaseous phase in BRAGFLO calculations, and using the values of f_{CO_2} and pH predicted for reactions among MgO, brine, and aqueous or gaseous CO_2 to calculate An solubilities.

Table MgO-1 provides the initial compositions of GWB and ERDA-6 brine and their compositions predicted by EQ3/6 for the An-solubility calculations for the CRA-2014 PA (Brush and Domski 2013b) after equilibration with (1) the MgO hydration and carbonation products brucite ($Mg(OH)_2$) and hydromagnesite (5424), respectively; (2) halite (NaCl) and anhydrite ($CaSO_4$), two of the most abundant minerals in the Salado; and (3) the An-bearing solids $Am(OH)_3$; hydrous, amorphous ThO_2; and $KNpO_2CO_3$. In addition to these solids, which are specified in the input files, EQ3/6 predicted that (1) the solids phase 5 and whewellite (Ca oxalate hydrate, or $CaC_2O_4 \cdot H_2O$) would precipitate from GWB; and (2) glauberite ($Na_2Ca(SO_4)_2$) and whewellite would precipitate from ERDA-6 brine if these brines equilibrate with brucite, hydromagnesite (5424), halite, and anhydrite. Note that the prediction that phase 5 would precipitate from GWB but not ERDA-6 brine is consistent with previous laboratory and modeling studies of the hydration of MgO carried out for the WIPP (see Sections MgO-4.1 and MgO-4.1.1). Note also that because oxalate (and other organic ligands) was included in these brines for the CRA-2014 PA calculations, Brush and Domski (Brush and Domski 2013b) predicted that whewellite would precipitate.

EQ3/6 predicts that equilibration of these brines with the solids listed above will (1) establish a total inorganic carbon (TIC) concentration of 3.79×10^{-4} M in GWB, and decrease the TIC concentration from 1.6×10^{-2} M to 4.55×10^{-4} M in ERDA-6 brine; (2) buffer f_{CO_2} at 3.14×10^{-6} atmospheres (atm) in both brines; and (3) establish a pH of 8.82 in GWB and increase the pH from 6.17 to 8.99 in ERDA-6 brine.

Equilibration of GWB and ERDA-6 brine with these solids will also change the concentrations of the major and other minor elements in these brines. In particular, the concentration of Mg in GWB will decrease from 1.02 to 0.330 M, but will increase from 0.019 to 0.136 M in ERDA-6 brine (Table MgO-1).

Table MgO- 1. Compositions of GWB and ERDA-6 Brine Predicted by EQ3/6 for the An-Solubility Calculations for the CRA-2014 PA (Brush and Domski 2013b) (M, Unless Otherwise Noted) before and after Equilibration with Brucite, Hydromagnesite, Halite, Anhydrite, Other Solids and Organics

Dissolved Element or Property	GWB before Reaction with Solids[a]	GWB after Reaction with Solids[b]	ERDA-6 Brine before Reaction with Solids[c]	ERDA-6 Brine after Reaction with Solids[d]

B(III)	0.158	0.186	0.063	0.0623
Na(I)	3.53	4.77	4.87	5.30
Mg(II)	1.02	0.330	0.019	0.136
K(I)	0.467	0.550	0.097	0.0960
Ca(II)	0.014	0.0111	0.012	0.0116
S(VI)	0.177	0.216	0.170	0.182
Cl(–I)	5.86	5.36	4.8	5.24
Br(–I)	0.0266	0.0313	0.011	0.0109
f_{CO2} (atm)	-	3.14×10^{-6}	-	3.14×10^{-6}
Ionic strength	-	6.44	-	5.99
pH[e] (std. units)	-	8.82	6.17	8.99
pcH	-	9.54	-	9.69
RH (%)[f]	-	73.5	-	74.7
TIC	-	3.79×10^{-4}	16	4.55×10^{-4}

[a] From Krumhansl et al. (1991) and Snider (2003b).

[b] From Brush and Domski (2013b, Table 5, 1 × Minimum).

[c] From Popielak et al. (1983).

[d] From Brush and Domski (2013b, Table 6, 1 × Minimum).

[e] The Pitzer scale is an unofficial pH scale consistent with pH values calculated using single-ion activity coefficients based on the Pitzer activity-coefficient model for brines and evaporite minerals of Harvie (Harvie et al. 1984), extended to include Nd(III), Am(III), and Cm(III); Th(IV); and Np (V). T. J. Wolery of Lawrence Livermore National Laboratory proposed the term "Pitzer scale" unofficially.

[f] Relative humidity.

MgO-5.2 Effects of MgO on Colloidal An Concentrations

The CRA-2009, Appendix MgO-2009, Section 5.2 , and U.S. DOE 2004, Appendix BARRIERS, Section BARRIERS-2.3.3 (U.S. DOE 2009) described the effects of MgO on colloidal An concentrations. There has been no change to the conceptual colloid model since the CRA-2009; however, a number of parameters have been updated for the CRA-2014 (Appendix SOTERM-2014, Section 3.8). Refer to the CCA, Appendix SOTERM (U.S. DOE 1996), for information on the colloid conceptual model.

MgO-5.2.1 Changes since the CRA-2009

In its Technical Support Document related to CRA-2009, Appendix MgO, the EPA (U.S. EPA 2010b) stated that "although the mineral-fragment colloids reported in the recent literature are not expected to be stable in WIPP brines, examination of the data used to develop the colloidal actinide source term model has shown that possible formation of mineral fragment colloids by MgO and its hydration and carbonation products under WIPP-relevant conditions has not been evaluated" (U.S. EPA 2010). This statement is partially in response to a study by Altmaier (Altmaier et al. 2004) that discussed the formation of colloids of magnesium chloride hydroxide hydrate, $Mg_2Cl(OH)_3 \cdot 4H_2O$, which is termed as phase 3 in cement literature, in their experiments in 4.5 M $MgCl_2$. The Altmaier (Altmaier et al. 2004) study raised the possibility that Mg-Cl-OH colloids could form in brines in the presence of MgO and that these colloids could sorb radionuclides and transport them. Therefore, the investigation into the presence or absence of Mg-Cl-OH colloids under the WIPP relevant conditions was necessary, as the presence of such colloids could have an effect on the actinide source term.

Since the CRA-2009, a series of experiments has been developed to investigate the potential formation of Mg-Cl-OH colloids under WIPP-relevant conditions and, if formed, the capacity of such colloids to sorb Th(IV) as mineral-fragment colloids in the WIPP source term (Xiong and Kim 2011). For GWB in the presence of MgO, the thermodynamically favored Mg-Cl-OH phase is $Mg_3Cl(OH)_5 \cdot 4H_2O$, termed as phase 5 in cement literature; no Mg-Cl-OH phase is thermodynamically favored in ERDA-6 in the presence of MgO (Xiong and Lord 2008). These experiments are in progress and results will be reported as they are available. As part of this effort, the study of Altmaier (Altmaier et al. 2004) was critically evaluated. Based on the results of this analysis it can be concluded that the formation of Mg-Cl-OH mineral fragment colloids in the Altmaier (Altmaier et al. 2004) study was an artifact of the experimental setup. The colloids formed due to the drastic pH shift when two disequilibrium solutions (concentrated $MgCl_2$ brine containing dissolved Th-nitrate and NaOH solution) were mixed. This "rapid precipitation" process that lead to the formation of colloids would not be expected to form within an actual system. These conclusions were substantiated in personal communication with Dr. Marcus Altmaier (Sassani 2013).

MgO-5.3 Effects of MgO on Other Near-Field Processes and Conditions

Section MgO-5.3.1, Section MgO-5.3.2, and Section MgO-5.3.3 are based on the text in the CRA-2004, Appendix BARRIERS, Section BARRIERS-2.3.4.1 , Section BARRIERS-2.3.4.2, and Section BARRIERS-2.3.4.3.

MgO-5.3.1 Effects of MgO on Repository H2O Content

The hydration of periclase could consume significant quantities of H_2O in the WIPP (Reaction [MgO.1]). The carbonation of brucite to form hydromagnesite (5424) or, less likely, hydromagnesite (4323), will not release this H_2O unless hydromagnesite (5424) or (4323) goes on to form magnesite. Furthermore, even if large quantities of magnesite form during the 10,000-year regulatory period, there will still be large quantities of periclase available for hydration because the DOE is emplacing more MgO than necessary to consume all the CO_2 that would be produced by microbial activity should all the CPR materials in TRU waste and waste containers be consumed.

MgO-5.3.1.1 Changes since the CRA-2009

During its completeness review of the CRA-2009, the EPA identified implementation of a more comprehensive H_2O budget for WIPP disposal rooms as a possible improvement in the WIPP PA (U.S. EPA 2010). Previous PAs (e.g., the 1997 PAVT, and the CRA-2004 PABC) included the effects of H_2O consumption and hydrogen (H_2) production by anoxic corrosion of steels and other iron-base (Fe-base) alloys in steel waste containers and in steels and other alloys in the waste. These PAs also included production of various gases by microbial consumption of CPR materials; and implicitly included hydrogen sulfide (H_2S) and CO_2 consumption by sulfidation of steels and other Fe-base alloys and carbonation of MgO, respectively. However, it was assumed that microbial consumption of CPR materials, sulfidation of steels and other Fe-base alloys, and MgO carbonation neither consumed nor produced H_2O (Camphouse 2013).

The CRA-2014 PA included: (1) hydration of periclase (MgO) to form brucite, which consumes H_2O; (2) carbonation of brucite to form hydromagnesite, which neither consumes nor produces H_2O; and (3) the reaction of hydromagnesite to form magnesite ($MgCO_3$) and brucite, which releases H_2O (Camphouse 2013). The reaction of hydromagnesite to magnesite was included because hydromagnesite is thermodynamically unstable with respect to magnesite and thus might proceed to a

significant extent during the 10,000-year WIPP regulatory period. Another possible hydromagnesite-magnesite reaction, which consumes CO_2 and releases H_2O but does not produce brucite (Appendix MgO-2009, Equation MgO.9 (U.S. DOE 2009)), was not included in the CRA-2014 PA. Appendix PA-2014 provides additional details regarding the inclusion of MgO hydration and carbonation in the near-field H_2O budget and the results of this change.

MgO-5.3.2 Effects of MgO on Gas Generation

The two gas-producing processes included in WIPP PA are anoxic corrosion of steels and other Fe-base alloys, which will produce H_2, and microbial consumption of CPR materials, which will produce mainly CO_2, hydrogen sulfide (H_2S), and methane (CH_4).

MgO-5.3.2.1 Gas Generation from Anoxic Corrosion

Appendix MgO-2009, Section 5.3.2.1 (U.S. DOE 2009) provided a description of the effects of MgO on gas generation from anoxic corrosion of steels and other Fe-base alloys. Since the CRA-2009, a new series of steel and lead corrosion experiments has been conducted (Roselle 2009, Roselle 2010, Roselle 2011a, Roselle 2011b, and Roselle 2013). The object of these experiments has been to determine steel and lead corrosion rates under more WIPP-relevant conditions. In these experiments, steel and lead coupons were immersed in brines under WIPP-relevant conditions using a continuous gas flow-through system. The experimental apparatus maintained the following conditions: pO_2 less than 5 parts per million (ppm); temperature of 26 °C; relative humidity at 78% ± 10%; and a range of CO_2 concentrations (0, 350, 1500 and 3500 ppm, balance N_2). Four high-ionic-strength brines were used: GWB, ERDA-6 brine, GWB with organic ligands (EDTA, acetate, citrate, and oxalate), and ERDA-6 brine with the same ligands. The composition of the experimental brines used was that calculated by Brush (Brush 2005) for brines equilibrated with MgO, halite and anhydrite. Therefore, the anoxic corrosion experiments of Roselle (Roselle 2009, Roselle 2010, Roselle 2011a, and Roselle 2011b) incorporated the effects of MgO on brine chemistry.

MgO-5.3.2.2 Microbial Gas Generation

Experiments by Leonard (Leonard et al 1999) on the potential toxicity of MgO to WIPP-relevant microorganisms suggested that MgO inhibited growth at concentrations above 0.5 grams per liter (g/L), but only in the absence of a pH buffer. The effects of MgO on microbial gas generation in this study were inconclusive. Appendix MgO-2009, Section MgO-5.3.2.2 (U.S. DOE 2009) reviewed studies of the potential toxicity of MgO to non-WIPP microorganisms.

No additional studies of the effects of MgO on microbial gas generation by WIPP-relevant microorganisms under expected WIPP conditions have been carried out since Leonard (Leonard et al 1999). However, WIPP-specific data obtained by Swanson (Swanson et al 2012) demonstrate that many WIPP-relevant microbes, especially haloarchaea, grow well at high $MgCl_2$ concentrations (~1.0 M) and can tolerate pH up to 9.5.

MgO-5.3.3 Effects of MgO on Room Closure

Appendix MgO-2009, Section 5.3.3 (U.S. DOE 2009) described the effects of MgO on room closure. There is no new information since the CRA-2009 on the effects of MgO on this process.

MgO-5.4 Effects of MgO on Far-Field An Transport

The CRA-2009, Appendix MgO-2009, Section 5.4 (U.S. DOE 2009) discussed the effects of MgO on far-field An transport. In particular, this discussion focused on the effects of MgO on the matrix distribution coefficients (K_ds) for dissolved thorium (Th), uranium (U), Pu, and americium (Am) in the Culebra member of the Rustler Formation. Since the CRA-2009, there have been changes in these K_ds; however, there have been no changes in the effects of MgO on these K_ds.

MgO-6.0 The MgO Excess Factor

The CRA-2009, Appendix MgO-2009, Section MgO-6.0 (U.S. DOE 2009) provided a detailed description of the MgO excess factor and its use in the WIPP. The MgO excess factor is defined as the ratio of the total amount of MgO to be emplaced in the WIPP divided by the total amount required to consume all of the CO_2 produced by microbial activity should all of the CPR materials in the repository be consumed. There have been no changes in the MgO excess factor since the CRA-2009.

MgO-7.0 References

(*Indicates a reference that has not been previously submitted.)

Altmaier, M., V. Neck, and T. Fanghänel. 2004. "Solubility and Colloid Formation of Th(IV) in Concentrated NaCl and MgCl2 Solution," Radiochimica Acta. Vol. 92, 537-543.* [Author]

Babb, S.C., and C.F. Novak. 1997. User's Manual for FMT Version 2.3: A Computer Code Employing the Pitzer Activity Coefficient Formalism for Calculating Thermodynamic Equilibrium in Geochemical Systems to High Electrolyte Concentrations. ERMS 243037. WIPP Performance Assessment. Albuquerque, NM: Sandia National Laboratories. [PDF / Author]

Bates, R.L., and J.A. Jackson, eds. 1984. Dictionary of Geological Terms. 3rd ed. New York: Anchor-Doubleday. [Author]

Brush, L.H. 1996. Memorandum to M.S. Tierney (Subject: Ranges and Probability Distributions of Kds for Dissolved Pu, Am, U, Th, and Np in the Culebra for the PA Calculations to Support the CCA). 10 June 1996. ERMS 238801. Albuquerque, NM: Sandia National Laboratories. [PDF / Author]

Brush, L.H. 2005. Results of Calculations of Actinide Solubilities for the WIPP Performance Assessment Baseline Calculations (May 18). ERMS 539800. Carlsbad, NM: Sandia National Laboratories. [PDF / Author]

Brush, L.H., and P.S. Domski. 2013a. Calculation of Organic-Ligand Concentrations for the WIPP CRA-2014 PA. Analysis Report, January 14, 2013. ERMS 559005. Carlsbad, NM: Sandia National Laboratories.* [PDF / Author]

Brush, L.H., and P.S. Domski. 2013b. Prediction of Baseline Actinide Solubilities for the WIPP CRA-2014 PA. Analysis Report, January 21, 2013. ERMS 559138. Carlsbad, NM: Sandia National Laboratories.* [PDF / Author]

Brush, L.H., P.S. Domski, and Y.-L. Xiong. 2012. Analysis Plan for WIPP Near-Field Geochemical Process Modeling. AP-153, Rev. 1, February 8, 2012. ERMS 556960. Carlsbad, NM: Sandia National Laboratories.* [PDF / Author]

Brush, L.H., and L.J. Storz. 1996. Memorandum to M.S. Tierney (Subject: Revised Ranges and Probability Distributions of Kds for Dissolved Pu, Am, U, Th, and Np in the Culebra for the PA Calculations to Support the CCA). 24 July 1996. ERMS 238231. Albuquerque, NM: Sandia National Laboratories. [PDF / Author]

Brush, L.H., and Y. Xiong. 2003a. Calculation of Actinide Solubilities for the WIPP Compliance Recertification Application (May 8). ERMS 529131. Carlsbad, NM: Sandia National Laboratories. [PDF / Author]

Brush, L.H., and Y. Xiong. 2003b. Calculation of Actinide Solubilities for the WIPP Compliance Recertification Application (March 20). AP-098. ERMS 526862. Carlsbad, NM: Sandia National Laboratories. [PDF / Author]

Brush, L.H., and Y. Xiong. 2003c. Calculation of Actinide Solubilities for the WIPP Compliance Recertification Application (Rev. 1, April 14). AP 098. ERMS 527714. Carlsbad, NM: Sandia National Laboratories. [PDF / Author]

Brush, L.H., and Y. Xiong. 2003d. Calculation of Organic Ligand Concentrations for the WIPP Compliance Recertification Application (April 14). ERMS 527567. Carlsbad, NM: Sandia National Laboratories. [PDF / Author]

Brush, L.H., and Y. Xiong, 2005a. Calculation of Actinide Solubilities for the WIPP Performance-Assessment Baseline Calculations (Rev 0, April 4). AP-120. ERMS 539255. Carlsbad, NM: Sandia National Laboratories. [PDF / Author]

Brush, L.H., and Y. Xiong, 2005b. Calculation of Organic-Ligand Concentrations for the WIPP Performance-Assessment Baseline Calculations (May 4). ERMS 539635. Carlsbad, NM: Sandia National Laboratories. [PDF / Author]

Brush, L.H., Y.-L. Xiong, and J.J. Long. 2009. Results of the Calculations of Actinide Solubilities for the CRA-2009 PABC. Analysis Report, October 7, 2009. ERMS 552201. Carlsbad, NM: Sandia National Laboratories.* [PDF / Author]

Camphouse, R.C. 2013. Analysis Plan for the 2014 WIPP Compliance Recertification Application Performance Assessment. AP-164. January 31, 2013. Carlsbad, NM: Sandia National Laboratories.* [PDF / Author]

Chavez, A.V. 2013. E-mail message to Laurence H. Brush (Subject: RE: "Change in MgO Bag Amounts and Sample Information; Attachement: "Larry Brush MgO Factor 062413 Rev. 1"), 10 October 2013. Carlsbad, NM: Nuclear Waste Partnership LLC.* [PDF / Author]

Clayton, D.J., R.C. Camphouse, J.W. Garner, A.E. Ismail, T.B. Kirchner, K.L. Kuhlman, and M.B. Nemer. 2010. Summary Report of the CRA-2009 Performance Assessment Baseline Calculation. ERMS 553039. Carlsbad, NM: Sandia National Laboratories.* [PDF / Author]

Deng, H., Y. Xiong, M. Nemer, and S. Johnsen. 2009. Experimental Work Conducted on MgO Long-Term Hydration: 2008 Milestone Report. May 27, 2009. ERMS 551421. Carlsbad, NM: Sandia National Laboratories.* [PDF / Author]

Deng, H., Y. Xiong, and M. Nemer. 2007. Experimental Work Conducted on MgO Characterization and Hydration, Milestone Report. ERMS 546570. Carlsbad, NM: Sandia National Laboratories. [PDF / Author]

Franco, J.R. 2012. "Planned Change Notice for Placement of MgO Supersacks," letter to A. Perrin with enclosure (analysis of an alternative placement scheme for MgO supersacks), February 14, 2012. Carlsbad, NM: Carlsbad Field Office.* [PDF / Author]

Freyer, D. 2012. Sorel Cement as Geochemical Barrier in Salt Formations, Proceedings of the International Workshops ABC-Salt (II) and HiTAC 2011. Eds. Altmaier, M., C. Bube, B. Kienzler, V. Metz, and D.T. Reed. 2012. KIT-SR 7625. Karlsruhe, Germany: Karlsruher Institut für Technologie. 29.* [Author]

Harvie, C.E., N. Møller, and J.H. Weare. 1984. "The Prediction of Mineral Solubilities in Natural Waters: The Na-K-Mg-Ca-H-Cl-SO4-OH-HCO3-CO3-CO2-H2O System to High Ionic Strengths at 25 °C," Geochimica et Cosmochimica Acta. Vol. 48, no. 4, 723-751.* [PDF / Author]

Kanney, J.F., and E.D. Vugrin. 2006. Memorandum to D.S. Kessel (Subject: Updated Analysis of Characteristic Time and Length Scales for Mixing Processes in the WIPP Repository to Reflect the CRA-2004 PABC Technical Baseline and the Impact of Supercompacted Mixed Waste and Heterogeneous Waste Emplacement). 31 August 2006. ERMS 544248. Carlsbad, NM: Sandia National Laboratories. [PDF / Author]

Kouba, S. E-mail message to Laurence H. Brush (Subject: RE: MgO Emplacement Factor as of December 31, 2012; Attachment: CBFO_Emplacement_Statistics-12-31-2012.txt), 8 October 2013. Carlsbad, NM: Nuclear Waste Partnership LLC.* [PDF / Author]

Krumhansl, J.L., J.W. Kelly, H.W. Papenguth, and R.V. Bynum. 1997. Memorandum to E.J. Nowak (Subject: MgO Acceptance Criteria). 10 December 1997. ERMS 248997. Albuquerque, NM: Sandia National Laboratories. [PDF / Author]

Krumhansl, J.L., K.M. Kimball, and C.L. Stein. 1991. Intergranular Fluid Compositions from the Waste Isolation Pilot Plant (WIPP), Southeastern New Mexico. SAND90-0584. Albuquerque, NM: Sandia National Laboratories. [PDF / Author]

Leigh, C., J. Kanney, L. Brush, J. Garner, G. Kirkes, T. Lowry, M. Nemer, J. Stein, E. Vugrin, S. Wagner, and T. Kirchner. 2005. 2004 Compliance Recertification Application Performance Assessment Baseline Calculation (Revision 0). ERMS 541521. Carlsbad, NM: Sandia National Laboratories. [PDF / Author]

Leonard, P.A., B.A. Strietelmeier, L. Pansoy-Hjelvik, R. Villareal. 1999. Microbial Characterization for the Source-Term Waste Test Program (STTP) at Los Alamos. Proceedings of the Waste Management Conference, February 1999. LA-UR-99-709. [PDF / Author]

Marcinowski, F. 2001. Letter to I.R. Triay (1 Enclosure). 11 January 2001. ERMS 519362. Washington DC: U.S. Environmental Protection Agency, Radiation Protection Division. [PDF / Author]

Marcinowski, F. 2004. Letter to R.P. Detwiler (Subject: Approving the DOE's Request to Dispose of Compressed (Supercompacted) Waste from the Advanced Mixed Waste Treatment Program in the

WIPP). 26 March 2004. ERMS 534327. Washington, DC: U.S. Environmental Protection Agency, Office of Air and Radiation. [PDF / Author]

Molecke, M.A. 1983. A Comparison of Brines Relevant to Nuclear Waste Experimentation. SAND83-0516. Albuquerque, NM: Sandia National Laboratories. [PDF / Author]

Novak, C.F. 1997. Memorandum to R.V. Bynum (Subject: Calculation of Actinide Solubilities in WIPP SPC and ERDA-6 Brines under MgO Backfill Scenarios Containing either Nesquehonite or Hydromagnesite as the Mg-CO3 Solubility-Limiting Phase). 21 April 1997. ERMS 246124. Albuquerque, NM: Sandia National Laboratories. [PDF / Author]

Novak, C.F., R.C. Moore, and R.V. Bynum. 1996. Prediction of Dissolved Actinide Concentrations in Concentrated Electrolyte Solutions: A Conceptual Model and Model Results for the Waste Isolation Pilot Plant (WIPP). SAND96-2695C. ERMS 238628. Presentation at the 1996 International Conference on Deep Geological Disposal of Radioactive Waste, September 16-19, 1996, Winnipeg, Manitoba. [Author]

Papenguth, H.W. 1999. Memorandum to M.G. Marietta (Subject: Evaluation of Candidate MgO Materials for Use as Backfill at WIPP). 12 November 1999. ERMS 520314. Albuquerque, NM: Sandia National Laboratories. [PDF / Author]

Peake, T. 2012. "Magnesium Oxide Supersack Size Reduction and Alternative Emplacement Plan," e-mail to J.R. Franco, July 13, 2012. Washington, DC: U.S. Environmental Protection Agency Office of Radiation and Indoor Air.* [PDF / Author]

Popielak, R.S., R.L. Beauheim, S.R. Black, W.E. Coons, C.T. Ellingson, and R.L. Olsen. 1983. Brine Reservoirs in the Castile Formation, Waste Isolation Pilot Plant Project, Southeastern New Mexico. TME 3153. Carlsbad, NM: U.S. Department of Energy, WIPP Project Office. [PDF / Author]

Roselle, G.T. 2009. Iron and Lead Corrosion in WIPP-Relevant Conditions: Six Month Results. Milestone report, October 7, 2009. ERMS 546084. Carlsbad, NM: Sandia National Laboratories.* [PDF / Author]

Roselle, G.T. 2010. Iron and Lead Corrosion in WIPP-Relevant Conditions: 12 Month Results. Milestone report, October 14, 2010. ERMS 554383. Carlsbad, NM: Sandia National Laboratories.* [PDF / Author]

Roselle, G.T. 2011a. Iron and Lead Corrosion in WIPP-Relevant Conditions: 18 Month Results. Milestone report, January 5, 2011. ERMS 554715. Carlsbad, NM: Sandia National Laboratories.* [PDF / Author]

Roselle, G.T. 2011b. Iron and Lead Corrosion in WIPP-Relevant Conditions: 24 Month Results. Milestone report, May 3, 2011. ERMS 555246. Carlsbad, NM: Sandia National Laboratories.* [PDF / Author]

Roselle, G.T. 2013. Determination of Corrosion Rates from Iron/Lead Corrosion Experiments to be used for Gas Generation Calculations, [Revision 1]. Analysis report, January 23, 2013. ERMS 559077. Carlsbad, NM: Sandia National Laboratories.* [PDF / Author]

Sassani, D. 2013. "Our discussion on intrinsic Th colloids and Mg-Cl-OH colloids." Email from David Sassani to Gregory Roselle. ERMS 560114.* [PDF / Author]

Snider, A.C. 2003a. "Hydration of Magnesium Oxide in the Waste Isolation Pilot Plant." Sandia National Laboratories Technical Baseline Reports; WBS 1.3.5.3, Compliance Monitoring; WBS 1.3.5.4, Repository Investigations; Milestone RI 03-210; January 31, 2003 (pp. 4.2-1 through 4.2-6). ERMS 523189. Carlsbad, NM: Sandia National Laboratories. [PDF / Author]

Snider, A.C. 2003b. Verification of the Definition of Generic Weep Brine and the Development of a Recipe for This Brine. ERMS 527505. Carlsbad, NM: Sandia National Laboratories. [PDF / Author]

Snider, A.C., and Y. Xiong. 2002a. "Carbonation of Magnesium Oxide." Sandia National Laboratories Technical Baseline Reports; WBS 1.3.5.3, Compliance Monitoring; WBS 1.3.5.4, Repository Investigations; Milestone RI130; July 31, 2002 (pp. 4.1-1 through 4.1-28). ERMS 523189. Carlsbad, NM: Sandia National Laboratories. [PDF / Author]

Snider, A.C., and Y.-L. Xiong. 2002b. Experimental Study of WIPP Engineered Barrier MgO at Sandia National Laboratories Carlsbad Facility (Rev. 2, October 2). TP 00-07. ERMS 523957. Carlsbad, NM: Sandia National Laboratories. [PDF / Author]

Snider, A.C., Y.-L. Xiong, and N.A. Wall. 2004. Experimental Study of WIPP Engineered Barrier MgO at Sandia National Laboratories Carlsbad Facility (Rev. 3, August 26). TP 00-07. ERMS 536591. Carlsbad, NM: Sandia National Laboratories. [PDF / Author]

Swanson, J.S., D.T. Reed, D.A. Ams, D.M. Norden, and K.A. Simmons. 2012. Status Report on the Microbial Characterization of Halite and Groundwater Samples from the WIPP. Report LCO-ACP-12, LA-UR 12-22824. Carlsbad, NM: Los Alamos National Laboratory. [PDF / Author]

Triay, I. 2000. Letter to F. Marcinowski (Subject: Requesting EPA Approval of the Elimination of MgO Minisacks from the WIPP). 21 July 2001. ERMS 519362. Carlsbad, NM: Carlsbad Area Office. [PDF / Author]

U.S. Department of Energy (DOE). 1996. Title 40 CFR Part 191 Compliance Certification Application for the Waste Isolation Pilot Plant (October). 21 vols. DOE/CAO-1994-2184. Carlsbad, NM: Carlsbad Area Office. [Author]

U.S. Department of Energy (DOE). 2000. MgO Mini-Sack Elimination Proposal (July 21). ERMS 519362. Carlsbad, NM: Carlsbad Area Office. [PDF / Author]

U.S. Department of Energy (DOE). 2004. Title 40 CFR Part 191 Compliance Recertification Application for the Waste Isolation Pilot Plant (March). 10 vols. DOE/WIPP 2004-3231. Carlsbad, NM: Carlsbad Field Office. [Author]

U.S. Department of Energy (DOE). 2009. Title 40 CFR Part 191 Subparts B and C Compliance Recertification Application for the Waste Isolation Pilot Plant, DOE/WIPP 09-3424. Carlsbad, NM: Carlsbad Field Office.* [Author]

U.S. Environmental Protection Agency (EPA). 1993. 40 CFR Part 191 Environmental Radiation Protection Standards for the Management and Disposal of Spent Nuclear Fuel, High-Level and Transuranic Radioactive Wastes; Final Rule. Federal Register, vol. 58: 66398-416. [PDF / Author]

U.S. Environmental Protection Agency (EPA). 1998a. CARD No. 44: Engineered Barriers. Compliance Application Review Documents for the Criteria for the Certification and Recertification of the Waste Isolation Pilot Plant's Compliance with the 40 CFR 191 Disposal Regulations: Final

Certification Decision (May) (pp. 44-1 through 44-36). Washington, DC: Office of Radiation and Indoor Air. [PDF / Author]

U.S. Environmental Protection Agency (EPA). 1998b. 40 CFR Part 194: Criteria for the Certification and Recertification of the Waste Isolation Pilot Plant's Compliance with the Disposal Regulations: Certification Decision; Final Rule. Federal Register, vol. 63 (May 18, 1998): 27353-406. [PDF / Author]

U.S. Environmental Protection Agency (EPA). 1998c. "CARD No. 23: Models and Computer Codes." Compliance Application Review Documents for the Criteria for the Certification and Recertification of the Waste Isolation Pilot Plant's Compliance with the 40 CFR 191 Disposal Regulations: Final Certification Decision (May) (pp. 23-1 through 23-93). EPA 402-R-97-013. Washington, DC: Office of Radiation and Indoor Air. [PDF / Author]

U.S. Environmental Protection Agency (EPA). 1998d. Technical Support Document for Section 194.23: Models and Computer Codes. Washington, DC: Office of Radiation and Indoor Air. [PDF / Author]

U.S. Environmental Protection Agency (EPA). 1998e. Technical Support Document for Section 194.23: Parameter Justification Report (May). Washington, DC: Office of Radiation and Indoor Air. [PDF / Author]

U.S. Environmental Protection Agency (EPA). 2001. Approval of Elimination of Minisacks. Washington, DC: Office of Radiation and Indoor Air. [PDF / Author]

U.S. Environmental Protection Agency (EPA). 2004. Discussion of Major Issues Associated with EPA's Compressed Waste Review. ERMS 534327. Washington, DC: Office of Air and Radiation. [PDF / Author]

U.S. Environmental Protection Agency (EPA). 2010a. Emplacement Inspection Report, EPA Inspection No. EPA-WIPP-6.10-29c, of the Waste Isolation Pilot Plant, June 29 to July 1, 2010, Docket NO: A-98-49, Item: II-B3-112.* [PDF / Author]

U.S. Environmental Protection Agency (EPA). 2010b. Technical Support Document for Section 194.24: Evaluation of the Compliance Recertification Actinide Source Term, Backfill Efficacy, and Culebra Dolomite Distribution Coefficient Values (Revision 1). EPA Air Docket A-98-49, Item II-B1-25. Washington, DC: Office of Air and Radiation.* [Author]

Wall, N.A. 2005. Preliminary Results for the Evaluation of Potential New MgO (January 27). ERMS 538514. Carlsbad, NM: Sandia National Laboratories. [PDF / Author]

Wang, Y. 1998. WIPP PA Validation Document for FMT (Version 2.4), Document Version 2.4. ERMS 251587. Carlsbad, NM: Sandia National Laboratories. [PDF / Author]

Wang, Y., and C.R. Bryan. 2000. Experimental Study of WIPP MgO Backfill at Sandia National Laboratories Carlsbad Facility (Rev. 0, July 11). TP 00-07. ERMS 512216. Carlsbad, NM: Sandia National Laboratories. [PDF / Author]

Wang, Y., C.R. Bryan, and N.A. Wall. 2001. Experimental Study of WIPP MgO Backfill at Sandia National Laboratories Carlsbad Facility (Rev. 1, June 22). TP 00-07. ERMS 518747. Carlsbad, NM: Sandia National Laboratories. [PDF / Author]

Washington TRU Solutions (WTS). 2003. Specification for Prepackaged MgO Backfill. Specification D-0101, Rev. 5. October 31, 2003. Carlsbad, NM: Washington TRU Solutions. [PDF / Author]

Washington TRU Solutions (WTS). 2005. Specification for Prepackaged MgO Backfill. Specification D-0101, Rev. 7. May 12, 2005. Carlsbad, NM: Washington TRU Solutions. [PDF / Author]

Washington TRU Solutions (WTS). 2009a. Engineering Change Order (ECO) 12137. January 15, 2009. Carlsbad, NM: Washington TRU Solutions.* [PDF / Author]

Washington TRU Solutions (WTS). 2009b. Specification for Prepackaged MgO Backfill. Specification D-0101, Rev. 8. February 11, 2009. Carlsbad, NM: Washington TRU Solutions.* [PDF / Author]

Westinghouse Waste Isolation Division (WID). 1997. Dose Assessment of Hand Emplacement of MgO Sacks around CH Waste 7-Packs at the Waste Isolation Pilot Plant (April). WIPP Radiological Control Position Paper 97-05. Carlsbad, NM: Westinghouse WID. [PDF / Author]

Wolery, T.J. 2008. Analysis Plan for EQ3/6 Analytical Studies. AP-140, Rev. 0, May 15, 2008. ERMS 548930. Carlsbad, NM: Sandia National Laboratories. [PDF / Author]

Wolery, T.J., Y.-L. Xiong, and J.J. Long. 2010. Verification and Validation Plan/Validation Document for EQ3/6 Version 8.0a for Actinide Chemistry, Document Version 8.10. ERMS 550239. Carlsbad, NM: Sandia National Laboratories.* [PDF / Author]

Xiong, Y.-L. 2011a. Email to J. Long (Subject: Release of EQ3/6 Database DATA0.FM1). 9 March 2011. ERMS 555152. Carlsbad, NM: Sandia National Laboratories.* [PDF / Author]

Xiong, Y.-L. 2011b. WIPP Verification and Validation Plan/Validation Document for EQ3/6 Version 8.0a for Actinide Chemistry, Revision 1. Supersedes ERMS 550239. May 12, 2011. ERMS 555358. Carlsbad, NM: Sandia National Laboratories.* [PDF / Author]

Xiong, Y.-L. 2011c. Experimental Determination of Solubility Constant of Hydromagnesite (5424) in NaCl Solutions up to 4.4 m at Room Temperature, Chemical Geology. Vol. 284, nos. 3-4, 262-269.* [Author]

Xiong, Y.-L., and S. Kim. 2011. Experimental Investigation of Absence or Presence of Colloids of Magnesium Chloride Hydroxide Hydrate (Phase 5) in the WIPP Generic Weep Brine (GWB) Under the WIPP Relevant Conditions at Sandia National Laboratories Carlsbad Facility TP 12-01. ERMS 556785. Carlsbad, NM: Sandia National Laboratories.* [PDF / Author]

Xiong, Y.-L., H.-R. Deng, M.B. Nemer, and S. Johnsen. 2009. Thermodynamic Data for Phase 5 ($Mg_3Cl(OH)_5 \cdot 4H_2O$) Determined from Solubility Experiments. Memorandum to L.H. Brush, May 18, 2009. ERMS 551294. Carlsbad, NM: Sandia National Laboratories.* [PDF / Author]

Xiong, Y.-L., H.-R. Deng, M.B. Nemer, and S. Johnsen. 2010. Experimental Determination of the Solubility Constant for Magnesium Chloride Hydroxide Hydrate ($Mg_3Cl(OH)_5 \cdot 4H_2O$, Phase 5) at Room Temperature, and Its Importance to Nuclear Waste Isolation in Geological Repositories in Salt Formations, Geochimica et Cosmochimica Acta. Vol. 74, no. 16, 4605-4611.* [Author]

Title 40 CFR Part 191
Subparts B and C
Compliance Recertification Application 2014
for the
Waste Isolation Pilot Plant

Appendix MON-2014
WIPP Monitoring Programs

United States Department of Energy
Waste Isolation Pilot Plant

Carlsbad Field Office
Carlsbad, New Mexico

Compliance Recertification Application 2014
Appendix MON-2014

Table of Contents

List of Tables

Acronyms and Abbreviations

CARD Compliance Application Review Document

CBFO Carlsbad Field Office

CCA Compliance Certification Application

CFR Code of Federal Regulations

cm centimeter

CMP Compliance Monitoring Program

CRA Compliance Recertification Application

DBDSP Delaware Basin Drilling Surveillance Program

DOE U.S. Department of Energy

DRZ disturbed rock zone

EPA U.S. Environmental Protection Agency

FEP feature, event, or process

ft feet

GMP Geotechnical Monitoring Program

GDMPP Groundwater Detection Monitoring Program Plan

GWMP Groundwater Monitoring Program

GWMPP Groundwater Monitoring Program Plan

kg kilogram

km kilometer

m meter

M&OC Management and Operating Contractor

mi mile

NMED New Mexico Environment Department

PA performance assessment

QA quality assurance

QAPD Quality Assurance Program Document

SMP Subsidence Monitoring Program

WIPP Waste Isolation Pilot Plant

WQSP Water Quality Sampling Program

WDS Waste Data System

The page intentionally left blank.

MON-1.0 Introduction

This appendix to the 2014 Compliance Recertification Application (CRA-2014) describes a specific monitoring program that was developed to meet commitments contained in the U.S. Department of Energy's (DOE's) application to the U.S. Environmental Protection Agency (EPA), which demonstrated compliance with radioactive waste disposal regulations 40 CFR Part 191 Subparts B and C and the certification criteria in 40 CFR Part 194. This appendix does not address monitoring activities intended to demonstrate compliance with 40 CFR Part 191 Subpart A.

The monitoring activities described are performed as assurance measures to detect substantial and detrimental deviations from expected disposal system performance. This program consists of a preclosure and postclosure monitoring program using monitoring techniques that do not jeopardize the isolation of the waste. The program must be conducted until the DOE and the EPA agree there are no significant concerns to be addressed by further monitoring. The long-term performance expectations for the disposal system are derived from conceptual models, scenarios, and assumptions developed for the Waste Isolation Pilot Plant (WIPP) performance assessment (PA).

The activities performed for the overall monitoring programs at the WIPP facility comprehensively address the range of regulatory requirements at departmental, state, and federal levels. This appendix addresses activities relevant to monitoring the disposal system. This document provides an overview of the Compliance Monitoring Program (CMP) and specifically describes how:

- The 10 compliance monitoring parameters are derived from the data.
- Information and data are extracted from the various WIPP monitoring and sampling programs.
- The assessments are made against repository performance expectations.
- The results are reported to the EPA.

On January 3, 2002, the DOE Carlsbad Field Office (CBFO) submitted a letter to the EPA (Triay 2002). This letter requested Appendix MON be rewritten to incorporate the portions of Appendices Environmental Monitoring Plan (EMP), Groundwater Surveillance Program Plan (GWMP), Geotechnical Monitoring Plan (GTMP), Subsidence Monitoring Plan (SMP), and Delaware Basin Drilling Monitoring Plan (DMP) required to demonstrate compliance with 40 CFR § 191.14(b) (U.S. EPA 1993) in accordance with the criteria established by 40 CFR § 194.42 (U.S. EPA 1996). The EPA approved the request in a letter to CBFO on March 15, 2002 (Marcinowski 2002).

MON-1.1 Compliance Monitoring Program

This appendix describes the CMP for the WIPP facility. Compliance monitoring concentrates on the following areas:

- The Geotechnical Engineering Program
- The Groundwater Monitoring Program (GWMP)
- The Delaware Basin Drilling Surveillance Program (DBDSP)
- The Subsidence Monitoring Program (SMP)

- Waste Inventory Monitoring Based on Waste Data System (WDS)

The data and information collected since the 2009 Compliance Recertification Application (CRA-2009) (U.S. DOE 2009a) for the above-listed programs are recorded or referenced in Appendix DATA-2014. The descriptions provided in this appendix are specific to the CMP and, thus, the requirements of section 191.14(b) and section 194.42.

MON-1.2 Preclosure and Postclosure Monitoring

The requirements of 40 CFR § 191.14, section 194.42, the initial EPA certification (U.S. EPA 1998a), the 2006 Recertification (U.S. EPA 2006), and the 2010 Recertification (U.S. EPA 2010) serve as the regulatory basis for preclosure and postclosure monitoring. These requirements specify that disposal systems must be monitored to detect substantial and detrimental deviation from expected disposal system performance.

MON-1.3 Monitoring Assessment

The DOE was required by 40 CFR § 194.42(a) to perform an analysis that would determine the effects of various parameters on the performance of the disposal system, and to use the results in preclosure and postclosure monitoring plans. The disposal system performance analysis identified 10 monitoring parameters, listed in Section MON-2.1, to be monitored and assessed within the CMP. The discussion of preclosure monitoring activities for these 10 parameters includes the following:

- Identifying activities required to comply with the monitoring requirements of the EPA's certification and recertification of compliance with Part 191 Subparts B and C during the preclosure phase of the project

- Identifying organizations that generate the monitoring data, organizations that convert the data to monitoring parameters and assess the results against expected results, and the organization that reports the results of the assessments to the EPA

- Identifying the compliance monitoring schedule

- Providing an overview of quality assurance (QA) requirements applicable to the CMP

MON-1.4 Appendix Summary

Section MON-2.0 identifies the monitoring requirements of Part 191 Subparts B and C in keeping with the criteria of Part 194. Section MON-3.0 describes the preclosure monitoring program associated with each monitoring parameter, the monitoring schedules, and program outputs. Section MON 4-0 describes the planned postclosure monitoring. Section MON-5.0 describes the QA requirements applicable to the CMP. Section MON-6.0 describes the process of communicating and reporting CMP results and evaluations.

MON-2.0 Compliance Monitoring Program Requirements

The DOE's preclosure and postclosure CMP defines programs to assess the performance of specific aspects of the disposal system. The relevant monitoring requirements are identified in:

- Section 191.14(b)
- Section 194.42
- The May 18, 1998, 40 CFR Part 194 Criteria for the Certification and Recertification of the Waste Isolation Pilot Plant's Compliance with the Disposal Regulations: Certification Decision, Section VIII.D.4 , Monitoring (U.S. EPA 1998a)
- The CRA-2004, Chapter 7.0, Section 7.2
- The CRA-2009, Section 42.0 , Monitoring (40 CFR § 194.42)

MON-2.1 Compliance Certification/Recertification

The original approach used to develop the CMP was based on the results of the parameter analysis documented in the Compliance Certification Application (CCA), Chapter 7.0, and Appendix MON, Attachment MONPAR (U.S. DOE 1996). The EPA documented its approval of the DOE monitoring approach in the compliance certification decision (U.S. EPA 1998a) and Compliance Application Review Document (CARD) 42 (U.S. EPA 1998b). In the CRA-2004, Appendix MON-2004 was rewritten to incorporate portions of Appendices EMP, GWMP, GTMP, SMP, and DMP that were not revised for the CRA-2004. The DOE reassessed the CCA, Appendix MON, Attachment MONPAR, for the CRA-2004 and determined the original conclusions and monitoring parameters identified in MONPAR remain valid and unchanged (Kirkes and Wagner 2003). For the CRA-2009, the DOE once again assessed the original MONPAR analysis used to determine which monitoring parameters should be included in the CMP. Based on the review of operational activities, conditions, monitoring data, PA, and experimental programs that occurred since the CRA-2004, the reassessment states, "the conclusions of the MONPAR analysis remain valid and its conclusions continue to be adequate for inclusion in the CRA-2009″ (Wagner 2008). An assessment of the program was made again in 2013 to determine if changes should be made to the CMP. This assessment determined that the conclusions of the original MONPAR assessment remain valid; therefore no changes are needed to the program (Wagner 2013). The annual compliance monitoring reports also concluded that no changes to the monitoring program are recommended (Wagner and Hillesheim 2008 and Wagner and Hillesheim 2009; Wagner and Kuhlman 2010; Wagner, Kuhlman and Johnson 2011 and Wagner, Kuhlman and Johnson 2012).

The EPA-approved monitoring approach recognizes that the DOE will monitor 10 parameters. These parameters are:

1. Creep closure and stresses
2. Extent of brittle deformation
3. Initiation of brittle deformation
4. Displacement of deformation features
5. Change in Culebra Dolomite Member of the Rustler Formation (hereafter referred to as Culebra) groundwater composition
6. Change in Culebra groundwater flow

7. Drilling rate

8. Probability of encountering a Castile Formation (hereafter referred to as the Castile) brine reservoir

9. Subsidence

10. Waste activity

All of the above parameters are being monitored during the preclosure period.

The CRA-2004, Appendix MON-2004, Attachment A, describes the DOE's plans for postclosure monitoring. The DOE will revisit this plan for postclosure monitoring before the end of WIPP facility operations.

The monitoring parameters that have related PA parameters include:

- Drilling rate
- Probability of encountering a Castile brine reservoir
- Change in Culebra groundwater flow
- Change in Culebra groundwater composition
- Waste activity

The other monitoring parameters are related to either the EPA's list of potential monitoring parameters in 40 CFR 194.42 or screening decisions for repository features, events, or processes (FEPs). Table MON-1 describes the related PA parameters and the related FEPs.

The data used to determine the 10 monitoring parameters of the CMP are generated by 5 separate monitoring programs (described in Sections MON-3.1, MON-3.2, MON-3.3, MON-3.4, and MON-3.5). Each monitoring program focuses on the collection of field data. The programs that generate or evaluate the data are described in Section MON-6.0. Results from each monitoring program are documented individually in annual reports (see Appendix DATA-2014), while the assessment results of the 10 parameters are documented and reported in a compliance monitoring parameter assessment reports (Wagner and Hillesheim 2008 and Wagner and Hillesheim 2009; Wagner and Kuhlman 2010; Wagner, Kuhlman and Johnson 2011 and Wagner, Kuhlman and Johnson 2012).

As stated earlier, if any of the data, parameters, or observations are not consistent with expectations as defined in Section MON-6.1.1, the CMP process requires addressing concerns and developing recommendations. Results from monitoring programs will be generated on an ongoing basis throughout the operational period of the repository. Compliance monitoring data are provided to the cognizant individuals and organizations within the project and evaluated for their significance, and the evaluation results and data summaries are reported to the EPA. Section MON-6.0 describes the process of communicating and reporting CMP results and evaluations.

Table MON- 1. Monitoring Parameters

Monitoring Parameter	Monitoring Program	Frequency of Data Collection and Reporting	Related PA Parameter	Related FEPs	Evaluation Cycle
Creep Closure and Stresses	Geotechnical Monitoring Program (GMP)	Various data calls from weekly to monthly based on repository conditions, instrumentation, and data collection system. Data are reported annually.	Not directly related to a PA parameter. May provide a short-term (operational) observation of the geomechanical response of repository excavation. Can provide confidence in the creep closure model.	Salt creep, excavation-induced stress changes, changes in stress field, pressurization.	Data are evaluated annually and during recertification
Extent of Brittle Deformation	GMP	Various data calls from weekly to monthly based on repository conditions, instrumentation, and data collection system. Data are reported annually.	Not directly related to a PA parameter. Can provide confidence in the long-term behavior of the disturbed rock zone (DRZ), as modeled. Intrinsic shaft DRZ permeability and effective shaft seal permeability is calculated from this parameter.	DRZ, roof falls, consolidation of seals.	Data are evaluated annually and during recertification.
Initiation of Brittle Deformation	GMP	Various data calls from weekly to monthly based on repository conditions, instrumentation, and data collection system. Data are reported annually.	Not directly related to a PA parameter. Can provide confidence in the anhydrite fracture model implemented in the BRAGFLO code. May provide related repository observation data on initiation or displacement of major brittle deformation features in the roof or surrounding rock.	Disruption due to gas effects.	Data are evaluated annually and during recertification.
Displacement of Deformation Features	GMP	Various data calls from weekly to monthly based on repository conditions, instrumentation, and data collection system. Data are reported annually.	Not directly related to a PA parameter. Provides related repository operational data on initiation or displacement of major brittle deformation features in the roof or surrounding rock.	Stability of open panel.	Data are evaluated annually and during recertification.

Monitoring Parameter	Monitoring Program	Frequency of Data Collection and Reporting	Related PA Parameter	Related FEPs	Evaluation Cycle
Culebra Groundwater Composition	Groundwater Monitoring Program (GWMP)	Data are collected annually and reported annually.	Average Culebra brines composition and matrix distribution coefficient for uranium (IV, VI), plutonium (III, IV), thorium (IV), americium (III). Matrix distribution coefficient is not a sensitive PA parameter.	Groundwater geochemistry, actinide sorption.	Data are evaluated annually and during recertification.
Change in Culebra Groundwater Flow	GWMP	Data are collected monthly and reported annually.	Culebra transmissivity, fracture and matrix porosity, fracture spacing, dispersivity, and climate index. Changes in Culebra groundwater flow are important to performance and incorporated into the PA.	Groundwater flow and recharge.	Data are evaluated annually and during recertification.
Drilling Rate	DBDSP	As well records are received (weekly and monthly basis). Data are reported annually.	Required PA parameter per 40 CFR § 194.33. The Drilling Rate is important to performance and incorporated into the PA.	Drilling Fluid Flow	Data are evaluated annually and during recertification
Probability of Encountering a Castile Brine Reservoir	DBDSP	As drilling records are received. . Data are reported annually.	Probability of Encountering a Castile Brine Reservoir	Drilling Fluid Flow	Data are evaluated annually and during recertification
Subsidence	SMP	Data are reported annually or as determined necessary by the DOE.	Not directly related to a PA parameter. Can provide spatial information on surface subsidence (if any) over the influence area of the underground openings during operations.	Changes to groundwater flow due to mining effects; subsidence baseline.	Data are evaluated annually or as determined necessary by the DOE.

Monitoring Parameter	Monitoring Program	Frequency of Data Collection and Reporting	Related PA Parameter	Related FEPs	Evaluation Cycle
Waste Activity	Waste Inventory Monitoring Based on WDS	Continually updated as waste is approved for shipment to the WIPP and emplaced. . Data are reported annually.	Waste Activity	Waste Inventory Monitoring Based on WDS	Data are evaluated annually and during recertification

The 10 parameters above are called *compliance monitoring parameters*. As discussed previously, the EPA determined during the original WIPP certification and the 2004 and 2009 recertifications that these parameters met the regulatory monitoring requirements.

MON-3.0 Preclosure Compliance Monitoring

This section describes the preclosure CMP and the resulting data. The 10 parameters, associated monitoring program for each, frequency of data collection and reporting, related PA parameters, and related FEPs decisions used to support the PA are listed in Table MON-1.

MON-3.1 Geotechnical Engineering Program Plan

The WIPP Geotechnical Engineering Program Plan (Nuclear Waste Partnership LLC 2012a) defines the field programs and investigations carried out by the Geotechnical Engineering Section within the Management and Operating Contractor (M&OC). The Geotechnical Engineering Program provides geologic information related to geotechnical characteristics and assesses the stability and performance of the underground facility. The geotechnical monitoring activities identified in Table MON-1 are included as part of the WIPP Geotechnical Engineering Program Plan. This plan provides for the collection of data as described in the Geomechanical Monitoring Program and the Geosciences Program.

MON-3.1.1 Geomechanical Monitoring Program

The data collected as part of the Geomechanical Monitoring Program is usedto validate the WIPP design, track short-term and long-term geotechnical performance behavior of underground openings, and support routine safety and stability evaluations of the excavations. From an operational point of view, geomechanical data are used to identify areas of potential instability allow corrective action to be taken in a timely manner. For underground opening behavior, in situ data were used to model long-term disposal system performance. Geomechanical monitoring instrumentation generates data related to the following four parameters:

1. Creep closure and stresses
2. Extent of brittle deformation
3. Initiation of brittle deformation
4. Displacement of deformation feature

MON-3.1.1.1 Scope

The activities associated with the Geomechanical Monitoring Program are designed to:

- Maintain and augment the geotechnical instrumentation system in the WIPP underground and upgrade the automatic data acquisition system as necessary.
- Monitor geotechnical instrumentation on a regular basis and maintain a current database of instrument readings.
- Evaluate the geotechnical instrumentation data and prepare regular reports that document the data and analyses describing the stability and performance of underground openings.
- Recommend corrective or preventive measures to ensure excavation stability and safe operation of the facility.

MON-3.1.1.2 Schedule

The process by which geomechanical monitoring of an area is initiated may vary as part of operational excavation monitoring or research testing. Installation and monitoring of the instruments is governed by approved WIPP procedures. Instrumentation is monitored remotely using data loggers, or is read manually. Routine tasks are carried out according to approved WIPP procedures. Activities which are in development, or which are not expected to be performed routinely, are performed in accordance with industry standards and individual activity plans that supplement the Geotechnical Engineering Program Plan.

Remotely polled instruments are connected to a surface computer through a system of cables, termination boxes, and data loggers. Manually read instruments are monitored using electronic read-out boxes and mechanical measuring devices. Instrumentation is located in the shafts and drifts, including tape extensometer stations, convergence meters, borehole extensometers, piezometers, embedment strain gauges, stress gauges, inclinometers, load cells, and crack meters. Monitoring data are collected on a quarterly basis at a minimum, but more frequent readings may be collected as determined by the cognizant engineer or cognizant manager. Instruments are read as designated in Table MON-1.

MON-3.1.1.3 Program Output

Data analysis is performed on an annual basis and is published annually in the Geotechnical Analysis Report (U.S. DOE 2009b, U.S. DOE 2010a, U.S. DOE 2011a, and U.S. DOE 2012a).

An assessment of convergence measurements and geotechnical observations is made after each round of data collection. The results of each assessment are distributed to affected underground repository operations, engineering, and safety managers.

MON-3.1.2 Geosciences Program

Geosciences activities document existing geologic conditions and characteristics and monitor for changes resulting from the excavations. These activities generate data related to the following four parameters:

1. Creep closure and stresses

2. Extent of brittle deformation

3. Initiation of brittle deformation

4. Displacement of deformation features

MON-3.1.2.1 Scope

The Geosciences Program implements field activities such as geologic mapping of the facility and near-surface stratigraphic horizons, core logging, and geophysical surveys. These activities generate data used in monitoring the repository and in rock mechanics studies. Information from the Geosciences Program is used to document the existing geologic conditions and characteristics and to monitor for changes resulting from excavations. Activities associated with this program include geologic and fracture mapping, maintenance of a facility for the storage of geologic samples (the Core Library), seismic monitoring and evaluation, and other activities performed as needed. These activities characterize, demonstrate the continuity of, and document the geology at the site.

MON-3.1.2.2 Schedule

The following activities are performed on the indicated schedule:

- Seismic Monitoring. Regional seismic monitoring and evaluation are conducted by the New Mexico Institute of Mining and Technology. The network is operated continuously and monitoring results are reported quarterly.

- Geologic Mapping. Geologic mapping is conducted in newly excavated areas and in other areas when deemed necessary by the cognizant engineer or Geotechnical Engineering Manager.

- At a minimum, a complete analysis of geotechnical data is performed annually. The geotechnical activities will continue throughout the operational period.

MON-3.1.2.3 Program Output

Data analysis is performed on an annual basis and is published annually in the Geotechnical Analysis Report (U.S. DOE 2009b, U.S. DOE 2010a, U.S. DOE 2011a, and U.S. DOE 2012a).

MON-3.2 Groundwater Monitoring Program

Groundwater monitoring at the WIPP facility is carried out under the WIPP Groundwater Monitoring Program Plan (GWMPP) (Nuclear Waste Partnership LLC 2012b). The purpose of the GWMP is to collect groundwater data from numerous wells located at and near the facility.

The Culebra is the focus of the GWMP. It has been extensively studied during past hydrologic characterization programs, and was found to be the most likely hydrologic pathway to the accessible environment or compliance point for any potential human-intrusion-caused release scenario.

Data obtained through the GWMP are also used to support the following two monitoring parameters:

1. Culebra groundwater composition

2. Culebra groundwater flow parameters

Details on how the program is implemented are provided in the GWMPP (Nuclear Waste Partnership LLC 2012b).

On January 31, 2012, the New Mexico Environment Department (NMED) submitted a letter from Dave Martin, Cabinet Secretary, to Edward Ziemianski, Interim Manager of the Carlsbad Field Office, and Farok Sharif, Washington TRU Solutions, transmitting a Class 2 Permit Modification Request, EPA I.D. Number NM4890139088-TSDF (NMED 2012a). As a result of this modification, changes were made to the Culebra Water Quality Sampling Program. The groundwater composition sampling frequency and the method for reporting the change in the groundwater flow parameter was changed. Prior to 2012, sampling was conducted semi-annually. The sampling frequency was changed to annual sampling, based on 15 years of data that indicated little or no change in constituent concentrations. The change also aligned the 40 CFR § 194.42 Compliance Monitoring Program requirements with the WIPP Groundwater Detection Monitoring Program Plan (GDMPP) as defined in the WIPP Hazardous Waste Facility Permit (NMED 2012b).

MON-3.2.1 Scope

The GWMPP addresses requirements for sample collection, groundwater surface elevation monitoring, groundwater flow direction monitoring, data management, and reporting of groundwater monitoring data. It also identifies analytical parameters selected to assess groundwater quality.

Six Culebra wells were drilled as part of the WIPP GWMP: Water Quality Sampling Program (WQSP) wells WQSP-1 through WQSP-6. Water samples are collected from these wells and analyzed for certain chemical and physical parameters. This activity generates data in support of the Culebra Groundwater Composition parameter, which calls for analysis of the following ions:

Cations: Ca^{2+}, K^{+}, Na^{+}, Mg^{2+}

Anions: Cl^{-}, HCO_3^{-}, SO_4^{2-}

Water level data are collected to assess changes in Culebra groundwater flow. Water level measurements are tracked over time using WQSP wells and other wells that are widely distributed across the WIPP area to monitor potentiometric surface and groundwater flow directions. If changes in water level(s) occur, the cause is investigated, and any potential impact on the long-term performance of the repository is assessed.

MON-3.2.1.1 Sampling and Reporting for Water Quality

Sampling for water quality is performed at six groundwater monitoring wells. The Culebra is monitored using wells WQSP-1 through WQSP-6. It should be noted that the program previously monitored well WQSP-6a in the Dewey Lake Red Beds Formation. However, the change in the WIPP GDMPP introduced through a NMED Class 2 Permit Modification Request removed this well from the sampling and reporting program.

Field parameter measurements are used by the sampling team to determine when purged groundwater is representative of the undisturbed native groundwater of the Culebra. After well stabilization, final samples are collected for submittal to analytical laboratories. The field indicator parameters are pH, temperature, specific conductance, and specific gravity. Each well is purged no more than three well

bore volumes, or until field parameters stabilize, whichever occurs first. Well stabilization occurs when field-analyzed parameters are within ± 5% of three consecutive measurements. Should field parameters not stabilize after 3 well bore volumes have been purged, a notation is made in the field data sheets, where appropriate, and final samples are obtained.

When the field indicator parameters have stabilized, indicating that the sample is representative of the Culebra, final samples are collected in the appropriate type of container for the specific analysis to meet state and federal groundwater requirements. The final samples are submitted to a laboratory for analysis. Section MON-3.2.1 lists the analytes needed to support the PA parameter.

Samples are tracked and managed in accordance with WIPP facility standard operating procedures to assure samples are analyzed within prescribed time periods.

MON-3.2.1.2 Sampling and Reporting for Water Level Fluctuations

Water level measurements are taken in the six groundwater monitoring wells (WQSP-1 through WQSP-6) and other available WIPP wells in the monitoring network (Appendix HYDRO-2014, Figure HYDRO-1. Location of WIPP Wells and Well pads). The water level monitoring will be used to identify water level fluctuations.

In addition to the water level measurements, groundwater density is determined in the wells on an annual basis. This density is used to convert the water level measurements to equivalent freshwater heads for developing potentiometric surface maps.

MON-3.2.2 Schedule

Background water quality in both the upgradient and downgradient monitoring wells has been established for the WIPP facility. The six WQSP monitoring wells constructed for the GWMP are sampled on an annual basis to compare to the baseline water quality. Prior to 2012, sampling was conducted semi-annually. The sampling frequency was changed to an annual basis, based on 15 years of data that indicated little or no change in constituent concentrations. The change also aligned the 40 CFR 194.42 Compliance Monitoring Program requirements with the WIPP GDMPP. The change in the WIPP GDMPP was introduced through a NMED Class 2 Permit Modification Request.

The groundwater level is measured by monitoring the wells on at least a monthly basis. Groundwater level measurements are monitored and collected for other WIPP wells, as well as for the WQSP wells. The water levels are determined monthly in at least one accessible, completed interval at each available well pad, and quarterly in redundant wells at well pads where two or more wells are completed in the same interval. Groundwater level measurements are primarily used to examine changes in groundwater flow rate and direction to identify any changes pertinent to compliance.

The characteristics of the GWMP, such as the frequency of sampling and the location of the sampled wells, will be reevaluated if significant changes are observed in the groundwater flow direction or gradient. Reporting frequencies are listed in Table MON-2.

Table MON- 2. WIPP GWMP Sample Collection and Water Level Reporting Frequency

Type of Well	Frequency
Water Quality Sampling	
WQSP wells (six)	Annually

Water Level Monitoring	
WQSP wells (six)	Monthly and before sampling events
Other available WIPP wells	Monthly and quarterly on selected wells

MON-3.2.3 Program Outputs

The groundwater samples are analyzed to quantify Culebra groundwater parameters and water quality parameters listed in Section MON-3.2.1.

The GWMP also generates Culebra water level data. The data and results of the GWMP are summarized and published on an annual basis in the WIPP Annual Site Environmental Report (U.S. DOE 2008a, U.S. DOE 2009c, U.S. DOE 2010b, U.S. DOE 2011b, and U.S. DOE 2012b).

MON-3.3 Delaware Basin Drilling Surveillance Program

The DBDSP is described in the Delaware Basin Drilling Surveillance Plan (Nuclear Waste Partnership LLC 2012c). This plan provides the framework for the surveillance of drilling activities within the Delaware Basin, with specific emphasis on the nine-township area surrounding the WIPP site. The DBDSP mandates the collection of information related to the following two parameters:

1. Probability of encountering a Castile brine reservoir

2. Drilling rate

In addition to the parameters listed above, the DBDSP collects information on the following activities:

- Borehole plugging
- Enhanced recovery
- Natural gas storage
- Solution mining
- Potash mining
- Seismic events

MON-3.3.1 Scope

The DBDSP is to provide for active surveillance of drilling activities within the Delaware Basin. The WIPP PA includes the impacts of drilling on the performance of the disposal system. The number of deep boreholes drilled per square kilometer is a parameter used in PA calculations for inadvertent intrusion scenarios. This parameter is based on actual drilling rates within the Delaware Basin over the last 100 years, as required by 40 CFR § 194.33 (U.S. EPA 1996).

The results of the DBDSP continue to expand the existing database. The results of this program are used to detect any substantial deviations from the assumptions used in the previous PA (see Section MON-3.3.2, Table MON-3). Collecting additional information about resource exploration and

exploitation activities and practices in the Delaware Basin provides information to determine whether the drilling scenarios, assumptions, and probabilities used in the PA will continue to be valid for each five-year recertification of the WIPP disposal system.

Drilling information for the study area is obtained through commercially available electronic databases and the records of government agencies. The electronic database is updated weekly to reflect drilling activities in the Delaware Basin. Records of government agencies are updated as they become available.

MON-3.3.2 Schedule

Table MON-3 shows the frequency of DBDSP data collection.

Table MON- 3. DBDSP Data Collection Schedule

Information Collected	Frequency
Borehole plugging	Weekly
Enhanced recovery	Monthly
Gas storage	Annually
Solution mining	Annually
Potash mining	Annually
Seismic events	Quarterly
Drilling-related	Weekly
Probability of encountering a Castile brine reservoir	Weekly
Drilling rate calculations	Quarterly

MON-3.3.3 Program Outputs

DBDSP results are used to update and maintain a database of drilling activities and related practices in the Delaware Basin. For the nine-township area surrounding the WIPP dispoal system, the DBDSP updates and maintains a database containing the following information:

- Plugging and abandonment activities, including descriptions of plugging configurations
- The fraction of plugged and abandoned boreholes that are sealed
- Well conversion activities (injection, disposal, water)
- Injection well operations (disposal and secondary recovery)
- Drilling activities, including borehole depths, diameters, and type and amount of drilling fluid
- Ownership of state and federal minerals and hydrocarbon leases within the area
- Occurrences of pressurized brine within the Castile

Data collected and recorded as a result of the DBDSP are reported annually in the Delaware Basin Monitoring Annual Report (U.S. DOE 2008b, U.S. DOE 2009d, U.S. DOE 2010c, U.S. DOE 2011c, and U.S. DOE 2012c).

MON-3.4 Subsidence Monitoring Program

The SMP is described in detail in the WIPP Underground and Surface Surveying Program (Nuclear Waste Partnership LLC 2012d). Subsidence monitoring measures vertical movement of the land surface relative to a reference location using state-of-the-art leveling equipment. The technique used to monitor subsidence involves measuring the vertical height difference between two or more markers placed on a surface a known distance away from each other using a leveling survey. A reference benchmark is used as the standard and the relative movement of the other benchmark(s) is measured to detect vertical movement over time. Subsidence measurements are relative because the reference is fixed only with respect to the subsidence marker(s).

MON-3.4.1 Scope

The activities associated with the SMP are designed to:

- Provide time-related spatial information on surface subsidence within 152.4 meters (m) (500 feet (ft)) surrounding the waste shaft during the operational phase of the repository
- Provide time-related spatial information on surface subsidence over the influence area of the underground openings for comparison with subsidence predictions
- Maintain a database of subsidence data

With current technology, vertical elevation can be measured at a precision of 0.0305 centimeters (cm) (0.001 ft). Subsidence monitoring was chosen by the DOE as a long-term monitoring tool because it effectively meets the requirements in section 191.14(b). Subsidence monitoring is conducted to detect substantial and detrimental deviations from expected repository performance by comparing actual subsidence to predicted subsidence.

Subsidence data currently being compiled will be compared to subsidence predictions. In addition, subsidence monitoring during the operational phase generates data to establish a baseline against which long-term subsidence data and information may be evaluated.

MON-3.4.2 Schedule

Subsidence surveys are performed annually throughout the operations period. After closure of the repository, subsidence surveys will be performed at 10-year intervals for at least 100 years or until no further useful information may be obtained through continued monitoring.

MON-3.4.3 Program Outputs

The SMP generates annual surface subsidence data for 24.14 kilometers (km) (15 miles (mi)) of leveling loops through 48 monuments. Results are reported annually in the WIPP Subsidence Monument Leveling Survey (U.S. DOE 2008c, U.S. DOE 2009e, U.S. DOE 2010d, U.S. DOE 2011d, U.S. DOE 2012d, and U.S. DOE 2012e).

MON-3.5 Waste Inventory Monitoring Based on WIPP Waste Data System

Information on the waste activity parameter is measured or estimated by generator sites through waste characterization activities. Sites are required to report certain information in the WIPP WDS, formerly called the WIPP Waste Information System, or WWIS. Reports are generated to tabulate key waste parameters for waste that has been emplaced in the WIPP repository. The waste activity parameter includes tracking the total waste material parameter weights and curie content of the 10 radionuclides listed in Section MON-3.5.3.

MON-3.5.1 Scope

Radionuclide inventory data and material parameter weights for every container of waste placed in the WIPP underground repository are submitted to the WDS database at the time waste is certified for shipment to the WIPP facility. The waste activity parameters being tracked and reported include radiological activity (in curies) emplaced during the 40 CFR § 194.4(b)(4) (U.S. EPA 1996) reporting period and the cumulative activity since waste was first emplaced in the repository. The radionuclides being tracked (in curies) include:

- americium-241
- plutonium-238
- plutonium-239
- plutonium-240
- plutonium-242
- uranium-233
- uranium-234
- uranium-238
- strontium-90
- cesium-137

The material parameter weights that are annually tracked and reported in the section 194.4(b)(4) report include:

- A repository maximum limit for emplaced cellulose, plastic and rubber materials of 2.2×10^7 kg
- A repository minimum for emplaced ferrous metals of 2×10^7 kg
- A repository minimum for emplaced nonferrous metals of 2×10^3 kg

MON-3.5.2 Schedule

A current collection of radionuclide inventory data and material parameter weights for the WIPP is maintained within the WDS, and data reports can be generated at any time.

MON-3.5.3 Program Outputs

The data collected for the waste activity parameter is tracked by the WDS. The WDS annually generates a Waste Emplacement Summary Report that is submitted each November to the EPA in the annual 40 CFR § 194.4(b)(4) report (U.S. DOE 2008d, U.S. DOE 2009f, U.S. DOE 2010e, U.S. DOE 2011e, and U.S. DOE 2012f). . In addition, to aid the EPA, an EPA Dashboard is available on the WDS for their use and they can call up any of the following reports at their discretion.

• Container Query

• Nuclide Report

• Waste Emplacement Report

• Summary of Waste Emplacement Inventory Report

• Emplacement By container Type Report

• Emplacement History Overview

MON-4.0 Postclosure (Long Term) Monitoring

The final Postclosure Monitoring Plan will be developed prior to final facility closure (sealing of the shafts), but will not be implemented until after facility closure. When the final Postclosure Monitoring Plan is written, the historic monitoring data collected per the requirements of this Preclosure Monitoring Plan that will support postclosure monitoring will be analyzed.

MON-5.0 Monitoring Programs Quality Assurance Requirements

The quality of the work performed under the DOE CMP is accomplished per the criteria of 40 CFR § 194.22(a)(2)(ii) (U.S. EPA 1996) and controlled by the application of the CBFO Quality Assurance Program Document (QAPD) (U.S. DOE 2010f). Waste information is controlled by implementing the relevant quality assurance requirements at generator sites.

In addition to the management requirements, such as document and record control established in the QAPD, requirements related to sampling and monitoring activities are specified. In particular, the following two sections of the QAPD are directly related to the performance of monitoring work and the control of samples:

- Section 2.4 - Inspection and Testing
  - Qualification of personnel
  - Inspection
  - Test requirements
  - Monitoring, measuring, testing, and data collection
  - Use and control of measuring and test equipment

- Calibration

- Section 4.0 - Sample Control Requirements
  - Sample control
  - Sample identification
  - Handling, storing, and shipping samples
  - Disposition of nonconforming samples

WIPP monitoring programs are subject to EPA inspections in accordance with 40 CFR § 194.21 (U.S. EPA 1996).

The CMP relies on the individual monitoring plan's QA program to ensure compliance with DOE WIPP requirements for data quality assessments, objectives, and analyses. Each sampling and monitoring program is implemented through individual implementation plans, which include the QA descriptions, objectives, and references to the applicable governing QA document.

MON-6.0 Reporting and Assessment

Information flow is controlled to ensure important monitoring results are communicated to the appropriate individuals and groups.

MON-6.1 Monitoring Data Reporting

The monitoring programs that generate data used in the CMP are implemented and coordinated by the M&OC.

MON-6.1.1 CMP Assessment Report

The results of the CMP are reported in the compliance assessment report (Wagner and Hillesheim 2008 and Wagner and Hillesheim 2009; Wagner and Kuhlman 2010; Wagner, Kuhlman and Johnson 2011 and Wagner, Kuhlman and Johnson 2012). The Sandia National Laboratories Annual Compliance Monitoring Parameter Assessment Reports are provided to the EPA with each recertification as references to Appendix DATA.

The CMP results may indicate two general cases: normal or expected conditions, in which results are generally consistent with existing data, parameter values, and conceptual models; and anomalous conditions, in which results are inconsistent with existing data, parameter values, or conceptual models. The DOE determines whether these results are consistent with expected conditions modeled in the PA or screening decisions used to support the compliance determination. The report also recommends if the CMP should be modified based on results of the monitoring programs.

MON-6.1.2 External Reporting

The DOE reviews the recommendations of the M&OC and the Scientific Advisor to evaluate their significance. Significance is determined based on consideration of the following criteria:

- Containment requirements established pursuant to 40 CFR § 191.13 (U.S. EPA 1993) are, or are expected to be, exceeded.

- Releases from previously emplaced waste that lead to committed effective doses that are, or are expected to be, in excess of those established pursuant to 40 CFR § 191.15 (U.S. EPA 1993) (not including emissions from operations covered pursuant to Part 191 Subpart A).

- Releases that have caused, or are expected to cause, concentrations of radionuclides (or estimated doses due to radionuclides in underground sources of drinking water in the accessible environment) to exceed the limits established pursuant to Part 191 Subpart C.

If monitoring results meet any of these criteria, the results are considered significant. Significant monitoring results are promptly reported to the EPA. The report is accompanied by a recommended course of action, including the appropriate external reporting. If the monitoring results exceed or possibly exceed containment requirements or release limits as specified in 40 CFR § 194.4(b)(3)(ii), the CBFO will immediately cease emplacement of waste in the WIPP repository and notify the EPA within 24 hours.

If the DOE discovers a condition or activity that differs significantly from what is indicated in the most recent compliance application, but does not involve conditions or activities listed in section 194.4(b)(3)(ii), then the difference shall be reported in writing to the EPA within 10 calendar days of discovery. For normal conditions where monitoring results are within expectations, the CMP assessment documents these conditions (Wagner and Hillesheim 2008 and Wagner and Hillesheim 2009; Wagner and Kuhlman 2010; Wagner, Kuhlman and Johnson 2011 and Wagner, Kuhlman and Johnson 2012) .

MON-7.0 References

(*Indicates a reference that has not been previously submitted.)

Kirkes, R. and S. Wagner. 2003. MONPAR Reassessment. ERMS 533098. Carlsbad, NM: Sandia National Laboratories. [PDF / Author]

Marcinowski, F. 2002. Letter to I.R. Triay. 15 March 2002. Washington, DC: U.S. Environmental Protection Agency, Office of Air and Radiation. [PDF / Author]

New Mexico Environment Department (NMED). 2012a. Letter from Dave Martin, Cabinet Secretary, to Edward Ziemianski, Interim Manager of the Carlsbad Field Office, and Farok Sharif, Washington TRU Solutions (Subject: Approval and Partial Denial of Permit Modification Requests to Update Ventilation Langauge, Add a Shielded Container, and Revise the WIPP Groudwater Detection Monitoring Program Plan, WIPP Hazardous Waste Facility Permit, EPA I.D. Number NM4890139088). 31 January 2012.* [PDF / Author]

New Mexico Environment Department (NMED). 2012b. WIPP Hazardous Waste Facility Permit, May 8, 2012, Part 5 - Groundwater Detection Monitoring. Carlsbad, NM: U.S. Department of Energy. [PDF / Author]

Nuclear Waste Partnership LLC (NWP). 2012a. WIPP Geotechnical Engineering Program Plan (Rev. 7, November 19). WP 07 1. Carlsbad, NM: Carlsbad Field Office.* [PDF / Author]

Nuclear Waste Partnership LLC (NWP). 2012b. WIPP Groundwater Monitoring Program Plan (Rev. 12, November 30). WP 02 1. Carlsbad, NM: Carlsbad Field Office.* [PDF / Author]

Nuclear Waste Partnership LLC (NWP). 2012c. Delaware Basin Drilling Surveillance Plan (Rev. 5, November 27). WP 02-PC.02. Carlsbad, NM: Carlsbad Field Office.* [PDF / Author]

Nuclear Waste Partnership LLC (NWP). 2012d. WIPP Underground and Surface Surveying Program (Rev. 6, November 30). WP 09 ES.01. Carlsbad, NM: Carlsbad Field Office.* [PDF / Author]

Triay, I.R. 2002. Letter to F. Marcinowski (1 Enclosure). 3 January 2002. Carlsbad, NM: U.S. Department of Energy, Carlsbad Field Office. [PDF / Author]

U.S. Department of Energy (DOE). 1996. Title 40 CFR Part 191 Compliance Certification Application for the Waste Isolation Pilot Plant (October). 21 vols. DOE/CAO-1996-2184. Carlsbad, NM: Carlsbad Field Office. [Author]

U.S. Department of Energy (DOE). 2008a. WasteIsolation Pilot Plant Annual Site Environmental Report: Calendar Year 2007 (September). DOE/WIPP 08-2225. Carlsbad, NM: Carlsbad Field Office.* [PDF / Author]

U.S. Department of Energy (DOE). 2008b. Delaware Basin Monitoring Annual Report (September 2008). DOE/WIPP-08-2308. Carlsbad, NM: Carlsbad Field Office.* [PDF / Author]

U.S. Department of Energy (DOE). 2008c. WIPP Subsidence Monument Leveling Survey 2007 (December). DOE/WIPP-08-2293. Carlsbad, NM: Carlsbad Field Office.* [PDF / Author]

U.S. Department of Energy (DOE). 2008d. Annual Change Report 2007/2008 (November 15). DOE/WIPP 0408-3317. Carlsbad, NM: Carlsbad Field Office.* [PDF / Author]

U.S. Department of Energy (DOE). 2009a. Title 40 CFR Part 191 Compliance Recertification Application for the Waste Isolation Pilot Plant (March). DOE/WIPP 2009-3424. Carlsbad, NM: Carlsbad Field Office.* [Author]

U.S. Department of Energy (DOE). 2009b. Geotechnical Analysis Report for July 2007 - June 2008 (March). 2 vols. DOE/WIPP 09-3177. Carlsbad, NM: Carlsbad Field Office.* [PDF / Author]

U.S. Department of Energy (DOE). 2009c. Waste Isolation Pilot Plant Annual Site Environmental Report: Calendar Year 2008. DOE/WIPP 09-2225. Carlsbad, NM: Carlsbad Field Office.* [PDF / Author]

U.S. Department of Energy (DOE). 2009d. Delaware Basin Monitoring Annual Report (September 2009). DOE/WIPP 09-2308. Carlsbad, NM: Carlsbad Field Office.* [PDF / Author]

U.S. Department of Energy (DOE). 2009e. WIPP Subsidence Monument Leveling Survey 2008 (December). DOE/WIPP 09-2293. Carlsbad, NM: Carlsbad Field Office.* [PDF / Author]

U.S. Department of Energy (DOE). 2009f. Annual Change Report 2008/2009(November 13). DOE/WIPP 09-0335. Carlsbad, NM: Carlsbad Field Office.* [PDF / Author]

U.S. Department of Energy (DOE). 2010a. Geotechnical Analysis Report for July 2008 - June 2009 (April). 2 vols. DOE/WIPP 10-3177. Carlsbad, NM: Carlsbad Field Office.* [PDF / Author]

U.S. Department of Energy (DOE). 2010b. Waste Isolation Pilot Plant Annual Site Environmental Report: Calendar Year 2009. DOE/WIPP 10-2225. Carlsbad, NM: Carlsbad Field Office.* [PDF / Author]

U.S. Department of Energy (DOE). 2010c. Delaware Basin Monitoring Annual Report (September 2010). DOE/WIPP-10-2308. Carlsbad, NM: Carlsbad Field Office.* [PDF / Author]

U.S. Department of Energy (DOE). 2010d. WIPP Subsidence Monument Leveling Survey 2009 (December). DOE/WIPP-10-2293. Carlsbad, NM: Carlsbad Field Office.* [PDF / Author]

U.S. Department of Energy (DOE). 2010e. Annual Change Report 2009/2010 (November). DOE/WIPP-10-1660. Carlsbad, NM: Carlsbad Field Office.* [PDF / Author]

U.S. Department of Energy (DOE). 2010f. Quality Assurance Program Document (Revision 11, June). DOE/CBFO-94-1012. Carlsbad, NM: Carlsbad Field Office. [PDF / Author]

U.S. Department of Energy (DOE). 2011a. Geotechnical Analysis Report for July 2009-June 2010 (March). 2 vols. DOE/WIPP 11-3177. Carlsbad, NM: Carlsbad Field Office.* [PDF / Author]

U.S. Department of Energy (DOE). 2011b. Waste Isolation Pilot Plant Annual Site Environmental Report: Calendar Year 2010. DOE/WIPP 11-2225. Carlsbad, NM: Carlsbad Field Office.* [PDF / Author]

U.S. Department of Energy (DOE). 2011c. Delaware Basin Monitoring Annual Report (September 2011). DOE/WIPP-11-2308. Carlsbad, NM: Carlsbad Field Office.* [PDF / Author]

U.S. Department of Energy (DOE). 2011d. WIPP Subsidence Monument Leveling Survey 2010 (December). DOE/WIPP-11-2293. Carlsbad, NM: Carlsbad Field Office.* [PDF / Author]

U.S. Department of Energy (DOE). 2011e. Annual Change Report 2010/2011 (August). DOE/WIPP-11-3479. Carlsbad, NM: Carlsbad Field Office.* [PDF / Author]

U.S. Department of Energy (DOE). 2012a. Geotechnical Analysis Report for July 2010 to June 2011 (May). DOE/WIPP-12-3408. Carlsbad, NM: Carlsbad Field Office.* [PDF / Author]

U.S. Department of Energy (DOE). 2012b. Waste Isolation Pilot Plant Annual Site Environmental Report Calendar Year 2011. DOE/WIPP 12-3489. Carlsbad, NM: Carlsbad Field Office.* [PDF / Author]

U.S. Department of Energy (DOE). 2012c. Delaware Basin Monitoring Annual Report (September 2012). DOE/WIPP-12-2308. Carlsbad, NM: Carlsbad Field Office.* [PDF / Author]

U.S. Department of Energy (DOE). 2012d. WIPP Subsidence Monument Leveling Survey 2011 (December). DOE/WIPP 12-2293. Carlsbad, NM: Carlsbad Field Office.* [PDF / Author]

U.S. Department of Energy (DOE). 2012e. WIPP Subsidence Monument Leveling Survey 2012 (December). DOE/WIPP 12-3497. Carlsbad, NM: Carlsbad Field Office.* [PDF / Author]

U.S. Department of Energy (DOE). 2012f. Annual Change Report 2011/2012: 7 (October). DOE/WIPP-12-3496. Carlsbad, NM: Carlsbad Field Office.* [PDF / Author]

U.S. Environmental Protection Agency (EPA). 1993. 40 CFR Part 191: Environmental Radiation Protection Standards for the Management and Disposal of Spent Nuclear Fuel, High-Level and Transuranic Radioactive Wastes; Final Rule. Federal Register, vol. 58 (December 20, 1993): 66398-416. [PDF / Author]

U.S. Environmental Protection Agency (EPA). 1996. 40 CFR Part 194: Criteria for the Certification and Recertification of the Waste Isolation Pilot Plant's Compliance with the 40 CFR Part 191 Disposal Regulations; Final Rule. Federal Register, vol. 61 (February 9, 1996): 5223-45. [PDF / Author]

U.S. Environmental Protection Agency (EPA). 1998a. 40 CFR Part 194: Criteria for the Certification and Recertification of the Waste Isolation Pilot Plant's Compliance with the Disposal Regulations: Certification Decision; Final Rule. Federal Register, vol. 63 (May 18, 1998): 27353-406. [PDF / Author]

U.S. Environmental Protection Agency (EPA). 1998b. CARD No. 42: Monitoring. Compliance Application Review Document Number 42 for the Criteria for the Certification and Recertification of the Waste Isolation Pilot Plant's Compliance with the 40 CFR 191 Disposal Regulations: Final Certification Decision (May) (pp. 42-1 through 42-24). Washington, DC: Office of Radiation and Indoor Air. [PDF / Author]

U.S. Environmental Protection Agency (EPA). 2006. 40 CFR Part 194: Criteria for the Certification and Recertification of the Waste Isolation Pilot Plant's Compliance with the Disposal Regulations: Recertification Decision (Final Notice). Federal Register, vol. 71 (April 10, 2006): 18010-021.* [PDF / Author]

U.S. Environmental Protection Agency (EPA). 2010. 40 CFR Part 194: Criteria for the 15 Certification and Recertification of the Waste Isolation Pilot Plant's Compliance with the 16 Disposal Regulations: Recertification Decision; Final Rule. Federal Register, vol. 75 17 (November 18, 2010): 70584-595.* [PDF / Author]

Wagner, S.W. 2008. Reassessment of MONPAR Analysis for Use in the 2009 Compliance Recertification Application. ERMS 548948. Carlsbad, NM: Sandia National Laboratories. [PDF / Author]

Wagner, S.W. and M. Hillesheim. 2008. Sandia National Laboratories Annual Compliance Monitoring Parameter Assessment for 2008 (January). WBS 1.3.1. Carlsbad, NM.* [PDF / Author]

Wagner, S.W. and M. Hillesheim. 2009. Sandia National Laboratories Annual Compliance Monitoring Parameter Assessment for 2009 (January). WBS 1.3.1. Carlsbad, NM. * [PDF / Author]

Wagner, S.W. and K. Kuhlman 2010. Sandia National Laboratories Annual Compliance Monitoring Parameter Assessment for 2010 (November). WBS 1.3.1. Carlsbad, NM.* [PDF / Author]

Wagner, S.W., K.L. Kuhlman., and P.B. Johnson. 2011. Sandia National Laboratories Annual Compliance Monitoring Parameter Assessment for 2011 (December). WBS 1.3.1. Carlsbad, NM.* [PDF / Author]

Wagner, S.W., K.L. Kuhlman. and P.B. Johnson. 2012. Sandia National Laboratories Annual Compliance Monitoring Parameter Assessment for 2012 (November).* [PDF / Author]

Wagner, S.W. 2013. Reassessment of MONPAR Analysis for Use in the 2014 Compliance Recertification Application. ERMS 560164. Carlsbad, NM: Sandia National Laboratories.* [PDF / Author]

Title 40 CFR Part 191
Subparts B and C
Compliance Recertification Application 2014 for the

Waste Isolation Pilot Plant

Appendix PA-2014
Performance Assessment

United States Department of Energy
Waste Isolation Pilot Plant

Carlsbad Field Office
Carlsbad, New Mexico

Compliance Recertification Application 2014

Appendix PA

Table of Contents

List of Figures

List of Tables

Acronyms and Abbreviations

% percent

AIC active institutional control

C Celsius

CCA Compliance Certification Application

CCDF complementary cumulative distribution function

CDF cumulative distribution function

CFR Code of Federal Regulations

CH-TRU contact-handled transuranic

Ci curies

CL confidence Limit

CPR cellulosic, plastic, and rubber

CRA Compliance Recertification Application

DBR direct brine release

DDZ drilling damaged zone

DOE U.S. Department of Energy

DP disturbed repository performance

DRZ disturbed rock zone

E deep drilling scenario

EPA U.S. Environmental Protection Agency

ERDA U.S. Energy Research and Development Administration

FEP feature, event, and process

FMT Fracture-Matrix Transport

FVW fraction of excavated repository volume occupied by waste

gal gallon

GWB Generic Weep Brine

in inch

J Joule

K Kelvin

K_d distribution coefficient

kg kilogram

km kilometer

km^2 square kilometers

L liter

LHS Latin hypercube sampling

LWB Land Withdrawal Boundary

M mining scenario

m meter

m^2 square meters

m^3 cubic meters

MB marker bed

ME mining and drilling scenario

mol mole

MPa megapascal

MTHM metric tons of heavy metal

MWd megawatt-days

N Newton

Pa Pascal

PA performance assessment

PABC performance assessment baseline calculation

PAVT Performance Assessment Verification Test

PCC partial correlation coefficient

PCS panel closure system

PDE partial differential equation

PDF probability distribution function

PIC passive institutional control

RH-TRU remote-handled transuranic

RKS Redlich-Kwong-Soave

RoR Rest of Repository

ROM run-of-mine

s second

s^2 seconds squared

SCF/d standard cubic feet per day

SMC Salado Mass Concrete

SNL Sandia National Laboratories

SRC standardized regression coefficient

T-field transmissivity field

TRU transuranic

TVD Total Variation Diminishing

UP undisturbed repository performance

WIPP Waste Isolation Pilot Plant

yr year

Elements and Chemical Compounds

Al aluminum

Am americium

C carbon

$C_6H_{10}O_5$ generic formula for CPR

Ca calcium

CH_4 methane

Cm curium

CO_2 carbon dioxide

Cr chromium

Cs cesium

Fe iron

H_2 hydrogen gas

H_2O water

H_2S hydrogen sulfide

I iodine

Mg magnesium

$Mg(OH)_2$ brucite

$Mg_5(CO_3)_4(OH)_2 \cdot 4H_2O$ hydromagnesite (5424)

MgO magnesium oxide, or periclase

Mn manganese

Ni nickel

NO_3^- nitrate

Np neptunium

Pb lead

Pm promethium

Pu plutonium

Ra radium

Sn tin

SO_4 sulfate

SO_4^{2-} sulfate ion

Sr strontium

Tc technetium

Th thorium

U uranium

V vanadium

PA-1.0 Introduction

This appendix presents the mathematical models used to evaluate performance of the Waste Isolation Pilot Plant (WIPP) disposal system and the results of these models for the 2014 Compliance Recertification Application (CRA-2014) Performance Assessment (PA). The term PA signifies an analysis that (1) identifies the processes and events that might affect the disposal system; (2) examines the effects of these processes and events on the performance of the disposal system; and (3) estimates the cumulative releases of radionuclides, considering the associated uncertainties, caused by all significant processes and events (section 191.12 [U.S. EPA 1993]). PA is designed to address three primary questions about the WIPP:

Q1: What processes and events that might affect the disposal system could take place at the WIPP site over the next 10,000 years?

Q2: How likely are the various processes and events that might affect the disposal system to take place at the WIPP site over the next 10,000 years?

Q3: What are the consequences of the various processes and events that might affect the disposal system that could take place at the WIPP site over the next 10,000 years?

In addition, accounting for uncertainty in the parameters of the PA models leads to a further question:

Q4: How much confidence should be placed in answers to the first three questions?

These questions give rise to a methodology for quantifying the probability distribution of possible radionuclide releases from the WIPP repository over the next 10,000 years and characterizing the uncertainty in that distribution due to imperfect knowledge about the parameters contained in the models used to predict releases. The containment requirements of section 191.13 require this probabilistic methodology.

This appendix is organized as follows: Section PA-1.1 summarizes changes made to the WIPP PA since the CRA-2009 PA (Clayton et al. 2008). Section PA-2.0 gives an overview and describes the overall conceptual structure of the CRA-2014 PA. The WIPP PA is designed to address the requirements of section 191.13, and thus involves three basic entities: (1) models for both the physical processes that take place at the WIPP site and the estimation of potential radionuclide releases that may be associated with these processes, (2) a probabilistic characterization of the uncertainty in the models and parameters that underlay the WIPP PA (to account for epistemic uncertainty), and (3) a probabilistic characterization of different futures that could occur at the WIPP site over the next 10,000 years (to account for aleatory uncertainty). Section PA-1.1 is supplemented by Appendix SCR-2014, which documents the results of the screening process for features, events, and processes (FEPs) that are retained in the conceptual models of repository performance, including those FEPs which have been modified since CRA-2009.

Section PA-3.0 describes the probabilistic characterization of different futures and summarizes the stochastic variables that represent future drilling and mining events in the PA. This characterization plays an important role in the construction of the complementary cumulative distribution function (CCDF) specified in section 191.13. Regulatory guidance and extensive review of the WIPP site identified exploratory drilling for natural resources and the mining of potash as the only significant disruptions at the WIPP site with the potential to affect radionuclide releases to the accessible environment.

Section PA-4.0 presents the mathematical models for both the physical processes that take place at the WIPP and the estimation of potential radionuclide releases. The mathematical models implement the conceptual models as prescribed in section 194.23, and permit the construction of the CCDF specified in section 191.13. Models presented in Section PA-4.0 include two-phase (i.e., gas and brine) flow in the vicinity of the repository; radionuclide transport in the Salado Formation (hereafter referred to as the Salado); releases to the surface at the time of a drilling intrusion due to cuttings, cavings, spallings, and direct brine releases (DBRs); brine flow in the Culebra Dolomite Member of the Rustler Formation (hereafter referred to as the Culebra); and radionuclide transport in the Culebra. Section PA-4.0 is supplemented by Appendices MASS-2014, TFIELD-2014, and PORSURF-2014. Appendix MASS-2014 discusses the modeling assumptions used in the WIPP PA. Appendix TFIELD-2014 discusses the generation of the transmissivity fields (T-fields) used to model groundwater flow in the Culebra. Appendix PORSURF-2014 presents results from modeling the effects of excavated region closure, waste consolidation, and gas generation in the repository.

Section PA-5.0 discusses the probabilistic characterization of parameter uncertainty, and summarizes the uncertain variables incorporated into the CRA-2014 PA, the distributions assigned to these variables, and the correlations between variables. Section PA-5.0 is supplemented by Kicker and Herrick (Kicker and Herrick 2013) and Appendix SOTERM-2014. Kicker and Herrick (Kicker and Herrick 2013) catalogs the full set of parameters used in the CRA-2014 PA. Appendix SOTERM-2014 describes the actinide source term for the WIPP performance calculations, including the mobile concentrations of actinides that may be released from the repository in brine.

Section PA-6.0 summarizes the computational procedures used in the CRA-2014 PA, including sampling techniques, sample size, statistical confidence for mean CCDF, generation of sample, generation of individual futures, construction of CCDFs, calculations performed with the models discussed in Section PA-4.0, construction of releases for each future, and the sensitivity analysis techniques in use.

Section PA-7.0 presents the results of the PA for an undisturbed repository. Releases from the undisturbed repository are determined by radionuclide transport in brine flowing from the repository to the Land Withdrawal Boundary (LWB) through the marker beds (MBs) or shafts. Releases in the undisturbed scenario are used to demonstrate compliance with the individual and groundwater protection requirements in 40 CFR Part 191 (section 194.51 and section 194.52).

Section PA-8.0 presents PA results for a disturbed repository. As discussed in Section PA-2.3.1, the only future events and processes in the analysis of disturbed repository performance are those associated with mining and deep drilling. Release mechanisms include direct releases at the time of the intrusion via cuttings, cavings, spallings, and DBR, and long-term releases via radionuclide transport up abandoned boreholes to the Culebra and thence to the LWB.

Section PA-9.0 presents the set of CCDFs resulting from the CRA-2014 PA. This material supports Section 194.34 of CRA-2014, which demonstrates compliance with the containment requirements of section 191.13. Section PA-9.0 presents the most significant output variables from the PA models, accompanied by sensitivity analyses to determine which subjectively uncertain parameters are most influential in the uncertainty of PA results.

The results of the PA for CRA-2014, as documented in Section PA-7.0, Section PA-8.0, and Section PA-9.0, confirm that direct releases from drilling intrusions are the major contributors to radionuclide releases to the accessible environment. In addition, the CRA-2014 PA results demonstrate that the WIPP continues to comply with the quantitative containment requirements in section 191.13(a).

The overall structure of Appendix PA-2014 is identical with that of the Appendix PA-2009 (U.S. DOE 2009). This appendix follows the approach used by Helton et al. (1998) to document the mathematical models used in the Compliance Certification Application (CCA) PA and the results of that analysis. Much of the content of this appendix derives from Helton et al. (1998); these authors' contributions are gratefully acknowledged.

PA-1.1 Changes since the CRA-2009 PA

As part of its review of the CRA-2009 (U.S. DOE 2009), the U.S. Environmental Protection Agency (EPA) requested changes to the CRA-2009 PA (Cotsworth 2009) including updates to the repository waste inventory, actinide solubilities, Culebra transmissivity fields, drilling parameters, and matrix partition coefficients. These changes were incorporated into the CRA-2009 Performance Assessment Baseline Calculation (CRA-2009 PABC) (Clayton et al. 2010). Repository performance with these requested changes was subsequently assessed by the EPA, and the WIPP was recertified in 2010 (U.S. EPA 2010a). The CRA-2009 PABC is the current regulatory baseline for the WIPP. The U.S. Department of Energy (DOE) continues to use the same PA methodology as in the CCA and the CRA-2009 PABC because changes that have been made since the EPA first certified the WIPP in 1998 do not impact PA methodology. A detailed presentation for the CCA PA methodology is provided in (Helton et al. (1998), Section 2).

In addition to including applicable changes from CRA-2009 incorporated in the CRA-2009 PABC, the CRA-2014 PA is updated based on new information since the CRA-2009 PABC. Information on the implementation of these updates is contained in Camphouse et al. (Camphouse et al.2013). Changes included in the CRA-2014 PA relative to the CRA-2009 PA are summarized in Table PA-1. Culebra transmissivity fields and matrix partition coefficients were updated as part of the CRA-2009 PABC; these updates are carried forward to the CRA-2014 PA. Updates to Culebra transmissivity fields (T-fields) and matrix partition coefficients are included in Table PA-1 for the sake of completeness as they are changes made since the CRA-2009 PA. Other changes between the CRA-2009 PA and the CRA-2009 PABC have been superseded by new information since the CRA-2009 PABC. The random seeds used in the CRA-2009 PABC are also used in the CRA-2014 PA. Use of the CRA-2009 PABC random seeds (and parameter ordering as applicable) results in identical sampled values for sampled parameters that are common to the CRA-2009 PABC and the CRA-2014 PA.

This section ends with motivations for and brief descriptions of each of the updates developed for and included in the CRA-2014 PA.

Table PA- 1. Changes since the CRA-2009 PA Incorporated in the CRA-2014 PA

WIPP Project Change	Summary of Change and Cross-Reference
Culebra Transmissivity Fields (Carried over from CRA-2009 PABC)	Culebra transmissivity fields are updated based on revised hydrogeologic factors for the Culebra (Appendix HYDRO-2014, Attachment TFIELD-2014).
Updated Culebra Matrix Partition Coefficients (Carried over from CRA-2009 PABC)	Updated to account for higher organic ligand concentrations in the WIPP waste inventory (Clayton 2009).
Panel Closure Design	The Option D panel closure system (PCS) design is replaced with the run-of-mine panel closure system (ROMPCS) design (see Sections PA-1.1.1 and PA-4.2.8).
Added Volume in the Repository Experimental Region	A volume of 60,335 cubic meters (m^3) is added to the volume of the WIPP experimental region for Salt Disposal Investigation experiments (see Section PA-1.1.2).
Probability of Encountering Pressurized Brine during a Drilling Intrusion	A revised distribution is used for WIPP PA parameter GLOBAL:PBRINE (see Section PA-1.1.3).
Refinement to Steel Corrosion Rate	A revised distribution is used for WIPP PA parameter STEEL:CORRMCO2 (see Section PA-1.1.4).
Updated Waste Shear Strength	A revised distribution is used for WIPP PA parameter BOREHOLE:TAUFAIL (see Section PA-1.1.5).
Updated Waste Inventory Information	Inventory parameters in the CRA-2014 PA are updated to reflect information collected through December 31, 2011 (see Section PA-1.1.6).

Drilling Rate	The drilling rate increased from 59.8 to 67.3 boreholes per square kilometer (km^2) over 10,000 years (see Section PA-1.1.7). Borehole plugging pattern probabilities are also updated.
Refined Water Balance Implementation	The repository water balance implementation is refined to include the major gas and brine producing and consuming reactions in the existing conceptual model (see Sections PA-1.1.8 and PA-4.2.5).
Variable Brine Volume	Radionuclide concentrations in brine are dependent on the volume of brine in the repository at the time of intrusion (see Section PA-1.1.9).
Radionuclide Solubilities and their Uncertainty	Radionuclide baseline solubilities are updated to reflect the organic ligand content in the CRA-2014 PA waste inventory, and are calculated for several brine volumes. Solubility uncertainties are updated based on recently available results in published literature (see Section PA-1.1.10 and SOTERM-2014, Section 5.0).
Updated Colloid Parameters	Colloid parameters in the CRA-2014 are updated to reflect data presented in Reed et al. (Reed et al. 2013) (see section PA 1.1.11).

The CRA-2014 PA is comprised of four individual cases, with a subset of the changes listed in Table PA-1 incorporated into the first three. This was done in order to evaluate the effects of various individual, and combined, changes. The fourth case includes all changes listed in Table PA-1. A thorough description of the four cases, and the changes included in them, is given in Camphouse (Camphouse 2013d). CRA-2014 PA results included in this appendix correspond to the fourth case where all changes listed in Table PA-1 are included in the PA. Results from each of the individual cases can be found in the appropriate individual CRA-2014 PA analysis packages. Citations for this additional documentation are included in the references section of this appendix, and are indicated in the list below.

- Unit Loading Calculation (Kicker and Zeitler 2013a)
- Inventory Screening Analysis (Kicker and Zeitler 2013b)
- Parameter Sampling (Kirchner 2013a)
- Salado Flow (Camphouse 2013c)
- Direct Brine Release Volumes (Malama 2013)
- Cuttings, Cavings, and Spallings (Kicker 2013)
- Radionuclide Transport (Kim 2013a)
- Actinide Mobilization (Kim 2013b)
- CCDF Normalized Releases (Zeitler 2013)
- Run Control (Long 2013)

PA-1.1.1 Replacement of Option D with the ROMPCS

The WIPP waste panel closures comprise a feature of the repository that has been represented in the WIPP PA regulatory compliance demonstration since the CCA (U.S. DOE 1996). The 1998 rulemaking that certified the WIPP to receive transuranic (TRU) waste required the DOE to implement the Option D PCS at the WIPP. Following the selection of the Option D panel closure design in 1998, the DOE has reassessed the engineering of the panel closure and established a revised design which is simpler, cheaper, easier to construct, and equally effective at performing its operational period isolating function. The DOE has submitted a planned change request to the EPA requesting that EPA modify Condition 1 of the Final Certification Rulemaking for 40 CFR Part 194 (U.S. EPA 1998a) for the WIPP, and that a revised panel closure design be approved for use in all panels (U.S. DOE 2011a). The revised panel closure design, denoted as the ROMPCS, is comprised of 100 feet of run-of-mine (ROM) salt with barriers at each end. A PA was executed to quantify WIPP repository performance impacts associated with the replacement of the approved Option D PCS design with the ROMPCS (Camphouse et al. 2012a). It was found that long-term WIPP performance with the ROMPCS design is similar to that seen with Option D. The ROMPCS design is implemented in the CRA-2014 PA, and is further discussed in Section PA-4.2.8.

PA-1.1.2 Additional Mined Volume in the Repository North End

Following the recertification of the WIPP in November 2010, the DOE submitted a planned change notice to the EPA that justified additional excavation to the WIPP experimental area (U.S. DOE 2011b) for the Salt Disposal Investigations (SDI) project. A performance assessment was undertaken to determine the impact of the additional excavation on the long-term performance of the facility (Camphouse et al. 2011). Impacts were determined via a direct comparison to results obtained in the CRA-2009 PABC. It was found that total normalized releases were indistinguishable from those obtained in the CRA-2009 PABC, and remained below regulatory release limits. After reviewing the DOE proposal and written responses to questions related to the effects of increasing the mined area, the EPA found that the mining phase of the SDI activities will not adversely impact WIPP waste handling activities, air monitoring, disposal operations, or long-term repository performance (U.S. EPA 2011). An additional excavated volume of 60,335 m^3 in the WIPP experimental area is included in the CRA-2014 PA Salado flow model in an identical fashion to that done in Camphouse et al. (Camphouse et al. 2011).

PA-1.1.3 Refinement to the Probability of Encountering Pressurized Brine

Penetration into a region of pressurized brine during a WIPP drilling intrusion can have significant consequences with respect to releases. The WIPP PA parameter GLOBAL:PBRINE (hereafter PBRINE) is used to specify the probability that a drilling intrusion into the

excavated region of the repository encounters a region of pressurized brine below the repository. Parameter PBRINE has historically been an uncertain parameter in the WIPP PA, and its initial development was the result of an analysis of Time Domain Electromagnetics (TDEM) data (Rechard et al. 1991; Peake 1998). A framework that provides a quantitative argument for refinement of parameter PBRINE has been developed since the CRA-2009 PABC (Kirchner et al. 2012). The refinement of PBRINE results from a re-examination of the TDEM data while also including a greatly expanded set of drilling data for locations adjacent to the WIPP site than were available when the original analysis was performed in 1998. The refinement is based on a sub-region that has a high-density cluster of drilling intrusions. The resulting subset of data is used to provide a conservative estimate of the probability of brine pocket intrusion based solely on the drilling data and to estimate a probability of encountering a brine pocket given that a well is drilled into a TDEM-identified region, that is a region with high conductivity. The distribution for PBRINE that results from this framework is used in the CRA-2014 PA, and is listed in Kicker and Herrick (Kicker and Herrick 2013), Table 4.

PA-1.1.4 Refinement to the Corrosion Rate of Steel

The interaction of steel in the WIPP with repository brines will result in the formation of hydrogen (H_2) gas due to anoxic corrosion of the metal. The rate of H_2 gas generation will depend on the corrosion rate and the type of corrosion products formed. Wang and Brush (Wang and Brush 1996a) provided estimates of gas-generation parameters for the long-term WIPP PA based on experimental work of Telander and Westerman (1997). A new series of steel and lead corrosion experiments has been conducted with the aim of determining steel and lead corrosion rates under WIPP-relevant conditions. Telander and Westerman measured H_2 generation rates directly and from those measurements were able to calculate metal corrosion rates. In contrast, the new experiments directly measure metal corrosion rates. A description of the new experiments and the use of their results to determine an updated steel corrosion rate are presented in Roselle (Roselle 2013). The WIPP PA parameter STEEL:CORRMCO2 represents the anoxic steel corrosion rate for brine-inundated steel in the absence of microbially produced carbon dioxide (CO_2). Based on the newly obtained experimental corrosion data and its subsequent analysis, Roselle (Roselle 2013) recommends that both the distribution type and values for parameter STEEL:CORRMCO2 be changed to reflect the new experimental data. The revised steel corrosion parameter is used in the CRA-2014 PA, and is listed in Kicker and Herrick (Kicker and Herrick 2013), Table 4.

PA-1.1.5 Refinement to the Effective Shear Strength of WIPP Waste

The WIPP PA includes scenarios in which human intrusion results in a borehole intersecting the repository. During the intrusion, drilling mud flowing up the borehole will apply a hydrodynamic shear stress on the borehole wall. Erosion of the wall material can occur if this stress is high enough, resulting in a release of radionuclides being carried up the borehole with the drilling mud. In this intrusion event, the drill bit would penetrate repository waste, and the drilling mud would flow up the borehole in a predominately vertical direction. In order to experimentally simulate these conditions, a flume was designed and constructed. In the flume experimental apparatus, eroding fluid enters a vertical channel from the bottom and flows past a specimen of surrogate WIPP waste. Experiments were conducted to determine the erosive impact on surrogate waste materials that were developed to represent WIPP waste that is 50%, 75%, and 100% degraded by weight. A description of the vertical flume, the experiments conducted in it, and conclusions to be drawn from those experiments are discussed in Herrick et al. (Herrick et al. 2012). The WIPP PA parameter BOREHOLE:TAUFAIL is used to represent the effective shear strength for erosion of WIPP waste. Based on experimental results that realistically simulate the effect of a drilling intrusion on an accepted surrogate waste material, as well as analyses of existing data, Herrick (Herrick 2013) recommends a refinement to parameter BOREHOLE:TAUFAIL be used in the CRA-2014 PA. The refined distribution used for the effective waste shear strength in the CRA-2014 PA is listed in Kicker and Herrick (Kicker and Herrick 2013), Table 4.

PA-1.1.6 Waste Inventory Update

The waste information used in the CRA-2014 PA is updated from that used in the CRA-2009 PABC calculations. The Performance Assessment Inventory Report (PAIR) - 2012 (Van Soest 2012) was released on November 29, 2012. The PAIR - 2012 contains updated estimates to the anticipated radionuclide content and non-radionuclide constituents, scaled to a full repository, based on inventory information collected through December 31, 2011. The WIPP PA inventory parameters are updated in the CRA-2014 PA to account for this new information. Waste inventory parameters used in the CRA-2014 PA are discussed further in Kicker and Zeitler (Kicker and Zeitler 2013b).

PA-1.1.7 Updated Drilling Rate and Plugging Pattern Parameters

The WIPP regulations require that current drilling practices are assumed for future inadvertent intrusions in WIPP PA. The DOE continues to survey drilling activity in the Delaware Basin in accordance with the criteria established in 40 CFR 194.33. Results for the year 2012 are documented in the 2012 Delaware Basin Monitoring Annual Report (U.S. DOE 2012). Plugging pattern probabilities and the drilling rate are updated in the CRA-2014 PA to include information assembled through year 2012, and are developed in Camphouse (Camphouse 2013d). Drilling rate and plugging pattern probabilities correspond to parameters GLOBAL:LAMBDAD, GLOBAL:ONEPLG, GLOBAL:TWOPLG, and GLOBAL:THREEPLG, and their CRA-2014 PA values are listed in Kicker and Herrick (Kicker and Herrick 2013), Table 38.

PA-1.1.8 Refinement to Repository Water Balance

The saturation and pressure history of the repository are used throughout PA. Along with flow in and out of the repository, the saturation and pressure are influenced by the reaction of materials placed in the repository with the surrounding environment. As part of the review of the CRA-2009, the EPA noted several issues for possible additional investigation, including the potential implementation of a more detailed repository water balance (U.S. EPA 2010b). The repository water balance implementation is refined in the CRA-2014 PA in order to include

the major gas and brine producing and consuming reactions in the existing conceptual model. Development of the revised water balance implementation is given in Clayton (Clayton 2013), and is further discussed in Section PA-4.2.5.

PA-1.1.9 Variable Brine Volume

To date, the minimum brine volume necessary for a DBR has been used as an input to the radionuclide solubility calculation. The entire organic ligand inventory was assumed to be dissolved in the minimum necessary brine volume, and the resulting organic ligand concentrations were then used in the calculation of radionuclide solubilities. As the organic ligand inventory has increased over time, the use of a constant organic ligand concentration in brine that is independent of the actual volume of brine present in the repository has resulted in overall mass-balance errors. For large repository brine volumes, the use of ligand concentrations that correspond to the minimum brine volume necessary for a DBR yields greater quantities of dissolved organics in brine than are present in the waste inventory. The result is higher actinide concentrations in brine than are physically attainable when repository brine volumes are large. As a result, the calculation of baseline radionuclide solubilities is extended in the CRA-2014 so that they are dependent on the concentration of organic ligands, which vary with the actual volume of brine present in the repository (Brush and Domski 2013a). Brine volumes of 1x, 2x, 3x, 4x, and 5x the minimum requisite repository brine volume for a DBR (17,400 m^3) (Clayton 2008b) are used in the calculation of baseline radionuclide solubilities in the CRA-2014 (Brush and Domski 2013b). The organic ligand waste inventory is assumed to be dissolved in each of these multiples of the minimum necessary brine volume. The resulting organic ligand concentrations, now dependent on a range of brine volume, are then used to calculate baseline radionuclide solubilities corresponding to each brine volume. This approach keeps ligand mass constant over realized brine volumes, rather than keeping ligand concentration constant over realized brine volumes. The variable brine volume implementation results in five baseline solubilities for actinides in the +III, +IV, and +V oxidation states, with these baseline solubilities being calculated for both Salado and Castile brines (see materials SOLMOD3, SOLMOD4, and SOLMOD5 in Kicker and Herrick (Kicker and Herrick 2013), Table 27). Radionuclide concentrations prescribed for a DBR volume in a given vector realization are obtained by interpolating between concentrations calculated for the integer multiples of the minimum necessary DBR volume (WIPP Performance Assessment 2010).

PA-1.1.10 Updated Radionuclide Solubilities and Uncertainty

The solubilities of actinide elements are influenced by the chemical components of the waste (for example, organic ligands). With the release of the PAIR - 2012 (Van Soest 2012), updated information on the amount of various chemical components in the waste is available. To incorporate this updated information, parameters used to represent baseline actinide solubilities are updated in the CRA-2014 PA. Baseline radionuclide solubilities are calculated in the CRA-2014 PA using multiples of the minimum brine volume necessary for a DBR to occur, as discussed in Section PA-1.1.9. Additional experimental results have been published in the literature since the CRA-2009 PABC, and this new information is used in the CRA-2014 PA to enhance the uncertainty ranges and probability distributions for actinide solubilities. More discussion of radionuclide solubilities and their associated uncertainties is given in Brush and Domski (Brush and Domski 2013b and Brush and Domski 2013c) and Appendix SOTERM-2014, Section 5.0.

PA-1.1.11 Updated Colloid Parameters

Colloid parameters are updated in the CRA-2014 PA to incorporate recently available data given in Reed et al. (Reed et al. 2013). Actinide colloid enhancement parameters were re-assessed and updated, as appropriate, to reflect recent literature and more extensive WIPP-specific data. The CRA-2014 PA contains no changes to the WIPP colloid model developed for the CCA.

PA-2.0 Overview and Conceptual Structure of the PA

Because of the amount and complexity of the material presented in Appendix PA-2014, an introductory summary is provided below, followed by detailed discussions of the topics in the remainder of this section, which is organized as follows:

Section PA-2.1 - Overview of PA

Section PA-2.2 - The conceptual structure of the PA used to evaluate compliance with the containment requirements

Section PA-2.3 - The overall methodology used to develop FEPs, the screening methodology applied to the FEPs, the results of the screening process, and the development of the scenarios considered in the system-level consequence analysis

PA-2.1 Overview of Performance Assessment

A demonstration of future repository performance is required by the disposal standards in Part 191. These standards invoke a PA demonstration that potential cumulative releases of radionuclides to the accessible environment over a 10,000-year period after disposal are less than specified limits based on the nature of the materials disposed (section 191.13). The PA is used to determine the effects of all significant processes and events that may affect the disposal system, consider the associated uncertainties of the processes and events, and estimate the probable cumulative releases of radionuclides. The PA analyses supporting this determination must be quantitative and consider uncertainties caused by all significant processes and events that may affect the disposal system, including future inadvertent human intrusion into the repository. A quantitative PA is conducted using a series of coupled computer models in which epistemic parameter uncertainties are addressed by a stratified Monte Carlo sampling procedure on selected input parameters, and uncertainties related to future intrusion events are addressed using simple random sampling.

The foundations of PA are a thorough understanding of the disposal system and the possible future interactions of the repository, waste, and surrounding geology. The DOE's confidence in the results of PA is based in part on the strength of the original research done during site characterization, experimental results used to develop and confirm parameters and models, and robustness of the facility design.

As required by regulation, results of the PA are displayed as CCDFs showing the probability that cumulative radionuclide releases from the disposal system will exceed the values calculated for scenarios considered in the analysis. These CCDFs are calculated using reasonable and, in some cases, conservative conceptual models based on the scientific understanding of the disposal system's behavior. Parameters used in these models are derived from experimental data, field observations, and relevant technical literature. Parameters updated in the CRA-2014 PA are discussed in Section PA-1.1 and summarized in Table PA-1.

PA-2.1.1 Undisturbed Repository Mechanics

An evaluation of undisturbed repository performance, which is defined to exclude human intrusion and unlikely disruptive natural events, is required by regulation (see section 191.15 and section 191.24). Evaluations of past and present natural geologic processes in the region indicate that none has the potential to breach the repository within 10,000 years (see the CCA, Appendix SCR, Section SCR.1). Disposal system behavior is dominated by the coupled processes of rock deformation surrounding the excavation, fluid flow, and waste degradation. Each of these processes can be described independently, but the extent to which they occur is affected by the others.

Rock deformation immediately around the repository begins as soon as an excavation creates a disturbance in the stress field. Stress relief results in some degree of brittle fracturing and the formation of a disturbed rock zone (DRZ), which surrounds excavations in all deep mines including the WIPP repository. For the WIPP, the DRZ is characterized by an increase in permeability and porosity, and it may ultimately extend a few meters (m) from the excavated region. Salt will also deform by creep processes resulting from deviatoric stress, causing the salt to move inward and fill voids. Salt creep will continue until deviatoric stress is dissipated and the system is once again at stress equilibrium (see the CRA-2004, Chapter 6.0, Section 6.4.3.1).

The ability of salt to creep, thereby healing fractures and filling porosity, is one of its fundamental advantages as a medium for geologic disposal of radioactive waste, and one reason it was recommended by the National Academy of Sciences (see the CCA, Chapter 1.0, Section 1.3). Salt creep provides the mechanism for crushed salt compaction in the shaft seal system, yielding properties approaching those of intact salt within 200 years (see the CCA, Appendix SEAL, Appendix D, Section D5.2). Salt creep will also cause the DRZ surrounding the shaft to heal rapidly around the concrete components of the seal system. In the absence of elevated gas pressure in the repository, salt creep would also substantially compact the waste and heal the DRZ around the disposal region. Fluid pressures can become large enough through the combined effect of salt creep reducing pore volumes, and gas generation from waste degradation processes, to maintain significant porosity (greater than 20%) within the disposal room throughout the performance period (see also the CRA-2004, Chapter 6.0, Section 6.4.3).

Characterization of the Salado indicates that fluid flow from the far field does not occur on time scales of interest in the absence of an artificially imposed hydraulic gradient (see the CRA-2004, Chapter 2.0, Section 2.1.3.4 for a description of Salado investigations). This lack of fluid flow is the second fundamental reason for choosing salt as a medium for geologic disposal of radioactive waste. Lack of fluid flow is a result of the extremely low permeability of evaporite rocks that make up the Salado. Excavating the repository has disturbed the natural hydraulic gradient and rock properties, resulting in some fluid flow. Small quantities of interstitial brine present in the Salado move toward regions of low hydraulic potential, and brine seeps are observed in the underground repository. The slow flow of brine from halite into more permeable anhydrite MBs, and then through the DRZ into the repository, is expected to continue as long as the hydraulic potential within the repository is below that of the far field. The repository environment will also include gas, so the fluid flow must be modeled as a two-phase process. Initially, the gaseous phase will consist primarily of air trapped at the time of closure, although other gases may form from waste degradation. In the PA, the gaseous phase pressure will rise due to creep closure, gas generation, and brine inflow, creating the potential for flow from the excavated region (see also the CRA-2004, Chapter 6.0, Section 6.4.3.2).

An understanding of waste degradation processes indicates that the gaseous phase in fluid flow and the repository's pressure history will be far more important than if the initial air were the only gas present. Waste degradation can generate significant additional gas by two processes (see also the CRA-2004, Chapter 6.0, Section 6.4.3.3 for historical perspective):

1. The generation of hydrogen (H_2) gas by anoxic corrosion of steels, other iron (Fe)-based alloys, and aluminum (Al) and Al-based alloys

2. The generation of carbon dioxide (CO_2) and hydrogen sulfide (H_2S) by anaerobic microbial consumption of waste containing cellulosic, plastic, and rubber (CPR) materials

Coupling these gas-generation reactions to fluid-flow and salt-creep processes is complex. Gas generation will increase fluid pressure in the repository, thereby decreasing the hydraulic gradient between the far field and the excavated region and inhibiting the processes of brine inflow. This also reduces the deviatoric stress and will therefore reduce the salt creep. Anoxic corrosion will also consume brine as it breaks down water to oxidize steels and other Fe-based alloys and release H_2. Thus, corrosion has the potential to be a self-limiting process, in that as it consumes all water in contact with steels and other Fe-based alloys, it will cease. Microbial reactions also require water, either in brine or the gaseous phase. In the CRA-2009 PABC, it was assumed that microbial reactions neither consume nor produce water. For the CRA-2014 PA, the same biodegradation pathways are included as implemented in the CRA-2009 PA, but the consumption or generation of water from reactions other than anoxic corrosion are also considered (see Section PA-4.2.5).

The total volume of gas generated by corrosion and microbial consumption may be sufficient to result in repository pressures that approach lithostatic. Sustained pressures above lithostatic are not physically reasonable within the disposal system because the more brittle anhydrite layers are expected to fracture if sufficient gas is present. The conceptual model implemented in the PA causes anhydrite MB permeability and porosity to increase rapidly as pore pressure approaches and exceeds lithostatic. This conceptual model for pressure-dependent

fracturing approximates the hydraulic effect of pressure-induced fracturing and allows gas and brine to move more freely within the MBs at higher pressures (see the CRA-2004, Chapter 6.0, Section 6.4.5.2).

Overall, the behavior of the undisturbed disposal system will result in extremely effective isolation of the radioactive waste. Concrete, clay, and asphalt components of the shaft seal system will provide an immediate and effective barrier to fluid flow through the shafts, isolating the repository until salt creep has consolidated the compacted crushed salt components and permanently sealed the shafts. Around the shafts, the DRZ in halite layers will heal rapidly because the presence of the solid material within the shafts will provide rigid resistance to creep. The DRZ around the shaft, therefore, will not provide a continuous pathway for fluid flow (see the CRA-2004, Chapter 6.0, Section 6.4.4). Similarly, the run-of-mine salt in each panel closure will reconsolidate and resist creep, leading to a build-up of compressive stress which in turn will cause healing of the DRZ locally. In PA, it is conservatively assumed that the DRZ does not heal around either the disposal region or the operations and experimental regions, and pathways for fluid flow may exist indefinitely to the overlying and underlying anhydrite layers (e.g., MB 139 and Anhydrites A and B). Some quantity of brine will be present in the repository under most conditions and may contain actinides mobilized as both dissolved and colloidal species. Gas generation by corrosion and microbial degradation is expected to occur, and will result in elevated pressures within the repository. Fracturing due to high gas pressures may enhance gas and brine migration from the repository, but gas transport will not contribute to the release of actinides from the disposal system. Brine flowing out of the waste disposal region through anhydrite layers may transport actinides as dissolved and colloidal species. However, the quantity of actinides that may reach the accessible environment boundary through the interbeds during undisturbed repository performance is insignificant and has no effect on the compliance determination. In addition, no migration of radionuclides is expected to occur vertically through the Salado (see Section PA-7.0, and Kim (2013a)).

PA-2.1.2 Disturbed Repository Mechanics

The WIPP PA is required by the performance standards to consider scenarios that include intrusions into the repository by inadvertent and intermittent drilling for resources. The probability of these intrusions is based on a future drilling rate. This rate was calculated using the method outlined in Section 33, which analyzes the past record of drilling events in the Delaware Basin. Active institutional controls (AICs) are assumed to prevent intrusion during the first 100 years after closure (section 194.41). Future drilling practices are assumed to be the same as current practice, also consistent with regulatory criteria. These practices include the type and rate of drilling, emplacement of casing in boreholes, and the procedures implemented when boreholes are plugged and abandoned (section 194.33).

Human intrusion by drilling may cause releases from the disposal system through five mechanisms:

1. Cuttings, which include material intersected by the rotary drilling bit

2. Cavings, which include material eroded from the borehole wall during drilling

3. Spallings, which include solid material carried into the borehole during rapid depressurization of the waste disposal region

4. DBRs, which include contaminated brine that may flow to the surface during drilling

5. Long-term brine releases, which include the contaminated brine that may flow through a borehole after it is abandoned

The first four mechanisms immediately follow an intrusion event and are collectively referred to as direct releases. The accessible environment boundary for these releases is the ground surface. The fifth mechanism, actinide transport by long-term groundwater flow, begins when concrete plugs are assumed to degrade in an abandoned borehole and may continue throughout the regulatory period. The accessible environment boundary for these releases is the lateral subsurface limit of the controlled area (CRA-2004, Chapter 6.0, Section 6.0.2.3).

Repository conditions prior to intrusion correspond to those of the undisturbed repository. As an intrusion provides a pathway for radionuclides to reach the ground surface and enter the geological units above the Salado, additional processes are included to model the disturbed repository. These processes include the mobilization of radionuclides as dissolved and colloidal species in repository brine and groundwater flow, and subsequent actinide transport in the overlying units. Flow and transport in the Culebra are of particular interest because it is the most transmissive unit above the repository. Thus, the Culebra is a potential pathway for lateral migration of contaminated brine in the event of a drilling intrusion accompanied by significant flow up the intrusion borehole (see the CRA-2004, Chapter 6.0, Section 6.4.6.2).

PA-2.1.2.1 Cuttings and Cavings

In a rotary drilling operation, the volume of material brought to the surface as cuttings is calculated as the cylinder defined by the thickness of the unit and the diameter of the drill bit. The quantity of radionuclides released as cuttings is therefore a function of the activity of the intersected waste and the diameter of the intruding drill bit. The DOE uses a constant value of 0.31115 m (12.25 inches [in]), consistent with bits currently used at the WIPP depth in the Delaware Basin (see the CRA-2004, Chapter 6.0, Section 6.4.12.5). The intersected waste activity may vary depending on the type of waste intersected. The DOE considers random penetrations into remote-handled transuranic (RH-TRU) waste and each of the 451 different waste streams (see Kicker and Zeitler 2013a) identified for contact-handled transuranic (CH-TRU) waste.

The volume of particulate material eroded from the borehole wall by the drilling fluids and brought to the surface as cavings may be affected by the drill bit diameter, effective shear resistance of the intruded material, speed of the drill bit, viscosity of the drilling fluid and rate at which it is circulated in the borehole, and other properties related to the drilling process. During the intrusion, drilling mud flowing up the borehole will apply a hydrodynamic shear stress on the borehole wall. Erosion of the wall material can occur if this stress is high enough,

resulting in a release of radionuclides being carried up the borehole with the drilling mud. In this intrusion event, the drill bit would penetrate repository waste, and the drilling mud would flow up the borehole in a predominately vertical direction. In order to experimentally simulate these conditions, a flume was designed and constructed (Herrick et al. 2012). In the flume experimental apparatus, eroding fluid enters a vertical channel from the bottom and flows past a specimen of surrogate WIPP waste. Experiments were conducted to determine the erosive impact on surrogate waste materials that were developed to represent WIPP waste that is 50%, 75%, and 100% degraded by weight. The DOE used newly available data from these experiments to develop the effective shear strength of WIPP waste in the CRA-2014 PA (Camphouse et al. 2013). The quantity of radionuclides released as cavings depends on the volume of eroded material and its activity, which is treated in the same manner as the activity of cuttings (see also Section PA-4.5 and Section PA-6.8.2.1).

PA-2.1.2.2 Spallings

Unlike releases from cuttings and cavings, which occur with every modeled borehole intrusion, spalling releases can only occur if pressure in the waste-disposal region is sufficiently high (greater than 10 megapascals (Mpa)). At these high pressures, gas flow toward the borehole may be sufficiently rapid to cause additional solid material to enter the borehole. If spalling occurs, the volume of spalled material will be affected by the physical properties of the waste, such as its tensile strength and particle diameter. Since the CCA, a revised conceptual model for the spallings phenomena has been developed (see Appendix PA-2004, Section PA-4.6 , and Attachment MASS-2004, Section MASS-16.1.3). Model development, execution, and sensitivity studies necessitated implementing parameter values pertaining to waste characteristics, drilling practices, and physics of the process. The parameter range for particle size was derived by expert elicitation (Carlsbad Area Office Technical Assistance Contractor 1997).

The quantity of radionuclides released as spalled material depends on the volume of spalled waste and its activity. Because spalling may occur at a greater distance from the borehole than cuttings and cavings, spalled waste is assumed to have the volume-averaged activity of CH-TRU waste, rather than the sampled activities of individual waste streams. The low permeability of the region surrounding the RH-TRU waste means it is isolated from the spallings process and does not contribute to the volume or activity of spalled material (see also Section PA-4.6 and Section PA-6.8.2.2 for further description of the spallings model).

PA-2.1.2.3 Direct Brine Flow

Radionuclides may be released to the accessible environment if repository brine enters the borehole during drilling and flows to the ground surface. The quantity of radionuclides released by direct brine flow depends on the volume of brine reaching the ground surface and the concentration of radionuclides contained in the brine. DBRs will not occur if repository pressure is below the hydrostatic pressure in the borehole, assumed to be 8 MPa in the WIPP PA. At higher repository pressures, mobile brine present in the repository will flow toward the borehole. If the volume of brine flowing from the repository into the borehole is small, it will not affect the drilling operation, and flow may continue until the driller reaches the base of the evaporite section and installs casing in the borehole (see also Section PA-4.7 and Section PA-6.8.2.3).

PA-2.1.2.4 Mobilization of Actinides in Repository Brine

Actinides may be mobilized in repository brine in two principal ways:

1. As dissolved species
2. As colloidal species

The solubilities of actinides depend on their oxidation states, with the more reduced forms (for example, III and IV oxidation states) being less soluble than the oxidized forms (V and VI). Conditions within the repository will be strongly reducing because of large quantities of metallic Fe in the steel containers and the waste, and-in the case of plutonium (Pu)-only the lower-solubility oxidation states (Pu(III) and Pu (IV)) will persist. Microbial activity will also help create reducing conditions. Solubilities also vary with pH. The DOE is therefore emplacing MgO in the waste-disposal region to ensure conditions that reduce uncertainty and establish low actinide solubilities. MgO consumes CO_2 and buffers pH, lowering actinide solubilities in the WIPP brines (see Appendix SOTERM-2014, Section SOTERM-2.3.2 and Appendix MgO-2014, Section MgO-5.1). Solubilities in the PA are based on the chemistry of brines that might be present in the waste-disposal region, reactions of these brines with the MgO engineered barrier, and strongly reducing conditions produced by anoxic corrosion of steels and other Fe-based alloys.

The waste contains organic ligands that could increase actinide solubilities by forming complexes with dissolved actinide species. However, these organic ligands also form complexes with other dissolved metals, such as magnesium (Mg), calcium (Ca), Fe, lead (Pb), vanadium (V), chromium (Cr), manganese (Mn), and nickel (Ni), that will be present in repository brines due to corrosion of steels and other Fe-based alloys. The CRA-2014 PA speciation and solubility calculations include the effect of organic ligands but not the beneficial effect of competition with Fe, Pb, V, Cr, Mn, and Ni (Appendix SOTERM-2014, Section SOTERM-2.3.6 and Section SOTERM-4.6, and Brush and Domski (Brush and Domski 2013a)).

Colloidal transport of actinides has been examined, and four types of colloids have been determined to represent the possible behavior at the WIPP. These include microbial colloids, humic substances, actinide intrinsic colloids, and mineral fragments. Concentrations of actinides mobilized as these colloidal forms are included in the estimates of total actinide concentrations used in PA (see Appendix SOTERM-2014, Section SOTERM-3.9).

PA-2.1.2.5 Long-Term Brine Flow up an Intrusion Borehole

Long-term releases to the ground surface or groundwater in the Rustler Formation (hereafter referred to as the Rustler) or overlying units may occur after the borehole has been plugged and abandoned. In keeping with regulatory criteria, borehole plugs are assumed to have properties consistent with current practice in the basin. Thus, boreholes are assumed to have concrete plugs emplaced at various locations. Initially, concrete plugs effectively limit fluid flow in the borehole. However, under most circumstances, these plugs cannot be expected to remain fully effective indefinitely. For the purposes of PA, discontinuous borehole plugs above the repository are assumed to degrade 200 years after emplacement. From then on, the borehole is assumed to fill with a silty-sand-like material containing degraded concrete, corrosion products from degraded casing, and material that sloughs into the hole from the walls. Of six possible plugged borehole configurations in the Delaware Basin, three are considered either likely or adequately representative of other possible configurations; one configuration (a two-plug configuration) is explicitly modeled in the flow and transport model (see Section PA-3.7 and Appendix MASS-2014, Section MASS-15.3).

If sufficient brine is available in the repository, and if pressure in the repository is higher than in the overlying units, brine may flow up the borehole following plug degradation. In principle, this brine could flow into any permeable unit or to the ground surface if repository pressure were high enough. For modeling purposes, brine is allowed to flow only into the higher-permeability units and to the surface. Lower-permeability anhydrite and mudstone layers in the Rustler are treated as if they were impermeable to simplify the analysis while maximizing the amount of flow into units where it could potentially contribute to disposal system releases. Model results indicate that essentially all flow occurs into the Culebra, which has been recognized since the early stages of site characterization as the most transmissive unit above the repository and the most likely pathway for subsurface transport (see also the CRA-2004, Chapter 2.0, Section 2.2.1.4.1.2).

PA-2.1.2.6 Groundwater Flow in the Culebra

Site characterization activities in the units above the Salado have focused on the Culebra. These activities have shown that the direction of groundwater flow in the Culebra varies somewhat regionally, but in the area that overlies the repository, flow is southward. These characterization and modeling activities conducted in the units above the Salado confirm that the Culebra is the most transmissive unit above the Salado. The Culebra is the unit into which actinides are likely to be introduced from long-term flow up an abandoned borehole. Regional variation in the Culebra's groundwater flow direction is influenced by the transmissivity observed, as well as the lateral (facies) changes in the lithology of the Culebra in the groundwater basin where the WIPP is located. Groundwater flow in the Culebra is affected by the presence of fractures, fracture fillings, and vuggy pore features (see Appendix HYDRO-2014 and the CRA-2004, Chapter 2.0, Section 2.1.3.5). Other laboratory and field activities have focused on the behavior of dissolved and colloidal actinides in the Culebra. Members of the public suggested that karst formation and processes may be a possible alternative conceptual model for flow in the Rustler. Karst may be thought of as voids in near-surface or subsurface rock created by water flowing when rock is dissolved. Public comments stated that karst could develop interconnected "underground rivers" that may enhance the release of radioactive materials from the WIPP. Because of this comment, the EPA required the DOE to perform a thorough reexamination of all historical data, information, and reports, both those by the DOE and others, to determine if karst features or development had been missed during previous work done at the WIPP. The DOE's findings are summarized in Lorenz (Lorenz 2006a and Lorenz 2006b). The EPA also conducted a thorough reevaluation of karst and of the work done during the CCA (U.S. EPA 2006a). The EPA's reevaluation of historical evidence and recent work by the DOE did not show even the remotest possibility of an "underground river" near the WIPP, nor did it change the CCA conclusions. Therefore, the EPA believed karst was not a viable alternative model at the WIPP. For a more complete discussion of the reevaluation of karst, see CARD 14/15 (U.S. EPA 2006b) and Lorenz (Lorenz 2006a and Lorenz 2006b).

Basin-scale regional modeling of three-dimensional groundwater flow in the units above the Salado demonstrates that it is appropriate, for the purposes of estimating radionuclide transport, to conceptualize the Culebra as a two-dimensional confined aquifer (see the CRA-2004, Chapter 2.0, Section 2.2.1.1). Uncertainty in the flow field is incorporated by using 100 different geostatistically based T-fields, each of which is consistent with available head and transmissivity data and with updated information on geologic factors potentially affecting transmissivity in the Culebra (see TFIELD-2014).

Groundwater flow in the Culebra is modeled as a steady-state process, but two mechanisms considered in the PA could affect flow in the future. Potash mining in the McNutt Potash Zone (hereafter referred to as the McNutt) of the Salado, which occurs now in the Delaware Basin outside the controlled area and may continue in the future, could affect flow in the Culebra if subsidence over mined areas causes fracturing or other changes in rock properties (see the CRA-2004, Chapter 6.0, Section 6.3.2.3). Climatic changes during the next 10,000 years may also affect groundwater flow by altering recharge to the Culebra (see the CRA-2004, Chapter 6.0, Section 6.4.9, and the CCA, Appendix CLI).

Consistent with regulatory criteria of section 194.32, mining outside the controlled area is assumed to occur in the near future, and mining within the controlled area is assumed to occur with a probability of 1 in 100 per century (adjusted for the effectiveness of AICs during the first 100 years after closure). Consistent with regulatory guidance, the effects of mine subsidence are incorporated in PA by increasing the transmissivity of the Culebra over the areas identified as mineable by a factor sampled from a uniform distribution between 1 and 1000 (U.S. EPA 1996a, p. 5229). T-fields used in PA are therefore adjusted and steady-state flow fields calculated accordingly, once for mining that occurs only outside the controlled area, and once for mining that occurs both inside and outside the controlled area (Appendix TFIELD-2014, Section 9.0). Mining outside the controlled area is considered in both undisturbed and disturbed repository performance.

The extent to which the climate will change during the next 10,000 years and how such change will affect groundwater flow in the Culebra are uncertain. Regional three-dimensional modeling of groundwater flow in the units above the Salado indicates that flow velocities in the Culebra may increase by a factor of 1 to 2.25 for reasonably possible future climates (see the CCA, Appendix CLI). This uncertainty is incorporated in PA by scaling the calculated steady-state-specific discharge within the Culebra by a sampled parameter within this range.

PA-2.1.2.7 Actinide Transport in the Culebra

Field tests have shown that the Culebra is best characterized as a double-porosity medium for estimating contaminant transport in groundwater (see the CRA-2004, Chapter 2.0, Section 2.2.1.4.1.2, and Appendix HYDRO-2014, Section 7.1). Groundwater flow and advective transport of dissolved or colloidal species and particles occurs primarily in a small fraction of the rock's total porosity and corresponds to the porosity of open and interconnected fractures and vugs. Diffusion and slower advective flow occur in the remainder of the porosity, which is associated with the low-permeability dolomite matrix. Transported species, including actinides (if present), will diffuse into this porosity.

Diffusion from the advective porosity into the dolomite matrix will retard actinide transport through two mechanisms. Physical retardation occurs simply because actinides that diffuse into the matrix are no longer transported with the flowing groundwater. Transport is interrupted until the actinides diffuse back into the advective porosity. In situ tracer tests have demonstrated this phenomenon (Meigs et al. 2000). Chemical retardation also occurs within the matrix as actinides are sorbed onto dolomite grains. The relationship between sorbed and liquid concentrations is assumed to be linear and reversible. The distribution coefficients (K_ds) that characterize the extent to which actinides will sorb on dolomite were based on experimental data (see the CRA-2004, Chapter 6.0, Section 6.4.6.2).

PA-2.1.2.8 Intrusion Scenarios

Human intrusion scenarios evaluated in the PA include both single intrusion events and combinations of multiple boreholes. Two different types of boreholes are considered: those that penetrate a region of pressurized brine in the underlying Castile Formation (hereafter referred to as the Castile), and those that do not.

The presence of brine pockets under the repository is speculative, but on the basis of current information cannot be ruled out. A pressurized brine pocket was encountered at the WIPP-12 borehole within the controlled area to the north of the disposal region, and other pressurized brine pockets associated with regions of deformation in the Castile have been encountered elsewhere in the Delaware Basin (see the CRA-2004, Chapter 2.0, Section 2.2.1.2.2). In the CRA-2009 PABC, the DOE represented the probability of encountering a pressurized brine pocket during a drilling intrusion as being uncertain, with a range from 0.01 to 0.60. A framework that provides a quantitative argument for refinement of this probability has been developed since the CRA-2009 PABC (Kirchner et al. 2012). The probability of a pressurized brine pocket encounter that results from this refinement is represented as an uncertain parameter, with a range from 0.06 to 0.19.

The primary consequence of penetrating a pressurized brine pocket is the supply of an additional source of brine beyond that which might flow into the repository from the Salado. Direct releases at the ground surface resulting from the first repository intrusion would be unaffected by additional Castile brine, even if it flowed to the surface, because brine moving straight up a borehole will not significantly mix with waste. However, the presence of Castile brine could significantly increase radionuclide releases in two ways. First, the volume of contaminated brine that could flow to the surface may be greater for a second or subsequent intrusion into a repository that has already been connected by a previous borehole to a Castile reservoir. Second, the volume of contaminated brine that may flow up an abandoned borehole after plug degradation may be greater for combinations of two or more boreholes that intrude the same panel if one of the boreholes penetrates a pressurized brine pocket. Both processes are modeled in PA.

PA-2.1.3 Compliance Demonstration Method

The DOE uses PA to demonstrate continued regulatory compliance of the WIPP. The PA process comprehensively considers the FEPs relevant to disposal system performance (see Appendix SCR-2014). Those FEPs shown by screening analyses to potentially affect performance are included in quantitative calculations using a system of coupled computer models to describe the interaction of the repository with the natural system, both with and without human intrusion. Uncertainty in parameter values is incorporated in the analysis by a Monte Carlo approach, in which multiple simulations (or realizations) are completed using sampled values for the imprecisely known input parameters (see the CRA-2004, Chapter 6.0, Section 6.1.5). Distribution functions characterize the state of knowledge for these parameters, and each realization of the modeling system uses a different set of sampled input values. A sample size of 300 results in 300 different values of each parameter. Thus, there are 300 different sets (vectors) of input parameter values. These 300 vectors are divided among 3 replicates. Quality assurance activities demonstrate that the parameters, software, and analysis used in PA are the result of a rigorous process conducted under controlled conditions (section 194.22).

Of the FEPs considered, exploratory drilling for natural resources has been identified as the only disruption with sufficient likelihood and consequence of impacting releases from the repository. For each vector of parameters values, 10,000 possible futures are constructed, where a single future is defined as a series of intrusion events that occur randomly in space and time (Section PA-2.2). Each of these futures is assumed to have an equal probability of occurring; hence a probability of 0.0001. Cumulative radionuclide releases from the disposal system are calculated for each future, and CCDFs are constructed by sorting the releases from smallest to largest and then summing the probabilities across the future. Mean CCDFs are then computed for the three replicates of sampled parameters (Section PA-2.2). The key metric for regulatory compliance is the overall mean CCDF for total releases in combination with its confidence limits (CL).

PA-2.2 Conceptual Structure of the PA

This section outlines the conceptual structure of the WIPP PA with an emphasis on how its development is guided by regulatory requirements. The conceptual structure of the CRA-2014 PA is identical to that of the CRA-2009 PA.

PA-2.2.1 Regulatory Requirements

The methodology employed in PA derives from the EPA's standard for the geologic disposal of radioactive waste, Environmental Radiation Protection Standards for the Management and Disposal of Spent Nuclear Fuel, High-Level and Transuranic Radioactive Wastes (Part 191) (U.S. EPA 1993), which is divided into three subparts. Subpart A applies to a disposal facility prior to decommissioning and establishes

standards for the annual radiation doses to members of the public from waste management and storage operations. Subpart B applies after decommissioning and sets probabilistic limits on cumulative releases of radionuclides to the accessible environment for 10,000 years (section 191.13) and assurance requirements to provide confidence that section 191.13 will be met (section 191.14). Subpart B also sets limits on radiation doses to members of the public in the accessible environment for 10,000 years of undisturbed repository performance (section 191.15). Subpart C limits radioactive contamination of groundwater for 10,000 years after disposal (section 191.24). The DOE must demonstrate a reasonable expectation that the WIPP will continue to comply with the requirements of Part 191 Subparts B and C as a necessary condition for WIPP recertification.

The following is the central requirement in Part 191 Subpart B, and the primary determinant of the PA methodology (U.S. EPA 1985, p. 38086).

> § 191.13 Containment Requirements:
>
> (a) Disposal systems for spent nuclear fuel or high-level or transuranic radioactive wastes shall be designed to provide a reasonable expectation, based upon performance assessments, that cumulative releases of radionuclides to the accessible environment for 10,000 years after disposal from all significant processes and events that may affect the disposal system shall:
>
> (1) Have a likelihood of less than one chance in 10 of exceeding the quantities calculated according to Table 1 (Appendix A); and
>
> (2) Have a likelihood of less than one chance in 1,000 of exceeding ten times the quantities calculated according to Table 1 (Appendix A).
>
> (b) Performance assessments need not provide complete assurance that the requirements of 191.13(a) will be met. Because of the long time period involved and the nature of the events and processes of interest, there will inevitably be substantial uncertainties in projecting disposal system performance. Proof of the future performance of a disposal system is not to be had in the ordinary sense of the word in situations that deal with much shorter time frames. Instead, what is required is a reasonable expectation, on the basis of the record before the implementing agency, that compliance with 191.13(a) will be achieved.

Section 191.13 (a) refers to "quantities calculated according to Table 1 (Appendix A)," which means a normalized radionuclide release to the accessible environment based on the type of waste being disposed, the initial waste inventory, and the size of release that may occur (U.S. EPA 1985, Appendix A). Table 1 of Appendix A specifies allowable releases (i.e., release limits) for individual radionuclides and is reproduced as Table PA-2. The WIPP is a repository for TRU waste, which is defined as "waste containing more than 100 nanocuries of alpha-emitting TRU isotopes, with half-lives greater than twenty years, per gram of waste" (U.S. EPA 1985, p. 38084). The normalized release R for TRU waste is defined by

$$R = \sum_i \left(\frac{Q_i}{L_i} \right) \left(\frac{1 \times 10^6 \text{ Ci}}{C} \right) \quad \text{(PA.1)}$$

where Q_i is the cumulative release of radionuclide i to the accessible environment during the 10,000-year period following closure of the repository (curies [Ci]), L_i is the release limit for radionuclide i given in Table PA-2 (Ci), and C is the amount of TRU waste emplaced in the repository (Ci). In the CRA-2014 PA, $C = 2.06 \times 10^6$ Ci (Kicker and Zeitler 2013b, Section 2). Further, "accessible environment" means (1) the atmosphere, (2) land surfaces, (3) surface waters, (4) oceans, and (5) all of the lithosphere beyond the controlled area. "Controlled area" means (1) a surface location, to be identified by passive institutional controls (PICs), that encompasses no more than 100 square kilometers (km^2) and extends horizontally no more than 5 kilometers (km) in any direction from the outer boundary of the original radioactive waste's location in a disposal system, and (2) the subsurface underlying such a location (section 191.12).

Table PA- 2. Release Limits for the Containment Requirements (U.S. EPA 1985, Appendix A, Table 1)

Radionuclide	Release Limit Li per 1000 MTHM[a] or Other Unit of Waste[b]
Americium-241 or -243	100
Carbon-14	100
Cesium-135 or -137	1,000
Iodine-129	100
Neptunium-237	100
Pu-238, -239, -240, or -242	100
Radium-226	100
Strontium-90	1,000
Technetium-99	10,000
Thorium (Th) -230 or -232	10
Tin-126	1,000
Uranium (U) -233, -234, -235, -236, or -238	100
Any other alpha-emitting radionuclide with a half-life greater than 20 years	100
Any other radionuclide with a half-life greater than 20 years that does not emit alpha particles	1,000

Radionuclide	Release Limit Li per 1000 MTHM[a] or Other Unit of Waste[b]

a Metric tons of heavy metal (MTHM) exposed to a burnup between 25,000 megawatt-days (MWd) per metric ton of heavy metal (MWd/MTHM) and 40,000 MWd/MTHM.
b An amount of TRU waste containing one million Ci of alpha-emitting TRU radionuclides with half-lives greater than 20 years.

PAs are the basis for addressing the containment requirements. To help clarify the intent of Part 191, the EPA promulgated 40 CFR Part 194, Criteria for the Certification and Recertification of the Waste Isolation Pilot Plant's Compliance with the Part 191 Disposal Regulations. There, an elaboration on the intent of section 191.13 is prescribed.

> § 194.34 Results of performance assessments.
>
> (a) The results of performance assessments shall be assembled into "complementary, cumulative distributions functions" (CCDFs) that represent the probability of exceeding various levels of cumulative release caused by all significant processes and events.
>
> (b) Probability distributions for uncertain disposal system parameter values used in performance assessments shall be developed and documented in any compliance application.
>
> (c) Computational techniques, which draw random samples from across the entire range of the probability distributions developed pursuant to paragraph (b) of this section, shall be used in generating CCDFs and shall be documented in any compliance application.
>
> (d) The number of CCDFs generated shall be large enough such that, at cumulative releases of 1 and 10, the maximum CCDF generated exceeds the 99th percentile of the population of CCDFs with at least a 0.95 probability.
>
> (e) Any compliance application shall display the full range of CCDFs generated.
>
> (f) Any compliance application shall provide information which demonstrates that there is at least a 95% level of statistical confidence that the mean of the population of CCDFs meets the containment requirements of § 191.13 of this chapter.

The DOE's PA methodology uses information about the disposal system and waste to evaluate performance over the 10,000-year regulatory time period. To accomplish this task, the FEPs with potential to affect the future of the WIPP are first defined (Section PA-2.3.1). Next, scenarios that describe potential future conditions in the WIPP are formed from logical groupings of retained FEPs (Section PA-2.3.2). The scenario development process results in a probabilistic characterization for the likelihood of different futures that could occur at the WIPP (Section PA-2.2.2). Using the retained FEPs, models are developed to estimate the radionuclide releases from the repository (Section PA-2.2.3). Finally, uncertainty in model parameters is characterized probabilistically (Section PA-2.2.4).

PA-2.2.2 Probabilistic Characterization of Different Futures

As discussed in Section PA-2.3.1, the CCA PA scenario development process for the WIPP identified exploratory drilling for natural resources as the only disruption with sufficient likelihood and consequence of impacting releases from the repository (see the CCA, Appendix SCR). In addition, Part 194 specifies that the occurrence of mining within the LWB must be included in the PA. These requirements have not changed for the CRA-2014 PA. As a result, the projection of releases over the 10,000 years following closure of the WIPP is driven by the nature and timing of intrusion events.

The collection of all possible futures $\mathbf{x}_{st}$ forms the basis for the probability space ($\mathcal{S}_{st}$, $\mathbb{S}_{sc}$, p_{st}) characterizing aleatory uncertainty, where $\mathcal{S}_{st} = \{\mathbf{x}_{st} : \mathbf{x}_{st}$ is a possible future of the WIPP$\}$, $\mathbb{S}_{sc}$ is a suitably restricted collection of sets of futures called "scenarios" (Section PA-3.10), and p_{st} is a probability measure for the elements of $\mathcal{S}_{st}$. A possible future, $\mathbf{x}_{st,i}$, is thus characterized by the collection of intrusion events that occur in that future:

$$\mathbf{x}_{st,i} = [\underbrace{(t_1, e_1, l_1, b_1, p_1, \mathbf{a}_1)}_{1^{st}\text{ intrusion}}, \underbrace{(t_2, e_2, l_2, b_2, p_2, \mathbf{a}_2)}_{2^{nd}\text{ intrusion}}, \ldots, \underbrace{(t_n, e_n, l_n, b_n, p_n, \mathbf{a}_n)}_{n^{th}\text{ intrusion}}, t_{min}] \quad \text{(PA.2)}$$

where

- n is the number of drilling intrusions
- t_j is the time (year) of the j^{th} intrusion
- l_j designates the location of the j^{th} intrusion
- e_j designates the penetration of an excavated or nonexcavated area by the j^{th} intrusion
- b_j designates whether or not the j^{th} intrusion penetrates pressurized brine in the Castile Formation
- p_j designates the plugging procedure used with the j^{th} intrusion (i.e., continuous plug, two discrete plugs, three discrete plugs)
- $\mathbf{a}_j$ designates the type of waste penetrated by the j^{th} intrusion (i.e., no waste, CH-TRU waste, RH-TRU waste and, for CH-TRU waste, the waste streams encountered)
- t_{min} is the time at which potash mining occurs within the LWB

The subscript *st* indicates that aleatory (i.e., stochastic) uncertainty is being considered. The subscript *i* indicates that the future $\mathbf{x}_{st}$ is one of many sample elements from $\mathcal{S}_{st}$.

The probabilistic characterization of n, t_j, l_j, and e_j is based on the assumption that drilling intrusions will occur randomly in time and space at a constant average rate (i.e., follow a Poisson process); the probabilistic characterization of b_j derives from assessed properties of

brine pockets; the probabilistic characterization of $\mathbf{a}_j$ derives from the volumes of waste emplaced in the WIPP in relation to the volume of the repository; and the probabilistic characterization of p_j derives from current drilling practices in the sedimentary basin (i.e., the Delaware Basin) in which the WIPP is located. A vector notation is used for $\mathbf{a}_j$ because it is possible for a given drilling intrusion to miss the waste or to penetrate different waste types (CH-TRU and RH-TRU), as well as to encounter different waste streams in the CH-TRU waste. Further, the probabilistic characterization for t_{min} follows from the criteria in Part 194 that the occurrence of potash mining within the LWB should be assumed to occur randomly in time (i.e., follow a Poisson process with a rate constant of $\lambda_m = 10^{-4}\ \mathrm{yr}^{-1}$), with all commercially viable potash reserves within the LWB extracted at time t_{min}. In practice, the probability measure p_{st} is defined by specifying probability distributions for each component of $\mathbf{x}_{st}$, as discussed further in Section PA-3.0.

PA-2.2.3 Estimation of Releases

Based on the retained FEPs (Section PA-2.3.1), release mechanisms include direct transport of material to the surface at the time of a drilling intrusion (i.e., cuttings, spallings, and brine flow) and release subsequent to a drilling intrusion due to brine flow up a borehole with a degraded plug (i.e., groundwater transport). The quantities of releases are determined by the state of the repository through time, which is determined by the type, timing, and sequence of prior intrusion events. For example, pressure in the repository is an important determinant of spallings, and the amount of pressure depends on whether the drilling events that have occurred penetrated brine pockets and how long prior to the current drilling event the repository was inundated.

Computational models for estimating releases were developed using the retained FEPs; these models are summarized in Figure PA-1. These computational models implement the conceptual models representing the repository system as described in section 194.23 and the mathematical models for physical processes presented in Section PA-4.0. Most of the computational models involve the numerical solution of partial differential equations (PDEs) used to represent processes such as material deformation, fluid flow, and radionuclide transport.

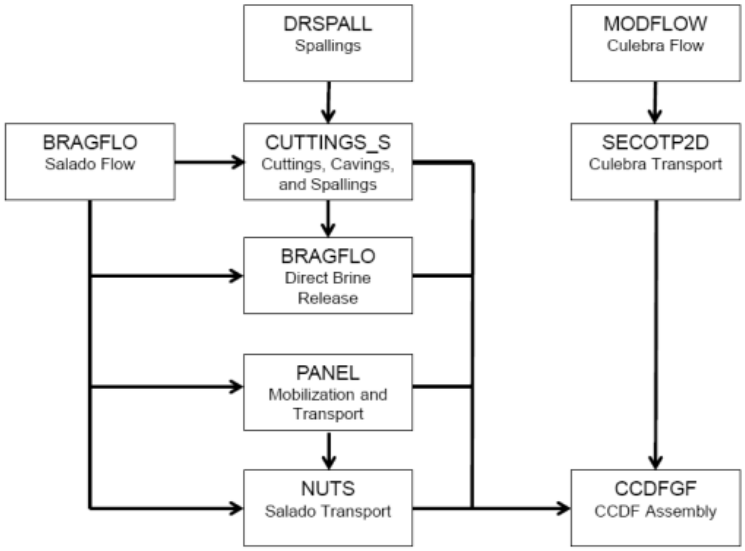

Figure PA- 1. Computational Models Used in PA

The collection of computation models can be represented abstractly as a function $f(\mathbf{x}_{st} \mid \mathbf{v}_{su})$, which quantifies the release that could result from the occurrence of a specific future $\mathbf{x}_{st}$ and a specific set of values for model parameters $\mathbf{v}_{su}$. Because the future of the WIPP is unknown, the values of $f(\mathbf{x}_{st} \mid \mathbf{v}_{su})$ are uncertain. Thus, the probability space $(\mathcal{S}_{st}, \mathbb{S}_{sc}, p_{st})$, together with the function $f(\mathbf{x}_{st} \mid \mathbf{v}_{su})$, give rise to the CCDF specified in section 191.13 (a), as illustrated in Figure PA-2. The CCDF represents the probability that a release from the repository greater than R will be observed, where R is a point on the abscissa (x-axis) of the graph (Figure PA-2).

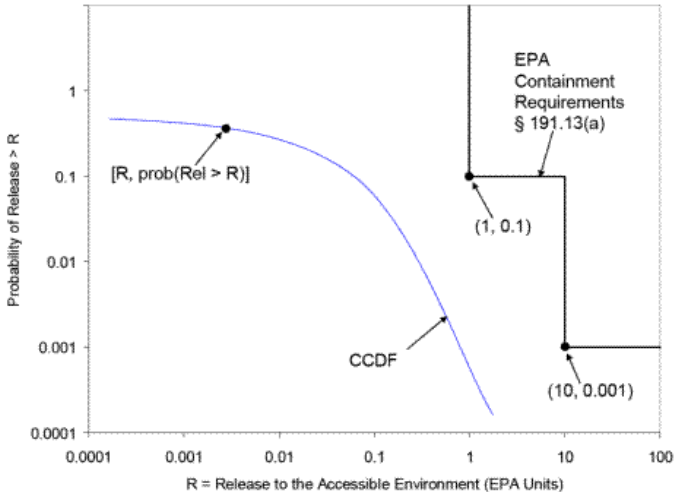

Figure PA- 2. Construction of the CCDF Specified in 40 CFR Part 191 Subpart B

Formally, the CCDF depicted in Figure PA-2 results from an integration over the probability space (S_{st} , $\mathbb{S}_{sc}$, p_{st}):

$$prob(rel > R|\mathbf{v}_{su}) = \int_{S_{st}} \delta_R(f(\mathbf{x}_{st}|\mathbf{v}_{su}))\, d_{st}(\mathbf{x}_{st}|\mathbf{v}_{su})\, dV_{st} \quad \text{(PA.3)}$$

where $\delta_R(f(\mathbf{x}_{st}|\mathbf{v}_{su})) = 1$ if $f(\mathbf{x}_{st}|\mathbf{v}_{su}) > R$, $\delta_R(f(\mathbf{x}_{st}|\mathbf{v}_{su})) = 0$ if $f(\mathbf{x}_{st}|\mathbf{v}_{su}) \le R$, and $d_{st}(\mathbf{x}_{st}|\mathbf{v}_{su})$ is the probability density function associated with the probability space (S_{st} , $\mathbb{S}_{sc}$, p_{st}). In practice, the integral in Equation (PA.3) is evaluated by a Monte Carlo technique, where a random sample $\mathbf{x}_{st,i}$, $i = 1, nR$, (where nR is the number of releases) is generated from S_{st} consistent with the probability distribution p_{st} . Using this random sample, Equation (PA.3) is numerically evaluated as

$$prob(rel > R|\mathbf{v}_{su}) = \int_{S_{su}} \delta_R(f(\mathbf{x}_{st}|\mathbf{v}_{su}))\, d_{st}(\mathbf{x}_{st}|\mathbf{v}_{su})\, dV_{st}$$

$$\cong \sum_{i=1}^{nR} \delta_R(f(\mathbf{x}_{st,i}|\mathbf{v}_{su}))/nR \quad \text{(PA.4)}$$

The models in Figure PA-1 are too complex to permit a closed-form evaluation of the integral in Equation (PA.4) that defines the CCDF specified in Part 191. In the WIPP PA, these probability distribution functions (PDFs) are constructed using Monte Carlo simulation to sample the entire possible set of release outcomes. As long as the sampling is conducted properly and a sufficient number of samples is collected, the PDF of the sample should successfully approximate the PDF of the sample "universe" of all possible releases.

In PA, the number of samples nR used to construct a CCDF is 10,000. However, the models in Figure PA-1 are also too computationally intensive to permit their evaluation for each of these 10,000 futures. Due to this constraint, the models in Figure PA-1 are evaluated for a relatively small number of specific scenarios, and the results of these evaluations are used to construct CCDFs. The representative scenarios are labeled E0, E1, E2, and E1E2, and are defined in Section PA-3.10; the procedure for constructing a CCDF from these scenarios is described in Section PA-6.6.

PA-2.2.4 Probabilistic Characterization of Parameter Uncertainty

If the parameters used in the process-level models of Figure PA-1 were precisely known and if the models could accurately predict the future behavior of the repository, the evaluation of repository performance alone would be sufficient to answer the first three questions related to repository performance. However, the models do not perfectly represent the dynamics of the system and their parameters are not precisely known. Therefore, it is necessary to estimate the confidence one has in the CCDFs being constructed. The confidence in the CCDFs is established using Monte Carlo methods to evaluate how the uncertainty in the model parameters impacts the CCDFs or releases. The probabilistic characterization of the uncertainty in the model parameters is the outcome of the data development effort for the WIPP, summarized in Section 6.0 of Kicker and Herrick (Kicker and Herrick 2013).

Formally, uncertainty in the parameters that underlie the WIPP PA can be characterized by a second probability space (S_{su} , $\mathbb{S}_{sc}$, p_{su}), where the sample space S_{su} is defined by

$S_{su} = \{\mathbf{v}_{su}: \mathbf{v}_{su}$ is a sampled vector of parameter values$\}$ (PA.5)

The subscript *su* indicates that epistemic (i.e., subjective) uncertainty is being considered. An element $\mathbf{v}_{su} \in \mathbf{S}_{su}$ is a vector $\mathbf{v}_{su} = v_{su,1}, v_{su,2}, \ldots, v_{su,N})$ of length *N*, where each element $v_{su,k}$ is an uncertain parameter used in the models to estimate releases. In practice, the probability measure p_{su} is defined by specifying probability distributions for each element of $\mathbf{v}_{su}$, discussed further in Section PA-5.0.

If the actual value for $\mathbf{v}_{su}$ were known, the CCDF resulting from evaluation of Equation (PA.4) could be determined with certainty and compared with the criteria specified in Part 191. However, given the complexity of the WIPP site, the 10,000-year period under consideration, and the state of knowledge about the natural and engineered system, values for $\mathbf{v}_{su}$ are not known with certainty. Rather, the uncertainty in $\mathbf{v}_{su}$ is characterized probabilistically, as described above, leading to a distribution of CCDFs (Figure PA-3), with each CCDF resulting from one of many vectors of values of $\mathbf{v}_{su}$. The uncertainty associated with the parameters is termed epistemic uncertainty, and has been referred to in WIPP PA documentation as subjective uncertainty.

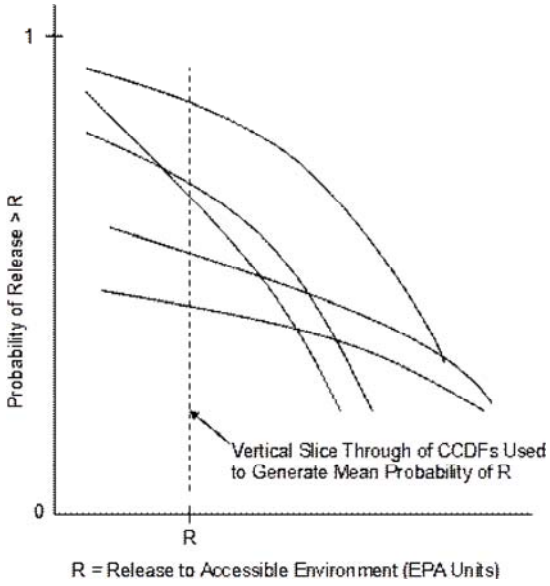

Figure PA- 3. Distribution of CCDFs Resulting from Possible Values for the Sampled Parameters

The WIPP PA uses a Monte Carlo procedure for evaluating the effects of epistemic uncertainty on releases. The procedure involves sampling the distributions assigned to the uncertain parameters and generating a CCDF of releases based on the results of the process-level models generated using those parameters values. By repeating this process many times, a distribution of the CCDFs can be constructed. The requirements of section 191.13 are evaluated, in part, using the mean probability of release. The overall mean probability curve is created by averaging across the CCDFs for releases, i.e., averaging the CCDFs across vertical slices (Figure PA-3) (a formal definition is provided in Helton et al. 1998). In addition, confidence limits on the mean are computed using standard t-statistics. The proximity of these curves to the boundary line in Figure PA-2 indicates the confidence with which Part 191 will be met. Confidence is also established by examining the distribution of the CCDFs in relation to the release limits.

The WIPP PA uses a stratified sampling design called LHS (McKay, Beckman, and Conover 1979) to generate a sample $\mathbf{v}_{su}$, $i = 1, \ldots, nLHS$, from $\mathbf{S}_{su}$ consistent with the probability distribution p_{su}. LHS is an efficient scheme for sampling the range of a distribution using a relatively small sample. Based on order statistics, the sample size of $nLHS = 300$ replicates would provide coverage of 99% of the CCDF distribution with a confidence of 95%.

In Part 194, the EPA decided that the statistical portion of the determination of compliance with Part 191 will be based on the sample mean. The LHS sample sizes should be demonstrated operationally to improve (reduce the size of) the confidence interval for the estimated mean. The underlying principle is to show convergence of the mean (U.S. EPA 1996b, p. 8-41).

The DOE has chosen to demonstrate repeatability of the mean and to address the associated criteria of Part 194 using an operational approach of multiple replication, as proposed by Iman (Iman 1982). The complete set of PA calculations was repeated three times with all aspects of the analysis identical except for the random seed used to initiate the LHS procedure. Thus, PA results are available for 3 replicates, each based on an independent set of 100 LHS vectors drawn from identical distributions for imprecisely known parameters and propagated through an identical modeling system. This technique of multiple replication allows the adequacy of the sample size chosen in the Monte Carlo analysis to be evaluated and provides a suitable measure of confidence in the mean CCDF estimation used to demonstrate compliance with section 191.13 (a).

PA-2.3 PA Methodology

This section addresses scenarios formed from FEPs that were retained for PA calculations, and introduces the specification of scenarios for consequence analysis.

PA-2.3.1 Identification and Screening of FEPs

The EPA has provided criteria concerning the scope of PAs in section 194.32. In particular, criteria relating to the identification of potential processes and events that may affect disposal system performance are provided in section 194.32(e), which states

> Any compliance application(s) shall include information which:
>
> (1) Identifies all potential processes, events or sequences and combinations of processes and events that may occur during the regulatory time frame and may affect the disposal system;
>
> (2) Identifies the processes, events or sequences and combinations of processes and events included in performance assessments; and
>
> (3) Documents why any processes, events or sequences and combinations of processes and events identified pursuant to paragraph (e)(1) of this section were not included in performance assessment results provided in any compliance application.

Section 32 of this application fulfills these criteria by documenting the DOE's identification, screening, and screening results of all potential processes and events consistent with the criteria specified in section 194.32(e). The first two steps in scenario development involve identifying and screening FEPs that are potentially relevant to the performance of the disposal system. The FEPs screening arguments used for the CRA-2014 PA are described in Section 32 and Appendix SCR-2014.

PA-2.3.2 Scenario Development and Selection

Logic diagrams illustrate the formation of scenarios for consequence analysis from combinations of events that remain after FEP screening (Cranwell et al. 1990) (Figure PA-4). Each scenario shown in Figure PA-4 is defined by a combination of occurrence and nonoccurrence for all potentially disruptive events. Disruptive events are defined as those that create new pathways or significantly alter existing pathways for fluid flow and, potentially, radionuclide transport within the disposal system. Each of these scenarios also contains a set of features and nondisruptive events and processes that remain after FEP screening. As shown in Figure PA-4, undisturbed repository performance (UP) and disturbed repository performance (DP) scenarios are considered in consequence modeling for the WIPP PA. The UP scenario is used for compliance assessments (section 194.54 and section 194.55). The M scenario is for future mining within the site boundary. Potash mining outside the site boundary is included in all scenarios. Important aspects of UP and DP scenarios are summarized in this section.

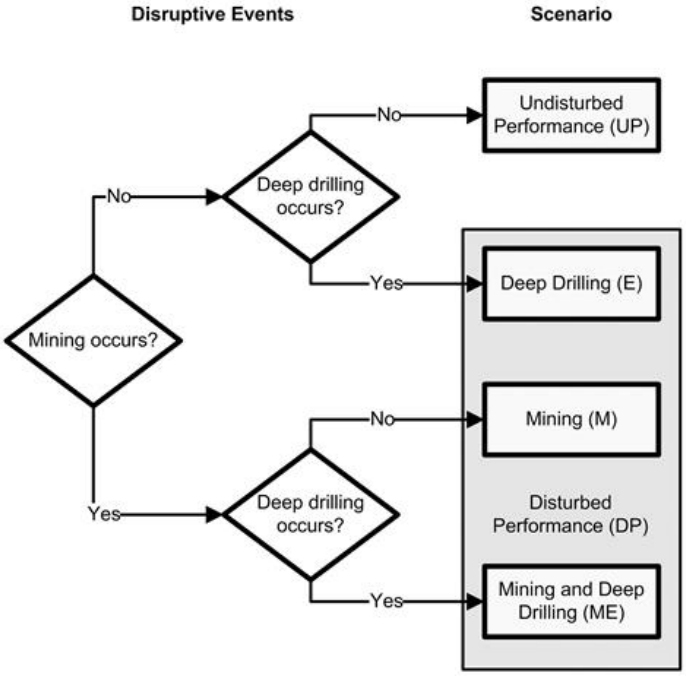

Figure PA- 4. Logic Diagram for Scenario Analysis

PA-2.3.2.1 Undisturbed Repository Performance

The UP scenario is defined in section 191.12 to mean "the predicted behavior of a disposal system, including consideration of the uncertainties in predicted behavior, if the disposal system is not disrupted by human intrusion or the occurrence of unlikely natural events." For compliance assessments with respect to the Individual and Groundwater Protection Requirements (section 191.15; Appendix IGP-2009), it is only necessary to consider the UP scenario. The UP scenario is also considered with DP scenario for PA with respect to the containment requirements (section 191.13).

No potentially disruptive natural events and processes are likely to occur during the regulatory time frame. Therefore, all naturally occurring events and processes retained for scenario construction are nondisruptive and are considered part of the UP scenario. Mining outside the LWB is assumed at the end of AIC for all scenarios. The mining scenario (M) involves future mining within the controlled area. The disturbed repository deep drilling scenario (E) involves at least one deep drilling event that intersects the waste disposal region. The M

scenario and the E scenario may both occur in the future. The DOE calls a future in which both of these events occur the mining and drilling scenario (ME). More detailed descriptions are found in Section PA-2.3.2.2.

The potential effects of future deep drilling and/or mining within the controlled area are the only natural features and waste- (and repository-) induced FEPs retained after screening that are included in the DP scenario, but excluded in the UP scenario. Among the most significant FEPs that will affect the UP scenario within the disposal system are excavation-induced fracturing, gas generation, salt creep, and MgO in the disposal rooms.

- The repository excavation and consequent changes in the rock stress field surrounding the excavated opening will create a DRZ immediately adjacent to excavated openings. The DRZ will exhibit mechanical and hydrological properties different than those of the intact rock.
- Organic material in the waste may degrade because of microbial activity, and brine will corrode metals in the waste and waste containers, with concomitant generation of gases. Gas generation may result in pressures sufficient to both maintain or develop fractures and change the fluid flow pattern around the waste disposal region.
- At the repository depth, salt creep will tend to heal fractures and reduce the permeability of the DRZ, the crushed salt component of the shaft seals, and the ROM salt in the panel closures to near that of the host rock salt.
- The MgO engineered barrier emplaced in the disposal rooms will react with CO_2 and maintain mildly alkaline conditions. Metal corrosion in the waste and waste containers will maintain reducing conditions. These effects will maintain low radionuclide solubility.

Radionuclides can become mobile as a result of waste dissolution and colloid generation following brine flow into the disposal rooms. Colloids may be generated from the waste (humics, mineral fragments, microbes, and actinide intrinsic colloids) or from other sources (humics, mineral fragments, and microbes).

Conceptually, there are several pathways for radionuclide transport within the undisturbed disposal system that may result in releases to the accessible environment (Figure PA-5). Contaminated brine may migrate away from the waste-disposal panels if pressure within the panels is elevated by gas generated from corrosion or microbial consumption. Radionuclide transport may occur laterally, through the anhydrite interbeds toward the subsurface boundary of the accessible environment in the Salado, or through access drifts or anhydrite interbeds to the base of the shafts. In the latter case, if the pressure gradient between the panels and overlying strata is sufficient, contaminated brine may migrate up the shafts. As a result, radionuclides may be transported directly to the ground surface, or laterally away from the shafts through permeable strata such as the Culebra, toward the subsurface boundary of the accessible environment. These conceptual pathways are shown in Figure PA-5.

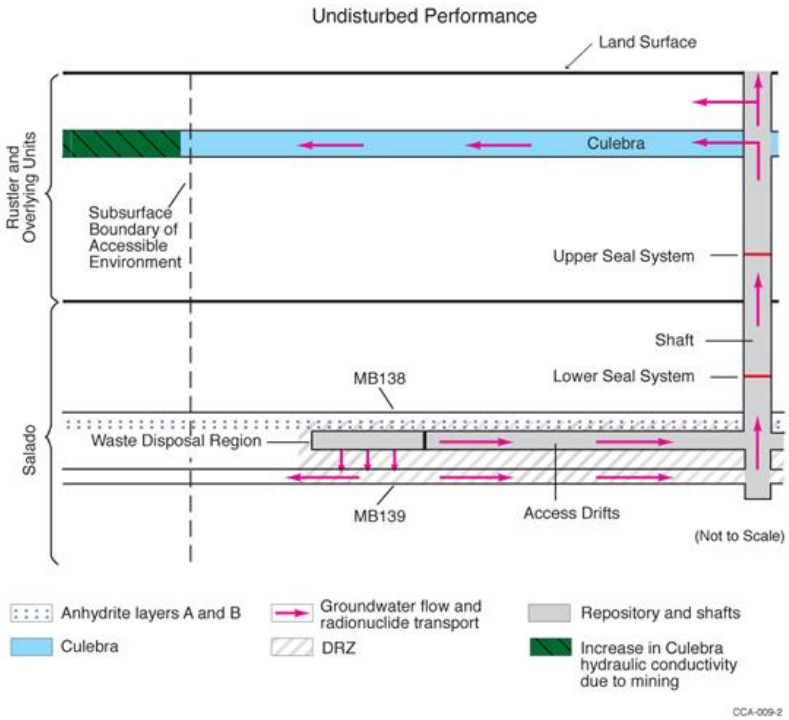

Figure PA- 5. Conceptual Release Pathways for the UP Scenario

The modeling system described in Section PA-4.0 includes potential radionuclide transport along other pathways, such as migration through Salado halite. However, the natural properties of the undisturbed system make radionuclide transport to the accessible environment via these other pathways unlikely.

PA-2.3.2.2 Disturbed Repository Performance

Assessments for compliance with section 191.13 need to consider the potential effects of future disruptive natural and human-initiated events and processes on the performance of the disposal system. No potentially disruptive natural events and processes are considered sufficiently likely to require inclusion in analyses of either the UP or DP scenario. The only future human-initiated events and processes retained after FEP screening are those associated with mining and deep drilling (but not the subsequent use of a borehole) within the controlled area or LWB when institutional controls cannot be assumed to eliminate the possibility of such activities (Section PA-3.2 and the CRA-2004, Chapter 6.0, Section 6.4.12.1). In total, 21 disturbed repository FEPs associated with future mining and deep drilling have been identified. These FEPs were assigned a screening designator of the DP scenario.

For evaluating the consequences of disturbed repository performance, the DOE has defined the M scenario, the E scenario, and the ME scenario. These scenarios are described in the following sections.

PA-2.3.2.2.1 Disturbed Repository M Scenario

The M scenario involves future mining within the controlled area. Consistent with the criteria stated by the EPA in section 194.32(b) for PA calculations, the effects of potential future mining within the controlled area are limited to changes in hydraulic conductivity of the Culebra that result from subsidence (as described in Section PA-3.9). The modeling system used for the M scenario is similar to that developed for the UP scenario, but with a modified Culebra T-field in the controlled area to account for the mining effects.

Radionuclide transport may be affected in the M scenario if a head gradient between the waste disposal panels and the Culebra causes brine contaminated with radionuclides to move from the waste disposal panels to the base of the shafts and up to the Culebra. The changes in the Culebra T-field may affect the rate and direction of radionuclide transport within the Culebra. Features of the M scenario are illustrated in Figure PA-6.

Three disturbed repository FEPs (H13, H37, and H57 in Appendix SCR-2004, Table SCR-1) are related to the occurrence and effects of future mining.

PA-2.3.2.2.2 Disturbed Repository E Scenario

The disturbed repository E scenario involves at least one deep drilling event that intersects the waste disposal region. The EPA provides criteria for analyzing the consequences of future drilling events in PA in section 194.33(c).

> Performance assessments shall document that in analyzing the consequences of drilling events, the Department assumed that:
>
> (1) Future drilling practices and technology will remain consistent with practices in the Delaware Basin at the time a compliance application is prepared. Such future drilling practices shall include, but shall not be limited to: the types and amounts of drilling fluids; borehole depths, diameters, and seals; and the fraction of such boreholes that are sealed by humans; and
>
> (2) Natural processes will degrade or otherwise affect the capability of boreholes to transmit fluids over the regulatory time frame.

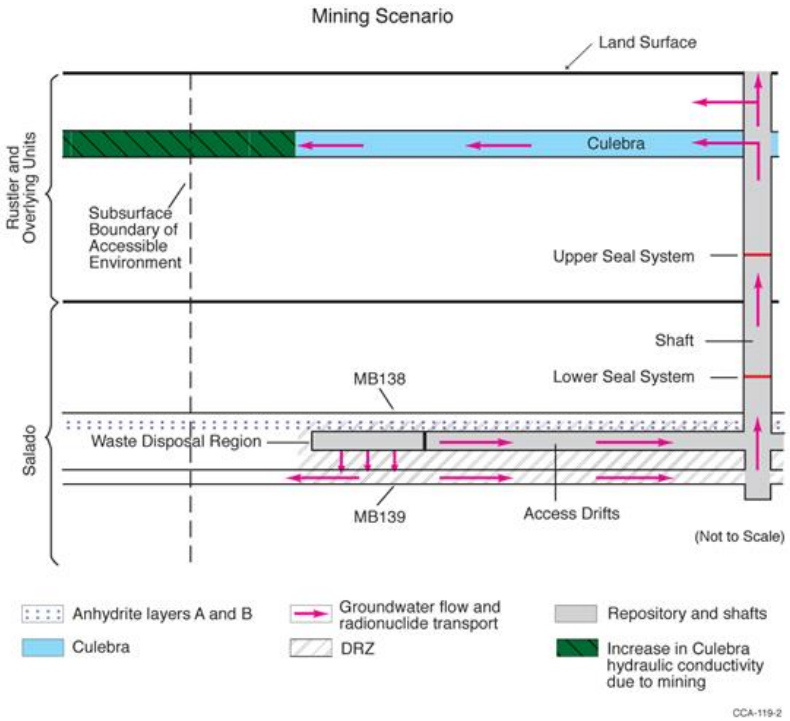

Figure PA- 6. Conceptual Release Pathways for the Disturbed Repository M Scenario

Consistent with these criteria, there are several pathways for radionuclides to reach the accessible environment in the E scenario. Before any deep drilling intersects the waste, potential release pathways are identical to those in the undisturbed repository scenario.

If a borehole intersects the waste in the disposal rooms, releases to the accessible environment may occur as material entrained in the circulating drilling fluid is brought to the surface. Particulate waste brought to the surface may include cuttings, cavings, and spallings. During drilling, contaminated brine may flow up the borehole and reach the surface, depending on fluid pressure within the waste disposal panels.

When abandoned, the borehole is assumed to be plugged in a manner consistent with current practices in the Delaware Basin as prescribed in section 194.33(c)(1). An abandoned intrusion borehole with degraded casing and/or plugs may provide a pathway for fluid flow and contaminant transport from the intersected waste panel to the ground surface if the fluid pressure within the panel is sufficiently greater than hydrostatic. Additionally, if brine flows through the borehole to overlying units, such as the Culebra, it may carry dissolved and colloidal actinides that can be transported laterally to the accessible environment by natural groundwater flow in the overlying units.

Alternatively, the units intersected by an intrusion borehole may provide sources for brine flow to a waste panel during or after drilling. For example, in the northern Delaware Basin, the Castile, which underlies the Salado, contains isolated volumes of brine at fluid pressures greater than hydrostatic (as discussed in the CRA-2004, Chapter 2.0, Section 2.2.1.2.2). The WIPP-12 borehole penetration of one of these volumes provided data on one pressurized brine pocket within the controlled area. The location and properties of brine pockets cannot be reliably predicted; thus, the possibility of a deep borehole penetrating both a waste panel and a brine reservoir is accounted for in consequence analysis of the WIPP, as discussed in the CRA-2004, Chapter 6.0, Section 6.4.8. Such a borehole could provide a connection for brine flow from the Castile to the waste panel, thus increasing fluid pressure and brine volume in the waste panel.

A borehole that is drilled through a disposal room pillar, but does not intersect waste, could also penetrate the brine reservoir underlying the waste disposal region. Such an event would, to some extent, depressurize the brine reservoir, and thus would affect the consequences of any subsequent reservoir intersections. The PA does not take credit for possible brine reservoir depressurization.

The DOE has distinguished two types of deep drilling events by whether or not the borehole intersects a Castile brine reservoir. A borehole that intersects a waste disposal panel and penetrates a Castile brine reservoir is designated an E1 event. A borehole that intersects a waste panel but does not penetrate a Castile brine reservoir is designated an E2 event. The consequences of deep drilling intrusions depend not only on the type of a drilling event, but on whether the repository was penetrated by an earlier E2 event or flooded due to an earlier E1 event. The PA also does not take credit for depressurization of brine reservoirs from multiple drilling intrusions. These scenarios are described in order of increasing complexity in the following sections.

PA-2.3.2.2.3 The E2 Scenario

The E2 scenario is the simplest scenario for inadvertent human intrusion into a waste disposal panel. In this scenario, a panel is penetrated by a drill bit; cuttings, cavings, spallings, and brine flow releases may occur; and brine flow may occur in the borehole after it is plugged and abandoned. Sources for brine that may contribute to long-term flow up the abandoned borehole are the Salado or, under certain conditions, the units above the Salado. An E2 scenario may involve more than one E2 drilling event, although the flow and transport model configuration developed for the E2 scenario evaluates the consequences of futures that have only one E2 event. Features of the E2 scenario are illustrated in Figure PA-7.

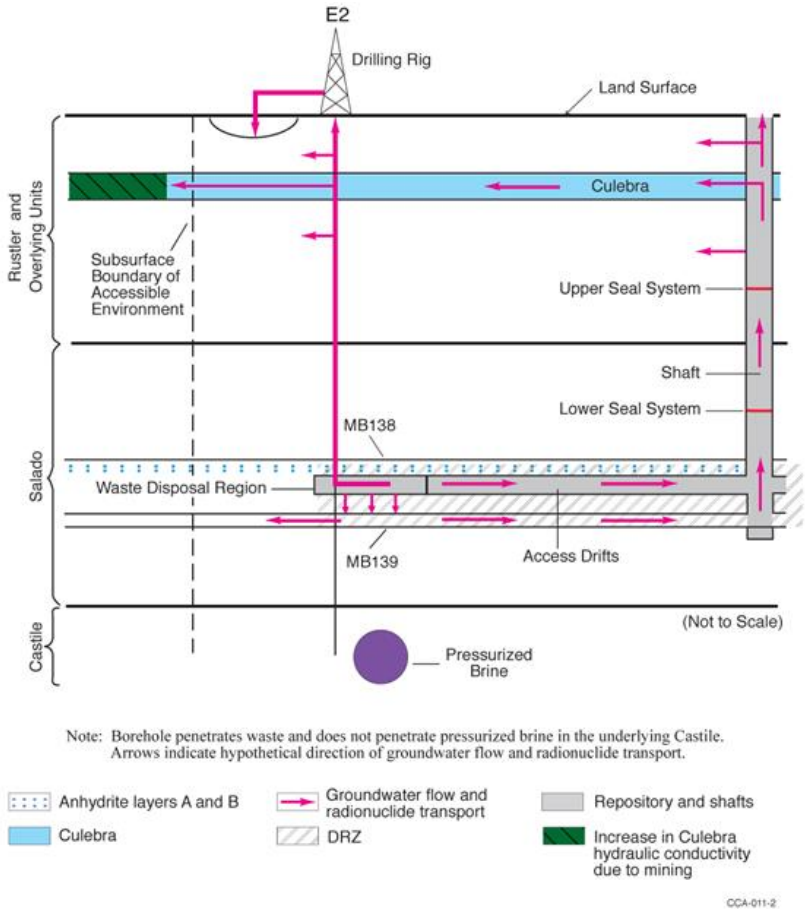

Figure PA- 7. Conceptual Release Pathways for the Disturbed Repository Deep Drilling E2 Scenario

PA-2.3.2.2.4 The E1 Scenario

Any scenario with exactly one inadvertent penetration of a waste panel that also penetrates a Castile brine reservoir is called E1. Features of this scenario are illustrated in Figure PA-8.

Sources of brine in the E1 scenario are the brine reservoir, the Salado, and, under certain conditions, the units above the Salado. However, the brine reservoir is conceptually the dominant source of brine in this scenario. The flow and transport model configuration developed for the E1 scenario evaluates the consequences of futures that have only one E1 event.

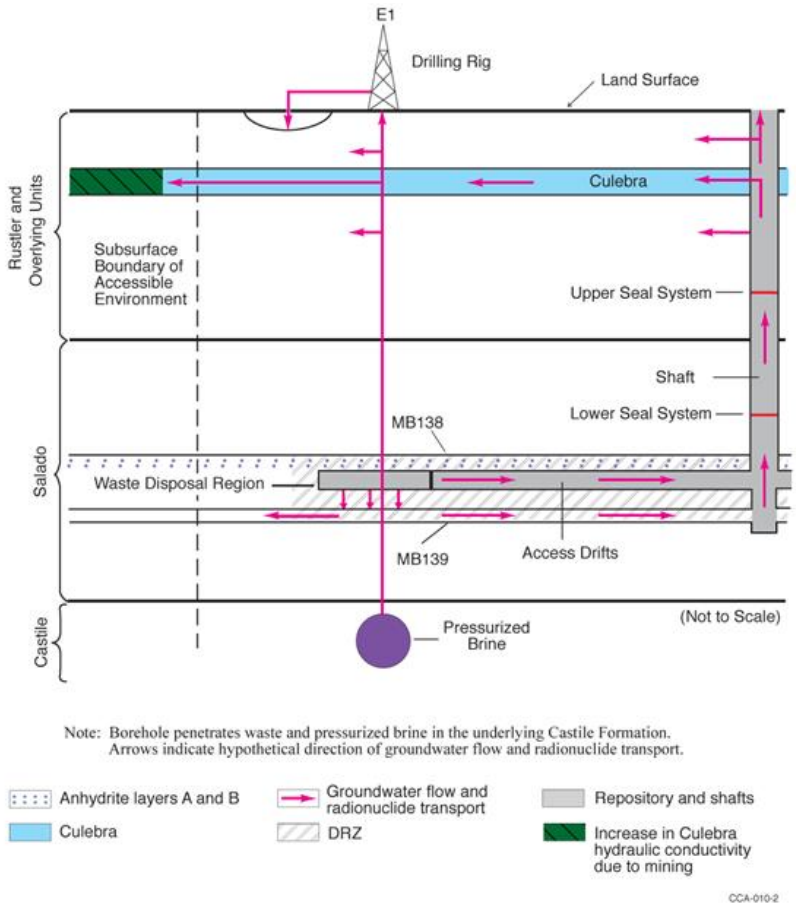

Figure PA- 8. Conceptual Release Pathways for the Disturbed Repository Deep Drilling E1 Scenario

PA-2.3.2.2.5 The E1E2 Scenario

The E1E2 scenario is defined as all futures with multiple penetrations of a waste panel of which at least one intrusion is an E1. One example of this scenario, with a single E1 event and a single E2 event penetrating the same panel, is illustrated in Figure PA-9. However, the E1E2 scenario can include many possible combinations of intrusion times, locations, and types of event (E1 or E2). The sources of brine in this scenario are those listed for the E1 scenario, and multiple E1 sources may be present. The E1E2 scenario has a potential flow path not present in the E1 or E2 scenarios: flow from an E1 borehole through the waste to another borehole. This flow path has the potential to (1) bring large quantities of brine in direct contact with waste and (2) provide a less restrictive path for this brine to flow to the units above the Salado (via multiple boreholes) compared to either the individual E1 or E2 scenarios. It is both the presence of brine reservoirs and the potential for flow through the waste to other boreholes that make this scenario different from combinations of E2 boreholes in terms of potential consequences.

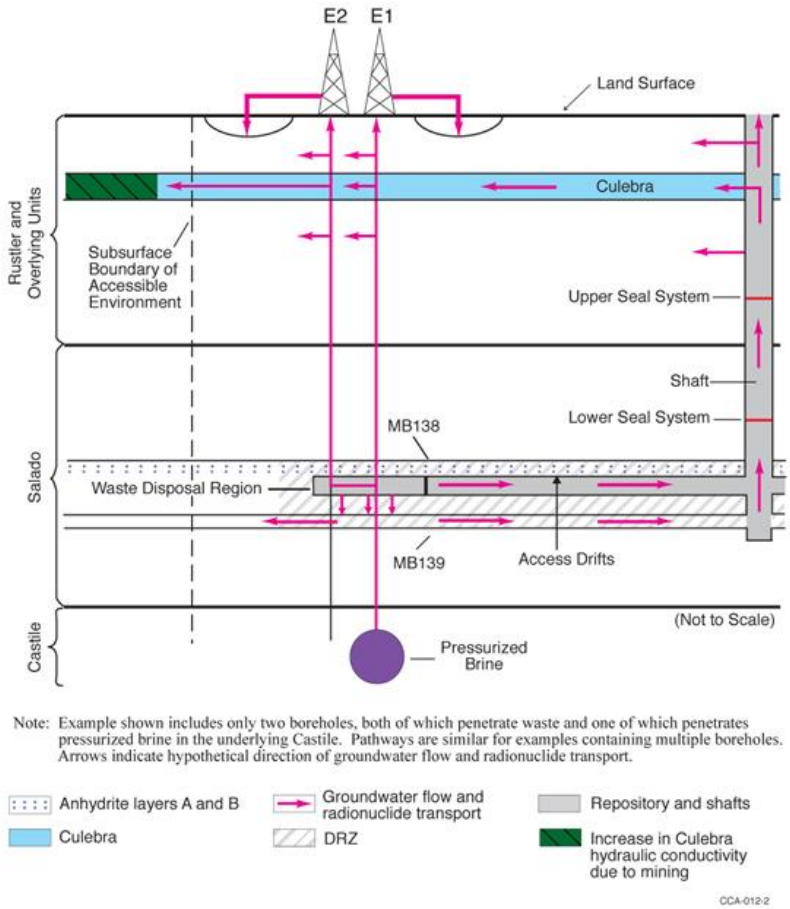

Figure PA- 9. Conceptual Release Pathways for the Disturbed Repository Deep Drilling E1E2 Scenario

PA-2.3.2.3 Disturbed Repository ME Scenario

The M scenario and the E scenario may both occur in the future. The DOE calls a future in which both of these events occur the ME scenario. The occurrence of both mining and deep drilling do not create processes beyond those already described separately for the M and E scenarios. For example, the occurrence of mining does not influence any of the interactions between deep boreholes and the repository or brine reservoirs, nor does the occurrence of drilling impact the effects of mining on Culebra hydrogeology.

PA-2.3.2.4 Scenarios Retained for Consequence Analysis

The scenarios described in Section PA-2.3.2.1, Section PA-2.3.2.2, and Section PA-2.3.2.3 have been retained for consequence analysis to determine compliance with the containment requirements in section 191.13. The modeling systems used to evaluate the consequences of these undisturbed and disturbed scenarios are discussed in Section PA-2.3.3.

PA-2.3.3 Calculation of Scenario Consequences

Calculating scenario consequences requires quantitative modeling. This section discusses the conceptual and computational models and some parameter values used to estimate the consequence of the scenarios described in Section PA-2.3.2. Additional discussion of conceptual models and modeling assumptions is provided in Section PA-4.0. Additional descriptions of sampled parameter values are included in Kicker and Herrick (Kicker and Herrick 2013).

A single modeling system was used to represent the disposal system and calculate the CCDFs. The modeling system, however, can be conveniently described in terms of various submodels, with each describing a part of the overall system. The models used in the WIPP PA, as in other complex analyses, exist at four different levels.

1. **Conceptual models** are a set of qualitative assumptions that describe a system or subsystem for a given purpose. At a minimum, these assumptions concern the geometry and dimensionality of the system, initial and boundary conditions, time dependence, and the nature of the relevant physical and chemical processes. The assumptions should be consistent with one another and with existing information within the context of the given purpose.

2. **Mathematical models** represent the processes at the site. The conceptual models provide the context within which these mathematical models must operate, and define the processes they must characterize. The mathematical models are predictive in the sense that, once provided with the known or assumed properties of the system and possible perturbations to the system, they predict the response of

the system. The processes represented by these mathematical models include fluid flow, mechanical deformation, radionuclide transport in groundwater, and removal of waste through intruding boreholes.

3. **Numerical models** are developed to approximate mathematical model solutions because most mathematical models do not have closed-form solutions.

4. **Computational models** generally refer to the implementation of the numerical models in the computer code with specific initial and boundary conditions and parameter values. The complexity of the system requires computer codes to solve the numerical models.

Parameters are values necessary in mathematical, numerical, or computational models. Data are descriptors of the physical system being considered, normally obtained by experiment or observation. The distinction between data and parameters can be subtle. Parameters are distinct from data, however, for three reasons: (1) Data may be evaluated, statistically or otherwise, to generate model parameters to account for uncertainty in data. (2) Some parameters have no relation to the physical system, such as the parameters in a numerical model to determine when an iterative solution scheme has converged. (3) Many model parameters are applied at a different scale than one directly observed or measured in the physical system. The distinction between data and parameter values is described further in Kicker and Herrick (Kicker and Herrick 2013) and Tierney (Tierney 1990), where distribution derivations for specific parameters are given.

PA-3.0 Probabilistic Characterization of Futures

The PA for the WIPP identifies uncertainty in parameters and uncertainty in future events as distinctly different entities and requires sampling to be conducted in two dimensions. One dimension focuses on characterizing the uncertainty in terms of the probability that various possible futures will occur at the WIPP site over the next 10,000 years. The other dimension characterizes the uncertainty due to lack of knowledge about the precise values of model parameters appropriate for the WIPP repository. Each dimension of the analysis is characterized by a probability space. Monte Carlo methods are used with the WIPP PA modeling system to sample each of the two probability spaces.

Characterizing the probability distribution for the first dimension of the PA depends on identifying the kinds of events that could impact releases from the repository over the next 10,000 years. Screening analyses of possible future events concluded that the only significant events with the potential to affect radionuclide releases to the accessible environment are drilling and mining within the LWB (Appendix SCR-2004, Section SCR-5.0). Consequently, modeling the future states of the repository focuses on representing the occurrences and effects of these two events. CCDFGF uses stochastic processes to simulate intrusion events by drilling and the occurrence of mining for natural resources. CCDFGF assembles the results from the deterministic models and selects the most appropriate scenario data provided by these models to use as the simulation of a 10,000-year future progresses. Ten thousand potential futures are simulated and used to create distributions of potential releases, and then compiled into a single CCDF of potential releases.

The WIPP PA is required not only to estimate the likelihood of future releases, but to establish statistical confidence in those estimates. Confidence is established using the second dimension of the analysis, which is based on the evaluation of uncertainty in the values of some of the parameters of the deterministic models. This uncertainty is assumed to represent a lack of knowledge about the true values of the parameters, and is labeled epistemic uncertainty. Epistemic uncertainty can be viewed as the representation of potential systematic errors in the results. The impact of epistemic uncertainty on the results is determined by generating 300 sets of parameter values using a stratified random sampling design, LHS, and then running the deterministic models and CCDFGF with each set of sampled parameters. Thus, 300 CCDFs are generated by CCDFGF. The 300 simulations are organized as 3 replicates of 100 vectors each. Because the uncertainty assigned to the parameters represents a lack of knowledge, this epistemic uncertainty could theoretically be reduced by collecting data to improve knowledge about the parameters. Epistemic uncertainty is represented in the projections of potential releases from the repository by the variability among the 300 CCDFs.

The WIPP PA modeling system consists of a set of coupled deterministic models (BRAGFLO, PANEL, NUTS, SECOTP2D, and CUTTINGS_S) that provide scenario-specific results to the code CCDFGF (Figure PA-1). CCDFGF is, in contrast, a stochastic simulation model used to simulate potential futures of repository performance where drilling and mining intrusions can impact the state of the repository and produce release events. CCDFGF implements the timing of intrusions as stochastic events, thus incorporating the aleatory uncertainty associated with projections of future events. This section describes how aleatory uncertainty is implemented in PA. Epistemic uncertainty is discussed in Section PA-6.0.

PA-3.1 Probability Space

As discussed in Section PA-2.2.2, aleatory uncertainty is defined by the possible futures $\mathbf{x}_{st,i}$ conditional on the set i of parameters used in Equation (PA.2). Section PA-3.2, Section PA-3.3, Section PA-3.4, Section PA-3.5, Section PA-3.6, Section PA-3.7, Section PA-3.8, and Section PA-3.9 describe the individual components t_j, e_j, l_j, b_j, p_j, $\mathbf{a}_j$, and t_{min} of $\mathbf{x}_{st,i}$ and their associated probability distributions. The concept of a scenario as a subset of the sample space of $\mathbf{x}_{st,i}$ is discussed in Section PA-3.10. The procedure used to sample the individual elements $\mathbf{x}_{st,i}$ is described in Section PA-6.5.

PA-3.2 AICs and PICs

The AICs and PICs will be implemented at the WIPP site to deter human activity detrimental to repository performance. The AICs and PICs are described in detail in the CRA-2004, Chapter 7.0 and in appendices referenced in Chapter 7.0. Permanent markers will be constructed to inform future populations of the location of the WIPP, and part of the marker system will be a berm that defines the active areas of the repository. In this section, the impact of AICs and PICs on PA is described.

The AICs will be implemented at the WIPP after final facility closure to control site access and ensure that activities detrimental to disposal system performance do not occur within the controlled area. The AICs will preclude human intrusion in the disposal system. A 100-year limit on the effectiveness of AICs in PA is established in section 191.14 (a). Because of the regulatory restrictions and the nature of the AICs that will be implemented, PA assumes there are no inadvertent human intrusions or mining in the controlled area for 100 years following repository closure.

The PICs are designed to deter inadvertent human intrusion into the disposal system. Only minimal assumptions were made about the nature of future society when designing the PICs to comply with the assurance requirements. The preamble to Part 194 limits any credit for PICs in deterring human intrusion to 700 years after disposal (U.S. EPA 1996a, p. 5231). Although the DOE originally took credit for PICs in the CCA PA, it has not taken credit since. Not including PICs is a conservative implementation, as no credit is taken for a beneficial component of the system.

PA-3.3 Drilling Intrusion

As described in Section PA-2.3.2.2, drilling intrusions in PA are assumed to occur randomly in time and space following a Poisson process. Specifically, the drilling rate considered within the area marked by a berm as part of the system for PICs (Kicker and Herrick 2013, Table 38) is 6.73×10^{-3} intrusions per square kilometer per year ($km^{-2}\ yr^{-1}$). AICs are assumed to prevent any drilling intrusions for the first 100 years after the decommissioning of the WIPP (Section PA-3.2). In the computational implementation of PA, it is convenient to represent the Poisson process for drilling intrusions by its corresponding rate term $\lambda_d(t)$ for intrusions into the area marked by the berm. Specifically,

$$\lambda_d(t) = \begin{cases} 0 & 0 \le t < 100\,yr \\ (0.6285\,km^2)\left(6.73\times10^{-3}\,km^{-2}yr^{-1}\right) = 4.23\times10^{-3}\,yr^{-1} & 100 \le t \le 10{,}000\,yr \end{cases} \quad \text{(PA.6)}$$

where 0.6285 km^2 is the area enclosed by the berm (Kicker and Herrick 2013, Table 37) and t is the elapsed time (in years) since decommissioning the WIPP.

The function $\lambda_d(t)$ defines the parameter of the exponential distribution that gives rise to the times of intrusions, t_j of Equation (PA.2). In the computational implementation of the analysis, the exponential distribution is randomly sampled to define the times between successive drilling intrusions (Figure PA-10 and Section PA-6.5). A key assumption of the exponential distribution is that events are independent of each other, so the occurrence of one event has no effect on the occurrence of the next event. The process giving rise to such events is sometimes called a Poisson process because the distribution of such events over a fixed interval of time is a Poisson distribution. Due to the 10,000-year regulatory period specified in section 191.13, t_j is assumed to be bounded above by 10,000 years in the definition of $\mathbf{x}_{st,i}$. Further, t_j is bounded below by 100 years as defined in Equation (PA.6).

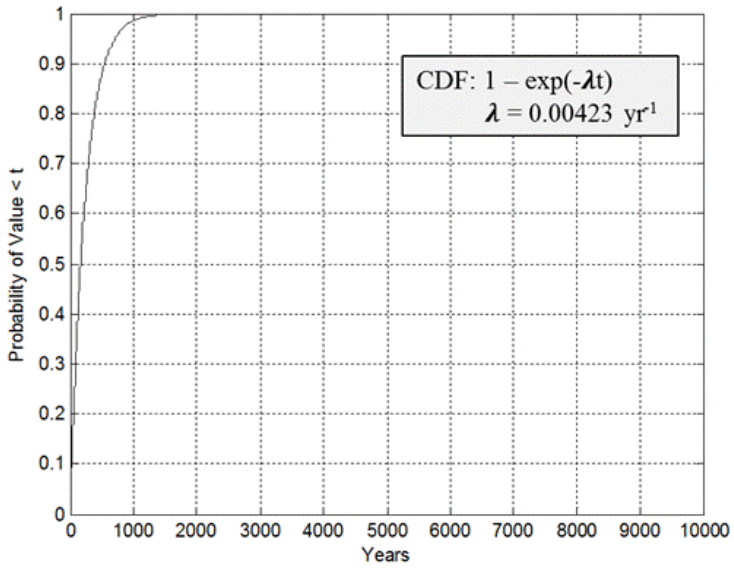

Figure PA- 10. CDF for Time Between Drilling Intrusions

PA-3.4 Penetration of Excavated/Nonexcavated Area

The variable e_j is a designator for whether or not the j^{th} drilling intrusion penetrates an excavated, waste-filled area of the repository: $e_j = 0$ or 1 implies penetration of a nonexcavated or excavated area, respectively. The corresponding probabilities $P[e_j = 0]$ and $P[e_j = 1]$ for $e_j = 0$ and $e_j = 1$ are

$$pEx_1 = P[e_j = 1] = 0.1273 \text{ km}^2 / 0.6285 \text{ km}^2 = 0.203 \quad \text{(PA.7)}$$

$$pEx_0 = P[e_j = 0] = 1 - pEx_1 = 0.797 \quad \text{(PA.8)}$$

where 0.1273 km^2 and 0.6285 km^2 are the excavated area of the repository and the area of the berm, respectively (Kicker and Herrick 2013, Table 37).

PA-3.5 Drilling Location

Locations of drilling intrusions through the excavated, waste-filled area of the repository are discretized to the 144 locations in Figure PA-11. Assuming that a drilling intrusion occurs within the excavated area, it is assumed to be equally likely to occur at each of these 144 locations. Thus, the probability pL_k that drilling intrusion j will occur at location l_k, k = 1, 2, …, 144 in Figure PA-11 is

$$pL_{k,k=1,2,3} = P[k = 1] = P[k = 2] = \ldots = P[k = 144] = 1/144 = 6.94 \times 10^{-3} \quad \text{(PA.9)}$$

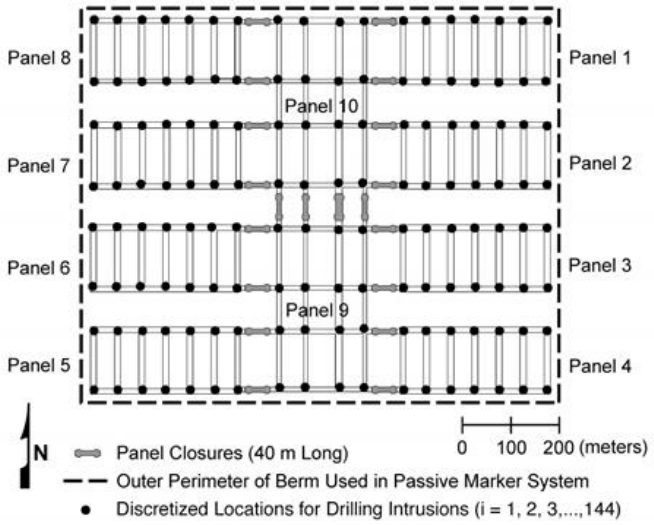

Figure PA- 11. Discretized Locations for Drilling Intrusions

PA-3.6 Penetration of Pressurized Brine

The conceptual models for the Castile include the possibility that pressurized brine reservoirs underlie the repository (Section PA-4.2.10). The variable b_j is a designator for whether or not the j^{th} drilling intrusion penetrates pressurized brine, where $b_j = 0$ signifies nonpenetration and $b_j = 1$ signifies penetration of pressurized brine. In the CRA-2014 PA, the probability of encountering pressurized brine during a drilling intrusion has been refined from that used in the CRA-2009 PABC. Specifically, the probability $pB_1 = P[b_j = 1]$ in the CRA-2014 PA is sampled from a normal distribution ranging from 0.06 to 0.19 (see Section PA-1.1.3 and Kirchner et al. 2012).

PA-3.7 Plugging Pattern

Three borehole plugging patterns, p_k, are considered in PA: (1) p_1, a full concrete plug through the Salado to the Bell Canyon Formation (hereafter referred to as Bell Canyon), (2) p_2, a two-plug configuration with concrete plugs at the Rustler/Salado interface and the Castile/Bell Canyon interface, and (3) p_3, a three-plug configuration with concrete plugs at the Rustler/ Salado, Salado/Castile, and Castile/Bell Canyon interfaces. The DOE continues to survey drilling activity in the Delaware Basin in accordance with the criteria established in section 194.33. Results for the year 2012 are documented in the 2012 Delaware Basin Monitoring Annual Report (U.S. DOE 2012). Drilling parameters are updated in the CRA-2014 PA to include information assembled through year 2012. The probability that a given drilling intrusion will be sealed with plugging pattern p_k, k= 1, 2, 3, is given by pPL_k, where $pPL_1 = P[k = 1] = 0.04$, $pPL_2 = P[k = 2] = 0.594$, $pPL_3 = P[k = 3] = 0.366$ (Kicker and Herrick 2013, Table 38).

PA-3.8 Activity Level

The waste intended for disposal at the WIPP is represented by 528 distinct waste streams, with 451 of these waste streams designated as CH-TRU waste and 77 designated as RH-TRU waste (Kicker and Zeitler 2013a). For the CRA-2014 PA, the 77 separate RH-TRU waste streams are represented by a single, combined RH-TRU waste stream, as has been done in all previous PAs. The activity levels for the waste streams are given in Kicker and Herrick 2013, Tables B-1 and B-2. Each waste container emplaced in the repository contains waste from a single CH-TRU waste stream. Waste packaged in 55-gallon (gal) drums is stacked 3 drums high within the repository. Although waste in other packages (e.g., standard waste boxes, 10-drum overpacks, etc.) may not be stacked 3 high, PA assumes that each drilling intrusion into CH-TRU waste intersects 3 different waste streams. In contrast, all RH-TRU waste is represented by a single waste stream, and so each drilling

intrusion through RH-TRU waste is assumed to intersect this single waste stream. Appendix MASS-2014, Section MASS-19.0 examines the sensitivity of PA results to the assumption that three waste streams are intersected by each drilling intrusion into CH-TRU waste.

The vector $\mathbf{a}_j$ characterizes the type of waste penetrated by the j^{th} drilling intrusion. Specifically,

$\mathbf{a}_j = 0$ if $e_j = 0$ (PA.10)

(i.e., if the i^{th} drilling intrusion does not penetrate an excavated area of the repository)

$\mathbf{a}_j = 1$ if $e_j = 1$ and RH-TRU is penetrated (PA.11)

$\mathbf{a}_j = [iCH_{j1}, iCH_{j2}, iCH_{j3}]$ if $e_j = 1$ and CH-TRU is penetrated (PA.12)

where iCH_{j1}, iCH_{j2}, and iCH_{j3} are integer designators for the CH-TRU waste streams intersected by the j^{th} drilling intrusion (i.e., each of iCH_{j1}, iCH_{j2}, and iCH_{j3} is an integer between 1 and 451).

Whether the j^{th} intrusion penetrates a nonexcavated or excavated area is determined by the probabilities pE_0 and pE_1 discussed in Section PA-3.4. The type of waste penetrated is determined by the probabilities pCH and pRH. The excavated area used for disposal of CH-TRU waste (aCH) is 1.115×10^5 square meters (m^2) and the area used for disposal of RH-TRU waste (aRH) is 1.576×10^4 m^2 (Kicker and Herrick 2013, Table 37), for a total disposal area of $aEX = aCH + aRH = 1.273 \times 10^5$ m^2. Given that the j^{th} intrusion penetrates an excavated area, the probabilities pCH and pRH of penetrating CH-TRU and RH-TRU waste are given by

$$pCH = P[\text{CH waste area penetrated}] = aCH / aEX = (1.115 \times 10^5\ \text{m}^2) / (1.273 \times 10^5\ \text{m}^2) = 0.876$$

(PA.13)

$$pRH = P[\text{RH waste area penetrated}] = aRH / aEX = (1.576 \times 10^4\ \text{m}^2) / (1.273 \times 10^5\ \text{m}^2) = 0.124$$

(PA.14)

As indicated in this section, the probabilistic characterization of $\mathbf{a}_j$ depends on a number of individual probabilities. Specifically, pEx_0 and pEx_1 determine whether a nonexcavated or excavated area is penetrated (Section PA-3.5). Probabilities pCH and pRH determine whether CH-TRU or RH-TRU waste is encountered, given penetration of an excavated area. The individual waste stream volumes in Kicker and Herrick (Kicker and Herrick 2013), Tables B-1 and B-2 are used to determine the specific waste streams iCH_{j1}, iCH_{j2}, and iCH_{j3} encountered, given a penetration of CH-TRU waste. The probability of encountering a particular CH-TRU waste stream is computed as the ratio of the volume of that waste stream to the volume of CH-TRU waste.

PA-3.9 Mining Time

Full mining of known potash reserves within the LWB is assumed to occur at time t_{min}. The occurrence of mining within the LWB in 10,000 years in the absence of institutional controls is specified as following a Poisson process with a rate of $\lambda_m = 1 \times 10^{-4}\ \text{yr}^{-1}$ (parameter GLOBAL:MINERT in Kicker and Herrick 2013, Table 38). However, this rate can be reduced by AICs and PICs. Specifically, AICs are assumed to result in no possibility of mining for the first 100 years after decommissioning of the WIPP. In PA, PICs do not affect the mining rate. Thus, the mining rate $\lambda_m(t)$ is

$$\lambda_m(t) = 0\ \text{yr}^{-1} \quad \text{for } 0 \le t < 100\ \text{yrs} \quad \text{(PA.15)}$$

$$\lambda_m(t) = 1 \times 10^{-4}\ \text{yr}^{-1} \quad \text{for } 100 \le t \le 10{,}000\ \text{yrs} \quad \text{(PA.16)}$$

where t is the elapsed time since decommissioning of the WIPP.

In the computational implementation of the analysis, $\lambda_m(t)$ is used to define the distribution of time to mining. The use of $\lambda_m(t)$ to characterize t_{min} is analogous to the use of λ_d to characterize the t_j, except that only one mining event is assumed to occur (i.e., $\mathbf{x}_{st,i}$ contains only one value for t_{min}) in order to be consistent with guidance given in Part 194 that mining within the LWB should be assumed to remove all economically viable potash reserves. Due to the 10,000-year regulatory period specified in section 191.13, t_{min} is assumed to be bounded above by 10,000 years in the definition of $\mathbf{x}_{st,i}$.

PA-3.10 Scenarios and Scenario Probabilities

A scenario is a subset of the sample space for aleatory uncertainty. The underlying goal of scenario definition is to define the state of repository conditions prior to and following intrusion events. Scenarios are specific cases of inputs or system states that are selected to cover the range of possible cases. Given the complexity of the futures $\mathbf{x}_{st,i}$ (see Equation (PA.2)), many different scenarios can be defined. The computational complexity of the function $f(\mathbf{x}_{st} | \mathbf{v}_{su})$ in Section PA-2.2.3 limits evaluation to only a few intrusion scenarios. As presented in Section PA-2.3.2, PA considers four fundamental intrusion scenarios:

E0 = no drilling intrusion through an excavated area of the repository

E1 = a drilling intrusion through an excavated area of the repository that penetrates pressurized brine in the Castile

E2 = a drilling intrusion through an excavated area of the repository that does not penetrate pressurized brine in the Castile

E1E2 = two or more previous intrusions, at least one of which is an E1 intrusion

These definitions of intrusion scenarios capture the most important events impacting the state of the repository: whether or not the repository is inundated by the penetration of a brine pocket, and whether or not there exists a possible route of release upward via a borehole. The state of the repository is also designated as E0, E1, E2, or E1E2. Scenarios for some of the process-level models consist of a single intrusion scenario occurring at specific times. CCDFGF is used to simulate multiple intrusions over 10,000 years (see section PA-3.11).

If only the intrusion scenarios controlled the state of the repository, then the state would be defined by the sequence of drilling events alone. However, CCDFGF also considers the impact of plugging pattern on boreholes. A borehole with a full plugging pattern that penetrates the waste area is also assumed to have no impact, and leaves the repository in its previous state, including the undisturbed state (see Section PA-6.8.4.1 and Figure PA-33 for more details). Thus, an E2 intrusion event into an E0 repository will result in an E0 state if a full plugging pattern is used, or an E2 state otherwise. An E1 intrusion subsequent to an E2 intrusion will leave the repository in an E1E2 state, where it will remain, regardless of subsequent intrusions. It is therefore important to distinguish between the type of intrusion, listed above, and the state of the repository.

The probability that no excavated area will be penetrated during the 10,000-year interval can be computed using a distribution of the number of penetration events and the probability that a drilling event will penetrate the excavated area. For the Poisson distribution of drilling events, the probability of there being n events in the 10,000-year history is

$$\frac{e^{-\lambda_d \times 9900}(\lambda_d \times 9900)^n}{n!} \text{ for } n = 1, 2, 3, \ldots \quad \text{(PA.17)}$$

where λ_d is the mean drilling rate per year in the period following the period of AICs, 9,900 is the number of years in which drilling can occur after the institutional control period of 100 years, and n is the number of drilling events. The probability of having n events all within the nonexcavated area is $pEx_0{}^n$, or specifically 0.797^n. Thus, the probability of having only events in the nonexcavated area over 10,000 years, i.e., having no drilling intrusions into the excavated area, is just the sum across all n of the products of the probability of having exactly n drilling events and the probability that all n events penetrate the unexcavated area:

$$\sum_{n=1}^{\infty} \frac{e^{-\lambda_d \times 9900}(\lambda_d \times 9900)^n}{n!} pEx_0^n = e^{-\lambda_d \times 9900 \times pEx_0} \quad \text{(PA.18)}$$

The calculated probability becomes

$\exp[-0.203(4.23\times10^{-3})(10000-100)] = 2.03\times10^{-4}$ (PA.19)

This probability is the lower bound on the probability of the repository being in an E0 state, given that it does not include the consideration of the plugging pattern.

The probability of a single E1, E2, or E1E2 intrusion over 10,000 years is relatively small. Assuming that pB_1 takes on its mean value of 0.127 (see Section PA-3.6), and ignoring the impact of the plugging pattern, for a constant rate of drilling, λ_d, these equations are

$\exp[-9900 \; \&\#120640; _d pEx_1](9900 \; \&\#120640; _d pEx_1)pB_1 = 2.2\times10^{-4}$ (PA.20)

and

$\exp[-9900 \; \&\#120640; _d pEx_1](9900 \; \&\#120640; _d pEx_1)pB_0 = 1.5\times10^{-3}$ (PA.21)

respectively, where ($pEx_1 \times \lambda_d$) represents the annual rate of drilling into the excavated region of the repository which is multiplied by *9900* to give the frequency per 9,900 years. The probability of an intrusion into the excavated area is subsequently multiplied by the probability of hitting or missing a brine pocket. In this form, it can be seen that the term for the probability for intrusion is equivalent to the PDF of the Poisson distribution for $n = 1$:

$$f(n) = \frac{e^{-\lambda}\lambda^n}{n!} \quad \text{(PA.22)}$$

The expressions defining the probability of being in the E0 state after 10,000 years and of having a single E1 or E2 intrusion event after 10,000 years are relatively simple because the scenarios E0, E1, and E2 are relatively simple. The scenario E1E2 is more complex and, as a result, computing its probability is also more complex. Closed-form formulas for the probabilities of quite complex scenarios can be derived, but they are very complicated and involve large numbers of iterated integrals (Helton 1993).

PA-3.11 CCDF Construction

CCDFGF simulates histories that can have many intrusion events (WIPP Performance Assessment 2010). The process-level models evaluate the releases at a small number of specific times for each of the four intrusion scenarios. Releases from the repository are calculated using results from these fundamental scenarios (Section PA-6.7 and Section PA-6.8). Releases for an arbitrary future are estimated from the results of these fundamental scenarios (Section PA-6.8); these releases are used to construct CCDFs by Equation (PA.4).

The WIPP PA uses the Monte Carlo approach to construct the CCDF indicated in Equation (PA.4). The Monte Carlo approach generates releases for 10,000 possible futures. CCDFs are constructed by treating the 10,000 releases values as order statistics; each release is assigned a probability of 1×10^{-4}, and the CCDF can be constructed by plotting the complement of the sum of the probabilities ordered by the release value. The CRA-2014 PA uses the same approach as the CRA-2009 PA.

PA-4.0 Estimation of Releases

This section describes how releases to the accessible environment are estimated for a particular future in PA.

PA-4.1 Results for Specific Futures

The function $f(\mathbf{x}_{st,i})$ estimates the radionuclide releases to the accessible environment associated with each of the possible futures ($\mathbf{x}_{st,i}$) that could occur at the WIPP site over the next 10,000 years. In practice, $f(\mathbf{x}_{st,i})$ is quite complex and is constructed by the models implemented in computer programs used to simulate important processes and releases at the WIPP. In the context of these models, $f(\mathbf{x}_{st,i})$ has the form

$$\begin{aligned} f(\mathbf{x}_{st,i}) = {} & f_C(\mathbf{x}_{st,i}) + f_{SP}\left[\mathbf{x}_{st,i}, f_B(\mathbf{x}_{st,i})\right] + f_{DBR}\left[\mathbf{x}_{st,i}, f_B(\mathbf{x}_{st,i})\right] \\ & + f_{MB}\left[\mathbf{x}_{st,i}, f_B(\mathbf{x}_{st,i})\right] + f_{DL}\left[\mathbf{x}_{st,i}, f_B(\mathbf{x}_{st,i})\right] + f_S\left[\mathbf{x}_{st,i}, f_B(\mathbf{x}_{st,i})\right] \\ & + f_{ST}\left[f_{MF}(\mathbf{x}_{st,0}), f_{NP}\left[\mathbf{x}_{st,i}, f_B(\mathbf{x}_{st,i})\right]\right] \end{aligned} \quad \text{(PA.23)}$$

where

$\mathbf{x}_{st,i}$ ~ particular future under consideration

$\mathbf{x}_{st,0}$ ~ future involving no drilling intrusions but a mining event at the same time t_{min} as in x_{st}

$f_C(\mathbf{x}_{st,i})$ ~ cuttings and cavings release to accessible environment for $\mathbf{x}_{st,i}$ calculated with CUTTINGS_S

$f_B(\mathbf{x}_{st,i})$ ~ two-phase flow in and around the repository calculated for $\mathbf{x}_{st,i}$ with BRAGFLO; in practice, $f_B(\mathbf{x}_{st,i})$ is a vector containing a large amount of information, including pressure and brine saturation in various geologic members

$f_{SP}\left[\mathbf{x}_{st,i}, f_B(\mathbf{x}_{st,i})\right]$ ~ spallings release to accessible environment for $\mathbf{x}_{st,i}$ calculated with the spallings model contained in DRSPALL and CUTTINGS_S; this calculation requires repository conditions calculated by $f_B(\mathbf{x}_{st,i})$ as input

$f_{DBR}\left[\mathbf{x}_{st,i}, f_B(\mathbf{x}_{st,i})\right]$ ~ DBR to accessible environment for $\mathbf{x}_{st,i}$ also calculated with BRAGFLO; this calculation requires repository conditions calculated by $f_B(\mathbf{x}_{st,i})$ as input

$f_{MB}\left[\mathbf{x}_{st,i}, f_B(\mathbf{x}_{st,i})\right]$ ~ release through anhydrite MBs to accessible environment for $\mathbf{x}_{st,i}$ calculated with NUTS; this calculation requires flows in and around the repository calculated by $f_B(\mathbf{x}_{st,i})$ as input

$f_{DL}\left[\mathbf{x}_{st,i}, f_B(\mathbf{x}_{st,i})\right]$ ~ release through Dewey Lake to accessible environment for $\mathbf{x}_{st,i}$ calculated with NUTS; this calculation requires flows in and around the repository calculated by $f_B(\mathbf{x}_{st,i})$ as input

$f_S\left[\mathbf{x}_{st,i}, f_B(\mathbf{x}_{st,i})\right]$ ~ release to land surface due to brine flow up a plugged borehole for $\mathbf{x}_{st,i}$ calculated with NUTS; this calculation requires flows in and around the repository calculated by $f_B(\mathbf{x}_{st,i})$ as input

$f_{MF}(\mathbf{x}_{st,0})$ ~ flow field in the Culebra calculated for $\mathbf{x}_{st,0}$ with MODFLOW; $\mathbf{x}_{st,0}$ is used as an argument to f_{MF} because drilling intrusions are assumed to cause no perturbations to the flow field in the Culebra

$f_{NP}\left[\mathbf{x}_{st,i}, f_B(\mathbf{x}_{st,i})\right]$ ~ release to Culebra for $\mathbf{x}_{st,i}$ calculated with NUTS or PANEL as appropriate; this calculation requires flows in and around the repository calculated by $f_B(\mathbf{x}_{st,i})$ as input

$f_{ST}\left[f_{MF}(\mathbf{x}_{st,0}), f_{NP}\left[\mathbf{x}_{st,i}, f_B(\mathbf{x}_{st,i})\right]\right]$ ~ groundwater transport release through Culebra to accessible environment calculated with SECOTP2D. This calculation requires MODFLOW results (i.e., $f_{MF}(\mathbf{x}_{st,0})$) and NUTS or PANEL results (i.e., $f_{NP}\left[\mathbf{x}_{st,i}, f_B(\mathbf{x}_{st,i})\right]$) as input

The remainder of this section describes the mathematical structure of the mechanistic models that underlie the component functions of $f(\mathbf{x}_{st,i})$ in Equation (PA.23).

The Monte Carlo CCDF construction procedure, implemented in the code CCDFGF (WIPP Performance Assessment 2010), uses a sample of size $nS = 10{,}000$ in PA. The individual programs that estimate releases do not run fast enough to allow this many evaluations of f. As a result, a two-step procedure is being used to evaluate f in calculating the summation in Equation (PA.23). First, f and its component functions are evaluated with the procedures (i.e., models) described in this section for a group of preselected futures. Second, values of $f(\mathbf{x}_{st})$ for the randomly selected futures $\mathbf{x}_{st,i}$ used in the numerical evaluation of the summation in Equation (PA.23) are then constructed from results obtained in the first step. These constructions are described in Section PA-6.7 and Section PA-6.8, and produce the evaluations of $f(\mathbf{x}_{st})$ that are actually used in Equation (PA.23).

For notational simplicity, the functions on the right-hand side of Equation (PA.23) will typically be written with only $\mathbf{x}_{st}$ as an argument (e.g., $f_{SP}(\mathbf{x}_{st})$ and will be used instead of $f_{SP}[\mathbf{x}_{st}, f_B(\mathbf{x}_{st})]$). However, the underlying dependency on the other arguments will still be present.

The major topics considered in this chapter are two-phase flow in the vicinity of the repository as modeled by BRAGFLO (i.e., f_B) (Section PA-4.2), radionuclide transport in the vicinity of the repository as modeled by NUTS (i.e., $f_{MB}, f_{DL}, f_S, f_{NP}$) (Section PA-4.3), radionuclide transport in the vicinity of the repository as modeled by PANEL (i.e., f_{NP}) (Section PA-4.4), cuttings and cavings releases to the surface as modeled by CUTTINGS_S (i.e., f_C) (Section PA-4.5), spallings releases to the surface as modeled by DRSPALL and CUTTINGS_S (i.e., f_{SP}) (Section PA-4.6), DBRs to the surface as modeled by BRAGFLO (i.e., f_{DBR}) (Section PA-4.7), brine flow in the Culebra as modeled by MODFLOW (i.e., f_{MF}) (Section PA-4.8), and radionuclide transport in the Culebra as modeled by SECOTP2D (i.e., f_{ST}) (Section PA-4.9).

PA-4.2 Two-Phase Flow: BRAGFLO

Quantifying the effects of gas and brine flow on radionuclide transport from the repository requires a two-phase (brine and gas) flow code. The two-phase flow code BRAGFLO is used to simulate gas and brine flow in and around the repository (Camphouse 2013a and Camphouse 2013b). Additionally, the BRAGFLO code incorporates the effects of disposal room consolidation and closure, gas generation, and rock fracturing in response to gas pressure. This section describes the mathematical models on which BRAGFLO is based, the representation of the repository in the model, and the numerical techniques employed in the solution.

PA-4.2.1 Mathematical Description

Two-phase flow in the vicinity of the repository is represented by the following system of two conservation equations, two constraint equations, and three equations of state:

Gas Conservation

$$\nabla \cdot \left[\frac{\alpha \rho_g K_g k_{rg}}{\mu_g}\left(\nabla P_g + \rho_g g \nabla h\right)\right] + \alpha q_g + \alpha q_{ug} = \alpha \frac{\partial\left(\phi \rho_g S_g\right)}{\partial t} \quad \text{(PA.24)}$$

Brine Conservation

$$\nabla \cdot \left[\frac{\alpha \rho_b K k_{rb}}{\mu_b}\left(\nabla P_b + \rho_b g \nabla h\right)\right] + \alpha q_b + \alpha q_{ub} = \alpha \frac{\partial\left(\phi \rho_b S_b\right)}{\partial t} \quad \text{(PA.25)}$$

Saturation Constraint

$$S_g + S_b = 1 \quad \text{(PA.26)}$$

Capillary Pressure Constraint

$$P_c = P_g - P_b = P_c(S_b) \quad \text{(PA.27)}$$

Gas Density

ρ_g (determined by Redlich-Kwong-Soave (RKS) equation of state; see Equation (PA.51))
(PA.28)

Brine Density

$$\rho_b = \rho_{b0} \exp\left[c_b\left(P_b - P_{b0}\right)\right] \quad \text{(PA.29)}$$

Formation Porosity

$$\phi = \phi_0 \exp\left[c_r\left(P_b - P_{b0}\right)\right] \quad \text{(PA.30)}$$

where

g = acceleration due to gravity (meters per second squared [m])
h = vertical distance from a reference location (m)
k_{rl} = relative permeability (dimensionless) to fluid l, $l = b$ (brine), g (gas)
P_c = capillary pressure in Pascals (Pa)
P_l = pressure of fluid l (Pa)
q_{rl} = rate of production (or consumption, if negative) of fluid l due to chemical reaction (kilograms per cubic meter per seconds [kg/m^3/s])
q_l = rate of injection (or removal, if negative) of fluid l (kg/m^3/s)
S_l = saturation of fluid l (dimensionless)
t = time (s)
α = geometry factor (m)
ρ_l = density of fluid l (kg/m^3)
μ_l = viscosity of fluid l (Pa s)
ϕ = porosity (dimensionless)
ϕ_0 = reference (i.e., initial) porosity (dimensionless)
P_{b0} = reference (i.e., initial) brine pressure (Pa), constant in Equation (PA.29) and spatially variable in Equation (PA.30)
ρ_0 = reference (i.e., initial) brine density (kg/m^3)
c_ϕ = pore compressibility (Pa^{-1})
c_b = brine compressibility (Pa^{-1})
K = permeability of the material (m^2), isotropic for PA (Howarth and Christian-Frear 1997)

For the brine transport Equation (PA.25), the intrinsic permeability of the material is used. For the gas transport Equation (PA.24), the permeability K is modified to account for the Klinkenberg effect (Klinkenberg 1941). Specifically,

$$K_g = \left(1 + \frac{bK^a}{P_g}\right) \quad \text{(PA.31)}$$

where a and b are gas and formation-dependent constants. Values of $a = -0.3410$ and $b = 0.2710$ were determined from data obtained for MB 139 (Christian-Frear 1996), with these values used for all material regions in Figure PA-12.

The conservation equations are valid in one (i.e., $\nabla = [\partial/\partial x]$), two (i.e., $\nabla = [\partial/\partial x, \partial/\partial y]$), and three (i.e., $\nabla = [\partial/\partial x, \partial/\partial y, \partial/\partial z]$) dimensions. In PA, the preceding system of equations is used to model two-phase fluid flow within the two-dimensional region shown in Figure PA-12. The details of this system are discussed below.

The α term in Equation (PA.24) and Equation (PA.25) is a dimension-dependent geometry factor and is specified by

α = area normal to flow direction in one-dimensional flow (i.e., $\Delta y\, \Delta z$; units = m^2)
= thickness normal to flow plane in two-dimensional flow (i.e., Δz; units = m)
= 1 in three-dimensional flow (dimensionless) (PA.32)

PA uses a two-dimensional geometry to compute two-phase flow in the vicinity of the repository, and as a result, α is the thickness of the modeled region (i.e., Δz) normal to the flow plane (Figure PA-12). Due to the use of the two-dimensional grid in Figure PA-12, α is spatially dependent, with the values used for α defined in the column labeled "Δz." Specifically, α increases with distance away from the repository edge in both directions to incorporate the increasing pore volume through which fluid flow occurs. The method used in PA, called rectangular flaring, is illustrated in Figure PA-13 and ensures that the total volume surrounding the repository is conserved in the numerical grid. The equations and method used to determine α for BRAGFLO grids used in the WIPP PA were developed by Stein (Stein 2002).

The h term in Equation (PA.24) and Equation (PA.25) defines vertical distance from a reference point. In PA, this reference point is taken to be the center of MB 139 at the location of the shaft (i.e., $(x_{ref}, y_{ref}) = (23664.9\text{ m}, 378.685\text{ m})$, which is the center of cell 1272 in Figure PA-14). Specifically, h is defined by

$$h(x,y) = (x - x_{ref})\sin\theta + (y - y_{ref})\cos\theta \quad \text{(PA.33)}$$

where θ is the inclination of the formation in which the point (x, y) is located. In PA, the Salado is modeled as having an inclination of 1 degree from north to south, and all other formations are modeled as being horizontal. Thus, $\theta = 1$ degree for points within the Salado, and $\theta = 0$ degrees otherwise. Treating the Salado as an inclined formation and treating the Castile, Castile brine reservoir, Rustler, and overlying units as horizontal creates discontinuities in the grid at the lower and upper boundaries of the Salado. However, this treatment does not create a computational problem, since the Salado is isolated from vertical flow; its upper boundary adjoins the impermeable Los Medaños Member (formerly referred to as the Unnamed Member) at the base of the Rustler, and its lower boundary adjoins the impermeable Castile.

In the solution of Equation (PA.24), Equation (PA.25), Equation (PA.26), Equation (PA.27), Equation (PA.28), Equation (PA.29) and (PA.30), S_b and S_g are functions of location and time. Thus, P_c, k_{rb}, and k_{rg} are functions of the form $P_c(x, y, t)$, $k_{rb}(x, y, t)$, and $k_{rg}(x, y, t)$. In the computational implementation of the solution of the preceding equations, flow of phase l out of a computational cell (Figure PA-

14) cannot occur when $S_l(x, y, t) \le S_{lr}(x, y, t)$, where S_{lr} denotes the residual saturation for phase l. The values used for S_{lr}, $l = b, g$ are summarized in Table PA-3.

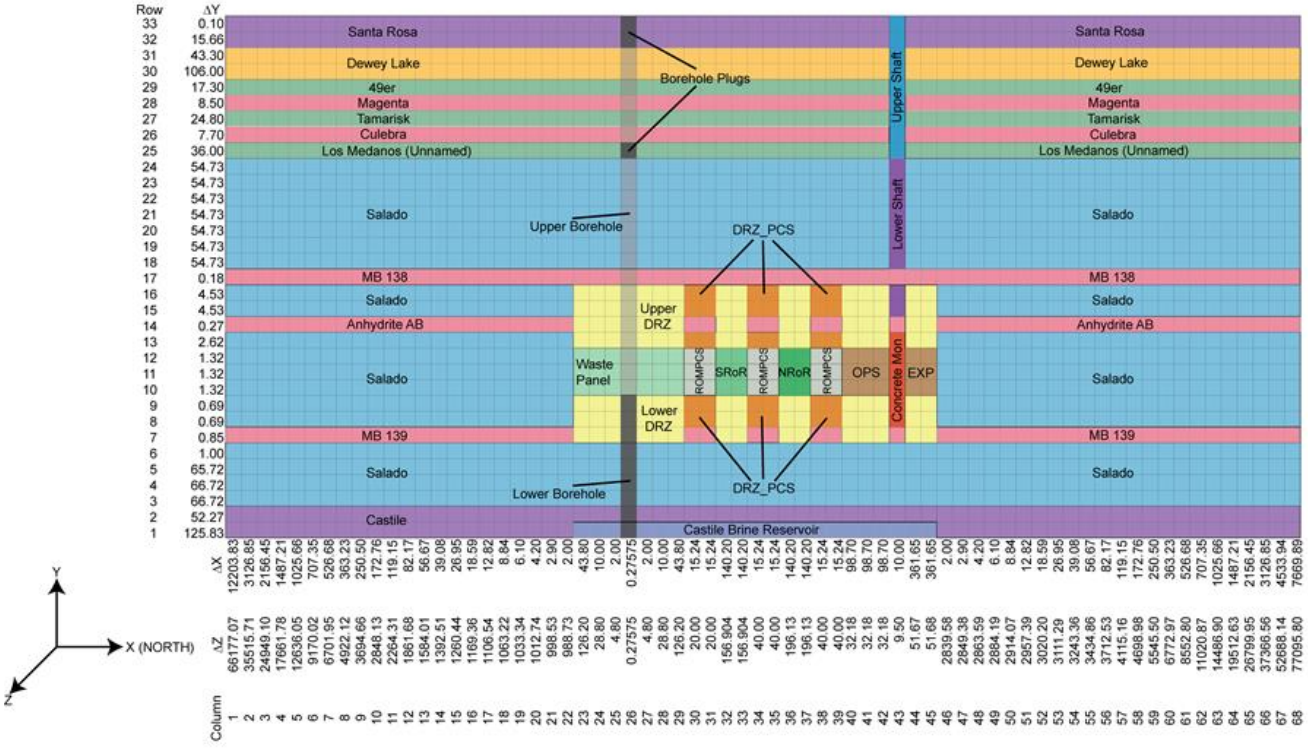

Figure PA- 12. Computational Grid Used in BRAGFLO for PA

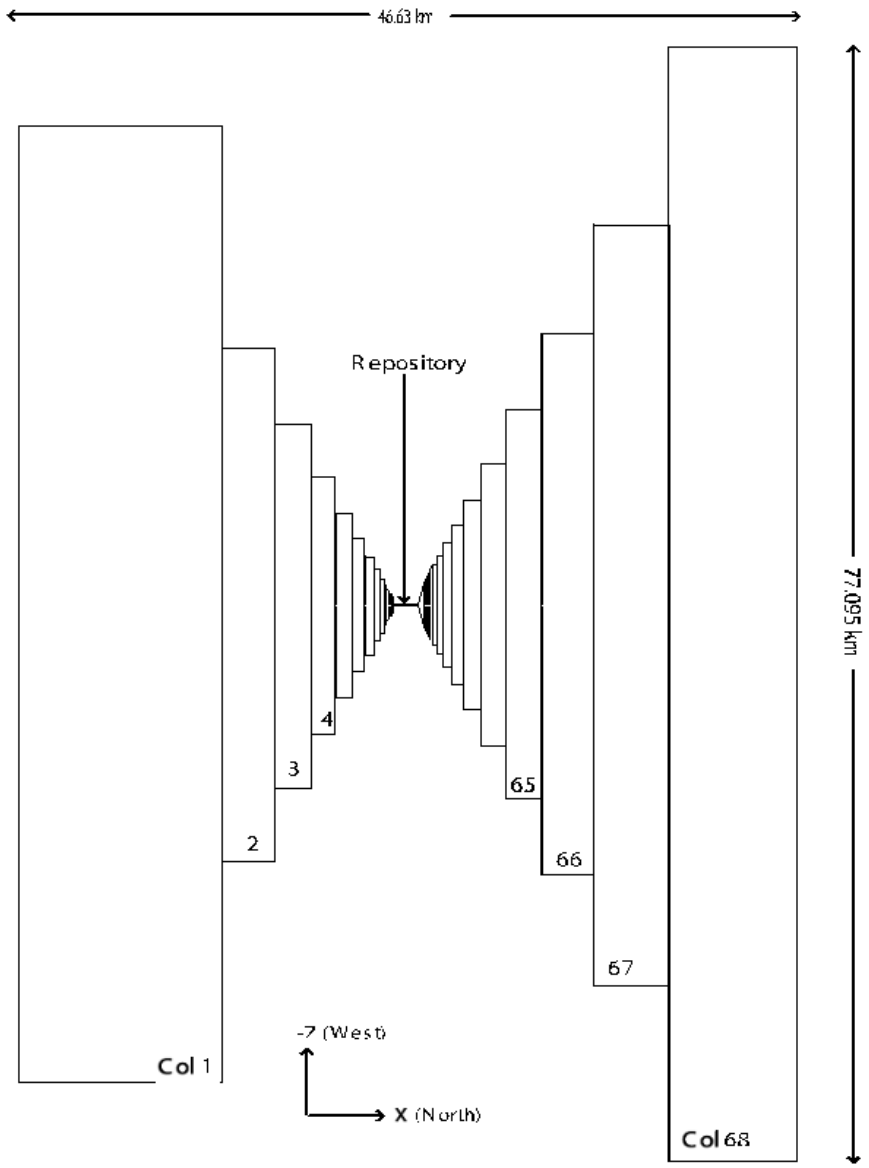

Figure PA- 13. Definition of Element Depth in BRAGFLO Grid

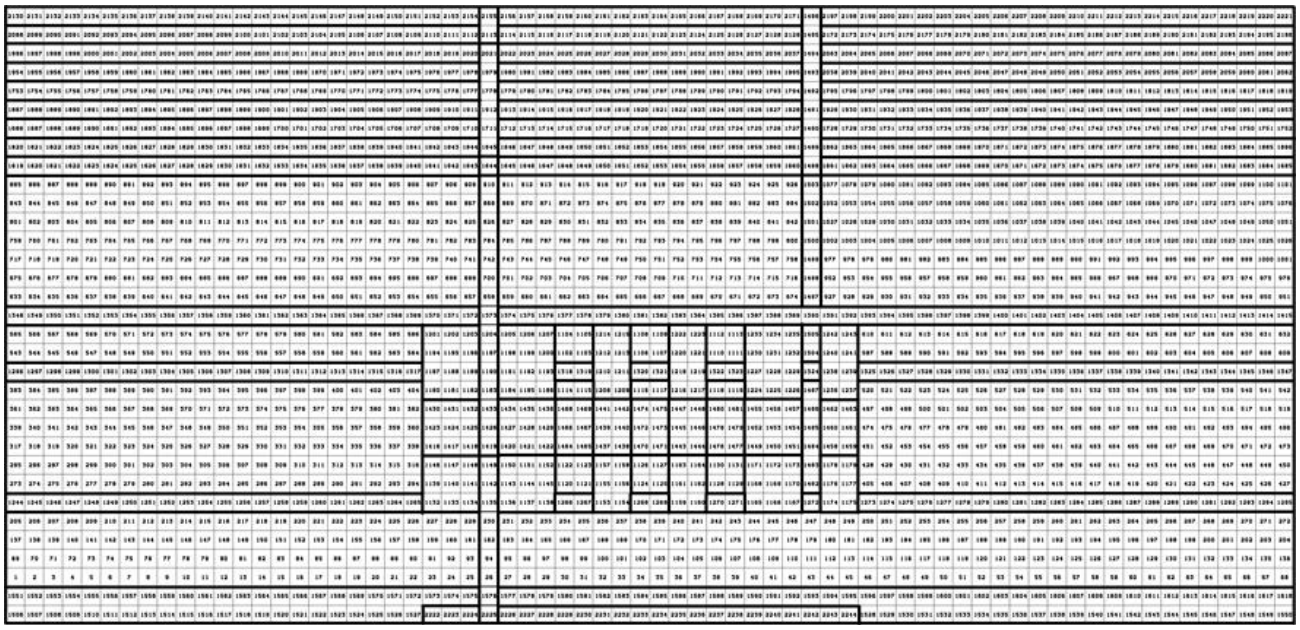

Figure PA- 14. BRAGFLO Grid Cell Indices

Table PA- 3. Parameter Values Used in Representation of Two-Phase Flow

Table PA-3. Parameter Values Used in Representation of Two-Phase Flow (Continued)

Region	Material	Material Description	Brooks-Corey Pore Distribution (PORE_DIS)[a] λ	Threshold Pressure Linear Parameter (PCT_A)[a] a	Threshold Pressure Exponential Parameter (PCT_EXP)[a] η	Residual Brine Saturation (SAT_RBRN)[a] *Sbr*	Residual Gas Saturation (SAT_RGAS)[a] *Sgr*	Porosity (POROSITY)[a] $\phi 0$	Pore Compressibility[a] c_ϕ, Pa^{-1}	Intrinsic Permeability (PRMX_LOG)[a] k, m^2
Region	Material	Material Description	Brooks-Corey Pore Distribution (PORE_DIS)[a] λ	Threshold Pressure Linear Parameter (PCT_A)[a] a	Threshold Pressure Exponential Parameter (PCT_EXP)[a] η	Residual Brine Saturation (SAT_RBRN)[a] *Sbr*	Residual Gas Saturation (SAT_RGAS)[a] *Sgr*	Porosity (POROSITY)[a] $\phi 0$	Pore Compressibility[a] c_ϕ, Pa^{-1}	Intrinsic Permeability (PRMX_LOG)[a] k, m^2
Salado	S_HALITE	Undisturbed halite	0.7	0.56	– 0.346	0.3	0.2	HALPOR[b]	f(HALCOMP)[b,d]	10^x, x = HALPRM[b]
DRZ	DRZ_0	DRZ, – 5 to 0 years	0.7	0.0	0.0	0.0	0.0	f(HALPOR)[b,c]	f(HALCOMP)[b,d]	$1.0 \times 10\text{-}17$
	DRZ_1	DRZ, 0 to 10,000 years	0.7	0.0	0.0	0.0	0.0	f(HALPOR)[b,c]	f(HALCOMP)[b,d]	10^x, x = DRZPRM[b]
MB 138	S_MB138	Anhydrite MB in Salado	ANHBCEXP[b]	0.26	– 0.348	ANRBSAT[b]	ANRGSSAT[b]	0.011	f(ANHCOMP)[b,d]	10^x, x = ANHPRM[b]
Anhydrite AB	S_ANH_AB	Anhydrite layers A and B in Salado	ANHBCEXP[b]	0.26	– 0.348	ANRBSAT[b]	ANRGSSAT[b]	0.011	f(ANHCOMP)[b,d]	10^x, x = ANHPRM[b]
MB 139	S_MB139	Anhydrite MB in Salado	ANHBCEXP[b]	0.26	– 0.348	ANRBSAT[b]	ANRGSSAT[b]	0.011	f(ANHCOMP)[b,d]	10^x, x = ANHPRM[b]
Waste Panel	CAVITY_1	Single waste panel, – 5 to 0 years	NA[e]	NA[e]	NA[e]	0.0	0.0	1.0	0.0	1.0×10^{-10}
	WAS_AREA	Single waste panel, 0 to 10,000 years	2.89	0.0	0.0	WRBRNSAT[b]	WRGSSAT[b]	0.848[f]	0.0	2.4×10^{-13}
Rest of Repository (SRoR and NRoR)	CAVITY_2	RoR, – 5 to 0 years	NA[e]	NA[e]	NA[e]	0.0	0.0	1.0	0.0	1.0×10^{-10}
	REPOSIT	RoR, 0 to 10,000 years	2.89	0.0	0.0	WRBRNSAT[b]	WRGSSAT[b]	0.848[f]	0.0	2.4×10^{-13}
Ops	CAVITY_3	Operations area, – 5 to 0 years	NA[e]	NA[e]	NA[e]	0.0	0.0	1.0	0.0	1.0×10^{-10}
	OPS_AREA	Operations area, 0 to 10,000 years	NA[e]	NA[e]	NA[e]	0.0	0.0	0.18	0.0	1.0×10^{-11}
Exp	CAVITY_3	Experimental area, – 5 to 0 years	NA[e]	NA[e]	NA[e]	0.0	0.0	1.0	0.0	1.0×10^{-10}

Table PA-3. Parameter Values Used in Representation of Two-Phase Flow (Continued)

Region	Material	Material Description	Brooks-Corey Pore Distribution (PORE_DIS)[a] λ	Threshold Pressure Linear Parameter (PCT_A)[a] a	Threshold Pressure Exponential Parameter (PCT_EXP)[a] η	Residual Brine Saturation (SAT_RBRN)[a] Sbr	Residual Gas Saturation (SAT_RGAS)[a] Sgr	Porosity (POROSITY)[a] $\phi 0$	Pore Compressibility[a] c_ϕ, Pa^{-1}	Intrinsic Permeability (PRMX_LOG)[a] k, m^2
Exp	EXP_AREA	Experimental area, 0 to 10,000 years	NA[e]	NA[e]	NA[e]	0.0	0.0	0.18	0.0	1.0×10^{-11}
Castile	IMPERM_Z	Castile	0.7	0.0	0.0	0.0	0.0	0.005	0.0	1.0×10^{-35}
Castile Brine Reservoir	CASTILER	Brine Reservoir in Castile	0.7	0.56	– 0.346	0.2	0.2	f(BPCOMP)[b,g]	f(BPCOMP)[b,d]	10^x, x = BPPRM[b]
Culebra	CULEBRA	Culebra Member of Rustler	0.6436	0.26	– 0.348	0.08363	0.07711	0.151	6.622517×10^{-10}	7.72681×10^{-14}
Magenta	MAGENTA	Magenta Member of Rustler	0.6436	0.26	– 0.348	0.08363	0.07711	0.138	1.915942×10^{-9}	6.309576×10^{-16}
Dewey Lake	DEWYLAKE	Dewey Lake Redbeds	0.6436	0.0	0.0	0.08363	0.07711	0.143	6.993007×10^{-8}	5.011881×10^{-17}
Santa Rosa	SANTAROS	Santa Rosa Formation	0.6436	0.0	0.0	0.08363	0.07711	0.175	5.714286×10^{-8}	1.0×10^{-10}
Los Medaños	UNNAMED	Los Medaños Member of Rustler	0.7	0.0	0.0	0.2	0.2	0.181	0.0	1.0×10^{-35}
Tamarisk	TAMARISK	Tamarisk Member of Rustler	0.7	0.0	0.0	0.2	0.2	0.064	0.0	1.0×10^{-35}
Forty-niner	FORTYNIN	Forty-niner Member of Rustler	0.7	0.0	0.0	0.2	0.2	0.082	0.0	1.0×10^{-35}
DRZ_PCS	DRZ_0	DRZ, -5 to 0 years	0.7	0.0	0.0	0.0	0.0	f(HALPOR)[b,c]	f(HALCOMP)[b,d]	1.0×10^{-17}
	DRZ_1	DRZ, 0 to 200 years	0.7	0.0	0.0	0.0	0.0	f(HALPOR)[b,c]	f(HALCOMP)[b,d]	10^x, x = DRZPRM[b]
	DRZ_PCS	DRZ above/below the panel closures, 200 to 10,000 years	0.7	0.0	0.0	0.0	0.0	f(HALPOR)[b,c]	f(HALCOMP)[b,d]	10^x, x = DRZPCPRM[b]

a Parenthetical parameter names are property names for the corresponding material, as indicated in Table PA-17 .

b Uncertain variable; see Table PA-17.
c See Equation (PA.34).
d See Equation (PA.37); f_0 can also be defined by an uncertain variable.
e These materials are using relative permeability model = 11; see Table PA-4.
f Initial value of porosity f_0; porosity changes dynamically to account for creep closure (see Section PA-4.2.3).
g See Equation (PA.35).

Table PA-3. Parameter Values Used in Representation of Two-Phase Flow (Continued)

Region	Material	Material Description	Brooks-Corey Pore Distribution (PORE_DIS)[a] λ	Threshold Pressure Linear Parameter (PCT_A)[a] a	Threshold Pressure Exponential Parameter (PCT_EXP)[a] η	Residual Brine Saturation (SAT_RBRN)[a] Sbr	Residual Gas Saturation (SAT_RGAS)[a] Sgr	Porosity (POROSITY)[a] $\phi 0$	Pore Compressibility[a] c_ϕ, Pa^{-1}	Intrinsic Permeability (PRMX_LOG)[a] k, m^2
ROMPCS	CAVITY_4	Panel closures, -5 to 0 years	NA[e]	NA[e]	NA[e]	0.0	0.0	1.0	0.0	1.0×10^{-10}
	PCS_T1	Panel closures, 0 to 100 years	T1PDIS[b]	0.0	0.0	T1SRBRN[b]	T1SRGAS[b]	T1POROS[b]	f(T1POROS)[b,d]	10^x, x = T1PRMX[b]
	PCS_T2	Panel closures, 100 to 200 years	T1PDIS[b]	0.0	0.0	T1SRBRN[b]	T1SRGAS[b]	T2POROS[b]	f(T2POROS)[b,d]	f(T2POROS)
	PCS_T3	Panel closures, 200 to 10,000 years	T1PDIS[b]	0.0	0.0	T1SRBRN[b]	T1SRGAS[b]	T3POROS[b]	f(T3POROS)[b,d]	f(T3POROS)
CONC_MON	CAVITY_4	Concrete monolith portion of shaft seals, – 5 to 0 years	NA[e]	NA[e]	NA[e]	0.0	0.0	1.0	0.0	1.0×10^{-10}
	CONC_MON	Concrete monolith portion of shaft seals, 0 to 10,000 years	0.94	0.0	0.0	SHURBRN[b]	SHURGAS[b]	0.05	1.2×10^{-9}	1.0×10^{-14}
Upper Shaft	CAVITY_4	Upper portion of shaft seals, – 5 to 0 years	NA[e]	NA[e]	NA[e]	0.0	0.0	1.0	0.0	1.0×10^{-10}

Table PA-3. Parameter Values Used in Representation of Two-Phase Flow (Continued)

Region	Material	Material Description	Brooks-Corey Pore Distribution (PORE_DIS)[a] λ	Threshold Pressure Linear Parameter (PCT_A)[a] a	Threshold Pressure Exponential Parameter (PCT_EXP)[a] η	Residual Brine Saturation (SAT_RBRN)[a] *Sbr*	Residual Gas Saturation (SAT_RGAS)[a] *Sgr*	Porosity (POROSITY)[a] ϕ_0	Pore Compressibility[a] c_ϕ, Pa^{-1}	Intrinsic Permeability (PRMX_LOG)[a] k, m^2
	SHFTU	Upper portion of shaft seals, 0 to 10,000 years	CONBCEXP[b]	0.0	0.0	SHURBRN[b]	SHURGAS[b]	0.005	2.05×10^{-8}	10^x, x = SHUPRM[b]

a Parenthetical parameter names are property names for the corresponding material, as indicated in Table PA-17 .

b Uncertain variable; see Table PA-17.
c See Equation (PA.34).
d See Equation (PA.37); f_0 can also be defined by an uncertain variable.
e These materials are using relative permeability model = 11; see Table PA-4.
f Initial value of porosity f_0; porosity changes dynamically to account for creep closure (see Section PA-4.2.3).
g See Equation (PA.35).

Table PA-3. Parameter Values Used in Representation of Two-Phase Flow (Continued)

Region	Material	Material Description	Brooks-Corey Pore Distribution (PORE_DIS)[a] λ	Threshold Pressure Linear Parameter (PCT_A)[a] a	Threshold Pressure Exponential Parameter (PCT_EXP)[a] η	Residual Brine Saturation (SAT_RBRN)[a] *Sbr*	Residual Gas Saturation (SAT_RGAS)[a] *Sgr*	Porosity (POROSITY)[a] ϕ_0	Pore Compressibility[a] c_ϕ, Pa^{-1}	Intrinsic Permeability (PRMX_LOG)[a] k, m^2
Lower Shaft	CAVITY_4	Lower portion of shaft seals, − 5 to 0 years	NA[c]	NA[c]	NA[c]	0.0	0.0	1.0	0.0	1.0×10^{-10}
	SHFTL_T1	Lower portion of shaft seals, 0 to 200 years	CONBCEXP[b]	0.0	0.0	SHURBRN[b]	SHURGAS[b]	0.005	4.28×10^{-9}	10^x, x = SHLPRM1[b]
	SHFTL_T2	Lower portion of shaft seals, 200 to 10,000 years	CONBCEXP[b]	0.0	0.0	SHURBRN[b]	SHURGAS[b]	0.005	4.28×10^{-9}	10^x, x = SHLPRM2[b]
Borehole plugs	CONC_PLG	Concrete borehole plug, before plug degradation	0.94	0.0	0.0	0.0	0.0	0.32	1.1875×10^{-9}	10^x, x = PLGPRM[b]
	BH_SAND	Borehole after plug degradation, 200 years after intrusion	0.94	0.0	0.0	0.0	0.0	0.32	0.0	10^x, x = BHPRM[b]
Upper Borehole	BH_OPEN	Borehole above repository before plug degradation	0.7	0.0	0.0	0.0	0.0	0.32	0.0	1.0×10^{-9}
	BH_SAND	Borehole after plug degradation, 200 years after intrusion	0.94	0.0	0.0	0.0	0.0	0.32	0.0	10^x, x = BHPRM[b]
Lower Borehole	BH_OPEN	Borehole below repository before creep closure	0.7	0.0	0.0	0.0	0.0	0.32	0.0	1.0×10^{-9}
	BH_CREEP	Borehole below repository after creep closure, 1,000 years after intrusion	0.94	0.0	0.0	0.0	0.0	0.32	0.0	$10^x/10$, x = BHPRM[a]

a Parenthetical parameter names are property names for the corresponding material, as indicated in Table PA-17 .

b Uncertain variable; see Table PA-17.
c See Equation (PA.34).
d See Equation (PA.37); f_0 can also be defined by an uncertain variable.
e These materials are using relative permeability model = 11; see Table PA-4.
f Initial value of porosity f_0; porosity changes dynamically to account for creep closure (see Section PA-4.2.3).
g See Equation (PA.35).

Values for ϕ_0 and c_ϕ (Equation (PA.30)) are also given in Table PA-3. Initial porosity ϕ_0 for the DRZ is a function of the uncertain parameter for initial halite porosity ϕ_{0H} (HALPOR; see Table PA-17) and is given by Martell (Martell 1996a) and Bean (Bean et al 1996), Section 4:

$$\phi_0 = \phi_{0H} + 0.0029 \quad \text{(PA.34)}$$

Initial porosity ϕ_0 of the Castile brine reservoir is calculated from the uncertain sampled parameter for the bulk Castile rock compressibility (BPCOMP; see Table PA-17), according to the following relationship:

$$\phi_0 = \frac{BPCOMP}{1.0860 \times 10^{-12}} \quad \text{(PA.35)}$$

where 1.0860×10^{-10} is a scaling constant that ensures that the productivity ratio, PR, remains constant at 2.0×10^{-3} m^3/Pa. The productivity ratio PR is computed by

$$PR = V \frac{BPCOMP}{\phi_0} \quad \text{(PA.36)}$$

where V is the volume of the grid block representing the Castile brine reservoir in Figure PA-12. Because of this relationship, the initial porosity of the brine reservoir ranges from 0.1842 to 0.9208. This range of porosity is not meant to represent an actual reservoir, but rather allows a reservoir to supply a volume of brine to the repository in the event of an E1 intrusion consistent with observed brine flows in the Delaware Basin.

The compressibility c_ϕ in Equation (PA.30) and Table PA-3 is pore compressibility. Compressibility is treated as uncertain for Salado anhydrite, Salado halite, and regions of pressurized brine in the Castile. However, the sampled value for each of these variables corresponds to bulk compressibility rather than to the pore compressibility actually used in the calculation. Assuming all of the change in volume during compression occurs in the pore volume, the conversion from bulk compressibility C_r to pore compressibility C_ϕ is approximated by

$$C_\phi = \frac{C_r}{\phi_0} \quad \text{(PA.37)}$$

where ϕ_0 is the initial porosity in the region under consideration.

The primary model used in PA for capillary pressure P_c and relative permeability k_{rl} is a modification of the Brooks-Corey model (Brooks and Corey 1964). In this model, P_c, k_{rb}, and k_{rg} are defined by

$$P_c = P_t(k) / S_{e2}^{1/\lambda} \quad \text{(PA.38)}$$

$$k_{rb} = S_{e1}^{(2+3\lambda)/\lambda} \quad \text{(PA.39)}$$

$$k_{rg} = (1 - S_{e2})^2 \left(1 - S_{e2}^{(2+\lambda)/\lambda}\right) \quad \text{(PA.40)}$$

where

λ = pore distribution parameter (dimensionless)
$P_t(k)$ = capillary threshold pressure (Pa) as a function of intrinsic permeability k (Webb 1992)
$= \alpha k^\eta$ (PA.41)
S_{e1} = effective brine saturation (dimensionless) without correction for residual gas saturation
$= (S_b - S_{br}) / (1 - S_{br})$ (PA.42)
S_{e2} = effective brine saturation (dimensionless) with correction for residual gas saturation
$= (S_b - S_{br}) / (1 - S_{gr} - S_{br})$ (PA.43)

The values used for λ, α, η, S_{br}, S_{gr}, and k are summarized in Table PA-3. The statement that the Brooks-Corey model is in use means that P_c, k_{rb}, and k_{rg} are defined by Equation (PA.38), Equation (PA.39) and Equation (PA.40).

In the anhydrite MBs, either the Brooks-Corey model or the van Genuchten-Parker model is used as determined by the subjectively uncertain parameter ANHBCVGP (see Table PA-17). A linear model is used to represent two-phase flow in an open borehole (i.e., for the first 200 years after a drilling intrusion for boreholes with two-plug or three-plug configurations, in the open cavities [CAVITY_1, . . , CAVITY_4], and for the experimental and operations areas). This is discussed further below.

In the van Genuchten-Parker model, P_c, k_{rb}, and k_{rg} are defined by (van Genuchten 1978)

$$P_c = P_{VGP} \left(S_{e2}^{-1/m} - 1\right)^{1-m} \quad \text{(PA.44)}$$

$$k_{rb} = S_{e1}^{1/2} \left[1 - \left(1 - S_{e1}^{1/m}\right)^m\right]^2 \quad \text{(PA.45)}$$

$$k_{rg} = (1 - S_{e2})^{1/2} \left(1 - S_{e2}^{1/m}\right)^{2m} \quad \text{(PA.46)}$$

where $m = \lambda/(1 + \lambda)$ and the capillary pressure parameter P_{VGP} is determined by requiring that the capillary pressures defined in Equation (PA.38) and Equation (PA.44) are equal at an effective brine saturation of $S_{e2} = 0.5$ (Webb 1992). The van Genuchten-Parker model is only used for the anhydrite MBs in the Salado and uses the same values for λ, S_{br}, and S_{gr} as the Brooks-Corey model (Table PA-3).

In the linear model used for the open borehole (RELP_MOD = 5), P_c, k_{rb}, and k_{rg} are defined by

$P_c = 0, k_{rb} = S_{e1}, k_{rg} = 1 - S_{e1}$ (PA.47)

Another linear model (RELP_MOD = 11) is used for the open cavities (CAVITY_1, . . . , CAVITY_4) for the −5 to 0 year portion of the simulation (see Section PA-4.2.2) and the experimental and operations areas (t = 0 to 10,000 years) which, in PA, are modeled without a time-dependent creep closure:

$k_{ri} = 0 \quad for \quad S_l < S_{lr}$ (PA.48)

$k_{ri} = \frac{(S_l - S_{lr})}{tol} \quad for \quad S_{lr} \le S_l \le S_{lr} + tol$ (PA.49)

$k_{ri} = 1 \quad for \quad S_l > S_{lr} + tol$ (PA.50)

where l = gas or brine and tol is a tolerance (slope) over which the relative permeability changes linearly from 0 to 1. In PA, $tol = 1 \times 10^{-2}$ (dimensionless). Thus, the relative permeabilities are ~ 1 for saturations away from residual saturation.

Capillary pressure P_c for both the van Genuchten-Parker and Brooks-Corey models becomes unbounded as brine saturation S_b approaches the residual brine saturation, S_{br}. To avoid unbounded values, P_c is capped at 1×10^8 Pa in selected regions (Table PA-4).

Gas density is computed using the RKS equation of state, with the gas assumed to be pure H_2. For a pure gas, the RKS equation of state has the form (Walas 1985, pp. 43−54)

$P_g = \frac{RT}{V - b} - \frac{a\alpha}{V(V + b)}$ (PA.51)

where

R = gas constant = 8.31451 Joules (J) mole (mol)$^{-1}$ K^{-1}
T = temperature (K) = 300.15 K (= 30 °C; 81 °F)
V = molar volume (m^3 mol^{-1})
$a = 0.42747\, R^2\, T^2_{crit} / P_{crit}$
$b = 0.08664\, RT_{crit} / P_{crit}$

$\alpha = \left[1 + \left(0.48508 + 1.55171\omega - 0.15613\omega^2\right)\left(1 - T_r^{0.5}\right)\right]^2$
$\approx 1.202 \exp\left(-0.30288 T_r\right)$ for H_2 (Graboski and Daubert 1979)
T_{crit} = critical temperature (K)
P_{crit} = critical pressure (Pa)
$T_r = T / T_{crit}$ = reduced temperature
ω = acentric factor
= 0 for H_2 (Graboski and Daubert 1979)

Table PA- 4. Models for Relative Permeability and Capillary Pressure in Two-Phase Flow

Material	Relative Permeability[a] (RELP_MOD)	Capillary Pressure[b] (CAP_MOD)	Material	Relative Permeability[a] (RELP_MOD)	Capillary Pressure[b] (CAP_MOD)
BH_OPEN	5	1	MAGENTA	4	2
BH_SAND	4	1	OPS_AREA	11	1
BH_CREEP	4	1	PCS_T1	4	1
CASTILER	4	2	PCS_T2	4	1
CAVITY_1	11	1	PCS_T3	4	1
CAVITY_2	11	1	REPOSIT	12	1
CAVITY_3	11	1	SANTAROS	4	1
CAVITY_4	11	1	SHFTU	4	1
CONC_MON	4	2	SHFTL_T1	4	1
CONC_PLG	4	1	SHFTL_T2	4	1

CULEBRA	4	2	S_ANH_AB	ANHBCVGP[c]	2
DEWYLAKE	4	1	S_HALITE	4	2
DRZ_0	4	1	S_MB138	ANHBCVGP[c]	2
DRZ_1	4	1	S_MB139	ANHBCVGP[c]	2
DRZ_PCS	4	1	TAMARISK	4	1
EXP_AREA	11	1	UNNAMED	4	1
FORTYNIN	4	1	WAS_AREA	12	1
IMPERM_Z	4	1			

[a] Relative permeability model, where 4 = Brooks-Corey model given by Equation (PA.38) , Equation (PA.39) and Equation (PA.40), 5 = linear model given by Equation (PA.47), 11 = linear model given by Equation (PA.48), Equation (PA.49) and Equation (PA.50), 12 = modified Brooks-Corey model to account for cutoff saturation (Camphouse 2013b), and ANHBCVGP = use of Brooks-Corey or van Genuchten-Parker model treated as a subjective uncertainty.

[b] Capillary pressure model, where 1 = capillary pressure is unbounded, 2 = P_c bounded above by 1×10^8 Pa as S_b approaches S_{br}.

[c] See ANHBCVGP in Table PA-17.

In order to account for quantum effects in H_2, effective critical temperature and pressure values of $T_{crit} = 43.6$ K and $P_{crit} = 2.047 \times 10^6$ Pa are used instead of the true values for these properties (Prausnitz 1969). Equation (PA.51) is solved for molar volume V. The gas density ρ_g then is given by

$$\rho_g = \frac{M_{w,H_2}}{V} \quad \text{(PA.52)}$$

where M_{w,H_2} is the molecular weight of H_2 (i.e., 2.01588×10^{-3} kg/mol; see Weast 1969, p. B-26).

Brine density ρ_b is defined by Equation (PA.29), with $\rho_{b0} = 1230.0$ kg/m^3 at a pressure of $P_{b0} = 1.0132 \times 10^5$ Pa and $c_b = 2.5 \times 10^{-10}$ Pa^{-1} (Roberts 1996). Porosity, ϕ, is used as defined by Equation (PA.30) with two exceptions: in the repository (see Section PA-4.2.3) and in the DRZ and MBs subsequent to fracturing (see Section PA-4.2.4). The values of ϕ_0 and c_ϕ used in conjunction with Equation (PA.30) are listed in Table PA-3. The reference pressure P_{b0} in Equation (PA.30) is spatially variable and corresponds to the initial pressures $P_b(x, y, -5)$ (here, −5 means at time equal to −5 years; see Section PA-4.2.2). The gas and brine viscosities μ_l, $l = g, b$ in Equation (PA.24) and Equation (PA.25) were assumed to have values of $\mu_g = 8.93 \times 10^{-6}$ Pa s (H2:VISCO; see Vargaftik 1975) and $\mu_b = 2.1 \times 10^{-3}$ Pa s (BRINESAL:VISCO; see McTigue 1993).

The terms q_g, q_{rg}, q_b, and q_{rb} in Equation (PA.24) and Equation (PA.25) relate to well injection or removal (i.e., q_g, q_b) and reaction, production, or consumption (i.e., q_{rg}, q_{rb}) of gas and brine, with positive signs corresponding to injection or production and negative signs corresponding to removal or consumption. In the long-term Salado flow calculations, no injection or removal of gas or brine is calculated using q_g and q_b. Thus, q_g and q_b are equal to zero. That is, after an intrusion, the borehole is treated as a porous media, rather than a point source or sink of brine and gas. Furthermore, the mass and pressure lost to a DBR during the intrusion is conservatively ignored in the BRAGFLO calculations. In the DBR calculations discussed in Section PA-4.7, q_g and q_b are used to describe injection and production wells in the DBR grid.

More detail on the definition of q_{rg} and q_{rb} is provided in Section PA-4.2.5.

PA-4.2.2 Initial Conditions

In each two-phase flow simulation, a short period of time representing disposal operations is simulated. This period of time is called the start-up period, and covers 5 years from $t = -5$ years to 0 years, corresponding to the amount of time a typical panel is expected to be open during disposal operations. All grid locations require initial brine pressure and gas saturation at the beginning of the simulation (t = –5 years).

The Rustler and overlying units (except in the shaft) are modeled as horizontal with spatially constant initial pressure in each layer (see Figure PA-12). Table PA-5 lists the initial brine pressure, P_b, and gas saturation, S_g, for the Rustler.

The Salado (Mesh Rows 3-24 in Figure PA-12) is assumed to dip uniformly $\theta = 1$ degree downward from north to south (right to left in Figure PA-12). Except in the repository excavations and the shaft, brine is initially assumed (i.e., at −5 years) to be in hydrostatic equilibrium relative to an uncertain initial pressure $P_{b,ref}$ (SALPRES; see Table PA-17) at a reference point located at shaft center at the elevation of the midpoint of MB 139, which is the center of Cell 1272 in Figure PA-14. This gives rise to the condition

$$P_b(x, y, -5) = P_{b,ref} + \frac{1}{c_b} \ln\left[\frac{\rho_b(x, y, -5)}{\rho_{b0}}\right] \quad \text{(PA.53)}$$

$$\rho_b(x, y, -5) = \frac{1}{g\, c_b \left[y_e - \Phi\left(x_{ref}, y_{ref}, -5\right)\right] + \frac{1}{g\, c_b\, \rho_{b0}}} \quad \text{(PA.54)}$$

$$\Phi\left(x_{ref}, y_{ref}, -5\right) = y_{ref} + \frac{1}{g\, c_b}\left[\frac{1}{\rho_{b0}} - \frac{1}{\rho_b\left(x_{ref}, y_{ref}, -5\right)}\right] \quad \text{(PA.55)}$$

$$\rho_b\left(x_{ref}, y_{ref}, -5\right) = \rho_{b0} \exp\left[-c_b\left(P_{b,ref} - P_{b0}\right)\right] \quad \text{(PA.56)}$$

$$y_e = y_{ref} + h(x, y) \quad \text{(PA.57)}$$

Table PA- 5. Initial Conditions in the Rustler

Name	Mesh Row (Figure PA-12)	P_b (x, y, -5), Pa	S_g (x, y, -5)
Santa Rosa	33	1.013250×10^5	$1 - S_b = 0.916$ (S_b = SANTAROS:SAT_IBRN)[a]
Santa Rosa	32	1.013250×10^5	$1 - S_b = 0.916$ (S_b = SANTAROS:SAT_IBRN)[a]
Dewey Lake	31	1.013250×10^5	$1 - S_b = 0.916$ (S_b = SANTAROS:SAT_USAT)[a]
Dewey Lake[c]	30	7.355092×10^5	$1 - S_b = 0.916$ (S_b = SANTAROS:SAT_USAT)[a]
Forty-niner[c]	29	1.47328×10^6	0[b]
Magenta	28	9.465×10^5 (MAGENTA:PRESSURE)	0[b]
Tamarisk[c]	27	1.82709×10^6	0[b]
Culebra	26	9.141×10^5 (CULEBRA:PRESSURE)	0[b]
Los Medaños [c]	25	2.28346×10^6	0[b]

[a] The names in parenthesis are parameters in the WIPP PA Parameter Database.

[b] The Rustler is assumed to be fully saturated. This initial condition is set in the program ICSET. See (Nemer and Clayton 2008), Section 3.2.

[c] These pressures are calculated in the ALGEBRA1 step analogously to Equation (PA.53), using the brine density of 1220 kg/m^3. See subsequent discussion taking $\theta = 0$ and the reference point (x_{ref}, y_{ref}) at the top of the Dewey Lake. See the ALGEBRA input file ALG1_BF_CRA09.INP in library LIBCRA09_BF, class CRA09-1 on the WIPP PA cluster for details. See (Nemer and Clayton 2008), Section 4.1.7 for details on the ALGEBRA1 step.

where

$h(x, y)$ is defined in Equation (PA.33)
$\rho_{b0} = 1220$ kg/m^3 (BRINESAL:DNSFLUID)
$c_b = 3.1 \times 10^{-10}$ Pa^{-1} (BRINESAL:COMPRES)
$g = 9.80665$ meters per second squared (m/s^2)
$P_{b,ref} = 1.01325 \times 10^5$ Pa (BRINESAL:REF_PRES)
P_{b0} = sampled far-field pressure in the undisturbed halite (S_HALITE:PRESSURE)

In the Salado, initial gas saturation $S_g(x, y, -5) = 0$ (see Nemer and Clayton 2008, Section 4.1.6). The Castile (Mesh Rows 1 and 2) is modeled as horizontal and initial brine pressure is spatially constant within each layer (no dip), except that the brine reservoir is treated as a different material from the rest of the Castile and has a different initial pressure, which is a sampled parameter. Specifically, outside the brine reservoir, pressure is calculated using Equation (PA.53) with no dip ($\theta = 0$) in the ALGEBRA1 step. Within the reservoir, $P_b(x, y, -5) = BPINTPRS$, the uncertain initial pressure in the reservoir (see Table PA-17). Initial gas saturation $S_g(x, y, -5) = 0$.

Within the shaft (areas Upper Shaft, Lower Shaft, and CONC_MON) and panel closures (areas ROMPCS), $P_b(x, y, -5) = 1.01325 \times 10^5$ Pa and $S_g(x, y, -5) = 1$. Within the excavated area (Waste Panel, South RoR, and North RoR, Ops and Exp), $P_b(x, y, -5) = 1.01325 \times 10^5$ Pa and $S_g(x, y, -5) = 1$.

At the end of the initial five-year start-up period and the beginning of the regulatory period ($t = 0$ years), brine pressure and gas saturation are reset in the shaft, panel closures, and excavated areas. In the shaft (areas Upper Shaft, Lower Shaft, and CONC_MON), $P_b(x, y, 0) = 1.01325 \times 10^5$ Pa and $S_g(x, y, 0) = 1 \times 10^{-7}$. In the panel closures, $P_b(x, y, 0) = 1.01325 \times 10^5$ Pa and $S_g(x, y, 0) = 1$ - PCS_T1:SAT_RBRN, where PCS_T1:SAT_RBRN is a sampled parameter having a minimum of 0.0 and a maximum of 0.6. In the waste disposal regions (areas Waste Panel, South RoR, and North RoR), $P_b(x, y, 0) = 1.28039 \times 10^5$ Pa and $S_g(x, y, 0) = 0.985$ (see WAS_AREA:SAT_IBRN). The initial pressure in the waste disposal regions is greater than atmospheric pressure (1.01325×10^5 Pa) to account for the incremental pressure generated by faster initial microbial gas generation rates observed during laboratory experiments

(Nemer and Stein 2005, Sections 3.2 and 5.5.2). In the other excavated areas, $P_b(x, y, 0) = 1.01325 \times 10^5$ Pa and $S_g(x, y, 0) = 1.0$. The value of initial pressure in the waste disposal regions is identical with that used in the CRA-2009 PABC (Clayton et al. 2010).

PA-4.2.3 Creep Closure of Repository

Salt creep occurs naturally in the Salado halite in response to deviatoric stress. Inward creep of rock is generally referred to as creep closure. Creep closure of excavated regions begins immediately from excavation-induced deviatoric stress. If the rooms were empty, closure would proceed to the point where the void volume created by the excavation would be eliminated as the surrounding formation returned to a uniform stress state. In the waste disposal region, inward creep of salt causes consolidation of the waste, and this waste consolidation continues until the load on the surrounding rock reached lithostatic, and the deviatoric stress is removed, at which point salt creep and waste consolidation ceases. The amount of waste consolidation that occurs and the time it takes to consolidate are governed by the waste properties (e.g., waste strength, modulus, etc.), the surrounding rock properties, the dimensions and location of the room, and relative quantities of brine and gas present.

The porosity of the waste disposal regions and neighboring access drifts (i.e., Waste Panel, South RoR, and North RoR in Figure PA-12) is assumed to change through time due to creep closure of the halite surrounding the excavations. The equations on which BRAGFLO is based do not incorporate this type of deformation. Therefore, the changes in repository porosity due to halite deformation are modeled in a separate analysis with the geomechanical program SANTOS, which implements a quasi-static, large-deformation, finite-element procedure (Stone 1997). Interpolation procedures are then used with the SANTOS results to define porosity (ϕ) within the repository as a function of time, pressure, and gas generation rate.

For more information on the generation of the porosity surface for BRAGFLO in PA, see Appendix PORSURF-2014.

PA-4.2.4 Fracturing of MBs and DRZ

Fracturing within the anhydrite MBs (i.e., regions MB 138, Anhydrite AB, and MB 139 in Figure PA-12) and in the DRZ (region DRZ in Figure PA-12) is assumed to occur at brine pressures slightly above lithostatic pressure, and is implemented through a pressure-dependent compressibility $c_r(P_b)$ (Mendenhall and Gerstle 1995). Specifically, MB fracturing begins at a brine pressure of

$$P_{bi} = P_{b0} + \Delta P_i \quad \text{(PA.58)}$$

where P_{bi} and P_{b0} are spatially dependent (i.e., $P_{b0} = P(x, y, 0)$ as in Section PA-4.2.2) and $\Delta P_i = 2 \times 10^5$ Pa (see S_MB138:PI_DELTA in Kicker and Herrick 2013, Table 22)

Fracturing ceases at a pressure of

$$P_{ba} = P_{b0} + \Delta P_a \quad \text{(PA.59)}$$

and a fully fractured porosity of

$$\phi(P_{ba}) = \phi_a = \phi_0 + \Delta\phi_a \quad \text{(PA.60)}$$

where $\Delta P_a = 3.8 \times 10^6$ Pa (see S_MB138:PF_DELTA in Kicker and Herrick 2013, Table 22), ϕ_0 is spatially dependent (Table PA-3), and $\Delta\phi_a = 0.04$, 0.24, and 0.04 for anhydrite materials S_MB138, S_ANH_AB, and S_MB139, respectively (see e.g. S_MB138:DPHIMAX in Kicker and Herrick 2013, Table 22).

Once fractured, compressibility c_r becomes a linear function

$$c_r(P_b) = c_r + \left(\frac{P_b - P_{bi}}{P_{ba} - P_{bi}}\right)(c_{ra} - c_r) \quad \text{(PA.61)}$$

of brine pressure for $P_{bi} \le P_b \le P_{ba}$, with c_{ra} defined so that the solution ϕ of

$$\frac{d\phi}{dP_b} = c_{ra}(P_b)\phi, \quad \text{where} \quad \phi(P_{bi}) = \phi_0 \exp\left[c_r(P_{bi} - P_{b0})\right] \quad \text{(PA.62)}$$

satisfies $\phi(P_{ba}) = \phi_a$; specifically, c_{ra} is given by

$$c_{ra} = c_r\left[1 - \frac{2(P_{ba} - P_{b0})}{P_{ba} - P_{bi}}\right] + \left[\frac{2}{P_{ba} - P_{bi}}\right]\ln\left(\frac{\phi_a}{\phi_0}\right) \quad \text{(PA.63)}$$

The permeability $k_f(P_b)$ of fractured material at brine pressure P_b is related to the permeability of unfractured material at brine pressure P_{bi} by

$$k_f(P_b) = \left[\frac{\phi(P_b)}{\phi(P_{bi})}\right]^n k \quad \text{(PA.64)}$$

where k is the permeability of unfractured material (i.e., at P_{bi}) and n is defined so that $k_f(P_{ba}) = 1 \times 10^{-9}$ m^2 (i.e., n is a function of k, which is an uncertain input to the analysis; see ANHPRM in Table PA-17). When fracturing occurs, $k_f(P_b)$ is used instead of k in the definition of the permeability for the fractured areas of the anhydrite MBs.

Fracturing is also modeled in the DRZ region in Figure PA-12. The fracture model implementation is the same as for the anhydrite materials. In this case, fracturing would be in halite rather than anhydrite, but because of the limited extent of the DRZ and the proximity of the nearby interbeds, this representation was deemed acceptable by the Salado Flow Peer Review panel (Caporuscio, Gibbons, and Oswald 2003).

PA-4.2.5 Gas Generation and Brine Production

Gas production is assumed to result from anoxic corrosion of steel and the microbial degradation of CPR materials. Thus, the gas generation rate q_{rg} in Equation (PA.24) is of the form

$$q_{rg} = q_{rgc} + q_{rgs} + q_{rgm} \quad \text{(PA.65)}$$

where q_{rgc} is the rate of gas production per unit volume of waste (kg/m^3/s) due to anoxic corrosion of Fe-base metals, q_{rgs} is the rate of gas production per unit volume of waste (kg/m^3/s) due to sulfidation of Fe-base metals, and q_{rgm} is the rate of gas production per unit volume of waste (kg/m^3/s) due to microbial degradation of CPR materials. Furthermore, the brine production rate q_{rb} in Equation (PA.25) is of the form

$$q_{rb} = q_{rbc} + q_{rbs} + q_{rbm} + q_{rbh} + q_{rbhc} \quad \text{(PA.66)}$$

where q_{rbc} is the rate of brine production per unit volume of waste (kg/m^3/s) due to anoxic corrosion of Fe-base metals, q_{rbs} is the rate of brine production per unit volume of waste (kg/m^3/s) due to sulfidation of Fe-base metals, q_{rbm} is the rate of brine production per unit volume of waste (kg/m^3/s) due to microbial degradation of CPR materials, q_{rbh} is the rate of brine production per unit volume of waste (kg/m^3/s) due to hydration of MgO, and q_{rbhc} is the rate of brine production per unit volume of waste (kg/m^3/s) due to hydromagnesite conversion to magnesite (developed in Clayton 2013).

Chemical reactions are assumed to take place only within the waste disposal regions (i.e., Waste Panel, South RoR, and North RoR in Figure PA-12) and all the generated gas is assumed to have the same properties as H_2 (see discussion in Appendix MASS-2014, Section MASS-3.2). In PA, the consumable materials are assumed to be homogeneously distributed throughout the waste disposal regions (i.e., the concentration of Fe-base metals, CPR materials and MgO in the waste area is not spatially dependent). A separate analysis examined the potential effects on PA results of spatially varying Fe-base metal and CPR material concentrations, and concluded that PA results are not affected by representing these materials with spatially varying concentrations (see Appendix MASS-2014, Section MASS-19.0).

The rates q_{rgc}, q_{rgs}, q_{rgm}, q_{rbc}, q_{rbs}, q_{rbm}, q_{rbh}, q_{rbhc} (kg/m^3/s) are defined by

gas generation by corrosion

$$q_{rgc} = \left\{R_{ci} S_{b,eff} + R_{ch} S_g^*\right\} D_c \rho_{Fe} X_c \left(H_2|Fe\right) M_{H_2} \quad \text{(PA.67)}$$

gas generation by sulfidation

$$q_{rgs} = q_{rgm} X_m (H_2S|C) X_s (H_2|Fe) \quad \text{(PA.68)}$$

microbial gas generation

$$q_{rgm} = \left(R_{mi} S_{b,eff} + R_{mh} S_g^*\right) D_c X_m (H_2|C) M_{H_2} B_{fc} \quad \text{(PA.69)}$$

brine production by corrosion

$$q_{rbc} = q_{rgc} X_c (H_2O|H_2) M_{H_2O} / M_{H_2} \quad \text{(PA.70)}$$

brine production by sulfidation

$$q_{rbs} = q_{rgs} X_s (H_2O|H_2) M_{H_2O} / M_{H_2} \quad \text{(PA.71)}$$

microbial brine production

$$q_{rbm} = q_{rgm} X_m (H_2O|H_2) M_{H_2O} / M_{H_2} \quad \text{(PA.72)}$$

brine production by MgO hydration

$$q_{rbh} = \left(R_{hi}S_{b,eff} + R_{hh}S_g^*\right)D_m X_h(H_2O|MgO)M_{H_2O}$$ (PA.73)

brine production by hydromagnesite conversion to magnesite

$$q_{rbhc} = R_{hc}D_{HM}X_{hc}(H_2O|HM)M_{H_2O}$$ (PA.74)

where

D_s = surface area concentration of steel in the repository (m^2 surface area steel/ m^3 disposal volume)
D_c = mass concentration of cellulosics in the repository (kg biodegradable material/m^3 disposal volume)
D_m = mass concentration of MgO in the repository (kg MgO/m^3 disposal volume)
D_{HM} = mass concentration of hydromagnesite in the repository (kg hydromagnesite /m^3 disposal volume)
M_{H_2} = molecular weight of H_2 (kg H_2/mol H_2), 2.02×10^{-3} kg/mol (Lide 1991, pp. 1-7, 1-8)
M_{H_2O} = molecular weight of water (H_2O) (kg H_2O/mol H_2O), 1.80×10^{-2} kg/mol (Lide 1991, pp. 1-7, 1-8)
R_{ci} = corrosion rate under inundated conditions (m/s)
R_{ch} = corrosion rate under humid conditions (m/s)
R_{mi} = rate of cellulose biodegradation under inundated conditions (mol $C_6H_{10}O_5$/kg $C_6H_{10}O_5$/s)
R_{mh} = rate of cellulose biodegradation under humid conditions (mol $C_6H_{10}O_5$/kg $C_6H_{10}O_5$/s)
R_{hi} = MgO hydration rate under inundated conditions (mol MgO/kg MgO/s)
R_{hh} = MgO hydration rate under humid conditions (mol MgO/kg MgO/s)
R_{hc} = rate of hydromagnesite conversion to magnesite (mol hydromagnesite/kg hydromagnesite/s)
$S_{b,eff}$ = effective brine saturation due to capillary action in the waste materials (see Equation (PA.99) in Section PA-4.2.6)

$$S_g^* = \begin{cases} 1 - S_{b,eff} & \text{if } S_{b,eff} > 0 \\ 0 & \text{if } S_{b,eff} = 0 \end{cases}$$

$X_c(H_2|Fe)$ = stoichiometric coefficient for gas generation due to corrosion of steel, i.e., moles of H_2 produced by the corrosion of 1 mole of Fe (mol H_2/mol Fe)
$X_s(H_2|Fe)$ = stoichiometric coefficient for gas generation due to sulfidation of steel, i.e., moles of H_2 produced by the sulfidation of 1 mole of Fe (mol H_2/mol Fe)
$X_m(H_2S|C)$ = stoichiometric coefficient for H_2S microbial degradation of cellulose, i.e., moles of H_2S generated per mole of carbon consumed by microbial action (mol H_2S/mol C)
$X_m(H_2|C)$ = stoichiometric coefficient for H_2 microbial degradation of cellulose, i.e., moles of H_2 generated per mole of carbon consumed by microbial action (mol H_2/mol C)
$X_c(H_2O|H_2)$ = stoichiometric coefficient for brine production due to corrosion of steel, i.e., moles of H_2O produced per mole of H_2 generated by corrosion (mol H_2O/mol H_2)
$X_s(H_2O|H_2)$ = stoichiometric coefficient for brine production due to sulfidation of steel, i.e., moles of H_2O produced per mole of H_2 generated by sulfidation (mol H_2O/mol H_2)
$X_m(H_2O|H_2)$ = stoichiometric coefficient for brine production due to microbial degradation of cellulose, i.e., moles of H_2O produced per mole of H_2 generated by microbial degradation of cellulose (mol H_2O/mol H_2)
$X_h(H_2O|MgO)$ = stoichiometric coefficient for brine production due to MgO hydration, i.e., moles of H_2O produced per mole of MgO generated by hydration (mol H_2O/mol MgO)
$X_{hc}(H_2O|HM)$ = stoichiometric coefficient for brine production due to hydromagnesite conversion to magnesite, i.e., moles of H_2O produced per mole of hydromagnesite converted to magnesite (mol H_2O/mol hydromagnesite)
ρ_{Fe} = molar density of steel (mol/m^3), 1.41×10^5 mol/m^3 (Telander and Westerman 1993)
B_{fc} = parameter (WAS_AREA:BIOGENFC, discussed in detail later in this section) uniformly sampled from 0 to 1, used to account for the uncertainty in whether microbial gas generation could be realized in the WIPP at experimentally measured rates.

The reactions are assumed to continue until the associated substrate (i.e., steel, cellulose, MgO, etc.) is exhausted (i.e., zero order kinetics are assumed). The terms $S_{b,eff}$ and S_g^*, which are functions of location and time, correct for the amount of substrate exposed to inundated and humid conditions, respectively. All the corrosion and microbial action is assumed to cease when no brine is present, which is the reason that 0 replaces $S_g = 1$ in the definition of S_g^*. In PA, $R_{ch} = 0$ and R_{ci}, R_{mh}, R_{mi}, R_{hi}, R_{hh}, and R_{hc} are defined by uncertain variables (see WGRCOR, WGRMICH, WGRMICI, BRUCITEC, BRUCITES, BRUCITEH and HYMAGCON in Table PA-17). However, R_{mh} is now sampled based on the sampled value of R_{mi}: see Nemer and Clayton (Nemer and Clayton 2008, Section 5.1.3). The calculations of D_s, D_c, D_m, D_{HM}, X_c (H_2|Fe), X_s (H_2|Fe), X_m (H_2S|C), X_m (H_2|C), X_c (H_2O|H_2), X_s (H_2O|H_2), X_m (H_2O|H_2), X_h (H_2O|MgO), X_{hc} (H_2O|HM), and B_{fc} are discussed below.

The concentration D_s in Equation (PA.67) is defined by

$$D_s = A_d n_d / V_R \quad \text{(PA.75)}$$

where

A_d = surface area of steel associated with a waste disposal drum (m^2/drum)
V_R = initial volume of a single room in the repository (m^3)
n_d = ideal number of waste drums that can be close-packed into a single room

In PA, A_d = 6 m^2/drum (REFCON:ASDRUM), V_R = 3,644 m^3 (REFCON:VROOM), and n_d = 6804 drums (REFCON:DRROOM).

The biodegradable materials to be disposed at the WIPP consist of cellulosic materials, plastics, and rubbers. Cellulosics have been demonstrated experimentally to be the most biodegradable of these materials (Francis, Gillow, and Giles 1997). The occurrence of significant microbial gas generation in the repository will depend on whether (1) microbes capable of consuming the emplaced organic materials will be present and active, (2) sufficient electron acceptors will be present and available, and (3) enough nutrients will be present and available.

In the CRA-2004, the probability that microbial gas generation could occur was assigned a value of 0.5. During the CRA-2004 PABC, the EPA (Cotsworth 2005) indicated that the probability that microbial gas generation could occur (WMICDFLG) should be set equal to 1 in PA calculations. To comply with the EPA's letter, in the CRA-2004 PABC and the CRA-2009 PA the parameter WMICDFLG was changed so that the probability that microbial gas generation could occur was set to 1 while preserving the previous probability distribution on whether CPR could be degraded. The same approach is used in the CRA-2014 PA. This is summarized in Table PA-6, and is discussed further in Nemer and Stein (Nemer and Stein 2005), Section 5.4.

Table PA- 6. Probabilities for Biodegradation of Different Organic Materials (WAS_AREA:PROBDEG) in the CRA-2014 PA

WAS_AREA:PROBDEG	Meaning	Probability CRA-2014
0	No microbial degradation can occur	0.0
1	Biodegradation of only cellulose can occur	0.75
2	Biodegradation of all CPR materials can occur	0.25

Because there are significant uncertainties in whether the experimentally observed gas-generation rates could be realized in the WIPP repository, during the CRA-2004 PABC the EPA agreed to allow the DOE to multiply the sampled microbial rates by a parameter (WAS_AREA:BIOGENFC) uniformly sampled from 0 to 1 (B_{fc}). This is discussed further in Nemer, Stein, and Zelinski (Nemer, Stein, and Zelinski 2005), Section 4.2.2. The same approach is used in the CRA-2014 PA.

In cases where biodegradation of rubbers and plastics occur, rubbers and plastics are converted to an equivalent quantity of cellulosics based on their carbon equivalence (Wang and Brush 1996a). This produces the density calculation

$$D_c = \begin{cases} m_{cel} / V_R & \text{for biodegradation of cellulosics only} \\ \left(m_{cel} + m_r + 1.7 m_p\right) / V_R & \text{for biodegradation of CPR materials} \end{cases} \quad \text{(PA.76)}$$

where m_{cel} is the mass of cellulosics (kg), m_r is the mass of rubbers (kg), and m_p is the mass of plastics (kg).

Mass values for CPR materials can be found in Kicker and Herrick (Kicker and Herrick 2013), Table 26.

The most plausible iron corrosion reactions after closure of the WIPP are believed to be (Wang and Brush 1996a)

$Fe + 2H_2O = Fe(OH)_2 + H_2$ (PA.77)

$3Fe + 4H_2O = Fe_3O_4 + 4H_2$ (PA.78)

When normalized to 1 mole of Fe and linearly weighted by the factors x and $1-x$ $(0 \le x \le 1)$, the two preceding reactions become

$$Fe + \left(\frac{4+2x}{3}\right)H_2O = \left(\frac{4-x}{3}\right)H_2 + xFe(OH)_2 + \left(\frac{1-x}{3}\right)Fe_3O_4 \quad \text{(PA.79)}$$

where x and $1-x$ are the fractions of Fe consumed in the reactions in Equation (PA.77) and Equation (PA.78), respectively. Although magnetite (Fe_3O_4) has been observed to form on Fe as a corrosion product in low-Mg anoxic brines at elevated temperatures (Telander and Westerman 1997) and in oxic brine (Haberman and Frydrych 1988), there is no evidence that it will form at WIPP repository temperatures. If Fe_3O_4 were to form, H_2 would be produced (on a molar basis) in excess of the amount of Fe consumed. However, anoxic corrosion experiments (Telander and Westerman 1993) did not indicate the production of H_2 in excess of the amount of Fe consumed. Therefore, the

stoichiometric factor x in Reaction (PA.79) is set to 1.0 (i.e., $x = 1$), which implies that Reaction (PA.77) represents corrosion. Thus, the stoichiometric factor for corrosion is

$$X_c(H_2|Fe) = (4-x)/3 = 1 \text{ mol/mol} \quad \text{(PA.80)}$$

which implies that one mole of H_2 is produced for each mole of Fe consumed, and the stoichiometric factor for brine consumption is

$$X_c(H_2O|H_2) = (4+2x)/3 = 2 \text{ mol/mol} \quad \text{(PA.81)}$$

which implies that two moles of H_2O are consumed for each mole of H_2 produced.

The most plausible biodegradation reactions after closure of the WIPP are believed to be (Wang and Brush 1996a)

denitrification $C_6H_{10}O_5 + 4.8H^+ + 4.8NO_3^- = 7.4H_2O + 6CO_2 + 2.4N_2$ (PA.82)

sulfate reduction $C_6H_{10}O_5 + 6H^+ + 3SO_4^{2-} = 5H_2O + 6CO_2 + 3H_2S$ (PA.83)

methanogenesis $C_6H_{10}O_5 + H_2O = 3CH_4 + 3CO_2$ (PA.84)

However, in the CRA-2004 PABC, the EPA (Cotsworth 2005) directed the DOE to remove methanogenesis (Equation (PA.84)) from PA. The EPA cited the presence of calcium sulfate as gypsum and anhydrite in the bedded salt surrounding the repository as possible sources of sulfate. These sources of sulfate would, if accessible, promote sulfate reduction (Equation PA.83), which is energetically and kinetically favored over methanogenesis. In response, the DOE removed methanogenesis from PA. The removal of methanogenesis is discussed fully in Nemer and Zelinski (Nemer and Zelinski 2005). Methanogenesis is also removed in the CRA-2014 PA.

The average stoichiometry of Reaction (PA.82), Reaction (PA.83), and Reaction (PA.84), is

$C_6H_{10}O_5/6$ + microbes = y (mol) gas + z (mol) H_2O + unknowns (PA.85)

where the average stoichiometric factors y and z represent the number of moles of gas (assumed to be H_2) and brine produced from each mole of carbon consumed, respectively. In PA, the CO_2 is ignored, as it is assumed to be consumed by reactions with magnesium materials in the repository. The factors depend on the extent of the individual biodegradation pathways. Then, $X_m(H_2|C)$ is equal to y and $X_m(H_2O|H_2)$ is equal to the ratio of z to y.

In the absence of methanogenesis, y and z from Equation (PA.85) become

$$y = \frac{2.4}{6}F_{NO3} + \frac{3}{6}F_{SO4} \quad \text{(PA.86)}$$

$$z = \frac{7.4}{6}F_{NO3} + \frac{5}{6}F_{SO4} \quad \text{(PA.87)}$$

where F_{NO3} is the fraction of carbon consumed through the denitrification reaction and F_{SO4} is the fraction of carbon consumed by sulfate reduction. F_{NO3} is calculated by comparing the quantity of NO_3^- (mols) initially present in the repository (M°_{NO3} , 2.74×10^7 mol, Kicker and Herrick 2013, Table 31) and the moles of carbon that could be consumed by biodegradation. F_{SO4} is then just one minus F_{NO3} . Since, $X_m(H_2S|C)$ only considers H_2S, this stoichiometric factor is

$$X_m(H_2S|C) = \frac{3}{6}F_{SO4} \quad \text{(PA.88)}$$

With biodegradation by sulfate reduction, hydrogen sulfide (H_2S) is produced. The reactions of iron and its corrosion products with H_2S are modeled as

$Fe(s) + H_2S(g) \rightarrow FeS(s) + H_2(g)$, (PA.89)

$Fe(OH)_2(s) + H_2S(g) \rightarrow FeS(s) + 2H_2O(l)$ (PA.90)

In PA it is assumed that Reaction (PA.90) kinetically dominates Reaction (PA.89), and so based on Reaction (PA.90)

$$X_s(H_2|Fe) = -1/1 = -1 \text{ mol/mol} \quad \text{(PA.91)}$$

$$X_s(H_2O|H_2) = 2/-1 = -2 \text{ mol/mol} \quad \text{(PA.92)}$$

To provide added assurance of WIPP performance, a sufficient amount of MgO is added to the repository to remove CO_2 (Bynum et al. 1997). MgO is emplaced in the repository such that there are at least 1.2 moles of MgO per mole of carbon in the repository (see Appendix MgO-2009, Section MgO-6.2.4.6). MgO in polypropylene "supersacks" is emplaced on top of the three-layer waste stacks to create

conditions that reduce actinide solubilities in the repository (see Appendix MgO-2014, Section MgO-2.1.1 and Appendix SOTERM-2014, Section SOTERM-2.3). The mass concentration of MgO in the repository is calculated by

$$D_m = 1.2 D_c M_{MgO} / M_c \quad \text{(PA.93)}$$

where

M_{MgO} = molecular weight of MgO (kg MgO/mol MgO), 4.03×10^{-2} kg/mol (Lide 1997, pp. 4-68)
M_c = molecular weight of cellulosics (kg cellulosics/mol cellulosics), 2.70×10^{-2} kg/mol

If brine flows into the repository, MgO will react with water in brine and in the gaseous phase to produce brucite ($Mg[OH]_2$)

$MgO + H_2O(aq \text{ and/or } g) \rightarrow Mg(OH)_2$ (PA.94)

In this equation, "aq and/or g" indicates that the H_2O reacts with MgO present in the aqueous phase (brine) and/or the gaseous phase and so

$$X_h(H_2O|MgO) = -1/1 = -1 \ mol/mol \quad \text{(PA.95)}$$

The brucite will react with essentially all of the CO_2 that could be produced by complete microbial consumption of the CPR materials in the waste, and will create hydromagnesite (Appendix MgO-2014, Section MgO-5.1 and Appendix SOTERM-2014, Section SOTERM-2.3)

$5\ Mg(OH)_2 + 4\ CO_2(g) \rightarrow Mg_5(CO_3)_4(OH)_2 \cdot 4\ H_2O$ (PA.96)

Since hydromagnesite is not thermodynamically stable under repository conditions, it is expected to dehydrate to form magnesite.

$Mg_5(CO_3)_4(OH)_2{:}4\ H_2O(s) \rightarrow 4\ MgCO_3(s) + Mg(OH)_2(s) + 4\ H_2O(l)$. (PA.97)

and so

$$X_{hc}(H_2O|HM) = 4/1 = 4 \ mol/mol \quad \text{(PA.98)}$$

The mass concentration of hydromagnesite, D_{HM} , is calculated dynamically and is a function of the biodegradation rate and hydromagnesite conversion to magnesite rate.

PA-4.2.6 Capillary Action in the Waste

Capillary action (wicking) is the ability of a material to carry a fluid by capillary forces above the level it would normally seek in response to gravity. In the current analysis, this phenomena is accounted for by defining an effective saturation given by

$$S_{b,eff} = \begin{cases} S_b - S_{min} + S_{wick}\left\{1 - \mathrm{Exp}\left[200\alpha\left(\mathrm{Max}\left(S_b - S_{min}, 0\right)\right)^2\right]\right\} & \text{if } 0 < S_b \le 1 - S_{wick} + S_{min} \\ 0 & \text{if } S_b \le S_{min} \\ 1 & \text{if } S_b > 1 - S_{wick} + S_{min} \end{cases}$$

(PA.99)

where

$S_{b,eff}$ = effective brine saturation
S_b = brine saturation
S_{wick} = wicking saturation
S_{min} = minimum brine saturation at which code can run in the waste-filled areas
α = smoothing parameter = –1000

The effective saturation, $S_{b,eff}$, given by Equation (PA.99) approaches zero as S_b approaches a small value S_{min} . In simulations where Fe corrosion dried out the repository, the time required to complete the simulation can be quite long. In order to speed up the code and increase robustness, the parameter S_{min} was added as part of the CRA-2009 PA. For PA, S_{min} = 0.015, which is small enough to not affect the results, while greatly reducing run time. This is explained fully in Nemer and Clayton (Nemer and Clayton 2008), Section 5.2.2.

The effective saturation is used on a grid block basis within all waste regions (Waste Panel, South RoR, and North RoR in Figure PA-12). The wicking saturation, S_{wick} , is treated as an uncertain variable (see WASTWICK in Table PA-17). The effective brine saturation $S_{b,eff}$ is currently used only to calculate chemical reaction rates, and does not directly affect the two-phase flow calculations.

PA-4.2.7 Shaft Treatment

The WIPP excavation includes four shafts that connect the repository region to the surface: the air intake shaft, salt handling shaft, waste handling shaft, and exhaust shaft. In PA, these four shafts are modeled as a single shaft. The rationale for this modeling treatment is set forth in Sandia National Laboratories (1992), Volume 5, Section 2.3.

The shaft seal model included in the PA grid (Column 43 in Figure PA-12) is the simplified shaft model used in the CRA-2009 PA. The simplified shaft seal model used in PA is described by Stein and Zelinski (Stein and Zelinski 2003) and is briefly discussed below; this model was approved by the Salado Flow Peer Review Panel (Caporuscio, Gibbons, and Oswald 2003).

The planned design of the shaft seals involves numerous materials, including earth, crushed salt, clay, asphalt, and Salado Mass Concrete (SMC) (see the CCA, Appendix SEAL). The design is intended to control both short-term and long-term fluid flow through the Salado portion of the shafts. For the CCA PA, each material in the shaft seal was represented in the BRAGFLO grid. Analysis of the flow results from the CCA PA and the subsequent CCA Performance Assessment Verification Test (PAVT) (Sandia National Laboratories 1997; U.S. DOE 1997) indicated that no significant flows of brine or gas occurred in the shaft during the 10,000-year regulatory period. As a result of these analyses, a simplified shaft seal model was developed for the CRA-2004 PA.

A conceptual representation of the simplified shaft seal system used in PA is shown in Figure PA-15. The simplified model divides the shaft into three sections: an upper section (shaft seal above the Salado), a lower section (within the Salado), and a concrete monolith section within the repository horizon. A detailed discussion of how the material properties were assigned for the simplified shaft seal model is included in James and Stein (James and Stein 2003). The permeability value used to represent the upper and lower sections is defined as the harmonic mean of the component materials' permeability in the detailed shaft seal model (including permeability adjustments made for the DRZ assumed to surround the lower shaft seal section within the Salado). Porosity is defined as the thickness-weighted mean porosity of the component materials. Other material properties are described in James and Stein (James and Stein 2003).

The lower section of the shaft experiences a change in material properties at 200 years. This change simulates the consolidation of seal materials within the Salado and significantly decreases permeability. This time was chosen as a conservative overestimate of the amount of time expected for this section of the shaft to become consolidated. The concrete monolith section of the shaft is unchanged from the CCA PA and is represented as being highly permeable for 10,000 years to ensure that fluids can access the north end (operations and experimental areas) in the model. In three thin regions at the stratigraphic position of the anhydrite MBs, the shaft seal is modeled as MB material (Figure PA-15). This model feature is included so that fluids flowing in the DRZ and MB fractures can access the interbeds to the north of the repository "around" the shaft seals. Because these layers are so thin, they have virtually no effect on the effective permeability of the shaft seal itself.

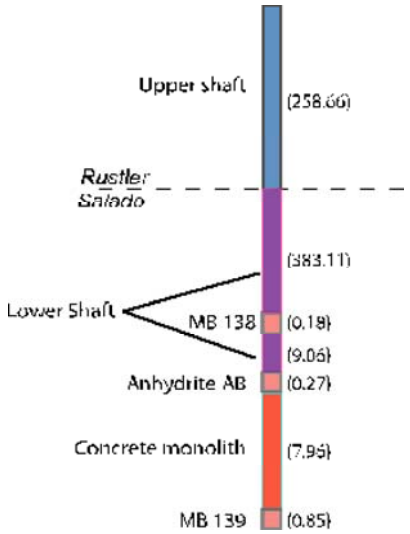

Figure PA- 15. Schematic View of the Simplified Shaft Model (numbers on right indicate length in meters)

The simplified shaft model was tested in the AP-106 analysis (Stein and Zelinski 2003), which supported the Salado Flow Peer Review (Caporuscio, Gibbons, and Oswald 2003). The results of the AP-106 analysis demonstrate that vertical brine flow through the simplified shaft model is comparable to brine flows seen through the detailed shaft model used in the CCA PA and subsequent CCA PAVT calculations.

PA-4.2.8 ROMPCS

The WIPP waste panel closures comprise a feature of the repository that has been represented in WIPP PA regulatory compliance demonstration since the CCA. Following the selection of the Option D panel closure design in 1998, the DOE has reassessed the engineering of the panel closure and established a revised design which is simpler, easier to construct, and equally effective at performing its operational-period isolating function. The revised design is the ROMPCS, and is comprised of 100 feet of ROM salt with barriers at each end (Figure PA-16). The barriers consist of ventilation bulkheads, and are similar to those used in the panels as room closures. The ventilation bulkheads are designed to restrict air flows and prevent personnel access into waste-filled areas during the operational phase of the repository. The ventilation bulkheads are expected to have no significant impact on long-term performance of the panel closures and are therefore not

included in the representation of the ROMPCS. Option D explosion walls fabricated from concrete blocks have been emplaced in the entries of waste panels 1, 2, and 5. It is expected that these walls will not be significant structures after the initial 100-year time period, due to the brittle, non-plastic behavior of concrete. The already emplaced explosion walls are therefore expected to have no significant impact on long-term panel closure performance, and so are also not included in the representation of the ROMPCS. Consequently, the ROMPCS is modeled as consisting of 100 feet of ROM salt in the WIPP PA.

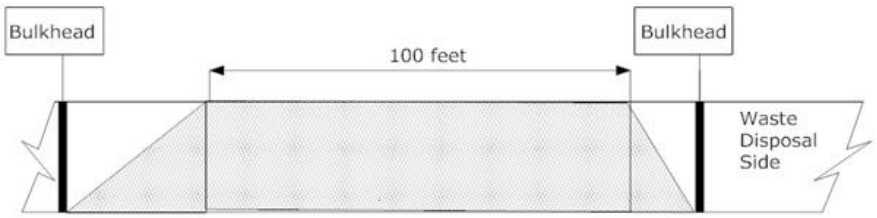

(a) Panel closure with 100 feet of ROM salt between two ventilation bulkheads

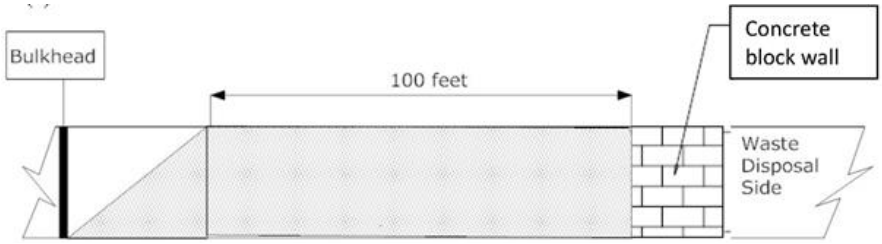

(b) Panel closure with 100 feet of ROM salt between a ventilation bulkhead and explosion wall

Figure PA- 16. Schematic Diagram of the ROMPCS

Material parameters and timings used to represent the ROMPCS are developed to account for the following physical processes and accepted rock mechanics principles:

1. Creep closure of the salt rock surrounding panel entries will cause consolidation of ROM salt emplaced in panel entries.
2. Eventually, the ROM salt comprising the closures will approach a condition similar to intact salt.
3. As ROM salt reaches higher fractional densities during consolidation, back stress will be imposed on the surrounding rock mass leading to eventual healing of the DRZ.
4. DRZ healing above and below the ROM salt panel closures will reduce DRZ porosity and permeability in those areas.

ROMPCS properties are based on three time periods (see Camphouse et al. 2012a, Camphouse 2013c, and Camphouse et al. 2013) to capture the temporal dependence of the physical processes listed above. Consequently, the ROMPCS is represented by three materials, with each material representing the ROMPCS for a portion of the 10,000-year regulatory period. Material PCS_T1 represents the ROMPCS for the first 100 years after facility closure. Material PCS_T2 models the ROMPCS from 100 to 200 years. Finally, material PCS_T3 represents the ROMPCS from years 200 to 10,000. For the first 200 years post-closure, the DRZ above and below the ROMPCS maintains the same properties as specified to the DRZ surrounding the disposal rooms (PA material DRZ_1). After 200 years, the DRZ above and below the ROMPCS is modeled as having healed, and is represented by material DRZ_PCS(see Figure PA-12 and Appendix MASS-2014, Section 4.1.3). Material DRZ_1 has the same properties in the CRA-2014 PA as were assigned to it in the CRA-2009 PABC. The permeability of material DRZ_PCS is modified slightly in the CRA-2014 PA as compared to the CRA-2009 PABC (see Appendix PA-2009, Section 4.2.8.3 for a discussion of material DRZ_PCS used in the CRA-2009 PABC). The healing of the DRZ region above and below the ROMPCS will not yield a higher permeability than that above the rooms. A relationship is implemented in the CRA-2014 PA to enforce that the permeability of material DRZ_PCS is never greater than the permeability of material DRZ_1. The constraint placed on the permeability for DRZ_PCS is that DRZ_PCS:PRMX ≤ DRZ_1:PRMX, and likewise in the y and z directions. If the sampled permeability for DRZ_PCS is greater than that obtained for DRZ_1, then DRZ_PCS retains the DRZ_1 permeability. The uncertainty distributions specified for the permeabilities of materials DRZ_1 and DRZ_PCS in the CRA-2014 PA are identical to those used in the CRA-2009 PABC.

As developed in Camphouse et al. (Camphouse et al. 2012b), permeability and porosity values are obtained through sampling for ROMPCS material PCS_T1. Porosity values are sampled for materials PCS_T2 and PCS_T3 and then used to calculate permeability values for these materials. The relationship used to calculate the permeability of material PCS_T2 is of the form

$$k_2 = 10^{(-21.187(1-\phi_2)+1.5353+\alpha)}$$

where k_2 is the calculated permeability for PCS_T2, ϕ_2 is the sampled PCS_T2 porosity value, and α is sampled from a normal distribution having a mean of 0, a standard deviation of 0.86,

and truncated at ±2 standard deviations. An analogous relationship is used for PCS_T3, and is of the form

$$k_2 = 10^{(-21.187(1-\phi_2)+1.5353+\alpha)}$$

Overlap in the porosity ranges for materials PCS_T1 and PCS_T2 potentially results in an increase in panel closure porosity during the transition from PCS_T1 to PCS_T2 at 100 years, a non-physical result. To prevent this possibility, the porosity for PCS_T2 is conditionally sampled so that PCS_T2:POROSITY ≤ PCS_T1:POROSITY for all vectors. For similar reasons, the porosity for material PCS_T3 is conditionally sampled so that PCS_T3:POROSITY ≤ PCS_T2:POROSITY. Similar constraints are placed on the calculated permeabilities for materials PCS_T2 and PCS_T3. The calculated permeability value for PCS_T2 is constrained such that PCS_T2:PRMX ≤ PCS_T1:PRMX. If the calculated permeability for PCS_T2 is greater than the sampled permeability for PCS_T1, then PCS_T2 retains the sampled PCS_T1 permeability. The same is true for the calculated permeabilities in the y and z directions. A similar constraint is placed on the calculated permeability for PCS_T3 in order to prevent non-physical instantaneous increases in panel closure permeability at 200 years. The constraint placed on the calculated permeability for PCS_T3 is that PCS_T3:PRMX ≤ PCS_T2:PRMX, and likewise in the x and y directions. If the calculated permeability for PCS_T3 is greater than the permeability for PCS_T2, then PCS_T3 retains the sampled PCS_T2 permeability. Uncertain parameters representing the ROMPCS are listed in Kicker and Herrick (Kicker and Herrick 2013), Table 4.

PA-4.2.9 Borehole Model

The major disruptive event in PA is the penetration of the repository by a drilling intrusion. The same numerical grid is used for undisturbed and borehole intrusion scenarios. In the undisturbed scenario (see Section PA-6.7.1), grid cells corresponding to the intrusion location have the material properties of the neighboring stratigraphic or excavated modeling unit. There is no designation in the borehole grid except for the reduced lateral dimensions of this particular column of grid cells.

In the scenarios simulating drilling disturbance, cells corresponding to the intrusion location start out with the same material properties as in the undisturbed scenario. At the time of intrusion, these cells are reassigned borehole material properties. The drilling intrusion is modeled by modifying the permeability of the grid blocks in Column 26 of Figure PA-12 (values listed in Table PA-7). Furthermore, the drilling intrusion is assumed to produce a borehole with a diameter of 12.25 in. (0.31115 m) (Vaughn 1996; Howard 1996), borehole fill is assumed to be incompressible, capillary effects are ignored, residual gas and brine saturations are set to zero, and porosity is set to 0.32 (see materials CONC_PLG, BH_OPEN, BH_SAND, and BH_CREEP in Table PA-3). When a borehole that penetrates pressurized brine in the Castile is simulated (i.e., an E1 intrusion), the permeability modifications indicated in Table PA-7 extend from the ground surface (i.e., Grid Cell 2155 in Figure PA-14) to the base of the pressurized brine (i.e., Grid Cell 2225 in Figure PA-14). When a borehole that does not penetrate pressurized brine in the Castile is under consideration (i.e., an E2 intrusion), the permeability modifications indicated in Table PA-7 stop at the floor of the intruded waste panel (i.e., Grid Cell 1419 in Figure PA-14).

PA-4.2.10 Castile Brine Reservoir

High-pressure Castile brine was encountered in several WIPP-area boreholes, including the WIPP-12 borehole within the controlled area and the U.S. Energy Research and Development Administration (ERDA)-6 borehole northeast of the site. Consequently, the conceptual model for the Castile includes the possibility that brine reservoirs underlie the repository. The E1 and E1E2 scenarios include borehole penetration of both the repository and a brine reservoir in the Castile.

Unless a borehole penetrates both the repository and a brine reservoir in the Castile, the Castile is conceptually unimportant to PA because of its expected low permeability. Two regions are specified in the disposal system geometry of the Castile horizon: the Castile (Rows 1 and 2 in Figure PA-12) and a reservoir (Row 1, Columns 23 to 45 in Figure PA-12). The Castile region has an extremely low permeability, which prevents it from participating in fluid flow processes.

Table PA- 7. Permeabilities for Drilling Intrusions Through the Repository

Time After Intrusion	Assigned Permeabilities
0-200 years	Concrete plugs are assumed to be emplaced at the Santa Rosa (i.e., a surface plug with a length of 15.76 m; corresponds to Grid Cells 2113, 2155 in Figure PA-14) and the Los Medaños Member of the Rustler (i.e., a plug at the top of the Salado with a length of 36 m; corresponds to Grid Cell 1644 in Figure PA-14). Concrete plugs are assumed to have a permeability log-uniformly sampled between 10^{-19} m^2 to 10^{-17} m^2 (see material CONC_PLG in Kicker and Herrick (2013), Table 4). The open portions of the borehole are assumed to have a permeability of 1×10^{-9} m^2.
200-1200 years	Concrete plugs are assumed to fail after 200 years (U.S. DOE 1995). An entire borehole is assigned a permeability typical of silty sand log-uniformly sampled between $10^{-16.3}$ m^2 and 10^{-11} m^2 (see parameter BHPRM and material BH_SAND in Kicker and Herrick 2013, Table 4).
> 1200 years	Permeability of borehole reduced by one order of magnitude in the Salado beneath the repository due to creep closure of borehole (Thompson et al. 1996) (i.e., $k = 10^{x}/10$, x = BHPRM, in Grid Cells 2225, 1576, 26, 94, 162, 230, 1135, 1142, 1149 of Figure PA-14) (see material BH_CREEP in Kicker and Herrick 2013, Table 4).

It is unknown whether a brine reservoir exists below the repository. As a result, the conceptual model for the brine reservoirs is somewhat different from those for known major properties of the natural barrier system, such as stratigraphy. The principal difference is that a reasonable treatment of the uncertainty of the existence of a brine reservoir requires assumptions about the spatial distribution of such reservoir and the probability of intersection (see Appendix MASS-2014, Section MASS.17.0). A range of probabilities for a borehole hitting a brine reservoir is used (see Section PA-3.6).

In addition to the stochastic uncertainty in the location and hence in the probability of intersecting reservoirs, there is also uncertainty in the properties of reservoirs. The manner in which brine reservoirs would behave if penetrated is captured by parameter ranges and is

incorporated in the BRAGFLO calculations of disposal system performance. The conceptual model for the behavior of such a brine reservoir is discussed below. The properties specified for brine reservoirs are pressure, permeability, compressibility, and porosity, and are sampled from parameter ranges (see Table PA-17).

Where they exist, Castile brine reservoirs in the northern Delaware Basin are believed to be fractured systems, with high-angle fractures spaced widely enough that a borehole can penetrate through a volume of rock containing a brine reservoir without intersecting any fractures, and therefore not producing brine. Castile brine reservoirs occur in the upper portion of the Castile (Popielak et al. 1983). Appreciable volumes of brine have been produced from several reservoirs in the Delaware Basin, but there is little direct information on the areal extent of the reservoirs or the existence of the interconnection between them. Data from WIPP-12 and ERDA-6 indicate that fractures have a variety of apertures and permeabilities, and they deplete at different rates. Brine occurrences in the Castile behave as reservoirs; that is, they are bounded systems.

PA-4.2.11 Numerical Solution

Determining gas and brine flow in the vicinity of the repository requires solving the two nonlinear PDEs in Equation (PA.24), Equation (PA.25), Equation (PA.26), Equation (PA.27), Equation (PA.28), Equation (PA.29) and Equation (PA.30) on the computational domain in Figure PA-12, along with evaluating appropriate auxiliary conditions. The actual unknown functions in this solution are P_b and S_g, although the constraint conditions also give rise to values for P_g and S_b. As two dimensions in space and one dimension in time are in use, P_b, P_g, S_b, and S_g are functions of the form $P_b(x, y, t)$, $P_g(x, y, t)$, $S_b(x, y, t)$, and $S_g(x, y, t)$.

Solving Equation (PA.24), Equation (PA.25), Equation (PA.26), Equation (PA.27), Equation (PA.28), Equation (PA.29) and Equation (PA.30) requires both initial value and boundary value conditions for P_b and S_g. The initial value conditions for P_b and S_g are given in Section PA-4.2.2. As indicated there, the calculation starts at time $t = -5$ years, with a possible resetting of values at $t = 0$ years, which corresponds to final waste emplacement and sealing of the repository. The boundary conditions are such that no brine or gas moves across the exterior grid boundary (Table PA-8). This Neumann-type boundary condition is maintained for all time. Further, BRAGFLO allows the user to maintain a specified pressure and/or saturation at any grid

Table PA- 8. Boundary Value Conditions for P_g and P_b

Boundaries below (Row 1, y = 0 m) and above (Row 33, y = 1039 m) system for $0 \le x \le 46630$ m (Columns 1-68) and -5 yr ≤ t. Below, *j* refers to the unit normal vector in the positive *y* direction.	
$\left(\nabla P_g + \rho_g g \nabla h\right)\Big\vert_{(x,y,t)} \cdot \mathbf{j} = 0$ Pa / *m*	No gas flow condition
$\left(\nabla P_b + \rho_b g \nabla h\right)\Big\vert_{(x,y,t)} \cdot \mathbf{j} = 0$ Pa / *m*	No brine flow condition
Boundaries at left (Column 1, *x* = 0 m) and right (Column 68, *x* = 46630 m) of system for $0 \le y \le 1039$ m (Rows 1-33) and -5 yr ≤ t. Below, *i* refers to the unit normal vector in the positive x direction.	
$\left(\nabla P_g + \rho_g g \nabla h\right)\Big\vert_{(x,y,t)} \cdot \mathbf{i} = 0$ Pa / *m*	No gas flow condition
$\left(\nabla P_b + \rho_b g \nabla h\right)\Big\vert_{(x,y,t)} \cdot \mathbf{i} = 0$ Pa / *m*	No brine flow condition

block. This is not a boundary condition and is not required to close the problem. This feature is used to specify Dirichlet-type conditions at the surface grid blocks (Columns 1-68, Row 33, Figure PA-12) and at the far-field locations in the Culebra and Magenta (Columns 1 and 68, Row 26, and Columns 1 and 68, Row 28, Figure PA-12). These auxiliary conditions are summarized in Table PA-9.

Table PA- 9. Auxiliary Dirichlet Conditions for S_g and P_b

Surface Grid Blocks	
$S_g(i, j, t) = 0.08363$	Columns 1-42, 44-68, Row 33, -5 yr ≤ t Saturation is not forced at the shaft cell on the surface because its saturation is reset to 1.0 at t = 0 yr.
$P_b(i, j, t) = 1.01 \times 10^5$ Pa	Columns 1-68, row 33, -5 yr ≤ t
Culebra and Magenta Far Field	
$P_b(i, 26, t) = 9.14 \times 10^5$ Pa	i = 1 and 68, j = 26, -5 yr ≤ t (Culebra)
$P_b(i, 28, t) = 9.47 \times 10^5$ Pa	i = 1 and 68, j = 28, -5 yr ≤ t (Magenta)

A fully implicit finite-difference procedure is used to solve Equation (PA.24), Equation (PA.25), Equation (PA.26), Equation (PA.27), Equation (PA.28), Equation (PA.29) and Equation (PA.30). The associated discretization of the gas mass balance equation is given by

$$\frac{1}{\Delta x_i}\left\{\frac{1}{x_{i+1}-x_i}\left[\frac{\alpha\rho_g k_x k_{rg}}{\mu_g}\right]_{i+1/2,j}^{n+1}\left(\Phi^{x-}_{g_{i+1,j}}-\Phi^{x+}_{g_{i,j}}\right)^{n+1}\right.$$

$$\left.-\frac{1}{x_i-x_{i-1}}\left[\frac{\alpha\rho_g k_x k_{rg}}{\mu_g}\right]_{i-1/2,j}^{n+1}\left(\Phi^{x-}_{g_{i,j}}-\Phi^{x+}_{g_{i-1,j}}\right)^{n+1}\right\}$$

$$+\frac{1}{\Delta y_j}\left\{\frac{1}{y_{j+1}-y_j}\left[\frac{\alpha\rho_g k_y k_{rg}}{\mu_g}\right]_{i,j+1/2}^{n+1}\left(\Phi^{y-}_{g_{i,j+1}}-\Phi^{y-}_{g_{i,j}}\right)^{n+1}\right.$$

$$\left.-\frac{1}{y_j-y_{j-1}}\left[\frac{\alpha\rho_g k_y k_{rg}}{\mu_g}\right]_{i,j-1/2}^{n+1}\left(\Phi^{y-}_{g_{i,j}}-\Phi^{y+}_{g_{i,j-1}}\right)^{n+1}\right\}$$

$$+\alpha_{i,j}q^{n+1}_{g_{i,j}}+\alpha_{i,j}q^{n+1}_{rg_{i,j}}-\frac{\left(\alpha\phi\rho_g S_g\right)^{n+1}_{i,j}-\left(\alpha\phi\rho_g S_g\right)^{n}_{i,j}}{\Delta t}=0 \quad \text{(PA.100)}$$

where Φ represents the phase potentials given by

$$\Phi^{x+}_{g_{i,j}}=P_{g_{i,j}}+\rho_{g_{i+1/2,j}}g h_{i,j},\quad \Phi^{x-}_{g_{i,j}}=P_{g_{i,j}}+\rho_{g_{i-1/2,j}}g h_{i,j}$$

and

$$\Phi^{y+}_{g_{i,j}}=P_{g_{i,j}}+\rho_{g_{i,j+1/2}}g h_{i,j},\quad \Phi^{y-}_{g_{i,j}}=P_{g_{i,j}}+\rho_{g_{i,j-1/2}}g h_{i,j}$$

the subscripts are defined by

i = x-direction grid index
j = y-direction grid index
$i\pm 1/2$ = x-direction grid block interface
$j\pm 1/2$ = y-direction grid block interface
x_i = grid block center in the x-coordinate direction (m)
y_j = grid block center in the y-coordinate direction (m)
Δx_i = grid block length in the x-coordinate direction (m)
Δy_j = grid block length in the y-coordinate direction (m)

the superscripts are defined by

n = index in the time discretization, known solution time level
n+1 = index in the time discretization, unknown solution time level

and the interblock densities are defined by

$$\rho_{g_{i+1/2,j}}=\frac{\Delta x_{i+1,j}}{\Delta x_{i,j}+\Delta x_{i+1,j}}\rho_{g_{i,j}}+\frac{\Delta x_{i,j}}{\Delta x_{i,j}+\Delta x_{i+1,j}}\rho_{g_{i+1,j}}$$

$$\rho_{g_{i-1/2,j}}=\frac{\Delta x_{i,j}}{\Delta x_{i-1,j}+\Delta x_{i,j}}\rho_{g_{i-1,j}}+\frac{\Delta x_{i-1,j}}{\Delta x_{i-1,j}+\Delta x_{i,j}}\rho_{g_{i,j}}$$

$$\rho_{g_{i,j+1/2}}=\frac{\Delta y_{i,j+1}}{\Delta y_{i,j}+\Delta y_{i,j+1}}\rho_{g_{i,j}}+\frac{\Delta y_{i,j}}{\Delta y_{i,j}+\Delta y_{i,j+1}}\rho_{g_{i,j+1}}$$

$$\rho_{g_{i,j-1/2}}=\frac{\Delta y_{i,j}}{\Delta y_{i,j-1}+\Delta y_{i,j}}\rho_{g_{i,j-1}}+\frac{\Delta y_{i,j-1}}{\Delta y_{i,j-1}+\Delta y_{i,j}}\rho_{g_{i,j}}$$

The interface values of k_{rg} in Equation (PA.100) are evaluated using upstream weighted values (i.e., the relative permeabilities at each grid block interface are defined to be the relative permeabilities at the center of the adjacent grid block with the highest potential). Further, interface values for $\alpha \rho_g k_x / \mu_g$ and $\alpha \rho_g k_y / \mu_g$ are obtained by harmonic averaging of adjacent grid block values for these expressions. Currently all materials are isotropic, i.e. $k_x = k_y = k_z$.

The discretization of the brine mass balance equation is obtained by replacing the subscript for gas, *g*, by the subscript for brine, *b*. As a reminder, P_g and S_b are replaced in the numerical implementation with the substitutions indicated by Equation (PA.27) and Equation (PA.26), respectively. Wells are not used in the conceptual model for long-term Salado flow calculations, but they are used for DBR calculations. Thus, for long-term Salado flow calculations, the terms q_g and q_b are zero. For long-term Salado flow calculations, the wellbore is not treated by a well model, but rather is explicitly modeled within the grid as a distinct material region (i.e., Upper Borehole and Lower Borehole in Figure PA-12).

The resultant coupled system of nonlinear brine and gas mass balance equations is integrated in time using the Newton-Raphson method with upstream weighting of the relative permeabilities, as previously indicated. The primary unknowns at each computational cell center are brine pressure and gas saturation.

PA-4.2.12 Gas and Brine Flow across Specified Boundaries

The Darcy velocity vectors $v_g(x, y, t)$ and $v_b(x, y, t)$ for gas and brine flow ($m^3/m^2/s$ = m/s) are defined by the expressions

$$v_g(x,y,t) = k k_{rg} \left(\nabla P_g + \rho_g g \nabla h \right) / \mu_g \quad \text{(PA.101)}$$

and

$$v_b(x,y,t) = k k_{rb} \left(\nabla P_b + \rho_b g \nabla h \right) / \mu_b \quad \text{(PA.102)}$$

Values for v_g and v_b are obtained and saved as the numerical solution of Equation (PA.24), Equation (PA.25), Equation (PA.26), Equation (PA.27), Equation (PA.28), Equation (PA.29) and Equation (PA.30) is carried out. Cumulative flows of gas, $C_g(t, B)$, and brine, $C_b(t, B)$, from time 0 to time *t* across an arbitrary boundary *B* in the domain of (Figure PA-12) is then given by

$$C_l(t,B) = \int_0^t \left[\int_B \alpha(x,y) v_l(x,y,t) \cdot n(x,y) \, ds \right] dt \quad \text{(PA.103)}$$

for $l = g, b$, where $\alpha(x, y)$ is the geometry factor defined in Equation (PA.32), $n(x, y)$ is an outward-pointing unit normal vector, and $\int_B ds$ denotes a line integral. As an example, *B* could correspond to the boundary of the waste disposal regions in Figure PA-12. The integrals defining $C_g(t, B)$ and $C_b(t, B)$ are evaluated using the Darcy velocities defined by Equation (PA.101) and Equation (PA.102). Due to the dependence of gas volume on pressure, $C_g(t, B)$ is typically calculated in moles or cubic meters at standard temperature and pressure, which requires an appropriate change of units for v_g in the calculation of $C_l(t,B)$.

PA-4.2.13 Additional Information

Additional information on BRAGFLO and its use in the CRA-2014 PA can be found in the BRAGFLO user's manual (Camphouse 2013b), the BRAGFLO design document (Camphouse 2013a) and the analysis package for the Salado flow calculations in the CRA-2014 PA (Camphouse 2013c).

PA-4.3 Radionuclide Transport in the Salado: NUTS

The NUTS code is used to model radionuclide transport in the Salado. NUTS models radionuclide transport within all regions for which BRAGFLO computes brine and gas flow, and for each realization uses as input the corresponding BRAGFLO velocity field, pressures, porosities, saturations, and other model parameters, including, for example, the geometrical grid, residual saturation, material map, and compressibility. Of the radionuclides that are transported vertically due to an intrusion or up the shaft, without reaching the surface as a DBR, it is assumed that the lateral radionuclide transport is in the most transmissive unit, the Culebra. Therefore, the radionuclide transport through the Dewey Lake to the accessible environment and to the land surface due to long-term flow are set to zero.

The PA uses NUTS in two different modes. First, the code is used in a computationally fast *screening* mode to identify those BRAGFLO realizations for which it is unnecessary to do full transport calculations because the amount of contaminated brine that reaches the Culebra or the LWB within the Salado is insufficient to significantly contribute to the total integrated release of radionuclides from the disposal system. For the remaining realizations, which have the possibility of consequential release, a more computationally intensive calculation of each radionuclide's full transport is performed (see Section PA-6.7.2).

This section describes the model used to compute radionuclide transport in the Salado for E0, E1, and E2 scenarios (defined in Section PA-2.3.2). The model for transport in the E1E2 scenario, which is computed using the PANEL code, is described in Section PA-4.4.

NUTS models radionuclide transport by advection (see Appendix MASS-2014, Section MASS-12.5). NUTS disregards sorptive and other retarding effects throughout the entire flow region. Physically, some degree of retardation must occur at locations within the repository and

the geologic media; it is therefore conservative to ignore retardation processes. NUTS also ignores reaction-rate aspects of dissolution and colloid formation processes, and mobilization is assumed to occur instantaneously. Neither molecular nor mechanical dispersion is modeled in NUTS. These processes are assumed to be insignificant compared to advection, as discussed further in Appendix MASS-2014, Section MASS-12.5.

Colloidal actinides are subject to retardation by chemical interaction between colloids and solid surfaces and by clogging of small pore throats (i.e., by sieving). There will be some interaction of colloids with solid surfaces in the anhydrite interbeds. Given the low permeability of intact interbeds, it is likely that pore apertures will be small and some sieving will occur. However, colloidal particles, if not retarded, are transported slightly more rapidly than the average velocity of the bulk liquid flow. Because the effects on transport of slightly increased average pore velocity and retarded interactions with solid surfaces and sieving offset one another, the DOE assumes residual effects of these opposing processes will be either small or beneficial, and does not incorporate them when modeling actinide transport in the Salado interbeds.

If brine in the repository moves into interbeds, it is likely that mineral precipitation reactions will occur. Precipitated minerals may contain actinides as trace constituents. Furthermore, colloidal-sized precipitates will behave like mineral-fragment colloids, which are destabilized by brines, quickly agglomerating and settling by gravity. The beneficial effects of precipitation and coprecipitation are neglected in PA.

Fractures, channeling, and viscous fingering may also impact transport in Salado interbeds, which contain natural fractures. Because of the low permeability of unfractured anhydrite, most fluid flow in interbeds will occur in fractures. Even though some properties of naturally fractured interbeds are characterized by in situ tests, uncertainty exists in the characteristics of the fracture network that may be created with high gas pressure in the repository. The PA modeling system accounts for the possible effects on porosity and permeability of fracturing by using a fracturing model (see Section PA-4.2.4). The processes and effects associated with fracture dilation or fracture propagation not already captured by the PA fracture model are negligible (see the CCA, Appendix MASS, Section MASS.13.3 and Appendix MASS, Attachment 13.2). Of those processes not already incorporated, channeling has the greatest potential effect.

Channeling is the movement of fluid through the larger-aperture sections of a fracture network with locally high permeabilities. It could locally enhance actinide transport. However, it is assumed that the effects of channeled flow in existing or altered fractures will be negligible for the length and time scales associated with the disposal system. The DOE believes this assumption is reasonable because processes are likely to occur that limit the effectiveness of channels or the dispersion of actinides in them. First, if gas is present in the fracture network, it will be present as a nonwetting phase and will occupy theportions of the fracture network with relatively large apertures, where the highest local permeabilities will exist. The presence of gas thus removes the most rapid transport pathways from the contaminated brine and decreases the impact of channeling. Second, brine penetrating the Salado from the repository is likely to be completely miscible with in situ brine. Because of miscibility, diffusion or other local mixing processes will probably broaden fingers (reduce concentration gradients) until the propagating fingers are indistinguishable from the advancing front.

Gas will likely penetrate the liquid-saturated interbeds as a fingered front, rather than a uniform front. Fingers form when there is a difference in viscosity between the invading fluid (gas) and the resident fluid (liquid brine), and because of channeling effects. This process does not affect actinide transport, however, because actinides of interest are transported only in the liquid phase, which will not displace gas in the relatively high-permeability regions due to capillary effects.

PA-4.3.1 Mathematical Description

The following system of PDEs is used to model radionuclide transport in the Salado:

$$-\nabla \cdot \alpha \mathbf{v}_b C_{bl} + \alpha S_l = \alpha \frac{\partial}{\partial t}\left(\phi S_b C_{bl}\right) + \left(\alpha \phi S_b C_{bl}\right)\lambda_l - \alpha \phi S_b \sum_{p \in P(l)} C_{bp}\lambda_p \quad \text{(PA.104)}$$

$$-S_l = \frac{\partial}{\partial t}\left(C_{sl}\right) + C_{sl}\lambda_l - \sum_{p \in P(l)} C_{sp}\lambda_p \quad \text{(PA.105)}$$

for l = 1, 2, …, n_R, where

$\mathbf{v}_b$ = Darcy velocity vector ($m^3/m^2/s$ = m/s) for brine (supplied by BRAGFLO from solution of Equation (PA.102))
C_{bl} = concentration (kg/m^3) of radionuclide l in brine
C_{sl} = concentration (kg/m^3) of radionuclide l in solid phase (i.e., not in brine), with concentration defined with respect to total (i.e., bulk) formation volume (only used in repository; see Figure PA-12)
S_l = linkage term ($kg/m^3/s$) due to dissolution/precipitation between radionuclide l in brine and in solid phase (see Equation (PA.106))
ϕ = porosity (supplied by BRAGFLO from solution of Equation (PA.24), Equation (PA.25), Equation (PA.26), Equation (PA.27), Equation (PA.28), Equation (PA.29) and Equation (PA.30))
S_b = brine saturation (supplied by BRAGFLO from solution of Equation (PA.24), Equation (PA.25), Equation (PA.26), Equation (PA.27), Equation (PA.28), Equation (PA.29) and Equation (PA.30))
λ_l = decay constant (s^{-1}) for radionuclide l
$P(l)$ = {p: radionuclide p is a parent of radionuclide l}
n_R = number of radionuclides,

and α is the dimension-dependent geometry factor in Equation (PA.32). PA uses a two-dimensional representation for fluid flow and radionuclide transport in the vicinity of the repository, with α defined by the element depths in Figure PA-12. Although omitted for brevity, the terms α, $\boldsymbol{v}_b$, C_{bl}, C_{sl}, S_l, S_b, and ϕ are functions $\alpha(x,y)$, $\boldsymbol{v}_b(x,y,t)$, $C_{bl}(x,y,t)$, $C_{sl}(x,y,t)$, $S_l(x,y,t)$, $S_b(x,y,t)$, and $\phi(x,y,t)$ of time t and the spatial variables x and y. Equation (PA.104) and Equation (PA.105) are defined and solved on the same computational grid (Figure PA-12) used by BRAGFLO for the solution of Equation (PA.24), Equation (PA.25), Equation (PA.26), Equation (PA.27), Equation (PA.28), Equation (PA.29) and Equation (PA.30).

Radionuclides are assumed to be present in both brine (Equation (PA.104)) and in an immobile solid phase (Equation (PA.105)), although radionuclide transport takes place only by brine flow (Equation (PA.104)). Maximum radionuclide concentrations are calculated for elements dissolved in Salado and Castile brines for oxidation states III, IV, and V. Maximum concentrations are dependent on the dissolved solubility (mols per liter mol/L) for each brine type and oxidation state, as well as the uncertainty associated with the dissolved solubility. Dissolved solubilities and their uncertainties are developed in Brush and Domski (Brush and Domski 2013b and Brush and Domski 2013c), and are listed in Kicker and Herrick (Kicker and Herrick 2013), Table 27, Table A-8 , and Table A-9. Only the maximum concentration corresponding to the minimum brine volume of 17,400 m^3 is used in Salado transport calculations due to the computational expense associated with NUTS. This approach is conservative as it maximizes the concentration of actinides that are potentially transported across the LWB.

The maximum radionuclide concentration is assumed to equilibrate instantly for each element (Am, Pu, U, Th). Then each individual radionuclide equilibrates between the brine and solid phases based on the maximum concentration of the radionuclide and the mole fractions of other isotopes included in the calculation. The linkage between the brine and solid phases in Equation (PA.104) and Equation (PA.105) is accomplished by the term S_l, where

$$S_l = \begin{cases} \delta(\tau - t)\, Dif\left(S_T, C_{b,El(l)}\right) MF_{sl} & \text{if } 0 \le Dif\left(S_T, C_{b,El(l)}\right) \le \dfrac{C_{s,El(l)}}{\phi S_b} \text{ and } 0 < S_b \\ \delta(\tau - t)\left[\dfrac{C_{s,El(l)}}{\phi S_b}\right] MF_{sl} & \text{if } 0 \le \dfrac{C_{s,El(l)}}{\phi S_b} < Dif\left(S_T, C_{b,El(l)}\right) \text{ and } 0 < S_b \\ \delta(\tau - t)\, Dif\left(S_T, C_{b,El(l)}\right) MF_{bl} & \text{if } Dif\left(S_T, C_{b,El(l)}\right) < 0 \text{ and } 0 < S_b \\ 0 & \text{otherwise} \end{cases}$$

(PA.106)

where

$S_T\left[Br(t), Ox(l), El(l)\right]$ = maximum concentration (kg/m^3) of element $El(l)$ in oxidation state $Ox(l)$ in brine type $Br(t)$, where $El(l)$ denotes the element of which radionuclide l is an isotope, $Ox(l)$ denotes the oxidation state in which element $El(l)$ is present, and $Br(t)$ denotes the type of brine present in the repository at time t.

$C_{p,El(l)}$ = concentration (kg/m3) of element $El(l)$ in brine ($p = b$) or solid ($p = s$), which is equal to the sum of concentrations of radionuclides that are isotopes of same element as radionuclide l, where $k \in El(l)$ only if k is an isotope of element $El(l)$:

$$C_{p,El(l)} = \sum_{k \in El(l)} C_{p,k} \quad \text{(PA.107)}$$

$Dif\left(S_T, C_{b,El(l)}\right)$ = difference (kg/m^3) between maximum concentration of element $El(l)$ in brine and existing concentration of element $El(l)$ in brine

$$Dif\left(S_T, C_{b,El(l)}\right) = S_T\left[Br(t), Ox(l), El(l)\right] - C_{b,El(l)} \quad \text{(PA.108)}$$

MF_{pl} = mole fraction of radionuclide l in phase p, where $p = b$ (brine) or $p = s$ (solid)

$$MF_{pl} = C_{pl} CM_l \Big/ \sum_{k \in El(l)} C_{pk} CM_k \quad \text{(PA.109)}$$

CM_l = conversion factor (mol/kg) from kilograms to moles for radionuclide l

$\delta(\tau - t)$ = Dirac delta function (s^{-1}) ($\delta(\tau - t) = 0$ if $\tau \neq t$ and $\int_{-\infty}^{\infty} \delta(\tau - t)\, d\tau = 1$)

The terms S_l, S_b, $C_{p,El(l)}$, MF_{pl}, and ϕ are functions of time t and the spatial variables x and y, although the dependencies are omitted for brevity. The Dirac delta function, $\delta(\tau - t)$, appears in Equation (PA.106) to indicate that the adjustments to concentration are implemented instantaneously within the numerical solution of Equation (PA.104) and Equation (PA.105) whenever a concentration imbalance is observed.

The velocity vector $\boldsymbol{v}_b$ in Equation (PA.104) and Equation (PA.105) is defined in Equation (PA.102) and is obtained from the numerical solution of Equation (PA.24), Equation (PA.25), Equation (PA.26), Equation (PA.27), Equation (PA.28), Equation (PA.29) and Equation (PA.30). If B denotes an arbitrary boundary (e.g., the LWB) in the domain of Equation (PA.104) and Equation (PA.105) (as shown in Figure PA-12), the cumulative transport of $C_l(t, B)$ of radionuclide l from time 0 to time t across B is given by

$$C_l(t,B) = \int_0^t \left[\int_B v_b(x,y,t) C_l(x,y,t) \alpha(x,y) \cdot \boldsymbol{n}(x,y) ds \right] dt \quad \text{(PA.110)}$$

where $\boldsymbol{n}(x, y)$ is an outward-pointing unit normal vector and $\int_B ds$ denotes a line integral over B.

Equation (PA.104) and Equation (PA.105) models advective radionuclide transport due to the velocity vector $\boldsymbol{v}_b$.

PA-4.3.2 Radionuclides Transported

Since the solution of Equation (PA.104) and Equation (PA.105) for many radionuclides and decay chains is computationally very expensive, the number of radionuclides for direct inclusion in the analysis is initially reduced using the algorithm shown in Figure PA-17. The number of radionuclides included in the transport calculations is then further reduced by combining those with similar decay and transport properties. The CRA-2014 PA uses the same reduction algorithm as the CCA PA (see the CCA, Appendix WCA); the algorithm was found to be acceptable in the CCA review (U.S. EPA 1998a, Section 4.6.1.1).

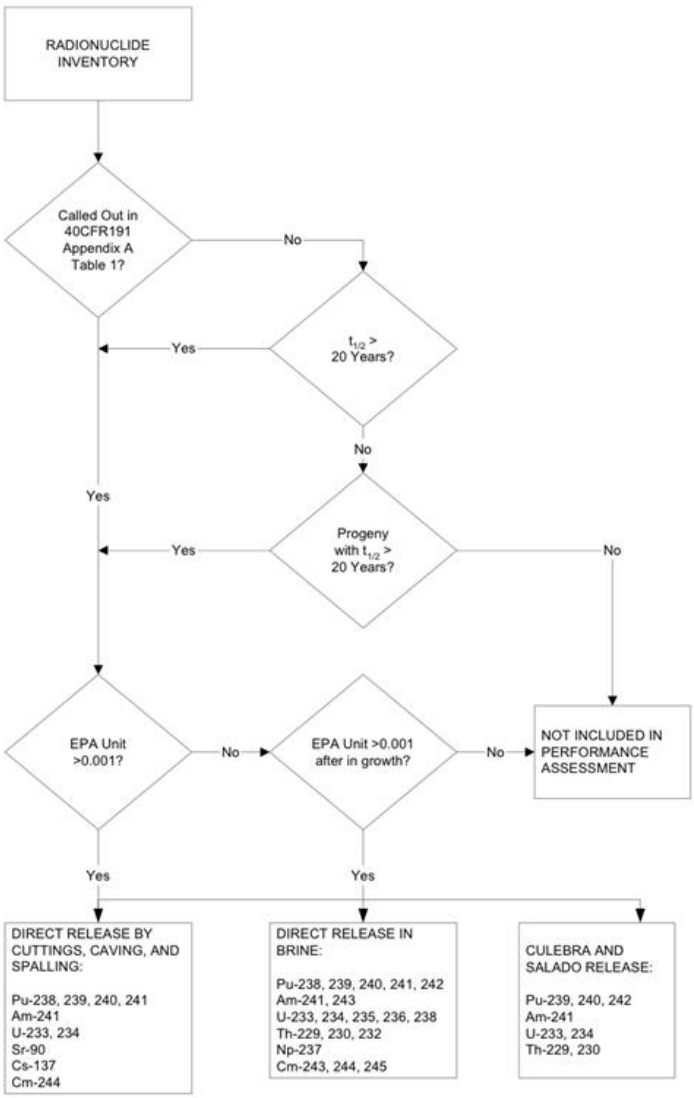

Figure PA- 17. Selecting Radionuclides for the Release Pathways Conceptualized by PA

Using Figure PA-17, the number of radionuclides initially included in the decay calculations is 29. These radionuclides are the same as those in the CRA-2009 PABC, and belong to the following decay chains:

$$^{242}\mathrm{Pu} \rightarrow {}^{238}\mathrm{U} \rightarrow {}^{234}\mathrm{U} \rightarrow {}^{230}\mathrm{Th} \rightarrow {}^{226}\mathrm{Ra} \rightarrow {}^{210}\mathrm{Pb} \quad \begin{matrix} & & {}^{238}\mathrm{Pu} \\ & & \downarrow \end{matrix} \quad \text{(PA.111)}$$

$$^{243}\mathrm{Am} \rightarrow {}^{239}\mathrm{Pu} \rightarrow {}^{235}\mathrm{U} \rightarrow {}^{231}\mathrm{Pa} \quad \begin{matrix} {}^{243}\mathrm{Cm} \\ \downarrow \end{matrix} \quad \text{(PA.112)}$$

$$^{252}\mathrm{Cf} \rightarrow {}^{248}\mathrm{Cm} \rightarrow {}^{244}\mathrm{Pu} \rightarrow {}^{240}\mathrm{Pu} \rightarrow {}^{236}\mathrm{U} \rightarrow {}^{232}\mathrm{Th} \rightarrow {}^{228}\mathrm{Ra} \quad \begin{matrix} & & & & {}^{244}\mathrm{Cm} \\ & & & & \downarrow \end{matrix} \quad \text{(PA.113)}$$

$$^{245}\mathrm{Cm} \rightarrow {}^{241}\mathrm{Pu} \rightarrow {}^{241}\mathrm{Am} \rightarrow {}^{237}\mathrm{Np} \rightarrow {}^{233}\mathrm{U} \rightarrow {}^{229}\mathrm{Th} \quad \text{(PA.114)}$$

Radionuclides considered in the decay calculations that do not belong to one of the decay chains listed above are ^{147}Pm, ^{137}Cs, and ^{90}Sr. In addition, some intermediates with extremely short half-lives, such as ^{240}U, were omitted from the decay chains.

Further simplification of the decay chains is possible based on the total inventories. Releases of radionuclides whose inventories total less than one EPA unit are essentially insignificant, as any release that transports essentially all of a given species outside the LWB will be dominated by the releases of other species with much larger inventories. In addition, ^{137}Cs and ^{90}Sr can be omitted because their concentrations drop to below 1 EPA unit within 150 years, which makes it improbable that a significant release of these radionuclides will occur.

After the reduction of radionuclides outlined inFigure PA-17 and the paragraph above, the following 10 radionuclides remained from the decay chains shown:

$$\left\{{}^{242}\mathrm{Pu}, {}^{238}\mathrm{Pu}\right\} \rightarrow {}^{234}\mathrm{U} \rightarrow {}^{230}\mathrm{Th} \quad \text{(PA.115)}$$

$$^{239}\mathrm{Pu} \quad \text{(PA.116)}$$

$$^{240}\mathrm{Pu} \quad \text{(PA.117)}$$

$$^{241}\mathrm{Pu} \rightarrow {}^{241}\mathrm{Am} \rightarrow {}^{233}\mathrm{U} \rightarrow {}^{229}\mathrm{Th} \quad \text{(PA.118)}$$

^{238}Pu does not significantly affect transport calculations because of its short half-life (87.8 years). The remaining nine radionuclides were then further reduced by combining those with similar decay and transport properties. In particular, ^{234}U, ^{230}Th, and ^{239}Pu were used as surrogates for the groups {^{234}U, ^{233}U}, {^{230}Th, ^{229}Th}, and {^{242}Pu, ^{240}Pu, ^{239}Pu}, with the initial inventories of ^{234}U, ^{230}Th, and ^{239}Pu being increased to account for the additional radionuclide(s) in each group.

In increasing the initial inventories, the individual radionuclides were combined (or "lumped" together) on either a mole or curie basis (i.e., moles added and then converted back to curies, or curies added directly (see Kicker and Zeitler 2013b)). In each case, the method that maximized the combined inventory was used; thus, ^{233}U was added to ^{234}U, ^{240}Pu to ^{239}Pu, and ^{229}Th to ^{230}Th by curies, while ^{242}Pu was added to ^{239}Pu by moles. In addition, ^{241}Pu was added to ^{241}Am by moles because ^{241}Pu has a half-life of 14 years and will quickly decay to ^{241}Am. The outcome of this process was the following set of five radionuclides in three simplified decay chains:

$$^{241}\mathrm{Am};\ {}^{238}\mathrm{Pu} \rightarrow {}^{234}\mathrm{U} \rightarrow {}^{230}\mathrm{Th};\ {}^{239}\mathrm{Pu} \quad \text{(PA.119)}$$

which were then used with Equation (PA.104) and Equation (PA.105) for transport in the vicinity of the repository. The development of these "lumped" radionuclide inventories is done in Kicker and Zeitler (Kicker and Zeitler 2013b), and the results are listed in Kicker and Herrick (Kicker and Herrick 2013), Table 29. These "lumped" radionuclides closely approximate the activity of the total normalized waste inventory (Kim 2013b).

PA-4.3.3 NUTS Tracer Calculations

All BRAGFLO realizations are first evaluated using NUTS in a screening mode to identify those realizations for which a significant release of radionuclides to the LWB cannot occur. The screening simulations consider an infinitely soluble, nondecaying, nondispersive, and nonsorbing species as a tracer element. The tracer is given a unit concentration in all waste disposal areas of 1 kg/m^3. If the amount of tracer that reaches the selected boundaries (the top of the Salado and the LWB within the Salado) does not exceed a cumulative mass of 10^{-7} kg within 10,000 years, it is assumed there is no consequential release to these boundaries. If the cumulative mass outside the boundaries within

10,000 years exceeds 10^{-7} kg, a complete transport analysis is conducted. The value of 10^{-7} kg is selected because, regardless of the isotopic composition of the release, it corresponds to a normalized release less than 10^{-6} EPA units, the smallest release displayed in CCDF construction (Stockman 1996). The largest normalized release would be 9.98×10^{-7} EPA units, corresponding to 10^{-7} kg of ^{241}Am if the release was entirely ^{241}Am.

PA-4.3.4 NUTS Transport Calculations

For BRAGFLO realizations with greater than 10^{-7} kg reaching the boundaries in the tracer calculations, NUTS models the transport of five different radionuclide species (^{241}Am, ^{239}Pu, ^{238}Pu, ^{234}U, and ^{230}Th). These radionuclides represent a larger number of radionuclides; as discussed in Section PA-4.3.2, radionuclides were grouped together based on similarities, such as isotopes of the same element and those with similar half-lives, to simplify the calculations. For transport purposes, solubilities are lumped to represent both dissolved and colloidal forms. These groupings simplify and expedite calculations.

PA-4.3.5 Numerical Solution

Equation (PA.104) and Equation (PA.105) are numerically solved by the NUTS program (WIPP Performance Assessment 1997a) on the same computational grid (Figure PA-12) used by BRAGFLO for the solution of Equation (PA.24), Equation (PA.25), Equation (PA.26), Equation (PA.27), Equation (PA.28), Equation (PA.29), and Equation (PA.30). In the solution procedure, Equation (PA.104) and Equation (PA.105) are numerically solved with $S_l = 0$ for each time step, with the instantaneous updating of concentrations indicated in Equation (PA.106) and the appropriate modification to C_{sl} in Equation (PA.105) taking place after the time step. The solution is carried out for the five radionuclides indicated in Equation (PA.119).

The initial value and boundary value conditions used with Equation (PA.104) and Equation (PA.105) are given in Table PA-10. At time $t = 0$ (corresponding to the year 2033), the total inventory of each radionuclide is assumed to be in brine; the solubility constraints associated with Equation (PA.106) then immediately adjust the values for $C_{bl}(x, y, t)$ and $C_{sl}(x, y, t)$ for consistency with the constraints imposed by $S_T(Br, Ox, El)$ and available radionuclide inventory.

The n_R PDEs in Equation (PA.104) and Equation (PA.105) are discretized in two dimensions and then developed into a linear system of algebraic equations for numerical implementation. The following conventions are used in the representation of each discretized equation:

- The subscript b is dropped from C_{bl}, so that the unknown function is represented by C_l.
- A superscript n denotes time t_n, with the assumption that the solution C_l is known at time t_n and is to be propagated to time t_{n+1}.
- The grid indices are i in the x-direction and j in the y-direction, and are the same as the BRAGFLO grid indices.

Table PA- 10. Initial and Boundary Conditions for $C_{bl}(x, y, t)$ and $C_{sl}(x, y, t)$

Initial Conditions for $C_{bl}(x, y, t)$ and $C_{sl}(x, y, t)$
$C_{bl}(x, y, t) = A_l(0)/V_b(0)$ if (x, y) is a point in the repository (i.e., areas Waste Panel, South RoR and North RoR, in Figure PA-12), where $A_l(0)$ is the amount (kg) of radionuclide l present at time $t = 0$ and $V_b(0)$ is the amount (m^3) of brine in repository at time $t = 0$ (from solution of Equation (PA.24), Equation (PA.25), Equation (PA.26), Equation (PA.27), Equation (PA.28), Equation (PA.29) and Equation (PA.30) with BRAGFLO) for all (x, y). = 0 otherwise. $C_{sl}(x, y, t)$ = 0 if (x, y) is a point in the repository.
Boundary Conditions for $C_{bl}(x, y, t)$
$f_l(B,t) = \int_B \mathbf{v}_b(x,y,t)\, C_{bl}(x,y,t)\, \alpha(x,y) \cdot \mathbf{n}(x,y)\, ds$, where B is any subset of the outer boundary of the computational grid in Figure PA-12, $f_l(B,t)$ is the flux (kg/s) at time t of radionuclide l across B, $\mathbf{v}_b(x, y, t)$ is the Darcy velocity ($m^3/m^2/s$) of brine at (x, y) on B and is obtained from the solution of Equation (PA.24) Equation (PA.25), Equation (PA.26), Equation (PA.27), Equation (PA.28), Equation (PA.29), and Equation (PA.30) by BRAGFLO, $\mathbf{n}(x, y)$ denotes an outward-pointing unit normal vector, and $\int_B ds$ denotes a line integral along B.

- Fractional indices refer to quantities evaluated at grid block interfaces.
- Each time step by NUTS is equal to 20 BRAGFLO time steps because BRAGFLO stores results (here, v_b, ϕ, and S_b) every 20 time steps.

The following finite-difference discretization is used for the l^{th} equation in each grid block (i, j):

$$q^{n+1}_{b,i+1/2,j}C^{n+1}_{l,i+1/2,j} - q^{n+1}_{b,i-1/2,j}C^{n+1}_{l,i-1/2,j} + q^{n+1}_{b,i,j+1/2}C^{n+1}_{l,i,j+1/2} - q^{n+1}_{b,i,j-1/2}C^{n+1}_{l,i,j-1/2} =$$

$$\frac{V_{R,i,j}}{\Delta t}\left[\left\{\phi_{l,j}S_{b_{l,j}}C_{l,i,j}\right\}^{n+1} - \left\{\phi_{l,j}S_{b_{l,j}}C_{l,i,j}\right\}^{n}\right]$$
$$+V_{R,i,j}\left\{\phi_{l,j}S_{b_{l,j}}C_{l,i,j}\right\}^{n+1}\lambda_l - V_{R,i,j}\left(\phi_{l,j}S_{b_{l,j}}\right)^{n+1}\sum_{p\in P(l)}C^{n+1}_{p,i,j}\lambda_p \qquad \text{(PA.120)}$$

where q_b is the grid block interfacial brine flow rate (m^3/s) and V_R is the grid block volume (m^3). The quantity q_b is based on v_b and α in Equation (PA.104) and Equation (PA.105), and the quantity V_R is based on grid block dimensions (Figure PA-12) and α.

The interfacial values of concentration in Equation (PA.120) are discretized using the one-point upstream weighting method (Aziz and Settari 1979), which results in

$$q^{n+1}_{b,i-1/2,j}\left(\omega_{i+1}C^{n+1}_{l,i,j} + (1-\omega_{i+1})C^{n+1}_{l,i-1,j}\right) - q^{n+1}_{b,i-1/2,j}\left(\omega_i C^{n+1}_{l,i-1,j} + (1-\omega_i)C^{n+1}_{l,i,j}\right)$$
$$+q^{n+1}_{b,i,j+1/2}\left(\omega_{j+1}C^{n+1}_{l,i,j} + (1-\omega_{j+1})C^{n+1}_{l,i,j+1}\right) - q^{n+1}_{b,i,j-1/2}\left(\omega_j C^{n+1}_{b,i,j-1} + (1-\omega_j)C^{n+1}_{l,i,j}\right) =$$

$$\frac{V_{R,i,j}}{\Delta t}\left[\left\{\phi_{l,j}S_{b_{l,j}}C_{l,i,j}\right\}^{n+1} - \left\{\phi_{l,j}S_{b_{l,j}}C_{l,i,j}\right\}^{n}\right] + V_{R,i,j}\left\{\phi_{l,j}S_{b_{l,j}}C_{l,i,j}\right\}^{n+1}\lambda_l$$
$$- V_{R,i,j}\left(\phi_{l,j}S_{b_{l,j}}\right)^{n+1}\sum_{p\in P(l)}C^{n+1}_{p,i,j}\lambda_p \qquad \text{(PA.121)}$$

where ω derives from the upstream weighting for flow between adjacent grid blocks and is defined by

$$\omega_i = \begin{cases} 1 & \text{if flow is from grid block } (i-1,j) \text{ to grid block } (i,j) \\ 0 & \text{otherwise} \end{cases}$$

$$\omega_j = \begin{cases} 1 & \text{if flow is from grid block } (i,j-1) \text{ to grid block } (i,j) \\ 0 & \text{otherwise} \end{cases}$$

By collecting similar terms, Equation (PA.121) can be represented by the linear equation

$$AC^{n+1}_{l,i,j-1} + BC^{n+1}_{l,i-1,j} + DC^{n+1}_{l,i,j} + EC^{n+1}_{l,i+1,j} + FC^{n+1}_{l,i,j+1} = R_{l,i,j} \qquad \text{(PA.122)}$$

where

$$A = -\omega_j q^{n+1}_{b,i,j-1/2} \qquad B = -\omega_i q^{n+1}_{b,i-1/2,j}$$
$$E = (1-\omega_{i+1})\,q^{n+1}_{b,i+1/2,j} \qquad F = (1-\omega_{j+1})\,q^{n+1}_{b,i,j+1/2}$$

$$D = -(1-\omega_j)\,q^{n+1}_{b,i,j-1/2} - (1-\omega_i)\,q^{n+1}_{b,i-1/2,j} + \omega_{j+1}q^{n+1}_{b,i,j+1/2} + \omega_{i+1}q^{n+1}_{b,i+1/2,j}$$
$$-\left(\frac{V_{R,i,j}}{\Delta t} - V_{R,i,j}\lambda_l\right)\left\{\phi_{l,j}S_{b_{l,j}}\right\}^{n+1}$$

$$R_{l,i,j} = -\frac{V_{R,i,j}}{\Delta t}\left\{\phi_{l,j}S_{b_{l,j}}C_{l,i,j}\right\}^{n} - V_{R,i,j}\left(\phi_{l,j}S_{b_{l,j}}\right)^{n+1}\sum_{p\in P(l)}C^{n+1}_{p,i,j}\lambda_p$$

Given the form of Equation (PA.122), the solution of Equation (PA.104) and Equation (PA.105) has now been reduced to the solution of $n_R \times n_G$ linear algebraic equations in $n_R \times n_G$ unknowns, where n_R is the number of equations for each grid block (i.e., the number of radionuclides) and n_G is the number of grid blocks into which the spatial domain is discretized (Figure PA-12).

The system of PDEs in Equation (PA.104) and Equation (PA.105) is strongly coupled because of the contribution from parental decay to the equation governing the immediate daughter. Consequently, a sequential method is used to solve for the radionuclide concentrations by starting at the top of a decay chain and working down from parent to daughter. This implies that when solving Equation (PA.122) for the l^{th} isotope concentration, all parent concentrations occurring in the right-hand-side term R are known. The system of equations is then linear in the concentrations of the l^{th} isotope. As a result, solving Equation (PA.104) and Equation (PA.105) is reduced from the solution of one

algebraic equation at each time step with $n_R \times n_G$ unknowns to the solution of n_R algebraic equations each with n_G unknowns at each time step, which can result in a significant computational savings.

The matrix resulting from one-point upstream weighting has the following structural form for a 3 ´ 3 system of grid blocks, and a similar structure for a larger number of grid blocks:

	1	2	3	4	5	6	7	8	9
1	X	X	0	X					
2	X	X	X	0	X				
3	0	X	X	0	0	X			
4	X	0	0	X	X	0	X		
5		X	0	X	X	X	0	X	
6			X	0	X	X	0	0	X
7				X	0	0	X	X	0
8					X	0	X	X	X
9						X	0	X	X

where X designates possible nonzero matrix entries, and 0 designates zero entries within the banded structure. All entries outside of the banded structure are zero. Because of this structure, a banded direct elimination solver (Aziz and Settari 1979, Section 8.2.1) is used to solve the linear system for each radionuclide. The bandwidth is minimized by first indexing equations in the coordinate direction with the minimum number of grid blocks. The coefficient matrix is stored in this banded structure, and all infill coefficients calculated during the elimination procedure are contained within the band structure. Therefore, for the matrix system in two dimensions, a pentadiagonal matrix of dimension $I_{BW} \times n_G$ is inverted instead of a full $n_G \times n_G$ matrix, where I_{BW} is the bandwidth.

The numerical implementation of Equation (PA.105) enters the solution process through updates to the radionuclide concentrations in Equation (PA.121) between each time step, as indicated in Equation (PA.106). The numerical solution of Equation (PA.104) and Equation (PA.105) also generates the concentrations required to numerically evaluate the integral that defines $C_l(t, B)$ in Equation (PA.110).

PA-4.3.6 Additional Information

Additional information on NUTS and its use in WIPP PA can be found in the NUTS users manual (WIPP Performance Assessment 1997a) and in the analysis package of Salado transport calculations for the CRA-2014 PA (Kim 2013a). Furthermore, additional information on dissolved and colloidal actinides is given in Appendix SOTERM-2014, Section SOTERM-5.0.

PA-4.4 Radionuclide Transport in the Salado: PANEL

This section describes the model used to compute radionuclide transport in the Salado for the E1E2 scenario. The model for transport in E0, E1, and E2 scenarios is described in Section PA-4.3.

PA-4.4.1 Mathematical Description

A relatively simple mixed-cell model is used for radionuclide transport in the vicinity of the repository after an E1E2 intrusion, when connecting flow between two drilling intrusions into the same waste panel is assumed to take place. With this model, the amount of radionuclide *l* contained in a waste panel is represented by

$$\frac{dA_l}{dt} = -v_b C_{bl} - \lambda_l A_l + \sum_{p \in P(l)} \lambda_p A_p \qquad \text{(PA.123)}$$

where

$A_l(t)$ = amount (mol) of radionuclide *l* in waste panel at time *t*

$C_{bl}(t)$ = concentration (mol/m^3) of radionuclide *l* in brine in waste panel at time *t* (Equation (PA.124) and Equation (PA.125))

$v_b(t)$ = rate (m^3/s) at which brine flows out of the repository at time *t* (supplied by BRAGFLO from solution of Equation (PA.102))

and λ_l and $P(l)$ are defined in conjunction with Equation (PA.104) and Equation (PA.105).

The brine concentration C_{bl} in Equation (PA.123) is defined by

$$C_{bl}(t) = S_l\left[Br, Ox, El\right] MF_l(t)$$
$$if \quad S_l\left[Br(t), Ox, El\right] \le \sum_{k \in El(l)} A_k(t) / V_b(t) \qquad \text{(PA.124)}$$

$$= A_l(t) / V_b(t) \quad \text{if} \sum_{k \in El(l)} A_k(t) / V_b(t) < S_T[Br, Ox, El] \tag{PA.125}$$

where

$MF_l(t)$ = mole fraction of radionuclide l in waste panel at time t

$$= \frac{A_l(t)}{\sum_{k \in El(l)} A_k(t)} \tag{PA.126}$$

$V_b(t)$ = volume (m^3) of brine in waste panel at time t (supplied by BRAGFLO from solution of Equation (PA.24), Equation (PA.25), Equation (PA.26), Equation (PA.27), Equation (PA.28), Equation (PA.29), and Equation (PA.30))

and $S_T[Br, Ox, El]$ is the maximum concentration expressed in units of mol/L. Quantity $C_{bl}(t)$ is defined to be the maximum concentration S_T if there is sufficient radionuclide inventory in the waste panel to generate this concentration (Equation (PA.124)); otherwise, $C_{bl}(t)$ is defined by the concentration that results when all the relevant element in the waste panel is placed in solution (Equation (PA.125)). The dissolved and colloidal actinides equilibrate instantly for each element.

Given r_b and C_{bl}, evaluation of the integral

$$R_l(t) = \int_0^t C_{bl}(\tau) r_b(\tau) d\tau \tag{PA.127}$$

provides the cumulative release $R_l(t)$ of radionuclide l from the waste panel through time t.

PA-4.4.2 Numerical Solution

Equation (PA.123) is numerically evaluated by the PANEL model (WIPP Performance Assessment 1998b) using a discretization based on time steps of 50 years or less. Specifically, Equation (PA.123) is evaluated with the approximation

$$A_l(t_{n+1}) = A_l(t_n) - \left[\int_{t_n}^{t_{n+1}} r_b(\tau) d\tau\right] C_{bl}(t_n) - A_l(t_n) \exp(-\lambda_l \Delta t) + G_l(t_n, t_{n+1}) \tag{PA.128}$$

where

$G_l(t_n, t_{n+1})$ = gain in radionuclide l due to the decay of precursor radionuclides between t_n

and t_{n+1} (see Equation (PA.129)), $\Delta t = t_{n+1} - t_n = 50\ yr$.

As the solution progresses, values for $C_{bl}(t_n)$ are updated in consistency with Equation (PA.124) and Equation (PA.125), and the products $r_b(t_n) C_{bl}(t_n)$ are accumulated to provide an approximation to R_l in Equation (PA.127).

The term $G_l(t_n, t_{n+1})$ in Equation (PA.128) is evaluated with the Bateman equations (Bateman 1910), with PANEL programmed to handle decay chains of up to five (four decay daughters for a given radionuclide). As a single example, if radionuclide l is the third radionuclide in a decay chain (i.e., $l = 3$) and the two preceding radionuclides in the decay chain are designated by $l = 1$ and $l = 2$, then

$$G_3(t_n, t_{n+1}) = \frac{\lambda_2 A_2(t_n)}{(\lambda_3 - \lambda_2)}\left[\exp(-\lambda_2 \Delta t) - \exp(-\lambda_3 \Delta t)\right] + \lambda_1 \lambda_2 A_1(t_n)\left\{\frac{\exp(-\lambda_1 \Delta t)}{(\lambda_2 - \lambda_1)(\lambda_3 - \lambda_1)} + \frac{\exp(-\lambda_2 \Delta t)}{(\lambda_3 - \lambda_2)(\lambda_1 - \lambda_2)} + \frac{\exp(-\lambda_3 \Delta t)}{(\lambda_1 - \lambda_3)(\lambda_2 - \lambda_3)}\right\} \tag{PA.129}$$

in Equation (PA.128).

PA-4.4.3 Implementation in PA

The preceding model is used in two ways in PA. First, Equation (PA.127) estimates releases to the Culebra associated with E1E2 intrusion scenarios (see Section PA-6.7.3). Second, radionuclide concentrations are calculated that correspond to multiples of the minimum brine volume (17,400 m^3) necessary for a DBR. Concentrations corresponding to the minimum brine volume comprise the S_l term indicated in Equation (PA.106) used in the NUTS calculations for Salado transport. Concentrations calculated over the range of brine volumes are used to determine releases when a volume of brine is released to the ground surface during a drilling intrusion.

For E1E2 intrusions, the initial amount A_l of radionuclide l is the inventory of the decayed isotope at the time of the E1 intrusion. PANEL calculates the inventory of each of the 29 radioisotopes throughout the regulatory period. The initial concentration C_{bl} of radionuclide l is computed by Equation (PA.123), Equation (PA.124), and Equation (PA.125). For the DBR calculations, the initial amount A_l of radionuclide l is the inventory of the isotope at the time of repository closure.

PA-4.4.4 Additional Information

Additional information on PANEL and its use in the CRA-2014 PA calculations can be found in the PANEL user's manual (WIPP Performance Assessment 2003a), the analysis package for PANEL calculations (Kim 2013b), and the analysis package for Salado transport calculations in the CRA-2014 PA (Kim 2013a).

PA-4.5 Cuttings and Cavings to Surface: CUTTINGS_S

Cuttings are waste solids contained in the cylindrical volume created by the cutting action of the drill bit passing through the waste, while cavings are additional waste solids eroded from the borehole by the upward-flowing drilling fluid within the borehole. The releases associated with these processes are computed within the CUTTINGS_S code (WIPP Performance Assessment 2003b). The mathematical representations used for cuttings and cavings are described in this section.

PA-4.5.1 Cuttings

The uncompacted volume of cuttings removed and transported to the surface in the drilling fluid, V_{cut}, is given by

$$V_{cut} = AH_i = \pi D^2 H_i / 4 \quad \text{(PA.130)}$$

where A is the drill bit area (m^2), H_i is the initial (or uncompacted) repository height (3.96 m) (see parameter BLOWOUT:HREPO in Kicker and Herrick 2013, Table 5), and D is the drill-bit diameter (0.31115 m) (see parameter BOREHOLE:DIAMMOD in Kicker and Herrick 2013, Table 5). For drilling intrusions through RH-TRU waste, H_i = 0.509 m is used (see parameter REFCON:HRH in Kicker and Herrick 2013, Table 37).

PA-4.5.2 Cavings

The cavings component of the direct surface release is caused by the shearing action of the drilling fluid on the waste as it flows up the borehole annulus. Like the cuttings release, the cavings release is assumed to be independent of the conditions that exist in the repository during a drilling intrusion.

The final diameter of the borehole depends on the diameter of the drillbit and on the extent to which the actual borehole diameter exceeds the drill-bit diameter. Although a number of factors affect erosion within a borehole (Chambre Syndicale de la Recherche et de la Production du Petrole et du Gaz Naturel 1982), the most important is the fluid shear stress on the borehole wall (i.e., the shearing force per unit area, N/m^2) resulting from circulating drilling fluids (Darley 1969, Walker and Holman 1971). As a result, PA estimates cavings removal with a model based on the effect of shear stress on the borehole diameter. In particular, the borehole diameter is assumed to grow until the shear stress on the borehole wall is equal to the shear strength of the waste, which is the limit below which waste erosion ceases.

The final eroded diameter D_f (m) of the borehole through the waste determines the total volume V (m^3) of uncompacted waste removed to the surface by circulating drilling fluid. Specifically,

$$V = V_{cut} + V_{cav} = \pi D_f^2 H_i / 4 \quad \text{(PA.131)}$$

where V_{cav} is the volume (m^3) of waste removed as cavings.

Most borehole erosion is believed to occur in the vicinity of the drill collar (Figure PA-18) because of decreased flow area and consequent increased mud velocity (Rechard, Iuzzolino, and Sandha 1990, Letters 1a and 1b, App. A). An important determinant of the extent of this erosion is whether the flow of the drilling fluid in the vicinity of the collar is laminar or turbulent. PA uses Reynolds numbers to distinguish between the occurrence of laminar flow and turbulent flow. The Reynolds number is the ratio between inertial and viscous (or shear) forces in a fluid, and can be expressed as (Fox and McDonald 1985)

$$\mathrm{Re} = \frac{\rho_f D_e v}{\eta} \quad \text{(PA.132)}$$

where Re is the Reynolds number (dimensionless), ρ_f is the fluid density (kg/m^3), D_e is the equivalent diameter (m), $v = \|\mathbf{v}\|$ is the fluid speed ($m\ s^{-1}$), and η is the fluid viscosity ($kg\ m^{-1}\ s^{-1}$).

Typically, ρ_f, v, and η are averages over a control volume with an equivalent diameter of D_e, where $\rho_f = 1.21 \times 10^3$ kg/m^3 (see parameter DRILLMUD:DNSFLUID in Kicker and Herrick 2013, Table 5), v = 0.7089 m s^{-1} (based on 40 gal/min/in of drill diameter) (Berglund 1992), and $D_e = 2(R - R_i)$, as shown in Figure PA-18. The diameter of the drill collar (i.e., $2R_i$ in Figure PA-18) is 8.0 in = 0.2032 m

(Kicker 2013). The determination of η is discussed below. PA assumes that Reynolds numbers less than 2100 are associated with laminar flow, while Reynolds numbers greater than 2100 are associated with turbulent flow (Walker 1976).

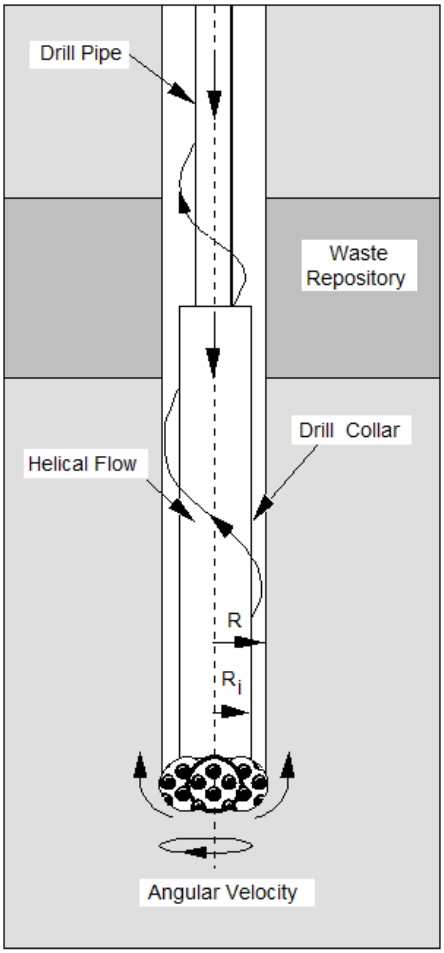

Figure PA- 18. Detail of Rotary Drill String Adjacent to Drill Bit

Drilling fluids are modeled as non-Newtonian, which means that the viscosity η is a function of the shear rate within the fluid (i.e., the rate at which the fluid velocity changes normal to the flow direction, m/s/m). PA uses a model proposed by Oldroyd (1958) to estimate the viscosity of drilling fluids. As discussed in the *Drilling Mud and Cement Slurry Rheology Manual* (Chambre Syndicale de la Recherche et de la Production du Petrole et du Gaz Naturel 1982), the Oldroyd model leads to the following expression for the Reynolds number associated with the helical flow of a drilling fluid within an annulus:

$$\mathrm{Re} = \frac{0.8165 \rho_f D_e v}{\eta_\infty} \quad \text{(PA.133)}$$

where ρ_f, D_e, and v are defined as in Equation (PA.132), and η_∞ is the asymptotic value for the derivative of the shear stress (τ, kg m^{-1} s^{-2}) with respect to the shear rate (Γ, s^{-1}) obtained as the shear rate increases (i.e., $\eta_\infty = d\tau / d\Gamma$ as $\Gamma \to \infty$). PA uses Equation (PA.133) to determine whether drilling fluids in the area of the drill collar are undergoing laminar or turbulent flow.

The Oldroyd model assumes that the shear stress τ is related to the shear rate Γ through the relationship

$$\tau = \eta_0 \left(\frac{1 + \sigma_2 \Gamma^2}{1 + \sigma_1 \Gamma^2} \right) \Gamma \quad \text{(PA.134)}$$

where η_0 is the asymptotic value of the viscosity (kg m^{-1} s^{-1}) that results as the shear rate Γ approaches zero, and σ_1 and σ_2 are constants (s^2). The expression leads to

$$\eta_\infty = \eta_0 \left(\frac{\sigma_2}{\sigma_1} \right) \quad \text{(PA.135)}$$

PA uses values of $\eta_0 = 1.834 \times 10^{-2}$ kg m^{-1} s^{-1}, $\sigma_1 = 1.082 \times 10^{-6}$ s^2, and $\sigma_2 = 5.410 \times 10^{-7}$ s^2 (Berglund 1996), from which viscosity in the limit of infinite shear rate is found to be $\eta_\infty = 9.17 \times 10^{-3}$ kg m^{-1} s^{-1}. The quantity η_∞ is comparable to the plastic viscosity of the fluid (Chambre Syndicale de la Recherche et de la Production du Petrole et du Gaz Naturel 1982).

As previously indicated, different models are used to determine the eroded diameter D_f of a borehole depending on whether flow in the vicinity of the drill collar is laminar or turbulent. The model for borehole erosion in the presence of laminar flow is described next, and then the model for borehole erosion in the presence of turbulent flow is described.

PA-4.5.2.1 Laminar Flow Model

As shown by Savins and Wallick (1966), the shear stresses associated with the laminar helical flow of a non-Newtonian fluid, as a function of the normalized radius, r, can be expressed as

$$\tau(R,r) = \sqrt{\left(\frac{C}{r^2}\right)^2 + \left[\frac{RJ}{2r}\left(r^2 - \lambda^2\right)\right]^2} \quad \text{(PA.136)}$$

for $R_i/R \le r \le 1$, where R_i and R are the inner and outer radii within which the flow occurs, as indicated in Figure PA-18; $\tau(R, \rho)$ is the shear stress (kg m^{-1} s^{-2}) at a radial distance ΔR beyond the inner boundary (i.e., at $r = (R_i + \Delta R)/R$); and the variables C, J, and λ depend on R and satisfy conditions Equation (PA.138), Equation (PA.139) and Equation (PA.140). The shear stress at the outer radius R is given by

$$\tau(R,1) = \sqrt{C^2 + \left[\frac{RJ}{2}\left(1 - \lambda^2\right)\right]^2} \quad \text{(PA.137)}$$

As previously indicated, the borehole radius R is assumed to increase as a result of erosional processes until a value of R is reached at which $\tau(R, 1)$ is equal to the shear strength of the waste. In PA, the shear strength of the waste is represented by the uncertain parameter BOREHOLE:TAUFAIL that has a minimum of 2.22 Pa and a maximum of 77.0 Pa (see Kicker and Herrick 2013, Table 4). Computationally, determining the eroded borehole diameter R associated with a particular value of the waste shear strength requires repeated evaluation of $\tau(R, 1)$, as indicated in Equation (PA.137), until a value of R is determined for which $\tau(R, 1)$ equals the shear strength.

The quantities C, J, and λ must satisfy the following three conditions (Savins and Wallick 1966) for Equation (PA.137) to be valid:

$$\int_{R_i/R}^{1} \left(\frac{x^2 - \lambda^2}{\eta x}\right) dx = 0 \quad \text{(PA.138)}$$

$$C\int_{R_i/R}^{1} \frac{dx}{\eta x^3} = \Delta\Omega \quad \text{(PA.139)}$$

$$J\int_{R_i/R}^{1} \left(\frac{(R_i/R)^2 - x^2}{\eta x}\right)\left(\frac{x^2 - \lambda^2}{\eta x}\right) dx = -\frac{2Q}{\pi R^4} \quad \text{(PA.140)}$$

where η, the drilling fluid viscosity (kg m^{-1} s^{-1}), is a function of R and ρ; $\Delta\Omega$ is the drill string angular velocity (rad s^{-1}); and Q is the drilling fluid flow rate (m^3 s^{-1}).

The viscosity η in Equation (PA.138), Equation (PA.139) and Equation (PA.140) is introduced into the analysis by assuming that the drilling fluid follows the Oldroyd model for shear stress in Equation (PA.134). By definition of the viscosity η,

$$\tau = \eta\Gamma \quad \text{(PA.141)}$$

and from Equation (PA.134)

$$\Gamma^2 = \frac{\eta - \eta_0}{\eta_0\sigma_2 - \eta\sigma_1} \quad \text{(PA.142)}$$

thus the expression in Equation (PA.136) can be reformulated as

$$\frac{\eta^2(\eta - \eta_0)^2}{(\eta_0\sigma_2 - \eta\sigma_1)^2} = \left(\frac{C}{r^2}\right)^2 + \left[\frac{RJ}{2r}\left(r^2 - \lambda^2\right)\right]^2 \quad \text{(PA.143)}$$

As discussed by Savins and Wallick (1966) and Berglund (1992), the expressions in Equation (PA.138), (Equation (PA.139) and Equation (PA.140) and Equation (PA.142) can be numerically evaluated to obtain C, J, and λ for use in Equation (PA.136) and Equation (PA.137). In PA, the drill string angular velocity $\Delta\Omega$ is treated as an uncertain parameter (see DOMEGA in Table PA-17), and

$$Q = v\left(\pi R^2 - \pi R_i^2\right) \quad \text{(PA.144)}$$

where $v = 0.7089$ m s^{-1} as used in Equation (PA.132), and η_0, σ_1, and σ_2 are defined as in Equation (PA.134) and Equation (PA.135).

PA-4.5.2.2 Turbulent Flow Model

The model for borehole erosion in the presence of turbulent flow is now described. Unlike the theoretically derived relationship for erosion in the presence of laminar flow, the model for borehole erosion in the presence of turbulent flow is empirical. In particular, pressure loss for axial flow in an annulus under turbulent flow conditions can be approximated by (Chambre Syndicale de la Recherche et de la Production du Petrole et du Gaz Naturel 1982)

$$\Delta P = \frac{2fL\rho_f v^2}{0.8165 D_e} \quad \text{(PA.145)}$$

where ΔP is the pressure change (Pa), f is the Fanning friction factor (dimensionless), L is the distance (m) over which pressure change ΔP occurs, and ρ_f, v, and D_e are defined in Equation (PA.132).

For turbulent pipe flow, f is empirically related to the Reynolds number Re defined in Equation (PA.132) by (Whittaker 1985)

$$\frac{1}{\sqrt{f}} = -4\log_{10}\left(\frac{\varepsilon}{3.72D} + \frac{1.255}{\mathrm{Re}\sqrt{f}}\right) \quad \text{(PA.146)}$$

where D is the inside diameter (m) of the pipe and ε is a "roughness term" equal to the average depth (m) of pipe wall irregularities. In the absence of a similar equation for flow in an annulus, Equation (PA.146) is used in PA to define f for use in Equation (PA.145), with D replaced by the effective diameter $D_e = 2(R - R_i)$ and ε equal to the average depth of irregularities in the waste-borehole interface. In the present analysis, $\varepsilon = 0.025$ m (parameter WAS_AREA:ABSROUGH in Kicker and Herrick 2013, Table 26), which exceeds the value often selected in calculations involving very rough concrete or riveted steel piping (Streeter 1958).

The pressure change ΔP in Equation (PA.145) and the corresponding shear stress τ at the walls of the annulus are approximately related by

$$(\Delta P)\pi\left(R^2 - R_i^2\right) = 2\pi L\tau(R + R_i) \quad \text{(PA.147)}$$

where $\pi\left(R^2 - R_i^2\right)$ is the cross-sectional area of the annulus (see Figure PA-18) and $2\pi L(R + R_i)$ is the total surface area of the annulus. Rearranging Equation (PA.145) and using the relationship in Equation (PA.141) yields

$$\tau(R) = \frac{f\rho_f v^2}{2(0.8165)} \quad \text{(PA.148)}$$

which was used in the CCA to define the shear stress at the surface of a borehole of radius R. The radius R enters into Equation (PA.138), Equation (PA.139) and Equation (PA.140) through the use of $D = 2(R - R_i)$ in the definition of f in Equation (PA.146). As with laminar flow, the borehole radius R is assumed to increase until a value of $\tau(R)$ is reached that equals the sample value for the shear strength of the waste (i.e., the uncertain parameter WTAUFAIL in Table PA-17). Computationally, the eroded borehole diameter is determined by solving Equation (PA.148) for R under the assumption that $\tau(R)$ equals the assumed shear strength of the waste.

For the CRA-2004 PA, a slight modification to the definition of τ in Equation (PA.148) was made to account for drill string rotation when fluid flow in the vicinity of the drill collars is turbulent (Abdul Khader and Rao 1974; Bilgen, Boulos, and Akgungor 1973). Specifically, an axial flow velocity correction factor (i.e., a rotation factor), F_r, was introduced into the definition of τ. The correction factor F_r is defined by

$$F_r = v2100 / v \quad \text{(PA.149)}$$

where $v2100$ is the norm of the flow velocity required for the eroded diameters to be the same for turbulent and laminar flow at a Reynolds number of Re = 2100, and is obtained by solving

$$\tau_{fan} = \frac{f\rho_f v_{2100}^2}{2(0.8165)} \quad \text{(PA.150)}$$

for $v2100$ with D in the definition of f in Equation (PA.146) assigned the final diameter value that results for laminar flow at a Reynolds number of Re = 2100 (that is, the D in $D_e = 2(R - R_i) = D - 2R_i$ obtained from Equation (PA.133) with Re = 2100). The modified definition of τ is

$$\tau(R) = \frac{f\rho_f(F_r v)^2}{2(0.8165)} \quad \text{(PA.151)}$$

and results in turbulent and laminar flow with the same eroded diameter at a Reynolds number of 2100, where PA assumes that the transition between turbulent and laminar flow takes place.

PA-4.5.2.3 Calculation of Rf

The following algorithm was used to determine the final eroded radius R_f of a borehole and incorporates a possible transition from turbulent to laminar fluid flow within a borehole:

Step 1. Use Equation (PA.133) to determine an initial Reynolds number Re, with R initially set to the drill-bit radius, $R_0 = 0.31115$ m (parameter BOREHOLE:DIAMMOD in Kicker and Herrick 2013, Table 5).

Step 2. If Re < 2100, the flow is laminar and the procedure in Section PA-4.5.2.1 is used to determine R_f. Because any increase in the borehole diameter will cause the Reynolds number to decrease, the flow will remain laminar and there is no need to consider the possibility of turbulent flow as the borehole diameter increases, with the result that R_f determined in this step is the final eroded radius of the borehole.

Step 3. If Re ≥ 2100, then the flow is turbulent, and the procedure discussed in Section PA-4.5.2.2 is used to determine R_f. Once R_f is determined, the associated Reynolds number Re is recalculated using Equation (PA.133) and $R = R_f$. If the recalculated Re > 2100, a transition from turbulent to laminar flow cannot take place, and the final eroded radius is R_f determined in this step. If not, go to Step 4.

Step 4. If the Reynolds number Re with the new R_f in Step 3 satisfies the inequality Re ≤ 2100, a transition from turbulent to laminar flow is assumed to have taken place. In this case, R_f is recalculated assuming laminar flow, with the outer borehole radius R initially defined to be the radius associated with Re = 2100. In particular, the initial value for R is given by the radius at which the transition from laminar to turbulent flow takes place:

$$R = R_i + \frac{2100\eta_\infty}{2(0.8165)v\rho} \quad \text{(PA.152)}$$

which is obtained from Equation (PA.133) by solving for R with Re = 2100. A new value for R_f is then calculated with the procedure discussed in Section PA-4.5.2.1 for laminar flow, with this value of R_f replacing the value from Step 3 as the final eroded diameter of the borehole.

Step 5. Once R_f is known, the amount of waste removed to the surface is determined using Equation (PA.131) with $D_f = 2R_f$.

PA-4.5.3 Additional Information

Additional information on CUTTINGS_S and its use in the CRA-20014 PA to determine cuttings and cavings releases can be found in the CUTTINGS_S user's manual (WIPP Performance Assessment 2003b) and in the analysis package for cuttings and cavings releases (Kicker 2013).

PA-4.6 Spallings to Surface: DRSPALL and CUTTINGS_S

Spallings are waste solids introduced into a borehole by the movement of waste-generated gas towards the lower-pressure borehole. In engineering literature, the term "spalling" describes the dynamic fracture of a solid material, such as rock or metal (Antoun et al. 2003). In the WIPP PA, the spallings model describes a series of processes, including tensile failure of solid waste, fluidization of failed material, entrainment into the wellbore flow, and transport up the wellbore to the land surface. Spallings releases could occur when pressure differences between the repository and the wellbore cause solid stresses in the waste exceeding the waste material strength and gas velocities sufficient to mobilize failed waste material.

The spallings model is described in the following sections. Presented first are the primary modeling assumptions used to build the conceptual model. Next, the mathematical model and its numerical implementation in the computer code DRSPALL are described. Finally, implementation of the spallings model in the WIPP PA by means of the code CUTTINGS_S is discussed.

PA-4.6.1 Summary of Assumptions

Assumptions underlying the spallings model include the future state of the waste, specifications of drilling equipment, and the driller's actions at the time of intrusion. Consistent with the other PA models, the spallings model assumes massive degradation of the emplaced waste through mechanical compaction, corrosion, and biodegradation. Waste is modeled as a homogeneous, isotropic, weakly consolidated

material with uniform particle size and shape. The rationale for selecting the spallings model material properties is addressed in detail by Hansen et al. (Hansen et al. 1997) and Hansen, Pfeifle, and Lord (Hansen, Pfeifle, and Lord 2003).

Drilling equipment specifications, such as bit diameter and drilling mud density, are based on surveys of drillers in the Delaware Basin (Hansen, Pfeifle, and Lord 2003). Assumptions about the driller's actions during the intrusion are conservative. Typically, the drilling mud density is controlled to maintain a slightly "overbalanced" condition so that the mud pressure is always slightly higher than the fluid pressures in the formation. If the borehole suddenly passes through a high-pressure zone, the well can quickly become "underbalanced," with a resulting fluid pressure gradient driving formation fluids into the wellbore. This situation is known as a *kick* and is of great concern to drillers because a violent kick can lead to a blowout of mud, gas, and oil from the wellbore, leading to equipment damage and worker injury. Standard drilling practice is to watch diligently for kicks. The first indicator of a kick is typically an increase in mud return rate, leading to an increase in mud pit volume (Frigaard and Humphries 1997). Downhole monitors detect whether the kick is air, H_2S, or brine. If the kick fluid is air, the standard procedure is to stop drilling and continue pumping mud in order to circulate the air pocket out. If the mud return rate continues to grow after drilling has stopped and the driller believes that the kick is sufficiently large to cause damage, the well may be shut in by closing the blowout preventer. Once shut in, the well pressure may be bled off slowly and mud weight eventually increased and circulated to offset the higher formation pressure before drilling continues. The spallings model simulates an underbalanced system in which a gas kick is assured, and the kick proceeds with no intervention from the drill operation. Therefore, drilling and pumping continue during the entire blowout event.

PA-4.6.2 Conceptual Model

The spallings model calculates transient repository and wellbore fluid flow before, during, and after a drilling intrusion. To simplify the calculations, both the wellbore and the repository are modeled by one-dimensional geometries. The wellbore assumes a compressible Newtonian fluid consisting of a mixture of mud, gas, salt, and waste solids; viscosity of the mixture varies with the fraction of waste solids in the flow. In the repository, flow is viscous, isothermal, compressible single-phase (gas) flow in a porous medium.

The wellbore and repository flows are coupled by a cylinder of porous media before penetration, and by a cavity representing the bottom of the borehole after penetration. Schematic diagrams of the flow geometry prior to and after penetration are shown in Figure PA-19 and Figure PA-20, respectively. The drill bit moves downward as a function of time, removing salt or waste material. After penetration, waste solids freed by drilling, tensile failure, and associated fluidization may enter the wellbore flow stream at the cavity forming the repository-wellbore boundary.

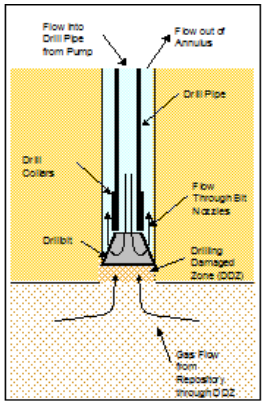

Figure PA- 19. Schematic Diagram of the Flow Geometry Prior to Repository Penetration

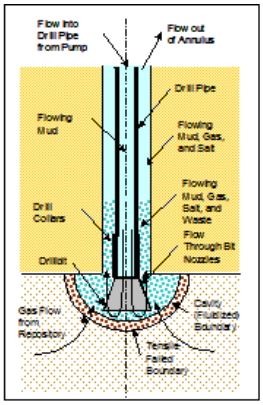

Figure PA- 20. Schematic Diagram of the Flow Geometry After Repository Penetration

PA-4.6.2.1 Wellbore Flow Model

Flow in the well is modeled as a one-dimensional pipe flow with cross-sectional areas corresponding to the appropriate flow area at a given position in the well, as shown in Figure PA-21 and Figure PA-22. This model is conceptually similar to that proposed by Podio and Yang (Podio and Yang 1986) for use in the oil and gas industry. Drilling mud is added at the wellbore entrance by the pump. Flow through the drill bit is treated as a choke with cross-sectional area appropriate for the bit nozzle area. At the annulus output to the surface, the mixture is ejected at a constant atmospheric pressure. The gravitational body force acts in its appropriate direction based on position before or after the bit.

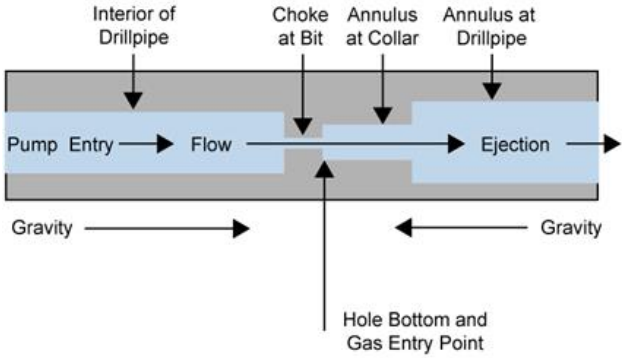

Figure PA- 21. Effective Wellbore Flow Geometry Before Bit Penetration

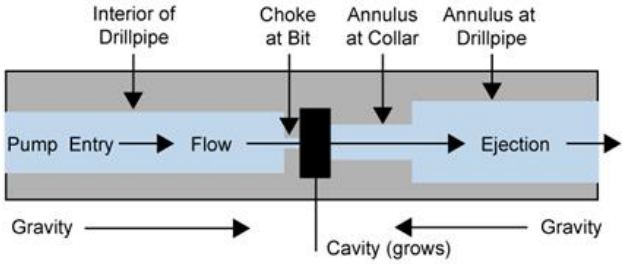

Figure PA- 22. Effective Wellbore Flow Geometry After Bit Penetration

Prior to drill bit penetration into the repository, gas from the repository can flow through drilling-damaged salt into the well. After penetration, the cavity at the bottom of the wellbore couples the wellbore flow and the repository flow models; gas and waste material can exit the repository domain into the cavity. The cavity radius increases as waste materials are moved into the wellbore.

The system of equations representing flow in the wellbore consists of four equations for mass conservation, one for each phase (salt, waste, mud, and gas); one equation for conservation of total momentum; two equations relating gas and mud density to pressure; the definition of density for the fluid mixture; and one constraint imposed by the fixed volume of the wellbore. The conservation of mass and momentum is described by

$$\frac{\partial}{\partial t}\left(\rho_q V_q\right)+\frac{\partial}{\partial z}\left(\rho_q V_q u\right)=S_q \quad \text{(PA.153)}$$

$$\frac{\partial}{\partial t}\left(\rho V u\right)+\frac{\partial}{\partial z}\left(\rho V u^2\right)=-V\left(\frac{\partial P}{\partial z}-\rho g+F\right)+S_{mom} \quad \text{(PA.154)}$$

where

q = phase (w for waste, s for salt, m for mud, and g for gas)
V_q = volume (m^3) of phase q
V = total volume (m^3)
ρ_q = density (kg/m^3) of phase q, constant for salt and waste (2,180 and 2,650 kg/m^3, respectively) and pressure-dependent for gas and mud (see Equation (PA.155) and Equation (PA.156))
ρ = density of fluid mixture (kg/m^3) determined by Equation (PA.157)
u = velocity (m/s) of fluid mixture in wellbore
t = time (s)
z = distance (m) from inlet at top of well
S_q = rate of mass (kg/s) in phase q entering and exiting wellbore domain at position z (Equation (PA.168))
S_{mom} = rate of momentum ($kg\ m/s^2$) entering and exiting wellbore domain at position z (Equation (PA.171))
P = pressure (Pa) at position z
g = standard gravity ($9.8067\ kg/m/s^2$)
F = friction loss using pipe flow model ($kg/m^2/s^2$) determined by Equation (PA.159)

Gas is treated as isothermal and ideal, so the pressure and density are related by Boyle's law:

$$\frac{\rho}{\rho_{g,0}} = \frac{P}{P_{atm}} \quad \text{(PA.155)}$$

where $\rho_{g,0}$ is the density of H_2 gas at atmospheric pressure and 298 K (8.24182×10^{-2} kg/m^3).

The mud is assumed to be a compressible fluid, so

$$\rho_m = \rho_{m,0}\left[1 + c_m\left(P - P_{atm}\right)\right] \quad \text{(PA.156)}$$

where $\rho_{m,0}$ is the density of the mud at atmospheric pressure (1,210 kg/m^3) and c_m is the compressibility of the mud (3.1×10^{-10} Pa^{-1}).

The density of the fluid mixture is determined from the densities and volumes occupied by the phases:

$$\rho = \frac{\rho_g V_g + \rho_m V_m + \rho_s V_s + \rho_w V_w}{V} \quad \text{(PA.157)}$$

The volume of each phase is constrained by the fixed total volume of the wellbore:

$$V = V_g + V_m + V_s + V_w \quad \text{(PA.158)}$$

The friction loss is a standard formulation for pipe flow (Fox and McDonald 1985), where the head loss per unit length is given as

$$F = \frac{\Delta P}{L} = \frac{f \rho u^2}{2 d_h} \quad \text{(PA.159)}$$

where the hydraulic diameter d_h is given by

$$d_h = \frac{4A}{\pi(D_i + D_o)} \quad \text{(PA.160)}$$

with D_i and D_o being the inner and outer diameters, respectively. In PA, D_o = 0.31115 m throughout the domain. From the bit to the top of the collar, D_i = 0.2032 m; above the collar, D_i = 0.1143 m. The area A is calculated as the area of the annulus between the outer and inner radii:

$$A = \frac{\pi}{4}\left(D_o^2 - D_i^2\right) \quad \text{(PA.161)}$$

Thus, d_h = 0.108 m from the bit to the top of the collar, and d_h = 0.197 m above the collar.

The Darcy friction factor f in Equation (PA.159) is determined by the method of Colebrook (Fox and MacDonald 1985). In the laminar regime, which is assumed to be characterized by Reynolds numbers below 2100 (Walker 1976),

$$f = \frac{64}{\mathrm{Re}} \quad \text{(PA.162)}$$

and in the turbulent regime (Re > 2100)

$$\frac{1}{\sqrt{f}} = -2.0 \log_{10}\left(\frac{\varepsilon}{3.72 d_h} + \frac{2.51}{\mathrm{Re}\sqrt{f}}\right) \quad \text{(PA.163)}$$

where $\mathrm{Re} = \frac{u \rho d_h}{\eta}$ is the Reynolds number of the mixture, and η is the viscosity calculated in Equation (PA.164), below. As the wellbore mixture becomes particle-laden, the viscosity of the mixture is determined from an empirical relationship developed for proppant slurry flows in channels for the oil and gas industry (Barree and Conway 1995). Viscosity is computed by an approximate slurry formula based on the volume fraction of waste solids:

$$\eta = \eta_0\left(1 - \frac{w}{w_{\max}}\right)^3 \quad \text{(PA.164)}$$

where η_0 is a base mixture viscosity (9.17×10^{-3} Pa s), $w = V_w / V$ is the current volume fraction of waste solids, w_{max} is an empirically determined maximal volume fraction above which flow is choked (0.615), and s is an empirically determined constant (−1.5) (Hansen, Pfeifle, and Lord 2003).

PA-4.6.2.1.1 Wellbore Initial Conditions

Initial conditions in the wellbore approximate mixture flow conditions just prior to waste penetration. The wellbore is assumed to contain only mud and salt. Initial conditions for the pressure, fluid density, volume fractions of mud and salt, and the mixture velocity are set by the following algorithm:

Step 1. Set pressure in the wellbore to hydrostatic: $P(z) = P_{atm} - \rho_{m,0} gz$.

Step 2. Set mud density using Equation (PA.156).

Step 3. Set mixture velocity: $u(z) = R_m / A(z)$, where R_m is the volume flow rate of the pump (0.0202 m^3/s), and $A(z)$ is the cross-sectional area of the wellbore.

Step 4. Set volume of salt in each cell: $V_{s,i} = R_{drill} A_{bit} \Delta z_i / u_i$, where R_{drill} is the rate of drilling (0.004445 m/s), $A_{bit} = \pi d_{bit}^2 / 4$ is the area of the bottom of the wellbore, Δz_i is the i-th zone size, u_i is the mixture velocity in the i-th zone, and d_{bit} is the diameter of the bit (0.31115 m).

Step 5. Set volume fraction of mud in each cell: $V_{m,i} = V_i - V_{s,i}$.

Step 6. Recalculate mixture density using Equation (PA.157), assuming no waste or gas in the wellbore.

The initial conditions set by this algorithm approximate a solution to the wellbore flow (Equation (PA.153) and Equation (PA.154)) for constant flow of mud and salt in the well. The approximation rapidly converges to a solution for wellbore flow if steady-state conditions are maintained (WIPP Performance Assessment 2003c).

PA-4.6.2.1.2 Wellbore Boundary Conditions

For simplicity, DRSPALL does not model flow of mud down the pipe to the bit. Mass can enter the wellbore below the drill bit and exit at the wellbore outlet. Below the bit, mud, salt, gas, and waste can enter the wellbore. PA assumes a constant volume of mud flow down the drilling pipe; therefore, the source term for mud, $S_{m,in}$, is set by the volumetric flow rate of the pump R_m (0.0202 m^3/s) and the density of the mud at the bottom of the wellbore:

$$S_{m,in} = \rho_m R_m \quad \text{(PA.165)}$$

Until the drill bit penetrates the repository, salt enters the wellbore at a constant rate:

$$S_{s,in} = \rho_s R_{drill} A_{bit} \quad \text{(PA.166)}$$

Additional mass enters the wellbore by gas flow from the repository ($S_{gas,in}$) and spalling of waste material ($S_{w,in}$); these mass sources are discussed in Section PA-4.6.2.3. The outlet of the wellbore is set to atmospheric pressure. Mass exiting the wellbore is determined from the mixture velocity, the area of the outlet A_{out} (0.066 m^2), and the density and volume fraction of each phase at the outlet of the wellbore:

$$S_{q,out} = \rho u_{out} A_{out} \frac{V_q}{V} \quad \text{(PA.167)}$$

Finally, the net change in mass and momentum for phase q is

$$S_q = S_{q,in} - S_{q,out} \quad \text{(PA.168)}$$

$$S_{mom,in} = \frac{\rho_{0,m}}{A_p} R_{mudpump} \quad \text{(PA.169)}$$

The outlet of the wellbore is set to atmospheric pressure. Momentum exiting the wellbore is determined from the fluid velocity and the area of the outlet A_{out} (0.066 m^2):

$$S_{mom,out} = -\rho A_{out} u_{out}^2 \quad \text{(PA.170)}$$

No momentum is added by mass flow into the wellbore from the repository; thus

$$S_{mom} = S_{mom,in} - S_{mom,out}$$ (PA.171)

PA-4.6.2.2 Repository Flow Model

The repository is modeled as a radially symmetric domain. A spherical coordinate system is used for most DRSPALL calculations. In a few circumstances, cylindrical coordinates are used in PA calculations, where spall volumes are large enough that spherical coordinates are not representative of the physical process (Lord, Rudeen, and Hansen 2003). The design document for DRSPALL (WIPP Performance Assessment 2003d) provides details on implementing the repository flow model in cylindrical coordinates.

Flow in the repository is transient, compressible, viscous, and single-phase (gas) flow in a porous medium. Gas is treated as isothermal and ideal. The equations governing flow in the repository are the equation of state for ideal gases (written in the form of Boyle's law for an ideal gas at constant temperature), conservation of mass, and Darcy's law with the Forchheimer correction (Aronson 1986, Whitaker 1996):

$$\frac{\rho_g}{\rho_{g,0}} = \frac{P}{P_{atm}}$$ (PA.172)

$$\phi \frac{\partial \rho_g}{\partial t} + \nabla \cdot (\rho_g u) = 0$$ (PA.173)

$$\nabla P = -\frac{\eta_g}{k}(1+F)u$$ (PA.174)

where

P = pressure in pore space (Pa)
ρ_g = density of gas (kg/m^3)
u = velocity of gas in pore space (m/s)
ϕ = porosity of the solid (unitless)
η_g = gas viscosity (8.934×10^{-6} Pa s)
k = permeability of waste solid (m^2)
F = Forchheimer correction (unitless)

The Forchheimer correction is included in Equation (PA.174) to account for inertia in the flowing gas, which becomes important at high gas velocities (Ruth and Ma 1992). When the Forchheimer coefficient is zero, Equation (PA.174) reduces to Darcy's law. A derivation of Equation (PA.174) from the Navier-Stokes equations is given by Whitaker (1996); the derivation suggests that F is a linear function of gas velocity for a wide range of Reynolds numbers.

In PA, the Forchheimer correction takes the form

$$F = \beta_{nd} \rho u$$ (PA.175)

where β_{nd} is the non-Darcy coefficient, which depends on material properties such as the tortuosity and area of internal flow channels, and is empirically determined (Belhaj et al. 2003). DRSPALL uses a value from Li et al. (2001) that measured high-velocity nitrogen flow through porous sandstone wafers, giving the result

$$\beta_{nd} = \frac{1.15 \times 10^{-6}}{k\phi}$$ (PA.176)

Equation (PA.172), Equation (PA.173) and Equation (PA.174) combine into a single equation for pressure in the porous solid:

$$\frac{\partial P}{\partial t} = \frac{k'}{2\phi\eta_g} \nabla^2 P^2 + \frac{1}{2\phi\eta_g} \nabla P^2 \cdot \nabla k'$$ (PA.177)

where

$$k' = \frac{k}{1+F} = \frac{k}{1+\beta_{nd}\rho u}$$ (PA.178)

and the Laplacian operator in a radially symmetric coordinate system is given by

$$\nabla^2 = \frac{1}{r^{n-1}} \frac{\partial}{\partial r}\left(r^{n-1} \frac{\partial}{\partial r} \right)$$ (PA.179)

where $n = 2$ and $n = 3$ for polar and spherical coordinates, respectively.

In DRSPALL, the permeability of the waste solid is a subjectively uncertain parameter that is constant for waste material that has not failed and fluidized. In a region of waste that has failed, the permeability increases as the waste fluidizes by a factor of $1 + F_f$, where F_f is the fraction of failed material that has fluidized and is based on the fluidization relaxation time. This approximately accounts for the material bulking as it fluidizes.

Initial pressure in the repository is set to a constant value P_{ff}. A no-flow boundary condition is imposed at the outer boundary ($r = R$):

$\nabla P(R) = 0$ (PA.180)

At the inner boundary ($r = r_{cav}$), the pressure is specified as $P(r_{cav}, t) = P_{cav}(t)$, where $P_{cav}(t)$ is defined in the next section. The cavity radius r_{cav} increases as drilling progresses and waste material fails and moves into the wellbore; calculation of r_{cav} is described in Section PA-4.6.2.3.3.

PA-4.6.2.3 Wellbore to Repository Coupling

Prior to penetration, a cylinder of altered-permeability salt material with diameter equal to the drill bit is assumed to connect the bottom of the wellbore to the repository. At the junction of the repository and this cylinder of salt, a small, artificial cavity is used to determine the boundary pressure for repository flow. After penetration, the cavity merges with the bottom of the wellbore to connect the wellbore to the repository.

PA-4.6.2.3.1 Flow Prior to Penetration

The cylinder of salt connecting the wellbore to the repository is referred to as the drilling damaged zone (DDZ) in Figure PA-19. The permeability of the DDZ, k_{DDZ}, is 1×10^{-14} m^2. The spallings model starts with the bit 0.15 m above the repository; the bit advances at a rate of $R_{drill} = 0.004445$ m/s.

To couple the repository to the DDZ, the model uses an artificial pseudo-cavity in the small hemispherical region of the repository below the wellbore with the same surface area as the bottom of the wellbore (Figure PA-22). The pseudo-cavity is a numerical device that smoothes the discontinuities in pressure and flow that would otherwise occur upon bit penetration of the repository. The pseudo-cavity contains only gas, and is initially at repository pressure. The mass of gas in the cavity m_{cav} is given by

$$\frac{dm_{cav}}{dt} = S_{rep} - S_{g,in} \quad \text{(PA.181)}$$

where

S_{rep} = gas flow from repository into pseudo-cavity (kg/s); see Equation (PA.182)
$S_{g,in}$ = gas flow from pseudo-cavity through DDZ into wellbore (kg/s); see Equation (PA.183)

Flow from the repository into the pseudo-cavity is given by

$$S_{rep} = \rho_{g,rep} u_{rep} \phi A_{cav} \quad \text{(PA.182)}$$

where

$\rho_{g,rep}$ = gas density in repository at cavity surface (kg/m^3) = $\rho_g(r_{cav})$
u_{rep} = gas velocity (m/s) in repository at cavity surface = $u(r_{cav})$
ϕ = porosity of waste (unitless)
A_{cav} = surface area of hemispherical part of the cavity (m^2)
= $\pi d_{bit}^2 / 4$, where d_{bit} is the diameter of the bit (m)

Flow out of the pseudo-cavity through the DDZ and into the wellbore is modeled as steady-state using Darcy's Law:

$$S_{g,in} = \frac{k_{DDZ} \pi M_w}{2\eta_g RTL} \left(\frac{d_{bit}}{2}\right)^2 \left(P_{cav}^2 - P_{BH}^2\right) \quad \text{(PA.183)}$$

where

η_g = viscosity of H_2 gas (8.934×10^{-6} Pa s)
M_w = molecular weight of H_2 gas (0.00202 kg / mol)
R = ideal gas constant (8.314 J/mol K)
T = repository temperature (constant at 300 K (27 ºC; 80 ºF))

L = length (m) of DDZ (from bottom of borehole to top of repository)
P_{cav} = pressure in pseudo-cavity (Pa)
P_{BH} = pressure at bottom of wellbore (Pa)

A justification for using this steady-state equation is provided in the design document for DRSPALL (WIPP Performance Assessment 2003d). The pseudo-cavity is initially filled with gas at a pressure of P_{ff}. The boundary pressure on the well side (P_{BH}) is the pressure immediately below the bit, determined by Equation (PA.153) and Equation (PA.154). The pressure in the pseudo-cavity (P_{cav}) is determined by the ideal gas law:

$$P_{cav} = \frac{m_{cav} R_0 T}{V_{cav}} \quad \text{(PA.184)}$$

where m_{cav} is the number of moles of gas in the cavity and the cavity volume V_{cav} is given by

$$V_{cav} = \frac{\pi d_{bit}^3}{24\sqrt{2}} \quad \text{(PA.185)}$$

In PA, the drilling rate into the ground is assumed constant at 0.004445 m/s; thus $L = L_i$ - 0.004445t until $L = 0$, at which time the bit penetrates the waste. The term L_i is the distance from the bit to the waste at the start of calculation (0.15 m).

PA-4.6.2.3.2 Flow After Penetration

After waste penetration, the bottom of the wellbore is modeled as a hemispherical cavity in the repository, the radius of which grows as drilling progresses and as material fails and moves into the cavity. Gas, drilling mud, and waste are assumed to thoroughly mix in this cavity; the resulting mixture flows around the drill collars and then up the annulus between the wellbore and the drill string. Gas flow from the repository into the cavity is given by Equation (PA.182); however, A_{cav} is now dependent on the increasing radius of the cavity (see Section PA-4.6.2.3.3). Mudflow into the cavity from the wellbore is given by Equation (PA.165). Waste flow into the cavity is possible if the waste fails and fluidizes; these mechanisms are discussed in Section PA-4.6.2.3.4 and Section PA-4.6.2.3.5. Pressure in the cavity is equal to that at the bottom of the wellbore, and is computed by Equation (PA.184).

PA-4.6.2.3.3 Cavity Volume After Penetration

The cylindrical cavity of increasing depth created by drilling is mapped to a hemispherical volume at the bottom of the wellbore to form the cavity. This mapping maintains equal surface areas in order to preserve the gas flux from the repository to the wellbore. The cavity radius from drilling is thus

$$r_{drill} = \sqrt{\frac{d_{bit}^2 + 4 d_{bit} \Delta H}{8}} \quad \text{(PA.186)}$$

where ΔH is the depth of the drilled cylinder. In PA, the drilling rate into the ground is assumed constant at 0.004445 m/s; thus ΔH = 0.004445t until $\Delta H = H$, the height of compacted waste (m). Since the initial height of the repository is 3.96 m, H is computed from the porosity ϕ by $H = 3.96(1-\phi_0)/(1-\phi)$, where ϕ_0 is the initial porosity of a waste-filled room.

The cavity radius r_{cav} is increased by the radius of failed and fluidized material r_{fluid}, which is the depth to which fluidization has occurred beyond the drilled radius. That is,

$$r_{cav} = r_{drill} + r_{fluid} \quad \text{(PA.187)}$$

PA-4.6.2.3.4 Waste Failure

Gas flow from the waste creates a pressure gradient within the waste, which induces elastic stresses in addition to the far-field confining stress. These stresses may lead to tensile failure of the waste material, an assumed prerequisite to spallings releases. While the fluid calculations using Equation (PA.172), Equation (PA.173) and Equation (PA.174) are fully transient, the elastic stress calculations are assumed to be quasi-static (i.e., sound-speed phenomena in the solid are ignored). Elastic effective stresses are (Jaeger and Cook 1969)

$$\sigma_r(r) = \sigma_{sr}(r) + \sigma_{ff}\left(1 - \left(\frac{r_{cav}}{r}\right)^3\right) + P(r_{cav})\left(\frac{r_{cav}}{r}\right)^3 - \beta P(r) \quad \text{(PA.188)}$$

$$\sigma_\theta(r) = \sigma_{s\theta}(r) + \sigma_{ff}\left[1 + \frac{1}{2}\left(\frac{r_{cav}}{r}\right)^2\right] - \frac{P(r_{cav})}{2}\left(\frac{r_{cav}}{r}\right)^3 - \beta P(r) \quad \text{(PA.189)}$$

where β is Biot's constant (assumed here to be 1.0) and σ_{ff} is the confining far-field stress (assumed constant at 14.8 MPa).

The flow-related radial and tangential stresses (σ_{sr} and $\sigma_{s\theta}$, respectively) are computed by equations analogous to differential thermal expansion (Timoshenko and Goodier 1970):

$$\sigma_{sr}(r) = \frac{2\beta}{r^3}\left(\frac{1-2\upsilon}{1-\upsilon}\right)\int_{r_{cav}}^{r}\left(P(s)-P_{ff}\right)s^2 ds \quad \text{(PA.190)}$$

$$\sigma_{s\theta}(r) = -\beta\left(\frac{1-2\upsilon}{1-\upsilon}\right)\left(\frac{1}{r^3}\int_{r_{cav}}^{r}\left(P(s)-P_{ff}\right)s^2 ds - \left(P(r)-P_{ff}\right)\right) \quad \text{(PA.191)}$$

where P_{ff} is the initial repository pressure and υ is Poisson's ratio (0.38).

Since stresses are calculated as quasi-static, an initial stress reduction caused by an instantaneous pressure drop at the cavity face propagates instantaneously through the waste. The result of calculating Equation (PA.188) can be an instantaneous early-time tensile failure of the entire repository if the boundary pressure is allowed to change suddenly. This is nonphysical and merely a result of the quasi-static stress assumption, combined with the true transient pore pressure and flow-related stress equations. To prevent this nonphysical behavior, tensile failure propagation is limited by a tensile failure velocity (1000 m/s; see Hansen et al. 1997). This limit has no quantitative effect on results, other than to prevent nonphysical tensile failure.

At the cavity face, Equation (PA.188) and Equation (PA.190) evaluate to zero, consistent with the quasi-static stress assumption. This implies that the waste immediately at the cavity face cannot experience tensile failure; however, tensile failure may occur at some distance into the waste material. Consequently, the radial effective stress σ_r is averaged from the cavity boundary into the waste over a characteristic length L_t (0.02 m). If this average radial stress $\overline{\sigma_r}$ is tensile and its magnitude exceeds the material tensile strength ($|\overline{\sigma_r}| >$ TENSLSTR), the waste is no longer capable of supporting radial stress and fails, permitting fluidization. The waste tensile strength is an uncertain parameter in the analysis (see TENSLSTR in Table PA-11).

Equation (PA.189) and Equation (PA.191) evaluate shear stresses in the waste. DRSPALL does not use the waste shear stresses to calculate waste failure for spall releases. These stresses are included in this discussion for completeness.

PA-4.6.2.3.5 Waste Fluidization

Failed waste material is assumed to be disaggregated, but not in motion; it remains as a porous, bedded material lining the cavity face, and is treated as a continuous part of the repository from the perspective of the porous flow calculations. The bedded material may be mobilized and enter the wellbore if the gas velocity in the failed material (see Equation (PA.174)) exceeds a minimum fluidization velocity, U_f. The minimum fluidization velocity is determined by solving the following quadratic equation (Cherimisinoff and Cherimisinoff 1984, Ergun 1952)

$$\frac{1.75}{a\phi^3}\left\{\frac{d_p U_f \rho_g}{\eta_g}\right\}^2 + 150\left(\frac{1-\phi}{a^2\phi^3}\right)\left\{\frac{d_p U_f \rho_g}{\eta_g}\right\} = \frac{d_p^3 \rho_g\left(\rho_w-\rho_g\right)g}{\eta_g^2} \quad \text{(PA.192)}$$

where

a = particle shape factor (unitless)
d_p = particle diameter (m)

Fluidization occurs in the failed material to the depth at which gas velocity does not exceed the fluidization velocity; this depth is denoted by r_{fluid} and is used to determine cavity radius (Section PA-4.6.2.3.3). If fluidization occurs, the gas and waste particles mix into the cavity at the bottom of the wellbore. Because this mixing cannot be instantaneous, which would be nonphysical (much as allowing instantaneous tensile failure propagation would be nonphysical), a small artificial relaxation time, equal to the cavity radius r_{cav} divided by the superficial gas velocity $u(r_{cav})$, is imposed upon the mixing phenomenon. The fluidized material is released into the cavity uniformly over the relaxation time.

PA-4.6.3 Numerical Model

The numerical model implements the conceptual and mathematical models described above (Section PA-4.6.2). Both the wellbore and the repository domain calculations use time-marching finite differences. These are part of a single computational loop and therefore use the same time step. The differencing schemes for the wellbore and repository calculations are similar, but not identical.

PA-4.6.3.1 Numerical Method-Wellbore

The wellbore is zoned for finite differencing, as illustrated in Figure PA-23, which shows zones, zone indices, grid boundaries, volumes, and interface areas. The method is Eulerian: zone boundaries are fixed, and fluid flows across the interfaces by advection. Quantities are zone-centered and in tegration is explicit in time.

To reduce computation time, an iterative scheme is employed to update the wellbore flow solution. The finite-difference scheme first solves Equation (PA.153) and Equation (PA.154) for the mass of each phase in each grid cell and the momentum in each grid cell.

The updated solution to Equation (PA.153) and Equation (PA.154) is then used to compute the volume of each phase, the pressure, and the mixture velocity in each grid cell.

All of the materials (mud, salt, gas, and waste) are assumed to move together as a mixture. Because fluid moves through the cell boundaries, the calculation requires a value for the flow through each cell boundary during a time step. These values are obtained by averaging the fluid velocities at the zone centers, given by

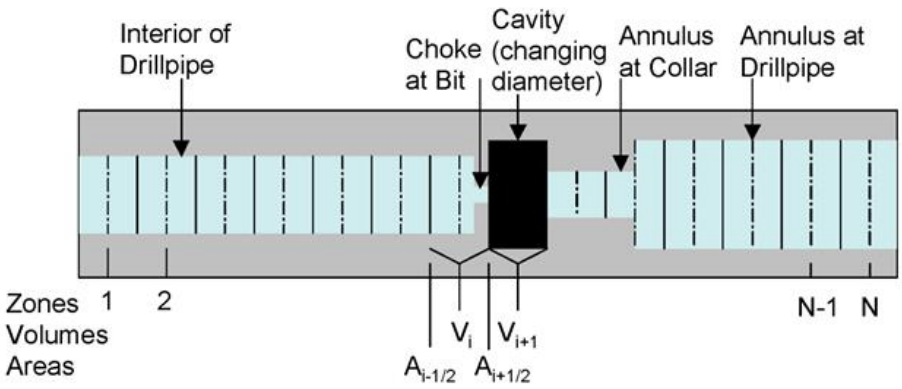

Figure PA- 23. Finite-Difference Zoning for Wellbore

$$u_{i+1/2} = \frac{1}{2}\left(u_{i+1}^{n-1} + u_i^{n-1}\right) \quad \text{(PA.193)}$$

The mass transport equation, prior to any volume change, becomes

$$V_i\ \rho_i^* = V_i \rho_i^{n-1} - \left(A_{i+1/2}\rho_{i+1/2}^{n-1} u_{i+1/2} - A_{i-1/2}\rho_{i-1/2}^{n-1} u_{i-1/2}\right)\Delta t + S_{m,i}\Delta t \quad \text{(PA.194)}$$

Here, the source terms $S_{m,i}$ correspond to material entering or exiting at the pump, cavity, and surface. The "upwind" zone-centered densities are used for the interfaces values, $\rho_{i+1/2}^{n-1}$ and $\rho_{i-1/2}^{n-1}$.

Finally, any changed volumes are incorporated and numerical mass diffusion is added for stability:

$$V_i \rho_i^n = V_i \rho_i^* + \Delta x_i s \sum_{q \in \{w,m,s,g\}} \zeta_q D_{i,q} \quad \text{(PA.195)}$$

where

$$D_{i,q} = \left[A_{i+1/2}\left(\left\{\rho f_q\right\}_{i+1}^{n-1} - \left\{\rho f_q\right\}_i^{n-1}\right) - A_{i-1/2}\left(\left\{\rho f_q\right\}_i^{n-1} - \left\{\rho f_q\right\}_{i-1}^{n-1}\right)\right]$$

and ζ_q is the diffusion coefficient for phase q. The density ρf_q for phase q being diffused is calculated from the mixture density, ρ, and the mass fraction, f_q, of phase q in the referenced cell ($f_q = \rho V_{q,i} / \rho V_i$). The numerical diffusion coefficient ζ_q is chosen empirically for stability. Separate diffusion coefficients could be used for the different materials (mud, gas, etc.); however, sufficient stability is obtained by diffusing only mud and salt using the same coefficient ($\zeta_m = \zeta_s = 0.0001$ and $\zeta_w = \zeta_g = 0$).

Momentum is differenced as

$$V_i(\rho u)_i^* = V_i(\rho u)_i^{n-1} - \Delta t\left\{A_{i+1/2}(\rho u)_{i+1/2}^{n-1} u_{i+1/2} - A_{i-1/2}(\rho u)_{i-1/2}^{n-1} u_{i-1/2}\right\}$$
$$- V_i \Delta t\left(\frac{P_{i+1}^{n-1} - P_{i-1}^{n-1}}{2\Delta z} - \rho_i^{n-1} g + F_i^{n-1}\right) + S_{mom,i}\Delta t, \quad \text{(PA.196)}$$

where the dissipation term F_i^{n-1} is obtained from Equation (PA.159) and is constrained by

$$\left|F_l^{n-1}\right| \le \left| \frac{p_{l+1}^{n-1} - p_{l-1}^{n-1}}{2\Delta x} - \rho_l^{n-1} g \right| \quad \text{(PA.197)}$$

and the sign of F_l^{n-1} is chosen to oppose flow. Finally, numerical momentum diffusion is added without distinguishing between phases in the mixture (ρ is the mixture density):

$$V_l\ (\rho u)_l^n = V_l\ (\rho u)_l^* - \zeta_p \Delta x_l \left[A_{l+1/2} \left((\rho u)_{l+1}^{n-1} - (\rho u)_l^{n-1} \right) - A_{l-1/2} \left((\rho u)_l^{n-1} - (\rho u)_{l-1}^{n-1} \right) \right]$$

(PA.198)

In PA, $\zeta_p = 0.01$.

Equation (PA.156), Equation (PA.157), and Equation (PA.158) comprise a simultaneous system of equations for the volumes of gas and mud and the pressure in the wellbore. The volumes of salt and waste are known, since they are considered incompressible. Equation (PA.156) and Equation (PA.157) combine into a quadratic equation for gas volume:

$$aV_g^2 + bV_g - c = 0 \quad \text{(PA.199)}$$

where

$$a = 1 - c_m P_{atm},$$
$$b = c_m P_{atm} V_{g,0} - aV^* + V_{m,0},$$
$$c = V^* c_m P_{atm} V_{g,0},$$
$$V_{g,0} = m_g / \rho_{g,0},$$
$$V_{m,0} = m_m / \rho_{m,0},$$
$$V^* = V_m + V_g = V - V_s - V_w$$

The volume of the mud phase follows from Equation (PA.156) and the pressure from Equation (PA.155). Once the mixture density in each cell (ρ_i) is updated by Equation (PA.157), the mixture velocity in each cell (u_i) is computed by

$$u_i = \frac{(\rho u)_i}{\rho_i} \quad \text{(PA.200)}$$

where the quantity ρu is determined by Equation (PA.198).

PA-4.6.3.2 Numerical Method-Repository

The time integration method for the repository flow is implicit, with spatial derivatives determined after the time increment. This method requires the inversion of a matrix for the entire repository, which is usually straightforward. The implicit scheme is unconditionally stable. However, it is still necessary to use small time steps to ensure gradient accuracy.

The numerical method follows Press et al. (1989). For simplicity, the equations are presented for constant zone size, although DRSPALL implements difference equations that allow for a variable zone size. Near the cavity, a small, constant zone size is used, and then zones are allowed to grow geometrically as the outer boundary is approached. This procedure greatly increases computational efficiency without sacrificing accuracy in the region of interest.

For an isothermal ideal gas, the pseudopressure ψ is defined as

$$\psi = \frac{P^2}{\eta} \quad \text{(PA.201)}$$

Using Equation (PA.201), Equation (PA.177) is expanded to

$$\frac{\partial \psi}{\partial t} = D(\psi) \left[\frac{\partial^2 \psi}{\partial r^2} + \frac{(m-1)}{r} \frac{\partial \psi}{\partial r} + \frac{1}{k'} \frac{\partial k'}{\partial r} \frac{\partial \psi}{\partial r} \right] \quad \text{(PA.202)}$$

where $D(\psi) = \frac{k'}{\phi}\sqrt{\frac{\psi}{\eta}} = \frac{k'P}{\phi\eta}$; Equation (PA.202) is then converted to a difference equation by treating $D(\psi)$ as constant over a zone, using its zone-centered value at the current time D_j^n:

$$\frac{\psi_j^{n+1}-\psi_j^n}{\Delta t} = \frac{D_j^n}{\Delta r}\left[\frac{\psi_{j+1}^{n+1}-2\psi_j^{n+1}+\psi_{j-1}^{n+1}}{\Delta r} + \frac{(m-1)\left(\psi_{j+1}^{n+1}-\psi_{j-1}^{n+1}\right)}{2r_j} + \frac{\left(k_{j+1}'^{n+1}-k_{j-1}'^{n+1}\right)\left(\psi_{j+1}^{n+1}-\psi_{j-1}^{n+1}\right)}{4k'\Delta r}\right] \quad \text{(PA.203)}$$

Collecting similar terms in ψ leads to a tridiagonal system:

$-\alpha_1\psi_{j-1}^{n+1} + (1+2\alpha)\psi_j^{n+1} - \alpha_2\psi_{j+1}^{n+1} = \psi_j^n$, j = 1,2…. (PA.204)

where

$$\alpha = \frac{D_j^n \Delta t}{(\Delta r)^2}$$

$$\alpha_1 = \left(\frac{D_j^n}{\Delta r}\right)\left(\frac{1}{\Delta r} - \frac{(m-1)}{2r_j} - \frac{k_{i+1}'^{n+1}-k_{i-1}'^{n+1}}{4k'\Delta r}\right)\Delta t$$

$$\alpha_2 = \left(\frac{D_j^n}{\Delta r}\right)\left(\frac{1}{\Delta r} + \frac{(m-1)}{2r_j} + \frac{k_{i+1}'^{n+1}-k_{i-1}'^{n+1}}{4k'\Delta r}\right)\Delta t$$

Equation (PA.204) may be solved by simplified LU decomposition, as presented in Press et al. (1989).

The boundary condition at the inner radius is implemented by noting that for $i = 1$ (the first intact or nonfluidized cell), ψ_{i-1} is the cavity pseudopressure, which is known, and therefore can be moved to the right-hand side of Equation (PA.204):

$(1+2\alpha)\psi_1^{n+1} - \alpha_2\psi_2^{n+1} = \psi_1^n + \alpha_1\psi_{cav}^{n+1}$ (PA.205)

The far-field boundary condition is a zero gradient, which is implemented by setting $\psi_{j+1}^{n+1} = \psi_j^{n+1}$ in Equation (PA.205), recognizing that $1+2\alpha = 1+\alpha_1+\alpha_2$ and rearranging, which gives

$-\alpha_1\psi_{j-1}^{n+1} + (1+\alpha_1)\psi_j^{n+1} = \psi_j^n$ (PA.206)

where j is the index of the last computational cell.

PA-4.6.3.3 Numerical Method-Wellbore to Repository Coupling

The term u_{rep}, appearing in Equation (PA.182), is the gas velocity in the repository at the waste-cavity interface and is determined from the pressure gradient inside the waste. DRSPALL uses the pressure ($P1$) at the center of the first numerical zone in the waste to determine u_{rep}:

$$u_{rep} = \frac{k(P_1 - P_{cav})}{\eta_g \phi \Delta r} \quad \text{(PA.207)}$$

PA-4.6.4 Implementation in the PA

During development of the spallings model, a total of five parameters were determined to be both uncertain and potentially significant to model results (Hansen, Pfeifle, and Lord 2003; Lord and Rudeen 2003). All five parameters relate to the repository conditions or the state of the waste at the time of intrusion. Table PA-11 lists the uncertain parameters in the DRSPALL calculations; these parameters are also listed in Table PA-17.

Table PA- 11. Uncertain Parameters in the DRSPALL Calculations

Quantity	Property	Implementation
Repository Pressure	REPIPRES	Initial repository pressure (Pa); spall calculated for values of 10, 12, 14, and 14.8 MPa. Defines initial repository pressure in Equation (PA.177) (see Section PA-4.6.2.2) and P_{ff} in Equation (PA.190).
Repository Permeability	REPIPERM	Permeability (m^2) of waste, implemented by parameter SPALLMOD/REPIPERM. Log-uniform distribution from 2.4×10^{-14} to 2.4×10^{-12}. Defines k in Equation (PA.174).
Repository Porosity	REPIPOR	Porosity (dimensionless) of waste, implemented by parameter SPALLMOD/REPIPOR. Uniform distribution from 0.35 to 0.66. Defines ϕ in Equation (PA.173).
Particle Diameter	PARTDIAM	Particle diameter of waste (m) after tensile failure, implemented by parameter SPALLMOD/PARTDIAM. Log-uniform distribution from 0.001 to 0.1 (m). Defines d_p in Equation (PA.192).
Tensile Strength	TENSLSTR	Tensile strength of waste (Pa), implemented by parameter SPALLMOD/TENSLSTR. Uniform distribution from 0.12 MPa to 0.17 MPa. Defines maximum $\bar{\sigma}_T$ for Section PA-4.6.2.3.4.

The computational requirements of DRSPALL prohibit calculation of spall volumes for all possible combinations of initial conditions and parameter values. Since repository pressure is a time-dependent value computed by the BRAGFLO model (see Section PA-4.2), DRSPALL calculations were performed for a small number of pressures. Sensitivity studies showed that spall does not occur at pressures below 10 MPa; this value was used as the lower bound on pressure. In DRSPALL, the repository pressure cannot exceed the far-field confining stress (14.8 MPa); consequently, 14.8 MPa was used as the upper bound on pressure. Computations were also performed for intermediate pressures of 12 and 14 MPa. The remaining four parameters listed in Table PA-11 are treated as subjectively uncertain. The uncertainty represented by these parameters pertains to the future state of the waste, which is modeled in PA as a homogeneous material with uncertain properties (see Section PA-5.0).

Spall volumes are computed for each combination of initial pressure and sample element, for a total of $4 \times 300 = 1{,}200$ model runs. Although repository porosity could be treated as an initial condition (using the time-dependent value computed by BRAGFLO), to reduce the number of computational cases and ensure that extreme porosity values were represented, repository porosity was included as a sampled parameter.

The spallings submodel of the code CUTTINGS_S uses the DRSPALL results to compute the spall volume for a given initial pressure P. If $P < 10$ MPa or $P > 14.8$ MPa, the spall volume is the value computed for REPIPRES = 10 MPa or REPIPRES = 14.8 MPa, respectively. If P falls between 10 and 14.8 MPa, the spall volume is constructed by linear interpolation between the DRSPALL results for pressures that bracket P.

PA-4.6.5 Additional Information

Additional information on DRSPALL and its use in PA to determine spallings releases can be found in the DRSPALL user's manual (WIPP Performance Assessment 2003e) and in the analysis package for spallings releases (Kicker 2013). Additional information on the construction of spall volumes by the code CUTTINGS_S can be found in the CUTTINGS_S design document (WIPP Performance Assessment 2003f).

PA-4.7 DBR to Surface: BRAGFLO

This section describes the model for DBR volumes, which are volumes of brine released to the surface at the time of a drilling intrusion. DBR volumes are calculated by the code BRAGFLO, the same code used to compute two-phase flow in and around the repository (see Section PA-4.2).

PA-4.7.1 Overview of Conceptual Model

DBRs could occur if the pressure in the repository at the time of a drilling intrusion exceeds 8 MPa, which is the pressure exerted by a column of brine-saturated drilling fluid at the depth of the repository (Stoelzel and O'Brien 1996). For repository pressures less than 8 MPa, no DBRs are assumed to occur. However, even if the repository pressure exceeds 8 MPa at the time of a drilling intrusion, a DBR is not assured, as there might not be sufficient mobile brine in the repository to result in movement towards the borehole. Brine saturation in the repository must exceed the residual brine saturation of the waste material. The residual brine saturation is sampled from a uniform distribution ranging from 0.0 to 0.552 in the CRA-2014 PA.

DBRs are estimated for the following cases: (1) an initial intrusion into the repository into either a lower (down-dip), middle, or upper (up-dip) panel; (2) an intrusion into a waste panel preceded by an E1 intrusion into either the same waste panel, an adjacent panel, or a nonadjacent panel; and (3) an intrusion into a waste panel preceded by an E2 intrusion into either the same waste panel, an adjacent panel, or a nonadjacent panel (see Section PA-6.7). To determine releases for the above cases, the DBR calculations use a computational grid that explicitly includes all 10 waste panels (Figure PA-24).

For perspective, the following list provides a comparison of the BRAGFLO mesh for the Salado flow calculations (Figure PA-12) and the DBR mesh used for the DBR calculations (Figure PA-24):

1. The DBR mesh is defined in the areal plane with the z dimension (height) one element thick; the BRAGFLO mesh is defined as a cross section, with multiple layers in height and the thickness (y dimension) one element thick.

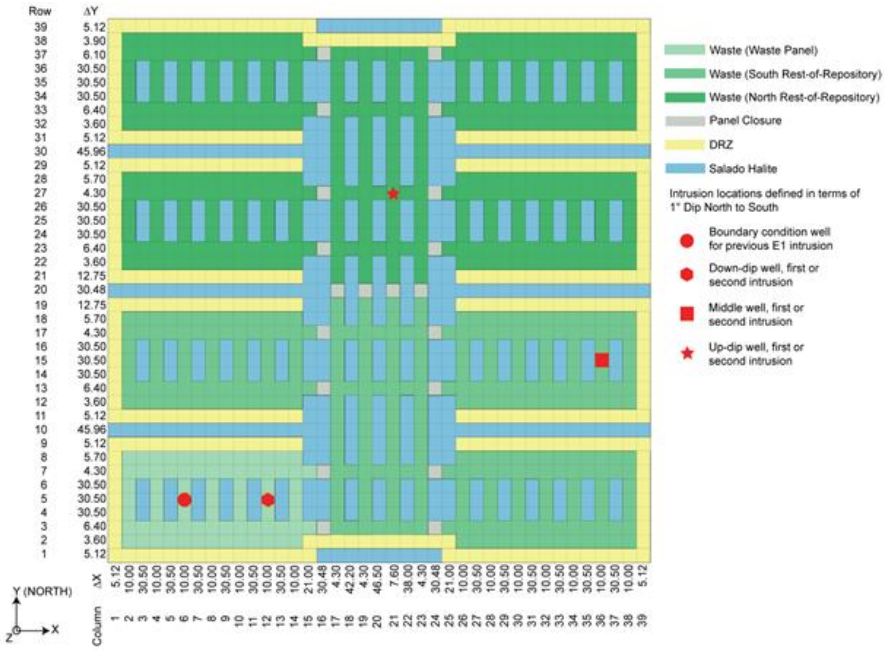

Figure PA- 24. DBR Grid Used in PA

2. The DBR mesh uses constant thickness, while the BRAGFLO mesh uses rectangular flaring to account for three-dimensional volumes in a two-dimensional grid (Figure PA-13).

3. The DBR mesh represents flow only in the waste area. The BRAGFLO model includes the surrounding geology as well as the entire WIPP excavation (including operations, experimental, and shaft regions).

4. Local scale heterogeneities are included in the DBR mesh, including the salt pillars, rooms, panel closures, and passageways that contain waste. These are not fully represented in the BRAGFLO mesh.

5. The DRZ is included in both models, but exists above and below the excavated regions in the BRAGFLO model, whereas the DRZ surrounds the waste rooms on the sides of the DBR mesh.

6. Both models include a one-degree formation dip through the excavated regions (Equation (PA.33)).

The DBRs are assumed to take place over a relatively short period of time (i.e., 3 to 4.5 days; see Section PA-4.7.8) following the drilling intrusion. The initial value conditions for determining DBR volumes are obtained by mapping solutions of Equation (PA.24), Equation (PA.25), Equation (PA.26), Equation (PA.27), Equation (PA.28), Equation (PA.29), and Equation (PA.30) obtained from BRAGFLO with the computational grid in Figure PA-12 onto the grid in Figure PA-24.

In concept, theDBR for a drilling intrusion has the form

$$DBR = \int_0^{t_e} rDBR(t)\,dt \quad \text{(PA.208)}$$

where

DBR = DBR volume (m^3) for drilling intrusion
$rDBR(t)$ = rate (m^3) at time t at which brine flows up intruding borehole
t = elapsed time (s) since drilling intrusion
t_e = time (s) at which DBR ends

The definition of $rDBR(t)$ is discussed in the following sections. It is based on the two-phase flow relationships in Equation (PA.24), Equation (PA.25), Equation (PA.26), Equation (PA.27), Equation (PA.28), Equation (PA.29), and Equation (PA.30) and use of the Poettmann-Carpenter correlation (Poettmann and Carpenter 1952) to determine a boundary pressure at the connection between the intruding borehole and the repository. The time t_e is based on current drilling practices in the Delaware Basin (Section PA-4.7.8).

PA-4.7.2 Linkage to Two-Phase Flow Calculation

The mesh in Figure PA-24 was linked to the mesh in Figure PA-12 by subdividing the waste disposal area in the mesh in Figure PA-12 into three regions (Figure PA-25). The upper region represents the northern rest of repository (North RoR) area in Figure PA-12. The middle region represents the southern rest of repository (South RoR) area in Figure PA-12. The lower region represents the farthest down-dip repository area (Waste Panel) in Figure PA-12 that contained waste and thus corresponds to the single down-dip waste panel. The linkage between the solutions to Equation (PA.24), Equation (PA.25), Equation (PA.26), Equation (PA.27), Equation (PA.28), Equation (PA.29), and Equation (PA.30) and the DBR calculations was made by assigning quantities calculated by BRAGFLO for each region in Figure PA-12 to the corresponding waste region in Figure PA-24.

The height of the grid in Figure PA-24 was assigned a value that corresponded to the crushed height, h (m), of the waste as predicted by the solution of Equation (PA.24), Equation (PA.25), Equation (PA.26), Equation (PA.27), Equation (PA.28), Equation (PA.29) and Equation (PA.30). Specifically,

$$h = h_i \frac{1-\phi_i}{1-\phi} \quad \text{(PA.209)}$$

where h_i and ϕ_i are the initial height (m) and porosity of the waste and ϕ is the volume-averaged porosity of the waste at the particular time under consideration (Section PA-4.2.3). The areas designated panel closures, DRZ, and impure halite in Figure PA-24 were assigned the same pressures and saturations as the corresponding grid blocks in the 10,000-year BRAGFLO calculations. Moreover, panel closure areas in the DBR calculation were assigned the same porosity and permeability values as the corresponding grid blocks in the 10,000-year BRAGFLO calculation.

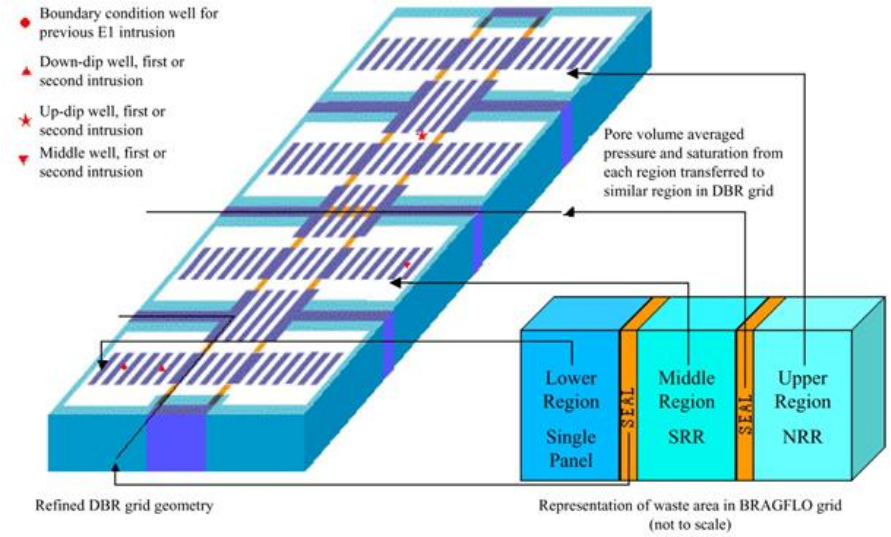

Figure PA- 25. Assignment of Initial Conditions for DBR Calculation

The initial brine pressure $p_b(x, y, 0)$ and gas saturation $S_g(x, y, 0)$ in the grid in Figure PA-24 are assigned by

$$p_b(x,y,0) = \frac{\int_R \tilde{p}_b(\tilde{x},\tilde{y},t_{int})\,dV}{\int_R dV} \quad \text{(PA.210)}$$

$$S_g(x,y,0) = \frac{\int_R \tilde{S}_g(\tilde{x},\tilde{y},t_{int})\,dV}{\int_R dV} \quad \text{(PA.211)}$$

where (x, y) designates a point in the grid in Figure PA-24, $\tilde{p}_b$ and $\tilde{S}_g$ denote solutions to Equation (PA.24), Equation (PA.25), Equation (PA.26), Equation (PA.27), Equation (PA.28), Equation (PA.29), and Equation (PA.30), $\tilde{x}$ and $\tilde{y}$ denote the variables of integration, t_{int} is the time at which the drilling intrusion occurs, and R corresponds to the region in the BRAGFLO computational grid (Figure PA-12) that is mapped into the region in the DBR computational grid (Figure PA-24) that contains the point (x, y) (Figure PA-25). Note that t_{int} defines a time in the solution of Equation (PA.24), Equation (PA.25), Equation (PA.26), Equation (PA.27), Equation (PA.28), Equation (PA.29), and Equation (PA.30); $t = 0$ defines the start time for the DBR calculation and corresponds to t_{int} in the solution of Equation (PA.24), Equation (PA.25), Equation (PA.26), Equation (PA.27), Equation (PA.28), Equation (PA.29), and Equation (PA.30).

The initial porosity $\phi(x, y, 0)$ of DRZ regions in the DBR grid (Figure PA-24) is set by the equation listed in Table PA-12. In Table PA-12, $h(t_{int})$ is the height of the repository at the time of intrusion (typically 1 to 1.5 m; corresponds to h in Equation (PA.24), Equation (PA.25), Equation (PA.26), Equation (PA.27), Equation (PA.28), Equation (PA.29), and Equation (PA.30)), $h_{DRZ,i}$ is the effective DRZ height (43.50

m) that results in the DRZ in Figure PA-24 having the same pore volume as the initial pore volume of the DRZ in Figure PA-12, and $\phi_{DRZ,i}$ is the initial porosity of the DRZ (see Table PA-3). The initial porosities of panel closure and Salado halite regions are set to their corresponding values in the 10,000-year BRAGFLO run at the time of intrusion. The initial porosity of waste regions in the DBR grid is set to the average porosity of the intruded panel, the south rest-of-repository, and the north rest-of-repository at the time of intrusion.

Table PA- 12. Initial DRZ Porosity in the DBR Calculation

Grid Region	Initial Porosity
DRZ	$\phi_{DRZ,i}\frac{h_{DRZ,i}}{h_1(t_{int})}$

PA-4.7.3 Conceptual Representation for Flow Rate rDBR(t)

The driving force that would give rise to the DBR is a difference between waste panel pressure, p_w (Pa), and the flowing bottomhole pressure in the borehole, p_{wf} (Pa), at the time of the intrusion. The flowing bottomhole pressure p_{wf}, defined as the dynamic pressure at the inlet of the intruding borehole to the waste panel, is less than the static pressure p_w due to friction and acceleration effects. The rate at which brine and gas are transported up the intruding borehole is determined by the difference $p_w - p_{wf}$ and a productivity index J_p for the intruded waste panel (Mattax and Dalton 1990, p. 79):

$$q_p(t) = J_p\left[p_w(t) - p_{wf}\right] \quad \text{(PA.212)}$$

where

$q_p(t)$ = flow rate (m^3/s) at time t for phase p ($p = b \sim$ brine, $p = g \sim$ gas)

J_p = productivity index ($m^3/Pa \cdot s$) for phase p

and p_w and p_{wf} are defined above. As indicated by the inclusion/exclusion of a dependence on t, the terms J_p and p_{wf} are constant during the determination of $q_p(t)$ for a particular drilling intrusion in the present analysis, and $p_w(t)$ changes as a function of time. In concept, the DBR is given by

$$DBR = \int_0^{t_c} rDBR(t)\,dt = \int_0^{t_c} J_b\left[p_w(t) - p_{wf}\right]dt \quad \text{(PA.213)}$$

once J_b (brine), p_w, and p_{wf} are determined. Section PA-4.7.4 discusses the determination of J_p (for both gas and brine), Section PA-4.7.5 presents the numerical determination of p_w and DBR, and the determination of p_{wf} is discussed in Section PA-4.7.6. The associated gas release is given by the corresponding integral with J_g (gas) rather than J_b (brine). In the computational implementation of the analysis, DBR is determined as part of the numerical solution of the system of PDEs that defines p_w (Section PA-4.7.5).

PA-4.7.4 Determination of Productivity Index Jp

In a radial drainage area with uniform saturation, which is assumed to be valid throughout the DBR, the following representation for J_p can be determined from Darcy's law (Mattax and Dalton 1990, p. 79; Williamson and Chappelear 1981; Chappelear and Williamson 1981):

$$J_p = \frac{2\pi k k_{rp} h}{\mu_p\left[\ln\left(\frac{r_e}{r_w}\right) + s + c\right]} \quad \text{(PA.214)}$$

where

k = absolute permeability (assumed to be constant through time at 2.4×10^{-13} m^2)

k_{rp} = relative permeability to phase p (calculated with modified Brooks-Corey model in Equation (PA.145), Equation (PA.146), and Equation (PA.147) and brine and gas saturations, S_b and S_g, obtained by mapping solutions of Equation (PA.24), Equation (PA.25), Equation (PA.26), Equation (PA.27), Equation (PA.28), Equation (PA.29), and Equation (PA.30) obtained with the grid in Figure PA-12 onto the grid in Figure PA-24)

h = crushed panel height (Equation (PA.209))

μ_p = viscosity of fluid phase (assumed to be constant through time with $\mu_b = 1.8 \times 10^{-3}$ Pa·s, and $\mu_g = 8.92 \times 10^{-6}$ Pa·s [Kaufmann 1960])

r_e = external drainage radius (for use with the rectangular grid blocks in Figure PA-24, r_e is taken to be the equivalent areal radius; see Equation (PA.215))

r_w = wellbore radius (assumed to be constant through time at 0.1556 m (Gatlin 1960, Table 14.7)

c = –0.50 for pseudo-steady-state flow

s = skin factor, which is used to incorporate flow stimulation caused by cavings and spallings release (see Equation (PA.216))

In the present analysis,

$$r_s = \sqrt{(\Delta x)(\Delta y)/\pi}$$ (PA.215)

where Δx is the x dimension (m) and Δy is the y dimension (m) of the grid block containing the down-dip well in Figure PA-24 (Δx = 10 m and Δy = 30.5 m).

The skin factor s is derived from the cavings and spallings release. Due to the uncertainty in the cavings and spallings parameters, the calculated solid release volume can vary for each realization. The skin factor is calculated for each realization, based on the calculated solid release volume, through the following petroleum engineering well testing relationship (Lee 1982, pp. 5-7):

$$s = \left(\frac{k}{k_s} - 1\right) \ln\left(\frac{r_s}{r_w}\right)$$ (PA.216)

where

k_s = permeability (m^2) of an open channel as a result of spallings releases (assumed to be infinite)
r_s = effective radius (m) of the wellbore with the cuttings, cavings, and spallings volume removed

The effective radius r_s is obtained by converting the cuttings, cavings, and spallings volume removed into a cylinder of equal volume with the initial height of the waste (h_i), and then computing the radius of the cylinder:

$$r_s = \sqrt{\frac{V_s}{h_i \pi}}$$ (PA.217)

and substitution of r_s into Equation (PA.216) with $k_s = \infty$ yields

$$s = (-1) \ln\left(\frac{\sqrt{\frac{V_s}{h_i \pi}}}{r_w}\right)$$ (PA.218)

PA-4.7.5 Determination of Waste Panel Pressure pw(t) and DBR

The repository pressure $p_w(t)$ in Equation (PA.213) after a drilling intrusion is determined with the same system of nonlinear PDEs discussed in Section PA-4.2. These equations are solved numerically by the code BRAGFLO used with the computational grid in Figure PA-24 and assumptions (i.e., parameter values, initial value conditions, and boundary value conditions) appropriate for representing brine flow to an intruding borehole over a relatively short time period immediately after the intrusion (e.g., 3 to 4.5 days). Due to the short time periods under consideration, the model for DBR does not include gas generation due to either corrosion or microbial action or changes in repository height due to creep closure.

Although the determination of DBR can be conceptually represented by the integral in Equation (PA.208), in the numerical implementation of the analysis, DBR is determined within the numerical solution of the system of PDEs that defines $p_b(x, y, t)$.

With the specific assumptions for DBR, Equation (PA.24) , Equation (PA.25), Equation (PA.26), Equation (PA.27), Equation (PA.28), Equation (PA.29), and Equation (PA.30) become

Gas Conservation $\nabla \cdot \left[\frac{\alpha \rho_g K_g k_{rg}}{\mu_g}\left(\nabla p_g + \rho_g g \nabla h\right)\right] = \alpha \frac{\partial\left(\phi \rho_g S_g\right)}{\partial t}$ (PA.219)

Brine Conservation $\nabla \cdot \left[\frac{\alpha \rho_b K_b k_{rb}}{\mu_b}\left(\nabla p_b + \rho_b g \nabla h\right)\right] = \alpha \frac{\partial\left(\phi \rho_b S_b\right)}{\partial t}$ (PA.220)

Saturation Constraint $S_g + S_b = 1$ (PA.221)

Capillary Pressure Constraint $p_g - p_b = 0$ (PA.222)

Gas Density ρ_g determined by RKS equation of state (Equation (PA.52)) (PA.223)

Brine Density $\rho_b = \rho_{b0} \exp\left[c_b\left(p_b - p_{b0}\right)\right]$ (PA.224)

Formation Porosity $\phi = \phi_0 \exp\left[c_\phi \left(p_b - p_{b0}\right)\right]$ (PA.225)

with all symbols having the same definitions as in Equation (PA.24), Equation (PA.25), Equation (PA.26) Equation (PA.27), Equation (PA.28), Equation (PA.29), and Equation (PA.30).

The primary differences between the BRAGFLO calculations described in Section PA-4.2 and the BRAGFLO calculations described in this section are in the computational meshes (Figure PA-24 and Figure PA-12), initial values (Table PA-3 and Section PA-4.7.2), and boundary conditions (Table PA-13). In particular, brine and gas flow associated with intruding boreholes in the DBR calculations are incorporated by the assignment of appropriate boundary conditions. Specifically, brine flow up an intruding borehole is incorporated into Equation (PA.219), Equation (PA.220), Equation (PA.221), Equation (PA.222), Equation (PA.223), Equation (PA.224), and Equation (PA.225) by using the Poettmann-Carpenter wellbore model to determine the pressure at the outflow point in a waste panel (Figure PA-24), with this pressure entering the calculation as a boundary value condition (Table PA-13). The details of this determination are discussed in Section PA-4.7.6. Furthermore, for calculations that assume a prior E1 intrusion, the effects of this intrusion are also incorporated into the analysis by specifying a pressure as a boundary condition (Table PA-13). The determination of this pressure is discussed in Section PA-4.7.6.

Table PA- 13. Boundary Conditions for p_b and S_g in DBR Calculations

(x, y) on Upper (Northern) or Lower (Southern) Boundary in Figure PA-24, $t \geq 0$	
$\left(\nabla p_g + \rho_g g \nabla h\right)\big\|_{(x,y,t)} \cdot \mathbf{j} = 0$ *Pa/m*	No gas flow condition
$\left(\nabla p_b + \rho_b g \nabla h\right)\big\|_{(x,y,t)} \cdot \mathbf{j} = 0$ *Pa/m*	No brine flow condition
(x, y) on Right (Eastern) or Left (Western) Boundary in Figure PA-24, $t \geq 0$	
$\left(\nabla p_g + \rho_g g \nabla h\right)\big\|_{(x,y,t)} \cdot \mathbf{i} = 0$ *Pa/m*	No gas flow condition
$\left(\nabla p_b + \rho_b g \nabla h\right)\big\|_{(x,y,t)} \cdot \mathbf{i} = 0$ *Pa/m*	No brine flow condition
(x, y) at Location of Drilling Intrusion under Consideration (see indicated points in Figure PA-24), $t \geq 0$	
$p_b(x, y, t) = p_{wf}$ (see Section PA-4.7)	Constant pressure condition
(x, y) at Location of Prior Drilling Intrusion into Pressurized Brine (see indicated point in Figure PA-24), $t \geq 0$	
$p_b(x, y, t) = p_{wE1}$ (see Section PA-4.7.7)	Constant pressure condition

PA-4.7.6 Boundary Value Pressure pwf

The boundary value pressure p_{wf} at the inlet of the intruding borehole is defined by a system of equations of the following form:

$$\frac{dp}{dh} = G\left(q_b\left[p(0)\right], q_g\left[p(0)\right], p(h), h\right), \quad 0 \leq h \leq 655m \quad \text{(PA.226)}$$

$$p(655) = 1.013 \times 10^5 \ Pa \quad \text{(PA.227)}$$

$$q_b\left[p(0)\right] = J_b\left[p_w - p(0)\right] \quad \text{(PA.228)}$$

$$q_g\left[p(0)\right] = J_g\left[p_w - p(0)\right] \quad \text{(PA.229)}$$

where $p(h)$ is pressure (Pa) at elevation h in the borehole, with $h = 0$ m corresponding to the entry point of the borehole into the waste panel and $h = 655$ m corresponding to the land surface (Figure PA-26); G is a function (Pa/m) characterizing the change of pressure with elevation in the borehole; $p(655)$ is an initial value condition requiring that pressure at the land surface (i.e., the outlet point of the borehole) be equal to atmospheric pressure; q_b [$p(0)$] and q_g [$p(0)$] define brine and gas flow rates (m^3/s) into the borehole; J_b and J_g are productivity indexes (m^3/Pa s) (see Equation (PA.214); and p_w is the pressure (Pa) in the repository at the time of the drilling intrusion.

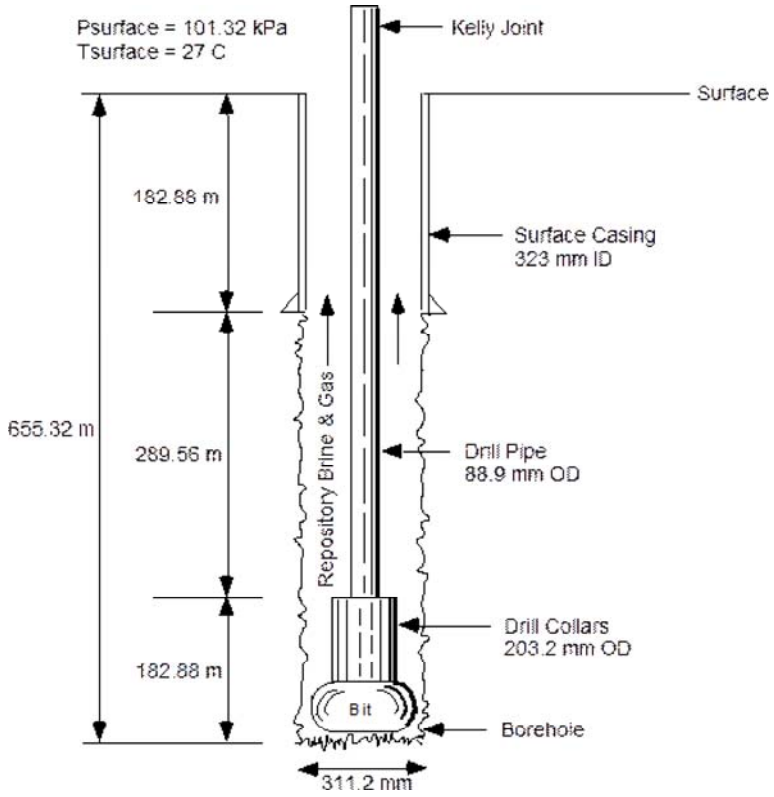

Figure PA- 26. Borehole Representation Used for Poettmann-Carpenter Correlation

The boundary value pressure p_{wf} is defined by

$$p_{wf} = p(0) \quad \text{(PA.230)}$$

Thus, p_{wf} is determined by the numerical solution of Equation (PA.226) for $p(0)$ subject to the constraints in Equation (PA.227), Equation (PA.228), and Equation (PA.229).

The pressure p_w corresponds to the pressure $p_w(0)$, and is obtained from the solution of Equation (PA.24), Equation (PA.25), Equation (PA.26), Equation (PA.27), Equation (PA.28), Equation (PA.29), and Equation (PA.30) with the computational grid in Figure PA-12 (see Section PA-4.7.2). The production indexes J_b and J_g are defined in Equation (PA.214). Thus, the only quantity remaining to be specified in Equation (PA.226), Equation (PA.227), Equation (PA.228), and Equation (PA.229) is the function G.

Brine and gas flow up a borehole is governed by complex physics dependent on frictional effects and two-phase fluid properties. This phenomenon has been widely studied in the petroleum industry and many modeling procedures have been developed to predict flow rates and pressures in vertical two-phase pipe flow (i.e., to define G in Equation (PA.226)) (Brill and Beggs 1986). For this analysis, the Poettmann-Carpenter model (Poettmann and Carpenter 1952; Welchon, Bertuzzi, and Poettmann 1962) was used to define G because it accounts for multiphase frictional effects based on empirical (i.e., field) data from flowing wells, is one of the few modeling approaches that included annular flow data in its development, and is relatively easy to implement. Specifically, the Poettmann-Carpenter model defines G by

$$G\left(q_b\left[p(0)\right], q_g\left[p(0)\right], p(h), h\right) = gm(h) + f'\left(m(h), D(h), q_b\left[p(0)\right]\right) gm(h) F^2(h) / D^5(h) \quad \text{(PA.231)}$$

where

g = acceleration due to gravity (9.8 m/s^2)
$m(h)$ = density (kg/m^3) of fluids (i.e., gas and brine) in wellbore at elevation h (Note: $m(h)$ is a function of $q_b[p(0)]$ and $q_g[p(0)]$; see Equation (PA.232))
$f'\left(m(h), D(h) q_b\left[p(0)\right]\right)$ = empirically defined scale factor (m/s^2) (Note: f' is the scale factor in the Poettmann-Carpenter model for fluid flow in a wellbore [Poettmann and Carpenter 1952]; see discussion below)

$F(h)$ = flow rate (m^3/s) of fluids (i.e., gas and brine) in wellbore at elevation h (Note: $F(h)$ is a function of $q_b[p(0)]$ and $q_g[p(0)]$; see Equation (PA.233))

$D(h)$ = effective diameter (m) of wellbore (see Equation (PA.236))

The first term, $gm(h)$, in Equation (PA.231) results from the contribution of elevation to pressure; the second term results from frictional effects (Poettmann and Carpenter 1952). The fluid density $m(h)$ at elevation h is given by

$$m(h) = \frac{q_b[p(0)]\rho_b[p(0)] + q_g[p(0)]\rho_g[p(0)]}{F(h)} \quad \text{(PA.232)}$$

where

$$F(h) = q_b[p(0)] + \frac{z(h)\,p(h)}{p(0)} q_g[p(0)] \quad \text{(PA.233)}$$

and

$\rho_b[p(0)]$ = density (kg/m^3) of brine at pressure $p(0)$ and temperature 300.1 K, which is fixed at 1230 kg/m^3

$\rho_g[p(0)]$ = density (kg/m^3) of H_2 at pressure $p(0)$ and temperature 300.1 K (see Equation (PA.234))

$z(h)$ = z-factor for compressibility of H_2 at elevation h (Note: $z(h)$ is a function of $p(h)$; see Equation (PA.235)), and $q_b[p(0)]$ and $q_g[p(0)]$ are defined in Equation (PA.226), Equation (PA.227), Equation (PA.228), and Equation (PA.229)

The gas density in Equation (PA.232) is obtained from the universal gas law, $PV = nRT$, by

$$\rho_g[p(0)] = C_{m,kg}\frac{n}{V} = C_{m,kg}\frac{P}{RT} \quad \text{(PA.234)}$$

where n is the amount of gas (mol) in a volume V, $C_{m,kg}$ is the conversion factor from moles to kilograms for H_2 (i.e., 2.02×10^{-3} kg/mol), $P = p(0)$, $R = 8.3145$ J/mol K, and $T = 300.1$ K. The z-factor is given by

$$z(h) = 1 + \left(8.54 \times 10^{-8}\ \text{Pa}^{-1}\right) p(h) \quad \text{(PA.235)}$$

and was obtained from calculations performed with the SUPERTRAPP program (Ely and Huber 1992) for pure H_2 and a temperature of 300.1 K (Stoelzel and O'Brien 1996, Figure 4.7.4). The preceding approximation to $z(h)$ was obtained by fitting a straight line between the results for pressures of 0 psi and 3000 psi and a H_2 mole fraction of 1 in Stoelzel and O'Brien (1996, Figure 4.7.4); the actual calculations used the more complex, but numerically similar, regression model given in Stoelzel and O'Brien (1996, Figure 4.7.4). The numerator and denominator in Equation (PA.232) involve rates, with the time units canceling to give $m(h)$ in units of kg/m^3.

The effective diameter $D(h)$ in Equation (PA.231) is defined with the hydraulic radius concept. Specifically,

$$D^5(h) = \left[D_o(h) + D_i(h)\right]^2 \left[D_o(h) - D_i(h)\right]^3 \quad \text{(PA.236)}$$

where $D_i(h)$ and $D_o(h)$ are the inner and outer diameters (m) of the wellbore at elevation $h(m)$ (see Figure PA-26). The factor f' in Equation (PA.231) is a function of $m(h)$, $D(h)$, and $q_b[p(0)]$.

Subsequent to submittal of the CCA PA, it was discovered that the factor of 2π was omitted from Equation (PA.214). This error was determined to be of no consequence to the CCA PA conclusions (Hadgu et al. 1999) and was corrected in the CRA-2004 PA. As a consequence of the error correction, the regression models used to determine the boundary pressure p_{wf} were recalculated (Hadgu et al. 1999). The corrected regression models are reported in this appendix.

The following iterative procedure based on the bisection method was used to approximate solutions to Equation (PA.226), Equation (PA.227), Equation (PA.228), and Equation (PA.229).

Step 1. Estimate $p(0)$ using a bisection algorithm:

The initial guess for $p(0)$ is the midpoint $\frac{1}{2}p_w$ of interval $[0, p_w]$, where p_w is the pressure in the repository at the time of the drilling intrusion used in Equation (PA.226), Equation (PA.227), Equation (PA.228), and Equation (PA.229).

The next guess for $p(0)$ is at the midpoint of either $\left[0, \frac{1}{2} p_w\right]$ or $\left[\frac{1}{2} p_w, p_w\right]$, depending on whether the resultant approximation to $p(655)$ is above or below atmospheric pressure.

Subsequent guesses for $p(0)$ are made in a similar manner.

Step 2. Use $p(0)$, known values for J_b, J_g, and p_w, and Equation (PA.226), Equation (PA.227), Equation (PA.228), and Equation (PA.229) to determine $q_b[p(0)]$ and $q_g[p(0)]$.

Step 3. Use the bisection method with $\Delta h = 25$ ft = 7.62 m and appropriate changes in annular diameter (Figure PA-26) to determine $p(655)$ (i.e., $p(h + \Delta h) = p(h) + G(q_b[p(0)], q_g[p(0)], p(h), h), \Delta h)$).

Step 4. Stop if $p(655)$ is within 0.07% of atmospheric pressure (i.e., if $|1.013 \times 10^5 \, Pa - p(655)| \leq 70 \, Pa$). Otherwise, return to Step 1 and repeat process.

The preceding procedure is continued until the specified error tolerance (i.e., 0.07%) has been met. The computational design of the PA has the potential to require more than 23,000 separate DBR calculations (3 replicates × 5 scenarios × 3 drilling locations × 100 vectors × 5 to 6 intrusion times per scenario). In concept, each of these cases requires the solution of Equation (PA.226), Equation (PA.227), Equation (PA.228), and Equation (PA.229) with the iterative procedure just presented to obtain the boundary value condition $p_{wf} = p(0)$ (Table PA-13). To help hold computational costs down, $p(0)$ was calculated for approximately 2,000 randomly generated vectors of the form

$$\mathbf{v} = \left[p_w, h, S_{br}, S_{gr}, S_b, A_i\right] \quad \text{(PA.237)}$$

where p_w is the repository pressure (used in definition of $q_b[p(0)]$ and $q_g[p(0)]$ in Equation (PA.226), Equation (PA.227), Equation (PA.228), and Equation (PA.229)), h is the crushed height of the repository (used in definition of J_p in Equation (PA.214)), S_{br} and S_{gr} are the residual saturations for gas and brine in the repository (used in definition of k_{rp} in Equation (PA.214)), S_b is the saturation of brine in the repository (used in definition of k_{rp} in Equation (PA.214)), and A_i is the equivalent area of material removed by cuttings, cavings, and spallings (used in definition of skin factor s in Equation (PA.218)). The outcomes of these calculations were divided into three cases:

1. Mobile brine only (i.e., $k_{rg} = 0$ in Equation (PA.219))

2. Brine-dominated flow (i.e., $k_{rb} > k_{rg}$)

3. Gas-dominated flow (i.e., $k_{rg} > k_{rb}$)

Regression procedures were then used to fit algebraic models that can be used to estimate $p(0)$. These regression models were then used to determine $p(0)$, and hence, p_{wf}. The resulting three regression models (or curve fit equations) for flowing bottomhole pressure (p_{wf}) are as follows:

1. For a system with only mobile brine ($k_{rg} = 0$)

$$p_{wf} = a + bx + cy + dx^2 + ey^2 + fxy + gx^3 + hy^3 + ixy^2 + jx^2y \quad \text{(PA.238)}$$

where $x = \log(j_b)$ and $y = p_w$ (= repository pressure), the coefficients in Equation (PA.238) were determined to be

$a = 3.2279346 \times 10^{11}$
$b = 9.4816648 \times 10^{10}$
$c = -6.2002715 \times 10^{3}$
$d = 9.2450601 \times 10^{9}$
$e = 4.1464475 \times 10^{-6}$
$f = -1.2886068 \times 10^{3}$
$g = 2.9905582 \times 10^{8}$
$h = 1.0857041 \times 10^{-14}$
$i = 4.7119798 \times 10^{-7}$
$j = -6.690712 \times 10^{-1}$

with a resulting coefficient of determination $R^2 = 0.974$.

2. For brine-dominated flow ($k_{rb} > k_{rg}$)

$$p_{wf} = \frac{a + bx + cx^2 + dy}{1 + ex + fx^2 + gx^3 + hy} \quad \text{(PA.239)}$$

where $x = \log\left(\frac{k_{rg}}{k_{rb}}\right)$ and $y = p_w$ (= repository pressure), the coefficients in Equation (PA.239) were determined to be

$a = 1.6065077 \times 10^{6}$
$b = 2.6243397 \times 10^{6}$
$c = 2.4768899 \times 10^{6}$
$d = -5.3635476 \times 10^{-2}$
$e = 7.0815693 \times 10^{-1}$
$f = 3.8012696 \times 10^{-1}$
$g = 4.1916956 \times 10^{-3}$
$h = -2.4887085 \times 10^{-8}$

with a resulting coefficient of determination $R^2 = 0.997$.

3. For gas-dominated flow ($k_{rg} > k_{rb}$)

$$p_{wf} = a + b\frac{1}{x} + cy + d\frac{1}{x^2} + ey^2 + f\frac{x}{y} + g\frac{1}{x^3} + hy^3 + i\frac{y^2}{x} + j\frac{y}{x^2} \quad \text{(PA.240)}$$

where $x = \log(j_g)$ and $y = p_w$ (= repository pressure), the coefficients in Equation (PA.240) were determined to be

$a = -1.0098405 \times 10^{9}$
$b = -2.3044622 \times 10^{10}$
$c = 9.8039146$
$d = -1.7426466 \times 10^{11}$
$e = 1.8309137 \times 10^{-7}$
$f = 1.7497064 \times 10^{2}$
$g = -4.3698224 \times 10^{11}$
$h = -1.4891198 \times 10^{-16}$
$i = 1.3006196 \times 10^{-6}$
$j = 7.5744833 \times 10^{2}$

with a resulting coefficient of determination $R^2 = 0.949$.

PA-4.7.7 Boundary Value Pressure pwE1

Some of the DBR calculations are for a drilling intrusion that has been preceded by an E1 intrusion in either the same waste panel, an adjacent waste panel, or a nonadjacent waste panel (Section PA-6.7.6). The effects of these prior E1 intrusions are incorporated into the solution of Equation (PA.219), Equation (PA.220), Equation (PA.221), Equation (PA.222), Equation (PA.223), Equation (PA.224), and Equation (PA.225), and hence into the DBR, by specifying a boundary pressure p_{wE1} at the location of the E1 intrusion into the repository (Table PA-13).

Two cases are considered for the definition of p_{wE1}: (1) an open borehole between the brine pocket and the repository and (2) a borehole filled with silty-sand-like material between the brine pocket and the repository. The first case corresponds to the situation in which the drilling intrusion occurs within 200 years of a prior drilling intrusion that penetrated the pressurized brine pocket, and the second case corresponds to the situation in which the drilling intrusion occurs more than 200 years after a prior drilling intrusion that penetrated the pressurized brine pocket.

PA-4.7.7.1 Solution for Open Borehole

In this case, p_{wE1} is set equal to the flowing well pressure p_{wfBP} of an open borehole between the brine pocket and the repository, and is given by

$$Q = f_1\left(p_{BP}, p_{wfBP}\right) \quad \text{(PA.241)}$$

$$Q = f_2\left(p_{wfBP}, p_{wfBI}\right) \quad \text{(PA.242)}$$

$$Q = f_3\left(p_{wfBI}, p_{wfBO}\right) \quad \text{(PA.243)}$$

where

p_{BP} = pressure (Pa) in brine pocket

p_{wfBP} = flowing well pressure (Pa) at outlet from brine pocket

p_{wfBI} = flowing well pressure (Pa) at inlet to repository from brine pocket

p_{wfBO} = flowing well pressure (Pa) at outlet from repository due to intruding borehole (Note: The boreholes associated with p_{wfBI} and p_{wfBO} arise from different drilling intrusions and hence are at different locations; see Figure PA-24)

Q = brine flow rate (m^3/s) from brine pocket to repository, through repository, and then to surface

and f_1, f_2, and f_3 are linear functions of their arguments. In the development, p_{BP} and p_{wfBO} are assumed to be known, with the result that Equation (PA.241), Equation (PA.242), and Equation (PA.243) constitutes a system of three linear equations in three unknowns (i.e., p_{wfBP}, p_{wbFI} and Q) that can be solved to obtain p_{wfBI}. In the determination of p_{wfBI} for use in a particular solution of Equation (PA.219), Equation (PA.220), Equation (PA.221), Equation (PA.222), Equation (PA.223), Equation (PA.224),and Equation (PA.225), p_{BP} is the pressure in the brine pocket at the time of the intrusion obtained from the solution of Equation (PA.24), Equation (PA.25), Equation (PA.26), Equation (PA.27), Equation (PA.28), Equation (PA.29), and Equation (PA.30) with BRAGFLO, and p_{wfBO} is the flowing well pressure obtained from conditions at the time of the intrusion (from the solution of Equation (PA.24), Equation (PA.25), Equation (PA.26), Equation (PA.27), Equation (PA.28), Equation (PA.29), and Equation (PA.30)) and the solutions of the Poettmann-Carpenter model embodied in Equation (PA.238), Equation (PA.239), and Equation (PA.240) (i.e., given pressure, k_{rg} and k_{rb} at the time of the intrusion, and J_p, p_{wfBO} is determined from the regression models indicated in Equation (PA.238), Equation (PA.239), and Equation (PA.240)).

The definition of Equation (PA.241), Equation (PA.242), and Equation (PA.243) is now discussed. Equation (PA.241) characterizes flow out of the brine pocket into an open borehole and has the form (Williamson and Chappelear 1981, Chappelear and Williamson 1981)

$$Q = \left(\frac{2\pi k_{BP} h_{BP}}{\mu \left[\ln\left(r_{eBP} / r_w \right) - 0.5 \right]} \right) \left(p_{BP} - p_{wfBP} \right) \quad \text{(PA.244)}$$

where

k_{BP} = brine pocket permeability (m^2)

h_{BP} = effective brine pocket height (m)

r_{eBP} = effective brine pocket radius (m)

r_w = wellbore radius (m)

μ = brine viscosity (Pa s)

In the present analysis, k_{BP} is an uncertain analysis input (see BHPRM in Table PA-17); h_{BP} = 125.83 m; r_{eBP} = 114 m (Stoelzel and O'Brien 1996), which corresponds to the size of the largest brine pocket that could fit under one waste panel; r_w = (8.921 in.)/2 = 0.1133 m, which is the inside radius of a 9 5/8 in. outside diameter casing (Gatlin 1960, Table 14.7); $\mu = 1.8 \times 10^{-3}$ Pa s; and p_{BP} is determined from the solution of Equation (PA.24), Equation (PA.25), Equation (PA.26), Equation (PA.27), Equation (PA.28), Equation (PA.29), and Equation (PA.30), as previously indicated.

Equation (PA.242) characterizes flow up an open borehole from the brine pocket to the repository and is based on Poiseuille's Law (Prasuhn 1980, Eqs. 7-21, 7-22). Specifically, Equation (PA.242) has the form

$$Q = \left[\frac{\pi D^4}{128 \mu \left(y_{BP} - y_{rep} \right)} \right] \left[\left(p_{wfBP} - p_{wfBI} \right) + g\rho \left(y_{rep} - y_{BP} \right) \right] \quad \text{(PA.245)}$$

where

D = wellbore diameter (m)

y_{rep} = elevation of repository (m) measured from surface

y_{BP} = elevation of brine pocket (m) measured from surface

g = acceleration due to gravity (9.8 m/s^2)

ρ = density of brine (kg/m^3)

and the remaining symbols have already been defined.

In the present analysis, $D = 2r_w$ = 0.2266 m, ρ = 1230 kg/m^3, and $y_{BP} - y_{rep}$ = 247 m. With the preceding values,

$$128\mu \left(y_{BP} - y_{rep} \right) / \pi D^4 = 6.87 \times 10^3 \text{ Pa s} / m^3 \quad \text{(PA.246)}$$

$$g\rho\left(y_{rep}-y_{BP}\right)=2.98\times10^{6}\ \text{Pa} \quad \text{(PA.247)}$$

Thus,

$$p_{wfBI}=p_{wfBP}-2.98\times10^{6}\ \text{Pa} \quad \text{(PA.248)}$$

when Q is small ($\leq 0.1\ m^3/s$). When appropriate, this approximation can be used to simplify the construction of solutions to Equation (PA.241), Equation (PA.242), and Equation (PA.243).

Equation (PA.243) characterizes flow through the repository from the lower borehole to the bottom of the borehole associated with the drilling intrusion under consideration and has the same form as Equation (PA.244). Specifically,

$$Q=\left(\frac{2\pi k_{rep}h_{rep}}{\mu\left[\ln\left(r_{e,rep}/r_{w}\right)-0.5\right]}\right)\left(p_{wfBI}-p_{wfBO}\right) \quad \text{(PA.249)}$$

where

k_{rep} = repository permeability (m^2)

h_{rep} = repository height (m)

$r_{e,rep}$ = effective repository radius (m)

and the remaining symbols have already been defined. In the present analysis, $k_{rep} = 2.4 \times 10^{-13}\ m^2$; h_{rep} at the time of the drilling intrusion under consideration is obtained from the solution of Equation (PA.24), Equation (PA.25), Equation (PA.26), Equation (PA.27), Equation (PA.28), Equation (PA.29), and Equation (PA.30) (see Equation (PA.209)); and $r_{e,rep}$ is the same as the radius r_e defined in Equation (PA.215). As previously indicated, p_{wfBO} is obtained from the solutions to the Poettmann-Carpenter model summarized in Equation (PA.238), Equation (PA.239), and Equation (PA.240).

Three equations (i.e., Equation (PA.244), Equation (PA.245), and Equation (PA.249)) with three unknowns (i.e., p_{wfBP}, p_{wfBI} and Q) have now been developed. The solution for p_{wfBI} defines the initial value $p_{wE\,1}$ in Table PA-13. When the simplification in Equation (PA.248) is used, the resultant solution for p_{wfBI} is

$$p_{wfBI}=\frac{p_{wfBO}+\left(p_{BP}-2.98\times10^{6}\right)K_1}{1+K_1} \quad \text{(PA.250)}$$

where

$$K_1=\frac{k_{BP}h_{BP}\left[\ln\left(\frac{r_{e,rep}}{r_w}\right)-\frac{1}{2}\right]}{k_{rep}h_{rep}\left[\ln\left(\frac{r_{eBP}}{r_w}\right)-\frac{1}{2}\right]} \quad \text{(PA.251)}$$

and -2.98×10^6 comes from Equation (PA.247). The expression in Equation (PA.251) was used to define $p_{wE\,1}$ in the CCA for the determination of DBRs resulting from a drilling intrusion that occurred within 200 years of a preceding E1 intrusion (see Table PA-7). The same approach was used for the CRA-2014 PA.

PA-4.7.7.2 Solution for Sand-Filled Borehole

The determination of the pressure p_{wfBI}, with the assumption that a borehole filled with silty-sand-like material connects the brine pocket and the repository, is now considered. The approach is similar to that used for the open borehole, except that Equation (PA.241) and Equation (PA.242) are replaced by a single equation based on Darcy's Law. Specifically, flow from the brine pocket to the repository is represented by

$$Q=\frac{k_{BH}A_{BH}\left[\left(p_{wfBP}-p_{wfBI}\right)+g\rho\right]}{\mu\left(y_{BP}-y_{rep}\right)} \quad \text{(PA.252)}$$

where

k_{BH} = borehole permeability (m^2)

A_{BH} = borehole cross-sectional area (m^2)

and the remaining symbols have been previously defined. In the present analysis, k_{BH} is an uncertain input (see BHPRM in Table PA-17) and A_{BH} is defined by the assumption that the borehole diameter is the same as the drill bit diameter (i.e., 12.25 in. = 0.31115 m).

The representation for flow from the brine pocket inlet point through the repository to the outlet point associated with the drilling intrusion under consideration remains as defined in Equation (PA.249). Thus, two equations (i.e., Equation (PA.249) and Equation (PA.252)) and two unknowns (i.e., p_{wfBI} and Q) are under consideration. Solution for p_{wfBI} yields

$$p_{wfBI} = \frac{p_{wfBO} + K_2 p_{BP} - 2.98 \times 10^6 K_2}{1 + K_2} \quad \text{(PA.253)}$$

where

$$K_2 = \frac{\pi k_{BH} r_w^2 \left[\ln\left(\frac{r_{gBP}}{r_w} \right) - \frac{1}{2} \right]}{2\pi l_{rep} k_{rep} \left(y_{BP} - y_{rep} \right)} \quad \text{(PA.254)}$$

and -2.98×10^6 comes from Equation (PA.247). The expression in Equation (PA.254) was used to define p_{wE1} in the determination of DBRs for a drilling intrusion that occurred more than 200 years after a preceding E1 intrusion (see Table PA-7).

PA-4.7.8 End of DBR

The CRA-2014 PA has 23,400 cases that potentially require solution of Equation (PA.219), Equation (PA.220), Equation (PA.221), Equation (PA.222), Equation (PA.223), Equation (PA.224) and Equation (PA.225) to obtain the DBR volume (see Section PA-6.7.6). However, the DBR was set to zero without solution of Equation (PA.219), Equation (PA.220), Equation (PA.221), Equation (PA.222), Equation (PA.223), Equation (PA.224), and Equation (PA.225) when there was no possibility of a release (i.e., at the time of the intrusion, the intruded waste panel had either a pressure less than 8 MPa or a brine saturation below the residual brine saturation S_{br}).

If there is little or no gas flow associated with brine inflow into the borehole during drilling in the Salado Formation, the current industry practice is to allow the brine to "seep" into the drilling mud and be discharged to the mud pits until the salt section is cased. If there is a significant amount of gas flow, it is possible that the driller will lose control of the well. In such cases, DBRs will take place until the gas flow is brought under control. Two possibilities exist: (1) the driller will regain control of the well when the gas flow drops to a manageable level, and (2) aggressive measures will be taken to shut off the gas flow before it drops to a manageable level. Experience at the South Culebra Bluff Unit #1, which blew out in January 1978, suggests that approximately 11 days may be needed to bring a well under control. It took 11 days to assemble the equipment and personnel needed to bring that well under control.

A reevaluation of the current drilling practices, including a review of the historic information and interviews with current drilling personnel in the WIPP area, has been conducted (Kirkes 2007). This analysis found

1. The South Culebra Bluff #1 is not a suitable analogue for a hypothetical WIPP blowout.

2. Basing the WIPP maximum DBR parameter on the single most catastrophic blowout event in the region's history does not reasonably represent "current drilling practice" as directed by regulations.

3. Well-known drilling procedures are sufficient to stop or *kill* a WIPP blowout under the most extreme anticipated pressures in hours, not days.

4. Using 4.5 days for a maximum DBR duration is still quite conservative, in that it assumes flow into the wellbore continues throughout the kill procedure and casing/cementing procedures, even though this assumption is not consistent with current practice.

Therefore, for the CRA-2009 PA, a value of 4.5 days was used for the maximum value used for t_e . This value is also used in the CRA-2014 PA.

Given the preceding, t_e is defined by

$$t_e = \begin{cases} \max\{3\text{ d}, t_f\} & \text{if } t_f \le 4.5\text{ d} \\ 4.5\text{ d} & \text{if } t_f > 4.5\text{ d} \end{cases} \quad \text{(PA.255)}$$

in PA, where t_f is the time at which the gas flow out of the well drops below 1×10^5 standard cubic feet per day (SCF/d). As a reminder, gas flow out of the repository in the intruding borehole, and hence t_e , is determined as part of the solution to Equation (PA.219), Equation (PA.220), Equation (PA.221), Equation (PA.222), Equation (PA.223), Equation (PA.224), and Equation (PA.225).

PA-4.7.9 Numerical Solution

As previously indicated, the BRAGFLO program is used to solve Equation (PA.219), Equation (PA.220), Equation (PA.221), Equation (PA.222), Equation (PA.223), Equation (PA.224), and Equation (PA.225) with the computational grid in Figure PA-24, the initial value conditions in Section PA-4.7.2, the boundary value conditions in Table PA-13, and parameter values appropriate for modeling DBRs. Thus, the numerical procedures in use for Equation (PA.219), Equation (PA.220), Equation (PA.221), Equation (PA.222), Equation (PA.223), Equation (PA.224), and Equation (PA.225) are the same as those described in Section PA-4.2.11 for the solution of Equation (PA.24), Equation (PA.25), Equation (PA.26), Equation (PA.27), Equation (PA.28), Equation (PA.29), and Equation (PA.30).

In this solution, the boundary value conditions associated with drilling intrusions (i.e., p_{wf} and p_{wE1} in Table PA-13) are implemented through the specification of fluid withdrawal terms (i.e., q_g and q_b in Equation (PA.24), Equation (PA.25), Equation (PA.26), Equation (PA.27), Equation (PA.28), Equation (PA.29), and Equation (PA.30)), rather than as predetermined boundary value conditions. With this implementation, the representations in Equation (PA.219) and Equation (PA.220) for gas and brine conservation become

$$\nabla \cdot \left[\frac{\alpha \rho_g K_g k_{rg}}{\mu_g}\left(\nabla p_g + \rho_g g \nabla h\right)\right] + \alpha q_g = \alpha \frac{\partial\left(\phi \rho_g S_g\right)}{\partial t} \quad \text{(PA.256)}$$

$$\nabla \cdot \left[\frac{\alpha \rho_b K_b k_{rb}}{\mu_b}\left(\nabla p_b + \rho_b g \nabla h\right)\right] + \alpha q_b = \alpha \frac{\partial\left(\phi \rho_b S_b\right)}{\partial t} \quad \text{(PA.257)}$$

and the constraints in Equation (PA.219), Equation (PA.220), Equation (PA.221), Equation (PA.222), Equation (PA.223), Equation (PA.224), and Equation (PA.225) remain unchanged. As used in Equation (PA.256) and Equation (PA.257), q_g and q_b are independent of the computational grid in use (Figure PA-24). In practice, q_g and q_b are defined with a productivity index (see Equation (PA.214)) that is a function of the specific computational grid in use, with the result that these definitions are only meaningful in the context of the computational grid that they are intended to be used with. This specificity results because q_g and q_b as used in Equation (PA.256) and Equation (PA.257) are defined on a much smaller scale than can typically be implemented with a reasonably sized computational grid. As a result, the values used for q_g and q_b in the numerical solution of Equation (PA.256) and Equation (PA.257) must incorporate the actual size of the grid in use.

In the solution of Equation (PA.256) and Equation (PA.257) with the computational grid in Figure PA-24, q_g is used to incorporate gas flow out of the repository, and q_b is used to incorporate both brine inflow to the repository from a pressurized brine pocket and brine flow out of the repository. For gas flow out of the repository,

$$q_g(x,y,t) = \frac{k k_{rg}(x,y,t)\left[p_g(x,y,t) - p_{wf}\right]}{\mu_g\left[\ln(r_e / r_w) + s + c\right]} \quad \text{(PA.258)}$$

if (x, y) is at the center of the grid cell containing the drilling intrusion (Figure PA-24), and $q_g(x, y, t) = 0$ (kg/m^3)/s otherwise, where k, k_{rg}, μ_g, r_e, r_w, s, and c are defined in conjunction with Equation (PA.214), p_g is gas pressure, and p_{wf} is the flowing well pressure at the outlet borehole (i.e., the boundary value condition in Table PA-13). The factor h in Equation (PA.214) is the crushed height of the repository as indicated in Equation (PA.214) and defines the factor α in Equation (PA.256) and Equation (PA.257). In the numerical solution, $q_g(x, y, t)$ defines $q_{g_{i,j}}^{n+1}$ in Equation (PA.100), with $q_{g_{i,j}}^{n+1}$ having a nonzero value only when i, j correspond to the grid cell containing the borehole through which gas outflow is taking place (i.e., the grid cells containing the down-dip, middle, and up-dip wells in Figure PA-24).

For brine flow,

$$q_b(x,y,t) = \frac{k k_{rb}(x,y,t)\left[p_b(x,y,t) - p_{wf}\right]}{\mu_b\left[\ln(r_e / r_w) + s + c\right]} \quad \text{(PA.259)}$$

if (x, y) is at the center of the grid cell containing the drilling intrusion through which brine outflow from the repository is taking place (Figure PA-24);

$$q_b(x,y,t) = \frac{k k_{rb}(x,y,t)\left[p_{wE1} - p_b(x,y,t)\right]}{\mu_b\left[\ln(r_e / r_w) + c\right]} \quad \text{(PA.260)}$$

if (x, y) is at the center of the grid cell containing a prior drilling intrusion into a pressurized brine pocket (Figure PA-24), where p_{wE1} is the boundary value condition defined in Table PA-13; and $q_b(x, y, t) = 0$ otherwise. In the numerical solution of Equation (PA.256), $q_g(x, y, t)$ defines $q_{b_{i,j}}^{n+1}$ in a discretization for Equation (PA.257) that is equivalent to the discretization for Equation (PA.256) shown in Equation (PA.100), with $q_{b_{i,j}}^{n+1}$ having a nonzero value only when i, j correspond to the grid cell containing the borehole through which brine outflow is taking place (i.e., the grid cells containing the down-dip, middle, and up-dip wells in Figure PA-24), in which case, Equation (PA.259)

defines $q_{b_{i,j}}^{n+1}$, or when *i, j* corresponds to the grid cell containing the borehole through which brine inflow to the repository from a pressurized brine pocket is taking place (i.e., the grid cell containing the E1 intrusion in Figure PA-24), in which case Equation (PA.260) defines $q_{b_{i,j}}^{n+1}$.

PA-4.7.10 Additional Information

Additional information on BRAGFLO and its use in the CRA-2014 PA to determine DBRs can be found in the analysis package for DBR (Malama 2013) and in the BRAGFLO user's manual (Camphouse 2013b).

PA-4.8 Groundwater Flow in the Culebra Dolomite

Extensive site characterization and modeling activities conducted in the WIPP vicinity have confirmed that the Culebra Dolomite Member of the Rustler Formation is the most transmissive geologic unit above the Salado. Thus, the Culebra is the unit into which actinides are most likely to be introduced from long-term flow up a hypothetical abandoned borehole.

The Culebra's regional variation in groundwater flow direction is influenced by the distribution of rock types in the groundwater basin where the WIPP is located. Site characterization activities have shown that the direction of groundwater flow in the Culebra varies somewhat regionally, but in the area that overlies the site, flow is generally southward. Site characterization activities have also demonstrated that there is no evidence of karst groundwater systems in the controlled area, although groundwater flow in the Culebra is affected by the presence of fractures, fracture fillings, and vuggy pore features.

Basin-scale regional modeling of three-dimensional groundwater flow in the units above the Salado demonstrates that it is appropriate, for the purposes of estimating radionuclide transport, to conceptualize the Culebra as a two-dimensional confined aquifer. Groundwater flow in the Culebra is modeled as a steady-state process, but uncertainty in the flow field is incorporated in the analysis by using 100 different geostatistically based T-fields. The T-fields are initially constructed to be consistent with available head, transmissivity, and well testing data. Each T-field is subsequently modified to incorporate impacts of uncertain future processes (potash mining and climate change), as described below.

Potash mining in the McNutt Potash Zone (hereafter referred to as the McNutt) of the Salado, which occurs now in the Delaware Basin outside the controlled area and may continue in the future, could affect flow in the Culebra if subsidence over mined areas causes fracturing or other changes in rock properties. Consistent with regulatory criteria, mining outside the controlled area is assumed to occur in the near future, and mining within the controlled area is assumed to occur with a probability of 1 in 100 per century (adjusted for the effectiveness of AICs during the first 100 years following closure). Consistent with regulatory guidance, the effects of mine subsidence are incorporated in the PA by increasing the transmissivity of the Culebra over the areas identified as mineable by a factor sampled from a uniform distribution between 1 and 1000. T-fields used in the PA are therefore adjusted to account for this and steady-state flow fields calculated accordingly, once for mining that occurs only outside the controlled area, and once for mining that occurs both inside and outside the controlled area. Mining outside the controlled area is considered in both undisturbed and disturbed performance.

Climatic changes during the next 10,000 years may also affect groundwater flow by altering recharge to the Culebra. The extent to which the climate will change during the next 10,000 years and how such a change will affect groundwater flow in the Culebra are uncertain. However, regional three-dimensional modeling of groundwater flow in the units above the Salado indicates that flow velocities in the Culebra may increase by a factor of 1 to 2.25 for reasonably possible future climates (Corbet and Swift 1996a and Corbet and Swift 1996b). This uncertainty is incorporated in the PA by scaling the calculated steady-state specific discharge within the Culebra by a sampled parameter within this range.

PA-4.8.1 Mathematical Description

Groundwater flow in the Culebra is represented by the PDE

$$S = \left(\frac{\partial h}{\partial t}\right) = \nabla \cdot (b\mathbf{K}\nabla h) - Q \quad \text{(PA.261)}$$

where

S = medium storativity (dimensionless),
h = hydraulic head (m),
t = time (s),
b = aquifer thickness (m),
$\mathbf{K}$ = hydraulic conductivity tensor (m/s),
Q = source/sink term expressed as the volumetric flux per unit area ($(m^3/m^2)/s = m/s$).

Further, the Culebra is assumed to be two-dimensional with isotropic hydraulic conductivity. As a result, $\mathbf{K}$ is defined by

$$\mathbf{K}(x,y) = k(x,y)\begin{bmatrix} 1 & 0 \\ 0 & 1 \end{bmatrix} \quad \text{(PA.262)}$$

where $k(x, y)$ is the hydraulic conductivity (m/s) at the point (x, y). The following simplifying assumptions are also made: fluid flow in the Culebra is at steady state (i.e., $\partial h/\partial t = 0$), and source and sink effects arising from borehole intrusions and infiltration are negligible (i.e., $Q = 0$). Given these assumptions, Equation (PA.261) simplifies to

$$\nabla \cdot (b\mathbf{K}\nabla h) = 0 \quad \text{(PA.263)}$$

which is the equation actually solved to obtain fluid flow in the Culebra. In PA, $b = 7.75$ m, and $k(x, y)$ in Equation (PA.262) is a function of an imprecisely known T-field, as discussed in Section PA-4.8.2.

PA-4.8.2 Implementation in the PA

This section describes the salient features of the Culebra flow field calculation implementation. One should note, however, that this implementation has not been changed for the CRA-2014 PA. Culebra flow results obtained in the CRA-2009 PABC (see Kuhlman 2010) are also used in the CRA-2014 PA as none of the changes implemented in the CRA-2014 PA impact Culebra flow results. The CRA-2009 PABC Culebra flow calculations included updated transmissivity fields from those used in the CRA-2009 PA. This section reflects the updated T-fields used in the CRA-2009 PABC and the CRA-2014 PA.

The first step in the analysis of fluid flow in the Culebra is to generate T-fields $T(x, y)$ (m^2/s) for the Culebra and to characterize the uncertainty in these fields. This was accomplished by generating a large number of plausible T-fields. A description of the method used to construct these T-fields is included in Appendix TFIELD-2014. A brief outline of the method is presented below.

The T-fields used for PA are based on several types of information, including a regression model developed on WIPP-site geologic data, measured head levels in the Culebra for the year 2007, and multi-well drawdown pumping tests. The process that led to the final T-fields used in the PA is discussed below.

Geologic data, including (1) depth to the top of the Culebra, (2) reduction in thickness of the upper Salado by dissolution, (3) presence of gypsum cements in the Culebra, (4) interpretation of high-diffusivity connections between wells from multi-well pumping tests, and (5) the spatial distribution of halite in the Rustler below and above the Culebra, were used to define a geologic regression model that relates transmissivity at any location to a set of geologically defined parameters.

Base T-fields are defined for a modeling domain measuring 28.4 km east-west by 30.7 km north-south using a method of stochastic simulation. The base T-fields were constructed from information on the depth to the Culebra, indicator functions defining the location of Salado dissolution, halite occurrence, presence of gypsum cements, and high transmissivity zones.

The base T-fields are calibrated to a steady-state snapshot of water-level data in 44 wells from the year 2007, and nine transient pumping test responses. Calibration is automated using the parameter estimation program PEST (Doherty 2002). PEST iteratively changes pilot points in transmissivity (T), horizontal T anisotropy, storativity, and recharge to minimize an objective function. MODFLOW 2000 (Harbaugh et al. 2000) is run 10 times for each forward iteration in order to compute the predicted flow solution against observed data. The objective function minimized by PEST is a combination of the weighted sum of the squared residuals between the measured and modeled heads and drawdowns and a second weighted sum of the squared differences in the estimated transmissivity between pairs of pilot points. The second weighted sum is intended to keep the parameter fields as homogeneous as possible, providing numerical stability when estimating more parameters than data.

The calibrated T-fields produced by PEST and MODFLOW are screened according to specific acceptance criteria (see Appendix TFIELD, Section 5.3.4). Calibrated T-fields that meet the acceptance criteria are modified for the partial and full mining scenarios. This modification increases transmissivity by a random factor between 1 and 1000 in areas containing potash reserves, as described below. Steady-state flow simulations are then run using the mining-modified T-fields.

Because radionuclide transport calculations are performed using a uniform 50 × 50 m grid, the final step in the flow simulation is to run MODFLOW with a 50 × 50 m grid to calculate the flow fields required for the transport code. The hydraulic conductivities for the refined grid are obtained by dividing each 100 × 100 m cell used in the T-field calculations into four 50 × 50 m cells. The conductivities assigned to each of the four cells are equal to the conductivity of the larger cell (Leigh, Beauheim, and Kanney 2003).

The hydraulic conductivity $k(x, y)$ in Equation (PA.262) is defined in terms of the T-fields $T(x, y)$ by

$$k(x, y) = T(x, y)/b \quad \text{, (PA.264)}$$

where b is the Culebra thickness - a constant 7.5 m.

Fluid flow is determined (using MODFLOW to solve Equation (PA.263)) for two different cases: (1) a partial mining case (only mining of potash deposits outside the LWB), and (2) a full mining case (mining of potash deposits both inside and outside the LWB). The model domains and mining-affected areas for these two cases in the CRA-2009 PABC are also used in the CRA-2014 PA, and are shown in Figure PA-27. As specified by guidance in 40 CFR Part 194, potash mining increases the Culebra's hydraulic conductivity in the vicinity of such mining by an uncertain factor with a value between 1 and 1000. As specified in section 194.32 and described in Section PA-3.9, economic potash reserves outside the LWB are assumed to have been fully mined by the end of the 100-year period of AICs, after which the occurrence of potash mining within the LWB follows a Poisson process with a rate constant of $\lambda_m = 1 \times 10^{-4}\ \text{yr}^{-1}$.

In the partial mining case, the hydraulic conductivity $k_{PM}(x, y)$ is defined by Equation (PA.264) inside the WIPP boundary and by $k_{PM}(x, y) = k(x, y) \times MF$ outside the WIPP boundary, where MF is determined by the uncertain parameter CTRANSFM (see Table PA-17). In the full mining case, the hydraulic conductivity is defined by $k_{FM}(x, y) = k(x, y) \times MF$ in all areas of the modeling domain.

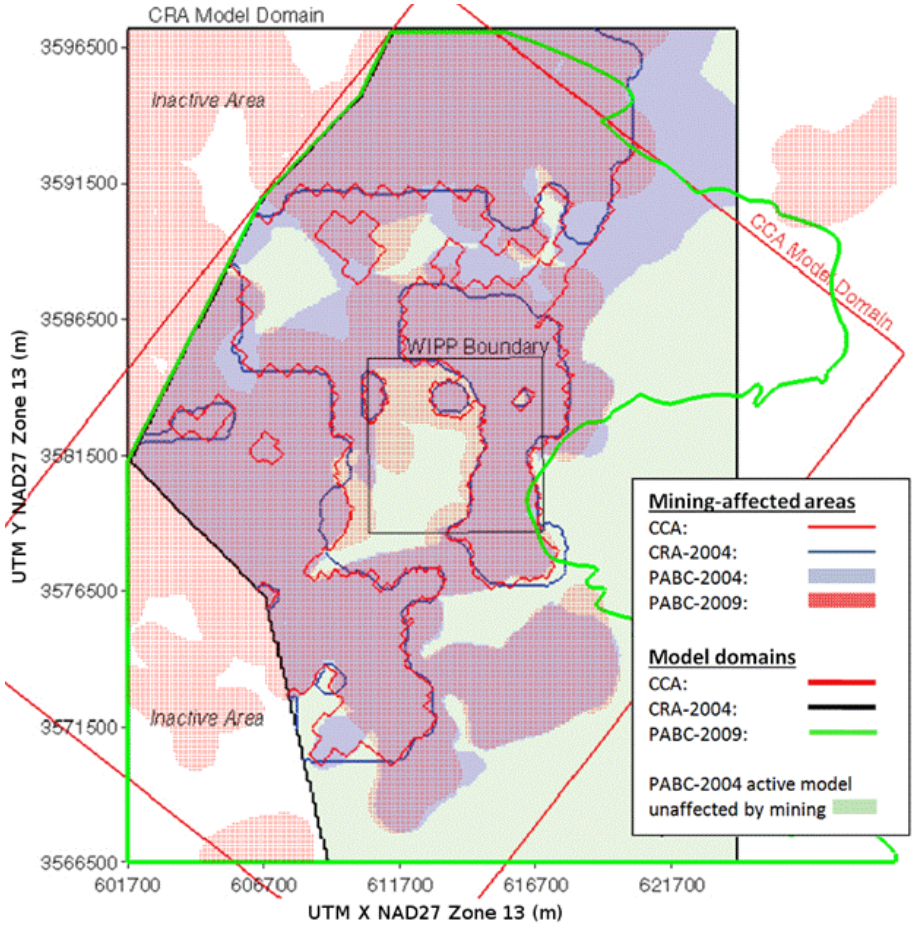

Figure PA- 27. Areas of Potash Mining in the McNutt Potash Zone

In turn , $k_{PM}(x, y)$ and $k_{FM}(x, y)$ result in the following definition for the hydraulic conductivity tensor **K**:

$$\mathbf{K}_i(x,y) = k_i(x,y)\begin{bmatrix} 1 & 0 \\ 0 & A(x,y) \end{bmatrix}, \; i = PM, FM \quad \text{(PA.265)}$$

In the analysis, Equation (PA.263) is solved with each of the preceding definitions of $\mathbf{K}_i$ to obtain characterizations of fluid flow in the Culebra for partially-mined conditions and fully mined conditions.

The determination of fluid flow in the Culebra through the solution of Equation (PA.263) does not incorporate the potential effects of climate change on fluid flow. Such effects are incorporated into the analysis by an uncertain scale factor to introduce the potential effects of climate change into the analysis (Corbet and Swift 1996a and Corbet and Swift 1996b). Specifically, the Darcy fluid velocity $v_i(x, y)$ actually used in the radionuclide transport calculations is given by

$$\mathbf{v}_i(x,y) = \left[u_i(x,y), v_i(x,y)\right] = SFC\left[\mathbf{K}_i(x,y)\nabla h_i(x,y)\right]^T, \; i = PM, FM \quad \text{(PA.266)}$$

where $u_i(x, y)$ and $v_i(x, y)$ represent Darcy fluid velocities (m/s) at the point (x, y) in the x and y directions, respectively; $\nabla h_i(x, y)$ is obtained from Equation (PA.263) with $\mathbf{K} = \mathbf{K}_i$; and SFC is a scale factor used to incorporate the uncertainty that results from possible climate changes. The scale factor SFC is determined by the uncertain parameter CCLIMSF (see Table PA-17).

PA-4.8.3 Computational Grids and Boundary Value Conditions

The representation for fluid flow in the Culebra in Equation (PA.263) is evaluated on a numerical grid 28.4 km east-west by 30.7 km north-south, aligned with the compass directions (Figure PA-28). The modeling domain is discretized into 68,768 uniform 100 × 100 m cells. The northern model boundary is slightly north of the northern end of Nash Draw, 12 km (7.4 miles) north of the northern WIPP site boundary,

and about 1 km (0.62 miles) north of Intrepid Potash's east tailings pile. The eastern boundary lies in a low-transmissivity region that contributes little flow to the modeling domain. The southern boundary lies 12.2 km south of the southern WIPP site boundary, far enough from the WIPP site to have little effect on transport rates on the site. The western model boundary passes through the Mosaic (formerly International Minerals and Chemicals) tailings pond (Laguna Uno; see Hunter 1985) due west of the WIPP site in Nash Draw.

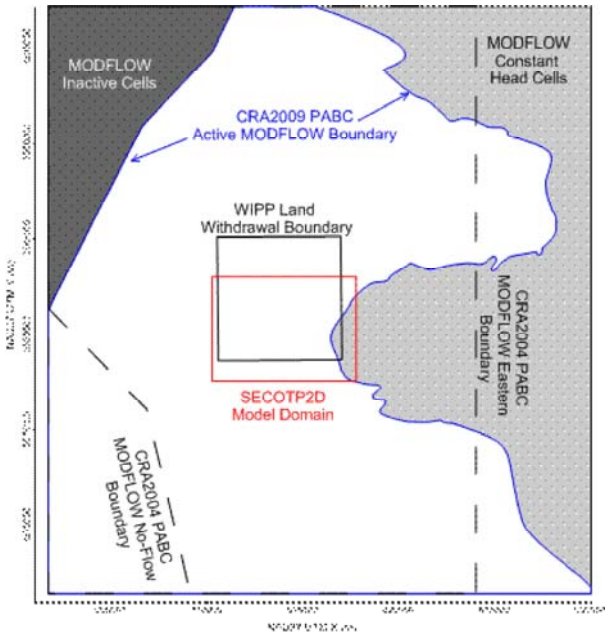

Figure PA- 28. Modeling Domain for Groundwater Flow (MODFLOW) and Radionuclide Transport (SECOTP2D) in the Culebra

Two types of boundary conditions are specified: constant-head and no-flow (Figure PA-28). MODFLOW boundaries used in the CRA-2009 PABC are also used in the CRA-2014 PA. Constant-head conditions along the eastern boundary of the model domain (the irregular blue line in Figure PA-28) are specified to the land surface elevation. Constant head conditions along the northern, southern, and western boundaries were obtained from a polynomial fit to 2007 heads. The western model boundary passes through the Mosaic tailings pond (Laguna Uno) due west of the WIPP site in Nash Draw. A no-flow boundary is specified in the model from this tailings pond up the axis of Nash Draw to the northeast, reflecting the concept that groundwater flows down the axis of Nash Draw, forming a groundwater divide. Thus, the northwestern corner of the modeling domain is specified as inactive cells in MODFLOW, and the specified head cells in the eastern portion of the MODFLOW domain are essentially inactive, since their heads are specified, not computed.

PA-4.8.4 Numerical Solution

The flow model in Equation (PA.263) is evaluated on the computational grid described in Section PA-4.8.3 using MODFLOW 2000 (Harbaugh et al. 2000). MODLFOW discretizes the flow equation with a second-order difference procedure (McDonald and Harbaugh 1988, p. 126). Specifically, the discretized form of Equation (PA.263) is

$$0 = CR_{i,j-1/2}\left(h_{i,j-1} - h_{i,j}\right) + CR_{i,j+1/2}\left(h_{i,j+1} - h_{i,j}\right) + CC_{i-1/2,j}\left(h_{i-1,j} - h_{i,j}\right) + CC_{i+1/2,j}\left(h_{i+1,j} - h_{i,j}\right) \quad \text{(PA.267)}$$

where CR and CC are the row and column hydraulic conductances at the cell interface between node i, j and a neighboring node (m^2/s). Since the grid is uniform, the hydraulic conductance is simply the harmonic mean of the hydraulic conductivity in the two neighboring cells multiplied by the aquifer thickness. For example, the hydraulic conductance between cells (i, j) and $(i, j - 1)$ is given by $CR_{i,j-1/2}$, and the hydraulic conductance between cells (i, j) and $(i + 1, j)$ is given by $CC_{i+1/2,j}$:

$$CR_{i,j-1/2} = \frac{2k_{i,j}k_{i,j-1}}{k_{i,j} + k_{i,j-1}} \times b \quad \text{and} \quad CC_{i+1/2,j} = \frac{2k_{i,j}k_{i+1,j}}{k_{i,j} + k_{i+1,j}} \times b$$

where $k_{i,j}$ is the hydraulic conductivity in cell i, j (m/s) and b is the aquifer thickness (m).

Figure PA-29 illustrates the cell numbering convention used in the finite-difference grid for MODFLOW. The determination of h is then completed by the solution of the linear system of equations in Equation (PA.267) for the unknown heads $h_{i,j}$. Fluxes at cell interfaces are calculated from the values for $h_{i,j}$ internally in MODFLOW.

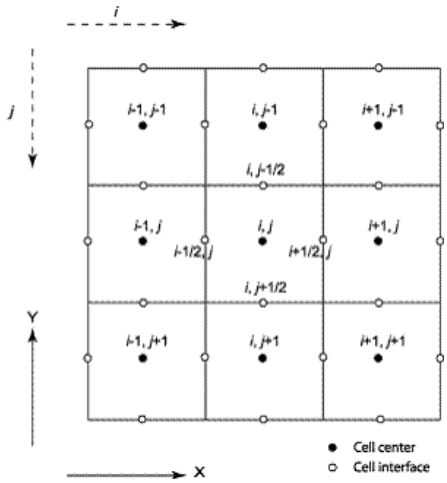

Figure PA- 29. Finite-Difference Grid Showing Cell Index Numbering Convention Used by MODFLOW

PA-4.8.5 Additional Information

Additional information on MODFLOW and its use in the WIPP PA to determine fluid flow in the Culebra can be found in the MODFLOW-2000 user's manual (Harbaugh et al. 2000) and in Hart et al. (Hart et al. 2009). Calculation of the flow fields used in the CRA-2014 PA is presented in Kuhlman (2010).

PA-4.9 Radionuclide Transport in the Culebra Dolomite

Extensive laboratory and field investigations have focused on the physical mechanisms influencing transport in the Culebra, as well as the behavior of dissolved and colloidal actinides in the Culebra. Field tests have confirmed the Culebra can be characterized as a double-porosity medium to estimate groundwater radionuclide transport. Groundwater flow and advective transport of dissolved or colloidal species and particles occur primarily in a small fraction of the rock's total porosity corresponding to the porosity of open and interconnected fractures and vugs. Diffusion and (much slower) advective flow occur in the remainder of the porosity, which is associated with the low-permeability dolomite matrix. Transported species, including actinides, if present, will diffuse into this porosity.

Diffusion from the advective porosity into the dolomite matrix will retard actinide transport by two mechanisms. Physical retardation occurs simply because actinides that diffuse into the matrix are no longer transported with the flowing groundwater, so transport is interrupted until they diffuse back into the advective porosity. In situ tracer tests have been conducted to demonstrate this phenomenon (Meigs, Beauheim, and Jones 2000). Chemical retardation also occurs within the matrix as actinides are sorbed onto dolomite grains. The relationship between sorbed and liquid concentrations is assumed to be linear and reversible. The distribution coefficients (K_d) that characterize the extent to which actinides will sorb on dolomite are based on experimental data. After their review of the CCA, the EPA required the DOE to use the same ranges, but to change the distribution of K_ds from uniform to loguniform. The EPA further requested changes to the lower limits of the distributions of K_d in the CRA-2009 PABC (Kelly 2009).

Modeling, supported by field tests and laboratory experiments, indicates that physical and chemical retardation will be extremely effective in reducing the transport of dissolved actinides in the Culebra. Experimental work has demonstrated that transport of colloidal actinides is not a significant mechanism in the Culebra (Papenguth 1996). As a result, actinide transport through the Culebra to the subsurface boundary of the controlled area is not a significant pathway for releases from the WIPP, although it continues to be computed in PA. As discussed in Section PA-9.0, the location of the mean CCDF that demonstrates compliance with the containment requirements of section 191.13 is determined almost entirely by direct releases at the ground surface during drilling (cuttings, cavings, DBRs, and spallings).

Radionuclide transport in the Culebra is computed using the SECOTP2D computer code (WIPP Performance Assessment 1997b). The mathematical equations solved by SECOTP2D and the numerical methods used in the code are described in the following sections.

PA-4.9.1 Mathematical Description

Radionuclide transport in the Culebra is described by a parallel-plate, dual-porosity model (Meigs and McCord 1996). The parallel-plate, dual-porosity conceptualization assumes that the numerous fractures within the formation are aligned in a parallel fashion and treats the fractured porous media as two overlapping continua: one representing the fractures and the other representing the surrounding porous rock matrix (see Figure PA-30). In this model, one system of PDEs is used to represent advective transport in fractures within the Culebra and another PDE system is used to represent diffusive transport and sorption in the matrix that surrounds the fractures.

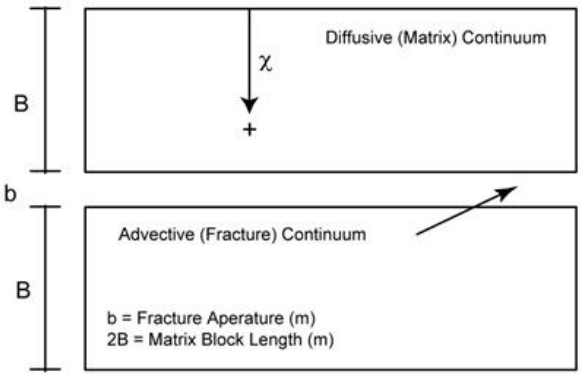

Figure PA- 30. Parallel-Plate, Dual-Porosity Conceptualization

PA-4.9.1.1 Advective Transport in Fractures

The PDE system used to represent advective transport in fractures is given by (WIPP Performance Assessment 1997b)

$$\nabla \cdot \left[\phi \mathbf{D}_k \nabla C_k - \mathbf{v} C_k\right] = \phi R_k \left(\frac{\partial C_k}{\partial t}\right) + \phi R_k \lambda_k C_k - \phi R_{k-1} \lambda_{k-1} C_{k-1} - Q_k - \Gamma_k \quad \text{(PA.268)}$$

for k = 1, 2, …, *nR*, where

nR = number of radionuclides under consideration
C_k = concentration of radionuclide *k* in brine (kg/m^3)
$\mathbf{D}_k$ = hydrodynamic dispersion tensor (m^2/s)
$\mathbf{v}$ = Darcy velocity (i.e., specific discharge) of brine (m/s = (m^3/m^2)/s)
ϕ = advective (i.e., fracture) porosity (dimensionless)
R_k = advective retardation coefficient (dimensionless)
λ_k = decay constant for radionuclide k (s^{-1})
Q_k = injection rate of radionuclide *k* per unit bulk volume of formation ((kg/s)/m^3) (Note: $Q_k > 0$ corresponds to injection into the fractures)
Γ_k = mass transfer rate of radionuclide *k* per unit bulk volume of formation due to diffusion between fractures and surrounding matrix ((kg/s)/m^3) (Note: $\Gamma_k > 0$ corresponds to diffusion into fractures)

The Darcy velocity **v** is obtained from the solution of Equation (PA.263); specifically, **v** is defined by the relationship in Equation (PA.266). The advective porosity ϕ, defined as the ratio of the interconnected fracture pore volume to the total volume, is determined by an uncertain parameter (see CFRCPOR in Table PA-17).

The hydrodynamic dispersion tensor is defined by (WIPP Performance Assessment 1997b; Bear 1972)

$$\mathbf{D}_k = \frac{1}{\|\mathbf{v}\|\phi}\begin{bmatrix} u & -v \\ v & u \end{bmatrix}\begin{bmatrix} \alpha_L & 0 \\ 0 & \alpha_T \end{bmatrix}\begin{bmatrix} u & v \\ -v & u \end{bmatrix} + \tau D_k^* \begin{bmatrix} 1 & 0 \\ 0 & 1 \end{bmatrix} \quad \text{(PA.269)}$$

where α_L and α_T are the longitudinal and transverse dispersivities (m); *u* and *v* are the *x* and *y* components of $\mathbf{v}$ (i.e., $\mathbf{v} = [u, v]$); $\mathbf{D}_k^*$ is the free water molecular diffusion coefficient (m^2 s^{-1}) for radionuclide *k*; and τ is the advective tortuosity, defined as the ratio of the true length of the flow path of a fluid particle to the straight-line distance between the starting and finishing points of the particle's motion. As in the CCA PA (Helton et al. 1998), the CRA-2014 PA uses $\alpha_L = \alpha_T = 0$ m and $\tau = 1$. Thus, the definition of $\mathbf{D}_k$ used in PA reduces to

$$\mathbf{D}_k = \mathbf{D}_k^* \begin{bmatrix} 1 & 0 \\ 0 & 1 \end{bmatrix} \quad \text{(PA.270)}$$

The diffusion coefficients, D*k, for the oxidation states of the radionuclides under consideration are shown in Table PA-14 (see parameters PU+3:MD0, PU+4:MD0, and U+6:MD0 in Kicker and Herrick 2013, Table 27). The existence of Pu in the (III) or (IV) oxidation state (i.e., as Pu(III) or Pu(IV)) and the existence of U in the (IV) or (VI) oxidation state (i.e., as U(IV) or U(VI)) is determined by an uncertain parameter (see WOXSTAT in Table PA-17).

Table PA- 14. Radionuclide Culebra Transport Diffusion Coefficients

Oxidation State	III	IV	VI
Diffusion Coefficient (m^2/s)	3.00×10^{-10}	1.53×10^{-10}	4.26×10^{-10}

The advective retardation coefficient R_k is defined by

$$R_k = 1 + (1-\phi)\rho_A K_{Ak} / \phi \quad \text{(PA.271)}$$

where

ρ_A = surface area density of fractures in Culebra (m^2/m^3 = 1/m) (i.e., surface area of fractures (m^2) divided by volume of fractures (m^3))
K_{Ak} = surface area distribution coefficient ((kg/m^2)/(kg/m^3) = m) (i.e., concentration of radionuclide k sorbed on fracture surfaces (kg/m^2) divided by concentration of radionuclide k dissolved in brine within fractures (kg/m^3))

Following the logic used in the CCA (Helton et al. 1998), $K_{Ak} = 0$ and thus $R_k = 1$ are used in the PA.

In concept, the term Q_k in Equation (PA.268) provides the link between the releases to the Culebra calculated with NUTS and PANEL (Section PA-6.7) and transport within the Culebra. In the computational implementation of PA, radionuclide transport calculations in the Culebra were performed for unit radionuclide releases to the Culebra, and the outcomes of these calculations were used to construct the release to the accessible environment associated with time-dependent releases into the Culebra derived from NUTS and PANEL calculations (Section PA-6.8.3). The definition of Q_k is discussed in more detail in Section PA-4.9.1.4.

The initial condition for Equation (PA.268) is

$$C_k(x,y,0) = 0 \text{ kg/m}^3 \quad \text{(PA.272)}$$

Furthermore, the boundary value conditions for Equation (PA.268) are defined at individual points on the boundary of the grid in Figure PA-28 on the basis of whether the flow vector $\mathbf{v} = [u, v]$ defines a flow entering the grid or leaving the grid. The following Neumann boundary value condition is imposed at points (x, y) where flow leaves the grid:

$$\nabla C_k(x,y,t) \cdot n(x,y) = 0 \left(\text{kg/m}^3\right)/\text{m}^3 \quad \text{(PA.273)}$$

where $n(x, y)$ is an outward-pointing unit normal vector defined at (x, y). The following Dirichlet boundary value condition is imposed at points (x, y) where flow enters the grid:

$$C_k(x,y,t) = 0 \text{ kg/m}^3 \quad \text{(PA.274)}$$

PA-4.9.1.2 Diffusive Transport in the Matrix

The system of PDEs used to represent diffusive transport in the matrix surrounding the fractures is given by (WIPP Performance Assessment 1997b)

$$\frac{\partial}{\partial \chi}\left(\phi' D'_k \frac{\partial C'_k}{\partial \chi}\right) = \phi' R'_k \left(\frac{\partial C'_k}{\partial t}\right) + \phi' R'_k \lambda_k C'_k - \phi' R'_{k-1} \lambda_{k-1} C'_{k-1} \quad \text{(PA.275)}$$

where χ is the spatial coordinate in Figure PA-30, D'_k is the matrix diffusion coefficient (m^2/s) for radionuclide k defined by $D'_k = D^*_k \tau'$, and τ' is the matrix tortuosity. The remaining terms have the same meaning as those in Equation (PA.268), except that the prime denotes properties of the matrix surrounding the fractures. A constant value ($\tau' = 0.11$) for the matrix (i.e., diffusive) tortuosity is used in PA (Meigs 1996). The matrix (i.e., diffusive) porosity ϕ' is an uncertain input to the analysis (see CMTRXPOR in Table PA-17). The matrix retardation R'_k is defined by

$$R'_k = 1 + (1-\phi')\rho_s K_{dk} / \phi' \quad \text{(PA.276)}$$

where ρ_s is the particle density (kg/m^3) of the matrix and K_{dk} is the distribution coefficient ((Ci/kg)/(Ci/m^3) = m^3/kg) for radionuclide k in the matrix. The density ρ_s is assigned a value of 2.82×10^3 kg/m^3 (Martell 1996b). The distribution coefficients K_{dk} are uncertain inputs to the analysis and dependent on the uncertain oxidation state of the relevant element (see CMKDAM3, CMKDPU3, CMKDPU4, CMKDTH4, CMKDU4, CMKDU6, and WOXSTAT in Table PA-17).

The initial and boundary value conditions used in the formulation of Equation (PA.275) are

$$C'_k(x,y,\chi,0) = 0 \text{ kg/m}^3 \quad \text{(PA.277)}$$

$$\partial C'_k(x,y,0,t)/\partial z = 0 \text{ kg/m}^2 \quad \text{(PA.278)}$$

$$C'_k(x,y,B,t) = C_k(x,y,t) \quad \text{(PA.279)}$$

where (x, y) corresponds to a point in the domain on which Equation (PA.268) is solved and B is the matrix half-block length (m) in Figure PA-30 (i.e., $2B$ is the thickness of the matrix between two fractures). The initial condition in Equation (PA.277) means that no radionuclide is present in the matrix at the beginning of the calculation. The boundary value condition in Equation (PA.278) implies that no radionuclide movement can take place across the centerline of a matrix block separating two fractures. The boundary value condition in Equation (PA.279) ensures that the dissolved radionuclide concentration in the matrix at the boundary with the fracture is the same as the dissolved radionuclide concentration within the fracture. The matrix half-block length B is an uncertain input to the analysis (see CFRACSP in Table PA-17).

PA-4.9.1.3 Coupling Between Fracture and Matrix Equations

The linkage between Equation (PA.268) and Equation (PA.275) is accomplished through the term Γ_k, defining the rate at which radionuclide k diffuses across the boundary between a fracture and the adjacent matrix (see Figure PA-30). Specifically,

$$\Gamma_k = -\frac{2\phi}{b}\left(\phi' D_k^f \left.\frac{\partial C_k^f}{\partial \chi}\right|_{\chi=\chi}\right) \quad \text{(PA.280)}$$

where b is the fracture aperture (m) defined by

$$b = \phi B(1-\phi) \quad \text{(PA.281)}$$

PA-4.9.1.4 Source Term

As already indicated, Equation (PA.268) and Equation (PA.275) are solved for unit radionuclide releases to the Culebra. Specifically, a release of 1 kg of each of the four lumped radionuclides (^{241}Am, ^{234}U, ^{230}Th, and ^{239}Pu) under consideration was assumed to take place over a time interval from 0 to 50 years, with this release taking place into the computational cell WPAC, located at the center of the Waste Panel Area in Figure PA-28, that has dimensions of 50 m × 50 m. The volume of this cell is given by

$$V = (50m)(50m)(4m) = 1\times 10^4\ m^3 \quad \text{(PA.282)}$$

where 4 m is the effective thickness of the Culebra Dolomite (Meigs and McCord 1996). As a result, $Q_k(x, y, t)$ has the form

$$Q_k(x,y,t) = \frac{1\ kg}{(1\times 10^4\ m^3)(50\ yr)(3.16\times 10^7\ s/yr)} = 6.33\times 10^{-14}\ kg/m^3/s \quad \text{(PA.283)}$$

for $0 \le t \le 50$ yr and (x, y) in cell WPAC, and $Q_k(x, y, t) = 0$ (kg/m^3/s) otherwise.

PA-4.9.1.5 Cumulative Releases

If $\mathcal{B}$ denotes an arbitrary boundary (e.g., the LWB) in the domain of Equation (PA.268) (i.e., Figure PA-28), then the cumulative transport of $C_k(t, B)$ of radionuclide k from time 0 to time t across $\mathcal{B}$ is given by

$$C_k(t,B) = \int_0^t \left[\int_{\mathcal{B}} \left\{v(x,y)C_k(x,y,\tau) - \phi D_k(x,y,t)\nabla C_k(x,y,\tau)\right\} b \cdot n(x,y)\, ds\right] d\tau \quad \text{(PA.284)}$$

where h is the thickness of the Culebra (4 m), f is the advective porosity in Equation (PA.268), $n(x, y)$ is an outward pointing unit normal vector, and $\int_B ds$ denotes a line integral over B.

PA-4.9.2 Numerical Solution

The numerical solution to the coupled PDE system represented by Equation (PA.268) and Equation (PA.275) is computed using SECOTP2D, an implicit finite-volume code for the simulation of multispecies reactive transport. A high-level description of the numerical procedures implemented in SECOTP2D follows, with more detail available in WIPP Performance Assessment (1997b).

PA-4.9.2.1 Discretization of Fracture Domain

The fracture domain is discretized in space using the block-centered finite-difference method indicated in Figure PA-31. In this formulation, cell concentrations are defined at grid block centers while the velocity components $[u, v]$ are defined on grid cell faces. A uniform mesh with 50 m × 50 m cells is used for the spatial discretization. Ghost cells are placed outside the problem domain for the purpose of implementing boundary conditions. The temporal discretization is accomplished using variable time step sizes.

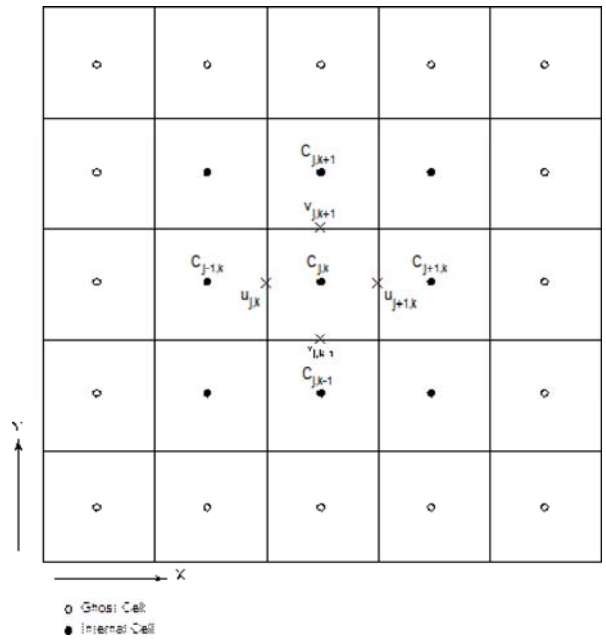

Figure PA- 31. Schematic of Finite-Volume Staggered Mesh Showing Internal and Ghost Cells

The dispersive term, $\nabla \cdot (\phi D_k \nabla C_k)$, in Equation (PA.268) is approximated using a second-order central difference formula (Fletcher 1988).

The advective term , $\nabla \cdot \mathbf{v} C_k$, is approximated using the Total Variation Diminishing (TVD) method (Sweby 1984). The TVD method provides a way of accurately resolving advection-dominated transport problems without the occurrence of nonphysical oscillations commonly present in second-order solutions. This method invokes a weighted upstream differencing scheme that locally adjusts the weighting to prevent oscillatory behavior and maximize solution accuracy. The weighting parameters are known as the TVD flux limiters $\Phi(x, y, r)$, where r is a function of the concentration gradient and direction of flow. PA uses the van Leer TVD limiter (Sweby 1984, p. 1005), which is defined as

$$\Phi(x,y,r) = \max\left\{0, \min\left\{2r, \frac{r+|r|}{1+|r|}\right\}\right\} \quad \text{(PA.285)}$$

At locations where u (i.e., the Darcy velocity in the x direction) is positive, r is defined at the j -1/2, k interface by

$$r_{j-1/2,k} = \frac{\partial C/\partial x|_{j-3/2,k}}{\partial C/\partial x|_{j-1/2,k}} \quad \text{(PA.286)}$$

and at locations where u is negative, r is defined by

$$r_{j-1/2,k} = \frac{\partial C/\partial x|_{j+1/2,k}}{\partial C/\partial x|_{j-1/2,k}} \quad \text{(PA.287)}$$

Similar definitions are made for r at the j, k -1/2 interface in the y-direction with v (i.e., the Darcy velocity in the y direction) used instead of u.

Because Φ_k is a function of C_k, the discretized set of equations is nonlinear. This nonlinearity is addressed by treating the flux limiters explicitly (i.e., time lagged). Explicit treatment of the limiter functions, however, can lead to oscillatory and sometimes unstable solutions when the Courant number exceeds unity ($Cr > 1$), where Cr is defined by

$$Cr = \max\{Cr_x, Cr_y\}, \quad \text{where } Cr_x = |u|\Delta t/\phi\Delta x \text{ and } Cr_y = |v|\Delta t/\phi\Delta y$$

(PA.288)

To avoid this behavior, the application of the TVD method is restricted to regions in which the Courant numbers are less than one. In regions where $Cr > 1$, a first-order full upwinding scheme is invoked, which is unconditionally stable and nonoscillatory.

The discretized form of Equation (PA.268) can be expressed in a delta formulation as

$$\left(\mathbf{I}+\mathbf{L}_{xx}+\mathbf{L}_{yy}+\mathbf{S}\right)\Delta\mathbf{C}^{n+1}=\mathbf{RHS}^{n} \quad \text{(PA.289)}$$

where $\mathbf{I}$ is the identity matrix, $\mathbf{L}_{xx}$ and $\mathbf{L}_{yy}$ are finite-difference operators in the x and y directions, $\mathbf{S}$ is an implicit source term that accounts for decay and mass transfer between the matrix and the fracture, **RHS** consists of the right-hand-side known values at time level n, and $\Delta\mathbf{C}_{n}+1=\mathbf{C}_{n}+1-\mathbf{C}_{n}$. Direct inversion of Equation (PA.289) for a typical Culebra transport problem is very computationally intensive, requiring large amounts of memory and time. To reduce these requirements, the operator in Equation (PA.289) is factored as follows:

$$\left(\mathbf{I}+\mathbf{L}_{xx}+\alpha_{x}\mathbf{S}\right)\left(\mathbf{I}+\mathbf{L}_{yy}+\alpha_{y}\mathbf{S}\right)\Delta\mathbf{C}^{n+1}=\mathbf{RHS}^{n} \quad \text{(PA.290)}$$

where a_x and a_y are constants that must sum to one (i.e., $a_x + a_y = 1$). The left-hand sides in Equation (PA.289) and Equation (PA.290) are not equivalent, with the result that the factorization of Equation (PA.289) and Equation (PA.290) is referred to as an approximate factorization (Fletcher 1988). The advantage of approximately factoring Equation (PA.289) is that the resulting equation consists of the product of two finite-difference operators that are easily inverted independently using a tridiagonal solver. Hence, the solution to the original problem is obtained by solving a sequence of problems in the following order:

$$\left(\mathbf{I}+\mathbf{L}_{xx}+\alpha_{x}\mathbf{S}\right)\Delta\bar{\mathbf{C}}=\mathbf{RHS}^{n} \quad \text{(PA.291)}$$

$$\left(\mathbf{I}+\mathbf{L}_{yy}+\alpha_{y}\mathbf{S}\right)\Delta\mathbf{C}^{n+1}=\Delta\bar{\mathbf{C}} \quad \text{(PA.292)}$$

$$\mathbf{C}^{n+1}=\mathbf{C}^{n}+\Delta\mathbf{C}^{n+1} \quad \text{(PA.293)}$$

PA-4.9.2.2 Discretization of Matrix Equation

The nonuniform mesh used to discretize the matrix equation is shown in Figure PA-32. Straightforward application of standard finite-difference or finite-volume discretizations on nonuniform meshes results in truncation error terms that are proportional to the mesh spacing variation (Hirsch 1988). For nonuniform meshes, the discretization can be performed after a transformation from the Cartesian physical space (χ) to a stretched Cartesian computational space (ξ). The transformation is chosen so that the nonuniform grid spacing in physical space is transformed to a uniform spacing of unit length in computational space (the computational space is thus a one-dimensional domain with a uniform mesh). The transformed equations contain metric coefficients that must be discretized, introducing the mesh size influence into the difference formulas. Standard unweighted differencing schemes can then be applied to the governing equations in the computational space.

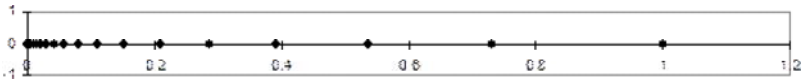

Figure PA- 32. Illustration of Stretched Grid Used for Matrix Domain Discretization

The SECOTP2D code applies such a coordinate transformation to the nonuniform diffusion domain mesh, solving the transformed system of equations in the uniform computational space. The transformed matrix equation is written as

$$\phi' R'_k \frac{\partial \dot{C}'_k}{\partial t} - \frac{\partial \dot{F}'_v}{\partial \xi'} = -\phi' R'_k \lambda_k \dot{C}'_k + \phi' R'_{k-1} \lambda_{k-1} \dot{C}'_{k-1} \quad \text{(PA.294)}$$

where

$$\dot{C}'_k = \frac{C'_k}{J} \quad \text{(PA.295)}$$

$$\dot{F}'_v = D' \xi'_x \frac{\partial C'_k}{\partial \xi'} \quad \text{(PA.296)}$$

In the uniform computational space, a first-order backwards difference formula is used to approximate the temporal derivative, while a second-order accurate central difference is used to approximate spatial derivatives.

PA-4.9.2.3 Fracture-Matrix Coupling

The equations for the fracture and the matrix are coupled through the mass transfer term, Γ_k. In the numerical solution, these equations are coupled in a fully implicit manner and solved simultaneously. A procedure outlined in Huyakorn, Lester, and Mercer (1983) was adapted and redeveloped for an approximate factorization algorithm with the delta formulation and a finite-volume grid. The coupling procedure consists of three steps:

Step 1. Write the mass transfer term Γ_k in a delta (Δ) form.

Step 2. Evaluate Δ terms that are added to the implicit part of the fracture equation. This is accomplished using the inversion process (LU factorization) in the solution of the matrix equation. After the construction of the lower tridiagonal matrix L and the intermediate solution, there is enough information to evaluate the Δ terms. This new information is fed into the fracture equation that is subsequently solved for concentrations in the fracture at the new time level (n+1).

Step 3. Construct the boundary condition for the matrix equation at the fracture-matrix interface using fracture concentrations at the (n+1) time level. Matrix concentrations are then obtained using the upper tridiagonal matrix U by back substitution. A detailed description of this technique and its implementation is given in the SECOTP2D user's manual (WIPP Performance Assessment 1997b).

PA-4.9.2.4 Cumulative Releases

The cumulative transport $C_k(t, B)$ of individual radionuclides across specified boundaries indicated in Equation (PA.284) is also accumulated during the numerical solution of Equation (PA.268) and Equation (PA.275).

PA-4.9.3 Additional Information

Because neither the Culebra flow fields nor the random seed used in LHS sampling have been changed from the CRA-2009 PABC, the radionuclide transport calculations from the CRA-2009 PABC were used in the CRA-2014 PA. Additional information on SECOTP2D and its use to determine radionuclide transport in the Culebra can be found in the SECOTP2D user's manual (WIPP Performance Assessment 1997b) and in the CRA-2009 PABC analysis package for radionuclide transport in the Culebra Dolomite (Kuhlman 2010).

PA-5.0 Probabilistic Characterization of Subjective Uncertainty

This section summarizes the treatment of uncertainty in the CRA-2014 PA parameters. This uncertainty gives rise to the epistemic uncertainty in the CCDFs defined in Section PA-2.2.4.

PA-5.1 Probability Space

As discussed in Section PA-2.2.4, the statement of confidence in the CCDFs of releases from the CRA-2014 PA is based on a probabilistic characterization of the uncertainty in important input parameters to the analysis. The probability distribution for each parameter is based on all available knowledge about the parameter, including measurements, and describes a degree of belief as to the appropriate range of the parameter value. This degree of belief depends on the numerical, spatial, and temporal resolution of the models selected for use in PA (Section PA-4.0). Correlations and other dependencies between imprecisely known variables are also possible. These relationships represent observed or logical dependencies between the possible parameter values.

The probability space that characterizes epistemic uncertainty can be represented as ($\mathbb{S}_{su}$, $\mathbb{S}_{su}$, p_{su}). The subscript *su* indicates that epistemic (i.e., subjective) uncertainty is being considered. The individual elements of $\mathbb{S}_{su}$ are vectors $\mathbf{v}_{su}$ of the form

$$\mathbf{v}_{su} = [v_1, v_2, \ldots, v_{nv}] \quad \text{(PA.297)}$$

where each v_j is an imprecisely known input to the analysis, and nv is the number of such inputs.

The uncertainty in the v_j , and hence in $\mathbf{v}_{su}$, is characterized by developing a distribution

$$D_j, \; j = 1, 2, \ldots, nV \quad \text{(PA.298)}$$

for each v_j . It is the distributions in Equation (PA.297) and any associated correlations between the v_j that define ($\mathbb{S}_{su}$, $\mathbb{S}_{su}$, p_{su}).

The uncertain parameters incorporated into the CRA-2014 PA are discussed in Section PA-5.2, and the distributions and correlations assigned to these variables are described in Section PA-6.4 and Kicker and Herrick (Kicker and Herrick 2013), Table 4. Finally, a discussion of the concept of a scenario is given in Section PA-5.3.

PA-5.2 Variables Included for Subjective Uncertainty

The CRA-2014 PA identified 63 imprecisely known variables for inclusion in the analysis (see Kicker and Herrick 2013, Table 4). Most of the uncertain variables in the CRA-2014 PA were also treated as uncertain in the CRA-2009 PA. Most uncertain parameter additions and removals in the CRA-2014 PA relative to the CRA-2009 PA are due to the replacement of the Option D panel closure system with the ROMPCS and the refinement to the water budget implementation that includes MgO hydration. Table PA-15 and Table PA-16 list the additions and removals between the sets of uncertain parameters in the CRA-2009 PA and the CRA-2014 PA. All subjectively uncertain variables incorporated into the CRA-2014 PA are used as input to the models discussed in Section PA-2.2.3 and Section PA-4.0.

Table PA- 15. Sampled Parameters Added Since the CRA-2009 PA

Material	Property	Description

PCS_T1	PRMX_LOG	$\log_{10}$ of intrinsic permeability, X direction
PCS_T1	SAT_RGAS	Residual gas saturation
PCS_T1	SAT_RBRN	Residual brine saturation
PCS_T1	PORE_DIS	Brooks-Corey pore distribution parameter
PCS_T1	POROSITY	Porosity
PCS_T2	POROSITY	Porosity
PCS_T2	POR2PERM	Quantity used to calculate intrinsic permeability using sampled porosity values
PCS_T3	POROSITY	Porosity
WAS_AREA	BRUCITEC	MgO inundated hydration rate in ERDA-6 brine
WAS_AREA	BRUCITES	MgO inundated hydration rate in Generic Weep Brine (GWB)
WAS_AREA	BRUCITEH	MgO humid hydration rate
WAS_AREA	HYMAGCON	Rate of conversion of hydromagnesite to magnesite

Table PA- 16. Sampled Parameters Removed Since the CRA-2009 PA

Material	Property	Description
CELLULS	FBETA	Factor beta for microbial reaction rates
CONC_PCS	PRMX_LOG	$\log_{10}$ of intrinsic permeability, X direction
CONC_PCS	SAT_RGAS	Residual gas saturation
CONC_PCS	SAT_RBRN	Residual brine saturation
CONC_PCS	PORE_DIS	Brooks-Corey pore distribution parameter

Each uncertain variable is assigned a distribution that characterizes the subjective uncertainty in that variable. Distributions for each parameter are described in Kicker and Herrick (Kicker and Herrick 2013) Table 4, which also contains documentation for each of the 63 parameters sampled by the LHS code during the PA. The set of subjectively uncertain variables are listed in Table PA-17. The input files used for PA code STEPWISE use short names for input parameters rather than material:property designations used in other codes. These short names are required because of a limitation in the length of variable names in STEPWISE. The short names used in STEPWISE are listed in Table PA-17 under the "Name" column, and are taken from Table 1 of Kirchner (2013b).

Table PA- 17. Variables Representing Epistemic Uncertainty in the CRA-2014 PA

Material	Property	Name	Description
AM+3	MKD_AM	CMKDAM3	Matrix distribution coefficient (m^3/kg) for Am in the III oxidation state. Defines K_{dk} in Equation (PA.276).
BH_SAND	PRMX_LOG	BHPERM	Logarithm of intrinsic permeability (m^2) of the silty-sand-filled borehole (Table PA-7). Used in regions Upper Borehole and Lower Borehole in Figure PA-12.
BOREHOLE	DOMEGA	DOMEGA	Drill string angular velocity (rad/s). Defines $\Delta\Omega$ in Equation (PA.139).
BOREHOLE	TAUFAIL	WTAUFAIL	Shear strength of waste (Pa). Defines $\tau(R, 1)$ in Equation (PA.137).
CASTILER	COMP_RCK	BPCOMP	Bulk compressibility (Pa^{-1}) of Castile brine reservoir. Defines c_{fB} in Equation (PA.35) for region CASTILER of Figure PA-12.
CASTILER	PRESSURE	BPINTPRS	Initial brine pore pressure in the Castile brine reservoir (region CASTILER in Figure PA-12).
CASTILER	PRMX_LOG	BPPRM	Logarithm of intrinsic permeability (m^2) of the Castile brine reservoir. Used in region CASTILER in Figure PA-12.
CONC_PLG	PRMX_LOG	PLGPRM	Logarithm of intrinsic permeability (m^2) of the concrete borehole plugs (Table PA-7). Used in region Borehole Plugs in Figure PA-12.
CULEBRA	APOROS	CFRACPOR	Culebra fracture (i.e., advective) porosity (dimensionless). Defines ϕ in Equation (PA.268).
CULEBRA	DPOROS	CMTRXPOR	Culebra matrix (i.e., diffusive) porosity (dimensionless). Defines ϕ' in Equation (PA.275).

CULEBRA	HMBLKLT	CFRACSP	Culebra fracture spacing (m). Equal to half the distance between fractures (i.e., the Culebra half-matrix-block length).
CULEBRA	MINP_FAC	CTRANSFM	Multiplier (dimensionless) applied to transmissivity of the Culebra within the LWB after mining of potash reserves. Defines *MF* in Equation (PA.261) (see Section PA-4.8.2).
DRZ_1	PRMX_LOG	DRZPRM	Logarithm of intrinsic permeability (m^2) of the DRZ. Used in regions Upper DRZ and Lower DRZ in Figure PA-12.
DRZ_PCS	PRMX_LOG	DRZPCPRM	Logarithm of intrinsic permeability (m^2) of the DRZ immediately above and below the panel closure (Section PA-4.2.8). Used in region DRZ_PCS in Figure PA-12.
GLOBAL	CLIMTIDX	CCLIMSF	Climate scale factor (dimensionless) for Culebra flow field. Defines *SFC* in Equation (PA.266).
GLOBAL	OXSTAT	WOXSTAT	Indicator variable for elemental oxidation states (dimensionless). WOXSTAT <= 0.5 indicates radionuclides in lower oxidation states. WOXSTAT >0.5 indicates radionuclides in higher oxidation states.

Table PA-17. Variables Representing Epistemic Uncertainty in the CRA-2014 PA (Continued)

Material	Property	Name	Description
GLOBAL	PBRINE	PBRINE	Probability that a drilling intrusion penetrates pressurized brine in the Castile. Defines pB_1; see Section PA-3.6.
GLOBAL	TRANSIDX	CTRAN	Indicator variable for selecting T-field. See Section PA-4.8.2.
PCS_T1	PORE_DIS	T1PDIS	Brooks-Corey pore distribution parameter
PCS_T1	POROSITY	T1POROS	Effective porosity
PCS_T1	PRMX_LOG	T1PRMX	Log of intrinsic permeability, X-direction
PCS_T1	SAT_RBRN	T1SRBRN	Residual Brine Saturation
PCS_T1	SAT_RGAS	T1SRGAS	Residual Gas Saturation
PCS_T2	POR2PERM	T2P2PERM	Distribution used to calculate permeability from sampled porosity values
PCS_T2	POROSITY	T2POROS	Effective porosity
PCS_T3	POROSITY	T3POROS	Effective porosity
PHUMOX3	PHUMCIM	WPHUMOX3	Ratio (dimensionless) of concentration of actinides attached to humic colloids to dissolved concentration of actinides for oxidation state III in Castile brine.
PU+3	MKD_PU	CMKDPU3	Matrix distribution coefficient (m^3/kg) for Pu in III oxidation state. Defines K_{dk} in Equation (PA.276).
PU+4	MKD_PU	CMKDPU4	Matrix distribution coefficient (m^3/kg) for Pu in IV oxidation state. Defines K_{dk} in Equation (PA.276).
S_HALITE	COMP_RCK	HALCROCK (previously HALCOMP)	Bulk compressibility of halite (Pa^{-1}). Defines c_r in Equation (PA.37) for Salado region of Figure PA-12.
S_HALITE	POROSITY	HALPOR	Halite porosity (dimensionless). Defines ϕ_0 in Equation (PA.30) for Salado region in Figure PA-12.
S_HALITE	PRESSURE	SALPRES	Initial brine pore pressure (Pa) in the Salado halite, applied at an elevation consistent with the intersection of MB 139. Defines $p_{b,ref}$ for Equation (PA.53) for Salado region in Figure PA-12.
S_HALITE	PRMX_LOG	HALPRM	Logarithm of intrinsic halite permeability (m^2). Used in region Salado in Figure PA-12.
S_MB139	PORE_DIS	ANHBCEXP	Brooks-Corey pore distribution parameter for anhydrite (dimensionless). Defines λ in Equation (PA.38), Equation (PA.39), and Equation (PA.40) for regions MB 138, Anhydrite AB, and MB 139 of Figure PA-12 for use with Brooks-Corey model; defines λ in $m = \lambda/(1+\lambda)$ in Equation (PA.44), Equation (PA.45), and Equation (PA.46) for use with van Genuchten-Parker model in the same regions.
S_MB139	PRMX_LOG	ANHPRM	Logarithm of intrinsic anhydrite permeability (m^2). Used in regions MB 138, Anhydrite AB, and MB 139 in Figure PA-12.

Table PA-17. Variables Representing Epistemic Uncertainty in the CRA-2014 PA (Continued)

Material	Property	Name	Description
S_MB139	RELP_MOD	ANHBCVGP	Indicator for relative permeability model (dimensionless) for regions MB 138, Anhydrite AB, and MB 139 in Figure PA-12. See Table PA-4.
S_MB139	SAT_RBRN	ANRBRSAT	Residual brine saturation in anhydrite (dimensionless). Defines S_{br} in Equation (PA.43) for regions MB 138, Anhydrite AB, and MB 139 in Figure PA-12.
SHFTL_T1	PRMX_LOG	SHLPRM2	Logarithm of intrinsic permeability (m^2) of lower shaft-seal materials for the first 200 years after closure. Used in Lower Shaft region in Figure PA-12.
SHFTL_T2	PRMX_LOG	SHLPRM3	Logarithm of intrinsic permeability (m^2) of lower shaft-seal materials from 200 years to 10,000 years after closure. Used in Lower Shaft region in Figure PA-12.
SHFTU	PRMX_LOG	SHUPRM	Logarithm of intrinsic permeability (m^2) of upper shaft-seal materials. Used in Upper Shaft region in Figure PA-12.
SHFTU	SAT_RBRN	SHURBRN	Residual brine saturation in upper shaft-seal materials (dimensionless). Defines S_{br} in Equation (PA.43) for Upper Shaft region in Figure PA-12.
SHFTU	SAT_RGAS	SHURGAS	Residual gas saturation in upper shaft-seal materials (dimensionless). Defines S_{gr} in Equation (PA.42) for Upper Shaft region in Figure PA-12.
SOLMOD3	SOLVAR	WSOLVAR3	Solubility multiplier (dimensionless) for III oxidation states. Used by ALGEBRA prior to PANEL (Section PA-4.4, Brush and Domski 2013c).
SOLMOD4	SOLVAR	WSOLVAR4	Solubility multiplier (dimensionless) for IV oxidation states. Used by ALGEBRA prior to PANEL (Section PA-4.4, Brush and Domski 2013c).
SPALLMOD	PARTDIAM	SPPDIAM (previously SPLPTDIA, WPRTDIAM)	Particle diameter of waste (m) after tensile failure, implemented by parameter SPALLMOD/PARTDIAM. Loguniform distribution from 0.001 to 0.1 (m). Defines d_p in Equation (PA.192).
SPALLMOD	REPIPERM	REPIPERM	Waste permeability of gas (m^2) local to intrusion borehole. Defines k in Equation (PA.174).
SPALLMOD	REPIPOR	SPLRPOR	Waste porosity (dimensionless) at time of drilling intrusion. Defines ϕ in Equation (PA.173).
SPALLMOD	TENSLSTR	TENSLSTR	Tensile strength (Pa) of waste. Defines $\bar{\sigma}_T$ in Section PA-4.6.2.3.4.
STEEL	CORRMCO2	WGRCOR	Rate of anoxic steel corrosion (m/s) under brine-inundated conditions with no CO_2 present. Defines R_{ci} in Equation (PA.67) for areas Waste Panel, South RoR, and North RoR in Figure PA-12.
TH(IV)	MKD_TH	CMKDTH4	Matrix distribution coefficient (m^3/kg) for Th in IV oxidation state. Defines K_{dk} in Equation (PA.276).
U(IV)	MKD_U	CMKDU4	Matrix distribution coefficient (m^3/kg) for U in IV oxidation state. Defines K_{dk} in Equation (PA.276).
U(VI)	MKD_U	CMKDU6	Matrix distribution coefficient (m^3/kg) for U in VI oxidation state. Defines K_{dk} in Equation (PA.276).
WAS_AREA	BIOGENFC	WBIOGENF	Probability of obtaining sampled microbial gas generation rates.
WAS_AREA	BRUCITEC	WBRUITEC	Waste emplacement area and waste,MgO inundated hydration rate in ERDA-6 brine
WAS_AREA	BRUCITEH	WBRUITEH	Waste emplacement area and waste,MgO humid hydration rate
WAS_AREA	BRUCITES	WBRUITES	Waste emplacement area and waste,MgO inundated hydration rate in GWB
WAS_AREA	GRATMICH	WGRMICH	Rate of CPR biodegradation (mol $C_6H_{10}O_5$ / kg $C_6H_{10}O_5$ /s) under anaerobic, humid conditions.
WAS_AREA	GRATMICI	WGRMICI	Rate of CPR biodegradation (mol $C_6H_{10}O_5$ / kg $C_6H_{10}O_5$ /s) under anaerobic, brine-inundated conditions.
WAS_AREA	HYMAGCON	WHYMAGC	Waste emplacement area rate of conversion of hydromagnesite to magnesite

Table PA-17. Variables Representing Epistemic Uncertainty in the CRA-2014 PA (Continued)

Material	Property	Name	Description
WAS_AREA	PROBDEG	WMICDFLG	Index for model of CPR material microbial degradation (dimensionless). Used in Waste Panel, South RoR, and North RoR areas in Figure PA-12.
WAS_AREA	SAT_RBRN	WRBRNSAT	Residual brine saturation in waste (dimensionless). Defines S_{br} in Equation (PA.42) for Waste Panel, South RoR, and North RoR areas in Figure PA-12; also used in waste material in Figure PA-24 for DBR calculation; see Section PA-4.7.
WAS_AREA	SAT_RGAS	WRGSSAT	Residual gas saturation in waste (dimensionless). Defines S_{gr} in Equation (PA.43) for Waste Panel, South RoR, and North RoR areas in Figure PA-12; also used in waste material in Figure PA-24 for DBR calculation; see Section PA-4.7.
WAS_AREA	SAT_WICK	WASTWICK	Increase in brine saturation of waste due to capillary forces (dimensionless). Defines S_{wick} in Equation (PA.99) for Waste Panel, South RoR, and North RoR areas in Figure PA-12.

PA-5.3 Separation of Aleatory and Epistemic Uncertainty

PA uses the term *scenario* to refer to specific types of events within the sample space for aleatory uncertainty (E0, E1, E2, or E1E2; see Section PA-3.10). This definition is consistent with the concept that a scenario is something that could happen in the future. A future contains events of the form defined in Equation (PA.2) and is associated with a probability, one that characterizes the likelihood that a possible future will match the occurrences that will take place at the WIPP over the next 10,000 years. In contrast, the probability associated with a specific vector $\mathbf{v}_{su}$, i.e., a specific set of parameter values, characterizes a degree of belief that the vector contains the appropriate values for the 63 uncertain variables in CRA-2014 PA. The distribution of epistemic vectors defines the impact of parameter uncertainty over the full range of possible futures and is used to establish confidence in the results.

PA-6.0 Computational Procedures

This section outlines the computational procedures used to execute the CRA-2014 PA. First, the sampling procedures applied to evaluate performance accounting for epistemic and aleatory uncertainty are outlined. The mechanistic calculations used to evaluate the function $f(\mathbf{x}_{st})$ in Equation (PA.23) are tabulated, followed by a description of the algorithms used to compute releases. This section concludes with a discussion of sensitivity analysis techniques used to identify which uncertain parameters are primary contributors to the uncertainty in the PA results.

PA-6.1 Sampling Procedures

Extensive use is made of sampling procedures in PA. In particular, simple random sampling is used to generate individual CCDFs (Section PA-2.2.3) and LHS is used to assess the effects of imprecisely known model parameters (Section PA-2.2.4).

Using simple random sampling, a possible future, $\mathbf{x}_{st,i,k}$, is characterized by the collection of intrusion events occurring in that future (see Section PA-2.2.2). The subscript *st* denotes that intrusion is modeled as a stochastic (or random) process, the subscript *i* indicates that the future is one of many possible futures, and the subscript *k* indicates that the vector of uncertain parameter sampled values is one of many such vectors. The *nR* sets of values (possible futures) are selected according to the joint probability distribution for the elements of $\mathbb{S}_{st}$ as defined by ($\mathbb{S}_{st}$, $\mathbb{S}_{st}$, p_{st}). In practice, the joint probability distribution is defined by specifying a distribution D_j for each element x_j of $\mathbb{S}_{st}$. Points from different regions of the sample space occur in direct relationship to the probability of occurrence of these regions. Furthermore, each sample element is selected independently of all other sample elements. The values selected using simple random sampling provide unbiased estimates for means, variances, and distributions of the variables. The collection of *nR* samples can be denoted as a vector $\mathbf{x}_{st,k}$:

$$\mathbf{x}_{st,k} = \left[\mathbf{x}_{st,1,k}, \mathbf{x}_{st,2,k}, \ldots, \mathbf{x}_{st,nR,k}\right] \quad \text{(PA.299)}$$

The WIPP PA code CCDFGF is used to simulate possible futures based on the values of the variables sampled. These variables control the stochastic processes defined within CCDFGF, such as the time when a drilling intrusion can take place, where that drilling intrusion is located, and whether the drilling intrusion encounters an excavated area. The code CCDFGF is capable of generating and evaluating thousands of possible futures; PA uses a sample size (*nR*) of 10,000 to generate a distribution of possible repository releases. This sample size is sufficient to estimate the 0.999 quantile for the distribution of releases to the accessible environment.

LHS is used to sample the parameters for which distributions of epistemic uncertainty were defined to integrate over the probability space for subjective uncertainty ($\mathbb{S}_{su}$, $\mathbb{S}_{su}$, p_{su}). This technique was first introduced by McKay, Beckman, and Conover (1979). In LHS, the range of each uncertain parameter v_j is divided into *nLHS* intervals of equal probability and one value is selected at random from each interval. The *nLHS* values thus obtained for v_1 are paired at random without replacement with the *nLHS* values obtained for v_2. These *nLHS*

pairs are combined in a random manner without replacement with the *nLHS* values of v_3 to form *nLHS* triples. This process is continued until a set of *nLHS* *nV*-tuples is formed. These *nV*-tuples are of the form

$$\mathbf{v}_{stu,k} = \left[v_{k,1}, v_{k,2}, \ldots, v_{k,nV} \right], \; k = 1, \ldots, nLHS \quad \text{(PA.300)}$$

and constitute the Latin hypercube sample. The individual v_j s must be independent of each other for the preceding construction procedure to work. For more information about LHS and a comparison with other sampling techniques, see Helton and Davis (Helton and Davis 2003).

LHS stratifies the sampling to ensure that the sampled values cover the full range of each v_j in the *nLHS* samples. LHS provides unbiased estimates for means and distribution functions of each sampled variable (McKay, Beckman, and Conover 1979). In particular, uncertainty and sensitivity analysis results obtained with LHS are robust even when relatively small samples (i.e., *nLHS* = 50 to 200) are used (Iman and Helton 1988 and Iman and Helton 1991; Helton et al. 1995).

When sampling for both aleatory uncertainty and epistemic uncertainty are considered, the joint sample space, $\mathbf{x}$, consists of a vector of *nLHS* vectors of possible futures:

$$\mathbf{x} = \left[\mathbf{x}_{st,1}, \mathbf{x}_{st,2}, \ldots, \mathbf{x}_{st,nLHS} \right] \quad \text{(PA.301)}$$

The differences between the *nLHS* futures are due to the uncertainty in the v_j, i.e. the epistemic uncertainty in model parameters.

PA-6.2 Sample Size for Incorporation of Subjective Uncertainty

Section 194.34(d) states that

> The number of CCDFs generated shall be large enough such that, at cumulative releases of 1 and 10, the maximum CCDF generated exceeds the 99th percentile of the population of CCDFs with at least a 0.95 probability.

For an LHS of size *nLHS*, the preceding guidance is equivalent to the inequality

$$1 - 0.99^{nLHS} > 0.95 \quad \text{(PA.302)}$$

which results in a minimum value of 298 for *nLHS*. PA uses a total sample size of 300 to represent the epistemic uncertainty. As discussed in the next section, the 300 samples are divided among 3 replicates of size 100 each to demonstrate convergence of the mean for the population of CCDFs.

PA-6.3 Statistical Confidence on Mean CCDF

Section 194.34(f) states,

> Any compliance assessment shall provide information which demonstrates that there is at least a 95% level of statistical confidence that the mean of the population of CCDFs meets the containment requirements of § 191.13 of this chapter.

Given that LHS is used, the confidence intervals required by section 194.34(f) are obtained with a replicated sampling technique proposed by Iman (Iman 1982). In this technique, the sampling in Equation (PA.303) is repeated *nS* times with different random seeds. These samples lead to a sequence $\bar{P}_r(R)$, $r = 1, 2, \ldots, nS$ of estimated mean exceedance probabilities, where $\bar{P}_r(R)$ defines the mean CCDF obtained for sample *r* (i.e., $\bar{P}_r(R)$ is the mean probability that a normalized release of size *R* will be exceeded; see Section PA-2.2.4) and *nS* is the number of independent samples generated with different random seeds. The seed of the random number generator determines the sequence of the numbers it generates. Then,

$$\bar{P}(R) = \sum_{r=1}^{nS} \bar{P}_r(R) / nS \quad \text{(PA.303)}$$

and

$$SE(R) = \left\{ \sum_{r=1}^{nS} \left[\bar{P}_r(R) - \bar{P}(R) \right]^2 / nS(nS-1) \right\}^{1/2} \quad \text{(PA.304)}$$

provide an additional estimate of the mean CCDF and an estimate of the standard error ($SE(R)$) associated with the mean exceedance probabilities. The t-distribution with $nS - 1$ degrees of freedom can be used to place confidence intervals around the mean exceedance probabilities for individual *R* values (i.e., around $\bar{P}(R)$). Specifically, the $1 - \alpha$ confidence interval is given by $\bar{P}_r(R) \pm t_{1-\alpha/2} SE(R)$, where $t_{1-\alpha/2}$ is the $1 - \alpha/2$ quantile of the t-distribution with $nS - 1$ degrees of freedom (e.g., $t_{1-\alpha/2} = 4.303$ for $\alpha = 0.05$ and $nS = 3$). The same procedure can also be used to place pointwise confidence intervals around percentile curves. The mean and its standard error could equally well be computed from one replicate of size 300. However, the use of three replicates, each with its own random seed, minimizes the impact

of any one seed used in random number generation. The three replicates have also been useful in evaluating the presence of spurious correlations among parameters and releases in the sensitivity analyses.

PA-6.4 Generation of Latin Hypercube Samples

The LHS program (WIPP Performance Assessment 2005) is used to produce three independently generated Latin hypercube samples of size *nLHS* = 100 each, for a total of 300 sample elements. Each individual replicate is a Latin hypercube sample of the form

$$\mathbf{v}_{SR,k} = \left[v_{k,1}, v_{k,2}, \ldots, v_{k,nV} \right], \; k = 1, 2, \ldots, nLHS = 100 \quad \text{(PA.305)}$$

In the context of the replicated sampling procedure described in Section PA-6.2, *nS* = 3 replicates of 100 are used. For notational convenience, the replicates are designated by R1, R2, and R3.

The restricted pairing technique described in Section PA-6.1 is used to induce requested correlations and also to assure that uncorrelated variables have correlations close to zero. The variable pairs (S_HALITE:PRMX_LOG, S_HALITE:COMP_RCK) and (CASTILER: PRMX_LOG, CASTILER:COMP_RCK) are assigned rank correlations of –0.99 and –0.75, respectively. All other variable pairs are assigned rank correlations of zero. The restricted pairing technique successfully produces these correlations (Table PA-18). Correlated variables have correlations that are close to their specified values.

Table PA- 18. Observed and Expected Correlations Between Variable Pairs (S_HALITE:COMP_RCK, S_HALITE:PRMX_LOG) and (CASTILER:COMP_RCK ,CASTILER:PRMX_LOG)

Replicate	Between		Expected Correlation	Observed Correlation
1	CASTILER:COMP_RCK	CASTILER:PRMX_LOG	-0.75	-0.7281
	S_HALITE:COMP_RCK	S_HALITE:PRMX_LOG	-0.99	-0.9869
2	CASTILER:COMP_RCK	CASTILER:PRMX_LOG	-0.75	-0.7242
	S_HALITE:COMP_RCK	S_HALITE:PRMX_LOG	-0.99	-0.9907
3	CASTILER:COMP_RCK	CASTILER:PRMX_LOG	-0.75	-0.7252
	S_HALITE:COMP_RCK	S_HALITE:PRMX_LOG	-0.99	-0.9834

The code LHS_EDIT (Kirchner 2013a) was used to enforce a conditional relationship between three pairs of variables. The relationships were WAS_AREA:GRATMICH ≤ WAS_AREA:GRATMICI (Clayton 2008a, Nemer and Stein 2005) and PCS_T3: POROSITY ≤ PCS_T2: POROSITY ≤ PCS_T1:POROSITY (Camphouse 2013d). The relationships were enforced by modifying values in the LHS transfer file, thus making the conditioned values available for use in the sensitivity analysis. For each pair of variables LHS_EDIT rescales the sampled value of the parameter to the left of the ≤ symbol to the new "controlled" value using the equation

$$v_i' = \frac{v_i - U_{V,lower}}{U_{V,upper} - U_{V,lower}} \times \left\{ \min(x_i, U_{V,upper}) - U_{V,lower} \right\} + U_{V,lower} \quad \text{(PA.306)}$$

where v_i' is the conditioned value of the left hand variable, v_i is the sampled value of that variable, x_i is the sampled value of the right hand variable, and $U_{V,lower}$ and $U_{V,upper}$ are the bounds of the distribution assigned to the left hand variable. This method preserves the probability associated with the value of the left hand variable.

PA-6.5 Generation of Individual Futures

Simple random sampling (Section PA-6.1) is used to generate 10,000 possible futures that are then used to construct CCDFs of potential releases. Table PA-19 outlines the algorithm used to generate a single future in PA.

Table PA- 19. Algorithm to Generate a Single Future

1. Sample $t_{i,1}$ with a time dependent λ_d given by $\lambda_d(t) = \begin{cases} 0 & \text{if } 0 \le t \le t_A \\ \lambda_d & \text{if } t > t_A \end{cases}$ where t_A = 100 yr (i.e., time at which administrative control ends) and $\lambda_d = 4.23 \times 10^{-3}$ yr^{-1} (see Section PA-3.3). The index i is the number of the future and 1 represents the first intrusion event.
2. Sample $e_{i,1}$ with a probability of $p[E0] = 0.797$ that the intrusion will be in an unexcavated area and a probability of $p[E1] = 0.203$ that the intrusion will be in an excavated area (see Section PA-3.4).
3. Sample $l_{i,1}$ with a probability of $p[L_j] = 6.94 \times 10^{-3}$ for each of the j = 1, 2, …, 144 nodes in Figure PA-11 (see Section PA-3.5).
4. Sample $b_{i,1}$ with a probability of $p[B_1]$ that the intrusion will penetrate pressurized brine (see Section PA-3.6). $p[B_1]$ is sampled from a normal distribution ranging from 0.06 to 0.19.

5. Sample $p_{i,1}$ with probabilities of $p[PL1] = 0.04$, $p[PL2] = 0.594$, and $p[PL3] = 0.366$ that plugging pattern 1, 2, or 3, respectively, will be used (see Section PA-3.7).
6. Sample the activity level $\mathbf{a}_{i,1}$ (see Section PA-3.8).
6.1 Penetration of nonexcavated area (i.e., $e_{i,1} = 0$): $\mathbf{a}_{i,1} = a_{i,1} = 0$.
6.2 Penetration of excavated area (i.e., $e_{i,1} = 1$): Sample to determine if intrusion penetrates RH-TRU or CH- TRU waste with probabilities of $p[RH] = 0.124$ and $p[CH] = 0.876$ of penetrating RH-TRU and CH-TRU waste, respectively.
6.3 Penetration of RH-TRU waste: $\mathbf{a}_{i,1} = a_{i,1} = 1$.
6.4 Penetration of CH-TRU waste: Use probabilities $p[CH_j]$ of intersecting waste stream j, $j = 1, 2, \ldots, 451$, (see Kicker and Zeitler 2013a) to independently sample three intersected waste streams $iCH1$, $iCH2$, $iCH3$ (i.e., each of $iCH1$, $iCH2$, $iCH3$ is an integer between 1 and 451). Then, $\mathbf{a}_{i,1} = [2, iCH1, iCH2, iCH3]$.
7. Repeat Steps 1 - 6 to determine properties (i.e., $t_{i,j}$, $e_{i,j}$, $l_{i,j}$, $b_{i,j}$, $p_{i,j}$, $\mathbf{a}_{i,j}$) of the j^{th} drilling intrusion.
8. Continue until $t_{n+1} > 10{,}000$ yr; the n intrusions thusly generated define the drilling intrusions associated with $\mathbf{x}_{st,i}$.
9. Sample t_{min} with a time dependent λ_m given by $\lambda_m(t) = \begin{cases} 0 & \text{if } 0 \le t \le t_A \\ \lambda_m & \text{if } t > t_A \end{cases}$ where $t_A = 100$ yr and $\lambda_m = 1 \times 10^{-4}$ yr^{-1} (see Section PA-3.9).

For each vector of the LHS sample, a total of $nS = 10{,}000$ individual futures of the form

$$\mathbf{x}_{st,i} = \left[\left(t_{L1}, e_{L1}, l_{L1}, b_{L1}, p_{L1}, \mathbf{a}_{L1}\right), \left(t_{L2}, e_{L2}, l_{L2}, b_{L2}, p_{L2}, \mathbf{a}_{L2}\right), \ldots, \left(t_{LK}, e_{LK}, l_{LK}, b_{LK}, p_{LK}, \mathbf{a}_{LK}\right), t_{t,min}\right], i = 1, 2, \ldots, nR = 10{,}000 \quad \text{(PA.307)}$$

are generated in the construction of all CCDFs for that LHS vector. As 300 LHS vectors are used in the analysis and 10,000 futures are sampled for each LHS vector, the total number of futures used in the analysis for CCDF construction is 3×10^6.

The drilling rate λ_d is used to generate the times at which drilling intrusions occur. For a Poisson process with a constant λ_d (i.e., a stationary process), the cumulative distribution function (CDF) for the time Δt between the successive events is given by (Ross 1987, p. 113)

$$prob(t \le \Delta t) = 1 - \exp(-\lambda_d \Delta t) \quad \text{(PA.308)}$$

A uniformly distributed random number r_1 is selected from [0, 1]. Then, solution of

$$r_1 = 1 - \exp(-\lambda_d t_1) \quad \text{(PA.309)}$$

for t_1 gives the time of the first drilling intrusion. An initial period of 100 years of administrative control is assumed; thus 100 years is added to the t_1 obtained in Equation (PA.309) to obtain the time of the first drilling intrusion. Selecting a second random number r_2 and solving

$$r_2 = 1 - \exp(-\lambda_d \Delta t_1) \quad \text{(PA.310)}$$

for Δt_1 gives the time interval between the first and second drilling intrusions, with the outcome that $t_2 = t_1 + \Delta t_1$. This process continues until t_{n+1} exceeds 10,000 years. The times $t_1, t_2, \ldots, t_n$ then constitute the drilling times in that possible future..

The mining time t_{min} is sampled in a manner similar to the drilling times. Additional uniformly distributed random numbers from [0,1] are used to generate the elements e_j , l_j , b_j , p_j , $\mathbf{a}_j$ of $\mathbf{x}_{st,i}$ from their assigned distributions (see Section PA-2.2.2).

PA-6.6 Construction of CCDFs

In PA, the sampling of individual futures (Section PA-6.5) and associated CCDF construction is carried out by the CCDFGF program (WIPP Performance Assessment 2010). The sampled futures $\mathbf{x}_{st,i}$ in Equation (PA.307) are used to construct CCDFs for many different quantities (e.g., cuttings and cavings releases, spallings releases, DBRs, etc.). The construction process is the same for each quantity. For notational convenience, assume that the particular quantity under consideration can be represented by a function $f(\mathbf{x}_{st,i})$, with the result that 10,000 values

$$f(\mathbf{x}_{st,i}), \text{ i} = 1, 2, \ldots, 10{,}000 \quad \text{(PA.311)}$$

are available for use in CCDF construction. Formally, the resultant CCDF is defined by the expression in Equation (PA.3). In practice, the desired CCDF is obtained after ordering $f(\mathbf{x}_{st,i})$ from smallest to largest or largest to smallest, as described below.

PA uses a binning procedure in CCDF construction to simplify sorting the individual $f(\mathbf{x}_{st,i})$ and to reduce the number of plot points. Specifically, the range of $f(\mathbf{x}_{st,i})$ is divided into intervals (i.e., bins) by the specified points

$$f_{min} = b_0 < b_1 < b_2 < \ldots < b_n = f_{max} \quad \text{(PA.312)}$$

where f_{min} is the minimum value of $f(\mathbf{x}_{st,i})$ to be plotted (typically 10^{-6} or 10^{-5} for an EPA-normalized release), f_{max} is the maximum value of f to be plotted (typically 100 for an EPA-normalized release), n is the number of bins in use, and the b_i are typically loguniformly distributed with 20 values per order of magnitude. A counter nB_j is used for each interval $[b_j 1, b_j]$. All counters are initially set to zero. Then, as individual values $f(\mathbf{x}_{st,i})$ are generated, the counter nB_j is incremented by 1 when the inequality

$$b_{j-1} < f(\mathbf{x}_{st,i}) \le b_j \quad \text{(PA.313)}$$

is satisfied. When necessary, f_{max} is increased in value so that the inequality $f(\mathbf{x}_{st,i}) < f$max will always be satisfied. Once the 10,000 values for $f(\mathbf{x}_{st,i})$ have been generated, a value of nB_j exists for each interval $[b_j - 1, b_j]$. The quotient

$$pB_j = nB_j / 10,000 \quad \text{(PA.314)}$$

provides an approximation to the probability that $f(\mathbf{x}_{st,i})$ will have a value that falls in the interval $[b_j - 1, b_j]$. The resultant CCDF is then defined by the points

$$\left[b_j, prob\{value > b_j\}\right] = \left\{b_j, \sum_{k=j+1}^{n} pB_k\right\} \quad \text{(PA.315)}$$

for $j = 0, 1, 2, \ldots, n-1$, where $prob(value > b_j)$ is the probability that a value greater than b_j will occur.

The binning technique produces histograms that are difficult to read when multiple CCDFs appear in a single plot. As the number of futures is increased and the bins are refined, the histogram CCDF should converge to a continuous CCDF as additional points are used in its construction. The continuous CCDF is approximated by drawing diagonal lines from the left end of one bin to the left end of the next bin.

When multiple CCDFs appear in a single plot, the bottom of the plot becomes very congested as the individual CCDFs drop to zero on the abscissa. For this reason, each CCDF stops at the largest observed consequence value among the 10,000 values calculated for that CCDF. Stopping at the largest consequence value, rather than the left bin boundary of the bin that contains this value, permits the CCDF to explicitly show the largest observed consequence. Because a sample size of 10,000 is used in the generation of CCDFs for comparison with the EPA release limits, the probability corresponding to the largest observed consequence is typically 10^{-4}.

PA-6.7 Mechanistic Calculations

In the CRA-2014 PA, calculations were performed with the models described in Section PA-4.0 for selected elements of S_{st} (see Section PA-3.10), and the results were used to determine the releases to the accessible environment for the large number (i.e., 10,000) of randomly sampled futures used to estimate individual CCDFs. The same set of mechanistic calculations was performed for each LHS element. This section summarizes the calculations performed with each of the models described in Section PA-4.0; Section PA-6.8 outlines the algorithms used to construct releases for the randomly sampled elements $\mathbf{x}_{st,i}$ of S_{st} from the results of the mechanistic calculations. Long (2013) documents execution of the calculations and archiving of calculation results.

PA-6.7.1 BRAGFLO Calculations

The BRAGFLO code (Section PA-4.2) computes two-phase (brine and gas) flow in and around the repository. BRAGFLO results are used as initial conditions in the models for Salado transport (implemented in NUTS and PANEL), spallings (implemented in CUTTINGS_S), and DBR (also calculated by BRAGFLO). Thus, the BRAGFLO scenarios are used to define scenarios for other codes.

The four fundamental scenarios for the CRA-2014 PA (Section PA-3.10) define four categories of calculations to be performed with BRAGFLO (i.e., E0, E1, E2, and E1E2). These four fundamental scenarios were expanded into six general scenarios by specifying the time of drilling intrusions. Table PA-20 summarizes the specific scenarios used in the CRA-2014 PA. A total of 6 scenarios × nR × $nLHS$ = 6 × 3 × 100 = 1,800 BRAGFLO calculations were conducted for the CRA-2014 PA.

Table PA- 20. BRAGFLO Scenarios in the CRA-2014 PA

Fundamental Scenario (Section PA-3.10)	Specific Scenario	Time of Drilling Intrusion(s)
E0: no drilling intrusions.	S1-BF	N/A
E1: single intrusion through an excavated area of the repository that penetrates pressurized brine in the Castile.	S2-BF	350 years
	S3-BF	1,000 years
	S4-BF	350 years

Fundamental Scenario (Section PA-3.10)	Specific Scenario	Time of Drilling Intrusion(s)
E2: single intrusion through an excavated area of the repository that does not penetrate pressurized brine in the Castile.	S5-BF	1,000 years
E1E2: two intrusions into the same waste panel, the first being an E2 intrusion and the second being an E1 intrusion.	S6-BF	1,000 years for E2 intrusion 2,000 years for E1 intrusion

Values for the activity level $\mathbf{a}_1$ and mining time t_{min} are not needed for the mechanistic calculations; these values are used in the construction of the releases from the results of the mechanistic calculations (Section PA-6.8). Although a value for drilling location l_1 is not specified, a drilling location is required for the BRAGFLO calculations. If equivalent grids were used in the definition of $\mathbf{x}_{st,i}$ (Figure PA-11) and in the numerical solution of the PDEs on which BRAGFLO is based (Figure PA-12), the location of the drilling intrusion used in the BRAGFLO calculations could be specified as a specific value for l_1, which in turn would correspond to one of the 144 locations in Figure PA-11 designated by l in the definition of $\mathbf{x}_{st,i}$. However, as these grids are not the same, a unique pairing between a value for l_1 and the location of the drilling intrusion used in the computational grid employed with BRAGFLO is not possible. The BRAGFLO computational grid divides the repository into a lower waste panel (Waste Panel area), a middle group of four waste panels (South RoR area), and an upper group of five waste panels (North RoR area), with the drilling intrusion taking place through the center of the lower panel (Figure PA-12). Thus, in the context of the locations in Figure PA-11 potentially indexed by l_1, the drilling intrusions in Scenarios S2-S5 occur at a location in Panel 5, which is the southernmost panel. In Scenario S6, both intrusions occur at a location in Panel 5, with the effects of flow between the two boreholes implemented through assumptions involving the time-dependent behavior of borehole permeability (Table PA-7).

PA-6.7.2 NUTS Calculations

For Scenarios S1-BF to S5-BF, radionuclide transport through the Salado is computed by the code NUTS (Section PA-4.3) using the flow fields computed by BRAGFLO. Two types of calculations are performed with NUTS. First, a set of screening calculations identifies elements of the sample from S_{su} for which radionuclide transport through the Salado to the LWB or Culebra is possible. The screening calculations identify a subset of the sample from S_{su} for which transport is possible and for which release calculations are performed. Screening calculations are performed for BRAGFLO Scenarios S1-BF to S5-BF, for a total of 1,500 screening calculations with NUTS. For each vector that is retained (based on the screening calculations), release calculations are performed for a set of intrusion times.

Table PA-21 lists five scenarios for release calculations corresponding to the five BRAGFLO scenarios. Each NUTS scenario uses the flow field computed for the corresponding BRAGFLO scenario. The intrusion times for the NUTS scenarios are accommodated by shifting the BRAGFLO flow fields in time so that the NUTS and BRAGFLO intrusions coincide. For example, the NUTS S3 scenario with an intrusion at 3,000 years requires a flow field for the time interval between (3,000 years and 10,000 years); this scenario uses the BRAGFLO S3-BF scenario flow field for the time interval between (1,000 years and 8,000 years).

Table PA- 21. NUTS Release Calculations in the CRA-2014 PA

NUTS Scenario	Number of Vectors with Releases				Flow field	Intrusion Time (t1)
	R1	R2	R3	Total		
S1	0	0	0	0	BRAGFLO S1-BF scenario	N/A
S2	87	88	92	267	BRAGFLO S2-BF scenario	E1 intrusion at 100 and 350 years
S3	79	81	81	241	BRAGFLO S3-BF scenario	E1 intrusion at 1,000, 3,000, 5,000, 7,000, or 9,000 years
S4	19	22	20	61	BRAGFLO S4-BF scenario	E2 intrusion at 100 and 350 years
S5	17	22	16	55	BRAGFLO S5-BF scenario	E2 intrusion at 1,000, 3,000, 5,000, 7,000, or 9,000 years

Values for the variables indicating intrusion into an excavated area (e_1), penetration of pressurized brine (b_1), plugging pattern (p_1), and drilling location (l_1) are the same as in the corresponding BRAGFLO scenario. Values for the activity level $\mathbf{a}_1$ and mining time t_{min} are not specified for the NUTS scenarios.

PA-6.7.3 PANEL Calculations

As outlined in Section PA-4.4, the code PANEL is used to estimate releases to the Culebra associated with E1E2 scenarios and to estimate radionuclide concentrations in brine for use in estimating DBRs. An E1E2 scenario assumes two drilling intrusions into the same waste panel: the first an E2 intrusion (Table PA-20) occurring at time t_1 and the second an E1 intrusion (Table PA-20) occurring at time t_2. PANEL calculations are performed for t_2 = 100, 350, 1,000, 2,000, 4,000, 6,000, and 9,000 years using the flow field produced by the single BRAGFLO calculation for Scenario S6-BF, for a total of $7 \times nR \times nLHS = 7 \times 3 \times 100 = 2{,}100$ PANEL calculations. The BRAGFLO flow field is shifted forward or backward in time as appropriate so that the time of the second intrusion (t_2) coincides with the flow field. The shifting of the BRAGFLO flow field results in values for the time (t_1) of the first intrusion (E2) for the PANEL calculations given by

$$t_1 = \max\{100yr,\ t_2 - 1200yr\} \quad \text{(PA.316)}$$

where the restriction that t_1 cannot be less than 100 years results from the definition of $\mathbf{x}_{st,i}$, which does not allow negative intrusion times, and from the assumption of 100 years of administrative control during which there is no drilling (i.e., $\lambda_d(t) = 0\ \mathrm{yr}^{-1}$ for $0 \le t \le 100$ yr; see Equation (PA.6)). Under this convention, the definition of Scenario S6-BF for the BRAGFLO calculations differs from what is actually done computationally because t_1 does not always precede t_2 by 1,000 years in the PANEL calculation. Values for the other variables defining the element $\mathbf{x}_{st,i}$ of S_{st} for the PANEL E1E2 scenarios are the same as in the BRAGFLO S6-BF scenario.

Calculating radionuclide concentrations is not specific to any BRAGFLO scenarios because BRAGFLO computes two phase flow, not radionuclide transport. Radionuclide concentrations in brine are calculated using baseline solubilities corresponding to 1x, 2x, 3x, 4x, and 5x the minimum brine volume (17,400 m^3, Clayton 2008c) necessary for a DBR. The concentration calculations compute the mobilized activity in two different brines (Castile and Salado) and are performed at 100; 125; 175; 350; 1,000; 3,000; 5,000; 7,500; and 10,000 years for a total of 2 (brine types) × 5 (brine volumes) × 9 (times) × nR = 270 calculations.

PA-6.7.4 DRSPALL Calculations

The code DRSPALL calculates the spallings volume produced by gas buildup within the repository. Because of the computational expense associated with running the code, rather than evaluating all possible pressures for each vector, a set of four pressures is evaluated for each vector in each replicate. These values are then passed to CUTTINGS_S to act as a lookup table used by the latter code to linearly interpolate the spallings volume as a function of the repository pressure. DRSPALL does not compute releases to the environment, which is computed by the CUTTINGS_S code. A total of 4 pressures × nR × $nLHS$ = 4 × 3 × 100 = 1,200 DRSPALL calculations were performed. As none of the changes implemented for the CRA-2014 PA affected the DRSPALL calculations, the results from the CRA-2004 PABC DRSPALL calculations that were used in the CRA-2009 PA are also used in the CRA-2014 PA.

PA-6.7.5 CUTTINGS_S Calculations

The code CUTTINGS_S computes the volumes of solids removed from the repository by cuttings and cavings (see Section PA-4.5) and spallings (see Section PA-4.6). PA code CUTTINGS_S is also used as a transfer program between the BRAGFLO Salado flow calculation and the BRAGFLO DBR calculation. Results obtained by BRAGFLO for each realization in scenarios S1-BF to S5-BF are used to initialize the flow field properties necessary for the calculation of DBRs. This requires that results obtained on the BRAGFLO grid be mapped appropriately to the DBR grid. Code CUTTINGS_S is used to transfer the appropriate scenario results obtained with BRAGFLO to the DBR calculation. As a result, intrusion scenarios and times used in the calculation of spallings volumes correspond to those used in the calculation of DBRs. Table PA-22 lists the CUTTINGS_S calculations performed for the CRA-2014 PA, totaling 78 × nR × $nLHS$ = 78 × 3 × 100 = 23,400 CUTTINGS_S calculations. These scenarios and intrusion times are also used in the calculation of DBRs, and are given the -DBR modifier to avoid confusion with the 6 scenarios used in BRAGLO Salado flow modeling.

Table PA- 22. CUTTINGS_S Release Calculations in the CRA-2014 PA

Scenario	Description
S1-DBR	Intrusion into lower, middle, or upper waste panel in undisturbed (i.e., E0 conditions) repository at 100; 350; 1,000; 3,000; 5,000; or 10,000 years: 18 combinations.
S2-DBR	Initial E1 intrusion at 350 years followed by a second intrusion into the same, adjacent, or nonadjacent waste panel at 550; 750; 2,000; 4,000; or 10,000 years: 15 combinations.
S3-DBR	Initial E1 intrusion at 1,000 years followed by a second intrusion into the same, adjacent, or nonadjacent waste panel at 1,200; 1,400; 3,000; 5,000; or 10,000 years: 15 combinations.
S4-DBR	Initial E2 intrusion at 350 years followed by a second intrusion into the same, adjacent, or nonadjacent waste panel at 550; 750; 2,000; 4,000; or 10,000 years: 15 combinations.
S5-DBR	Initial E2 intrusion at 1,000 years followed by a second intrusion into the same, adjacent, or nonadjacent waste panel at 1,200; 1,400; 3,000; 5,000; or 10,000 years: 15 combinations.

The CUTTINGS_S S1-DBR scenario computes volumes of solid material released from the initial intrusion in the repository. Initial conditions for the CUTTINGS_S S1-DBR scenario are taken from the results of the BRAGFLO S1-DBR scenario during the intrusion of Waste Panel, South RoR, and North RoR areas in Figure PA-12, corresponding to the lower, middle, and upper waste panels. In this scenario, the excavated area is penetrated ($e_1 = 1$) and the drilling location (l_1) is defined as one of the nodes (Figure PA-11) in the appropriate panel of Figure PA-24. The actual locations where the intrusions are assumed to occur correspond to the points in Figure PA-24 designated "Down-dip well," "Middle well," and "Up-dip well" for the lower, middle, and upper waste panel, respectively. Values for the variables indicating penetration of pressurized brine (b_1), plugging pattern (p_1), activity level ($\mathbf{a}_1$), and mining time (t_{min}) are not specified for the CUTTINGS_S S1 scenario.

The other CUTTINGS_S scenarios (Scenarios S2-DBR to S5-DBR) compute volumes of solids released by a second or subsequent intrusion. Initial conditions are taken from the results of the corresponding BRAGFLO scenario at the time of the second intrusion. As in the BRAGFLO scenarios, the first intrusion occurs in the lower waste panel (Waste Panel area in Figure PA-12), so the drilling location (l_1) is defined as one of the nodes in Panel 5 (Figure PA-11). The second intrusion occurs in the same waste panel as the first intrusion (area Waste Panel in Figure PA-12), an adjacent waste panel (South RoR area in Figure PA-12), or a nonadjacent waste panel (North RoR area in Figure PA-12); hence the drilling location (l_2) is defined as one of the nodes (Figure PA-11) in the appropriate panel of Figure PA-24.

The activity level for the first intrusion $a1$ takes a value that indicates CH-TRU waste penetration (i.e., $\mathbf{a}1 = [2, CH_{11}, CH_{12}, CH_{13}]$), but the specific waste streams penetrated (i.e. CH_{11}, CH_{12}, CH_{13}) are not specified (see Section PA-6.8.2.1). For the second intrusion, the excavated area is penetrated ($e_2 = 1$) and the drilling location (l_2) is defined as one of the nodes in the appropriate panel (Figure PA-11), as

described above. As for the first intrusion, the activity level $\mathbf{a}_2$ only indicates CH-TRU waste penetration. Values for the other variables defining the first intrusion (e_1, b_1, and p_1) are the same as in the corresponding BRAGFLO scenario. Values for the other variables defining the second intrusion (b_2 and p_2) and the mining time t_{min} are not specified for the CUTTINGS_S scenarios.

PA-6.7.6 BRAGFLO Calculations for DBR Volumes

Volumes of brine released to the surface during an intrusion are calculated using BRAGFLO, as described in Section PA-4.7. Calculations of DBR volumes were conducted for the same scenarios as CUTTINGS_S (Table PA-22). Thus, the elements of $\mathcal{S}_{st}$ described in Section PA-6.7.5 also characterize the elements for which DBR volumes are computed. A total of 23,400 BRAGFLO calculations were performed.

PA-6.7.7 MODFLOW Calculations

As described in Section PA-4.8, the MODFLOW calculations produce flow fields in the Culebra for two categories of conditions: partially mined conditions in the vicinity of the repository and fully mined conditions in the vicinity of the repository (Figure PA-27). As specified in section 194.32(b), partially mined conditions are assumed to exist by the end of the administrative control period (i.e., at 100 years after closure). After the time that mining occurs within the LWB (t_{min} ; see Section PA-3.9), fully mined conditions are assumed for the remainder of the 10,000-year regulatory period. The flow fields for partially mined conditions are calculated by MODFLOW using the T-fields for partially mined conditions (see Section PA-4.8.2). Additional MODFLOW calculations determine the flow fields for fully mined conditions and are performed using the T-fields for fully mined conditions. Thus, a total of $2 \times nR \times nLHS = 2 \times 3 \times 100 = 600$ MODFLOW calculations were performed (Table PA-23). The procedure for performing the Culebra transport calculations has remained the same since CRA-2009, but the T-fields used in the flow calculation were developed for CRA-2009 PABC using new data and a new peer-reviewed calibration approach (see Appendix TFIELD-2014). These T-fields are also used in the CRA-2014 PA. The definition of the extent of potash reserves, used to determine the areas partial and full mining factors are applied to, was also updated for CRA-2009 PABC PA (see Appendix TFIELD-2014). The potash extent definition was also used in the CRA-2014 PA.

Table PA- 23. MODFLOW Scenarios in the CRA-2014 PA

MODFLOW: 600 Flow-Field Calculations
PM: Partially mined conditions in vicinity of repository
FM: Fully mined conditions in vicinity of repository
Total calculations = $2 \times nR \times nLHS = 2 \times 3 \times 100 = 600$
Note: Only 100 calibrated T-fields were constructed with PEST and MODFLOW for use in the analysis. The T-fields are an input to the calculation of flow fields. In each replicate, the T-field used for a particular flow field was assigned using an index value (CTRAN; see Table PA-17) included in the LHS.

PA-6.7.8 SECOTP2D Calculations

The SECOTP2D calculations are performed for the same elements $\mathbf{x}_{st,0}$ and $\mathbf{x}_{st,m}$ of $\mathcal{S}_{st}$ defined in Section PA-6.7.7 for the MODFLOW calculations, giving a total of $2 \times nR \times nLHS = 2 \times 3 \times 100 = 600$ SECOTP2D calculations (Table PA-24). In CRA-2009 PABC PA Culebra transport calculations, the lower limits of the matrix distribution coefficient (K_d) distributions were decreased several orders of magnitude, as requested by the EPA (Kelly 2009). Lower limits of the K_d ranges for Am(III) and Pu(III) were reduced from 2.0E-2 to 5.0E-3 m^3/kg; lower limits for Pu(IV), Th(IV), and U(IV) were reduced from 7.0E-1 to 5.0E-4 m^3/kg; the lower limit for U(VI) was not changed. Lower K_d values result in smaller retardation coefficients, and were requested to reflect the increase in organic ligand content in the WIPP inventory. The CRA-2009 PABC PA calculations used are unchanged in the CRA-2014 PA.

Table PA- 24. SECOTP2D Scenarios in the CRA-2014 PA

SECOTP2D: 600 Calculations
PM: Partially mined conditions in vicinity of repository
FM: Fully mined conditions in vicinity of repository
Total calculations = $2 \times nR \times nLHS = 2 \times 3 \times 100 = 600$
Note: Each calculation includes a unit release for each of four radionuclides: ^{241}Am, ^{239}Pu, ^{230}Th, and ^{234}U.

PA-6.8 Computation of Releases

The mechanistic computations outlined in Section PA-6.7 are used to compute releases for each sampled element $\mathbf{x}_{st,i}$ of $\mathcal{S}_{st}$. Releases from the repository can be partitioned into three categories: undisturbed releases, which may occur in futures without drilling intrusions; direct releases, which occur at the time of a drilling event; and long-term releases, which occur as a consequence of a history of drilling intrusions. For a given future ($\mathbf{x}_{st,i}$ of $\mathcal{S}_{st}$ in Equation (PA.307)) other than undisturbed conditions ($\mathbf{x}_{st,0}$), the direct and long-term releases are computed by the code CCDFGF (WIPP Performance Assessment 2010) from the results of the mechanistic calculations summarized in Section PA-6.7, performed with the models presented in Section PA-4.0. Releases from an undisturbed repository are computed from the results of the NUTS S1 scenario (Section PA-6.7.2).

PA-6.8.1 Undisturbed Releases

Repository releases for the futures ($\mathbf{x}_{st,0}$) in which no drilling intrusions occur are computed by the NUTS release calculations for E0 conditions (Table PA-21). The NUTS model computes the activity of each radionuclide that reaches the accessible environment during the regulatory period via transport through the MBs, the Dewey Lake Red Beds and land surface due to brine flow up a plugged borehole. These releases are represented as $f_{MB}[\mathbf{x}_{st,0}, f_B(\mathbf{x}_{st,0})]$, $f_{DL}[\mathbf{x}_{st,0}, f_B(\mathbf{x}_{st,0})]$ and $f_S[\mathbf{x}_{st,0}, f_B(\mathbf{x}_{st,0})]$ in Equation (PA.23). The undisturbed releases for the CRA-2014 PA are summarized in Section PA-7.2.

PA-6.8.2 Direct Releases

Direct releases include cuttings, cavings, spallings, and DBRs. The model for each direct release component computes a volume (solids or liquid) released directly to the surface for each drilling intrusion. These volumes are combined with an appropriate concentration of activity in the released waste. Summary information for the CRA-2014 PA direct releases are given in Section PA-8.5.

PA-6.8.2.1 Construction of Cuttings and Cavings Releases

Each drilling intrusion encountering waste is assumed to release a volume of solid material as cuttings, as described in Section PA-4.5.1. The uncompacted volume of waste removed by cuttings (V_{cut}) is computed by Equation (PA.130). In addition, drilling intrusions that encounter CH-TRU waste may release additional solid material as cavings, as described in Section PA-4.5.2. The uncompacted volume of material removed by cuttings and cavings combined ($V = V_{cut} + V_{cav}$) is computed by Equation (PA.131). For a drilling intrusion that encounters RH-TRU waste, the final eroded diameter D_f in Equation (PA.131) is equal to the bit diameter in Equation (PA.130). In PA, all drilling intrusions assume a drill bit diameter of 0.31115 m (see parameter BOREHOLE:DIAMMOD in Kicker and Herrick 2013, Table 5).

The uncompacted volume of material removed is not composed entirely of waste material; rather, the uncompacted volume includes MgO and any void space initially present around the waste containers. The volume of waste removed (V_w) is determined by multiplying the uncompacted volume by the fraction of excavated repository volume (FVW) occupied by waste, thus

$$V_w = V \times FVW \quad \text{(PA.317)}$$

where $FVW = 0.385$ for CH-TRU waste and $FVW = 1.0$ for RH-TRU waste (see parameters REFCON:FVW and REFCON:FVRW in Kicker and Herrick 2013, Table 37). The activity in the material released by cuttings and cavings is determined by stochastically selecting a subset of all waste streams. The vector ($\mathbf{a}_j$) described in Section PA-3.8 determines which type of waste (CH-TRU or RH-TRU) and which waste streams are selected. The activity per cubic meter of waste stream volume is computed for each waste stream at a discrete set of times accounting for radioactive decay and ingrowth by the code EPAUNI. The results of the CRA-2014 PA EPAUNI calculations are presented in Kicker and Zeitler (Kicker and Zeitler 2013a). Activities at other times are determined by linear interpolation. The cuttings and cavings release $f_C(\mathbf{x}_{st,i})$ is the product of the average activity per cubic meter (C_r, computed as the average activity over the waste streams comprising the selected subset with the assumption that each waste stream contributes an equal volume to the release) and the volume of waste released (Equation (PA.318)):

$$f_C(\mathbf{x}_{st,i}) = V_w \times C_r \quad \text{(PA.318)}$$

PA-6.8.2.2 Construction of Spallings Releases

Spallings releases are calculated for all intrusions that encounter CH-TRU waste. The construction of the spallings release $f_{SP}(\mathbf{x}_{st,i})$ is nearly identical to that described in Section PA-6.8.2.3 for the calculation of DBRs, except that volumes of solid material released will be used rather than volumes of brine. These solid releases are calculated with the spallings submodel of the CUTTINGS_S program for the combinations of repository condition, location relative to previous intrusions, and time between intrusions listed in Table PA-22. Linear interpolation determines the releases for other combinations of repository condition, location, and time between intrusions (WIPP Performance Assessment 2003b).

The concentration of radionuclides in the spallings release volume is computed as the average activity per cubic meter in the CH-TRU waste at the time of intrusion. Activities in each waste stream are computed at a discrete set of times by the code EPAUNI (Kicker and Zeitler 2013a); activities at other times are determined by linear interpolation.

PA-6.8.2.3 Construction of DBRs

DBRs (also termed blowout releases) are calculated for all intrusions that encounter CH-TRU waste. DBRs $f_{DBR}(\mathbf{x}_{st,i})$ are constructed from the volume of brine released (V_{DBR}) to the surface (Equation (PA.208)) and the concentrations of radionuclides in that volume of brine (C_{bl}, see Equation (PA.105)). Brine volume released to the surface is computed by BRAGFLO (Section PA-4.7.3) for the times listed in Table PA-22; brine volumes released for intrusions at other times are computed by linear interpolation (WIPP Performance Assessment 2003a).

Calculating DBR volumes distinguishes between the first intrusion and subsequent intrusions. The release volumes for the initial intrusion (E0 repository conditions) are further distinguished by the panel group (upper, middle, and lower). As shown in Table PA-22, BRAGFLO computes release volumes for the initial intrusion at a series of intrusion times; the release volume for the initial intrusion at other times is computed by linear interpolation (WIPP Performance Assessment 2010). Release volumes for subsequent intrusions are distinguished by the current state of the repository (E1 or E2) and the relative distance between the panel intruded by the current borehole and the panel of the

initial intrusion (same, adjacent, nonadjacent). The algorithms for determining repository conditions and distance between intrusions are described in Section PA-6.7.5.

As indicated in Table PA-22, DBR volumes for a second intrusion are computed by BRAGFLO for combinations of repository condition, distance between intrusions, and time between intrusions. Brine release volumes for other combinations of condition, distance, and time are computed by linear interpolation (WIPP Performance Assessment 2010). Brine releases from the third and subsequent intrusions are computed as if the current intrusion was the second intrusion into the repository.

Radionuclide concentrations in brine (C_{bl}) are calculated by PANEL (Section PA-6.7.3) for the times listed in Table PA-21 and multiples of 1x, 2x, 3x, 4x, and 5x the minimum brine volume necessary for a DBR (17,400 m^3); concentrations at other times (and other brine volumes) are computed by linear interpolation (WIPP Performance Assessment 2010). The type of intrusion (E1 or E2) determines the brine (Salado or Castile brine) selected for the concentration calculation; Castile brine is used for E1 intrusions, and Salado brine is used for E2 intrusions.

The DBR is computed as the product of the release concentration and the volume, V_{DBR}:

$$f_{DBR}(\mathbf{x}_{st,i}) = V_{DBR} \times C_{bl} \quad \text{(PA.319)}$$

PA-6.8.3 Radionuclide Transport Through the Culebra

One potential path for radionuclides to leave the repository is through the boreholes to the Culebra, then through the Culebra to the LWB (Kim 2013a). As indicated in Table PA-21, the NUTS and PANEL models are used to estimate radionuclide transport through boreholes to the Culebra $f_{NP}(\mathbf{x}_{st,i})$ for a fixed set of intrusion times; releases to the Culebra for intrusions at other times are determined by linear interpolation (WIPP Performance Assessment 2010). NUTS computes the release to the Culebra over time for E1 and E2 boreholes; PANEL computes the release to the Culebra for an E1E2 borehole.

Each borehole may create a pathway for releases to the Culebra. The first E1 or E2 borehole in each panel creates a release path, with the radionuclide release taken from the appropriate NUTS data. Subsequent E2 boreholes into a panel with only E2 boreholes do not cause additional releases; the WIPP PA assumes that a subsequent E2 borehole into a panel having only earlier E2 intrusions does not provide a significant source of additional brine, and thus does not release additional radionuclides to the Culebra.

An E1E2 borehole results from the combination of two or more intrusions into the same panel, at least one of which is an E1 intrusion. A subsequent E1 borehole changes the panel's condition to E1E2, as does an E2 borehole into a panel that has an earlier E1 intrusion. Once E1E2 conditions exist in a panel, they persist throughout the regulatory period. However, releases from a panel with E1E2 conditions are restarted for each subsequent E1 intrusion into that panel, since additional E1 intrusions may introduce new volumes of brine to the panel.

Releases to the Culebra are summed across all release pathways to the Culebra to obtain total releases to the Culebra $r_k(t)$ for the k^{th} radionuclide at each time t. Releases to the Culebra include both dissolved radionuclides and radionuclides sorbed to colloids. The WIPP PA assumes that radionuclides sorbed to humic colloids disassociate and transport, as do dissolved radionuclides; it is also assumed that other colloid species do not transport in the Culebra (see Appendix SOTERM-2014, Section SOTERM-4.6). The release to the Culebra is partitioned into dissolved and colloid species by multiplying $r_k(t)$ by radionuclide-specific factors for the fraction dissolved and the fraction on colloids. Dissolved radionuclides are always transported through the Culebra.

Radionuclide transport through the Culebra is computed by the code SECOTP2D (Section PA-4.9) for partially mined and fully mined conditions, as indicated in Table PA-24. These computations assume a 1 kg source of each radionuclide placed in the Culebra between 0 and 50 years and result in the fraction of each source $f_{m,k}(t)$, where m is the mining condition and k is the index for the radionuclide, reaching the LWB at each subsequent time t. For convenience, the time-ordering of the data from SECOTP2D is reversed so that the fraction $f_{m,k}(t)$ associated with year $t = 200$, for example, represents the release at the boundary at year 10,000 for a release occurring between 150 and 200 years.

The total release through the Culebra $R_{Cul,k}$ is calculated for the k^{th} radionuclide by

$$R_{Cul,k} = \sum_{t_i \le t_{min}} r_k(t_i) f_{PM,k}(t_i) + \sum_{t_i > t_{min}} r_k(t_i) f_{FM,k}(t_i) \quad \text{(PA.320)}$$

where $r_k(t_i)$ is the release of the k^{th} radionuclide to the Culebra in kg at time t_i, and $f_{PM,k}(t_i)$ and $f_{FM,k}(t_i)$ are the fractions of a unit source placed in the Culebra in the interval (t_{i-1}, t_i) that reaches the LWB by the end of the 10,000-year regulatory period for partially mined and fully mined conditions within the LWB, respectively. The function $f_{m,k}(t)$ ($m = PM, FM$) changes when mining is assumed to occur within the LWB; hence the sum in the equation above is evaluated in two parts, where t_{min} is the time that mining occurs. The total releases through the Culebra $f_{ST}(\mathbf{x}_{st,i})$ are computed by converting the release of each radionuclide $R_{Cul,k}$ from kg to EPA units, then summing over all radionuclides.

PA-6.8.4 Determining Initial Conditions for Direct and Transport Releases

A sequence of intrusions into the repository can change the conditions in and around the repository and, hence, affect releases from subsequent intrusions. This section describes how panel and repository conditions are determined for a given intrusion.

PA-6.8.4.1 Determining Repository and Panel Conditions

Direct releases by DBR and spallings, and subsequent releases by radionuclide transport, require determining the conditions in the intruded panel and the repository at the time of the intrusion. One of three conditions is assigned to the repository:

- E0 the repository is undisturbed by drilling,
- E1 the repository has at least one E1 intrusion, or
- E2 the repository has one or more E2 intrusions, but no E1 intrusions.

In addition, each panel is assigned one of four conditions:

- E0 the excavated regions of the panel have not been intruded by drilling,
- E1 the panel has one previous E1 intrusions (intersecting a brine reservoir in the Castile),
- E2 the panel has one or more previous E2 intrusions (none intersect brine reservoirs), or
- E1E2 the panel has at least two previous intrusions, at least one of which is an E1 intrusion.

Repository conditions are used to determine direct releases for each intrusion by DBRs and spallings. Panel conditions are used to determine releases by transport through the Culebra.

When an intrusion into CH-TRU waste occurs, the stochastic variables in Table PA-19 are used in the algorithm shown in Figure PA-33 to determine the type of the intrusion (E1 or E2). The type of the intrusion is used to update the conditions for the intruded panel and the repository before stepping forward in time to the next intrusion.

PA-6.8.4.2 Determining Distance from Previous Intrusions

Direct releases by DBR and spallings require determining the distance between the panel hit by the current intrusion and the panels hit by previous intrusions. In PA, the 10 panels are divided into three groups: lower, consisting of only Panel 5; middle, including Panels 3, 4, 6, and 9; and upper, including Panels 1, 2, 7, 8, and 10, as shown in Figure PA-25. These divisions are consistent with the repository representation in the BRAGFLO model for Salado flow (Section PA-4.2) and for DBRs (Section PA-4.7).

The initial intrusion can occur in any of the 10 actual waste panels, so the direct releases for the initial intrusion are modeled as if the initial intrusion occurred in a lower, middle, or upper waste panel based on the division discussed above. Initial conditions for direct releases from subsequent intrusions are modeled by one of three cases: lower, middle, and upper, corresponding to the three panel groups shown in Figure PA-25 and listed in Table PA-22. The lower case represents a second intrusion into a previously intruded panel. The middle case represents an intrusion into an undisturbed panel that is adjacent to a previously disturbed panel. The upper case represents an intrusion into an undisturbed panel that is not adjacent to a previously disturbed panel. Adjacent panels share one side in common, and nonadjacent panels share no sides in common.

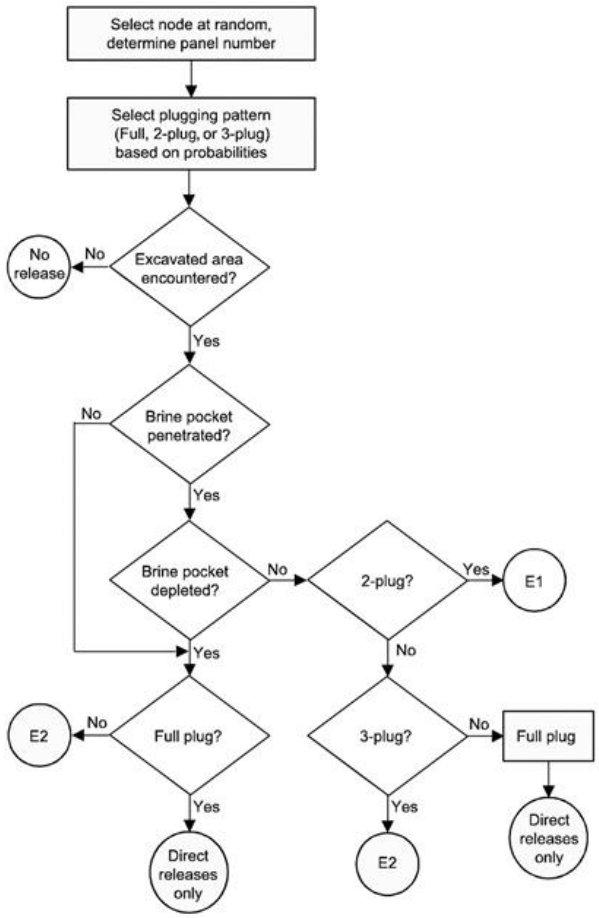

Figure PA- 33. Logic Diagram for Determining the Intrusion Type

The time and location of the previous intrusion is used to determine distance from the current intrusion and depends on the repository condition, which is determined by the intrusion of greatest consequence across all panels prior to the current intrusion. E1 intrusions are assumed to be of greater consequence than E2 intrusions. The previous intrusion is selected by finding the closest panel (same, adjacent, nonadjacent) whose intrusion condition, excluding the current intrusion, is equal to the repository condition. The time of the previous intrusion is the time of the most recent intrusion with the greatest consequence and closest distance. Likewise, the condition of each panel is equal to the intrusion of greatest consequence into the panel prior to the current intrusion.

PA-6.8.5 CCDF Construction

For each vector $\mathbf{v}_{su,k}$ in the space of subjective uncertainty, the code CCDFGF samples a sequence $\mathbf{x}_{st,i}$, $i = 1, 2, \ldots, nR$ of futures. In PA, $nR = 10{,}000$; this number of futures is sufficient to adequately estimate the mean CCDF of total releases for comparison with the boundary line specified in section 191.13, as demonstrated in Section PA-9.0. A release $f(\mathbf{x}_{st,i})$ for each future is then constructed as described in Section PA-6.8.1, Section PA-6.8.2, and Section PA-6.8.3. Once the $f(\mathbf{x}_{st,i})$ are evaluated, the CCDF can be approximated as indicated in Equation (PA.321).

$$prob(Rel > R) = \int_{\mathbf{v}_{su}} \delta_R\left[f(\mathbf{x}_{st,i})\right] d_{su}(\mathbf{x}_{st,i})\, d\mathbf{v}_{su} \cong \sum_{i=1}^{nR} \delta_R\left[f(\mathbf{x}_{st,i})\right] / nR \quad \text{(PA.321)}$$

A binning technique is used to construct the desired CCDF: the consequence axis is divided into a sequence of bins, and the number of values for $f(\mathbf{x}_{st,i})$ falling in each bin is accumulated. In addition, all values for $f(\mathbf{x}_{st,i})$ are saved and subsequently ordered to provide an alternative method for constructing the CCDFs. In addition to the total CCDF for all releases, it will be possible to obtain CCDFs for individual release modes (e.g., cuttings, spallings, DBRs, to Culebra, through MBs, through Culebra). The logic diagram for CCDF production is shown in Figure PA-34.

The CCDF construction indicated in this section is for a single sample element $\mathbf{v}_{su,k}$ of the form indicated in conjunction with Equation (PA.305). Repeated generation of CCDFs for individual sample elements $\mathbf{v}_{su,k}$, i.e. for the vectors representing epistemic uncertainty in the model results, will lead to the distribution of complete CCDFs.

PA-6.9 Sensitivity Analysis

Evaluating one or more of the models discussed in Section PA-4.0 with the LHS in Equation (PA.305) creates a mapping

$\{\mathbf{v}_{su,k}, \mathbf{y}_{su,k}\}$, k = 1, 2, …, nLHS (PA.322)

from analysis inputs (i.e., $\mathbf{v}_{su,k}$) to analysis results (i.e., $y(\mathbf{v}_{su,k})$), where $\mathbf{y}_{su,k}$ denotes the results obtained with the model or models under consideration. In other words, for each vector of parameters samples, there is a corresponding CCDF of releases, $y(\mathbf{v}_{su,k})$. A vector notation is used for y because, in general, a large number of predicted results are produced by each of the models used in PA. Sensitivity analysis explores the mapping in Equation (PA.322) to determine how the uncertainty in individual elements of $\mathbf{v}_{su,k}$ affects the uncertainty in individual elements of $y(\mathbf{v}_{su,k})$. Understanding how uncertainty in analysis inputs affects analysis results aids in understanding PA and improving the models for future PAs. In some cases, sensitivity analysis results are based on pooling the results obtained for the three replicated LHSs (i.e., R1, R2, R3) discussed in Section PA-6.4. In other cases, the sensitivity analysis is based on the results for each replicate, and statistics are compared across the three replicates. Note that pooling LHS replicates that include correlated variables can introduce a small bias into the statistics, although there are methods that allow for correlated variables when pooling replicates (Sallaberry, Helton, and Hora 2006).

Three principal techniques are used in the sensitivity analysis: scatterplots, regression analyses to determine standardized regression coefficients and partial correlation coefficients, and stepwise regression analyses. Each technique is briefly discussed.

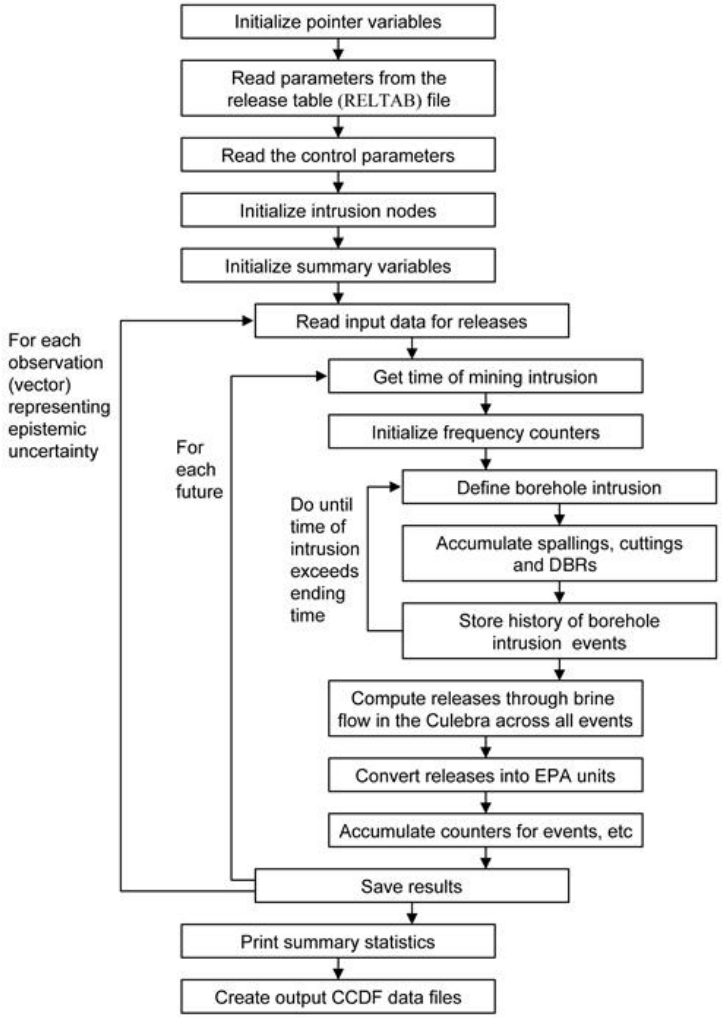

Figure PA- 34. Processing of Input Data to Produce CCDFs

PA-6.9.1Scatterplots

Scatterplots, the simplest sensitivity analysis technique, are performed by plotting the points

$\{v_{k,j}, y_k\}$, $k = 1, 2, \ldots, nLHS$ (PA.323)

for each element v_j of $\mathbf{S}_{su}$. The resulting plots can reveal relationships between y and the elements of $\mathbf{S}_{su}$. Scatterplots can be effective at revealing nonlinear relationships or threshold values. Examining such plots when LHS is used can be particularly revealing because of the

full stratification over the range of each input variable. Iman and Helton (Iman and Helton 1988) provide an example where the scatterplots revealed a rather complex pattern of variable interactions.

PA-6.9.2 Regression Analysis

A more formal investigation of the mapping in Equation (PA.322) can be based on regression analysis. In this approach, a model of the form

$$y = b_0 + \sum_{j=1}^{n} b_j x_j \quad \text{(PA.324)}$$

is developed from the mapping between analysis inputs and analysis results shown in Equation (PA.322), where the x_j are the input variables under consideration and the b_j are coefficients that must be determined. The coefficients b_j and other aspects of the regression model's construction in Equation (PA.324) can indicate the importance of the individual variables x_j with respect to the uncertainty in y. The PA employs the method of least squares to determine the coefficients b_j (Myers 1986).

Often the regression in Equation (PA.324) is performed after the input and output variables are normalized to mean zero and standard deviation one. The resulting coefficients b_j are called standardized regression coefficients (SRCs). When the x_j are independent, the absolute value of the SRCs can provide a measure of variable importance. Specifically, the coefficients provide a measure of importance based on the effect of moving each variable away from its expected value by a fixed fraction of its standard deviation while retaining all other variables at their expected values.

Partial correlation coefficients (PCCs) can also measure the linear relationships between the output variable y and the individual input variables. The PCC between y and an individual variable x_p is obtained through a sequence of regression models. First, the following two regression models are constructed:

$$\hat{y} = b_0 + \sum_{\substack{j=1 \\ j \neq p}}^{n} b_j x_j \text{ and } \hat{x}_p = c_0 + \sum_{\substack{j=1 \\ j \neq p}}^{n} c_j x_j \quad \text{(PA.325)}$$

The results of the two preceding regressions are then used to define the new variables $y - \hat{y}$ and $x_p - \hat{x}_p$. By definition, the PCC between y and x_p is the correlation coefficient between $y - \hat{y}$ and $x_p - \hat{x}_p$. Thus, the PCC provides a measure of the linear relationship between y and x_p with the linear effects of the other variables removed.

Regression and correlation analyses often perform poorly when the relationships between the input and output variables are nonlinear. This is not surprising, as such analyses assume linear relationships between variables. The problems associated with poor linear fits to nonlinear data can be avoided by use of the rank transformation (Iman and Conover 1979). The rank transformation is a simple concept: data are replaced with their corresponding ranks, and then the usual regression and correlation procedures are performed on these ranks. Specifically, the smallest value of each variable is assigned Rank 1, the next largest value is assigned Rank 2, and so on up to the largest value, which is assigned the rank m, where m denotes the number of observations. The analysis is then performed with these ranks used as the values for the input and output variables. A formal development of PCCs and the relationships between PCCs and SRCs is provided by Iman, Shortencarier, and Johnson (Iman, Shortencarier, and Johnson 1985).

PA-6.9.3 Stepwise Regression Analysis

Stepwise regression analysis provides an alternative to constructing a regression model containing all the input variables. With this approach, a sequence of regression models is constructed. The first regression model contains the single input variable with the largest impact on the uncertainty in the output variable (i.e., the input variable that has the largest correlation with the output variable y). The second regression model contains the two input variables with the largest impact on the output variable: the input variable from the first step, plus whichever of the remaining variables has the largest impact on uncertainty not accounted for by the first variable (i.e., the input variable that has the largest correlation with the uncertainty in y that cannot be accounted for by the first variable). Additional models in the sequence are defined in the same manner, until further models are unable to meaningfully increase the amount of uncertainty that can be accounted for in the output variable.

Stepwise regression analysis can provide insights into the importance of the individual variables. First, the order in which the variables are selected in the stepwise procedure indicates their importance, with the most important variable being selected first, the next most important variable being selected second, and so on. Second, the R^2 values at successive steps of the analysis also measure variable importance by indicating how much of the uncertainty in the dependent variable can be accounted for by all variables selected at each step. When the input variables are uncorrelated, the differences in the R^2 values for the regression models constructed at successive steps equals the fraction of the total uncertainty in the output variable accounted for by the individual input variable added at each step. Third, the absolute values of the SRCs in the individual regression models indicate variable importance. Further, the sign of an SRC indicates whether the input and output variable tend to increase and decrease together (a positive coefficient) or tend to move in opposite directions (a negative coefficient).

PA-7.0 Results for the Undisturbed Repository

The PA tabulates releases from the repository for undisturbed conditions. Releases from the undisturbed repository to the accessible environment fall under two sets of protection requirements. The first, as set forth in section 191.15, protects individuals from radiological exposure; the second, in 40 CFR Part 191 Subpart C, protects groundwater resources from contamination. This section shows how the WIPP complies with these two requirements by presenting brine and gas flow (BRAGFLO) and radionuclide transport (NUTS) results from modeling the undisturbed repository. For the undisturbed repository, radionuclide transport through the repository shafts to the Culebra, and lateral radionuclide transport through the marker beds and across the LWB, are the only potential release mechanisms. The results discussed in Section PA-7.2 show that there are no releases to the accessible environment from the undisturbed repository. Results of the CRA-2014 PA for the undisturbed repository are summarized in Camphouse et al. (Camphouse et al. 2013). The overall structure of the CRA-2014 PA is summarized in Section PA-1.1.

PA-7.1 Salado Flow

This section summarizes the Salado flow calculation results for the undisturbed (S1-BF) scenario (see Table PA-20 for an explanation of the BRAGFLO scenarios). The Salado flow model represents the repository as five regions in the numerical grid: three waste-filled regions (the Waste Panel, South RoR, and North RoR in Figure PA-12) and two excavated regions with no waste (the operations area and experimental area in Figure PA-12). A detailed presentation of the CRA-2014 PA Salado flow results can be found in Camphouse (Camphouse 2013c).

In undisturbed conditions, pressure strongly influences the extent to which contaminated brine might migrate from the repository to the accessible environment. Pressures and brine saturations in repository waste regions are important quantities relevant to direct release mechanisms considered in the WIPP PA. Spallings releases depend directly on repository pressure. Direct brine releases (DBRs) depend on both repository pressure and brine saturation. Waste region pressures and brine saturations obtained for undisturbed conditions are used to generate initial conditions for the spallings and DBR models (Section PA-8.5.2 and Section PA-8.5.3, respectively). Consequently, results for these quantities in the undisturbed repository can impact results seen for the disturbed scenarios investigated in the WIPP PA.

Figure PA-35 through Figure PA-40 show the waste region pressures for scenario S1-BF of the CRA-2014 PA. Overall mean pressure curves shown for the CRA-2009 PABC and the CRA-2014 PA are obtained by forming the average of all 300 vector realizations. Over time, repository pressures increase due to several factors: rapid initial creep closure of rooms, initial inflow of brine causing gas generation due to corrosion, and availability of CPR material to produce gas by microbial degradation. Changes included in the CRA-2014 PA yield a reduction in the mean pressure calculated for undisturbed repository waste areas as compared to the CRA-2009 PABC. The expanded mined volume in the repository experimental area contributes somewhat to this reduction, but it is primarily due to reduced gas generation seen in the CRA-2014 PA results. The revised iron corrosion rate utilized in the CRA-2014 PA results in slower gas production due to iron corrosion (on average). The addition of MgO chemistry in the revised water balance implementation also reduces the amount of free water available for gas production by iron corrosion and microbial degradation of cellulose. The sequestration of free water further reduces gas production, and consequently pressure, in repository waste areas (Camphouse 2013c).

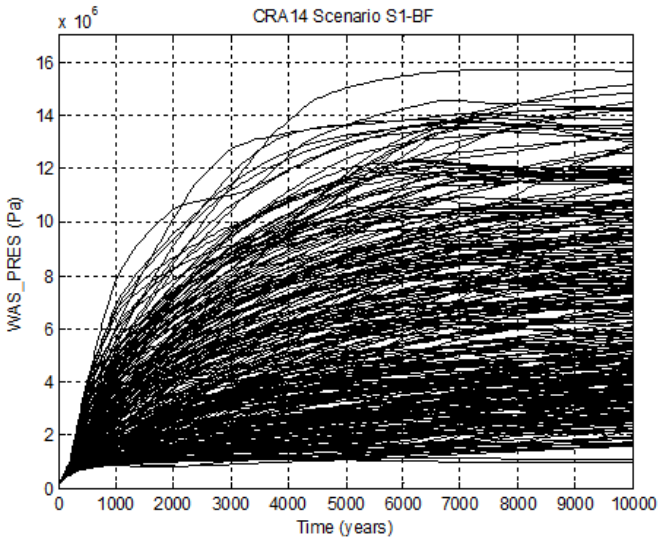

Figure PA- 35. Horsetail Plot of Waste Panel Pressure, Scenario S1-BF, CRA-2014 PA

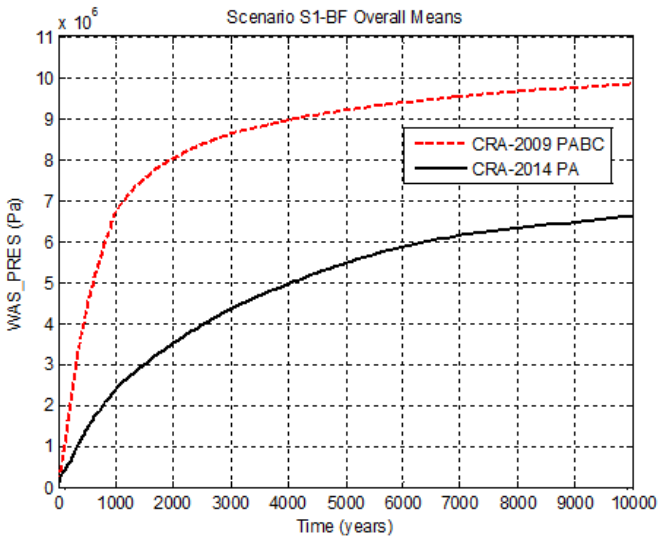

Figure PA- 36. Overall Means of Waste Panel Pressure, Scenario S1-BF

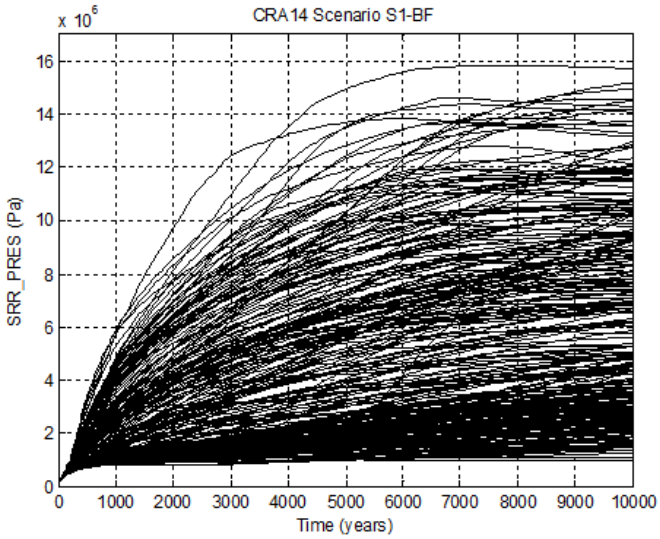

Figure PA- 37. Horsetail Plot of SRoR Pressure, Scenario S1-BF, CRA-2014 PA

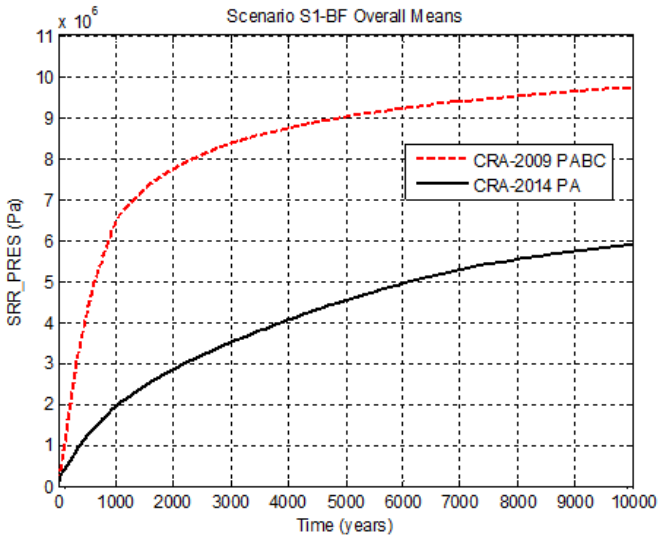

Figure PA- 38. Overall Means of SRoR Pressure, Scenario S1-BF

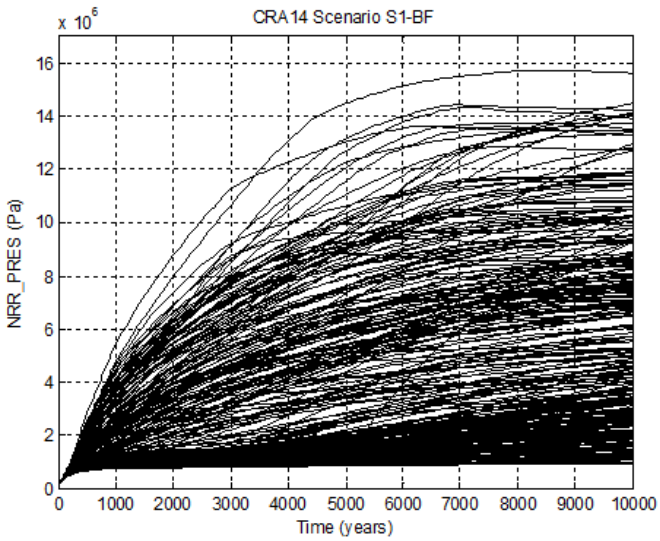

Figure PA- 39. Horsetail Plot of NRoR Pressure, Scenario S1-BF, CRA-2014 PA

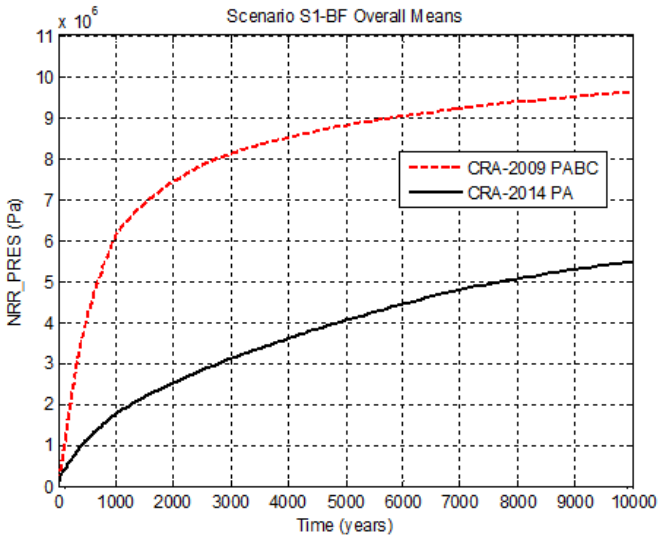

Figure PA- 40. Overall Means of NRoR Pressure, Scenario S1-BF

The trend toward waste region pressure reduction in the CRA-2014 PA yields a corresponding increase (on average) in cumulative brine inflow to repository waste regions (cumulative brine inflow includes inflow from the surrounding rock and adjacent panels). Increases in waste region brine inflow are more pronounced for waste panels at lower elevation due to the 1° dip in elevation north-to-south that is implemented in the Salado flow model. The changes in brine inflow to repository waste regions have a direct impact on the brine saturations calculated for those areas. Waste region brine saturations obtained in the CRA-2014 PA are shown in Figure PA-41 to Figure PA-46. Overall mean brine saturation curves shown for the CRA-2009 PABC and the CRA-2014 PA are obtained by forming the average of all 300 vector realizations. As seen in Figure PA-41 to Figure PA-46, brine saturations tend to be higher in the waste panel at lowest elevation, with brine saturations typically being lower in the SRoR and NRoR than those seen in the separately modeled waste panel. Moreover, waste areas at higher elevation, such as the SRoR and the NRoR, have lower mean brine saturations in the CRA-2014 PA results as compared to the CRA-2009 PABC, especially in the first 2000 years. This is due to water sequestration in the refined water balance implementation and the combination of the 1-degree repository downdip and more permeable panel closures at early times. Waste panels at lowest elevation, such as the separately modeled waste panel in BRAGFLO, have a lower mean brine saturation at early times as compared to the CRA-2009 PABC. However, the mean waste panel brine saturation gradually increases until it becomes greater than that seen in the CRA-2009 PABC at roughly 750 years. As the SRoR and NRoR together represent nine of the ten repository waste panels, the sequestration of brine in the refined water budget implementation yields a repository that tends to be drier overall for undisturbed conditions as compared to the CRA-2009 PABC (Camphouse 2013c).

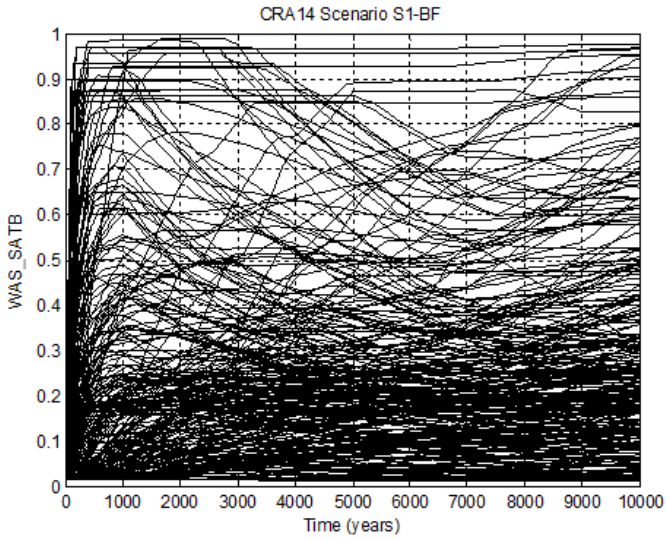

Figure PA- 41. Horsetail Plot of Waste Panel Brine Saturation, Scenario S1-BF, CRA-2014 PA

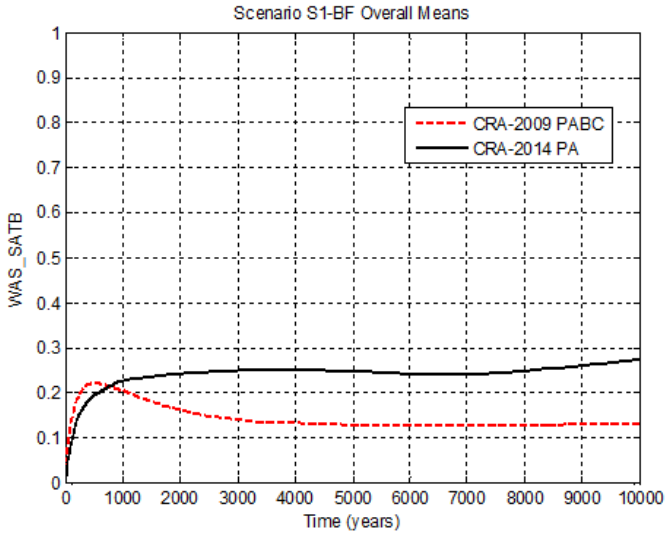

Figure PA- 42. Overall Means of Waste Panel Brine Saturation, Scenario S1-BF

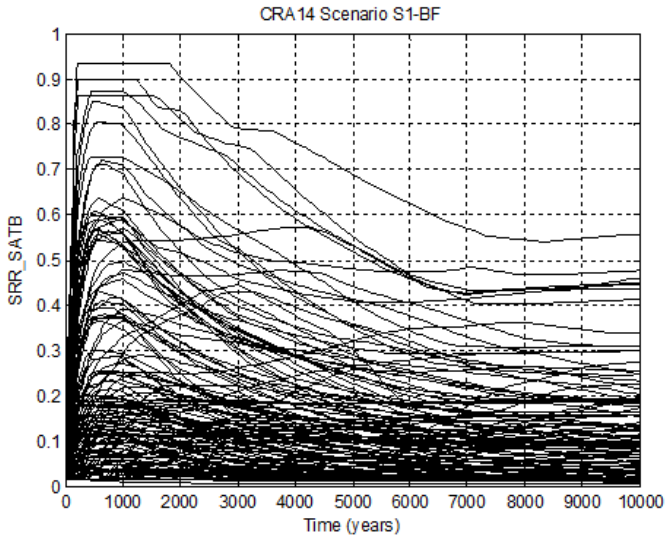

Figure PA- 43. Horsetail Plot of SRoR Brine Saturation, Scenario S1-BF, CRA-2014 PA

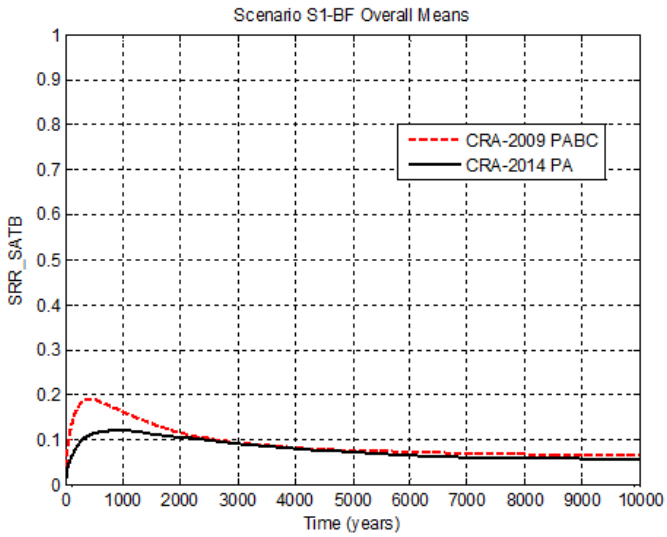

Figure PA- 44. Overall Means of SRoR Brine Saturation, Scenario S1-BF

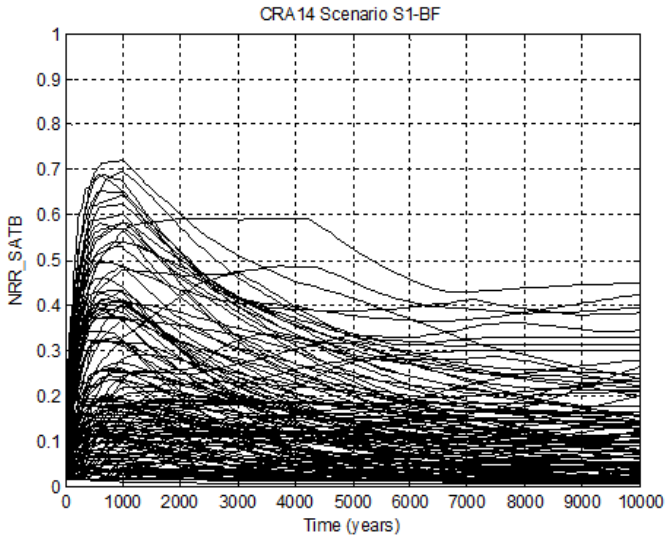

Figure PA- 45. Horsetail Plot of NRoR Brine Saturation, Scenario S1-BF, CRA-2014 PA

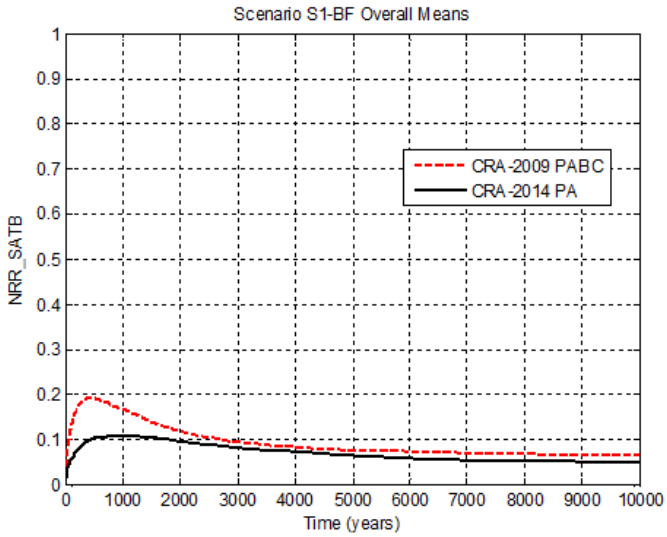

Figure PA- 46. Overall Means of NRoR Brine Saturation, Scenario S1-BF

The repository shaft is modeled in the WIPP PA as being directly between the operations and experimental regions of the repository. Consequently, the pressure in these repository regions impacts the volume of brine moved up the shaft toward the ground surface, shown in Figure PA-47 and Figure PA-48. The trend toward lower pressure in repository waste regions in the CRA-2014 PA translates to a similar trend toward pressure reduction in the repository operations and experimental regions. The trend toward lower pressure in these areas results in an overall reduction to the mean cumulative brine flow up the shaft in the CRA-2014 PA.

In the CRA-2009 PABC, vector 53 of replicate 1 had the highest total cumulative brine flow to the LWB for the undisturbed repository. It was the only vector that was screened in as a source of radionuclide transport through the Salado marker beds and across the LWB in the NUTS calculation. Vector 53 of replicate 1 also has the highest cumulative brine flow to the LWB for the undisturbed repository in the CRA-2014 PA. However, the maximum brine outflow across the LWB associated with this vector is reduced in the CRA-2014 PA due to reduced pressures seen for the undisturbed repository in the CRA-2014 PA. In addition, brine flow across the LWB for this vector starts at roughly 6,500 years post-closure in the CRA-2014 PA as compared to roughly 3,000 years post-closure in the CRA-2009 PABC (Figure PA-49).

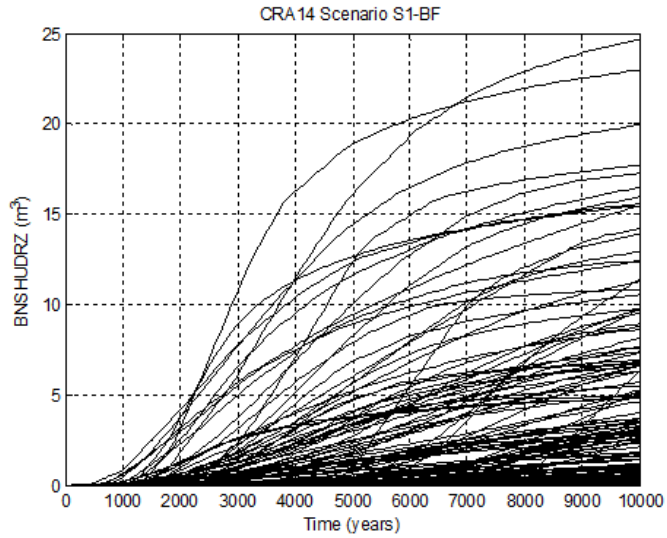

Figure PA- 47. Horsetail Plot of Brine Flow up the Shaft, Scenario S1-BF, CRA-2014 PA

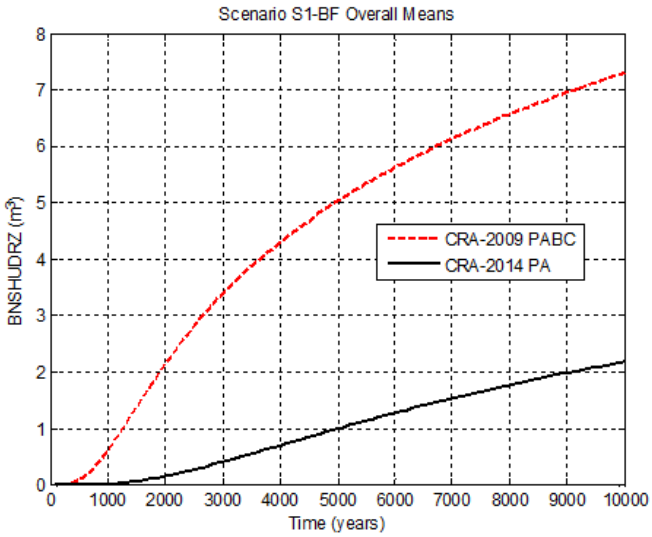

Figure PA- 48. Overall Means of Brine Flow up the Shaft, Scenario S1-BF

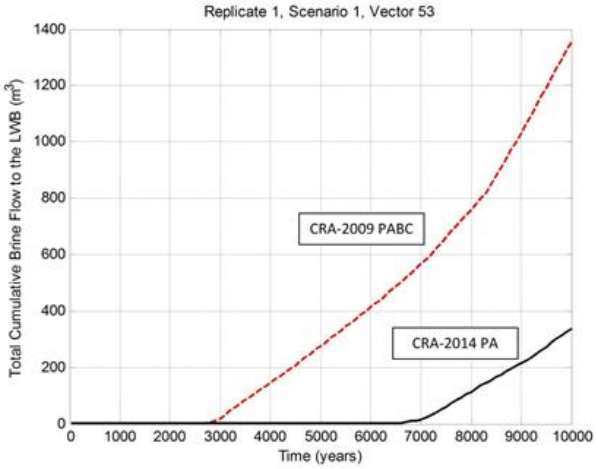

Figure PA- 49. Comparision of Brine Flow Across the LWB, Scenario S1-BF, CRA-2009 PABC and CRA-2014 PA

PA-7.2 Radionuclide Transport

This section summarizes the radionuclide transport results for the undisturbed repository, both up the shaft to the Culebra and through the Salado to the LWB. Radionuclide transport in the undisturbed scenario is calculated by the code NUTS. Kim (Kim 2013a) presents a detailed analysis of the NUTS results for the CRA-2014 PA.

Screening runs using a conservative tracer determine which vectors have the potential to transport radionuclides to the accessible environment. Full Salado transport simulations are then performed for all screened-in vectors that have the potential to transport radionuclides to the accessible environment. In the CRA-2009 PABC, only vector 53 of replicate 1 was screened in for the radionuclide transport calculation in the undisturbed scenario. In the CRA-2014 PA, no vectors exceeded the NUTS screening step for the undisturbed repository (Kim and Camphouse 2013). As discussed in the preceding section, vector 53 of replicate 1 also has the highest cumulative brine flow to the LWB for the undisturbed repository in the CRA-2009 PA and the CRA-2014 PA. However, the maximum brine outflow across the LWB associated with this vector is reduced in the CRA-2014 PA due to reduced pressures seen for the undisturbed repository. Brine outflows across the LWB associated with this vector also begin at later times in the CRA-2014 PA. Consequently, no vectors exceeded the NUTS screening criterion, resulting in no radionuclide transport through the Salado to the LWB in the CRA-2014 PA. Similarly, no vectors showed radionuclide transport through the shafts to the Culebra (Kim 2013a).

As no radionuclide transport to the accessible environment occurred in the CRA-2014 PA, there are no releases associated with the undisturbed scenario in the CRA-2014 PA.

PA-8.0 Results for a Disturbed Repository

The WIPP repository might be disturbed by exploratory drilling for natural resources during the 10,000-year regulatory period. Drilling could create additional pathways for radionuclide transport, especially in the Culebra, and could release material directly to the surface. In

addition, mining for potash within the LWB might alter flow in the overlying geologic units and locally accelerate transport through the Culebra. The disturbed scenarios used in PA modeling capture the range of possible releases resulting from drilling and mining.

Total releases are computed by the code CCDFGF. Total releases comprise transport releases and direct releases. Transport releases generally involve movement of radionuclides up an abandoned borehole into the Culebra, then through the Culebra to the LWB. Transport of radionuclides to the Culebra is computed using the codes NUTS and PANEL (see Section PA-6.7.2 and Section PA-6.7.3) using the brine flows computed by BRAGFLO (see Section PA-6.7.1). Radionuclide transport through the Culebra is computed by the code SECOTP2D (see Section PA-6.7.8) using flow fields calculated by MODFLOW (see Section PA-6.7.7).

Direct releases occur at the time of a drilling intrusion and include releases of solids (cuttings, cavings, and spallings) computed using the code CUTTINGS_S (see Section PA-6.7.4) and DBRs computed using BRAGFLO (see Section PA-6.7.6). Pressure and brine saturation within the waste areas are used as initial conditions for the direct release models. Results from the undisturbed repository (see Section PA-7.0) are used as the initial conditions for the first intrusion. To calculate initial conditions for subsequent intrusions, and to compute the source of radionuclides for transport in the Culebra, BRAGFLO uses a set of drilling scenarios to calculate conditions within the repository after an intrusion (see Section PA-6.7.6).

This section first summarizes the scenarios used to represent drilling intrusions and the resulting repository conditions calculated by BRAGFLO. Transport releases are presented next, followed by cuttings, cavings, spallings, and DBRs. The CRA-2014 PA results obtained for the disturbed repository are summarized in Camphouse et al. (Camphouse et al.2013).

PA-8.1 Drilling Scenarios

As shown in Table PA-20, the PA considers two types of drilling intrusions: E1 and E2. The E1 intrusion scenario represents the possibility that a borehole creates a pathway between the repository and a pressurized brine reservoir located within the underlying Castile formation. The E2 intrusion scenario represents a borehole that intrudes into the repository, but does not connect the repository with an underlying brine reservoir. Repository conditions are calculated for the E1 intrusion scenario at 350 and 1,000 years, and are referred to as the BRAGFLO S2-BF and S3-BF scenarios, respectively. The BRAGFLO Scenarios S4-BF and S5-BF represent E2 intrusions that occur at 350 and 1,000 years, respectively. An additional BRAGFLO scenario, S6-BF, simulates the effects of an E2 intrusion at 1,000 years followed by an E1 intrusion 1,000 years later into the same panel.

PA-8.2 Mining Scenarios

Long-term releases within the Culebra could be influenced by future mining activities that remove all the known potash reserves within the LWB and cause the transmissivity within the overlying Culebra to change (see Section PA-4.8). The full mining of known potash reserves within the LWB in the absence of AICs and PICs is modeled as a Poisson process, with a rate of 10^{-4} yr^{-1} (see Section PA-3.9). For any particular future, this rate is used to determine a time at which full mining has occurred. Flow fields are calculated for the Culebra for two conditions: partial mining, which assumes all potash has been mined from reserves outside the LWB; and full mining, which assumes all reserves have been mined both inside and outside the LWB. Radionuclide transport through the Culebra uses the partial-mining flow fields prior to the time at which full mining has occurred and the full-mining flow fields after that time.

PA-8.3 Salado Flow

This section summarizes the results of the Salado flow calculations for the disturbed scenarios. Camphouse (Camphouse 2013c) provides a detailed presentation of BRAGFLO results obtained in the CRA-2014 PA.

PA-8.3.1 Salado Flow Results for E1 Intrusion Scenarios

Results are now presented for disturbed scenario S2-BF. Results presented for this scenario are representative of those calculated for E1 intrusion scenarios (scenarios S2-BF and scenario S3-BF), with the only difference being the time of intrusion. In the results that follow, trends discussed for scenario S2-BF also apply to scenario S3-BF. Results presented in this section are limited to those calculated for the intruded waste panel. Quantities calculated for the SRoR and NRoR in scenario S2-BF are similar to those calculated and previously discussed for undisturbed conditions because the panel closures in the CRA-2014 PA are tighter than the Option D closures in the CRA-2009 PABC.

Scenario S2-BF represents an E1 intrusion at 350 years. The horsetail plot of waste panel pressure obtained for the 300 vector realizations of the CRA-2014 PA is shown in Figure PA-50. The overall mean waste panel pressure curves obtained in the CRA-2014 PA and the CRA-2009 PABC are plotted together in Figure PA-51. The reduction in pressure (on average) for the undisturbed repository translates to lower porosity (on average) in repository waste regions at the time of intrusion (Camphouse 2013c). The trend toward reduced porosity at the time of intrusion results in increased pressure in the waste panel after it is connected to highly pressurized Castile brine during the intrusion, because of the reduced volume for the brine to flow into. The replacement of the Option D PCS with the ROMPCS that has "tighter" long-term properties also contributes to this pressure increase. The mean waste panel pressure obtained in the CRA-2014 PA remains higher than that seen in the CRA-2009 PABC for a period of time after the intrusion, but eventually falls below the CRA-2009 PABC result at roughly 6200 years (Figure PA-51). The impact of the revised iron corrosion rate implemented in the CRA-2014 PA results in a reduction (on average) to the rate of gas production due to iron corrosion. Gas generation due to iron corrosion is the dominant gas production mechanism in both the CRA-2014 PA and the CRA-2009 PABC. The reduction (on average) in the rate of gas production due to iron corrosion in the CRA-2014 PA yields a corresponding decrease in the rate of mean gas generation in the waste panel, resulting in the eventual reduction in waste region pressure as compared to the CRA-2009 PABC.

The reduction in mean waste panel pressure in the CRA-2014 PA for the undisturbed repository allows for increased brine inflow to the waste panel up to the time of intrusion. The increased brine inflow to the waste panel has a direct impact on waste panel brine saturation. The horsetail plot of waste panel brine saturation obtained in the CRA-2014 PA is shown in Figure PA-52. The overall mean waste panel brine saturation curves obtained in the CRA-2014 PA and the CRA-2009 PABC are plotted together in Figure PA-53. The increased mean waste panel brine inflow seen in the CRA-2014 PA as compared to the CRA-2009 PABC results in a corresponding increase in the CRA-2014 PA mean waste panel brine saturation following the E1 intrusion at 350 years.

Brine flow up the intrusion borehole potentially results in contaminated brine being transported to the ground surface following the intrusion as well as lateral transport of contaminated brine through the Culebra and across the LWB. The horsetail plot of cumulative brine flow up the intrusion borehole obtained in the CRA-2014 PA is shown in Figure PA-54. Overall means for this quantity obtained in the CRA-2014 PA and the CRA-2009 PABC are plotted together in Figure PA-55. The increased waste panel brine saturation in the CRA-2014 PA results, combined with the increase in mean waste panel pressure for a period of time after the intrusion, yields an increase in the overall mean obtained for brine flow up the intrusion borehole in the CRA-2014 PA as compared to the CRA-2009 PABC.

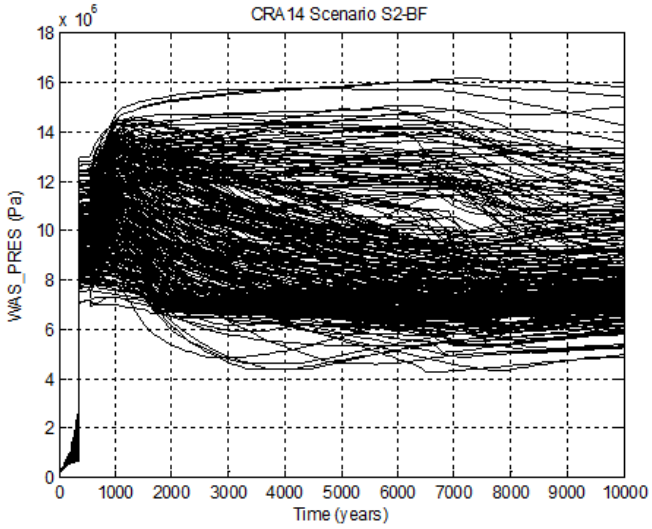

Figure PA- 50. Horsetail Plot of Waste Panel Pressure in the CRA-2014 PA, Scenario S2-BF

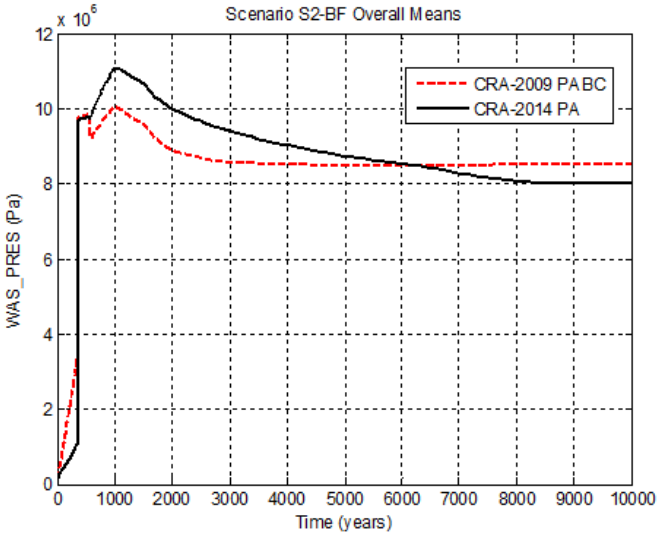

Figure PA- 51. Overall Means of Waste Panel Pressure, Scenario S2-BF

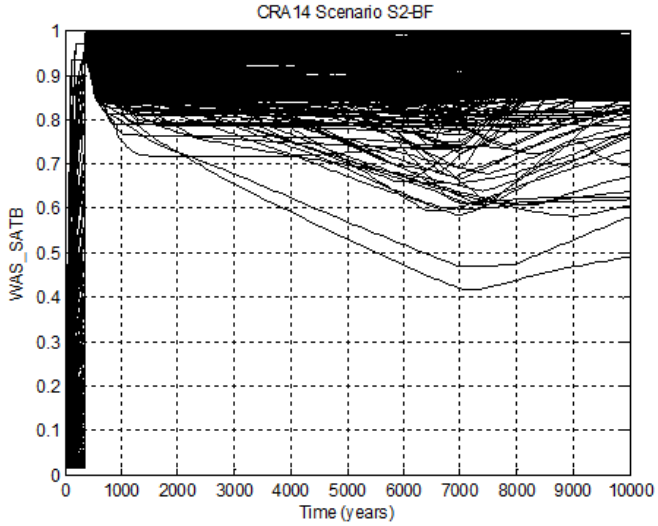

Figure PA- 52. Horsetail Plot of Waste Panel Brine Saturation in the CRA-2014 PA, Scenario S2-BF

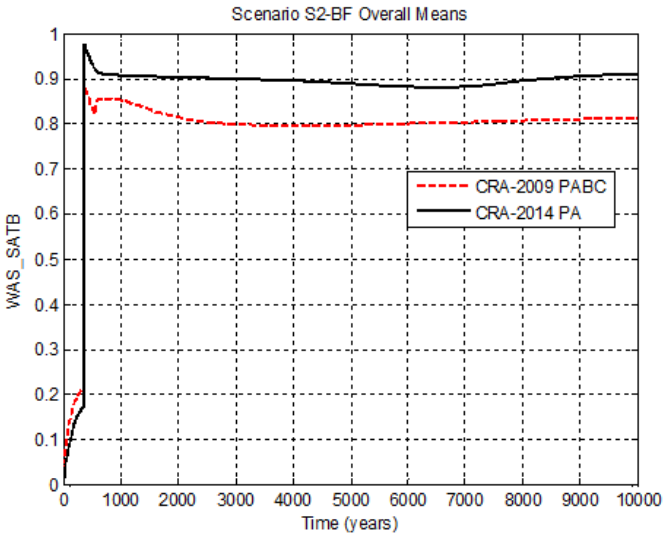

Figure PA- 53. Overall Means of Waste Panel Brine Saturation, Scenario S2-BF

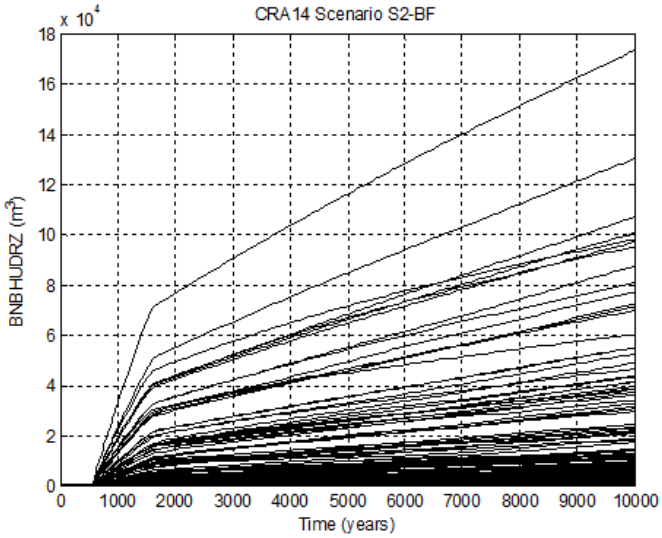

Figure PA- 54. Horsetail Plot of Cumulative Brine Flow up the Intrusion Borehole in the CRA-2014 PA, Scenario S2-BF

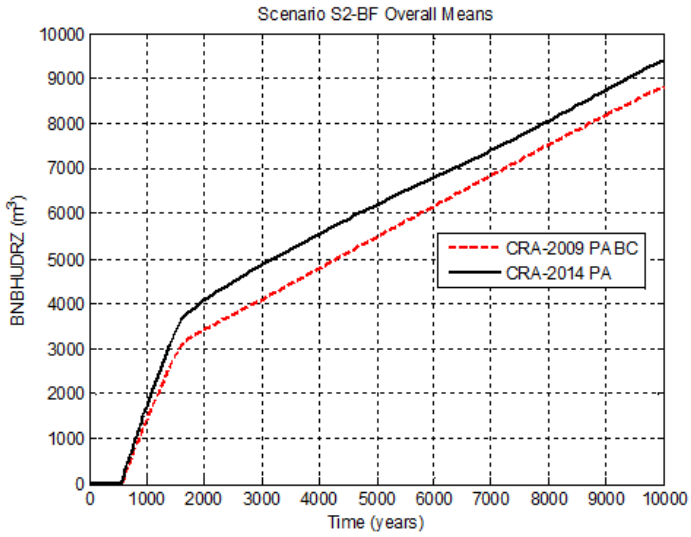

Figure PA- 55. Overall Means of Brine Flow up the Borehole, Scenario S2-BF

PA-8.3.2 Salado Flow Results for E2 Intrusion Scenarios

Results are now presented for disturbed scenario S4-BF. Scenario S4-BF represents an E2 intrusion at 350 years. Results presented for this scenario are representative of those calculated for E2 intrusion scenarios (scenarios S4-BF and scenario S5-BF), with the only difference being the time of intrusion. In the results that follow, trends discussed for scenario S4-BF also apply to scenario S5-BF. Results presented in this section are limited to those calculated for the intruded waste panel. Quantities calculated for the SRoR and NRoR are similar to those calculated and previously discussed for undisturbed conditions because of the tighter panel closures.

The horsetail plot of waste panel pressure obtained for the 300 vector realizations of scenario S4-BF in the CRA-2014 PA is shown in Figure PA-56. The overall means of waste panel pressure obtained in the CRA-2014 PA and the CRA-2009 PABC are plotted together in Figure PA-57. The refined iron corrosion rate and water budget implementation utilized in the CRA-2014 PA result in a reduction in the overall mean waste panel pressure as compared to the CRA-2009 PABC for undisturbed conditions. Consequently, at the time of the E2 intrusion, the mean waste panel pressure is lower in the CRA-2014 PA result than in the CRA-2009 PABC, and is also lower 200 years later when the borehole plugs fail. The result is a lower scenario S4-BF mean pressure in the CRA-2014 PA than in the CRA-2009 PABC. The trend toward reduced pressure in the CRA-2014 PA scenario S4-BF results in a corresponding trend toward increased brine flow to the waste panel prior to the E2 intrusion at 350 years, as well as increased brine inflow to the panel after the borehole plugs fail at 550 years. As seen in the results for the undisturbed repository, brine sequestration due to MgO hydration yields a reduced mean brine saturation in the waste panel prior to the intrusion at 350 years, even though the brine inflow at early times is higher in the CRA-2014 PA result. The increased inflow of brine following the intrusion yields an increased mean brine saturation in the CRA-2014 PA results as more brine becomes available in the waste panel than can be sequestered by MgO hydration. The horsetail plot of waste panel brine saturation obtained in scenario S4-BF in the CRA-2014 PA is shown in Figure PA-58. The overall means of waste panel brine saturation obtained in the CRA-2014 PA and the CRA-2009 PABC are plotted together in Figure PA-59. The mean cumulative brine flow up the intrusion borehole is similar, but slightly higher, in the CRA-2014 PA as compared to the CRA-2009 PABC. The horsetail plot of cumulative brine flow up the intrusion borehole obtained in scenario S4-BF of the CRA-2014 PA is shown in Figure PA-60. Overall means for this quantity obtained in the CRA-2014 PA and the CRA-2009 PABC are plotted together in Figure PA-61.

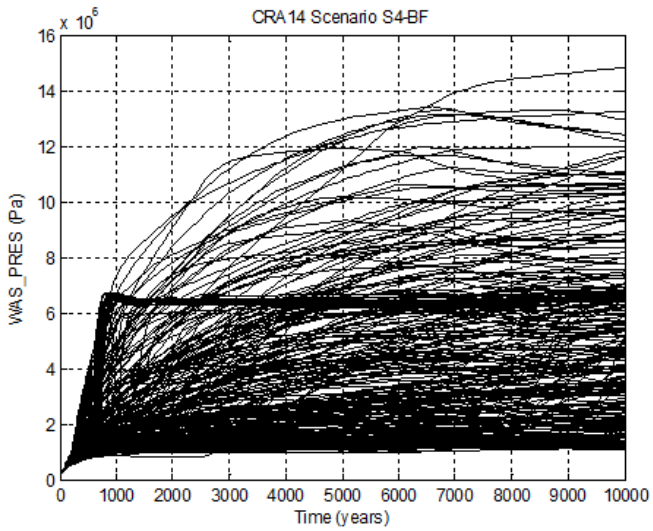

Figure PA- 56. Horsetail Plot of Waste Panel Pressure in the CRA-2014 PA, Scenario S4-BF

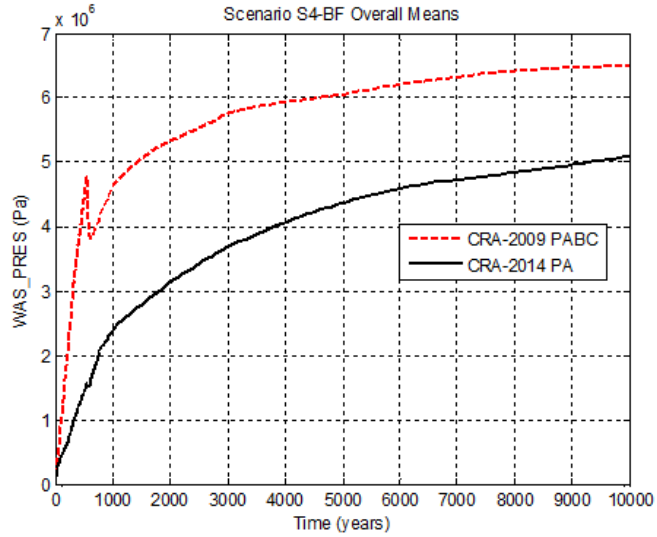

Figure PA- 57. Overall Means of Waste Panel Pressure, Scenario S4-BF

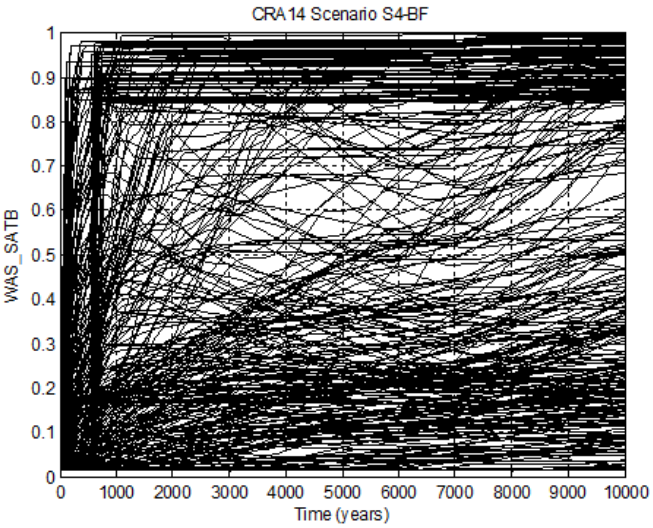

Figure PA- 58. Horsetail Plot of Waste Panel Brine Saturation in the CRA-2014 PA, Scenario S4-BF

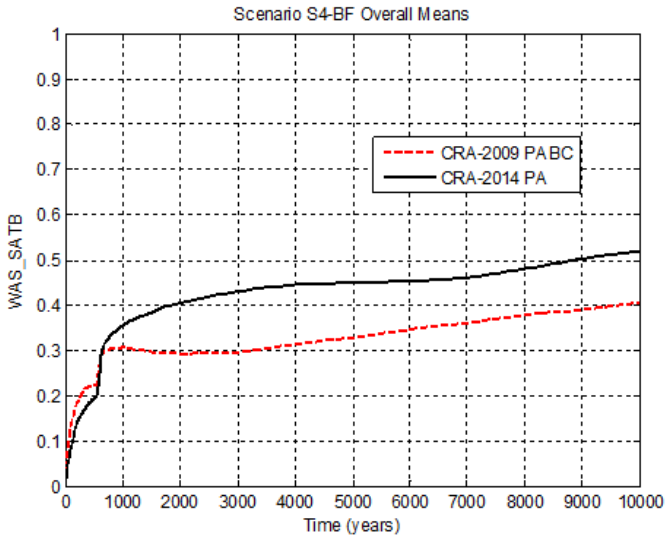

Figure PA- 59. Overall Means of Waste Panel Brine Saturation, Scenario S4-BF

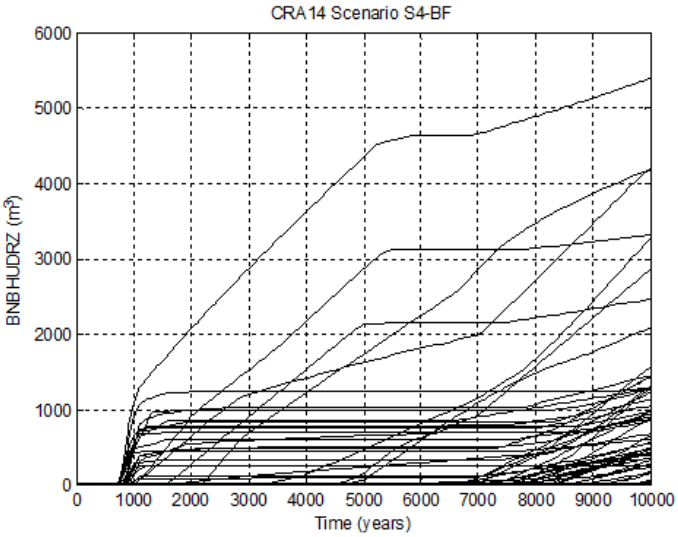

Figure PA- 60. Horsetail Plot of Cumulative Brine Flow up the Intrusion Borehole in the CRA-2014 PA, Scenario S4-BF

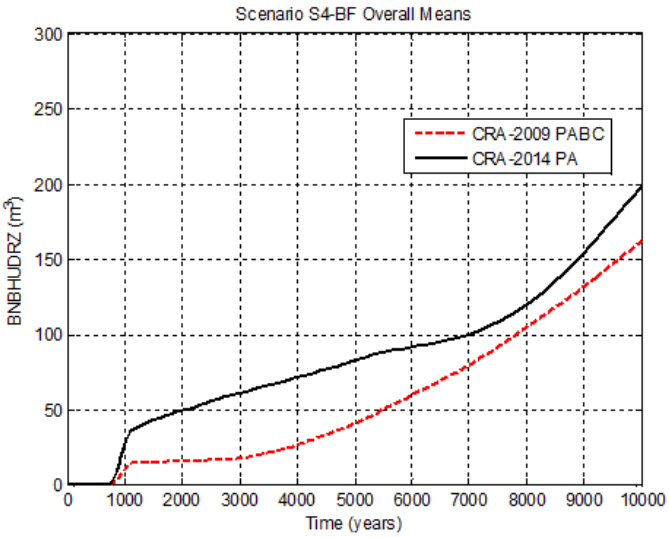

Figure PA- 61. Overall Means of Brine Flow up the Borehole, Scenario S4-BF

PA-8.3.3 Salado Flow Results for the Multiple Intrusion Scenario

BRAGFLO scenario S6-BF models an E2 intrusion occurring at 1000 years, followed by an E1 intrusion into the same panel at 2000 years. Calculated brine flows up the intrusion borehole obtained in scenario S6-BF are used in PA code PANEL to determine the radionuclide source term to the Culebra for the multi-intrusion case. The overall mean of cumulative brine flow up the intrusion borehole in scenario S6-BF (Figure PA-63) is increased in the CRA-2014 PA as compared to the CRA-2009 PABC, with the increase similar to that seen for the E1 intrusion results (Figure PA-55). The horsetail plot of cumulative brine flow up the intrusion borehole obtained in the CRA-2014 PA for scenario S6-BF is shown in Figure PA-62.

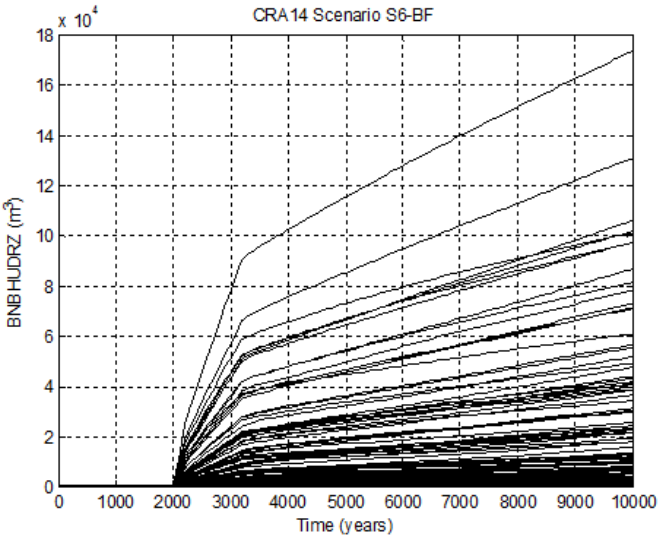

Figure PA- 62. Horsetail Plot of Cumulative Brine Flow up the Intrusion Borehole in the CRA-2014 PA, Scenario S6-BF

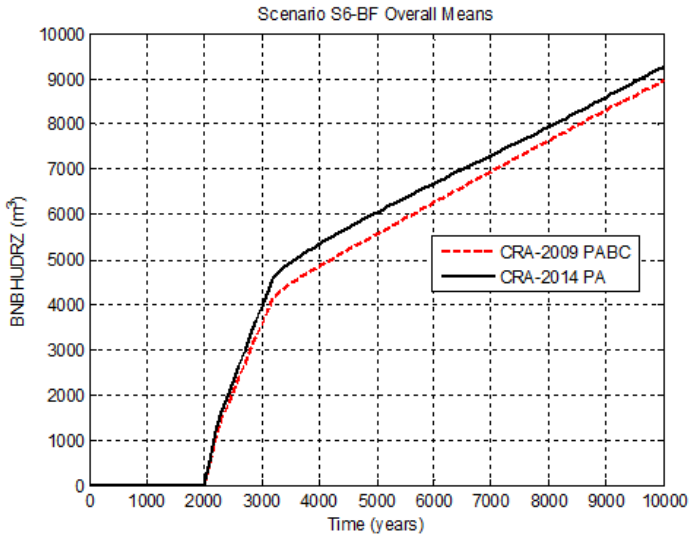

Figure PA- 63. Overall Means of Brine Flow up the Borehole, Scenario S6-BF

PA-8.4 Radionuclide Transport

In the disturbed scenarios, radionuclide transport in the Salado is calculated by the code NUTS (see Section PA-6.7.2). Radionuclide transport from the Salado to the Culebra is calculated by NUTS and PANEL (see Section PA-6.7.2 and Section PA-6.7.3). Radionuclide transport within the Culebra is calculated by SECOTP2D (see Section PA-6.7.8). For all radionuclide transport calculations, mobilized concentrations of radionuclides in Salado and Castile brines are computed by the code PANEL (see Section PA-6.7.3).

This section summarizes the radionuclide transport results for the disturbed scenarios. Camphouse (Camphouse 2013c) describes the brine and gas flow in the Salado. Detailed analysis of the radionuclide transport in the Salado is presented in Kim (2013a). Kim (2013b) provides an analysis of the mobilized concentrations of radionuclides in Salado and Castile brines. Appendix TFIELD-2014 and Kuhlman (2010) present an analysis of the flow and radionuclide transport within the Culebra.

PA-8.4.1 Radionuclide Mobilized Concentrations

The code PANEL calculates the time-varying concentration of radionuclides mobilized in brine, either as dissolved isotopes or as isotopes sorbed to mobile colloids (see Equation (PA.124) and Equation (PA.125)). Two different brines are considered: GWB, a magnesium-rich interstitial brine present in the Salado Formation; and ERDA-6, a sodium-rich brine in the Castile. Radionuclide solubility in the two brines can be considerably different. Before an E1 intrusion, PA assumes that the brine in the repository is GWB; after an E1 intrusion, brine in the repository is assumed to be ERDA-6. Baseline radionuclide solubilities are calculated using multiples of the minimum brine volume (17,400 m^3) necessary for a DBR to occur (Brush and Domski 2013b). Brine volumes of 1x, 2x, 3x, 4x, and 5x this minimum necessary brine volume are used in the calculation of baseline radionuclide solubilities in ERDA-6 brine and GWB, and these solubilities are listed in Kicker and Herrick (Kicker and Herrick 2013), Table 27.

Figure PA-64 and Figure PA-65 show the concentration of radioactivity mobilized in Salado brine as a function of time for all vectors in replicate 1 of the CRA-2014 PA. Figure PA-64 shows results obtained using baseline solubilities corresponding to the minimum brine volume of 17,400 m^3 (denoted as BV1 in that figure). Figure PA-65 shows results obtained using baseline solubilities corresponding to 5x the minimum brine volume (denoted as BV5 in that figure). Analogous results for Castile brine are shown in Figure PA-66 and Figure PA-67. As seen in those figures, radionuclide concentrations are reduced by roughly a factor of four from the minimum brine volume (BV1) to five times the minimum brine volume (BV5). Concentrations are expressed as EPA units/m^3 to combine the radioactivity of different isotopes. At early times (before 2000 years), the total mobilized concentrations (in both Salado and Castile brines) have their highest values because of the contribution of americium. After about 4000 years, the contribution from americium is much reduced because of the decay of ^{241}Am. After about 4000 years, the total mobilized concentrations are dominated by plutonium, with concentrations of uranium and thorium being orders of magnitude lower (Kim 2013b).

The CRA-2014 PA results for total mobilized concentrations show a similar variability to what was obtained in the CRA-2009 PABC. However, total mobilized concentrations obtained in the CRA-2014 PA decrease as the brine volume increases. This trend is expected to reduce releases associated with large DBR volumes in the CRA-2009 PABC.

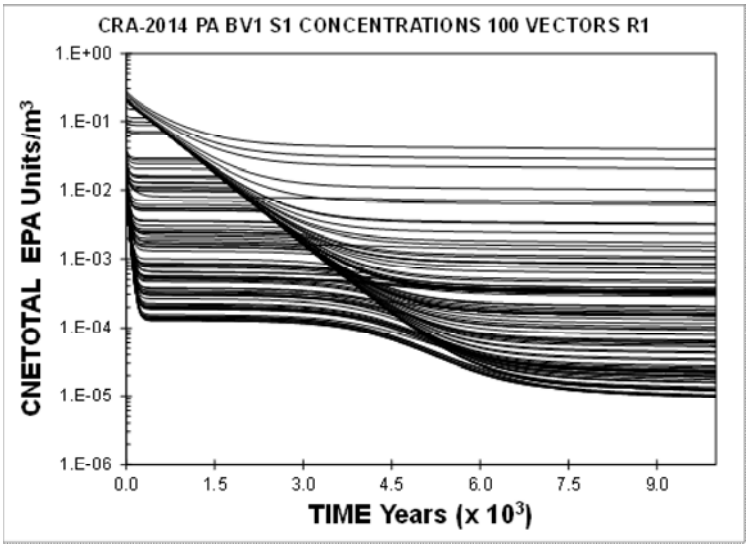

Figure PA- 64. CRA-2014 PA Total Mobilized Concentrations in Salado Brine, Replicate 1, BV1

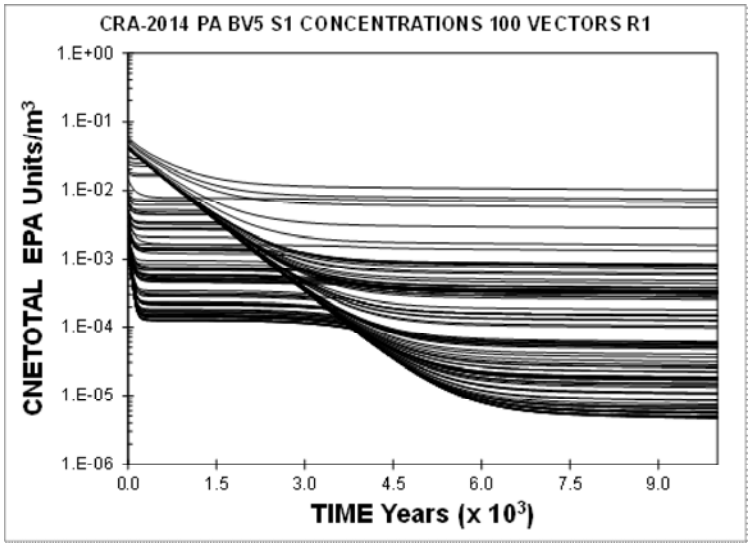

Figure PA- 65. CRA-2014 PA Total Mobilized Concentrations in Salado Brine, Replicate 1, BV5

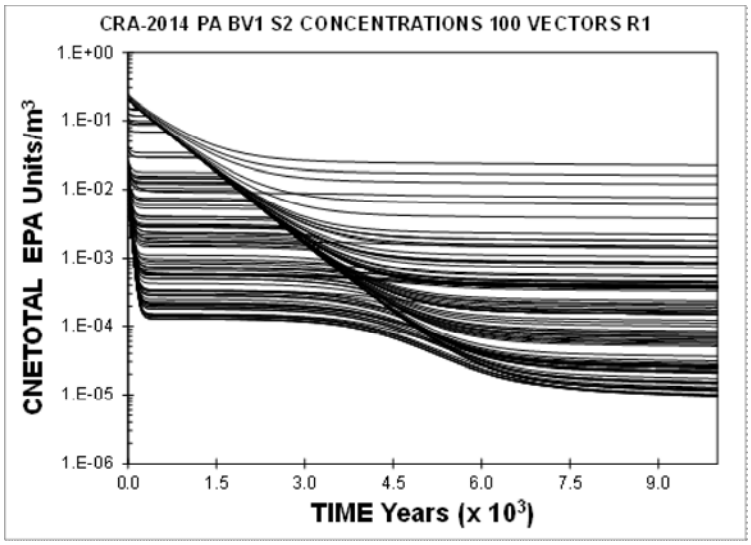

Figure PA- 66. CRA-2014 PA Total Mobilized Concentrations in Castile Brine, Replicate 1, BV1

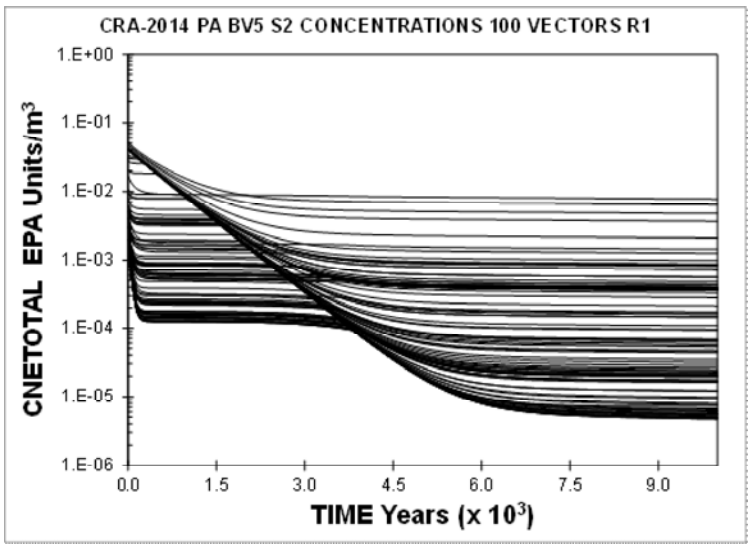

Figure PA- 67. CRA-2014 PA Total Mobilized Concentrations in Castile Brine, Replicate 1, BV5

PA-8.4.2 Transport through MBs and Shaft

In the disturbed scenarios, none of the 300 realizations obtained in the CRA-2014 PA resulted in releases through the the markerbeds that exceed the screening limit of 1×10^{-7} kg/m^3. In the CRA-2009 PABC, vector 53 of replicate 1 exceeded this limit for scenario S2-BF. As was the case in the CRA-2009 PABC, no realization showed transport of radionuclides through the shaft to the Culebra in the CRA-2014 PA.

PA-8.4.3 Transport to the Culebra

Radionuclide transport to the Culebra via a single intrusion borehole (disturbed scenarios S2-BF, S3-BF, S4-BF, and S5-BF) is modeled with the code NUTS (Section PA-4.3). Transport to the Culebra in the multiple intrusion scenario (S6-BF) is modeled with the code PANEL (Section PA-4.4). Detailed discussion of the radionuclide transport to the Culebra calculations can be found in Kim (Kim 2013a).

Figure PA-68 through Figure PA-72 show cumulative radioactivity transported up the borehole to the Culebra for the intrusion scenarios modeled with BRAGFLO. Transport to the Culebra is larger and occurs for more vectors in the S2-BF, S3-BF and S6-BF scenarios (with E1 intrusions) than in the S4-BF or S5-BF scenarios (E2 intrusions only). Most transport to the Culebra occurs over a relatively short period of time immediately after the borehole intrusion. For some E2 cases the releases are delayed because of the need to build up sufficient gas pressure. For the multiple intrusion scenario (S6-BF), only 5 vectors show radionuclide transport resulting from the E2 intrusion at 1,000 years; most radionuclide transport occurs immediately after the E1 intrusion at 2,000 years.

Radionuclide transport releases to the Culebra obtained in the CRA-2014 PA exhibit larger maximum and average values than were obtained in the CRA-2009 PABC (Kim 2013a). As seen in the Salado flow results already discussed, brine flows up the intrusion borehole are larger (on average) in the CRA-2014 PA than in the CRA-2009 PABC. Only the baseline radionuclide solubilities corresponding to the minimum brine volume necessary for a DBR are used in the CRA-2014 PA Salado transport calculation to keep the computational expense associated with NUTS calculations at a feasible level. Baseline solubilities corresponding to this volume of brine in the CRA-2009 PABC and the CRA-2014 PA are similar. However, the mean and maximum values of the solubility uncertainty distribution for +IV actinides increased in the CRA-2014 PA. This, combined with the overall trend toward increased brine flow up the intrusion borehole, results in a trend toward increased radionuclide transport releases to the Culebra for CRA-2014 PA disturbed scenarios.

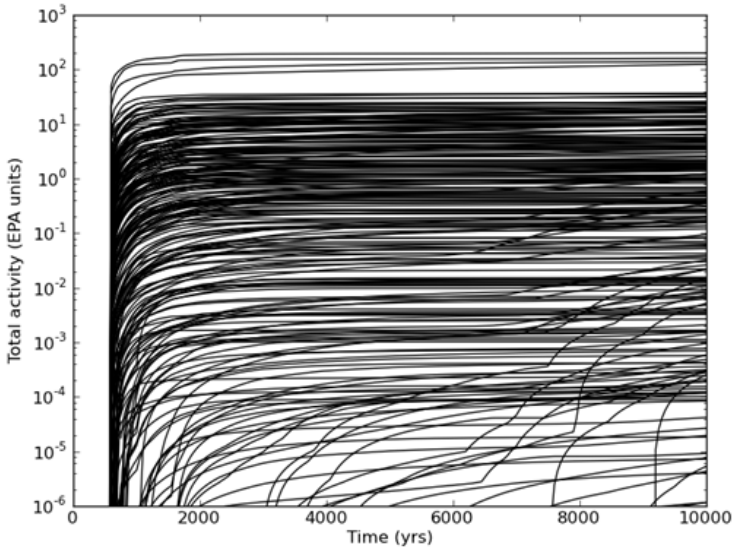

Figure PA- 68. CRA-2014 PA Cumulative Transport Release to the Culebra, Scenario S2-BF

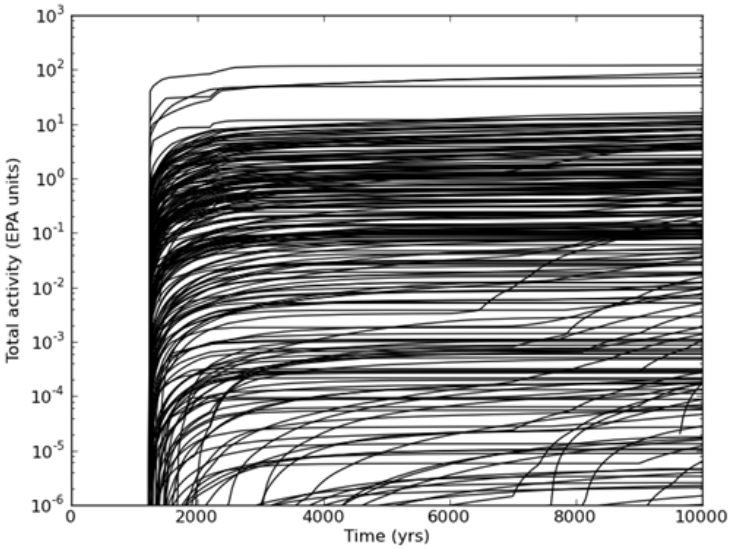

Figure PA- 69. CRA-2014 PA Cumulative Transport Release to the Culebra, Scenario S3-BF

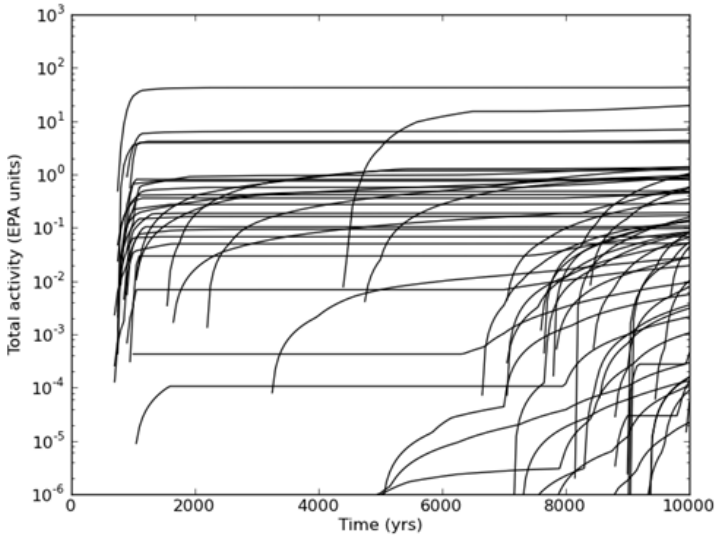

Figure PA- 70. CRA-2014 PA Cumulative Transport Release to the Culebra, Scenario S4-BF

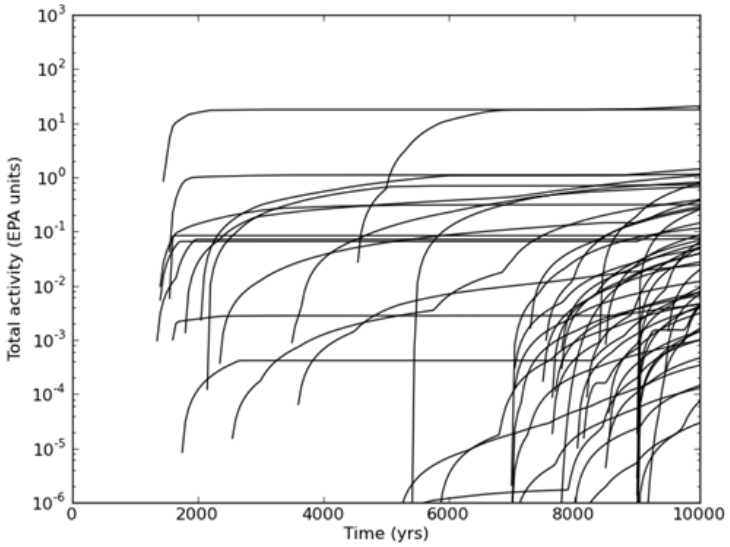

Figure PA- 71. CRA-2014 PA Cumulative Transport Release to the Culebra, Scenario S5-BF

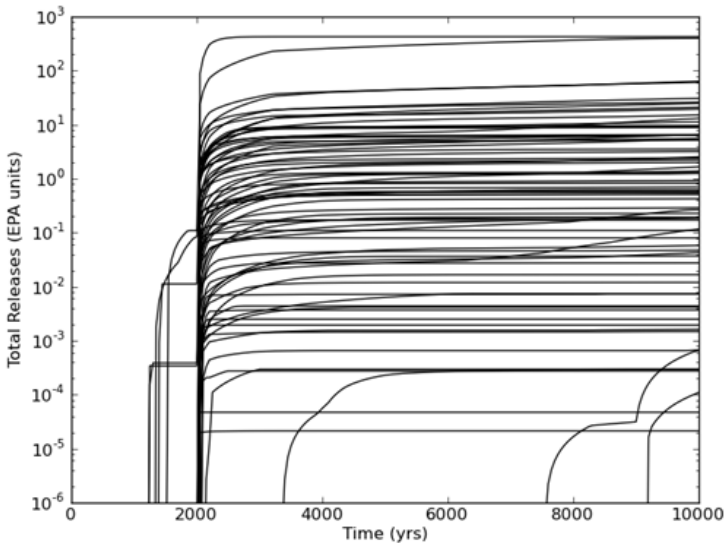

Figure PA- 72. CRA-2014 PA Cumulative Transport Release to the Culebra, Scenario S6-BF

PA-8.4.4 Transport through the Culebra

As none of the changes included in the CRA-2014 PA impact Culebra transport, the CRA-2014 PA uses Culebra transport results obtained in the CRA-2009 PABC. The CRA-2009 PABC Culebra transport calculation included a number of changes as compared to Culebra transport results used in the CRA-2009 PA. These changes included:

1. Changes in the definition of minable potash
2. Reductions to the lower limits of the matrix distribution coefficients (K_d) for Am(III), Pu(III), Pu(IV), Th(IV), and U(IV)
3. Updates to the Culebra transmissivity fields

Radionuclide transport through the Culebra for a given set of uncertain parameters is calculated with the code SECOTP2D (see Section PA-6.7.8). Note that the total release of radionuclides across the LWB at the Culebra for given futures is calculated with the code CCDFGF by convolving the SECOTP2D results with the radionuclide transport to the Culebra calculated by NUTS and PANEL. This section discusses the SECOTP2D results; total releases through the Culebra are presented in Section PA-9.4.

Culebra radionuclide transport calculations were performed for three replicates of 100 vectors each for both partial-mining and full-mining scenarios (600 total simulations). Each of the 600 radionuclide transport simulations used a unique flow field computed separately with the code MODFLOW 2000 (see Kuhlman 2010). The partial-mining scenario assumes the extraction of all potash reserves outside the LWB, while the full-mining scenario assumes that all potash reserves both inside and outside the LWB are exploited.

In each radionuclide transport simulation, 1 kg of each of four radionuclides (^{241}Am, ^{234}U, ^{230}Th, and ^{239}Pu) are released in the Culebra above the center of the waste panel area. Radionuclide transport of the ^{230}Th daughter product of ^{234}U decay is calculated and tracked as a separate species. In the following discussion, ^{230}Th will refer to the ^{234}U daughter product and ^{230}ThA will refer to that released at the waste panel area.

For the three replicates included in the CRA-2014 PA, the number of vectors with cumulative releases greater than 10^{-9} kg criterion, established in the CCA, is shown in Table PA-25 for each radionuclide, under partial and full mining conditions. All SECOTP2D results, regardless of magnitude, are included in the calculation of releases from the Culebra. Under partial and full mining conditions, ^{234}U has the highest number of vectors that surpassed the 10^{-9} kg criterion, while ^{241}Am has the least number of vectors. A considerable increase is observed in the full mining scenario compared with the partial mining scenario, due to the increased proximity of the potash reserves within the LWB to the repository, which are extracted in the full mining scenario (Kuhlman 2010).

Table PA- 25. Number of Realizations with Radionuclide Transport to the LWB

# of vectors	Partial Mining			Full Mining		
	R1	R2	R3	R1	R2	R3
^{241}Am	0	0	0	8	10	3
^{239}Pu	3	1	1	20	27	22
^{234}U	11	14	12	48	50	47
^{230}Th	5	10	6	36	38	42
^{230}ThA	2	3	0	21	31	29

PA-8.5 Direct Releases

Direct releases occur at the time of a drilling intrusion, and include cuttings and cavings, spallings, and DBRs. This section presents an analysis of the volume released by each mechanism.

Kicker (Kicker 2013) provides additional information about the cuttings, cavings, and spallings releases calculated for the CRA-2014 PA. Malama (2013) provides a detailed analysis of DBRs in the CRA-2014 PA.

PA-8.5.1 Cuttings and Cavings

Cuttings and cavings are the solid waste material removed from the repository and carried to the surface by the drilling fluid during borehole drilling. Cuttings are the materials removed directly by the drill bit, and cavings are the material eroded from the walls of the borehole by shear stresses from the circulating drill fluid. The volume of cuttings and cavings material removed from a single drilling intrusion into the repository is assumed to be in the shape of a cylinder. The code CUTTINGS_S calculates the area of the base of this cylinder, and cuttings and cavings results in this section are reported in terms of these areas. The volumes of cuttings and cavings removed can be calculated by multiplying these areas with the initial repository height 3.96 m (BLOWOUT:HREPO).

The drill bit diameter (parameter BOREHOLE:DIAMMOD) is specified to be 0.31115 meters in both the CRA-2009 PABC and the CRA-2014 PA. A cuttings area of 0.0760 m^2 is obtained for all vectors in both the CRA-2009 PABC and the CRA-2014 PA as both analyses use the same constant drill bit diameter value. A refined distribution for parameter BOREHOLE:TAUFAIL is implemented in the CRA-2014 PA, and is listed in Kicker and Herrick (Kicker and Herrick 2013), Table 4. A loguniform distribution having a minimum of 0.05 Pa, a mean of 10.5 Pa, and a maximum of 77.0 Pa was used to represent uncertainty in parameter BOREHOLE:TAUFAIL in the CRA-2009 PABC. A uniform distribution having a minimum of 2.22 Pa, a mean of 39.61 Pa, and a maximum of 77.0 Pa is used for this parameter in the CRA-2014 PA. Parameter BOREHOLE:TAUFAIL is used to represent the effective shear strength for erosion of WIPP waste (see Section PA-4.5.2); changes to it potentially impact cavings release areas.

Cuttings and cavings area statistics calculated in the CRA-2014 PA are shown in Table PA-26. The refinement to parameter BOREHOLE:TAUFAIL used in the CRA-2014 PA results in a shift toward a lower mean cavings area as well as a decrease in the overall number of vectors with nonzero cavings area in the CRA-2014 PA as compared to the PABC-2009.

Table PA- 26. CRA-2014 PA Cavings Area Statistics

Replicate	Minimum (m^2)	Maximum (m^2)	Mean (m^2)	Number of Vectors without Cavings
R1	0.0	0.090	0.01	50
R2	0.0	0.090	0.01	44
R3	0.0	0.075	0.01	50

The uncertainty in cavings area arises primarily from the uncertainty in the shear strength of the waste (Kicker 2013). Lower shear strengths tend to result in larger cavings releases, and hence larger cuttings and cavings releases.

PA-8.5.2 Spallings

Calculating the volume of solid waste material released to the surface due to spallings from a single drilling intrusion into the repository is a two-part procedure. The code DRSPALL calculates the spallings volumes from a single drilling intrusion at four values of repository pressure (10, 12, 14, and 14.8 MPa). Following this, spallings volumes from a single intrusion are calculated using the code CUTTINGS_S; this code linearly interpolates the spallings volumes calculated using DRSPALL, based on the pressure calculated by BRAGFLO. Results from both of these calculations are documented in this section.

PA-8.5.2.1 DRSPALL Results

None of the changes implemented in the CRA-2014 PA affect the DRSPALL calculations, so the DRSPALL results used in the CRA-2009 PA were also used in the CRA-2014 PA. These results were generated by running DRSPALL for each of 100 vectors in 3 replicates and for 4 values of repository pressure (10, 12, 14, and 14.8 MPa; see Section PA-4.6.4). No spallings occurred at 10 MPa for any vector.

The uncertainty in the spallings volumes arises from four uncertain variables in the DRSPALL calculations: waste permeability, waste porosity, waste tensile strength, and waste particle diameter after tensile failure (Table PA-11). Figure PA-73 indicates that the largest spallings volumes occur when waste permeability is less than 1.0×10^{-13} m^2, but larger permeability values result in a higher frequency of nonzero spallings volumes. This observation can be explained as follows: the higher permeability values sampled result in smaller tensile stresses and less tensile failure, but promote fluidization. Lower permeability leads to greater tensile stresses and tensile failure, but failed material may not be able to fluidize at this low permeability.

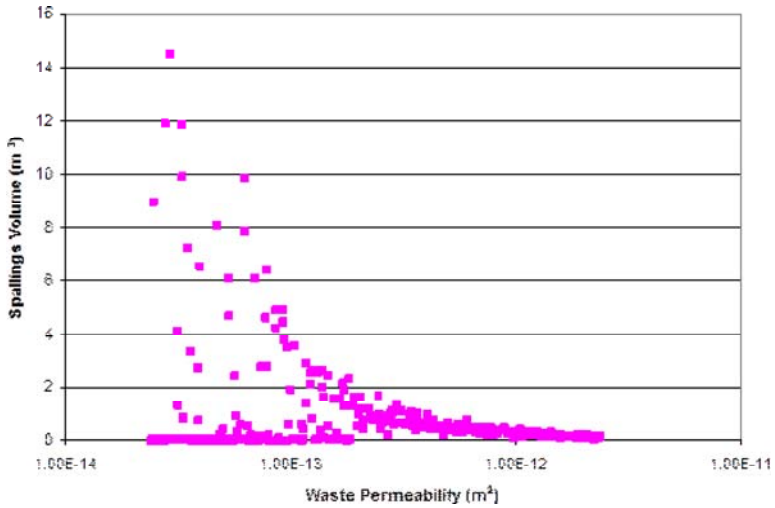

Figure PA- 73. Scatterplot of Waste Permeability Versus Spallings Volume, CRA-2014 PA

Smaller particle diameter values (see Figure PA-74) tend to result in larger spallings volumes and a higher frequency of nonzero spallings volumes. The uncertainty in the spallings volumes from a single intrusion is largely determined by the uncertainty in these two parameters. Obvious correlations between spallings volumes and the other two parameters could not be established.

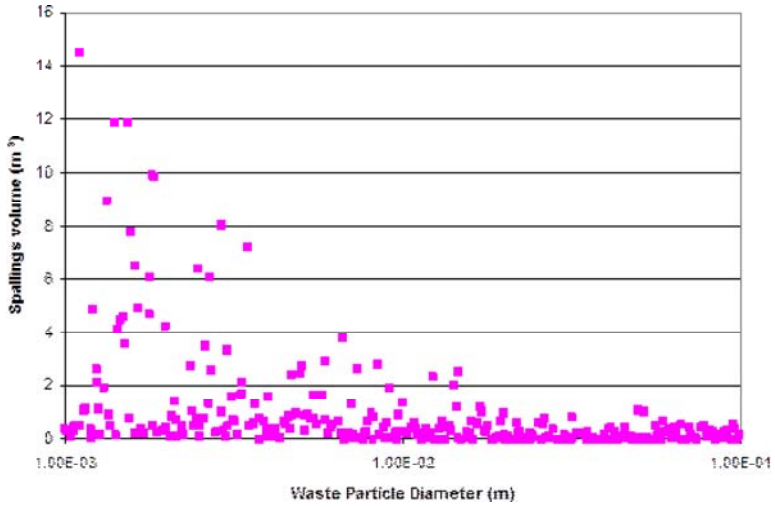

Figure PA- 74. Scatterplot of Waste Particle Diameter Versus Spallings Volume, CRA-2014 PA

PA-8.5.2.2 CUTTINGS_S Results

Two factors directly affect the CUTTINGS_S calculation of spallings volumes for the drilling scenarios: the volumes calculated by DRSPALL and the repository pressures calculated by BRAGFLO.

Table PA-27 summarizes the statistics for the CRA-2014 PA spallings volumes. Results presented in that table are assessed over all three replicates, times, vectors, and drilling locations. The maximum spallings volumes obtained for scenarios S1-DBR, S4-DBR, and S5-DBR (see Table PA-22) are reduced in the CRA-2014 PA as compared to the CRA-2009 PABC. The same is also true of the average release volumes obtained for these scenarios. Scenario S1-DBR corresponds to an intrusion into a theretofore undisturbed repository. Scenarios S4-DBR and S5-DBR correspond to a subsequent intrusion into a repository that has already undergone an earlier E2 intrusion. From the Salado flow results already discussed, repository waste regions trend toward lower pressure in the CRA-2014 PA for undisturbed conditions and E2 intrusion scenarios. This translates directly to reductions in spallings release volumes for scenarios S1-DBR, S4-DBR, and S5-DBR. For E1 intrusion scenarios, the mean pressure in the intruded panel is increased in the CRA-2014 PA for a period of time after the intrusion, but eventually falls below that seen in the CRA-2009 PABC. Scenarios S2-DBR and S3-DBR correspond to a subsequent intrusion into a repository that has already undergone a previous E1 intrusion. The trend toward higher waste panel pressure for a period of time after the initial E1 intrusion results in greater maximum spallings release volumes for scenarios S2-DBR and S3-DBR, although the average nonzero spallings volumes are quite similar for the S2-DBR and S3-DBR scenarios. The overall trend in the CRA-2014 PA is toward lower waste region pressure as compared to the CRA-2009 PABC. The result is a reduction in the number of realizations that result in a nonzero spallings release volume in all scenarios as compared to the CRA-2009 PABC.

Table PA- 27. CRA-2014 PA Spallings Volume Statistics

Scenario	Maximum Volume (m3)		Average Nonzero Volume (m3)		Number of Nonzero Volumes	
	CRA-2009 PABC	CRA-2014 PA	CRA-2009 PABC	CRA-2014 PA	CRA-2009 PABC	CRA-2014 PA
S1-DBR	4.91	1.67	0.40	0.32	466	112
S2-DBR	8.29	9.69	0.44	0.43	352	278
S3-DBR	7.97	9.13	0.38	0.45	351	170
S4-DBR	2.26	1.67	0.37	0.26	161	55
S5-DBR	1.93	1.67	0.38	0.28	233	66

Spallings releases are also a function of intrusion location. From the Salado flow results already discussed, the trend is toward reduced pressure in the south and north rest-of-repository regions in the CRA-2014 PA. This corresponds to reductions in spallings releases in those regions. The trend toward lower pressure is also evident for the intruded southernmost panel, except for E1 intrusion scenarios. For E1 scenarios, the mean pressure in the intruded panel is increased in the CRA-2014 PA for a period of time after the intrusion, but eventually falls below that seen in the CRA-2009 PABC. The result is a larger maximum spallings release for intrusions into the lower region in the CRA-2014 PA. The overall trend toward lower waste region pressure yields a reduction in the number of nonzero spallings volumes at all intrusion locations.

PA-8.5.3 DBRs

DBRs to the surface can occur during or shortly after a drilling intrusion. For each element of the Latin hypercube sample, the code BRAGFLO calculates volumes of brine released for a total of 78 combinations of intrusion time, intrusion location, and initial conditions (see Section PA-6.7.6). Initial conditions for the DBR calculations are obtained from the BRAGFLO Salado flow model results from Scenarios S1-BF through S5-BF. Salado flow model results from the S1-BF scenario (Section PA-7.1) are used as initial conditions for DBR when modeling a first intrusion into the repository that may have a DBR. Salado flow model results from the S2-BF through S5-BF scenarios (Section PA-8.3) are used as initial conditions for DBR when modeling second or subsequent drilling intrusions that may have a DBR.

Summary statistics of the calculated DBR volumes in the CRA-2014 PA are shown in Table PA-28. Results presented in that table are assessed over all three replicates, times, vectors, and drilling locations. As was also the case in the CRA-2009 PABC, release volumes that are less than the screening criterion of 1×10^{-7} m^3, established in the CCA, are considered to be inconsequential and are not included in the tally of vectors that result in DBR release volumes in the CRA-2014 PA calculations.

Table PA- 28. CRA-2014 PA DBR Volume Statistics

Scenario	Number of Nonzero Volumes		Maximum volume (m^3)		Average nonzero volume (m^3)	
	CRA-2009 PABC	CRA-2014 PA	CRA-2009 PABC	CRA-2014 PA	CRA-2009 PABC	CRA-2014 PA
S1-DBR	369	220	27.60	47.31	0.10	0.22
S2-DBR	1179	1140	48.20	58.02	2.80	3.78
S3-DBR	926	988	40.60	55.09	1.50	2.65
S4-DBR	211	104	20.40	36.77	0.10	0.15
S5-DBR	314	133	21.10	36.60	0.10	0.17

There is a reduction in the overall number of vectors that result in a DBR release volume in the CRA-2014 PA as compared to the CRA-2009 PABC. From the Salado flow results already presented, changes included in the CRA-2014 PA result in most of the repository being drier (on average) and under lower pressure (on average) than was the case in the CRA-2009 PABC. Mean brine saturations and pressures are lower in the south and north rest-of-repository in the CRA-2014 PA as compared to the CRA-2009 PABC. The result is an overall reduction in the number of vectors that satisfy the two necessary conditions (see Section PA-4.7.1) for a nonzero DBR volume.

There is a consistent increase in the maximum DBR volumes from the CRA-2009 PABC to the CRA-2014 PA. For undisturbed conditions, as well as all intrusion scenarios, increases are seen in the mean brine saturation of the southernmost waste panel in the CRA-2014 PA Salado flow results. For undisturbed and E2 intrusions scenarios, increases in the mean waste panel brine saturation are accompanied by decreases in the mean waste panel pressure. However, increased brine saturation can result in larger maximum DBR volumes for vectors that also satisfy the DBR necessary condition for pressure. For E1 intrusion scenarios, the increase in the mean brine saturation of the southernmost waste panel is accompanied by increased mean pressure for a period of time after the intrusion. The result is larger maximum DBR volumes for E1 intrusion scenarios.

DBR volume trends observed in the CRA-2014 PA are consistent with those found in prior analyses with regard to drilling location. DBRs are less likely to occur in intrusions situated in the up-dip (upper) drilling locations than in the down-dip (lower) drilling location. Of all the intrusions that had a non-zero DBR volume in the CRA-2014 PA, 82.4% occurred in the lower location. Of all the intrusions that have a

non-zero DBR volume and occur during a down-dip (lower) drilling intrusion, 89.9% are found in scenarios S2-DBR and S3-DBR. DBR results obtained in the CRA-2014 PA continue to demonstrate that the majority of non-zero DBR volumes occur when there is a previous E1 intrusion within the same panel. In addition to DBRs being less likely to occur for drilling intrusions in the up-dip (upper) locations, DBR volumes from such intrusions tend to be much smaller than those from lower drilling intrusions. For all three replicates of the CRA-2014 PA, the maximum DBR volume for the upper drilling location is 5.1 m^3 compared to 58.0 m^3 for the lower drilling location. These observations support the conclusion that intrusions into the lower location are the primary source for significant DBRs.

The combination of relatively high pressure and brine saturation in the intruded panel is required for direct brine release to the surface. Figure PA-75 shows a scatter plot of DBR volume versus pressure in the intruded panel at different intrusion times for scenario S2-DBR, replicate 1, lower drilling intrusion for the CRA-2014 PA. In that figure, symbols indicate the value of the mobile brine saturation, defined as brine saturation minus residual brine saturation in the waste. As prescribed by the conceptual model, there are no DBRs until pressures exceed the 8 MPa vertical line in the figure. Figure PA-75 shows a clustering of the data about a linear trend (dashed line in the figure).

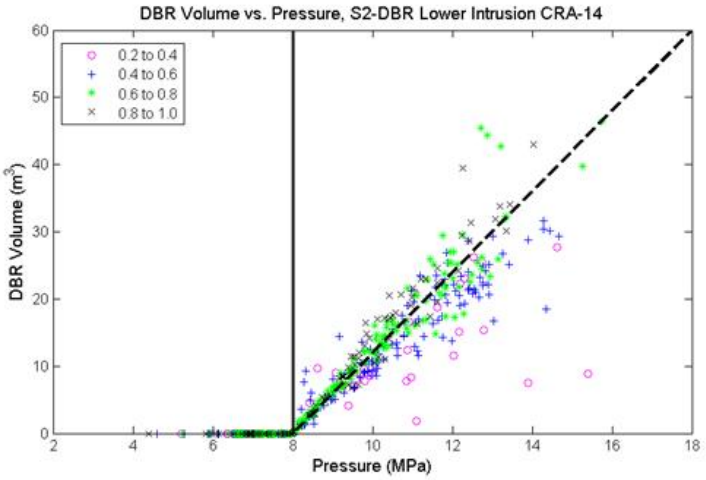

Figure PA- 75. Sensitivity of DBR Volumes to Pressure and Mobile Brine Saturation, Replicate R1, Scenario S2, Lower Intrusion, CRA-2014 PA. (Symbols indicate the range of mobile brine saturation given in the legend.)

PA-9.0 Normalized Releases

The radioactive waste disposal regulations of Part 191, Subparts B and C include containment requirements for radionuclides. The containment requirements of section 191.13 specify that releases from a disposal system to the accessible environment must not exceed the release limits set forth in 40 CFR Part 191, Appendix A, Table 1. As set forth in section 194.34, the results of PA are required to be expressed as CCDFs of total releases.

This section discusses each of the four categories of releases that constitute the total release: cuttings and cavings, spallings, DBRs, and transport releases, followed by the total normalized releases for the CRA-2014 PA. A comparison between the CRA-2014 PA and the CRA-2009 PABC results is also presented. In summary, despite the changes and corrections made between the CRA-2009 PABC and the CRA-2014 PA, there were no major changes in the overall pattern of releases. Cuttings, cavings, and DBRs remain the most significant pathways for release of radioactive material to the land surface. Contributions to total releases from spallings and Culebra transport are much less significant. The resulting CCDFs of total normalized releases for the CRA-2014 PA are within the regulatory limits defined in section 191.13.

Rank regression analysis was used to evaluate the sensitivity of the normalized releases to the sampled parameters. The predicted error sum of squares (PRESS) was computed to detect over-fitting of the regression model to the data. Over-fitting can occur when the regression methodology causes the fit to favor specific points rather than the general shape of the data curve. In such a case the minimum value of PRESS may occur earlier than the last step in the regression analysis. No such condition was observed in any of the rank correlation analyses performed in the CRA-2014 PA. Details of the sensitivity analysis performed in the CRA-2014 PA can be found in Kirchner (Kirchner 2013b).

PA-9.1 Cuttings and Cavings

The overall mean CCDFs for cuttings and cavings releases from the CRA-2014 PA and the CRA-2009 PABC are shown in Figure PA-76. Overall, cuttings and cavings normalized releases calculated for the CRA-2014 PA are smaller than those for the CRA-2009 PABC. The activity of the CRA-2014 waste inventory is greater (in EPA units) over time than that implemented in the CRA-2009 PABC (Kicker and Zeitler 2013a). The drilling rate per unit area is also increased in the CRA-2014 PA, which increases the number of drilling events into repository waste areas. Although the changes in waste inventory and drilling rate both serve to increase cuttings and cavings releases, the effect of the CRA-2014 PA waste shear strength refinement is to reduce cavings release volumes, and hence cuttings and cavings volumes

overall (Kicker 2013), enough so that normalized releases due to cuttings and cavings in the CRA-2014 PA fall below those seen in the CRA-2009 PABC (Zeitler 2013).

The uncertainty in mean cuttings and cavings releases is primarily due to the uncertainty in the cuttings and cavings volume. Cuttings volume is controlled by the drill bit diameter whereas cavings volume depends on waste shear strength and, to a much smaller extent, the angular velocity of the drill string (Kicker 2013). The rank regression analysis showed that waste shear strength (BOREHOLE:TAUFAIL) controls about 65% of the variability in mean cuttings and cavings releases in replicate 1 of the CRA-2014 PA, as compared to 98% in replicate 1 of the CRA-2009 PABC. This difference is undoubtedly due to the change in the distribution of BOREHOLE:TAUFAIL from a loguniform distribution to a uniform distribution of somewhat smaller range (Kirchner 2013b).

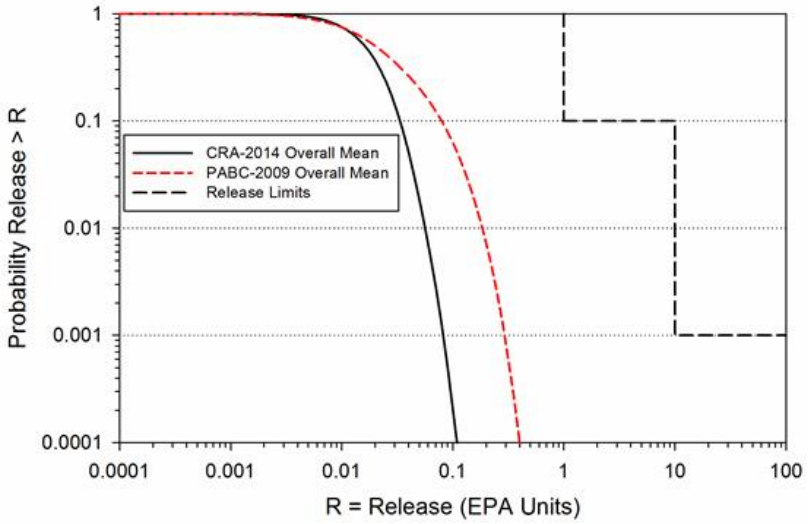

Figure PA- 76. Overall Mean CCDFs for Cuttings and Cavings Releases: CRA-2014 PA and CRA-2009 PABC

PA-9.2 Spallings

Figure PA-77 shows the overall mean spallings release CCDFs from the CRA-2014 PA and the CRA-2009 PABC. Spallings release volumes directly depend on repository pressure at the time of intrusion. Despite the modified panel closure system, which serves to increase waste panel pressures (on average), the updated steel corrosion rate, additional excavation in the WIPP experimental area, and the updated repository water balance implementation each contribute to a trend toward decreased waste panel pressures in the CRA-2014 PA. This trend toward lower waste panel pressure directly translates to a trend toward decreased spallings release volumes from the PABC-2009 to the CRA-2014 PA (Kicker 2013). The result is an overall reduction in spallings normalized releases, despite an increase in waste inventory activity, due to a decrease in the number of nonzero spallings volumes (Zeitler 2013).

The rank regression analysis indicates that the dominant uncertain parameters with regard to the uncertainty in spallings releases in the CRA-2014 PA include the particle diameter for disaggregated waste (SPALLMOD:PARTDIAM) and the initial brine pressure in the Castile

(CASTILER:PRESSURE). The intial brine pressure in the Castile impacts waste region pressures following E1 drilling intrusions which, in turn, impacts spallings release volumes and their frequency. Waste fluidization during a drilling intrusion is a function of waste particle diameter. The dominant uncertain parameter with regard to the uncertainty in spallings releases in the CRA-2009 PABC was the effective porosity of intact halite (S_HALITE:POROSITY). The number of vectors with zero spallings release volumes in the CRA-2014 PA was high enough to reduce the effectiveness of the regression analysis. A large number of zero values in the data tend to negate the assumption of linear regression that errors (residuals) are normally distributed. In addition, the distribution of zeros along the independent axis can exert a lot of influence on the slope of the regression model (Kirchner 2013b).

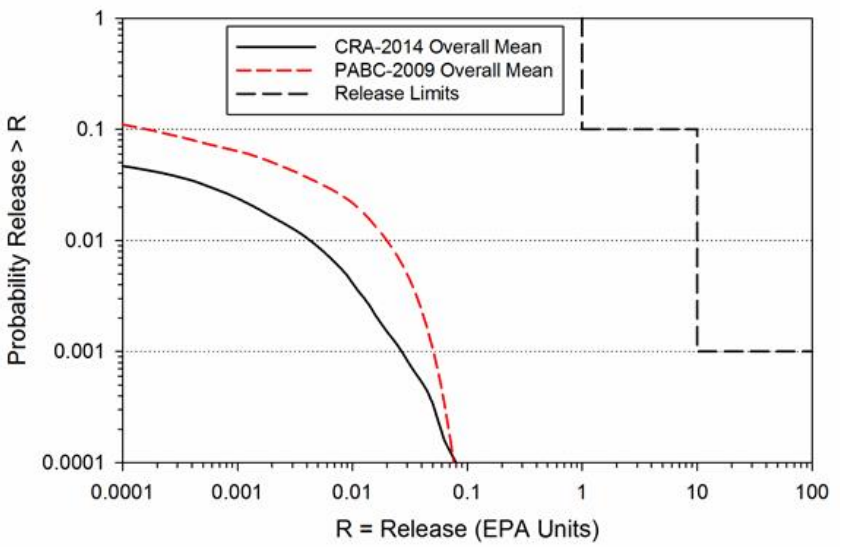

Figure PA- 77. Overall Mean CCDFs for Spallings Releases: CRA-2014 PA and CRA 2009 PABC

PA-9.3 Direct Brine

The overall mean CCDFs for DBRs from the CRA-2014 PA and the CRA-2009 PABC are shown in Figure PA-78. Overall, there is a decrease in normalized DBRs from the CRA-2009 PABC to the CRA-2014 PA. Several changes included in the CRA-2014 PA contribute to this reduction. The refinement to the probability that a drilling intrusion results in a pressurized brine pocket encounter (parameter GLOBAL:PBRINE) yields an overall reduction to DBR volumes in the CRA-2014 PA CCDFGF results (Zeitler 2013). The variable brine volume implementation maps radionuclide mobilized concentrations in brine to volumes of brine released. Radionuclide mobilized concentrations in brine decrease for the +III actinides as brine volume increases in the CRA-2014 PA (see Section PA-8.4.1), whereas mobilized concentrations in brine remained fixed (for each vector) in the CRA-2009 PABC, regardless of the actual brine volume being released. There is a consistent increase in maximum DBR volumes from the CRA-2009 PABC to the CRA-2014 PA (see Section PA-8.5.3). However, the variable brine volume implementation results in overall lower mobilized radionuclide concentrations in these larger brine volumes. The revised steel corrosion rate and water balance implementation used in the CRA-2014 PA also lead to an overall reduction in the number of vectors that satisfy the two necessary conditions for a DBR. In total, the combined impact of changes included in the CRA-2014 PA is an overall net reduction to normalized direct brine releases as compared to the CRA-2009 PABC.

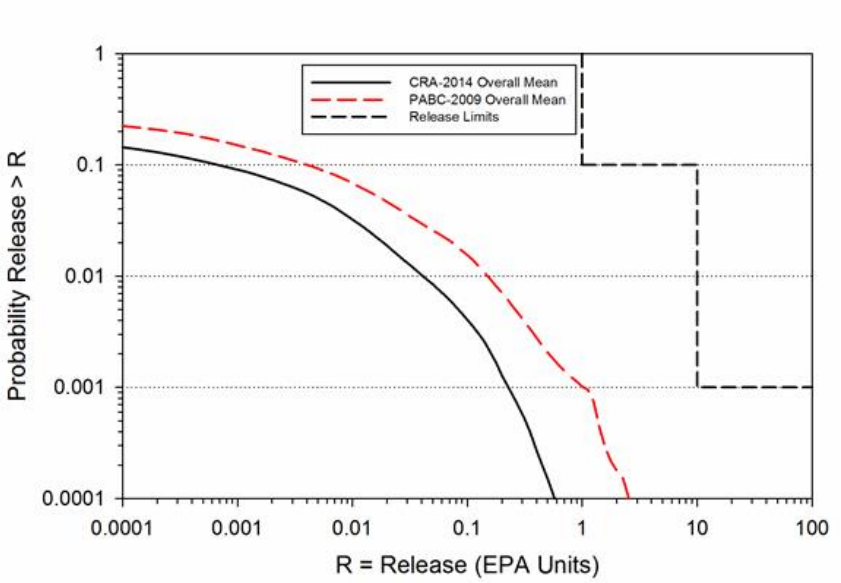

Figure PA- 78. Overall Mean CCDFs for DBRs: CRA-2014 PA and CRA-2009 PABC

The CRA-2009 PABC analysis showed that four variables (SOLMOD3:SOLVAR, CASTILER:PRESSURE, STEEL:CORRMCO2 and GLOBAL:PBRINE in Kicker and Herrick 2013, Table 4) accounted for more than 50% of the uncertainty in DBR. Variable SOLMOD3:SOLVAR is the WIPP PA parameter representing solubility uncertainty for radionuclides in the +III oxidation state. Quantity CASTILER:PRESSURE represents brine pressure in the Castile brine reservoir implemented in the WIPP PA. STEEL:CORRMCO2 represents the inundated corrosion rate for steel in the absence of CO_2. The WIPP PA parameter GLOBAL:PBRINE represents the probability that a drilling intrusion in an excavated repository area encounters pressurized brine. SOLMOD3:SOLVAR and

CASTILER:PRESSURE are ranked first and second in importance, respectively, in all three replicates of the CRA-2014 PA. However, in the CRA-2014 PA STEEL:CORRMCO2 did not enter the regression model for any replicate, and GLOBAL:PBRINE entered the regression models of replicates 2 and 3 only in steps 5 and 13, respectively. This reduction in importance for GLOBAL:PBRINE and STEEL:CORRMCO2 is most likely related to the reduction in the ranges of the distributions assigned to these two parameters (Kirchner 2013b).

PA-9.4 Groundwater Transport

Figure PA-79 shows the mean CCDFs for normalized releases due to transport through the Culebra for the CRA-2014 PA and the CRA-2009 PABC. As seen in that figure, mean releases from the Culebra decrease from the CRA-2009 PABC to the CRA-2014 PA. Relatively few vectors (roughly 10%) contribute to nonzero Culebra transport releases (Zeitler 2013). The upper limit of the distribution for parameter GLOBAL:PBRINE has decreased from the CRA-2009 PABC to the CRA-2014 PA while the lower limit has increased. As discussed for the radionuclide transport results of Section PA-8.4.3, radionuclide transport releases to the Culebra are most likely to occur during an E1 intrusion. The refinement of the PBRINE distribution, which sets the probability that an E1 drilling intrusion occurs in a given future, results in increased Culebra transport releases for some vectors (as the PBRINE lower limit has increased) and decreases in others (as the PBRINE upper limit has decreased). The net effect is a reduction in the mean CCDF for normalized Culebra transport releases in the CRA-2014 PA as compared to the CRA-2009 PABC.

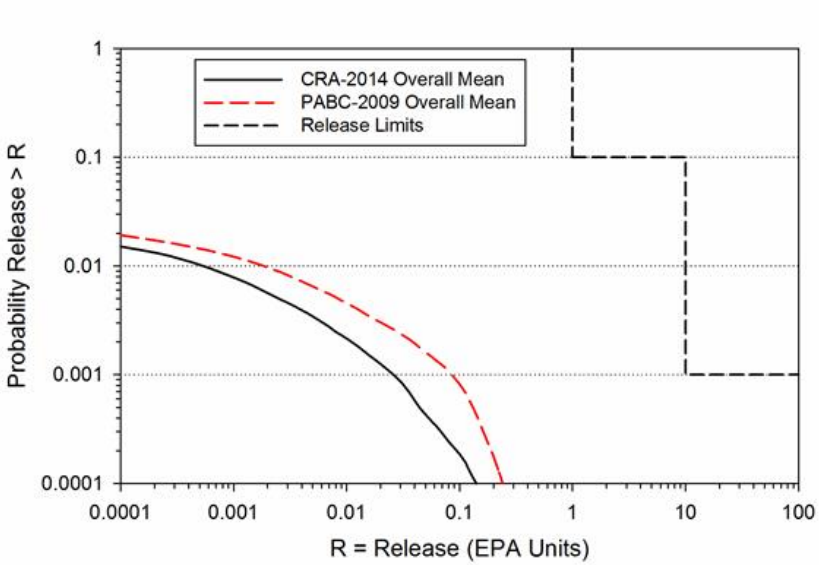

Figure PA- 79. Mean CCDFs for Releases from the Culebra: CRA-2014 PA and CRA-2009 PABC

Zero Culebra transport releases are due, for the most part, to transport rates frequently being too small to enable contaminants to reach the LWB within the 10,000-year regulatory period. The times of the intrusions giving rise to flows *to* the Culebra are also likely to influence whether or not such releases occur. These times are not represented in the "sampled" input parameters and thus cannot be associated with the releases in a sensitivity analysis. Changes in the releases from the Culebra are not due to changes in the rate of transport because 1) the flow fields used in the CRA-2014 analysis are the same as those used in the CRA-2009 PABC analysis, and 2) there were no changes in the matrix distribution coefficients (K_d) for the radionuclides, so there was no change in the retardation during transport. The increase in the drilling rate may have caused some vectors to have releases that previously had none because of having earlier intrusion times in some futures, thus providing the time needed to have the radionuclides reach the LWB. In the CRA-2009 PABC the percentages of the vectors for replicates 1, 2 and 3 having zero releases were 9%, 7% and 6% respectively. In the CRA-2014 these percentages were 5%, 6% and 2%. However, in both analyses the same 32 vectors across the three replicates had releases exceeding 0.0001 EPA units (Kirchner 2013b).

PA-9.5 Total Normalized Releases

Total normalized releases for the CRA-2014 PA are presented in this section and subsequently compared to results obtained in the CRA-2009 PABC. Total releases are calculated by totaling the releases from each release pathway: cuttings and cavings releases, spallings releases, DBRs, and transport releases (there were no undisturbed releases to contribute to total release). CRA-2014 PA CCDFs for total releases obtained in replicates 1, 2, and 3 are plotted together in Figure PA-80.

The overall mean CCDF is computed as the arithmetic mean of the mean CCDFs from each replicate. To quantitatively determine the sufficiency of the sample size, a confidence interval is computed about the overall mean CCDF using the Student's t-distribution and the mean CCDFs from each replicate. Figure PA-81 shows 95% confidence intervals about the overall mean. The CCDF and confidence intervals lie below and to the left of the limits specified in section 191.13(a). Thus, the WIPP continues to comply with the containment requirements of Part 191.

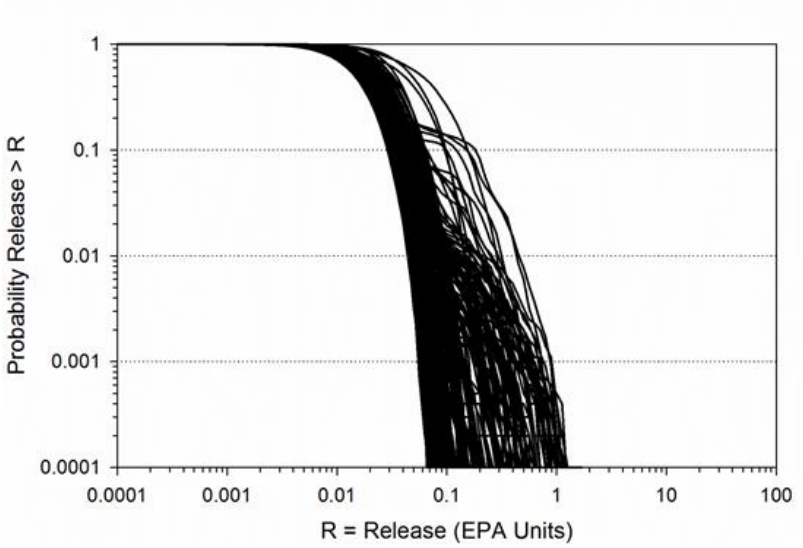

Figure PA- 80. Total Normalized Releases, Replicates R1, R2, and R3, CRA-2014 PA

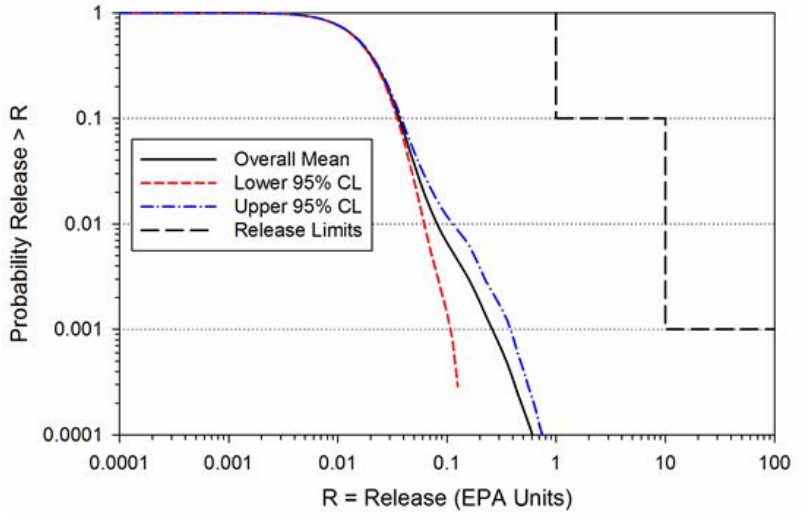

Figure PA- 81. Confidence Interval on Overall Mean CCDF for Total Normalized Releases, CRA-2014 PA

Mean CCDFs of the individual release mechanisms that comprise total normalized releases are plotted together in Figure PA-82, as well as the CRA-2014 PA total release overall mean. As seen in that figure, total normalized releases obtained in the CRA-2014 PA are dominated by cuttings and cavings releases and DBRs. Contributions to total releases from spallings and Culebra transport are much less significant. The rank regression analysis shows that the waste shear strength is the leading uncertain parameter associated with cuttings and cavings releases, and controls about 65% of mean cuttings and cavings releases in the CRA-2014 PA (Kirchner 2013b). For DBRs, the rank regression analysis shows that the solubility multiplier that represents uncertainty in solubility limits for all actinides in the III oxidation state (parameter SOLMOD3:SOLVAR) is ranked first in importance (Kirchner 2013b). The dominant release mechanisms of the CRA-2014 PA are consistent with those found in the CRA-2009 PABC, as are the leading uncertain parameters associated with those mechanisms.

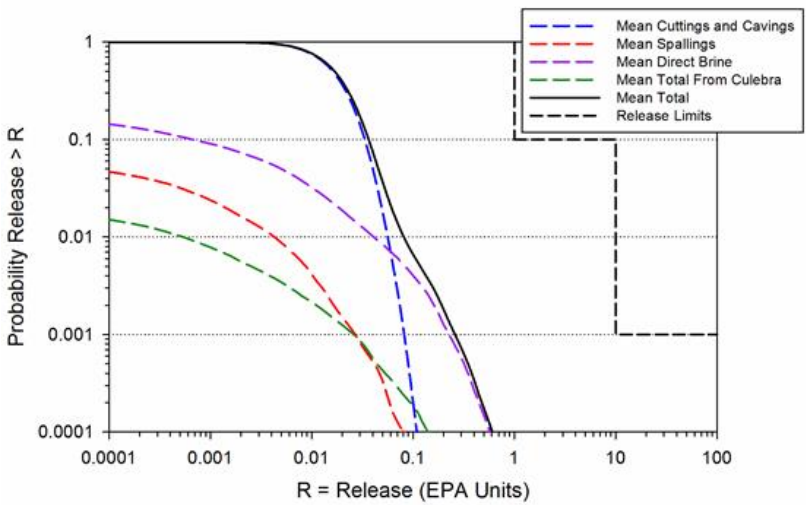

Figure PA- 82. Comparison of Overall Means for Release Componenets of the CRA-2014 PA

Overall means for total normalized releases obtained in the CRA-2009 PABC and the CRA-2014 PA are plotted together in Figure PA-83. Overall, total normalized releases decrease from the CRA-2009 PABC to the CRA-2014 PA as each contributing component is reduced in the CRA-2014 PA.

A comparison of the statistics on the overall mean for total normalized releases obtained in the CRA-2009 PABC and the CRA-2014 PA can be seen in Table PA-29. At probabilities of 0.1 and 0.001, values obtained for the mean total release are lower for the CRA-2014 PA.

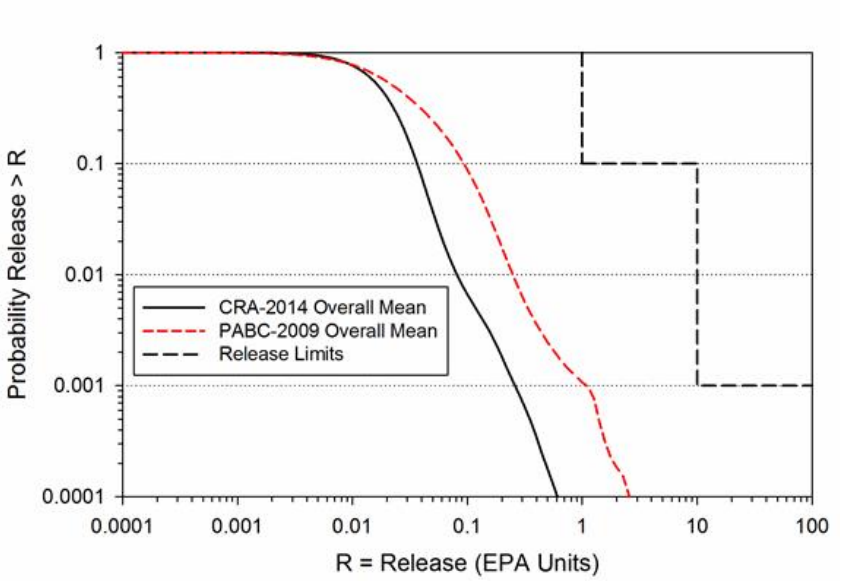

Figure PA- 83. CRA-2014 PA and CRA-2009 PABC Overall Mean CCDFs for Total Normalized Releases

Table PA- 29. CRA-2014 PA and CRA-2009 PABC Statistics on the Overall Mean for Total Normalized Releases in EPA Units at Probabilities of 0.1 and 0.001

Probability	Analysis	Mean Total Release	Lower 95% CL	Upper 95% CL	Release Limit
0.1	CRA-2014 PA	0.0367	0.0352	0.0384	1
	CRA-2009 PABC	0.0937	0.0908	0.0959	1
0.001	CRA-2014 PA	0.261	0.109	0.384	10
	CRA-2009 PABC	1.10	0.372	1.77	10

PA-10.0 References

(*Indicates a reference that has not been previously submitted.)

Abdul Khader, M.H., and H.S. Rao. 1974. "Flow Through Annulus with Large Radial Clearance." American Society of Civil Engineers, Journal of the Hydraulics Division, vol. 100, no. HY1: 25-39. [Author]

Antoun, T., L. Seanman, D.R. Curran, G.I. Kanel, S.V. Razorenor, and A.V. Utkin. 2003. Spall Fracture. New York: Springer-Verlag. [Author]

Aronson, D.G. 1986. The Porous Medium Equation. Nonlinear Diffusion Problems. Lecture Notes in Mathematics 1224. New York: Springer-Verlag. [Author]

Aziz, K., and A. Settari. 1979. Petroleum Reservoir Simulation. New York: Elsevier. [Author]

Barree, R.D., and M.W. Conway. 1995. "Experimental and Numerical Modeling of Convective Proppant Transport." Journal of Petroleum Technology, vol. 47 (March): 216-22. [Author]

Bateman, H. 1910. "The Solution of a System of Differential Equations Occurring in the Theory of Radio-Active Transformations." Proceedings of the Cambridge Philosophical Society, vol. 15: 423-27. [Author]

Bean, J.E., M.E. Lord, D.A. McArthur, R.J. MacKinnon, J.D. Miller, and J.D. Schreiber. 1996. Analysis Package for the Salado Flow Calculations (Task 1) of the Performance Assessment Analysis Supporting the Compliance Certification Application (CCA). ERMS 420238. Albuquerque, NM: Sandia National Laboratories. (EPA Air Docket A-93-02, Item II-G-08). [PDF / Author]

Bear, J. 1972. Dynamics of Fluids in Porous Media. New York: Dover. [Author]

Beauheim, R.L. 2003. AP-100 Task 1: Development and Application of Acceptance Criteria for Culebra Transmissivity (T) Fields, Analysis Report. ERMS 531136. Carlsbad, NM: Sandia National Laboratories. [PDF / Author]

Belhaj, H.A., K.R. Agha, A.M. Nouri, S.D. Butt, H.F. Vaziri, and M.R. Islam. 2003. Numerical Simulation of Non-Darcy Flow Utilizing the New Forchheimer's Diffusivity Equation. SPE 81499. Paper presented at the SPE 13th Middle East Oil Show & Conference, Bahrain, April 2003. [Author]

Berglund, J.W. 1992. Mechanisms Governing the Direct Removal of Wastes from the Waste Isolation Pilot Plant Repository Caused by Exploratory Drilling. SAND92-7295. Albuquerque, NM: Sandia National Laboratories. [PDF / Author]

Berglund, J.W. 1996. Analysis Package for the Cuttings and Spallings Calculations (Task 5 and 6) of the Performance Assessment Calculation Supporting the Compliance Certification Application (CCA), AP-015 and AP-016. ERMS 240521. Albuquerque, NM: Sandia National Laboratories. [PDF / Author]

Bilgen, E., R. Boulos, and A.C. Akgungor. 1973. "Leakage and Frictional Characteristics of Turbulent Helical Flow In Fine Clearance." Journal of Fluids Engineering, Transactions of the ASME, Series I, vol. 95: 493-97. [Author]

Brill, J.P., and H.D. Beggs. 1986. Two-Phase Flow in Pipes. 5th ed. Tulsa: University of Tulsa. [Author]

Brooks, R.H., and A.T. Corey. 1964. Hydraulic Properties of Porous Media. Hydrology Paper No. 3. ERMS 241117. Fort Collins, CO: Colorado State University. [PDF / Author]

Brush, L.H. and P. Domski. 2013a. Calculation of Organic-Ligand Concentrations for the WIPP CRA-2014 PA. ERMS 559005. Carlsbad, NM: Sandia National Laboratories.* [PDF / Author]

Brush, L.H. and P. Domski. 2013b. Prediction of Baseline Actinide Solubilities for the WIPP CRA-2014 PA. ERMS 559138. Carlsbad, NM: Sandia National Laboratories.* [PDF / Author]

Brush, L.H. and P. Domski. 2013c. Uncertainty Analysis of Actinide Solubilities for the WIPP CRA-2014 PA, Revision 1. ERMS 559712. Carlsbad, NM: Sandia National Laboratories.* [PDF / Author]

Bynum, R.V., C. Stockman, Y. Wang, A. Peterson, J. Krumhansl, J. Nowak, J. Cotton, M.S.Y. Chu, and S.J. Patchett. 1997. "Implementation of Chemical Controls Through a Backfill System for the Waste Isolation Pilot Plant (WIPP)." SAND96-2656C. Proceedings of the Sixth International Conference on Radioactive Waste Management and Environmental Remediation, ICEM '97, Singapore, October 12-16, 1997 (pp. 357-61). Eds. R. Baker, S. Slate, and G. Benda. New York: American Society of Mechanical Engineers. [Author]

Camphouse, R. 2013a. Design Document Criteria and Design Document for BRAGFLO, Version 6.02. ERMS 558660. Carlsbad, NM: Sandia National Laboratories.* [PDF / Author]

Camphouse, R. 2013b. Users Manual Criteria and User's Manual for BRAGFLO, Version 6.02. ERMS 558663. Carlsbad, NM: Sandia National Laboratories.* [PDF / Author]

Camphouse, R. 2013c. Analysis Package for Salado Flow Modeling Done in the 2014 Compliance Recertification Application Performance Assessment (CRA-2014 PA). ERMS 559980. Carlsbad, NM: Sandia National Laboratories.* [PDF / Author]

Camphouse, R. 2013d. Analysis Plan for the 2014 WIPP Compliance Recertification Application Performance Assessment. ERMS 559198. Carlsbad, NM: Sandia National Laboratories.* [PDF / Author]

Camphouse, R.C., D.C. Kicker, T.B. Kirchner, J.J. Long, and J.J. Pasch. 2011. Impact Assessment of SDI Excavation on Long-Term WIPP Performance. ERMS 555824. Carlsbad, NM: Sandia National Laboratories.* [PDF / Author]

Camphouse, R.C., D. Kicker, T. Kirchner, J. Long, B. Malama, and T. Zeitler. 2012a. Summary Report and Run Control for the 2012 WIPP Panel Closure System Performance Assessment. ERMS 558365. Carlsbad, NM: Sandia National Laboratories.* [PDF / Author]

Camphouse, R.C., M. Gross, C. Herrick, D. Kicker, and B. Thompson. 2012b. Recommendations and Justifications of Parameter Values for the Run-of-Mine Salt Panel Closure System Design Modeled in the PCS-2012 PA. Memo to WIPP Records Center dated May 3, 2012. ERMS 557396. Carlsbad, NM: Sandia National Laboratories.* [PDF / Author]

Camphouse, R., D. Kicker, S. Kim, T. Kirchner, J. Long, B. Malama, T. Zeitler. 2013. Summary Report for the 2014 WIPP Compliance Recertification Application Performance Assessment. ERMS 560252. Carlsbad, NM: Sandia National Laboratories.* [PDF / Author]

Caporuscio, F., J. Gibbons, and E. Oswald. 2003. Waste Isolation Pilot Plant: Salado Flow Conceptual Models Final Peer Review Report. ERMS 526879. Carlsbad, NM: Carlsbad Area Office, Office of Regulatory Compliance. [PDF / Author]

Carlsbad Area Office Technical Assistance Contractor (CTAC). 1997. Expert Elicitation on WIPP Waste Particle-Size Distribution(s) During the 10,000-Year Regulatory Post-Closure Period (Final Report, June 3). ERMS 541365. Carlsbad, NM: U.S. Department of Energy. [PDF / Author]

Chambre Syndicale de la Recherche et de la Production du Petrole et du Gaz Naturel. 1982. Drilling Mud and Cement Slurry Rheology Manual. English translation. Houston: Gulf Publishing. [Author]

Chappelear, J.E., and A.S. Williamson. 1981. "Representing Wells in Numerical Reservoir Simulation: Part 2-Implementation." Society of Petroleum Engineers Journal, vol. 21: 339-44. [Author]

Cherimisinoff, N.P., and P.N. Cherimisinoff. 1984. Hydrodynamics of Gas-Solids Fluidization. Houston, TX: Gulf Publishing. [Author]

Christian-Frear, T.L. 1996. Salado Halite Permeability from Room Q Analysis. ERMS 414996. Albuquerque, NM: Sandia National Laboratories. [PDF / Author]

Clayton, D.J. 2007. Corrections to Input Files for DBR PABC Calculations. ERMS 546311. Carlsbad, NM: Sandia National Laboratories. [PDF / Author]

Clayton, D.J. 2008a. Analysis Plan for the Performance Assessment for the 2009 Compliance Recertification Application (Revision 1). AP-137. ERMS 547905. Carlsbad, NM: Sandia National Laboratories. [PDF / Author]

Clayton, D.J. 2008b. Memorandum to L. Brush (Subject: Update to the Calculation of the Minimum Brine Volume for a Direct Brine Release). 2 April 2008. ERMS 548522. Carlsbad, NM: Sandia National Laboratories.* [PDF / Author]

Clayton, D.J. 2009. Update to Kd Values for the PABC-2009. ERMS 552395. Carlsbad, NM: Sandia National Laboratories.* [PDF / Author]

Clayton, D.J. 2013. Justification of Chemistry Parameters for Use in BRAGFLO for AP-164, Revision 1. ERMS 559466. Carlsbad, NM: Sandia National Laboratories.* [PDF / Author]

Clayton, D.J., S. Dunagan, J.W. Garner, A.E. Ismail, T.B. Kirchner, G.R. Kirkes, and M.B. Nemer. 2008. Summary Report of the 2009 Compliance Recertification Application Performance Assessment. ERMS 548862. Carlsbad, NM: Sandia National Laboratories. [PDF / Author]

Clayton, D.J., R.C. Camphouse, J.W. Garner, A.E. Ismail, T.B. Kirchner, K.L. Kuhlman, M.B. Nemer. 2010. Summary Report of the CRA-2009 Performance Assessment Baseline Calculation. ERMS 553039. Carlsbad, NM: Sandia National Laboratories.* [PDF / Author]

Corbet, T.F., and P.M. Knupp. 1996. The Role of Regional Groundwater Flow in the Hydrogeology of the Culebra Member of the Rustler Formation at the Waste Isolation Pilot Plant (WIPP), Southeastern New Mexico. SAND96-2133. Albuquerque, NM: Sandia National Laboratories. [PDF / Author]

Corbet, T., and P. Swift. 1996a. Memorandum to M.S. Tierney (Subject: Distribution for Non-Salado Parameter for SECOFL2D: Climate Index). 12 April 1996. ERMS 237465. Albuquerque, NM: Sandia National Laboratories. [PDF / Author]

Corbet, T., and P. Swift. 1996b. Parameters Required for SECOFL2D: Climate Index. Record Package. ERMS 237465. Albuquerque, NM: Sandia National Laboratories. [PDF / Author]

Cotsworth, E. 2005. Letter to U.S. Department of Energy (1 Enclosure). March 4, 2005. ERMS 538858. Washington, DC: U.S. Environmental Protection Agency, Office of Air and Radiation. [PDF / Author]

Cotsworth, E. 2009. EPA Letter on CRA-2009 First Set of Completeness Comments. ERMS 551444. Washington, DC: U.S. Environmental Protection Agency, Office of Radiation and Indoor Air.* [PDF / Author]

Cranwell, R.M., R.V. Guzowski, J.E. Campbell, and N.R. Ortiz. 1990. Risk Methodology for Geologic Disposal of Radioactive Waste: Scenario Selection Procedure. NUREG/CR-1667. SAND80-1429. ERMS 226750. Albuquerque, NM: Sandia National Laboratories. [PDF / Author]

Darley, H.C.H. 1969. "A Laboratory Investigation of Borehole Stability." JPT Journal of Petroleum Technology, July: 883-92. [Author]

Doherty, J. 2002. Design Document (DD) for PEST Version 5.5. ERMS 523970. Los Alamos, NM: Los Alamos National Laboratories. [PDF / Author]

Ely, J.F., and M.L. Huber. 1992. NIST Thermophysical Properties of Hydrocarbon Mixtures Database (SUPERTRAPP), Version 1.0, User's Guide. ERMS 242589. Gaithersburg, MD: U.S. Department of Commerce, National Institute of Standards and Technology, Standard Reference Data Program. [Author]

Ergun, S. 1952. "Fluid Flow Through Packed Columns." Chemical Engineering Progress, vol. 48: 89-94. [Author]

Fletcher, C.A.J. 1988. Computational Techniques for Fluid Dynamics. 2nd ed. Vols. 1 and 2. New York: Springer-Verlag. [Author]

Fox, R.W., and A.T. McDonald. 1985. Introduction to Fluid Mechanics. 3rd ed. New York: Wiley. [Author]

Francis, A.J., J.B. Gillow, and M.R. Giles. 1997. Microbial Gas Generation Under Expected Waste Isolation Pilot Plant Repository Conditions. SAND96-2582. Albuquerque, NM: Sandia National Laboratories. [PDF / Author]

Frigaard, I.A., and N.L. Humphries. 1997. "High Penetration Rates: Hazards and Well Control-A Case Study." Proceedings, March 1997 Society of Petroleum Engineers/International Association of Drilling Contractors Drilling Conference (SPE paper 37953). Amsterdam: Society of Petroleum Engineers. [Author]

Gatlin, C. 1960. Petroleum Engineering: Drilling and Well Completions. Englewood Cliffs, NJ: Prentice-Hall. [Author]

Graboski, M.S., and T.E. Daubert. 1979. A Modified Soave Equation of State for Phase Equilibrium Calculations: 3: Systems Containing Hydrogen. Industrial and Engineering Chemistry Process Design and Development, vol. 18: 300-06. [Author]

Haberman, J.H., and D.J. Frydrych. 1988. "Corrosion Studies of A216 Grade WCA Steel in Hydrothermal Magnesium-Containing Brines." Materials Research Society Symposium Proceedings: Scientific Basis for Nuclear Waste Management XI (pp. 761-72). Eds. M.J. Apted and R.E. Westerman. Pittsburgh: Materials Research Society. [Author]

Hadgu, T., P. Vaughn, J. Bean, D. Johnson, J. Johnson, K. Aragon, and J. Helton. 1999. Memorandum to M. Marietta (Subject: Modifications to the 96 CCA Direct Brine Release Calculations). 2 November 1999. ERMS 511276. Carlsbad, NM: Sandia National Laboratories. [PDF / Author]

Hansen, F.D., M.K. Knowles, T.W. Thompson, M. Gross, J.D. McLennan, and J.F. Schatz. 1997. Description and Evaluation of a Mechanistically Based Conceptual Model for Spall. SAND97-1369. Albuquerque, NM: Sandia National Laboratories. [PDF / Author]

Hansen, F.D., T.W. Pfeifle, and D.L. Lord. 2003. Parameter Justification Report for DRSPALL. ERMS 531057. Carlsbad, NM: Sandia National Laboratories. [PDF / Author]

Harbaugh, A.W., E.R. Banta, M.C. Hill, and M.G. McDonald. 2000. MODFLOW-2000: The U.S. Geological Survey Modular Ground-Water Model-User Guide to Modularization Concepts and the Ground-Water Flow Process. Open File Report 00-92. Reston, VA: U.S. Geological Survey. [PDF / Author]

Hart, D., R. Beauheim, and S. McKenna. 2009. Analysis Report for Task 7 of AP-114: Calibration of Culebra Transmissivity Fields. ERMS 552391. Carlsbad, NM: Sandia National Laboratories.* [PDF / Author]

Helton, J.C. 1993. "Drilling Intrusion Probabilities for Use in Performance Assessment for Radioactive Waste Disposal." Reliability Engineering and System Safety, vol. 40: 259-75. [Author]

Helton, J.C., J.D. Johnson, M.D. McKay, A.W. Shiver, and J.L. Sprung. 1995. "Robustness of an Uncertainty and Sensitivity Analysis of Early Exposure Results with the MACCS Reactor Accident Consequence Model." Reliability Engineering and System Safety, vol. 48, no. 2: 129-48. [Author]

Helton, J.C., J.E. Bean, J.W. Berglund, F.J. Davis, K. Economy, J.W. Garner, J.D. Johnson, R.J. MacKinnon, J. Miller, D.G. O'Brien, J.L. Ramsey, J.D. Schreiber, A. Shinta, L.N. Smith, D.M. Stoelzel, C. Stockman, and P. Vaughn. 1998. Uncertainty and Sensitivity Analysis Results Obtained in the 1996 Performance Assessment for the Waste Isolation Pilot Plant. SAND98-0365. Albuquerque, NM: Sandia National Laboratories. [PDF / Author]

Helton, J.C., and F.J. Davis. 2003. "Latin Hypercube Sampling and the Propagation of Uncertainty in Analyses of Complex Systems." Reliability Engineering and System Safety. vol. 81, no. 1: 23-69. [Author]

Herrick, C.G., M.D. Schuhen, D.M. Chapin, and D.C. Kicker. 2012. Determining the Hydrodynamic Shear Strength of Surrogate Degraded TRU Waste Materials as an Estimate for the Lower Limit of the Performance Assessment Parameter TAUFAIL. ERMS 558479. Carlsbad, NM: Sandia National Laboratories.* [PDF / Author]

Herrick, C.G. 2013. Memorandum to C. Camphouse (Subject: Follow-up to Questions Concerning TAUFAIL Flume Testing Raised during the November 14-15, 2012 Technical Exchange Between the DOE and EPA). 23 January 2013. ERMS 559081. Carlsbad, NM: Sandia National Laboratories.* [PDF / Author]

Hirsch, C. 1988. "Numerical Computation of Internal and External Flows." Fundamentals of Numerical Discretization. Vol. 1. Chichister, UK: John Wiley & Sons. [Author]

Howard, B.A. 1996. Memorandum to Sandia National Laboratories (Subject: Performance Assessment Parameter Input). 23 February 1996. ERMS 247595. Carlsbad, NM: Westinghouse Electric Corporation. [PDF / Author]

Howarth, S.M., and T. Christian-Frear. 1997. Porosity, Single-Phase Permeability, and Capillary Pressure Data from Preliminary Laboratory Experiments on Selected Samples from Marker Bed 139 at the Waste Isolation Pilot Plant. SAND94-0472/1/2/3. Albuquerque, NM: Sandia National Laboratories. [PDF / Author]

Hunter, R.L. 1985. A Regional Water Balance for the Waste Isolation Pilot Plant (WIPP) Site and Surrounding Area. SAND84-2233. Albuquerque, NM: Sandia National Laboratories. [PDF / Author]

Huyakorn, P.S., B.H. Lester, and J.W. Mercer. 1983. "An Efficient Finite Element Technique for Modelling Transport in Fractured Porous Media: 1. Single Species Transport." Water Resources Research, vol. 19: 841-54. [Author]

Iman, R.L. 1982. "Statistical Methods for Including Uncertainties Associated with the Geologic Isolation of Radioactive Waste Which Allow for a Comparison with Licensing Criteria." Proceedings of the Symposium on Uncertainties Associated with the Regulation of the Geologic Disposal of High-Level Radioactive Waste, March 9-13, 1981 (pp. 145-57). Ed. D.C. Kocher. NUREG/CP-0022, CONF-810372. Washington, DC: U.S. Nuclear Regulatory Commission, Directorate of Technical Information and Document Control. [Author]

Iman, R.L., M.J. Shortencarier, and J.D. Johnson. 1985. A FORTRAN 77 Program and User's Guide for the Calculation of Partial Correlation and Standardized Regression Coefficients. SAND85-0044. NUREG/CR-4122. Albuquerque, NM: Sandia National Laboratories. [PDF / Author]

Iman, R.L., and W.J. Conover. 1979. "The Use of the Rank Transform in Regression." Technometrics, vol. 21: 499-509. [Author]

Iman, R.L., and W.J. Conover. 1982. "A Distribution-Free Approach to Inducing Rank Correlation Among Input Variables." Communications in Statistics: Simulation and Computation, vol. B11, no. 3: 311-34. [Author]

Iman, R.L., and J.C. Helton. 1988. "An Investigation of Uncertainty and Sensitivity Analysis Techniques for Computer Models." Risk Analysis, vol. 8: 71-90. [Author]

Iman, R.L., and J.C. Helton. 1991. "The Repeatability of Uncertainty and Sensitivity Analyses for Complex Probabilistic Risk Assessments." Risk Analysis, vol. 11: 591-606. [Author]

Jaeger, J.C. and N.G.W. Cook. 1969. Fundamentals of Rock Mechanics, Chapman and Hall Ltd., London, England.* [Author]

James, S.J., and J. Stein. 2003. Analysis Report for the Development of a Simplified Shaft Seal Model for the WIPP Performance Assessment (Rev 1). ERMS 525203. Carlsbad, NM: Sandia National Laboratories. [PDF / Author]

Kaufmann, D.W., ed. 1960. Sodium Chloride: The Production and Properties of Salt and Brine. American Chemical Society Monograph 145. New York: Reinhold. [Author]

Kelly, T. 2009. EPA Third Letter Requesting Additional Information on the CRA-2009. ERMS 552374. Washington, DC: U.S. EPA Office of Radiation and Indoor Air.* [PDF / Author]

Kicker, D. 2013. Analysis Package for Cuttings, Cavings, and Spallings: 2014 Complinace Recertification Application Performance Assessment (CRA-2014 PA). ERMS 560060. Carlsbad, NM: Sandia National Laboratories.* [PDF / Author]

Kicker, D. and C. Herrick. 2013. Parameter Summary Report for the 2014 Compliance Recertification Application. Carlsbad, NM: Sandia National Laboratories.* [PDF / Author]

Kicker, D. and and T. Zeitler. 2013a. Analysis Package for EPA Unit Loading Calculations for the 2014 Compliance Recertification Application Performance Assessment (CRA-2014 PA). ERMS 560065. Carlsbad, NM: Sandia National Laboratories.* [PDF / Author]

Kicker, D. and and T. Zeitler. 2013b. Radionuclide Inventory Screening Analysis for the 2014 Compliance Recertification Application Performance Assessment (CRA-2014 PA). ERMS 559257. Carlsbad, NM: Sandia National Laboratories.* [PDF / Author]

Kim, S. 2013a. Analysis Package for Salado Transport Calculations: CRA-2014 Performance Assessment. ERMS 560174. Carlsbad, NM: Sandia National Laboratories.* [PDF / Author]

Kim, S. 2013b. Analysis Package for PANEL: CRA-2014 Performance Assessment. ERMS 560174. Carlsbad, NM: Sandia National Laboratories. [PDF / Author]

Kim, S. and R. Camphouse. 2013. Marker Bed Concentrations and Radium-226 Concentration for Undisturbed NUTS Scenario in AP-164. Memorandum to SNL WIPP Records Center dated April 25, 2013. ERMS 559914. Carlsbad, NM: Sandia National Laboratories.* [PDF / Author]

Kirchner, T. 2013a. Generation of the LHS Samples for the CRA-2014 (AP-164) PA Calculations. ERMS 559950. Carlsbad, NM: Sandia National Laboratories.* [PDF / Author]

Kirchner, T. 2013b. Sensitivity of the CRA-2014 Performance Assessment Releases to Parameters. ERMS 560043. Carlsbad, NM: Sandia National Laboratories.* [PDF / Author]

Kirchner, T., T. Zeitler, and R. Kirkes. 2012. Evaluating the Data in Order to Derive a Value for GLOBAL:PBRINE. Memorandum to Sean Dunagan dated December 11, 2012. ERMS 558724. Carlsbad, NM: Sandia National Laboratories.* [PDF / Author]

Kirkes, R. 2007. Evaluation of the Duration of Direct Brine Release in WIPP Performance Assessment (Revision 0). ERMS 545988. Carlsbad, NM: Sandia National Laboratories. [PDF / Author]

Klinkenberg, L.J. 1941. The Permeability of Porous Media to Liquids and Gases (pp. 200-13). API Drilling and Production Practice. ERMS 208556. Albuquerque, NM: Sandia National Laboratories. [PDF / Author]

Kuhlman, K. 2010. Analysis Report for the CRA-2009 PABC Culebra Flow and Transport Calculations. ERMS 552951. Carlsbad, NM: Sandia National Laboratories.* [PDF / Author]

Lee, J. 1982. Well Testing. SPE Textbook Series Vol. 1. New York: Society of Petroleum Engineers of AIME. [Author]

Leigh, C., R. Beauheim, and J. Kanney. 2003. SNL WIPP Analysis Plan AP-100, Revision 0, Analysis Plan for Calculation of Culebra Flow and Transport, Compliance Recertification Application. ERMS 530172. Carlsbad, NM: Sandia National Laboratories. [PDF / Author]

Li, D., R.K. Svec, T.W. Engler, and R.B. Grigg. 2001. Modeling and Simulation of the Wafer Non-Darcy Flow Experiments. SPE 68822. Paper presented at the SPE Western Regional Meeting, Bakersfield, CA, March 26-30. [Author]

Lide, D.R., ed. 1991. CRC Handbook of Chemistry and Physics. 72nd ed. Boca Raton: CRC Press. [Author]

Long, J. 2013. Execution of Performance Assessment Codes for the CRA-2014 Performance Assessment. ERMS 560016. Carlsbad, NM: Sandia National Laboratories. [PDF / Author]

Lord, D.L., D.K. Rudeen, and C.W. Hansen. 2003. Analysis Package for DRSPALL: Compliance Recertification Application Part I: Calculation of Spall Volume. ERMS 532766. Carlsbad, NM: Sandia National Laboratories. [PDF / Author]

Lord, D.L., and D.K. Rudeen. 2003. Sensitivity Analysis Report: Parts I and II: DRSPALL Version 1.00: Report for Conceptual Model Peer Review July 7-11. ERMS 524400. Carlsbad, NM: Sandia National Laboratories. [PDF / Author]

Lorenz, J.C. 2006a. Assessment of the Potential for Karst in the Rustler Formation at the WIPP Site. SAND2005-7303. Albuquerque, NM: Sandia National Laboratories.* [PDF / Author]

Lorenz, J.C. 2006b. Assessment of the Geological Evidence for Karst in the Rustler Formation at the WIPP Site. Caves and Karst of Southeastern New Mexico (pp. 243-52). L. Land, V.W.* [Author]

Lowry, T. 2003. Analysis Package for Salado Transport Calculations: Compliance Recertification Application (Revision 0). ERMS 530163. Carlsbad, NM: Sandia National Laboratories. [PDF / Author]

Lowry, T.S. 2005. Analysis Package for Salado Transport Calculations: CRA-2004 PA Baseline Calculation. ERMS 541084. Carlsbad, NM: Sandia National Laboratories. [PDF / Author]

Malama, B. 2013. Analysis Package for Direct Brine Releases: CRA-2014 Performance Assessment (CRA-2014 PA). ERMS 560069. Carlsbad, NM: Sandia National Laboratories.* [PDF / Author]

Martell, M. 1996a. Memorandum to C. Lattier (Subject: Additional Information for the DRZ [Disturbed Rock Zone] Porosity). 14 November 1996. ERMS 242257. Albuquerque, NM: Sandia National Laboratories. [PDF / Author]

Martell, M. 1996b. Memorandum to C. Lattier (Subject: Additional Information for the Culebra Transport Parameter Id: 843, idpram: DNSGRAIN, idmtrl: CULEBRA, WIPP Data Entry Form 464 at WPO # 32689). 10 December 1996. ERMS 232689. Albuquerque, NM: Sandia National Laboratories. [PDF / Author]

Mattax, C.C., and R.L. Dalton. 1990. Reservoir Simulation. SPE Monograph 13. Richardson, TX: Henry L. Doherty Memorial Fund of Society of Petroleum Engineers, Inc. [Author]

McDonald, M.G., and A.W. Harbaugh. 1988. "A Modular Three-Dimensional Finite-Difference Ground-Water Flow Model." U.S. Geological Survey Techniques of Water-Resources Investigations. Book 6, Chap. A1. U.S. Government Printing Office. [Author]

McKay, M.D., R.J. Beckman, and W.J. Conover. 1979. "A Comparison of Three Methods for Selecting Values of Input Variables in the Analysis of Output from a Computer Code." Technometrics, vol. 21: 239-45. [Author]

McKenna, S.A., and D.B. Hart. 2003. Analysis Report: Task 4 of AP-088 Conditioning of Base T-Fields to Transient Heads. ERMS 531124. Albuquerque, NM: Sandia National Laboratories. [PDF / Author]

McTigue, D.F. 1993. Permeability and Hydraulic Diffusivity of Waste Isolation Pilot Plant Repository Salt Inferred from Small-Scale Brine Inflow Experiments. SAND92-1911. Albuquerque, NM: Sandia National Laboratories. [PDF / Author]

Meigs, L. 1996. Memorandum to J. Ramsey (Subject: Non-Salado: Diffusive Tortuosity for the Culebra Dolomite). 16 May 1996. ERMS 238940. Albuquerque, NM: Sandia National Laboratories. [PDF / Author]

Meigs, L., and J. McCord. 1996. Physical Transport in the Culebra Dolomite. ERMS 239167. Albuquerque, NM: Sandia National Laboratories. [PDF / Author]

Meigs, L., R.L. Beauheim, and T.L. Jones (eds). 2000. Interpretations of Tracer Tests Performed in the Culebra Dolomite at the Waste Isolation Pilot Plant Site. SAND97-3109. Albuquerque, NM: Sandia National Laboratories. [PDF / Author]

Mendenhall, F.T., and W. Gerstle. 1995. WIPP Anhydrite Fracture Modeling, Systems Prioritization Method - Iteration 2 Baseline Position Paper: Disposal Room and Cutting Models. ERMS 239830. Albuquerque, NM: Sandia National Laboratories. [PDF / Author]

Myers, R.H. 1986. Classical and Modern Regression with Applications. Boston: Duxbury. [Author]

Nemer, M.B. 2007. Effects of Not Including Emplacement Materials in CPR Inventory on Recent PA Results. ERMS 545689. Carlsbad, NM: Sandia National Laboratories. [PDF / Author]

Nemer, M.B., and D.J. Clayton. 2008. Analysis Package for Salado Flow Modeling, 2009 Compliance Recertification Application Calculation. ERMS 548607. Carlsbad, NM: Sandia National Laboratories. [PDF / Author]

Nemer, M.B., and J.S. Stein. 2005. Analysis Package for BRAGFLO, 2004 Compliance Recertification Application Performance Assessment Baseline Calculation (June 28). ERMS 540527. Carlsbad, NM: Sandia National Laboratories. [PDF / Author]

Nemer, M.B., J.S. Stein, and W. Zelinski. 2005. Analysis Report for BRAGFLO Preliminary Modeling Results With New Gas Generation Rates Based Upon Recent Experimental Results. ERMS 539437. Carlsbad, NM: Sandia National Laboratories. [PDF / Author]

Nemer, M.B. and W. Zelinski. 2005. Analysis Report for BRAGFLO Modeling Results with the removal of Methanogenesis from the Microbial-Gas-Generation Model. ERMS 538748. Carlsbad, NM: Sandia National Laboratories. [PDF / Author]

Oldroyd, J.G. 1958. "Non-Newtonian Effects in Steady Motion of Some Idealized Elastico-Viscous Liquids." Proceedings of the Royal Society of London: Series A: Mathematical and Physical Sciences, vol. 245, no. 1241: 278-97. ERMS 243211. [Author]

Papenguth, H.W. 1996. Parameter Record Package for Colloid Actinide Retardation Parameters. WPO 38173, Sandia WIPP Central Files (SWCF). [PDF / Author]

Peake, Thomas. 1998. Technical Report Review of TDEM Analysis of WIPP Brine Pockets. Washington, DC: U. S. Environmental Protection Agency, Office of Radiation and Indoor Air.* [PDF / Author]

Podio, A.L., and A.P. Yang. 1986. Well Control Simulator for IBM Personal Computer. IADC/SPE 14737. Paper presented at the International Association of Drilling Engineers/Society of Petroleum Engineers Drilling Conference. Dallas, TX, February 10-12. [Author]

Poettmann, F.H., and P.G. Carpenter. 1952. "Multiphase Flow of Gas, Oil, and Water Through Vertical Flow Strings with Application to the Design of Gas-lift Installations." Drilling and Production Practice (1952): 257-317. [Author]

Popielak, R.S., R.L. Beauheim, S.R. Black, W.E. Coons, C.T. Ellingson, and R.L. Olsen. 1983. Brine Reservoirs in the Castile Formation Waste Isolation Pilot Plant (WIPP) Project Southeastern New Mexico. TME-3153. Carlsbad, NM: Westinghouse Electric Corp. [PDF / Author]

Prasuhn, A.L. 1980. Fundamentals of Fluid Mechanics. Englewood Cliffs, NJ: Prentice-Hall. [Author]

Prausnitz, J.M. 1969. Molecular Thermodynamics of Fluid-Phase Equilibria. Englewood Cliffs, NJ: Prentice-Hall. [Author]

Press, W.H., B.P. Flannery, S.A. Teukolsky, and W.T. Vetterling. 1989. Numerical Recipes in Pascal: The Art of Scientific Computing. Cambridge: Cambridge U P. [Author]

Rechard, R. P., A. C. Peterson, J. D. Schreiber, H. J. Iuzzolino, M. S. Tierney and J. S. Sandha. 1991. Preliminary comparison with 40 CFR Part 191, Subpart B for the Waste Isolation Pilot Plant, December 1991; Volume 3: Reference Data. Albuquerque, NM: Sandia National Laboratories.* [PDF / Author]

Rechard, R.P., H. Iuzzolino, and J.S. Sandha. 1990. Data Used in Preliminary Performance Assessment of the Waste Isolation Pilot Plant (1990). SAND89-2408. Albuquerque, NM: Sandia National Laboratories. [PDF / Author]

Reed, D.J., J. Swanson, J.-F. Lucchini and M. Richman. 2013. Intrinsic, Mineral and Microbial Colloid Enhancement Parameters for the WIPP Actinide Source Term. ERMS 559200. LCO-ACP-18. Carlsbad, NM: Los Alamos Laboratory.* [PDF / Author]

Roberts, R. 1996. Salado: Brine Compressibility. Records Package. ERMS 412842. Albuquerque, NM: Sandia National Laboratories. [PDF / Author]

Roselle, G.T. 2013. Determination of Corrosion Rates from Iron/Lead Corrosion Experiments to be used for Gas Generation Calculations. ERMS 559077. Carlsbad, NM: Sandia National Laboratories.* [PDF / Author]

Ross, S.M. 1987. Introduction to Probability and Statistics for Engineers and Scientists. New York: John Wiley & Sons. [Author]

Ruth, D., and H. Ma. 1992. "On the Derivation of the Forchheimer Equation by Means of the Averaging Theorem." Transport in Porous Media, vol. 7: 255-64. [Author]

Sallaberry, C.J., J.C. Helton, and S.C. Hora. 2006. Extension of Latin Hypercube Samples with Correlated Variables. SAND2006-6135. Albuquerque, NM: Sandia National Laboratories. [PDF / Author]

Sandia National Laboratories (SNL). 1992. Preliminary Performance Assessment for the Waste Isolation Pilot Plant, December 1992. 5 vols. SAND92-0700/1-5. Albuquerque, NM: Sandia National Laboratories. [PDF / Author]

Sandia National Laboratories (SNL). 1997. Summary of Uncertainty and Sensitivity Analysis Results for the EPA-Mandated Performance Assessment Verification Test. ERMS 420667. Albuquerque, NM: Sandia National Laboratories. [PDF / Author]

Savins, J.G., and G.C. Wallick. 1966. "Viscosity Profiles, Discharge Rates, Pressures, and Torques for a Rheologically Complex Fluid in a Helical Flow." A.I.Ch.E. Journal, vol. 12: 357-63. [Author]

Stein, J.S. 2002. Memorandum to M.K. Knowles (Subject: Methodology behind the TBM BRAGFLO Grid), 13 May 2002. ERMS 522373. Carlsbad, NM: Sandia National Laboratories. [PDF / Author]

Stein, J.S. and W. Zelinski. 2003. Analysis Report for: Testing of a Proposed BRAGFLO Grid to be used for the Compliance Recertification Application Performance Assessment Calculations. ERMS 526868. Carlsbad, NM: Sandia National Laboratories. [PDF / Author]

Stockman, C., A. Shinta, and J. Garner, J. 1996. Analysis Package for the Salado Transport Calculations (Task 2) of the Performance Assessment Analysis Supporting the Compliance Certification Application. ERMS 422314. Carlsbad, NM: Sandia National Laboratories. [PDF / Author]

Stoelzel, D.M., and D.G. O'Brien. 1996. Analysis Package for the BRAGFLO Direct Release Calculations (Task 4) of the Performance Assessment Calculations Supporting the Compliance Certification Application (CCA), AP-029, Brine Release Calculations. ERMS 240520. Albuquerque, NM: Sandia National Laboratories. [PDF / Author]

Stone, C.M. 1997. SANTOS-A Two-Dimensional Finite Element Program for the Quasistatic, Large Deformation, Inelastic Response of Solids. SAND90-0543. Albuquerque, NM: Sandia National Laboratories. [PDF / Author]

Streeter, V.L. 1958. Fluid Mechanics. 2nd ed. New York: McGraw-Hill. [Author]

Sweby, P.K. 1984. "High Resolution Schemes Using Flux Limiters for Hyperbolic Conservation Laws." SIAM Journal on Numerical Analysis, vol. 21: 995-1011. [Author]

Telander, M.R., and R.E. Westerman. 1993. Hydrogen Generation by Metal Corrosion in Simulated Waste Isolation Pilot Plant Environments: Progress Report for the Period November 1989 Through December 1992. SAND92-7347. Albuquerque, NM: Sandia National Laboratories. [PDF / Author]

Telander, M.R., and R.E. Westerman. 1997. Hydrogen Generation by Metal Corrosion in Simulated Waste Isolation Pilot Plant Environments. SAND96-2538. Albuquerque, NM: Sandia National Laboratories. [PDF / Author]

Thompson, T.W., W.E. Coons, J.L. Krumhansl, and F.D. Hansen. 1996. Inadvertent Intrusion Borehole Permeability (July). ERMS 241131. Albuquerque, NM: Sandia National Laboratories. [PDF / Author]

Tierney, M.S. 1990. Constructing Probability Distributions of Uncertain Variables in Models of the Performance of the Waste Isolation Pilot Plant: the 1990 Performance Simulations. SAND 90-2510. Albuquerque, NM: Sandia National Laboratories. [PDF / Author]

Timoshenko, S.P., and J.N. Goodier. 1970. Theory of Elasticity. 3rd ed. New York: McGraw-Hill. [Author]

Trovato, E.R. 1997. Letter to A. Alm (6 Enclosures). 19 March 1997. ERMS 245835. Washington, DC: U.S. Environmental Protection Agency, Office of Air and Radiation. [PDF / Author]

U.S. Department of Energy (DOE). 1995. Waste Isolation Plant Sealing System Design Report. DOE/WIPP-95-3117. Carlsbad, NM: U.S. Department of Energy, Carlsbad Area Office. [PDF / Author]

U.S. Department of Energy (DOE). 1996. Title 40 CFR Part 191 Compliance Certification Application for the Waste Isolation Pilot Plant (October). 21 vols. DOE/CAO 1996-2184. Carlsbad, NM: U.S. Department of Energy, Carlsbad Area Office. [Author]

U.S. Department of Energy (DOE). 1997. Supplemental Summary of EPA-Mandated Performance Assessment Verification Test (All Replicates) and Comparison with the Compliance Certification Application Calculations (August 8). WPO 46702. ERMS 414879. Carlsbad, NM: U.S. Department of Energy, Carlsbad Area Office. [PDF / Author]

U.S. Department of Energy (DOE). 2004. Title 40 CFR Part 191 Compliance Recertification Application for the Waste Isolation Pilot Plant (March). 10 vols. DOE/WIPP 2004-3231. Carlsbad, NM: U.S. Department of Energy, Carlsbad Field Office. [Author]

U.S. Department of Energy (DOE). 2009. Title 40 CFR Part 191 Compliance Recertification Application for the Waste Isolation Pilot Plant. DOE/WIPP 09-3424. Carlsbad, NM: U.S. Department of Energy, Carlsbad Field Office. [Author]

U.S. Department of Energy (DOE). 2011a. Panel Closure System Design, Planned Change Request to the EPA 40 CFR Part 194 Certification of the Waste Isolation Pilot Plant. Carlsbad, NM: U.S. Department of Energy, Carlsbad Field Office.* [PDF / Author]

U.S. Department of Energy (DOE). 2011b. Letter from E. Ziemianski to J. Edwards (Subject: Notification of Intent to Begin the Salt Disposal Investigations). 11 August 2011. Carlsbad, NM: U.S. Department of Energy, Carlsbad Field Office.* [PDF / Author]

U.S. Department of Energy (DOE). 2012. Delaware Basin Monitoring Annual Report. DOE/WIPP-12-2308. Carlsbad, NM: Carlsbad Field Office.* [PDF / Author]

U.S. Environmental Protection Agency (EPA). 1985. 40 CFR 191: Environmental Standards for the Management and Disposal of Spent Nuclear Fuel, High-Level and Transuranic Radioactive Wastes; Final Rule. Federal Register, vol. 50 (September 19, 1985): 38066-089. [PDF / Author]

U.S. Environmental Protection Agency (EPA). 1993. "40 CFR 191: Environmental Radiation Protection Standards for the Management and Disposal of Spent Nuclear Fuel, High-Level and Transuranic Radioactive Wastes; Final Rule." Federal Register, vol. 58 (December 20, 1993): 66398-416. [PDF / Author]

U.S. Environmental Protection Agency (EPA). 1996a. "40 CFR Part 194: Criteria for the Certification and Recertification of the Waste Isolation Pilot Plant's Compliance with the 40 CFR Part 191 Disposal Regulations; Final Rule." Federal Register, vol. 61 (February 9, 1996): 5223-45. [PDF / Author]

U.S. Environmental Protection Agency (EPA). 1996b. Background Information Document for 40 CFR Part 194 (January). EPA 402-R-96-002. Washington, DC: Office of Radiation and Indoor Air. [PDF / Author]

U.S. Environmental Protection Agency (EPA). 1998a. "40 CFR Part 194: Criteria for the Certification and Recertification of the Waste Isolation Pilot Plant's Compliance with the Disposal Regulations: Certification Decision; Final Rule." Federal Register, vol. 63 (May 18, 1998): 27353-406. [PDF / Author]

U.S. Environmental Protection Agency (EPA). 1998b. Technical Support Document for 194.23: Parameter Justification Report (May). Washington, DC: Office of Radiation and Indoor Air. [PDF / Author]

U.S. Environmental Protection Agency (EPA). 1998c. Technical Support Document for 194.32: Scope of Performance Assessments (May). Washington, DC: Office of Radiation and Indoor Air. [PDF / Author]

U.S. Environmental Protection Agency (EPA). 2005. Teleconference with U.S. Department of Energy (DOE), Sandia National Laboratories (SNL), and Los Alamos National Laboratory (LANL), Carlsbad, NM. March 2, 2005. [PDF / Author]

U.S. EPA. 2006a. Technical Support Document for Section 194.14/15: Evaluation of Karst at the WIPP Site (March). Washington, DC: Office of Radiation and Indoor Air. [PDF / Author]

U.S. EPA. 2006b. Recertification CARD No. 14/15: Content of Certification Application and Compliance Recertification Application(s). Compliance Application Review Documents for the Criteria for the Certification and Recertification of the Waste Isolation Pilot Plant's Compliance with the 40 CFR 191 Disposal Regulations: Final Recertification Decision (March) (pp. 14/15-1 through 14/15-34, pp. 14-A-1 through 14-A-3, and pp. 15-A-1 through 15-A-17). Washington, DC: Office of Radiation and Indoor Air. [PDF / Author]

U.S. Environmental Protection Agency (EPA). 2010a. "40 CFR Part 194 Criteria for the Certification and Recertification of the Waste Isolation Pilot Plant's Compliance With the Disposal Regulations: Recertification Decision." Federal Register No. 222, Vol. 75, pp. 70584-70595, November 18, 2010.* [PDF / Author]

U.S. Environmental Protection Agency (EPA). 2010b. Technical Support Document for Section 194.24, Evaluation of the Compliance Recertification Actinide Source Term, Backfill Efficacy and Culebra Dolomite Distribution Coefficient Values (Revision 1), November 2010.* [PDF / Author]

U.S. Environmental Protection Agency (EPA). 2011. Letter from Jonathan Edwards to Ed Ziemianski dated November 17, 2011.* [PDF / Author]

Van Genuchten, R. 1978. Calculating the Unsaturated Hydraulic Conductivity with a New Closed-Form Analytical Model. Report 78-WR-08. ERMS 249486. Princeton: Princeton University, Department of Civil Engineering, Water Resources Program. [PDF / Author]

Van Soest, G.D. 2012. Performance Assessment Inventory Report - 2012. LA-UR-12-26643. Carlsbad, NM: Los Alamos National Laboratory.* [PDF / Author]

Vargaftik, N.B. 1975. Tables on the Thermophysical Properties of Liquids and Gases in Normal and Dissociated States. 2nd ed. Washington, DC: Hemisphere. [Author]

Vaughn, P. 1996. Memorandum (with attachments) to M. Tierney (Subject: WAS_AREA and REPOSIT SAT_RBRN Distribution). 13 February 1996. ERMS 234902. Albuquerque, NM: Sandia National Laboratories. [PDF / Author]

Walas, S.M. 1985. Phase Equilibria in Chemical Engineering. Boston: Butterworth. [Author]

Walker, R.E. 1976. "Hydraulic Limits are Set by Flow Restrictions." Oil and Gas Journal, vol. 74, no. 40: 86-90. [Author]

Walker, R.E., and W.E. Holman. 1971. "Computer Program Predicting Drilling-Fluid Performance." Oil and Gas Journal, vol. 69, no. 13: 80-90. [Author]

Wang, Y., and L. Brush. 1996a. Memorandum to M. Tierney (Subject: Estimates of Gas-Generation Parameters for the Long-Term WIPP Performance Assessment). 26 January 1996. ERMS 231943. Albuquerque, NM: Sandia National Laboratories. [PDF / Author]

Wang, Y., and L. Brush. 1996b. Memorandum to M. Tierney (Subject: Modify the Stoichiometric Factor y in BRAGFLO to Include the Effect of MgO Added to WIPP Repository as Backfill). 23 February 1996. ERMS 232286. Albuquerque, NM: Sandia National Laboratories. [PDF / Author]

Weast, R.C., ed. 1969. Handbook of Chemistry and Physics. 50th ed. Cleveland: Chemical Rubber Pub. Co. [Author]

Webb, S.W. 1992. Appendix A: Uncertainty Estimates for Two-Phase Characteristic Curves for 1992 40 CFR 191 Calculations, Preliminary Performance Assessment for the Waste Isolation Pilot Plant, December 1992 (pp. A-147 through A-155). Volume 3: Model Parameters. SAND92-0700/3. Albuquerque, NM: Sandia National Laboratories. [PDF / Author]

Welchon, J.K., A.F. Bertuzzi, and F.H. Poettmann. 1962. Wellbore Hydraulics. Petroleum Production Handbook (pp. 31-1 through 31-36). Eds. T.C. Frick and R.W. Taylor. Dallas: Society of Petroleum Engineers of AIME. [Author]

Whittaker, A., ed. 1985. Theory and Application of Drilling Fluid Hydraulics. Boston: International Human Resources Development Corporation. [Author]

Whitaker, S. 1996. "The Forchheimer Equation: A Theoretical Development." Transport in Porous Media, vol. 25: 27-61. [Author]

Williamson, A.S., and J.E. Chappelear. 1981. "Representing Wells in Numerical Reservoir Simulation: Part 1-Theory." Society of Petroleum Engineers Journal, vol. 21: 323-38. [Author]

WIPP Performance Assessment. 1997a. User's Manual for NUTS, Version 2.05. ERMS 246002. Albuquerque, NM: Sandia National Laboratories. [PDF / Author]

WIPP Performance Assessment. 1997b. User's Manual for SECOTP2D, Version 1.41. ERMS 245734. Albuquerque, NM: Sandia National Laboratories. [PDF / Author]

WIPP Performance Assessment. 1998a. Design Document for PANEL (Version 4.00). ERMS 52169. Carlsbad, NM: Sandia National Laboratories. [PDF / Author]

WIPP Performance Assessment. 2003a. User's Manual for PANEL Version 4.02. ERMS 526652. Carlsbad, NM: Sandia National Laboratories. [PDF / Author]

WIPP Performance Assessment. 2003b. User's Manual for CUTTINGS_S, Version 5.10. ERMS 532340. Albuquerque, NM: Sandia National Laboratories. [PDF / Author]

WIPP Performance Assessment. 2003c. Verification and Validation Plan and Validation Document for DRSPALL (Version 1.00). ERMS 524782. Carlsbad, NM: Sandia National Laboratories. [PDF / Author]

WIPP Performance Assessment. 2003d. Design Document for DRSPALL (Version 1.00). ERMS 529878. Carlsbad, NM: Sandia National Laboratories. [PDF / Author]

WIPP Performance Assessment. 2003e. User's Manual for DRSPALL Version 1.00. ERMS 524780. Carlsbad, NM: Sandia National Laboratories. [PDF / Author]

WIPP Performance Assessment. 2003f. Design Document for CUTTINGS (Version 5.10). [PDF / Author]

WIPP Performance Assessment. 2005. User's Manual for LHS, Version 2.42. ERMS 538374. Carlsbad, NM: Sandia National Laboratories. [PDF / Author]

WIPP Performance Assessment. 2010. Design Document Criteria, User's ManualCriteria and Design Document and User's Manual for CCDFGF, Version 6.0. ERMS 552386. Carlsbad, NM: Sandia National Laboratories.* [PDF / Author]

Zeitler, T. 2013. Analysis Package for CCDFGF: 2014 Compliance Recertification Application Performance Assessment (CRA-2014 PA), Revision 0. ERMS 560074. Carlsbad, NM: Sandia National Laboratories.* [PDF / Author]

Title 40 CFR Part 191
Subparts B and C
Compliance Recertification Application 2014
for the
Waste Isolation Pilot Plant

Appendix PORSURF-2014
Porosity Surface

United States Department of Energy
Waste Isolation Pilot Plant

Carlsbad Field Office
Carlsbad, New Mexico

Compliance Recertification Application 2014
Appendix PORSURF-2014

Table of Contents

List of Figures

This page intentionally left blank.

Acronyms and Abbreviations

CCA Compliance Certification Application

CFR Code of Federal Regulations

CRA Compliance Recertification Application

DOE U.S. Department of Energy

EPA U.S. Environmental Protection Agency

f scaling factor for the gas generation rate

K Kelvin

m meter

mol mole

MPa megapascal

N number of moles

N_{drums} number of waste drums in a room

p pressure

PA Performance Assessment

Pa pascal

ϕ porosity

R universal gas constant

r gas generation rate

s second

T absolute temperature

t time

V volume

WIPP Waste Isolation Pilot Plant

yr year

This page intentionally left blank.

PORSURF-1.0 Introduction

Both creep closure of the salt and the presence of either brine or gas in the U.S. Department of Energy (DOE) Waste Isolation Pilot Plant (WIPP) waste disposal region influence time-dependent changes in void volume in the waste disposal area. As a consequence, these processes influence two-phase fluid flow of brine and gases through the disposal area and its capacity for storing fluids. For performance assessment (PA), a porosity surface method is used to indirectly couple mechanical closure with two-phase fluid flow calculations implemented in the BRAGFLO code (see Appendix PA-2014, Section PA-4.2). The porosity surface approach is used because current codes are not capable of fully coupling creep closure, waste consolidation, brine availability, and gas production and migration. The porosity surface method incorporates the results of closure calculations obtained from the SANTOS code, a quasistatic, large deformation, finite element structural analysis code (Stone 1997a). The adequacy of the method is documented in Freeze (Freeze 1996), who concludes that the approximation is valid so long as the rate of room pressurization in final calculations is bounded by the room pressurization history used to develop the porosity surface.

The porosity surface used in the Compliance Recertification Application (CRA) of 2014 (CRA-2014) PA is the same surface used for the Compliance Certification Application (CCA) (U.S. DOE 1996), the CRA of 2004 (CRA-2004) (U.S. DOE 2004), and the CRA of 2009 (CRA-2009) (U.S. DOE 2009). Consequently, the models and parameters used to calculate this surface are unchanged from the CCA PA. For information on the porosity surface used in the CCA PA, see the CCA, Appendix PORSURF (U.S. DOE 1996).

A separate analysis considered the potential effects on repository performance of uncertainty in the porosity surface (U.S. DOE 2009, Appendix MASS-2009, Section MASS-21.0). Uncertainty in the porosity surface can arise from heterogeneity in the rigidity of waste packages and from uncertain spatial arrangements of waste in the repository. The analysis considered four porosity surfaces, including the surface from the CCA, which represented various bounding combinations of waste package rigidity and waste initial porosity. The analysis concluded that uncertainty in the porosity surface did not have significant effects on repository performance, and recommended the continued use of the CCA porosity surface in PA.

PORSURF-2.0 Creep Closure Method

Creep closure is accounted for in BRAGFLO by changing the porosity of the waste disposal area according to a table of porosity values, termed the porosity surface. The porosity surface is generated using SANTOS, a nonlinear finite element code. Disposal room porosity is calculated over time, for different rates of gas generation and gas production potential, to construct a three-dimensional porosity surface representing changes in porosity as a function of pressure and time over the 10,000-year simulation period.

The completed porosity surface is compiled in tabular form and is used in the solution of the gas and brine mass balance equations presented in Appendix PA-2014, Section PA-4.2.1. Porosity is interpolated from the porosity surface corresponding to the calculated gas pressure at time step t_n . This is done iteratively, as decreases in the porosity will increase the pressure. The closure data provided by SANTOS can be viewed as a series of surfaces, with any gas generation history computed by BRAGFLO constrained to fall on this surface. Various techniques described in Freeze, Larson, and Davies (Freeze, Larson, and Davies 1995) were used to check the validity of this approach, and it was found to be a reasonable representation of the behavior observed in the complex models.

In SANTOS, the gas pressure in the disposal room at time t_n is computed from the ideal gas law by the following relationship:

$$p_g = \frac{NRT}{V}$$

where N is the number of moles of gas at time t_n , R is the universal gas constant (8.31 m^3·Pa/mol·K), T is the absolute temperature in kelvins (K) (constant at 300 K), and V is the free volume of the room at time t_n . The number of moles of gas is computed as

$$N_t = N_{t-1} + N_{drums} \times f \times r(t) \times (t_n - t_{n-1})$$

where $r(t)$ is the gas generation rate (mol/drum/yr) at time t for the scaling factor f and N_{drums} is the number of drums of waste in the room (6804 drums/room). The base gas generation rate in SANTOS is

$$r(t) = \begin{cases} 2\ mol/drum/yr, & 0 \le t \le 550\ yr \\ 1\ mol/drum/yr, & 550\ yr < t \le 1050\ yr \end{cases}$$

The base gas generation rate $r(t)$ is representative of relatively high gas production rates from both microbial degradation of cellulosic, plastic, and rubber materials and from anoxic corrosion of iron-based metals (Appendix PA-2014, Section PA-4.2.5 ; Butcher 1997a; Roselle 2013). To provide a range of SANTOS results that spans the possible range of pressure computed by BRAGFLO, the gas generation rate is varied by the scaling factor *f*. Thirteen values of *f* are used to construct the porosity surface: *f* = 0.0, 0.025, 0.05, 0.1, 0.2, 0.4, 0.5, 0.6, 0.8, 1.0, 1.2, 1.6, and 2.0. The condition *f* = 0 represents the state of the repository when no gas is produced; *f* = 2 represents twice the base gas generation rate.

In SANTOS, gas generation is included to introduce a range of values for gas pressure during room closure, thereby capturing its effects. The use of the scaling factor *f* ensures that SANTOS results span a wide range of possible gas generation rates and potentials.

PORSURF-3.0 Conceptual Model for Porosity Surface

The ability of salt to deform with time, eliminate voids, and create an impermeable barrier around the waste was one of the principal reasons for locating the WIPP repository in a bedded salt formation (National Academy of Sciences National Research Council 1957, pp. 4,5). The creep closure process is a complex and interdependent series of events starting after a region within the repository is excavated. Immediately upon excavation, the equilibrium state of the rock surrounding the repository is disturbed, and the rock begins to deform and return to equilibrium. At equilibrium, deformation eventually ceases as the waste region has undergone as much compaction as is possible under the prevailing lithostatic stress field and the differential stresses in the salt approach zero.

Creep closure of a room begins immediately upon excavation and causes the volume of the cavity to decrease. If the room were empty, rather than partially filled with waste, closure would proceed until the void volume created by the excavation is eliminated; the surrounding halite would then return to its undisturbed, uniform stress state. In a waste-filled room, the rock will contact the waste and the rate of closure will decrease as the waste compacts and stiffens. Closure will eventually cease when the waste can take the full overburden load without further deformation. Initially, unconsolidated waste can support only small loads, but as the room continues to close after contact with the waste, the waste will consolidate and support a greater portion of the overburden load.

The presence of gas in the room will retard the closure process due to pressure buildup. As the waste consolidates, pore volume is reduced and pore pressure increases (using the ideal gas law). In this process, the waste can be considered to be a skeleton structure immersed in a pore fluid (the gas). As the pore pressure increases, less overburden weight is carried by the skeleton, and more support is provided by the gas. If the gas pressure increases to lithostatic pressure, the pore pressure alone is sufficient to support the overburden.

PORSURF-4.0 SANTOS Numerical Analyses

Computing repository creep closure is a particularly challenging structural engineering problem because the rock surrounding the repository continually deforms with time until equilibrium is reached. Not only is the deformation of the salt inelastic, but it also involves large deformations that are not customarily addressed with conventional structural deformation codes. In addition, the formation surrounding the repository is heterogeneous in composition, containing various parting planes and interbeds with different properties than the salt.

Waste deformation is also nonlinear, with large strains, and the response of a waste-filled room is complicated by the presence of gas. These complex characteristics of the materials making up the repository and its surroundings require the use of highly specialized constitutive models. Appropriate models have been built into the SANTOS code over a number of years. Principal components of these models include the following:

1. Disposal Room Configuration and Idealized Stratigraphy. Disposal room dimensions, computational configuration, and idealized stratigraphy are defined in the CCA, Appendix PORSURF, Attachment 1. The idealized stratigraphy is reproduced in Figure PORSURF-1.

2. Discretized Finite Element Model. A two-dimensional plane strain model, shown in Figure PORSURF-2, is used for the SANTOS analyses. The discretized model represents the room as one of an infinite number of rooms located at the repository horizon. The model contains 1,680 quadrilateral uniform-strain elements and 1,805 nodal points. Contact surfaces between the emplaced waste and the surfaces of the room are addressed. The justification for this model and additional detail on initial and boundary conditions are provided in the CCA, Appendix PORSURF, Attachment 1.

3. Geomechanical Models. Mechanical material response models and their corresponding property values are assigned to each region of the configuration. These models include:

A. A combined transient-secondary creep constitutive model for clean and argillaceous halite

B. An inelastic constitutive model for anhydrite

C. A volumetric plasticity model for the emplaced waste

D. Material properties are provided in the CCA, Appendix PORSURF, Attachment 1.

Continual testing and reviews of computer codes by the DOE and the U.S. Environmental Protection Agency (EPA) from before the CCA have shown that the use of SANTOS and its models are adequate for WIPP porosity surface calculations (e.g., Argüello and Holland 1996; WIPP PA 2003; U.S. EPA 2005).

The results of the SANTOS calculations are illustrated in Figure PORSURF-3 and Figure PORSURF-4. Figure PORSURF-3 shows disposal room porosity as a function of time for various values of the gas generation scaling factor f. Figure PORSURF-4 shows disposal room pressure as a function of time for various values of f. When $f = 0$, no gas is present in the disposal room; thus, disposal room pressure is zero for all times. This pressure curve is omitted from Figure PORSURF-4.

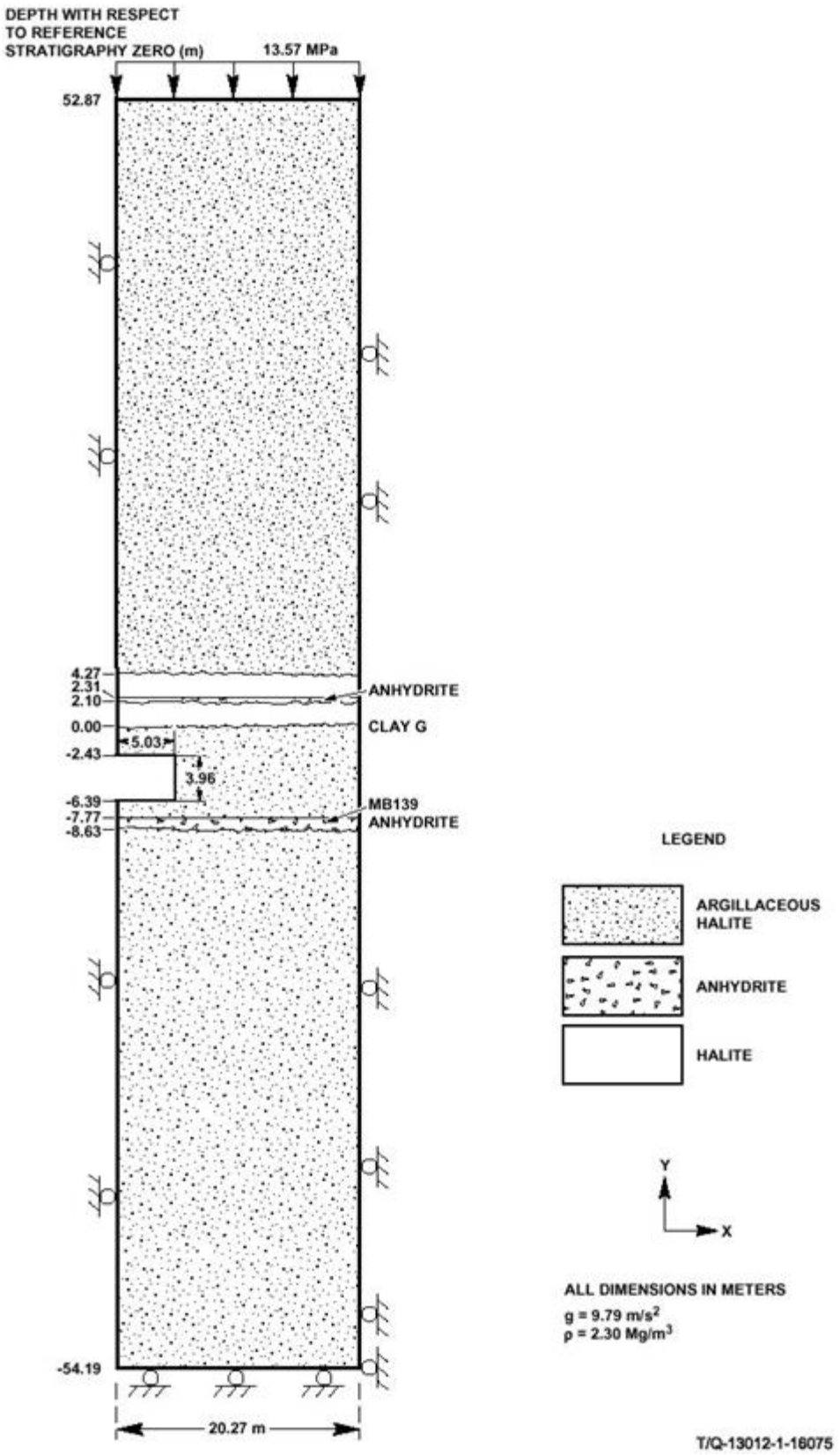

Figure PORSURF- 1. Stratigraphy Used for the Porosity Surface Calculations

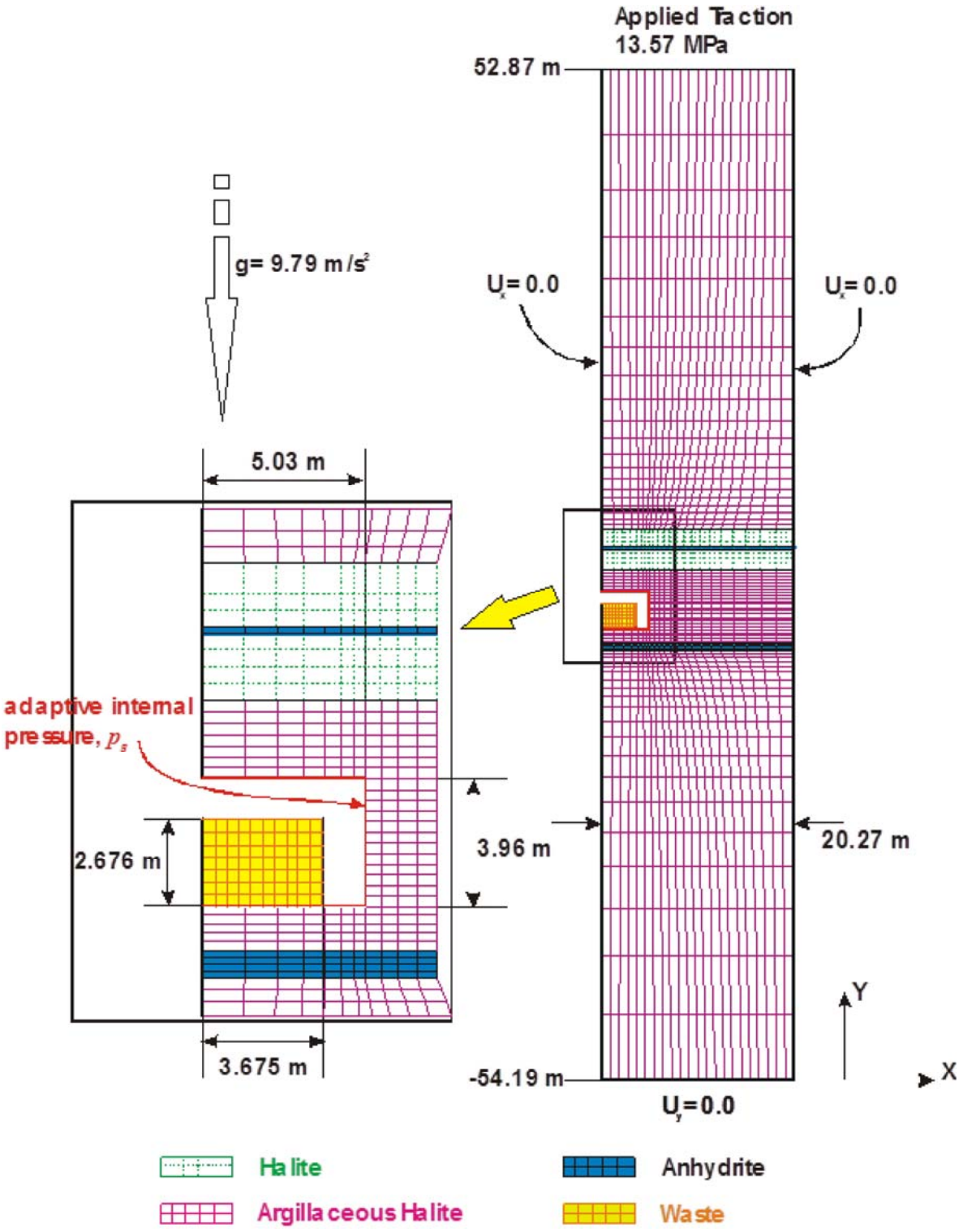

Figure PORSURF- 2. Mesh Discretization and Boundary Conditions Used for the Porosity Surface Calculations

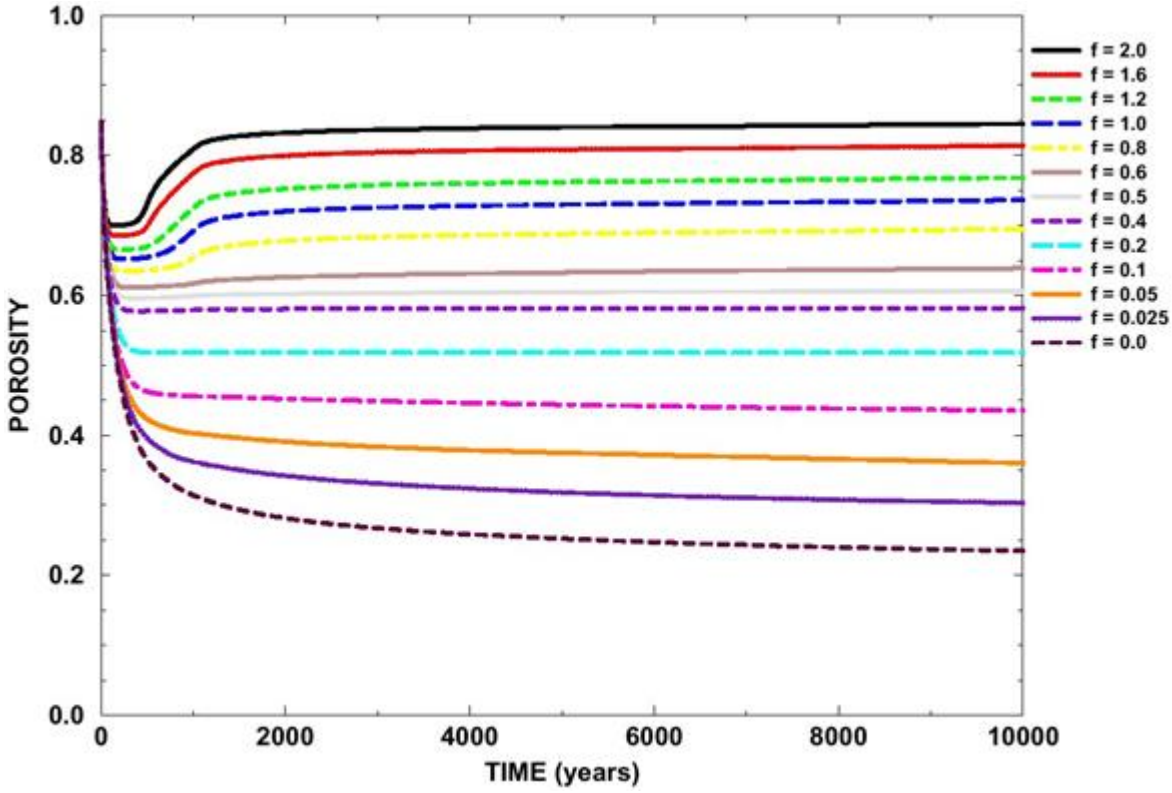

Figure PORSURF- 3. Disposal Room Porosity for Various Values of the Scaling Factor *f*

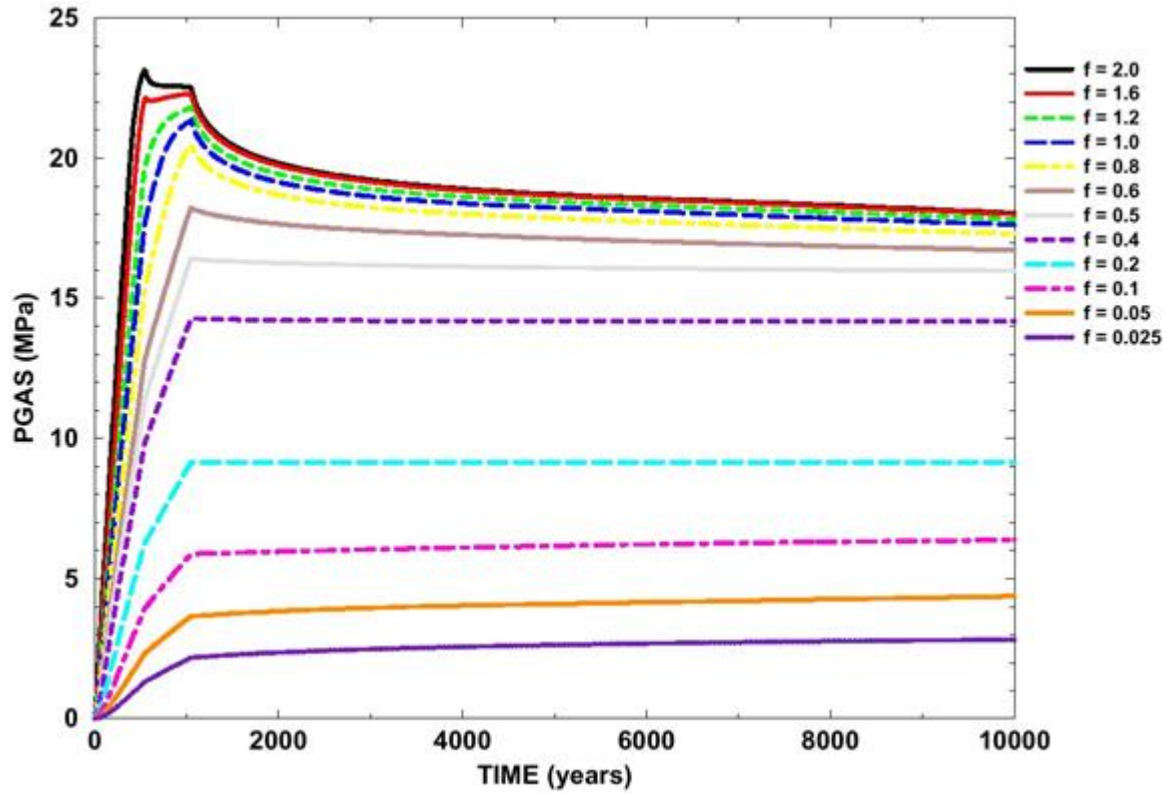

Figure PORSURF- 4. Disposal Room Pressure for Various Values of the Scaling Factor *f*

PORSURF-5.0 Implementation of Porosity Surface in BRAGFLO

As outlined above, the SANTOS program is used to calculate time-dependent porosities and pressures in the repository for a range of gas generation rates determined by the scaling factor *f*. Calculation with each value of *f* results in the porosity and pressure curves in Figure PORSURF-3 and Figure PORSURF-4.

The porosity calculated by SANTOS is the intrinsic, or true, porosity, which is defined as the ratio of the void volume to the current volume of a (deformable) element of waste. In contrast, porosity in BRAGFLO is defined as the ratio of void volume to the original volume of an element of waste. Mathematically, the BRAGFLO porosity, ϕ_B, and the intrinsic porosity in SANTOS, ϕ, are defined as

$$\phi_B = \frac{V_{void}}{V_0}$$

$$\phi = \frac{V_{void}}{V}$$

where V_{void} is the current void volume, V_0 is the original (total) volume, and V is the current (total) volume of a waste element.

The porosities shown in Figure PORSURF-3 are the porosities calculated by SANTOS to be used in BRAGFLO. The BRAGFLO porosities are related to the porosities calculated by SANTOS by correcting for deformation of the waste during repository closure. The relationship between ϕ_B and ϕ is given by

$$\phi_B = \frac{1-\phi_0}{1-\phi}\phi$$

where ϕ_0 is the initial porosity of the waste. Note that the values of ϕ_B and ϕ are equal at the initial porosity before the waste starts to compact.

Brine pressures p_b (t) obtained in the waste disposal regions are used in conjunction with the results in Figure PORSURF-3 and Figure PORSURF-4 to estimate porosity in the waste-filled regions for the BRAGFLO calculations. In the CRA-2014 PA, brine pressure and gas pressure are set as equal in the waste-filled regions, i.e., capillary pressure is not included (see Appendix PA-2014, Section PA-4.2). This is unchanged from the CCA and previous two CRA PAs.

Given a value for $p(t)$, BRAGFLO looks at the porosity surface to find indices for times in the porosity table so that

$$t_1 \le t \le t_2$$

Next, BRAGFLO determines whether the current pressure is above the pressure curve in the interpolation table corresponding to the maximum *f* value or corresponding to the minimum *f* value in the table. If p lies above the curve formed by the points $(t_1, p(t_1, f_{\max}))$ and $(t_2, p(t_2, f_{\max}))$, the porosity is calculated by interpolation using the following formula:

$$\phi = \phi(t_1, f_{\max}) + \frac{\phi(t_2, f_{\max}) - \phi(t_1, f_{\max})}{t_2 - t_1}(t - t_1)$$

Similarly, if p lies below the curve formed by the points $(t_1, p(t_1, f_{\min}))$ and $(t_2, p(t_2, f_{\min}))$, the porosity is calculated by interpolation using the following formula:

$$\phi = \phi(t_1, f_{\min}) + \frac{\phi(t_2, f_{\min}) - \phi(t_1, f_{\min})}{t_2 - t_1}(t - t_1)$$

For values of p that do not lie above or below the maximum and minimum $p(t, f)$ curves in the interpolation table, BRAGFLO finds f values f_1 and f_2 so that the point (t, p) lies between two curves $(t, p(t, f_1))$ and $(t, p(t, f_2))$. This is illustrated in Figure PORSURF-5.

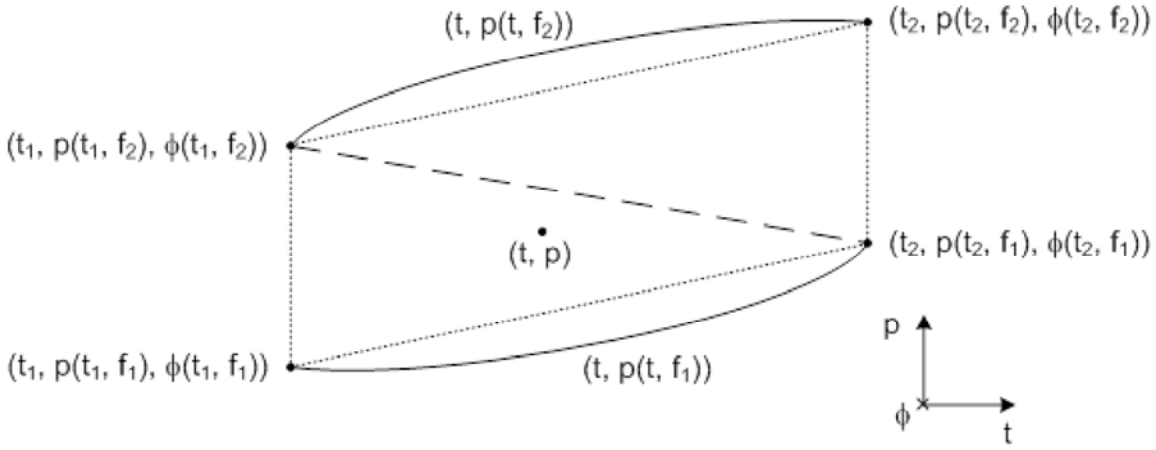

Figure PORSURF- 5. Location of Points in Porosity Table around Point (t, p)

Interpolation is performed on the triangle formed by the set of points that encloses the point (t, p). For example, in Figure PORSURF-5, the points constituting the lower triangle would be used for interpolation. Interpolation on the triangle is calculated from the areas of the three triangles in the plane of t and p that can be formed from the point (t, p) and the vertices of the enclosing triangle, as illustrated in Figure PORSURF-6. The porosity is then calculated from

$$\phi(t, p) = \frac{A_1}{A}\phi(t_1, f_2) + \frac{A_2}{A}\phi(t_1, f_1) + \frac{A_3}{A}\phi(t_2, f_1)$$

where A is the total area of the triangles $(A_1 + A_2 + A_3)$ in Figure PORSURF-6.

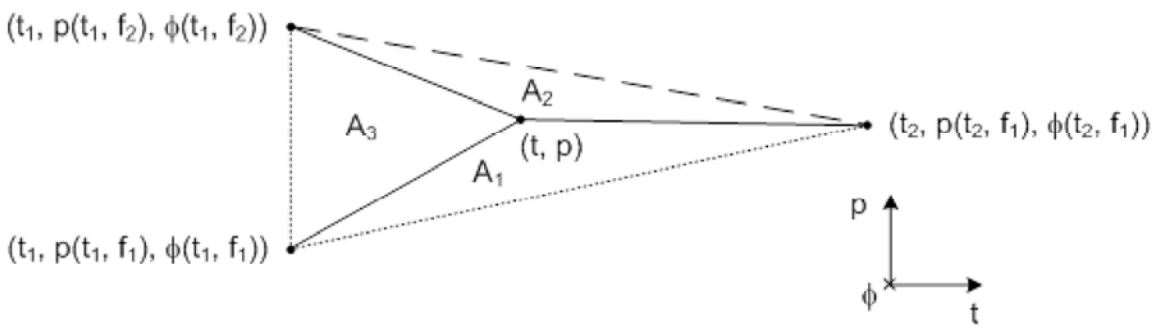

Figure PORSURF- 6. Triangular Interpolation to Determine the Porosity at (*t*, *p*)

At $t = 0$ (i.e., immediately after the operational period; see Appendix PA-2014, Section PA-4.2), interpolation is performed using the points $(t_1, p(t_1, f_1), \phi(t_1, f_1))$, $(t_2, p(t_2, f_1), \phi(t_2, f_1))$, and $(t_2, p(t_2, f_2), \phi(t_2, f_2))$. This is because at $t = 0$, the two points vertically separated in Figure PORSURF-6 at t_1 are equal (the porosity is equal to the initial value at $t = 0$ for all values of f).

PORSURF-6.0 Dynamic Closure of the North End and Hallways

The porosity surface method is not used to model the north end of the repository occupied by the experimental and operational regions. During development of the CCA PA, a supporting analysis compared brine and gas flow results for two models for closure of the north end of the repository: a dynamic closure model and a baseline model, in which the porosity and permeability of these regions were held constant (Vaughn, Lord, and MacKinnon 1995). The study examined the effect of these two approaches on brine releases to the accessible environment for both disturbed and undisturbed conditions, as well as the effects on brine pressures and brine saturations in the modeled regions. The study concluded that the baseline case (assuming constant low porosity and high permeability) consistently led to either similar or more conservative brine pressures and brine saturations, thereby overestimating potential releases relative to the dynamic consolidation case. Consequently, PA uses the simplifying case of constant porosity and permeability in the north end of the repository, rather than modeling dynamic closure of these areas.

PORSURF-7.0 Additional Information

The following attachments were included in the CCA, Appendix PORSURF (U.S. DOE 1996) to document additional details of the porosity surface method:

1. The CCA, Appendix PORSURF, Attachment 1, *Proposed Model for the Final Porosity Surface Calculations*. This memo documents preliminary configuration and constitutive property values for the final porosity surface calculations. Tables in the memo include elastic and creep properties for clean halite and argillaceous halite, volumetric strain data and material constants used in the volumetric-plasticity model for waste, and elastic and Drucker-Prager constants assigned to anhydrite Marker Bed 139. This attachment was supplemented and updated subsequent to the CCA by Butcher (Butcher 1997a and Butcher 1997b).

2. The CCA, Appendix PORSURF, Attachment 2, *Baseline Inventory Assumptions for the Final Porosity Surface Calculations*. This memo discusses the effect of changes in the Transuranic Waste Baseline Inventory Report on the SANTOS analyses.

3. The CCA, Appendix PORSURF, Attachment 3, *Corrosion and Microbial Gas Generation Potentials*. This memo discusses the rationale for the base gas production potentials of 1,050 mol per drum for corrosion and 550 mol per drum for microbial decay in the SANTOS analyses.

4. The CCA, Appendix PORSURF, Attachment 4, *Resolution of Remaining Issues for the Final Disposal Room Calculations*. This memo provides additional detail on the disposal room elevation, determination of plastic constants for transuranic waste, and determination of SANTOS input constants for clean halite, argillaceous halite, and anhydrite.

5. The CCA, Appendix PORSURF, Attachment 5, *Sample SANTOS Input File for Disposal Room Analysis*. A representative sample input file is provided in this attachment. This listing does not include the adaptive pressure boundary condition subroutine used to calculate the gas pressure in a disposal room (Stone 1997b).

6. The CCA, Appendix PORSURF, Attachment 6, *Final Porosity Surface Data*. This attachment provides SANTOS results for selected gas generation scaling factors $f = 0.5$, 1.0, and 2.0. This attachment was updated and published as a formal SAND report (Stone 1997b) subsequent to submittal of the CCA.

7. The CCA, Appendix PORSURF, Attachment 7, *SANTOS - A Two-Dimensional Finite Element Program for the Quasistatic, Large Deformation, Inelastic Response of Solids*. This report documents the SANTOS code.

PORSURF-8.0 References

(*Indicates a reference that has not been previously submitted.)

Argüello, J.G. and J.F. Holland. 1996. SANTOS - Verification and Qualification Document. ERMS 235675. Albuquerque, NM: Sandia National Laboratories. [PDF / Author]

Butcher, B.M. 1997a. A Summary of the Sources of Input Parameter Values for the Waste Isolation Pilot Plant Final Porosity Surface Calculations. SAND97-0796. Albuquerque, NM: Sandia National Laboratories. [PDF / Author]

Butcher, B.M. 1997b. Waste Isolation Pilot Plant Disposal Room Model. SAND97-0794. Albuquerque, NM: Sandia National Laboratories. [PDF / Author]

Freeze, G.A. 1996. Repository Closure-Reasoned Argument for FEP Issue DR12. ERMS 413328. Albuquerque, NM: Sandia National Laboratories. [PDF / Author]

Freeze, G.A., K.W. Larson, and P.B. Davies. 1995. Coupled Multiphase Flow and Closure Analysis of Repository Response to Waste-Generated Gas at the Waste Isolation Pilot Plant (WIPP). SAND93-1986. Albuquerque, NM: Sandia National Laboratories. [PDF / Author]

National Academy of Sciences-National Research Council (NAS-NRC). 1957. The Disposal of Radioactive Waste on Land. Publication 519. Washington, DC: National Academy of Sciences. [Author]

Roselle, G.T. 2013. Determination of Corrosion Rates from Iron/Lead Corrosion Experiments to be used for Gas Generation Calculations, Rev. 1. ERMS 559077. Carlsbad, NM: Sandia National Laboratories.* [PDF / Author]

Stone, C.M. 1997a. SANTOS - A Two-Dimensional Finite-Element Program for the Quasistatic, Large Deformation, Inelastic Response of Solids. SAND90-0543. Albuquerque, NM: Sandia National Laboratories. [PDF / Author]

Stone, C.M. 1997b. Final Disposal Room Structural Response Calculations. SAND97-0795. Albuquerque, NM: Sandia National Laboratories. [PDF / Author]

U.S. Department of Energy. (DOE) 1996. Title 40 CFR Part 191 Compliance Certification Application for the Waste Isolation Pilot Plant. 21 vols. DOE/CAO 1996-2184. Carlsbad, NM: Carlsbad Area Office. [Author]

U.S. Department of Energy. (DOE) 2004. Title 40 CFR Part 191 Compliance Recertification Application for the Waste Isolation Pilot Plant. 10 vols. DOE/WIPP 2004-3231. Carlsbad, NM: Carlsbad Field Office. [Author]

U.S. Department of Energy. (DOE) 2009. Title 40 CFR Part 191 Compliance Recertification Application for the Waste Isolation Pilot Plant. DOE/WIPP 09-3424. Carlsbad, NM: Carlsbad Field Office. [Author]

U.S. Environmental Protection Agency. (EPA) 2005. Technical Support Document for Section 194.27: SANTOS Computer Code in WIPP Performance Assessment. Docket No.: A-98-49, II-B1-17. Washington, DC: U.S. EPA Office of Radiation and Indoor Air. [PDF / Author]

Vaughn, P., M. Lord, and R. MacKinnon. 1995. DR-3: Dynamic Closure of the North-End and Hallways. Summary Memorandum of Record to D.R. Anderson; Subject: FEP Screening Issue DR-3; dated December 21, 1995. ERMS 230794. Albuquerque, NM: Sandia National Laboratories. [PDF / Author]

WIPP PA. 2003. Verification and Validation Plan/Validation Document for SANTOS (Version 2.1.7). ERMS 530091. Carlsbad, NM: Sandia National Laboratories. [PDF / Author]

Title 40 CFR Part 191
Subparts B and C
Compliance Recertification Application 2014
for the
Waste Isolation Pilot Plant

Appendix SCR-2014
Feature, Event, and Process Screening for PA

United States Department of Energy
Waste Isolation Pilot Plant

Carlsbad Field Office
Carlsbad, New Mexico

Compliance Recertification Application 2014
Appendix SCR-2014
Feature, Event, and Process Screening for PA

Table of Contents

List of Figures

List of Tables

This page intentionally left blank.

Acronyms and Abbreviations

μm micrometer

AIC active institutional controls

Bq becquerels

°C degrees centigrade

CAG Compliance Application Guidance

CCA Compliance Certification Application

CCDF complementary cumulative distribution function

CDF cumulative distribution function

CFR Code of Federal Regulations

CH-TRU contact-handled transuranic

Ci curie

cm centimeter

CRA Compliance Recertification Application

DBDSP Delaware Basin Drilling Surveillance Program

DFR driving force ratio

DOE U.S. Department of Energy

DP disturbed performance

DRZ disturbed rock zone

EP event and process

EPA U.S. Environmental Protection Agency

ERMS Electronic Record Management System

°F degrees Fahrenheit

FEP feature, event, and process

FLAC Fast Lagrangian Analysis Continua

FSU Florida State University

ft foot/feet

ft^2 square foot

ft^3 cubic foot

g gram

gal gallon

gpm gallons per minute

H human-initiated

HCN historic, current, and near-future

hr hour

IB inside boundary

in. inch/inches

K_d retardation distribution coefficient

kg kilogram

kg/m^3 kilograms per cubic meter

km kilometer

km^2 square kilometer

kW kilowatt

L liter

lb/gal pounds per gallon

LWA Land Withdrawal Act

m meter

m^2 square meter

m^3 cubic meter

Ma BP million years before present

MB marker bed

MeV megaelectron volt

mi mile

mL milliliter

MPa megapascal

MPI Mississippi Potash Inc.

mV millivolt

N natural

OB outside boundary

oz ounce

PA performance assessment

PABC Performance Assessment Baseline Calculation

PAVT Performance Assessment Verification Test

PCN planned change notice

PIC passive institutional control

ppm parts per million

psi pounds per square inch

psia pounds per square inch absolute

RH-TRU remote-handled transuranic

s second

SDDI Salt Defense Disposal Investigations

SDI Salt Disposal Investigations

SKI Statens Kärnkraftinspektion

SO-C screened-out consequence

SO-P screened-out probability

SO-R screened-out regulatory

T-field transmissitivity field

TRU transuranic

UP undisturbed performance

V volt

W waste and repository-induced

W watt

W/Ci watts per curie

W/g watts per gram

WIPP Waste Isolation Pilot Plant

yd^3 cubic yard

yr year

yrs years

Elements and Chemical Compounds

Al aluminum

Am americium

An actinide

CH_4 methane

CO_2 carbon dioxide

Cs cesium

EDTA ethylenediaminetetraacetate

Fe iron

MgO magnesium oxide

Np neptunium

Pm promethium

Pu plutonium

Rn radon

Sr strontium

Th thorium

U uranium

SCR-1.0 Introduction

The U.S. Department of Energy (DOE) has developed the Waste Isolation Pilot Plant (WIPP) in southeastern New Mexico for the disposal of transuranic (TRU) wastes generated by defense programs. In May of 1998, the U.S. Environmental Protection Agency (EPA) certified that the WIPP would meet the disposal standards (U.S. EPA 1998a, p. 27405) established in 40 CFR Part 191 Subparts B and C (U.S. EPA 1993), thereby allowing the WIPP to begin waste disposal operations. This certification was based, in part, on performance assessment (PA) calculations that were included in the DOE's Compliance Certification Application (CCA) (U.S. DOE 1996). These calculations demonstrate that the cumulative releases of radionuclides to the accessible environment will not exceed those allowed by the EPA standard.

The WIPP Land Withdrawal Act (LWA) (U.S. Congress 1992) requires the WIPP to be recertified (demonstrating continued compliance with the disposal standards) every five years (yrs). As such, the DOE prepared the 2004 Compliance Recertification Application (CRA-2004) (U.S. DOE 2004), which demonstrated that the WIPP complied with the EPA's requirements for radioactive waste disposal. The CRA-2004 included changes to the WIPP long-term compliance baseline since the CCA. As a result of the CRA-2004 and information provided in response to specific requests, the EPA recertified the WIPP on March 29, 2006 (U.S. EPA 2006). Subsequently, this recertification process was repeated by the DOE with its submittal of the CRA-2009 (U.S. DOE 2009). Again, the EPA carefully reviewed the application, and after requesting additional information and calculations, recertified that the WIPP continued to comply with the long-term disposal requirements of 40 CFR Part 191 and the compliance criteria of 40 CFR Part 194 (U.S. EPA 1996a) in November 2010 (U.S. EPA 2010a). Currently, and in compliance with the requirements for periodic recertification, the DOE has prepared the CRA-2014, which documents changes since the CRA-2009, and demonstrates compliance with the long-term disposal requirements of 40 CFR Part 191 and the compliance criteria of 40 CFR Part 194.

To assure that PA calculations account for important aspects of the disposal system, features, events, and processes (FEPs) considered to be potentially important to the disposal system are identified. These FEPs are used as a tool for determining what phenomena and components of the disposal system are dealt with in PA calculations. For the WIPP CCA, a systematic process was used to compile, analyze, screen, and document FEPs for use in PA. The FEP screening process used in the CCA, the CRA-2004, the CRA-2009, and this CRA-2014 is described in detail in the CCA, Chapter 6.0, Section 6.2. For recertification applications, this process evaluates any new information that may have impacts on or present inconsistencies to those screening arguments and decisions presented since the last certification or recertification. The FEPs baseline is managed according to Sandia Activity/Project Specific Procedure 9-4, *Performing FEPs Baseline Impact Assessment for Planned or Unplanned Changes* (Revision 3) (Kirkes 2013a). For the CRA-2014, a reassessment of FEPs concluded that of the 245 FEPs considered for the CRA-2009, 184 have not been changed and 61 have been updated with new information. Of the 61 updated FEPs, one has also had its screening decision changed. Therefore, there are 245 WIPP FEPs for the CRA-2014.

SCR-2.0 Basis for FEPs Screening Process

SCR-2.1 Requirement for FEPs

The origin of FEPs is related to the EPA's radioactive waste disposal standard's requirement to use PA methodology. The DOE was required to demonstrate that the WIPP complied with the containment requirements of section 191.13 (U.S. EPA 1993). These requirements state that the DOE must use PA to demonstrate that radionuclide releases from the disposal system during the 10,000 yrs following closure will fall below specified limits. The PA analyses supporting this determination must be quantitative and must consider uncertainties caused by all significant processes and events that may affect the disposal system, including inadvertent human intrusion into the repository during the future. The scope of PA is further defined by the EPA at section 194.32 (U.S. EPA 1996a), which states,

> Any compliance application(s) shall include information which:
>
> (1) Identifies all potential processes, events or sequences and combinations of processes and events that may occur during the regulatory time frame and may affect the disposal system;
>
> (2) Identifies the processes, events or sequences and combinations of processes and events included in performance assessments; and
>
> (3) Documents why any processes, events or sequences and combinations of processes and events identified pursuant to paragraph (e)(1) of this section were not included in performance assessment results provided in any compliance application.

Therefore, the PA methodology includes a process that compiles a comprehensive list of the FEPs that are potentially relevant to disposal system performance. Those FEPs shown by screening analysis to have the potential to affect performance are represented in scenarios and quantitative calculations using a system of linked computer models to describe the interaction of the repository with the natural system, both with and without human intrusion. For the CCA, the DOE first compiled a comprehensive list of FEPs, which was then subjected to a screening process that eventually lead to the set of FEPs used in PA to demonstrate the WIPP's compliance with the long-term disposal standards.

SCR-2.2 FEPs List Development for the CCA

As a starting point, the DOE assembled a list of potentially relevant FEPs from the compilation developed by Stenhouse, Chapman, and Sumerling (Stenhouse, Chapman, and Sumerling 1993) for the Swedish Nuclear Power Inspectorate (Statens Kärnkraftinspektion, or SKI). The SKI list was based on a series of FEP lists developed for other disposal programs and is considered the best-documented and most comprehensive starting point for the WIPP. For the SKI study, an initial raw FEP list was compiled based on nine different FEP identification studies.

The compilers of the SKI list eliminated a number of FEPs as irrelevant to the particular disposal concept under consideration in Sweden. These FEPs were reinstated for the WIPP effort, and several FEPs on the SKI list were subdivided to facilitate screening for the WIPP. Finally, to ensure comprehensiveness, other FEPs specific to the WIPP were added based on review of key project documents and broad examination of the preliminary WIPP list by both project participants and stakeholders. The initial unedited list is contained in the CCA, Appendix SCR, Attachment 1. The initial unedited FEP list was restructured and revised to derive the comprehensive WIPP FEP list used

in the CCA. The number of FEPs was reduced to 237 in the CCA to eliminate the ambiguities and duplications presented in a generic list. Restructuring the list did not remove any substantive issues from the discussion. As discussed in more detail in the CCA, Appendix SCR, Attachment 1, the following steps were used to reduce the initial unedited list to the appropriate WIPP FEP list used in the CCA.

- References to subsystems were eliminated because the SKI subsystem classification was not appropriate for the WIPP disposal concept. For example, in contrast to the Swedish disposal concept, canister integrity does not have a role in post-operational performance of the WIPP, and the terms near-field, far-field, and biosphere were not unequivocally defined for the WIPP site.

- Duplicate FEPs were eliminated. Duplicate FEPs arose in the SKI list because individual FEPs could act in different subsystems. FEPs had a single entry in the CCA list whether they were applicable to several parts of the disposal system or to a single part only (for example, the FEP Gas Effects). Disruption appears in the seals, backfill, waste, canister, and near-field subsystems in the initial FEP list. These FEPs were represented by a single FEP, Disruption Due to Gas Effects.

- FEPs that were not relevant to the WIPP design or inventory were eliminated. Examples include FEPs related to high-level waste, copper canisters, and bentonite backfill.

- FEPs relating to engineering design changes were eliminated because they were not relevant to a compliance application based on the DOE's design for the WIPP.

- FEPs relating to constructional, operational, and decommissioning errors were eliminated. The DOE has administrative and quality control procedures to ensure that the facility will be constructed, operated, and decommissioned properly.

- Detailed FEPs relating to processes in the surface environment were aggregated into a small number of generalized FEPs. For example, the SKI list includes the biosphere FEPs Inhalation of Salt Particles, Smoking, Showers and Humidifiers, Inhalation and Biotic Material, Household Dust and Fumes, Deposition (Wet and Dry), Inhalation and Soils and Sediments, Inhalation and Gases and Vapors (Indoor and Outdoor), and Suspension in Air, which were represented by the FEP Inhalation.

- FEPs relating to the containment of hazardous metals, volatile organic compounds, and other chemicals not regulated by Part 191 were not included.

- A few FEPs were renamed to be consistent with terms used to describe specific WIPP processes (for example, Wicking, Brine Inflow).

These steps resulted in a list of WIPP-relevant FEPs retained for further consideration in the first certification PA. These FEPs were screened to determine which would be included in the PA models and scenarios for the CCA PA. As mentioned in Section SCR-1.0, the FEPs baseline is managed by procedure to be systematically reviewed and updated prior to each recertification application. As a result of this process, the CRA-2004 included 235 WIPP FEPs, and both the CRA-2009 and CRA-2014 include 245 WIPP FEPs. These evaluations are documented in Wagner et al. (Wagner et al. 2003), Kirkes (Kirkes 2008), and Kirkes (Kirkes 2013b), respectively.

SCR-2.3 Criteria for Screening of FEPs and Categorization of Retained FEPs

The purpose of FEP screening is to identify those FEPs that should be accounted for in PA calculations, and those FEPs that need not be considered further. The DOE's process of removing FEPs from consideration in PA calculations involved the structured application of explicit screening criteria. The criteria used to screen out FEPs are explicit regulatory exclusion (SO-R), probability (SO-P), or consequence (SO-C). All three criteria are derived from regulatory requirements. FEPs not screened out as SO-R, SO-P, or SO-C were retained for inclusion in PA calculations and are classified as either undisturbed performance (UP) or disturbed performance (DP) FEPs.

SCR-2.3.1 Regulation (SO-R)

Specific FEP screening criteria are stated in Part 191 and Part 194. Such screening criteria relating to the applicability of particular FEPs represent screening decisions made by the EPA. That is, in the process of developing and demonstrating the feasibility of the Part 191 standard and the Part 194 criteria, the EPA considered and made conclusions on the relevance, consequence, and probability of particular FEPs occurring. In so doing, it allowed some FEPs to be eliminated from consideration.

SCR-2.3.2 Probability of Occurrence of a FEP Leading to Significant Release of Radionuclides (SO-P)

Low-probability events can be excluded on the basis of the criterion provided in section 194.32(d), which states, "performance assessments need not consider processes and events that have less than one chance in 10,000 of occurring over 10,000 years." In practice, for most FEPs screened out on the basis of low probability of occurrence, it has not been possible to estimate a meaningful quantitative probability. In the absence of quantitative probability estimates, a qualitative argument was used.

SCR-2.3.3 Potential Consequences Associated with the Occurrence of the FEPs (SO-C)

The DOE recognizes two uses for this criterion:

1. FEPs can be eliminated from PA calculations on the basis of insignificant consequence. Consequence can refer to effects on the repository or site or to radiological consequence. In particular, section 194.34 (a) (U.S. EPA 1996a) states, "The results of performance assessments shall be assembled into 'complementary, cumulative distribution functions' (CCDFs) that represent the probability of exceeding various levels of cumulative release caused by all significant processes and events." The DOE has omitted events and processes (EPs) from PA calculations where there is a reasonable expectation that the remaining probability distribution of cumulative releases would not be significantly changed by such omissions.

2. FEPs that are potentially beneficial to subsystem performance may be eliminated from PA calculations if necessary to simplify the analysis. This argument may be used when there is uncertainty as to exactly how the FEP should be incorporated into assessment calculations or when incorporation would incur unreasonable difficulties.

In some cases, the effects of the particular event or process occurring, although not necessarily insignificant, can be shown to lie within the range of uncertainty of another FEP already accounted

for in the PA calculations. In such cases, the event or process may be included in PA calculations implicitly, within the range of uncertainty associated with the included FEP.

Although some FEPs could be eliminated from PA calculations on the basis of more than one criterion, the most practical screening criterion was used for classification. In particular, a regulatory screening classification was used in preference to a probability or consequence screening classification. FEPs that have not been screened out based on any of the three criteria were included in the PA.

SCR-2.3.4 UP FEPs

FEPs classified as UP are accounted for in calculations of UP of the disposal system. UP is defined in section 191.12 (U.S. EPA 1993) as "the predicted behavior of a disposal system, including consideration of the uncertainties in predicted behavior, if the disposal system is not disrupted by human intrusion or the occurrence of unlikely natural events." The UP FEPs are accounted for in the PA calculations to evaluate compliance with the containment requirements in section 191.13. Undisturbed PA calculations are also used to demonstrate compliance with the individual and groundwater protection requirements of section 191.15 (U.S. EPA 1993) and Part 191 Subpart C, respectively.

SCR-2.3.5 DP FEPs

The FEPs classified as DP are accounted for only in assessment calculations for DP. The DP FEPs that remain following the screening process relate to the potential disruptive effects of future drilling and mining events in the controlled area. Consideration of both DP and UP FEPs is required to evaluate compliance with section 191.13.

SCR-2.4 FEPs Categories and Timeframes

In the following sections, FEPs are discussed under the categories Natural FEPs, Human-Induced EPs, and Waste- and Repository-Induced FEPs. Identifiers (IDs) of Natural FEPs begin with "N," IDs of Human-Induced EPs begin with "H," and IDs of Waste- and Repository-Induced FEPs begin with "W." The FEPs are also considered within time frames during which they may occur. Because of the regulatory requirements concerning human activities, two time periods were used when evaluating human-induced EPs. These time frames were defined as Historical, Current, and Near-Future Human Activities (HCN) and Future Human Activities (Future). These time frames are also discussed in Section SCR-2.4.2.

SCR-2.4.1 Description of Natural FEPs

Natural FEPs are those that relate to hydrologic, geologic, and climate conditions that have the potential to affect long-term performance of the WIPP disposal system over the regulatory time frame. These FEPs do not include the impacts of other human-related activities such as the effect of boreholes on FEPs related to natural changes in groundwater chemistry. Only natural FEPs are included in the screening process.

Consistent with section 194.32(d), the DOE has screened out several natural FEPs from PA calculations on the basis of a low probability of occurrence at or near the WIPP site. In particular, natural events for which there is no evidence indicating that they have occurred within the Delaware Basin have been screened on this basis. For FEPs analysis, the probabilities of occurrence of these

events are assumed to be zero. Quantitative, nonzero probabilities for such events, based on numbers of occurrences, cannot be ascribed without considering regions much larger than the Delaware Basin, thus neglecting established geological understanding of the FEPs that occur within particular geographical provinces.

In considering the overall geological setting of the Delaware Basin, the DOE has eliminated many FEPs from PA calculations on the basis of low consequence. FEPs that have had little effect on the characteristics of the region in the past are expected to be of low consequence for the regulatory time period.

SCR-2.4.2 Description of Human-Induced EPs

Human-induced EPs (Human EPs) are those associated with human activities in the past, present, and future. The EPA provided guidance in their regulations concerning which human activities are to be considered, their severity, and the manner in which to include them in the future predictions.

The scope of PAs is clarified with respect to human-induced EPs in section 194.32. At section 194.32 (a), the EPA states,

> Performance assessments shall consider natural processes and events, mining, deep drilling, and shallow drilling that may affect the disposal system during the regulatory time frame.

Thus, PAs must include consideration of human-induced EPs relating to mining and drilling activities that might take place during the regulatory time frame. In particular, PAs must consider the potential effects of such activities that might take place within the controlled area at a time when institutional controls cannot be assumed to completely eliminate the possibility of human intrusion.

Further criteria concerning the scope of PAs are provided at section 194.32(c):

> Performance assessments shall include an analysis of the effects on the disposal system of any activities that occur in the vicinity of the disposal system prior to disposal and are expected to occur in the vicinity of the disposal system soon after disposal. Such activities shall include, but shall not be limited to, existing boreholes and the development of any existing leases that can be reasonably expected to be developed in the near future, including boreholes and leases that may be used for fluid injection activities.

In order to implement the criteria in section 194.32 relating to the scope of PAs, the DOE has divided human activities into three categories: (1) human activities currently taking place and those that took place prior to the time of the compliance application, (2) human activities that might be initiated in the near future after submission of the compliance application, and (3) human activities that might be initiated after repository closure. The first two categories of EPs, corresponding to the HCN time frame, are considered under UP, and EPs in the third category, which belong to the Future time frame, may lead to DP conditions. A description of these three categories follows.

1. Historical and current human activities include resource-extraction activities that have historically taken place and are currently taking place outside the controlled area. These activities are of potential significance insofar as they could affect the geological, hydrological, or geochemical characteristics of the disposal system or groundwater flow pathways outside the disposal system. Current human activities taking place within the controlled area are essentially those associated with development of the WIPP repository. Historic human activities include existing boreholes.

2. Near-future human activities include resource-extraction activities that may be expected to occur outside the controlled area based on existing plans and leases. Thus, the near future includes the expected lives of existing mines and oil and gas fields, and the expected lives of new mines and oil and gas fields that the DOE expects will be developed based on existing plans and leases. These activities are of potential significance insofar as they could affect the geological, hydrological, or geochemical characteristics of the disposal system or groundwater flow pathways outside the disposal system. The only human activities expected to occur within the controlled area in the near future are those associated with development of the WIPP repository. The DOE expects that any activity initiated in the near future, based on existing plans and leases, will be initiated prior to repository closure. Activities initiated prior to repository closure are assumed to continue until their completion.

3. Future human activities include activities that might be initiated within or outside the controlled area after repository closure. This includes drilling and mining for resources within the disposal system at a time when institutional controls cannot be assumed to completely eliminate the possibility of such activities. Future human activities could influence the transport of contaminants within and outside the disposal system by directly removing waste from the disposal system or altering the geological, hydrological, or geochemical characteristics of the disposal system.

SCR-2.4.2.1 Scope of Future Human Activities in PA

PAs must consider the effects of future human activities on the performance of the disposal system. The EPA has provided criteria relating to future human activities in section 194.32(a), which limits the scope of consideration of future human activities in PAs to mining and drilling.

SCR-2.4.2.1.1 Criteria Concerning Future Mining

The EPA provides the following additional criteria concerning the type of future mining that should be considered by the DOE in section 194.32(b):

> Assessments of mining effects may be limited to changes in the hydraulic conductivity of the hydrogeologic units of the disposal system from excavation mining for natural resources. Mining shall be assumed to occur with a one in 100 probability in each century of the regulatory time frame. Performance assessments shall assume that mineral deposits of those resources, similar in quality and type to those resources currently extracted from the Delaware Basin, will be completely removed from the controlled area during the century in which such mining is randomly calculated to occur. Complete removal of such mineral resources shall be assumed to occur only once during the regulatory time frame.

Thus, consideration of future mining may be limited to mining within the controlled area at the locations of resources that are similar in quality and type to those currently extracted from the Delaware Basin. Potash is the only resource that has been identified within the controlled area in quality similar to that currently mined from underground deposits elsewhere in the Delaware Basin. The hydrogeological impacts of future potash mining within the controlled area are accounted for in calculations of the DP of the disposal system. Consistent with section 194.32(b), all economically recoverable resources in the vicinity of the disposal system (outside the controlled area) are assumed to be extracted in the near future.

SCR-2.4.2.1.2 Criteria Concerning Future Drilling

With respect to consideration of future drilling, in the preamble to Part 194, the EPA

> …reasoned that while the resources drilled for today may not be the same as those drilled for in the future, the present rates at which these boreholes are drilled can nonetheless provide an estimate of the future rate at which boreholes will be drilled.

Criteria concerning the consideration of future deep and shallow drilling in PAs are provided in section 194.33 (U.S. EPA 1996a). The EPA also provides a criterion in section 194.33(d) concerning the use of future boreholes subsequent to drilling:

> With respect to future drilling events, performance assessments need not analyze the effects of techniques used for resource recovery subsequent to the drilling of the borehole.

Thus, PAs need not consider the effects of techniques used for resource extraction and recovery that would occur subsequent to the drilling of a borehole in the future. These activities are screened SO-R.

The EPA provides an additional criterion that limits the severity of human intrusion scenarios that must be considered in PAs. In section 194.33(b)(1) the EPA states,

> Inadvertent and intermittent intrusion by drilling for resources (other than those resources provided by the waste in the disposal system or engineered barriers designed to isolate such waste) is the most severe human intrusion scenario.

SCR-2.4.2.1.3 Screening of Future Human EPs

Future Human EPs accounted for in PA calculations for the WIPP are those associated with mining and deep drilling within the controlled area at a time when institutional controls cannot be assumed to completely eliminate the possibility of such activities. All other future Human EPs, if not eliminated from PA calculations based on regulation, have been eliminated based on low consequence or low probability. For example, the effects of future shallow drilling within the controlled area were eliminated from CCA PA calculations on the basis of low consequence to the performance of the disposal system.

SCR-2.4.3 Description of Waste- and Repository-Induced FEPs

The waste- and repository-induced FEPs are those that relate specifically to the waste material, waste containers, shaft seals, magnesium oxide (MgO) backfill, panel closure system (PCS), repository structures, and investigation boreholes. All FEPs related to radionuclide chemistry and radionuclide migration are included in this category. The FEPs related to radionuclide transport resulting from future borehole intersections of the WIPP excavation are defined as waste- and repository-induced FEPs.

SCR-3.0 FEPs

The reassessment of FEPs (Kirkes 2013b) results in a new FEPs baseline for CRA-2014. As discussed in Section SCR-1.0, 184 of the 245 WIPP FEPs have not changed since the CRA-2009. However, 61 FEPs required updates to their FEP descriptions and/or screening arguments, one of which has also had its screening decision changed. The single screening decision change does not result in a new

FEP incorporated into PA calculations; the particular FEP will now be screened out of PA. Thus, the CRA-2014 considers 245 WIPP FEPs.

Table SCR-1 outlines the results of the assessment, and subsequent sections of this document present the actual screening decisions and supporting arguments. Those FEPs not separated by gridlines in the first column of Table SCR-1 have been addressed by group because of close similarity with other FEPs within that group. This grouping process was formerly used in the CCA and also by the EPA in its Technical Support Document for section 194.32 (U.S. EPA 1998b).

Table SCR- 1. FEPs Summary for CRA-2014

EPA FEP I.D.[a,b,c,d]	FEP Name	Screening Argument Update?	Screening Decision Changed?	Screening Classification
N1	Stratigraphy	No change	No	UP
N2	Brine Reservoirs	Updated by new PA parameter GLOBAL:PBRINE	No	DP
N3	Changes in Regional Stress	No change	No	SO-C
N4	Regional Tectonics	No change	No	SO-C
N5	Regional Uplift and Subsidence	No change	No	SO-C
N6	Salt Deformation	No change	No	SO-P
N7	Diapirism	No change	No	SO-P
N8	Formation of Fractures	No change	No	SO-P UP (Repository)
N9	Changes in Fracture Properties	No change	No	SO-C UP (Near Repository)
N10	Formation of New Faults	No change	No	SO-P
N11	Fault Movement	No change	No	SO-P
N12	Seismic Activity	Updated with new seismic data	No	UP
N13	Volcanic Activity	No change	No	SO-P
N14	Magmatic Activity	No change	No	SO-C
N15	Metamorphic Activity	No change	No	SO-P
N16	Shallow Dissolution	No change	No	UP
N18	Deep Dissolution	No change	No	SO-P
N20	Breccia Pipes	No change	No	SO-P
N21	Collapse Breccias	No change	No	SO-P
N22	Fracture Infills	No change	No	SO-C - Beneficial
N23	Saturated Groundwater Flow	No change	No	UP
N24	Unsaturated Groundwater Flow	No change	No	UP
N25	Fracture Flow	No change	No	UP

Table SCR- 1. FEPs Summary for CRA-2014

EPA FEP I.D.[a ,b ,c, d]	FEP Name	Screening Argument Update?	Screening Decision Changed?	Screening Classification
N27	Effects of Preferential Pathways	No change	No	UP
N26	Density Effects on Groundwater Flow	No change	No	SO-C
N28	Thermal Effects on Groundwater Flow	No change	No	SO-C
N29	Saline Intrusion (Hydrogeological Effects)	No change	No	SO-P
N30	Freshwater Intrusion (Hydrogeological Effects)	No change	No	SO-P
N31	Hydrological Response to Earthquakes	No change	No	SO-C
N32	Natural Gas Intrusion	No change	No	SO-P
N33	Groundwater Geochemistry	No change	No	UP
N34	Saline Intrusion (Geochemical Effects)	No change	No	SO-C
N38	Effects of Dissolution	No change	No	SO-C
N35	Freshwater Intrusion (Geochemical Effects)	No change	No	SO-C
N36	Changes in Groundwater Eh	No change	No	SO-C
N37	Changes in Groundwater pH	No change	No	SO-C
N39	Physiography	No change	No	UP
N40	Impact of a Large Meteorite	No change	No	SO-P
N41	Mechanical Weathering	No change	No	SO-C
N42	Chemical Weathering	No change	No	SO-C
N43	Aeolian Erosion	No change	No	SO-C
N44	Fluvial Erosion	No change	No	SO-C
N45	Mass Wasting (Erosion)	No change	No	SO-C
N46	Aeolian Deposition	No change	No	SO-C
N47	Fluvial Deposition	No change	No	SO-C
N48	Lacustrine Deposition	No change	No	SO-C
N49	Mass Wasting (Deposition)	No change	No	SO-C
N50	Soil Development	No change	No	SO-C
N51	Stream and River Flow	No change	No	SO-C
N52	Surface Water Bodies	No change	No	SO-C
N53	Groundwater Discharge	No change	No	UP
N54	Groundwater Recharge	No change	No	UP

Table SCR- 1. FEPs Summary for CRA-2014

EPA FEP I.D.[a ,b ,c, d]	FEP Name	Screening Argument Update?	Screening Decision Changed?	Screening Classification
N55	Infiltration	No change	No	UP
N56	Changes in Groundwater Recharge and Discharge	No change	No	UP
N57	Lake Formation	No change	No	SO-C
N58	River Flooding	No change	No	SO-C
N59	Precipitation (e.g., Rainfall)	No change	No	UP
N60	Temperature	No change	No	UP
N61	Climate Change	No change	No	UP
N62	Glaciation	No change	No	SO-P
N63	Permafrost	No change	No	SO-P
N64	Seas and Oceans	No change	No	SO-C
N65	Estuaries	No change	No	SO-C
N66	Coastal Erosion	No change	No	SO-C
N67	Marine Sediment Transport and Deposition	No change	No	SO-C
N68	Sea Level Changes	No change	No	SO-C
N69	Plants	No change	No	SO-C
N70	Animals	No change	No	SO-C
N71	Microbes	No change	No	SO-C (UP - for colloidal effects and gas generation)
N72	Natural Ecological Development	No change	No	SO-C
H1	Oil and Gas Exploration	Updated with new drilling rate	No	SO-C (HCN) DP (Future)
H2	Potash Exploration	No change	No	SO-C (HCN) DP (Future)
H4	Oil and Gas Exploitation	Updated with new drilling rate	No	SO-C (HCN) DP (Future)
H8	Other Resources	No change	No	SO-C (HCN) DP (Future)
H9	Enhanced Oil and Gas Recovery	No change	No	SO-C (HCN) DP (Future)
H3	Water Resources Exploration	Updated with most recent monitoring information	No	SO-C (HCN) SO-C (Future)
H5	Groundwater Exploitation	Updated with most recent monitoring information	No	SO-C (HCN) SO-C (Future)

Table SCR- 1. FEPs Summary for CRA-2014

EPA FEP I.D.[a,b,c,d]	FEP Name	Screening Argument Update?	Screening Decision Changed?	Screening Classification
H6	Archaeological Investigations	No change	No	SO-R (HCN) SO-R (Future)
H7	Geothermal	No change	No	SO-R (HCN) SO-R (Future)
H10	Liquid Waste Disposal	No change	No	SO-R (HCN) SO-R (Future)
H11	Hydrocarbon Storage	No change	No	SO-R (HCN) SO-R (Future)
H12	Deliberate Drilling Intrusion	No change	No	SO-R (HCN) SO-R (Future)
H13	Conventional Underground Potash Mining	No change	No	UP (HCN) DP (Future)
H14	Other Resources (Mining For)	No change	No	SO-C (HCN) SO-R (Future)
H15	Tunneling	No change	No	SO-R (HCN) SO-R (Future)
H16	Construction of Underground Facilities (For Example Storage, Disposal, Accommodation)	No change	No	SO-R (HCN) SO-R (Future)
H17	Archaeological Excavations	No change	No	SO-C (HCN) SO-R (Future)
H18	Deliberate Mining Intrusion	No change	No	SO-R (HCN) SO-R (Future)
H19	Explosions for Resource Recovery	No change	No	SO-C (HCN) SO-R (Future)
H20	Underground Nuclear Device Testing	No change	No	SO-C (HCN) SO-R (Future)
H21	Drilling Fluid Flow	No change	No	SO-C (HCN) DP (Future)
H22	Drilling Fluid Loss	No change	No	SO-C (HCN) DP (Future)
H23	Blowouts	Updated with new parameter GLOBAL:PBRINE	No	SO-C (HCN) DP (Future)
H24	Drilling-Induced Geochemical Changes	No change	No	UP (HCN) DP (Future)
H25	Oil and Gas Extraction	No change	No	SO-C (HCN) SO-R (Future)
H26	Groundwater Extraction	No change	No	SO-C (HCN) SO-R (Future)
H27	Liquid Waste Disposal-Outside Boundary (OB)	No change	No	SO-C (HCN) SO-C (Future)

Table SCR- 1. FEPs Summary for CRA-2014

EPA FEP I.D.[a,b,c,d]	FEP Name	Screening Argument Update?	Screening Decision Changed?	Screening Classification
H28	Enhanced Oil and Gas Production-OB	No change	No	SO-C (HCN) SO-C (Future)
H29	Hydrocarbon Storage-OB	No change	No	SO-C (HCN) SO-C (Future)
H60	Liquid Waste Disposal-Inside Boundary (IB)	No change	No	SO-R (HCN) SO-R (Future)
H61	Enhanced Oil and Gas Production-IB	No change	No	SO-R (HCN) SO-R (Future)
H62	Hydrocarbon Storage-IB	No change	No	SO-R (HCN) SO-R (Future)
H30	Fluid-Injection Induced Geochemical Changes	No change	No	UP (HCN) SO-R (Future)
H31	Natural Borehole Fluid Flow	Updated to reflect new plugging probabilities	No	SO-C (HCN) SO-C (Future, holes not penetrating waste panels) DP (Future, holes penetrating panels)
H32	Waste-Induced Borehole Flow	Updated to reflect new plugging probabilities	No	SO-R (HCN) DP (Future)
H34	Borehole-Induced Solution and Subsidence	No change	No	SO-C (HCN) SO-C (Future)
H35	Borehole-Induced Mineralization	No change	No	SO-C (HCN) SO-C (Future)
H36	Borehole-Induced Geochemical Changes	No change	No	UP (HCN) DP (Future) SO-C (for units other than the Culebra)
H37	Changes in Groundwater Flow Due to Mining	No change	No	UP (HCN) DP (Future)
H38	Changes in Geochemistry Due to Mining	No change	No	SO-C (HCN) SO-R (Future)
H39	Changes in Groundwater Flow Due to Explosions	No change	No	SO-C (HCN) SO-R (Future)
H40	Land Use Changes	No change	No	SO-R (HCN) SO-R (Future)
H41	Surface Disruptions	No change	No	UP (HCN) SO-C (Future)
H42	Damming of Streams or Rivers	No change	No	SO-C (HCN) SO-R (Future)
H43	Reservoirs	No change	No	SO-C (HCN) SO-R (Future)

Table SCR- 1. FEPs Summary for CRA-2014

EPA FEP I.D.[a,b,c,d]	FEP Name	Screening Argument Update?	Screening Decision Changed?	Screening Classification
H44	Irrigation	No change	No	SO-C (HCN) SO-R (Future)
H45	Lake Usage	No change	No	SO-R (HCN) SO-R (Future)
H46	Altered Soil or Surface Water Chemistry by Human Activities	No change	No	SO-C (HCN) SO-R (Future)
H47	Greenhouse Gas Effects	No change	No	SO-R (HCN) SO-R (Future)
H48	Acid Rain	No change	No	SO-R (HCN) SO-R (Future)
H49	Damage to the Ozone Layer	No change	No	SO-R (HCN) SO-R (Future)
H50	Coastal Water Use	No change	No	SO-R (HCN) SO-R (Future)
H51	Sea Water Use	No change	No	SO-R (HCN) SO-R (Future)
H52	Estuarine Water Use	No change	No	SO-R (HCN) SO-R (Future)
H53	Arable Farming	No change	No	SO-C (HCN) SO-R (Future)
H54	Ranching	No change	No	SO-C (HCN) SO-R (Future)
H55	Fish Farming	No change	No	SO-R (HCN) SO-R (Future)
H56	Demographic Change and Urban Development	No change	No	SO-R (HCN) SO-R (Future)
H57	Loss of Records	No change	No	NA (HCN) DP (Future)
H58	Solution Mining for Potash	Updated with information regarding solution mining activities in the region	No	SO-R (HCN) SO-R (Future)
H59	Solution Mining for Other Resources	Updated with new information regarding brine wells in the region	No	SO-C (HCN) SO-C (Future)
W1	Disposal Geometry	Updated with new information regarding additional mined area used for experiments	No	UP

Table SCR- 1. FEPs Summary for CRA-2014

EPA FEP I.D.[a,b,c,d]	FEP Name	Screening Argument Update?	Screening Decision Changed?	Screening Classification
W2	Waste Inventory	Updated to reflect the inventory data sources used for the CRA-2014 PA	No	UP
W3	Heterogeneity of Waste Forms	Updated to reflect the inventory data sources used for the CRA-2014 PA	No	DP
W4	Container Form	Updated to reflect the inventory data sources used for the CRA-2014 PA	No	SO-C - Beneficial
W5	Container Material Inventory	Updated to reflect the inventory data sources used for the CRA-2014 PA	No	UP
W6	Shaft Seal Geometry	No change	No	UP
W7	Shaft Seal Physical Properties	No change	No	UP
W109	Panel Closure Geometry	Updated with new information on panel closure design	No	UP
W110	Panel Closure Physical Properties	Updated with new information on panel closure design	No	UP
W8	Shaft Seal Chemical Composition	No change	No	SO-C Beneficial
W111	Panel Closure Chemical Composition	Updated with new information on panel closure design	No	SO-C Beneficial
W9	Backfill Physical Properties	No change	No	SO-C
W10	Backfill Chemical Composition	Updated to reflect implementation of water balance in PA	No	UP
W11	Post-Closure Monitoring	No change	No	SO-C
W12	Radionuclide Decay and In-Growth	No change	No	UP
W13	Heat from Radioactive Decay	Updated to reflect the inventory used for the CRA-2014 PA	No	SO-C

Table SCR- 1. FEPs Summary for CRA-2014

EPA FEP I.D.[a,b,c,d]	FEP Name	Screening Argument Update?	Screening Decision Changed?	Screening Classification
W14	Nuclear Criticality: Heat	Updated to reflect the inventory used for the CRA-2014 PA	No	SO-P
W15	Radiological Effects on Waste	Updated to reflect the inventory used for the CRA-2014 PA	No	SO-C
W16	Radiological Effects on Containers	Updated to reflect the inventory used for the CRA-2014 PA	No	SO-C
W17	Radiological Effects on Shaft Seals	Updated to reflect the inventory used for the CRA-2014 PA	No	SO-C
W112	Radionuclide Effects on Panel Closures	Updated to reflect the inventory used for the CRA-2014 PA	No	SO-C
W18	Disturbed Rock Zone (DRZ)	Updated to include new panel closure implementation	No	UP
W19	Excavation-Induced Changes in Stress	Updated to include new panel closure implementation	No	UP
W20	Salt Creep	Updated to include new panel closure implementation	No	UP
W21	Changes in the Stress Field	Updated to include new panel closure implementation	No	UP
W22	Roof Falls	No change	No	UP
W23	Subsidence	No change	No	SO-C
W24	Large Scale Rock Fracturing	No change	No	SO-P
W25	Disruption Due to Gas Effects	No change	No	UP
W26	Pressurization	Updated to reference new corrosion experiments and associated parameters	No	UP
W27	Gas Explosions	No change	No	UP

Table SCR- 1. FEPs Summary for CRA-2014

EPA FEP I.D.[a,b,c,d]	FEP Name	Screening Argument Update?	Screening Decision Changed?	Screening Classification
W28	Nuclear Explosions	Updated to reflect the inventory used for the CRA-2014 PA	No	SO-P
W29	Thermal Effects on Material Properties	Updated to reflect the inventory used for the CRA-2014 and planned thermal experiments	No	SO-C
W30	Thermally-Induced Stress Changes	Updated to reflect the inventory used for the CRA-2014 and planned thermal experiments	No	SO-C
W31	Differing Thermal Expansion of Repository Components	Updated to reflect the inventory used for the CRA-2014 and planned thermal experiments	No	SO-C
W72	Exothermic Reactions	Updated to reflect the inventory used for the CRA-2014 and planned thermal experiments	No	SO-C
W73	Concrete Hydration	Updated to reflect the inventory used for the CRA-2014 and planned thermal experiments	No	SO-C
W32	Consolidation of Waste	No change	No	UP
W36	Consolidation of Shaft Seals	No change	No	UP
W37	Mechanical Degradation of Shaft Seals	No change	No	UP
W39	Underground Boreholes	No change	No	UP
W113	Consolidation of Panel Closures	Updated screening argument with new information regarding panel closure composition	No	UP

Table SCR- 1. FEPs Summary for CRA-2014

EPA FEP I.D.[a,b,c,d]	FEP Name	Screening Argument Update?	Screening Decision Changed?	Screening Classification
W114	Mechanical Degradation of Panel Closures	Updated screening argument with new information regarding panel closure composition	No	UP
W33	Movement of Containers	Updated to reference new inventory data	No	SO-C
W34	Container Integrity	No change	No	SO-C Beneficial
W35	Mechanical Effects of Backfill	No change	No	SO-C
W40	Brine Inflow	Updated to reflect water balance implementation in PA	No	UP
W41	Wicking	Updated to reflect water balance implementation in PA	No	UP
W42	Fluid Flow Due to Gas Production	Updated to reflect water balance implementation in PA and new steel corrosion rates	No	UP
W43	Convection	Updated to reflect planned thermal experiments	No	SO-C
W44	Degradation of Organic Material	Updated to reference new inventory data	No	UP
W45	Effects of Temperature on Microbial Gas Generation	Updated to reference new inventory data	No	UP
W48	Effects of Biofilms on Microbial Gas Generation	Updated to reference new inventory data	No	UP
W46	Effects of Pressure on Microbial Gas Generation	No change	No	SO-C

Table SCR- 1. FEPs Summary for CRA-2014

EPA FEP I.D.[a,b,c,d]	FEP Name	Screening Argument Update?	Screening Decision Changed?	Screening Classification
W47	Effects of Radiation on Microbial Gas Generation	Updated with new radionuclide inventory and information related to the EPA request for additional information on CRA-2009	No	SO-C
W49	Gases from Metal Corrosion	Updated to reference new corrosion experiments and inventory	No	UP
W51	Chemical Effects of Corrosion	Updated to reference new corrosion experiments and inventory	No	UP
W50	Galvanic Coupling (Within the Repository)	No change	No	SO-C
W52	Radiolysis of Brine	No change	No	SO-C
W53	Radiolysis of Cellulose	Screening argument updated with new radionuclide inventory	No	SO-C
W54	Helium Gas Production	Screening argument updated with new radionuclide inventory	No	SO-C
W55	Radioactive Gases	Updated to reference new inventory data	No	SO-C
W56	Speciation	Reference made to new solubility calculations based on new inventory components	No	UP in disposal rooms and Culebra. SO-C elsewhere, and SO-C Beneficial in cementitious seals
W57	Kinetics of Speciation	No change	No	SO-C
W58	Dissolution of Waste	No change	No	UP
W59	Precipitation of Secondary Minerals	No change	No	SO-C Beneficial
W60	Kinetics of Precipitation and Dissolution	No change	No	SO-C

Table SCR- 1. FEPs Summary for CRA-2014

EPA FEP I.D.[a,b,c,d]	FEP Name	Screening Argument Update?	Screening Decision Changed?	Screening Classification
W61	Actinide Sorption	No change	No	UP in the Culebra and Dewey Lake; SO-C-Beneficial in the disposal room, shaft seals, panel closures, and other geologic units.
W62	Kinetics of Sorption	No change	No	UP in the Culebra and Dewey Lake; SO-C-Beneficial in the disposal room, shaft seals, panel closures, and other geologic units.
W63	Changes in Sorptive Surfaces	No change	No	UP
W64	Effects of Metal Corrosion	No change	No	UP
W66	Reduction-Oxidation Kinetics	No change	No	UP
W65	Reduction-Oxidation Fronts	No change	No	SO-P
W67	Localized Reducing Zones	No change	No	SO-C
W68	Organic Complexation	Updated to reflect implementation of variable brine volume in PA	No	UP
W69	Organic Ligands	Updated to reflect implementation of variable brine volume, new inventory data	No	UP
W71	Kinetics of Organic Complexation	No change	No	SO-C
W70	Humic and Fulvic Acids	No change	No	UP
W74	Chemical Degradation of Shaft Seals	No change	No	UP
W76	Microbial Growth on Concrete	No change	No	UP
W115	Chemical Degradation of Panel Closures	Updated screening argument with new panel closure materials	Yes	SO-P
W75	Chemical Degradation of Backfill	No change	No	SO-C
W77	Solute Transport	No change	No	UP
W78	Colloid Transport	No change	No	UP

Table SCR- 1. FEPs Summary for CRA-2014

EPA FEP I.D.[a,b,c,d]	FEP Name	Screening Argument Update?	Screening Decision Changed?	Screening Classification
W79	Colloid Formation and Stability	No change	No	UP
W80	Colloid Filtration	No change	No	UP
W81	Colloid Sorption	No change	No	UP
W82	Suspensions of Particles	No change	No	DP
W83	Rinse	No change	No	SO-C
W84	Cuttings	No change	No	DP
W85	Cavings	Updated with new waste shear strength data	No	DP
W86	Spallings	Updated with new water balance implementation	No	DP
W87	Microbial Transport	No change	No	UP
W88	Biofilms	No change	No	SO-C Beneficial
W89	Transport of Radioactive Gases	Updated to reference CRA-2014 inventory data	No	SO-C
W90	Advection	No change	No	UP
W91	Diffusion	No change	No	UP
W92	Matrix Diffusion	No change	No	UP
W93	Soret Effect	Updated based on new inventory data	No	SO-C
W94	Electrochemical Effects	No change	No	SO-C
W95	Galvanic Coupling (Outside the Repository)	No change	No	SO-P
W96	Electrophoresis	No change	No	SO-C
W97	Chemical Gradients	No change	No	SO-C
W98	Osmotic Processes	No change	No	SO-C
W99	Alpha Recoil	No change	No	SO-C
W100	Enhanced Diffusion	No change	No	SO-C
W101	Plant Uptake	No change	No	SO-R (for section 191.13) SO-C (for section 191.15)
W102	Animal Uptake	No change	No	SO-R (for section 191.13) SO-C (for section 191.15)

Table SCR- 1. FEPs Summary for CRA-2014

EPA FEP I.D.[a,b,c,d]	FEP Name	Screening Argument Update?	Screening Decision Changed?	Screening Classification
W103	Accumulation in Soils	No change	No	SO-C Beneficial (for section 191.13) SO-C (for section 191.15)
W104	Ingestion	No change	No	SO-R SO-C (for section 191.15)
W105	Inhalation	No change	No	SO-R SO-C (for section 191.15)
W106	Irradiation	No change	No	SO-R SO-C (for section 191.15)
W107	Dermal Sorption	No change	No	SO-R SO-C (for section 191.15)
W108	Injection	No change	No	SO-R SO-C (for section 191.15)

[a] N = Natural FEP

[b] H = Human-induced event and process (EP)

[c] W = Waste- and Repository-induced FEP

[d] FEPs in this column that are not separated by rows represent FEPs that are similar in nature and are discussed and screened as a common group.

SCR-4.0 Screening of Natural FEPs

This section presents the screening arguments and decisions for natural FEPs. Natural FEPs may be important to the performance of the disposal system. Screening of natural FEPs is done in the absence of human influences on the FEPs. Of the 70 natural FEPs, 68 remain completely unchanged and two have been updated to include additional information. No screening decisions (classifications) for natural FEPs were changed, and no additional natural FEPs have been identified.

SCR-4.1 Geological FEPs

SCR-4.1.1 Stratigraphy

SCR-4.1.1.1 FEP Numbers: N1 and N2 FEP Titles: Stratigraphy(N1) Brine Reservoir (N2)

SCR-4.1.1.2 Screening Decision: UP (N1) DP (N2)

The *Stratigraphy* of the geological formations in the region of the WIPP is accounted for in PA calculations. The presence of *Brine Reservoirs* in the Castile Formation (hereafter referred to as the Castile) is accounted for in PA calculations.

SCR-4.1.1.2.1 Summary of New Information

Since the CRA-2009, new information has been gathered and analyzed that supports changing the probability that pressurized brine will be intercepted in WIPP intrusion scenarios. Kirchner et al. (Kirchner et al. 2012) describes the methodology and rationale for arriving at the updated parameter distribution for the PA parameter GLOBAL:PBRINE. This updated parameter does not change the screening argument or decision from the CRA-2009; brine reservoirs continue to be included in disturbed performance scenarios (DP).

SCR-4.1.1.2.2 Screening Argument

SCR-4.1.1.2.3

The stratigraphy and geology of the region around the WIPP, including the distribution and characteristics of pressurized brine reservoirs in the Castile, are discussed in detail in the CCA, Chapter 2.0, Section 2.1.3. The stratigraphy of the geological formations in the region of the WIPP is accounted for in PA calculations through the setup of the model geometries (Appendix PA-2014, Section PA-4.2.1). The presence of brine reservoirs is accounted for in the treatment of inadvertent drilling (Appendix PA-2014, Section PA-4.2.10).

SCR-4.1.2 Tectonics

SCR-4.1.2.1 FEP Numbers: N3, N4, and N5 FEP Titles: Changes in Regional Stress (N3) Regional Tectonics (N4) Regional Uplift and Subsidence (N5)

SCR-4.1.2.1.1 Screening Decision: SO-C

The effects of *Regional Tectonics*, *Regional Uplift* and *Subsidence*, and *Change in Regional Stress* have been eliminated from PA calculations on the basis of low consequence to the performance of the disposal system.

SCR-4.1.2.1.2 Summary of New Information

No new information that affects the screening of this FEP has been identified since the CRA-2009.

SCR-4.1.2.1.3 Screening Argument

Regional tectonics encompasses two related issues of concern: the overall level of regional stress and whether any significant changes in regional stress might occur.

The tectonic setting and structural features of the area around the WIPP are described in the CCA, Chapter 2.0, Section 2.1.5. In summary, there is no geological evidence for Quaternary regional tectonics in the Delaware Basin. The eastward tilting of the region has been dated as mid-Miocene to Pliocene by King (King 1948, pp. 120–21) and is associated with the uplift of the Guadalupe Mountains to the west. Fault zones along the eastern margin of the basin, where it flanks the Central Basin Platform, were active during the Late Permian. Evidence for this includes the displacement of the Rustler Formation (hereafter referred to as the Rustler) observed by Holt and Powers (Holt and

Powers 1988, pp. 4–14) and the thinning of the Dewey Lake Redbeds Formation (hereafter referred to as the Dewey Lake) reported by Schiel (Schiel 1994). There is, however, no surface displacement along the trend of these fault zones, indicating that there has been no significant Quaternary movement. Other faults identified within the evaporite sequence of the Delaware Basin are inferred by Barrows' figures in Borns et al. (Borns et al. 1983, pp. 58–60) to be the result of salt deformation rather than regional tectonic processes. According to Muehlberger, Belcher, and Goetz (1978, p. 338), the nearest faults on which Quaternary movement has been identified lie to the west of the Guadalupe Mountains and are of minor regional significance. The effects of regional tectonics and changes in regional stress have therefore been eliminated from PA calculations on the basis of low consequence to the performance of the disposal system.

There are no reported stress measurements from the Delaware Basin, but a low-level, regional stress regime with low deviatoric stress has been inferred from the geological setting of the area (see the CCA, Chapter 2.0, Section 2.1.5). The inferred low level of regional stress and the lack of Quaternary tectonic activity indicate that regional tectonics and any changes in regional stress will be minor and therefore of low consequence to the performance of the disposal system. Even if rates of regional tectonic movement experienced over the past 10 million yrs continue, the extent of regional uplift and subsidence over the next 10,000 yrs would only be approximately 1 meter (m) (about several feet [ft]]). This amount of uplift or subsidence would not lead to a breach of the Salado because the salt would deform plastically to accommodate this slow rate of movement. Uniform regional uplift or a small increase in regional dip consistent with this past rate could give rise to downcutting by rivers and streams in the region. The extent of this downcutting would be little more than the extent of uplift, and reducing the overburden by 1 or 2 m would have no significant effect on groundwater flow or contaminant transport in units above or below the Salado. Thus, the effects of regional uplift and subsidence have been eliminated from PA calculations on the basis of low consequence to the performance of the disposal system.

SCR-4.1.2.1.4 Tectonic Setting and Site Structural Features

The DOE has screened out, on the basis of either probability or consequence or both, all tectonic, magmatic, and structural processes. The screening discussions can be found in the CCA, Appendix SCR. The information needed for this screening is included here and covers (1) regional tectonic processes such as subsidence, uplift, and basin tilting; (2) magmatic processes such as igneous intrusion and events such as volcanism; and (3) structural processes such as faulting and loading and unloading of the rocks because of long-term sedimentation or erosion. Discussions of structural events, such as earthquakes, are considered to the extent that they may create new faults or activate old faults. The seismicity of the area is considered in the CCA, Chapter 2.0, Section 2.6 for the purposes of determining seismic design parameters for the facility.

SCR-4.1.2.1.5 Tectonics

The processes and features included in this section are those more traditionally considered part of tectonics-processes that develop the broad-scale features of the earth. Salt dissolution is a different process that can develop some features resembling those of tectonics.

Most broad-scale structural elements of the area around the WIPP developed during the Late Paleozoic (see the CCA, Appendix GCR, pp. 3-58 through 3-77). There is little historical or geological evidence of significant tectonic activity in the vicinity, and the level of stress in the region is low. The entire region tilted slightly during the Tertiary, and activity related to Basin and Range

tectonics formed major structures southwest of the area. Seismic activity is specifically addressed in a separate section.

Broad subsidence began in the area as early as the Ordovician, developing a sag called the Tobosa Basin. By Late Pennsylvanian to Early Permian time, the Central Basin Platform developed (see the CCA, Chapter 2.0, Figure 2-19), separating the Tobosa Basin into two parts: the Delaware Basin to the west and the Midland Basin to the east. The Permian Basin refers to the collective set of depositional basins in the area during the Permian Period. Southwest of the Delaware Basin, the Diablo Platform began developing either in the Late Pennsylvanian or Early Permian. The Marathon Uplift and Ouachita tectonic belt limited the southern extent of the Delaware Basin.

According to Brokaw et al. (Brokaw et al. 1972, p. 30), pre-Ochoan sedimentary rocks in the Delaware Basin show evidence of gentle downwarping during deposition, while Ochoan and younger rocks do not. A relatively uniform eastward tilt, generally from about 14 to 19 meters per kilometer (m/km) (75 to 100 ft per mile [ft/mi]), has been superimposed on the sedimentary sequence. King (King 1948, pp. 108 and 121) generally attributes the uplift of the Guadalupe and Delaware mountains along the west side of the Delaware Basin to the later Cenozoic, though he also notes that some faults along the west margin of the Guadalupe Mountains have displaced Quaternary gravels.

King (King 1948, p. 144) also infers the uplift from the Pliocene-age deposits of the Llano Estacado. Subsequent studies of the Ogallala of the Llano Estacado show that it varies in age from Miocene (about 12 million yrs before present) to Pliocene (Hawley 1993). This is the most likely range for uplift of the Guadalupe Mountains and broad tilting to the east of the Delaware Basin sequence.

Analysis of the present regional stress field indicates that the Delaware Basin lies within the Southern Great Plains stress province. This province is a transition zone between the extensional stress regime to the west and the region of compressive stress to the east. An interpretation by Zoback and Zoback (Zoback and Zoback 1991, p. 350) of the available data indicates that the level of stress in the Southern Great Plains stress province is low. Changes to the tectonic setting, such as the development of subduction zones and a consequent change in the driving forces, would take much longer than 10,000 yrs to occur.

To the west of the Southern Great Plains province is the Basin and Range province, or Cordilleran Extension province, where according to Zoback and Zoback (Zoback and Zoback 1991, pp. 348-51) normal faulting is the characteristic style of deformation. The eastern boundary of the Basin and Range province is marked by the Rio Grande Rift. Sanford, Jakasha, and Cash (Sanford, Jakasha, and Cash 1991, p. 230) note that, as a geological structure, the Rift extends beyond the relatively narrow geomorphological feature seen at the surface, with a magnetic anomaly at least 500 km (300 mi) wide. On this basis, the Rio Grande Rift can be regarded as a system of axial grabens along a major north-south trending structural uplift (a continuation of the Southern Rocky Mountains). The magnetic anomaly extends beneath the Southern Great Plains stress province, and regional-scale uplift of about 1,000 m (3,300 ft) over the past 10 million yrs also extends into eastern New Mexico.

To the east of the Southern Great Plains province is the large Mid-Plate province that encompasses central and eastern regions of the conterminous United States and the Atlantic basin west of the Mid-Atlantic Ridge. The Mid-Plate province is characterized by low levels of paleo- and historic seismicity. Where Quaternary faulting has occurred, it is generally strike-slip and appears to be associated with the reactivation of older structural elements.

Zoback et al. (Zoback et al. 1991) report no stress measurements from the Delaware Basin. The stress field in the Southern Great Plains stress province has been defined from borehole measurements in west Texas and from volcanic lineaments in northern New Mexico. These measurements were interpreted by Zoback and Zoback (Zoback and Zoback 1991, p. 353) to indicate that the least principal horizontal stress is oriented north-northeast and south-southwest and that most of the province is characterized by an extensional stress regime.

There is an abrupt change between the orientation of the least principal horizontal stress in the Southern Great Plains and the west-northwest orientation of the least principal horizontal stress characteristic of the Rio Grande Rift. In addition to the geological indications of a transition zone as described above, Zoback and Zoback (Zoback and Zoback 1980, p. 6134) point out that there is also evidence for a sharp boundary between these two provinces. This is reinforced by the change in crustal thickness from about 40 km (24 mi) beneath the Colorado Plateau to about 50 km (30 mi) or more beneath the Southern Great Plains east of the Rio Grande Rift. The base of the crust within the Rio Grande Rift is poorly defined but is shallower than that of the Colorado Plateau (Thompson and Zoback 1979, p. 152). There is also markedly lower heat flow in the Southern Great Plains (typically < 60 m W m $^{-2}$) reported by Blackwell, Steele, and Carter (1991, p. 428) compared with that in the Rio Grande Rift (typically > 80 m W m $^{-2}$) reported by Reiter, Barroll, and Minier (Reiter, Barroll, and Minier 1991, p. 463).

On the eastern boundary of the Southern Great Plains province, there is only a small rotation in the direction of the least principal horizontal stress. There is, however, a change from an extensional, normal faulting regime to a compressive, strike-slip faulting regime in the Mid-Plate province. According to Zoback and Zoback (Zoback and Zoback 1980, p. 6134), the available data indicate that this change is not abrupt and that the Southern Great Plains province can be viewed as a marginal part of the Mid-Plate province.

SCR-4.1.3 Structural FEPs

SCR-4.1.3.1 Deformation

SCR-4.1.3.1.1 FEP Numbers: N6 and N7 FEP Titles: Salt Deformation (N6) Diapirism (N7)

SCR-4.1.3.1.1.1 Screening Decision: SO-P

Natural *Salt Deformation* and *Diapirism* at the WIPP site over the next 10,000 yrs on a scale severe enough to significantly affect performance of the disposal system have been eliminated from PA calculations on the basis of low probability of occurrence.

SCR-4.1.3.1.1.2 Summary of New Information

No new information that affects the screening of this FEP has been identified since the CRA-2009.

SCR-4.1.3.1.1.3 Screening Argument

Some of the evaporites in the northern Delaware Basin have been deformed and it has been proposed that the likely mechanism for deformation is gravity foundering of the more dense anhydrites in less dense halite (e.g., Anderson and Powers 1978; Jones 1981; Borns et al. 1983; Borns 1987). Diapirism occurs when the deformation is penetrative, i.e., halite beds disrupt overlying anhydrites. As

Anderson and Powers (Anderson and Powers 1978) suggested, this may have happened northeast of the WIPP at the location of drillhole ERDA-6. This is the only location where diapirism has been suggested for the evaporites of the northern Delaware Basin. The geologic situation suggests that deformation occurred before the Miocene-Pliocene Ogallala Formation was deposited (Jones 1981). Mechanical modeling is consistent with salt deformation occurring over about 700,000 yrs to form the deformed features known in the northern part of the WIPP site (Borns et al. 1983). The DOE drew the conclusion that evaporites at the WIPP site deform too slowly to affect performance of the disposal system.

Because brine reservoirs appear to be associated with deformation, Powers et al. (Powers et al. 1996) prepared detailed structure elevation maps of various units from the base of the Castile upward through the evaporites in the northern Delaware Basin. Drillholes are far more numerous for this study than at the time of the study by Anderson and Powers (Anderson and Powers 1978). Subdivisions of the Castile appear to be continuous in the vicinity of ERDA-6 and at ERDA-6. There is little justification for interpreting diapiric piercement at that site. The location and distribution of evaporite deformation in the area of the WIPP site is similar to that proposed by earlier studies (e.g., Anderson and Powers 1978; Borns et al. 1983; Borns and Shaffer 1985).

Surface domal features at the northwestern end of Nash Draw were of undetermined origin prior to WIPP investigations (e.g., Vine 1963), but extensive geophysical studies were conducted of these features as part of early WIPP studies (see Powers 1996). Two of the domal features were drilled, demonstrating that they had a solution-collapse origin (breccia pipes) and were not related in any way to salt diapirism (Snyder and Gard 1982).

A more recent study of structure for the Culebra Dolomite Member of the Rustler Formation (hereafter referred to as the Culebra) (Powers 2003) shows that the larger deformation associated with deeper units is reflected by the Culebra, although the structural relief is muted. In addition, evaporite deformation in the northern part of the WIPP site, associated with the area earlier termed the "disturbed zone" (Powers et al. 1978), is hardly observable on a map of Culebra structure (Powers 2003). There is no evidence of more recent deformation at the WIPP site based on such maps.

Deformed salt in the lower Salado and upper strata of the Castile has been encountered in a number of boreholes around the WIPP site; the extent of existing salt deformation is summarized in the CCA, Chapter 2.0, Section 2.1.6.1, and further detail is provided in the CCA, Appendix DEF.

A number of mechanisms may result in salt deformation: in massive salt deposits, buoyancy effects or diapirism may cause salt to rise through denser, overlying units; and in bedded salt with anhydrite or other interbeds, gravity foundering of the interbeds into the halite may take place. Results from rock mechanics modeling studies (see the CCA, Appendix DEF) indicate that the time scale for the deformation process is such that significant natural deformation is unlikely to occur at the WIPP site over any time frame significant to waste isolation. Thus, natural salt deformation and diapirism severe enough to alter existing patterns of groundwater flow or the behavior of the disposal system over the regulatory period has been eliminated from PA calculations on the basis of low probability of occurrence over the next 10,000 yrs.

SCR-4.1.3.2 Fracture Development

SCR-4.1.3.2.1 FEP Number: N8 FEP Title: Formation of Fractures

SCR-4.1.3.2.1.1 Screening Decision: SO-P, UP (Repository)

Formation of Fractures has been eliminated from PA calculations on the basis of a low probability of occurrence over 10,000 yrs. The *Formation of Fractures* near the repository is accounted for in PA through treatment of the DRZ.

SCR-4.1.3.2.1.2 Summary of New Information

No new information that affects the screening of this FEP has been identified since the CRA-2009.

SCR-4.1.3.2.1.3 Screening Argument

The formation of fractures requires larger changes in stress than are required for changes to the properties of existing fractures to overcome the shear and tensile strength of the rock. It has been concluded from the regional tectonic setting of the Delaware Basin that no significant changes in regional stress are expected over the regulatory period. The EPA agrees that fracture formation in the Rustler is likely a result of halite dissolution and subsequent overlying unit fracturing loading/unloading, as well as the syn- and postdepositional processes. Intraformational postdepositional dissolution of the Rustler has been ruled out as a major contributor to Rustler salt distribution and thus to new fracture formation based on work by Holt and Powers in the CCA (Appendix DEF, Section DEF3.2) and Powers and Holt (Powers and Holt 1999 and Powers and Holt 2000), who believe that depositional facies and syndepositional dissolution account for most of the patterns on halite distribution in the Rustler. The argument against developing new fractures in the Rustler during the regulatory period appears reasonable. The formation of new fracture sets in the Culebra has therefore been eliminated from PA calculations on the basis of a low probability of occurrence over 10,000 yrs.

Repository-induced fracturing of the DRZ and Salado interbeds is accounted for in PA calculations.

A mechanism such as salt diapirism could develop fracturing in the Salado, but there is little evidence of diapirism in the Delaware Basin. Salt deformation has occurred in the vicinity of the WIPP, and fractures have developed in deeper Castile anhydrites as a consequence. Deformation rates are slow, and it is highly unlikely that this process will induce significant new fractures in the Salado during the regulatory time period. Surface domal features at the northwestern end of Nash Draw were of undetermined origin prior to WIPP investigations (e.g., Vine 1963), but extensive geophysical studies were conducted of these features as part of early WIPP studies (see Powers 1996). Two of the domal features were drilled, demonstrating that they had a solution-collapse origin (breccia pipes) and were not related in any way to salt diapirism (Snyder and Gard 1982).

SCR-4.1.3.2.2 FEP Number: N9 FEP Title: Changes in Fracture Properties

SCR-4.1.3.2.2.1 Screening Decision: SO-C, UP (near repository)

Naturally induced *Changes in Fracture Properties* that may affect groundwater flow or radionuclide transport in the region of the WIPP have been eliminated from PA calculations on the basis of low consequence to the performance of the disposal system. *Changes in Fracture Properties* near the repository are accounted for in PA calculations through treatment of the DRZ.

SCR-4.1.3.2.2.2 Summary of New Information

No new information that affects the screening of this FEP has been identified since the CRA-2009.

SCR-4.1.3.2.2.3 Screening Argument

Groundwater flow in the region of the WIPP and transport of any released radionuclides may take place along fractures. The rate of flow and the extent of transport will be influenced by fracture characteristics. Changes in fracture properties could arise through natural changes in the local stress field; for example, through tectonic processes, erosion or sedimentation changing the amount of overburden, dissolution of soluble minerals along beds in the Rustler or upper Salado, or dissolution or precipitation of minerals in fractures.

Tectonic processes and features (changes in regional stress [N3]; tectonics [N4]; regional uplift and subsidence [N5]; salt deformation [N6]; diapirism [N7]) have been screened out of PA. These processes are not expected to significantly change the character of fractures during the regulatory period.

Surface erosion or deposition (e.g., N41-N49) are not expected to significantly change the overburden on the Culebra during the regulatory period. The relationship between Culebra transmissivity and depth is significant (Holt and Yarbrough 2002; Holt and Powers 2002), but the potential change to Culebra transmissivity based on deposition or erosion from these processes over the regulatory period is insignificant.

Shallow dissolution (N16), where soluble beds from the upper Salado or Rustler are removed by groundwater, has been extensively considered. There are no direct effects on the Salado at depths of the repository. Extensive study of the upper Salado and Rustler halite units (Holt and Powers 1988; the CCA, Appendix FAC; Powers and Holt 1999 and Powers and Holt 2000; Powers 2003) indicates little potential for dissolution at the WIPP site during the regulatory period. Existing fracture properties are expressed through the relationship between Culebra transmissivity values and geologic factors at and near the WIPP site (Holt and Yarbrough 2002; Holt and Powers 2002, p. 215). These have been incorporated into the transmissivity values for the CRA-2009 Performance Assessment Baseline Calculation (PABC).

Mineral precipitation within fractures (N22) is expected to be beneficial to performance, and it has been screened out on the basis of low consequence. Natural dissolution of fracture fillings within the Culebra is incorporated within FEP N16 (Shallow Dissolution). There is no new information on the distribution of fracture fillings within the Culebra. The effects of fracture fillings are also expected to be represented in the distribution of Culebra transmissivity values around the WIPP site and are thus incorporated into PA.

Repository-induced fracturing of the DRZ and Salado interbeds is accounted for in PA calculations (UP), and is discussed further in FEPs W18 and W19.

SCR-4.1.3.2.3 FEP Numbers: N10 and N11 FEP Titles: Formation of New Faults (N10) Fault Movement (N11)

SCR-4.1.3.2.3.1 Screening Decision: SO-P

Naturally induced *Fault Movement* and *Formation of New Faults* of sufficient magnitude to significantly affect the performance of the disposal system have been eliminated from PA calculations on the basis of low probability of occurrence over 10,000 yrs.

SCR-4.1.3.2.3.2 Summary of New Information

No new information that affects the screening of this FEP has been identified since the CRA-2009.

SCR-4.1.3.2.3.3 Screening Argument

Faults are present in the Delaware Basin in both the units underlying the Salado and in the Permian evaporite sequence (see the CCA, Section 2.1.5.3). According to Powers et al. (Powers et al. 1978 included in the CCA, Appendix GCR), there is evidence that movement along faults within the pre-Permian units affected the thickness of Early Permian strata, but these faults did not exert a structural control on the deposition of the Castile, the Salado, or the Rustler. Fault zones along the margins of the Delaware Basin were active during the Late Permian Period. Along the eastern margin, where the Delaware Basin flanks the Central Basin Platform, Holt and Powers (Holt and Powers 1988; also included in the CCA, Appendix FAC) note that there is displacement of the Rustler, and Schiel (Schiel 1994) notes that there is thinning of the Dewey Lake. There is, however, no surface displacement along the trend of these fault zones, indicating that there has been no significant Quaternary movement. Muehlberger et al. (Muehlberger et al. 1978, p. 338) note that the nearest faults on which Quaternary movement has been identified lie to the west of the Guadalupe Mountains.

The WIPP is located in an area of tectonic quiescence. Seismic monitoring conducted for the WIPP since the CCA continues to record small events at distance from the WIPP, and these events are mainly in areas associated with resource production (see Section SCR-4.1.3.2.4.2 for more information on seismic events in the area). The absence of Quaternary fault scarps and the general tectonic setting and understanding of its evolution indicate that large-scale, tectonically induced fault movement within the Delaware Basin can be eliminated from PA calculations on the basis of low probability over 10,000 yrs. The stable tectonic setting also allows the formation of new faults within the basin over the next 10,000 yrs to be eliminated from PA calculations on the basis of low probability of occurrence.

Evaporite dissolution at or near the WIPP site has the potential for developing fractures in the overlying beds. Three zones with halite (top of Salado, M1/H1 of the Los Medaños Member, and M2/H2 of the Los Medaños Member) underlie the Culebra at the site (Powers 2003). The upper Salado is present across the site, and there is no indication that dissolution of this area will occur in the regulatory period or cause faulting at the site. The Los Medaños units show both mudflat facies and halite-bearing facies within or adjacent to the WIPP site (Powers 2003). Although the distribution of halite in the Rustler is mainly the result of depositional facies and syndepositional dissolution (Holt and Powers 1988; Powers and Holt 1999 and Powers and Holt 2000), the possibility of past or future halite dissolution along the margins cannot be ruled out (Holt and Powers 1988; Beauheim and Holt 1990). If halite in the lower Rustler has been dissolved along the depositional margin, it has not occurred recently or has been of no consequence, as there is no indication on the surface or in Rustler structure of new (or old) faults in this area (e.g., Powers et al. 1978, Powers 2003).

The absence of Quaternary fault scarps and the general tectonic setting and understanding of its evolution indicate that large-scale, tectonically induced fault movement within the Delaware Basin can be eliminated from PA calculations on the basis of low probability over 10,000 yrs. The stable tectonic setting also allows the formation of new faults within the basin over the next 10,000 yrs to be eliminated from PA calculations on the basis of low probability of occurrence.

SCR-4.1.3.2.4 FEP Number: N12 FEP Title: Seismic Activity

SCR-4.1.3.2.4.1 Screening Decision: UP

The post-closure effects of *Seismic Activity* on the repository and the DRZ are accounted for in PA calculations.

SCR-4.1.3.2.4.2 Summary of New Information

Since the CCA, a much more rigorous seismic monitoring system has been developed by the New Mexico Institute of Mining and Technology (NMIMT). This enhanced monitoring network has greatly increased the sensitivity and detection capability of previous systems. Beginning in 2007, the Delaware Basin Drilling Surveillance Program (DBDSP) also improved its seismic database, allowing the identification and incorporation of data previously unavailable. Using this expanded database, the DBDSP identified 703 seismic events recorded within approximately 300 km (187 mi) from the WIPP site, most of which (85%) occurred in close proximity to the Dagger Draw gas field, during the 2002 - 2007 timeframe. During the current CRA-2014 monitoring period (October 2007 through December 2012) there were 543 seismic events recorded within approximately 300 km (187 mi) of the WIPP site. One notable seismic event occurred on March 18, 2012, with a magnitude of 2.4. This seismic event was associated with a potash mine roof fall. This event occurred 14 km (9 mi) southwest of the WIPP site (Callicoat 2013). No damage was identified at the WIPP site. With the continued collection of additional data, it is increasingly clear that the overwhelming majority of these seismic events are anthropogenic in nature.

SCR-4.1.3.2.4.3 Screening Argument

The following subsections present the screening argument for seismic activity (groundshaking).

SCR-4.1.3.2.4.4 Causes of Seismic Activity

Seismic activity describes transient ground motion that may be generated by several energy sources. There are two possible causes of seismic activity that could potentially affect the WIPP site: natural and human-induced. Natural seismic activity is caused by fault movement (earthquakes) when the buildup of strain in rock is released through sudden rupture or movement. Human-induced seismic activity may result from a variety of surface and subsurface activities, such as explosions (H19 and H20), mining (H13, H14, H58, and H59), fluid injection (H28), and fluid withdrawal (H25).

SCR-4.1.3.2.4.5 Groundshaking

Ground vibration and the consequent shaking of buildings and other structures are the most obvious effects of seismic activity. Once the repository and shafts have been sealed, however, existing surface structures will be dismantled. Postclosure PAs are concerned with the effects of seismic activity on the closed repository.

In regions of low and moderate seismic activity, such as the Delaware Basin, rocks behave elastically in response to the passage of seismic waves, and there are no long-term changes in rock properties. The effects of earthquakes beyond the DRZ have been eliminated from PA calculations on the basis of low consequence to the performance of the disposal system. An inelastic response, such as cracking, is only possible where there are free surfaces, as in the roof and walls of the repository prior to closure by creep. Seismic activity could, therefore, have an effect on the properties of the DRZ.

An assessment of the extent of damage in underground excavations caused by groundshaking depends largely on observations from mines and tunnels. Because such excavations tend to take place in rock

types more brittle than halite, these observations cannot be related directly to the behavior of the WIPP. According to Wallner (Wallner 1981, p. 244), the DRZ in brittle rock types is likely to be more highly fractured and hence more prone to spalling and rockfalls than an equivalent zone in salt. Relationships between groundshaking and subsequent damage observed in mines will therefore be conservative with respect to the extent of damage induced at the WIPP by seismic activity.

Dowding and Rozen (Dowding and Rozen 1978) classified damage in underground structures following seismic activity and found that no damage (cracks, spalling, or rockfalls) occurred at accelerations below 0.2 gravities (g) and that only minor damage occurred at accelerations up to 0.4 g. Lenhardt (Lenhardt 1988, p. 392) showed that a magnitude 3 earthquake would have to be within 1 km (0.6 mi) of a mine to result in falls of loose rock. The risk of seismic activity in the region of the WIPP reaching these thresholds is discussed below.

SCR-4.1.3.2.4.6 Seismic Risk in the Region of the WIPP

Prior to the introduction of a seismic monitoring network in 1960, most recorded earthquakes in New Mexico were associated with the Rio Grande Rift, although small earthquakes were detected in other parts of the region. In addition to continued activity in the Rio Grande Rift, the instrumental record has shown a significant amount of seismic activity originating from the Central Basin Platform and a number of small earthquakes in the Los Medaños area. Seismic activity in the Rio Grande Rift is associated with extensional tectonics in that area. Seismic activity in the Central Basin Platform may be associated with natural earthquakes, but there are also indications that this activity occurs in association with oil-field activities such as fluid injection. Small earthquakes in the Los Medaños region have not been precisely located, but may be the result of mining activity in the region. The CCA, Chapter 2.0, Section 2.6.2 contains additional discussion of seismic activity and risk in the WIPP region.

The instrumental record was used as the basis of a seismic risk study primarily intended for design calculations of surface facilities rather than for postclosure PAs. The use of this study to define probable ground accelerations in the WIPP region over the next 10,000 yrs is based on the assumptions that hydrocarbon extraction and potash mining will continue in the region and that the regional tectonic setting precludes major changes over the next 10,000 yrs.

Three source regions were used in calculating seismic risk: the Rio Grande Rift, the Central Basin Platform, and part of the Delaware Basin province (including the Los Medaños). Using conservative assumptions about the maximum magnitude event in each zone, the study indicated a return period of about 10,000 yrs (annual probability of occurrence of 10^{-4}) for events producing ground accelerations of 0.1 g. Ground accelerations of 0.2 g would have an annual probability of occurrence of about 5×10^{-6}.

The results of the seismic risk study and the observations of damage in mines caused by groundshaking give an estimated annual probability of occurrence of between 10^{-8} and 10^{-6} for events that could increase the permeability of the DRZ. The DRZ is accounted for in PA calculations as a zone of permanently high permeability (see Appendix PA-2014, Section PA-4.2.4); this treatment is considered to account for the effects of any potential seismic activity.

SCR-4.1.4 Crustal Process

SCR-4.1.4.1 FEP Number: N13 FEP Title: Volcanic Activity

SCR-4.1.4.1.1 Screening Decision: SO-P

Volcanic Activity has been eliminated from PA calculations on the basis of low probability of occurrence over 10,000 yrs.

SCR-4.1.4.1.2 Summary of New Information

No new information that affects the screening of this FEP has been identified since the CRA-2009.

SCR-4.1.4.1.3 Screening Argument

The Paleozoic and younger stratigraphic sequences within the Delaware Basin are devoid of locally derived volcanic rocks. Volcanic ashes (dated at 13 million yrs and 0.6 million yrs) do occur in the Gatuña Formation (hereafter referred to as the Gatuña), but these are not locally derived. Within eastern New Mexico and northern, central, and western Texas, the closest Tertiary volcanic rocks with notable areal extent or tectonic significance to the WIPP are approximately 160 km (100 mi) to the south in the Davis Mountains volcanic area. The closest Quaternary volcanic rocks are 250 km (150 mi) to the northwest in the Sacramento Mountains. No volcanic rocks are exposed at the surface within the Delaware Basin.

Volcanic activity is associated with particular tectonic settings: constructive and destructive plate margins, regions of intraplate rifting, and isolated hot-spots in intraplate regions. The tectonic setting of the WIPP site and the Delaware Basin is remote from plate margins, and the absence of past volcanic activity indicates the absence of a major hot spot in the region. Intraplate rifting has taken place along the Rio Grande some 200 km (120 mi) west of the WIPP site during the Tertiary and Quaternary Periods. Igneous activity along this rift valley is comprised of sheet lavas intruded on by a host of small-to-large plugs, sills, and other intrusive bodies. However, the geological setting of the WIPP site within the large and stable Delaware Basin allows volcanic activity in the region of the WIPP repository to be eliminated from performance calculations on the basis of low probability of occurrence over the next 10,000 yrs.

SCR-4.1.4.2 FEP Number: N14 FEP Title: Magmatic Activity

SCR-4.1.4.2.1 Screening Decision: SO-C

The effects of *Magmatic A ctivity* have been eliminated from the PA calculations on the basis of low consequence to the performance of the disposal system.

SCR-4.1.4.2.2 Summary of New Information

No new information that affects the screening of this FEP has been identified since the CRA-2009.

SCR-4.1.4.2.3 Screening Argument

Magmatic activity is defined as the subsurface intrusion of igneous rocks into country rock. Deep intrusive igneous rocks crystallize at depths of several kilometers (several miles) and have no surface or near-surface expression until considerable erosion has taken place. Alternatively, intrusive rocks may form from magma that has risen to near the surface or in the vents that give rise to volcanoes and lava flows. Magma near the surface may be intruded along subvertical and subhorizontal discontinuities (forming dikes and sills, respectively), and magma in volcanic vents may solidify as plugs. The formation of such features close to a repository or the existence of a recently intruded rock mass could impose thermal stresses, inducing new fractures or altering the hydraulic characteristics of existing fractures.

The principal area of magmatic activity in New Mexico is the Rio Grande Rift, where extensive intrusions occurred during the Tertiary and Quaternary Periods. The Rio Grande Rift, however, is in a different tectonic province than the Delaware Basin, and its magmatic activity is related to the extensional stress regime and high heat flow in that region.

Within the Delaware Basin, there is a single identified outcrop of a lamprophyre dike about 70 km (40 mi) southwest of the WIPP (see the CCA, Chapter 2.0, Section 2.1.5.4 and the CCA, Appendix GCR for more detail). Closer to the WIPP site, similar rocks have been exposed within potash mines some 15 km (10 mi) to the northwest, and igneous rocks have been reported from petroleum exploration boreholes. Material from the subsurface exposures has been dated at around 35 million yrs. Some recrystallization of the host rocks took place alongside the intrusion, and there is evidence that minor fracture development and fluid migration also occurred along the margins of the intrusion. However, the fractures have been sealed, and there is no evidence that the dike acted as a conduit for continued fluid flow.

Aeromagnetic surveys of the Delaware Basin have shown anomalies that lie on a linear southwest-northeast trend that coincides with the surface and subsurface exposures of magmatic rocks. There is a strong indication, therefore, of a dike or a closely related set of dikes extending for at least 120 km (70 mi) across the region (see the CCA, Chapter 2.0, Section 2.1.5.4). The aeromagnetic survey conducted to delineate the dike showed a magnetic anomaly that is several kilometers (several miles) wide at depth and narrows to a thin trace near the surface. This pattern is interpreted as the result of an extensive dike swarm at depths of less than approximately 4.0 km (2.5 mi) near the Precambrian basement, from which a limited number of dikes have extended towards the surface.

Magmatic activity has taken place in the vicinity of the WIPP site in the past, but the igneous rocks have cooled over a long period. Any enhanced fracturing or conduits for fluid flow have been sealed by salt creep and mineralization. Continuing magmatic activity in the Rio Grande Rift is too remote from the WIPP location to be of consequence to the performance of the disposal system. Thus, the effects of magmatic activity have been eliminated from PA calculations on the basis of low consequence to the performance of the disposal system.

SCR-4.1.4.2.4 FEP Number: N15 FEP Title: Metamorphic Activity

SCR-4.1.4.2.4.1 Screening Decision: SO-P

Metamorphic A ctivity has been eliminated from PA calculations on the basis of low probability of occurrence over the next 10,000 yrs.

SCR-4.1.4.2.4.1 Summary of New Information

No new information that affects the screening of this FEP has been identified since the CRA-2009.

SCR-4.1.4.2.4.2 Screening Argument

Metamorphic activity, that is, solid-state recrystallization changes to rock properties and geologic structures through the effects of heat and/or pressure, requires depths of burial much greater than the depth of the repository. Regional tectonics that would result in the burial of the repository to the depths at which the repository would be affected by metamorphic activity have been eliminated from PA calculations on the basis of low probability of occurrence; therefore, metamorphic activity has also been eliminated from PA calculations on the basis of low probability of occurrence over the next 10,000 yrs.

SCR-4.1.5 Geochemical Processes

SCR-4.1.5.1 FEP Number: N16 FEP Title: Shallow Dissolution (including lateral dissolution)

SCR-4.1.5.1.1 Screening Decision: UP

Shallow Dissolution is accounted for in PA calculations.

SCR-4.1.5.1.2 Summary of New Information

No new information that affects the screening of this FEP has been identified since the CRA-2009.

SCR-4.1.5.1.3 Screening Argument

This section discusses a variety of styles of dissolution that have been active in the region of the WIPP or in the Delaware Basin. A distinction has been drawn between shallow dissolution involving circulation of groundwater, mineral dissolution in the Rustler and at the top of the Salado in the region of the WIPP, and deep dissolution taking place in the Castile and the base of the Salado. Dissolution will initially enhance porosities, but continued dissolution may lead to compaction of the affected units with a consequent reduction in porosity. Compaction may result in fracturing of overlying brittle units and increased permeability. Extensive dissolution may create cavities (karst) and result in the total collapse of overlying units. This topic is discussed further in the CCA, Chapter 2.0, Section 2.1.6.2.

SCR-4.1.5.1.4 Shallow Dissolution

In the region around the WIPP, shallow dissolution by groundwater flow has removed soluble minerals from the upper Salado as well as the Rustler to form Nash Draw; extensive solution within the closed draw has created karst features including caves and dolines in the sulfate beds of the Rustler (see Lee 1925; Bachman 1980, Bachman 1985, and Bachman 1987a). An alluvial doline drilled at WIPP 33, about 850 m (2800 ft) west of the WIPP site boundary, is the nearest karst feature known in the vicinity of the site. Upper Salado halite dissolution in Nash Draw resulted in fracture propagation upward through the overlying Rustler (Holt and Powers 1988). The margin of dissolution

of halite from the upper Salado has commonly been placed west of the WIPP site, near, but east of, Livingston Ridge, the eastern boundary of Nash Draw. Halite occurs in the Rustler east of Livingston Ridge, with the margin generally progressively eastward in higher stratigraphic units (e.g., Snyder 1985; Powers and Holt 1995). The distribution of halite in the Rustler has commonly been attributed to shallow dissolution (e.g., Powers et al. 1978; Lambert 1983; Bachman 1985; Lowenstein 1987). During early studies for the WIPP, the variability of Culebra transmissivity in the vicinity of the WIPP was commonly attributed to the effects of Rustler halite dissolution and changes in fracturing as a consequence.

After a detailed sedimentologic and stratigraphic investigation of WIPP cores, shafts, and geophysical logs from the region around the WIPP, the distribution of halite in the Rustler was attributed to depositional and syndepositional processes rather than postdepositional dissolution (Holt and Powers 1988; Powers and Holt 2000). Rustler exposures in shafts for the WIPP revealed extensive sedimentary structures in clastic units (Holt and Powers 1984, Holt and Powers 1986, and Holt and Powers 1990), and the suite of features in these beds led these investigators (Holt and Powers 1988; Powers and Holt 1990 and Powers and Holt 2000) to reinterpret the clastic units. They conclude that the clastic facies represent mainly mudflat facies tracts adjacent to a salt pan. Although some halite was likely deposited in mudflat areas proximal to the salt pan, it was largely removed by syndepositional dissolution, as indicated by soil structures, soft sediment deformation, bedding, and small-scale vertical relationships (Holt and Powers 1988; Powers and Holt 1990, Powers and Holt 1999 and Powers and Holt 2000). The depositional margins of halite in the Rustler are the likely points for past or future dissolution (e.g., Holt and Powers 1988; Beauheim and Holt 1990). Cores from drillholes at the H-19 drillpad near the Tamarisk Member halite margin show evidence of some dissolution of halite in the Tamarisk (Mercer et al. 1998), consistent with these predictions. The distribution of Culebra transmissivity values is not considered related to dissolution of Rustler halite, and other geological factors (e.g., depth, upper Salado dissolution) correlate well with Culebra transmissivity (e.g., Powers and Holt 1995; Holt and Powers 2002).

Since the CCA was completed, the WIPP has conducted additional work on shallow dissolution, principally of the upper Salado, and its possible relationship to the distribution of transmissivity values for the Culebra as determined through testing of WIPP hydrology wells.

Analysis Plan 088 (AP-088) (Beauheim 2002) noted that potentiometric surface values for the Culebra in many monitoring wells were outside the uncertainty ranges used to calibrate models of steady-state heads for the unit. AP-088 directed the analysis of the relationship between geological factors and values of transmissivity at Culebra wells. The relationship between geological factors, including dissolution of the upper Salado as well as limited dissolution in the Rustler, and Culebra transmissivity has been used to evaluate differences between assuming steady-state Culebra heads and changing heads.

Task 1 for AP-088 (Powers 2003) evaluated geological factors, including shallow dissolution in the vicinity of the WIPP site related to Culebra transmissivity. A much more extensive drillhole geological database was developed than was previously available, utilizing sources of data from WIPP, potash exploration, and oil and gas exploration and development. The principal findings related to shallow dissolution are (1) a relatively narrow zone (~ 200 - 400 m [656 - 1,312 ft] wide) could be defined as the margin of dissolution of the upper Salado in much of the area around the WIPP, (2) the upper Salado dissolution margin commonly underlies surface escarpments such as Livingston Ridge, and (3) there are possible extensions or reentrants of incipient upper Salado dissolution extending eastward from the general dissolution margin. The WIPP site proper is not affected by this process.

Culebra transmissivity correlates well with depth or overburden, which affects fracture apertures (Powers and Holt 1995; Holt and Powers 2002; Holt and Yarbrough 2002). Dissolution of the upper Salado appears to increase transmissivity by one or more orders of magnitude (Holt and Yarbrough 2002). Because there is no indication of upper Salado dissolution at the WIPP site, Holt and Yarbrough (Holt and Yarbrough 2002) did not include this factor for the WIPP site in estimates of base transmissivity values for the WIPP site and surroundings.

The effects of shallow dissolution (including the impacts of lateral dissolution) have been included in PA calculations in the derivation of transmissivity fields for Culebra flow and transport.

SCR-4.1.5.2 FEP Numbers: N18, N20, and N21 FEP Titles: Deep Dissolution (N18) Breccia Pipes (N20) Collapse Breccias (N21)

SCR-4.1.5.2.1 Screening Decision: SO-P

Deep Dissolution and the formation of associated features (for example, solution chimneys or *Breccia P ipes*, *Collapse B reccias*) at the WIPP site have been eliminated from PA calculations on the basis of low probability of occurrence over the next 10,000 yrs.

SCR-4.1.5.2.2 Summary of New Information

No new information that affects the screening of this FEP has been identified since the CRA-2009.

SCR-4.1.5.2.3 Screening Argument

This section discusses a variety of styles of dissolution that have been active in the region of the WIPP or in the Delaware Basin. A distinction has been drawn between shallow dissolution, involving circulation of groundwater and mineral dissolution in the Rustler and at the top of the Salado in the region of the WIPP, and deep dissolution taking place in the Castile and the base of the Salado. Dissolution will initially enhance porosities, but continued dissolution may lead to compaction of the affected units with a consequent reduction in porosity. Compaction may result in fracturing of overlying brittle units and increased permeability. Extensive dissolution may create cavities (karst) and result in the total collapse of overlying units. This topic is discussed further in the CCA, Chapter 2.0, Section 2.1.6.2.

SCR-4.1.5.2.4 Deep Dissolution

Deep dissolution is limited to processes involving dissolution of the Castile or basal Salado and features such as breccia pipes (also known as solution chimneys) associated with this process (see the CCA, Chapter 2.0, Section 2.1.6.2). Deep dissolution is distinguished from shallow and lateral dissolution not only by depth, but also by the origin of the water. Dissolution by groundwater from deep water-bearing zones can lead to the formation of cavities. Collapse of overlying beds leads to the formation of collapse breccias if the overlying rocks are brittle, or to deformation if the overlying rocks are ductile. If dissolution is extensive, breccia pipes or solution chimneys may form above the cavity. These pipes may reach the surface or pass upwards into fractures and then into microcracks that do not extend to the surface. Breccia pipes may also form through the downward percolation of meteoric waters, as discussed earlier. Deep dissolution is of concern because it could accelerate contaminant transport through the creation of vertical flow paths that bypass low-permeability units in

the Rustler. If dissolution occurred within or beneath the waste panels themselves, there could be increased circulation of groundwater through the waste, as well as a breach of the Salado host rock.

Features identified as being the result of deep dissolution are present along the northern and eastern margins of the Delaware Basin. In addition to features that have a surface expression or that appear within potash mine workings, deep dissolution has been cited by Anderson et al. (Anderson et al. 1972, p. 81) as the cause of lateral variability within evaporite sequences in the lower Salado.

Exposures of the McNutt Potash Member of the Salado within a mine near Nash Draw have shown a breccia pipe containing cemented brecciated fragments of formations higher in the stratigraphic sequence. At the surface, this feature is marked by a dome, and similar domes have been interpreted as dissolution features. The depth of dissolution has not been confirmed, but the collapse structures led Anderson (Anderson 1978, p. 52) and Snyder et al. (Snyder et al. 1982, p. 65) to postulate dissolution of the Capitan Limestone at depth; collapse of the Salado, Rustler, and younger formations; and subsequent dissolution and hydration by downward percolating waters. San Simon Sink (see the CCA, Chapter 2.0, Section 2.1.6.2), some 35 km (20 mi) east-southeast of the WIPP site, has also been interpreted as a solution chimney. Subsidence has occurred there in historical times according to Nicholson and Clebsch (Nicholson and Clebsch 1961, p. 14), suggesting that dissolution at depth is still taking place. Whether this is the result of downward-percolating surface water or deep groundwater has not been confirmed. The association of these dissolution features with the inner margin of the Capitan Reef suggest that they owe their origins, if not their continued development, to groundwaters derived from the Capitan Limestone.

SCR-4.1.5.2.5 Dissolution within the Castile and Lower Salado

The Castile contains sequences of varved anhydrite and carbonate (that is, laminae deposited on a cyclical basis) that can be correlated between several boreholes. On the basis of these deposits, a basin-wide uniformity in the depositional environment of the Castile evaporites was assumed. The absence of varves from all or part of a sequence and the presence of brecciated anhydrite beds have been interpreted by Anderson et al. (Anderson et al.1972) as evidence of dissolution. Holt and Powers (the CCA, Appendix FAC) have questioned the assumption of a uniform depositional environment and contend that the anhydrite beds are lateral equivalents of halite sequences without significant postdepositional dissolution. Wedges of brecciated anhydrite along the margin of the Castile have been interpreted by Robinson and Powers (Robinson and Powers 1987, p. 78) as gravity-driven clastic deposits, rather than the result of deep dissolution.

Localized depressions at the top of the Castile and inclined geophysical marker units at the base of the Salado have been interpreted by Davies (Davies 1983, p. 45) as the result of deep dissolution and subsequent collapse or deformation of overlying rocks. The postulated cause of this dissolution was circulation of undersaturated groundwaters from the Bell Canyon Formation (hereafter referred to as Bell Canyon). Additional boreholes (notably WIPP-13, WIPP-32, and DOE-2) and geophysical logging led Borns and Shaffer (Borns and Shaffer 1985) to conclude that the features interpreted by Davies as being dissolution features are the result of irregularities at the top of Bell Canyon. These irregularities led to localized depositional thickening of the Castile and lower Salado sediments.

SCR-4.1.5.2.6 Collapse Breccias at Basin Margins

Collapse breccias are present at several places around the margins of the Delaware Basin. Their formation is attributed to relatively fresh groundwater from the Capitan Limestone that forms the

margin of the basin. Collapse breccias corresponding to features on geophysical records that have been ascribed to deep dissolution have not been found in boreholes away from the margins. These features have been reinterpreted as the result of early dissolution prior to the deposition of the Salado.

SCR-4.1.5.2.7 Summary of Deep Dissolution

Deep dissolution features have been identified within the Delaware Basin, but only in marginal areas underlain by Capitan Reef. There is a low probability that deep dissolution will occur sufficiently close to the waste panels over the regulatory period to affect groundwater flow in the immediate region of the WIPP. Deep dissolution at the WIPP site has therefore been eliminated from PA calculations on the basis of low probability of occurrence over the next 10,000 yrs.

SCR-4.1.5.3 FEP Number: N22 FEP Title: Fracture Infill

SCR-4.1.5.3.1 Screening Decision: SO-C - Beneficial

The effects of *Fracture I nfill* have been eliminated from PA calculations on the basis of beneficial consequence to the performance of the disposal system.

SCR-4.1.5.3.2 Summary of New Information

No new information that affects the screening of this FEP has been identified since the CRA-2009.

SCR-4.1.5.3.3 Screening Argument

SCR-4.1.5.3.3.1 Mineralization

Precipitation of minerals as fracture infills can reduce hydraulic conductivities. The distribution of infilled fractures in the Culebra closely parallels the spatial variability of lateral transmissivity in the Culebra. The secondary gypsum veins in the Rustler have not been dated. Strontium isotope studies (Siegel et al. 1991, pp. 5-53 to 5-57) indicate that the infilling minerals are locally derived from the host rock rather than extrinsically derived, and it is inferred that they reflect an early phase of mineralization and are not associated with recent meteoric waters.

Stable isotope geochemistry in the Rustler has also provided information on mineral stabilities in these strata. Both Chapman (Chapman 1986, p. 31) and Lambert and Harvey (Lambert and Harvey 1987, p. 207) imply that the mineralogical characteristics of units above the Salado have been stable or subject to only minor changes under the various recharge conditions that have existed during the past 0.6 million yrs-the period since the formation of the Mescalero caliche and the establishment of a pattern of climate change and associated changes in recharge that led to present-day hydrogeological conditions. No changes in climate are expected other than those experienced during this period, and for this reason, no changes are expected in the mineralogical characteristics other than those expressed by the existing variability of fracture infills and diagenetic textures. Formation of fracture infills will reduce transmissivities and will therefore be of beneficial consequence to the performance of the disposal system.

SCR-4.2 Subsurface Hydrological FEPs

SCR-4.2.1 Groundwater Characteristics

SCR-4.2.1.1 FEP Numbers: N23, N24, N25, and N27 FEP Titles: Saturated Groundwater Flow (N23) Unsaturated Groundwater Flow (N24) Fracture Flow (N25) Effects of Preferential Pathways (N27)

SCR-4.2.1.1.1 Screening Decision: UP

Saturated Groundwater Flow, Unsaturated Groundwater Flow, Fracture Flow, and Effects of Preferential Pathways are accounted for in PA calculations.

SCR-4.2.1.1.2 Summary of New Information

No new information that affects the screening of these FEPs has been identified since the CRA-2009.

SCR-4.2.1.1.3 Screening Argument

Saturated groundwater flow, unsaturated groundwater flow, and fracture flow are accounted for in PA calculations. Groundwater flow is discussed in the CCA, Chapter 2.0, Section 2.2.1; and Chapter 6.0, Section 6.4.5 and Section 6.4.6.

The hydrogeologic properties of the Culebra are also spatially variable. This variability, including the effects of preferential pathways, is accounted for in PA calculations in the estimates of transmissivity and aquifer thickness.

SCR-4.2.1.2 FEP Number: N26 FEP Title: Density Effect on Groundwater Flow

SCR-4.2.1.2.1 Screening Decision: SO-C

Density Effects on Groundwater Flow has been eliminated from PA calculations on the basis of low consequence to the performance of the disposal system.

SCR-4.2.1.2.2 Summary of New Information

No new information that affects the screening of this FEP has been identified since the CRA-2009.

SCR-4.2.1.2.3 Screening Argument

The most transmissive unit in the Rustler, and hence the most significant potential pathway for transport of radionuclides to the accessible environment, is the Culebra. The properties of Culebra groundwaters are not homogeneous, and spatial variations in groundwater density (the CCA, Chapter 2.0, Section 2.2.1.4.1.2) could influence the rate and direction of groundwater flow. A comparison of the gravity-driven flow component and the pressure-driven component in the Culebra, however, shows that only in the region to the south of the WIPP are head gradients low enough for density gradients to be significant (Davies 1989, p. 53). Accounting for this variability would rotate groundwater flow vectors towards the east (down-dip) and hence fluid in the high-transmissivity zone would move away from the zone. Excluding brine density variations within the Culebra from PA

calculations is therefore a conservative assumption, and density effects on groundwater flow have been eliminated from PA calculations on the basis of low consequence to the performance of the disposal system.

SCR-4.2.2 Changes in Groundwater Flow

SCR-4.2.2.1 FEP Number: N28 FEP Title: Thermal Effects on Groundwater Flow

SCR-4.2.2.1.1 Screening Decision: SO-C

Natural Thermal Effects on Groundwater Flow have been eliminated from PA calculations on the basis of low consequence to the performance of the disposal system.

SCR-4.2.2.1.2 Summary of New Information

No new information that affects the screening of this FEP has been identified since the CRA-2009.

SCR-4.2.2.1.3 Screening Argument

The geothermal gradient in the region of the WIPP has been measured at about 30 degrees centigrade (°C) (54 degrees Fahrenheit [°F]) per kilometer (50 °C [90 °F] per mile). Given the generally low permeability in the region and the limited thickness of units in which groundwater flow occurs (for example, the Culebra), natural convection will be too weak to have a significant effect on groundwater flow. No natural FEPs have been identified that could significantly alter the temperature distribution of the disposal system or give rise to thermal effects on groundwater flow. Such effects have therefore been eliminated from PA calculations on the basis of low consequence to the performance of the disposal system.

SCR-4.2.2.2 FEP Number: N29 FEP Title: Saline Intrusion (hydrogeological effects)

SCR-4.2.2.2.1 Screening Decision: SO-P

Changes in groundwater flow arising from *Saline I ntrusion* have been eliminated from PA calculations on the basis of low probability of occurrence over 10,000 yrs.

SCR-4.2.2.2.2 Summary of New Information

No new information that affects the screening of this FEP has been identified since the CRA-2009.

SCR-4.2.2.2.3 Screening Argument

No natural events or processes have been identified that could result in saline intrusion into units above the Salado or cause a significant increase in fluid density. Natural saline intrusion has therefore been eliminated from PA calculations on the basis of low probability of occurrence over the next 10,000 yrs. Saline intrusion arising from human events such as drilling into a pressurized brine pocket is discussed in FEPs H21 through H24 (Section SCR-5.2.1.4).

SCR-4.2.2.3 FEP Number: N30 FEP Title: Freshwater Intrusion (hydrogeological effects)

SCR-4.2.2.3.1 Screening Decision: SO-P

Changes in groundwater flow arising from *Freshwater I ntrusion* have been eliminated from PA calculations on the basis of low probability of occurrence over 10,000 yrs.

SCR-4.2.2.3.2 Summary

No new information that affects the screening of this FEP has been identified since the CRA-2009.

SCR-4.2.2.3.2.1 Screening Argument

A number of FEPs, including climate change, can result in changes in infiltration and recharge (see discussions for FEPs N53 through N55, Section SCR-4.5.3.1). These changes will affect the height of the water table and, hence, could affect groundwater flow in the Rustler through changes in head gradients. The generally low transmissivity of the Dewey Lake and the Rustler, however, will prevent any significant changes in groundwater density from occurring within the Culebra over the timescales for which increased precipitation and recharge are anticipated. No other natural events or processes have been identified that could result in freshwater intrusion into units above the Salado or cause a significant decrease in fluid density. Freshwater intrusion has therefore been eliminated from PA calculations on the basis of low probability of occurrence over the next 10,000 yrs.

SCR-4.2.2.4 FEP Number: N31 FEP Title: Hydrological Response to Earthquakes

SCR-4.2.2.4.1 Screening Decision: SO-C

Hydrological Response to E arthquakes has been eliminated from PA calculations on the basis of low consequence to the performance of the disposal system.

SCR-4.2.2.4.2 Summary of New Information

No new information that affects the screening of this FEP has been identified since the CRA-2009.

SCR-4.2.2.4.3 Screening Argument

SCR-4.2.2.4.3.1 Hydrological Effects of Seismic Activity

There are a variety of hydrological responses to earthquakes. Some of these responses, such as changes in surface-water flow directions, result directly from fault movement. Others, such as changes in subsurface water chemistry and temperature, probably result from changes in flow pathways along the fault or fault zone. According to Bredehoeft et al. (Bredehoeft et al. 1987, p. 139), further away from the region of fault movement, two types of changes to groundwater levels may take place as a result of changes in fluid pressure.

- The passage of seismic waves through a rock mass causes a volume change, inducing a transient response in the fluid pressure, which may be observed as a short-lived fluctuation of the water level in wells.

- Changes in volume strain can cause long-term changes in water level. A buildup of strain occurs prior to rupture and is released during an earthquake. The consequent change in fluid pressure may be manifested by the drying up or reactivation of springs some distance from the region of the epicenter.

Fluid-pressure changes induced by the transmission of seismic waves can produce changes of up to several meters (several yards) in groundwater levels in wells, even at distances of thousands of kilometers from the epicenter. These changes are temporary, however, and levels typically return to pre-earthquake levels in a few hours or days. Changes in fluid pressure arising from changes in volume strain persist for much longer periods, but they are only potentially consequential in tectonic regimes where there is a significant buildup of strain. The regional tectonics of the Delaware Basin indicates that such a buildup has a low probability of occurring over the next 10,000 yrs (see FEPs N3 and N4, Section SCR-4.1.2.1).

The expected level of seismic activity in the region of the WIPP will be of low consequence to the performance of the disposal system in terms of groundwater flow or contaminant transport. Changes in groundwater levels resulting from more distant earthquakes will be too short in duration to be significant. Thus, hydrological response to earthquakes has been eliminated from PA calculations on the basis of low consequence to the performance of the disposal system.

SCR-4.2.2.5 FEP Number: N32 FEP Title: Natural Gas Intrusion

SCR-4.2.2.5.1 Screening decision: SO-P

Changes in groundwater flow arising from *Natural Gas Intrusion* have been eliminated from PA calculations on the basis of low probability of occurrence over 10,000 yrs.

SCR-4.2.2.5.2 Summary of New Information

No new information that affects the screening of this FEP has been identified since the CRA-2009.

SCR-4.2.2.5.2.1 Screening Argument

Hydrocarbon resources are present in formations beneath the WIPP (the CCA, Chapter 2.0, Section 2.3.1.2), and natural gas is extracted from the Morrow Formation. These reserves are, however, some 4,200 m (14,000 ft) below the surface, and no natural events or processes have been identified that could result in natural gas intrusion into the Salado or the units above. Natural gas intrusion has therefore been eliminated from PA calculations on the basis of low probability of occurrence over the next 10,000 yrs.

SCR-4.3 Subsurface Geochemical FEPs

SCR-4.3.1 Groundwater Geochemistry

SCR-4.3.1.1 FEP Number: N33 FEP Title: Groundwater Geochemistry

SCR-4.3.1.1.1 Screening Decision: UP

Groundwater Geochemistry in the hydrological units of the disposal system is accounted for in PA calculations.

SCR-4.3.1.1.2 Summary of New Information

No new information that affects the screening of this FEP has been identified since the CRA-2009.

SCR-4.3.1.1.3 Screening Argument

The most important aspect of groundwater geochemistry in the region of the WIPP in terms of chemical retardation and colloid stability is salinity. Groundwater geochemistry is discussed in detail in the CCA, Chapter 2.0, Section 2.2 and Section 2.4 and summarized here. The Delaware Mountain Group, Castile, and Salado contain basinal brines. Waters in the Castile and Salado are at or near halite saturation. Above the Salado, groundwaters are also relatively saline, and groundwater quality is poor in all of the permeable units. Waters from the Culebra vary spatially in salinity and chemistry. They range from saline sodium chloride-rich waters to brackish calcium sulfate-rich waters. In addition, a range of magnesium-to-calcium ratios has been observed, and some waters reflect the influence of potash mining activities, having elevated potassium-to-sodium ratios. Waters from the Santa Rosa are generally of better quality than those from the Rustler. Salado and Castile brine geochemistry is accounted for in PA calculations of the actinide (An) source term (the CCA, Chapter 6.0, Section 6.4.3.4). Culebra brine geochemistry is accounted for in the retardation factors used in PA calculations of actinide transport (see the CCA, Chapter 6.0, Section 6.4.6.2).

SCR-4.3.1.2 FEP Numbers: N34 and N38 FEP Titles: Saline Intrusion (N34) Effects of Dissolution (N38)

SCR-4.3.1.2.1 Screening Decision: SO-C

The effects of *Saline I ntrusion* and *Dissolution* on groundwater chemistry have been eliminated from PA calculations on the basis of low consequence to the performance of the disposal system.

SCR-4.3.1.2.2 Summary of New Information

No new information that affects the screening of this FEP has been identified since the CRA-2009.

SCR-4.3.1.2.3 Screening Argument

Saline intrusion and effects of dissolution are considered together in this discussion because dissolution of minerals such as halite (NaCl), anhydrite ($CaSO_4$), or gypsum ($CaSO_4 \cdot 2H_2O$) (N38)

could - in the most extreme case - increase the salinity of groundwaters in the Culebra to levels characteristic of those expected after saline intrusion (N34).

No natural events or processes have been identified that could result in saline intrusion into units above the Salado. Injection of Castile or Salado brines into the Culebra as a result of human intrusion, an anthropogenically induced event, was included in past PA calculations. Laboratory studies carried out to evaluate radionuclide transport in the Culebra following human intrusion produced data that can also be used to evaluate the consequences of natural saline intrusion.

The possibility that dissolution of halite, anhydrite, or gypsum might result in an increase in the salinity of low- to moderate-ionic-strength groundwaters in the Culebra also appears unlikely, despite the presence of halite in the Los Medaños under most of the WIPP site (Siegel and Lambert 1991, Figure 1-13), including the expected Culebra off-site transport pathway (the direction of flow from the point(s) at which brines from the repository would enter the Culebra, flow towards the south or south-southeast, and eventually to the boundary of the WIPP site). (The Los Medaños Member of the Rustler, formerly referred to as the unnamed lower member of the Rustler, underlies the Culebra.) A dissolution-induced increase in the salinity of Culebra groundwaters is unlikely because (1) the dissolution of halite is known to be rapid; (2) (moderate-ionic-strength) groundwaters along the off-site transport pathway (and at many other locations in the Culebra) have had sufficient time to dissolve significant quantities of halite, if this mineral is present in the subjacent Los Medaños and if Culebra fluids have been in contact with it; and (3) the lack of high-ionic-strength groundwaters along the off-site transport pathway (and elsewhere in the Culebra) implies that halite is present in the Los Medaños but Culebra fluids have not contacted it, or that halite is not present in the Los Medaños. Because halite dissolves so rapidly if contacted by undersaturated solutions, this conclusion does not depend on the nature and timing of Culebra recharge (i.e., whether the Rustler has been a closed hydrologic system for several thousand to a few tens of thousands of yrs, or is subject to significant modern recharge).

Nevertheless, saline intrusion would not affect the predicted transport of thorium (Th), uranium (U), plutonium (Pu), and americium (Am) in the Culebra. This is because (1) the laboratory studies that quantified the retardation of Th, U, Pu, and Am for the CCA PA were carried out with both moderate-ionic-strength solutions representative of Culebra groundwaters along the expected off-site transport pathway and high-ionic-strength solutions representative of brines from the Castile and the Salado (Brush 1996; Brush and Storz 1996); and (2) the results obtained with the Castile and Salado brines were - for the most part - used to predict the transport of Pu(III) and Am(III); Th(IV), U(IV), Np(IV), and Pu(IV); and U(VI). The results obtained with the saline solutions were used for these actinide oxidation states because the extent to which saline and Culebra brines will mix along the offsite transport pathway in the Culebra was unclear at the time of the CCA PA; therefore, Brush (Brush 1996) and Brush and Storz (Brush and Storz 1996) recommended that PA use the results that predict less retardation. In the case of Pu(III) and Am(III); Th(IV), U(IV), Np(IV), and Pu(IV); and U(VI), the retardation distribution coefficient (K_ds) obtained with the saline solutions were somewhat lower than those obtained with the Culebra fluids. The K_ds used in the CRA-2014 are the same as used in the CRA-2009 PABC.

Finally, it is important to reiterate that the use of results from laboratory studies with saline solutions to predict radionuclide transport in the Culebra for previous PAs and the CRA-2014 PA implement the effects of saline intrusion caused by human intrusion, not natural saline intrusion. The conclusions that natural saline intrusion is unlikely, that significant dissolution is unlikely, and that these events or processes would have no significant consequence - in the unlikely event that they occur - continue to be valid.

SCR-4.3.1.3 FEP Numbers: N35, N36, and N37 FEP Titles: Freshwater Intrusion (Geochemical Effects) (N35) Change in Groundwater Eh (N36) Changes in Groundwater pH (N37)

SCR-4.3.1.3.1 Screening Decision: SO-C

The effects of *Freshwater Intrusion* on groundwater chemistry have been eliminated from PA calculations on the basis of low consequence to the performance of the disposal system. *Changes in Groundwater Eh* and *Changes in Groundwater pH* have been eliminated from PA calculations on the basis of low consequence to the performance of the disposal system.

SCR-4.3.1.3.2 Summary of New Information

No new information that affects the screening of this FEP has been identified since the CRA-2009.

SCR-4.3.1.3.3 Screening Argument

Natural changes in the groundwater chemistry of the Culebra and other units that resulted from saline intrusion or freshwater intrusion could potentially affect chemical retardation and the stability of colloids. Changes in groundwater Eh andgroundwater pH could also affect the migration of radionuclides (see FEPs W65 to W70, Section SCR-6.5.5.2 , Section SCR-6.5.5.3, Section SCR-6.5.6.1, and Section SCR-6.5.6.2). No natural EPs have been identified that could result in saline intrusion into units above the Salado, and the magnitude of any natural temporal variation from the effects of dissolution on groundwater chemistry, or because of changes in recharge, is likely to be no greater than the present spatial variation. These FEPs related to the effects of future natural changes in groundwater chemistry have been eliminated from PA calculations on the basis of low consequence to the performance of the disposal system. See Appendix SOTERM-2014, Section 2.3.1 for a discussion of WIPP brine chemistry.

The most likely mechanism for (natural) freshwater intrusion into the Culebra (N35), changes in groundwater Eh (N36), and changes in groundwater pH (N37) is (natural) recharge of the Culebra. (Other FEPs consider possible anthropogenically induced recharge). These three FEPs are closely related because an increase in the rate of recharge could reduce the ionic strength(s) of Culebra groundwaters, possibly enough to saturate the Culebra with (essentially) fresh water, at least temporarily. Such a change in ionic strength could, if enough atmospheric oxygen remained in solution, also increase the Eh of Culebra groundwaters enough to oxidize Pu from the relatively immobile III and IV oxidation states (Pu(III) and Pu(IV)) - the oxidation states expected under current conditions (Brush 1996; Brush and Storz 1996) - to the relatively mobile V and VI oxidation states (Pu(V) and Pu(VI)). Similarly, recharge of the Culebra with freshwater could also change the pH of Culebra groundwaters from the currently observed range of about 6 to 7 to mildly acidic values, thus (possibly) decreasing the retardation of dissolved Pu and Am. (These changes in ionic strength, Eh, and pH could also affect mobilities of Th, U, and neptunium (Np), but the long-term performance of the WIPP is much less sensitive to the mobilities of these radioelements than to those of Pu and Am.)

There is still considerable uncertainty regarding the extent and timing of recharge to the Culebra. Lambert (Lambert 1986), Lambert and Carter (Lambert and Carter 1987), and Lambert and Harvey (Lambert and Harvey 1987) used a variety of stable and radiogenic isotopic-dating techniques to conclude that the Rustler (and the Dewey Lake) have been closed hydrologic systems for several

thousand to a few tens of thousands of yrs. In other words, the last significant recharge of the Rustler occurred during the late Pleistocene in response to higher levels of precipitation and infiltration associated with the most recent continental glaciation of North America, and the current flow field in the Culebra is the result of the slow discharge of groundwater from this unit. Other investigators have agreed that it is possible that Pleistocene recharge has contributed to present-day flow patterns in the Culebra, but that current patterns are also consistent with significant current recharge (Haug et al. 1987; Davies 1989). Still others (Chapman 1986 and Chapman 1988) have rejected Lambert's interpretations in favor of exclusively modern recharge, at least in some areas. For example, the low salinity of Hydrochemical Zone B south of the WIPP site could represent dilution of Culebra groundwater with significant quantities of recently introduced meteoric water (see Siegel et al. 1991, pp. 2-57-2-62 and Figure 2-17 for definitions and locations of the four hydrochemical facies in the Culebra in and around the WIPP site).

Past hydrogeological investigations into the cause and effect from observed water-level rises in the Culebra led to a revised groundwater conceptual model (Appendix TFIELD-2014, Section 3.0). Continuing hydrogeological studies have seen responses to precipitation events in Culebra wells. This is not to say, however, that present-day rainfall actually enters the Culebra wherever a pressure response to rainfall is observed. Rather, the rainfall reaches a water table in a higher stratigraphic unit that is in sufficient hydraulic communication with the Culebra to transmit a *pressure* response rapidly. It takes a much longer time for water or dissolved constituents to move through the subsurface than it takes a pressure wave to propagate through a saturated porous medium (Appendix HYDRO-2014, Section 7.1).

However, the justification of this screening decision does not depend on this issue. If recharge occurs mainly during periods of high precipitation (pluvials) associated with periods of continental glaciation, the consequences of such recharge are likely reflected in the ranges of geochemical conditions currently observed in the Culebra as a whole, as well as along the likely offsite transport pathway (the direction of flow from the point(s) at which brines from the repository would enter the Culebra in the event of human intrusion to the south or south-southeast and eventually to the boundary of the WIPP site). Hence, the effects of recharge, (possible) freshwater intrusion, and (possible) concomitant changes in groundwater Eh and pH can be screened out on the basis of low consequence to the performance of the far-field barrier. The reasons for the conclusion that the effects of pluvial recharge are inconsequential (i.e., are already included among existing variations in geochemical conditions) are (1) as many as 50 continental glaciations and associated pluvials have occurred since the late Pliocene Epoch 2.5 million yrs ago (2.5 Ma BP); (2) the glaciations and pluvials that have occurred since about 0.5 to 1 Ma BP have been significantly more severe than those that occurred prior to 1 Ma BP (see, for example, Servant 2001); and (3) conditions in the Culebra are favorable for retardation of actinides despite the effects of as many as 50 periods of recharge.

It is also worth noting that the choice of the most recent glacial maximum as an upper limit for possible climatic changes during the 10,000-year (yr) WIPP regulatory period (Swift et al. 1991; the CCA, Appendix CLI) established conservative upper limits for precipitation and recharge of the Culebra at the WIPP site. The review by Swift et al. (Swift et al. 1991), later incorporated in the CCA, Appendix CLI, provides evidence that precipitation in New Mexico did not attain its maximum level (about 60-100% of current precipitation) until a few thousand yrs before the last glacial maximum. Swift et al. (Swift et al. 1991) pointed out,

> Prior to the last glacial maximum 22 to 18 ka BP, evidence from mid- Wisconsin faunal assemblages in caves in southern New Mexico, including the presence of extralimital species such as the desert tortoise that are now restricted to warmer climates, suggests warm summers and mild, relatively dry winters

(Harris 1987, 1988). Lacustrine evidence confirms the interpretation that conditions prior to and during the glacial advance that were generally drier than those at the glacial maximum. Permanent water did not appear in what was later to be a major lake in the Estancia Valley in central New Mexico until sometime before 24 ka BP (Bachhuber 1989). Late-Pleistocene lake levels in the San Agustin Plains in western New Mexico remained low until approximately 26.4 ka BP, and the $\delta\ ^{18}O$ record from ostracode shells suggests that mean annual temperatures at that location did not decrease significantly until approximately 22 ka BP (Phillips et al. 1992).

Therefore, it is likely that precipitation and recharge did not attain levels characteristic of the most recent glacial maximum until about 70,000 to 75,000 yrs after the last glaciations had begun. High-resolution, deep-sea $\delta\ ^{18}O$ data (and other data) reviewed by Servant (Servant 2001, Figure 1 and Figure 2) support the conclusion that, although the volume of ice incorporated in continental ice sheets can expand rapidly at the start of a glaciation, attainment of maximum volume does not occur until a few thousand or a few tens of thousands of yrs prior to the termination of the approximately 100,000-yr glaciations that have occurred during the last 0.5 to 1 Ma BP. Therefore, it is unlikely that precipitation and recharge will reach their maximum levels during the 10,000-yr regulatory period.

If, on the other hand, significant recharge occurs throughout both phases of the glacial-interglacial cycles, the conclusion that the effects of pluvial and modern recharge are inconsequential (i.e., are already reflected by existing variations in geochemical conditions) is also still valid. The effects of future natural changes in groundwater chemistry have been eliminated from PA calculations on the basis of low consequence to the performance of the disposal system.

SCR-4.4 Geomorphological FEPs

SCR-4.4.1 Physiography

SCR-4.4.1.1 FEP Number: N39 FEP Title: Physiography

SCR-4.4.1.1.1 Screening Decision: UP

Relevant aspects of the *Physiography*, geomorphology, and topography of the region around the WIPP are accounted for in PA calculations.

SCR-4.4.1.1.2 Summary of New Information

No new information that affects the screening of this FEP has been identified since the CRA-2009.

SCR-4.4.1.1.3 Screening Argument

Physiography and geomorphology are discussed in detail in the CCA, Chapter 2.0, Section 2.1.4, and are accounted for in the setup of the PA calculations (the CCA, Chapter 6.0, Section 6.4.2).

SCR-4.4.1.2 FEP Number: N40 FEP Title: Impact of a Large Meteorite

SCR-4.4.1.2.1 Screening Decision: SO-P

Disruption arising from the *Impact of a Large Meteorite* has been eliminated from PA calculations on the basis of low probability of occurrence over 10,000 yrs.

SCR-4.4.1.3 Summary of New Information

No new information that affects the screening of this FEP has been identified since the CRA-2009.

SCR-4.4.1.4 Screening Argument

Meteors frequently enter the earth's atmosphere, but most of these are small and burn up before reaching the ground. Of those that reach the ground, most produce only small impact craters that would have no effect on the postclosure integrity of a repository 650 m (2,150 ft) below the ground surface. While the depth of a crater may be only one-eighth of its diameter, the depth of the disrupted and brecciated material is typically one-third of the overall crater diameter (Grieve 1987, p. 248). Direct disruption of waste at the WIPP would only occur with a crater larger than 1.8 km (1.1 mi) in diameter. Even if waste were not directly disrupted, the impact of a large meteorite could create a zone of fractured rocks beneath and around the crater. The extent of such a zone would depend on the rock type. For sedimentary rocks, the zone may extend to a depth of half the crater diameter or more (Dence et al. 1977, p. 263). The impact of a meteorite causing a crater larger than 1 km (0.6 mi) in diameter could thus fracture the Salado above the repository.

Geological evidence for meteorite impacts on earth is rare because many meteorites fall into the oceans and erosion and sedimentation serve to obscure craters that form on land. Dietz (Dietz 1961) estimated that meteorites that cause craters larger than 1 km (0.6 mi) in diameter strike the earth at the rate of about one every 10,000 yrs (equivalent to about 2×10^{-13} impacts per square kilometer (km^2) per yr). Using observations from the Canadian Shield, Hartmann (1965, p. 161) estimated a frequency of between 0.8×10^{-13} and 17×10^{-13} impacts/km^2/yr for impacts causing craters larger than 1 km (0.6 mi). Frequencies estimated for larger impacts in studies reported by Grieve (Grieve 1987, p. 263) can be extrapolated to give a rate of about 1.3×10^{-12} impacts/km^2/yr for craters larger than 1 km (0.6 mi). It is commonly assumed that meteorite impacts are randomly distributed across the earth's surface, although Halliday (1964, pp. 267-277) calculated that the rate of impact in polar regions would be some 50 to 60 percent of that in equatorial regions. The frequencies reported by Grieve (Grieve 1987) would correspond to an overall rate of about 1 per 1,000 yrs on the basis of a random distribution.

Assuming the higher estimated impact rate of 17×10^{-13} impacts per square kilometer per yr for impacts leading to fracturing of sufficient extent to affect a deep repository, and assuming a repository footprint of 1.4 km × 1.6 km (0.9 mi × 1.0 mi) for the WIPP, yields a frequency of about 4×10^{-12} impacts per yr for a direct hit above the repository. This impact frequency is several orders of magnitude below the screening threshold of 10^{-4} per 10,000 yrs provided in section 194.32(d).

Meteorite hits directly above the repository footprint are not the only impacts of concern, however, because large craters may disrupt the waste panels even if the center of the crater is outside the repository area. It is possible to calculate the frequency of meteorite impacts that could disrupt a deep repository such as the WIPP by using the conservative model of a cylinder of rock fractured to a depth equal to one-half the crater diameter, as shown in the CCA, Appendix SCR, Figure SCR-1. The area within which a meteorite could impact the repository is calculated by

$$S_D = \left(L + 2 \times \frac{D}{2}\right) \times \left(W + 2 \times \frac{D}{2}\right), \quad \text{(SCR.1)}$$

where

L = length of the repository footprint (km)

W = width of the repository footprint (km)

D = diameter of the impact crater (km)

S_D = area of the region where the crater would disrupt the repository (km^2)

There are insufficient data on meteorites that have struck the earth to derive a distribution function for the size of craters directly. Using meteorite impacts on the moon as an analogy, however, Grieve (Grieve 1987, p. 257) derived the following distribution function:

$$F_D \propto D^{-1.8} \quad \text{(SCR.2)}$$

where

F_D = frequency of impacts resulting in craters larger than D (impacts/km^2/yr).

If $f(D)$ denotes the frequency of impacts giving craters of diameter D, then the frequency of impacts giving craters larger than D is

$$F_D = \int_D^{\infty} f(D)\,dD \quad \text{(SCR.3)}$$

and

$$f(D) = F_1 \times 1.8 \times D^{-2.8}, \quad \text{(SCR.4)}$$

where

F_1 = frequency of impacts resulting in craters larger than 1 km (impacts/km^2/yr)

$f(D)$ = frequency of impacts resulting in craters of diameter D ((impacts/km^2/yr)

The overall frequency of meteorite impacts, in the size range of interest, that could disrupt or fracture the repository is thus given by

$$N = \int_{2h}^{M} f(D) \times S_D dD, \quad \text{(SCR.5)}$$

where

h = depth to repository (kilometers),

M = maximum size of meteorite considered (kilometers)

N = frequency of impacts leading to disruption of the repository (impacts per yr), and

$$N = 1.8F_1\left[\frac{(M)^{0.2}-(2h)^{0.2}}{0.2} - LW\frac{(M)^{-1.8}-(2h)^{-1.8}}{1.8} - (L+W)\frac{(M)^{-0.8}-(2h)^{-0.8}}{0.8}\right] \quad \text{(SCR.6)}$$

Conservatively using the size (933 km [550 mi]) of the largest known asteroid, Ceres (Tedesco 1992), for the maximum size considered and if it is assumed that the repository is located at a depth of 650 m (2,150 ft) and has a footprint area of 1.4 km × 1.6 km (0.9 mi × 1.0 mi) and that meteorites creating craters larger than 1 km in diameter hit the earth at a frequency (F_1) of 17×10^{-13} impacts/km^2/yr, then Equation (SCR.6) gives a frequency of approximately 5.6×10^{-11} impacts per yr for impacts disrupting the repository. If impacts are randomly distributed over time, this corresponds to a probability of 5.6×10^{-7} over 10,000 yrs.

Similar calculations have been performed that indicate rates of impact of between 10^{-12} and 10^{-13} per yr for meteorites large enough to disrupt a deep repository (see, for example, Hartmann 1979, Kärnbränslesakerhet 1978, Claiborne and Gera 1974, Cranwell et al. 1990, and Thorne 1992). Meteorite impact can thus be eliminated from PA calculations on the basis of low probability of occurrence over 10,000 yrs.

Assuming a random or nearly random distribution of meteorite impacts, cratering at any location is inevitable given sufficient time. Although repository depth and host-rock lithology may reduce the consequences of a meteorite impact, there are no repository locations or engineered systems that can reduce the probability of impact over 10,000 yrs.

SCR-4.4.1.5 FEP Number: N41 and N42 FEP Titles: Mechanical Weathering (N41) Chemical Weathering (N42)

SCR-4.4.1.5.1 Screening Decision: SO-C

The effects of *Chemical Weathering* and *Mechanical Weathering* have been eliminated from PA calculations on the basis of low consequence to the performance of the disposal system.

SCR-4.4.1.5.2 Summary of New Information

No new information that affects the screening of these FEPs has been identified since the CRA-2009.

SCR-4.4.1.5.3 Screening Argument

Mechanical weathering and chemical weathering are assumed to be occurring at or near the surface around the WIPP site through processes such as exfoliation and leaching. The extent of these processes is limited and they will contribute little to the overall rate of erosion in the area or to the availability of material for other erosional processes. The effects of chemical weathering and mechanical weathering have been eliminated from PA calculations on the basis of low consequence to the performance of the disposal system.

SCR-4.4.1.6 FEP Numbers: N43, N44, and N45 FEP Titles: Aeolian Erosion (N43) Fluvial Erosion (N44) Mass Wasting (N45)

SCR-4.4.1.6.1 Screening Decision: SO-C

The effects of *Fluvial Erosion*, *Aeolian Erosion*, and *Mass Wasting* in the region of the WIPP have been eliminated from PA calculations on the basis of low consequence to the performance of the disposal system.

SCR-4.4.1.6.2 Summary of New Information

No new information has been identified that affects the screening of these FEPs since the CRA-2009.

SCR-4.4.1.6.3 Screening Argument

The geomorphological regime on the Mescalero Plain (Los Medaños) in the region of the WIPP is dominated by aeolian processes. Dunes are present in the area, and although some are stabilized by vegetation, aeolian erosion will occur as they migrate across the area. Old dunes will be replaced by new dunes, and no significant changes in the overall thickness of aeolian material are likely to occur.

Currently, precipitation in the region of the WIPP is too low (about 33 centimeters [cm] [13 inches (in.)] per yr) to cause perennial streams, and the relief in the area is too low for extensive sheet flood erosion during storms. An increase in precipitation to around 61 cm (24 in.) per yr in cooler climatic conditions could result in perennial streams, but the nature of the relief and the presence of dissolution hollows and sinks will ensure that these streams remain small. Significant fluvial erosion is not expected during the next 10,000 yrs.

Mass wasting (the downslope movement of material caused by the direct effect of gravity) is important only in terms of sediment erosion in regions of steep slopes. In the vicinity of the WIPP, mass wasting will be insignificant under the climatic conditions expected over the next 10,000 yrs.

Erosion from wind, water, and mass wasting will continue in the WIPP region throughout the next 10,000 yrs at rates similar to those occurring at present. These rates are too low to affect the performance of the disposal system significantly. Thus, the effects of fluvial erosion, aeolian erosion, and mass wasting have been eliminated from PA calculations on the basis of low consequence to the performance of the disposal system.

SCR-4.4.1.7 FEP Number: N50 FEP Title: Soil Development

SCR-4.4.1.7.1 Screening Decision: SO-C

Soil Development has been eliminated from PA calculations on the basis of low consequence to the performance of the disposal system.

SCR-4.4.1.7.2 Summary of New Information

No new information that affects the screening of this FEP has been identified since the CRA-2009.

SCR-4.4.1.7.3 Screening Argument

The Mescalero caliche is a well-developed calcareous remnant of an extensive soil profile across the WIPP site and adjacent areas. Although this unit may be up to 3 m (10 ft) thick, it is not continuous and does not prevent infiltration to the underlying formations. At Nash Draw, this caliche, dated in Lappin et al. (Lappin et al. 1989, pp. 2-4) at 410,000 to 510,000 yrs old, is present in collapse blocks, indicating some growth of Nash Draw in the late Pleistocene. Localized gypsite spring deposits about 25,000 yrs old occur along the eastern flank of Nash Draw, but the springs are not currently active. The Berino soil, interpreted as 333,000 yrs old (Rosholt and McKinney 1980, Table 5), is a thin soil horizon above the Mescalero caliche. The persistence of these soils on the Livingston Ridge and the lack of deformation indicates the relative stability of the WIPP region over the past half-million yrs.

Continued growth of caliche may occur in the future but will be of low consequence in terms of its effect on infiltration. Other soils in the area are not extensive enough to affect the amount of infiltration that reaches underlying aquifers. Soil development has been eliminated from PA calculations on the basis of low consequence to the performance of the disposal system.

SCR-4.5 Surface Hydrological FEPs

SCR-4.5.1 Depositional Processes

SCR-4.5.1.1 FEP Numbers: N46, N47, N48, and N49 FEP Titles: Aeolian Deposition (N46) Fluvial Deposition (47) Lacustrine Deposition (N48) Mass Waste (Deposition) (N49)

SCR-4.5.1.1.1 Screening Decision: SO-C

The effects of *Aeolian Deposition*, *Fluvial Deposition*, and *Lacustrine Deposition* and sedimentation in the region of the WIPP have been eliminated from PA calculations on the basis of low consequence to the performance of the disposal system.

SCR-4.5.1.1.2 Summary of New Information

No new information that affects the screening of these FEPs has been identified since the CRA-2009.

SCR-4.5.1.1.3 Screening Argument

The geomorphological regime on the Mescalero Plain (Los Medaños) in the region of the WIPP is dominated by aeolian processes, but although some dunes are stabilized by vegetation, no significant changes in the overall thickness of aeolian material are expected to occur. Vegetational changes during periods of wetter climate may further stabilize the dune fields, but aeolian deposition is not expected to significantly increase the overall thickness of the superficial deposits.

The limited extent of water courses in the region of the WIPP, under both present-day conditions and under the expected climatic conditions, will restrict the amount of fluvial deposition and lacustrine deposition in the region.

Mass wasting (deposition) may be significant if it results in dams or modifies streams. In the region around the WIPP, the Pecos River forms a significant water course some 19 km (12 mi) away, but the broadness of its valley precludes either significant mass wasting or the formation of large impoundments.

Sedimentation from wind, water, and mass wasting is expected to continue in the WIPP region throughout the next 10,000 yrs at the low rates similar to those occurring at present. These rates are too low to significantly affect the performance of the disposal system. Thus, the effects of aeolian deposition, fluvial deposition, and lacustrine deposition and sedimentation resulting from mass wasting have been eliminated from PA calculations on the basis of low consequence.

SCR-4.5.2 Streams and Lakes

SCR-4.5.2.1 FEPs Number: N51 FEPs Title: Stream and River Flow

SCR-4.5.2.1.1 Screening Decision: SO-C

Stream and River Flow has been eliminated from PA calculations on the basis of low consequence to the performance of the disposal system.

SCR-4.5.2.1.2 Summary of New Information

No new information that affects the screening of this FEP has been identified since the CRA-2009.

SCR-4.5.2.1.3 Screening Argument

No perennial streams are present at the WIPP site, and there is no evidence in the literature indicating that such features existed at this location since the Pleistocene (see, for example, Powers et al. 1978; Bachman 1974, Bachman 1981, and Bachman 1987b). The Pecos River is approximately 19 km (12 mi) from the WIPP site and more than 90 m (300 ft) lower in elevation. Stream and river flow has been eliminated from PA calculations on the basis of low consequence to the performance of the disposal system.

SCR-4.5.2.2 FEP Number: N52 FEP Title: Surface Water Bodies

SCR-4.5.2.2.1 Screening Decision: SO-C

The effects of *Surface Water Bodies* have been eliminated from PA calculations on the basis of low consequence to the performance of the disposal system.

SCR-4.5.2.2.2 Summary of New Information

No new information that affects the screening of this FEP has been identified since the CRA-2009.

SCR-4.5.2.2.3 Screening Argument

No standing surface water bodies are present at the WIPP site, and there is no evidence in the literature indicating that such features existed at this location during or after the Pleistocene (see, for example, Powers et al. 1978, and Bachman 1974, Bachman 1981, and Bachman 1987b). In Nash Draw, lakes and spoil ponds associated with potash mines are located at elevations 30 m (100 ft) below the elevation of the land surface at the location of the waste panels. There is no evidence in the literature to suggest that Nash Draw was formed by stream erosion or was at any time the location of a deep body of standing water, although shallow playa lakes have existed there at various times. Based on these factors, the formation of large lakes is unlikely and the formation of smaller lakes and ponds is of little consequence to the performance of the disposal system. The effects of surface water bodies have therefore been eliminated from PA calculations on the basis of low consequence to the performance of the disposal system.

SCR-4.5.3 Groundwater Recharge and Discharge

SCR-4.5.3.1 FEP Numbers: N53, N54, and N55 FEP Titles: Groundwater Discharge (N53) Groundwater Recharge (N54) Infiltration (N55)

SCR-4.5.3.1.1 Screening Decision: UP

Groundwater Recharge, Groundwater Discharge, and Infiltration are accounted for in PA calculations.

SCR-4.5.3.1.2 Summary of New Information

No new information that affects the screening of these FEPs has been identified since the CRA-2009.

SCR-4.5.3.1.3 Screening Argument

The groundwater basin described in the CCA, Chapter 2.0, Section 2.2.1.4 is governed by flow from areas where the water table is high to areas where the water table is low. The height of the water table is governed by the amount of groundwater recharge reaching the water table, which in turn is a function of the vertical hydraulic conductivity and the partitioning of precipitation between evapotranspiration, runoff, and infiltration. Flow within the Rustler is also governed by the amount of groundwater discharge that takes place from the basin. In the region around the WIPP, the principal discharge areas are along Nash Draw and the Pecos River. Groundwater flow modeling accounts for infiltration, recharge, and discharge (the CCA, Chapter 2.0, Section 2.2.1.4 and Chapter 6.0, Section 6.4.10.2).

SCR-4.5.3.2 FEP Number: N56 FEP Title: Changes in Groundwater Recharge and Discharge

SCR-4.5.3.2.1 Screening Decision: UP

Changes in Groundwater Recharge and Discharge arising as a result of climate change are accounted for in PA calculations.

SCR-4.5.3.2.2 Summary of New Information

No new information that affects the screening of this FEP has been identified since the CRA-2009.

SCR-4.5.3.2.3 Screening Argument

Changes in recharge may affect groundwater flow and radionuclide transport in units such as the Culebra and Magenta dolomites. Changes in the surface environment driven by natural climate change are expected to occur over the next 10,000 yrs (see FEPs N59 to N63). Groundwater basin modeling (the CCA, Chapter 2.0, Section 2.2.1.4) indicates that a change in recharge will affect the height of the water table in the area of the WIPP, and that this will in turn affect the direction and rate of groundwater flow.

The present-day water table in the vicinity of the WIPP is within the Dewey Lake at about 980 m (3,215 ft) above mean sea level (the CCA, Chapter 2.0, Section 2.2.1.4.2.1). An increase in recharge relative to present-day conditions would raise the water table, potentially as far as the local ground surface. Similarly, a decrease in recharge could result in a lowering of the water table. The low transmissivity of the Dewey Lake and the Rustler ensures that any such lowering of the water table will be at a slow rate, and lateral discharge from the groundwater basin is expected to persist for several thousand yrs after any decrease in recharge. Under the anticipated changes in climate over the next 10,000 yrs, the water table will not fall below the base of the Dewey Lake, and dewatering of the Culebra is not expected to occur during this period (the CCA, Chapter 2.0, Section 2.2.1.4).

Changes in groundwater recharge and discharge are accounted for in PA calculations through definition of the boundary conditions for flow and transport in the Culebra (the CCA, Chapter 6.0, Section 6.4.9, and Appendix PA-2014, Section PA-4.8.3).

SCR-4.5.3.3 FEP Numbers: N57 and N58 FEP Titles: Lake Formation (N57) River Flooding (N58)

SCR-4.5.3.3.1 Screening Decision: SO-C

The effects of *River Flooding* and *Lake Formation* have been eliminated from PA calculations on the basis of low consequence to the performance of the disposal system.

SCR-4.5.3.3.2 Summary of New Information

No new information that affects the screening of this FEP has been identified since the CRA-2009.

SCR-4.5.3.3.3 Screening Argument

Intermittent flooding of stream channels and the formation of shallow lakes will occur in the WIPP region over the next 10,000 yrs. These may have a short-lived and local effect on the height of the water table, but are unlikely to affect groundwater flow in the Culebra.

Future occurrences of playa lakes or other longer-term floods will be remote from the WIPP and will have little consequence on system performance in terms of groundwater flow at the site. There is no reason to believe that any impoundments or lakes could form over the WIPP site itself. Thus, river flooding and lake formationhave been eliminated from PA calculations on the basis of low consequence to the performance of the disposal system.

SCR-4.6 Climate EPs

SCR-4.6.1 Climate and Climate Changes

SCR-4.6.1.1 FEP Numbers: N59 and N60 FEP Titles: Precipitation (N59) Temperature (N60)

SCR-4.6.1.1.1 Screening Decision: UP

Precipitation and Temperature are accounted for in PA calculations.

SCR-4.6.1.1.2 Summary of New Information

No new information that affects the screening of this FEP has been identified since the CRA-2009.

SCR-4.6.1.1.3 Screening Argument

The climate and meteorology of the region around the WIPP are described in the CCA, Section 2.5.2. Precipitation in the region is low (about 33 cm [13 in.] per yr) and temperatures are moderate with a mean annual temperature of about 63 °F (17 °C). Precipitation and temperature are important controls on the amount of recharge that reaches the groundwater system and are accounted for in PA calculations by use of a sampled parameter for scaling flow velocity in the Culebra (see Appendix PA-2014, Section PA-4.8).

SCR-4.6.1.2 FEP Number: N61 FEP Title: Climate Change

SCR-4.6.1.2.1 Screening Decision: UP

Climate Change is accounted for in PA calculations.

SCR-4.6.1.2.2 Summary of New Information

No new information that affects the screening of this FEP has been identified since the CRA-2009.

SCR-4.6.1.2.3 Screening Argument

Climate changes are instigated by changes in the earth's orbit and by feedback mechanisms within the atmosphere and hydrosphere. Models of these mechanisms, combined with interpretations of the geological record, suggest that the climate will become cooler and wetter in the WIPP region during the next 10,000 yrs as a result of natural causes. Other changes, such as fluctuations in radiation intensity from the sun and variability within the many feedback mechanisms, will modify this climatic response to orbital changes. The available evidence suggests that these changes will be less extreme than those arising from orbital fluctuations.

The effect of a change to cooler and wetter conditions is considered to be an increase in the amount of recharge, which in turn will affect the height of the water table (see FEPs N53 through N56, Section SCR-4.5.3.1 and SCR-4.5.3.2). The height of the water table across the groundwater basin is an

important control on the rate and direction of groundwater flow within the Culebra (see the CCA, Chapter 2.0, Section 2.2.1.4), and hence potentially on transport of radionuclides released to the Culebra through the shafts or intrusion boreholes. Climate change is accounted for in PA calculations through a sampled parameter used to scale groundwater flow velocity in the Culebra (see Appendix PA-2014, Section PA-4.8).

SCR-4.6.1.3 FEP Numbers: N62 and N63 FEP Titles: Glaciation (N62) Permafrost (N63)

SCR-4.6.1.3.1 Screening Decision: SO-P

Glaciation and the effects of *Permafrost* have been eliminated from PA calculations on the basis of low probability of occurrence over 10,000 yrs.

SCR-4.6.1.3.2 Summary of New Information

No new information that affects the screening of these FEPs has been identified since the CRA-2009.

SCR-4.6.1.3.3 Screening Argument

No evidence exists to suggest that the northern part of the Delaware Basin has been covered by continental glaciers at any time since the beginning of the Paleozoic Era. During the maximum extent of continental glaciation in the Pleistocene Epoch, glaciers extended into northeastern Kansas at their closest approach to southeastern New Mexico. There is no evidence that alpine glaciers formed in the region of the WIPP during the Pleistocene glacial periods.

According to the theory that relates the periodicity of climate change to perturbations in the earth's orbit, a return to a full glacial cycle within the next 10,000 yrs is highly unlikely (Imbrie and Imbrie 1980, p. 951).

Thus, glaciation has been eliminated from PA calculations on the basis of low probability of occurrence over the next 10,000 yrs. Similarly, a number of processes associated with the proximity of an ice sheet or valley glacier, such as permafrost and accelerated slope erosion (solifluction) have been eliminated from PA calculations on the basis of low probability of occurrence over the next 10,000 yrs.

SCR-4.7 Marine FEPs

SCR-4.7.1 Seas, Sedimentation, and Level Changes

SCR-4.7.1.1 FEP Numbers: N64 and N65 FEP Titles: Seas and Oceans (N64) Estuaries (N65)

SCR-4.7.1.1.1 Screening Decision: SO-C

The effects of *Estuaries* and *Seas and Oceans* have been eliminated from PA calculations on the basis of low consequence to the performance of the disposal system.

SCR-4.7.1.1.2 Summary of New Information

No new information that affects the screening of these FEPs has been identified since the CRA-2009.

SCR-4.7.1.1.3 Screening Argument

The WIPP site is more than 800 km (480 mi) from the Pacific Ocean and from the Gulf of Mexico. Estuaries and seas and oceans have therefore been eliminated from PA calculations on the basis of low consequence to the disposal system.

SCR-4.7.1.2 FEPs Numbers: N66 and N67 FEPs Titles: Coastal Erosion (N66) Marine Sediment Transport and Deposition (N67)

SCR-4.7.1.2.1 Screening Decision: SO-C

Coastal Erosion and *Marine Sediment Transport and Deposition* have been eliminated from PA calculations on the basis of low consequence to the performance of the disposal system.

SCR-4.7.1.2.2 Summary of New Information

No new information that affects the screening of these FEPs has been identified since the CRA-2009.

SCR-4.7.1.2.3 Screening Argument

The WIPP site is more than 800 km (480 mi) from the Pacific Ocean and Gulf of Mexico. The effects of coastal erosion and marine sediment transport and deposition have therefore been eliminated from PA calculations on the basis of low consequence to the performance of the disposal system.

SCR-4.7.1.3 FEP Number: N68 FEP Title: Sea Level Changes

SCR-4.7.1.3.1 Screening Decision: SO-C

The effects of both short-term and long-term *Sea Level Changes* have been eliminated from PA calculations on the basis of low consequence to the performance of the disposal system.

SCR-4.7.1.3.2 Summary of New Information

No new information that affects the screening of this FEP has been identified since the CRA-2009.

SCR-4.7.1.3.3 Screening Argument

The WIPP site is some 1,036 m (3,400 ft) above sea level. Global sea level changes may result in sea levels as much as 140 m (460 ft) below that of the present day during glacial periods, according to Chappell and Shackleton (Chappell and Shackleton 1986, p. 138). This can have marked effects on coastal aquifers. During the next 10,000 yrs, the global sea level can be expected to drop towards this glacial minimum, but this will not affect the groundwater system in the vicinity of the WIPP. Short-term changes in sea level, brought about by events such as meteorite impact, tsunamis, seiches, and

hurricanes may raise water levels by several tens of meters. Such events have a maximum duration of a few days and will have no effect on the surface or groundwater systems at the WIPP site. Anthropogenic-induced global warming has been conjectured by Warrick and Oerlemans (Warrick and Oerlemans 1990, p. 278) to result in longer-term sea level rise. The magnitude of this rise, however, is not expected to be more than a few meters, and such a variation will have no effect on the groundwater system in the WIPP region. Thus, the effects of both short-term and long-term sea level changes have been eliminated from PA calculations on the basis of low consequence to the performance of the disposal system.

SCR-4.8 Ecological FEPs

SCR-4.8.1 Flora and Fauna

SCR-4.8.1.1 FEP Numbers: N69 and N70 FEP Titles: Plants (N69) Animals (N70)

SCR-4.8.1.1.1 Screening Decision: SO-C

The effects of the natural *Plants* and *Animals* (flora and fauna) in the region of the WIPP have been eliminated from PA calculations on the basis of low consequence to the performance of the disposal system.

SCR-4.8.1.1.2 Summary of New Information

No new information that affects the screening of this FEP has been identified since the CRA-2009.

SCR-4.8.1.1.3 Screening Argument

The terrestrial and aquatic ecology of the region around the WIPP is described in the CCA, Chapter 2.0, Section 2.4.1. The plants in the region are predominantly shrubs and grasses. The most conspicuous animals in the area are jackrabbits and cottontail rabbits. The effects of this flora and fauna in the region have been eliminated from PA calculations on the basis of low consequence to the performance of the disposal system.

SCR-4.8.1.2 FEP Number: N71 FEP Title: Microbes

SCR-4.8.1.2.1 Screening Decision: SO-C (UP for colloidal effects and gas generation)

The effects of *Microbes* on the region of the WIPP have been eliminated from PA calculations on the basis of low consequence to the performance of the disposal system.

SCR-4.8.1.2.2 Summary of New Information

No new information that affects the screening of this FEP has been identified since the CRA-2009.

SCR-4.8.1.2.3 Screening Argument

Microbes are presumed to be present within the thin soil horizons and in groundwater (Gillow et al. 2000; Swanson and Simmons 2013; Appendix SOTERM-2014, Section 2.4.1). The adsorption of actinides, or their analogs, onto microbial surfaces is dependent upon many factors, including biomass concentration, organism type, actinide oxidation state, the presence of complexing agents, matrix ionic strength and pH. These factors, for the key An(III) and An(IV) oxidation states, were accounted for under WIPP-relevant conditions (Reed et al. 2013; Appendix SOTERM-2014, Section 3.9). These biocolloids are relatively large in size (>0.3 μ) and exhibit relatively low sorption when compared to the inorganic and organic complexants also present. The density of microbial cells as colloidal particles will be limited by their low relative sorption and will be rapidly reduced by filtration in the Culebra because of their relative large size, leading to the conclusion that microbial colloids will have an insignificant impact on radionuclide transport in the Culebra. A similar conclusion is also observed in other deep geologic disposal concepts (e.g., for the Swedish granite concept (Pederson 1999)).

SCR-4.8.1.3 FEP Number: N72 FEP Title: Natural Ecological Development

SCR-4.8.1.3.1 Screening Decision: SO-C

The effects of *Natural Ecological Development* likely to occur in the region of the WIPP have been eliminated from PA calculations on the basis of low consequence to the performance of the disposal system.

SCR-4.8.1.3.2 Summary of New Information

No new information that affects the screening of this FEP has been identified since the CRA-2009.

SCR-4.8.1.3.3 Screening Argument

The region around the WIPP is sparsely vegetated as a result of the climate and poor soil quality. Wetter periods are expected during the regulatory period, but botanical records indicate that, even under these conditions, dense vegetation will not be present in the region (Swift 1992; see the CCA, Appendix CLI, p. 17). The effects of the indigenous fauna are of low consequence to the performance of the disposal system and no natural events or processes have been identified that would lead to a change in this fauna that would be of consequence to system performance. Natural ecological development in the region of the WIPP has therefore been eliminated from PA calculations on the basis of low consequence to the performance of the disposal system.

SCR-5.0 Screening of Human-Induced EPs

The following section presents screening arguments and decisions for human-induced EPs. Table SCR-1 provides summary information regarding changes to human-induced EPs since the CCA. Of the 61 human-induced EPs included in the CRA-2014, 52 remain unchanged, and 9 were updated with new information.

SCR-5.1 Human-Induced Geological EPs

SCR-5.1.1 Drilling

SCR-5.1.1.1 FEP Numbers: H1, H2, H4, H8, and H9 FEP Titles: Oil and Gas Exploration (H1) Potash Exploration (H2) Oil and Gas Exploitation (H4) Other Resources (drilling for) (H8) Enhanced Oil and Gas Recovery (drilling for) (H9)

SCR-5.1.1.1.1 Screening Decision: SO-C (HCN) DP (Future)

The effects of historical, current, and near-future drilling associated with Oil and Gas Exploration, Potash Exploration, Oil and Gas Exploitation, Drilling for Other Resources, and Drilling for Enhanced Oil and Gas Recovery has been eliminated from PA calculations on the basis of low consequence to the performance of the disposal system (see screening discussion for H21, H22, and H23). Oil and gas exploration, potash exploration, oil and gas exploitation, drilling for other resources, and enhanced oil and gas recovery in the future is accounted for in DP scenarios through incorporation of the rate of future drilling as specified in section 194.33.

SCR-5.1.1.1.2 Summary of New Information

The CRA-2014 will use an updated drilling rate as required by section 194.33. This new rate does not change the screening argument or decision for FEPs H1, Oil and Gas Exploration, H4, Oil and Gas Exploitation, H8, Other Resources, and H9, Enhanced Oil and Gas Recovery. This updated deep drilling rate is implemented through the PA parameter GLOBAL:LAMBDAD. For the CRA-2014, the value for this parameter is 6.73×10^{-3} boreholes per km^2 per yr. This is an increase to the value of 5.98×10^{-3} boreholes per km^2 per yr used in the CRA-2009 PABC. Additionally, further exploitation of the existing oil leases in Section 31 (beneath the southeast corner of the WIPP site) has occurred via horizontal drilling.

SCR-5.1.1.1.3 Historical, Current, and Near-Future Human EPs

Resource exploration and exploitation are the most common reasons for drilling in the Delaware Basin and are the most likely reasons for drilling in the near future. The WIPP location has been evaluated for the occurrence of natural resources in economic quantities. Powers et al. (Powers et al. 1978) (the CCA, Appendix GCR, Chapter 8) investigated the potential for exploitation of potash, hydrocarbons, caliche, gypsum, salt, uranium, sulfur, and lithium. Also, in 1995, the New Mexico Bureau of Mines and Mineral Resources performed a reevaluation of the mineral resources at and within 1.6 km (1 mi) around the WIPP site (New Mexico Bureau of Mines and Mineral Resources 1995). While some resources do exist at the WIPP site, for the HCN time frames, such drilling is assumed to only occur outside the WIPP site boundary, with the exception of horizontal wells beneath Section 31 (the southwest corner of the WIPP site). Oil leases that pre-existed the withdrawal of land by the Federal government for the WIPP in Section 31 were not condemned, as it was determined that production of these resources could be conducted without adverse effects to the WIPP. As such, the DOE only controls from the surface to 6,000 ft (1,829 m) below ground surface. Operators have continued to produce these leases and four new horizontal wells have been drilled beneath this section since the last recertification application. This continued development and production is consistent with the expectations of the DOE and the EPA (U.S. EPA 1998c). These wells originate outside the WIPP boundary and transition to horizontal orientation at depths below 6,000 ft (1,829 m). The vertical portion of these drill holes lie outside the WIPP boundary. Therefore, it is not expected that vertical wells will be initiated within the WIPP site during the HCN time frame. This assumption is based on current federal ownership and management of the WIPP during operations, and assumed effectiveness of institutional controls for the 100-yr period immediately following site closure.

Drilling associated with oil and gas exploration and oil and gas exploitation currently takes place in the vicinity of the WIPP. For example, gas is extracted from reservoirs in the Morrow Formation, some 4,200 m (14,000 ft) below the surface, and oil is extracted from shallower units within the Delaware Mountain Group, some 2,150 to 2,450 m (7,000 to 8,000 ft) below the surface.

Potash resources in the vicinity of the WIPP are discussed in the CCA, Chapter 2.0, Section 2.3.1.1. Throughout the Carlsbad Potash District, commercial quantities of potash are restricted to the McNutt, which forms part of the Salado above the repository horizon. Potash exploration and evaluation boreholes have been drilled within and outside the controlled area. Such drilling will continue outside the WIPP land withdrawal boundary, but no longer occurs within the boundary because rights and controls have been transferred to the DOE. Moreover, drilling for the evaluation of potash resources within the boundary will not occur throughout the time period of active institutional controls (AICs).

Drilling for other resources has taken place within the Delaware Basin. For example, sulfur extraction using the Frasch process began in 1969 and continued for three decades at the Culberson County Rustler Springs mine near Orla, Texas. In addition, brine wells have been in operation in and about the Delaware Basin for at least as long. Solution mining processes for sulfur, salt (brine), potash, or any other mineral are not addressed in this FEP; only the drilling of the borehole is addressed here. Resource extraction through solution mining and any potential effects are evaluated in Section SCR-5.2.2.3 (*Solution Mining for Potash* [H58]). Nonetheless, the drilling activity associated with the production of other resources is not notably different than drilling for petroleum exploration and exploitation.

Drilling for the purposes of reservoir stimulation and subsequent enhanced oil and gas recovery does take place within the Delaware Basin, although systematic, planned waterflooding has not taken place near the WIPP. Instead, injection near the WIPP consists of single-point injectors, rather than broad, grid-type waterflood projects (Hall et al. 2013). In the vicinity of the WIPP, fluid injection usually takes place using boreholes initially drilled as producing wells. Therefore, regardless of the initial intent of a deep borehole, whether in search of petroleum reserves or as an injection point, the drilling event and associated processes are virtually the same. These drilling-related processes are addressed more fully in Section SCR-5.2.1.1 (*Drilling Fluid Flow* [H21]), Section SCR-5.2.1.2 (*Drilling Fluid Loss* [H22]), and Section SCR-5.2.1.3 (*Blowouts* [H23]). Discussion on the effects subsequent to drilling a borehole for the purpose of enhancing oil and gas recovery is discussed in Section SCR-5.2.1.6 *(Enhanced Oil and Gas Production [H28]).*

In summary, drilling associated with oil and gas exploration, potash exploration, oil and gas exploitation, enhanced oil and gas recovery, and drilling associated with Other Resources has taken place and is expected to continue in the Delaware Basin. The potential effects of existing and possible near-future boreholes on fluid flow and radionuclide transport within the disposal system are discussed in FEPs H25 through H36 (Section SCR-5.2.1.5, Section SCR-5.2.1.6, Section SCR-5.2.1.7, Section SCR-5.2.1.8, Section SCR-5.2.1.9, Section SCR-5.2.1.10, Section SCR-5.2.1.11, Section SCR-5.2.1.12, and Section SCR-5.2.1.13), where low-consequence screening arguments are provided.

SCR-5.1.1.1.4 Future Human EPs

Criteria in section 194.33 require the DOE to examine the historical rate of drilling for resources in the Delaware Basin. Thus, consistent with section 194.33(b)(3)(i), the DOE has used the historical

record of deep drilling associated with oil and gas exploration, potash exploration, oil and gas exploitation, enhanced oil and gas recovery, and drilling associated with other resources (sulfur exploration) in the Delaware Basin in calculations to determine the rate of future deep drilling in the Delaware Basin (see Section 33 of this application).

SCR-5.1.1.2 FEP Numbers: H3 and H5 FEP Titles: Water Resources Exploration (H3) Groundwater Exploitation (H5)

SCR-5.1.1.2.1 Screening Decision: SO-C (HCN) SO-C (Future)

The effects of HCN and future drilling associated with *Water Resources Exploration* and *Groundwater Exploitation* have been eliminated from PA calculations on the basis of low consequence to the performance of the disposal system. Historical shallow drilling associated with *Water Resources Exploration* and *Groundwater Exploitation* is accounted for in calculations to determine the rate of future shallow drilling.

SCR-5.1.1.2.2 Summary of New Information

The Delaware Basin Monitoring Program records and tracks the development of deep and shallow wells within the vicinity of the WIPP. An updated shallow drilling rate of 2.88×10^{-3} boreholes per km^2 per yr was calculated in the Delaware Basin Monitoring Annual Report (U.S. DOE 2012). While this information has been updated since the last recertification, it does not result in a change in the screening arguments or decisions of these FEPs.

SCR-5.1.1.2.3 Screening Argument

Drilling associated with water resources exploration and groundwater exploitation has taken place and is expected to continue in the Delaware Basin. For the most part, water resources in the vicinity of the WIPP are scarce. Elsewhere in the Delaware Basin, potable water occurs in places while some communities rely solely on groundwater sources for drinking water. Even though water resources exploration and groundwater exploitation occur in the Basin, all such exploration/exploitation is confined to shallow drilling that extends no deeper than the Rustler. Thus, it will not impact repository performance because of the limited drilling anticipated in the future and the sizeable thickness of low-permeability Salado salt between the waste panels and the shallow groundwaters. Given the limited groundwater resources and minimal consequence of shallow drilling on performance, the effects of HCN and future drilling associated with water resources exploration and groundwater exploitation have been eliminated from PA calculations on the basis of low consequence to the performance of the disposal system. The screening argument therefore remains the same as given previously in the CCA.

Although shallow drilling for water resources exploration and groundwater exploitation have been eliminated from PA calculations, the DBDSP continues to collect drilling data related to water resources, as well as other shallow drilling activities. As shown in the DBDSP 2012 Annual Report (U.S. DOE 2012), the total number of shallow water wells in the Delaware Basin is currently 2,296, compared to 2,331 shallow water wells reported in the CCA. This decrease of 35 wells is attributed primarily to the reclassification of water wells to other types of shallow boreholes. Based on these data, the shallow drilling rate for water resources exploration and groundwater exploitation is

essentially the same as reported in the CCA. The distribution of groundwater wells in the Delaware Basin was included in the CCA, Appendix USDW, Section USDW.3.

SCR-5.1.1.2.4 Historical, Current, and Near-Future Human EPs

Water is currently extracted from formations above the Salado, as discussed in the CCA, Chapter 2.0, Section 2.3.1.3. The distribution of groundwater wells in the Delaware Basin is included in the CCA, Appendix USDW, Section USDW.3. Water resources explorationand groundwater exploitation are expected to continue in the Delaware Basin.

In summary, drilling associated with water resources exploration, groundwater exploitation, potash exploration, oil and gas exploration, oil and gas exploitation, enhanced oil and gas recovery, and drilling to explore other resources has taken place and is expected to continue in the Delaware Basin. The potential effects of existing and possible near-future boreholes on fluid flow and radionuclide transport within the disposal system are discussed in Section SCR-5.2, where low-consequence screening arguments are provided.

SCR-5.1.1.2.5 Future Human EPs

Criteria in section 194.33 require that, to calculate the rates of future shallow and deep drilling in the Delaware Basin, the DOE should examine the historical rate of drilling for resources in the Delaware Basin.

Shallow drilling associated with water, potash, sulfur, oil, and gas extraction has taken place in the Delaware Basin over the past 100 yrs. However, of these resources, only water and potash are present at shallow depths (less than 655 m (2,150 ft) below the surface) within the controlled area. Thus, consistent with section 194.33(b)(4), the DOE includes drilling associated with water resources exploration, potash exploration, and groundwater exploitation in calculations to determine the rate of future shallow drilling in the Delaware Basin. However, the effects of such events are not included in PA calculations because of low consequence to the performance of the disposal system.

SCR-5.1.1.3 FEP Numbers: H6, H7, H10, H11, and H12 FEP Titles: Archeological Investigations (H6) Geothermal Energy Production (H7) Liquid Waste Disposal (H10) Hydrocarbon Storage (H11) Deliberate Drilling Intrusion (H12)

SCR-5.1.1.3.1 Screening Decision: SO-R (HCN) SO-R (Future)

Drilling associated with Archeological Investigations, Geothermal Energy Production, Liquid Waste Disposal, Hydrocarbon Storage, and Deliberate Drilling Intrusion have been eliminated from PA calculations on regulatory grounds.

SCR-5.1.1.3.2 Summary of New Information

No new information that affects the screening of these FEPs has been identified since the CRA-2009.

SCR-5.1.1.3.3 Screening Argument

SCR-5.1.1.3.3.1 Historic, Current, and Near-Future EPs

No drilling associated with archeology or geothermal energy production has taken place in the Delaware Basin. Consistent with the future states assumptions in section 194.25(a) (U.S. EPA 1996), such drilling activities have been eliminated from PA calculations on regulatory grounds.

While numerous archeological sites exist at and near the WIPP site, drilling for archeological purposes has not occurred. Archeological investigations have only involved shallow surface disruptions, and do not require deeper investigation by any method, drilling or otherwise. Geothermal energy is not considered to be a potentially exploitable resource because economically attractive geothermal conditions do not exist in the northern Delaware Basin.

Oil and gas production byproducts are disposed of underground in the WIPP region, but such liquid waste disposal does not involve drilling of additional boreholes (see H27, Section SCR-5.2.1.6); therefore drilling of boreholes for the explicit purpose of disposal has not occurred.

Hydrocarbon storage takes place in the Delaware Basin, but it involves gas injection through existing boreholes into depleted reservoirs (see, for example, Burton et al. 1993, pp. 66-67). Therefore, drilling of boreholes for the explicit purpose of hydrocarbon storag*e* has not occurred.

Consistent with section 194.33(b)(1), all near-future Human EPs relating to deliberate drilling intrusion into the WIPP excavation have been eliminated from PA calculations on regulatory grounds.

SCR-5.1.1.3.3.2 Future Human EPs

Consistent with section 194.33 and the future states assumptions in section 194.25(a), drilling for purposes other than resource recovery (such as WIPP site investigation) and drilling activities that have not taken place in the Delaware Basin over the past 100 yrs need not be considered in determining future drilling rates. Thus, drilling associated with archeological investigations, geothermal energy production, liquid waste disposal, hydrocarbon storage, and deliberate drilling intrusion have been eliminated from PA calculations on regulatory grounds.

SCR-5.1.2 Excavation Activities

SCR-5.1.2.1 FEP Number: H13 FEP Title: Conventional Underground Potash Mining

SCR-5.1.2.1.1 Screening Decision: UP (HCN) DP (Future)

As prescribed by section 194.32(b), the effects of HCN and future *Conventional Underground Potash Mining* are accounted for in PA calculations (see also FEP H37).

SCR-5.1.2.1.2 Summary of New Information

No new information that affects the screening of this FEP has been identified since the CRA-2009.

SCR-5.1.2.1.3 Screening Argument

Potash is the only known economically viable resource in the vicinity of the WIPP that is recovered by underground mining (see the CCA, Chapter 2.0, Section 2.3.1). Potash is mined extensively by conventional techniques in the region east of Carlsbad and up to 2.4 km (1.5 mi) from the boundaries of the controlled area of the WIPP. According to existing plans and leases (see the CCA, Chapter 2.0, Section 2.3.1.1), potash mining is expected to continue in the vicinity of the WIPP in the near future. The DOE assumes that all economically recoverable potash in the vicinity of the disposal system will be extracted in the near future, although there are no economical reserves above the WIPP waste panels (Griswold and Griswold 1999).

In summary, conventional underground potash mining is currently taking place and is expected to continue in the vicinity of the WIPP in the near future. The potential effects of HCN and future conventional underground potash mining are accounted for in PA calculations as prescribed by section 194.32(b), and as further described in the supplementary information to Part 194 Subpart C, "Compliance Certification and Recertification" and in the Compliance Application Guidance (CAG), Subpart C, § 194.32, Scope of Performance Assessments.

SCR-5.1.2.2 FEP Number: H14 FEP Title: Other Resources (mining for)

SCR-5.1.2.2.1 Screening Decision: SO-C (HCN) SO-R (Future)

HCN *Mining for Other Resources* has been eliminated from PA calculations on the basis of low consequence to the performance of the disposal system. Future *Mining for Other Resources* has been eliminated from PA calculations on regulatory grounds.

SCR-5.1.2.2.2 Summary of New Information

No new information that affects the screening of this FEP has been identified since the CRA-2009.

SCR-5.1.2.2.3 Screening Argument

Potash is the only known economically viable resource in the vicinity of the WIPP that is recovered by underground mining. Potash is mined extensively in the region east of Carlsbad and up to 5 km (3.1 mi) from the boundaries of the controlled area. According to existing plans and leases, potash mining is expected to continue in the vicinity of the WIPP in the near future. The DOE assumes that all economically recoverable potash in the vicinity of the disposal system will be extracted in the near future. Excavation for resources other than potash and archaeological excavations have taken place or are currently taking place in the Delaware Basin. These activities have not altered the geology of the controlled area significantly, and have been eliminated from PA calculations for the HCN timeframe on the basis of low consequence to the performance of the disposal system.

Potash is the only resource that has been identified within the controlled area in a quality similar to that currently mined elsewhere in the Delaware Basin. Future mining for other resources has been eliminated from PA calculations on the regulatory basis of section 194.25(a).

SCR-5.1.2.3 FEP Numbers: H15 and H16 FEP Titles: Tunneling (H15) Construction of Underground Facilities (H16)

SCR-5.1.2.3.1 Screening Decision: SO-R (HCN) SO-R (Future)

Consistent with section 194.33(b)(1), near-future, human-induced EPs relating to *Tunneling* into the WIPP excavation and *Construction of Underground Facilities* have been eliminated from PA calculations on regulatory grounds. Furthermore, consistent with section 194.25(a), future human-induced EPs relating to *Tunneling* into the WIPP excavation and *Construction of Underground Facilities* have been eliminated from PA calculations on regulatory grounds.

SCR-5.1.2.3.2 Summary

No new information that affects the screening of this FEP has been identified since the CRA-2009.

SCR-5.1.2.3.3 Screening Argument

No tunneling or construction of underground facilities (for example, storage, disposal, accommodation [i.e., dwellings]) has taken place in the Delaware Basin. Mining for potash occurs (a form of tunneling), but is addressed specifically in (Section SCR-5.1.2.1 (*Conventional Underground Potash Mining* [H13])). Gas storage does take place in the Delaware Basin, but it involves injection through boreholes into depleted reservoirs, and not excavation (see, for example, Burton et al. 1993, pp. 66-67).

Because tunneling and construction of underground facilities (other than the WIPP) have not taken place in the Delaware Basin, and consistent with the future-states assumptions in section 194.25(a), such excavation activities have been eliminated from PA calculations on regulatory grounds.

SCR-5.1.2.4 FEP Number: H17 FEP Title: Archeological Excavations

SCR-5.1.2.4.1 Screening Decision: SO-C (HCN) SO-R (Future)

HCN *Archaeological Excavations* have been eliminated from PA calculations on the basis of low consequence to the performance of the disposal system. Future *Archaeological Excavations* into the disposal system have been eliminated from PA calculations on regulatory grounds.

SCR-5.1.2.4.2 Summary of New Information

No new information that affects the screening of this FEP has been identified since the CRA-2009.

SCR-5.1.2.4.3 Screening Argument

Archeological excavations have occurred at or near the WIPP, but involved only minor surface disturbances. These archaeological excavations may continue into the foreseeable future as other archeological sites are discovered. These activities have not altered the geology of the controlled area significantly, and have been eliminated from PA calculations on the basis of low consequence to the performance of the disposal system for the HCN timeframe.

Also, consistent with section 194.32(a), which limits the scope of consideration of future human actions to mining and drilling, future archaeological excavations have been eliminated from PA calculations on regulatory grounds.

SCR-5.1.2.5 FEP Number: H18 FEP Title: Deliberate Mining Intrusion

SCR-5.1.2.5.1 Screening Decision: SO-R (HCN) SO-R (Future)

Consistent with section 194.33(b)(1), near-future, human-induced EPs relating to *Deliberate Mining Intrusion* into the WIPP excavation have been eliminated from PA calculations on regulatory grounds. Furthermore, consistent with section 194.33(b)(1), future human-induced EPs relating to *Deliberate Mining Intrusion* into the WIPP excavation have been eliminated from PA calculations on regulatory grounds.

SCR-5.1.2.5.2 Summary of New Information

No new information that affects the screening of this FEP has been identified since the CRA-2009.

SCR-5.1.2.5.3 Screening Argument

Consistent with section 194.33(b)(1), all future human-related EPs relating to deliberate mining intrusion into the WIPP excavation have been eliminated from PA calculations on regulatory grounds.

SCR-5.1.3 Subsurface Explosions

SCR-5.1.3.1 FEPs Number: H19 FEP Title: Explosions for Resource Recovery

SCR-5.1.3.1.1 Screening Decision: SO-C (HCN) SO-R (Future)

Historical underground *Explosions for Resource Recovery* have been eliminated from PA calculations on the basis of low consequence to the performance of the disposal system. Future underground *Explosions for Resource Recovery* have been eliminated from PA calculations on regulatory grounds.

SCR-5.1.3.1.2 Summary of New Information

No new information that affects the screening of this FEP has been identified since the CRA-2009.

SCR-5.1.3.1.3 Screening Argument

This section discusses subsurface explosions associated with resource recovery that may result in pathways for fluid flow between hydraulically conductive horizons. The potential effects of explosions on the hydrological characteristics of the disposal system are discussed in Section SCR-5.2.3.1 (*Changes in Groundwater Flow Due to Explosions* [H39]).

SCR-5.1.3.1.4 Historical, Current, and Near-Future Human EPs

Neither small-scale nor regional-scale explosive techniques to enhance the formation of hydraulic conductivity form a part of current mainstream oil- and gas-production technology. Instead, controlled perforating and hydrofracturing are used to improve the performance of oil and gas boreholes in the Delaware Basin. However, small-scale explosions have been used in the past to fracture oil- and natural-gas-bearing units to enhance resource recovery. The size of explosion used to fracture an oil- or gas-bearing unit is limited by the need to contain the damage within the unit being exploited. In the area surrounding the WIPP, the stratigraphic units with oil and gas resources are too deep for explosions to affect the performance of the disposal system. Thus, the effects of explosions for resource recovery have been eliminated from PA calculations on the basis of low consequence to the performance of the disposal system.

Potash mining is currently taking place and is expected to continue in the vicinity of the WIPP in the near future. Potash is mined extensively in the region east of Carlsbad and up to 2.4 km (1.3 mi) from the boundaries of the controlled area. In earlier yrs, conventional drill, blast, load, and rail-haulage methods were used. Today, continuous miners similar to those used in coal-mining have been adapted to fit the potash-salt formations. Hence, drilling and blasting technology is not used in the present day potash mines. Thus, the effects of explosions for resource recovery have been eliminated from PA calculations on the basis of low consequence to the performance of the disposal system.

Consistent with section 194.33(d), PAs need not analyze the effects of techniques used for resource recovery subsequent to the drilling of a future borehole. Therefore, future underground explosions for resource recovery have been eliminated from PA calculations on regulatory grounds.

SCR-5.1.3.2 FEPs Number: H20 FEP Title: Underground Nuclear Device Testing

SCR-5.1.3.2.1 Screening Decision: SO-C (HCN) SO-R (Future)

Historical *Underground Nuclear Device Testing* has been eliminated from PA calculations on the basis of low consequence to the performance of the disposal system. Future *Underground Nuclear Device Testing* has been eliminated from PA calculations on regulatory grounds.

SCR-5.1.3.2.2 Summary of New Information

No new information that affects the screening of this FEP has been identified since the CRA-2009.

SCR-5.1.3.2.3 Screening Argument

SCR-5.1.3.2.3.1 Historical, Current, and Near-Future Human EPs

The Delaware Basin has been used for an isolated nuclear test. This test, Project Gnome (Rawson et al. 1965), took place in 1961 at a location approximately 13 km (8 mi) southwest of the WIPP waste disposal region. Project Gnome was decommissioned in 1979.

The primary objective of Project Gnome was to study the effects of an underground nuclear explosion in salt. The Gnome experiment involved the detonation of a 3.1 kiloton nuclear device at a depth of 360 m (1,190 ft) in the bedded salt of the Salado. The explosion created an approximately spherical cavity of about 27,000 cubic meters (m^3) (950,000 cubic ft [ft^3]) and caused surface displacements in a radius of 360 m (1,180 ft). No earth tremors perceptible to humans were reported at distances over 40 km (25 mi) from the explosion. A zone of increased permeability was observed to extend at least

46 m (150 ft) laterally from and 105 m (344 ft) above the point of the explosion. The test had no significant effects on the geological characteristics of the WIPP disposal system. Thus, historical underground nuclear device testing has been eliminated from PA calculations on the basis of low consequence to the performance of the disposal system. Due to a moratorium on underground nuclear testing, there are no existing plans for underground nuclear device testing in the vicinity of the WIPP in the near future.

SCR-5.1.3.2.3.2 Future Human EPs

The criterion in section 194.32(a) relating to the scope of PAs limits the consideration of future human actions to mining and drilling. Therefore, future underground nuclear device testing has been eliminated from PA calculations on regulatory grounds.

SCR-5.2 Subsurface Hydrological and Geochemical EPs

SCR-5.2.1 Borehole Fluid Flow

SCR-5.2.1.1 FEP Number: H21 FEP Title: Drilling Fluid Flow

SCR-5.2.1.1.1 Screening Decision: SO-C (HCN) DP (Future)

Drilling Fluid Flow associated with historical, current, near-future, and future boreholes that do not intersect the waste disposal region has been eliminated from PA calculations on the basis of low consequence to the performance of the disposal system. The possibility of a future deep borehole penetrating a waste panel, such that drilling-induced flow results in transport of radionuclides to the land surface or to overlying hydraulically conductive units, is accounted for in PA calculations. The possibility of a deep borehole penetrating both the waste disposal region and a Castile brine reservoir is accounted for in PA calculations.

SCR-5.2.1.1.2 Summary of New Information

No new information that affects the screening of this FEP has been identified since the CRA-2009.

SCR-5.2.1.1.3 Screening Argument

Borehole circulation fluid could be lost to thief zones encountered during drilling, or fluid could flow from pressurized zones through the borehole to the land surface (blowout) or to a thief zone. Such drilling-related EPs could influence groundwater flow and, potentially, radionuclide transport in the affected units. Future drilling within the controlled area could result in direct releases of radionuclides to the land surface or transport of radionuclides between hydraulically conductive units.

Movement of brine from a pressurized zone through a borehole into potential thief zones such as the Salado interbeds or the Culebra could result in geochemical changes and altered radionuclide migration rates in these units.

SCR-5.2.1.1.3.1 Historical, Current, and Near-Future Human EPs

Drilling fluid flow is a short-term event that can result in the flow of pressurized fluid from one geologic stratum to another. However, long-term flow through abandoned boreholes would have a

greater hydrological impact in the Culebra than a short-term event like drilling-induced flow outside the controlled area. Wallace (Wallace 1996a) analyzed the potential effects of flow through abandoned boreholes in the future within the controlled area, and concluded that interconnections between the Culebra and deep units could be eliminated from PA calculations on the basis of low consequence. Thus, the HCN of drilling fluid flow associated with boreholes outside the controlled area has been screened out on the basis of low consequence to the performance of the disposal system.

As discussed in FEPs H25 through H36 (Section SCR-5.2.1.5, Section SCR-5.2.1.6, Section SCR-5.2.1.7, Section SCR-5.2.1.8, Section SCR-5.2.1.9, Section SCR5.2.1.10, Section SCR-5.2.1.11, Section SCR-5.2.1.12, and Section SCR-5.2.1.13), drilling associated with water resources exploration, groundwater exploitation, potash exploration, oil and gas exploration, oil and gas exploitation, enhanced oil and gas recovery, and drilling to explore other resources has taken place or is currently taking place outside the controlled area in the Delaware Basin. These drilling activities are expected to continue in the vicinity of the WIPP in the near future.

SCR-5.2.1.1.3.2 Future Human EPs

For the future, drill holes may intersect the waste disposal region and their effects could be more profound. Thus, the possibility of a future borehole penetrating a waste panel, so that drilling fluid flow and, potentially, blowout results in transport of radionuclides to the land surface or to overlying hydraulically conductive units, is accounted for in PA calculations.

The units intersected by the borehole may provide sources for fluid flow (brine, oil, or gas) to the waste panel during drilling. In the vicinity of the WIPP, the Castile that underlies the Salado contains isolated volumes of brine at fluid pressures greater than hydrostatic. A future borehole that penetrates a Castile brine reservoir could provide a connection for brine flow from the reservoir to the waste panel, thus increasing fluid pressure and brine volume in the waste panel. The possibility of a deep borehole penetrating both a waste panel and a brine reservoir is accounted for in PA calculations.

Penetration of an underpressurized unit underlying the Salado could result in flow and radionuclide transport from the waste panel to the underlying unit during drilling, although drillers would minimize such fluid loss to a thief zone through the injection of materials to reduce permeability or through the use of casing and cementing. Also, the permeabilities of formations underlying the Salado are less than the permeability of the Culebra (Wallace 1996a). Thus, the consequences associated with radionuclide transport to an underpressurized unit below the waste panels during drilling will be less significant, in terms of disposal system performance, than the consequences associated with radionuclide transport to the land surface or to the Culebra during drilling. Through this comparison, drilling events that result in penetration of underpressurized units below the waste-disposal region have been eliminated from PA calculations on the basis of beneficial consequence to the performance of the disposal system.

SCR-5.2.1.2 FEP Number: H22 FEP Title: Drilling Fluid Loss

SCR-5.2.1.2.1 Screening Decision: SO-C (HCN) DP (Future)

Drilling Fluid Loss associated with HCN and future boreholes that do not intersect the waste disposal region has been eliminated from PA calculations on the basis of low consequence to the performance of the disposal system. The possibility of a future *Drilling Fluid L oss* into waste panels is accounted for in PA calculations.

SCR-5.2.1.2.2 Summary of New Information

No new information that affects the screening of this FEP has been identified since the CRA-2009.

SCR-5.2.1.2.3 Screening Argument

Drilling fluid loss is a short-term event that can result in the flow of pressurized fluid from one geologic stratum to another. Large fluid losses would lead a driller to inject materials to reduce permeability, or it would lead to the borehole being cased and cemented to limit the loss of drilling fluid. Assuming such operations are successful, drilling fluid loss in the near future outside the controlled area will not significantly affect the hydrology of the disposal system. Thus, drilling fluid loss associated with historical, current, and near-future boreholes has been eliminated from PA calculations on the basis of low consequence to the performance of the disposal system.

In evaluating the potential consequences of drilling fluid loss to a waste panel in the future, two types of drilling events need to be considered - those that intercept pressurized fluid in underlying formations such as the Castile (defined in the CCA, Chapter 6.0, Section 6.3.2.2 as E1 events), and those that do not (E2 events). A possible hydrological effect would be to make a greater volume of brine available for gas generation processes and thereby increase gas volumes at particular times in the future. For either type of drilling event, on the basis of current drilling practices, the driller is assumed to pass through the repository rapidly. Relatively small amounts of drilling fluid loss might not be noticed and might not give rise to concern. Larger fluid losses would lead to the driller injecting materials to reduce permeability, or to the borehole being cased and cemented, to limit the loss of drilling fluid.

For boreholes that intersect pressurized brine reservoirs, the volume of fluid available to flow up a borehole will be significantly greater than the volume of any drilling fluid that could be lost. This greater volume of brine is accounted for in PA calculations, and is allowed to enter the disposal room (see the CCA, Chapter 6.0, Section 6.4.7). Thus, the effects of drilling fluid loss will be small by comparison to the potential flow of brine from pressurized brine reservoirs. Therefore, the effects of drilling fluid loss for E1 drilling events have been eliminated from PA calculations on the basis of low consequence to the performance of the disposal system.

The consequences of drilling fluid loss into waste panels in the future are accounted for in PA calculations for E2 events.

SCR-5.2.1.2.3.1 Historical, Current, and Near-Future Human EPs

Drilling fluid flow will not affect hydraulic conditions in the disposal system significantly unless there is substantial drilling fluid loss to a thief zone, such as the Culebra. Typically, zones into which significant borehole circulation fluid is lost are isolated through injection of materials to reduce permeability or through casing and cementing programs. Assuming such operations are successful, drilling fluid loss in the near future outside the controlled area will not affect the hydrology of the disposal system significantly and be of no consequence.

SCR-5.2.1.2.3.2 Future Human EPs

The consequences of drilling within the controlled area in the future will primarily depend on the location of the borehole. Potentially, future deep drilling could penetrate the waste disposal region.

Hydraulic and geochemical conditions in the waste panel could be affected as a result of drilling fluid loss to the panel.

Penetration of an underpressurized unit underlying the Salado could result in flow and radionuclide transport from the waste panel to the underlying unit during drilling, although drillers would minimize such fluid loss to a thief zone through the injection of materials to reduce permeability or through the use of casing and cementing. Also, the permeabilities of formations underlying the Salado are less than the permeability of the Culebra (Wallace 1996a). Thus, the consequences associated with radionuclide transport to an underpressurized unit below the waste panels during drilling will be less significant, in terms of disposal system performance, than the consequences associated with radionuclide transport to the land surface or to the Culebra during drilling. Through this comparison, drilling events that result in penetration of underpressurized units below the waste-disposal region have been eliminated from PA calculations on the basis of beneficial consequence to the performance of the disposal system.

For boreholes that do not intersect pressurized brine reservoirs (but do penetrate the waste-disposal region), the treatment of the disposal room implicitly accounts for the potential for greater gas generation resulting from drilling fluid loss. Thus, the hydrological effects of drilling fluid loss for E2 drilling events are accounted for in PA calculations within the conceptual model of the disposal room for drilling intrusions.

SCR-5.2.1.3 FEP Number: H23 FEP Title: Blowouts

SCR-5.2.1.3.1 Screening Decision: SO-C (HCN) DP (Future)

Blowouts associated with HCN and future boreholes that do not intersect the waste disposal region have been eliminated from PA calculations on the basis of low consequence to the performance of the disposal system. The possibility of a future deep borehole penetrating a waste panel such that drilling-induced flow results in transport of radionuclides to the land surface or to overlying hydraulically conductive units is accounted for in PA calculations. The possibility of a deep borehole penetrating both the waste disposal region and a Castile brine reservoir is accounted for in PA calculations.

SCR-5.2.1.3.2 Summary of New Information

Blowouts are implemented in PA through the parameter GLOBAL:PBRINE, which represents the probability of an inadvertent intrusion borehole encountering pressurized brine beneath the repository. This parameter has been updated based on new data and analysis as reported in Kirchner et al. (Kirchner et al. 2012). This parameter update does not change the screening argument or decision; H23 *Blowouts* continue to be classified as DP for the future timeframe.

SCR-5.2.1.3.3 Screening Argument

Blowouts are short-term events that can result in the flow of pressurized fluid from one geologic stratum to another. For the near future, a blowout may occur in the vicinity of the WIPP but is not likely to affect the disposal system because of the distance from the well to the waste panels, assuming that AICs are in place which restrict borehole installation to outside the WIPP boundary. *Blowouts* associated with HCN and future boreholes that do not intersect the waste disposal region have been eliminated from PA calculations on the basis of low consequence to the performance of the

disposal system. For the future, the drill holes may intersect the waste disposal region and these effects could be more profound. Thus, *blowouts* are included in the assessment of future activities and their consequences are accounted for in PA calculations.

Fluid could flow from pressurized zones through the borehole to the land surface (*blowout*) or to a thief zone. Such drilling-related EPs could influence groundwater flow and, potentially, radionuclide transport in the affected units. Movement of brine from a pressurized zone through a borehole into potential thief zones such as the Salado interbeds or the Culebra could result in geochemical changes and altered radionuclide migration rates in these units.

SCR-5.2.1.3.3.1 Historical, Current, and Near-Future Human EPs

Drilling associated with water resources exploration, groundwater exploitation, potash exploration, oil and gas exploration, oil and gas exploitation, enhanced oil and gas recovery, and drilling to explore other resources has taken place or is currently taking place outside the controlled area in the Delaware Basin. These drilling activities are expected to continue in the vicinity of the WIPP in the near future.

Naturally occurring brine and gas pockets have been encountered during drilling in the Delaware Basin. Brine pockets have been intersected in the Castile (as discussed in the CCA, Chapter 2.0, Section 2.2.1.2). Gas blowouts have occurred during drilling in the Salado. Usually, such events result in brief interruptions in drilling while the intersected fluid pocket is allowed to depressurize through flow to the surface (for a period lasting from a few hours to a few days). Drilling then restarts with an increased drilling mud weight. Under these conditions, blowouts in the near future will cause isolated hydraulic disturbances, but will not affect the hydrology of the disposal system significantly.

Potentially, the most significant disturbance to the disposal system could occur if an uncontrolled blowout during drilling resulted in substantial flow through the borehole from a pressurized zone to a thief zone. For example, if a borehole penetrates a brine reservoir in the Castile, brine could flow through the borehole to the Culebra over the long term, and, as a result, could affect hydraulic conditions in the Culebra. The potential effects of such an event can be compared to the effects of long-term fluid flow from deep overpressurized units to the Culebra through abandoned boreholes. Wallace (Wallace 1996a) analyzed the potential effects of flow through abandoned boreholes in the future within the controlled area and concluded that interconnections between the Culebra and deep units could be eliminated from PA calculations on the basis of low consequence. Long-term flow through abandoned boreholes would have a greater hydrological impact in the Culebra than short-term, drilling-induced flow outside the controlled area. Thus, the effects of fluid flow during drilling in the near future have been eliminated from PA calculations on the basis of low consequence to the performance of the disposal system.

In summary, blowouts associated with historical, current, and near-future boreholes have been eliminated from PA calculations on the basis of low consequence to the performance of the disposal system.

SCR-5.2.1.3.3.2 Future Human EPs-Boreholes that Intersect the Waste Disposal Region

The consequences of drilling within the controlled area in the future will depend primarily on the location of the borehole. Potentially, future deep drilling could penetrate the waste disposal region. If the borehole intersects the waste in the disposal rooms, radionuclides could be transported as a result of drilling fluid flow: releases to the accessible environment may occur as material entrained in the circulating drilling fluid is brought to the surface. Also, during drilling, contaminated brine may flow

up the borehole and reach the surface, depending on fluid pressure within the waste disposal panels; blowout conditions could prevail if the waste panel were sufficiently pressurized at the time of intrusion.

SCR-5.2.1.3.3.3 Hydraulic Effects of Drilling-Induced Flow

The possibility of a future borehole penetrating a waste panel, so that drilling fluid flow and, potentially, blowout results in transport of radionuclides to the land surface or to overlying hydraulically conductive units, is accounted for in PA calculations.

The units intersected by the borehole may provide sources for fluid flow (brine, oil, or gas) to the waste panel during drilling. In the vicinity of the WIPP, the Castile that underlies the Salado contains isolated volumes of brine at fluid pressures greater than hydrostatic. A future borehole that penetrates a Castile brine reservoir could provide a connection for brine flow from the reservoir to the waste panel, thus increasing fluid pressure and brine volume in the waste panel. The possibility of a deep borehole penetrating both a waste panel and a brine reservoir is accounted for in PA calculations.

Future boreholes could affect the hydraulic conditions in the disposal system. Intersection of pockets of pressurized gas and brine would likely result in short-term, isolated hydraulic disturbances, and will not affect the hydrology of the disposal system significantly. Potentially the most significant hydraulic disturbance to the disposal system could occur if an uncontrolled blowout during drilling resulted in substantial flow through the borehole from a pressurized zone to a thief zone. For example, if a borehole penetrates a brine reservoir in the Castile, brine could flow through the borehole to the Culebra, and, as a result, could affect hydraulic conditions in the Culebra. The potential effects of such an event can be compared to the effects of long-term fluid flow from deep overpressurized units to the Culebra through abandoned boreholes. Wallace (Wallace 1996a) analyzed the potential effects of such interconnections in the future within the controlled area (but that do not intersect waste), and concluded that flow through abandoned boreholes between the Culebra and deep units could be eliminated from PA calculations on the basis of low consequence.

SCR-5.2.1.4 FEP Number: H24 FEP Title: Drilling-Induced Geochemical Changes

SCR-5.2.1.4.1 Screening Decision: UP (HCN) DP (Future)

Drilling-Induced Geochemical Changes that occur within the controlled area as a result of HCN and future drilling-induced flow are accounted for in PA calculations.

SCR-5.2.1.4.2 Summary of New Information

No new information that affects the screening of this FEP has been identified since the CRA-2009.

SCR-5.2.1.4.3 Screening Argument

Borehole circulation fluid could be lost to thief zones encountered during drilling, or fluid could flow from pressurized zones through the borehole to the land surface (blowout) or to a thief zone. Such drilling-related EPs could influence groundwater flow and, potentially, radionuclide transport in the affected units. Future drilling within the controlled area could result in direct releases of radionuclides to the land surface or transport of radionuclides between hydraulically conductive units.

Movement of brine from a pressurized zone through a borehole and into potential thief zones such as the Salado interbeds or the Culebra, could result in geochemical changes and altered radionuclide migration rates in these units.

SCR-5.2.1.4.3.1 Historical, Current, and Near-Future Human EPs

Drilling associated with resource exploration, exploitation, and recovery has taken place or is currently taking place outside the controlled area in the Delaware Basin. These drilling activities are expected to continue in the vicinity of the WIPP in the near future. Chemical changes induced by such drilling are discussed below.

SCR-5.2.1.4.3.2 Geochemical Effects of Drilling-Induced Flow-HCN

Radionuclide migration rates are governed by the coupled effects of hydrological and geochemical processes (see discussions in FEPs W77 through W100, Section SCR-6.6.1.1 , Section SCR-6.6.1.2, Section SCR-6.6.2.1, Section SCR-6.6.3.1, Section SCR-6.6.3.2, Section SCR-6.6.4.1, Section SCR-6.7.1.1, Section SCR-6.7.2.1, Section SCR-6.7.3.1, Section SCR-6.7.4.1, Section SCR-6.7.4.2, Section SCR-6.7.4.3, Section SCR-6.7.5.1, Section SCR-6.7.5.2, Section SCR-6.7.5.3, and Section SCR-6.7.5.4). Human EPs outside the controlled area could affect the geochemistry of units within the controlled area if they occur sufficiently close to the edge of the controlled area. Movement of brine from a pressurized reservoir in the Castile through a borehole into potential thief zones, such as the Salado interbeds or the Culebra, could cause drilling-induced geochemical changes resulting in altered radionuclide migration rates in these units through their effects on colloid transport and sorption (colloid transport may enhance radionuclide migration, while radionuclide migration may be retarded by sorption).

The treatment of colloids in PA calculations is described in the CCA, Chapter 6.0, Section 6.4.3.6 and Section 6.4.6.2.2. The repository and its contents provide the main source of colloids in the disposal system. By comparison, Castile brines have relatively low total colloid concentrations. Therefore, changes in colloid transport in units within the controlled area as a result of HCN drilling-induced flow have been eliminated from PA calculations on the basis of low consequence to the performance of the disposal system.

Sorption within the Culebra is accounted for in PA calculations as discussed in the CCA, Chapter 6.0, Section 6.4.6.2. The sorption model comprises an equilibrium, sorption isotherm approximation, employing K_ds applicable to dolomite in the Culebra (Appendix PA-2004, Attachment MASS, Section MASS-15.2). The cumulative distribution functions (CDFs) of K_ds used in PA were modified in the CRA-2009 PABC as a result of EPA comments (Clayton 2009). These values are also used in the CRA-2014. Any changes in sorption geochemistry in the Culebra within the controlled area as a result of HCN drilling-induced flow are accounted for in PA calculations.

Sorption within the Dewey Lake is accounted for in PA calculations, as discussed in the CCA, Chapter 6.0, Section 6.4.6.6. It is assumed that the sorptive capacity of the Dewey Lake is sufficiently large to prevent any radionuclides that enter the Dewey Lake from being released over 10,000 yrs (Wallace et al. 1995). Sorption within other geological units of the disposal system has been eliminated from PA calculations on the basis of beneficial consequence to the performance of the disposal system. The effects of changes in sorption in the Dewey Lake and other units within the controlled area as a result of HCN drilling-induced flow have been eliminated from PA calculations on the basis of low consequence to the performance of the disposal system.

SCR-5.2.1.4.3.3 Future Human EPs - Boreholes that Intersect the Waste Disposal Region

The consequences of drilling within the controlled area in the future will primarily depend on the location of the borehole. Future deep drilling could potentially penetrate the waste disposal region. If the borehole intersects the waste in the disposal rooms, radionuclides could be transported as a result of drilling fluid flow and geochemical conditions in the waste panel could be affected as a result of drilling induced geochemical changes.

SCR-5.2.1.4.3.4 Future Human EPs - Boreholes That Do Not Intersect the Waste Disposal Region

Future boreholes that do not intersect the waste disposal region could nevertheless encounter contaminated material by intersecting a region into which radionuclides have migrated from the disposal panels, or could affect hydrogeological conditions within the disposal system. Consistent with the containment requirements in section 191.13(a), PAs need not evaluate the effects of the intersection of contaminated material outside the controlled area.

Movement of brine from a pressurized reservoir in the Castile, through a borehole and into thief zones such as the Salado interbeds or the Culebra could result in drilling-induced geochemical changes and altered radionuclide migration rates in these units.

SCR-5.2.1.4.3.5 Geochemical Effects of Drilling-Induced Flow

Movement of brine from a pressurized reservoir in the Castile through a borehole into thief zones, such as the Salado interbeds or the Culebra, could cause geochemical changes resulting in altered radionuclide migration rates in these units through their effects on colloid transport and sorption.

The contents of the waste disposal panels provide the main source of colloids in the disposal system. Thus, consistent with the discussion in FEPs H21, H22, and H23 (Section SCR-5.2.1.1, Section SCR-5.2.1.2, and SCR-5.2.1.3), colloid transport as a result of drilling-induced flow associated with future boreholes that do not intersect the waste disposal region has been eliminated from PA calculations on the basis of low consequence to the performance of the disposal system.

As discussed in FEPs H21, H22, and H23 (Section SCR-5.2.1.1, Section SCR-5.2.1.2, and SCR-5.2.1.3), sorption within the Culebra is accounted for in PA calculations. The sorption model accounts for the effects of changes in sorption in the Culebra as a result of drilling-induced flow associated with boreholes that do not intersect the waste disposal region.

Consistent with the screening discussion in FEPs H21, H22, and H23 (Section SCR-5.2.1.1, Section SCR-5.2.1.2, and SCR-5.2.1.3), the effects of changes in sorption in the Dewey Lake within the controlled area as a result of drilling-induced flow associated with boreholes that do not intersect the waste disposal region have been eliminated from PA calculations on the basis of low consequence to the performance of the disposal system. Sorption within other geological units of the disposal system has been eliminated from PA calculations on the basis of beneficial consequence to the performance of the disposal system.

In summary, the effects of drilling-induced geochemical changes that occur within the controlled area as a result of HCN and future drilling-induced flow are accounted for in PA calculations. Those that occur outside the controlled area have been eliminated from PA calculations.

SCR-5.2.1.5 FEP Numbers: H25 and H26 FEP Titles: Oil and Gas Extraction Groundwater Extraction

SCR-5.2.1.5.1 Screening Decision: SO-C (HCN) SO-R (Future)

HCN *Groundwater Extraction* and *Oil and Gas Extraction* outside the controlled area has been eliminated from PA calculations on the basis of low consequence to the performance of the disposal system. *Groundwater Extraction* and *Oil and Gas Extraction* through future boreholes has been eliminated from PA calculations on regulatory grounds.

SCR-5.2.1.5.2 Summary of New Information

No new information that affects the screening of this FEP has been identified since the CRA-2009.

SCR-5.2.1.5.2.1 Screening Argument

The extraction of fluid could alter fluid-flow patterns in the target horizons, or in overlying units as a result of a failed borehole casing. Also, the removal of confined fluid from oil- or gas-bearing units can cause compaction in some geologic settings, potentially resulting in subvertical fracturing and surface subsidence.

SCR-5.2.1.5.2.2 Historical, Current, and Near-Future Human EPs

As discussed in FEPs H25 through H36, water, oil, and gas production are the only activities involving fluid extraction through boreholes that have taken place or are currently taking place in the vicinity of the WIPP. These activities are expected to continue in the vicinity of the WIPP in the near future.

Groundwater extraction outside the controlled area from formations above the Salado could affect groundwater flow. The Dewey Lake contains a productive zone of saturation south of the WIPP site. Several wells operated by the J.C. Mills Ranch south of the WIPP produce water from the Dewey Lake to supply livestock (see the CCA, Chapter 2.0, Section 2.2.1.4.2.1). Water has also been extracted from the Culebra at the Engle Well approximately 9.66 km (6 mi) south of the controlled area to provide water for livestock. Additionally, a water well at the Sandia National Laboratories wellpad SNL-14 also provides livestock water for the Mills ranch. This well is approximately 3,000 ft (0.9 km) from the WIPP site boundary.

If contaminated water intersects a well while it is producing, then contaminants could be pumped to the surface. Consistent with the containment requirements in section 191.13(a), PAs need not evaluate radiation doses that might result from such an event. However, compliance assessments must include any such events in dose calculations for evaluating compliance with the individual protection requirements in section 191.15. For undisturbed conditions, there are no radionuclide releases to units above the Salado, and therefore no releases to the accessible environment or producing water wells in the area (Appendix IGP-2014 and Section 53).

Pumping from wells at the J.C. Mills Ranch may have resulted in reductions in hydraulic head in the Dewey Lake within southern regions of the controlled area, leading to increased hydraulic head gradients. However, these changes in the groundwater flow conditions in the Dewey Lake will have no significant effects on the performance of the disposal system, primarily because of the sorptive

capacity of the Dewey Lake (see the CCA, Chapter 6.0, Section 6.4.6.6). Retardation of any radionuclides that enter the Dewey Lake will be such that no radionuclides will migrate through the Dewey Lake to the accessible environment within the 10,000-yr regulatory period.

The effects of groundwater extraction from the Culebra from a well 9.66 km (6 mi) south of the controlled area have been evaluated by Wallace (Wallace 1996b), using an analytical solution for Darcian fluid flow in a continuous porous medium. Wallace (Wallace 1996b) showed that such a well pumping at about 1.9 liters (L) (0.5 gallon [gal]) per minute for 10,000 yrs will induce a hydraulic head gradient across the controlled area of about 4×10^{-5}. The hydraulic head gradient across the controlled area currently ranges from between 0.001 to 0.007. Therefore, pumping from the Engle Well will have only minor effects on the hydraulic head gradient within the controlled area even if pumping were to continue for 10,000 yrs. Thus, the effects of HCN groundwater extraction outside the controlled area have been eliminated from PA calculations on the basis of low consequence to the performance of the disposal system.

Oil and gas extraction outside the controlled area could affect the hydrology of the disposal system. However, the horizons that act as oil and gas reservoirs are sufficiently below the repository for changes in fluid-flow patterns to be of low consequence, unless there is fluid leakage through a failed borehole casing. Also, oil and gas extraction horizons in the Delaware Basin are well-lithified rigid strata, so oil and gas extraction is not likely to result in compaction and subsidence (Brausch et al. 1982, pp. 52, 61). Furthermore, the plasticity of the salt formations in the Delaware Basin will limit the extent of any fracturing caused by compaction of underlying units. Thus, neither the extraction of gas from reservoirs in the Morrow Formation (some 4,200 m (14,000 ft) below the surface), nor extraction of oil from the shallower units within the Delaware Mountain Group (about 1,250 to 2,450 m (about 4,000 to 8,000 ft) below the surface) will lead to compaction and subsidence. In summary, historical, current, and near-future oil and gas extraction outside the controlled area has been eliminated from PA calculations on the basis of low consequence to the performance of the disposal system.

SCR-5.2.1.5.2.3 Future Human EPs

Consistent with section 194.33(d), PAs need not analyze the effects of techniques used for resource recovery subsequent to the drilling of a future borehole. Therefore, groundwater extraction and oil and gas extraction through future boreholes have been eliminated from PA calculations on regulatory grounds.

SCR-5.2.1.6 FEP Numbers: H27, H28, and H29 FEP Titles: Liquid Waste Disposal - OB (H27) Enhanced Oil and Gas Production - OB (H28) Hydrocarbon Storage - OB (H29)

SCR-5.2.1.6.1 Screening Decision: SO-C (HCN) SO-C (Future)

The hydrological effects of HCN fluid injection (*Liquid Waste Disposal*, *Enhanced Oil and Gas Production*, and *Hydrocarbon Storage*) through boreholes outside the controlled area have been eliminated from PA calculations on the basis of low consequence to the performance of the disposal system. *Liquid Waste Disposal*, *Enhanced Oil and Gas Production*, and *Hydrocarbon Storage* in the future have been eliminated from PA calculations based on low consequence.

SCR-5.2.1.6.2 Summary of New Information

No new information that affects the screening of this FEP has been identified since the CRA-2009.

SCR-5.2.1.6.3 Screening Argument

The injection of fluids could alter fluid-flow patterns in the target horizons or, if there is accidental leakage through a borehole casing, in any other intersected hydraulically conductive zone. Injection of fluids through a leaking borehole could also result in geochemical changes and altered radionuclide migration rates in the thief units.

SCR-5.2.1.6.3.1 Historical, Current, and Near-Future Human EPs

The only historical and current activities involving fluid injection through boreholes in the Delaware Basin areenhanced oil and gas production (waterflooding or carbon dioxide (CO_2) injection), hydrocarbon storage (gas reinjection), and liquid waste disposal (byproducts from oil and gas production). These fluid injection activities are expected to continue in the vicinity of the WIPP in the near future.

Hydraulic fracturing of oil- or gas-bearing units is currently used to improve the performance of hydrocarbon reservoirs in the Delaware Basin. Fracturing is induced during a short period of high-pressure fluid injection, resulting in increased hydraulic conductivity near the borehole. Normally, this controlled fracturing is confined to the pay zone and is unlikely to affect overlying strata.

Secondary production techniques, such as waterflooding, that are used to maintain reservoir pressure and displace oil are currently employed in hydrocarbon reservoirs in the Delaware Basin (Brausch et al. 1982, pp. 29-30). Tertiary recovery techniques, such as CO_2 miscible flooding, have been implemented with limited success in the Delaware Basin, but CO_2 miscible flooding is not an attractive recovery method for reservoirs near the WIPP (Melzer 2013). Even if CO_2 flooding were to occur, the effects, if any, would be very similar to those associated with waterflooding.

Reinjection of gas for storage currently takes place at one location in the Delaware Basin in a depleted gas field in the Morrow Formation at the Washington Ranch near Carlsbad Caverns (Burton et al. 1993, pp. 66-67; Appendix DATA-2004, Attachment A). This field is too far from the WIPP site to have any effect on WIPP groundwaters under any circumstances. Disposal of liquid by-products from oil and gas production involves injection of fluid into depleted reservoirs. Such fluid injection techniques result in repressurization of the depleted target reservoir and mitigates any effects of fluid withdrawal.

The most significant effects of fluid injection would arise from substantial and uncontrolled fluid leakage through a failed borehole casing. The highly saline environment of some units can promote rapid corrosion of well casings and may result in fluid loss from boreholes.

SCR-5.2.1.6.3.2 Hydraulic Effects of Leakage through Injection Boreholes

The Vacuum Field (located in the Capitan Reef, some 30 km [20 mi] northeast of the WIPP site) and the Rhodes-Yates Field (located in the back reef of the Capitan, some 70 km (45 mi) southeast of the WIPP site) have been waterflooded for 40 yrs with confirmed leaking wells, which have resulted in brine entering the Salado and other formations above the Salado (see, for example, Silva 1994, pp. 67-68). Currently, saltwater disposal takes place in the vicinity of the WIPP into formations below the Castile. However, leakages from saltwater disposal wells or waterflood wells in the near future in the vicinity of the WIPP are unlikely to occur because of the following:

- There are significant differences between the geology and lithology in the vicinity of the disposal system and that of the Vacuum and Rhodes-Yates Fields. The WIPP is located in the Delaware Basin in a fore-reef environment, where a thick zone of anhydrite and halite (the Castile) exists. In the vicinity of the WIPP, oil is produced from the Brushy Canyon Formation at depths greater than 2,100 m (7,000 ft). By contrast, the Castile is not present at either the Vacuum or the Rhodes-Yates Field, which lie outside the Delaware Basin. Oil production at the Vacuum Field is from the San Andres and Grayburg Formations at depths of approximately 1,400 m (4,500 ft), and oil production at the Rhodes-Yates Field is from the Yates and Seven Rivers Formations at depths of approximately 900 m (3,000 ft). Waterflooding at the Rhodes-Yates Field involves injection into a zone only 60 m (200 ft) below the Salado. There are more potential thief zones below the Salado near the WIPP than at the Rhodes-Yates or Vacuum Fields; the Salado in the vicinity of the WIPP is therefore less likely to receive any fluid that leaks from an injection borehole. Additionally, the oil pools in the vicinity of the WIPP are characterized by channel sands with thin net pay zones, low permeabilities, high irreducible water saturations, and high residual oil saturations. Therefore, waterflooding of oil fields in the vicinity of the WIPP on the scale of that undertaken in the Vacuum or the Rhodes-Yates Field is unlikely.

- New Mexico state regulations require the emplacement of a salt isolation casing string for all wells drilled in the potash enclave, which includes the WIPP area, to reduce the possibility of petroleum wells leaking into the Salado. Also, injection pressures are not allowed to exceed the pressure at which the rocks fracture. The injection pressure gradient must be kept below 4.5×10^3 pascals per meter above hydrostatic if fracture pressures are unknown. Such controls on fluid injection pressures limit the potential magnitude of any leakages from injection boreholes.

- Recent improvements in well completion practices and reservoir operations management have reduced the occurrences of leakages from injection wells. For example, injection pressures during waterflooding are typically kept below about 23×10^3 pascals per meter to avoid fracture initiation. Also, wells are currently completed using cemented and perforated casing, rather than the open-hole completions used in the early Rhodes-Yates wells.

Any injection well leakages that do occur in the vicinity of the WIPP in the near future are more likely to be associated with liquid waste disposal than waterflooding. Disposal typically involves fluid injection though old and potentially corroded well casings and does not include monitoring to the same extent as waterflooding. Such fluid injection could affect the performance of the disposal system if sufficient fluid leaked into the Salado interbeds to affect the rate of brine flow into the waste disposal panels.

Stoelzel and O'Brien (Stoelzel and O'Brien 1996) evaluated the potential effects on the disposal system of leakage from a hypothetical salt water disposal borehole near the WIPP. Stoelzel and O'Brien (Stoelzel and O'Brien 1996) used the two-dimensional BRAGFLO model (vertical north-south cross-section) to simulate saltwater disposal to the north and to the south of the disposal system. The disposal system model included the waste disposal region, the marker beds (MBs) and anhydrite intervals near the excavation horizon, and the rock strata associated with local oil and gas developments. A worst-case simulation was run using high values of borehole and anhydrite permeability and a low value of halite permeability to encourage flow to the disposal panels via the anhydrite. The boreholes were assumed to be plugged immediately above the Salado (consistent with the plugging configurations described in the CCA, Chapter 6.0, Section 6.4.7.2). Saltwater disposal

into the Upper Bell Canyon was simulated, with annular leakage through the Salado. A total of approximately 7×10^5 m^3 (2.47×10^7 ft^3) of brine was injected through the boreholes during a 50-yr simulated disposal period. In this time, approximately 50 m^3 (1,765.5 ft^3) of brine entered the anhydrite interval at the horizon of the waste disposal region. For the next 200 yrs, the boreholes were assumed to be abandoned (with open-hole permeabilities of 1×10^{-9} square meters (m^2) (4×10^{-8} $in.^2$)). Cement plugs (of permeability 1×10^{-17} m^2 (4×10^{-16} $in.^2$)) were assumed to be placed at the injection interval and at the top of the Salado. Subsequently, the boreholes were prescribed the permeability of silty sand (see the CCA, Chapter 6.0, Section 6.4.7.2), and the simulation was continued until the end of the 10,000-yr regulatory period. During this period, approximately 400 m^3 (14,124 ft^3) of brine entered the waste disposal region from the anhydrite interval. This value of cumulative brine inflow is within the bounds of the values generated by PA calculations for the UP scenario. During the disposal well simulation, leakage from the injection boreholes would have had no significant effect on the inflow rate at the waste panels.

Stoelzel and Swift (Stoelzel and Swift 1997) expanded on Stoelzel and O'Brien's (Stoelzel and O'Brien 1996) work by considering injection for a longer period of time (up to 150 yrs) and into deeper horizons at higher pressures. They developed two computational models (a modified cross-sectional model and an axisymmetric radial model) that are alternatives to the cross-sectional model used by Stoelzel and O'Brien (Stoelzel and O'Brien 1996). Rather than repeat the conservative and bounding approach used by Stoelzel and O'Brien (Stoelzel and O'Brien 1996), Stoelzel and Swift (Stoelzel and Swift 1997) focused on reasonable and realistic conditions for most aspects of the modeling, including setting parameters that were sampled in the CCA at their median values. Model results indicate that, for the cases considered, the largest volume of brine entering MB 139 (the primary pathway to the WIPP) from the borehole is approximately 1,500 m^3 (52,974 ft^3), which is a small enough volume that it would not affect Stoelzel and O'Brien's (Stoelzel and O'Brien 1996) conclusion even if it somehow all reached the WIPP. Other cases showed from 0 to 600 m^3 (21,190 ft^3) of brine entering MB 139 from the injection well. In all cases, high-permeability fractures created in the Castile and Salado anhydrite layers by the modeled injection pressures were restricted to less than 400 m (1,312 ft) from the wellbore, and did not extend more than 250 m in MB 138 and MB 139.

No flow entered MB 139, nor was fracturing of the unit calculated to occur away from the borehole, in cases in which leaks in the cement sheath had permeabilities of $10^{-12.5}$ m^2 (corresponding to the median value used to characterize fully degraded boreholes in the CCA) or lower. The cases modeled in which flow entered MB 139 from the borehole and fracturing occurred away from the borehole required injection pressures conservatively higher than any currently in use near the WIPP and either 150 yrs of leakage through a fully degraded cement sheath or 10 yrs of simultaneous tubing and casing leaks from a waterflood operation. These conditions are not likely to occur in the future. If leaks like these do occur from brine injection near the WIPP, however, results of the Stoelzel and Swift (Stoelzel and Swift 1997) modeling study indicate that they will not affect the performance of the repository.

Thus, the hydraulic effects of leakage through HCN boreholes outside the controlled area have been eliminated from PA calculations on the basis of low consequence to the performance of the disposal system.

SCR-5.2.1.6.3.3 Effects of Density Changes Resulting from Leakage Through Injection Boreholes

Leakage through a failed borehole casing during a fluid injection operation in the vicinity of the WIPP could alter fluid density in the affected unit, which could result in changes in fluid flow rates and directions within the disposal system. Disposal of oil and gas production byproducts through boreholes could increase fluid densities in transmissive units affected by leakage in the casing. Operations such as waterflooding use fluids derived from the target reservoir, or fluids with a similar composition, to avoid scaling and other reactions. Therefore, the effects of leakage from waterflood boreholes would be similar to leakage from disposal wells.

Denser fluids have a tendency to sink relative to less dense fluids, and, if the hydrogeological unit concerned has a dip, there will be a tendency for the dense fluid to travel in the downdip direction. If this direction is the same as the direction of the groundwater pressure gradient, there would be an increase in flow velocity, and conversely, if the downdip direction is opposed to the direction of the groundwater pressure gradient, there would be a decrease in flow velocity. In general terms, taking account of density-related flow will cause a rotation of the flow vector towards the downdip direction that is dependent on the density contrast and the dip.

Wilmot and Galson (Wilmot and Galson 1996) showed that brine density changes in the Culebra resulting from leakage through an injection borehole outside the controlled area will not affect fluid flow in the Culebra significantly. Potash mining activities assumed on the basis of regulatory criteria to occur in the near future outside the controlled area will have a more significant effect on modeled Culebra hydrology. The distribution of existing leases suggests that near-future mining will take place to the north, west, and south of the controlled area (see the CCA, Chapter 2.0, Section 2.3.1.1). The effects of such potash mining are accounted for in calculations of UP of the disposal system (through an increase in the transmissivity of the Culebra above the mined region, as discussed in FEPs H37, H38, and H39 [Section SCR-5.2.2.1, Section SCR-5.2.2.2, and Section SCR-5.2.3.1]). Groundwater modeling that accounts for potash mining shows a change in the fluid pressure distribution and a consequent shift of flow directions towards the west in the Culebra within the controlled area (Wallace 1996c). A localized increase in fluid density in the Culebra resulting from leakage from an injection borehole would rotate the flow vector towards the downdip direction (towards the east).

Wilmot and Galson (Wilmot and Galson 1996) compared the relative magnitudes of the freshwater head gradient and the gravitational gradient and showed that the density effect is of low consequence to the performance of the disposal system. According to Darcy's Law, flow in an isotropic porous medium is governed by the gradient of fluid pressure and a gravitational term

$$\bar{v} = -\frac{k}{\mu}\left[\nabla p - \rho \bar{g}\right] \quad \text{(SCR.7)}$$

where

v = Darcy velocity vector (m s^{-1})

k = intrinsic permeability (m^2)

μ = fluid viscosity (Pa s)

∇p = gradient of fluid pressure (Pa m^{-1})

ρ = fluid density (kg m^{-3})

g = gravitational acceleration vector (m s^{-2})

The relationship between the gravity-driven flow component and the pressure-driven component can be shown by expressing the velocity vector in terms of a freshwater head gradient and a density-related elevation gradient

$$\bar{v} = -K\left[\nabla H_f + \frac{\Delta\rho}{\rho_f}\nabla E\right] \quad \text{(SCR.8)}$$

where

K = hydraulic conductivity (m s^{-1})

∇H_f = gradient of freshwater head

$\Delta\rho$ = difference between actual fluid density and reference fluid density (kg m^{-3})

ρ_f = density of freshwater (kg m^{-3})

∇E = gradient of elevation

Davies (Davies 1989, p. 28) defined a driving force ratio (DFR) to assess the potential significance of the density gradient

$$DFR = \frac{\Delta\rho\left|\nabla E\right|}{\rho_f\left|\nabla H_f\right|} \quad \text{(SCR.9)}$$

and concluded that a DFR of 0.5 can be considered an approximate threshold at which density-related gravity effects may become significant (Davies 1989, p. 28).

The dip of the Culebra in the vicinity of the WIPP is about 0.44 degrees or 8 m/km (26 ft/mi) to the east (Davies 1989, p. 42). According to Davies (Davies 1989, pp. 47-48), freshwater head gradients in the Culebra between the waste panels and the southwestern and western boundaries of the accessible environment range from 4 m/km (13 ft/mi) to 7 m/km (23 ft/mi). Only small changes in gradient arise from the calculated effects of near-future mining. Culebra brines have densities ranging from 998 to 1,158 kilograms per cubic meter (kg/m^3) (998 to 1,158 parts per million [ppm]) (Cauffman et al. 1990, Table E1.b). Assuming the density of fluid leaking from a waterflood borehole or a disposal well to be 1,215 kg/m^3 (1,215 ppm) (a conservative high value similar to the density of Castile brine [Popielak et al. 1983, Table C-2]) leads to a DFR of between 0.07 and 0.43. These values of the DFR show that density-related effects caused by leakage of brine into the Culebra during fluid injection operations are not significant.

In summary, the effects of HCN fluid injection (liquid waste disposal, enhanced oil and gas production, and hydrocarbon storage) through boreholes outside the controlled area have been eliminated from PA calculations on the basis of low consequence to the performance of the disposal system.

SCR-5.2.1.6.3.4 Geochemical Effects of Leakage through Injection Boreholes

Injection of fluids through a leaking borehole could affect the geochemical conditions in thief zones, such as the Salado interbeds or the Culebra. Such fluid injection-induced geochemical changes could alter radionuclide migration rates within the disposal system in the affected units if they occur sufficiently close to the edge of the controlled area through their effects on colloid transport and sorption.

The majority of fluids injected (for example, during brine disposal) have been extracted locally during production activities. Because they have been derived locally, their compositions are similar to fluids currently present in the disposal system, and they will have low total colloid concentrations compared to those in the waste disposal panels (see FEPs discussion for H21 through H24, Section SCR-5.2.1.1 , Section SCR-5.2.1.2, Section SCR-5.2.1.3, and SCR-5.2.1.4). The repository will remain the main source of colloids in the disposal system. Therefore, colloid transport as a result of HCN fluid injection has been eliminated from PA calculations on the basis of low consequence to the performance of the disposal system.

As discussed in FEPs H21 through H24 (Section SCR-5.2.1.1, Section SCR-5.2.1.2, Section SCR-5.2.1.3, and SCR-5.2.1.4), sorption within the Culebra is accounted for in PA calculations. The sorption model used accounts for the effects of any changes in sorption in the Culebra as a result of leakage through HCN injection boreholes.

Consistent with the screening discussion in FEPs H21 through H24, the effects of changes in sorption in the Dewey Lake within the controlled area as a result of leakage through HCN injection boreholes have been eliminated from PA calculations on the basis of low consequence to the performance of the disposal system. Sorption within other geological units of the disposal system has been eliminated from PA calculations on the basis of beneficial consequence to the performance of the disposal system.

Non-locally derived fluids could be used during hydraulic fracturing operations. However, such fluid-injection operations would be carefully controlled to minimize leakage to thief zones. Therefore, any potential geochemical effects of such leakages have been eliminated from PA calculations on the basis of low consequence to the performance of the disposal system.

SCR-5.2.1.6.3.5 Future Human EPs

Consistent with section 194.33(d), PAs need not analyze the effects of techniques used for resource recovery subsequent to the drilling of a future borehole within the site boundary. Liquid waste disposal (byproducts from oil and gas production), enhanced oil and gas production, and hydrocarbon storage are techniques associated with resource recovery and are expected to continue into the future outside the site boundary. Analyses have shown that these activities have little consequence on repository performance (Stoelzel and Swift 1997). Therefore, activities such as liquid waste disposal, enhanced oil and gas production, and hydrocarbon storage outside the site boundary have been eliminated from PA calculations on the basis of low consequence.

SCR-5.2.1.7 FEP Numbers: H60, H61, and H62 FEP Titles: Liquid Waste Disposal - IB (H60) Enhanced Oil and Gas Production - IB (H61) Hydrocarbon Storage - IB (H62)

SCR-5.2.1.7.1 Screening Decision: SO-R (HCN) SO-R (Future)

The hydrological effects of HCN fluid injection (*Liquid Waste Disposal*, *Enhanced Oil and Gas Production*, and *Hydrocarbon Storage*) through boreholes inside the controlled area have been eliminated from PA calculations on regulatory grounds (section 194.25(a)). *Liquid Waste Disposal*, *Enhanced Oil and Gas Production*, and *Hydrocarbon Storage* (within the controlled area) in the future have been eliminated from PA calculations on regulatory grounds (section 194.33(d)).

SCR-5.2.1.7.2 Summary of New Information

No new information that affects the screening of this FEP has been identified since the CRA-2009.

SCR-5.2.1.7.3 Screening Argument

The injection of fluids in a borehole within the WIPP boundary could alter fluid-flow patterns in the target horizons or, if there is accidental leakage through a borehole casing, in any other intersected hydraulically conductive zone. Injection of fluids through a leaking borehole within the WIPP boundary could also result in geochemical changes and altered radionuclide migration rates in the thief units.

SCR-5.2.1.7.3.1 Historical, Current, and Near-Future Human EPs

Injection of fluids for the purposes of liquid disposal, enhanced oil and gas production, or hydrocarbon storage has not occurred within the WIPP boundary. Therefore, based on the future states assumption provided by section 194.25(a), it is assumed that such activities will not occur within the near-future time frame, which includes the period of WIPP AICs. These activities are excluded from PA calculations on regulatory grounds.

SCR-5.2.1.7.3.2 Future Human EPs

The provisions of section 194.33(d) state, "that performance assessments need not analyze the effects of techniques used for resource recovery subsequent to the drilling of the borehole." Therefore, the future injection of fluids for the purposes of liquid disposal, enhanced oil and gas production, and hydrocarbon storage within the WIPP boundary have been excluded from PA calculations on regulatory grounds.

SCR-5.2.1.8 FEP Number: H30 FEP Title: Fluid Injection-Induced Geochemical Changes

SCR-5.2.1.8.1 Screening Decision: UP (HCN) SO-R (Future)

Geochemical changes that occur inside the controlled area as a result of fluid flow associated with HCN fluid injection are accounted for in PA calculations. Geochemical changes resulting from fluid injection in the future inside the controlled area have been eliminated from PA calculations on regulatory grounds.

SCR-5.2.1.8.2 Summary of New Information

No new information that affects the screening of this FEP has been identified since the CRA-2009.

SCR-5.2.1.8.3 Screening Argument

The injection of fluids could alter fluid-flow patterns in the target horizons or, if there is accidental leakage through a borehole casing, in any other intersected hydraulically conductive zone. Injection of fluids through a leaking borehole could also result in geochemical changes and altered radionuclide migration rates in the thief units.

SCR-5.2.1.8.3.1 Geochemical Effects of Leakage through Injection Boreholes

Injection of fluids through a leaking borehole could affect the geochemical conditions in thief zones, such as the Salado interbeds or the Culebra. Such fluid injection-induced geochemical changes could alter radionuclide migration rates within the disposal system in the affected units if they occur sufficiently close to the edge of the controlled area through their effects on colloid transport and sorption.

The majority of fluids injected (for example, during brine disposal) have been extracted locally during production activities. Because they have been derived locally, their compositions are similar to fluids currently present in the disposal system, and they will have low total colloid concentrations compared to those in the waste disposal panels (see FEPs H21 through H24, Section SCR-5.2.1.1 , Section SCR-5.2.1.2, Section SCR-5.2.1.3, and SCR-5.2.1.4). The repository will remain the main source of colloids in the disposal system. Therefore, colloid transport as a result of HCN fluid injection has been eliminated from PA calculations on the basis of low consequence to the performance of the disposal system.

As discussed in FEPs H21 through H24 (Section SCR-5.2.1.1, Section SCR-5.2.1.2, Section SCR-5.2.1.3, and SCR-5.2.1.4), sorption within the Culebra is accounted for in PA calculations. The sorption model used accounts for the effects of any changes in sorption in the Culebra as a result of leakage through HCN injection boreholes.

Consistent with the screening discussion in FEPs H21 through H24, the effects of changes in sorption in the Dewey Lake within the controlled area as a result of leakage through HCN injection boreholes have been eliminated from PA calculations on the basis of low consequence to the performance of the disposal system. Sorption within other geological units of the disposal system has been eliminated from PA calculations on the basis of beneficial consequence to the performance of the disposal system.

Non-locally derived fluids could be used during hydraulic fracturing operations. However, such fluid injection operations would be carefully controlled to minimize leakage to thief zones. Therefore, any potential geochemical effects of such leakages have been eliminated from PA calculations on the basis of low consequence to the performance of the disposal system.

SCR-5.2.1.8.3.2 Future Human EPs

Consistent with section 194.33(d), PAs need not analyze the effects of techniques used for resource recovery subsequent to the drilling of a future borehole. Liquid waste disposal (byproducts from oil and gas production), enhanced oil and gas production, and hydrocarbon storage are techniques associated with resource recovery. Therefore, the use of future boreholes for such activities and fluid injection-induced geochemical changes have been eliminated from PA calculations on regulatory grounds.

SCR-5.2.1.9 FEP Number: H31 FEP Title: Natural Borehole Fluid Flow (H31)

SCR-5.2.1.9.1 Screening Decision: SO-C (HCN) SO-C (Future, holes not penetrating waste panels) DP (Future, holes through waste panels)

The effects of *Natural Borehole Fluid Flow* through existing or near-future abandoned boreholes, known or unknown, have been eliminated from PA calculations on the basis of low consequence to the performance of the disposal system. *Natural Borehole Fluid Flow* through a future borehole that intersects a waste panel is accounted for in PA calculations. The effects of *Natural Borehole Fluid Flow* through a future borehole that does not intersect the waste-disposal region have been eliminated from PA calculations on the basis of low consequence to the performance of the disposal system.

SCR-5.2.1.9.2 Summary of New Information

Probabilities for the various borehole types used in PA have been updated based on information gathered by the Delaware Basin Monitoring Program. These updated probabilities do not impact or change the screening arguments or decisions, but are incorporated into PA in an effort to reflect current technologies and methods used in industry. These PA parameters are described in Camphouse (Camphouse 2013a).

SCR-5.2.1.9.3 Screening Argument

Abandoned boreholes could provide pathways for fluid flow and, potentially, contaminant transport between any intersected zones. For example, such boreholes could provide pathways for vertical flow between transmissive units in the Rustler, or between the Culebra and units below the Salado, which could affect fluid densities, flow rates, and flow directions.

Movement of fluids through abandoned boreholes could result in borehole-induced geochemical changes in the receiving units such as the Salado interbeds or Culebra, and thus alter radionuclide migration rates in these units.

Potentially, boreholes could provide pathways for surface-derived water or groundwater to percolate through low-permeability strata and into formations containing soluble minerals. Large-scale dissolution through this mechanism could lead to subsidence and to changes in groundwater flow patterns. Also, fluid flow between hydraulically conductive horizons through a borehole may result in changes in permeability in the affected units through mineral precipitation.

SCR-5.2.1.9.3.1 Historical, Current, and Near-Future Human EPs

Abandoned water, potash, oil, and gas exploration and production boreholes exist within and outside the controlled area. Most of these boreholes have been plugged in some way, but some have simply been abandoned. Over time, even the boreholes that have been plugged may provide hydraulic connections among the units they penetrate as the plugs degrade. The DOE assumes that records of past and present drilling activities in New Mexico are largely accurate and that evidence of most boreholes would be included in these records. However, the potential effects of boreholes do not change depending on whether their existence is known, hence flow through undetected boreholes and flow through detected boreholes can be evaluated together.

SCR-5.2.1.9.3.2 Hydraulic Effects of Flow through Abandoned Boreholes

Fluid flow and radionuclide transport within the Culebra could be affected if deep boreholes result in hydraulic connections between the Culebra and deep, overpressurized or underpressurized units, or if boreholes provide interconnections for flow between shallow units.

SCR-5.2.1.9.3.3 Connections Between the Culebra and Deeper Units

Fluid flow and radionuclide transport within the Culebra could be affected if deep boreholes result in hydraulic connections between the Culebra and deep, overpressurized or underpressurized units. Over the past 80 yrs, a large number of deep boreholes have been drilled within and around the controlled area (see the CCA, Chapter 6.0, Section 6.4.12.2). The effects on the performance of the disposal system of long-term hydraulic connections between the Culebra and deep units depends on the locations of the boreholes. In some cases, changes in the Culebra flow field caused by interconnections with deep units could decrease lateral radionuclide travel times to the accessible environment.

As part of an analysis to determine the impact of such interconnections, Wallace (Wallace 1996a) gathered information on the pressures, permeabilities, and thicknesses of potential oil- or gas-bearing sedimentary units; such units exist to a depth of about 5,500 m (18,044 ft) in the vicinity of the WIPP. Of these units, the Atoka, some 4,000 m (13,123 ft) below the land surface, has the highest documented pressure of about 64 megapascals (MPa) (9,600 pounds per square inch [psi]), with permeability of about 2×10^{-14} m^2 (2.1×10^{-13} square ft [ft^2]) and thickness of about 210 m (689 ft). The Strawn, 3,900 m (12,795 ft) below the land surface, has the lowest pressures (35 MPa [5,000 psi], which is lower than hydrostatic) and highest permeability (10^{-13} m^2 [1.1×10^{-12} ft^2]) of the deep units, with a thickness of about 90 m (295 ft).

PA calculations indicate that the shortest radionuclide travel times to the accessible environment through the Culebra occur when flow in the Culebra in the disposal system is from north to south. Wallace (Wallace 1996a) ran the steady-state SECOFL2D model with the PA data that generated the shortest radionuclide travel times (with and without mining in the controlled area) but perturbed the flow field by placing a borehole connecting the Atoka to the Culebra just north of the waste disposal panels and a borehole connecting the Culebra to the Strawn just south of the controlled area. The borehole locations were selected to coincide with the end points of the fastest flow paths modeled, which represents an unlikely worst-case condition. Although the Atoka is primarily a gas-bearing unit, Wallace (Wallace 1996a) assumed that the unit is brine saturated. This assumption is conservative because it prevents two-phase flow from occurring in the Culebra, which would decrease the water permeability and thereby increase transport times. It was conservatively assumed that the pressure in the Atoka would not have been depleted by production before the well was plugged and abandoned. Furthermore, it was conservatively assumed that all flow from the Atoka would enter the Culebra and not intermediate or shallower units, and that flow from the Culebra could somehow enter the Strawn despite intermediate zones having higher pressures than the Culebra. The fluid flux through each borehole was determined using Darcy's Law, assuming a borehole hydraulic conductivity of 10^{-4} m/s (for a permeability of about 10^{-11} m^2 [1.1×10^{-10} ft^2]) representing silty sand, a borehole radius of 0.25 m (.82 ft), and a fluid pressure in the Culebra of 0.88 MPa (132 psi) at a depth of about 200 m (650 ft). With these parameters, the Atoka was calculated to transmit water to the Culebra at about 1.4×10^{-5} m^3/s (0.22 gallons per minute [gpm]), and the Strawn was calculated to receive water from the Culebra at about 1.5×10^{-6} m^3/s (0.024 gpm).

Travel times through the Culebra to the accessible environment were calculated using the SECOFL2D velocity fields for particles released to the Culebra above the waste panels, assuming no retardation by sorption or diffusion into the rock matrix. Mean Darcy velocities were then determined from the distance each radionuclide traveled, the time taken to reach the accessible environment, and the effective Culebra porosity. The results show that, at worst, interconnections between the Culebra and deep units under the unrealistically conservative assumptions listed above could cause less than a twofold increase in the largest mean Darcy velocity expected in the Culebra in the absence of such interconnections.

These effects can be compared to the potential effects of climate change on gradients and flow velocities through the Culebra. As discussed in the CCA, Chapter 6.0, Section 6.4.9 and Corbet and Knupp (Corbet and Knupp 1996), the maximum effect of a future, wetter climate would be to raise the water table to the ground surface. This would raise heads and gradients in all units above the Salado. For the Culebra, the maximum change in gradient was estimated to be about a factor of 2.1. The effect of climate change is incorporated in compliance calculations through the Climate Index, which is used as a multiplier for Culebra groundwater velocities. The Climate Index has a bimodal distribution, with the range from 1.00 to 1.25 having a 75% probability, and the range from 1.50 to 2.25 having a 25% probability. Because implementation of the Climate Index leads to radionuclide releases through the Culebra that are orders of magnitude lower than the regulatory limits, the effects of flow between the Culebra and deeper units through abandoned boreholes can be screened out on the basis of low consequence.

SCR-5.2.1.9.3.4 Connections Between the Culebra and Shallower Units

Abandoned boreholes could also provide interconnections for long-term fluid flow between shallow units (overlying the Salado). Abandoned boreholes could provide pathways for downward flow of water from the Dewey Lake and/or Magenta to the Culebra because the Culebra hydraulic head is lower than the hydraulic heads of these units. Magenta freshwater heads are as much as 45 m (148 ft) higher than Culebra freshwater heads. Because the Culebra is generally at least one order of magnitude more transmissive than the Magenta at any location, a connection between the Magenta and Culebra would cause proportionally more drawdown in the Magenta head than rise in the Culebra head. For example, for a one-order-of-magnitude difference in transmissivity and a 45-m (148-ft) difference in head, the Magenta head would decrease by approximately 40 m (131 ft) while the Culebra head increased by 5 m (16 ft). This head increase in the Culebra would also be a localized effect, decreasing with radial distance from the leaking borehole. The primary flow direction in the Culebra across the WIPP site is from north to south, with the Culebra head decreasing by approximately 20 m (66 ft) across this distance. A 5-m (16-ft) increase in Culebra head at the northern WIPP boundary would, therefore, increase gradients by at most 25%.

The Dewey Lake freshwater head at the WQSP-6 pad is 55 m (180 ft) higher than the Culebra freshwater head. Leakage from the Dewey Lake could have a greater effect on Culebra head than leakage from the Magenta if the difference in transmissivity between the Dewey Lake and Culebra observed at the WQSP-6 pad, where the Dewey Lake is two orders of magnitude more transmissive than the Culebra (Beauheim and Ruskauff 1998), persists over a wide region. However, the saturated, highly transmissive zone in the Dewey Lake has only been observed south of the WIPP disposal panels. A connection between the Dewey Lake and the Culebra south of the panels would tend to decrease the north-south gradient in the Culebra across the site, not increase it.

In any case, leakage of water from overlying units into the Culebra could not increase Culebra heads and gradients as much as might result from climate change, discussed above. Because implementation

of the Climate Index leads to radionuclide releases through the Culebra that are orders of magnitude lower than the regulatory limits, the effects of flow between the Culebra and shallower units through abandoned boreholes can be screened out on the basis of low consequence.

SCR-5.2.1.9.3.5 Changes in Fluid Density Resulting from Flow Through Abandoned Boreholes

Leakage from historical, current, and near-future abandoned boreholes that penetrate pressurized brine pockets in the Castile could give rise to fluid density changes in affected units. Wilmot and Galson (Wilmot and Galson 1996) showed that brine density changes in the Culebra resulting from leakage through an abandoned borehole would not have a significant effect on the Culebra flow field. A localized increase in fluid density in the Culebra resulting from leakage from an abandoned borehole would rotate the flow vector towards the downdip direction (towards the east). A comparison of the relative magnitudes of the freshwater head gradient and the gravitational gradient, based on an analysis similar to that presented in Section SCR-5.2.1.6 (FEPs H27, H28, and H29), shows that the density effect is of low consequence to the performance of the disposal system.

SCR-5.2.1.9.3.6 Future Human EPs

The EPA provides criteria for analysis of the consequences of future drilling events in section 194.33 (c). Consistent with these criteria, the DOE assumes that after drilling is complete, the borehole is plugged according to current practice in the Delaware Basin (see the CCA, Chapter 6.0, Section 6.4.7.2, and Camphouse 2013a). Degradation of casing and/or plugs may result in connections for fluid flow and, potentially, contaminant transport between connected hydraulically conductive zones. The long-term consequences of boreholes drilled and abandoned in the future will primarily depend on the location of the borehole and the borehole casing and plugging methods used.

SCR-5.2.1.9.3.7 Hydraulic Effects of Flow Through Abandoned Boreholes

A future borehole that penetrates a Castile brine reservoir could provide a connection for brine flow from the reservoir to the waste panel, thus increasing fluid pressure and brine volume in the waste panel. Long-term natural borehole fluid flow through such a borehole is accounted for in PA calculations (see the CCA, Chapter 6.0, Section 6.4.8).

Deep, abandoned boreholes that intersect the Salado interbeds near the waste disposal panels could provide pathways for long-term radionuclide transport from the waste panels to the land surface or to overlying units. The potential significance of such events were assessed by the WIPP PA Department (1991, B-26 to B-27), which examined single-phase flow and transport between the waste panels and a borehole intersecting MB 139 outside the DRZ. The analysis assumed an in situ pressure of 11 MPa in MB 139, a borehole pressure of 6.5 MPa (975 psi) (hydrostatic) at MB 139, and a constant pressure of 18 MPa (2,700 psi) as a source term in the waste panels representing gas generation. Also, MB 139 was assigned a permeability of approximately 3×10^{-20} m^2 (3.2×10^{-19} ft^2) and a porosity of 0.01%. The disturbed zone was assumed to exist in MB 139 directly beneath the repository only and was assigned a permeability of 1.0×10^{-17} m^2 (1.1×10^{-16} ft^2) and a porosity of 0.055%. Results showed that the rate of flow through a borehole located just 0.25 m (0.8 ft) outside the DRZ would be more than two orders of magnitude less than the rate of flow through a borehole located within the DRZ because of the contrast in permeability. Thus, any releases of radionuclides to the accessible environment through deep boreholes that do not intersect waste panels would be insignificant compared to the releases that would result from transport through boreholes that intersect waste panels. Thus, radionuclide transport through deep boreholes that do not intersect waste panels has

been eliminated from PA calculations on the basis of low consequence to the performance of the disposal system.

SCR-5.2.1.9.3.8 Fluid Flow and Radionuclide Transport in the Culebra

Fluid flow and radionuclide transport within the Culebra could be affected if future boreholes result in hydraulic connections between the Culebra and either deeper or shallower units. Over the 10,000-yr regulatory period, a large number of deep boreholes could be drilled within and around the controlled area (see the CCA, Chapter 6.0, Section 6.4.12.2). The effects on the performance of the disposal system of long-term hydraulic connections between the Culebra and deeper or shallower units would be the same as those discussed above for historic, current, and near-future conditions. Thus, the effects of flow between the Culebra and deeper or shallower units through abandoned future boreholes can be screened out on the basis of low consequence.

SCR-5.2.1.9.3.9 Changes in Fluid Density Resulting from Flow Through Abandoned Boreholes

A future borehole that intersects a pressurized brine reservoir in the Castile could also provide a source for brine flow to the Culebra in the event of borehole casing leakage, with a consequent localized increase in fluid density in the Culebra. The effect of such a change in fluid density would be to increase any density-driven component of groundwater flow. If the downdip direction, along which the density-driven component would be directed, is different from the direction of the groundwater pressure gradient, there would be a slight rotation of the flow vector towards the downdip direction. The groundwater modeling presented by Davies (Davies 1989, p. 50) indicates that a borehole that intersects a pressurized brine pocket and causes a localized increase in fluid density in the Culebra above the waste panels would result in a rotation of the flow vector slightly towards the east. However, the magnitude of this effect would be small in comparison to the magnitude of the pressure gradient (see screening argument for FEPs H27, H28, and H29, Section SCR-5.2.1.6 , where this effect is screened out on the basis of low consequence).

SCR-5.2.1.10 FEP Number: H32 FEP Title: Waste-Induced Borehole Flow

SCR-5.2.1.10.1 Screening Decision: SO-R (HCN) DP (Future)

Waste-induced flow through boreholes drilled in the near future has been eliminated from PA calculations on regulatory grounds. *Waste-Induced Borehole Flow* through a future borehole that intersects a waste panel is accounted for in PA calculations.

SCR-5.2.1.10.2 Summary of New Information

Probabilities for the various borehole types used in PA have been updated based on information gathered by the Delaware Basin Monitoring Program. These updated probabilities do not impact or change the screening arguments or decisions, but are incorporated into PA in an effort to reflect current technologies and methods used in industry. These PA parameters are described in Camphouse (Camphouse 2013a).

SCR-5.2.1.10.3 Screening Argument

Abandoned boreholes could provide pathways for fluid flow and, potentially, contaminant transport between any intersected zones. For example, such boreholes could provide pathways for vertical flow

between transmissive units in the Rustler, or between the Culebra and units below the Salado, which could affect fluid densities, flow rates, and flow directions.

Continued resource exploration and production in the near future will result in the occurrence of many more abandoned boreholes in the vicinity of the controlled area. Institutional controls will prevent drilling (other than that associated with the WIPP development) from taking place within the controlled area in the near future. Therefore, no boreholes will intersect the waste disposal region in the near future, and waste-induced borehole flow in the near future has been eliminated from PA calculations on regulatory grounds.

SCR-5.2.1.10.3.1 Future Human EPs

The EPA provides criteria concerning analysis of the consequences of future drilling events in section 194.33(c). Consistent with these criteria, the DOE assumes that after drilling is complete, the borehole is plugged according to current practice in the Delaware Basin (see the CCA, Chapter 6.0, Section 6.4.7.2 and Camphouse 2013a). Degradation of casing and/or plugs may result in connections for fluid flow and, potentially, contaminant transport between connected hydraulically conductive zones. The long-term consequences of boreholes drilled and abandoned in the future will primarily depend on the location of the borehole and the borehole casing and plugging methods used.

SCR-5.2.1.10.3.2 Hydraulic Effects of Flow Through Abandoned Boreholes

An abandoned future borehole that intersects a waste panel could provide a connection for contaminant transport away from the repository horizon. If the borehole has degraded casing and/or plugs, and the fluid pressure within the waste panel is sufficient, radionuclides could be transported to the land surface. Additionally, if brine flows through the borehole to overlying units, such as the Culebra, it may carry dissolved and colloidal actinides that can be transported laterally to the accessible environment by natural groundwater flow in the overlying units. Long-term waste-induced borehole flow is accounted for in PA calculations (see Appendix PA-2014, Section PA-2.1.2.5).

SCR-5.2.1.11 FEP Number: H34 FEP Title: Borehole-Induced Solution and Subsidence

SCR-5.2.1.11.1 Screening Decision: SO-C (HCN) SO-C (Future)

The effects of *Borehole-Induced Solution and Subsidence* associated with existing, near-future, and future abandoned boreholes have been eliminated from PA calculations on the basis of low consequence to the performance of the disposal system.

SCR-5.2.1.11.2 Summary of New Information

No new information that affects the screening of this FEP has been identified since the CRA-2009.

SCR-5.2.1.11.3 Screening Argument

Potentially, boreholes could provide pathways for surface-derived water or groundwater to percolate through low-permeability strata and into formations containing soluble minerals. Large-scale dissolution through this mechanism could lead to subsidence and to changes in groundwater flow patterns. Also, fluid flow between hydraulically conductive horizons through a borehole may result in changes in permeability in the affected units through mineral precipitation.

SCR-5.2.1.11.3.1 Historical, Current, and Near-Future Human EPs

SCR-5.2.1.11.3.1.1 Borehole-Induced Solution and Subsidence

During the period covered by HCN FEPs, drilling within the land withdrawn for the WIPP will be controlled, and boreholes will be plugged according to existing regulations. Under these circumstances and during this time period, borehole-induced solution and subsidence at the WIPP is eliminated from PA calculations on the basis of no consequence to the disposal system.

Outside the area withdrawn for the WIPP, drilling has been regulated, but conditions of historical and existing boreholes are highly variable. Borehole-induced solution and subsidence may occur in these areas, although it is expected to be limited and should not affect the disposal system, as discussed in the following paragraphs.

Three features are required for significant borehole-induced solution and subsidence to occur: a borehole, an energy gradient to drive unsaturated (with respect to halite) water through the evaporite-bearing formations, and a conduit to allow migration of brine away from the site of dissolution. Without these features, minor amounts of halite might be dissolved in the immediate vicinity of a borehole, but percolating water would become saturated with respect to halite and stagnant in the bottom of the drillhole, preventing further dissolution.

At, and in the vicinity of the WIPP site, drillholes penetrating into but not through the evaporite-bearing formations have little potential for dissolution. Brines coming from the Salado and Castile, for example, have high total dissolved solids and are likely to precipitate halite, not dissolve more halite during passage through the borehole. Water infiltrating from the surface or near-surface units may not be saturated with halite. For drillholes with a total depth in halite-bearing formations, there is little potential for dissolution because the halite-bearing units have very low permeability and provide little outlet for the brine created as the infiltrating water fills the drillhole. ERDA-9 is the deepest drillhole in the immediate vicinity of the waste panels at the WIPP; the bottom of the drillhole is in the uppermost Castile, with no known outlet for brine at the bottom.

Drillholes penetrating through the evaporite-bearing formations provide possible pathways for circulation of water. Underlying units in the vicinity of the WIPP site with sufficient potentiometric levels or pressures to reach or move upward through the halite units generally have one of two characteristics: (1) high-salinity brines, which limit or eliminate the potential for dissolution of evaporites, or (2) are gas producers. Wood et al. (Wood et al. 1982) analyzed natural processes of dissolution of the evaporites by water from the underlying Bell Canyon. They concluded that brine removal in the Bell Canyon is slow, limiting the movement of dissolution fronts or the creation of natural collapse features. Existing drillholes that are within the boundaries of the withdrawn land and also penetrate through the evaporites are not located in the immediate vicinity of the waste panels or WIPP workings.

There are three examples in the region that appear to demonstrate the process for borehole-induced solution and subsidence, but the geohydrologic setting and drillhole completions differ from those at or near the WIPP.

An example of borehole-induced solution and subsidence occurred in 1980 about 160 km (100 mi) southeast of the WIPP site (outside the Delaware Basin) at the Wink Sink (Baumgardner et al. 1982; Johnson 1989), where percolation of shallow groundwater through abandoned boreholes, dissolution of the Salado, and subsidence of overlying units led to a surface collapse feature 110 m (360 ft) in

width and 34 m (110 ft) deep. At the Wink Sink, the Salado is underlain by the Tansill, Yates, and Capitan Formations, which contain vugs and solution cavities through which brine could migrate. Also, the hydraulic head of the Santa Rosa (the uppermost aquifer) is greater than those of the deep aquifers (Tansill, Yates, and Capitan), suggesting downward flow if a connection were established. A second sink (Wink Sink 2) formed in May 2002, near the earlier sink (Johnson et al. 2003). Its origin is similar to the earlier sink. By February 2003, Wink Sink 2 had enlarged by surface collapse to a length of about 305 m (1,000 ft) and a width of about 198 m (650 ft).

A similar, though smaller, surface collapse occurred in 1998 northwest of Jal, New Mexico (Powers 2000). The most likely cause of collapse appears to be dissolution of Rustler, and possibly Salado, halite as relatively low salinity water from the Capitan Reef circulated through breaks in the casing of a deep water supply well. Much of the annulus behind the casing through the evaporite section was uncemented, and work in the well at one time indicated bent and ruptured casing. The surface collapse occurred quickly, and the sink was initially about 23 m (75 ft) across and a little more than 30 m (100 ft) deep. By 2001, the surface diameter was about 37 m (120 ft), and the sink was filled with collapse debris to about 18 m (60 ft) below the ground level (Powers, in press).

The sinkholes near Wink, Texas and Jal, New Mexico, occurred above the Capitan Reef (which is by definition outside the Delaware Basin), and the low-salinity water and relatively high potentiometric levels of the Capitan Reef appear to be integral parts of the process that formed these sinkholes. They are reviewed as examples of the process of evaporite dissolution and subsidence related to circulation in drillholes. Nevertheless, the factors of significant low salinity water and high potentiometric levels in units below the evaporites do not appear to apply at the WIPP site.

Beauheim (Beauheim 1986) considered the direction of natural fluid flow through boreholes in the vicinity of the WIPP. Beauheim (Beauheim 1986, p. 72) examined hydraulic heads measured using drill stem tests in the Bell Canyon and the Culebra at well DOE-2 and concluded that the direction of flow in a cased borehole open only to the Bell Canyon and the Culebra would be upward. Bell Canyon waters in the vicinity of the WIPP site are saline brines (e.g., Lambert 1978; Beauheim et al. 1983; Mercer et al. 1987), limiting the potential for dissolution of the overlying evaporites. However, dissolution of halite in the Castile and the Salado would increase the relative density of the fluid in an open borehole, causing a reduction in the rate of upward flow. The direction of borehole fluid flow could potentially reverse, but such a flow could be sustained only if sufficient driving pressure, porosity, and permeability exist for fluid to flow laterally within the Bell Canyon. A further potential sink for Salado-derived brine is the Capitan Limestone. However, the subsurface extent of the Capitan Reef is approximately 16 km (10 mi) from the WIPP at its closest point, and this unit will not provide a sink for brine derived from boreholes in the vicinity of the controlled area. A similar screening argument is made for natural deep dissolution in the vicinity of the WIPP (see N16 and N18, Section SCR-4.1.5.1 and Section SCR-4.1.5.2).

The effects of borehole-induced solution and subsidence through a waste panel are considered below. The principal effects of borehole-induced solution and subsidence in the remaining parts of the disposal system should be to change the hydraulic properties of the Culebra and other rocks in the system. The features are local (limited lateral dimensions) and commonly nearly circular. If subsidence occurs along the expected travel path and the transmissivity of the Culebra is increased, as in the calculations conducted by Wallace (Wallace 1996c), the travel times should increase. If the transmissivity along the expected flow path decreased locally as a result of such a feature, the flow path should be lengthened by travel around the feature. Thus, the effects of borehole-induced solution and subsidence around existing abandoned boreholes, and boreholes drilled and abandoned in the

near-future, have been eliminated from PA calculations on the basis of low consequence to the performance of the disposal system.

SCR-5.2.1.11.3.2 Future Human EPs

The EPA provides criteria concerning analysis of the consequences of future drilling events in section 194.33(c). Consistent with these criteria, the DOE assumes that after drilling is complete the borehole is plugged according to current practice in the Delaware Basin (see Appendix PA-2014, Section PA-2.1.2.5). Degradation of casing and/or plugs may result in connections for fluid flow and, potentially, contaminant transport between connected hydraulically conductive zones. The long-term consequences of boreholes drilled and abandoned in the future will primarily depend on the location of the borehole and the borehole casing and plugging methods used.

SCR-5.2.1.11.3.2.1 Borehole-Induced Solution and Subsidence

Future boreholes that do not intersect the WIPP excavation do not differ in long-term behavior or consequences from existing boreholes, and can be eliminated from PA on the basis of low consequence to the performance of the disposal system.

The condition of more apparent concern is a future borehole that intersects the WIPP excavation. Seals and casings are assumed to degrade, connecting the excavation to various units. For a drillhole intersecting the excavation, but not connecting to a brine reservoir or to formations below the evaporites, downward flow is limited by the open volume of the disposal room(s), which is dependent with time, gas generation, or brine inflow to the disposal system from the Salado.

Maximum dissolution, and maximum increase in borehole diameter, will occur at the top of the Salado; dissolution will decrease with depth as the percolating water becomes salt saturated. Eventually, degraded casing and concrete plug products, clays, and other materials will fill the borehole. Long-term flow through a borehole that intersects a waste panel is accounted for in DP calculations by assuming that the borehole is eventually filled by such materials, which have the properties of a silty sand (see Appendix PA-2014, Section PA-2.1.2.5). However, these calculations assume that the borehole diameter does not increase with time. Under the conditions assumed in the CCA for an E2 drilling event at 1,000 yrs, about 1,000 m^3 (35,316 ft^3) would be dissolved from the lower Rustler and upper Salado. If the dissolved area is approximately cylindrical or conical around the borehole, and the collapse/subsidence propagates upward as occurred in breccia pipes (e.g., Snyder and Gard 1982), the diameter of the collapsed or subsided area through the Culebra and other units would be a few tens of meters across. Changes in hydraulic parameters for this small zone should slow travel times for any hypothesized radionuclide release, as discussed for HCN occurrences. This does not change the argument for low consequence due to borehole-induced solution and subsidence for these circumstances.

If a drillhole through a waste panel and into deeper evaporites intercepts a Castile brine reservoir, the brine has little or no capability of dissolving additional halite. The Castile brine flow is considered elsewhere as part of DP. There is, however, no *Borehole-Induced Solution and Subsidence* under this circumstance, and therefore there is no effect on performance because of this EP.

If a borehole intercepts a waste panel and also interconnects with formations below the evaporite section, fluid flow up or down is determined by several conditions and may change over a period of time (e.g., as dissolution increases the fluid density in the borehole). Fluid flow downward is not a concern for performance, as fluid velocities in units such as the Bell Canyon are slow and should not

be of concern for performance (Wilson et al. 1996). As with boreholes considered for HCN, the local change in hydraulic parameters, if it occurs along the expected flow path, would be expected to cause little change in travel time and should increase the travel time.

In summary, the effects of borehole-induced solution and subsidence around future abandoned boreholes have been eliminated from PA calculations on the basis of low consequence to the performance of the disposal system.

SCR-5.2.1.12 FEP Number: H35 FEP Title: Borehole-Induced Mineralization

SCR-5.2.1.12.1 Screening Decision: SO-C (HCN) SO-C (Future)

The effects of *Borehole-Induced Mineralization*, associated with existing, near-future, and future abandoned boreholes, have been eliminated from PA calculations on the basis of low consequence to the performance of the disposal system.

SCR-5.2.1.12.2 Summary of New Information

No new information that affects the screening of this FEP has been identified since the CRA-2009.

SCR-5.2.1.12.3 Screening Argument

Abandoned boreholes could provide pathways for fluid flow and, potentially, contaminant transport between any intersected zones. For example, such boreholes could provide pathways for vertical flow between transmissive units in the Rustler, or between the Culebra and units below the Salado, which could affect fluid densities, flow rates, and flow directions.

Movement of fluids through abandoned boreholes could result in borehole-induced geochemical changes in the receiving units, such as the Salado interbeds or Culebra, and thus alter radionuclide migration rates in these units.

Potentially, boreholes could provide pathways for surface-derived water or groundwater to percolate through low-permeability strata and into formations containing soluble minerals. Large-scale dissolution through this mechanism could lead to subsidence and to changes in groundwater flow patterns. Also, fluid flow between hydraulically conductive horizons through a borehole may result in changes in permeability in the affected units through mineral precipitation.

SCR-5.2.1.12.3.1 Borehole-Induced Mineralization

Fluid flow between hydraulically conductive horizons through a borehole may result in changes in permeability in the affected units through mineral precipitation. For example:

- Limited calcite precipitation may occur as the waters mix in the Culebra immediately surrounding the borehole, and calcite dissolution may occur as the brines migrate away from the borehole as a result of variations in water chemistry along the flow path.
- Gypsum may be dissolved as the waters mix in the Culebra immediately surrounding the borehole but may precipitate as the waters migrate through the Culebra.

The effects of these mass transfer processes on groundwater flow depend on the original permeability structure of the Culebra rocks and the location of the mass transfer. The volumes of minerals that may precipitate or dissolve in the Culebra as a result of the injection of Castile or Salado brine through a borehole will not affect the existing spatial variability in the permeability field significantly.

Predicted radionuclide transport rates in the Culebra assume that the dolomite matrix is diffusively accessed by the contaminants. The possible inhibition of matrix diffusion by secondary mineral precipitation on fracture walls as a result of mixing between brines and Culebra porewater was addressed by Wang (Wang 1998). Wang showed that the volume of secondary minerals precipitated because of this mechanism was too small to significantly affect matrix porosity and accessibility.

Consequently, the effects ofborehole-induced mineralization on permeability and groundwater flow within the Culebra, as a result of brines introduced via any existing abandoned boreholes and boreholes drilled and abandoned in the near future, have been eliminated from PA calculations on the basis of low consequence to the performance of the disposal system.

SCR-5.2.1.12.4 Future Human EPs

The EPA provides criteria concerning analysis of the consequences of future drilling events in section 194.33(c). Consistent with these criteria, the DOE assumes that after drilling is complete the borehole is plugged according to current practice in the Delaware Basin (see DOE 2012, Section 2.7 , and Appendix PA-2014, Section PA 2.1.2.5). Degradation of casing and/or plugs may result in connections for fluid flow and, potentially, contaminant transport between connected hydraulically conductive zones. The long-term consequences of boreholes drilled and abandoned in the future will primarily depend on the location of the borehole and the borehole casing and plugging methods used.

SCR-5.2.1.12.4.1 Borehole-Induced Mineralization

Fluid flow between hydraulically conductive horizons through a future borehole may result in changes in permeability in the affected units through mineral precipitation. However, the effects of mineral precipitation as a result of flow through a future borehole in the controlled area will be similar to the effects of mineral precipitation as a result of flow through an existing or near-future borehole (see FEP H32, Section SCR-5.2.1.10). Thus, borehole-induced mineralization associated with flow through a future borehole has been eliminated from PA calculations on the basis of low consequence to the performance of the disposal system.

SCR-5.2.1.13 FEP Number: H36 FEP Title: Borehole-Induced Geochemical Changes

SCR-5.2.1.13.1 Screening Decision: UP (HCN) DP (Future) SO-C for units other than the Culebra

Geochemical changes that occur inside the controlled area as a result of long-term flow associated with HCN and future abandoned boreholes are accounted for in PA calculations.

SCR-5.2.1.13.2 Summary of New Information

No new information that affects the screening of this FEP has been identified since the CRA-2009.

SCR-5.2.1.13.3 Screening Argument

Abandoned boreholes could provide pathways for fluid flow and, potentially, contaminant transport between any intersected zones. For example, such boreholes could provide pathways for vertical flow between transmissive units in the Rustler, or between the Culebra and units below the Salado, which could affect fluid densities, flow rates, and flow directions.

Movement of fluids through abandoned boreholes could result in borehole-induced geochemical changes in the receiving units such as the Salado interbeds or Culebra, and thus alter radionuclide migration rates in these units.

SCR-5.2.1.13.3.1 Geochemical Effects of Borehole Flow

Movement of fluids through abandoned boreholes could result in borehole-induced geochemical changes in the receiving units such as the Salado interbeds or Culebra. Such geochemical changes could alter radionuclide migration rates within the disposal system in the affected units if they occur sufficiently close to the edge of the controlled area, or if they occur as a result of flow through existing boreholes within the controlled area through their effects on colloid transport and sorption.

The contents of the waste disposal panels provide the main source of colloids in the disposal system. Thus, consistent with the discussion in Section SCR-5.2.1.4 (*Borehole-Induced Geochemical Changes* [H24]), colloid transport as a result of flow through existing and near-future abandoned boreholes has been eliminated from PA calculations on the basis of low consequence to the performance of the disposal system.

As discussed in H24, sorption within the Culebra is accounted for in PA calculations. The sorption model used accounts for the effects of changes in sorption in the Culebra as a result of flow through existing and near-future abandoned boreholes.

Consistent with the screening discussion in Section SCR-5.2.1.4, the effects of changes in sorption in the Dewey Lake inside the controlled area as a result of flow through existing and near-future abandoned boreholes have been eliminated from PA calculations on the basis of low consequence to the performance of the disposal system. Sorption within other geological units of the disposal system has been eliminated from PA calculations on the basis of beneficial consequence to the performance of the disposal system.

SCR-5.2.1.13.4 Future Human EPs

The EPA provides criteria concerning analysis of the consequences of future drilling events in section 194.33(c). Consistent with these criteria, the DOE assumes that after drilling is complete the borehole is plugged according to current practice in the Delaware Basin (see DOE 2012, Section 2.7 , and Appendix PA-2014, Section PA-3.7). Degradation of casing and/or plugs may result in connections for fluid flow and, potentially, contaminant transport between connected hydraulically conductive zones. The long-term consequences of boreholes drilled and abandoned in the future will primarily depend on the location of the borehole and the borehole casing and plugging methods used.

SCR-5.2.1.13.4.1 Geochemical Effects of Flow Through Abandoned Boreholes

Movement of fluids through abandoned boreholes could result in borehole-induced geochemical changes in the receiving units, such as the Salado interbeds or Culebra. Such geochemical changes

could alter radionuclide migration rates within the disposal system in the affected units through their effects on colloid transport and sorption.

The waste disposal panels provide the main source of colloids in the disposal system. Colloid transport within the Culebra as a result of long-term flow associated with future abandoned boreholes that intersect the waste disposal region are accounted for in PA calculations, as described in the CCA, Chapter 6.0, Section 6.4.3.6 and Section 6.4.6.2.1. Consistent with the discussion in Section SCR-5.2.1.4, colloid transport as a result of flow through future abandoned boreholes that do not intersect the waste disposal region has been eliminated from PA calculations on the basis of low consequence to the performance of the disposal system. The Culebra is the most transmissive unit in the disposal system and it is the most likely unit through which significant radionuclide transport could occur. Therefore, colloid transport in units other than the Culebra, as a result of flow through future abandoned boreholes, has been eliminated from PA calculations on the basis of low consequence to the performance of the disposal system.

As discussed in Section SCR-5.2.1.4, sorption within the Culebra is accounted for in PA calculations. The sorption model accounts for the effects of changes in sorption in the Culebra as a result of flow through future abandoned boreholes.

Consistent with the screening discussion in Section SCR-5.2.1.4, the effects of changes in sorption in the Dewey Lake within the controlled area as a result of flow through future abandoned boreholes have been eliminated from PA calculations on the basis of low consequence to the performance of the disposal system. Sorption within other geological units of the disposal system has been eliminated from PA calculations on the basis of beneficial consequence to the performance of the disposal system.

SCR-5.2.2 Excavation-Induced Flow

SCR-5.2.2.1 FEP Number: H37 FEP Title: Changes in Groundwater Flow Due to Mining

SCR-5.2.2.1.1 Screening Decision: UP (HCN) DP (Future)

Changes in Groundwater Flow due to *Mining* (HCN and future) are accounted for in PA calculations.

SCR-5.2.2.1.2 Summary of New Information

No new information that affects the screening of this FEP has been identified since the CRA-2009.

SCR-5.2.2.1.3 Screening Argument

Excavation activities may result in hydrological disturbances of the disposal system. Subsidence associated with excavations may affect groundwater flow patterns through increased hydraulic conductivity within and between units. Fluid flow associated with excavation activities may also result in changes in brine density and geochemistry in the disposal system.

SCR-5.2.2.1.3.1 Historical, Current, and Near-Future Human EPs

Currently, potash mining is the only excavation activity currently taking place in the vicinity of the WIPP that could affect hydrogeological or geochemical conditions in the disposal system. Potash is mined in the region east of Carlsbad and up to 5 km (3.1 mi) from the boundaries of the controlled area. Mining of the McNutt Potash Zone in the Salado is expected to continue in the vicinity of the WIPP (see the CCA, Chapter 2.0, Section 2.3.1.1): the DOE assumes that all economically recoverable potash in the vicinity of the WIPP (outside the controlled area) will be extracted in the near future.

SCR-5.2.2.1.3.2 Hydrogeological Effects of Mining

Potash mining in the Delaware Basin typically involves constructing vertical shafts to the elevation of the ore zone and then extracting the minerals in an excavation that follows the trend of the ore body. Potash has been extracted using conventional room-and-pillar mining, secondary mining where pillars are removed, and modified long-wall mining methods. Mining techniques used include drilling and blasting (used for mining langbeinite) and continuous mining (commonly used for mining sylvite). The DOE (Westinghouse 1994, pp. 2-17 to 2-19) reported investigations of subsidence associated with potash mining operations located near the WIPP. The reported maximum total subsidence at potash mines is about 1.5 m (5 ft), representing up to 66% of initial excavation height, with an observed angle of draw from the vertical at the edge of the excavation of 58 degrees. The DOE (Westinghouse 1994 pp. 2-22 to 2-23) found no evidence that subsidence over local potash mines had caused fracturing sufficient to connect the mining horizon to water-bearing units or the surface. However, subsidence and fracturing associated with mining in the McNutt in the vicinity of the WIPP may allow increased recharge to the Rustler units and affect the lateral hydraulic conductivity of overlying units, such as the Culebra, which could influence the direction and magnitude of fluid flow within the disposal system. Such changes in groundwater flow due to mining are accounted for in calculations of UP of the disposal system. The effects of any increased recharge that may be occurring are, in effect, included by using the hydraulic heads measured to calibrate Culebra transmissivity fields (T-fields) and calculate transport through those fields (Appendix TFIELD-2014).

Potash mining, and the associated processing outside the controlled area, have changed fluid densities within the Culebra, as demonstrated by the areas of higher densities around boreholes WIPP-27 and WIPP-29 (Davies 1989, p. 43). Transient groundwater flow calculations (Davies 1989, pp. 77-81) show that brine density variations to the west of the WIPP site caused by historical and current potash processing operations will not persist because the rate of groundwater flow in this area is fast enough to flush the high-density groundwaters to the Pecos River. These calculations also show that accounting for the existing brine density variations in the region east of the WIPP site, where hydraulic conductivities are low, would have little effect on the direction or rate of groundwater flow. Therefore, changes in fluid densities from historical and current human EPs have been eliminated from PA calculations on the basis of low consequence to the performance of the disposal system.

The distribution of existing leases and potash grades suggests that near-future mining will take place to the north, west, and south of the controlled area (see the CCA, Appendix DEL). A localized increase in fluid density in the Culebra, in the mined region or elsewhere outside the controlled area, would rotate the flow vector towards the downdip direction (towards the east). A comparison of the relative magnitudes of the pressure gradient and the density gradient (based on an analysis identical to that presented for fluid leakage to the Culebra through boreholes) shows that the density effect is of low consequence to the performance of the disposal system.

SCR-5.2.2.1.4 Future Human EPs

Consistent with section 194.32(b), consideration of future mining may be limited to potash mining within the disposal system. Within the controlled area, the McNutt provides the only potash of appropriate quality. The extent of possible future potash mining within the controlled area is discussed in the CCA, Chapter 2.0, Section 2.3.1.1. Criteria concerning the consequence modeling of future mining are provided in section 194.32(b): the effects of future mining may be limited to changes in the hydraulic conductivity of the hydrogeologic units of the disposal system. Thus, consistent with section 194.32(b), changes in groundwater flow due to mining within the controlled area are accounted for in calculations of the DP of the disposal system (see the CCA, Chapter 6.0, Section 6.4.6.2.3).

SCR-5.2.2.2 FEP Number: H38 FEP Title: Changes in Geochemistry Due to Mining

SCR-5.2.2.2.1 Screening Decision: SO-C (HCN) SO-R (Future)

Changes in Geochemistry due to Mining (HCN) have been eliminated from PA calculations on the basis of low consequence to the performance of the disposal system. Future *Changes in Geochemistry due to Mining* have been eliminated from PA calculations on regulatory grounds.

SCR-5.2.2.2.2 Summary of New Information

No new information that affects the screening of this FEP has been identified since the CRA-2009.

SCR-5.2.2.2.3 Screening Argument

SCR-5.2.2.2.3.1 Historical, Current, and Near-Future Human EPs

Potash mining is the only excavation activity currently taking place in the vicinity of the WIPP that could affect hydrogeological or geochemical conditions in the disposal system. Potash is mined in the region east of Carlsbad and up to 5 km (1.5 mi) from the boundaries of the controlled area. Mining of the McNutt in the Salado is expected to continue in the vicinity of the WIPP (see the CCA, Chapter 2.0, Section 2.3.1.1): the DOE assumes that all economically recoverable potash in the vicinity of the WIPP (outside the controlled area) will be extracted in the near future.

SCR-5.2.2.2.3.2 Geochemical Effects of Mining

Fluid flow associated with excavation activities may result in geochemical disturbances of the disposal system. Some waters from the Culebra reflect the influence of current potash mining, having elevated potassium to sodium ratios. However, potash mining has had no significant effect on the geochemical characteristics of the disposal system. Solution mining, which involves the injection of freshwater to dissolve the ore body, can be used for extracting sylvite. The impact on the WIPP of neighboring potash mines was examined in greater detail by D'Appolonia (D'Appolonia 1982). D'Appolonia noted that attempts to solution mine sylvite in the Delaware Basin failed because of low ore grade, thinness of the ore beds, and problems with heating and pumping injection water. See discussion in Section SCR-5.1.2.1 (*Conventional Underground Potash Mining* [H13]). Thus, changes in geochemistry due to mining (HCN) have been eliminated from PA calculations on the basis of low consequence to the performance of the disposal system.

SCR-5.2.2.2.3.3 Future Human EPs

Consistent with section 194.32(b), consideration of future mining may be limited to potash mining within the disposal system. Within the controlled area, the McNutt provides the only potash of appropriate quality. The extent of possible future potash mining within the controlled area is discussed in the CCA, Chapter 2.0, Section 2.3.1.1. Criteria concerning the consequence modeling of future mining are provided in section 194.32(b): the effects of future mining may be limited to changes in the hydraulic conductivity of the hydrogeologic units of the disposal system. Thus, consistent with section 194.32(b), changes in groundwater flow as a result of mining within the controlled area are accounted for in calculations of the DP of the disposal system (see the CCA, Chapter 6.0, Section 6.4.6.2.3). Other potential effects, such as changes in geochemistry due to mining, have been eliminated from PA calculations on regulatory grounds.

SCR-5.2.2.3 FEP Number H58 FEP Title: Solution Mining for Potash

SCR-5.2.2.3.1 Screening Decision: SO-R (HCN) SO-R (Future)

HCN and future *Solution Mining for Potash* has been eliminated from PA calculations on regulatory grounds. HCN and future solution mining for other resources has been eliminated from PA calculations on the basis of low consequence to the performance of the disposal system.

SCR-5.2.2.3.2 Summary of New Information

The prospect of using solution-mining techniques for extracting potash has been identified and considered in the region since the mid-1990s. After a lengthy planning and permitting period, Intrepid Potash, Inc., recently began flooding the abandoned mine workings of the old Eddy Potash mine in an effort to extract residual potash (sylvite) from the mine pillars. This potash is unrecoverable through conventional methods due to mine stability issues as discussed below. The extent of solutioning will be north of the Delaware Basin boundary, and is therefore beyond the region of interest for the WIPP Project. The initiation of this project does not invalidate current screening arguments and decisions, because the actual solution activity is outside the Delaware Basin. The screening argument has been updated with details of this new project and additional justification for the current screening decision.

SCR-5.2.2.3.3 Screening Argument

The potash reserves evaluated by Griswold and Griswold (Griswold and Griswold 1999) and New Mexico Bureau of Mines and Mineral Resources (New Mexico Bureau of Mines and Mineral Resources 1995) at the WIPP are of economic importance in only two ore zones; the 4^{th} and the 10^{th} contain two minerals of economic importance, langbeinite and sylvite. The ore in the 10^{th} ore zone is primarily sylvite with some langbeinite and the ore in the 4th zone is langbeinite with some sylvite. Langbeinite falls between gypsum and polyhalite in solubility and dissolves at a rate 1000 times slower than sylvite (Heyn 1997). Halite, the predominate gangue mineral present, is much more soluble than the langbeinite. Because of the insolubility of langbeinite, sylvite is the only potash ore in the WIPP vicinity that could be mined using a solution mining process. Mining for sylvite by solutioning would cause the langbeinite to be lost because conventional mining could not be done in conjunction with a solution mining process.

Typically, solution mining is used for potash:

When deposits are at depths in excess of 914 m (3,000 ft) and rock temperatures are high, or are geologically too complex to mine profitably using conventional underground mining techniques

To recover the potash pillars at the end of a mine's life

When a mine is unintentionally flooded with waters from underlying or overlying rock strata and conventional mining is no longer feasible

Communiqués with IMC Global (Heyn 1997; Prichard 2003) indicated that rock temperature is critical to the success of a solution-mining endeavor. Mosaic Potash's (previously IMC Global) solution mines in Michigan and Saskatchewan are at depths of around 914 m (3,000 ft) or greater, at which rock temperatures are higher. The ore zones at the WIPP are shallow, at depths of 457 to 549 m (1,500 to 1,800 ft), with fairly cool rock temperatures. Prichard (Prichard 2003) states that solution mining is energy intensive and the cool temperature of the rock would add to the energy costs. In addition, variable concentrations of confounding minerals (such as kainite and leonite) will cause problems with the brine chemistry.

Douglas W. Heyn (chief chemist of IMC Kalium) provided written testimony to the EPA related to the Agency's rulemaking activities on the CCA. Heyn concluded that "the rational choice for extracting WIPP potash ore reserves would be by conventional room and pillar mechanical means" (Heyn 1997). It is the opinion of IMC Global that no company will ever attempt solution mining of the ores in or near the WIPP (Heyn 1997; Prichard 2003).

The impact on the WIPP of neighboring potash mines and the possible effects of solution mining for potashor other evaporite minerals were examined in detail by D'Appolonia (D'Appolonia 1982). According to D'Appolonia (D'Appolonia 1982), and in agreement with Heyn (Heyn 1997) of IMC Global, Inc., solution mining of langbeinite is not technically feasible because the ore is less soluble than the surrounding evaporite minerals. Serious technical and economic obstacles exist that render solution mining for potash very unlikely in the immediate vicinity of the WIPP. Expectedly, no operational example of this technology exists within the Delaware Basin; that is, solution mining for potash in not considered a current practice in the area. For this reason, consideration of solution mining on the disposal system in the future may be excluded on regulatory grounds. For example, the EPA stated in their Response to Comments, Section 8 , Issue GG (EPA 1998d):

> …However, the Agency emphasizes that, in accordance with the WIPP compliance criteria, solution mining does not need to be included in the PA. As previously discussed, potash solution mining is not an ongoing activity in the Delaware Basin. Section 194.32(b) of the rule limits assessment of mining effects to excavation mining. Thus the solution mining scenarios proposed are excluded on regulatory grounds after repository closure. Prior to or soon after disposal, solution mining is an activity that could be considered under Section 194.32(c). However, DOE found that potash solution mining is not an ongoing activity in the Delaware Basin; and one pilot project examining solution mining in the Basin is not substantive evidence that such mining is expected to occur in the near future. (Even if mining were assumed to occur in the near future, the proposed scenarios would not be possible because, even though solution mining might occur, there would be no intruding borehole to provide a pathway into the repository: active institutional controls would preclude such drilling during the first 100 years after disposal.) Furthermore, Section 194.33 (d) states that PA need not analyze the effects of techniques used for resource recovery (e.g. solution mining) after a borehole is drilled in the future.

Conventional mining activities will continue to be incorporated into the WIPP PA as directed by the EPA CAG (U.S. EPA 1996b). Because the potash mines in the vicinity of the WIPP are in their mature (declining) stages of production, solution mining may be used in the future for extraction of remaining pillars, as is being done in the Intrepid Potash, Inc. project just outside the Delaware Basin.

Nonetheless, at the time of this FEP reassessment, this technology is not being employed within the Delaware Basin and a screening based on the future states assumption at section 194.25(a) is appropriate for this mining technique at this time. While a regulatory screening (SO-R) is currently appropriate, if a potash solution mining project were to exist within the vicinity of the WIPP (within the Delaware Basin), the DOE has effectively argued that the consequences of such activity would be of low consequence, and addressed by conventional mining FEPs. In a response to the Environmental Evaluation Group comment, the DOE effectively argued that, "If solution mining for potash were undertaken in the vicinity of the WIPP it could result in subsidence. However, performance assessment calculations already assume that widespread subsidence will occur as a result of potash mining in the near future. The assumed extent of subsidence and its effects on the hydraulic conductivity of Culebra are independent of the mining methods used (underground excavation or solution mining)." (U.S. EPA 1998d).

SCR-5.2.2.4 FEP Number: H59 FEP Title: Solution Mining for Other Resources

SCR-5.2.2.4.1 Screening Decision: SO-C (HCN) SO-C (Future)

HCN and future *Solution Mining for Other Resources* have been eliminated from PA calculations on the basis of low consequence to the performance of the disposal system.

SCR-5.2.2.4.2 Summary of New Information

Brine well information provided in Table SCR-2 has been updated based on new information from the DBDSP (U.S. DOE 2012). The CRA-2009 reported 12 active brine wells within the Delaware Basin. For the CRA-2014 the DBDSP again reports 12 active brine wells, although they are not the same 12 as reported in 2009. Two previously active wells have been taken out of service and plugged and abandoned. Alternatively, there have been two new brine wells put into service during this period, leaving the total active brine wells at 12. Updated information is also provided that describes brine well collapses in southeast New Mexico.

SCR-5.2.2.4.3 Screening Argument

Brine wells (solution mining for brine) exist within the Delaware Basin, although none within the vicinity of the WIPP. Sulfur extraction using the Frasch process began in 1969 and continued for three decades at the Culberson County Rustler Springs mine near Orla, Texas. Solution mining for the purposes of creating a storage cavity has not occurred within the New Mexico portion of the Delaware Basin.

SCR-5.2.2.4.4 Solution Mining for Brine

Oil and gas reserves in the Delaware Basin are located in structures within the Delaware Mountain Group and lower stratigraphic units. Boreholes drilled to reach these horizons pass through the Salado and Castile that comprise thick halite and other evaporite units. To avoid dissolution of the halite units during drilling and prior to casing of the borehole, the fluid used for lubrication, rotating the drilling-bit cutters, and transporting cuttings (drilling mud) must be saturated with respect to halite. Most oil- and gas-field drilling operations in the Delaware Basin therefore use saturated brine (10 to 10.5 pounds per gallon [lb/gal]) as a drilling fluid until reaching the Bell Canyon, where intermediate casing is set.

One method of providing saturated brine for drilling operations is solution mining, whereby fresh water is pumped into the Salado, allowed to reach saturation with respect to halite, and then recovered. This manufactured brine is then transported to the drilling site by water tanker.

Two principal techniques are used for solution mining: single-borehole operations and doublet or two-borehole operations.

Table SCR- 2. Delaware Basin Brine Well Status

County	Location	API No.	Well Name and No.	Operator	CRA-2009 Status	CRA-2014 Status†
Eddy	22S-26E-36	3001521842	City of Carlsbad #WS-1	Key Energy Services	Active Brine Well	Plugged Brine Well
Eddy	22S-27E-03	3001520331	Tracy #3	Ray Westall	Plugged Brine Well	Plugged Brine Well
Eddy	22S-27E-17	3001522574	Eugenie #WS-1	I & W Inc	Active Brine Well	Plugged Brine Well
Eddy	22S-27E-17	3001523031	Eugenie #WS-2	I & W Inc	Plugged Brine Well	Plugged Brine Well
Eddy	22S-27E-23	3001528083	Dunaway #1	Mesquite SWD, Inc.	Active Brine Well	Active Brine Well
Eddy	22S-27E-23	3001538084	Dunaway #2	Mesquite SWD, Inc.	--	Active Brine Well
Loving	Blk 29-03	4230110142	Lineberry Brine Station #1	Chance Properties	Active Brine Well	Active Brine Well
Loving	Blk 01-82	4230130680	Chapman Ford #BR1	Herricks & Son Co.	Plugged Brine Well	Plugged Brine Well
Loving	Blk 33-80	4230180318	Mentone Brine Station #1D	Basic Energy Services	Active Brine Well	Active Brine Well
Loving	Blk 29-28	4230180319	East Mentone Brine Station #1	Permian Brine Sales, Inc.	Plugged Brine Well	Plugged Brine Well
Loving	Blk 01-83	4230180320	North Mentone #1	Chance Properties	Active Brine Well	Active Brine Well
Reeves	Blk 56-30	4238900408	Orla Brine Station #1D	Mesquite SWD Inc.	Active Brine Well	Active Brine Well
Reeves	Blk 04-08	4238920100	North Pecos Brine Station #WD-1	Chance Properties	Active Brine Well	Active Brine Well
Reeves	Blk 07-21	4238980476	Coyanosa Brine Station #1	Chance Properties	Active Brine Well	Active Brine Well
Ward	Blk 17-20	4247531742	Pyote Brine Station #WD-1	Chance Properties	Active Brine Well	Active Brine Well
Ward	Blk 01-13	4247534514	Quito West Unit #207	Seaboard Oil Co.	Active Brine Well	Active Brine Well
Ward	Blk 34-200	4247520329	Barstow Brine Station #1	Basic Energy Services, LP	--	Active Brine Well
Ward	Blk 34-174	4247582265	Barstow Brine Station #1	Energy Equity Company	Active Brine Well	Active Brine Well

† **Bold type** indicates a change from CRA-2009.

In single-borehole operations, a borehole is drilled into the upper part of the halite unit. After casing and cementing this portion of the borehole, the borehole is extended, uncased, into the halite formation. An inner pipe is installed from the surface to the base of this uncased portion of the borehole. During operation, fresh water is pumped down the annulus of the borehole. This dissolves halite over the uncased portion of the borehole, and saturated brine is forced up the inner tube to the surface.

In doublet operations, a pair of boreholes are drilled, cased, and cemented into the upper part of the halite unit. The base of the production well is set some feet below the base of the injection well. In the absence of natural fractures or other connections between the boreholes, hydrofracturing is used to induce fractures around the injection well. During operation, fresh water is pumped down the injection well. This initially dissolves halite from the walls of the fractures and the resulting brine is then pumped from the production well. After a period of operation a cavity develops between the boreholes as the halite between fractures is removed. Because of its lower density, fresh water injected into this cavity will rise to the top and dissolve halite from the roof of the cavity. As the brine density increases it sinks within the cavern and saturated brine is extracted from the production well.

SCR-5.2.2.4.4.1 Current Brine Wells within the Delaware Basin

Brine wells are classified as Class II injection wells. In the Delaware Basin, the process includes injecting fresh water into a salt formation to create a saturated brine solution which is then extracted and utilized as a drilling agent. These wells are tracked by the DBDSP on a continuing basis. Supplemental information provided to the EPA in 1997 showed 11 brine wells in the Delaware Basin. Since that time, additional information has shown that there are 16 brine wells within the Delaware basin, of which 4 are plugged and abandoned. This results in 12 currently active brine wells. Table SCR-2 provides information on these wells. While these wells are within the Delaware Basin, none are within the vicinity of the WIPP. The nearest operating brine well is the Dunaway #1, which is approximately 22 mi (35.4 km) from the WIPP.

Two New Mexico operating brine wells collapsed in 2008, causing surface sinkholes. A subsurface cavern associated with a brine well 17.3 mi (27.8 km) southeast of Artesia, New Mexico collapsed on July 16, 2008. Later, on November 3, 2008 a brine well collapsed near Loco Hills, New Mexico. Both of these wells are located outside the Delaware Basin. These collapses prompted the New Mexico Energy, Minerals, and Natural Resources Secretary to issue a six-month moratorium on new brine wells, and also prompted a reevaluation of New Mexico Oil Conservation Division (NMOCD) rules and policies regarding brine wells. The state reviewed all active brine wells and determined that the Eugenie #WS-1, located within the city limits of Carlsbad, (approximately 30 mi (48 km) from the WIPP) was at risk of collapse. Due to these concerns, the Eugenie #1 was plugged and removed from service in late 2008. The NMOCD has since contracted a private engineering firm to install monitoring equipment at the Eugenie #1 site to warn of imminent collapse. The NMOCD continues to gather information regarding this and all brine wells in the state to assess the future risk of collapses from existing wells and the potential impacts. The division is also considering redefining the allowable criteria for the proper siting, construction, operation, and closure of brine operations.

SCR-5.2.2.4.5 Solution Mining for Other Minerals

Currently, there are no ongoing solution mining activities within the vicinity of the WIPP. The Rustler Springs sulfur mine located in Culberson County, Texas, began operations in 1969 and continued until it was officially closed in 1999. This mine used the Frasch process (superheated water injection) to extract molten sulfur (Cunningham 1999).

SCR-5.2.2.4.6 Solution Mining for Gas Storage

No gas storage cavities have been solution mined within the New Mexico portion of the Delaware Basin. Five gas storage facilities exist within the general vicinity of the WIPP; however, only one is within the Delaware basin. This one New Mexico Delaware Basin facility uses a depleted gas

reservoir for storage and containment; it was not solution mined (see Appendix DATA-2004, Attachment A, Section DATA-A-5.4).

SCR-5.2.2.4.7 Solution Mining for Disposal

Solution mining can be used to create a disposal cavity in bedded salt. Such disposal cavities can be used for the disposal of naturally occurring radioactive material or other wastes. No such cavities have been mined or operated within the vicinity of the WIPP.

SCR-5.2.2.4.8 Effects of Solution Mining

SCR-5.2.2.4.8.1 Subsidence

Regardless of whether the single-borehole or two-borehole technique is used for solution mining, the result is a subsurface cavity which could collapse and lead to subsidence of overlying strata. In a response to the Environmental Evaluation Group comment, the DOE effectively argued that, "If solution mining for potash were undertaken in the vicinity of the WIPP it could result in subsidence. However, performance assessment calculations already assume that widespread subsidence will occur as a result of potash mining in the near future. The assumed extent of subsidence and its effects on the hydraulic conductivity of Culebra are independent of the mining methods used (underground excavation or solution mining)." (U.S. EPA 1998d). While this FEP is primarily concerned with solution mining for other minerals (not potash), this argument holds for the removal of any mineral via the solution process (i.e., brine production).

SCR-5.2.2.4.8.2 Hydrogeological Effects

In regions where solution mining takes place, the hydrogeology could be affected in a number ways:

- Subsidence above a large dissolution cavity could change the vertical and lateral hydraulic conductivity of overlying units.
- Extraction of fresh water from aquifers for solution mining could cause local changes in pressure gradients.
- Loss of injected fresh water or extracted brine to overlying units could cause local changes in pressure gradients.

The potential for subsidence to take place above solution mining operations in the region of Carlsbad, New Mexico is discussed above. Some subsidence could occur in the future if brine operations continue at existing wells. Resulting fracturing may change permeabilities locally in overlying formations. However, because of the restricted scale of the solution mining at a particular site, and the distances between such wells, such fracturing will have no significant effect on hydrogeology near the WIPP.

Solution mining operations in the Delaware Basin extract water from shallow aquifers so that, even if large drawdowns are permitted, the effects on the hydrogeology will be limited to a relatively small area around the operation. Since all the active operations are more than 32 km (20 mi) from the WIPP, there will be no significant effects on the hydrogeology near the WIPP.

Discharge plans for solution mining operations typically include provision for annual mechanical integrity tests at one and one-half the normal operating pressure for four hours (New Mexico Oil Conservation Division 1994). Thus, the potential for loss of integrity and consequent leakage of freshwater or brine to overlying formations is low. If, despite these annual tests, large water losses did take place from either injection or production wells, the result would be low brine yields and remedial actions would most likely be taken by the operators.

SCR-5.2.2.4.8.3 Geochemical Effects

Solution mining operations could affect the geochemistry of surface or subsurface water near the operation if there were brine leakage from storage tanks or production wells. Discharge plans for solution mining operations specify the measures to be taken to prevent leakage and to mitigate the effects of any that do take place. These measures include berms around tanks and annual mechanical integrity testing of wells (New Mexico Oil Conservation Division 1994). The potential for changes in geochemistry is therefore low, and any brine losses that did take place would be limited by remedial actions taken by the operator. In the event of leakage from a production well, the effect on geochemistry of overlying formation waters would be localized and, given the distance of such wells from the WIPP site, such leakage would have no significant effect on geochemistry near the WIPP.

SCR-5.2.2.4.9 Conclusion of Low Consequence

Brine production through solution mining takes place in the Delaware Basin, and the DOE assumes it will continue in the near future. Because of the existence of these solution operations, it is not possible to screen this activity based on the provisions of section 194.25(a). However, despite oil and gas exploration and production taking place in the vicinity of the WIPP site, the nearest operating solution mine is more than 32 km (20 mi) from the WIPP site. These locations are too far from the WIPP site for any changes in hydrogeology or geochemistry, from subsidence or fresh water or brine leakage, to affect the performance of the disposal system. Thus, the effects of HCN and future solution mining for other resources in the Delaware Basin can be eliminated from PA calculations on the basis of low consequence to the performance of the disposal system.

SCR-5.2.3 Explosion-Induced Flow

SCR-5.2.3.1 FEP Number: H39 FEPs Title: Changes in Groundwater Flow Due to Explosions

SCR-5.2.3.1.1 Screening Decision: SO-C (HCN) SO-R (Future)

Changes in Groundwater Flow due to Explosions (HCN) have been eliminated from PA calculations on the basis of low consequence to the performance of the disposal system. Changes in groundwater flow that may be caused by future explosions have been eliminated from PA calculations on regulatory grounds.

SCR-5.2.3.1.2 Summary of New Information

No new information that affects the screening of this FEP has been identified since the CRA-2009.

SCR-5.2.3.1.3 Screening Argument

SCR-5.2.3.1.3.1 Historical, Current, and Near-Future Human EPs

The small-scale explosions that have been used in the Delaware Basin to fracture oil- and natural-gas-bearing units to enhance resource recovery have been too deep to have disturbed the hydrology of the disposal system (see FEP H19, Section SCR-5.1.3.1).

Also, as discussed in Section SCR-5.1.3.2 (*Underground Nuclear Device Testing* [H20]), the Delaware Basin has been used for an isolated nuclear test (Project Gnome), approximately 13 km (8 mi) southwest of the WIPP waste disposal region. An induced zone of increased permeability was observed to extend 46 m (150 ft) laterally from the point of the explosion. The increase in permeability was primarily associated with motions and separations along bedding planes, the major preexisting weaknesses in the rock. This region of increased permeability is too far from the WIPP site to have had a significant effect on the hydrological characteristics of the disposal system. Thus, changes in groundwater flow due to explosions in the past have been eliminated from PA calculations on the basis of low consequence to the performance of the disposal system.

SCR-5.2.3.1.3.2 Future Human EPs

The criterion in section 194.32(a) relating to the scope of PAs limits the consideration of future human actions to mining and drilling. Also, consistent with section 194.33(d), PAs need not analyze the effects of techniques used for resource recovery subsequent to the drilling of a future borehole. Therefore, changes in groundwater flow due to explosions in the future have been eliminated from PA calculations on regulatory grounds.

SCR-5.3 Geomorphological EPs

SCR-5.3.1 Land Use Changes

SCR-5.3.1.1 FEP Number: H40 FEP Title: Land Use Changes

SCR-5.3.1.1.1 Screening Decision: SO-R (HCN) SO-R (Future)

Land Use Changes have been eliminated from PA calculations on regulatory grounds.

SCR-5.3.1.1.2 Summary of New Information

No new information that affects the screening of this FEP has been identified since the CRA-2009.

SCR-5.3.1.1.3 Screening Argument

This section discusses surface activities that could affect the geomorphological characteristics of the disposal system and result in changes in infiltration and recharge conditions. The potential effects of water use and control on disposal system performance are discussed in FEPs H42 through H46 (Section SCR-5.4.1.1, Section SCR-5.4.1.2, and Section SCR-5.4.1.3).

SCR-5.3.1.1.4 Historical, Current, and Near-Future Human EPs

Surface activities that take place at present in the vicinity of the WIPP site include those associated with potash mining, oil and gas reservoir development, water extraction, and grazing. Additionally, a number of archeological investigations have taken place within the controlled area that were aimed at protecting and preserving cultural resources. Elsewhere in the Delaware Basin, sand, gravel, and caliche are produced through surface quarrying. The only surface activity that has the potential to affect the disposal system is potash tailings, salt tailings (both potash and WIPP), and effluent disposal. Potash tailings ponds may act as sources of focused recharge to the Dewey Lake and Rustler units.

Three potash tailings piles/ponds are in operation that might be influencing groundwater flow at the WIPP site. These are the Mississippi Potash Inc. (MPI) East tailings pile, approximately 10 km (6 mi) due north of the WIPP, the MPI West tailings pile in the northwest arm of Nash Draw, and the IMC Kalium tailings pile, approximately 10 km (6 mi) due west of the WIPP in Nash Draw. These tailings piles have been in operation for decades-disposal at the MPI East site, the youngest of the piles, began in 1965. Brine disposal at these locations affects Rustler groundwaters in Nash Draw, as shown by the hydrochemical facies D waters described by Siegel et al. (1991, p. 2-61). Brine disposal also affects heads in Nash Draw, and these head effects likely propagate to the WIPP site as well. These effects, however, predate water-level monitoring for the WIPP and have been implicitly included when defining boundary heads for Culebra flow models. The Culebra T-fields developed for the CRA-2009 PABC (also used in this CRA-2014) include data gathered since 2000 to define model boundary conditions. Thus, the effects of brine disposal at the tailings piles can be considered to be included in PA calculations. These effects are expected to continue in the near future.

The Delaware Basin monitoring program monitors land use activities in the WIPP vicinity. This program has not identified new planned uses for land in the vicinity of the WIPP (U.S. DOE 2012). Therefore, consistent with the criteria in section 194.32(c) and section 194.54(b) (U.S. EPA 1996a), land use changes in the near future in the vicinity of the WIPP have been eliminated from PA calculations on regulatory grounds.

SCR-5.3.1.1.5 Future Human EPs

The criterion in section 194.25(a), concerned with predictions of the future states of society, requires that compliance assessments and PAs "shall assume that characteristics of the future remain what they are at the time the compliance application is prepared, provided that such characteristics are not related to hydrogeologic, geologic or climatic conditions." Therefore, no future land use change*s* need be considered in the vicinity of the WIPP, and they have been eliminated from PA calculations on regulatory grounds.

SCR-5.3.1.2 FEP Number: H41 FEP Title: Surface Disruptions

SCR-5.3.1.2.1 Screening Decision: UP (HCN) SO-C (Future)

The effects of HCN *Surface Disruptions* are accounted for in PA calculations. The effects of future *Surface Disruptions* have been eliminated from PA calculations on the basis of low consequence.

SCR-5.3.1.2.2 Summary of New Information

No new information that affects the screening of this FEP has been identified since the CRA-2009.

SCR-5.3.1.2.3 Screening Argument

This section discusses surface activities that could affect the geomorphological characteristics of the disposal system and result in changes in infiltration and recharge conditions. The potential effects of water use and control on disposal system performance are discussed in FEPs H42 through H46.

SCR-5.3.1.2.4 Historical, Current, and Near-Future Human EPs

Most surface activities have no potential to affect the disposal system and are, therefore, screened out on the basis of low consequence (e.g., archaeological excavations and arable farming). However, the effects of activities capable of altering the disposal system (disposal of potash effluent) are included in the modeling of current conditions (i.e., heads) at and around the site. Discussion regarding these anthropogenic effects is found in the CRA-2004, Chapter 2.0, Section 2.2.1.4.2.2.

Surface activities that take place at present in the vicinity of the WIPP site include those associated with potash mining, oil and gas reservoir development, water extraction, and grazing. Additionally, a number of archeological investigations have taken place within the controlled area that were aimed at protecting and preserving cultural resources. Elsewhere in the Delaware Basin, sand, gravel, and caliche are produced through surface quarrying. The only surface activity that has the potential to affect the disposal system is potash tailings, salt tailings (both potash and WIPP), and effluent disposal. Potash tailings ponds may act as sources of focused recharge to the Dewey Lake and Rustler units.

Three potash tailings piles/ponds are in operation that might be influencing groundwater flow at the WIPP site. These are the MPI East tailings pile, approximately 10 km (6 mi) due north of the WIPP, the MPI West tailings pile in the northwest arm of Nash Draw, and the IMC Kalium tailings pile, approximately 10 km (6 mi) due west of the WIPP in Nash Draw. These tailings piles have been in operation for decades-disposal at the MPI East site, the youngest of the piles, began in 1965. Brine disposal at these locations affects Rustler groundwaters in Nash Draw, as shown by the hydrochemical facies D waters described by Siegel et al. (Siegel et al. 1991, p. 2-61). Brine disposal also affects heads in Nash Draw, and these head effects likely propagate to the WIPP site as well. These effects, however, predate water-level monitoring for the WIPP and have been implicitly included when defining boundary heads for Culebra flow models. The Culebra T-fields developed for the CRA-2009 PABC (also used in this CRA-2014) include data gathered since 2000 to define model boundary conditions. Thus, the effects of brine disposal at the tailings piles can be considered to be included in PA calculations. These effects are expected to continue in the near future.

SCR-5.3.1.2.5 Future Human EPs

Future tailings ponds, if situated in Nash Draw, are expected to change Culebra (and Magenta) heads, similar to existing ones. Future tailings ponds outside of Nash Draw would not be expected to alter Culebra heads because leakage from the ponds would not be able to propagate through the low-permeability lower Dewey Lake clastics and Rustler anhydrites overlying the Culebra during the 100 yrs or less that such a pond might be in operation. Because PA calculations already include the present-day effects of tailings ponds in Nash Draw on heads, as well as the effects of future potash mining on the permeability of the Culebra (which has much greater potential to alter flow than

changes in head), future surface disruptions affecting hydrologic or geologic conditions (such as potash tailings ponds) may be screened out on the basis of low consequence.

SCR-5.4 Surface Hydrological EPs

SCR-5.4.1 Water Control and Use

SCR-5.4.1.1 FEP Numbers: H42, H43, and H44 FEP Titles: Damming of Streams and Rivers (H42) Reservoirs (H43) Irrigation (H44)

SCR-5.4.1.1.1 Screening Decision: SO-C (HCN) SO-R (Future)

The effects of HCN *Damming of Streams and Rivers*, *Reservoirs*, and *Irrigation* have been eliminated from PA calculations on the basis of low consequence to the performance of the disposal system. Future *Damming of Streams and Rivers*, *Reservoirs*, and *Irrigation* have been eliminated from PA calculations on regulatory grounds.

SCR-5.4.1.1.2 Summary of New Information

No new information that affects the screening of this FEP has been identified since the CRA-2009.

SCR-5.4.1.1.3 Screening Argument

Irrigation and damming, as well as other forms of water control and use, could lead to localized changes in recharge, possibly leading to increased heads locally, thereby affecting flow directions and velocities in the Rustler and Dewey Lake.

SCR-5.4.1.1.4 Historical, Current, and Near-Future Human EPs

In the WIPP area, two topographically low features, the Pecos River and Nash Draw, are sufficiently large to warrant consideration for damming. Dams and reservoirs already exist along the Pecos River. However, the Pecos River is far enough from the waste panels (19 km [12 mi]) that the effects of damming of streams and rivers and reservoirs can be eliminated from PA calculations on the basis of low consequence to the performance of the disposal system. Nash Draw is not currently dammed, and based on current hydrological and climatic conditions, there is no reason to believe it will be dammed in the near future.

Irrigation uses water from rivers, lakes, impoundments, and wells to supplement the rainfall in an area to grow crops. Irrigation in arid environments needs to be efficient and involves the spreading of a relatively thin layer of water for uptake by plants, so little water would be expected to infiltrate beyond the root zone. However, some water added to the surface may infiltrate and reach the water table, affecting groundwater flow patterns. Irrigation currently takes place on a small scale within the Delaware Basin but not in the vicinity of the WIPP, and the extent of irrigation is not expected to change in the near future. Such irrigation has no significant effect on the characteristics of the disposal system. Thus, the effects of irrigationhave been eliminated from PA calculations on the basis of low consequence to the performance of the disposal system.

SCR-5.4.1.1.5 Future Human EPs

The EPA has provided criteria relating to future human activities in section 194.32(a) that limit the scope of consideration of future human actions in PAs to mining and drilling. Therefore, the effects of future damming of streams and rivers, reservoirs, and irrigation have been eliminated from PA calculations on regulatory grounds.

SCR-5.4.1.2 FEP Number: H45 FEP Title: Lake Usage

SCR-5.4.1.2.1 Screening Decision: SO-R (HCN) SO-R (Future)

The effects of *Lake Usage* have been eliminated from PA calculations on regulatory grounds.

SCR-5.4.1.2.2 Summary of New Information

No new information that affects the screening of this FEP has been identified since the CRA-2009.

SCR-5.4.1.2.3 Screening Argument

Irrigation and damming, as well as other forms of water control and use, could lead to localized changes in recharge, possibly leading to increased heads locally, thereby affecting flow directions and velocities in the Rustler and Dewey Lake. Surface activities, such as those associated with potash mining, could also affect soil and surface water chemistry. Note that the potential effects of geomorphological changes through land use are discussed in Section SCR-5.3.1.1 and Section SCR-5.3.1.2.

SCR-5.4.1.2.4 Historical, Current, and Near-Future Human EPs

As discussed in the CCA, Chapter 2.0, Section 2.2.2, there are no major natural lakes or ponds within 8 km (5 mi) of the site. To the northwest, west, and southwest, Red Lake, Lindsey Lake, and Laguna Grande de la Sal are more than 8 km (5 mi) from the site, at elevations of 914 to 1,006 m (3,000 to 3,300 ft). Laguna Gatuña, Laguna Tonto, Laguna Plata, and Laguna Toston are playas more than 16 km (10 mi) north and are at elevations of 1,050 m (3,450 ft) or higher.

Waters from these lakes are of limited use. Therefore human activities associated with lakes have been screened out of PA calculations based on regulatory grounds supported by section 194.32(c) and section 194.54(b).

SCR-5.4.1.2.5 Future Human EPs

The EPA has provided criteria relating to future human activities in section 194.32(a) that limit the scope of consideration of future human actions in PAs to mining and drilling. Therefore, the effects of future lake usage have been eliminated from PA calculations on regulatory grounds.

SCR-5.4.1.3 FEP Number: H46 FEP Title: Altered Soil or Surface Water Chemistry by Human Activities

SCR-5.4.1.3.1 Screening Decision: SO-C (HCN) SO-R (Future)

The effects of HCN *Altered Soil or Surface Water Chemistry by Human Activities* have been eliminated from PA calculations on the basis of low consequence to the performance of the disposal system. Future *Altered Soil or Surface Water Chemistry by Human Activities* have been eliminated from PA calculations on regulatory grounds.

SCR-5.4.1.3.2 Summary of New Information

No new information that affects the screening of this FEP has been identified since the CRA-2009.

SCR-5.4.1.3.3 Screening Argument

Irrigation and damming, as well as other forms of water control and use, could lead to localized changes in recharge, possibly leading to increased heads locally, thereby affecting flow directions and velocities in the Rustler and Dewey Lake. Surface activities, such as those associated with potash mining, could also affect soil and surface water chemistry.

SCR-5.4.1.3.4 Historical, Current, and Near-Future Human EPs

Potash mining effluent and runoff from oil fields have altered soil and surface water chemistry in the vicinity of the WIPP. However, the performance of the disposal system will not be sensitive to soil and surface water chemistry. Therefore, altered soil or surface water chemistry by human activities has been eliminated from PA calculations on the basis of low consequence to the performance of the disposal system. The effects of effluent from potash processing on groundwater flow are discussed in H37 (Section SCR-5.2.2.1).

SCR-5.4.1.3.5 Future Human EPs

The EPA has provided criteria relating to future human activities in section 194.32(a) that limit the scope of consideration of future human actions in PAs to mining and drilling. Therefore, the effects of future altered soil or surface water chemistry by human activities have been eliminated from PA calculations on regulatory grounds.

SCR-5.5 Climatic EPs

SCR-5.5.1 Anthropogenic Climate Change

SCR-5.5.1.1 FEP Numbers: H47, H48, and H49

FEP Titles: *Greenhouse Gas Effects* (H47)
Acid Rain (H48)
Damage to the Ozone Layer (N49)

SCR-5.5.1.1.1 Screening Decision: SO-R (HCN) SO-R (Future)

The effects of anthropogenic climate change (*Acid Rain*, *Greenhouse Gas Effects*, and *Damage to the Ozone Layer*) have been eliminated from PA calculations on regulatory grounds.

SCR-5.5.1.1.2 Summary of New Information

No new information that affects the screening of this FEP has been identified since the CRA-2009.

SCR-5.5.1.1.3 Anthropogenic Climate Change

The effects of the current climate and natural climatic change are accounted for in PA calculations, as discussed in the CCA, Chapter 6.0, Section 6.4.9, and Appendix PA-2014, Section PA-4.8. However, human activities may also affect the future climate and thereby influence groundwater recharge in the WIPP region. The effects of anthropogenic climate change may be on a local to regional scale (acid rain) or on a regional to global scale (greenhouse gas effects and damage to the ozone layer). Of these anthropogenic effects, only the greenhouse gas effect could influence groundwater recharge in the WIPP region. However, consistent with the future states assumptions in section 194.25, compliance assessments and PAs need not consider indirect anthropogenic effects on disposal system performance. Therefore, the effects of anthropogenic climate change have been eliminated from PA calculations on regulatory grounds.

SCR-5.6 Marine EPs

SCR-5.6.1 Marine Activities

SCR-5.6.1.1 FEP Numbers: H50, H51, and H52 FEP Titles: Costal Water Use (H50) Seawater Use (H51) Estuarine Water Use (H52)

SCR-5.6.1.1.1 Screening Decision: SO-R (HCN) SO-R (Future)

HCN, and future *Coastal Water Use*, *Seawater Use*, and *Estuarine Water Use* have been eliminated from PA calculations on regulatory grounds.

SCR-5.6.1.1.2 Summary of New Information

No new information that affects the screening of this FEP has been identified since the CRA-2009.

SCR-5.6.1.1.3 Screening Argument

This section discusses the potential for human EPs related to marine activities to affect infiltration and recharge conditions in the vicinity of the WIPP.

SCR-5.6.1.1.4 Historical, Current, and Near-Future Human EPs

The WIPP site is more than 800 km (480 mi) from the nearest seas, and hydrological conditions in the vicinity of the WIPP have not been affected by marine activities. Furthermore, consistent with the criteria in section 194.32(c) and section 194.54(b), consideration of HCN human activities is limited to those activities that have occurred or are expected to occur in the vicinity of the disposal system.

Therefore, Human EPs related to marine activities (such as coastal water use, seawater use, and estuarine water use) have been eliminated from PA calculations on regulatory grounds.

SCR-5.6.1.1.5 Future Human EPs

The EPA has provided criteria relating to future human activities in section 194.32(a) that limit the scope of consideration of future human actions in PAs to mining and drilling. Therefore, the effects of future marine activities (such as coastal water use, seawater use, and estuarine water use) have been eliminated from PA calculations on regulatory grounds.

SCR-5.7 Ecological EPs

SCR-5.7.1 Agricultural Activities

SCR-5.7.1.1 FEP Numbers: H53, H54, and H55 FEP Titles: Arable Farming (H53) Ranching (H54) Fish Farming (H55)

SCR-5.7.1.1.1 Screening Decision: SO-C (HCN) (H53, H54) SO-R (HCN) (H55) SO-R (Future) (H53, H54, H55)

The effects of HCN *Ranching* and *Arable Farming* have been eliminated from PA calculations on the basis of low consequence to the performance of the disposal system. The effects of changes in future *Ranching* and *Arable Farming* practices have been eliminated from PA calculations on regulatory grounds. *Fish Farming* has been eliminated from PA calculations on regulatory grounds.

SCR-5.7.1.1.2 Summary of New Information

No new information that affects the screening of this FEP has been identified since the CRA-2009.

SCR-5.7.1.1.3 Screening Argument

Agricultural activities could affect infiltration and recharge conditions in the vicinity of the WIPP. Also, application of acids, oxidants, and nitrates during agricultural practice could alter groundwater geochemistry.

SCR-5.7.1.1.4 Historical, Current, and Near-Future Human EPs

Grazing leases exist for all land sections immediately surrounding the WIPP and grazing occurs within the controlled area (see the CCA, Chapter 2.0, Section 2.3.2.2). Although grazing and related crop production have had some control on the vegetation at the WIPP site, these activities are unlikely to have affected subsurface hydrological or geochemical conditions. The climate, soil quality, and lack of suitable water sources all mitigate against agricultural development of the region in the near future. Therefore, the effects of HCN ranching and arable farming have been eliminated from PA calculations on the basis of low consequence to the performance of the disposal system. Consistent with the criteria in section 194.32(c) and section 194.54(b), agricultural activities, such as fish farming, that have not taken place and are not expected to take place in the near future in the vicinity of the WIPP have been eliminated from PA calculations on regulatory grounds.

SCR-5.7.1.1.5 Future Human EPs

The EPA has provided criteria relating to future human activities in section 194.32(a) that limit the scope of consideration of future human activities in PAs to mining and drilling. Also, the criterion in section 194.25(a) concerned with predictions of the future states of society requires that compliance assessments and PAs "shall assume that characteristics of the future remain what they are at the time the compliance application is prepared." Therefore, the effects of changes in future agricultural practices (such as ranching, arable farming, and fish farming) have been eliminated from PA calculations on regulatory grounds.

SCR-5.7.2 Social and Technological Development

SCR-5.7.2.1 FEP Number: H56 FEP Title: Demographic Change and Urban Development

SCR-5.7.2.1.1 Screening Decision: SO-R (HCN) SO-R (Future)

Demographic Change and Urban Development in the near future and in the future have been eliminated from PA calculations on regulatory grounds.

SCR-5.7.2.1.2 Summary of New Information

No new information that affects the screening of this FEP has been identified since the CRA-2009.

SCR-5.7.2.1.3 Screening Argument

Social and technological changes in the future could result in the development of new communities and new activities in the vicinity of the WIPP that could have an impact on the performance of the disposal system.

Demography in the WIPP vicinity is discussed in the CCA, Chapter 2.0, Section 2.3.2.1. The community nearest to the WIPP site is the town of Loving, 29 km (18 mi) west-southwest of the site center. There are no existing plans for urban developments in the vicinity of the WIPP in the near future. Furthermore, the criterion in section 194.25(a), concerned with predictions of the future states of society, requires that compliance assessments and PAs "shall assume that characteristics of the future remain what they are at the time the compliance application is prepared." Therefore, demographic change and urban development in the vicinity of the WIPP and technological developments have been eliminated from PA calculations on regulatory grounds.

SCR-5.7.2.2 FEP Number: H57 FEP Title: Loss of Records

SCR-5.7.2.2.1 Screening Decision: Not Applicable (N/A) (HCN) DP (Future)

Loss of Records in the future is accounted for in PA calculations.

SCR-5.7.2.2.2 Summary of New Information

No new information that affects the screening of this FEP has been identified since the CRA-2009.

SCR-5.7.2.2.3 Screening Argument

Because the DOE will maintain control for the current period throughout the active institutional period (100 yrs after closure), inadvertent drilling intrusion resulting from the loss of records is not applicable during the HCN period. However, PAs must consider the potential effects of human activities that might take place within the controlled area at a time when institutional controls cannot be assumed to eliminate completely the possibility of human intrusion. Consistent with section 194.41 (b) (U.S. EPA 1996a), the DOE assumes no credit for AICs for more than 100 yrs after disposal. Also, consistent with section 194.43(c) (U.S. EPA 1996a), the DOE originally assumed in the CCA that passive institutional controls (PICs) do not eliminate the likelihood of future human intrusion entirely. The provisions at section 194.43(c) allow credit for PICs by reducing the likelihood of human intrusions for several hundred yrs. In U.S. DOE 1996a, the DOE took credit for these controls that include records retention by reducing the probability of intrusion for the first 600 yrs after active controls cease. The EPA disallowed this credit during the original certification (U.S. EPA 1998a). The DOE no longer takes credit for PICs in PA, effectively assuming that all public records and archives relating to the repository are lost 100 yrs after closure. Therefore, the DOE continues to include the loss of records FEP within PA and does not include credit for PICs.

SCR-6.0 Waste and Repository-Induced FEPs

This section presents screening arguments and decisions for waste- and repository-induced FEPs. There are 114 waste- and repository-induced FEPs used in the CRA-2014. Of these, 64 remain unchanged since the CRA-2009 and 50 were updated with new information.

SCR-6.1 Waste and Repository Characteristics

SCR-6.1.1 Repository Characteristics

SCR-6.1.1.1 FEP Number: W1 FEP Title: Disposal Geometry

SCR-6.1.1.1.1 Screening Decision: UP

The WIPP repository *Disposal Geometry* is accounted for in PA calculations.

SCR-6.1.1.1.2 Summary of New Information

The CRA-2014 will include repository changes that alter the disposal geometry. Additional tunnels in the northern region of the repository have been mined to accommodate experiments planned in the future. These experiments are not expected to affect FEPs current screening decisions, or expected repository performance. This additional mined volume (60,335 m^3) will be represented within the appropriate PA codes and models as described in Camphouse (Camphouse 2013a). This change does not affect the screening argument or decision. This FEP remains classified UP.

SCR-6.1.1.2 Screening Argument

Disposal geometry is described in the CRA-2004, Chapter 3.0, Section 3.2 and is accounted for in the setup of PA calculations (the CRA-2004, Chapter 6.0, Section 6.4.2).

SCR-6.1.2 Waste Characteristics

SCR-6.1.2.1 FEP Number: W2 and W3 FEP Title: Waste Inventory Heterogeneity of Waste Forms

SCR-6.1.2.1.1 Screening Decision: UP (W2) DP (W3)

The *Waste Inventory* and *Heterogeneity of Waste Forms* are accounted for in PA calculations.

SCR-6.1.2.1.2 Summary of New Information

The waste inventory used for the CRA-2014 PA calculations has been updated as provided in Kicker and Zeitler (Kicker and Zeitler 2013). Since these FEPs are accounted for in PA, inventory-related parameters may differ from those used in previous PAs; however, the screening decisions have not changed and these FEPs are represented in PA calculations.

SCR-6.1.2.1.3 Screening Argument

Waste characteristics, comprising the waste inventory and heterogeneity of waste forms, are described in the CCA, Appendix BIR. The waste inventory is accounted for in PA calculations in deriving the dissolved actinide source term and gas generation rates. The distribution of contact-handled transuranic (CH-TRU) and remote-handled transuranic (RH-TRU) waste within the repository leads to room-scale heterogeneity of the waste forms, which is accounted for in PA calculations when considering the potential activity of waste material encountered during inadvertent borehole intrusion (Appendix PA-2014, Section PA-3.8).

SCR-6.1.3 Container Characteristics

SCR-6.1.3.1 FEP Number: W4 FEP Title: Container Form

SCR-6.1.3.1.1 Screening Decision: SO-C - Beneficial

The *Container Form* has been eliminated from PA calculations on the basis of beneficial consequence to the performance of the disposal system.

SCR-6.1.3.1.2 Summary of New Information

The physical form of the containers is conservatively ignored in performance calculations. However, certain aspects of the container (material composition) are accounted for in PA. The waste inventory for the CRA-2014 has been updated as detailed in Van Soest (Van Soest 2012) and contains masses of container materials. While the physical form of containers will be conservatively ignored for waste containment properties (SO-C Beneficial), other aspects of the containers will be included and updated per this new waste inventory. As such, changes represented in the inventory used for this application do not affect this FEP or its screening decision.

SCR-6.1.3.1.3 Screening Argument

The container form has been eliminated from PA calculations on the basis of its beneficial effect on retarding radionuclide release. The PA assumes instantaneous container failure and waste dissolution consistent with the source-term model, even though WIPP performance calculations show that a significant fraction of steel and other Fe-base materials will remain undegraded over 10,000 yrs (see Helton et al. 1998). All these undegraded container materials will (1) prevent contact between brine and radionuclides; (2) decrease the rate and extent of radionuclide transport because of high tortuosity along the flow pathways and, as a result, increase opportunities for metallic iron (Fe) and corrosion products to beneficially reduce radionuclides to lower oxidation states. Therefore, the container form can be eliminated on the basis of its beneficial effect on retarding radionuclide transport. In the CCA, Appendix WCL, a minimum quantity of metallic Fe was specified to ensure sufficient reactants to reduce radionuclides to lower and less soluble oxidation states. This requirement is met as long as there are no substantial changes in container materials. The inventory used for the CRA-2014 contains 3.69×10^7 kg of steel in packaging (includes containers) materials. This value is up slightly from 3.59×10^7 kg reported in 2008 (Van Soest 2012). Therefore, the current inventory estimate indicates that there is a sufficient quantity of metallic iron to ensure reduction of radionuclides to lower and less soluble oxidation states.

SCR-6.1.3.2 FEP Number: W5 FEP Title: Container Material Inventory

SCR-6.1.3.2.1 Screening Decision: UP

The *Container Material Inventory* is accounted for in PA calculations.

SCR-6.1.3.2.2 Summary of New Information

The masses of container materials associated with the waste inventory for the CRA-2014 have been updated as detailed in Van Soest (Van Soest 2012).

SCR-6.1.3.2.3 Screening Argument

The container material inventory is described in Van Soest (Van Soest 2012) and is accounted for in PA calculations through the estimation of gas generation rates (see Appendix PA-2014, Section PA-4.2.5). In the CCA, Appendix WCL, a minimum quantity of metallic Fe was specified to ensure sufficient reactants to reduce radionuclides to lower and less soluble oxidation states. This requirement is met as long as there are no substantial changes in container materials. The inventory used for the CRA-2014 contains 3.69×10^7 kg of steel in packaging (includes containers) materials. This value is up slightly from 3.59×10^7 kg reported in 2008 (Van Soest 2012).

SCR-6.1.4 Seal Characteristics

SCR-6.1.4.1 FEP Numbers: W6, W7, W109, and W110 FEP Titles: Shaft Seal Geometry (W6) Shaft Seal Physical Properties (W7) Panel Closure Geometry (W109) Panel Closure Physical Properties (W110)

SCR-6.1.4.1.1 Screening Decision: UP

The Shaft Seal Geometry, Shaft Seal Physical Properties, Panel Closure Geometry, and Panel Closure Properties are accounted for in PA calculations.

SCR-6.1.4.1.2 Summary of New Information

The CRA-2014 PA includes a new PCS design constructed of run-of-mine (ROM) salt, rather than the previously planned "Option D" concrete PCS. The physical dimensions of the new ROM salt PCS are also different than the "Option D" PCS. These changes affect the implementation of both W109 *Panel Closure Geometry* and W110 *Panel Closure Physical Properties*. The manner in which these changes are implemented in PA is described in Camphouse (Camphouse 2013a).

SCR-6.1.4.1.3 Screening Argument

Shaft seal characteristics, including shaft seal geometry, and physical properties are described in the CCA, Chapter 3.0, Section 3.3.2. The ROMPCS geometry and physical properties are described in Camphouse et al. (Camphouse et al. 2012). These repository elements are accounted for in PA calculations through the representation of the seal system and panel closures in BRAGFLO and the permeabilities assigned to the shaft seal and panel closure materials (see Appendix PA-2014, Section PA-4.2.7 and Section PA-4.2.8).

SCR-6.1.4.2 FEP Numbers: W8, W111 FEP Titles: Shaft Seal Chemical Composition (W8) Panel Closure Chemical Composition (W111)

SCR-6.1.4.2.1 Screening Decision: SO-C Beneficial

The *Shaft Seal Chemical Composition* has been eliminated from PA calculations on the basis of beneficial consequence to the performance of the disposal system.

SCR-6.1.4.2.2 Summary of New Information

The CRA-2014 includes the new ROM salt PCS. While the proposed PCS design does not include the same concrete elements as the previously planned Option D, it is still considered conservative to ignore any sorptive properties potentially present in the new design.

SCR-6.1.4.2.3 Screening Argument

The effect of shaft seal chemical composition and panel closure chemical composition on actinide speciation and mobility has been eliminated from PA calculations on the basis of beneficial consequence to the performance of the disposal system.

SCR-6.1.4.2.4 Repository Seals (Shaft and Panel Closures)

Certain repository materials have the potential to interact with groundwater and significantly alter the chemical speciation of any radionuclides present. In particular, extensive use of cementitious materials in the shaft seals may have the capacity to buffer groundwaters to extremely high pH (for example, Bennett et al. 1992, pp. 315 - 325). At high pH values, the speciation and adsorption

behavior of many radionuclides is such that their dissolved concentrations are reduced in comparison with near-neutral waters. This effect reduces the migration of radionuclides in dissolved form.

Several publications describe strong actinide (or actinide analog) sorption by cement (Altenheinhaese et al. 1994; Wierczinski et al. 1998; Pointeau et al. 2001), or sequestration by incorporation into cement alteration phases (Gougar et al. 1996; Dickson and Glasser 2000). These provide support for the screening argument that chemical interactions between the cement seals and the brine will be of beneficial consequence to the performance of the disposal system.

For the PCS, choosing to ignore any sorptive properties potentially present in the new design does not create an inconsistency within the current model. Radionuclide concentrations in brine are modeled to remain constant throughout each vector and are not reduced through sorption by any closure component, regardless of its composition, even though impurities in the host rock (such as clays) have sorptive properties as well as corrosion products expected to be present in the repository.

The effects of cementitious materials in shaft seals on groundwater chemistry have been eliminated from PA calculations on the basis of beneficial consequence to the performance of the disposal system.

SCR-6.1.5 Backfill Characteristics

SCR-6.1.5.1 FEP Number: W9 FEP Title: Backfill Physical Properties

SCR-6.1.5.1.1 Screening Decision: SO-C

Backfill Physical Properties have been eliminated from PA calculations on the basis of low consequence to the performance of the disposal system.

SCR-6.1.5.1.2 Summary of New Information

No new information that affects the screening of this FEP has been identified since the CRA-2009.

SCR-6.1.5.1.3 Screening Argument

A chemical backfill is being added to the disposal room to buffer the chemical environment. The backfill characteristics were previously described in the CCA, Appendix BACKwith additional information contained in Appendix BARRIERS-2004, Section BARRIERS-2.3.4.3. The mechanical and thermal effects of backfill are discussed in W35 (Section SCR-6.3.5.4) and W72 (Section SCR-6.3.4.1) respectively, where they have been eliminated from PA calculations on the basis of low consequence to the performance of the disposal system. Backfill will result in an initial permeability for the disposal room lower than that of an empty cavity, so neglecting the hydrological effects of backfill is a conservative assumption with regard to brine inflow and radionuclide migration. Thus, backfill physical properties have been eliminated from PA calculations on the basis of low consequence to the performance of the disposal system.

SCR-6.1.5.2 FEP Number: W10 FEP Title: Backfill Chemical Composition

SCR-6.1.5.2.1 Screening Decision: UP

The *Backfill Chemical Composition* is accounted for in PA calculations.

SCR-6.1.5.2.2 Summary of New Information

The CRA-2014 PA contains a refinement of water balance within the repository. This refinement is implemented within the Chemical Conditions Conceptual Model, and will include the major gas- and brine-producing and consuming reactions within the existing model, one of which is MgO hydration (see Camphouse 2013a). This model enhancement does not change the screening argument or decision for this FEP, but is mentioned here for completeness.

SCR-6.1.5.2.3 Screening Argument

A chemical backfill is added to the disposal room to buffer the chemical environment. The backfill characteristics are described in Appendix MgO-2009, Section MgO-3.0. The mechanical and thermal effects of backfill are discussed in W35 (Section SCR-6.3.5.4) and W72 (Section SCR-6.3.4.1), respectively, where they have been eliminated from PA calculations on the basis of low consequence to the performance of the disposal system. Backfill chemical composition is accounted for in PA calculations in deriving the dissolved and colloidal actinide source terms (see Appendix SOTERM-2014, Section SOTERM-2.3 , -3.9, -4.6, and -4.7, Appendix MgO-2009, Section MgO-5.0 , and Brush and Domski 2013a) and in the production of gas within the repository.

SCR-6.1.6 Post-Closure Monitoring Characteristics

SCR-6.1.6.1 FEPs Number: W11 FEP Title: Post-Closure Monitoring

SCR-6.1.6.1.1 Screening Decision: SO-C

The potential effects of *Post-Closure Monitoring* have been eliminated from PA calculations on the basis of low consequence to the performance of the disposal system.

SCR-6.1.6.1.2 Summary of New Information

No new information that affects the screening of this FEP has been identified since the CRA-2009.

SCR-6.1.6.1.3 Screening Argument

Post-closure monitoring is required by section 191.14(b) (U.S. EPA 1993) as an assurance requirement to "detect substantial and detrimental deviations from expected performance." The DOE has designed the monitoring program (see the CCA, Appendix MON) so that the monitoring methods employed are not detrimental to the performance of the disposal system (section 194.42(d)) (U.S. EPA 1996a). Nonintrusive monitoring techniques are used so that post-closure monitoring would not impact containment or require remedial activities. In summary, the effects of monitoring have been

eliminated from PA calculations on the basis of low consequence to the performance of the disposal system.

SCR-6.2 Radiological FEPs

SCR-6.2.1 Radioactive Decay and Heat

SCR-6.2.1.1 FEP Number: W12 FEP Title: Radionuclide Decay and Ingrowth

SCR-6.2.1.1.1 Screening Decision: UP

Radionuclide decay and ingrowthare accounted for in PA calculations.

SCR-6.2.1.1.2 Summary of New Information

No new information that affects the screening of this FEP has been identified since the CRA-2009.

SCR-6.2.1.1.3 Screening Argument

Radionuclide decay and ingrowth are accounted for in PA calculations (see Appendix PA-2014, Section PA-4.3).

SCR-6.2.1.2 FEP Number: W13 FEP Title: Heat From Radioactive Decay

SCR-6.2.1.2.1 Screening Decision: SO-C

The effects of temperature increases as a result of *Heat From Radioactive Decay* have been eliminated from PA calculations on the basis of low consequence to the performance of the disposal system.

SCR-6.2.1.2.2 Summary of New Information

The radionuclide inventory used for the CRA-2014 PA calculations (Kicker and Zeitler 2013) is lower than previously estimated for the CCA. Thus, all CRA-2014 radioactive decay heat screening arguments are bounded by the previous CCA screening arguments.

SCR-6.2.1.2.3 Screening Argument

Radioactive decay of the waste emplaced in the repository will generate heat. The importance of heat from radioactive decay depends on the effects that the induced temperature changes would have on mechanics (W29 - W31, Section SCR-6.3.4.1), fluid flow (W40 and W41, Section SCR-6.4.1.1), and geochemical processes (W44 through W75, Section SCR-6.5.1.1 , Section SCR-6.5.1.2, Section SCR-6.5.1.3, Section SCR-6.5.1.4, Section SCR-6.5.1.5, Section SCR-6.5.1.6, Section SCR-6.5.1.7, Section SCR-6.5.1.8, Section SCR-6.5.1.9, Section SCR-6.5.2.1, Section SCR-6.5.2.2, Section SCR-6.5.3.1, Section SCR-6.5.4.1, Section SCR-6.5.5.1, Section SCR-6.5.5.2, Section SCR-6.5.5.3, Section SCR-6.5.6.1, Section SCR-6.5.7.1, Section SCR-6.5.7.1, and Section SCR-6.5.7.2). For

example, extreme temperature increases could result in thermally induced fracturing, regional uplift, or thermally driven flow of gas and brine in the vicinity of the repository.

The design basis for the WIPP requires that the thermal loading does not exceed 10 kilowatts (kW) per acre. Transportation restrictions also require that the thermal power generated by waste in an RH-TRU container shall not exceed 300 watts (U.S. Nuclear Regulatory Commission 2002).

The DOE has conducted numerous studies related to heat from radioactive decay. The following presents a brief summary of these past analyses. First, a numerical study to calculate induced temperature distributions and regional uplift is reported in DOE (U.S. DOE 1980, pp. 9-149 through 9-150). This study involved estimation of the thermal power of CH-TRU waste containers. The DOE (U.S. DOE 1980, p. 9-149) analysis assumed the following:

- All CH-TRU waste drums and boxes contain the maximum permissible quantity of Pu. The fissionable radionuclide content for CH-TRU waste containers was assumed to be no greater than 200 grams (g) per 0.21 m^3 (7 ounces [oz] per 7.4 ft^3) drum and 350 g/1.8 m^3 (12.3 oz/63.6 ft^3) standard waste box (^{239}Pu fissile gram equivalents).

- The Pu in CH-TRU waste containers is weapons grade material producing heat at 0.0024 watts per gram (W/g). Thus, the thermal power of a drum is approximately 0.5 W, and that of a box is approximately 0.8 W.

- Approximately 3.7×10^5 m^3 (1.3×10^7 ft^3) of CH-TRU waste are distributed within a repository enclosing an area of 7.3×10^5 m^2 (7.9×10^6 ft^2). This is a conservative assumption in terms of quantity and density of waste within the repository, because the maximum capacity of the WIPP is 1.756×10^5 m^3 (6.2×10^6 ft^3) for all waste (as specified by the LWA) to be placed in an enclosed area of approximately 5.1×10^5 m^2 (16 mi^2).

- Half of the CH-TRU waste volume is placed in drums and half in boxes so that the repository will contain approximately 900,000 drums and 900,000 boxes. Thus, a calculated thermal power of 0.7 W/m^2 (2.8 kW/acre) of heat is generated by the CH-TRU waste.

- Insufficient RH-TRU waste would be emplaced in the repository to influence the total thermal load.

Under these assumptions, Thorne and Rudeen (Thorne and Rudeen 1981) estimated the long-term temperature response of the disposal system to waste emplacement. Calculations assumed a uniform initial power density of 2.8 kW/acre (0.7 W/m^2) which decreases over time. Thorne and Rudeen (Thorne and Rudeen 1981) attributed this thermal load to RH-TRU waste, but the DOE (U.S. DOE 1980) more appropriately attributed this thermal load to CH-TRU waste based on the assumptions listed above. Thorne and Rudeen (Thorne and Rudeen 1981) estimated the maximum rise in temperature at the center of a repository to be 1.6 °C (2.9 °F) at 80 yrs after waste emplacement.

More recently, Sanchez and Trellue (Sanchez and Trellue 1996) estimated the maximum thermal power of an RH-TRU waste container. The Sanchez and Trellue (Sanchez and Trellue 1996) analysis involved inverse shielding calculations to evaluate the thermal power of an RH-TRU container corresponding to the maximum permissible surface dose of 1,000 rem per hour (rem/hr). The following calculational steps were taken in the Sanchez and Trellue (Sanchez and Trellue 1996) analysis:

- Calculate the absorbed dose rate for gamma radiation corresponding to the maximum surface dose equivalent rate of 1,000 rem/hr. Beta and alpha radiation are not included in this calculation because such particles will not penetrate the waste matrix or the container in significant quantities. Neutrons are not included in the analysis because the maximum dose rate from neutrons is 270 millirems/hr, and the corresponding neutron heating rate will be insignificant.

- Calculate the exposure rate for gamma radiation corresponding to the absorbed dose rate for gamma radiation.

- Calculate the gamma flux density at the surface of a RH-TRU container corresponding to the exposure rate for gamma radiation. Assuming the gamma energy is 1.0 megaelectron volts, the maximum allowable gamma flux density at the surface of a RH-TRU container is about 5.8×10^8 gamma rays/cm^2/seconds (s).

- Determine the distributed gamma source strength, or gamma activity, in an RH-TRU container from the surface gamma flux density. The source is assumed to be shielded such that the gamma flux is attenuated by the container and by absorbing material in the container. The level of shielding depends on the matrix density. Scattering of the gamma flux, with loss of energy, is also accounted for in this calculation through inclusion of a gamma buildup factor. The distributed gamma source strength is determined assuming a uniform source in a right cylindrical container. The maximum total gamma source (gamma curies [Ci]) is then calculated for a RH-TRU container containing 0.89 m^3 (31.4 ft^3) of waste. For the waste of greatest expected density (about 6,000 kg/m^3 (360 lb/ft^3), the gamma source is about 2×10^4 Ci/m^3 (566 Ci/ft^3).

- Calculate the total Ci load of a RH-TRU container (including alpha and beta radiation) from the gamma load. The ratio of the total Ci load to the gamma Ci load was estimated through examination of the radionuclide inventory presented in the CCA, Appendix BIR. The gamma Ci load and the total Ci load for each radionuclide listed in the WIPP BIR were summed. Based on these summed loads the ratio of total Ci load to gamma Ci load of RH-TRU waste was calculated to be 1.01.

- Calculate the thermal load of a RH-TRU container from the total Ci load. The ratio of thermal load to Ci load was estimated through examination of the radionuclide inventory presented in the CCA, Appendix BIR. The thermal load and the total Ci load for each radionuclide listed in the WIPP inventory were summed. Based on these summed loads the ratio of thermal load to Ci load of RH-TRU waste was calculated to be about 0.0037 watts per curie (W/Ci). For a gamma source of 2×10^4 Ci/m^3 (566 Ci/ft^3), the maximum permissible thermal load of a RH-TRU container is about 70 W/m^3 (2 W/ft^3). Thus, the maximum thermal load of a RH-TRU container is about 60 W, and the transportation limit of 300 W will not be achieved.

Note that Sanchez and Trellue (Sanchez and Trellue 1996) calculated the average thermal load for a RH-TRU container to be less than 1 W. Also, the total RH-TRU heat load is less than 10% of the total heat load in the WIPP. Thus, the total thermal load of the RH-TRU waste will not significantly affect the average rise in temperature in the repository resulting from decay of CH-TRU waste.

Temperature increases will be greater at locations where the thermal power of an RH-TRU container is 60 W, if any such containers are emplaced. Sanchez and Trellue (Sanchez and Trellue 1996) estimated the temperature increase at the surface of a 60 W RH-TRU waste container. Their analysis involved solution of a steady-state thermal conduction problem with a constant heat source term of 70 W/m^3 (2 W/ft^3). These conditions represent conservative assumptions because the thermal load will decrease with time as the radioactive waste decays. The temperature increase at the surface of the container was calculated to be about 3 °C (5.4 °F).

In summary, previous analyses have shown that the average temperature increase in the WIPP repository caused by radioactive decay of the emplaced CH- and RH-TRU waste will be less than 2 ° C (3.6 °F). Temperature increases of about 3 °C (5.4 °F) may occur in the vicinity of RH-TRU containers with the highest allowable thermal load of about 60 W (based on the maximum allowable surface dose equivalent for RH-TRU containers). Potential heat generation from nuclear criticality is discussed in Section SCR-6.2.1.3 and exothermic reactions and the effects of repository temperature changes on mechanics are discussed in the set of FEPs grouped as W29, W30, W31, W72, and W73 (Section SCR-6.3.4.1). These FEPs have been eliminated from PA calculations on the basis of low consequence to the performance of the disposal system.

Additionally, WIPP transportation restrictions and WIPP design basis loading configurations do not allow the thermal load of the WIPP to exceed 10 kW/acre (NRC 2002). Transportation requirements restrict the thermal load from RH-TRU waste containers to no more than 300 W per container (NRC 2002). However, the limit on the surface dose equivalent rate of the RH-TRU containers (1,000 rem/hr) is more restrictive and equates to a thermal load of only about 60 W per container. Based on the thermal loads permitted, the maximum temperature rise in the repository from radioactive decay heat should be less than 2 °C (3.6 °F).

The previous FEPs screening arguments for the CCA used a bounding radioactivity heat load of 0.5 W/drum for the CH-TRU waste containers. With a total CH-TRU volume of 168,500 m^3 (~5,950,000 ft^3) this corresponds to approximately 810,000 55-gal drum equivalents with a corresponding heat load of > 400 kW used for the CCA FEPs screening arguments. From Sanchez and Trellue (Sanchez and Trellue 1996), it can be seen that a realistic assessment of the heat load, based on radionuclide inventory data in the Transuranic Waste Baseline Inventory Report is less than 100 kW. Thus, the CCA FEPs incorporate a factor of safety of at least four, and heat loads from the CRA-2014 inventory would be even less.

SCR-6.2.1.3 FEPs Number: W14 FEPs Title: Nuclear Criticality: Heat

SCR-6.2.1.3.1 Screening Decision: SO-P

Nuclear Criticality has been eliminated from PA calculations on the basis of low probability of occurrence over 10,000 yrs.

SCR-6.2.1.3.2 Summary of New Information

The screening argument for this FEP has been updated to reference the inventory used in the CRA-2014. The arguments and conclusions have not been changed as a result of this new information.

SCR-6.2.1.3.3 Screening Argument

Nuclear criticality refers to a sustained fission reaction that may occur if fissile radionuclides reach both a sufficiently high concentration and total mass (where the latter parameter includes the influence of enrichment of the fissile radionuclides). In the subsurface, the primary effect of a nuclear reaction is the production of heat.

Nuclear criticality (near and far field) was eliminated from PA calculations for the WIPP for waste contaminated with TRU radionuclides. The probability for criticality within the repository is low (there are no mechanisms for concentrating fissile radionuclides dispersed amongst the waste). Possible mechanisms for concentration in the waste disposal region include high solubility, compaction, sorption, and precipitation. First, the maximum solubility of ^{239}Pu in the WIPP repository, the most abundant fissile radionuclide, is orders of magnitude lower than necessary to create a critical solution. The same is true for ^{235}U, the other primary fissile radionuclide. Second, the waste is assumed to be compacted by repository processes to one fourth its original volume. This compaction is still an order of magnitude too disperse (many orders of magnitude too disperse if neutron absorbers that prevent criticality (for example, ^{238}U) are included). Third, any potential sorbents in the waste would be fairly uniformly distributed throughout the waste disposal region; consequently, concentration of fissile radionuclides in localized areas through sorption is improbable. Fourth, precipitation requires significant localized changes in brine chemistry; small local variations are insufficient to separate substantial amounts of ^{239}Pu from other actinides in the waste disposal region (for example, 11 times more ^{238}U is present than ^{239}Pu).

Criticality away from the repository (following an inadvertent human intrusion) has a low probability because (1) the amount of fissile material transported from the repository is small; (2) host rock media have small porosities (insufficient for the generation of a sizable precipitation zone); and (3) no credible mechanism exists for concentrating fissile material during transport (the natural tendency is for transported material to be dispersed). As discussed in the CRA-2004, Chapter 6.0, Section 6.4.6.2, and Appendix PA-2004, Attachment MASS, Section MASS-15.0 , the dolomite porosity consists of intergranular porosity, vugs, microscopic fractures, and macroscopic fractures. As discussed in the CRA-2004, Chapter 6.0, Section 6.4.5.2, porosity in the MBs consists of partially healed fractures that may dilate as pressure increases. Advective flow in both units occurs mostly through macroscopic fractures. Consequently, any potential deposition through precipitation or sorption is constrained by the depth to which precipitation and sorption occur away from fractures. This geometry is not favorable for fission reactions and eliminates the possibility of criticality. Thus, nuclear criticality has been eliminated from PA calculations on the basis of low probability of occurrence.

Additionally, screening arguments made in Rechard et al. (Rechard et al. 1996) are represented in greater detail in Rechard et al. (Rechard et al. 2000 and Rechard et al. 2001). A major finding among the analysis results in the screening arguments is the determination that fissile material would need to be reconcentrated by three orders of magnitude in order to be considered in a criticality scenario. Because inventory values reported in Kicker and Zeitler (Kicker and Zeitler 2013) are below that used in previous calculations, screening analyses for nuclear criticality are conservatively bounded by the previous CCA screening arguments (Rechard et al. 1996, Rechard et al. 2000, and Rechard et al. 2001).

SCR-6.2.2 Radiological Effects on Material Properties

SCR-6.2.2.1 FEP Numbers: W15, W16, W17, and W112 FEP Titles: Radiological Effects on Waste(W15) Radiological Effects on Containers (W16) Radiological Effects on Shaft Seals (W17) Radiological Effects on Panel Closures (W112)

SCR-6.2.2.1.1 Screening Decision: SO-C

Radiological Effects on the properties of the *Waste*, *Containers*, *Shaft Seals*, and *Panel Closures* have been eliminated from PA calculations on the basis of low consequence to the performance of the disposal system.

SCR-6.2.2.1.2 Summary of New Information

The screening arguments for these FEPs have been updated to include references to the radionuclide inventory used for CRA-2014 PA calculations.

SCR-6.2.2.1.3 Screening Argument

Ionizing radiation can change the physical properties of many materials. Strong radiation fields could lead to damage of waste matrices, brittleness of the metal containers, and disruption of any crystalline structure in the seals. The low level of activity of the waste in the WIPP is unlikely to generate a strong radiation field. According to the inventory data presented in Van Soest (Van Soest 2012) and Kicker and Zeitler (Kicker and Zeitler 2013), the overall activity for all TRU radionuclides has decreased from 3.44×10^6 Ci reported in the CCA, to 2.48×10^6 Ci in the CRA-2004, to 2.32×10^6 Ci in the CRA-2009, to 2.06×10^6 Ci for the CRA-2014. This decrease will not change the original screening argument. Furthermore, PA calculations assume instantaneous container failure and waste dissolution according to the source-term model (see the CCA, Chapter 6.0, Section 6.4.3.4, Section 6.4.3.5, and Section 6.4.3.6). Therefore, radiological effects on the properties of the waste, container, shaft seals, and panel closures have been eliminated from PA calculations on the basis of low consequence to the performance of the disposal system.

SCR-6.3 Geological and Mechanical FEPs

SCR-6.3.1 Excavation-Induced Changes

SCR-6.3.1.1 FEP Numbers: W18 and W19 FEP Titles: Disturbed Rock Zone (W18) Excavation-Induced Change in Stress (W19)

SCR-6.3.1.1.1 Screening Decision: UP

Excavation-induced host rock fracturing through formation of a *Disturbed Rock Zone* and *Changes in Stress* are accounted for in PA calculations.

SCR-6.3.1.1.2 Summary of New Information

Implementation of the new ROM salt PCS in PA requires new parameters for the DRZ above the PCS. Modifications to relevant parameters are described in Camphouse (Camphouse 2013a). These

changes are downstream of the FEPs screening process, and will not change the screening decision; these FEPs will remain classified UP.

SCR-6.3.1.1.3 Screening Argument

Construction of the repository has caused local excavation-induced changes in stress in the surrounding rock as discussed in the CCA, Chapter 3.0, Section 3.3.1.5. Excavation-induced changes in stress has led to failure of intact rock around the opening, creating a DRZ of fractures. On completion of the WIPP excavation, the extent of the induced stress field perturbation will be sufficient to have caused dilation and fracturing in the anhydrite layers "a" and "b," MB 139, and, possibly, MB 138. The creation of the DRZ around the excavation and the disturbance of the anhydrite layers and MBs will alter the permeability and effective porosity of the rock around the repository, providing enhanced pathways for flow of gas and brine between the waste-filled rooms and the nearby interbeds. This excavation-induced, host-rock fracturing is accounted for in PA calculations (the CCA, Chapter 6.0, Section 6.4.5.3).

SCR-6.3.1.2 FEP Numbers: W20 and W21 FEP Titles: Salt Creep(W20) Change in the Stress Field (W21)

SCR-6.3.1.2.1 Screening Decision: UP

Salt Creep in the Salado and any resultant *Changes in the Stress Field* are accounted for in PA calculations.

SCR-6.3.1.2.2 Summary of New Information

Salt creep and changes in stress will affect the consolidation of the ROM salt PCS over time. Modifications to relevant parameters are described in Camphouse (Camphouse 2013a). These changes are downstream of the FEPs screening process, and will not change the screening decision; these FEPs will remain classified UP.

SCR-6.3.1.2.3 Screening Argument

Salt creep will lead to changes in the stress field, compaction of the waste and containers, and consolidation of the long-term components of the sealing system. It will also tend to close fractures in the DRZ, leading to reductions in porosity and permeability, increases in pore fluid pressure, and reductions in fluid flow rates in the repository. Salt creep in the Salado is accounted for in PA calculations (the CCA, Chapter 6.0, Section 6.4.3.1). The long-term repository seal system relies on the consolidation of the crushed-salt seal material and healing of the DRZ around the shaft seals and in and around the panel closures to achieve a low permeability under stresses induced by salt creep. Shaft seal and panel closure performance is discussed further in Section SCR-6.3.5.1 (FEPs W36, W37, W113, and W114).

SCR-6.3.1.3 FEP Number: W22 FEP Title: Roof Falls

SCR-6.3.1.3.1 Screening Decision: UP

The potential effects of *Roof Ralls* on flow paths are accounted for in PA calculations.

SCR-6.3.1.3.2 Summary of New Information

No new information that affects the screening of this FEP has been identified since the CRA-2009.

SCR-6.3.1.3.3 Screening Argument

Instability of the DRZ could lead to localized roof falls in the first few hundred yrs. If instability of the DRZ causes roof falls, development of the DRZ may be sufficient to disrupt the anhydrite layers above the repository, which may create a zone of rock containing anhydrite extending from the interbeds toward a waste-filled room. Fracture development is most likely to be induced as the rock stress and strain distributions evolve because of creep. In the long term, the effects of roof falls in the repository are likely to be minor because salt creep will reduce the void space and the potential for roof falls as well as promote healing of any roof material that has fallen into the rooms. However, because of uncertainty in the process by which the disposal room DRZ heals, the flow model used in PA assumes that a higher permeability zone remains for the long term. Thus, the potential effects of roof falls on flow paths are accounted for in PA calculations through appropriate ranges of the parameters describing the DRZ.

SCR-6.3.1.4 FEP Numbers: W23 and W24 FEP Titles: Subsidence (W23) Large Scale Rock Fracturing (W24)

SCR-6.3.1.4.1 Screening Decision(s): SO-C (W23) SO-P (W24)

Fracturing within units overlying the Salado and surface displacement caused by *Subsidence* associated with repository closure have been eliminated from PA calculations on the basis of low consequence to the performance of the disposal system. The potential for excavation- or repository-induced *Subsidence* to create *Large Scale Rock Fracturing* and fluid flow paths between the repository and units overlying the Salado has been eliminated from PA calculations on the basis of the low probability of occurrence over 10,000 yrs.

SCR-6.3.1.4.2 Summary of New Information

No new information that affects the screening of this FEP has been identified since the CRA-2009.

SCR-6.3.1.4.3 Screening Argument

Instability of the DRZ could lead to localized roof falls in the first few hundred yrs. If instability of the DRZ causes roof falls, development of the DRZ may be sufficient to disrupt the anhydrite layers above the repository, which may create a zone of rock containing anhydrite extending from the interbeds toward a waste-filled room. Fracture development is most likely to be induced as the rock stress and strain distributions evolve because of creep and the local lithologies. In the long term, the effects of roof falls in the repository are likely to be minor because salt creep will reduce the void space and the potential for roof falls as well as promote healing of any roof material that has fallen into the rooms. Because of uncertainty in the process by which the disposal room DRZ heals, the flow model used in PA assumed that a higher-permeability zone remained for the long term. The CCA

PAVT modified the DRZ permeability to a sampled range. Thus, the potential effects of roof falls on flow paths are accounted for in PA calculations through appropriate ranges of the parameters describing the DRZ.

The amount of subsidence that can occur as a result of salt creep closure or roof collapse in the WIPP excavation depends primarily on the volume of excavated rock, the initial and compressed porosities of the various emplaced materials (waste, backfill, panel and drift closures, and seals), the amount of inward creep of the repository walls, and the gas and fluid pressures within the repository. The DOE (Westinghouse 1994) has analyzed potential excavation-induced subsidence with the primary objective of determining the geomechanical advantage of backfilling the WIPP excavation. The DOE (Westinghouse 1994, pp. 3-4 through 3-23) used mass conservation calculations, the influence function method, the National Coal Board empirical method, and the two-dimensional, finite-difference-code, Fast Lagrangian Analysis of Continua (FLAC) to estimate subsidence for conditions ranging from no backfill to emplacement of a highly compacted crushed-salt backfill. The DOE (Westinghouse 1994, pp. 2-17 to 2-23) also investigated subsidence at potash mines located near the WIPP site to gain insight into the expected subsidence conditions at the WIPP and to calibrate the subsidence calculation methods.

Subsidence over potash mines will be much greater than subsidence over the WIPP because of the significant differences in stratigraphic position, depth, extraction ratio, and layout. The WIPP site is located stratigraphically lower than the lowest potash mine, which is near the base of the McNutt. At the WIPP site, the base of the McNutt is about 150 m (490 ft) above the repository horizon. The WIPP rock extraction ratio in the waste disposal region will be about 22%, as compared to 65% for the lowest extraction ratios within potash mines investigated by the DOE (Westinghouse 1994, p. 2-17).

The DOE (Westinghouse 1994, p. 2-22) reported the maximum total subsidence at potash mines to be about 1.5 m (5 ft). This level of subsidence has been observed to have caused surface fractures. However, the DOE (Westinghouse 1994, p. 2-23) found no evidence that subsidence over potash mines had caused fracturing sufficient to connect the mining horizon to water-bearing units or the land surface. The level of disturbance caused by subsidence above the WIPP repository will be less than that associated with potash mining and thus, by analogy, will not create fluid flow paths between the repository and the overlying units.

The various subsidence calculation methods used by the DOE (Westinghouse 1994, pp. 3-4 to 3-23) provided similar and consistent results, which support the premise that subsidence over the WIPP will be less than subsidence over potash mines. Estimates of maximum subsidence at the land surface for the cases of no backfill and highly compacted backfill are 0.62 m (2 ft) and 0.52 m (1.7 ft), respectively. The mass conservation method gave the upper bound estimate of subsidence in each case. The surface topography in the WIPP area varies by more than 3 m (10 ft), so the expected amount of repository-induced subsidence will not create a basin, and will not affect surface hydrology significantly. The DOE (Westinghouse 1994, Table 3-13) also estimated subsidence at the depth of the Culebra using the FLAC model for the case of an empty repository (containing no waste or backfill). The FLAC analysis assumed the Salado to be halite and the Culebra to have anhydrite material parameters.

Maximum subsidence at the Culebra was estimated to be 0.56 m (1.8 ft). The vertical strain was concentrated in the Salado above the repository. Vertical strain was less than 0.01% in units overlying the Salado and was close to zero in the Culebra (Westinghouse 1994, Figure 3-40). The maximum horizontal displacement in the Culebra was estimated to be 0.02 m (0.08 ft), with a maximum tensile

horizontal strain of 0.007%. The DOE (Westinghouse 1994, 4-1 to 4-2) concluded that the induced strains in the Culebra will be uniformly distributed because no large-scale faults or discontinuities are present in the vicinity of the WIPP. Furthermore, strains of this magnitude would not be expected to cause extensive fracturing.

At the WIPP site, the Culebra transmissivity varies spatially over approximately five orders of magnitude (see Appendix TFIELD-2009, Figure TFIELD-64). Where transmissive horizontal fractures exist, hydraulic conductivity in the Culebra is dominated by flow through the fractures. An induced tensile vertical strain may result in an increase in fracture aperture and corresponding increases in hydraulic conductivity. The magnitude of increase in hydraulic conductivity can be estimated by approximating the hydrological behavior of the Culebra with a simple conceptual model of fluid flow through a series of parallel fractures with uniform properties. A conservative estimate of the change in hydraulic conductivity can be made by assuming that all the vertical strain is translated to fracture opening (and none to rock expansion). This method for evaluating changes in hydraulic conductivity is similar to that used by the EPA in estimating the effects of subsidence caused by potash mining (Peake 1996; U.S. EPA 1996c).

The equivalent porous medium hydraulic conductivity, K (m/s), of a system of parallel fractures can be calculated assuming the cubic law for fluid flow (Witherspoon et al. 1980):

$$K = \frac{w^3 \rho g N}{12 \mu D} \quad \text{(SCR.10)}$$

where w is the fracture aperture, ρ is the fluid density (taken to be 1,000 kg/m^3), g is the acceleration due to gravity (9.81 m/s^2 (32 ft) per second squared), μ is the fluid viscosity (taken as 0.001 pascal seconds), D is the effective Culebra thickness (7.7 m (26.3 ft)), and N is the number of fractures. For 10 fractures with a fracture aperture, w, of 6×10^{-5} m (2×10^{-4} ft), the Culebra hydraulic conductivity, K, is approximately 7 m per yr (2×10^{-7} m (6.5×10^{-7} ft) per second). The values of the parameters used in this calculation are within the range of those expected for the Culebra at the WIPP site (Appendix TFIELD-2009).

The amount of opening of each fracture as a result of subsidence-induced tensile vertical strain, ε, (assuming rigid rock), is $D\varepsilon/N$ meters. Thus, for a vertical strain of 0.0001, the fracture aperture, w, becomes approximately 1.4×10^{-4} m. The Culebra hydraulic conductivity, K, then increases to approximately 85 m (279 ft) per yr (2.7×10^{-6} m (8.9×10^{-6} ft) per second). Thus, on the basis of a conservative estimate of vertical strain, the hydraulic conductivity of the Culebra may increase by an order of magnitude. In PA calculations, multiple realizations of the Culebra T-fields are generated as a means of accounting for spatial variability and uncertainty . A change in hydraulic conductivity of one order of magnitude through vertical strain is within the range of uncertainty incorporated in the Culebra T-fields through these multiple realizations. Thus, changes in the horizontal component of Culebra hydraulic conductivity resulting from repository-induced subsidence have been eliminated from PA calculations on the basis of low consequence.

A similar calculation can be performed to estimate the change in vertical hydraulic conductivity in the Culebra as a result of a horizontal strain of 0.00007 m/m (Westinghouse 1994, p. 3-20). Assuming this strain to be distributed over about 1,000 fractures (neglecting rock expansion), with zero initial aperture, in a lateral extent of the Culebra of about 800 m (2,625 ft) (Westinghouse 1994, Figure 3-39), then the subsidence-induced fracture aperture is approximately 6×10^{-5} m (1.9×10^{-4} ft).

Using the values for ρ, g, and μ, above, the vertical hydraulic conductivity of the Culebra can then be calculated, through an equation similar to above, to be 7 m (23 ft) per yr (2×10^{-7} m (6.5×10^{-7} ft) per second). Thus, vertical hydraulic conductivity in the Culebra may be created as a result of repository-induced subsidence, although this is expected to be insignificant.

In summary, as a result of observations of subsidence associated with potash mines in the vicinity of the WIPP, the potential for subsidence to create fluid flow paths between the repository and units overlying the Salado has been eliminated from PA calculations on the basis of low probability. The effects of repository-induced subsidence on hydraulic conductivity in the Culebra have been eliminated from PA calculations on the basis of low consequence to the performance of the disposal system.

SCR-6.3.2 Effects of Fluid Pressure Changes

SCR-6.3.2.1 FEP Numbers: W25 and W26 FEP Titles: Disruption Due to Gas Effects (W25) Pressurization (W26)

SCR-6.3.2.1.1 Screening Decision: UP

The mechanical effects of gas generation through *Pressurization* and *Disruption Due to Gas Effects* flow are accounted for in PA calculations.

SCR-6.3.2.1.2 Summary of New Information

Iron corrosion experiments (Wall and Enos 2006) have been completed since the CRA-2009 that provide new corrosion rates for expected WIPP-relevant conditions (Roselle 2013). These rates are implemented with a new parameter distribution type and values for the parameter STEEL:CORRMCO2. This parametric change does not affect the screening argument, decision, or the implementation of gas generation (pressurization) within PA models.

SCR-6.3.2.1.3 Screening Argument

The mechanical effects of gas generation, including the slowing creep closure of the repository because of gas pressurization and the fracturing of interbeds in the Salado through disruption due to gas effects are accounted for in PA calculations (the CCA, Chapter 6.0, Section 6.4.5.2 and Section 6.4.3.1).

SCR-6.3.3 Effects of Explosions

SCR-6.3.3.1 FEP Number: W27 FEP Title: Gas Explosions

SCR-6.3.3.1.1 Screening Decision: UP

The potential effects of *Gas Explosions* are accounted for in PA calculations.

SCR-6.3.3.1.2 Summary of New Information

No new information that affects the screening of this FEP has been identified since the CRA-2009.

SCR-6.3.3.1.3 Screening Argument

Explosive gas mixtures could collect in the head space above the waste in a closed panel. The most explosive gas mixture potentially generated will be a mixture of hydrogen, methane (CH_4), and oxygen, which will convert to CO_2 and water on ignition. This means that there is little likelihood of a gas explosion in the long term because the rooms and panels are expected to become anoxic and oxygen depleted. Compaction through salt creep will also greatly reduce any void space in which the gas can accumulate. Analysis (see Appendix BARRIERS-2004, Attachment PCS) indicates that the most explosive mixture of hydrogen, CH_4, and oxygen will be present in the void space approximately 20 yrs after panel-closure emplacement. This possibility of an explosion prior to the occurrence of anoxic conditions is considered in the design of the operational panel closure. The effect of such an explosion on the DRZ is expected to be no more severe than a roof fall, which is accounted for in the PA calculations (FEP W22).

SCR-6.3.3.2 FEP Number: W28 FEP Title: Nuclear Explosions

SCR-6.3.3.2.1 Screening Decision: SO-P

Nuclear Explosions have been eliminated from PA calculations on the basis of low probability of occurrence over 10,000 yrs.

SCR-6.3.3.2.2 Summary of New Information

This FEP has been updated to include the most recent inventory information as presented in Kicker and Zeitler (Kicker and Zeitler 2013). This new information does not change the screening argument or decision for this FEP.

SCR-6.3.3.2.3 Screening Argument

Nuclear explosions have been eliminated from PA calculations on the basis of low probability of occurrence over 10,000 yrs. For a nuclear explosion to occur, a critical mass of Pu would have to undergo rapid compression to a high density. Even if a critical mass of Pu could form in the system, there is no mechanism for rapid compression. Inventory information used for the CRA-2014 is presented in Kicker and Zeitler (Kicker and Zeitler 2013). The updated inventory information for the CRA-2014 shows a reduction of TRU radionuclides from previous estimates. Thus, current criticality screening arguments are conservatively bounded by the previous CCA screening arguments (Rechard et al. 1996, Rechard et al. 2000, and Rechard et al. 2001).

SCR-6.3.4 Thermal Effects

SCR-6.3.4.1 FEP Numbers: W29, W30, W31, W72, and W73 FEP Titles: Thermal Effects on Material Properties (W29) Thermally-Induced Stress Changes (W30) Differing Thermal Expansion of Repository Components (W31) Exothermic Reactions (W72) Concrete Hydration (W73)

SCR-6.3.4.1.1 Screening Decision: SO-C

The effects of *Thermally-Induced Stress*, *Differing Thermal Expansion of Repository Components*, and *Thermal Effects on Material Properties* in the repository have been eliminated from PA calculations on the basis of low consequence to performance of the disposal system.

The thermal effects of *Exothermic Reactions*, including *Concrete Hydration*, have been eliminated from PA calculations on the basis of low consequence to the performance of the disposal system.

SCR-6.3.4.1.2 Summary of New Information

This FEP has been updated to include the most recent inventory information as presented in Van Soest (Van Soest 2012). Thermal calculations have been updated with the updated quantities of reactants and provided below. Additionally, planned Salt Disposal Investigations (SDI) experiments as detailed in Patterson (Patterson 2011) or the Salt Defense Disposal Investigations (SDDI) (Franco 2012) will place heaters in newly excavated tunnels in the northern experimental region of the WIPP. Mining has been completed, but heater tests have not yet commenced. An evaluation conducted by Kuhlman (Kuhlman 2011) for the SDI planned change notice (PCN) shows that any thermal pulse from these experiments will be very minimal, on the order of 0.02 °C or less. Therefore, the screening argument and decision for this FEP is unaffected by the conduct of these experiments.

SCR-6.3.4.1.3 Screening Argument

Thermally induced stress could result in pathways for groundwater flow in the DRZ, in the anhydrite layers and MBs, and through seals, or it could enhance existing pathways. Conversely, elevated temperatures will accelerate the rate of salt creep and mitigate fracture development. Thermal expansion could also result in uplift of the rock and ground surface overlying the repository, and thermal buoyancy forces could lift the waste upward in the salt rock.

The distributions of thermal stress and strain changes depend on the induced temperature field and the differing thermal expansion of components of the repository, which depends on the components' elastic properties. Thermal effects on material properties (such as permeability and porosity) could potentially affect the behavior of the repository.

Exothermic reactions in the WIPP repository include MgO hydration, MgO carbonation, aluminum (Al) corrosion, and cement hydration (Bennett et al. 1996). Wang (Wang 1996) has shown that the temperature rise by an individual reaction is proportional to $\sqrt{VM}$, where V is the maximum rate of brine inflow into a waste panel for a reaction limited by brine inflow (or a specified maximum reaction rate for a reaction limited by its own kinetics) and M is the quantity of the reactant. MgO hydration, cement hydration, and Al corrosion are assumed to be limited by brine inflow because they all consume water and have high reaction rates. The amounts of reactants are tabulated in Table SCR-3.

Table SCR- 3. Changes in Inventory Quantities from the CCA to the CRA-20 14

Inventory	CCA	CRA-2004	CRA-2009	CRA-2014
MgO (tons)	85,600[a]	72,760 (because of the elimination of mini-sacks)[a]	59,385[e]	51,430[h]

Cellulosics (tons)	5,940[b]	8,120[c]	8,907[f]	5,127[i]
Plastics (tons)	3,740[b]	8,120[c]	10,180[f]	10,487[i]
Rubber (tons)	1,100[b]	1,960[c]	1,885[f]	1,379[i]
Aluminum alloys (tons)	1,980[b]	1,960[c]	2,030[f]	504[i]
Cement (tons)	8,540[b]	9,971[d]	13,888[g]	11872[j]

[a] U.S. DOE (U.S. DOE 2000a)

[b] U.S. DOE (U.S. DOE 1996b). Only CH-TRU wastes are considered. Total volume of CH-TRU wastes is 1.1×10^5 m^3. This is not scaled to WIPP disposal volume.

[c] Appendix DATA-2004, Attachment F. Only CH-TRU wastes are considered. Total volume of CH-TRU waste is 1.4×10^5 m^3. This is not scaled to WIPP disposal volume.

[d] This estimate is derived from data in Leigh (Leigh 2003) includes both reacted and unreacted cement. (1.2×10^7 kg × 1.4 × 10^5/168485/1000 kg/ton = 9971 tons cement).

[e] This estimate is derived by assuming that Panel 1 has an MgO excess factor of 1.95, three panel equivalents have a 1.67 excess factor, and the remaining 6 panel equivalents have a 1.2 excess factor, resulting in a 1.416 projected excess factor for a full repository. The projected excess factor is then multiplied by the equivalent cellulose value of 28,098 × (40.3/27) (the MgO molar ratio).

[f] This value is derived using material densities reported in Leigh et al. (Leigh et al. 2005b) ,and total CH-TRU waste volume (1.45×10^5 m^3 reported in Leigh et al. (Leigh et al. 2005a)).

[g] This value is derived from data in Leigh (Leigh 2003) and Leigh et al. (Leigh et al. 2005a). ((1.2×10^7 kg) × 39/29 × ($1.45 \times$ 10^5)/168485/1000 kg/ton = 13,888 tons cement).

[h] This estimate is derived by assuming that Panel 1 has an MgO excess factor of 1.95, three panel equivalents have a 1.67 excess factor, and the remaining 6 panel equivalents have a 1.2 excess factor, resulting in a 1.416 projected excess factor for a full repository. The projected excess factor is then multiplied by the equivalent cellulose value of 24,334 × (40.3/27) (the MgO molar ratio).

[i] This value is derived from Van Soest (Van Soest 2012) and contains CH, RH, packaging, and emplacement materials.

[j] This value is derived from Van Soest (Van Soest 2012) and contains reacted and unreacted cements for both CH and RH wastes.

Similarly, MgO carbonation, which consumes CO_2, is limited by CO_2 generation from microbial degradation. Given a biodegradation rate constant, the total CO_2 generated per yr is proportional to the total quantity of biodegradable materials in the repository. Using the computational methods in Wang and Brush (Wang and Brush 1996a and Wang and Brush 1996b), the inventory of biodegradable materials has been changed from 23,884 (8,120 + 1.7 × 8,120 + 1,960) tons for the CRA-2004[1] to 28,098 (8,907 + 1.7 × 10,180 + 1,885) tons of equivalent cellulosics for the CRA-2009.[1] For the CRA-2014, this value changes to 24,334 (5,127 + 1.7 × 10,487 + 1,379) tons of equivalent cellulosics. This decrease in biodegradable materials corresponds to a proportional decrease in CO_2 generation, all other factors (such as brine saturation) being equal. For MgO carbonation and microbial degradation, the calculated temperature rises have been updated for the changes in both microbial gas generation and waste inventory and are presented in Table SCR-4.

Temperature rises (^{o}C) by exothermic reactions are revised as follows:

CCA conditions following a drilling event show that Al corrosion could, at most, result in a short-lived (two yrs) temperature increase of about 6 °C (10.8 °F) above ambient room temperature (about 27 °C (80 °F)) (Bennett et al. 1996). A temperature rise of 6 °C (10.8 °F) represented the maximum that could occur as a result of any combination of exothermic reactions occurring simultaneously. Revised maximum temperature rises by exothermic reactions for CRA-2014 are still less than 12 ºC (22 °F) (as shown in Table SCR-4). Such small temperature changes cannot affect material properties. Thus, thermal effects on material properties in the repository have been eliminated from PA calculations on the basis of low consequence to the performance of the disposal system.

Table SCR- 4. CCA and CRA Exothermic Temperature Rises

Reactant	CCA[a]	CRA-2004[a]	CRA-2009[a]	CRA-2014[a]

Mgo hydration	< 4.5	< 4.7	< 4.2	< 3.9
Mgo carbonation	< 0.6	< 0.7	< 0.6	< 0.6
Microbial degradation	< 0.8	< 1.4	< 1.5	< 1.4
Aluminum corrosion	< 6.0	< 6.8	< 6.9	< 3.4
Cement hydration	< 2.0	< 2.5	< 3.0	< 2.7

[a] All values are in degrees Celsius.

All potential sources of heat and elevated temperature have been evaluated and found not to produce high enough temperature changes to affect the repository's performance. Sources of heat within the repository include radioactive decay and exothermic chemical reactions such as backfill hydration and metal corrosion. The rates of these exothermic reactions are limited by the availability of brine in the repository. In general, the various sources of heat do not appear to be great enough to jeopardize the performance of the disposal system.

SCR-6.3.5 Mechanical Effects on Material Properties

SCR-6.3.5.1 FEP Numbers: W32, W36, W37, W39, W113, and W114 FEP Titles: Consolidation of Waste (W32) Consolidation of Shaft Seals (W36) Mechanical Degradation of Shaft Seals (W37) Underground Boreholes (W39) Consolidation of Panel Closures (W113) Mechanical Degradation of Panel Closures (W114)

SCR-6.3.5.1.1 Screening Decision: UP

Consolidation of Waste is accounted for in PA calculations. Consolidation of Shaft Seals and Panel Closures and Mechanical Degradation of Shaft Seals and Panel Closures are accounted for in PA calculations. Flow through isolated, unsealed Underground Boreholes is accounted for in PA calculations.

SCR-6.3.5.1.2 Summary of New Information

The descriptions and screening arguments for FEPs W113 *Consolidation of Panel Closures* and W114 *Mechanical Degradation of Panel Closures* will be affected by the planned ROM salt PCS. These repository components will continue to be screened into PA calculations (UP), but their implementation will change as a result of new parameter values necessary to represent the expected physical properties and characteristics of the ROM salt PCS. No other changes are required.

SCR-6.3.5.1.3 Screening Argument

Consolidation of waste is accounted for in PA calculations in the modeling of creep closure of the disposal room (Appendix PA-2014, Section PA-4.2.3).

Consolidation of shaft seals, consolidation of the ROM salt PCS, mechanical degradation of shaft seals, and mechanical degradation of panel closures are accounted for in PA calculations through the permeability ranges assumed for the seal and closure systems (Appendix PA-2014, Section PA-4.2.7 and Section PA-4.2.8).

The site investigation program has also involved the drilling of boreholes from within the excavated part of the repository. Following their use for monitoring or other purposes, these underground

boreholes will be sealed where practical, and salt creep will also serve to consolidate the seals and to close the boreholes. Any boreholes that remain unsealed will connect the repository to anhydrite interbeds within the Salado, and thus provide potential pathways for radionuclide transport. PA calculations account for fluid flow to and from the interbeds by assuming that the DRZ has a permanently enhanced permeability that allows flow of repository brines into specific anhydrite layers and interbeds. This treatment is also considered to account for the effects of any unsealed boreholes.

SCR-6.3.5.2 FEP Number: W33 FEP Title: Movement of Containers

SCR-6.3.5.2.1 Screening Decision: SO-C

Movement of Containers has been eliminated from PA calculations on the basis of low consequence to the performance of the disposal system.

SCR-6.3.5.2.2 Summary of New Information

The FEP description has been updated to reflect new waste inventory data for the CRA-2014. Waste densities have decreased slightly since the CRA-2009. This inventory change has no impact upon the screening argument and decision for this FEP.

SCR-6.3.5.2.3 Screening Argument

Movement of waste containersplaced in salt may occur as a result of two buoyancy mechanisms (Dawson and Tillerson 1978): (1) the density contrast between the waste container and the surrounding salt, and (2) the temperature contrast between a salt volume that includes a heat source and the surrounding unheated salt. When the density of the waste container is greater than the density of the surrounding salt, the container sinks relative to the salt, whereas when the salt density is greater than the container density, the container rises relative to the salt. Similarly, when a discrete volume of salt within a large salt mass is heated, the heat raises the temperature of the discrete volume above that of the surrounding salt, thereby inducing density contrasts and buoyant forces that initiate upward flow of the heated salt volume. In a repository setting, the source of the heat may be radioactive decay of the waste itself or exothermic reactions of the backfill materials and waste constituents, e.g., MgO hydration, MgO carbonation, Al corrosion, cement hydration, and calcium oxide hydration.

For the CCA, the density of the compacted waste and the grain density of the halite in the Salado were assumed to be 2,000 kg/m^3 and 2,163 kg/m^3, respectively. Because this density contrast is small, the movement of containers relative to the salt was considered minimal, particularly when drag forces on the waste containers were also considered. In addition, vertical movement initiated in response to thermally induced density changes for high-level waste containers of a similar density to those at the WIPP were calculated to be approximately 0.35 m (1.1 ft) (Dawson and Tillerson 1978, p. 22). This calculated movement was considered conservative, given that containers at the WIPP will generate much less heat and will, therefore, move less. As a result, container movement was eliminated from PA calculations on the basis of low consequences to the performance of the disposal system.

The calculations performed for the DOE (U.S. DOE 1996a) were based on estimates of the waste inventory. However, with the initiation of waste disposal, actual waste inventory is tracked and future waste stream inventories have been refined. Based on an evaluation of these data, two factors may affect the conclusions reached in U.S. DOE (U.S. DOE 1996a) concerning container movement.

The first factor is changes in density of the waste form. According to CRA-2009 inventory data (Leigh et al. 2005a), the waste density has changed only slightly since that anticipated for the CCA. Most recent inventory data provided in Van Soest (Van Soest 2012) show slight decreases in overall waste densities (see Van Soest 2012, Table 6-3). Some future waste streams may, however, be more highly compacted, perhaps having a density roughly three times greater than that assumed in the CCA, while others may be less dense. In calculations of container movement, Dawson and Tillerson (Dawson and Tillerson 1978, p. 22) varied container density by nearly a factor of 3 (from 2,000 kg/m^3 (125 lb/ft^3) to 5,800 kg/m^3 (362 lb/ft^3)) and found that an individual dense container could move vertically as much as about 28 m (92 ft). Given the geologic environment of the WIPP, a container would likely encounter a dense stiff unit (such as an anhydrite stringer) that would arrest further movement far short of this upper bound; however, because of the massive thickness of the Salado salt, even a movement of 28 m (92 ft) would have little impact on performance.

The second inventory factor that could affect container movement is the composition of the waste (and chemical buffer) relative to its heat production. Radioactive decay, nuclear criticality, and exothermic reactions are three possible sources of heat in the WIPP repository. According to Kicker and Zeitler (Kicker and Zeitler 2013) the TRU radionuclide inventory has decreased from 3.44×10^6 Ci reported in the CCA, to 2.48×10^6 Ci in the CRA-2004, to 2.32×10^6 Ci in the CRA-2009 to 2.06×10^6 Ci in the CRA-2014. Such a small change will not result in a significant deviation from the possible temperature rise predicted in the CCA. Additionally, and as shown in Section SCR-6.3.4.1 (FEPs W72 and W73), temperature rises from exothermic reactions are quite small (see Table SCR-4). Note that the revised maximum temperature increases caused by exothermic reactions are still less than 12 °C (22 °F).

Based on the small differences between the temperature and density assumed in the CCA and those determined using new inventory data (Van Soest 2012; Kicker and Zeitler 2013), the conclusion about the importance of container movement reported in the CCA will not be affected, even when more highly compacted future waste streams are considered. The effects of the revised maximum temperature rise and higher-density future waste streams on container movement are competing factors (high-density waste will sink, whereas the higher-temperature waste-salt volume will rise) that may result in even less movement. Therefore, movement of waste containers has been eliminated from PA calculations on the basis of low consequence.

SCR-6.3.5.3 FEP Number: W34 FEP Title: Container Integrity

SCR-6.3.5.3.1 Screening Decision: SO-C Beneficial

Container Integrity has been eliminated from PA calculations on the basis of beneficial consequence to the performance of the disposal system.

SCR-6.3.5.3.2 Summary of New Information

No new information that affects the screening of this FEP has been identified since the CRA-2009.

SCR-6.3.5.3.3 Screening Argument

Container integrity is required only for waste transportation. Past PA calculations show that a significant fraction of steel and other Fe-base materials will remain undegraded over 10,000 yrs (see,

for example, Helton et al. 1998). In addition, it is assumed in both CCA and CRA-2004 calculations that there is no microbial degradation of plastic container materials in 75% of PA realizations (Wang and Brush 1996). All these undegraded container materials will (1) prevent the contact between brine and radionuclides; and (2) decrease the rate and extent of radionuclide transport because of high tortuosity along the flow pathways and, as a result, increase opportunities for metallic iron and corrosion products to beneficially reduce radionuclides to lower oxidation states. Therefore, container integrity can be eliminated on the basis of its beneficial effect on retarding radionuclide transport. PA assumes instantaneous container failure and waste dissolution according to the source-term model.

SCR-6.3.5.4 FEP Number: W35 FEP Title: Mechanical Effects of Backfill

SCR-6.3.5.4.1 Screening Decision: SO-C

The *Mechanical Effects of Backfill* have been eliminated from PA calculations on the basis of low consequence to the performance of the disposal system.

SCR-6.3.5.4.2 Summary of New Information

No new information that affects the screening of this FEP has been identified since the CRA-2009.

SCR-6.3.5.4.3 Screening Argument

The chemical conditioners or backfill added to the disposal room will act to resist creep closure. However, calculations have shown that because of the high porosity and low stiffness of the waste and the high waste to potential backfill volume, inclusion of backfill does not significantly decrease the total subsidence in the waste emplacement area or disposal room (Westinghouse 1994). In 2001, the DOE eliminated MgO mini-sacks from the repository, reducing the total inventory from 85,600 short tons to 74,000 short tons, which reduced the potential backfill volume (U.S. EPA 2001). More recently, the required amount of MgO has been further reduced (Reyes 2008). Therefore, the mechanical effects of backfill have been eliminated from PA calculations on the basis of low consequence to the performance of the disposal system.

SCR-6.4 Subsurface Hydrological and Fluid Dynamic FEPs

SCR-6.4.1 Repository-Induced Flow

SCR-6.4.1.1 FEP Numbers: W40 and W41 FEP Titles: Brine Inflow (W40) Wicking (W41)

SCR-6.4.1.1.1 Screening Decision: UP

Two-phase brine and gas flow and capillary rise (wicking) in the repository and the Salado are accounted for in PA calculations.

SCR-6.4.1.1.2 Summary of New Information

Expected repository conditions vary based on factors such as contents of the repository, brine present, elapsed time since closure and the most recent hypothetical intrusion. These factors (and others) are considered interdependent and represent the complex interactions that might prevail over time in the repository environment. These interactions are accounted for in the Chemical Conditions Conceptual Model. As part of their review of the CRA-2009, the EPA noted that the existing treatment for water balance within the repository could be improved to include additional chemical reactions that affect the water balance within the repository (U.S. EPA 2010b). As such, the CRA-2014 PA calculations will include an improved treatment of water balance. The main objective of refining the repository water balance is to include the major gas and brine producing and consuming reactions within the existing conceptual model. This change in the implementation of repository water balance is considered a model enhancement as it adds additional reactions (MgO hydration, and the carbonation of brucite to form hydromagnesite) that represent transitional compounds in the reaction path. While these two FEPs are not directly related to this change, this new information is provided for completeness. Also, because this change in implementation will occur downstream of the FEP screening process, these FEPs remain classified UP.

SCR-6.4.1.1.3 Screening Argument

Brine inflow to the repository may occur through the DRZ, impure halite, anhydrite layers, or clay layers. Pressurization of the repository through gas generation could limit the amount of brine that flows into the rooms and drifts. Two-phase flow of brine and gas in the repository and the Salado is accounted for in PA calculations (Appendix PA-2014, Section PA-4.2).

Capillary rise (or wicking) is a potential mechanism for liquid migration through unsaturated zones in the repository. Capillary rise in the waste material could affect gas generation rates, which are dependent on water availability. Potential releases caused by drilling intrusion are also influenced by brine saturations and therefore by wicking. Capillary rise is therefore accounted for in PA calculations (Appendix PA-2014, Section PA-4.2).

SCR-6.4.2 Effects of Gas Generation

SCR-6.4.2.1 FEP Number: W42 FEP Title: Fluid Flow Due to Gas Production

SCR-6.4.2.1.1 Screening Decision: UP

Fluid Flow Due to Gas Production in the repository and the Salado is accounted for in PA calculations.

SCR-6.4.2.1.2 Summary of New Information

Refinement in the implementation of water balance as described above in SCR-6.4.1.1.2 will also affect the implementation of this FEP through the availability of water. Also, gas generation rates due to iron corrosion have been modified as a result of newly acquired experimental data (Roselle 2013) (see section SCR-6.3.2.1.2). Because this change is a refinement of a process already screened in, no other changes are necessary to this FEP. It remains classified UP.

SCR-6.4.2.1.3 Screening Argument

Pressurization of the repository through gas generation could limit the amount of brine that flows into the rooms and drifts. Gas may flow from the repository through the DRZ, impure halite, anhydrite layers, or clay layers. The amount of water available for reactions and microbial activity will impact the amounts and types of gases produced (W44 through W55, Section SCR-6.5.1.1 , Section SCR-6.5.1.2, Section SCR-6.5.1.3, Section SCR-6.5.1.4, Section SCR-6.5.1.5, Section SCR-6.5.1.6, Section SCR-6.5.1.7, Section SCR-6.5.1.8, and Section SCR-6.5.1.9). Gas generation rates, and therefore repository pressure, may change as the water content of the repository changes. Pressure changes and fluid flow due to gas production in the repository and the Salado are accounted for in PA calculations through modeling the two-phase flow (Appendix PA-2014, Section PA-4.2).

SCR-6.4.3 Thermal Effects

SCR-6.4.3.1 FEP Number: W43 FEP Title: Convection

SCR-6.4.3.1.1 Screening Decision: SO-C

Convection has been eliminated from PA calculations on the basis of low consequence to the performance of the disposal system.

SCR-6.4.3.1.2 Summary of New Information

Planned SDI experiments as detailed in Patterson (Patterson 2011) or the SDDI project (Franco 2012) will place heaters in newly excavated tunnels in the northern experimental region of the WIPP. Mining has been completed, but heater tests have not yet commenced. An evaluation conducted by Kuhlman (Kuhlman 2011) for the SDI PCN shows that any thermal pulse from these experiments will be very minimal, on the order of 0.02 °C or less. Therefore, the screening argument and decision for this FEP is unaffected by the conduct of these experiments.

SCR-6.4.3.1.3 Screening Argument

Temperature differentials in the repository could initiate convection. The resulting thermally induced brine flow or thermally-induced, two-phase flow could influence contaminant transport. Thermal gradients in the disposal rooms could potentially drive the movement of water vapor. For example, temperature increases around waste located at the edges of the rooms could cause evaporation of water entering from the DRZ. This water vapor could condense on cooler waste containers in the rooms and could contribute to brine formation, corrosion, and gas generation.

The characteristic velocity, *Vi*, for convective flow of fluid component *I* in an unsaturated porous medium is given by (from Hicks 1996)

$$V_i \approx -\frac{k_i}{\mu_i}\left(\alpha_i \rho_{i0} g \Delta T\right) \quad \text{(SCR.11)}$$

where α_i (per degree Kelvin) is the coefficient of expansion of the i^{th} component, k_i is the intrinsic permeability (m^2), μ_i is the fluid viscosity (pascal second), $\rho_{i\,0}$ (kg/m^3) is the fluid density at a reference point, g is the acceleration due to gravity, and ΔT is the change in temperature. This velocity may be evaluated for the brine and gas phases expected in the waste disposal region.

For a temperature increase of 10 °C (18 °F), the characteristic velocity for convective flow of brine in the DRZ around the concrete shaft seals is approximately 7×10^{-4} m (2.3×10^{-3} ft) per yr (2×10^{-11} m (6.6×10^{-11} ft) per second), and the characteristic velocity for convective flow of gas in the DRZ is approximately 1×10^{-3} m (3.2×10^{-3} ft) per yr (3×10^{-11} m (9.8×10^{-11} ft) per second) (Hicks 1996). For a temperature increase of 25 °C (45 °F), the characteristic velocity for convective flow of brine in the concrete seals is approximately 2×10^{-7} m (6.5×10^{-7} ft) per yr (6×10^{-15} m (1.9×10^{-14} ft) per second), and the characteristic velocity for convective flow of gas in the concrete seals is approximately 3×10^{-7} m (9.8×10^{-7} ft) per yr (8×10^{-15} m (2.6×10^{-4} ft) per second) (Hicks 1996). These values of Darcy velocity are much smaller than the expected values associated with brine inflow to the disposal rooms resulting from gas generation. In addition, the buoyancy forces generated by smaller temperature contrasts in the DRZ, resulting from backfill and radioactive decay will be short-lived and insignificant compared to the other driving forces for fluid flow. In summary, temperature changes in the disposal system will not cause significant thermal convection. Furthermore, the induced temperature gradients will be insufficient to generate water vapor and drive significant moisture migration.

The viscosity of pure water decreases by about 19% over a temperature range of between 27 °C (80 °F) and 38 °C (100 °F) (Batchelor 1973, p. 596). Although at a temperature of 27 °C (80 °F), the viscosity of Salado brine is about twice that of pure water (Rechard et al. 1990, p. A-19), the magnitude of the variation in brine viscosity between 27 °C (80 °F) and 38 °C (100 °F) will be similar to the magnitude of the variation in viscosity of pure water. The viscosity of air over this temperature range varies by less than 7% (Batchelor 1973, p. 594) and the viscosity of gas in the waste disposal region over this temperature range is also likely to vary by less than 7%. The Darcy fluid flow velocity for a porous medium is inversely proportional to the fluid viscosity. Thus, increases in brine and gas flow rates may occur as a result of viscosity variations in the vicinity of the concrete shaft seals. However, these viscosity variations will persist only for a short period in which temperatures are elevated, and, thus, the expected variations in brine and gas viscosity in the waste disposal region will not significantly affect the long-term performance of the disposal system.

For the CCA conditions following a drilling event, Al corrosion could, at most, result in a short-lived (two yrs) temperature increase of about 6 °C (10.8 °F). A temperature rise of 6 °C (10.8 °F) represented the maximum that could occur as a result of any combination of exothermic reactions occurring simultaneously. Revised maximum temperature rises by exothermic reactions for CRA-2014 are still less than 12 °C (22 °F) (as shown in Table SCR-4). Such small temperature changes cannot affect material properties and thermally induced flow.

In summary, temperature changes in the disposal system will not cause significant thermally induced two-phase flow. Thermal convection has been eliminated from PA calculations on the basis of low consequence to the performance of the disposal system.

SCR-6.5 Geochemical and Chemical FEPs

SCR-6.5.1 Gas Generation

SCR-6.5.1.1 FEP Numbers: W44, W45, and W48 FEP Titles: Degradation of Organic Material (W44) Effects of Temperature on Microbial Gas Generation (W45) Effects of Biofilms on Microbial Gas Generation (W48)

SCR-6.5.1.1.1 Screening Decision: UP

Microbial gas generation from Degradation of Organic Material is accounted for in PA calculations, and the Effects of Temperature on Microbial Gas Generation and the Effects of Biofilm Formation on Microbial Gas Generation are incorporated in the gas generation rates used.

SCR-6.5.1.1.2 Summary of New Information

These FEPs have been updated to be consistent with the latest inventory information and information resulting from an EPA request on the CRA-2009 (Kelly 2009). Clarifying statements have been added that reflect DOE's response to the EPA's request. The screening argument and decision are not affected by the updated information.

SCR-6.5.1.1.3 Screening Argument

Microbial breakdown of cellulosic material, and possibly plastics and other synthetic materials, will produce mainly CO_2 and CH_4 with minor amounts of nitrogen oxide, nitrogen, and hydrogen sulfide. The rate of microbial gas production will depend upon the nature of the microbial populations established, the prevailing conditions, and the substrates present. Microbial gas generation from degradation of organic material is accounted for in PA calculations. The latest data on microbial ecology at WIPP is given in Appendix SOTERM-2.4.1 and Swanson et al. (Swanson et al. 2012).

The following subsections discuss the effects of temperature, pressure, radiation, and biofilms on gas production rates via their control of microbial gas generation processes.

SCR-6.5.1.1.3.1 Effects of Temperature on Microbial Gas Generation

Calculations and experimental studies of induced temperature distributions within the repository have been undertaken and are described in FEPs W29, W30, and W31 (Section SCR-6.3.4.1). Numerical analysis suggests that the average temperature increase in the WIPP repository caused by radioactive decay of the emplaced CH-TRU and RH-TRU waste is likely to be less than 2 °C (3.6 °F) (FEP W13).

Temperature increases resulting from exothermic reactions are discussed in FEPs W72 and W73 (Section SCR-6.3.4.1). Potentially the most significant exothermic reactions are concrete hydration, backfill hydration, and aluminum corrosion. Hydration of the seal concrete could raise the temperature of the concrete to approximately 53 °C (127 °F) and that of the surrounding salt to approximately 38 °C (100 °F) one week after seal emplacement (W73).

As discussed in FEPs W72 and W73 (Section SCR-6.3.4.1), the maximum temperature rise in the disposal panels as a consequence of backfill hydration will be less than 3.9 °C (7.0 °F), resulting from brine inflow following a drilling intrusion into a waste disposal panel. Note that AICs will prevent drilling within the controlled area for 100 yrs after disposal. By this time, any heat generation by radioactive decay and concrete seal hydration will have decreased substantially, and the temperatures in the disposal panels will have decreased to close to initial values.

Under similar conditions following a drilling event, Al corrosion could, at most, result in a short-lived (two yrs) temperature rise of about 3.4 °C (6.1 °F) (see W72). These calculated maximum heat generation rates resulting from Al corrosion and backfill hydration could not occur simultaneously

because they are limited by brine availability; each calculation assumes that all available brine is consumed by the reaction of concern. Thus, the temperature rise of 12 °C (22 °F) represents the maximum that could occur as a result of any combination of exothermic reactions occurring simultaneously. Additionally, these reactions would be transient in nature and will not persist for long periods of time.

Relatively few data exist on the effects of temperature on microbial gas generation under expected WIPP conditions. Molecke (Molecke 1979, p. 4) summarized microbial gas generation rates observed during a range of experiments. Increases in temperature from ambient up to 40 °C (104 °F) or 50 °C (122 °F) were reported to increase gas production, mainly via the degradation of cellulosic waste under either aerobic or anaerobic conditions (Molecke 1979, p. 7). Above 70 °C (158 °F), however, gas generation rates were generally observed to decrease. The experiments were conducted over a range of temperatures and chemical conditions and for different substrates, representing likely states within the repository. Gas generation rates were presented as ranges with upper and lower bounds as estimates of uncertainty (Molecke 1979, p. 7). Molecke's work evaluated gas-generation rates over a range of temperatures, including those significantly higher than expected in the WIPP (up to 70 °C [158 °F]). Later experiments reported by Francis and Gillow (Francis and Gillow 1994) support the gas generation rate data reported by Molecke (Molecke 1979). These experiments investigated microbial gas generation under a wide range of possible conditions in the repository. These conditions included the presence of microbial inoculum, humid or inundated conditions, cellulosic substrates, additional nutrients, electron acceptors, bentonite, and initially oxic or anoxic conditions. These experiments were carried out at a temperature of 30 °C (86 °F). Gas generation rates used in the PA calculations are described in Appendix PA-2014, Section PA-4.2.5. The effects of temperature on microbial gas generation are implicitly incorporated in the gas generation rates used.

SCR-6.5.1.1.3.2 Effects of Biofilms on Microbial Gas Generation

The location of microbial activity within the repository is likely to be controlled by the availability of substrates and nutrients. Biofilms may develop on surfaces where nutrients are concentrated. They consist of one or more layers of cells with extracellular polymeric material, and serve to maintain an optimum environment for growth. Within such a biofilm ecosystem, nutrient retention and recycling maximize microbe numbers on the surface (see, for example, Stroes-Gascoyne and West 1994, pp. 9-10).

Biofilms can form on almost any moist surface, but their development is likely to be restricted in porous materials. Even so, their development is possible at locations throughout the disposal system. The effects of biofilms on microbial gas generationmay affect disposal system performance through control of microbial population size and their effects on radionuclide transport.

Molecke (Molecke 1979, p. 4) summarized microbial gas generation rates observed during a range of experimental studies. The experiments were conducted over a range of temperatures and chemical conditions and for different substrates representing likely states within the repository. However, the effect of biofilm formation in these experiments was uncertain. Molecke (Molecke 1979, p. 7), presented gas generation rates as ranges, with upper and lower bounds as estimates of uncertainty. Later experiments reported by Francis and Gillow (Francis and Gillow 1994) support the gas generation rate data reported by Molecke (Molecke 1979). Their experiments investigated microbial gas generation under a wide range of possible conditions in the repository. These conditions included the presence of microbial inoculum, humid or inundated conditions, cellulosic substrates, additional nutrients, electron acceptors, bentonite, and initially oxic or anoxic conditions. Under the more favorable conditions for microbial growth established during the experiments, the development of

populations of halophilic microbes and associated biofilms was evidenced by observation of an extracellular, carotenoid pigment, bacterioruberin, in the culture bottles (Francis and Gillow 1994, p. 59). Gas generation rates used in the PA calculations have been derived from available experimental data and are described in Appendix PA-2014, Section PA-4.2.5. The effects of biofilms on microbial gas generation rates are implicitly incorporated in the gas generation rates.

Biofilms may also influence contaminant transport rates through their capacity to retain and thus retard both the microbes themselves and radionuclides. This effect is not accounted for in PA calculations, but is considered potentially beneficial to calculated disposal system performance. Microbial transport is discussed in Section SCR-6.6.3.1.

SCR-6.5.1.2 FEP Number: W46 FEP Title: Effects of Pressure on Microbial Gas Generation

SCR-6.5.1.2.1 Screening Decision: SO-C

The *Effects of Pressure on Microbial Gas Generation* has been eliminated from PA calculations on the basis of low consequence to the performance of the disposal system.

SCR-6.5.1.2.2 Summary of New Information

No new information that affects the screening of this FEP has been identified since the CRA-2009.

SCR-6.5.1.2.3 Screening Argument

Directly relevant to WIPP conditions, the gas generation experiments with actual waste components at Argonne National Laboratory provide no indication of any enhancement of pressured nitrogen atmosphere (2,150 pounds per square inch absolute [psia]) on microbial gas generation (Felicione et al. 2001). In addition, microbial breakdown of cellulosic material, and possibly plastics and other synthetic materials in the repository, will produce mainly CO_2 and CH_4 with minor amounts of nitrogen oxide, nitrogen, and hydrogen sulfide. The accumulation of these gaseous species will contribute to the total pressure in the repository. Increases in the partial pressures of these reaction products could potentially limit gas generation reactions. However, such an effect is not taken into account in the WIPP PA calculations. The rate of microbial gas production will depend upon the nature of the microbial populations established, the prevailing conditions, and the substrates present. Microbial gas generation from degradation of organic material is accounted for in PA calculations.

Chemical reactions may occur depending on, among other things, the concentrations of available reactants, the presence of catalysts and the accumulation of reaction products, the biological activity, and the prevailing conditions (for example, temperature and pressure). Reactions that involve the production or consumption of gases are often particularly influenced by pressure because of the high molar volume of gases. The effect of high total pressures on chemical reactions is generally to reduce or limit further gas generation.

Few data exist from which the effects of pressure on microbial gas generation reactions that may occur in the WIPP can be assessed and quantified. Studies of microbial activity in deep-sea environments (for example, Kato et al. 1994, p. 94) suggest that microbial gas generation reactions are less likely to be limited by increasing pressures in the disposal rooms than are inorganic gas

generation reactions (for example, corrosion). Consequently, the effects of pressure on microbial gas generation have been eliminated from PA calculations on the basis of low consequence to the performance of the disposal system.

SCR-6.5.1.3 FEP Number: W47 FEP Title: Effects of Radiation on Microbial Gas Generation

SCR-6.5.1.3.1 Screening Decision: SO-C

The *Effects of Radiation on Microbial Gas Generation* has been eliminated from PA calculations on the basis of low consequence to the performance of the disposal system.

SCR-6.5.1.3.2 Summary of New Information

The FEP screening argument has been updated to reflect the radionuclide inventory used for CRA-2009 calculations, although the screening decision has not changed.

SCR-6.5.1.3.3 Screening Argument

Radiation may slow down microbial gas generation rates, but such an effect is not taken into account in the WIPP PA calculations. According to the inventory data presented in Leigh and Trone (Leigh and Trone 2005), the overall activity for all TRU radionuclides has decreased from 3.44×10^6 Ci reported in the CCA, to 2.48×10^6 Ci in the CRA-2004, to 2.32×10^6 Ci in the CRA-2009, to 2.06×10^6 Ci for the CRA-2014 (Kicker and Zeitler 2013). This decrease will not affect the original screening argument.

Experiments investigating microbial gas generation rates suggest that the effects of alpha radiation from TRU waste is not likely to have significant effects on microbial activity (Barnhart et al. 1980; Francis 1985). Consequently, the effects of radiation on microbial gas generation have been eliminated from PA calculations on the basis of low consequence to the performance of the disposal system.

SCR-6.5.1.4 FEP Numbers: W49 and W51 FEP Titles: Gases from Metal Corrosion Chemical Effects of Corrosion

SCR-6.5.1.4.1 Screening Decision: UP

Gas generation from metal corrosion is accounted for in PA calculations, and the effects of chemical changes from metal corrosion are incorporated in the gas generation rates used.

SCR-6.5.1.4.2 Summary of New Information

Metals present in the waste and waste containers have been updated for the CRA-2014 in Van Soest (Van Soest 2012). Iron corrosion experiments (Wall and Enos 2006) have been completed since the CRA-2009 that provide new corrosion rates for expected WIPP-relevant conditions (Roselle 2013). These rates are implemented with a new parameter distribution type and values for the parameter

STEEL:CORRMCO2. This parametric change does not affect the screening argument, decision, or the implementation of gas generation within PA models.

SCR-6.5.1.4.3 Screening Argument

Oxic corrosion of waste drums and metallic waste will occur at early times following closure of the repository and will deplete its oxygen content. Anoxic corrosion will follow the oxic phase and will produce hydrogen while consuming water. Gases from metal corrosion are accounted for in PA calculations.

The predominant chemical effect of corrosion reactions on the environment of disposal rooms will be to lower the oxidation state of the brines and maintain reducing conditions.

Molecke (Molecke 1979, p. 4) summarized gas generation rates that were observed during a range of experiments. The experiments were conducted over a range of temperatures and chemical conditions representing likely states within the repository. Later experiments reported by Telander and Westerman (Telander and Westerman 1993) support the gas generation rate data reported by Molecke (Molecke 1979). Their experiments investigated gas generation from corrosion under a wide range of possible conditions in the repository. The studies included corrosion of low-carbon steel waste packaging materials in synthetic brines, representative of intergranular Salado brines at the repository horizon, under anoxic (reducing) conditions.

Gas generation rates used in the PA calculations have been derived from available experimental data and are described in Appendix PA-2014, Section PA-4.2.5. Recently completed iron corrosion experiments were analyzed by Roselle (Roselle 2013) and result in new iron corrosion rates which in turn affect the rate of gas generation from this process. The effects of chemical changes from metal corrosion are, therefore, accounted for in PA calculations.

SCR-6.5.1.5 FEP Number: W50 FEP Title: Galvanic Coupling (within the repository)

SCR-6.5.1.5.1 Screening Decision: SO-C

The effects of *Galvanic Coupling* have been eliminated from PA calculations on the basis of low consequence to the performance of the disposal system.

SCR-6.5.1.5.2 Summary of New Information

No new information that affects the screening of this FEP has been identified since the CRA-2009.

SCR-6.5.1.5.3 Screening Argument

Galvanic coupling (i.e., establishing an electrical current through chemical processes) could lead to the propagation of electric potential gradients between metals in the waste form, canisters, and other metals external to the waste form, potentially influencing corrosion processes, gas generation rates, and chemical migration.

Metallic ore bodies external to the repository are nonexistent (see the CCA, Appendix GCR) and therefore galvanic coupling between the waste and metals external to the repository would not occur.

However, a variety of metals will be present within the repository as waste metals and containers, creating a potential for formation of galvanic cells over short distances. As an example, the presence of copper could influence rates of hydrogen gas production resulting from the corrosion of iron. The interactions between metals depend upon their physical disposition and the prevailing solution conditions, including pH and salinity. Good physical and electrical contact between the metals is critical to the establishment of galvanic cells.

Consequently, given the preponderance of iron over other metals within the repository and the likely passivation of many nonferrous materials, the influence of these electrochemical interactions on corrosion, and therefore on gas generation, is expected to be minimal. Therefore, the effects of galvanic coupling have been eliminated from PA calculations on the basis of low consequence.

SCR-6.5.1.6 FEP Number: W52 FEP Title: Radiolysis of Brine

SCR-6.5.1.6.1 Screening Decision: SO-C

Gas generation from *Radiolysis of Brine* has been eliminated from PA calculations on the basis of low consequence to the performance of the disposal system.

SCR-6.5.1.6.2 Summary of New Information

No new information that affects the screening of this FEP has been identified since the CRA-2009.

SCR-6.5.1.6.3 Screening Argument

Radiolysis of brine in the WIPP disposal rooms, and of water in the waste, will lead to the production of gases and may significantly affect the oxygen content of the rooms. This, in turn, will affect the prevailing chemical conditions and potentially the concentrations of radionuclides that may be mobilized in the brines.

The overall reaction for the radiolysis of water in the waste and brine is

$H_2O \rightarrow H_2 + ½\ O_2$. (SCR.12)

However, the production of intermediate oxygen-bearing species that may subsequently undergo reduction will lead to reduced oxygen gas yields. The remainder of this section is concerned with the physical effects of gas generation by radiolysis of brine.

Reed et al. (Reed et al. 1993) studied radiolytic gas generation during experiments lasting between 155 and 182 days. These experiments involved both synthetic brines similar to those sampled from the Salado at the WIPP repository horizon, and brines occurring in reservoirs in the Castile, as well as real brines sampled from the Salado in the repository workings. The brines were spiked with ^{239}Pu (VI) at concentrations between 6.9×10^{-9} and 3.4×10^{-4} molal. During these relatively short-term experiments, hydrogen gas was observed as the product of radiolysis. Oxygen gas was not observed; this was attributed to the formation of intermediate oxygen-bearing species. However, given sufficient exposure to alpha-emission, oxygen production may reach 50% that of hydrogen.

An estimate of the potential rate of gas generation caused by the radiolysis of brine, R_{RAD}, can be made by making the following assumptions:

- Gas production occurs following the reaction above, so that 1.5 moles of gas are generated for each mole of water consumed
- Gas production occurs as a result of the alpha decay of ^{239}Pu
- ^{239}Pu concentrations in the disposal room brines are controlled by solubility equilibria
- All of the dissolved Pu is ^{239}Pu

R_{RAD} is then given by

$$R_{RAD} = \frac{Y_g C_{Pu} SA_{Pu} \overline{E}_\alpha V_B}{N_D N_A} \quad \text{(SCR.13)}$$

$$R_{RAD} = \frac{\left(\frac{1.5 \text{ molecule gas}}{\text{molecule } H_2O}\right)\left(3.15\times10^{7}\ \frac{\text{s}}{\text{yr}}\right)\left(3\times10^{-4}\ \frac{\text{mol}}{\text{L}}\right)\left(5.42\times10^{11}\ \frac{\text{Bq}}{\text{mol}}\right)\left(5.15\times10^{6}\ \frac{\text{eV}}{\text{dis}}\right)\left(\frac{1.5\ H_2O}{100\ \text{eV}}\right)(4.36\times10^{5}\ \text{L})}{(8\times10^{5}\ \text{drums})\left(6.022\times10^{23}\ \frac{\text{molecules}}{\text{mole}}\right)}$$

$$= 0.533 \text{ mol·drum}^{-1}\text{/yr} \quad \text{(SCR.14)}$$

Y_g = radiolytic gas yield, in number of moles of gas produced per number of water molecules consumed

C_{Pu} = maximum dissolved concentration of plutonium (molar)

SA_{Pu} = specific activity of ^{239}Pu (5.42×10^{11} becquerels (Bq) per mole)

$\overline{E}_\alpha$ = average energy of α-particles emitted during ^{239}Pu decay (5.15×10^6 eV)

G = number of water molecules split per 100 eV of energy transferred from alpha-particles

V_B = volume of brine in the repository (L)

N_D = number of CH-TRU drums in the repository ($\sim 8 \times 10^5$)

N_A = Avogadro constant (6.022×10^{23} molecules per mole)

The value of *G* used in this calculation has been set at 0.015, the upper limit of the range of values observed (0.011 to 0.015) during experimental studies of the effects of radiation on WIPP brines (Reed et al. 1993). A maximum estimate of the volume of brine that could potentially be present in the disposal region has been made from its excavated volume of 436,000 m^3 (520,266 cubic yards [yd^3]). This estimate, in particular, is considered to be highly conservative because it makes no allowance for creep closure of the excavation, or for the volume of waste and backfill that will be emplaced, and takes no account of factors that may limit brine inflow. These parameter values lead to

an estimate of the potential rate of gas production caused by the radiolysis of brine of 0.6 moles per drum per yr or less.

Assuming ideal gas behavior and repository conditions of 30 °C (86 °F) and 14.8 MPa (lithostatic pressure), this is equivalent to approximately 6.8×10^4 L (1.8×10^4 gal) per yr.

Potential gas production rates from other processes that will occur in the repository are significantly greater than this. For example, under water-saturated conditions, microbial degradation of cellulosic waste has the potential to yield between 1.3×10^6 and 3.8×10^7 L (3.4×10^5 and 1.0×10^7 gal) per yr; anoxic corrosion of steels has the potential to yield up to 6.3×10^5 L (1.6×10^5 gal) per yr.

In addition to the assessment of the potential rate of gas generation by radiolysis of brine given above, a study of the likely consequences on disposal system performance has been undertaken by Vaughn et al. (Vaughn et al. 1995). A model was implemented in BRAGFLO to estimate radiolytic gas generation in the disposal region according to the equation above.

A set of BRAGFLO simulations was performed to assess the magnitude of the influence of the radiolysis of brine on contaminant migration to the accessible environment. The calculations considered radiolysis of water by 15 isotopes of Th, Pu, U, and Am. Conditional CCDFs of normalized contaminated brine releases to the Culebra via a human intrusion borehole and the shaft system, as well as releases to the subsurface boundary of the accessible environment via the Salado interbeds, were constructed and compared to the corresponding baseline CCDFs calculated excluding radiolysis. The comparisons indicated that radiolysis of brine does not significantly affect releases to the Culebra or the subsurface boundary of the accessible environment under disturbed or undisturbed conditions (Vaughn et al. 1995). Although the analysis of Vaughn et al. (Vaughn et al. 1995) used data that are different than those used in the PA calculations, estimates of total gas volumes in the repository are similar to those considered in the analysis performed by Vaughn et al. (Vaughn et al. 1995).

Therefore, gas generation by radiolysis of brine has been eliminated from PA calculations on the basis of low consequence to the performance of the disposal system.

SCR-6.5.1.7 FEP Number: W53 FEP Title: Radiolysis of Cellulose

SCR-6.5.1.7.1 Screening Decision: SO-C

Gas generation from *Radiolysis of Cellulose* has been eliminated from PA calculations on the basis of low consequence to the performance of the disposal system.

SCR-6.5.1.7.2 Summary of New Information

This FEP has been updated with new inventory data related to cellulose content. Decreasing waste inventory values indicate that radiolysis of cellulose will not be a significant process. The screening argument and decision are not affected by this change in inventory information.

SCR-6.5.1.7.3 Screening Argument

Molecke (Molecke 1979) compared experimental data on gas production rates caused by radiolysis of cellulose and other waste materials with gas generation rates by other processes, including bacterial (microbial) waste degradation. The comparative gas generation rates reported by Molecke (Molecke 1979, p. 4) are given in terms of most probable ranges, using units of moles per yr per drum, for drums of 0.21 m^3 (0.27 yd^3) in volume. A most probable range of 0.005 to 0.011 moles per yr per drum is reported for gas generation caused by radiolysis of cellulosic material (Molecke 1979, p. 4). As a comparison, a most probable range of 0.0 to 5.5 moles per yr per drum is reported for gas generation by bacterial degradation of waste.

The data reported by Molecke (Molecke 1979) are consistent with more recent gas generation investigations made under the WIPP program, and indicate that radiolysis of cellulosic materials will generate significantly less gas than other gas generation processes. Gas generation from radiolysis of cellulosics therefore can be eliminated from PA calculations on the basis of low consequence to the performance of the disposal system.

Radiolytic gas generation is controlled by the radioactivity of wastes and the waste properties. According to the new inventory presented in Leigh and Trone (Leigh and Trone 2005), the overall activity for all TRU radionuclides has decreased from 3.44×10^6 Ci reported in the CCA, to 2.48×10^6 Ci in the CRA-2004, to 2.32×10^6 Ci in the CRA-2009 to 2.06×10^6 Ci in the CRA-2014 (Kicker and Zeitler 2013). Such decreasing activity levels imply that the radiolytic effects will be decreased from those presented in the CCA.

Radiolytic gas generation is also limited by transportation requirements, which state that the hydrogen generated in the innermost layer of confinement must be no more than 5% over 60 days (U.S. DOE 2000b). Thus, the maximum rate allowed for transportation is 0.21 m^3/drum × 5% × 1,000 L/m^3/60 days × 365 days/yr = 61 L/drum/yr, smaller than the maximum microbial gas generation rate. Note that this estimate is very conservative and the actual rates are even smaller. This result is consistent with the general consensus within the international research community that the effect of radiolytic gas generation on the long-term performance of a low/intermediate level waste repository is negligible (Rodwell et al. 1999).

SCR-6.5.1.8 FEP Number: W54 FEP Title: Helium Gas Production

SCR-6.5.1.8.1 Screening Decision: SO-C

Gas generation from helium production has been eliminated from PA calculations on the basis of low consequence to the performance of the disposal system.

SCR-6.5.1.8.2 Summary of New Information

The updated information for the WIPP disposal inventory indicates that the expected WIPP-scale radionuclide activity (2.06 million Ci of TRU isotopes) (Kicker and Zeitler 2013) is less than previously estimated in the Transuranic Waste Baseline Inventory Report, Revision 3 (U.S. DOE 1996b). Thus, the helium gas production argument for CRA-2014is conservatively bounded by the CCA screening argument. The FEP screening argument and screening decision remain unchanged.

SCR-6.5.1.8.3 Screening Argument

Helium gas production will occur by the reduction of α-particles (helium nuclei) emitted from the waste. The maximum amount of helium that could be produced can be calculated from the number of α-particles generated during radioactive decay. The α-particles are converted to helium gas by the following reaction:

$^4He^{2+} + 2e^- \rightarrow He(g)$ (SCR.15)

For the screening argument used in the CCA, the inventory *(I)* that may be emplaced in the repository is approximately 4.07 million Ci or 1.5×10^{17} Bq (see the CCA, Appendix BIR). Assuming that the inventory continues to yield α-particles at this rate throughout the 10,000-yr regulatory period, the maximum rate of helium gas produced (R_{He}) may be calculated from

$$R_{He} = \frac{I\left(\frac{1\ He\ atom}{\alpha - decay}\right)}{N_A} \quad \text{(SCR.16)}$$

R_{He} is the rate of helium gas production in the repository (mole per second).

I is the waste inventory, 1.5×10^{17} Bq, assuming that 1 Bq is equal to 1 α-decay per second, and N_A is Avogadro's constant (6.022×10^{23} atoms per mole). These assumptions regarding the inventory lead to maximum estimates for helium production because some of the radionuclides will decay by beta and gamma emission.

R_{He} is approximately 5.5×10^{-7} moles per second based on an α-emitting inventory of 4.07 million Ci (much greater than current inventory estimates) (Kicker and Zeitler 2013). Assuming ideal gas behavior and repository conditions of 30 °C (86 °F) and 14.8 MPa or 146 atmospheres (lithostatic pressure) yields approximately 1.3 L (0.34 gal) per yr.

The effects of helium gas production have been eliminated from PA calculations on the basis of low consequence to the performance of the disposal system.

SCR-6.5.1.9 FEP Number: W55 FEP Title: Radioactive Gases

SCR-6.5.1.9.1 Screening Decision: SO-C

The formation and transport of *Radioactive Gases* has been eliminated from PA calculations on the basis of low consequence to the performance of the disposal system.

SCR-6.5.1.9.2 Summary of New Information

This FEP has been updated with references to the latest inventory information.

SCR-6.5.1.9.3 Screening Argument

Based on the composition of the anticipated waste inventory, as described in Van Soest (Van Soest 2012), the radioactive gases that will be generated in the repository are radon (Rn) and ^{14}C-labeled CO_2 and CH_4.

Van Soest (Van Soest 2012) indicates that a small amount of ^{14}C (0.01 Ci) will be disposed in the WIPP. This amount is insignificant in comparison with the section 191.13 cumulative release limit for ^{14}C.

Notwithstanding this comparison, consideration of transport of radioactive gases could potentially be necessary in respect of the section 191.15 individual protection requirements. ^{14}C may partition into CO_2 and CH_4 formed during microbial degradation of cellulosic and other organic wastes (for example, rubbers and plastics). However, total fugacities of CO_2 in the repository are expected to be very low because of the action of the MgO backfill, which will lead to incorporation of CO_2 in solid magnesite. Similarly, interaction of CO_2 with cementitious wastes will limit CO_2 fugacities by the formation of solid calcium carbonate. Thus, because of the formation of solid carbonate phases in the repository, significant transport of ^{14}C as carbon dioxide-14 has been eliminated from PA calculations on the basis of low consequence to the performance of the disposal system.

Potentially significant volumes of CH_4 may be produced during the microbial degradation of cellulosic waste. However, volumes of methane-14 will be small given the low total inventory of ^{14}C and the tendency of ^{14}C to be incorporated into solid carbonate phases in the repository. Therefore, although transport of ^{14}C could occur as methane-14, this effect has been eliminated from the current PA calculations on the basis of low consequence to the performance of the disposal system.

Rn gas will contain proportions of the alpha emitters ^{219}Rn, ^{220}Rn, and ^{222}Rn. All of these have short half-lives, but ^{222}Rn is potentially the most important because it is produced from the abundant waste isotope, ^{238}Pu, and because it has the longest half-life of the radon isotopes (≈ 4 days). ^{222}Ra will exhibit secular equilibrium with its parent^{226}Rn, which has a half-life of 1600 yrs. Consequently,^{222}Rn will be produced throughout the 10,000-yr regulatory time period. Conservative analysis of the potential ^{222}Rn inventory suggests activities of less than 716 Ci at 10,000 yrs (Bennett 1996).

Direct comparison of the estimated level of ^{222}Rn activity with the release limits specified in section 191.13 cannot be made because the release limits do not cover radionuclides with half-lives less than 20 yrs. For this reason, production of Rn gas can be eliminated from the PA calculations on regulatory grounds. Notwithstanding this regulatory argument, the small potential Rn inventory means that the formation and transport of Rn gas can also be eliminated from PA calculations on the basis of low consequence to the performance of the disposal system.

SCR-6.5.2 Speciation

SCR-6.5.2.1 FEP Number: W56 FEP Title: Speciation

SCR-6.5.2.1.1 Screening Decision: UP - Disposal Room UP - Culebra SO-C - Beneficial - Shaft Seals

Chemical *Speciation* is accounted for in PA calculations in the estimates of radionuclide solubility in the disposal rooms and the degree of chemical retardation estimated during contaminant transport. The effects of cementitious seals on chemical *Speciation* have been eliminated from PA calculations on the basis of beneficial consequence to the performance of the disposal system.

SCR-6.5.2.1.2 Summary of New Information

Actinide solubilities have been recalculated for the CRA-2014 (Brush and Domski 2013a; Brush and Domski 2013b; and Brush and Domski 2013c) based on the latest inventory components as provided in Van Soest (Van Soest 2012). These new solubilities do not affect the screening arguments or decisions below.

SCR-6.5.2.1.3 Screening Argument

Chemical speciation refers to the form in which elements occur under a particular set of chemical or environmental conditions. Conditions affecting chemical speciation include the temperature, pressure, and salinity (ionic strength) of the water in question. The importance of chemical speciation lies in its control of the geochemical reactions likely to occur and the consequences for actinide mobility.

SCR-6.5.2.1.3.1 Disposal Room

The concentrations of radionuclides that dissolve in any brines present in the disposal rooms after repository closure will depend on the stability of the chemical species that form under the prevailing conditions (for example, temperature, pressure, and ionic strength). The method used to derive radionuclide solubilities in the disposal rooms (see Brush and Domski 2013a) considers the expected conditions. The MgO backfill will buffer pH values in the disposal room to between 9 and 10. Thus, chemical *Speciation* is accounted for in PA calculations in the estimates of radionuclide solubility in the disposal rooms.

SCR-6.5.2.1.3.2 Repository (Shaft) Seals

Certain repository materials, including the cementitious components of the shaft seals, have the potential to interact with groundwater and significantly alter the chemical speciation of any radionuclides present. In particular, extensive use of cementitious materials in the seals may have the capacity to buffer groundwater to extremely high pH (for example, Bennett et al. 1992, pp. 315-25). At high pH values, the speciation and adsorption behavior of many radionuclides is such that their dissolved concentrations are reduced in comparison with near-neutral waters. This effect reduces the migration of radionuclides in dissolved form. The effects of cementitious seals on groundwater chemistry have been eliminated from PA calculations on the basis of beneficial consequence to the performance of the disposal system.

SCR-6.5.2.1.3.3 Culebra

Chemical speciation will affect actinide retardation in the Culebra. The dependence of An retardation on speciation in the Culebra is accounted for in PA calculations by sampling over ranges of K_ds. The ranges of K_ds are based on the range of groundwater compositions and speciation in the Culebra, including consideration of nonradionuclide solutes. The methodology used to simulate sorption in the Culebra is described in Appendix PA-2014, Section PA-4.9.

SCR-6.5.2.2 FEP Number: W57 FEP Title: Kinetics of Speciation

SCR-6.5.2.2.1 Screening Decision: SO-C

The effects of reaction kinetics in chemical speciation reactions have been eliminated from PA calculations on the basis of low consequence to the performance of the disposal system.

SCR-6.5.2.2.2 Summary of New Information

No new information has been identified that affects the screening of this FEP since the CRA-2009.

SCR-6.5.2.2.3 Screening Argument

Chemical speciation of actinides describes the composition and relative distribution of dissolved species, such as the hydrated metal ion, or complexes, whether with organic or inorganic ligands. Conditions affecting chemical speciation include temperature, ionic strength, ligand concentration, and pH of the solution. Some ligands, such as hydroxide, may act to decrease An solubility, while others, such as citrate, frequently have the opposite influence, often increasing An solubility.

SCR-6.5.2.2.4 Disposal Room Equilibrium Conditions

The concentrations of radionuclides that can be dissolved in brines within the disposal rooms will depend on the thermodynamic stabilities and solubilities of the respective metal complexes. Geochemical modeling using the code EQ3/6 to determine the brine solubilities of radionuclides takes into account the expected conditions, including temperature, ionic strength, pH, and ligand concentration. The chemical speciation at equilibrium is accounted for in PA calculations in the estimates of radionuclide solubility in the disposal rooms.

SCR-6.5.2.2.5 Kinetics of Complex Formation

The waste that is emplaced within the WIPP contains radionuclides, including actinides or An-bearing materials in solid phases, e.g., metal oxides, salts, coprecipitated solids, and contaminated objects. In the event of contact with brine, the solution phase concentration of dissolved radionuclides is controlled both by the solution composition and by the kinetics of dissolution of the solid phases, effectively approaching equilibrium from undersaturation. Solution complexation reactions of most metal ions with common inorganic ligands, such as carbonate and hydroxide, and with organic ligands such as acetate, citrate, oxalate, and ethylene diamine tetra-acetate (EDTA) are kinetically very fast, reaching equilibrium in fractions of a second, an inconsequentially short time increment on the scale of the 10,000-yr regulatory period. Reactions of these types are generally so fast that special techniques must be adopted to measure the reaction rates; as a practical matter, the reaction rate is limited by the mixing rate when metal solutions are combined with ligand solutions. As a result, the rate of approach to an equilibrium distribution of solution species takes place much more rapidly than dissolution, making the dissolution reaction the rate-limiting step. The effects of reaction kinetics in aqueous systems are discussed by Lasaga et al. (Lasaga et al. 1994), who suggest that in contrast to many heterogeneous reactions, homogeneous aqueous geochemical speciation reactions involving relatively small inorganic species occur rapidly and are accurately described by thermodynamic equilibrium models that neglect explicit consideration of reaction kinetics.

For that reason, the rate at which solution species approach equilibrium distribution is of no consequence to repository performance. Kinetics of chemical speciation may be eliminated from PA calculations on the basis of no consequence.

SCR-6.5.3 Precipitation and Dissolution

SCR-6.5.3.1 FEP Numbers: W58, W59, and W60 FEP Titles: Dissolution of Waste (W58) Precipitation of Secondary Minerals (W59) Kinetics of Precipitation and Dissolution (W60)

SCR-6.5.3.1.1 Screening Decision: UP - W58 SO-C Beneficial - W59 SO-C - W60

Waste dissolution and the release of radionuclides in the disposal rooms are accounted for in PA calculations. The formation of radionuclide-bearing precipitates from groundwaters and brines and the associated retardation of contaminants have been eliminated from PA calculations on the basis of beneficial consequence to the performance of the disposal system. The effect of reaction kinetics in controlling the rate of waste dissolution within the disposal rooms has been eliminated from PA calculations on the basis of beneficial consequence to the performance of the disposal system.

SCR-6.5.3.1.2 Summary of New Information

No new information has been identified that affects the screening of these FEPs since the CRA-2009.

SCR-6.5.3.1.3 Screening Argument

Dissolution of waste and precipitation of secondary minerals control the concentrations of radionuclides in brines and can influence rates of contaminant transport. Waste dissolution is accounted for in PA calculations. The formation of radionuclide-bearing precipitates from groundwaters and brines and the associated retardation of contaminants have been eliminated from PA calculations on the basis of beneficial consequence to the performance of the disposal system. Results of actinide studies that in some in some cases identify phase formation are provided in Appendix SOTERM-2014, Section 3.0. These results do not affect the screening arguments or decisions.

At low temperatures, precipitation and dissolution reactions are caused by changes in fluid chemistry that result in chemical undersaturation or oversaturation (Bruno and Sandino 1987). Precipitation can be divided into two stages: nucleation and crystal growth. Following nucleation, growth rates depend on the rates of surface processes and the transport of materials to the growth site. Mineral dissolution often depends on whether a surface reaction or transport of material away from the reaction site acts as the rate-controlling process. The former case may cause selective dissolution along crystallographically controlled features, whereas the latter may induce rapid bulk dissolution (Berner 1981). Thus, a range of kinetic behaviors will be exhibited by different mineral precipitation and dissolution reactions in geochemical systems.

SCR-6.5.3.1.3.1 Disposal Room

The waste that is emplaced within the WIPP contains radionuclides, including actinides or An-bearing materials in solid phases, e.g., metal oxides, salts, coprecipitated solids, and contaminated objects. In the event of contact with brine, the solution phase concentration of dissolved radionuclides is controlled both by the solution composition and the kinetics of dissolution of the solid phases, effectively approaching equilibrium from undersaturation. Solution complexation reactions of most metal ions with common inorganic ligands, such as carbonated and hydroxide, and with organic

ligands such as acetate, citrate, oxalate, and EDTA are kinetically very fast, reaching equilibrium in less than 1 s, which is infinitesimally small on the time scale of the 10,000-yr regulatory period. The rate at which thermodynamic equilibrium is approached between solution composition and the solubility-controlling solid phases will be limited by rate of dissolution of the solid materials in the waste. As a result, until equilibrium is reached, the solution concentration of the actinides will be lower than the concentration predicted based upon equilibrium of the solution phase components with the solubility-limiting solid phases. The WIPP An source term model, which describes interactions of the waste and brine, is described in detail in the CCA, Chapter 6.0, Section 6.4.3.5. The assumption of instantaneous equilibrium in waste dissolution reactions is a conservative approach, yielding maximum concentration estimates for radionuclides in the disposal rooms because a time-weighted average resulting from a kinetically accurate estimate of solution compositions would have lower concentrations at early times. Waste dissolution at the thermodynamic equilibrium solubility limit is accounted for in PA calculations. However, the kinetics of dissolution within the disposal rooms has been eliminated from PA calculations on the basis of beneficial consequence to the performance of the disposal system.

SCR-6.5.3.1.3.2 Geological Units

During groundwater flow, radionuclide precipitation processes that occur will lead to reduced contaminant transport. No credit is given in PA calculations to the potentially beneficial occurrence of precipitation of secondary minerals. The formation of radionuclide-bearing precipitates from groundwaters and brines and the associated retardation of contaminants have been eliminated from PA calculations on the basis of beneficial consequence to disposal system performance. As a result, kinetics of precipitation has also been eliminated from PA calculations because no credit is taken for precipitation reactions.

SCR-6.5.4 Sorption

SCR-6.5.4.1 FEP Numbers: W61, W62, and W63 FEP Titles: Actinide Sorption (W61) Kinetics of Sorption (W62) Changes in Sorptive Surfaces (W63)

SCR-6.5.4.1.1 Screening Decision: UP - (W61, W62) In the Culebra and Dewey Lake SO-C - Beneficial - (W61, W62) In the Disposal Room, Shaft Seals, Panel Closures, Other Geologic Units UP - (W63)

Sorption within the disposal rooms, which would serve to reduce radionuclide concentrations, has been eliminated from PA calculations on the basis of beneficial consequence to the performance of the disposal system. The effects of sorption processes in shaft seals and panel closures have been eliminated from PA calculations on the basis of beneficial consequence to the performance of the disposal system. Sorption within the Culebra and the Dewey Lake is accounted for in PA calculations. Sorption processes within other geological units of the disposal system have been eliminated from PA calculations on the basis of beneficial consequence to the performance of the disposal system. Mobile adsorbents (for example, microbes and humic acids), and the sorption of radionuclides at their surfaces, are accounted for in PA calculations in the estimates of the concentrations of actinides that may be carried. The potential effects of reaction kinetics in adsorption processes and of *Changes in Sorptive Surfaces* are accounted for in PA calculations.

SCR-6.5.4.1.2 Summary of New Information

No new information has been identified that affects the screening of these FEPs since the CRA-2009.

SCR-6.5.4.1.3 Screening Argument

Sorption may be defined as the accumulation of matter at the interface between a solid and an aqueous solution. Within PA calculations, including those made for the WIPP, the use of isotherm representations of An sorption prevails because of their computational simplicity in comparison with other models (Serne 1992, pp. 238−39). New mineral colloid and biosorption data for colloid formation have been used to update colloidal enhancement factors (see Appendix SOTERM-2014, Section SOTERM 3.9). This new information does not change the screening arguments, decisions, or implementation of these FEPs within PA.

The mechanisms that control the kinetics of sorption processes are, in general, poorly understood. Often, sorption of inorganic ions on mineral surfaces is a two-step process consisting of a short period (typically minutes) of diffusion-controlled, rapid uptake, followed by slower processes (typically weeks to months) including surface rearrangement, aggregation and precipitation, and solid solution formation (Davis and Kent 1990, p. 202). Available data concerning rates of sorption reactions involving the important radionuclides indicate that, in general, a range of kinetic behavior is to be expected.

The relevance to the WIPP of sorption reaction kinetics lies in their effects on chemical transport. Sorption of waste contaminants to static surfaces of the disposal system, such as seals and host rocks, acts to retard chemical transport. Sorption of waste contaminants to potentially mobile surfaces, such as colloids, however, may act to enhance chemical transport, particularly if the kinetics of contaminant desorption are slow or the process is irreversible (nonequilibrium).

The following subsections discuss sorption in the disposal rooms, shaft seals, panel closures, the Culebra, and other geological units of the WIPP disposal system. Sorption on colloids, microbes, and particulate material is also discussed.

SCR-6.5.4.1.3.1 Disposal Room

The concentrations of radionuclides that dissolve in waters entering the disposal room will be controlled by a combination of sorption and dissolution reactions. However, because sorption processes are surface phenomena, the amount of material likely to be involved in sorption mass transfer processes will be small relative to that involved in the bulk dissolution of waste. The WIPP PA calculations therefore assume that dissolution reactions control radionuclide concentrations. Sorption on waste, containers, and backfill within the disposal rooms, which would serve to reduce radionuclide concentrations, has been eliminated from PA calculations on the basis of beneficial consequence to the performance of the disposal system.

SCR-6.5.4.1.4 Shaft Seals and Panel Closures

The CCA, Chapter 3.0 and Appendix SEAL describe the seals that are to be placed at various locations in the access shafts and waste panel access tunnels. The materials to be used include crushed salt, bentonite clay, and cementitious grouts. Of these, the latter two in particular possess significant sorption capacities. No credit is given for the influence of sorption processes that may occur in seal materials and their likely beneficial effects on radionuclide migration rates. The effects of sorption

processes in shaft seals and panel closures have been eliminated from PA calculations on the basis of beneficial consequence to the performance of the disposal system.

SCR-6.5.4.1.4.1 Culebra

Sorption within the Culebra is accounted for in PA calculations as discussed in the CCA, Chapter 6.0, Section 6.4.6.2. The model used comprises an equilibrium, sorption isotherm approximation, employing constructed CDFs of K_ds applicable to dolomite in the Culebra. The potential effects of reaction kinetics in adsorption processes are encompassed in the ranges of K_ds used. The geochemical speciation of the Culebra groundwaters and the effects of changes in sorptive surfaces are implicitly accounted for in PA calculations for the WIPP in the ranges of K_ds used.

SCR-6.5.4.1.4.2 Other Geological Units

During groundwater flow, any radionuclide sorption processes that occur between dissolved or colloidal actinides and rock surfaces will lead to reduced rates of contaminant transport. The sorptive capacity of the Dewey Lake is sufficiently large to prevent any radionuclides that enter it from being released to the accessible environment over 10,000 yrs (Wallace et al. 1995). Thus, sorption within the Dewey Lake is accounted for in PA calculations, as discussed in the CCA, Chapter 6.0, Section 6.4.6.6. No credit is given to the potentially beneficial occurrence of sorption in other geological units outside the Culebra. Sorption processes within other geological units of the disposal system have been eliminated from PA calculations on the basis of beneficial consequence to the performance of the disposal system.

SCR-6.5.4.1.4.3 Sorption on Colloids, Microbes, and Particulate Material

The interactions of sorption processes with colloidal, microbial, or particulate transport are complex. Neglecting sorption of contaminants on immobile surfaces in the repository shafts and Salado (for example, the clays of the Salado interbeds) is a conservative approach because it leads to overestimated transport rates. However, neglecting sorption on potentially mobile adsorbents (for example, microbes and humic acids) cannot be shown to be conservative with respect to potential releases, because mobile adsorbents may act to transport radionuclides sorbed to them. Consequently, the concentrations of actinides that may be carried by mobile adsorbents are accounted for in PA calculations (see the CCA, Chapter 6.0, Section 6.4.3.6).

SCR-6.5.5 Reduction-Oxidation Chemistry

SCR-6.5.5.1 FEP Numbers: W64 and W66 FEP Titles: Effects of Metal Corrosion Reduction-Oxidation Kinetics

SCR-6.5.5.1.1 Screening Decision: UP

The effects of reduction-oxidation reactions related to metal corrosion on reduction-oxidation conditions are accounted for in PA calculations. Reduction-oxidation reaction kinetics are accounted for in PA calculations.

SCR-6.5.5.1.2 Summary of New Information

No new information has been identified that affects the screening of these FEPs since the CRA-2009.

SCR-6.5.5.1.3 Screening Argument

SCR-6.5.5.1.3.1 Reduction-Oxidation Kinetics

In general, investigation of the reduction-oxidation couples present in aqueous geochemical systems suggests that most reduction-oxidation reactions are not in thermodynamic equilibrium (Wolery 1992, p. 27). The lack of data characterizing the rates of reactions among trace element reduction-oxidation couples leads to uncertainty in elemental speciation. This uncertainty in reduction-oxidation kineticsis accounted for in PA calculations in the dissolved An source term model (see Appendix SOTERM-2014, Section SOTERM-4.3), which estimates the probabilities that particular actinides occur in certain oxidation states. New data regarding reduction of plutonium by iron in WIPP brine are summarized in Appendix SOTERM-2014, Section 3.6.2. This new information does not affect the screening argument or decision for these FEPs.

SCR-6.5.5.1.3.2 Corrosion

Other than gas generation, which is discussed in FEPs W44 through W55, the main effect of metal corrosion will be to influence the chemical conditions that prevail within the repository. Ferrous metals will be the most abundant metals in the WIPP, and these will corrode on contact with any brines entering the repository. Initially, corrosion will occur under oxic conditions owing to the atmospheric oxygen present in the repository at the time of closure. However, consumption of the available oxygen by corrosion reactions will rapidly lead to anoxic (reducing) conditions. These changes and controls on conditions within the repository will affect the chemical speciation of the brines and may affect the oxidation states of the actinides present. Changes to the oxidation states of the actinides will lead to changes in the concentrations that may be mobilized during brine flow. The oxidation states of the actinides are accounted for in PA calculations by the use of parameters that describe probabilities that the actinides exist in particular oxidation states and, as a result, the likely An concentrations. Therefore, the effects of metal corrosion are accounted for in PA calculations.

SCR-6.5.5.2 FEP Number: W65 FEP Title: Reduction-Oxidation Fronts

SCR-6.5.5.2.1 Screening Decision: SO-P

The migration of *Reduction-Oxidation Fronts* through the repository has been eliminated from PA calculations on the basis of low probability of occurrence over 10,000 yrs.

SCR-6.5.5.2.2 Summary of New Information

No new information has been identified that affects the screening of this FEP since the CRA-2009.

SCR-6.5.5.2.3 Screening Argument

The development of reduction-oxidation fronts in the disposal system may affect the chemistry and migration of radionuclides. Reduction-oxidation fronts separate regions that may be characterized, in broad terms, as having different oxidation potentials. On either side of a reduction-oxidation front, the behavior of reduction-oxidation-sensitive elements may be controlled by different geochemical reactions. Elements that exhibit the greatest range of oxidation states (for example, U, Np, and Pu) will be the most affected by reduction-oxidation front development and migration. The migration of reduction-oxidation fronts may occur as a result of diffusion processes, or in response to groundwater

flow, but will be restricted by the occurrence of heterogeneous buffering reactions (for example, mineral dissolution and precipitation reactions). Indeed, these buffering reactions cause the typically sharp, distinct nature of reduction-oxidation fronts.

Of greater significance is the possibility that the flow of fluids having different oxidation potentials from those established within the repository might lead to the development and migration of a large-scale reduction-oxidation front. Reduction-oxidation fronts have been observed in natural systems to be the loci for both the mobilization and concentration of radionuclides, such as U. For example, during investigations at two U deposits at Poços de Caldas, Brazil, U was observed by Waber (Waber 1991) to be concentrated along reduction-oxidation fronts at the onset of reducing conditions by its precipitation as U oxide. In contrast, studies of the Alligator Rivers U deposit in Australia by Snelling (Snelling 1992) indicated that the movement of the relatively oxidized weathered zone downwards through the primary ore body as the deposit was eroded and gradually exhumed led to the formation of secondary uranyl-silicate minerals and the mobilization of U in its more soluble U(VI) form in near-surface waters. The geochemical evidence from these sites suggests that the reduction-oxidation fronts had migrated only slowly, at most on the order of a few tens of meters per million yrs. These rates of migration were controlled by a range of factors, including the rates of erosion, infiltration of oxidizing waters, geochemical reactions, and diffusion processes.

The migration of large-scale reduction-oxidation front through the repository as a result of regional fluid flow is considered unlikely over the regulatory period on the basis of comparison with the slow rates of reduction-oxidation front migration suggested by natural system studies. This comparison is considered conservative because the relatively impermeable nature of the Salado suggests that reduction-oxidation front migration rates at the WIPP are likely to be slower than those observed in the more permeable lithologies of the natural systems studied. Large-scale reduction-oxidation fronts have therefore been eliminated from PA calculations on the basis of low probability of occurrence over 10,000 yrs.

SCR-6.5.5.3 FEP Number: W67 FEP Title: Localized Reducing Zones

SCR-6.5.5.3.1 Screening Decision: SO-C

The formation of *Localized Reducing Zones* has been eliminated from PA calculations on the basis of low consequence to the performance of the disposal system.

SCR-6.5.5.3.2 Summary of New Information

No new information has been identified that affects the screening of this FEP since the CRA-2009.

SCR-6.5.5.3.3 Screening Argument

The dominant reduction reactions in the repository include steel corrosion and microbial degradation. The following bounding calculation shows that molecular diffusion alone will be sufficient to mix brine chemistry over a distance of meters and therefore the formation of localized reducing zones in the repository is of low consequence.

The diffusion of a chemical species in a porous medium can be described by Fick's equation (e.g., Richardson and McSween 1989, p.132):

$$\frac{\partial C}{\partial t} = \frac{\partial}{\partial X}\left(D_{eff}\frac{\partial C}{\partial X}\right) \quad \text{(SCR.17)}$$

where C is the concentration of the diffusing chemical species, t is the time, X is the distance, and D_{eff} is the effective diffusivity of the chemical species in a given porous medium. D_{eff} is related to the porosity (ϕ) of the medium by (e.g., Oelkers 1996):

$$D_{eff} = \phi^2 D \quad \text{(SCR.18)}$$

where D is the diffusivity of the species in pure solution. The D values for most aqueous species at room temperatures fall into a narrow range, and 10^{-5} cm^2 (1.5×10^{-6} $in.^2$) per s is a good approximation (e.g., Richardson and McSween 1989, p.138). From the WIPP PA calculations (Bean et al. 1996, p.7-29; WIPP Performance Assessment 1993, Equation B-8), the porosity in the WIPP waste panels after room closure is calculated to be 0.4 to 0.7. From Equation (SCR.19), the effective diffusivity D_{eff} in the waste is estimated to be 2 - 5 × 10^{-6} cm^2 (7×10^{-7} $in.^2$) per second (= 6 - 16 × 10^{-3} m^2/yr).

Given a time scale of T, the typical diffusion penetration distance (L) can be determined by scaling:

$$L = \sqrt{D_{eff} T} \quad \text{(SCR.19)}$$

Using Equation (SCR.20), the diffusion penetration distance in the WIPP can be calculated as a function of diffusion time, as shown in Figure SCR-1.

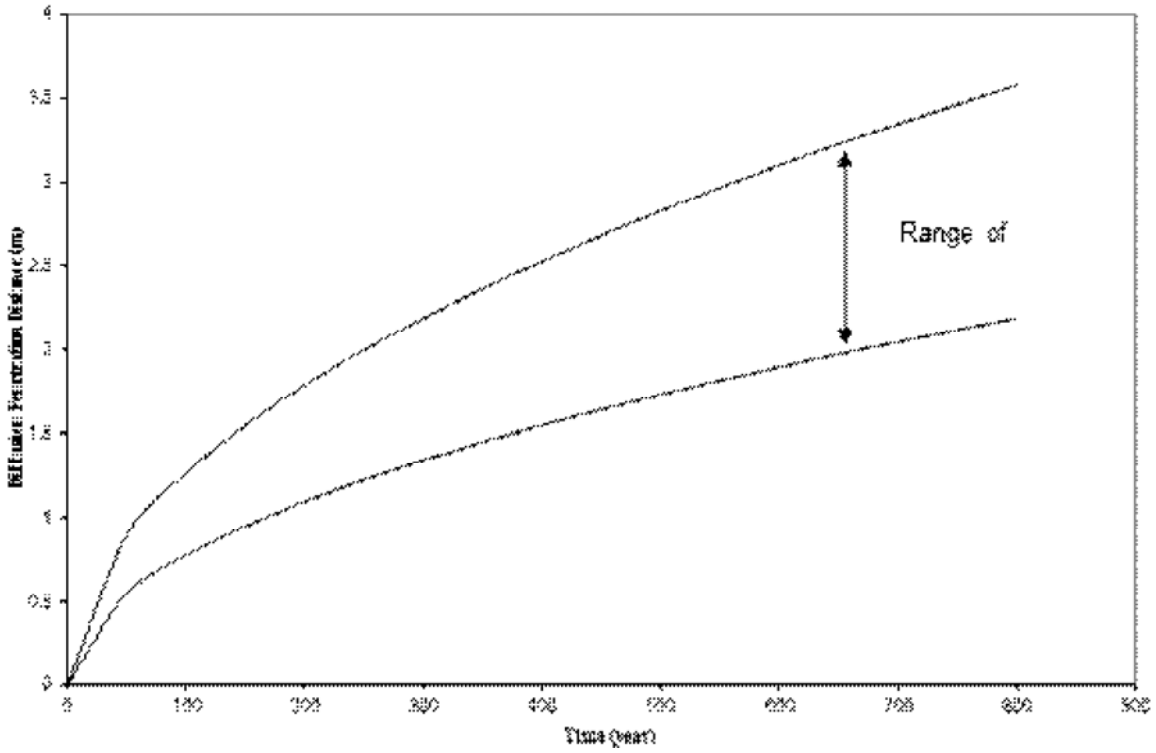

Figure SCR- 1. Diffusion Penetration Distance in the WIPP as a Function of Diffusion Time

Direct brine release requires the repository gas pressure to be at least 8 MPa (Stoelzel et al. 1996). The CRA-2014 calculations show that it will take at least 1000 yrs for the repository pressure to reach this critical value by gas generation processes (see Camphouse 2013b, Figure 6-3). Over this time scale, according to Equation (SCR.20) and Figure SCR-1, molecular diffusion alone can mix brine composition effectively at least over a distance of ~ 1 m (3.3 ft).

The above calculation assumes diffusion only through liquid water. This assumption is applicable to steel corrosion, the humid rate of which is zero. Note that microbial reactions can also consume or release gaseous species. The diffusion of a gaseous species is much faster than an aqueous one. Thus, molecular diffusion can homogenize microbial reactions even at a much larger scale.

The height of waste stacks in the repository after room closure (h) can be calculated by:

$$h = \frac{h_0(1-\phi_0)}{1-\phi} \quad \text{(SCR.20)}$$

where h_0 and ϕ_0 are the initial height of waste stacks and the initial porosity of wastes, which are assumed to be 3.96 m and 0.848, respectively, in the WIPP PA. For ϕ = 0.4 - 0.7, h is estimated to be 1.0 to 2.0 m. This means that molecular diffusion alone can homogenize redox reaction in the vertical dimension of the repository. Therefore, the formation of localized reducing zones is unlikely. The general repository environment will become reducing shortly after room closure because of metal corrosion and microbial reactions. Therefore, localized reducing zones can be eliminated from PA calculations on the basis of low consequence to the disposal system.

SCR-6.5.6 Organic Complexation

SCR-6.5.6.11 FEP Numbers: W68, W69, and W71 FEP Titles: Organic Complexation (W68) Organic Ligands (W69) Kinetics of Organic Complexation (W71)

SCR-6.5.6.1.1 Screening Decision: UP - W68 and W69 SO-C - W71

The effects of anthropogenic *Organic Complexation* reactions, including the effects of *Organic Ligands*, humic, and fulvic acids, have been incorporated in the PA calculations. The kinetics of organic ligand complexation is screened out because the rate at which organic ligands are complexed to actinide is so fast that it has no consequence to repository performance.

SCR-6.5.6.1.2 Summary of New Information

These FEPs have been updated with references to the newest waste inventory (Van Soest 2012) and the most recent solubility calculations (Brush and Domski 2013a). The CRA-2014 PA includes improved treatment of the amount of brine within the repository such that it more accurately represents dissolved radionuclide concentrations over a range of possible brine volumes (see Camphouse 2013a). This change in the implementation of brine volume is considered a model enhancement as it corrects a mass balance issue that was present in previous PAs. FEPs related to this improvement (W68 and W69) continue to be screened in as UP.

SCR-6.5.6.1.3 Screening Argument

From a PA standpoint, the most important actinides are Th, U, Np, Pu, and Am. Dissolved Th, U, Np, Pu, and Am will essentially speciate entirely as Th(IV), U(IV) or U(VI), Np(IV) or Np(V), Pu(III) or Pu(IV), and Am(III) under the strongly reducing conditions expected as a result of the presence of Fe (II) and microbes (see Appendix SOTERM-2014, Section SOTERM-4.3). New WIPP-specific data on the effects of organic complexation on neodymium and thorium are summarized in Appendix SOTERM-2014, Section 3.8.2. This new information does not affect the screening argument or decision for these FEPs.

Some organic ligands can increase the actinide solubilities. An estimate of masses of the complexing agents in the TRU solidified waste forms scheduled for disposal in the WIPP is presented in Van Soest (Van Soest 2012). Acetate, citrate, oxalate, and EDTA were determined to be the only water-soluble and actinide-complexing organic ligands present in significant quantities in the inventory. These ligands and their complexation with actinides (Th(IV), U(VI), Np(V), and Am(III)) in a variety of ionic strength media were studied at Florida State University (FSU) (Choppin et al. 2001). The FSU studies showed that acetate, citrate, oxalate, and EDTA are capable of significantly enhancing dissolved An concentrations. Lactate behavior was also studied at FSU because it appeared in the preliminary inventory of nonradioactive constituents of the TRU waste to be emplaced in the WIPP (Brush 1990); lactate did not appear in the current inventory (Van Soest 2012).

Although the FSU experimental work on organic ligands complexation showed that acetate, citrate, oxalate, and EDTA are capable of significantly enhancing dissolved An concentrations, SNL did not include the results in the FMT calculations for the CCA PA because (1) the thermodynamic database for organic complexation of actinides was not considered adequate at the time, and (2) side-calculations using thermodynamic data for low-ionic-strength NaCl solutions showed that transition metals (in particular iron, nickel, chromium, vanadium, and manganese present in waste drum steel) would compete effectively with the actinides for the binding sites on the organic ligands, thus preventing significant complexation of actinides.

The solubilities of the actinides are calculated using EQ3/6, a software package for calculating actinide concentration limits based on thermodynamic parameters. The parameters for EQ3/6 are derived both from experimental investigations specifically designed to provide parameter values for this model and from the published literature. The CRA-2014 calculations include the effects of organic ligands (acetate, citrate, EDTA, and oxalate) on actinide solubilities in the EQ3/6 calculations (Brush and Domski 2013b). The EQ3/6 database includes all of the results of experimental studies (Choppin et al. 2001) required to predict the complexation of dissolved An(III), An(IV), and An(V) species by acetate, citrate, EDTA, and oxalate (Giambalvo 2002a and Giambalvo 2002b).

Solution complexation reactions of most metal ions with common inorganic ligands, such as carbonate and hydroxide, and with organic ligands, such as acetate, citrate, oxalate, and EDTA, are kinetically very fast, reaching equilibrium in fractions of a second, an inconsequentially short time increment on the scale of the 10,000-yr regulatory period. Reactions of these types are generally so fast that special techniques must be adopted to measure the reaction rates; as a practical matter, the reaction rate is limited by the mixing rate when metal solutions are combined with ligand solutions.

For that reason, the rate at which organic ligands are complexed to actinide is of no consequence to repository performance. Kinetics of organic complexation may be eliminated from PA calculations on the basis of no consequence.

Organic ligands can also influence potential retardation of radionuclides in geologic materials. Organic ligand concentration in repository brine could reduce K_ds in the Culebra. The impact of

organic ligands on K_d ranges used in radionuclide transport calculations was included in PA for the CRA-2009 PABC (Kuhlman 2010). The CRA-2014 uses these revised ranges.

SCR-6.5.6.2 FEP Number: W70 FEP Title: Humic and Fulvic Acids

SCR-6.5.6.2.1 Screening Decision: UP

The presence of *Humic Acids* and *Fulvic Acids* is incorporated in PA calculations.

SCR-6.5.6.2.2 Summary of New Information

No new information has been identified that affects the screening of this FEP since the CRA-2009.

SCR-6.5.6.2.3 Screening Argument

The occurrence of humic acids and fulvic acids is incorporated in PA calculations in the models for radionuclide transport by humic colloids (see Appendix PA-2014, Section PA-4.3).

SCR-6.5.7 Chemical Effects on Material Properties

SCR-6.5.7.1 FEP Numbers: W74, W76, and W115 FEP Titles: Chemical Degradation of Shaft Seals (W74) Microbial Growth on Concrete (W76) Chemical Degradation of Panel Closures (W115)

SCR-6.5.7.1.1 Screening Decision: UP (W74 and W76) SO-P (W115)

The effects of *Chemical Degradation of Shaft Seals*, and *Microbial Growth on Concrete* are accounted for in PA calculations. *Chemical Degradation of Panel Closures* has been screened out based on low probability.

SCR-6.5.7.1.2 Summary of New Information

The CRA-2014 PA represents a new panel closure system constructed of run-of-mine (ROM) salt. Historically, FEP W115 *Chemical Degradation of Panel Closures* has been included in past PA calculations (classified UP), due to the potential for concrete to degrade in the repository environment. However, because the new PCS will be constructed of ROM salt, it is no longer appropriate to include in PA calculations because, unlike the concrete in the Option D panel closure, the ROM salt will not be susceptible to chemical degradation. The ROM salt closure will be identical to the host rock chemistry, which will be at chemical equilibrium with any brine from the near field. In the event brine were present that differed significantly from the host rock chemistry, the PCS material will not be preferentially degraded from that of the host rock.

SCR-6.5.7.1.3 Screening Argument

The concrete used in the shaft seal systems will degrade as a result of chemical reaction with the infiltrating groundwater. Degradation could lead to an increase in permeability of the seal system. The main uncertainties with regard to cement degradation rates at the WIPP are the effects of groundwater

chemistry, the exact nature of the cementitious phases present, and the rates of brine infiltration. The PA calculations take a conservative approach to these uncertainties by assuming a large increase in permeability of the concrete seals only a few hundred yrs after closure. These permeability values are based on seal design considerations and consider the potential effects of degradation processes. Therefore, the effects of chemical degradation of shaft seals are accounted for in PA calculations through the CDFs used for seal material permeabilities. The panel closures are planned to be constructed of ROM salt. Due to the salt construction, chemical degradation is not expected to occur to the ROM salt PCS.

Concrete can be inhabited by alkalophilic bacteria, which could produce acids, thereby accelerating the seal degradation process. Nitrification processes, which will produce nitric acid, tend to be aerobic, and will be further limited at the WIPP by the low availability of ammonium in the brines (Pedersen and Karlsson 1995, p. 75). Because of the limitations on growth caused by the chemical conditions, it is likely that the effects of microbial growth on concrete will be small. The effects of such microbial activity on seal properties are, therefore, implicitly accounted for in PA calculations through the CDFs used for seal material permeabilities.

SCR-6.5.7.2 FEP Number: W75 FEP Title: Chemical Degradation of Backfill

SCR-6.5.7.2.1 Screening Decision: SO-C

The effects on material properties of the *Chemical Degradation of Backfill* have been eliminated from PA calculations on the basis of low consequence.

SCR-6.5.7.2.2 Summary of New Information

No new information has been identified that affects the screening of this FEP since the CRA-2009.

SCR-6.5.7.2.3 Screening Argument

Degradation of the chemical conditioners or backfill added to the disposal room is a prerequisite of their function in buffering the chemical environment of the disposal room. However, the chemical reactions (Snider 2001) and dissolution involved will change the physical properties of the material. Because the mechanical and hydraulic characteristics of the backfill have been eliminated from PA calculations on the basis of low consequence to the performance of the disposal system, the effects of the chemical degradation of backfill on material properties have been eliminated from PA calculations on the same basis.

SCR-6.6 Contaminant Transport Mode FEPs

SCR-6.6.1 Solute and Colloid Transport

SCR-6.6.1.1 FEP Number: W77 FEP Title: Solute Transport

SCR-6.6.1.1.1 Screening Decision: UP

Transport of dissolved radionuclides is accounted for in PA calculations.

SCR-6.6.1.1.2 Summary of New Information

No new information has been identified that affects the screening of this FEP since the CRA-2009.

SCR-6.6.1.1.3 Screening Argument

Solute transport may occur by advection, dispersion, and diffusion down chemical potential gradients, and is accounted for in PA calculations (see Appendix PA-2014, Section PA-4.3).

SCR-6.6.1.2 FEP Numbers: W78, W79, W80, and W81 FEP Titles: Colloidal Transport (W78) Colloidal Formation and Stability (W79) Colloidal Filtration (W80) Colloidal Sorption (W81)

SCR-6.6.1.2.1 Screening Decision: UP

Formation of colloids, transport of colloidal radionuclides, and colloid retardation through filtration and sorption are accounted for in PA calculations.

SCR-6.6.1.2.2 Summary of New Information

No new information has been identified that affects the screening of these FEPs since the CRA-2009.

SCR-6.6.1.2.3 Screening Argument

Colloids typically have sizes of between 1 nm and 1 μm and may form stable dispersions in groundwaters. Colloid formation and stability depends on their composition and the prevailing chemical conditions (for example, salinity). Depending on their size, colloid transport may occur at different rates than those of fully dissolved species. They may be physically excluded from fine porous media, and their migration may be accelerated through fractured media in channels where velocities are greatest. However, they can also interact with the host rocks during transport and become retarded. These interactions may be of a chemical or physical nature and include electrostatic effects leading to colloid sorption, and sieving leading to colloid filtration and pore blocking. Colloidal formation and stability is accounted for in PA calculations through estimates of colloid numbers in the disposal room based on the prevailing chemical conditions (Appendix SOTERM-2014, Section SOTERM-4.6). Colloidal sorption, colloidal filtration, and colloidal transport in the Culebra are accounted for in PA calculations (CCA Section 6.4.6.2.2). New WIPP-relevant data regarding colloid formation and transport can be found in Appendix SOTERM-2014, Section 3.9. This information does not affect the screening argument or decision for this FEP.

SCR-6.6.2 Particle Transport

SCR-6.6.2.1 FEP Numbers: W82, W83, W84, W85, and W86 FEP Titles: Suspension of Particles (W82) Rinse (W83) Cuttings (W84) Cavings (W85) Spallings (W86)

SCR-6.6.2.1.1 Screening Decision: DP W82, W84, W85, W86 SO-C W83

The formation of particulates through *R inse* and subsequent transport of radionuclides in groundwater and brine has been eliminated from PA calculations for undisturbed conditions on the basis of low consequence to the performance of the disposal system. The transport of radionuclides as particulates (cuttings, cavings, and spallings) during penetration of the repository by a borehole, is accounted for in PA calculations.

SCR-6.6.2.1.2 Summary of New Information

Recent experiments (Herrick et al. 2012) on surrogate waste materials has resulted in new parameter values for the shear strength of waste. This parameter directly affects the amount of cavings (W85) during intrusion scenarios. Additionally, the improved implementation of water balance (Camphouse 2013a) within the repository may indirectly affect spallings (W86). These enhancements are downstream of the screening process and will not affect either of these FEPs; they remain included in disturbed scenarios and are classified DP.

SCR-6.6.2.1.3 Screening Argument

Suspensions of particles that have sizes larger than colloids are unstable because the particles undergo gravitational settling. It is unlikely that brine flow will be rapid enough within the WIPP disposal rooms to generate particulate suspensions through rinse and transport under undisturbed conditions. Mobilization of suspensions would effect a local and minor redistribution of radionuclides within the room and would not result in increased radionuclide transport from the repository. The formation of particulates through rinse and transport of radionuclides in groundwater and brine has been eliminated from PA calculations for undisturbed conditions on the basis of low consequence to the performance of the disposal system.

Inadvertent human intrusion into the repository by a borehole could result in transport of waste material to the ground surface through drilling-induced flow and blowouts (FEPs H21 and H23, Section SCR-5.2.1.1 and Section SCR-5.2.1.3). This waste could include material intersected by the drill bit (cuttings), material eroded from the borehole wall by circulating drilling fluid (cavings), and material that enters the borehole as the repository depressurizes (spallings). Transport of radionuclides by these materials and in brine is accounted for in PA calculations and is discussed in Appendix PA-2014, Sections PA-4.5 and PA-4.6.

SCR-6.6.3 Microbial Transport

SCR-6.6.3.1 FEP Number: W87 FEP Title: Microbial Transport

SCR-6.6.3.1.1 Screening Decision: UP

Transport of radionuclides bound to microbes is accounted for in PA calculations.

SCR-6.6.3.1.2 Summary of New Information

No new information has been identified that affects the screening of this FEP since the CRA-2009.

SCR-6.6.3.1.3 Screening Argument

Microbes will be introduced into the disposal rooms during the operational phase of the repository and will also occur naturally in geological units throughout the disposal system. Because of their colloidal size, microbes, and any radionuclides bound to them, may be transported at different rates than radionuclides in solution. Microbial transport of radionuclides is accounted for in PA calculations (Appendix SOTERM-2014, Section SOTERM-3.9.2.3 and Reed et al. (Reed et al. 2013). New data on the formation of biocolloids is summarized in Appendix SOTERM-2014, Section 3.9.2.3 and Reed et al. (Reed et al. 2013). This information does not affect the screening argument or decision for this FEP.

SCR-6.6.3.2 FEP Number: W88 FEP Title: Biofilms

SCR-6.6.3.2.1 Screening Decision: SO-C Beneficial

The effects of *Biofilms* on microbial transport have been eliminated from PA calculations on the basis of beneficial consequence to the performance of the disposal system.

SCR-6.6.3.2.2 Summary of New Information

No new information has been identified that affects the screening of this FEP since the CRA-2009.

SCR-6.6.3.2.3 Screening Argument

Microbes will be introduced into the disposal rooms during the operational phase of the repository and will also occur naturally in geological units throughout the disposal system.

Biofilms may influence microbial and radionuclide transport rates through their capacity to retain, and therefore retard, both the microbes themselves and radionuclides. The formation of biofilms in deep subsurface environments such as in the WIPP is controversial. Since the microbial degradation experiments at Brookhaven National Laboratory bracket expected repository conditions, the potential effect of biofilms formation on microbial degradation and transport, if any, has been captured in the PA parameters derived from those experiments (Francis and Gillow 1994; Francis et al. 1997; Francis and Gillow 2000; Gillow and Francis 2001a and Gillow and Francis 2001b; Gillow and Francis 2002a and Gillow and Francis 2002b). As a matter of fact, no apparent formation of stable biofilms was observed in the Brookhaven National Laboratory experiments. The formation of biofilms tends to reduce cell suspension and mobility. Additional information on the microbial ecology of WIPP is provided in Appendix SOTERM-2014, Section 2.4.1. This effect has been eliminated from PA calculations on the basis of beneficial consequence to the performance of the disposal system.

SCR-6.6.4 Gas Transport

SCR-6.6.4.1 FEP Number: W89 FEP Title: Transport of Radioactive Gases

SCR-6.6.4.1.1 Screening Decision: SO-C

The *Transport of Radioactive Gases* has been eliminated from PA calculations on the basis of low consequence to the performance of the disposal system.

SCR-6.6.4.1.2 Summary of New Information

This FEP discussion has been updated to include recent inventory information. This new information does not affect the screening argument or decision for this FEP.

SCR-6.6.4.1.3 Screening Argument

The production and potential transport of radioactive gases are eliminated from PA calculations on the basis of low consequence to the performance of the disposal system. Transportable radioactive gases are comprised mainly of isotopes of Rn and ^{14}C. Rn gases are eliminated from PA because their inventory is small (<4 Ci) (Van Soest 2012), and their half-lives are short (<4 days), resulting in insignificant potential for release from the repository.

SCR-6.7 Contaminant Transport Processes

SCR-6.7.1 Advection

SCR-6.7.1.1 FEP Number: W90 FEP Title: Advection

SCR-6.7.1.1.1 Screening Decision: UP

Advection of contaminants is accounted for in PA calculations.

SCR-6.7.1.1.2 Summary of New Information

No new information has been identified that affects the screening of this FEP since the CRA-2009.

SCR-6.7.1.1.3 Screening Argument

Advection (that is, the transport of dissolved and solid material by flowing fluid) is accounted for in PA calculations (Appendix PA-2014, Section PA-4.3).

SCR-6.7.2 Diffusion

SCR-6.7.2.1 FEP Numbers: W91 and W92 FEP Titles: Diffusion(W91) Matrix Diffusion (W92)

SCR-6.7.2.1.1 Screening Decision: UP

Diffusion of contaminants and retardation by *Matrix Diffusion* are accounted for in PA calculations.

SCR-6.7.2.1.2 Summary of New Information

No new information has been identified that affects the screening of this FEP since the CRA-2009.

SCR-6.7.2.1.3 Screening Argument

Diffusion (that is, the movement of molecules or particles both parallel to and transverse to the direction of advection in response to Brownian forces) and, more specifically matrix diffusion, whereby movement is transverse to the direction of advection within a fracture and into the surrounding rock matrix, are accounted for in PA calculations (Appendix PA-2014, Section PA-4.9).

SCR-6.7.3 Thermochemical Transport Phenomena

SCR-6.7.3.1 FEP Number: W93 FEP Title: Soret Effect

SCR-6.7.3.1.1 Screening Decision: SO-C

The effects of thermochemical transport phenomena (the *Soret Effect*) have been eliminated from PA calculations on the basis of low consequence to the performance of the disposal system.

SCR-6.7.3.1.2 Summary of New Information

This FEP has been updated with new thermal heat rise values for Al corrosion and MgO hydration, based on the latest inventory data (Van Soest 2012). These values continue to be low and do not affect the screening argument or decision for this FEP.

SCR-6.7.3.1.3 Screening Argument

According to Fick's law, the diffusion flux of a solute is proportional to the solute concentration gradient. In the presence of a temperature gradient there will also be a solute flux proportional to the temperature gradient (the Soret Effect). Thus, the total solute flux, J, in a liquid phase may be expressed as

$$J = -D\bar{\nabla}C - ND\bar{\nabla}T \quad \text{(SCR.21)}$$

where C is the solute concentration, T is the temperature of the liquid, D is the solute diffusion coefficient, and

$$N = S_T C(1-C) \quad \text{(SCR.22)}$$

in which S_T is the Soret coefficient. The mass conservation equation for solute diffusion in a liquid is then

$$\frac{\partial C}{\partial t} = \nabla \cdot (D\nabla C + ND\nabla T) \quad \text{(SCR.23)}$$

When temperature gradients exist in solutions with both light and heavy solute molecules, the heavier molecules tend to concentrate in the colder regions of the solution. Typically, large temperature gradients are required for Soret diffusion to be significant compared to Fickian diffusion.

Radioactive decay, nuclear criticality, and exothermic reactions are three possible sources of heat in the WIPP repository. The U.S. DOE (U.S. DOE 1980) estimated that radioactive decay of CH-TRU waste will result in a maximum temperature rise at the center of the repository of 1.6 °C (2.9 °F) at 80

yrs after waste emplacement. Sanchez and Trellue (Sanchez and Trellue 1996) have shown that the total thermal load of RH-TRU waste will not significantly affect the average temperature increase in the repository. Temperature increases of about 3 °C (5.4 °F) may occur at the locations of RH-TRU containers with maximum thermal power (60 W). Such temperature increases are likely to be short-lived on the time scale of the 10,000-yr regulatory period because of the rapid decay of heat-producing nuclides in RH-TRU waste, such as ^{137}Cs (cesium), ^{90}Sr (strontium), ^{241}Pu, and ^{147}Pm (promethium), whose half-lives are approximately 30, 29, 14, and 3 yrs, respectively. Soret diffusion generated by such temperature gradients will be negligible compared to other radionuclide transport mechanisms.

Temperature increases resulting from exothermic reactions are discussed in Section SCR-6.3.4.1. The maximum temperature rise in the disposal panels will be less than 3.9 °C (7.0 °F) as a consequence of MgO hydration. Note that AICs will prevent drilling within the controlled area for 100 yrs after disposal. Heat generation by radioactive decay and concrete seal hydration will have decreased substantially after 100 yrs, and the temperatures in the disposal panels will have decreased nearly to the temperature of the undisturbed host rock.

If the repository were to be inundated following a drilling intrusion, Al corrosion could, at most, result in a short-lived (two yrs) temperature increase of about 3.4 °C (6.1 °F). These calculated maximum heat generation rates resulting from Al corrosion and backfill hydration could not occur simultaneously because they are limited by brine availability; each calculation assumes that all available brine is consumed by the reaction of concern. Thus, the temperature rise of 3.9 °C (7.0 °F) represents the maximum that could occur as a result of a combination of exothermic reactions occurring simultaneously. Temperature increases of this magnitude will not result in significant Soret diffusion within the disposal system.

The limited magnitude and spatial scale of temperature gradients in the disposal system indicate that Soret diffusion will be insignificant, allowing the effects of thermochemical transport (Soret Effect) to be eliminated from PA calculations on the basis of low consequence to the performance of the disposal system.

SCR-6.7.4 Electrochemical Transport Phenomena

SCR-6.7.4.1 FEP Number: W94 FEP Title: Electrochemical Effects

SCR-6.7.4.1.1 Screening Decision: SO-C

The effects of electrochemical transport phenomena caused by electrochemical reactions have been eliminated from PA calculations on the basis of low consequence to the performance of the disposal system.

SCR-6.7.4.1.2 Summary of New Information

No new information that affects the screening of this FEP has been identified since the CRA-2009.

SCR-6.7.4.1.3 Screening Argument

The variety of waste metals and metal packaging in the repository may allow galvanic cells spanning short distances to be established. The interactions among the metals depend upon their physical characteristics and the chemical conditions in the repository. For example, good physical and electrical contact, which is critical to the establishment of galvanic cells, may be impeded by electrically nonconductive waste materials. Additionally, in order to establish a galvanic cell, it is necessary that the metals have different values for standard reduction potentials. For example, a galvanic cell is not expected to be formed by contact of two segments of metals with identical compositions. As a result, galvanic cells can only be established by contact of dissimilar metals, as might happen because of contact between a waste drum and the contents, or between contents within a waste package. The localized nature of electrochemical transport is restricted to the size scale over which galvanic cells can develop, i.e., on the order of size of waste packages. Since the possible range of transport is restricted by the physical extent of galvanic activity, electrochemical effects cannot act as long-range transport mechanisms for radionuclides and therefore are of no consequence to the performance of the repository.

SCR-6.7.4.2 FEP Number: W95 FEP Title: Galvanic Coupling (outside the repository)

SCR-6.7.4.2.1 Screening Decision: SO-P

The effects of *Galvanic Coupling* between the waste and metals external to the repository on transport have been eliminated from PA calculations on the basis of low probability of occurrence over 10,000 yrs.

SCR-6.7.4.2.2 Summary of New Information

No new information that affects the screening of this FEP has been identified since the CRA-2009.

SCR-6.7.4.2.3 Screening Argument

With regard to the WIPP, galvanic coupling refers to the establishment of galvanic cells between metals in the waste form, canisters, and other metals external to the waste form.

Long-range electric potential gradients may exist in the subsurface as a result of groundwater flow and electrochemical reactions. The development of electric potential gradients may be associated with the weathering of sulfide ore bodies, variations in rock properties at geological contacts, bioelectric activity associated with organic matter, natural corrosion reactions, and temperature gradients in groundwater. With the exception of mineralization potentials associated with metal sulfide ores, the magnitude of electric potentials is usually less than about 100 millivolts (mV) and the potentials tend to average to zero over distances of several thousand feet (Telford et al. 1976). Metals external to the waste form can include natural metallic ore bodies in the host rock. However, metallic ore bodies and metallic sulfide ores do not exist in the region of the repository (the CCA, Appendix GCR). As a result, galvanic coupling between the waste and metallic materials outside the repository cannot occur. Therefore, galvanic coupling is eliminated from PA calculations on the basis of low probability of occurrence over 10,000 yrs.

SCR-6.7.4.3 FEP Number: W96 FEP Title: Electrophoresis

SCR-6.7.4.3.1 Screening Decision: SO-C

The effects of electrochemical transport phenomena caused by *Electrophoresis* have been eliminated from PA calculations on the basis of low consequence to the performance of the disposal system.

SCR-6.7.4.3.2 Summary of New Information

No new information that affects the screening of this FEP has been identified since the CRA-2009.

SCR-6.7.4.3.3 Screening Argument

Long range (in terms of distance) electric potential gradients may exist in the subsurface as a result of groundwater flow and electrochemical reactions. The development of potentials may be associated with the weathering of sulfide ore bodies, variations in rock properties at geological contacts, bioelectric activity associated with organic matter, natural corrosion reactions, and temperature gradients in groundwater. With the exception of mineralization potentials associated with metal sulfide ores, the magnitude of such potentials is usually less than about 100 mV and the potentials tend to average to zero over distances of several thousand feet (Telford et al. 1976, p. 458). Short range potential gradients caused by the corrosion of metals within the waste may be set up over distances that are restricted to the size scale of the waste packages.

A variety of metals will be present within the repository as waste metals and metal packaging, which may allow electrochemical cells to be established over short distances. The types of interactions that will occur depend on the metals involved, their physical characteristics, and the prevailing solution conditions. Electrochemical cells that may be established will be small relative to the size of the repository, limiting the extent to which migration of contaminants by electrophoresis can occur. The electric field gradients will be of small magnitude and confined to regions of electrochemical activity in the area immediately surrounding the waste material. As a result, electrophoretic effects on migration behavior caused by both long and short range potential gradients have been eliminated from PA calculations on the basis of low consequence to the performance of the disposal system.

SCR-6.7.5 Physiochemical Transport Phenomena

SCR-6.7.5.1 FEP Number: W97 FEP Title: Chemical Gradients

SCR-6.7.5.1.1 Screening Decision: SO-C

The effects of enhanced diffusion across *Chemical Gradients* have been eliminated from PAs on the basis of low consequence to the performance of the disposal system.

SCR-6.7.5.1.2 Summary of New Information

No new information that affects the screening of this FEP has been identified since the CRA-2009.

SCR-6.7.5.1.3 Screening Argument

Chemical gradients within the disposal system, whether induced naturally or resulting from repository material and waste emplacement, may influence the transport of contaminants. Gradients will exist at interfaces between different repository materials and between repository and geological materials. Distinct chemical regimes will be established within concrete seals and adjoining host rocks. Similarly, chemical gradients will exist between the waste and the surrounding rocks of the Salado. Other chemical gradients may exist because of the juxtaposition of relatively dilute groundwaters and brines or between groundwaters with different compositions. Natural gradients currently exist between different groundwaters in the Culebra.

Enhanced diffusion is a possible consequence of chemical gradients that occur at material boundaries. However, the distances over which enhanced diffusion could occur will be small in comparison to the size of the disposal system. Processes that may be induced by chemical gradients at material boundaries include the formation or destabilization of colloids. For example, cementitious materials that will be emplaced in the WIPP as part of the waste and the seals contain colloidal-sized materials, such as calcium-silicate-hydrate gels, and alkaline pore fluids. Chemical gradients will exist between the pore fluids in the cementitious materials and the less alkaline surroundings. Chemical interactions at these interfaces may lead to the generation of colloids of the inorganic, mineral fragment type. Colloidal compositions may include calcium oxide, calcium hydroxide, calcium-aluminum silicates, calcium-silicate-hydrate gels, and silica. Experimental investigations of the stability of inorganic, mineral fragment colloidal dispersions have been carried out as part of the WIPP colloid-facilitated actinide transport program (Papenguth and Behl 1996). More recently, the colloidal enhancement parameters for mineral, intrinsic, and microbial colloids were reassessed for the actinide source term for the CRA-2014 PA (Reed et al. 2013). The most important observations for mineral colloids are: (1) there is no evidence for the formation of significant amounts of magnesium-derived mineral colloid species, and (2) iron oxides can lead to long-term and relatively small plutonium mineral colloids in these brine systems, and the concentrations observed are within the current enhancement parameter values (Reed et al. 2013, Section 4.3). Based on these observations, there are no changes in the mineral colloid enhancement parameters for the actinide source term in the CRA-2014 PA. These new results for mineral colloids do not affect the screening decision for this FEP.

SCR-6.7.5.2 FEP Number: W98 FEP Title: Osmotic Processes

SCR-6.7.5.2.1 Screening Decision: SO-C

The effects of *Osmotic Processes* have been eliminated from PA calculations on the basis of beneficial consequence to the performance of the disposal system.

SCR-6.7.5.2.2 Summary of New Information

No new information that affects the screening of this FEP has been identified since the CRA-2009.

SCR-6.7.5.2.3 Screening Argument

Osmotic processes, i.e., diffusion of water through a semipermeable or differentially permeable membrane in response to a concentration gradient, may occur at interfaces between waters of different salinities. Osmotic processes can occur if waters of different salinities and/or compositions exist on

either side of a particular lithology such as clay, or a lithological boundary that behaves as a semipermeable membrane. At the WIPP, clay layers within the Salado may act as semipermeable membranes across which osmotic processes may occur.

In the absence of a semipermeable membrane, water will move from the more dilute water into the more saline water. However, the migration of dissolved contaminants across an interface may be restricted depending upon the nature of the membrane. A hydrological gradient across a semipermeable membrane may either enhance or oppose water movement by osmosis depending on the direction and magnitude of the gradient. Dissolved contaminants that cannot pass through a semipermeable membrane may be moved towards the membrane and concentrated along the interface when advection dominates over osmosis and reverse osmosis occurs. Thus, both osmosis and reverse osmosis can restrict the migration of dissolved contaminants and possibly lead to concentration along interfaces between different water bodies. The effects of osmotic processes have been eliminated from PA calculations on the basis of beneficial consequence to the performance of the disposal system.

SCR-6.7.5.3 FEP Number: W99 FEP Title: Alpha Recoil

SCR-6.7.5.3.1 Screening Decision: SO-C

The effects of *Alpha Recoil* processes on radionuclide transport have been eliminated from PA calculations on the basis of low consequence to performance of the disposal system.

SCR-6.7.5.3.2 Summary of New Information

No new information that affects the screening of this FEP has been identified since the CRA-2009.

SCR-6.7.5.3.3 Screening Argument

Alpha particles are emitted with sufficiently high energies that daughter nuclides recoil appreciably to conserve system momentum. For example, ^{238}U decays to ^{234}Th with emission of a 4.1 megaelectron volt (MeV) alpha particle. The law of conservation of momentum requires that the daughter nuclide, ^{234}Th, recoils in the opposite direction with an energy of approximately 0.07 MeV. The energy is great enough to break chemical bonds or cause ^{234}Th to move a short distance through a crystal lattice. If the ^{234}Th is close enough to the surface of the crystal, it will be ejected into the surroundings. ^{234}Th decays to ^{234}Pa which decays to ^{234}U with respective half-lives of 24.1 days and 1.17 minutes. The recoil and decay processes can lead to the apparent preferential dissolution or leaching of ^{234}U relative to ^{238}U from crystal structures and amorphous or adsorbed phases. Preferential leaching may be enhanced because of radiation damage to the host phase resulting from earlier radioactive decay events. Consequently, ^{234}U sometimes exhibits enhanced transport behavior relative to ^{238}U.

The influence of alpha recoil processes on radionuclide transport through natural geologic media is dependent on many site-specific factors, such as mineralogy, geometry, and microstructure of the rocks, as well as geometrical constraints on the type of groundwater flow, e.g., porous or fracture flow. Studies of natural radionuclide-bearing groundwater systems often fail to discern a measurable effect of alpha-recoil processes on radionuclide transport above the background uncertainty introduced by the spatial heterogeneity of the geological system. Consequently, the effects of the

alpha recoil processes that occur on radionuclide transport are thought to be minor. These effects have therefore been eliminated from PA calculations on the basis of low consequence to the performance of the disposal system.

SCR-6.7.5.4 FEP Number: W100 FEP Title: Enhanced Diffusion

SCR-6.7.5.4.1 Screening Decision: SO-C

Enhanced diffusion is a possible consequence of chemical gradients that occur at material boundaries. However, the distances over which enhanced diffusion could occur will be small in comparison to the size of the disposal system. Therefore, the effects of *Enhanced Diffusion* across chemical gradients at material boundaries have been eliminated from PAs on the basis of low consequence to the performance of the disposal system.

SCR-6.7.5.4.2 Summary of New Information

No new information that affects the screening of this FEP has been identified since the CRA-2009.

SCR-6.7.5.4.3 Screening Argument

Enhanced diffusion only occurs where there are higher than average chemical gradients. The spatial extent of chemical gradients should be quite limited and as enhanced diffusion occurs, it will tend to reduce the chemical gradient. Thus, the driving force for the enhanced diffusion will be reduced and eventually eliminated as the system approaches steady state or equilibrium conditions. Because of the limited spatial extent of enhanced diffusion, its effect on radionuclide transport should be small.

Processes that may be induced by chemical gradients at material boundaries include the formation or destabilization of colloids. For example, cementitious materials, emplaced in the WIPP as part of the waste and the seals, contain colloidal-sized phases such as calcium-silicate-hydrate gels and alkaline pore fluids. Chemical gradients will exist between the pore fluids in the cementitious materials and the less-alkaline surroundings. Chemical interactions at these interfaces may lead to the generation of colloids of the inorganic, mineral-fragment type. Colloidal compositions may include calcium and MgO, calcium hydroxide, calcium-aluminum silicates, calcium-silicate-hydrate gels, and silica. Concentrations of colloidal suspensions originating from concrete within the repository are considered in PA calculations even though expected to be extremely low.

Distinct interfaces between waters of different salinities and different densities may limit mixing of the water bodies and affect flow and contaminant transport. Such effects have been eliminated from PA calculations on the basis of low consequence to the performance of the disposal system.

The effects of enhanced diffusion across chemical gradients at material boundaries have been eliminated from PAs on the basis of low consequence to the performance of the disposal system.

SCR-6.8 Ecological FEPs

SCR-6.8.1 Plant, Animal, and Soil Uptake

SCR-6.8.1.1 FEP Numbers: W101, W102, and W103 FEP Titles: Plant Uptake (W101) Animal Uptake (W102) Accumulation in Soils (W103)

SCR-6.8.1.1.1 Screening Decision: SO-R for section 191.13 - W101, W102 SO-C Beneficial for section 191.13 - W103 SO-C for section 191.15 - W101, W102, W103

Plant Uptake, *Animal Uptake*, and *Accumulation in Soils* have been eliminated from compliance assessment calculations for section 191.15 on the basis of low consequence. *Plant Uptake* and *Animal Uptake* in the accessible environment have been eliminated from PA calculations for section 191.13 on regulatory grounds. *Accumulation in Soils* within the controlled area has been eliminated from PA calculations for section 191.13 on the basis of beneficial consequences.

SCR-6.8.1.1.2 Summary of New Information

No new information has been identified that affects the screening of these FEPs since the CRA-2009.

SCR-6.8.1.1.3 Screening Argument

The results of the calculations presented in Section 34, "Results of Performance Assessment," show that releases to the accessible environment under undisturbed conditions are restricted to lateral releases through the DRZ at repository depth. Thus, for evaluating compliance with the EPA's individual protection requirements in section 191.15, FEPs that relate to plant uptake, animal uptake, and accumulation in soils have been eliminated from compliance assessment calculations on the basis of low consequence.

PAs for evaluating compliance with the EPA's cumulative release requirements in section 191.13 need not consider radionuclide migration in the accessible environment. Therefore, FEPs that relate to plant uptake and animal uptake in the accessible environment have been eliminated from PA calculations on regulatory grounds. Accumulation in soils that may occur within the controlled area would reduce releases to the accessible environment and can, therefore, be eliminated from PA calculations on the basis of beneficial consequence.

SCR-6.8.2 Human Uptake

SCR-6.8.2.1 FEP Numbers: W104, W105, W106, W107, and W108 FEP Titles: Ingestion (W104) Inhalation (W105) Irradiation (W106) Dermal Sorption (W107) Injection (W108)

SCR-6.8.2.1.1 Screening Decision: SO-R SO-C for section 191.15

Ingestion, *Inhalation*, *Irradiation*, *Dermal Sorption*, and *Injection* have been eliminated from compliance assessment calculations for section 191.15 and Part 191 Subpart C on the basis of low consequence. FEPs that relate to human uptake in the accessible environment have been eliminated from PA calculations for section 191.13 on regulatory grounds.

SCR-6.8.2.1.2 Summary of New Information

No new information has been identified that affects the screening of these FEPs since the CRA-2009.

SCR-6.8.2.1.3 Screening Argument

As described in Section 54, "Scope of Compliance Assessments," releases to the accessible environment under undisturbed conditions are restricted to lateral migration through anhydrite interbeds within the Salado. Because of the bounding approach taken for evaluating compliance with the EPA's individual protection requirements in section 191.15 and the groundwater protection requirements in Part 191 Subpart C (see Section 54), FEPs that relate to human uptake by ingestion, inhalation, irradiation, dermal sorption, and injection have been eliminated from compliance assessment calculations on the basis of low consequence.

PAs for evaluating compliance with the EPA's cumulative release requirements in section 191.13 need not consider radionuclide migration in the accessible environment. Therefore, FEPs that relate to human uptake in the accessible environment have been eliminated from PA calculations on regulatory grounds.

SCR-7.0 References

(*Indicates a reference that has not been previously submitted.)

Altenheinhaese, C. H., H. Bischoff, L. Fu, J. Mao, and G. Marx. 1994. "Adsorption of Actinides on Cement Compounds." Journal of Allows and Compounds, vol. 213: 553-56. [Author]

Anderson, R.Y. 1978. Deep Dissolution of Salt, Northern Delaware Basin, New Mexico. Report to Sandia National Laboratories. ERMS 229530. Albuquerque, NM: Sandia National Laboratories. [PDF / Author]

Anderson, R.Y., W.E. Dean, Jr., D.W. Kirkland, and H.I. Snider. 1972. "Permian Castile Varved Evaporite Sequence, West Texas and New Mexico." ERMS 241261. Geological Society of America Bulletin, vol. 83, no. 1: 59-85. [Author]

Anderson, R.Y., and D.W. Powers. 1978. "Salt Anticlines in Castile-Salado Evaporite Sequence, Northern Delaware Basin." Geology and Mineral Deposits of Ochoan Rocks in Delaware Basin and Adjacent Areas: New Mexico Bureau of Mines and Mineral Resources (pp. 79-84), Circular 159. ERMS 241419. G.S. Austin, ed. [Author]

Bachhuber, F.W. 1989. "The Occurrence and Paleolimnologic Significance of Cutthroat Trout (Oncorhynchus clarki) in Pluvial Lakes of the Estancia Valley, Central New Mexico." Geological Society of America Bulletin, vol. 101: 1543-51. [Author]

Bachman, G.O. 1974. Geologic Processes and Cenozoic History Related to Salt Dissolution in Southeastern New Mexico. Open-File Report 74-194. ERMS 243249. Denver, CO: U.S. Geological Survey. [PDF / Author]

Bachman, G.O. 1980. Regional Geology and Cenozoic History of Pecos Region, Southeastern New Mexico. Open-File Report 80-1099. ERMS 241268. Denver, CO: U.S. Geological Survey. [PDF / Author]

Bachman, G.O. 1981. Geology of Nash Draw, Eddy County, New Mexico. Open-File Report 81-31. ERMS 241265. Denver, CO: U.S. Geological Survey. [PDF / Author]

Bachman, G.O. 1985. Assessment of Near-Surface Dissolution at and Near the Waste Isolation Pilot Plant (WIPP), Southeastern New Mexico. SAND84-7178. ERMS 224609. Albuquerque, NM: Sandia National Laboratories. [PDF / Author]

Bachman, G.O. 1987a. "Stratigraphy and Dissolution of the Rustler Formation." The Rustler Formation at the WIPP Site: Report of a Workshop on the Geology and Hydrology of the Rustler Formation as it Relates to the WIPP Project (pp. 16-25). ERMS 249769. L. Chaturvedi, ed. Carlsbad, NM, March 1985. Santa Fe, NM: EEG-34, Environmental Evaluation Group. [Author]

Bachman, G.O. 1987b. Karst in Evaporites in Southeastern New Mexico. SAND86-7078. ERMS 224006. Albuquerque, NM: Sandia National Laboratories. [PDF / Author]

Barnhart, B.J., R. Hallet, D.E. Caldwell, E. Martinez, and E.W. Campbell. 1980. Potential Microbial Impact on Transuranic Wastes under Conditions Expected in the Waste Isolation Pilot Plant (WIPP): Annual Report, October 1, 1978-September 30, 1979. LA-8297-PR. ERMS 241220. Los Alamos, NM: Los Alamos Scientific Laboratory. [PDF / Author]

Batchelor, G.K. 1973. An Introduction to Fluid Dynamics. ERMS 243337. Cambridge: Cambridge UP, London, UK. [Author]

Baumgardner, R.W., Jr., A.D. Hoadley, and A.G. Goldstein. 1982. Formation of the Wink Sink, a Salt Dissolution and Collapse Feature, Winkler County, Texas. Report of Investigations No. l14. Austin, TX: Bureau of Economic Geology. [Author]

Bean, J.E., M.E., Lord, D.A. McArthur, R.J. MacKinnon, J.D. Miller, and J.D. Schreiber. 1996. Analysis Package for the Salado Flow Calculations (Task 1) of the Performance Assessment Analysis Supporting the Compliance Certification Application. ERMS 420238. (EPA Air Docket A-93-02, Item II-G-08). Albuquerque, NM: Sandia National Laboratories. [PDF / Author]

Beauheim, R.L. 1986. Hydraulic-Test Interpretations for Well DOE-2 at the Waste Isolation Pilot Plant (WIPP) Site. SAND86-1364. ERMS 227656. Albuquerque, NM: Sandia National Laboratories. [PDF / Author]

Beauheim, R.L. 2002. Analysis Plan for Evaluation of the Effects of Head Changes on Calibration of Culebra Transmissivity Fields: Analysis Plan AP-088. (Rev. 1). ERMS 522085. Carlsbad, NM: Sandia National Laboratories. [PDF / Author]

Beauheim, R.L. and Holt, R.M. 1990. Hydrogeology of the WIPP site, in Powers, D.W., Holt, R.M., Beauheim, R.L., and Rempe, N., eds., Geological and Hydrological Studies of Evaporites in the Northern Delaware Basin for the Waste Isolation Pilot Plant (WIPP): Guidebook 14. ERMS 246378. Geological Society of America (Dallas Geological Society), p. 45-78. [Author]

Beauheim, R.L., B.W. Hassinger, and J.A. Klaiber. 1983. Basic Data Report for Borehole Cabin Baby-1 Deepening and Hydrologic Testing, Waste Isolation Pilot Plant (WIPP) Project, Southeastern New Mexico. WTSD-TME-020. ERMS 241315. Carlsbad, NM: Westinghouse Electric Corporation. [PDF / Author]

Beauheim, R.L., and G.J. Ruskauff. 1998. Analysis of Hydraulic Tests of the Culebra and Magenta Dolomites and Dewey Lake Redbeds Conducted at the Waste Isolation Pilot Plant Site. SAND98-0049. ERMS 251839. Albuquerque, NM: Sandia National Laboratories. [PDF / Author]

Bennett, D. 1996. Formation and Transport of Radioactive Gases. Summary Memorandum of Record for GG-8 and RNT-26. 16 May 1996. SWCF-A 1.2.07.3: PA: QA: TSK: GG-8, RNT-26. ERMS 415478. Albuquerque, NM: Sandia National Laboratories. [PDF / Author]

Bennett, D.G., D. Read, M. Atkins, and F.P. Glasser. 1992. "A Thermodynamic Model for Blended Cements II: Cement Hydrate Phases; Thermodynamic Values and Modeling Studies." ERMS 241221. Journal of Nuclear Materials, vol. 190: 315-15. [Author]

Bennett, D., Y. Wang, and T. Hicks. 1996. Memorandum to Distribution (Subject: An Evaluation of Heat Generation Processes for the WIPP). 20 August 1996. ERMS 240635. Albuquerque, NM: Sandia National Laboratories. [PDF / Author]

Berner, R.A. 1981. "Kinetics of Weathering and Diagenesis, in Kinetics of Geochemical Processes." Reviews in Mineralogy, vol. 8: 111-33. ERMS 241361. A.C. Lasaga, and R.J. Kirkpatrick, eds. Washington, DC: Mineralogical Society of America. [Author]

Blackwell, D.D., J.L. Steele, and L.S. Carter. 1991. "Heat-Flow Patterns of the North American Continent: A Discussion of the Geothermal Map of North America." Neotectonics of North America (pp. 423-436). ERMS 241460. D.B. Slemmons, E.R. Engdahl, M.D. Zoback, and D.D. Blackwell, eds. Boulder, CO: Geological Society of America. [Author]

Borns, D.J. 1987. "Structural Development of Evaporites in the Northern Delaware Basin." Guidebook 18: Geology of the Western Delaware Basin, West Texas and Southeastern New Mexico (pp. 80-97). ERMS 235759. D.W Powers and W.C. James, eds. El Paso, TX: El Paso Geological Society. [Author]

Borns, D.J., L.J. Barrows, D.W. Powers, and R.P. Snyder. 1983. Deformation of Evaporites Near the Waste Isolation Pilot Plant (WIPP) Site. SAND82-1069. ERMS 227532. Albuquerque, NM: Sandia National Laboratories. [PDF / Author]

Borns, D.J., and S.E. Shaffer. 1985. Regional Well-Log Correlation in the New Mexico Portion of the Delaware Basin. SAND83-1798. ERMS 224511. Albuquerque, NM: Sandia National Laboratories. [PDF / Author]

Brausch, L.M., A.K. Kuhn, J.K. Register. 1982. Natural Resources Study, Waste Isolation Pilot Plant (WIPP) Project, Southeastern New Mexico. WTSD-TME-3156. ERMS 239094. Carlsbad, NM: U.S. Department of Energy. [PDF / Author]

Bredehoeft, J.D., F.S. Riley, and E.A. Roeloffs. 1987. "Earthquakes and Groundwater." ERMS 241635. Earthquakes and Volcanoes, vol. 19, no. 4: 138-46. [Author]

Brokaw, A.L., C.L. Jones, M.E. Cooley, and W.H. Hays. 1972. Geology and Hydrology of the Carlsbad Potash Area, Eddy and Lea Counties, New Mexico. ERMS 243356. Open File Report 4339-1. Denver, CO: U.S. Geological Survey. [PDF / Author]

Bruno, J. and A. Sandino. 1987. Radionuclide Co-Precipitation. SKB Technical Report, no. 87-23. ERMS 241222. Stockholm: Swedish Nuclear Fuel and Waste Management Co. [PDF / Author]

Brush, L.H. 1990. Test Plan for Laboratory and Modeling Studies of Repository and Radionuclide Chemistry for the Waste isolation Pilot Plant. SAND90-0266. ERMS 225053. Albuquerque, NM: Sandia National Laboratories. [PDF / Author]

Brush, L.H. 1996. Memorandum to M.S. Tierney(Subject: Ranges and Probability Distributions of Kds for Dissolved Pu, Am, U, Th, and Np in the Culebra for the PA Calculations to Support the CCA). 10 June 1996. ERMS 238801. Albuquerque, NM: Sandia National Laboratories. [PDF / Author]

Brush, L.H. and L.J. Storz. 1996. Memorandum to M.S. Tierney (Subject: Revised Ranges and Probability Distributions of Kds for Dissolved Pu, Am, U, Th, and Np in the Culebra for the PA Calculations to Support the CCA). July 24, 1996. ERMS 241561. Albuquerque, NM: Sandia National Laboratories. [PDF / Author]

Brush, L. H. and P. Domski. 2013a. Prediction of Baseline Actinide Solubilities for the WIPP CRA-2014 PA. ERMS 559138. Carlsbad, NM: Sandia National Laboratories.* [PDF / Author]

Brush, L. H. and P. Domski. 2013b. Calculation of Organic-Ligand Concentrations for the WIPP CRA-2014 PA. ERMS 559005. Carlsbad, NM: Sandia National Laboratories.* [PDF / Author]

Brush, L. H. and P. Domski. 2013c. Uncertainty Analysis of Actinide Solubilities for the WIPP CRA-2014 PA, Revision 1. ERMS 559712. Carlsbad, NM: Sandia National Laboratories.* [PDF / Author]

Burton, P.L., J.W. Adams, and C. Engwall. 1993. "History of the Washington Ranch, Eddy County, New Mexico." New Mexico Geological Society Guidebook. 44th Field Conference, Carlsbad Region, New Mexico and West Texas. D.W. Love, J.W. Hawley, B.S. Kues, J.W. Adams, G.W. Austin, and J.M. Barker, eds. ERMS 241273. Roswell, NM: New Mexico Geological Society. [Author]

Callicoat, J. 2013. "Seismic Activity Within the Delaware Basin 2012". Inter-office memo to file. February 13, 2013. RES:13:107. Carlsbad, NM: Nuclear Waste Partnership LLC.* [PDF / Author]

Camphouse, R.C., M. Gross, C.G. Herrick, D.C. Kicker, and B. Thompson. 2012. Recommendations and Justifications of Parameter Values for the Run-of-Mine Salt Panel Closure System Design Modeled in the PCS-2012 PA. Memo to WIPP Records Center dated May 3, 2012. ERMS 557396. Carlsbad NM: Sandia National Laboratories. [PDF / Author]

Camphouse, R.C. 2013a. Analysis Plan for the 2014 WIPP Compliance Recertification Application Performance Assessment. ERMS 559198. Carlsbad, NM: Sandia National Laboratories.* [PDF / Author]

Camphouse, R.C. 2013b. BRAGFLO Analysis Report for the CRA-2014 Performance Assessment Calculations. Carlsbad, NM: Sandia National Laboratories.* [PDF / Author]

Cauffman, T.L., A.M. LaVenue, and J.P. McCord. 1990. Ground-Water Flow Modeling of the Culebra Dolomite, Volume II: Data Base. SAND89-7068/2. ERMS 210551. Albuquerque, NM: Sandia National Laboratories. [PDF / Author]

Chapman, J.B. 1986. Stable Isotopes in Southeastern New Mexico Groundwater: Implications for Dating Recharge in the WIPP Area, EEG-35, DOE/AL/10752-35. ERMS 241274. Santa Fe, NM: Environmental Evaluation Group. [PDF / Author]

Chapman, J.B. 1988. Chemical and Radiochemical Characteristics of Groundwater in the Culebra Dolomite, Southeastern New Mexico. EEG-39. ERMS 241223. Santa Fe, NM: New Mexico Environmental Evaluation Group. [PDF / Author]

Chappell, J. and N.J. Shackleton. 1986. "Oxygen Isotopes and Sea Level." ERMS 241275. Nature, vol. 324, no. 6093: 137-40. [Author]

Choppin, G.R., A.H. Bond, M. Borkowski, M.G. Bronikowski, J.F. Chen, S. Lis, J. Mizera, O. Pokrovsky, N.A. Wall, Y.X. Xia, and R.C. Moore. 2001. Waste Isolation Pilot Plant Actinide Source Term Test Program: Solubility Studies and Development of Modeling Parameters. SAND99-0943. ERMS 518556. Albuquerque, NM: Sandia National Laboratories. [PDF / Author]

Claiborne, H.C., and F. Gera. 1974. Potential Containment Failure Mechanisms and Their Consequences at a Radioactive Waste Repository in Bedded Salt in New Mexico. ORNL-TM-4639. ERMS 241224. Oak Ridge, TN: Oak Ridge National Laboratory. [PDF / Author]

Clayton, D.J. 2009. Update to the Kd values for the PABC-2009. ERMS 552395. Carlsbad, NM: Sandia National Laboratories.* [PDF / Author]

Corbet, T.F. and P.M. Knupp. 1996. The Role of Regional Groundwater Flow in the Hydrogeology of the Culebra Member of the Rustler Formation at the Waste Isolation Pilot Plant (WIPP), Southeastern New Mexico. SAND96-2133. ERMS 243482. Albuquerque, NM: Sandia National Laboratories. [PDF / Author]

Cranwell, R.M., R.V. Guzowski, J.E. Campbell, and N.R. Ortiz.. 1990. Risk Methodology for Geologic Disposal of Radioactive Waste: Scenario Selection Procedure. NUREG/CR-1667. SAND80-1429. ERMS 226750. Albuquerque, NM: Sandia National Laboratories. [PDF / Author]

Cunningham, C. 1999. "End of the Santa Fe Trail." ERMS 530223. Sulfur, no. 264. September-October 1999. [Author]

D'Appolonia Consulting Engineers, Inc. 1982. Natural Resources Study - Waste Isolation Pilot Plant (WIPP) Project, Southeastern New Mexico (January). NM78-648-813A. Albuquerque, NM: D'Appolonia Consulting Engineers, Inc. [PDF / Author]

Davies, P.B. 1983. "Assessing the Potential for Deep-Seated Salt Dissolution and Subsidence at the Waste Isolation Pilot Plant (WIPP)." State of New Mexico Environmental Evaluation Group Conference, WIPP Site Suitability for Radioactive Waste Disposal, Carlsbad, NM, May 12-13, 1983. ERMS 229533. Albuquerque, NM: Sandia National Laboratories. [PDF / Author]

Davies, P.B. 1989. Variable Density Ground-Water Flow and Paleohydrology in the Waste Isolation Pilot Plant (WIPP) Region, Southeastern New Mexico. Open File Report 88-490. ERMS 238854. Denver, CO: U.S. Geological Survey. [PDF / Author]

Davis, J.A. and D.B. Kent. 1990. "Surface Complexation Modeling in Aqueous Geochemistry." Mineral-Water Interface Geochemistry. ERMS 241473. M.F. Hochella and A.F. White, eds. Reviews in Mineralogy vol. 23: pp. 177-260. Washington, DC: Mineralogical Society of America. [Author]

Dawson, P.R. and J.R. Tillerson. 1978. Nuclear Waste Canister Thermally Induced Motion. SAND78-0566. ERMS 227328. Albuquerque, NM: Sandia National Laboratories. [PDF / Author]

Dence, M.R., R.A.F. Grieve, and P.B. Robertson. 1977. "Terrestrial Impact Structures: Principal Characteristics and Energy Considerations." Impact and Explosion Cratering: Planetary and Terrestrial Implications (pp. 247-75). D.J. Roddy, R.O. Pepin, and R.B. Merrill, eds. New York: Permagon. [Author]

Dickson, C.L. and F.P. Glasser. 2000. "Cerium (III, IV) in Cement-Implications for Actinide (III, IV) Immobilization." Cement and Concrete Research, vol. 30: 1619-23. [Author]

Dietz, R.S. 1961. Astroblemes. ERMS 241226. Scientific American, vol. 205, no. 2: 50-58. [Author]

Dowding, C.H. and A. Rozen. 1978. "Damage to Rock Tunnels from Earthquake Shaking." ERMS 241350. Journal of the Geotechnical Engineering Division, American Society of Civil Engineers, vol. 104, No. GT2: 175-91. [Author]

Francis, A.J. 1985. "Low-Level Radioactive Wastes in Subsurface Soils," in Soil Reclamation Processes: Microbiological Analyses and Applications. ERMS 241227. R.L. Tate, III and D.A. Klein, eds. New York: Marcel Dekker, Inc. (pp. 279-331). [Author]

Francis, A.J. and J.B. Gillow. 1994. Effects of Microbial Gas Processes on Generation Under Expected Waste Isolation Pilot Plant Repository Conditions, Progress Report through 1992. SAND93-7036. ERMS 210673. Albuquerque, NM: Sandia National Laboratories. [PDF / Author]

Francis, A.J. and J.B. Gillow. 2000. Memorandum to Y. Wang (Subject: Progress Report: Microbial Gas Generation Program). 6 January 2000. ERMS 509352. Upton, NY: Brookhaven National Laboratory. [PDF / Author]

Francis A.J., J.B. Gillow, and M.R. Giles. 1997. Microbial Gas Generation under Expected Waste Isolation Pilot Plant Repository Conditions. SAND96-2582. ERMS 244125. Albuquerque, NM: Sandia National Laboratories. [PDF / Author]

Franco, J.R. 2012. "Notice of Revisions to the Salt Disposal Investigations Testing Concepts." Letter to J. Edwards, U.S. Environmental Protection Agency, Washington, D.C. June 20, 2012. U.S. Department of Energy, Carlsbad, NM: Carlsbad Area Office.* [PDF / Author]

Giambalvo, E.R. 2002a. Memorandum to L.H. Brush (Subject: Recommended Parameter Values for Modeling Organic Ligands in WIPP Brines). 25 July 2002. ERMS 522981. Carlsbad, NM: Sandia National Laboratories. [PDF / Author]

Giambalvo, E.R. 2002b. Memorandum to L.H. Brush (Subject: Recommended m0/RT Values for Modeling the Solubility of Oxalate Solids in WIPP Brines). 31 July 2002. ERMS 523057. Carlsbad, NM: Sandia National Laboratories. [PDF / Author]

Gillow, J.B., M. Dunn, A.J. Francis, D.A. Lucero, and H.W. Papenguth. 2000. "The Potential of Subterranean Microbes in Facilitating Actinide Migration at the Grimsel Test Site and Waste Isolation Pilot Plant," Radiochemica Acta, vol. 88: 769-774. [Author]

Gillow, J.B. and A.J. Francis. 2001a. "Re-Evaluation of Microbial Gas Generation under Expected Waste Isolation Pilot Plant Conditions: Data Summary Report, January 24, 2001." Sandia National Laboratories Technical Baseline Reports, WBS 1.3.5.4, Repository Investigations Milestone RI010, January 31, 2001 (pp. 19-46). ERMS 516749. Carlsbad, NM: Sandia National Laboratories. [PDF / Author]

Gillow, J.B. and A.J. Francis. 2001b. "Re-Evaluation of Microbial Gas Generation under Expected Waste Isolation Pilot Plant Conditions: Data Summary and Progress Report (February 1 - July 13, 2001), July 16, 2001, Rev. 0." Sandia National Laboratories Technical Baseline Reports, WBS 1.3.5.4, Repository Investigations Milestone R1020, July 31, 2001 (pp. 3-1 through 3-21). ERMS 518970. Carlsbad, NM: Sandia National Laboratories. [PDF / Author]

Gillow, J.B. and A.J. Francis. 2002a. "Re-Evaluation of Microbial Gas Generation under Expected Waste Isolation Pilot Plant Conditions: Data Summary and Progress Report (July 14, 2001 - January 31, 2002), January 22, 2002." Sandia National Laboratories Technical Baseline Reports, WBS 1.3.5.3, Compliance Monitoring; WBS 1.3.5.4, Repository Investigations, Milestone RI110, January 31, 2002 (pp. 2.1-1 through 2.1-26). ERMS 520467. Carlsbad, NM: Sandia National Laboratories. [PDF / Author]

Gillow, J.B. and A.J. Francis. 2002b. "Re-Evaluation of Microbial Gas Generation under Expected Waste Isolation Pilot Plant Conditions: Data Summary and Progress Report (February 1 - July 15, 2002), July 18, 2002." Sandia National Laboratories Technical Baseline Reports, WBS 1.3.5.3, Compliance Monitoring; WBS 1.3.5.4, Repository Investigations, Milestone RI130, July 31, 2002 (pp. 3.1-1 through 3.1-A10). ERMS 523189. Carlsbad, NM: Sandia National Laboratories. [PDF / Author]

Gougar, M.L.D., B.E. Scheetz, and D.M. Roy. 1996. "Ettringite and C-S-H Portland Cement Phases for Waste Ion Immobilization: A Review." Waste Management, vol. 16, no. 4: 295-303. [Author]

Gray, J.L. 1991. Letter to W. Price (Subject: Carlsbad Brine Well Collapse and Subsidence Investigation, Simon Environmental Services Project No. 502-939-01). September 25, 1991. ERMS 549576. Norman, OK: Simon Environmental Services. [PDF / Author]

Grieve, R.A.F. 1987. "Terrestrial Impact Structures." ERMS 241228. Annual Review of Earth and Planetary Sciences, vol. 15: 245-70. [Author]

Griswold, G.B. and J.E. Griswold. 1999. "Method of Potash Reserve Evaluation" in New Mexico Bureau of Mines & Mineral Resources (pp. 33-67), Circular 207 (1999). [Author]

Hall, R.K., D. R. Creamer, S.G. Hall, and L.S. Melzer. 2013. Water Injection in WIPP Vicinity: Current Practices, Failure Rates and Future Operations. (July). Midland, TX: Russell K. Hall and Associates, Inc. [PDF / Author]

Halliday, I. 1964. "The Variation in the Frequency of Meteorite Impact with Geographic Latitude." ERMS 241229. Meteoritics, vol. 2, no. 3: 271-278. [Author]

Harris, A.H. 1987. "Reconstruction of Mid-Wisconsin Environments in Southern New Mexico," National Geographic Research, vol. 3, no. 2: 142-51. [Author]

Harris, A.H. 1988. "Late Pleistocene and Holocene Microtus (pitymys) (Rodentia: cricetidae) in New Mexico." Journal of Vertebrate Paleontology, vol. 8, no. 3: 307-13. [Author]

Hartmann, W.K. 1965. "Terrestrial and Lunar Flux of Large Meteorites in the Last Two Billion Years." ERMS 241230. Icarus, vol. 4, no. 2: 157−65. [Author]

Hartmann, W.K. 1979. Long-Term Meteorite Hazards to Buried Nuclear Waste Report 2, in Assessment of Effectiveness of Geologic Isolation Systems: A Summary of FY-1978 Consultant

Input for Scenario Methodology Development. ERMS 241232. B.L. Scott, G.L. Benson, R.A. Craig, and M.A. Harwell, eds. PNL-2851. Richland, WA: Pacific Northwest Laboratory. [PDF / Author]

Haug, A., V.A. Kelley, A.M. LaVenue, and J.F. Pickens. 1987. Modeling of Ground-Water Flow in the Culebra Dolomite at the Waste Isolation Pilot Plant (WIPP) Site: Interim Report, SAND86-7167. ERMS 228486. Albuquerque, NM: Sandia National Laboratories. [Author]

Hawley, J.W. 1993. "The Ogallala and Gatuña Formation in the Southeastern New Mexico and West Texas." ERMS 241431. New Mexico Geological Society, Forty-Fourth Annual Field Conference, Carlsbad, NM, October 6-9, 1993 (pp. 261-69). D.W. Love et al., eds. Socorro, NM: New Mexico Geological Society. [Author]

Helton, J.C., J.E. Bean, J.W. Berglund, F.J. Davis, K. Economy, J.W. Garner, J.D. Johnson, R.J., MacKinnon, J. Miller, D.G. O'Brien, J.L. Ramsey, J.D. Schreiber, A. Shinta, L.N. Smith, D.M. Stoelzel, C. Stockman, and P. Vaughn. 1998. Uncertainty and Sensitivity Analysis Results Obtained in the 1996 Performance Assessment for the Waste Isolation Pilot Plant. SAND98-0365. ERMS 252619. Albuquerque, NM: Sandia National Laboratories. [PDF / Author]

Herrick, C.G., M.D. Schuhen, D.M. Chapin, and D.C. Kicker. 2012. Determining the Hydrodynamic Shear Strength of Surrogate Degraded TRU Waste Materials as an Estimate for the Lower limit of the Performance Assessment Parameter TAUFAIL. ERMS 558479. Carlsbad, NM: Sandia National Laboratories.* [PDF / Author]

Heyn, D.W. 1997. Letter from IMC Kalium to the U.S. EPA on Potash Solution Mining at WIPP Site. 26 February 1997. ERMS 530221. Washington, DC. [PDF / Author]

Hickerson, A.L. 1991. Letter to V. Pierce (B&E Inc., Carlsbad, New Mexico). 12 April 1991. Odessa, TX. [PDF / Author]

Hicks, T.W. 1996. "Thermal Convection and Effects of Thermal Gradients," Summary Memorandum of Record for GG-4 and S-10. Memorandum. 29 May 1996. SWCF-A 1.2.07.3: PA: QA: TSK: S10,GG4. ERMS 411687. Albuquerque, NM: Sandia National Laboratories. [PDF / Author]

Hicks, T.W. 1997a. Memorandum from T. Hicks to P. Swift. 6 March 1997. "Solution Mining for Potash." [PDF / Author]

Hicks, T.W. 1997b. Memorandum from T.W. Hicks to P.N. Swift. 7 March 1997. "Solution Mining for Brine." [PDF / Author]

Holt, R.M. and D. W. Powers. 1984. Geotechnical Activities in the Waste Handling Shaft, Waste Isolation Pilot Plant (WIPP) Project, Southeastern New Mexico: WTSD-TME 038. ERMS 241347. Carlsbad, NM: U.S. Department of Energy. [PDF / Author]

Holt, R.M. and D.W. Powers. 1986. Geotechnical Activities in the Exhaust Shaft, Waste Isolation Pilot Plant (WIPP) Project, Southeastern New Mexico: DOE-WIPP 86-008. ERMS 241696. Carlsbad, NM: U.S. Department of Energy. [PDF / Author]

Holt, R.M. and D.W. Powers. 1988. Facies Variability and Post-Depositional Alteration within the Rustler Formation in the Vicinity of the Waste Isolation Pilot Plant, Southeastern New Mexico. DOE/WIPP 88-004. ERMS 242145. Carlsbad, NM: U.S. Department of Energy. [PDF / Author]

Holt, R.M. and D.W. Powers. 1990. Geotechnical Activities in the Air Intake Shaft, Waste Isolation Pilot Plant. WIPP-DOE 90-051. Carlsbad, NM: U.S. Department of Energy. [PDF / Author]

Holt, R.M. and D.W. Powers. 2002. "Impact of Salt Dissolution on the Transmissivity of the Culebra Dolomite Member of the Rustler Formation, Delaware Basin Southeastern New Mexico." Geological Society of America Abstracts with Programs, vol. 34, no. 6: 215. [Author]

Holt, R.M. and L. Yarbrough. 2002. Analysis Report: Task 2 of AP-088; Estimating Base Transmissivity Fields (July 8). ERMS 523889. Carlsbad, NM: Sandia National Laboratories. [PDF / Author]

Imbrie, J. and J.Z. Imbrie. 1980. "Modeling the Climatic Response to Orbital Variations." ERMS 241338. Science, vol. 207, no. 4434: 943-953. [Author]

Johnson, K.S. 1989. "Development of the Wink Sink in West Texas, USA, Due to Salt Dissolution and Collapse." Environmental Geology and Water Science, vol. 14: 81-92. [Author]

Johnson, K.S., E.W. Collins, and S. Seni. 2003. "Sinkholes and Land Subsidence due to Salt Dissolution near Wink, West Texas, and Other Sites in West Texas and New Mexico." Evaporite Karst and Engineering/Environmental Problems in the United States (pp. 183-96). K.T. Johnson and J.T. Neal, eds. Norman, OK: Oklahoma Geological Survey. [Author]

Jones, C.L. 1981. Geologic Data for Borehole ERDA-6, Eddy County, New Mexico. ERMS 242321. Open-File Report 81-468. Denver, CO: U.S. Geological Society. [PDF / Author]

Kärnbränslesakerhet. 1978. Handling of Spent Nuclear Fuel and Final Storage of Vitrified High Level Reprocessing Waste. ERMS 242406. Stockholm: Kärnbränslesakerhet. [PDF / Author]

Kato, C., T. Sato, M. Smorawinska, and K. Horikoshi. 1994. "High Pressure Conditions Stimulate Expression of Chloramphenicol Acetyltransferase Regulated by the Iac Promoter in Escherichia coli." ERMS 241233. FEMS Microbiology Letters, vol. 122, nos. 1-2: 91-96. [Author]

Kicker, D.C. and T. Zeitler. 2013. Radionuclide Inventory Screening Analysis for the 2014 Compliance Recertification Application Performance Assessment (CRA-2014 PA), (Revision 0, February 19). ERMS 559257. Carlsbad, NM: Sandia National Laboratories. [PDF / Author]

King, P.B. 1948. Geology of the Southern Guadalupe Mountains, Texas. ERMS 241749. Professional Paper 215. Washington, DC: U.S. Geological Survey. [PDF / Author]

Kirchner, T., T. Zeitler, and R. Kirkes. 2012. Evaluating the Data in Order to Derive a Value for GLOBAL:PBRINE. Memorandum to Sean Dunagan dated December 11, 2012. ERMS 558724. Carlsbad, NM: Sandia National Laboratories. [PDF / Author]

Kirkes, G.R. 2008. Features, Events and Processes Assessment for the Compliance Recertification Application-2009 (Revision 0). ERMS 550489. Carlsbad, NM: Sandia National Laboratories. [PDF / Author]

Kirkes, G.R. 2013a. Activity/Project Specific Procedure SP 9-4: Performing FEPs Baseline Impact Assessments for Planned or Unplanned Changes (Revision 3, June 19). Carlsbad, NM: Sandia National Laboratories.* [PDF / Author]

Kirkes, G.R. 2013b. Features, Events and Processes Assessment for the Compliance Recertification Application-2014 (Revision 0). ERMS 560488. Carlsbad, NM: Sandia National Laboratories.* [PDF / Author]

Kuhlman, K.L. 2010. Analysis Report for the CRA-2009 PABC Culebra Flow and Transport Calculations. ERMS 549013. Carlsbad, NM: Sandia National Laboratories. [PDF / Author]

Kuhlman, K.L. 2011. "SDI Heater Testing Long-Term Thermal Effects Calculation." Analysis Report for AP-156, Revision 0, May 27. ERMS 555622. Carlsbad, NM: Sandia National Laboratories.* [PDF / Author]

Lambert, S.J. 1978. "The Geochemistry of Delaware Basin Groundwaters." ERMS 504429. Geology and Mineral Deposits of Ochoan Rocks in Delaware Basin and Adjacent Areas. G.S. Austin, ed. Circular 159. Socorro, NM: New Mexico Bureau of Mines and Mineral Resources. [Author]

Lambert, S.J. 1983. Dissolution of Evaporites in and Around the Delaware Basin, Southeastern New Mexico and West Texas. SAND82-0461. ERMS 227520. Albuquerque, NM: Sandia National Laboratories. [PDF / Author]

Lambert, S.J. 1986. Stable-Isotope Studies of Groundwaters in Southeastern New Mexico, The Rustler Formation at the WIPP Site, EEG-34. SAND85-1978C. Santa Fe, NM: New Mexico Environmental Evaluation Group. [Author]

Lambert, S.J. and J.A. Carter. 1987. Uranium-Isotope Systematics in Groundwaters of the Rustler Formation, Northern Delaware Basin, Southeastern New Mexico. Principles and Methods. SAND87-0388. ERMS 245158. Albuquerque, NM: Sandia National Laboratories. [PDF / Author]

Lambert, S.J. and D.M. Harvey. 1987. Stable-Isotope Geochemistry of Groundwaters in the Delaware Basin of Southeastern New Mexico. SAND87-0138. WPO 24150. ERMS 224150. Albuquerque, NM: Sandia National Laboratories. [PDF / Author]

Lappin, A.R., R.L. Hunter, D.P. Garber, P.B. Davies, R.L. Beauheim, D.J. Borns, L.H. Brush, B.M. Butcher, T. Cauffman, M.S.Y. Chu, L.S. Gomez, R.V. Guzowski, H.J. Iuzzolino, V. Kelley, S.J. Lambert, M.G. Marietta, J.M. Mercer, E.J. Nowak, J. Pickens, R.P. Rechard, M. Reeves, K.L. Robinson, and M.D. Siegel (eds.). 1989. Systems Analysis, Long-Term Radionuclide Transport, and Dose Assessments, Waste Isolation Pilot Plant (WIPP), Southeastern New Mexico. SAND89-0462. ERMS 210281. Albuquerque, NM: Sandia National Laboratories. [PDF / Author]

Lasaga, A.C., J.M. Soler, J. Ganor, T.E. Burch, and K.L. Nagy. 1994. "Chemical Weathering Rate Laws and Global Geochemical Cycles." ERMS 241234. Geochimica et Cosmochimica Acta, vol. 58, no. 10: 2361-2386. [Author]

Lee, W.T. 1925. "Erosion by Solution and Fill." ERMS 252969. Contributions to Geography in the United States: U.S. Geological Survey Bulletin 760-C (pp. 107-21). [Author]

Leigh, C.D. 2003. Estimate of Portland Cement in TRU Waste for Disposal in WIPP for the Compliance Recertification Application. September 15, 2003. ERMS 531562. Carlsbad, NM: Sandia National Laboratories. [PDF / Author]

Leigh, C. and J. Trone. 2005. Calculation of the Waste Unit Factor for the Performance Assessment Baseline Calculation (Revision 0). ERMS 539613. Carlsbad, NM: Sandia National Laboratories. [PDF / Author]

Leigh, C., J. Trone, and B. Fox. 2005. TRU Waste Inventory for the 2004 Compliance Recertification Application Performance Assessment Baseline Calculation (Revision 1). ERMS 541118. Carlsbad, NM: Sandia National Laboratories. [PDF / Author]

Leigh, C., J. Kanney, L. Brush, J. Garner, G. Kirkes, T. Lowry, M. Nemer, J. Stein, E. Vugrin, S. Wagner and T. Kirchner. 2005. 2004 Compliance Recertification Application Performance Assessment Baseline Calculation (Revision 0). ERMS 541521. Carlsbad, NM: Sandia National Laboratories. [PDF / Author]

Lenhardt, W.A. 1988. "Damage Studies at a Deep Level African Gold Mine." Rockbursts & Seismicity in Mines, Proceeding of the Second International Symposium, Minneapolis, MN, June 8-10, 1988 (pp. 391-93). C. Fairhurst, ed. Brookfield, VT: A.A. Balkema. [Author]

Loken, M.C. 1994. SMC Thermal Calculations, RSI Calculation No. A141-GE-05. ERMS 242834. Prepared for Parsons Brinckerhoff, San Francisco, CA. Rapid City, SD: RE/SPEC, Inc. [PDF / Author]

Loken, M.C. and R. Chen. 1994. Rock Mechanics of SMC, RSI Calculation No. A141-GE-07. ERMS 242835. Prepared for Parsons Brinckerhoff, San Francisco, CA. Rapid City, SD: RE/SPEC, Inc. [PDF / Author]

Lowenstein, T.K. 1987. Post Burial Alteration of the Permian Rustler Formation Evaporites, WIPP Site, New Mexico: Textural, Stratigraphic and Chemical Evidence. EEG-36, DOE/AL/10752-36. ERMS 241237. Santa Fe, NM: Environmental Evaluation Group. [PDF / Author]

Melzer, L.S. 2013. An Updated Assessment of the CO2-Enhanced Oil Recovery Potential in the Vicinity of the Waste Isolation Pilot Plant (June). Midland, TX: Melzer Consulting.* [PDF / Author]

Mercer, J.W., R.L. Beauheim, R.P. Snyder, and G.M. Fairer. 1987. Basic Data Report for Drilling and Hydrologic Testing of Drillhole DOE-2 at the Waste Isolation Pilot Plant (WIPP) Site. SAND86-0611. ERMS 227646. Albuquerque, NM: Sandia National Laboratories. [PDF / Author]

Mercer, J.W., D.L. Cole, and R.M. Holt. 1998. Basic Data Report for Drillholes on the H-019 Hydropad (WIPP). SAND98-0071. ERMS 252240. Albuquerque, NM: Sandia National Laboratories. [PDF / Author]

Molecke, M.A. 1979. Gas Generation from Transuranic Waste Degradation. SAND79-0911C. ERMS 228093. Albuquerque, NM: Sandia National Laboratories. [Author]

Muehlberger, W.R., R.C. Belcher, and L.K. Goetz. 1978. "Quaternary Faulting on Trans-Pecos, Texas." ERMS 241238. Geology, vol. 6, no. 6: 337-340. [Author]

New Mexico Bureau of Mines and Mineral Resources (NMBMMR). 1995. Final Report Evaluation of Mineral Resources at the Waste Isolation Pilot Plant (WIPP) Site. March 31, 1995. 4 vols. ERMS 239149. Socorro, NM: New Mexico Bureau of Mines and Mineral Resources, Campus Station. [PDF / Author]

New Mexico Oil Conservation Division (OCD). 1994. "Attachment to Discharge Plan BW-26 Approval Salado Brine Sales No. 3 Brine Facility Discharge Plan Requirements." Attachment to letter from W.J. LeMay, (Oil Conservation Division, Santa Fe, New Mexico) to W.H. Brininstool (Salado Brine Sales, Jal, New Mexico). 12 January 1994. [PDF / Author]

Nicholson, A., Jr. and A. Clebsch, Jr. 1961. "Geology and Ground-Water Conditions in Southern Lea County, New Mexico." ERMS 241583. Ground-Water Report 6. Socorro, NM: New Mexico Bureau of Mines and Mineral Resources. [Author]

Oelkers, E. H. 1996. "Physical and Chemical Properties of Rocks and Fluids for Chemical Mass Transport Calculations." Reviews in Mineralogy, vol. 34: 131-191. [Author]

Papenguth, H.W. and Y.K. Behl. 1996. Test Plan for Evaluation of Colloid-Facilitated Actinide Transport at the Waste Isolation Pilot Plant (16 January). TP 96-01. ERMS 417319. Albuquerque, NM: Sandia National Laboratories. [PDF / Author]

Patterson, R.L. 2011. Inputs and Information for the SDI Thermal Test Planned Change Notice. Letter and attachment to P. Shoemaker, C. Stroud, and S. Patchet. May 16, 2011. U.S. Department of Energy Waste Isolation Pilot Plant. ERMS 555495. Carlsbad, NM: Carlsbad Area Office.* [PDF / Author]

Peake, T. 1996. Memorandum to Public Rulemaking Docket A-92-56 (Subject: WIPP-Examination of Mining and Hydraulic Conductivity). 31 January 1996. ERMS 241239. Washington, DC: U.S. Environmental Protection Agency. [PDF / Author]

Pedersen, K. 1999. "Subterranean Microorganisms and Radioactive Waste Disposal in Sweden." Engineering Geology, vol. 52: 163-176. [Author]

Pedersen, K. and F. Karlsson. 1995. Investigations of Subterranean Microorganisms: Their Importance for Performance Assessment of Radioactive Waste Disposal. SKB Technical Report 95-10. Stockholm, Sweden: Swedish Nuclear Fuel and Waste Management Co. [PDF / Author]

Phillips, F.M., A.R. Campbell, C. Kruger, P.S. Johnson, R. Roberts, and E. Keyes. 1992. A Reconstruction of the Water Balance in Western United States Lake Basins in Response to Climate Change, New Mexico Water Resources Research Institute Report 269. Las Cruces, NM: New Mexico Water Resources Research Institute. [Author]

Pointeau, I., B. Piriou, M. Fedoroff, M.G. Barthes, N. Marmier, and F. Fromage. 2001. "Sorption Mechanisms of Eu3+ on CSH Phases of Hydrated Cements." Journal of Colloid and Interface Science, vol. 236, no. 2: 252-259. [Author]

Popielak, R.S., R.L. Beauheim, S.R. Black, W.E. Coons, C.T. Ellingson, and R.L. Olsen. 1983. Brine Reservoirs in the Castile Formation, Waste Isolation Pilot Plant (WIPP) Project, Southeastern New Mexico. TME-3153. ERMS 242085. Carlsbad, NM: U.S. Department of Energy. [PDF / Author]

Powers, D.W. 1996. Tracing Early Breccia Pipe Studies, Waste Isolation Pilot Plant, Southeastern New Mexico: A Study of the Documentation Available and Decision-Making During the Early Years of WIPP. SAND94-0991. ERMS 230968. Albuquerque, NM: Sandia National Laboratories. [PDF / Author]

Powers, D.W., J.M. Sigda, and R.M. Holt. 1996. Probability of Intercepting a Pressurized Brine Reservoir under the WIPP. ERMS 240199. Carlsbad, NM: Sandia National Laboratories. [PDF / Author]

Powers, D.W. 2000. Evaporites, Casing Requirements, Water-Floods, and Out-of-Formation Waters: Potential for Sinkhole Developments: Technical Class - Sinkholes And Unusual Subsidence Over Solution-Mined Caverns And Salt And Potash Mines. San Antonio, TX: Solution Mining Research Institute. [Author]

Powers, D.W. 2003. Analysis Report, Task 1 of AP-088: Construction of Geologic Contour Maps (January). ERMS 522086. Albuquerque, NM: Sandia National Laboratories. [Author]

Powers, D.W. Evaporites, Casing Requirements, Water-Floods, and Out-of-Formation Waters: Potential for Sinkhole Developments: Circular (in press). Norman, OK: Oklahoma Geological Survey. [Author]

Powers, D.W. and R.M. Holt. 1990. "Sedimentology of the Rustler Formation near the Waste Isolation Pilot Plant (WIPP) Site." Geological and Hydrological Studies of Evaporites in the Northern Delaware Basin for the Waste Isolation Pilot Plant (WIPP), New Mexico (pp. 79-106). Geological Society of America Field Trip No. 14 Guidebook. Dallas, TX: Dallas Geological Society. [Author]

Powers, D.W. and R.M. Holt. 1995. Regional Processes Affecting Rustler Hydrogeology. ERMS 244173. Carlsbad, NM: Sandia National Laboratories. [PDF / Author]

Powers, D.W. and R.M. Holt. 1999. "The Los Medaños Member of the Permian (Ochoan) Rustler Formation." ERMS 532368. New Mexico Geology, vol. 21, no. 4: 97-103. [Author]

Powers, D.W. and R.M. Holt. 2000. "The Salt that Wasn't There: Mudflat Facies Equivalents to Halite of the Permian Rustler Formation, Southeastern New Mexico." ERMS 532369. Journal of Sedimentary Research, vol. 70, 29-39. [Author]

Powers, D.W., S.J. Lambert, S.E. Shaffer, I.R. Hill, and W.D. Weart, eds. 1978. Geological Characterization Report, Waste Isolation Pilot Plant (WIPP) Site, Southeastern New Mexico. SAND78-1596. ERMS 205448 (vol. 1). ERMS 205448 (vol. 2). Albuquerque, NM: Sandia National Laboratories. [PDF / Author]

Powers, D.W., J.M. Sigda, and R.M. Holt. 1996. Probability of Intercepting a Pressurized Brine Reservoir under the WIPP. ERMS 240199. Albuquerque, NM: Sandia National Laboratories. [PDF / Author]

Prichard, D.A. 2003. E-mail to Mary-Alena Martell (Subject: Potash Solution Mining at WIPP). 6 April 2003. ERMS 525161. Carlsbad, NM: IMC Global, Inc. [PDF / Author]

Rawson, D., C. Boardman, and N. Jaffe-Chazan. 1965. Project Gnome, the Environment Created by a Nuclear Explosion in Salt. PNE-107F. ERMS 241242. Lawrence Radiation Laboratory, University of California, Livermore, CA. Springfield, VA: National Technical Information Service. [PDF / Author]

Rechard, R.P., H. Iuzzolino, and J.S. Sandha. 1990. Data Used in Preliminary Performance Assessment of the Waste Isolation Pilot Plant (1990). SAND89-2408. ERMS 227724. Albuquerque, NM: Sandia National Laboratories. [PDF / Author]

Rechard, R.P., C.T. Stockman, L.C. Sanchez, H.R. Trellue, J.S. Rath, and J. Liscum-Powell. 1996. RNT-1: Nuclear Criticality in Near Field and Far Field. FEP Screening Argument. ERMS 240818. Albuquerque, NM: Sandia National Laboratories. [PDF / Author]

Rechard, R.P., L.C. Sanchez, C.T. Stockman, and H.R. Trellue. 2000. Consideration of Nuclear Criticality When Disposing of Transuranic Waste at the Waste Isolation Pilot Plant. SAND99-2898. ERMS 514911. Albuquerque, NM: Sandia National Laboratories. [PDF / Author]

Rechard, R.P., L.C. Sanchez, H.R. Trellue, and C.T. Stockman. 2001. Unfavorable Conditions for Nuclear Criticality Following Disposal of Transuranic Waste at the Waste Isolation Pilot Plant. Nuclear Technology, vol. 136, (October 2001): 99-129. [Author]

Reed, D.T., S. Okajima, L.H. Brush, and M.A. Molecke. 1993. "Radiolytically-Induced Gas Production in Plutonium-Spiked WIPP Brine, Scientific Basis for Nuclear Waste Management XVI," Materials Research Society Symposium Proceedings, Boston, MA, November 30 - December 4, 1992. C.G. Interrante and R.T. Pabalan, eds. SAND92-7283C. ERMS 228637. Materials Research Society, Pittsburgh, PA. Vol. 294, pp. 431-438. [Author]

Reed, D.T., J.S. Swanson, J-F. Lucchini, and M.K. Richmann. 2013. Intrinsic, Mineral, and Microbial Colloid Enhancement Parameters for the WIPP Actinide Source Term. Report LCO-ACP-18, LA-UR 13-20858. Carlsbad, NM: Los Alamos National Laboratory.* [PDF / Author]

Reiter, M., M.W. Barroll, and J. Minier. 1991. "An Overview of Heat Flow in Southwestern United States and Northern Chihuahua, Mexico." ERMS 241575. Neotectonics of North America (pp. 457-66). D.B. Slemmons, E.R. Engdahl, M.D. Zoback, and D.D. Blackwell, eds. Boulder, CO: Geological Society of America. [Author]

Reyes, J. 2008. Letter to D.C. Moody (5 Enclosures). 11 February 2008. Washington, DC: U.S. Environmental Protection Agency, Office of Air and Radiation. [PDF / Author]

Richardson, S. M. and H.Y. McSween, Jr. 1989. Geochemistry: Pathways and Processes. Prentice Hall. [Author]

Robinson, J.Q. and D.W. Powers. 1987. "A Clastic Deposit Within the Lower Castile Formation, Western Delaware Basin, New Mexico." ERMS 241368. Geology of the Western Delaware Basin, West Texas and Southeastern New Mexico (pp. 69-79). D.W. Powers and W.C. James, eds. El Paso, TX: El Paso Geological Society Guidebook 18, El Paso Geological Society. [Author]

Rodwell, W.R., A.W. Harris, S.T. Horseman, P. Lalieux, W. Muller, Amaya L. Ortiz, and K. Pruess. 1999. Gas Migration and Two-Phase Flow through Engineered and Geological Barriers for a Deep Repository for Radioactive Waste. A Joint EC/NEA Status Report. EC, European Commission Report EUR 19122 EN. [Author]

Rosholt, J.N. and C.R. McKinney. 1980. "Uranium Series Disequilibrium Investigations related to the WIPP Site, New Mexico, Part II, Uranium Trend Dating of Surficial Deposits and Gypsum Spring Deposits near WIPP Site, New Mexico," Open-File Report 80-879. Denver, CO: U.S. Geological Survey. [PDF / Author]

Sanchez, L.C. and H.R. Trellue. 1996. "Estimation of Maximum RH-TRU Thermal Heat Load for WIPP." Memorandum to T. Hicks (Galson Sciences Ltd.). 17 January 1996. ERMS 231165. Albuquerque, NM: Sandia National Laboratories. [PDF / Author]

Sanford, A.R., L.H. Jakasha, and D.J. Cash. 1991. "Seismicity of the Rio Grand Rift in New Mexico." ERMS 241571. Neotectonics of North America (pp. 229-44). D.B. Slemmons, E.R. Engdahl, M.D. Zoback, and D.D. Blackwell, eds. Boulder, CO: Geological Society of America. [Author]

Schiel, K.A. 1994. "A New Look at the Age, Depositional Environment and Paleogeographic Setting of the Dewey Lake Formation (Late Permian)." ERMS 220465. West Texas Geological Society Bulletin, vol. 33, no. 9: 5-13. [Author]

Serne, R.J. 1992. "Current Adsorption Models and Open Issues Pertaining to Performance Assessment." In Proceedings of the DOE/Yucca Mountain Site Characterization Project Radionuclide Adsorption Workshop at Los Alamos National Laboratory, September 11-12, 1990. ERMS 241243. Comp. J.A. Canepa. LA-12325-C. Los Alamos, NM: Los Alamos National Laboratory. 43-74. [PDF / Author]

Servant, J. 2001. "The 100 kyr Cycle of Deglaciation During the Last 450 kyr: A New Interpretation of Oceanic and Ice Core Data." Global and Planetary Change, vol. 29: 121-133. [Author]

Siegel, M.D., S.J. Lambert, and K.L. Robinson, eds. 1991. Hydrogeochemical Studies of the Rustler Formation and Related Rocks in the Waste Isolation Pilot Plant Area, Southeastern New Mexico. SAND88-0196. ERMS 225624. Albuquerque, NM: Sandia National Laboratories. [PDF / Author]

Silva, M.K. 1994. Implications of the Presence of Petroleum Resources on the Integrity of the WIPP. ERMS 241470. EEG-55. Albuquerque, NM: Environmental Evaluation Group. [PDF / Author]

Snelling, A.A. 1992. Alligator Rivers Analogue Project Final Report, Volume 2, Geologic Setting. ERMS 241471. UK DOE Report DOE/HMIP/RR/92/072, SKI Report SKI TR, vol. 92:20-2. Her Majesty's Inspectorate of Pollution of the Department of the Environment, London. Stockholm, Sweden: Swedish Nuclear Fuel and Waste Management Co. [PDF / Author]

Snider, A.C. 2001. "The Hydration of Magnesium Oxide in the Waste Isolation Pilot Plant, December 2001." Boston, MA: MRS Fall 2001 Conference. [Author]

Snyder, R.P. 1985. Dissolution of Halite and Gypsum, and Hydration of Anhydrite to Gypsum, Rustler Formation, in the Vicinity of the Waste Isolation Pilot Plant, Southeastern New Mexico. Open-File Report 85-229. Denver, CO: U.S. Geological Survey. [PDF / Author]

Snyder, R.P. and L.M. Gard, Jr. 1982. Evaluation of Breccia Pipes in Southeastern New Mexico and Their Relation to the Waste Isolation Pilot Plant (WIPP) Site. ERMS 241244. Open-File Report 82-968. Denver, CO: U.S. Geological Society. [PDF / Author]

Stenhouse, M.J., N.A. Chapman, and T.J. Sumerling. 1993. SITE-94 Scenario Development FEP Audit List Preparation: Methodology and Presentation. SKI Technical Report 93:27. ERMS 241371. Stockholm: Swedish Nuclear Power Inspectorate. [PDF / Author]

Stoelzel, D.M. and D.G. O'Brien. 1996. The Effects of Salt Water Disposal and Waterflooding on WIPP. Summary Memorandum of Record for NS-7a. ERMS 240837. Albuquerque, NM: Sandia National Laboratories. [PDF / Author]

Stoelzel, D.M. and P.N. Swift. 1997. Supplementary Analyses of the Effect of Salt Water Disposal and Waterflooding on the WIPP. ERMS 244158. Albuquerque, NM: Sandia National Laboratories. [PDF / Author]

Stroes-Gascoyne, S. and J.M. West. 1994. Microbial Issues Pertaining to the Canadian Concept for the Disposal of Nuclear Fuel Waste. AECL Report No. AECL-10808, COG-93-54. Atomic Energy of Canada Ltd. Manitoba, Canada: Whiteshell Labs, Pinawa. ERMS 241639. [PDF / Author]

Swift, P.N., W.D. Weart, S. G. Bertram-Howrey, R.V. Guzowski, K.F. Brinster, and S.B. Pasztor. 1991. Long-Term Climate Variability at the Waste Isolation Pilot Plant, Background Information Presented to the Expert Panel on Inadvertent Human Intrusion into the Waste Isolation Pilot Plant. R.V. Guzowski and M.M. Gruebel, eds. SAND91-0928. Albuquerque, NM: Sandia National Laboratories. [PDF / Author]

Swift, P.N. 1992. Long-Term Climate Variability at the Waste Isolation Pilot Plant, Southeastern New Mexico, USA. SAND91-7055. ERMS 227093. Albuquerque, NM: Sandia National Laboratories. [PDF / Author]

Swanson, J.S., D.T. Reed, D.A. Ams, D.M. Norden, and K.A. Simmons. 2012. Status Report on the Microbial Characterization of Halite and Groundwater Samples from the WIPP. Report LCO-ACP-12, LA-UR 12-22824. Carlsbad, NM: Los Alamos National Laboratory.* [PDF / Author]

Swanson, J.S. and K.A. Simmons. 2013. Update on Microbial Characterization of WIPP Groundwaters. Report LCO-ACP-20, LA-UR 13-20623. Carlsbad, NM: Los Alamos National Laboratory.* [PDF / Author]

Tedesco, E.F. 1992. "Ceres." McGraw-Hill Encyclopedia of Science & Technology. 1992 ed. Vol. 3. p. 443. [Author]

Telander, M.R. and R.E. Westerman. 1993. Hydrogen Generation by Metal Corrosion in Simulated Waste Isolation Pilot Plant Environments: Progress Report for the Period November 1989 through 1992. SAND92-7347. ERMS 223456. Albuquerque, NM: Sandia National Laboratories. [PDF / Author]

Telford, W.M., L.P. Geldart, R. E. Sheriff, and D.A. Keys. 1976. Applied Geophysics. Cambridge, MA: Cambridge UP. [Author]

Thompson, G.A. and M.L. Zoback. 1979. "Regional Geophysics of the Colorado Plateau." ERMS 241603. Tectonophysics, vol. 61, nos. 1-3: 149-81. [Author]

Thorne, B.J. and D.K. Rudeen. 1981. Regional Effects of TRU Repository Heat. SAND80-7161. WPO 10281. ERMS 210281. Albuquerque: Sandia National Laboratories. [PDF / Author]

Thorne, M.C. 1992. Dry Run 3 - A Trial Assessment of Underground Disposal of Radioactive Wastes Based on Probabilistic Risk Analysis - Volume 8: Uncertainty and Bias Audit. ERMS 241245. DOE/HMIP/RR/92.040. London: Her Majesty's Inspectorate of Pollution (HMIP) of the Department of the Environment. [PDF / Author]

U.S. Congress. 1992. Waste Isolation Pilot Plant Land Withdrawal Act. ERMS 239105. Public Law 102-579, October 1992. 102nd Congress, Washington, DC. [PDF / Author]

U.S. Department of Energy (DOE). 1980. Final Environmental Impact Statement, Waste Isolation Pilot Plant (October). 2 vols. DOE/EIS-0026. ERMS 238835 and ERMS 238838. Washington, DC: U.S. Department of Energy. [PDF / Author]

U.S. Department of Energy (DOE). 1996a. Title 40 CFR Part 191 Compliance Certification Application for the Waste Isolation Pilot Plant (October). 21 vols. DOE/CAO-1996-2184. Carlsbad, NM: Carlsbad Field Office. [Author]

U.S. Department of Energy (DOE). 1996b. Transuranic Waste Baseline Inventory Report (Revision 3). DOE/CAO-95-1121. ERMS 243330. U.S. Department of Energy, Carlsbad, NM. [PDF / Author]

U.S. Department of Energy (DOE). 1999. Waste Isolation Pilot Plant 1998 Site Environmental Report. DOE/WIPP 99-2225. Carlsbad, NM: Carlsbad Area Office. [PDF / Author]

U.S. Department of Energy (DOE). 2000a. MgO Mini-Sack Elimination Proposal (July 21). ERMS 519362. Carlsbad, NM: Carlsbad Area Office. [PDF / Author]

U.S. Department of Energy (DOE). 2000b. TRUPACT-II Authorized Methods for Payload Control (Revision 19b). March 2000. Carlsbad, NM: Washington TRU Solutions, LLC. [Author]

U.S. Department of Energy (DOE). 2004. Title 40 CFR Part 191 Compliance Recertification Application for the Waste Isolation Pilot Plant (March). 10 vols. DOE/WIPP 2004-3231. Carlsbad, NM: Carlsbad Field Office. [Author]

U.S. Department of Energy (DOE). 2010. Response to the Environmental Protection Agency October 19, 2009 Letter on the 2009 Compliance Recertification Application. Enclosure 1, Item 3-23-8. February 19, 2010. Carlsbad, NM: Carlsbad Field Office. [PDF / Author]

U. S. Environmental Protection Agency (EPA). 1993. "40 CFR Part 191: Environmental Radiation Protection Standards for the Management and Disposal of Spent Nuclear Fuel, High-Level and Transuranic Radioactive Wastes; Final Rule." Federal Register, vol. 58 (December 20, 1993): 66398-416. [PDF / Author]

U.S. Environmental Protection Agency (EPA). 1996a. "40 CFR Part 194: Criteria for the Certification and Recertification of the Waste Isolation Pilot Plant's Compliance With the 40 CFR Part 191 Disposal Regulations; Final Rule." Federal Register, vol. 61 (February 9, 1996): 5224-45. [PDF / Author]

U.S. Environmental Protection Agency (EPA). 1996b. Compliance Application Guidance for 40 CFR Part 194 (March 29). EPA 402-R-95-014. ERMS 239159. Washington, DC: Office of Radiation and Indoor Air. [PDF / Author]

U.S. Environmental Protection Agency (EPA). 1996c. Criteria for the Certification and Re-Certification of the Waste Isolation Pilot Plant's Compliance with the 40 CFR Part 191 Disposal Regulations, Background Information Document for 40 CFR Part 194. 402-R-96-002. Washington, DC: Office of Radiation and Indoor Air. [PDF / Author]

U.S. Environmental Protection Agency (EPA). 1998a. "40 CFR Part 194: Criteria for the Certification and Recertification of the Waste Isolation Pilot Plant's Compliance with the Disposal Regulations; Certification Decision; Final Rule." Federal Register, vol. 63 (May 18, 1998): 27353-406. [PDF / Author]

U.S. Environmental Protection Agency (EPA). 1998b. Technical Support Document for Section 193.32: Scope of Performance Assessments (May). Washington, DC: Office of Radiation and Indoor Air. [PDF / Author]

U.S. Environmental Protection Agency (EPA). 1998c. "CARD No. 33: Consideration of Drilling Events in Performance Assessments." Compliance Application Review Documents for the Criteria for the Certification and Recertification of the Waste Isolation Pilot Plant's Compliance with the 40 CFR 191 Disposal Regulations: Final Certification Decision (May) (pp. 33-1 through 33-31). Washington, DC: Office of Radiation and Indoor Air.* [PDF / Author]

U.S. Environmental Protection Agency (EPA). 1998d. Response to Comments: Criteria for the Certification and Recertification of the Waste Isolation Pilot Plant's Compliance with the 40 CFR Part 191 Disposal Regulations (May). Washington, DC: Office of Radiation and Indoor Air. [PDF / Author]

U.S. Environmental Protection Agency (EPA). 2001. Approval for the elimination of magnesium oxide mini-sacks from the Waste Isolation Pilot Plant. ERMS 519362. Letter from Frank Marcinowski, EPA to Dr. Ines Triay, DOE. Washington, DC: Office of Radiation and Indoor Air. [PDF / Author]

U.S. Environmental Protection Agency (EPA). 2006. Criteria for the Certification and Recertification of the Waste Isolation Pilot Plant's Compliance with the 40 CFR Part 191 Disposal Regulations: Recertification Decision. EPA-HQ-OAR-2004-0025. Washington, DC: Office of Radiation and Indoor Air. [PDF / Author]

U.S. Environmental Protection Agency (EPA). 2010a. "40 CFR Part 194 Criteria for the Certification and Recertification of the Waste Isolation Pilot Plant's Compliance with the Disposal Regulations: Rectification Decision; Final Notice." Federal Register, vol. 75 (November 18, 2010): 70584 - 595. [PDF / Author]

U.S. Environmental Protection Agency (EPA). 2010b. Technical Support Document for Section 194.24, Evaluation for the Compliance Recertification Actinide Source Term, Backfill Efficacy and Culebra Dolomite Distribution Coefficient Values (Revision 1). November 2010. Washington, DC: Office of Radiation and Indoor Air. [PDF / Author]

U.S. Nuclear Regulatory Commission (NRC). 2002. Model RH-TRU 72-B Package Certificate of Compliance Number 9212, Revision 2. December 27, 2002. Washington, DC: U.S. Nuclear Regulatory Commission. [PDF / Author]

Vaughn, P., M. Lord, J. Garner, and R. MacKinnon. 1995. "Radiolysis of Brine." Errata to Summary Memorandum of Record GG-1, SWCF-A:1.1.6.3:PA:QA:TSK:GG1,S7. 21 December 1995. ERMS 230786. Albuquerque, NM: Sandia National Laboratories. [PDF / Author]

Vine, J.D. 1963. Surface Geology of the Nash Draw Quadrangle, Eddy County, New Mexico. ERMS 239558. Bulletin 1141-B. Washington, DC: U.S. Geological Survey. [PDF / Author]

Waber, N. 1991. Mineralogy, Petrology and Geochemistry of the Poços de Caldas Analogue Study Sites, Minas Gerais, Brazil, I:. Osamu Utsumi Uranium Mine. Nagra Report NTB-90-20. Baden, Switzerland: National Genossen Schaft für die Lagerung Radioaktiver Abfalle (NAORA). [PDF / Author]

Wagner, S., R. Kirkes, and M.A. Martell. 2003. Features, Events and Processes: Reassessment for Recertification Report. ERMS 530184. Carlsbad, NM: Sandia National Laboratories. [PDF / Author]

Wakeley, L.D., P.T. Harrington, and F.D. Hansen. 1995. Variability in Properties of Salado Mass Concrete. SAND94-1495. ERMS 222744. Albuquerque, NM: Sandia National Laboratories. [PDF / Author]

Wall, N.A. and S.A. Mathews. 2005. Sustainability of Humic Acids in the Presence of Magnesium Oxide. Applied Geochemistry, vol. 20: 1704-13.* [Author]

Wall, N.A. and D. Enos. 2006. Iron and Lead Corrosion in WIPP-Relevant Conditions, TP 06-02, Rev. 1. ERMS 5432238. Carlsbad NM: Sandia National Laboratories. [PDF / Author]

Wallace, M. 1996a. "Leakage from Abandoned Boreholes." Summary Memorandum of Record for NS-7b, SWCF-A 1.1.6.3:PA:QA:TSK:NS-7b. ERMS 240819. Albuquerque, NM: Sandia National Laboratories. [PDF / Author]

Wallace, M. 1996b. "Pumping from the Culebra Outside the Controlled Area." Summary Memorandum of Record for NS-5. SWCF-A 1.1.6.3:PA:QA:TSK:NS-5. ERMS 240831. Albuquerque, NM: Sandia National Laboratories. [PDF / Author]

Wallace, M. 1996c. Records Package for Screening Effort NS11: Subsidence Associated with Mining Inside or Outside the Controlled Area (November 21). ERMS 412918. Carlsbad, NM: Sandia National Laboratories. [PDF / Author]

Wallace, M., R. Beauheim, C. Stockman, M. A. Martell, K. Brinster, R. Wilmot, and T. Corbert. 1995. "Dewey Lake Data Collection and Compilation." Summary Memorandum of Record for NS-1, SWCF-A 1.1.6.3:PA:QA:TSK:NS-1. ERMS 222508. Albuquerque: Sandia National Laboratories. [PDF / Author]

Wallner, M. 1981. "Critical Examination of Conditions for Ductile Fracture in Rock Salt." ERMS 241372. Proceedings of the Workshop on Near-Field Phenomena in Geologic Repositories for Radioactive Waste, Seattle, WA, August 31-September 3, 1981 (pp. 243-53). Paris: Organisation for Economic Co-operation and Development. [Author]

Wang, Y. 1996. Memorandum to Internal Distribution(Subject: Evaluation of the Thermal Effect of MgO Hydration for the Long-Term WIPP Performance Assessment). 9 May 1996. ERMS 237743. Albuquerque, NM: Sandia National Laboratories. [PDF / Author]

Wang, Y. 1998. Memorandum to Malcolm D. Siegel (Subject: On the Matrix Pore Plugging Issue). 8 August 1998. ERMS 421858. Albuquerque, NM: Sandia National Laboratories. [PDF / Author]

Wang, Y. and L.H. Brush. 1996a. Memorandum to M.S. Tierney (Subject: Estimates of Gas-Generation Parameters for the Long-Term WIPP Performance Assessment). 26 January 1996. ERMS 231943. Albuquerque, NM: Sandia National Laboratories. [PDF / Author]

Wang, Y. and L.H. Brush. 1996b. Memorandum to M.S. Tierney (Subject: Modify the Stoichiometric Factor y in the BRAGFLO to Include the Effect of MgO Added to WIPP Repository as a Backfill). 23 February 1996. ERMS 232286. Albuquerque, NM: Sandia National Laboratories. [PDF / Author]

Warrick, R. and J. Oerlemans. 1990. Sea Level Rise, in Climate Change: The IPCC Scientific Assessment (pp. 257-81). J.T. Houghton, G.J. Jenkins, and J.J. Ephraums, eds. Sweden: Intergovernmental Panel on Climate Change. [Author]

Westinghouse Electric Corporation. 1994. Backfill Engineering Analysis Report, Waste Isolation Pilot Plant. WPO 37909. ERMS 237909. Carlsbad, NM: Westinghouse Electric Corporation. [PDF / Author]

Wierczinski, B., S. Helfer, M. Ochs, and G. Skarnemark. 1998. "Solubility Measurements and Sorption Studies of Thorium in Cement Pore Water." Journal of Alloys and Compounds, vol. 271: 272−76. [Author]

Wilmot, R.D. and D.A. Galson. 1996. Memorandum of Record for NS17 and NS18, SWCF-A 1.1.6.3:PA:QA:TSK; NS-17, NS-18 (Subject: Human-Initiated Brine Density Changes). ERMS 238748. Albuquerque, NM: Sandia National Laboratories. [PDF / Author]

Wilson, C., D. Porter, J. Gibbons, E. Oswald, G. Sjoblom, and F. Caporuscio. 1996. Conceptual Models Supplementary Peer Review Report (December). ERMS 243153. Carlsbad, NM: Carlsbad Area Office. [PDF / Author]

WIPP Performance Assessment Department. 1991. Preliminary Comparison with 40 CFR Part 191, Subpart B for the Waste Isolation Pilot Plant, December 1991, Volume 1: Methodology and Results. SAND91-0893/1. ERMS 226404. Albuquerque, NM: Sandia National Laboratories, WIPP Performance Assessment Department. [PDF / Author]

WIPP Performance Assessment Department. 1993. Preliminary Performance Assessment for the Waste Isolation Pilot Plant, December 1992, Volume 4: Uncertainty and Sensitivity Analyses for 40 CFR 191, Subpart B. SAND92-0700/4.UC-721. ERMS 223599. Albuquerque, NM: Sandia National Laboratories. [PDF / Author]

Witherspoon, P.A., J.S.Y., Wang, K. Iwai, and J.E. Gale. 1980. "Validity of Cubic Law for Fluid Flow in a Deformable Rock Fracture." ERMS 238853. Water Resources Research, vol. 16: 1016−24. [Author]

Wolery, T.J. 1992. EQ3NR-A Computer Program for Geochemical Aqueous Speciation Solubility Calculations: Theoretical Manual, User's Guide, and Related Documentation (Version 7.0). UCRL-MA-110662 PT III. Berkeley, CA: Lawrence Livermore National Laboratory. [PDF / Author]

Wood, B.J., R.E. Snow, D.J. Cosler, and S. Haji-Djafari. 1982. Delaware Mountain Group (DMG) Hydrology - Salt Removal Potential, Waste Isolation Pilot Plant (WIPP) Project, Southeastern New Mexico. TME 3166. ERMS 241602. Albuquerque NM: U.S. Department of Energy. [PDF / Author]

Zoback, M.D. and M.L. Zoback. 1991. "Tectonic Stress Field of North America and Relative Plate Motions." ERMS 241601. Neotectonics of North America (pp. 339-66). D.B. Slemmons, E.R. Engdahl, M.D. Zoback, and D.D. Blackwell, eds. Boulder, CO: Geological Society of America. [Author]

Zoback, M.L. and Zoback, M.D. 1980. "State of Stress in the Conterminous United States." ERMS 241600. Journal of Geophysical Research, vol. 85, no. B11: 6113-56. [PDF / Author]

Zoback, M.L., M.D. Zoback, J. Adams, S. Bell, M. Suter, G. Suarez, C. Estabrook, and M. Magee. 1991. Stress Map of North America. Continent Scale Map CSM-5, Scale 1:5,000,000. Boulder, CO: Geological Society of America. [Author]

[1] The 1.7 molar conversion rate for plastic is based on analyses presented in Wang and Brush (1996a and 1996b).

Title 40 CFR Part 191
Subparts B and C
Compliance Recertification Application 2014
for the
Waste Isolation Pilot Plant

Appendix SOTERM-2014
Actinide Chemistry Source Term

United States Department of Energy
Waste Isolation Pilot Plant

Carlsbad Field Office
Carlsbad, New Mexico

Compliance Recertification Application 2014 Appendix SOTERM-2014
Actinide Chemistry Source Term

Table of Contents

List of Figures

List of Tables

Acronyms and Abbreviations

% percent

α alpha particle

A_γ Debye-Hückel parameter

a_i activity of a chemical species

µ, or µm micrometer, micron

µs microsecond

am amorphous

aq aqueous

ASTP Actinide Source Term Program

atm atmosphere

β (apparent) stability constant, or beta particle

Bq becquerel

BRAGFLO Brine and Gas Flow code

C Celsius; centigrade; concentration

CAPHUM maximum (cap) actinide concentration associated with mobile humic colloids

CAPMIC maximum actinide concentration that could be associated with microbes

CCA Compliance Certification Application

CFR Code of Federal Regulations

Ci Curie

CMC carboxymethylcellulose

CN coordination number

coll colloid

CONCINT actinide concentration associated with mobile actinide intrinsic colloids

CONCMIN actinide concentration associated with mobile mineral fragment colloids

CPR cellulosic, plastic, and rubber materials

C_{Pu} maximum concentration of all combined isotopes of Pu

cr crystalline phase

CRA Compliance Recertification Application

DBR direct brine release

D-H Debye-Hückel theory

DNA deoxyribonucleic acid

DOE U.S. Department of Energy

DRZ disturbed rock zone

E_0 or E_h potential

EDTA ethylenediaminetetraacetic acid

EDS energy dispersive x-ray spectroscopy

EPA U.S. Environmental Protection Agency

ERDA Energy Research and Development Administration

EQ3/6 software program for geochemical modeling of aqueous systems

eV electron volt

EXAFS Extended X-Ray Absorption Fine Structure

F Fahrenheit

f_{CO_2} fugacity of carbon dioxide

f(I) Debye-Hückel function

f'(I) derivative of the Debye-Hückel function

FMT Fracture-Matrix Transport

ft foot/feet

γ gamma radiation or activity coefficient

g gaseous, or gram, or gravity of Earth

G molecular yield in molecules/100 eV of absorbed ionizing radiation

g/L gram per liter

g/mL gram per milliliter

GBq giga becquerel

GWB Generic Weep Brine

h hours

HEXS high-energy X-ray scattering

hyd hydrated

I ionic strength

ICP-MS inductively coupled plasma-mass spectrometry

ISA isosaccharinic acid

K degree Kelvin or stability constant

kDa kilo Dalton

kg kilogram

K_d dissociation constant

km kilometer

K_s solubility constantK_{sp} solubility product

λ_{ij} second-order interaction coefficient

L liter

LANL Los Alamos National Laboratory

LANL-CO Los Alamos National Laboratory - Carlsbad Operations

LET Linear Energy Transfer

log logarithm

$\log_{10}$ logarithm base 10

LWB land withdrawal boundary

μ_{ijk} third-order interaction coefficient

m meter, molal

M mole per liter

m^2 square meter

m^3 cubic meter

mg milligram

mM millimole per liter

mol mole

molec molecule

MPa megapascal

mV millivolt

n neutron, or number

N degree of polymerization number

nm nanometer

NONLIN Sandia code

N_S Adsorption site density (sites/nm^2)

NUTS Nuclide Transport System code

OXSTAT oxidation state parameter

P pressure

PA performance assessment

PABC Performance Assessment Baseline Calculation

PANEL Program used in PA

PAVT Performance Assessment Verification Test

pC_{H+} or pcH Negative logarithm of H^+ concentration in moles per liter

pCO_2 Partial pressure of carbon dioxide

pH negative logarithm of H^+ activity

PHUMCIM Proportionality constant for the actinide concentration associated with mobile humic colloids, in Castile brine

PHUMSIM Proportionality constant for the actinide concentration associated with mobile humic colloids, in Salado brine

pK_a negative logarithm of the dissociation constant of an acid

pm picometer

pmH negative logarithm of H^+ concentration in molal

ppm parts per million

PROPMIC proportionality constant describing the bioassociation of actinides with mobile microorganisms

ref reference

RH relative humidity

rpm revolutions per minute

s solid or second

SECOTP2D computer program that simulates single or multiple component radionuclide transport in fractures or granular aquifers

SEM scanning electron microscope

$S_{i,b}$ solubility calculated for oxidation state i in brine b

SIT Specific Ion Interaction theory

SNL Sandia National Laboratories

SOTERM Actinide Chemistry Source Term (WIPP)

SPC Salado Primary Constituents

SRB sulfate-reducing bacteria

SU_i solubility uncertainty sampled from a distribution unique to each oxidation state i

T temperature

$t_{½}$ half-life

TDS total dissolved solid

TR-LIF Time-resolved laser induced fluorescence

TRU transuranic

V volt, or vanadium

w with

WIPP Waste Isolation Pilot Plant

WWIS WIPP Waste Information System

XANES X-Ray Absorption Near Edge Structure

XRD X-Ray Diffraction

yr year

z_i charge of the specie "i"

Elements and Chemical Compounds

Am Americium

Am(II) Americium in the +2 oxidation state

Am(III) Americium in the +3 oxidation state

Am(IV) Americium in the +4 oxidation state

Am(V) Americium in the +5 oxidation state

Am(VI) Americium in the +6 oxidation state

Am^{2+} Americium cation - Aqueous form of the americium in the +2 oxidation state that only exists as a transient

Am^{3+} Americium cation - Aqueous form of the americium in the +3 oxidation state

Am^{4+} Americium cation - Aqueous form of the americium in the +4 oxidation state

$Am(Cl)_n^{(3-n)}$ Americium (III) chloride complex with n = 1 or 2

$Am(CO_3)_n^{(3-2n)}$ Americium (III) carbonate complex with n=1, 2, 3 or 4

Am OH CO_3 Americium (III) carbonato hydroxide

AmO_2^{+} Americium oxo-cation - Aqueous form of the americium in the +5 oxidation state

AmO_2^{2+} Americium oxo-cation - Aqueous form of the americium in the +6 oxidation state

AmO_2OH Americium (V) oxide hydroxide

$AmOH^{2+}$ Americium (III) hydroxide cation - (1:1) complex

$Am(OH)_2^{+}$ Americium (III) hydroxide cation - (1:2) complex

$Am(OH)_3$ Americium hydroxide

$Am(OH)_4^{-}$ Americium (III) hydroxide anion - (1:4) complex

$Am(OH)_n^{(3-n)}$ Americium (III) hydroxide ion - (n:3-n) complex

$AmPO_4$ Americium (III) phosphate

$Am(SO_4)_n^{(3-2n)}$ Americium (III) sulfate complex with n = 1 or 2

$[An]_p$ Concentration of an adsorbed actinide element (mol/particle)

An Actinide

An(III) General actinide in the +3 oxidation state

An(IV) General actinide in the +4 oxidation state

An(V) General actinide in the +5 oxidation state

An(VI) General actinide in the +6 oxidation state

An^{3+} Aqueous form of the actinide in the +3 oxidation state

An^{4+} Aqueous form of the actinide in the +4 oxidation state

An^{n+} Aqueous form of the actinide in the +n oxidation state

$An_2(CO_3)_3$ Actinide (III) carbonate - (2:3) complex

$An_2(CO_3)_2^{2+}$ Actinide (III) carbonate iaon - (2:2) complex

$AnB_4O_7^{+}$ Actinide (III) tetraborate ion - (1:1) complex

$AnCl^{2+}$ Actinide (III) chloride ion - (1:1) complex

$An(CO_3)^{+}$ Actinide (III) carbonate ion - (1:1) complex

$An(CO_3)_2^{-}$ Actinide (III) carbonate ion - (1:2) complex

$An(CO_3)_3^{3-}$ Actinide (III) carbonate ion - (1:3) complex

$AnCO_3OH$ Actinide (III) carbonate hydroxide

$AnL^{(n+m)}$ Complex of an actinide with a charge n and an organic ligand L with a charge m

$An(V)O_2^+$ or AnO_2^+ Aqueous form of the actinide in the +5 oxidation state

$An(VI)O_2^{2+}$ or AnO_2^{2+} Aqueous form of the actinide in the +6 oxidation state

$AnOH^{2+}$ Actinide (III) hydroxide cation - (1:1) complex

$An(OH)_3$ Hydroxide of the actinide (III)

$AnPO_4$ Actinide (III) phosphate

$AnSO_4^+$ Actinide (III) sulfate ion - (1:1) complex

$B_3O_3(OH)_4^-$ Hydroxy polynuclear form of boric acid

$B_4O_7^{2-}$ Tetraborate anion

$B(OH)_x^{3-x}$ Hydroxyborate ions

Br^- Bromide anion

[C] Concentration of species *C* in solution

[C_0] Concentration of a chosen standard state

C Carbon or concentration

$C_6H_{10}O_5$ Cellulose

CH_4 Methane

$CH_3CO_2^-$ Acetate anion

$(CH_2CO_2)_2C(OH)(CO_2)^{3-}$ Citrate anion

$(CH_2CO_2)_2N(CH_2)_2N(CH_2CO_2)_2^{4-}$ Ethylenediaminetetraacetate (EDTA) anion

$C_2O_4^{2-}$ Oxalate anion

Ca Calcium

Ca^{2+} Calcium cation

$CaCl_2$ Calcium chloride

$CaCO_3$ Calcium carbonate

$CaMg(CO_3)_2$ Dolomite, calcium magnesium carbonate

$Ca[M(OH)_3]^{2+}$ Calcium metal (III) hydroxide cation - (1:1:3) complex

$Ca_2[M(OH)_4]^{3+}$ Calcium metal (III) hydroxide cation - (2:1:4) complex

$Ca_3[M(OH)_6]^{3+}$ Calcium metal (III) hydroxide cation - (3:1:6) complex

$Ca_p[Cm(OH)_n]^{3+2p-n}$ Calcium curium (III) hydroxide ion - (p:n:3+2p-n) complex

$Ca_4[Pu(OH)_8]^{4+}$ Calcium plutonium (IV) hydroxide cation complex

$CaSO_4$ Anhydrite, calcium sulfate

$CaSO_4 \cdot 2H_2O$ Gypsum, hydrated calcium sulfate

$Ca_4[Th(OH)_8]^{4+}$ Calcium thorium (IV) hydroxide cation complex

Cl Chlorine

Cl^- Chloride ion

Cl_2 Chlorine

Cl_2^- Chlorine free radical

Cl_3^- Chlorine anion

$ClBr^-$ Chloride bromide radical

ClO^- Hypochlorite anion

ClO_2^- Chlorite anion

ClO_3^- Chlorate anion

ClO_4^- Perchlorate anion

Cm Curium

Cm(III) Curium in the +3 oxidation state

Cm(IV) Curium in the +4 oxidation state

Cm^{3+} Curium cation - Aqueous form of the curium at the +3 oxidation state

$Cm_m(OH)_{3m}$ Curium hydroxide polymer

$Cm(OH)_3$ Curium hydroxide

$Cm(OH)_4^-$ Curium (III) hydroxide anion - (1:4) complex

CO_2 Carbon dioxide

CO_3^{2-} Carbonate anion

Cr Chromium

Cs Cesium

F^- Fluoride

Fe Iron

Fe(0), Fe^0 Zero-valent iron, metallic iron

$FeCO_3$ Iron (II) carbonate, ferrous carbonate

$Fe_2(OH)_3Cl$ Iron -hibbingite, ferrous chloride trihydroxide

Fe_3O_4 Magnetite, iron (II,III) oxide

Fe^{2+} Aqueous form of the iron in the +2 oxidation state, ferrous anion

Fe^{3+} Aqueous form of the iron in the +3 oxidation state, ferric anion

Fe(II) Iron in the +2 oxidation state

$Fe(II)(OH)_2$ Ferrous hydroxide

Fe(III) Iron in the +3 oxidation state

$Fe(III)_2Fe(II)_4(OH)_{12}CO_3 \cdot 2H_2O$ Green rust

$Fe(OH)_3$ Ferric hydroxide

$Fe(OH)_2 \cdot (x-2)H_2O$ Hydrated ferrous hydroxide

FeOOH Goethite, iron oxide hydroxide

FeS Iron (II) sulfideH Hydrogen

H^+ Hydrogen cation

H_2 Hydrogen

HPO_4^{2-} Hydrogenphosphate anion

HCO_3^- Bicarbonate anion, hydrogen carbonate anion

H_2O Water

H_2O_2 Hydrogen peroxide

HOBr Hypobromous acid

HOCl Hypochlorous acid

$H_2PO_4^-$ Dihydrogen phosphate anion

H_2S Hydrogen sulfide

K Potassium

K^+ Potassium cation

KCl Potassium chloride

$K_2MgCa_2(SO_4)_4 \cdot 2H_2O$ Polyhalite

$KNpO_2CO_3 \cdot 2H_2O$ Hydrated potassium neptunium (V) carbonate - (1:1:1) complex

$K_3NpO_2(CO_3)_2 \cdot 0.5H_2O$ Hydrated potassium neptunium (V) carbonate - (3:1:2) complex

KOH Potassium hydroxide

K_2SO_4 Potassium sulfate

$K_2U_2O_7$ Potassium diuranate

Li^+ Lithium ion

M(III) Metal in the +3 oxidation state

Mg Magnesium

Mg^{2+} Magnesium cation

$MgCl_2$ Magnesium chloride

$Mg_3(OH)_5Cl \cdot 4H_2O$ Magnesium chloride hydroxide hydrate

$MgCO_3$ Magnesite, magnesium carbonate

$Mg_5(CO_3)_4(OH)_2 \cdot 4H_2O$ Hydromagnesite

$Mg_2(OH)_3Cl \cdot 4H_2O$ Magnesium chloride hydroxide hydrate, magnesium oxychloride

MgO Periclase, magnesium oxide

$Mg(OH)_2$ Brucite, magnesium hydroxide

Mn Manganese

N_2 Nitrogen

Na Sodium

Na^+ Sodium cation

NaBr Sodium bromide

NaCl Sodium chloride

$NaClO_4$ Sodium perchlorate

NaOH Sodium hydroxide

Na_2SO_4 Sodium sulfate

$Na_2S_2O_4$ Sodium hydrosulfite

$NaAm(CO_3)_2$ Sodium americium (III) carbonate

NaCl Halite, sodium chloride

$NaHCO_3$ Sodium bicarbonate

$NaNpO_2CO_3 \cdot 3.5H_2O$ Hydrated sodium neptunium (V) carbonate - (1:1:1) complex

$Na_3NpO_2(CO_3)_2$ Sodium neptunium (V) carbonate - (3:1:2) complex

NaOH Sodium hydroxide

$Na_2U_2O_7 \cdot xH_2O$ Sodium diuranate hydrate

Nd Neodymium

Nd(III) Neodymium in the +3 oxidation state

$Nd(OH)_3$ Neodymium (III) hydroxide

Ni Nickel

Ni^{2+} Nickel (II) cation

NO_3^- Nitrate anion

Np Neptunium

Np(IV) Neptunium in the +4 oxidation state

Np(V) Neptunium in the +5 oxidation state

Np(VI) Neptunium in the +6 oxidation state

Np^{4+} Neptunium cation - Aqueous form of the neptunium at the +4 oxidation state

NpO_2 Neptunium (IV) oxide

NpO_2^+ or $Np(V)O_2^+$ Neptunyl cation - Aqueous form of the neptunium at the +5 oxidation state

NpO_2^{2+} or $Np(VI)O_2^{2+}$ Neptunyl cation - Aqueous form of the neptunium at the +6 oxidation state

NpO_5^{3-} Neptunyl anion - Aqueous form of the neptunium at the +7 oxidation state$NpO_2CO_3^-$ Neptunium (V) carbonate ion - (1:1) complex

$NpO_2(CO_3)_2^{3-}$ Neptunium (V) carbonate ion - (1:2) complex

$NpO_2(CO_3)_3^{5-}$ Neptunium (V) carbonate ion - (1:3) complex

$Np(OH)_3$ Neptunium (III) hydroxide

$Np(OH)_4$ Neptunium (IV) hydroxide

$Np(OH)_5^-$ Neptunium (IV) hydroxide ion - (1:5) complex

NpO_2OH Neptunium (V) hydroxide

$NpO_2(OH)_2$ Neptunium (VI) hydroxide

$NpO_2(OH)_2^-$ Neptunium (V) hydroxide ion - (1:2) complexO Oxygen

O_2 Molecular oxygen

OBr^- Hypobromite anion

OCl^- Hypochlorite anion

OH Hydroxide

OH^- Hydroxide anion

OH· Hydroxyl radical

Pb Lead

Pb^{2+} Lead cation - Aqueous form of the lead at the +2 oxidation state

Pb^{4+} Lead cation - Aqueous form of the lead at the +4 oxidation state

$PbCl_2$ Lead (II) chloride

$PbCO_3$ Lead (II) carbonate

$[Pb_6O(OH)_6]^{4+}$ Lead (II) polyoxyhydroxide cation

PbO Lead (II) oxide

PO_4^{3-} Phosphate anion

$(PbOH)_2CO_3$ Lead (II) hydroxide carbonate

PbS Lead (II) sulfide

$PbSO_4$ Lead (II) sulfate

Pu Plutonium

Pu(III) Plutonium in the +3 oxidation state

Pu(IV) Plutonium in the +4 oxidation state

Pu(V) Plutonium in the +5 oxidation state

Pu(VI) Plutonium in the +6 oxidation state

Pu(VII) Plutonium in the +7 oxidation state

Pu^{3+} Plutonium cation - Aqueous form of the plutonium at the +3 oxidation state

Pu^{4+} Plutonium cation - Aqueous form of the plutonium at the +4 oxidation state

$Pu(CO_3)^+$ Plutonium (III) carbonate ion - (1:1) complex

$Pu(CO_3)_2^-$ Plutonium (III) carbonate ion - (1:2) complex

$Pu(CO_3)_3^{3-}$ Plutonium (III) carbonate ion - (1:3) complex

PuF_2^{2+} Plutonium (IV) fluoride cation

PuO_2 Plutonium (IV) dioxide

PuO_{2+x} Oxidized plutonium (IV) dioxide

PuO_2CO_3 Plutonium (VI) carbonate

$PuO_2CO_3^-$ Plutonium (V) carbonate ion - (1:1) complex

$PuO_2(CO_3)_2^{3-}$ Plutonium (V) carbonate ion - (1:2) complex

$PuO_2(CO_3)_2^{2-}$ Plutonium (VI) carbonate ion - (1:2) complex

$PuO_2(CO_3)_3^{4-}$ Plutonium (VI) carbonate ion - (1:3) complex

PuO_2F^+ Plutonium (VI) oxofluoride cation

PuO_2^+ or $Pu(V)O_2^+$ Plutonyl cation - Aqueous form of the plutonium at the +5 oxidation state

PuO_2^{2+} or $Pu(VI)O_2^{2+}$ Plutonyl cation - Aqueous form of the plutonium at the +6 oxidation state

$PuO_2(OH)_2$ Plutonium (VI) hydroxide

$PuO_3 \cdot xH_2O$ Plutonium (VI) trioxide-hydrate

$Pu(OH)_3$ Plutonium (III) hydroxide

$Pu(OH)_3^+$ Plutonium (IV) hydroxide cation - (1:3) complex

$Pu(OH)_4$ Plutonium (IV) hydroxide

$[Pu(H_2O)_m]^{n+}$ Hydrolysis complex of plutonium

$[Pu(O)Pu(O)Pu(O)...]_n$ Plutonium polymer

S^{2-} Sulfide anion

SO_4^{2-} Sulfate anion

Sr Strontium

Th Thorium

Th(IV) Thorium in the +4 oxidation state

Th^{3+} Thorium cation - Aqueous form of the thorium at the +3 oxidation state

Th^{4+} Thorium cation - Aqueous form of the thorium at the +4 oxidation state

$Th(CO_3)_5^{6-}$ Thorium (IV) pentacarbonyl ion complex

$ThISA_2^{2+}$ Thorium (IV) isosaccharinic acid ion - (1:2) complex

ThO_2 Thorium dioxide

$Th(OH)^{3+}$ Thorium (IV) hydroxide ion - (1:1) complex

$Th(OH)_2^{2+}$ Thorium (IV) hydroxide ion - (1:2) complex

$Th(OH)_3^{+}$ Thorium (IV) hydroxide ion - (1:3) complex

$Th_4(OH)_{12}^{4+}$ Thorium (IV) hydroxide ion - (4:12) complex

$Th_6(OH)_{15}^{9+}$ Thorium (IV) hydroxide ion - (6:9) complex

$Th(OH)_4$ Thorium hydroxide

$Th(OH)(CO_3)_4^{5-}$ Thorium (IV) hydroxide carbonate ion - (1:1:4) complex

$Th(OH)_2(CO_3)_2^{2-}$ Thorium (IV) hydroxide carbonate ion - (1:2:2) complex

$Th(OH)_3CO_3^{-}$ Thorium (IV) hydroxide carbonate ion - (1:3:1) complex

$Th(OH)_2SO_4$ Thorium (IV) hydroxide sulfate ion - (1:2:1) complex

$Th(OH)_4ISA_2^{2-}$ Thorium (IV) hydroxide isosaccharinic acid ion - (1:4:2) complex

$Th(SO_4)_3^{2-}$ Thorium (IV) sulfate ion - (1:3) complex

$Th(SO_4)_2$ Thorium (IV) sulfate

$Th(SO_4)_2 \cdot K_2SO_4 \cdot 4H_2O$, $Th(SO_4)_2 \cdot 2K_2SO_4 \cdot 2H_2O$, $Th(SO_4)_2 \cdot 3.5K_2SO_4$ Hydrated potassium thorium (IV) sulfate complex

$Th(SO_4)_2 \cdot Na_2SO_4 \cdot 6H_2O$ Hydrated sodium thorium (IV) sulfate complex

U Uranium

U(III) Uranium in the +3 oxidation state

U(IV) Uranium in the +4 oxidation state

U(V) Uranium in the +5 oxidation state

U(VI) Uranium in the +6 oxidation state

U^{3+} Uranium cation - Aqueous form of the uranium at the +3 oxidation state

U^{4+} Uranium cation - Aqueous form of the uranium at the +4 oxidation state

UO_2 Uraninite, uranium (IV) dioxide

UO_2^{2+} or $U(VI)O_2^{2+}$ Uranyl cation - Aqueous form of the uranium at the +6 oxidation state

UO_2CO_3 Rutherfordine, uranium (VI) carbonate

$UO_2(CO_3)_2^{2-}$ Uranium (VI) carbonate ion - (1:2) complex

$UO_2(CO_3)_3^{4-}$ Uranium (VI) carbonate ion - (1:3) complex or triscarbonato complex

$(UO_2)_3(CO_3)_6^{6-}$ Uranium (VI) carbonate ion - (3:6) complex

$(UO_2)_2(CO_3)(OH)_3^{-}$ Uranium (VI) carbonate hydroxide ion - (2:1:3) complex

$(UO_2)_{11}(CO_3)_6(OH)_{12}^{2-}$ Uranium (VI) carbonate hydroxide ion - (11:6:12) complex

$UO_2(OH)_3^-$ Uranium (VI) hydroxide ion - (1:3) complex

$UO_2(OH)_4^{2-}$ Uranium (VI) hydroxide ion - (1:4) complex

$U(OH)_4$ Uranium (IV) hydroxide

$UO_2.xH_2O$ Hydrous uranium (IV) dioxide

$(UO_2)(OH)_2 \cdot xH_2O$ or $UO_3 \cdot xH_2O$ Schoepite, hydrated uranium trioxide

V Vanadium

ZrO_2 Zirconium dioxide

SOTERM-1.0 Introduction

Appendix SOTERM-2014 (Actinide Chemistry Source Term) is a summary of the U.S. Department of Energy's (DOE's) understanding of the Waste Isolation Pilot Plant (WIPP) chemical conditions, assumptions, and processes; the underlying actinide chemistry; and the resulting actinide concentrations that were calculated based on this repository chemistry. This appendix supplements Appendix PA-2014 in the 2014 Compliance Recertification Application (CRA-2014). The results summarized here are based, in part, on various assumptions about the chemical conditions in the repository, and calculations, that were included in the formulation of the baseline used for the CRA-2014 Performance Assessment (PA). The WIPP-related geochemical experimental results obtained within and outside of the WIPP project since the CRA-2009 was submitted are also summarized.

Actinide release from the WIPP is a critical performance measure for the WIPP as a transuranic (TRU) waste repository. There are a number of potential pathways for actinide release considered by the WIPP PA; these are discussed in detail in Appendix PA-2014. Quantifying the impact of these releases contributes directly to assessing compliance with 40 CFR Part 191 (U.S. EPA 1993).

In the undisturbed scenario for PA, actinide releases up the shafts or laterally through the marker beds are insignificant in all realizations and have no impact on compliance (Appendix PA-2014, Section 7). The self-sealing of the salt and the reducing anoxic environment in the repository provide the primary mechanisms for geologic isolation of the TRU waste in the undisturbed scenario. For the disturbed scenarios, actinide releases can occur as a result of inadvertent human intrusions (i.e., boreholes drilled into or through the repository). For example, direct brine release (DBR) to the accessible environment may occur during a drilling intrusion, or actinides may be transported up a borehole to the Culebra Dolomite Member of the Rustler Formation and then move laterally through the Culebra to the Land Withdrawal Boundary (LWB). The potential for human intrusions makes it important to assess the range of possible repository conditions and actinide concentrations associated with the disturbed scenarios.

This appendix focuses on the actinide source term used to calculate actinide release from the WIPP for DBR and transport through the Salado Formation and Culebra. This actinide source term is the sum of the soluble and colloidal species in brine. Direct release of actinide particulates to the surface resulting from cuttings, cavings, and spallings is not considered part of the actinide source term because these particulate releases do not depend on the mobilized actinide concentrations in brine.

The relative importance of radioelements (Camphouse et al. 2013) that significantly contribute to the actinide source term, and consequently impact the long-term performance of the WIPP, which is unchanged since the CRA-2009 Performance Assessment Baseline Calculation (PABC) (Clayton et al. 2010), is:

$$Pu \approx Am >> U > Th >> Np, Cm, \text{and fission products} \quad \text{(SOTERM.1)}$$

The TRU components for this list of radionuclides are the alpha (α)-emitting isotopes of plutonium (Pu), americium (Am), neptunium (Np), and curium (Cm) with half-lives greater than 20 years. These TRU actinides make up the waste unit factor used to calculate the normalized release from the WIPP in U.S. Environmental Protection Agency (EPA) units, as required by 40 CFR Part 191. In SOTERM, the chemistry of thorium (Th) and uranium (U) is also discussed, since these actinides are present in the WIPP waste and their chemistry is analogous to the TRU components.

This appendix has the following overall organization:

- An overview of key near-field conditions and biogeochemical processes is presented in Section SOTERM-2.0.
- An updated literature review and summary of WIPP-relevant results for the key actinides is given in Section SOTERM-3.0.

- A summary of the WIPP actinide PA approach and assumptions, along with the calculated actinide solution concentrations, is provided in Section SOTERM-4.0.

- The PA implementation of the dissolved and colloidal components of the source term is described in Section SOTERM-5.0.

Each of these sections identifies important changes and/or new information since the CRA-2009 (U.S. DOE 2009) and the CRA-2009 PABC (Clayton et al. 2010).

SOTERM-2.0 Expected WIPP Repository Conditions, Chemistry, and Processes

The pre-emplacement and post-emplacement near-field processes and conditions that could affect actinide concentrations in the WIPP are discussed in this section. An up-front summary of the current WIPP chemistry model assumptions and conditions is given in Table SOTERM-1. An up-front summary of the assumptions/role of the engineered barrier and key WIPP-relevant processes is given in Table SOTERM-2. The anticipated inventory of key waste, packaging and emplacement materials in the WIPP is summarized in Table SOTERM-3. All of these are discussed in more detail in the following sections. Emphasis in the detailed description is placed on how these processes and conditions in the repository could affect the concentrations of dissolved and colloi dal actinide species in brine.

Overall, there are relatively few changes in the WIPP repository conditions, chemistry, and processes since the CRA-2009 and the CRA-2009 PABC. New data that support the current WIPP position in some areas were obtained. A preview of these data is given below.

Changes in WIPP repository conditions, chemistry and processes since the CRA 2009 and CRA-2009 PABC:

1) New inventory data, based on the 2012 annual inventory (Van Soest 2012) exist on the amounts of lead, iron and the cellulosic, plastic and rubber (CPR) material in the WIPP. This is summarized in Table SOTERM-3.
2) The minimum brine volume for DBR, which is unchanged at 17,400 m^3, is the basis of a variable brine volume PA implementation (Section SOTERM-2.2.4; Appendix PA-2014, Section 1.1.9).
3) Brine chemistry and actinide solubilities are now being calculated using EQ3/6 rather than the Fracture Matrix Transport (FMT) program, although the database is essentially the same. This is discussed in Section SOTERM-2.3.1.
4) Modeling and experimental studies to further evaluate the transitional brine chemistry between Generic Weep Brine (GWB) and Energy Research and Development Administration Well-6 (ERDA-6) brines were completed and are described in Section SOTERM-2.3.1. These data support past and ongoing WIPP specific research, but do not impact the WIPP PA.
5) The potential concentration of organic chelating agents has been updated based on new inventory data (Van Soest 2012; Brush and Domski 2013b). These new concentrations are discussed in section SOTERM-2.3.6.
6) Gas generation rates due to corrosion were recalculated based on the new WIPP relevant corrosion rates (Roselle 2013; Section SOTERM-2.3.4; Appendix PA-2014, Section 1.1.4).
7) A Significant amount of new data was obtained on the WIPP microbial ecology (Section SOTERM-2.4.1). This new information is centered on indigenous microorganisms in salt from the WIPP and those present in briny groundwaters in the area of the WIPP. Some progress was also made on the aerobic biodegradation of organic chelating agents and the bioassociation of WIPP specific isolates. Although this has provided more insight to the nature of indigenous halophilic microorganisms, we do not have a complete understanding of this microbial ecology and these results have not led to a change in the WIPP microbial model.

Table SOTERM- 1. Summary of Current WIPP Chemistry Model Assumptions and Conditions

Repository Condition or Parameter	CRA-2014 PA Assumptions	SOTERM-2014 Section
Ambient Geochemistry	Predominantly halite of the Salado Formation, with anhydrite interbeds and inclusions.	2.1
Temperature	Ambient temperature is 28 °C (82 °F). An increase of up to 3 °C (5.4 ° F) is possible as a result of the emplacement of TRU waste.	2.2.2
Humidity	~70 percent (%) relative humidity (RH) at the repository temperature.	2.2.3
Water Content	Host rock is groundwater-saturated with inclusions in the salt that range from 0.057% to 3% by mass. Repository is initially unsaturated until a borehole intrusion occurs. Depending on pressure and intrusion scenarios, the first intrusion will occur between 100 and 1000 years (yrs).	2.2.3
Pressure	A maximum pressure in the repository of about 15 megapascals (MPa) (148 atmospheres [atm]), equivalent to the lithostatic stress at	2.2.1

Repository Condition or Parameter	CRA-2014 PA Assumptions	SOTERM-2014 Section
	the repository level; a hydrostatic pressure of about 8 MPa (79.0 atm) at the bottom of an intrusion borehole at repository depth.	
Gas Phase	Initially air/oxic at repository closure, but rapidly transitions to an anoxic atmosphere dominated by hydrogen with smaller amounts of methane and nitrogen. Trace amounts of carbon dioxide, hydrogen sulfide, and other microbial gases may be present.	2.2.3 2.4.1
Disturbed Rock Zone (DRZ)	Upper bound of 12 meters (m) above the repository and 2 m below the repository horizon.	2.2.5
Minimum Brine Volume for DBR	The calculated minimum volume of brine from any source needed for DBR release is 17,400 cubic meters (m^3). This volume is the basis of the variable brine volume approach now used in PA.	2.2.4
WIPP Brine	High-ionic-strength brine that varies with pH and reaction with MgO but is bracketed by GWB and ERDA-6 brine formulations used in the WIPP project.	2.3.1
pH	The expected pH is about 9 (ionic-strength-corrected measured pH (pC_{H+}) of 9.5) and controlled by MgO. The borate and carbonate present add to the brine buffer capacity.	2.3.2

Table SOTERM-2. Assumptions/Role of the Engineered Barrier, Emplaced Waste, and Key WIPP Subsurface Processes

Barrier or Process	CRA-2014 Assumptions and Role in PA	SOTERM-2014 Section
MgO	Engineered barrier for the WIPP that will sequester carbon dioxide (CO_2) and control increases and decreases in pH by the precipitation of brucite, hydromagnesite, and magnesite.	2.3.3
Corrosion	Container steel and metals in WIPP waste will react to remove oxygen and produce hydrogen.	2.3.4
Iron and Lead Chemistry	The chemistry of iron and lead, which are added to the repository, contributes to our overall understanding of the chemistry of actinides in brine, but this chemistry is selectively implemented in PA.	2.3.4 and 2.3.5
Organic Chelating Agents	The four organic chelating agents addressed by PA are acetate, oxalate, citrate and ethylenediaminetetraacetic acid (EDTA). These are assumed to not degrade under the expected WIPP conditions; their solubility is defined by their inventory (except for oxalate, which is solubility limited); these complex actinides and increase their solubility in the source term.	2.3.6
CPR	These materials are introduced to the WIPP as waste, packaging material and emplacement material. Their biodegradation leads to the formation of carbon dioxide that dissolves in brine to form bicarbonate/carbonate species that impact pH and complex actinides.	2.3.7
Microbial Effects	Gas generation, primarily carbon dioxide and hydrogen sulfide, resulting from the biodegradation of CPR materials and creation of reducing conditions, including bioreduction of actinide elements from higher oxidation states. Microbial processes are assumed to occur in all PA realizations.	2.4.1
Radiolysis	Localized oxidizing effects possible near high-activity actinides, but overall radiolytic processes are overwhelmed by the in-room chemistry.	2.4.2

Table SOTERM- 3. Total Projected Waste, Packaging and Cement Material in the WIPP Repository (Van Soest 2012)

Material	Source/Type	*Amount (kg)	Total (kg)
Iron-based metals/alloys	Waste	1.22×10^7	4.91×10^7
	Packaging	3.69×10^7	

Aluminum-based metals/alloys	Waste	4.57×10^5	4.57×10^5
Lead	Packaging	8.28×10^3	8.28×10^3
	Waste	3.66×10^6	
Cellulosics	Packaging	7.23×10^5	4.65×10^6
	Emplacement	2.6×10^5	
	Waste	5.50×10^6	
Plastics	Packaging	2.77×10^6	9.51×10^6
	Emplacement	1.25×10^6	
Rubber	Waste	1.18×10^6	1.25×10^6
	Packaging	7.33×10^4	
	Waste	1.03×10^7	
CPR Total	Packaging	3.57×10^6	1.54×10^7
	Emplacement	1.51×10^6	
Cement	Reacted	4.22×10^6	1.08×10^7
	Combination	6.55×10^6	
MgO	Emplacement	N/A	51,430 tons
Organic Ligands (all from waste)	Acetate	9.96×10^3	2.41×10^4
	Acetic Acid	1.41×10^4	
	Oxalate	6.50×10^2	1.85×10^4
	Oxalic Acid	1.78×10^4	
	Citrate	2.55×10^3	7.78×10^3
	Citric Acid	5.23×10^3	
	EDTA	3.76×10^2	3.76×10^2

*Includes remote-handled and contact-handled waste sources when applicable.

SOTERM-2.1 Ambient Geochemical Conditions

The ambient geochemical conditions are discussed in detail in the Compliance Certification Application (CCA) (U.S. DOE 1996) and the CRA-2004, Chapter 2 and Chapter 6, Section 6.4.3 (U.S. DOE 2004). The Salado, which is the host formation, is predominantly pure halite (NaCl), with interbeds (marker beds) consisting mainly of anhydrite ($CaSO_4$). The nearly pure halite contains accessory evaporite minerals such as anhydrite ($CaSO_4$), gypsum ($CaSO_4 \cdot 2H_2O$), polyhalite ($K_2MgCa_2(SO_4)_4 \cdot 2H_2O$), magnesite ($MgCO_3$), and clays. Small quantities of intergranular (grain-boundary) brines and intragranular brines (fluid inclusions) are associated with the salt at the repository horizon. These brines are highly concentrated solutions (ionic strength up to 8 moles per liter [M]) of predominantly sodium (Na^+), magnesium (Mg^{2+}), potassium (K^+), chloride (Cl^-), and sulfate (SO_4^{2-}), with smaller amounts of calcium (Ca^{2+}), carbonate (CO_3^{2-}), and borate ($B(OH)_4^-$ and/or $B_4O_7^{2-}$). These brines have been in contact with the Salado evaporite minerals since their deposition (estimated to be 250 million years) and are saturated with respect to these minerals.

Underlying the Salado is the Castile Formation, composed of alternating units of interlaminated carbonate, anhydrite, and nearly pure halite. The Castile in the vicinity of the WIPP site is known to contain localized brine reservoirs with sufficient pressure to force brine to the surface if penetrated by a borehole. Castile brines are predominantly saturated NaCl solutions containing Ca^{2+} and SO_4^{2-}, as well as small concentrations of other elements, and are about eight times more concentrated than seawater. Overlying the Salado in the vicinity of the WIPP site is the Culebra Dolomite Member of the Rustler Formation, a fractured dolomite ($CaMg(CO_3)_2$) layer. It is significant because it is expected to be the most transmissive geologic pathway to the accessible environment. Culebra brines are generally more dilute than the Salado and Castile brines, and are predominantly NaCl with K^+, Mg^{2+}, Ca^{2+}, SO_4^{2-}, and CO_3^{2-}. More detailed information on the distribution of Culebra brine salinity in the WIPP site and vicinity can be found in Appendix HYDRO-2014.

SOTERM-2.2 Repository Conditions

Repository conditions that could potentially affect actinide solubility are briefly summarized in this section. These include repository pressure, repository temperature, water content and relative humidity, the minimum free volume for actinide release (effective porosity), and the extent of the DRZ.

SOTERM-2.2.1 Repository Pressure

The preexcavation lithostatic pressure (Stein 2005; Appendix PA-2014, Section 4.2.4) in the WIPP at repository depth is about 15 MPa (148 atm). This pressure can be reestablished after repository closure due to salt creep and gas generation, but there are a number of PA vectors that predict pressure may not be fully restored even by the end of the 10,000-yr period of WIPP performance, and final pressures may range from 6 to 15 MPa (in the undisturbed scenario) and from 0.1 to 15 MPa (in the disturbed scenarios) considered in the CRA-2014 PA. In this context, the pressure in the repository after closure cannot significantly exceed the far-field confining stress of about 15 MPa.

DBR can occur when the pressure in the repository at the time of a drilling intrusion exceeds 8 MPa and a sufficient amount of brine has already flowed into the repository (see related discussions in Section SOTERM-2.2.4, Stein (Stein 2005) and Clayton (Clayton 2008)). Eight MPa is the pressure exerted by a column of brine-saturated drilling fluid at the depth of the repository (Stoelzel and O'Brien 1996). For repository pressures less than 8 MPa, no DBRs are assumed to occur because the fluid pressure in the repository cannot eject the drilling fluid from the borehole. There is also no DBR until the brine volume exceeds the minimum brine volume (see Section SOTERM-2.2.4) needed to fill the effective porosity present in the compacted TRU waste.

The range of pressures expected in the WIPP will not likely have an impact on actinide solubility. The maximum pressure possible (~15 MPa) is well below pressures needed to affect the solution chemistry, and is not expected to have a significant effect on actinide solubilities or processes that lead to the association of actinides with colloidal particles. For these reasons, the effect of pressure on actinide solubility is not considered in the WIPP PA.

SOTERM-2.2.2 Repository Temperature

The ambient pre-emplacement temperature at the WIPP repository horizon is 27 degrees centigrade (ºC) (80 degrees Farenheit (ºF)) (Bennett et al. 1996). The emplacement of TRU waste in the WIPP introduces possible exothermic reactions: MgO hydration, MgO carbonation, microbial degradation, aluminum corrosion and cement hydration. The potential contributions of each of these processes were re-evaluated for the CRA-2014 (see Appendix SCR-2014, Section 6.3.4.1.3) and leads to a maximum possible temperature increase of up to 39 ºC (12 ºC increase). These elevated temperatures are expected to persist for a short period of time, perhaps a few years or decades. This is also discussed in Sanchez and Trellue (Sanchez and Trellue 1996) and Wang and Brush (Wang and Brush 1996). For the purposes of PA, the temperature of the WIPP underground repository is assumed to be constant with time at 300 Kelvin (K) (27 ºC [80 ºF]) (Appendix PA-2014, Section 4.2.2).

Actinide solubilities were calculated in the WIPP PA using thermodynamic and laboratory data measured at 25 ºC [77 ºF]. The expected effect of the slightly elevated temperature in the WIPP on actinide concentrations is relatively small, especially when compared to other uncertainties inherent in the measurement and calculation of the actinide solubilities and colloidal concentrations. For this reason, the very small effect of temperature on actinide solubility was not considered in the WIPP PA calculations.

SOTERM-2.2.3 Water Content and Relative Humidity

A key argument for the WIPP as a TRU waste repository is that the self-sealing of the salt will limit the availability and transport of water into and through the repository, and correspondingly minimize the potential release of TRU nuclides from the repository. In all the undisturbed repository scenarios considered by PA, no significant release of actinides from the WIPP is predicted (Appendix PA-2014, Section 7). There is, however, groundwater in the WIPP, even in undisturbed scenarios, that is potentially available to interact with the TRU waste. The salt surrounding the waste is groundwater-saturated with both intergranular and intragranular water. The amount of water present as inclusions in the salt is effectively used as an uncertain parameter in PA calculations with a range of 0.057 to 3 weight % based on what was measured in preexcavation salt (Skokan et al. 1987; Powers et al. 1978). In PA (Appendix PA-2014, Section 4.2.4) this is done indirectly by sampling a range in the halite porosity for the intact and DRZ salt (0.001 to 0.0519 and 0.0038 to 0.0548 respectively - see Ismail 2007). Available brine can seep into the repository horizon and fill the pore volume of the transuranic (TRU) waste in the excavated areas. The presence of some brine in the WIPP prior to brine saturation leads to an environment that will contain an atmosphere of up to about 70% RH, defined by the vapor pressure of saturated brine at the repository temperature. This water vapor pressure will be present, at least in part, until brine saturation occurs as a result of some human intrusions or brine seepage into the excavated area.

The presence of a humid environment in the WIPP prior to brine saturation may have a transitory effect on actinide solubilities. These transitory/temporary phases are not considered in the WIPP PA because they will be rapidly overwhelmed by the in-room chemistry and higher reactivity of the waste components should brine inundation or saturation occur.

SOTERM-2.2.4 Minimum Repository Brine Volume and Variable Brine Volume Implementation

The minimum brine volume is the lowest amount of brine needed for a DBR to occur during an intrusion scenario. Two criteria must be met:

1) Volume-averaged pressure in the vicinity of the repository encounter by drilling must exceed the drilling fluid hydrostatic pressure
2) Brine saturation in the repository must exceed the residual saturation of the waste material

The minimum brine volume is given by the following:

Minimum brine volume = (median sampled residual brine saturation)

x (consolidated void volume)

x (equivalent repository rooms) (SOTERM.2)

This was most recently recalculated by Clayton (Clayton 2008) to be 17,400 m^3. This 17,400 m^3 value corresponds to a consolidated void volume of 523.1 m^3, 120.3 equivalent rooms in the repository, and a median value for the sampled residual brine saturation of 0.276. These parameters were calculated based on the method recommended by Stein (Stein 2005), except that the drilling fluid hydrostatic pressure (8 MPa) was used rather than the lowest pressure realization at 10,000 years. This change makes the minimum volume calculation more consistent with the DBR conceptual model.

The minimum repository brine volume has two important potential impacts on calculating actinide concentrations in the WIPP. The first is that the predicted inventory of some actinides, when fully dissolved in this brine volume, lead to concentrations that are below their predicted solubility, most importantly Np and Cm. In this context, they are assumed to be fully dissolved in the brine and since their inventory-limited concentration is small, the impact on the calculated actinide release is insignificant. The second impact is on the predicted concentration of key organic and inorganic complexants that coexist with the TRU species in WIPP waste. The maximum concentrations of acetate, citrate, and EDTA (see Section SOTERM-2.3.6) are defined by their fully dissolved concentration in this minimum brine volume.

SOTERM-2.2.5 DRZ

The DRZ is a zone immediately surrounding the excavated repository that has been altered by the construction of the repository. A more detailed discussion of the DRZ can be found in Appendix PA-2014, Section 4.2.4. In the Brine and Gas Flow (BRAGFLO) code, the Upper DRZ has a height of about 12 m (39 feet [ft]) and the Lower DRZ has a depth of about 2.2 m (7.2 ft). The creation of this DRZ disturbs the anhydrite layers and marker beds and alters the permeability and effective porosity of the rock around the excavated areas, providing enhanced pathways for the flow of gas and brine between the waste-filled rooms and the nearby interbeds.

The DRZ is important to the calculation of dissolved actinide concentrations because it potentially makes the minerals in the interbeds "available" for reaction with the TRU and emplaced waste components. The most important of these minerals is the calcium sulfate (anhydrite) that could function as a source of sulfate for processes in the repository subsequent to brine inundation. Currently, sulfate is assumed to be available from the DRZ into the waste area, which prolongs microbial sulfate reduction processes in the WIPP.

SOTERM-2.3 Repository Chemistry

Brine present in the WIPP will react with emplaced TRU waste, waste components, and the engineered barrier material to establish the brine chemistry that will define actinide solubilities and colloid formation. At the repository horizon, the brine composition will be defined by a combination of factors that include the initial composition of the in-flow brine; reactions that control pH; and the extent to which this brine is altered by equilibration with the waste components, emplaced container materials, and the waste-derived organic chelating agents that can dissolve in the brine. An overview of this repository chemistry is given in this section.

SOTERM-2.3.1 WIPP Brine

Salado brine will enter the repository after closure, and can be supplemented by Castile brine in some human intrusion scenarios. It is also possible that groundwater from the Rustler and Dewey Lake Formation could flow down the borehole into the repository, mix with the waste, and then be forced back up a borehole. The majority of WIPP-specific solubility studies since the CRA-2004 were performed using brines that bracket the expected range in brine composition. Including brine mixing in PA has been considered and rejected because using the end member brines (i.e., GWB or ERDA-6 brines) brackets the median values and uncertainties for the solubility calculations.

In addition to using these end-member brines in PA, other simplifying assumptions are also made:

1. Any brine present in the repository is well mixed with waste.
2. Equilibria with halite and anhydrite, the most abundant Salado minerals at or near the stratigraphic horizon of the repository, are rapidly established.
3. Oxidation-reduction (redox) equilibria with waste materials are not assumed.
4. Brine compositions attained after equilibration of GWB or ERDA-6 with the MgO engineered barrier exist for the entire 10,000-year regulatory period.

The composition of brine in and around the WIPP site prior to waste emplacement was established by sampling the groundwater and intergranular inclusions in the Salado and Castile (Popielak et al. 1983; Snider 2003a). A number of synthetic brines that simulate these compositions were developed and have been used for WIPP laboratory studies (Lucchini et al. 2013c, Table 1). Currently, the two simulated brines that best represent these repository-relevant, end-member brines are: (1) GWB, which simulates intergranular (grain-boundary) brines from the Salado at or near the stratigraphic horizon of the repository (Snider 2003a); and (2) ERDA-6, which simulates brine from the ERDA-6 well, typical of fluids in Castile brine reservoirs (Popielak et al. 1983).

The reaction of GWB and ERDA-6 brines with MgO (brucite), halite, anyhydrite, and hydromagnesite leads to some potentially significant changes in the composition of the brine (Table SOTERM-4). These brines were reacted using EQ3/6 version 8.0a and database DATAA0.FMT.R2 (Brush and Domski 2013a). The most important of these changes for GWB brine is the lowering of the magnesium concentration from 1.02 to 0.330 M, a decrease in calcium concentration from 14 to 11.1 mM, and a pH of 8.82. For ERDA-6, there is a significant increase in the magnesium concentration from 19 to 136 millimoles per liter (mM), a decrease in total inorganic carbon from 16 to 0.455 mM, and an increase of the pH to 8.99 from 6.17. The pH associated with these MgO-reacted brines established the range of expected pH values in the WIPP for the calculation of actinide solubilities, and the composition of these reacted brines were used in PA to calculate actinide solubility in brine (Brush and Domski 2013a).

There are new data that validate the bracketing approach being used in the WIPP PA since the CRA-2009 submittal. Modeling (Brush et al. 2011) and experimental (Lucchini et al. 2013c) studies were conducted to investigate the pH dependency and the long-term stability of WIPP-specific brines. This was done to assess the validity of using the GWB and ERDA-6 formulations as bracketing brines in the solubility studies and establishes a broad-pH range comparison between modeling and experimental results.

The long-term stability of the unused GWB and ERDA-6 simulated brines (95% composition), used in actinide solubility studies showed no pattern of instability or precipitation. These results confirmed that the 95% formulations of the GWB and ERDA-6 brine were stable for up to six years and that the methods used for storage were appropriate and adequate during this time. The concentration of the brine components in the long-term uranium, neodymium and plutonium solubility and redox studies were also measured to determine their stability under the broader range of pH and experimental conditions used (pC_{H+} of 6-12, presence of actinides/analogs, presence of carbonate, presence of iron). Under this broader set of interactions, the only changes noted were the precipitation of borate and magnesium salts in the higher-pH ERDA-6 experiments ($pC_{H+} > 10$).

The effect of pC_{H+} on WIPP simulated brines was also investigated and modeled. GWB (100% formulation) was stepwise titrated up to $pC_{H+} \sim 13$, and the brine component concentrations were determined after 3-week equilibrations. These experimental results were compared with the predicted composition of the brine using the current WIPP brine model (Figures SOTERM-1 and SOTERM-2). Overall, there was good agreement between the experimental and the modeling results at $pC_{H+} \leq 10.5$ (which includes the pC_{H+} predicted for the expected conditions in the WIPP). The one exception to this is the decrease in tetraborate concentrations to $\sim 2 \times 10^{-3}$M between pC_{H+} of 10 and 10.5 (Figure SOTERM-1) since there are currently no Pitzer parameters for tetraborate in the WIPP model.

At $pC_{H+} \geq 10.5$, there were a number of explainable discrepancies noted between the experimental and modeling results for Mg^{2+}, Ca^{2+} and tetraborate (Figures SOTERM-1 and SOTERM-2). Specifically, calcium precipitation was only observed experimentally at $pC_{H+} > 10.5$; magnesium remains in solution above pC_{H+} 10.5 in the experiments performed and does not precipitate to the extent predicted by the model; and the tetraborate concentration goes through a minimum at pC_{H+} 9.75 that is also not captured in the modeling results. These results are explained by precipitation of calcium carbonate, as it was observed in the experiments of Kerber Schütz et al. (Kerber Schütz et al. 2011), and the resolubilization of magnesium due to a change in the speciation of tetraborate at high pC_{H+} (Schweitzer and Pesterfield 2010).

Overall, the modeling and experimental brine chemistry studies established a better understanding of the actinide-relevant brine chemistry over a wider range of experimental conditions than previously studied. GWB and ERDA-6 were confirmed as good "bracketing" brines for WIPP-relevant studies, as GWB brine transitions into ERDA-6 at $pC_{H+} \sim 10.5$. Relatively good agreement was found between the long-term experiments (using 95% formulation brines) and the titration experiments (using the 100% formulation GWB). All of these results effectively increase the robustness of the current WIPP model and provide a better foundation for future and ongoing WIPP-relevant actinide solubility studies.

Table SOTERM- 4. Composition of GWB and ERDA-6 Brine Before and After Reaction with Anhydrite, Brucite and Hydromagnesite. The reacted brine compositions were used to calculate actinide solubilities for the CRA-2014 PA.

Ion or property[a]	GWB Brine Composition[b]	GWB after reaction with MgO (phase 5), halite, and anhydrite[c]	ERDA-6 Brine Composition[d]	ERDA-6 after reaction with MgO (phase 5), halite, and anhydrite[c]
$B(OH)_x^{3-x}$ (see footnote e)	158 mM	186 mM	63 mM	62.3 mM
Na^+	3.53 M	4.77 M	4.87 M	5.30 M
Mg^{2+}	1.02 M	0.330 M	19 mM	136 mM
K^+	0.467 M	0.550 M	97 mM	96.0 mM
Ca^{2+}	14 mM	11.1 mM	12 mM	11.6 mM
SO_4^{2-}	177 mM	216 mM	170 mM	182 mM
Cl^-	5.86 M	5.36 M	4.8 M	5.24 M
Br^-	26.6 mM	31.3 mM	11 mM	10.9 mM
Total Inorganic C (as HCO_3^-)	Not reported	0.379 mM	16 mM	0.455 mM
pH	Not reported	8.82	6.17	8.99
Ionic Strength (M)	7.44	6.44	5.32	5.99

a - ions listed represent the total of all species with this ion.
b - From Snider 2003a
c - From Brush, Domski and Xiong 2011
d - From Popielak et al. 1983
e - Boron species will be present in brine as boric acid, hydroxyl polynuclear forms ($B_3O_3(OH)_4^-$, and/or borate forms (e.g., $B_4O_7^-$)

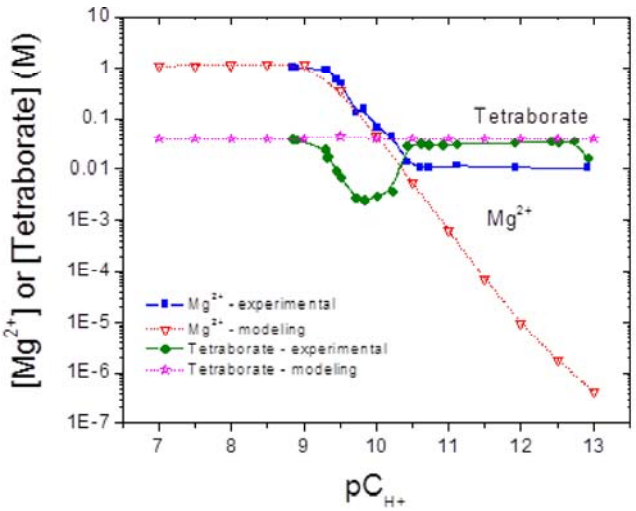

Figure SOTERM- 1. Comparison of Experimentally-measured (Lucchini et al. 2013c) and Model-predicted (Brush et al. 2011) Concentrations of Tetraborate and Mg^{2+} in GWB 100% Saturated Brine as a Function of pC_{H+}.

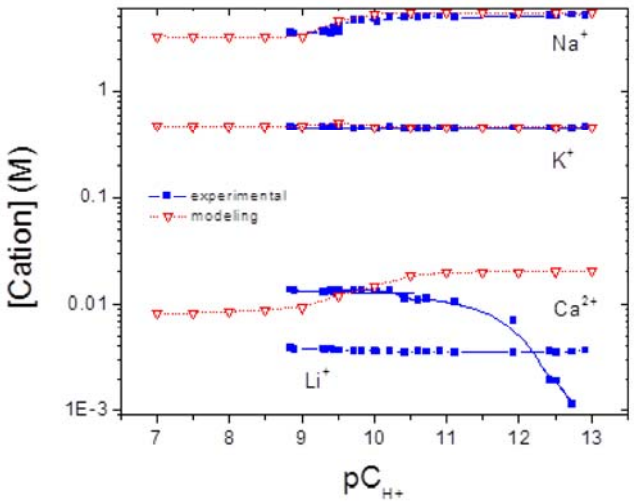

Figure SOTERM- 2. Comparison of Experimentally-measured (Lucchini et al. 2013c) and Model-predicted (Brush et al. 2011) Concentrations of Na^+, K^+, Ca^{2+} and Li^+ in GWB 100% Saturated Brine as a Function of pC_{H+}. Li^+ was not considered in the numerical simulation.

SOTERM-2.3.2 Brine pH and pH Buffering

The brine pH is a very critical parameter in defining the solubility of actinides under conditions where brine-mediated releases (DBR and transport through the Culebra) would be important in the WIPP. There are a number of highly-coupled processes that can influence the pH when the emplaced TRU waste is inundated with brine. The most important of these are the potential buffering capacity of the brine coming into the WIPP, the reactions of this brine with emplaced waste components (most notably reduced metals and organics), and microbial processes. The reactions of the emplaced MgO barrier material are expected to sufficiently control and define the pH when the repository is saturated with brine. Although there have been modeling and experimental studies to investigate the pH of WIPP-specific brines, there is no significant change in the key arguments for brine pH and pH buffering since the CRA-2009.

The range of brine composition that is likely to be present in the WIPP repository was discussed in Section SOTERM-2.3.1 (see also Table SOTERM-4). These brines have an intrinsic buffering capacity that is highest at pH 8.5-9. ERDA-6 brine, although it has an ambient pH of 6.2, contains a number of constituents that, in the pH range of 8-10, add buffer capacity to the reacted brine: carbonate/bicarbonate (16 mM), borate (63 mM), and divalent cations that tend to react with hydroxide or carbonate to influence pH (Ca^{2+} at 12 mM, and Mg^{2+} at 19 mM). The pK_a for boric acid and dissolved carbonate/bicarbonate species are 9.0 and 9.67, respectively, which explains the tendency of this brine to maintain the pH in the range of 8-10. Operationally, the simulated ERDA-6 brines prepared in the laboratory have relatively high buffering capacity, and significant changes in brine concentrations and pH are not routinely observed once the pH is experimentally defined (Lucchini et al. 2013c). An operational pH range for ERDA-6 has been defined as having an upper limit of pH ~10, which is the pH at which a cloud point (indicating magnesium (Mg) precipitation) is observed. The pre-excavation ambient ERDA-6-like brine will naturally add to the buffering capacity of the WIPP brine due to its acid-base components and will establish a relatively high buffer capacity at the mildly alkaline conditions expected in the WIPP.

The expected pH in the WIPP in the event of brine saturation, however, will be defined by the reaction of the Castile ERDA-6-like brine with the waste components and barrier material. This was re-evaluated as part of the documentation for the CRA-2014 PA (Brush et al. 2011; Table SOTERM-4; Brush and Domski 2013a; Lucchini et al. 2013c). The hydration and carbonation reactions of MgO are discussed extensively in Appendix MgO-2009. In PA, the following two reactions combine to define f_{CO2} and the pH:

$$5Mg(OH)_2 + 4CO_2(aq \text{ or } g) \leftrightarrows Mg_5(CO_3)_4(OH)_2 \cdot 4H_2O \text{ (SOTERM.3)}$$

$$Mg(OH)_2 \leftrightarrows Mg^{2+} + 2OH^- \text{ (SOTERM.4)}$$

Calcite formation (see reaction SOTERM.5) may also occur (see Figure SOTERM-2). This reaction is not considered in PA and remains a conservatism in the current PA model.

$$Mg(OH)_2 + Ca^{2+} + CO_2(aq \text{ or } g) \leftrightarrows CaCO_3 + Mg^{2+} + H_2O(aq \text{ or } g) \text{ (SOTERM.5)}$$

In PA, all vectors assume microbial activity consume organic material to produce CO_2 (see more detailed discussion in Section SOTERM-2.4.1.1). Carbon dioxide production, if not for its sequestration by MgO, would over time acidify any brine present in the repository and increase the solubility of the actinides relative to that predicted for near-neutral and mildly basic conditions. Current

repository assumptions lead to a calculated f_{CO2} of 3.14 x 10^{-6} atm ($10^{-5.50}$ atm) in both GWB and ERDA-6 and a predicted pH of 8.82 and 8.99 respectively. These f_{CO2} and pH values were used in the actinide speciation and solubility calculations for all CRA-2014 PA vectors.

There are no new WIPP-specific results to report that explicitly address the MgO buffering of the WIPP brine since the CRA-2009. The brine titration experiments and calculations that were performed were described in section 2.3.1. These data are consistent with experimental results published previously by the German program (Altmaier et al. 2003) that were discussed more extensively in Appendix SOTERM-2009, section 2.3.2. All of these data suggest that MgO controls the pH to a pH = 9 ± 1. In this context, it is predicted that brine pH will remain between 8 and 10 under the range of expected conditions in the WIPP.

SOTERM-2.3.3 Selected MgO Chemistry and Reactions

MgO is the bulk, granular material emplaced in the WIPP as an engineered barrier. The MgO currently being placed in the WIPP contains 96 ± 2 mol % reactive constituents (i.e., periclase and lime) (Deng et al. 2006; Reyes 2008). The amount of MgO emplaced in the WIPP is currently calculated based on the estimated CPR content with an excess factor of 1.2, and it is estimated that in excess of 50,000 metric tons will be emplaced in the WIPP by the time of repository closure.

The chemistry of MgO is critical to the overall performance of the WIPP and is discussed in detail in Appendix MgO-2009. The most recent data are described in Xiong and Lord (Xiong and Lord 2008). The MgO, as the engineered barrier in the WIPP repository design, has two important functions that directly support the PA calculation of actinide concentrations in brine:

1. Sequester the excess CO_2 produced by the microbial consumption of CPR material and establish/maintain a low f_{CO2} in the repository (see reaction SOTERM.3). This is currently estimated to be $10^{-5.5}$ atm for GWB and ERDA-6 brine.

2. Establish and buffer the brine pH by maintaining a magnesium solution concentration that reacts with hydroxide (see reaction SOTERM.4) to buffer the pH at about 9. This was part of the pH discussion in Section SOTERM-2.3.2. This buffering removes uncertainty from the actinide concentration calculations.

Initially, MgO will undergo hydration to generate brucite ($Mg(OH)_2$). In time, brucite will react further to form magnesium chloride hydroxide hydrate (e.g., $Mg_3(OH)_5Cl{\cdot}4H_2O$) in Salado brine (Appendix MgO-2014, section MgO-4.1). These phases combine to control the concentration of magnesium in high-magnesium brine (for example, GWB). The existence of magnesium as an aqueous (aq) cation in equilibrium with excess magnesium minerals helps to establish the solution pH.

For the reaction of MgO with GWB brine, PA uses a magnesium concentration of ~0.33 M (Table SOTERM-4), which is supported by experimental results showing a magnesium concentration ~0.3 M (Lucchini et al. 2013c). This reaction was also investigated by Altmaier et al. (Altmaier et al. 2003) and Harvie, Møller, and Weare (Harvie, Møller, and Weare 1984). Snider also noted that the rate of MgO hydration is most likely linked to mineral phase changes between hydrated magnesium oxychloride and brucite (Snider 2003b). The existence of the hydrated magnesium oxychloride phase was inferred from scanning electron microscope (SEM) images, coupled with an energy dispersive x-ray spectroscopy system (EDS), to identify Mg-Cl phases. The Altmaier and Harvie studies showed that the hydration reaction was a solid-phase transformation between brucite and hydrated magnesium oxychloride that depends not on magnesium concentration, but on chloride concentration, with an invariant point predicted at 1.8 m MgCl concentration and a -log m_{H+} = 8.95.

The most important role of the MgO engineered barrier is to sequester carbon dioxide to maintain a low f_{CO2} in the repository. Microbial consumption of CPR materials could produce significant quantities of CO_2. Under these conditions, brucite and magnesium chloride hydroxide hydrate will react with the CO_2 generated. Both laboratory and modeling studies predict that the following carbonation reaction will buffer $f_{CO\ 2}$ at a value of $10^{-5.50}$ atm in both GWB and ERDA-6:

$$5Mg(OH)_2 + 4CO_2(aq \text{ or } g) \leftrightarrows Mg_5(CO_3)_4(OH)_2 \cdot 4H_2O \text{ (SOTERM.6)}$$

This reaction effectively removes excess CO_2 from the repository and bicarbonate/carbonate from the brine. The initial product of MgO carbonation reaction is $Mg_5(CO_3)_4(OH)_2{\cdot}4H_2O$. This is converted into $MgCO_3$, which is the expected stable mineral form of magnesium carbonate in the WIPP, according to Reaction SOTERM.7:

$$Mg_5(CO_3)_4(OH)_2 \cdot 4H_2O + CO_2(aq \text{ or } g) + 10\ H_2O \leftrightarrows 5\ MgCO_3{\cdot}3H_2O \text{ (SOTERM.7)}$$

Reaction SOTERM.6 is slow and it is estimated that hundreds to thousands of years (Appendix MgO-2009; Clayton 2013) are needed for the conversion of hydromagnesite to magnesite. Consumption of CO_2 will prevent the brine acidification, and magnesium carbonate precipitation will maintain low carbonate concentration in the WIPP brine to avoid the formation of highly soluble actinide species with carbonate complexes. Although MgO will consume essentially all CO_2, residual quantities in equilibrium with magnesite under the WIPP conditions will persist in the aqueous and gaseous phases.

The importance of magnesium chemistry, and correspondingly the chemistry associated with the emplaced MgO on the calculation of actinide concentrations in brine is clear. MgO sequesters CO_2 and minimizes the buildup of carbonate in brine. At the expected

pH, carbonate forms strong complexes with the An(III), An(IV), and An(VI) oxidation states. An increased carbonate concentration in brine would significantly increase actinide solubilities. Additionally, MgO helps establish the pH in brine. The removal of CO_2 prevents a decrease in the pH that could also significantly increase actinide solubility. An additional beneficial effect of MgO is to maintain a solution concentration of Mg^{2+} that will precipitate as brucite to keep the pH in the 8-10 range. The presence of MgO leads to a more predictable chemistry that lowers the uncertainty when calculating actinide concentrations in the WIPP brine.

SOTERM-2.3.4 Iron Chemistry and Corrosion

The WIPP repository will contain a large quantity of reduced iron due to the use of iron-based containers for much of the emplaced TRU waste. Currently, it is estimated that the WIPP will contain over 49,000 metric tons of iron (Van Soest 2012) when all the waste is emplaced. The presence of this reduced metal will have an important role in the establishment of reducing conditions in the WIPP by removing oxygen. Reduced iron species (aqueous Fe(II) and Fe(0, II)-valent minerals) are important because they will reduce higher-valent actinides in the WIPP, leading to lower actinide solubilities (Section SOTERM-3.6; Reed et al. 2009; Reed et al. 2006). The role of iron in the WIPP PA is unchanged since the CRA-2009, although new data on WIPP-specific corrosion rates were obtained that are now the basis of gas generation rates due to corrosion (Appendix PA-2014, Section1.1.4).

The chemistry of iron will have a pronounced effect on WIPP-relevant actinide chemistry in many ways. The linkages of iron chemistry to the redox chemistry are well established in the literature (Farrell et al. 1999; Fredrickson et al. 2000; Qui et al. 2001; Nakata et al. 2004; Behrends and Van Cappellen 2005). Iron will establish reducing conditions conducive to the overall reduction of higher-valent actinide species and precipitate an iron sulfide phase that removes sulfide from solution. Additionally, iron species could sequester carbon dioxide and compete with actinides for organic and inorganic complexants, although there is no explicit credit taken for this in the WIPP PA.

It is expected that oxic corrosion of steels and aerobic microbial consumption of CPR materials will quickly consume the limited amount of oxygen (O_2) trapped within the repository at the time of closure. After O_2 is consumed, anoxic corrosion of metals will occur (Brush 1990; Brush 1995; Wang and Brush 1996; Roselle 2013). In all of the vectors for the 2009 PA, the CRA-2009 PABC, the 2004 PA, the CRA-2004 PABC, the CCA PA, and the EPA's CCA 1997 Performance Assessment Verification Test (PAVT), there were significant amounts of uncorroded steels and other Fe-base alloys in the repository throughout the 10,000-yr regulatory period. The WIPP-specific experiments (Telander and Westerman 1993; Telander and Westerman 1997) showed that steels and other Fe-based alloys will corrode by the following reactions:

$$Fe + (x)H_2O \leftrightarrows Fe(OH)_2 \cdot (x\text{-}2)H_2O + H_2 \text{; (SOTERM.8)}$$

$$3Fe + 4H_2O \leftrightarrows Fe_3O_4 + 4H_2 \text{; (SOTERM.9)}$$

$$Fe + H_2O + CO_2 \leftrightarrows FeCO_3 + H_2 \text{; and (SOTERM.10)}$$

$$Fe + H_2S \leftrightarrows FeS + H_2 . \text{ (SOTERM.11)}$$

Since the experiments of Telander and Westerman (Telander and Westerman 1993; Telander and Westerman 1997), a new series of steel and lead corrosion experiments has been conducted (Roselle 2009, Roselle 2010, Roselle 2011a, Roselle 2011b, and Roselle 2013). The object of these experiments has been to determine steel and lead corrosion rates under WIPP-relevant conditions. Telander and Westerman (Telander and Westerman 1993; Telander and Westerman 1997) measured H_2 generation rates directly and from those measurements were then able to calculate metal corrosion rates. However, the new experiments directly measured metal corrosion rates based on mass loss (Roselle 2013). These new experiments showed that it is possible for other corrosion products (e.g., green rust, hibbingite, etc.) to form (Roselle 2009, Roselle 2010, Roselle 2011a, Roselle 2011b, and Roselle 2013; Nemer et al. 2011). In fact, Roselle (Roselle 2013) states that green rust is the most likely corrosion product in experiments with low atmospheric CO_2 concentrations (<350 ppm). At higher concentrations of CO_2 (>1500 ppm) iron carbonate was seen as the major corrosion product (forming via SOTERM.10). Assuming an idealized formula for green rust as $[Fe(III)_2Fe(II)_4(OH)_{12}CO_3 \cdot 2H_2O]$, then the corrosion reaction would be written as:

$$6\ Fe + CO_2 + 15\ H_2O \leftrightarrows Fe(III)_2Fe(II)_4(OH)_{12}CO_3 \cdot 2H_2O + 7\ H_2 \text{ (SOTERM.12)}$$

Roselle (Roselle 2013) determined corrosion rates for steel inundated in brine in the absence of CO_2. Based on these rates, a new distribution was presented whose mean value is nearly an order of magnitude less than the previous value determined by Wang and Brush (Wang and Brush 1996). Based on these new corrosion rates, there will still be significant amounts of uncorroded steels and other Fe-base alloys in the repository throughout the 10,000-yr regulatory period.

In reducing environments, reduced iron phases (Fe(II) oxides and zero valent iron) and aqueous ferrous iron will be present. These are all reducing agents towards key actinide species (Table SOTERM-5) and will help establish the predominance of lower-valent actinides in the WIPP. The concentration of ferrous iron could be relatively high in the WIPP brine, although its solubility has not yet been explicitly determined. There are also many potential reactions that could control and/or define the iron chemistry. The expectation is that ferrous hydroxide will control the solubility of iron, leading to a predicted solubility in the range of 10^{-6} M to

10^{-4} M for pH between 8.5 and 10.5 (Refait and Génin 1994). A similar range of iron solubility in brines was observed by Nemer et al. (Nemer et al. 2011) in experiments where Fe-hibbingite, $Fe_2(OH)_3Cl$, was the solubility controlling phase.

Table SOTERM- 5. Redox Half-Reaction Potentials for Key Fe, Pb, Pu, and U Reactions at 25 oC and I<1 (Morss, Edelstein, and Fuger 2006, Chapter 23)

Metal Species Reduced	E_o (Acidic) (V)	E_o at pH = 8 (V)
$Pb^{4+} \rightarrow Pb^{2+}$	1.69	2.47
$PuO_2^{+} \rightarrow Pu^{4+}$	1.170	0.70
$PuO_2^{2+} \rightarrow PuO_2^{+}$	0.916	0.60
$Fe(OH)_3(s) \rightarrow Fe^{2+}$	Not Applicable	0.1
$FeOOH(s) \rightarrow FeCO_3(s)$	Not Applicable	-0.05
$UO_2^{2+} \rightarrow U^{4+}$	0.338	-0.07
$Pu^{4+} \rightarrow Pu^{3+}$	0.982	-0.39
$Pb^{2+} \rightarrow Pb$	-0.1251	-0.54
$Fe^{3+} \rightarrow Fe^{2+}$	0.77	-0.86
$Fe(II)(OH)_2 \rightarrow Fe(0)$	-0.44	-0.89
$U^{4+} \rightarrow U^{3+}$	-0.607	-1.95

Three important reactions of iron are considered. The first is the reaction of metallic iron with carbon dioxide to form strongly insoluble ferrous carbonate. The solubility product of this salt is log K = -10.8 at I = 0 (NIST 2004), and it is much smaller than magnesium carbonate. This suggests that the presence of iron will likely remove CO_2 from the repository more effectively than MgO due to its lower solubility product. This reaction is not included in the WIPP PA because the CO_2 reacts sufficiently with MgO (so the Fe reaction is not needed) and the DOE does not have sufficient data on the iron carbonation reaction.

The second is the reaction of iron and ferrous ions with the hydrogen sulfide that could be generated in the repository by sulfate-reducing microbes. This will lead to a very insoluble ferrous sulfide precipitate with a solubility product of log K_s = -17.2 (NIST 2004). This helps remove sulfide, which can complex actinides, from brine. This reaction is assumed to occur instantaneously in the PA.

Finally, iron species form strong complexes with organic ligands. The strongest of these complexes is with EDTA. The net effect is that dissolved iron species will compete with actinides for organic ligands, and in many cases out-compete the actinides to counteract the potential enhancement of actinide solubility that would otherwise occur. This reaction is not currently included in the PA because the DOE does not have sufficient data on the reactions that form iron EDTA complexes. Work is currently underway to obtain the necessary thermodynamic parameters for future input into the model.

SOTERM-2.3.5 Chemistry of Lead in the WIPP

Lead is present in the repository in the metallic form as part of the waste and waste packaging. The currently anticipated inventory in waste packaging is approximately 8.3 metric tons (Van Soest 2012). The reactivity of zero-valent lead is greatly mitigated by the formation of a thin, coherent, protective oxide, oxycarbonate, chloride, or sulfate protective layer. Metallic lead also reacts slowly with water at room temperature and undergoes corrosion to form oxides and oxyhydroxides. Under slightly alkaline conditions, the hydrolysis of lead leads to formation of a poly-oxyhydroxide cation, $[Pb_6O(OH)_6]^{4+}$. The following reactions are possible under WIPP-relevant conditions:

$$2Pb + O_2 \leftrightarrows 2PbO \quad \text{(SOTERM.13)}$$

$$2PbO + H_2O + CO_2 \leftrightarrows (PbOH)_2CO_3 \quad \text{(SOTERM.14)}$$

$$Pb + H_2O + CO_2 \leftrightarrows PbCO_3 + H_2 \quad \text{(SOTERM.15)}$$

$$Pb + H_2S \leftrightarrows PbS + H_2 \quad \text{(SOTERM.16)}$$

$$Pb^{2+} + 2Cl^{-} \leftrightarrows PbCl_2 \quad \text{(SOTERM.17)}$$

$$Pb^{2+} + SO_4^{2-} \leftrightarrows PbSO_4 \quad \text{(SOTERM.18)}$$

$$5Pb^{2+} + PbO + 6OH^{-} \leftrightarrows [Pb_6O(OH)_6]^{4+} \quad \text{(SOTERM.19)}$$

The corrosion of lead in WIPP-relevant conditions was studied extensively by Roselle (Roselle 2009, Roselle 2010, Roselle 2011a, Roselle 2011b, and Roselle 2013). In these experiments, lead coupons were immersed in the WIPP brines (GWB and ERDA-6) under anoxic conditions and a range of atmospheric CO_2 concentrations. Results from multiyear experiments show formation of Pb-Ca carbonate phase at CO_2 > 350 ppm. No corrosion product buildup was observed in the absence of CO_2; however, coupons were discolored due to the likely formation of lead oxide. Corrosion rates for lead in the absence of CO_2 were similar to those measured for steel (Roselle 2013).

The solubility of lead in the WIPP brine is expected to be low, due in part to the passivation process, but also because of insoluble solids formation. Strong oxidants (e.g., radiolysis products) may locally enhance the dissolution of lead, but alkaline brine, which contains chlorides and carbonate/bicarbonate species, will overwhelm radiolytic effects to maintain a low concentration of lead in the brine. In solution, lead will exist as Pb^{2+} species that are redox-active toward high-valent actinides (see Table SOTERM-5) and will help establish and maintain reducing conditions in the brine.

Lead, as was the case with iron, can influence the redox chemistry (see Table SOTERM-5) and precipitate carbonate and sulfide from the WIPP brine. This leads to a redox chemistry that will help maintain reducing conditions and effectively lower carbonate concentration. Both of these will potentially lower actinide solubility in the WIPP. These impacts are not considered in the WIPP PA due to a lack of sufficient data, and this remains a conservatism in the WIPP model.

SOTERM-2.3.6 Organic Chelating Agents

Organic chelating agents are used in the processing and cleanup/decontamination of actinides throughout the DOE complex. For this reason, they are often present as co-contaminants with the TRU component in the WIPP waste. Some of these chelating agents strongly complex actinides and have a significant effect on their solubility in brine. In this context, four organic chelating agents-oxalate, acetate, citrate, and EDTA-are tracked as part of the WIPP inventory process, and the potential effects of these complexants on the calculated actinide solubilities were evaluated as part of the CRA-2014 WIPP PA (Brush and Domski 2013a and Brush and Domski 2013b).

The potential concentrations of the key organic ligands in the WIPP used in the CRA-2014 PA were calculated by Brush and Domski (Brush and Domski 2013b) and are based on the 2012 WIPP inventory data (Van Soest 2012). The organic concentrations for the minimum brine volume used in the CRA-2009 PABC and CRA-2014 PA (see section SOTERM-2.2.4) are summarized in Table SOTERM-6. In the WIPP PA implementation, variable brine volume concentrations will be used as described in Brush and Domski (Brush and Domski 2013a).

Table SOTERM- 6. Comparison of the Concentrations of Organic Ligands in WIPP Brine Used in the CRA-2009 PABC and the CRA-2014 PA

Organic Ligand	CRA-2009 PABC Maximum Anticipated Concentration (M) [b]	CRA-2014 PA Maximum Anticipated Concentration (M) [c]
Acetate	1.94×10^{-2}	2.30×10^{-2}
Oxalate[a]	1.73×10^{-2}	1.18×10^{-2}
Citrate	2.38×10^{-3}	2.33×10^{-3}
EDTA	6.47×10^{-5}	7.40×10^{-5}

a - the concentration of oxalate may be limited by its solubility, not inventory, in ERDA-6 brine.
b - Brush and Xiong 2005a
c - Brush and Domski 2013b

Dissolved metals will compete with the actinides to form organic complexes. As the metals in the repository corrode, additional transition metal ions will dissolve into the brine. These ionic species include iron (Fe) and lead (Pb). Other steel constituents, such as nickel (Ni), chromium (Cr), vanadium (V), and manganese (Mn), may also be present. Additionally, divalent cations in the brine, most importantly Mg^{2+} and Ca^{2+}, will also form complexes with these chelating agents and compete with the actinide species. The stability constants for Mg^{2+}, Ca^{2+}, Fe^{2+}, Pb^{2+}, and Ni^{2+} and deprotonation constants for the organic acids are shown in Table SOTERM-7 (NIST 2004). These formation constants, in many respects, follow the same trends as the actinide species with respect to the strength of the complexant (e.g., EDTA > citrate >> oxalate and acetate). When present in high enough concentrations, these metals will compete with the actinide to form complexes and effectively lower the effect of organic complexation on actinide solubility. However, this is not included in the PA and remains as a conservatism in the WIPP actinide concentration model.

Table SOTERM- 7. Apparent Stability Constants for Organic Ligands with Selected Metals (NIST 2004)

Organic Ligand	pK_a	Metal	Ionic Strength (m)	$\log_{10} \beta_1$

EDTA	k_1 8.86-9.05 k_2 6.10-7.02 k_3 2.79-2.54 k_4 2.05-2.20	Fe^{2+} Ni^{2+} Pb^{2+} Mg^{2+} Ca^{2+}	0.1 0.1 0.1 1 1	14.3 18.4 18 8.61 9.68
Citrate	k_1 5.58-5.30 k_2 4.25-4.38 k_3 2.85-3.06	Fe^{2+} Ni^{2+} Pb^{2+} Mg^{2+} Ca^{2+}	0.1 0.1 1.0 0.1 0.1	4.4 5.18 4.44 3.43 3.48
Oxalate	k_1 3.74-4.23 k_2 1.15-1.43	Fe^{2+} Ni^{2+} Pb^{2+} Mg^{2+} Ca^{2+}	1.0 0.1 1.0 0.1 0.1	3.05 4.16 4.20 2.75 2.46
Acetate	k_1 4.52-4.99	Fe^{2+} Ni^{2+} Pb^{2+} Mg^{2+} Ca^{2+}	3.0 0.1 0.1 0.1 0.1	0.54 0.88 2.15 0.51 0.55

There are two final, but important, observations about the organic chelating agents present in the WIPP. First, they are expected to have very different tendencies toward biodegradation, based on extensive experience with soil bacteria in the literature (Banaszak, Rittmann and Reed. 1998; Reed, Deo and Rittmann 2010). Microbial activity, based on many general observations with soil bacteria, will likely readily degrade citrate, oxalate, and acetate to very low (submicromolar) steady-state concentrations. This important degradation pathway is not as certain for EDTA, which tends to resist biodegradation in most groundwater. These degradation pathways have, however, not been demonstrated for the halophiles typically present in the WIPP, and it is currently assumed in the WIPP PA that no degradation pathways for these organic complexants, microbiological or chemical, exist.

The second important observation is that these chelating agents, under WIPP-relevant conditions, are expected to help establish reducing conditions in the WIPP because they tend to reduce higher-valent actinides. This has been demonstrated in the WIPP brine for Np(V) and Pu(V/VI), but was not observed for U(VI) (Reed et al. 1998). These chelating agents also tend to oxidize III actinides to IV, which would have a beneficial effect on actinide solubility in the WIPP because the actinides in the IV oxidation state are approximately 10 times less soluble than actinides in the III oxidation state. These potentially beneficial effects of organic chelating agents on actinide speciation are also currently not included in the WIPP PA and remain a conservatism in the WIPP model.

SOTERM-2.3.7 CPR in WIPP Waste

The WIPP waste contains a relatively high amount of organic material, since much of the waste is residue from laboratory operations where CPR materials were widely used. Current estimates project over 14,000 metric tons of plastic and cellulosic materials with about 1,250 metric tons of rubber material in the WIPP (Van Soest 2012; Table SOTERM-3). This organic material is important from the perspective of repository performance in that it provides an organic "feedstock" for microbial activity that could lead to gas generation (carbon dioxide, hydrogen, hydrogen sulfide, and possibly methane), as well as degradation products that can complex actinides or form pseudocolloids. CPR degradation is represented in the PA to evaluate these potential impacts on the actinide concentrations and release.

SOTERM-2.4 Important Post-emplacement Processes

There are three important post-emplacement processes that take place in the WIPP after repository closure. These are metal corrosion, microbiological effects, and radiolysis. Metal corrosion was already discussed as part of the iron chemistry section (Section SOTERM-2.3.4). Microbiological effects and radiolysis are br iefly discussed in this section.

SOTERM-2.4.1 Microbial Effects in the WIPP

Microbiological processes can have a significant effect on many aspects of subsurface chemical and geochemical processes. This, particularly as it relates to contaminant transport and remediation, has been well established for soil bacteria in low-ionic-strength

and near-surface groundwaters (Reed, Deo and Rittmann 2010; Banaszak, Rittmann and Reed 1998). In the WIPP, as a result of the high-ionic-strength brines present, halophilic microorganisms will predominate. In prior recertifications, what was understood about halophilic organisms under WIPP-relevant conditions was established through a series of long-term studies conducted as part of the Actinide Source Term Program (ASTP) project by researchers at Brookhaven (Brush 1990; Francis and Gillow 1994; Brush 1995; Wang and Brush 1996). This, since CRA-2009, was significantly extended by newer studies (Swanson et al. 2012; Swanson et al. 2013a; Swanson et al. 2013b; Swanson and Simmons 2013). Although this new information has increased our understanding of microbial processes in the WIPP, there are no changes to the WIPP microbial model proposed for the CRA-2014.

The potential effects of microbial activity on the fate and transport of actinide metals from deep geological waste repositories have been well described (McCabe 1990; Lloyd and Macaskie 2002; Pedersen 2002; Wang and Francis 2005) and may include 1) gas generation from the degradation of organic waste components, 2) the creation of a reducing environment from oxygen consumption, 3) redox reactions with metals and oxyanions, 4) the generation of organic ligands from the incomplete degradation of organic waste components, and 5) the mobilization of actinides adsorbed onto organism surfaces.

The WIPP PA considers gas generation, since it leads to CO_2 formation and increased dissolved carbonate, and biocolloid formation to have the largest potential impact on the mobile concentration of actinides in the source term. Because of the scarcity of data during the time of earlier certification efforts (Barnhart et al. 1978a, Barnhart et al. 1979b, Barnhart et al. 1979c and Barnhart et al. 1979d), there are high levels of conservatism in the current WIPP microbial model and there are no proposed changes to this model in the CRA-2014. This conservatism is attributed to the high uncertainty about microbial processes in hypersaline systems since these are not well studied and because microbial processes attributed to low-ionic strength environments were conferred upon the organisms that inhabit salt-based repositories. In fact, we are finding that organisms indigenous to hypersaline environments, such as the WIPP and its environs, are not as metabolically diverse as is typically seen with their low ionic strength counterparts and are, therefore, far less likely to play a large role in waste transformation. There is still uncertainty about what organisms may predominate should brine inundation occur, but it is becoming clear that non-halophilic organisms introduced with emplaced waste are unlikely to survive the near-field conditions. The microbial model assumptions that are used in the WIPP PA are discussed extensively elsewhere (Appendix PA-2014, Sections 2.1.1 and 4.2.5; U.S. EPA 2006). In this section we provide an updated view of the WIPP microbial ecology, present some new experimental results and discuss these in the context of some of our current PA assumptions. These results increase the DOE's overall understanding of the microbial ecology in the WIPP and suggest that the current WIPP PA assumptions about microbial gas generation are conservatively high.

SOTERM-2.4.1.1 Microbial Ecology in the WIPP

Hypersaline conditions result in a unique microbial ecology due to the thermodynamic constraints imposed upon the organisms inhabiting such environments. Survival in hypersaline systems depends on an organism's ability to maintain osmotic balance with its external environment (Oren 2006).

If the energetic cost of this maintenance exceeds the benefit of a given metabolic reaction, that reaction will not proceed. As a result, microbial metabolic processes are limited to the following at salt concentrations greater than 2.5 M NaCl, the cut-off for extremely halophilic microorganisms: oxygenic and anoxygenic photosynthesis; aerobic respiration; denitrification; fermentation; manganese, arsenite, and selenate reduction; dissimilatory sulfate reduction with incomplete organic oxidation; methanogenesis from methylated amines; acetogenesis; and chemolithotrophic oxidation of sulfur compounds (see Figure SOTERM-3; Oren 1999 and Oren 2011). All of these processes are either energetically favorable or are performed by organisms that maintain osmotic balance by a less costly strategy.

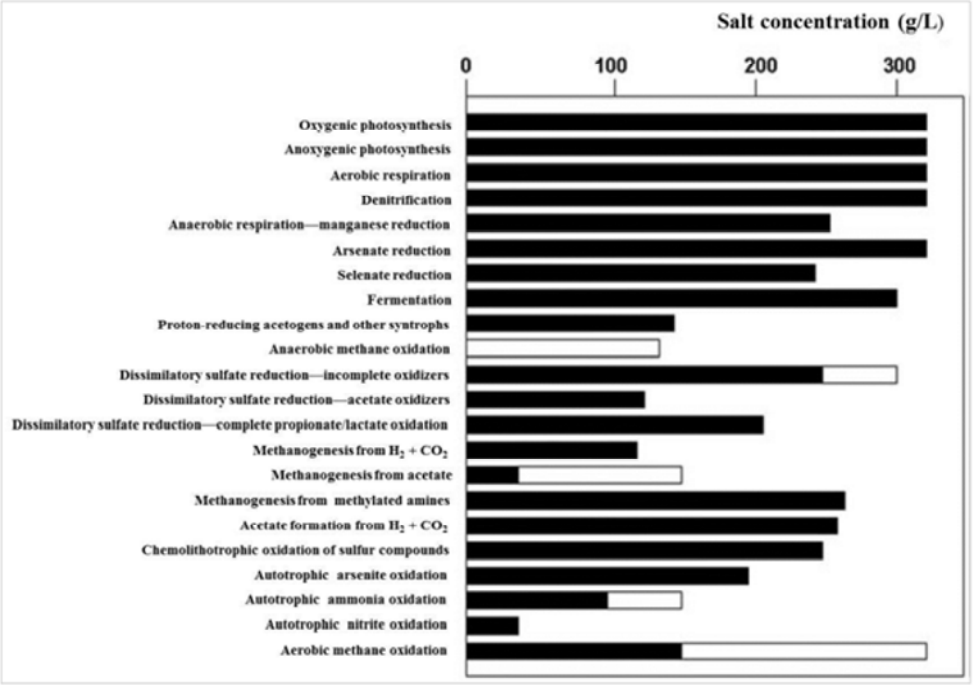

Figure SOTERM- 3. Approximate Upper Salt Concentration Limits for the Occurrence of Selected Microbial Processes (from Oren 2011). Solid bars are derived from laboratory experimental data using pure cultures; open bars are taken from in situ measurements of possible microbial activity.

Apart from these thermodynamic constraints, the repertoire of potential microbial metabolic pathways within the WIPP is limited even further by 1) physical confinement of the repository without input of exogenous electron acceptors (especially oxygen), moisture (i.e., brine), or light; 2) high ionic strength; 3) high pH; and 4) nonideal substrates. These factors may restrict or effectively eliminate many capabilities.

Thus, microbial activity within the repository should be considered as varying in time and space (Swanson et al. 2012; Swanson and Simmons 2013). Obligate aerobic and extremely halophilic organisms may dominate the initial oxic environment, followed by the low-probability appearance of extremely halophilic anaerobes. In regard to space variation, extreme halophiles will dominate the near-field; while the salinity gradient will dictate the level of halophilism of organisms found within the far-field. Recent work on the characterization of microorganisms at the WIPP has supported these time and space assumptions and will be reviewed below (Swanson et al. 2012; Swanson and Simmons 2013).

Variation in time

Aerobic respiration by haloarchaea will be predominant immediately after repository closure and will remain so until oxygen levels decrease from the corrosion of iron canisters and less importantly, due to microbial activity. Once oxygen has been depleted, nitrate, organic acids, and sulfate will be present as potential electron acceptors.

While most haloarchaea are obligate aerobes, some are capable of nitrate reduction and fermentation of small organics, such as amino acids. However, once conditions become anaerobic, haloarchaeal numbers will decrease and cells will become dormant. The longevity of these organisms entrapped in fluid inclusions or in interstitial brines is well documented; thus, they will be present throughout repository history but are not likely to be active because of unfavorable conditions (Norton and Grant 1988; Mormile et al. 2003; Schubert et al. 2009; Schubert et al. 2010).

Halophilic, aerobic fungi and bacteria have also been isolated from WIPP halite (Swanson et al., 2012; Swanson and Simmons 2013; Gunde-Cimermann et al. 2009). These organisms may survive the early oxic and moist conditions of the repository prior to inundation, but are unlikely to survive in stringent WIPP brines that exceed either their sodium or magnesium tolerances. In anaerobic enrichments of WIPP halite, fungal hyphae did not elongate and spores did not grow, and eventually the fungi died off (Swanson and Simmons 2013).

Bacteria have only been isolated from WIPP halite under aerobic, low-salt conditions, although they may grow in up to 3.4 M NaCl (Swanson et al. 2012). A halophilic denitrifier, *Halomonas* sp. WIPP 1A, was isolated from previous studies, but its actual source is unknown (Francis et al. 2000). Sulfate reducers (*Bacteria*) have thus far not been found in subsurface halite. Gillow and Francis (Gillow and Francis 2006) noted a sulfide precipitate in their long-term incubations, which they attributed to the presence of sulfate-reducing bacteria (SRB); however, these incubations were also inoculated with brine lake sediment, the most likely source of these organisms. SRBs have been found in other hypersaline environments (i.e., brine lakes, solar salterns; Porter et al. 2007;

Sørensen et al. 2009). Their presence in seeps or in the underlying Castile formation brines is unknown. Sulfate is present in Castile brine and is also formed from the dissolution of anhydrite present in the halite interbeds.

Variation in space

The variation of microbial communities in space concerns the near-field versus intermediate-field versus far-field and reflects the variation in ionic strength in these spaces. With differing ionic strength comes differing community compositions and, hence, different metabolic potential.

Extremely halophilic archaea and some few bacteria may survive at the NaCl concentrations expected in the near-field. Incubations of WIPP halite under high-salt conditions (4.7 M NaCl) yielded only archaeal isolates (Swanson et al. 2012), and these survive in the WIPP brine. The intermediate-field, an area of hypothetical mixing of the repository soup and Culebra groundwater, should support the growth of these same and other haloarchaea and also halophilic bacteria and fungi. The Culebra is considered to be the most likely pathway for actinide migration from the repository, in the low-probability event of a breach into the WIPP horizon (U.S. DOE 2011), and is therefore considered as the far-field. This space has been shown to be dominated by a range of moderately halophilic and halotolerant bacteria, whose diversity decreases as ionic strength increases (Swanson and Simmons 2013).

This distinction in space is important in that waste transformation will occur more readily in the presence of bacteria than archaea. Metabolic activities shown to occur in the far-field include aerobic respiration, fermentation, nitrate reduction, iron reduction, and sulfate reduction; while still other processes are energetically feasible-reduction of other oxyanions, chemolithotrophy (oxidation of ammonium, sulfide), methanogenesis at lower salt concentrations, and methanotrophy (Oren 1999, Oren 2008, and Oren 2011; Swanson et al. 2012; Swanson and Simmons 2013).

Influence of Substrate

Ideal substrates for haloarchaea include small organics, such as amino acids, acetate, glucose, and often citrate (Oren 2006). Organic complexing agents-acetate, oxalate, citrate, and EDTA-will be the predominant low-molecular-weight carbon substrates, but cellulosics may contribute significantly to the carbon inventory. The availability of these substrates will depend upon their dissolved concentrations in brine, which are expected to be at or below the current inventory-predicted levels (Table SOTERM-6). The WIPP haloarchaea are capable of degrading acetate, citrate, and oxalate in aerobic brines (Swanson et al. 2013a; Swanson et al. 2013b) but there is as yet no evidence for anaerobic degradation. In the far-field, acetate and citrate degraders are present, but the fates of oxalate and EDTA have not been studied (Swanson and Simmons 2013).

Organisms introduced in waste

If soil has been introduced into waste containers, it may contain diverse microorganisms capable of many different types of metabolism, and some may even be halotolerant. Spore-forming organisms may survive in spore form for extremely long periods of time, but they will not likely vegetate. Even a halophilic *Virgibacillus* sp. isolated from WIPP groundwater was unable to grow at NaCl concentrations above 17.5%, at which point it sporulated (Swanson et al. 2012). Although the survival of soil organisms at expected WIPP ionic strength has not been shown, gas generation was reported in incubations of soil and TRU-simulated waste in brine (Caldwell et al. 1988); however, results were equivocal, and microbes were never looked for in the samples.

In spite of conditions inconducive to significant microbial activity, the theoretical possibility of such an occurrence must be taken into consideration by PA, and the current knowledge of the microbial ecology at the WIPP should not affect these assessments other than to underscore the conservatism of the model.

SOTERM-2.4.1.2 WIPP-related Microbial Degradation of CPR

The generation of gas from the degradation of cellulose in waste repositories is an important process that is difficult to reliably predict. The WIPP PA considers this process to be a guaranteed occurrence, which is a very conservative approach, that proceeds completely to carbon dioxide and water (Appendix PA-2014, Section 4.2.5) if the following conditions are met: 1) microorganisms capable of degrading cellulose are present at repository closure, 2) these organisms can survive for a significant length of time, and 3) sufficient water, electron acceptors, and nutrients are available to support their activity (Brush 1995). The reality is that cellulose degradation is a complex process requiring the concerted efforts of many different groups of organisms, few of which are either found or would survive in the WIPP. Additionally, the degradation process differs between aerobic and anaerobic environments, as the organisms within those spaces utilize different mechanisms for hydrolysis (Lynd et al. 2002; Wilson 2011).

Sources of cellulose in hypersaline habitats include dead algal biomass and halophytic debris. Many halophilic microorganisms possessing cellulase activity or capable of growth on cellulosic substrates have been reported. Two fungi isolated from WIPP halite, one with documented ligninolytic capability (*Cladosporium*; Cronin and Post 1977; Gunde-Cimerman et al. 2009), were capable of growth on Kimwipes and using carboxymethylcellulose (CMC) as the sole carbon source (Swanson and Simmons 2013). Moderately halophilic bacteria, including organisms similar to those isolated from the WIPP environs-e.g., *Halomonas* sp., *Virgibacillus* sp., and *Salinicoccus* sp.-have also exhibited cellulase activity (Rohban et al. 2009), and an extremely halophilic bacterium, *Marinimicrobium haloxylanilyticum*, was found to degrade CMC in up to 22% NaCl. A mixed culture, presumably archaea, enriched from WIPP halite adhered to and altered Kimwipe fibers, as observed microscopically (Vreeland et al. 1998).

Of the above, the bacteria and fungi are unlikely to survive in the WIPP brines, and all are obligately aerobic. Only one anaerobic, cellulolytic microorganism has been isolated from a hypersaline environment-*Halocella halocellulolytica* (Simankova and Zavarzin 1992; Simankova et al. 1993). This organism degrades cellulose (filter paper) in concentrations of NaCl up to 20%. Thus, it is unlikely that any significant anaerobic cellulose degradation will occur in the WIPP near-field, but lower salinities may permit utilization in the far-field.

Early studies on gas generation were carried out as part of the Actinide Source Term Program (ASTP) at Los Alamos National Laboratory, and later studies took place at Brookhaven National Laboratory. While inconclusive, these studies support the general opinion that organisms introduced into the WIPP along with emplaced waste will not be able to survive in high ionic strength media.

Later studies showed gas generation from cellulose degradation, and these were used as the basis for the WIPP PA assumptions (Francis and Gillow 1993; Francis et al. 1997; Gillow and Francis 2006). These studies used a mixed inoculum, including brine lake sediment and water, underground brine seep, and halite. Because of the relatively rich inoculum, the rates of gas generation measured can be considered optimistic. Sediments are rich in organisms, including anaerobes, even in hypersaline systems. Even so, these studies provide a more realistic scenario than the earlier studies, especially since expected WIPP conditions were better known at the time of design.

The presence of exogenous cellulolytic bacteria introduced in the waste drums themselves cannot be ruled out and, in fact, these organisms have been detected in simulated waste pits (Field et al. 2010). If any moisture were present in the drums, these organisms may have had a chance to cause initial cellulose breakdown to products more easily metabolized by cellulase-producing bacteria should they come into contact with these by-products during early oxic periods. Again, these organisms are unlikely to survive or be active in brine, although some are likely to be halotolerant.

Cellulase-producing haloarchaea, including *Haloarcula*, *Halobacterium*, and *Halorubrum* spp., have been isolated previously from hypersaline salt lakes and salterns (Birbir et al. 2007). While these organisms are likely to thrive at high ionic strength, their use of cellulose by-products will be limited, once again, to early oxic periods.

Still, complex organics may be more recalcitrant to degradation in anaerobic, hypersaline systems. Cellulose fibers have been preserved in fluid inclusions extracted from WIPP halite, suggesting that this type of high-molecular weight organic is recalcitrant to degradation at high salt concentrations, possibly owing to the lack of ionizing radiation, water available for hydrolysis, and microbial activity (Griffith et al. 2008).

The current PA approach to account for CPR degradation, although there are many reasons that a much lower extent of biodegradation should occur, remains conservative in that it assumes that the biodegradation of all cellulosic and plastic material is guaranteed. This adds to the overall conservatism of the WIPP actinide source term model.

SOTERM-2.4.1.3 Bioreduction of Multivalent Actinides

The microbially induced reduction of higher-valent actinides would be an important beneficial effect for the WIPP, in that lower-valent actinide species are less soluble. This has recently been the focus of much research due to its expected role in microbially mediated remediation and containment of subsurface contaminants (Banaszak, Rittman, and Reed 1998; Banaszak et al. 1999; Lloyd, Young, and Macaskie 2000; Reed et al. 2007; Icopini, Boukhalfa, and Neu 2007; Francis, Dodge, and Gillow 2008). For soil bacteria, there is no question that biotic mechanisms that lead to the reduction of actinides exist under a wide range of anaerobic subsurface conditions.

There are, however, very few data concerning metal reduction in hypersaline environments (Sorokin and Muyzer 2010; Emmerich et al. 2012). This is likely due to the low solubility of oxidized metal species in these systems; thus, the data are generally limited to lower ionic strength systems, insoluble metal oxides in sediments, or metals associated with particulate organic matter or associated with microbial mats. The ability of WIPP-indigenous microorganisms to reduce metals is again divided between near-field and far-field spaces.

Both *Clostridium* spp. and sulfate-reducing bacteria with metal-reducing capability have been detected in the Culebra and could be capable of directly reducing higher-valent actinides in the far-field (Swanson et al. 2012; Swanson and Simmons 2013). Additionally, the indirect reduction of iron by either fermenting *Halanaerobium* spp. or SRB was shown to precipitate iron-sulfide complexes by lowering the redox potential or reducing sulfate, respectively, in iron-amended enrichment incubations. The reduction of iron by other SRB and fermenters has been shown previously in hypersaline sediments (Emmerich et al. 2012).

In the near-field, however, it is less likely that direct biotic processes will cause actinide reduction since haloarchaea have not been shown to directly reduce metals.

The potentially beneficial effects of bioreduction to lower the solubility of multivalent actinides are not considered in the WIPP PA. There remains high uncertainty about this process for halophilic microorganisms and there is not yet definitive WIPP-specific data to explain and support this reduction pathway.

SOTERM-2.4.1.4 Current WIPP PA Model for the Biodegradation of CPR

There is no change from the CRA-2009 in the CPR microbial degradation model proposed in the CRA-2014. There are no new gas generation rates, and the implementation and basis of the gas generation rates has not changed (Appendix PA-2014, Section 4.2.5).

Currently, microbial activity is considered in all PA vectors. The presence of this microbial activity means it is assumed that microbes may consume 100% of the cellulosic materials in the repository, and that there is a probability of 0.25 that microbes may consume the plastic and rubber materials. Thus, there is microbial consumption of cellulosic materials, but not of plastic or rubber materials, in 75% of the PA realizations (vectors), and microbial consumption of CPR materials in 25% of the vectors.

Microbial consumption of CPR materials could affect the actinide source term in four ways:

1) Productionof significant quantities of CO_2, which could acidify the brine in the absence of an MgO buffer or increase the solubility of actinides by increasing carbonate levels that complex some actinides at the expected mildly alkaline pH

2) Bioreduction of higher-valent actinide species leading to lower-valent, less-soluble actinide species

3) Degradation of solubilizing organic ligands, leading to lower actinide solubility

4) Increased biomass that may lead to the formation of microbial colloids that increase the amount of actinide pseudocolloids in the brine

The effect of CO_2 production is discussed in this section. The remaining three effects are implicitly considered in the analyses that address the oxidation-state distributions (Section SOTERM-4.3), the effects of organic ligands (Section SOTERM-2.3.6), and the effects of colloids (Section SOTERM-3.9). The simplifications used in the PA calculations for all four of these effects are discussed at the end of this section.

Microbial activity, if it occurs to a significant extent in the WIPP, would consume CPR materials by the following sequential reactions (Brush 1990; Francis and Gillow 1994; Brush 1995; Wang and Brush 1996; Francis 1998):

$$C_6H_{10}O_5 + 4.8H^+ + 4.8NO_3^- \rightarrow 7.4H_2O + 6CO_2 + 2.4N_2; \text{ (SOTERM.20)}$$

$$C_6H_{10}O_5 + 6H^+ + 3SO_4^{2-} \rightarrow 5H_2O + 6CO_2 + 3H_2S; \text{ (SOTERM.21)}$$

$$C_6H_{10}O_5 + H_2O \rightarrow 3CH_4 + 3CO_2. \text{ (SOTERM.22)}$$

Methanogenesis, described by reaction SOTERM.22, is not included as a degradation pathway because it is assumed that the sulfate present in the DRZ is always available. This exclusion is considered a conservative assumption relative to the amount of carbon dioxide that could be produced. In effect, the CRA-2014 PA assumes that an excess of sulfate is always available to sustain sulfate-reduction as a mode of respiration. When unlimited sulfate is available from natural sources in the host rock, 4% of the gas generation occurs through denitrification and 96% occurs by way of sulfate reduction. The omission of methanogenesis is now further supported by the fact that this process has been shown unfavorable at the ionic strengths expected in the WIPP (Oren 2011, also see discussion in Section SOTERM-2.4.1.1). Microbial consumption of CPR materials, therefore, is assumed to produce significant quantities of CO_2, which could in turn acidify any brine present in the repository and increase the solubilities of the actinides relative to those predicted for neutral and mildly basic conditions. Therefore, the DOE is emplacing MgO in the repository to decrease actinide solubilities by consuming essentially all of the CO_2 that could be produced by microbial consumption of CPR materials, and by buffering (controlling) the f_{CO_2} and pH within ranges that are favorable from the standpoint of actinide speciation and solubility (see Section SOTERM-2.3.2).

Three effects of microbial consumption of CPR materials are recognized in the system performance modeling. A simplification has been made so the effects will be time-independent after 100 years. These effects are

1. CO_2 production: With the addition of excess MgO, the effects of CO_2 production are minimized, and it is assumed that the system may be modeled using the brucite-hydromagnesite ($Mg_5(CO_3)_4(OH)_2 \cdot 4H_2O$) buffer.

2. Redox effects: After 100 years, the repository will have a reducing environment. This is, in part, established by the postclosure microbial consumption of oxygen, but is also due to the corrosion of steel. This combined effect leads to the formation of an anoxic reducing environment in the WIPP.

3. Biocolloid formation: Production of microbial colloids is possible and may contribute to the formation of colloidal species that add to the actinide source-term concentration in DBR release.

SOTERM-2.4.2 Radiolysis Effects in the WIPP

Radiolysis effects in the WIPP are caused by the interaction of ionizing radiation and particles (neutrons, α, β, and γ) with the gases, brines, and materials present in the repository. These effects have not been extensively studied under WIPP-related conditions, but there is a fairly good general understanding of their extent and nature. For most conditions expected in the WIPP, radiolytic effects are predicted to be transient and insignificant. In this context, there is a recognition that although radiolysis can lead to localized conditions and effects that could oxidize multivalent actinides, the brine chemistry, metal corrosion, and microbiological activity will combine to very rapidly overwhelm these effects. For this reason, radiolysis effects on actinide solubility are not explicitly included in the WIPP PA to calculate actinide concentrations. More specifics on the overall mechanisms, brine radiation chemistry, and potential radiolytic effects on actinide speciation are given in this section.

There are no new data on the radiolysis of brine systems since the CRA-2009. Radiolytic effects continue to be low in importance for transuranic waste under WIPP-relevant conditions and data obtained (see section SOTERM-3.6) on Pu-Fe systems show that the iron chemistry and expected reducing conditions prevail over radiolytic processes.

SOTERM-2.4.2.1 Radiation Chemistry of Brine Systems

The radiolysis of high-ionic-strength brine systems has not been extensively studied, but some studies exist (Büppelman, Kim, and Lierse 1988; Kim et al. 1994; Kelm, Pashalidis, and Kim 1999; Ershov et al. 2002). The many components in the brine systems of interest to the WIPP will lead to relatively complex radiation chemistry and the formation of numerous transients and free radicals.

In contrast to this, the radiation chemistry of pure and dilute aqueous systems has been extensively investigated, and detailed reviews of this research have been published (Draganic and Draganic 1971; Spinks and Woods 1990). The irradiation of pure water leads to the formation of molecular hydrogen peroxide (H_2O_2) and hydrogen (H_2). These molecular yields are relatively insensitive to a wide range of conditions in dilute systems for a given type of ionizing radiation. Molecular yields are G_{H2} = 0.45 molecule (molec)/100 electron-volt (eV) and G_{H2O2} = 0.7 molec/100 eV for low Linear Energy Transfer (LET) ionizing radiation (β, and γ) and G_{H2} = 1.6 molec/100 eV and G_{H2O2} = 1.5 molec/100 eV for high LET radiation (α and neutrons). The radiolytic formation of hydrogen in the WIPP brine due to self-irradiation effects of ^{239}Pu was established and a molecular yield of G_{H2} = 1.4 molec/100 eV was measured (Reed et al. 1993). This yield is consistent with the high LET literature, even though the irradiations were performed in brine.

The high concentrations of electron and free radical scavengers present in the WIPP brine have a pronounced effect on the radiation chemistry. Most importantly, halides react with the hydroxyl radical (OH·) or act as scavengers (such as Cl^- or Br^-) to gradually lower the molecular yield of H_2O_2 as the concentration of the scavengers is increasing (Kelm, Pashalidis, and Kim 1999). In this context, oxidizing transient species are "chemically" stored as oxychlorides and oxybromides, leading to a shift towards more oxidizing conditions. Figure SOTERM-4 gives an overview of the radiolytic pathways and mechanisms that are likely (Buppelmann, Kim, and Lierse 1988). In NaCl brine, the formation of chloride species (ClO^-, HOCl, Cl_2, and Cl_3^-) is favored, instead of H_2O_2 (Büppelmann, Kim, and Lierse 1988).

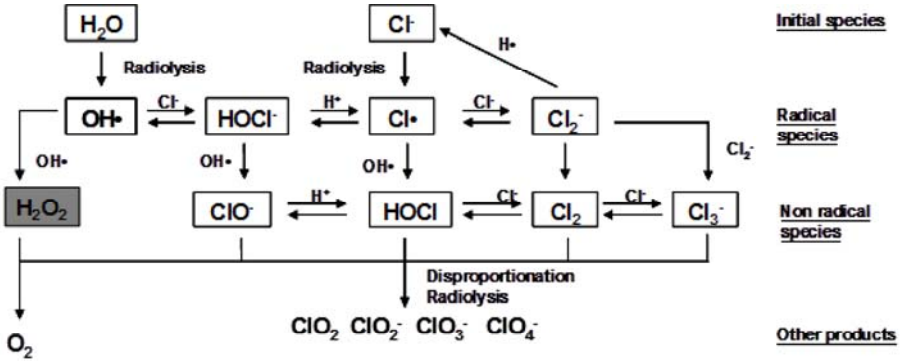

Figure SOTERM- 4. NaCl Brine Radiolysis Species and Suggested Mechanism of Production. The formation of chloride species (ClO^-, HOCl, Cl_2, and Cl_3^-) is favored instead of H_2O_2 (based on data in Büppelmann, Kim, and Lierse 1988).

Kelm, Pashalidis, and Kim (Kelm, Pashalidis, and Kim 1999) showed that the formation of hypochlorite ion increases with the chloride concentration and the dose (Figure SOTERM-5) in NaCl brine. The authors found that in solutions containing 37 gigabecquerel (GBq)/liter (L) of ^{238}Pu, the hypochlorite concentration increases with time (dose) and appears to approach a steady state (see Figure SOTERM-5). At a constant dose rate, the maximum hypochlorite concentration depends on the chloride concentration. It was also observed that hypochlorite ion generation was negligible when chloride concentrations were smaller than 2 M.

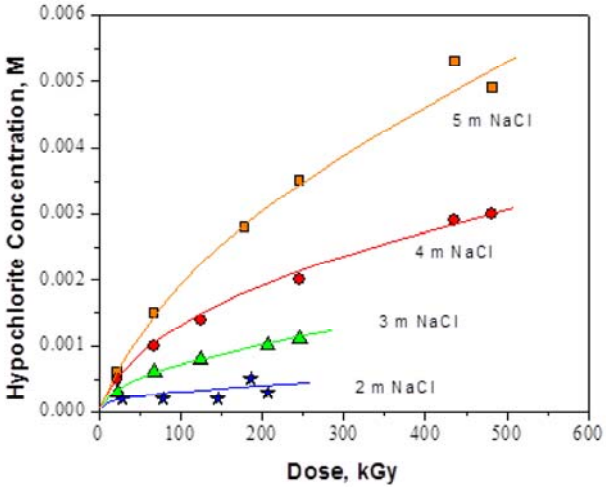

Figure SOTERM- 5. Radiolytic Formation of Hypochlorite Ion in Solutions of Various NaCl Concentrations at a Constant Alpha Activity of 37 GBq/L at pH~12 (based on data in Kelm, Pashalidis, and Kim 1999)

In the WIPP brine, however, some solutes other than chloride may play a role. Ershov et al. (Ershov et al. 2002) showed that small amounts of bromide in natural brines under radiolysis can give Cl_2^-, $ClBr^-$, and Br^- radical anions at the radical step, and then mixed halogen molecules and trihalide ions by radical recombination at the molecular step (Ershov et al. 2002). The hydrolysis of mixed halogen molecules can then result in the formation of hypobromite (OBr^-) (acidic form: hypobromous acid [HOBr]), a starting substance to more stable bromates of higher oxidation state (Ershov et al. 2002).

Some WIPP-specific experiments were performed to establish the key radiolytic product in GWB and ERDA-6 brine (Lucchini et al. 2010a). This study confirms that hydrogen peroxide (H_2O_2) and hypochlorite ion (OCl^-) are unstable in these WIPP brines, due in part to metallic impurities in the brine. There was, however, an accelerated decomposition of these species when bromide (Br^-) was present, which is the case for both ERDA-6 and GWB brines. Here, OCl^- readily and stoichiometricly reacted with Br^- to form hypobromite ion (OBr^-), which appeared to be the most important radiolytic transient observed under these conditions. OBr^-, like OCl^-, is also an oxidizing species (E^o=0.76V), that will likely lead to the oxidation of multivalent actinides in the WIPP, but this reactivity has not been established experimentally under representative WIPP conditions (Lucchini et al. 2010a).

In the WIPP, most of the brine radiolysis is caused by the deposition of alpha particles from the TRU isotopes present in the WIPP waste. The range (distance traveled until the alpha particle's energy is lost) of these alpha particles is very short (<40 microns) and radiolysis of the brine solution will take place at the solid-liquid interface. Locally, the concentration of oxidative radiolytic products of brine, such as hypochlorite, chlorite, chlorate, and products of their reaction with brine components (e.g., hypobromite) may be high, and they may directly interact with the radioactive surface. These "very-near" radiolytic effects, however, are expected to be quickly mitigated by the bulk brine chemistry and the reaction of reducing agents (e.g., reduced iron) with the oxidizing molecular products formed.

SOTERM-2.4.2.2 Potential Radiolytic Effects on Actinide Speciation and Solubility

A buildup of oxidizing radiolytic products in brine may increase the redox potential of the brine (Büppelmann, Kim, and Lierse 1988), and consequently directly generate higher-valent actinide species. Alternatively, these radiolytic products could be inserted into some solid actinide phases. For example, Kim et al. (Kim et al. 1994) studied the solubility of schoepite, $(UO_2)(OH)_2 \cdot xH_2O$, with hypochlorite ion in 0.1M NaCl at 25 °C (77 °F), in CO_2-free atmosphere (Kim et al. 1994). Their X-Ray Diffraction (XRD) patterns of the residual precipitates showed the introduction of the hypochlorite ion in precipitates. Kim et al. (Kim et al. 1994) observed that the presence of hypochlorite ion in the initial schoepite structure enhanced the solubility of the solid 10 to 100 times in the range of pH 6.0-9.8, compared with its solubility in the absence of hypochlorite ion (Kim et al. 1994). However, this effect was reduced when the molar ratio $[ClO^-]/[UO_2^{2+}]$ increased. This scenario is unlikely to occur in the WIPP because the potential buildup of oxidizing radiolytic products generated in brine is readily overwhelmed by the overall reducing capacity of the site (reduced metals and microbial processes).

The buildup of oxidizing radiolytic products due to brine radiolysis has also been shown to significantly affect the solution chemistry of Am. For example, Am(III) was oxidized to the more soluble forms of Am, namely AmO_2^+ and AmO_2^{2+} (Magirius, Carnall, and Kim 1985; Katz, Seaborg, and Morss 1986; Stadler and Kim 1988; and Meyer et al. 2002). Magirius, Carnall, and Kim (Magirius, Carnall, and Kim 1985) reported on the radiation effects exerted upon a 5 M NaCl solution at the pH 8 to 9 range using precipitated $Am(OH)_3$ at a concentration of 1.03×10^{-3} M (1.07 curie [Ci]/L). They observed that the precipitate began to show

discoloration, changing from pink Am^{3+} to brown AmO_2^+, within 24 hours (h), with quantitative oxidation of all the Am to AmO_2^+ within 1 week. Because Pu is more readily oxidized than Am, the expectation is that Pu could also be oxidized in irradiated brine. The metastability of Pu(VI) in the WIPP brine when no reducing agents were present was established and attributed to self-radiolysis effects of the ^{239}Pu isotope used (Reed, Okajima, and Richmann 1994; Reed et al. 2006).

Stadler and Kim (Stadler and Kim 1988) also report the existence of higher oxidation states of Am, due to self radiolysis. Solubility experiments on $Am(OH)_3$(solid[s]) in 3 M NaCl resulted in much higher Am concentrations than was calculated from the solubility product. This difference was assigned to the radiolytic oxidation of Am^{3+} to AmO_2^+. Spectrophotometric evidence of AmO_2^+ species in solution was reported. The authors report the value of $\log_{10}K_{S,0} = -9.3 \pm 0.5$ for the reaction

$$AmO_2OH(s) \leftrightarrows AmO_2^+ + OH^- \text{ (SOTERM.23)}$$

The solubility product of $AmO_2OH(s)$ is in general agreement with other solubility studies on different pentavalent actinides.

These results show there is clearly a potential for oxidized, higher-valent actinides to form in brine when no reducing agents are present. This, however, needs to be interpreted in the context of the strong reducing agents and processes that will predominate in the WIPP, such as bioreduction (Section SOTERM-2.4.1.2), iron reduction (Section SOTERM-2.3.4), and reduction by organic complexants (Section SOTERM-2.3.6). The WIPP-specific data show that the presence of reduced iron (Fe(II/0)) leads to a rapid reduction of Pu(VI) to Pu(IV) species under a wide range of anoxic conditions (Reed et al. 2006; Reed et al. 2009; Section SOTERM-3.6). These results are expected to extend to the Am(V) system, since this species is more readily reduced than Pu (V/VI). Reduced iron will also react with radiolytically generated oxidizing species, such as hypochlorite or hypobromite, to prevent their buildup in the brine solution with time. In summary, these WIPP-specific results show that the reductants present in WIPP waste (reduced metals and organics) will overwhelm potential radiolytic effects under the expected conditions in the WIPP, and a significant and sustained radiolytic enhancement of actinide solubilities is not predicted.

SOTERM-3.0 WIPP-Relevant Actinide Chemistry

The speciation of actinides under WIPP-relevant conditions defines the source term for actinide release from the WIPP in release scenarios where dissolved actinide concentrations are important (e.g., DBR and transport through the Salado or Culebra). The key factors that establish the concentrations of dissolved actinides under subsurface conditions are known. The most important of these factors for the WIPP repository are:

1. Actinide redox chemistry is a critical factor in establishing the concentration of actinides in brine. The solubility of reduced actinides (III and IV oxidation states) is significantly lower than oxidized forms (V and/or VI). In this context, the reduced-metal chemistry and microbial processes that establish and maintain reducing conditions in the WIPP are important.
2. The complexation of each actinide species is a critical factor in defining its solubility. For a given oxidation state, the inorganic and organic complexes present will define the solubility of the actinide. These complexants are in the preemplacement environment, are part of the TRU waste that is emplaced, or are produced as a result of subsurface processes, most notably microbial and corrosion processes.
3. Intrinsic and pseudoactinide colloid formation is a critical factor in defining the overall solution concentration of each actinide. The contribution of actinide colloids to the concentration of actinides in the WIPP is predicted to be significant. Many of the key TRU species in their expected oxidation states tend to form colloids or strongly associate with the non-actinide colloids present (e.g., microbial, humic and mineral).

The WIPP PA approach that was established in the initial WIPP license application (U.S. DOE 1996), and continued through the CRA-2014 PA calculations (Camphouse et al. 2013), accounts for all three of these key factors.

The PA concept of actinide speciation in the WIPP is well grounded in what has been observed for actinide contaminants in near-surface groundwater. In natural systems, the following inorganic ligands are potentially important complexants of radionuclides in solution: CO_3^{2-}/HCO_3^-, OH^-, $C1^-$, SO_4^{2-}/S^{2-}, fluoride (F^-), and phosphate. Additionally, anthropogenic and bioderived chelating agents can strongly bind actinide species and will compete with the inorganic complexants present. Lastly, the tendencies of actinides to form intrinsic colloids and strongly associate or bind with colloidal particles are also well established. The relative importance of these complexants and processes depends on the pH, radionuclide oxidation state present, the presence of other metals, and the relative ligand concentrations. There are a number of general reviews on various aspects of actinide environmental chemistry (Allard 1982; Choppin, Liljenzin, and Rydberg 2004 [pp. 94-112]; Clark, Hobart, and Neu 1995; Banaszak, Rittmann, and Reed 1998; Runde 2000; Nitsche et al. 1992; Reed, Deo and Rittmann 2010; Runde and Neu 2010).

For the anoxic, reducing, and mildly basic brine systems expected in the WIPP, the most important inorganic complexants are expected to be carbonate/bicarbonate and hydroxide. There are also important organic complexants that coexist in TRU waste with the potential to strongly influence actinide solubility. In this context, the relative importance of actinides and overall oxidation state with respect to their potential release from the WIPP is:

Actinides: Pu ≈ Am >> U > Th >> Np ≈ Cm (SOTERM.24)

Actinide Oxidation State: An(III) > An(IV) >> An(VI) >> An(V) (SOTERM.25)

In the CRA-2014 PA (Appendix PA-2014, Section 8.4), the contribution of Pu, Am, U, Th, Cm, and Np is expressly considered, although only Pu and Am contribute significantly to TRU release from the WIPP. The III oxidation state is the most important oxidation state based on current WIPP PA assumptions that Am always exists in the III state, Pu exists in the III state in ~50% of the vectors, and the III oxidation state is more soluble than the IV (see Section SOTERM-4.0 and Tables SOTERM-20 and SOTERM-24).

In this section, an update of the literature and a summary of new WIPP-specific data is provided (when available) for all the actinides that contribute in one way or another to PA. Section SOTERM-3.1 gives a summary of changes since the CRA-2009 and CRA-2009 PABC; Section SOTERM-3.2 gives an overview of the projected and current inventory of actinides in the WIPP; Section SOTERM-3.3, Section SOTERM-3.4, Section SOTERM-3.5, Section SOTERM-3.6 and SOTERM-3.7 contain an overview of the relevant environmental chemistry and WIPP-specific results for Th, U, Np, Pu, and Am/Cm, respectively; Section SOTERM-3.8 pertains to the complexation of actinides by organic chelating agents in the WIPP; and Section SOTERM-3.9 provides an overview of the potential for the formation of actinide colloids in the WIPP. An up-front overview of the current assumptions and understanding of WIPP actinide chemistry is given in Table SOTERM-8. The PA implementation of this actinide environmental chemistry is discussed in Section SOTERM-4.0 and Section SOTERM-5.0.

SOTERM-3.1 Changes in Actinide Chemistry Information since the CRA-2009 and the CRA-2009 PABC

Overall, there are few significant changes in the CRA-2014 general approach and assumptions used to understand and predict actinide behavior in the WIPP from a PA perspective. The following key assumptions are continued:

- Oxidation state distributions for the TRU actinides, and correspondingly, assumptions regarding their solubility calculations using redox-invariant analogs, have not changed.
- The approach used to calculate solubilities for Pu and Am oxidation states, which are the key actinides from the perspective of PA, have not changed. EQ3/6, rather than FMT, however, is now being used to calculate these solubilities with the WIPP actinide database.
- Inventory assumptions regarding the amounts of organic chelating agents and actinides in TRU waste are being updated annually.
- The WIPP colloidal model that accounts for intrinsic, mineral fragment, microbial and humic colloidal enhancements has not changed.

Table SOTERM- 8. Overview of the WIPP PA View/Role and Relevant Environmental Chemistry of the Key Actinide Species in the WIPP (References for Each Actinide are Provided in the Following Sections)

Actinide	WIPP PA View/Role	Environmental Chemistry
Thorium	Not a TRU component. Currently included in PA calculations, but not a significant contributor to actinide release. Used as an oxidation-state invariant analog for the IV actinides. Th data are used in EQ3/6 to calculate the solubility of Pu(IV), Np(IV), and U(IV).	Exists as Th^{4+} complexes and is sparingly soluble under a wide range of environmental conditions. Th has a high tendency towards intrinsic colloid formation.
Uranium	Not a TRU component. Potentially useful as a VI analog for Pu(VI) species. Currently, U is conservatively assumed to be U(VI) in 50% of the PA vectors (set at a 1 mM solubility) and U(IV) in 50% of the PA vectors. It is not predicted to be a significant contributor to actinide release (based on Ci).	Exists as UO_2^{2+} and U^{4+} species that are strongly correlated with redox conditions. Can form highly insoluble U(VI) and U(IV) phases. Can persist up to mM concentrations in near-surface groundwater.
Neptunium	TRU component. Currently included in the PA calculations, but not a significant contributor to actinide release. Assumed to be IV in 50% of the PA vectors and V in 50% of the PA vectors. Expected to predominate in the IV oxidation state under the conditions expected in the WIPP.	Mobile and relatively soluble as the NpO_2^{+} species under oxidizing conditions. Is fairly insoluble and immobile as Np^{4+} under reducing conditions.
Plutonium	TRU component. Major contributor to actinide release calculations. Assumed to be IV in 50% of PA vectors and III in the other 50% of PA vectors.	Relatively immobile and insoluble as a subsurface contaminant. Persists as Pu^{4+} except under biomediated, strongly reducing conditions where Pu^{3+} species may be formed. If transported, this will likey be primarily through colloidal mechanisms.
Americium	TRU component. Major contributor to actinide release calculations. Exists in the III oxidation state in all vectors and its thermodynamic data are used by EQ3/6 for all III oxidation state calculations. Significant colloidal contribution due to strong association as a pseudocolloid.	Relatively immobile and insoluble as a subsurface contaminant. Persists as Am^{3+} complexes under a wide range of environmental conditions.
Curium		

Actinide	WIPP PA View/Role	Environmental Chemistry
	Small quantities of ^{243}Cm, ^{245}Cm, and ^{248}Cm are present in the WIPP. ^{244}Cm, although present, is not a TRU waste component due to its <20 year half-life. These are very minor contributors to actinide release. Chemistry is analogous to Am(III).	Not a very significant concern as a subsurface contaminant. Has the same chemistry as Am, so it will persist as a Cm^{3+} species.
Organic Chelating Agents	The effects of EDTA, citrate, oxalate, and acetate on actinide solubility are considered in the WIPP PA. These are present in the WIPP waste and it is assumed that they are neither destroyed nor created by WIPP-relevant subsurface processes.	EDTA can persist under a wide range of environmental conditions and strongly chelates actinides. Citrate, oxalate, and acetate will likely be degraded due to microbial activity.
Actinide Colloids	Intrinsic and pseudocolloids with actinides are formed. These are accounted for in the WIPP PA and add to the conservatism of the actinide concentrations calculated.	Importance and role of An colloid-facilitated transport are the subject of much ongoing debate. The key issue within the WIPP is the potential contribution of colloids to the actinide source term and not their ability to facilitate actinide transport.

There are new data, within and outside the WIPP project, that continue to support and/or expand the robustness of the current PA assumptions. The most important of these are:

- New WIPP-specific data that confirm the predominance of lower-valent plutonium in long-term, iron-dominated brine systems.
- The solubility of An(IV) in simulated WIPP brines over a wide range of conditions was experimentally determined using Th (IV) as an analog for Pu(IV). These data support current PA solubilities for the IV actinides.
- The effect of the complexation of organic chelating agents on actinide (III/IV) oxidation states was experimentally determined. Relatively strong complexation effects are noted with An(III) that is consistent with current WIPP modeling.
- The solubility of U(VI) as a function of carbonate was determined and shown to be well below the current EPA-set limit of 1 mM.
- The colloidal enhancement parameters were re-evaluated and new parameter recommendations were made. Experiments specific to intrinsic, microbial, and to a lesser extent mineral fragment colloids are reported. These data, although incomplete, provide stronger supporting data for the current WIPP colloid model. The specific changes are described in more detail in Section SOTERM-3.9.
- A variable brine volume approach was implemented in PA to calculate actinide solubility. This extends the minimum brine volume approach used in CRA-2009.

SOTERM-3.2 Actinide Inventory in the WIPP

The actinide inventory for the WIPP, based on the Performance Assessment Inventory Report - 2012 (Van Soest 2012), is given in Table SOTERM-9. This is the inventory used in CRA-2014. Also included in this table is the calculated inventory-limited solubility of the various actinides and radionuclides considered by the WIPP PA.

Over long time frames, only Pu and Am are expected to make a significant contribution to releases from the WIPP (see time profile in Table SOTERM-10), although the relative contribution of Am decreases significantly after 1000 years due to its half-life. Curium (Cm), which is predominantly present as ^{244}Cm, is well below the calculated solubility for III actinides when fully dissolved and, with its very short half-life (18.11 years), will not be important beyond the 100-year period of institutional control. Although some cesium (Cs) and strontium (Sr) is initially present in the WIPP, these fission products can only contribute significantly to the overall release from the WIPP for the first 100 years of repository history and are not significant beyond the period of institutional control.

Table SOTERM- 9. WIPP Radionuclide Inventory (Van Soest 2012) Decay-Corrected to 2033. This Inventory was used in the CRA-2014 PA Calculations.

Selected Radionuclides	Activity (Ci)	Amount (kg)	Element-Specific Inventory (all reported isotopes)	Inventory-Defined Solubility Limit[a] (M)
Actinides				
^{229}Th	1.40	6.57×10^{-3}	7.04 Ci 1.35×10^{4} Kg	>> Solubility
^{230}Th	4.14	0.2		
^{232}Th	1.50	1.35×10^{4}		

Selected Radionuclides	Activity (Ci)	Amount (kg)	Element-Specific Inventory (all reported isotopes)	Inventory-Defined Solubility Limit[a] (M)
^{233}U	139	14.2		
^{234}U	242	38.3		
^{235}U	76.4	3.49×10^{4}	528 Ci 2.26×10^{5} Kg	>> Solubility
^{236}U	5.44	83.2		
^{238}U	64.8	1.91×10^{5}		
^{237}Np	23.2	32.5	23.2 Ci 32.5 Kg	8×10^{-6} M (≥ projected solubility)
^{238}Pu	6.01×10^{5}	34.7		
^{239}Pu	5.74×10^{5}	9.13×10^{3}		
^{240}Pu	1.75×10^{5}	762	2.02×10^{6}Ci 1.20×10^{4} Kg	>> Solubility
^{241}Pu	6.63×10^{5}	6.38		
^{242}Pu	8.09×10^{3}	2.04×10^{3}		
^{244}Pu	0.0101	0.567		
^{241}Am	7.05×10^{5}	203	7.05×10^{5} Ci 203 Kg	5×10^{-5} M (≥ projected solubility)
^{243}Am	51.2	0.254		
^{244}Cm	9.97×10^{3}	0.122	9.97×10^{3} Ci 0.122 Kg	~ 3 x 10^{-8} M
Fission Products[b]				
^{137}Cs	2.35×10^{5}	2.67	2.35×10^{5} Ci 2.67 Kg	1×10^{-6} M
^{90}Sr	2.09×10^{5}	1.51	2.09×10^{5} Ci 1.51 Kg	1×10^{-6} M

a Moles in the inventory divided by the minimum brine volume (17,400 m^3)
b Fission products are not TRU, but are considered in the PA to calculate overall release

Table SOTERM-10. Time-dependence of Radionuclide Inventory (Van Soest 2012)

Element	2033 (0 years) Ci (Kg)	2133 (100 years) Ci (Kg)	3033 (1000 years) Ci (Kg)	12033 (10,000 years) Ci (Kg)
Th	7.04 (1.35×10^{4})	8.52 (1.35×10^{4})	22.5 (1.35×10^{4})	127 (1.35×10^{4})
U	528 (2.26×10^{5})	645 (2.26×10^{5})	746 (2.26×10^{5})	769 (2.28×10^{5})
Np	23.2 (32.5)	44.8 (62.9)	140 (197)	170 (238)
Pu	2.02×10^{6} (1.20×10^{4})	1.03×10^{6} (1.19×10^{4})	7.24×10^{5} (1.16E4)	5.00×10^{5} (9.12×10^{3})
Am	7.05×10^{5} (203)	6.20×10^{5} (179)	1.47×10^{5} (42.4)	21.1 (0.0994)
Cm	9.97×10^{3}	216	2.32×10^{-13}	0.00

	(0.122)	(2.65×10^{-3})	(2.84×10^{-18})	(0.00)
Cs	2.35×10^{5} (2.67)	2.33×10^{4} (0.265)	2.17×10^{-5} (2.46×10^{-10})	0.00 (0.00)
Sr	2.09×10^{5} (1.51)	1.78×10^{4} (0.129)	4.21×10^{-6} (3.05×10^{-11})	0.00 (0.00)

SOTERM-3.3 Thorium Chemistry

Th is not a TRU component, although an estimated 13.5 metric tons of Th will be in the WIPP. The release of Th as the ^{230}Th isotope was calculated in the CRA-2014 PA and does not significantly contribute to the overall release of activity from the WIPP. Th is, however, important for the WIPP in that it is used as a redox-invariant analog for the IV actinides (Pu(IV), Np(IV), and U (IV)), and Th complexation data are used in the EQ3/6 code for the An(IV) solubility calculations (Section SOTERM-4.1).

SOTERM-3.3.1 Thorium Environmental Chemistry

Th, under a wide range of conditions, has one stable oxidation state in aqueous solutions: the Th^{4+} tetravalent ion. For this reason, the environmental chemistry of Th is understood from the perspective of the solubility and complexation of this species, which is also the species expected to be present in the WIPP environment when DBR and transport release scenarios are important.

Other oxidation states for Th in aqueous systems have been reported. Klapötke and Schulz (Klapötke and Schulz 1997) suggested a Th^{3+} species as a somewhat stable species in slightly acidic solution but this is not correct; it has been discounted because the proposed reaction for the species' formation is shown to be thermodynamically impossible, and the azido-chloro Th^{4+} complex was incorrectly assigned to the Th^{3+} species (Ionova, Madic, and Guillaumont 1998).

The hydrolysis of Th^{4+}, as is true for all An(IV) species in the WIPP, is complex and a critically important interaction in defining the overall solubility of Th. This was recently investigated by Ekberg et al. (Ekberg et al. 2000), Rai et al. (Rai et al. 2000), Moulin et al. (Moulin et al. 2001), and Okamoto, Mochizuki, and Tsushim (Okamoto, Mochizuki, and Tsushim 2003), and was critically reviewed by Neck and Kim (Neck and Kim 2001) and Moriyama et al. (Moriyama et al. 2005). The authors have proposed a comprehensive set of thermodynamic constants that extends to all tetravalent actinides. The solubility products were determined for amorphous (am) $Th(OH)_4$ (Neck et al. 2002; Altmaier et al. 2005 and Altmaier et al. 2006) and for crystalline ThO_2 (Neck et al. 2003), as well as for specific ion interaction theory parameters (Neck, Altmaier, and Fanghänel 2006). The thermodynamic stability constants are listed in Table SOTERM-11.

Table SOTERM- 11. Thermodynamic Stability Constants for Key Th Hydrolytic Species

Hydrolytic Reaction/Species	Stability Constant
Mononuclear Species	
$Th(OH)_{4,am} \leftrightarrows Th^{4+} + 4OH^-$	$\log K_{s,am} = -47.8 \pm 0.3$
$Th(OH)_{4,cr} \leftrightarrows Th^{4+} + 4OH^-$	$\log K_{s,cr} = -53.2 \pm 0.4$
$Th^{4+} + OH^- \leftrightarrows Th(OH)^{3+}$	$\log \beta^0_{\ 1} = 11.8 \pm 0.2$
$Th^{4+} + 2OH^- \leftrightarrows Th(OH)_2^{\ 2+}$	$\log \beta^0_{\ 2} = 22.0 \pm 0.6$
$Th^{4+} + 3OH^- \leftrightarrows Th(OH)_3^{\ +}$	$\log \beta^0_{\ 3} = 31 \pm 1$
$Th^{4+} + 4OH^- \leftrightarrows Th(OH)_{4,aq}$	$\log \beta^0_{\ 4} = 38.5 \pm 1$
Polynuclear Species	
$4Th^{4+} + 12OH^- \leftrightarrows Th_4(OH)_{12}^{\ 4+}$	$\log \beta^0_{\ 4,12} = 141$
$6Th^{4+} + 15OH^- \leftrightarrows Th_6(OH)_{15}^{\ 9+}$	$\log \beta^0_{\ 6,15} = 176$

Discrepancies in the ThO_2(cr) solubility were recently studied (Vandenborre et al. 2010) and assigned to the different forms of material present: bulk ThO_2(cr) grains (80%) and $ThO_x(OH)_y(H_2O)_z$(s) grain boundaries (20%). The hydrated material may originate from the initial grain-boundary oxide materials, which are more sensitive to humidity than the bulk materials. The solubilities of these two phases are quite different and together with the "local solubility" (the most active sites) were used to explain the discrepancies noted.

The presence of carbonate in solution greatly increases the solubility of thorium dioxide (ThO_2). An increase by one order of magnitude of the carbonate concentration in the range of 0.1 - 2 M leads to a five-order-of-magnitude increase in the Th(IV)

solubility due to the formation of mono- and penta-carbonate complexes. Östhols, Bruno, and Grenthe (Östhols, Bruno, and Grenthe 1994) proposed the following equilibrium reactions and the corresponding stability constants:

$$ThO_2 + H^+ + H_2O + CO_3^{2-} \leftrightarrows Th(OH)_3CO_3^- \log K_{131} = 6.11 \pm 0.19 \text{ (SOTERM.26)}$$

$$ThO_2 + 4H^+ + 5\,CO_3^{2-} \leftrightarrows Th(CO_3)_5^{6-} + 2H_2O \log K_{105} = 42.12 \pm 0.32 \text{ (SOTERM.27)}$$

This speciation scheme, however, was criticized in recent work (Altmaier et al. 2005) because it overpredicts the dependency of Th solubility on carbonate and underpredicts the effect of hydrolysis at higher pH. That hydrolysis prevails at pH >10 is supported by detailed experimental results (Figure SOTERM-6). These data are explained by the predominance in this system of $Th(OH)(CO_3)_4^{5-}$ complex rather than $Th(CO_3)_5^{6-}$. A greater role for other ternary complexes of thorium (e.g., $Th(OH)_2(CO_3)_2^{2-}$), which are also likely to be present in the WIPP conditions, is also proposed, and formation constants for these complexation reactions are reported. The use of the pentacarbonyl complex for the IV actinides in the WIPP PA, for these reasons, is a conservative assumption that overpredicts the solubility of the IV oxidation state at pH > 10. A correction in the FMT database, now in the EQ3/6 database, to the value of the $Th(OH)_4$(aqueous [aq]) to be consistent with Neck et al. (Neck et al. 2002) was incorporated into the CRA-2004 PABC and there are no new changes in this speciation scheme in CRA-2014.

The dissolution of crystalline ThO_2 in low ionic strength media and the effect of carbonate and calcium concentration on the solubility of thorium were investigated at alkaline pH (Kim et al. 2010). The observed thorium concentration in the groundwater was greater than predicted. This discrepancy was explained by the authors as the result of colloid formation. Carbonate affected the observed thorium solubility as expected. There was no calcium enhancement of the thorium solubility until a calcium concentration of 1.25 mM.

Oxyanions such as phosphate and, to a lesser extent, sulfate, also form Th^{4+} complexes that can precipitate at pH <5. The effect of phosphate on solubility of microcrystalline ThO_2 is very limited. The stability constants for $Th^{4+}/H_2PO_4^-$ and Th^{4+}/HPO_4^{2-} were reported (Langmuir and Herman 1980). Overall, the role of these oxyanions is expected to be unimportant for the mildly basic brines (pH ~8-10) present in the WIPP.

A new perturbation to the understanding of Th speciation, as well as other actinides in the IV oxidation state, is the recent observation that Ca, and to a lesser extent, magnesium (Mg), enhances Th solubility at pH >10 when carbonate is present (see Figure SOTERM-7). In recent publications, the formation of $Ca_4[Th(OH)_8]^{4+}$ and $Ca_4[Pu(OH)_8]^{4+}$ ion pairs in alkaline $CaCl_2$ solution is reported (Brendebach et al. 2007; Altmaier, Neck, and Fanghänel 2008). These species cause a rapid increase in the solubility of all tetravalent actinides at pH greater than 11. This increased solubility is only observed at $CaCl_2$ concentrations above 0.5 M for Th(IV), and correspondingly above 2 M for Pu(IV) species. This effect can be discounted for the WIPP PA because Ca concentrations in the WIPP are predicted to be approximately 14 mM or less with a pH of approximately 8.7. These are both well below the levels needed to see a significant effect for both Th and Pu.

Actinides in the IV oxidation state, because of the complexity of their solution chemistry and very high tendency towards hydrolysis, form colloidal species in groundwater. The potential effect of colloid formation on solubility of Th(IV) in concentrated NaCl and $MgCl_2$ solution was recently published by Altmaier, Neck, and Fanghänel (Altmaier, Neck, and Fanghänel 2004) and is shown in Figure SOTERM-8. In neutral-to-alkaline solutions, colloids could be formed as Th oxyhydroxide with $\log [Th]_{(colloid\ [coll])} = -6.3 \pm 0.5$, independent of ionic strength. In Mg solutions, the formation of pseudocolloids (i.e., Th(IV))sorbed onto $Mg_2(OH)_3Cl \cdot 4H_2O$(coll) led to an apparent increase of the total Th concentration up to 10^{-5} M (Walther 2003; Degueldre and Kline 2007; Bundschuh et al. 2000). For these reasons, colloid formation is addressed in the WIPP PA.

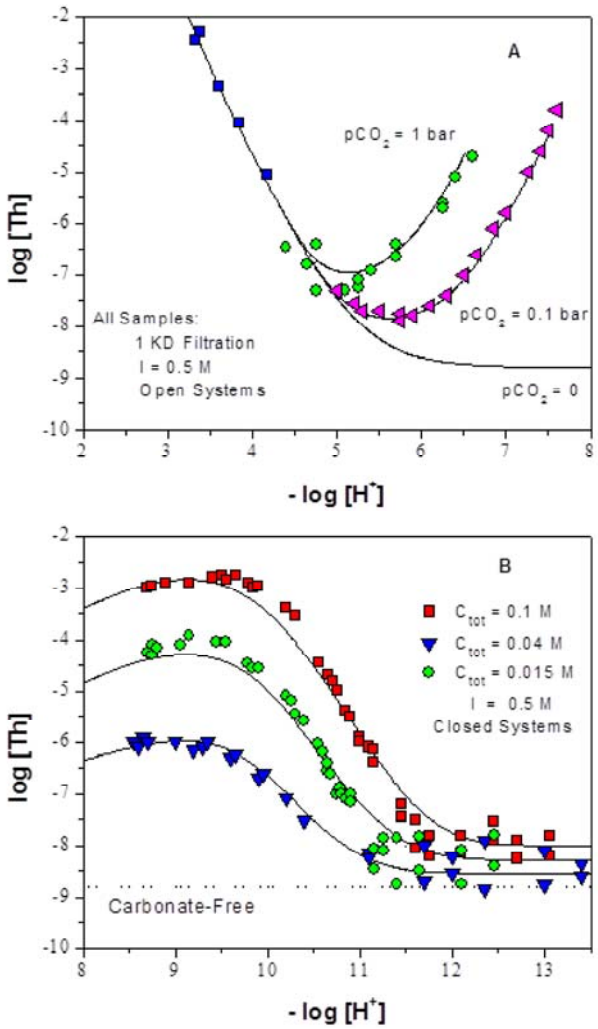

Figure SOTERM- 6. Solubility of Amorphous Th(IV) Oxyhydroxide as a Function of Carbonate Concentration in 0.5 M for (A) pH = 2-8 and (B) pH = 8-13.5. The solid lines are the calculated solubilities (based on data in Altmaier et al. 2005).

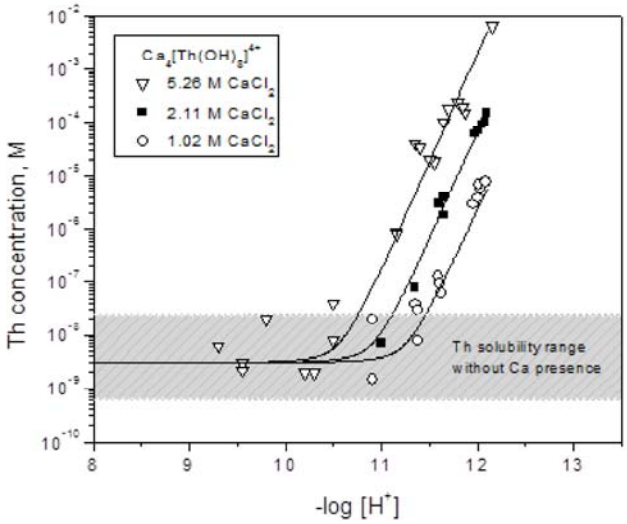

Figure SOTERM- 7. Effect of Calcium-carbonate Ternary Complexes on the Solubility of Th(IV) in Brine (Altmaier 2011).

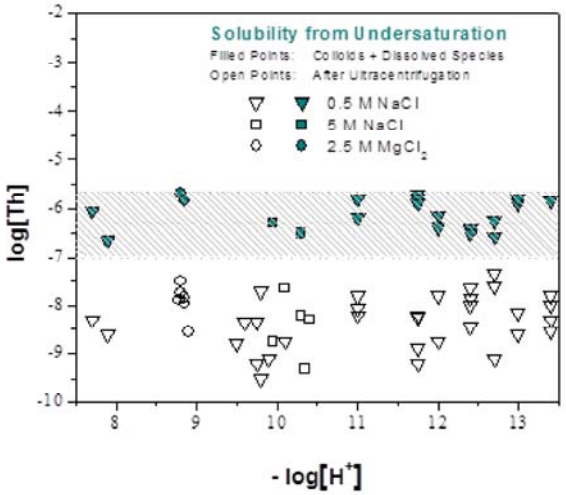

Figure SOTERM- 8. Solubility of $Th(OH)_4(am)$ Determined from Undersaturation in 0.5 NaCl, 5.0 M NaCl, and 2.5 M $MgCl_2$. Filled Points: Total Th Concentrations (Including Colloids); Open Points: Th Concentrations Measured after Ultracentrifugation at 90,000 Revolutions Per Minute (5×10^5 g) (based on data in Altmaier, Neck, and Fanghänel 2004).

SOTERM-3.3.2 WIPP-Specific Results since the CRA-2009 and the CRA-2009 PABC

A study to establish the solubility of thorium under WIPP-specific conditions was completed since CRA-2009. These experiments were performed in carbonate-free and carbonate-containing WIPP simulated brine to establish the effects of carbonate, pC_{H+} and time on thorium (IV) solubility and are published in a report entitled "Solubility of An(IV) in WIPP Brine, Thorium Analog Studies in WIPP Simulated Brine" (Borkowski et al. 2012).

The results obtained are shown in Figure SOTERM-9. After 2 years of equilibration in carbonate-free brine, the measured solubility of thorium was $6\text{-}7\times10^{-7}$ M and was essentially independent of pH and brine composition over the 6.5 to 11.5 pC_{H+} range investigated. Sequential filtration to ~ 10 nm pore size had little effect on the measured concentration. Subsequent ultracentrifugation up to 1,000,000 g resulted in up to a 40% colloidal fraction (but typically 20% or less), indicating that there was much less intrinsic colloid formation than reported in Altmaier, Neck and Fanghänel (2004) - see Figure SOTERM-8. The steady-state thorium concentrations measured, however, are consistent with literature reports for simplified brine systems (Altmaier, Neck and Fanghänel 2004) but show a significantly lower extent of aggregation to form intrinsic colloids.

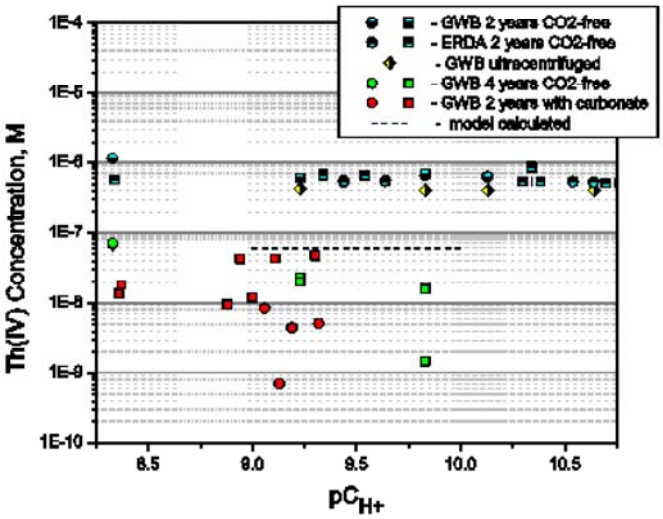

Figure SOTERM- 9. The Concentration of Thorium Measured in WIPP Simulated Brine (GWB and ERDA-6) as a Function of Time, Filtration and the Presence of Carbonate. Square symbols represent an undersaturation approach, whereas the circles represent the oversaturation approach. Although

high, but metastable, concentrations were initially present, in time the measured concentrations decreased and are at or below the WIPP model-predicted values (Borkowski et al. 2012).

After an additional 2 years of equilibration, the thorium concentration in carbonate-free GWB significantly decreased (green points in the figure). For pC_{H+} in the range of 7.5 to 8.3 (not all data shown in Figure SOTERM-9), some samples did not show a change in the thorium concentration, but others showed a decrease of over one order of magnitude and were similar to the thorium concentrations measured in GWB containing 10^{-2} and 10^{-3} M carbonate.

The presence of carbonate, at a concentration that is ten-fold greater than expected in the WIPP, had little/no effect on the measured thorium concentrations. After two years of equilibration, the thorium concentrations measured from under- and oversaturation in GWB did not depend on carbonate concentration. Concentrations measured from oversaturation were 2.5 orders of magnitude greater than those measured from undersaturation, indicating that metastable states can persist for long periods of time. The trend in the oversaturation data (see Figure SOTERM-9) is consistant with the literature data (Altmaier et al. 2005). In the undersaturation experiments, which are more relevant to the WIPP situation, the average thorium concentration was 2×10^{-8} M and continued to decrease at $pC_{H+} > 9$. The oversaturation experiments showed a similar trend and at $pC_{H+} > 9$ the thorium concentrations decreased to below 10^{-8} M. These results reproduce, to some extent, the trends reported in the literature (Altmaier et al. 2005), but the much higher ionic strength solutions used in our experiments shift our pH profile to a lower pC_{H+} value by approximately 1 pH unit.

At the expected WIPP repository pC_{H+}(~ 9.5), in the presence of carbonate, the thorium concentrations in GWB brine were 2×10^{-8} M or lower. This concentration trend suggests that at repository conditions the mixed thorium hydroxy-carbonato complexes do not play any role in the thorium solubility at $pC_{H+} > 9$.

The sequential filtration of thorium in the carbonate system (see Figure SOTERM-10) led to a dissolved thorium concentration of $2\text{-}6\times10^{-8}$ M in GWB. In ERDA-6 brine, however, the dissolved thorium concentration was about ten-fold greater and it is apparent that steady state thorium concentration was not achieved. The colloidal thorium species appear to be very small, less than 10 kDa (~5 nm). Overall, the truly dissolved thorium concentration was $3(\pm2) \times 10^{-8}$ M. The average total thorium concentration consisted of a dissolved fraction of 30 - 60% and a colloidal fraction of 40 - 70%.

The WIPP-specific thorium solubility results just summarized support the ongoing WIPP recertification effort in three important ways: 1) they provide empirical solubilities over a broad range of conditions that improve the robustness of the WIPP PA model, 2) they resolve and address published literature data in simplified brine systems that appeared to disagree with the current WIPP PA approach, and 3) they provide an input that will help establish the intrinsic colloidal enhancement factors for IV actinides. There is general agreement between our data and results reported in the literature for simplified brine systems, although we are seeing a far lower colloidal fraction in the total concentrations measured. After 4 years of equilibration, our measured solubilities are slightly lower (by a factor of ~ 2) than the solubilities calculated in the WIPP PA - this is well within the order of magnitude uncertainty typically observed between the calculated and measured solubilities in complex brine systems.

A key motivation in the WIPP thorium solubility and speciation studies was to explain the reports in the literature that very high colloidal fractions are present in high ionic-strength brine systems (mainly Altmaier et al. 2004). The WIPP-specific data show that there are colloids present in these systems, but these are much less than what was reported. The explanation for this is a combination of the differences in brine composition (sodium chloride brine vs. GWB/ERDA-6) between the two studies and the presence of MgO colloids in the Altmaier study where mineral fragment colloids were likely formed (which is counted as part of their colloidal fraction). Perhaps a more important result in the WIPP-specific studies is the observation that there is an equilibration between the intrinsic colloidal fraction and the dissolved species. This equilibrium shifts to a lower overall solubility with time that is now consistent with WIPP modeling predictions. This long-term shift defines these higher initial and essentially pH independent values for thorium solubility (Figure SOTERM-9 and SOTERM-8) that were obtained in both the German and WIPP data as metastable concentrations of thorium and explains the apparent discrepancy between model-predictions and experimental results. These solubility data support the current WIPP PA assumptions on An(IV) solubility and extend past project data to a broader range of pH and carbonate levels. These results also note that Ca-enhanced hydroxyl complexation can greatly increase the solubility of actinides (IV), something that has only been understood in the last couple of years; however, this complexation requires relatively high pH in combination with very high Ca levels, something that is not expected in the WIPP. The expected pH and dissolved Ca levels in the WIPP predict no effect on An(IV) dissolved concentration due to formation of this complex.

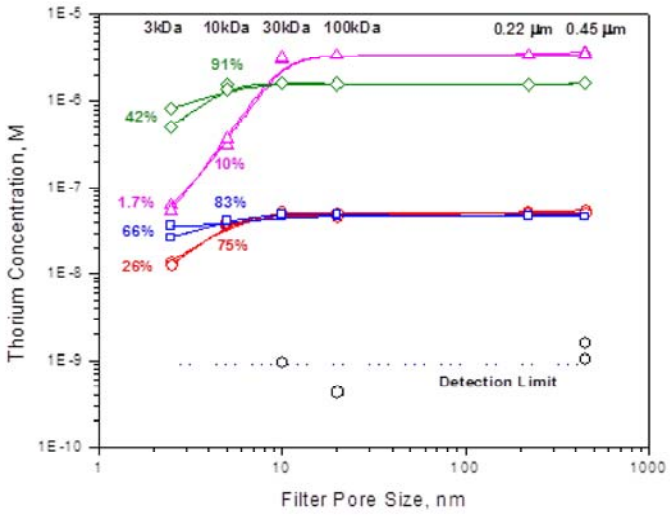

Figure SOTERM- 10. Thorium Concentration in Simulated WIPP Brine as a Function of Pore Size. Ultrafilters used are given at the top of the figure and correlate with the filter pore size on the x axis. The % numbers shown correspond to the % of thorium that passed through the filter for each data point.

SOTERM-3.4 Uranium Chemistry

Uranium is not a TRU component but is, by mass, the predominant actinide in the WIPP. Current estimates predict that ~226 metric tons will be placed in the repository (Van Soest 2012), but this is believed to be a high estimate since uranium content in waste is often indirectly determined. By mass, approximately 85% of this will be the ^{238}U isotope, with minor amounts of ^{233}U, ^{234}U, ^{235}U, and ^{236}U. Uranium does not contribute significantly to actinide release through cuttings/cavings and spallings because of its low specific activity (1.22×10^{4}Bq.g^{-1}). Uranium release can occur through the Culebra in very small amounts because of its potentially high solubility and low partition coefficient (K_d) in the VI oxidation state.

Uranium release, as the ^{234} U isotope, was calculated in the CRA-2014 PA. In the WIPP PA, the oxidation state distribution assumption is that U speciates as U(IV) in the reduced PA vectors and as U(VI) in the oxidized vectors (Section SOTERM-4.1). The concentration for U(VI) is currently set at 1 mM (U.S. EPA 2005), since there is no An(VI) model in the WIPP. U(IV) solubility is calculated using the Th(IV) speciation data in the WIPP model.

SOTERM-3.4.1 Uranium Environmental Chemistry

Uranium is by far the most studied of the actinides under environmentally relevant conditions. An extensive review of this chemistry, as it relates to the WIPP case, was completed in 2009 (Lucchini et al 2010a; U.S DOE 2009), and is updated herein. More general reviews can be found (Morss, Edelstein, and Fuger 2006; Guillaumont et al. 2003; Runde and Neu 2010). An overview of U environmental chemistry is presented in this section.

SOTERM-3.4.1.1 Uranium Subsurface Redox Chemistry

Uranium can theoretically exist in aqueous solution in the III, IV, V, and VI oxidation states (Hobart 1990; Keller 1971 [pp. 195-215]; Clark, Hobart and Neu 1995). In the environment, however, only the IV and VI oxidation states, which exist as U^{4+} and UO_2^{2+} species, are present. U^{3+}, should it be formed, is metastable and readily oxidized in aqueous solution, and U(V) only exists as a very short-lived transient that instantaneously disproportionates to form U(IV) and U(VI) species. The corresponding reduction potential diagram for U at pH = 0, 8, and 14 is given in Figure SOTERM-11 (Morss, Edelstein, and Fuger 2006).

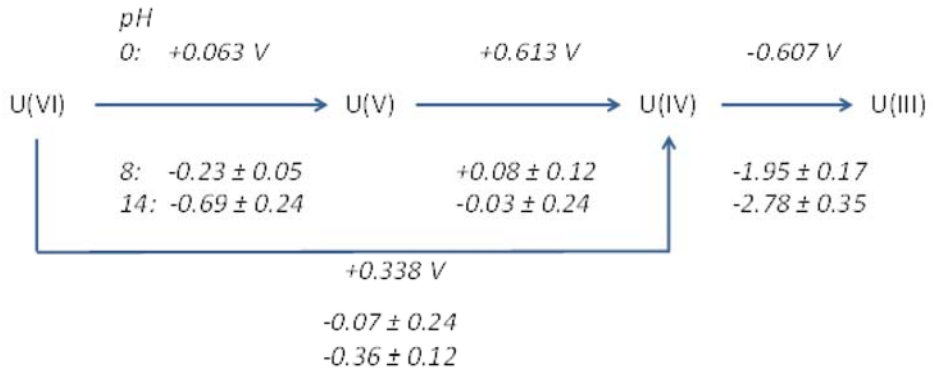

Figure SOTERM- 11. Reduction Potential Diagram for U at pH = 0, 8, and 14 (Based on Data in Morss, Edelstein, and Fuger 2006). For the expected reducing and mildly basic pH conditions in the WIPP, U(IV) is predicted to be the predominant oxidation state.

Under oxidizing subsurface conditions typical of most near-surface groundwater, U(VI) as UO_2^{2+} uranyl complexes is the predominant oxidation state and is not easily reduced geochemically. Thermodynamically, uranyl species are stable even under mildly reducing conditions and are not reduced by some Fe(II) phases (see Table SOTERM-5). In anoxic WIPP brine experiments with a hydrogen overpressure, uranyl persists as a stable hydrolytic or carbonate complex for over two years (Reed and Wygmans 1997).

In the anoxic and strongly reducing environment expected in the WIPP, however, potential reduction pathways exist. The two most important of these reduction pathways are reaction of uranyl with reduced iron phases (Fe[0/II]), and bioreduction by anaerobic microorganisms (e.g., metal and sulfate reducers). For these reasons, U(IV) is the oxidation state expected to predominate in the WIPP when brine inundation occurs.

The use of iron barriers in the removal of uranyl from groundwater is well established and has been reported for the removal of U (VI) from groundwater using zero-valent iron barriers (Gu et al. 1998; Fiedor et al. 1998; Farrell et al. 1999) and iron corrosion products formed in saline solution (Grambow et al. 1996). However, in those studies, it was unclear whether the removal of uranyl (UO_2^{2+}) resulted from reductive precipitation or from adsorption onto/incorporation into the iron corrosion products (Gu et al. 1998). In their experiments under saline conditions, Grambow et al. (Grambow et al. 1996) found that a large percentage of U was rapidly adsorbed onto the iron corrosion products consisting of over 97% hydrous Fe(II) oxide, and very little U(IV) was found. Recently, Myllykylä and Ollila (Myllykylä and Ollila 2011) observed the presence of U(IV) after adding an excess of Fe(II) to 0.01M NaCl and 0.002M $NaHCO_3$ solutions containing U(VI) inside an anaerobic glovebox.

Under anoxic conditions, Trolard et al. (Trolard et al. 1997) established that the corrosion of steel and iron generates Fe(II)/Fe(III) hydroxide species known as green rusts. Green rusts contain a certain amount of nonhydroxyl anions (carbonate, halides, or sulfate); they have a high specific surface area (Cui and Spahiu 2002) and a high cation sequestration capacity (O'Loughlin et al. 2003). They are considered metastable oxidation products of Fe(II) to magnetite Fe_3O_4 and Fe(III) oxyhydroxides (e.g., goethite α-FeOOH) (O'Loughlin et al. 2003). They could be generated by iron corrosion in the WIPP brines (Wang et al. 2001). A few experimental studies demonstrate that U(VI) is reduced to U(IV) by green rusts (Dodge et al. 2002; O'Loughlin et al. 2003).

Recent studies suggest that magnetite stoichiometry can significantly influence the extent of U(VI) reduction (Latta et al. 2012). Latta et al. (Latta et al. 2012) demonstrated that stoichiometric and partially oxidized magnetite ($Fe^{2+}/Fe^{3+} \geq 0.38$) reduce U(VI) to U(IV) in UO_2 nanoparticles in 2mM $NaHCO_3$ solution at pH 7.2, whereas with more oxidized magnetite ($Fe^{2+}/Fe^{3+} < 0.38$), possibly sorbed U(VI) is the dominant phase observed. Atomistic simulations conducted by Kerisit, Felmy and Ilton (Kerisit, Felmy and Ilton 2011), supported by existing Extended X-Ray Absorption Fine Structure (EXAFS) data provide strong evidence for the structural incorporation of U in Fe (hydro)oxides. The complexity of the U-Fe-H_2O-CO_2 system can explain the lack of a predominant mechanism (reduction-precipitation or adsorption/incorporation) for the removal of U(VI) in the presence of iron phases (Du et al. 2011; Ilton et al. 2012; Singer et al. 2012a; Singer et al. 2012b).

Banaszak, Rittmann, and Reed (Banaszak, Rittmann, and Reed 1998) have reviewed the important role of microbial processes in the reduction of multivalent metals under anaerobic/reducing conditions. For uranyl in particular, several studies exist that show that U(VI) is reduced to U(IV) species under a wide range of conditions (Lovley et al. 1991; Lovley et al. 1993; Barton et al. 1996; Huang et al. 1998; Abdelouas et al. 2000; Bender et al. 2000; Fredrickson et al. 2000; Suzuki et al. 2003). Most of this work pertains to groundwater bacteria, and is not directly applicable to the WIPP.

There are relatively few studies that investigate the interaction of U with the halophiles that are more typically present in the WIPP brine (Francis et al. 2004). Some WIPP-relevant research was done (Francis et al. 2000), but this work was mostly focused on gas

generation, not actinide interactions. It remains to be demonstrated that the mechanisms leading to the bioreduction of U(VI) also extend to the microbes present in the WIPP.

SOTERM-3.4.1.2 Solubility of U(IV)

Tetravalent U is expected to be the dominant oxidation state in the WIPP as a result of the reducing conditions that will prevail. The solubility of U(IV) under these conditions is analogous to that observed for Th (see Section SOTERM-3.3) and is, in fact, calculated in the WIPP PA with the Th(IV) database.

Experimentally, in solution, U^{4+} is readily oxidized to UO_2^{2+}. This occurs even when only trace levels of oxygen exist that are often below the limit of detection by most laboratory instrumentation. This explains why there are relatively few studies of U^{4+}. It is also problematic because there are very large discrepancies in the literature as a result of experimental artifact. In particular, there are a number of published results (Rai, Felmy, and Ryan 1990; Gayer and Leider 1957; Ryan and Rai 1983; Tremain et al. 1981; Casas et al. 1998) that suggest amphotericity for U^{4+} at pH >10. This, however, likely resulted from combined effects of two experimental artifacts: (1) oxidation to UO_2^{2+}, which is much more soluble, and (2) the presence of carbonate, which is a strong complexant of U^{4+}.

The solubility of U(IV) phases were also determined in simplified brines under conditions that relate to the WIPP (Rai et al. 1997; Rai et al. 1998; Yajima, Kawamura, and Ueta 1995; Torrero et al. 1994). These data are shown in Figure SOTERM-12. Rai et al. (Rai et al. 1997) determined the solubility of freshly precipitated $UO_2 \cdot xH_2O$(am) in NaCl and $MgCl_2$ solutions of various ionic strengths. They estimate the concentration of $U(OH)_4$(aq) in equilibrium with $UO_2 \cdot xH_2O$(am) to be about $10^{-8.0}$ M, and a number of data with greater concentrations in the neutral and alkaline range are ascribed to the presence of U(VI) in solution. This is in fair agreement with the value of $10^{-(8.7 \pm 0.4)}$ M proposed by Yajima, Kawamura, and Ueta (Yajima, Kawamura, and Ueta 1995). It is important to note that U(IV) concentrations at pH >5 show no significant dependence on the initial solid phase; both fresh precipitates in oversaturation experiments or electrodeposited microcrystalline UO_2(s) in undersaturation experiments gave the same results (Torrero et al. 1994).

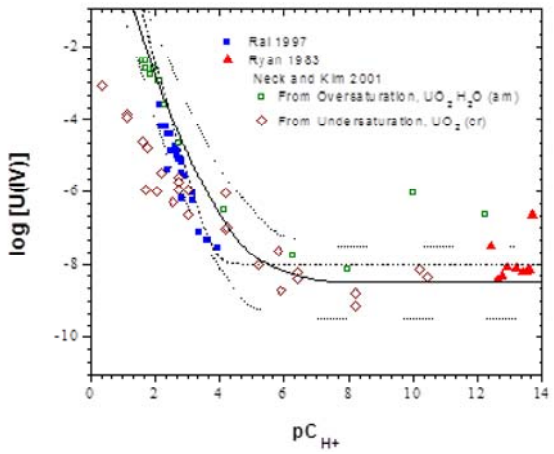

Figure SOTERM- 12. Solubility of UO_2(s) as a Function of pH at 20-25 ºC (68-77 °F) in 1M NaCl (based on Neck and Kim 2001). The experimental data are from Ryan and Rai (1983), Rai et al. (1997), and Neck and Kim (2001). The solid line is calculated by Neck with Log K_{sp} = (-54.5 ± 1.0) and the hydrolysis constants selected in Neck and Kim (2001). The dotted lines show the range of uncertainty. The dashed line is calculated with the model proposed by Rai et al. (1997).

SOTERM-3.4.1.3 Speciation and Solubility of U(VI)

U(VI) phases and aqueous species, although not expected to predominate in the WIPP, could be present due to the localized effects of radiolysis (see Section SOTERM-2.4.2). The WIPP PA currently makes the conservative assumption that U(VI) species predominate in 50% of the PA vectors. The solubility of U(VI) is, however, not explicitly calculated in the WIPP PA, since there is no model for actinides in the VI oxidation state. The potential contribution of U(VI) species to the overall solubility of U in the WIPP is implicitly considered in the WIPP PA in the 1 mM value for U solubility (U.S. EPA 2005). Prior to this, the solubility of U was defined as 1.2×10^{-5} M based on an assessment of the literature and existing WIPP-relevant experimental data by Hobart and Moore (Hobart and Moore 1996).

The solubility of U(VI) in the WIPP is expected to be defined by the combined contribution of two processes: hydrolysis with oxyhydroxide phase formation, and carbonate complexation with U carbonate phase formation. These are both very complex

systems, and there are many proposed speciation schemes. In carbonate-free or low-carbonate solutions, the speciation of U(VI) is dominated by hydrolysis.

Yamazaki et al. (Yamazaki et al. 1992) conducted U(VI) solubility experiments from both oversaturation and undersaturation in a synthetic brine at pC_{H+} values ranging from 6.4 to 12.4. The composition of this synthetic brine was close to the composition of the WIPP GWB brine, with higher concentrations of NaCl, NaBr, KCl and $MgCl_2$ and ionic strength ~6 M. This synthetic brine initially contained 0.11 mM of bicarbonate HCO_3^-, but the solution treatment (continuous nitrogen gas flow above the solution) likely removed some of the carbonate from solution before the later uranium additions and prevented any CO_2 uptake during the experiment. The results obtained at the pC_{H+} closest to WIPP repository conditions with no further carbonate additions are listed in Table SOTERM-12. Uranium (VI) concentrations of approximately 10^{-7} M were observed at pC_{H+} = 10.4 and 12.4 when nitrogen gas was continuously passing over the solutions to minimize CO_2 uptake. Despite extensive precipitation of brucite $Mg(OH)_2$ at these high pC_{H+} values, the solubility-controlling phase at $pC_{H+} \geq 9.3$ was found to be potassium diuranate $K_2U_2O_7$.

Diaz-Arocas and Grambow (Diaz-Arocas and Grambow 1998) investigated uranium (VI) solubility in NaCl solutions up to 5 M at 25 °C and different basic pH values, under an argon atmosphere using an oversaturation approach. Their uranium concentration equilibria in 5 M NaCl are presented in Table SOTERM-12. At pH ≥ 7.5, poorly crystalline sodium-uranates, identified by XRD, were formed in solutions. Diaz-Arocas and Grambow indicated that the solubility of this phase was about 3×10^{-5} M at pC_{H+} = 8.9 in 5 M sodium chloride in the absence of carbonate.

Carbonate, as CO_3^{2-}, has a significant effect on the solubility of U(VI) (Clark, Hobart and Neu 1995; Guillaumont et al. 2003). In the absence of competing complexing ligands, carbonate complexation will dominate the speciation of the uranyl ion under near-neutral pH conditions as long as there is ample carbonate-bicarbonate available (Clark, Hobart and Neu 1995). Complexation constants for binary U(VI) carbonate complexes at I = 0 M and 25 ºC (77 °F) are listed in Table SOTERM-12 (Guillaumont et al. 2003).

Table SOTERM- 12. Solubility of U(VI) in High-Ionic-Strength Media

U(VI) Concentration (M)	pC_{H+}	Solution	Time (days)	Solid	Reference
$(2.8 \pm 1.8) \times 10^{-5}$	8.9	5M NaCl	≈ 50	$Na_{0.68}UO_{3.34} \cdot (2.15\pm0.10)H_2O$	Diaz-Arocas and Grambow 1998
$(8.2 \pm 4.6) \times 10^{-5}$	7.6	5M NaCl	≈ 110	$Na_{0.45}UO_{3.23} \cdot (4.5\pm0.1) H_2O$	Diaz-Arocas and Grambow 1998
$(4.2 \pm 1.9) \times 10^{-4}$	7.1	5M NaCl	≈ 170	$Na_{0.29}UO_{3.15} \cdot (2.9\pm0.2) H_2O$	Diaz-Arocas and Grambow 1998
$(2.8 \pm 0.9) \times 10^{-6}$	6.5	5M NaCl	≈ 170	$Na_{0.14}UO_{3.07} \cdot (2.5\pm0.1) H_2O$	Diaz-Arocas and Grambow 1998
$(1.82 \pm 0.01) \times 10^{-3}$	8.4	Brine (air atmosphere)	100	α-schoepite (oversaturation)	Yamazaki et al. 1992
$(1.81 \pm 0.01) \times 10^{-3}$	8.4	Brine (air atmosphere)	100	α-schoepite (oversaturation)	Yamazaki et al. 1992
$(1.40 \pm 0.05) \times 10^{-3}$	8.4	Brine (air atmosphere)	244	α-schoepite (undersaturation)	Yamazaki et al. 1992
$(1.80 \pm 0.05) \times 10^{-3}$	8.4	Brine (air atmosphere)	244	α-schoepite (undersaturation)	Yamazaki et al. 1992
$(3.8 \pm 0.4) \times 10^{-7}$	10.4	Brine (initial 0.11mM HCO_3^-)	150	$Mg(OH)_2$ and $K_2U_2O_7$ (oversaturation)	Yamazaki et al. 1992
$(3.1 \pm 0.3) \times 10^{-7}$	10.4	Brine (initial 0.11mM HCO_3^-)	150	$Mg(OH)_2$ and $K_2U_2O_7$ (oversaturation)	Yamazaki et al. 1992
$(1.7 \pm 1.4) \times 10^{-7}$	8.1	ERDA-6	705	To be determined (oversaturation)	Lucchini et al. 2013b
$(9.9 \pm 3.0) \times 10^{-8}$	9.6	ERDA-6	705	To be determined (oversaturation)	Lucchini et al. 2013b
$(3.1 \pm 1.3) \times 10^{-8}$	10.5	ERDA-6	705	To be determined (oversaturation)	Lucchini et al. 2013b
$(2.1 \pm 0.6) \times 10^{-6}$	7.4	GWB	705	To be determined (oversaturation)	Lucchini et al. 2013b
$(4.3 \pm 1.3) \times 10^{-6}$	8.2	GWB	705	To be determined (oversaturation)	Lucchini et al. 2013b
$(8.1 \pm 2.4) \times 10^{-7}$	9.2	GWB	705	To be determined (oversaturation)	Lucchini et al. 2013b
$(2.7 \pm 0.5) \times 10^{-7}$	8.0	ERDA-6 (initial 2mM carbonate)	994	To be determined (oversaturation)	Lucchini et al. 2013a
$(3.2 \pm 1.0) \times 10^{-5}$	8.8	ERDA-6 (initial 2mM carbonate)	994	To be determined (oversaturation)	Lucchini et al. 2013a
$(3.5 \pm 2.8) \times 10^{-8}$	12.1	ERDA-6 (initial 2mM carbonate)	994	To be determined (oversaturation)	Lucchini et al. 2013a
$(2.6 \pm 0.8) \times 10^{-6}$	7.6	GWB	994	To be determined (oversaturation)	Lucchini et al. 2013a

U(VI) Concentration (M)	pC_{H+}	Solution	Time (days)	Solid	Reference
$(7.1 \pm 1.4) \times 10^{-7}$	9.0	(initial 2mM carbonate) GWB (initial 2mM carbonate)	994	To be determined (oversaturation)	Lucchini et al. 2013a

Table SOTERM- 13. Complexation Constants for Binary U(VI) Carbonate Complexes at I = 0 M and 25 ºC (Guillaumont et al. 2003)

Reaction and Solubility Product for UO_2CO_3(crystalline [cr])	
$UO_2CO_3(cr) \rightleftharpoons UO_2^{2+} + CO_3^{2-}$	Log $K^0_{SP(cr)} = -14.76 \pm 0.02$
Reactions and Formation Constants β^0_{nq} for $(UO_2)_n(CO_3)_q^{2n-2q}$	
$UO_2^{2+} + CO_3^{2-} \rightleftharpoons UO_2CO_3(aq)$	Log $\beta^0_{11} = 9.94 \pm 0.03$
$UO_2^{2+} + 2\ CO_3^{2-} \rightleftharpoons UO_2(CO_3)_2^{2-}$	Log $\beta^0_{12} = 16.61 \pm 0.09$
$UO_2^{2+} + 3\ CO_3^{2-} \rightleftharpoons UO_2(CO_3)_3^{4-}$	Log $\beta^0_{13} = 21.84 \pm 0.04$
$3\ UO_2^{2+} + 6\ CO_3^{2-} \rightleftharpoons (UO_2)_3(CO_3)_6^{6-}$	Log $\beta^0_{36} = 55.6 \pm 0.5$

The three monomeric complexes of general formula $UO_2(CO_3)$, $UO_2(CO_3)_2^{2-}$, and $UO_2(CO_3)_3^{4-}$ are present under the appropriate conditions. There is also evidence from electrochemical, solubility, and spectroscopy data that support the existence of $(UO_2)_3(CO_3)_6^{6-}$, $(UO_2)_2(CO_3)(OH)_3^-$, and $(UO_2)_{11}(CO_3)_6(OH)_{12}^{2-}$ polynuclear species, which can only form under the conditions of high-metal-ion concentration or high ionic strength (Clark, Hobart and Neu 1995). At uranyl concentrations above 10^{-3} M, the trimeric cluster $(UO_2)_3(CO_3)_6^{6-}$ can also be present in significant concentrations. When the uranyl ion concentration begins to exceed the carbonate concentration, hydrolysis will play an increasingly important role (Clark, Hobart and Neu 1995).

It is generally accepted that the major complex in solution at high carbonate concentrations is $UO_2(CO_3)_3^{4-}$ (Kramer-Schnabel et al. 1992; Pepper et al. 2004). However, at I = 0.5 M and I = 3 M, the polynuclear $(UO_2)_3(CO_3)_6^{6-}$ species becomes an important competitor of $UO_2(CO_3)_3^{4-}$. Grenthe et al. (Grenthe et al. 1984) indicated that the formation of $(UO_2)_3(CO_3)_6^{6-}$ is favored at high ionic strengths as a result of possible stabilization of the complex by ions of the background electrolyte.

At high pH, Yamamura et al. (Yamamura et al. 1998) demonstrated that hydrolysis overwhelms carbonate complexation. The solubility of U(VI) was measured in highly basic solutions ($11 \leq pH \leq 14$) at an ionic strength of I = 0.5 - 2 M over a wide range of carbonate concentrations (10^{-3} - 0.5 M) using both oversaturation and undersaturation approaches. In the oversaturation experiments, the solubility of U(VI) decreased with increasing equilibration time from one week to one year and was explained as an increase in the crystallinity of the solid phase with aging. The solid phase was identified as $Na_2U_2O_7 \cdot xH_2O$ by XRD. The undersaturation experiments conducted for one month with the solid phase indicated a rapid equilibrium. These data were interpreted by considering the formation of $UO_2(OH)_3^-$, $UO_2(OH)_4^{2-}$, and $UO_2(CO_3)_3^{4-}$ (Yamamura et al. 1998).

A few experimental investigations were reported on the influence of carbonate on U(VI) solubility in highly saline solutions (Yamazaki et al. 1992; Reed and Wygmans 1997; Lin et al. 1998; Fanghänel and Neck 2002). Lin et al. (Lin et al. 1998) evaluated U(VI) solubilities with up to 5M NaCl in a range of carbonate concentrations. At carbonate-ion concentrations greater than 10^{-7} M, $UO_2(CO_3)_3^{4-}$ was the dominant U(VI) complex in solution. At higher CO_2 partial pressures, the solubility-controlling solid phase was found to be UO_2CO_3(s), whereas at lower partial pressures, sodium uranate was identified as the solid phase in NaCl-saturated solutions. This study, although interesting, is of questionable use to the WIPP because the details were not fully published.

Yamazaki et al. (Yamazaki et al. 1992) measured the solubility of U(VI) in synthetic brine and an air atmosphere. The results obtained at $pC_{H+} = 8.4$ using both oversaturation and undersaturation approaches are listed in Table SOTERM-12. At this pC_{H+} value, millimole concentrations of uranium were measured in solution. Solids obtained at $pC_{H+} = 8.4$ were identified as poorly crystalline schoepite ($UO_3 \cdot xH_2O$) by X-Ray Diffraction (XRD). Yamazaki carried out some calculations to model the competition between calcium and magnesium for carbonate complexation in order to interpret his experimental solubility data. He concluded that the uranium solubility decrease above $pC_{H+} = 8.4$ was related to a shift from the triscarbonato uranyl complex $UO_2(CO_3)_3^{4-}$ to the uranyl hydroxide complexes $UO_2(OH)_n^{2-n}$, as precipitation of calcium carbonate ($CaCO_3$) occurred, and to the conversion of schoepite to potassium diuranate.

The only U(VI) solubility values available in the literature that were obtained in the presence of carbonate under WIPP-relevant conditions were featured in the fiscal year 1997 year-end report by Reed and Wygmans (Reed and Wygmans 1997). The experiments were carried out in ERDA-6 brine at pH 8 and 10, and in G-Seep brine at pH 5 and 7. U(VI), Np(VI), and Pu(VI) were added to the brine samples. CO_3^{2-} (10^{-4} M) was also added to some of the samples. The experiments were conducted under a hydrogen atmosphere at 25 ± 5 °C. Concentrations and oxidation states of the actinides were monitored over time. The U(VI) concentration was stable at approximately 1×10^{-4} M when measured as a function of time in ERDA-6 brine at pH 10 in the presence of CO_3^{2-} (Reed and Wygmans 1997).

SOTERM-3.4.2 WIPP-Specific Results since the CRA-2009 and the CRA-2009 PABC

The solubility of U(VI) in the absence and the presence of carbonate was extensively studied since the CRA-2009 in simulated GWB and ERDA-6 brine (Lucchini et al. 2010a, Lucchini et al. 2010b, 2013 and 2013a). A summary of these results is shown in Figure SOTERM-13 and a comparison of these results with other solubility data in the literature is given in Table SOTERM-12. No U(IV) solubility studies were conducted since Th(IV) is the analog for the IV actinides.

In the absence of carbonate, the measured U(VI) solubilities were about 10^{-6} M in GWB brine at $pC_{H+} \geq 7$ and about 10^{-8} - 10^{-7} M in ERDA-6 at $pC_{H+} \geq 8$ (Lucchini et al. 2007, 2010a and 2010b). These results put an upper bound of ~10^{-6} M for the solubility of uranyl in the carbonate-free WIPP brines for the investigated range of experimental conditions. At the expected pC_{H+} in the WIPP (~9.5), the measured uranium solubility was between 10^{-7} M and 10^{-6} M. In the presence of carbonate, the highest uranium solubility obtained experimentally was ~ 10^{-4} M, under WIPP-related conditions (pC_{H+} ~ 9.5). It is important to note that this uranium solubility, in the absence of carbonate, was 10-100 times lower than published results. The uranium (VI) solubility experiments reported in two other relevant publications (Yamazaki et al.1992; Diaz-Arocas and Grambow 1998) were performed in brines close to the WIPP brine composition, but possibly with a less rigorous control of a carbon dioxide-free environment. The impact of carbonate concentration on the solubility of uranium (VI) in the two simulated WIPP brines can be explained in terms of three distinctive pC_{H+} regions.

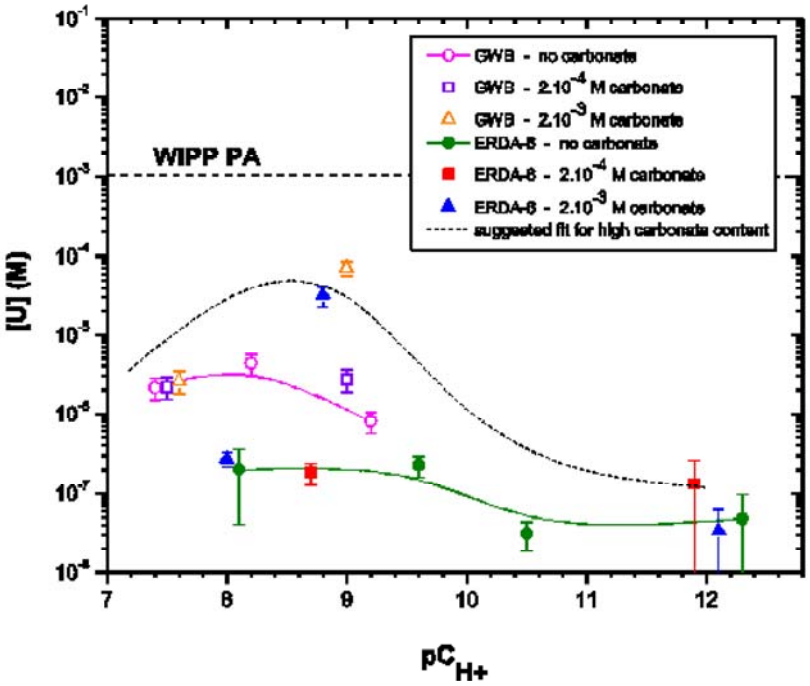

Figure SOTERM- 13. Uranium Concentration in ERDA-6 (Open Symbols) and GWB (filled symbols) versus pC_{H+}, in Nitrogen Controlled Atmosphere, in the Absence of Carbonate or in the Presence of Two Concentrations of Carbonate (2×10^{-4} M and 2×10^{-3} M) at the Beginning of the Experiments. The carbonate systems data correspond to 17 samplings performed over 994 days.

The first pC_{H+} region is $7.5 \leq pC_{H+} \leq 8$. In this pC_{H+} region, the uranium concentration was stable in both brines and independent of the carbonate concentration. However, there were small differences in the uranium solubility due to differences in the composition of the brine: ~ 10^{-6} M in GWB, and ~ 10^{-7} M in ERDA-6. These data indicated that there was no impact of carbonate in this pC_{H+} region ($7.5 \leq pC_{H+} \leq 8$), but there was certainly an effect due to one or more components of the brines that were present in higher amounts in GWB than in ERDA-6. Based on our investigation of neodymium solubility (Borkowski et al. 2010a), we postulated that borate may also play a role in defining the uranium (VI) solubility in this pC_{H+} region (see also Borkowski et al. 2010b). This possibility was confirmed experimentally (Lucchini, Borkowski and Richmann 2013; Lucchini et al. 2013a).

The second pC_{H+} region of interest, $8 \leq pC_{H+} \leq 10$, is directly relevant to the WIPP. In this pC_{H+} region, not only was there a compositional effect between the two brines studied (higher uranium concentrations in GWB than in ERDA-6 for identical carbonate content), but there was also an impact of carbonate on the observed uranium solubility in each brine. At high carbonate content (2×10^{-3} M in our experiments), the uranium concentrations reached 10^{-4} M, which was two or more orders of magnitude

higher than in the absence of carbonate. The low carbonate content data (2×10^{-4} M) did not reflect a strong influence of carbonate on uranium solubility, since the measured solubility was similar to the ones obtained in carbonate-free systems.

Lastly, the third pC_{H+} region of interest is at $10 \leq pC_{H+}$. In that pC_{H+} region, the uranium concentrations were stable around 10^{-7}-10^{-8} M. It is likely that hydrolysis overwhelmed any other possible effects on uranium solubility.

These newly obtained solubility data for uranium (VI) in the WIPP brine accomplished the following:

- Provided the first WIPP-relevant data for the VI actinide oxidation state that established the solubility of uranium (VI) over an extended pC_{H+} range for GWB and ERDA-6 brines in the absence or presence of carbonate

- Established an upper limit of ~ 10^{-6} M uranyl concentration at the reference pC_{H+} WIPP case in the absence of carbonate, and an upper limit of ~ 10^{-4} M uranyl concentration at the reference pC_{H+} WIPP case in the presence of 2 mM carbonate

- Confirmed a lack of significant amphotericity in the WIPP simulated brines at high pH values

- Demonstrated a small effect of borate complexation in the pC_{H+} range of 7.5 to 10

- Supported the current assumption in PA that the solubility of U(VI), under the expected range of conditions in the WIPP, will not exceed 1 mM

SOTERM-3.5 Neptunium Chemistry

The WIPP repository is projected to contain ~32.5 kg of Np, primarily as the ^{237}Np isotope (see Table SOTERM-8). Its inventory increases with time from the decay of ^{241}Am and the possibility of ^{238}U (n, 2n) reactions to 223 Kg at 1000y after emplacement. In the WIPP PA, Np speciates as Np(IV) in 50% of the PA vectors and as Np(V) in the other 50% of the PA vectors. The contribution of Np to actinide release from the WIPP was included in the CRA-2014 PA calculation, but its effect on release was negligible. Arguments have already been made that it should be excluded from consideration in the WIPP PA based on its low inventory (Brush and Garner 2005).

SOTERM-3.5.1 Neptunium Environmental Chemistry

The environmental chemistry of Np is somewhat unique in the actinide series as a result of the relatively high stability of the NpO_2^+ species, which is in the V oxidation state, under a wide range of conditions typically found in the subsurface. This oxidation state is prevalent when oxidizing conditions predominate (Hobart 1990). It is mobile because it has a relatively high solubility and it is not strongly sorbed or complexed. It does not hydrolyze strongly, with little or no measurable hydrolysis until pH >9 (Neck, Kim, and Kanellakopulos 1992; Itagaki et al. 1992). Much of the complexation data for inorganic and organic complexes for Np pertains to the V oxidation state for this reason (Lemire et al. 2001). The log K_{sp} for NpO_2OH (s) is 4.5 ± 0.06 (Neck, Kim, and Kanellakopulos 1992).

Np can, however, actually exist in up to five oxidation states in aqueous media. The redox potentials under basic conditions are (Martinot and Fuger 1985):

$$+0.58\ V + 0.6\ V + 0.3V\ -2.1V$$

$$NpO_5^{3-} \rightarrow NpO_2(OH)_2 \rightarrow NpO_2OH \rightarrow NpO_2 \rightarrow Np(OH)_3 \quad \text{(SOTERM.28)}$$

Only the Np(IV) and Np(VI) oxidation states, in addition to Np(V), can exist under the right conditions in reducing or oxidizing groundwater (Hobart 1990; Keller 1971 [pp. 195-215]; Clark, Hobart and Neu 1995). These exist as Np^{4+} complexes and NpO_2^{2+} complexes. Np(VI), unlike Np(V), is strongly hydrolyzed at near-neutral pH and is readily reduced by many constituents typically found in groundwater (e.g., organics and most reduced metals). For these reasons, it does not tend to persist in groundwater under most conditions.

Under reducing anoxic conditions, Np^{4+} species can predominate. These Np^{4+} species readily undergo hydrolysis and are comparable to Pu^{4+} in this regard. This system is highly irreversible and probably polymeric in nature, as is observed for Pu^{4+}. The measured solubility of Np^{4+} is $10^{-8.5}$ to $10^{-8.1}$ M with $Np(OH)_4$, not $Np(OH)_5^-$, as the predominant aqueous species (Rai and Ryan 1985; Eriksen et al. 1993). The importance and predominance of the Np(IV) oxidation state in reducing conditions is even more pronounced when anaerobic bacteria are present. Np(V) was readily reduced by sulfate-reducing bacteria (Banaszak, Reed, and Rittmann 1998) and methanogenic consortia (Banaszak et al. 1999), and precipitated as Np(IV) solids.

In WIPP-specific experiments (Reed and Wygmans1997), spectroscopic evidence for the reduction of Np(VI) to Np(V) in ERDA-6 (Castile) brine at pH 10 was observed along with complete reduction of Np(VI) to Np(V) in G-Seep (Salado) brine at pH 7 when no iron or microbial activity were present. In the presence of oxalate, citrate, and EDTA, rapid and complete reduction of Np(VI) to

Np(V) coupled with a slower formation of Np(IV) species was observed. The stability of Np(V) under these conditions is further confirmed by Neck, Runde, and Kim (Neck, Runde, and Kim 1995), who showed that Np(V) carbonate complexes are stable in 5M NaCl.

In the expected WIPP environment, however, where anoxic and reducing conditions with microbial activity and reduced iron are expected to be present, Np(IV) is expected to be the predominant oxidation state (Rai and Ryan 1985; Rai, Strickert, and McVay 1982; Kim et al. 1985; Pryke and Rees 1986). This is based on studies of the solubility of NpO_2OH in 1 M and 5 M NaCl solutions at pH 6.5, where the reduction of Np(V) to Np(IV) was observed (Kim et al. 1985; Neck, Kim, and Kanellakopulos 1992).

SOTERM-3.5.2 WIPP-Specific Results since the CRA-2009 and the CRA-2009 PABC

There are no new WIPP-relevant results on the chemistry and speciation of Np since CRA-2009 and the CRA-2009 PABC. Neptunium is not a key contributor to release from the WIPP.

SOTERM-3.6 Plutonium Chemistry

Plutonium is a key TRU component that contributes significantly to the potential for TRU release from the WIPP under all release mechanisms considered by PA. Pu isotopes, estimated to be ~12 metric tons at the time of closure, represent approximately 77% of the Ci content for actinides in TRU waste (see Table SOTERM-8) at emplacement. This changes with time to 62%, 83% and >99% at 100, 1000 and 10,000 years after emplacement due to radioactive decay and the relatively long half-life of ^{239}Pu. There are five isotopes of Pu that make a significant contribution to the Pu inventory, but ^{239}Pu, ^{238}Pu, and ^{241}Pu are the major contributors to the Ci content. Under the conditions expected in the WIPP, Pu(IV) is expected to be the predominant oxidation state (Weiner 1996). A more extensive review of Pu subsurface speciation issues as they pertain to the WIPP case was completed (Reed et al. 2009).

In the WIPP PA, all of the Pu is assumed to be reduced and present in the III or IV oxidation state. Half of the PA vectors contain 100% Pu(III), with the other half of the vectors containing 100% Pu(IV) species. Because the solubility of Pu(III) is roughly 10 times higher, the assumption that it is present is a conservatism built into the WIPP PA. The two higher-valent Pu oxidation states, Pu(V) and Pu(VI), are not considered in the PA because they cannot persist under the expected reducing and anoxic conditions in the WIPP.

SOTERM-3.6.1 Plutonium Environmental Chemistry

Generally, Pu can exist in oxidation states III, IV, V, VI, and VII (Katz, Seaborg, and Morss 1986, p. 781). Of these, only Pu(V), Pu(IV), and Pu(III) are expected to be important under environmentally relevant oxidizing and reducing conditions. Pu(VII) is very unstable and exists only in extremely basic solutions (for example, 7 M NaOH) that are not expected in the WIPP. Pu(VI) and Pu (V) can persist in the WIPP in the absence of reductants, but they are readily reduced in the presence of Fe(II/0) species, reduced by many organic chelators (Reed et al. 1998), and possibly reduced in anaerobic, biologically active systems (Reed et al. 2007; Icopini, Boukhalfa, and Neu 2007). The reduction of Pu(VI/V), under WIPP-relevant conditions, was shown by Clark and Tait (Clark and Tait 1996), Reed and Wygmans (1997), and Reed et al. (Reed et al. 2007). In this context, only Pu(III) and Pu(IV) oxidation state species are expected to be present under WIPP-related conditions.

SOTERM-3.6.1.1 Importance of Redox for Plutonium Speciation

The role and importance of redox reactions in determining actinide mobility and solubility are beyond question (Van Luik et al. 1987; Allard 1982; Choppin and Rao 1992). The redox potentials for the various oxidation states at pH 7 are (Cleveland 1979, pp. 11-46)

$$\underset{\text{+0.94 V}}{\underbrace{\underset{\text{+0.77 V}}{PuO_2(OH)_2\,(aq) \rightarrow PuO_2^{+}} \underset{\text{+1.11 V}}{\rightarrow} PuO_2{\cdot}H_2O\,(s)}} \underset{\text{-0.63 V}}{\rightarrow} Pu^{3+} \qquad \text{(SOTERM.29)}$$

A typical phase diagram for Pu in groundwater that illustrates the importance of redox is shown in Figure SOTERM-14.

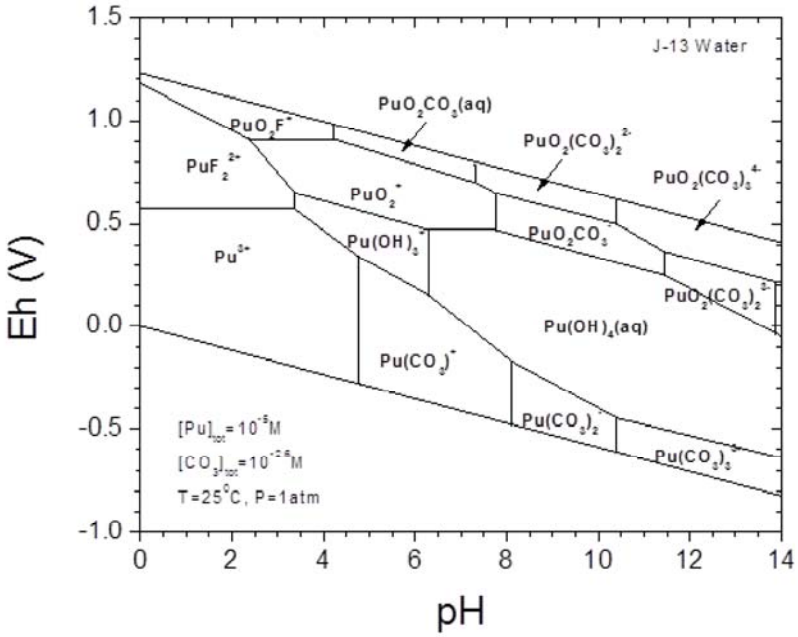

Figure SOTERM- 14. Speciation Diagram for Plutonium in Carbonated Low-Ionic-Strength Groundwater (Based on Data Presented in Runde et al. 2002). This illustrates the expected lower solubility of reduced Pu (III) and Pu(IV) phases, and suggests that the dominant Pu species in the pH 8-9 range are hydrolytic species with lesser contributions from carbonate.

Higher-valent Pu, specifically Pu(V) and Pu(VI), can be present in near-surface oxidizing groundwaters (Orlandini, Penrose, and Nelson 1986). The association of Pu(V) with organic colloidal material was proposed as the mechanism by which subsurface migration occurred. Pu(VI), in near-neutral systems, is strongly and irreversibly hydrolyzed (Okajima and Reed 1993). It is also readily reduced by organics and reduced metal species even when oxygen is present to form Pu(V), and is not generally stable under most groundwater-relevant conditions.

Pu(V), by analogy with Np(V), does not undergo hydrolysis until pH >7 and tends to form weak complexes. It readily disproportionates to form Pu(IV) and Pu(VI) at high concentrations and is relatively easy to reduce in the environment under anoxic conditions. Fe^{2+}(aq), Fe(II) minerals, and metallic iron reduce Pu(V) to Pu(IV).

In geochemical systems, redox control is often interpreted in terms of the iron, and in a broader sense, reduced metal, mineralogy, and associated aqueous chemistry (Sanchez, Murray, and Sibley 1985; White, Yee, and Flexser 1985). In the WIPP case, iron will undergo anoxic corrosion, producing Fe^{2+}. Both metallic iron (Fe^0) and Fe^{2+} have been shown to quantitatively reduce Pu(VI) in the WIPP brines to either Pu(IV) or Pu(III). Clark and Tait (Clark and Tait 1996) and Felmy et al. (Felmy et al. 1996) have experimentally observed the reduction of Pu(VI) carbonates by either Fe^0 or Fe^{2+} to Pu(IV). In the absence of carbonates, a quantitative reduction of Pu(VI) is also observed, but the oxidation state of the resulting species cannot be definitively determined because its concentration is below the lower detection limit of the oxidation state analytical process (about 10^{-9} M). However, since this concentration is well below the expected solubility of Pu(V) species, it was reasonably assumed that the Pu must have been reduced to either the IV or III oxidation state. Neretnieks (Neretnieks 1982) has shown that when dissolved actinides in moving groundwater came in contact with Fe(II), the actinides were reduced to a much-less-soluble oxidation state and precipitated.

Pu(III) is not predicted to be stable under the expected WIPP conditions. There are, however, some mechanisms identified in which Pu(III) species can be formed. Felmy et al. (Felmy et al. 1989) observed some Pu(III) in the WIPP brines at neutral and slightly basic conditions. PA conservatively takes account of these minor mechanisms by assuming that Pu is speciated as Pu(III) in 50% of the PA vectors.

General studies of Pu in brine have been done by a number of investigators (Büppelmann et al. 1986; Büppelmann, Kim, and Lierse 1988; Clark, Hobart, and Neu 1995; Nitsche et al. 1992; Nitsche et al. 1994; Pashalidis et al. 1993; Villareal, Bergquist, and Leonard 2001; Reed et al. 1993; Reed, Okajima, and Richmann 1994; Reed and Wygmans 1997). There has also been an assessment of the actinide chemistry in the WIPP CCA (Oversby 2000; Brush, Moore, and Wall 2001; U.S. EPA 2006). These studies confirm reduction of higher-valent Pu under the expected WIPP conditions and establish the key speciation trends for Pu in the WIPP (see Figure SOTERM-15). These trends are captured in the WIPP PA through analogy with Am(III) for Pu(III) and with Th(IV) for Pu(IV).

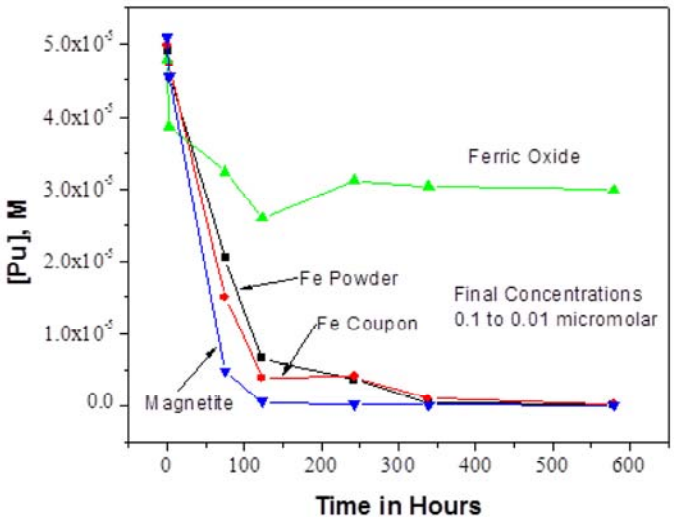

Figure SOTERM- 15. The Concentration of Pu as a Function of Time in the Presence of Iron Powder, Iron Coupon, Ferric Oxide, and Magnetite (Mixed Iron Oxide) (Reed et al. 2009)

SOTERM-3.6.1.2 Bioreduction of Higher-Valent Plutonium

Comprehensive and critical reviews of how actinide species and microorganisms interact have been published (Banaszak, Rittmann, and Reed 1998; Neu, Ruggiero, and Francis 2002; Reed et al. 2010). The likelihood that this could occur and recent results with Fe(III) reduction were discussed in Section SOTERM-2.4.1.4. Additionally, the important role of microbial activity through biotic transformations (Zitomer and Speece 1993; Banaszak, Rittmann, and Reed 1998; Rittmann, Banaszak, and Reed 2002; Reed et al. 2007) in defining oxidation state distribution of multivalent metals and actinides has been recognized.

Although the bioreduction of uranyl and neptunyl species is well established, there are relatively few studies of the bioreduction of plutonyl species. Reed et al. (Reed et al. 2007) demonstrate that *Shewanella alga*, a ubiquitous metal-reducing soil bacterium, reduces Pu(V) to Pu(III/IV) species. Icopini, Boukhalfa, and Neu (Icopini, Boukhalfa, and Neu 2007) have shown that *Geobacter* and *Shewanella oneidensis* also reduce higher-valent Pu to Pu(III/IV) species.

These Pu data are consistent with the oxidation state predictions in microbially active systems. It is particularly important to note that Pu(IV) is the expected oxidation state under a wide range of anoxic subsurface conditions, with no Pu(V) or Pu(VI) species expected. The recent Pu bioreduction results confirm that highly reducing conditions are being generated by metal-reducing bacteria under anaerobic growth conditions and support the current WIPP PA assumption that higher-valent actinides cannot persist when the concentration of dissolved actinides is important and microbial activity is prevalent.

There are no studies on the bioreduction of Pu(V/VI) under WIPP-relevant conditions (note discussion in Section SOTERM-2.4.1.4. Halophilic microorganisms (Gillow et al. 2000; Swanson and Simmons 2013; Swanson et al. 2012) typically found and expected to predominate in the WIPP environment have not been studied for their ability to reduce higher-valent actinides, although they will contribute to the establishment of reducing conditions in the WIPP.

SOTERM-3.6.1.3 Thermodynamic Stability of Higher-Valent Plutonium: PuO2+x

It has long been held that Pu oxide, as PuO_2, is the thermodynamically favored form of Pu oxide. This oxide is likely the predominant form of Pu in TRU waste and is believed to be the most important phase under WIPP-related conditions. In the last few years, however, there have been a number of studies that question this key and fundamental assumption.

Haschke, Allen, and Morales (Haschke, Allen, and Morales 2000) report that near-stoichiometric plutonium dioxide reacts with water vapor at temperatures between 25 °C and 350 °C (77 °F and 662 °F) according to the following reaction:

$$PuO_2(s) + xH_2O(g) \rightarrow PuO_{2+x}(s) + xH_2(g) \text{ (SOTERM.30)}$$

Here, water vapor is reduced by polycrystalline PuO_2 to produce hydrogen (H) and a previously unknown higher-oxide PuO_{2+x} with *x* as large as 0.27. If only Pu(IV) and Pu(V) are present in $PuO_{2.27}$, this oxide has 46% Pu(IV) and 54% Pu(V). Once formed, the PuO_{2+x} may dissolve in contact with groundwater to form aqueous PuO_2^{+} or PuO_2^{2+} species (Haschke and Ricketts 1995).

There remains some controversy about the mechanisms that led to the observation of higher-valent Pu in the PuO_{2+x}. This process only occurs under unsaturated conditions at high relative humidities. Haschke, Allen, and Morales (Haschke, Allen, and Morales 2000) argue that this conversion is due to a chemical reaction (that is, the above reaction has a Gibbs energy less than zero) rather than a radiolysis-induced reaction because the reaction rate is temperature dependent. However, there seems to be some

contribution from radiolysis in this process and this may be the dominant mechanism (LaVerne and Tandon 2002). Neither of these mechanisms are expected to impact WIPP repository performance.

The behavior of PuO_2 in contact with water was studied as a function of time by means of the short-lived isotope ^{238}Pu, as well as the longer-lived ^{239}Pu (Rai and Ryan 1982). This study concluded that crystalline PuO_2, amorphous PuO_2, and amorphous $PuO_3 \cdot xH_2O$ all convert to a material intermediate between crystalline PuO_2 and a hydrated amorphous material that contains both Pu(IV) and Pu(VI). These authors hypothesized that alpha particles generated by ^{238}Pu or ^{239}Pu irradiated water to generate OH radicals that reacted to form Pu(V) and/or Pu(VI) on the oxide surface. These observations are why the formation of localized oxidizing zones, where some higher-valent Pu can persist, is recognized in the WIPP PA. Reduction of these species, however, leads to a reformation of Pu(IV) hydrous oxide precipitates.

The overall issue of a thermodynamic driver for higher-valent Pu oxides, although it has received much recent attention in the literature, is not yet resolved, but has a relatively insignificant impact on the WIPP regardless of the mechanisms at work. A prolonged unsaturated phase in the WIPP could lead to the formation of some PuO_{2+x}, but this will be quickly overwhelmed in an aqueous environment and the higher-valent Pu will be reduced to Pu(III/IV) species, as described in Section SOTERM-3.5.1.1 and Section SOTERM-3.5.1.2. Both DBR and transport-release scenarios assume brine inundation and, correspondingly, the rapid introduction of reducing conditions.

SOTERM-3.6.2 WIPP-Specific Results since the CRA-2009 and the CRA-2009 PABC

Since the CRA-2009 and CRA-2009 PABC, the WIPP-specific Pu-Fe interaction studies (Reed et al. 2010) were extended in time to almost 6 years to establish the long-term oxidation state distribution of plutonium in these iron-dominated brine systems. In these investigations ^{242}Pu, initially as PuO_2^{2+}, was used to minimize radiolytic effects. Additionally these were done in two WIPP-relevant brines (see Table SOTERM-4): GWB as a high magnesium brine typical of MgO-reacted brine, and ERDA-6 as a high sodium chloride brine typical of brine found in the far field. The initial oxidation state was established using absorption spectrometry (Varian CARY 5000) and solids were prepared from these brines using established methods. Initially, only Pu(IV) was evident in the XANES analysis (see Figure SOTERM-16). This correlated with a plutonium concentration that was in the range of 2×10^{-9} M to as high as 1.5×10^{-7} M at the lower end of the pH range (pH = 7). These data agreed with the results obtained in a prior study after approximately two years when Pu-239 was the plutonium isotope (Reed et al. 2007). After ~5.8 years, these same solid samples were re-analyzed and found to be mostly Pu(III) with a small amount of Pu(IV) in a few samples (see Figure SOTERM-17 and Table SOTERM-14). The observation of Pu(III) in the solid phase correlated with an increase in the plutonium solution concentrations from 1×10^{-8} M to 3×10^{-7} M (see Figure SOTERM-18). This is a slight elevation in concentration, by a factor of ~ 2 to 5, when compared to the earlier Pu(IV)-relevant data. This increased solubility is also consistent with the phase transformation to Pu(III) since the solubility of Pu(III) is expected to be somewhat higher than Pu(IV).

The plutonium (III/IV) solids data show a qualitative correlation with the Fe(II)/Fe(III) ratio and measured redox potential (E_h). Experiments with less negative E_h also had a greater amount of Fe(III) and Pu(IV) species present in the system. This adds to the linkages seen by others between the iron and plutonium chemistry in subsurface conditions. Although these specific experiments were performed in brine, they are consistent with the correlation between iron chemistry and other metals observed in low ionic strength groundwater (Masue-Slowey et al. 2011; Holm and Curtiss 1989; Christensen et al. 2000). The overall reaction sequence is given by:

$$\text{Pu(V/VI)} \xrightarrow{\text{Rapid}} \text{Pu(IV)} \xrightarrow{\text{Slow}} \text{Pu(III/IV)} \qquad \text{(SOTERM.31)}$$

The predominance of Pu(III) at long times provides a strong data point on the reducing conditions that iron creates under WIPP-relevant conditions, but does not account for radiolytic impacts on E_h, and the effects of organic complexation which will stabilize Pu(IV) relative to Pu(III). These data, taken in context, strongly support the current WIPP PA assumption that Pu(III) and Pu(IV) will be prevalent in the WIPP and both oxidation states will contribute to the actinide source term.

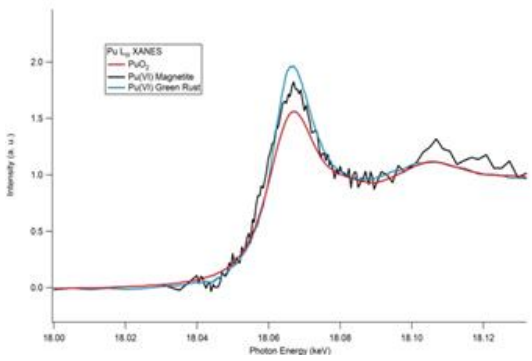

Figure SOTERM- 16. XANES Analysis of Plutonium Precipitates in the Magnetite and Iron Reduction Experiments at 3 Months. Pu(IV) phases were predominantly noted.

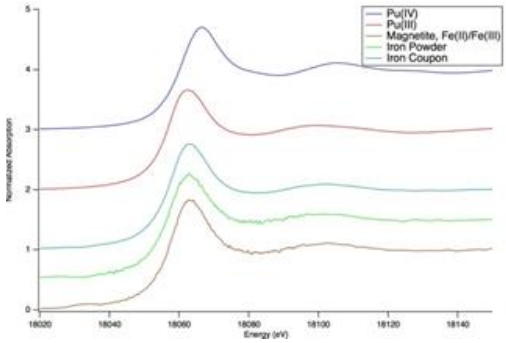

Figure SOTERM- 17. XANES Analysis of Solid Samples from the Pu-Fe Interactions Studies after ~ 6 Years. Pu(III) was the predominant oxidation state noted.

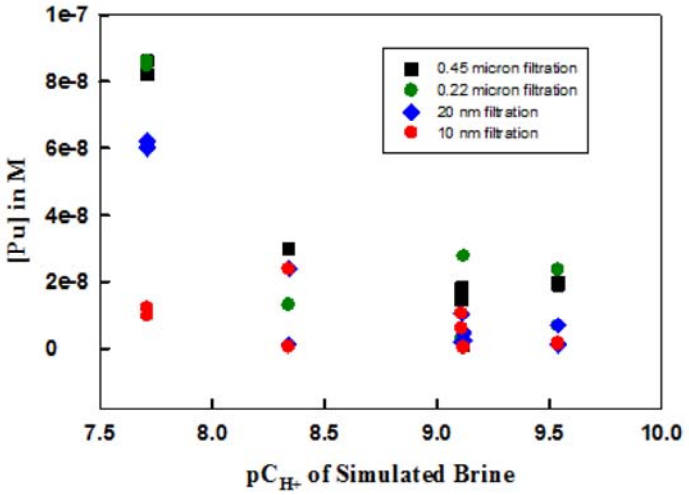

Figure SOTERM- 18. Effect of Filtration on the Measured Concentration of Plutonium as a Function of pC_{H+}. Data shown are 0.45 µ (black squares), 0.22µ (green circles), 20 nm (blue diamonds) and 10 nm (red circles) filtrations. Uncertainty in the filtration data, based on ICP-MS analyses, is estimated to be ± 20%. The concentration of 10 nm-filtered plutonium at pC_{H+} ~ 9.5 is 3 x 10^{-7} M.

Table SOTERM- 14. Qualitative Redox Indicators for Iron Interactions with Plutonium under Anoxic Conditions

Experiment	Description	[a] Oxidation State of Pu Solid	[b] $[Fe]_{total}$ in mM (% Fe^{2+} in solution)	[c] E_h Measured (± 3 mV)
PuFe23OX	ERDA-6 brine at pH ~9 with excess magnetite	~87% Pu(III), rest Pu(IV)	0.12 (25%)	-122 mV
PuFeCE8	ERDA-6 brine at pH ~8 with Fe coupon	~100% Pu(III)	ND	ND
PuFeCE10	ERDA-6 brine at pH ~ 9.6 with Fe coupon	~100% Pu(III)	0.27 (100%)	ND
PuFeP	ERDA-6 brine at pH~9 with excess Fe powder	~100% Pu(III)	0.18 (100%)	-175 mV
PuFeC	ERDA-6 brine at pH ~ 9 with Fe coupon	~90% Pu(III), rest Pu(IV)	0.18 (58%)	-110 mV
PuFeG7	GWB brine at pH ~6.7 with Fe coupon	~ 100% Pu(III)	12.62 (97%)	-210 mV

a.Pu(III) content established by XANES analysis of solids
b. Fe(II) content established by analysis using FerroZene®
c.Eh measurement made using an Orion combination ORP electrode
ND - not determined

SOTERM-3.7 Americium and Curium Chemistry

There are relatively small quantities of Am in TRU waste (see Table SOTERM-9), and this is anticipated to be ~ 0.203 metic tons at emplacement. The high activity of ^{241}Am ($t_{½}$ = 432 years, 3.443 Ci/g) makes Am a key contributor to potential actinide release from the WIPP at earlier times in repository history (~26% initially, decreasing to 17% and ~0% at 1000 and 10,000 years after emplacement). In the WIPP PA, Am is in the trivalent state in all vectors and the aqueous concentration consists of Am^{3+} complexes and colloidal species.

Cm is also present in very small quantities in the WIPP (Table SOTERM-9) and exists primarily as the ^{244}Cm isotope. The high activity of this isotope ($t_{½}$ = 18.11 years) makes Cm an important species in the WIPP at the very early stages of repository history. It is essentially unimportant for the PA because it has decayed away by the end of the 100-year period for active institutional controls. However, other Cm isotopes with longer half-lives are present in the inventory and are considered by the WIPP PA. The environmental chemistry of Am and Cm are very similar, and most of what is said in this section about the environmental chemistry of Am also applies to Cm.

A more detailed review of the literature for Am can be found as part of a WIPP report (Borkowski et al. 2008). The solubility of An (III) was measured in the WIPP brine over a wide range of conditions using Nd(III) as a redox-invariant analog. These data support current WIPP PA calculations for the solubility of Pu(III) and Am(III) in the WIPP brine and are also summarized in Borkowski et al. (Borkowski et al. 2008).

SOTERM-3.7.1 Americium and Curium Environmental Chemistry

Am is a 5f electron element and, like other elements of the actinide group, can exist in aqueous solution in several oxidation states. The electrode potentials for some Am couples are presented in Figure SOTERM-19. The trivalent state of Am is the most stable aqueous oxidation state (Katz, Seaborg, and Morss 1986, p. 912), and it is quite difficult to oxidize in aqueous solution (Hobart, Samhoun, and Peterson 1982). The trivalent Am ion has an ionic radius of 97.5 picometers (pm) (coordination number [CN]=6) and its chemical properties can be used as an analog for Pu(III), which has a similar ionic radius (100 pm at CN=6) and charge density, as well as for Cm(III) (97 pm at CN=6).

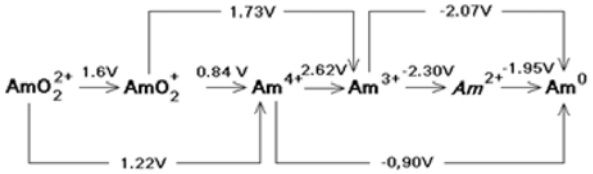

Figure SOTERM- 19. Redox Potential for Some Am Redox Couples (Silva et al. 1995, p. 74)

The *Am(II)* species is italicized to stress that it is only a transient species. As discussed by Martinot and Fuger (Martinot and Fuger 1985), there is evidence for the formation of *Am(II)* in aqueous perchlorate solution in the pulse radiolysis experiment. The half-life of this species was estimated to be approximately 5 µs. This species is not observed during the electroreduction of Am(III) to the metal in noncomplexing media (David, Maslennikov, and Peretrukhin 1990).

Cm is also distinguished by the relatively great stability of the III oxidation state with respect to oxidation or reduction (Katz, Seaborg, and Morss 1986, p. 970). The stability of Cm(III) may be attributed to the half-filled f-shell electronic configuration ($5f^7$). The oxidation of Cm(III) is achieved only with the strongest oxidizing agents, and only one report claims evidence for an oxidation state higher than IV (Korpusov, Patrusheva, and Dolidze 1975). The Cm(III) to Cm(IV) transition has not been successfully induced by ozone or electrochemically, and the Cm(IV) phosphotungstate produced by oxidizing with peroxysulfate is considerably less stable than the Am(IV) analog (Katz, Seaborg, and Morss 1986, p. 971). In the reducing environment of the WIPP repository, any higher-valent Cm produced radiolytically would be unstable. For all these reasons, the predominant oxidation state for Cm in the WIPP environment is Cm(III).

Higher-valent Am species have also been noted. Am(IV) species, with an ionic radius estimated by Shannon (Shannon 1976) to be 85 pm, is only stable in the presence of strongly complexing anions such as carbonate, fluoride, phosphate, or phosphotungstate, and was never found in any appreciable amount in trivalent Am solutions.

The pentavalent and hexavalent dioxoamericium ions AmO_2^+ and AmO_2^{2+} can be generated under strongly oxidizing conditions. Free radicals produced from α particles in water readily reduce these dioxoamericium ions back to Am^{3+}. In concentrated NaCl solution, in which the radiolysis products are strong oxidants, pentavalent and hexavalent Am are the predominant species (Büppelmann et al. 1986). Without an oxidant, the pentavalent dioxoamericium ion slowly disproportionates to AmO_2^{2+} and Am^{3+}.

These higher oxidation states are not stable in natural waters and can be readily reduced by action of reductants naturally present in those waters.

The speciation of Am in groundwater under mildly alkaline conditions is primarily defined by hydrolysis and carbonate complexation. Hydrolysis is generally represented by the following reaction:

$$Am^{3+} + nH_2O \leftrightarrows Am(OH)_n^{(3-n)} + nH^+ \text{ (SOTERM.32)}$$

Silva measured the $^{243}Am(OH)_3$(crystalline [cr]) and $Nd(OH)_3$(cr) solubilities in 0.1 M $NaClO_4$ solution at 25 ± 1 °C within the pH range 6 to 10 (Silva et al. 1995, p. 79-97). This is the only study with Am hydroxide using an x-ray-characterized crystalline solid. The solid phase was prepared by rigorously controlled, high-temperature transformation of $Am(OH)_3$(am). Optical viewing by SEM of the solid samples at the end of the solubility experiments showed no changes in the crystal. The use of the ^{243}Am isotope diminished α-particle damage of the crystal as a result of the 17-times-lower specific activity compared to ^{241}Am. The weakness of this experiment was the relatively short equilibration time of only 48 days. A log (K_{sp}) of 16.6 ± 0.4 was obtained for the $Am(OH)_3$ phase. The corresponding hydrolysis constants are listed in Table SOTERM-15. Similar values for Nd(III) hydrolysis were derived from the $Nd(OH)_3$(cr) solubility measurements.

Stadler and Kim (Stadler and Kim 1988) investigate the pH dependence of $Am(OH)_3$(s) solubility in 0.1 M $NaClO_4$ and more concentrated Na chloride and perchlorate solutions at 25 ± 0.5 °C. The effect of α-induced radiolysis on solubility was also studied using different total concentrations of ^{241}Am. The solid phase was not characterized in this work. Although the solid used in this work was different than that used by Silva et al. (Silva et al. 1995, pp. 275-76), the reported solubility products are in agreement. It is unclear, however, if the same phase controls the Am solubility in these two cases, because of markedly different preparation conditions of the starting solids.

Kim et al. (Kim et al. 1984) measured the solubility of $Am(OH)_3$(s) at I = 0.1 and 0.3 M $NaClO_4$, in the absence of CO_2 and at $pCO_2 = 10^{-3.5}$ atm, and attributed the solubility measured in terms of contributions from the hydroxy, carbonato- and mixed Am hydroxy-carbonato complexes. No characterization of the solid was reported in this work, so it was assumed to be $AmCO_3OH$(s). Several investigators found that changes in the solid phase in aqueous suspensions of Am(III) hydroxide due to aging conditions become evident in hours and continue for weeks. Similar results were reported by Felmy, Rai, and Fulton (Felmy, Rai, and Fulton 1990). These authors measured the solubility of $AmCO_3OH$(cr) at $pCO_2 = 10^{-3}$ atm. The change in total Am concentration measured in this work as a function of pH was similar to that reported by Kim et al. (Kim et al. 1984). Similar plots for the solubility of Nd in 5 M NaCl were measured by Borkowski et al. (Borkowski et al. 2008); however, the Nd concentrations obtained for the comparable pC_{H+} values were two to three orders of magnitude greater as a result of the higher ionic strength present.

Table SOTERM- 15. Hydrolysis Constants of Am(III) (in Logarithmic Units) Corresponding to Equation SOTERM.32

$AmOH^{2+}$	$Am(OH)_2^+$	$Am(OH)_3$(aq)	Medium	Reference
-7.93 ± 0.35	-14.77 ± 0.25	-24.71 ± 0.11	0.1 M $NaClO_4$	Kim et al. 1984
-7.5 ± 0.3	-15.4 ± 0.4	-26.9 ± 0.5	0.1 M $NaClO_4$	Stadler and Kim 1988
-7.8 ± 0.4	-15.4 ± 0.5	-26.9 ± 0.5	0.1 M NaCl	Stadler and Kim 1988
-8.1 ± 0.3	-15.8 ± 0.4	-27.0 ± 0.5	0.6 M NaCl	Stadler and Kim 1988
-7.7 ± 0.3	-16.7 ± 0.7	-25.0 ± 0.3	0.1 M $NaClO_4$	Silva et al. 1995, p. 81
-6.9 ± 0.2		-23.8 ± 0.9	0.1 M $NaClO_4$	Rösch et al. 1989
<-8.2	-17.1 ± 0.7	<-27.0	I → 0	Rai et al. 1983
-6.40 ± 0.11	-13.40 ± 0.16	-20.31 ± 0.17	3 M $NaClO_4$	Pazukhin and Kochergin 1989
-7.0 ± 0.4	-15.1 ± 0.4	-26.4 ± 0.5	0.1 M $NaClO_4$	Silva et al. 1995, p. 294
-7.2 ± 0.5	-15.1 ± 0.7	-26.2 ± 0.5	I = 0.1 M	Neck et al. 2009, p. 1557

Am complexation by carbonate was extensively investigated by solvent extraction, spectrophotometry, electromigration, and solubility (Kim et al. 1984; Rösch et al. 1989; Felmy, Rai, and Fulton 1990; Meinrath and Kim 1991; Nitsche et al. 1995; Torretto et al. 1995). Many different soluble species have been proposed for the Am-water-carbonate system: pure carbonate, bicarbonate, and/or mixed hydroxy-carbonate complexes. Silva et al. (Silva et al. 1995) carefully studied and reinterpreted the literature data. It is the consensus in these studies that $Am(CO_3)_n^{(3-2n)}$, with n = 1, 2 and 3, are the predominant carbonate complexes. According to Silva et al. (Silva et al. 1995), there is no experimental evidence for the existence of a complex with n = 4 even at the highest carbonate concentrations. The report also suggests that there is no evidence for the formation of Am(III)-bicarbonate or hydroxy-

carbonate complexes in solution. These data are, however, in disagreement with the more recent work done by Fanghänel and Kim (Fanghänel and Kim 1998), which reports spectroscopic evidence for the formation of the n = 4 species.

Data reported by Kim et al. (Kim et al. 1984) indicate that up to pC_{H+} = ~8.0, the carbonate complexation does not affect the solubility of Am(III). Analysis of Yuci groundwaters by Chen et al. (Chen et al. 2010), with a composition and E_h intermediate to the Yucca Mountain J-13 and UE-25 well compositions, demonstrates an americium carbonate solubility of $1.8x10^{-9}$ M at pH = 7.0 and $1.2x10^{-9}$ M at pH = 8.5 when equilibrated against solid $AmOH(CO)_3$. The presence of 10^{-4}- 10^{-2} M carbonate was shown not to influence amercium solubility in the pH range of 8-10. For the higher pC_{H+}, the presence of carbonate in 0.1-0.3 M $NaClO_4$ increases solubility of Am(III) in relation to carbonate-free systems, and at pC_{H+} = 10 this difference is almost 4 orders of magnitude. The predominance of carbonate complexation is observed in the pC_{H+} range from 7.5 to 10. At higher pC_{H+}, hydrolysis predominates over carbonate complexation.

Neck et al. (Neck et al. 2009) used known data on the solubility of $Am(OH)_3$, the hydrolysis of Am(III) and Cm(III), additional data from an extensive solubility study of $Nd(OH)_3$(s) in NaCl, $MgCl_2$ and $CaCl_2$ media of various ionic strength media and time resolved laser induced fluorescence (TR-LIF) data for Cm(III) in alkaline $CaCl_2$ to evaluate a comprehensive set of standard-state equilibrium constants and ion interaction parameters for the specific ion interaction theory SIT and Pitzer equations at 25 ^oC in the M(III) - H^+ - Na^+ - Mg^{2+} - Ca^{2+} - Cl^- - OH^- - H_2O system. The solubility and hydrolysis behavior of Am(III), Cm(III) and Nd(III) in both calcium-free and calcium-containing solutions is consistently described using a model that includes the ternary Ca-M(III)-OH complexes $Ca[M(OH)_3]^{2+}$, $Ca_2[M(OH)_4]^{3+}$ and $Ca_3[M(OH)_6]^{3+}$. Data are presented in Neck Tables 1, 2 and 3 for the SIT and Pitzer parameters for this system. Solubility studies in NaCl - NaOH, $NaClO_4$ - NaOH, pure NaOH and KOH solutions up to pH = 14 showed no evidence for the formation of $Am(OH)_4^-$, which would increase the americium solubility at high pH. Study of the TR-LIF behavior of curium in alkaline solutions of various media at pH > 10 showed that $Cm(OH)_3$(aq), which would be expected to dominate the speciation at pH = 11-14, nor the complex $Cm(OH)_4^-$, could be detected, primarily due to low curium solubility. Almost all of the curium is present as $Cm_m(OH)_{3m}$ polymers or colloidal $Cm(OH)_3$(am). In alkaline $CaCl_2$ solutions at I = 0.1 - 3M and pH ~ 10.5, as opposed to the sodium-based media above, the behavior of curium is strikingly different. Cm(III) emission bands were observed caused by complexes with three, four and six OH^- ligands. These complexes, not found in NaCl - NaOH media, are stabilized by the association of Ca^{2+} ions, e.g., the ternary complexes $Ca_p[Cm(OH)_n]^{3+2p-n}$. Stability constants for the complexation reaction:

$$pCa^{2+} + Cm^{3+} + nH_2O = Ca_p[Cm(OH)_n]^{3+2p-n} + nH^+ \quad \text{(SOTERM.33)}$$

are log ${}^*\beta^o_{1,1,3}$ = -26.3 ± 0.5, log ${}^*\beta^o_{2,1,4}$ = -37.2 ± 0.6 and log ${}^*\beta^o_{3,1,6}$ = -60.7 ± 0.5. These reactions do not affect the WIPP case under current conditions.

An extensive series of experiments, reported for CRA-2009, were performed to determine the solubility of Nd(III) as an analog for Pu(III) and Am(III) solubility in the brine (Borkowski et al. 2008). In this study, the solubility was determined in GWB and ERDA-6 brine, over a pH range of 6-12, and as a function of carbonate concentration. These solubility data extended earlier studies in simplified brines to simulated WIPP brine compositions and cover a broader range of experimental conditions. A composite of literature and WIPP-specific data is shown in Figure SOTERM-20.

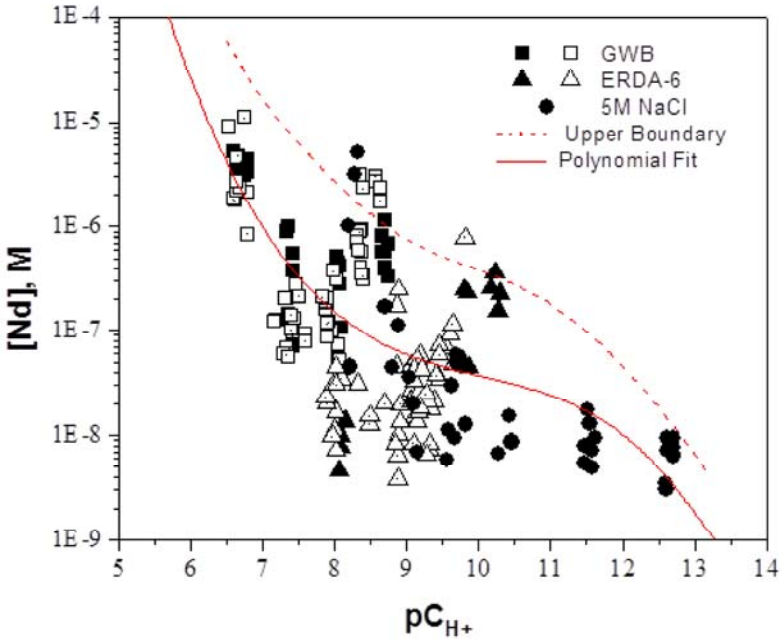

Figure SOTERM- 20. Composite of Nd Solubility Trends Under All Conditions Investigated (Borkowski et al. 2008). Open symbols correspond to undersaturation experiments and closed symbols correspond to oversaturation experiments.

SOTERM-3.7.2 WIPP-Specific Results since the CRA-2009 and the CRA-2009 PABC

There are no new WIPP-specific data since CRA-2009 and CRA-2009 PABC that is centered on the solubility of An(III) in brine. New data showing the impacts of organic complexation are summarized in section 3.8.

SOTERM-3.8 Complexation of Actinides by Organic Chelating Agents

The complexation of chelating agents with actinides has a significant impact on the concentrations of actinides in brine. At the pH of interest to the WIPP PA, only EDTA and citrate complex strongly enough to impact observed concentrations and this impact is mostly centered on the An(III) oxidation state.

SOTERM-3.8.1 Stability Constants for Organic Complexation with Actinides

The stability constants for organic ligand-actinide complexation were determined as part of the WIPP ASTP at Florida State University (Choppin et al. 1999). These data are summarized in Table SOTERM-16 and demonstrate some key trends in actinide complexation. For acetate, oxalate, and citrate, the strength of the complex formed is in the same order: IV > VI > III > V. For EDTA, the VI and III are switched. For the most part, the III and IV actinides, which are the two most important oxidation states in the WIPP, are strongly affected by organic complexation and thus can out-compete carbonate and hydrolysis if the organic concentrations are high enough. Of the four organic chelating agents considered, only citrate and EDTA are expected to form strong enough complexes to influence the speciation of actinides and potentially increase actinide concentrations under the expected conditions in the WIPP.

Table SOTERM- 16. Apparent Stability Constants for the Complexation of Organic Ligands with Actinides in NaCl Media (Choppin et al. 1999)

Organic Ligand	Actinide Ion	NaCl (molality)	$\log_{10} \beta_1$
Acetate	Am^{3+} Th^{4+} NpO_2^{+} UO_2^{2+}	0.3 to 5 0.3 to 5 0.3 to 5 0.3 to 4	1.44 - 2.2 3.68 - 4.18 1.05 - 1.8 2.23 - 3.09
Oxalate	Am^{3+} Th^{4+} NpO_2^{+} UO_2^{2+}	0.3 to 5 0.3 to 5 1.0 to 5.0 0.3 to 5	4.17 - 4.63 7.04 - 7.47 3.62 - 4.63 5.82 - 6.7
Citrate	Am^{3+}	0.3 to 5	4.84 - 5.9

	Th^{4+} NpO_2^{+} UO_2^{2+}	0.1 to 5 0.1 to 5 0.3 to 5	9.31 - 10.18 2.39 - 2.56 7.07 - 7.32
EDTA	Am^{3+} Th^{4+} NpO_2^{+} UO_2^{2+}	0.3 to 5 0.3 to 5 0.3 to 5 0.3 to 4	13.76 - 15.1 15.56 - 16.94 5.45 - 6.7 10.75 - 12.16

The possible impact of isosaccharinic acid (ISA) on thorium speciation was also considered. ISA is a chemical breakdown product of cellulosic material that has been shown to occur at pH>12. The two diastereoisomers, α- and β-isosaccharinic acids, are the products of chemical degradation of cellulosic materials in alkaline solutions. The alkaline degradation of different cellulosic materials was studied for the alkaline conditions that may exist in the initial stages of a cementitious repository (pH ~ 13.3). ISA is expected to be present in cement pore water, but it is strongly adsorbed to the cement surface. In the pore water, the concentration of ISA is expected to reach 10^{-4} M (Van Loon et al. 1997). The complexation data for ISA is very limited and there are no literature references for the tetravalent cations such as thorium. ISA is structurally a 2-hydroxycarboxylic acid; therefore, by analogy we can relate the complexation of thorium by ISA to the stability constants for Th(IV) with glycolic acid, lactic acid and 2-hydroxybutanoic acid (log K of 4.3, 4.2 and 3.8 respectively). Ligands with such low stability constants cannot outcompete An (IV) hydrolysis.

Rai et al. (Rai et al. 2000) developed a model for Th(IV) complexation with ISA. The major feature of their model is the predominance of thorium ternary complexes, e.g., $Th(OH)_4ISA_2^{2-}$, not $ThISA_2^{2+}$ complexes, as was proposed by Allard and Ekberg (Allard and Ekberg 2006a and Allard and Ekberg 2006b). According to Rai's model, mM ISA concentrations will not affect solubility of thorium. Data for higher ISA concentrations might be questionable, because Rai's model is based on 15 and 69 days equilibration times for ~10^{-6} M thorium concentrations. On the basis of our experiments and those published by German researchers, µM thorium concentrations can persist for years as a metastable state without ISA present. Complexes with a similar stoichiometry were also observed for uranium (VI) and the authors did not observe any enhanced solubility caused by ISA for pH in the range of 9.0 to 13.5 (Warwick et al. 2006).

For WIPP-related conditions, the occurrence of cellulosic chemical degradation pathways have a very low probability and, even if degradation occurs, the ISA formed will likely have a negligible effect on An(IV) solubility.

SOTERM-3.8.2 WIPP-specific Data on Organic Complexation Effects Since CRA-2009 and CRA-2009 PABC

The effect of organic complexation on the An(III) and An(IV) oxidation state were evaluated under WIPP-relevant conditions. EDTA and citrate had a strong effect on the An(III) solubility, but had essentially no impact on An(IV).

The effect of organic complexation on the solubility of Th(IV), as the An(IV) actinide analog, was determined in GWB brine in the presence of inventory-predicted organic concentration. The simultaneous presence of four organic chelating agents (2.42×10^{-3} M acetate, 3.02×10^{-2} oxalate, 3.62×10^{-3} citrate and 9.28×10^{-5} EDTA) led to a measured thorium solubility of 7.34×10^{-7} M in GWB brine at $pC_{H+} = 9.3$. This is in agreement with the 2-year solubility data (Borkowski et al., 2012) of 5×10^{-7} M and there is an order of magnitude agreement with the recently calculated thorium solubility for CRA-2014 (Brush and Domski 2013a). These experimental data confirm that there is no significant effect on the measured thorium solubility due to the presence of the organic chelators at or near their inventory-predicted limits.

The effect of organic complexation on the concentration of neodymium, as the An(III) analog, was also evaluated for each key chelating agent. These data are shown in Figure SOTERM-21. These data show a strong effect of citrate and EDTA where a 1:1 complex with the neodymium is being formed and the concentration of the neodymium is approximately the concentration of EDTA in ERDA-6 brine and ~ 50% of the concentration of EDTA in GWB brine.

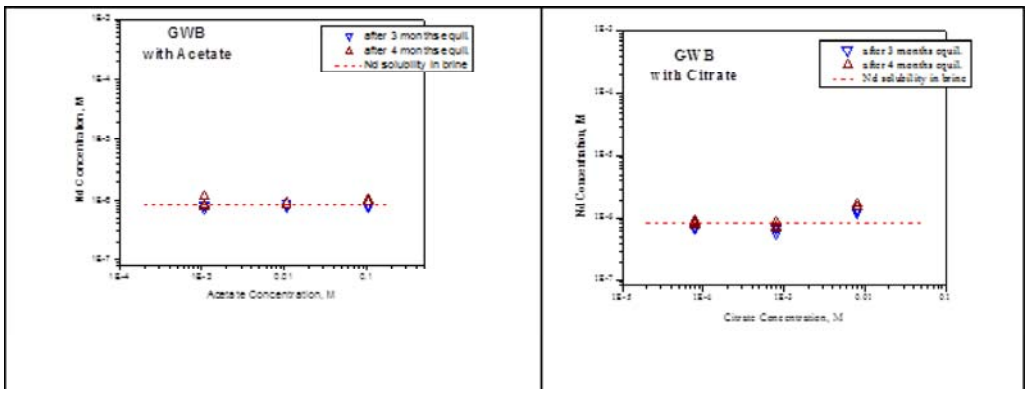

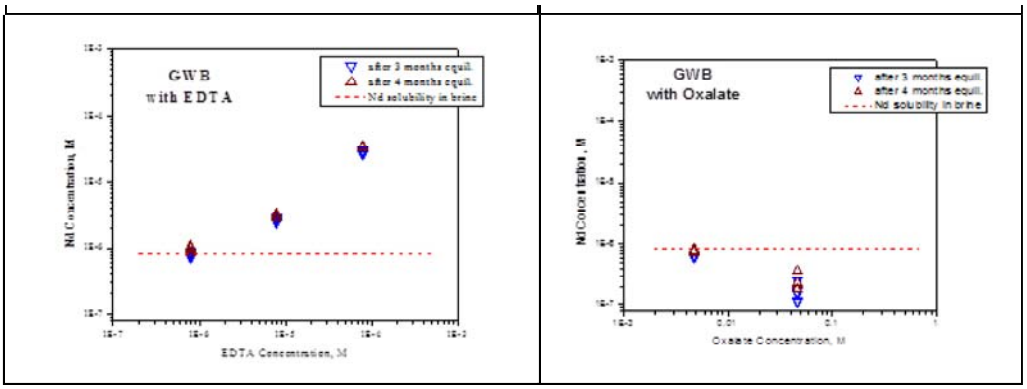

Figure SOTERM- 21. Effect of EDTA, Citrate, Oxalate and Acetate on the Solubility of Nd^{3+} in GWB Brine.

SOTERM-3.9 Actinide Colloids

The potential for colloidal species to have a role in defining the solution concentration and mobility of actinides in the WIPP was recognized early in the WIPP licensing process. This led to the development of a colloid model that accounts for these colloidal species. This model was based on an extensive literature review, some WIPP-specific experimental data, and some conservative simplifications that were extensively peer reviewed prior to the first license application (CCA). In this model, four types of colloids that could contribute to the actinide source term are identified: intrinsic, mineral, microbial and humic. The EPA found this model and approach to be satisfactory in the WIPP certification and subsequently in the CRA-2004 and CRA-2009 recertification. There has been essentially no change in this model since its initial certification by the EPA.

Actinide colloids in the WIPP are potentially important since the actinide source term is defined by the WIPP PA as the sum of contributions from dissolved actinide species and mobile colloidal actinide species (see U.S. DOE 2004, Appendix SOTERM-2004, and Reed et al. 2013) for a more detailed discussion of WIPP-relevant colloids). The importance of colloids in the migration and transport of actinide contaminants, although it continues to receive attention in the literature, remains somewhat controversial and difficult to prove. In this context, the consideration of colloidal enhancement of actinide concentrations by the WIPP PA is, at least in part, a conservatism that is built into the overall PA approach. In this context, the sorption of colloidal actinides onto fixed substrates and their filtration in low-porosity media will also reduce the mobile colloidal actinide source term, but no credit is currently being taken for this potentially significant reduction in colloidal concentrations.

Actinide colloids or pseudocolloids may be generated in the WIPP repository as a result of

1. Hydrolysis (intrinsic chemistry).

2. The interactions of dissolved actinide species with microbially derived colloids or colloids formed due to the corrosion of steel and waste constituents.

3. The hydrodynamic entrainment of colloidal-sized mineral fragments, as well as several other mechanisms.

The formation of colloids could enhance actinide release in two ways. First, increased actinide concentration will increase the magnitude of DBR release and the effective actinide source term concentration for transport through the Culebra. Second, colloids have very different transport properties than dissolved species, and are predicted to migrate more rapidly in the subsurface. This transport mechanism could enhance the overall actinide release in the WIPP through migration pathways in the Culebra member and the Salado.

The current WIPP colloidal model defines four potential colloidal contributions to the mobile actinide concentration that comprises the actinide source term:

Four potential types of colloids are recognized in the CCA and these definitions have not changed since then.

> *1. Mineral fragments are hydrophobic, hard-sphere particles that are kinetically stabilized or destabilized by electrostatic forces, and may consist of crystalline or amorphous solids. Mineral fragments may be made kinetically stable by coatings with steric stabilizers that prevent close contact. Mineral fragments may act as substrates for sorption of actinides or they may consist of precipitated or coprecipitated actinide solids.*
> *2. Actinide intrinsic colloids are macromolecules of actinides that, at least in some cases, may mature into a mineral-fragment-type of colloidal particle. When immature, they are hydrophilic; when mature, they become hydrophobic.*
> *3. Humic substances are hydrophilic, soft-sphere particles that are stabilized by salvation forces. They are often powerful substrates for uptake of metal cations and are relatively small (less than 100,000 atomic mass units).*

4. Microbes are relatively large colloidal particles that are stabilized by hydrophilic coatings on their surfaces, which behave as steric stabilizing compounds. They may act as substrates for extracellular actinide sorption or they may actively bioaccumulate actinides intracellularly.

In this section, the general environmental aspects of colloid-enhanced transport in the subsurface are discussed, along with an update of relevant WIPP-specific results since the CRA-2009 PABC.

SOTERM-3.9.1 Actinide Colloids in the Environment

The extent and potential formation of actinide colloids continues to be debated by researchers in the field. Since the CCA, there have been over 100 publications on actinide colloid chemistry that range in topics from real-system transport studies to the structure and inherent stability of actinide colloids. These remain largely focused on plutonium and its associated and very complex subsurface chemistry, but there are also studies on neptunium, americium, thorium and curium reported in the literature. It is also important to note that relatively few of these studies specifically address ionic-strength effects on colloid formation, stability and mobility. In this context, there are very few studies that in high ionic-strength systems (I > 5 M) and only a small fraction of these studies have direct application to the WIPP repository safety case.

A more extensive literature review is provided elsewhere (Reed et al. 2013). Key observations from the literature that impact the WIPP colloid model parameters are:

- A wide variety of actinide colloids are now noted to form in natural systems (see for example Khasanova et al. 2007). This differs somewhat from the conclusion made at the time of the CCA that only Pu colloids could form.

- Colloids that form in nature tend to be associated with iron colloidal species and tend to help immobilize rather than mobilize actinides. This is consistent with the WIPP model assumptions that only iron mineral colloids seem to form (see also new WIPP-specific date in section SOTERM-3.9.2). Colloidal species in the WIPP conceptualization primarily add to the source term concentration with only a small contribution to transport pathways through the Culebra.

- There are new data showing the existence of nanoclusters as an integral part of the aqueous speciation of some actinides. These are also seen in WIPP-specific brine systems (Reed et al. 2013; Section SOTERM-3.9.2).

- Bioassociation of actinides is observed in the literature and we have shown that this also extends to halophilic microorganisms (Figure SOTERM-22; Ams et al. 2013; Reed et al. 2013; Section SOTERM-3.9.2).

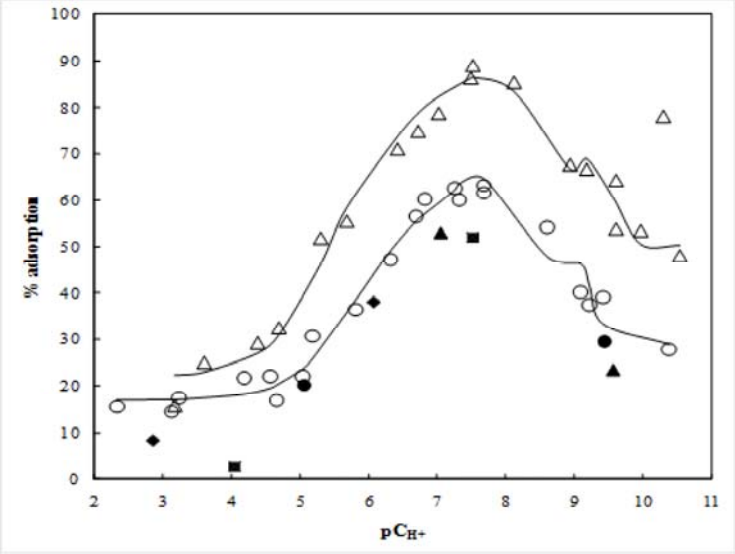

Figure SOTERM- 22. Experimental Data for Neptunium (V) Adsorption onto Chromohalobacter sp. as a Function of pH in 2 (Open Circles) and 4 (Open Triangles) M $NaClO_4$. Adsorption experiments were performed with 5 x 10^{-6} M total neptunium (V) and 5 grams per liter (g/L) (wet weight) bacteria (Ams et al. 2013). Solid curves represent best-fit calculated surface complexation models. Solid diamonds, squares, triangles, and circles represent the results of desorption experiments performed with 5 x 10^{-6} M total neptunium (V) and 5 g/L (wet weight) bacteria in 2 M $NaClO_4$.

Overall Impact of literature publications on the WIPP Colloid Model

Although there continues to be some progress made in the assessment of the colloidal issue as it applies to the potential subsurface migration of actinide species, there remains a great deal that is not well understood and substantive progress in this area is not likely in the very near future. The following general recommendations remain:

- It remains critical that the WIPP model continue to address the colloid issue.
- There is no literature evidence that the current four-colloid type model is inadequate; if anything it continues to be a conservative assumption built into the model.
- Current literature shows that colloidal species, intrinsic and mineral, of a number of actinides, not just plutonium, is observed - this is somewhat of a departure from the initial CCA literature survey conducted. These literature data, however, still do not explicitly address high ionic-strength systems.
- The structural data point towards intrinsic colloids that persist as very small (typically < 10nm) species.
- Biosorption data show that increased ionic-strength increased the extent of sorption and the overall trend with pH was to go through a maximum at about pH 8 and then decrease with increasing pH. At the predicted pC_{H+} of ~ 9.4 in the WIPP site, biosorption is in the range of ~ 40-65%.

SOTERM-3.9.2 WIPP-Specific Results since the CRA-2009 and CRA-2009 PABC

The mineral, intrinsic and microbial contribution to the WIPP mobile colloidal actinide source term model was re-examined in light of recent literature results and new WIPP-specific data (Reed et al. 2013). An extensive amount of work under WIPP-specific conditions was completed to re-assess the microbial colloid enhancement parameters. There were some discrepancies in the model in this area due to the lack of extensive WIPP-specific data at the time of the CCA. These experiments build on the more extensive understanding that we now have about the microbial ecology in the WIPP. Microbial colloid enhancement parameters based on these new data are recommended and these are, in general, more realistic and lead to a lower overall contribution of microorganisms to the actinide source term.

As a whole, the WIPP-specific data obtained since CRA-2009 provide the first WIPP-specific data on colloids since the time of the CCA. These data, although not complete, provide significant improvement in our understanding of the potential contribution of colloidal species to the actinide source term. Additionally, some inconsistencies between the known solution chemistry and literature observation are addressed. Updated parameters (see discussion in Section SOTERM-4.0) for the intrinsic, mineral and microbial colloid enhancement parameters are recommended.

SOTERM-3.9.2.1 Intrinsic and Mineral Colloids

The intrinsic and mineral colloidal fraction of the actinides and analogs investigated as part of the long-term solubility studies was determined to provide WIPP-specific data. The size fractionation was determined using ultrafiltration and, in some cases, ultracentrifugation methods down to ~ 2.5 nm. In almost all cases, <10 nm size nanospecies were observed and assigned to the intrinsic colloidal fraction. The >10 nm size fraction was also established and used to evaluate the existence of mineral colloids.

The size distribution of aqueous species was shown for thorium and plutonium(III) in Figures SOTERM-10 and SOTERM-18 respectively. Additionally, results were obtained for neodymium (Figure SOTERM-23), uranium (Figure SOTERM-24) and plutonium in more detail (Figure SOTERM-25). In most cases, there was no filtration effect above 10 nm with the notable exception of plutonium where iron was also present in solution. There was no evidence for Mg-derived colloidal contributions.

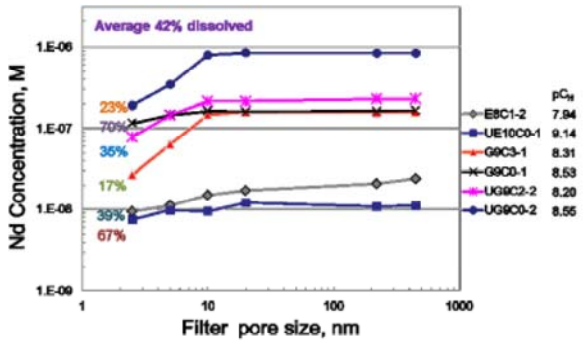

Figure SOTERM- 23. Sequential Filtration Results for the Long-term Neodymium Solubility Studies in Brine (E = ERDA-6; G = GWB) as a Function of Filter Pore Size for Different pC_{H+} and Brines. Significant filtration effects are only noted for filters that are 10 nm or smaller in size.

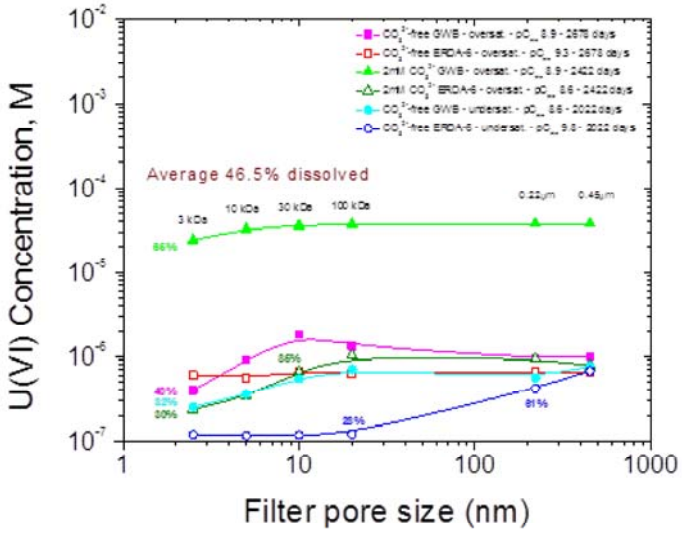

Figure SOTERM- 24. Concentration of Uranium Measured during Sequential Filtration as a Function of Different Pore Size Filters for Different Brine Solutions at Different pC_{H+}. Little/no filtration effect noted in all but one case above 10 nm filtration size.

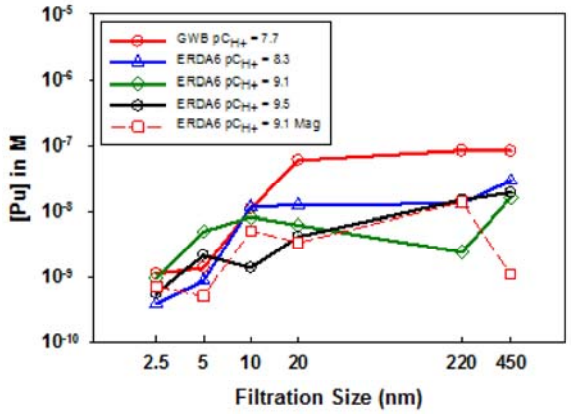

Figure SOTERM- 25. Sequential Filtration Data for the Pu-Fe Experiments as a Function of Filtration at Different pC_{H+} and Brine Composition. GWB and ERDA-6 brine experiments contained excess iron powder with the exception of the "mag" designated experiment in ERDA-6 that contained excess magnetite.

SOTERM-3.9.2.2 Humic Colloids

The stability of humic and fulvic acid in the WIPP brine was investigated (Wall et al. 2005) and found to be unstable in the presence of MgO. These results add to the conservatism of the WIPP colloid model in that it shows that humic colloids are not likely in the WIPP. There is, however, no change in the model parameter assumptions for this colloidal species.

SOTERM-3.9.2.3 Microbial colloids

Experiments to measure the bioassociation of the An(III) and An(IV) actinides with WIPP-relevant microorganisms were performed. These experiments were focused on the biosorption of the two most important actinide oxidation states, Nd(III) for An (III) and Th(IV) for An(IV), towards a representative halophilic bacteria and archaea. Redox-invariant analogs were used so that there was no question about the oxidation state being sorbed. These biosorption data are used to recalculate the PROPMIC microbial colloid enhancement parameter and, when combined with laboratory observations of microbial growth under WIPP-relevant conditions, a biomass-based CAPMIC value (see Section SOTERM-5.4).

The microorganisms used in the biosorption experiments are indigenous to the WIPP area. The bacterium used, *Chromohalobacter* sp., was isolated from brine retrieved from a shallow subsurface monitoring well incubated under aerobic conditions (Swanson et al. 2012; Ams et al. 2013). Although these are incubated aerobically, from the point of view of biosorption, the DOE expects these to be representative of anaerobically derived species. The origins of this water are believed to be a mixture of seepage from an above-ground, but now capped, mine tailings salt pile and actual groundwater flow through the Santa Rosa and Dewey Lake

contact (U.S. DOE 2011). Since then, this bacterium has also been isolated from incubations of WIPP halite at lower salt concentrations, and a Culebra groundwater incubated under aerobic, transitional, and nitrate-reducing conditions. The archaea utilized in these studies was *Halobacterium noricense*. This was isolated from incubations of halite in generic media and in the WIPP brines, detected in other subterranean salts worldwide (including Germany), requires 2.5-5 M NaCl, tolerates pH 6-10, and is 0.3-1.5 µm in size.

> The biosorption experiments are described in detail elsewhere (Reed et al. 2013). The biosorption of actinides towards microorganisms should correlate with their aqueous speciation. For this reason, it would be expected that similar oxidation states would exhibit similar biosorption behavior, at least to the extent that their aqueous speciation is similar.

Example biosorption data are shown for thorium in Figure SOTERM-26. It is notable that the biosorption data are different for bacteria and archaea and EDTA complexation can reduce the extent of biosorption noted. In both +3 and +4 cases and in both Francis' and LANL-CO work, the PROPMIC values obtained for *Archaea* are less than those for *Bacteria*.

Changes in approach for An(III/IV) Biosorption Enhancement Parameters

Based on the current understanding of halophilism and microbial ecology at the WIPP site, microbial enhancement parameters were determined based on five observations made in the biosorption and microbial growth-related experiments.

- First, an emphasis on the archaeal data for the near field was used since this presented the most realistic scenario of which organisms will be present. In PA, however, bacterial values were used.

- Second, the biosorption data obtained at the lowest pH values investigated (~ pC_{H+} = 8.5) are most reliable and should be the basis of the PROPMIC calculation. These have well correlated biomass dependencies (so sorption is the predominant process) and overall concentration stability. The higher pH data for both thorium and neodymium appear to have significant contributions from precipitation pathways, although this is clearly more evident in the thorium data.

- Third, it is more consistent with the overall WIPP actinide model to use actinide oxidation state rather than element to assign biosorption enhancement parameters - although element-specific values are also provided. In the PA implementation, the element-specific values were used.

- Fourth, CAPMIC values were changed for all elements to a concentration based on microbial biomass and sorption capacity. This adds more realism to the model and accounts for variability in the toxicity data - which was used in prior CRAs to determine this value.

- Fifth, a biomass-based number was used for CAPMIC. The new biomass-based CAPMICs are less than the total mobile values in the case of the +3 oxidation state.

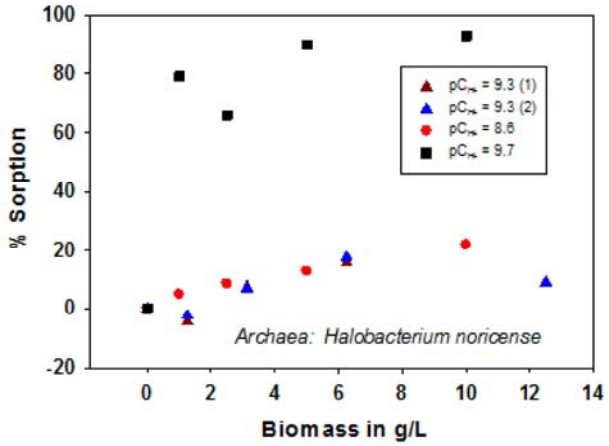

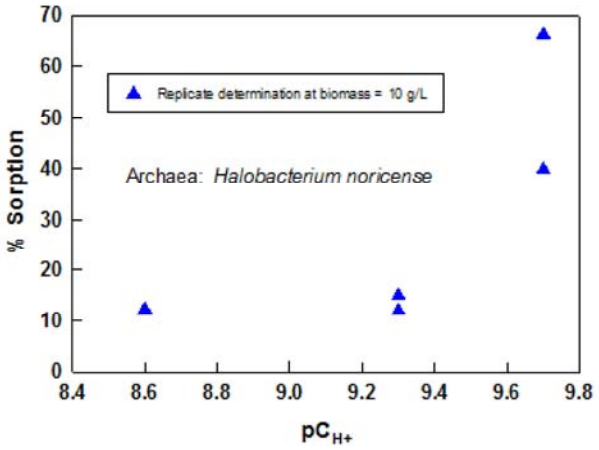

Figure SOTERM- 26. Biomass Dependency (top) and % Sorption (Bottom) of Thorium as a Function of pC_{H+} in pH-specific WIPP Brine. Reliance on lower-pH data was necessary due to the coupling of precipitation at the higher pHs investigated.

SOTERM-4.0 Calculation of the WIPP Actinide Source Term

The calculation of the WIPP dissolved-actinide source term was performed for the CRA-2014 PA (Brush and Domski 2013a) using the computer code EQ3/6 (Wolery 1992; Wolery and Daveler 1992; Wolery 2008; Wolery, Xiong and Long 2010) version 8.0a and the database DATA0.FMT.R2 (Xiong 2011a). A general description of the modeling approach to establish the actinide source term for the WIPP PA is described in this section.

Changes since the CRA-2009 and CRA-2009 PABC

There are essentially no significant changes in the approach and overall conceptual model used to determine the solubility of actinides in the WIPP since CRA-2009. There are some changes in the mechanics of this process that are noted here:

- FMT is no longer used. All solubility calculations are done with EQ3/6. The qualification of EQ3/6 was done as a precursor to this transition (Wolery 2008; Wolery, Xiong and Long 2010; Xiong 2011b). The Pitzer data set of chemical equations has not changed.
- The colloid enhancement parameters for the actinides were updated based on new WIPP-specific data and published literature (see Section SOTERM-3.9).
- Variable brine volume is now being implemented in PA (see SOTERM-5.1.4 and Brush and Domski 2013a).

SOTERM-4.1 Overview of WIPP Approach to Calculate Actinide Solubilities

The overall approach used to establish the actinides important in WIPP releases and calculate their solubilities for use in the WIPP PA is summarized in this section. This approach consists of the following:

- Assess the WIPP inventory and regulations that govern the application of the WIPP certification to determine the likely actinides of interest and, correspondingly, the key waste components that may affect their solubility.
- Establish a conceptual model for the key subsurface interactions and release mechanisms and using a combination of literature review and WIPP-specific experimental results to establish the likely oxidation state distribution, the species that affect actinide solubility and the parameters required to model the system at high ionic strength. This approach featured the following:

- Conservative assumptions, within the bounds of the conditions expected, for the oxidation state distribution.
- Use of redox-invariant analogs for multivalent actinides to determine formation constants and establish oxidation-specific solubilities.

- Use of the Pitzer activity-coefficient model and associated parameters to model solubilities at the high ionic strengths present. The Pitzer approach is recognized as the best approach for I > 0.3 M in brine systems.

- Calculate the solubility of the key actinides in the WIPP using the EQ3/6 code. The solubilities are modeled in reacted GWB and ERDA-6 brines and include the effects of organic complexation. This is expected to bracket the range in the composition of the brine expected.

- Establish the effects of colloids on the solubilities calculated.

- Tabulate and assign uncertainty distributions in the range of expected conditions and brine compositions to these solubility data. A new method for this is used in CRA-2014 (see Brush and Domski 2013c).

This range of possible solubilities for a wide range of possible conditions defines the actinide source term provided to the WIPP PA for the calculation of TRU release from the WIPP.

SOTERM-4.2 Use of Oxidation-State-Invariant Analogs

The solubility and speciation of multivalent actinides are often investigated with lanthanide and actinide analogs that mimic the property of interest but, for varying reasons, provide an advantage to the experimenter. The best example of this, used extensively in the WIPP modeling approach, is the use of redox-invariant analogs for the multivalent actinides, most notably Pu, to determine oxidation-state-specific properties (e.g., solubility or complexation). The advantage of these types of analogs is that they remove the uncertainty of oxidation-state change from the experiment, which is a complexity that can often lead to uncertain or incorrect interpretations of the results obtained.

For the TRU actinides, the redox-invariant analogs used are lanthanides or other actinides. Lanthanides, as 4f-electron elements, possess physical and chemical characteristics that make them good analogs for the actinides when they are redox-invariant under the conditions of the experiment. Correspondingly, actinides with their 5f-electron character also have good physical and chemical properties to be analogs for other actinides if they also have redox stability under WIPP-relevant conditions. This analog approach, although sometimes criticized in the literature, considerably simplifies experimental design and consequently improves the reliability of the experimental data (Choppin 1999).

A key argument for the use of analogs in WIPP-related experiments is that key complexants that define actinide solubility in the WIPP are hard-donor complexants (e.g., hydroxide, carbonate, borate, chloride, and/or sulfate). The use of lanthanides as analogs for actinides is based on observations in many extraction systems, along with the associated crystallographic data (Siekierski 1988) that show they are good analogs for compounds containing hard donor ligands (oxygen) where the cation-anion interactions are primarily electrostatic in nature. In this context, Nd(III) is a good analog for the chemical behavior of Am(III) and Pu(III) under most circumstances in the WIPP. Not only do these species have the same 3+ charge, they also have similar ionic radii for coordination number 6 (CN=6): 97.5 pm for Am^{3+}, 98.3 pm for Nd^{3+}, and 100 pm for Pu^{3+} (Shannon 1976). In this context, the magnitudes of electrostatic attractions between these metal ions and corresponding ligands will be similar, yielding comparable thermodynamic stabilities.

Th is used by the WIPP as a redox-invariant analog for Pu(IV), U(IV), and Np(IV). The use of the Th^{4+} stability constants to represent the other An(IV) species is conservative. Th^{4+} is the largest of the tetravalent actinide ions. It therefore has the lowest charge density and, correspondingly, relatively weaker ionic interactions when compared to the other tetravalent actinides. This is best exhibited by its lower tendency towards hydrolysis and intrinsic polymer formation relative to the other actinides (see Section SOTERM-3.2). For these reasons, the use of Th^{4+} as an analog is conservative, as Th will likely be the most soluble of the actinides in the tetravalent state under comparable WIPP-relevant conditions.

To a lesser extent, actinides are analogs for each other, depending on the oxidation state. Np(V), which has much greater redox stability than Pu(V) and much more favorable spectroscopy, is often used as an analog for Pu(V). U(VI), which is much more redox stable than Pu(VI) and Np(VI), is also used as an analog for these TRU actinides, although U(VI) is in fact a poor analog for Pu(VI) solubility. Am(III) and Cm(III) are also excellent analogs for Pu(III) as a result of their much greater redox stability and comparable ionic radii.

SOTERM-4.3 Actinide Inventory and Oxidation State Distribution in the WIPP

The actinide inventory used in CRA-2014 PA was the 2012 inventory that was summarized in Van Soest (Van Soest 2012). Key aspects of this were provided in Tables SOTERM-10 and SOTERM-11.

The oxidation states used by the WIPP PA to model actinide solubility are tabulated in Table SOTERM-17. Also included are the assumed abundance percent of each oxidation state and the speciation data set used in EQ3/6 for each oxidation state. This table is based on a general understanding of the corresponding actinide chemistry summarized in Section SOTERM-3.0.

Table SOTERM- 17. Oxidation States of the Actinides in the WIPP as Used in the CRA-2014 PA

Actinide Element	Oxidation States, Abundance (%), and Analog Used (If Any)				
	Oxidation State[a,b]				EQ3/6 Speciation Data Used
	III	IV	V	VI	
Thorium	-	100 %	-	-	Thorium
Uranium	-	50 %	-	50 %	1 mM assumed for VI, Th for IV
Neptunium	-	50%	50 %	-	Np for V Th for IV
Plutonium	50 %	50 %	-	-	Am for III Th for IV
Americium	100 %	-	-	-	Americium
Curium	100 %	-	-	-	Americium

a Oxidation state distributions (percentages) refer to the percent of PA vectors that have 100% of the specified oxidation state.
b In PA calculations the distribution of oxidation states is correlated for U, Np, and Pu such that the states for all three elements are simultaneously either in the lower oxidation state (U(IV), Np(IV), and Pu(III)) or in the higher oxidation state (U(VI), Np(V), and Pu(IV)).

A number of conservative assumptions are reflected in this table:

1. Use of 1 mM concentration for the solubility of U(VI). The actual solubility of U(VI) in the WIPP under the expected range of conditions is estimated to be <0.1 mM.

2. Use of Th as an analog for the IV actinides (see Section SOTERM-4.1 and Section SOTERM-3.2).

3. The assumption of a probability that 50% of the vectors have Pu(III) and 50% of the vectors have Pu(IV). The predominant Pu species expected is Pu(IV), although some Pu(III) is possible as a transient (see discussion in Section SOTERM-3.6). This is conservative because Pu(III) is approximately 6 to 10 times more soluble than corresponding Pu(IV) phases.

4. The assumption of a probability that 50% of the vectors have U(IV) and 50% of the vectors have U(VI). The predominant uranium species expected is U(IV), which is approximately four orders of magnitude less soluble than U(VI), based on current assumptions.

SOTERM-4.4 Actinide Speciation Reactions Used in EQ3/6

The version of the database used with the EQ3/6 code for the CRA-2014 PA was DATA0.FMT.R2 (Xiong 2011a). This was a conversion of the FMT database used in CRA-2009 into the EQ3/6 format and was extensively qualified (Wolery, Xiong and Long 2010). There were no significant changes to the speciation reactions and data used. For these reactions (see Wolery 1992 for a detailed discussion), log K is the log of the product of the activity of each reaction product (to the power of its coefficient) divided by the product of the activity of each reactant (to the power of its coefficient).

SOTERM-4.4.1 The III Actinides: Pu(III), Am(III), Cm(III)

The thermodynamic database for the III actinides currently used in EQ3/6 was described by Giambalvo (Giambalvo 2002a) and updated by Wolery (Wolery, Xiong and Long 2010). Nd, Am, and Cm are generally used to establish solubility of An(III) because, unlike plutonium, they have redox-stable trivalent oxidation states. Speciation and solubility data for the III actinides were parameterized for use in the Pitzer activity-coefficient model by Felmy et al. (Felmy et al. 1989) for the Na^+- Pu^{3+}-Cl^--H_2O system; by Felmy, Rai, and Fulton (Felmy, Rai, and Fulton 1990) for the Na^+-Am^{3+}-OH^--HCO_3^--H_2O system; by Rai, Felmy, and Fulton (Rai, Felmy, and Fulton 1995) for the Na^+-Am^{3+}-PO_4^{3-}-SO_4^{2-}-H_2O system; and by Rao et al. (Rao et al. 1996) for the Na^+-Nd^{3+}-CO_3^{2-}-HCO_3^--H_2O system. EQ3/6 uses the Am(III) data to calculate the solubility for all the III actinides. A diagram of the predominant species for Am is shown in Figure SOTERM-27.

The inorganic aqueous and solubility-limiting species featured in the model for Am(III) are

Am(III) Reactions	log K	
Am3+ + CO32- ⇆ AmCO3+	8.1	(SOTERM.34)
$Am^{3+} + 2CO_3^{2-} \leftrightarrows Am(CO_3)_2^-$	13.0	(SOTERM.35)
$Am^{3+} + 3CO_3^{2-} \leftrightarrows Am(CO_3)_3^{3-}$	15.2	(SOTERM.36)
$Am^{3+} + 4CO_3^{2-} \leftrightarrows Am(CO_3)_4^{5-}$	13.0	(SOTERM.37)

Am(III) Reactions	log K	
$Am^{3+} + OH^- \leftrightarrows AmOH^{2+}$	6.4	(SOTERM.38)
$Am^{3+} + 2OH^- \leftrightarrows Am(OH)_2^+$	12.3	(SOTERM.39)
$Am^{3+} + 3OH^- \leftrightarrows Am(OH)_3(aq)$	16.3	(SOTERM.40)
$Am^{3+} + Cl^- \leftrightarrows AmCl^{2+}$	0.24	(SOTERM.41)
$Am^{3+} + 2Cl^- \leftrightarrows AmCl_2^+$	-0.74	(SOTERM.42)
$Am^{3+} + SO_4^{2-} \leftrightarrows Am(SO_4)^+$	3.25	(SOTERM.43)
$Am^{3+} + 2SO_4^{2-} \leftrightarrows Am(SO_4)_2^-$	3.7	(SOTERM.44)
$Am^{3+} + OH^- + CO_3^{2-} \leftrightarrows AmOHCO_3(s)$	22.7	(SOTERM.45)
$Na^+ + Am^{3+} + 2CO_3^{2-} + 6H_2O \leftrightarrows NaAm(CO_3)_2 \cdot 6H_2O(s)$	21.4	(SOTERM.46)
$Am^{3+} + PO_4^{3-} \leftrightarrows AmPO_4(cr)$	24.8	(SOTERM.47)

In these reactions, "aq," "cr," and "s" are the abbreviations for aqueous, crystalline, and solid, respectively. The An(III) database was extended to mixed Na^+-CO_3^{2-}-Cl^-- media, and was shown to reproduce the independently measured solubility of $NaAm(CO_3)_2$ (s) in 5.6 M NaCl (Runde and Kim 1994) and the measured Nd(III) solubility in the WIPP brine (Borkowski et al. 2008).

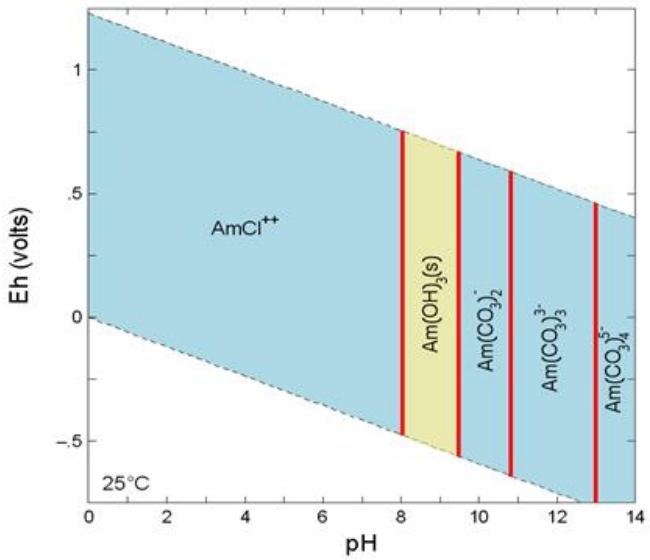

Figure SOTERM- 27. Predominant Am Species as a Function of pH and E_h Based on the Speciation Reactions 34 to 47 (Richmann 2008)

SOTERM-4.4.2 The IV Actinides: Th(IV), U(IV), Pu(IV), Np(IV)

The IV actinides addressed by the WIPP PA are Th(IV), U(IV), Pu(IV), and Np(IV). The variation in charge-to-radius ratio for the tetravalent actinides is greater than for actinides in other oxidation states (Cotton and Wilkinson 1988, pp. 11-46), and larger differences in the chemical behavior among the IV actinides is expected. The application of the Th(IV) model to the other IV species (U(IV), Np(IV), and Pu(IV)) is more uncertain, yet still conservative because Th(IV) is the most soluble of these elements under WIPP conditions. The model was evaluated against data for Pu(IV) and Np(IV) solubility and demonstrated to predict the chemical behavior of these actinides conservatively.

The thermodynamic database for the IV actinides currently used in EQ3/6 was described by Giambalvo (Giambalvo 2002b). Speciation and solubility data for Th(IV) were parameterized for the Pitzer activity-coefficient model for the Na^+-K^+ -Mg^{2+}-Cl^--SO_4^{2-}-CO_3^{2-}-HCO_3^- -OH^--H_2O system. This model requires the species Th^{4+}, $Th(OH)_2SO_4$ (s), $Th(SO_4)_3^{2-}$, $Th(SO_4)_2$ (aq), ThO_2, $Th(OH)_4$(aq), $Th(OH)_3CO_3^-$, and $Th(CO_3)_5^{6-}$ to describe the data pertinent to the WIPP (Felmy, Mason, and Rai 1991; Rabindra et

al. 1992; Felmy et al. 1996). A diagram of the predominant Th speciation, based on Reactions SOTERM.48 to 59, is shown in Figure SOTERM-28.

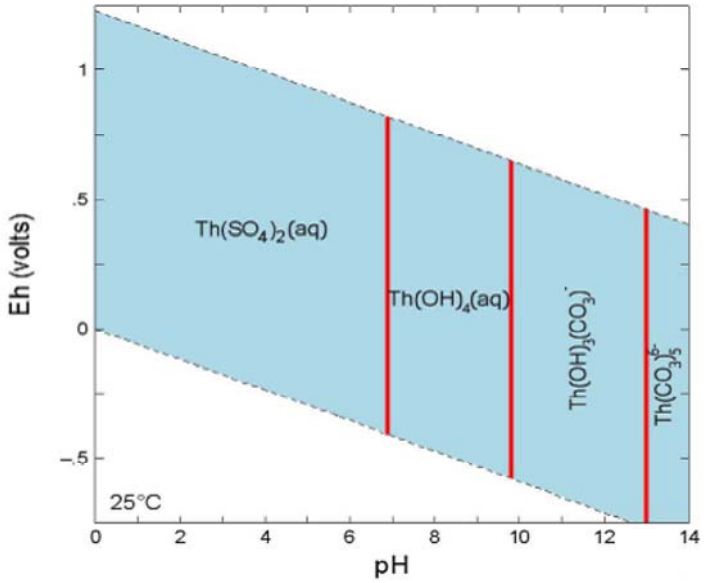

Figure SOTERM- 28. Predominant Species of Th as a Function of pH and Redox Conditions (Richmann 2008). Thorianite is predicted to predominate at the conditions expected in the WIPP repository.

The inorganic aqueous and solubility-limiting species featured in the IV model are:

Th(IV) Reactions	log K	
$ThO_2(am) + 2H_2O \leftrightarrows Th(OH)_4(aq)$	-7.0	(SOTERM.48)
$Th^{4+} + 4OH^- \leftrightarrows Th(OH)_4(aq)$	38.5	(SOTERM.49)
$Th^{4+} + 3OH^- + CO_3^{2-} \leftrightarrows Th(OH)_3CO_3^-$	38.3	(SOTERM.50)
$Th^{4+} + 5CO_3^{2-} \leftrightarrows Th(CO_3)_5^{6-}$	27.1	(SOTERM.51)
$Th^{4+} + 2SO_4^{2-} \leftrightarrows Th(SO_4)_2(aq);$	11.6	(SOTERM.52)
$Th^{4+} + 3SO_4^{2-} \leftrightarrows Th(SO_4)_3^{2-};$	12.4	(SOTERM.53)
$Th^{4+} + 2SO_4^{2-} + 9H_2O \leftrightarrows Th(SO_4)_2 \cdot 9H_2O(s);$	13.0	(SOTERM.54)
$Th^{4+} + 2SO_4^{2-} + 8H_2O \leftrightarrows Th(SO_4)_2 \cdot 8H_2O(s)$	12.9	(SOTERM.55)
$Th^{4+} + 2Na^+ + 3SO_4^{2-} + 6H_2O \leftrightarrows Th(SO_4)_2 \cdot Na_2SO_4 \cdot 6H_2O(s)$	17.6	(SOTERM.56)
$Th^{4+} + 2K^+ + 3SO_4^{2-} + 4H_2O \leftrightarrows Th(SO_4)_2 \cdot K_2SO_4 \cdot 4H_2O(s)$	18.1	(SOTERM.57)
$Th^{4+} + 4K^+ + 4SO_4^{2-} + 2H_2O \leftrightarrows Th(SO_4)_2 \cdot 2K_2SO_4 \cdot 2H_2O\ (s)$	21.2	(SOTERM.58)
$Th^{4+} + 7K^+ + 5.5SO_4^{2-} \leftrightarrows Th(SO_4)_2 \cdot 3.5K_2SO_4(s).$	24.7	(SOTERM.59)

SOTERM-4.4.3 The V Actinides: Np(V)

The only V actinide of interest to the WIPP is Np(V), which exists as the neptunyl ion, NpO_2^+. Pu(V), which can be formed under some conditions, is transitory and not expected to persist in significant quantities in the WIPP. The base model for Np(V) comes from Fanghänel, Neck, and Kim (Fanghänel, Neck, and Kim 1995), constructed for the German repository program.

The thermodynamic database for the V actinides currently used in EQ3/6 is described by Giambalvo (Giambalvo 2002c). Np(V) speciation and solubility were parameterized in the Pitzer activity-coefficient model for the Na^+-K^+ -Mg^{2+}-Cl^-- SO_4^{2-}-CO_3^{2-}-HCO_3^- -OH^--H_2O system. The model requires the aqueous species NpO_2^+, $NpO_2OH(aq)$, $NpO_2(OH)_2^-$, $NpO_2CO_3^-$, $NpO_2(CO_3)_2^{3-}$, and $NpO_2(CO_3)_3^{5-}$, and the solid species $NpO_2OH(am)$, $NpO_2OH(aged)$, $Na_3NpO_2(CO_3)_2(s)$, $KNpO_2CO_3 \cdot 2H_2O(s)$, $K_3NpO_2(CO_3)_2 \cdot 0.5H_2O(s)$, and $NaNpO_2CO_3 \cdot 3.5H_2O(s)$ to explain the available data. The predominant species for Np(V) are shown in Figure SOTERM-29.

The inorganic aqueous and solubility-limiting species used are:

Np(V) Reactions	log K	
$NpO_2^+ + OH^- \leftrightarrows NpO_2OH(aq)$	2.7	(SOTERM.60)
$NpO_2^+ + OH^- \leftrightarrows NpO_2OH(s, am)$	8.8	(SOTERM.61)
$NpO_2^+ + OH^- \leftrightarrows NpO_2OH(s, aged)$	9.5	(SOTERM.62)
$NpO_2^+ + 2OH^- \leftrightarrows NpO_2(OH)_2^-$	4.5	(SOTERM.63)
$NpO_2^+ + CO_3^{2-} \leftrightarrows NpO_2CO_3^-$	5.0	(SOTERM.64)
$NpO_2^+ + 2CO_3^{2-} \leftrightarrows NpO_2(CO_3)_2^{3-}$	6.4	(SOTERM.65)
$NpO_2^+ + 3CO_3^{2-} \leftrightarrows NpO_2(CO_3)_3^{5-}$	5.3	(SOTERM.66)
$Na^+ + NpO_2^+ + CO_3^{2-} + 3.5H_2O \leftrightarrows NaNpO_2(CO_3) \cdot 3.5H_2O(s)$	11.1	(SOTERM.67)
$3Na^+ + NpO_2^+ + 2CO_3^{2-} \leftrightarrows Na_3NpO_2(CO_3)_2(s)$	14.2	(SOTERM.68)
$K^+ + NpO_2^+ + CO_3^{2-} \leftrightarrows KNpO_2(CO_3)(s)$	13.6	(SOTERM.69)
$3K^+ + NpO_2^+ + 2CO_3^{2-} + 0.5H_2O \leftrightarrows K_3NpO_2(CO_3)_2 \cdot 0.5H_2O(s)$	-4.8	(SOTERM.70)

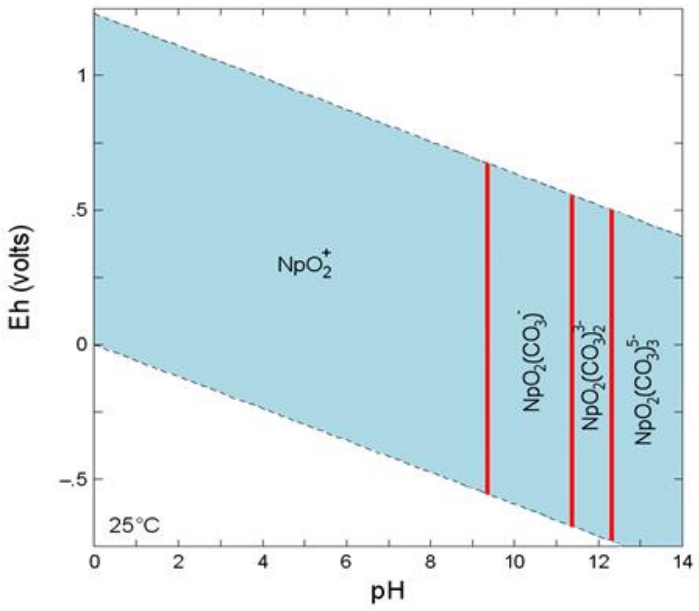

Figure SOTERM- 29. Predominant Species Diagram for Np as a Function of pH and E_h Based on the Np Speciation Data Reactions 60 to 70 (Richmann 2008)

SOTERM-4.4.4 The VI Actinides: U(VI)

The An(VI) EQ3/6 model has not been developed sufficiently for reliable use in predicting concentrations of this oxidation state in the WIPP brines under various solution conditions. Although uranyl carbonate can be successfully modeled, the hydrolysis behavior of U(VI) is quite complicated and no satisfactory predictive models applicable to WIPP-like conditions are yet available. Because the implementation of an MgO backfill limits the pmH and f_{CO2} to discrete values, empirical measurement of the solubility of U(VI) in WIPP and/or WIPP-like brines became practical. As documented in Hobart and Moore (Hobart and Moore 1996) and used in prior PA calculations, the solubility of U(VI) at pH 10, in the absence of carbonate, was determined to be 8.8×10^{-6} m. This is augmented by additional data from U(VI) solubility studies in WIPP-relevant carbonate-free brines reported in Section SOTERM-3.3.2 (Lucchini et al. 2010a; Lucchini et al. 2013a; Lucchini et al. 2013b). Here, the measured U(VI) solubility was 10^{-7} M to 10^{-6} M for GWB and ERDA-6 brine, respectively. The solubility of U(VI) currently used in the WIPP PA was established through discussions with the EPA to be 1 mM (U.S. EPA 2005) to account for the potential and expected effects of carbonate.

SOTERM-4.5 Calculations of Actinide Solubility Using the EQ3/6 Computer Code

Details of the implementation of EQ3/6 are described in more detail elsewhere (Wolery 2008; Wolery and Jarek 2003; Wolery, Xiong and Long 2010; Brush and Domski 2013a). EQ3/6 calculates chemical equilibrium for user-specified total element amounts in aqueous or aqueous/mineral geochemical systems. The EQ3/6 calculations of actinide solubility in the WIPP system performed for the WIPP PA included preequilibration with halite, anhydrite, brucite, and hydromagnesite (Brush and Domski 2013a), which are the minerals present in large quantities in the repository. The effects of the MgO backfill are realized by equilibrating brine with brucite, magnesite, and hydromagnesite.

SOTERM-4.5.1 Pitzer Approach for High-Ionic-Strength Brines

The Pitzer activity-coefficient model is substantially different in approach from the classic Debye-Hückel (D-H) theory of the behavior of ionic solutions. The latter is a theoretical approach to describing the behavior of dilute solutions; more importantly, because many ionic solutes do not behave ideally even at very low concentrations, D-H provides a means to calculate the activity, a_i , of a desired species. This is of great importance, as the Gibbs free energies of the various species in solution can be used to calculate solution equilibria if one knows the effective concentration of those species, i.e., their "activity" in solution. The activity of a given species i is tied to the molality of that species as $a_i = \gamma_i m_i$. Since the molality of species i is known, the unknown that must be calculated to determine a_i is, therefore, γ_i . The simplest form relating activity to molality from the D-H law is

$$\log \gamma_i = -A_\gamma z_i^2 \left(\frac{\sqrt{I}}{1+\sqrt{I}} \right) \quad \text{(SOTERM.71)}$$

where $A\gamma$ is the Debye-Hückel parameter, z_i is the charge of the ith species and I is the overall solution ionic strength. The fundamental difficulty with the D-H formalism is that even with extensions (Davies equation, B-dot equation)(Wolery 2008), the D-H law begins to deviate significantly from real solution behavior somewhere in the general region of I = 0.3 molal. As the WIPP brines (and many other highly concentrated ionic species of interest) are well above this level of ionic strength, many times with $I >$ 5, another description is required to properly describe the activities of the ionic species.

In 1973, Pitzer proposed a set of semiempirical equations to describe a_i . Pitzer (Pitzer 1973) wrote the Gibbs excess energy of a solution as a virial expansion, where a portion of the overall expansion can be tied down to a formalism similar to the D-H law and the majority of the remaining constants are empirically determined from measurements of the desired ions. The most general form of the equation is

$$\ln \gamma_i = \left(\frac{z_i^2}{2} \right) f'(I) + 2 \sum_j \lambda_{ij}(I) m_j + \sum_{jk} \left(\left(\frac{z_i^2}{2} \right) \lambda'_{ijk}(I) + 3\mu_{ijk} \right) m_j m_k \quad \text{, (SOTERM.72)}$$

where $f(I)$ is a Debye-Hückel function, $f'(I)$ is its derivative df/dI, the λ_{ij} are second-order interaction coefficients, $\lambda'_{ij}(I)$ is the derivative $d\lambda_{ij}/dI$, and the μ_{ijk} are third-order interaction coefficients. The experimentally observable values $\beta^{(0)}$, $\beta^{(1)}$, $\beta^{(2)}$, α_1, α_2, C^φ, and so forth are used to calculate the λ_{ij} and μ_{ijk} values needed to calculate γ_i (for more detail, see Wolery and Daveler 1992).

This approach has proven highly effective and has successfully described the behavior of solutions at high ionic strength. The disadvantage of this technique is that binary and ternary coefficients for the expansion are normally needed to completely describe all the activities of the different species; in addition, if the number of species in solution grows, the number of calculations grows that much faster, i.e., on the order of the cube of the number of species. This problem would be even worse, except that many of the terms describing neutral species can be legitimately neglected in geochemical systems.

This parameter-determination problem is of particular interest in the description of actinide behavior in the WIPP, since the GWB and ERDA-6 brines of interest contain a wide variety of ions in and of themselves, in addition to the actinides introduced into the repository. As a result of this, it was necessary to constrain the total number of possible species in solution, aqueous, solid or gas, and in addition, to determine Pitzer parameters for many species by analogy to others rather than by experimental measurement.

This is the basis of the parameter and species selection in the current database, DATA0.FMT.R2, which contains the parameters for those species incorporated into the limited species set description. In practice, this has worked well to describe solution behavior in the WIPP within a limited set of pH values at 25 ^{o}C.

SOTERM-4.5.2 Calculated Actinide Solubilities

The oxidation-state-specific actinide solubilities calculated for the CRA-2014 PA with EQ3/6 are summarized in Table SOTERM-18. For historical perspective, the calculated solubilities from prior PA analyses are also tabulated. In the CRA-2014 PA, the data are shown for two brines in the presence of organics, and as a function of equilibration with hydromagnesite. The hydromagnesite case is recognized by the project as the most relevant to the WIPP. It is important to note that, overall, the calculated solubilities have not changed much over time except for the effects of increased complexation of the An(III) actinides with organics as this inventory has increased.

As shown in Table SOTERM-18, the calculated solubility of the III actinides was 2.59×10^{-6} M to 1.48×10^{-6} M in the CRA-2014 PA (Brush and Domski 2013a). These data are also fairly consistent with recently measured results for Nd(III) solubility in brine (Borkowski et al. 2008). A somewhat broader range was noted historically: 2.88×10^{-7} M to 2.59×10^{-6} M. The expected solubility of the IV actinides ranges between 6.05×10^{-8} M and 7.02×10^{-8} M. This is also somewhat consistent with prior calculations and has increased slightly. Overall the solubility of the IV actinides is four to eight times lower than that predicted for the III actinides. The main reason for increases noted in CRA-2014 PA was the presence of organics in the brines.

Uncertainties in the solubility data and uncertainty in the NONLIN least-squares refinement, for Pitzer parameter determination, result in uncertainty in the model predictions. This distribution was sampled and used in PA as discussed in Section SOTERM-5.0 (Brush and Domski 2013c).

Four organic ligands are included in EQ3/6 calculations of actinide solubilities. These are acetate ($CH_3CO_2^-$), citrate [$(CH_2CO_2)_2C(OH)(CO_2)^{3-}$], EDTA [$(CH_2CO_2)_2N(CH_2)_2N(CH_2CO_2)_2^{4-}$], and oxalate ($C_2O_4^{2-}$). The current anticipated inventory of these complexing agents, with their inventory-limited solubilities in the WIPP, were summarized in Tables SOTERM-3 and SOTERM-7. These ligands are included in the solubility calculations because (1) approximately 60 organic compounds were identified among the nonradioactive constituents of the TRU waste to be emplaced in the WIPP (Brush 1990; Drez 1991; U.S. DOE 1996); (2) 10 of these 60 organic compounds could, if present in the WIPP, increase actinide solubilities because they are soluble in aqueous solutions such as the WIPP brines, and because they form complexes with dissolved actinides (Choppin 1988); and (3) of these 10 water-soluble organic ligands that form complexes with actinides, 4 (acetate, citrate, EDTA, and oxalate) are included in PA and tracked in the WIPP inventory (see the CCA, Appendix SOTERM, p. 96).

Table SOTERM- 18. Historical Actinide Solubilities Calculated for the CRA-2004 PABC, the CRA-2009 PABC and CRA-2014 PA (Brush and Domski 2013a, Table 13).

Actinide Oxidation State, and Brine	CRA-2004 PABC (M)	CRA-2009 PABC (M)	CRA-2014PA, 1× Minimum Brine Volume (M)	CRA-2014 PA, 5× Minimum Brine Volume (M)
III, GWB	3.87×10^{-7}	1.66×10^{-6}	2.59×10^{-6}	6.47×10^{-7}
III, ERDA-6	2.88×10^{-7}	1.51×10^{-6}	1.48×10^{-6}	3.92×10^{-7}
IV, GWB	5.64×10^{-8}	5.63×10^{-8}	6.05×10^{-8}	6.07×10^{-8}
IV, ERDA-6	6.79×10^{-8}	6.98×10^{-8}	7.02×10^{-8}	7.20×10^{-8}
V, GWB	3.55×10^{-7}	3.90×10^{-7}	2.77×10^{-7}	1.82×10^{-7}
V, ERDA-6	8.24×10^{-7}	8.75×10^{-7}	8.76×10^{-7}	6.44×10^{-7}

SOTERM-4.6 Calculation of Colloidal Contribution to Actinide Solution Concentrations

The importance and role of colloids in defining the concentration of actinides in the WIPP was discussed in Section SOTERM-3.9, and more extensive discussions of WIPP-related results are available (Reed et al. 2013; CCA Appendix SOTERM, Section 6). The PA conceptual approach used to account for colloidal enhancement of actinide concentrations was developed as part of the CCA and has not changed since this initial implementation. The four types of colloids identified as relevant to the WIPP are listed and described in Table SOTERM-19.

Three types of parameter values were determined: (1) constant concentration values, (2) concentration values proportional to the dissolved actinide concentration, and (3) maximum concentration values. These parameter types are summarized Table SOTERM-20 and were initially described in parameter record packages (Papenguth and Behl 1996; Papenguth 1996a; Papenguth 1996b; Papenguth 1996c).

For microbes, the proportionality relationship was made by element. For humic actinides, however, the relationship was made by oxidation state, rather than by element. For microbes and humic substances, the experiments described in the parameter record packages noted above also provided a basis to define upper limits of the actinide concentration that could be associated with each of those colloid types. For both humic and microbial actinides, the upper limit parameter was defined by element, rather than oxidation state, and is in units of molality. The use of the two upper limit parameters is slightly different, and is described in the sections below discussing humic substances and microbes.

Table SOTERM- 19. Classification of Four Colloid Types Considered by the WIPP PA

Mineral Fragment Colloids	Hydrophobic, hard-sphere particles that are kinetically stabilized or destabilized by electrostatic forces and may consist of crystalline or amorphous solids. Mineral fragments may be made kinetically stable by coatings with steric stabilizers that prevent close contact. Mineral fragments may act as substrates for sorption of actinides, or they may consist of precipitated or coprecipitated actinide solids.
Intrinsic Actinide Colloids	Intrinsic actinide colloids (also known as true colloids, real colloids, Type I colloids, and Eigenkolloide) are macromolecules of actinides that, at least in some cases, may mature into a mineral-fragment type of colloidal particle. When immature, they are hydrophilic; when mature, they become hydrophobic.
Humic Colloids	Humic substances are hydrophilic, soft-sphere particles that are stabilized by solvation forces. They are often powerful substrates for uptake of metal cations and are relatively small (less than 100,000 atomic mass units).
Microbial Colloids	Microbes are relatively large colloidal particles stabilized by hydrophilic coatings on their surfaces, which behave as steric stabilizing compounds. They may act as substrates for extracellular actinide sorption or actively bioaccumulate actinides intracellularly.

Table SOTERM- 20. Material and Property Names for Colloidal Parameters

Material	Property	Brief Description of Parameter
Th, U, Np, Pu, Am	CONCMIN	C oncentration of actinide associated with mobile mineral fragment colloids
Th, U, Np, Pu, Am	CONCINT	C oncentration of actinide associated with mobile intrinsic actinide colloids
Th, U, Np, Pu, Am	PROPMIC	P roportionality constant for concentration of actinides associated with mobile microbes
PHUMOX3 [a] PHUMOX4 PHUMOX5 PHUMOX6	PHUMCIM	P roportionality constant for concentration of actinides associated with mobile humic colloids; in Castile brine; actinide solubilities include organics (complexes with man-made organic ligands); solubilities were calculated assuming equilibrium with Mg-bearing minerals (brucite and hydromagnesite)
PHUMOX3 [a] PHUMOX4 PHUMOX5 PHUMOX6	PHUMSIM	P roportionality constant for concentration of actinides associated with mobile humic colloids; in Salado brine; actinide solubilities include organics (complexes with man-made organic ligands); solubilities were calculated assuming equilibrium with Mg-bearing minerals (brucite and hydromagnesite)
Th, U, Np, Pu, Am	CAPMIC	M aximum (cap) concentration of actinide associated with mobile microbes
Th, U, Np, Pu, Am	CAPHUM	M aximum (cap) concentration of actinide associated with mobile humic colloids

a Proportionality constant for actinide concentrations associated with mobile humic substances for PHUMOX3, for actinide elements with oxidation state *III* (that is, Pu(III) and Am(III)); PHUMOX4, oxidation state IV (Th(IV), U(IV), Np(IV), and Pu(IV)); PHUMOX5, oxidation state V (Np(V)); and PHUMOX6, oxidation state VI (U(VI)).

The colloid concentration factors used in the CRA-2014 PA are summarized in Table SOTERM-21. The general approach used to account for colloidal enhancement of actinide solubilities is described in detail in Appendix SOTERM-2014, Section 5.2 and Appendix PA-2014, Section 4.3. There were essentially no changes in the approach used from the CRA-2009 PABC although all the parameters were re-assessed.

Table SOTERM- 21. Colloid enhancement parameters used in CRA-2009 and CRA-2014 (Appendix SOTERM-2009; Reed et al. 2013)

Actinide	CONCMIN (Concentration on Mineral Fragments[a])	CONCINT (Concentration as Intrinsic Colloid[a]) (M)		PROPMIC (Proportion Sorbed on Microbes[b])		CAPMIC (Maximum Sorbed on Microbes[c]) (M)		Proportion Sorbed on Humics[b]		CAPHUM[d] (Maximum Sorbed on Humics[a])
								PHUMSIM (Salado) [d]	PHUMCIM (Castile) [d]	
CRA	2009 and 2014	2009	2014	2009	2014	2009	2014	2009 and 2014	2009 and 2014	2009 and 2014
Th(IV)	2.6×10^{-8}	0	2×10^{-8}	3.1	1.76	0.0019	2.3×10^{-6}	6.3	6.3	1.1×10^{-5}
U(IV)	2.6×10^{-8}	0	2×10^{-8}	0.0021	1.76	0.0021	2.3×10^{-6}	6.3	6.3	1.1×10^{-5}
U(VI)	2.6×10^{-8}	0	3×10^{-8}	0.0021	1.76	0.0021	2.3×10^{-6}	0.12	0.51	1.1×10^{-5}
Np(IV)	2.6×10^{-8}	0	2×10^{-8}	12.0	1.76	0.0027	2.3×10^{-6}	6.3	6.3	1.1×10^{-5}
Np(V)	2.6×10^{-8}	0	ND	12.0	1.76	0.0027	2.3×10^{-6}	9.1×10^{-4}	7.4×10^{-3}	1.1×10^{-5}
Pu(III)	2.6×10^{-8}	1×10^{-9}	2×10^{-8}	0.3	1.76	6.8×10^{-5}	2.3×10^{-6}	0.19	1.37[e]	1.1×10^{-5}
Pu(IV)	2.6×10^{-8}	1×10^{-9}	2×10^{-8}	0.3	1.76	6.8×10^{-5}	2.3×10^{-6}	6.3	6.3	1.1×10^{-5}
Am(III)	2.6×10^{-8}	0	4×10^{-9}	3.6	0.32	1.0	3.1×10^{-8}	0.19	1.37[e]	1.1×10^{-5}

a In units of moles colloidal actinide per liter - 2009 and 2014 parameters are the same
b In units of moles colloidal actinide per mole dissolved actinide
c In units of moles total mobile actinide per liter
d Humic colloid parameters for CRA-2009 and CRA-2014 are unchanged
e At 0.5 probability
NOTE: The colloidal source term is added to the dissolved source term to arrive at a total source term. Mineral fragments were provided with distributions, but the maximum was used as described in Appendix PA-2014, Section 8.4

SOTERM-5.0 Use of the Actinide Source Term in PA

The WIPP ASTP provided the parameters to construct the maximum dissolved and suspended colloidal actinide concentrations for use in modeling the mobilization and transport of actinides in the disposal system. In the WIPP PA, mobilization of radionuclides is represented by the PANEL code and transport of radionuclides within the repository and the Salado is represented by the Nuclide Transport System (NUTS) code (Appendix PA-2014, Section 6.7.3 and Section PA-6.7.2, respectively). A description of the simplifications, manipulations, and approach used in the PA to perform this modeling is discussed in this section.

SOTERM-5.1 Simplifications

The DOE has concentrated on those processes most likely to have a significant impact on system performance. Therefore, several simplifications were used in the modeling of radionuclide mobilization and transport in the CCA PA, the CCA PAVT, the CRA-2004 PA, the CRA-2004 PABC, the CRA-2009 PA, the CRA-2009 PABC and the CRA-2014 PA calculations. These include

- Using constant solubility parameters and constant colloidal parameters throughout the repository and regulatory period for a given realization
- Modeling only the isotopes most important to compliance
- Using the compositions of Castile and Salado brines (the end-member brines) to bracket the behavior of mixtures of these brines within the repository
- Sampling only the uncertain parameters with the most significant effect on repository performance
- Combining dissolved and colloidal species for transport within the disposal system, as modeled by NUTS and PANEL

SOTERM-5.1.1 Elements and Isotopes Modeled

Selection of isotopes for modeling mobilization and transport in the disposal system with NUTS and PANEL is described in Appendix PA-2014, Section PA-8.4. Runs of PANEL, the PA code that computes total mobilized radionuclide concentrations,

include 29 radionuclides in the decay calculations (Kim 2013b, Table 3 and Table 11). Runs of NUTS, the PA code that computes radionuclide transport within the Salado, are based on five radionuclides (^{230}Th, ^{234}U, ^{238}Pu, ^{239}Pu, and ^{241}Am) that represent groupings of radionuclides with similar decay and transport properties (Kim 2013a; Appendix PA-2014, Section PA-4.3.2). The number of radionuclides for transport calculations in NUTS has been reduced because calculations for the full WIPP inventory and decay chains would be very time consuming and because accurate results can be achieved with this limited set of radionuclides (Kicker and Zeitler 2013, Section 4).

Transport calculations in the Culebra use a reduced set of four radionuclides (^{230}Th, ^{234}U, ^{239}Pu, and ^{241}Am) for computational efficiency (Garner 1996). ^{238}Pu has been omitted from transport in the Culebra because its short half-life (87.7 years) means that little ^{238}Pu will enter the Culebra via brine flows up a borehole.

SOTERM-5.1.2 Use of Brine End Members

The general scenarios described in Appendix PA-2014, Section PA-2.3.2.2 and Section PA-8.3 and considered in the source term calculations may be categorized into three groups: (1) undisturbed performance (BRAGFLO S1 scenario); (2) intrusion through the repository and into the Castile, intersecting a pressurized brine reservoir (BRAGFLO S2, S3, and S6 scenarios); and (3) intrusion through the repository, but not into a pressurized brine reservoir (BRAGFLO S4 and S5 scenarios). The specific scenarios and the associated type of borehole intrusion considered by the WIPP PA are listed in Table SOTERM-22.

Table SOTERM- 22. WIPP PA Modeling Scenarios for the CRA-2014 PA (Garner and Leigh 2005; Leigh et al. 2005; Kim 2013a)

BRAGFLO Scenario	Description	Brine Used in PA
S1	E0 (Undisturbed Repository)	Salado (GWB)
S2	E1 intrusion at 350 years penetrates the repository and a brine pocket	Castile (ERDA-6)
S3	E1 intrusion at 1000 years penetrates the repository and a brine pocket	Castile (ERDA-6)
S4	E2 intrusion at 350 years penetrates the repository (only)	Salado (GWB)
S5	E2 intrusion at 1000 years penetrates the repository (only)	Salado (GWB)
S6	E2 intrusion at 1000 years penetrates the repository (only); E1 intrusion at 2000 years penetrates the repository and a brine pocket	Castile (ERDA-6)

Brine may enter the repository from three sources, depending on the nature of the borehole intrusion. Under all scenarios, brine may flow from the surrounding Salado through the DRZ and into the repository in response to the difference between the hydraulic head in the repository and in the surrounding formation. For the BRAGFLO S2 through S6 scenarios, in which a borehole is drilled into the repository, brine may flow down the borehole from the Rustler and/or the Dewey Lake. For the BRAGFLO S2, S3, and S6 scenarios, in which a pressurized Castile brine reservoir is intercepted, brine from the Castile may flow up the borehole into the repository.

As mentioned in Section SOTERM-2.3.1, the brines in the Salado and Castile have different compositions and the actinide solubilities are somewhat different in each of these end-member compositions.

The composition of the more dilute groundwaters from the Rustler and Dewey Lake are expected to change rapidly upon entering the repository as a result of fast dissolution of host Salado minerals from the walls and floor of the repository. These minerals comprise about 90-95% halite and about 1-2% each of polyhalite, gypsum, anhydrite, and magnesite (Brush 1990). Calculations titrating Salado rock into dilute brines using EQ3/6 (Wolery 1992; Wolery and Daveler 1992) show that gypsum, anhydrite, and magnesite saturate before halite. When halite saturates, the brine composition is very similar to that of Castile brine. One hundred times as much polyhalite must be added to the system before the resulting brine has a composition similar to Salado brines. These calculations indicate that if dilute brines dissolve away only the surfaces of the repository, they will obtain Castile-like compositions, but if they circulate through the Salado after saturating with halite, they may obtain compositions similar to Salado brine. Similarly, if Castile brine circulates through enough host rock, it may also approach Salado brine composition. In either case, the actual brine within the repository may be described as a mixture of the two concentrated-brine end members: Salado and Castile. This mixture, however, is very hard to quantify, because it is both temporally and spatially variable. Only in the undisturbed scenario is the mixture well defined as 100% Salado brine over the 10,000-year regulatory period. In this context, the Salado (GWB) and Castile (ERDA-6) brines bracket the range of expected brine compositions.

For a panel intersected by a borehole, the BRAGFLO calculations show that in the 10% of the repository represented by the BRAGFLO panel computational cells, the ratio of brine inflow that enters through the borehole versus through inflow from the host rock varies in time and depends on the sampled parameter values and scenario considered. This ratio was the only measure of brine mixing available to the source term runs in the CCA PA, the CCA PAVT, the CRA-2004 PA, the CRA-2004 PABC, the CRA-2009 PA, the CRA-2009 PABC, and the CRA-2014 PA calculations. As an estimate, this ratio (1) does not account for compositional changes that occur when H_2O is consumed by corrosion reactions or MgO hydration reactions; (2) does not resolve the details of

flow, diffusion, and brine interaction with internal pillars and the DRZ; and (3) is an average over one-tenth of the repository. It is expected that the fraction of Salado brine will be quite high in areas of the repository distant from the borehole and much lower near the borehole. Because radionuclide travel up the borehole can lead to significant release, the solubility of radionuclides near the borehole is important. Given these uncertainties, the DOE decided to use the Castile end-member composition to calculate radionuclide solubilities for scenarios where a borehole penetrates a brine reservoir, and to use the Salado end-member composition for scenarios where it does not (see Table SOTERM-22).

SOTERM-5.1.3 Sampling of Uncertain Parameters

The uncertain parameters to be sampled for the PA were selected based on the expected significance of their effect on repository performance. The following four parameters are sampled independently (Kim 2013a):

- The solubility uncertainty for oxidation state III (see discussion below and Figure SOTERM-30).
- The solubility uncertainty for oxidation state IV (see discussion below and Figure SOTERM- 31).
- The oxidation state for Pu, Np, and U. The sampled value is a flag that is "low" 50% of the time and "high" 50% of the time. If the flag is set to "high," Pu is assumed to be in the IV oxidation state, Np is assumed to be in the V oxidation state, and U is assumed to be in the VI oxidation state. If the flag is set to "low," Pu is assumed to be in the III oxidation state and Np and U are assumed to be in the IV oxidation state.
- The humic acid proportionality constant for the III oxidation state in Castile brine (see Table SOTERM-21 and Figure SOTERM-32).

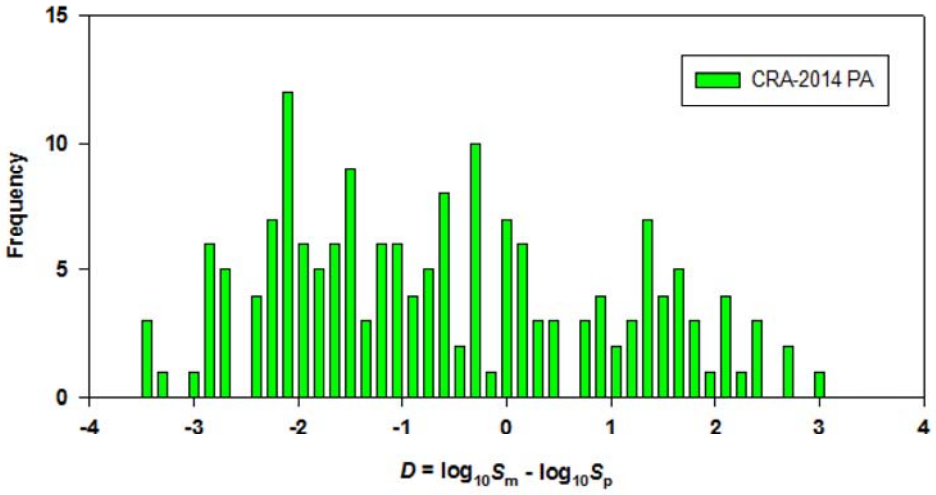

Figure SOTERM- 30. Frequency Distribution of the Difference of Experimental log Solubility ($log_{10}S_m$) from Model-Predicted Value ($log_{10}S_p$) for Nd(III) and Am(III). A total of 243 measured and predicted solubilities were compared (Brush and Domski 2013c).

As discussed by Garner and Leigh (Garner and Leigh 2005, Section 2.3), the solubility uncertainty for oxidation state V is zero. There is no uncertainty assigned to the solubility for oxidation state VI because the EPA specified a fixed, maximum solubility of 1×10^{-3} mol/L for U(VI).

Actinide solubilities for a single realization in the PA depend on (1) the oxidation state; (2) the brine for that realization (see Table SOTERM-22); and (3) the solution concentration uncertainty, as shown in Equation (SOTERM.73).

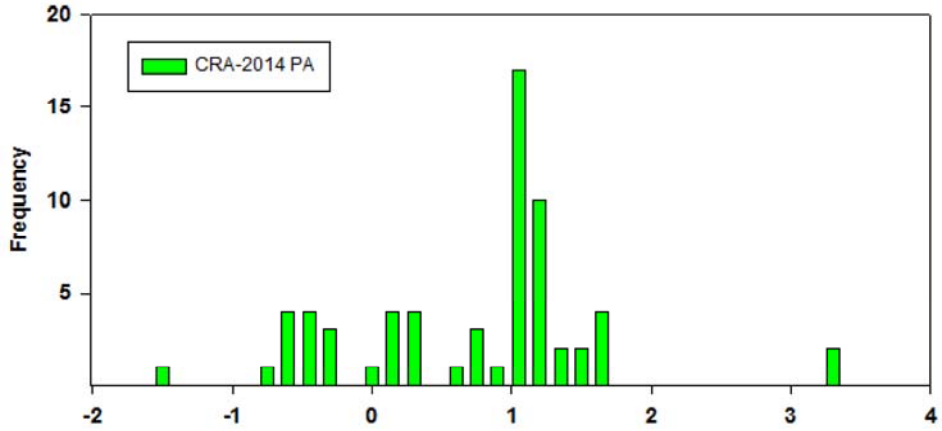

Figure SOTERM- 31. Frequency Distribution of the Deviation of Experimental log Solubility from Model-Predicted Value for all An(IV) Comparisons. A total of 45 measured and predicted solubilities were compared (Brush and Domski 2013c).

$$C_{i,b} = (S_{i,b}) \times (10^{SUi}) \text{ (SOTERM.73)}$$

$C_{i,b}$, used for every element in oxidation state i, is the concentration of oxidation state i and brine b. $S_{i,b}$ is the solubility calculated for oxidation state i in brine b with EQ3/6 (see Table SOTERM-18). SU_i is the solubility uncertainty sampled from a distribution unique to each oxidation state. Figure SOTERM-30 shows the distribution of SU values for oxidation state III. Figure SOTERM-31 shows the distribution of SU values for oxidation state IV. These distributions are calculated and documented in Brush and Domski (Brush and Domski 2013c).

Figure SOTERM-32 shows the cumulative distribution function for the humic-acid proportionality constant. All other humic-acid proportionality constants are constant values for both Castile and Salado brines, as shown in Table SOTERM-21.

SOTERM-5.1.4 Multiple Brine Volumes

Variable brine volume in the calculation of radionuclide concentrations in brine was implemented in the CRA-2014 PA. Radionuclide solubilities were calculated in terms of 1×, 2×, 3×, 4×, and 5× the minimum repository brine volume necessary for a DBR. Implementation of multiple brine volumes in PANEL calculations needs actinide solubilities that were calculated over multiple brine volumes by Brush and Domski (Brush and Domski 2013a). The calculated baseline actinide solubilities at 1× and 5× minimum brine volume are listed in Table SOTERM-19. A more detailed discussion of these results and the effects of variable brine volumes can be found in Brush and Domski (Brush and Domski 2013a).

SOTERM-5.1.5 Combining the Transport of Dissolved and Colloidal Species in the Salado

Dissolved and colloidal species may transport differently because of different diffusion rates, sorption onto stationary materials, and size-exclusion effects (filtration and hydrodynamic chromatography). With maximum molecular diffusion coefficients of about 4×10^{-10} m^2/s, actinides are estimated to diffuse about 10 m in 10,000 years, a negligible distance. Sorption and filtration have beneficial but unquantified effects on performance. Hydrodynamic chromatography may increase colloidal transport over dissolved transport by, at most, a factor of two for theoretically perfect colloidal-transport conditions. In the WIPP, the expected increase is much lower. Given the small or beneficial nature of these effects, they were not included in the CCA PA, the CCA PAVT, the CRA-2004 PA, the CRA-2004 PABC, the CRA-2009 PA, the CRA-2009 PABC, or the CRA-2014 PA calculations of radionuclide transport in the repository.

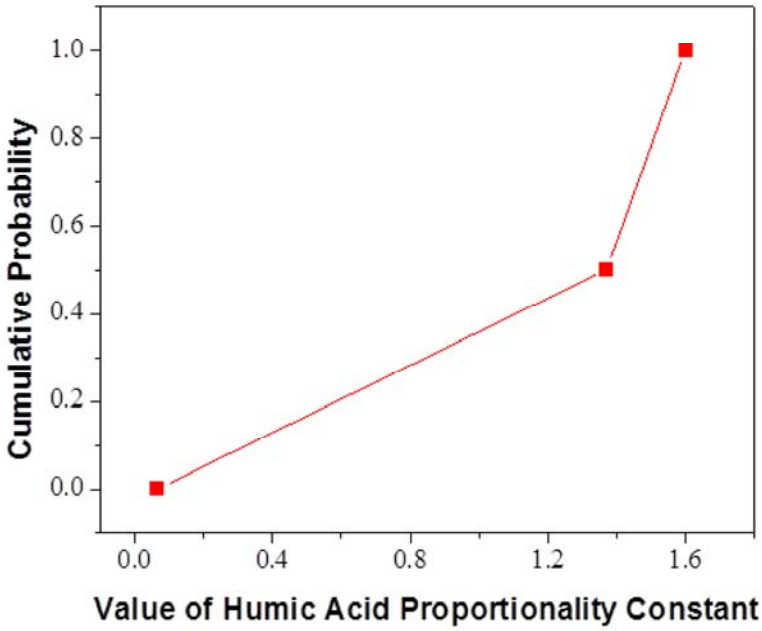

Figure SOTERM- 32. Cumulative Distribution Function for the Humic-Acid Proportionality Constant for the III Oxidation State in Castile Brine

SOTERM-5.2 Construction of the Source Term

Because PA does not differentiate dissolved from colloidal species for transport in the Salado, the total source term in the Salado is the sum of both components.. To model transport within the Culebra, however, this simplification was replaced by separating the mobilized actinides delivered to the Culebra by Salado transport codes into five components (dissolved, humic, microbial, mineral-fragment, and intrinsic colloids) to account for differences in their transport behavior. This is important because transport within the repository occurs through, at most, hundreds of meters of poorly defined waste undergoing decomposition, whereas transport through the Culebra occurs over kilometers in a relatively homogeneous (compared to waste) fractured dolomite.

The parameters required to construct the source term were as follows:

1. Solubilities for four oxidation states in Salado and Castile brines, the two brine end members.
2. Uncertainty distributions to be applied to the median solubilities for oxidation states III and IV.
3. A scheme for assigning sampled oxidation states ("low" or "high").
4. Colloidal concentrations or proportionality constants for each actinide (Th, U, Np, Pu, and Am) and an associated oxidation state for each of four colloid types.
5. Caps on the actinide concentrations that may be applied to two types of colloids (microbial and humic).
6. Cm is assigned the source term calculated for Am (i.e., it has the same solubility/speciation as Am up to its inventory limit).

Cm and Np are not explicitly transported in NUTS, although they are implicitly lumped with other modeled isotopes. They are, however, included in the PANEL calculations for use with the DBR calculations in PA.

These parameters are combined into a single maximum concentration for each modeled actinide in the PA calculations. The term "total mobilized concentration" is used for the combined concentrations of dissolved and colloidal species. The combined concentrations are not necessarily the actual concentrations, because the concentration may be lower as a result of inventory limits. Both NUTS and PANEL assume that the actinide concentrations specified by the total mobilized concentrations are attained instantaneously as long as sufficient inventory is available. When the inventory is insufficient, the actual mobilized concentration will be lower and is said to be inventory limited. The calculation of the total mobilized concentration is performed by PANEL for each of 100 sampled vectors in a replicate. A similar methodology to generate the combined maximum concentrations was used for the CCA PA, the CCA PAVT, the CRA-2004 PA, the CRA-2004 PABC, the CRA-2009 PA, the CRA-2009 PABC and the CRA-2014 PA.

All of the source term parameters and their associated distributions are entered into the PA parameter database. For each sampled parameter, the Latin Hypercube Sampling code uses the distribution from the PA parameter database to create 100 sampled values. These values are combined with the parameters that have constant values and stored in computational databases for each of the 100 vectors (i.e., 100 realizations), which constitute one replicate. For each realization, PANEL uses both the constant and sampled values for all of the source term parameters, and constructs the source term for NUTS and PANEL, as shown below. This process is repeated for scenarios using the Salado end-member total mobilized concentration and for scenarios using the Castile end-member total mobilized concentration.

$$\text{Dissolved} = \text{Baseline Solubility} \times 10^{\text{Sampled from Solubility Uncertainty Distribution}} \quad \text{(SOTERM.74)}$$

IF (Dissolved × Proportionality Constant of Humic Colloids < Humic Cap),

THEN Humic = Dissolved × Proportionality Constant of Humic Colloid, (SOTERM.75)

ELSE Humic = Humic Cap

Mineral = Database Concentration (a constant value) (SOTERM.76)

Intrinsic = Database Concentration (a constant value) (SOTERM.77)

Microbial_temp = Dissolved × Proportionality Constant of Microbial Colloids,

Total Mobile_temp = Dissolved + Humic + Microbial_temp + Mineral + Intrinsic

IF (Total Mobile_temp < Microbial Cap),

THEN Microbial = Microbial_temp, (SOTERM.78)

ELSE IF((Dissolved + Humic + Mineral + Intrinsic) > Microbial Cap),

THEN Microbial = 0

ELSE Microbial = Microbial Cap - (Dissolved + Humic + Mineral + Intrinsic)

Total Mobile = Dissolved + Humic + Microbial + Mineral + Intrinsic (SOTERM.79)

For actinides with more than one oxidation state, the oxidation state is specified by the oxidation-state parameter

IF (OXSTAT ≤ 0.5); THEN Lower Oxidation State,

ELSE Higher Oxidation State (SOTERM.80)

where OXSTAT is the oxidation-state parameter sampled from a uniform distribution between 0 and 1.

Solubility calculations are performed for Am(III), Th(IV), and Np(V) and the oxidation-state analogy is used to apply the values calculated for these elements/oxidation states to other actinide elements in the same oxidation states (if any). The total mobilized concentration and mobile fractions for Cm are set equal to the values for Am. In addition, the PA groups radioisotopes with similar decay and transport properties for the NUTS and SECOTP2D (component radionuclide transport in fractures or granular acquifers) transport calculations, as explained in Section SOTERM-5.1.5. For example, the U solubility is decreased to account for the shared solubility with the low-activity ^{238}U, which is not explicitly modeled, enabling NUTS to properly represent the effect of the U isotopes on compliance using the single lumped isotope ^{234}U (Appendix PA-2014, Section PA-4.3.2).

PANEL also calculates the fraction of each actinide mobilized by the five different mechanisms, as follows:

Fraction dissolved = Dissolved/Total Mobile (SOTERM.81)

Fraction on humics = Humic/Total Mobile (SOTERM.82)

Fraction in/on microbes = Microbial/Total Mobile (SOTERM.83)

Fraction on mineral fragments = Mineral/Total Mobile (SOTERM.84)

Fraction as intrinsic colloid = Intrinsic/Total Mobile (SOTERM.85)

SOTERM-5.3 Example Calculation of Actinide Solubility

As an example, for one realization in Salado brine, the sampled value for OXSTAT was 0.9, so Pu would be present in the IV state. The sampled value of the solubility uncertainty distribution was 0.09 for the IV state, which has a median brine solubility of 6.05×10^{-8} M. The humic proportionality constant for the IV oxidation state in Salado brine is 6.3, the microbial proportionality constant for Pu is 1.76, the humic cap is 1.1×10^{-5} M, the microbe cap for Pu is 2.3×10^{-6} M, the concentration of the actinide on mineral fragments is 2.6×10^{-8} M, and the Pu intrinsic-colloid concentration is 2×10^{-8} M.

For this realization, the maximum dissolved concentration of Pu(IV) used by the PA would be

$$C_{Pu} = (6.05 \times 10^{-8}) \times (10^{0.09}) = 7.44 \times 10^{-8} \text{ M. (SOTERM.86)}$$

(The calculations for this example have been rounded to two significant figures, although the PA would not round the intermediate or final values.) C_{Pu} is the maximum dissolved concentration of all combined isotopes of Pu.

The maximum humic-complexed Pu would be

$$(7.44 \times 10^{-8} \text{ M})(6.3 \text{ mol adsorbed per mol}) = 4.69 \times 10^{-7} \text{ M. (SOTERM.87)}$$

This value, however, does not exceed the cap for humic-mobilized Pu, 1.1×10^{-5} M. Therefore, in this case, the cap would not be used for the maximum humic-mobilized actinide concentration. Note that the humic-mobilized concentration of Pu exceeds the maximum dissolved concentration of Pu, which is usually the case.

The maximum microbial-mobilized Pu would be

$$(7.44 \times 10^{-8} \text{ M})(1.76 \text{ mol bioaccumulated per mol}) = 1.31 \times 10^{-7} \text{ M. (SOTERM.88)}$$

This value is less than the cap, 2.3×10^{-6} M, so the cap does not affect microbial-mobilized Pu for this realization.

The total mobilized concentration of Pu(IV) for this realization would then be the sum of the dissolved and colloidal contributions (see Equation [SOTERM.79]):

$$\text{Total Mobile} = \text{Dissolved} + \text{Humic} + \text{Microbial} + \text{Mineral} + \text{Intrinsic, (SOTERM.89)}$$

$$= 7.44 \times 10^{-8} + 4.69 \times 10^{-7} + 1.31 \times 10^{-7} + 2.6 \times 10^{-8} + 2.0 \times 10^{-8},$$

$$= 7.20 \times 10^{-7} \text{ M.}$$

SOTERM-5.4 Calculated Dissolved, Colloidal, and Total Actinide Solubilities

The output of the PANEL calculations is a computational database containing the source term and effective inventories. NUTS and PANEL both assume instantaneous dissolution and colloidal mobilization up to the solubility limits when sufficient inventory is present, as discussed in Appendix PA-2014, Section PA-4.3.4. Table SOTERM-23 shows the dissolved and colloidal components of the source term and the total mobile actinide concentrations obtained when median parameter values are used. For conservatism, 1× minimum brine volume was used because total mobilized concentration for a radionuclide decreases as the brine volume increases (Kim 2013a).

Table SOTERM- 23. Concentrations (M) of Dissolved, Colloidal, and Total Mobile Actinides Obtained Using Median Parameter Values for the CCA PAVT, CRA-2004 PABC, CRA-2009 PABC and CRA-2014 PAa

ıe	PAVT	CRA-2004 PABC	CRA-2009 PABC	CRA-2014 PA
	9.75×10^{-8}	3.61×10^{-7}	1.96×10^{-6}	3.46×10^{-7}
	7.48×10^{-8}	2.04×10^{-7}	9.87×10^{-7}	7.21×10^{-7}
	1.72×10^{-7}	5.64×10^{-7}	2.95×10^{-6}	1.07×10^{-6}
	1.06×10^{-8}	2.68×10^{-7}	1.78×10^{-6}	1.98×10^{-7}
	4.46×10^{-8}	4.75×10^{-7}	3.00×10^{-6}	6.65×10^{-7}
	5.52×10^{-8}	7.44×10^{-7}	4.79×10^{-6}	8.62×10^{-7}
	9.75×10^{-8}	3.61×10^{-7}	1.96×10^{-6}	3.46×10^{-7}
	3.96×10^{-7}	1.39×10^{-6}	7.45×10^{-6}	9.57×10^{-8}
	4.93×10^{-7}	1.75×10^{-6}	9.41×10^{-6}	4.42×10^{-7}
	1.06×10^{-8}	2.68×10^{-7}	1.78×10^{-6}	1.98×10^{-7}
	7.78×10^{-8}	1.34×10^{-6}	8.88×10^{-6}	3.01×10^{-7}

ıe	PAVT	CRA-2004 PABC	CRA-2009 PABC	CRA-2014 PA
	8.83×10^{-8}	1.61×10^{-6}	1.07×10^{-5}	4.98×10^{-7}
	1.06×10^{-8}	6.70×10^{-8}	1.70×10^{-8}	6.46×10^{-7}
	1.25×10^{-7}	6.56×10^{-7}	1.86×10^{-7}	4.12×10^{-6}
	1.36×10^{-7}	7.23×10^{-7}	2.03×10^{-7}	4.76×10^{-6}
	3.33×10^{-8}	8.07×10^{-8}	2.11×10^{-8}	7.50×10^{-7}
	3.39×10^{-7}	7.85×10^{-7}	2.24×10^{-7}	4.77×10^{-6}
	3.73×10^{-7}	8.65×10^{-7}	2.45×10^{-7}	5.52×10^{-6}

ım the WIPP PA Database http://tgw.sandia.gov/ and equations SOTERM.74 through SOTERM.79.

Table SOTERM-23. Concentrations (M) of Dissolved, Colloidal, and Total Mobile Actinides Obtained Using Median Parameter Values for the CCA PAVT, CRA-2004 PABC, CRA-2009 PABC and CRA-2014 PA[a] (*Continued*)

ınd Brine	PAVT	CRA-2004 PABC	CRA-2009 PABC	CRA-2014 PA
ıe	1.06×10^{-8}	6.70×10^{-8}	1.70×10^{-8}	6.46×10^{-7}
e	9.26×10^{-8}	4.48×10^{-7}	1.33×10^{-7}	4.13×10^{-6}
›rine	1.03×10^{-7}	5.15×10^{-7}	1.50×10^{-7}	4.77×10^{-6}
ıe	3.33×10^{-8}	8.07×10^{-8}	2.11×10^{-8}	7.50×10^{-7}
e	2.36×10^{-7}	5.35×10^{-7}	1.59×10^{-7}	4.78×10^{-6}
›rine	2.69×10^{-7}	6.15×10^{-7}	1.80×10^{-7}	5.53×10^{-6}
o brine	1.06×10^{-8}	6.70×10^{-8}	1.70×10^{-8}	6.46×10^{-7}
› brine	9.67×10^{-8}	4.69×10^{-7}	1.39×10^{-7}	4.12×10^{-6}
do brine	1.07×10^{-7}	5.36×10^{-7}	1.56×10^{-7}	4.76×10^{-6}
e brine	3.33×10^{-8}	8.07×10^{-8}	2.11×10^{-8}	7.50×10^{-7}
e brine	2.47×10^{-7}	5.60×10^{-7}	1.66×10^{-7}	4.77×10^{-6}
brine	2.80×10^{-7}	6.40×10^{-7}	1.87×10^{-7}	5.52×10^{-6}
ıe	7.07×10^{-6}	1.00×10^{-3}	1.00×10^{-3}	1.00×10^{-3}
e	8.89×10^{-7}	1.31×10^{-5}	1.31×10^{-5}	1.11×10^{-5}
›rine	7.96×10^{-6}	1.01×10^{-3}	1.01×10^{-3}	1.01×10^{-3}
ıe	7.15×10^{-6}	1.00×10^{-3}	1.00×10^{-3}	1.00×10^{-3}
e	3.69×10^{-6}	1.31×10^{-5}	1.31×10^{-5}	1.11×10^{-5}
›rine	1.08×10^{-5}	1.01×10^{-3}	1.01×10^{-3}	1.01×10^{-3}

etrieved from the WIPP PA Database http://tgw.sandia.gov/ and equations SOTERM.74 through SOTERM.79.

SOTERM-6.0 References

(*Indicates a reference that has not been previously submitted.)

Abdelouas, A., W. Lutze, W. Gong, E.H. Nuttall, B.A. Strietelmeier, and B.J. Travis. 2000. "Biological Reduction of Uranium in Groundwater and Subsurface Soil." The Science of the Total Environment, vol. 250: 21. [Author]

Allard, B. 1982. Solubilities of Actinides in Neutral or Basic Solutions. Actinides in Perspective. N. Edelstein, ed. New York: Pergamon. pp. 553-80. [Author]

Allard, S., and C. Ekberg. 2006a. "Complexing properties of a α-isosaccharinate: thorium." Radiochimica Acta 94, 537-540.* [Author]

Allard, S., and C. Ekberg. 2006b. "Complexing properties of α-isosaccharinate: stability constants, enthalpies and entropies of Th-complexation with uncertainty analysis." J. Solution Chem. 35, 1173-1186.* [Author]

Altmaier, M., V. Metz, V. Neck, R. Muller, and T. Fanghänel. 2003. "Solid-Liquid Equilibria of Mg(OH)2(cr) and Mg2(OH) 3Cl4H2O(cr) in the System Mg-Na-H-OH-Cl-H2O at 25ºC." Geochimica et Cosmochimica Acta, vol. 67: 3595-3601. [Author]

Altmaier, M., V. Neck, and Th. Fanghänel. 2004. "Solubility and Colloid formation of Th(IV) in concentrated NaCl and MgCl2 Solutions." Radiochimica Acta, vol. 92: 537-43. [Author]

Altmaier, M., V. Neck, and Th. Fanghänel. 2008. "Solubility of Zr(IV), Th(IV) and Pu(IV) hydrous oxides in CaCl2 solutions and the formation of ternary Ca-M(IV)-OH complexes." Radiochimica Acta vol. 96: (9-11) 541-550.* [Author]

Altmaier, M., V. Neck, M.A. Denecke, R. Yin, and Th. Fanghänel. 2006. "Solubility of ThO2 ·xH2O(am) and the Formation of Ternary Th(IV) Hydroxide-Carbonate Complexes in NaHCO3-Na2CO3 Solutions Containing 0-4M NaCl." Radiochimica Acta, vol. 94: 495-500. [Author]

Altmaier, M., V. Neck, R. Müller, and Th. Fanghänel. 2005. "Solubility of ThO2 xH2O(am) in Carbonate Solution and the Formation of Ternary Th(IV) Hydroxide-carbonate Complexes." Radiochimica Acta, vol. 93: 83-92. [Author]

Ams, D.A., J.S. Swanson, J. Szymanowski, J.B. Fein, M. Richmann, and D.T. Reed. 2013. "The Effect of High Ionic Strength on Neptunium (V) Adsorption to a halophilic bacterium." Geochimica et Comoschimica Acta, vol.: 110: 45-57.* [Author]

Banaszak, J.E., D.T. Reed, and B.E. Rittmann. 1998a. "Speciation-Dependent Toxicity of Neptunium(V) Towards Chelatobacter heintzii." Environmental Science and Technology, vol. 32: 1085-91. [Author]

Banaszak, J.E., B.E. Rittmann, and D.T. Reed. 1998b. Subsurface Interactions of Actinide Species and Microorganisms: Implications for the Bioremediation of Actinide-Organic Mixtures. ANL-98/26. Argonne, IL: Argonne National Laboratory. [Author]

Banaszak, J.E., S.M. Webb, B.E. Rittmann, J.-F. Gaillard, and D.T. Reed. 1999. "Fate of Neptunium in Anaerobic, Methanogenic Microcosm." Scientific Basis for Nuclear Waste Management XXII, vol. 556: 1141-49. [Author]

Barnhart, B.J., E.W. Campbell, J.M. Hardin, E. Martinez, D.E. Caldwell, and R. Hallett. 1978a. Potential microbial impact on transuranic wastes under conditions expected in the Waste Isolation Pilot Plant (WIPP). LA-7788-PR Progress Report, October-December 15, 1978. Los Alamos, NM: Los Alamos Scientific Laboratory.* [PDF / Author]

Barnhart, B.J., E.W. Campbell, J.M. Hardin, E. Martinez, D.E. Caldwell, and R. Hallett. 1979b. Potential microbial impact on transuranic wastes under conditions expected in the Waste Isolation Pilot Plant (WIPP). LA-7839-PR Progress Report, December 15, 1978-March 15, 1979. Los Alamos, NM: Los Alamos Scientific Laboratory.* [PDF / Author]

Barnhart, B.J., E.W. Campbell, E. Martinez, D.E. Caldwell, and R. Hallett. 1979c. Potential microbial impact on transuranic wastes under conditions expected in the Waste Isolation Pilot Plant (WIPP). LA-7918-PR Progress Report, March 15-June 15, 1979. Los Alamos, NM: Los Alamos Scientific Laboratory.* [PDF / Author]

Barnhart, B.J., E.W. Campbell, J.M. Hardin, E. Martinez, D.E. Caldwell, and R. Hallett. 1979d. Potential microbial impact on transuranic wastes under conditions expected in the Waste Isolation Pilot Plant (WIPP). LA-8297-PR Progress Report, October 1, 1978-September 30, 1979. Los Alamos, NM: Los Alamos Scientific Laboratory.* [PDF / Author]

Barton, L.L., K. Choudhury, B.M. Thomson, K. Steenhoudt, and A.R. Groffman. 1996. "Bacterial Reduction of Soluble Uranium: The First Step of In Situ Immobilization of Uranium." Radioactive Waste Management and Environmental Restoration, vol. 20: 141-51. [Author]

Behrends, T., and P. Van Cappellen. 2005. "Competition Between Enzymatic and Abiotic Reduction of Uranium(VI) under Iron Reducing Conditions." Chemical Geology, vol. 220: 315-27. [Author]

Bender, J., M.C. Duff, P. Phillips, and M. Hill. 2000. "Bioremediation and Bioreduction of Dissolved U(VI) by Microbial Mat Consortium Supported on Silica Gel Particles." Environmental Science and Technology, vol. 34: 3235-41. [Author]

Bennett, D., Y. Wang, and T. Hicks. 1996. Memorandum to Distribution (Subject: An Evaluation of Heat Generation Processes for the WIPP). 20 August 1996. ERMS 240635. Albuquerque, NM: Sandia National Laboratories.* [PDF / Author]

Birbir, M., B. Calli, B. Mertoglu, R. Bardavid, A. Oren, M. Ogmen and A. Ogan. 2007. "Extremely Halophilic Archaea from Tuz Lake, Turkey, and the Adjacent Kaldirim and Kayacik Salterns." World J. Microbiol Biotechnol, 23:309-316.* [Author]

Borkowski, M., J.-F. Lucchini, M.K. Richmann, and D.T. Reed. 2008. Actinide (III) Solubility in WIPP Brine: Data Summary and Recommendations. LCO-ACP-08, LANL\ACRSP Report, LA-14360. Los Alamos, NM: Los Alamos National Laboratory. [PDF / Author]

Borkowski, M. J-F. Lucchini, M.K. Richmann, and D.T. Reed. 2010a. Actinide (III) Solubility in WIPP Brine: Data Summary and Recommendations. Report LA-14360. Los Alamos, NM: Los Alamos National Laboratory.* [PDF / Author]

Borkowski, M., M.K. Richmann, D.T. Reed, and Y.-L. Xiong. 2010b. "Complexation of Nd(III) with Tetraborate Ion and Its Effect on Actinide(III) Solubility in WIPP Brine." Radiochimica Acta, vol.: 98.9-11 (2010): 577-582.* [Author]

Borkowski, M., M.K. Richmann, and J-F. Lucchini. 2012. Solubility of An(IV) in WIPP Brine: Thorium Analog Studies in WIPP Simulated Brine. Los Alamos Report LCO-ACP-17, LA-UR 12-24417. Carlsbad, NM: Los Alamos National Laboratory.* [PDF / Author]

Brendebach, B., M. Altmaier, J. Rothe, V. Neck, and M.A. Denecke. 2007. EXAFS Study of Aqueous Zr(IV) and Th(IV) Complexes in Alkaline CaCl2 Solutions: Ca3[Zr(OH)6]4+ and Ca4[Th(OH)8] 4+." Inorganic Chemistry, vol. 46: 6804-10. [Author]

Brush, L.H. 1990. Test Plan for Laboratory and Modeling Studies of Repository and Radionuclide Chemistry for the Waste Isolation Pilot Plant. SAND90-0266. ERMS 226015. Albuquerque, NM: Sandia National Laboratories. [PDF / Author]

Brush, L.H. 1995. Systems Prioritization Method-Iteration 2 Baseline Position Paper: Gas Generation in the Waste Isolation Pilot Plant (March 17). ERMS 228740. Albuquerque, NM: Sandia National Laboratories. [PDF / Author]

Brush, L.H., and J. Garner. 2005. Letter to D. Kessel (Subject: Additional Justification for the Insignificant Effect of Np on the Long-Term Performance of the WIPP). 21 February 2005. ERMS 538533. Albuquerque, NM: Sandia National Laboratories. [PDF / Author]

Brush, L.H., and P.S. Domski. 2013a. Prediction of Baseline Actinide Solubilities for the WIPP CRA-2014 PA. Analysis report, January 21, 2013. ERMS 559138. Carlsbad, NM: Sandia National Laboratories.* [PDF / Author]

Brush, L.H., and P.S. Domski. 2013b. Calculation of Organic-Ligand Concentrations for the WIPP CRA-2014 PA. Analysis report, January 14, 2013. ERMS 559005. Carlsbad, NM: Sandia National Laboratories.* [PDF / Author]

Brush, L.H., and P.S. Domski. 2013c. Uncertainty Analysis of Actinide Solubilities for the WIPP CRA-2014 PA, Rev. 1 Supercedes ERMS 559278. ERMS 559712. Albuquerque, NM: Sandia National Laboratories.* [PDF / Author]

Brush, L.H., and Y. Xiong. 2005a. Calculation of Organic-Ligand Concentrations for the WIPP Performance Assessment Baseline Calculations (May 4). ERMS 539635. Carlsbad, NM: Sandia National Laboratories. [PDF / Author]

Brush, L.H., and Y. Xiong. 2005b. Calculation of Actinide Solubilities for the WIPP Performance Assessment Baseline Calculations, Analysis AP-120, Rev. 0 (Rev. 0). AP-120. ERMS 539255. Carlsbad, NM: Sandia National Laboratories. [PDF / Author]

Brush, L.H., P.S. Domski, and Y.-L. Xiong. 2011 Predictions of the Compositions of Standard WIPP Brines as a Function of pcH for Laboratory Studies of the Speciation and Solubilities of Actinides. Analysis report, June 23, 2011. ERMS 555727 Carlsbad, NM: Sandia National Laboratories.* [PDF / Author]

Brush, L.H., R.C. Moore, and N.A. Wall. 2001. Response to EEG-77, Plutonium Chemistry under Conditions Relevant for WIPP Performance Assessment: Review of Experimental Results and Recommendations for Future Work, by V. Oversby. ERMS 517373. Carlsbad, NM: Sandia National Laboratories. [PDF / Author]

Bundschuh, T., R. Knopp, R. Müller, J.I. Kim, V. Neck, and Th. Fanghänel. 2000. "Application of LIBD to the Determination of the Solubility Product of Thorium(IV)-Colloids." Radiochimica Acta, vol. 88: 625-629. [Author]

Büppelmann, K., J.I. Kim, and Ch. Lierse. 1988. "The Redox Behavior of Pu in Saline Solutions under Radiolysis Effects." Radiochimica Acta, vol. 44/45: 65-70. [Author]

Büppelmann, K., S. Magirius, Ch. Lierse, and J.I. Kim. 1986. "Radiolytic Oxidation of Am (III) to Am (V) and Pu(IV) to Pu (VI) in Saline Solution." Journal of Less- Common Metals, vol. 122: 329-36. [Author]

Caldwell, D., R. Hallet, M. Molecke, E. Martinez, and B. Barnhart. 1988. Rates of CO2 Production From the Microbial Degradation of Transuranic Wastes Under Simulated Geologic Isolation Conditions. Report SAND87-7170. Carlsbad NM: Sandia National Laboratories.* [PDF / Author]

Camphouse, R.C., D.C. Kicker, S. Kim, T. Kirchner, J. Long, B. Malama, and T. Zeitler. 2013. Summary Report for the 2014 WIPP Compliance Recertification Application Performance Assessment. ERMS 560252. Carlsbad, NM: Sandia National Laboratories.* [PDF / Author]

Casas, I., J. De Pablo, J. Gimenez, M.E. Torrero, J. Bruno, E. Cera, R.J. Finch, and R.C. Ewing. 1998. "The Role of pe, pH, and Carbonate on the Solubility of UO2 and Uraninite under Nominally Reducing Conditions." Geochimica et Cosmochimica Acta, vol. 62: 2223-31. [Author]

Chen, T., Wang, X., Tian, W., Sun, M., Li, C., Liu, X., Wang, L., and C. Liu. 2010. "Solubility Analysis of Americium in Yuci Groundwater." Acta Physico-Chimica Sinica, vol. 26(4), 811-816.* [Author]

Choppin, G.R. 1988. Letter to L.H. Brush (Subject: Chemicals Listed Could Interact with Actinides). 29 December 1988. Tallahassee, FL: WIPP Central Files. [PDF / Author]

Choppin, G.R. 1999. "Utility of Oxidation State Analogs in the Study of Plutonium Behavior." Radiochimica Acta, vol. 85: 89-95. [Author]

Choppin, G.R., A.H. Bond, M. Borkowski, M.G. Bronikowski, J.G. Chen, S. Lis, J. Mizera, O. Pokrovski, N.A. Wall, Y.X. Xia, and R.C. Moore. 1999. WIPP Actinide Source Term Test Program: Solubility Studies and Development of Modeling Parameters. SAND 99-0943. Albuquerque, NM: Sandia National Laboratories. [PDF / Author]

Choppin, G.R., and L.F. Rao. 1992. Reduction of Neptunium(VI) by Organic Compounds. Transuranium Elements: A Half Century (pp. 262-75). L.R. Morss and J. Fuger, eds. Washington, DC: American Chemical Society. [Author]

Choppin, G.R., J. Liljenzin, and J.O. Rydberg. 2004. Radiochemistry and Nuclear Chemistry. 3rd ed. Woburn, MA: Butterworth-Heinenmann. [Author]

Christensen, T.H., P.L. Bjerg, S.A. Banwart, R. Jakobsen, G. Heron, and H-J. Albrechtsen. 2000. "Characterization of Redox Conditions in Groundwater Contaminant Plumes." Journal of Contaminant Hydrology, vol. 45: 165-241. [Author]

Clark, D.L., and C.D. Tait. 1996. Memorandum to Sandia WIPP Records Center (Subject: SWCF-A: 1.1.10.1.1: NQ: Actinide Source Term: LANL Monthly Reports). Sandia WIPP Central File A: WBS 1.1.10.1.1. WPO 31106. Albuquerque, NM: Sandia National Laboratories. [PDF / Author]

Clark, D.L., D.E. Hobart, and M.P. Neu. 1995. "Actinide Carbonate Complexes and Their Importance in Actinide Environmental Chemistry." Chemical Reviews, vol. 95: 25.* [Author]

Clayton, D.J. 2008. Memorandum to Larry Brush (Subject: Update to the Calculation of the Minimum Brine Volume for a Direct Brine Release). 2 April 2008. ERMS 548522. Carlsbad, NM: Sandia National Laboratories.* [PDF / Author]

Clayton, D.J. 2013. Justification of Chemistry Parameters for Use in BRAGFLO for AP-164, Revision 1. ERMS 559466. Carlsbad, NM: Sandia National Laboratories.* [PDF / Author]

Clayton, D.J., R.C. Camphouse, J.W. Garner, A.E. Ismail, T.B. Kirchner, K.L. Kuhlman, and M.B. Nemer. 2010. Summary Report of the CRA-2009 Performance Assessment Baseline Calculation. ERMS 553039. Carlsbad, NM: Sandia National Laboratories.* [PDF / Author]

Cleveland, J.M. 1979. The Chemistry of Plutonium. La Grange Park, IL: American Nuclear Society. [Author]

Cotton, F.A., and G. Wilkinson. 1988. Advanced Inorganic Chemistry. 5th ed. New York: Wiley. [Author]

Cronin, E., and F. Post. 1977. "Report of a Dematiaceous Hyphomycete From the Great Salt lake, Utah." Mycologia, 69: 846-847.* [Author]

Cui, D., and K. Spahiu. 2002. "The Reduction of U(VI) on Corroded Iron under Anoxic Conditions." Radiochimica Acta, vol. 90: 623-28. [Author]

David, F., A.G. Maslennikov, and V.P. Peretrukhin. 1990. "Electrochemical Reduction of Actinides ions in Aqueous solution: Application to Separations and Some Intermetallic Compound Synthesis." Journal of Radioanalytical Nuclear Chemistry, vol. 143: 415-26. [Author]

Degueldre, C., and A. Kline. 2007. "Study of Thorium Association and Surface Precipitation on Colloids." Earth and Planetary Science Letters, vol. 264: 104-13. [Author]

Deng, H., S. Johnson, Y. Xiong, G.T. Roselle, and M. Nemer. 2006. Analysis of Martin Marietta MagChem 10 WTS-60 MgO. ERMS 544712. Carlsbad, NM: Sandia National Laboratories. [PDF / Author]

Diaz-Arocas, P., and B. Grambow. 1998. "Solid-liquid Phase Equilibria of U(VI) in NaCl Solutions." Geochimica et Cosmochimica Acta, vol. 62: 245-63. [Author]

Dodge, C.J., A.J. Francis, J.B. Gillow, G.P. Halada, C. Eng, and C.R. Clayton. 2002. "Association of Uranium with Iron Oxides Typically Formed on Corroding Steel Surfaces." Environmental Science and Technology, vol. 36: 3504-11. [Author]

Draganic, I.G., and Z.D. Draganic. 1971. Primary Products of Water Radiolysis: Oxidizing Species-the Hydroxyl Radical and Hydrogen Peroxide. The Radiation Chemistry of Water (pp. 91-121). New York: Academic. [Author]

Drez, P.E. 1991. Preliminary Nonradionuclide Inventory of CH-TRU Waste, Preliminary Comparison with 40 CFR Part 191, Subpart B for the Waste Isolation Pilot Plant, December 1991. Volume 3: Reference Data (pp. A-43 through A-53). Eds. R.P. Rechard, A.C. Peterson, J.D. Schreiber, H.J. Iuzzolino, M.S. Tierney, and J.S. Sandha. SAND91-0893/3. Albuquerque, NM: Sandia National Laboratories. [PDF / Author]

Du, X., B. Boonchayaanant, W.-M. Wu, S. Fendorf, J. Bargar, and C.S. Criddle. 2011. "Reduction of Uranium(VI) by Soluble Iron (II) Conforms with Thermodynamic Predictions." Environmental Science & Technology, vol.45: 4718-25.* [Author]

Ekberg, C., Y. Albinsson, M.J. Comarmond, and P.L. Brown. 2000. "Studies on the Behavior of Thorium(IV)." Journal of Solution Chemistry, vol. 29, no. 1: 63-86. [Author]

Emmerich, M., A Bhansali, T. Lösekann-Behrens, C. Schröder, A. Kappler, and S. Behrens. 2012. "Abundance, Distribution, and Activity of Fe(II)-Oxidizing and Fe(III)-Reducing Microorginaism in Hypersaline Sediments of Lake Kasin, Sourthern Russia." Appl. Environ. Microbiol, 78(12): 4386-4399.* [Author]

Eriksen, T.E., P. Ndamamba, D. Cui, J. Bruno, M. Caceci, and K. Spahiu. 1993. SKB Technical Report 93-18. Stockholm: Svensk Kärnbränsleforsorjning AB. [Author]

Ershov, B.G., M. Kelm, E. Janata, A.V. Gordeev, and E. Bohnert. 2002. "Radiation-Chemical Effects in the Near-Field of a Final Disposal Site: Role of Bromine on the Radiolytic Processes in NaCl-Solutions." Radiochimica Acta, vol. 90: 617. [Author]

Fanghänel, Th., and J.I. Kim. 1998. "Spectoscopic Evaluation of Thermodynamics of Trivalent Actinides in Brines." Journal of Alloys and Compounds, vol. 271-273: 728-737. [Author]

Fanghänel, Th., and V. Neck. 2002. "Aquatic Chemistry and Solubility Phenomena of Actinide Oxides/hydroxides." Pure Applied Chemistry, vol. 74: 1895-1907. [Author]

Fanghänel, Th., V. Neck, and J.I. Kim. 1995. "Thermodynamics of Neptunium(V) in Concentrated Salt Solutions: II. Ion Interaction (Pitzer) Parameters for Np(V) Hydrolysis Species and Carbonate Complexes." Radiochimica Acta, vol. 69: 169-76. [Author]

Farrell, J., W.D. Bostick, R.J. Jarabeck, and J.N. Fiedor. 1999. "Uranium Removal from Ground Water Using Zero Valent Iron Media." Ground Water, vol. 37: 618-24. [Author]

Felmy, A.R., D. Rai, and R.W. Fulton. 1990. "The Solubility of AmOHCO3(cr) and the Aqueous Thermodynamics of the System Na+-Am3+-HCO3--CO32--OH-H2O." Radiochimica Acta, vol. 50: 193-204. [Author]

Felmy, A.R., D. Rai, J.AS. Schramke, and J.L. Ryan. 1989. "The Solubility of Plutonium Hydroxide in Dilute Solution and in High-Ionic Strength Chloride Brines." Radiochimica Acta, vol. 48: 29-35. [Author]

Felmy, A.R., D. Rai, S.M. Sterner, M.J. Mason, N.J. Hess, and S.D. Conradson. 1996. Thermodynamic Models for Highly Charged Aqueous Species: The Solubility of Th(IV) Hydrous Oxide in Concentrated NaHCO3 and Na2CO3 Solutions (August 14). ERMS 240226. Carlsbad, NM: Sandia National Laboratories. [PDF / Author]

Felmy, A.R., M.J. Mason, and D. Rai. 1991. "The Solubility of Hydrous Thorium(IV) Oxide in Chloride Media: Development of an Aqueous Ion-Interaction Model." Radiochimica Acta, vol. 55: 177-85. [Author]

Fiedor, J.N., W.D. Bostick, R.J. Jarabek, and J. Farrell. 1998. "Understanding the Mechanism of Uranium Removal from Groundwater by Zero-Valent Iron Using X-Ray Photoelectron Spectroscopy." Environmental Science and Technology, vol. 32: 1466-73. [Author]

Field, E., S. D'Imperio, A. Miller, M. VanEngelen, R. Gerlach, B. Lee, W. Apel, and B. Peyton. 2010. "Application of Molecular Techniques To Elucidate the Influence of Cellulosic Waste on the Bacterial Community Structure at a Simulated Low-Level-Radioactive-Waste Site." Appl. Environ. Microbiol., 76(10): 3106-3115.* [Author]

Francis, A.J. 1998. "Biotransformation of Uranium and Other Actinides in Radioactive Wastes." Journal of Alloys and Compounds, vol. 271-273: 78-84. [Author]

Francis, A.J., and J.B. Gillow. 1994. Effects of Microbial Processes on Gas Generation Under Expected Waste Isolation Pilot Plant Repository Conditions. Progress Report through 1992. SAND93-7036. WPO 26555. Albuquerque, NM: Sandia National Laboratories. [PDF / Author]

Francis, A.J., C.J. Dodge, and J. B. Gillow. 2008. "Reductive Dissolution of Pu(IV) by Costridium sp. under Anaerobic Conditions." Environmental Science and Technology, vol. 42: 2355-60. [Author]

Francis, A.J., C.J. Dodge, J.B. Gillow, and H.W. Papenguth. 2000. "Biotransformation of Uranium Compounds in High Ionic Strength Brine by a Halophilic Bacterium under Denitrifying Conditions." Environmental Science and Technology, vol. 34: 2311. [Author]

Francis, A.J., J.B. Gillow, and M.R. Giles. 1997. Microbial gas generation under expected Waste Isolation Pilot Plant repository conditions. SAND96-2582 Report. Albuquerque, NM: Sandia National Laboratories.* [PDF / Author]

Francis, A.J., J.B. Gillow, C.J. Dodge, R. Harris, T.J. Beveridge, and H.W. Papenguth. 2004. "Uranium Association with Halophilic and non-Halophilic Bacteria and Archaea." Radiochimica Acta, vol. 92: 481-88.* [Author]

Fredrickson, J.K., J.M. Zachara, D.W. Kennedy, M.C. Duff, Y.A. Gorby, S.W. Li, and K.M. Krupka. 2000. "Reduction of U(VI) in Goethite (α-FeOOH) Suspensions by a Dissimilatory Metal-Reducing Bacteria." Geochimica et. Cosmochimica Acta, vol. 64: 3085-98. [Author]

Garner, J.W. 1996. Radioisotopes to be Used in the 1996 CCA Calculations. ERMS 540572. Carlsbad, NM: Sandia National Laboratories. [PDF / Author]

Garner, J.W., and C. Leigh. 2005. Analysis Package for PANEL: CRA-2004 Performance Assessment Baseline Calculation (Revision 0). ERMS 540572. Albuquerque, NM: Sandia National Laboratories. [PDF / Author]

Gayer, K.H., and H. Leider. 1957. "The Solubility of Uranium (IV) Hydroxide in Solutions of Sodium Hydroxide and Perchloric Acid at 25°C." Canadian Journal of Chemistry, vol. 35: 5-7. [Author]

Giambalvo, E.R. 2002a. Memorandum to L.H. Brush (Subject: Recommended Parameter Values for Modeling An(III) Solubility in WIPP Brines). 25 July 2002. ERMS 522982. Carlsbad, NM: Sandia National Laboratories. [PDF / Author]

Giambalvo, E.R. 2002b. Memorandum to L.H. Brush (Subject: Recommended Parameter Values for Modeling An(IV) Solubility in WIPP Brines). 26 July 2002. ERMS 522986. Carlsbad, NM: Sandia National Laboratories. [PDF / Author]

Giambalvo, E.R. 2002c. Memorandum to L.H. Brush (Subject: Recommended Parameter Values for Modeling An(V) Solubility in WIPP Brines). 26 July 2002. ERMS 522990. Carlsbad, NM: Sandia National Laboratories. [PDF / Author]

Gillow, J.B., M. Dunn, A.J. Francis, D. A. Lucero, and H.W. Papenguth. 2000. "The Potential of Subterranean Microbes in Facilitating Actinide Migration at the Grimsel Test Site and Waste Isolation Pilot Plant." Radiochimica Acta, vol. 88: 769-74. [Author]

Gillow J.B.,and A.J. Francis. 2006. Microbial gas generation under expected Waste Isolation Pilot Plant Repository Conditions: Final Report. Report BNL-96148-2011-IR. Albuquerque, NM: Sandia National Laboratories.* [PDF / Author]

Grambow, B., E. Smailos, H. Geckeis, R. Muller, and H. Hentschel. 1996. "Sorption and Reduction of Uranium (VI) on Iron Corrosion Products under Reducing Saline Conditions." Radiochimica Acta, vol. 74: 149-54. [Author]

Grenthe, I., D. Ferri, F. Salvatore, and G. Riccio. 1984. "Studies on Metal Carbonate Equilibria. Part 10. A Solubility Study of the Complex Formation in the Uranium (VI)-Water-Carbon Dioxide (g) System at 25ºC." Journal of Chemical Society, Dalton Trans.: 2439-43. [Author]

Griffith, J., S. Wilcox, D. Powers, R. Nelson, and B. Baxter. 2008. "Discovery of Abundant Cellulose Microfibers Encased in 250 Ma Permian Halite: A Macromolecular Target in the Search for Life on Other Planet." Astrobiology, 8(2): 215-228.* [Author]

Gu, B., L. Liang, M.J. Dickey, X. Yin, and S. Dai. 1998. "Reductive Precipitation of Uranium (VI) by Zero-Valent Iron." Environmental Science and Technology, vol. 32: 3366-73. [Author]

Guillaumont, R., T. Fanghänel, J. Fuger, I. Grenthe, V. Neck, D.A. Palmer, and M.H. Rand. 2003. "Update on the Chemical Thermodynamics of Uranium, Neptunium, Plutonium, Americium and Technetium." F.I. Mompean, M. Illemassene, C. Domenech-Orti, and K. Ben Said, eds. Chemical Thermodynamics. Vol. 5. Amsterdam: Elsevier. [Author]

Gunde-Cimerman , N., J. Ramos, and A. Plemenitas. 2009. "Halotolerant and Halophilic Fungi." Mycological Research, 113: 1231-1241.* [Author]

Harvie, C.E., N. Møller, and J.H. Weare. 1984. "The Prediction of Mineral Solubilities in Natural Waters, The Na-K-Mg-Ca-H-Cl-SO4-OH-HCO3-CO2-H2O System to High Ionic Strengths at 25°C." Geochimica et Cosmochimica Acta, vol. 48: 723-51. [Author]

Haschke, J.M., and T.E. Ricketts. 1995. Plutonium Dioxide Storage: Conditions for Preparing and Handling. LA-12999. Los Alamos, NM: Los Alamos National Laboratory. [PDF / Author]

Haschke, J.M., T.H. Allen, and L.A. Morales. 2000. "Reaction of Plutonium Dioxide with Water: Formation and Properties of PuO2+x." Science, vol. 287: 285-87. [Author]

Hobart, D.E. 1990. Actinides in the Environment. Proceedings of the Robert A. Welch Foundation Conference on Chemical Research, No. XXXIV: 50 Years With Transuranium Elements (pp. 378-436). Houston, TX: Robert A. Welch Foundation. [Author]

Hobart, D.E., and R.C. Moore. 1996. Analysis of Uranium (VI) Solubility Data for WIPP Performance Assessment. (May 28, 1996). AP-028. Unpublished report. Albuquerque, NM: Sandia National Laboratories. [PDF / Author]

Hobart, D.E., K. Samhoun, and J. R. Peterson. 1982. "Spectroelectrochemical Studies of the Actinides: Stabilization of Americium (IV) in Aqueous Carbonate Solution." Radiochimica Acta, vol. 31: 139-45. [Author]

Holm, T.R., and C.D. Curtiss. 1989. "A Comparison of Oxidation-Reduction Potentials Calculated from the As(V)/As(III) and Fe (III)/Fe(II) Couples with Measured Platinum-Electrode Potentials in Groundwater." Journal of Contaminant Hydrology, vol. 5: 67-81.* [Author]

Huang, F.Y C., P.V. Brady, E.R. Lindgren, and P. Guerra. 1998. "Biodegradation of Uranium-Citrate Complexes: Implications for Extraction of Uranium from Soils." Environmental Science and Technology, vol. 32: 379. [Author]

Icopini, G.A., J. Boukhalfa, and M.P. Neu. 2007. "Biological Reduction of Np(V) and Np(V) Citrate by Metal-Reducing Bacteria." Environmental, Science, & Technology, vol. 41: 2764-69. [Author]

Ilton, E.S., J.S. Lezama Pacheco, J.R. Bargar, Z. Shi, J. Liu, L. Kovarik, M.H. Engelhard, and A.R. Felmy. 2012. "Reduction of U (VI) Incorporated in the Structure of Hematite." Environmental Science & Technology, vol.46: 9428-36.* [Author]

Ionova, G., C. Madic, and R. Guillamount. 1998. "About the Existence of Th(III) in Aqueous Solution." Polyhedron, vol. 17: 1991-95. [Author]

Ismail, A.E. 2007 Memorandum to File (Subject: Revised Porosity Estimates for the DRZ). 10 April 2007. ERMS 545755. Carlsbad NM: Sandia National Laboratories. [PDF / Author]

Itagaki, H., S. Nakayama, S. Tanaka, and M. Yamawaki. 1992. "Effect of Ionic Strength on the Solubility of Neptunium(V) Hydroxide." Radiochimica Acta, vol. 58/59: 61-66. [Author]

Katz, J.J., G.T. Seaborg, and L.R. Morss. 1986. The Chemistry of the Actinide Elements. 2nd ed. New York: Chapman and Hall. [Author]

Keller, C. 1971. The Chemistry of Transuranium Elements. Weinheim, Germany: Verlag Chemie. [Author]

Kelm, M., I. Pashalidis, and J.I. Kim. 1999. "Spectroscopic Investigation on the Formation of Hypochlorite by Alpha Radiolysis in Concentrated NaCl Solutions." Applied Radiation and Isotopes, vol. 51: 637-42. [Author]

Kerber Schütz, M., N. Lopes, A. Cenci, R. Ligabue, J. Dullius, S. Einloft, and J.M. Ketzer. 2011. "Effect of Time on the Carbonation Reaction of Saline Aquifers with Controlled pH." Energy Procedia, vol.4 :4546-51.* [Author]

Kerisit, S., A.R. Felmy, and E.S. Ilton. 2011. "Influence of Magnetite Stoichiometry on UVI Reduction." Environmental Science & Technology, vol.45: 2770-76.* [Author]

Khasanova, A.B., N.S. Shcherbina, S.N. Kalmykov, Yu.A. Teterin, and A.P. Novikov. 2007. "Sorption of Np(V), Pu(V), and Pu (VI) on Colloids of Fe(III) Oxides and Hydrous Oxides and MnO2." Radiochemistry, vol. 49: 419-25. [Author]

Kicker, D.C. and T. Zeitler. 2013. Radionuclide Inventory Screening Analysis for the 2014 Compliance Recertification Application Performance Assessment (CRA-2014 PA). ERMS 559257. Carlsbad, NM: Sandia National Laboratories.* [PDF / Author]

Kim, J.I., Ch. Apostolidis, G. Buckau, K. Buppelmann, B. Kanellakopulos, Ch. Lierse, S. Magirius, R. Stumpe, I. Hedler, Ch. Rahner, and W. Stoewer. 1985. Chemisches Verhalten von Np, Pu und Am in verschiedenen konzentrierten Salzloesunger = Chemical Behaviour of Np, Pu, and Am in Various Brine Solutions. RCM 01085. Munich, Germany: Institut für Radiochemie der Technische Universitaet Muenchen. (Available from National Technical Information Service, 555 Port Royal Road, Springfield, VA 22161, 703/487-4650 as DE857 2334.) [Author]

Kim, J.I., M. Bernkopf, Ch. Lierse, and F. Koppold. 1984. Hydrolysis Reactions of Am(III) and Pu(VI) Ions in Near-Neutral Solutions. Geochemical Behavior of Disposed Radioactive Waste (pp. 115-34). G.S. Barney, J.D. Navratill, and W.W. Schultz, eds. ACS Symposium Series No. 246. Washington, DC: American Chemical Society. [Author]

Kim, S. 2013a. Analysis Package for Salado Transport Calculations: CRA-2014 Performance Assessment. ERMS 560174. Carlsbad, NM: Sandia National Laboratories.* [PDF / Author]

Kim, S. 2013b. Analysis Package for PANEL: CRA-2014 Performance Assessment. ERMS 560056. Carlsbad, NM: Sandia National Laboratories.* [PDF / Author]

Kim, S.S., M.H. Baik, J.W. Choi, H.S. Shin, and J.I. Yun. 2010. "The dissolution of ThO2(cr) in carbonate solutions and a granitic groundwater." J. Radioanal. Nucl. Chem., 286: 91-97. [Author]

Kim, W.H., K.C. Choi, K.K. Park, and T.Y. Eom. 1994. "Effects of Hypochlorite Ion on the Solubility of Amorphous Schoepite at 25°C in Neutral to Alkaline Aqueous Solutions." Radiochimica Acta, vol. 66/67: 45-49. [Author]

Klapötke, T.M., and A. Schulz. 1997. "The First Observation of a Th3+ ion in Aqueous Solution." Polyhedron, vol. 16: 989-91. [Author]

Korpusov, G.V., E.N. Patrusheva, and M.S. Dolidze. 1975. "The Study of Extraction Systems and the Method of Separation of Trivalent Transuranium Elements Cm, Bk, and Cf." Soviet Radiochemistry, vol. 17: 230-36. [Author]

Kramer-Schnabel, U., H. Bischoff, R.H. Xi, and G. Marx. 1992. "Solubility Products and Complex Formation Equilibria in the Systems Uranyl Hydroxide and Uranyl Carbonate at 25°C and I=0.1M." Radiochimica Acta, vol. 56: 183-88. [Author]

Langmuir, D., and J.S. Herman. 1980. "Mobility of Thorium in Natural Waters at Low Temperatures." Geochimica et. Cosmochimica Acta, vol. 44: 1753-66. [Author]

Latta, D.E., C.A. Gorski, M.I. Boyanov, E.J. O'Loughlin, K.M. Kemner, and M.M. Scherer. 2012. "Influence of Magnetite Stoichiometry on UVI Reduction." Environmental Science & Technology, vol.46: 778-86.* [Author]

LaVerne, J.A., and L. Tandon. 2002. "H2 Production in the Radiolysis of Water on CeO2 and ZrO2." Journal of Physical Chemistry B, vol. 106: 380-86. [Author]

Leigh, C., J. Kanney, L. Brush, J. Garner, R. Kirkes, T. Lowry, M. Nemer, J. Stein, E. Vugrin, S. Wagner, and T. Kirchner. 2005. 2004 Compliance Recertification Application Performance Assessment Baseline Calculation (Revision 0). ERMS 541521. Carlsbad, NM: Sandia National Laboratories. [PDF / Author]

Lemire, R.J., J. Fuger, H. Nitsche, P. Potter, M.H. Rand, J. Rydberg, K. Spahiu, J.C. Sullivan, W.J. Ullman, P. Vitorge, and H. Wanner. 2001. Chemical Thermodynamics of Neptunium and Plutonium. Amsterdam: Elsevier. [Author]

Lin, M.R., P. Paviet-Hartmann, Y. Xu, and W.H. Runde. 1998. Uranyl Compounds in NaCl Solutions: Structure, Solubility and Thermodynamics. 216th ACS National Meeting: Preprints of Extended Abstracts, vol. 38: 208. Abstract for the National Meeting of the American Chemical Society, Division of Environmental Chemistry, Boston: 23-27 August. [Author]

Lloyd JR, and L.E. Macaskie. 2002. Biochemical basis of microbe-radionuclide interactions. In: Keith-Roach MJ, Livens FR, editors. Interactions of Microorganisms with Radionuclides. London: Elsevier Science Ltd. pp. 313-342.* [Author]

Lloyd, J.R., P. Yong, and L.E. Macaskie. 2000. "Biological Reduction and Removal of Np(V) by Two Microorganisms." Environmental Science and Technology, vol. 34: 1297-1301. [Author]

Lovley, D.R., E.E. Roden, E.J.P. Phillips, and J.C. Woodward. 1993. "Enzymatic Iron and Uranium Reduction by Sulfate-Reducing Bacteria." Marine Geology, vol. 113: 41. [Author]

Lovley, D.R., E.J.P. Phillips, Y.A. Gorbi, and E.R. Landa. 1991. "Microbial Reduction of Uranium." Nature, vol. 350: 413. [Author]

Lucchini, J.-F., H. Khaing, M. Borkowski, M.K. Richmann, and D.T. Reed. 2010a. Actinide (VI) Solubility in Carbonate-free WIPP Brine: Data Summary and Recommendations. LCO-ACP-10, LANL\ACRSP Report. LA-UR 10-00497. Los Alamos, NM: Los Alamos National Laboratory.* [PDF / Author]

Lucchini J.F., H. Khaing, and D.T. Reed. 2010b. Uranium (VI) Solubility in Carbonate-free ERDA-6 Brine. Scientific Basis for Nuclear Waste Management XXXIV, edited by K.L. Smith, S. Kroeker, B. Uberuaga, K.R. Whittle, Material Research Society Symposium Proceedings, vol.1265: 21-26.* [Author]

Lucchini, J.-F., M.K. Richmann, and M. Borkowski. 2013a. Uranium (VI) Solubility in WIPP Brine. LCO-ACP-14, LANL\ACRSP Report. LA-UR 13-20786. Los Alamos, NM: Los Alamos National Laboratory.* [PDF / Author]

Lucchini, J.-F., M. Borkowski, M.K. Richmann, and D.T. Reed. 2013b. "Uranium(VI) Solubility in carbonate-free WIPP Brine." Radiochim. Acta, 101, 391-398.* [Author]

Lucchini, J.-F., M. Borkowski, H. Khaing, M.K. Richmann, J. Swanson, K. Simmons, and D.T. Reed. 2013c. WIPP Actinide-Relevant Brine Chemistry. LCO-ACP-15, LANL\ACRSP Report. LA-UR 13-20620. Los Alamos, NM: Los Alamos National Laboratory.* [PDF / Author]

Lucchini, J.-F., M. Borkowski, M.K. Richmann, S. Ballard, and D.T. Reed. 2007. "Solubility of Nd3+ and UO22+ in WIPP Brine as Oxidation-State Invariant Analogs for Plutonium." Journal of Alloys and Compounds, vol. 444/445: 506-11. [Author]

Lynd, L., P. Weimer, W. van Zyl, and I. Pretorius. 2002. "Microbial Cellulose Utilization : Fundamentals and Biotechnology." Microbiology and Molecular Biology Reviews, 66(3): p. 506-577.* [Author]

Magirius, S., W.T. Carnall, and J.I. Kim. 1985. "Radiolytic Oxidation of Am(III) to Am(V) in NaCl Solution." Radiochimical Acta, vol. 38: 29-32. [Author]

Martinot, L., and J. Fuger. 1985. "The Actinides." Standard Potentials in Aqueous Solution (pp. 631-674). A.J. Bard, R. Parsons, and J. Jordan, eds. New York: Dekker. [Author]

Masue-Slowey, Y., B.D. Kocar, S.A.B. Jofré, K.U. Mayer, and S. Fendorf. 2011. "Transport Implications Resulting from Internal Redistribution of Arsenic and Iron within Constructed Soil Aggregates." Environmental Science and Technology, vol. 45(2): 582-588.* [Author]

McCabe, A. 1990. "The Potential Significance of Microbial Activity in Radioactive Waste Disposal." Experientia, 46: p. 779-787.* [Author]

Meinrath, G., and J.I. Kim. 1991. "The Carbonate Complexation of the Am(III) Ion." Radiochimica Acta, vol. 52/53: 29-34. [Author]

Meyer, D., S. Fouchard, E. Simoni, and C. DenAuwer. 2002. "Selective Dissolution of Am in Basic Media in the Presence of Ferricyanide Ions: a Mechanistic and Structural Study on Am(V) and Am(VI) Compounds." Radiochimica Acta, vol. 90: 253-58. [Author]

Moriyama, H., T. Sasaki, T. Kobayashi, and I. Takagi. 2005. "Systemics of Hydrolysis Constants of Tetravalent Actinide Ions." Journal of Nuclear Science and Technology, vol. 42-7: 626-35. [Author]

Mormile, M., M. Biesen, M. Gutierrez, A. Ventosa, J. Pavlovich, T. Onstott, and J. Fredrickson. 2003. "Isolation of Halobacterium Salinarum Retrieved Directly from Halite Brine Inclusions." Env. Microbiol., 5(11): 1094-1102.* [Author]

Morss, L.R., N. Edelstein, and J. Fuger. 2006. The Chemistry of the Actinide and Transactinide Elements. 3rd ed. New York: Springer. [Author]

Moulin, C., B. Amekraza, S. Hubert, and V. Moulin. 2001. "Study of Thorium Hydrolysis Species by Electrospray-Ionization Mass Spectrometry." Analytica Chimica Acta, vol. 441: 269-79. [Author]

Myllykylä, E., and K. Ollila. 2011. Reduction of Uranyl Carbonate and Hydroxide Complexes by Ferrous Ions in Aqueous Solution under Anaerobic Conditions. Abstract PA4-3, 13th International Conference on the Chemistry and Migration Behaviour of Actinides and Fission Products in the Geosphere Migration, Beijing, China, September 18-23, 2011.* [Author]

Nakata, K., S. Nagasaki, S. Tanaka, Y. Sakamoto, T. Tanaka, and H. Ogawa. 2004. "Reduction Rate of Neptunium(V) in Heterogeneous Solution with Magnetite." Radiochimica Acta, vol. 92: 145-49. [Author]

National Institute of Standards and Technology (NIST). 2004. Critical Stability Constants.Standard Reference Database 46 (Version 8.0). [Author]

Neck, V., and J.I. Kim. 2001. "Solubility and Hydrolysis of Tetravalent Actinides." Radiochimica Acta, vol. 89: 1-16. [Author]

Neck, V., J.I. Kim, and B. Kanellakopulos. 1992. "Solubility and Hydrolysis Behavior of Neptunium (V)." Radiochimica Acta, vol. 56:, 25-30. [Author]

Neck, V., M. Altmaier, and Th. Fanghänel. 2006. "Ion Interaction (SIT) Coefficients for the Th4+ Ion and Trace Activity Coefficients in NaClO4, NaNO3 and NaCl Solution Determined by Solvent Extraction with TBP." Radiochimica Acta, vol. 94: 501-07. [Author]

Neck, V., M. Altmaier, R. Müller, A. Bauer, Th. Fanghänel, and J.I. Kim. 2003. "Solubility of Crystalline Thorium Dioxide." Radiochimica Acta, vol. 91: 253-62. [Author]

Neck, V., M. Altmaier, T. Rabung, J. Lützenkirchen, and Th. Fänghanel. 2009. "Thermodynamics of Trivalent Actinides and Neodymium in NaCl, MgCl2, and CaCl2 Solutions: Solubility, Hydrolysis and Ternary Ca-M(III)-OH Complexes." Pure and Applied Chemistry, vol. 81(9), 1555-1568. [Author]

Neck, V., R. Müller., M. Bouby, M. Altmaier, J. Rothe, M.A. Denecke, and J.I. Kim. 2002. "Solubility of Amorphous Th(IV) Hydroxide: Application of LIBD to Determine the Solubility Product and EXAFS for Aqueous Speciation." Radiochimica Acta, vol. 90: 485-94. [Author]

Neck, V., W. Runde, and J.I. Kim. 1995. "Solid-Liquid Equilibria of Np(V) in Carbonate Solutions at Different Ionic Strengths: II." Journal of Alloys and Compounds, vol. 225: 295-302. [Author]

Nemer, M., Y. Xiong, A.E. Ismail, and J. Jang. 2011. "Solubility of Fe2(OH)3Cl (pure-iron end-member of hibbingite) in NaCl and Na2SO4 brines." Chemical Geology, v. 280, no. 1-2, 26-32.* [Author]

Neretnieks, I. 1982. The Movement of a Redox Front Downstream From a Repository for Nuclear Waste. KBS Report TR 82-16. Stockholm: Svensk Kärnbränsleforsorjning AB. [Author]

Neu, M.P., C.E. Ruggiero, and A.J. Francis. 2002. Bioinorganic Chemistry of Plutonium and Interactions of Plutonium with Microorganisms in Plants. Advances in Plutonium Chemistry (pp. 1967-2000). La Grange Park, IL: American Nuclear Society. [Author]

Nitsche, H., K. Roberts, K. Becraft, T. Prussin, D. Keeney, S. Carpenter, and D. Hobart. 1995. Solubility and Speciation Results from Over- and Under-saturation Experiments on Neptunium, Plutonium and Americium in water from Yucca Mountain Region Well UE-25p#1. Report LA-13017-MS. Los Alamos, NM: Los Alamos National Laboratory. [Author]

Nitsche, H., K. Roberts, R. Xi, T. Prussin, K. Becraft, I. Al Mahamid, H.B. Silber, S.A. Carpenter, R.C. Gatti, and C.F. Novak. 1994. "Long-Term Plutonium Solubility and Speciation Studies in a Synthetic Brine." Radiochimica Acta, vol. 66/67: 3. [Author]

Nitsche, H., K. Roberts, R.C. Gatti, T. Prussin, K. Becraft, S.C. Leung, S.A. Carpenter, and C.F. Novak. 1992. Plutonium Solubility and Speciation Studies in a Simulant of Air Intake Shaft Water from the Culebra Dolomite at the Waste Isolation Pilot Plant. SAND92-0659. WPO 23480. Albuquerque, NM: Sandia National Laboratories. [PDF / Author]

Norton, C., and W. Grant. 1988. "Survival of Halobacteria Within Fluid Inclusions in Salt Crystals." J. General Microbiology, 134: 1365-1373.* [Author]

O'Loughlin, E.J., S.D. Kelly, R.E. Cook, R. Csencsits, and K.M. Kemner. 2003. "Reduction of Uranium (VI) by Mixed Iron (II)/ Iron (III) Hydroxide (Green Rust): Formation of UO2 Nanoparticles." Environmental Science and Technology, vol. 37: 721-27. [Author]

Okajima, S., and D.T. Reed. 1993. "Initial Hydrolysis of Pu(VI)." Radiochimica Acta, vol. 60: 173-84. [Author]

Okamoto, Y., Y. Mochizuki, and S. Tsushim. 2003. "Theoretical Study of Hydrolysis Reactions of Tetravalent Thorium Ion." Chemical Physics Letters, vol. 373: 213-17. [Author]

Oren, A. 1999. "Bioenergetic Aspects of Halphilism." Microbiology and Molecular Biology Reviews, 63(2): 334-348.* [Author]

Oren, A. 2006. Life at high salt concentrations. In: Falkow S, Rosenberg E, Schleifer K-H, Stackebrandt E, Dworkin M, editors. The Prokaryotes. New York: Springer. pp. 263-282.* [Author]

Oren, A. 2008. "Microbial life at high salt concentrations: phylogenetic and metabolic diversity." Saline Systems, vol. 4:2. DOI: 10.1186/1746-1448-4-2.* [Author]

Oren, A. 2011. "Thermodynamic limits to microbial life at high salt concentrations." Environmental Microbiology, vol. 13: 1908-1923.* [Author]

Orlandini, J.A., W.R. Penrose, and D.M. Nelson. 1986. "Pu(V) as the Stable form of Oxidized Plutonium in Natural Waters." Marine Chemistry, vol. 18: 49-57. [Author]

Östhols, E., J. Bruno, and I. Grenthe. 1994. "On the Influence of Carbonate on Mineral Dissolution: III: The Solubility of Microcrystalline ThO2 in CO2-H2O Media." Geochimica et. Cosmochimica Acta, vol. 58: 613-623. [Author]

Oversby, V.M. 2000. Plutonium Chemistry under Conditions Relevant for WIPP Performance Assessment: Review of Experimental Results and Recommendations for Future Work (September). EEG-77. Albuquerque, NM: Environmental Evaluation Group. [Author]

Papenguth, H.W. 1996a. Letter to Christine T. Stockman (Subject: Parameter Record Package for Colloidal Actinide Source Term Parameters, Attachment A: Rationale for Definition of Parameter Values for Microbes). 7 May 1996. ERMS 235856. Carlsbad, NM: Sandia National Laboratories. [Author]

Papenguth, H.W. 1996b. Letter to Christine T. Stockman (Subject: Parameter Record Package for Colloidal Actinide Source Term Parameters, Attachment A: Rationale for Definition of Parameter Values for Humic Substances). 7 May 1996. ERMS 235855. Carlsbad, NM: Sandia National Laboratories. [PDF / Author]

Papenguth, H.W. 1996c. Letter to Christine T. Stockman (Subject: Parameter Record Package for Colloidal Actinide Source Term Parameters, Attachment A: Rationale for Definition of Parameter Values for Mineral Fragment Type Colloids). 7 May 1996. ERMS 235850. Carlsbad, NM: Sandia National Laboratories. [PDF / Author]

Papenguth, H.W., and Y.K. Behl. 1996. Test Plan for Evaluation of Colloid-Facilitated Actinide Transport at the Waste Isolation Pilot Plant (16 January). TP 96-01. ERMS 417319. Carlsbad, NM: Sandia National Laboratories. [PDF / Author]

Pashalidis, I., J.I. Kim, Ch. Lierse, and J.C. Sullivan. 1993. "The Chemistry of Pu in Concentrated Aqueous NaCl Solution: Effects of Alpha Self-Radiolysis and the Interaction Between Hypochlorite and Dioxoplutonium (VI)." Radiochimica Acta, vol. 60: 99. [Author]

Pazukhin, E.M., and S.M. Kochergin. 1989. "Stability Constants of Hydrolyzed Forms of Americium(III) and Solubility Product of its Hydroxide." Soviet Radiochemistry, vol. 31: 430-36. [Author]

Pedersen, K. 2002. Microbial processes in the disposal of high level radioactive waste 500m underground in Fennoscandian shield rocks. In: Keith-Roach MJ, Livens, FR, editors. Interactions of Microorganisms with Radionuclides. London: Elsevier Science Ltd. pp. 279-311.* [Author]

Pitzer, K.S. 1973. "Thermodynamics of Electrolytes. I. Theoretical Basis and General Equations." The Journal of Physical Chemistry, vol. 77(2): 268-277.* [Author]

Popielak, R.S., R.L. Beauheim, S.R. Black, W.E. Coons, C.T. Ellingson, and R.L. Olsen. 1983. Brine Reservoirs in the Castile Formation, Waste Isolation Pilot Plant Project, Southeastern New Mexico. TME 3153. Carlsbad, NM: U.S. Department of Energy. [PDF / Author]

Porter, D., A.N. Roychoudhury, and D. Cowan. 2007. "Dissimilatory Sulfate Reduction in Hypersaline Coastal Pans: Activity Across a Salinity Gradient." Geochimica et Cosmochimica Acta, 71: 5102-5116.* [Author]

Powers, D.W., S.J. Lambert, S.E. Shaffer, I.R. Hill, and W.D. Weart, eds. 1978. Geological Characterization Report, Waste Isolation Pilot Plant (WIPP) Site, Southeastern New Mexico. SAND78-1596. 2 vols. ERMS 205448. Albuquerque, NM: Sandia National Laboratories. [PDF / Author]

Pryke, D.C., and J.H. Rees. 1986. "Understanding the Behaviour of the Actinides Under Disposal Conditions: A Comparison between Calculated and Experimental Solubilities." Radiochimica Acta, vol. 40: 27-32. [Author]

Qui, S.R., C. Amrhein, M.L. Hunt, R. Pfeffer, B. Yakshinskiy, L. Zhang, T.E. Madey, and J.A. Yarmoff. 2001. "Characterization of Uranium Oxide Thin Films Grown from Solution onto Fe Surfaces." Applied Surface Science, vol. 181: 211-34. [Author]

Rabindra, N.R., K.M. Vogel, C.E. Good, W.B. Davis, L.N. Roy, D.A. Johnson, A.R. Felmy, and K.S. Pitzer. 1992. "Activity Coefficients in Electrolyte Mixtures: HCl + ThCl4 + H2O for 5-55 °C." Journal of Physical Chemistry, vol. 96: 11,065-072. [Author]

Rai, D., A.R. Felmy, and J.L. Ryan. 1990. "Uranium (VI) Hydrolysis Constants and Solubility Products of UO2.xH2O (am)." Inorganic Chemistry, vol. 29: 260-64. [Author]

Rai, D., A.R. Felmy, and R.W. Fulton. 1995. "Nd3+ and Am3+ Ion Interaction with Sulfate Ion and Their Influence on NdPO4(c) Solubility." Journal of Solution Chemistry, vol. 24: 879-95. [Author]

Rai, D., A.R. Felmy, N.J. Hess, and D.A. Moore. 1998. "A Thermodynamic Model for the Solubility of UO2(am) in the Aqueous K+-Na+-HCO3--CO32--OH--H2O System." Radiochimica Acta, vol. 82: 17-25. [Author]

Rai, D., A.R. Felmy, S.M. Sterner, D.A. Moore, M.J. Mason, and C.F. Novak. 1997. "The Solubility of Th(IV) and U(IV) Hydrous Oxides in Concentrated NaCl and MgCl2 Solutions." Radiochimica Acta, vol. 79: 239-47. [Author]

Rai, D., and J.L. Ryan. 1982. "Crystallinity and Solubility of Pu(IV) Oxide and Hydrous Oxide in Aged Aqueous Suspensions." Radiochimica Acta, vol. 30: 213-16. [Author]

Rai, D., and J.L. Ryan. 1985. "Neptunium (IV) Hydrous Oxide Solubility under Reducing and Carbonate Conditions." Inorganic Chemistry, vol. 24: 247-51. [Author]

Rai, D., D.A. Moore, C.S. Oakes, and M. Yui. 2000. "Thermodynamic Model for the Solubility of Thorium Dioxide in the Na+-Cl--OH--H2O System at 23 °C and 90°C." Radiochimica Acta, vol. 88: 297-306. [Author]

Rai, D., J.L. Ryan, D.A. Moore, and R.G. Strickert. 1983. "Am(III) Hydrolysis Constants and Solubility of Am(III) Hydroxide." Radiochimica Acta, vol. 33: 201-06. [Author]

Rai, D., R.G. Strickert, and G.L. McVay. 1982. "Neptunium Concentrations in Solutions Contacting Actinide-Doped Glass." Nuclear Technology, vol. 58: 69-76. [Author]

Rao, L., D. Rai, A.R. Felmy, R.W. Fulton, and C.F. Novak. 1996. "Solubility of NaNd(CO3)2·6H2O(c) in Concentrated NaCO3 and NaHCO3 Solutions." Radiochimica Acta, vol. 75: 141-47. [Author]

Reed, D.T., and D.R. Wygmans. 1997. Actinide Stability/Solubility in Simulated WIPP Brines (March 21). WPO44625. Argonne, IL: Argonne National Laboratory, Actinide Speciation and Chemistry Group, Chemical Technology Group. [Author]

Reed, D.T., J.-F. Lucchini, M. Borkowski, and M.K. Richmann. 2009. Reduction of Higher Valent Plutonium by Iron under Waste Isolation Pilot Plant (WIPP)- Relevant Conditions: Data Summary and Recommendations. LCO-ACP-09, LANL\ACRSP Report. Los Alamos, NM: Los Alamos National Laboratory. [PDF / Author]

Reed, D.T., J.-F. Lucchini, S.B. Aase, and A.J. Kropf. 2006. "Reduction of Plutonium (VI) in Brine under Subsurface Conditions." Radiochimica Acta, vol. 94: 591-97. [Author]

Reed, D.T., J.S. Swanson, J-F. Lucchini, and M.K. Richmann. 2013. Intrinsic, Mineral, and Microbial Colloid Enhancement Parameters for the WIPP Actinide Source Term. Report LCO-ACP-18, LA-UR 13-20858. Carlsbad, NM: Los Alamos National Laboratory.* [Author]

Reed, D.T., R. Deo, and B.E. Rittmann. 2010. Subsurface Interactions of Actinide Species and Microorganisms. In The Chemistry of the Actinide and Transactinide Elements by L.R. Morss, N.M. Edelstein and J. Fuger eds., Chapter 33. Netherlands: Springer Press, 2010.* [Author]

Reed, D.T., S. Okajima, and M.K. Richmann. 1994. "Stability and Speciation of Plutonium(VI) in WIPP Brine." Radiochimica Acta, vol. 66/67: 95-101. [Author]

Reed, D.T., S. Okajima, L.H. Brush, and M.A. Molecke. 1993. Radiolytically Induced Gas Production in Plutonium-Spiked WIPP Brine. Materials Research Society Symposium Proceedings (pp. 431-38). Vol. 294. Warrendale, PA: Materials Research Society. [Author]

Reed, D.T., S.B. Aase, D. Wygmans, and J. E. Banaszak. 1998. "The Reduction of Np(VI) and Pu(VI) by Organic Chelating Agents." Radiochimica Acta, vol. 82: 109-14. [Author]

Reed, D.T., S.E. Pepper, M.K. Richmann, G. Smith, R. Deo, and B.E. Rittmann. 2007. "Subsurface Bio-Mediated Reduction of Higher-Valent Uranium and Plutonium." Journal of Alloys and Compounds, vol. 444/445: 376-82. [Author]

Refait, Ph., and J.-M.R. Génin. 1994. "The Transformation of Chloride-Containing Green Rust One into Sulphated Green Rust Two by Oxidation in Mixed Cl- and SO42- Aqueous Media." Corrosion Science, vol. 36, no. 1: 55-65. [Author]

Richmann, M.K. 2008. Letter report to D. Reed (Subject: Eh/pH Diagrams for Am(III), Th(IV) and Np(V) Based on the FMT Database and Current PA Assumptions). 21 November 2008. Carlsbad, NM: Los Alamos National Laboratory. [PDF / Author]

Rittmann, B.E., J.E. Banaszak, and D.T. Reed. 2002. "Reduction of Np(V) and Precipitation of Np(IV) by an Anaerobic Microbial Consortium." Biodegradation, vol. 13: 329-42. [Author]

Rohban, R., M. Amoozegar, and A. Ventosa. 2009. "Screening and Isolation of Halophilic Bacteria Producing Extracellular Hydrolysis from Howz Soltan Lake, Iran." J. Ind. Microbiol. Biotechnol., 36: 333-340.* [Author]

Roselle, G.T. 2009. Iron and Lead Corrosion in WIPP-Relevant Conditions: Six Month Results. Milestone Report, October 7, 2009. ERMS 546084. Carlsbad, NM: Sandia National Laboratories.* [PDF / Author]

Roselle, G.T. 2010. Iron and Lead Corrosion in WIPP-Relevant Conditions: 12 Month Results. Milestone report, October 14, 2010. ERMS 554383. Carlsbad, NM: Sandia National Laboratories.* [PDF / Author]

Roselle, G.T. 2011a. Iron and Lead Corrosion in WIPP-Relevant Conditions: 18 Month Results. Milestone report, January 5, 2011. ERMS 554715. Carlsbad, NM: Sandia National Laboratories.* [PDF / Author]

Roselle, G.T. 2011b. Iron and Lead Corrosion in WIPP-Relevant Conditions: 24 Month Results. Milestone report, May 3, 2011. ERMS 555246. Carlsbad, NM: Sandia National Laboratories.* [PDF / Author]

Roselle, G.T. 2013. Determination of Corrosion Rates from Iron/Lead Corrosion Experiments to be Used for Gas Generation Calculations, Revision 1. Analysis report, January 23, 2013. ERMS 559077. Carlsbad, NM: Sandia National Laboratories.* [PDF / Author]

Runde, W. 2000. "The Chemical Interactions of Actinides in the Environment." Los Alamos Science, vol. 26: 330. [Author]

Runde, W., and J.I. Kim. 1994. Untersuchungen der Übertragbarkeit von Labordaten natürliche Verhältnisse. Chemisches Verhalten von drei- und fünfwertigem Americium in salinen NaCl-Lösungen. Report RCM-01094, Munich: Institut für Radiochemie, Technische Universität München. (Available from National Technical Information Service, 555 Port Royal Road, Springfield, VA, 22161, 703/487-4650 as DE 95752244.) [Author]

Runde, W., and M. Neu. 2010. Actinide Environmental Chemistry. In The Chemistry of the Actinide and Transactinide Elements by L.R. Morss, N.M. Edelstein and J. Fuger eds., Chapter 32. Netherlands: Springer Press, 2010.* [Author]

Runde, W., S.D. Conradson, D.W. Efurd, N. Lu, D.E. VanPelt, and C.D. Tait. 2002. "Solubility and Sorption of Redox-Sensitive Radionuclides (Np,Pu) in j-13 Water from the Yucca Mountain Site: Comparison Between Experiment and Theory." Applied Geochemistry, vol. 17: 837-53. [Author]

Ryan, J.L., and D. Rai. 1983. "The Solubility of Uranium (IV) Hydrous Oxide in Sodium Hydroxide Solutions under Reducing Conditions." Polyhedron, vol. 2: 947-52. [Author]

Sanchez, A.L., J.W. Murray, and T.H. Sibley. 1985. "The Adsorption of Plutonium IV and V on Geothite." Geochimica Cosmochimica Acta, vol. 49: 2297. [Author]

Sanchez, L.C., and H.R. Trellue. 1996. Memorandum to T. Hicks (Subject: Estimation of Maximum RH-TRU Thermal Heat Load for WIPP). 17 January 1996. WPO 31165. Albuquerque, NM: Sandia National Laboratories. [PDF / Author]

Schubert, B., T. Lowenstein, and M. Timofeeff. 2009. "Microscipic Identification of Prokaryotes in Modern and Ancient Halite, Saline Valley and Death Valley, California." Astrobiology 9(5): 467-482.* [Author]

Schubert, B., M. Timofeeff, T. Lowenstein, and J. Polle. 2010. "Dunaliella Cells in Fluid Incusions in Halite: Signficance for Long-term Survival of Prokaryotes." Geomicrobiology Journal, 27: 61-75.* [Author]

Schweitzer, G.K., and L.L. Pesterfield. 2010. Chapter 7: The Boron Group. The Aqueous Chemistry of the Elements. (pp. 150-154) Oxford, USA: Oxford University Press.* [Author]

Shannon, R.D. 1976. "Revised Effective Ionic Radii and Systematic Studies of Interatomic Distances in Halides and Chalcogenides." Acta Cryst, vol. A32: 751-67. [Author]

Siekierski, S. 1988. "Comparison of Yttrium, Lanthanides and Actinides in Respect to Unit Cell Volumes of Isostructural Compounds and Thermodynamic Functions of Complex Formation." Journal of Radioanalytical Nuclear Chemistry, vol. 122: 279-84. [Author]

Silva, R.J., G. Bidoglio, M.H. Rand, P.B. Robouch, H. Wanner, and I. Puigdomenech. 1995. Chemical Thermodynamics of Americium. Chemical Thermodynamics Series 2. New York Elsevier. [Author]

Simankova, M.V., and G.A. Zavarzin. 1992. "Anaerobic Degradation of Cellulose from Lake Sivash and Hypersaline Lagoons of the Arabat Spit." Microbiologiya, vol. 61: 288-292.* [Author]

Simankova, M.V., N. Chernych, G. Osipov and G. Zavarzin. 1993. "Halocella celluloytica gen. nov., sp. nov., a New Obligately Anaerobic, Halophilic, Cellulolytic bacterium." System. Appl. Microbio., 16: 385-389.* [Author]

Singer, D.M., S.M. Chatman, E.S. Ilton, K.M. Rosso, J.F. Banfield, and G.A. Waychunas. 2012a. "Identification of Simultaneous U (VI) Sorption Complexes and U(VI) Nanoprecipitates on the Magnetite (111) Surface." Environmental Science & Technology, vol.46: 3811-20.* [Author]

Singer, D.M., S.M. Chatman, E.S. Ilton, K.M. Rosso, J.F. Banfield, and G.A. Waychunas. 2012b. "U(VI) Sorption and Reduction Kinetics on the Magnetite (111) Surface." Environmental Science & Technology, vol.46: 3821-30.* [Author]

Skokan, C.K., M.C. Pfeifer, G.V. Keller, and H.T. Anderses. 1987. Studies of Electrical and Electromagnetic Methods for Characterizing Salt Properties at the WIPP Site, New Mexico. SAND87-7174. Carlsbad NM: Sandia National Laboratories. [PDF / Author]

Snider, A.C. 2003a. Verification of the Definition of Generic Weep Brine and the Development of a Recipe for This Brine. ERMS 527505. Carlsbad, NM: Sandia National Laboratories. [PDF / Author]

Snider, A.C. 2003b. Hydration of Magnesium Oxide in the Waste Isolation Pilot Plant. Materials Research Society Symposium Proceedings (pp. 665-70). Vol. 757. Warrendale, PA: Materials Research Society. [Author]

Sørensen, K., K. Reháková, E. Zapomělová, and A. Oren. 2009. "Distribution of Benthic Phototrophs, Sulfate Reducers, and Methanogens in Two Adjacent Saltern Evaporation Ponds in Eilat, Israel." Aquatic Microbial Ecology, vol. 56: 275-284.* [Author]

Sorokin D., and G. Muyzer. 2010. "Bacterial Dissimilatory MnO2 Reduction at Extremely Haloalkaline Conditions." Extremophiles, 14:41-46.* [Author]

Spinks, J.W.T., and R.J. Woods. 1990. Radiation Sources: The Interaction of Radiation with Matter. Introduction to Radiation Chemistry (pp. 243-313). New York: Wiley. [Author]

Stadler, S., and J.I. Kim. 1988. "Hydrolysis reactions of Am(III) and Am(V)." Radiochim. Acta, 44/45: 39-44. [Author]

Stein, J.S. 2005. Memorandum to L.H. Brush (Subject: Estimate of Volume of Brine in Repository that Leads to a Brine Release). 13 April 2005. ERMS 539372. Carlsbad, NM: Sandia National Laboratories. [PDF / Author]

Stoelzel, D.M., and D.G. O'Brien. 1996. Analysis Package for the BRAGFLO Direct Release Calculations (Task 4) of the Performance Assessment Analyses Supporting the Compliance Certification Application. AP-029. ERMS 240520. Albuquerque, NM: Sandia National Laboratories. [PDF / Author]

Suzuki, Y., S.D. Kelly, K.M. Kemner, and J.F. Banfield. 2003. "Microbial populations stimulated for hexavalent uranium reduction in uranium mine sediment." Applied and Environmental Microbiology, 69:1337-46.* [Author]

Swanson, J.S., and K.A. Simmons. 2013. Update on Microbial Characterization of WIPP Groundwaters. Report LCO-ACP-20, LA-UR 13-20623. Carlsbad, NM: Los Alamos National Laboratory.* [Author]

Swanson, J.S., D.M. Norden, H. Khaing, and D.T. Reed. 2013a. "Degradation of Organic Complexing Agents by Halophilic Microorganisms in Brines." Geomicrobiology Journal, 30: 189-98.* [Author]

Swanson, J.S., K.A. Simmons, D.M. Norden, and H. Khaing. 2013b. Biodegradation of Organic Complexing Agents by WIPP-indigenous Halophilic Microorganisms in Brines. Report LCO-ACP-19, LA-UR 13-20616. Carlsbad, NM: Los Alamos National Laboratory.* [Author]

Swanson, J.S., D.T. Reed, D.A. Ams, D.M. Norden, and K.A. Simmons. 2012. Status Report on the Microbial Characterization of Halite and Groundwater Samples from the WIPP. Report LCO-ACP-12, LA-UR 12-22824. Carlsbad, NM: Los Alamos National Laboratory.* [PDF / Author]

Telander, M.R., and R.E. Westerman. 1993. Hydrogen Generation by Metal Corrosion in Simulated Waste Isolation Pilot Plant Environments: Progress Report for the Period November 1989 Through December 1992. SAND92-7347. ERMS 223456. Albuquerque, NM: Sandia National Laboratories. [PDF / Author]

Telander, M.R., and R.E. Westerman. 1997. Hydrogen Generation by Metal Corrosion in Simulated Waste Isolation Pilot Plant Environments. SAND96-2538. Albuquerque, NM: Sandia National Laboratories. [PDF / Author]

Torrero, M.E., I. Casas, J. de Pablo, M.C.A. Sandino, and B.A. Grambow. 1994. "Comparison Between Unirradiated UO2(s) and Schoepite Solubilities in 1 M NaCl Medium." Radiochimica Acta, vol. 66/67: 29-35. [Author]

Torretto, P., K. Becraft, T. Prussin, K. Roberts, S. Carpenter, D. Hobart, and H. Nitsche. 1995. Solubility and Speciation Results from Oversaturation Experiments on Neptunium, Plutonium and Americium in a Neutral Electrolyte with a Total Carbonate Similar to Water from Yucca Mountain Region Well UE-25p#1. Report LA-13018-MS. Los Alamos, NM: Los Alamos National Laboratory. [PDF / Author]

Trolard, F., J.M.R. Genin, M. Abdelmoula, G. Bourrie, B. Humbert, and A. Herbillon. 1997. "Identification of a Green Rust mineral in a Reductomorphic Soil by Mossbauer and Raman Spectroscopies." Geochimica Cosmochimica Acta, vol. 63: 1107-11. [Author]

U.S. Department of Energy (DOE). 1996. Title 40 CFR Part 191 Compliance Certification Application for the Waste Isolation Pilot Plant (October). 21 vols. DOE/CAO-1996-2184. Carlsbad, NM: Carlsbad Field Office. [Author]

U.S. Department of Energy (DOE). 2004. Title 40 CFR Part 191 Compliance Recertification Application for the Waste Isolation Pilot Plant (March). 10 vols. DOE/WIPP 2004-3231. Carlsbad, NM: Carlsbad Field Office. [Author]

U.S. Department of Energy (DOE). 2009. Title 40 CFR Part 191 Subparts B and C Compliance Recertification Application 2009, Appendix PA, Attachment SOTERM. Carlsbad, NM: Carlsbad Field Office.* [PDF / Author]

U.S. Department of Energy (DOE). 2011. Waste Isolation Pilot Plant Annual Site Environmental Report for 2010. DOE/WIPP-11-2225. Carlsbad, NM: Carlsbad Field Office.* [PDF / Author]

U.S. Environmental Protection Agency (EPA). 1993. "40 CFR Part 191: Environmental Radiation Protection Standards for the Management and Disposal of Spent Nuclear Fuel, High-Level and Transuranic Radioactive Wastes; Final Rule." Federal Register, vol. 58 (December 20, 1993): 66398-416. [PDF / Author]

U.S. Environmental Protection Agency (EPA). 2005. Teleconference with U.S. Department of Energy (DOE), Sandia National Laboratories (SNL), and Los Alamos National Laboratory (LANL) (Subject: Change in U(VI) Solubility Assumption to a Concentration to 1 mM). 2 March 2005. [PDF / Author]

U.S. Environmental Protection Agency (EPA). 2006. Technical Support Document for Section 194.24: Evaluation of the Compliance Recertification Actinide Source Term and Culebra Dolomite Distribution Coefficient Values (March). Washington, DC: Office of Radiation and Indoor Air. [PDF / Author]

Van Loon, L.R., M.A. Glaus, S. Stallone, and A. Laube. 1997. Alkaline Degradation of Cellulose: Estimation of the Concentration of Isosaccharinic Acid in Cement Pore Water. Mat. Res. Soc. Symp. Proc. 506, 1009-1010.* [Author]

Van Luik, A.E., M.J. Apted, W.J. Bailey, J.H. Haberman, J.S. Shade, R.E. Guenther, R.J. Serne, E.R. Gilbert, R. Peters, and R.E. Williford. 1987. Spent Nuclear Fuel as a Waste Form for Geologic Disposal: Assessment and Recommendations on Data and Modeling Needs. PNL-6329. Richland, WA: Pacific Northwest Laboratories. [Author]

Van Soest, G. 2012. Performance Assessment Inventory Report - 2012 (PAIR 2012). INV-PA-12, LANL-CO\Inventory Report, Los Alamos, NM: Los Alamos National Laboratory.* [PDF / Author]

Vandenborre, J., B. Grambov, and A. Abdlouas. 2010. "Discrepancies in Thorium Oxide Solubility Values: Study of Attachment/Detachment Processes at the Solid/Solution Interface." Inorg. Chem., 49, 8736-8748.* [Author]

Villareal, R., J.M. Bergquist, and S.L. Leonard. 2001. The Actinide Source-Term Waste Test Program (STTP): Final Report. 3 vols. LA-UR-01-6822, LA-UR-01-6912, and LA-UR-01-6913. Los Alamos, NM: Los Alamos National Laboratory. [PDF / Author]

Vreeland R.H., A.F. Piselli Jr., S. McDonnough, and S.S. Meyers. 1998. "Distribution and diversity of halophilic bacteria in a subsurface salt formation." Extremophiles 2: 321-331.* [Author]

Wall, N.A., and S.A. Mathews. 2005. "Sustainability of Humic Acids in the Presence of Magnesium Oxide." Applied Geochemistry, vol. 20: 1704-13. [Author]

Walther, C. 2003. "Comparison of Colloid Investigations by Single Particle Analytical Techniques: A Case Study on Thorium-Oxyhydroxides." Colloids and Surfaces A: Physicochemical Engineering Aspects, vol. 217: 81-92. [Author]

Wang Y., and A.J. Francis. 2005. "Evaluation of microbial activity for long-term performance assessments of deep geologic nuclear waste repositories." Journal of Nuclear and Radiochemical Science 6: 43-50.* [Author]

Wang, Y., and L.H. Brush. 1996. Memorandum to M.S. Tierney (Subject: Estimates of Gas-Generation Parameters for the Long-Term WIPP Performance Assessment). 26 January 1996. ERMS 231943. Carlsbad, NM: Sandia National Laboratories. [PDF / Author]

Wang, Z., RC. Moore, A.R. Felmy, M.J. Mason, and R.K. Kukkadapu. 2001. "A study of the corrosion products of mild steel in high ionic strength brines." Waste Management 21:335-341.* [Author]

Warwick, P., N. Evans, and S.Vines. 2006. "Studies on some divalent metal α-isosaccharinic acid complexes." Radiochim. Acta 94, 363-368.* [Author]

Weiner, R. 1996. Technical memorandum to SWCF-A: Records Center (Subject: Documentation Package For: Oxidation State Distribution of Actinides in the Repository). 27 March 1996. ERMS 235194. Albuquerque, NM: Sandia National Laboratories. [Author]

White, A.F., A. Yee, and S. Flexser. 1985. "Surface Oxidation-Reduction Kinetics Associated with Experimental Basalt-Water Reactions at 25 °C." Chemical Geology, vol. 49: 73. [Author]

Wilson D. 2011. "Microbial Diversity of Cellulose Hydrolysis." Current Opinion in Microbiology (Ecology and Industrial Microbiology), 14: 259-263.* [Author]

Wolery, T.J. 1992. EQ3/6, A Software Package for Geochemical Modeling of Aqueous Systems: Package Overview and Installation Guide (Version 7.0). UCRL-MA-110662 PT 1. Livermore, CA: Lawrence Livermore National Laboratory. [Author]

Wolery, T.J. 2008. Analysis Plan for EQ3/6 Analytical Studies. AP-140, Rev. 0., 15 May 2008. ERMS 548930. Carlsbad, NM: Sandia National Laboratories.* [PDF / Author]

Wolery, T.J., and R.L. Jarek. 2003. Software User's Manual: EQ3/6, Version 8.0. Software Document No. 10813-UM-8.0-00. Albuquerque, NM: Sandia National Laboratories.* [PDF / Author]

Wolery, T.J., and S.A. Daveler. 1992. EQ3/6, A Computer Program for Reaction Path Modeling of Aqueous Geochemical Systems: Theoretical Manual, User's Guide, and Related Documentation (Version 7.0). UCRL-MA-110662-Pt. 4. Livermore, CA: Lawrence Livermore National Laboratory. [Author]

Wolery, T.J., Y.-L. Xiong, and J.J. Long. 2010. Verification and Validation Plan/Validation Document for EQ3/6 Version 8.0a for Actinide Chemistry, Document Version 8.10. ERMS 550239. Carlsbad, NM: Sandia National Laboratories.* [PDF / Author]

Xiong, Y.-L. 2011a. E-mail to Jennifer Long (Subject: Release of EQ3/6 Database DATA0.FM1). 9 March 2011. ERMS 555152. Carlsbad, NM: Sandia National Laboratories.* [PDF / Author]

Xiong, Y.-L. 2011b. WIPP Verification and Validation Plan/Validation Document for EQ3/6 Version 8.0a for Actinide Chemistry, Revision 1. Supersedes ERMS 550239. ERMS 555358. Carlsbad, NM: Sandia National Laboratories.* [PDF / Author]

Xiong, Y.-L., and A.S. Lord. 2008. "Experimental Investigations of the Reaction Path in the MgO-CO2-H2O System in Solution with Various Ionic Strengths, and Their Applications to Nuclear Waste Isolation." Applied Geochemistry, vol. 23: 1634-59. [Author]

Yajima, T., Y. Kawamura, and S. Ueta. 1995. Uranium(IV) Solubility and Hydrolysis Constants Under Reduced Conditions. Materials Research Society Symposium Proceedings, (pp. 1137-42). Vol. 353. Warrendale, PA: Materials Research Society. [Author]

Yamamura, T., A. Kitamura, A. Fukui, S. Nishikawa, T. Yamamoto, and H. Moriyama. 1998. "Solubility of U(VI) in Highly Basic Solutions." Radiochimica Acta, vol. 83: 139-146. [Author]

Yamazaki, H., B. Lagerman, V. Symeopoulos, and G.R. Choppin. 1992. "Solubility of Uranyl in Brine." Radioactive Waste Management, vol. 1992: 1607-11. [Author]

Zitomer, D.H., and R.E. Speece. 1993. "Sequential Environments for Enhanced Biotransformation of Aqueous Contaminants." Environmental Science and Technology, vol. 27: 227. [Author]

Title 40 CFR Part 191
Subparts B and C
Compliance Recertification Application 2014
for the
Waste Isolation Pilot Plant

Appendix TFIELD-2014
Transmissivity Fields

United States Department of Energy
Waste Isolation Pilot Plant

Carlsbad Field Office
Carlsbad, New Mexico

Compliance Recertification Application 2014
Appendix TFIELD-2014

Table of Contents

List of Figures

List of Tables

partial mining include 300 realizations, while no mining only includes 100 realizations.

Acronyms and Abbreviations

A transmissivity anisotropy [dimensionless]

AMSL above mean sea level

AP analysis plan

BLM Bureau of Land Management

CB Cabin Baby

CCA Compliance Certification Application

CDF cumulative distribution function

CFR Code of Federal Regulations

CRA Compliance Recertification Application

D diffusivity [m^2/s]

DOE U.S. Department of Energy

EPA U.S. Environmental Protection Agency

km kilometer

LWB Land Withdrawal Boundary

m meter

m^2 square meters

M/H mudstone/halite margin

m^2/s square meters per second

m^3/s cubic meters per second

m/yr meters per year

PA performance assessment

PABC performance assessment baseline calculation

R recharge [m/s]

RMSE root mean squared error

S storativity [dimensionless]

SNL Sandia National Laboratories

SSE sum of squared errors

SVD singular value decomposition

T transmissivity [m^2/s]

USGS U.S. Geological Survey

UTM Universal Transverse Mercator map projection

WIPP Waste Isolation Pilot Plant

TFIELD-1.0 Overview of the T-field Development, Calibration, and Mining Modification Process

Modeling the transport of radionuclides through the Culebra Dolomite Member of the Rustler Formation (hereafter referred to as the Culebra) is one component of the performance assessment (PA) performed for the U.S. Department of Energy (DOE) Waste Isolation Pilot Plant (WIPP) 2014 Compliance Recertification Application (CRA). Transport modeling in PA requires flow velocity results from the Culebra groundwater flow model. This Appendix describes the process used to develop and calibrate the input parameter fields for the Culebra flow model. Calibrated model parameters are referred to broadly as "T-fields" (transmissivity fields), although more parameters than just transmissivity (*T*) were calibrated as part of the CRA-2009 Performance Assessment Baseline Calculation (PABC) model (Clayton et al. 2010). This appendix describes the process followed for the CRA-2009 (PABC), which was a major change from the process followed for CRA-2004 PABC (Leigh et al. 2004), and involved a hydrology conceptual model peer review. The T-fields developed for CRA-2009 PABC were used unchanged in CRA-2014. Figures illustrating each calibrated T-field are given in Attachment A to this Appendix.

The work described in this Appendix was performed under two Sandia National Laboratories (SNL) analysis plans (APs): AP-114 (Beauheim 2008) and AP-144 (Kuhlman 2009). AP-114 (evaluation and recalibration of Culebra transmissivity fields) dealt with the development and calibration of the T-fields (including *T*, storativity (*S*), horizontal anisotropy (*A*), and vertical recharge (*R*)), in addition to development of T-field acceptance criteria. AP-144 (calculation of Culebra flow and transport) dealt with the modification of T-fields for the potential future effects of potash mining for use in the PA Culebra radionuclide transport calculations. The PA Culebra radionuclide transport calculations are not described in this Appendix, which focuses on the development and modification of the T-fields.

West of the WIPP, Culebra *T* is high where the Culebra overlies areas where the Salado Formation has been removed by dissolution (mostly in Nash Draw). East of the WIPP, Culebra *T* is low when the Culebra is bounded either above *or* below by halite in adjoining Rustler units. Further to the east, Culebra *T* is very low when the Culebra is bounded both above *and* below by halite in the Rustler. At the WIPP, between the high *T* in the west and low *T* in the east, Culebra *T* is observed to change significantly over short distances and is simulated in the WIPP Culebra flow model using a random mixture (i.e., stochastic patches) of high and low *T* zones, consistent with geologic and hydrologic observations. The geologic data discussed in Section TFIELD-2.0 are used to specify the boundaries of these Culebra conceptual model zones (Section TFIELD-3.0), which are then carried forward into the numerical implementation of the Culebra groundwater model (Section TFIELD-4.0).

The starting point in the T-field development process was to assemble and update information on geologic factors potentially affecting Culebra *T* (Section TFIELD-2.0). These factors include dissolution of the upper Salado Formation located below the Culebra, presence of gypsum cements, the thickness of overburden above the Culebra, and the spatial distribution of halite in the Rustler Formation both above and below the Culebra. Geologic information is available from hundreds of oil and gas wells and potash exploration holes in the vicinity of the WIPP site, while estimates of Culebra *T* are available from only 64 well locations. Details of the geologic data compilation are given in Powers (Powers 2002a, Powers 2002b and Powers 2003), updated in Powers (Powers 2007a and Powers 2007b), and summarized in Section TFIELD-2.0.

A two-part geologically based approach was used to generate base Culebra T-fields. In the first part (Section TFIELD-3.0), a conceptual model for geologic controls (i.e., soft data) on Culebra *T* was formalized and the hypothesized geologic controls were regressed against Culebra *T* estimates at monitoring wells to determine linear regression coefficients. The regression includes one continuously varying function, Culebra overburden thickness, and three indicator functions that assume values of 0 or 1 depending on the occurrence of open, interconnected fractures; Salado dissolution; and the presence or absence of halite in Rustler units bounding the Culebra.

In the second part (Section TFIELD-4.0), a method was developed for applying the linear regression model to predict Culebra *T* across the WIPP model area between the sparse observations at wells. The regression model was combined with the maps of geologic factors to create 1,000 stochastically varying base Culebra T-fields. Details about the development of the regression model and the creation of the base T-fields are given in Hart et al. (Hart et al. 2008). The conceptual model embodied in these 1,000 base Culebra T-fields was subject to peer review before model calibration proceeded (Section TFIELD-3.7). The peer review panel concluded the justification and scientific rigor of the methodology for preparing base T-fields were adequate (Burgess et al. 2008). A sample of 200 out of the 1,000 created base T-fields were calibrated following the process outlined in Section TFIELD-5.0, with the 100 best calibrated T-fields eventually chosen for use in PA radionuclide transport calculations.

Section TFIELD-5.0 presents details on the modeling approach used to calibrate the T-fields to both steady-state heads across the model domain and transient drawdown measurements from multi-well pumping tests. Heads measured in 42 Culebra observation wells around May 2007 were used to represent steady-state conditions in the Culebra, and drawdown responses in 67 total observation wells (62 unique locations) across nine pumping tests were used to provide transient calibration data. See Appendix HYDRO-2014 for more information on the Culebra monitoring well network and recent trends observed in Culebra water levels. Details on the steady-state heads are described in Johnson (Johnson 2009a and Johnson 2009b), and the transient drawdown data are summarized in Hart et al. (Hart et al. 2009). Assumptions made in modeling, the definition of an initial head distribution, assignment of boundary conditions, discretization of the spatial and temporal domain, weighting of the observations, and the use of PEST (Doherty 2000) with MODFLOW-2000 to calibrate the T-fields using a pilot-point method are described in detail in Hart et al. (Hart et al. 2009) and summarized in Section TFIELD-5.0. Section TFIELD-5.3.4 addresses the development and application of acceptance criteria to select the 100 best T-fields from the 200 calibrated T-fields. Acceptance was based on a combination of objective fit to both the steady-state and transient pumping test calibration data. Section TFIELD-5.4 provides summary statistics and other information for the 100 T-fields that were judged to be acceptably calibrated. Attachment A presents *T*, *S*, diffusivity (*D)*, and model-predicted flow speed for each of the chosen 100 realizations.

The data used in the construction (Sections TFIELD-3.0 and TFIELD-4.0) and calibration (Section TFIELD-5.0) of the T-fields were divided into three groups:

1. soft data only used in base T-field generation,
2. hard data used in both T-field generation and calibration, and
3. hard data only used in calibration.

This first group included geologic data (i.e., Salado dissolution, presence of gypsum cements in the Culebra, Culebra overburden thickness, and the locations of Rustler halite margins) and hydrologic

data (i.e., pairs of pumping and observation wells interpreted to have high diffusivity from multi-well pumping tests). The soft data were included in T-field generation because they were used to define boundaries also used in the calibration phase. The second group only included estimated *T* from single-well pumping tests, which were used directly in indicator kriging, indirectly in the overburden regression analysis, and directly as fixed pilot points in the calibration phase. The third group only included head and drawdown observations used as calibration targets. Some of these third group data were used in other analyses to estimate diffusivity values used as soft data (first group), but the drawdown data from multi-well pumping tests only appeared directly in the calibration phase.

Section TFIELD-6.0 discusses modifications of the T-fields performed to account for the effects of potash mining both within and outside the WIPP land withdrawal boundary. Potentially mining-affected areas were delineated, random transmissivity multipliers were applied to the transmissivity field in those areas, and particle tracks and travel times were computed (Kuhlman 2010). The flow fields produced by these mining-affected T-fields were input to the radionuclide transport model SECOTP2D used to compute both CRA-2009 PABC and CRA-2014 long-term PA releases (Appendix PA-2014). Section TFIELD-7.0 provides an executive summary of the development and modification of the Culebra T-fields.

TFIELD-2.0 Geologic Data

The work outlined in Section TFIELD-2.0 was performed as Task 1 under AP-114, Analysis Plan for Evaluation and Recalibration of Culebra Transmissivity Fields (Beauheim 2008). There were no changes to the model between CRA-2009 PABC and CRA-2014. Geologic data were updated to improve definition of geologic boundaries used to define zones as part of the process of creating new T-fields. Geologic boundaries were refined for CRA-2009 PABC using data from field investigations and newly obtained oil and gas well log data (Section TFIELD-2.2). The Salado dissolution margin bounds the high-*T* Culebra zone to the west in Nash Draw, and was only modified slightly for CRA-2009 PABC. The Rustler halite margins bound the very low-*T* Culebra zone to the east, and were modified significantly for CRA-2009 PABC. The confinement of the Culebra in the southeastern portion of Nash Draw was also investigated in AP-114 Task 1, to constrain the Culebra flow model inputs (Section TFIELD-2.3). Previous to CRA-2009 PABC, the Culebra groundwater flow model was only steady-state and did not include input parameters related to confinement or recharge. A model was developed regarding distribution of gypsum cements in the Culebra from available core data (Section TFIELD-2.3.3).

TFIELD-2.1 Culebra Hydrogeologic Setting

The Culebra Member of the Rustler Formation is considered as a potential long-term release pathway in WIPP PA because it is the most permeable laterally continuous geologic unit above the WIPP repository level (see Figure TFIELD 2-1 for general stratigraphy). Potential future human intrusion into the repository might connect the repository with the Culebra, which would then transport radionuclides to the accessible environment under natural flow conditions. The accessible environment is defined to be where the WIPP Land Withdrawal Boundary (LWB) intersects the Culebra in the subsurface.

The ability of the Culebra to advect groundwater and radionuclides to the accessible environment is affected by both depositional and post-depositional effects. The Culebra is believed to have been deposited quite uniformly over a wide area (the vertical thickness of the Culebra is quite uniform over lateral distances of many miles (e.g., Holt and Powers 1988)), but depositional effects include the presence of mudstone or halite layers in the Rustler Formation immediately above and below the Culebra. Post-depositional processes include dissolution of halite from the underlying Salado Formation and precipitation of vug- and pore-filling evaporates within the Culebra (see Figure TFIELD 2-2).

Understanding of the spatial distribution and thickness of halite in the Rustler Formation was improved for CRA-2009 PABC (compared to CRA-2009 (U.S. DOE 2009)) due to data obtained from analysis of geophysical logs from oil and gas wells. The lateral extent of Salado dissolution was modified slightly for CRA-2009 PABC, but remained largely similar to CRA-2009, with minor adjustments due to additional information for a few new WIPP wells (Powers 2007a and Powers 2007b).

Groundwater flow in the Culebra is generally from north to south at the WIPP site. Water levels in Culebra wells in Nash Draw (several miles to the west of the WIPP site) respond more rapidly to precipitation and behave differently than Culebra wells in the immediate vicinity of the WIPP site (Appendix HYDRO-2014, Section 7.1). Based on the north-south gradient currently observed at the WIPP, particle-tracking predictions from the WIPP waste panels through the Culebra result in flow towards the southern edge of the WIPP LWB.

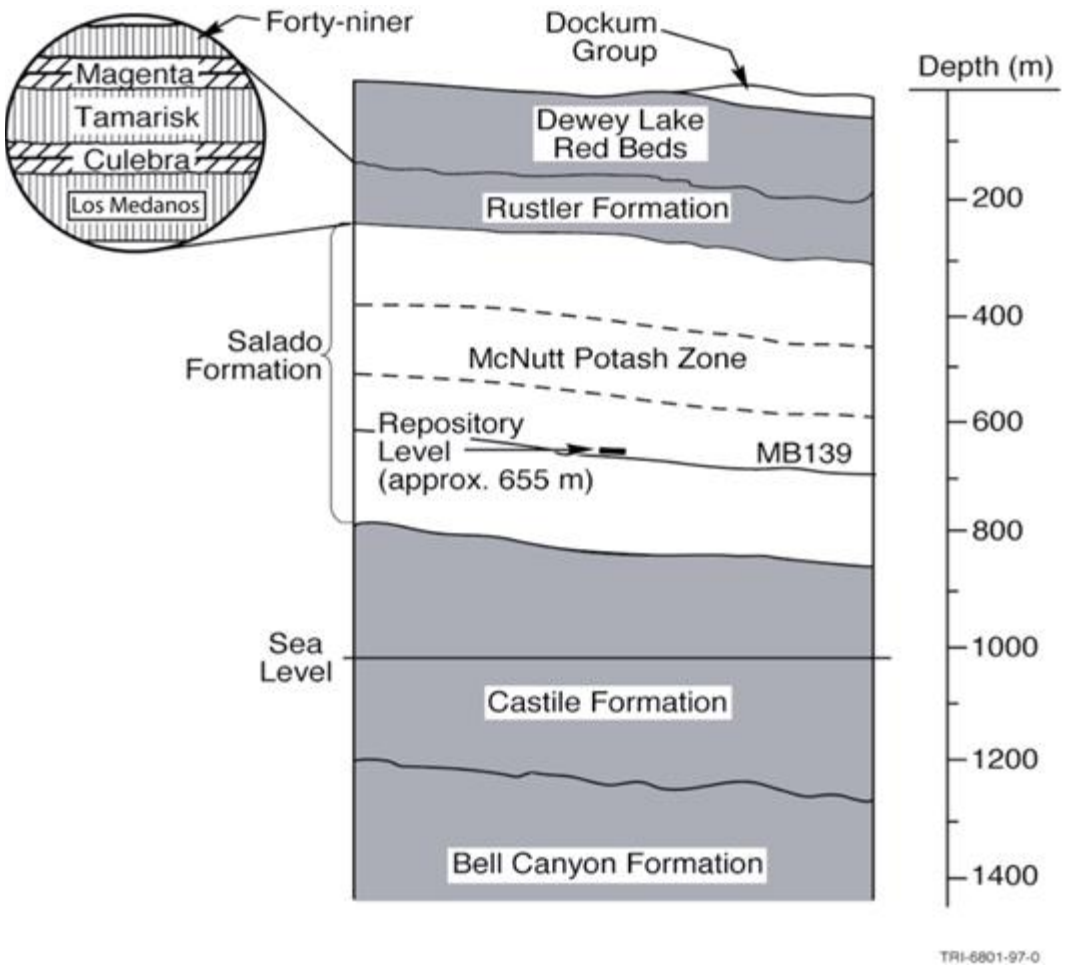

Figure TFIELD 2-1. Generalized Stratigraphy Near the WIPP

TFIELD-2.2 Refinement of Geologic Boundaries

The locations of the Rustler halite margins (Section TFIELD-2.2.1) and the Salado dissolution margin (Section TFIELD-2.2.2) both affect the conceptual model of Culebra *T* (see Figure TFIELD 2-1 for general relationships between the Rustler, the Salado and the WIPP repository). These were updated as part of the CRA-2009 PABC geologic study.

The presence of halite in the non-dolomite members of the Rustler Formation correlates strongly with estimates of Culebra *T*. Halite and anhydrite are found as pore-filling cements in the Culebra (reducing open fractures) when halite exists in layers above the Culebra, below the Culebra, or both (Figure TFIELD 2-2). When halite is found either above (H3) *or* below (H2) the Culebra, observed Culebra *T* is low. When halite exists both above *and* below the Culebra, observed Culebra *T* is extremely low.

North, south and west of the WIPP site, Cenozoic dissolution has affected the upper Salado Formation. Where this dissolution has occurred, the rocks overlying the Salado, including the Culebra, are strained (leading to larger apertures in existing fractures), fractured, collapsed, or brecciated (e.g., Beauheim and Holt 1990). All WIPP Culebra wells within the Salado dissolution zone have been interpreted to have high *T*. It is hypothesized that all regions affected by Salado dissolution have well-interconnected fractures and therefore high *T*.

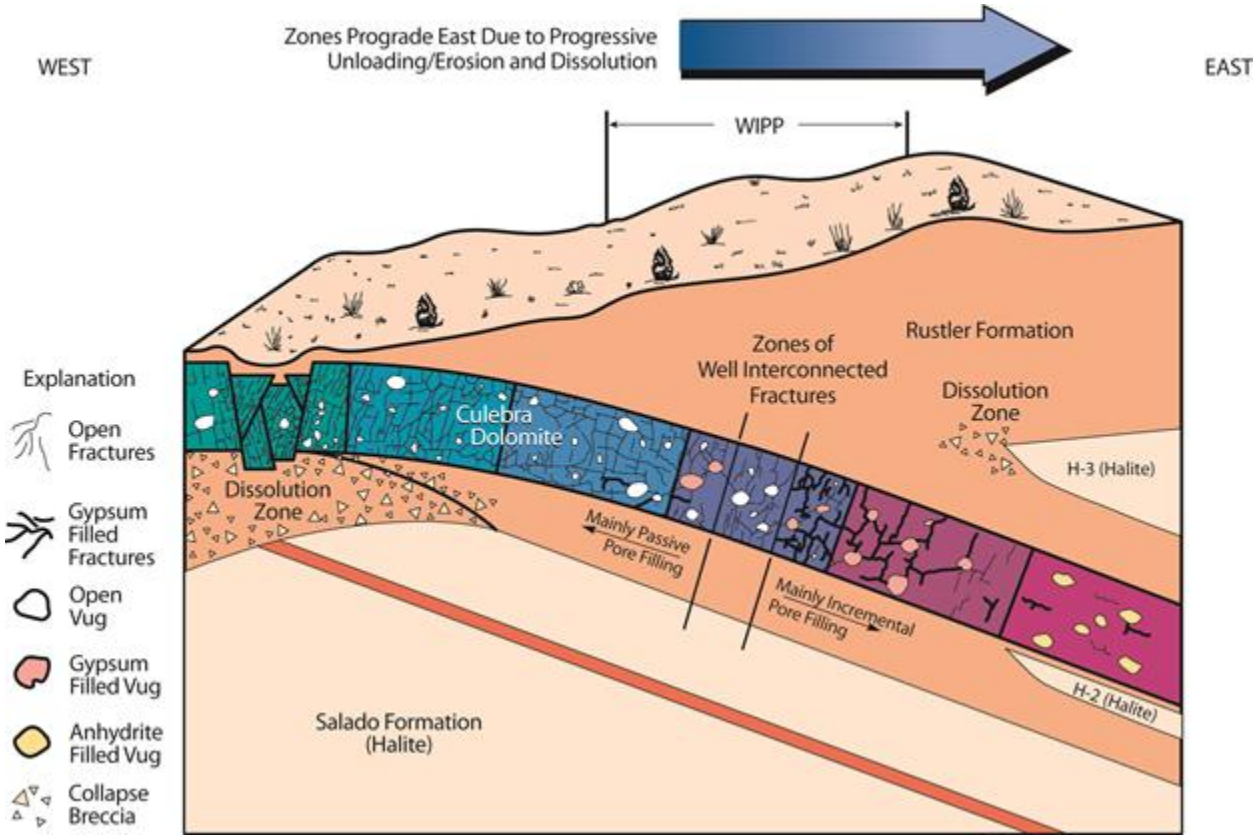

Figure TFIELD 2-2. WIPP Culebra Dolomite Conceptual Model. Culebra *T* decreases to the east (increasing overburden and halite) and increases to the west (fracturing due to underlying Salado dissolution). Halite appears both above (H-3) and below (H-2) the Culebra in the east. Primary groundwater flow direction through the Culebra is south.

TFIELD-2.2.1 Rustler Halite Margins

The Rustler Formation stratigraphic column given in Figure TFIELD 2-3 shows two types of geologic variability. Vertical stratigraphy places older formations below younger formations at the same location in space (e.g., the Los Medaños Member is older than the Culebra Member), while facies change place two units of similar age at different spatial locations, due to changes in depositional environments (e.g., Mudstone 4 (M4) and Halite 4 (H4) of the Forty-niner Member are of the same age, but occur in different locations).

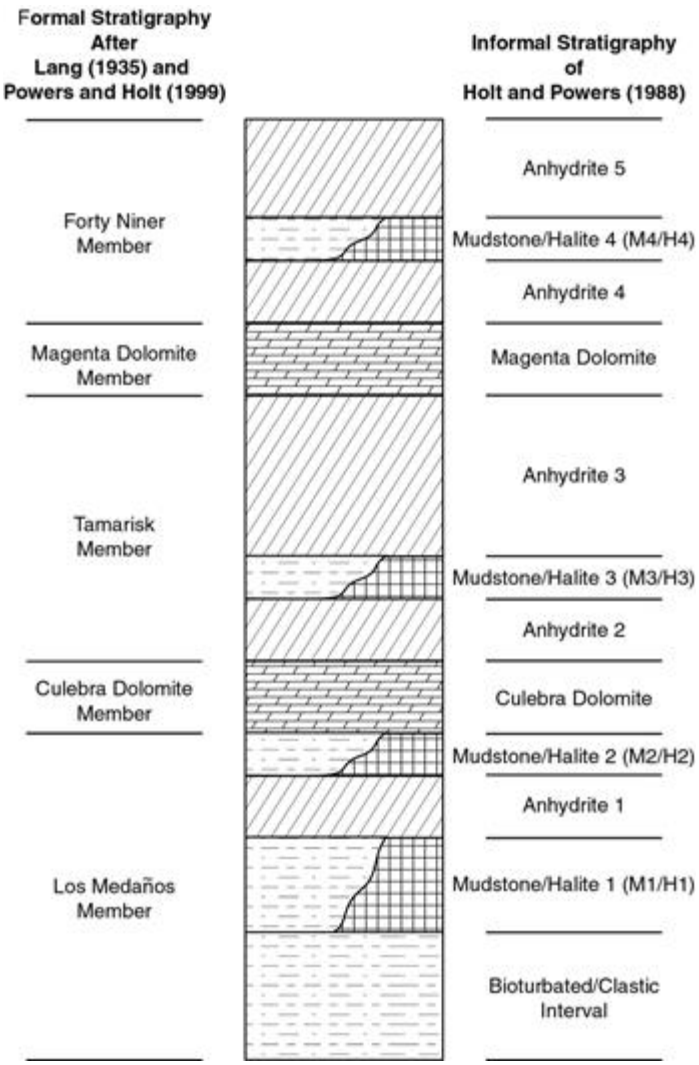

Figure TFIELD 2-3. Rustler Formation Stratigraphic Nomenclature

Powers (Powers 2002a and Powers 2002b) provided geologic data across the CRA-2004 PABC Culebra modeling domain that included maps of halite margins within the Rustler Formation. Those margins were largely based on work in Powers and Holt (Powers and Holt 1995), modified by some data collected from potash drillholes, especially in the northern area of the Culebra modeling domain. The observed distribution and thickness of halite in the Rustler is interpreted to be the result of sedimentary structures and facies relationships controlled by deposition, rather than the result of dissolution alone (Holt and Powers 1988; Powers and Holt 1999; Powers and Holt 2000). Before Holt and Powers (Holt and Powers 1988), many researchers incorrectly believed a uniform thickness of Rustler halite was deposited and later removed by dissolution in the areas near Nash Draw, leaving the observed mudstone layers as dissolution residue. Definitive data collected during WIPP air-intake shaft geologic mapping provided the basis for the current facies-based conceptual model used at the WIPP (Holt and Powers 1988). Some minor zones adjacent to the depositional margins have been interpreted as having undergone some post-depositional dissolution of halite, specifically the halite in the Tamarisk Member, but the extent of this Rustler halite dissolution is relatively minor (Beauheim and Holt 1990).

Significant changes to the locations of the M3/H3 and M2/H2 margins have been made for CRA-2009 in some areas since CRA-2004 (U.S. DOE 2004) as part of Task 1A of AP-114. The Rustler halite

margins used since CRA-2009 PABC are shown over a wide area in Figure TFIELD 2-4 through Figure TFIELD 2-7, as defined in Powers (Powers 2007a and Powers 2007b). Changes in the location of the halite margins were based mostly on newly obtained geophysical log data obtained from oil and gas exploration (both new and old wells), and a few hydrologic wells drilled by the WIPP program since 2003 (Powers 2007a).

Wells H-17 and H-12 (see Figure TFIELD 2-8), located where halite occurs in the Tamarisk Member (H3 interval; Figure TFIELD 2-6) but not in the Los Medaños Member (M2 interval; Figure TFIELD 2-5) of the Rustler Formation show low transmissivity. We assume high-transmissivity zones do not occur in the Culebra where H2 or H3 also occur. Margins near the WIPP remain nearly unchanged, and all modifications to the margins do not change the basic interpretation that the margins are the result of deposition and local syndepositional dissolution of halite, not regional halite dissolution from the Rustler (Holt and Powers 1988; Powers and Holt 2000; Powers et al. 2006). Core evidence from well SNL-8 shows limited brecciation of anhydrite 3 in the Tamarisk (Figure TFIELD 2-3) that is interpreted as an extension of a narrow margin along the H-3 margin where a limited amount of halite was dissolved after deposition (Powers 2009).

After refining the Rustler halite margin locations, all mudstone/halite margins now show similar gross trends (compare Figure TFIELD 2-4 through Figure TFIELD 2-7 and Figure TFIELD 2-8). Southeast of the WIPP, the margins are elongate roughly northwest to southeast. The gross trends of these margins are similar to the trend in the elevation of the top of Culebra (Figure TFIELD 2-9). As previously described (e.g., Holt and Powers 1988); Powers et al. (Powers et al. 2003), this northwest-to-southeast trending anticlinal feature is called the Divide anticline. Mudstone dominates along this trend in three of the mudstone-halite units of the Rustler (i.e., all except M1/H1).

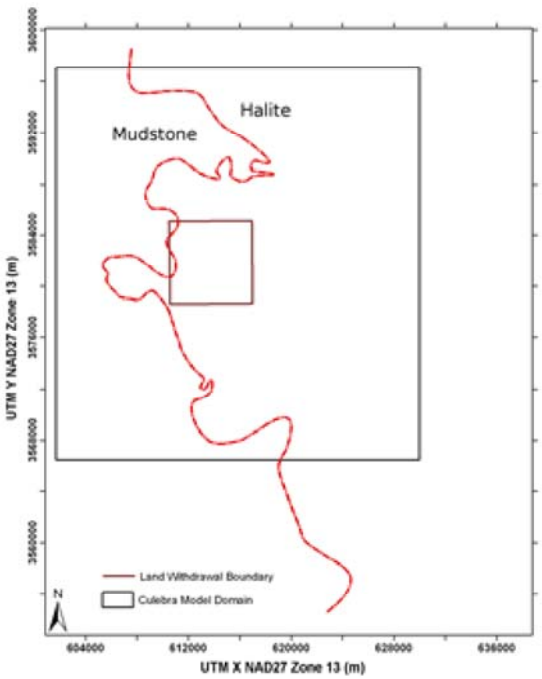

Figure TFIELD 2-4. M-1/H-1 Halite Margin In the Lower Los Medaños Member

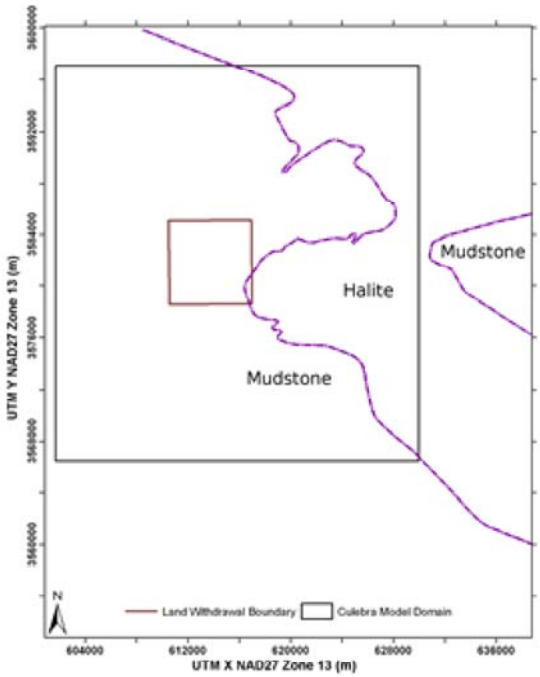

Figure TFIELD 2-5. M-2/H-2 Halite Margin In the Upper Los Medaños Member

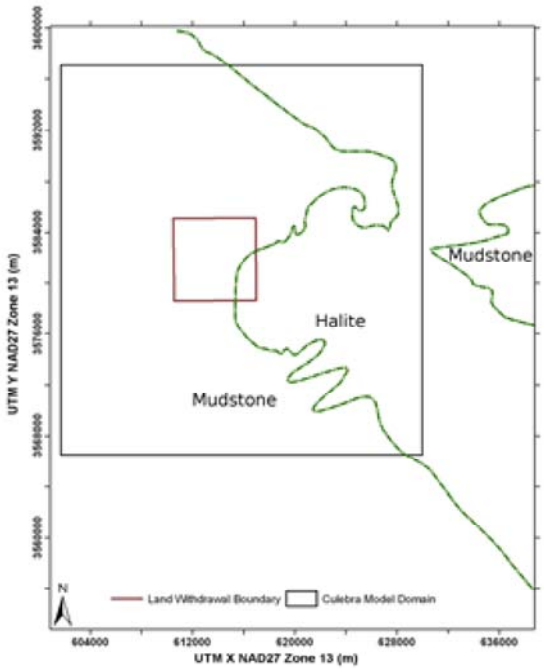

Figure TFIELD 2-6. M-3/H-3 Halite Margin In the Tamarisk Member

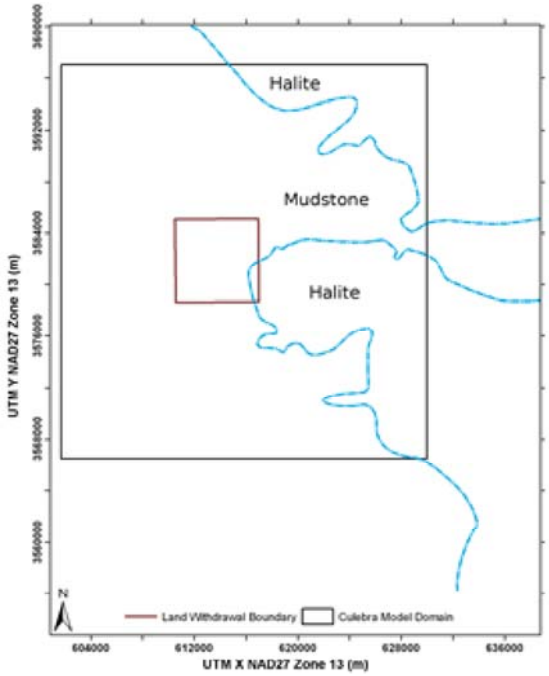

Figure TFIELD 2-7. M-4/H-4 Halite Margin In the Forty-niner Member

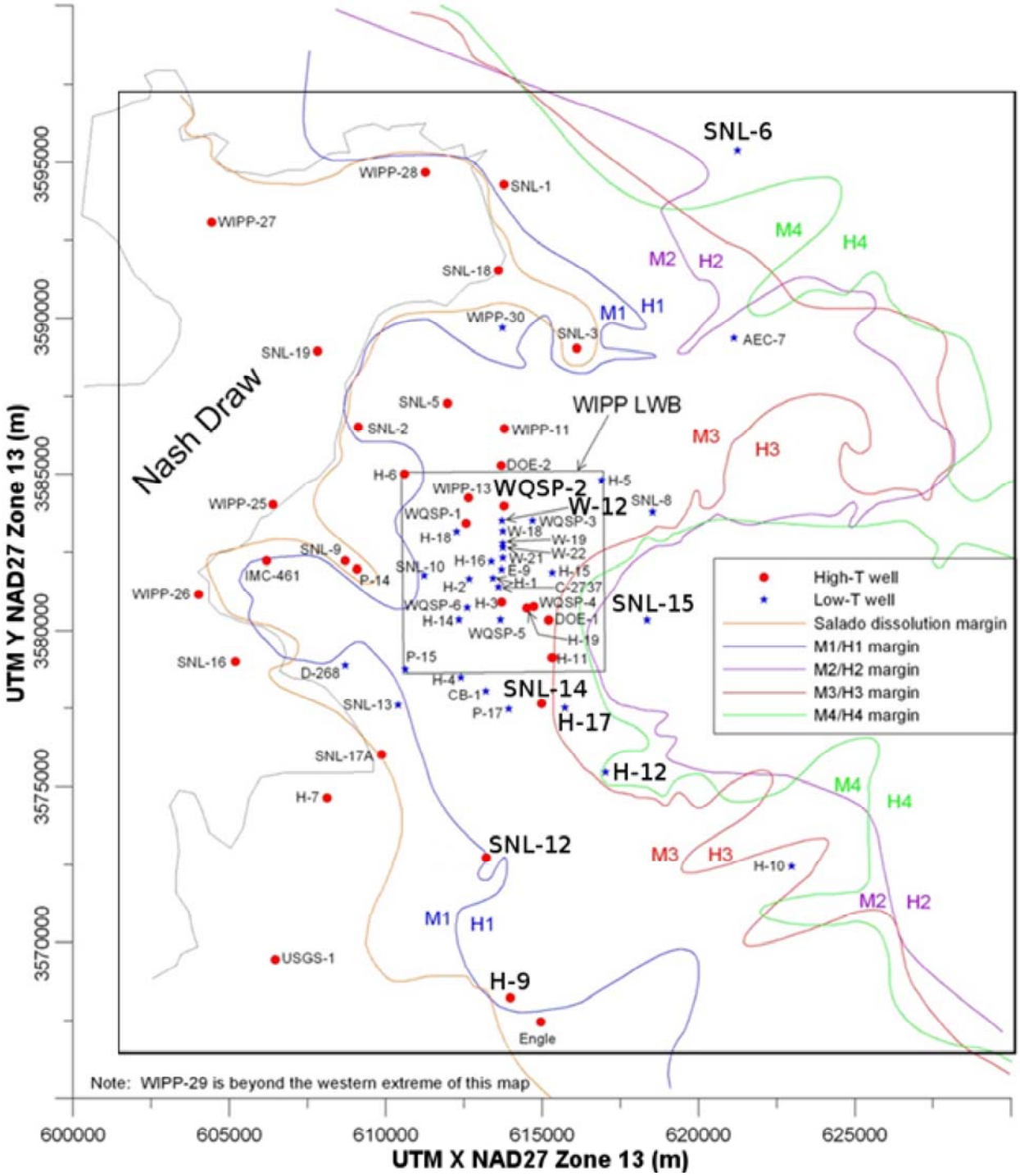

Figure TFIELD 2-8. Salado Dissolution Margin and Rustler Mudstone/Halite (M/H) Margins. WIPP Culebra wells with high or low transmissivity (*T*) are indicated. WIPP Culebra model extents indicated with large black rectangle. Wells mentioned in text are labeled using larger font.

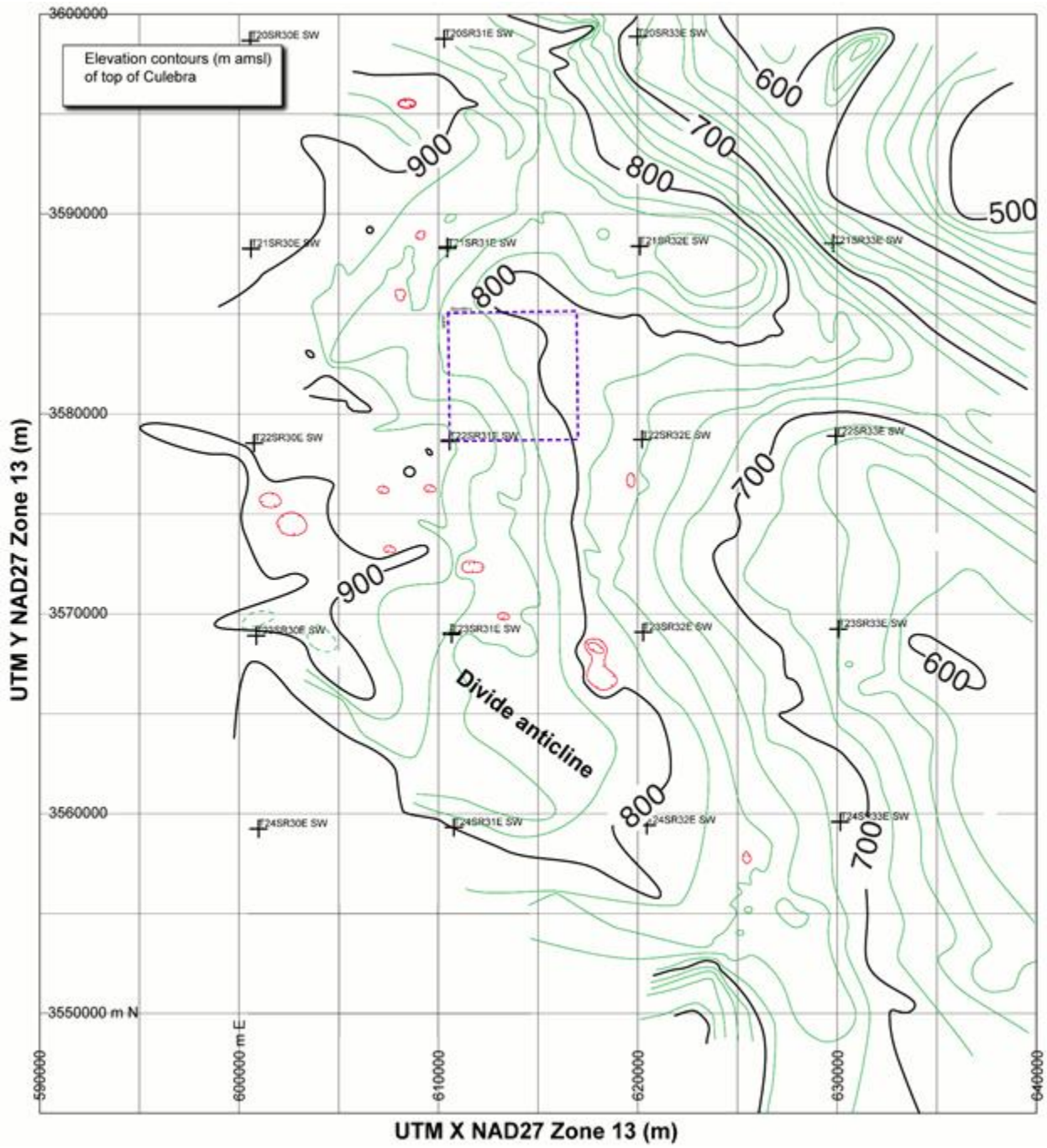

Figure TFIELD 2-9. Top Elevation (m Above Mean Sea Level (AMSL)) of the Culebra. WIPP LWB indicated with blue dashed line. Township (T) and Range (R) corners indicated with crosses.

TFIELD-2.2.2 Salado Dissolution

A margin marking the lateral extent of significant dissolution of upper Salado Formation halite for CRA-2004 PABC was inferred from significant local changes in thickness of the interval between the Culebra Dolomite and the Vaca Triste Sandstone Member of the Salado (Powers 2002a and Powers 2002b). For CRA-2009 PABC, the margin was modified to reflect information indicating embayments of the dissolution margin. Additional data were added south of the WIPP, with log cross

sections, to delineate the margin more accurately (Powers 2003). Some of these data are reflected in the simplified maps included in Powers et al. (Powers et al. 2003) and Holt et al. (Holt et al. 2005).

The Salado dissolution margin was updated for CRA-2009 (see Appendix G from the Analysis Report for Task 5 of AP-114 (Hart et al. 2008)) based on reinterpretation of geophysical borehole logs from oil and gas wells in the vicinity of H-9, which were not available for CRA-2004 PABC. This analysis placed H-9 east of the dissolution line, where previously it was considered to be within the area affected by Salado dissolution. The Salado dissolution margin is shown with the Rustler halite margins in Figure TFIELD 2-8, reflecting the change near H-9.

TFIELD-2.3 Confinement and Recharge in the Culebra

Field and map studies were performed to identify potential recharge locations south and west of the WIPP in the southeastern arm of Nash Draw (Powers 2006). This work also identified Culebra unconfined regions in the same geographic area. The boundaries to the west and south correspond to the model domain; the northern and eastern boundaries included the southeastern arm of Nash Draw and an area beyond the apparent eastern extent of the draw.

Five elements were identified as contributing to understanding recharge, which might be useful for modeling the possible effects of recharge to the Culebra in the study area:

1. extent of and relationship between surface drainage basins,
2. areas with differing Culebra confinement,
3. location and character of drainage channels within drainage basins,
4. location of specific recharge points (e.g., sinkholes), and
5. soil characteristics and rainfall infiltration across the study area.

Of these, the estimate of Culebra confinement is the most interpretive element. Drainage basins, channels and specific points of recharge are identified using surface topography features identifiable from maps, aerial photos, or field reconnaissance. Existing maps of soils, combined with surface reconnaissance and aerial photographs, permitted relatively direct assignment of soil properties controlling runoff. The degree of confinement of the Culebra in the study area, however, was not directly determinable from the surface data. As a result, a variety of surface features and well data were combined to estimate areas where the Culebra is less confined compared to conditions at the WIPP site, where there are more well-test and drillhole data.

TFIELD-2.3.1 Surface Drainage Basins

Drainage basin size and characteristics are important elements to determine how rainfall, infiltration, and runoff may contribute to recharge of near-surface Rustler hydrologic units in Nash Draw. Topographic maps, aerial photographs, and some field checking were used to define separate surface drainage basins.

The drainage basins are mainly separated by topographic divides and local lows or concentration points that can be distinguished on 7.5-minute quadrangle topographic maps supplemented by study of aerial photographs. Because Nash Draw is an area of significant evaporite karst (e.g., Powers and Owsley (Powers and Owsley 2003)), collapse features, caves, or sinkholes may capture local drainage

in smaller basins or subbasins wholly enclosed by another basin (Figure TFIELD 2-10). An example is drainage basin 7, which is wholly enclosed in drainage basin 6 (Figure TFIELD 2-10). These quite localized closed drainage basins in Nash Draw represent potential recharge locations for the Rustler Formation. Mapping the basins is the first step in understanding the complex geology and hydrology inside Nash Draw, which expresses itself as water-level fluctuations in some Culebra wells in and near Nash Draw (see hydrographs and references in Appendix HYDRO-2014).

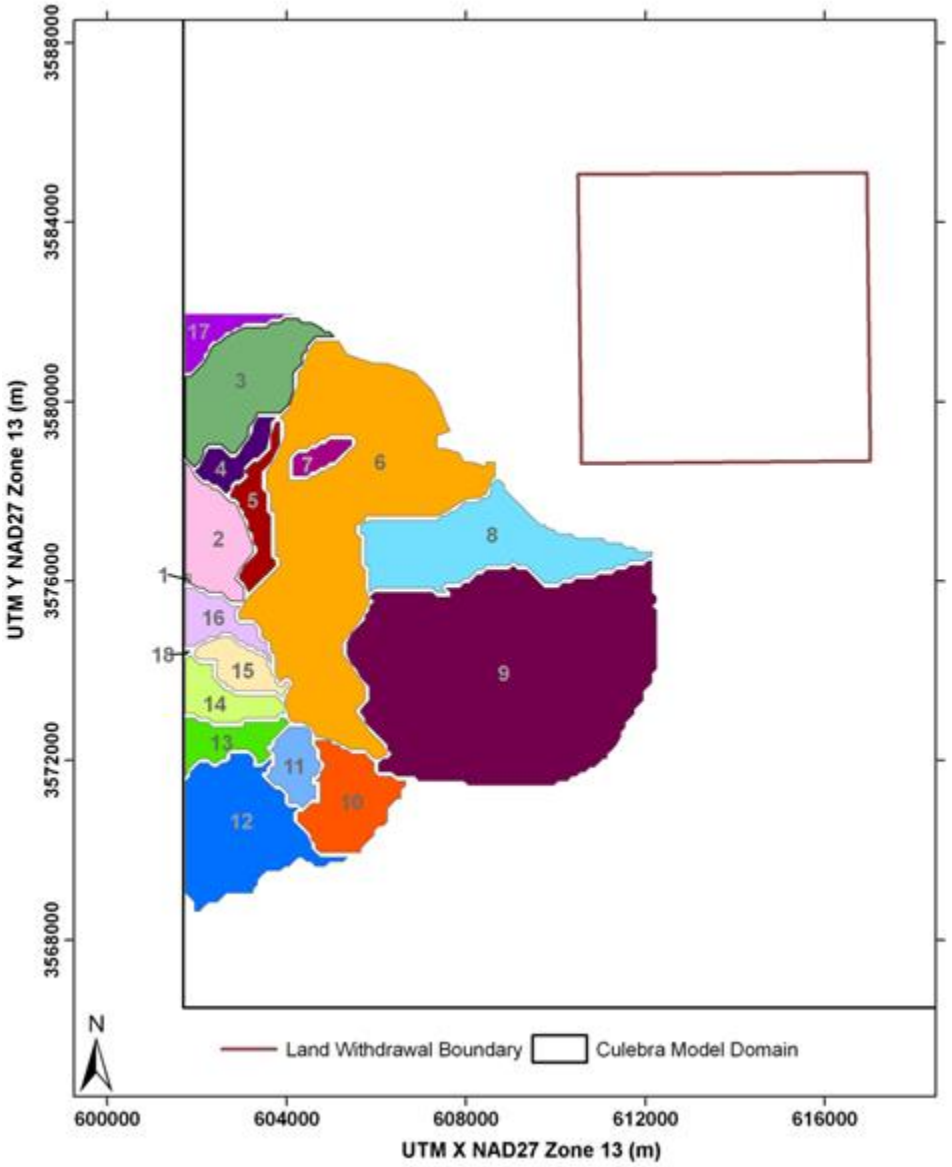

Figure TFIELD 2-10. Closed Drainage Sub-basins Identified in Southeastern Nash Draw. White areas are either outside Nash Draw or the study area.

TFIELD-2.3.2 Culebra Confinement

Across the WIPP site, the Culebra can be considered confined, with little potential for direct vertical recharge for the relatively short time period covered in the WIPP Culebra model calibration (i.e., the length of multi-well pumping tests). Within portions of Nash Draw, the Culebra is very shallow (i.e., only covered by portions of the highly fractured Tamarisk) and observed water levels show the Culebra responds to precipitation events in a very short time (Appendix HYDRO-2014). Due to the

interpretative nature of the confinement estimate, no numerical values of storativity were predicted from this geologic analysis, only zones of relatively higher or lower confinment, with an intermediate transition zone. The confined area has a relatively unambiguous definition, whereas the boundary between transition and unconfined is much more subjective.

The area of the Culebra considered confined (red in Figure TFIELD 2-11) is defined approximately by the interpreted margin of upper Salado halite dissolution (Powers et al. 2003). There is a significant increase in Culebra *T* values west and south of this margin, and this change is attributed to changes in fracture aperture associated with strain induced by dissolution. The transition zone (green in Figure TFIELD 2-11) includes areas where some data from wells indicate there is some vertical isolation of the Culebra, but information is less conclusive.

Most of the Culebra unconfined zone (blue in Figure TFIELD 2-11) is in central Nash Draw and out of the AP-114 Task 1 study area. The strategy for estimating relative Culebra confinement was to select areas where the Culebra is known or believed to be very shallow (≤30 meters (m) below ground surface) and where observed recharge points (caves, sinkholes, alluvial dolines) are believed to access units below the Magenta. Some large caves and sinkholes are developed in the Tamarisk gypsum beds and have a greater likelihood of providing hydraulic connection to the Culebra than similar openings in the Forty-niner gypsum beds. Many potash exploration holes within Nash Draw encountered lost-circulation zones, but the stratigraphic relationships of these zones to the Culebra are not well constrained. Thus, apart from the location from Livingston Ridge (the escarpment marking the eastern edge of the surface expression of Nash Draw) and the upper Salado dissolution margin, the factors determining confinement of the Culebra are generally qualitative.

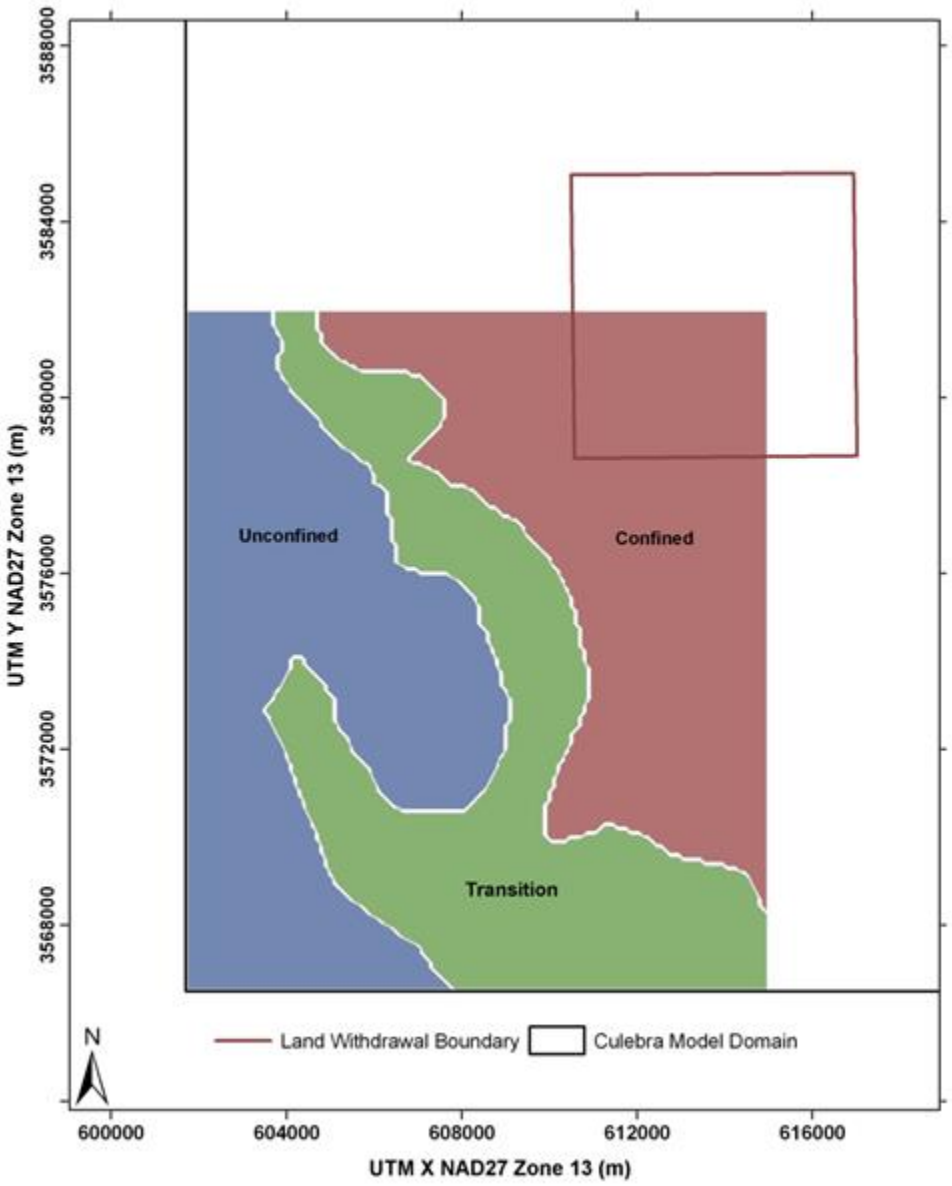

Figure TFIELD 2-11. Culebra Confinement Map for Southern Nash Draw Study Area. White areas are outside the Nash Draw geologic study area. Zones are shown over the entire model area in Figure TFIELD 5-3.

TFIELD-2.3.3 Gypsum Cements in the Culebra

The amount of gypsum cements in fractures and vuggy porosity within the Culebra is believed to be inversely related to Culebra *T* (Beauheim and Holt 1990). They postulated gypsum fracture fillings limited Culebra *T* by closing fracture apertures, filling critical fracture junctions. The postulated relationship remained qualitative because too few well locations had both measured T values and describable core. Since 1990, the Culebra has been cored and hydraulically tested at 24 additional locations, providing sufficient data to construct a quantitative model linking Culebra *T* with the presence of gypsum cements. No soft data on gypsum cements was used in T-field construction or calibration before CRA-2009 PABC.

In Appendix F of Hart et al. (Hart et al. 2008), a simple quantitative model was constructed relating Culebra gypsum content to *T*. Using units defined by Holt (Holt 1997), maps were developed to

illustrate spatial occurrence of gypsum in the Culebra. The maps used a gypsum index accounting for the relative Culebra gypsum content (Figure TFIELD 2-12 and Figure TFIELD 2-13). Using a critical value of the gypsum index, the high-*T*/low-*T* status of Culebra well locations were predicted with an accuracy >97% for WIPP well locations where both sufficient core and *T* estimates exist. These maps revealed that regions of no gypsum occur predominantly where Salado dissolution has affected the Culebra. The low-gypsum region in the southern WIPP LWB (Figure TFIELD 2-13) is similar to the high-diffusivity region defined by Beauheim (Beauheim 2007) (Figure TFIELD 4-2). Soft data were used to incorporate information about the influence of gypsum content on predicted Culebra *T*.

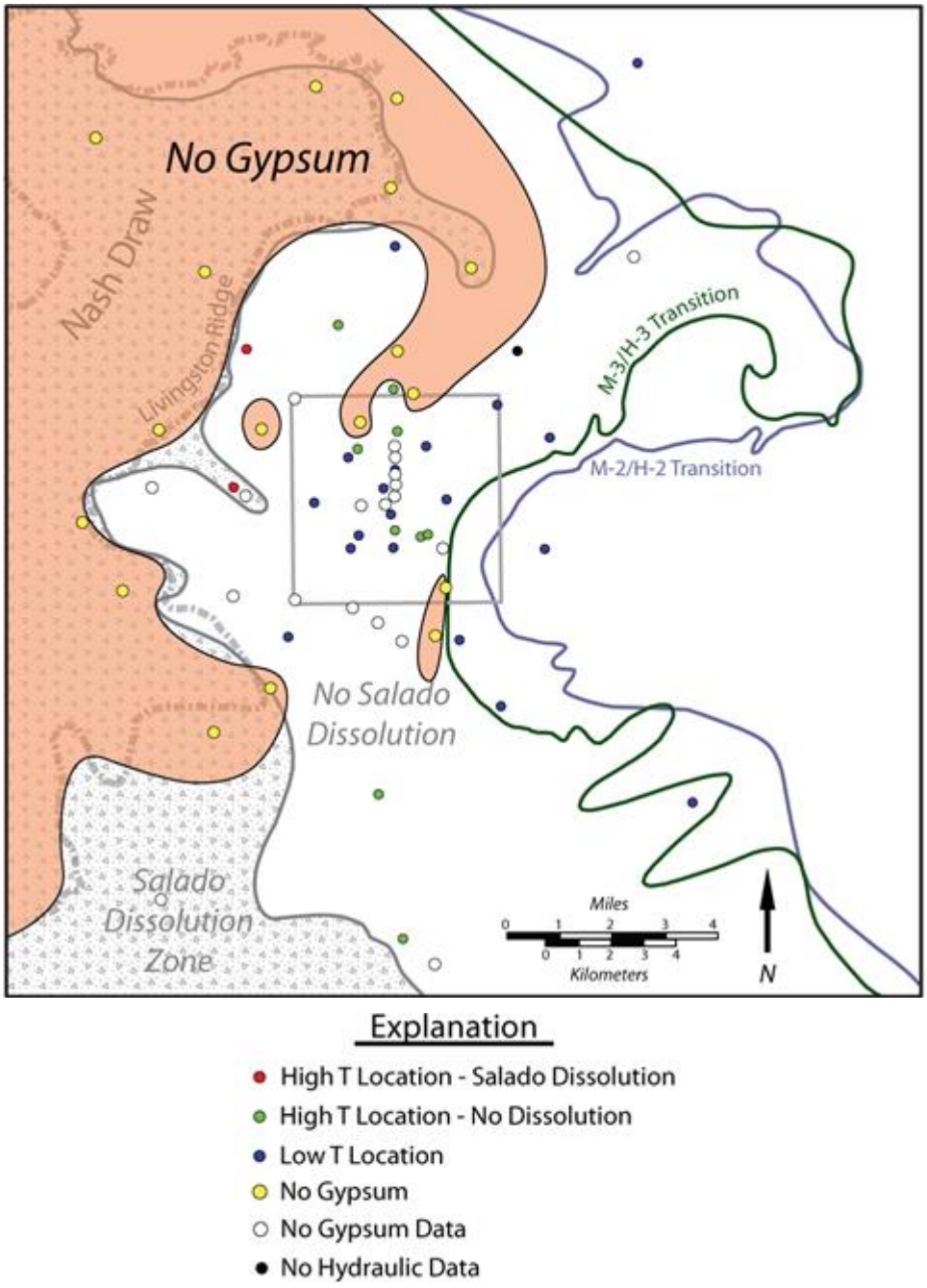

Figure TFIELD 2-12. Areas Where No Gypsum Has Been Found in Core Samples, Corresponding to a Greater Likelihood of Having Higher Culebra *T* Values

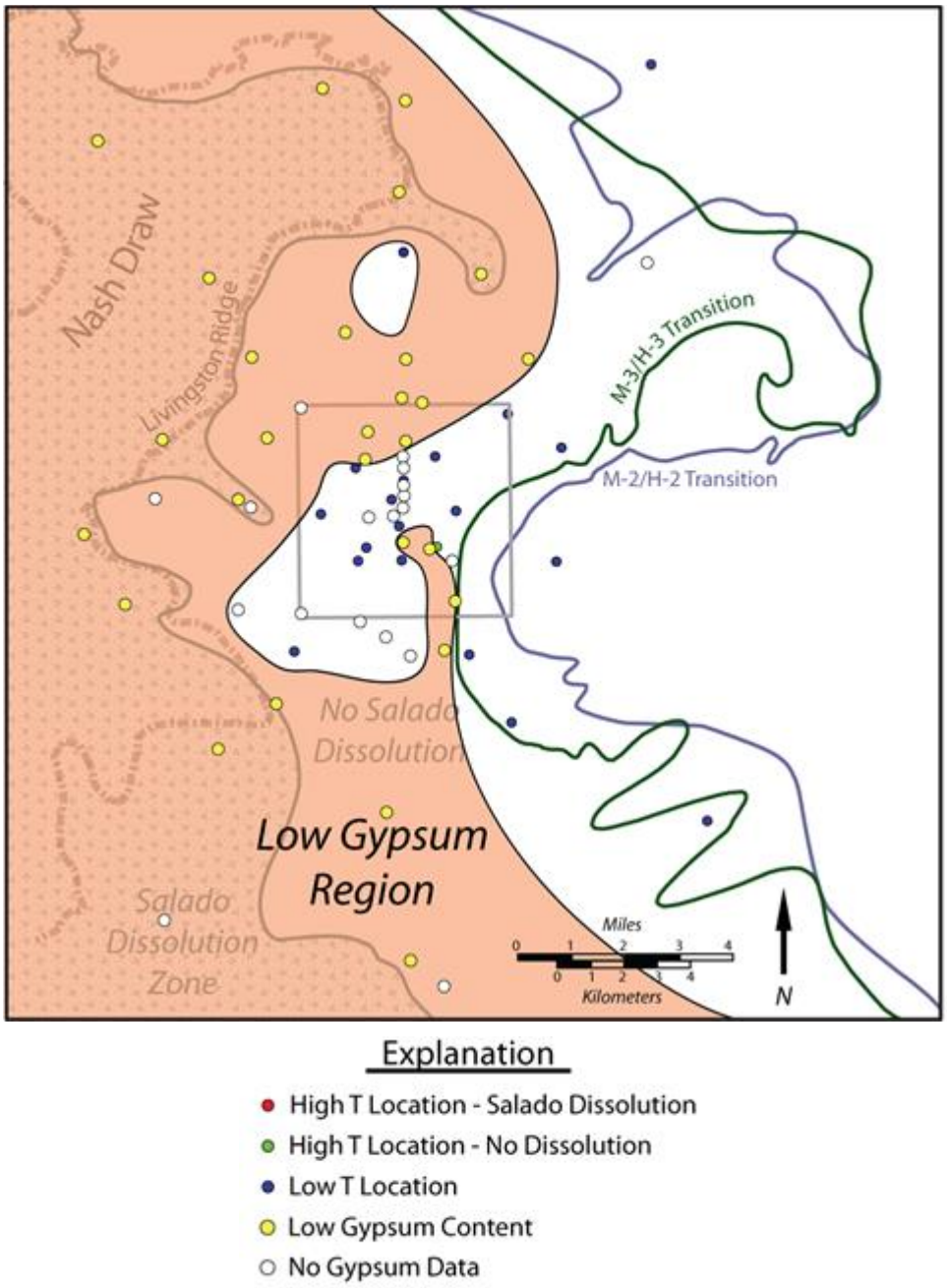

Figure TFIELD 2-13. Areas Where Wells Have Either No or Low Gypsum Content. The areas not shaded are likely to have high gypsum content and lower *T*.

TFIELD-3.0 T-Field Conceptual Model Refinement

The work outlined in Section TFIELD-3.0 was performed for CRA-2009 PABC under AP-114, Analysis Plan for Evaluation and Recalibration of Culebra Transmissivity Fields (Beauheim 2008), and still applies to CRA-2014. The conceptual model for base field creation was originally explained in Holt and Yarbrough (Holt and Yarbrough 2002), as Task 2, Subtask 1 of AP-088 for CRA-2004 PABC. Since then, the data supporting the conceptual model were updated and improved, but the model itself has changed very little. Any deviations of the CRA-2009 PABC model from the CRA-2009 model due to updates in data or process are discussed in this section. No updates have occurred for CRA-2014 since CRA-2009 PABC.

Figure TFIELD 2-2 illustrates the current geologic and hydrologic conceptual model of the Culebra dolomite in the vicinity of the WIPP site. Geologic controls on Culebra *T* were identified and a linear regression model relating these controls to *T* was constructed. The geology and geologic history of the Culebra has been described in detail elsewhere in the literature (Holt and Powers 1988; Beauheim and Holt 1990; Holt 1997). The following conceptual model was developed from this published work. Specifically, the model follows Holt (Holt 1997) in assuming variability in Culebra *T* is due strictly to post-depositional processes. Throughout the following discussion, the informal stratigraphic subdivisions of Holt and Powers (Powers 1988) are used to identify geologic units within the Rustler Formation, as listed in Figure TFIELD 2-3 and shown in map view for the Culebra model area in Figure TFIELD 2-8. The Culebra conceptual model given in this section passed a peer review (Burgess et al. 2008) before the calibration process in Section TFIELD-5.0 was begun.

It is hypothesized that Culebra *T* spatial distribution is a function of several geologic factors, some of which can be determined at a location using mapped geologic data, including:

1. Culebra overburden thickness,
2. fracture interconnection,
3. presence of gypsum cements in fractures and vuggy porosity,
4. dissolution of the upper Salado Formation below the Culebra, and
5. occurrence of halite in Rustler units above or below the Culebra.

High-*T* regions near the WIPP cannot be predicted using geologic data, as they represent areally persistent zones of well-interconnected fractures, and fracture interconnection cannot be observed or inferred from core or geophysical log data. Fracture interconnection is therefore treated as a stochastic process. Presence of gypsum cements in the Culebra, occurrence of Rustler halite, and Culebra overburden thickness instead varies slowly in space. These properties *can* be meaningfully mapped at the scale of the groundwater flow model.

TFIELD-3.1 Model Domain

The CRA-2009 PABC model domain was expanded to the east relative to the domain used for the CRA-2004 (U.S. DOE 2004) to reach an area where halite is present in all of the non-dolomite members of the Rustler Formation. This change was made to simplify the specification of the eastern boundary condition of the model. The current extent of the model domain is 601,700 to 630,000 m UTM X NAD27 and 3,566,500 to 3,597,100 m UTM Y NAD27. The domain was discretized into

100-m square cells, yielding a model 284 cells wide by 307 cells high. The Culebra was modeled as a single layer of uniform 7.75-m thickness (U.S. DOE 1996). The area covered by Figure TFIELD 2-8 corresponds to the model domain, showing the WIPP site boundary, the relevant geologic margins, and various Culebra monitoring wells. The model domain for CRA-2014 has not changed since CRA-2009 PABC.

TFIELD-3.2 Overburden Thickness

An inverse relationship was hypothesized between Culebra overburden thickness and Culebra *T*. Overburden thickness is a metric for two different controls on Culebra *T*. First, fracture apertures can be related to overburden thickness (e.g., Currie and Nwachukwu 1974), as lower *T* are found where Culebra depths are greater (Beauheim and Holt 1990; Holt 1997). Second, erosion of overburden leads to stress-relief fractures, and the amount of Culebra fracturing increases as the overburden thickness decreases (Holt 1997). The structure contour map of Culebra elevation (Figure TFIELD 2-9) has been constructed using geophysical logs from hundreds of oil and gas wells, and geologic information from more than 100 WIPP-related boreholes. The difference between the land surface elevation (as obtained from U.S. Geological Survey (USGS) topographic maps) and Culebra elevation is the overburden thickness (Figure TFIELD 3-1). Culebra overburden thickness ranges from near zero in the southern end of Nash Draw, to over 550 m in the northeastern corner of Figure TFIELD 3-1. The depth to the Culebra from the land surface defined the value of $d(x,y)$ for each cell in the Culebra model domain.

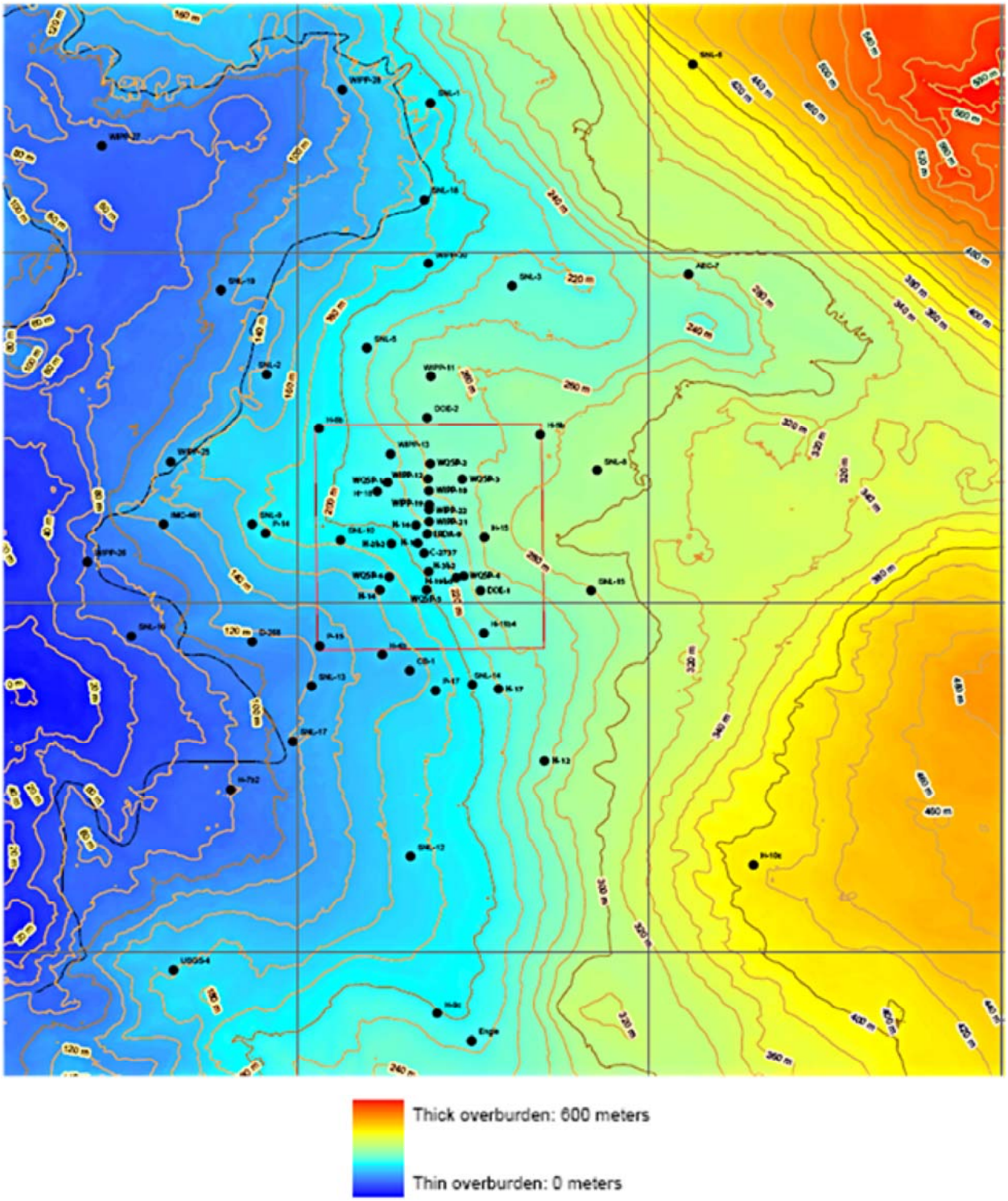

Figure TFIELD 3-1. Culebra Overburden Thickness Contours (m). Square is the WIPP LWB; irregular black outline west of WIPP is Nash Draw.

TFIELD-3.3 Fracture Interconnection

High-*T* zones within the Culebra are associated with interconnected fractures and occur randomly between areas bounded on the west by the Salado dissolution margin and on the east by H2 and/or H3 (the central area Zone 4 in Figure TFIELD 3-2). In these zones, fractures are well-interconnected, and

fracture interconnectivity is controlled by a complicated history of fracturing with several episodes of cement precipitation and dissolution (Beauheim and Holt 1990; Holt 1997). Unfortunately, no geologic metric for fracture interconnectivity was identifiable in cores or from subsurface geophysical logs, and fracture interconnectivity has only been identified from *in situ* hydraulic test data.

Because of this lack of a corresponding easy-to-map geologic metric for fracture interconnectivity, the spatial location of high-*T* zones was considered to be a stochastic process that could not be predicted deterministically. The spatial layout of these zones was simulated for CRA-2009 PABC using geostatistical indicator kriging with conditioning data (this was not changed for CRA-2014 since CRA-2009 PABC). This stochastic development of zones was a change from CRA-2004 PABC (Holt and Yarbrough 2002), where the only conditioning information was based on the *T* at wells. Information was added to the geostatistical model to increase the likelihood of high *T* being placed between two wells that hydraulic testing has revealed to be associated with larger diffusivity values. North of the WIPP site (i.e., south of WIPP-30) evidence exists for *both* high levels of gypsum in the Culebra and relatively high *D* between pumping/observation well pairs. In this unique region, the geologic conceptual model indicates there is slightly lower probability of being in a high-*T* zone than in other areas where a high *D* or high *T* estimate exists. Section TFIELD-4.2 discussed the process of merging hydraulic hard and soft data (single-well *T* estimates and multi-well *D* estimates, respectively) with geologic soft data on gypsum.

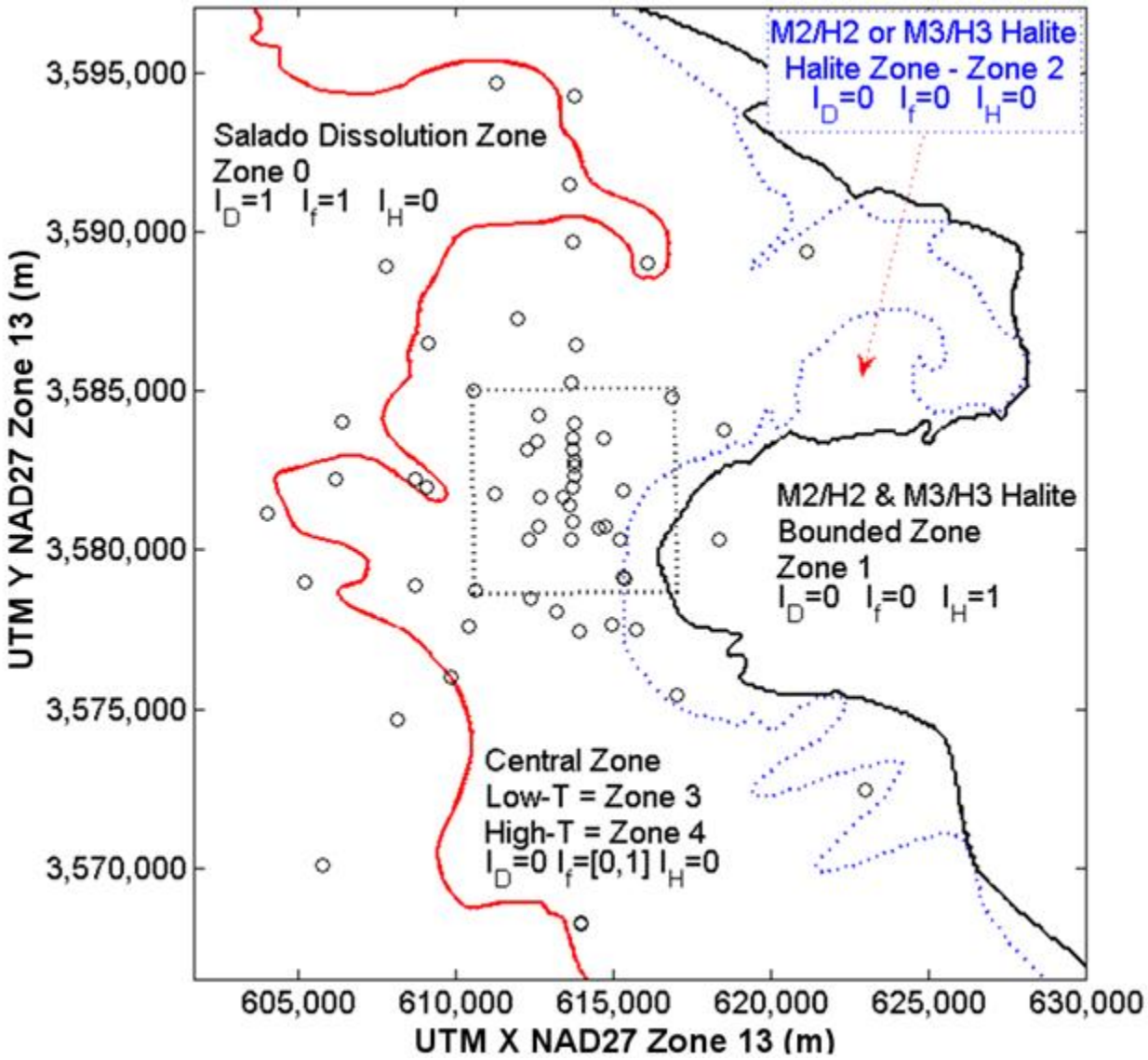

Figure TFIELD 3-2. Conceptual Model Zones With Indicator Values and Zone Numbers (Equation TFIELD 3.2). Zones 3 and 4 are distributed randomly between the Salado dissolution margin and westernmost M2/H3 or M3/H3 Rustler halite margins.

The Culebra *T* estimates at WIPP wells used in the CRA-2009 PABC modeling were the same as those used by Holt and Yarbrough (Holt and Yarbrough 2002), supplemented by more recent data reported from subsequent pumping tests (Roberts 2006 and 2007; Bowman and Roberts 2008). The $\log_{10}$ *T* data show a bimodal distribution in Figure TFIELD 3-3. Closely spaced wells sometimes show very different values; higher-*T* values are hypothesized to reflect the presence of well-interconnected fractures absent at lower-*T* locations. For example, wells WQSP-2 and WIPP-12 are only 454 m apart, but have *T* values differing by over two orders of magnitude (see blue star labeled W-12 and red circle labeled WQSP-2 in the north portion of the WIPP LWB in Figure TFIELD 2-8). Thus, the fractures present at WQSP-2 apparently do not extend to WIPP-12 or are not intersected by the WIPP-12 borehole. Well-interconnected fractures occur in regions affected by Salado dissolution (e.g., Nash Draw) and in areas with complicated cement dissolution and precipitation histories (e.g., high-*T* zones near the WIPP site). The natural break between the measured $\log_{10}$ *T* square meters per second (m^2/s) values at −5.4 (Holt and Yarbrough 2002) is illustrated with a vertical black line in

Figure TFIELD 3-3. The fracture-interconnection indicator (I_f) is defined in terms of this break (Equation TFIELD 3.1).

$$I_f = \begin{cases} 1, \log_{10} T(m^2/s) \geq -5.4 \\ 0, \log_{10} T(m^2/s) < -5.4 \end{cases} \quad \text{(TFIELD 3.1)}$$

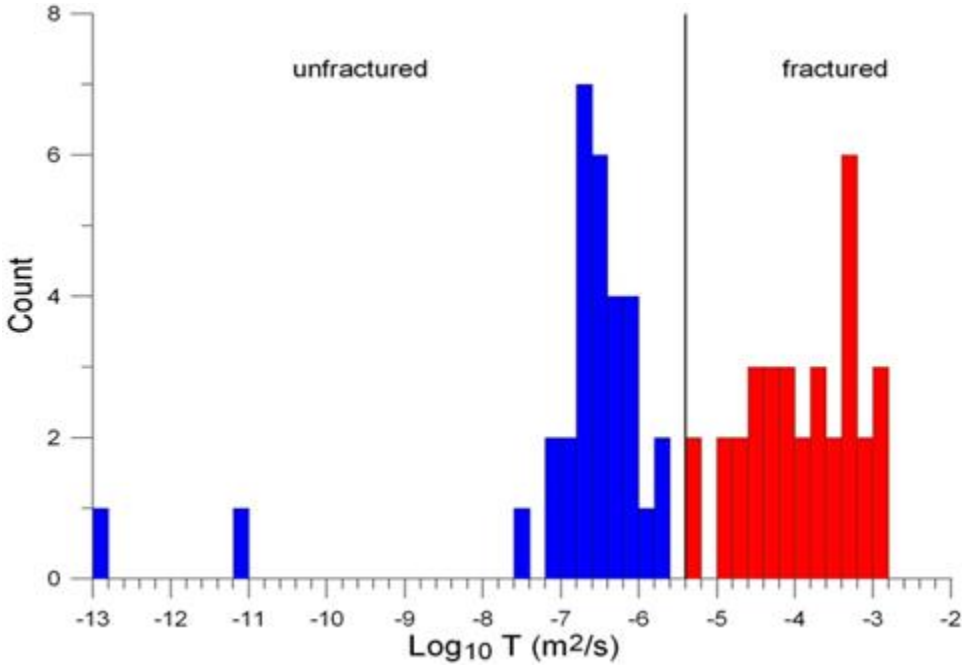

Figure TFIELD 3-3. Histogram of Log_{10} Culebra Transmissivity (T) Estimates at WIPP Wells from Single-well Tests

TFIELD-3.4 Salado Dissolution

Slight modification was made to the Salado dissolution margin used in CRA-2009 PABC, compared to CRA-2009, as outlined in Section TFIELD-2.2.2. No modifications were made for CRA-2014 since CRA-2009 PABC. The indicator variable for Salado dissolution is I_D, and was defined to be 1 in areas of the model domain where dissolution has occurred, and 0 elsewhere. The Salado dissolution margin is plotted with the Rustler halite margins in Figure TFIELD 2-8.

TFIELD-3.5 Rustler Halite Margins

The M2/H2 and M3/H3 Rustler halite margins were modified for CRA-2009 PABC compared to CRA-2009, as outlined in Section TFIELD-2.2.1. No modifications were made for CRA-2014 since CRA-2009 PABC. The margins are shown individually in Figure TFIELD 2-5 and Figure TFIELD 2-6, and together with the M1/H1 and M4/H4 Rustler halite margins and Salado dissolution margin in Figure TFIELD 2-8.

Wells SNL-6 and SNL-15 were drilled since Holt and Yarbrough (Holt and Yarbrough 2002). They are located east of the M2/H2 and M3/H3 halite margins, where halite is present in both intervals (see Figure TFIELD 2-8). As predicted by Holt (Holt 1997), the Culebra itself was partially cemented with halite at these locations, and estimated T were extremely low (Roberts 2007; Bowman and Roberts 2008). Based on these observations, Culebra T is assumed lower in the region where halite occurs

both above (in the M3/H3 interval) and below (in the M2/H2 interval), than the Culebra *T* where halite occurs in only one of these intervals. The indicator term I_H was defined to be 1 at any point where halite is present in both the M2/H2 and M3/H3 margins, and to be 0 elsewhere.

TFIELD-3.6 Transmissivity Regression Model

The following linear model for $Y(x,y) = \log_{10} T(x,y)$ was constructed

$$Y(x,y) = \begin{cases} \beta_1 + \beta_2 d(x,y) + \beta_3 + \beta_4 & Salado\ Dissolution & I_D = 1, I_f = 1, I_H = 0 \\ \beta_1 + \beta_2 d(x,y) + \beta_3 & Central\ High-T & I_D = 0, I_f = 1, I_H = 0 \\ \beta_1 + \beta_2 d(x,y) & Central\ Low-T & I_D = 0, I_f = 0, I_H = 0 \\ \beta_1 + \beta_2 d(x,y) & M2/H2 \mid M3/H3 & I_D = 0, I_f = 0, I_H = 0 \\ \beta_1 + \beta_2 d(x,y) + \beta_5 & M2/H2\ \&\ M3/H3 & I_D = 0, I_f = 0, I_H = 1 \end{cases} \quad \text{(TFIELD 3.2)}$$

where β_1 through β_5 are regression coefficients, the two-dimensional location vector (*x*,*y*) consists of NAD27 UTM Zone 13 *x* and *y* coordinates, *d*(*x*,*y*) is the Culebra overburden thickness (Figure TFIELD 3-1), I_f is an indicator of whether interconnected fractures are present in the Culebra, I_D is the Salado dissolution indicator, and I_H is the halite bounding indicator. In this model, | means logical or, while & means logical and. Regression coefficient β_1 is the intercept value for the linear model. Coefficient β_2 is the slope of *Y*(*x*,*y*)/*d*(*x*,*y*). The coefficients β_3, β_4, and β_5 represent adjustments to the intercept for the occurrence of interconnected fractures, Salado dissolution, and halite bounding, respectively. Although other types of linear models could have been developed, Equation TFIELD 3.2 is consistent with the conceptual model relating Culebra *T* to geologic controls, can be tested using published WIPP geologic and T estimates, and can be potentially verified with new Culebra wells.

Because there are only two data points for *T* in the zone where Culebra is bounded by halite, and both are significantly lower than any other *T* values in the model, the $\beta_5 I_H$ term in Equation TFIELD 3.2 was included to take into account the very low *T* zone. This was done to keep the conceptual model consistent for all zones, recognizing the base fields are primarily a starting point for subsequent calibration.

The combined results of the regression and the indicator kriging (Section TFIELD-4.3) were 1,000 base T-fields that shared certain geologic features, but were different from one another. This difference was provided by the stochastic placement of high-*T* areas in the central zone. These areas were placed using the GSLIB Sequential Indicator Simulation (SISIM) routine (qualified for use in WIPP PA according to NP 19-1 (Chavez 2006)). This routine used geostatistical methods to create stochastic indicator (Boolean value) fields.

TFIELD-3.7 Culebra Conceptual Model Peer Review

The Culebra conceptual model given in this section passed peer review before proceeding with the CRA-2009 PABC calibration of the Culebra T fields (Burgess et al. 2008). The peer review panel found the methodology presented here to be adequate, accurate, and valid enough to justify proceeding with the numerical implementation and calibration of the Culebra T-fields. The panel found the CRA-2009 PABC conceptual model to be greatly improved, compared to the Culebra conceptual model used in the Compliance Certification Application (CCA) (U.S. DOE 1996). The panel found the understanding of the physical processes connecting the Culebra groundwater geochemistry with the Culebra hydraulic properties to be insufficient. The peer review panel did not

feel this particular lack of understanding would be a problem in T-field development and calibration, due to the relatively high density of Culebra hydrologic data available at the WIPP site.

TFIELD-4.0 Base T-Field Construction

The work outlined in Section TFIELD-4.0 was performed under AP-114, Analysis Plan for Evaluation and Recalibration of Culebra *T* Fields (Beauheim 2008). This section discusses details associated with the incorporation of soft and hard data into the base T-field construction process. The base Culebra T-fields were the starting point for the calibration processes outlined in Section TFIELD-5.0. Aside from the definitions of some fixed parameter zones, all the parameters specified in the base T-field construction were allowed to be modified during the calibration process to produce model output that better matched observed steady-state and transient pressure observations. Inside the WIPP LWB there is a large amount of hard data to constrain the parameters of the groundwater model during calibration, while distant to the WIPP LWB the hard data are not sufficient to uniquely constrain the calibration. To help alleviate this problem, base T-field construction used soft data to provide additional constraints that could not be incorporated directly into the calibration process. Specification of soft data was used to create physically realistic starting points for the calibration. The starting point for the calibration has the most impact at locations distant to the WIPP LWB.

Kriging is a linear estimation process in the field of geostatistics that predicts an average value at locations without observations, using available observations and a model describing the variability of the function (i.e., the variogram, which is itself estimated from data). Indicator kriging is a specific form of the kriging where cutoffs are estimated (i.e., is the value above or below 1.0?), rather than a continuous value. Conditional stochastic simulation is a geostatistical approach for generating realizations that will have a common specified statistical structure specified through a variogram and data, but are otherwise random. Kriging predicts the mean and variance of a field, resulting in smooth mean fields. Kriging would be conceptually similar to generating many stochastic simulations and averaging the results. Conditional stochastic simulation with indicator kriging was used to predict location of high- and low-*T* areas
(is $\log_{10}$ T > −5.4 or < −5.4?), taking the model indicator variogram and various hard and soft data into account.

The constraints used to construct the base T-fields included a class-based linear regression relationship between $\log_{10}$ *T* and Culebra overburden within each type of well (see Section TFIELD-4.1) and geologic soft data such as the presence of halite in nearby units or gypsum cements in the Culebra (see Section TFIELD-4.2). The indicator variograms were constructed from these data (see Section TFIELD-4.3) and used to stochastically simulate the cutoff between high and low Culebra *T* (see Section TFIELD-4.4). The indicator kriging simulation result was a component of the base T-field construction (see Section TFIELD-4.5).

TFIELD-4.1 Step 1 - Linear Regression Analysis

The best fit to estimate *T* from single well tests was based on a multi-line regression analysis. The wells were separated into three groups: wells in the Salado dissolution zone, wells with low-*T* pumping test results, and wells with high-*T* pumping test results. Figure TFIELD 4-1 shows the $\log_{10}$ *T* values from pumping test results, the Culebra overburden thickness, and the regression lines fit to each group's data individually. The cutoff between low and high $\log_{10}$ *T* is −5.4. Wells located where the Culebra is bounded above and below by halite (SNL-6 and SNL-15) were considered outliers and were not included in the regression analysis. Instead, the $\beta_5 I_H$ term was chosen to yield values close to those interpreted from tests at SNL-6 and SNL-15 (presented in Appendix F of Hart et al. (Hart et al. 2008), Table F-1); this value was directly modified during the calibration stage in AP-114 Task 7

(Hart et al. 2009). The final regression equation for $Y = \log_{10} T$ (Equation TFIELD 4.1) and a table of the β values (Table TFIELD 4-1) resulted in a fit characterized by $R^2 = 0.92$ and $F = 216$.

$$Y(x,y) = \beta_1 + \beta_2 d(x,y) + \beta_3 I_f(x,y) + \beta_4 I_D(x,y) + \beta_5 I_H(x,y) + \varepsilon \quad \text{(TFIELD 4.1)}$$

The remainder (ε) represents the misfit between the regression model and observed data.

Table TFIELD 4-1. β-values for Regression Equation TFIELD 4.1

β_1	β_2	β_3	β_4	β_5
−5.69805	-3.48357×10^{-3}	2.06581	0.68589	−4.75095

The data and calculations were provided in Appendix A of Hart et al. (Hart et al. 2008).

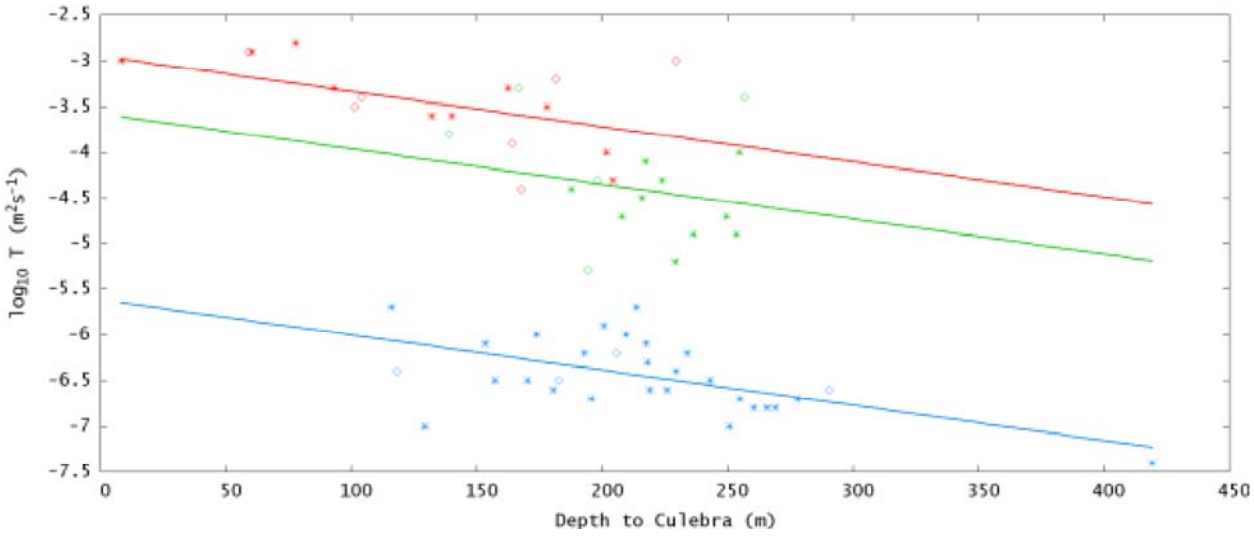

Figure TFIELD 4-1. Regression Lines for Low-*T* Wells (Blue), High-*T* and Non-dissolution Wells (Green), and Wells Within the Salado Dissolution Zone (Red). Open diamonds are wells new to the CRA-2009 PABC regression analysis (i.e., not included in CRA-2004 PABC).

TFIELD-4.2 Step 2 - Creation of Soft Data

Geologic and hydraulic information are included as soft data to maintain the geologic conceptual model through the stochastic indicator kriging simulations in Section TFIELD-4.4. Soft data define probabilities (P_{low}) a new well at a given point would have a low T value. For model cells that include wells where $\log_{10} T$ (m^2/s) has been estimated from single-well hydraulic tests, the observation is referred to as hard data to distinguish it from more indirect contributions to T values associated with soft data. Model cells where hard data (single-well test-derived $\log_{10} T$) is greater than −5.4 are assigned $P_{low} = 0$, while $P_{low} = 1$ for all cells containing low-T pumping test results. Estimated T used as hard data are presented in Table TFIELD 4-2, including coordinates, depth, and $\log_{10} T$ values used in regression model (from Listing A.1 of Appendix A in Hart et al. (Hart et al. 2008)).

Table TFIELD 4-2. Listing of Coordinates, Culebra Depth, and Log_{10} *T* Estimates from Single-well Tests (Hard Data) Used in Regression Model (Equation TFIELD 4.1)

Well	UTM *X* NAD27, Zone 13 (m)	UTM *Y* NAD27, Zone 13 (m)	depth to Culebra (m)	$\log_{10} T$ (m^2/s)
H-10b	622975	3572473	419.25	−7.4
P-15	610624	3578747	129.24	−7.0
WIPP-12	613710	3583524	250.7	−7.0
AEC-7	621126	3589381	269.14	−6.8
H-15	615315	3581859	265.79	−6.8
WQSP-3	614686	3583518	260.38	−6.8
H-12	617023	3575452	254.97	−6.7
H-5c	616903	3584802	277.82	−6.7
WIPP-30	613721	3589701	195.69	−6.7
H-17	615718	3577513	219.03	−6.6
SNL-8	618523	3583783	291.5	−6.6
WIPP-21	613743	3582319	225.85	−6.6
WQSP-6	612605	3580736	180.31	−6.6
CB-1	613191	3578049	157.27	−6.5
H-14	612341	3580354	170.23	−6.5
SNL-10	611217	3581777	182.58	−6.5
WIPP-18	613735	3583179	243.08	−6.5
SNL-13	610394	3577600	118.26	−6.4
WIPP-22	613739	3582653	229.51	−6.4
ERDA-9	613696	3581958	218.08	−6.3
C-2737	613597	3581401	205.74	−6.2
H-2c	612666	3581668	192.94	−6.2
WIPP-19	613739	3582782	233.93	−6.2
H-16	613369	3582212	217.46	−6.1
H-4c	612406	3578499	153.31	−6.1
H-1	613423	3581684	209.55	−6.0
P-17	613926	3577466	173.89	−6.0
WQSP-5	613668	3580353	200.67	−5.9
D-268	608702	3578877	115.98	−5.7
H-18	612264	3583166	213.57	−5.7
SNL-5	611970	3587285	194.16	−5.3
H-19b0	614514	3580716	229.2	−5.2
DOE-1	615203	3580333	253.44	−4.9
WQSP-4	614728	3580766	236.42	−4.9
H-3b1	613729	3580895	207.87	−4.7
WQSP-2	613776	3583973	249.72	−4.7
WQSP-1	612561	3583427	215.79	−4.5
H-6c	610610	3584983	187.61	−4.4
SNL-9	608705	3582238	167.64	−4.4
Engle	614953	3567454	204.22	−4.3
H-11b4	615301	3579131	223.93	−4.3
SNL-14	614973	3577643	198.12	−4.3
WIPP-13	612644	3584247	217.17	−4.1
DOE-2	613683	3585294	254.51	−4.0
H-9c	613974	3568234	201.78	−4.0
SNL-18	613606	3591536	163.98	−3.9
SNL-2	609113	3586529	138.99	−3.8
WIPP-25	606385	3584028	140.06	−3.6

Well	UTM *X* NAD27, Zone 13 (m)	UTM *Y* NAD27, Zone 13 (m)	depth to Culebra (m)	$\log_{10} T$ (m^2/s)
WIPP-28	611266	3594680	131.98	−3.6
P-14	609084	3581976	178	−3.5
SNL-17	609863	3576016	101.19	−3.5
SNL-19	607816	3588931	103.94	−3.4
WIPP-11	613791	3586475	256.95	−3.4
SNL-12	613210	3572728	166.73	−3.3
USGS-1	606462	3569459	162.44	−3.3
WIPP-27	604426	3593079	92.97	−3.3
SNL-1	613781	3594299	181.66	−3.2
SNL-3	616103	3589047	229.51	−3.0
WIPP-29	596981	3578694	8.23	−3.0
SNL-16	605265	3579037	58.83	−2.9
WIPP-26	604014	3581162	60.2	−2.9
H-7c	608095	3574640	77.88	−2.8

TFIELD-4.2.1 Halite Bounding

Two geologic margins, M2/H2 and M3/H3, were updated by Powers (2007a and 2007b), as summarized in Section TFIELD-2.2.1. Wells penetrating the Culebra in areas that are bounded both above and below by halite (e.g., SNL-6 and SNL-15) have been found to have very low *T* estimates, less than 10^{-11} m^2/s (Roberts 2007). Wells bounded by only one margin (e.g., H-12 and H-17) have lower than average *T* estimates.

Because high-*T* fractures are not predicted where halite is present in the Rustler, model cells located on the combined M2/H2 and M3/H3 margin were assigned $P_{low} = 1$. This ensured that no high-*T* areas were placed on the boundary itself, largely a cosmetic consistency fix. Additionally, regression results for all model cells in the halite zone were replaced with values directly from the regression equation; indicator values were only used in Zones 3 and 4, and were not used east of the Rustler halite margins in Zone 1 (Figure TFIELD 3-2).

TFIELD-4.2.2 Gypsum Cements

In all cases where sufficient core and *T* estimates exist, wells with no gypsum (Figure TFIELD 2-12) have high *T*, due to well-interconnected fractures. To account for this relationship, cells were assigned $P_{low} = 0.05$ where no gypsum is present. As seen in Figure TFIELD 2-12, this is a fairly large area. Rather than give all the cells in the area such a low P_{low} value, cells were selected from a regular grid at 1300-m spacing to receive soft data assignments (Figure TFIELD 4-3). A grid of 1300-m spacing was chosen to provide sufficient definition of the boundaries without overwhelming the SISIM geostatistical simulation with too many samples. The size of the matrix decomposed by SISM during estimation is proportional to the number of samples considered at each estimation location.

It was observed that in all cases where sufficient core and *T* estimates exist, wells outside of the low-gypsum region (Figure TFIELD 4-3) have low *T* because fracture interconnectivity is limited by gypsum cements. In the indicator kriging, areas outside of the low-gypsum region were assigned $P_{low} = 0.95$ to increase the likelihood of predicting low *T* in the simulation.

By definition, the areas of no-gypsum and high-gypsum content cannot overlap, therefore the high-gypsum data were sampled on the same grid used by the no-gypsum data. By using fractional likelihoods and sparse sampling, these soft data did not overwhelm the random sampling algorithm of

SISIM and allowed for greater variation between base field realizations. The high/low-gypsum content map is shown in Figure TFIELD 2-13. The low-gypsum region was not sampled, since it overlapped the no-gypsum region. Instead, the high-gypsum region was used. The area of high gypsum directly north of the WIPP LWB was sampled at 300-m spacing, to compensate for the diffusivity soft data described in the next section and produce model results more similar to observed Culebra behavior during pumping tests.

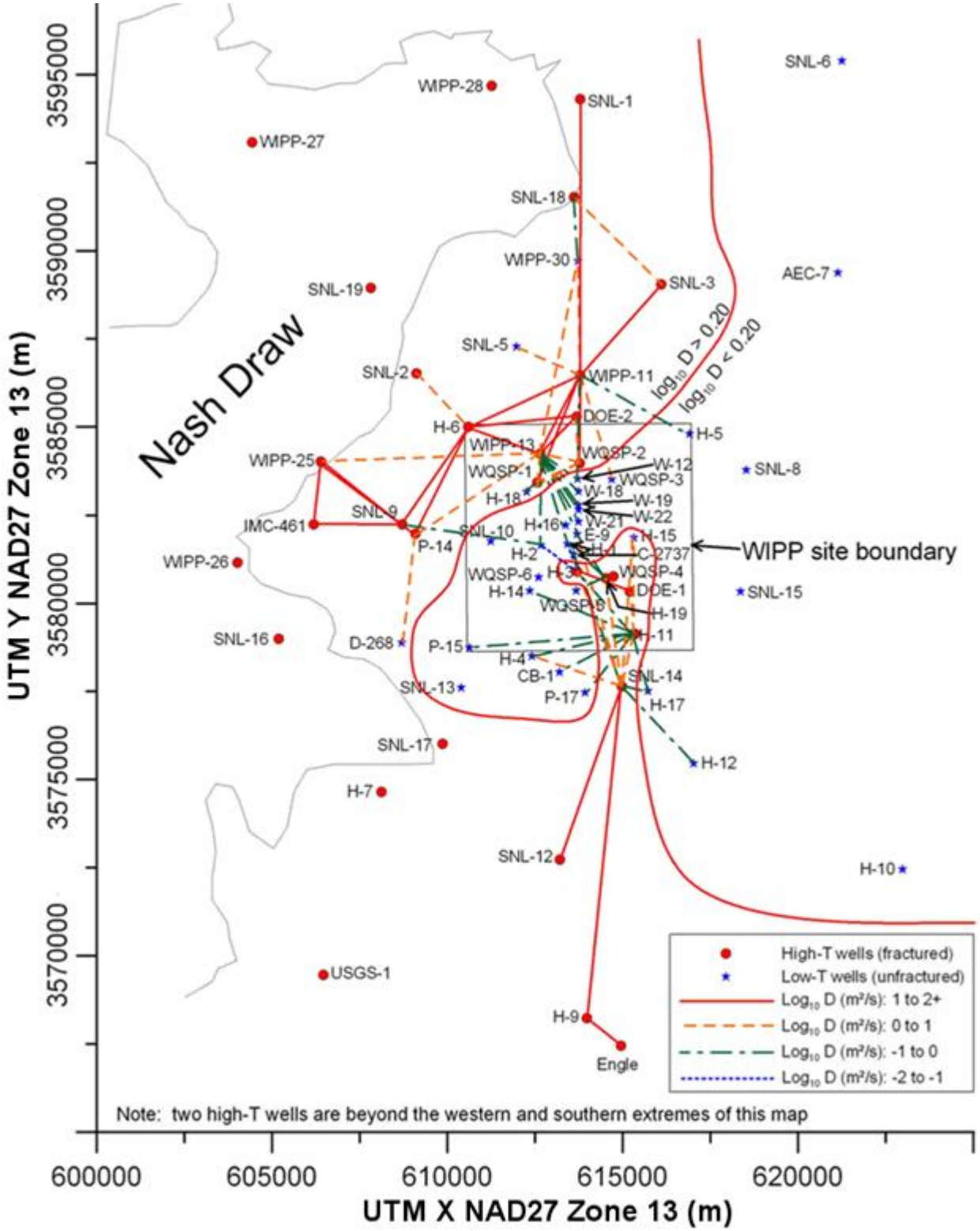

Figure TFIELD 4-2. Diffusivity Values Calculated Between Wells From Pumping Test Data. Connections where $\log_{10} D > 0.2$ are included as conditioning data with $P_{low} = 0.25$.

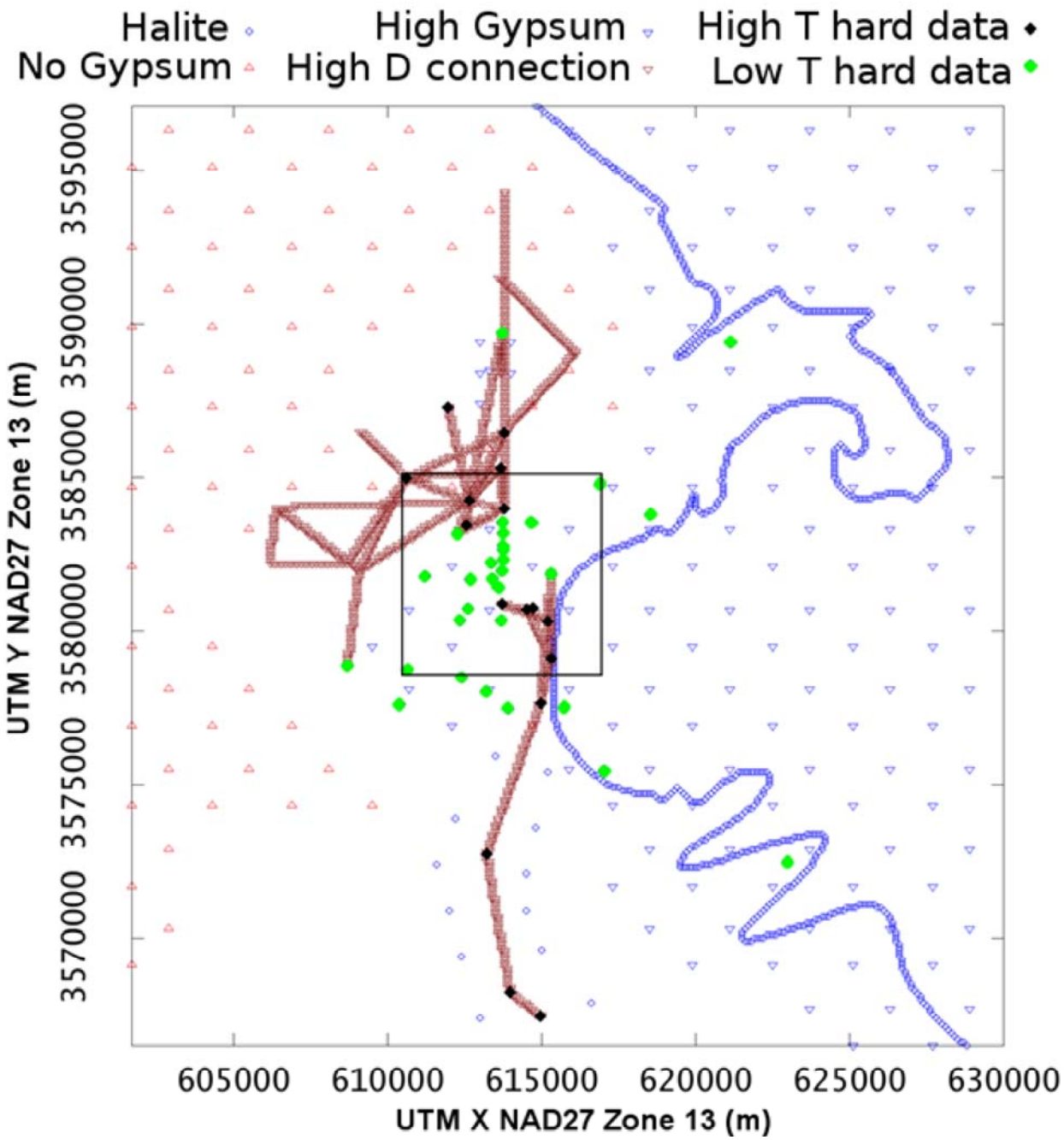

Figure TFIELD 4-3. Soft Data Points (Open Symbols) Generated During Step 2. Hard data points (filled symbols) are located at wells with single-well estimates of *T*. The black square is the WIPP LWB.

TFIELD-4.2.3 Diffusivity and Hydraulic Connections

Soft data were used to incorporate the degree of hydraulic connection observed between pairs of wells (pumping and observation wells) into the construction of the base fields. The diffusivity D (m^2/s) associated with the pumping and observation well pair was calculated from the results of many hydraulic tests conducted at the WIPP site (Beauheim 2007). A map of these values is shown in

Figure TFIELD 4-2, showing colored lines connecting pumping and observation wells involved in the nine pumping tests used in T-field calibration (pumping/observation wells listed in Table TFIELD 5-2). The model cells falling on a straight line connecting two wells with a calculated $\log_{10} D > 0.2$ (i.e., all red connecting lines and some orange dashed lines) were assigned $P_{low} = 0.25$ to account for the increased likelihood a cell on the connecting line would be high T (inverted maroon triangles in Figure TFIELD 4-3). Using $P_{low} = 0$ would have forced SISIM to create a direct path connecting two wells where a strong response to pumping was observed, and there is no geologic reason that these connections must be straight.

In addition to the high-T connection lines, a set of low-T points was placed roughly parallel to the SNL-14/SNL-12/H-9/Engle connection path to keep the high-T connection relatively narrow (blue circles in south central portion of Figure TFIELD 4-3). These points were assigned a $P_{low} = 1$, to ensure they would impact the indicator kriging simulation. Pumping SNL-14 in 2005 produced a strong response at H-9c nearly ten kilometers (km) to the south. During model development it was found the only way to recreate the observed response with the MODFLOW model was to incorporate a relatively narrow connecting zone of high T. Without adding some low-T points along the flanks of this path, SISIM tended to create a wide high-T area, which did not allow the drawdown response to propagate significantly from SNL-14 to H-9, as was observed. The observed response would be consistent with a narrow linear geological feature, which is difficult to simulate using the current MODFLOW model with 100-m grid spacing. These low-T points did not force the simulation to create a narrow high-T pathway in each realization, as many base fields still had large areas of high T that extend past these points. Fields generated with and without the narrow high-T pathway were modified through the calibration process, which included the SNL-14 pumping test data as calibration targets. This exercise was performed in an attempt to improve the ability of the base T fields to match observed data, since this might lead to fewer PEST iterations and quicker calibration times.

TFIELD-4.2.4 Combined Soft Data

The final combined soft data field is shown in Figure TFIELD 4-3. The soft data input files and calculation scripts are provided in Appendix B of Hart et al. (Hart et al. 2008).

Single-well estimates of T are hard data shown on the figure with filled diamonds (data listed in Table TFIELD 4-2). Hard data are combined here with soft data in base T-field creation, but appear again (without soft data) as fixed pilot points in the T-field calibration process (Section TFIELD-5.0). Filled green diamonds are wells with $\log_{10} T$ estimates ≤ -5.4 (m^2/s), and black filled diamonds are wells with $\log_{10} T$ estimates > -5.4 (m^2/s).

The grid of inverted open blue triangles in the east indicate areas with "high gypsum" (white area in Figure TFIELD 2-13), while the grid of open red triangles in the west indicates areas with "no gypsum" (peach area in Figure TFIELD 2-12).

Lines of closely spaced inverted brown triangles represent the connections between pumping and observation wells interpreted with a $\log_{10}$ diffusivity (D) > 0.2 m^2/s, including all solid red and some dashed orange lines in Figure TFIELD 4-2.

The open blue circles ("Halite" in the figure legend) are used in two ways to enforce high probability for low T in two different locations. The first use is the line of closely spaced open blue circles corresponding to M2/H2 or M3/H3; locations east of this line have either halite above or below the Culebra. This boundary marks the eastern edge of the random placement of high-T and low-T zones

(Zones 3 and 4 in Figure TFIELD 3-2). The second group, the open blue circles straddling the line connecting Engle, H-9, SNL-12, and SNL-14 (running south to north from the bottom middle of the figure), represents a low-*T* zone added to increase the contrast of the high-*T* zone along this line of south-to-north connectors, to better represent results observed in the SNL-14 multi-well pumping test.

TFIELD-4.3 Step 3 - Indicator Variography

The geostatistical indicator simulations done as part of the base T-field development are only utilized in the central section of the model domain, between the Salado dissolution area to the west and the low-*T* halite-sandwiched region to the east. Therefore, only wells in this middle section are used for construction of the indicator variogram. A total of 46 wells that provide information regarding $\log_{10} T$ were used in the calculation of the indicator variograms. The indicator value is determined by comparing each $\log_{10} T$ value to a threshold $\log_{10} T$ value,
$T_t = -5.4$,

$$I(x,y) = \begin{cases} 1 & if \log_{10} T < T_t \\ 0 & if \log_{10} T \geq T_t \end{cases} \quad \text{(TFIELD 4.2)}$$

Where $I(x,y)$ denotes the unitless indicator value at well location (x,y). The experimental indicator variogram was fit with a spherical variogram model, whose model parameters are given in Table TFIELD 4-3. Figure TFIELD 4-4 illustrates the experimental and model indicator variograms. The proportion of low-*T* values in the data set is 0.652. The variance of an indicator value is $(1 - p)p$, where p is the proportion of high or low values. The variance for these indicator data is 0.227 and is used directly as the sill in the variogram modeling (dashed horizontal line in Figure TFIELD 4-4). The parameters in Table TFIELD 4-3 are used as input to the SISIM program for creation of the stochastic component of the base T-fields. In an attempt to identify anisotropy, model variograms were calculated in both the NE-SW and NW-SE directions (see Appendix C of Hart et al. (Hart et al. 2008)). These directional variograms analyses were inconclusive, only omnidirectional (i.e., isotropic) variograms were used in the final analysis.

Table TFIELD 4-3. Variogram Parameters for Isotropic Fit to Indicator Data Variogram. Omnidirectional variogram calculated with a lag spacing of 500 m.

Parameter	Value
Model Type	Spherical
Nugget	0.0
Sill	0.227
Range	2195 m

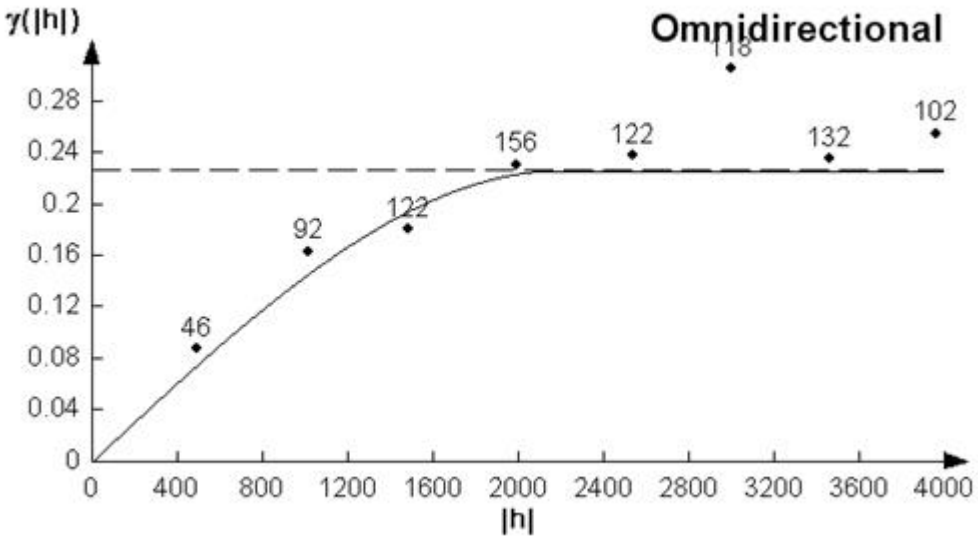

Figure TFIELD 4-4. Experimental Variogram (Dots) and Spherical Model (Line) for Indicator Values. *x*-axis is lag distance [meters], *y*-axis is the unitless indicator; numbers by dots indicate the number of pairs represented at each lag.

TFIELD-4.4 Step 4 - Conditional Indicator Simulation

With previous sections describing the indicator variogram model, hard *T* data values, and soft geologic and hydrologic data, stochastic realizations of high-*T* zones were constructed using the GSLIB program SISIM (Deutsch and Journel 1998). An example indicator field is given in Figure TFIELD 4-5. Maps summarizing statistics for the 1,000 resulting base T-fields are presented in Figure TFIELD 4-6 and Figure TFIELD 4-7. These figures show the impact the conditioning information had on the overall fields. The combined M2/H2 and M3/H3 margins have a standard deviation of 0 and are constant at the proper value as desired. Areas designated as higher likelihood of high *T* do show an average value that trends towards the high-*T* value (in this case, 0), but they still have a standard deviation that is non-zero, indicating that there is some variability in those areas. The same is true in areas outside the low-gypsum region. Additionally, areas with no conditioning information have higher standard deviations, indicating that high-*T* zone placement in those locations was allowed to be fully variable. Though there are some visible artifacts from the grids used in the average and standard deviation fields (locations of soft data points in Figure TFIELD 4-3 are discernible in Figure TFIELD 4-6 and Figure TFIELD 4-7), the individual realizations, such as Figure TFIELD 4-5, do not show these artifacts. Additionally, the majority of the artifacts occur outside the central zone, which is the only place the indicator fields are used. The indicator fields created by this process are the best possible combination of hydraulic and geologic conditioning given current data.

There is a relatively high density of hard data available inside the WIPP LWB, which significantly constrains the estimation process there. Geostatistical simulation is most useful to fill in large gaps near the edges of the model domain where a small number of observations exist. It must also be considered that these base-T fields are just a first guess for the model calibration process, which utilizes the single-well *T* and both the steady-state and multi-well pumping test drawdown data as calibration targets. Ultimately, these data drive the calibration, adjusting input parameters to better match observed data. See Section TFIELD-5.4 for figures and discussion illustrating the extent to which the input fields were adjusted to match the data (e.g., see Figure TFIELD 5-19).

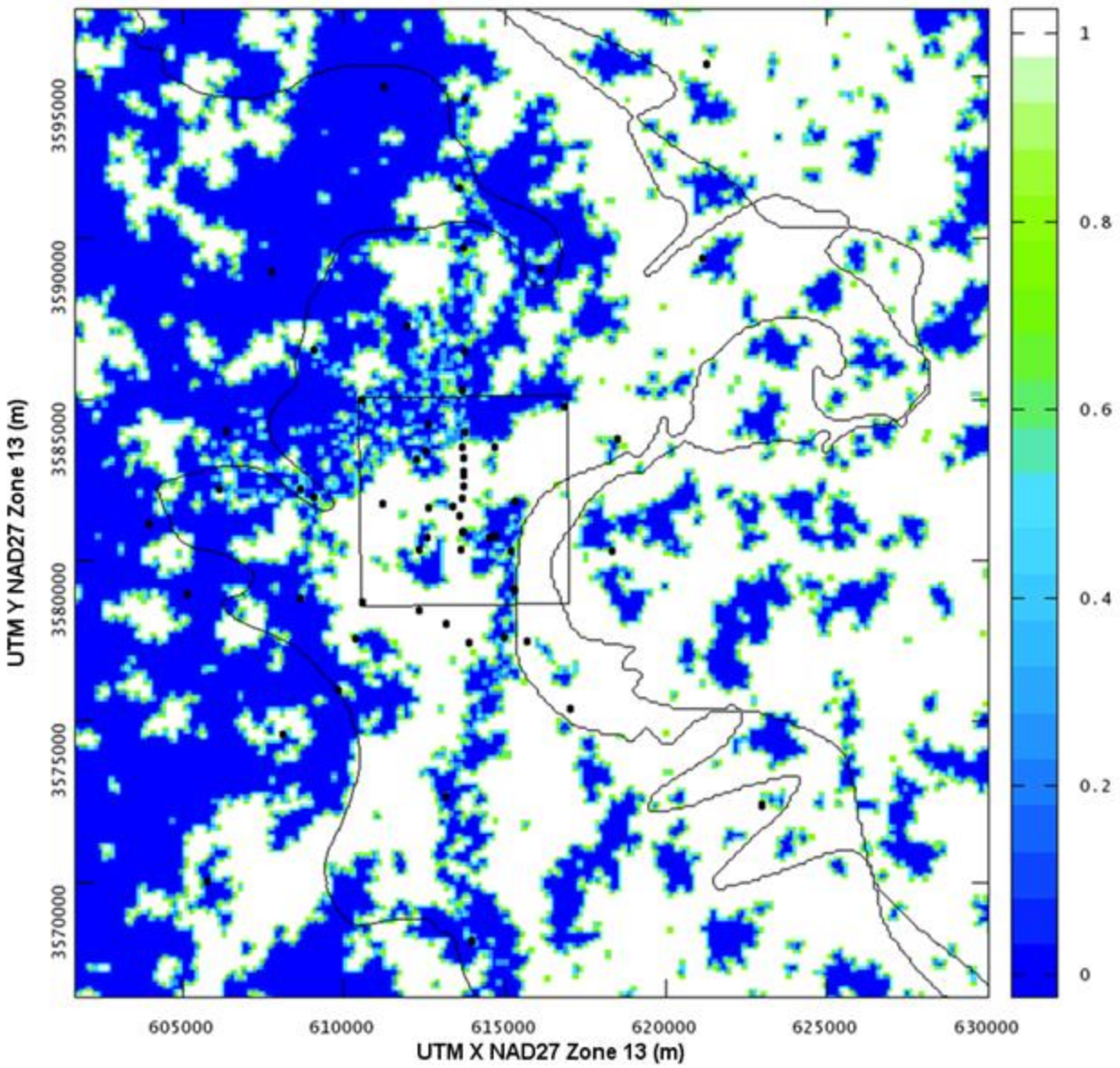

Figure TFIELD 4-5. Sample Indicator Field for Realization r123. 1 indicates low *T* and 0 indicates high *T*.

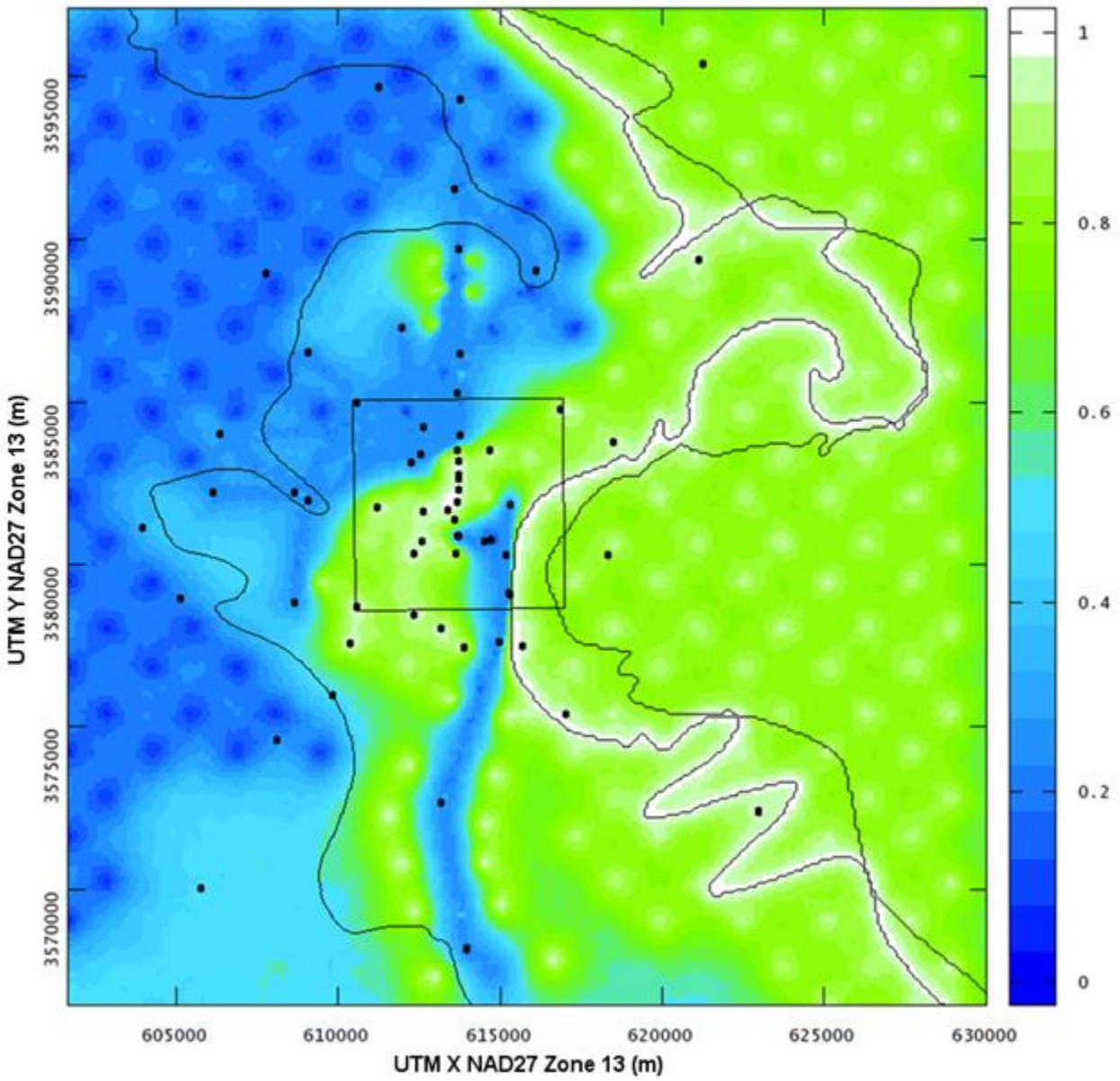

Figure TFIELD 4-6. Average Indicator Values Across All 1000 Base Realizations. 1 indicates low *T* and 0 indicates high *T*.

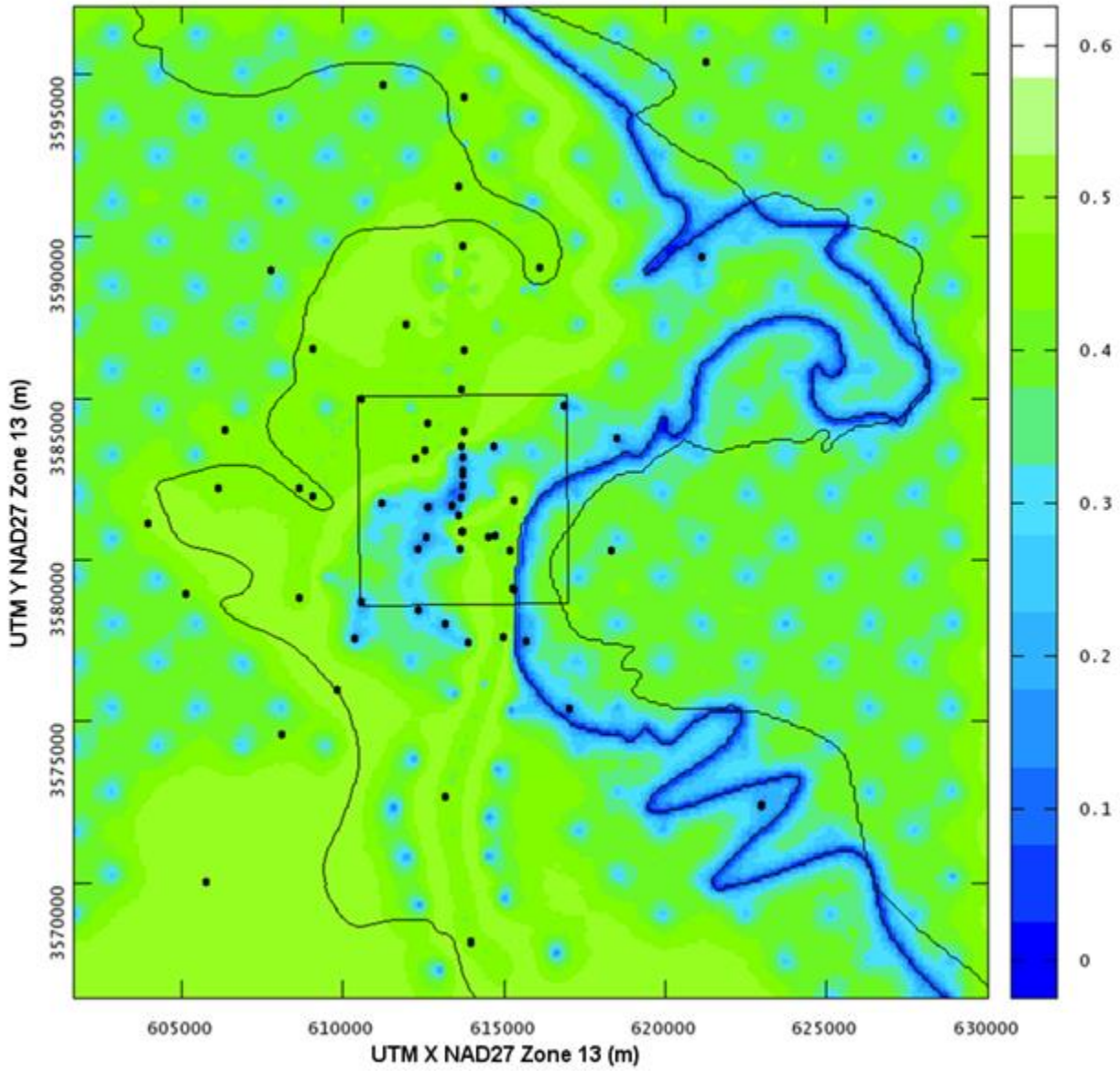

Figure TFIELD 4-7. Standard Deviation of Indicator Values Across All 1000 Base Realizations

TFIELD-4.5 Step 5 - Construction of Transmissivity Fields

Once the indicator fields were created, the T values were assigned using Equation TFIELD 4.1 using a Perl script. Equation TFIELD 4.3 was used to calculate $Y = \log_{10} T$ at each cell,

$$Y(x,y) = \boldsymbol{b}\,[Z(x,y)] + \boldsymbol{a}\,[Z(x,y)]\,d(x,y) \quad \text{(TFIELD 4.3)}$$

where $\boldsymbol{b}$ and $\boldsymbol{a}$ represent combinations of the β-coefficient based on the zone ($Z(x,y)$) of the cell. Table TFIELD 4-4 shows how the variables in the original linear regression equation (Equation TFIELD 4.1) were related to Equation TFIELD 4.3. Figure TFIELD 3-2 shows the indicator zone distribution.

Table TFIELD 4-4. Correlation of β and I Values from Equation TFIELD 4.1 to a and b Values in Equation TFIELD 4.3

Zone 0	Zone 1	Zone 2	Zone 3	Zone 4

	Salado	Halite 2	Halite	Central low T	Central high T
I_f	1	0	0	0	1
I_D	1	0	0	0	0
I_H	0	1	0	0	0
I_h	0	1	1	0	0
b	$\beta_1 + \beta_3 + \beta_4$	$\beta_1 + \beta_5$	β_1	β_1	$\beta_1 + \beta_3$
a	β_2	β_2	β_2	β_2	β_2

The Perl script was executed on all 1,000 realizations. A sample final base *T* field is presented in Figure TFIELD 4-8 for realization r123 (a random representative selection from the possible fields). The mean $\log_{10}$ *T*-field across all 1,000 realizations is presented in Figure TFIELD 4-9. The standard deviation of $\log_{10}$ *T* is presented in Figure TFIELD 4-10. Very low standard deviation occurs across the 1000 base realizations outside the stochastically sampled areas, including the higher *T* areas to the west and the lower *T* areas to the east (Figure TFIELD 4-10). These stochastically sampled areas are the main source of variability between the 1000 base realizations. The variability of the indicator variable across the realizations (Figure TFIELD 4-7) is one component of the variability observed in the final *T* values in the base *T* fields (plotted normalized to the range {0,1} in Figure TFIELD 4-10). The regression analysis produced variability in the predicted *T* values in a zone related to the variability in the overburden thickness.

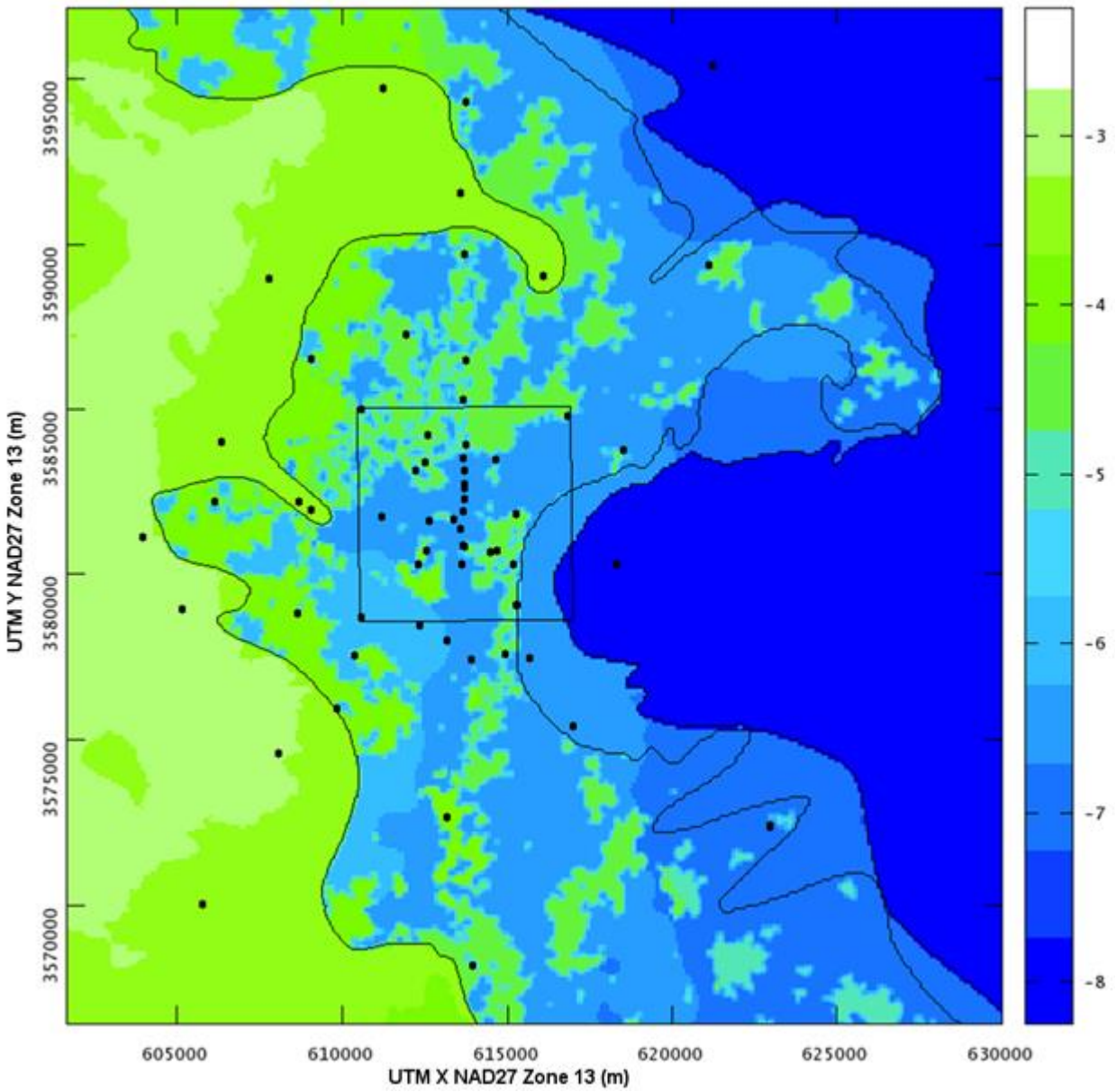

Figure TFIELD 4-8. Sample Log_{10} T (m^2/s) Base Field Realization r123

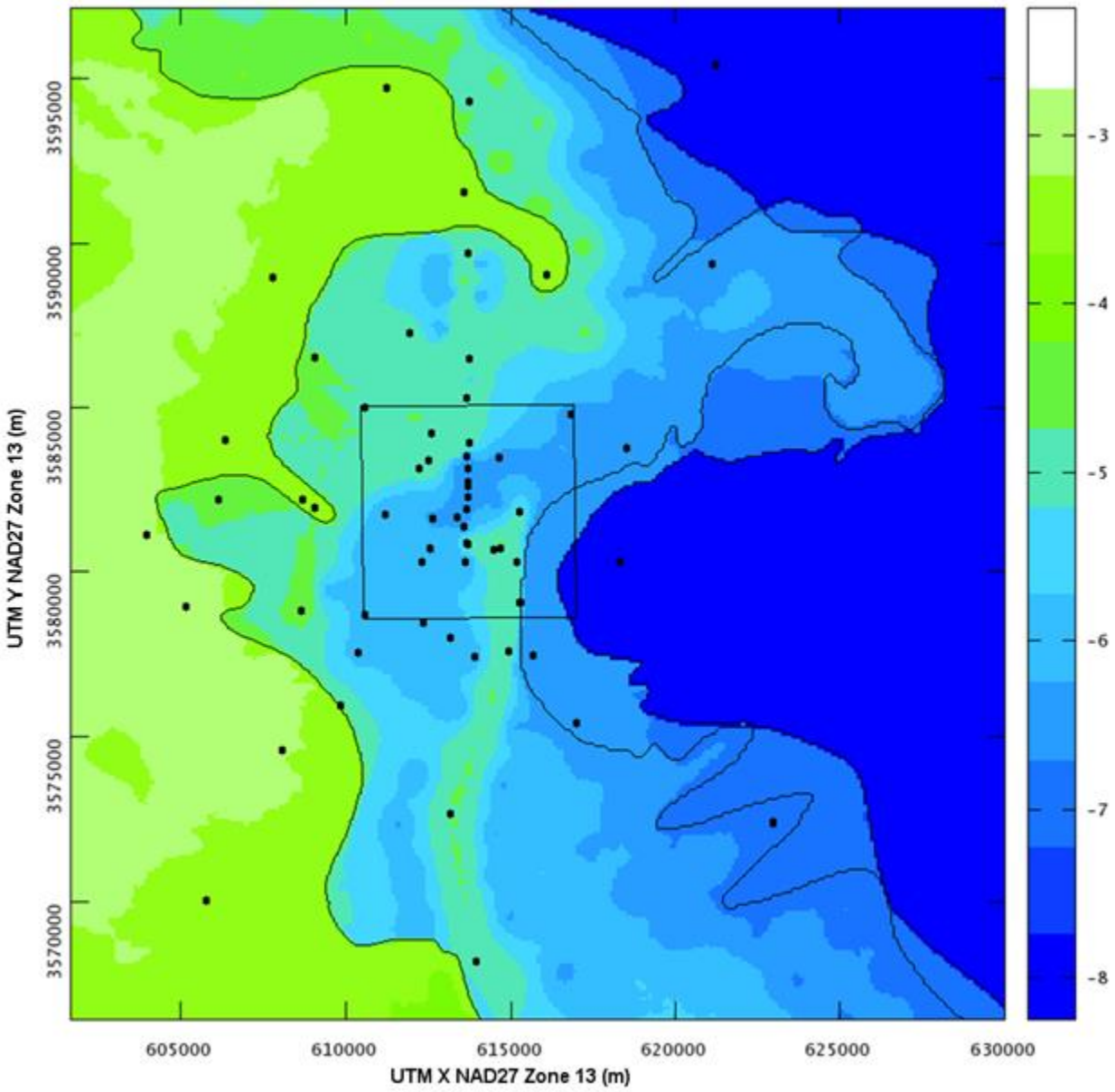

Figure TFIELD 4-9. Mean Log_{10} T (m^2/s) Values Across All 1000 Base Realizations

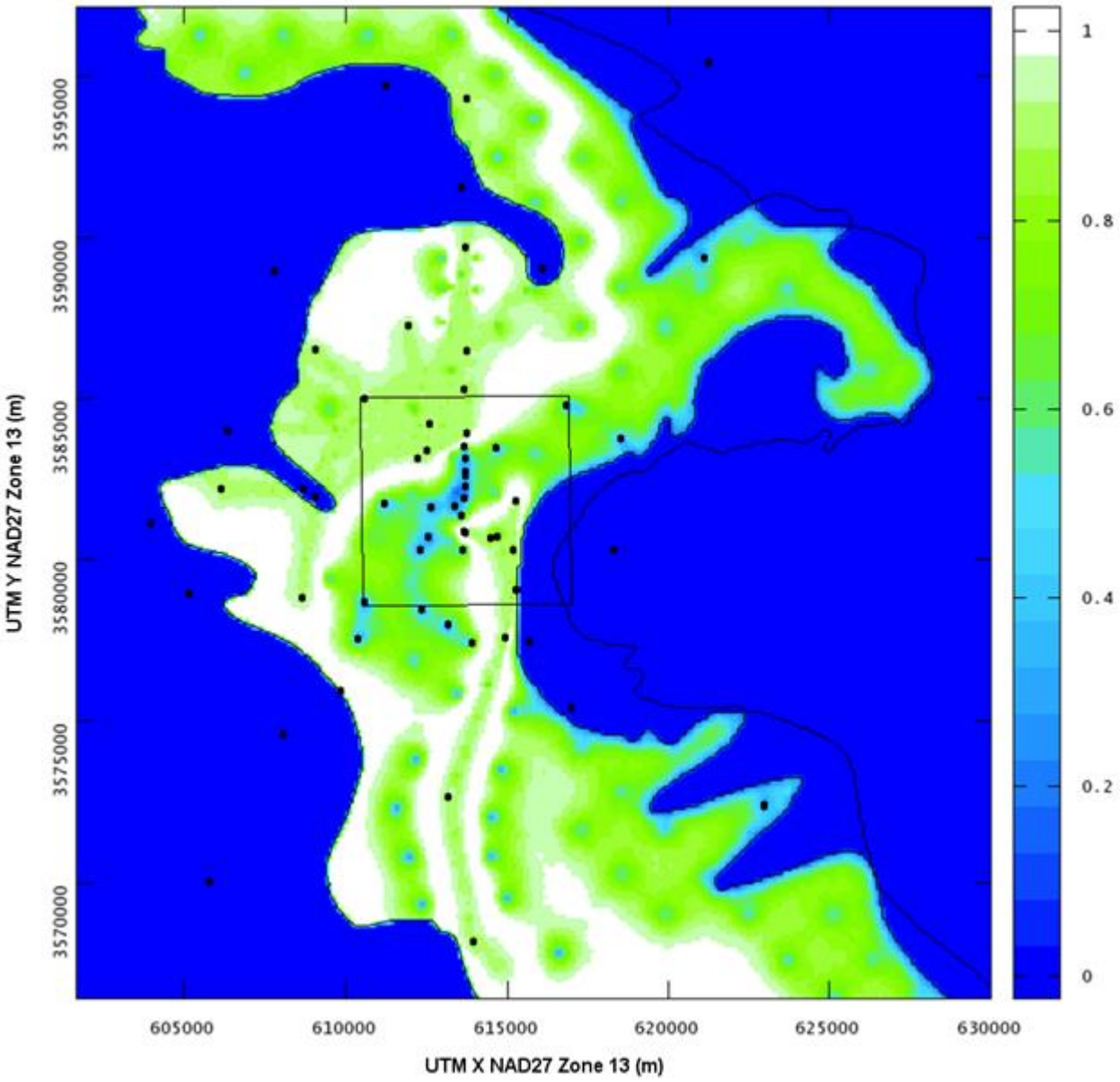

Figure TFIELD 4-10. Normalized Standard Deviation of Log_{10} *T* (m^2/s) Values Across All 1000 Base Realizations

TFIELD-5.0 T-Field Calibration

The work outlined in Section TFIELD-5.0 was performed under AP-114, Analysis Plan for Evaluation and Recalibration of Culebra T Fields (Beauheim 2008). The calibration of the T-fields used 200 of the 1,000 base fields from the results of AP-114 Task 5 (Hart et al. 2008, summarized in Section TFIELD-4.0) as starting points for the calibration process. More than 200 fields could not be calibrated, due to time constraints. Calibration is the process of systematically adjusting the input parameters to the MODFLOW model (fields of *T*, *A*, *S*, and *R*) to reduce the sum of the squared differences between field observations and MODFLOW model output (steady-state and transient head).

The pilot point calibration method was implemented using the parameter estimation software PEST. Automatic model calibration was utilized to make the process more easily documentable and reproducible, compared to manual calibration (i.e., trial and error). The MODFLOW model used to simulate groundwater flow through the Culebra contains a large number of active model cells for *T*, *A*, and *S* fields. Estimating each model element independently would require estimating hundreds of thousands of unknown parameters. The pilot point approach makes the calibration process more tractable by lowering the number of parameters to estimate. Instead of estimating each parameter in each model cell independently, parameter values are estimated at strategically placed pilot point locations. Parameter values at each model cell are then interpolated from the pilot points using kriging as a pre-processing step between parameter assignment by PEST and MODFLOW model execution. The pilot point approach allows mixing estimated and fixed pilot points (e.g., *T* pilot points at wells with single-well hydraulic test estimates of *T*). The pilot point approach was also used in CRA-2004 PABC and a variant of it was used (without PEST) in the CCA. Both steady-state and transient head calibration targets are discussed in Section TFIELD-5.1. The parameter zones, pilot point locations for each parameter, initial conditions, and boundary conditions are specified in Section TFIELD-5.2. The components of the MODFLOW model used with PEST, and the utilities required to pre-process and post-process the inputs and outputs from the model during the calibration are discussed in Section TFIELD-5.3. Finally, some post-calibration analysis of the results is presented in Section TFIELD-5.4.

The initial *T* values at pilot points were taken from the base fields. In addition to *T*, the horizontal *T* anisotropy (*A*), the storativity (*S*), and a linear section of recharge (*R*) were also calibrated. The same zone definitions used for developing the base *T* fields (see TFIELD-4.0) were used for *T* pilot points (although zone numbers changed), and similar zone definitions were used for anisotropy. Zones for storativity and recharge were based on other analyses completed in the area surrounding the WIPP site (see Section TFIELD-5.2.1). Pilot points were selected for each parameter and initial values were selected that were consistent with the conceptual model used to create the base fields (see Section TFIELD-5.2.2 and Section TFIELD-5.2.7).

A model variogram for *T* was created using the estimated *T* from single-well hydraulic tests. This variogram was also used for all parameters, as it was the only one that could be created from field data (see Section TFIELD-5.2.8). This variogram was used to create kriging factors that were then used to create continuous fields from the pilot point values. The *T*, *A*, *S*, and *R* fields were then used as inputs to the MODFLOW numerical model to produce simulated head and drawdown results (see Section TFIELD-5.2.10).

Once the MODFLOW models produced simulated drawdown and head results, the modeled results were compared to the field data for the tests that were modeled. The residual of an observation is

calculated in PEST as the weighted difference between measured and modeled data. Observation weights were selected to make the sum of the weighted steady-state head errors approximately equal to the sum of errors of four observation wells in a transient pumping test to approximately balance the steady-state and transient model-to-data misfits. The PEST optimization uses a single objective function, which is the sum of the steady-state and transient residuals. Because the improvement of model fit for steady-state heads might come at the expense of fit to transient pumping tests, a decision was made to balance the importance of the two groups in the calibration effort. The residuals were used by PEST to construct a finite-difference approximation of the Jacobian matrix. The Jacobian matrix is a measure of the sensitivity each model prediction has to each adjustable parameter, and is used to optimize the pilot point parameter values. The goal of the optimization is to minimize the objective function value, a measure of the misfit between model predictions and observed data (see Section TFIELD-5.2.9).

Because traditional construction of the Jacobian matrix requires at least $N_p + 1$ forward model calls (N_p parameters estimated in the calibration), using 1,100-plus parameters would be impossible without additional efficiency in the optimization. The PEST singular value decomposition (SVD) assist approach reduces the size of the Jacobian matrix by only using the most significant "super-parameters" that correspond to the eigenvectors with the largest singular values, estimated using the SVD of the Jacobian matrix. The SVD process required initial calculation of a full Jacobian matrix, but then reduced the subsequent number of required forward calls by a factor of four to six. The result was that three calls to PEST were required to calibrate the fields (see Figure TFIELD 5-1):

1. a single full Jacobian calculation, which required 1,100+ forward model calls;

2. an SVD calibration using the reduced parameter set that ran up to 50 iterations, requiring between 100 and 400 forward model calls per iteration; and

3. a final PEST run with the best parameter results to create the final fields corresponding to the best parameter values calculated during the SVD-assisted calibration.

Total calibration time for a single base field was approximately seven days using six processors (one master node and five slave nodes).

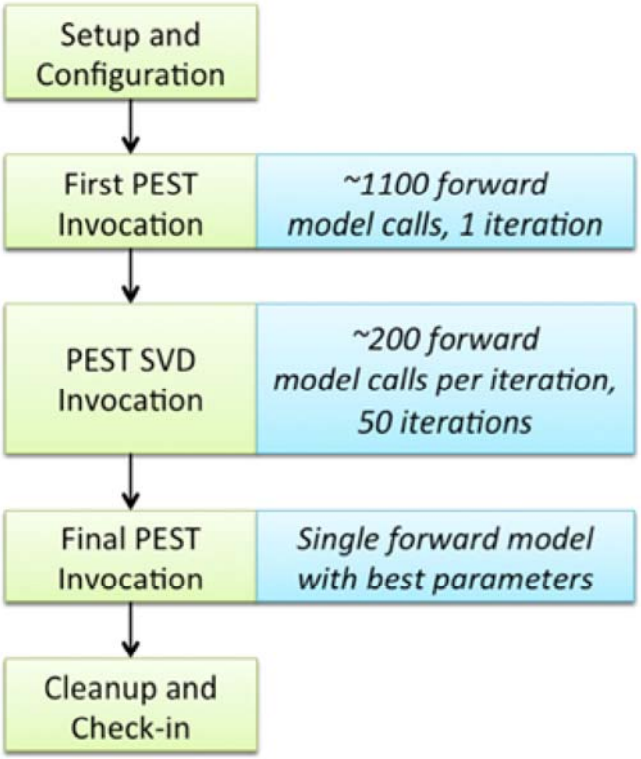

Figure TFIELD 5-1. Complete Calibration Process for a Single Realization

After approximately 140 fields had been calibrated, a few steady-state calibration targets were found to be incorrect by several meters. A total of 150 fields were calibrated using the incorrect targets, and an additional 50 fields were started using the corrected heads (Beauheim 2009; Johnson 2009a and Johnson 2009b). To deal with the incorrect values, a limited recalibration was performed on the results of the first 150 calibrations (see Section TFIELD-5.3.2). The same process that has been described was followed for the limited secondary calibration, but since the initial parameter values were taken from the calibrated results, only the necessary pilot point locations near the updated steady-state head values were allowed to be changed, and the SVD portion of the PEST recalibration was limited to 10 iterations. The end result was 200 fields, with 150 of these fields having undergone a secondary calibration to incorporate corrected field observation data. The impact of this change is discussed in Section TFIELD-5.3.3.

The end result of the calibration was the first 200 of the original 1,000 field sets (T, A, S, and R) calibrated to one set of steady-state heads and nine transient, multi-observation well pumping tests. More than 200 of the 1,000 base T-fields could not be calibrated due to time constraints associated with the calibration effort. Since the 1,000 base T-fields were generated randomly, the first 200 were in effect a random sample. The 100 best-calibrated fields (those with the smallest residuals) were selected as the final results from this task (see Section TFIELD-5.3.4). Several statistical analyses were performed on the fields themselves to generate average values and variances in the field results (Section TFIELD-5.4.1).

The complete calibrations were performed under quality-assurance run control with inputs and outputs stored in a version control repository on a central server. The calibrations required approximately six months of continuous runtime on a total of 80 processors. See Hart et al. (Hart et al. 2009) for details.

TFIELD-5.1 Model Calibration Targets

Two sets of head values were used for calibration of the Culebra flow model. The first dataset consists of 42 freshwater head values measured in May 2007, which were used as steady-state calibration targets (see Table TFIELD 5-1 for values used and see Johnson (Johnson 2009a and Johnson 2009b) for details). Appendix HYDRO-2014 shows the behavior of water levels in wells since 2007. The data in Appendix HYDRO-2014 support the continued use of 2007 water levels to represent steady-state conditions at the WIPP up to the CRA-2014 (see additional discussion in Appendix HYDRO-2014). The second dataset consists of drawdown data collected during 9 independent multi-well pumping tests conducted over a span of more than 20 years (see Table TFIELD 5-2 for lists of observation wells and relevant references).

The steady-state MODFLOW simulation is calibrated against data in Table TFIELD 5-1. Each of the nine transient pumping tests in Table TFIELD 5-2 are simulated as a separate MODFLOW model simulation. A "single" forward model run actually involved 10 individual MODFLOW simulations (1 steady-state and 9 transient simulations), each using the same input parameter fields, but different pumping configurations. Some wells appeared in multiple pumping tests (e.g., H-15, H-18, or ERDA-9). These wells had calibration targets associated with multiple transient forward simulations. The MODFLOW model is discussed more in Section TFIELD-5.2.10.

SNL-6 and SNL-15 are listed as steady-state targets in Table TFIELD 5-1, but they are located in the constant-head portion of the model domain and therefore their corresponding model-predicted values are not adjustable through changes in the *T* field.

Table TFIELD 5-1. Freshwater Head Observations Used as Steady-state Calibration Targets

Well Name	May 2007 head target (m AMSL)
C-2737	921.23
ERDA-9	924.88
H-2b2	929.62
H-3b2	918.68
H-4b	916.34
H-5b	939.12
H-6b	936.44
H-7b1	914.58
H-9c	912.8
H-10c	922.02
H-11b4	917.09
H-12	916.53
H-15	920.32
H-17	916.24
H-19b0	918.84
IMC-461	928.95
SNL-1	941.86
SNL-2	937.65
SNL-3	939.81
SNL-5	938.59
SNL-6	1110
SNL-8	929.94
SNL-9	932.05
SNL-10	931.54

Well Name	May 2007 head target (m AMSL)
SNL-12	915.24
SNL-13	918.19
SNL-14	916.33
SNL-15	1060
SNL-16	918.68
SNL-17A	916.78
SNL-18	939.87
SNL-19	937.58
USGS-4	911.11
WIPP-11	940.65
WIPP-13	939.78
WIPP-19	933.66
WIPP-25	937.57
WIPP-30	939.37
WQSP-1	938.28
WQSP-2	939.87
WQSP-3	936.43
WQSP-4	919.5
WQSP-5	918.18
WQSP-6	921.96

Table TFIELD 5-2. Summary of Transient Observations Used as Calibration Targets

Pumping Well(s)	Observation Wells[1]	Total # obs.	Reference
WQSP-2	H-18, DOE-2, WQSP-1, WIPP-13	77	Beauheim and Ruskauff 1998
H-19 and H-11	WQSP-5, H-1, H-15, DOE-1, ERDA-9, WIPP-21, H-3b2	143	Beauheim and Ruskauff 1998
WQSP-1	H-18, WIPP-13	36	Beauheim and Ruskauff 1998
WIPP-11	WQSP-2, WQSP-3, WIPP-12, SNL-9, SNL-5, H-6b, SNL-3, SNL-2, SNL-1, WIPP-30, WQSP-1, WIPP-13	250	Toll and Johnson 2006b; Roberts 2006
H-11	H-4b, H-12, H-14, H-15, H-17, DOE-1, CB-1, P-15, P-17, H-3b2	130	Beauheim 1989
WIPP-13	WIPP-19, WIPP-18, H-2b2, H-6b, WIPP-12, WIPP-25, DOE-2, WIPP-30, P-14	167	Beauheim 1987b
SNL-14	H-9c, H-4b, SNL-13, SNL-12, H-15, H-17, C-2737, ERDA-9, H-19b0, H-3b2, H-7, H-11b4	252	Toll and Johnson 2006a; Roberts 2006
P-14	D-268, H-18, WIPP-26, H-6b, WIPP-25	82	Beauheim and Ruskauff 1998
H-3	DOE-1, H-2b2, H-1, H-11b2	69	Beauheim 1987a

1. [1] See Figure TFIELD 4-2 for locations of pumping and observation wells and diffusivity values estimated from pumping tests.

TFIELD-5.2 Step 1 - Calibration Setup and Configuration

This step comprised the setup and configuration processes that were the same for every calibrated base field. Step 1 included the creation and definition of zones for each of the parameters and the selection of pilot point locations and initial values. Because of the stochastic nature of the transmissivity fields, unique zones are associated with each field, as defined in Hart et al. (Hart et al. 2008). The process to set up each field was the same, but certain elements, such as the exact number of pilot point locations used, were unique to each field.

The model domain and extent are identical to the domain defined in Section TFIELD-3.1. The base T-fields were taken from the results of Section TFIELD-4.5. Some model input files were created statically, and were used for every calibration. Some model input files were created dynamically for each calibration, but used the same variables and parameters in their creation.

TFIELD-5.2.1 Creation of Parameter Zones

Parameter zones were defined for each of the calibrated parameters. These zones or regions were defined to be consistent with the conceptual model for Culebra flow defined in Hart et al. (Hart et al. 2008) and summarized in Section TFIELD-3.0. The parameter zones were chosen to organize common pilot points groups together in the PEST calibration. Numerical values of parameter zones (i.e., zone numbers) are often different from those used in the conceptual model. Figure TFIELD 2-8 shows the different margins that define geologic zones and the locations of the Culebra wells that have been drilled in the vicinity of the WIPP.

TFIELD-5.2.1.1 Transmissivity Zones

The *T* zones were defined to be consistent with the zones used in the geologic model and soft data analysis (Section TFIELD-4.2). As shown in Figure TFIELD 5-2, a high-*T* zone exists to the west (zone 2), corresponding to the area of Salado dissolution, and a mixture of higher and lower *T* values corresponding to the stochastic zones (zone 0 and 1) provided in the base fields defined the center of the model domain. Unlike AP-114 Task 5 (Section TFIELD-4.5), where it was a separate zone, the area between the H2/M2 and H3/M3 margins (green in Figure TFIELD 5-2) was included in the same zone (zone 1) as the lower *T* stochastic areas provided by the base fields. The area east of both the H2/M2 and H3/M3 margins - where the Culebra is bounded both above and below by halite-cemented elements - was defined to be its own zone (zone 3), as was done in AP-114 Task 5. A no-flow boundary roughly follows the axis of Nash Draw defining the final region (zone 4), which is inactive and applies to all parameters.

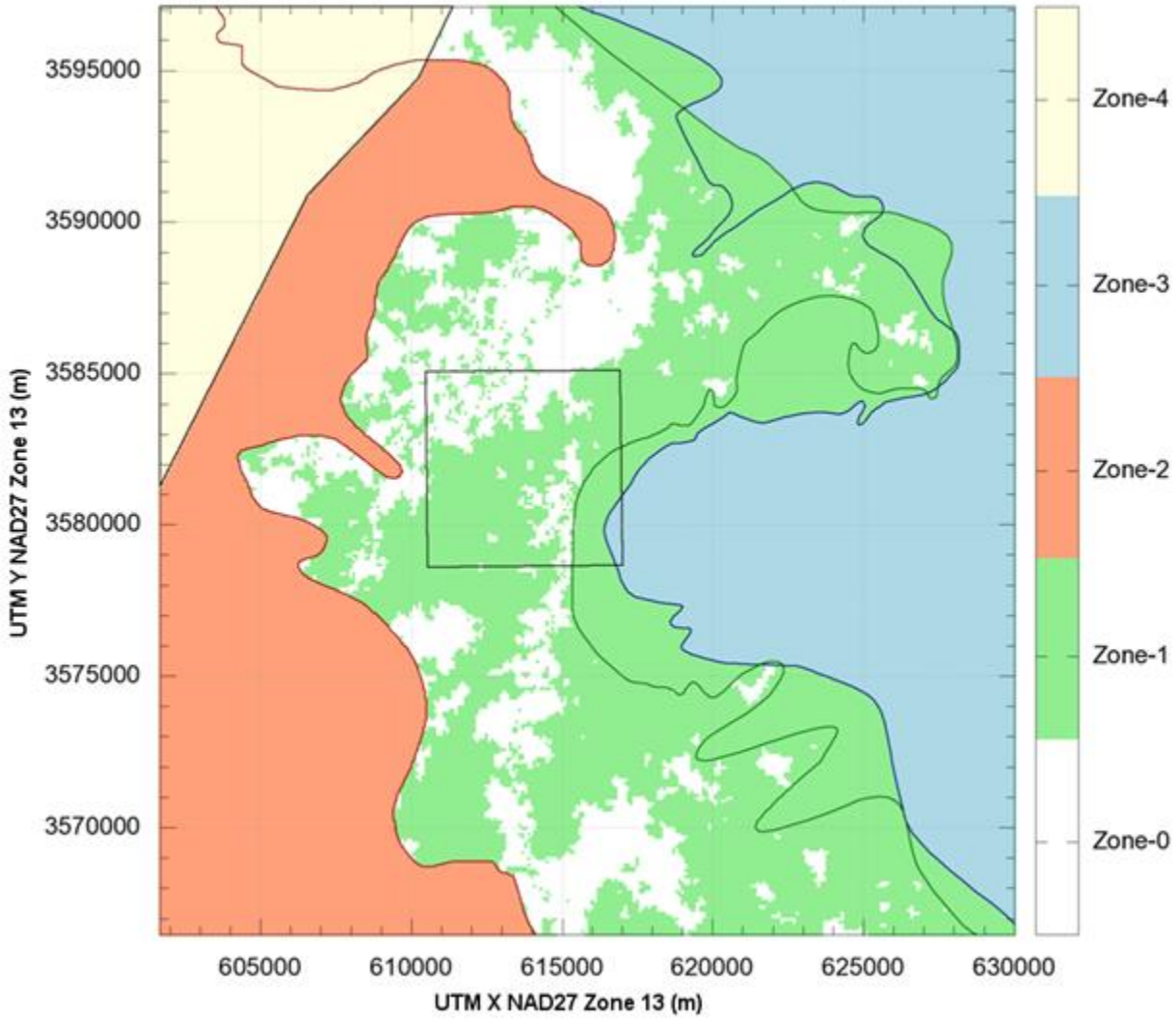

Figure TFIELD 5-2. Transmissivity Zone Map for a Single Realization. Zones 0 and 1 are the stochastic zones created in Hart et al. (2008); Zone 2 is the high-*T* Salado dissolution area; Zone 3 is the very low-*T* halite-bounded area; Zone 4 is the northwestern inactive area.

TFIELD-5.2.1.2 Horizontal Anisotropy Zones

The *T* anisotropy field used the same zones defined for *T*. The *T* values in the north-south (*y*) direction were calculated by multiplying the transmissivity value for the east-west (*x*) direction (given in the T-field) by the anisotropy value (*A*) at a given cell

$T_{NS} = T_{EW} A$. (TFIELD 5.1)

The map shown in Figure TFIELD 5-2 represents the zonation used for both *A* and *T*.

TFIELD-5.2.1.3 Storativity Zones

Besides the no-flow area (zone 4), four zones were defined for storativity estimation. The westernmost region (zone 2) is unconfined, as described in Powers et al. (Powers et al. 2006) (summarized in Section TFIELD-2.3.2). The largest area (zone 0) is fully confined, with its western boundary roughly following the Salado dissolution margin. The area between these two regions (zone

1) is the transition zone, where the Culebra is uncertainly confined. As with the *T* and *A* zones, the area east of both the H2/M2 and H3/M3 margins is a separate region (zone 3), but in this case storativity is simply held constant at the initial confined-zone value. A map of the storativity zones is shown in Figure TFIELD 5-3.

The unconfined zone was implemented as a zone of high confined storativity to simplify the numerical model by approximating the non-linear unconfined problem with a linear storativity one. By defining a much higher storativity value in the unconfined part of the domain, unconfined behavior can be approximately modeled using a confined numerical model, which is linear and executes quicker than the unconfined non-linear model. Since the unconfined or transition zone does not exist inside the WIPP LWB, this choice has little impact on interpretation of transient hydraulic tests there, and this choice has no impact on steady-state flow simulations (*S* is only used in transient simulations) used to predict radionuclide transport in PA.

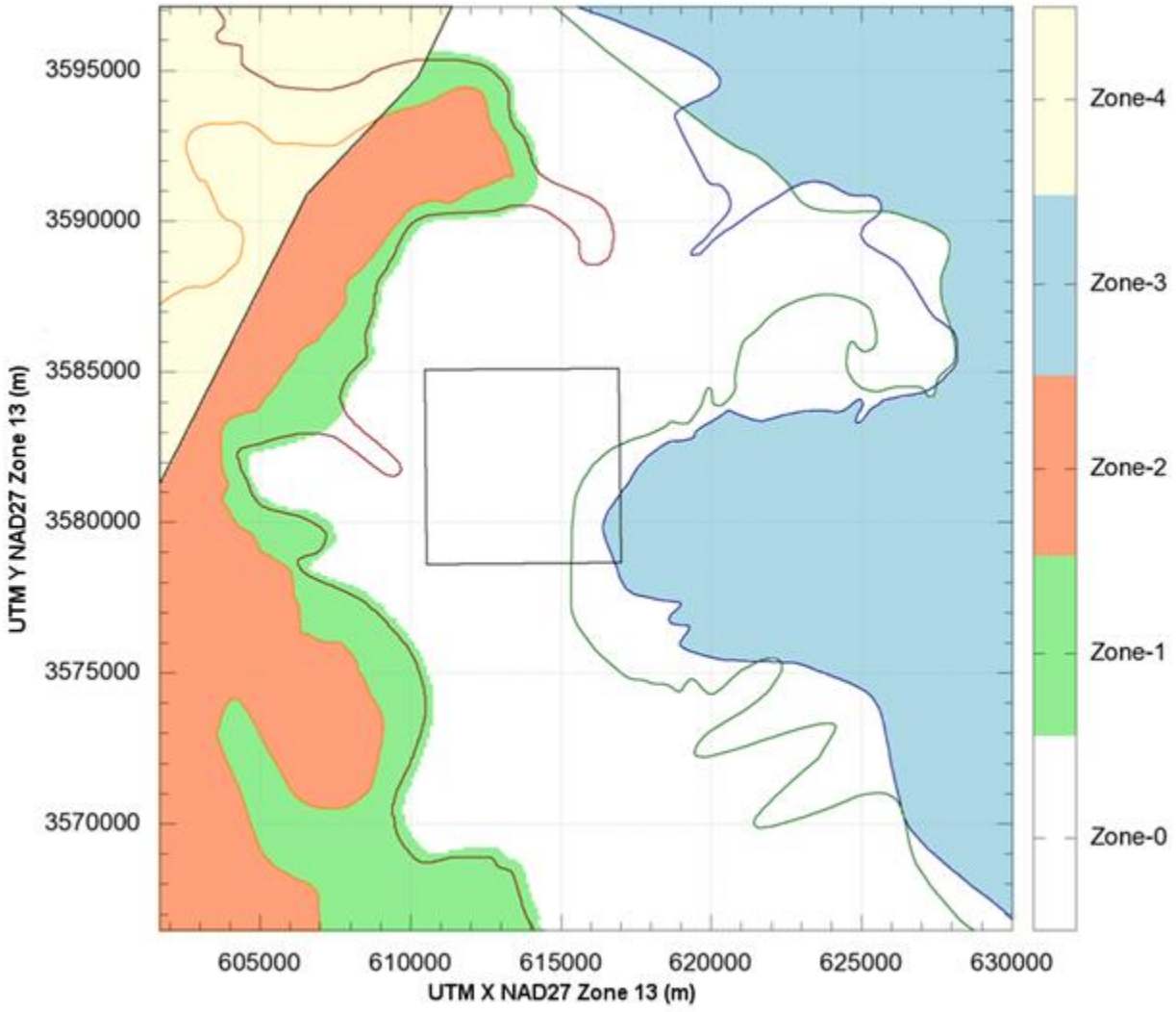

Figure TFIELD 5-3. Storativity Zones. Zone 0 is confined; Zone 1 is a transition between confined and unconfined; Zone 2 is unconfined; Zone 3 is confined and uncalibrated from the initial confined value; Zone 4 is inactive (no flow).

TFIELD-5.2.1.4 Recharge Zones

The conceptual model presented in Holt (Holt 1997) and Hart et al. (Hart et al. 2008) indicates that a groundwater divide exists somewhere southwest of the WIPP site. Previously in CRA-2004 PABC and CRA-2009, this groundwater divide was represented by extending the no-flow zone all the way to the southern boundary (McKenna and Hart 2003). Because the model used in this current task included the unconfined zone, it was decided to model the groundwater divide using recharge instead of a no-flow boundary. The areas of possible recharge were defined in AP-114 Task 1B (Powers 2006), summarized in Section TFIELD-2.3.1. Recharge values had to be extremely small (on the order of 10^{-11} m/s) to ensure convergence of steady-state MODFLOW simulations. Rather than try to determine which of the configurations presented in Task 1B was the "best" approximation, a similar simple approximation to the older no-flow approach was used. A recharge zone consisting of a line of cells extending NW to SE along the axis of the largest topographic feature (and roughly following the old no-flow boundary from McKenna and Hart (McKenna and Hart 2003) was used as the recharge zone. See Figure TFIELD 5-4 for a map of the recharge zone.

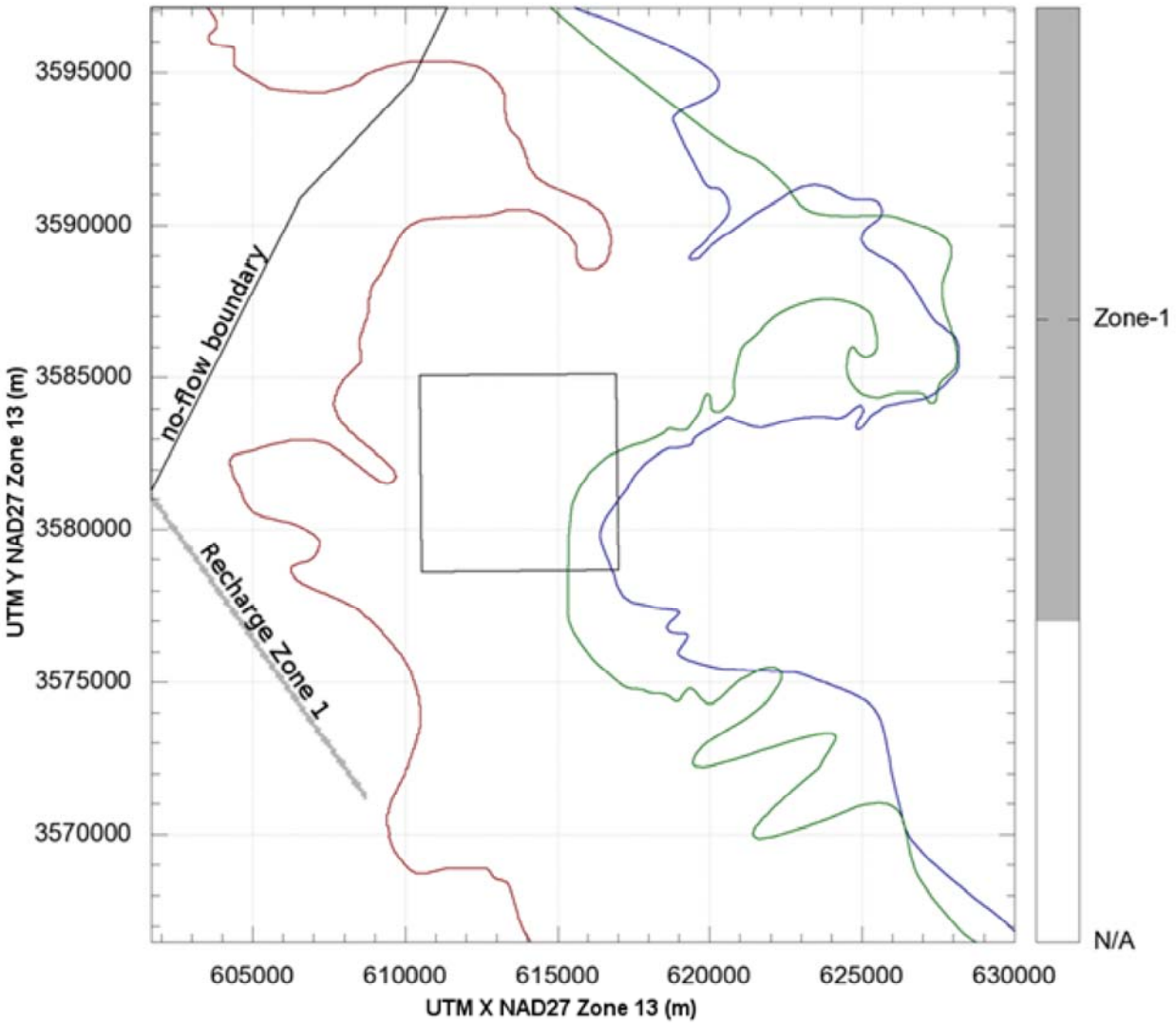

Figure TFIELD 5-4. Zone 1, the Zone of Non-zero Recharge. Zone 1 is the linear feature directed southeast from the center of the west edge of the model domain. The remaining model area has no recharge.

TFIELD-5.2.1.5 Flow, No-Flow, and Fixed-Head Zones

While the boundary conditions were not variable parameters in the calibration, the definition of the specified-head boundary conditions was an important part of the setup and configuration step. The no-flow zone in the northwest was defined to be the same as was used in AP-088 for CRA-2004 PABC. Though the *T* in this area is extremely low (10^{-13} to 10^{-11} m^2/s), there should be some flow exiting along the zone margin, however minute. Testing at SNL-6 and SNL-15 indicates that the hydraulic heads in this area may be recovering ultimately to levels above the land surface (Roberts 2007; Bowman and Roberts 2008; Appendix HYDRO-2014, Section 7.1). The "halite-sandwiched" zone east of either M2/H2 or M3/H3 was simultaneously made extremely low *T* and set to fixed-head values at the ground surface elevation. While this meant that the head values at SNL-6 and SNL-15 were no longer estimable, it was considered the simplest way to model the nearly stationary nature of the water in this zone using MODFLOW-2000. The flow zones are shown in Figure TFIELD 5-5, and the selection of the initial values is discussed in Section TFIELD-5.2.7. The northern, western, and southern flow boundaries were all fixed-head boundaries.

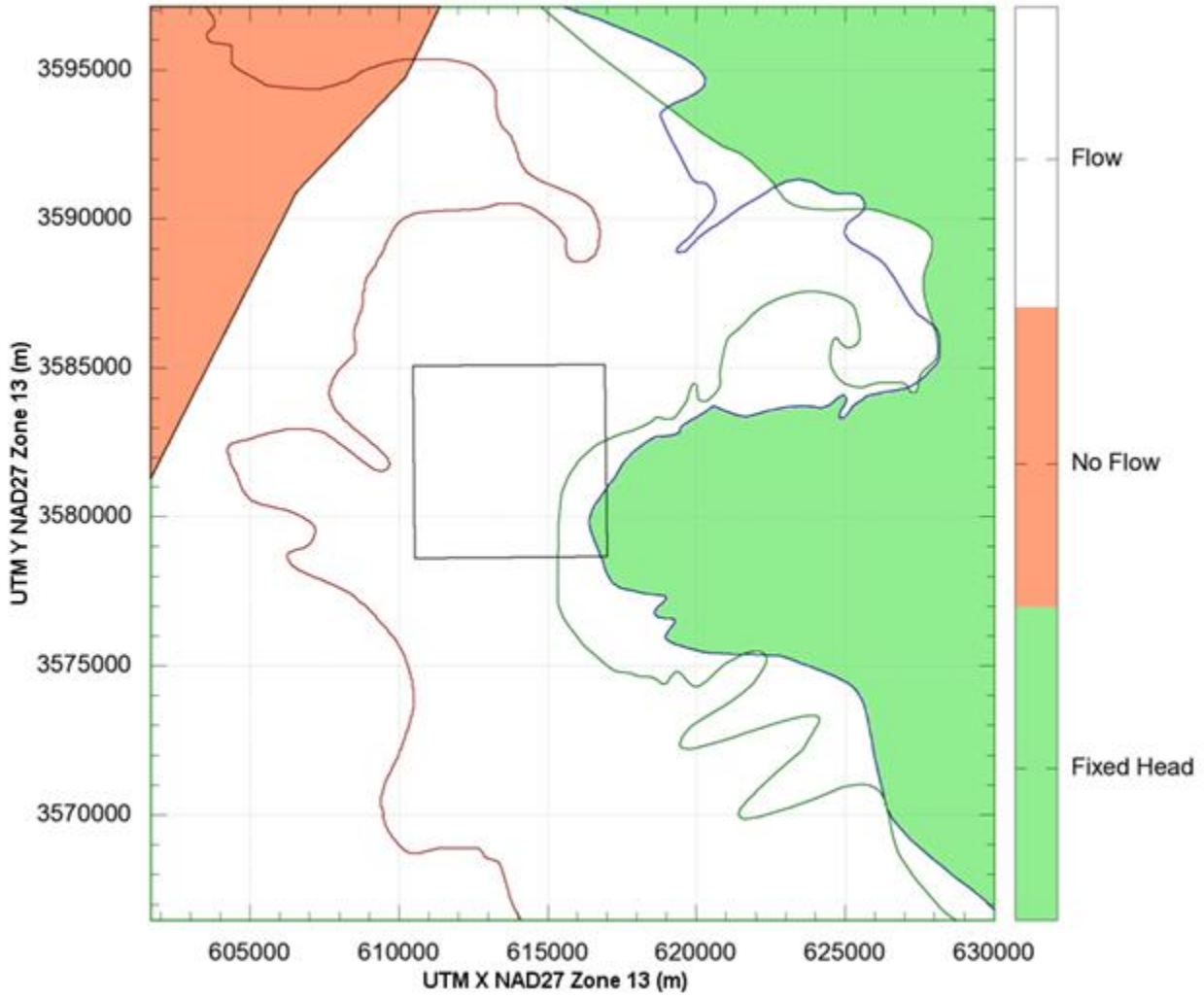

Figure TFIELD 5-5. Flow Zones. The fixed-head zone is green; the no-flow zone is salmon; the white area is normal flow. The fixed-head zone includes one cell along the northern, southern, and western boundaries.

TFIELD-5.2.2 Selection of Pilot Point Locations

Once the zones were defined, pilot point locations were selected. There were two types of pilot points, fixed and variable, and two placement approaches, gridded and linear. Selection of the points for each parameter required a combination of both types and approaches. The exact algorithm used to calculate placement is detailed in Hart et al. (Hart et al.2009), and resulted in the pilot point locations used and shown in Figure TFIELD 5-6 through Figure TFIELD 5-9.

TFIELD-5.2.3 Transmissivity-Specific Pilot Point Settings

In addition to pumping test wells, extra pilot points were placed in the transmissivity fields. These were included along the northern and southern boundaries to try to limit the effects that the fixed-head boundaries would have on transient pumping and the steady-state model results. The estimated *T* values from single-well pumping and slug tests were used as fixed *T* points that corresponded to the tested wells (see Table TFIELD 4-2 for test-derived transmissivity values). See Table TFIELD 5-3 for the ranges of pilot point values used, and see Figure TFIELD 5-6 for pilot point locations.

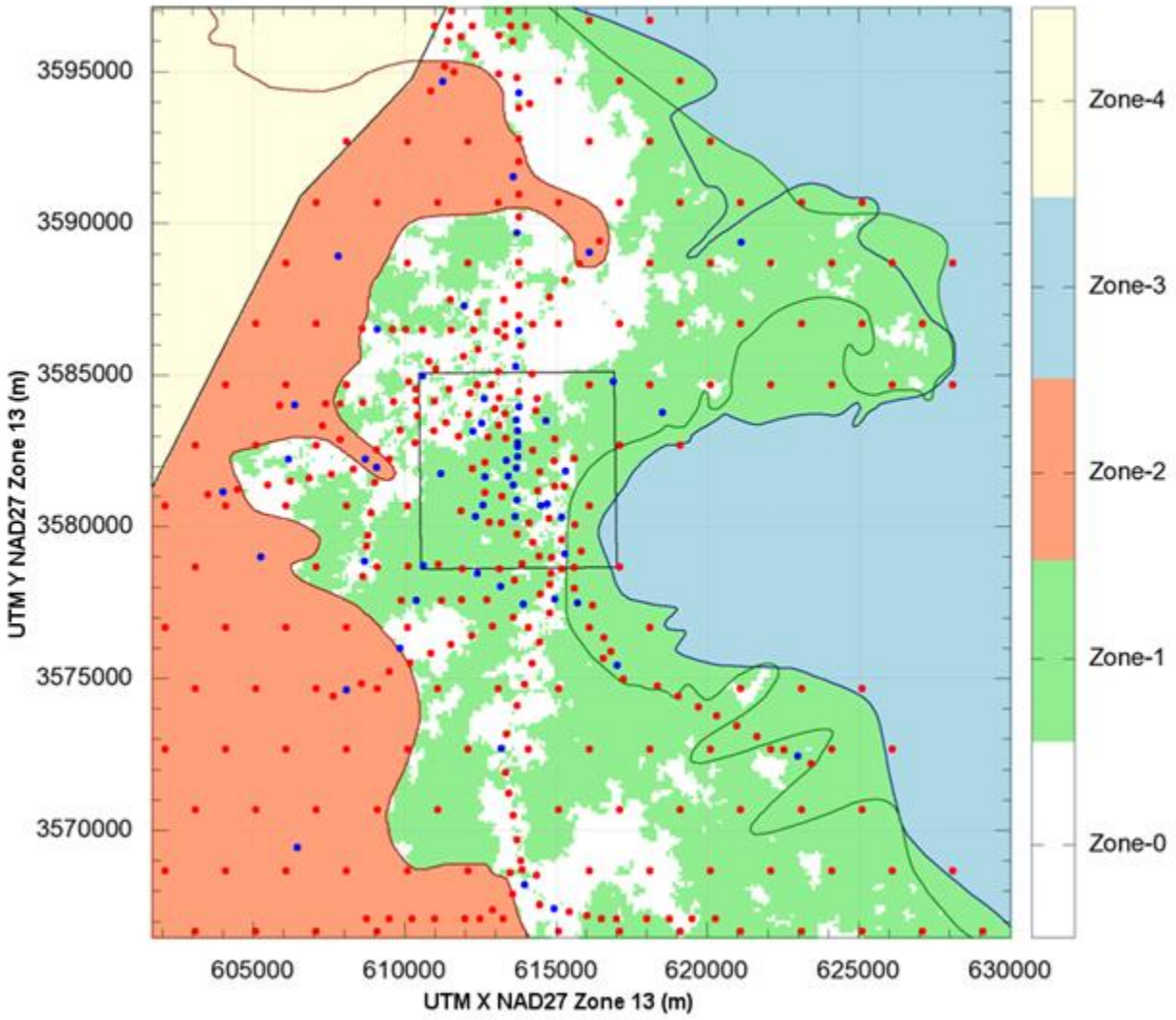

Figure TFIELD 5-6. Transmissivity Pilot Point Locations. Blue points are fixed values and red points are variable parameters. Zones correspond to a single realization.

Table TFIELD 5-3. Initial Values of Parameters at Pilot Points

Parameter	Zone	$\log_{10}$ Value[1]	Pilot Point $\log_{10}$ Calibration Limits
Transmissivity	Zone 0	$-0.003484\ d(x,y) - 3.6322$	[−19.0,−1.0]
	Zone 1	$-0.003484\ d(x,y) - 5.6981$	[−19.0,−1.0]
	Zone 2	$-0.003484\ d(x,y) - 2.9463$	[−19.0,−1.0]
	Zone 3	$-0.003484\ d(x,y) - 10.4490$	[−19.0,−1.0]
Anisotropy	All Zones	0.0	[−0.5, 0.5]
Storativity	Zone 0	−5.0	[−5.5,−4.5]
	Zone 1	−4.0	[−6.0,−0.5]
	Zone 2	−1.5	[−2.5,−0.5]
	Zone 3	−5.0	Fixed
Recharge	Zone 1	−11.0	[−19.0,−1.0]

[1] $d(x,y)$ is Culebra overburden thickness.

TFIELD-5.2.4 Anisotropy-Specific Pilot Point Settings

Anisotropy was unique because no fixed values and therefore no fixed pilot points were used. This result is due to the single-well tests not providing any estimate of anisotropy, and the multi-well tests providing too localized an estimate of anisotropy (only valid for a single cell or two in the model). See Figure TFIELD 5-7 for the locations of anisotropy pilot points.

TFIELD-5.2.5 Storativity-Specific Pilot Point Settings

The only variable storativity pilot points in the confined zone were along straight lines connecting pumping and observation wells in transient pumping tests. The gridded points were set as fixed values, since it was assumed there was no information allowing for effective calculation of storativity outside the transient tests. All pilot points located within the unconfined and transition zones were defined as variable. See Figure TFIELD 5-8 for the location of storativity pilot points.

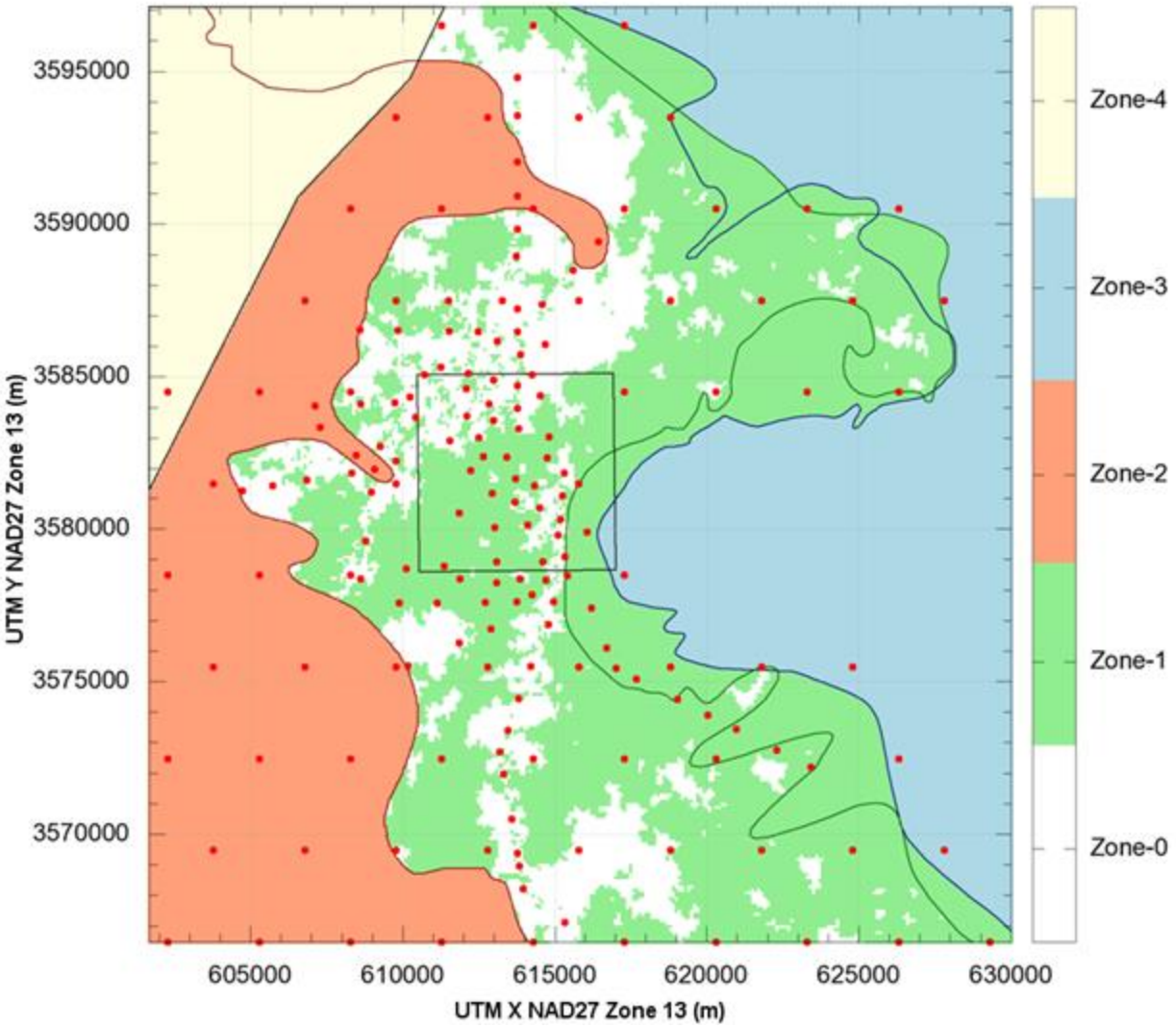

Figure TFIELD 5-7. Anisotropy Pilot Point Locations. All anisotropy pilot points were variable parameters. Zones correspond to a single realization.

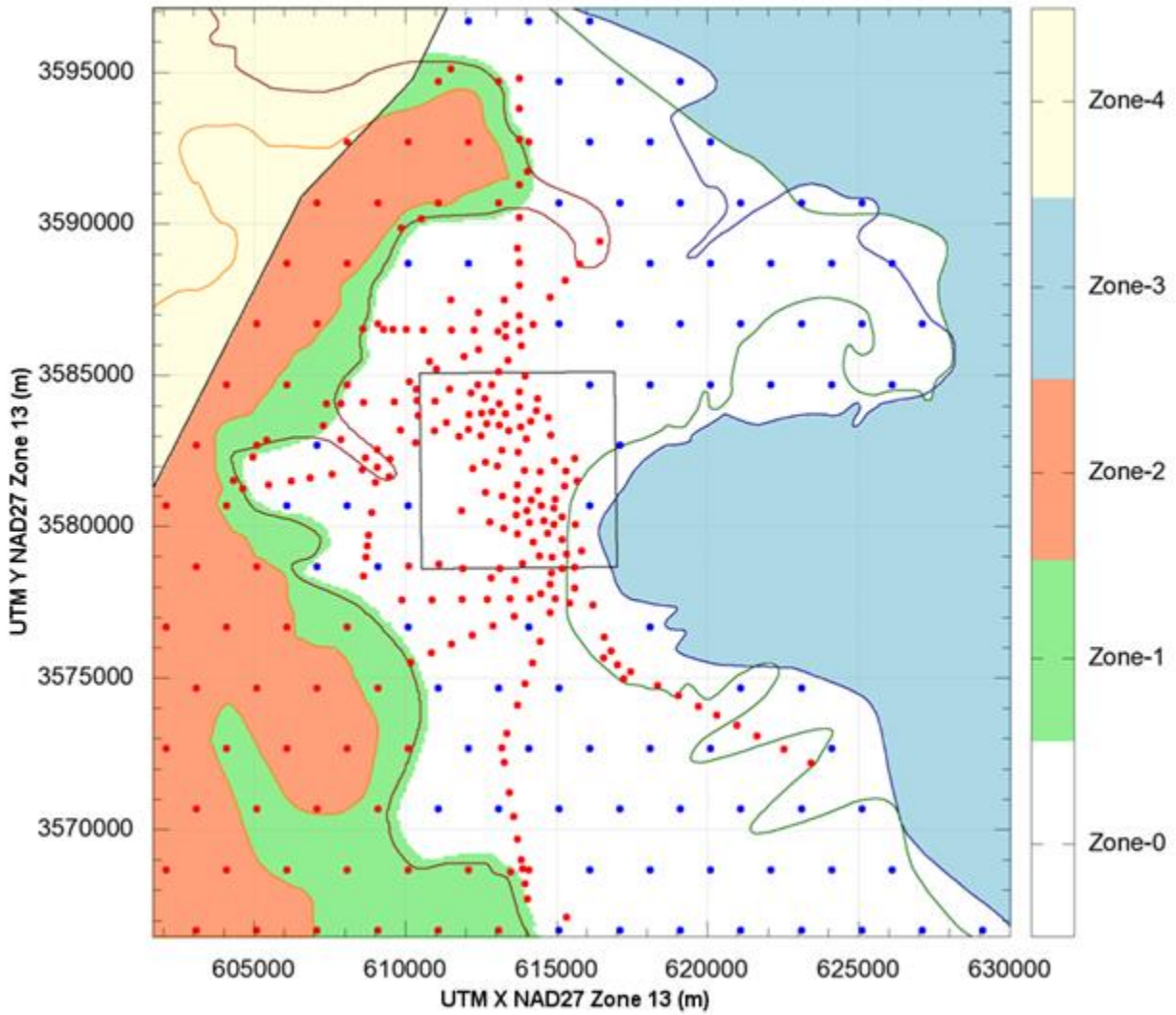

Figure TFIELD 5-8. Storativity Pilot Point Locations. Only pilot points along lines between wells in transient pumping tests and points in the unconfined zones (zones 1 and 2) were variable (red dots); the remaining pilot points were fixed (blue dots).

TFIELD-5.2.6 Recharge-Specific Pilot Point Settings

Because the recharge zone was a line, only four pilot points were needed in the entire zone. In this case, the pilot point nearest the western domain boundary was set as a fixed value of 10^{-30} m/s, which was interpreted as zero by the pre-processors to MODFLOW, and the other three were variable. See Figure TFIELD 5-9 for the location of the recharge pilot points.

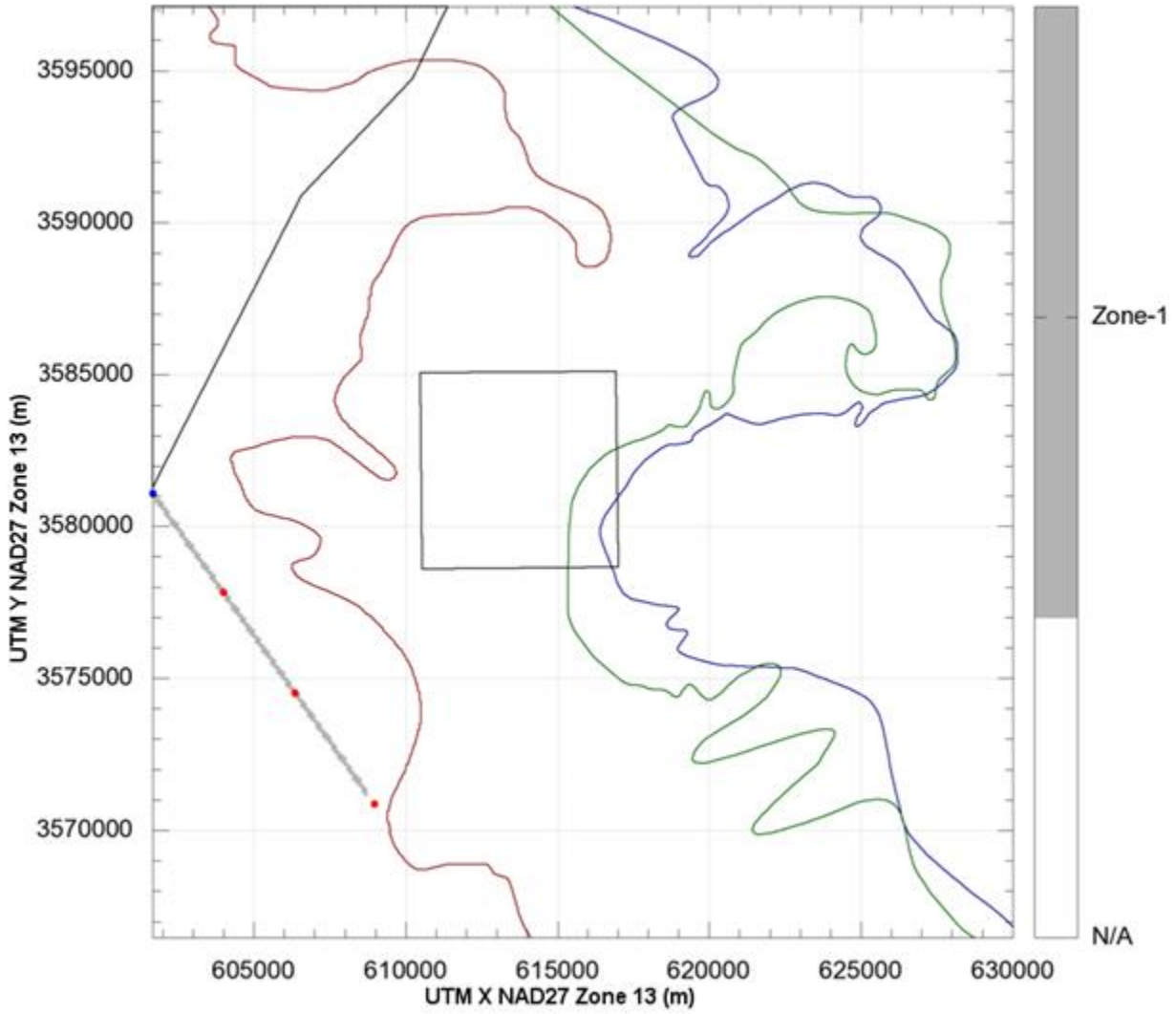

Figure TFIELD 5-9. Recharge Pilot Point Locations. The pilot point along the model domain boundary was fixed, while the other three points were variable.

TFIELD-5.2.7 Selection of Initial Values

Section TFIELD-5.2.7.1 discusses the initial values assigned to parameters before calibration, while TFIELD-5.2.7.2 discusses the assignment of a head field to the initial condition and certain specified-head boundary conditions in the groundwater flow model.

TFIELD-5.2.7.1 Parameter Initial Values

The initial values for each of the pilot points were defined according to the conceptual model and the values presented in Hart et al. (Hart et al. 2008), and summarized in Section TFIELD-3.0. For *T*, this meant that the same equation used to create the base *T* fields was used to define the initial values for the pilot points, based on their zone. Anisotropy was set to isotropic conditions ($A = 1$) for all points. Storativity was defined to start at 10^{-5} for the confined zone (the same value that was used for *S* in CRA-2004 PABC model AP-088), at 10^{-4} in the transition zone, and at $10^{-1.5}$ in the unconfined zone. Recharge was initialized as 10^{-11} m/s, a value found to be sufficiently small to allow MODFLOW to perform an initial run prior to PEST calibration. The zone-by-zone initial values for each parameter,

and the limits placed on the range the values could take in calibration, are presented in Table TFIELD 5-3. See Table TFIELD 4-2 for fixed *T* values.

TFIELD-5.2.7.2 Initial Head Field

Initial heads (H_0) were created using a multivariate equation based on normalized *x* and *y* coordinates ($-1 \le \{x,y\} \le +1$). The equation was designed to keep head along the northern boundary just above the measured head at SNL-1 and head along the southern boundary below the level measured at H-9c. These constraints were the defining factors on the constants in the equation that follows. This process was done only once, and the result was used as a static input file for all calibrations. The field was defined by the following equations

$$x = \left.\frac{i}{142}\right|_{i=-142,-141,\ldots 140,141}$$

$$y = \left.\frac{j}{142}\right|_{j=-153,-152,\ldots 152,153}$$

$$H_0(x,y) = 928 + 8\left[y + sign(y)\sqrt{|y|}\right] + 1.2\left(x^3 - x^2 - x\right) \quad \text{(TFIELD 5.2)}$$

where *sign*() is the sign of its argument (either +1 or -1) and $|y|$ is absolute value. For values east of both the H2/M2 and H3/M3 boundaries, the ground-surface elevation was used as the initial head value; see Appendix A of Hart et al. (Hart et al. 2009) for details. The resulting initial head field is shown in Figure TFIELD 5-10.

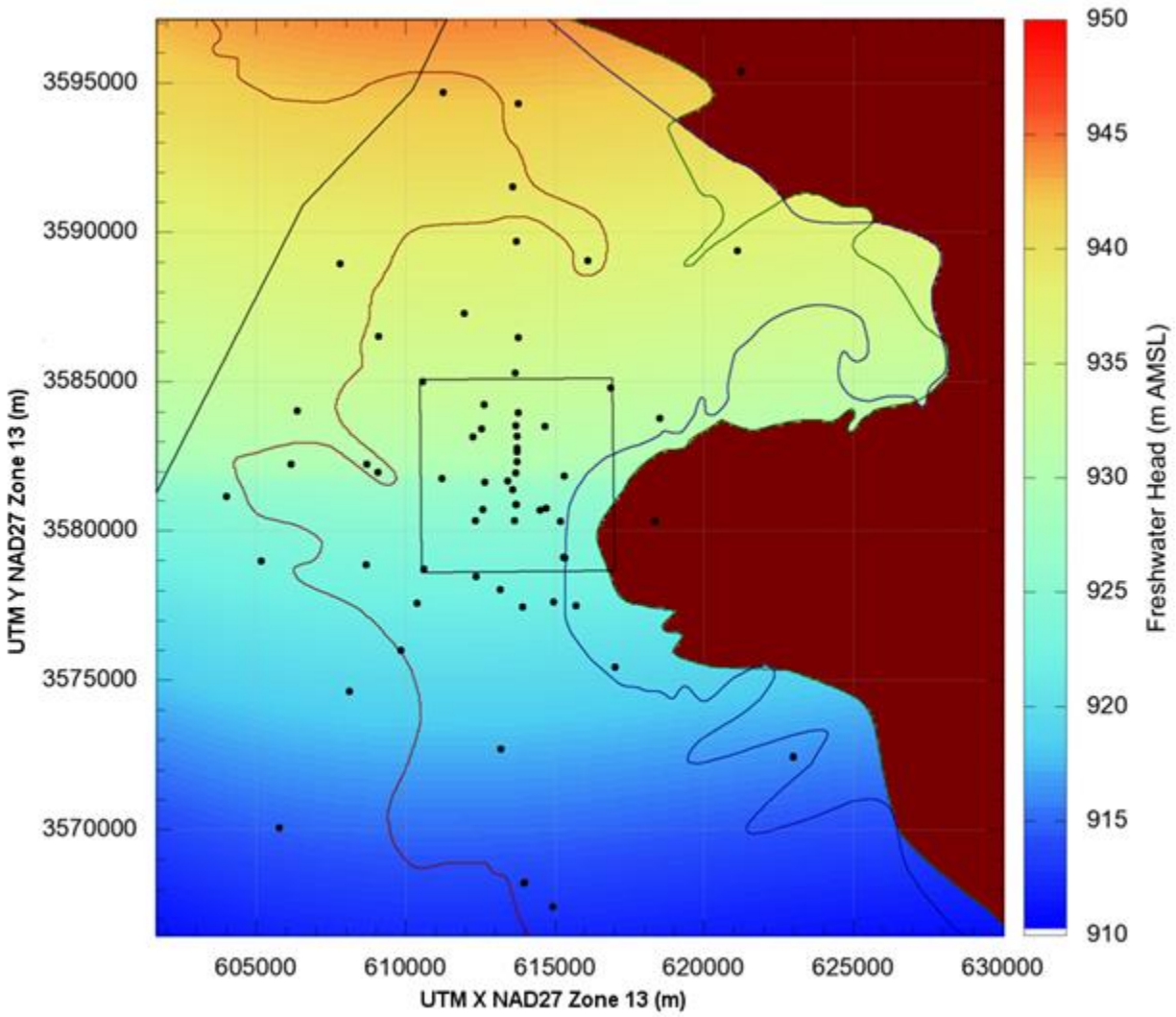

Figure TFIELD 5-10. Initial Head Values for Use in MODFLOW Steady-state Solution. Brick red head values were fixed at the ground surface elevation (>1,000 m AMSL).

TFIELD-5.2.8 Creation of Transmissivity Fields

Transmissivity fields are created from pilot points using kriging. Some pilot points are adjusted using PEST, while other pilot points are held fixed, because they correspond to estimated *T* values at wells with pumping tests. A variogram is needed to interpolate and extrapolate from the pilot points onto every element of the MODFLOW grid.

The transmissivity variogram (different from the indicator kriging variogram discussed in Section TFIELD-4.3) was created using transmissivity values estimated from well tests at 62 of the wells around the WIPP site. Wells outside the model domain and values at SNL-6 and SNL-15 were excluded from the calculation. The values at SNL-6 and SNL-15 are both several orders of magnitude lower than at the other wells, and are in a geologically distinct zone. While initial calculations showed that there was some statistical anisotropy, there were not sufficient measurements to create an anisotropic variogram. The complete steps for creating the variogram are presented in Hart et al. (Hart et al. 2009), Appendix B. The final parameters used are shown in Table TFIELD 5-4.

Table TFIELD 5-4. Parameters for *T* Model Variogram, Fitted to Transmissivity Data Using an Omnidirectional Variogram with Lag Spacing of 1,500 m

Parameter	Value
Model Type	Exponential
Nugget	0.02 $(\log_{10} T)^2$
Sill	1.95 $(\log_{10} T)^2$
Range	9,500 meters

TFIELD-5.2.9 Observations and Residuals

The observations (steady-state freshwater heads and pumping test drawdowns) used as calibration targets for PEST are summarized in Section TFIELD-5.1. Residuals are calculated as the difference between measured and model-generated freshwater heads or drawdowns. The PEST utility program MOD2OBS is used to extract the observations from model output at times and locations associated with each steady and transient observation.

TFIELD-5.2.10 MODFLOW Numerical Model

Inverse modeling (i.e., automatic calibration) requires a numerical model which generates results to compare against observed information. In this task, a MODFLOW 2000 (Harbaugh et al. 2000) flow model was developed for the Culebra that could use the base fields generated in Hart et al. (Hart et al. 2008) as inputs. As was done in CRA-2004 PABC (McKenna and Hart 2003), the link algebraic multi-grid (Mehl 2001) solver was used to increase speed and performance compared to other available solvers. In addition to *T*, it was decided to calibrate the local horizontal *T* anisotropy, storativity, and a strip zone of recharge as parameters in the calibration. Having these four parameters - *T*, *A*, *S*, and *R* - required a slightly more complex MODFLOW model implementation than was used in CRA-2004 PABC AP-088 (McKenna and Hart 2003). Specifically, both storativity and anisotropy were single values previously, and changing these to cell-by-cell values required the use of the layer property flow package instead of the block centered flow package used previously. Using recharge also required the addition of the recharge package; both packages are part of the standard MODFLOW distribution (Harbaugh et al. 2000). For the known information, steady-state heads from 2007 and drawdown results from nine different pumping tests performed between 1985 and 2008 were used as the measured data. A conceptual diagram of the MODFLOW model with its inputs and outputs is shown in Figure TFIELD 5-11.

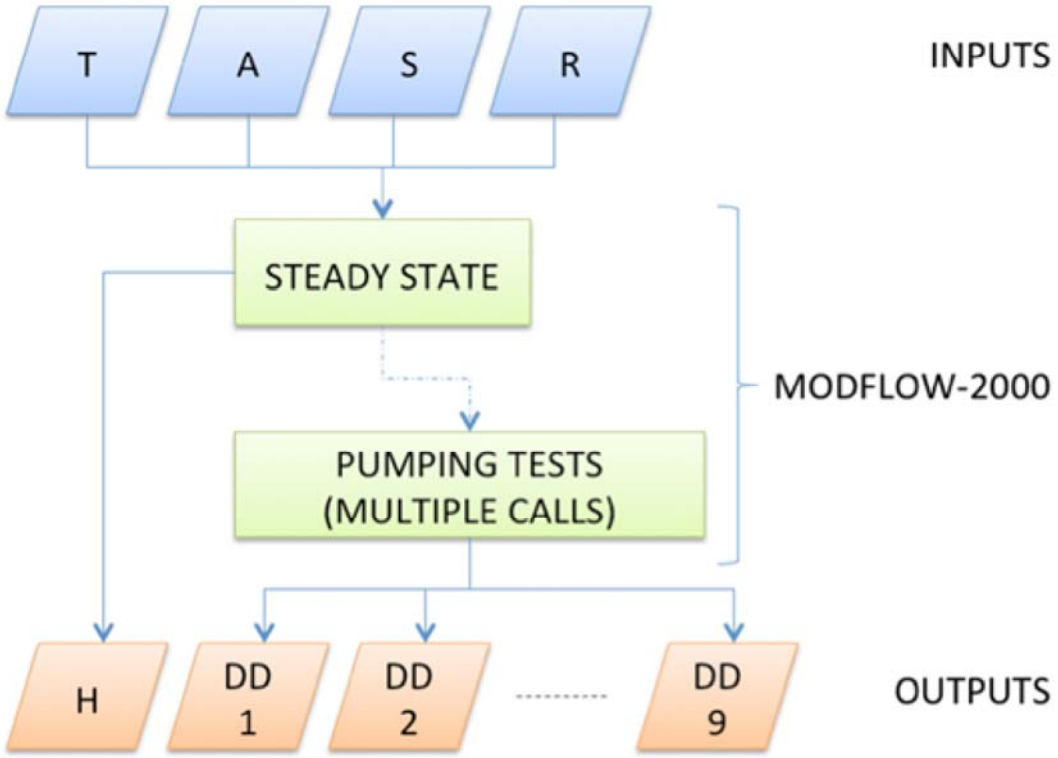

Figure TFIELD 5-11. Flow Chart Showing the Forward Model Used In the Model Calibration. *T*, *A*, *S*, and *R* are parameter fields. *H* represents the steady-state flow solution. *DD* $_1$-*DD* $_9$ represent transient drawdown computed for the 9 individual pumping tests from 9 separate forward simulations.

TFIELD-5.3 Step 2 -Calibration Process

The calibration process used multiple forward model calls to evaluate the impact that perturbing an input parameter has on model predictions at locations and times corresponding to observations. This process was computationally intensive, and involved 80 processors on 2 different computing clusters running for 6 months to calibrate 200 of the 1,000 base *T* fields.

TFIELD-5.3.1 PEST Calibration Process

The calibration process was done using the PEST inverse modeling software suite and its groundwater utilities. The steps involved in each forward model run during the PEST calibration are illustrated in Figure TFIELD 5-12; the complete calibration process is shown in Figure TFIELD 5-1.

The completed PEST simulation included the creation of the fields from the kriging factors and pilot points (PPK2FAC, FAC2REAL, REAL2MOD), the MODFLOW calls, and finally the observation extraction utilities (MOD2OBS and OBS2REAL), which extract modeled cell head or drawdown values from a binary MODFLOW output file. For SVD iterations, another preprocessor, PARCALC, is used to create the pilot point values from the super parameters (i.e., eigenvectors related to the largest eigenvalues - see description in TFIELD-5.0). The model script (model.sh), the REAL2MOD script, and the OBS2REAL script were written for this task, and are included in Appendix G of Hart et al. (Hart et al. 2009). PPK2FAC, FAC2REAL, and MOD2OBS are PEST utilities.

The first call to the PEST program was a single outer iteration to estimate the Jacobian matrix. This required over 1,100 forward model calls, one for each variable parameter value. Once the Jacobian matrix was calculated, the SVDAPREP program decomposed the Jacobian matrix into eigenvectors and kept the super parameters corresponding to the largest singular values. The result was a set of 100 to 300 super parameters that were then used with a 50-iteration PEST calibration. The termination criteria were:

1. a maximum of 50 iterations,
2. three successive iterations without an improvement in the objective function, or
3. a relative decrease of less than 0.001 in the objective function for three iterations.

Once termination criteria had been reached, the PEST program would output the best parameters to a file. This file was then used to create one final PEST control file, which issued a single model run with the best parameters as input. The results of this final call were then used to calculate the measures of fit and the final fields.

The run control details regarding the calibration process are presented in Appendix G of Hart et al. (Hart et al. 2009). Using the ReadScript.py run control system allowed automatic check-out of input files, execution, and check-in of the results to version control following calibration.

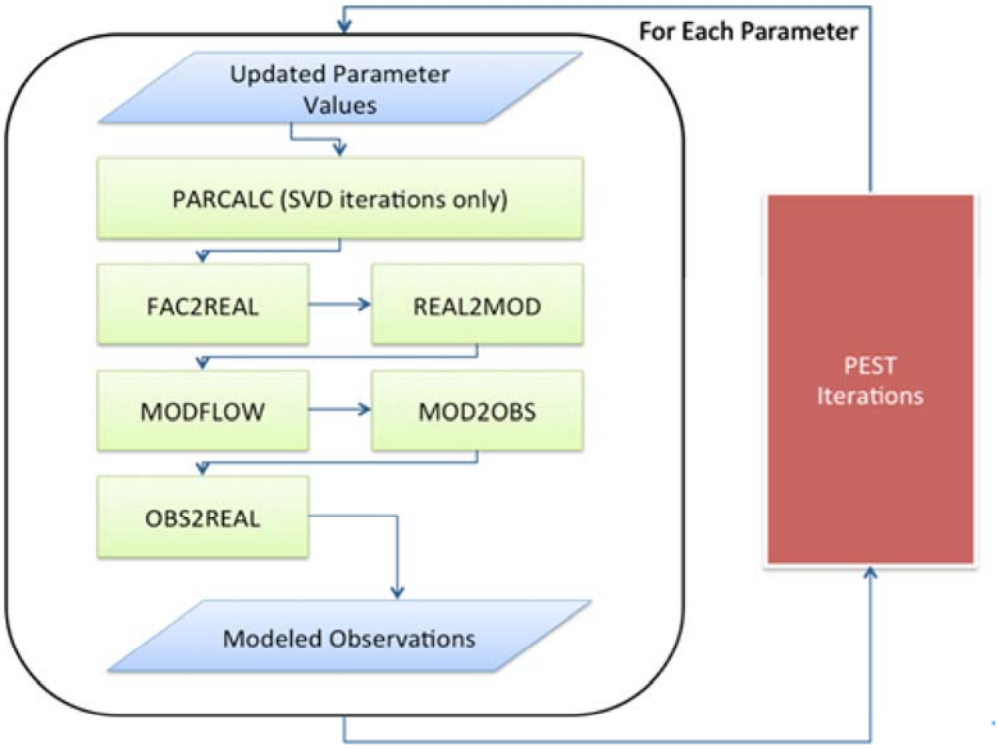

Figure TFIELD 5-12. Flowchart Illustrating the PEST Calibration Process

TFIELD-5.3.2 Calibrated Correction of Steady-State Head Values

Because some of the original steady-state calibration targets were incorrect, the fields that had already been calibrated to the incorrect data needed to be recalibrated to the new data. The two wells with the most significant changes, ERDA-9 and SNL-8, had more than one meter change from the old to new

values. At ERDA-9 the calibrations had consistently been unable to match the incorrect head value, which was too low compared to the higher corrected value. Without any recalibration, correcting the value for ERDA-9 produced better model fits.

TFIELD-5.3.2.1 Localized Recalibration in the Vicinity of SNL-8

The new calibration target for SNL-8 was based on a recalculation of the freshwater head (Johnson 2009a and Johnson 2009b). Because SNL-8 was not an observation well in any of the transient pumping tests, and because it was to the east and upgradient from the WIPP LWB, only a section of the fields were recalibrated to correct for the change in the calibration target at SNL-8. It was hoped that this would allow the *T*, *S*, *A* and *R* fields to change to match the SNL-8 head without requiring the week-long recalibration for each of the affected fields if the entire domain was recalibrated.

The recalibration process involved fixing all the parameters that had previously been calibrated, except for those parameters in a rectangular area around and upgradient from SNL-8. The complete area definition was 14 km east-west by 9 km north-south with the southwest corner at 616000 m X, 3580000 m Y UTM NAD27, and is shown in red on Figure TFIELD 5-13. All other aspects of the automatic calibration, including the forward model and the SVD assist process, were left the same. The resulting fields had significantly better fits to the steady-state heads, and little impact was seen on the transient test results (Table TFIELD 5-5).

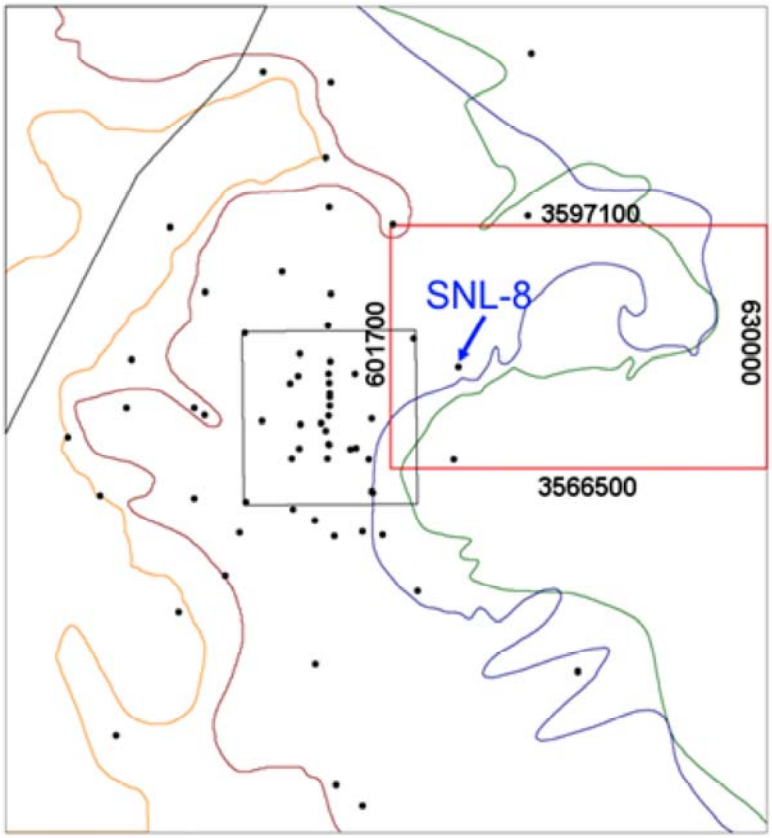

Figure TFIELD 5-13. Recalibration Boundary Shown in Red To the Northeast of the WIPP Site. Recalibration boundary limits are UTM *X* and *Y* NAD27 Zone 13 (m).

TFIELD-5.3.2.2 Continued Recalibration Activity

After examination of the acceptance criteria (discussed in the next section), some fields were recalibrated again, using the same recalibration process but holding none of the parameter values fixed at previously calculated values. This process essentially added some additional calibration iterations to these fields. This was only done on 15 fields that were now completely within the acceptance criteria for steady-state heads, and just outside the acceptance criteria for transient tests (Table TFIELD 5-5). The intent of this additional calibration was to increase the quality of the transient fits to get a total of 100 fields that met both the steady-state and transient calibration requirements. This secondary recalibration process was continued until 100 fields were obtained that met the requirements, and it did not always improve fits (i.e., in some cases the fields were already as fully calibrated, given the number of pilot points and observations and initial conditions).

Table TFIELD 5-5. Summary of Statistics Regarding Average Steady-state and Transient Errors Across Three Calibration Groups

	Steady-state Average Error (cm)			Pumping Response Average Error (cm)			
	Minimum	Average	Maximum	Minimum	Average	Maximum	n
A	45.6	68.9	195.0	12.9	16.4	34.2	135
B	50.5	73.8	115.3	12.5	16.5	23.0	50
C	57.8	66.1	72.8	13.9	15.4	17.4	15

A: Realizations with targeted recalibration near SNL-8.

B: Realizations with correct SNL-8 data.

C: Realizations recalibrated twice.

TFIELD-5.3.3 Evaluation of Impact of Multiple Calibration Processes

Because some fields were calibrated only once (set B: 50 fields following correction of the steady-state values), some fields were calibrated once and then underwent a localized recalibration (set A: the 135 first fields calibrated), and some fields even underwent a second round of calibration (set C: 15 fields), the impact this may have had on the final selection of fields was evaluated. Summaries of statistics for these calibration groups are given in Table TFIELD 5-5, while Appendix E of Hart et al. (Hart et al. 2009) contains the complete list of fields.

Because the final selection process did not look at which set of fields the results were taken from, the mix of fields should be similar to a random selection if the calibration processes were producing equivalent results. The random selection of fields from set B can be modeled as a binomial distribution with the p-value of 0.25 and $n = 100$. If the results are within the 95% confidence interval for a random selection of fields, then there should be between 17 and 33 fields selected from the set B. The final results used 83 fields from sets A and C, and the remaining 17 were selected from set B. This is within the confidence interval, so it is concluded that the different processes had no impact on the selection of the final fields. The selection of fields from set C versus those from set A can be modeled the same way, with a p-value of 0.10 and $n = 83$. The final selection included 10 from set C, which is within the confidence interval of 3 to 13 fields, and again the calibration process did not impact the field selection.

Because this mix of final fields is acceptable and came strictly from the cutoff values, and not from any deliberate attempt to select from one group or another, all 100 fields meeting the acceptance criteria are equally good and equally probable representations of the Culebra.

TFIELD-5.3.4 Selection of Best-Calibrated Fields

The selection criteria for the "best" calibrated fields consisted of comparing the absolute error of the modeled steady-state heads (sum of absolute values of residuals between model and data) to a cutoff value, and comparing the absolute average error of the modeled transient responses (sum of absolute values of errors at individual observation wells averaged through time) to a cutoff value. The steady-state and transient criteria were evaluated separately, and only fields that were less than the cutoff value for both sets of tests were selected as the final fields. The final cutoff values used were the mean value of the errors taken across all 200 fields, and are presented in Table TFIELD 5-6. The cutoffs were selected to choose approximately half of the fields. Using the mean values resulted in a set of 102 fields, so the two fields with the largest sum of the two metrics were discarded. In Figure TFIELD 5-14, the sum of the steady-state average errors was graphed against the sum of the transient pumping tests' average errors, and the selected and unselected fields are shown. The trend line shows graphically how PEST allows tradeoffs while keeping the improvement in errors as balanced as possible. The final field IDs are presented in Table TFIELD 5-7.

Table TFIELD 5-6. Cutoff Values for Final Field Selection

Test Type	Average Error Selection Cutoff
Steady State	0.699 m
Transient Pumping Response	0.164 m

Table TFIELD 5-7. Final Selected Field Identifiers

r001	r055	r207	r652
r002	r058	r256	r655
r004	r059	r260	r657
r006	r060	r273	r664
r007	r061	r276	r669
r009	r064	r279	r694
r010	r070	r298	r707
r012	r073	r327	r727
r013	r074	r328	r752
r017	r076	r361	r791
r024	r078	r431	r806
r027	r082	r440	r808
r028	r083	r465	r809
r029	r084	r486	r814
r032	r090	r489	r823
r034	r092	r506	r861
r037	r095	r508	r883
r038	r097	r511	r902
r040	r098	r515	r910
r041	r102	r522	r921
r045	r104	r568	r922
r051	r137	r571	r940

r052	r142	r631	r981
r053	r191	r634	r982
r054	r203	r640	r984

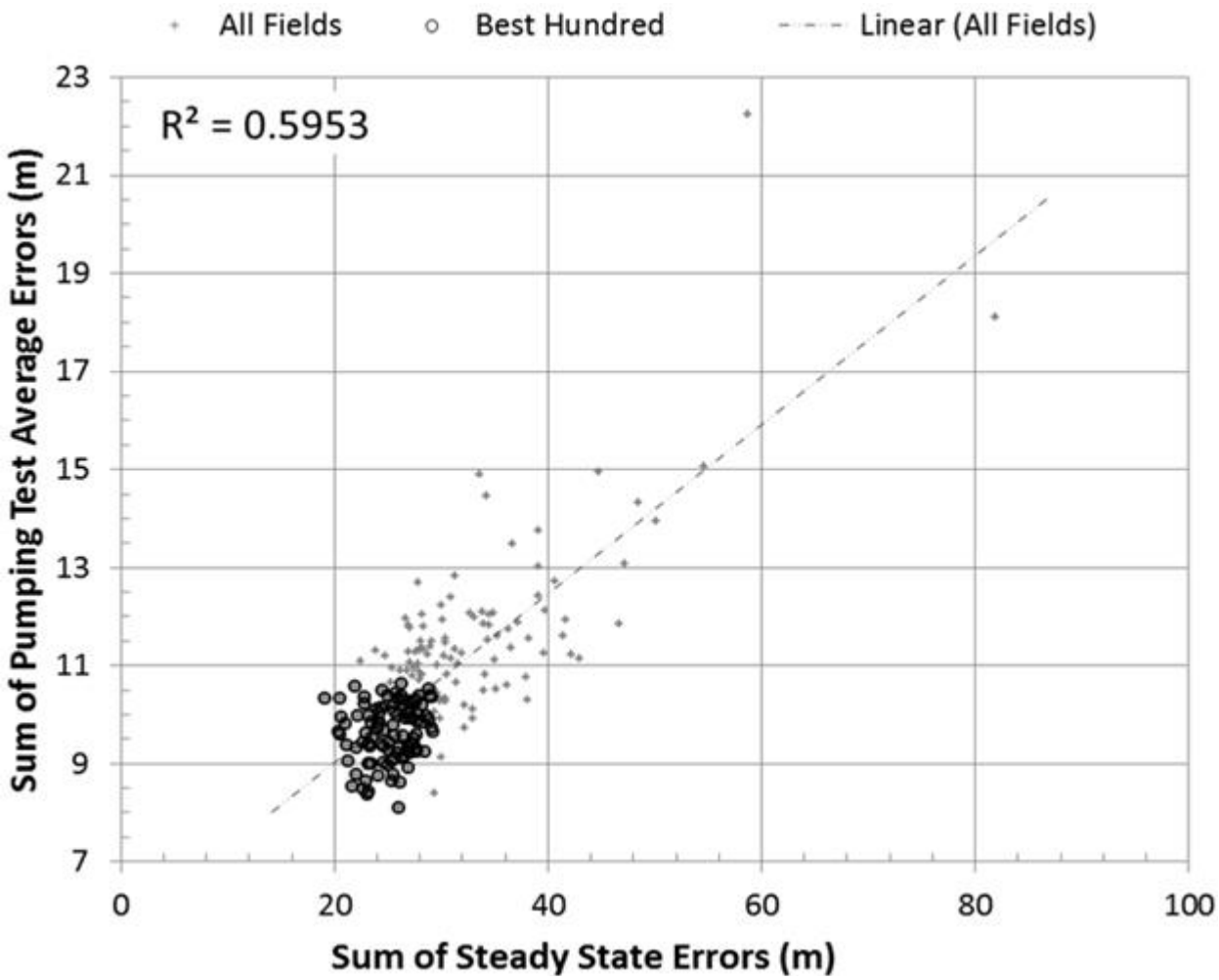

Figure TFIELD 5-14. Selection of Best Fields From All Fields by Weighted Sum of Steady-state Errors and Sum of Average Pumping Test Average Errors

TFIELD-5.4 Step 3 - Post-Calibration Analysis

The post-calibration analysis consisted of performing statistical analyses on the selected fields, and examining the calibrated forward model outputs. The full results of the steady-state forward model outputs are presented in Appendix C of AP-114 Task 7 (Hart et al. 2009), pumping test results are presented in Appendix D, and tabular results are presented in Appendix E of the same report. Calibrated model inputs and outputs for the 100 selected fields are presented in Attachment A to Appendix TFIELD.

TFIELD-5.4.1 Statistical Analysis of Resulting T, A, and S Fields

Plots of mean and standard deviation of the final 100 fields are given in Section TFIELD-5.4.1.1. The bulk *T* of the final calibrated fields are also compared to the bulk *T* of the base fields, using membership in the high or low *T* categories. Similarly, Sections TFIELD-5.4.1.2 and TFIELD-5.4.1.3 show summary statistics regarding the calibrated *S* and *R* fields, respectively.

TFIELD-5.4.1.1 Final Transmissivity and Anisotropy Fields

The T values presented in this section are the effective T values (T_e), which include A. Effective transmissivity was calculated as

$$\log_{10} T_e = \log_{10} T_{EW} + \tfrac{1}{2} \log_{10} A \quad \text{(TFIELD 5.3)}$$

which is the average of $\log_{10}$T in the north-south and east-west directions (see Equation TFIELD 5.1 in Section TFIELD-5.2.1.2). The bulk T_e, which is the average $\log_{10} T_e$ value of all cells in a given zone or zones, was calculated for the central and Salado dissolution region (zones 0-2) and compared to the bulk T_e of the same zones from the base fields. The eastern, very low-T region (zone 3) was compared separately. The bulk T_e values are shown in Table TFIELD 5-8. The mean effective T_e and the standard deviation of T_e are presented in map form in Figure TFIELD 5-15 and Figure TFIELD 5-16. The mean effective transmissivity map does not show the very low T zone east of the halite margins to improve the colormap contrast across the area around the WIPP site.

Because pilot point parameter values were essentially unconstrained for T (they were allowed to change across 18 orders of magnitude as shown in Table TFIELD 5-3), some areas in zones 0 and 1 could change from a low-T zone into the range generally considered high-T and vice versa. The defining value for high-T was set in AP-114 Task 5 (Hart et al. 2008) to be the bulk transmissivity value of the base fields: -5.41 $\log_{10}$ m^2/s. At each cell, the number of fields whose initial and final T values were in the high-T zone was calculated, and the maps of those numbers for the base and calibrated fields are presented in Figure TFIELD 5-17 and Figure TFIELD 5-18, respectively. The total number of fields where transmissivity effectively changed zones is represented graphically in Figure TFIELD 5-19 and Figure TFIELD 5-20. In these figures, the white regions define areas where no fields changed groups. The two measures shown in these sets of maps provide an indication of how the geologically based conceptual model used to create the base fields was altered by the steady-state and transient hydraulic information.

Table TFIELD 5-8. Bulk Log_{10} T_e Values Comparison

Base field bulk $\log_{10} T_e$ (Zones 0-2)	-5.41 $\log_{10}$ (m^2/s)
Calibrated field bulk $\log_{10} T_e$ (Zones 0-2)	-5.02 $\log_{10}$ (m^2/s)
Base field bulk $\log_{10} T_e$ (Zone 3)	-11.74 $\log_{10}$ (m^2/s)
Calibrated field bulk $\log_{10} T_e$ (Zone 3)	-10.47 $\log_{10}$ (m^2/s)

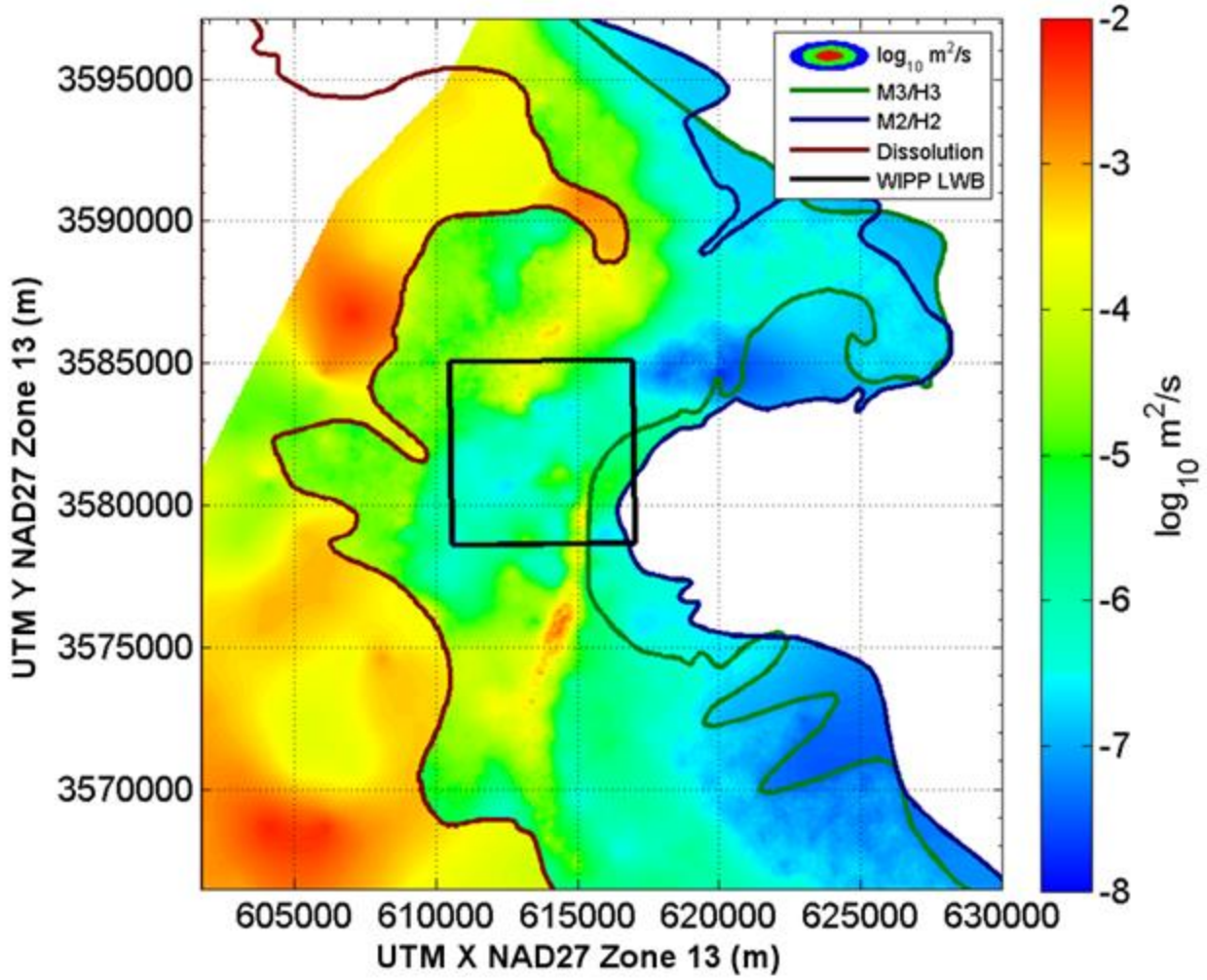

Figure TFIELD 5-15. Mean Effective Transmissivity (T_e) for Zones 0-2 Across the 100 Final Selected Fields. All 100 calibrated T_e fields are plotted in Appendix TFIELD Attachment A.

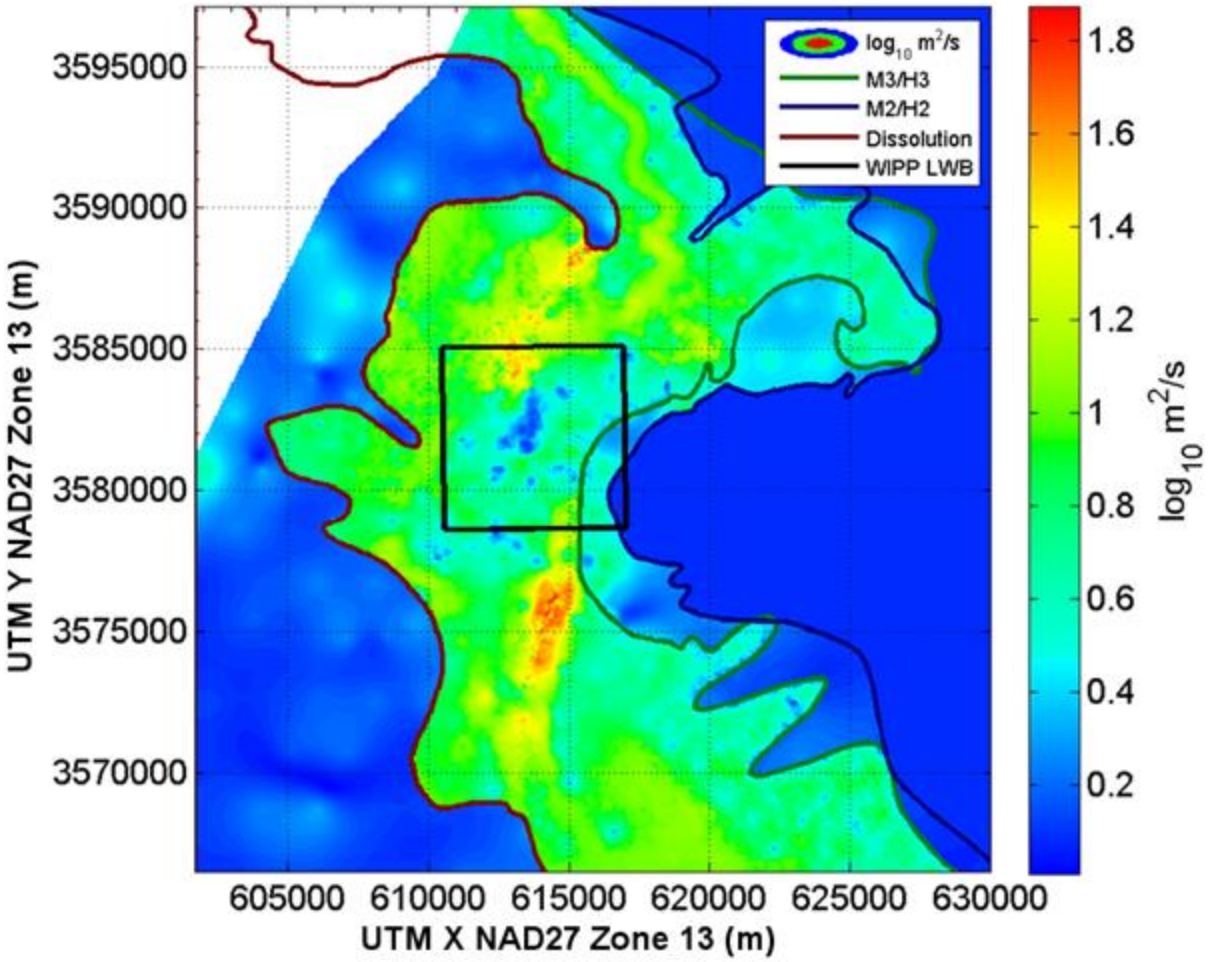

Figure TFIELD 5-16. Standard Deviation of Effective Transmissivity (T_e) for All Zones Across the 100 Final Selected Fields. All 100 calibrated T_e fields are plotted in Appendix TFIELD Attachment A.

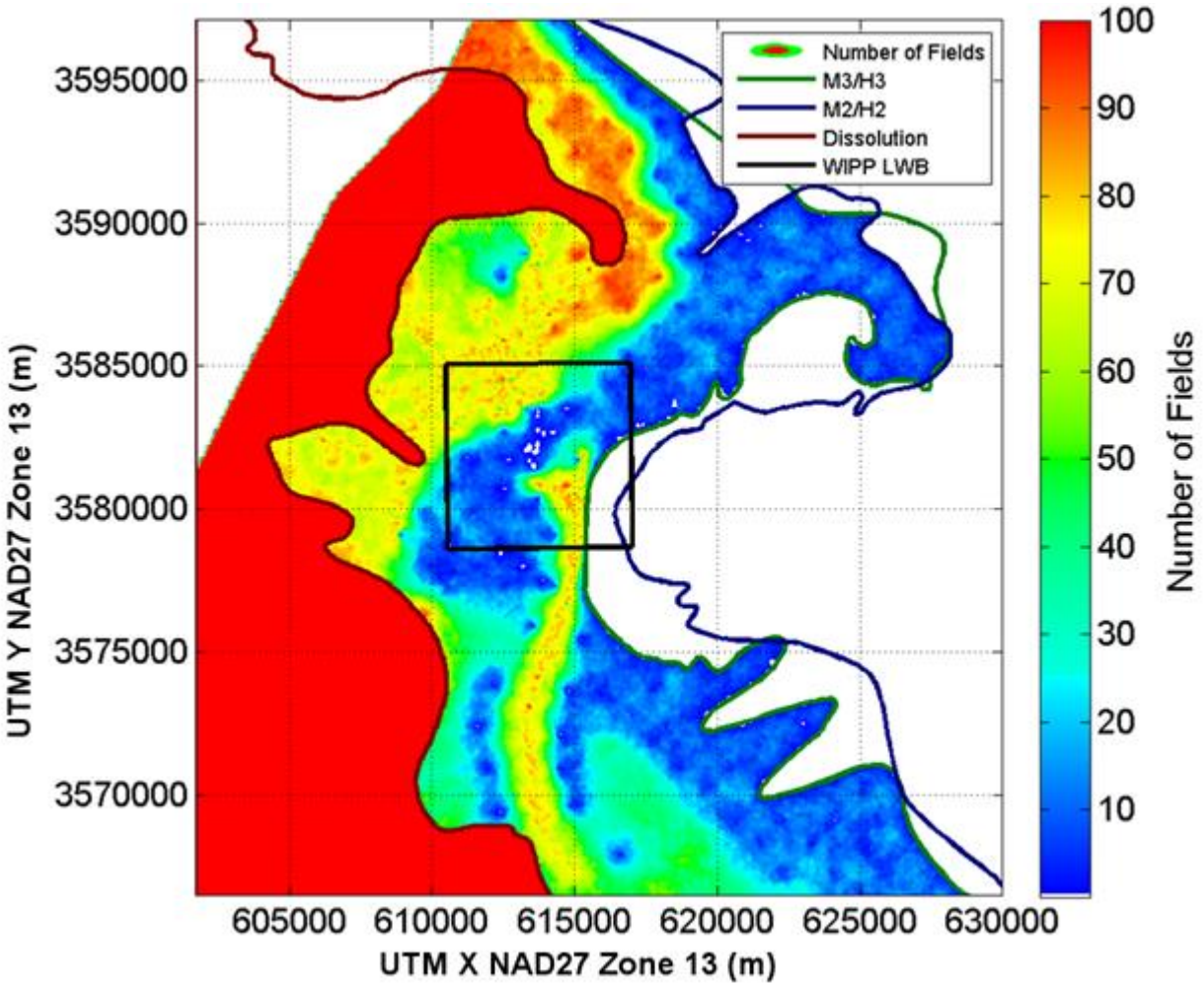

Figure TFIELD 5-17. High-*T* Zone Membership Calculated for the Base 100 *T* Fields Corresponding to the 100 Selected Calibrated Fields

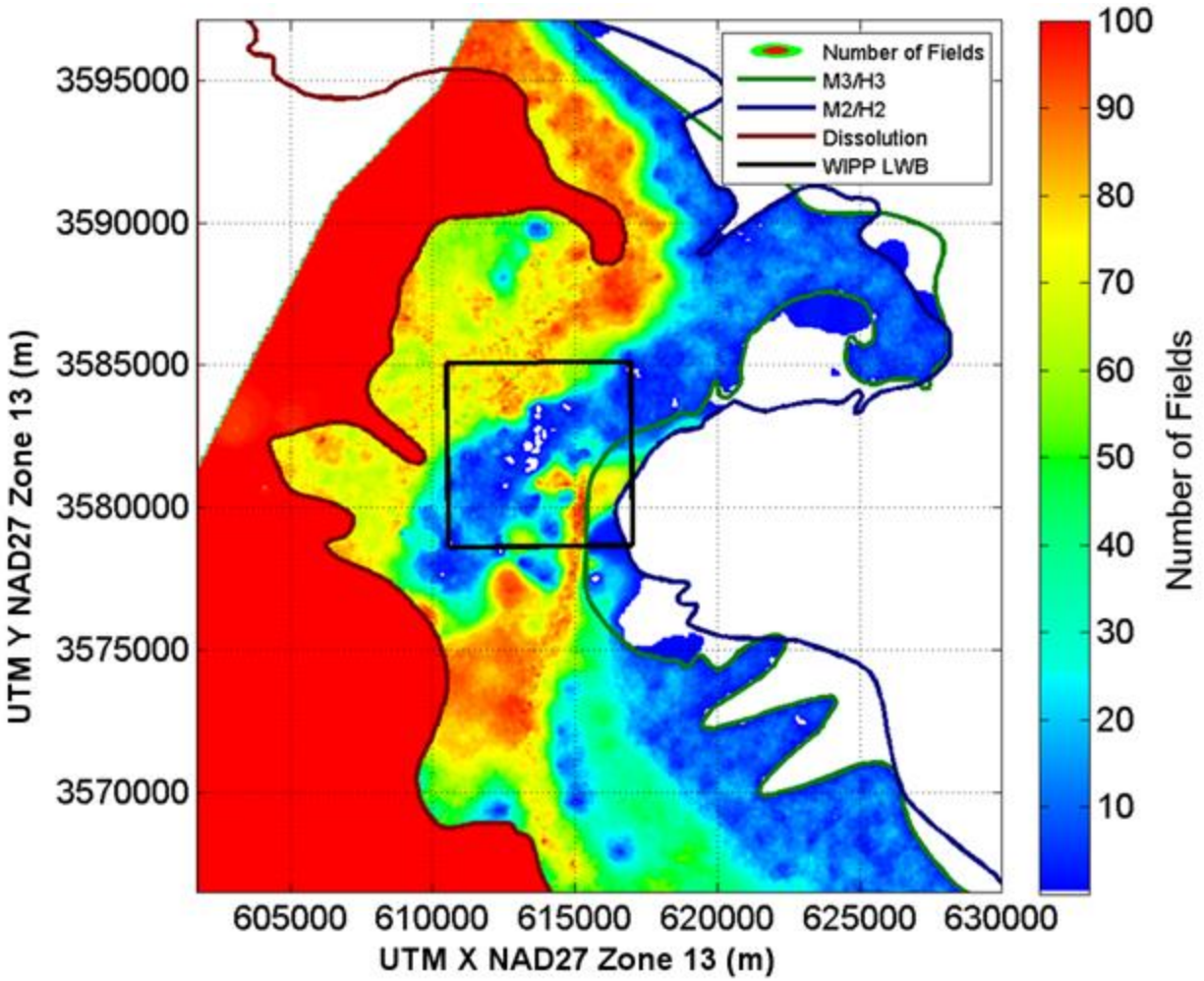

Figure TFIELD 5-18. High-*T* Zone Membership Calculated for the Calibrated *T* Values

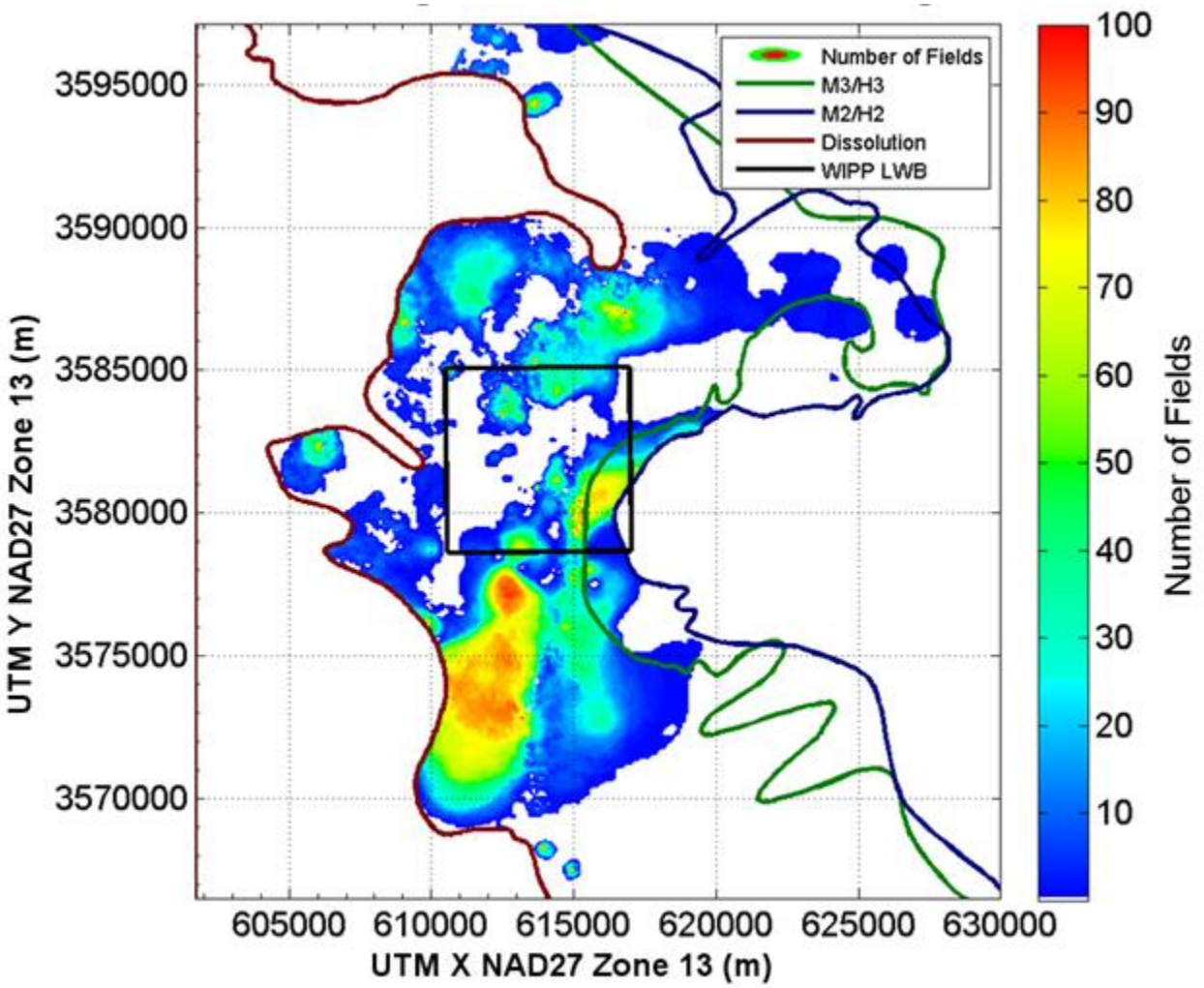

Figure TFIELD 5-19. Number of *T* Fields Where Low *T* Became High *T* Through PEST Calibration

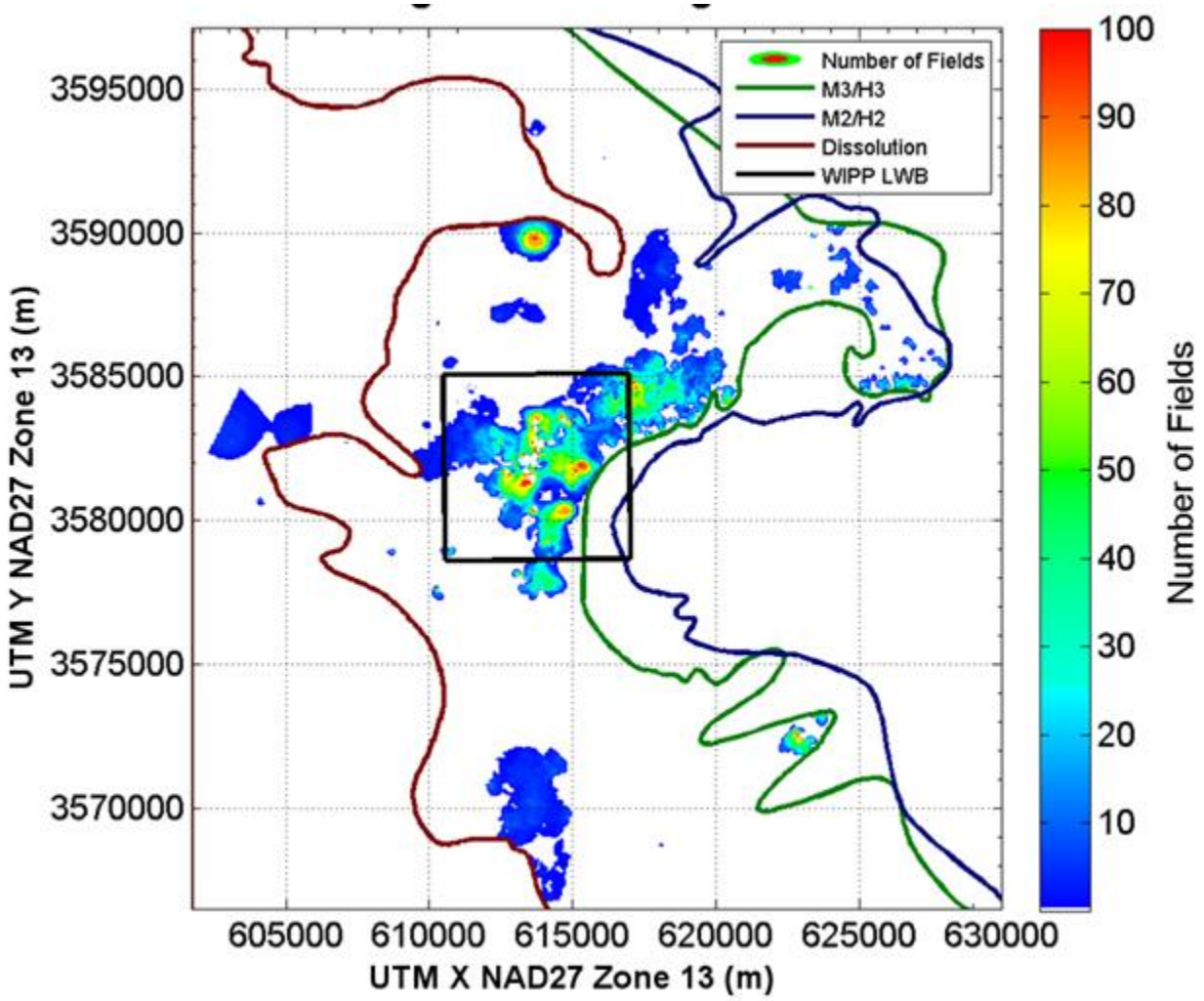

Figure TFIELD 5-20. Number of *T* Fields Where High *T* Became Low *T* Through PEST Calibration

TFIELD-5.4.1.2 Final Storativity Values

The mean and standard deviation of the final *S* fields are presented in Figure TFIELD 5-21 and Figure TFIELD 5-22. The mean *S* fields indicate that the overall *S* values in the confined and transitional zones did not change much from their initial values. Figure TFIELD 5-22 highlights the area northwest of P-14 with a red dashed oval. This area has high variability in estimated *S* across the 100 selected realizations. This may have some relation to the relatively poorer fits of the transient data for the WIPP-25 response to the P-14 pumping test in the model.

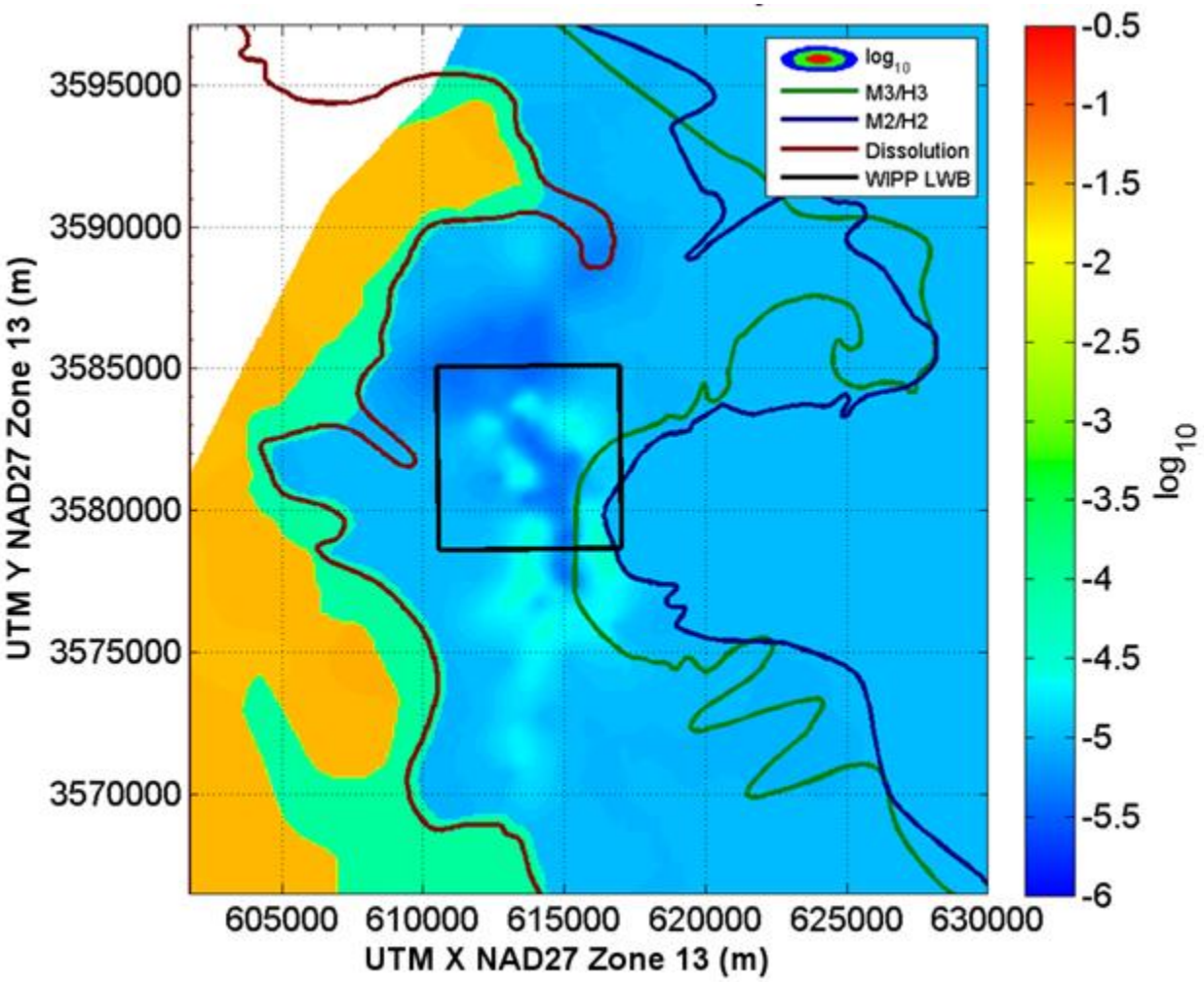

Figure TFIELD 5-21. Mean Storativity Values Across the 100 Final Calibrated Fields. Individual *S* fields are plotted in Appendix TFIELD Attachment A.

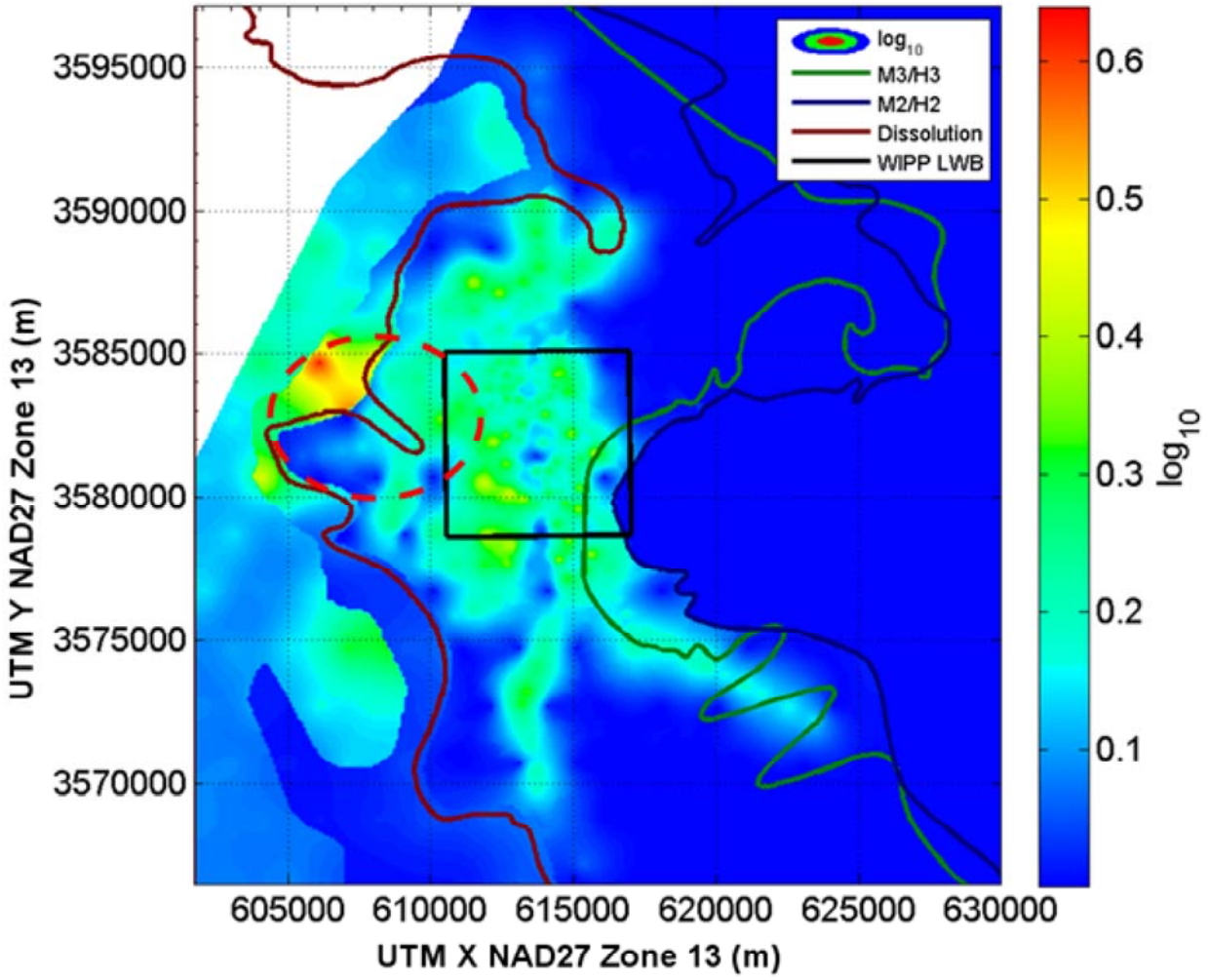

Figure TFIELD 5-22. Standard Deviation of Storativity Values Across the 100 Final Calibrated Fields. Red oval shows P-14 to WIPP-25 area of influence. Individual *S* fields are plotted in Appendix TFIELD Attachment A.

TFIELD-5.4.1.3 Final Recharge Values

The final recharge values were all less than the initial values of 10^{-11} m/s (3.2×10^{-4} meters per year (m/yr)). Compared to the other parameters, there was very little change in recharge. Because the recharge zone was linear, in addition to the cell-by-cell mapping, a view of the average, minimum and maximum recharge values is shown as a cross section in the cross-direction (across a row) as if looking from the south to the north through the domain in Figure TFIELD 5-23.

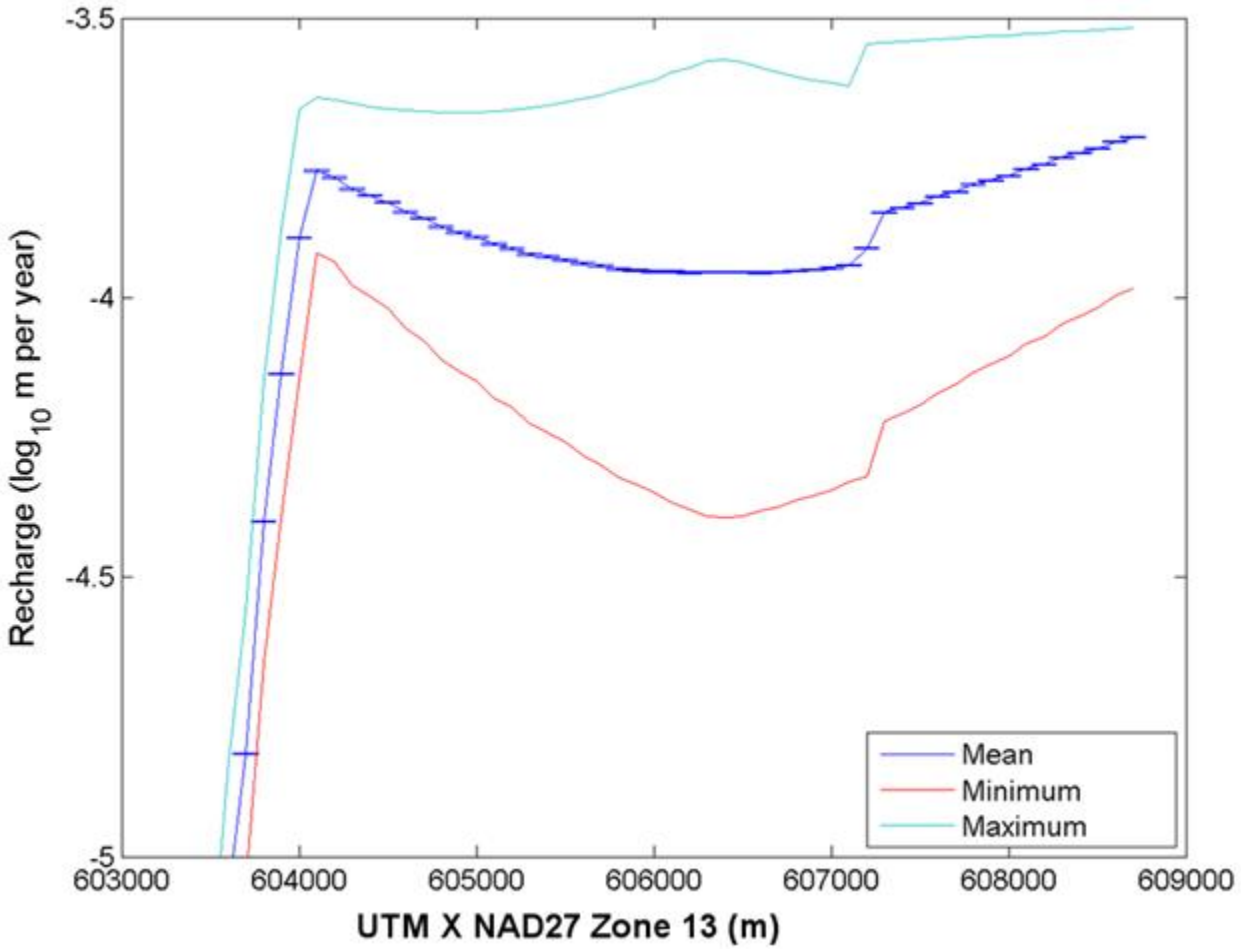

Figure TFIELD 5-23. Recharge as Viewed Through Columns From the South. The initial value was set at $10^{-3.5}$ m/year. The sharp dropoff to the west is the transition to the single fixed-recharge point of $10^{-11.5}$ m/year (interpreted as zero by REAL2MOD).

TFIELD-5.4.2 Forward Model Results Using the Calibrated Fields

The two main divisions of the results are the steady-state head results and the pumping test results. The results presented here only represent the 100 final selected fields, and therefore the maximum error is limited by the selection criteria described in Section TFIELD-5.3.4: an average steady-state error of less than 0.699 m and an average pumping test observation error of less than 0.164 m.

Figure TFIELD 5-24 shows the modeled steady-state head values plotted against the measured head values. The one-to-one correspondence line shows the ideal match, and the modeled results are presented as box-and-whisker plots at each observation well. Figure TFIELD 5-25 shows all 4,200 head errors across all 100 fields as a histogram of error values for steady-state head. Additional figures and tables summarizing steady-state calibration are presented in Appendix C of Hart et al. (Hart et al. 2009). The model-measurement misfit can be modeled as a zero-mean Gaussian distribution with a standard deviation of 0.10 m (McKenna and Wahi 2006). The measurement error distribution curve is included in Figure TFIELD 5-25.

Graphs for each of the transient pumping test results are presented in Appendix D of Hart et al. (2009). The average value of the error in the final fields ranged from 0.12 m to 0.164 m across all

tests, with an average error of 0.15 m. The maximum error for a single observation well ranged from 0.005 m to 2.5 m, with an average of 0.36 m as the maximum error at a given observation well.

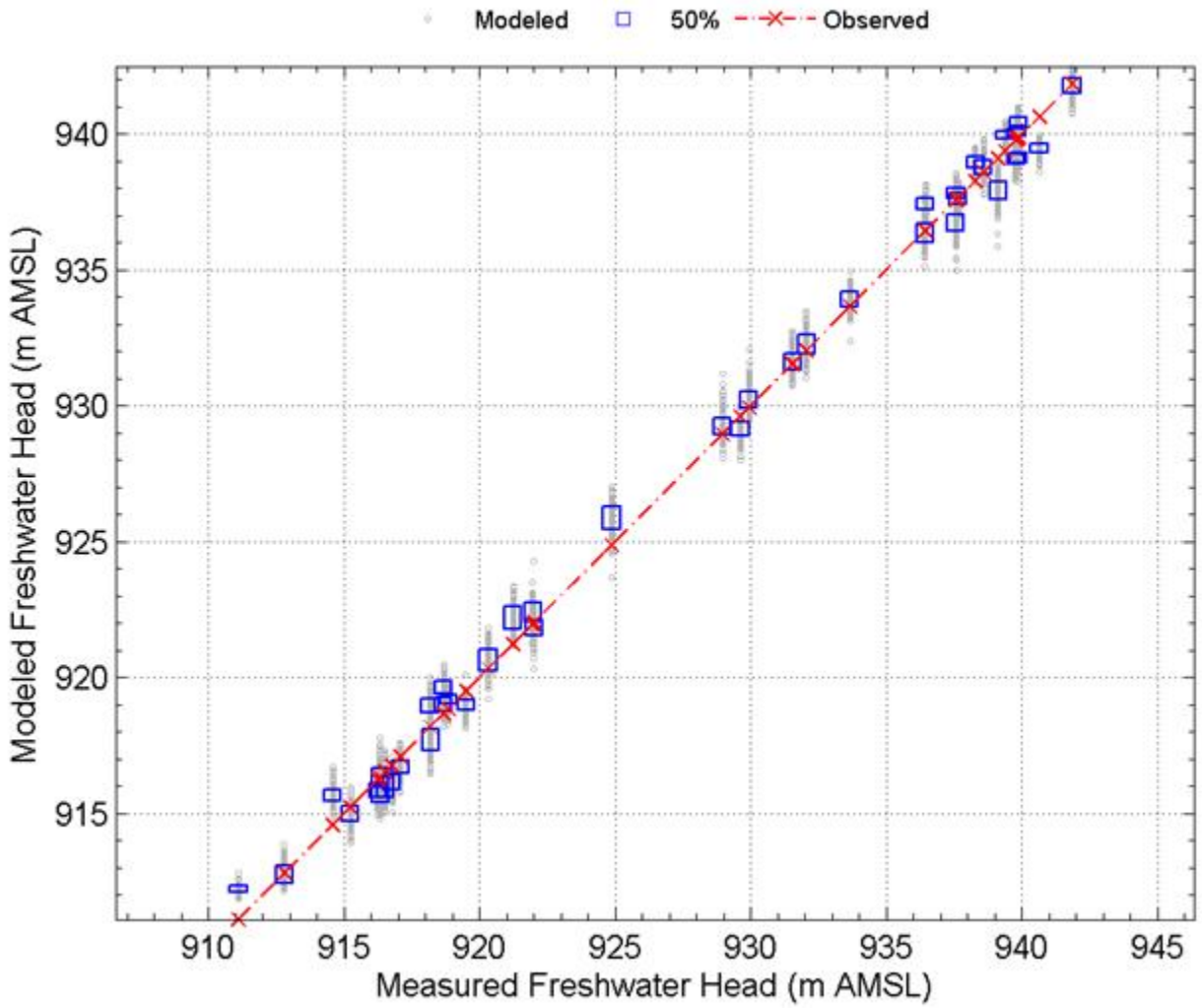

Figure TFIELD 5-24. Results for 42 Total Steady-state Head Measurements for the 100 Selected Fields (No SNL-6 or SNL-15). Observed heads are red ×'s along the diagonal line.

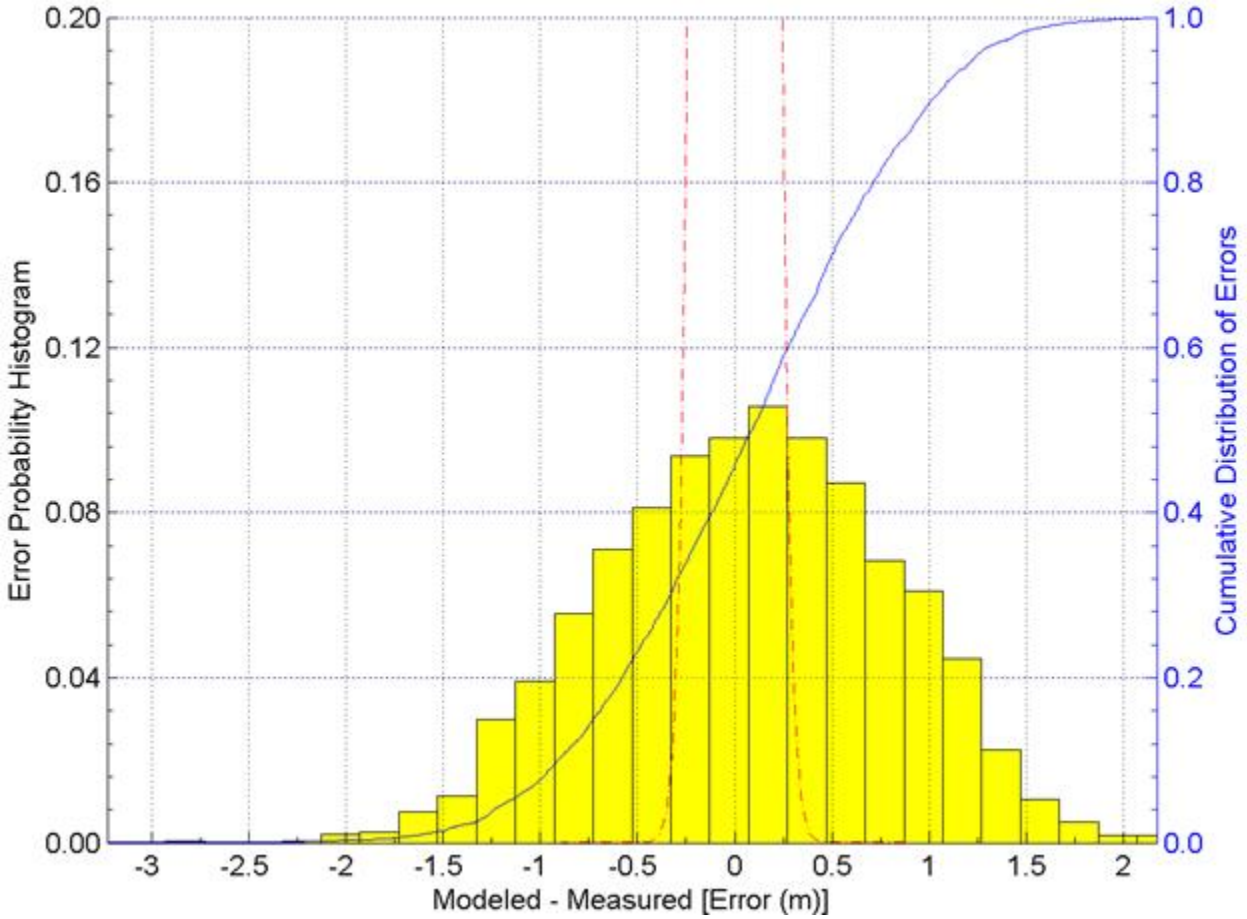

Figure TFIELD 5-25. Histogram of Steady-state Head Errors for the 100 Selected Fields (No SNL-6 or SNL-15). Red dashed line is the ±3σ section of the measurement error PDF. The slight skew to right is an artifact of the binning.

TFIELD-6.0 Culebra T-Field Mining Modifications

The work described in Section TFIELD-6.0 was completed under AP-144, Analysis Plan for the Calculation of Culebra Flow and Transport for CRA-2009 PABC (Kuhlman 2009). The modifications used for CRA-2009 PABC still apply to CRA 2014, and are therefore discussed here.

PA models two categories of mining-impacted transmissivity fields: partial mining with only mining outside the LWB, and full mining with regions both inside and outside the LWB mined.

The CRA-2009 PABC Culebra T-field mining modifications basically follow the procedure used in CRA-2004 PABC (Lowry and Kanney 2005), with two exceptions: 1) a new definition of the region containing minable potash is used, and 2) the new T-fields in Sections TFIELD-3.0 through TFIELD-5.0 are used as inputs. The procedure for the mining modification portion of the analysis is summarized below:

1. Obtain the sampled values for the random mining modification factor (100 vectors × 3 replicates);

2. Map potential areas of future potash mining onto the groundwater modeling domain for both full- and partial-mining scenarios;

3. Apply the mining modification factor to the 100 stochastically calibrated T-fields from AP-114 Task 7 (Hart et al. 2009), producing 600 mining-modified T-fields (100 vectors × 2 mining scenarios × 3 replicates);

4. Perform steady-state flow simulations for each of the 600 mining-modified T-fields using MODFLOW-2000; and

5. Perform particle tracking using the new mining-affected flow-fields to determine advective travel times to the WIPP LWB.

TFIELD-6.1 Overview

Potash mining in the region surrounding the WIPP involves underground excavation in the McNutt Potash zone of the upper Salado Formation, which is located stratigraphically above the WIPP repository horizon but below the Culebra Member of the Rustler Formation (see Figure TFIELD 2-1). It is hypothesized that subsidence due to collapse of the underground voids created in the McNutt potash zone during mining will lead to increased permeability in the Rustler Formation, due to increased fracturing, similar to the Salado dissolution zone effects in Figure TFIELD 2-2. The purpose of the mining scenario calculations is to determine the impact of potash mining on groundwater flow directions and transport velocities in the Culebra. This analysis largely represents a re-application of the methods used in CRA-2004 PABC (Lowry and Kanney 2005), with a few minor exceptions:

1. The definition of the regions where minable potash is believed to exist has been updated, as obtained from the Bureau of Land Management (BLM) (Cranston 2009).

2. The configuration of the MODFLOW model that mining modifications are being applied to has changed (see Sections TFIELD-3.0 through TFIELD-5.0).

3. The way the mining-modified areas interact with specified head areas of the flow model has changed, due to the change in the boundary conditions (there were no specified head areas inside the CRA-2004 PABC MODFLOW model).

This section describes the CRA-2009 PABC effort in characterizing mining effects in the Culebra and highlights the differences and additions relative to past calculations (Ramsey and Wallace 1996; Lowry 2003a, Lowry 2003b, and Lowry 2004). The reader is encouraged to review the past documents for further background information. There have been no changes to the mining modifications procedure or data for CRA-2014 since CRA-2009 PABC.

Starting with the 100 calibrated T-fields from Section TFIELD-5.0, T-fields are modified to reflect the effects of mining by multiplying the transmissivity value in cells that lie within designated mining zones by a random factor uniformly sampled between 1 and 1000. The range of this factor is set by the U.S. Environmental Protection Agency (EPA) in regulation 40 CFR 194.32(b) (U.S. EPA 1996). The scaling factor for each T-field is provided by Latin hypercube sampling (Kirchner 2010).

A forward steady-state flow simulation is run for each new T-field under each mining scenario (full and partial) across three replicates of mining factors, resulting in 600 simulations. Particle tracking is performed on both the 100 original and 600 modified flow-fields to compare the flow path and groundwater travel time from a point above the center of the WIPP disposal panels to the LWB. Cumulative distribution functions (CDFs) are produced for each mining scenario and compared to the undisturbed scenario. The CDFs indicate the probability a conservative tracer (i.e., a marked water particle) would reach the WIPP LWB during a given interval of time, flowing in the Culebra under a natural gradient. In addition to comparing travel times, particle-tracking directions are also examined to determine the effect on the regional flow direction in the WIPP area due to mining.

TFIELD-6.2 Model Domain, Boundary, and Initial Conditions

The eastern limit of the MODFLOW model domain used in the CRA-2009 PABC analysis (Hart et al. 2008) was extended eastward, compared to the MODFLOW domain used in the CRA-2004 PABC analysis. This change was made to locate the boundary in an area where halite is present in all of the non-dolomite members of the Rustler Formation, simplifying the specification of the eastern model boundary condition. See Section TFIELD-3.1 for CRA-2009 PABC MODFLOW model construction details.

TFIELD-6.2.1 Boundary and Initial Conditions

Like the model domain and discretization, the boundary and initial conditions used in CRA-2009 PABC are described fully in AP-114 Task 7 (Hart et al. 2009). Regional flow rates within the flow model are controlled by the boundary conditions and the hydraulic conductivity distribution. The regional gradient across the domain was approximately

(943.9 m - 911.6 m)/30.7 km = 0.00105 (TFIELD 6.1)

The gradient across the model domain was computed by averaging the constant heads along the northernmost portion of the northern boundary (row 1, columns 1-140, 943.9 m), subtracting the average heads along the entire southern boundary (911.6 m), and dividing by the north-south model domain extent (30.7 km). It was assumed that mining impacts would not significantly change this regional gradient and thus the specified initial conditions for the mining scenarios are identical to those in AP-114 Task 7 (Hart et al. 2009). In addition, the CCA, CRA-2004, and CRA-2004 PABC

all used this same conceptualization (keeping the outer boundary conditions fixed between the mining and non-mining scenarios). The same conceptualization was maintained in the CRA-2009 PABC model to facilitate comparisons between the different models.

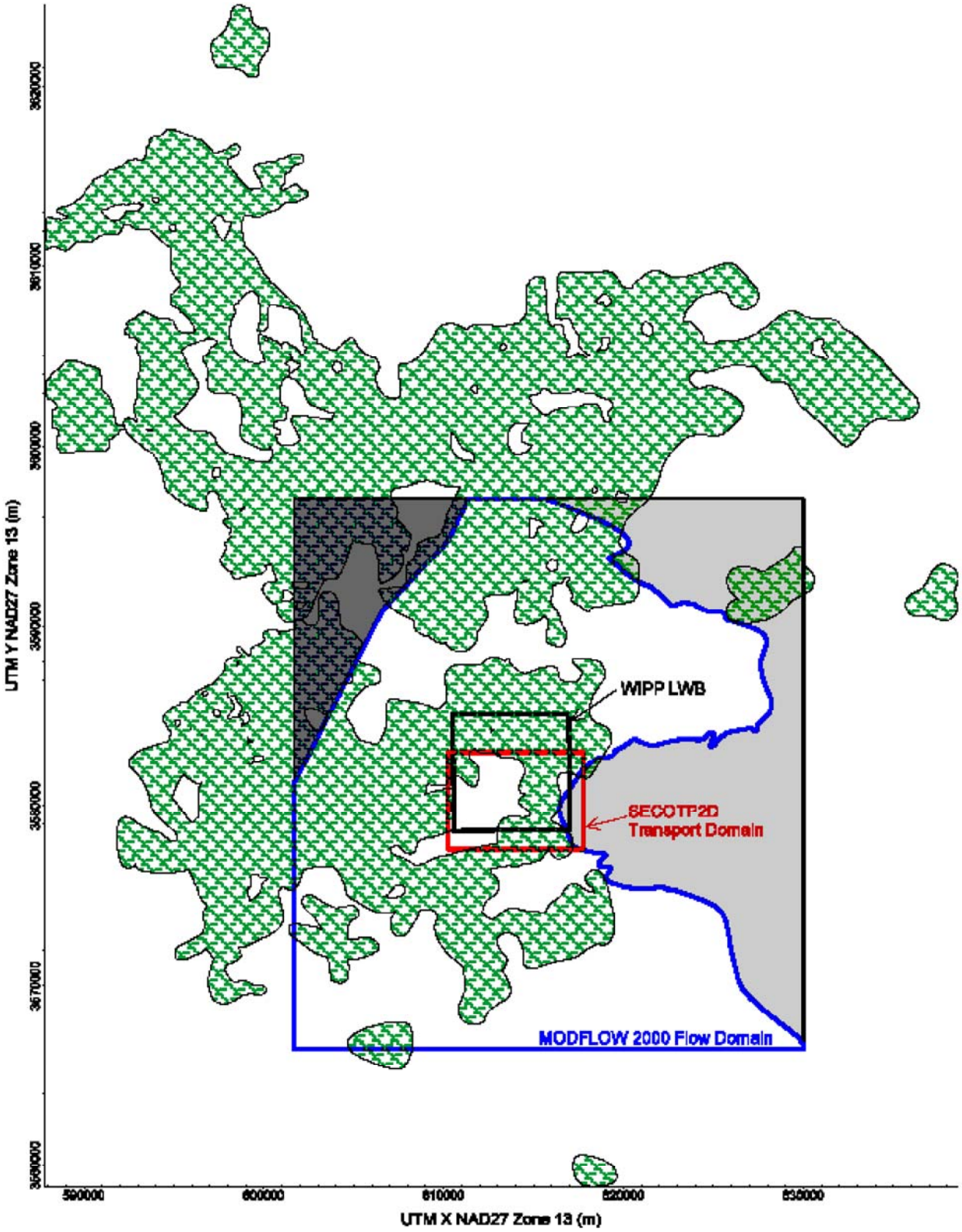

Figure TFIELD 6-1. Comparison of Minable Potash Area to the Flow and Transport Modeling Domains. Green hatches represent minable potash area (Cranston 2009).

TFIELD-6.2.2 Determination of Potential Mining Areas

The 2009 version of the BLM map delineating distribution of minable potash ore was obtained from BLM as an ESRI shapefile (Cranston 2009), plotted in Figure TFIELD 6-1. The process to convert this shapefile to a grid of integers corresponding to Culebra MODFLOW model cells (indicating whether a model cell was affected by mining or not) is explained in Appendix 1 of Kuhlman (Kuhlman 2010).

Since the potash-mining horizon is located in the Salado Formation below the Culebra, the areas disturbed by mining activities in the Culebra are larger than mined areas in the Salado due to angle-of-draw effects. Subsidence effects will not propagate up vertically, but instead will propagate up and out at 45° angles between horizontal and vertical. Based on an average distance from the McNutt potash zone to the Culebra, a 253-m-wide collar was added to the mining-impacted areas (consistent with that done previously; see Ramsey and Wallace (Ramsey and Wallace 1996) and Bertram (Bertram 1995). This was considered a conservative estimate of the angle-of-draw effects. To accommodate the angle of draw, the mining zone boundaries, as overlaid on the current model grid, were extended outward three cells (300 m) in the *x*- and *y*-directions, and two cells (283 m) in the diagonal directions (see Figure TFIELD 6-2 for an illustration of the mining-expansion stencil).

			A			
	A	A	A	A	A	
	A	A	A	A	A	
A	A	A	M	A	A	A
	A	A	A	A	A	
	A	A	A	A	A	
			A			

Figure TFIELD 6-2. Stencil Used to Model Cells Affected by Mining-related Subsidence (Blue Cells with A) Due to Mining in Red "M" Cell, Using 45° Angle of Draw

Figure TFIELD 6-3 shows the CRA-2009 PABC modeling domain and mining zones for the full-mining case in comparison to the 1996 CCA and the CRA-2004 delineations. The comparison of the current and previous partial-mining cases is shown in Figure TFIELD 6-4. A close-up of the WIPP site and the distribution of minable potash is shown in Figure TFIELD 6-5, which illustrates how the definition inside the WIPP LWB has changed significantly since CRA-2004 PABC. For CRA-2004 PABC, the closest minable potash was approximately 1,230 m from the center of the WIPP panels in the southeast direction; for CRA-2009 PABC, this distance was reduced to approximately 670 m (in a more easterly direction).

The output of this mining-area delineation was a mining effects indicator field. A value of 1 means the model cell lies within a potential mining-affected zone, and a value of 0 means that it is outside a potential mining-affected zone.

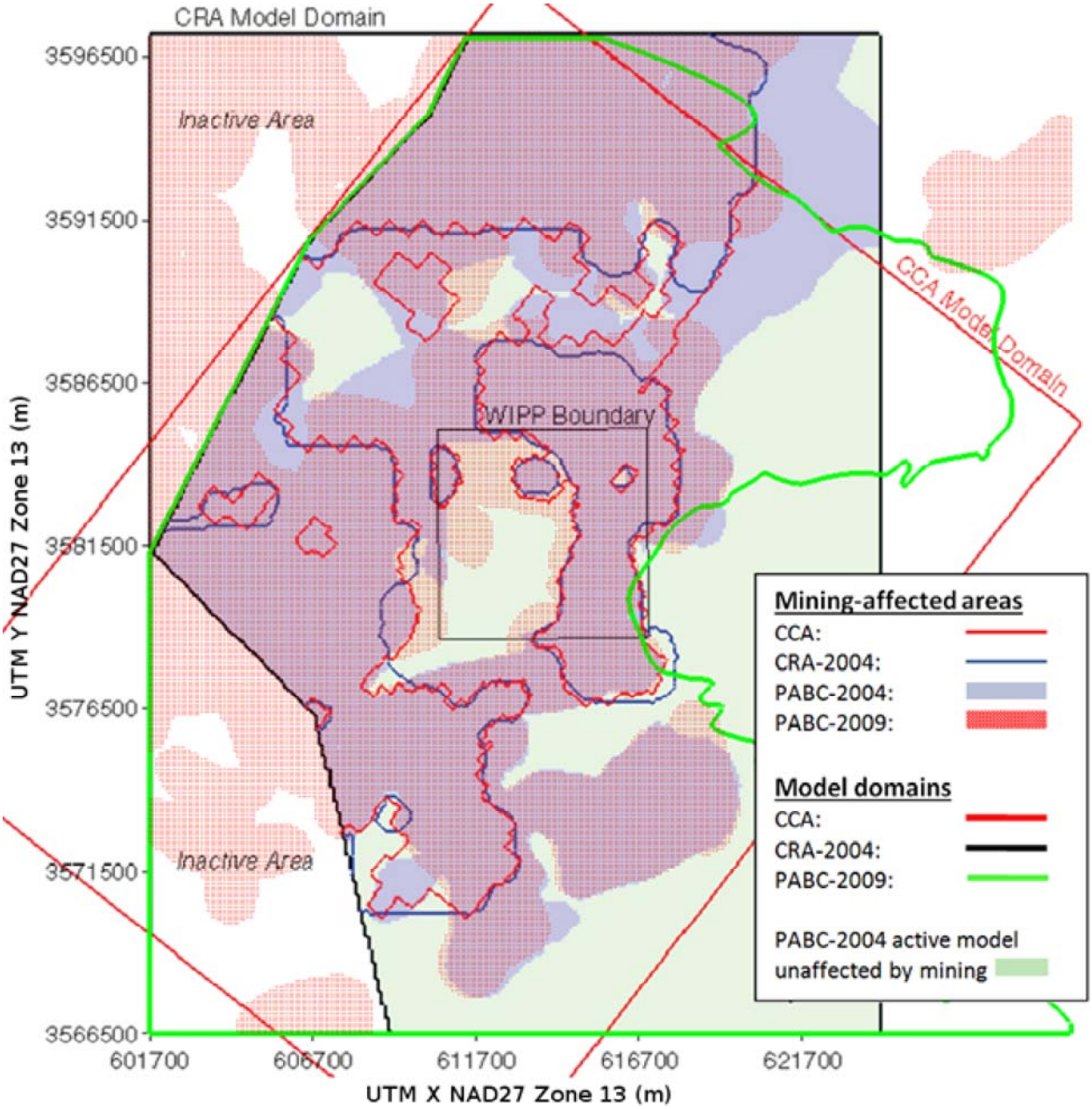

Figure TFIELD 6-3. Definitions of Mining-affected Areas in Full-mining Scenario Between Current and Previous Models. Base image is Figure 3.2 from Lowry and Kanney (2005). CRA-2009 PABC mining area (red stippled area) and model domain (green line) definitions are current definitions used in CRA-2014.

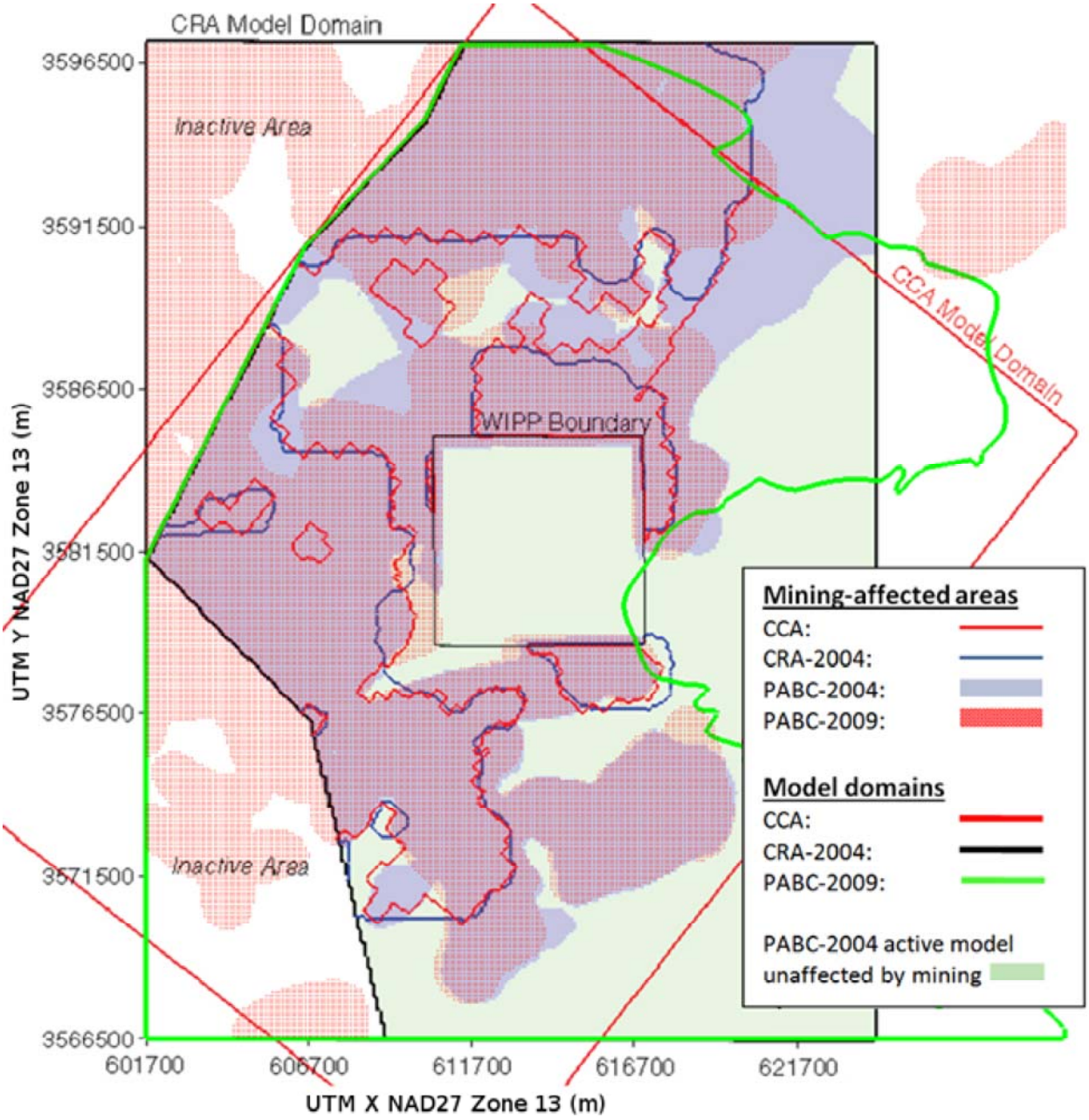

Figure TFIELD 6-4. Definitions of Partial-mining-affected Areas Between Current and Previous Applications. Base image is Figure 3.3 from Lowry and Kanney (2005). CRA-2009 PABC mining area (red stippled area) and model domain (green line) definitions are current definitions used in CRA-2014.

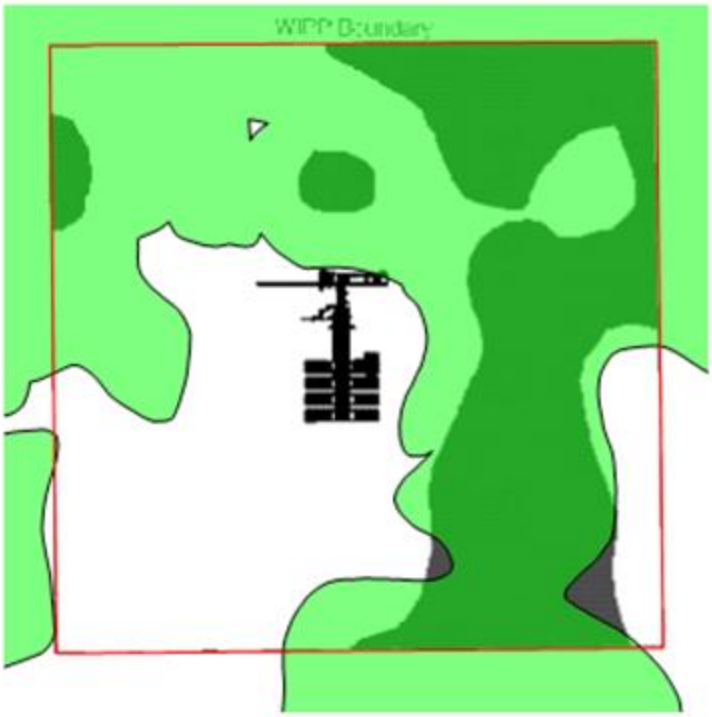

Figure TFIELD 6-5. Comparison of Minable Potash Distribution Inside the WIPP LWB for CRA-2004 PABC (Dark Gray) and CRA-2009 PABC (Translucent Green). The WIPP repository plan is shown for comparison, from Figure 3.6 of Lowry and Kanney (2005).

TFIELD-6.2.3 Use of Mining Zones in Forward Simulations

The calibration process in Section TFIELD-5.0 produced 100 sets of *T*, *A*, *S*, and *R* fields that each minimize the error between observed and model-calculated head distributions. To simulate the effects of mining, the field of *T* values from each realization was multiplied by its own unique mining scaling factor in areas of potential mining, and MODFLOW was re-run with these mining-modified T-fields to produce the mining-affected head and flow distributions. The other parameter fields (*S*, *A*, and *R*) were not modified in the process. The cell-by-cell flow budget files were used in particle tracking and radionuclide transport calculations. Three different sets of mining factors were used, each set forming a replicate (given here as R1, R2, and R3). Thus, for each mining scenario (full and partial), three sets of 100 mining-altered T-fields and related cell-by-cell flow budgets were produced.

TFIELD-6.2.4 Particle-Tracking Simulations

In each realization, a single conservative particle was tracked from the UTM NAD27 coordinate x = 6,135,975 m, y = 35,813,852 m (i.e., the Culebra location of monitoring well C-2737, directly above the center of the WIPP waste panels) to the LWB for each combination of T-field, replicate, and mining scenario using the SNL-developed particle-tracking code DTRKMF. Two main outputs were generated from the suite of particle tracks. First, plots were constructed showing the individual tracks for all 100 T-fields in each scenario for each replicate (six plots total). This allows visual comparison of the prevailing flow directions for the full- and partial-mining scenarios and the qualitative comparison of the variability of the tracking direction. Secondly, CDFs were constructed for each replicate and scenario, which describe the probability that a water particle will cross the LWB in a given amount of time. The six plots and the CDFs are presented in Section TFIELD-6.3.

TFIELD-6.3 Particle-Tracking Results

Particle tracks were computed using DTRKMF (Rudeen 2003), which uses the binary cell-by-cell flow budget files produced by MODFLOW-2000. In flow calculations, the full 7.75 m thickness of the Culebra is used, while for transport and particle-tracking purposes the thickness is reduced to 4.0 m to focus all flow through the lower, more permeable portion of the Culebra (Holt 1997). A value of 16% porosity was used for the particle-tracking calculations (parameter DPOROS). Porosity directly affects transport, but is not needed for the calibration of the flow model.

Particle tracking was performed to allow plotting and quantitative comparison between the two mining scenarios and the non-mining scenario, which was not used in the PA SECOTP2D radionuclide transport calculations. The particle-tracking results illustrate the advective pathway taken by a marked water particle. They do not take into consideration retardation, dispersion, or molecular diffusion, which may be accounted for in PA by radionuclide transport. The particle tracks also allow easier comparison of the 600 results (each a 1D trace) in a single plot, in contrast to showing 600 plots of concentrations (each a 2D field) produced from SECOTP2D.

TFIELD-6.3.1 Particle Travel Times

Compared to the non-mining scenario (results already given in AP-114 Task 7 (Hart et al. 2009)), the travel times for the partial-mining scenarios are longer, while travel times for the full-mining scenarios are shorter. The median travel time across all three replicates for the full-mining scenario is approximately 0.689 times the median travel time of the non-mined scenario (see Table TFIELD 6-1, Figure TFIELD 6-6, and Figure TFIELD 6-7 for summary statistics and comparison to CRA-2004 PABC results). All advective particle travel times are plotted, but it should be noted that the regulatory limit for radionuclide transport modeling is 10,000 years, taking into consideration retardation, diffusion, and dispersion (which do not apply to particle track modeling). The median travel time across all three replicates for the partial-mining scenario is 3.034 times greater than for the non-mining scenario. For CRA-2004 PABC, travel times in both the full- and partial-mining scenarios were slower (longer) than for the non-mining scenario. The CDFs for the full-, partial-, and non-mining scenarios are shown in Figure TFIELD 6-6. Travel times from CRA-2009 PABC for particles in the non-mining scenario are closer to CCA travel times than those from CRA-2004 PABC (Figure TFIELD 6-7).

Table TFIELD 6-1. Particle-tracking Travel-time Statistics from Center of the WIPP Panels to the WIPP LWB (Years). Global statistics for full and partial mining include 300 realizations, while no mining only includes 100 realizations.

		CRA-2009 PABC			CRA-2004 PABC		
Replicate	Statistic	Full	Partial	No Mining	Full	Partial	No Mining
R1	Median	5,138	22,581	N/A	64,026	117,815	N/A
	Max	200,260	91,119		2,175,165	2,727,191	
	Min	1,591	5,042		2,130	5,185	
R2	Median	4,956	21,999		80,801	148,489	
	Max	94,852	84,929		2,059,263	1,667,084	
	Min	1,421	5,037		2,463	4,855	
R3	Median	5,560	22,537		74,315	118,919	
	Max	93,172	86,758		1,779,512	3,128,693	
	Min	1,421	4,505		2,507	3,314	
Global	Median	5,084	22,376	7,374	70,170	131,705	18,289

	Max	200,260	91,119	73,912	2,175,165	3,128,693	101,205
	Min	1,421	4,505	2,618	2,130	3,314	3,111

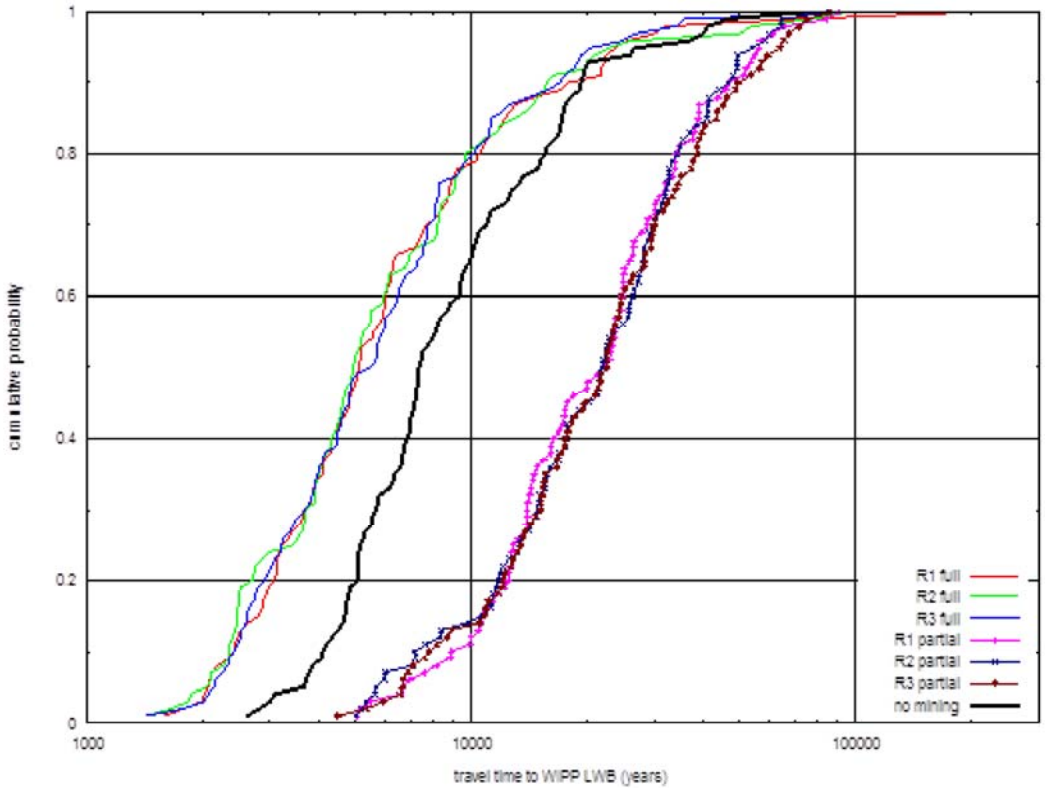

Figure TFIELD 6-6. CDF of Advective Particle Travel Times From the Center of the WIPP Waste Panels To the WIPP LWB for Full, Partial, and Non-mining Scenarios

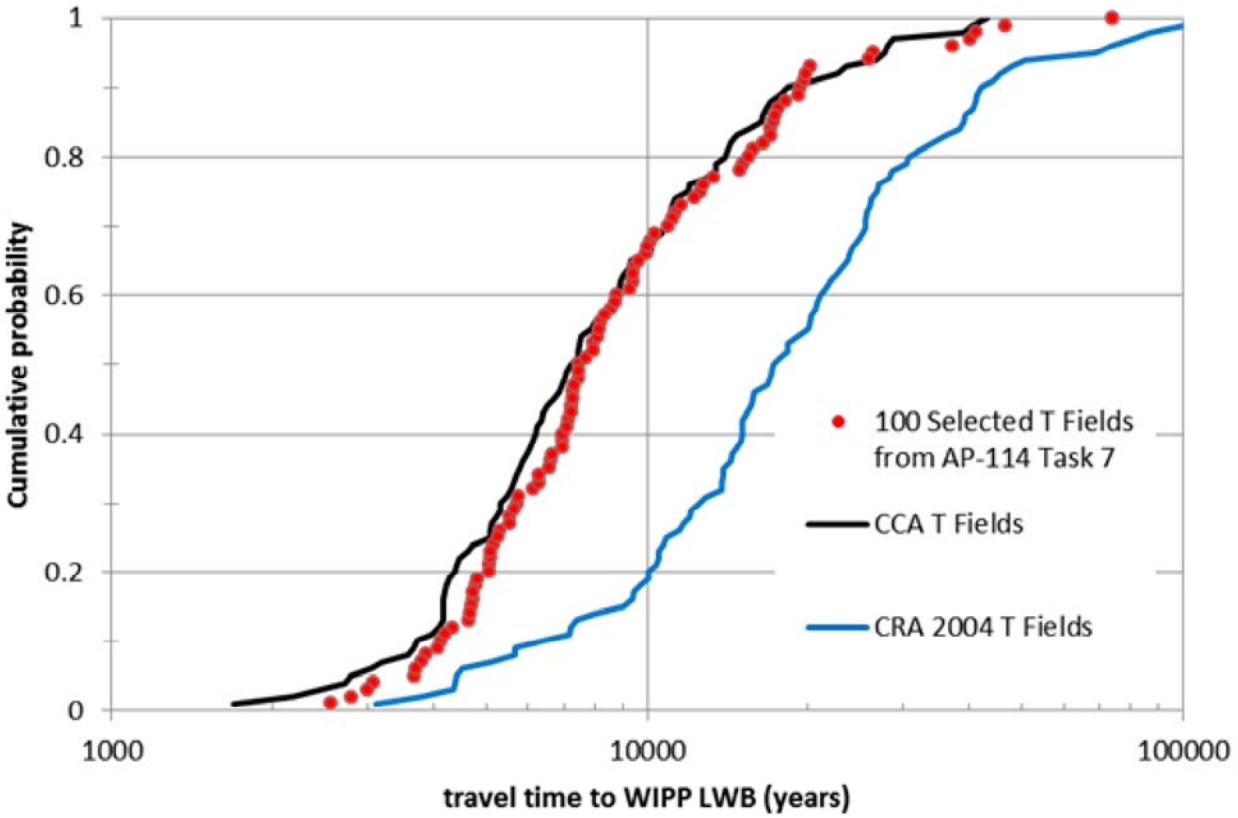

Figure TFIELD 6-7. Comparison of Advective Particle Travel Time CDFs for Non-mining Scenarios of CRA-2009 PABC, CRA-2004 PABC, and CCA. Travel times are from the center of the WIPP waste panels to the WIPP LWB.

TFIELD-6.3.2 Flow Directions

The particle track directions for the non-, full-, and partial-mining scenarios for CRA-2009 PABC are illustrated in Figure TFIELD 6-8 to Figure TFIELD 6-11. Figure TFIELD 6-13 shows the non-mining case particle tracks all the way to the edge of the MODFLOW model domain, rather than only to the WIPP LWB. Like past mining scenario calculations (i.e., CRA-2004 PABC), there is a strong similarity between the three replicates (R1, R2, and R3) for each scenario (full or partial mining), although the travel directions for the CRA-2009 PABC are different than for the CRA-2004 PABC (Lowry and Kanney 2005). A larger amount of minable ore exists inside the WIPP LWB, especially the ore immediately to the east of the particle release point. This leads to different effects of full mining on travel times compared to CRA-2004 PABC.

The high-T pathway in the southeastern portion of the WIPP site (Figure TFIELD 5-15) was more accurately represented in CRA-2009 PABC results, compared to CRA-2004 PABC results. This difference in the underlying flow field calibration is another source of difference between CRA-2004 PABC and CRA-2009 PABC particle-tracking results.

In CRA-2009 PABC, nearly all particles immediately go east to this boundary and then move south along it towards to the edge of the LWB at approximately x = 612.75 km (see Figure TFIELD 6-9 and Figure TFIELD 6-12). This is in contrast to the partial-mining scenario where the tracking directions are more similar to the non-mining scenario, but more evenly distributed spatially along the southern boundary. In the non-mining scenario, most of the particles exit near the high-transmissivity zone at approximately x = 615 km.

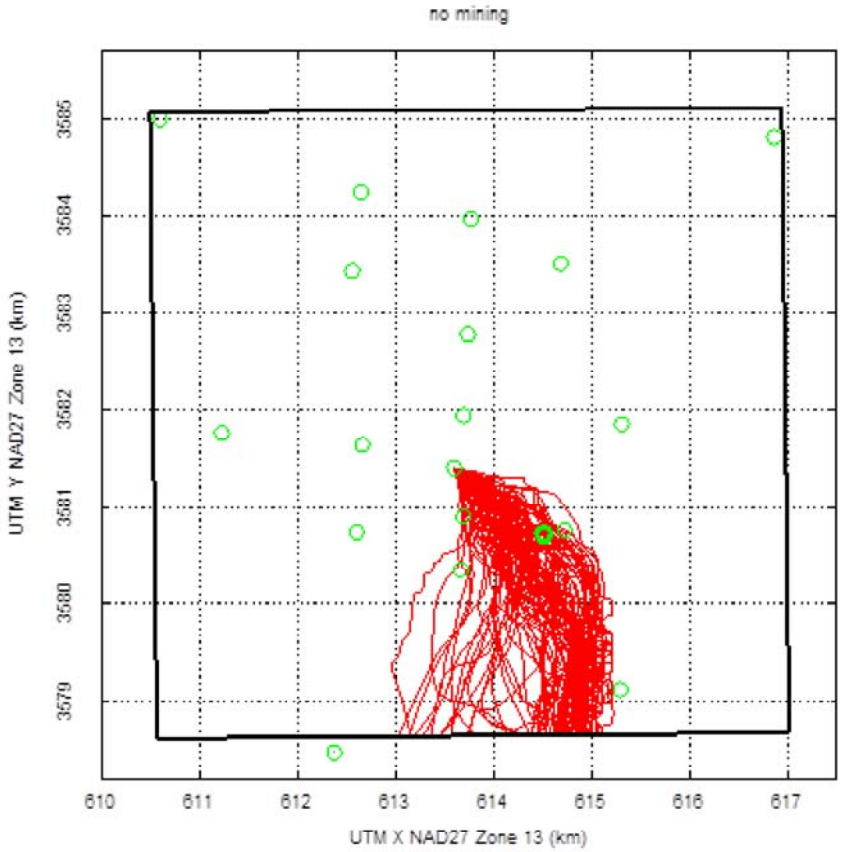

Figure TFIELD 6-8. 100 Particle Tracks for Non-mining Scenario. Black box is the WIPP LWB, green circles are Culebra monitoring well locations.

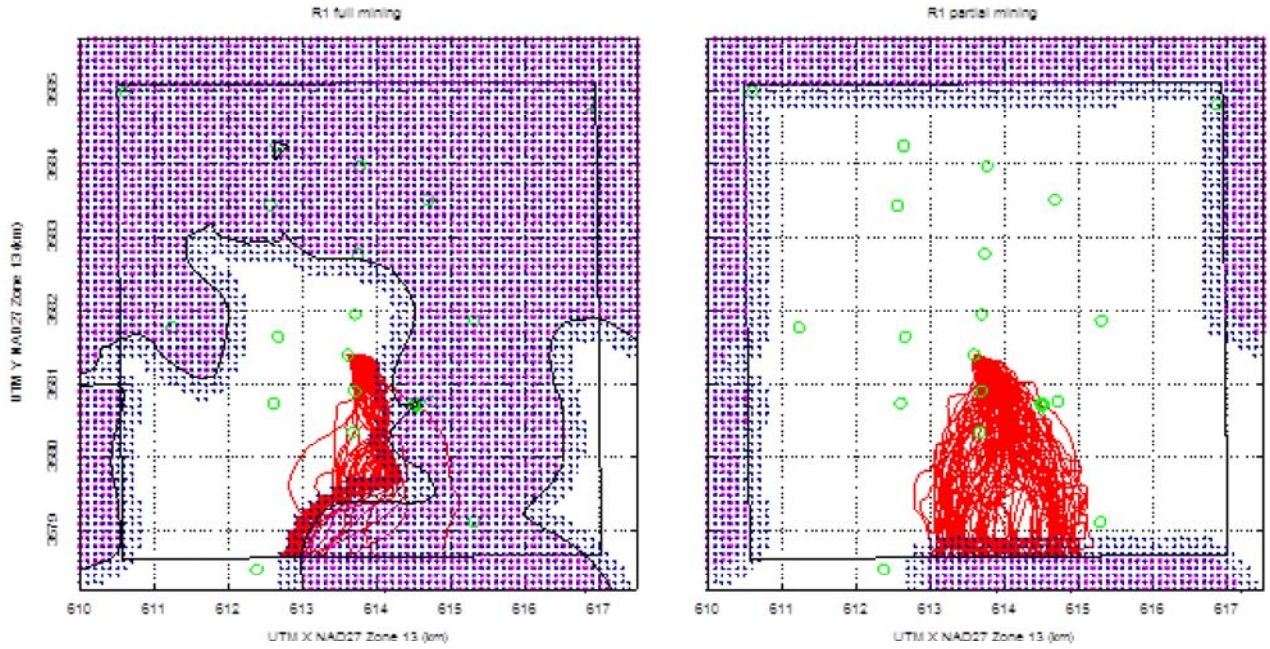

Figure TFIELD 6-9. 100 Particle Tracks Each for R1 Full and Partial Mining Scenarios. Small magenta squares and blue crosses indicate centers of MODFLOW cells located within potash and mining-affected areas, respectively; thin black line is minable potash.

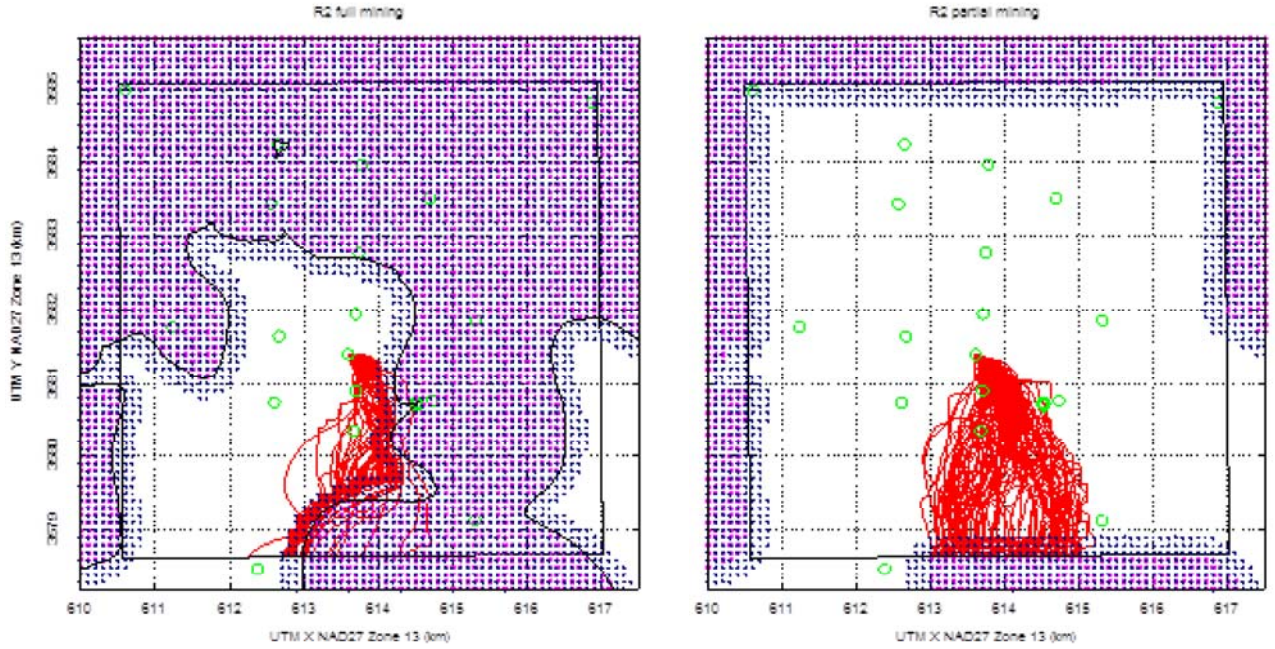

Figure TFIELD 6-10. 100 Particle Tracks Each for R2 Full- and Partial-mining Scenarios. Small magenta squares and blue crosses indicate centers of MODFLOW cells located within potash and mining-affected areas, respectively; thin black line is minable potash.

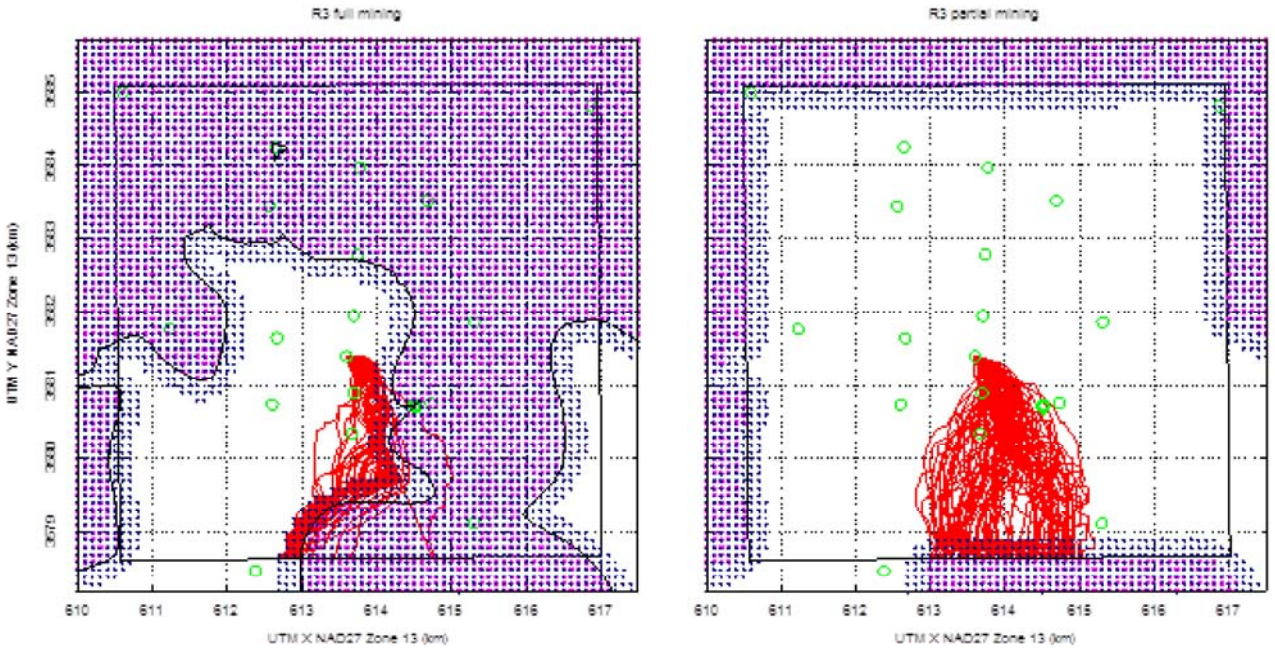

Figure TFIELD 6-11. 100 Particle Tracks Each for R3 Full- and Partial-mining Scenarios. Small magenta squares and blue crosses indicate centers of MODFLOW cells located within potash and mining-affected areas, respectively; thin black line is minable potash.

High-*T* areas corresponding to the mining-affected zones create preferential pathways through the system (e.g., see oranges and yellows in Figure TFIELD 6-14). These preferential pathways result in higher velocities and flow rates through the mining zone and therefore relatively slower velocities in the non-mined areas. In the partial-mining scenario, where there is no mining inside the WIPP LWB, the preferential pathway goes "around" the LWB, rather than through it (similar to behavior seen in both mining scenarios for CRA-2004 PABC). In the full-mining scenario, the potentially mined regions are closer to the release point than in CRA-2004 PABC (see Figure TFIELD 6-5 for comparison), giving the particles a high-*T* pathway from the release point to the LWB, resulting in shorter travel times than the non-mined scenario. This behavior is different from that predicted with the CRA-2004 PABC model. A comparison of the median, maximum, and minimum travel times for each scenario is presented in Table TFIELD 6-1.

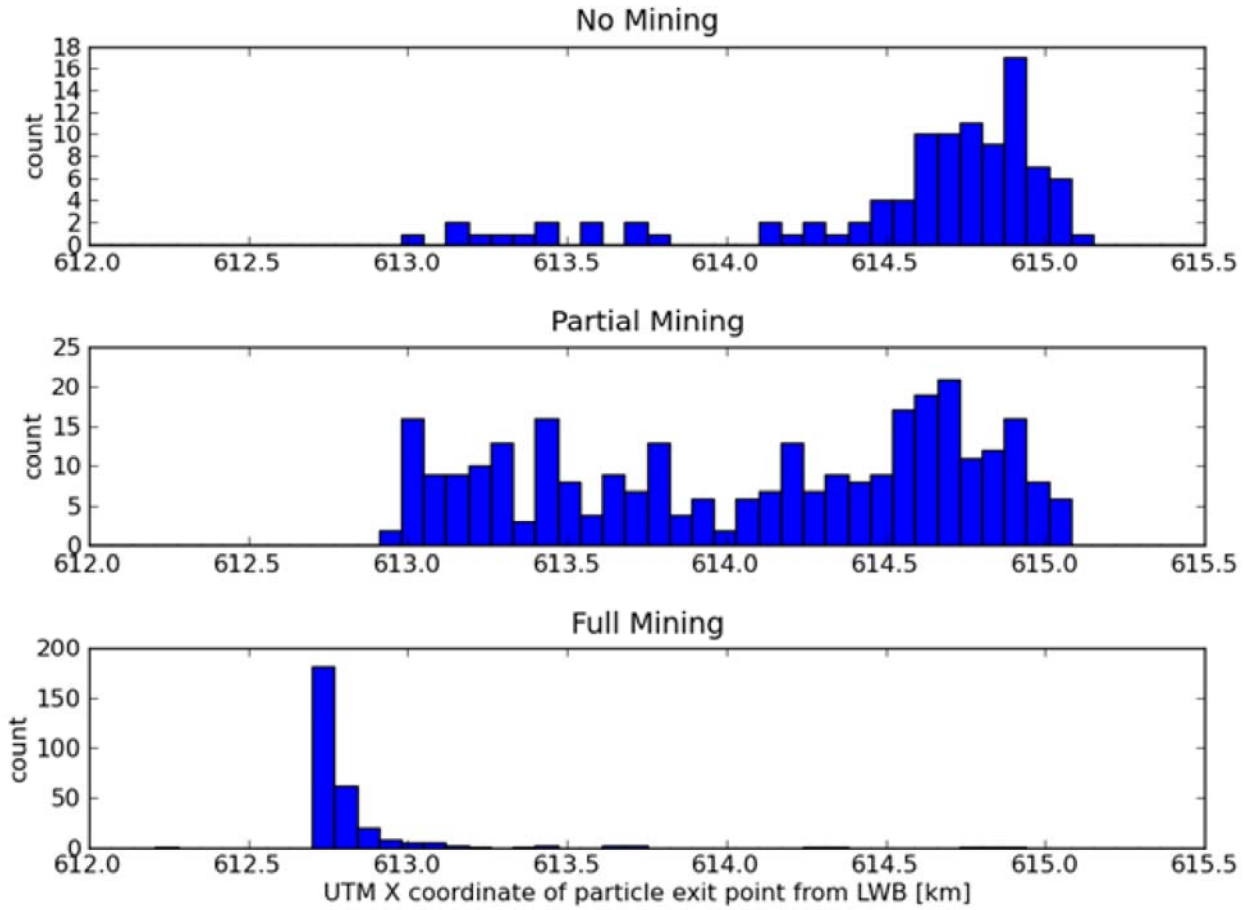

Figure TFIELD 6-12. Histograms of Particle *x*-coordinates at Exit Point From LWB. Full- and partial-mining include all three replicates (note different vertical scales between plots; no mining contains 100 particles while mining scenarios each include 300 particles).

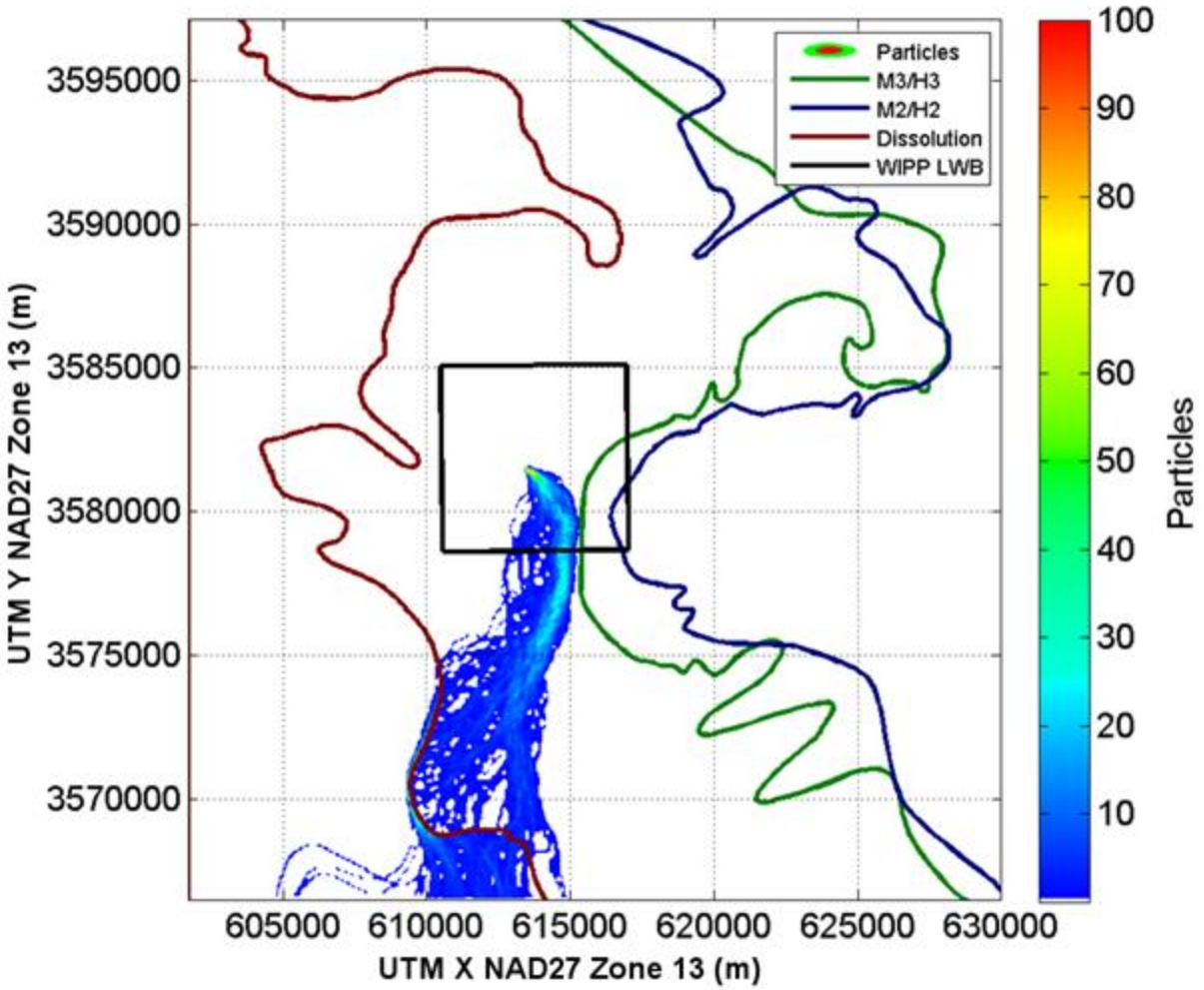

Figure TFIELD 6-13. Particle Counts in Each Cell Across All 100 Selected Realizations for Non-mining Scenario

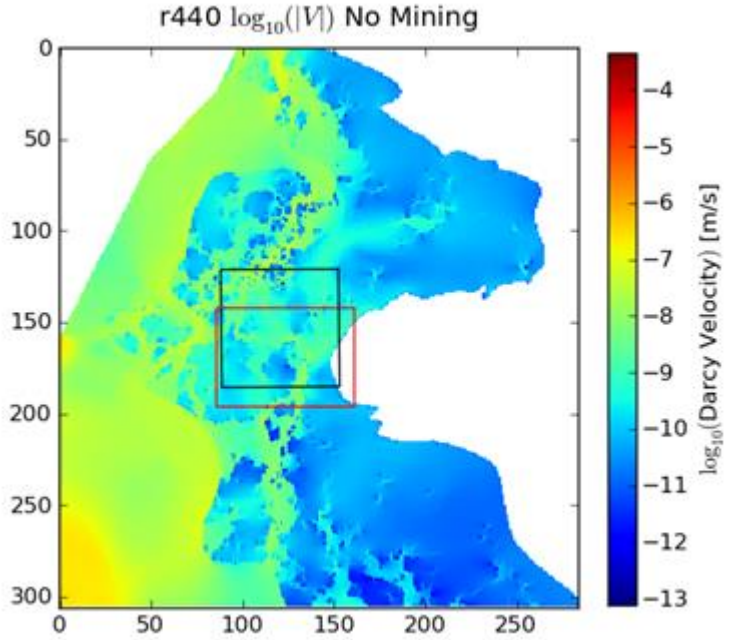

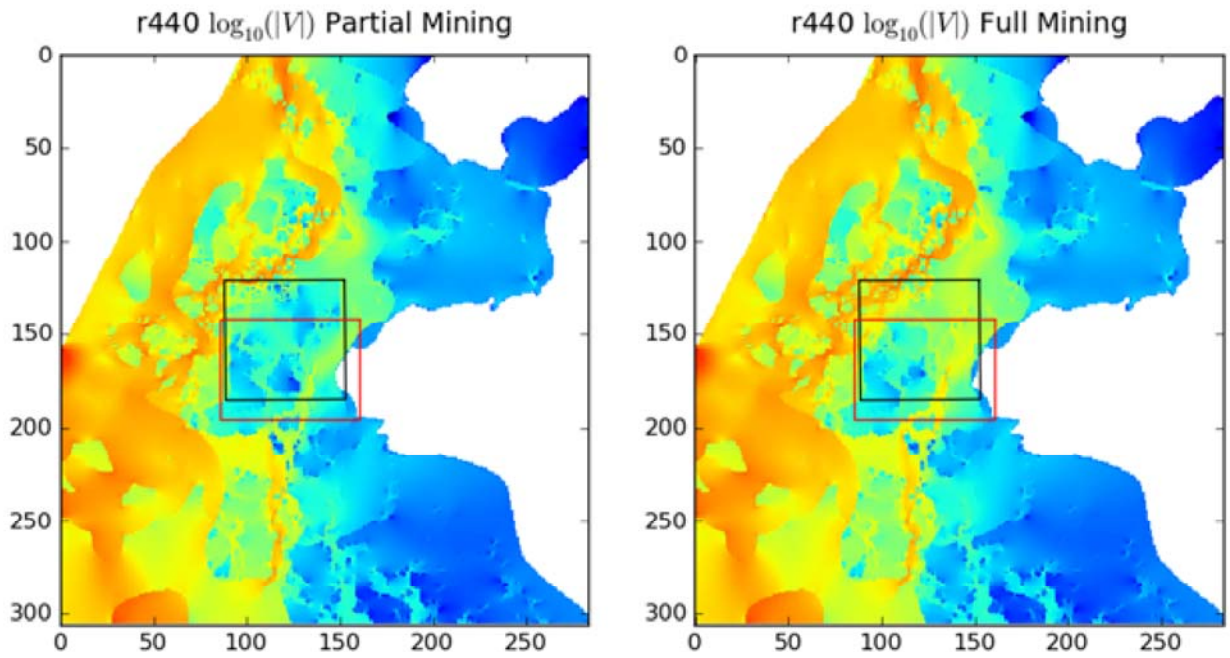

Figure TFIELD 6-14. Magnitude of Darcy Flux for a Single Realization (r440) for No, Partial, and Full-mining Scenarios Using Cell-based Coordinates. LWB (black) and SECOTP2D transport model domains (red) shown for reference.

TFIELD-6.3.3 Particle Speeds

Instantaneous speeds (the magnitude of particle velocities) were calculated from the DTRKMF particle locations and times using backwards finite differences,

$$v(t_{i+1}) = \frac{\sqrt{[x(t_i) - x(t_{i+1})]^2 + [y(t_i) - y(t_{i+1})]^2}}{t_{i+1} - t_i} \quad \text{(TFIELD 6.2)}$$

where a subscript i indicates the previous time step (a record or line in the DTRKMF output file) and a subscript i+1 is the current time step. This approach assumes a straight line connects the locations at the beginning and ends of the step, so it is potentially underestimating speeds, but step sizes are small and error should be minimal. These values should be used for qualitative comparisons between realizations and scenarios, rather than quantitative estimates of true particle velocities.

In Figure TFIELD 6-15 through Figure TFIELD 6-18, the color of the diamond indicates the particle velocity; the dots are located at the midpoint of the step, e.g., $x_{\text{midpt}} = \frac{1}{2}[x(t_i) + x(t_{i+1})]$, $y_{\text{midpt}} = \frac{1}{2}[y(t_i) + y(t_{i+1})]$. In the no-mining case (Figure TFIELD 6-15), the highest particle velocities are in the southeastern portion of the particle swarm, corresponding to the high-transmissivity pathway (Hart et al. 2009) exiting the LWB at approximately x = 614,750 m (Figure TFIELD 6-12). This high-T pathway has been observed in multi-well pumping tests, and was intentionally included in the soft data used to create the base T-fields (Section TFIELD-4.2.3). This high-T pathway was not as prevalent in the CRA-2004 PABC model calibration results.

The effects of the full-mining scenario are clearly evident in the left halves of Figure TFIELD 6-16 through Figure TFIELD 6-18. High particle velocities (yellows and oranges) are found along the margin of the mining-affected areas, where particles enter the increased-T region. For comparison, in

the partial-mining scenario the particles are relatively slowed down and more evenly distributed in the region between the release point and the southern WIPP LWB, with the only high velocities found in the high-*T* pathway in the southeast, similar to the no-mining scenario (Figure TFIELD 6-15).

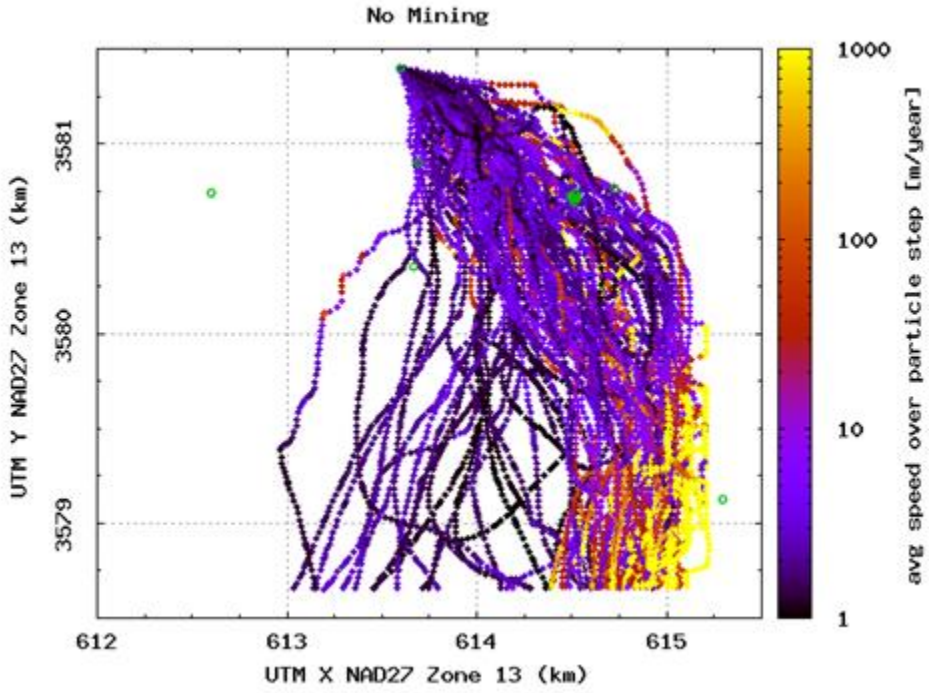

Figure TFIELD 6-15. Particle Speeds for Non-mining Scenario Computed from DTRKMF Results. Open symbols are Culebra well locations.

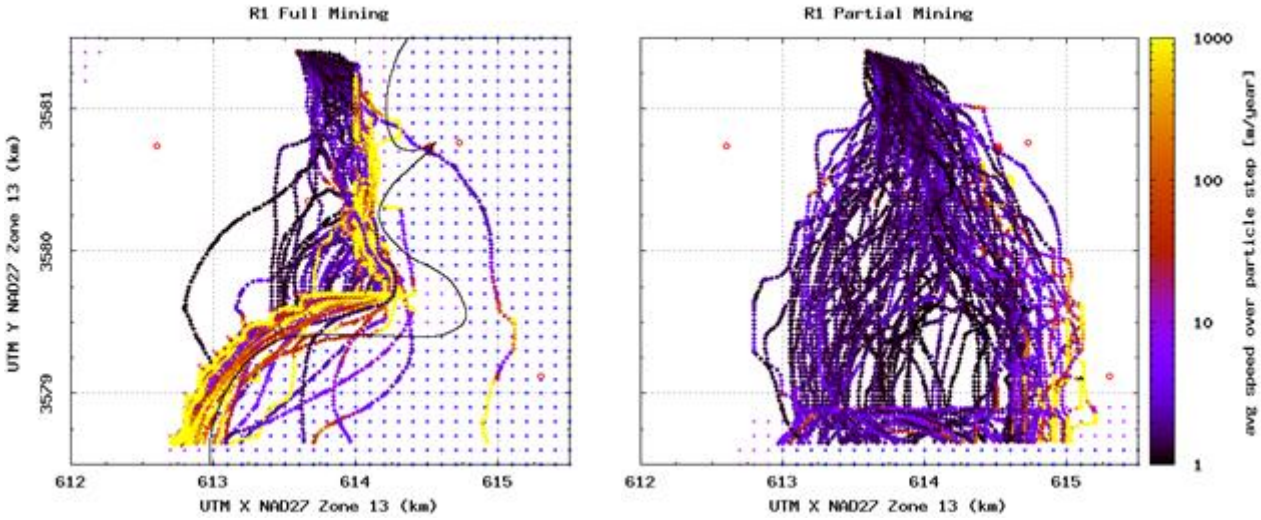

Figure TFIELD 6-16. Particle Speeds for R1, Computed From DTRKMF Results. Open symbols are Culebra well locations.

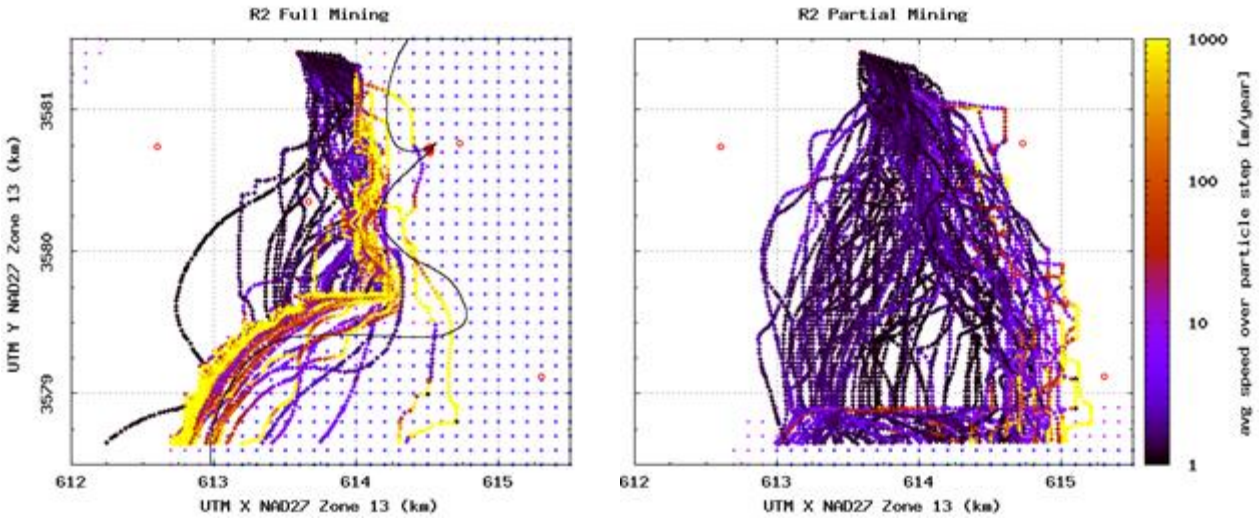

Figure TFIELD 6-17. Particle Speeds for R2, Computed From DTRKMF Results. Open symbols are Culebra well locations.

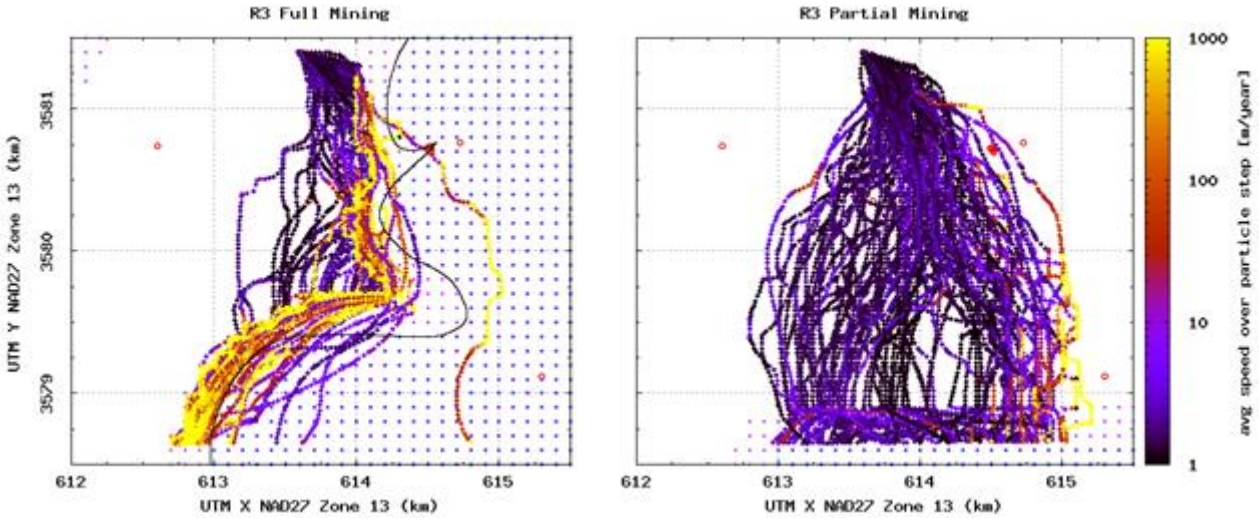

Figure TFIELD 6-18. Particle Speeds for R3, Computed from DTRKMF Results. Open symbols are Culebra well locations.

TFIELD-6.3.4 Particle-Tracking Discussion

Correlation analysis for the CRA-2009 PABC particle-tracking calculations shows that travel time and the random mining factor have weak positive correlation with the full-mining (Figure TFIELD 6-19) or partial-mining (Figure TFIELD 6-20) scenarios. Larger mining factors are weakly correlated with longer travel times. This is similar to what was observed for CRA-2004 PABC (Lowry and Kanney 2005). The high scatter in Figure TFIELD 6-19 and Figure TFIELD 6-20 indicates that the transmissivity spatial distribution plays the more significant role in determining the travel time than the mining factor does. See Appendix 1 of Kuhlman (Kuhlman 2010) for a cross-sectional comparison of transmissivity for each mining type, showing that the variability in the transmissivity due to calibration is on the same order as that due to mining for a single realization. The mining factor plays a weak but slightly larger role in explaining the observed variance for the partial-mining realizations (Figure TFIELD 6-20) than the full-mining realizations (Figure TFIELD 6-19), based on

the larger (but still relatively small) R^2 value for the straight-line fit of $\log_{10}$ travel times to mining factors.

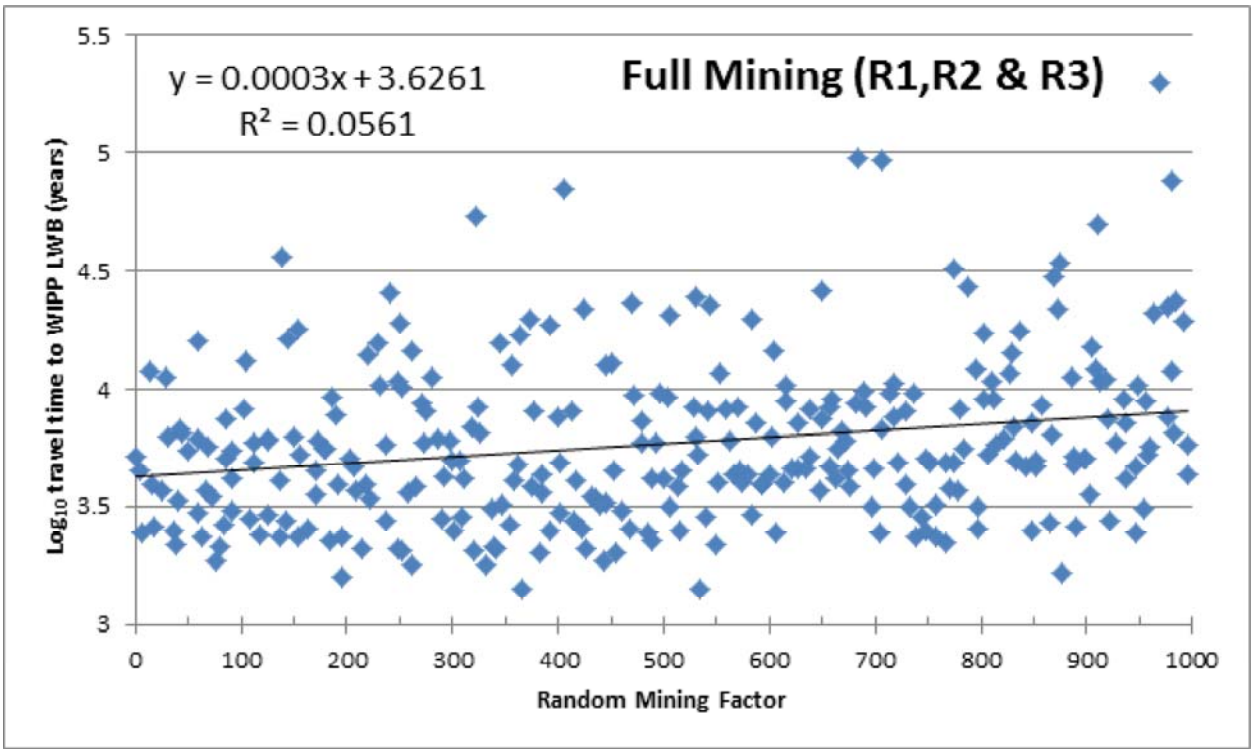

Figure TFIELD 6-19. Correlation of Mining Factor and Travel Time to the WIPP LWB for Full-mining Scenario (All Replicates)

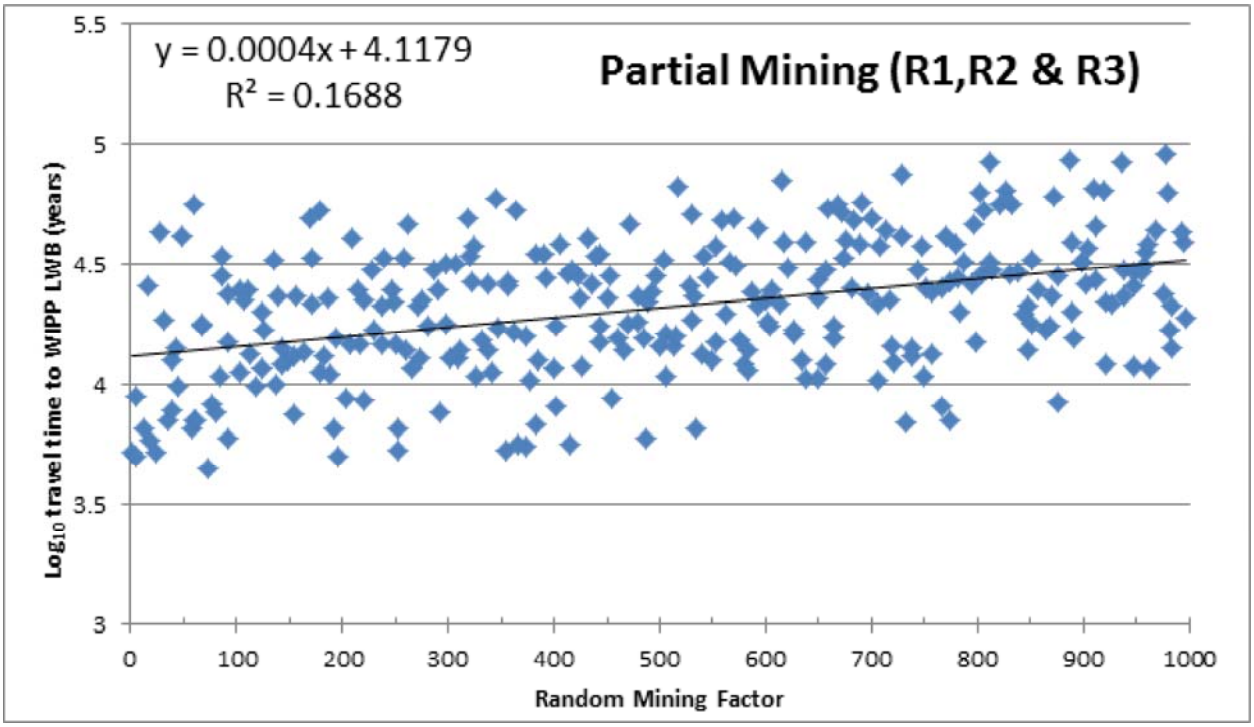

Figure TFIELD 6-20. Correlation of Mining Factor and Travel Time to the WIPP LWB for Partial-mining Scenario (All Replicates)

TFIELD-6.4 Mining Modification Summary

The 100 transmissivity fields resulting from calibration to both steady-state and transient observed freshwater heads in the Culebra (Section TFIELD-5.1) were modified to account for potential effects due to mining potash from the Salado Formation above the repository. A definition of the areal extent of minable potash was obtained from the BLM (Cranston 2009) and used to define areas where Culebra transmissivity was increased by a randomly sampled mining factor ($1 \leq$ `MINP_FACT` $\leq$ 1000). Two mining scenarios were developed: a full-mining scenario with all minable potash removed and a partial-mining scenario with only potash outside the WIPP LWB removed.

The mining-modified transmissivities were inputs to a MODFLOW flow model, which produced budget files used by DTRKMF to compute advective particle tracks from a release point at the center of the WIPP waste panels (C-2737) to the edge of the WIPP LWB. Results show that for the partial-mining scenario, the median particle travel time of 22,376 years is 3.03 times greater than for the non-mining scenario (7,374 years); the median particle travel time for the partial-mining scenario in CRA-2004 PABC was 7.06 times greater than for the non-mining scenario. In contrast to the CRA-2004 PABC, the full-mining scenario decreased median travel time to 5,084 years, a factor of 1.45 *faster* than for the non-mining scenario; the median particle travel time for the full-mining scenario in CRA-2004 PABC was 3.84 times *slower* than for the non-mining scenario. For the partial-mining scenario, the increase in transmissivity due to mining increases the relative flow rate through the mining zones, with a corresponding decrease in flow through the non-mining zones. This decrease in flow through the non-mining zones produces longer travel times for the partial-mining scenario. For the full-mining scenario, the potash definition from BLM (Cranston 2009) locates minable potash ore much closer to the C-2737 release point than in CRA-2004 PABC (see Figure TFIELD 6-5). This new shortened distance from the release point to the nearest minable potash (in the full-mining scenario) reverses the slowing-down trend observed in the CRA-2004 PABC analysis.

As in the CRA-2004 PABC calculations, a very weak positive correlation was found between the travel times and the random mining factor (the higher the random mining factor, the longer the particle travel time - see Figure TFIELD 6-19 and Figure TFIELD 6-20). As the mining factor is increased, the flow through the non-mining areas (including the C-2737 particle release location) is decreased, producing longer travel times and the positive correlation. Most of the advective particle travel time variability is due to differences in the base T-fields and their subsequent calibration, and not the random mining factor.

TFIELD-7.0 Summary

Observed Culebra transmissivities (*T*) have been related to four deterministic factors: the thickness of overburden above the Culebra, the presence or absence of dissolution of the upper Salado, the presence of gypsum cements, and the presence or absence of halite in units above and below the Culebra. Culebra *T* is also related to the occurrence of open, interconnected fractures that cannot be mapped as easily as the other three factors and therefore must be treated stochastically. A linear-regression model for Culebra *T* has been developed based on these factors that provided an excellent match to the observed data, and can be tested through the collection of additional data. This model was used to create 1000 stochastic realizations of the distribution of Culebra *T* (base T-fields) in the vicinity of the WIPP site.

A MODFLOW-2000 modeling domain was defined extending 30.7 km north-south and 28.4 km east-west, roughly centered on the WIPP site. This domain was discretized into 87,188 uniform 100-m square two-dimensional finite-difference cells. An inactive portion of the northwest corner of the domain is used to represent a no-flow boundary along the axis of Nash Draw. A low-permeability constant-head portion of the eastern section of the domain is used to represent the lithostatic pressure portion of the Culebra sandwiched above and below by Rustler halite units. Freshwater head observations in 42 monitoring wells from May 2007 were used as steady-state calibration targets. Drawdown observations in 62 observation wells, in response to 9 unique pumping tests, were used as transient calibration targets. A subset consisting of 100 of the 200 calibrated Culebra model realizations were selected based on their ability to simulate these observed heads.

The EPA requires that the potential effects of future potash mining be taken into account when evaluating the performance of the WIPP disposal system. Accordingly, *T* in the areas within the model domain where current or future mining might affect the Culebra were scaled by a random multiplier between 1 and 1,000 obtained from Latin hypercube sampling. A single multiplier was used for each T-field, applied first to the areas outside the WIPP LWB that might be mined to create a partial-mining T-field, and then to all areas (both inside and outside the WIPP LWB) to create a full-mining T-field. Three statistically similar replicates of mining multipliers were generated, leading to a total of 600 unique T-fields (100 calibrated realizations, 2 mining scenarios, and 3 replicates). The MODFLOW-2000 flow budgets were used from each realization as input for both advective particle tracking (DTRKMF) summarized here and radionuclide solute transport (SECOTP2D) used in WIPP PA.

The non-mined travel times from the center of the WIPP waste panels to the WIPP LWB are similar to those computed for the CCA and therefore faster than those computed for CRA-2004 PABC. The decrease in travel time to the LWB can be attributed to the presence of a consistent high-transmissivity pathway leaving the south-east portion of the LWB. The presence of this pathway is supported by observed drawdown data from the SNL-14 pumping test.

In the partial-mining case, particle tracks show increased travel times from the center of the WIPP waste panels to the WIPP LWB, compared to the non-mining scenario. In the full-mining case, particle tracks showed decreased travel times to the WIPP LWB, due to the close proximity of minable potash to the center of the WIPP waste panels.

TFIELD-8.0 References

(*Indicates a reference that has not been previously submitted.)

Beauheim, R.L. 1987a. Analysis of Pumping Tests of the Culebra Dolomite Conducted at the H-3 Hydropad at the Waste Isolation Pilot Plant (WIPP) Site. Albuquerque, NM: Sandia National Laboratories. SAND86-2311. [PDF / Author]

Beauheim, R.L. 1987b. Interpretation of the WIPP-13 Multipad Pumping Test of the Culebra Dolomite at the Waste Isolation Pilot Plant (WIPP) Site. Albuquerque, NM: Sandia National Laboratories. SAND87-2456. [PDF / Author]

Beauheim, R.L. 1989. Interpretation of H-11b4 Hydraulic Tests and the H-11 Multipad Pumping Test of the Culebra Dolomite at the Waste Isolation Pilot Plant (WIPP) Site. Albuquerque, NM: Sandia National Laboratories. SAND89-0536. [PDF / Author]

Beauheim, R.L. 2007. Diffusivity mapping of fracture interconnections. In Proceedings of the 2007 US EPA/NGWA Fractured Rock Conference. Westerville, OH, 2007. National Ground Water Association. [Author]

Beauheim, R.L. 2008. Analysis Plan for Evaluation and Recalibration of Culebra Transmissivity Fields AP-114, Revision 1. Carlsbad, NM: Sandia National Laboratories. [PDF / Author]

Beauheim, R.L. 2009. Changes to Culebra T-Field Calibration Procedures under AP-114 Task 7. Carlsbad, NM: Sandia National Laboratories. ERMS 551437. [PDF / Author]

Beauheim, R.L. and R.M. Holt. 1990. Geological and Hydrological Studies of Evaporites in the Northern Delaware Bains for the Waste Isolation Pilot Plant (WIPP). In D.W. Powers, R.M. Holt, R.L. Beauheim and N. Rempe, eds. Guidebook 14. Geological Society of America (Dallas Geological Society). pp.45-78. [Author]

Beauheim, R.L. and G.J. Ruskauff. 1998. Analysis of Hydraulic Tests of the Culebra and Magenta Dolomites and Dewey Lake Redbeds Conducted at the Waste Isolation Pilot Plant Site. Albuquerque, NM: Sandia National Laboratories. SAND98-0049. [PDF / Author]

Bertram, S.G. 1995. Record of FEP Screening Work, FEP ID#NS-11: Subsidence Associated with Mining Inside or Outside the Controlled Area. Carlsbad, NM: Sandia National Laboratories. ERMS 230761. [PDF / Author]

Bowman, D.O. and R.M. Roberts. 2008. Analysis Report for AP-070, Analysis of Hydraulic Tests Performed in IMC-461, SNL-6, H-11b2, H-15, and C-2737. Carlsbad, NM: Sandia National Laboratories. ERMS 539221. [Author]

Burgess, A., T. Doe, T. Lowenstein, and J.A. Thies. 2008. Waste Isolation Pilot Plant Culebra Hydrogeologicy Conceptual Model Peer Review Final Report. Carlsbad, NM: U.S. Department of Energy. ERMS 551513. [PDF / Author]

Chavez, M. 2006. NP 19-1 Software Requirements, Revision 12. Carlsbad, NM: Sandia National Laboratories. [PDF / Author]

Clayton, D.J., R.C. Camphouse, J.W. Garner, A.E. Ismail, T.B. Kirchner, K.L. Kuhlman, and M.B. Nemer. 2010. Summary Report of the CRA-2009 Performance Assessment Baseline Calculation. Carlsbad, NM: Sandia National Laboratories. ERMS 553039. [PDF / Author]

Cranston, C.C. 2009. Minable Potash Ore. Carlsbad, NM: Bureau of Land Management. ERMS 551120. [PDF / Author]

Currie, J.B. and S.O. Nwachukwu. 1974. Evidence on incipient fracture porosity in reservoir rocks at depth. Bulletin of Canadian Petroleum Geology. 22, pp.42-58. [Author]

Deutsch, C.V. and A.G. Journel. 1998. GSLIB: Geostatistical Software Library and User's Guide. 2nd ed. New York: Oxford University Press. [Author]

Doherty, J. 2000. PEST Manual. Brisbane, Australia: Watermark Numerical Computing. [Author]

Harbaugh, A.W., E.R. Banta, M.C. Hill, and M.G. McDonald 2000. MODFLOW 2000: The U.S. Geological Survey Modular Ground-Water Model User Guide. Reston, VA: U.S. Geological Survey. OFR 00-92. [PDF / Author]

Hart, D.B., R.L. Beauheim, and S.A. McKenna. 2009. Analysis Report for Task 7 of AP-114: Calibration of Culebra Transmissivity Fields. Carlsbad, NM: Sandia National Laboratories. ERMS 552391. [PDF / Author]

Hart, D.B., R.M. Holt, and S.A. McKenna. 2008. Analysis Report for Task 5 of AP-114: Generation of Revised Base Transmissivity Fields. Carlsbad, NM: Sandia National Laboratories. ERMS 549597. [PDF / Author]

Holt, R.M. 1997. Conceptual Model for Transport Processes in the Culebra Dolomite Member of the Rustler Formation. Albuquerque, NM: Sandia National Laboratories. SAND97-0194. [PDF / Author]

Holt, R.M., R.L. Beauheim, and D.W. Powers. 2005. Predicting fractured zones in the Culebra Dolomite. In B. Faybishenko, P.A. Witherspoon and J. Gale, eds. Dynamics of Fluids and Transport in Fractured Rock. American Geophysical Union. pp.103-16. [Author]

Holt, R.M. and D.W. Powers. 1988. Facies variability and post-depositional alteration within the Rustler Formation in the vicinity of the Waste Isolation Pilot Plant, southeastern New Mexico. Carlsbad, NM: Department of Energy. WIPP-DOE-88-004. [PDF / Author]

Holt, R.M. and L. Yarbrough. 2002. Analysis Report, Task 2 of AP-088, Estimating Base Transmissivity Fields. Carlsbad, NM: Sandia National Laboratories. ERMS 523889. [PDF / Author]

Johnson, P.B. 2009a. Potentiometric Surface, Adjusted to Equivalent Freshwater Heads, of the Culebra Dolomite Member of the Rustler Formation near the WIPP Site, Revision 1. Carlsbad, NM: Sandia National Laboratories. ERMS 548746. [PDF / Author]

Johnson, P.B. 2009b. Routine Calculations Report In Support of Task 6 of AP-114: Potentiometric Surface, Adjusted to Equivalent Freshwater Heads, of the Culebra Dolomite member of the Rustler Formation near the WIPP Site, Revision 2. Carlsbad, NM: Sandia National Laboratories. ERMS 551116. [PDF / Author]

Kirchner, T.B. 2010. Generation of the LHS Samples for the AP-145 (PABC09) PA Calculations. Carlsbad, NM: Sandia National Laboratories. ERMS 552905. [PDF / Author]

Kuhlman, K.L. 2009. AP-144 Analysis Plan for the Calculation of Culebra Flow and Transport for CRA2009PABC. Carlsbad, NM: Sandia National Laboratories. ERMS 551676. [PDF / Author]

Kuhlman, K.L. 2010. Analysis Report for the CRA-2009 PABC Culebra Flow and Transport Calculations (AP-144). Carlsbad, NM: Sandia National Laboratories. ERMS 552951. [PDF / Author]

Leigh, C.D., J.F. Kanney, L.H. Brush, J.W. Garner, G.R. Kirkes, T. Lowry, M.B. Nemer, J.S. Stein, E.D. Vugrin, S. Wagner, and T.B. Kirchner. 2004. 2004 Compliance Recertification Application Performance Assessment Baseline Calculation, Revision 0. Carlsbad, NM: Sandia National Laboratories. ERMS 541521. [PDF / Author]

Lowry, T.L. 2003a. Analysis Report, Task 5 of AP-088: Evaluation of Mining Scenarios. Carlsbad, NM: Sandia National Laboratories. ERMS 531138. [PDF / Author]

Lowry, T.L. 2003b. Analysis Report, Tasks 2 & 3 of AP-100: Grid Size Conversion and Generation of SECOTP2D Input. Carlsbad, NM: Sandia National Laboratories. ERMS 531137. [PDF / Author]

Lowry, T.S. 2004. Analysis Report for Inclusion of Omitted Areas in Mining Transmissivity Calculations in Response to EPA Comment G-11. Carlsbad, NM: Sandia National Laboratories. ERMS 538218. [PDF / Author]

Lowry, T.S. and J.F. Kanney. 2005. Analysis Report for the CRA-2004 PABC Culebra Flow and Transport Calculations. Carlsbad, NM: Sandia National Laboratories. ERMS 541508. [PDF / Author]

McKenna, S.A. and D.B. Hart. 2003. Analysis report for Task 4 of AP-088: Conditioning of Base T Fields to Transient Heads. Carlsbad, NM: Sandia National Laboratories. ERMS 531124. [PDF / Author]

McKenna, S.A. and A. Wahi. 2006. Local Hydraulic Gradient Estimator Analysis of Long-Term Monitoring Networks. Ground Water. 44(5), pp.723-31. [Author]

Mehl, S.W. 2001. MODFLOW-2000, The US Geological Survey Modular Ground-Water Model User Guide to the Link-AMG (LMG) Package for Solving Matrix Equations using an Algebraic Multigrid Solver. USGS (US Geological Survey). OFR 01-177. [PDF / Author]

Powers, D.W. 2002a. Analysis report Task 1 of AP-088, Construction of geologic contour maps. Carlsbad, NM: Sandia National Laboratories. ERMS 522085. [PDF / Author]

Powers, D.W. 2002b. Addendum to Analysis Report, Task 1 of AP-088, Construction of Geologic Contour Maps. Carlsbad, NM: Sandia National Laboratories. ERMS 523886. [PDF / Author]

Powers, D.W. 2003. Addendum 2 to Analysis report Task 1 of AP-088, Construction of geologic contour maps. Carlsbad, NM: Sandia National Laboratories. ERMS 522085. [PDF / Author]

Powers, D.W. 2006. Analysis Report Task 1B of AP-114: Identify possible area of recharge to the Culebra west and south of WIPP. Carlsbad, NM: Sandia National Laboratories. ERMS 547094. [PDF / Author]

Powers, D.W. 2007a. Analysis Report for Task 1A of AP-114: Refinement of Rustler Halite Margins Within the Culebra Modeling Domain. Carlsbad, NM: Sandia National Laboratories. ERMS 547559. [PDF / Author]

Powers, D.W. 2007b. Analysis Report for Task 1A of AP-114: refinement of Rustler Halite margins within the Culebra modeling domain. Carlsbad, NM: Sandia National Laboratories. ERMS 547559. [Author]

Powers, D.W. 2009. Basic Data Report for Drillhole SNL-8 (C-3150) (Waste Isolation Pilot Plant). DOE/WIPP 05-3324. Carlsbad, NM: U.S. Department of Energy. [PDF / Author]

Powers, D.W. and R.M. Holt. 1995. Regional geological processes affecting Ruster hydrogeology. IT Corporation for Westinghouse Electric Corporation. [PDF / Author]

Powers, D.W. and R.M. Holt. 1999. The Los Medanos Member of the Permian Rustler Formation. New Mexico Geology. 21(4), pp.97-103. [Author]

Powers, D.W. and R.M. Holt. 2000. The salt that wasn't there: mudflat facies equivalents to halite of the Permian Rustler Formation, southeastern New Mexico. Journal of Sedimentary Research, 70(1), pp.29-36. [Author]

Powers, D.W., R.M. Holt, R.L. Beauheim, and S.A. McKenna. 2003. Geologic factors related to the transmissivity of the Culebra Dolomite Member, Permian Rustler Formation, Delaware Basin, southeastern New Mexico. In K.S. Johnson and J.T. Neal, eds. Evaporite Karst and engineering/environmental problems in the United States. 109th ed. Oklahoma Geological Survey. pp.211-18. [Author]

Powers, D.W., R.M. Holt, R.L. Beauheim, and R.G. Richardson. 2006. Advances in depositional models of the Permian Rustler Formation, southeastern New Mexico. In Caves & Karst of Southeastern New Mexico. Fifty-seventh Annual Field Conference Guidebook ed. NM Geological Society. pp.267-76. [Author]

Powers, D.W. and D. Owsley. 2003. A field survey of evaporite karst along NM 128 realighment routes. In K.S. Johnson and J.T. Neal, eds. Evaporite karst and engineering / environmental problems in the United States. 109th ed. Oklahoma Geological Survey. pp.233-40. [Author]

Ramsey, J.L. and M. Wallace. 1996. Analysis Package for the Culebra Flow and Transport Calculations (Task 3) of the Performance Assessment Analyses Supporting the Compliance Certification Application. Carlsbad, NM: Sandia National Laboratories. ERMS 240516. [PDF / Author]

Roberts, R.M. 2006. Analysis Report for AP-070, Analysis of Culebra Pumping Tests Performed Between December 2003 and August 2005. Carlsbad, NM: Sandia National Laboratories. ERMS 543901. [PDF / Author]

Roberts, R.M. 2007. Analysis Report for AP-070, Analysis of Culebra Hydraulic Tests Performed Between June 2006 and September 2007. Carlsbad, NM: Sandia National Laboratories. ERMS 547418. [PDF / Author]

Rudeen, D.K. 2003. User's Manual for DTRKMF Version 1.00. Carlsbad, NM: Sandia National Laboratories. ERMS 523246. [PDF / Author]

Toll, N.J. and P.B. Johnson. 2006a. Routine Calculations Report In Support of Task 6 of AP-114, SNL-14 August 2005 Pumping Test Observation Well Data Processing, Summary of Files. Carlsbad, NM: Sandia National Laboratories. ERMS 543371. [PDF / Author]

Toll, N.J. and P.B. Johnson. 2006b. Routine Calculations Report In Support of Task 6 of AP-114, WIPP-11 February 2005 Pumping Test Observation Well Data Processing - Summary of Files. Carlsbad, NM: Sandia National Laboratories. ERMS 543651. [PDF / Author]

U.S. Department of Energy (DOE). 1996. Title 40 CFR Part 191 Compliance Certification Application for the Waste Isolation Pilot. Carlsbad, NM: U.S. Department of Energy Waste Isolation Pilot Plant, Carlsbad Area Office. DOE/CAO-1996-2184. [Author]

U.S. Department of Energy (DOE). 2004. Title 40 CFR Part 191 Subparts B and C Compliance Recertification Application for the Waste Isolation Pilot Plant. Carlsbad, NM: US Department of Energy Carlsbad Field Office. DOE/WIPP 2004-3231. [Author]

U.S. Department of Energy (DOE). 2009. Title 40 CFR Part 191 Subparts B and C Compliance Recertification Application for the Waste Isolation Pilot Plant. Carlsbad, NM: US Department of Energy Carlsbad Field Office. DOE/WIPP 2009-3424.* [Author]

U.S. Environmental Protection Agency (EPA). 1996. 40 CFR Part 194: Criteria for the Certification and Recertification of the Waste Isolation Pilot Plant's Compliance with 40 CFR Part 191 Disposal Regulations; Final Rule., 1996. Federal Register Vol 61, 5223-5245. [PDF / Author]

Title 40 CFR Part 191
Subparts B and C
Compliance Recertification Application 2014
for the
Waste Isolation Pilot Plant

Attachment A: TFIELD-2014 Visualization

United States Department of Energy
Waste Isolation Pilot Plant

Carlsbad Field Office
Carlsbad, New Mexico

Compliance Recertification Application 2014 Attachment A: TFIELD-2014 Visualization

This attachment contains figures for Appendix TFIELD-2014, related to the Culebra T-Field calibration process, performed as part of the 2009 Compliance Recertification Application (CRA-2009) Performance Assessment Baseline Calculation (PABC). These parameter inputs and outputs are used without modification in CRA-2014. The development of the input and output data is summarized in Appendix TFIELD-2014 and discussed in detail in Hart et al. (2009).

Hart, D.B., Beauheim, R.L. and McKenna, S.A. 2009. *Analysis Report for Task 7 of AP-114: Calibration of Culebra Transmissivity Fields*. Carlsbad, NM: Sandia National Laboratories. ERMS 552391.

Table of Contents

TFIELD Attachment A-1.0 100 Calibrated Hydraulic Conductivity Model Input Parameter Fields

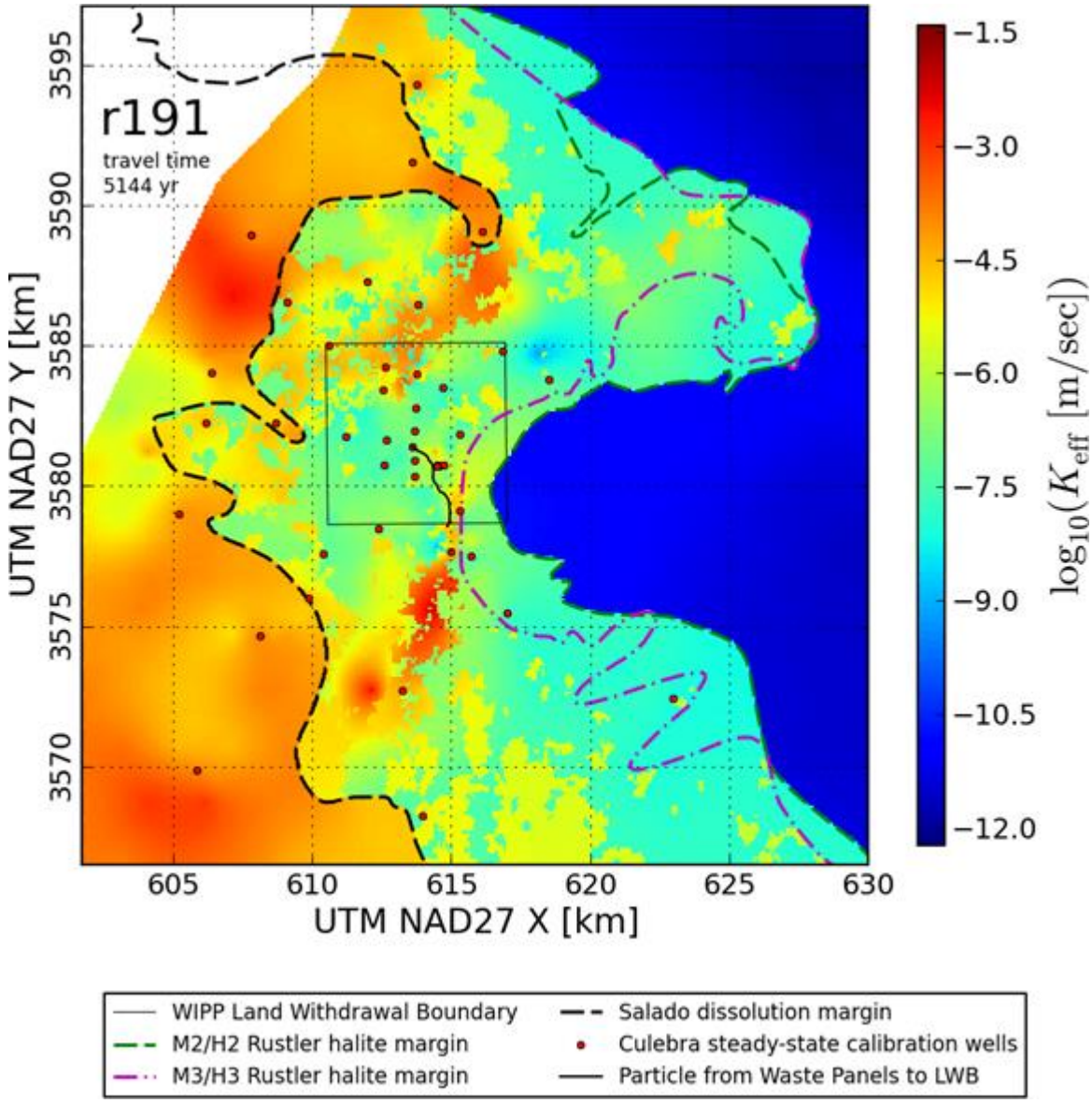
r191
travel time
5144 yr
UTM NAD27 Y [km]
3595
3590
3585
3580
3575
3570
605
610
615
620
625
630
UTM NAD27 X [km]
−1.5
−3.0
−4.5
−6.0
−7.5
−9.0
−10.5
−12.0
$\log_{10}(K_{\text{eff}}$ [m/sec])
WIPP Land Withdrawal Boundary
M2/H2 Rustler halite margin
M3/H3 Rustler halite margin
Salado dissolution margin
Culebra steady-state calibration wells
Particle from Waste Panels to LWB

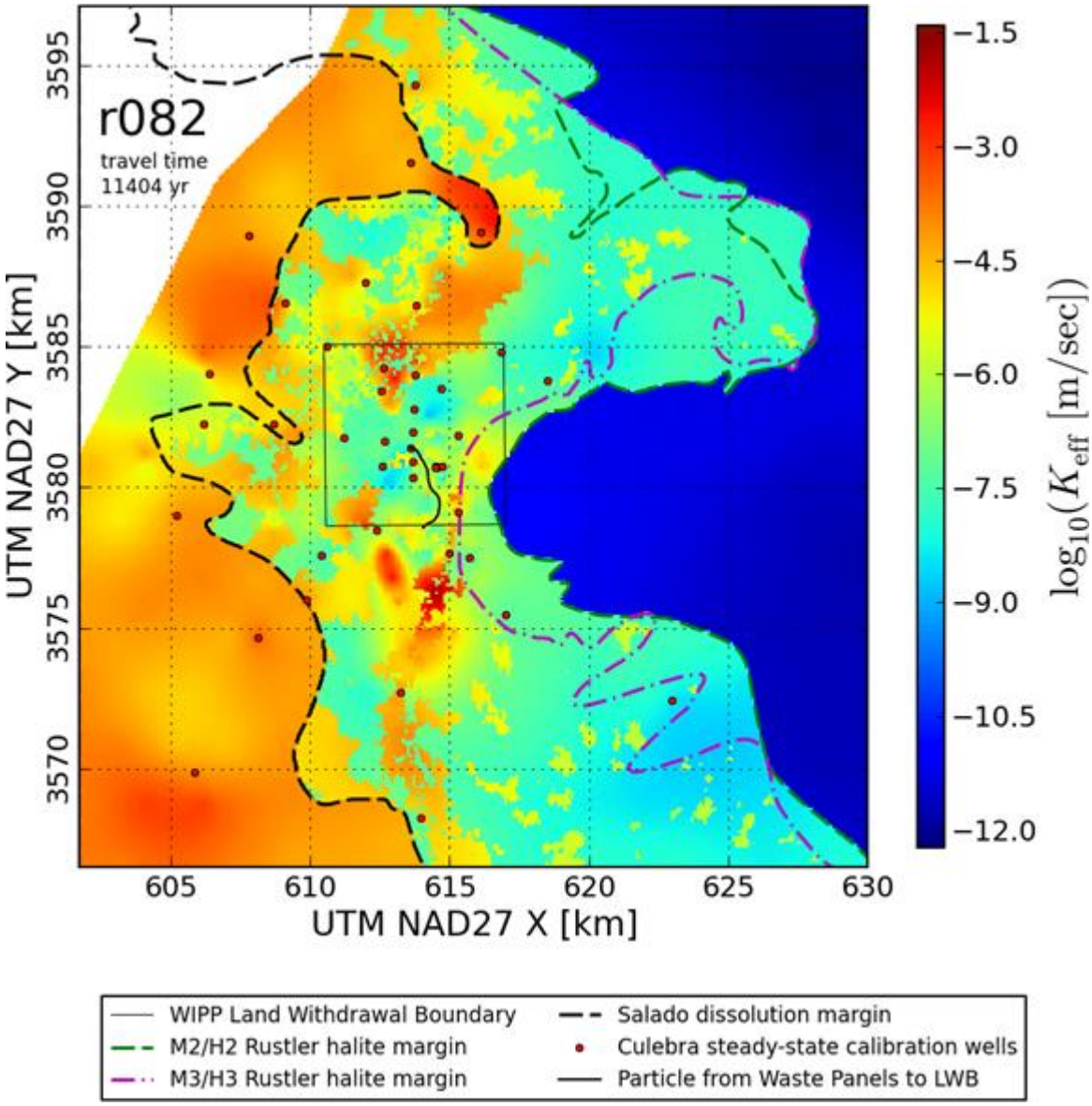
r082
travel time
11404 yr
UTM NAD27 Y [km]
3595
3590
3585
3580
3575
3570
605
610
615
620
625
630
UTM NAD27 X [km]
−1.5
−3.0
−4.5
−6.0
−7.5
−9.0
−10.5
−12.0
$\log_{10}(K_{\mathrm{eff}}\ [\mathrm{m/sec}])$
WIPP Land Withdrawal Boundary
M2/H2 Rustler halite margin
M3/H3 Rustler halite margin
Salado dissolution margin
Culebra steady-state calibration wells
Particle from Waste Panels to LWB

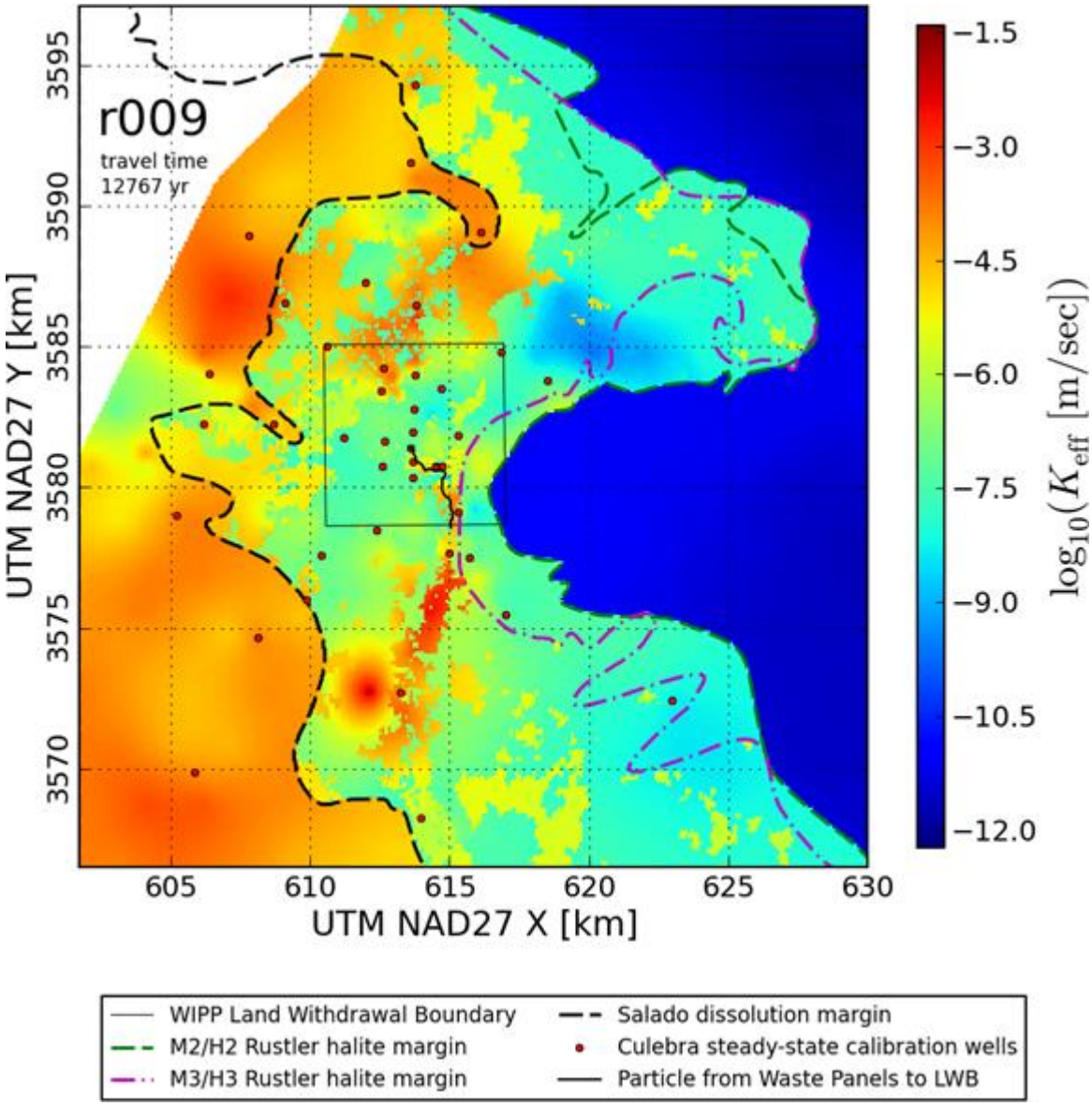
r009
travel time
12767 yr
UTM NAD27 Y [km]
3595
3590
3585
3580
3575
3570
605
610
615
620
625
630
UTM NAD27 X [km]
−1.5
−3.0
−4.5
−6.0
−7.5
−9.0
−10.5
−12.0
$\log_{10}(K_{\mathrm{eff}}\ [\mathrm{m/sec}])$
WIPP Land Withdrawal Boundary
M2/H2 Rustler halite margin
M3/H3 Rustler halite margin
Salado dissolution margin
Culebra steady-state calibration wells
Particle from Waste Panels to LWB

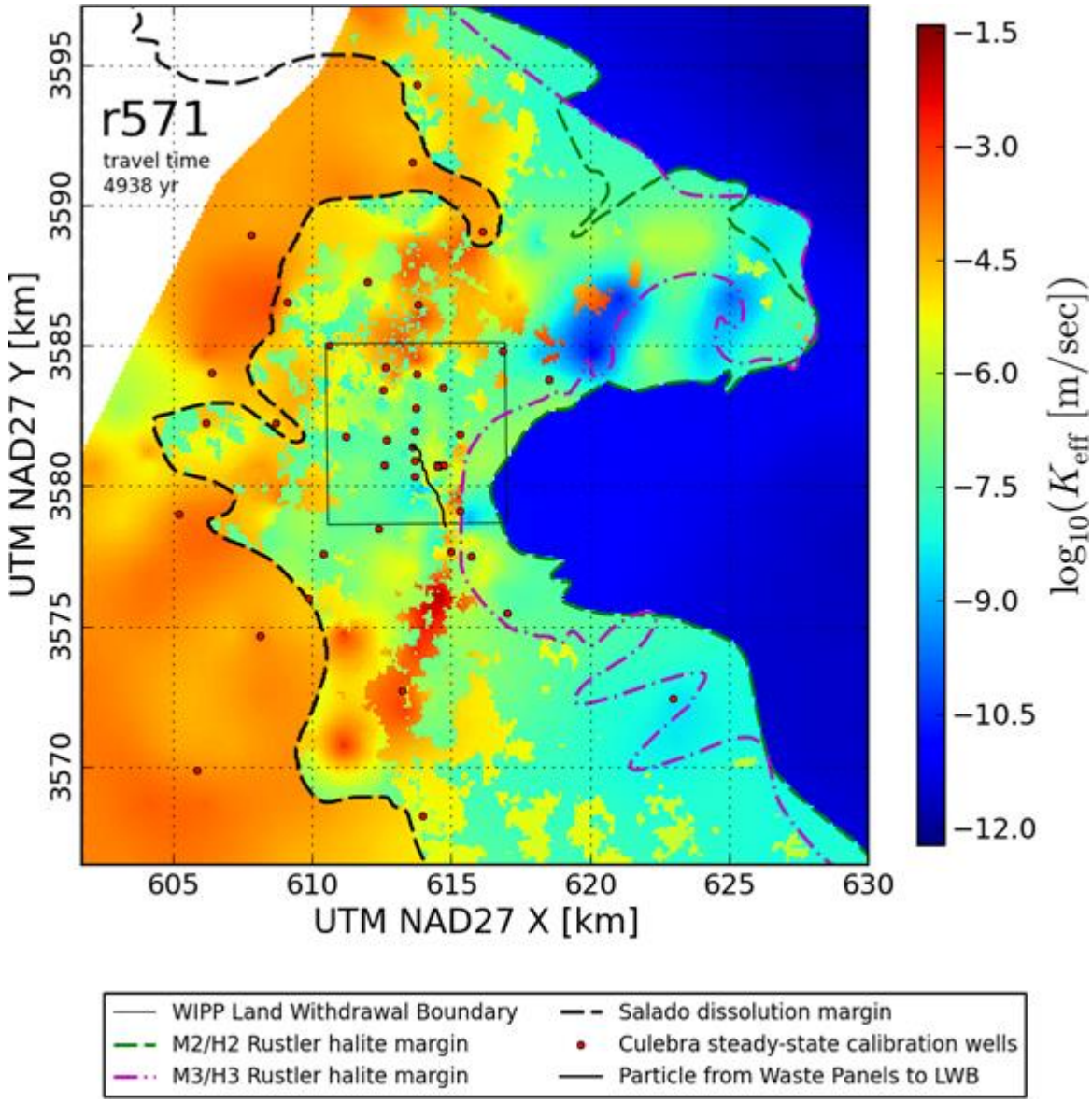
r571
travel time
4938 yr
UTM NAD27 Y [km]
3595
3590
3585
3580
3575
3570
605
610
615
620
625
630
UTM NAD27 X [km]
−1.5
−3.0
−4.5
−6.0
−7.5
−9.0
−10.5
−12.0
$\log_{10}(K_{\mathrm{eff}}\ [\mathrm{m/sec}])$
WIPP Land Withdrawal Boundary
M2/H2 Rustler halite margin
M3/H3 Rustler halite margin
Salado dissolution margin
Culebra steady-state calibration wells
Particle from Waste Panels to LWB

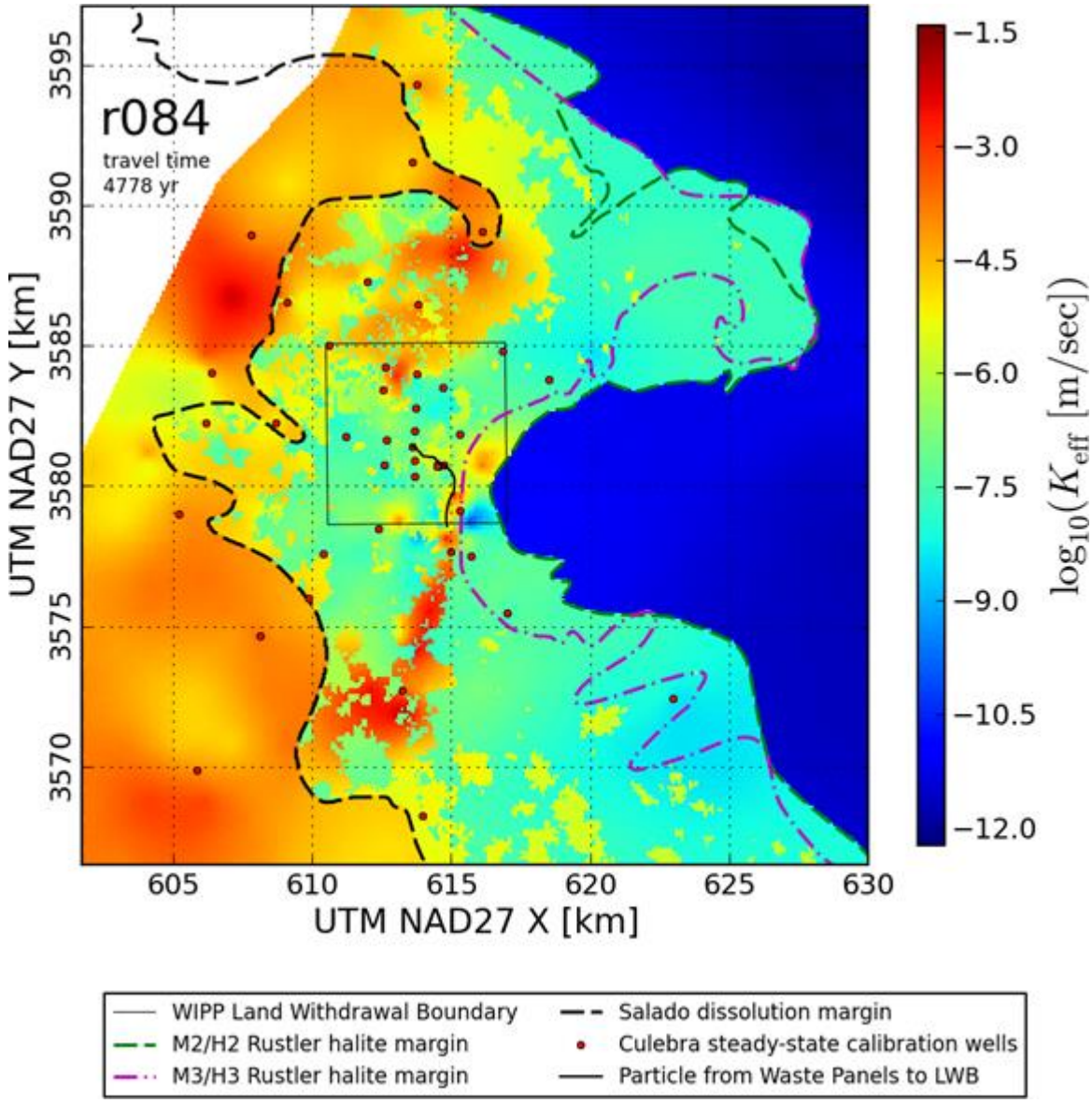
r084
travel time
4778 yr
UTM NAD27 Y [km]
3595
3590
3585
3580
3575
3570
605
610
615
620
625
630
UTM NAD27 X [km]
−1.5
−3.0
−4.5
−6.0
−7.5
−9.0
−10.5
−12.0
$\log_{10}(K_{\mathrm{eff}}\ [\mathrm{m/sec}])$
WIPP Land Withdrawal Boundary
M2/H2 Rustler halite margin
M3/H3 Rustler halite margin
Salado dissolution margin
Culebra steady-state calibration wells
Particle from Waste Panels to LWB

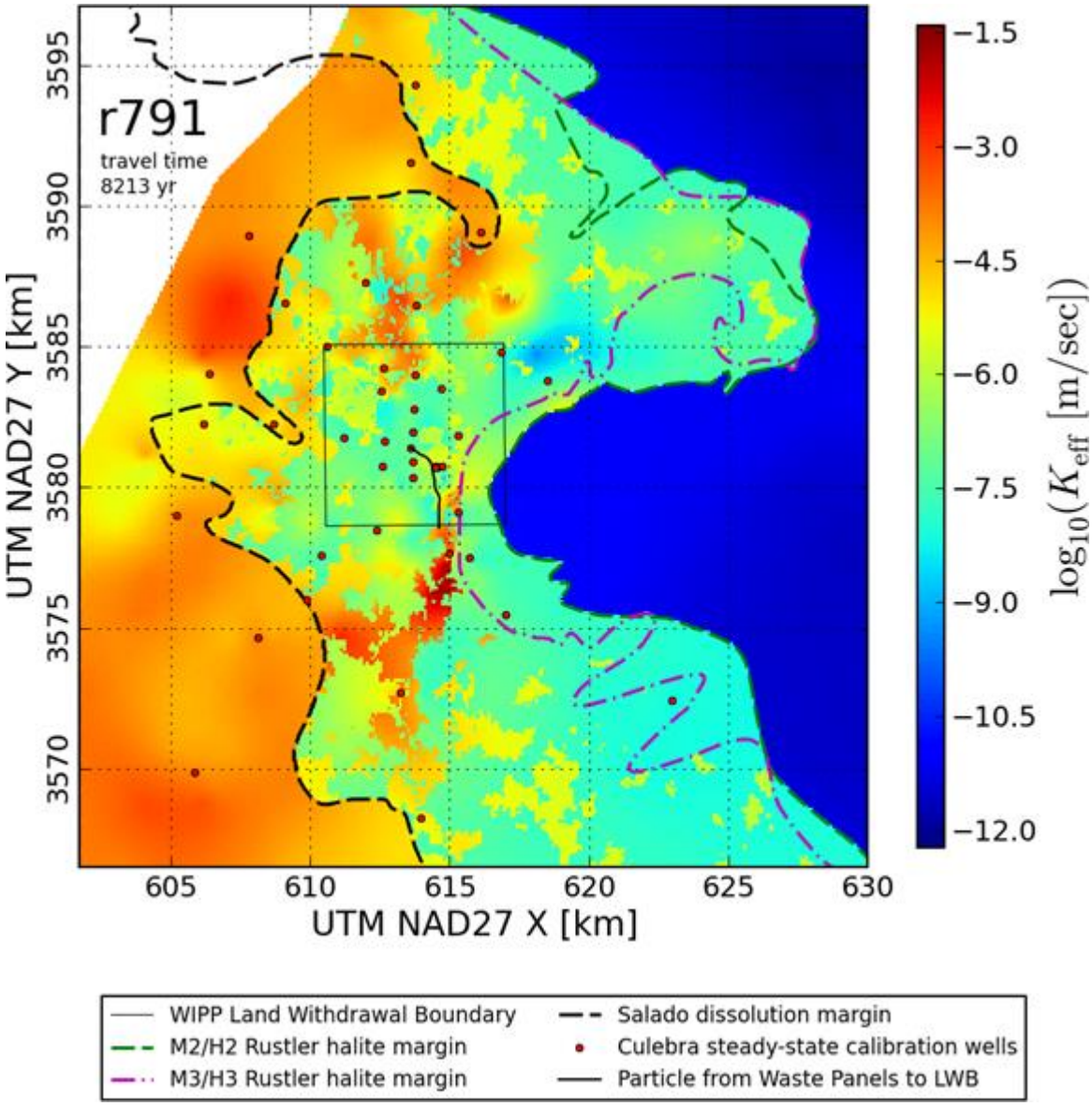
r791
travel time
8213 yr
UTM NAD27 Y [km]
3595
3590
3585
3580
3575
3570
605
610
615
620
625
630
UTM NAD27 X [km]
−1.5
−3.0
−4.5
−6.0
−7.5
−9.0
−10.5
−12.0
$\log_{10}(K_{\mathrm{eff}}\ [\mathrm{m/sec}])$
WIPP Land Withdrawal Boundary
M2/H2 Rustler halite margin
M3/H3 Rustler halite margin
Salado dissolution margin
Culebra steady-state calibration wells
Particle from Waste Panels to LWB

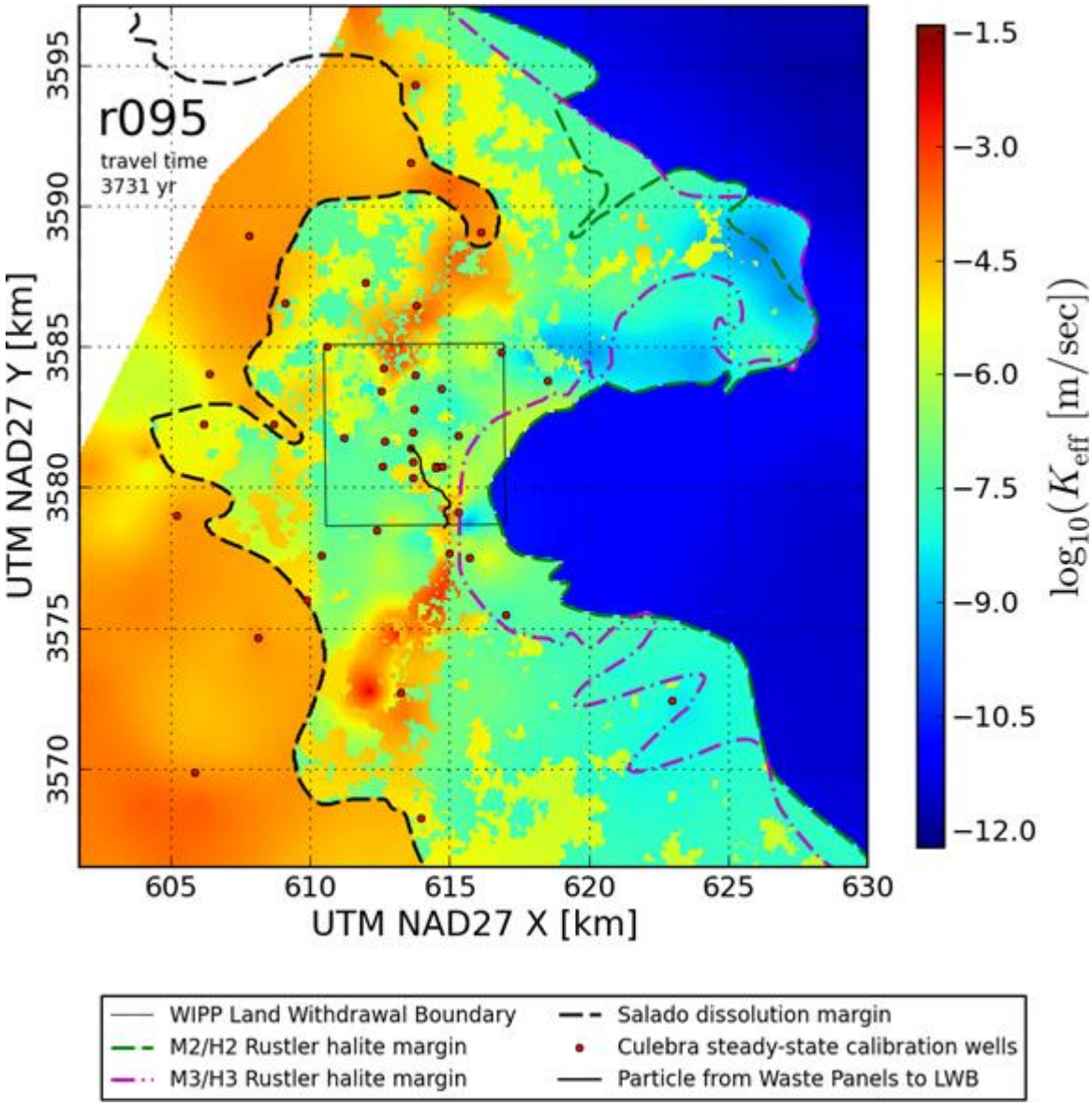
r095
travel time
3731 yr
UTM NAD27 Y [km]
3595
3590
3585
3580
3575
3570
605
610
615
620
625
630
UTM NAD27 X [km]
−1.5
−3.0
−4.5
−6.0
−7.5
−9.0
−10.5
−12.0
$\log_{10}(K_{\mathrm{eff}}\ [\mathrm{m/sec}])$
WIPP Land Withdrawal Boundary
M2/H2 Rustler halite margin
M3/H3 Rustler halite margin
Salado dissolution margin
Culebra steady-state calibration wells
Particle from Waste Panels to LWB

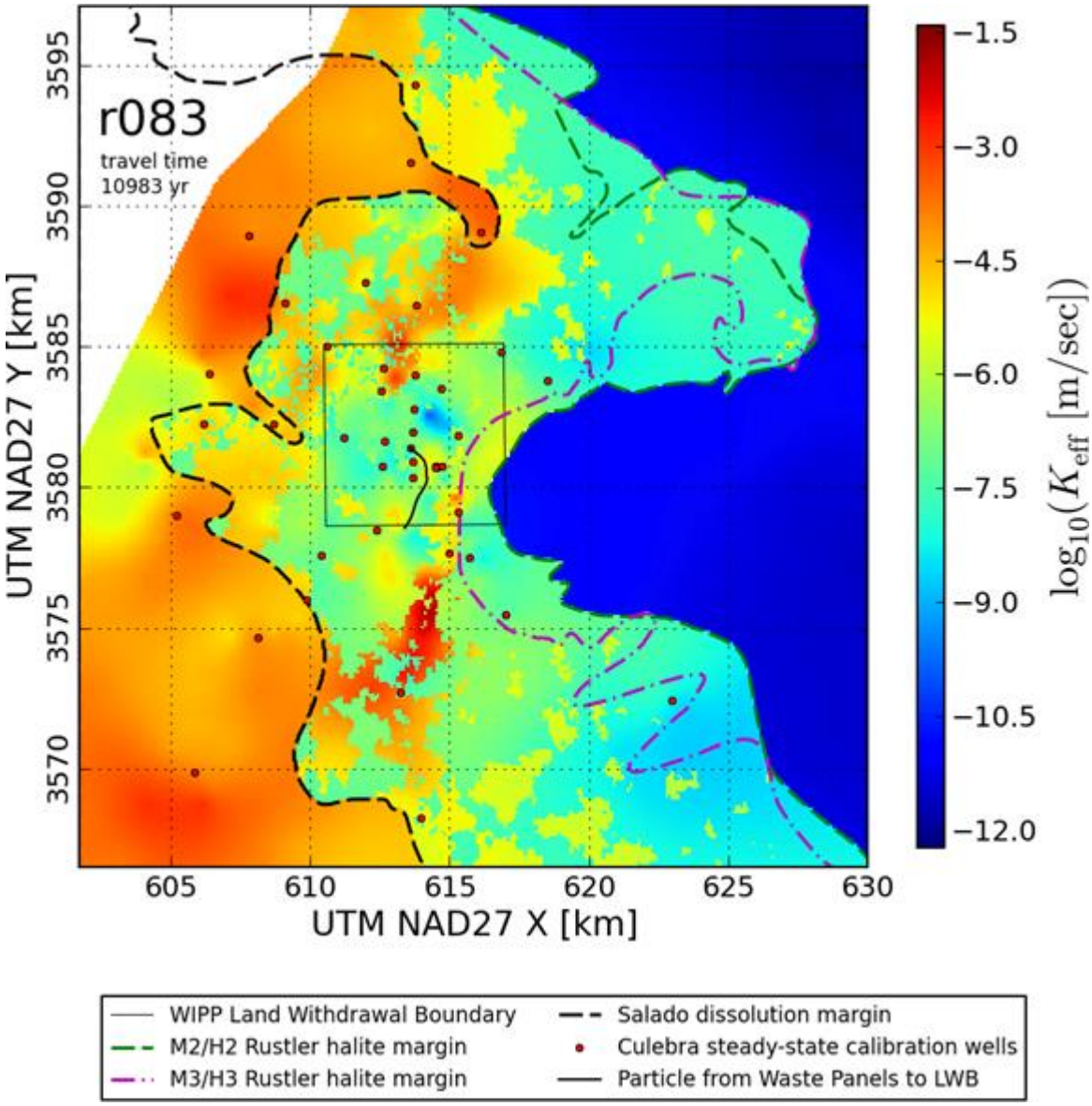
r083
travel time
10983 yr
UTM NAD27 Y [km]
3595
3590
3585
3580
3575
3570
605
610
615
620
625
630
UTM NAD27 X [km]
−1.5
−3.0
−4.5
−6.0
−7.5
−9.0
−10.5
−12.0
$\log_{10}(K_{\text{eff}}$ [m/sec])
WIPP Land Withdrawal Boundary
M2/H2 Rustler halite margin
M3/H3 Rustler halite margin
Salado dissolution margin
Culebra steady-state calibration wells
Particle from Waste Panels to LWB

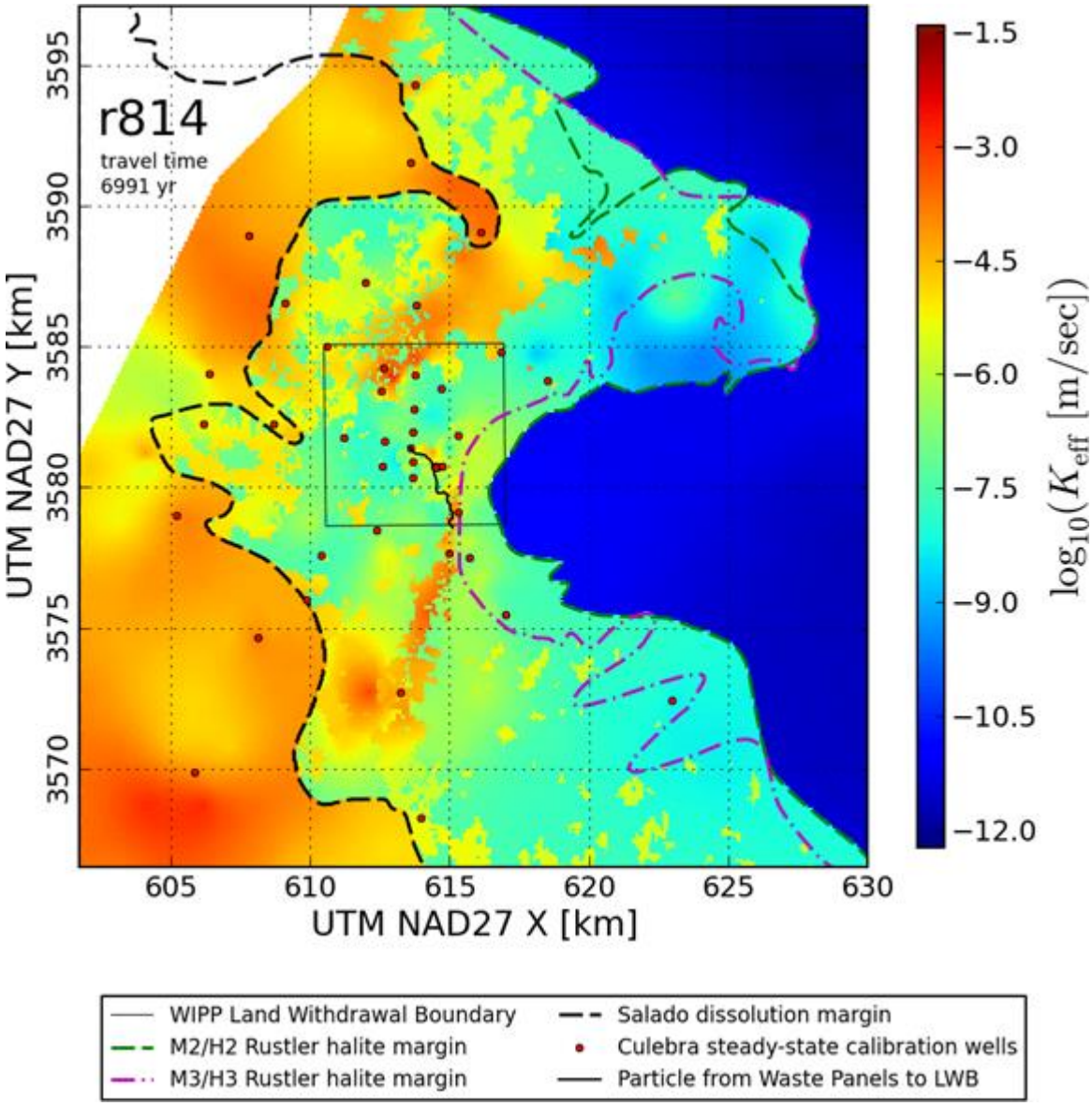
r814
travel time
6991 yr
UTM NAD27 Y [km]
3595
3590
3585
3580
3575
3570
605
610
615
620
625
630
UTM NAD27 X [km]
−1.5
−3.0
−4.5
−6.0
−7.5
−9.0
−10.5
−12.0
$\log_{10}(K_{\mathrm{eff}}\ [\mathrm{m/sec}])$
WIPP Land Withdrawal Boundary
M2/H2 Rustler halite margin
M3/H3 Rustler halite margin
Salado dissolution margin
Culebra steady-state calibration wells
Particle from Waste Panels to LWB

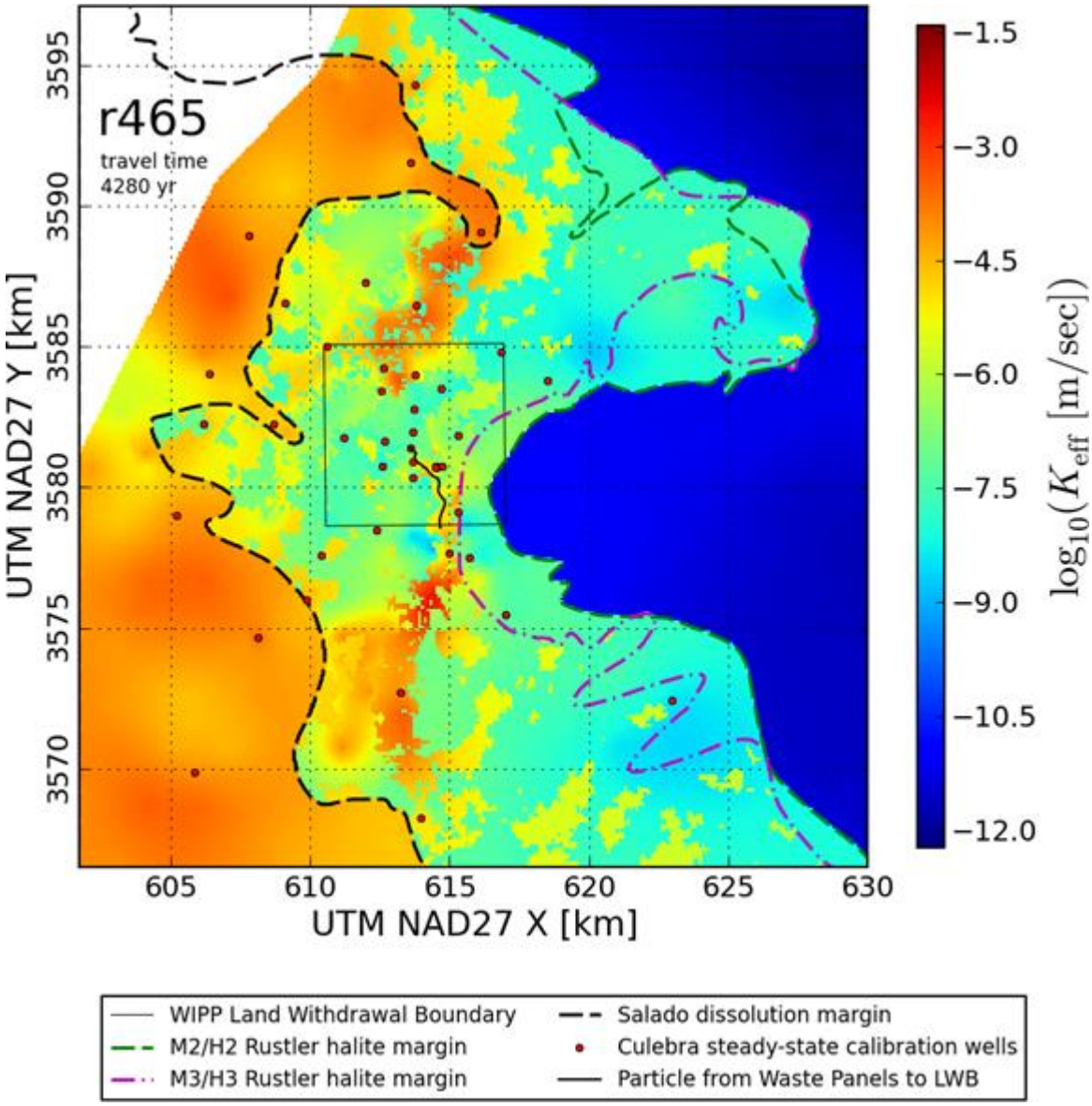
r465
travel time
4280 yr
UTM NAD27 Y [km]
3595
3590
3585
3580
3575
3570
605
610
615
620
625
630
UTM NAD27 X [km]
−1.5
−3.0
−4.5
−6.0
−7.5
−9.0
−10.5
−12.0
$\log_{10}(K_{\mathrm{eff}}\ [\mathrm{m/sec}])$
WIPP Land Withdrawal Boundary
M2/H2 Rustler halite margin
M3/H3 Rustler halite margin
Salado dissolution margin
Culebra steady-state calibration wells
Particle from Waste Panels to LWB

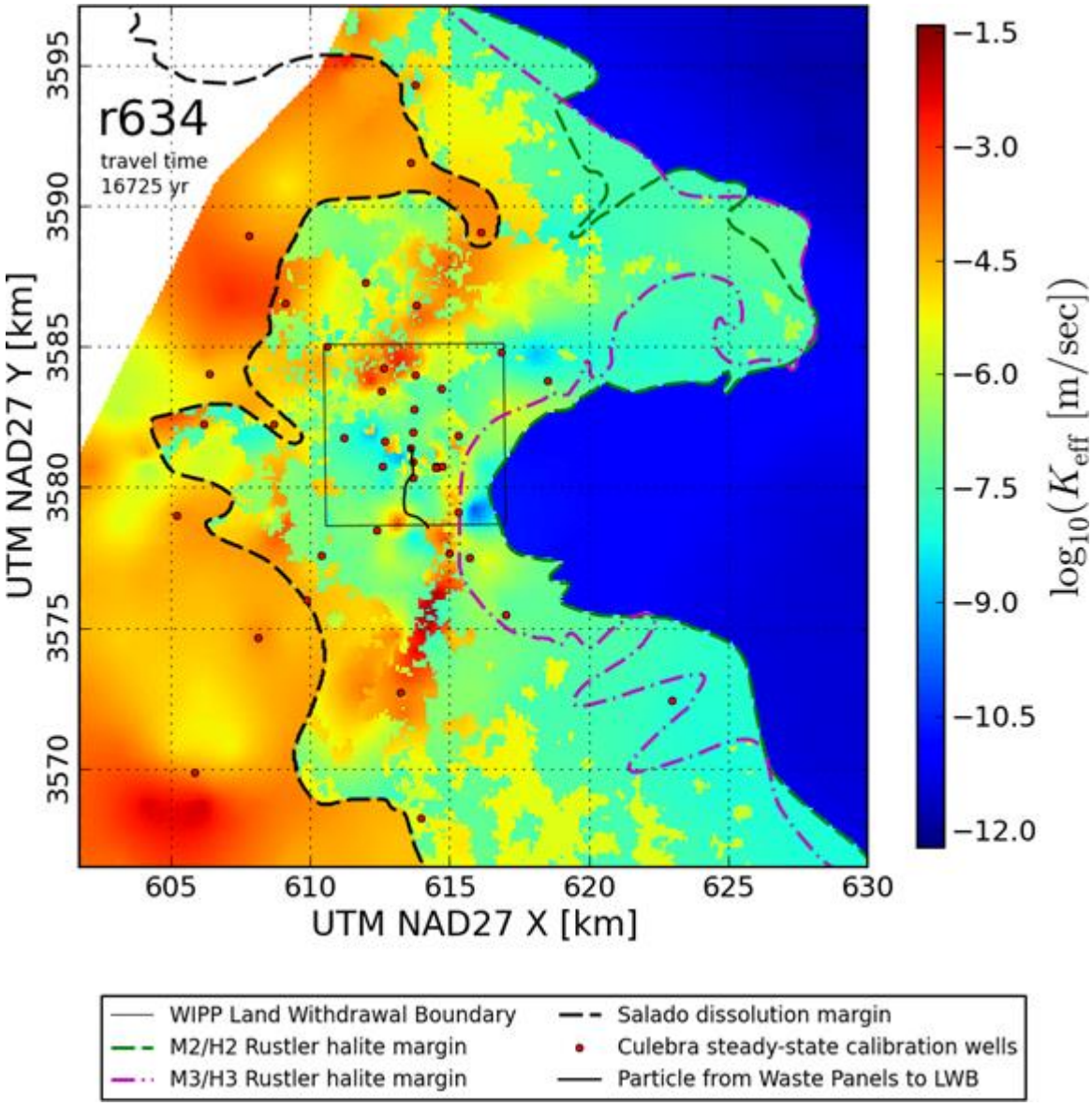
r634
travel time
16725 yr
UTM NAD27 Y [km]
3595
3590
3585
3580
3575
3570
605
610
615
620
625
630
UTM NAD27 X [km]
−1.5
−3.0
−4.5
−6.0
−7.5
−9.0
−10.5
−12.0
$\log_{10}(K_{\text{eff}}$ [m/sec])
WIPP Land Withdrawal Boundary
M2/H2 Rustler halite margin
M3/H3 Rustler halite margin
Salado dissolution margin
Culebra steady-state calibration wells
Particle from Waste Panels to LWB

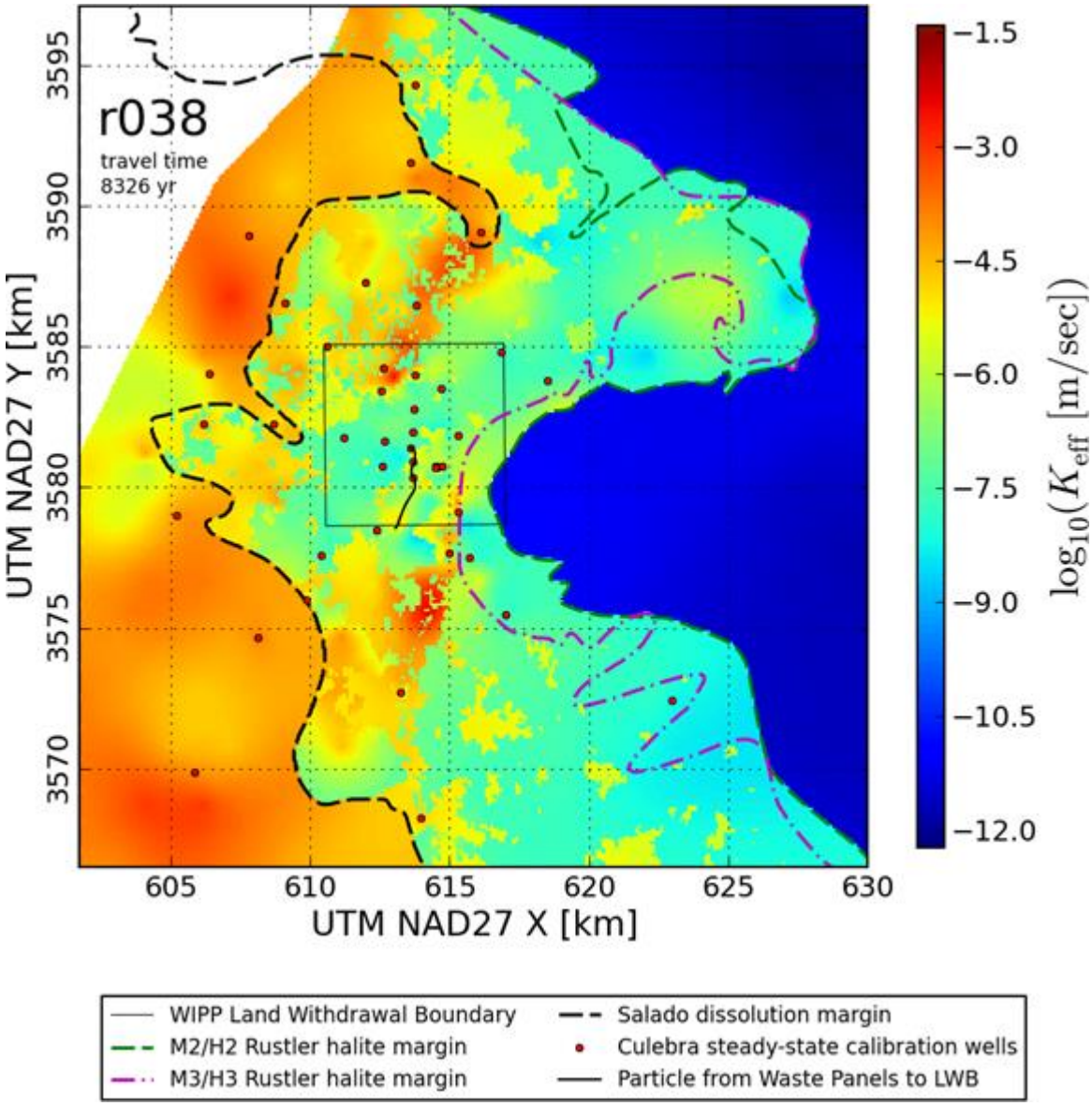
r038
travel time
8326 yr
UTM NAD27 Y [km]
3595
3590
3585
3580
3575
3570
605
610
615
620
625
630
UTM NAD27 X [km]
−1.5
−3.0
−4.5
−6.0
−7.5
−9.0
−10.5
−12.0
$\log_{10}(K_{\text{eff}}$ [m/sec])
WIPP Land Withdrawal Boundary
M2/H2 Rustler halite margin
M3/H3 Rustler halite margin
Salado dissolution margin
Culebra steady-state calibration wells
Particle from Waste Panels to LWB

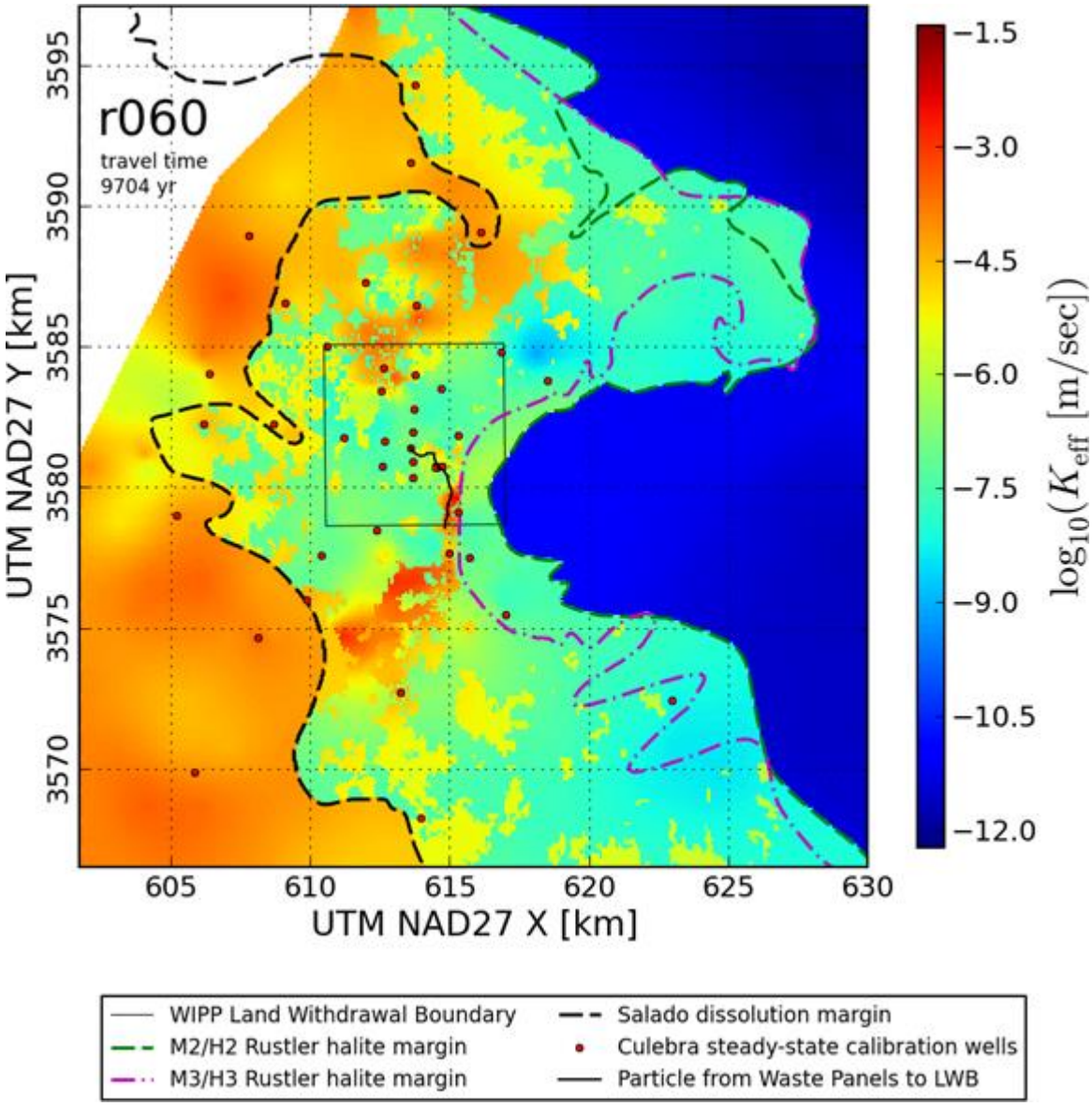
r060
travel time
9704 yr
UTM NAD27 Y [km]
3595
3590
3585
3580
3575
3570
605
610
615
620
625
630
UTM NAD27 X [km]
−1.5
−3.0
−4.5
−6.0
−7.5
−9.0
−10.5
−12.0
$\log_{10}(K_{\mathrm{eff}}\ [\mathrm{m/sec}])$
WIPP Land Withdrawal Boundary
M2/H2 Rustler halite margin
M3/H3 Rustler halite margin
Salado dissolution margin
Culebra steady-state calibration wells
Particle from Waste Panels to LWB

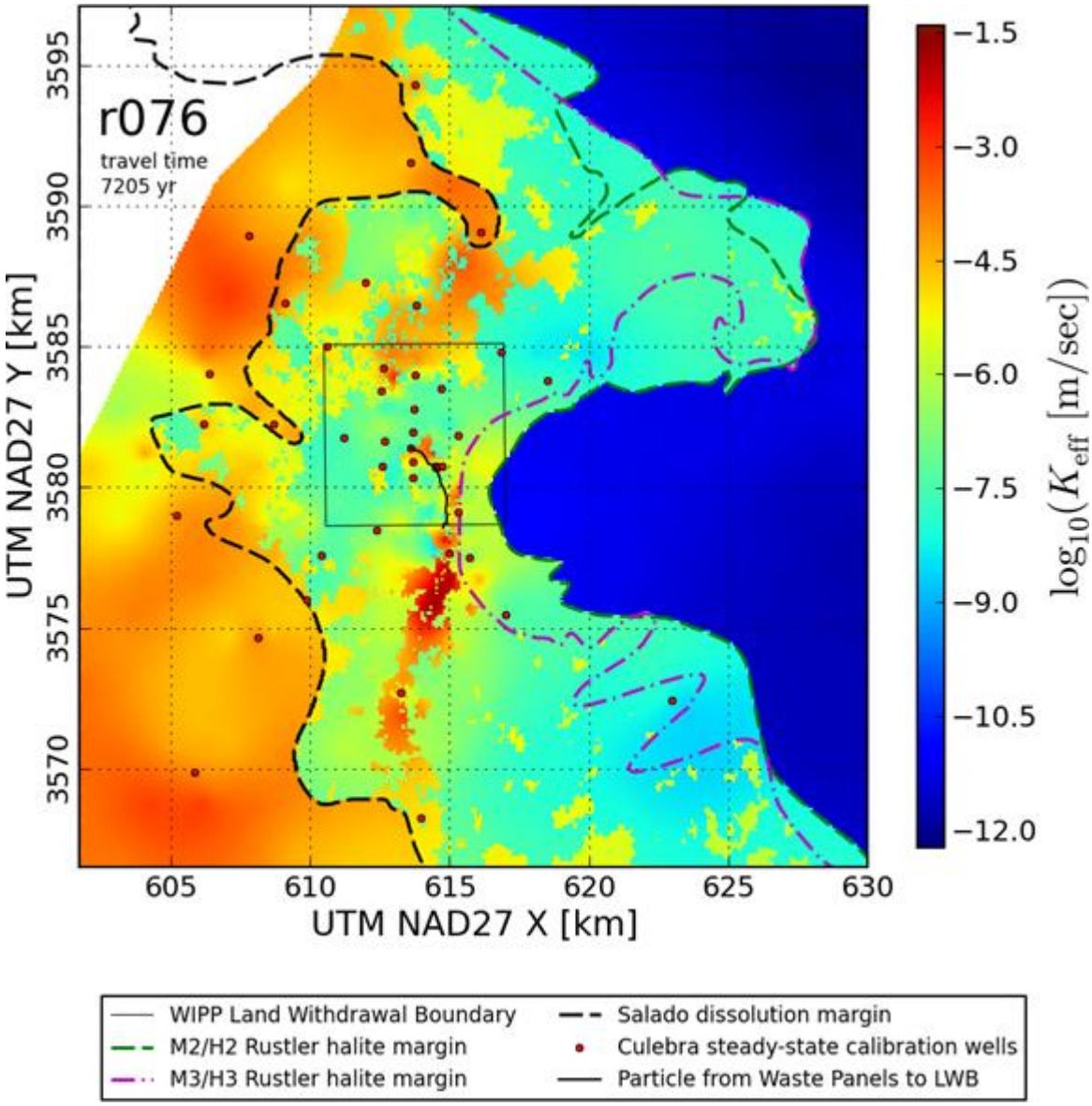
r076
travel time
7205 yr
UTM NAD27 Y [km]
3595
3590
3585
3580
3575
3570
605
610
615
620
625
630
UTM NAD27 X [km]
−1.5
−3.0
−4.5
−6.0
−7.5
−9.0
−10.5
−12.0
$\log_{10}(K_{\mathrm{eff}}\ [\mathrm{m/sec}])$
WIPP Land Withdrawal Boundary
M2/H2 Rustler halite margin
M3/H3 Rustler halite margin
Salado dissolution margin
Culebra steady-state calibration wells
Particle from Waste Panels to LWB

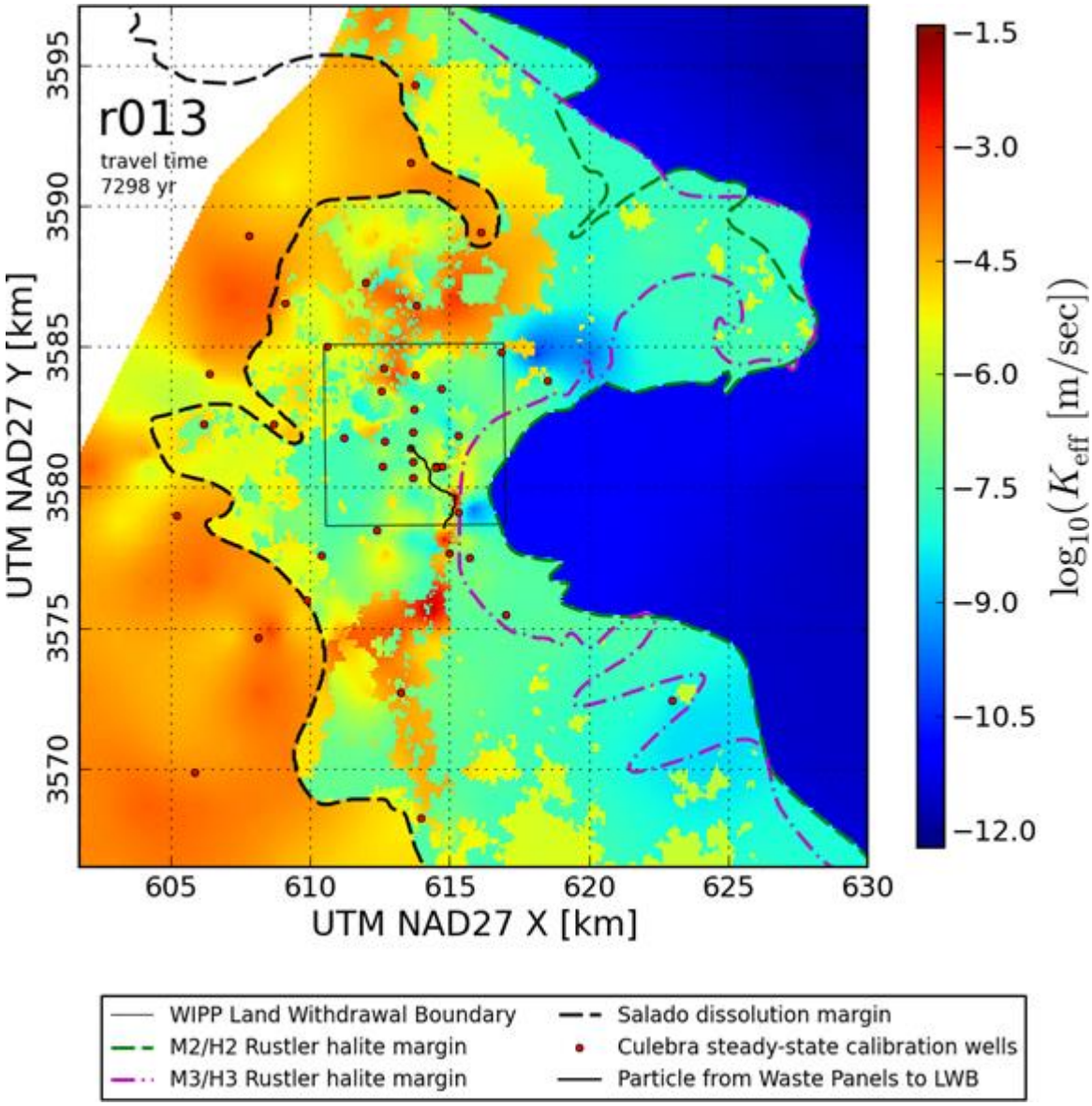
r013
travel time
7298 yr
UTM NAD27 Y [km]
3595
3590
3585
3580
3575
3570
605
610
615
620
625
630
UTM NAD27 X [km]
−1.5
−3.0
−4.5
−6.0
−7.5
−9.0
−10.5
−12.0
$\log_{10}(K_{\text{eff}}$ [m/sec])
WIPP Land Withdrawal Boundary
M2/H2 Rustler halite margin
M3/H3 Rustler halite margin
Salado dissolution margin
Culebra steady-state calibration wells
Particle from Waste Panels to LWB

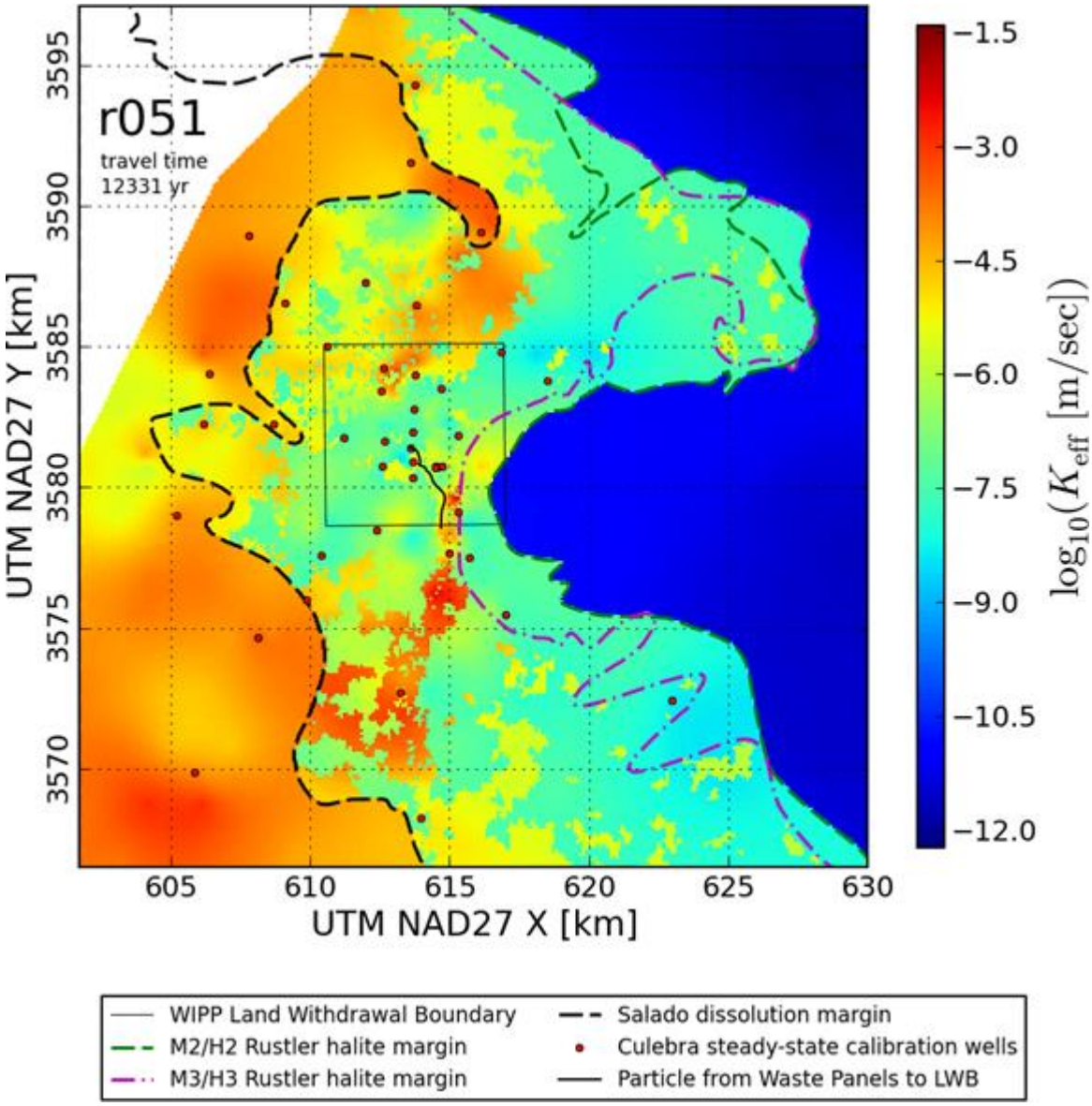
r051
travel time
12331 yr
UTM NAD27 Y [km]
3595
3590
3585
3580
3575
3570
605
610
615
620
625
630
UTM NAD27 X [km]
−1.5
−3.0
−4.5
−6.0
−7.5
−9.0
−10.5
−12.0
$\log_{10}(K_{\text{eff}}$ [m/sec])
WIPP Land Withdrawal Boundary
M2/H2 Rustler halite margin
M3/H3 Rustler halite margin
Salado dissolution margin
Culebra steady-state calibration wells
Particle from Waste Panels to LWB

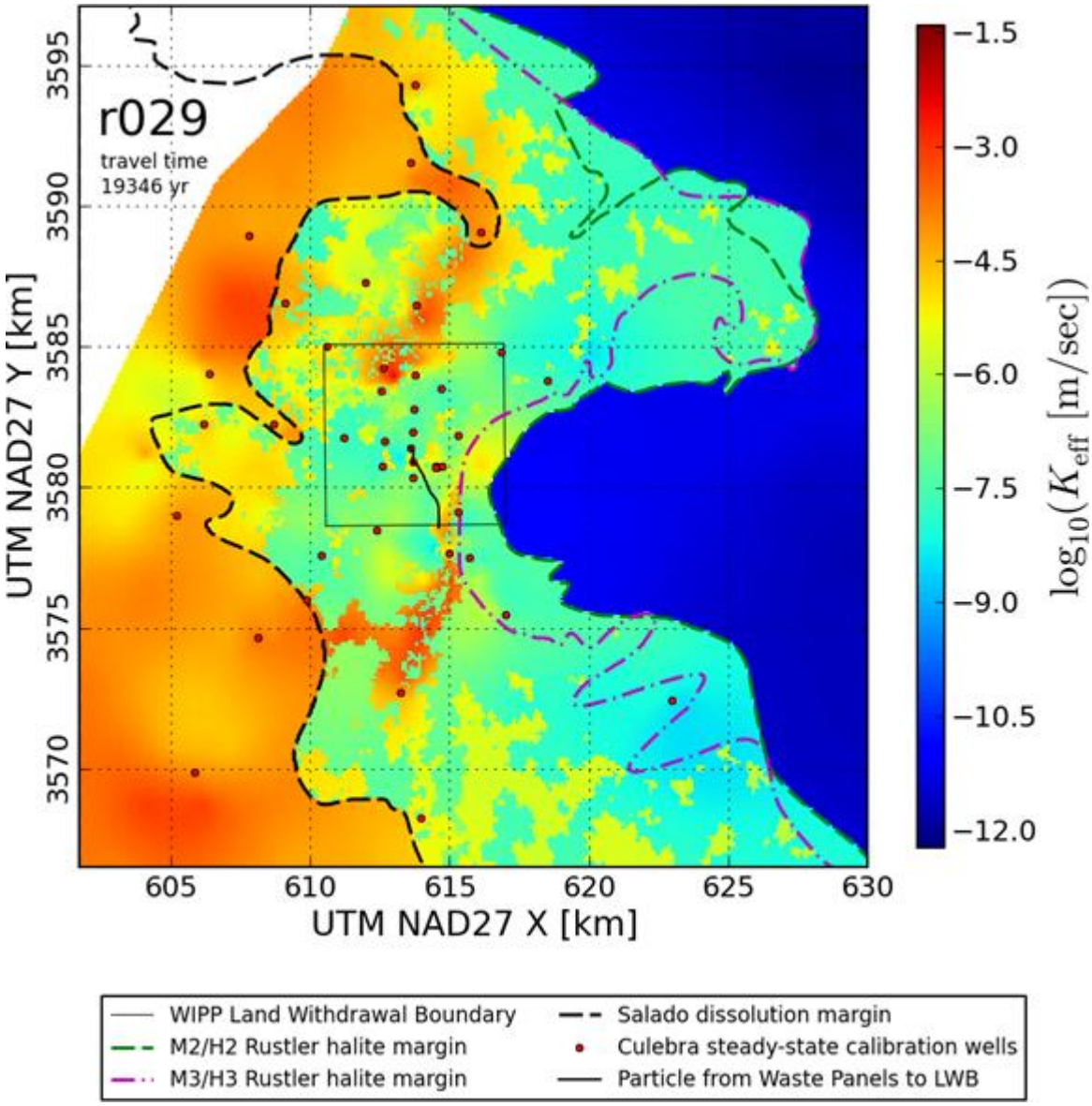
r029
travel time
19346 yr
UTM NAD27 Y [km]
3595
3590
3585
3580
3575
3570
605
610
615
620
625
630
UTM NAD27 X [km]
−1.5
−3.0
−4.5
−6.0
−7.5
−9.0
−10.5
−12.0
$\log_{10}(K_{\mathrm{eff}}$ [m/sec])
WIPP Land Withdrawal Boundary
M2/H2 Rustler halite margin
M3/H3 Rustler halite margin
Salado dissolution margin
Culebra steady-state calibration wells
Particle from Waste Panels to LWB

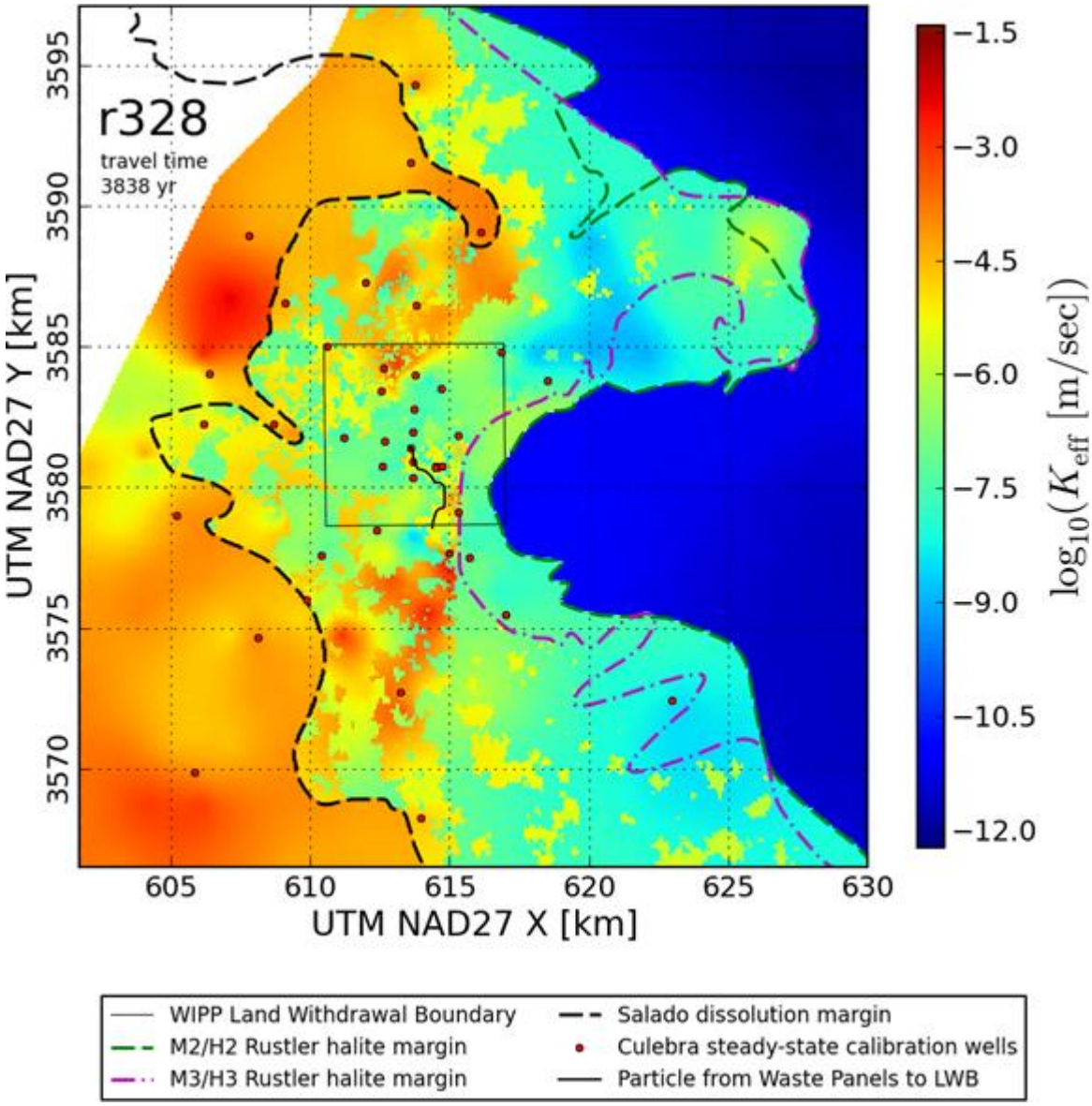
r328
travel time
3838 yr
UTM NAD27 Y [km]
3595
3590
3585
3580
3575
3570
605
610
615
620
625
630
UTM NAD27 X [km]
−1.5
−3.0
−4.5
−6.0
−7.5
−9.0
−10.5
−12.0
$\log_{10}(K_{\mathrm{eff}}\ [\mathrm{m/sec}])$
WIPP Land Withdrawal Boundary
M2/H2 Rustler halite margin
M3/H3 Rustler halite margin
Salado dissolution margin
Culebra steady-state calibration wells
Particle from Waste Panels to LWB

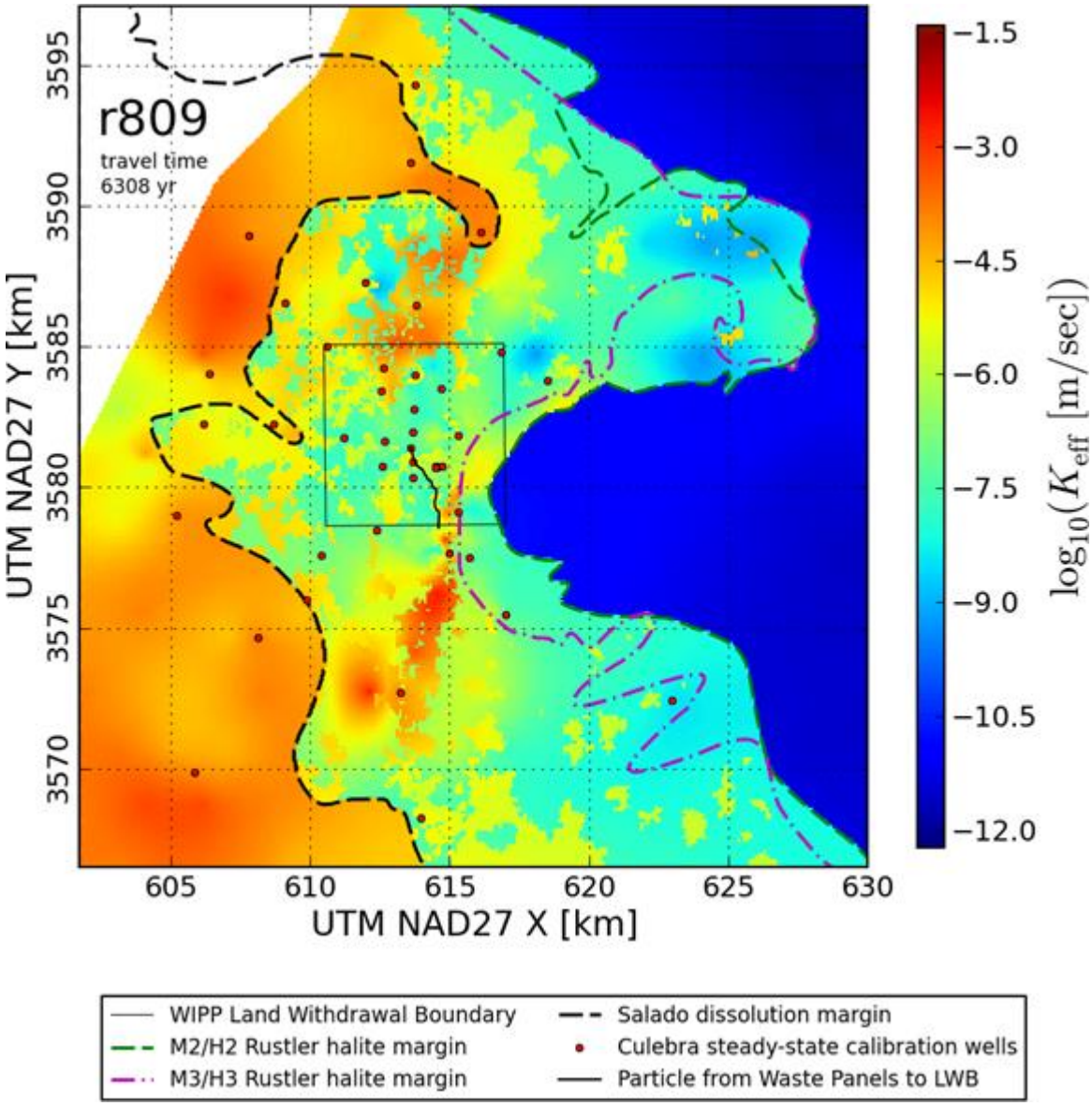
r809
travel time
6308 yr
UTM NAD27 Y [km]
3595
3590
3585
3580
3575
3570
605
610
615
620
625
630
UTM NAD27 X [km]
−1.5
−3.0
−4.5
−6.0
−7.5
−9.0
−10.5
−12.0
$\log_{10}(K_{\mathrm{eff}}\ [\mathrm{m/sec}])$
WIPP Land Withdrawal Boundary
M2/H2 Rustler halite margin
M3/H3 Rustler halite margin
Salado dissolution margin
Culebra steady-state calibration wells
Particle from Waste Panels to LWB

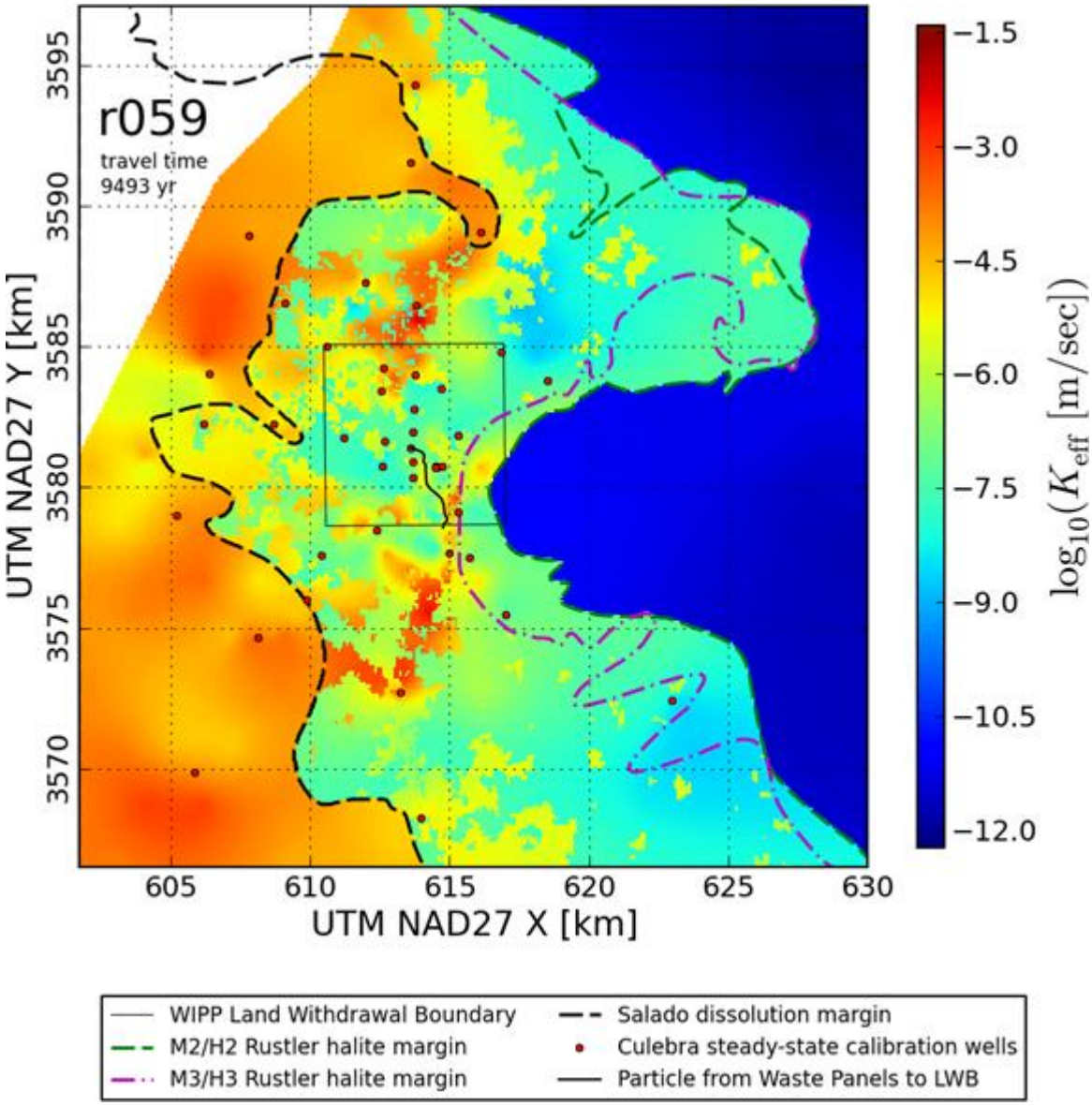
r059
travel time
9493 yr
UTM NAD27 Y [km]
3595
3590
3585
3580
3575
3570
605
610
615
620
625
630
UTM NAD27 X [km]
−1.5
−3.0
−4.5
−6.0
−7.5
−9.0
−10.5
−12.0
$\log_{10}(K_{\text{eff}}$ [m/sec])
WIPP Land Withdrawal Boundary
M2/H2 Rustler halite margin
M3/H3 Rustler halite margin
Salado dissolution margin
Culebra steady-state calibration wells
Particle from Waste Panels to LWB

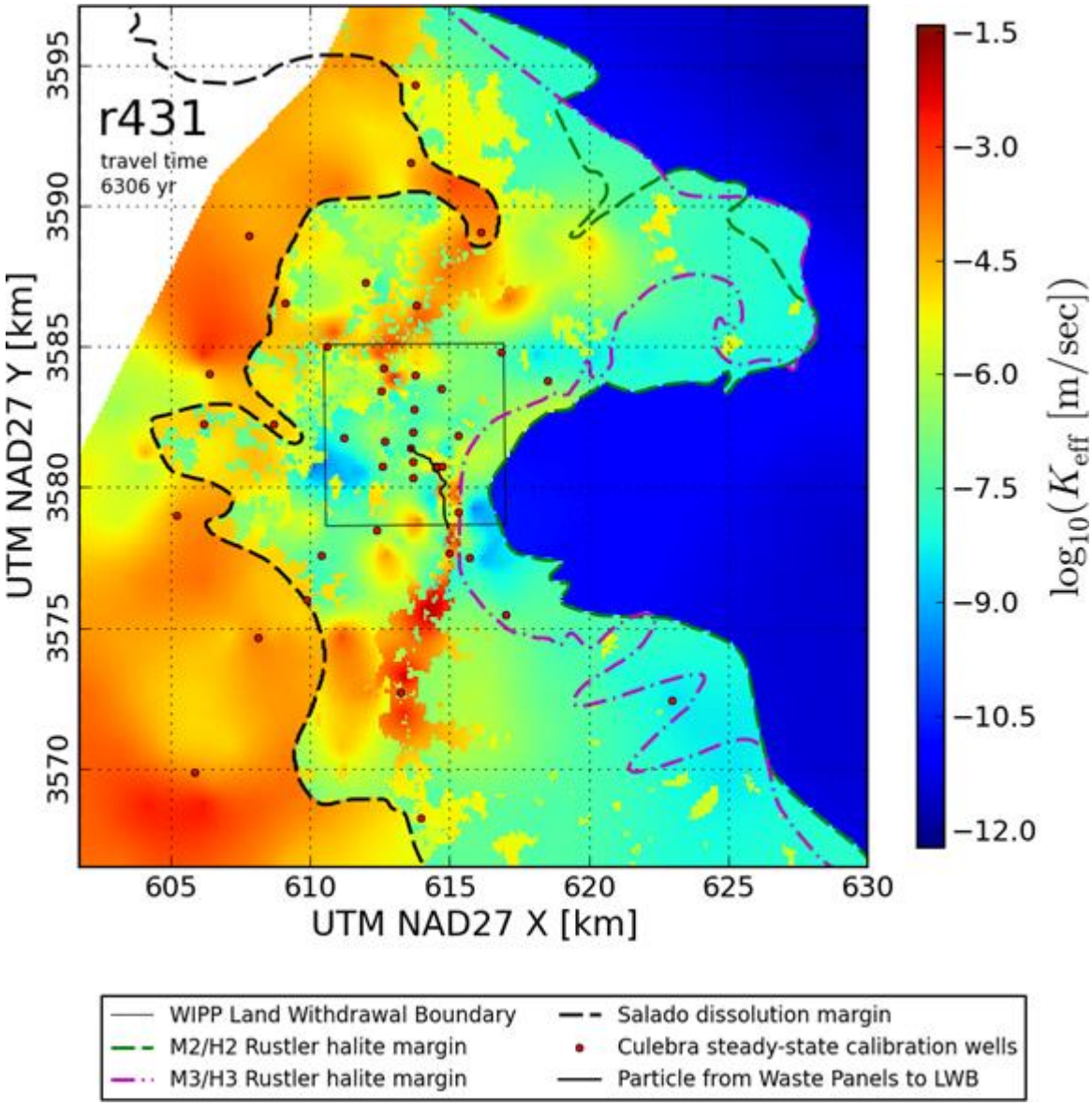
r431
travel time
6306 yr
UTM NAD27 Y [km]
3595
3590
3585
3580
3575
3570
605
610
615
620
625
630
UTM NAD27 X [km]
−1.5
−3.0
−4.5
−6.0
−7.5
−9.0
−10.5
−12.0
$\log_{10}(K_{\mathrm{eff}}\ [\mathrm{m/sec}])$
WIPP Land Withdrawal Boundary
M2/H2 Rustler halite margin
M3/H3 Rustler halite margin
Salado dissolution margin
Culebra steady-state calibration wells
Particle from Waste Panels to LWB

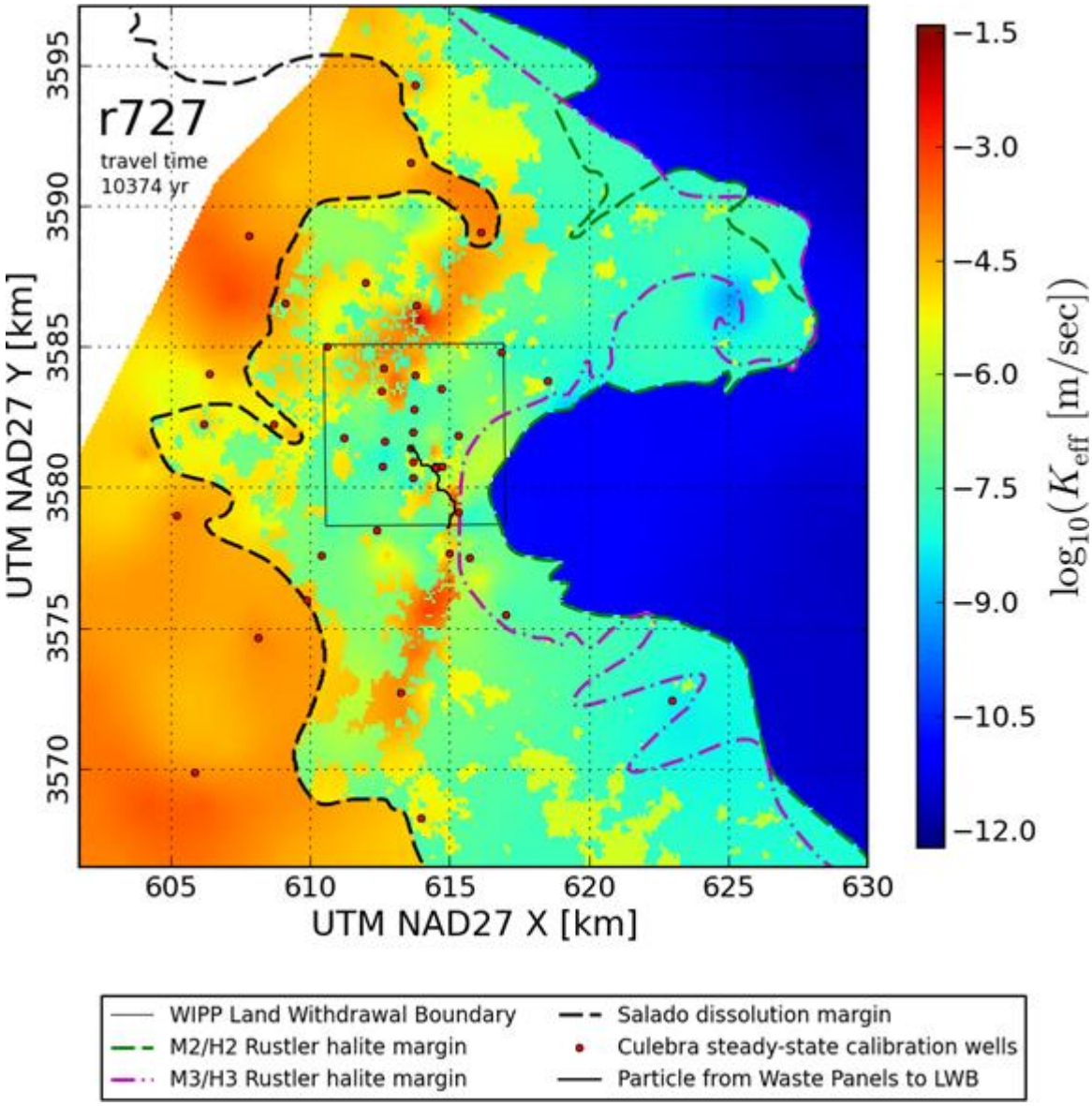
r727
travel time
10374 yr
UTM NAD27 Y [km]
3595
3590
3585
3580
3575
3570
605
610
615
620
625
630
UTM NAD27 X [km]
−1.5
−3.0
−4.5
−6.0
−7.5
−9.0
−10.5
−12.0
$\log_{10}(K_{\mathrm{eff}}\ [\mathrm{m/sec}])$
WIPP Land Withdrawal Boundary
M2/H2 Rustler halite margin
M3/H3 Rustler halite margin
Salado dissolution margin
Culebra steady-state calibration wells
Particle from Waste Panels to LWB

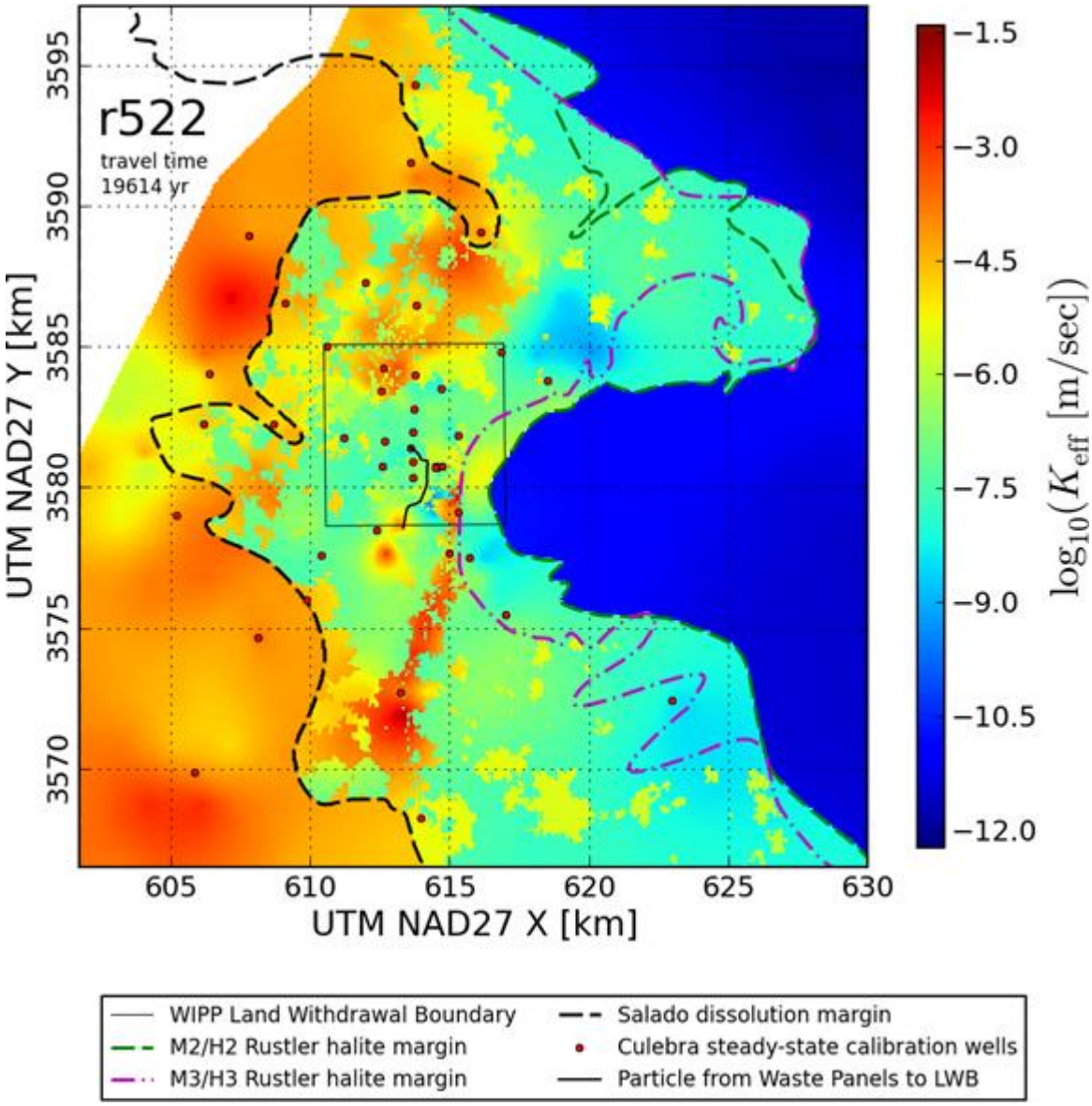
r522
travel time
19614 yr
UTM NAD27 Y [km]
3595
3590
3585
3580
3575
3570
605
610
615
620
625
630
UTM NAD27 X [km]
−1.5
−3.0
−4.5
−6.0
−7.5
−9.0
−10.5
−12.0
$\log_{10}(K_{\mathrm{eff}}\ [\mathrm{m/sec}])$
WIPP Land Withdrawal Boundary
M2/H2 Rustler halite margin
M3/H3 Rustler halite margin
Salado dissolution margin
Culebra steady-state calibration wells
Particle from Waste Panels to LWB

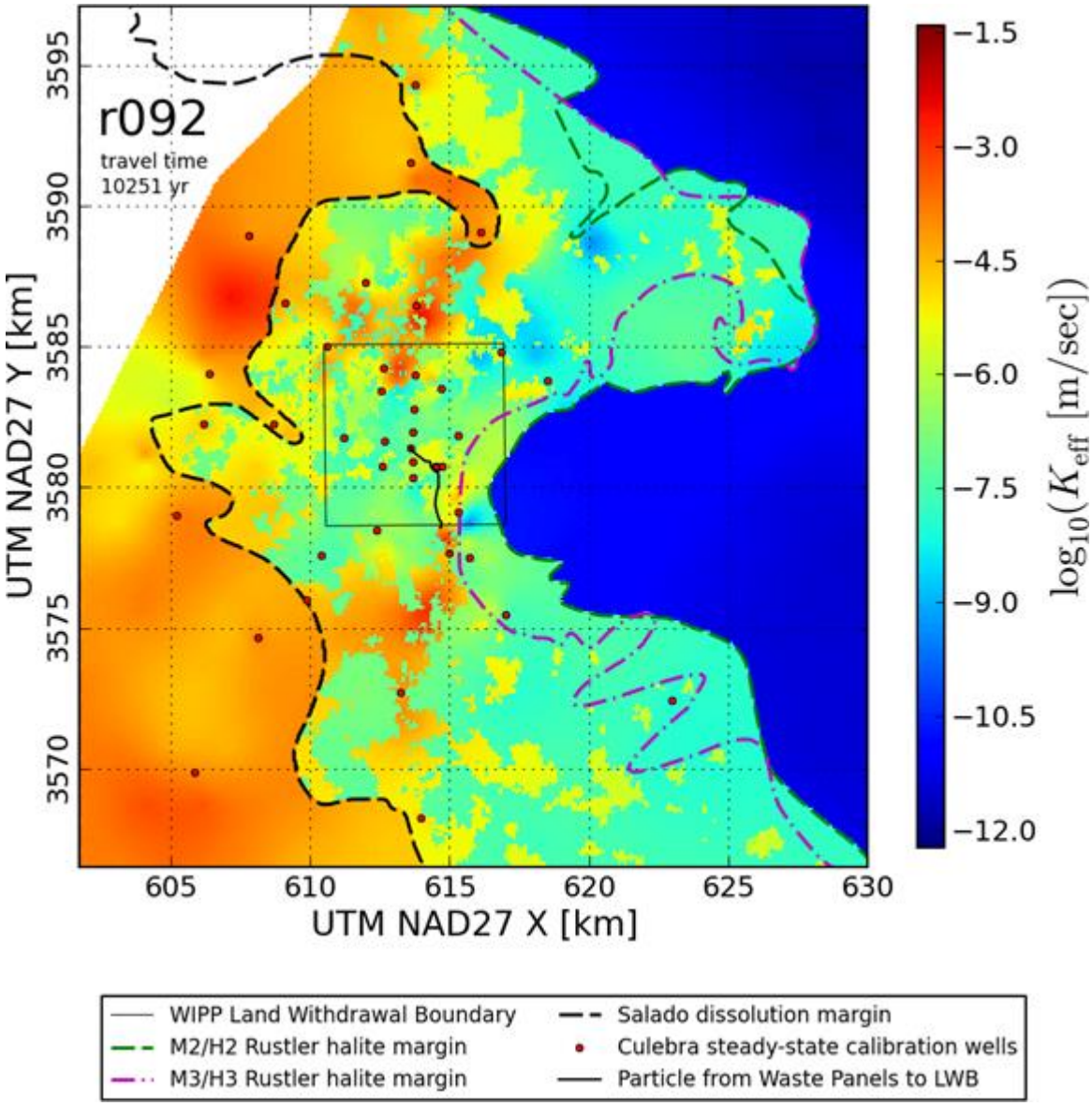
r092
travel time
10251 yr
UTM NAD27 Y [km]
3595
3590
3585
3580
3575
3570
605
610
615
620
625
630
UTM NAD27 X [km]
−1.5
−3.0
−4.5
−6.0
−7.5
−9.0
−10.5
−12.0
$\log_{10}(K_{\mathrm{eff}}\ [\mathrm{m/sec}])$
WIPP Land Withdrawal Boundary
M2/H2 Rustler halite margin
M3/H3 Rustler halite margin
Salado dissolution margin
Culebra steady-state calibration wells
Particle from Waste Panels to LWB

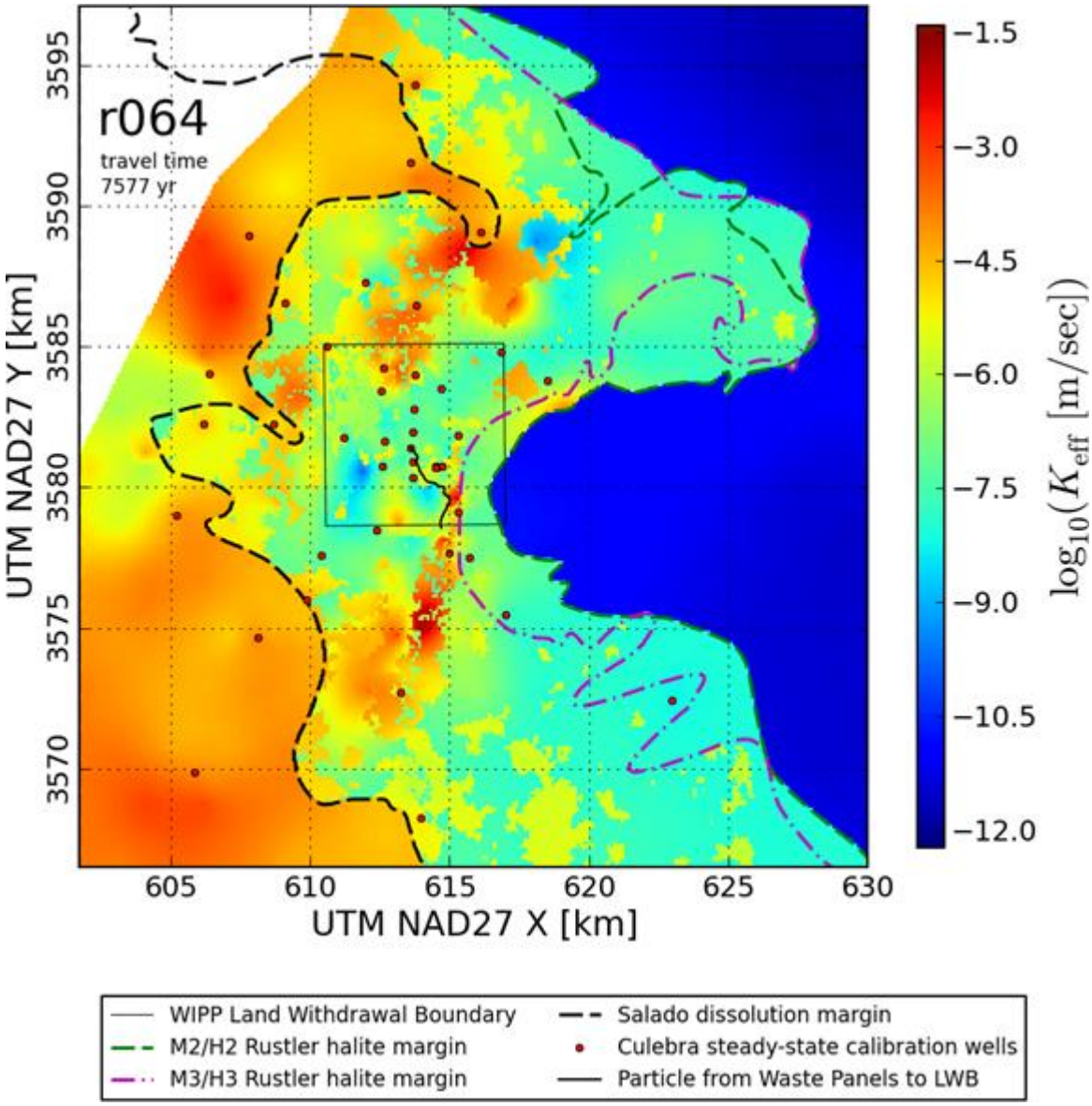
r064
travel time
7577 yr
UTM NAD27 Y [km]
3595
3590
3585
3580
3575
3570
605
610
615
620
625
630
UTM NAD27 X [km]
−1.5
−3.0
−4.5
−6.0
−7.5
−9.0
−10.5
−12.0
$\log_{10}(K_{\mathrm{eff}}\ [\mathrm{m/sec}])$
WIPP Land Withdrawal Boundary
M2/H2 Rustler halite margin
M3/H3 Rustler halite margin
Salado dissolution margin
Culebra steady-state calibration wells
Particle from Waste Panels to LWB

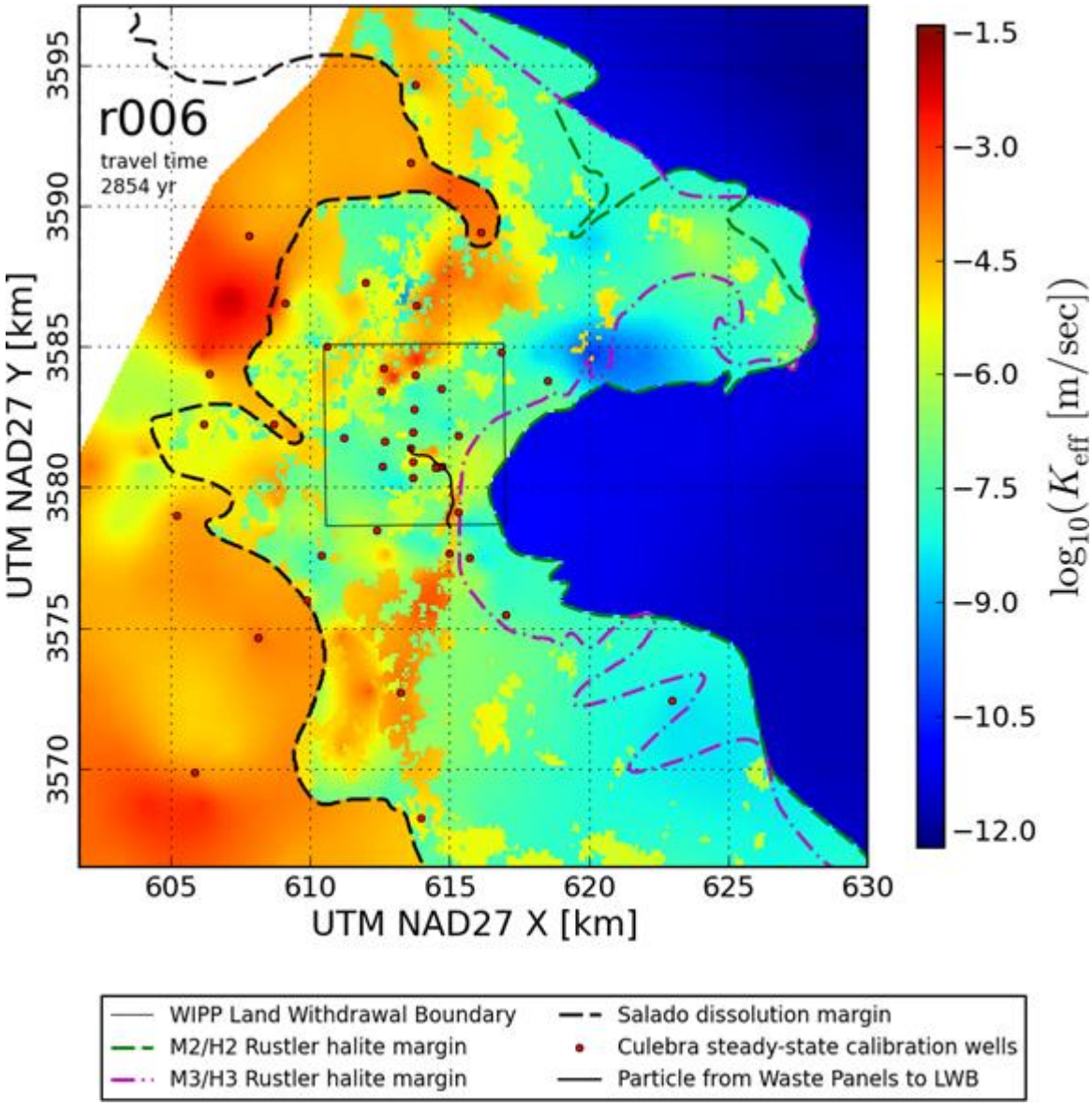
r006
travel time
2854 yr
UTM NAD27 Y [km]
3595
3590
3585
3580
3575
3570
605
610
615
620
625
630
UTM NAD27 X [km]
−1.5
−3.0
−4.5
−6.0
−7.5
−9.0
−10.5
−12.0
$\log_{10}(K_{\mathrm{eff}}$ [m/sec])
WIPP Land Withdrawal Boundary
M2/H2 Rustler halite margin
M3/H3 Rustler halite margin
Salado dissolution margin
Culebra steady-state calibration wells
Particle from Waste Panels to LWB

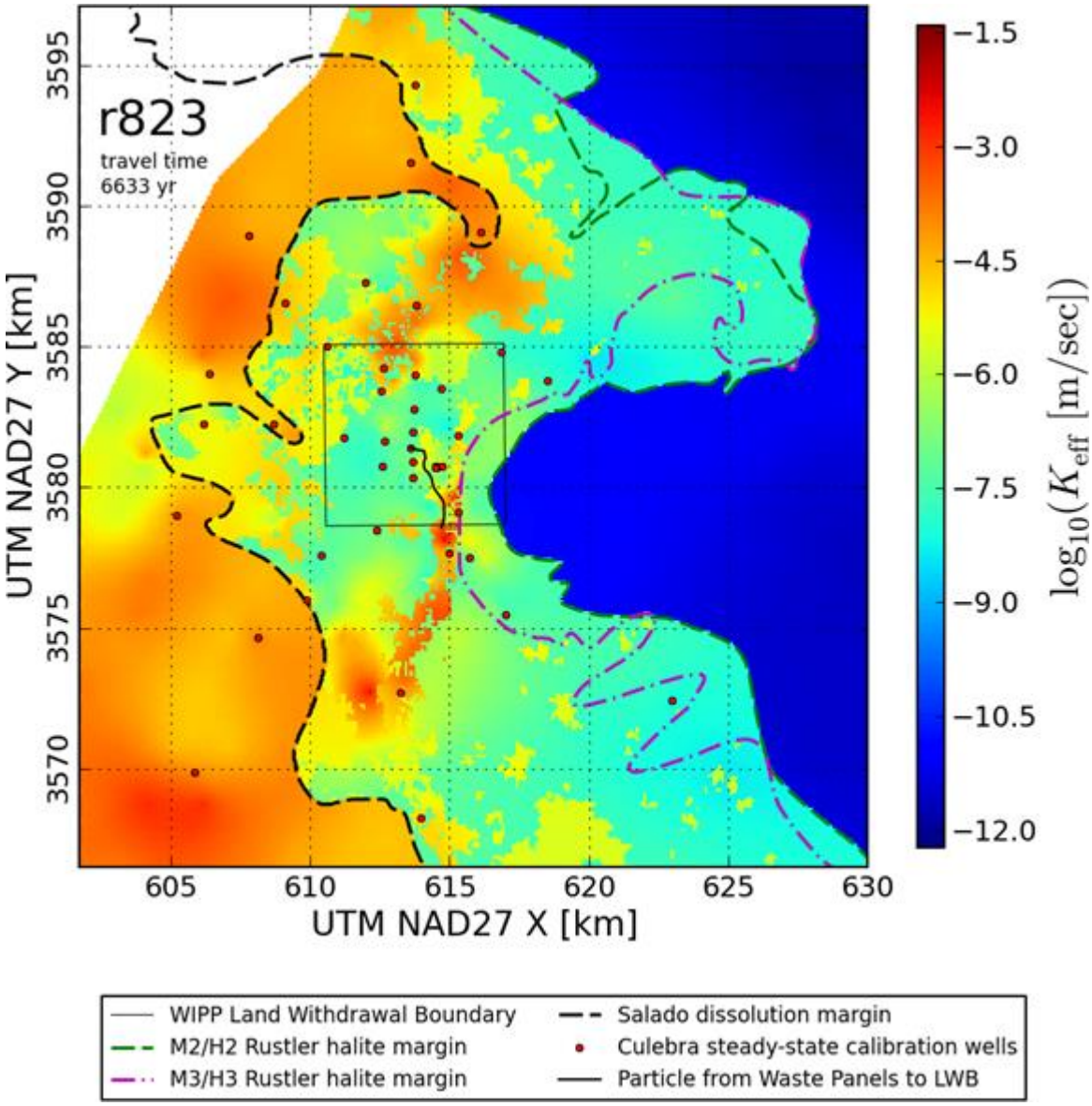
r823
travel time
6633 yr
UTM NAD27 Y [km]
3595
3590
3585
3580
3575
3570
605
610
615
620
625
630
UTM NAD27 X [km]
−1.5
−3.0
−4.5
−6.0
−7.5
−9.0
−10.5
−12.0
$\log_{10}(K_{\mathrm{eff}}\ [\mathrm{m/sec}])$
WIPP Land Withdrawal Boundary
M2/H2 Rustler halite margin
M3/H3 Rustler halite margin
Salado dissolution margin
Culebra steady-state calibration wells
Particle from Waste Panels to LWB

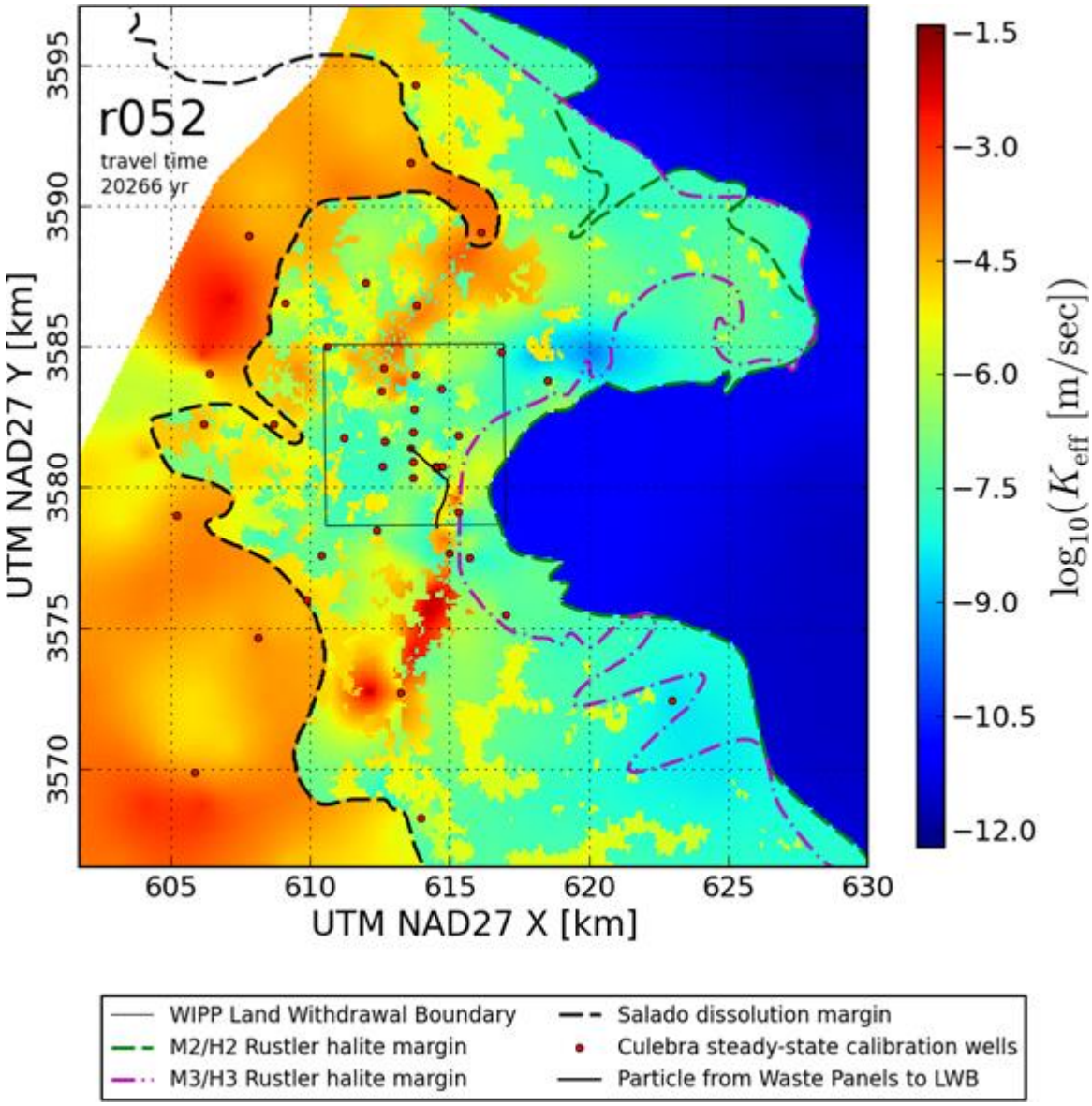
r052
travel time
20266 yr
UTM NAD27 Y [km]
3595
3590
3585
3580
3575
3570
605
610
615
620
625
630
UTM NAD27 X [km]
−1.5
−3.0
−4.5
−6.0
−7.5
−9.0
−10.5
−12.0
$\log_{10}(K_{\mathrm{eff}}\ [\mathrm{m/sec}])$
WIPP Land Withdrawal Boundary
M2/H2 Rustler halite margin
M3/H3 Rustler halite margin
Salado dissolution margin
Culebra steady-state calibration wells
Particle from Waste Panels to LWB

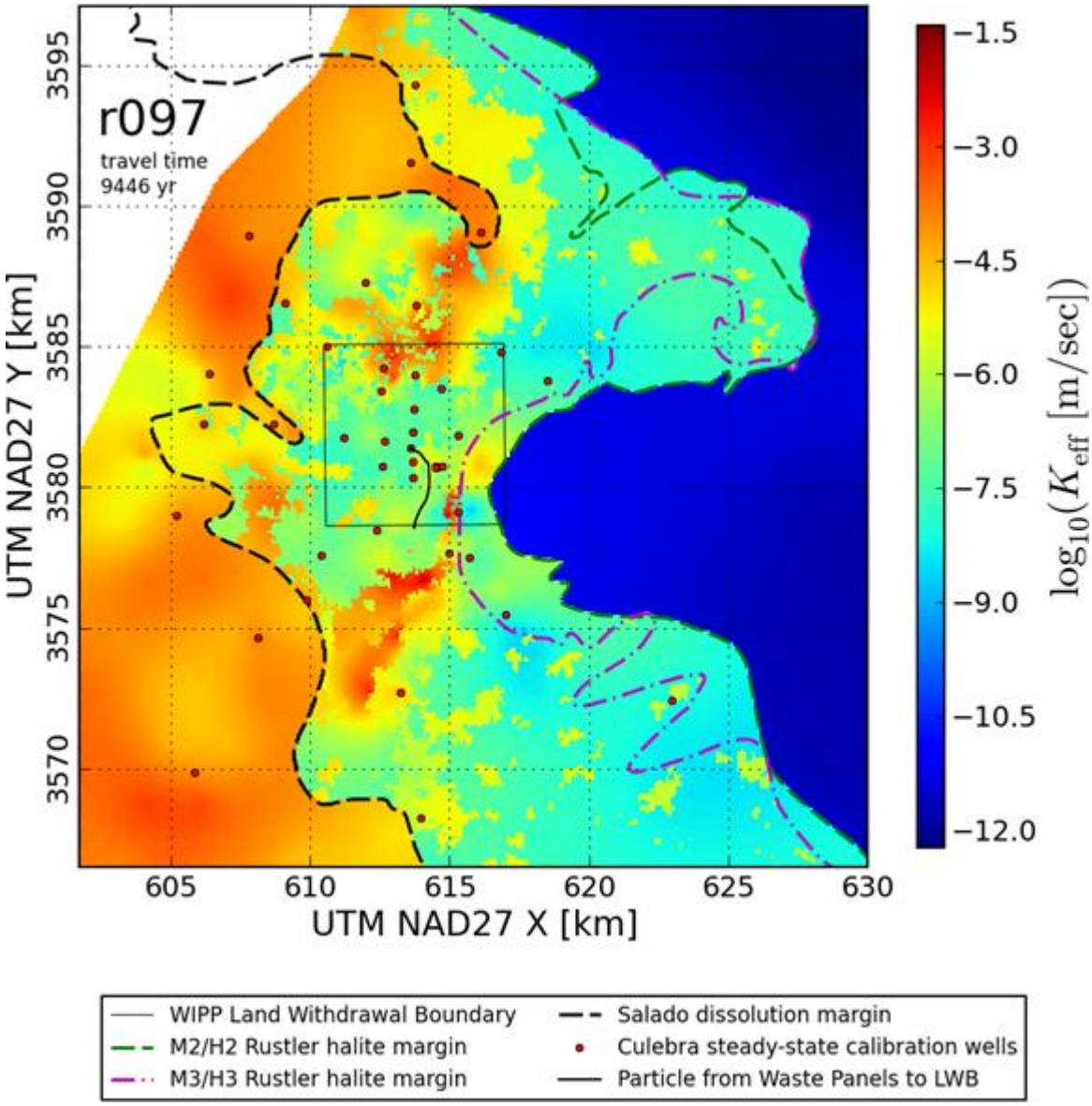
r097
travel time
9446 yr
UTM NAD27 Y [km]
3595
3590
3585
3580
3575
3570
605
610
615
620
625
630
UTM NAD27 X [km]
−1.5
−3.0
−4.5
−6.0
−7.5
−9.0
−10.5
−12.0
$\log_{10}(K_{\mathrm{eff}}\ [\mathrm{m/sec}])$
WIPP Land Withdrawal Boundary
M2/H2 Rustler halite margin
M3/H3 Rustler halite margin
Salado dissolution margin
Culebra steady-state calibration wells
Particle from Waste Panels to LWB

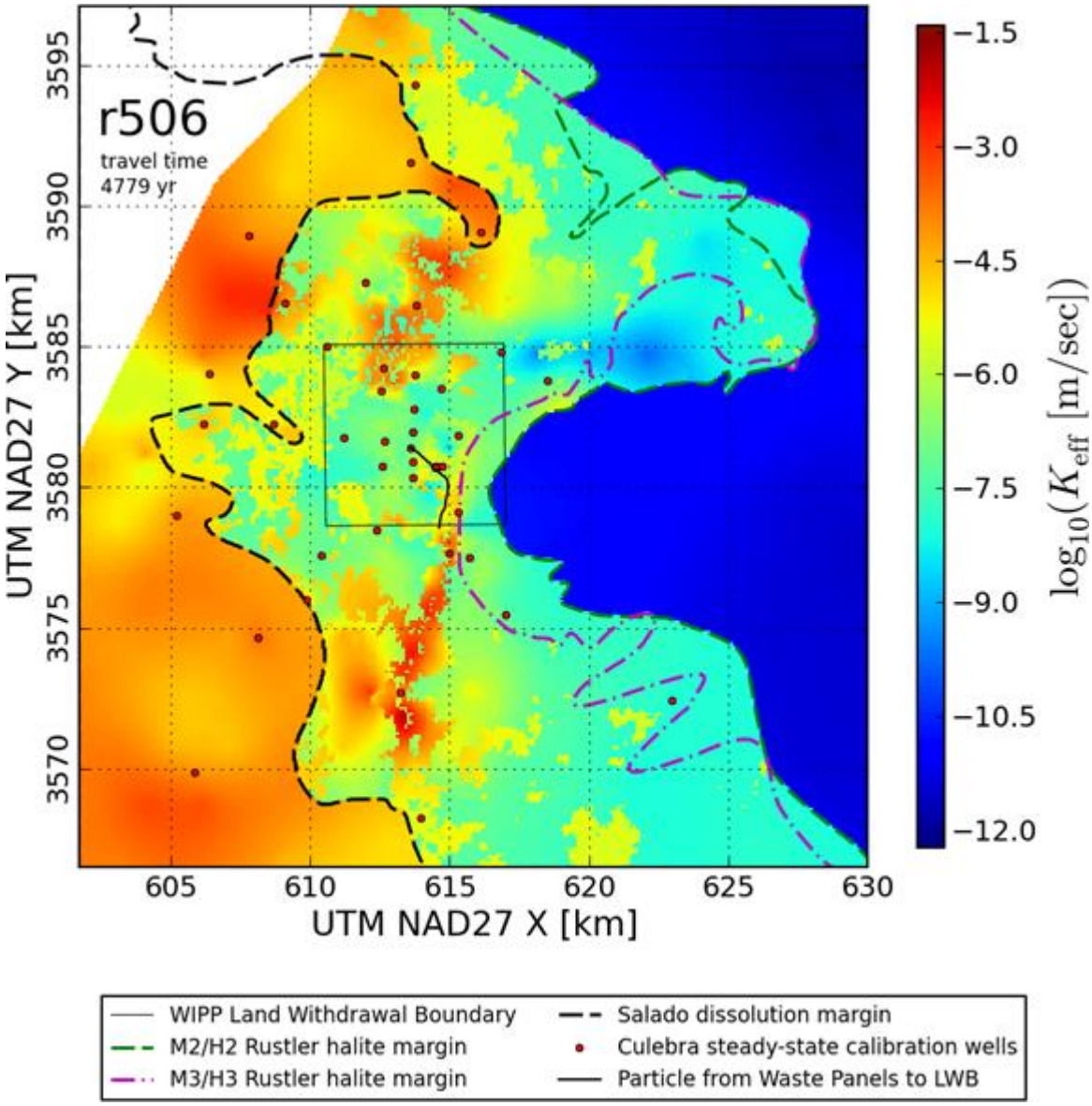
r506
travel time
4779 yr
UTM NAD27 Y [km]
3595
3590
3585
3580
3575
3570
605
610
615
620
625
630
UTM NAD27 X [km]
−1.5
−3.0
−4.5
−6.0
−7.5
−9.0
−10.5
−12.0
$\log_{10}(K_{\mathrm{eff}}\ [\mathrm{m/sec}])$
WIPP Land Withdrawal Boundary
M2/H2 Rustler halite margin
M3/H3 Rustler halite margin
Salado dissolution margin
Culebra steady-state calibration wells
Particle from Waste Panels to LWB

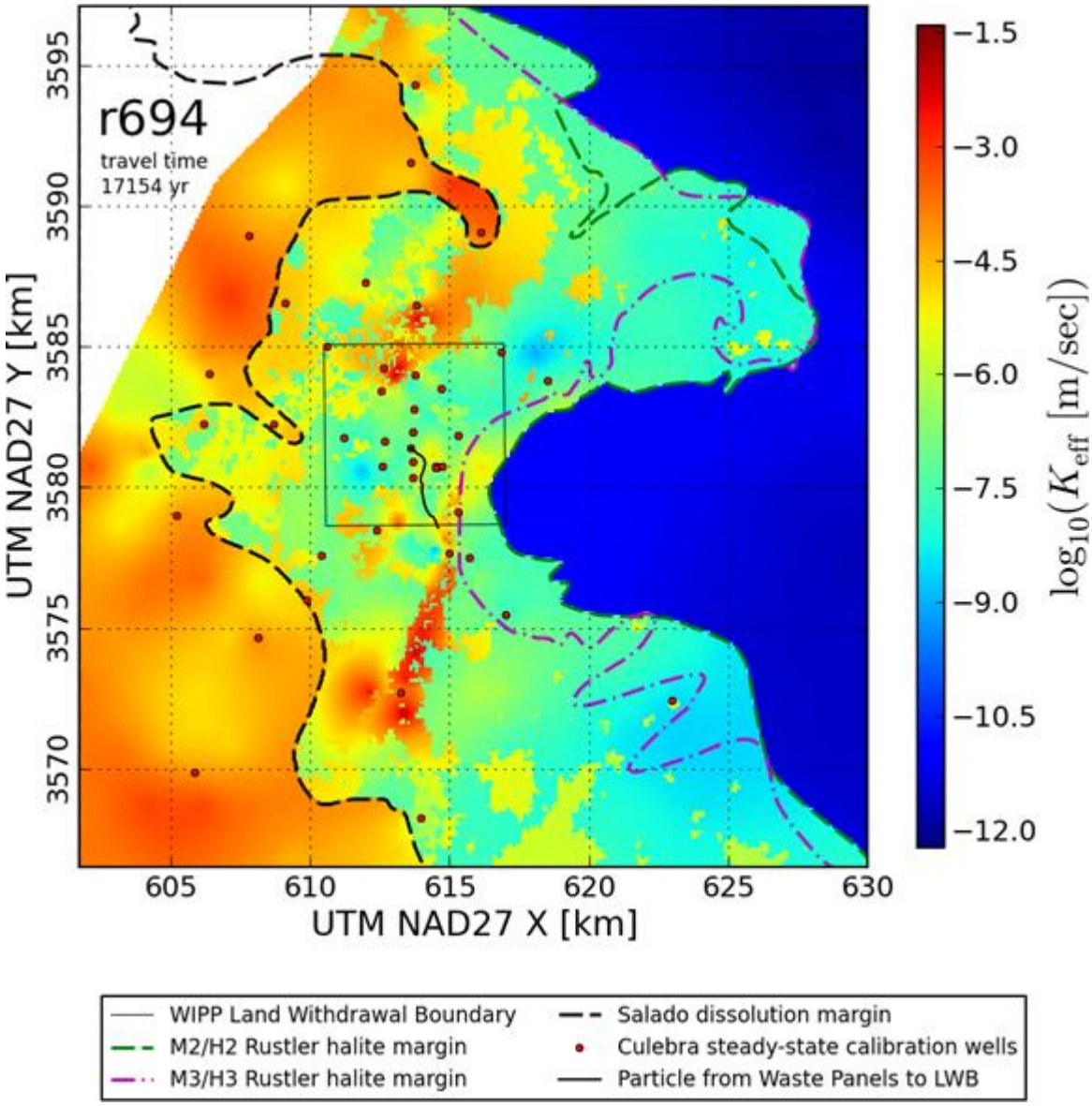
r694
travel time
17154 yr
UTM NAD27 Y [km]
3595
3590
3585
3580
3575
3570
605
610
615
620
625
630
UTM NAD27 X [km]
−1.5
−3.0
−4.5
−6.0
−7.5
−9.0
−10.5
−12.0
$\log_{10}(K_{\mathrm{eff}}\ [\mathrm{m/sec}])$
WIPP Land Withdrawal Boundary
M2/H2 Rustler halite margin
M3/H3 Rustler halite margin
Salado dissolution margin
Culebra steady-state calibration wells
Particle from Waste Panels to LWB

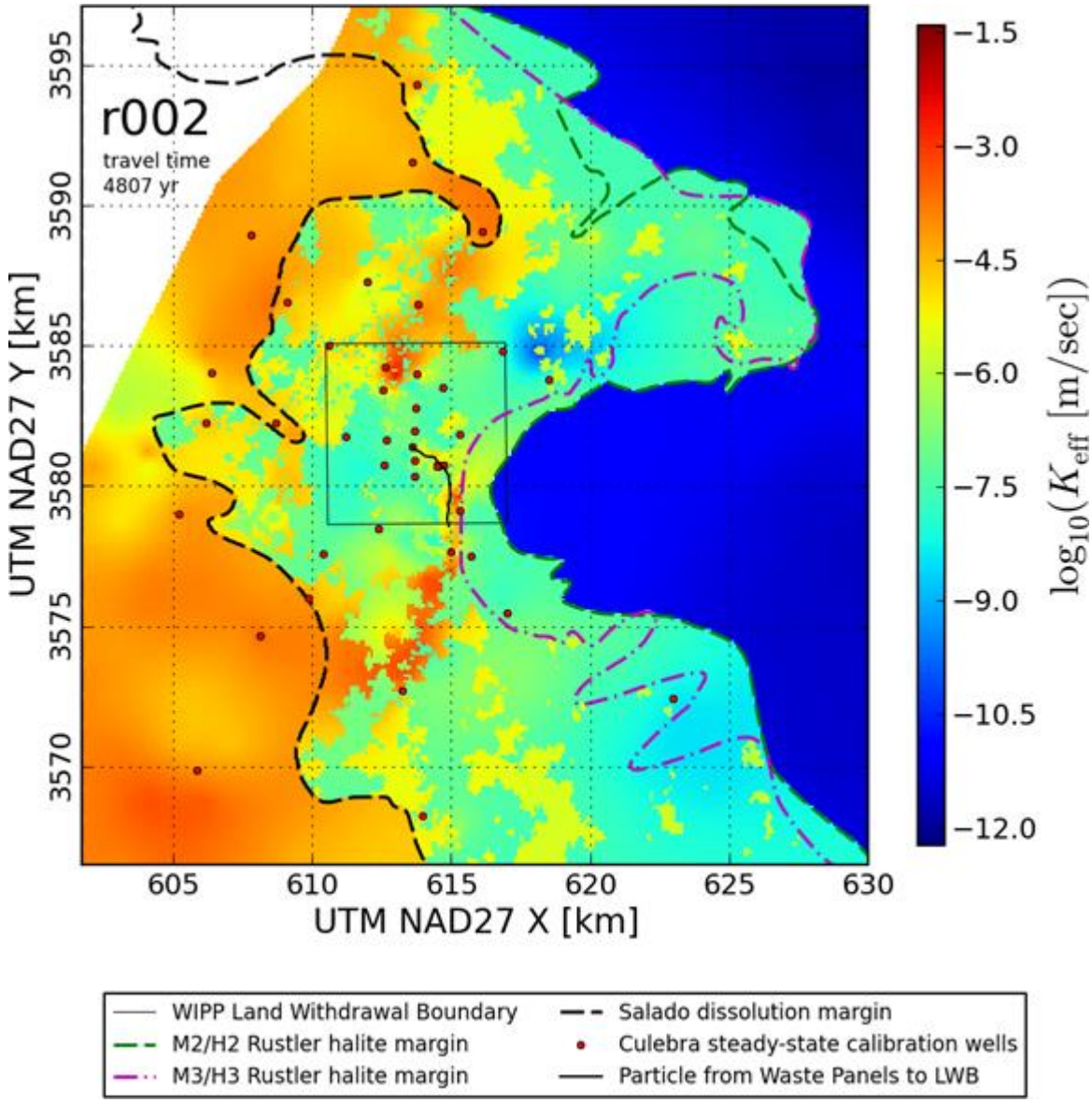
r002
travel time
4807 yr
UTM NAD27 Y [km]
3595
3590
3585
3580
3575
3570
605
610
615
620
625
630
UTM NAD27 X [km]
−1.5
−3.0
−4.5
−6.0
−7.5
−9.0
−10.5
−12.0
$\log_{10}(K_{\text{eff}}$ [m/sec])
WIPP Land Withdrawal Boundary
M2/H2 Rustler halite margin
M3/H3 Rustler halite margin
Salado dissolution margin
Culebra steady-state calibration wells
Particle from Waste Panels to LWB

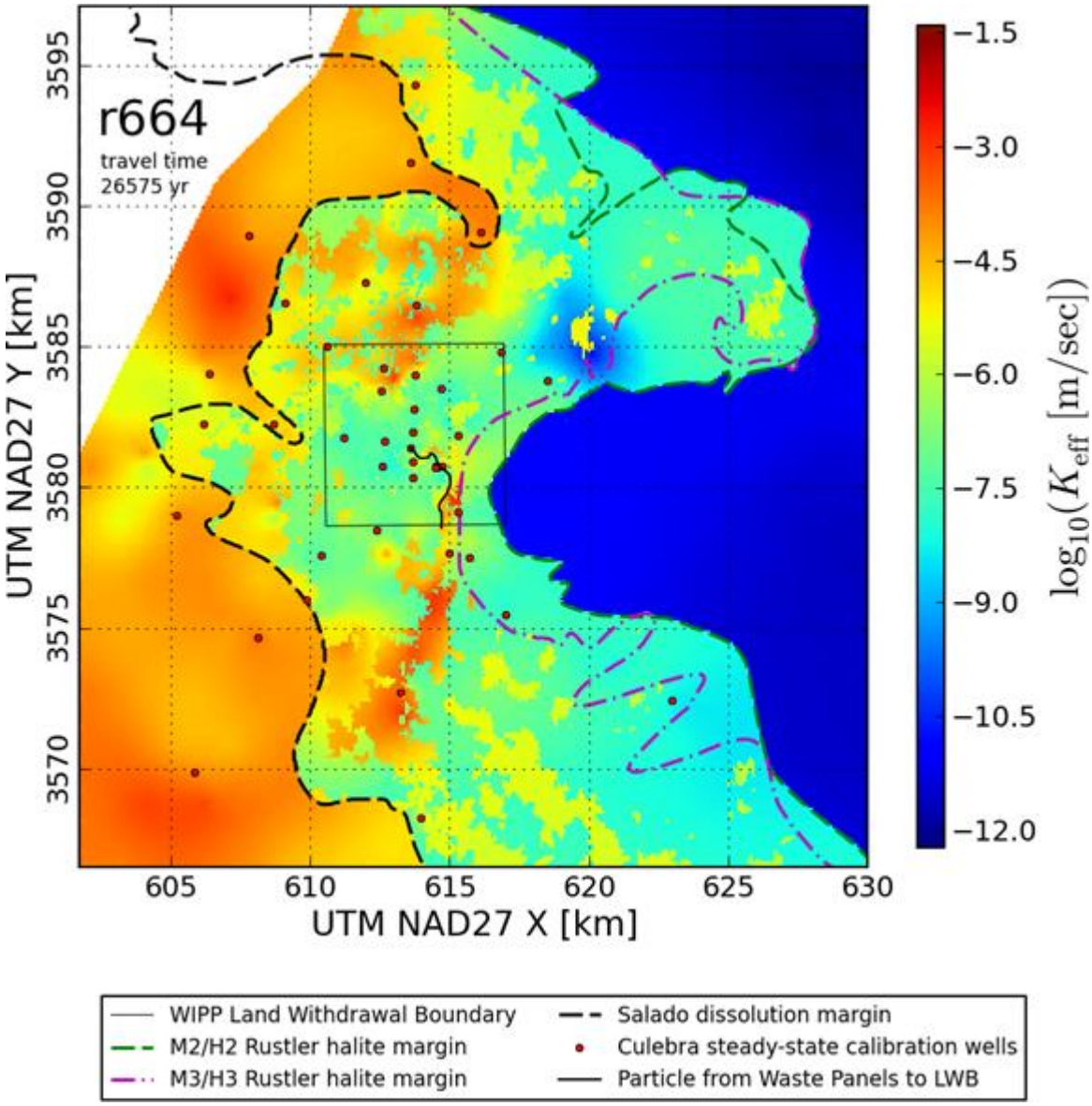
r664
travel time
26575 yr
UTM NAD27 Y [km]
3595
3590
3585
3580
3575
3570
605
610
615
620
625
630
UTM NAD27 X [km]
−1.5
−3.0
−4.5
−6.0
−7.5
−9.0
−10.5
−12.0
$\log_{10}(K_{\mathrm{eff}}$ [m/sec])
WIPP Land Withdrawal Boundary
M2/H2 Rustler halite margin
M3/H3 Rustler halite margin
Salado dissolution margin
Culebra steady-state calibration wells
Particle from Waste Panels to LWB

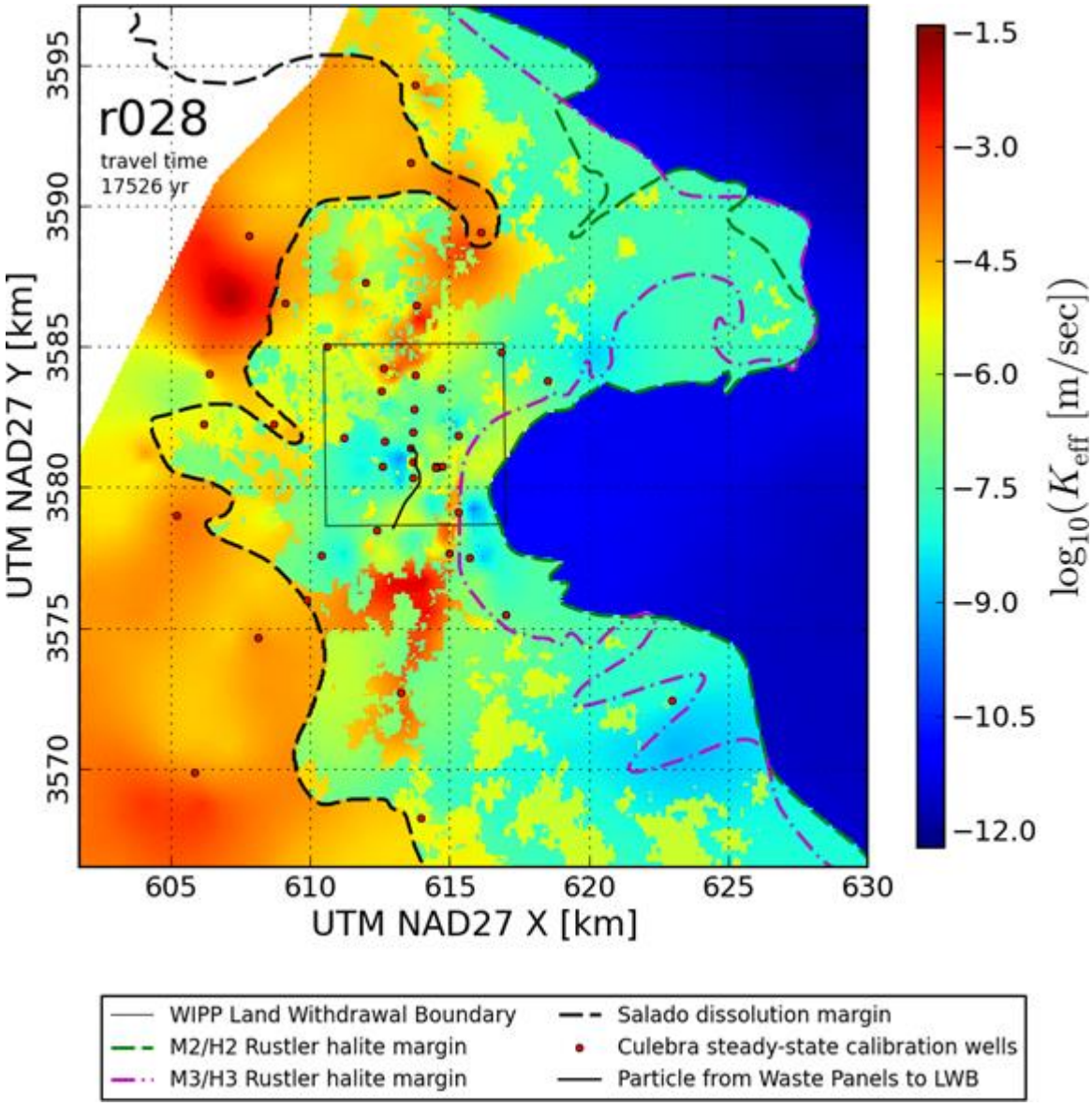
r028
travel time
17526 yr
UTM NAD27 Y [km]
3595
3590
3585
3580
3575
3570
605
610
615
620
625
630
UTM NAD27 X [km]
−1.5
−3.0
−4.5
−6.0
−7.5
−9.0
−10.5
−12.0
$\log_{10}(K_{\mathrm{eff}}\ [\mathrm{m/sec}])$
WIPP Land Withdrawal Boundary
M2/H2 Rustler halite margin
M3/H3 Rustler halite margin
Salado dissolution margin
Culebra steady-state calibration wells
Particle from Waste Panels to LWB

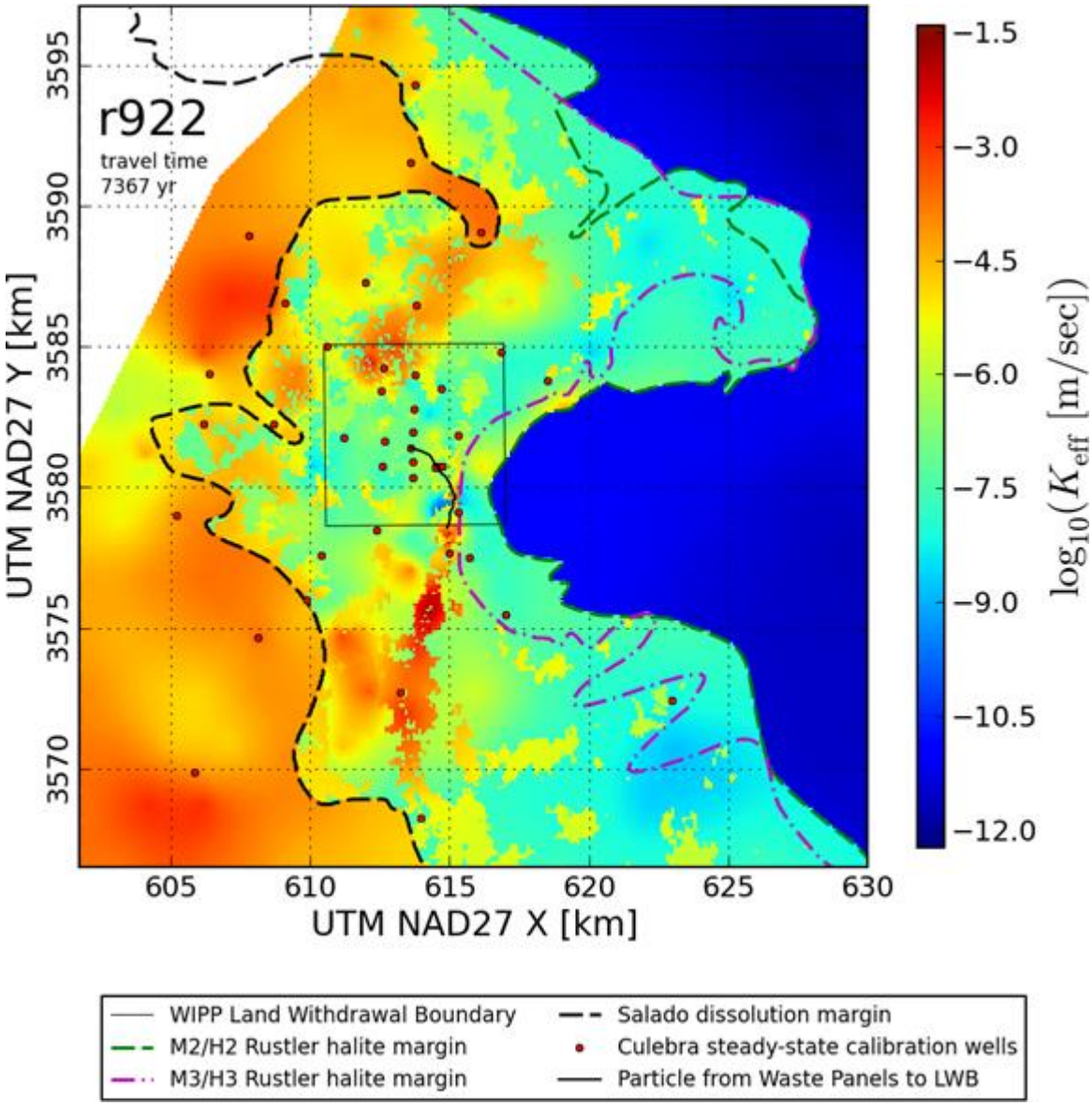
r922
travel time
7367 yr
UTM NAD27 Y [km]
3595
3590
3585
3580
3575
3570
605
610
615
620
625
630
UTM NAD27 X [km]
−1.5
−3.0
−4.5
−6.0
−7.5
−9.0
−10.5
−12.0
$\log_{10}(K_{\text{eff}}$ [m/sec])
WIPP Land Withdrawal Boundary
M2/H2 Rustler halite margin
M3/H3 Rustler halite margin
Salado dissolution margin
Culebra steady-state calibration wells
Particle from Waste Panels to LWB

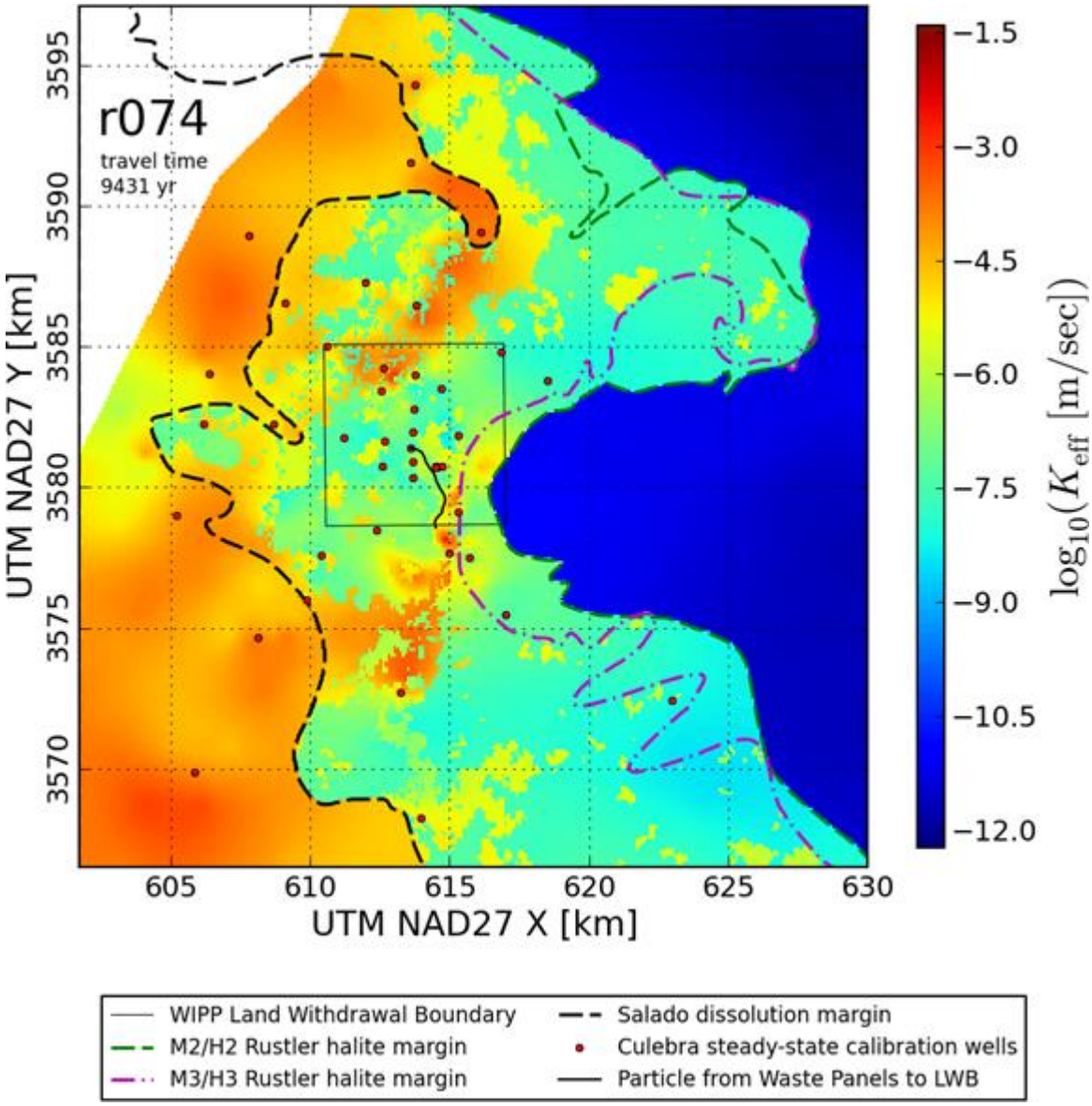
r074
travel time
9431 yr
UTM NAD27 Y [km]
3595
3590
3585
3580
3575
3570
605
610
615
620
625
630
UTM NAD27 X [km]
−1.5
−3.0
−4.5
−6.0
−7.5
−9.0
−10.5
−12.0
$\log_{10}(K_{\mathrm{eff}}\ [\mathrm{m/sec}])$
WIPP Land Withdrawal Boundary
M2/H2 Rustler halite margin
M3/H3 Rustler halite margin
Salado dissolution margin
Culebra steady-state calibration wells
Particle from Waste Panels to LWB

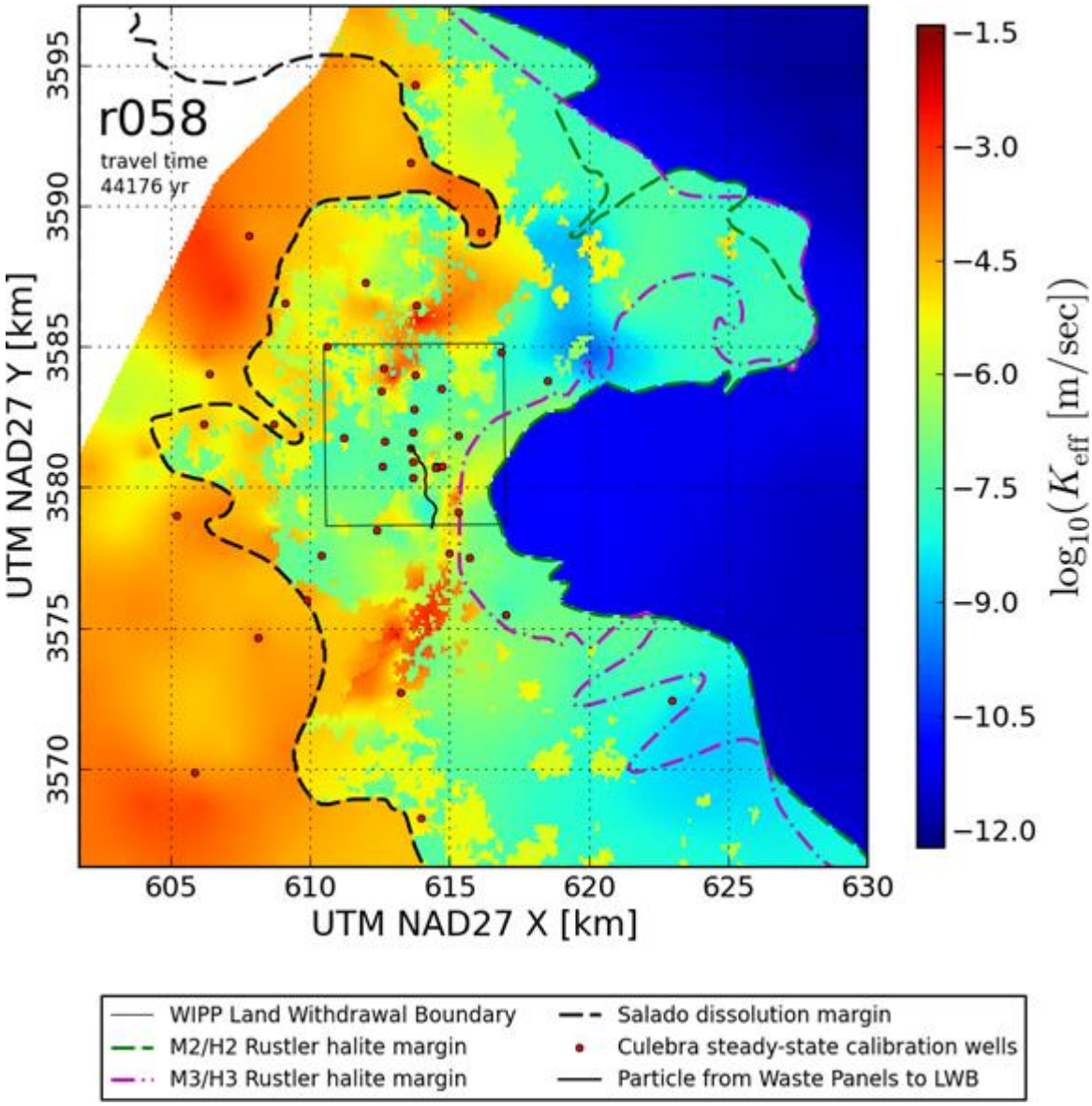
r058
travel time
44176 yr
UTM NAD27 Y [km]
3595
3590
3585
3580
3575
3570
605
610
615
620
625
630
UTM NAD27 X [km]
−1.5
−3.0
−4.5
−6.0
−7.5
−9.0
−10.5
−12.0
$\log_{10}(K_{\mathrm{eff}}\ [\mathrm{m/sec}])$
WIPP Land Withdrawal Boundary
M2/H2 Rustler halite margin
M3/H3 Rustler halite margin
Salado dissolution margin
Culebra steady-state calibration wells
Particle from Waste Panels to LWB

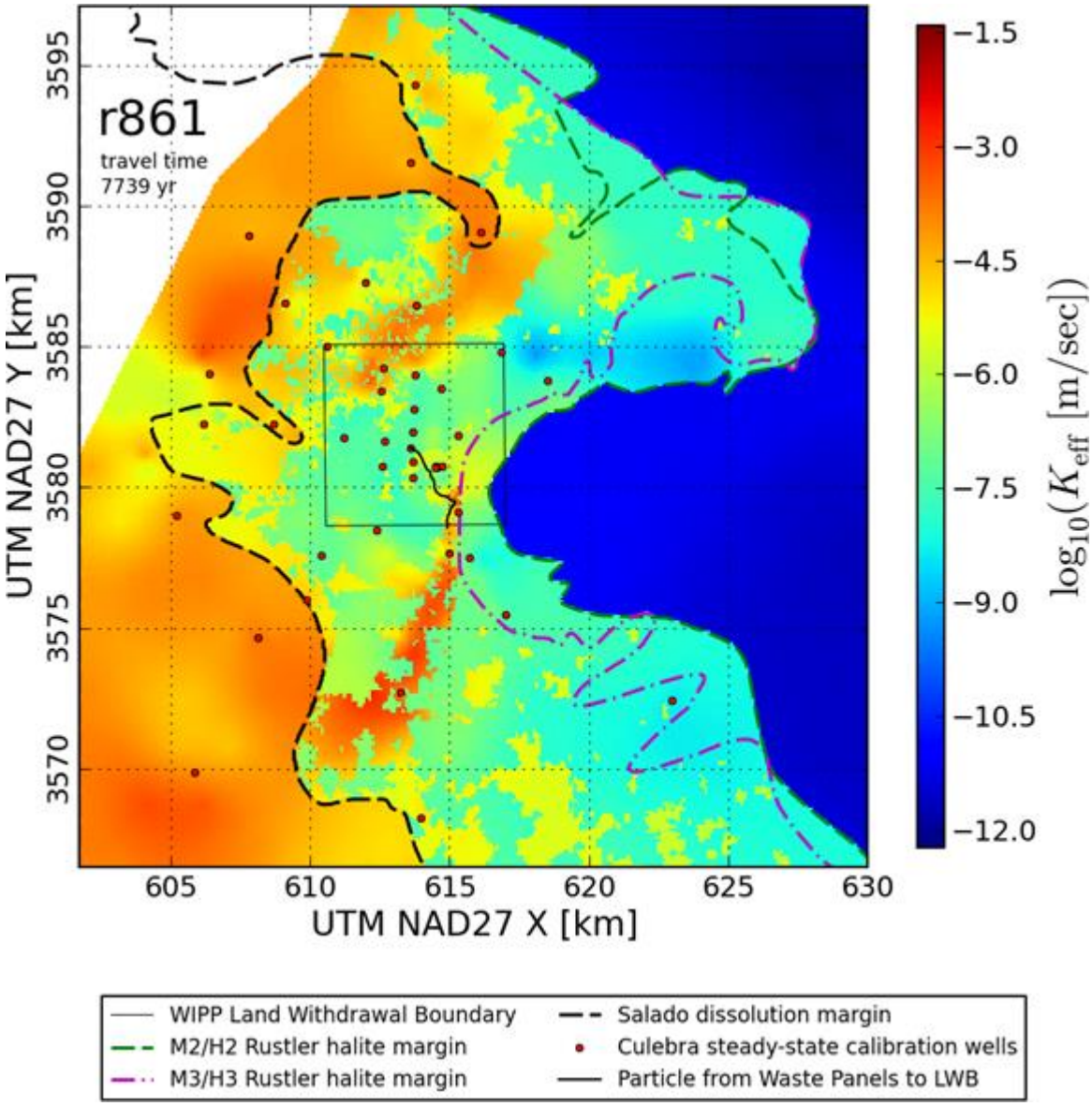
r861
travel time
7739 yr
UTM NAD27 Y [km]
3595
3590
3585
3580
3575
3570
605
610
615
620
625
630
UTM NAD27 X [km]
−1.5
−3.0
−4.5
−6.0
−7.5
−9.0
−10.5
−12.0
$\log_{10}(K_{\mathrm{eff}}\ [\mathrm{m/sec}])$
WIPP Land Withdrawal Boundary
M2/H2 Rustler halite margin
M3/H3 Rustler halite margin
Salado dissolution margin
Culebra steady-state calibration wells
Particle from Waste Panels to LWB

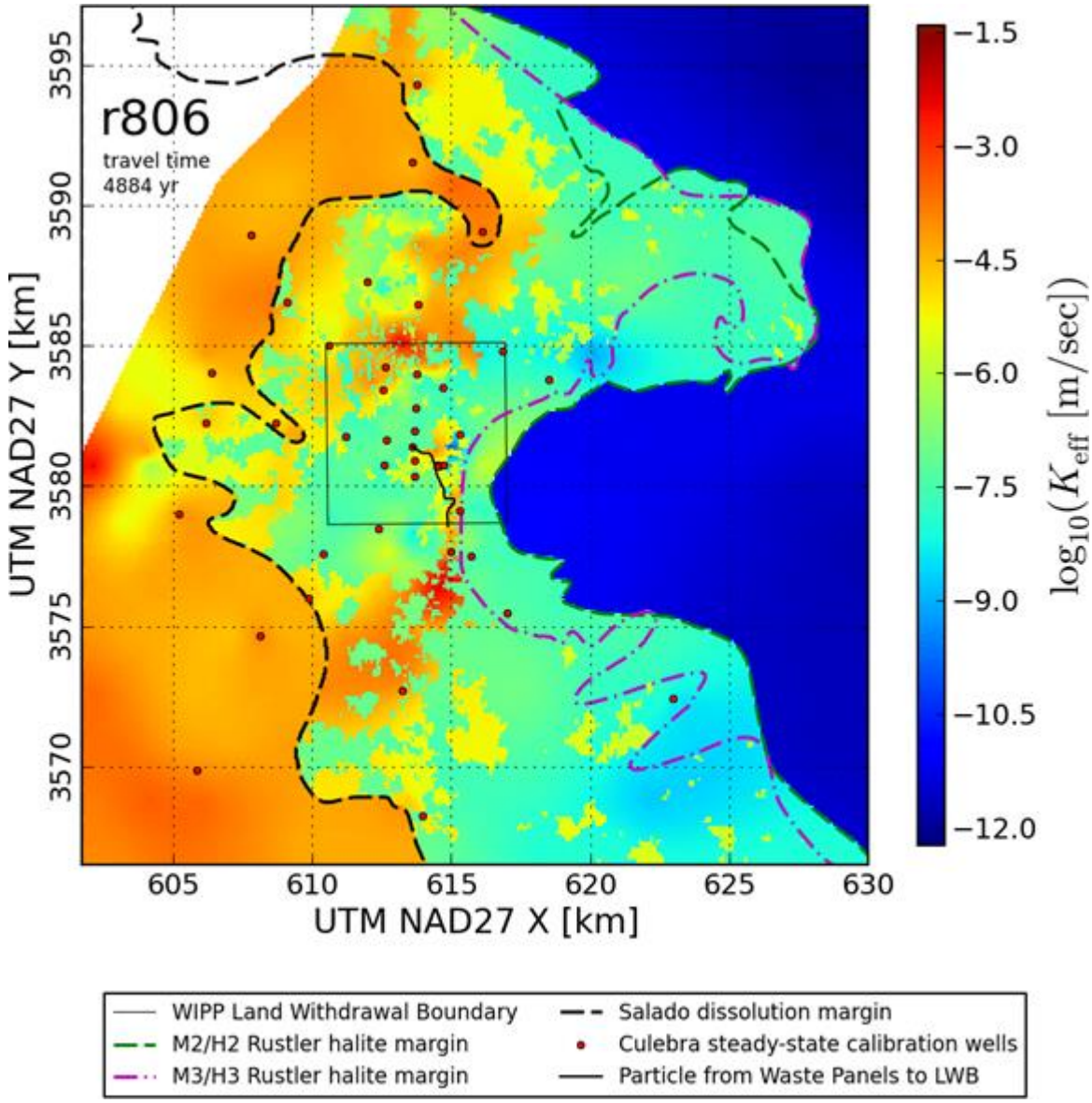
r806
travel time
4884 yr
UTM NAD27 Y [km]
3595
3590
3585
3580
3575
3570
605
610
615
620
625
630
UTM NAD27 X [km]
−1.5
−3.0
−4.5
−6.0
−7.5
−9.0
−10.5
−12.0
$\log_{10}(K_{\mathrm{eff}}\ [\mathrm{m/sec}])$
WIPP Land Withdrawal Boundary
M2/H2 Rustler halite margin
M3/H3 Rustler halite margin
Salado dissolution margin
Culebra steady-state calibration wells
Particle from Waste Panels to LWB

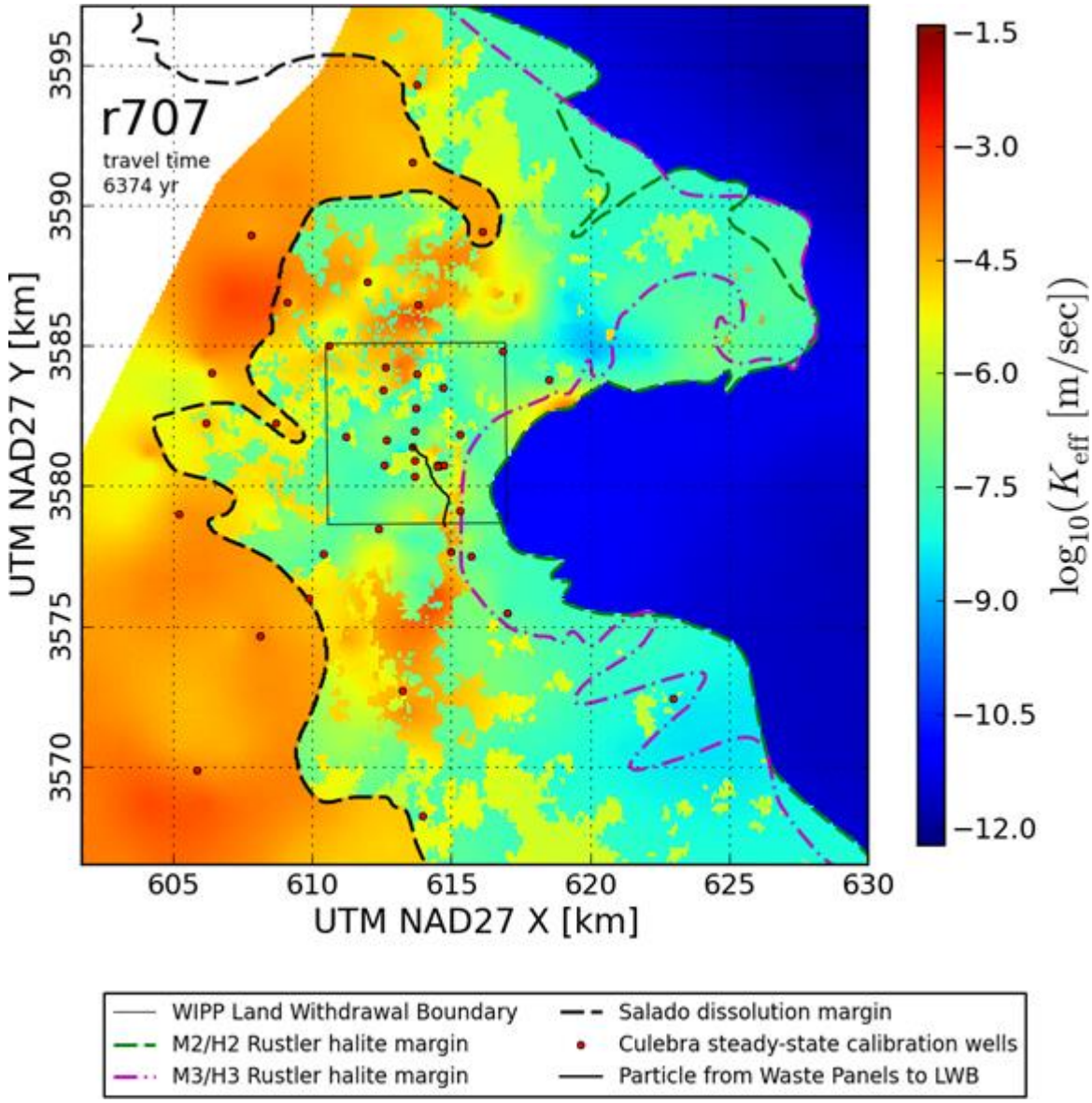
r707
travel time
6374 yr
UTM NAD27 Y [km]
3595
3590
3585
3580
3575
3570
605
610
615
620
625
630
UTM NAD27 X [km]
−1.5
−3.0
−4.5
−6.0
−7.5
−9.0
−10.5
−12.0
$\log_{10}(K_{\mathrm{eff}}\ [\mathrm{m/sec}])$
WIPP Land Withdrawal Boundary
M2/H2 Rustler halite margin
M3/H3 Rustler halite margin
Salado dissolution margin
Culebra steady-state calibration wells
Particle from Waste Panels to LWB

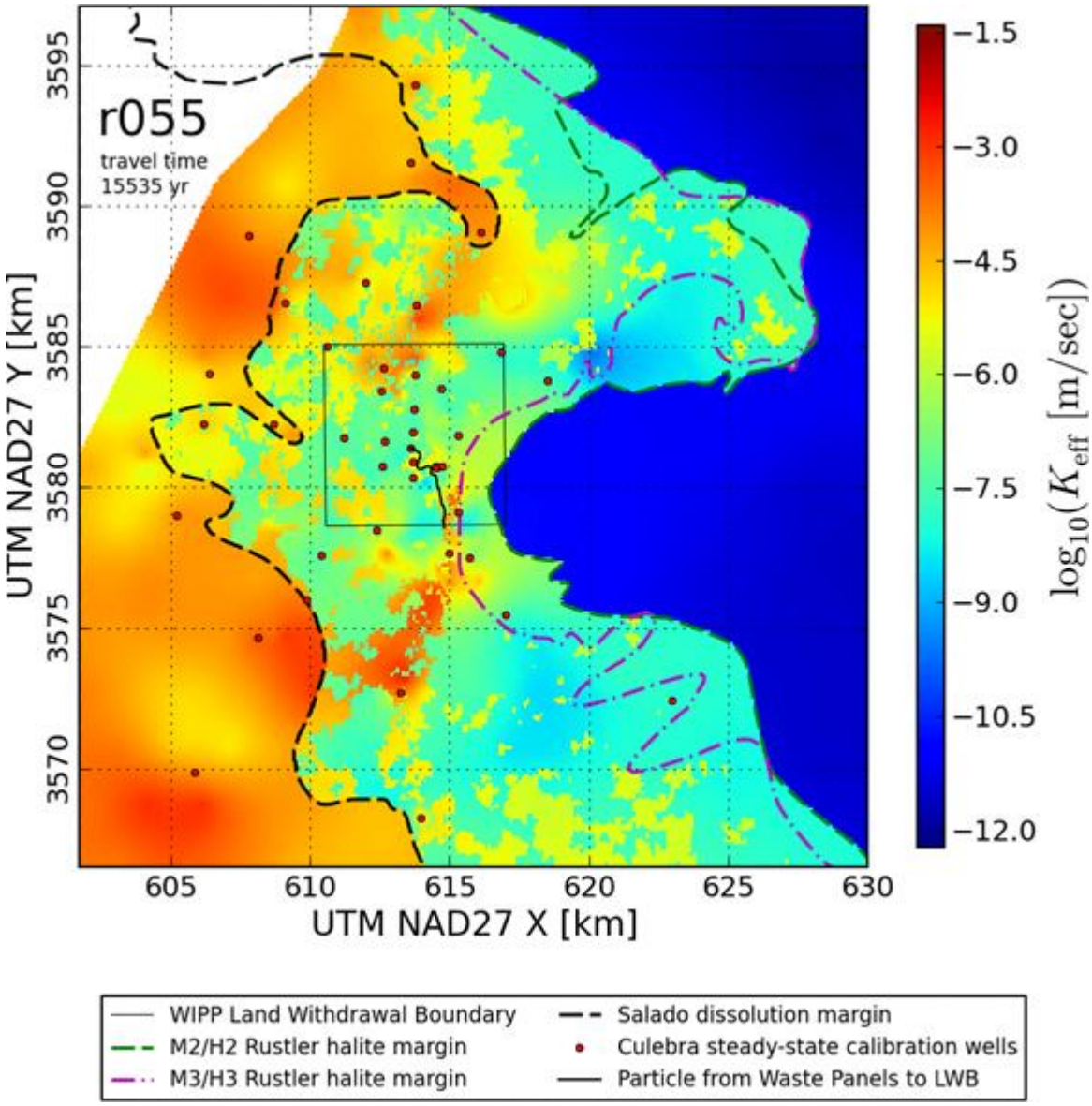
r055
travel time
15535 yr
UTM NAD27 Y [km]
3595
3590
3585
3580
3575
3570
605
610
615
620
625
630
UTM NAD27 X [km]
−1.5
−3.0
−4.5
−6.0
−7.5
−9.0
−10.5
−12.0
$\log_{10}(K_{\mathrm{eff}}\ [\mathrm{m/sec}])$
WIPP Land Withdrawal Boundary
M2/H2 Rustler halite margin
M3/H3 Rustler halite margin
Salado dissolution margin
Culebra steady-state calibration wells
Particle from Waste Panels to LWB

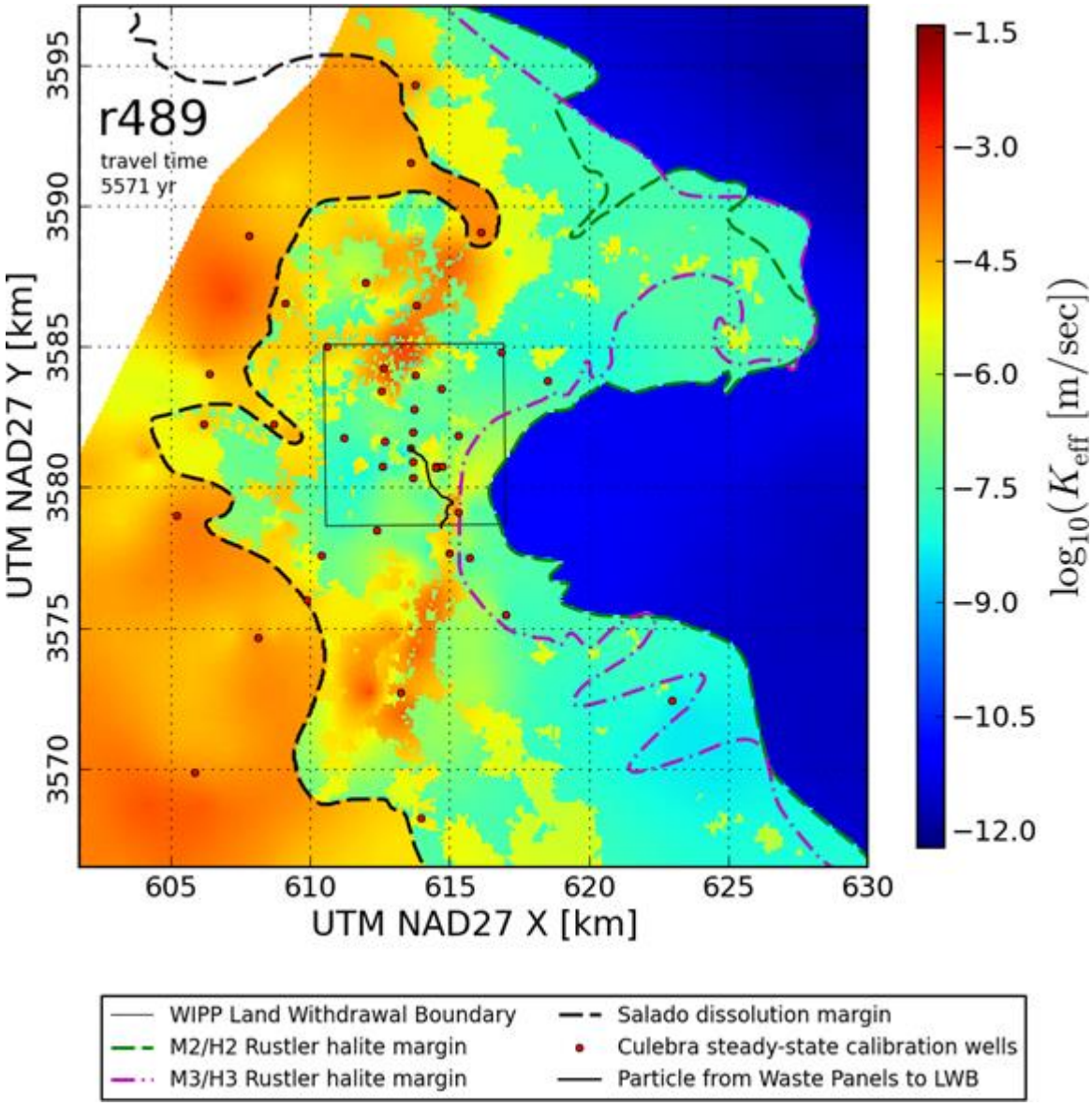
r489
travel time
5571 yr
UTM NAD27 Y [km]
3595
3590
3585
3580
3575
3570
605
610
615
620
625
630
UTM NAD27 X [km]
−1.5
−3.0
−4.5
−6.0
−7.5
−9.0
−10.5
−12.0
$\log_{10}(K_{\text{eff}}$ [m/sec])
WIPP Land Withdrawal Boundary
M2/H2 Rustler halite margin
M3/H3 Rustler halite margin
Salado dissolution margin
Culebra steady-state calibration wells
Particle from Waste Panels to LWB

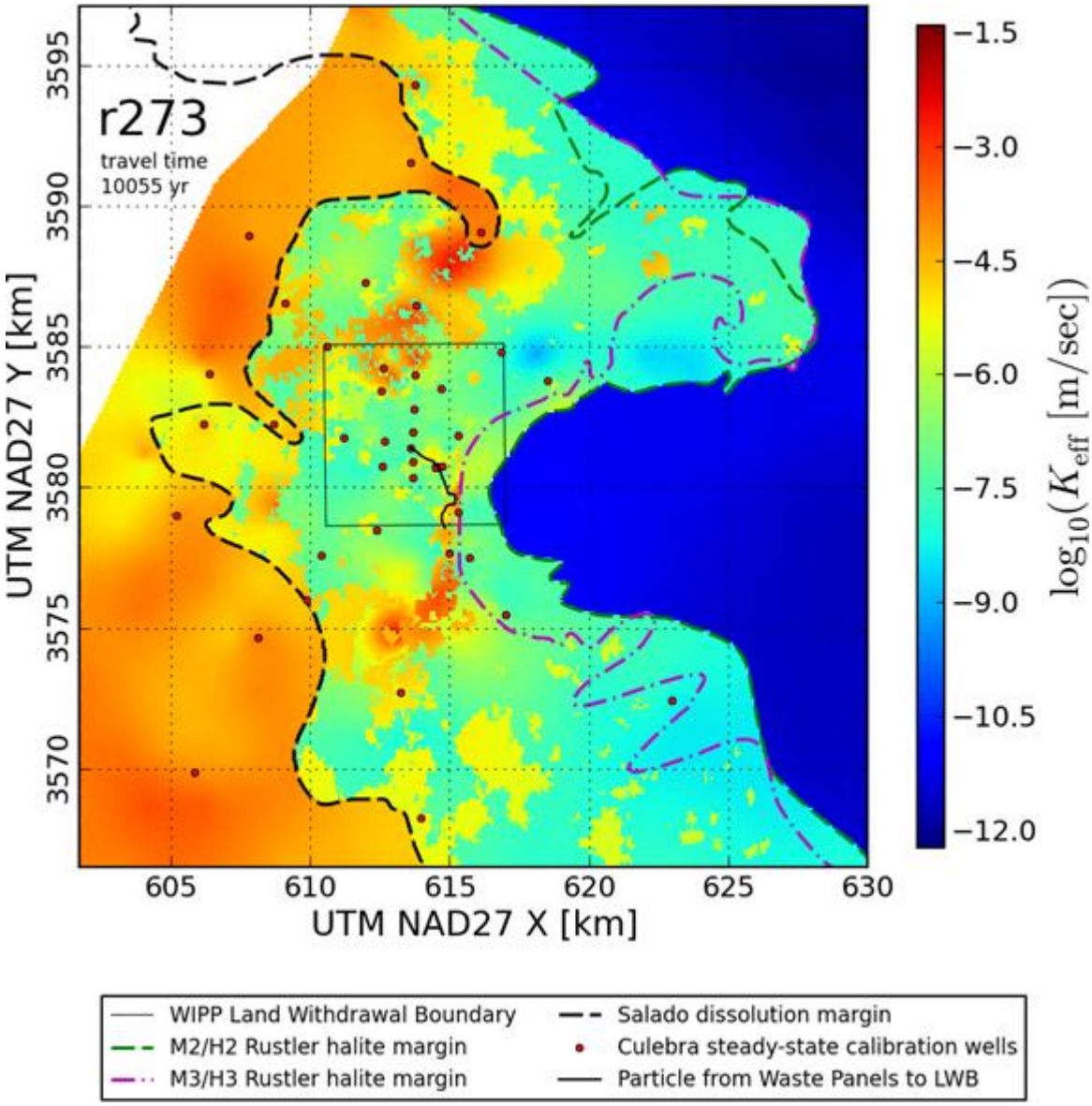
r273
travel time
10055 yr
UTM NAD27 Y [km]
3595
3590
3585
3580
3575
3570
605
610
615
620
625
630
UTM NAD27 X [km]
−1.5
−3.0
−4.5
−6.0
−7.5
−9.0
−10.5
−12.0
$\log_{10}(K_{\text{eff}}$ [m/sec])
WIPP Land Withdrawal Boundary
M2/H2 Rustler halite margin
M3/H3 Rustler halite margin
Salado dissolution margin
Culebra steady-state calibration wells
Particle from Waste Panels to LWB

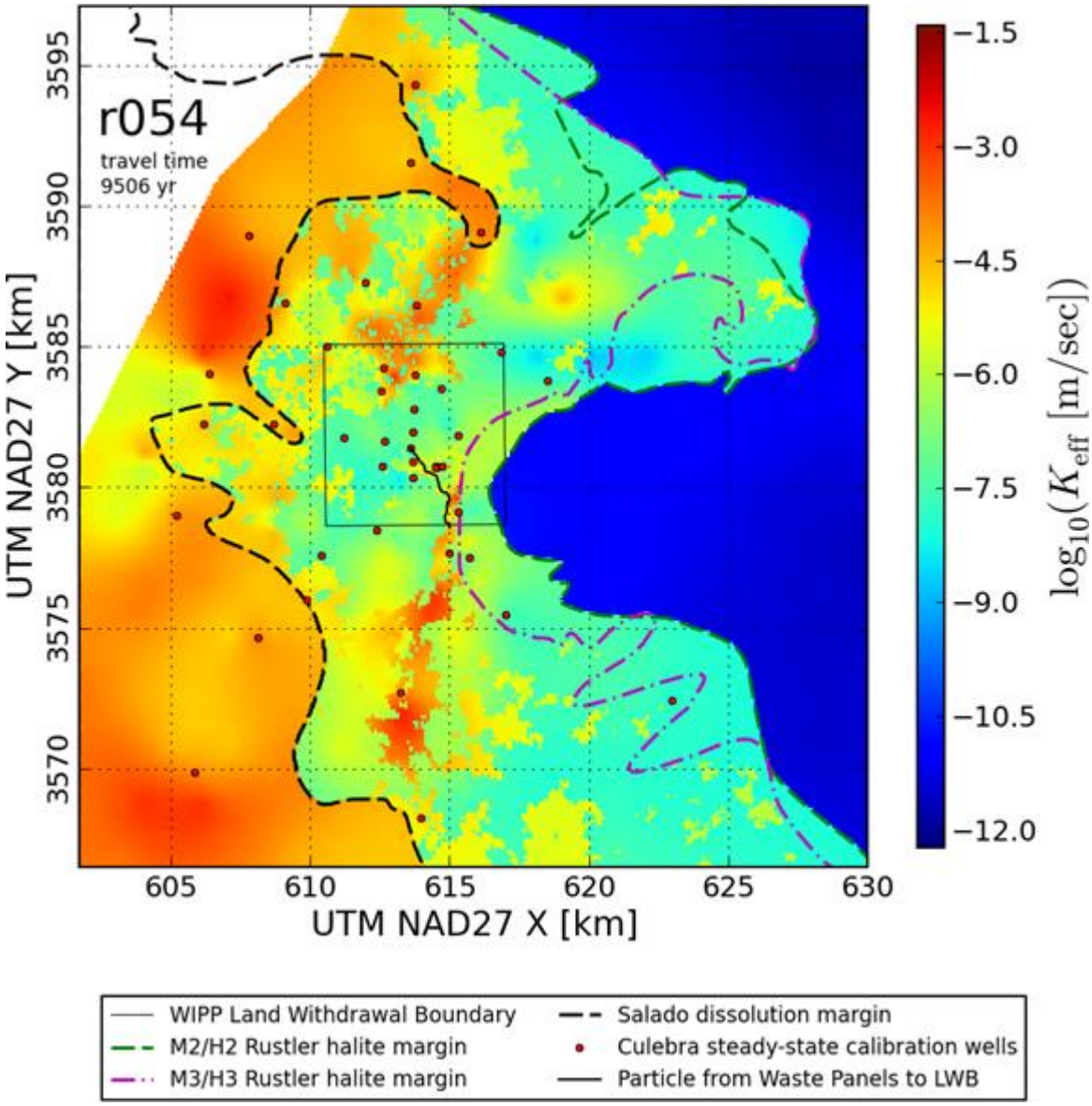
r054
travel time
9506 yr
UTM NAD27 Y [km]
3595
3590
3585
3580
3575
3570
605
610
615
620
625
630
UTM NAD27 X [km]
−1.5
−3.0
−4.5
−6.0
−7.5
−9.0
−10.5
−12.0
$\log_{10}(K_{\text{eff}}$ [m/sec])
WIPP Land Withdrawal Boundary
M2/H2 Rustler halite margin
M3/H3 Rustler halite margin
Salado dissolution margin
Culebra steady-state calibration wells
Particle from Waste Panels to LWB

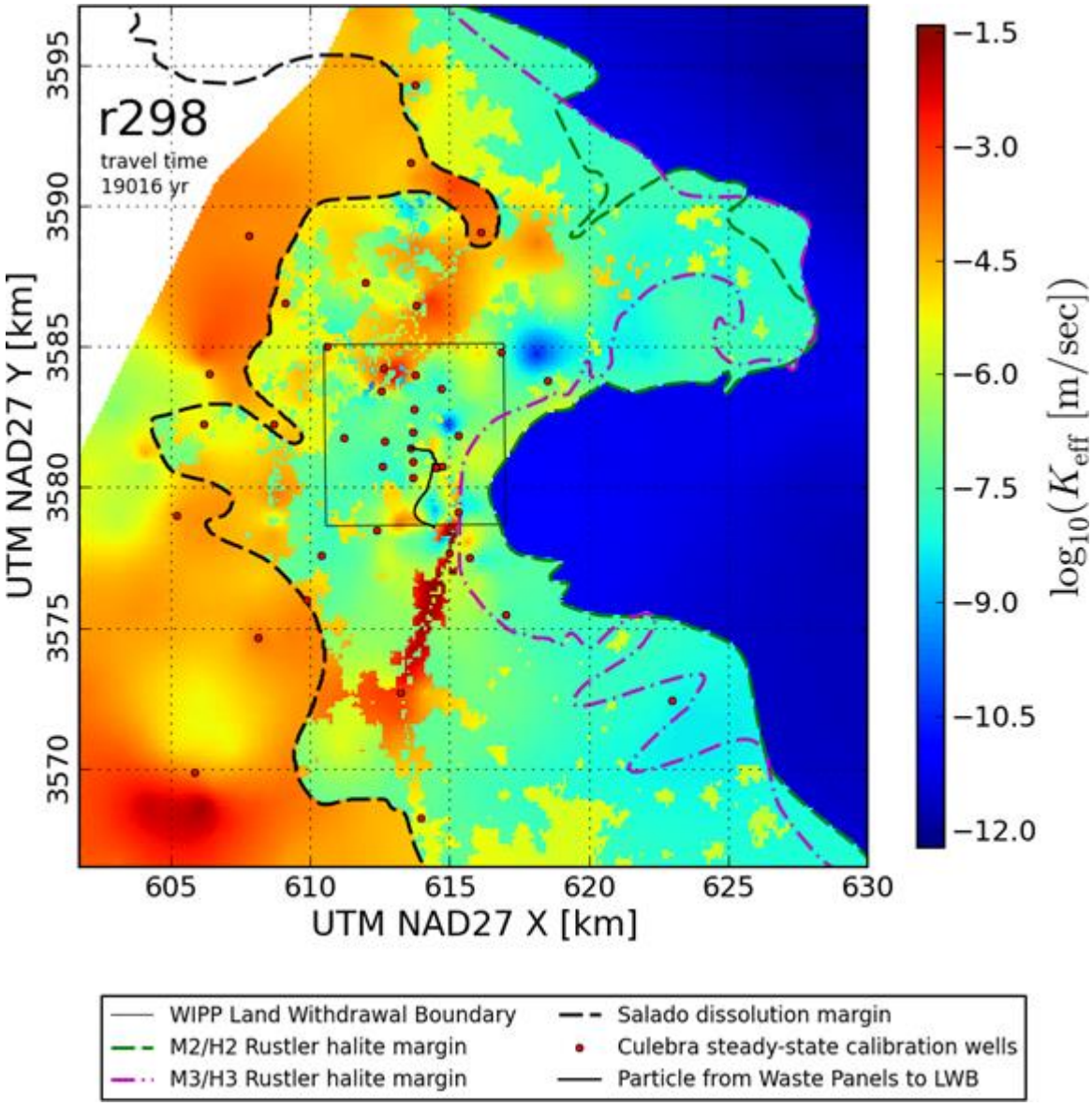
r298
travel time
19016 yr
UTM NAD27 Y [km]
3595
3590
3585
3580
3575
3570
605
610
615
620
625
630
UTM NAD27 X [km]
−1.5
−3.0
−4.5
−6.0
−7.5
−9.0
−10.5
−12.0
$\log_{10}(K_{\text{eff}}$ [m/sec])
WIPP Land Withdrawal Boundary
M2/H2 Rustler halite margin
M3/H3 Rustler halite margin
Salado dissolution margin
Culebra steady-state calibration wells
Particle from Waste Panels to LWB

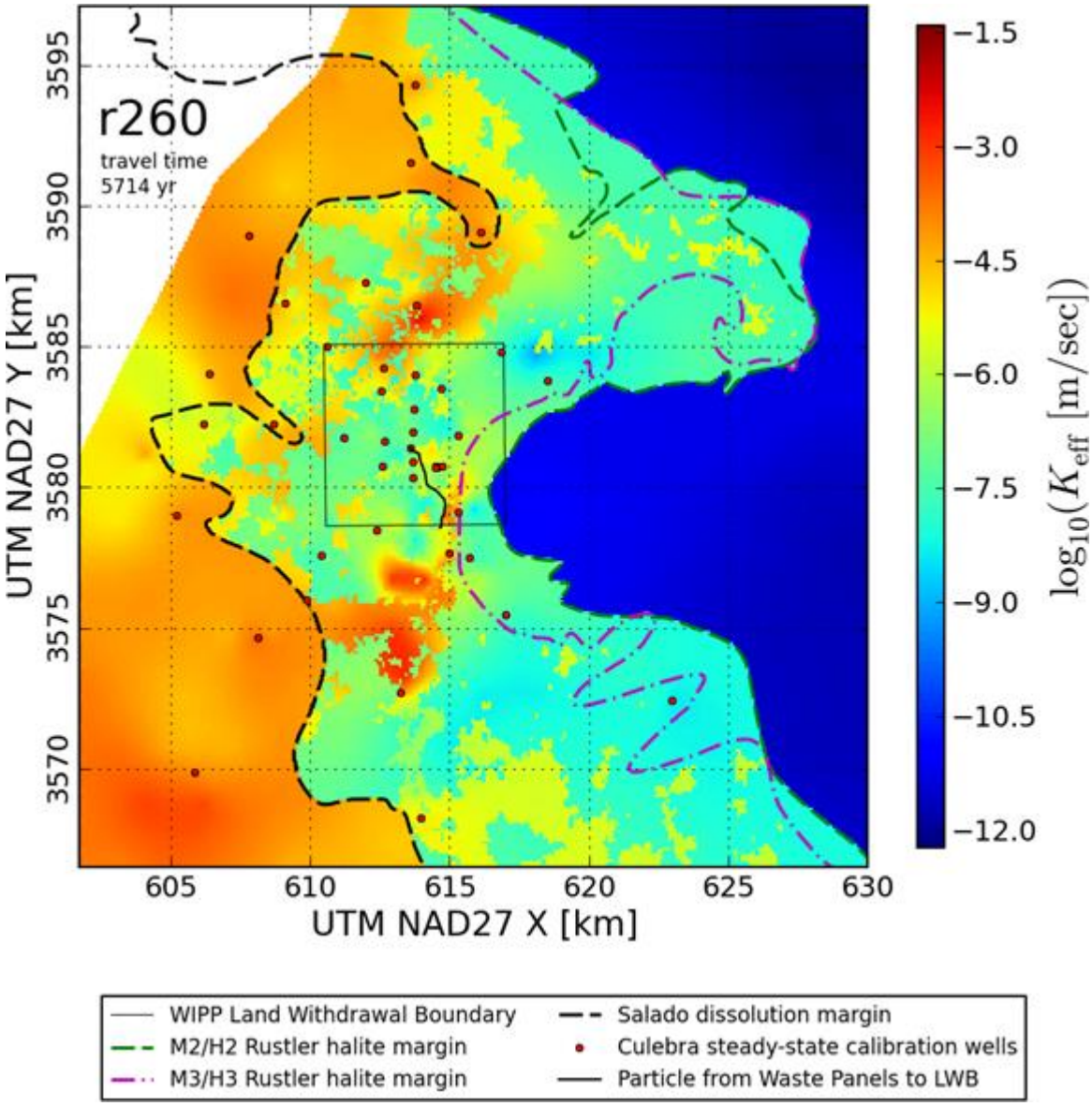
r260
travel time
5714 yr
UTM NAD27 Y [km]
3595
3590
3585
3580
3575
3570
605
610
615
620
625
630
UTM NAD27 X [km]
−1.5
−3.0
−4.5
−6.0
−7.5
−9.0
−10.5
−12.0
$\log_{10}(K_{\text{eff}}$ [m/sec])
WIPP Land Withdrawal Boundary
M2/H2 Rustler halite margin
M3/H3 Rustler halite margin
Salado dissolution margin
Culebra steady-state calibration wells
Particle from Waste Panels to LWB

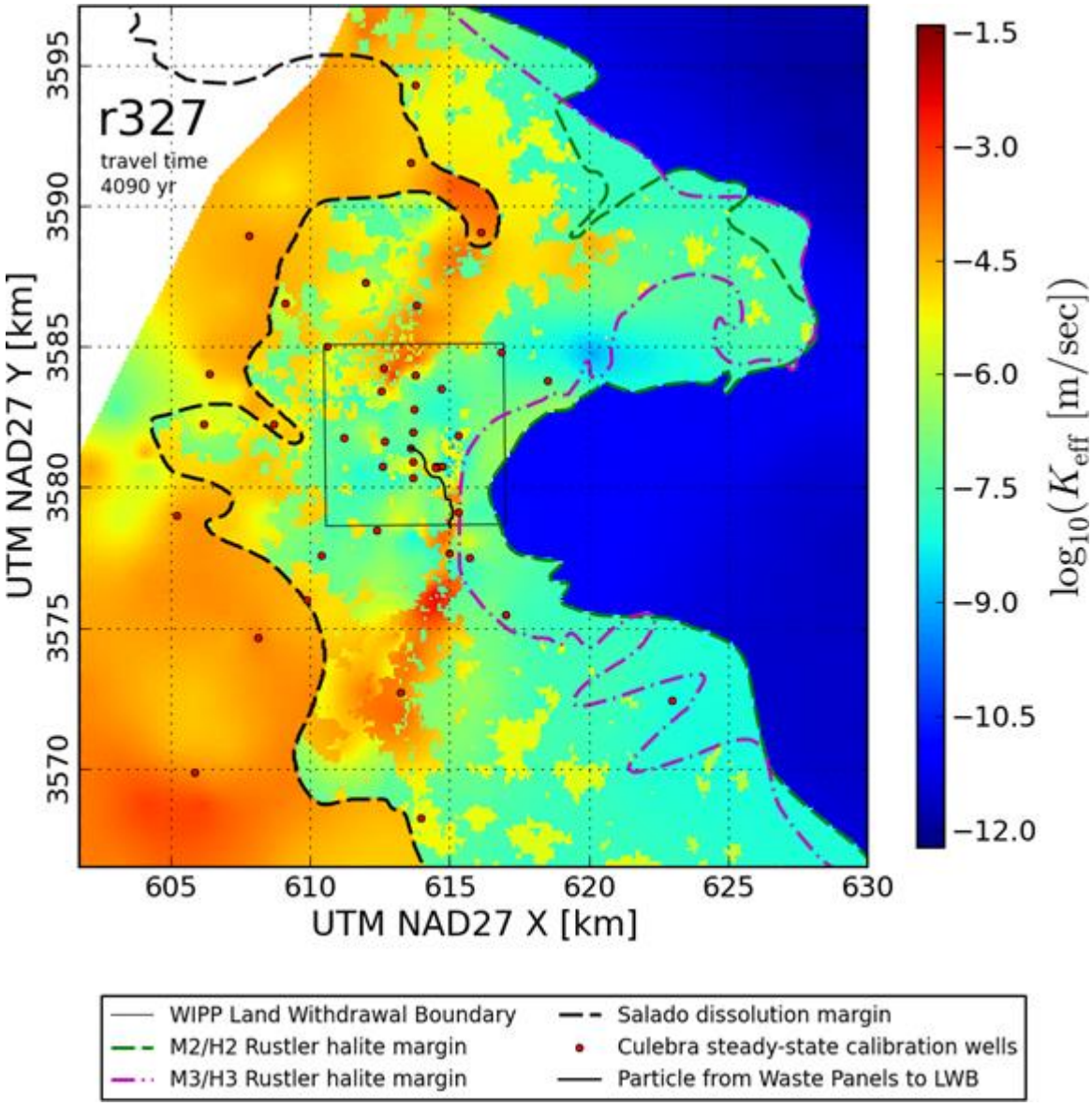
r327
travel time
4090 yr
UTM NAD27 Y [km]
3595
3590
3585
3580
3575
3570
605
610
615
620
625
630
UTM NAD27 X [km]
−1.5
−3.0
−4.5
−6.0
−7.5
−9.0
−10.5
−12.0
$\log_{10}(K_{\mathrm{eff}}\ [\mathrm{m/sec}])$
WIPP Land Withdrawal Boundary
M2/H2 Rustler halite margin
M3/H3 Rustler halite margin
Salado dissolution margin
Culebra steady-state calibration wells
Particle from Waste Panels to LWB

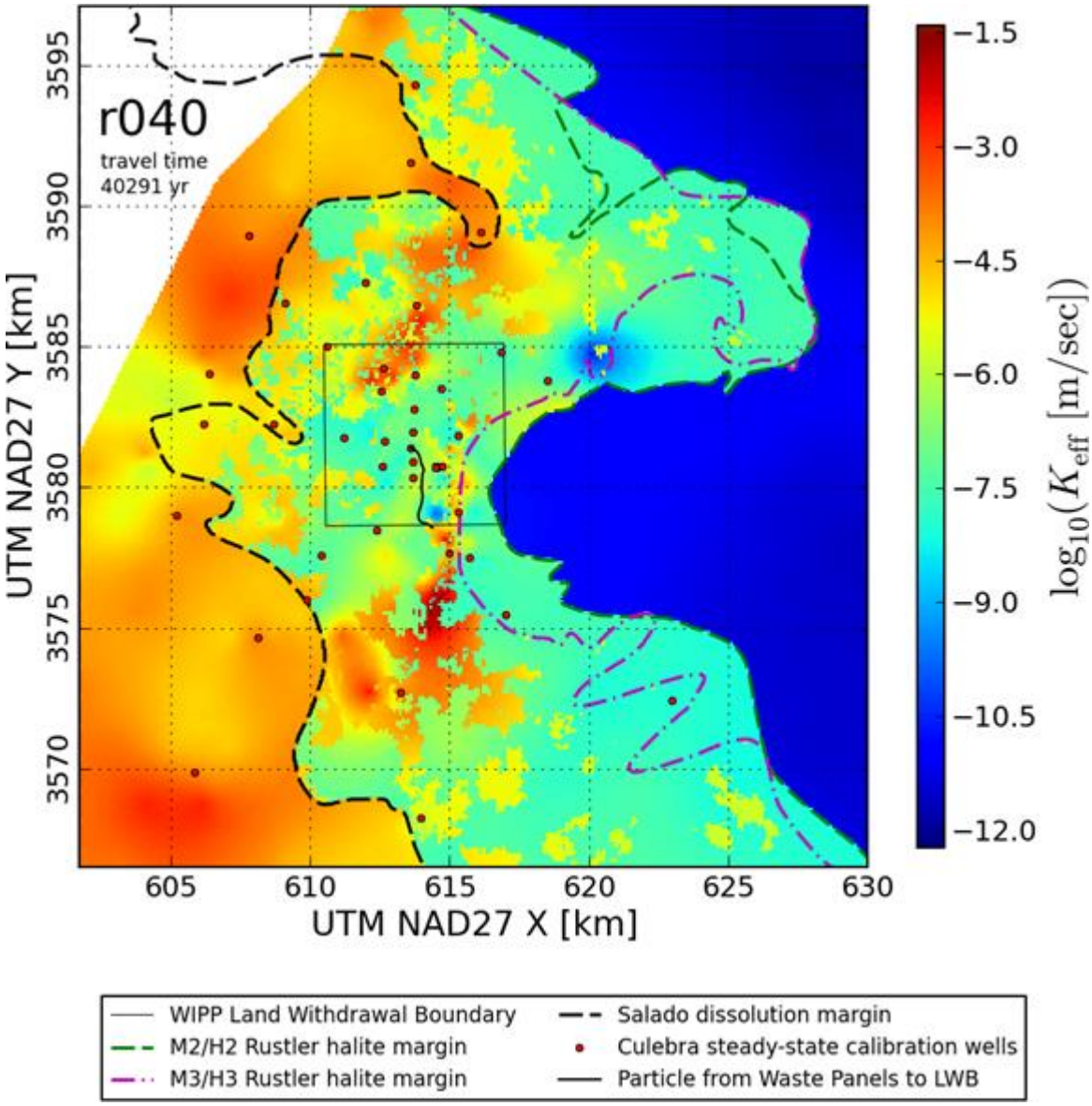
r040
travel time
40291 yr
UTM NAD27 Y [km]
3595
3590
3585
3580
3575
3570
605
610
615
620
625
630
UTM NAD27 X [km]
−1.5
−3.0
−4.5
−6.0
−7.5
−9.0
−10.5
−12.0
$\log_{10}(K_{\mathrm{eff}}\ [\mathrm{m/sec}])$
WIPP Land Withdrawal Boundary
M2/H2 Rustler halite margin
M3/H3 Rustler halite margin
Salado dissolution margin
Culebra steady-state calibration wells
Particle from Waste Panels to LWB

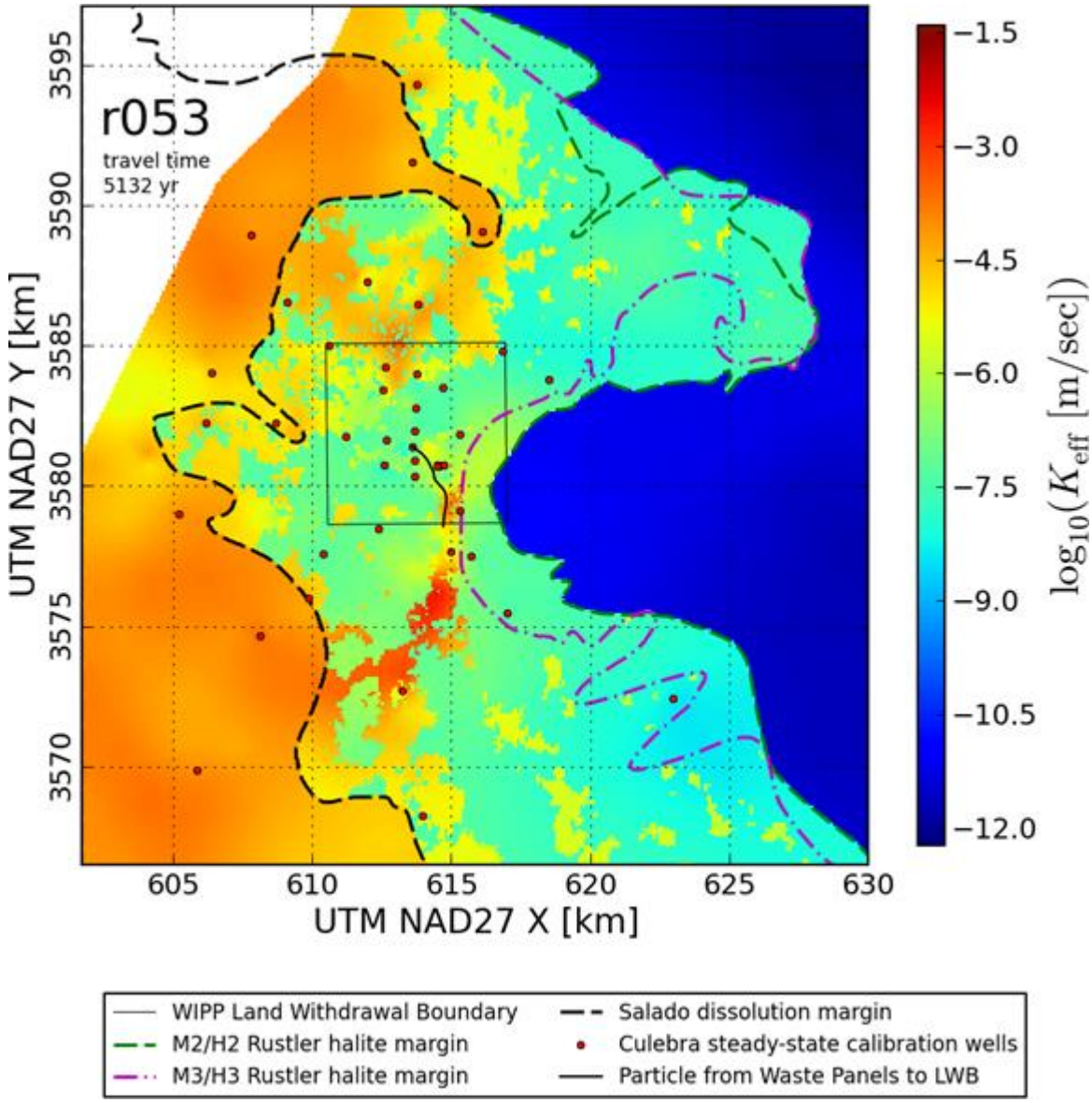
r053
travel time
5132 yr
UTM NAD27 Y [km]
3595
3590
3585
3580
3575
3570
605
610
615
620
625
630
UTM NAD27 X [km]
−1.5
−3.0
−4.5
−6.0
−7.5
−9.0
−10.5
−12.0
$\log_{10}(K_{\text{eff}}$ [m/sec])
WIPP Land Withdrawal Boundary
M2/H2 Rustler halite margin
M3/H3 Rustler halite margin
Salado dissolution margin
Culebra steady-state calibration wells
Particle from Waste Panels to LWB

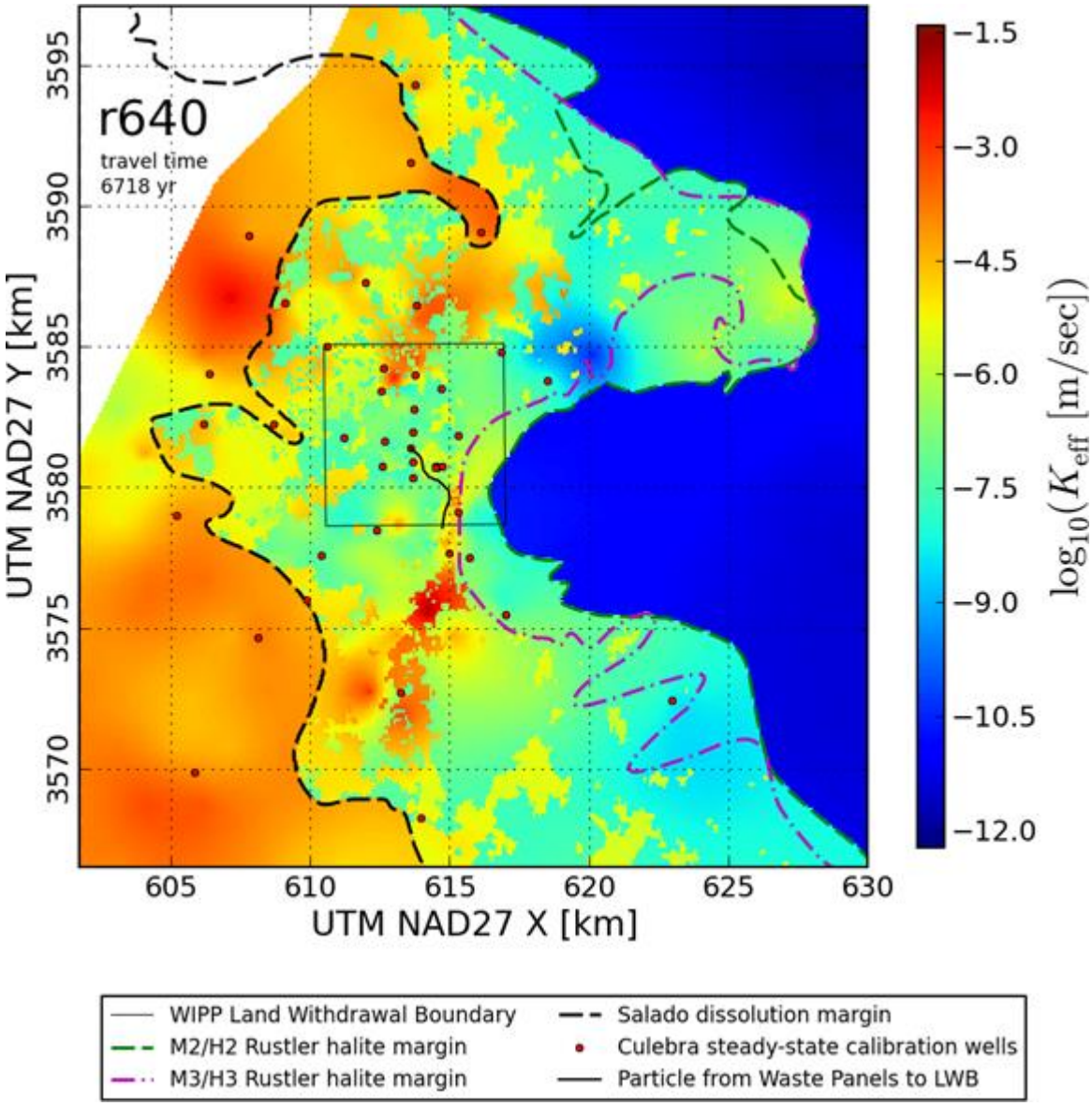
r640
travel time
6718 yr
UTM NAD27 Y [km]
3595
3590
3585
3580
3575
3570
605
610
615
620
625
630
UTM NAD27 X [km]
−1.5
−3.0
−4.5
−6.0
−7.5
−9.0
−10.5
−12.0
$\log_{10}(K_{\text{eff}}$ [m/sec])
WIPP Land Withdrawal Boundary
M2/H2 Rustler halite margin
M3/H3 Rustler halite margin
Salado dissolution margin
Culebra steady-state calibration wells
Particle from Waste Panels to LWB

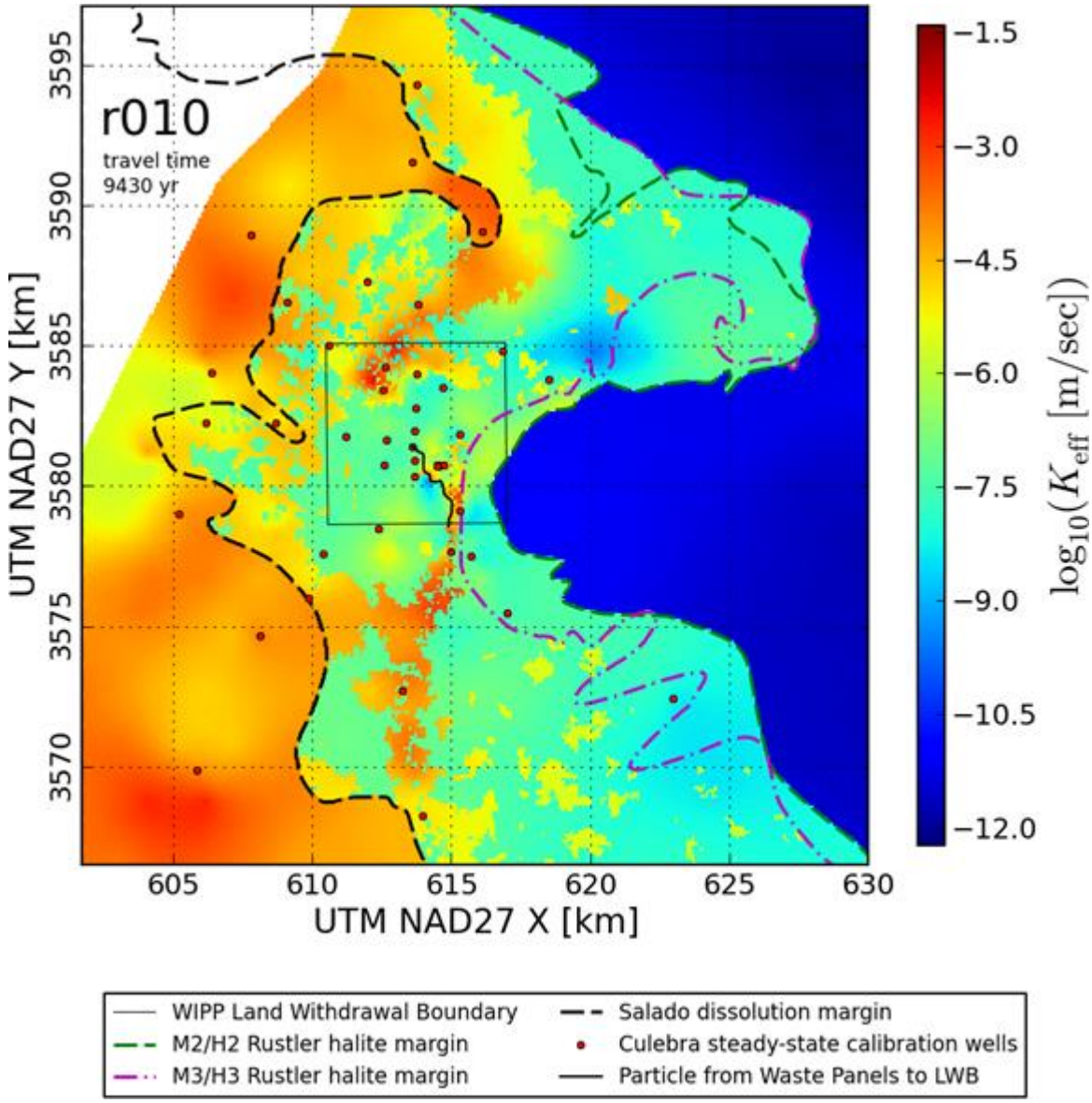
r010
travel time
9430 yr
UTM NAD27 Y [km]
3595
3590
3585
3580
3575
3570
605
610
615
620
625
630
UTM NAD27 X [km]
−1.5
−3.0
−4.5
−6.0
−7.5
−9.0
−10.5
−12.0
$\log_{10}(K_{\mathrm{eff}}\ [\mathrm{m/sec}])$
WIPP Land Withdrawal Boundary
M2/H2 Rustler halite margin
M3/H3 Rustler halite margin
Salado dissolution margin
Culebra steady-state calibration wells
Particle from Waste Panels to LWB

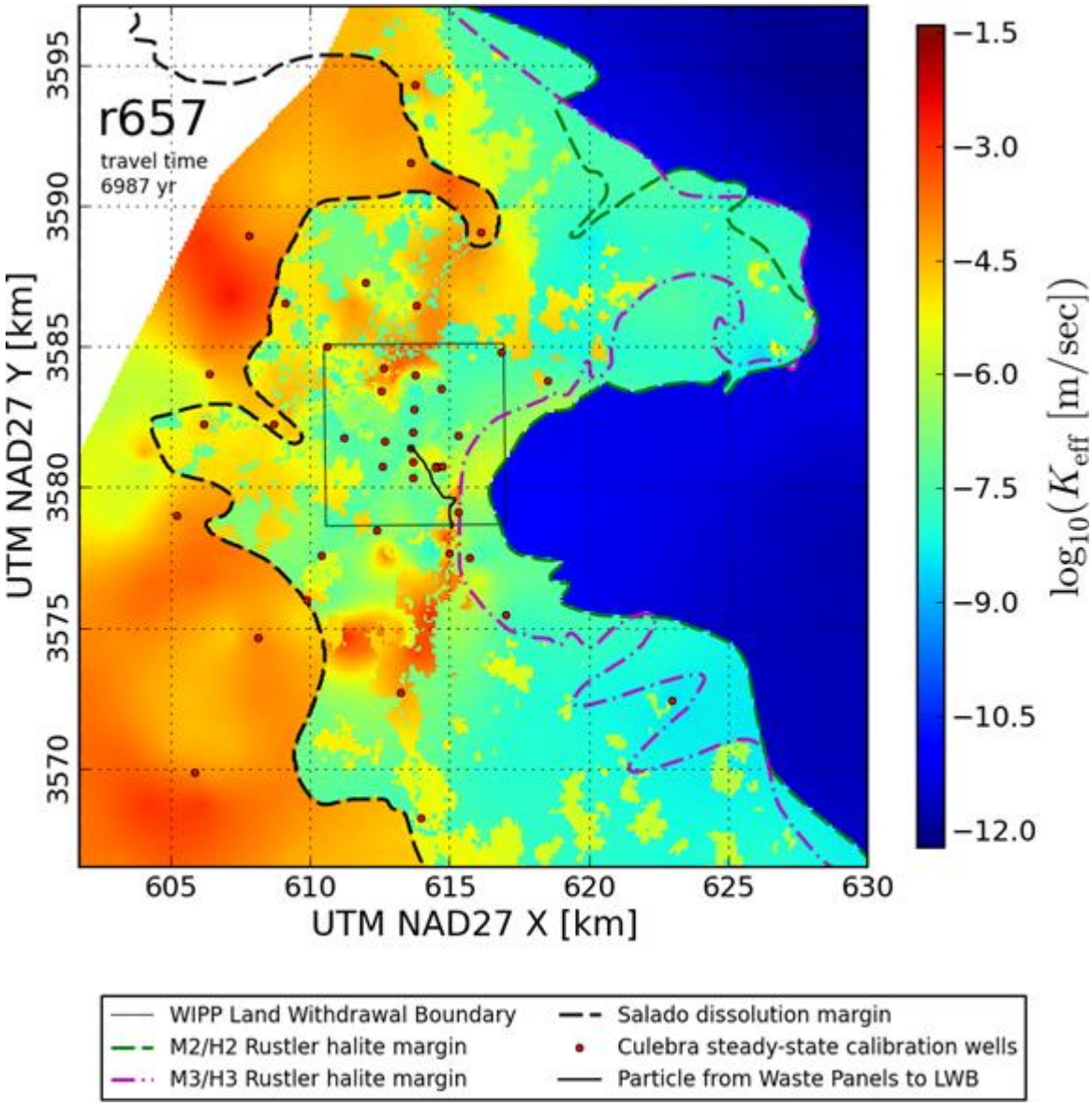
r657
travel time
6987 yr
UTM NAD27 Y [km]
3595
3590
3585
3580
3575
3570
605
610
615
620
625
630
UTM NAD27 X [km]
−1.5
−3.0
−4.5
−6.0
−7.5
−9.0
−10.5
−12.0
$\log_{10}(K_{\text{eff}}$ [m/sec])
WIPP Land Withdrawal Boundary
M2/H2 Rustler halite margin
M3/H3 Rustler halite margin
Salado dissolution margin
Culebra steady-state calibration wells
Particle from Waste Panels to LWB

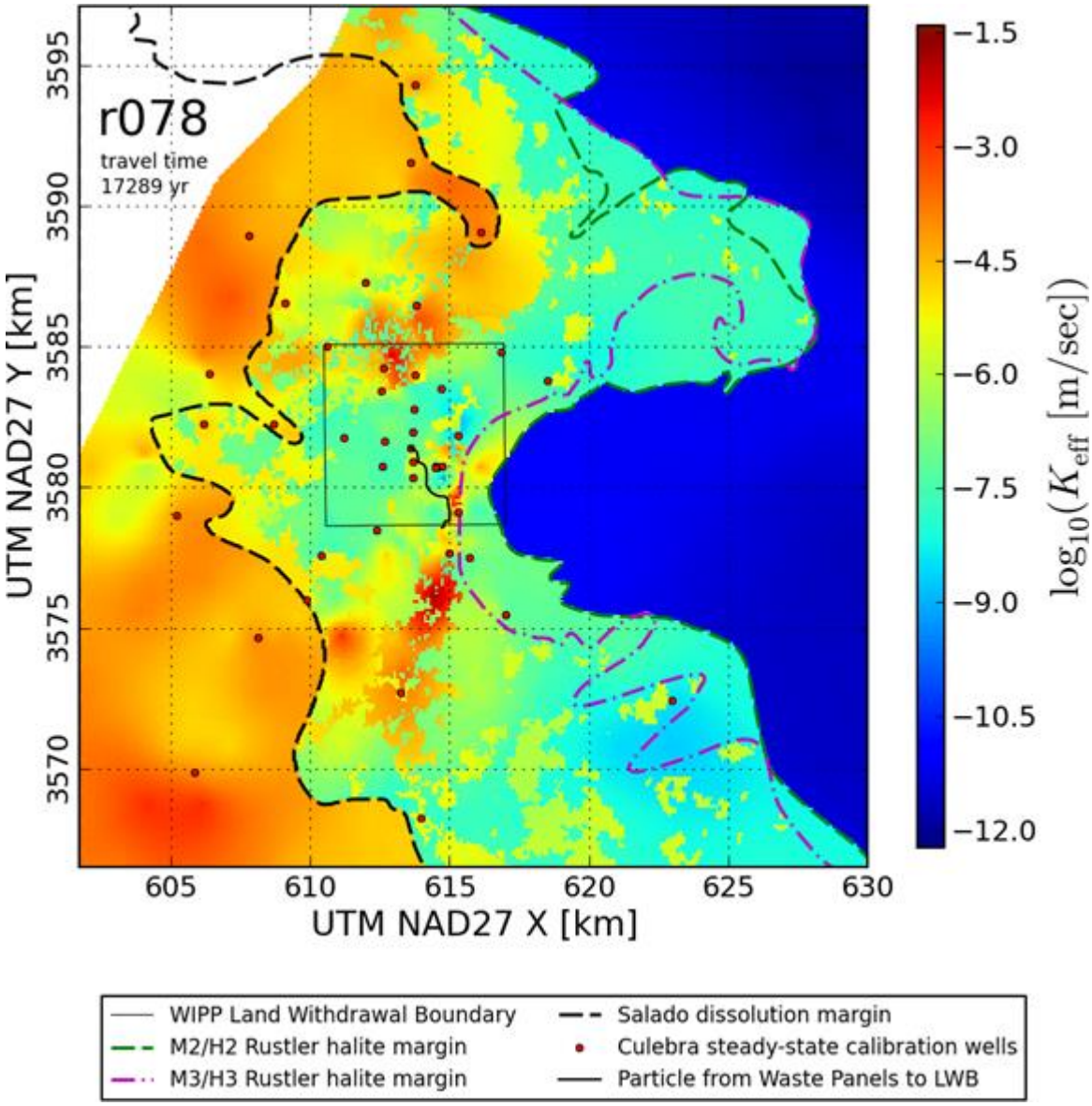
r078
travel time
17289 yr
UTM NAD27 Y [km]
3595
3590
3585
3580
3575
3570
605
610
615
620
625
630
UTM NAD27 X [km]
−1.5
−3.0
−4.5
−6.0
−7.5
−9.0
−10.5
−12.0
$\log_{10}(K_{\text{eff}}$ [m/sec])
WIPP Land Withdrawal Boundary
M2/H2 Rustler halite margin
M3/H3 Rustler halite margin
Salado dissolution margin
Culebra steady-state calibration wells
Particle from Waste Panels to LWB

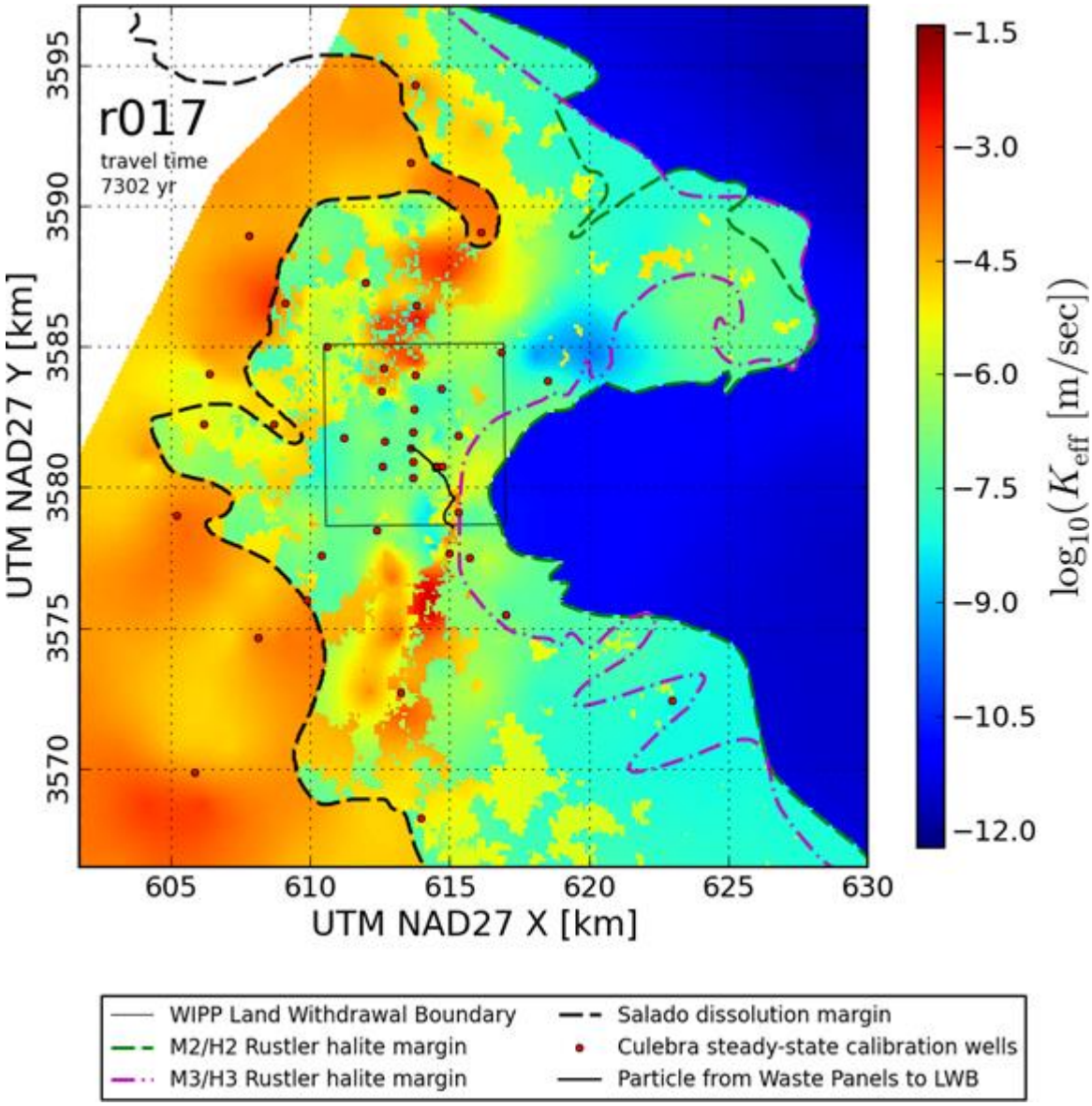
r017
travel time
7302 yr
UTM NAD27 Y [km]
3595
3590
3585
3580
3575
3570
605
610
615
620
625
630
UTM NAD27 X [km]
−1.5
−3.0
−4.5
−6.0
−7.5
−9.0
−10.5
−12.0
$\log_{10}(K_{\mathrm{eff}}\ [\mathrm{m/sec}])$
WIPP Land Withdrawal Boundary
M2/H2 Rustler halite margin
M3/H3 Rustler halite margin
Salado dissolution margin
Culebra steady-state calibration wells
Particle from Waste Panels to LWB

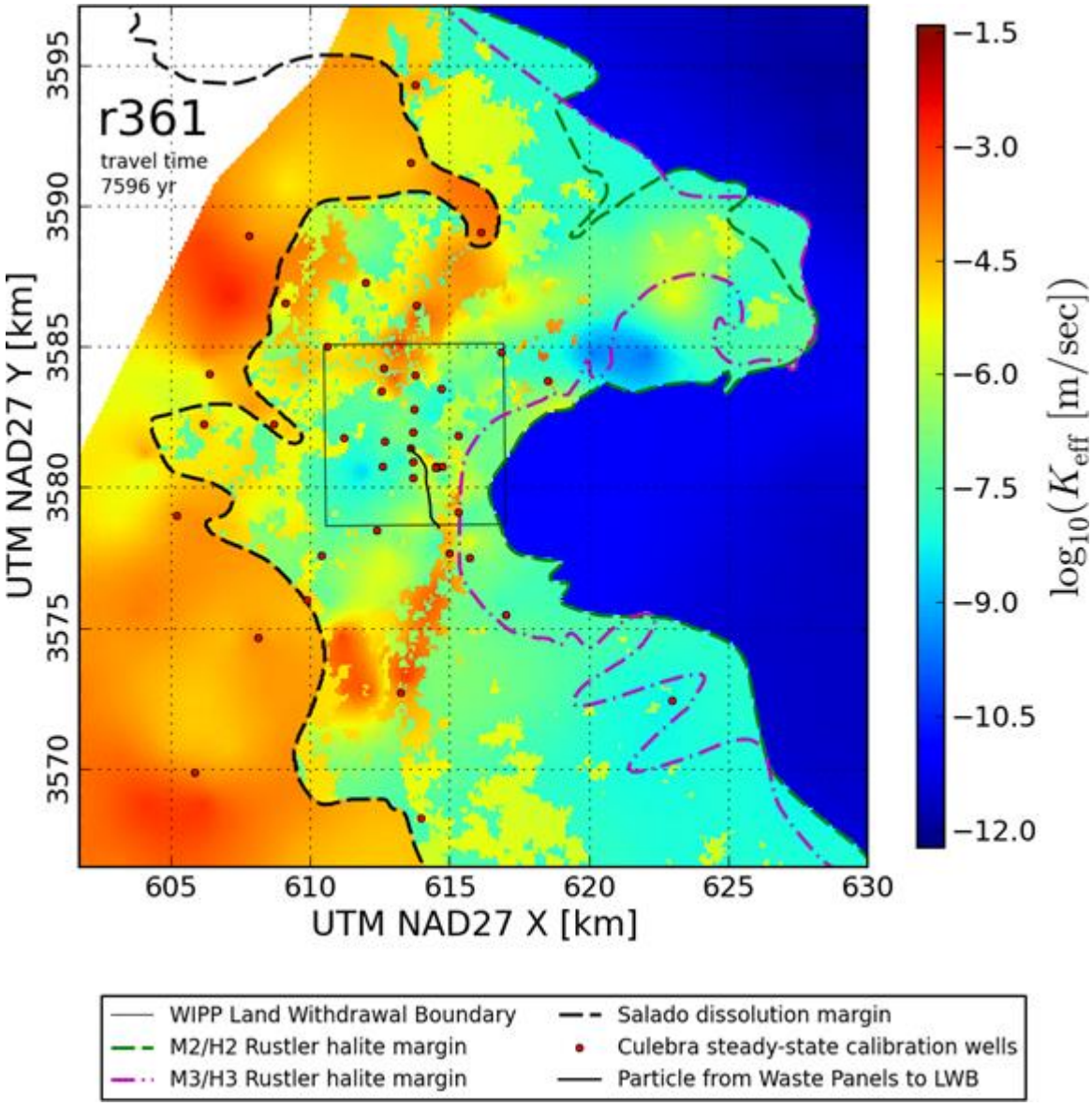
r361
travel time
7596 yr
UTM NAD27 Y [km]
3595
3590
3585
3580
3575
3570
605
610
615
620
625
630
UTM NAD27 X [km]
−1.5
−3.0
−4.5
−6.0
−7.5
−9.0
−10.5
−12.0
$\log_{10}(K_{\mathrm{eff}}\ [\mathrm{m/sec}])$
WIPP Land Withdrawal Boundary
M2/H2 Rustler halite margin
M3/H3 Rustler halite margin
Salado dissolution margin
Culebra steady-state calibration wells
Particle from Waste Panels to LWB

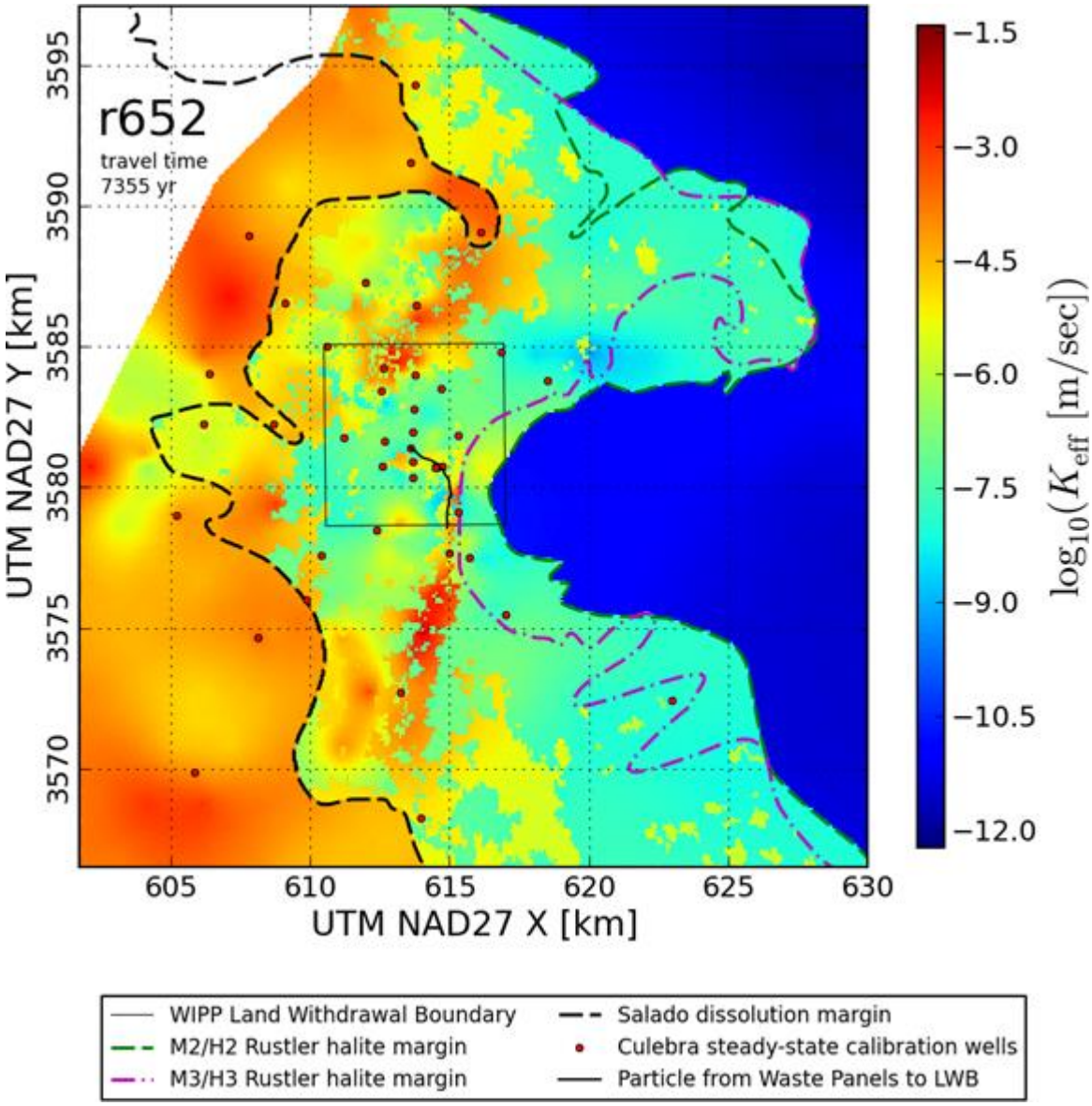
r652
travel time
7355 yr
UTM NAD27 Y [km]
3595
3590
3585
3580
3575
3570
605
610
615
620
625
630
UTM NAD27 X [km]
−1.5
−3.0
−4.5
−6.0
−7.5
−9.0
−10.5
−12.0
$\log_{10}(K_{\text{eff}}$ [m/sec])
WIPP Land Withdrawal Boundary
M2/H2 Rustler halite margin
M3/H3 Rustler halite margin
Salado dissolution margin
Culebra steady-state calibration wells
Particle from Waste Panels to LWB

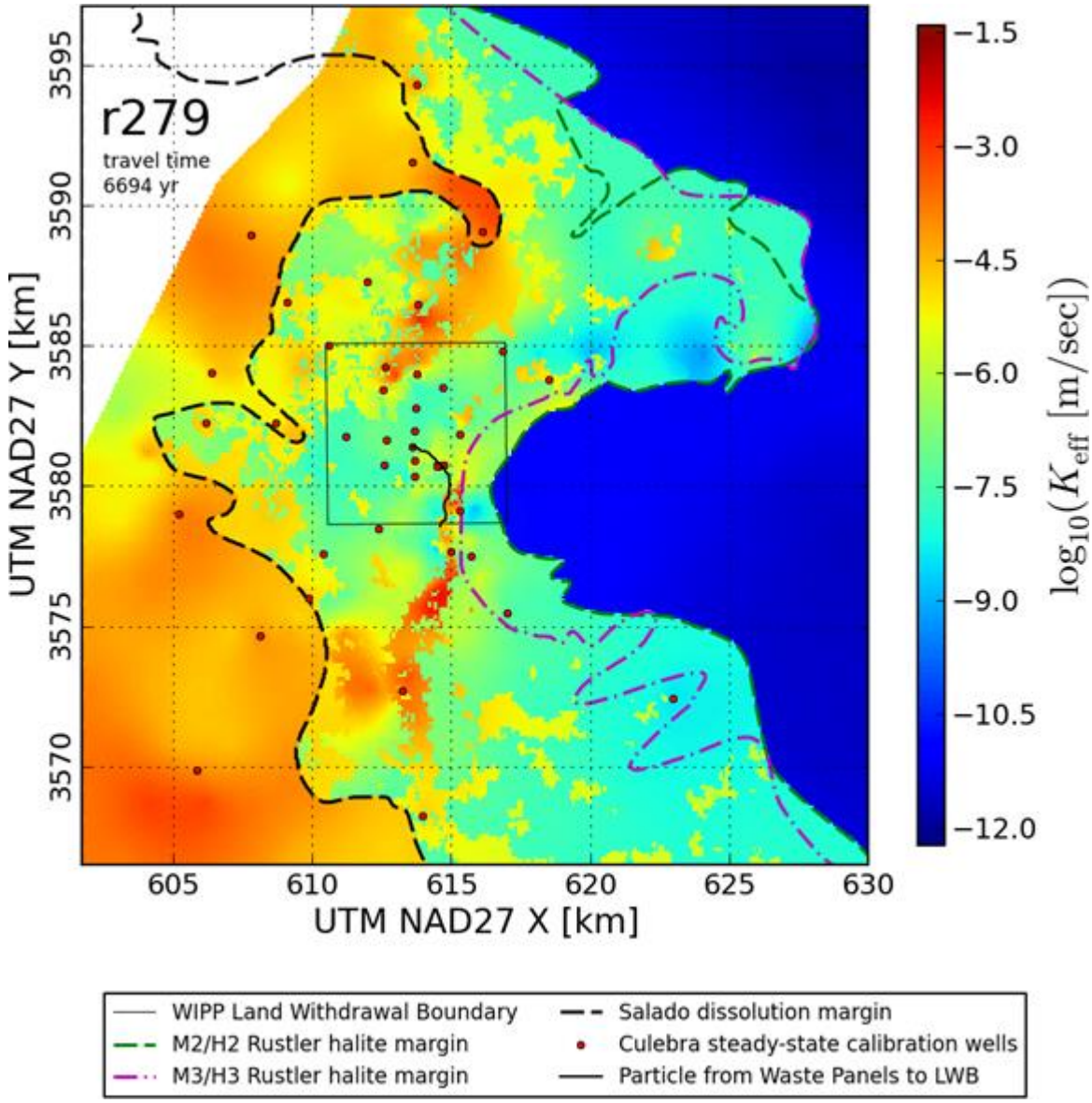
r279
travel time
6694 yr
UTM NAD27 Y [km]
3595
3590
3585
3580
3575
3570
605
610
615
620
625
630
UTM NAD27 X [km]
−1.5
−3.0
−4.5
−6.0
−7.5
−9.0
−10.5
−12.0
$\log_{10}(K_{\text{eff}}$ [m/sec])
WIPP Land Withdrawal Boundary
M2/H2 Rustler halite margin
M3/H3 Rustler halite margin
Salado dissolution margin
Culebra steady-state calibration wells
Particle from Waste Panels to LWB

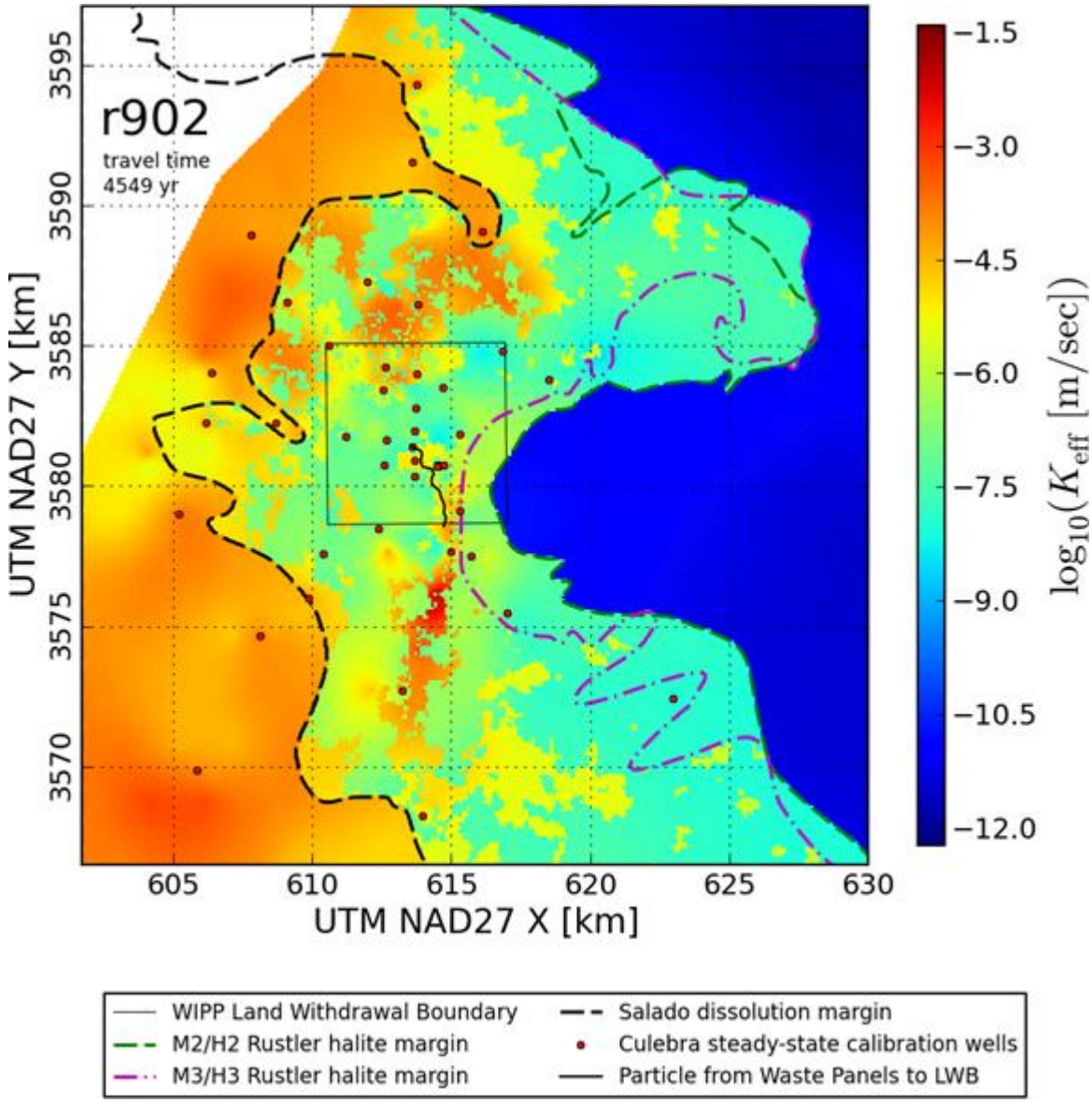
r902
travel time
4549 yr
UTM NAD27 Y [km]
3595
3590
3585
3580
3575
3570
605
610
615
620
625
630
UTM NAD27 X [km]
−1.5
−3.0
−4.5
−6.0
−7.5
−9.0
−10.5
−12.0
$\log_{10}(K_{\text{eff}}$ [m/sec])
WIPP Land Withdrawal Boundary
M2/H2 Rustler halite margin
M3/H3 Rustler halite margin
Salado dissolution margin
Culebra steady-state calibration wells
Particle from Waste Panels to LWB

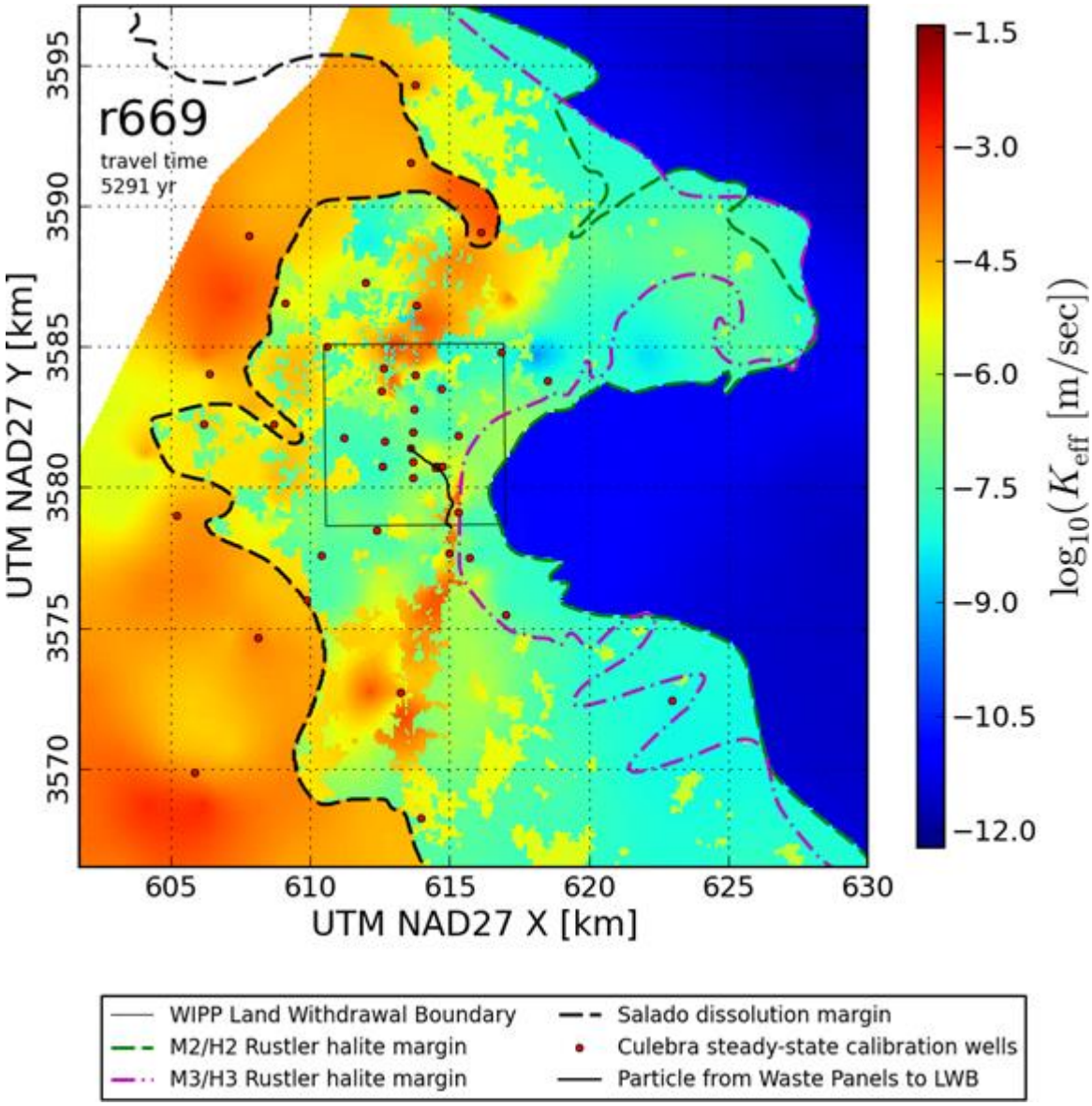
r669
travel time
5291 yr
UTM NAD27 Y [km]
3595
3590
3585
3580
3575
3570
605
610
615
620
625
630
UTM NAD27 X [km]
−1.5
−3.0
−4.5
−6.0
−7.5
−9.0
−10.5
−12.0
$\log_{10}(K_{\mathrm{eff}}\ [\mathrm{m/sec}])$
WIPP Land Withdrawal Boundary
M2/H2 Rustler halite margin
M3/H3 Rustler halite margin
Salado dissolution margin
Culebra steady-state calibration wells
Particle from Waste Panels to LWB

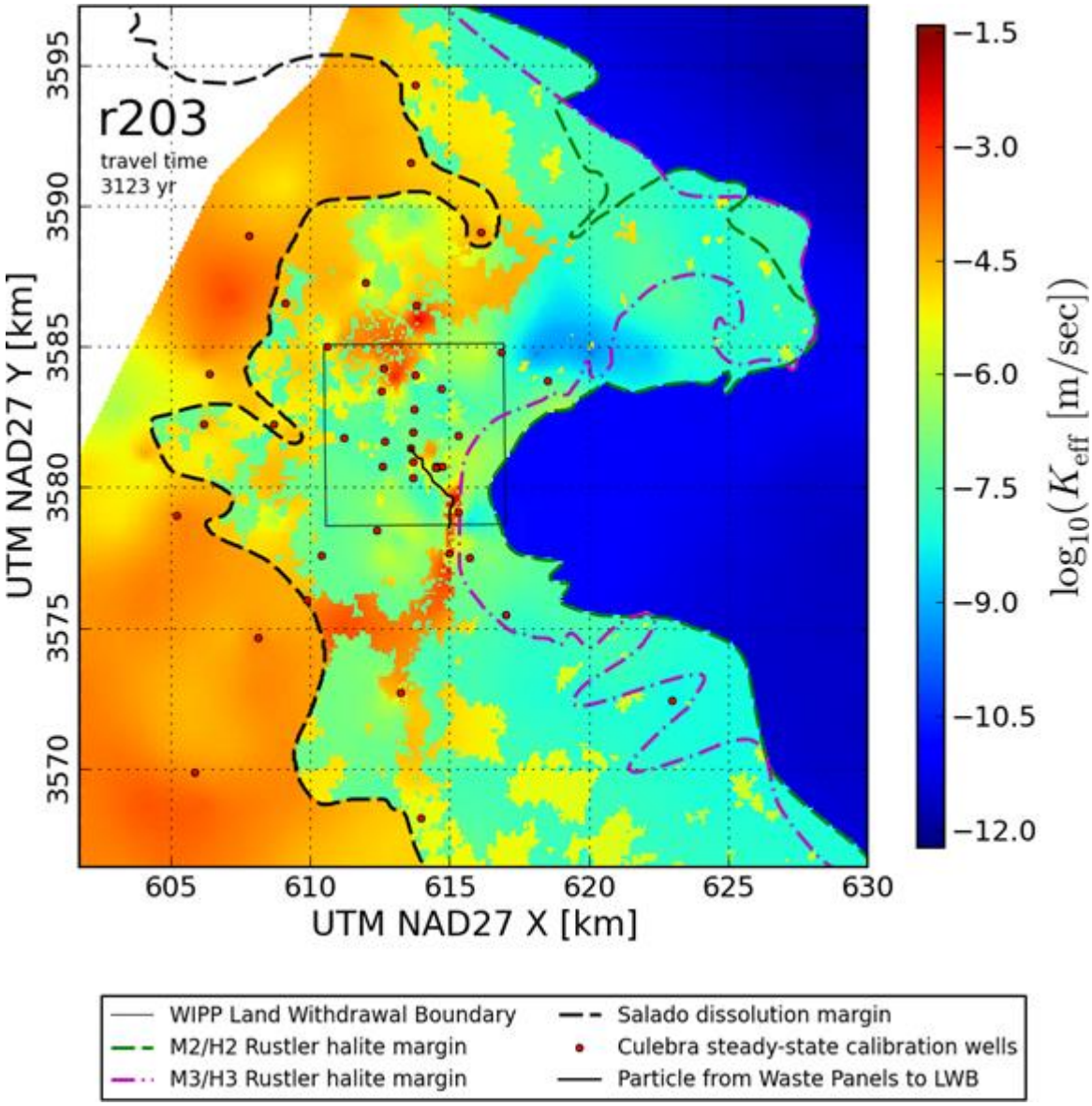
r203
travel time
3123 yr
UTM NAD27 Y [km]
3595
3590
3585
3580
3575
3570
605
610
615
620
625
630
UTM NAD27 X [km]
−1.5
−3.0
−4.5
−6.0
−7.5
−9.0
−10.5
−12.0
$\log_{10}(K_{\mathrm{eff}}\ [\mathrm{m/sec}])$
WIPP Land Withdrawal Boundary
M2/H2 Rustler halite margin
M3/H3 Rustler halite margin
Salado dissolution margin
Culebra steady-state calibration wells
Particle from Waste Panels to LWB

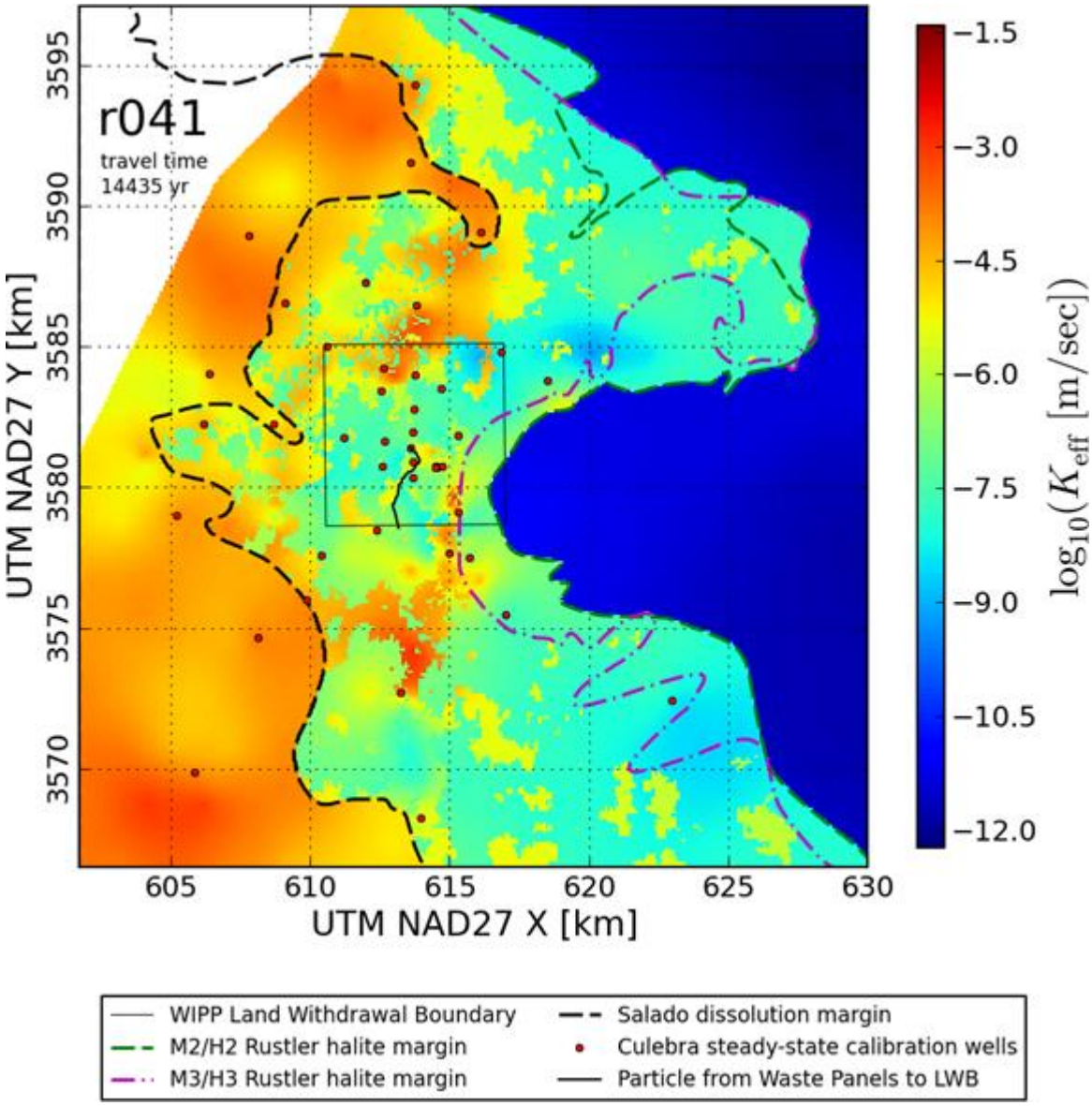
r041
travel time
14435 yr
UTM NAD27 Y [km]
3595
3590
3585
3580
3575
3570
605
610
615
620
625
630
UTM NAD27 X [km]
−1.5
−3.0
−4.5
−6.0
−7.5
−9.0
−10.5
−12.0
$\log_{10}(K_{\text{eff}}$ [m/sec])
WIPP Land Withdrawal Boundary
M2/H2 Rustler halite margin
M3/H3 Rustler halite margin
Salado dissolution margin
Culebra steady-state calibration wells
Particle from Waste Panels to LWB

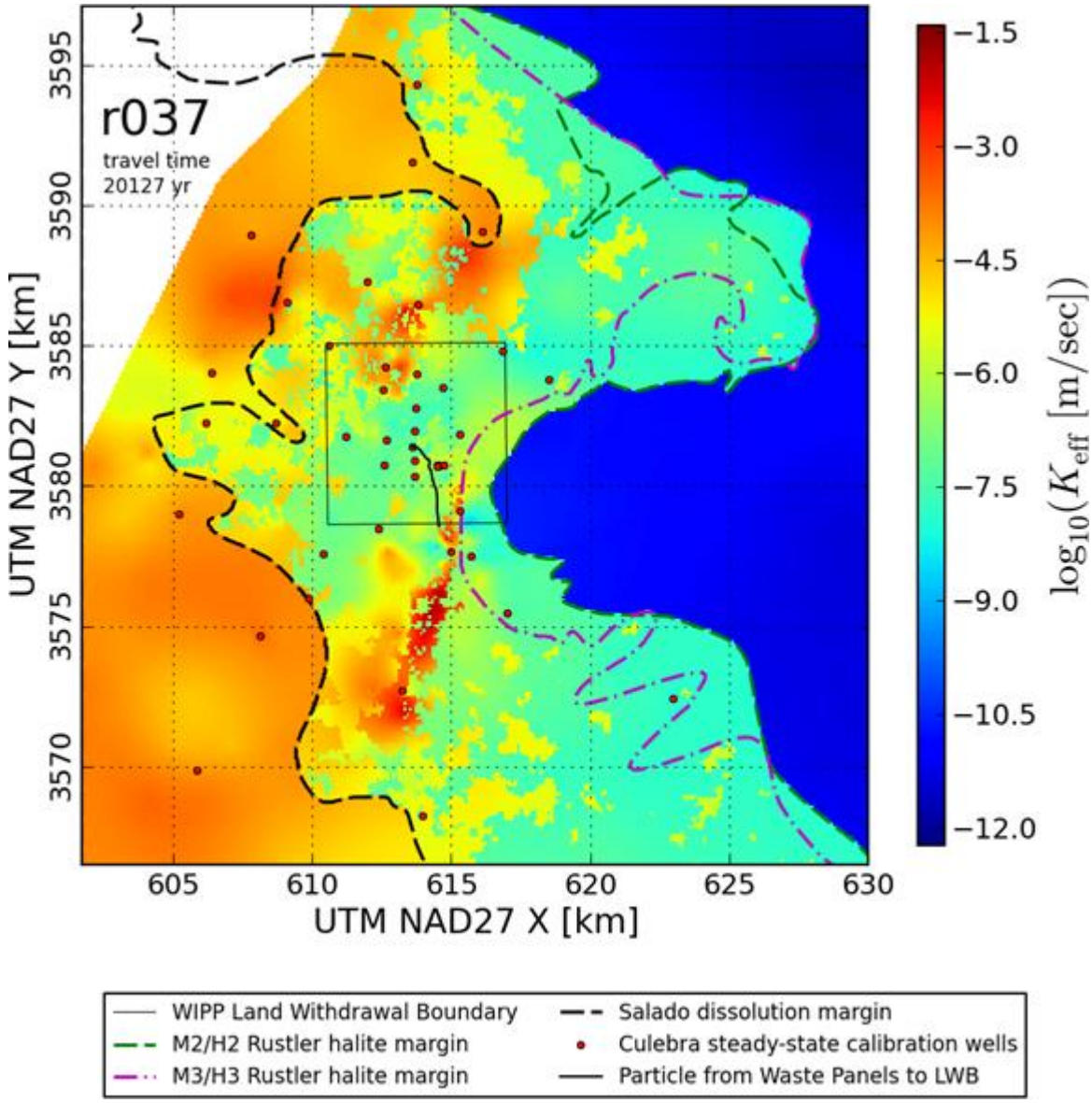
r037
travel time
20127 yr
UTM NAD27 Y [km]
3595
3590
3585
3580
3575
3570
605
610
615
620
625
630
UTM NAD27 X [km]
−1.5
−3.0
−4.5
−6.0
−7.5
−9.0
−10.5
−12.0
$\log_{10}(K_{\mathrm{eff}}\ [\mathrm{m/sec}])$
WIPP Land Withdrawal Boundary
M2/H2 Rustler halite margin
M3/H3 Rustler halite margin
Salado dissolution margin
Culebra steady-state calibration wells
Particle from Waste Panels to LWB

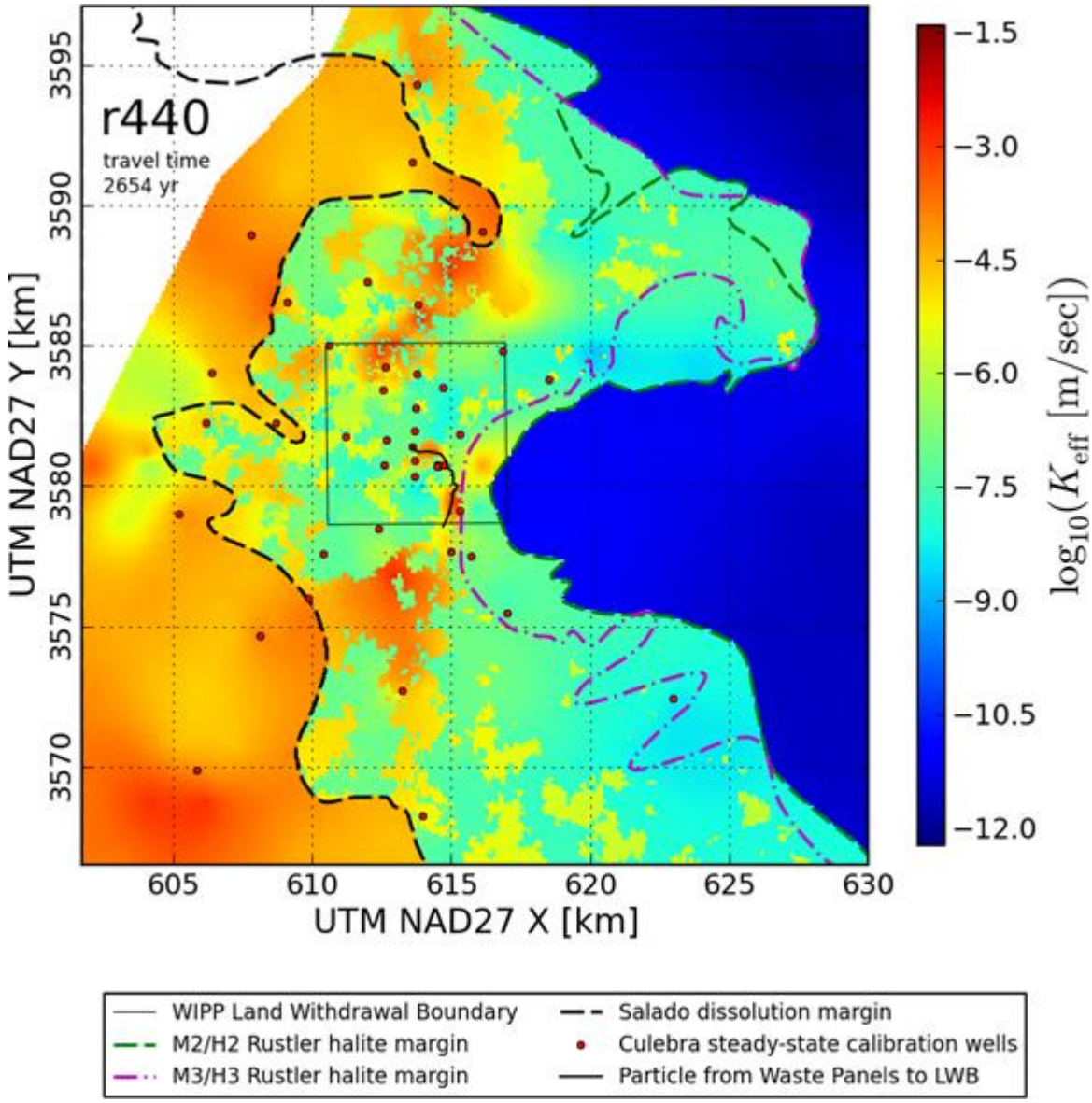
r440
travel time
2654 yr
UTM NAD27 Y [km]
3595
3590
3585
3580
3575
3570
605
610
615
620
625
630
UTM NAD27 X [km]
−1.5
−3.0
−4.5
−6.0
−7.5
−9.0
−10.5
−12.0
$\log_{10}(K_{\mathrm{eff}}\ [\mathrm{m/sec}])$
WIPP Land Withdrawal Boundary
M2/H2 Rustler halite margin
M3/H3 Rustler halite margin
Salado dissolution margin
Culebra steady-state calibration wells
Particle from Waste Panels to LWB

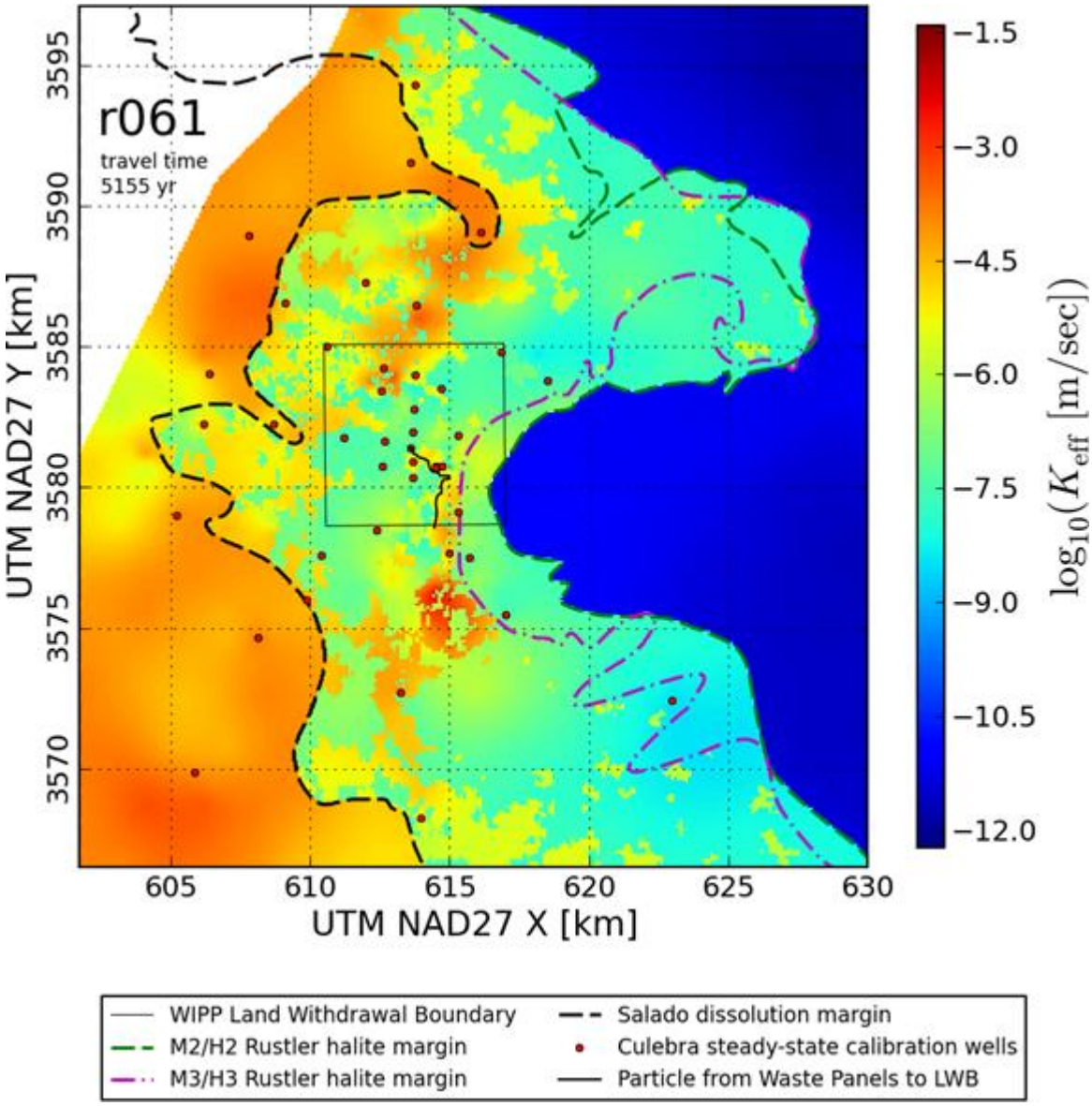
r061
travel time
5155 yr
UTM NAD27 Y [km]
3595
3590
3585
3580
3575
3570
605
610
615
620
625
630
UTM NAD27 X [km]
−1.5
−3.0
−4.5
−6.0
−7.5
−9.0
−10.5
−12.0
$\log_{10}(K_{\mathrm{eff}}\ [\mathrm{m/sec}])$
WIPP Land Withdrawal Boundary
M2/H2 Rustler halite margin
M3/H3 Rustler halite margin
Salado dissolution margin
Culebra steady-state calibration wells
Particle from Waste Panels to LWB

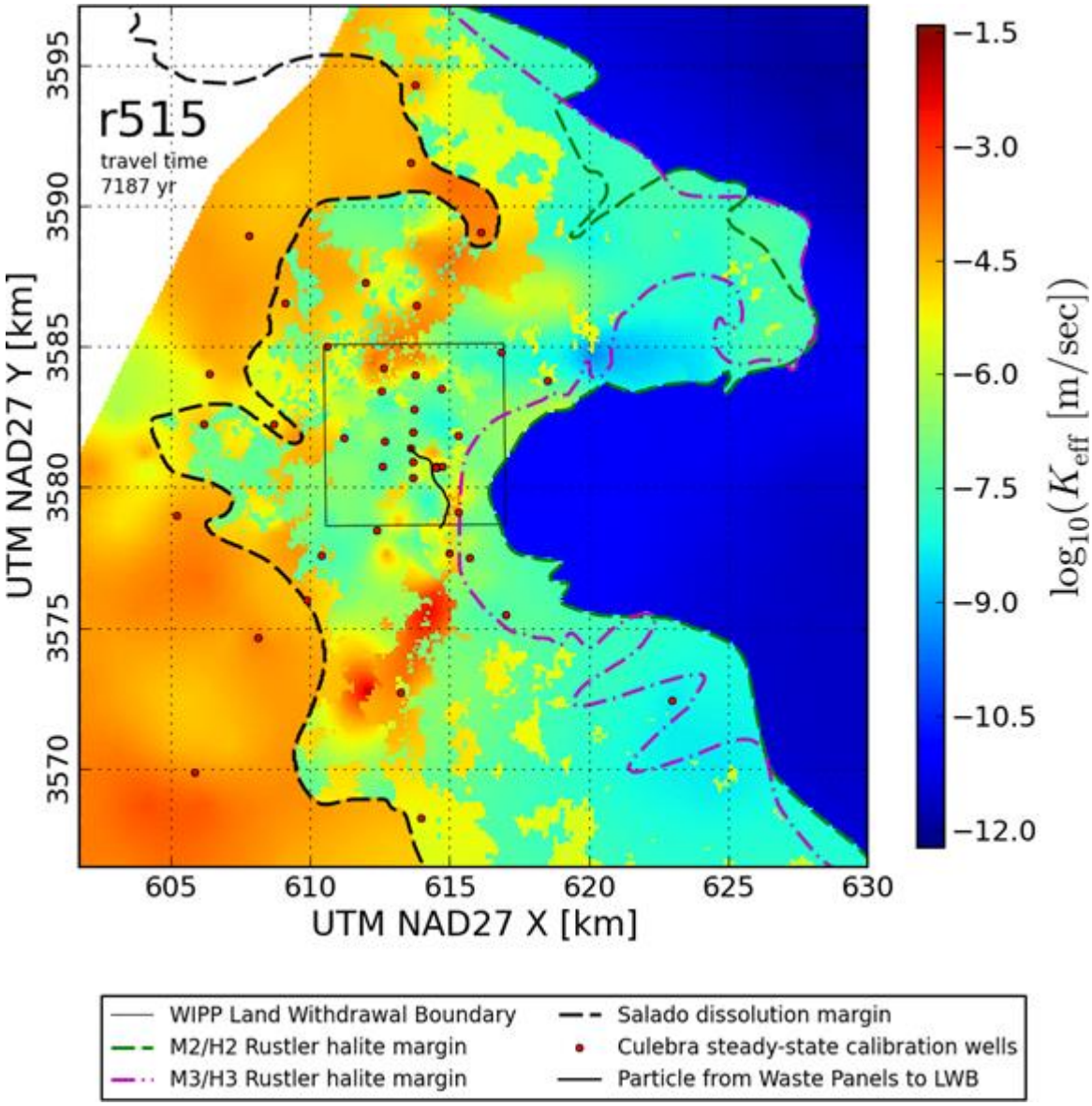
r515
travel time
7187 yr
UTM NAD27 Y [km]
3595
3590
3585
3580
3575
3570
605
610
615
620
625
630
UTM NAD27 X [km]
−1.5
−3.0
−4.5
−6.0
−7.5
−9.0
−10.5
−12.0
$\log_{10}(K_{\mathrm{eff}}\ [\mathrm{m/sec}])$
WIPP Land Withdrawal Boundary
M2/H2 Rustler halite margin
M3/H3 Rustler halite margin
Salado dissolution margin
Culebra steady-state calibration wells
Particle from Waste Panels to LWB

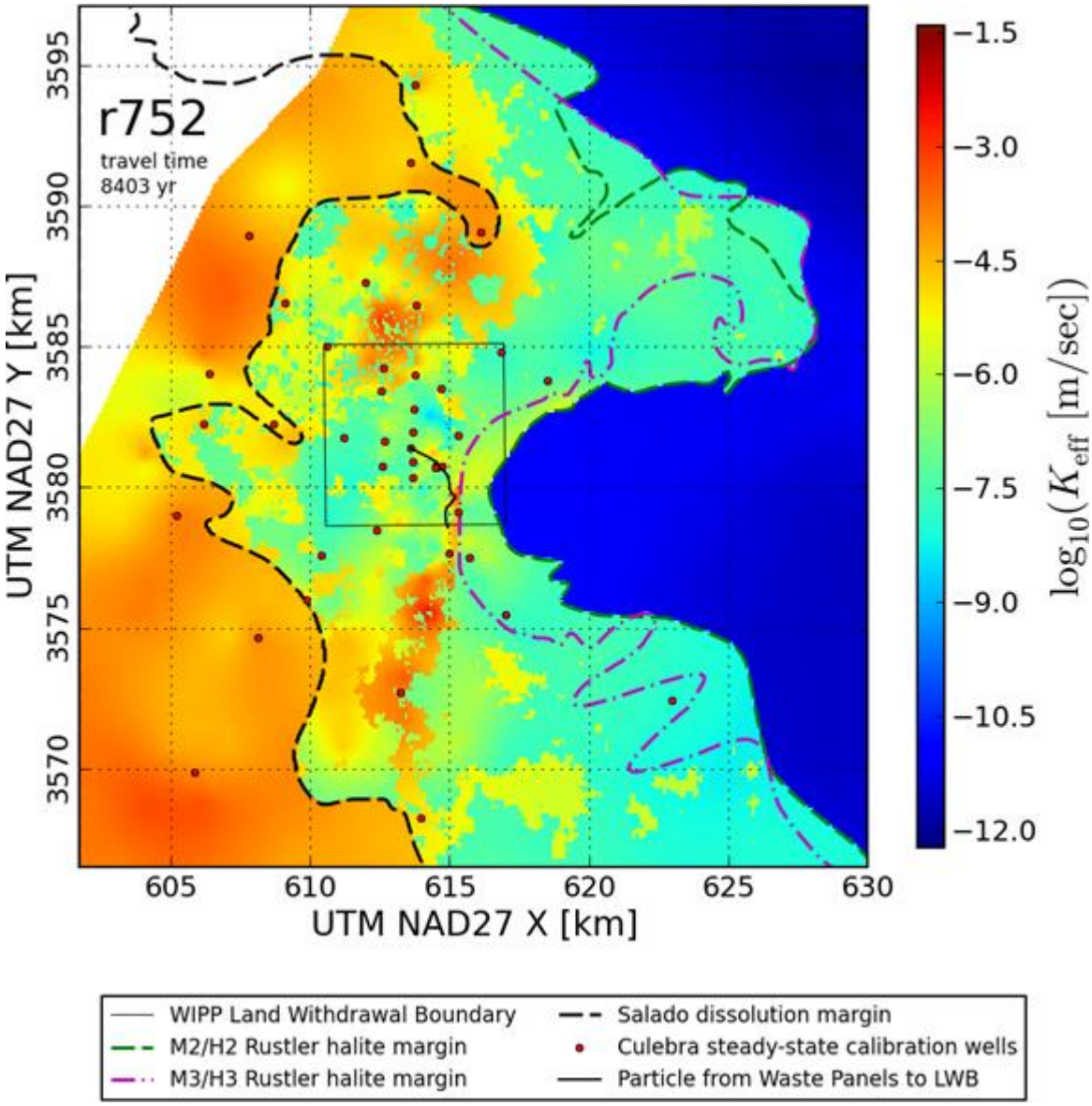
r752
travel time
8403 yr
UTM NAD27 Y [km]
3595
3590
3585
3580
3575
3570
605
610
615
620
625
630
UTM NAD27 X [km]
−1.5
−3.0
−4.5
−6.0
−7.5
−9.0
−10.5
−12.0
$\log_{10}(K_{\mathrm{eff}}\ [\mathrm{m/sec}])$
WIPP Land Withdrawal Boundary
M2/H2 Rustler halite margin
M3/H3 Rustler halite margin
Salado dissolution margin
Culebra steady-state calibration wells
Particle from Waste Panels to LWB

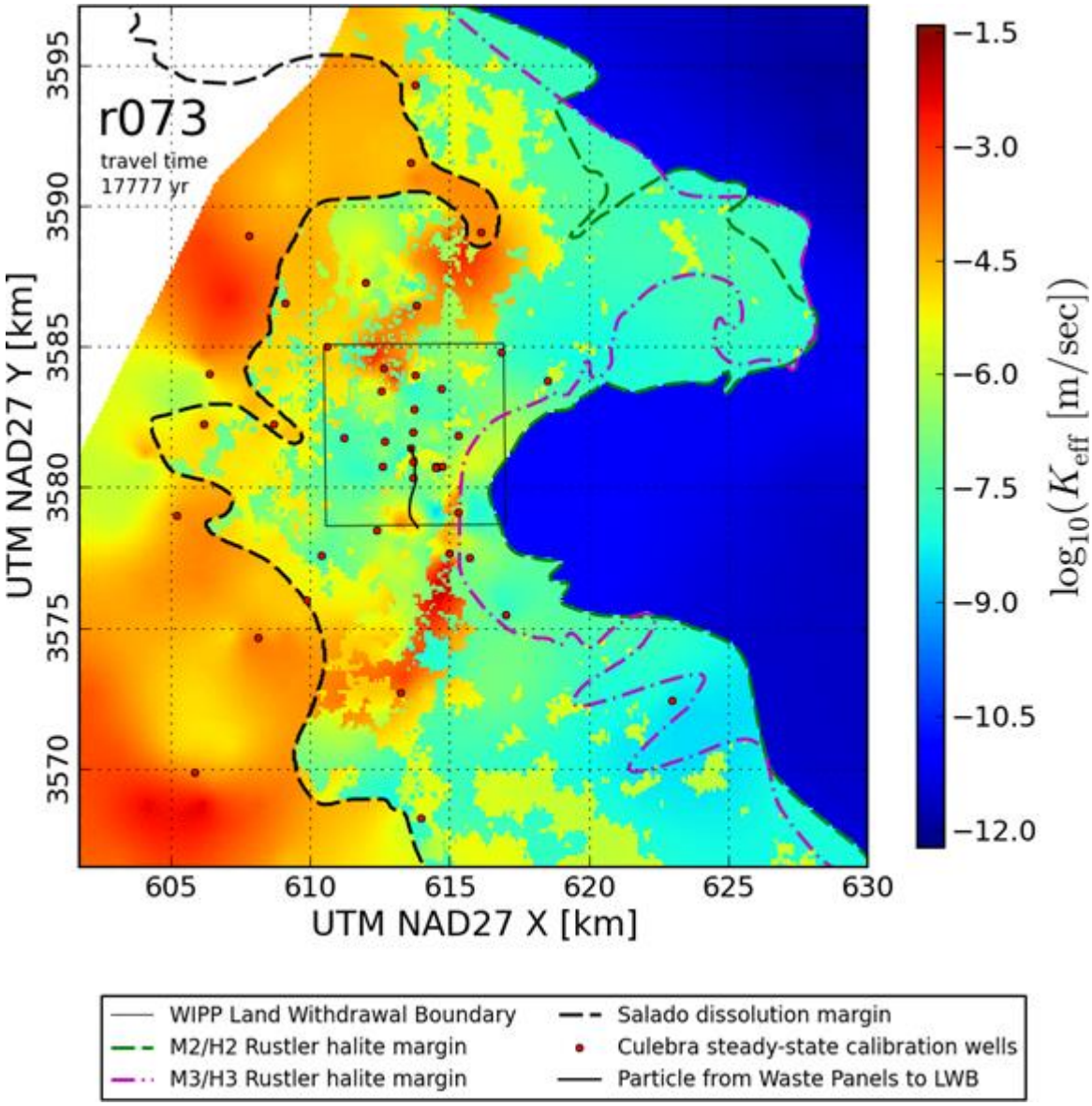
r073
travel time
17777 yr
UTM NAD27 Y [km]
3595
3590
3585
3580
3575
3570
605
610
615
620
625
630
UTM NAD27 X [km]
−1.5
−3.0
−4.5
−6.0
−7.5
−9.0
−10.5
−12.0
$\log_{10}(K_{\mathrm{eff}}\ [\mathrm{m/sec}])$
WIPP Land Withdrawal Boundary
M2/H2 Rustler halite margin
M3/H3 Rustler halite margin
Salado dissolution margin
Culebra steady-state calibration wells
Particle from Waste Panels to LWB

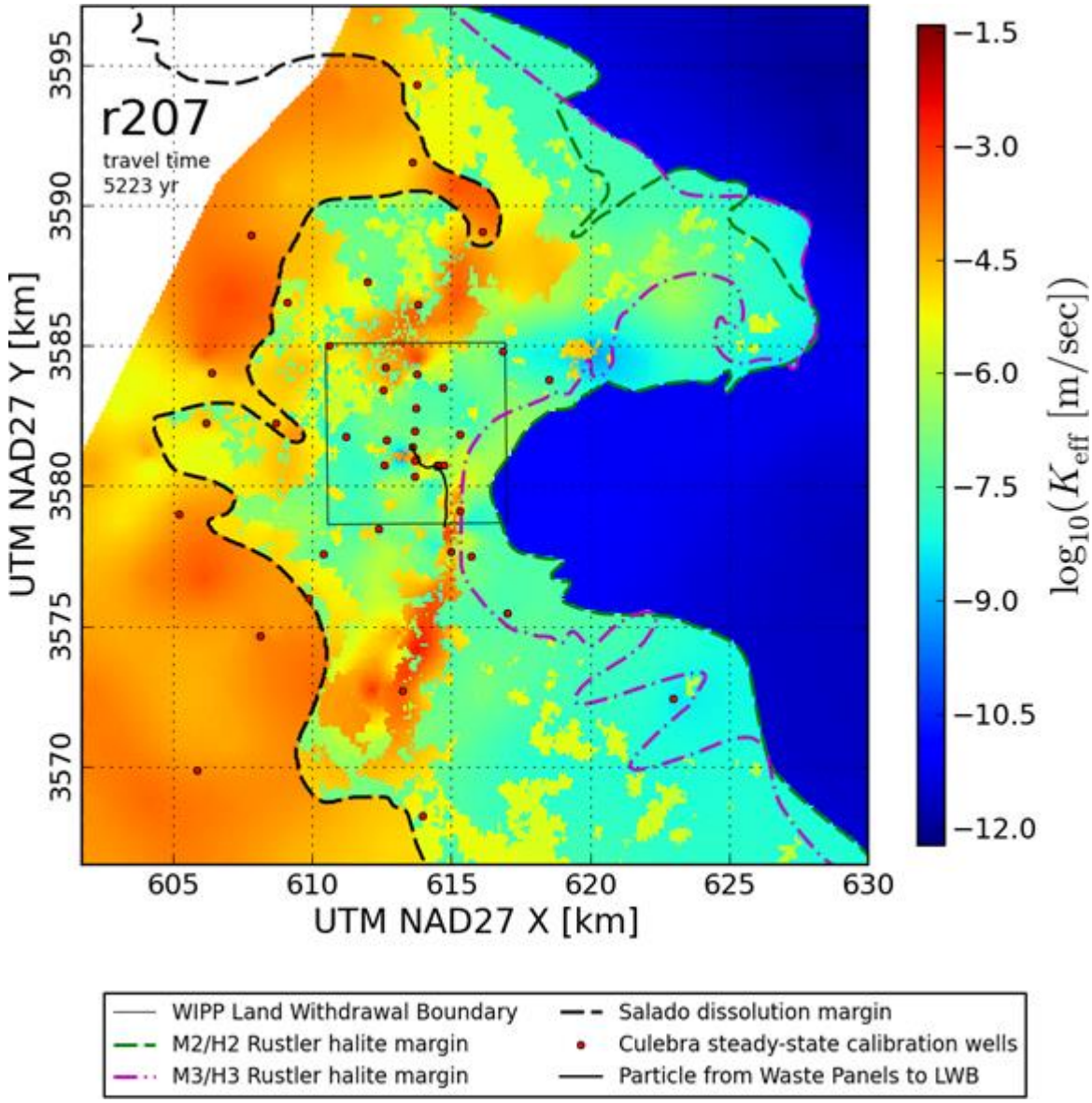
r207
travel time
5223 yr
UTM NAD27 Y [km]
3595
3590
3585
3580
3575
3570
605
610
615
620
625
630
UTM NAD27 X [km]
−1.5
−3.0
−4.5
−6.0
−7.5
−9.0
−10.5
−12.0
$\log_{10}(K_{\text{eff}}$ [m/sec])
WIPP Land Withdrawal Boundary
M2/H2 Rustler halite margin
M3/H3 Rustler halite margin
Salado dissolution margin
Culebra steady-state calibration wells
Particle from Waste Panels to LWB

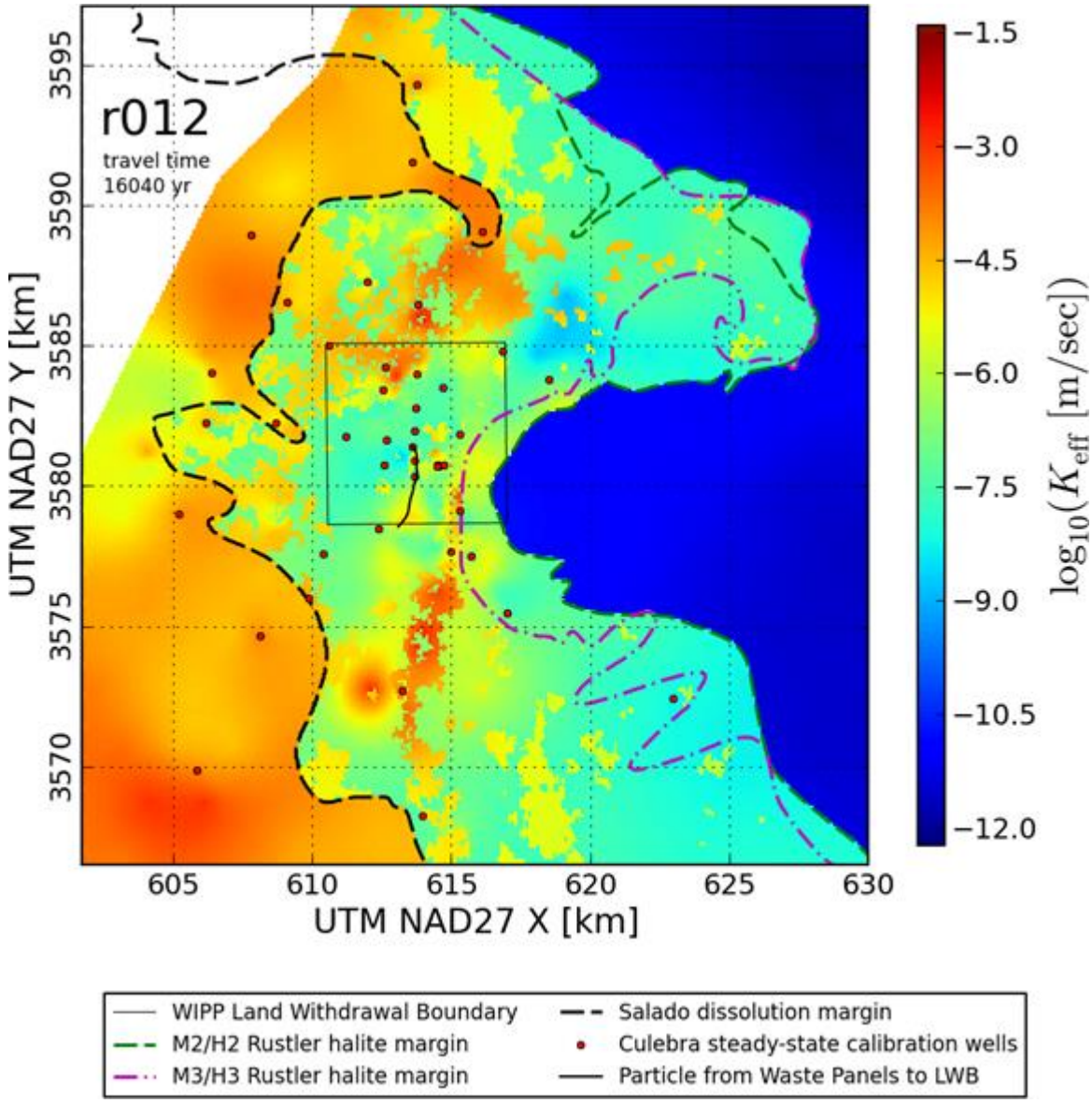
r012
travel time
16040 yr
UTM NAD27 Y [km]
3595
3590
3585
3580
3575
3570
605
610
615
620
625
630
UTM NAD27 X [km]
−1.5
−3.0
−4.5
−6.0
−7.5
−9.0
−10.5
−12.0
$\log_{10}(K_{\text{eff}}$ [m/sec])
WIPP Land Withdrawal Boundary
M2/H2 Rustler halite margin
M3/H3 Rustler halite margin
Salado dissolution margin
Culebra steady-state calibration wells
Particle from Waste Panels to LWB

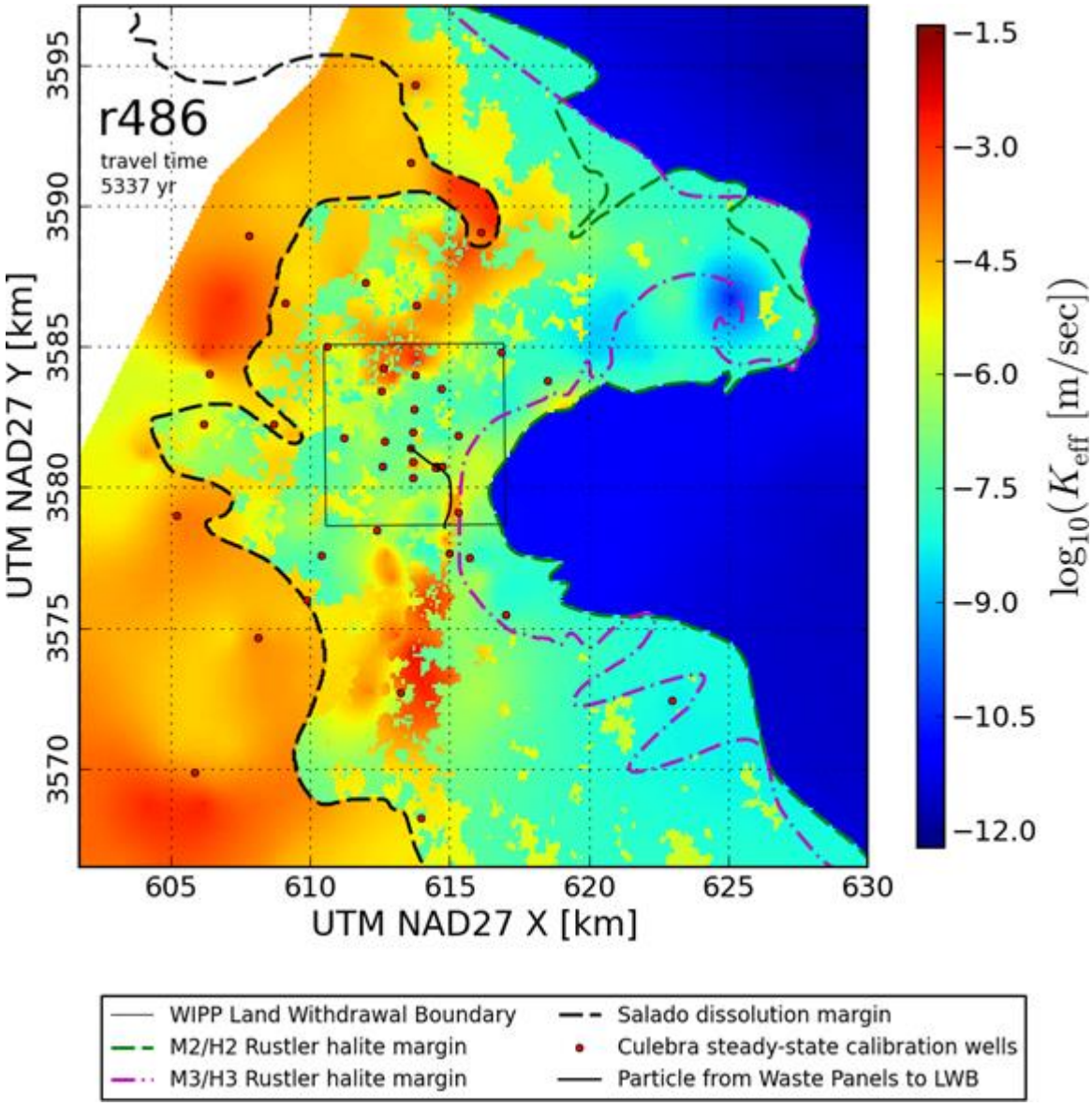
r486
travel time
5337 yr
UTM NAD27 Y [km]
3595
3590
3585
3580
3575
3570
605
610
615
620
625
630
UTM NAD27 X [km]
−1.5
−3.0
−4.5
−6.0
−7.5
−9.0
−10.5
−12.0
$\log_{10}(K_{\mathrm{eff}}\ [\mathrm{m/sec}])$
WIPP Land Withdrawal Boundary
M2/H2 Rustler halite margin
M3/H3 Rustler halite margin
Salado dissolution margin
Culebra steady-state calibration wells
Particle from Waste Panels to LWB

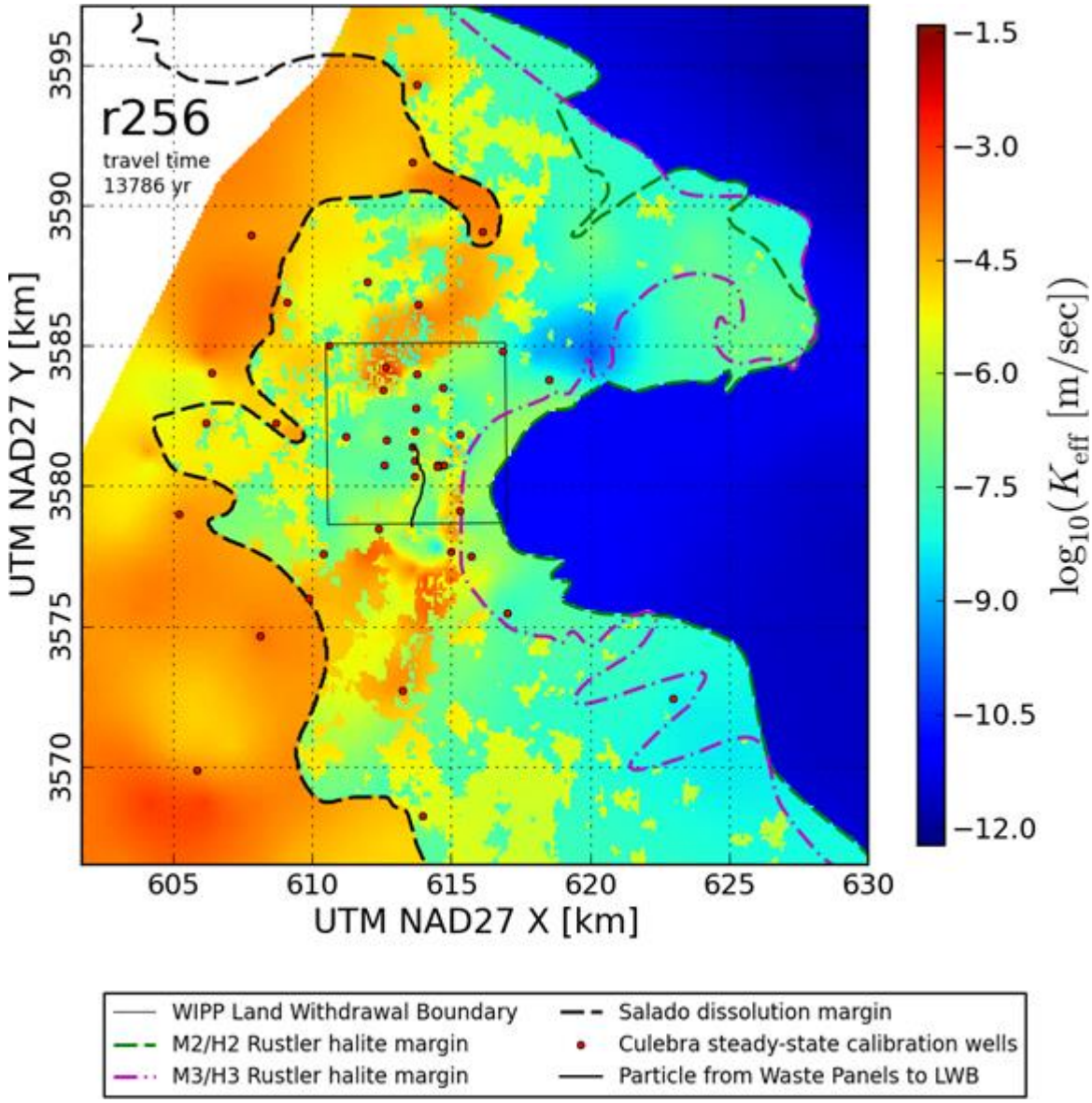
r256
travel time
13786 yr
UTM NAD27 Y [km]
3595
3590
3585
3580
3575
3570
605
610
615
620
625
630
UTM NAD27 X [km]
−1.5
−3.0
−4.5
−6.0
−7.5
−9.0
−10.5
−12.0
$\log_{10}(K_{\mathrm{eff}}\ [\mathrm{m/sec}])$
WIPP Land Withdrawal Boundary
M2/H2 Rustler halite margin
M3/H3 Rustler halite margin
Salado dissolution margin
Culebra steady-state calibration wells
Particle from Waste Panels to LWB

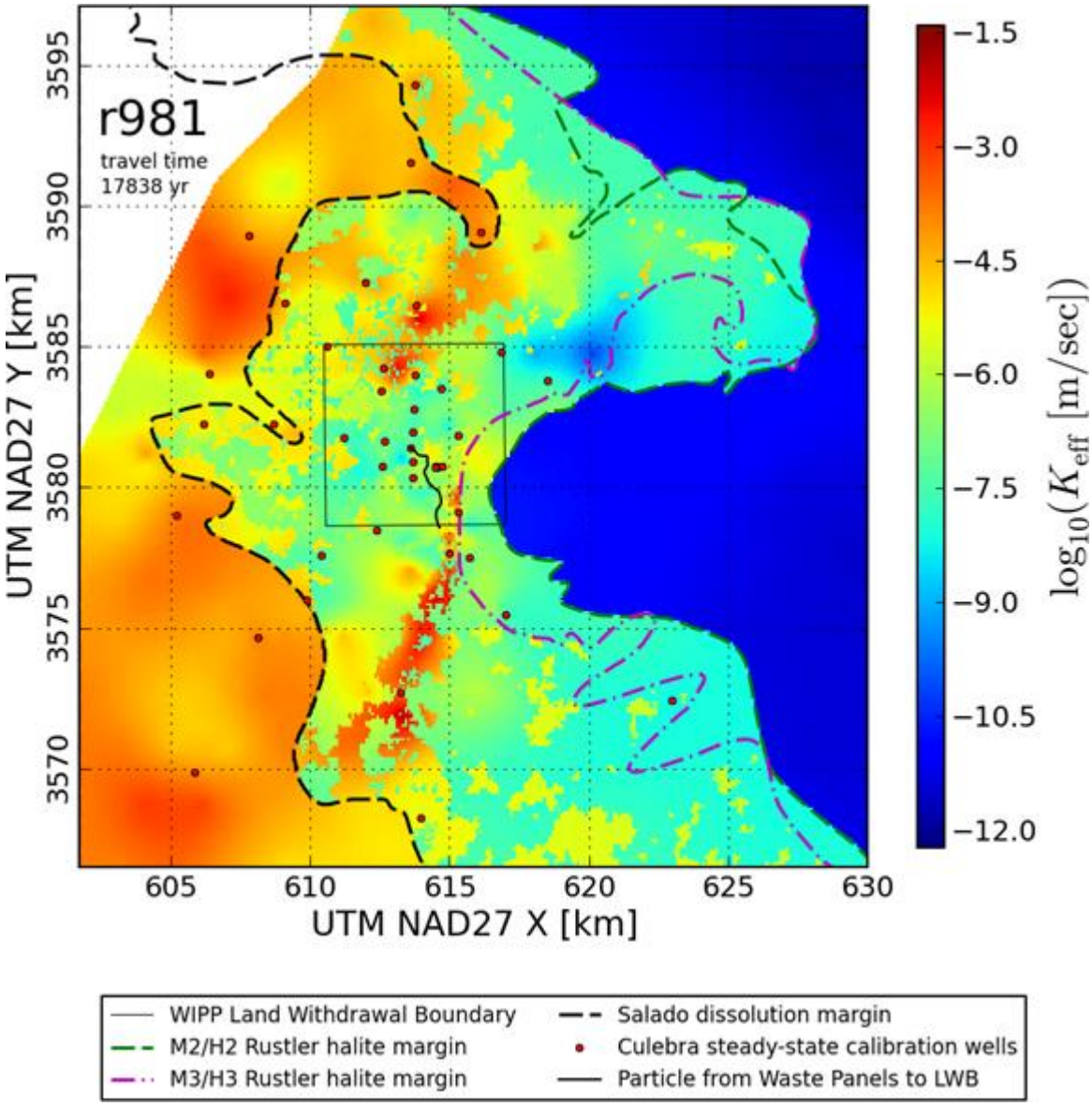
r981
travel time
17838 yr
UTM NAD27 Y [km]
3595
3590
3585
3580
3575
3570
605
610
615
620
625
630
UTM NAD27 X [km]
−1.5
−3.0
−4.5
−6.0
−7.5
−9.0
−10.5
−12.0
$\log_{10}(K_{\mathrm{eff}}\ [\mathrm{m/sec}])$
WIPP Land Withdrawal Boundary
M2/H2 Rustler halite margin
M3/H3 Rustler halite margin
Salado dissolution margin
Culebra steady-state calibration wells
Particle from Waste Panels to LWB

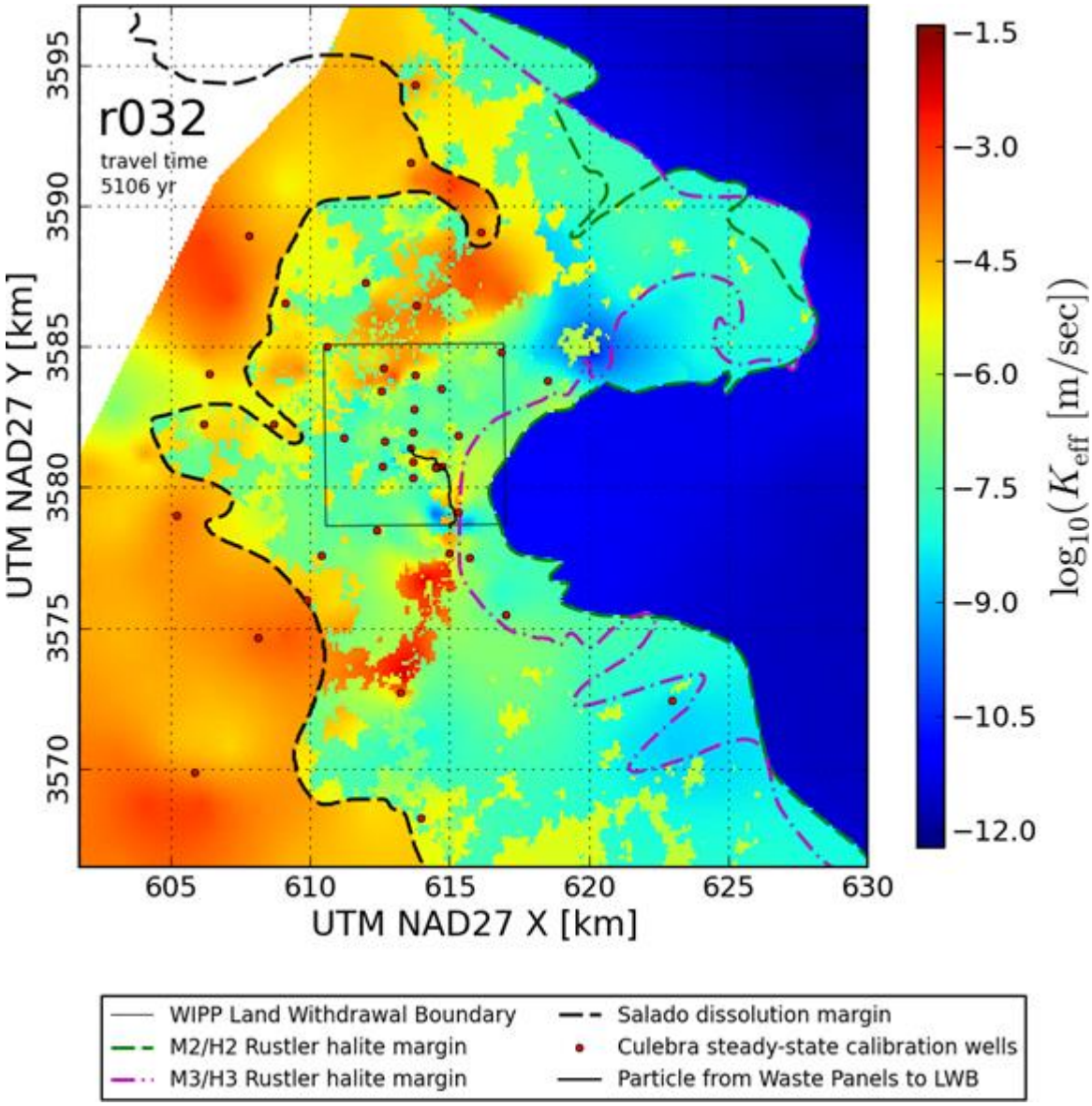
r032
travel time
5106 yr
UTM NAD27 Y [km]
3595
3590
3585
3580
3575
3570
605
610
615
620
625
630
UTM NAD27 X [km]
−1.5
−3.0
−4.5
−6.0
−7.5
−9.0
−10.5
−12.0
$\log_{10}(K_{\text{eff}}$ [m/sec])
WIPP Land Withdrawal Boundary
M2/H2 Rustler halite margin
M3/H3 Rustler halite margin
Salado dissolution margin
Culebra steady-state calibration wells
Particle from Waste Panels to LWB

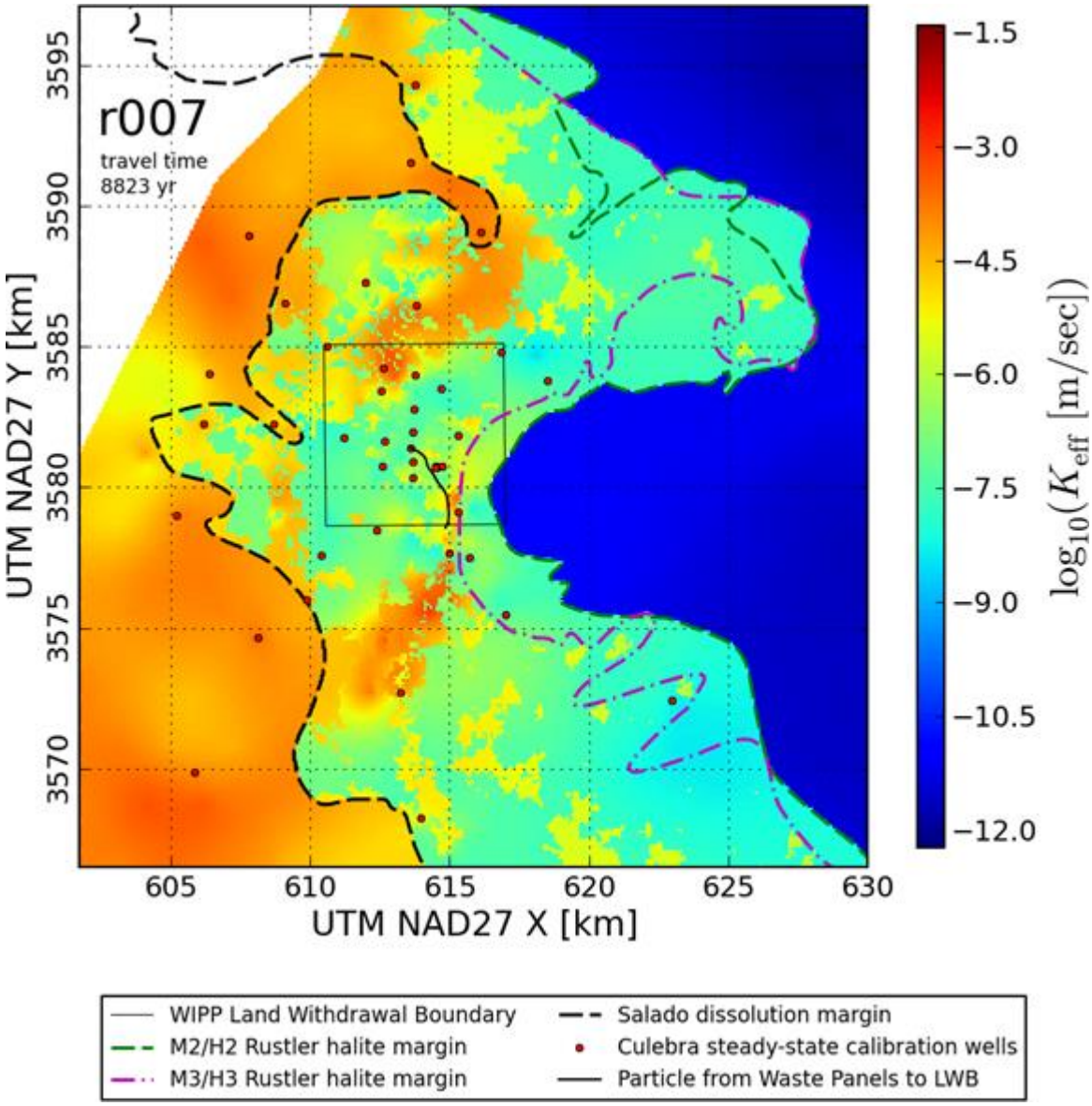
r007
travel time
8823 yr
UTM NAD27 Y [km]
3595
3590
3585
3580
3575
3570
605
610
615
620
625
630
UTM NAD27 X [km]
−1.5
−3.0
−4.5
−6.0
−7.5
−9.0
−10.5
−12.0
$\log_{10}(K_{\mathrm{eff}}\ [\mathrm{m/sec}])$
WIPP Land Withdrawal Boundary
M2/H2 Rustler halite margin
M3/H3 Rustler halite margin
Salado dissolution margin
Culebra steady-state calibration wells
Particle from Waste Panels to LWB

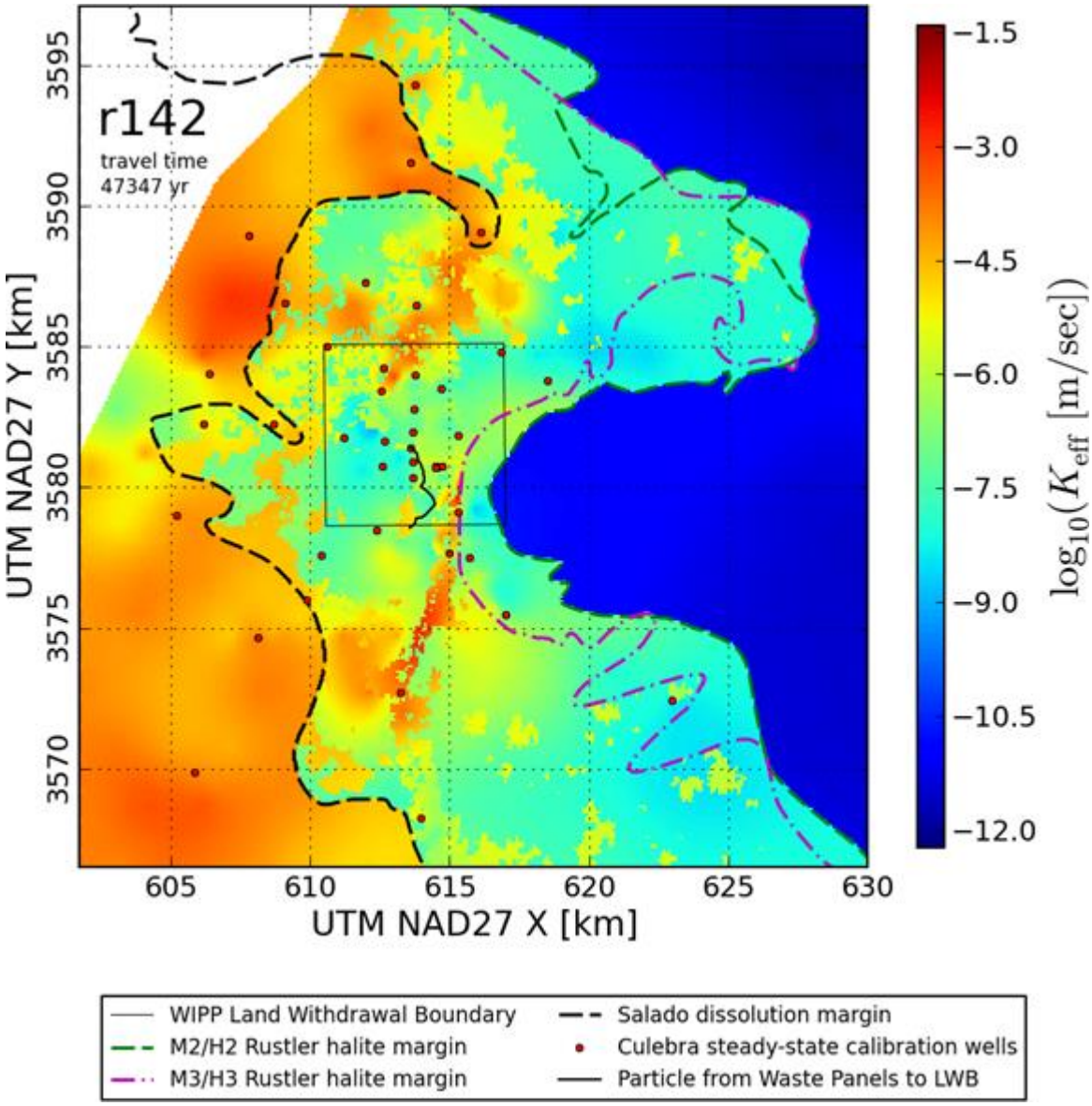
r142
travel time
47347 yr
UTM NAD27 Y [km]
3595
3590
3585
3580
3575
3570
605
610
615
620
625
630
UTM NAD27 X [km]
−1.5
−3.0
−4.5
−6.0
−7.5
−9.0
−10.5
−12.0
$\log_{10}(K_{\text{eff}}$ [m/sec])
WIPP Land Withdrawal Boundary
M2/H2 Rustler halite margin
M3/H3 Rustler halite margin
Salado dissolution margin
Culebra steady-state calibration wells
Particle from Waste Panels to LWB

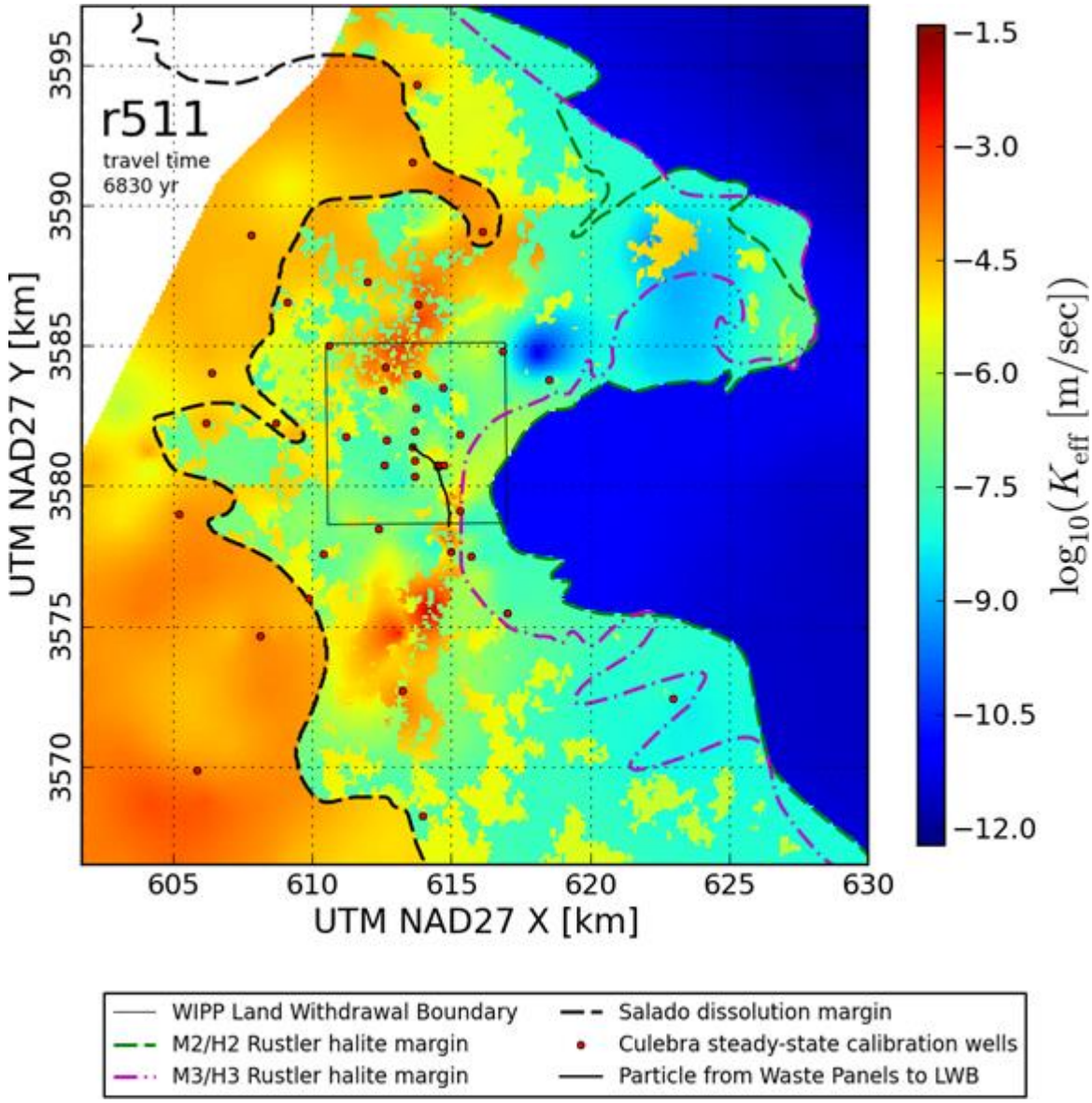
r511
travel time
6830 yr
UTM NAD27 Y [km]
3595
3590
3585
3580
3575
3570
605
610
615
620
625
630
UTM NAD27 X [km]
−1.5
−3.0
−4.5
−6.0
−7.5
−9.0
−10.5
−12.0
$\log_{10}(K_{\text{eff}}$ [m/sec])
WIPP Land Withdrawal Boundary
M2/H2 Rustler halite margin
M3/H3 Rustler halite margin
Salado dissolution margin
Culebra steady-state calibration wells
Particle from Waste Panels to LWB

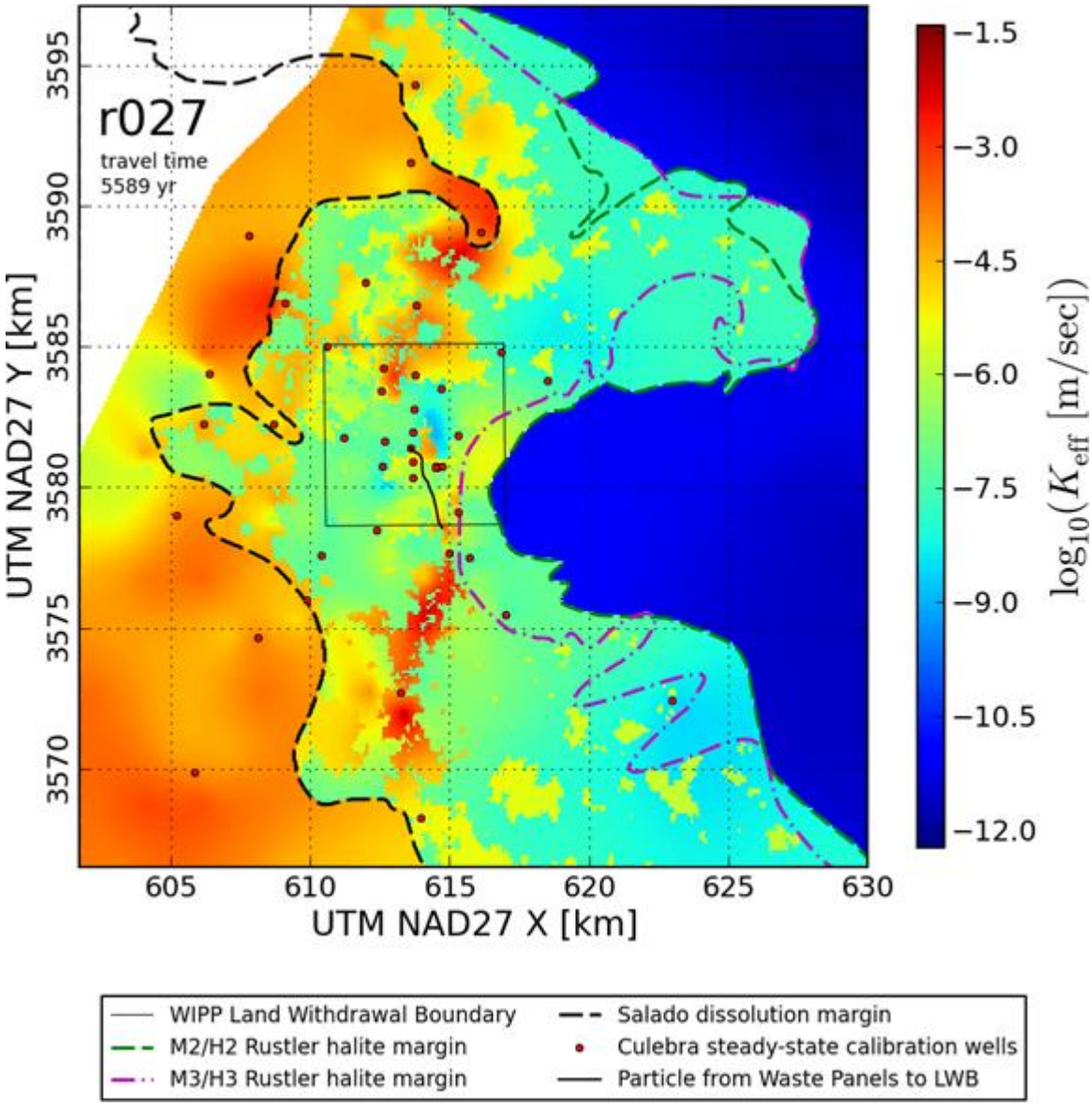
r027
travel time
5589 yr
UTM NAD27 Y [km]
3595
3590
3585
3580
3575
3570
605
610
615
620
625
630
UTM NAD27 X [km]
−1.5
−3.0
−4.5
−6.0
−7.5
−9.0
−10.5
−12.0
$\log_{10}(K_{\mathrm{eff}}\ [\mathrm{m/sec}])$
WIPP Land Withdrawal Boundary
M2/H2 Rustler halite margin
M3/H3 Rustler halite margin
Salado dissolution margin
Culebra steady-state calibration wells
Particle from Waste Panels to LWB

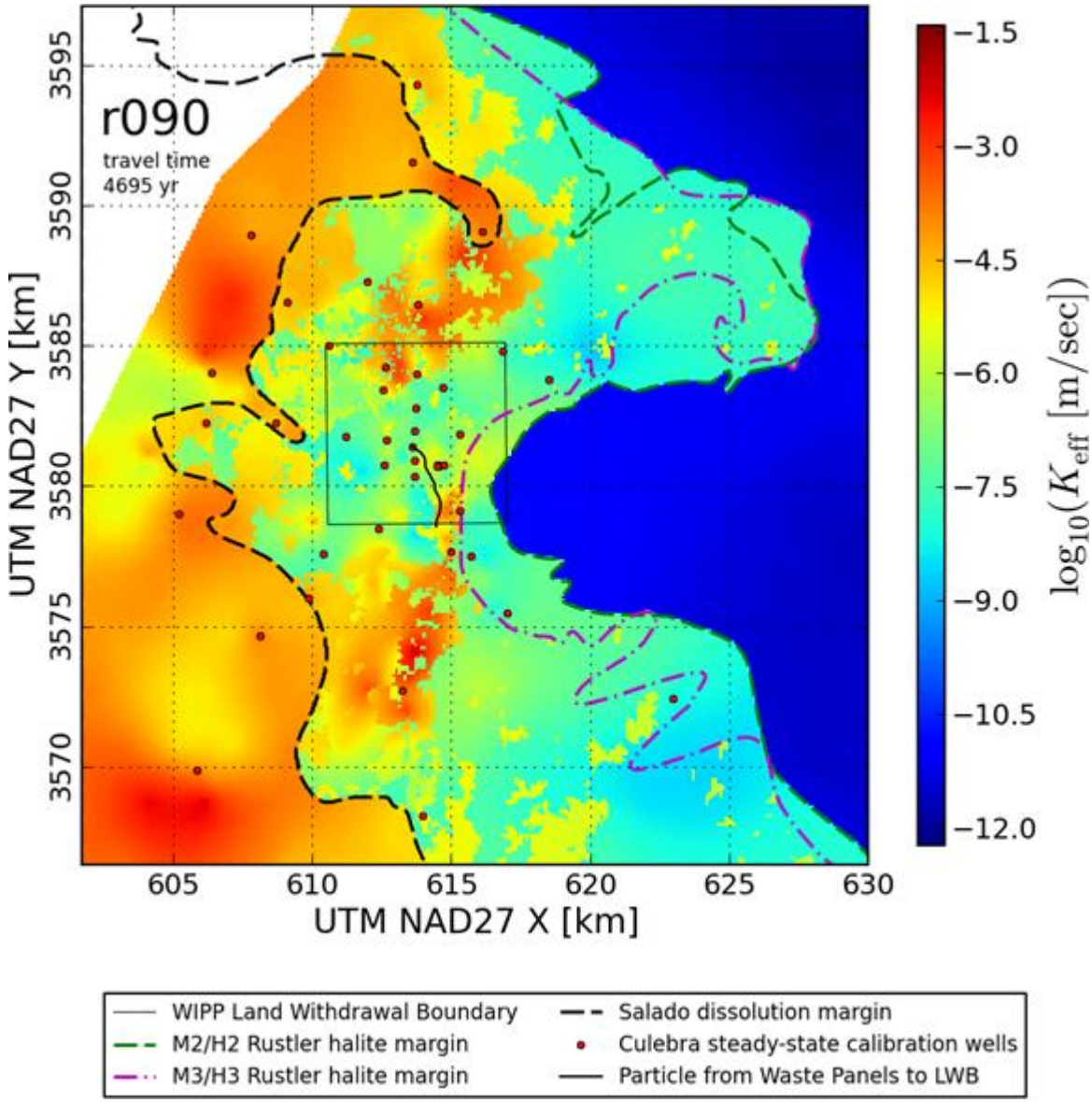
r090
travel time
4695 yr
UTM NAD27 Y [km]
3595
3590
3585
3580
3575
3570
605
610
615
620
625
630
UTM NAD27 X [km]
−1.5
−3.0
−4.5
−6.0
−7.5
−9.0
−10.5
−12.0
$\log_{10}(K_{\mathrm{eff}}\ [\mathrm{m/sec}])$
WIPP Land Withdrawal Boundary
M2/H2 Rustler halite margin
M3/H3 Rustler halite margin
Salado dissolution margin
Culebra steady-state calibration wells
Particle from Waste Panels to LWB

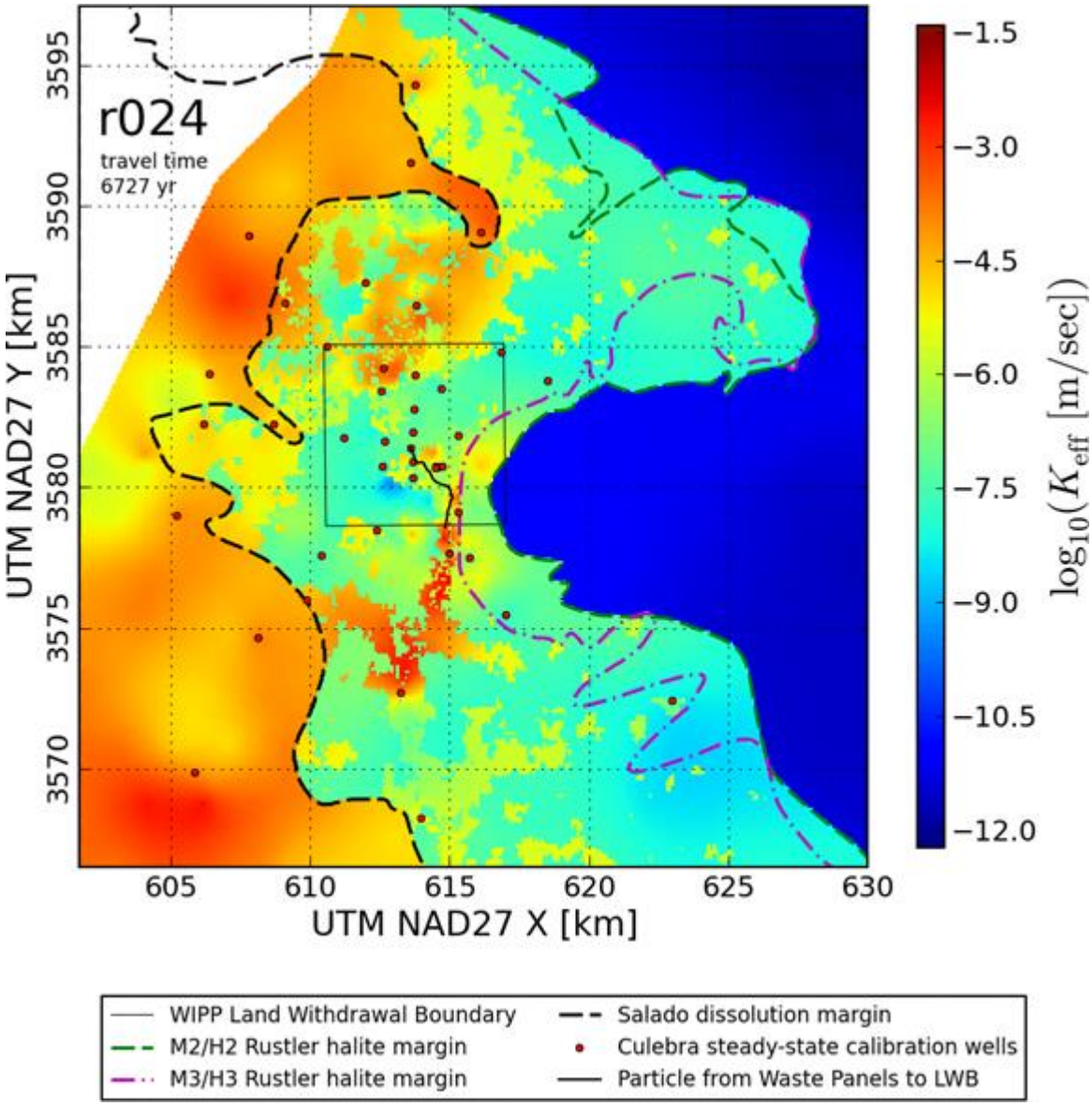
r024
travel time
6727 yr
UTM NAD27 Y [km]
3595
3590
3585
3580
3575
3570
605
610
615
620
625
630
UTM NAD27 X [km]
−1.5
−3.0
−4.5
−6.0
−7.5
−9.0
−10.5
−12.0
$\log_{10}(K_{\mathrm{eff}}$ [m/sec])
WIPP Land Withdrawal Boundary
M2/H2 Rustler halite margin
M3/H3 Rustler halite margin
Salado dissolution margin
Culebra steady-state calibration wells
Particle from Waste Panels to LWB

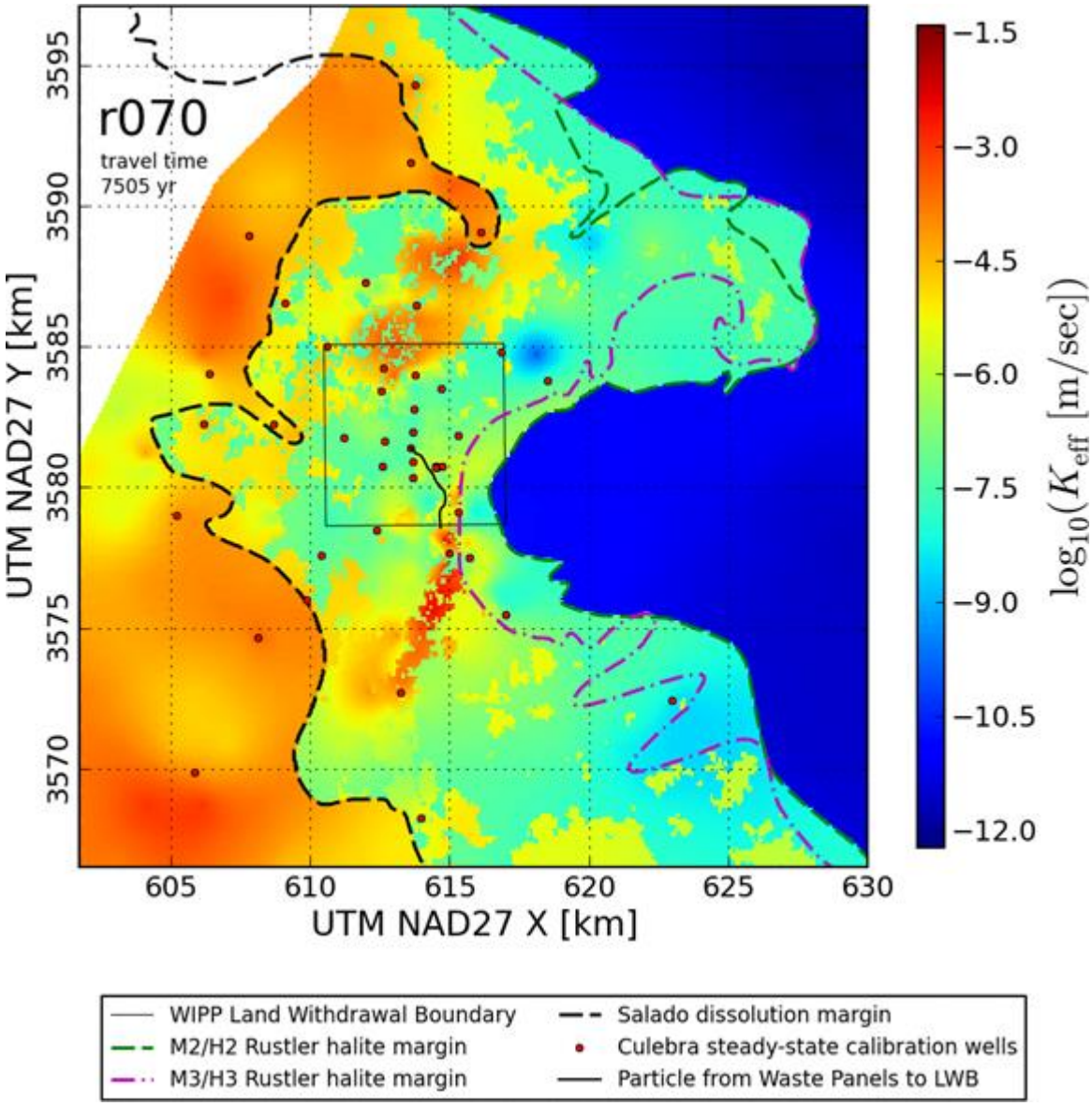
r070
travel time
7505 yr
UTM NAD27 Y [km]
3595
3590
3585
3580
3575
3570
605
610
615
620
625
630
UTM NAD27 X [km]
−1.5
−3.0
−4.5
−6.0
−7.5
−9.0
−10.5
−12.0
$\log_{10}(K_{\mathrm{eff}}\ [\mathrm{m/sec}])$
WIPP Land Withdrawal Boundary
M2/H2 Rustler halite margin
M3/H3 Rustler halite margin
Salado dissolution margin
Culebra steady-state calibration wells
Particle from Waste Panels to LWB

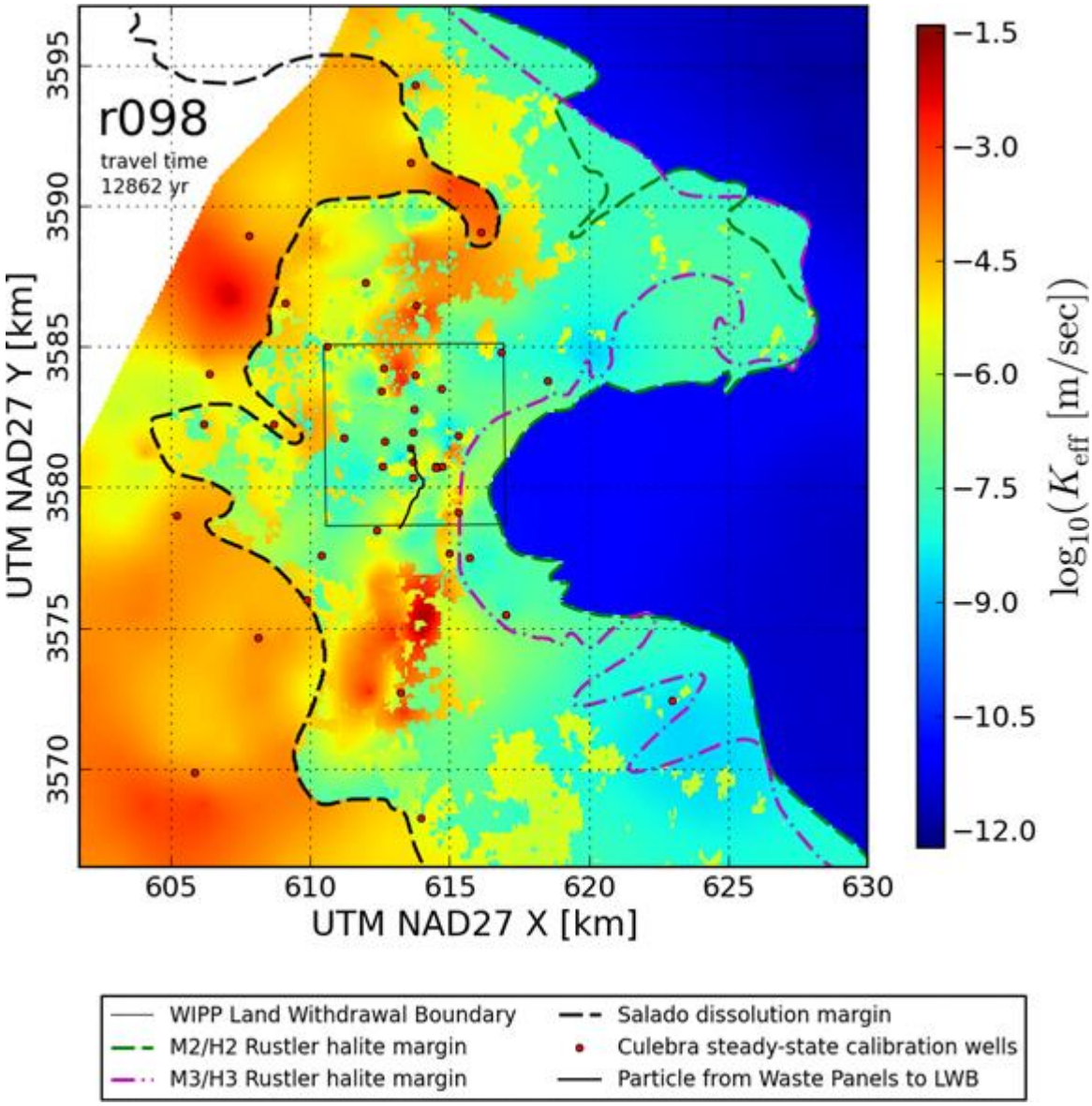
r098
travel time
12862 yr
UTM NAD27 Y [km]
3595
3590
3585
3580
3575
3570
605
610
615
620
625
630
UTM NAD27 X [km]
−1.5
−3.0
−4.5
−6.0
−7.5
−9.0
−10.5
−12.0
$\log_{10}(K_{\mathrm{eff}}\ [\mathrm{m/sec}])$
WIPP Land Withdrawal Boundary
M2/H2 Rustler halite margin
M3/H3 Rustler halite margin
Salado dissolution margin
Culebra steady-state calibration wells
Particle from Waste Panels to LWB

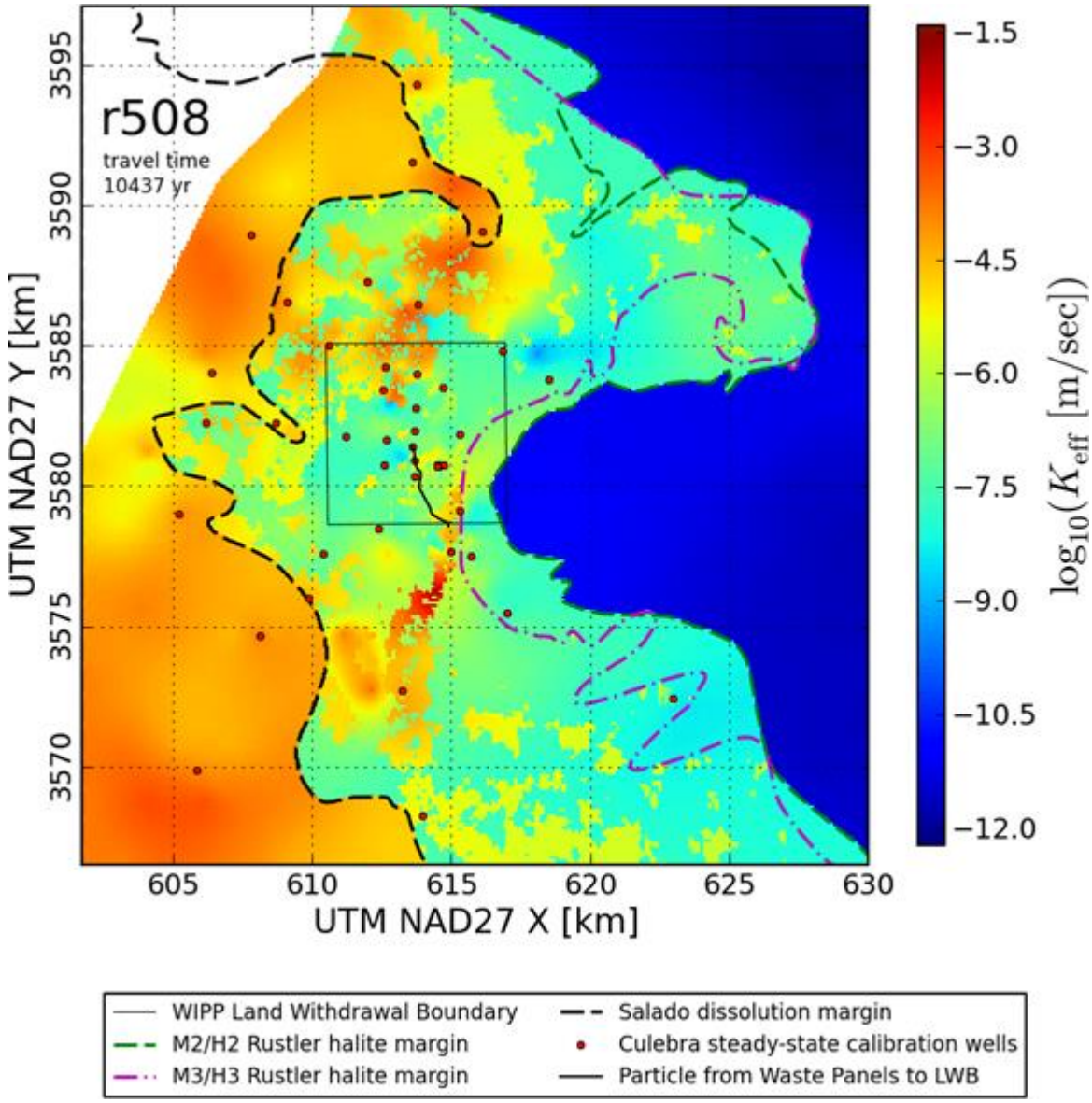
r508
travel time
10437 yr
UTM NAD27 Y [km]
3595
3590
3585
3580
3575
3570
605
610
615
620
625
630
UTM NAD27 X [km]
−1.5
−3.0
−4.5
−6.0
−7.5
−9.0
−10.5
−12.0
$\log_{10}(K_{\mathrm{eff}}\ [\mathrm{m/sec}])$
WIPP Land Withdrawal Boundary
M2/H2 Rustler halite margin
M3/H3 Rustler halite margin
Salado dissolution margin
Culebra steady-state calibration wells
Particle from Waste Panels to LWB

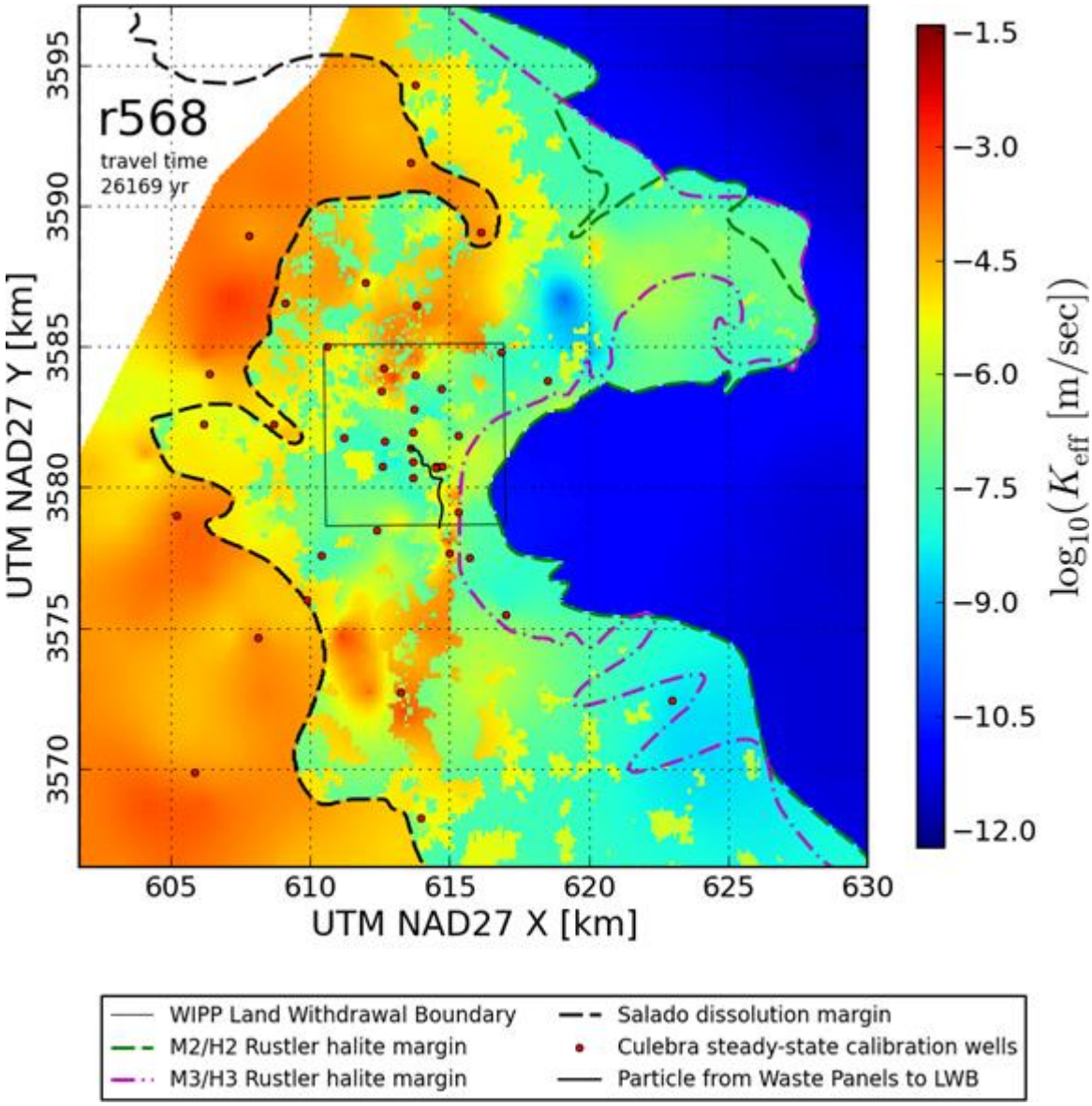
r568
travel time
26169 yr
UTM NAD27 Y [km]
3595
3590
3585
3580
3575
3570
605
610
615
620
625
630
UTM NAD27 X [km]
−1.5
−3.0
−4.5
−6.0
−7.5
−9.0
−10.5
−12.0
$\log_{10}(K_{\mathrm{eff}}\ [\mathrm{m/sec}])$
WIPP Land Withdrawal Boundary
M2/H2 Rustler halite margin
M3/H3 Rustler halite margin
Salado dissolution margin
Culebra steady-state calibration wells
Particle from Waste Panels to LWB

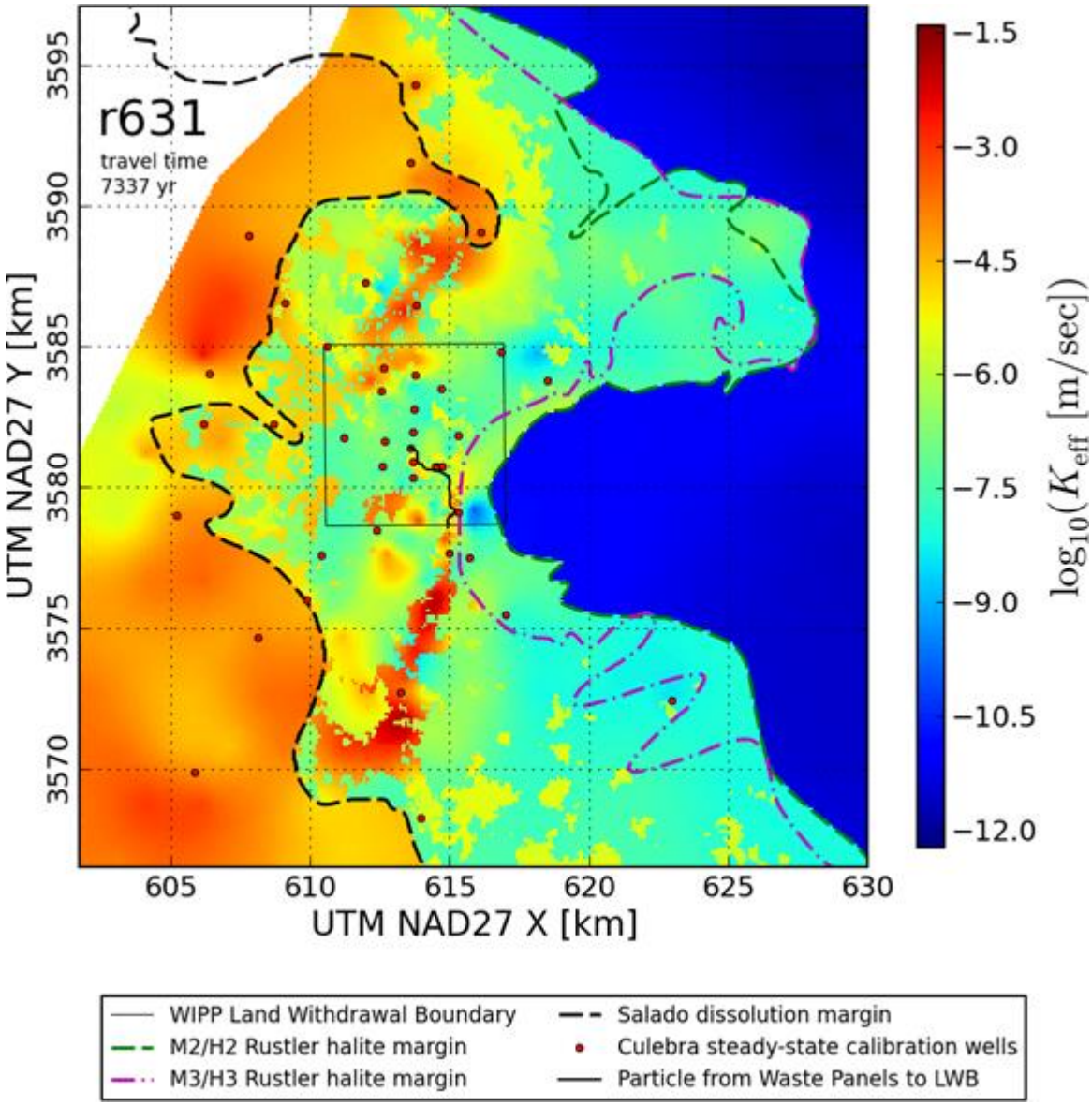
r631
travel time
7337 yr
UTM NAD27 Y [km]
3595
3590
3585
3580
3575
3570
605
610
615
620
625
630
UTM NAD27 X [km]
−1.5
−3.0
−4.5
−6.0
−7.5
−9.0
−10.5
−12.0
$\log_{10}(K_{\mathrm{eff}}\ [\mathrm{m/sec}])$
WIPP Land Withdrawal Boundary
M2/H2 Rustler halite margin
M3/H3 Rustler halite margin
Salado dissolution margin
Culebra steady-state calibration wells
Particle from Waste Panels to LWB

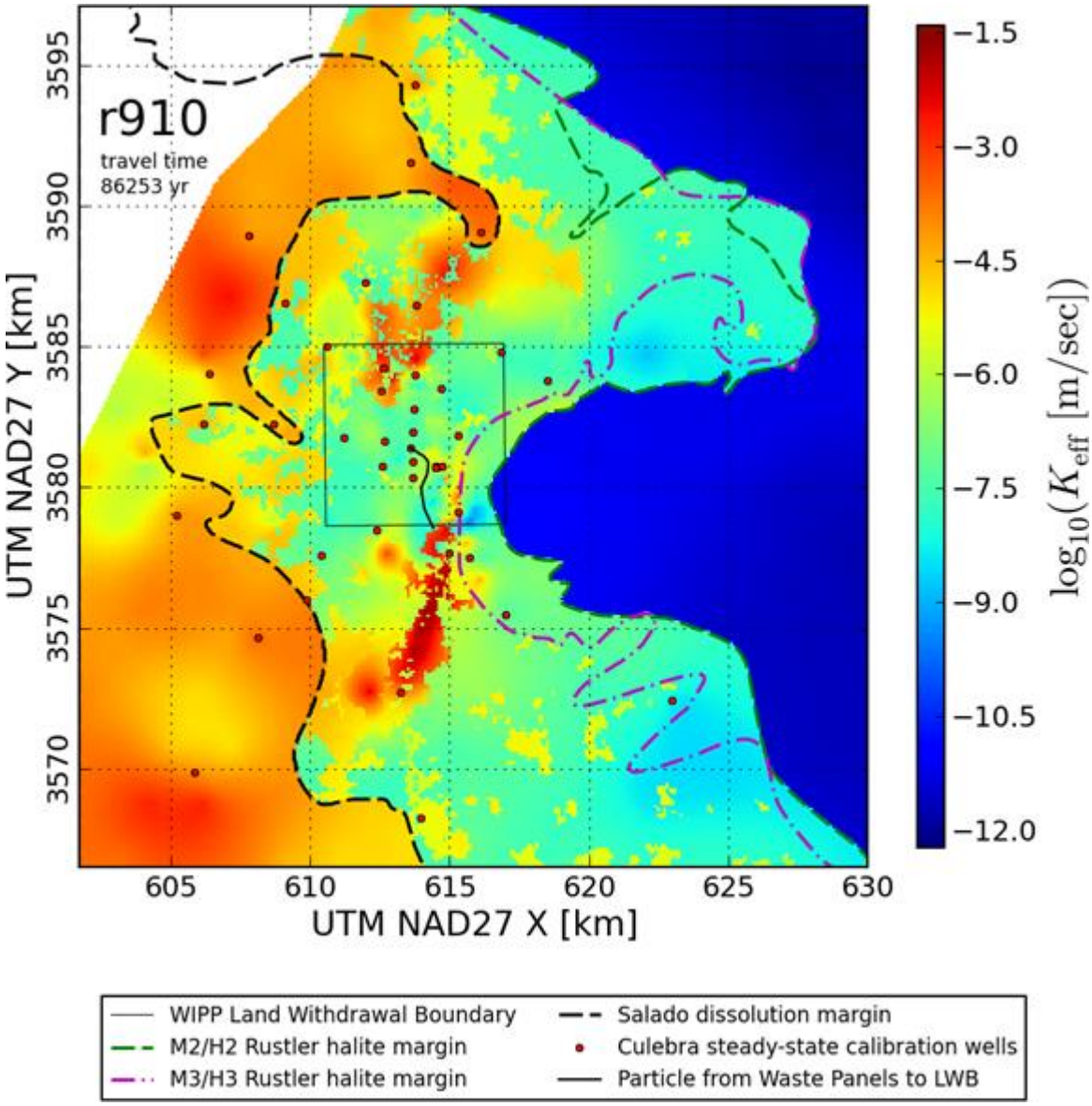
r910
travel time
86253 yr
UTM NAD27 Y [km]
3595
3590
3585
3580
3575
3570
605
610
615
620
625
630
UTM NAD27 X [km]
−1.5
−3.0
−4.5
−6.0
−7.5
−9.0
−10.5
−12.0
$\log_{10}(K_{\mathrm{eff}}\ [\mathrm{m/sec}])$
WIPP Land Withdrawal Boundary
M2/H2 Rustler halite margin
M3/H3 Rustler halite margin
Salado dissolution margin
Culebra steady-state calibration wells
Particle from Waste Panels to LWB

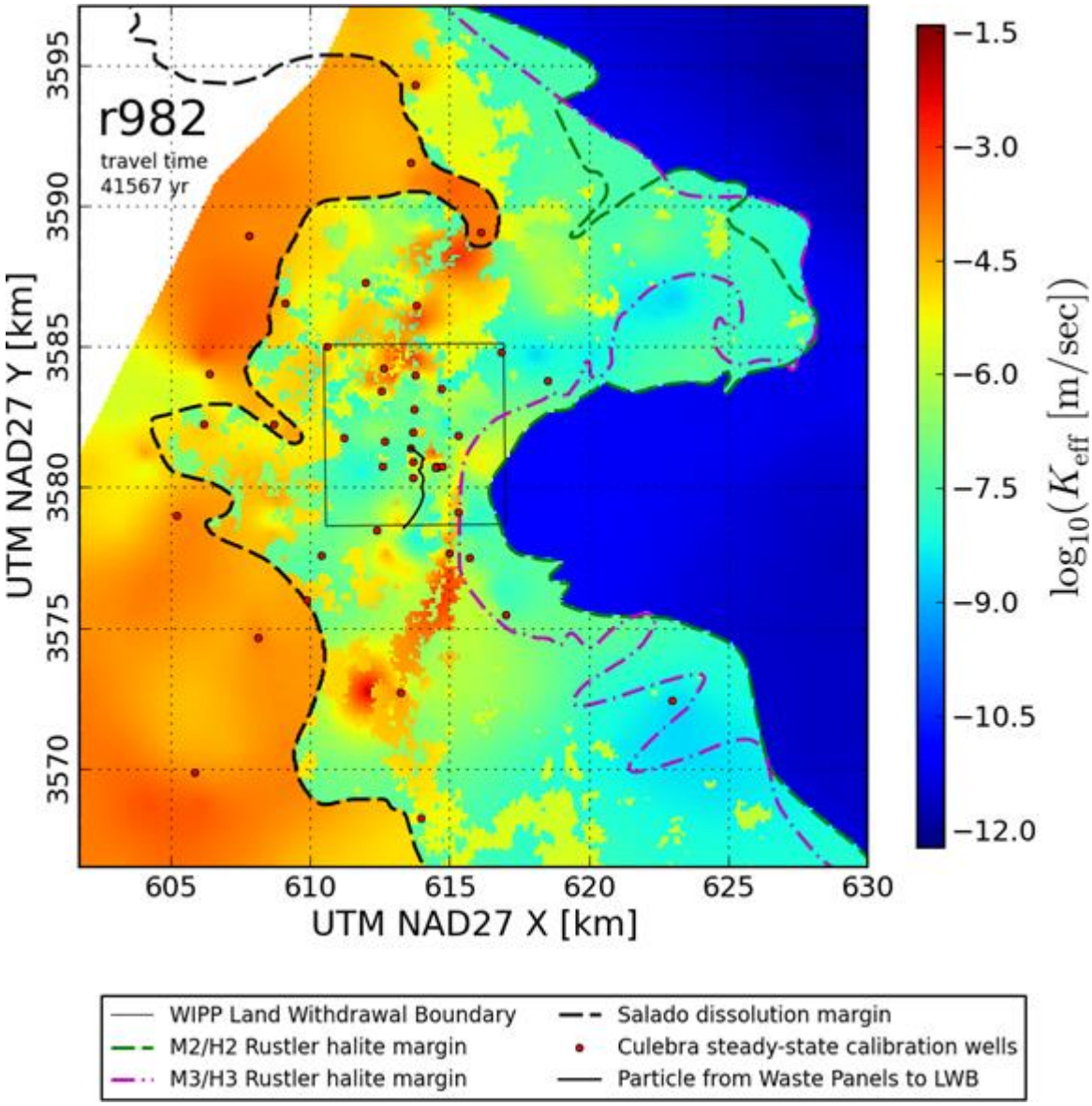
r982
travel time
41567 yr
UTM NAD27 Y [km]
3595
3590
3585
3580
3575
3570
605
610
615
620
625
630
UTM NAD27 X [km]
−1.5
−3.0
−4.5
−6.0
−7.5
−9.0
−10.5
−12.0
$\log_{10}(K_{\mathrm{eff}}\ [\mathrm{m/sec}])$
WIPP Land Withdrawal Boundary
M2/H2 Rustler halite margin
M3/H3 Rustler halite margin
Salado dissolution margin
Culebra steady-state calibration wells
Particle from Waste Panels to LWB

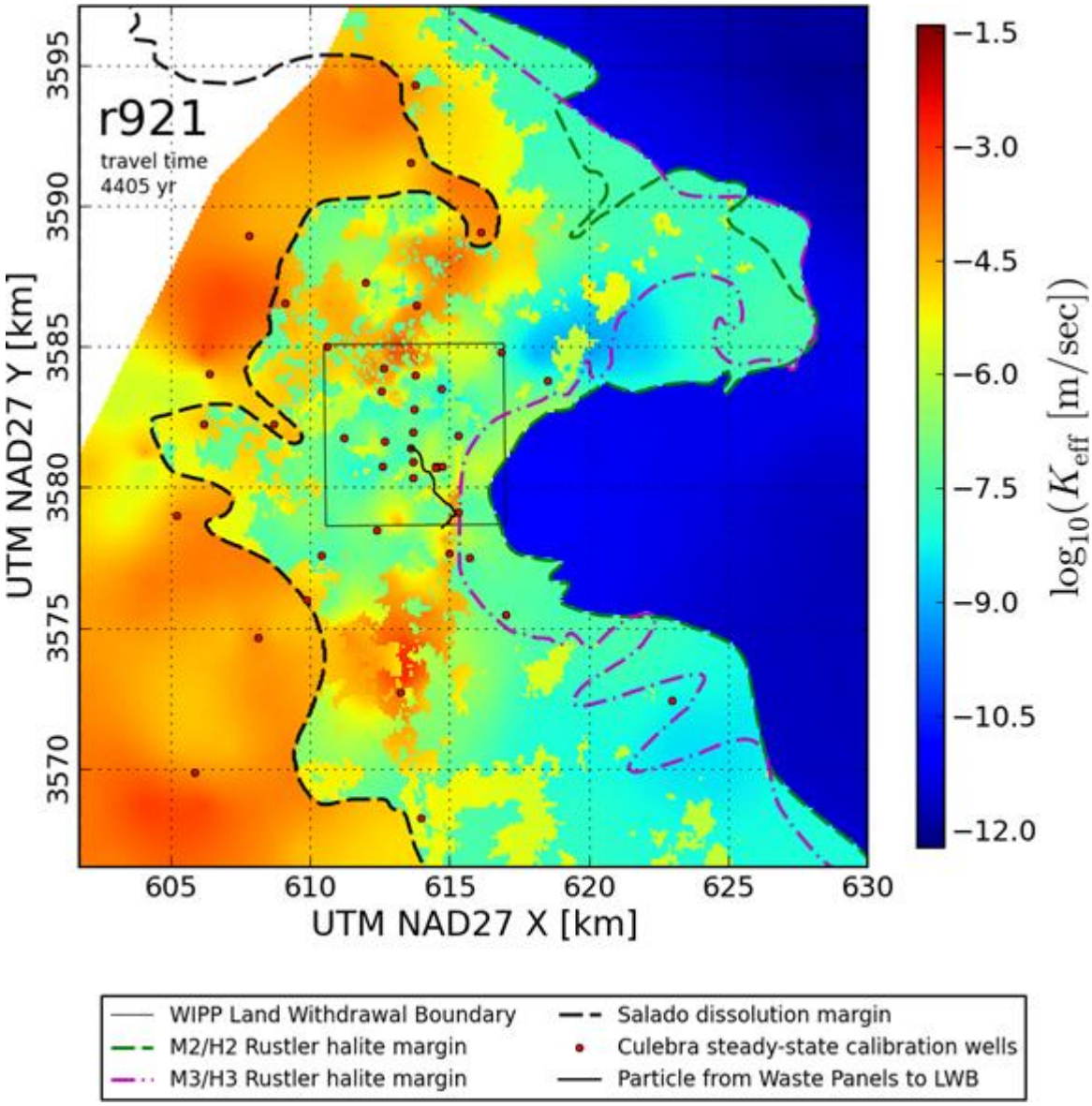
r921
travel time
4405 yr
UTM NAD27 Y [km]
3595
3590
3585
3580
3575
3570
605
610
615
620
625
630
UTM NAD27 X [km]
−1.5
−3.0
−4.5
−6.0
−7.5
−9.0
−10.5
−12.0
$\log_{10}(K_{\mathrm{eff}}\ [\mathrm{m/sec}])$
WIPP Land Withdrawal Boundary
M2/H2 Rustler halite margin
M3/H3 Rustler halite margin
Salado dissolution margin
Culebra steady-state calibration wells
Particle from Waste Panels to LWB

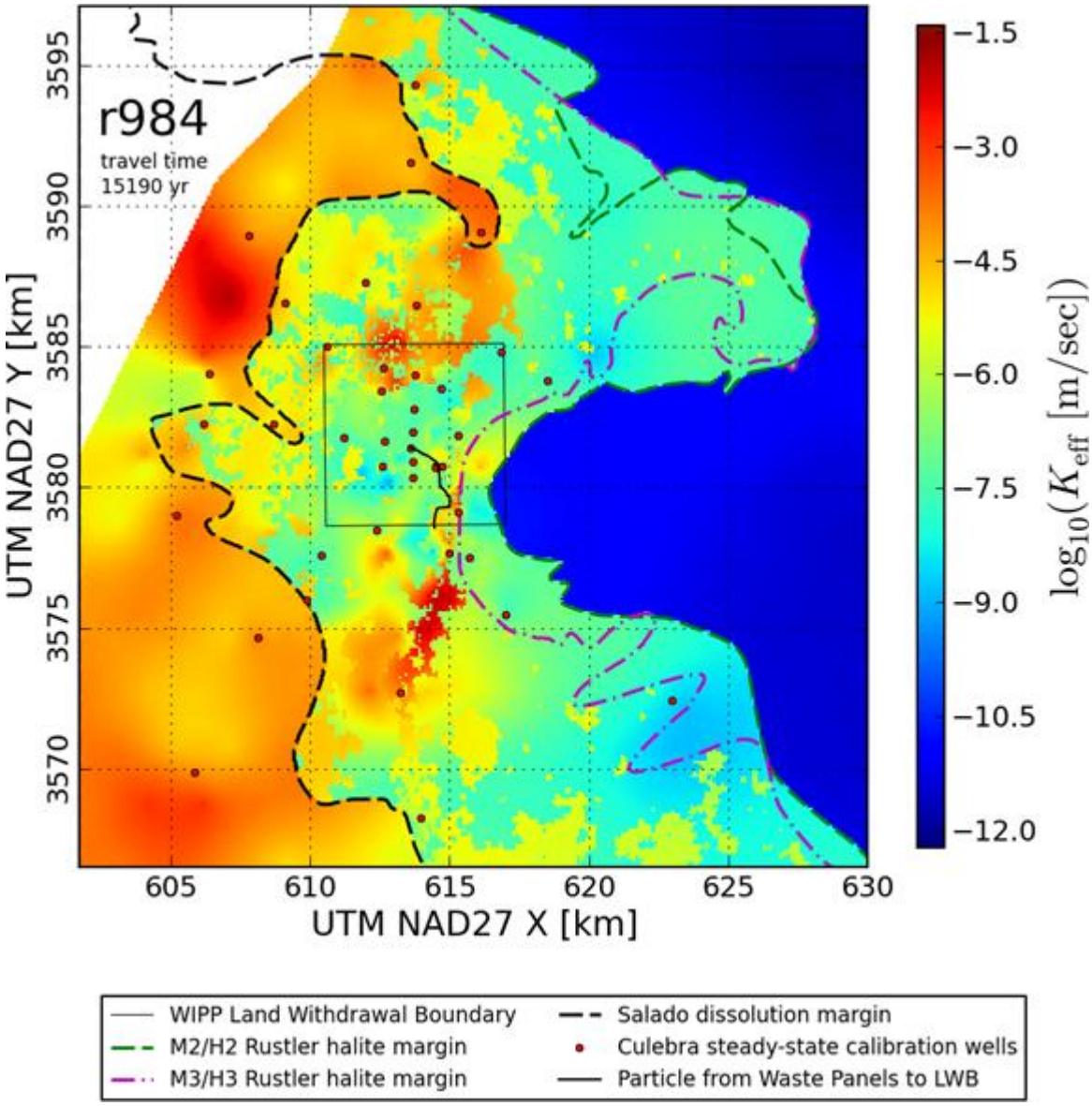
r984
travel time
15190 yr
UTM NAD27 Y [km]
3595
3590
3585
3580
3575
3570
605
610
615
620
625
630
UTM NAD27 X [km]
−1.5
−3.0
−4.5
−6.0
−7.5
−9.0
−10.5
−12.0
$\log_{10}(K_{\mathrm{eff}}\ [\mathrm{m/sec}])$
WIPP Land Withdrawal Boundary
M2/H2 Rustler halite margin
M3/H3 Rustler halite margin
Salado dissolution margin
Culebra steady-state calibration wells
Particle from Waste Panels to LWB

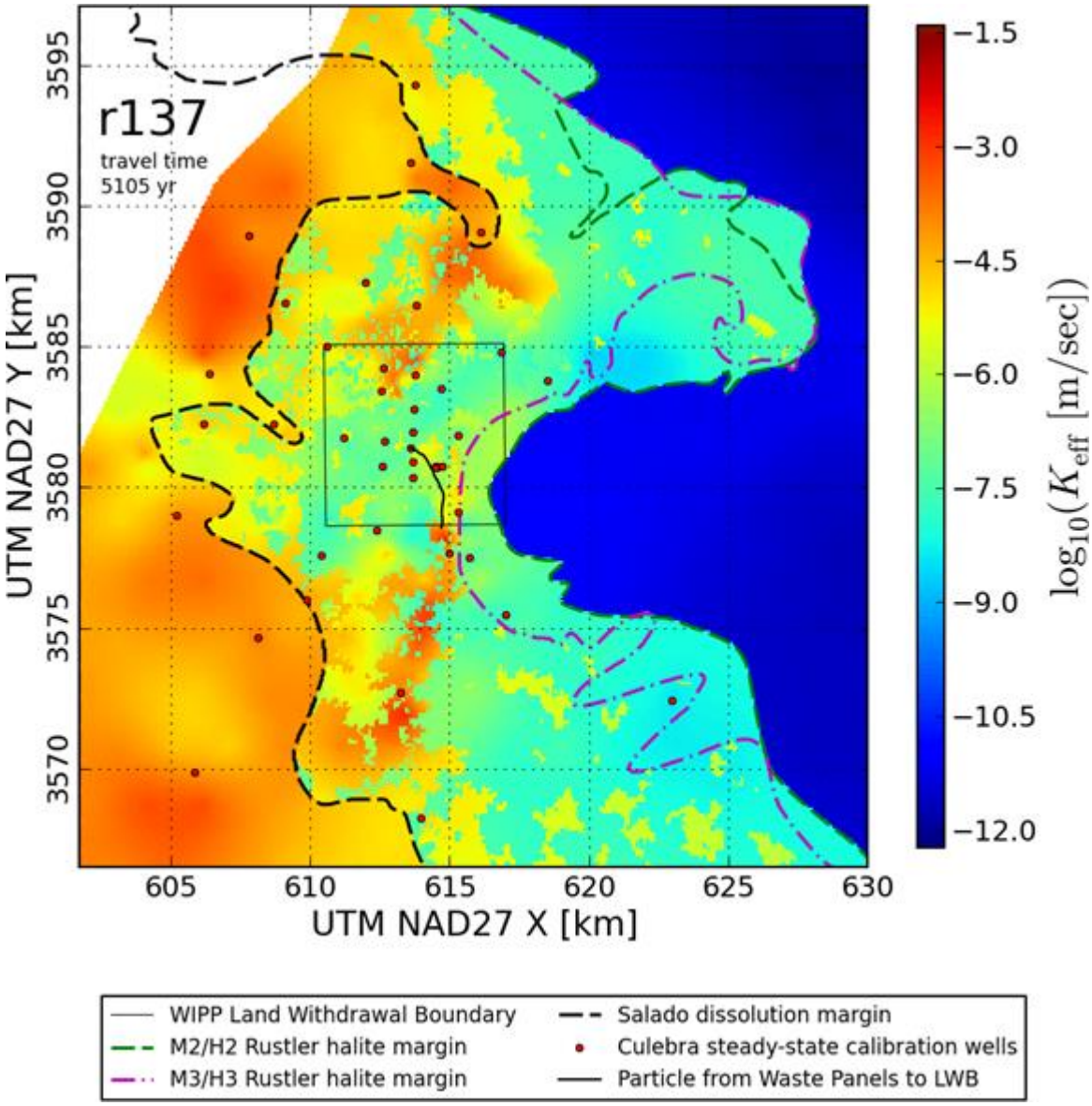
r137
travel time
5105 yr
UTM NAD27 Y [km]
3595
3590
3585
3580
3575
3570
605
610
615
620
625
630
UTM NAD27 X [km]
−1.5
−3.0
−4.5
−6.0
−7.5
−9.0
−10.5
−12.0
$\log_{10}(K_{\mathrm{eff}}$ [m/sec])
WIPP Land Withdrawal Boundary
M2/H2 Rustler halite margin
M3/H3 Rustler halite margin
Salado dissolution margin
Culebra steady-state calibration wells
Particle from Waste Panels to LWB

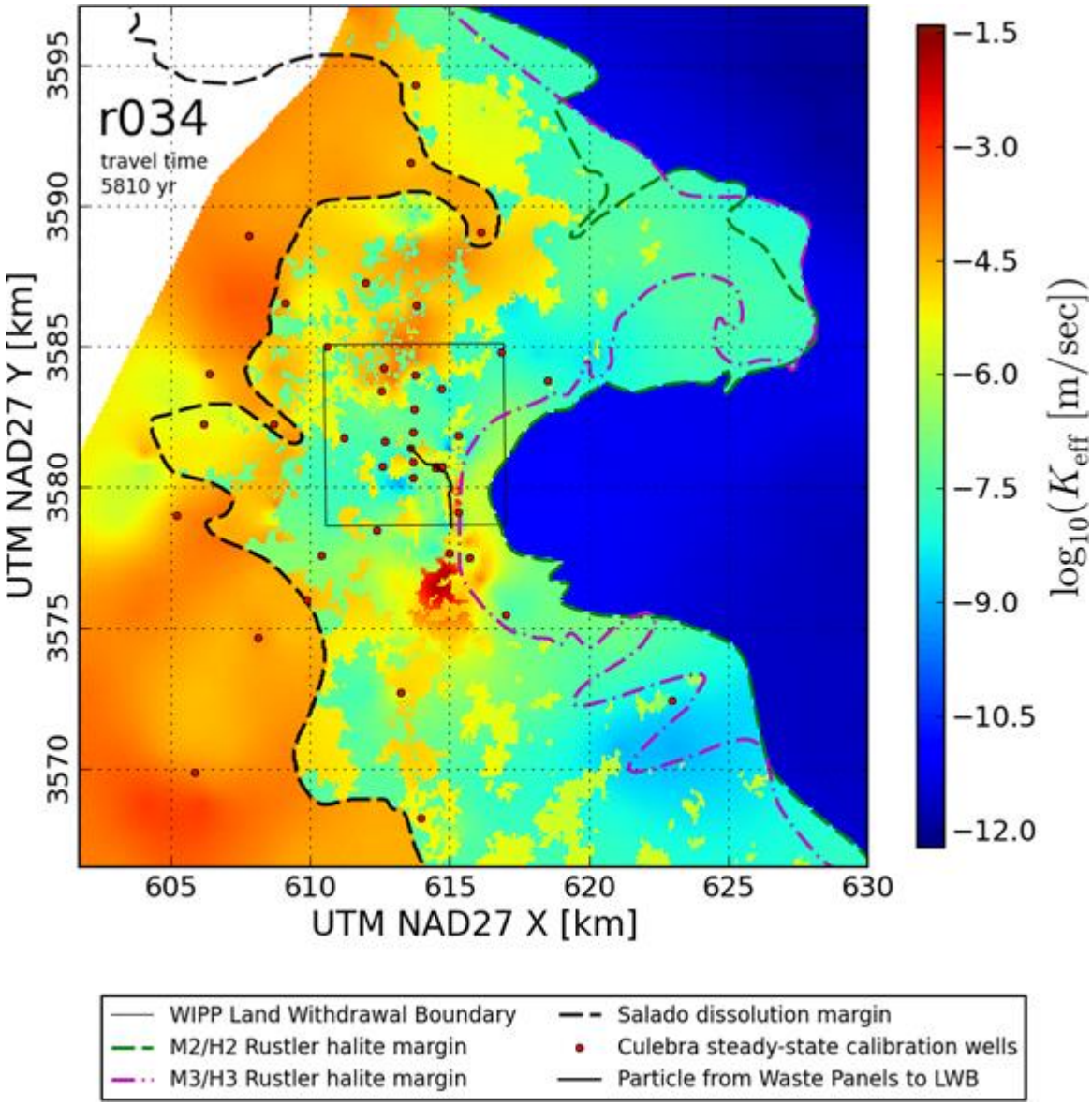
r034
travel time
5810 yr
UTM NAD27 Y [km]
3595
3590
3585
3580
3575
3570
605
610
615
620
625
630
UTM NAD27 X [km]
−1.5
−3.0
−4.5
−6.0
−7.5
−9.0
−10.5
−12.0
$\log_{10}(K_{\mathrm{eff}}\ [\mathrm{m/sec}])$
WIPP Land Withdrawal Boundary
M2/H2 Rustler halite margin
M3/H3 Rustler halite margin
Salado dissolution margin
Culebra steady-state calibration wells
Particle from Waste Panels to LWB

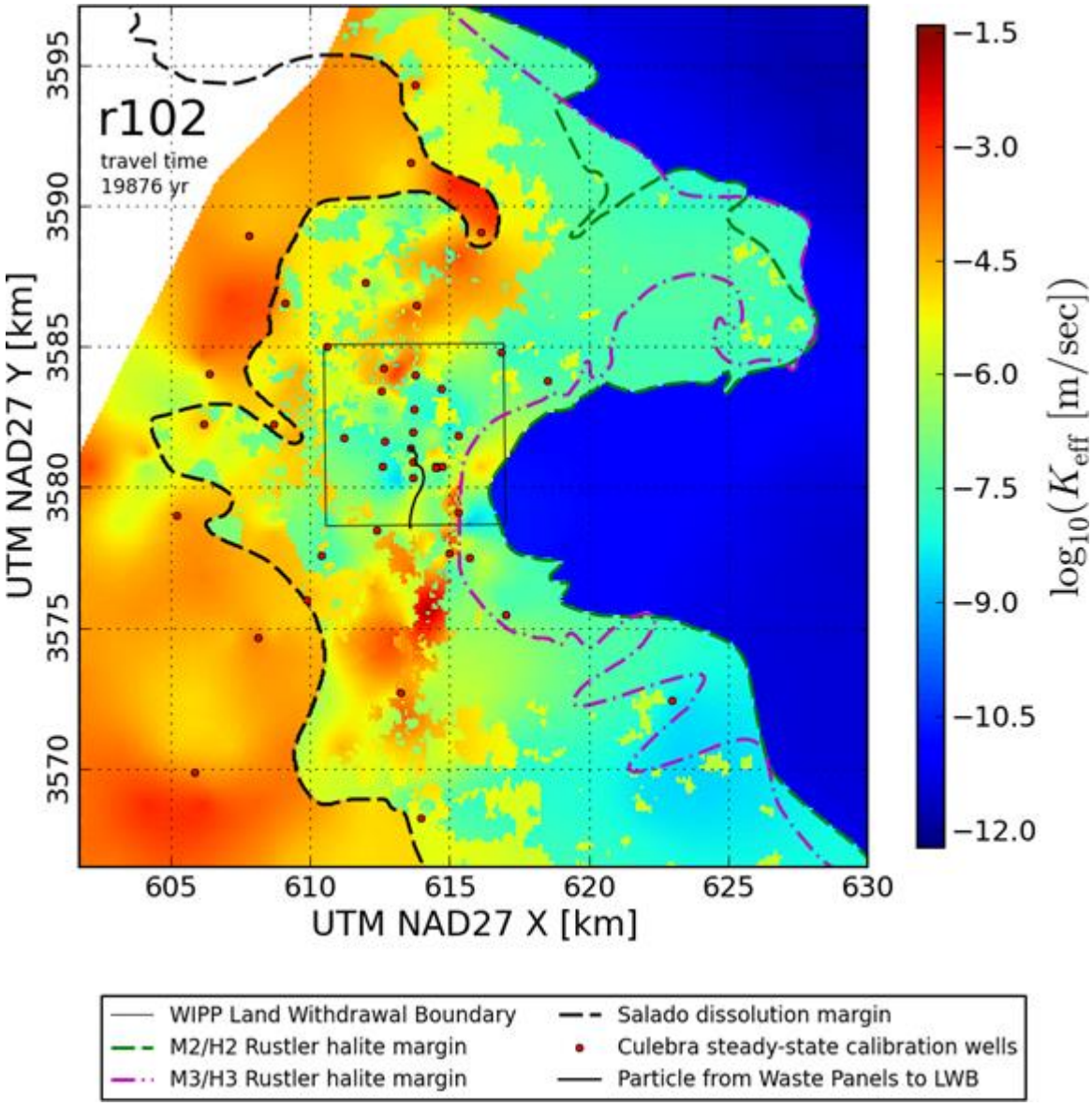
r102
travel time
19876 yr
UTM NAD27 Y [km]
3595
3590
3585
3580
3575
3570
605
610
615
620
625
630
UTM NAD27 X [km]
−1.5
−3.0
−4.5
−6.0
−7.5
−9.0
−10.5
−12.0
$\log_{10}(K_{\mathrm{eff}}\ [\mathrm{m/sec}])$
WIPP Land Withdrawal Boundary
M2/H2 Rustler halite margin
M3/H3 Rustler halite margin
Salado dissolution margin
Culebra steady-state calibration wells
Particle from Waste Panels to LWB

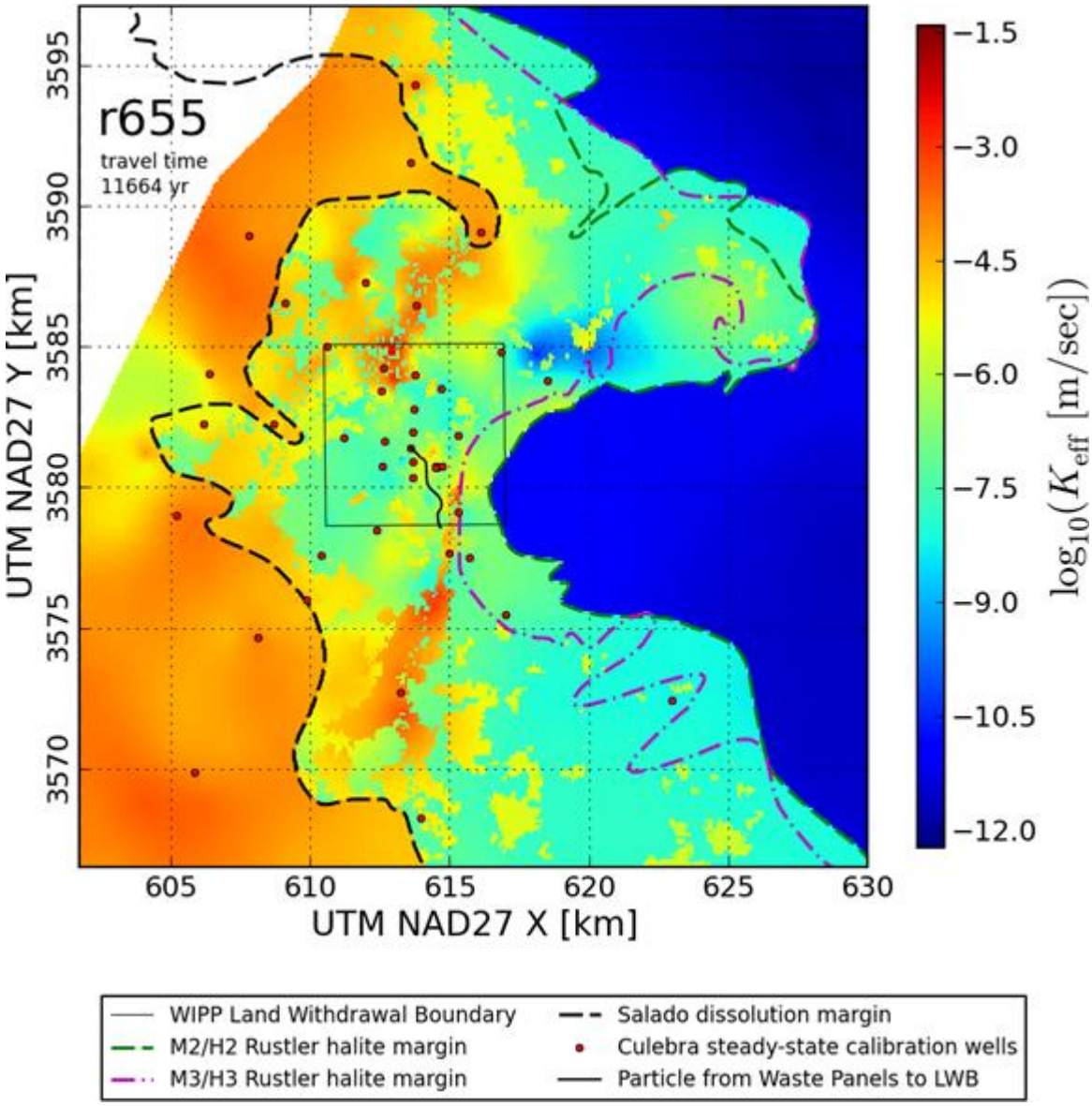
r655
travel time
11664 yr
UTM NAD27 Y [km]
3595
3590
3585
3580
3575
3570
605
610
615
620
625
630
UTM NAD27 X [km]
−1.5
−3.0
−4.5
−6.0
−7.5
−9.0
−10.5
−12.0
$\log_{10}(K_{\mathrm{eff}}\ [\mathrm{m/sec}])$
WIPP Land Withdrawal Boundary
M2/H2 Rustler halite margin
M3/H3 Rustler halite margin
Salado dissolution margin
Culebra steady-state calibration wells
Particle from Waste Panels to LWB

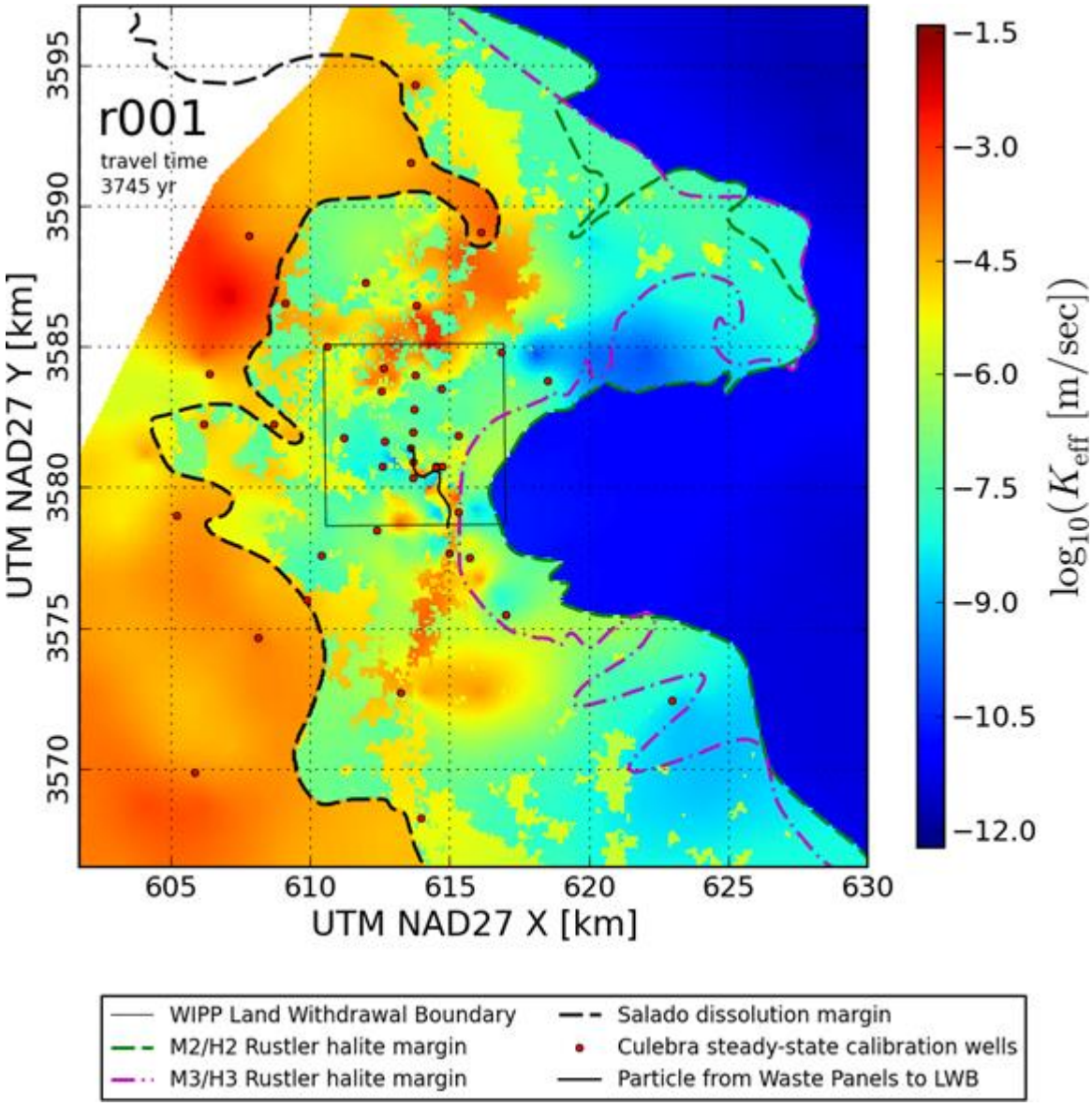
r001
travel time
3745 yr
UTM NAD27 Y [km]
3595
3590
3585
3580
3575
3570
605
610
615
620
625
630
UTM NAD27 X [km]
−1.5
−3.0
−4.5
−6.0
−7.5
−9.0
−10.5
−12.0
$\log_{10}(K_{\mathrm{eff}}\ [\mathrm{m/sec}])$
WIPP Land Withdrawal Boundary
M2/H2 Rustler halite margin
M3/H3 Rustler halite margin
Salado dissolution margin
Culebra steady-state calibration wells
Particle from Waste Panels to LWB

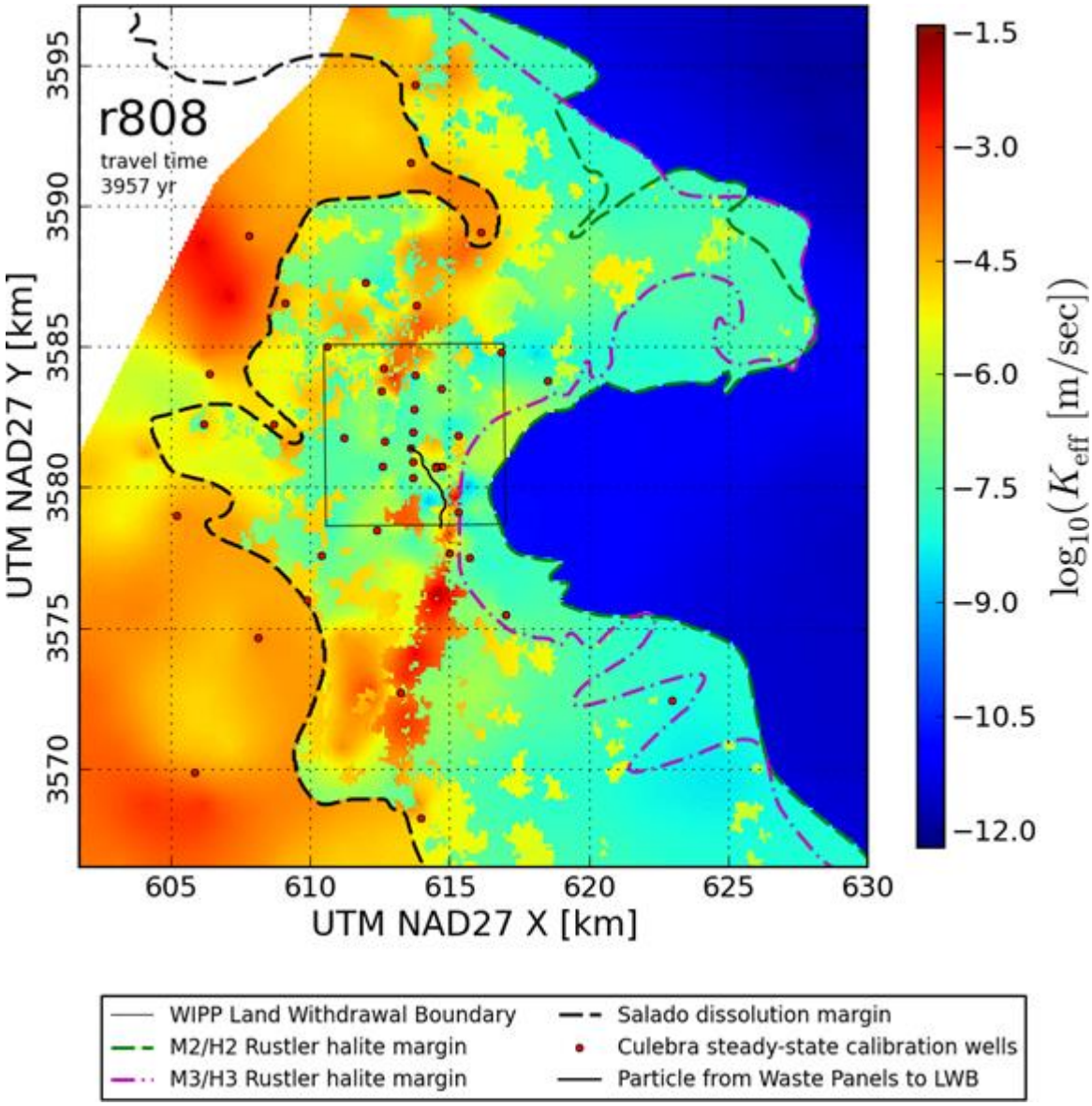
r808
travel time
3957 yr
UTM NAD27 Y [km]
3595
3590
3585
3580
3575
3570
605
610
615
620
625
630
UTM NAD27 X [km]
−1.5
−3.0
−4.5
−6.0
−7.5
−9.0
−10.5
−12.0
$\log_{10}(K_{\mathrm{eff}}\ [\mathrm{m/sec}])$
WIPP Land Withdrawal Boundary
M2/H2 Rustler halite margin
M3/H3 Rustler halite margin
Salado dissolution margin
Culebra steady-state calibration wells
Particle from Waste Panels to LWB

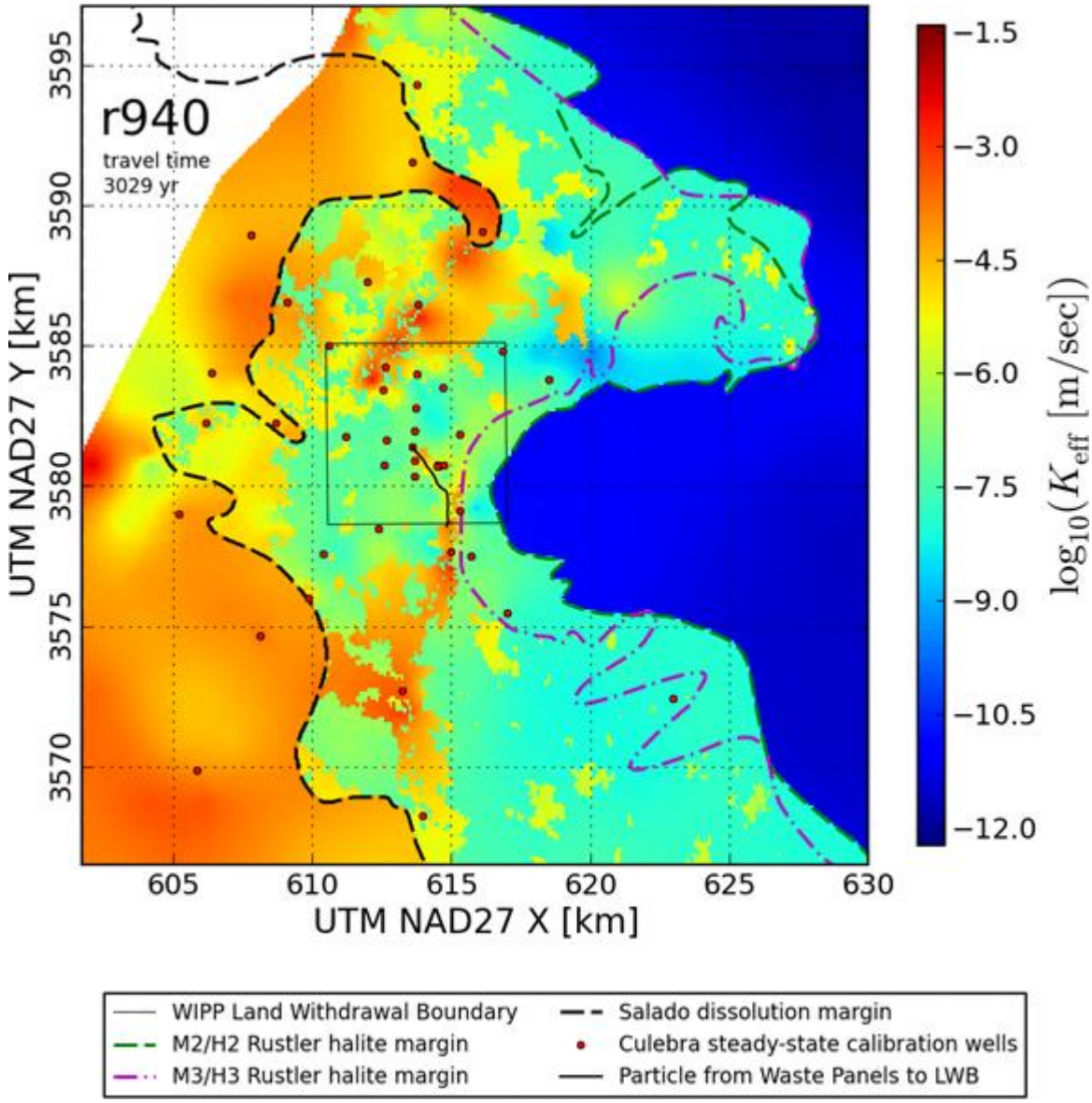
r940
travel time
3029 yr
UTM NAD27 Y [km]
3595
3590
3585
3580
3575
3570
605
610
615
620
625
630
UTM NAD27 X [km]
−1.5
−3.0
−4.5
−6.0
−7.5
−9.0
−10.5
−12.0
$\log_{10}(K_{\mathrm{eff}}\ [\mathrm{m/sec}])$
WIPP Land Withdrawal Boundary
M2/H2 Rustler halite margin
M3/H3 Rustler halite margin
Salado dissolution margin
Culebra steady-state calibration wells
Particle from Waste Panels to LWB

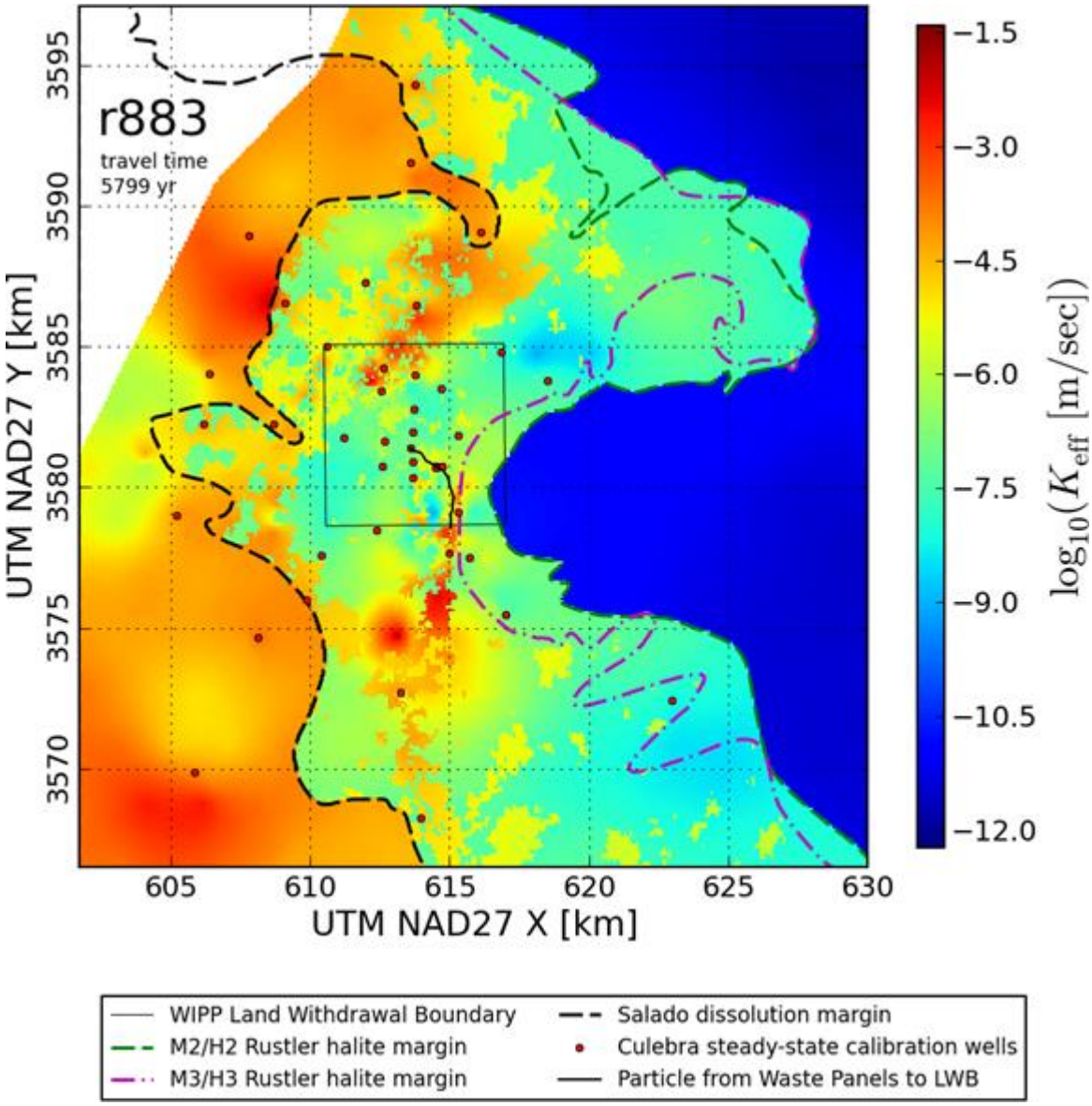
r883
travel time
5799 yr
UTM NAD27 Y [km]
3595
3590
3585
3580
3575
3570
605
610
615
620
625
630
UTM NAD27 X [km]
−1.5
−3.0
−4.5
−6.0
−7.5
−9.0
−10.5
−12.0
$\log_{10}(K_{\text{eff}}$ [m/sec])
WIPP Land Withdrawal Boundary
M2/H2 Rustler halite margin
M3/H3 Rustler halite margin
Salado dissolution margin
Culebra steady-state calibration wells
Particle from Waste Panels to LWB

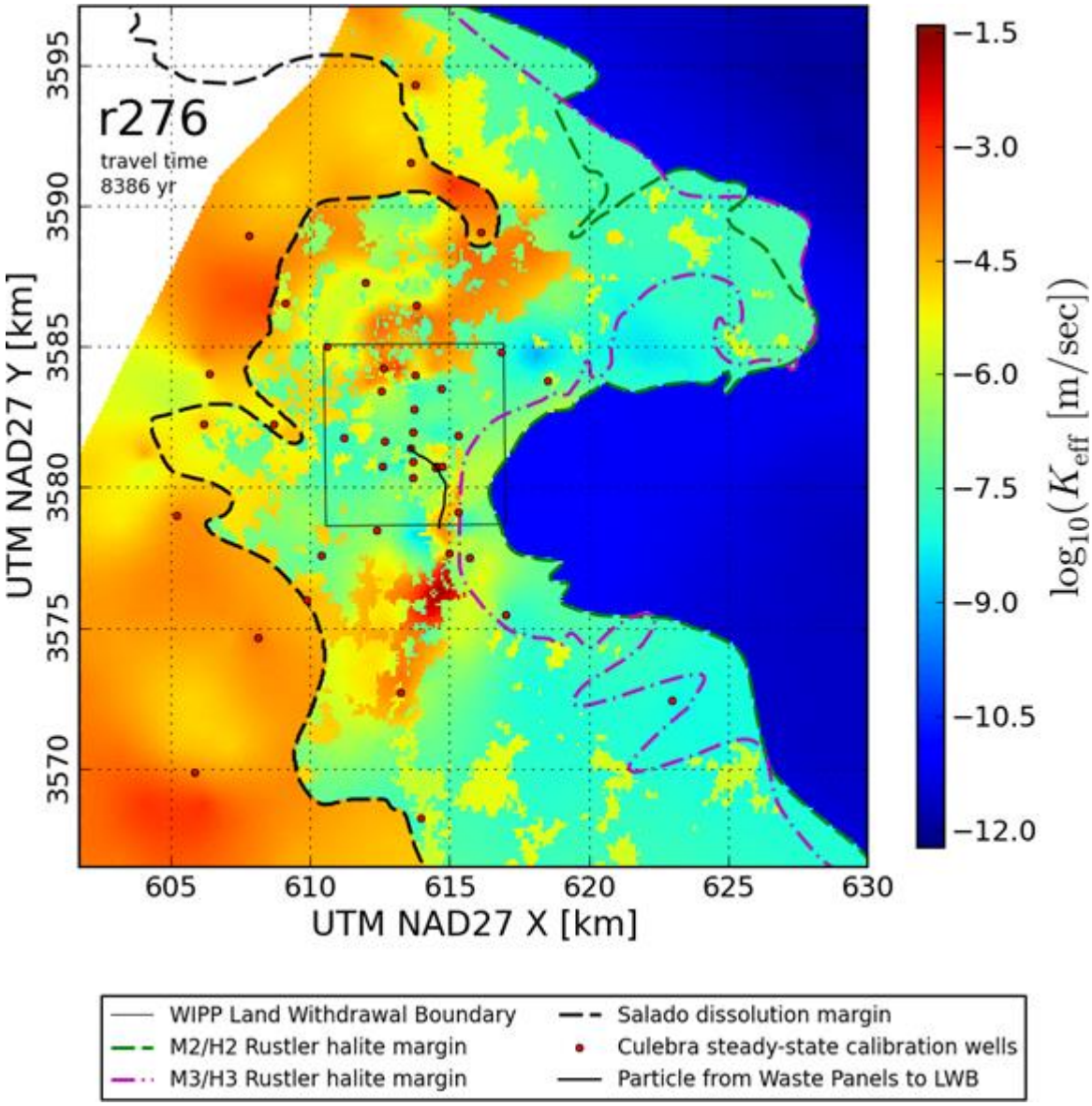
r276
travel time
8386 yr
UTM NAD27 Y [km]
3595
3590
3585
3580
3575
3570
605
610
615
620
625
630
UTM NAD27 X [km]
−1.5
−3.0
−4.5
−6.0
−7.5
−9.0
−10.5
−12.0
$\log_{10}(K_{\mathrm{eff}}\ [\mathrm{m/sec}])$
WIPP Land Withdrawal Boundary
M2/H2 Rustler halite margin
M3/H3 Rustler halite margin
Salado dissolution margin
Culebra steady-state calibration wells
Particle from Waste Panels to LWB

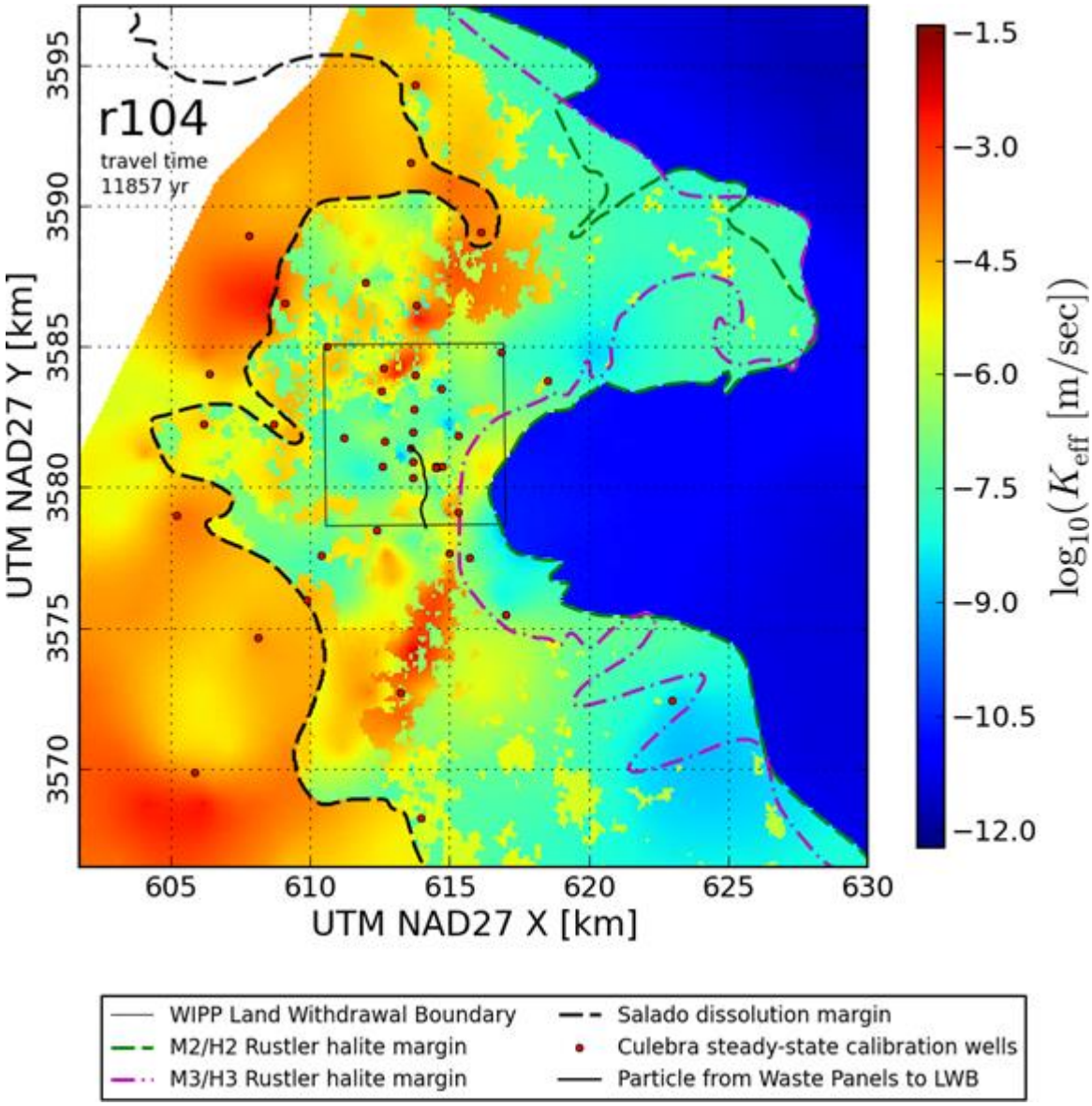
r104
travel time
11857 yr
UTM NAD27 Y [km]
3595
3590
3585
3580
3575
3570
605
610
615
620
625
630
UTM NAD27 X [km]
−1.5
−3.0
−4.5
−6.0
−7.5
−9.0
−10.5
−12.0
$\log_{10}(K_{\mathrm{eff}}\ [\mathrm{m/sec}])$
WIPP Land Withdrawal Boundary
M2/H2 Rustler halite margin
M3/H3 Rustler halite margin
Salado dissolution margin
Culebra steady-state calibration wells
Particle from Waste Panels to LWB

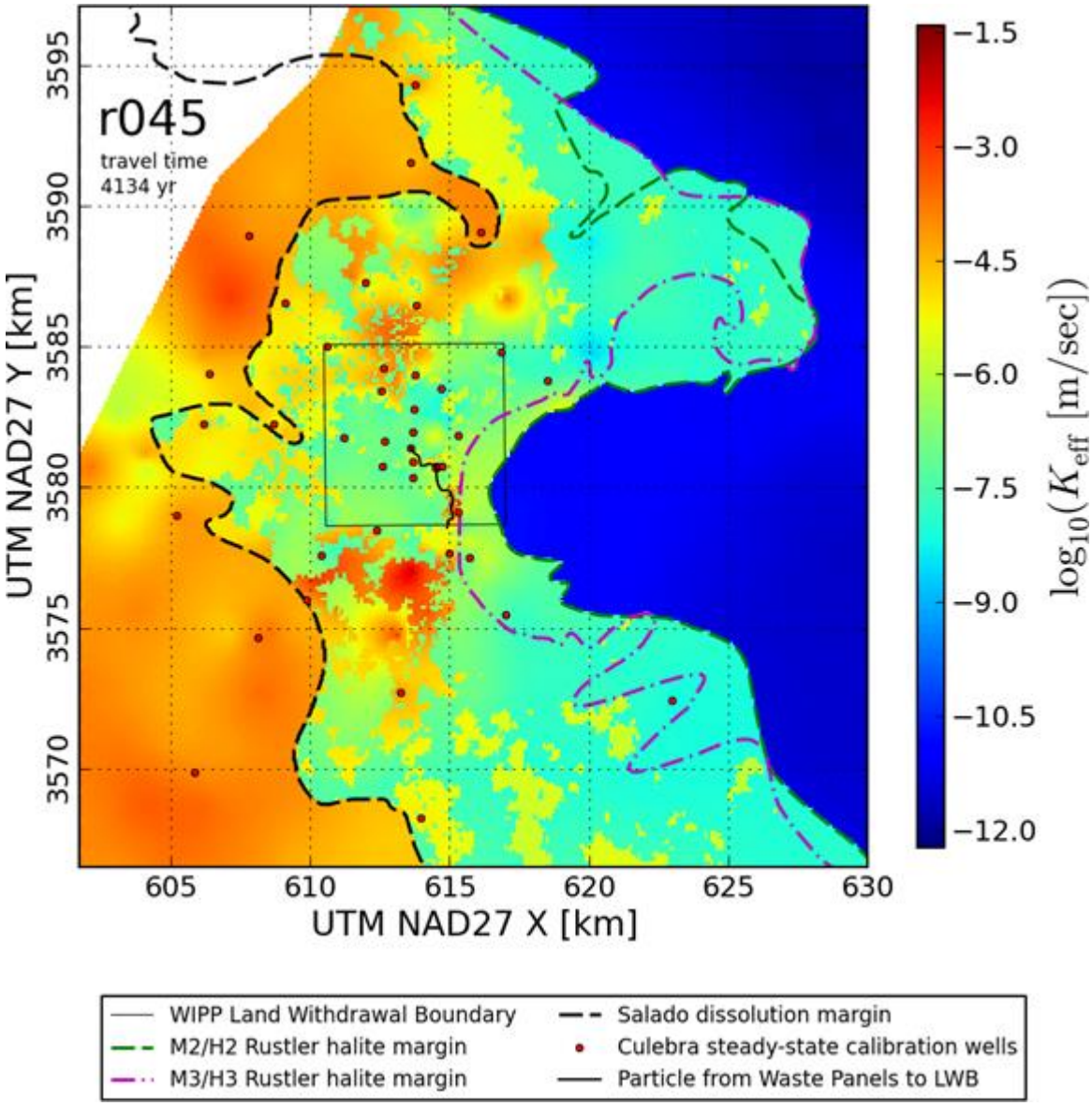
r045
travel time
4134 yr
UTM NAD27 Y [km]
3595
3590
3585
3580
3575
3570
605
610
615
620
625
630
UTM NAD27 X [km]
−1.5
−3.0
−4.5
−6.0
−7.5
−9.0
−10.5
−12.0
$\log_{10}(K_{\mathrm{eff}}\ [\mathrm{m/sec}])$
WIPP Land Withdrawal Boundary
M2/H2 Rustler halite margin
M3/H3 Rustler halite margin
Salado dissolution margin
Culebra steady-state calibration wells
Particle from Waste Panels to LWB

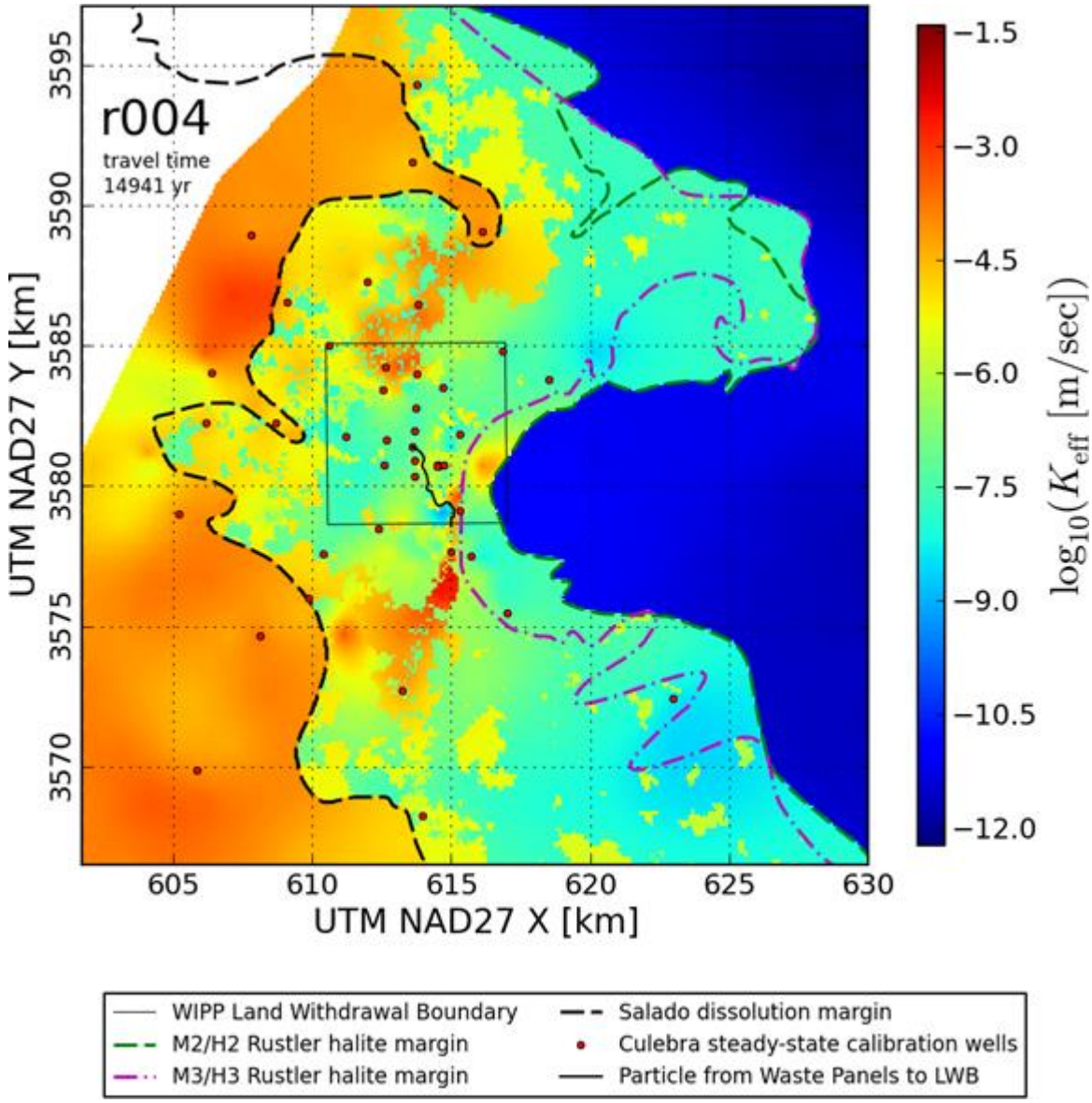

TFIELD Attachment A-2.0 100 Calibrated Specific Storage Model Input Parameter Fields

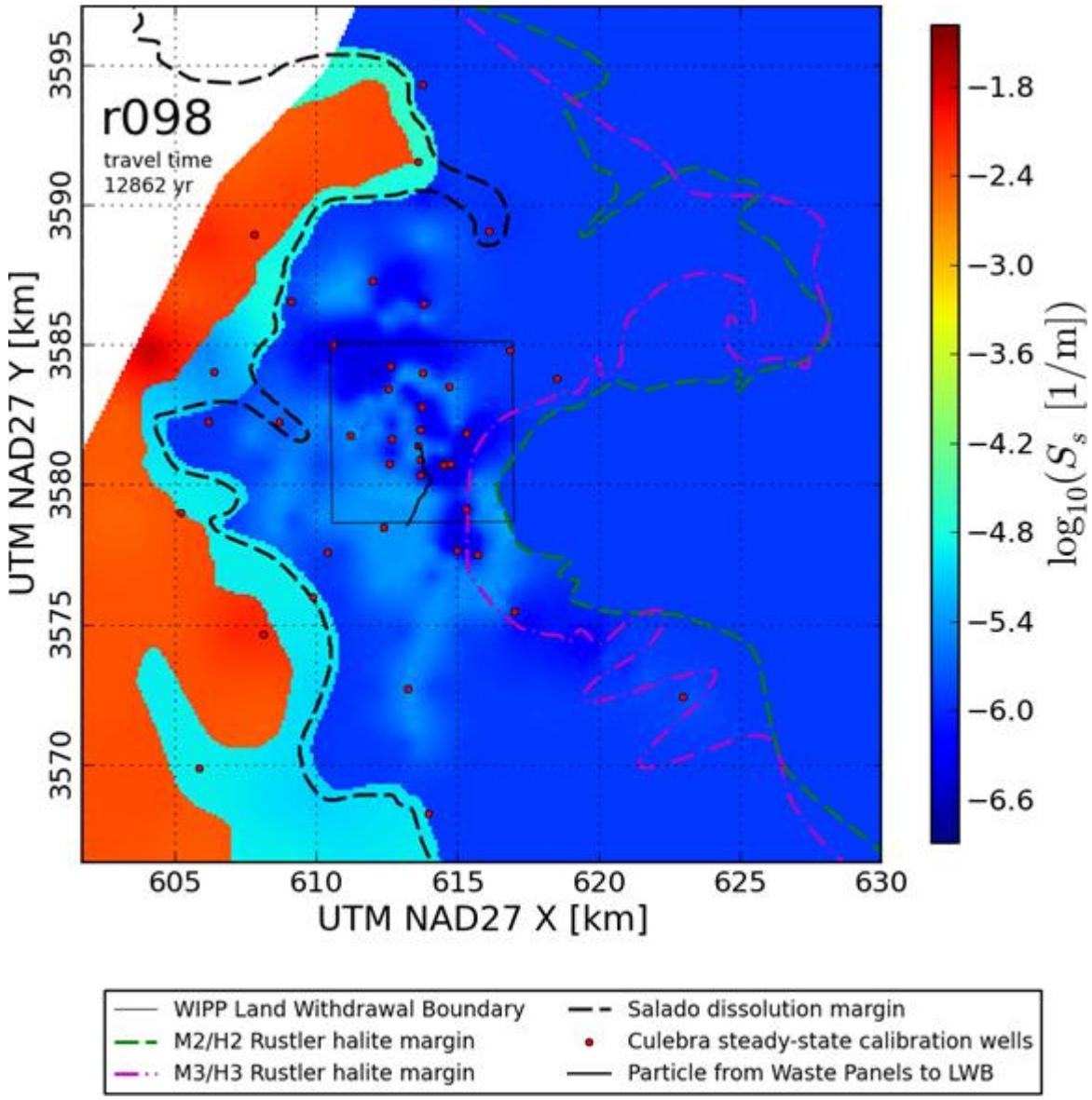
r098
travel time
12862 yr
UTM NAD27 Y [km]
3595
3590
3585
3580
3575
3570
605
610
615
620
625
630
UTM NAD27 X [km]
−1.8
−2.4
−3.0
−3.6
−4.2
−4.8
−5.4
−6.0
−6.6
$\log_{10}(S_s\ [1/\mathrm{m}])$
WIPP Land Withdrawal Boundary
M2/H2 Rustler halite margin
M3/H3 Rustler halite margin
Salado dissolution margin
Culebra steady-state calibration wells
Particle from Waste Panels to LWB

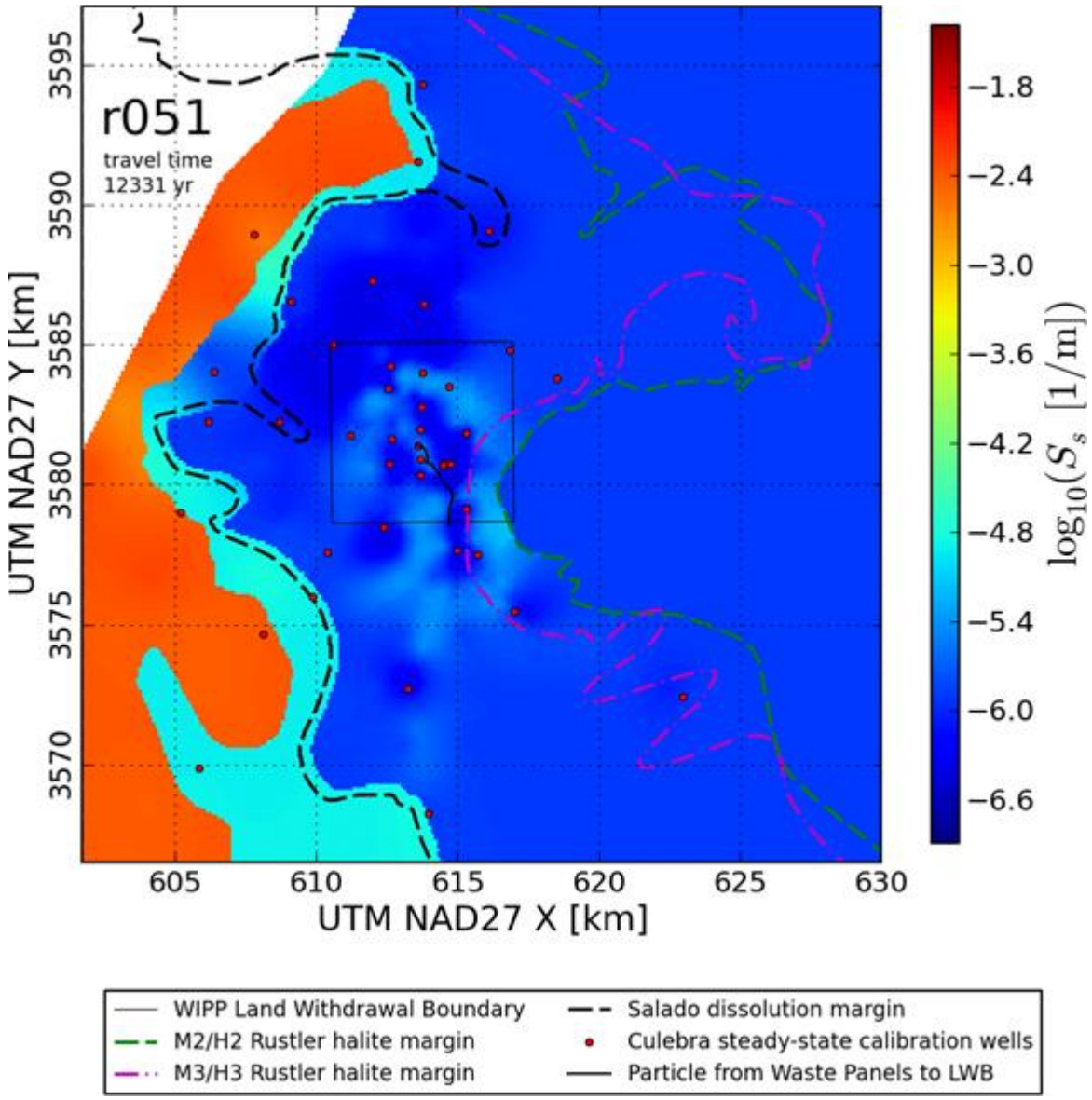
r051
travel time
12331 yr
UTM NAD27 Y [km]
3595
3590
3585
3580
3575
3570
605
610
615
620
625
630
UTM NAD27 X [km]
−1.8
−2.4
−3.0
−3.6
−4.2
−4.8
−5.4
−6.0
−6.6
$\log_{10}(S_s\ [1/\mathrm{m}])$
WIPP Land Withdrawal Boundary
M2/H2 Rustler halite margin
M3/H3 Rustler halite margin
Salado dissolution margin
Culebra steady-state calibration wells
Particle from Waste Panels to LWB

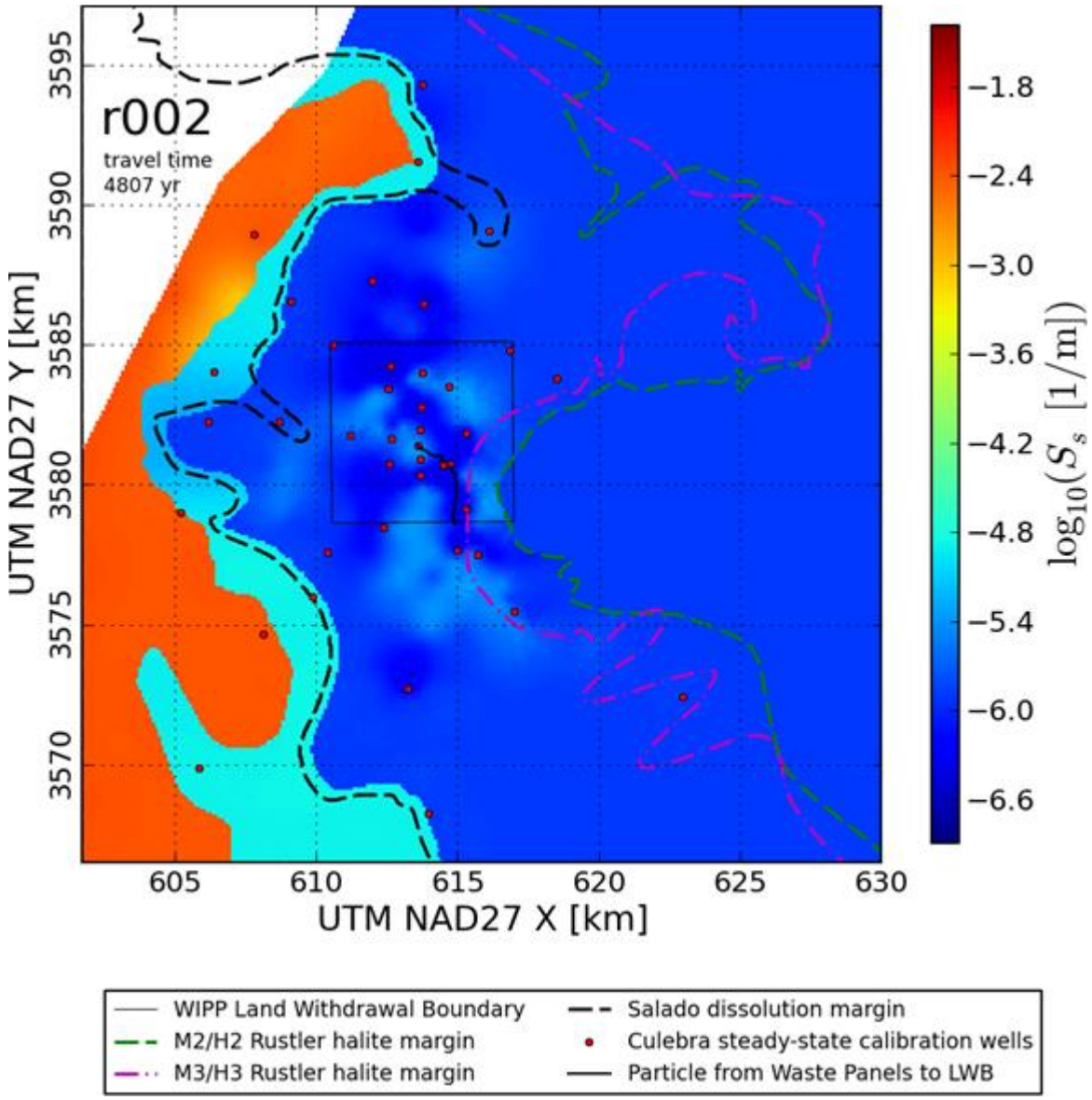
r002
travel time
4807 yr
UTM NAD27 Y [km]
3595
3590
3585
3580
3575
3570
605
610
615
620
625
630
UTM NAD27 X [km]
−1.8
−2.4
−3.0
−3.6
−4.2
−4.8
−5.4
−6.0
−6.6
$\log_{10}(S_s\ [1/\mathrm{m}])$
WIPP Land Withdrawal Boundary
M2/H2 Rustler halite margin
M3/H3 Rustler halite margin
Salado dissolution margin
Culebra steady-state calibration wells
Particle from Waste Panels to LWB

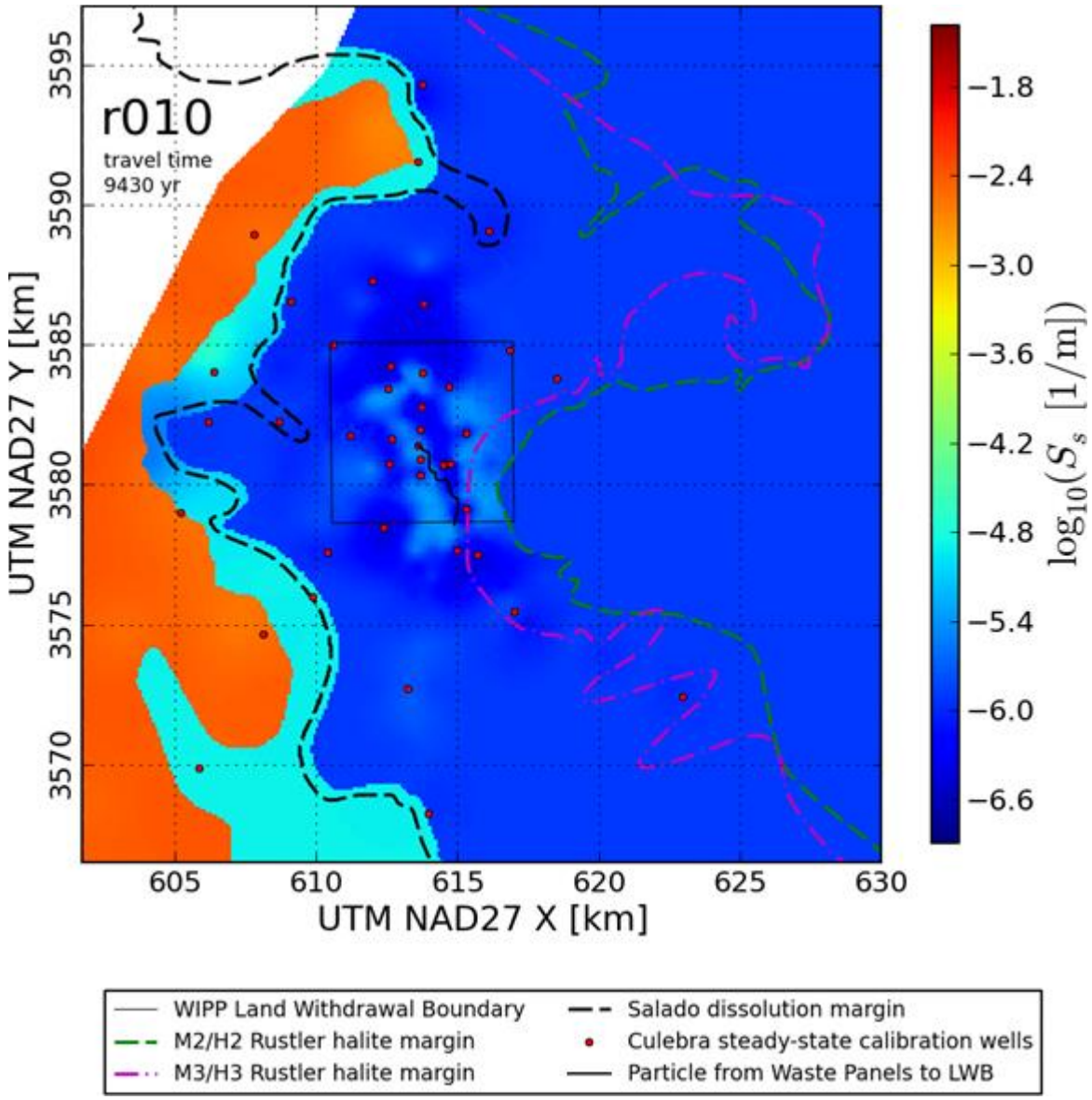
r010
travel time
9430 yr
UTM NAD27 Y [km]
3595
3590
3585
3580
3575
3570
605
610
615
620
625
630
UTM NAD27 X [km]
−1.8
−2.4
−3.0
−3.6
−4.2
−4.8
−5.4
−6.0
−6.6
$\log_{10}(S_s\ [1/\mathrm{m}])$
WIPP Land Withdrawal Boundary
M2/H2 Rustler halite margin
M3/H3 Rustler halite margin
Salado dissolution margin
Culebra steady-state calibration wells
Particle from Waste Panels to LWB

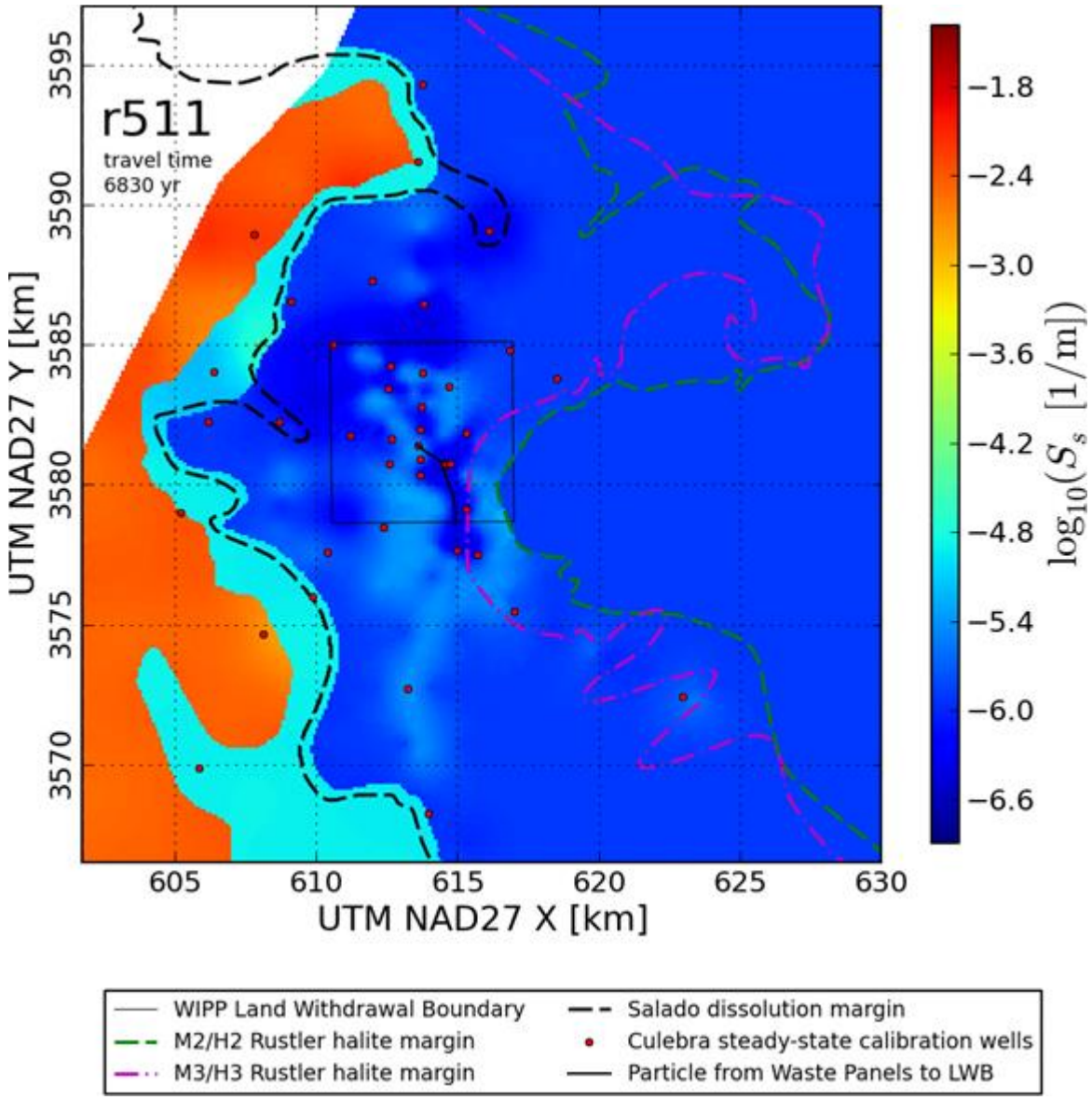
r511
travel time
6830 yr
UTM NAD27 Y [km]
3595
3590
3585
3580
3575
3570
605
610
615
620
625
630
UTM NAD27 X [km]
−1.8
−2.4
−3.0
−3.6
−4.2
−4.8
−5.4
−6.0
−6.6
$\log_{10}(S_s\ [1/\mathrm{m}])$
WIPP Land Withdrawal Boundary
M2/H2 Rustler halite margin
M3/H3 Rustler halite margin
Salado dissolution margin
Culebra steady-state calibration wells
Particle from Waste Panels to LWB

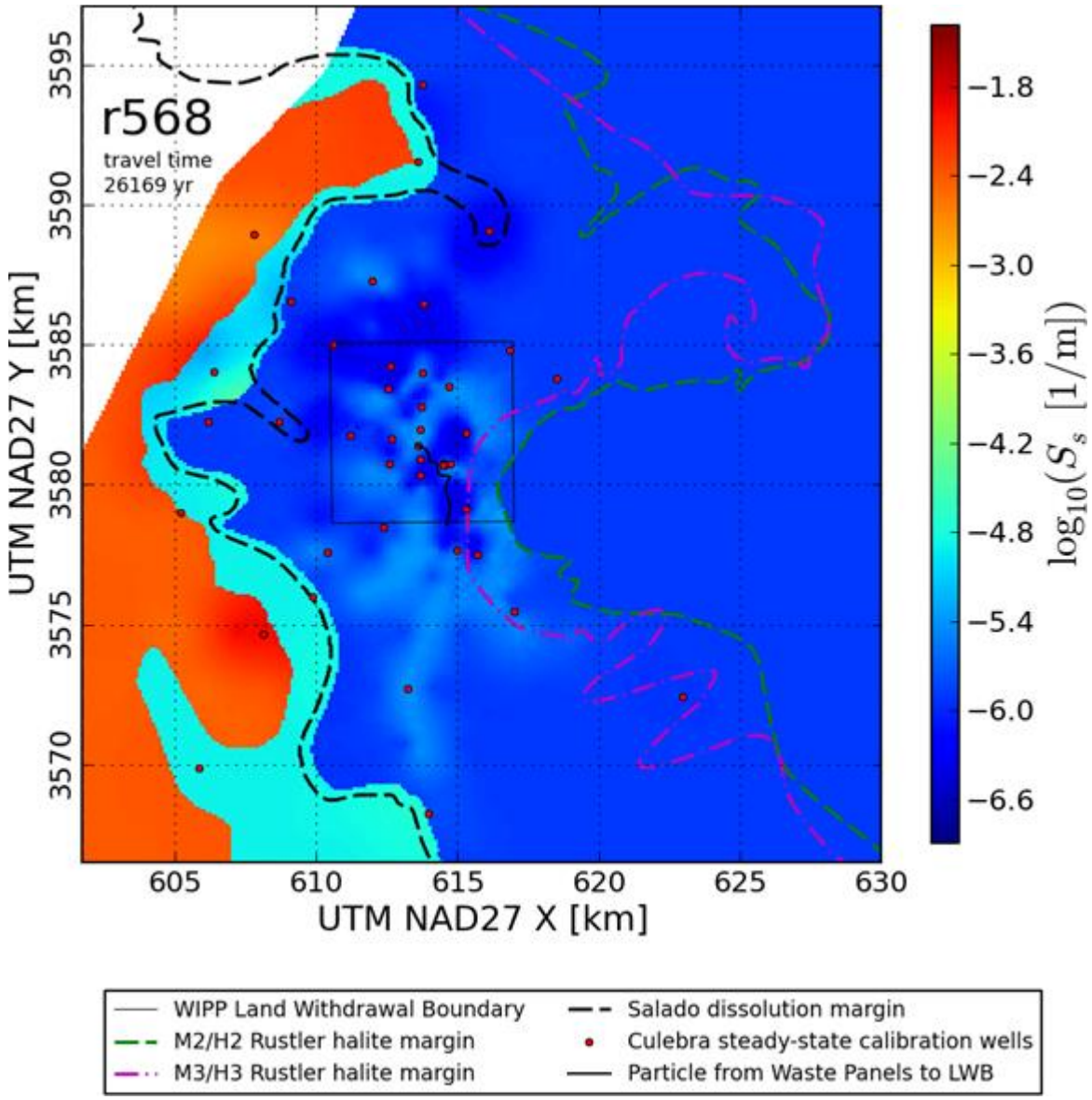
r568
travel time
26169 yr
UTM NAD27 Y [km]
3595
3590
3585
3580
3575
3570
605
610
615
620
625
630
UTM NAD27 X [km]
−1.8
−2.4
−3.0
−3.6
−4.2
−4.8
−5.4
−6.0
−6.6
$\log_{10}(S_s\ [1/\mathrm{m}])$
WIPP Land Withdrawal Boundary
M2/H2 Rustler halite margin
M3/H3 Rustler halite margin
Salado dissolution margin
Culebra steady-state calibration wells
Particle from Waste Panels to LWB

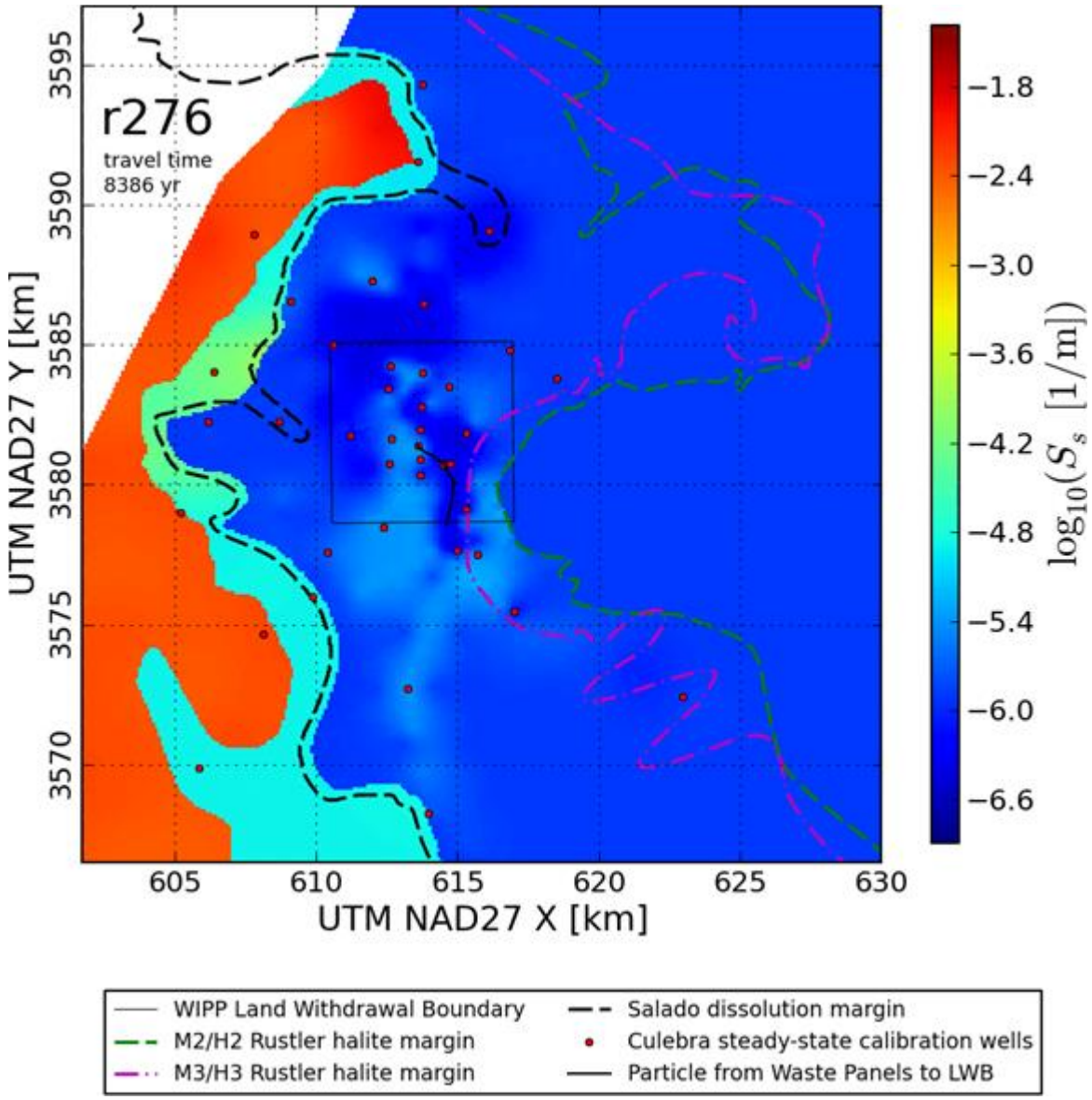
r276
travel time
8386 yr
UTM NAD27 Y [km]
3595
3590
3585
3580
3575
3570
605
610
615
620
625
630
UTM NAD27 X [km]
−1.8
−2.4
−3.0
−3.6
−4.2
−4.8
−5.4
−6.0
−6.6
$\log_{10}(S_s\ [1/\mathrm{m}])$
WIPP Land Withdrawal Boundary
M2/H2 Rustler halite margin
M3/H3 Rustler halite margin
Salado dissolution margin
Culebra steady-state calibration wells
Particle from Waste Panels to LWB

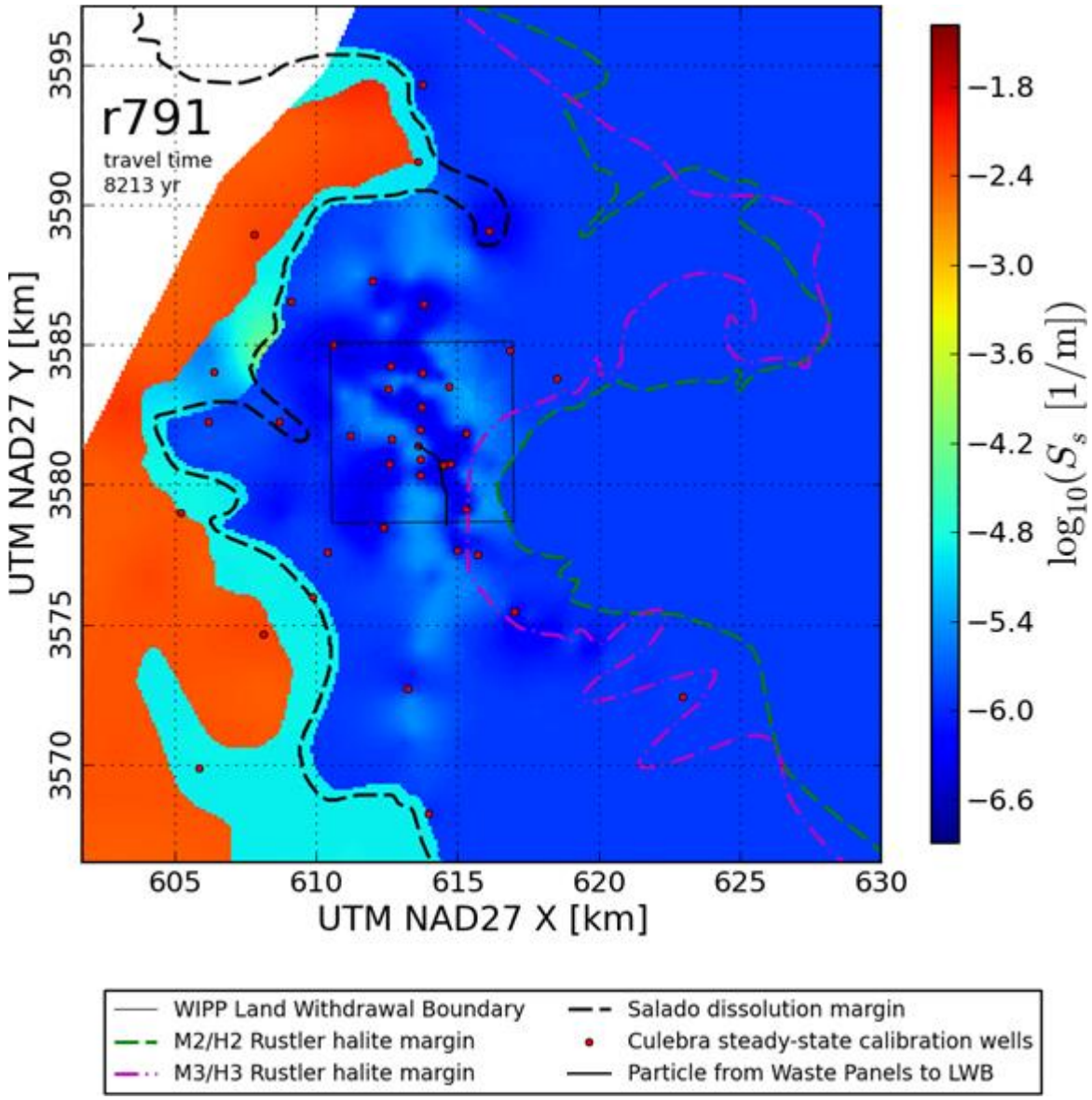
r791
travel time
8213 yr
UTM NAD27 Y [km]
3595
3590
3585
3580
3575
3570
605
610
615
620
625
630
UTM NAD27 X [km]
−1.8
−2.4
−3.0
−3.6
−4.2
−4.8
−5.4
−6.0
−6.6
$\log_{10}(S_s\ [1/\mathrm{m}])$
WIPP Land Withdrawal Boundary
M2/H2 Rustler halite margin
M3/H3 Rustler halite margin
Salado dissolution margin
Culebra steady-state calibration wells
Particle from Waste Panels to LWB

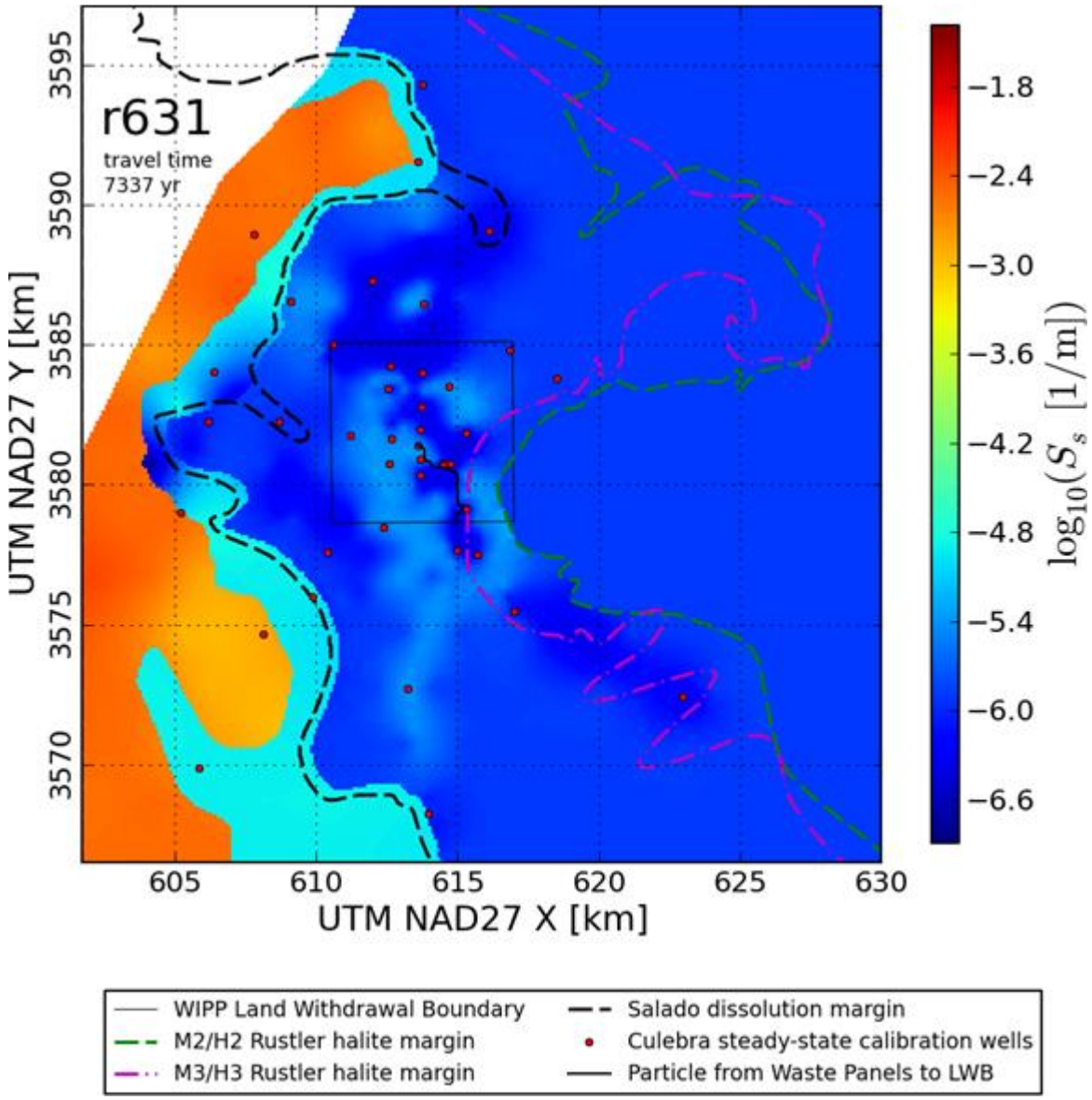
r631
travel time
7337 yr
UTM NAD27 Y [km]
3595
3590
3585
3580
3575
3570
605
610
615
620
625
630
UTM NAD27 X [km]
−1.8
−2.4
−3.0
−3.6
−4.2
−4.8
−5.4
−6.0
−6.6
$\log_{10}(S_s\ [1/\mathrm{m}])$
WIPP Land Withdrawal Boundary
M2/H2 Rustler halite margin
M3/H3 Rustler halite margin
Salado dissolution margin
Culebra steady-state calibration wells
Particle from Waste Panels to LWB

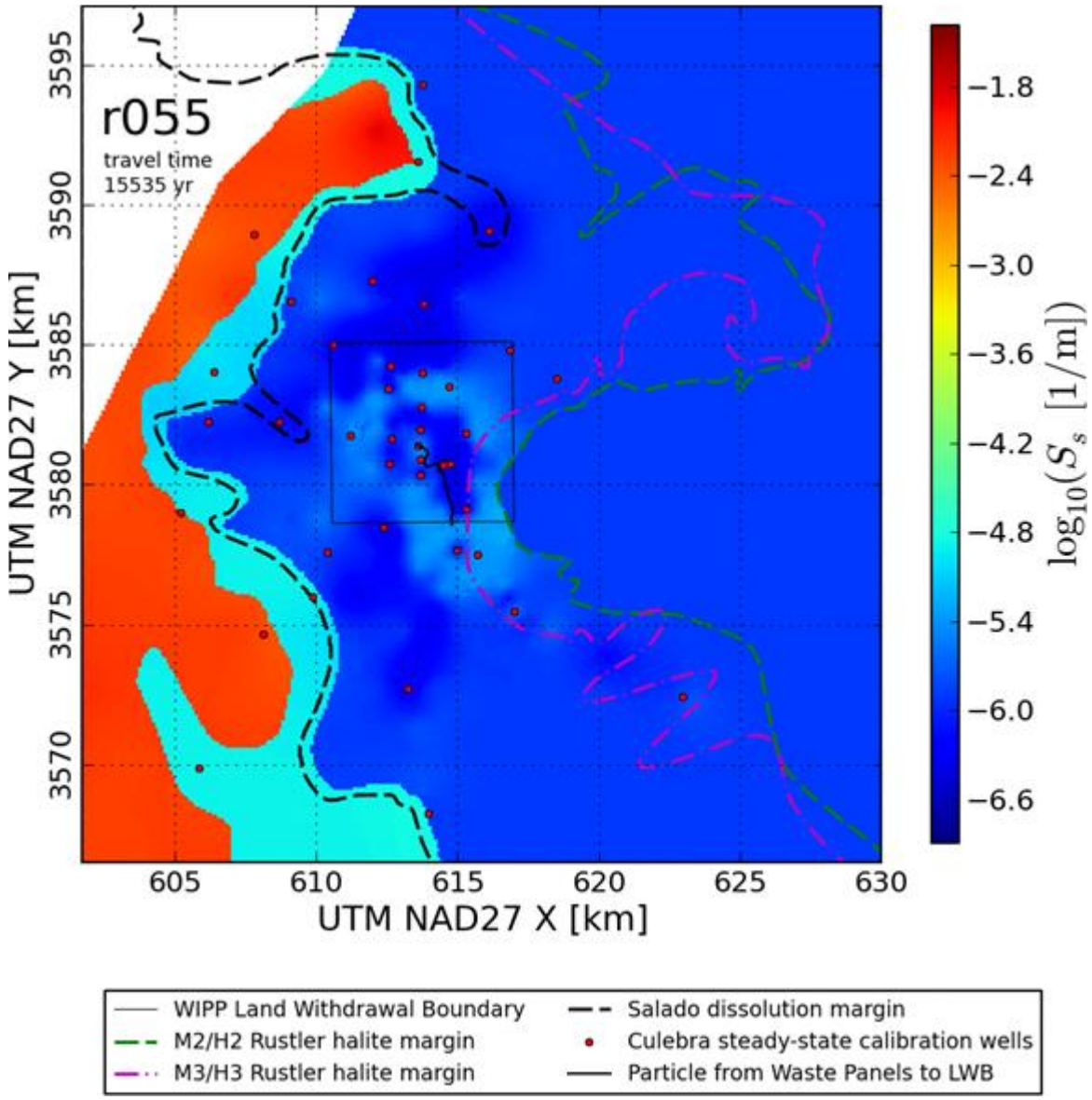
r055
travel time
15535 yr
UTM NAD27 Y [km]
3595
3590
3585
3580
3575
3570
605
610
615
620
625
630
UTM NAD27 X [km]
−1.8
−2.4
−3.0
−3.6
−4.2
−4.8
−5.4
−6.0
−6.6
$\log_{10}(S_s\ [1/\mathrm{m}])$
WIPP Land Withdrawal Boundary
M2/H2 Rustler halite margin
M3/H3 Rustler halite margin
Salado dissolution margin
Culebra steady-state calibration wells
Particle from Waste Panels to LWB

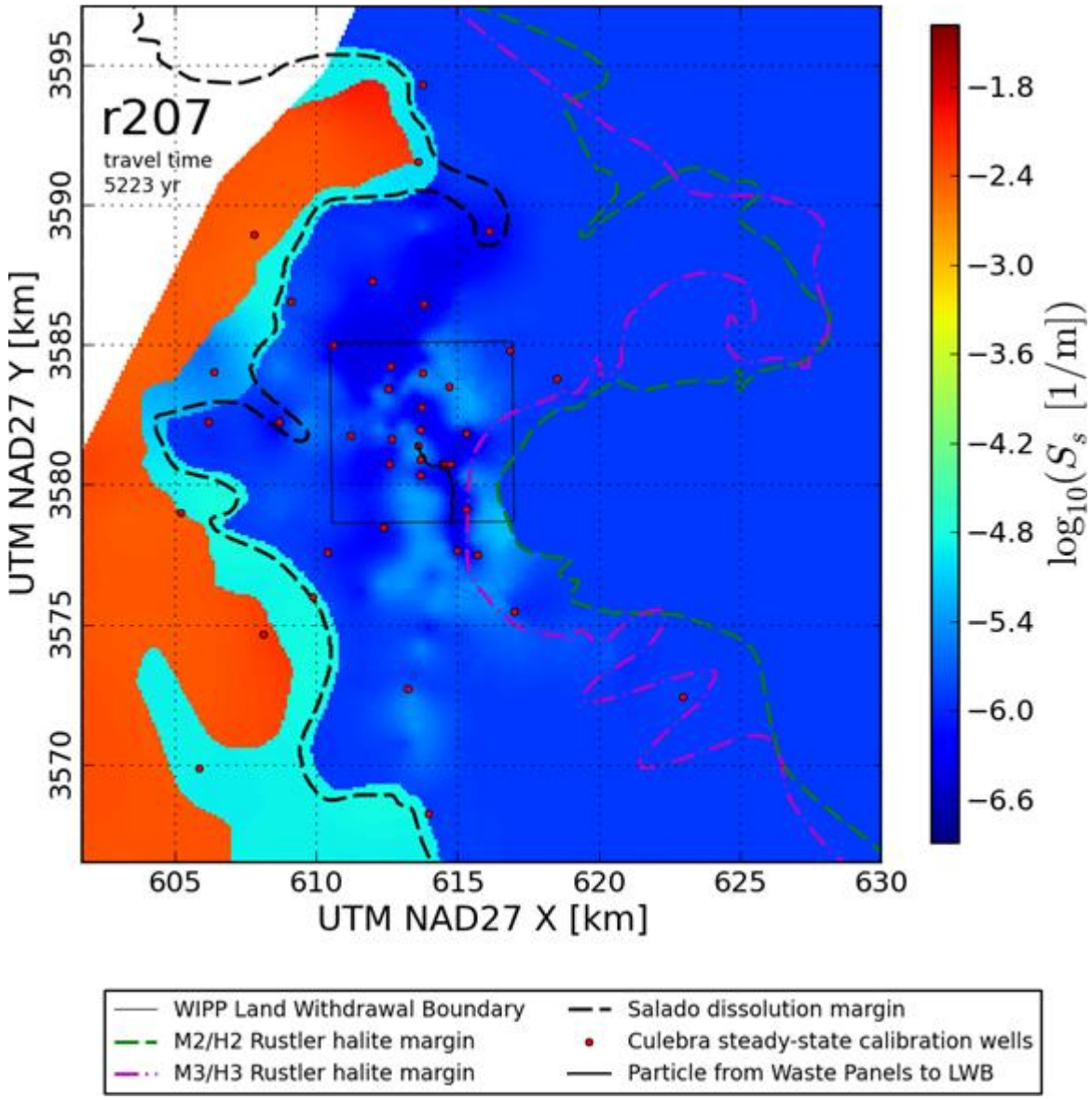
r207
travel time
5223 yr
UTM NAD27 Y [km]
3595
3590
3585
3580
3575
3570
605
610
615
620
625
630
UTM NAD27 X [km]
−1.8
−2.4
−3.0
−3.6
−4.2
−4.8
−5.4
−6.0
−6.6
$\log_{10}(S_s\ [1/\mathrm{m}])$
WIPP Land Withdrawal Boundary
M2/H2 Rustler halite margin
M3/H3 Rustler halite margin
Salado dissolution margin
Culebra steady-state calibration wells
Particle from Waste Panels to LWB

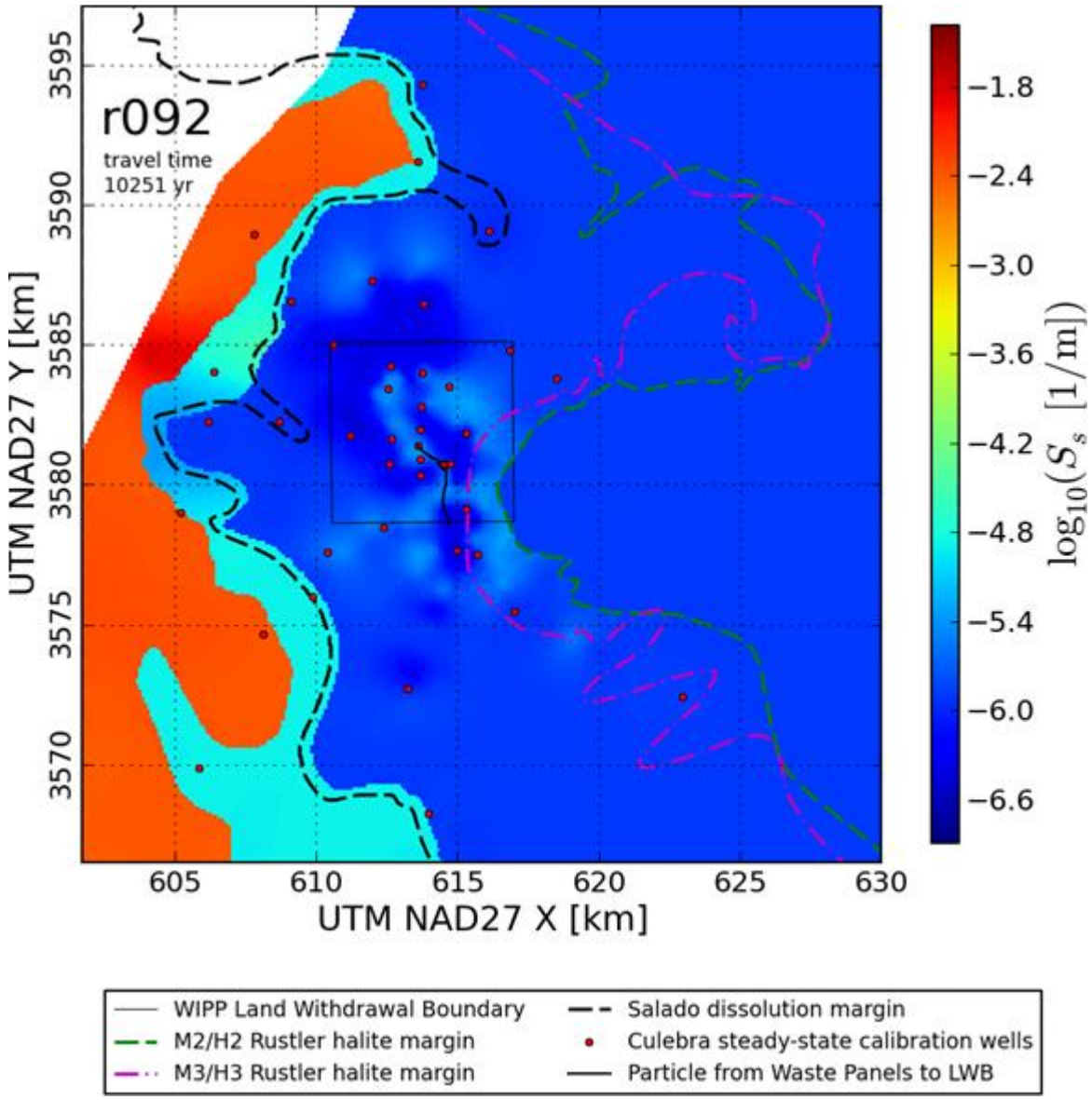
r092
travel time
10251 yr
UTM NAD27 Y [km]
3595
3590
3585
3580
3575
3570
605
610
615
620
625
630
UTM NAD27 X [km]
−1.8
−2.4
−3.0
−3.6
−4.2
−4.8
−5.4
−6.0
−6.6
$\log_{10}(S_s\ [1/\mathrm{m}])$
WIPP Land Withdrawal Boundary
M2/H2 Rustler halite margin
M3/H3 Rustler halite margin
Salado dissolution margin
Culebra steady-state calibration wells
Particle from Waste Panels to LWB

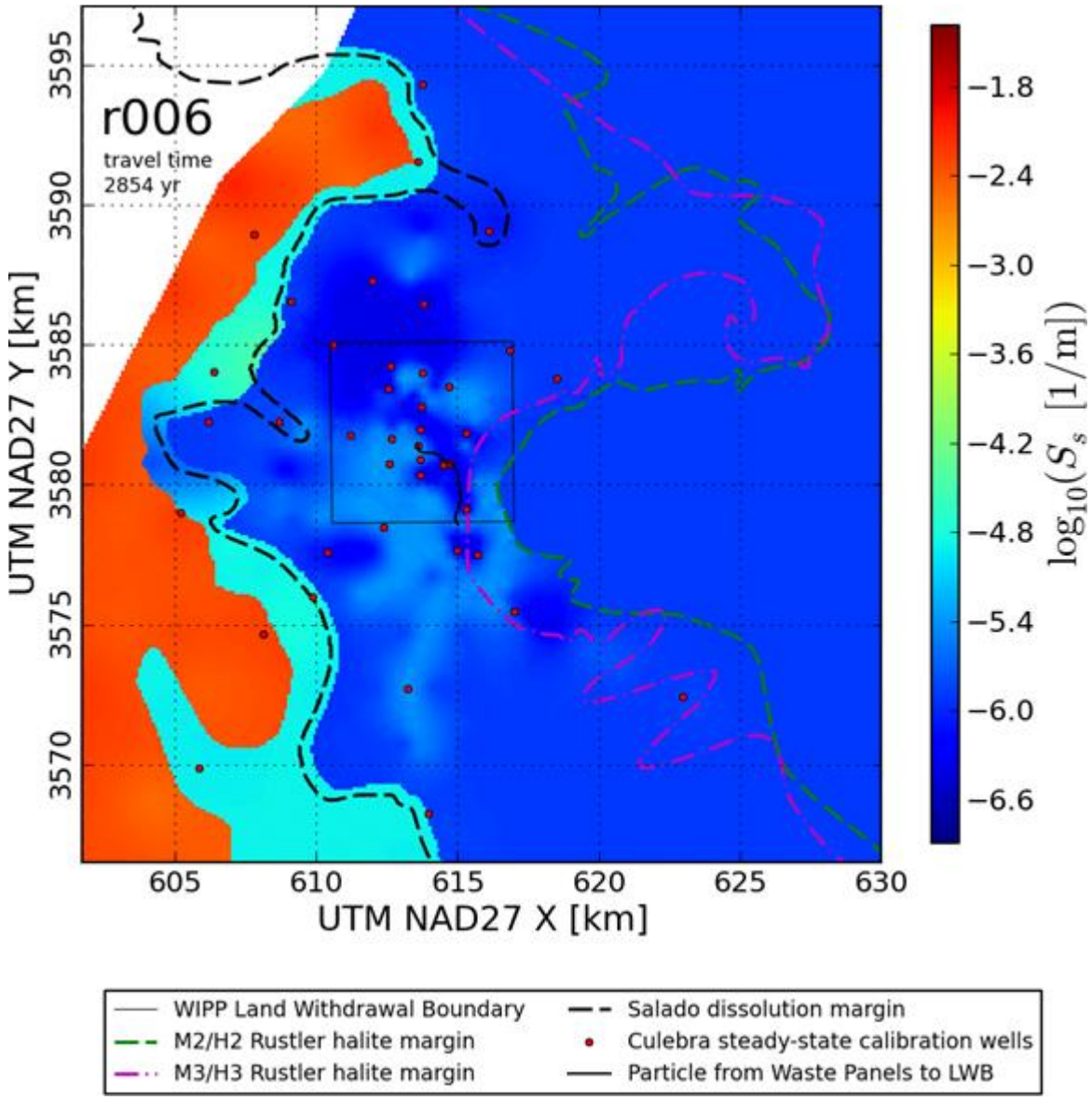
r006
travel time
2854 yr
UTM NAD27 Y [km]
3595
3590
3585
3580
3575
3570
605
610
615
620
625
630
UTM NAD27 X [km]
−1.8
−2.4
−3.0
−3.6
−4.2
−4.8
−5.4
−6.0
−6.6
$\log_{10}(S_s\ [1/\mathrm{m}])$
WIPP Land Withdrawal Boundary
M2/H2 Rustler halite margin
M3/H3 Rustler halite margin
Salado dissolution margin
Culebra steady-state calibration wells
Particle from Waste Panels to LWB

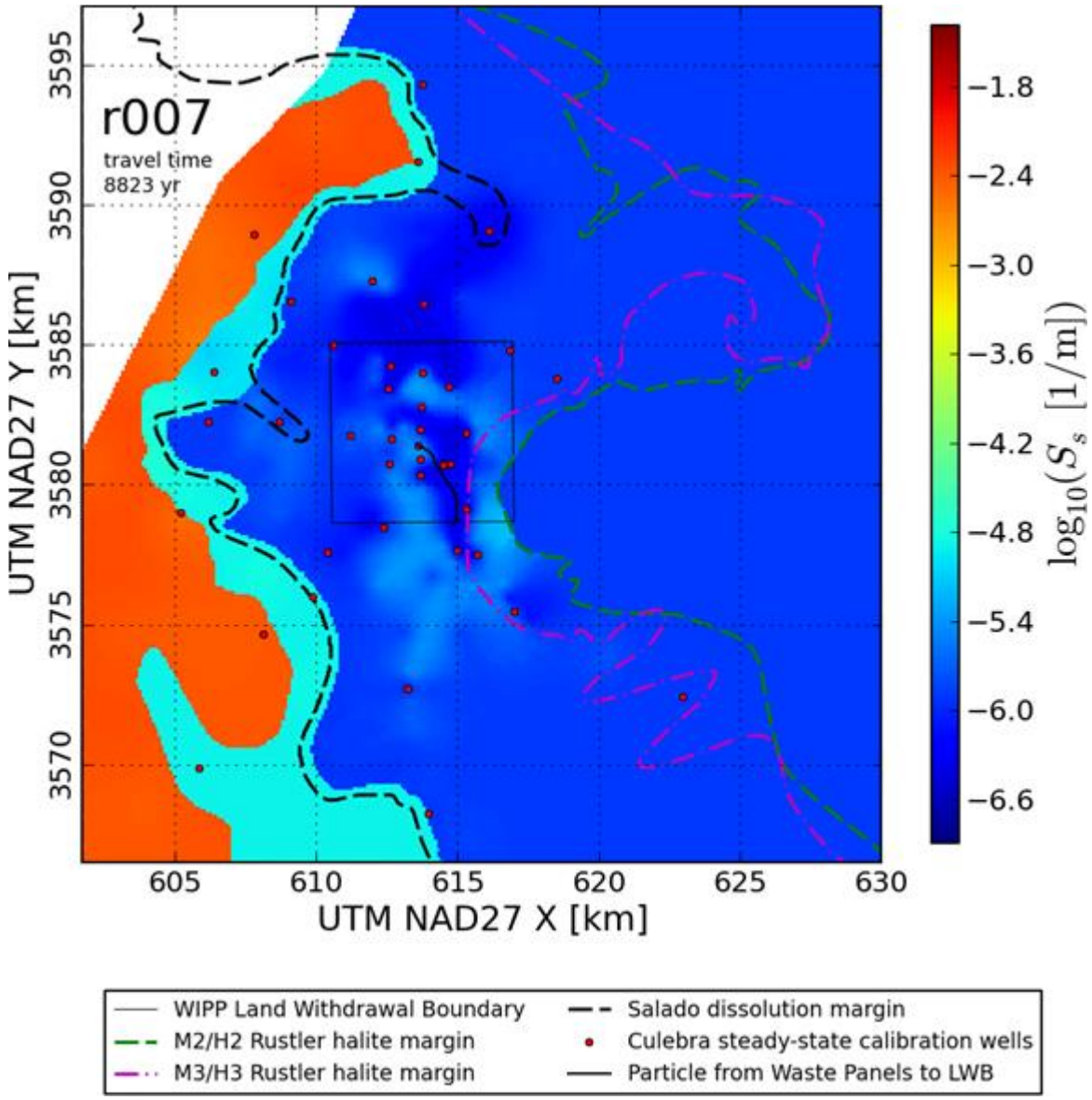
r007
travel time
8823 yr
UTM NAD27 Y [km]
3595
3590
3585
3580
3575
3570
605
610
615
620
625
630
UTM NAD27 X [km]
−1.8
−2.4
−3.0
−3.6
−4.2
−4.8
−5.4
−6.0
−6.6
$\log_{10}(S_s\ [1/\mathrm{m}])$
WIPP Land Withdrawal Boundary
M2/H2 Rustler halite margin
M3/H3 Rustler halite margin
Salado dissolution margin
Culebra steady-state calibration wells
Particle from Waste Panels to LWB

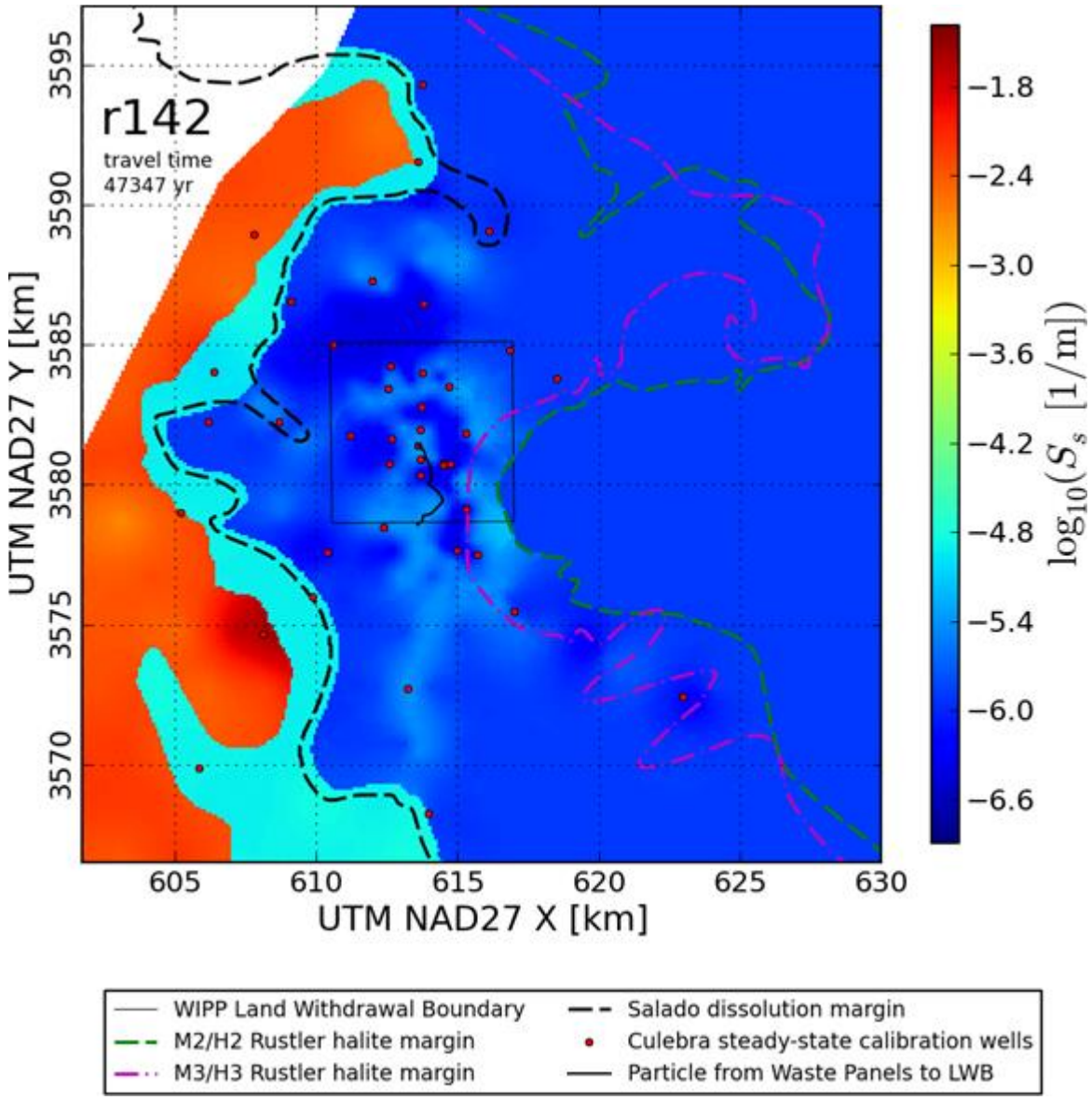
r142
travel time
47347 yr
UTM NAD27 Y [km]
3595
3590
3585
3580
3575
3570
605
610
615
620
625
630
UTM NAD27 X [km]
−1.8
−2.4
−3.0
−3.6
−4.2
−4.8
−5.4
−6.0
−6.6
$\log_{10}(S_s\ [1/\mathrm{m}])$
WIPP Land Withdrawal Boundary
M2/H2 Rustler halite margin
M3/H3 Rustler halite margin
Salado dissolution margin
Culebra steady-state calibration wells
Particle from Waste Panels to LWB

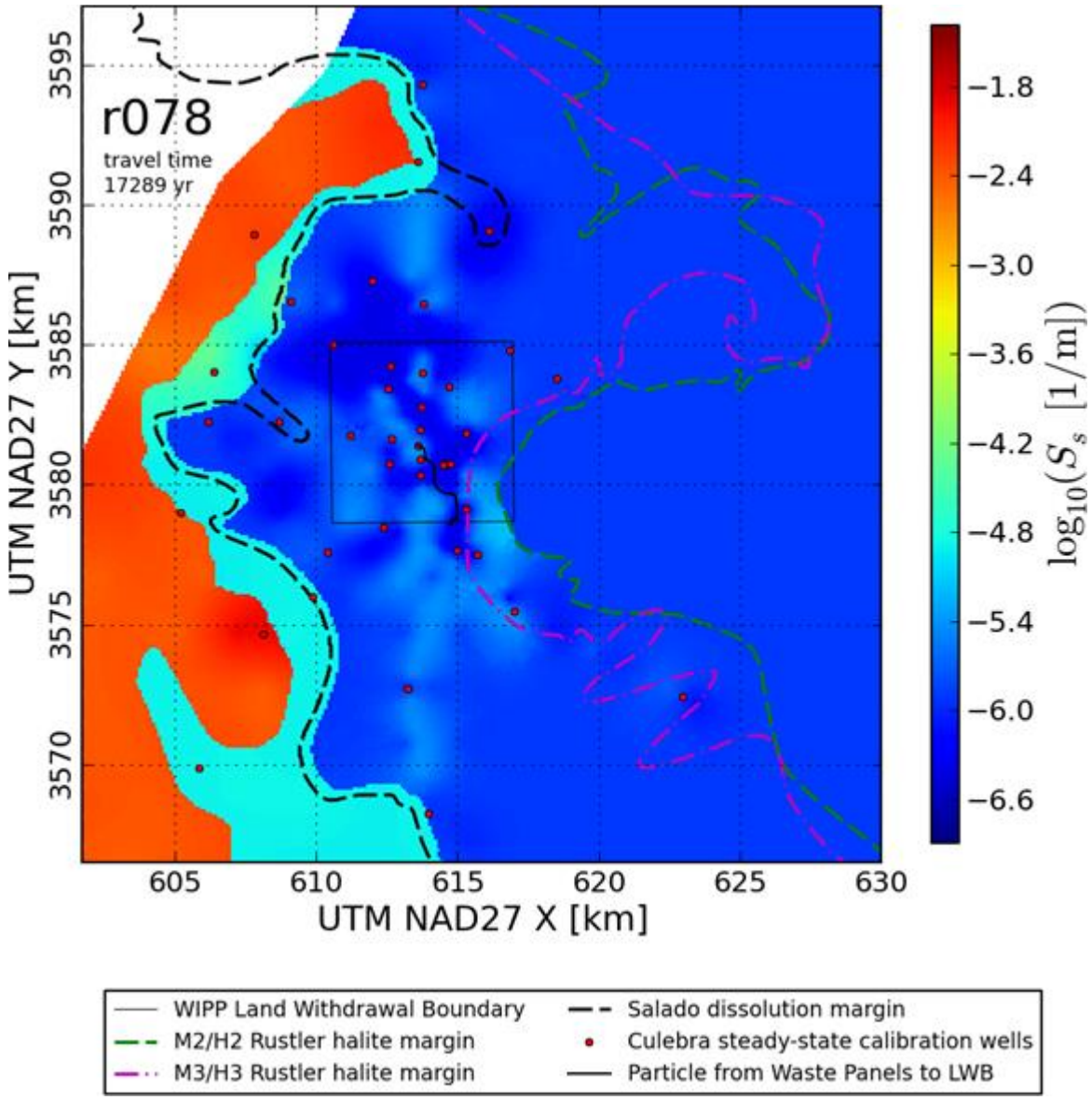
r078
travel time
17289 yr
UTM NAD27 Y [km]
3595
3590
3585
3580
3575
3570
605
610
615
620
625
630
UTM NAD27 X [km]
−1.8
−2.4
−3.0
−3.6
−4.2
−4.8
−5.4
−6.0
−6.6
$\log_{10}(S_s\ [1/\mathrm{m}])$
WIPP Land Withdrawal Boundary
M2/H2 Rustler halite margin
M3/H3 Rustler halite margin
Salado dissolution margin
Culebra steady-state calibration wells
Particle from Waste Panels to LWB

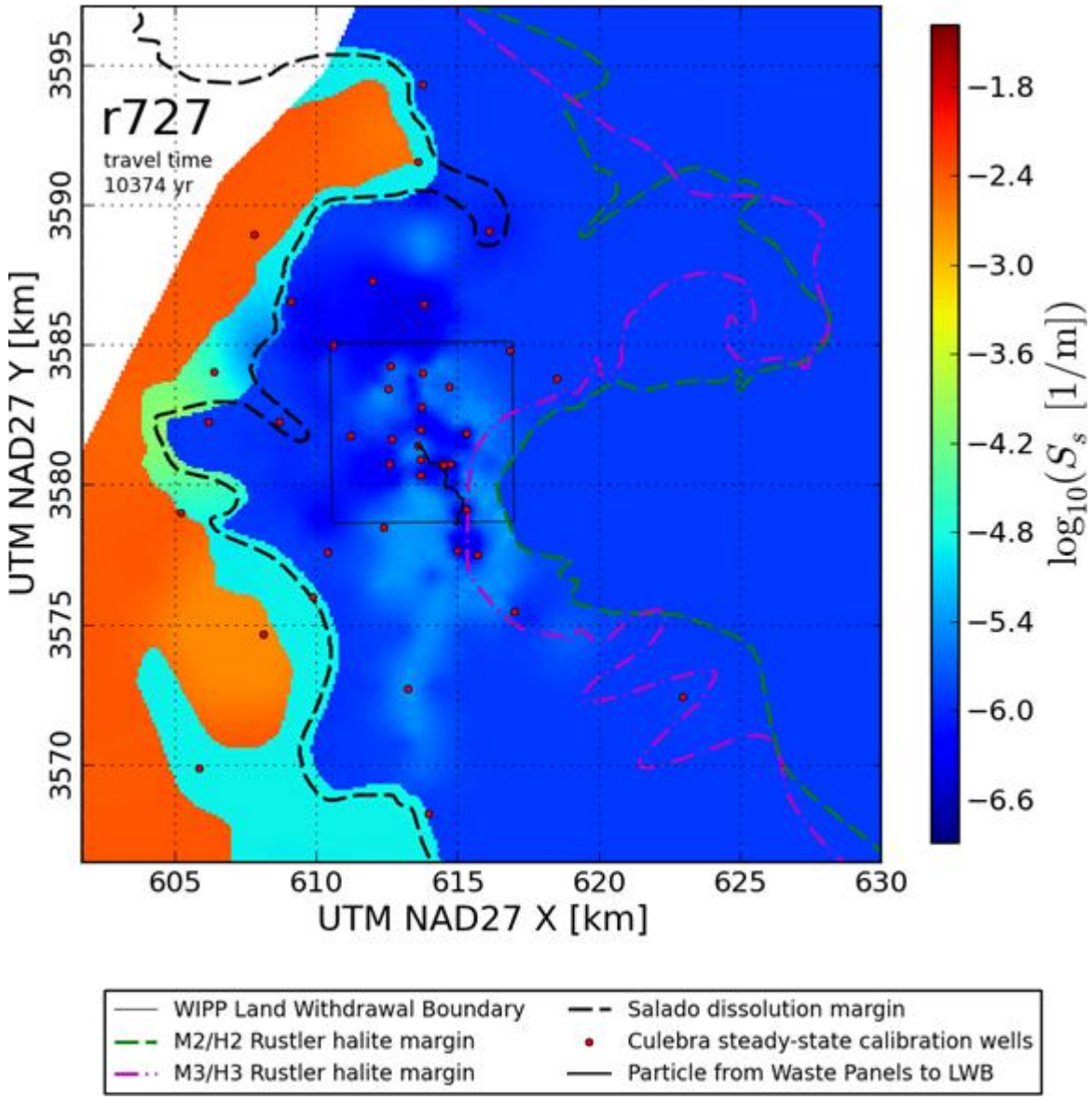
r727
travel time
10374 yr
UTM NAD27 Y [km]
3595
3590
3585
3580
3575
3570
605
610
615
620
625
630
UTM NAD27 X [km]
−1.8
−2.4
−3.0
−3.6
−4.2
−4.8
−5.4
−6.0
−6.6
$\log_{10}(S_s\ [1/\mathrm{m}])$
WIPP Land Withdrawal Boundary
M2/H2 Rustler halite margin
M3/H3 Rustler halite margin
Salado dissolution margin
Culebra steady-state calibration wells
Particle from Waste Panels to LWB

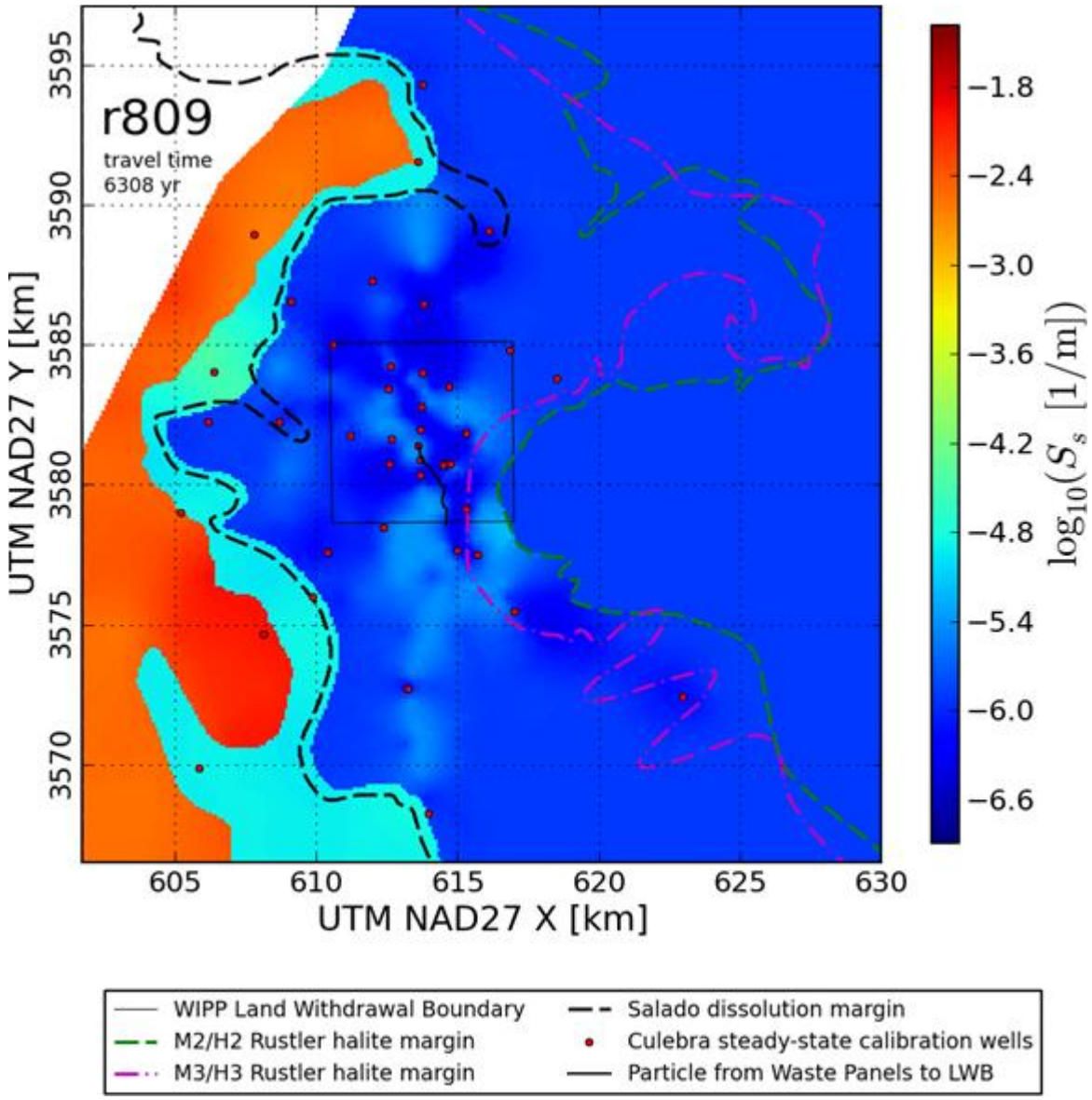
r809
travel time
6308 yr
UTM NAD27 Y [km]
3595
3590
3585
3580
3575
3570
605
610
615
620
625
630
UTM NAD27 X [km]
−1.8
−2.4
−3.0
−3.6
−4.2
−4.8
−5.4
−6.0
−6.6
$\log_{10}(S_s\ [1/\mathrm{m}])$
WIPP Land Withdrawal Boundary
M2/H2 Rustler halite margin
M3/H3 Rustler halite margin
Salado dissolution margin
Culebra steady-state calibration wells
Particle from Waste Panels to LWB

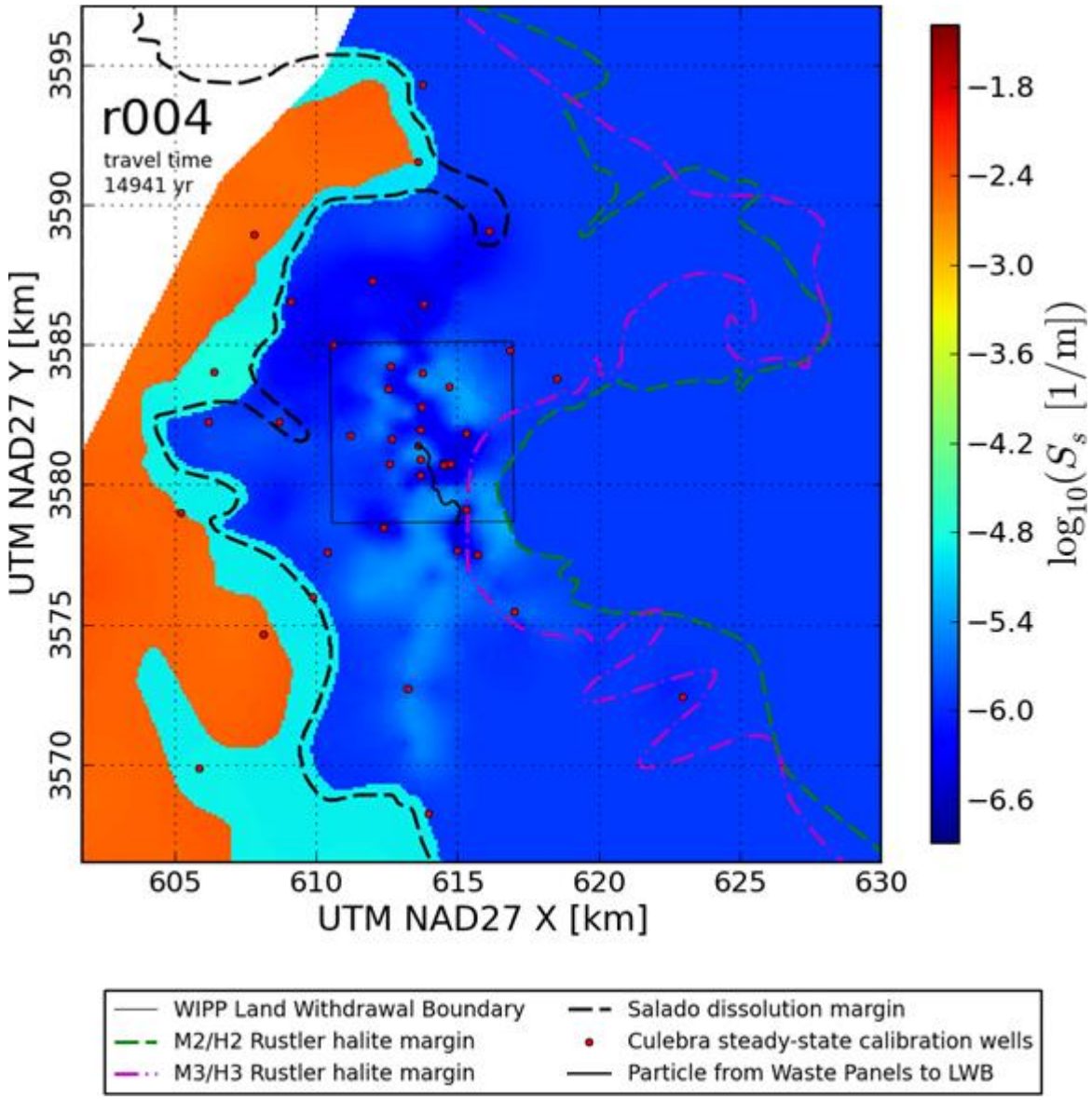
r004
travel time
14941 yr
UTM NAD27 Y [km]
3595
3590
3585
3580
3575
3570
605
610
615
620
625
630
UTM NAD27 X [km]
−1.8
−2.4
−3.0
−3.6
−4.2
−4.8
−5.4
−6.0
−6.6
$\log_{10}(S_s\ [1/\mathrm{m}])$
WIPP Land Withdrawal Boundary
M2/H2 Rustler halite margin
M3/H3 Rustler halite margin
Salado dissolution margin
Culebra steady-state calibration wells
Particle from Waste Panels to LWB

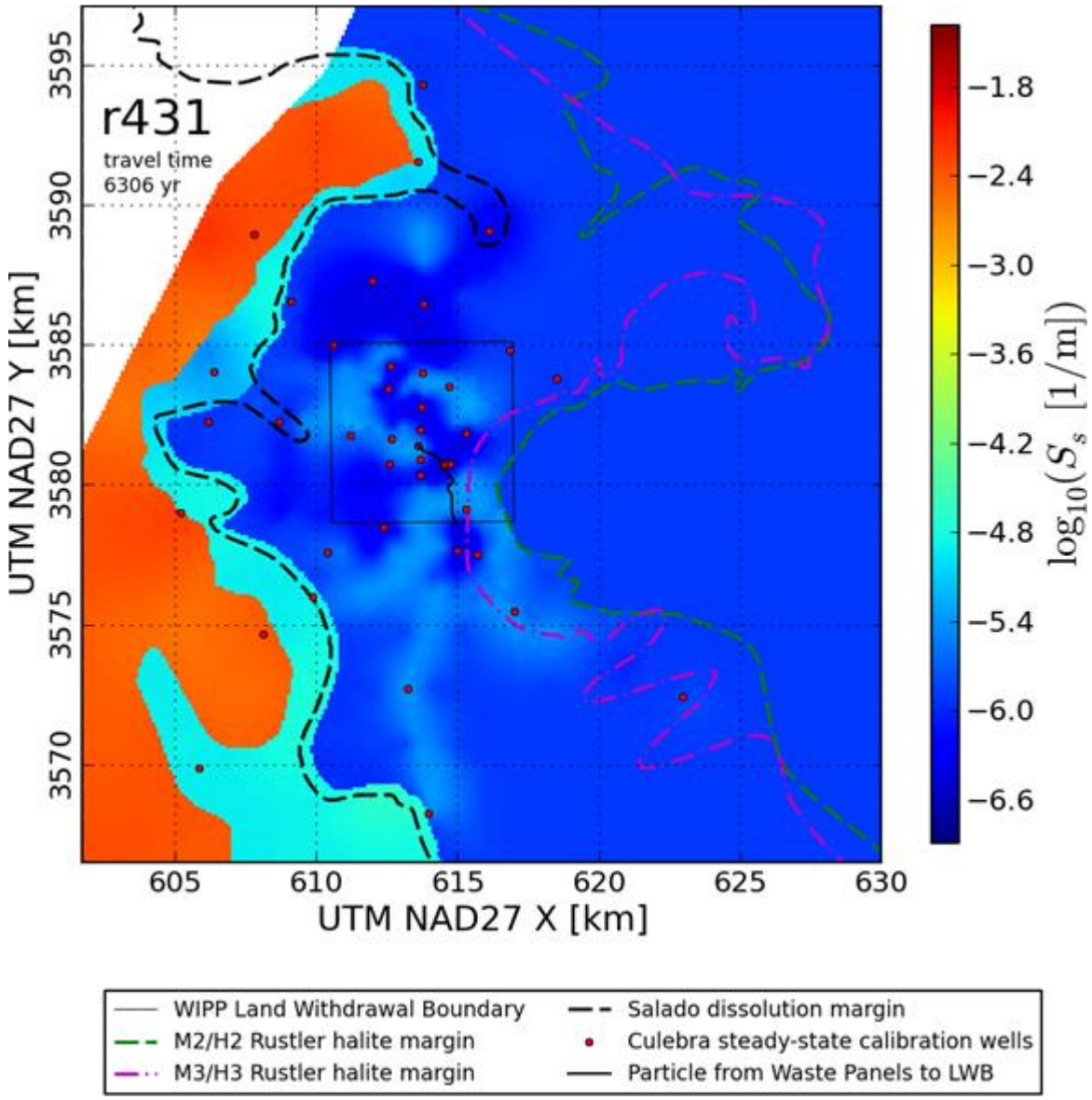
r431
travel time
6306 yr
UTM NAD27 Y [km]
3595
3590
3585
3580
3575
3570
605
610
615
620
625
630
UTM NAD27 X [km]
−1.8
−2.4
−3.0
−3.6
−4.2
−4.8
−5.4
−6.0
−6.6
$\log_{10}(S_s\ [1/\mathrm{m}])$
WIPP Land Withdrawal Boundary
M2/H2 Rustler halite margin
M3/H3 Rustler halite margin
Salado dissolution margin
Culebra steady-state calibration wells
Particle from Waste Panels to LWB

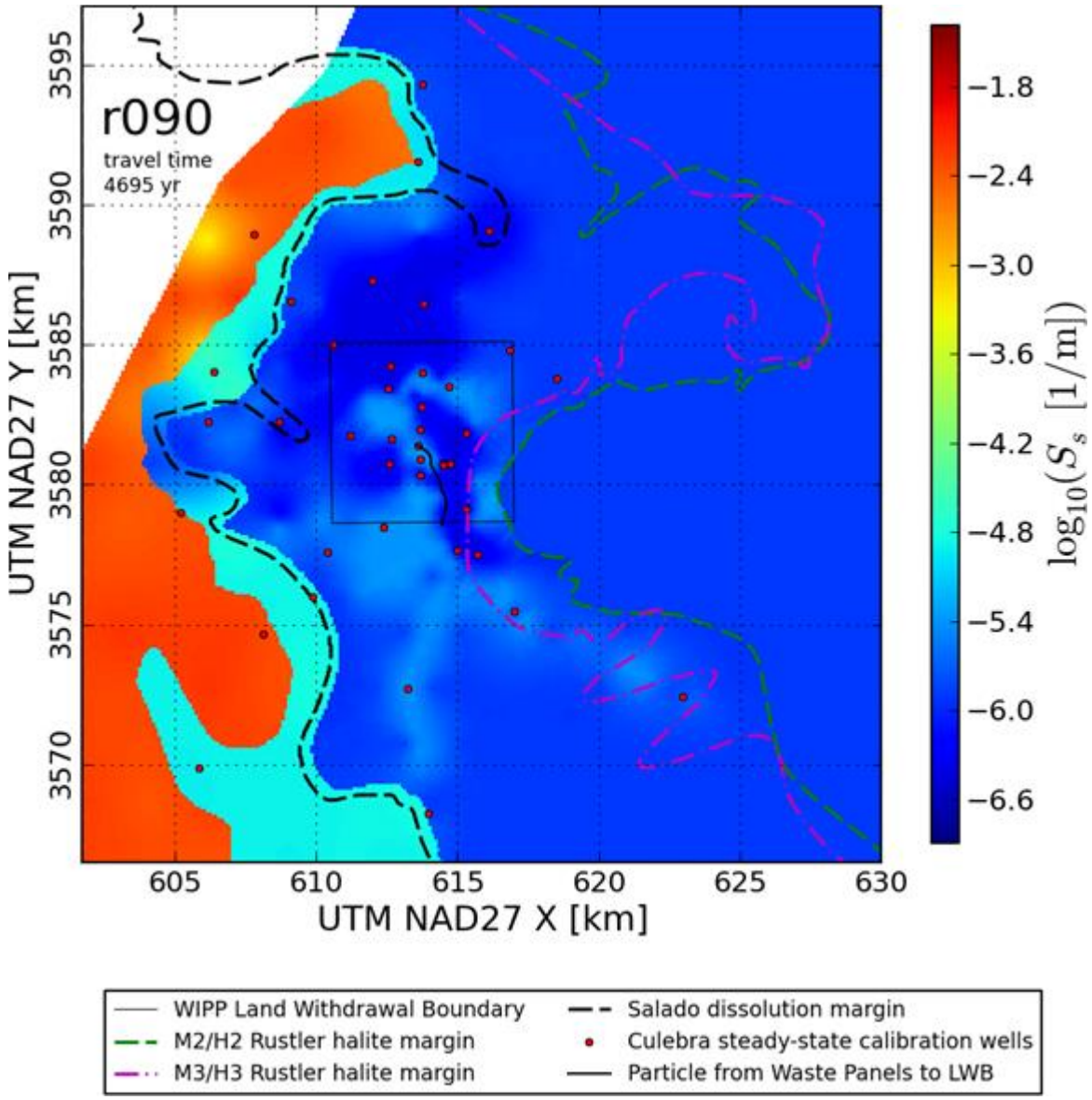
r090
travel time
4695 yr
UTM NAD27 Y [km]
3595
3590
3585
3580
3575
3570
605
610
615
620
625
630
UTM NAD27 X [km]
−1.8
−2.4
−3.0
−3.6
−4.2
−4.8
−5.4
−6.0
−6.6
$\log_{10}(S_s\ [1/\mathrm{m}])$
WIPP Land Withdrawal Boundary
M2/H2 Rustler halite margin
M3/H3 Rustler halite margin
Salado dissolution margin
Culebra steady-state calibration wells
Particle from Waste Panels to LWB

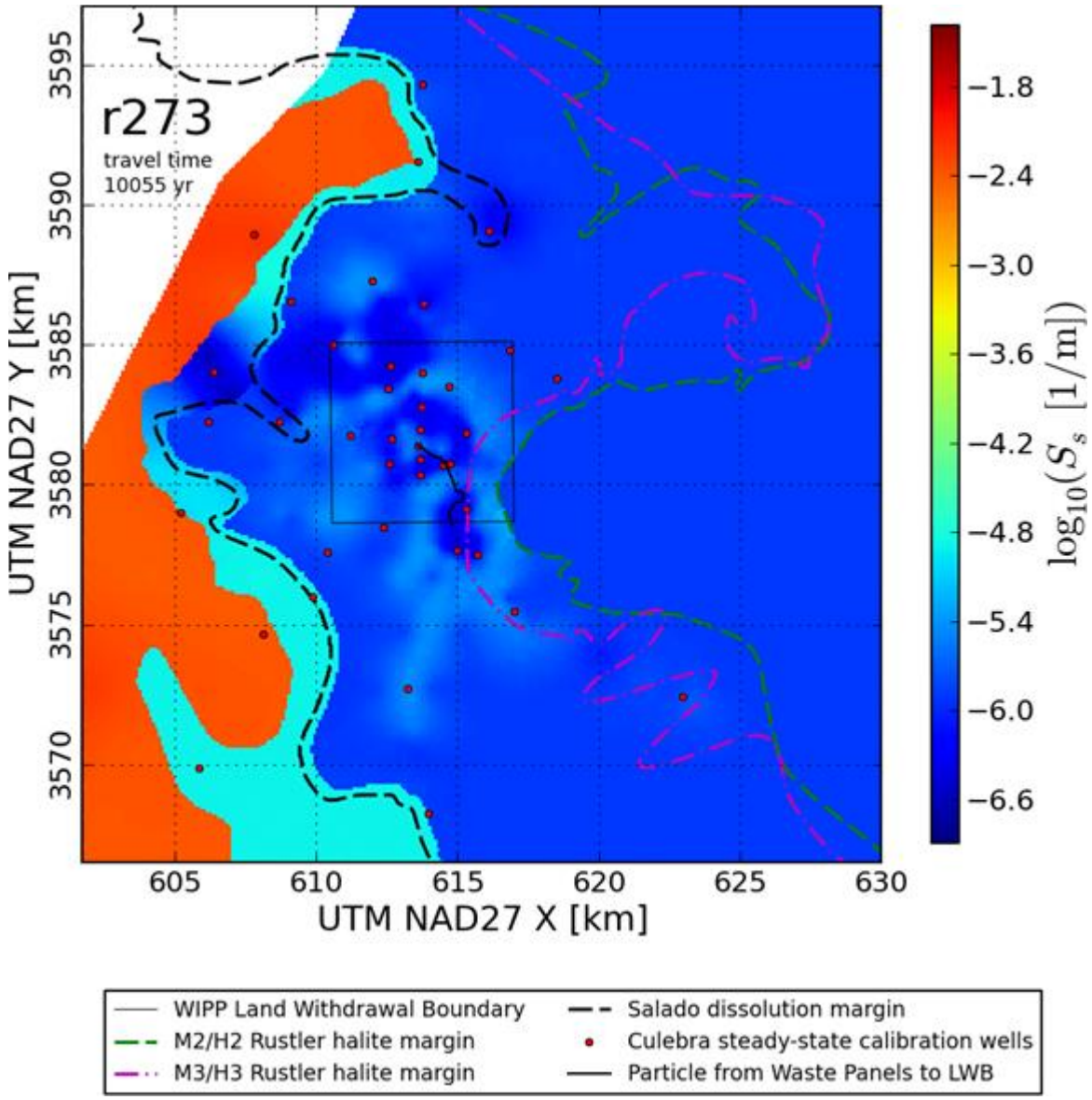
r273
travel time
10055 yr
UTM NAD27 Y [km]
3595
3590
3585
3580
3575
3570
605
610
615
620
625
630
UTM NAD27 X [km]
−1.8
−2.4
−3.0
−3.6
−4.2
−4.8
−5.4
−6.0
−6.6
$\log_{10}(S_s\ [1/\mathrm{m}])$
WIPP Land Withdrawal Boundary
M2/H2 Rustler halite margin
M3/H3 Rustler halite margin
Salado dissolution margin
Culebra steady-state calibration wells
Particle from Waste Panels to LWB

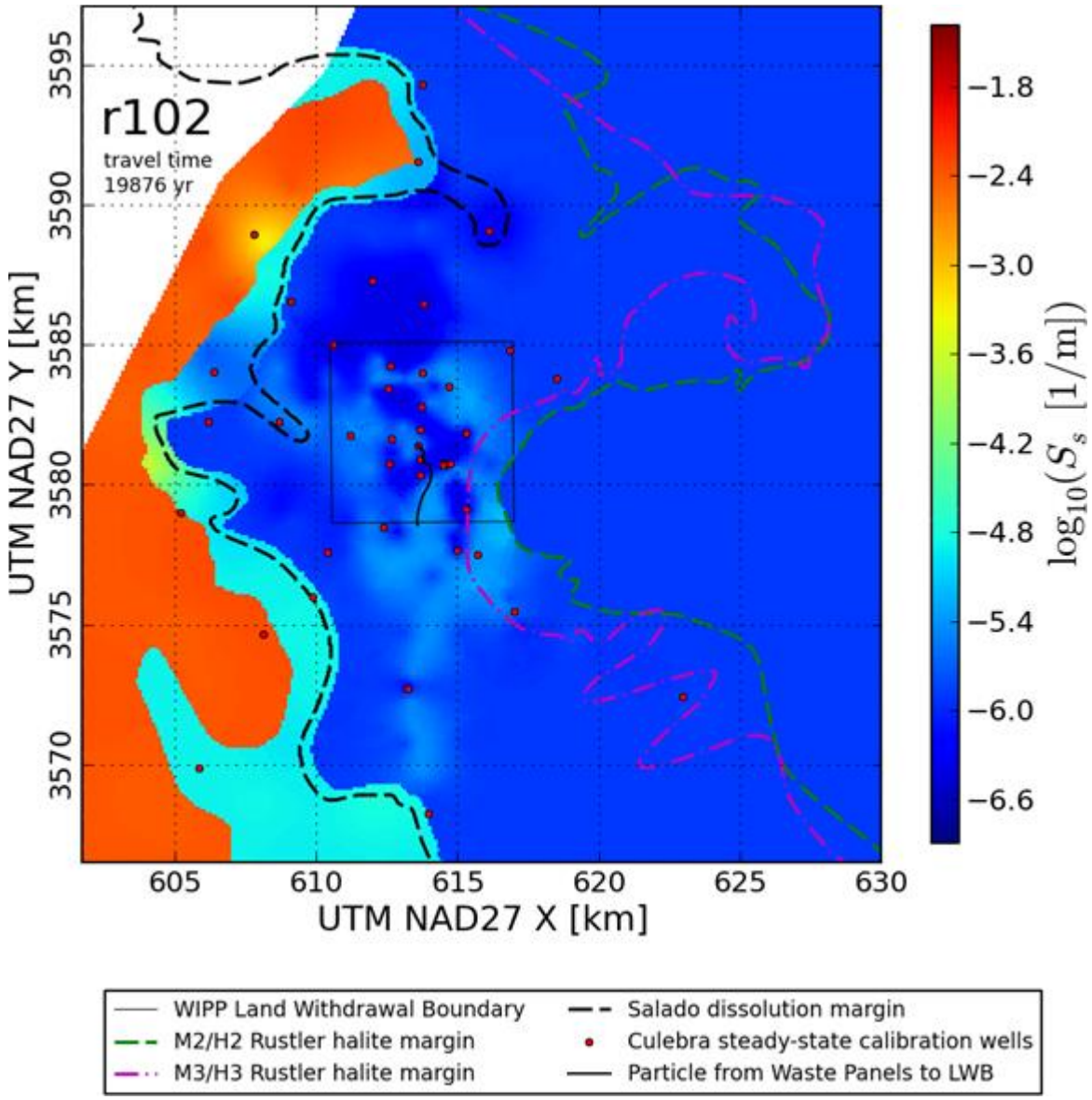
r102
travel time
19876 yr
UTM NAD27 Y [km]
3595
3590
3585
3580
3575
3570
605
610
615
620
625
630
UTM NAD27 X [km]
−1.8
−2.4
−3.0
−3.6
−4.2
−4.8
−5.4
−6.0
−6.6
$\log_{10}(S_s\ [1/\mathrm{m}])$
WIPP Land Withdrawal Boundary
M2/H2 Rustler halite margin
M3/H3 Rustler halite margin
Salado dissolution margin
Culebra steady-state calibration wells
Particle from Waste Panels to LWB

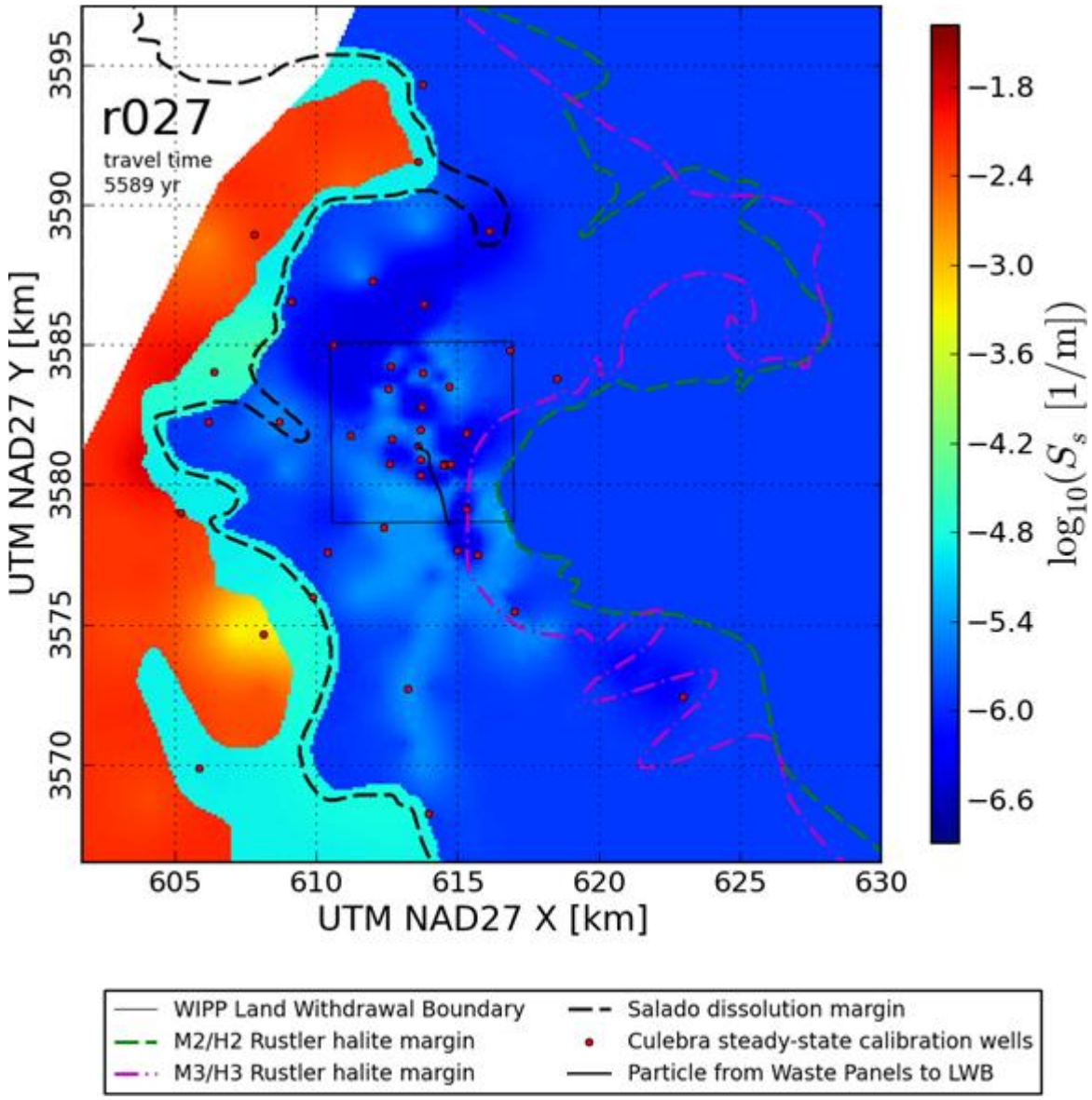
r027
travel time
5589 yr
UTM NAD27 Y [km]
3595
3590
3585
3580
3575
3570
605
610
615
620
625
630
UTM NAD27 X [km]
−1.8
−2.4
−3.0
−3.6
−4.2
−4.8
−5.4
−6.0
−6.6
$\log_{10}(S_s\ [1/\mathrm{m}])$
WIPP Land Withdrawal Boundary
M2/H2 Rustler halite margin
M3/H3 Rustler halite margin
Salado dissolution margin
Culebra steady-state calibration wells
Particle from Waste Panels to LWB

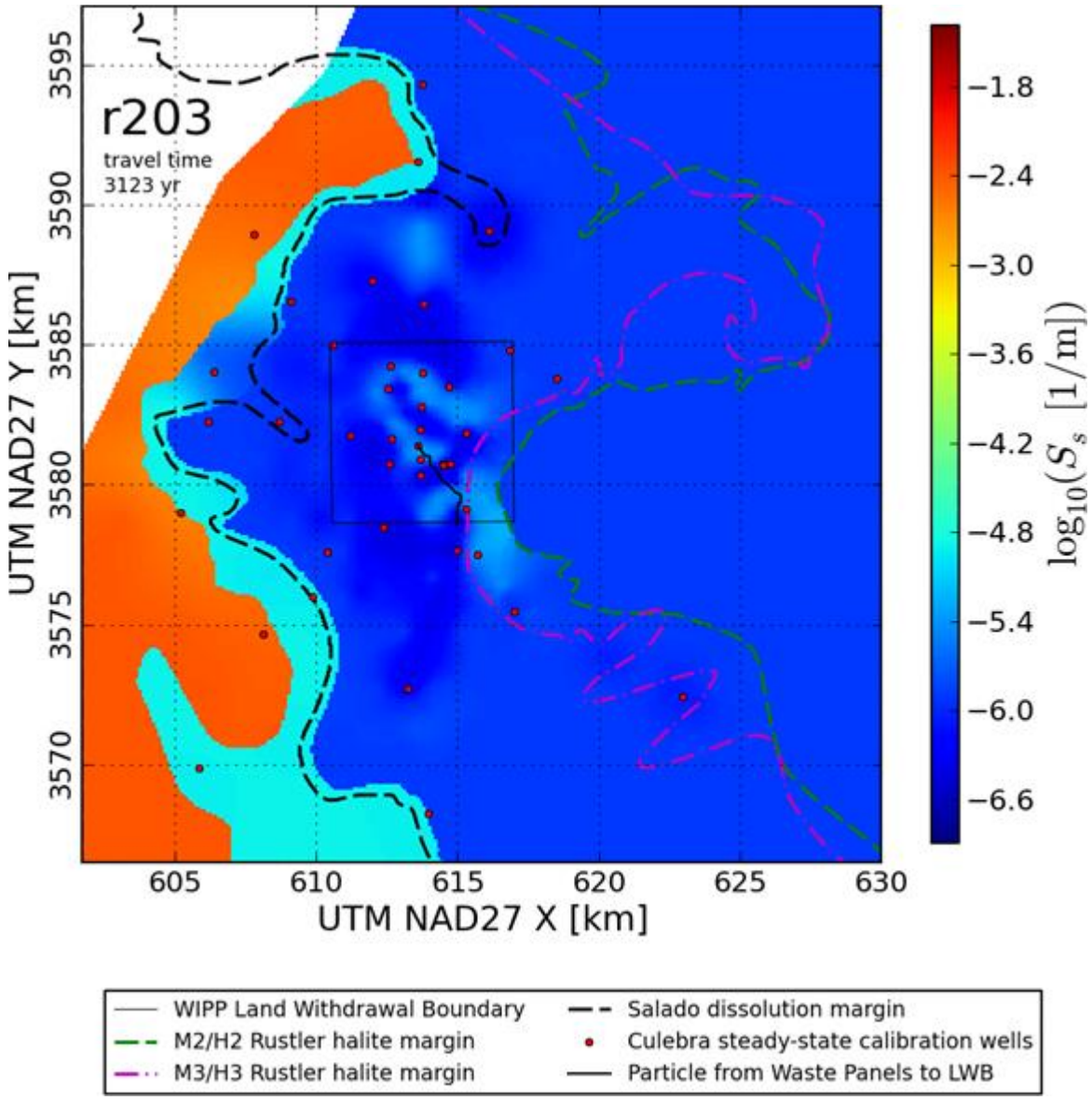
r203
travel time
3123 yr
UTM NAD27 Y [km]
3595
3590
3585
3580
3575
3570
605
610
615
620
625
630
UTM NAD27 X [km]
−1.8
−2.4
−3.0
−3.6
−4.2
−4.8
−5.4
−6.0
−6.6
$\log_{10}(S_s\ [1/\mathrm{m}])$
WIPP Land Withdrawal Boundary
M2/H2 Rustler halite margin
M3/H3 Rustler halite margin
Salado dissolution margin
Culebra steady-state calibration wells
Particle from Waste Panels to LWB

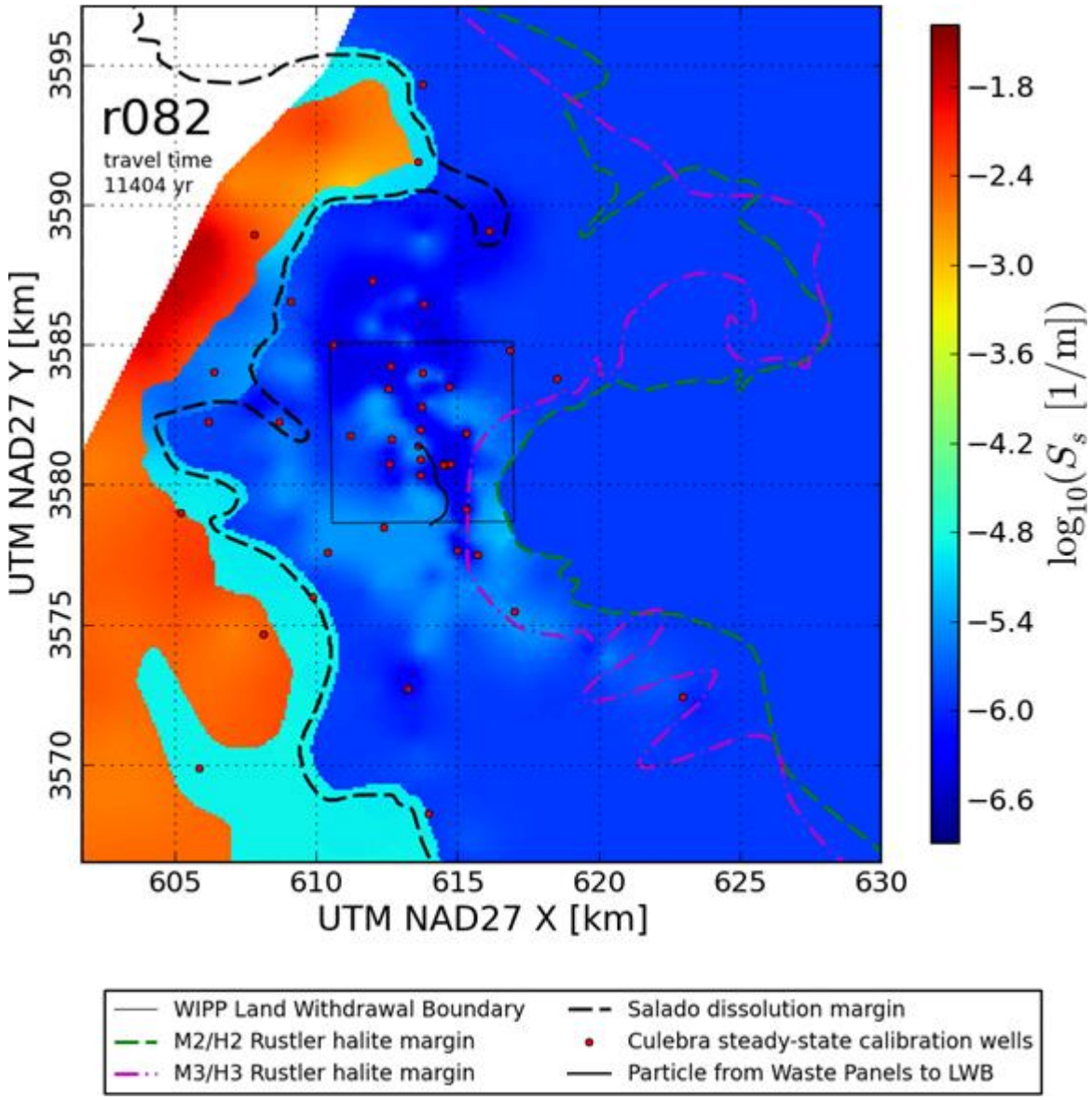
r082
travel time
11404 yr
UTM NAD27 Y [km]
3595
3590
3585
3580
3575
3570
605
610
615
620
625
630
UTM NAD27 X [km]
−1.8
−2.4
−3.0
−3.6
−4.2
−4.8
−5.4
−6.0
−6.6
$\log_{10}(S_s\ [1/\mathrm{m}])$
WIPP Land Withdrawal Boundary
M2/H2 Rustler halite margin
M3/H3 Rustler halite margin
Salado dissolution margin
Culebra steady-state calibration wells
Particle from Waste Panels to LWB

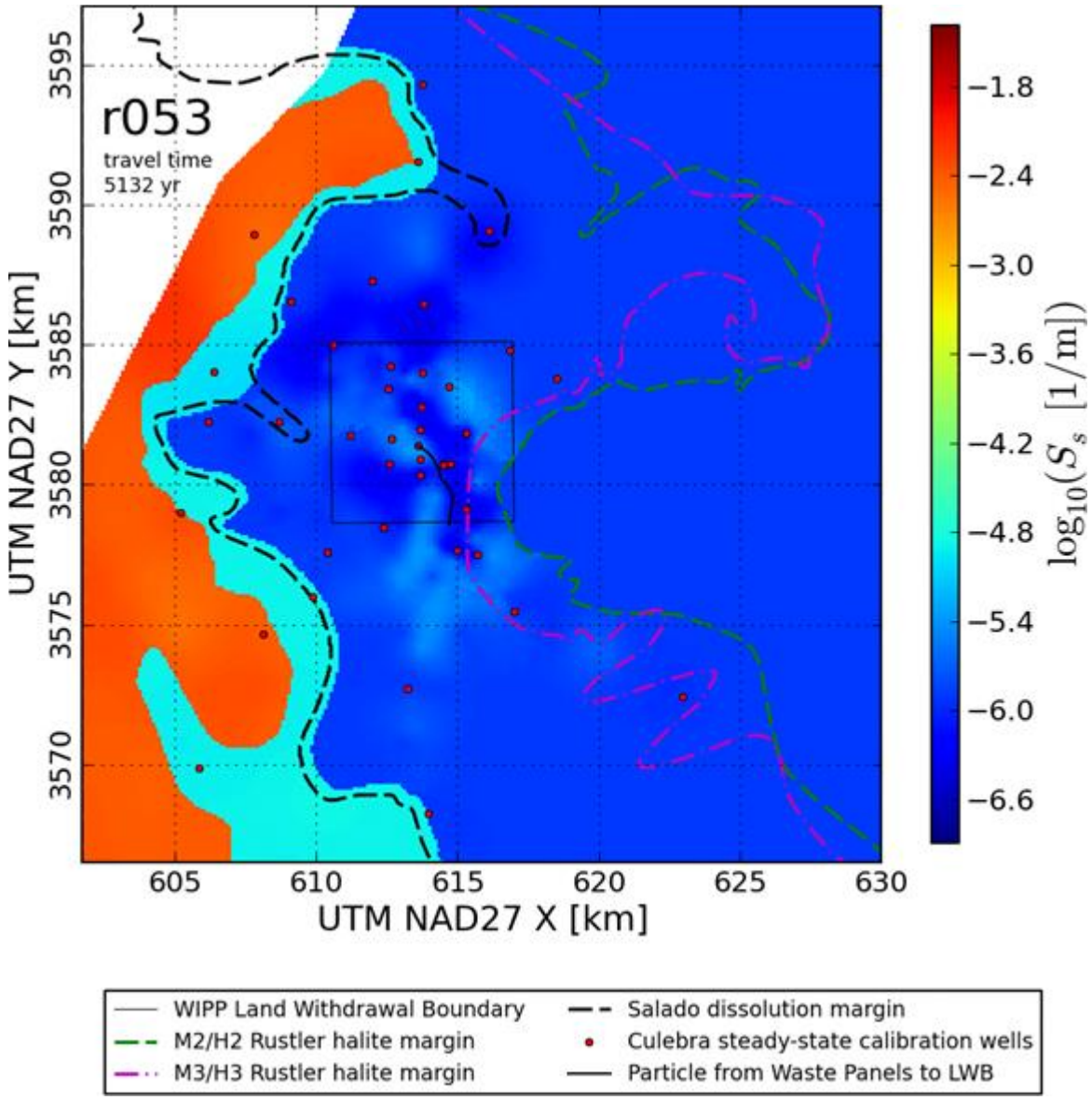
r053
travel time
5132 yr
UTM NAD27 Y [km]
3595
3590
3585
3580
3575
3570
605
610
615
620
625
630
UTM NAD27 X [km]
−1.8
−2.4
−3.0
−3.6
−4.2
−4.8
−5.4
−6.0
−6.6
$\log_{10}(S_s\ [1/\mathrm{m}])$
WIPP Land Withdrawal Boundary
M2/H2 Rustler halite margin
M3/H3 Rustler halite margin
Salado dissolution margin
Culebra steady-state calibration wells
Particle from Waste Panels to LWB

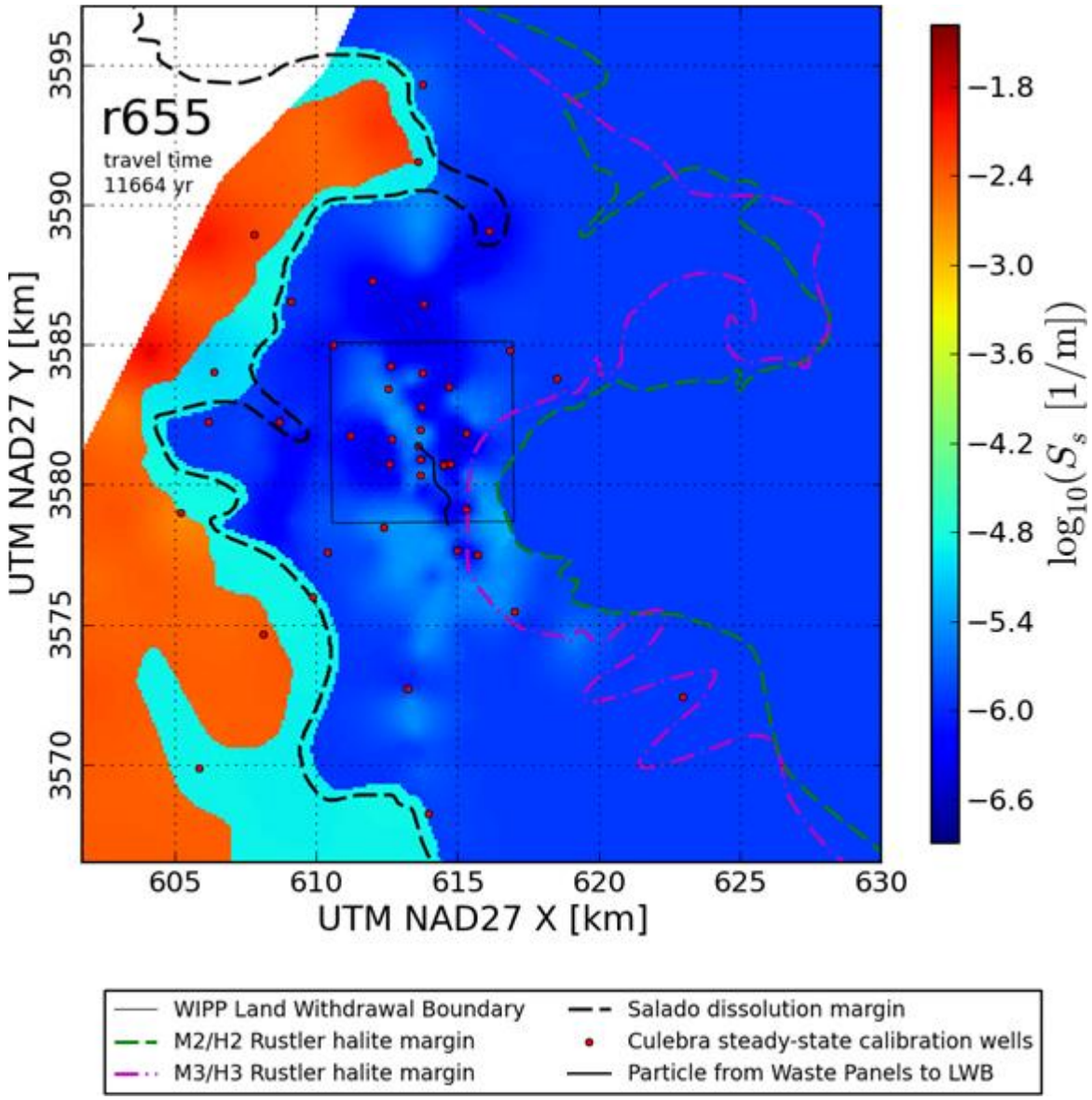
r655
travel time
11664 yr
UTM NAD27 Y [km]
3595
3590
3585
3580
3575
3570
605
610
615
620
625
630
UTM NAD27 X [km]
−1.8
−2.4
−3.0
−3.6
−4.2
−4.8
−5.4
−6.0
−6.6
$\log_{10}(S_s\ [1/\mathrm{m}])$
WIPP Land Withdrawal Boundary
M2/H2 Rustler halite margin
M3/H3 Rustler halite margin
Salado dissolution margin
Culebra steady-state calibration wells
Particle from Waste Panels to LWB

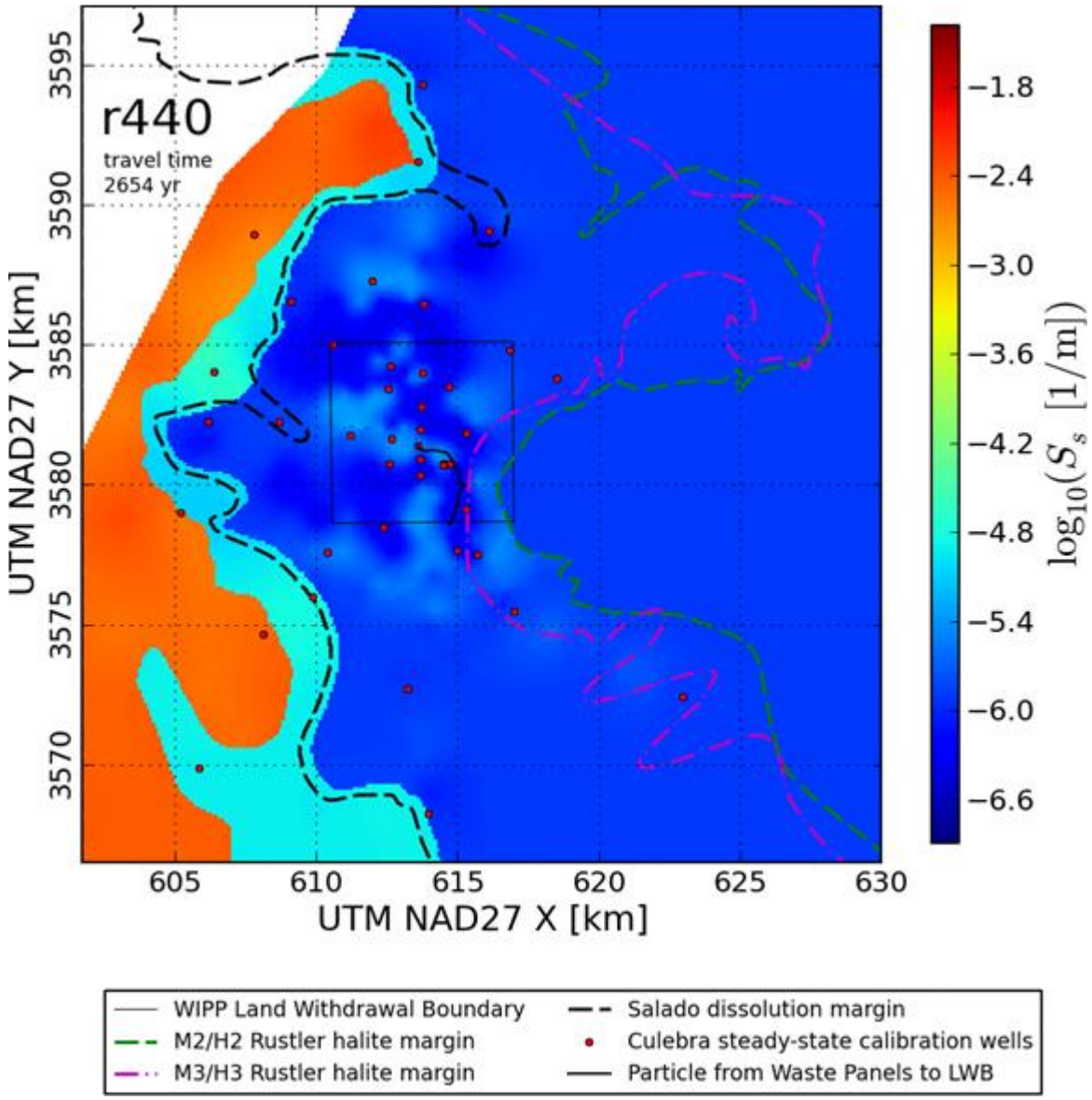
r440
travel time
2654 yr
UTM NAD27 Y [km]
3595
3590
3585
3580
3575
3570
605
610
615
620
625
630
UTM NAD27 X [km]
−1.8
−2.4
−3.0
−3.6
−4.2
−4.8
−5.4
−6.0
−6.6
$\log_{10}(S_s\ [1/\mathrm{m}])$
WIPP Land Withdrawal Boundary
M2/H2 Rustler halite margin
M3/H3 Rustler halite margin
Salado dissolution margin
Culebra steady-state calibration wells
Particle from Waste Panels to LWB

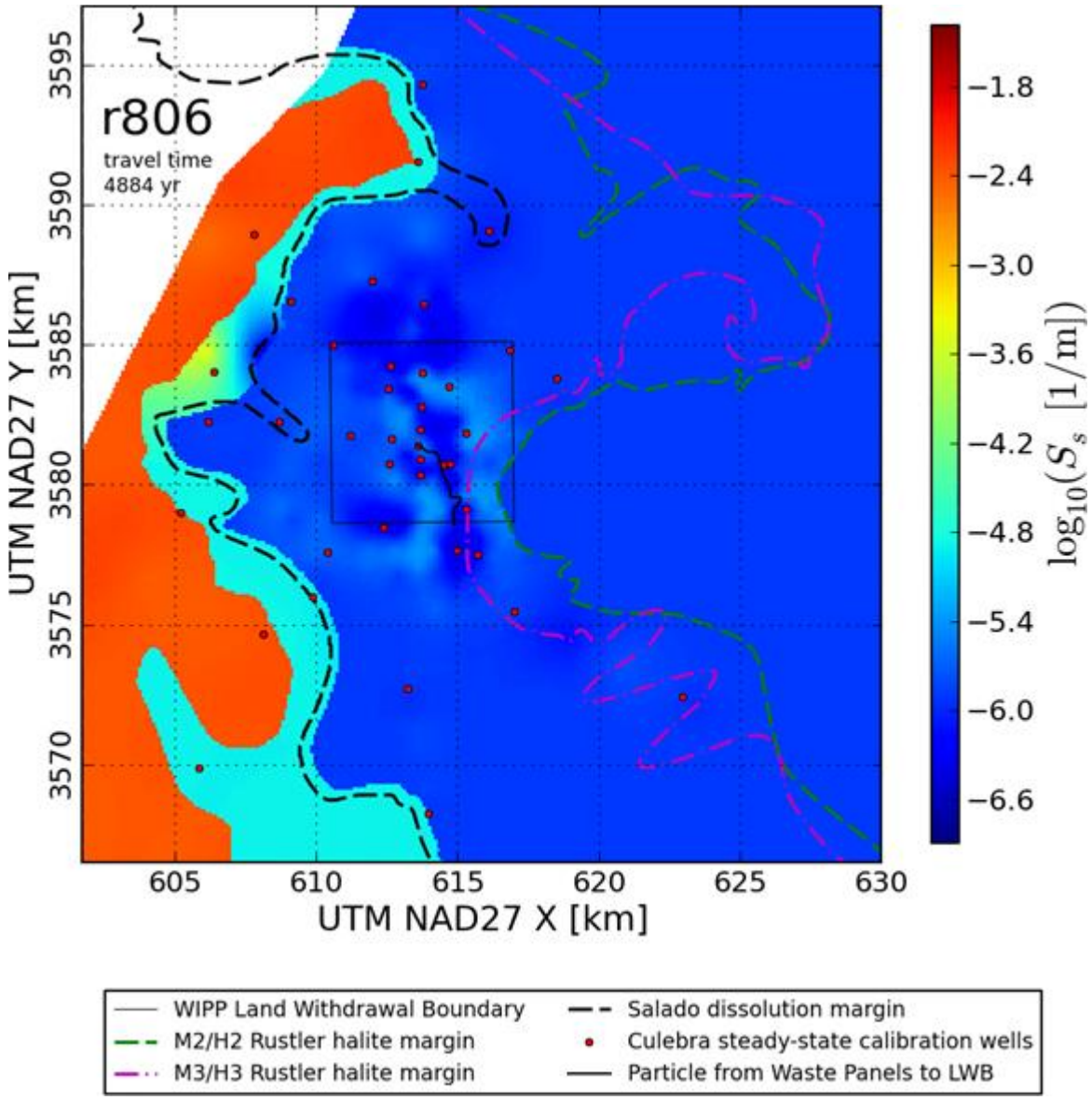
r806
travel time
4884 yr
UTM NAD27 Y [km]
3595
3590
3585
3580
3575
3570
605
610
615
620
625
630
UTM NAD27 X [km]
−1.8
−2.4
−3.0
−3.6
−4.2
−4.8
−5.4
−6.0
−6.6
$\log_{10}(S_s\ [1/\mathrm{m}])$
WIPP Land Withdrawal Boundary
M2/H2 Rustler halite margin
M3/H3 Rustler halite margin
Salado dissolution margin
Culebra steady-state calibration wells
Particle from Waste Panels to LWB

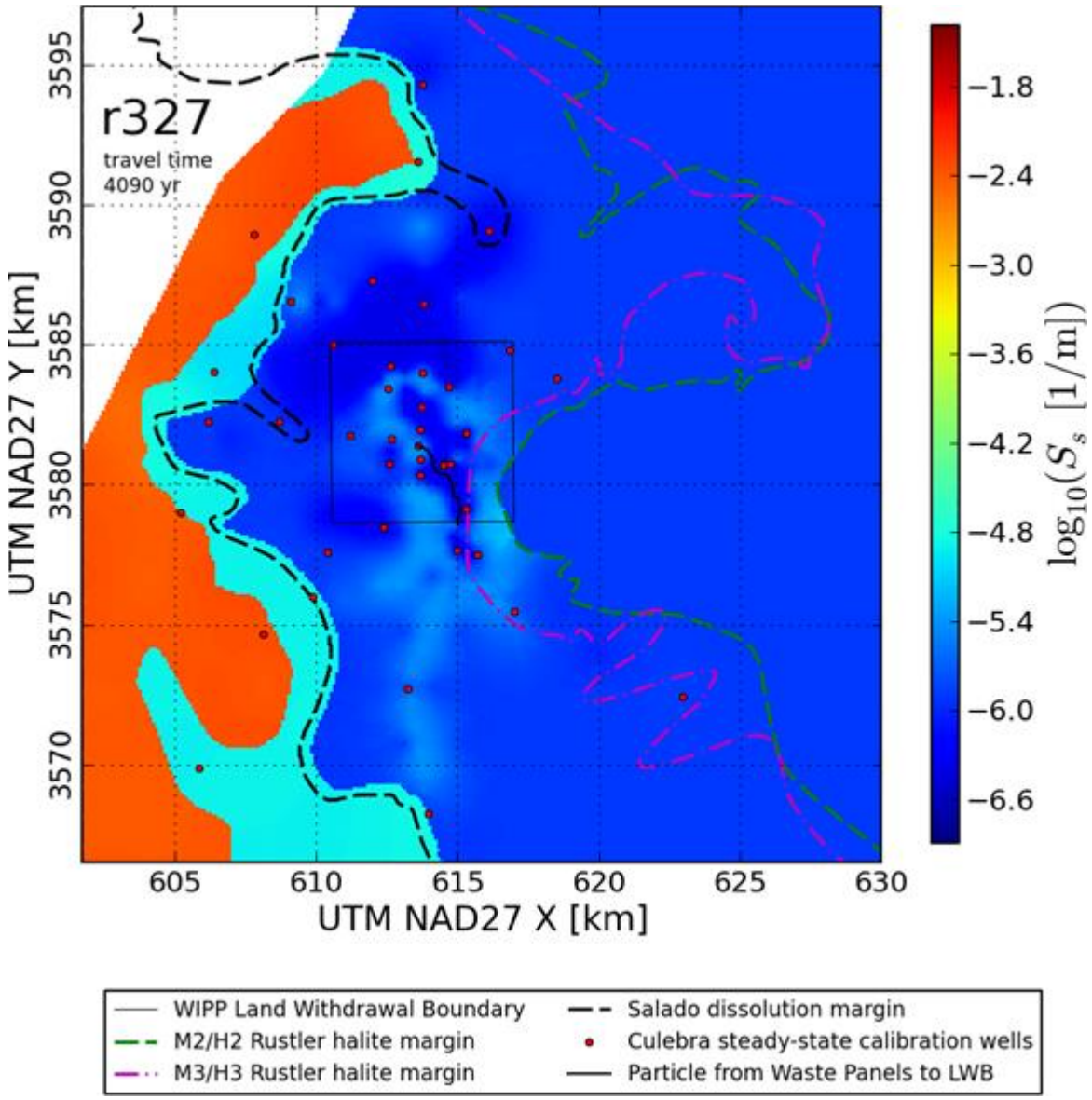
r327
travel time
4090 yr
UTM NAD27 Y [km]
3595
3590
3585
3580
3575
3570
605
610
615
620
625
630
UTM NAD27 X [km]
−1.8
−2.4
−3.0
−3.6
−4.2
−4.8
−5.4
−6.0
−6.6
$\log_{10}(S_s\ [1/\mathrm{m}])$
WIPP Land Withdrawal Boundary
M2/H2 Rustler halite margin
M3/H3 Rustler halite margin
Salado dissolution margin
Culebra steady-state calibration wells
Particle from Waste Panels to LWB

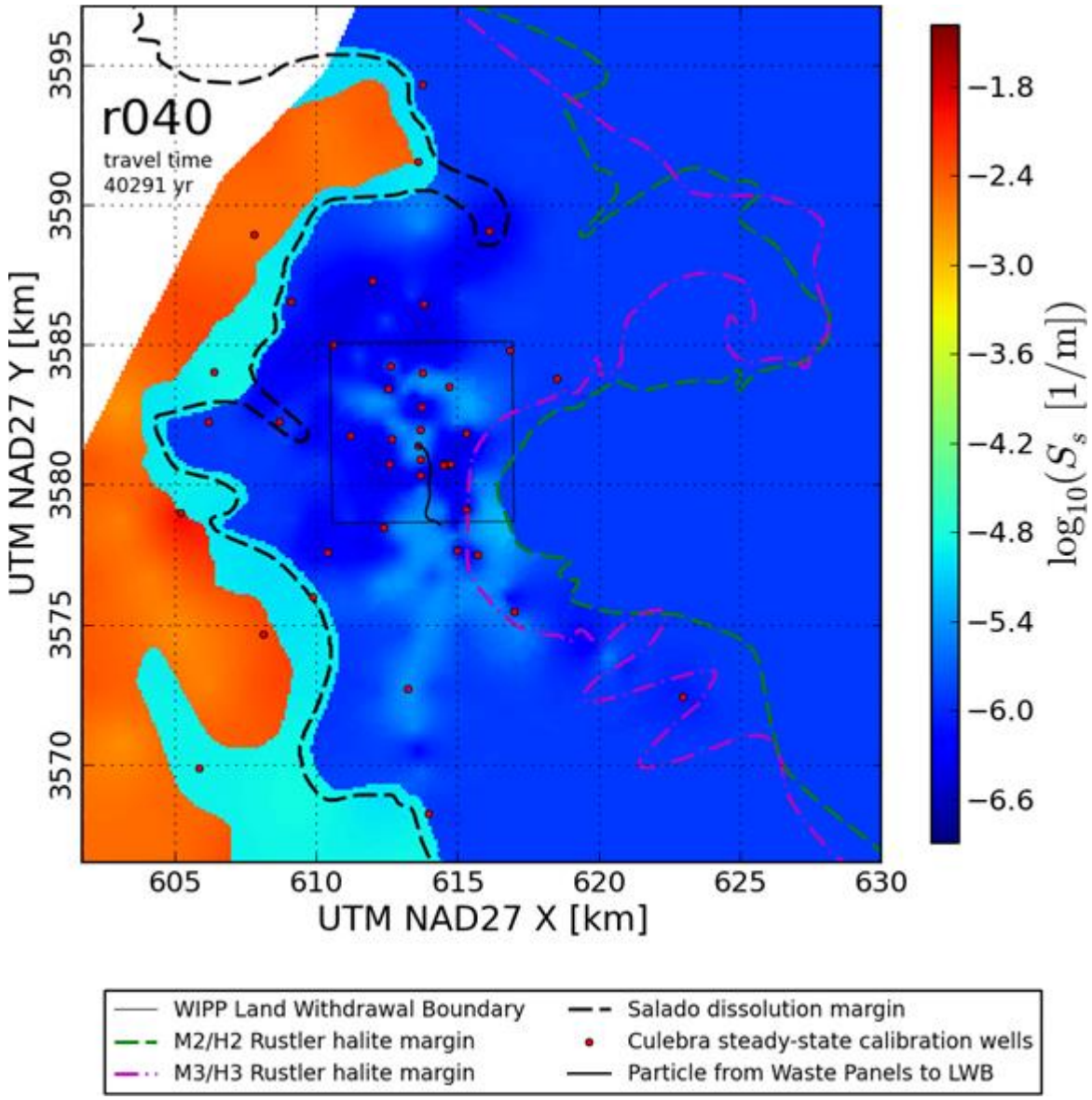
r040
travel time
40291 yr
UTM NAD27 Y [km]
3595
3590
3585
3580
3575
3570
605
610
615
620
625
630
UTM NAD27 X [km]
−1.8
−2.4
−3.0
−3.6
−4.2
−4.8
−5.4
−6.0
−6.6
$\log_{10}(S_s\ [1/\mathrm{m}])$
WIPP Land Withdrawal Boundary
M2/H2 Rustler halite margin
M3/H3 Rustler halite margin
Salado dissolution margin
Culebra steady-state calibration wells
Particle from Waste Panels to LWB

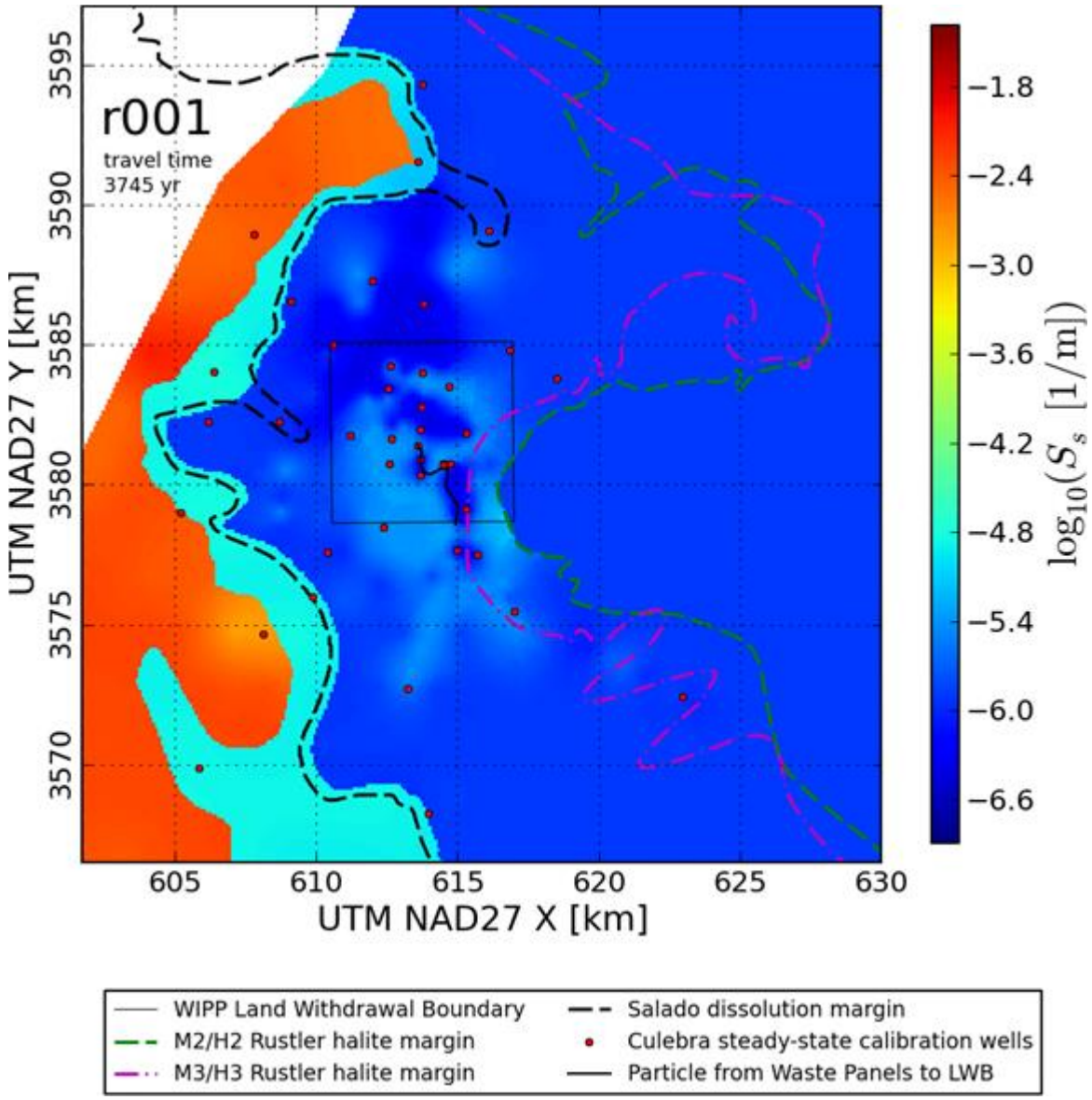
r001
travel time
3745 yr
UTM NAD27 Y [km]
3595
3590
3585
3580
3575
3570
605
610
615
620
625
630
UTM NAD27 X [km]
−1.8
−2.4
−3.0
−3.6
−4.2
−4.8
−5.4
−6.0
−6.6
$\log_{10}(S_s\ [1/\mathrm{m}])$
WIPP Land Withdrawal Boundary
M2/H2 Rustler halite margin
M3/H3 Rustler halite margin
Salado dissolution margin
Culebra steady-state calibration wells
Particle from Waste Panels to LWB

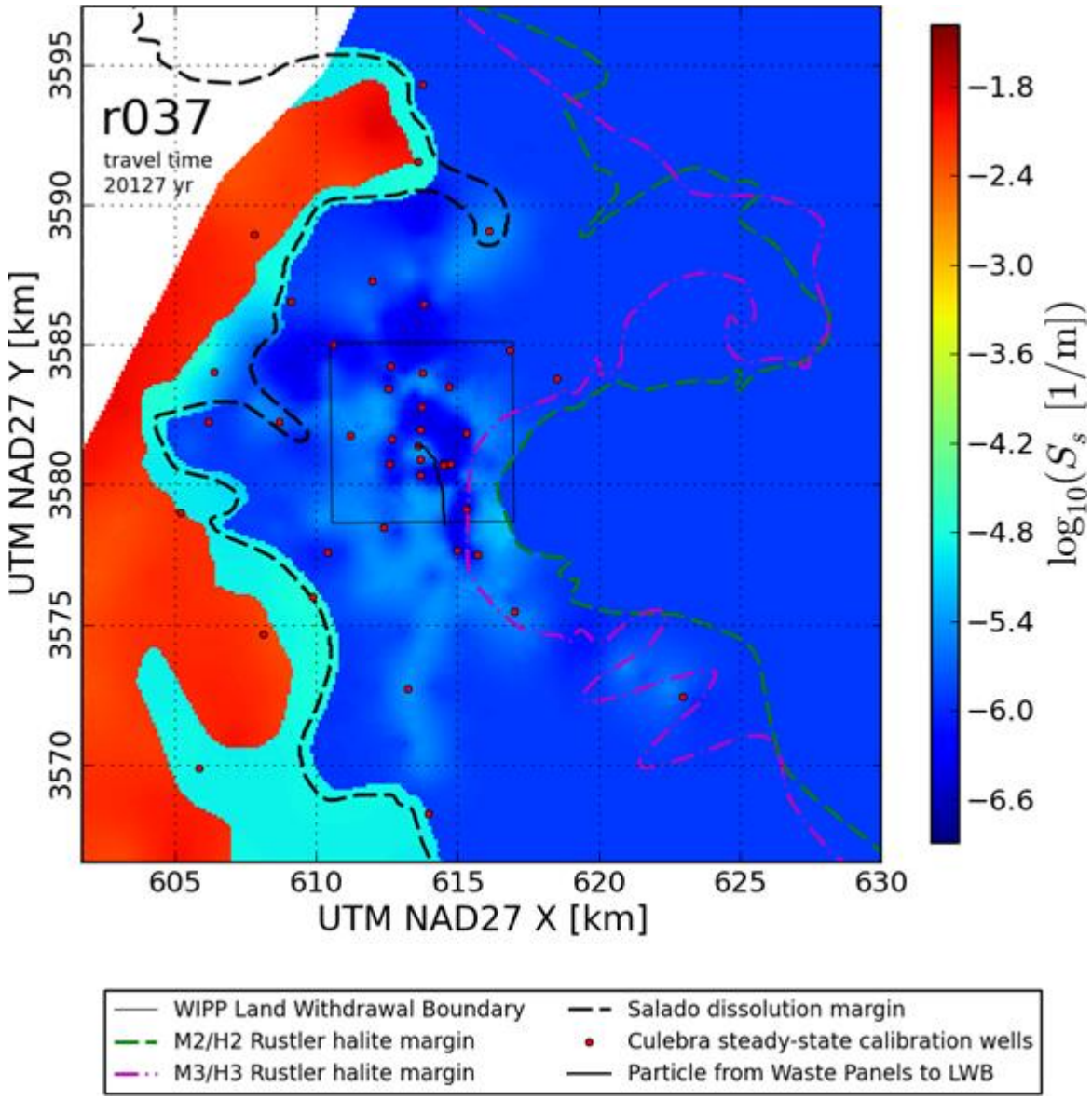
r037
travel time
20127 yr
UTM NAD27 Y [km]
3595
3590
3585
3580
3575
3570
605
610
615
620
625
630
UTM NAD27 X [km]
−1.8
−2.4
−3.0
−3.6
−4.2
−4.8
−5.4
−6.0
−6.6
$\log_{10}(S_s\ [1/\mathrm{m}])$
WIPP Land Withdrawal Boundary
M2/H2 Rustler halite margin
M3/H3 Rustler halite margin
Salado dissolution margin
Culebra steady-state calibration wells
Particle from Waste Panels to LWB

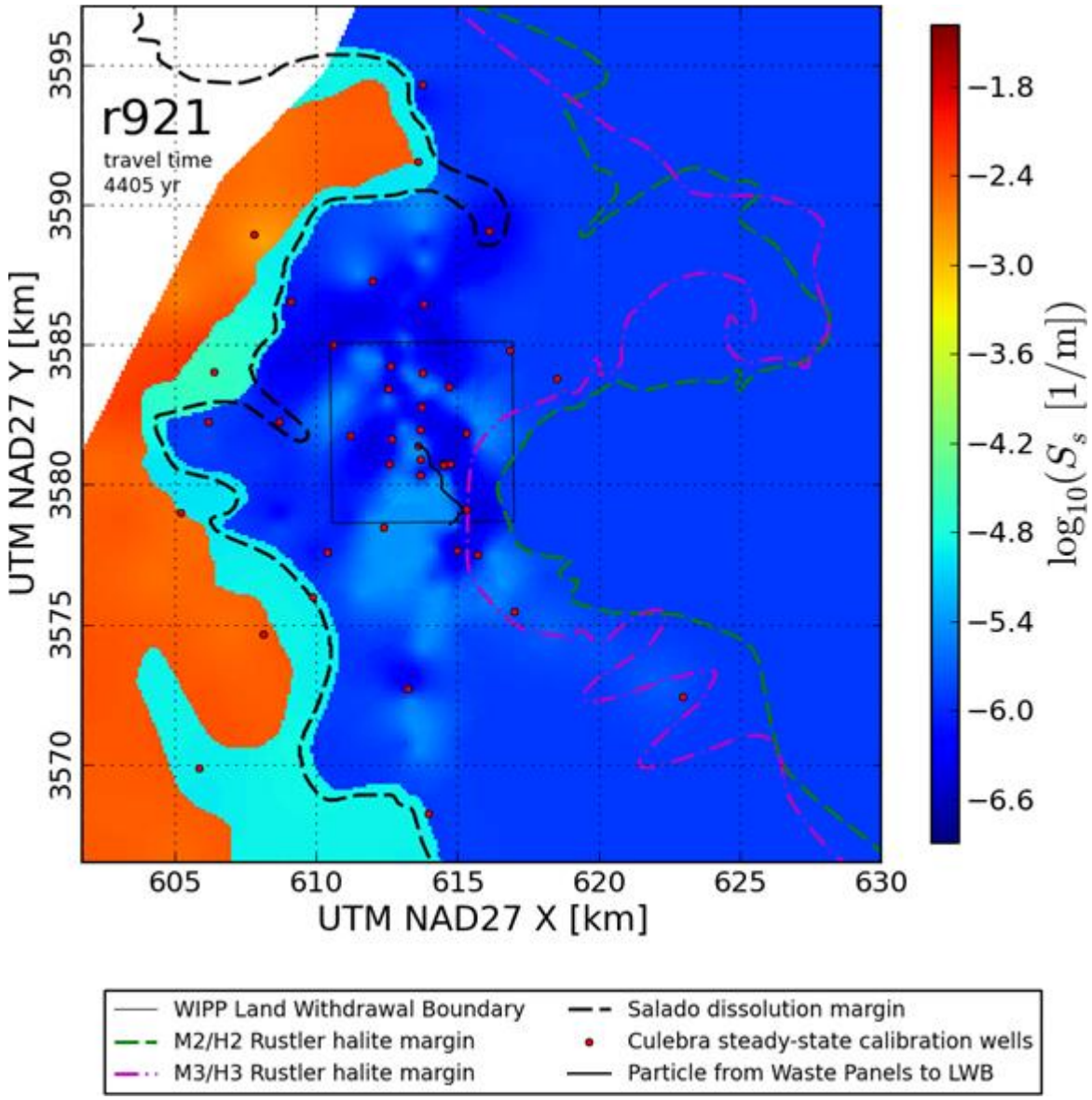
r921
travel time
4405 yr
UTM NAD27 Y [km]
3595
3590
3585
3580
3575
3570
605
610
615
620
625
630
UTM NAD27 X [km]
−1.8
−2.4
−3.0
−3.6
−4.2
−4.8
−5.4
−6.0
−6.6
$\log_{10}(S_s\ [1/\mathrm{m}])$
WIPP Land Withdrawal Boundary
M2/H2 Rustler halite margin
M3/H3 Rustler halite margin
Salado dissolution margin
Culebra steady-state calibration wells
Particle from Waste Panels to LWB

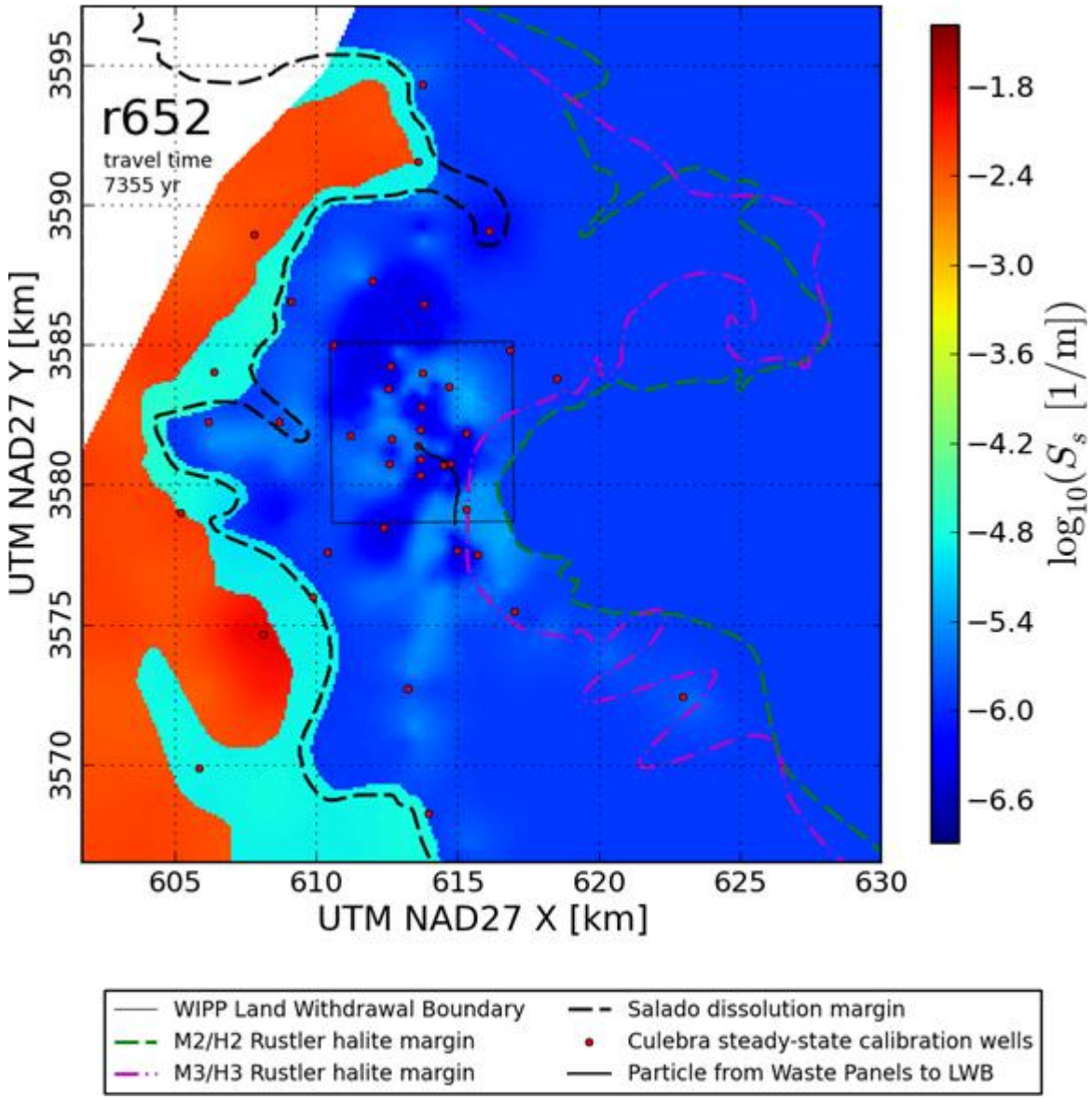
r652
travel time
7355 yr
UTM NAD27 Y [km]
3595
3590
3585
3580
3575
3570
605
610
615
620
625
630
UTM NAD27 X [km]
−1.8
−2.4
−3.0
−3.6
−4.2
−4.8
−5.4
−6.0
−6.6
$\log_{10}(S_s\ [1/\mathrm{m}])$
WIPP Land Withdrawal Boundary
M2/H2 Rustler halite margin
M3/H3 Rustler halite margin
Salado dissolution margin
Culebra steady-state calibration wells
Particle from Waste Panels to LWB

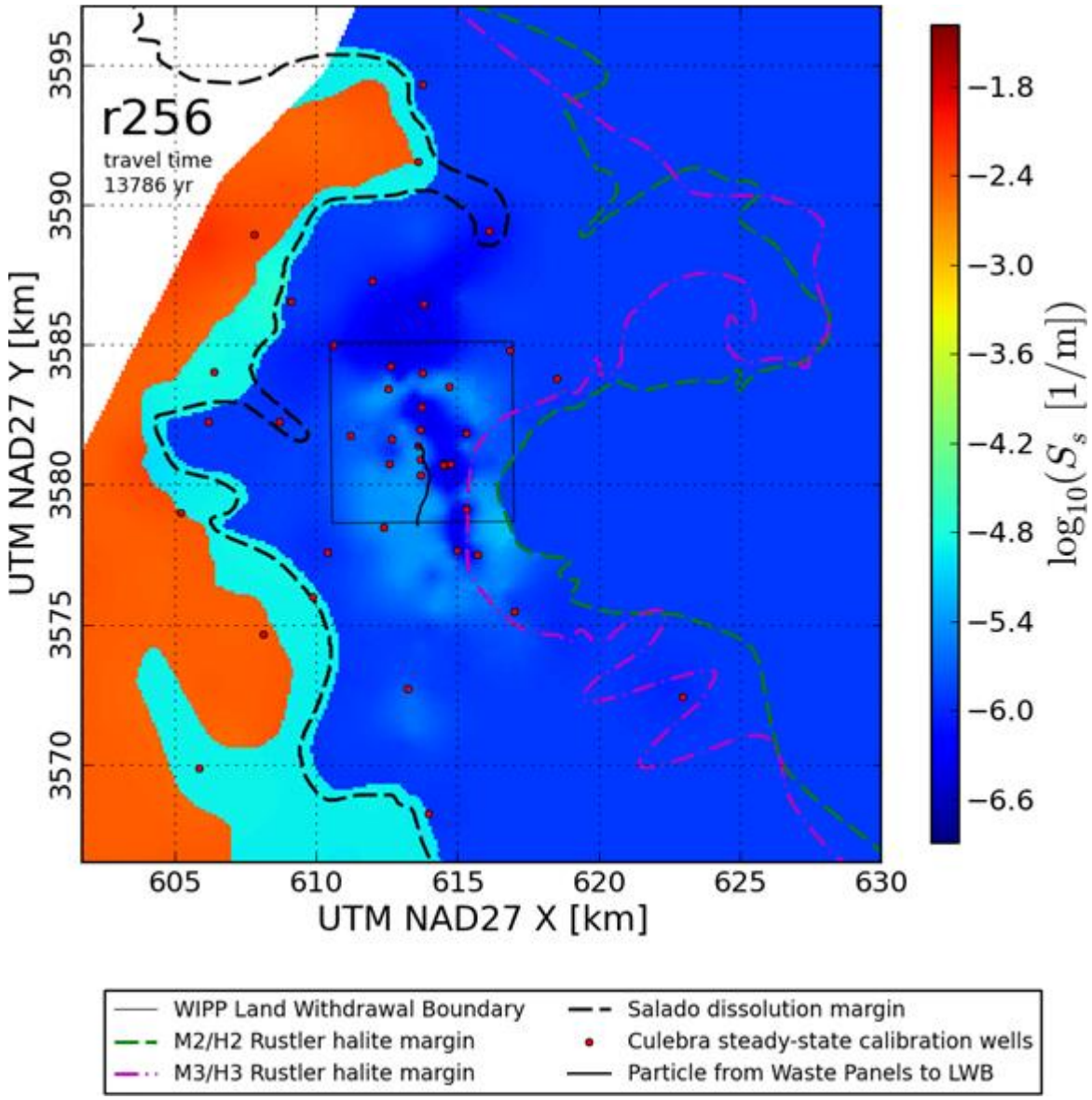
r256
travel time
13786 yr
UTM NAD27 Y [km]
3595
3590
3585
3580
3575
3570
605
610
615
620
625
630
UTM NAD27 X [km]
−1.8
−2.4
−3.0
−3.6
−4.2
−4.8
−5.4
−6.0
−6.6
$\log_{10}(S_s\ [1/\mathrm{m}])$
WIPP Land Withdrawal Boundary
M2/H2 Rustler halite margin
M3/H3 Rustler halite margin
Salado dissolution margin
Culebra steady-state calibration wells
Particle from Waste Panels to LWB

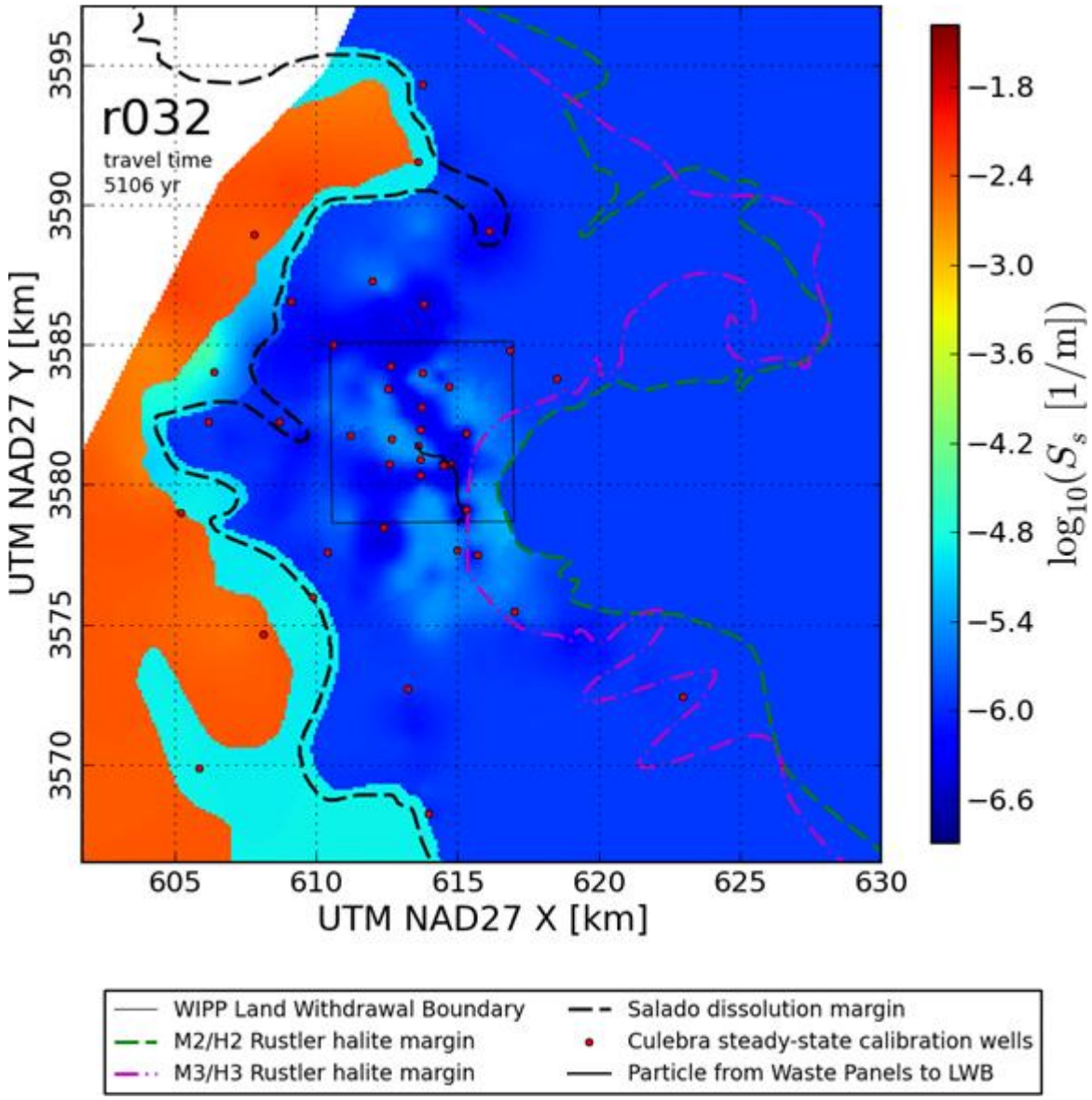
r032
travel time
5106 yr
UTM NAD27 Y [km]
3595
3590
3585
3580
3575
3570
605
610
615
620
625
630
UTM NAD27 X [km]
−1.8
−2.4
−3.0
−3.6
−4.2
−4.8
−5.4
−6.0
−6.6
$\log_{10}(S_s\ [1/\mathrm{m}])$
WIPP Land Withdrawal Boundary
M2/H2 Rustler halite margin
M3/H3 Rustler halite margin
Salado dissolution margin
Culebra steady-state calibration wells
Particle from Waste Panels to LWB

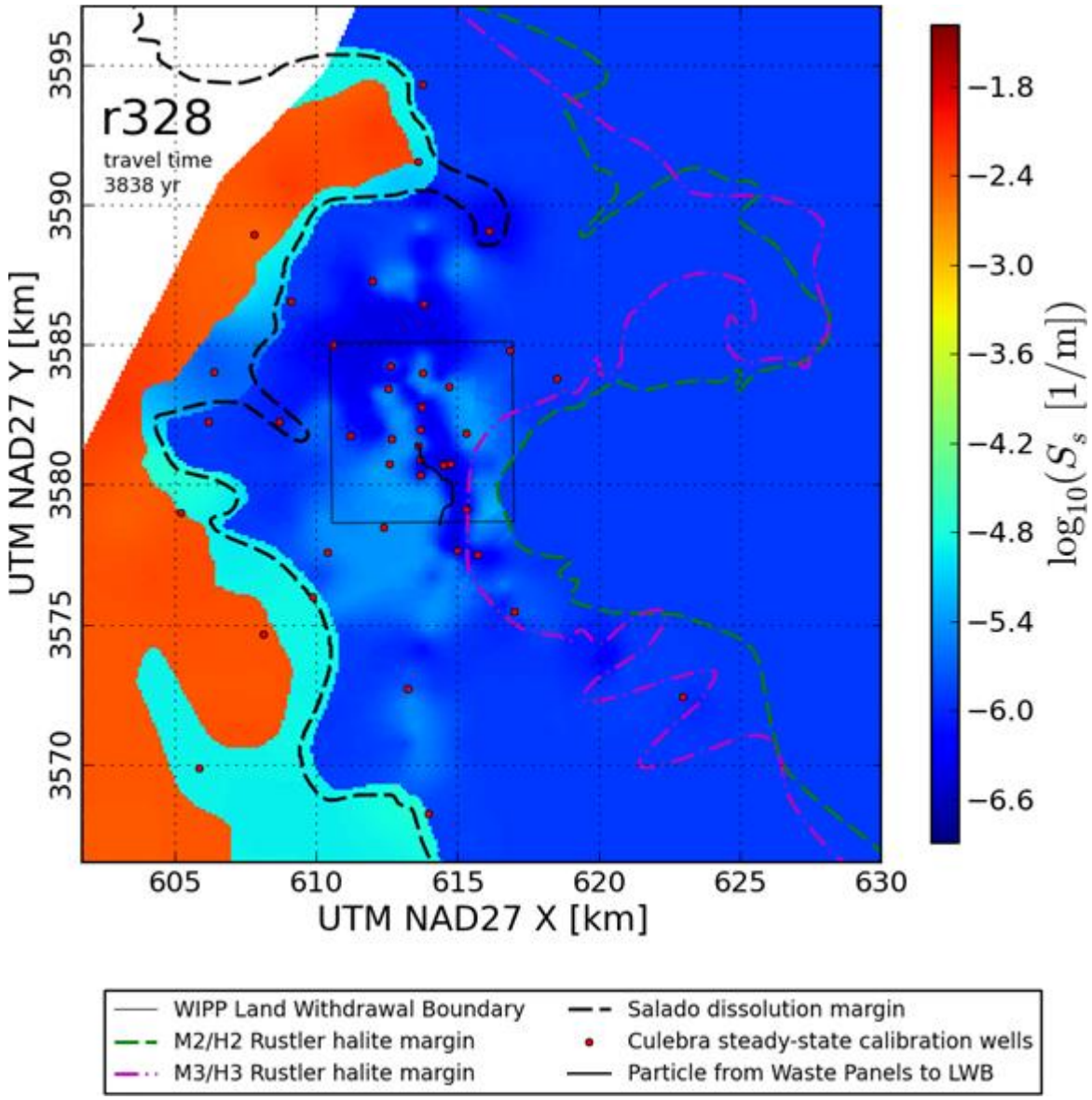
r328
travel time
3838 yr
UTM NAD27 Y [km]
3595
3590
3585
3580
3575
3570
605
610
615
620
625
630
UTM NAD27 X [km]
−1.8
−2.4
−3.0
−3.6
−4.2
−4.8
−5.4
−6.0
−6.6
$\log_{10}(S_s\ [1/\mathrm{m}])$
WIPP Land Withdrawal Boundary
M2/H2 Rustler halite margin
M3/H3 Rustler halite margin
Salado dissolution margin
Culebra steady-state calibration wells
Particle from Waste Panels to LWB

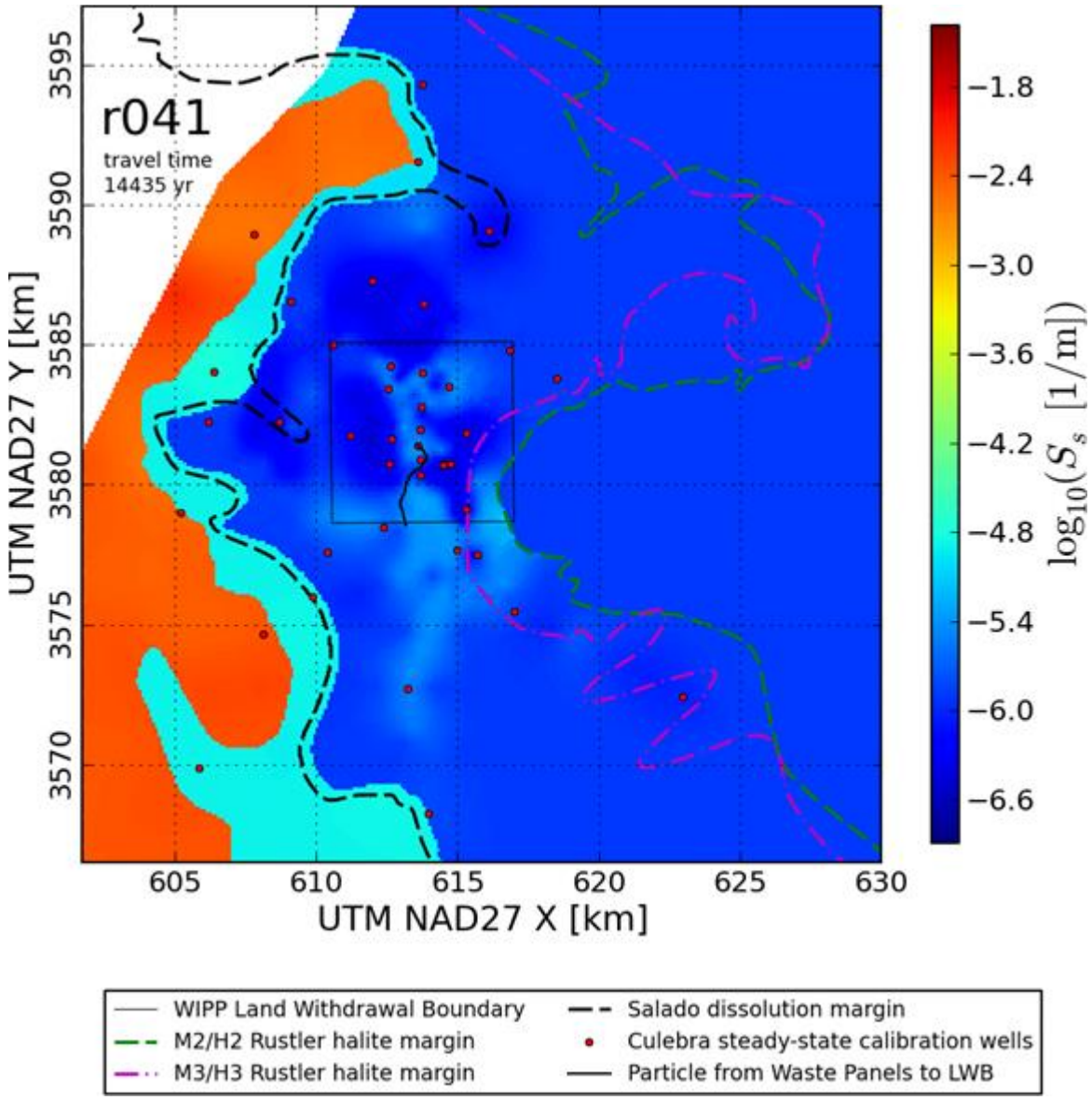
r041
travel time
14435 yr
UTM NAD27 Y [km]
3595
3590
3585
3580
3575
3570
605
610
615
620
625
630
UTM NAD27 X [km]
−1.8
−2.4
−3.0
−3.6
−4.2
−4.8
−5.4
−6.0
−6.6
$\log_{10}(S_s\ [1/\mathrm{m}])$
WIPP Land Withdrawal Boundary
Salado dissolution margin
M2/H2 Rustler halite margin
Culebra steady-state calibration wells
M3/H3 Rustler halite margin
Particle from Waste Panels to LWB

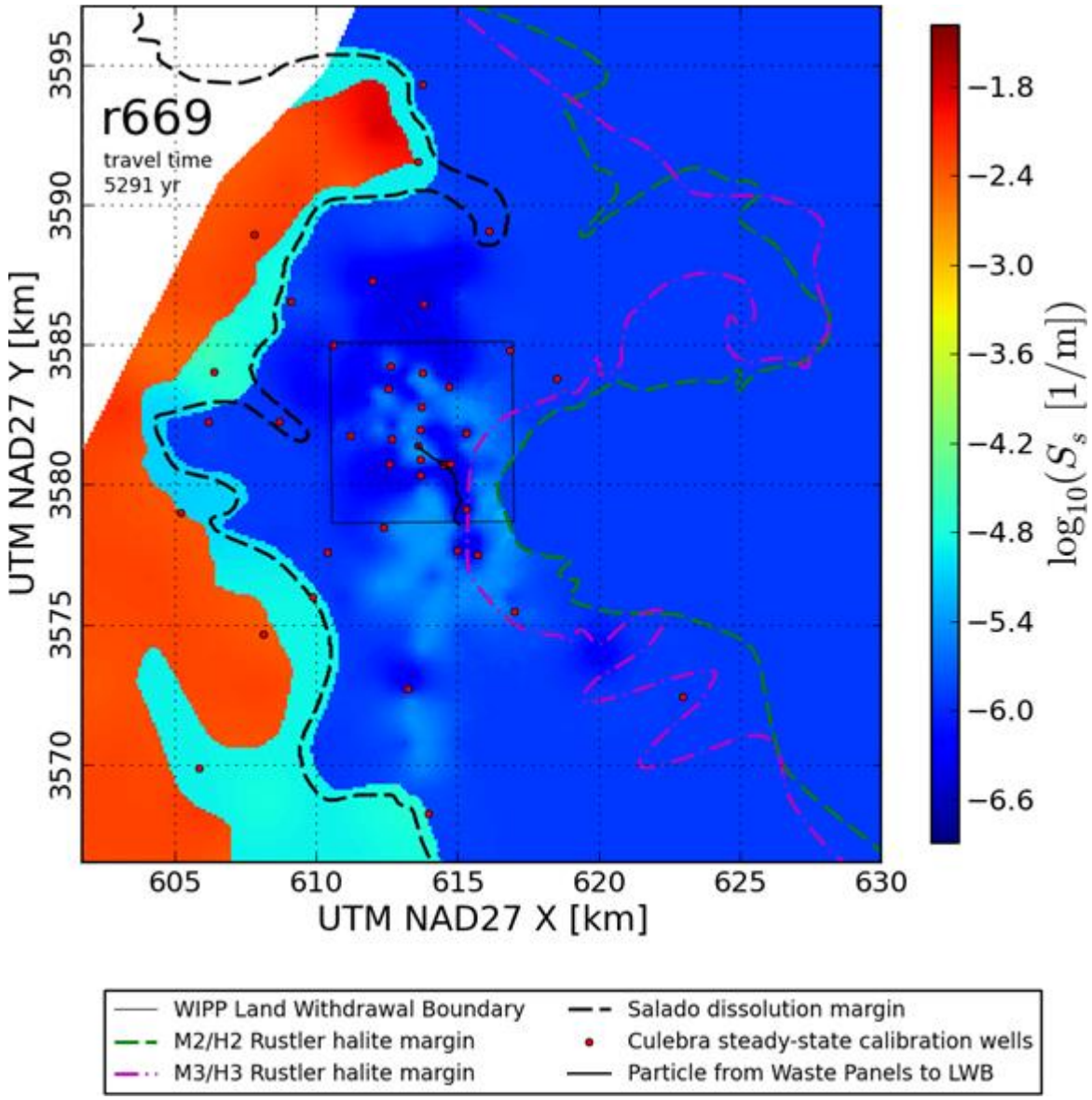
r669
travel time
5291 yr
UTM NAD27 Y [km]
3595
3590
3585
3580
3575
3570
605
610
615
620
625
630
UTM NAD27 X [km]
−1.8
−2.4
−3.0
−3.6
−4.2
−4.8
−5.4
−6.0
−6.6
$\log_{10}(S_s\ [1/\mathrm{m}])$
WIPP Land Withdrawal Boundary
M2/H2 Rustler halite margin
M3/H3 Rustler halite margin
Salado dissolution margin
Culebra steady-state calibration wells
Particle from Waste Panels to LWB

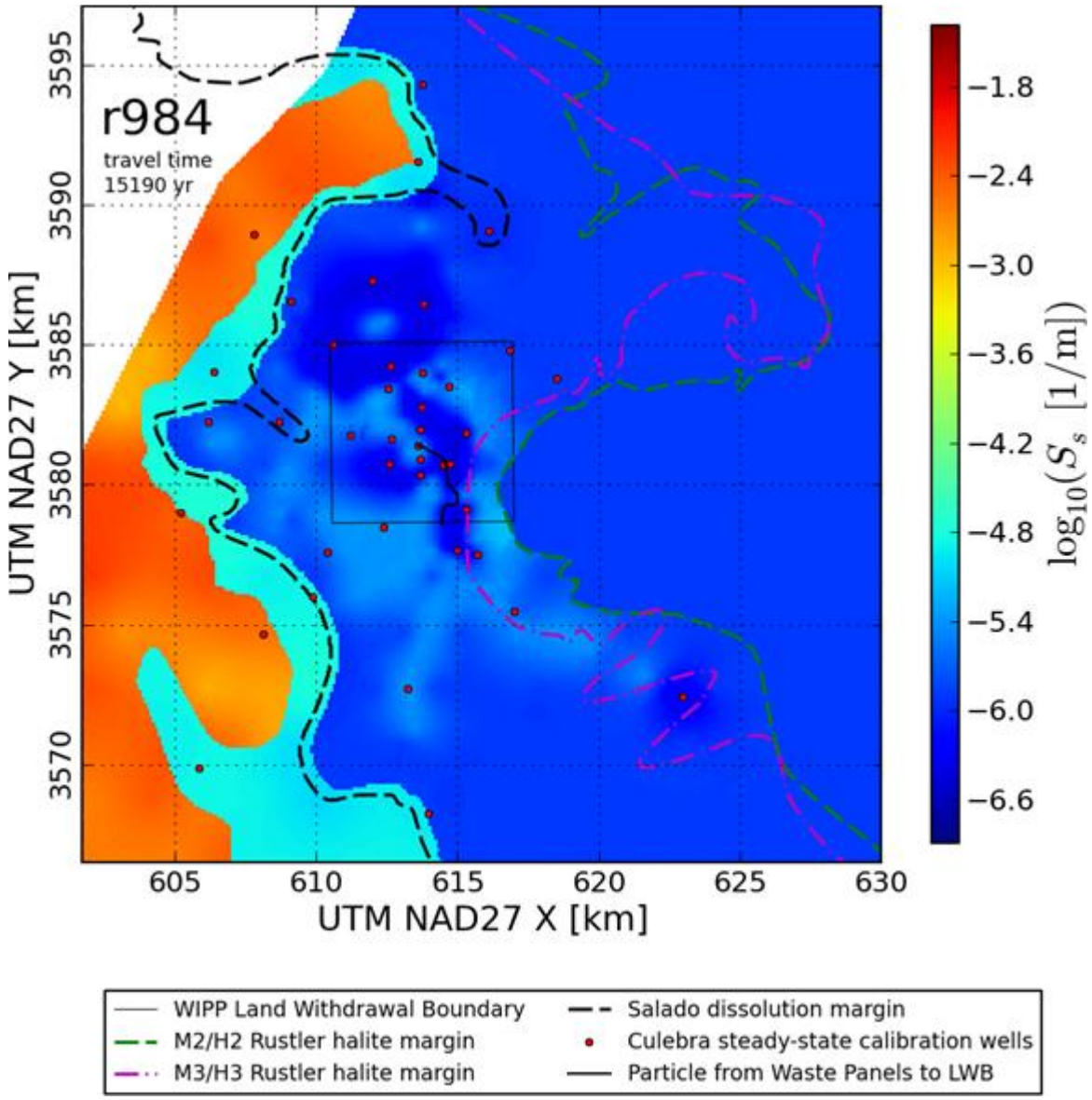
r984
travel time
15190 yr
UTM NAD27 Y [km]
3595
3590
3585
3580
3575
3570
605
610
615
620
625
630
UTM NAD27 X [km]
−1.8
−2.4
−3.0
−3.6
−4.2
−4.8
−5.4
−6.0
−6.6
$\log_{10}(S_s\ [1/\mathrm{m}])$
WIPP Land Withdrawal Boundary
M2/H2 Rustler halite margin
M3/H3 Rustler halite margin
Salado dissolution margin
Culebra steady-state calibration wells
Particle from Waste Panels to LWB

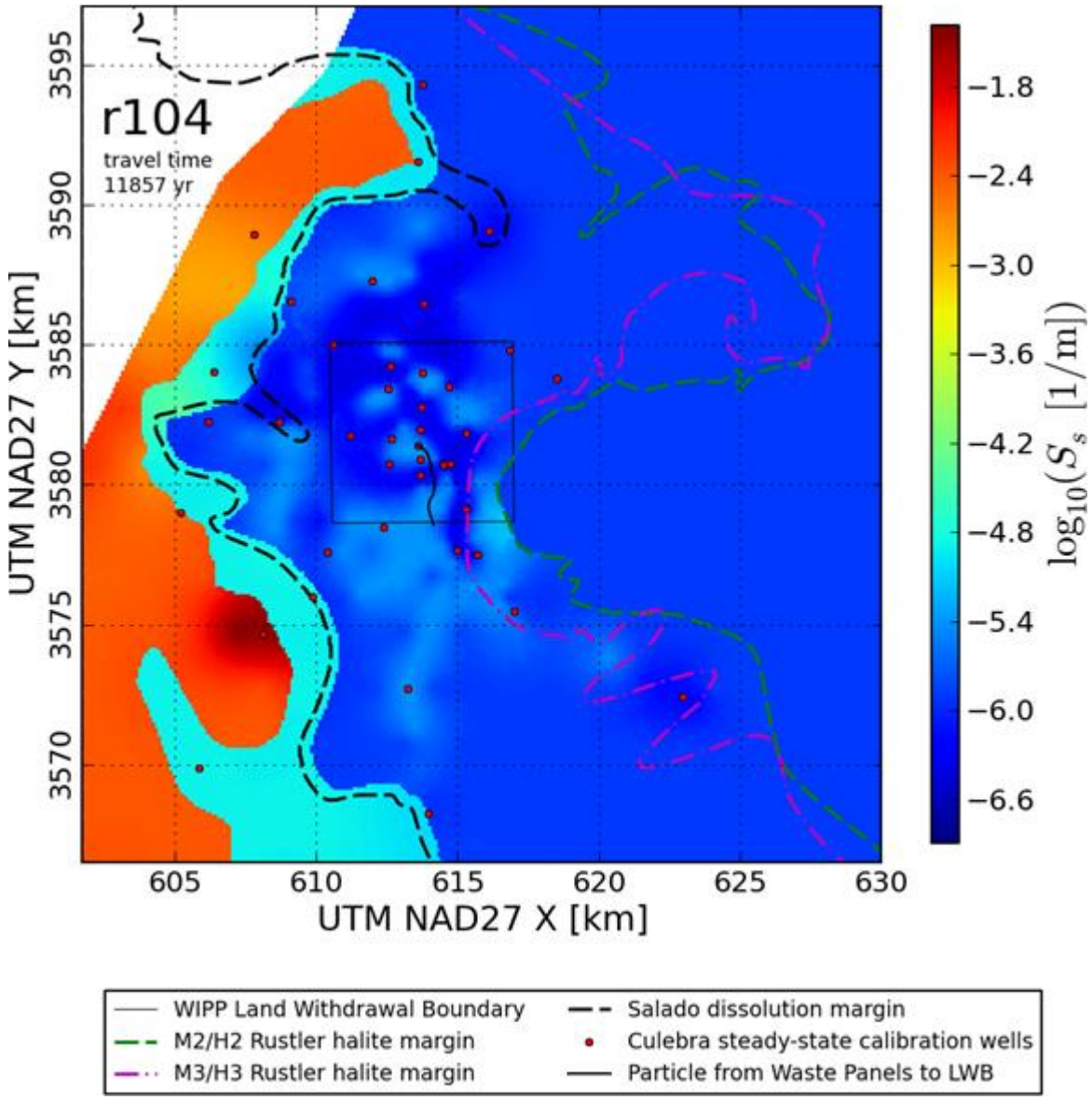
r104
travel time
11857 yr
UTM NAD27 Y [km]
3595
3590
3585
3580
3575
3570
605
610
615
620
625
630
UTM NAD27 X [km]
−1.8
−2.4
−3.0
−3.6
−4.2
−4.8
−5.4
−6.0
−6.6
$\log_{10}(S_s\ [1/\mathrm{m}])$
WIPP Land Withdrawal Boundary
M2/H2 Rustler halite margin
M3/H3 Rustler halite margin
Salado dissolution margin
Culebra steady-state calibration wells
Particle from Waste Panels to LWB

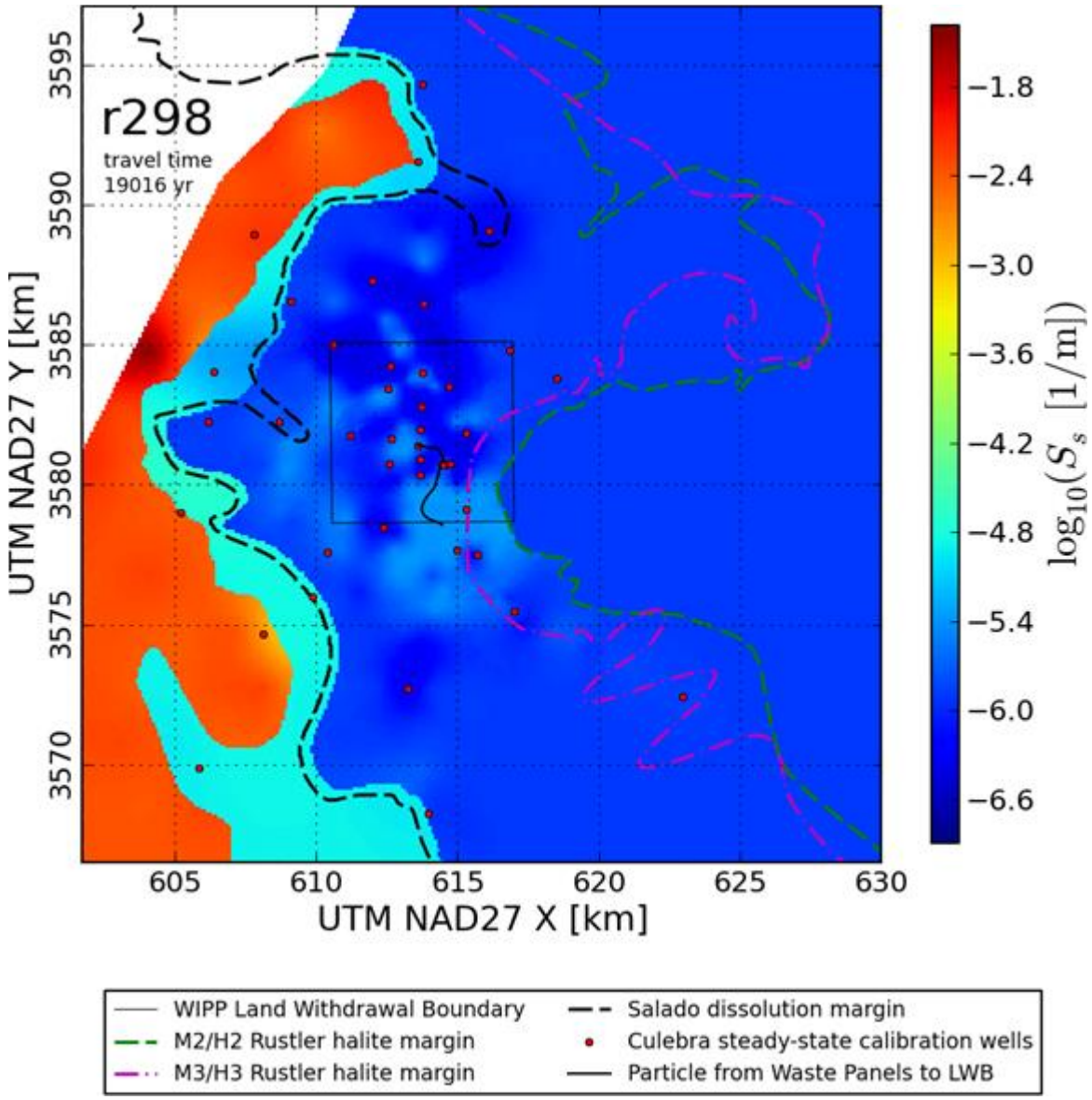
r298
travel time
19016 yr
UTM NAD27 Y [km]
3595
3590
3585
3580
3575
3570
605
610
615
620
625
630
UTM NAD27 X [km]
−1.8
−2.4
−3.0
−3.6
−4.2
−4.8
−5.4
−6.0
−6.6
$\log_{10}(S_s\ [1/\mathrm{m}])$
WIPP Land Withdrawal Boundary
M2/H2 Rustler halite margin
M3/H3 Rustler halite margin
Salado dissolution margin
Culebra steady-state calibration wells
Particle from Waste Panels to LWB

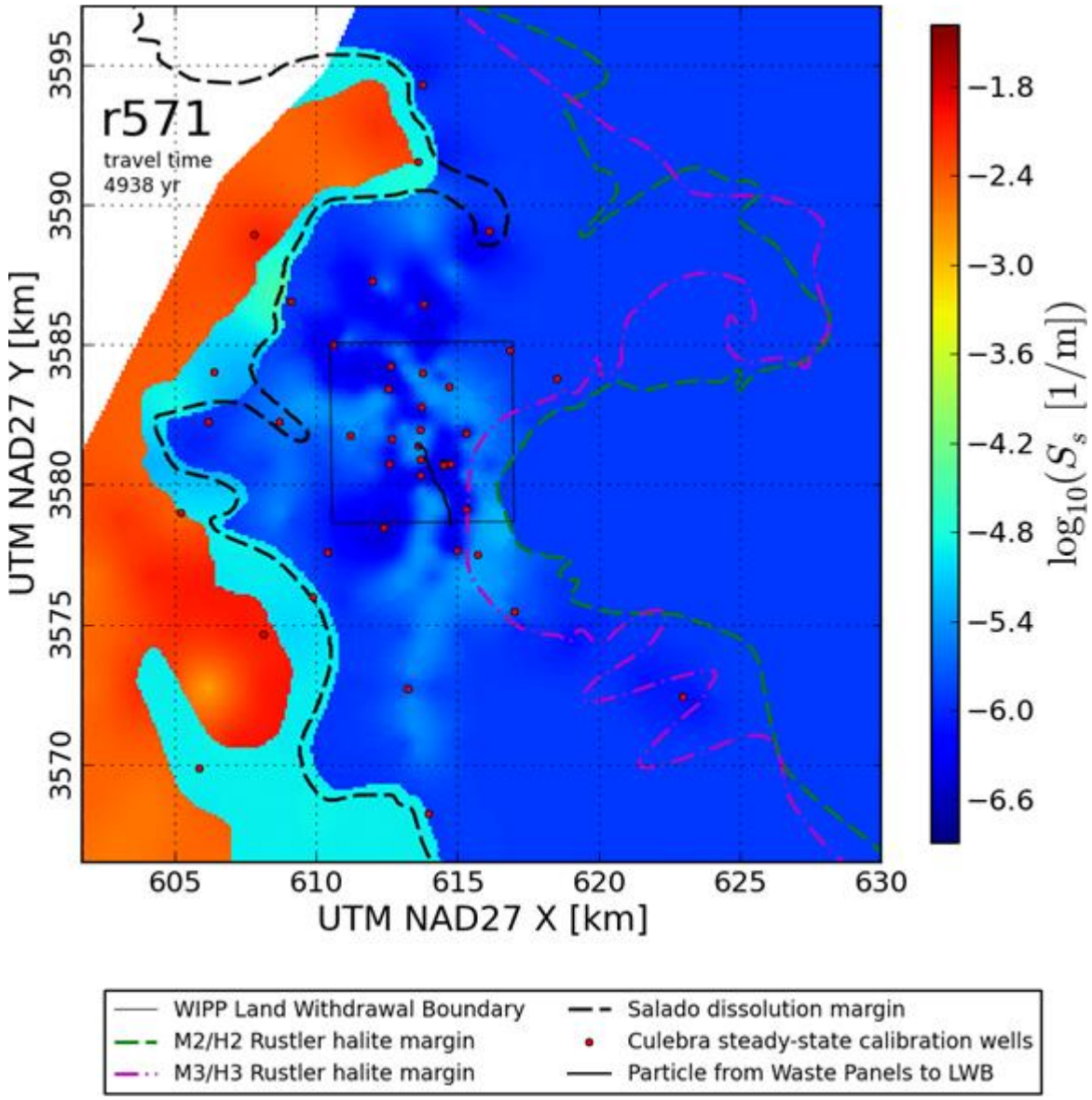
r571
travel time
4938 yr
UTM NAD27 Y [km]
3595
3590
3585
3580
3575
3570
605
610
615
620
625
630
UTM NAD27 X [km]
−1.8
−2.4
−3.0
−3.6
−4.2
−4.8
−5.4
−6.0
−6.6
$\log_{10}(S_s\ [1/\mathrm{m}])$
WIPP Land Withdrawal Boundary
M2/H2 Rustler halite margin
M3/H3 Rustler halite margin
Salado dissolution margin
Culebra steady-state calibration wells
Particle from Waste Panels to LWB

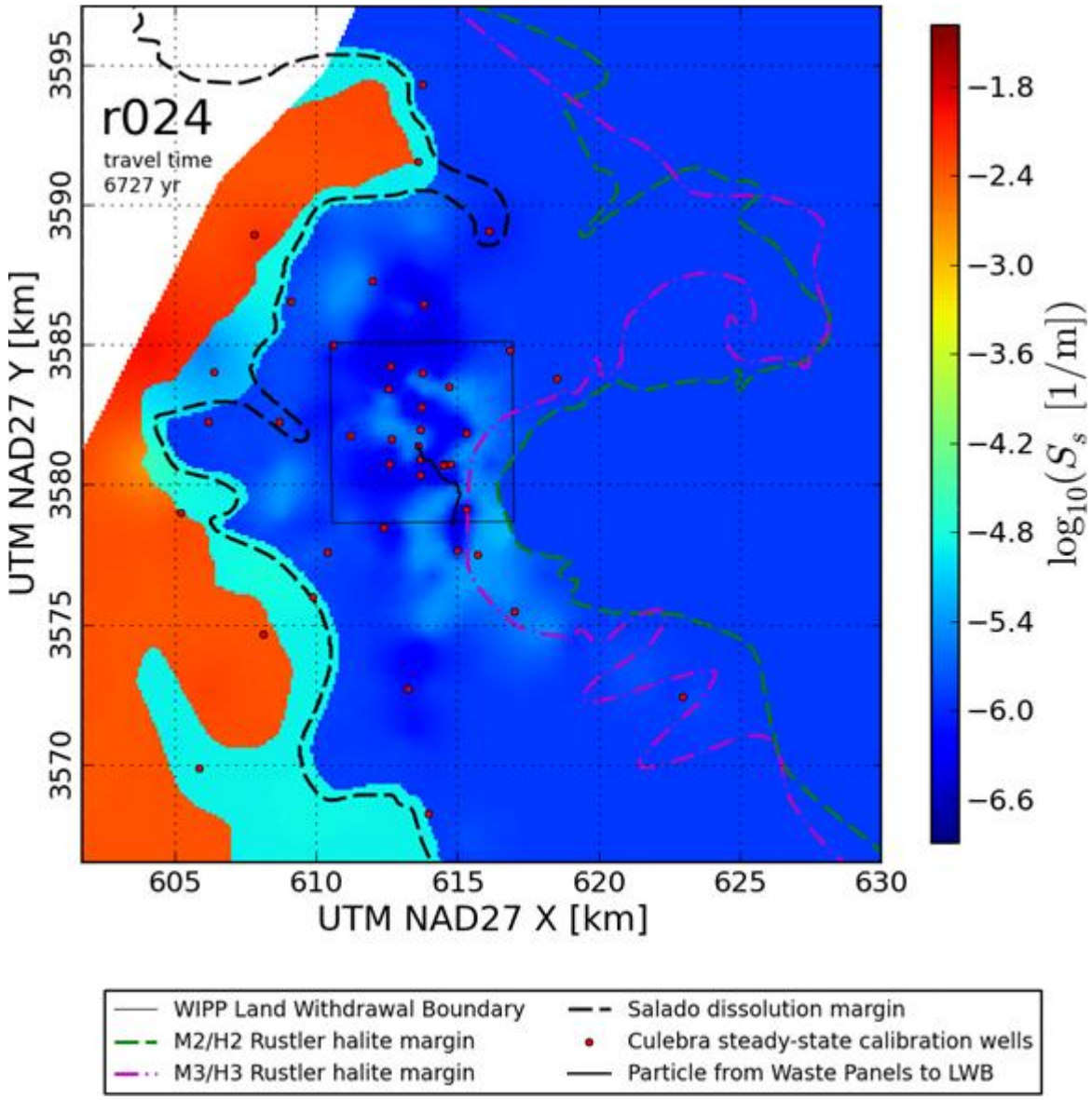
r024
travel time
6727 yr
UTM NAD27 Y [km]
3595
3590
3585
3580
3575
3570
605
610
615
620
625
630
UTM NAD27 X [km]
−1.8
−2.4
−3.0
−3.6
−4.2
−4.8
−5.4
−6.0
−6.6
$\log_{10}(S_s\ [1/\mathrm{m}])$
WIPP Land Withdrawal Boundary
M2/H2 Rustler halite margin
M3/H3 Rustler halite margin
Salado dissolution margin
Culebra steady-state calibration wells
Particle from Waste Panels to LWB

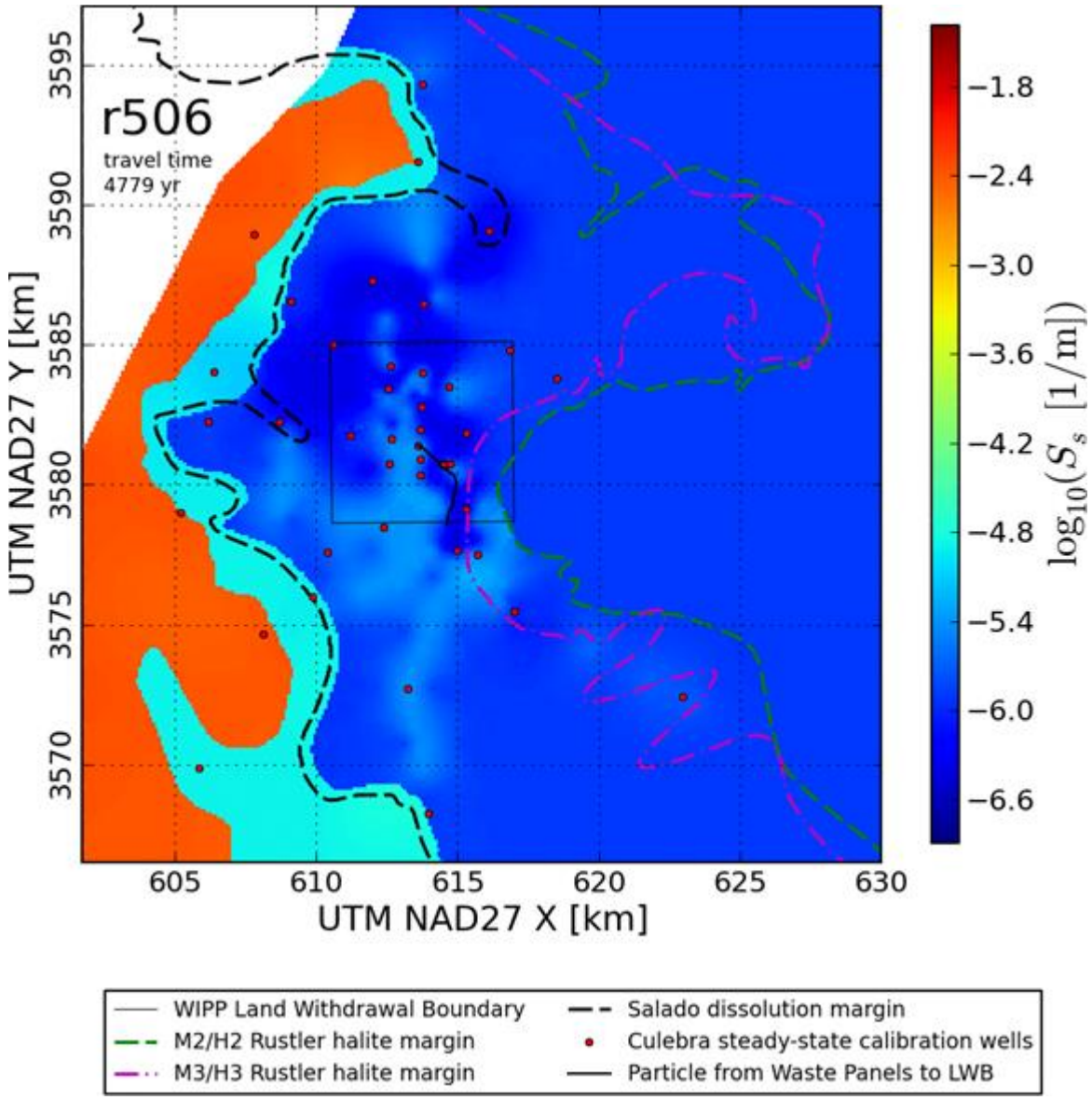
r506
travel time
4779 yr
UTM NAD27 Y [km]
3595
3590
3585
3580
3575
3570
605
610
615
620
625
630
UTM NAD27 X [km]
−1.8
−2.4
−3.0
−3.6
−4.2
−4.8
−5.4
−6.0
−6.6
$\log_{10}(S_s\ [1/\mathrm{m}])$
WIPP Land Withdrawal Boundary
M2/H2 Rustler halite margin
M3/H3 Rustler halite margin
Salado dissolution margin
Culebra steady-state calibration wells
Particle from Waste Panels to LWB

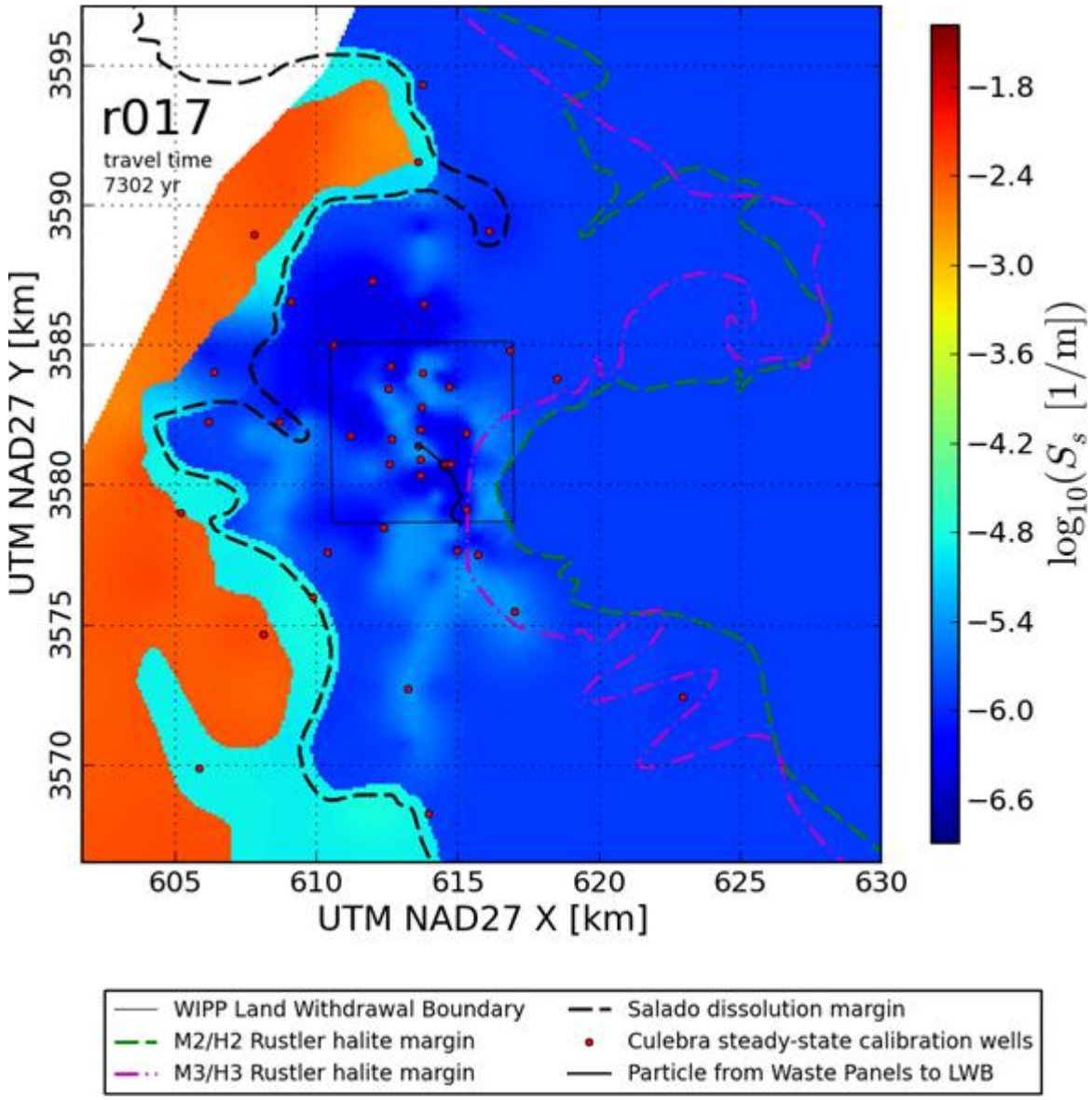
r017
travel time
7302 yr
UTM NAD27 Y [km]
3595
3590
3585
3580
3575
3570
605
610
615
620
625
630
UTM NAD27 X [km]
−1.8
−2.4
−3.0
−3.6
−4.2
−4.8
−5.4
−6.0
−6.6
$\log_{10}(S_s\ [1/\mathrm{m}])$
WIPP Land Withdrawal Boundary
M2/H2 Rustler halite margin
M3/H3 Rustler halite margin
Salado dissolution margin
Culebra steady-state calibration wells
Particle from Waste Panels to LWB

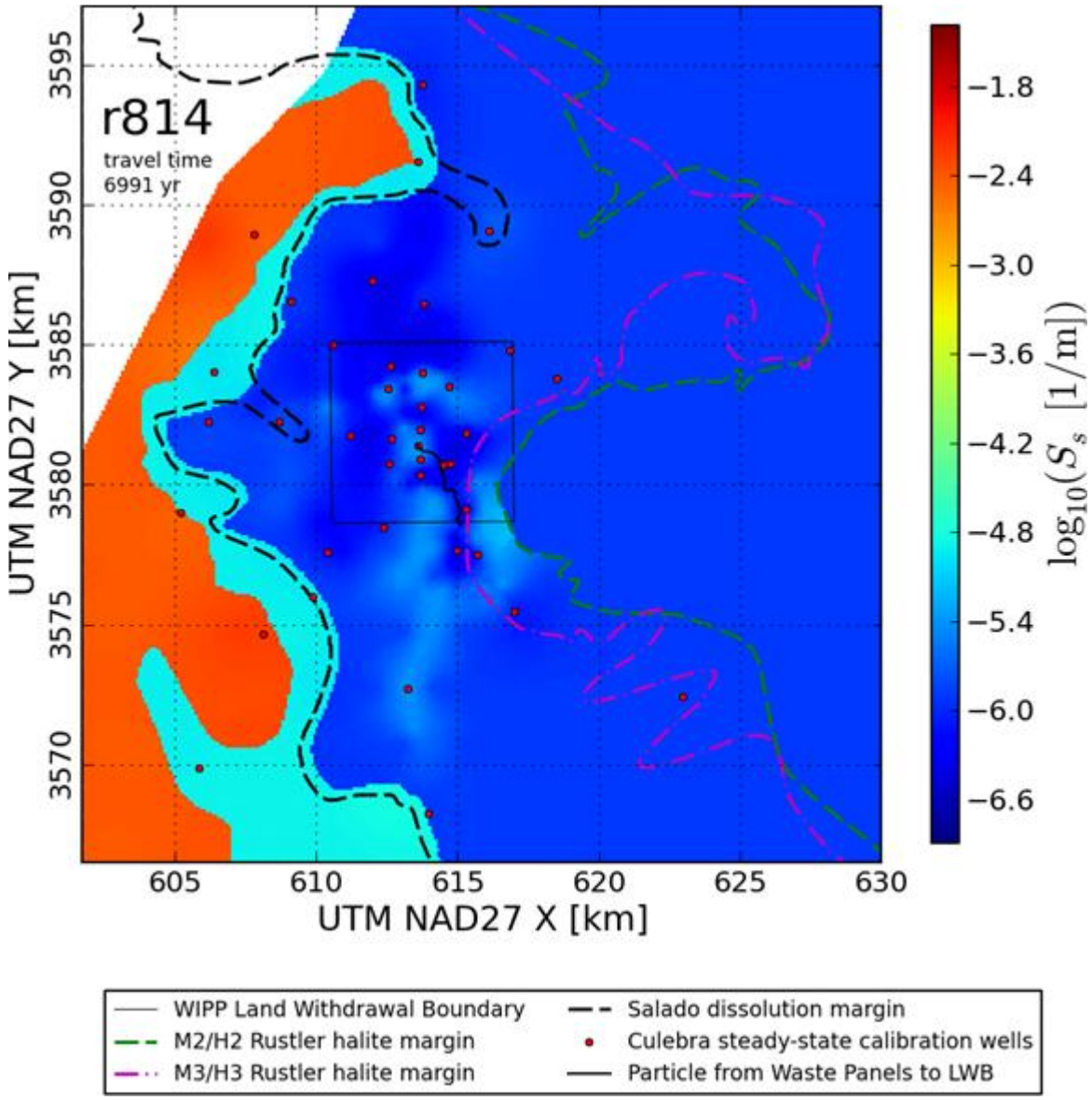
r814
travel time
6991 yr
UTM NAD27 Y [km]
3595
3590
3585
3580
3575
3570
605
610
615
620
625
630
UTM NAD27 X [km]
−1.8
−2.4
−3.0
−3.6
−4.2
−4.8
−5.4
−6.0
−6.6
$\log_{10}(S_s\ [1/\mathrm{m}])$
WIPP Land Withdrawal Boundary
M2/H2 Rustler halite margin
M3/H3 Rustler halite margin
Salado dissolution margin
Culebra steady-state calibration wells
Particle from Waste Panels to LWB

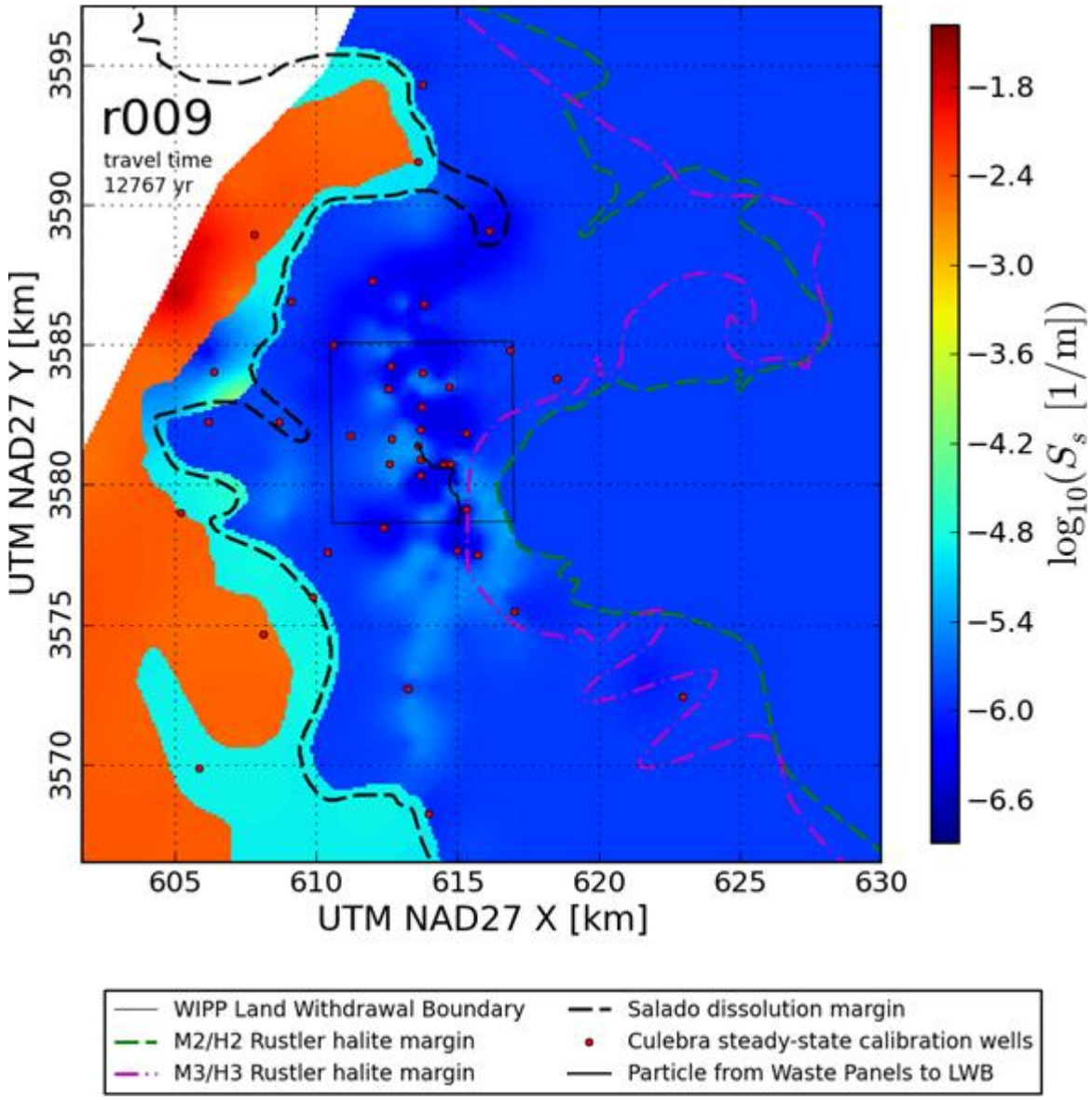
r009
travel time
12767 yr
UTM NAD27 Y [km]
3595
3590
3585
3580
3575
3570
605
610
615
620
625
630
UTM NAD27 X [km]
−1.8
−2.4
−3.0
−3.6
−4.2
−4.8
−5.4
−6.0
−6.6
$\log_{10}(S_s\ [1/\mathrm{m}])$
WIPP Land Withdrawal Boundary
M2/H2 Rustler halite margin
M3/H3 Rustler halite margin
Salado dissolution margin
Culebra steady-state calibration wells
Particle from Waste Panels to LWB

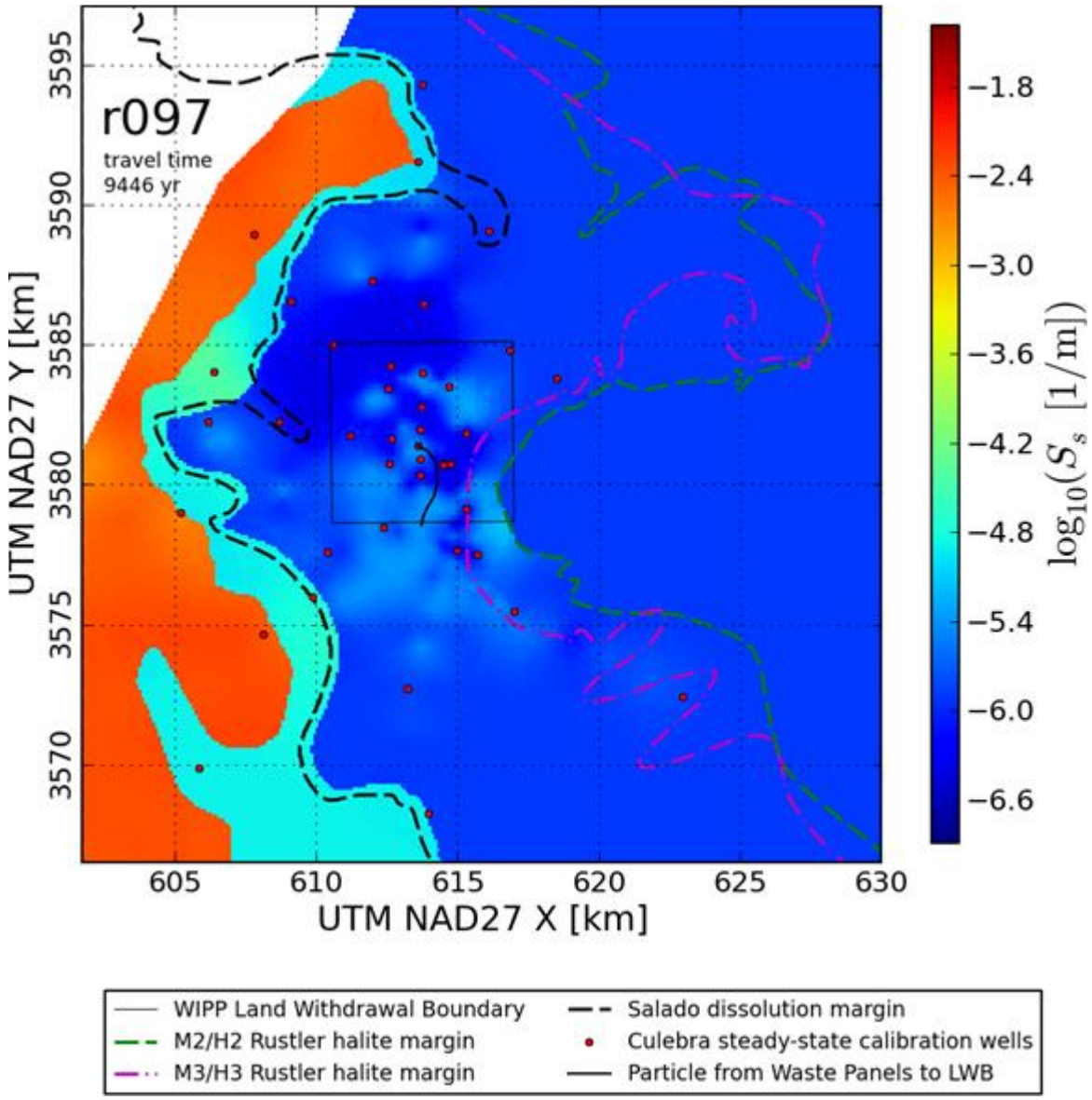
r097
travel time
9446 yr
UTM NAD27 Y [km]
3595
3590
3585
3580
3575
3570
605
610
615
620
625
630
UTM NAD27 X [km]
−1.8
−2.4
−3.0
−3.6
−4.2
−4.8
−5.4
−6.0
−6.6
$\log_{10}(S_s\ [1/\mathrm{m}])$
WIPP Land Withdrawal Boundary
M2/H2 Rustler halite margin
M3/H3 Rustler halite margin
Salado dissolution margin
Culebra steady-state calibration wells
Particle from Waste Panels to LWB

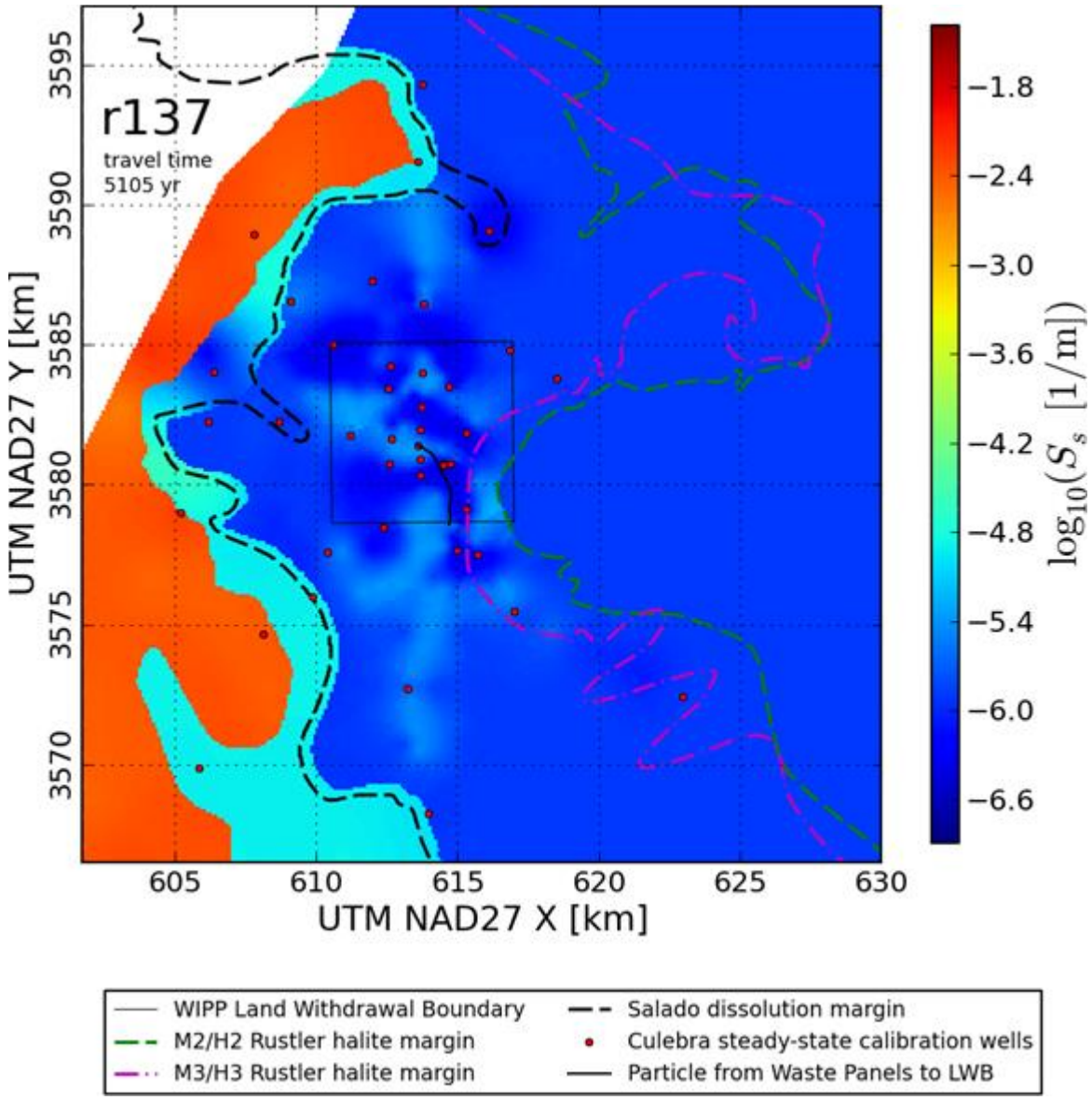
r137
travel time
5105 yr
UTM NAD27 Y [km]
3595
3590
3585
3580
3575
3570
605
610
615
620
625
630
UTM NAD27 X [km]
−1.8
−2.4
−3.0
−3.6
−4.2
−4.8
−5.4
−6.0
−6.6
$\log_{10}(S_s\ [1/\mathrm{m}])$
WIPP Land Withdrawal Boundary
M2/H2 Rustler halite margin
M3/H3 Rustler halite margin
Salado dissolution margin
Culebra steady-state calibration wells
Particle from Waste Panels to LWB

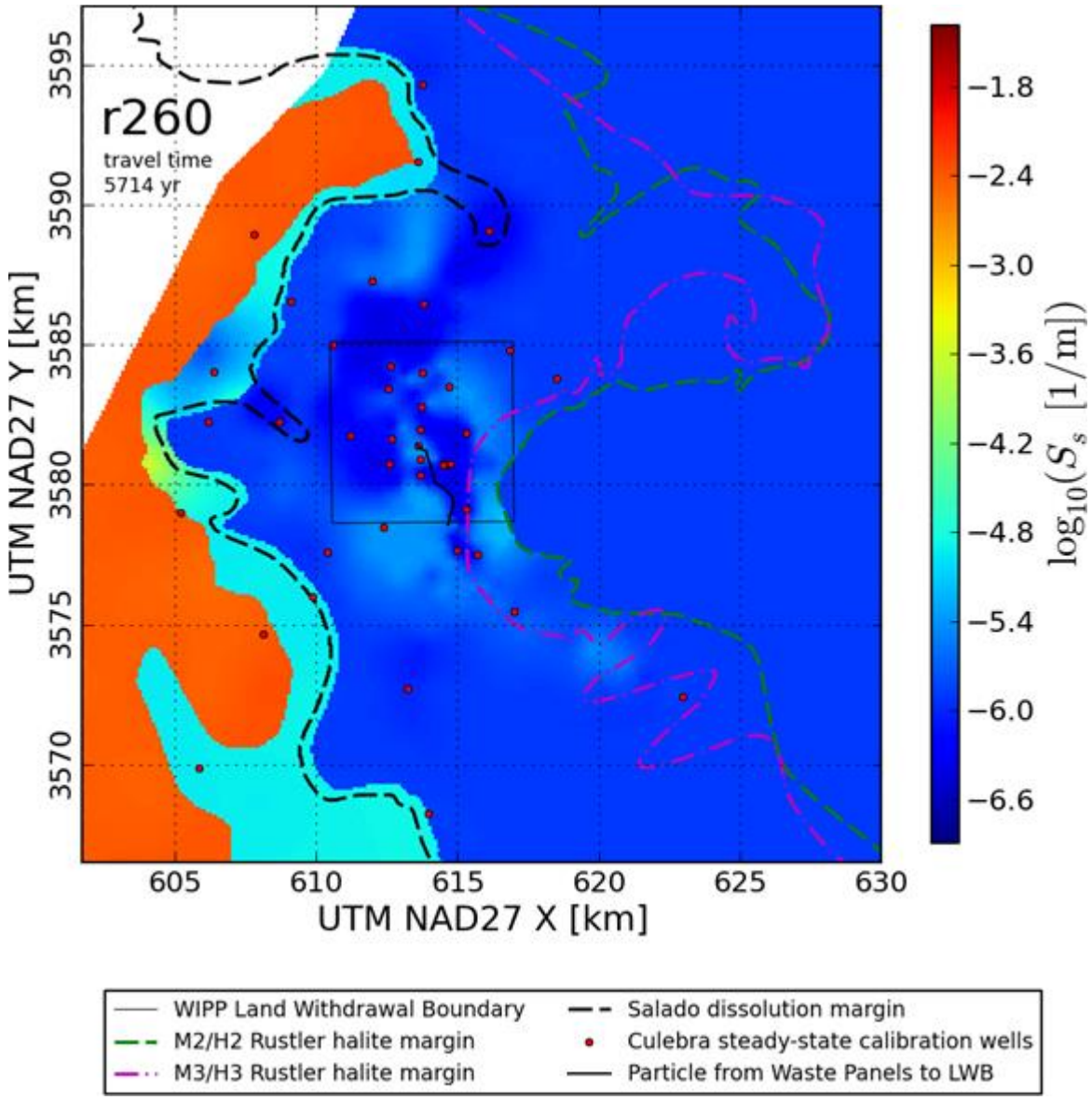
r260
travel time
5714 yr
UTM NAD27 Y [km]
3595
3590
3585
3580
3575
3570
605
610
615
620
625
630
UTM NAD27 X [km]
−1.8
−2.4
−3.0
−3.6
−4.2
−4.8
−5.4
−6.0
−6.6
$\log_{10}(S_s\ [1/\mathrm{m}])$
WIPP Land Withdrawal Boundary
M2/H2 Rustler halite margin
M3/H3 Rustler halite margin
Salado dissolution margin
Culebra steady-state calibration wells
Particle from Waste Panels to LWB

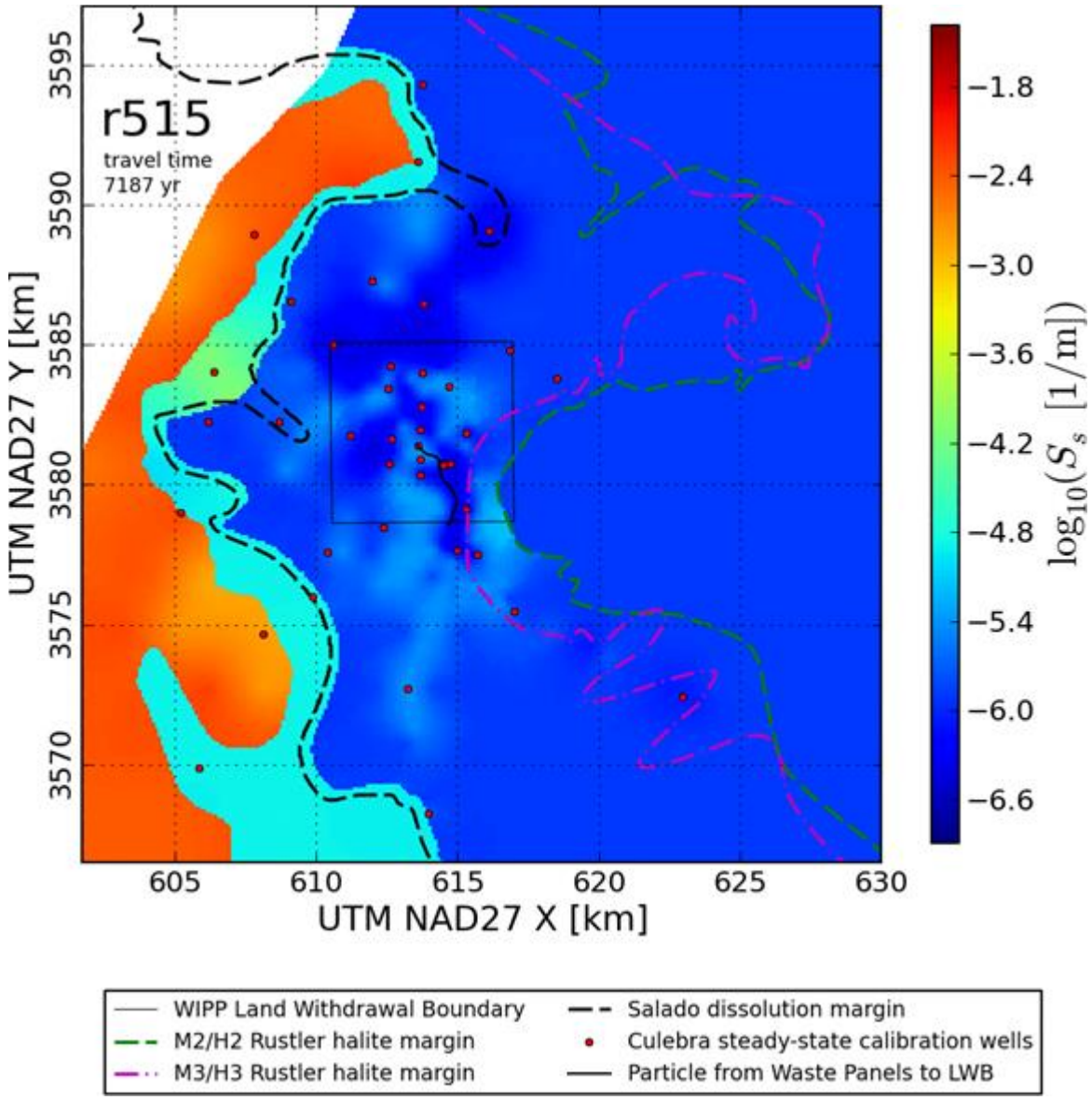
r515
travel time
7187 yr
UTM NAD27 Y [km]
3595
3590
3585
3580
3575
3570
605
610
615
620
625
630
UTM NAD27 X [km]
−1.8
−2.4
−3.0
−3.6
−4.2
−4.8
−5.4
−6.0
−6.6
$\log_{10}(S_s\ [1/\mathrm{m}])$
WIPP Land Withdrawal Boundary
M2/H2 Rustler halite margin
M3/H3 Rustler halite margin
Salado dissolution margin
Culebra steady-state calibration wells
Particle from Waste Panels to LWB

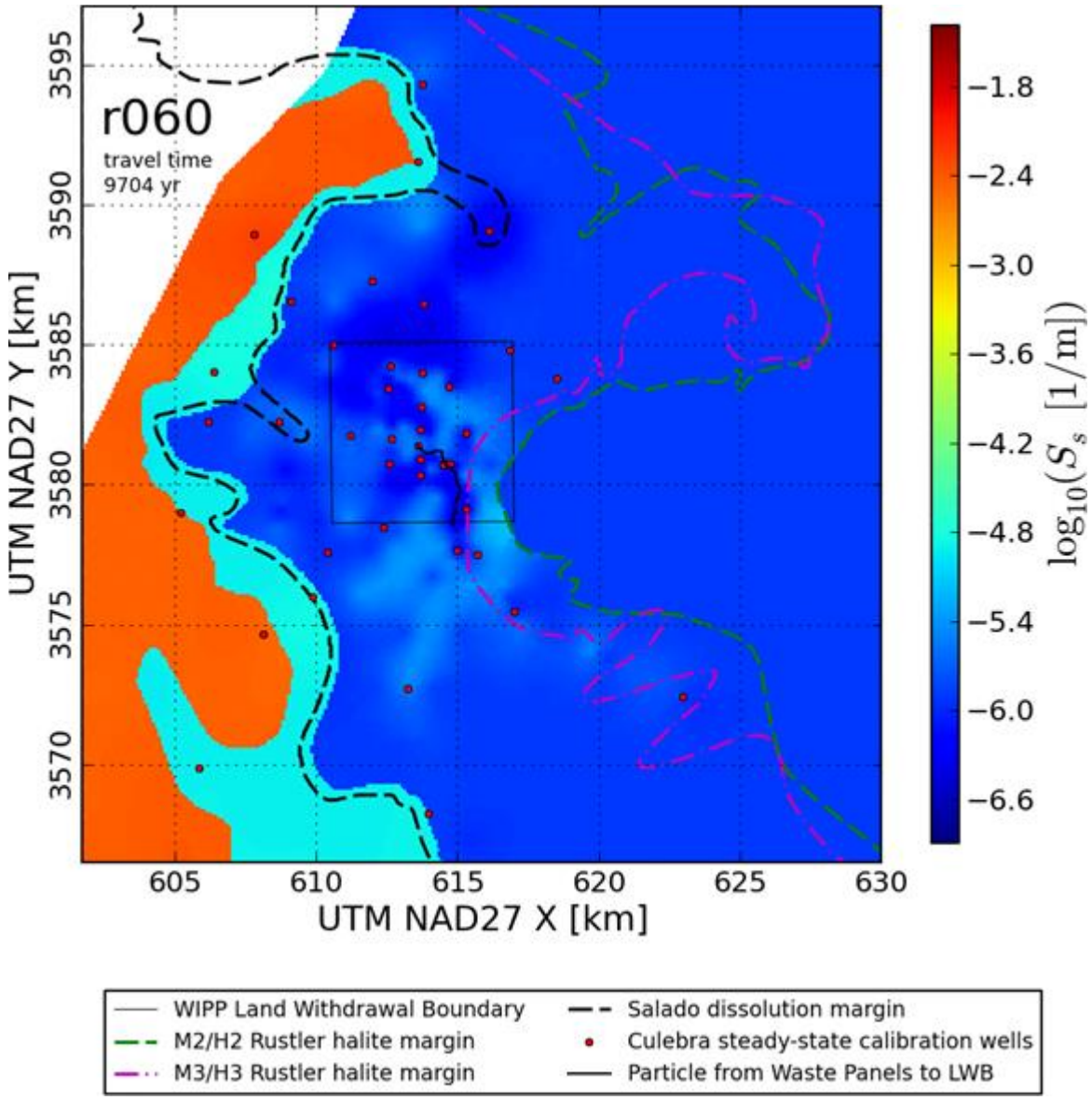
r060
travel time
9704 yr
UTM NAD27 Y [km]
3595
3590
3585
3580
3575
3570
605
610
615
620
625
630
UTM NAD27 X [km]
−1.8
−2.4
−3.0
−3.6
−4.2
−4.8
−5.4
−6.0
−6.6
$\log_{10}(S_s\ [1/\mathrm{m}])$
WIPP Land Withdrawal Boundary
M2/H2 Rustler halite margin
M3/H3 Rustler halite margin
Salado dissolution margin
Culebra steady-state calibration wells
Particle from Waste Panels to LWB

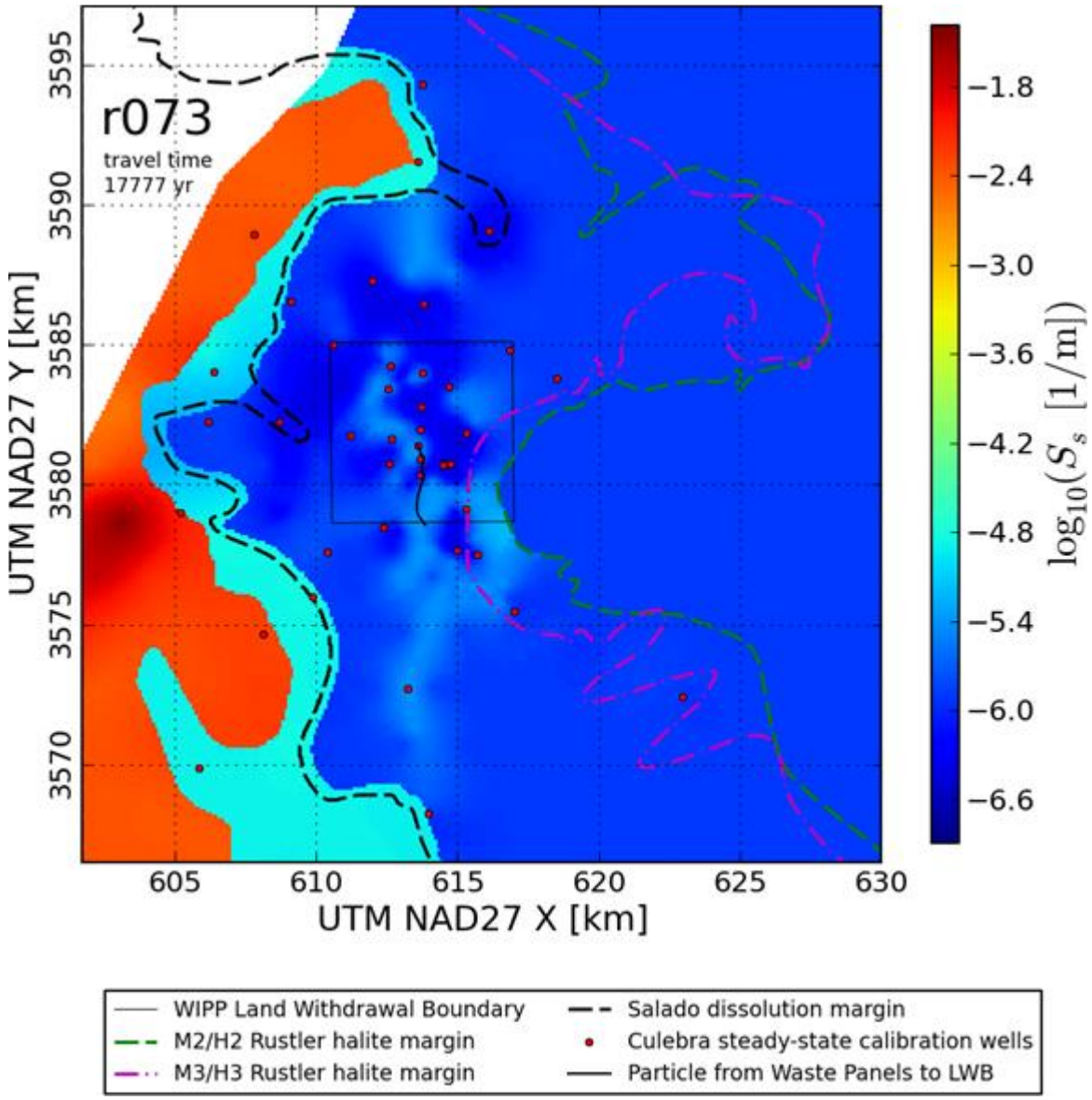
r073
travel time
17777 yr
UTM NAD27 Y [km]
3595
3590
3585
3580
3575
3570
605
610
615
620
625
630
UTM NAD27 X [km]
−1.8
−2.4
−3.0
−3.6
−4.2
−4.8
−5.4
−6.0
−6.6
$\log_{10}(S_s\ [1/\mathrm{m}])$
WIPP Land Withdrawal Boundary
M2/H2 Rustler halite margin
M3/H3 Rustler halite margin
Salado dissolution margin
Culebra steady-state calibration wells
Particle from Waste Panels to LWB

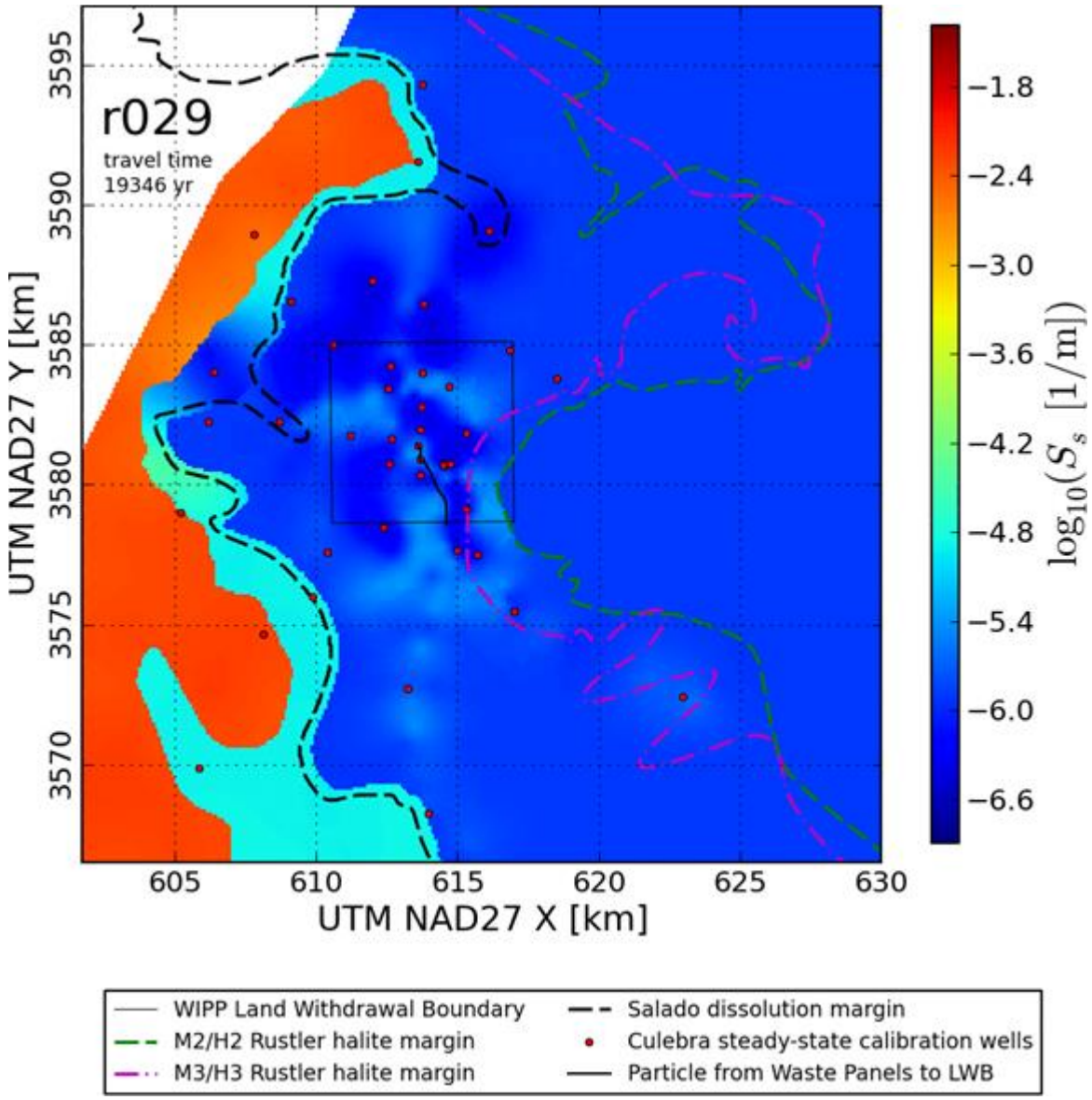
r029
travel time
19346 yr
UTM NAD27 Y [km]
3595
3590
3585
3580
3575
3570
605
610
615
620
625
630
UTM NAD27 X [km]
−1.8
−2.4
−3.0
−3.6
−4.2
−4.8
−5.4
−6.0
−6.6
$\log_{10}(S_s\ [1/\mathrm{m}])$
WIPP Land Withdrawal Boundary
M2/H2 Rustler halite margin
M3/H3 Rustler halite margin
Salado dissolution margin
Culebra steady-state calibration wells
Particle from Waste Panels to LWB

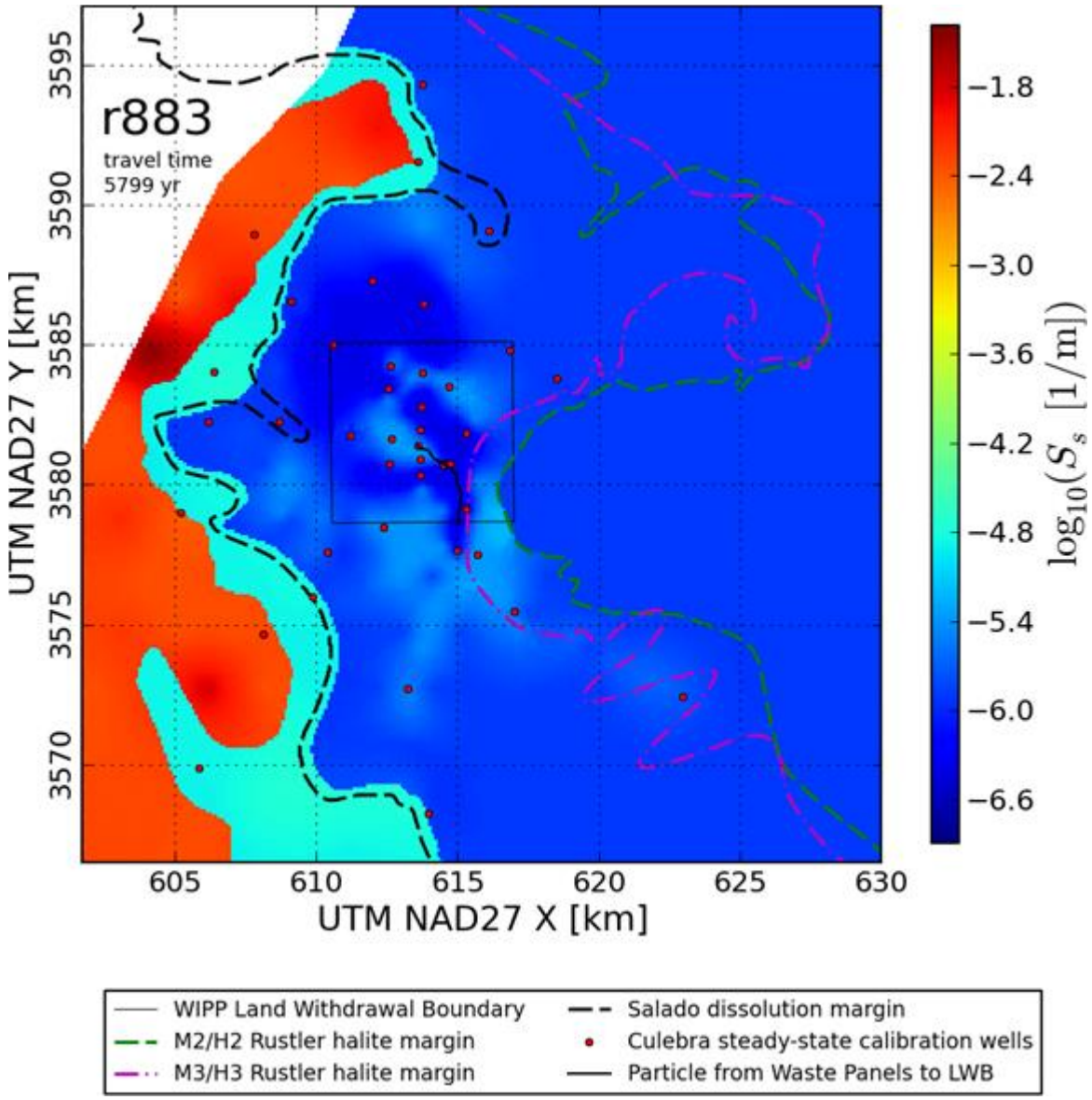
r883
travel time
5799 yr
UTM NAD27 Y [km]
3595
3590
3585
3580
3575
3570
605
610
615
620
625
630
UTM NAD27 X [km]
−1.8
−2.4
−3.0
−3.6
−4.2
−4.8
−5.4
−6.0
−6.6
$\log_{10}(S_s\ [1/\mathrm{m}])$
WIPP Land Withdrawal Boundary
M2/H2 Rustler halite margin
M3/H3 Rustler halite margin
Salado dissolution margin
Culebra steady-state calibration wells
Particle from Waste Panels to LWB

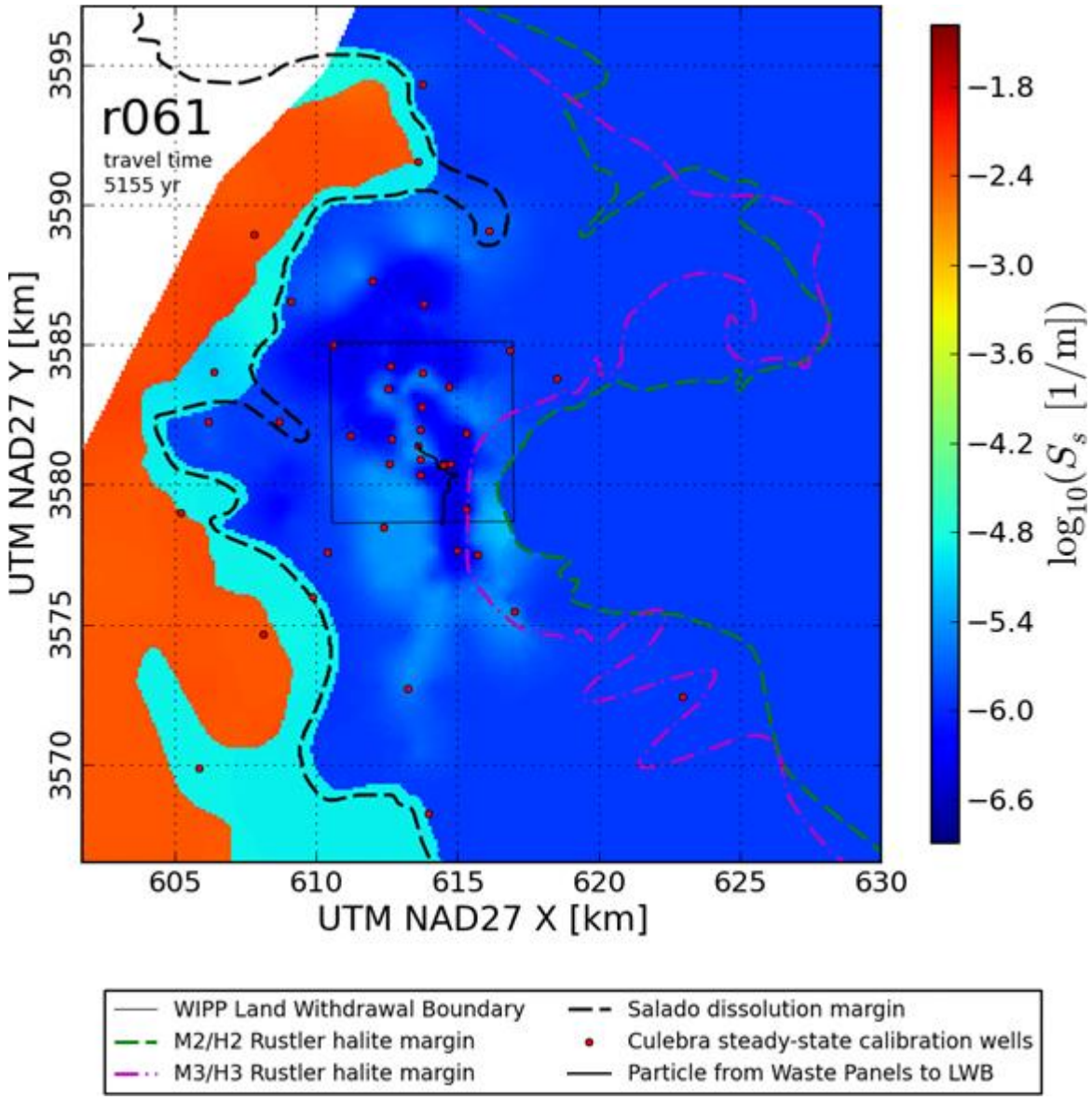
r061
travel time
5155 yr
UTM NAD27 Y [km]
3595
3590
3585
3580
3575
3570
605
610
615
620
625
630
UTM NAD27 X [km]
−1.8
−2.4
−3.0
−3.6
−4.2
−4.8
−5.4
−6.0
−6.6
$\log_{10}(S_s\ [1/\mathrm{m}])$
WIPP Land Withdrawal Boundary
M2/H2 Rustler halite margin
M3/H3 Rustler halite margin
Salado dissolution margin
Culebra steady-state calibration wells
Particle from Waste Panels to LWB

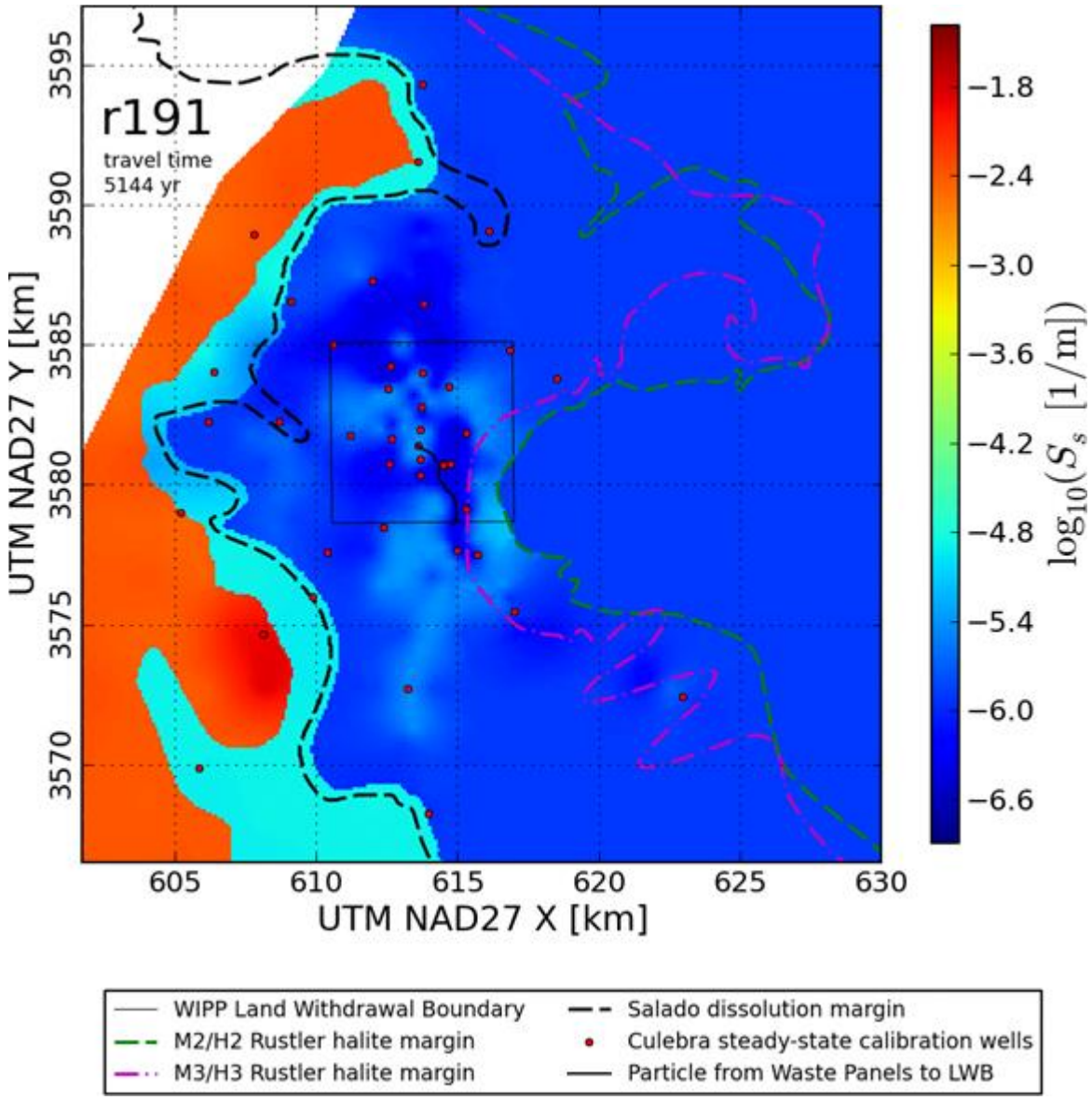
r191
travel time
5144 yr
UTM NAD27 Y [km]
3595
3590
3585
3580
3575
3570
605
610
615
620
625
630
UTM NAD27 X [km]
−1.8
−2.4
−3.0
−3.6
−4.2
−4.8
−5.4
−6.0
−6.6
$\log_{10}(S_s\ [1/\mathrm{m}])$
WIPP Land Withdrawal Boundary
M2/H2 Rustler halite margin
M3/H3 Rustler halite margin
Salado dissolution margin
Culebra steady-state calibration wells
Particle from Waste Panels to LWB

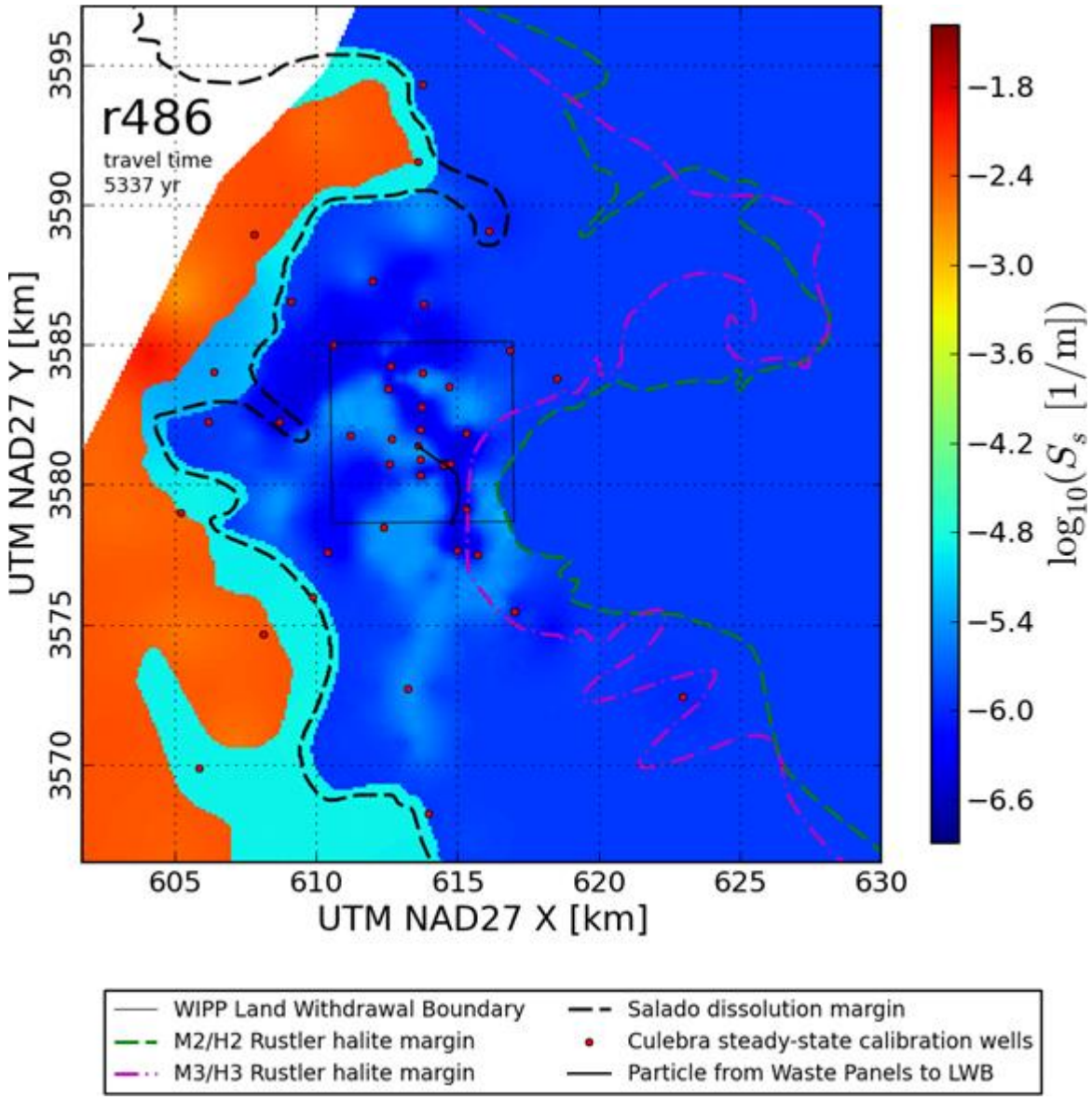
r486
travel time
5337 yr
UTM NAD27 Y [km]
3595
3590
3585
3580
3575
3570
605
610
615
620
625
630
UTM NAD27 X [km]
−1.8
−2.4
−3.0
−3.6
−4.2
−4.8
−5.4
−6.0
−6.6
$\log_{10}(S_s\ [1/\mathrm{m}])$
WIPP Land Withdrawal Boundary
M2/H2 Rustler halite margin
M3/H3 Rustler halite margin
Salado dissolution margin
Culebra steady-state calibration wells
Particle from Waste Panels to LWB

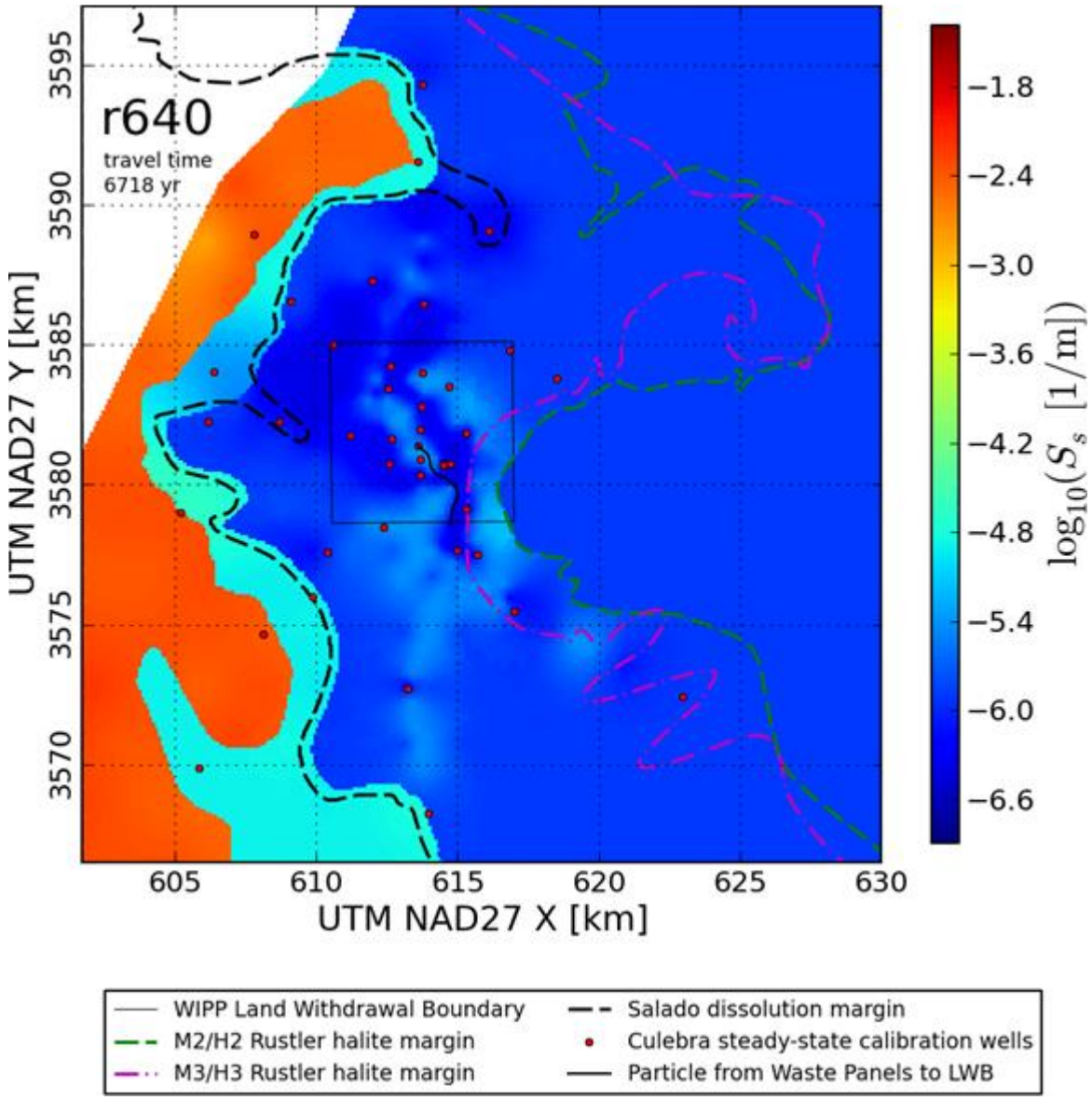
r640
travel time
6718 yr
UTM NAD27 Y [km]
3595
3590
3585
3580
3575
3570
605
610
615
620
625
630
UTM NAD27 X [km]
−1.8
−2.4
−3.0
−3.6
−4.2
−4.8
−5.4
−6.0
−6.6
$\log_{10}(S_s\ [1/\mathrm{m}])$
WIPP Land Withdrawal Boundary
M2/H2 Rustler halite margin
M3/H3 Rustler halite margin
Salado dissolution margin
Culebra steady-state calibration wells
Particle from Waste Panels to LWB

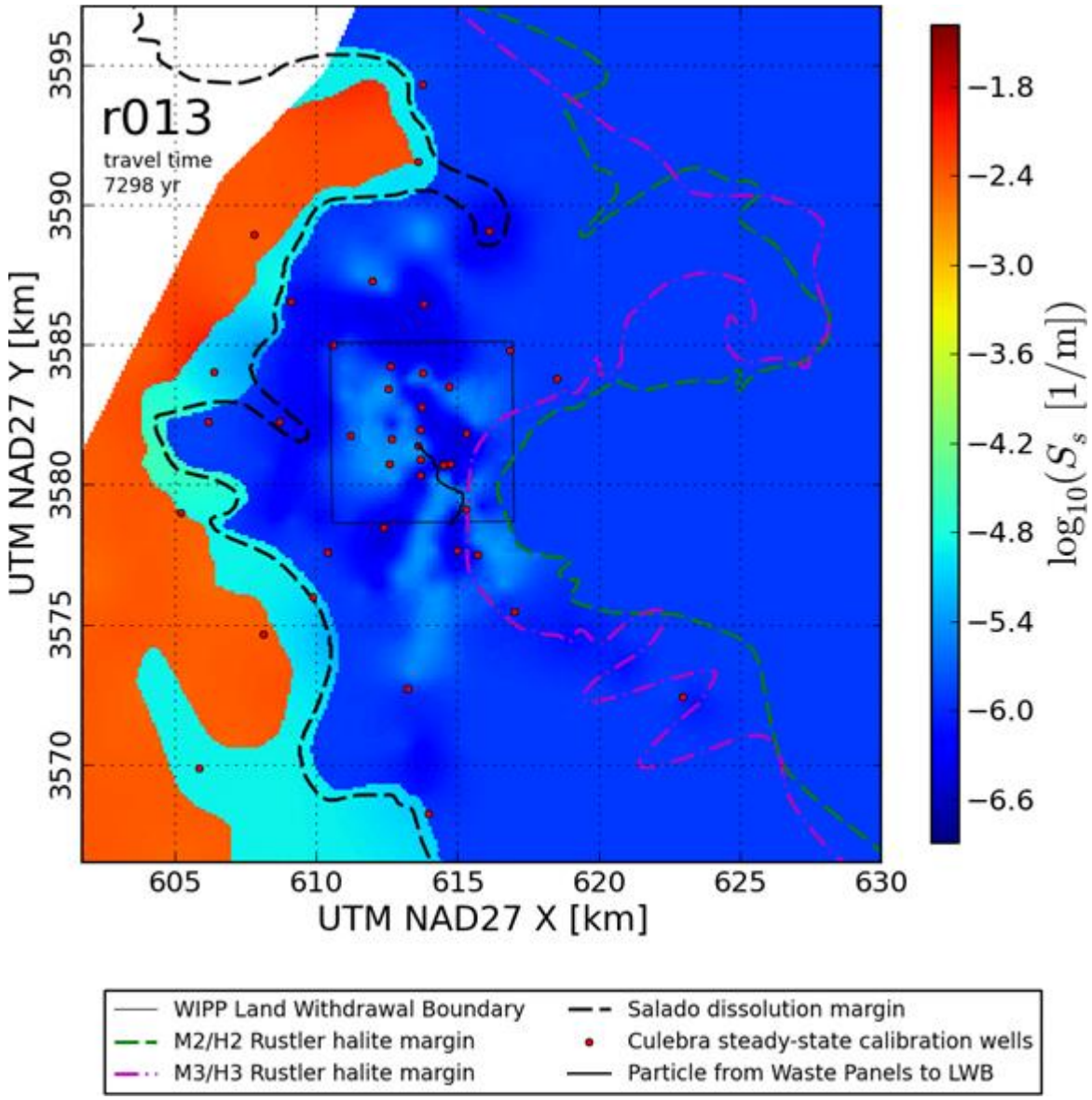
r013
travel time
7298 yr
UTM NAD27 Y [km]
3595
3590
3585
3580
3575
3570
605
610
615
620
625
630
UTM NAD27 X [km]
−1.8
−2.4
−3.0
−3.6
−4.2
−4.8
−5.4
−6.0
−6.6
$\log_{10}(S_s\ [1/\mathrm{m}])$
WIPP Land Withdrawal Boundary
M2/H2 Rustler halite margin
M3/H3 Rustler halite margin
Salado dissolution margin
Culebra steady-state calibration wells
Particle from Waste Panels to LWB

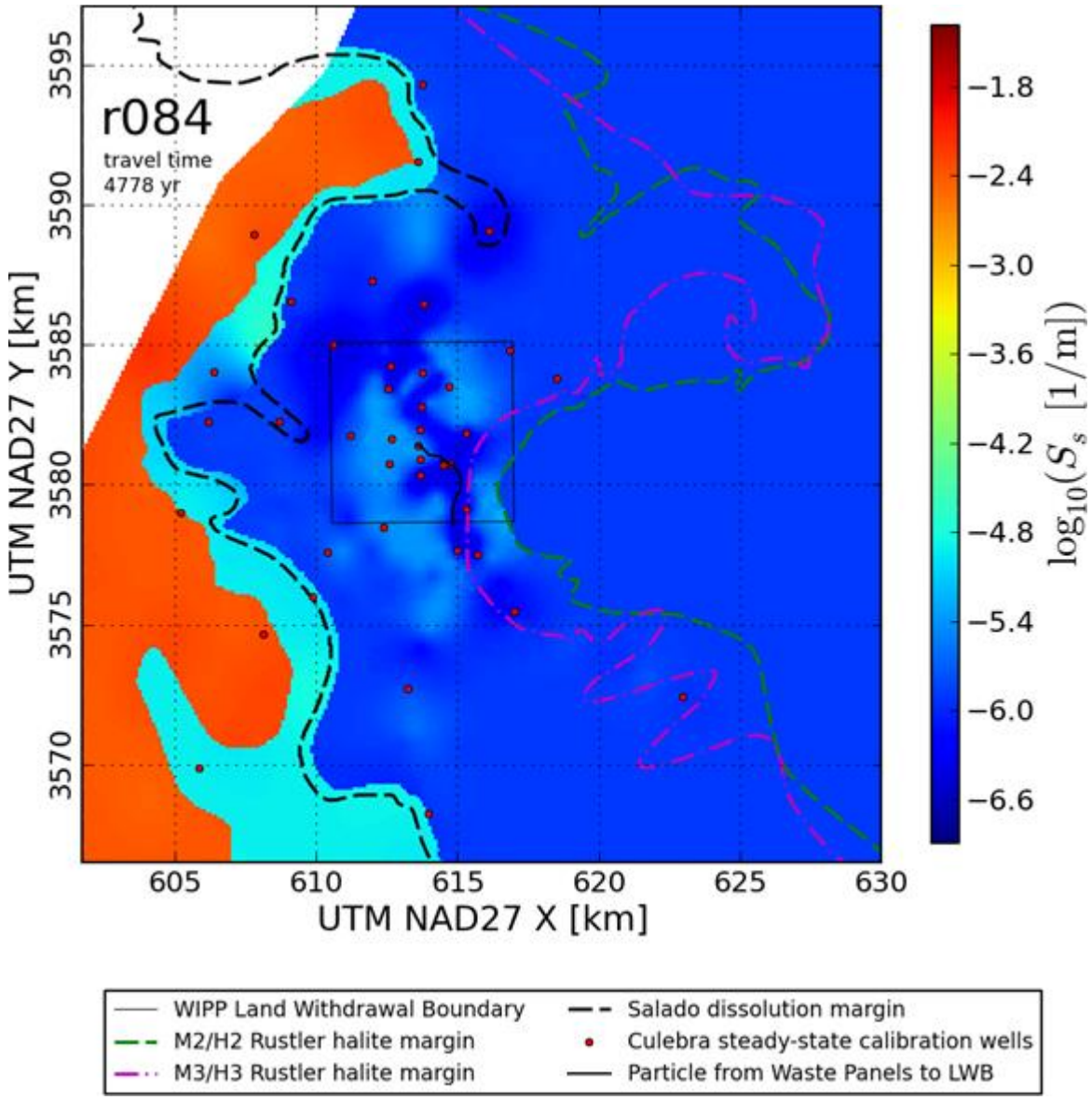
r084
travel time
4778 yr
UTM NAD27 Y [km]
3595
3590
3585
3580
3575
3570
605
610
615
620
625
630
UTM NAD27 X [km]
−1.8
−2.4
−3.0
−3.6
−4.2
−4.8
−5.4
−6.0
−6.6
$\log_{10}(S_s\ [1/\mathrm{m}])$
WIPP Land Withdrawal Boundary
M2/H2 Rustler halite margin
M3/H3 Rustler halite margin
Salado dissolution margin
Culebra steady-state calibration wells
Particle from Waste Panels to LWB

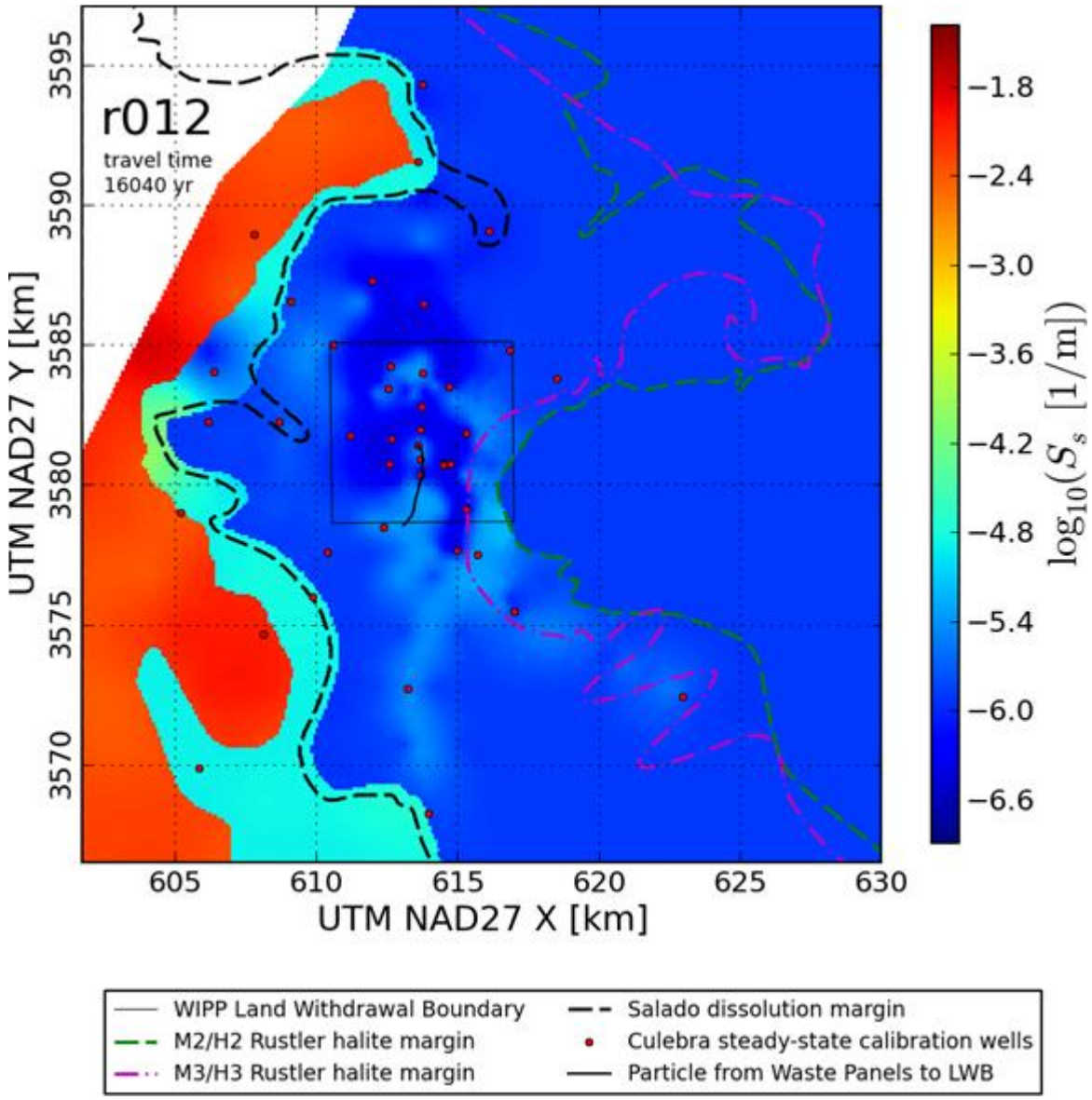
r012
travel time
16040 yr
UTM NAD27 Y [km]
3595
3590
3585
3580
3575
3570
605
610
615
620
625
630
UTM NAD27 X [km]
−1.8
−2.4
−3.0
−3.6
−4.2
−4.8
−5.4
−6.0
−6.6
$\log_{10}(S_s\ [1/\mathrm{m}])$
WIPP Land Withdrawal Boundary
M2/H2 Rustler halite margin
M3/H3 Rustler halite margin
Salado dissolution margin
Culebra steady-state calibration wells
Particle from Waste Panels to LWB

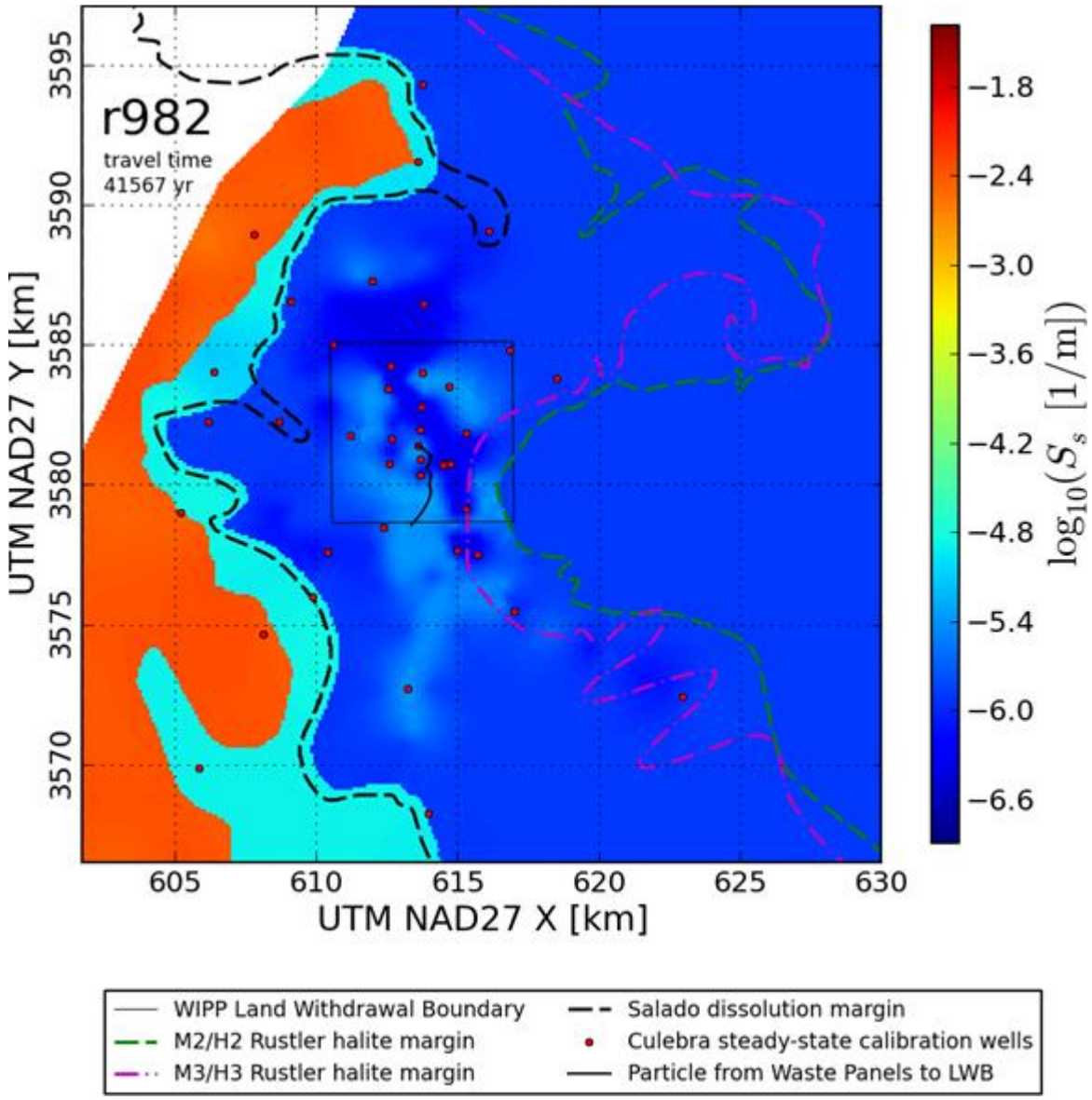
r982
travel time
41567 yr
UTM NAD27 Y [km]
3595
3590
3585
3580
3575
3570
605
610
615
620
625
630
UTM NAD27 X [km]
−1.8
−2.4
−3.0
−3.6
−4.2
−4.8
−5.4
−6.0
−6.6
$\log_{10}(S_s\ [1/\mathrm{m}])$
WIPP Land Withdrawal Boundary
M2/H2 Rustler halite margin
M3/H3 Rustler halite margin
Salado dissolution margin
Culebra steady-state calibration wells
Particle from Waste Panels to LWB

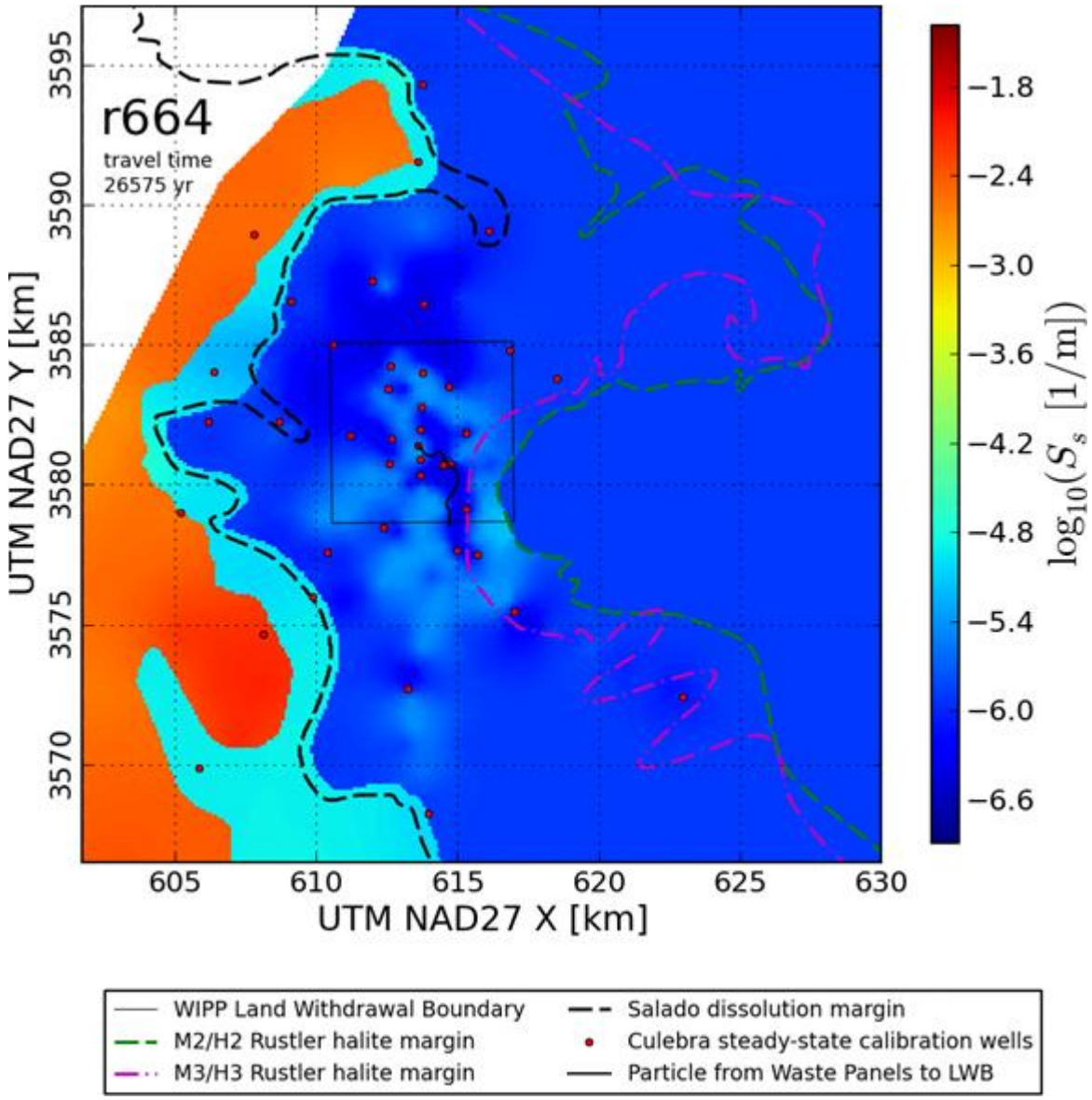
r664
travel time
26575 yr
UTM NAD27 Y [km]
3595
3590
3585
3580
3575
3570
605
610
615
620
625
630
UTM NAD27 X [km]
−1.8
−2.4
−3.0
−3.6
−4.2
−4.8
−5.4
−6.0
−6.6
$\log_{10}(S_s\ [1/\mathrm{m}])$
WIPP Land Withdrawal Boundary
M2/H2 Rustler halite margin
M3/H3 Rustler halite margin
Salado dissolution margin
Culebra steady-state calibration wells
Particle from Waste Panels to LWB

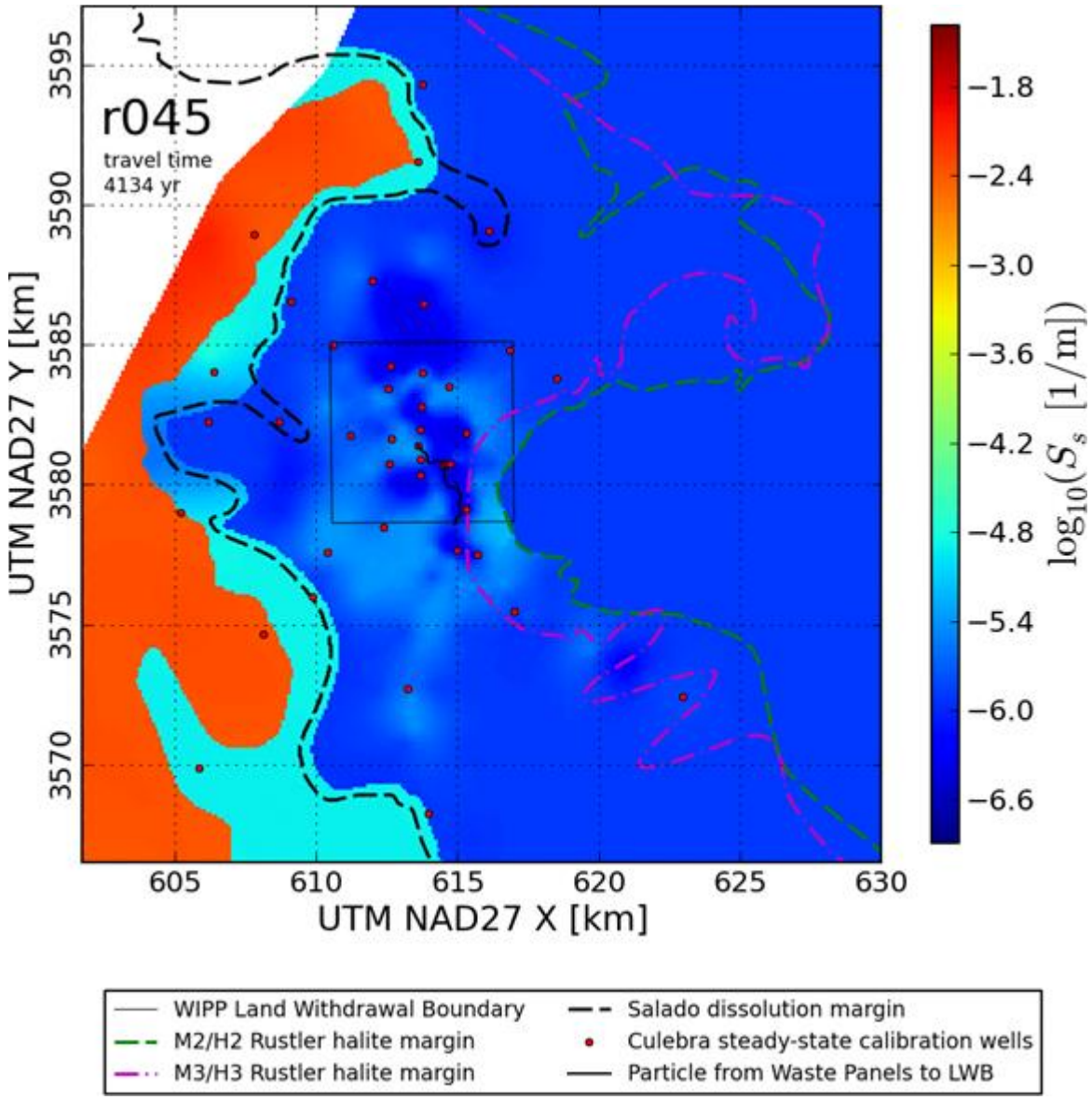
r045
travel time
4134 yr
UTM NAD27 Y [km]
3595
3590
3585
3580
3575
3570
605
610
615
620
625
630
UTM NAD27 X [km]
−1.8
−2.4
−3.0
−3.6
−4.2
−4.8
−5.4
−6.0
−6.6
$\log_{10}(S_s\ [1/\mathrm{m}])$
WIPP Land Withdrawal Boundary
M2/H2 Rustler halite margin
M3/H3 Rustler halite margin
Salado dissolution margin
Culebra steady-state calibration wells
Particle from Waste Panels to LWB

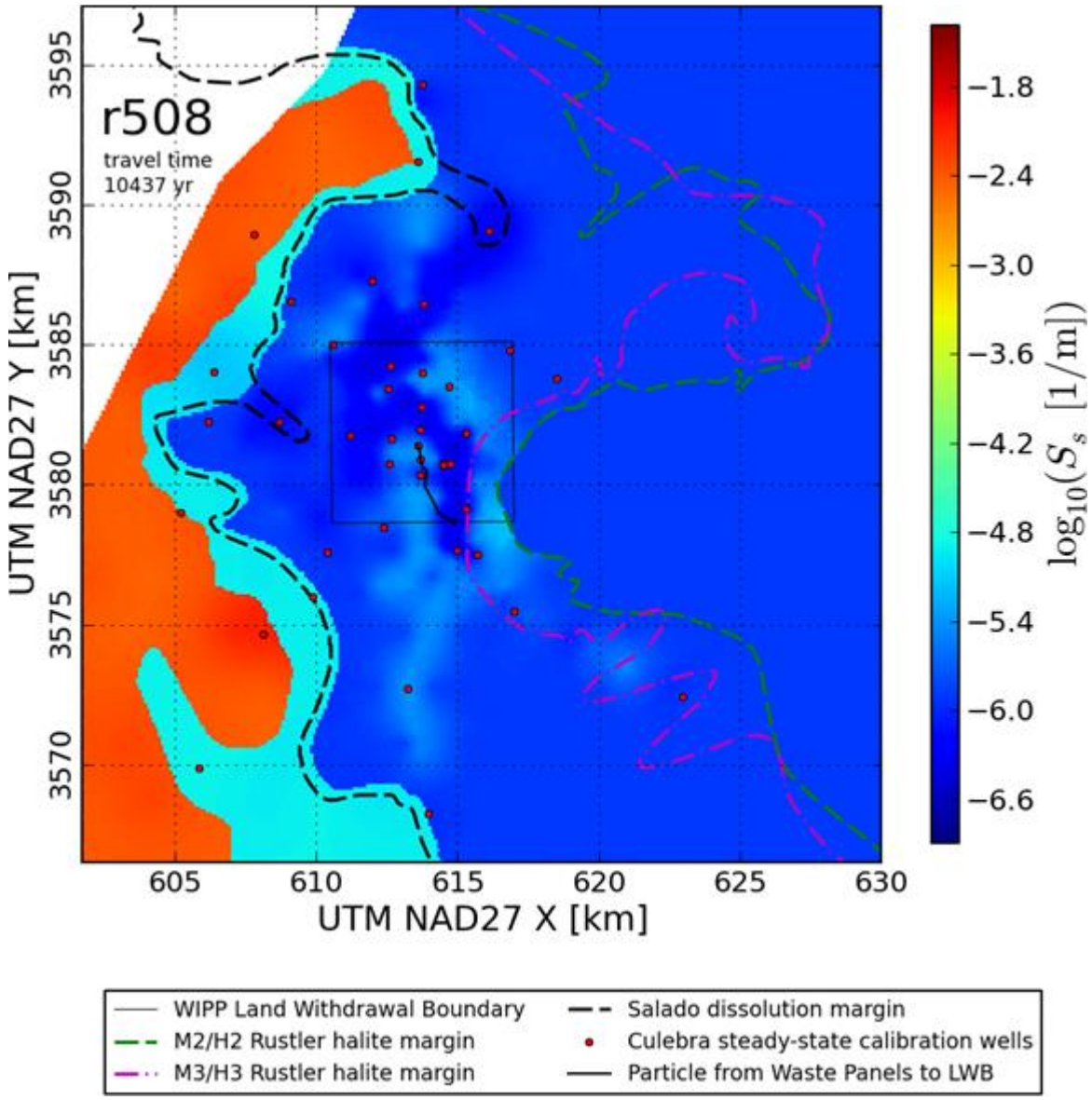
r508
travel time
10437 yr
UTM NAD27 Y [km]
3595
3590
3585
3580
3575
3570
605
610
615
620
625
630
UTM NAD27 X [km]
−1.8
−2.4
−3.0
−3.6
−4.2
−4.8
−5.4
−6.0
−6.6
$\log_{10}(S_s\ [1/\mathrm{m}])$
WIPP Land Withdrawal Boundary
M2/H2 Rustler halite margin
M3/H3 Rustler halite margin
Salado dissolution margin
Culebra steady-state calibration wells
Particle from Waste Panels to LWB

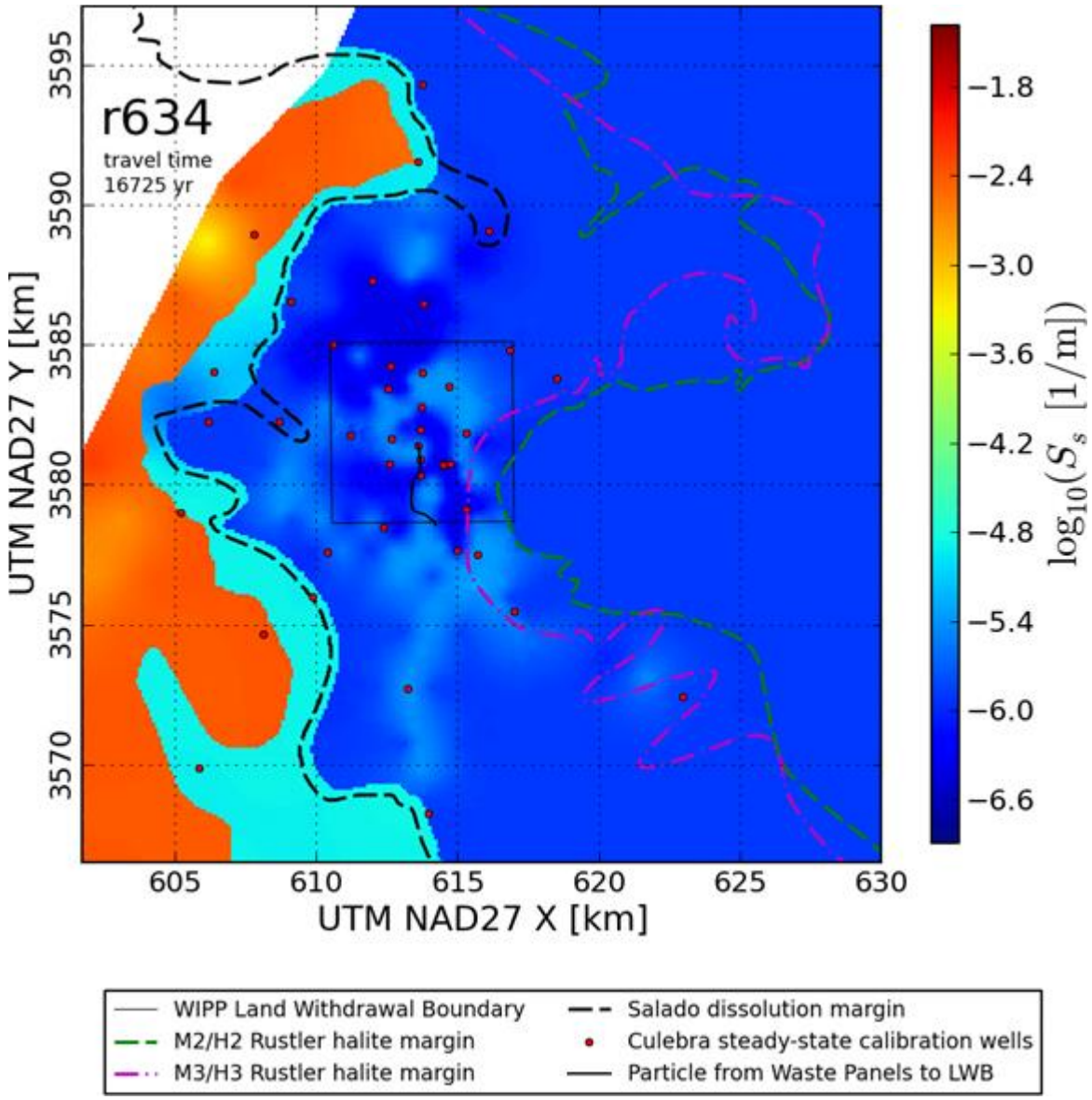
r634
travel time
16725 yr
UTM NAD27 Y [km]
3595
3590
3585
3580
3575
3570
605
610
615
620
625
630
UTM NAD27 X [km]
−1.8
−2.4
−3.0
−3.6
−4.2
−4.8
−5.4
−6.0
−6.6
$\log_{10}(S_s\ [1/\mathrm{m}])$
WIPP Land Withdrawal Boundary
M2/H2 Rustler halite margin
M3/H3 Rustler halite margin
Salado dissolution margin
Culebra steady-state calibration wells
Particle from Waste Panels to LWB

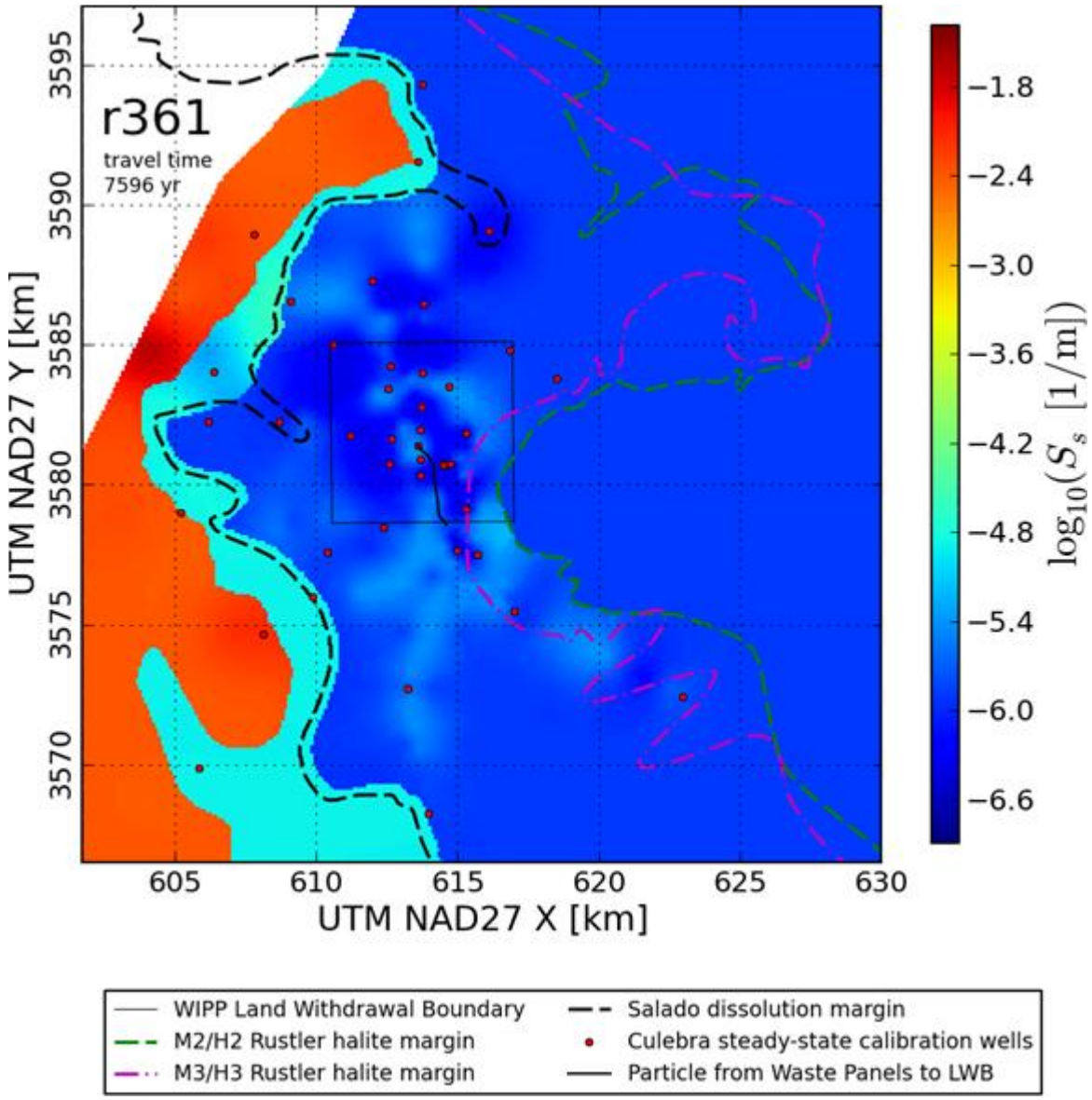
r361
travel time
7596 yr
UTM NAD27 Y [km]
3595
3590
3585
3580
3575
3570
605
610
615
620
625
630
UTM NAD27 X [km]
−1.8
−2.4
−3.0
−3.6
−4.2
−4.8
−5.4
−6.0
−6.6
$\log_{10}(S_s\ [1/\mathrm{m}])$
WIPP Land Withdrawal Boundary
M2/H2 Rustler halite margin
M3/H3 Rustler halite margin
Salado dissolution margin
Culebra steady-state calibration wells
Particle from Waste Panels to LWB

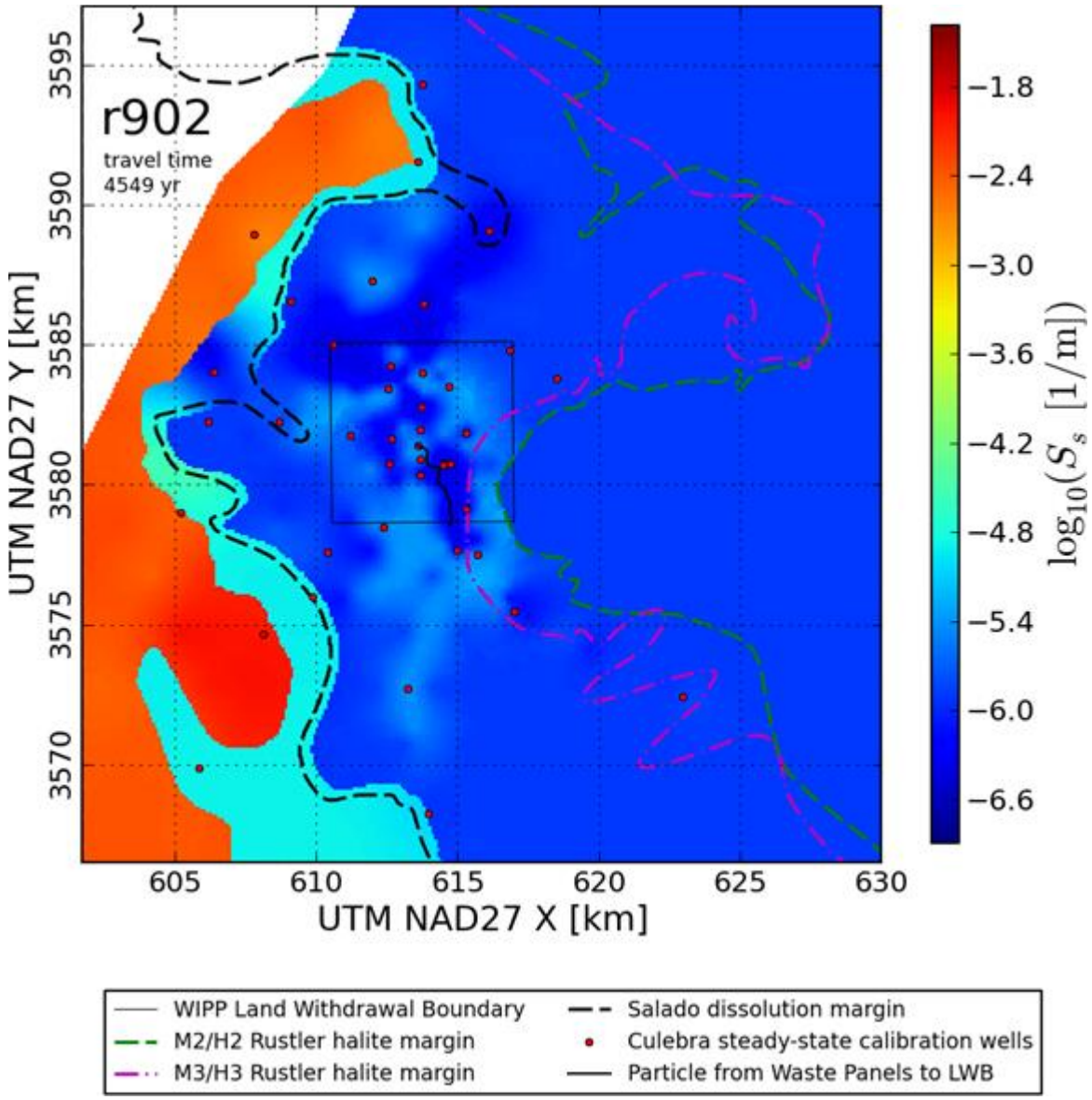
r902
travel time
4549 yr
UTM NAD27 Y [km]
3595
3590
3585
3580
3575
3570
605
610
615
620
625
630
UTM NAD27 X [km]
−1.8
−2.4
−3.0
−3.6
−4.2
−4.8
−5.4
−6.0
−6.6
$\log_{10}(S_s\ [1/\mathrm{m}])$
WIPP Land Withdrawal Boundary
M2/H2 Rustler halite margin
M3/H3 Rustler halite margin
Salado dissolution margin
Culebra steady-state calibration wells
Particle from Waste Panels to LWB

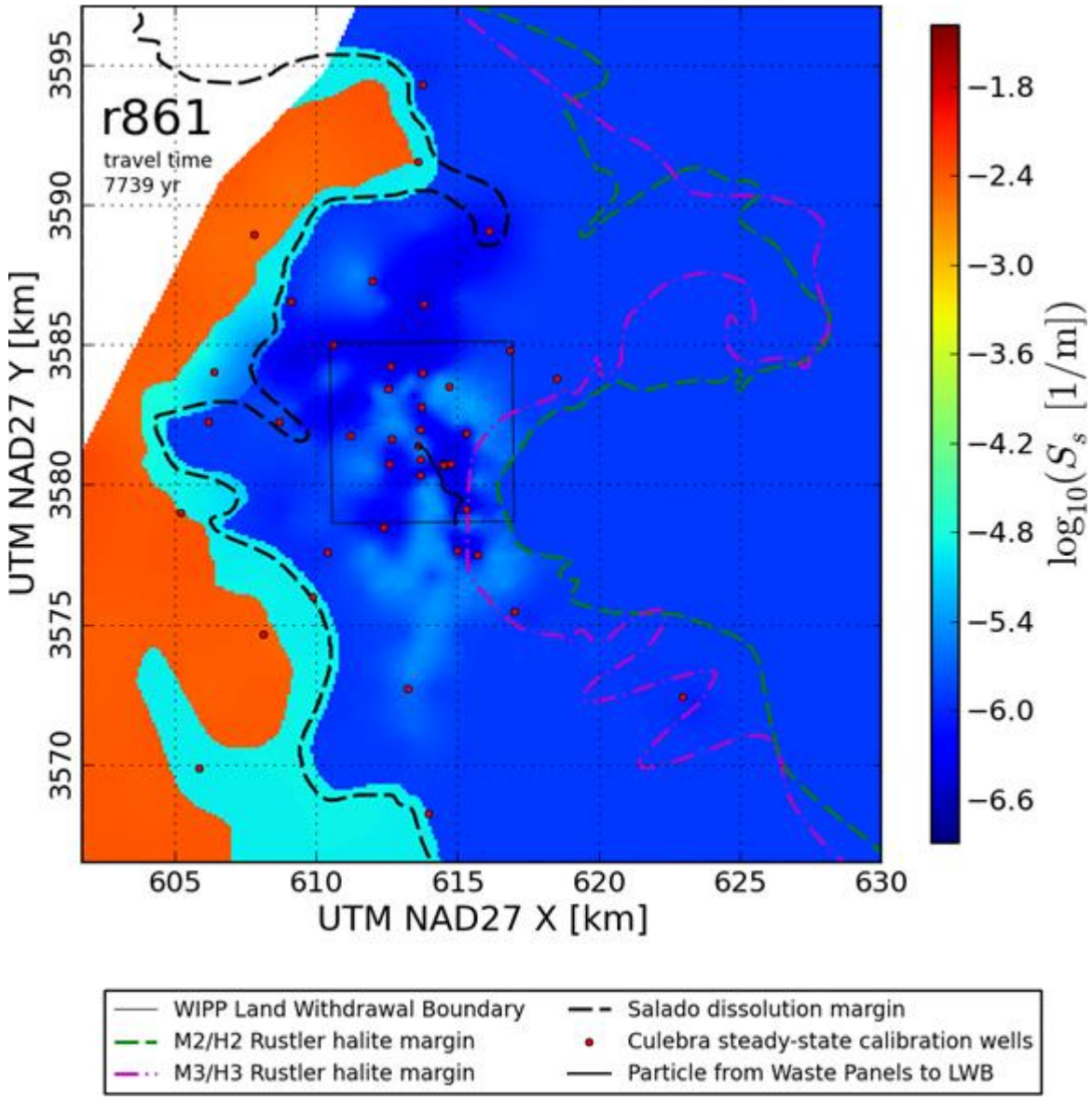
r861
travel time
7739 yr
UTM NAD27 Y [km]
3595
3590
3585
3580
3575
3570
605
610
615
620
625
630
UTM NAD27 X [km]
−1.8
−2.4
−3.0
−3.6
−4.2
−4.8
−5.4
−6.0
−6.6
$\log_{10}(S_s\ [1/\mathrm{m}])$
WIPP Land Withdrawal Boundary
M2/H2 Rustler halite margin
M3/H3 Rustler halite margin
Salado dissolution margin
Culebra steady-state calibration wells
Particle from Waste Panels to LWB

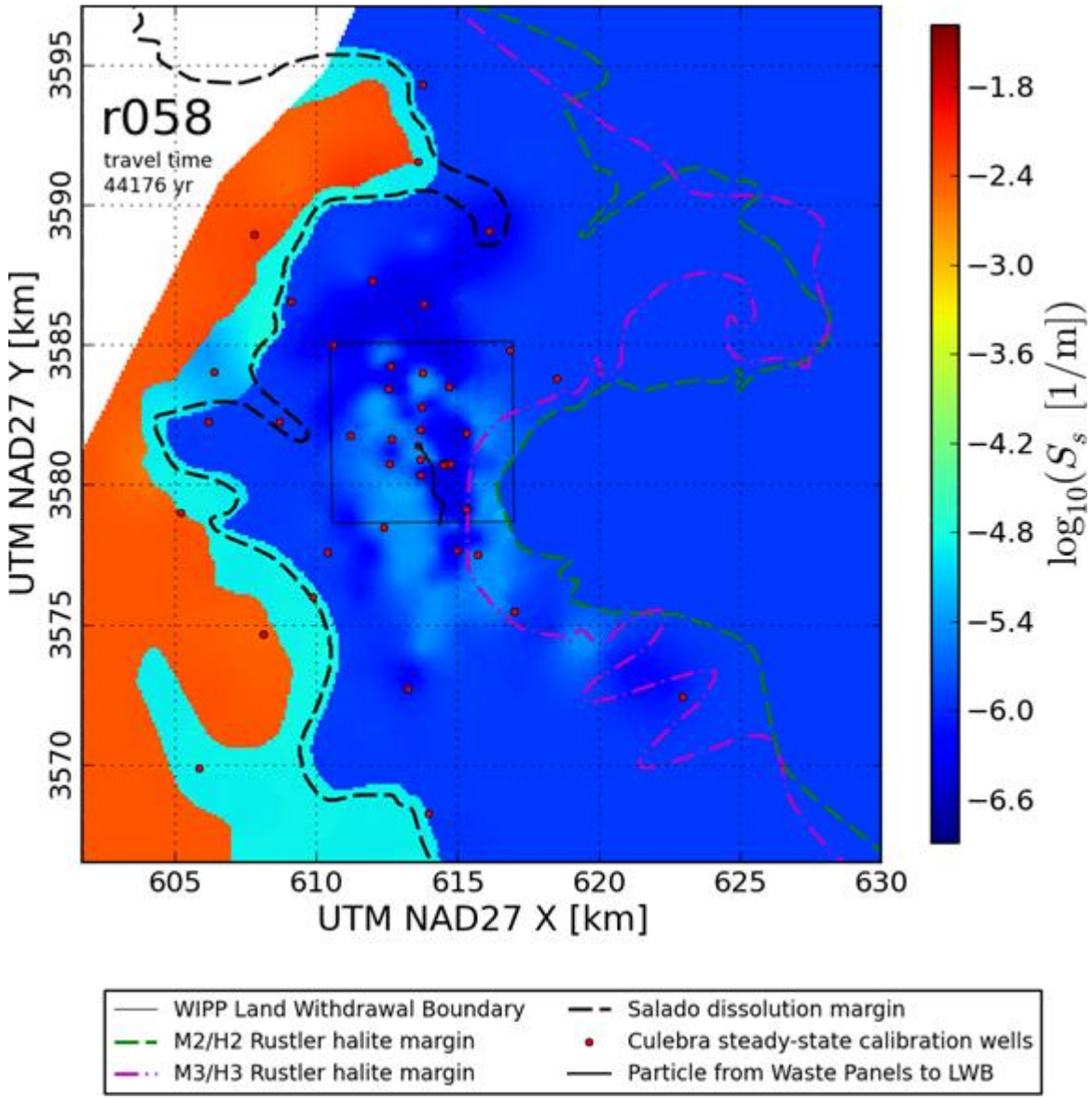
r058
travel time
44176 yr
UTM NAD27 Y [km]
3595
3590
3585
3580
3575
3570
605
610
615
620
625
630
UTM NAD27 X [km]
−1.8
−2.4
−3.0
−3.6
−4.2
−4.8
−5.4
−6.0
−6.6
$\log_{10}(S_s\ [1/\mathrm{m}])$
WIPP Land Withdrawal Boundary
M2/H2 Rustler halite margin
M3/H3 Rustler halite margin
Salado dissolution margin
Culebra steady-state calibration wells
Particle from Waste Panels to LWB

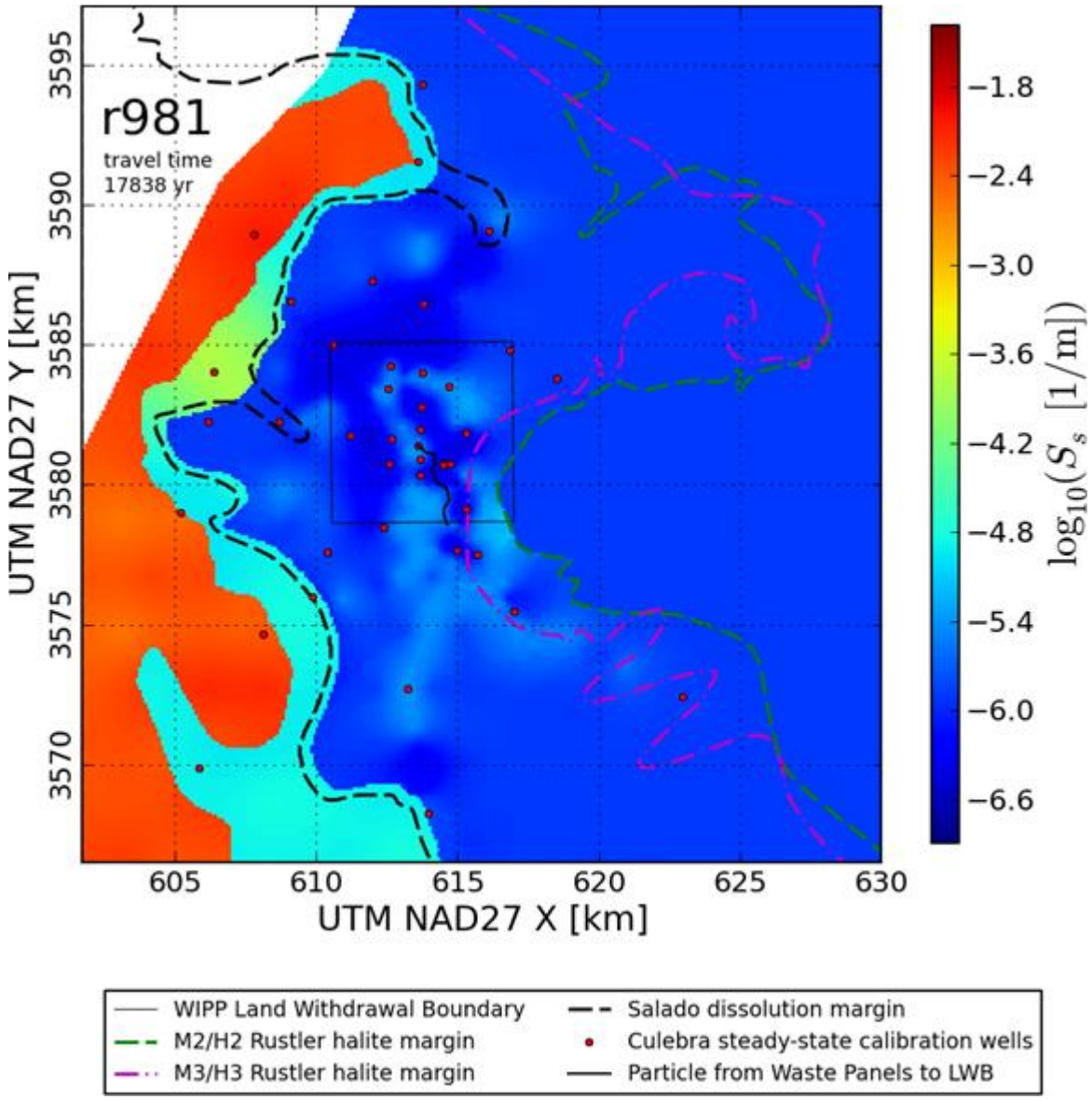
r981
travel time
17838 yr
UTM NAD27 Y [km]
3595
3590
3585
3580
3575
3570
605
610
615
620
625
630
UTM NAD27 X [km]
−1.8
−2.4
−3.0
−3.6
−4.2
−4.8
−5.4
−6.0
−6.6
$\log_{10}(S_s\ [1/\mathrm{m}])$
WIPP Land Withdrawal Boundary
M2/H2 Rustler halite margin
M3/H3 Rustler halite margin
Salado dissolution margin
Culebra steady-state calibration wells
Particle from Waste Panels to LWB

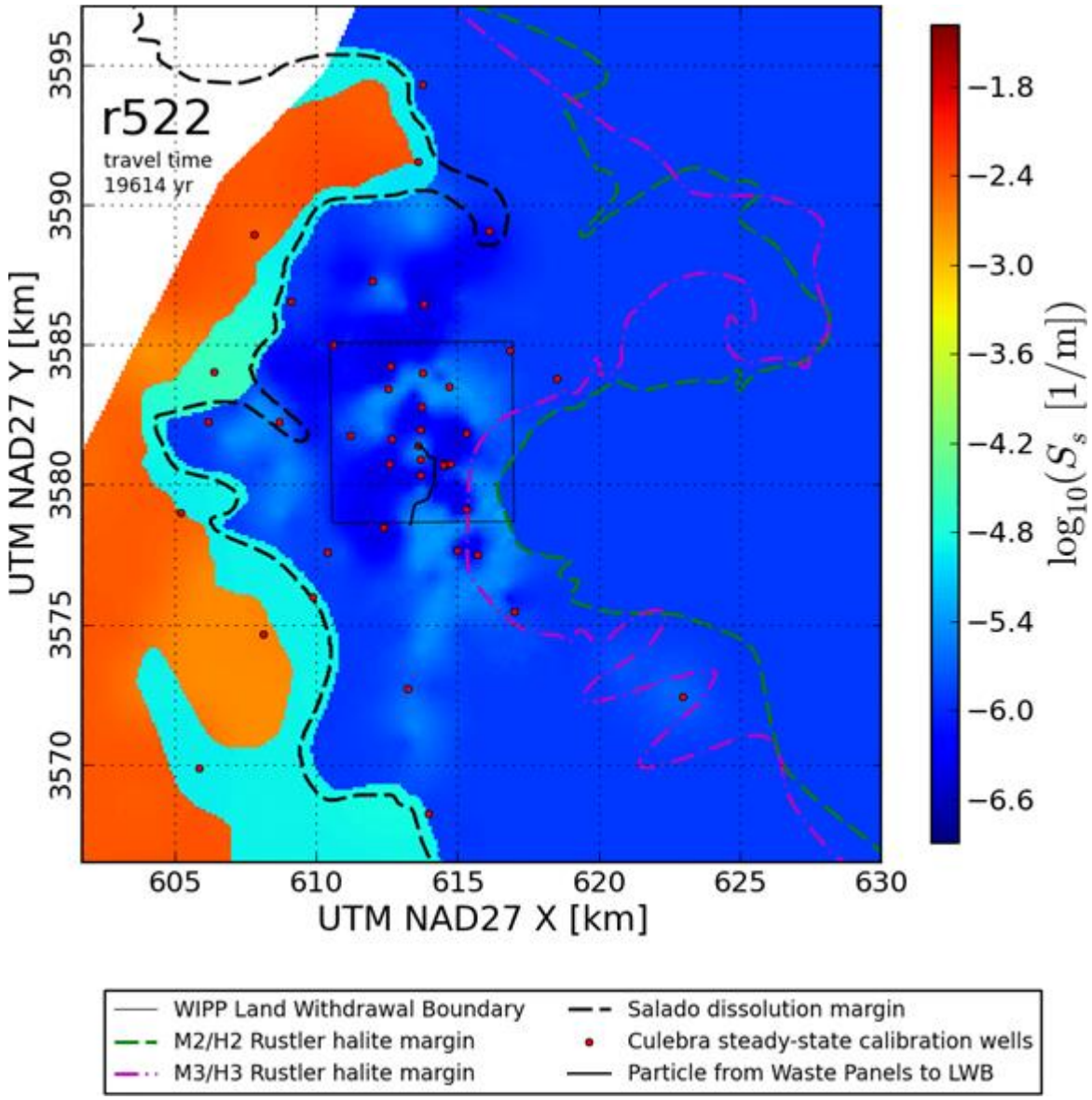
r522
travel time
19614 yr
UTM NAD27 Y [km]
3595
3590
3585
3580
3575
3570
605
610
615
620
625
630
UTM NAD27 X [km]
−1.8
−2.4
−3.0
−3.6
−4.2
−4.8
−5.4
−6.0
−6.6
$\log_{10}(S_s\ [1/\mathrm{m}])$
WIPP Land Withdrawal Boundary
M2/H2 Rustler halite margin
M3/H3 Rustler halite margin
Salado dissolution margin
Culebra steady-state calibration wells
Particle from Waste Panels to LWB

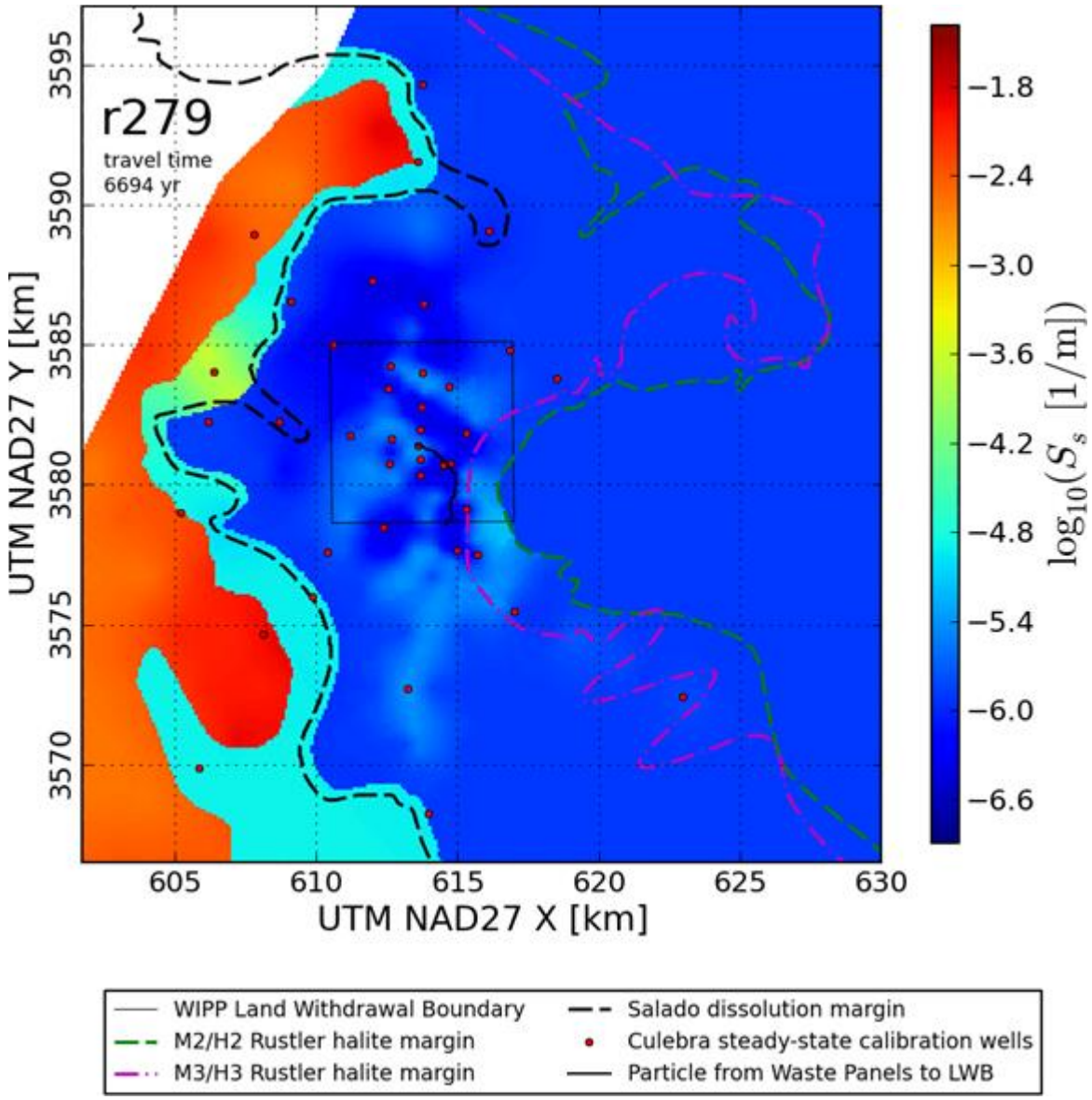
r279
travel time
6694 yr
UTM NAD27 Y [km]
3595
3590
3585
3580
3575
3570
605
610
615
620
625
630
UTM NAD27 X [km]
−1.8
−2.4
−3.0
−3.6
−4.2
−4.8
−5.4
−6.0
−6.6
$\log_{10}(S_s\ [1/\mathrm{m}])$
WIPP Land Withdrawal Boundary
M2/H2 Rustler halite margin
M3/H3 Rustler halite margin
Salado dissolution margin
Culebra steady-state calibration wells
Particle from Waste Panels to LWB

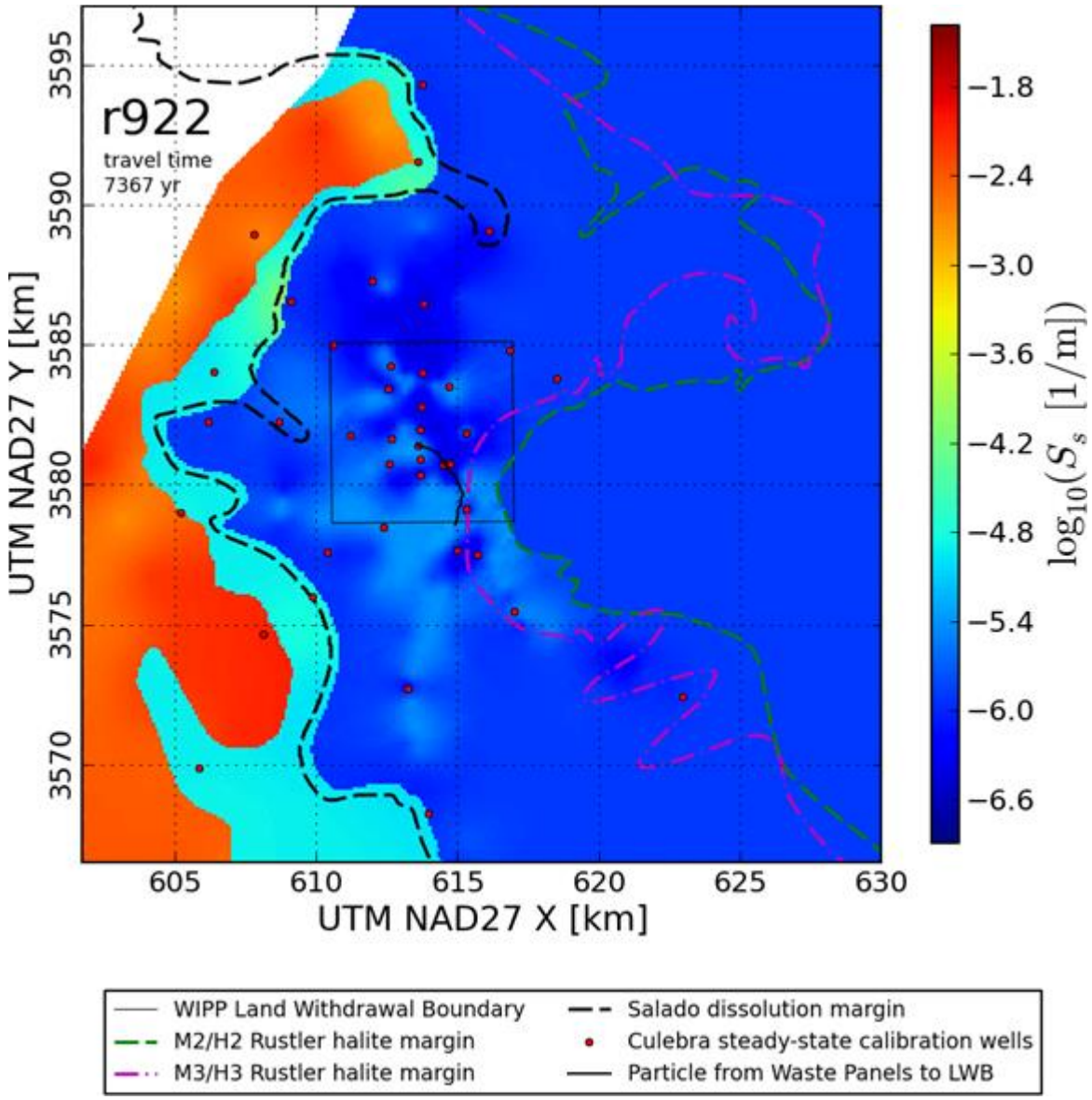
r922
travel time
7367 yr
UTM NAD27 Y [km]
3595
3590
3585
3580
3575
3570
605
610
615
620
625
630
UTM NAD27 X [km]
−1.8
−2.4
−3.0
−3.6
−4.2
−4.8
−5.4
−6.0
−6.6
$\log_{10}(S_s\ [1/\mathrm{m}])$
WIPP Land Withdrawal Boundary
M2/H2 Rustler halite margin
M3/H3 Rustler halite margin
Salado dissolution margin
Culebra steady-state calibration wells
Particle from Waste Panels to LWB

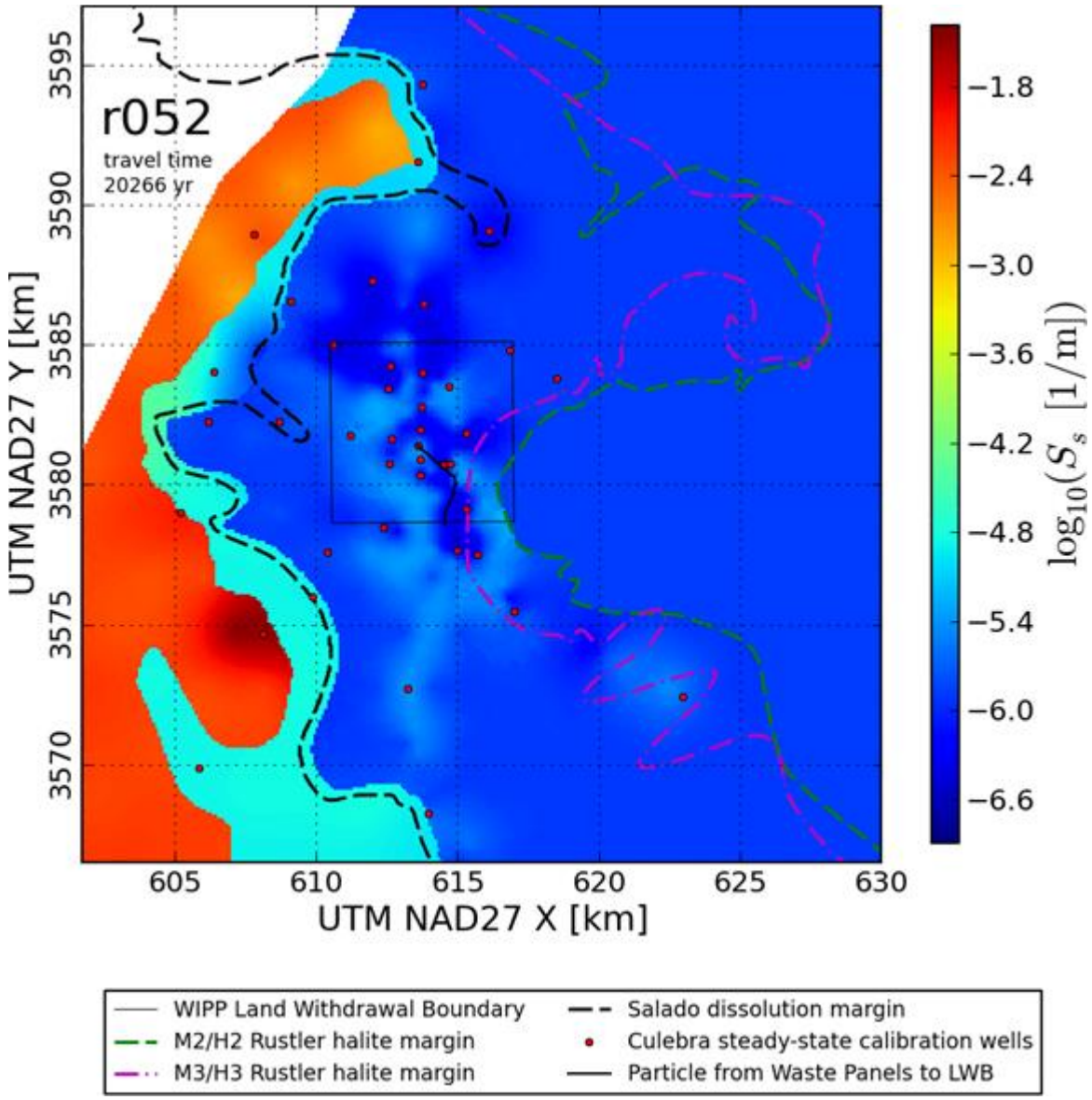
r052
travel time
20266 yr
UTM NAD27 Y [km]
3595
3590
3585
3580
3575
3570
605
610
615
620
625
630
UTM NAD27 X [km]
−1.8
−2.4
−3.0
−3.6
−4.2
−4.8
−5.4
−6.0
−6.6
$\log_{10}(S_s\ [1/\mathrm{m}])$
WIPP Land Withdrawal Boundary
M2/H2 Rustler halite margin
M3/H3 Rustler halite margin
Salado dissolution margin
Culebra steady-state calibration wells
Particle from Waste Panels to LWB

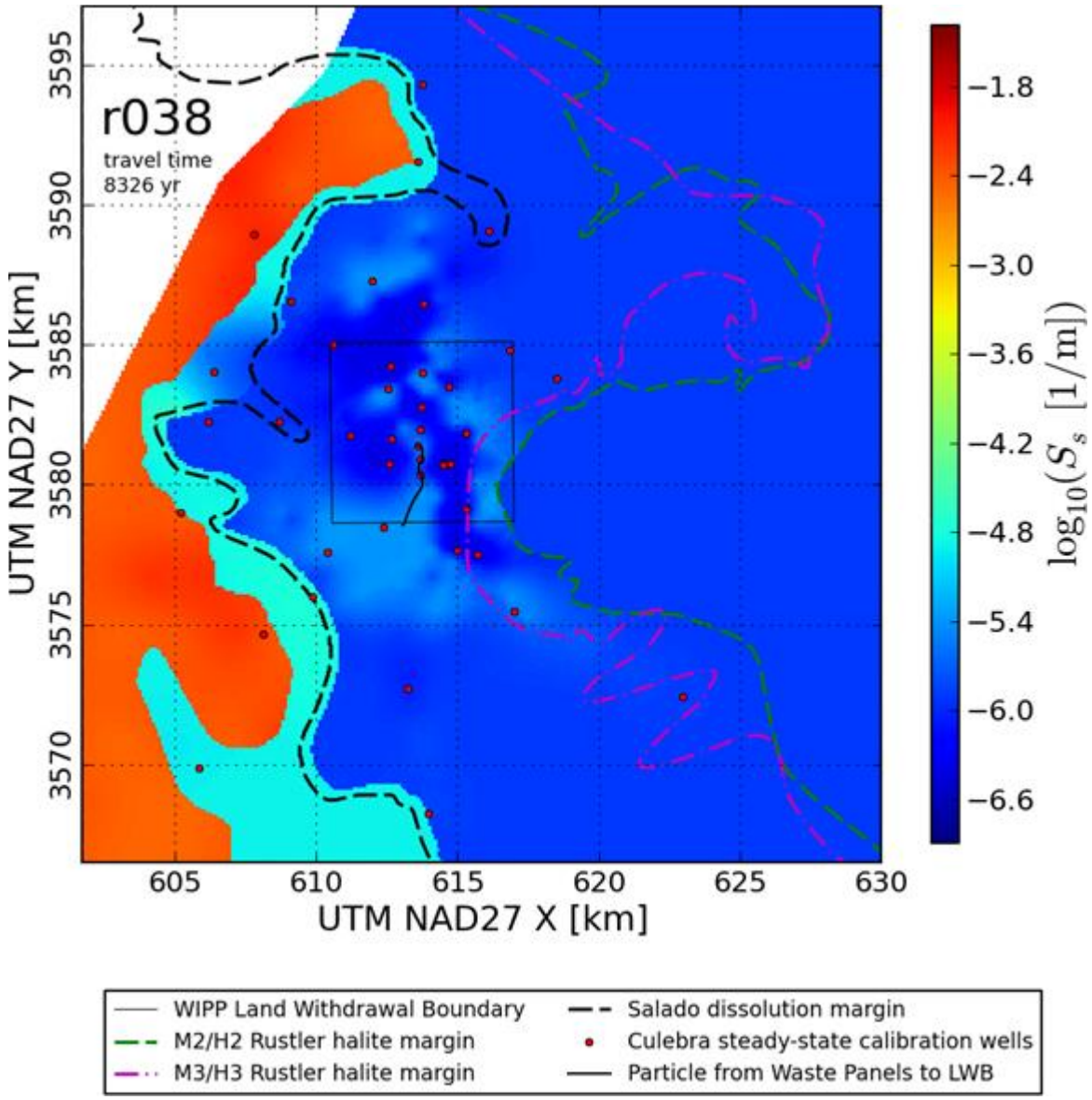
r038
travel time
8326 yr
UTM NAD27 Y [km]
3595
3590
3585
3580
3575
3570
605
610
615
620
625
630
UTM NAD27 X [km]
−1.8
−2.4
−3.0
−3.6
−4.2
−4.8
−5.4
−6.0
−6.6
$\log_{10}(S_s\ [1/\mathrm{m}])$
WIPP Land Withdrawal Boundary
M2/H2 Rustler halite margin
M3/H3 Rustler halite margin
Salado dissolution margin
Culebra steady-state calibration wells
Particle from Waste Panels to LWB

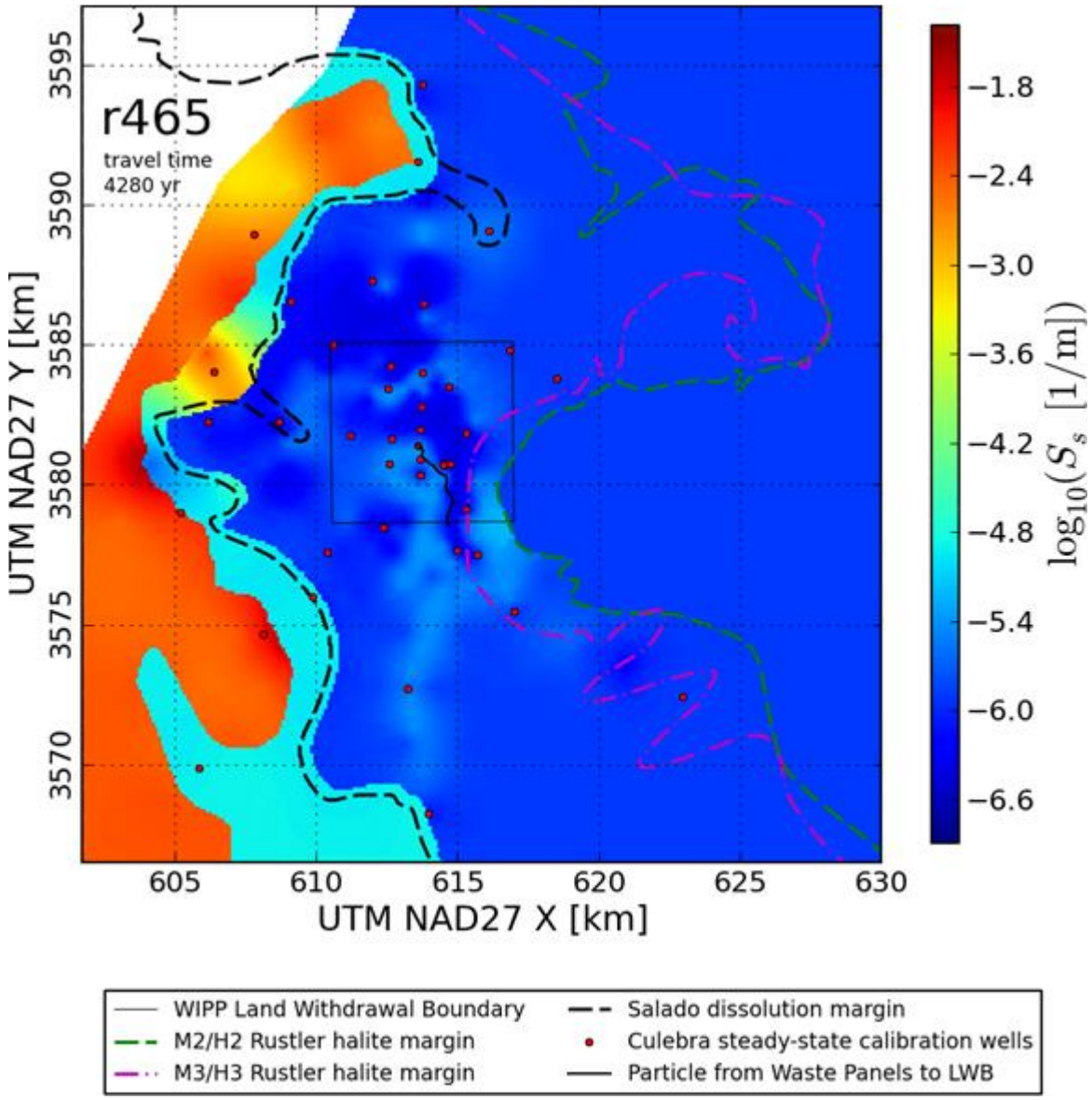
r465
travel time
4280 yr
UTM NAD27 Y [km]
3595
3590
3585
3580
3575
3570
605
610
615
620
625
630
UTM NAD27 X [km]
−1.8
−2.4
−3.0
−3.6
−4.2
−4.8
−5.4
−6.0
−6.6
$\log_{10}(S_s\ [1/\mathrm{m}])$
WIPP Land Withdrawal Boundary
M2/H2 Rustler halite margin
M3/H3 Rustler halite margin
Salado dissolution margin
Culebra steady-state calibration wells
Particle from Waste Panels to LWB

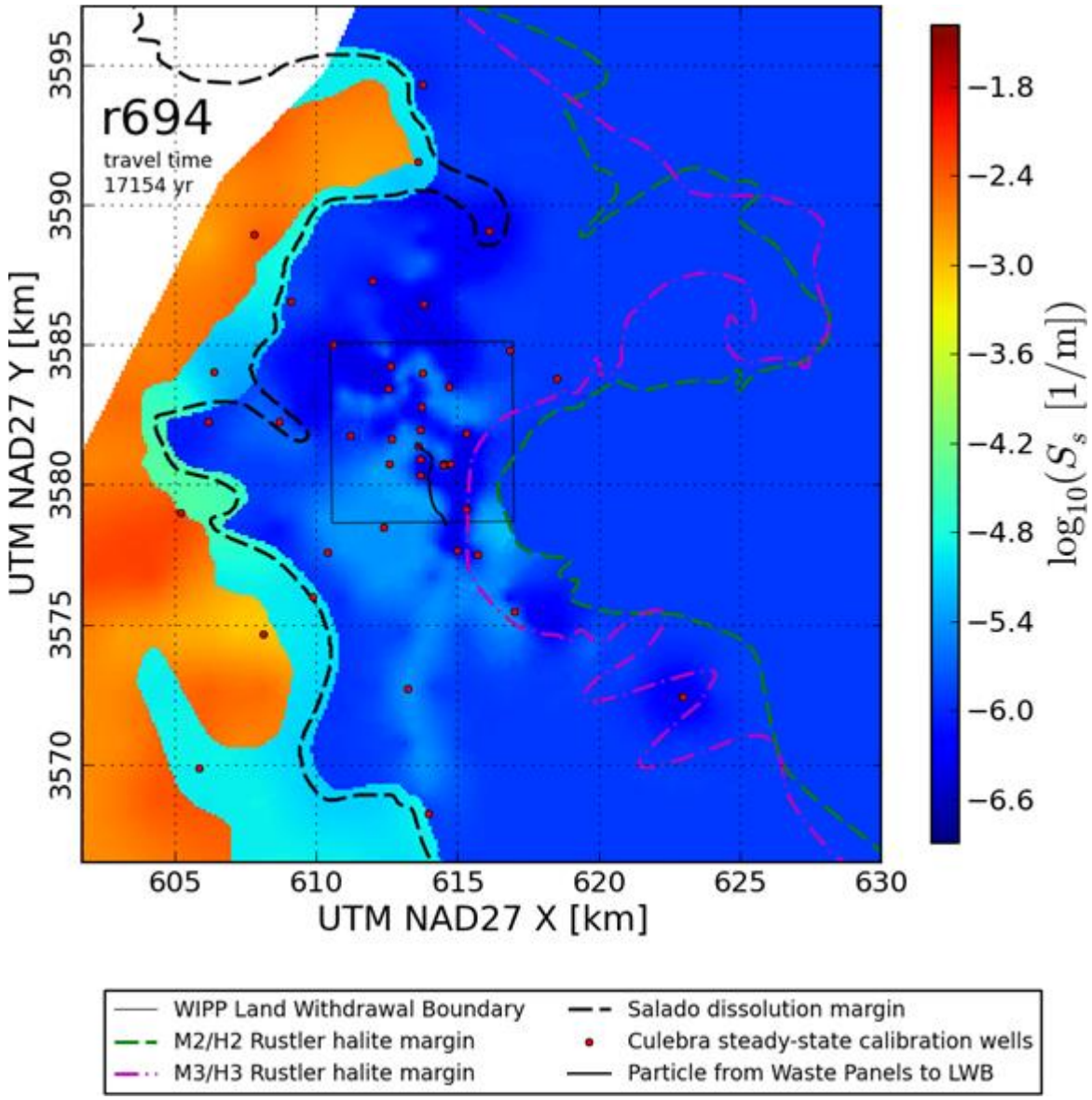
r694
travel time
17154 yr
UTM NAD27 Y [km]
3595
3590
3585
3580
3575
3570
605
610
615
620
625
630
UTM NAD27 X [km]
−1.8
−2.4
−3.0
−3.6
−4.2
−4.8
−5.4
−6.0
−6.6
$\log_{10}(S_s\ [1/\mathrm{m}])$
WIPP Land Withdrawal Boundary
M2/H2 Rustler halite margin
M3/H3 Rustler halite margin
Salado dissolution margin
Culebra steady-state calibration wells
Particle from Waste Panels to LWB

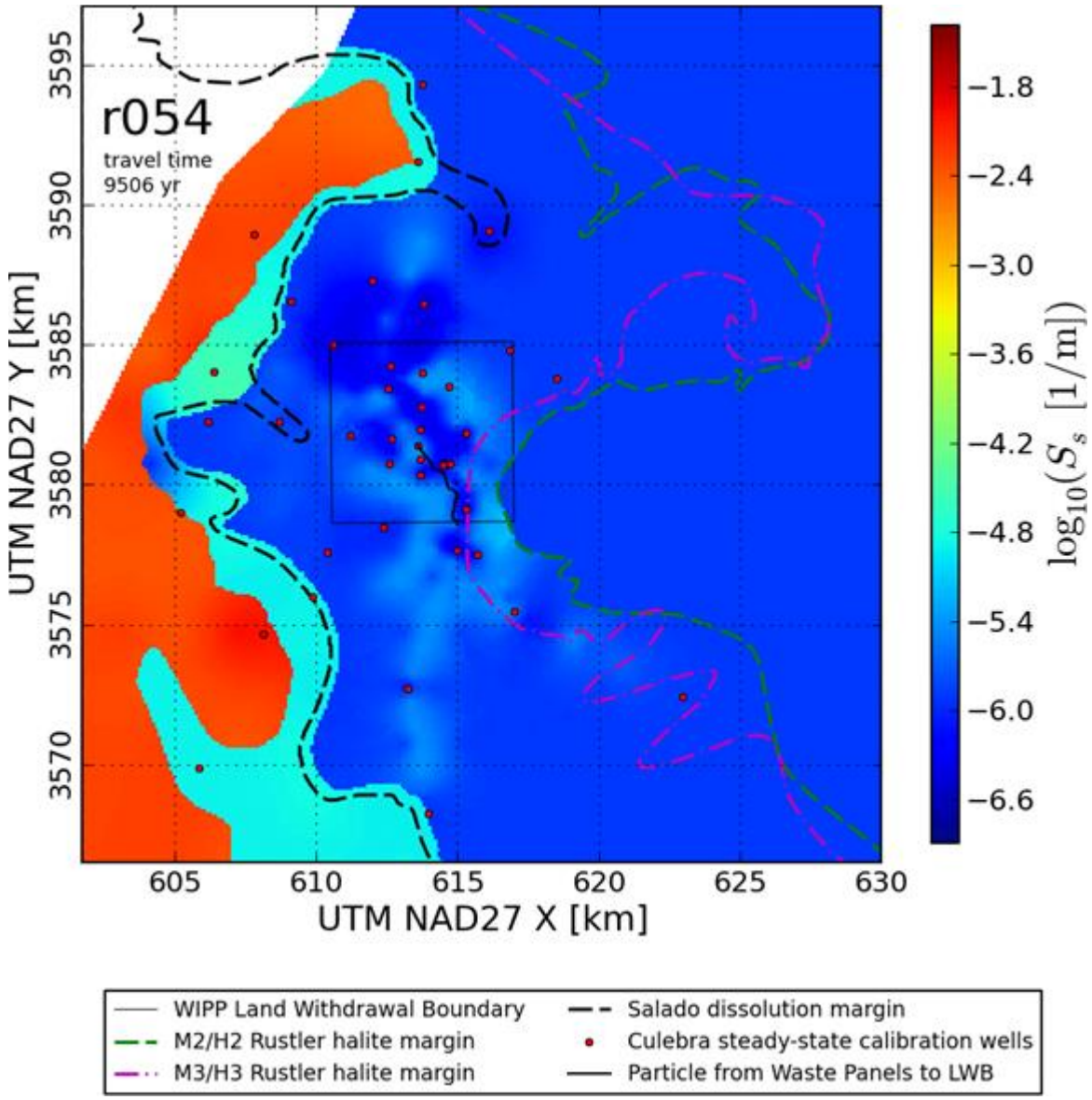
r054
travel time
9506 yr
UTM NAD27 Y [km]
3595
3590
3585
3580
3575
3570
605
610
615
620
625
630
UTM NAD27 X [km]
−1.8
−2.4
−3.0
−3.6
−4.2
−4.8
−5.4
−6.0
−6.6
$\log_{10}(S_s\ [1/\mathrm{m}])$
WIPP Land Withdrawal Boundary
M2/H2 Rustler halite margin
M3/H3 Rustler halite margin
Salado dissolution margin
Culebra steady-state calibration wells
Particle from Waste Panels to LWB

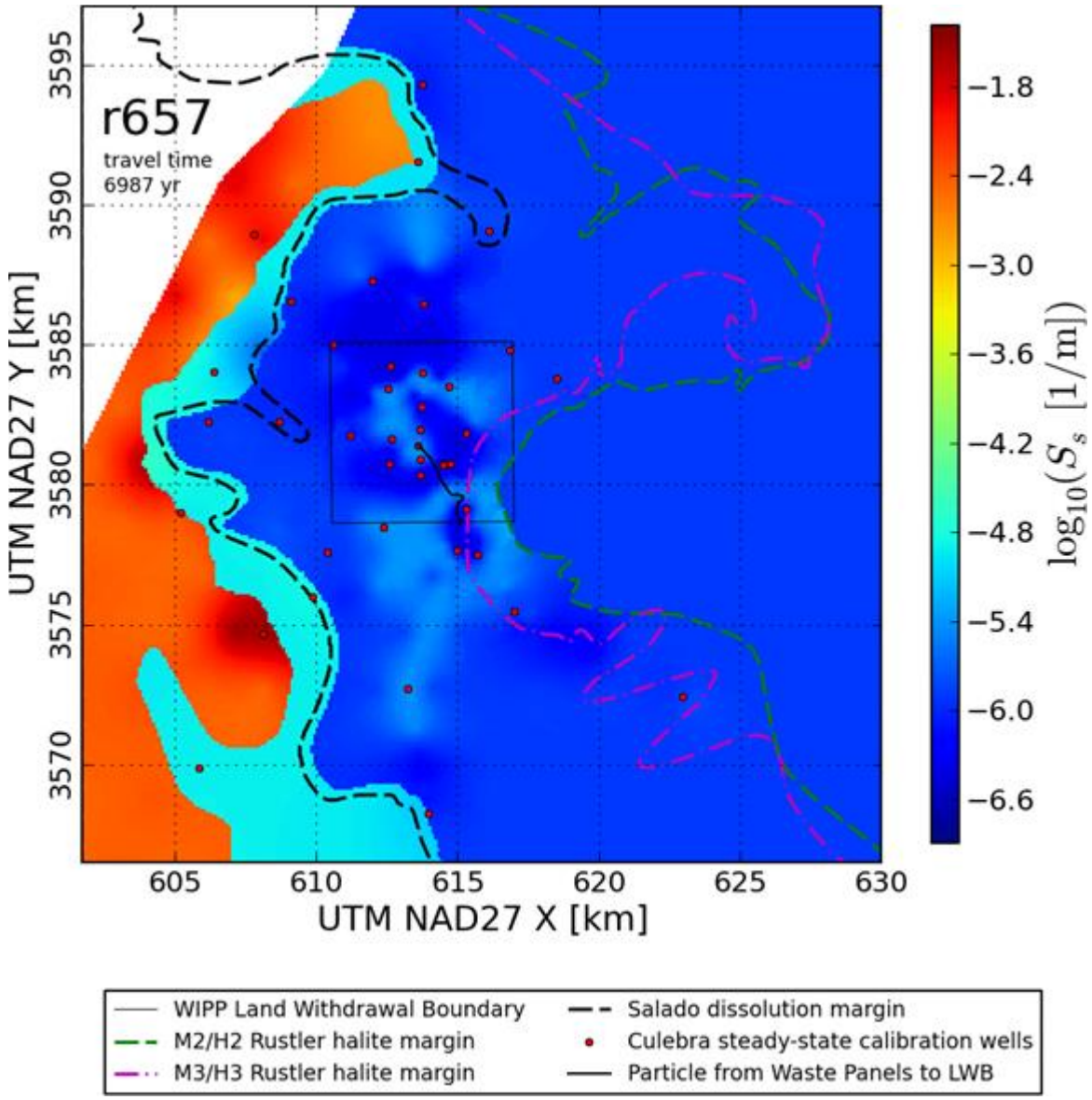
r657
travel time
6987 yr
UTM NAD27 Y [km]
3595
3590
3585
3580
3575
3570
605
610
615
620
625
630
UTM NAD27 X [km]
−1.8
−2.4
−3.0
−3.6
−4.2
−4.8
−5.4
−6.0
−6.6
$\log_{10}(S_s\ [1/\mathrm{m}])$
WIPP Land Withdrawal Boundary
M2/H2 Rustler halite margin
M3/H3 Rustler halite margin
Salado dissolution margin
Culebra steady-state calibration wells
Particle from Waste Panels to LWB

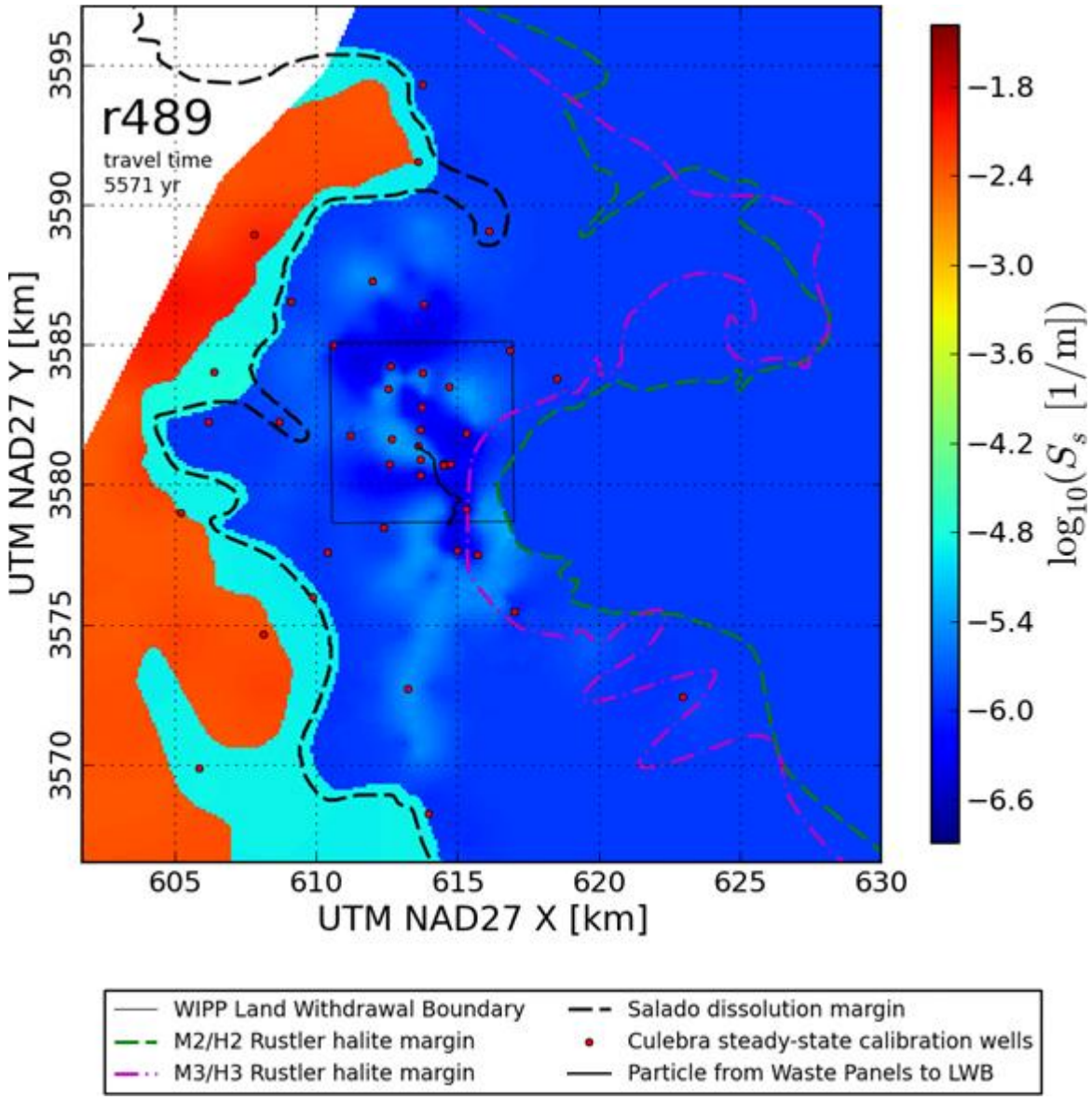
r489
travel time
5571 yr
UTM NAD27 Y [km]
3595
3590
3585
3580
3575
3570
605
610
615
620
625
630
UTM NAD27 X [km]
−1.8
−2.4
−3.0
−3.6
−4.2
−4.8
−5.4
−6.0
−6.6
$\log_{10}(S_s\ [1/\mathrm{m}])$
WIPP Land Withdrawal Boundary
M2/H2 Rustler halite margin
M3/H3 Rustler halite margin
Salado dissolution margin
Culebra steady-state calibration wells
Particle from Waste Panels to LWB

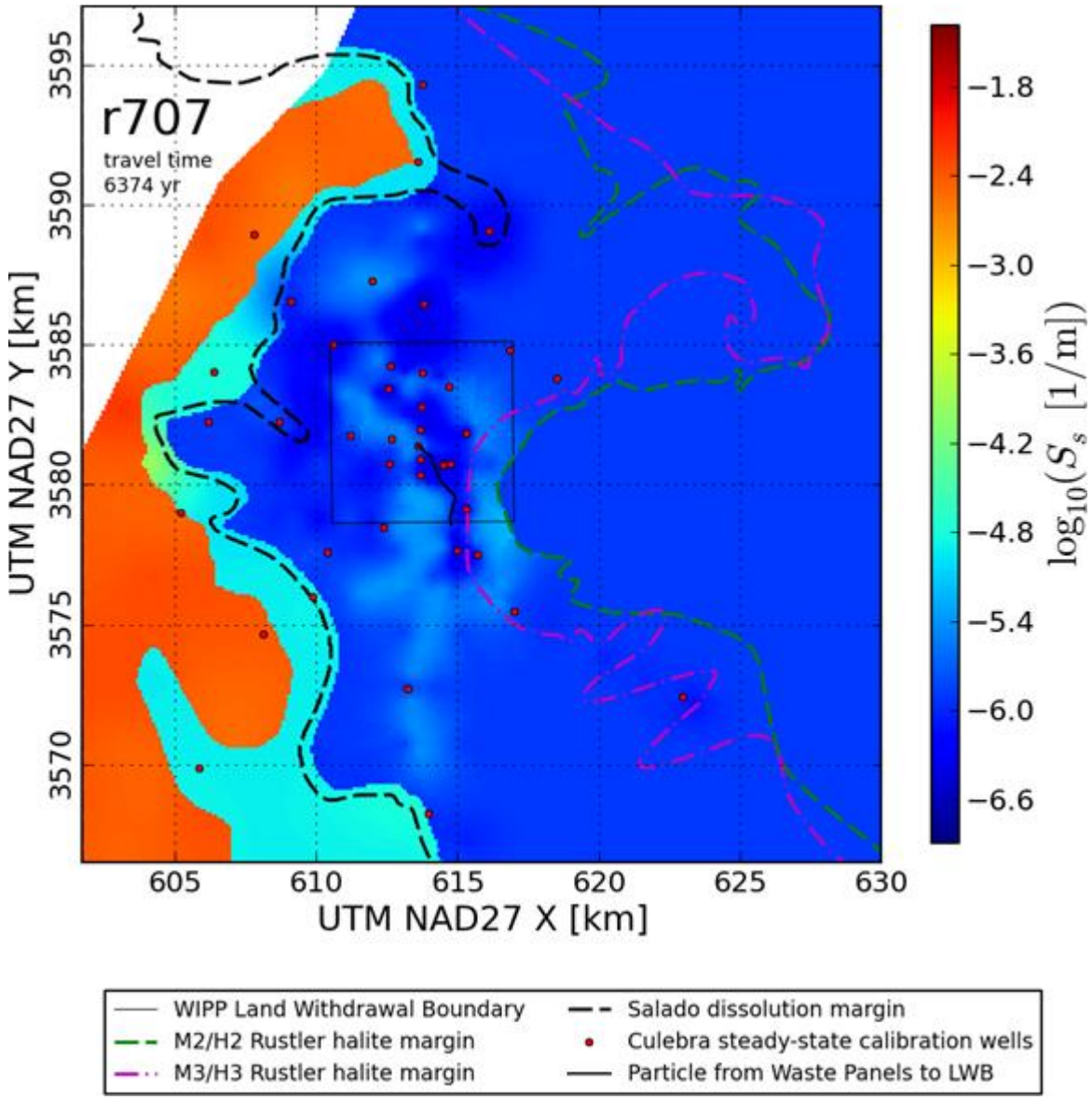
r707
travel time
6374 yr
UTM NAD27 Y [km]
3595
3590
3585
3580
3575
3570
605
610
615
620
625
630
UTM NAD27 X [km]
−1.8
−2.4
−3.0
−3.6
−4.2
−4.8
−5.4
−6.0
−6.6
$\log_{10}(S_s\ [1/\mathrm{m}])$
WIPP Land Withdrawal Boundary
M2/H2 Rustler halite margin
M3/H3 Rustler halite margin
Salado dissolution margin
Culebra steady-state calibration wells
Particle from Waste Panels to LWB

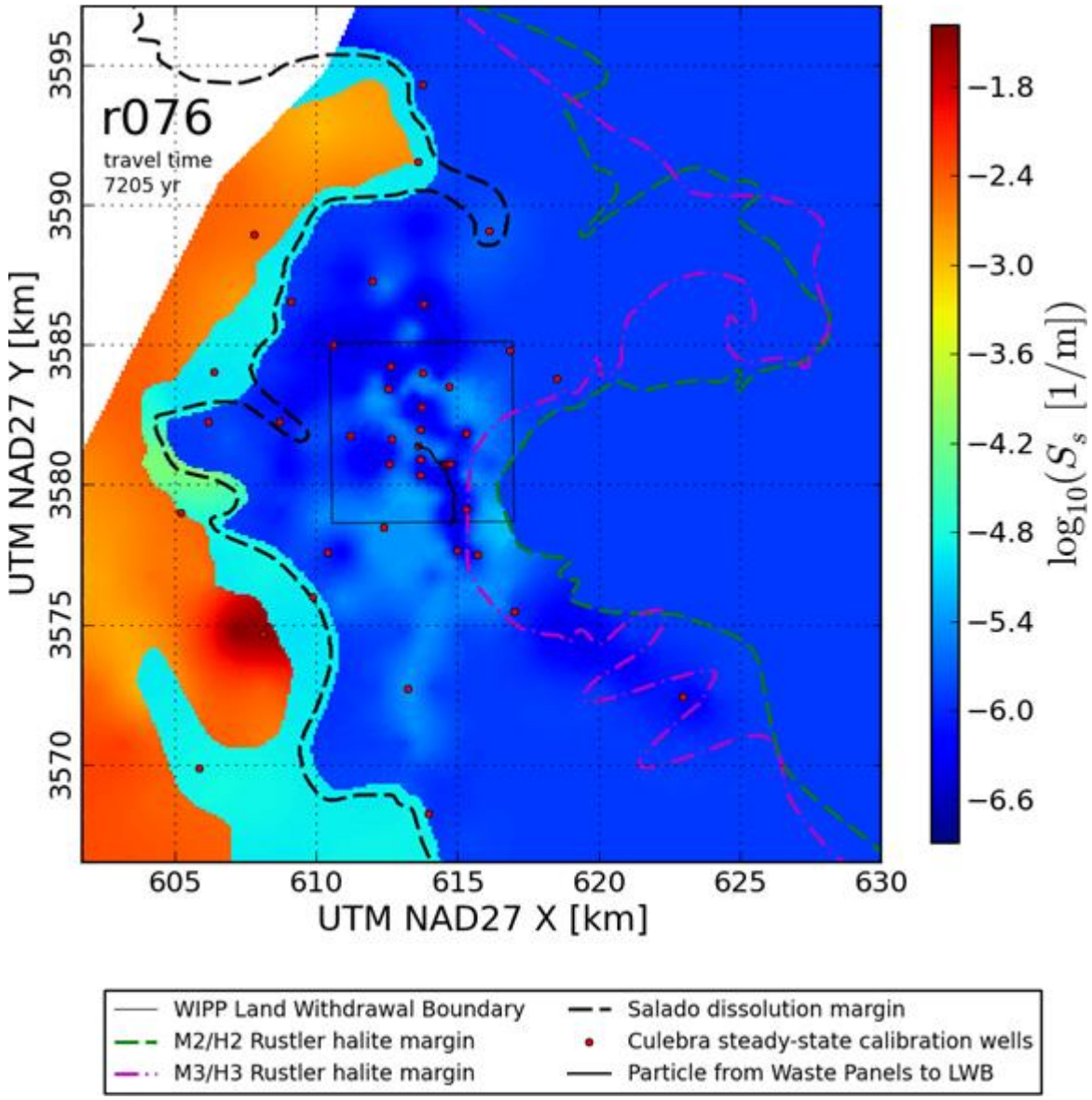
r076
travel time
7205 yr
UTM NAD27 Y [km]
3595
3590
3585
3580
3575
3570
605
610
615
620
625
630
UTM NAD27 X [km]
−1.8
−2.4
−3.0
−3.6
−4.2
−4.8
−5.4
−6.0
−6.6
$\log_{10}(S_s\ [1/\mathrm{m}])$
WIPP Land Withdrawal Boundary
M2/H2 Rustler halite margin
M3/H3 Rustler halite margin
Salado dissolution margin
Culebra steady-state calibration wells
Particle from Waste Panels to LWB

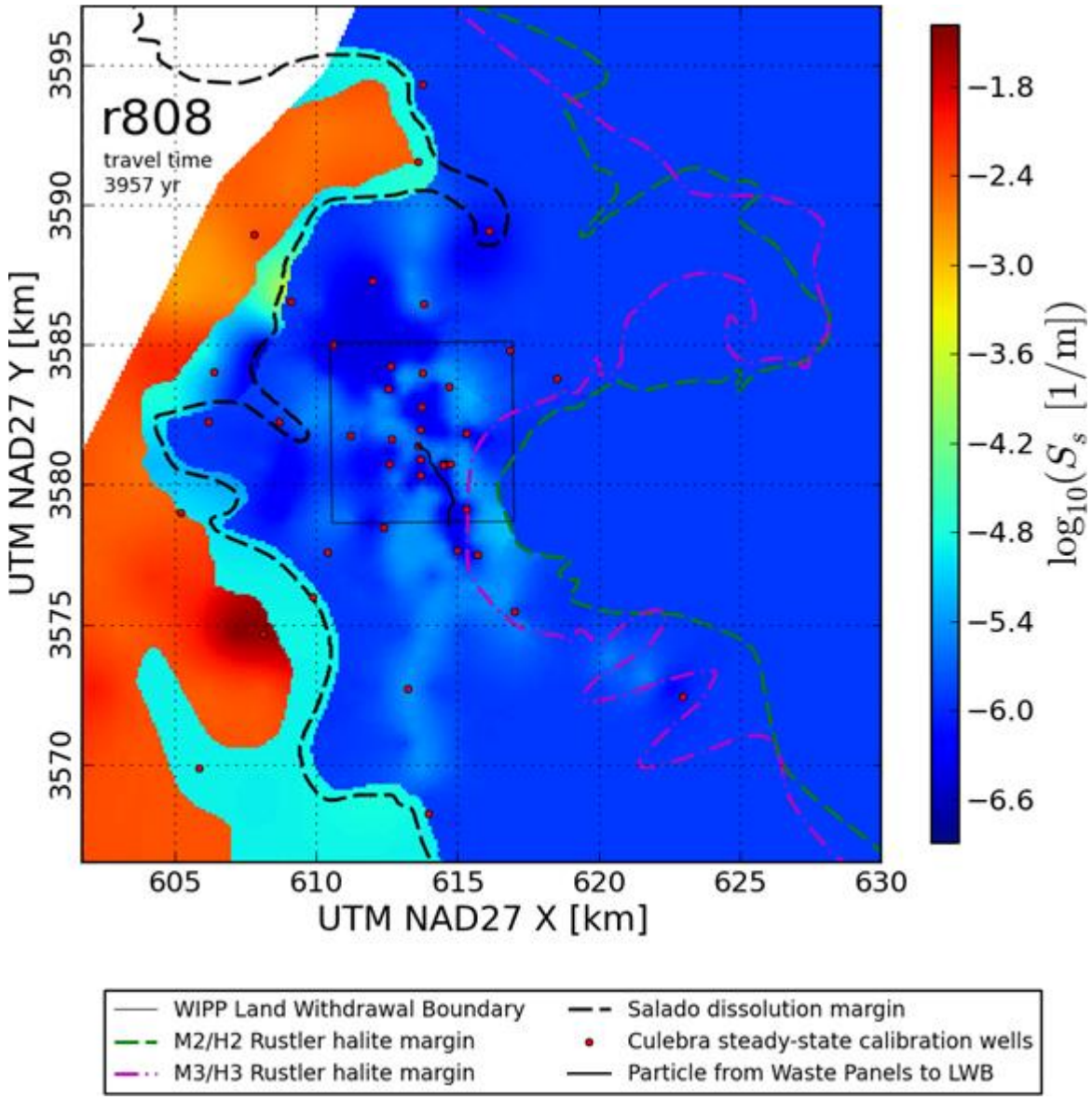
r808
travel time
3957 yr
UTM NAD27 Y [km]
3595
3590
3585
3580
3575
3570
605
610
615
620
625
630
UTM NAD27 X [km]
−1.8
−2.4
−3.0
−3.6
−4.2
−4.8
−5.4
−6.0
−6.6
$\log_{10}(S_s\ [1/\mathrm{m}])$
WIPP Land Withdrawal Boundary
M2/H2 Rustler halite margin
M3/H3 Rustler halite margin
Salado dissolution margin
Culebra steady-state calibration wells
Particle from Waste Panels to LWB

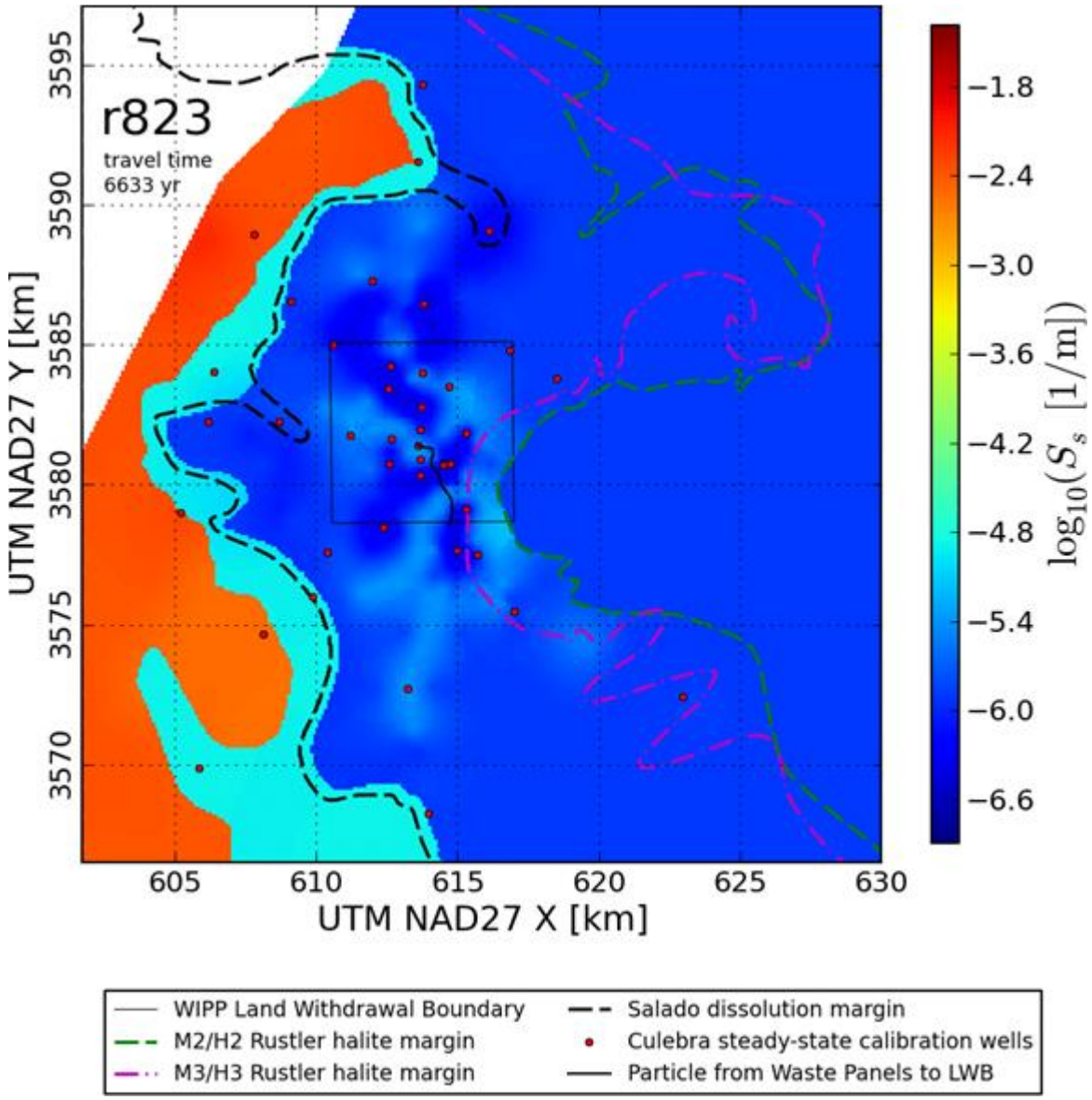
r823
travel time
6633 yr
UTM NAD27 Y [km]
3595
3590
3585
3580
3575
3570
605
610
615
620
625
630
UTM NAD27 X [km]
−1.8
−2.4
−3.0
−3.6
−4.2
−4.8
−5.4
−6.0
−6.6
$\log_{10}(S_s\ [1/\mathrm{m}])$
WIPP Land Withdrawal Boundary
M2/H2 Rustler halite margin
M3/H3 Rustler halite margin
Salado dissolution margin
Culebra steady-state calibration wells
Particle from Waste Panels to LWB

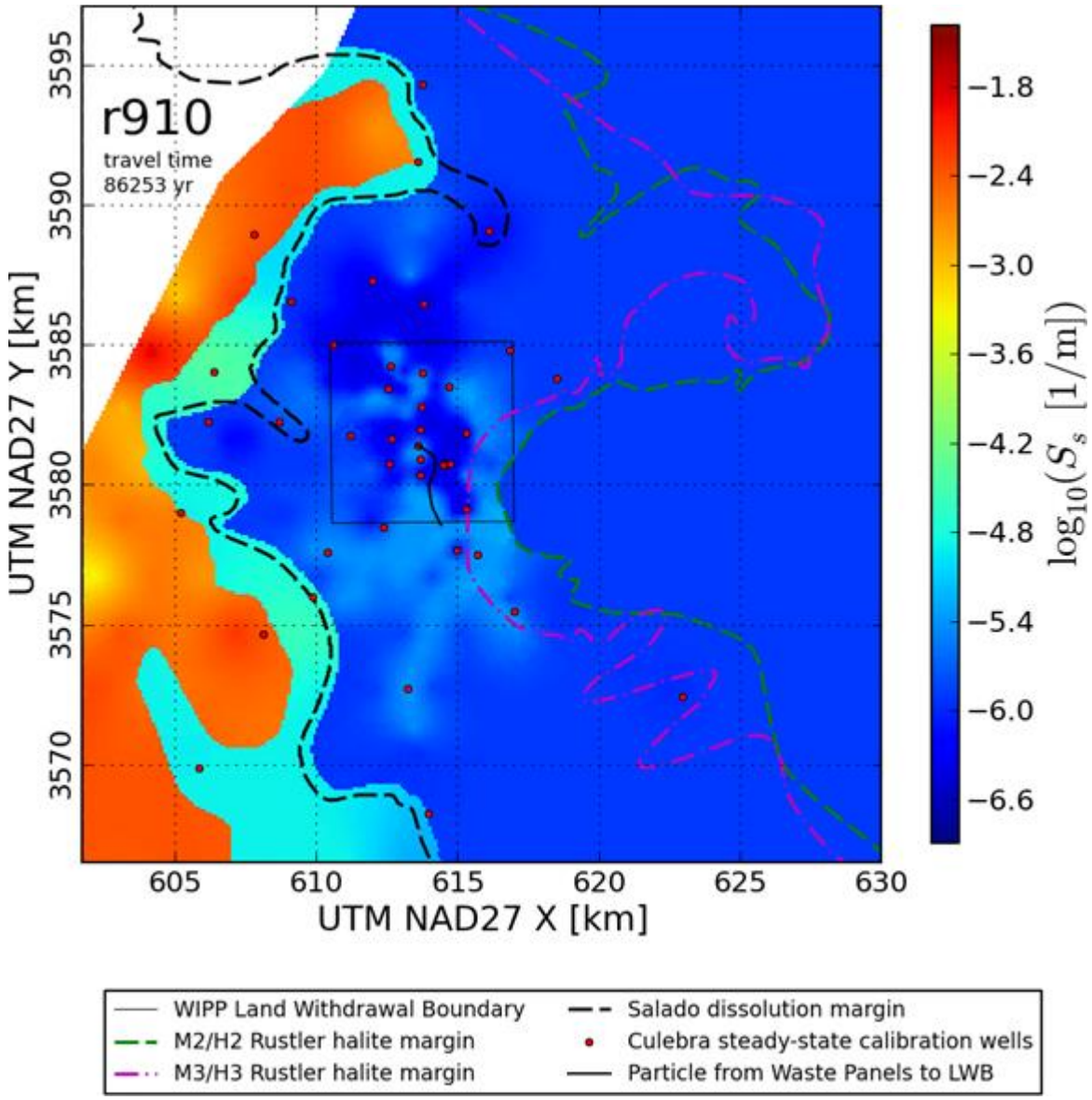
r910
travel time
86253 yr
UTM NAD27 Y [km]
3595
3590
3585
3580
3575
3570
605
610
615
620
625
630
UTM NAD27 X [km]
−1.8
−2.4
−3.0
−3.6
−4.2
−4.8
−5.4
−6.0
−6.6
$\log_{10}(S_s\ [1/\mathrm{m}])$
WIPP Land Withdrawal Boundary
M2/H2 Rustler halite margin
M3/H3 Rustler halite margin
Salado dissolution margin
Culebra steady-state calibration wells
Particle from Waste Panels to LWB

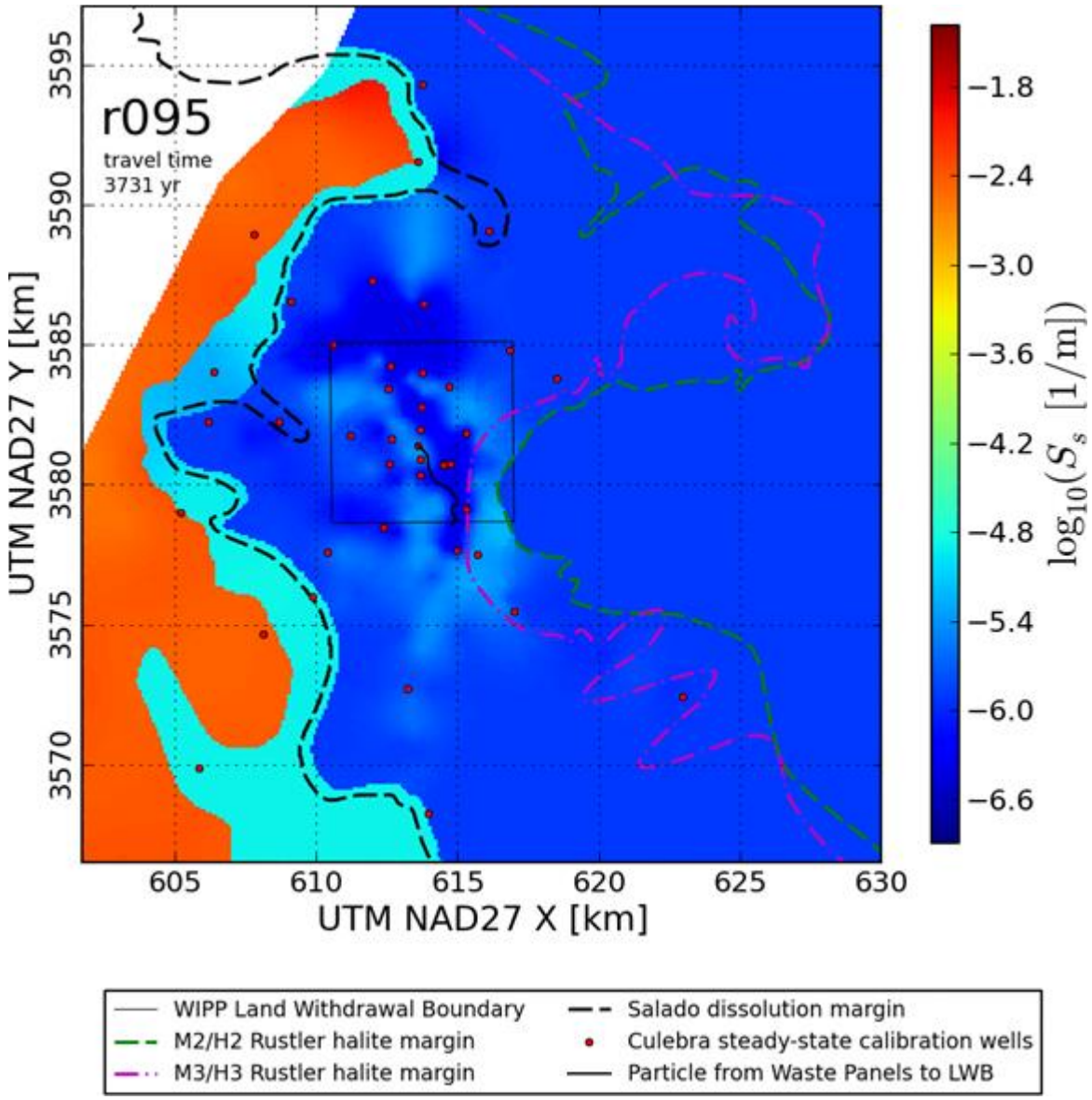
r095
travel time
3731 yr
UTM NAD27 Y [km]
3595
3590
3585
3580
3575
3570
605
610
615
620
625
630
UTM NAD27 X [km]
−1.8
−2.4
−3.0
−3.6
−4.2
−4.8
−5.4
−6.0
−6.6
$\log_{10}(S_s\ [1/\mathrm{m}])$
WIPP Land Withdrawal Boundary
M2/H2 Rustler halite margin
M3/H3 Rustler halite margin
Salado dissolution margin
Culebra steady-state calibration wells
Particle from Waste Panels to LWB

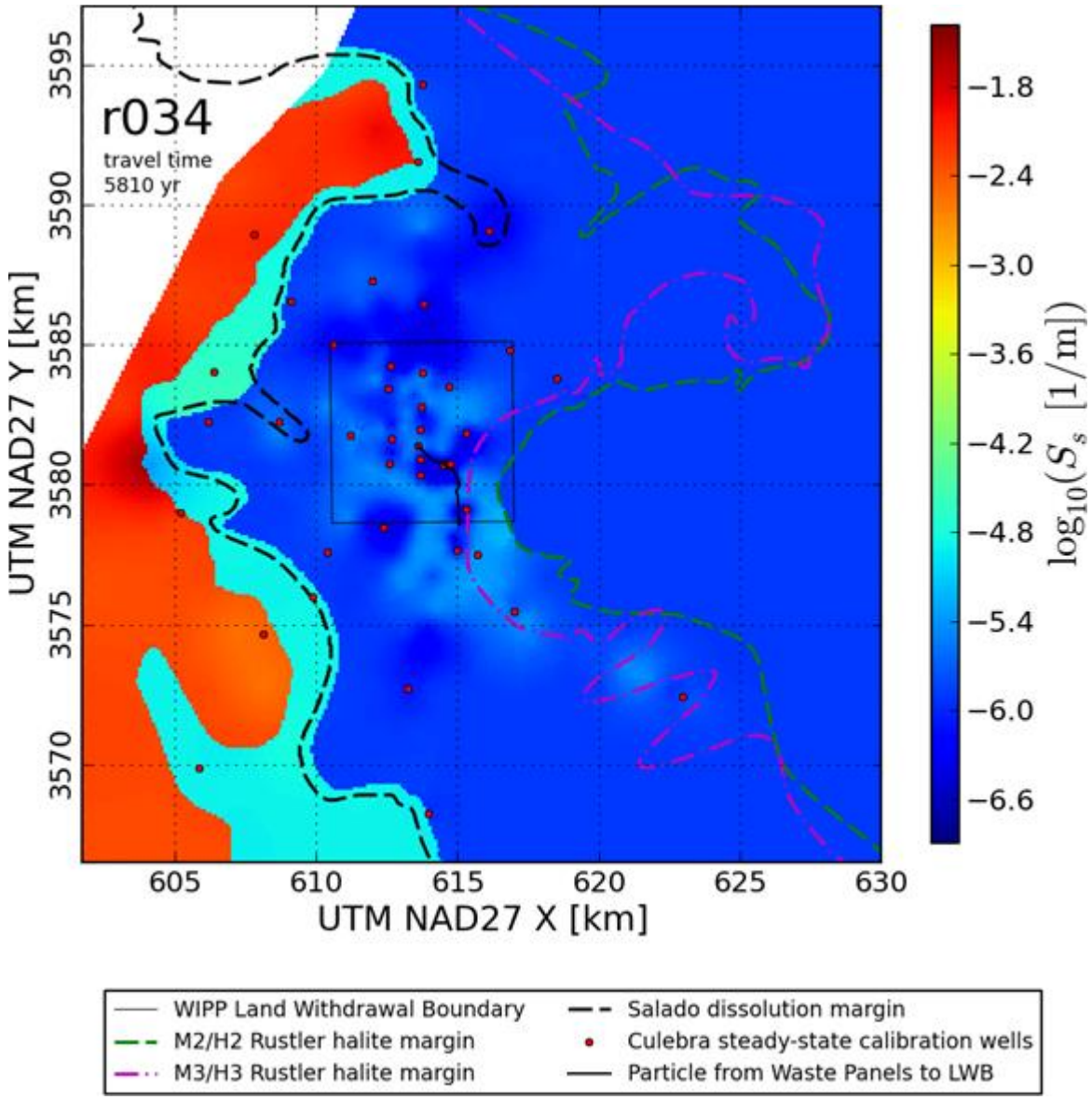
r034
travel time
5810 yr
UTM NAD27 Y [km]
3595
3590
3585
3580
3575
3570
605
610
615
620
625
630
UTM NAD27 X [km]
−1.8
−2.4
−3.0
−3.6
−4.2
−4.8
−5.4
−6.0
−6.6
$\log_{10}(S_s\ [1/\mathrm{m}])$
WIPP Land Withdrawal Boundary
M2/H2 Rustler halite margin
M3/H3 Rustler halite margin
Salado dissolution margin
Culebra steady-state calibration wells
Particle from Waste Panels to LWB

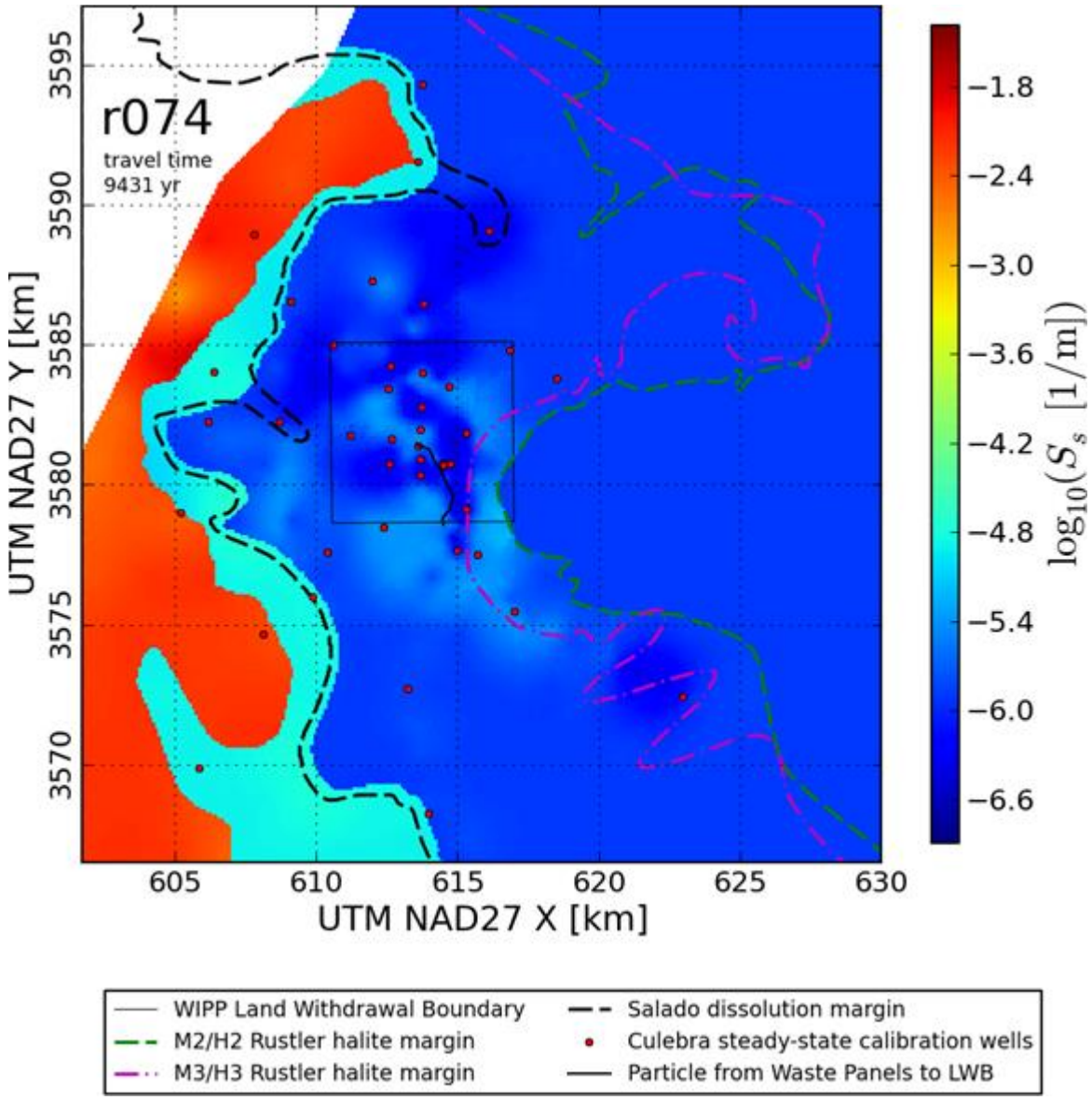
r074
travel time
9431 yr
UTM NAD27 Y [km]
3595
3590
3585
3580
3575
3570
605
610
615
620
625
630
UTM NAD27 X [km]
−1.8
−2.4
−3.0
−3.6
−4.2
−4.8
−5.4
−6.0
−6.6
$\log_{10}(S_s\ [1/\mathrm{m}])$
WIPP Land Withdrawal Boundary
M2/H2 Rustler halite margin
M3/H3 Rustler halite margin
Salado dissolution margin
Culebra steady-state calibration wells
Particle from Waste Panels to LWB

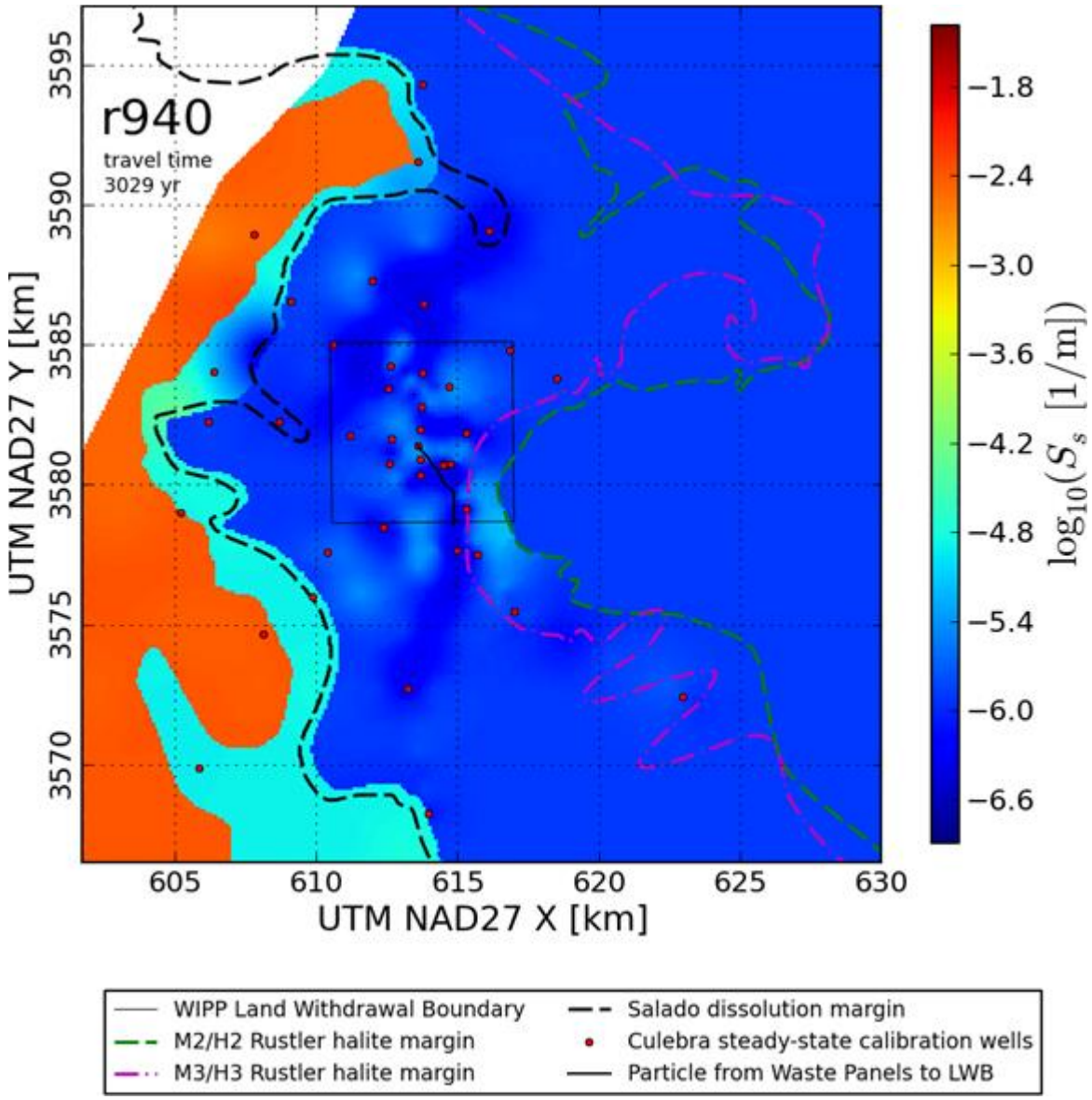
r940
travel time
3029 yr
UTM NAD27 Y [km]
3595
3590
3585
3580
3575
3570
605
610
615
620
625
630
UTM NAD27 X [km]
−1.8
−2.4
−3.0
−3.6
−4.2
−4.8
−5.4
−6.0
−6.6
$\log_{10}(S_s\ [1/\mathrm{m}])$
WIPP Land Withdrawal Boundary
M2/H2 Rustler halite margin
M3/H3 Rustler halite margin
Salado dissolution margin
Culebra steady-state calibration wells
Particle from Waste Panels to LWB

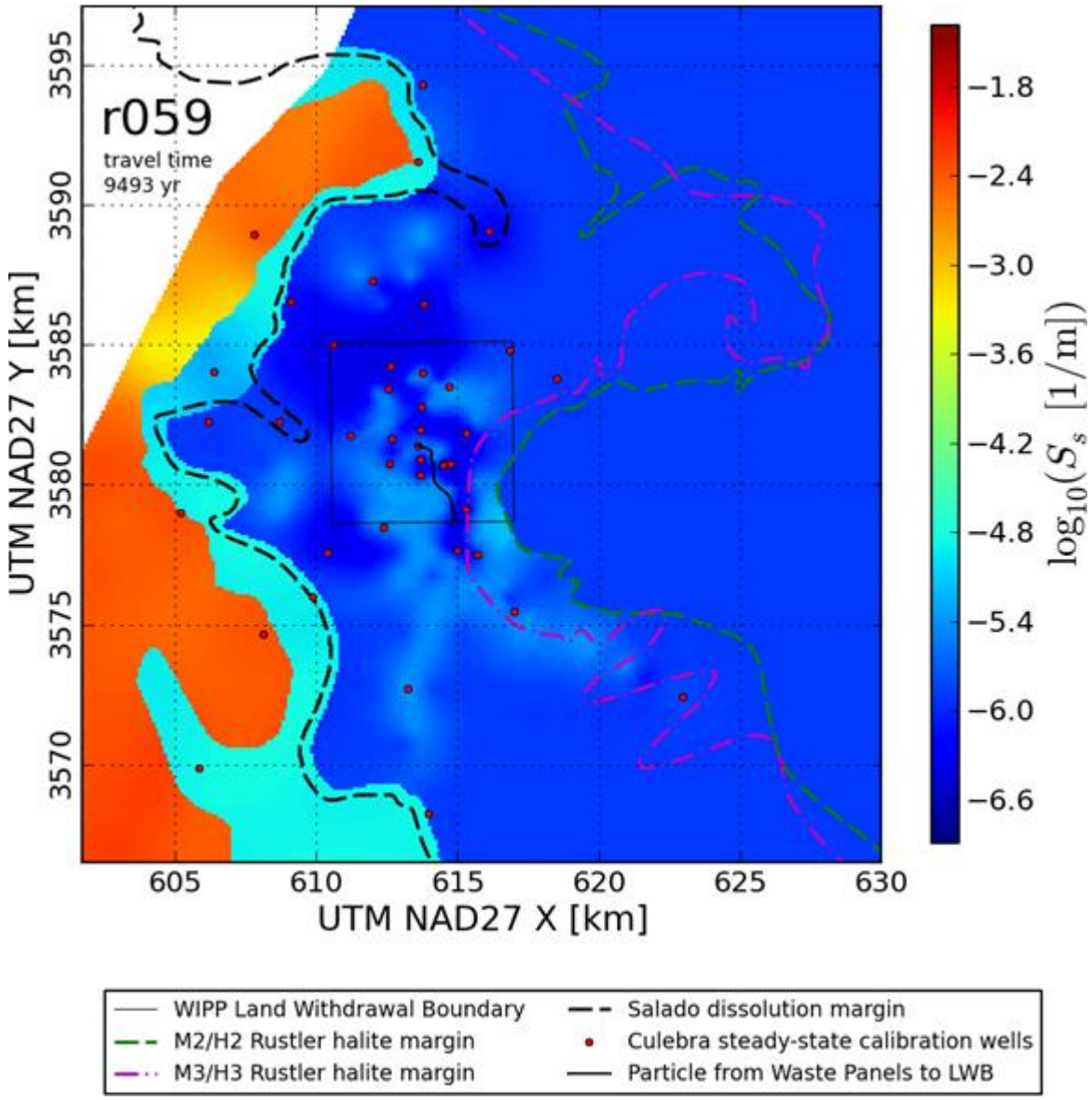
r059
travel time
9493 yr
UTM NAD27 Y [km]
3595
3590
3585
3580
3575
3570
605
610
615
620
625
630
UTM NAD27 X [km]
−1.8
−2.4
−3.0
−3.6
−4.2
−4.8
−5.4
−6.0
−6.6
$\log_{10}(S_s\ [1/\mathrm{m}])$
WIPP Land Withdrawal Boundary
M2/H2 Rustler halite margin
M3/H3 Rustler halite margin
Salado dissolution margin
Culebra steady-state calibration wells
Particle from Waste Panels to LWB

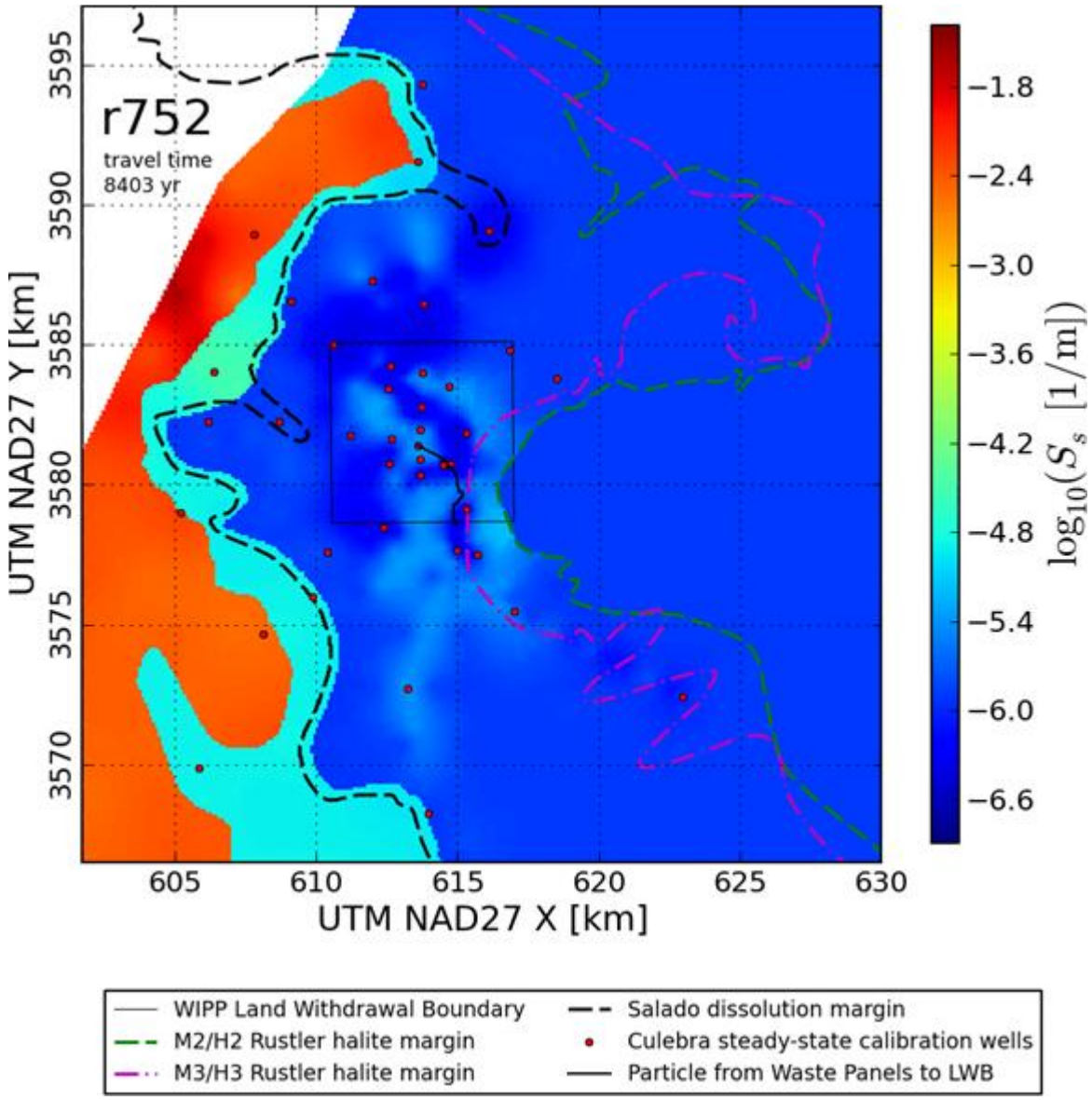
r752
travel time
8403 yr
UTM NAD27 Y [km]
3595
3590
3585
3580
3575
3570
605
610
615
620
625
630
UTM NAD27 X [km]
−1.8
−2.4
−3.0
−3.6
−4.2
−4.8
−5.4
−6.0
−6.6
$\log_{10}(S_s\ [1/\mathrm{m}])$
WIPP Land Withdrawal Boundary
M2/H2 Rustler halite margin
M3/H3 Rustler halite margin
Salado dissolution margin
Culebra steady-state calibration wells
Particle from Waste Panels to LWB

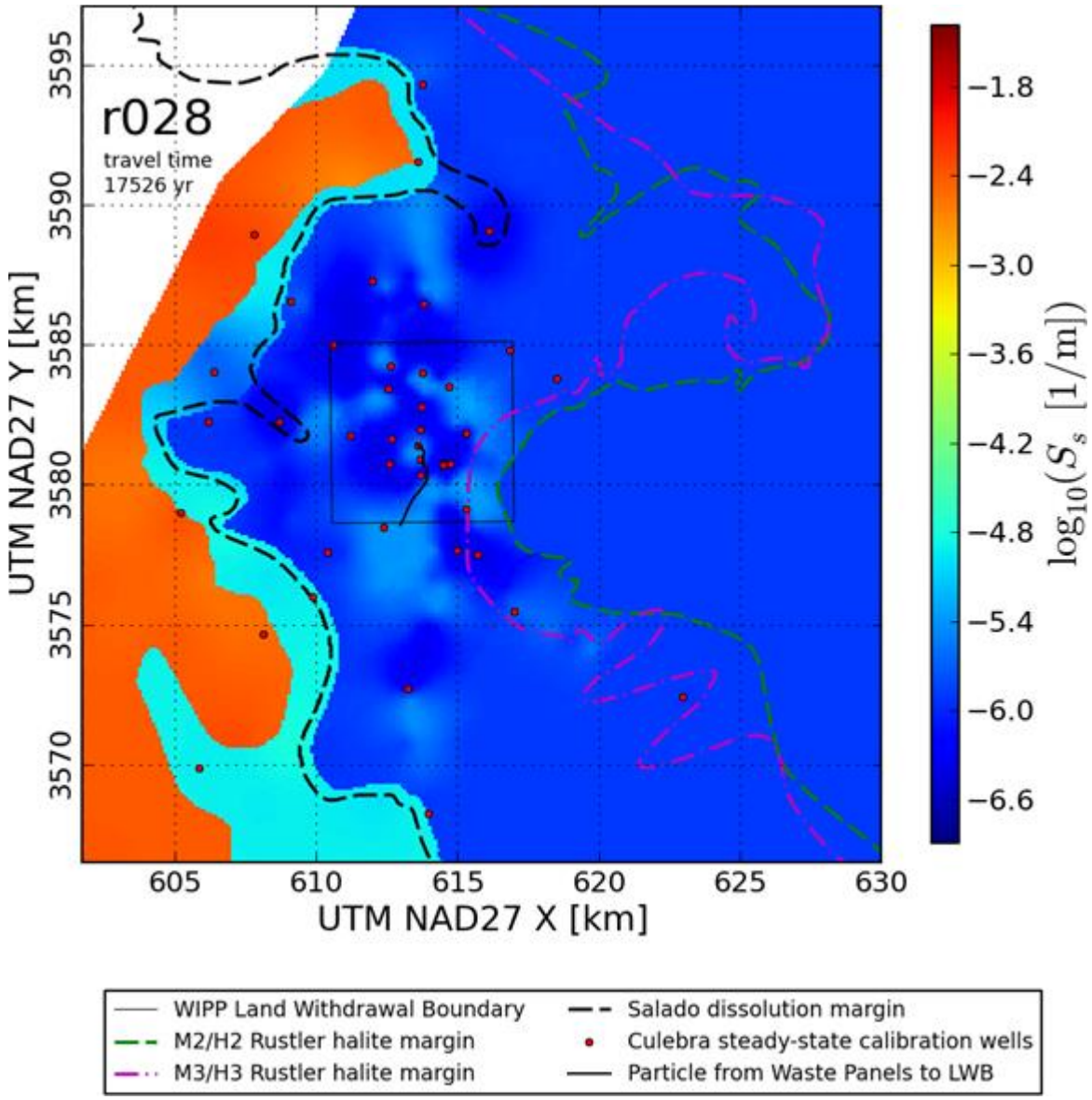
r028
travel time
17526 yr
UTM NAD27 Y [km]
3595
3590
3585
3580
3575
3570
605
610
615
620
625
630
UTM NAD27 X [km]
−1.8
−2.4
−3.0
−3.6
−4.2
−4.8
−5.4
−6.0
−6.6
$\log_{10}(S_s\ [1/\mathrm{m}])$
WIPP Land Withdrawal Boundary
Salado dissolution margin
M2/H2 Rustler halite margin
Culebra steady-state calibration wells
M3/H3 Rustler halite margin
Particle from Waste Panels to LWB

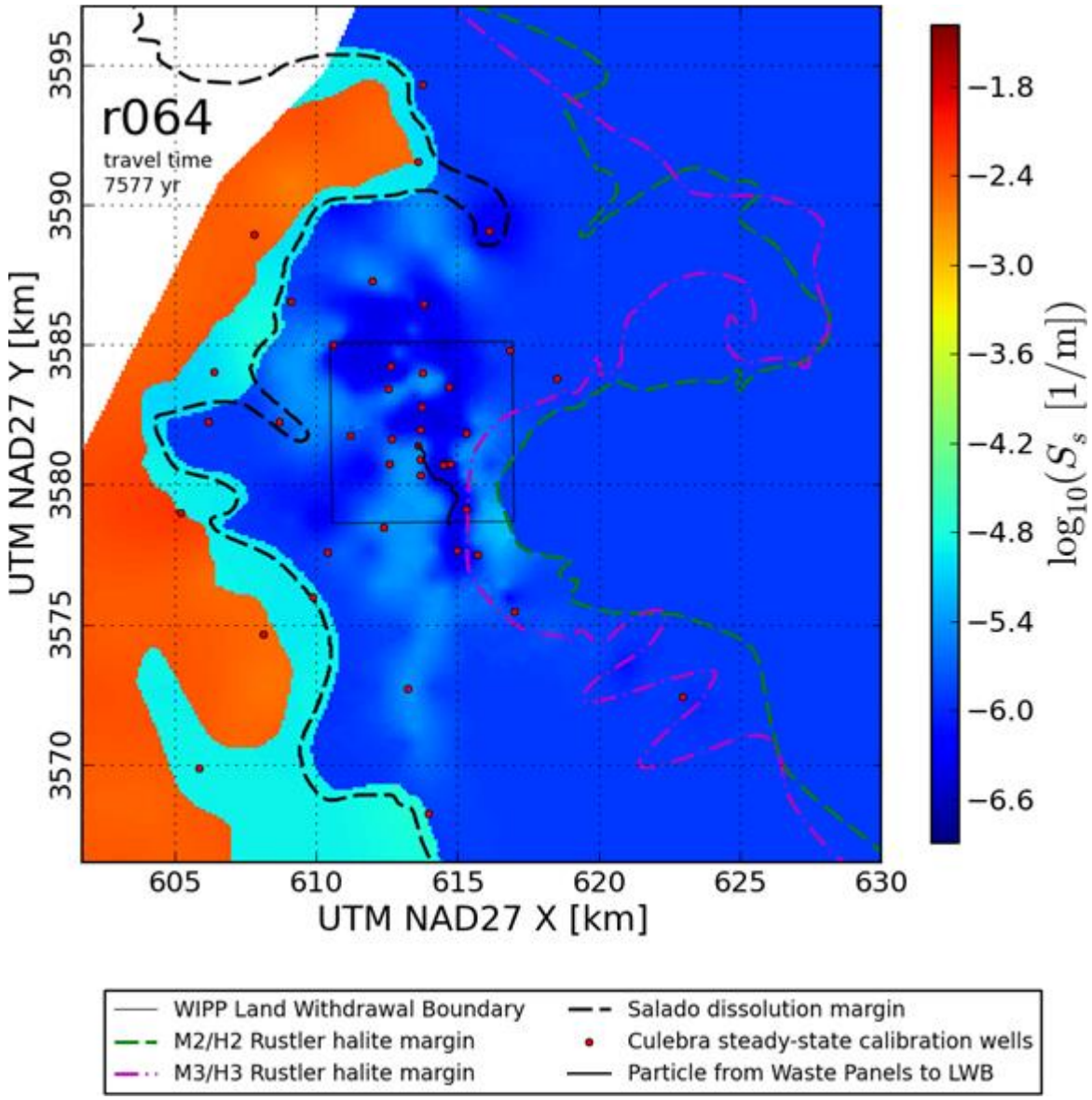
r064
travel time
7577 yr
UTM NAD27 Y [km]
3595
3590
3585
3580
3575
3570
605
610
615
620
625
630
UTM NAD27 X [km]
−1.8
−2.4
−3.0
−3.6
−4.2
−4.8
−5.4
−6.0
−6.6
$\log_{10}(S_s\ [1/\mathrm{m}])$
WIPP Land Withdrawal Boundary
M2/H2 Rustler halite margin
M3/H3 Rustler halite margin
Salado dissolution margin
Culebra steady-state calibration wells
Particle from Waste Panels to LWB

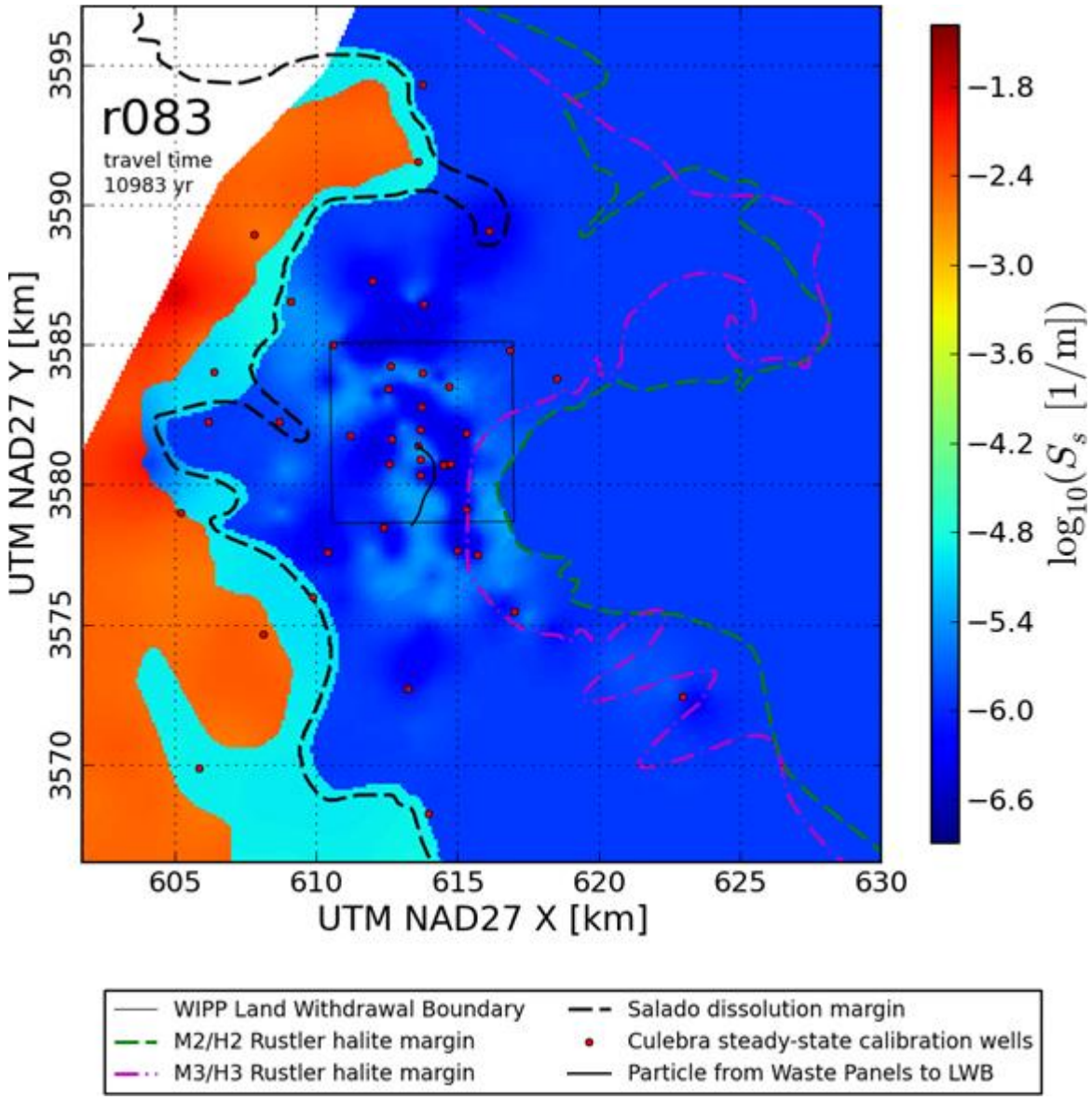
r083
travel time
10983 yr
UTM NAD27 Y [km]
3595
3590
3585
3580
3575
3570
605
610
615
620
625
630
UTM NAD27 X [km]
−1.8
−2.4
−3.0
−3.6
−4.2
−4.8
−5.4
−6.0
−6.6
$\log_{10}(S_s\ [1/\mathrm{m}])$
WIPP Land Withdrawal Boundary
M2/H2 Rustler halite margin
M3/H3 Rustler halite margin
Salado dissolution margin
Culebra steady-state calibration wells
Particle from Waste Panels to LWB

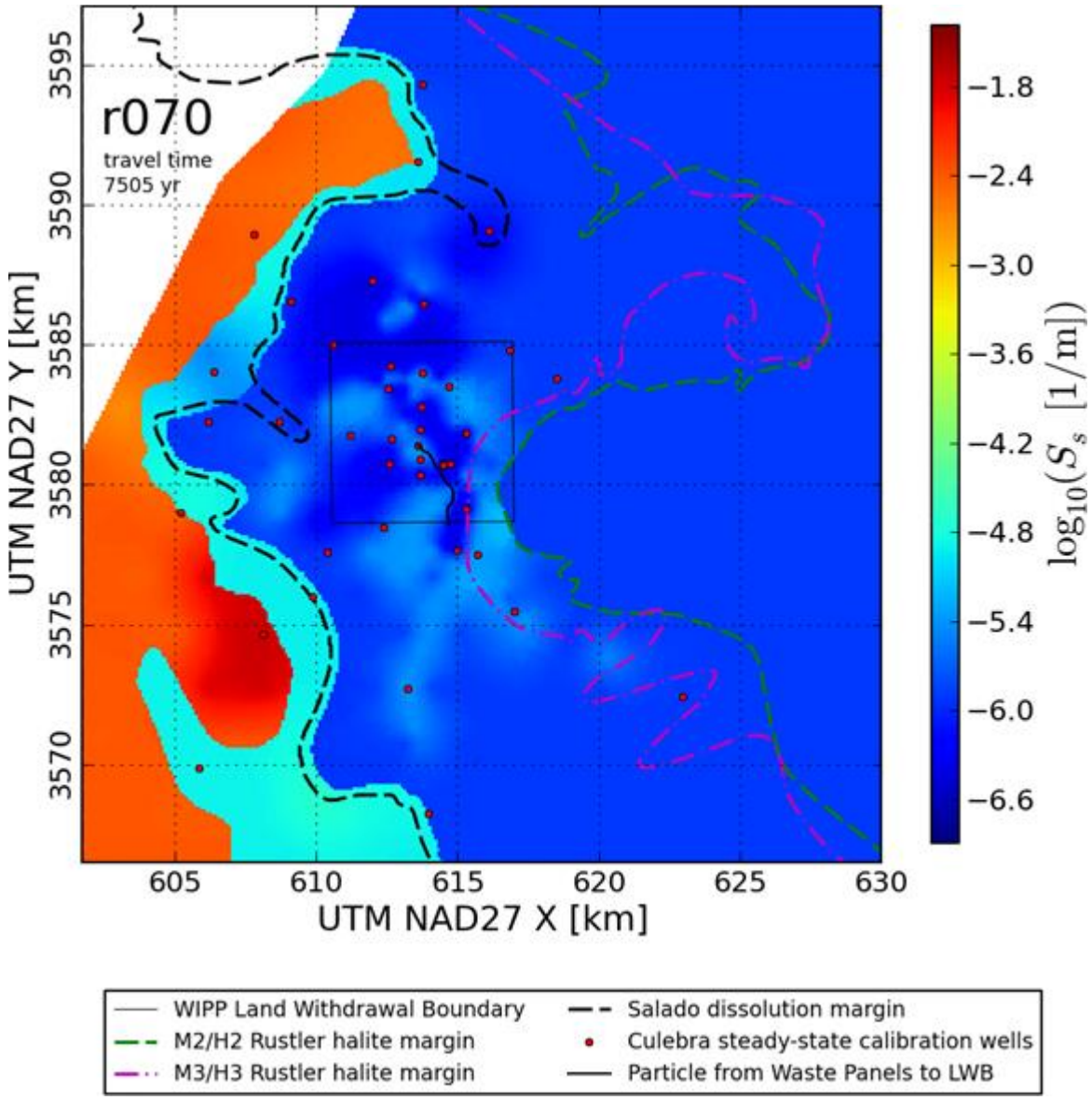

TFIELD Attachment A-3.0 100 Calibrated Hydraulic Diffusivity Model Input Parameter Fields

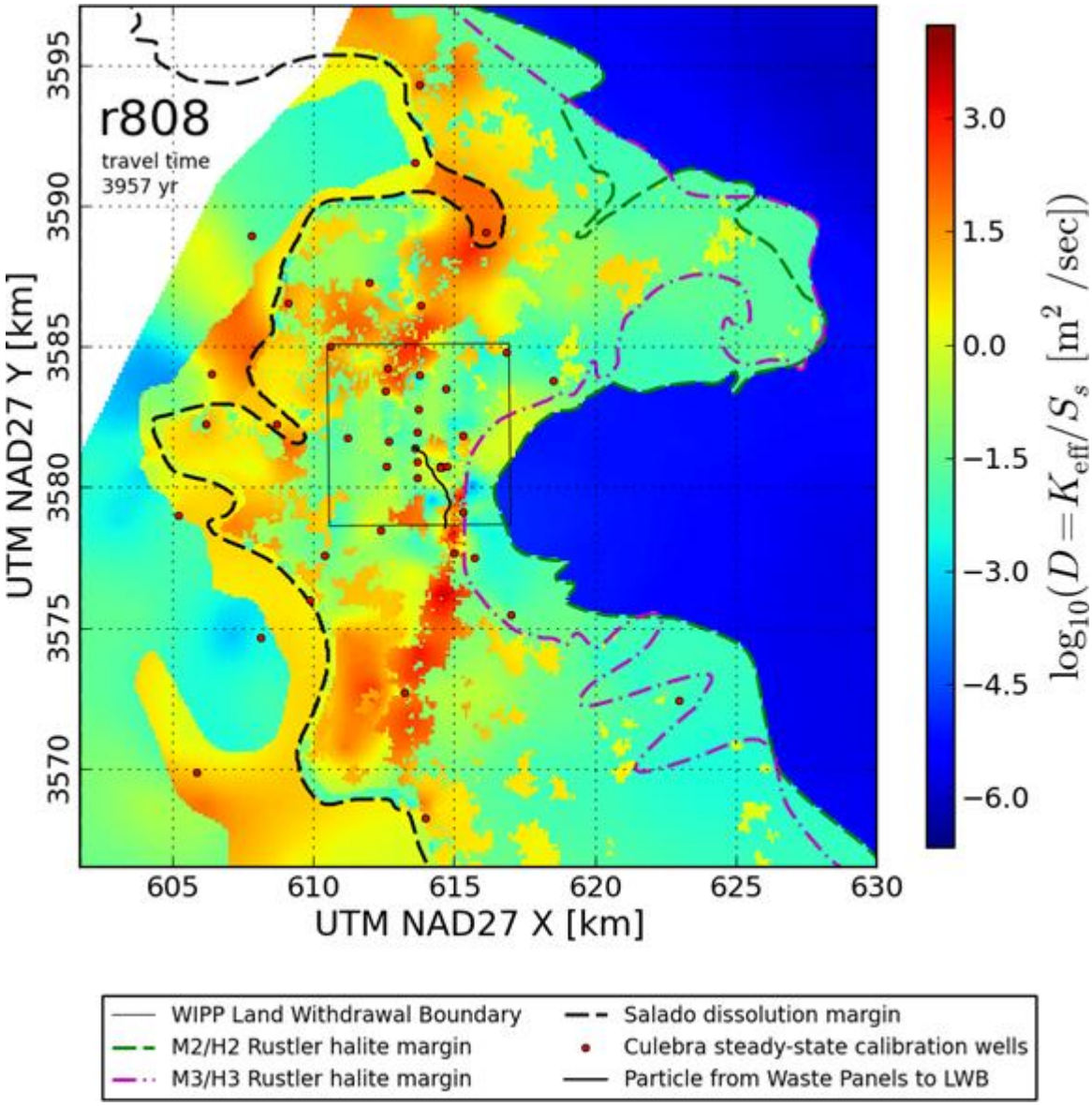
r808
travel time
3957 yr
UTM NAD27 Y [km]
3595
3590
3585
3580
3575
3570
605
610
615
620
625
630
UTM NAD27 X [km]
3.0
1.5
0.0
−1.5
−3.0
−4.5
−6.0
$\log_{10}(D = K_{\text{eff}}/S_s \ [\text{m}^2/\text{sec}])$
WIPP Land Withdrawal Boundary
M2/H2 Rustler halite margin
M3/H3 Rustler halite margin
Salado dissolution margin
Culebra steady-state calibration wells
Particle from Waste Panels to LWB

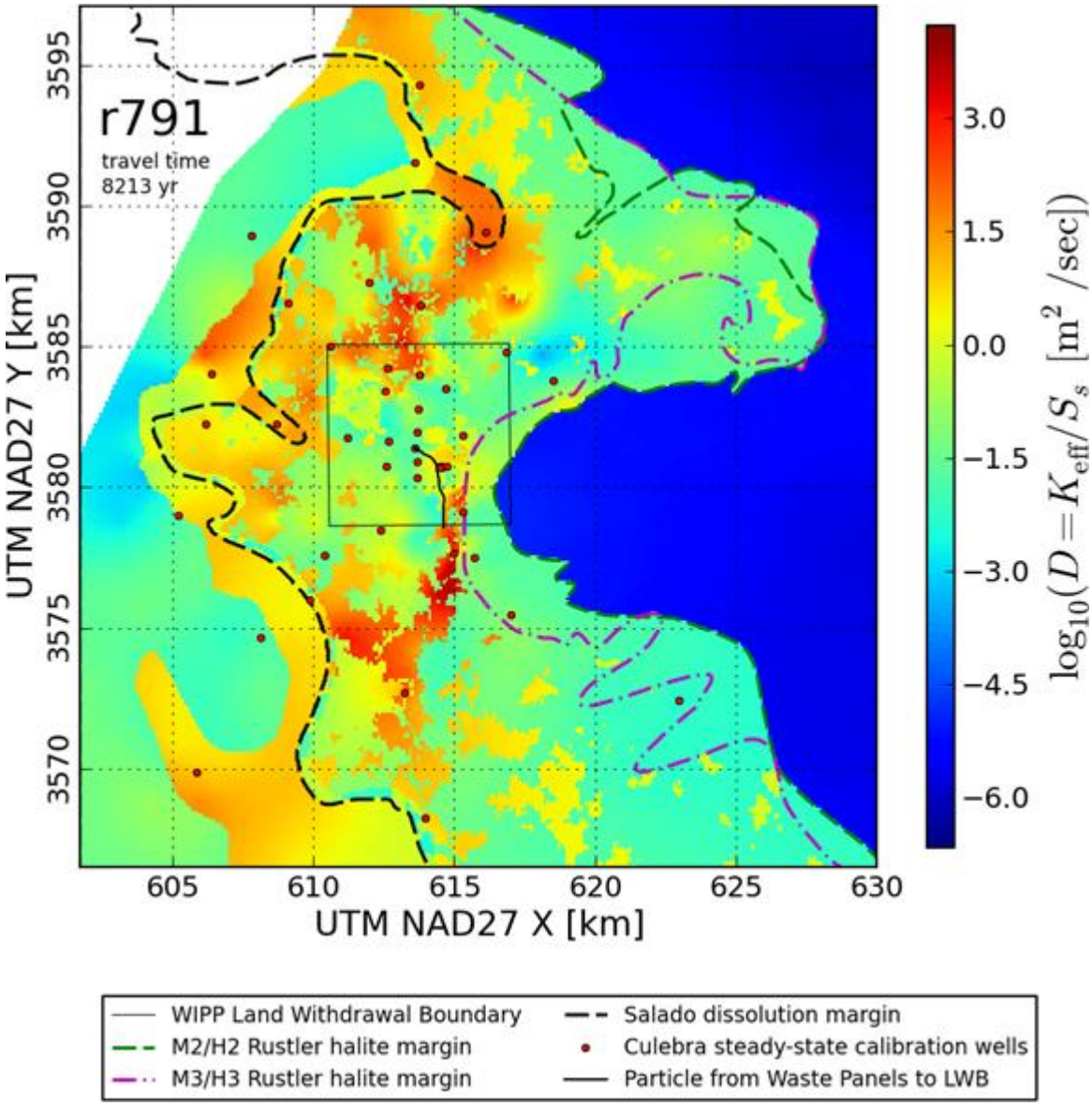
r791
travel time
8213 yr
UTM NAD27 Y [km]
3595
3590
3585
3580
3575
3570
605
610
615
620
625
630
UTM NAD27 X [km]
3.0
1.5
0.0
−1.5
−3.0
−4.5
−6.0
$\log_{10}(D = K_{\text{eff}}/S_s \ [\text{m}^2/\text{sec}])$
WIPP Land Withdrawal Boundary
M2/H2 Rustler halite margin
M3/H3 Rustler halite margin
Salado dissolution margin
Culebra steady-state calibration wells
Particle from Waste Panels to LWB

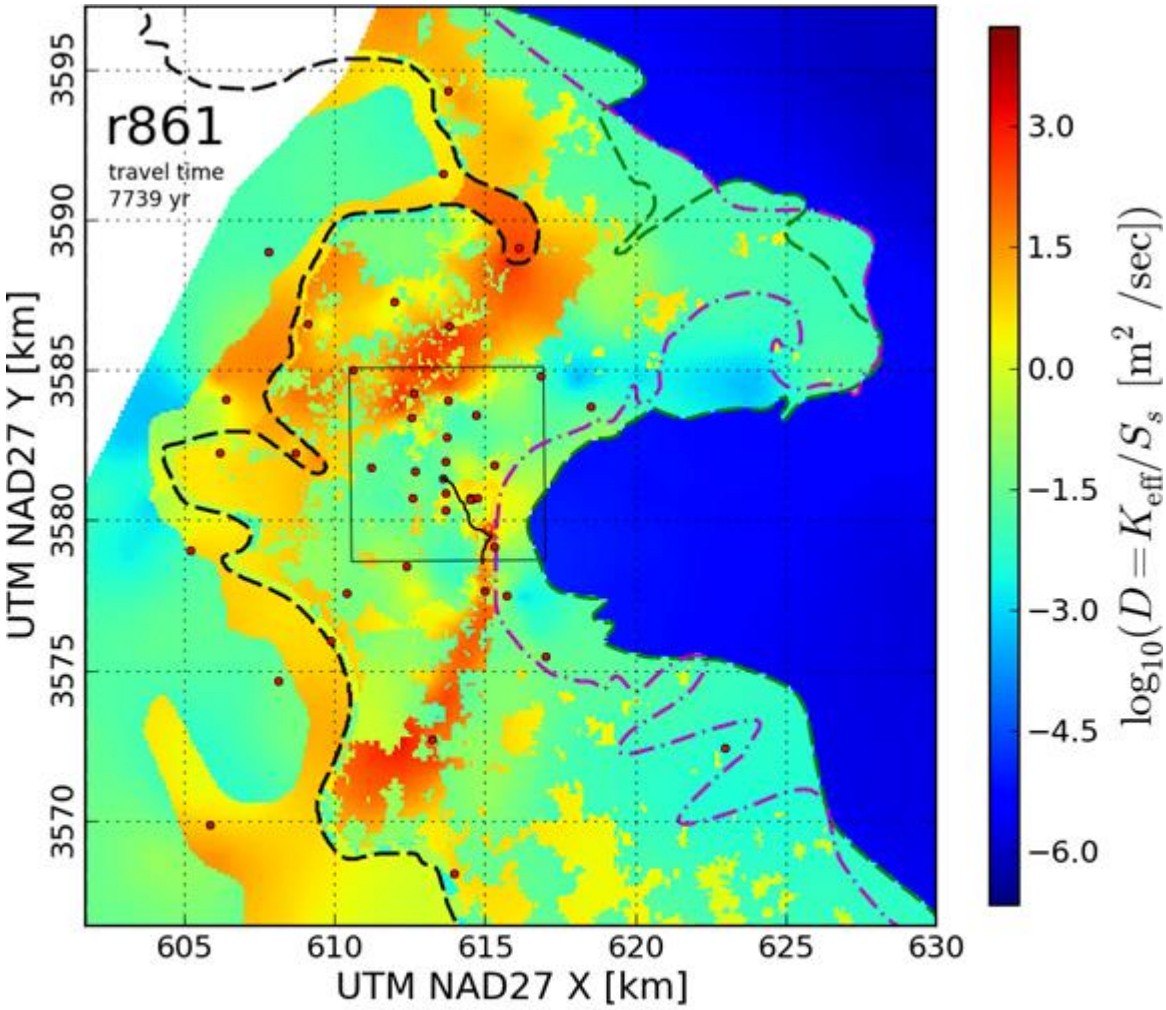
r861
travel time
7739 yr
UTM NAD27 Y [km]
3595
3590
3585
3580
3575
3570
605
610
615
620
625
630
UTM NAD27 X [km]
3.0
1.5
0.0
−1.5
−3.0
−4.5
−6.0
$\log_{10}(D = K_{\text{eff}}/S_s \ [\text{m}^2/\text{sec}])$
WIPP Land Withdrawal Boundary
M2/H2 Rustler halite margin
M3/H3 Rustler halite margin
Salado dissolution margin
Culebra steady-state calibration wells
Particle from Waste Panels to LWB

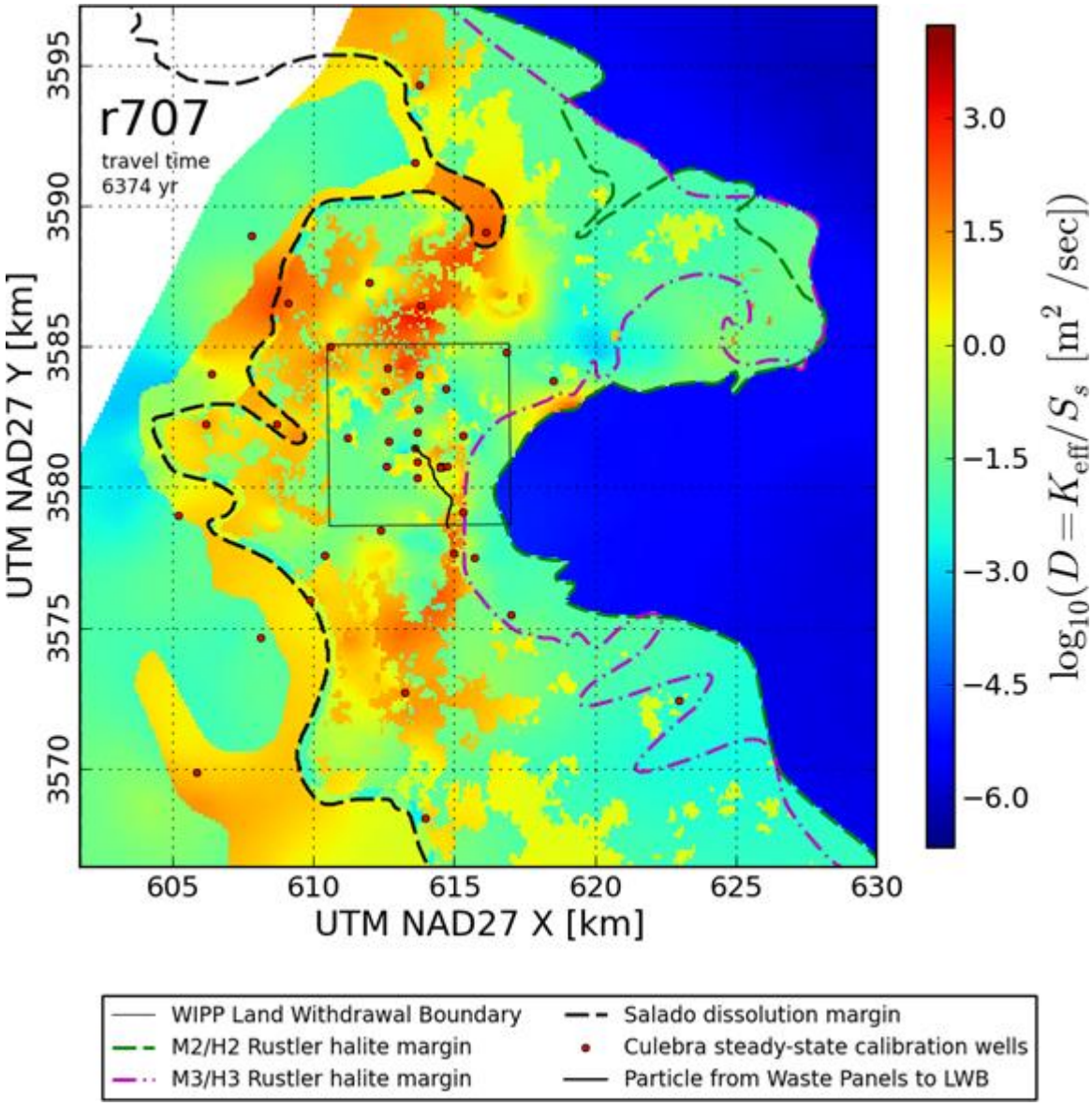
r707
travel time
6374 yr
UTM NAD27 Y [km]
3595
3590
3585
3580
3575
3570
605
610
615
620
625
630
UTM NAD27 X [km]
3.0
1.5
0.0
−1.5
−3.0
−4.5
−6.0
$\log_{10}(D = K_{\text{eff}}/S_s \ [\text{m}^2/\text{sec}])$
WIPP Land Withdrawal Boundary
M2/H2 Rustler halite margin
M3/H3 Rustler halite margin
Salado dissolution margin
Culebra steady-state calibration wells
Particle from Waste Panels to LWB

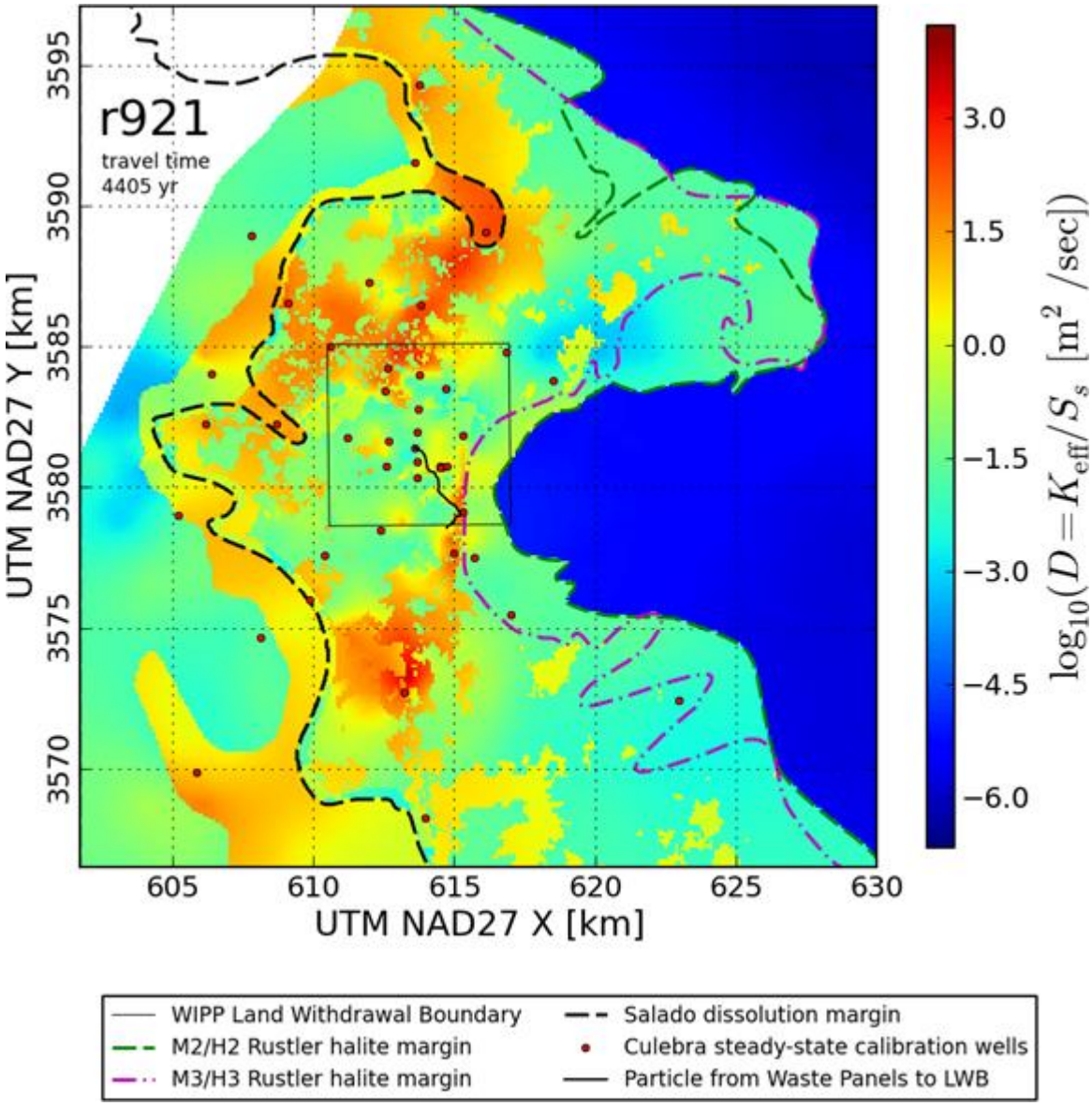
r921
travel time
4405 yr
UTM NAD27 Y [km]
3595
3590
3585
3580
3575
3570
605
610
615
620
625
630
UTM NAD27 X [km]
3.0
1.5
0.0
−1.5
−3.0
−4.5
−6.0
$\log_{10}(D = K_{\text{eff}}/S_s \ [\text{m}^2/\text{sec}])$
WIPP Land Withdrawal Boundary
M2/H2 Rustler halite margin
M3/H3 Rustler halite margin
Salado dissolution margin
Culebra steady-state calibration wells
Particle from Waste Panels to LWB

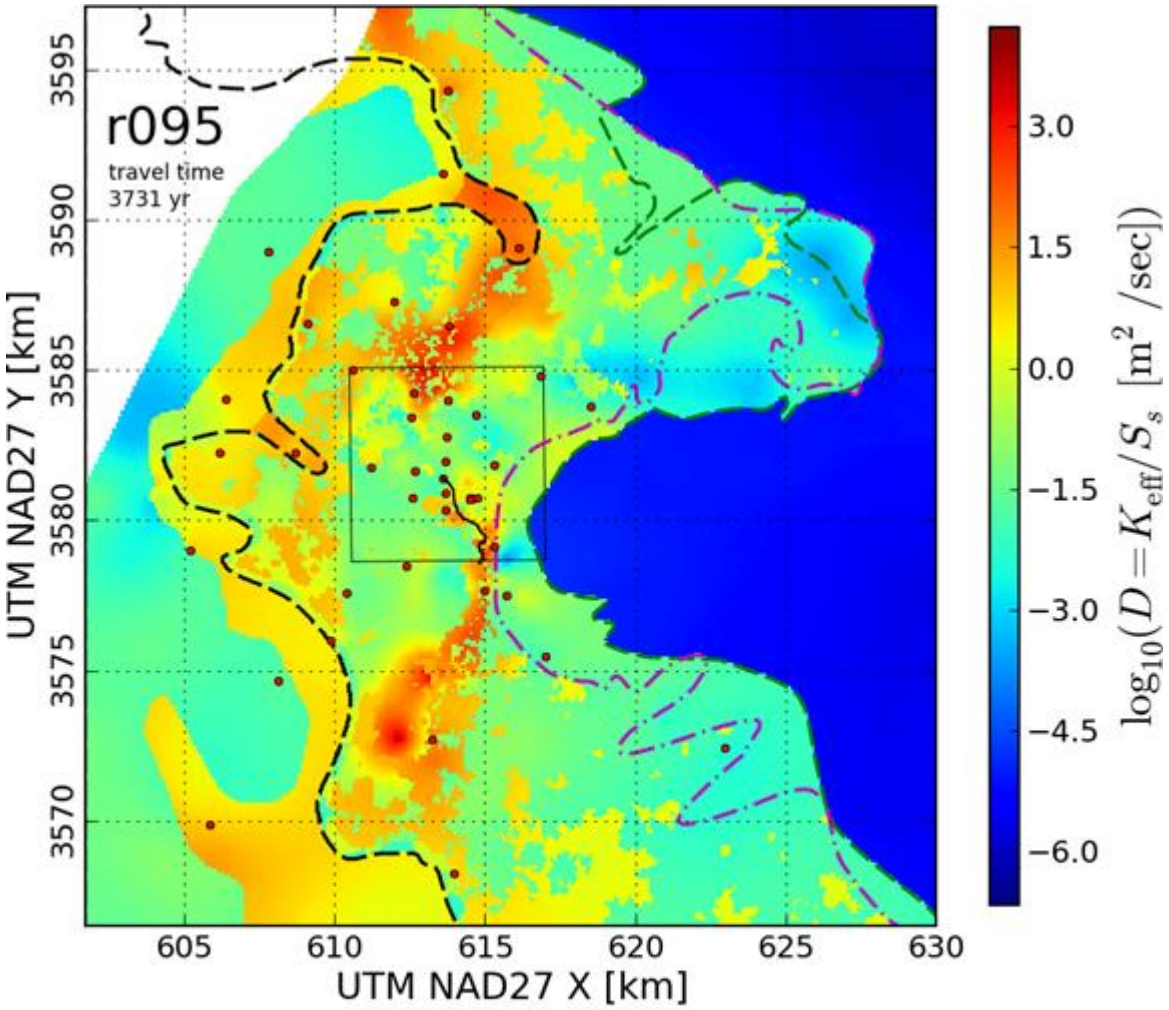
r095
travel time
3731 yr
UTM NAD27 Y [km]
3595
3590
3585
3580
3575
3570
605
610
615
620
625
630
UTM NAD27 X [km]
3.0
1.5
0.0
−1.5
−3.0
−4.5
−6.0
$\log_{10}(D = K_{\text{eff}}/S_s \ [\text{m}^2/\text{sec}])$
WIPP Land Withdrawal Boundary
M2/H2 Rustler halite margin
M3/H3 Rustler halite margin
Salado dissolution margin
Culebra steady-state calibration wells
Particle from Waste Panels to LWB

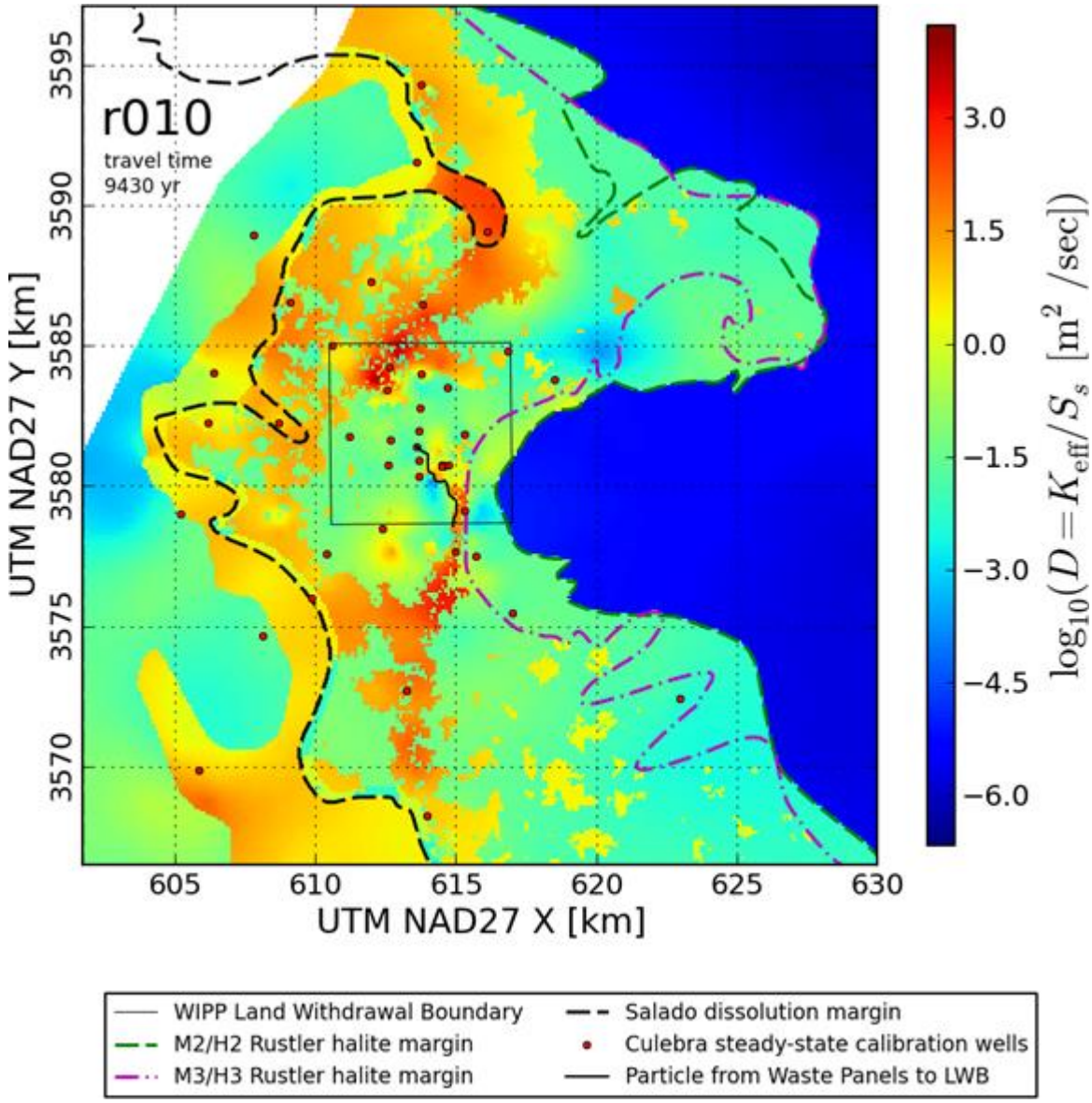
r010
travel time
9430 yr
UTM NAD27 Y [km]
3595
3590
3585
3580
3575
3570
605
610
615
620
625
630
UTM NAD27 X [km]
3.0
1.5
0.0
−1.5
−3.0
−4.5
−6.0
$\log_{10}(D = K_{\text{eff}}/S_s \ [\text{m}^2/\text{sec}])$
WIPP Land Withdrawal Boundary
M2/H2 Rustler halite margin
M3/H3 Rustler halite margin
Salado dissolution margin
Culebra steady-state calibration wells
Particle from Waste Panels to LWB

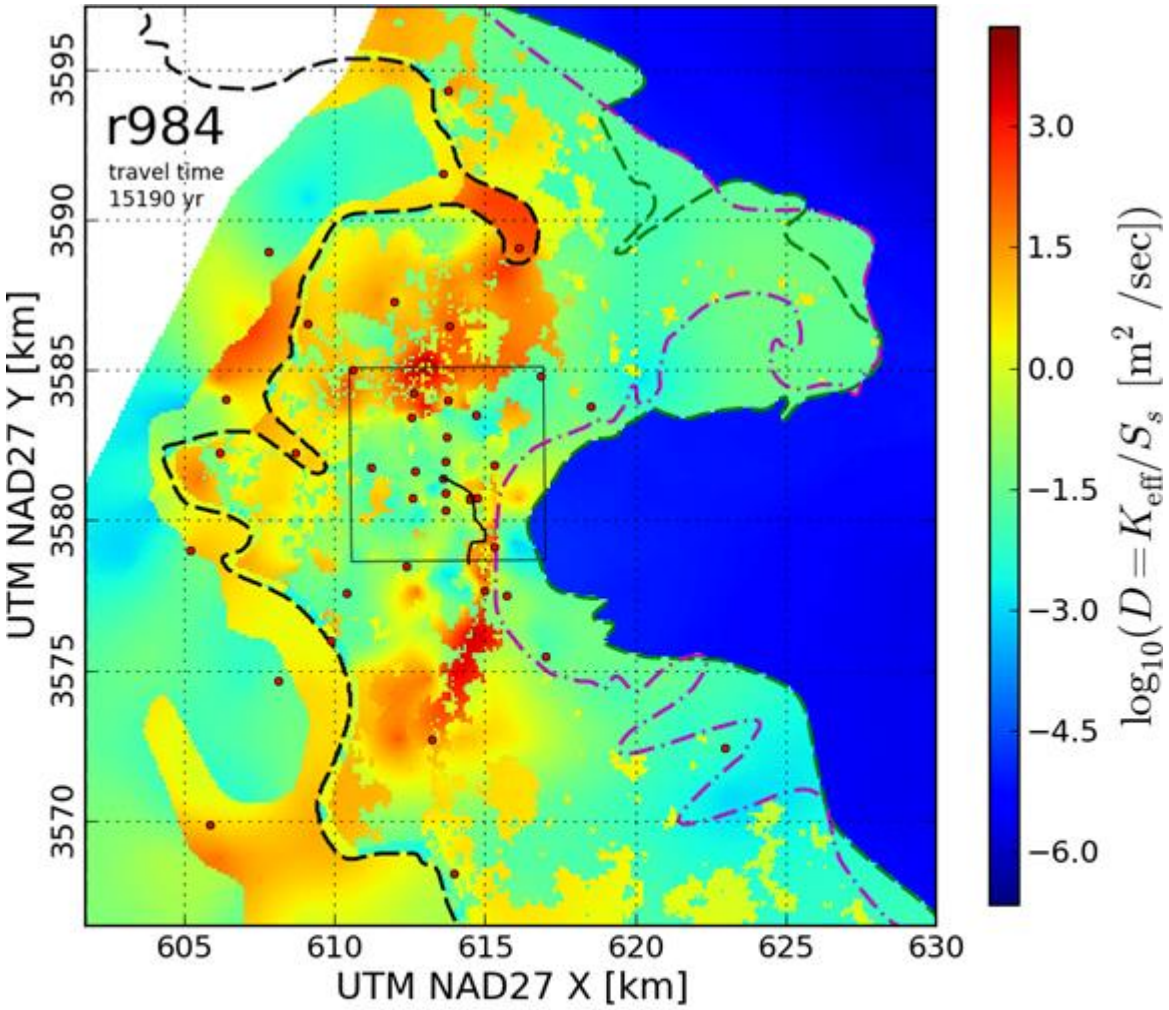
r984
travel time
15190 yr
UTM NAD27 Y [km]
3595
3590
3585
3580
3575
3570
605
610
615
620
625
630
UTM NAD27 X [km]
3.0
1.5
0.0
−1.5
−3.0
−4.5
−6.0
$\log_{10}(D = K_{\text{eff}}/S_s \ [\text{m}^2/\text{sec}])$
WIPP Land Withdrawal Boundary
M2/H2 Rustler halite margin
M3/H3 Rustler halite margin
Salado dissolution margin
Culebra steady-state calibration wells
Particle from Waste Panels to LWB

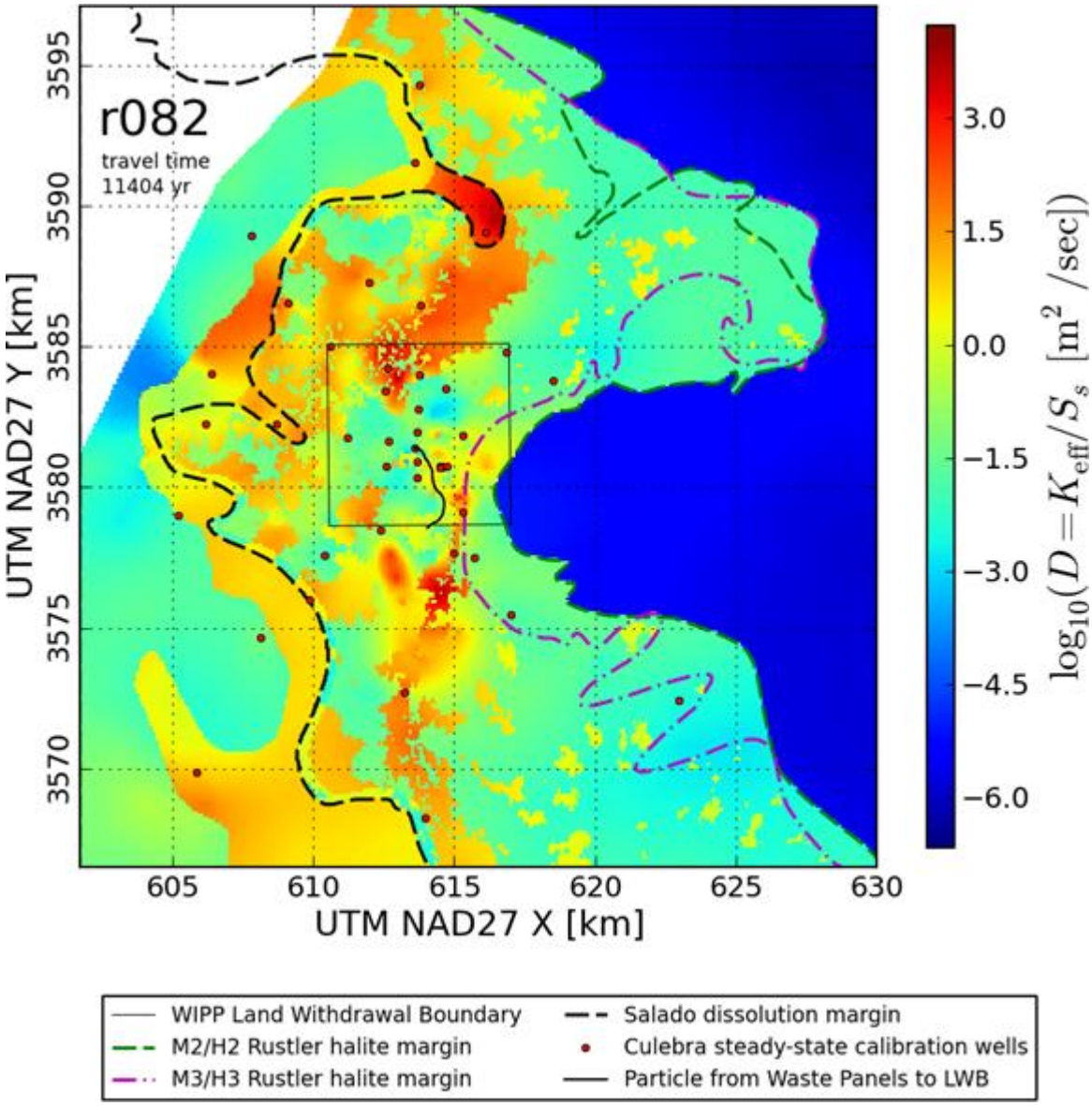
r082
travel time
11404 yr
UTM NAD27 Y [km]
3595
3590
3585
3580
3575
3570
605
610
615
620
625
630
UTM NAD27 X [km]
3.0
1.5
0.0
−1.5
−3.0
−4.5
−6.0
$\log_{10}(D = K_{\text{eff}}/S_s \ [\text{m}^2/\text{sec}])$
WIPP Land Withdrawal Boundary
M2/H2 Rustler halite margin
M3/H3 Rustler halite margin
Salado dissolution margin
Culebra steady-state calibration wells
Particle from Waste Panels to LWB

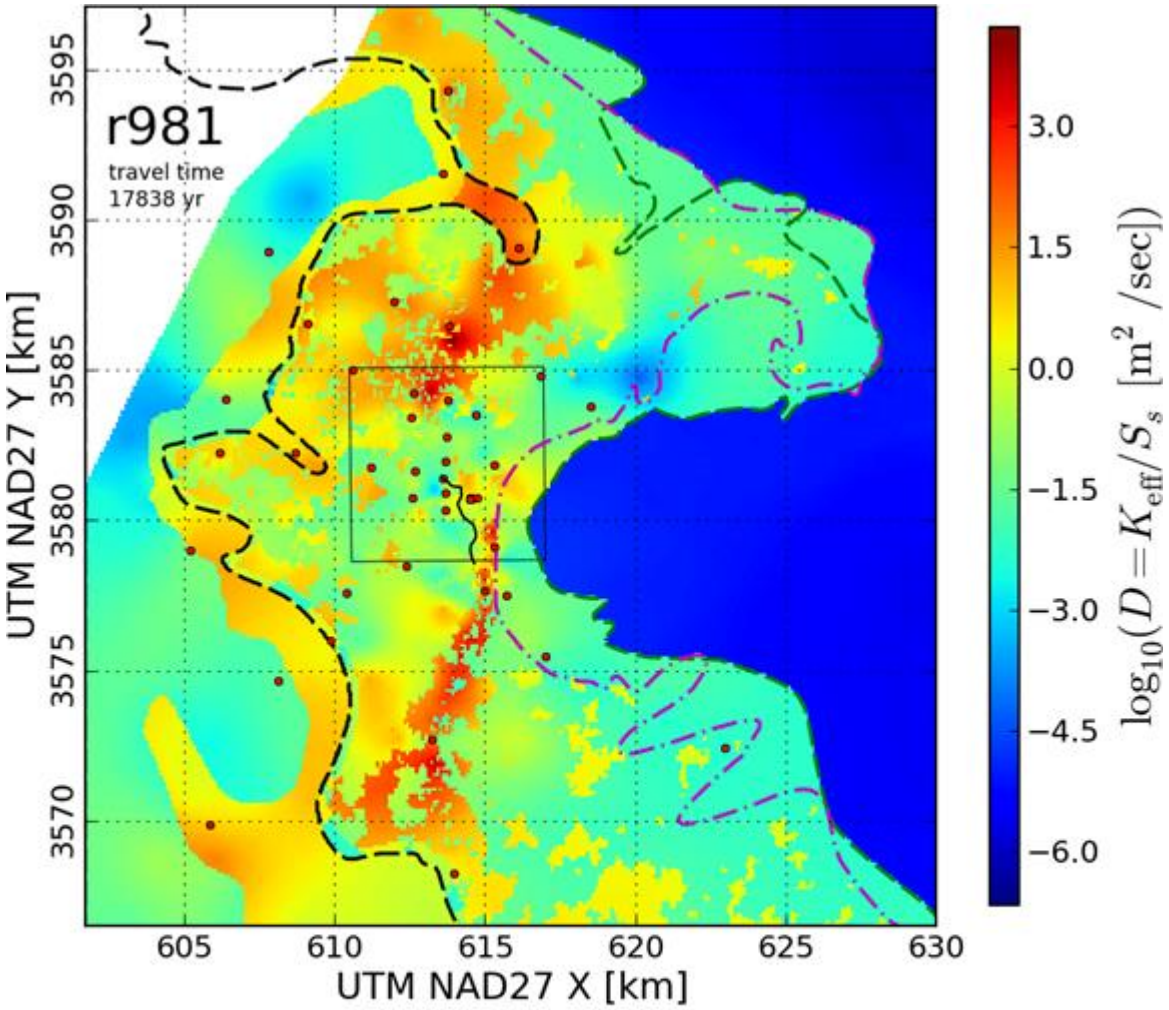
r981
travel time
17838 yr
UTM NAD27 Y [km]
3595
3590
3585
3580
3575
3570
605
610
615
620
625
630
UTM NAD27 X [km]
3.0
1.5
0.0
−1.5
−3.0
−4.5
−6.0
$\log_{10}(D = K_{\text{eff}}/S_s \ [\text{m}^2/\text{sec}])$
WIPP Land Withdrawal Boundary
M2/H2 Rustler halite margin
M3/H3 Rustler halite margin
Salado dissolution margin
Culebra steady-state calibration wells
Particle from Waste Panels to LWB

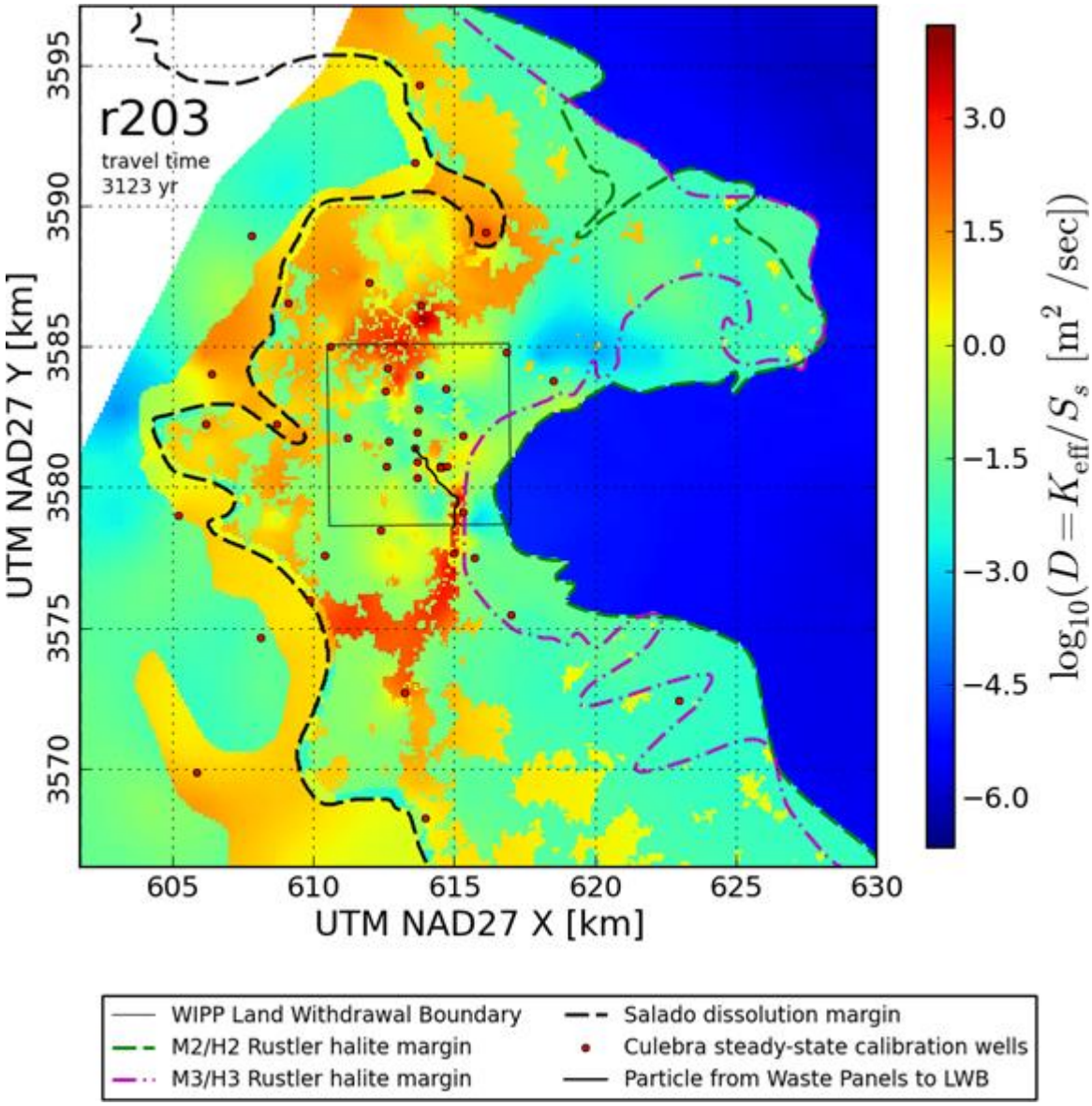
r203
travel time
3123 yr
UTM NAD27 Y [km]
3595
3590
3585
3580
3575
3570
605
610
615
620
625
630
UTM NAD27 X [km]
3.0
1.5
0.0
−1.5
−3.0
−4.5
−6.0
$\log_{10}(D = K_{\text{eff}}/S_s \ [\text{m}^2/\text{sec}])$
WIPP Land Withdrawal Boundary
M2/H2 Rustler halite margin
M3/H3 Rustler halite margin
Salado dissolution margin
Culebra steady-state calibration wells
Particle from Waste Panels to LWB

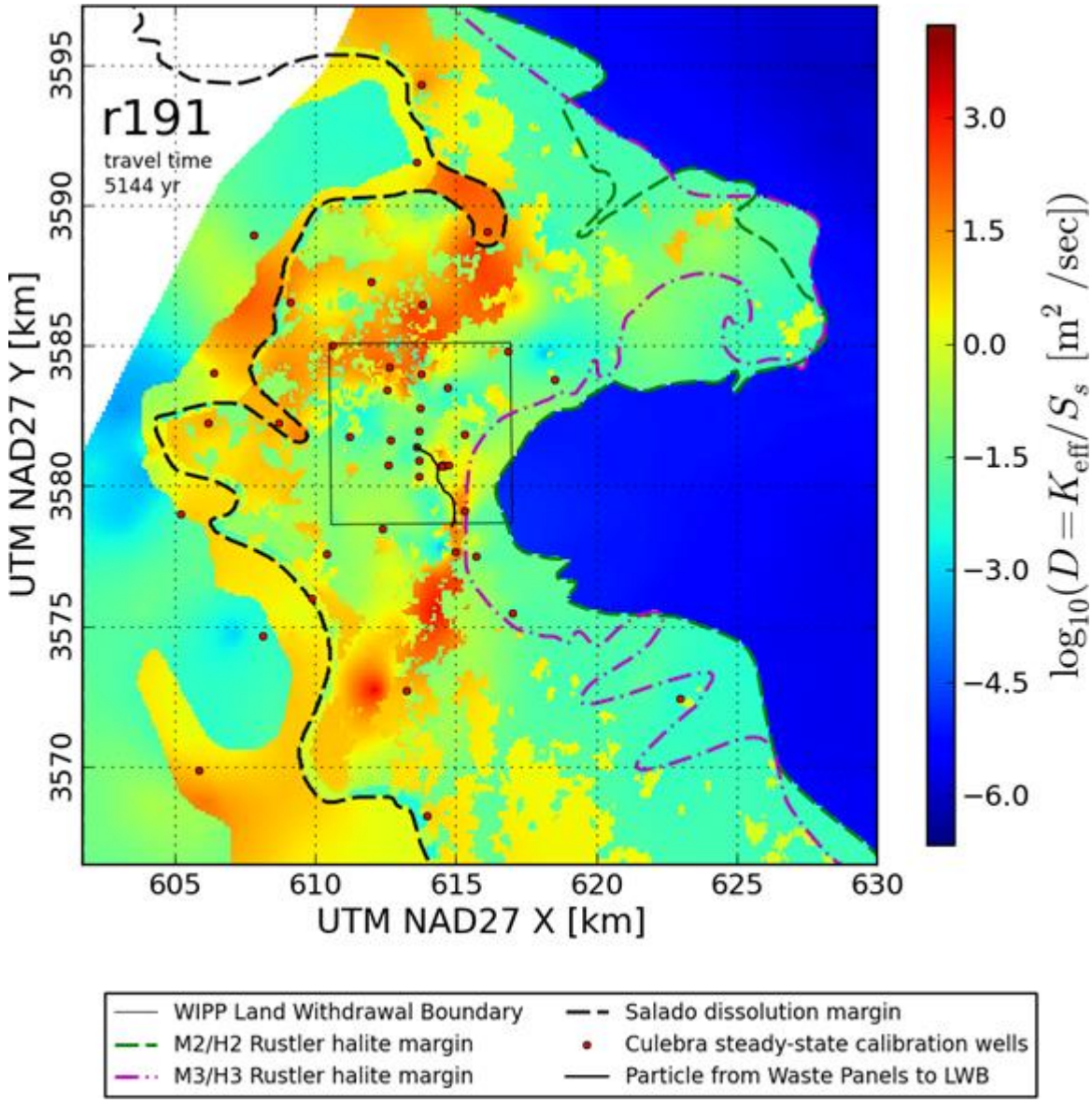
r191
travel time
5144 yr
UTM NAD27 Y [km]
3595
3590
3585
3580
3575
3570
605
610
615
620
625
630
UTM NAD27 X [km]
3.0
1.5
0.0
−1.5
−3.0
−4.5
−6.0
$\log_{10}(D = K_{\text{eff}}/S_s \ [\text{m}^2/\text{sec}])$
WIPP Land Withdrawal Boundary
M2/H2 Rustler halite margin
M3/H3 Rustler halite margin
Salado dissolution margin
Culebra steady-state calibration wells
Particle from Waste Panels to LWB

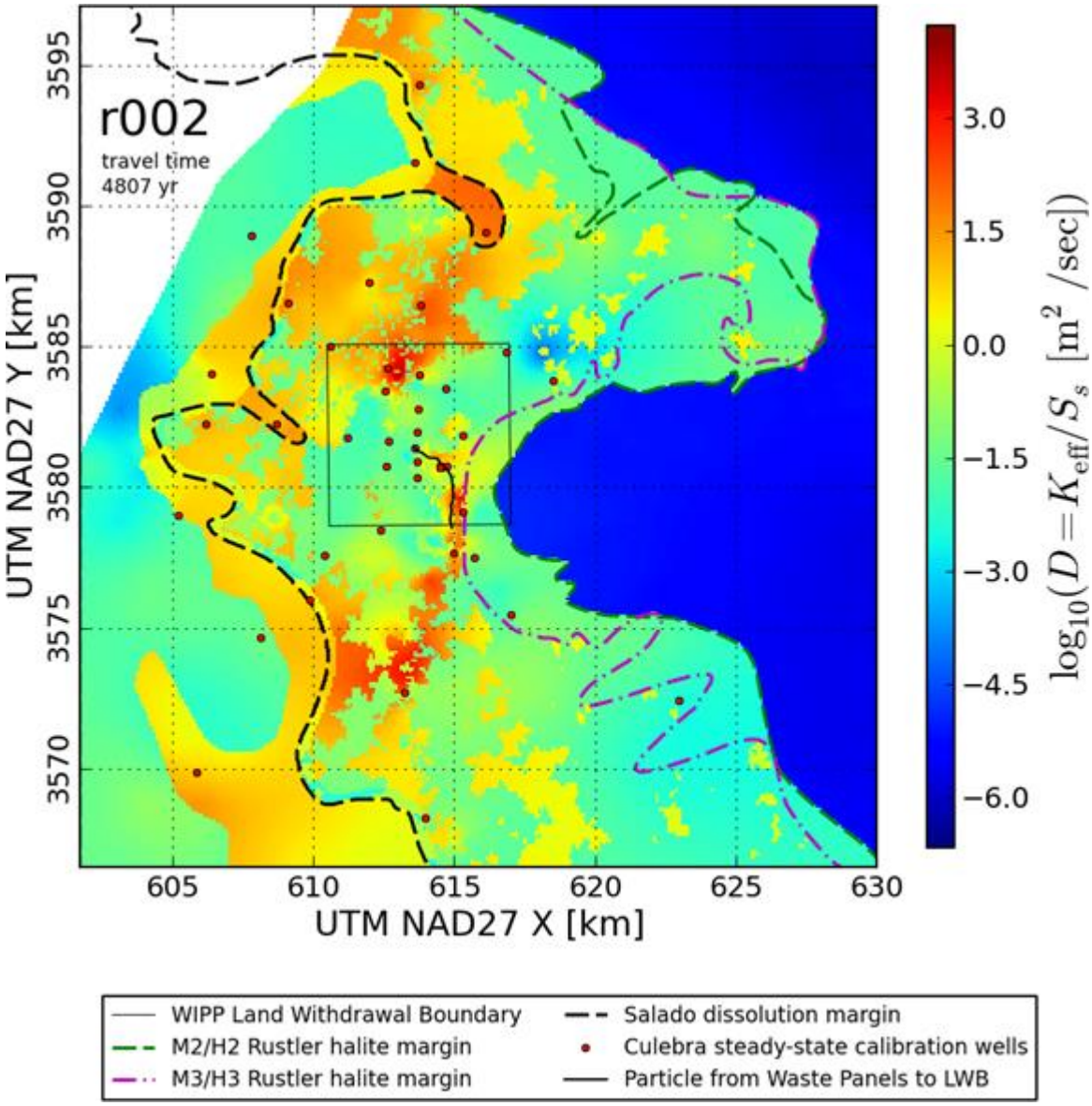
r002
travel time
4807 yr
UTM NAD27 Y [km]
3595
3590
3585
3580
3575
3570
605
610
615
620
625
630
UTM NAD27 X [km]
3.0
1.5
0.0
−1.5
−3.0
−4.5
−6.0
$\log_{10}(D = K_{\text{eff}}/S_s \ [\text{m}^2/\text{sec}])$
WIPP Land Withdrawal Boundary
M2/H2 Rustler halite margin
M3/H3 Rustler halite margin
Salado dissolution margin
Culebra steady-state calibration wells
Particle from Waste Panels to LWB

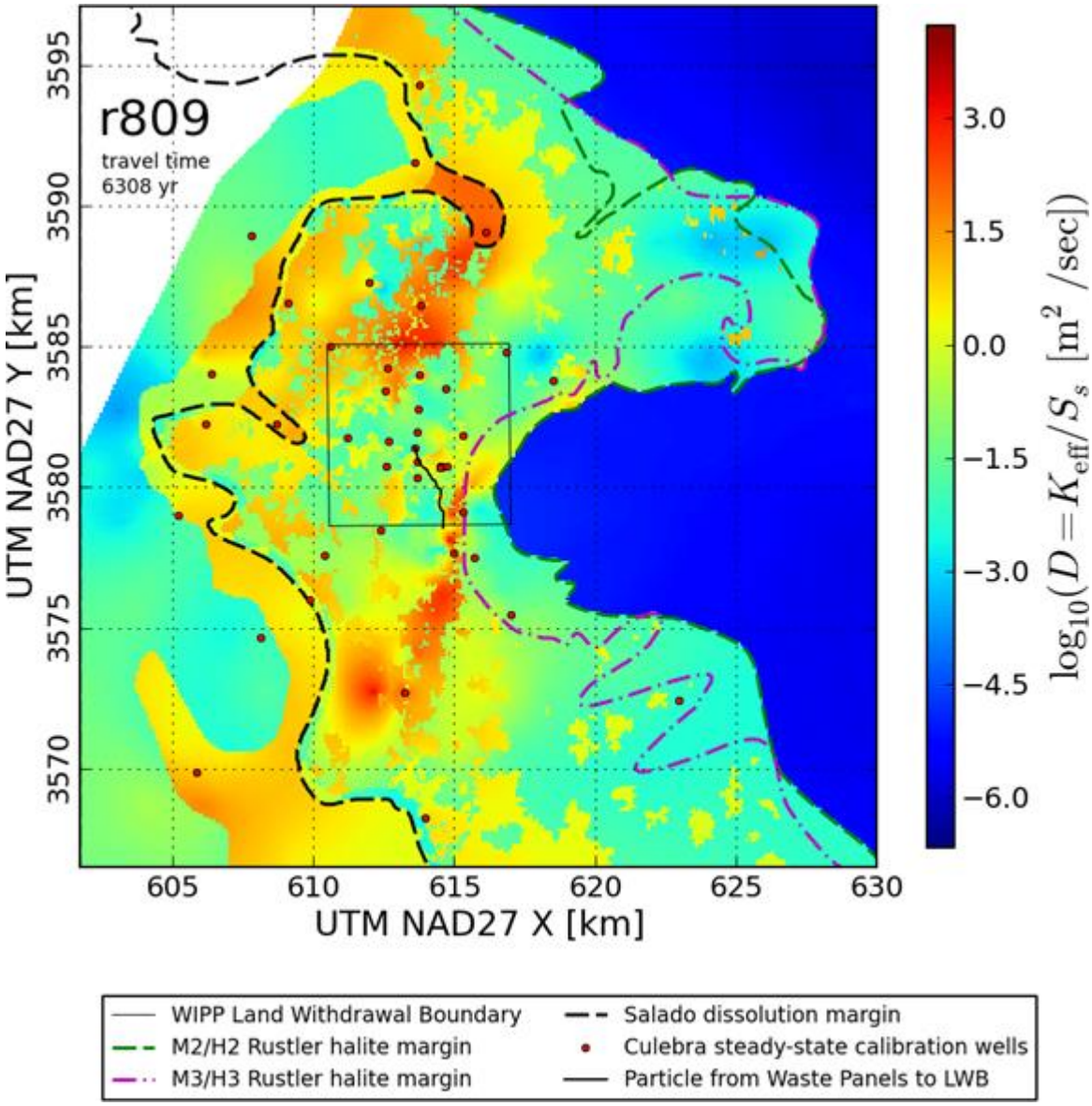
r809
travel time
6308 yr
UTM NAD27 Y [km]
3595
3590
3585
3580
3575
3570
605
610
615
620
625
630
UTM NAD27 X [km]
3.0
1.5
0.0
−1.5
−3.0
−4.5
−6.0
$\log_{10}(D = K_{\text{eff}}/S_s \ [\text{m}^2/\text{sec}])$
WIPP Land Withdrawal Boundary
M2/H2 Rustler halite margin
M3/H3 Rustler halite margin
Salado dissolution margin
Culebra steady-state calibration wells
Particle from Waste Panels to LWB

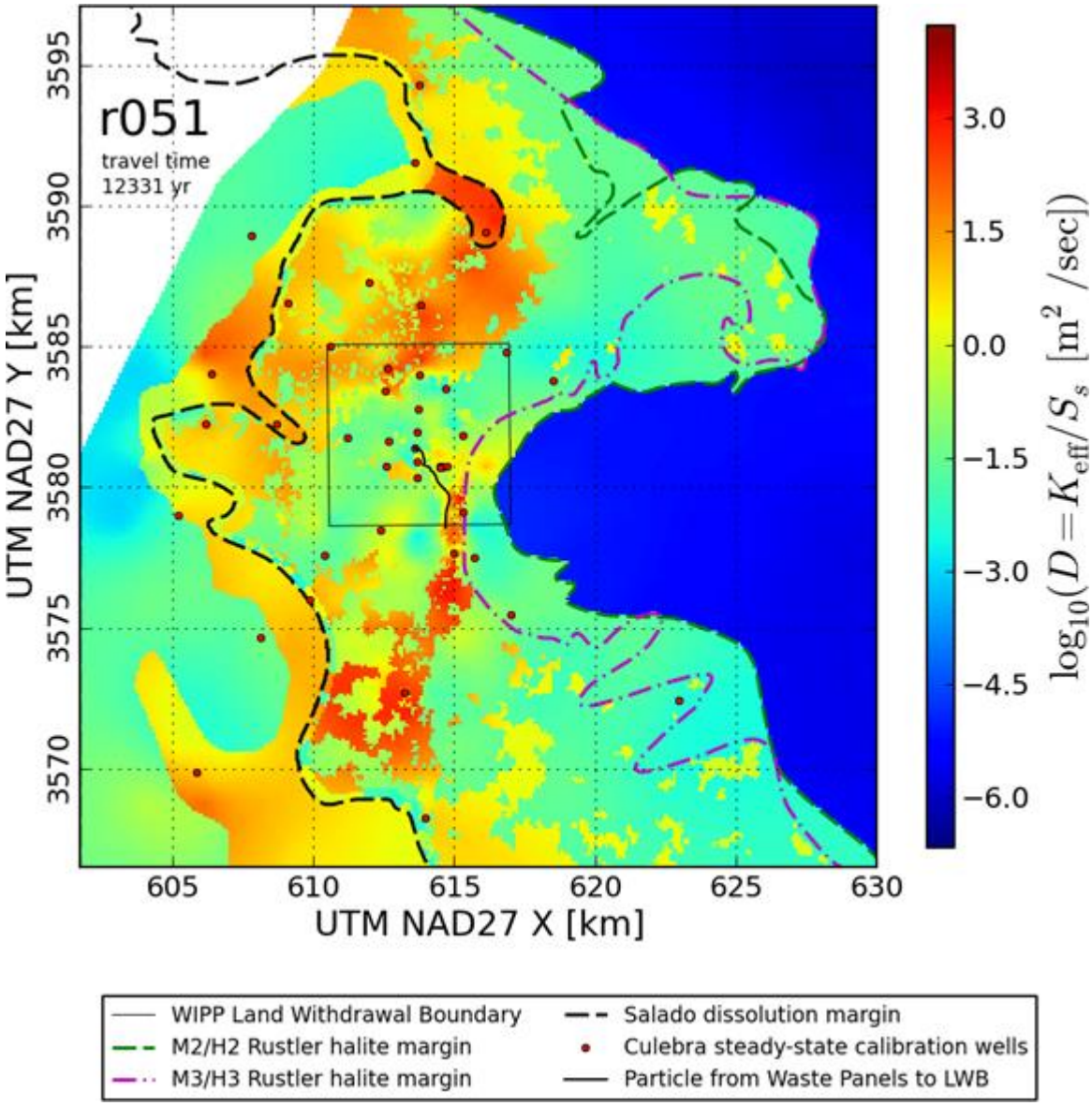
r051
travel time
12331 yr
UTM NAD27 Y [km]
3595
3590
3585
3580
3575
3570
605
610
615
620
625
630
UTM NAD27 X [km]
3.0
1.5
0.0
−1.5
−3.0
−4.5
−6.0
$\log_{10}(D = K_{\text{eff}}/S_s \ [\text{m}^2/\text{sec}])$
WIPP Land Withdrawal Boundary
M2/H2 Rustler halite margin
M3/H3 Rustler halite margin
Salado dissolution margin
Culebra steady-state calibration wells
Particle from Waste Panels to LWB

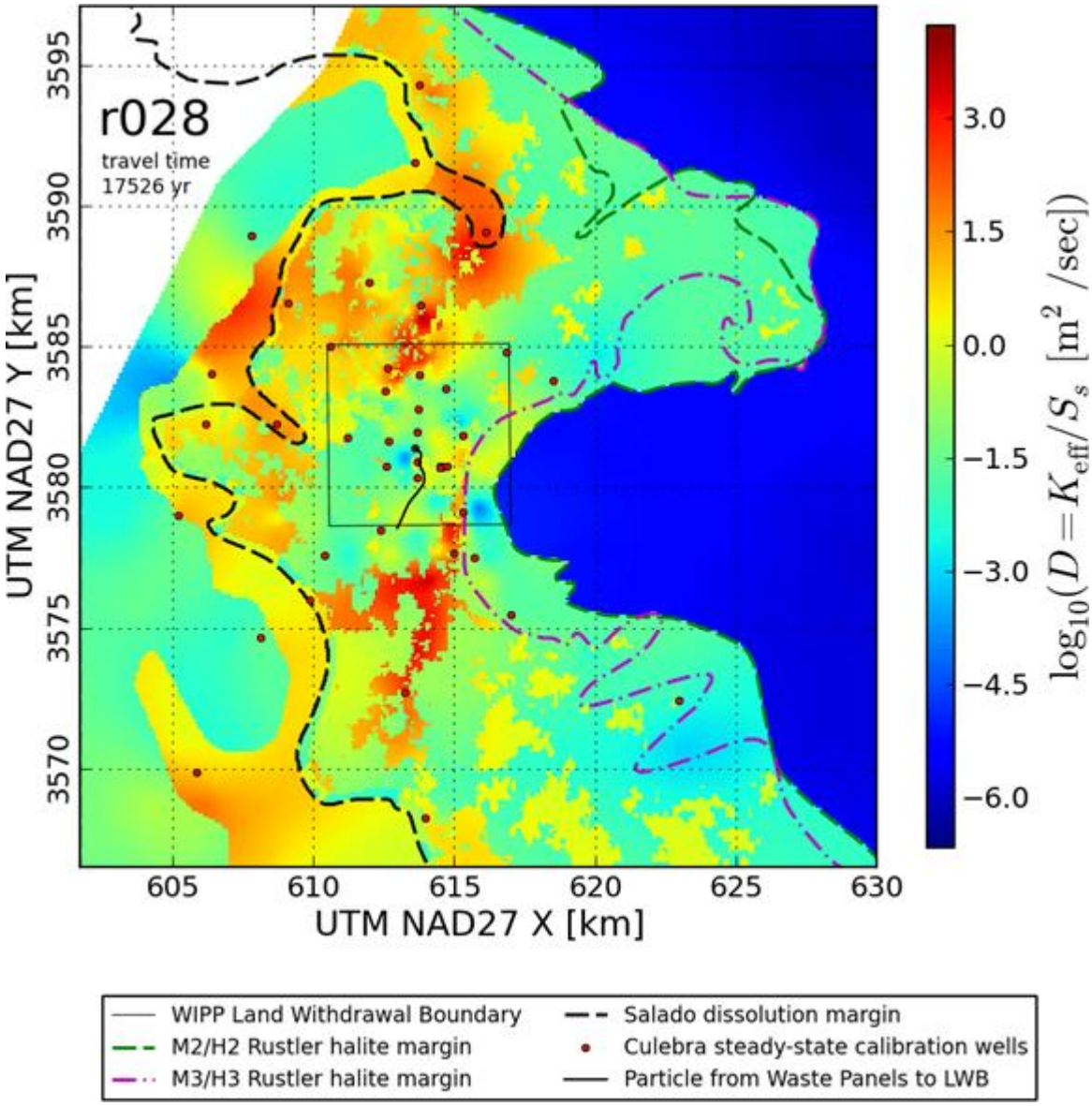
r028
travel time
17526 yr
UTM NAD27 Y [km]
3595
3590
3585
3580
3575
3570
605
610
615
620
625
630
UTM NAD27 X [km]
3.0
1.5
0.0
−1.5
−3.0
−4.5
−6.0
$\log_{10}(D = K_{\text{eff}}/S_s \ [\text{m}^2/\text{sec}])$
WIPP Land Withdrawal Boundary
M2/H2 Rustler halite margin
M3/H3 Rustler halite margin
Salado dissolution margin
Culebra steady-state calibration wells
Particle from Waste Panels to LWB

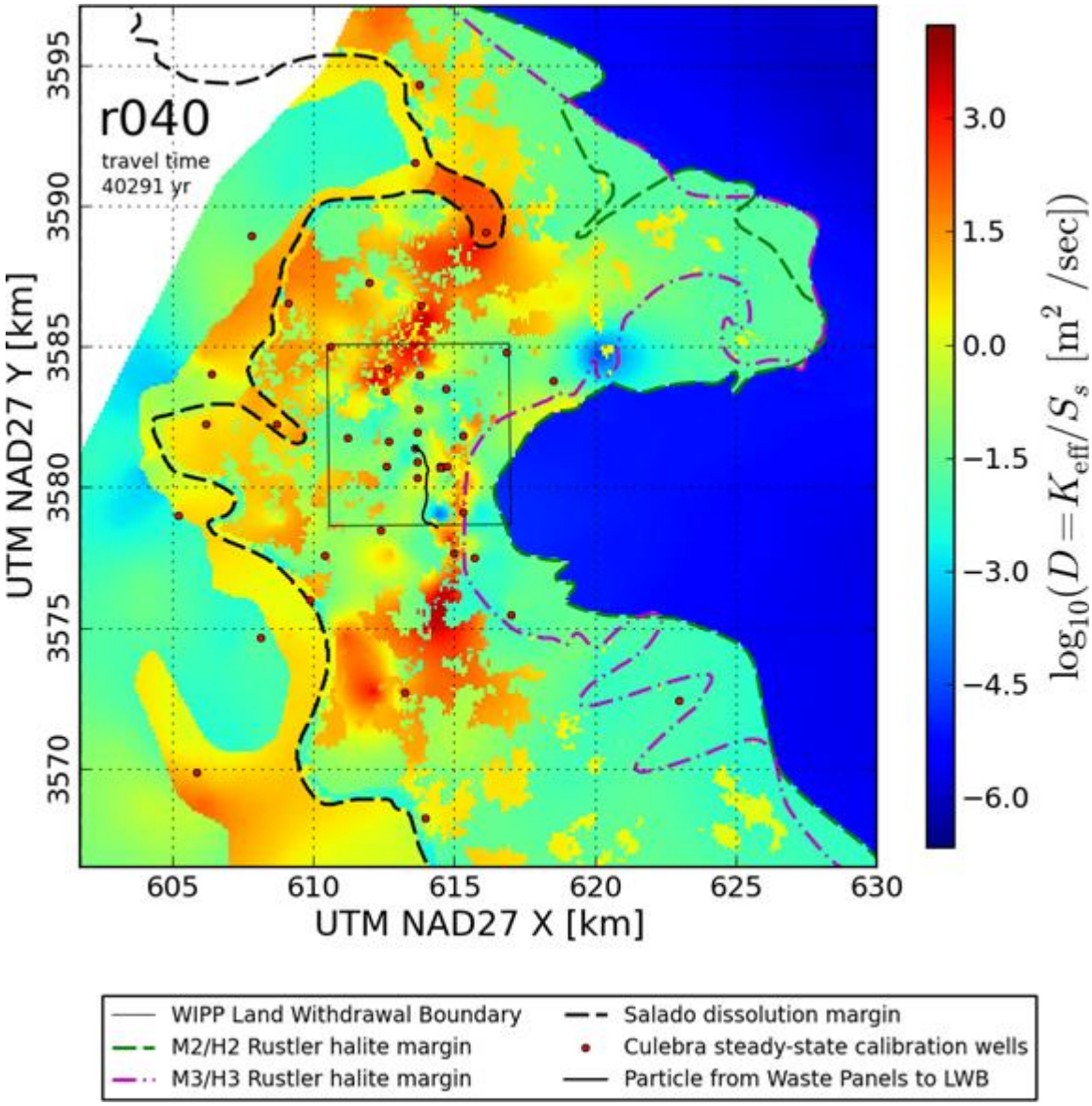
r040
travel time
40291 yr
UTM NAD27 Y [km]
3595
3590
3585
3580
3575
3570
605
610
615
620
625
630
UTM NAD27 X [km]
3.0
1.5
0.0
−1.5
−3.0
−4.5
−6.0
$\log_{10}(D = K_{\text{eff}}/S_s \ [\text{m}^2/\text{sec}])$
WIPP Land Withdrawal Boundary
M2/H2 Rustler halite margin
M3/H3 Rustler halite margin
Salado dissolution margin
Culebra steady-state calibration wells
Particle from Waste Panels to LWB

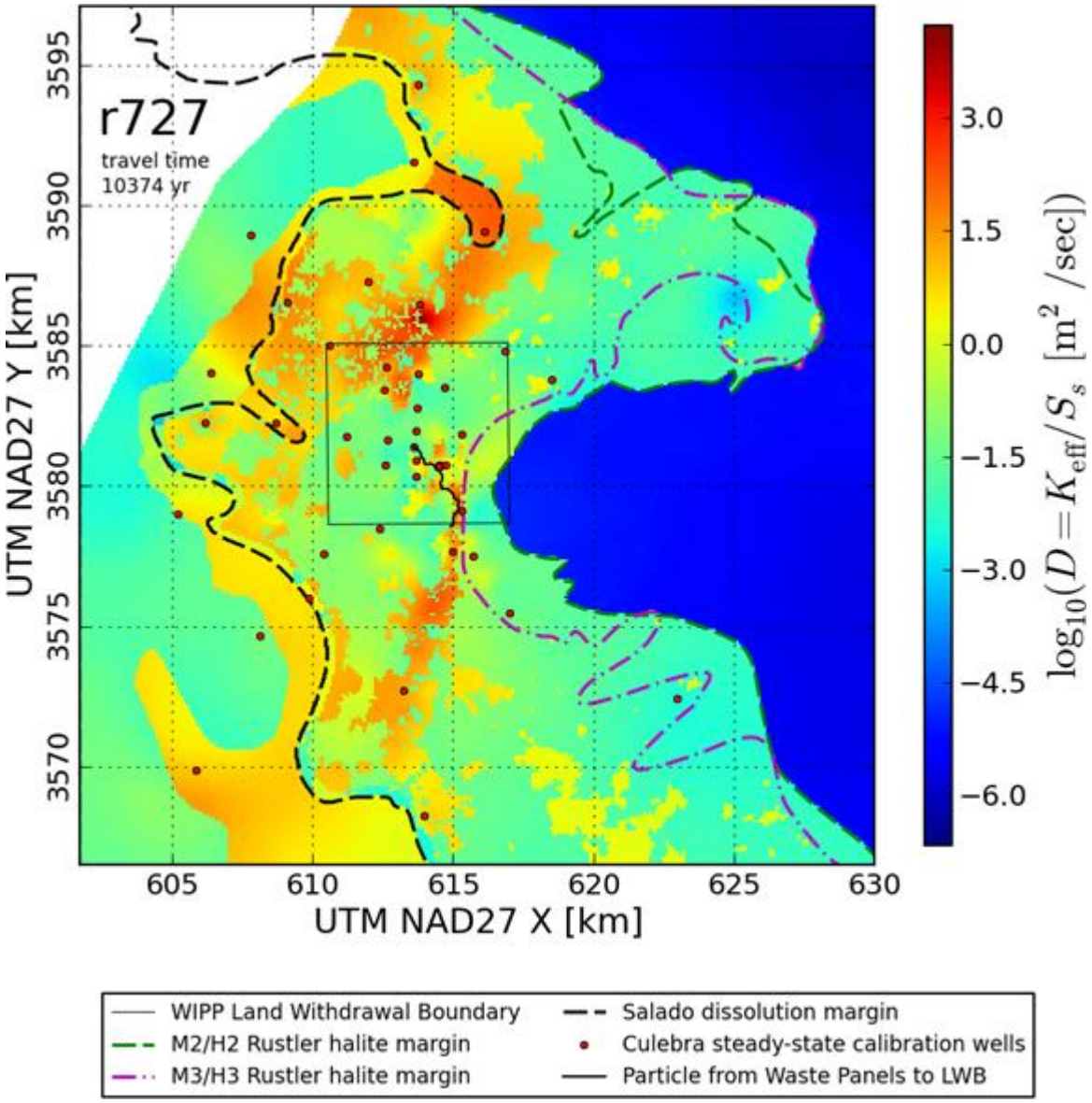
r727
travel time
10374 yr
UTM NAD27 Y [km]
3595
3590
3585
3580
3575
3570
605
610
615
620
625
630
UTM NAD27 X [km]
3.0
1.5
0.0
−1.5
−3.0
−4.5
−6.0
$\log_{10}(D = K_{\text{eff}}/S_s \ [\text{m}^2/\text{sec}])$
WIPP Land Withdrawal Boundary
M2/H2 Rustler halite margin
M3/H3 Rustler halite margin
Salado dissolution margin
Culebra steady-state calibration wells
Particle from Waste Panels to LWB

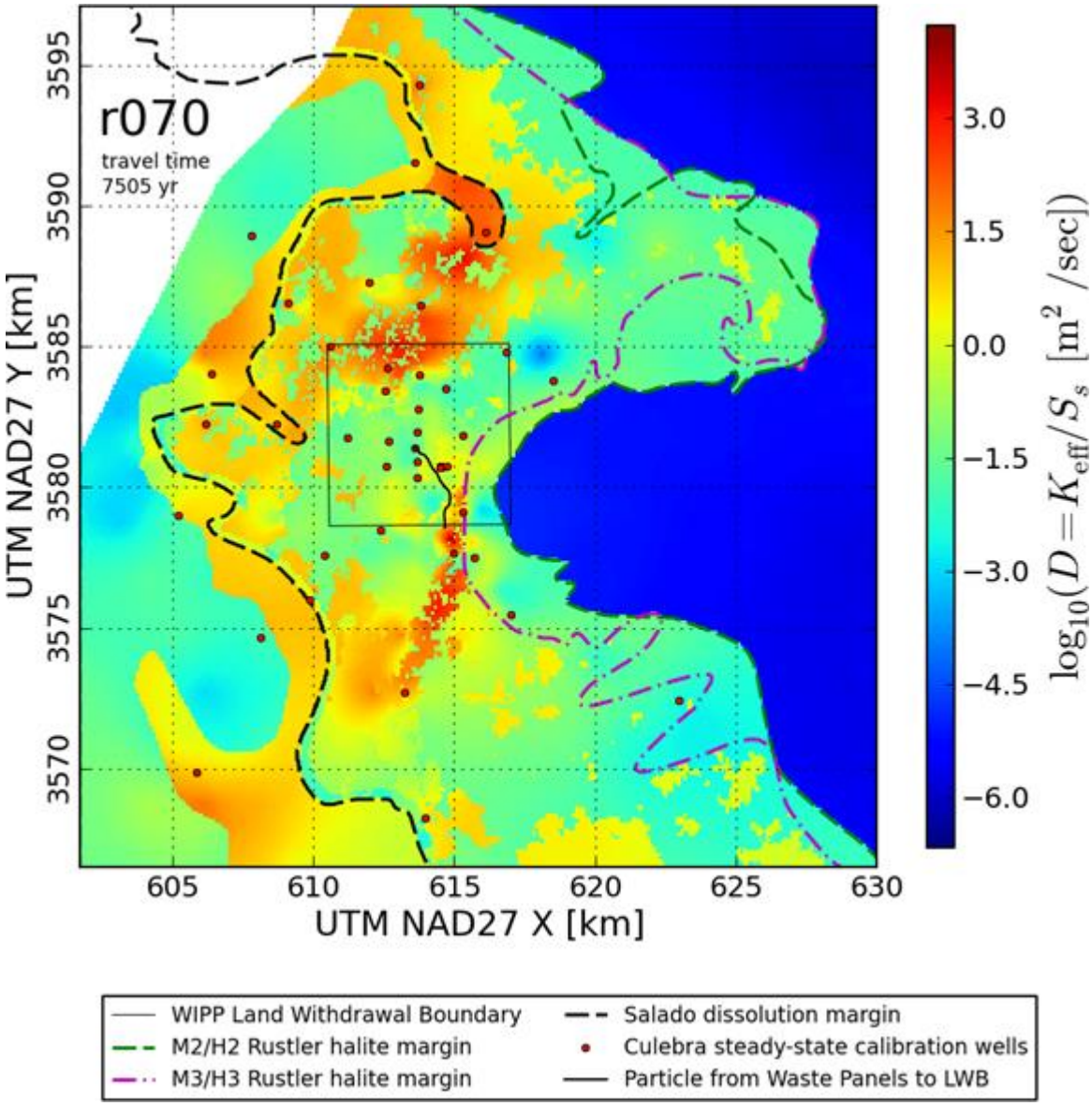
r070
travel time
7505 yr
UTM NAD27 Y [km]
3595
3590
3585
3580
3575
3570
605
610
615
620
625
630
UTM NAD27 X [km]
3.0
1.5
0.0
−1.5
−3.0
−4.5
−6.0
$\log_{10}(D = K_{\text{eff}}/S_s \ [\text{m}^2/\text{sec}])$
WIPP Land Withdrawal Boundary
M2/H2 Rustler halite margin
M3/H3 Rustler halite margin
Salado dissolution margin
Culebra steady-state calibration wells
Particle from Waste Panels to LWB

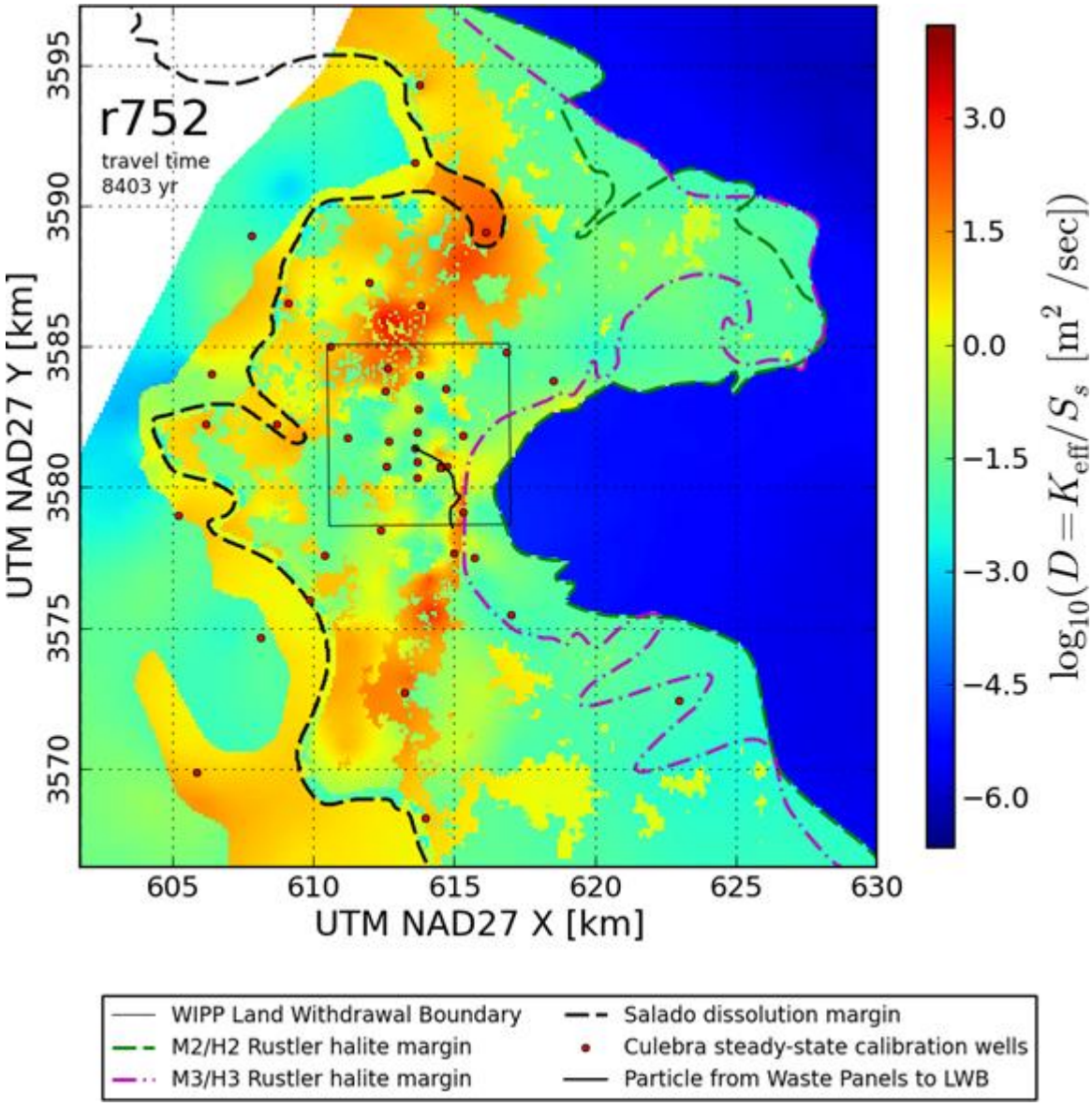
r752
travel time
8403 yr
UTM NAD27 Y [km]
3595
3590
3585
3580
3575
3570
605
610
615
620
625
630
UTM NAD27 X [km]
3.0
1.5
0.0
−1.5
−3.0
−4.5
−6.0
$\log_{10}(D = K_{\text{eff}}/S_s \ [\text{m}^2/\text{sec}])$
WIPP Land Withdrawal Boundary
M2/H2 Rustler halite margin
M3/H3 Rustler halite margin
Salado dissolution margin
Culebra steady-state calibration wells
Particle from Waste Panels to LWB

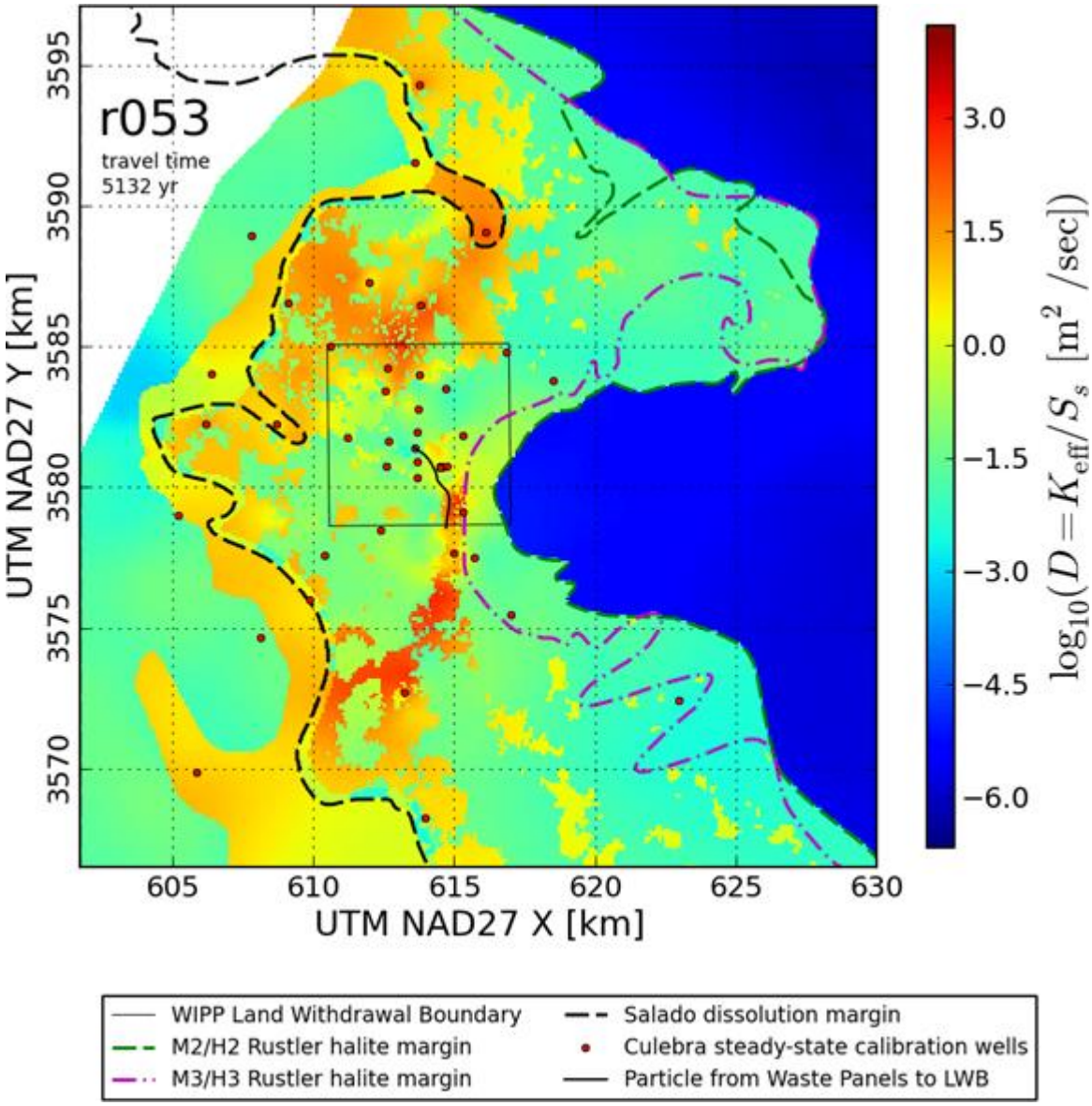
r053
travel time
5132 yr
UTM NAD27 Y [km]
3595
3590
3585
3580
3575
3570
605
610
615
620
625
630
UTM NAD27 X [km]
3.0
1.5
0.0
−1.5
−3.0
−4.5
−6.0
$\log_{10}(D = K_{\text{eff}}/S_s \ [\text{m}^2/\text{sec}])$
WIPP Land Withdrawal Boundary
M2/H2 Rustler halite margin
M3/H3 Rustler halite margin
Salado dissolution margin
Culebra steady-state calibration wells
Particle from Waste Panels to LWB

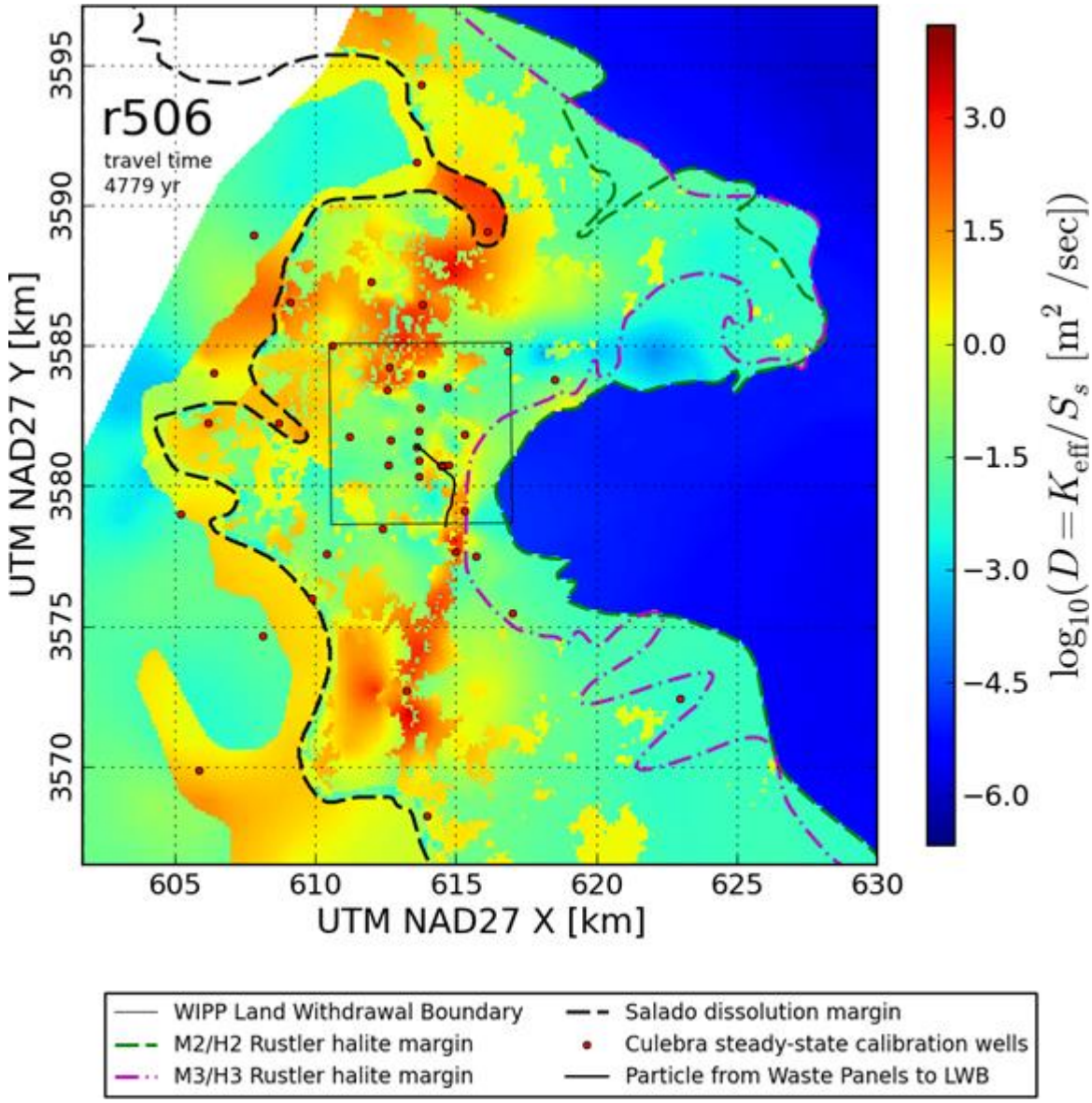
r506
travel time
4779 yr
UTM NAD27 Y [km]
3595
3590
3585
3580
3575
3570
605
610
615
620
625
630
UTM NAD27 X [km]
3.0
1.5
0.0
−1.5
−3.0
−4.5
−6.0
$\log_{10}(D = K_{\text{eff}}/S_s \ [\text{m}^2/\text{sec}])$
WIPP Land Withdrawal Boundary
M2/H2 Rustler halite margin
M3/H3 Rustler halite margin
Salado dissolution margin
Culebra steady-state calibration wells
Particle from Waste Panels to LWB

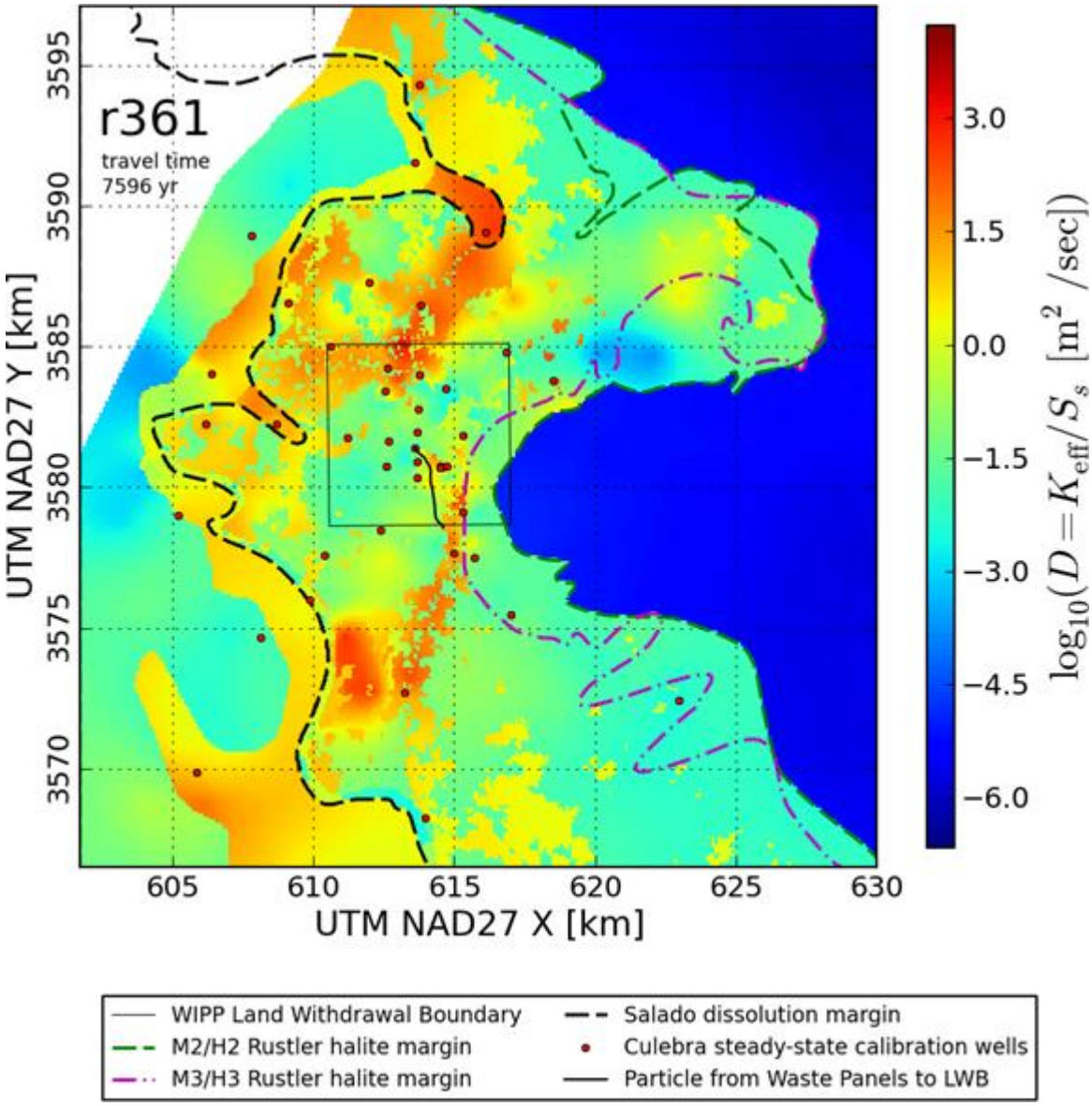
r361
travel time
7596 yr
UTM NAD27 Y [km]
3595
3590
3585
3580
3575
3570
605
610
615
620
625
630
UTM NAD27 X [km]
3.0
1.5
0.0
−1.5
−3.0
−4.5
−6.0
$\log_{10}(D = K_{\text{eff}}/S_s \ [\text{m}^2/\text{sec}])$
WIPP Land Withdrawal Boundary
M2/H2 Rustler halite margin
M3/H3 Rustler halite margin
Salado dissolution margin
Culebra steady-state calibration wells
Particle from Waste Panels to LWB

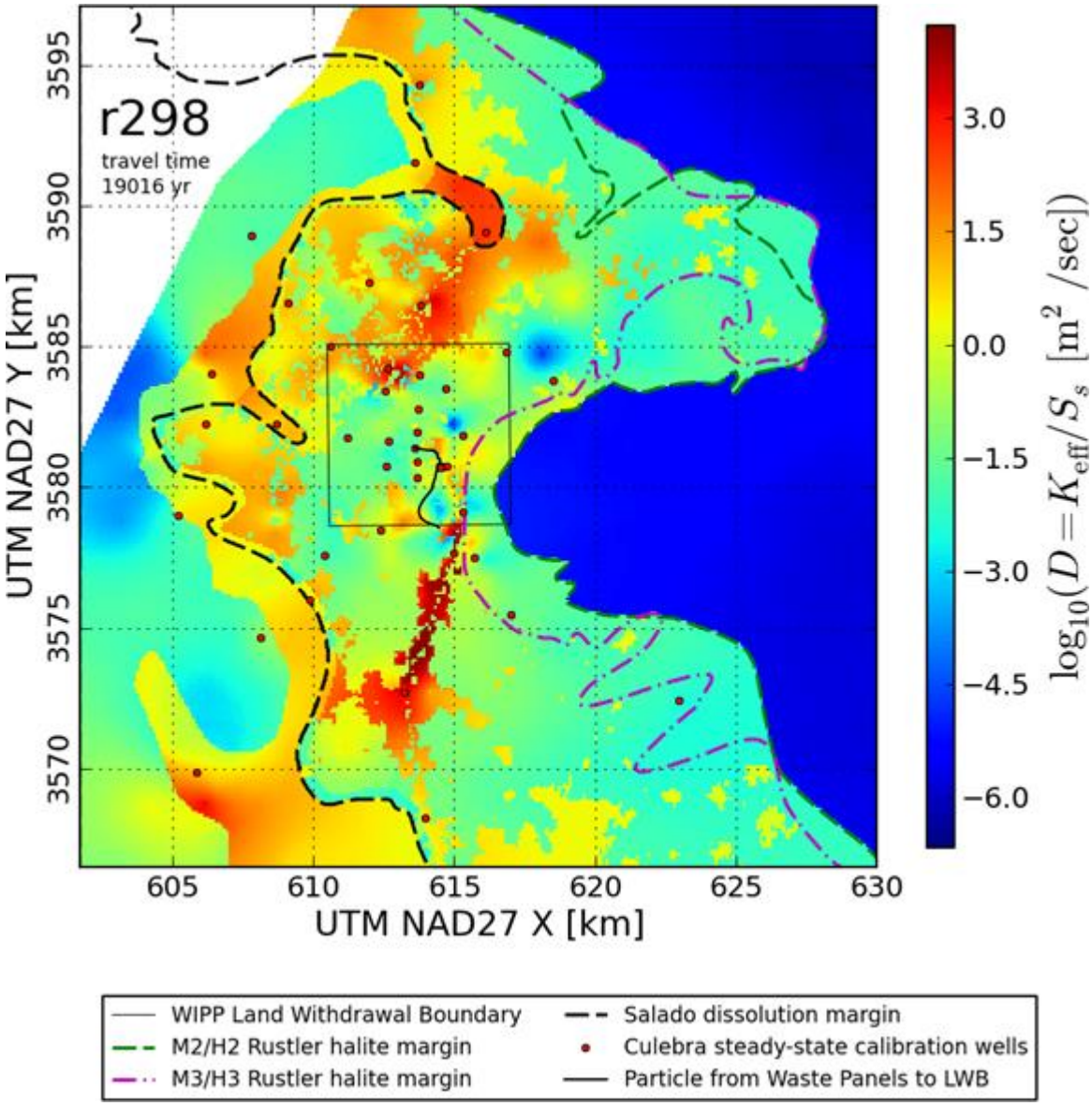
r298
travel time
19016 yr
UTM NAD27 Y [km]
3595
3590
3585
3580
3575
3570
605
610
615
620
625
630
UTM NAD27 X [km]
3.0
1.5
0.0
−1.5
−3.0
−4.5
−6.0
$\log_{10}(D = K_{\text{eff}}/S_s \ [\text{m}^2/\text{sec}])$
WIPP Land Withdrawal Boundary
M2/H2 Rustler halite margin
M3/H3 Rustler halite margin
Salado dissolution margin
Culebra steady-state calibration wells
Particle from Waste Panels to LWB

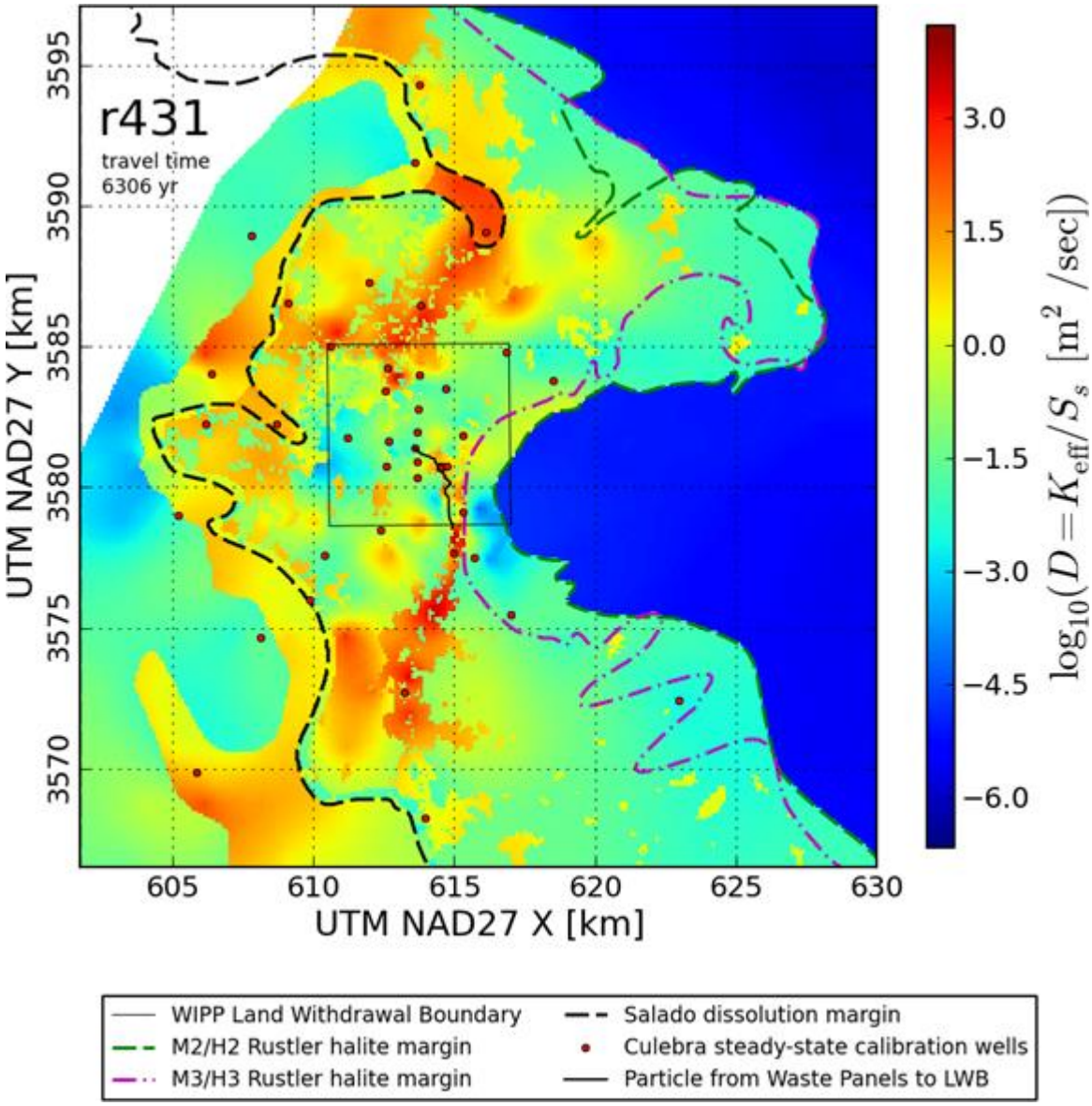
r431
travel time
6306 yr
UTM NAD27 Y [km]
3595
3590
3585
3580
3575
3570
605
610
615
620
625
630
UTM NAD27 X [km]
3.0
1.5
0.0
−1.5
−3.0
−4.5
−6.0
$\log_{10}(D = K_{\text{eff}}/S_s \ [\text{m}^2/\text{sec}])$
WIPP Land Withdrawal Boundary
M2/H2 Rustler halite margin
M3/H3 Rustler halite margin
Salado dissolution margin
Culebra steady-state calibration wells
Particle from Waste Panels to LWB

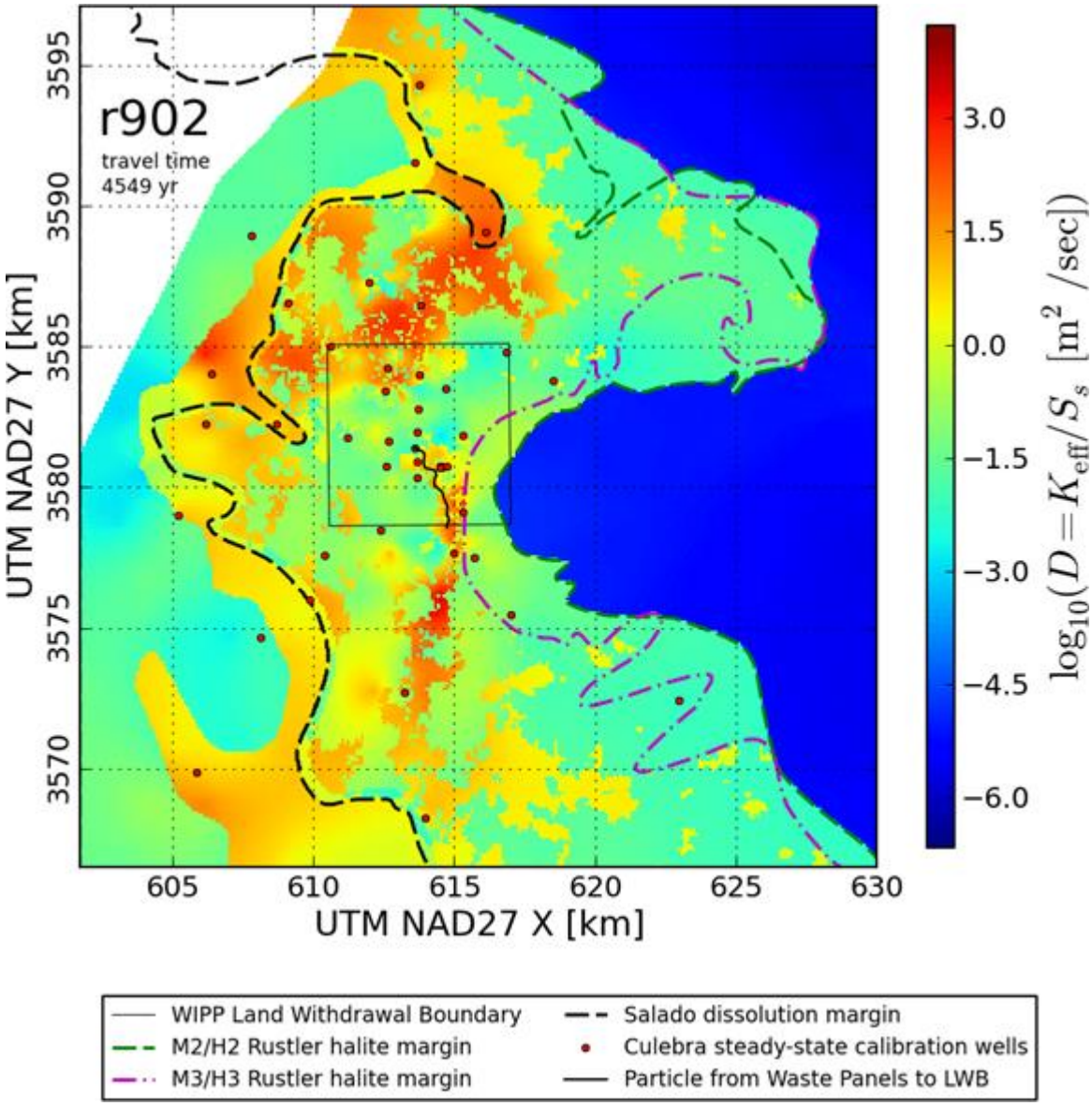
r902
travel time
4549 yr
UTM NAD27 Y [km]
3595
3590
3585
3580
3575
3570
605
610
615
620
625
630
UTM NAD27 X [km]
3.0
1.5
0.0
−1.5
−3.0
−4.5
−6.0
$\log_{10}(D = K_{\text{eff}}/S_s \ [\text{m}^2/\text{sec}])$
WIPP Land Withdrawal Boundary
M2/H2 Rustler halite margin
M3/H3 Rustler halite margin
Salado dissolution margin
Culebra steady-state calibration wells
Particle from Waste Panels to LWB

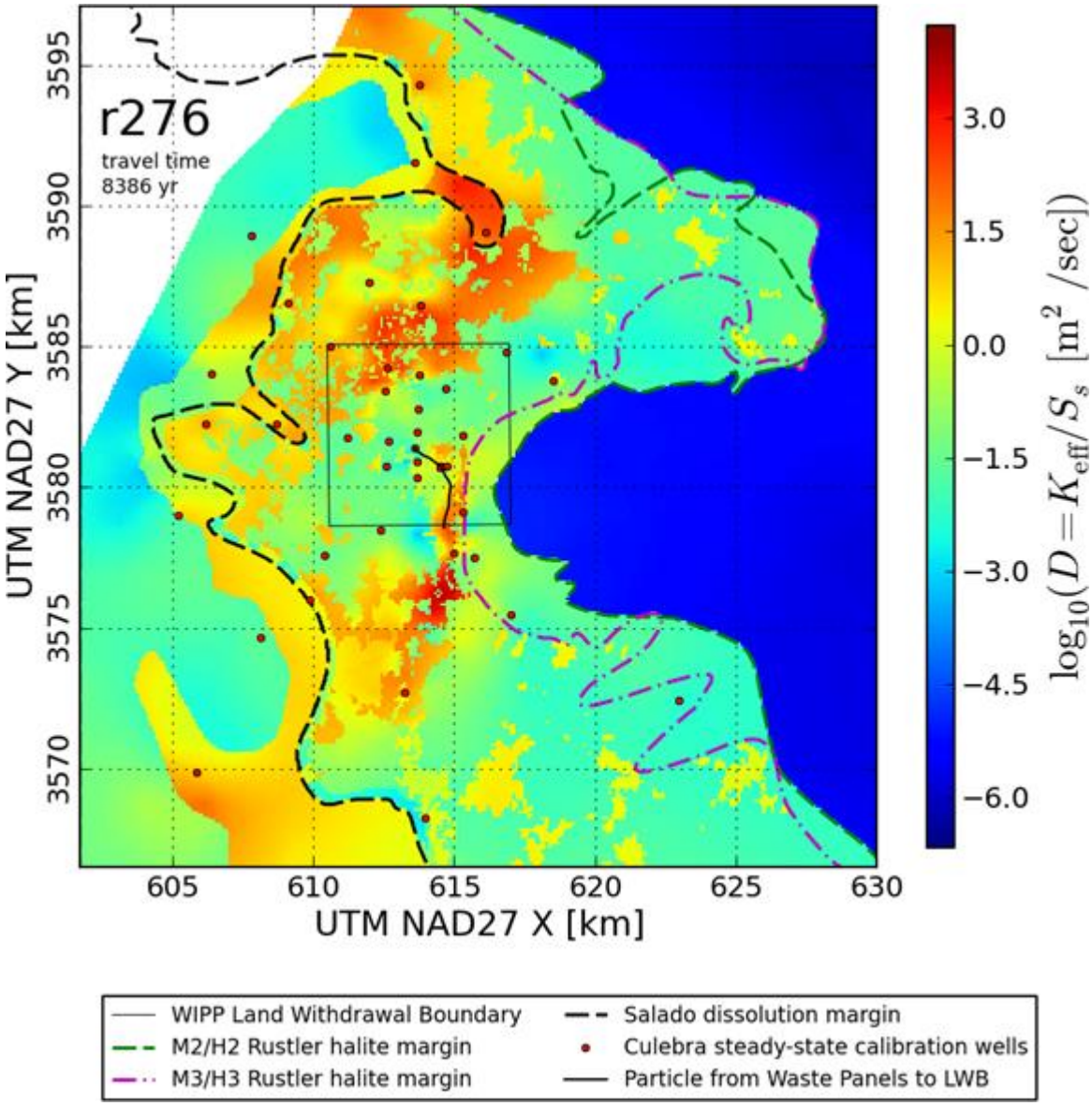
r276
travel time
8386 yr
UTM NAD27 Y [km]
3595
3590
3585
3580
3575
3570
605
610
615
620
625
630
UTM NAD27 X [km]
3.0
1.5
0.0
−1.5
−3.0
−4.5
−6.0
$\log_{10}(D = K_{\text{eff}}/S_s \ [\text{m}^2/\text{sec}])$
WIPP Land Withdrawal Boundary
M2/H2 Rustler halite margin
M3/H3 Rustler halite margin
Salado dissolution margin
Culebra steady-state calibration wells
Particle from Waste Panels to LWB

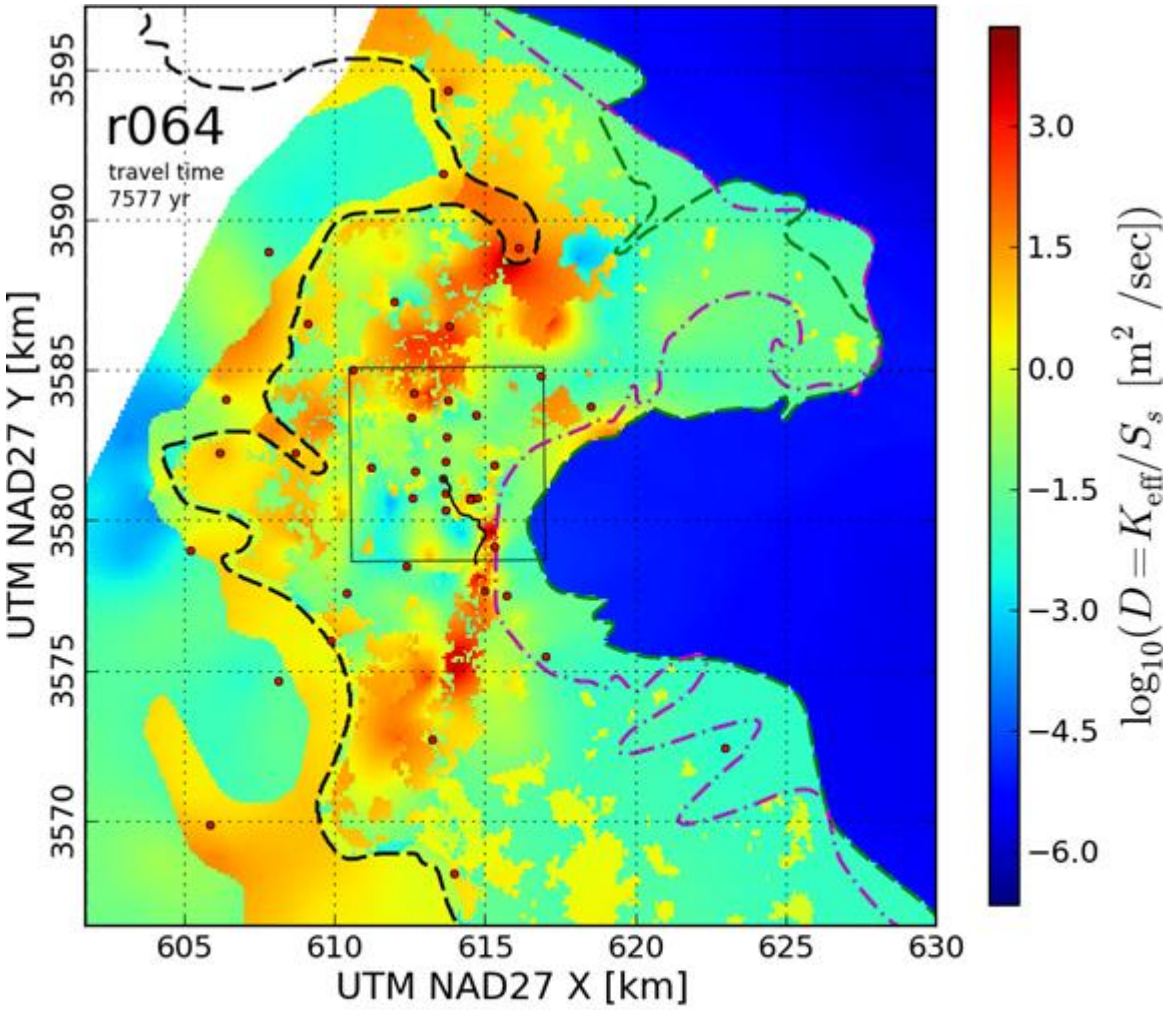
r064
travel time
7577 yr
UTM NAD27 Y [km]
3595
3590
3585
3580
3575
3570
605
610
615
620
625
630
UTM NAD27 X [km]
3.0
1.5
0.0
−1.5
−3.0
−4.5
−6.0
$\log_{10}(D = K_{\text{eff}}/S_s \ [\text{m}^2/\text{sec}])$
WIPP Land Withdrawal Boundary
M2/H2 Rustler halite margin
M3/H3 Rustler halite margin
Salado dissolution margin
Culebra steady-state calibration wells
Particle from Waste Panels to LWB

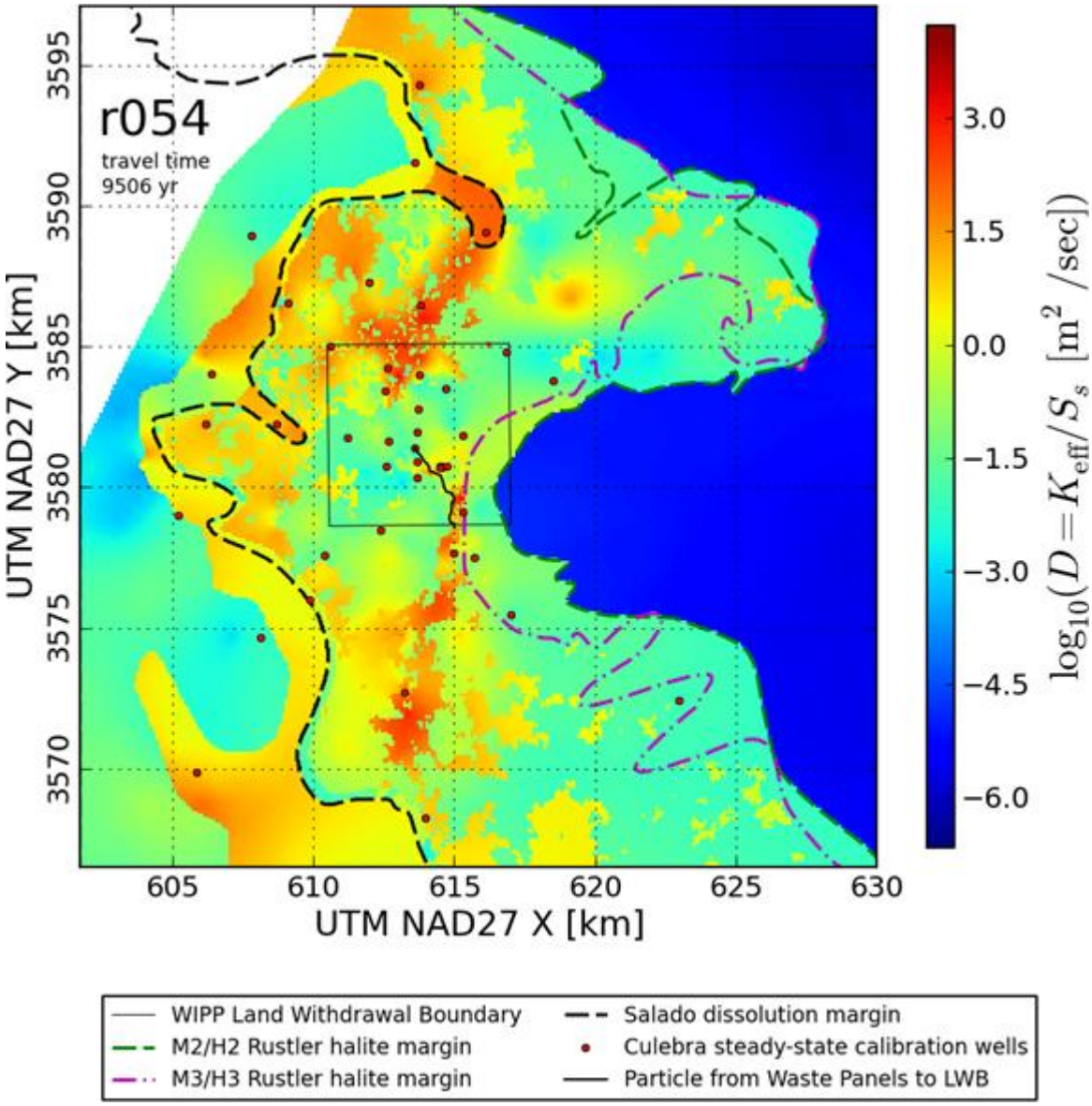
r054
travel time
9506 yr
UTM NAD27 Y [km]
3595
3590
3585
3580
3575
3570
605
610
615
620
625
630
UTM NAD27 X [km]
3.0
1.5
0.0
−1.5
−3.0
−4.5
−6.0
$\log_{10}(D = K_{\text{eff}}/S_s \ [\text{m}^2/\text{sec}])$
WIPP Land Withdrawal Boundary
M2/H2 Rustler halite margin
M3/H3 Rustler halite margin
Salado dissolution margin
Culebra steady-state calibration wells
Particle from Waste Panels to LWB

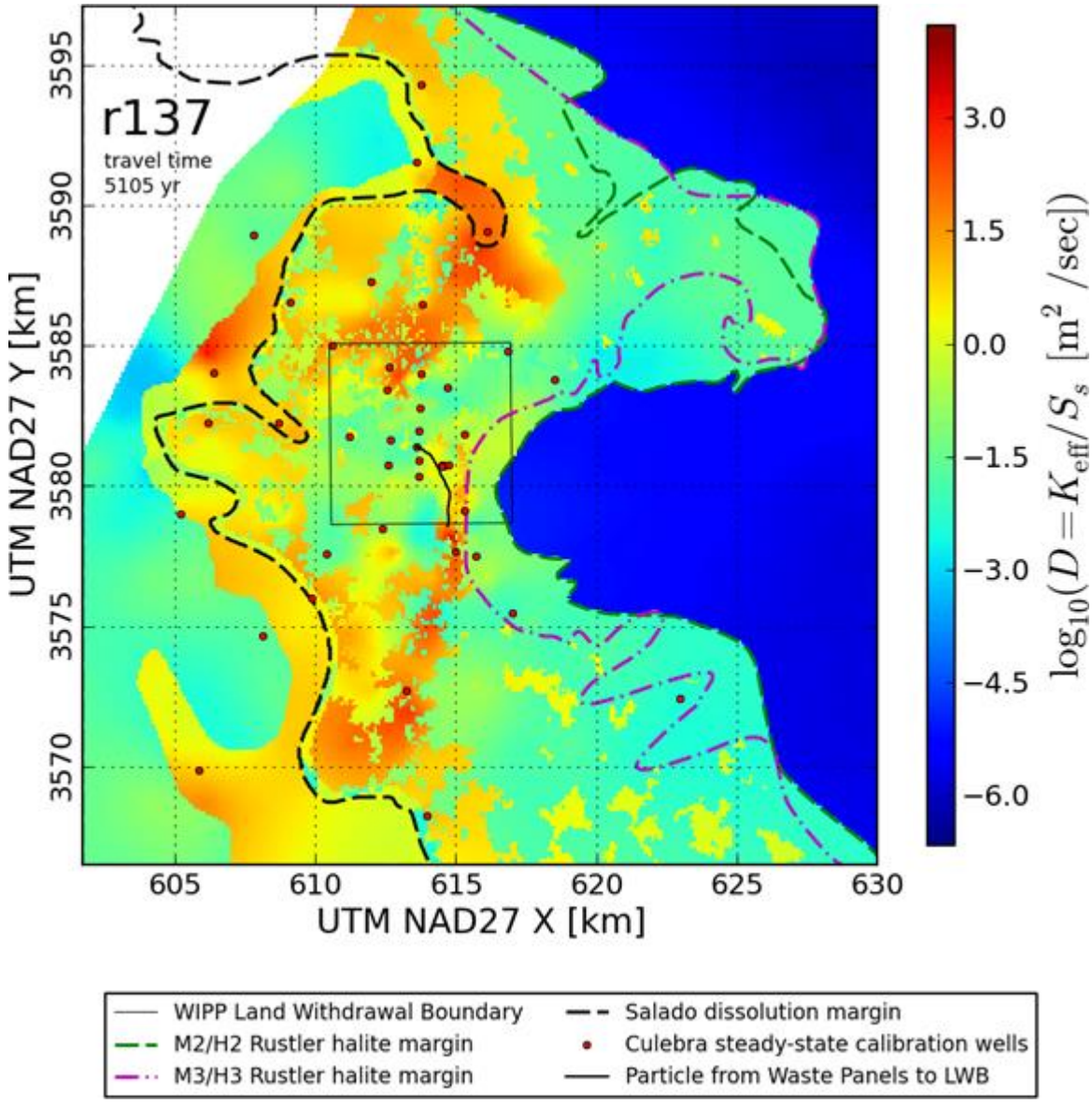
r137
travel time
5105 yr
UTM NAD27 Y [km]
3595
3590
3585
3580
3575
3570
605
610
615
620
625
630
UTM NAD27 X [km]
3.0
1.5
0.0
−1.5
−3.0
−4.5
−6.0
$\log_{10}(D = K_{\text{eff}}/S_s \ [\text{m}^2/\text{sec}])$
WIPP Land Withdrawal Boundary
M2/H2 Rustler halite margin
M3/H3 Rustler halite margin
Salado dissolution margin
Culebra steady-state calibration wells
Particle from Waste Panels to LWB

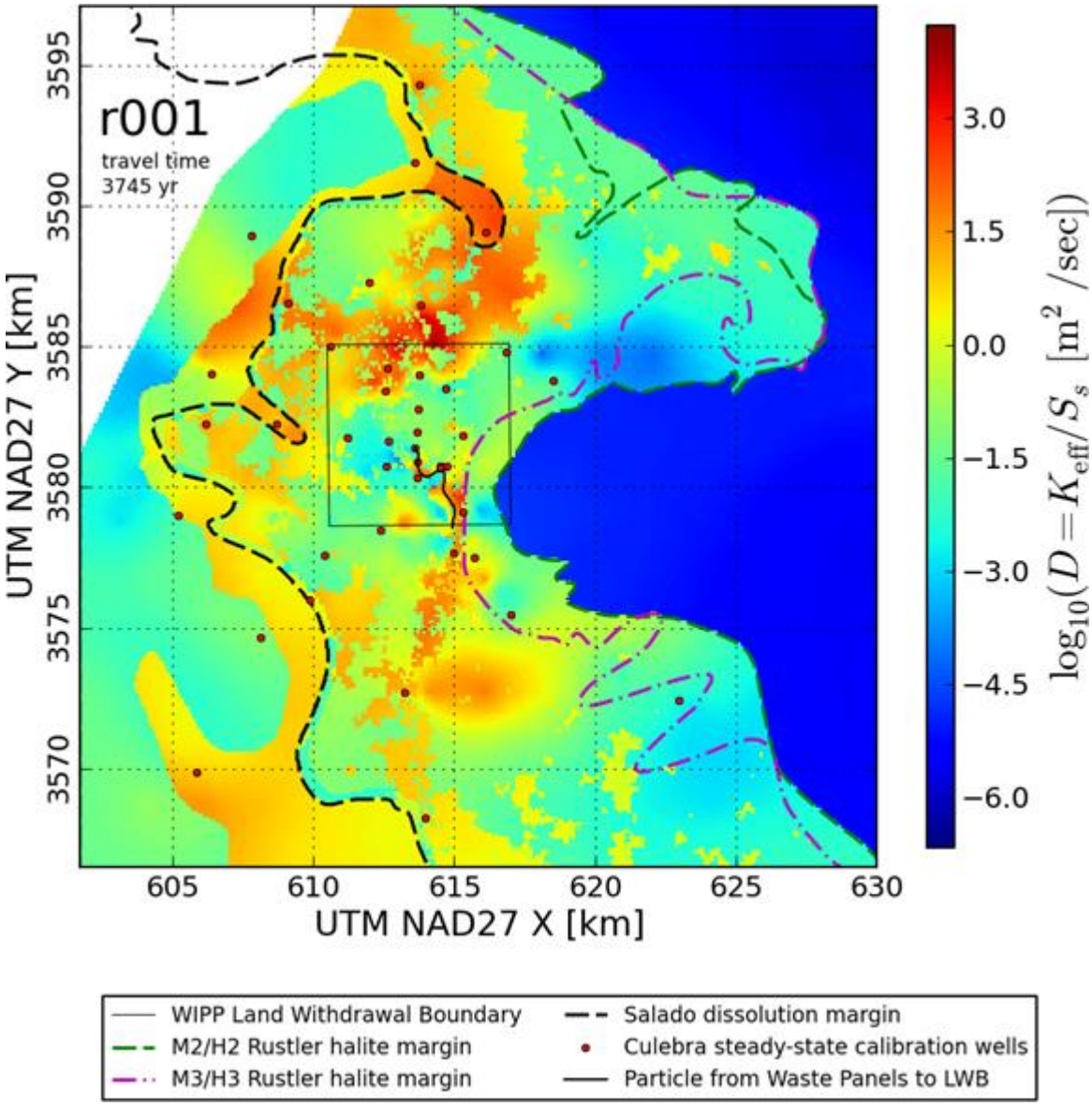
r001
travel time
3745 yr
UTM NAD27 Y [km]
3595
3590
3585
3580
3575
3570
605
610
615
620
625
630
UTM NAD27 X [km]
3.0
1.5
0.0
−1.5
−3.0
−4.5
−6.0
$\log_{10}(D = K_{\text{eff}}/S_s \ [\text{m}^2/\text{sec}])$
WIPP Land Withdrawal Boundary
M2/H2 Rustler halite margin
M3/H3 Rustler halite margin
Salado dissolution margin
Culebra steady-state calibration wells
Particle from Waste Panels to LWB

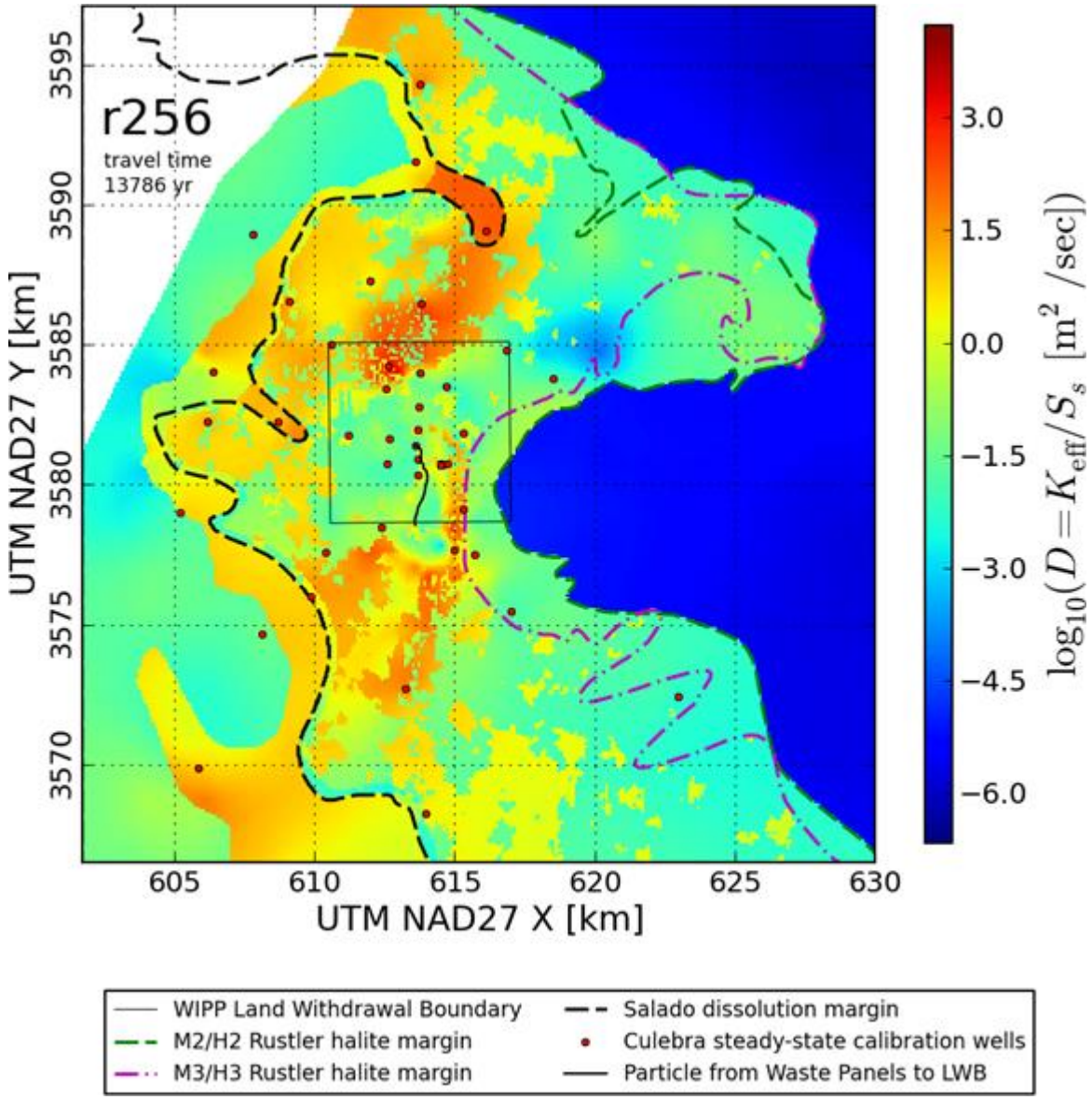
r256
travel time
13786 yr
UTM NAD27 Y [km]
3595
3590
3585
3580
3575
3570
605
610
615
620
625
630
UTM NAD27 X [km]
3.0
1.5
0.0
−1.5
−3.0
−4.5
−6.0
$\log_{10}(D = K_{\text{eff}}/S_s \ [\text{m}^2/\text{sec}])$
WIPP Land Withdrawal Boundary
M2/H2 Rustler halite margin
M3/H3 Rustler halite margin
Salado dissolution margin
Culebra steady-state calibration wells
Particle from Waste Panels to LWB

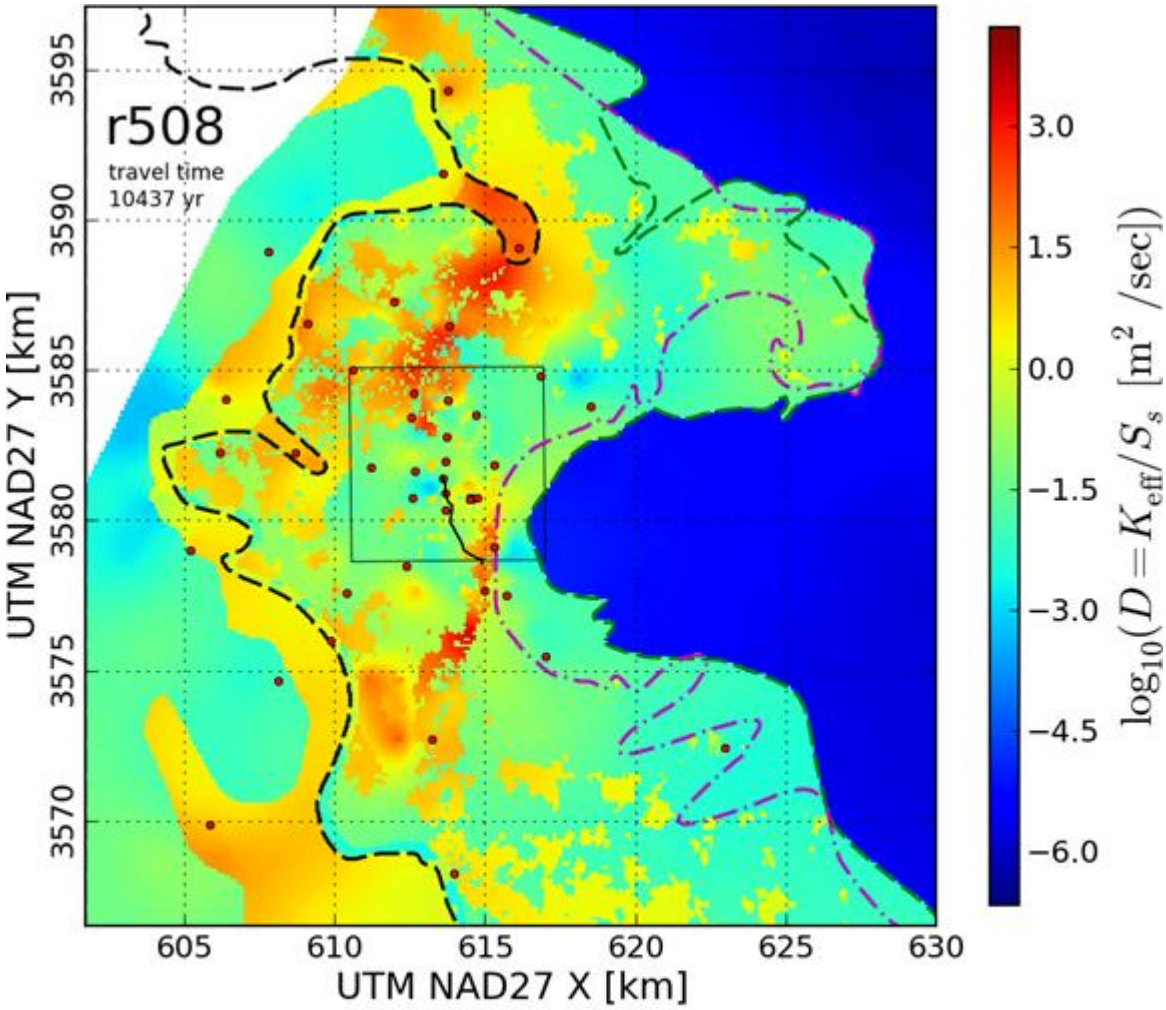
r508
travel time
10437 yr
UTM NAD27 Y [km]
3595
3590
3585
3580
3575
3570
605
610
615
620
625
630
UTM NAD27 X [km]
3.0
1.5
0.0
−1.5
−3.0
−4.5
−6.0
$\log_{10}(D = K_{\text{eff}}/S_s \ [\text{m}^2/\text{sec}])$
WIPP Land Withdrawal Boundary
M2/H2 Rustler halite margin
M3/H3 Rustler halite margin
Salado dissolution margin
Culebra steady-state calibration wells
Particle from Waste Panels to LWB

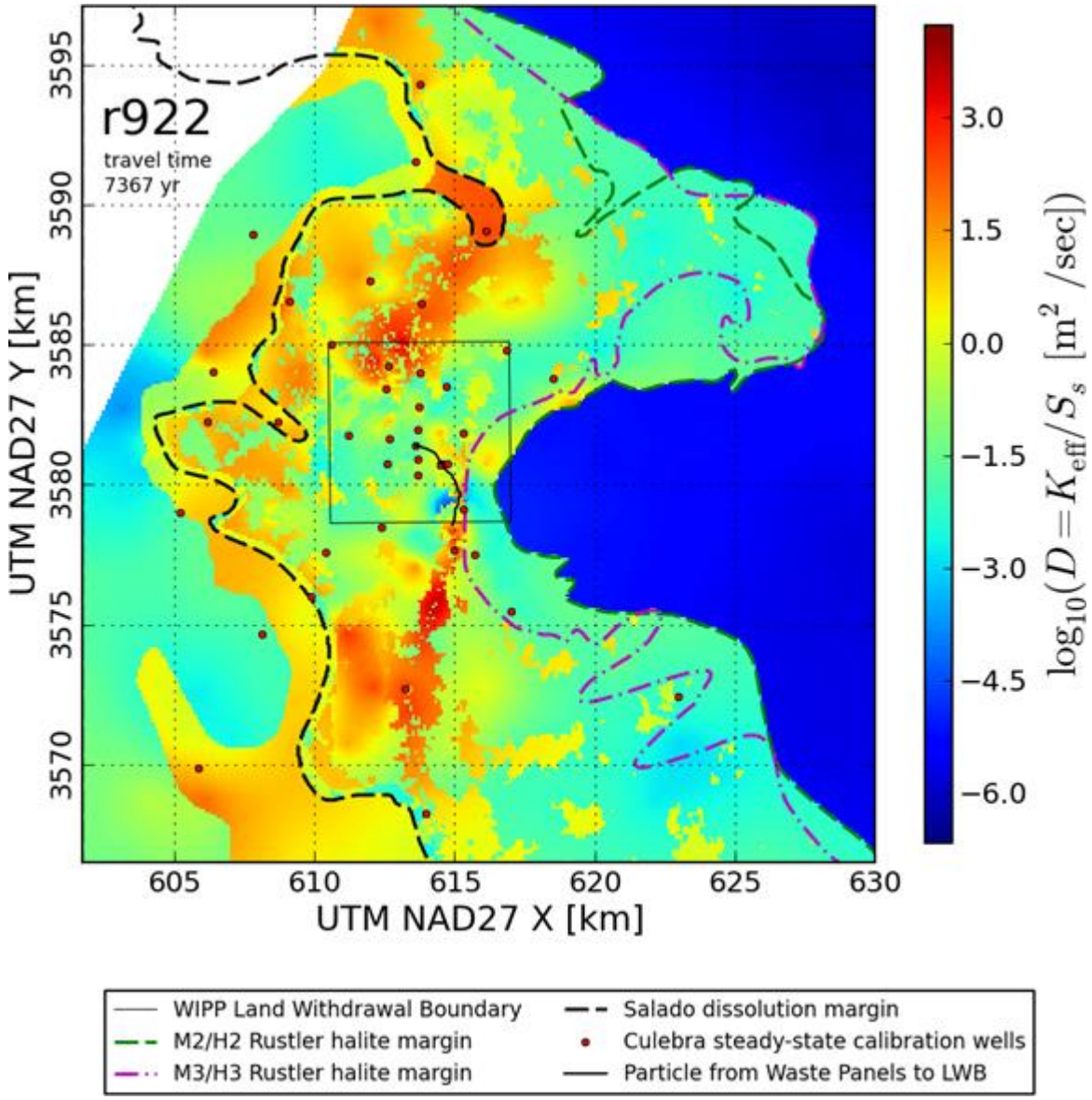
r922
travel time
7367 yr
UTM NAD27 Y [km]
3595
3590
3585
3580
3575
3570
605
610
615
620
625
630
UTM NAD27 X [km]
3.0
1.5
0.0
−1.5
−3.0
−4.5
−6.0
$\log_{10}(D = K_{\text{eff}}/S_s \ [\text{m}^2/\text{sec}])$
WIPP Land Withdrawal Boundary
M2/H2 Rustler halite margin
M3/H3 Rustler halite margin
Salado dissolution margin
Culebra steady-state calibration wells
Particle from Waste Panels to LWB

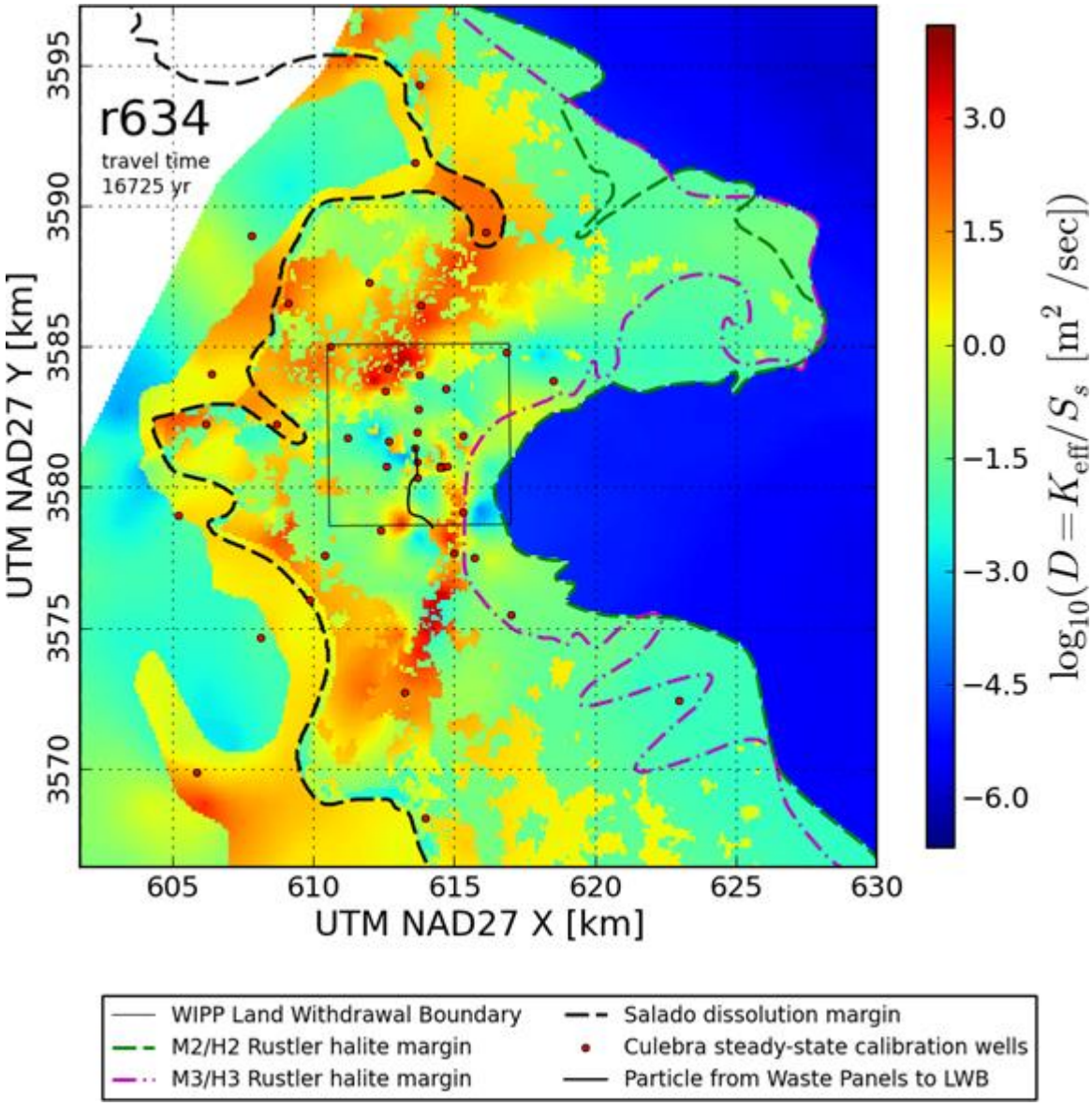
r634
travel time
16725 yr
UTM NAD27 Y [km]
3595
3590
3585
3580
3575
3570
605
610
615
620
625
630
UTM NAD27 X [km]
3.0
1.5
0.0
−1.5
−3.0
−4.5
−6.0
$\log_{10}(D = K_{\text{eff}}/S_s \ [\text{m}^2/\text{sec}])$
WIPP Land Withdrawal Boundary
M2/H2 Rustler halite margin
M3/H3 Rustler halite margin
Salado dissolution margin
Culebra steady-state calibration wells
Particle from Waste Panels to LWB

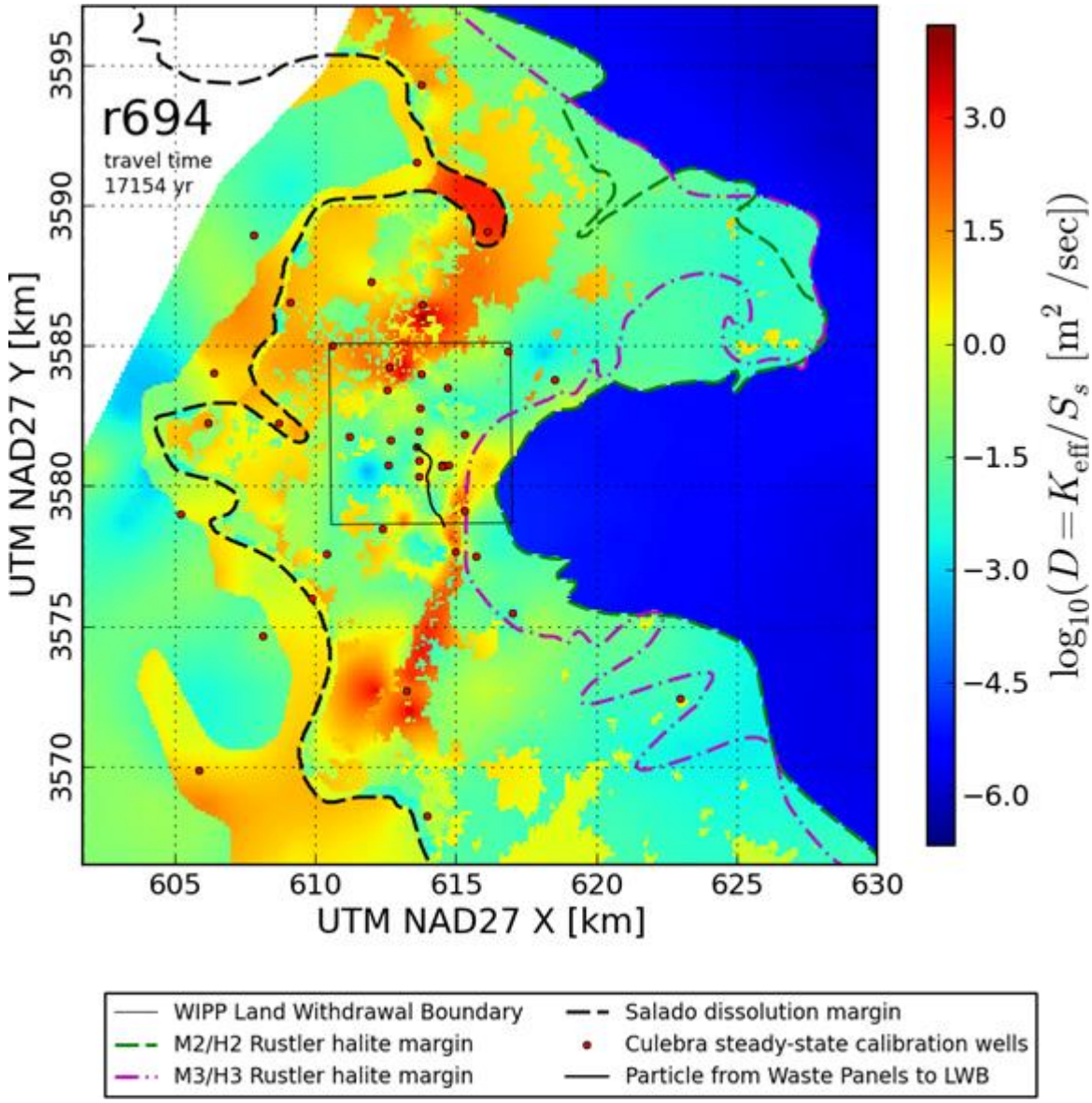
r694
travel time
17154 yr
UTM NAD27 Y [km]
3595
3590
3585
3580
3575
3570
605
610
615
620
625
630
UTM NAD27 X [km]
3.0
1.5
0.0
−1.5
−3.0
−4.5
−6.0
$\log_{10}(D = K_{\text{eff}}/S_s \ [\text{m}^2/\text{sec}])$
WIPP Land Withdrawal Boundary
M2/H2 Rustler halite margin
M3/H3 Rustler halite margin
Salado dissolution margin
Culebra steady-state calibration wells
Particle from Waste Panels to LWB

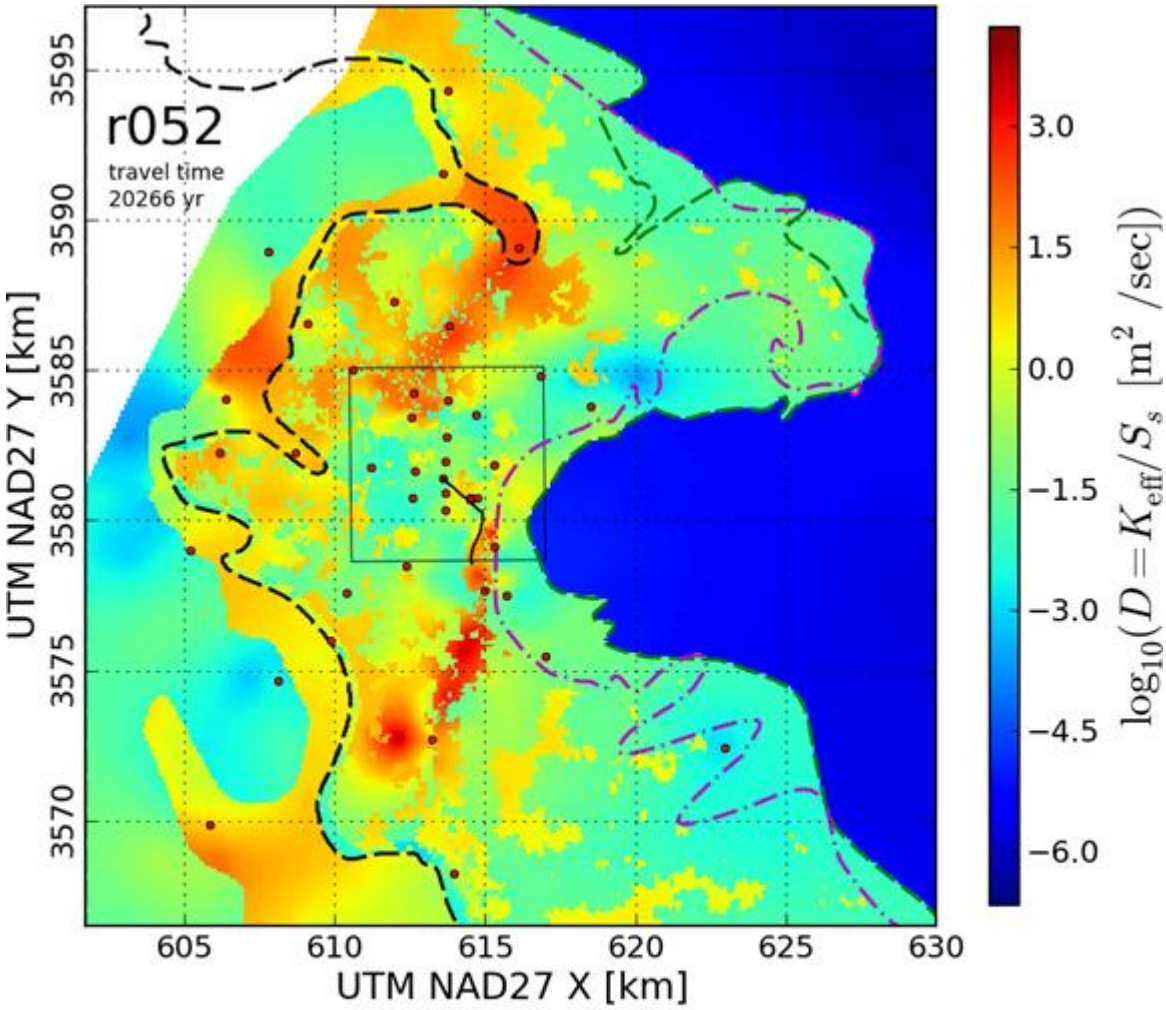
r052
travel time
20266 yr
UTM NAD27 Y [km]
3595
3590
3585
3580
3575
3570
605
610
615
620
625
630
UTM NAD27 X [km]
3.0
1.5
0.0
−1.5
−3.0
−4.5
−6.0
$\log_{10}(D = K_{\text{eff}}/S_s \ [\text{m}^2/\text{sec}])$
WIPP Land Withdrawal Boundary
M2/H2 Rustler halite margin
M3/H3 Rustler halite margin
Salado dissolution margin
Culebra steady-state calibration wells
Particle from Waste Panels to LWB

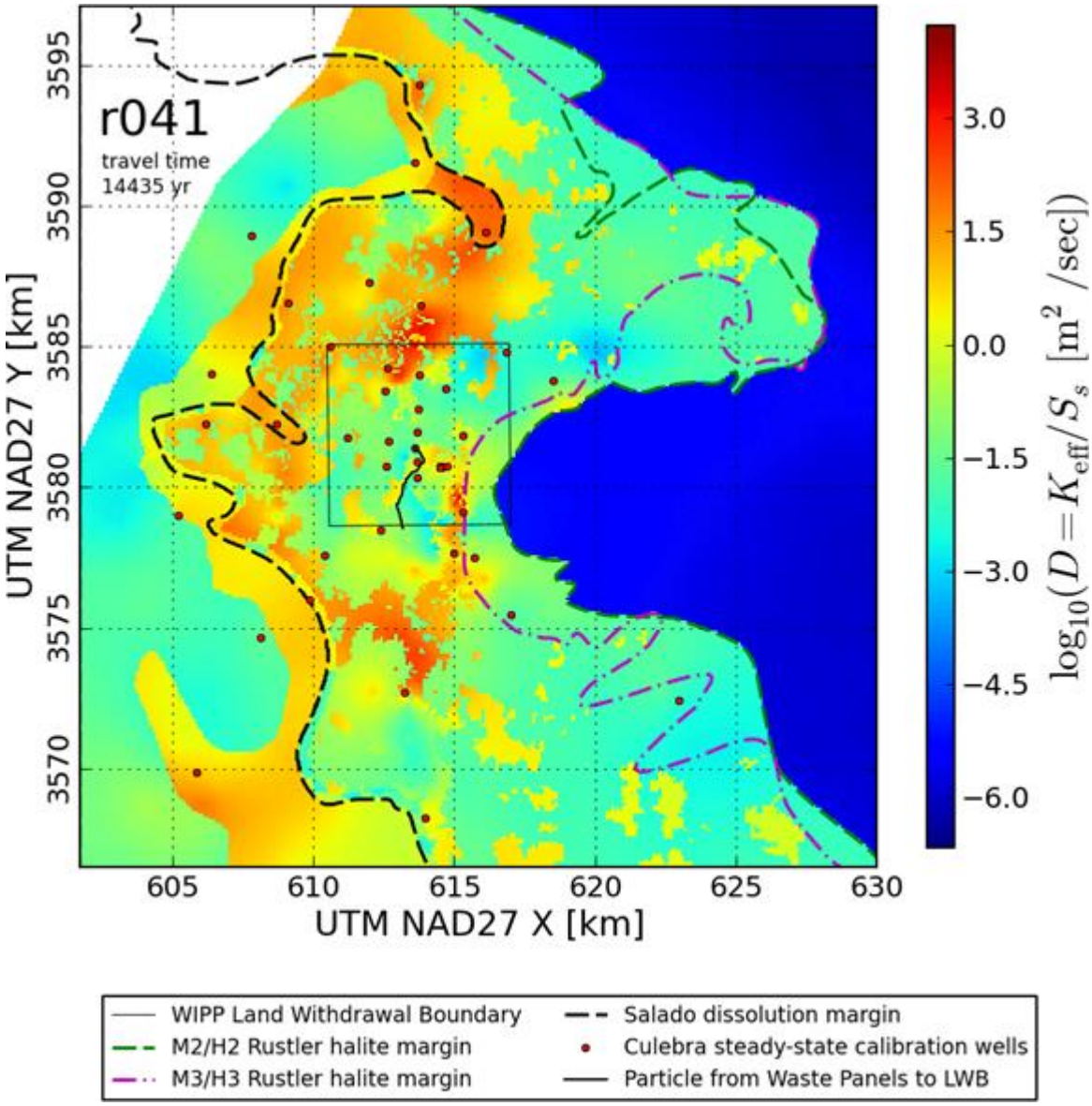
r041
travel time
14435 yr
UTM NAD27 Y [km]
3595
3590
3585
3580
3575
3570
605
610
615
620
625
630
UTM NAD27 X [km]
3.0
1.5
0.0
−1.5
−3.0
−4.5
−6.0
$\log_{10}(D = K_{\text{eff}}/S_s \ [\text{m}^2/\text{sec}])$
WIPP Land Withdrawal Boundary
M2/H2 Rustler halite margin
M3/H3 Rustler halite margin
Salado dissolution margin
Culebra steady-state calibration wells
Particle from Waste Panels to LWB

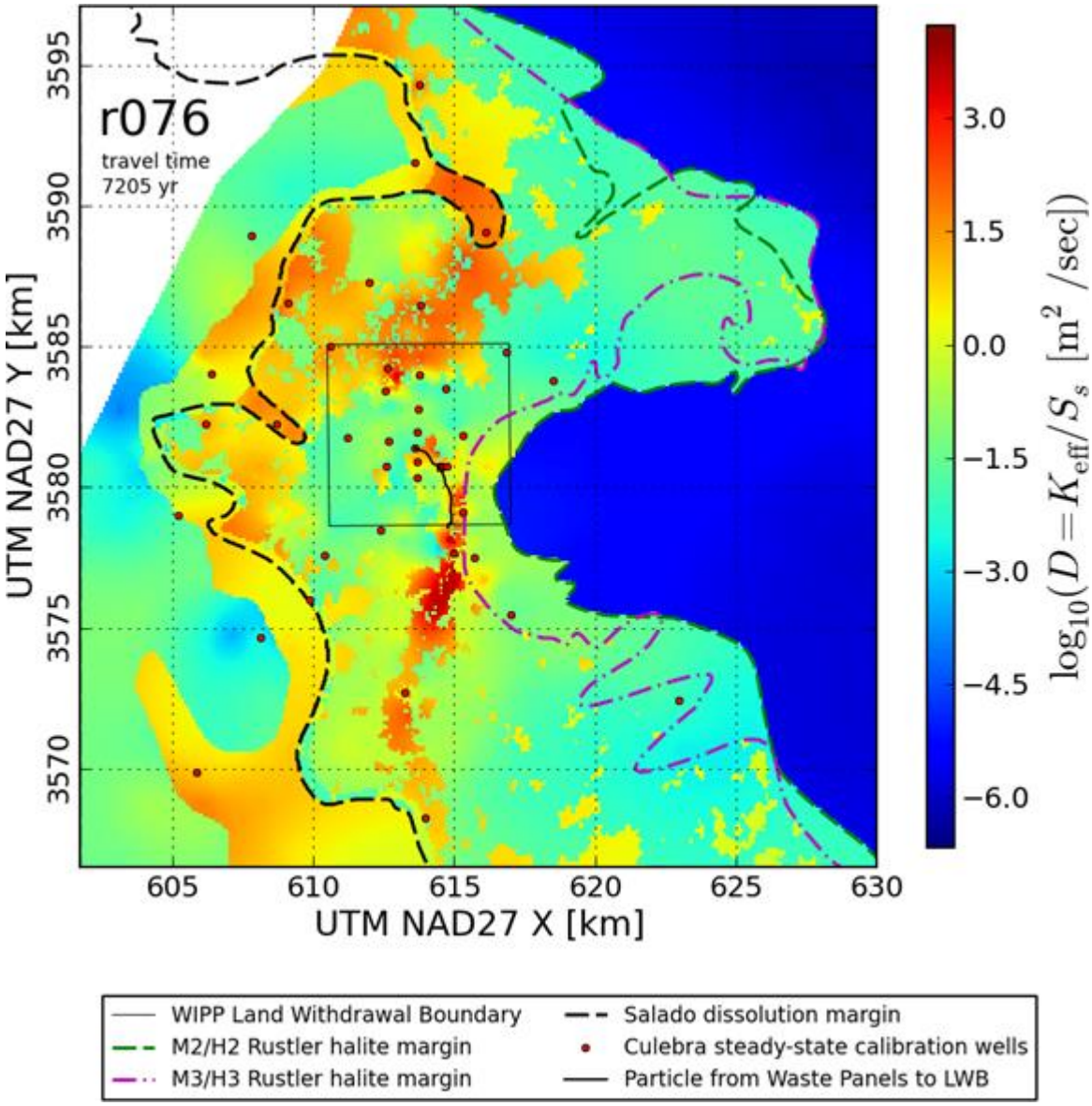
r076
travel time
7205 yr
UTM NAD27 Y [km]
3595
3590
3585
3580
3575
3570
605
610
615
620
625
630
UTM NAD27 X [km]
3.0
1.5
0.0
−1.5
−3.0
−4.5
−6.0
$\log_{10}(D = K_{\text{eff}}/S_s \ [\text{m}^2/\text{sec}])$
WIPP Land Withdrawal Boundary
M2/H2 Rustler halite margin
M3/H3 Rustler halite margin
Salado dissolution margin
Culebra steady-state calibration wells
Particle from Waste Panels to LWB

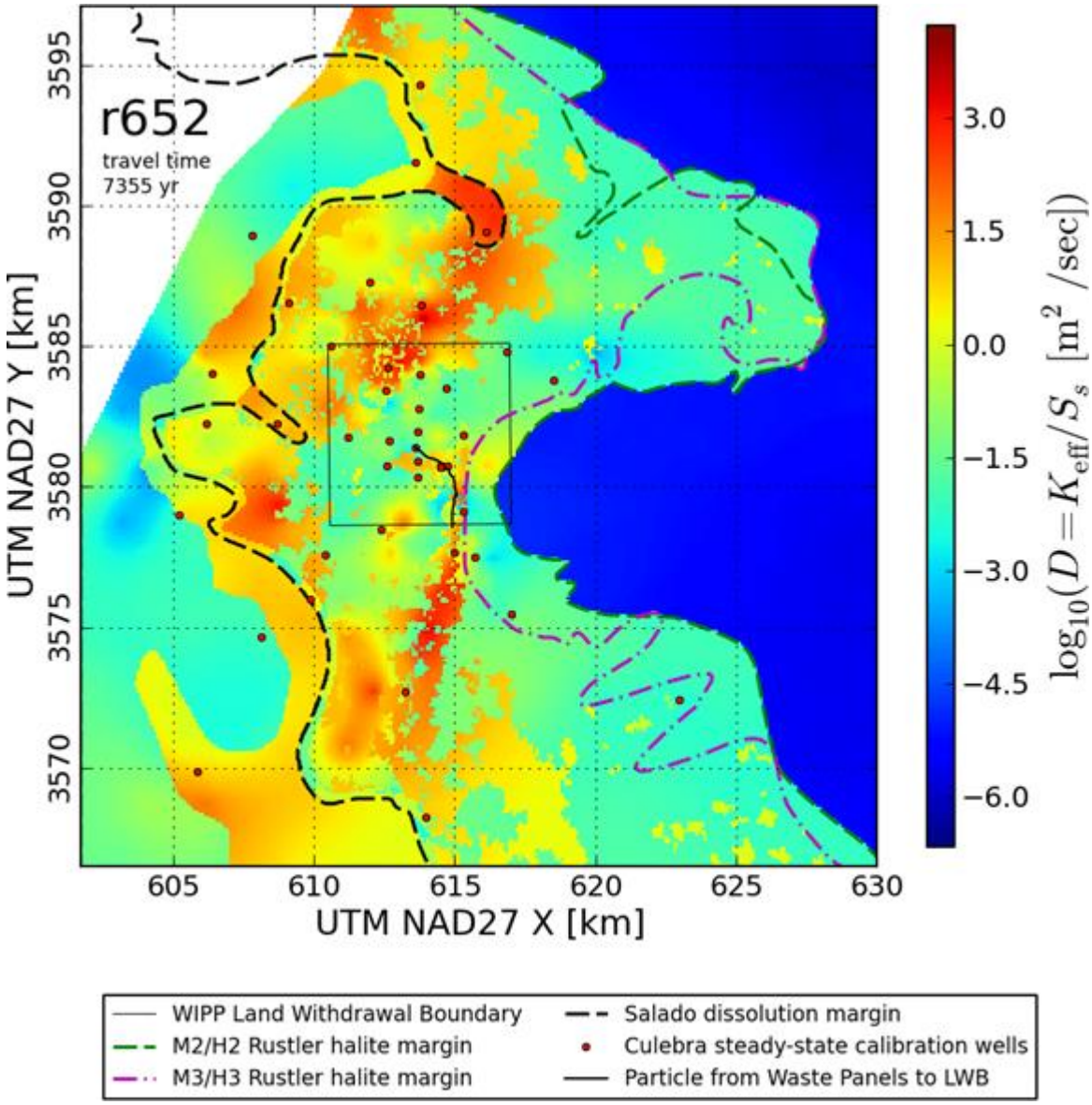
r652
travel time
7355 yr
UTM NAD27 Y [km]
3595
3590
3585
3580
3575
3570
605
610
615
620
625
630
UTM NAD27 X [km]
3.0
1.5
0.0
−1.5
−3.0
−4.5
−6.0
$\log_{10}(D = K_{\text{eff}}/S_s \ [\text{m}^2/\text{sec}])$
WIPP Land Withdrawal Boundary
M2/H2 Rustler halite margin
M3/H3 Rustler halite margin
Salado dissolution margin
Culebra steady-state calibration wells
Particle from Waste Panels to LWB

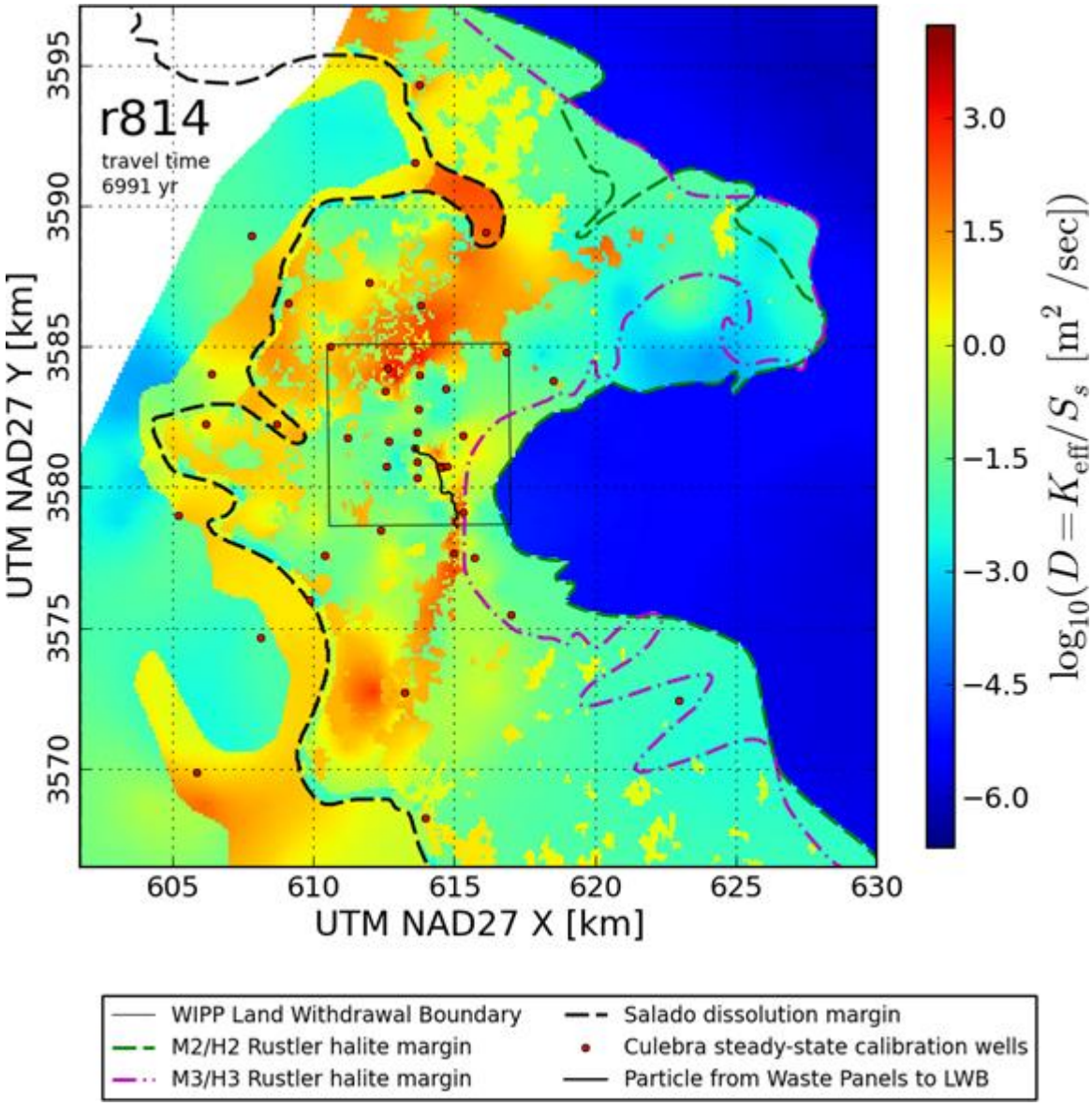
r814
travel time
6991 yr
UTM NAD27 Y [km]
3595
3590
3585
3580
3575
3570
605
610
615
620
625
630
UTM NAD27 X [km]
3.0
1.5
0.0
−1.5
−3.0
−4.5
−6.0
$\log_{10}(D = K_{\text{eff}}/S_s \ [\text{m}^2/\text{sec}])$
WIPP Land Withdrawal Boundary
M2/H2 Rustler halite margin
M3/H3 Rustler halite margin
Salado dissolution margin
Culebra steady-state calibration wells
Particle from Waste Panels to LWB

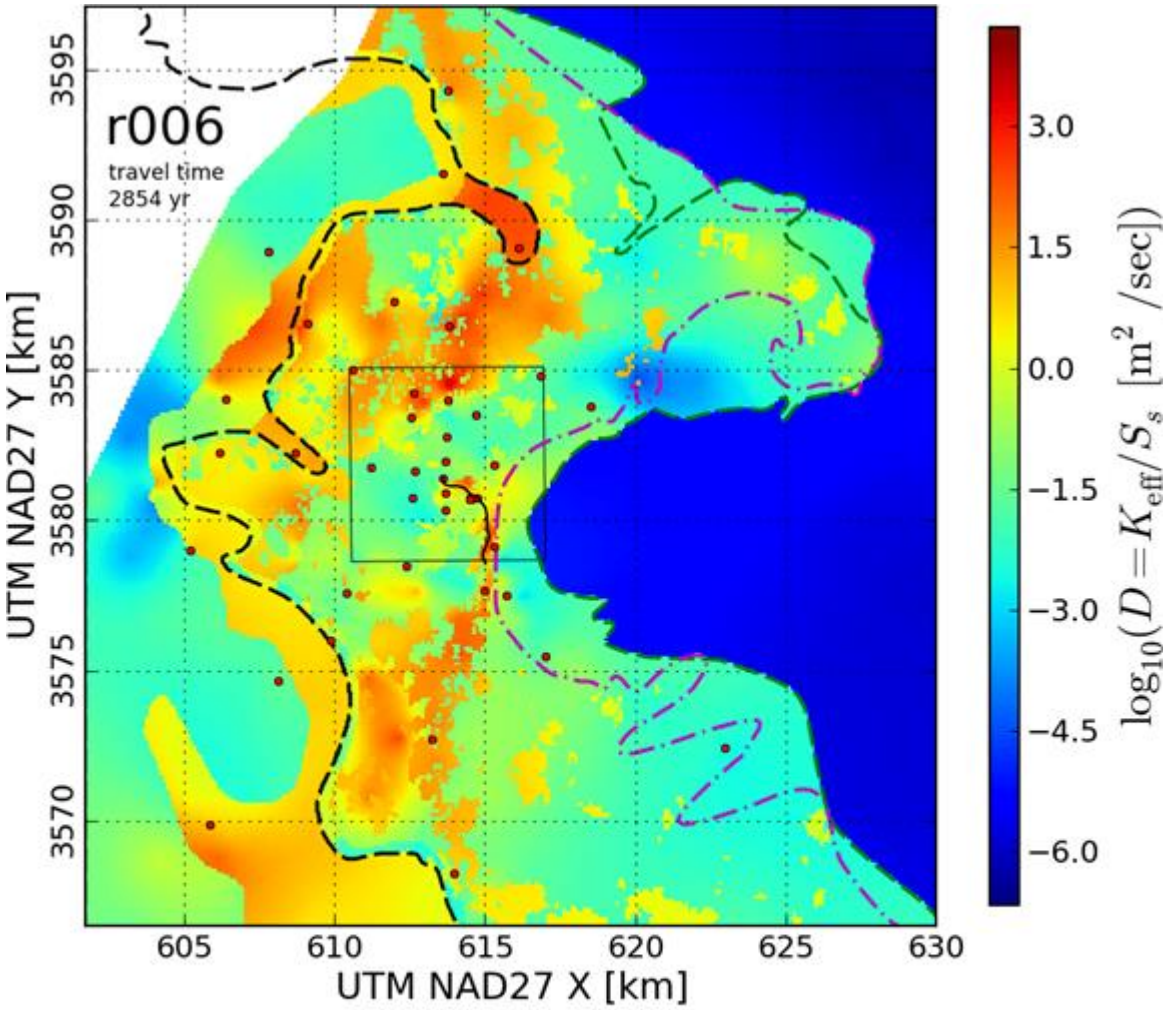
r006
travel time
2854 yr
UTM NAD27 Y [km]
3595
3590
3585
3580
3575
3570
605
610
615
620
625
630
UTM NAD27 X [km]
3.0
1.5
0.0
−1.5
−3.0
−4.5
−6.0
$\log_{10}(D = K_{\text{eff}}/S_s \ [\text{m}^2/\text{sec}])$
WIPP Land Withdrawal Boundary
M2/H2 Rustler halite margin
M3/H3 Rustler halite margin
Salado dissolution margin
Culebra steady-state calibration wells
Particle from Waste Panels to LWB

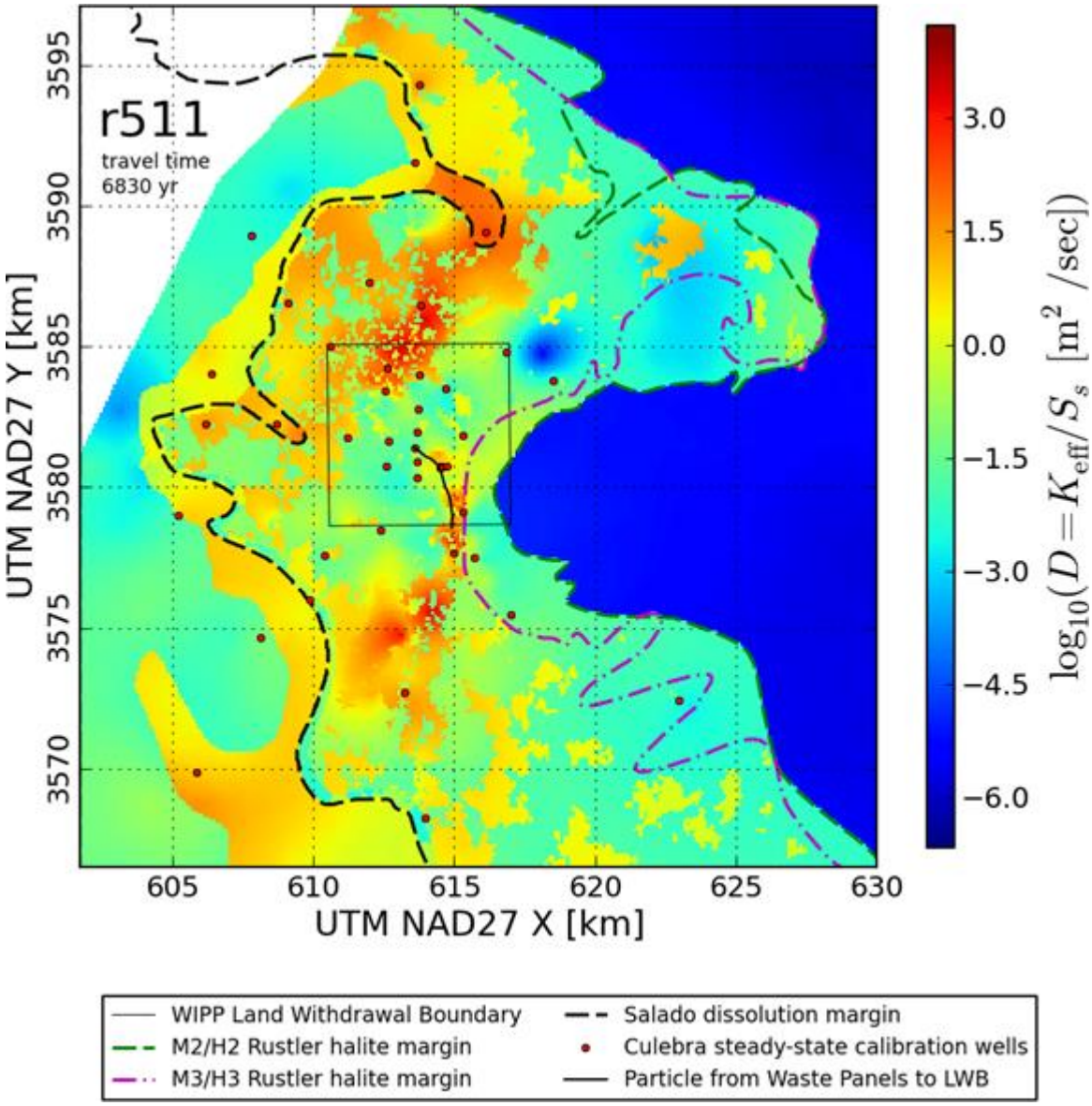
r511
travel time
6830 yr
UTM NAD27 Y [km]
3595
3590
3585
3580
3575
3570
605
610
615
620
625
630
UTM NAD27 X [km]
3.0
1.5
0.0
−1.5
−3.0
−4.5
−6.0
$\log_{10}(D = K_{\text{eff}}/S_s \ [\text{m}^2/\text{sec}])$
WIPP Land Withdrawal Boundary
M2/H2 Rustler halite margin
M3/H3 Rustler halite margin
Salado dissolution margin
Culebra steady-state calibration wells
Particle from Waste Panels to LWB

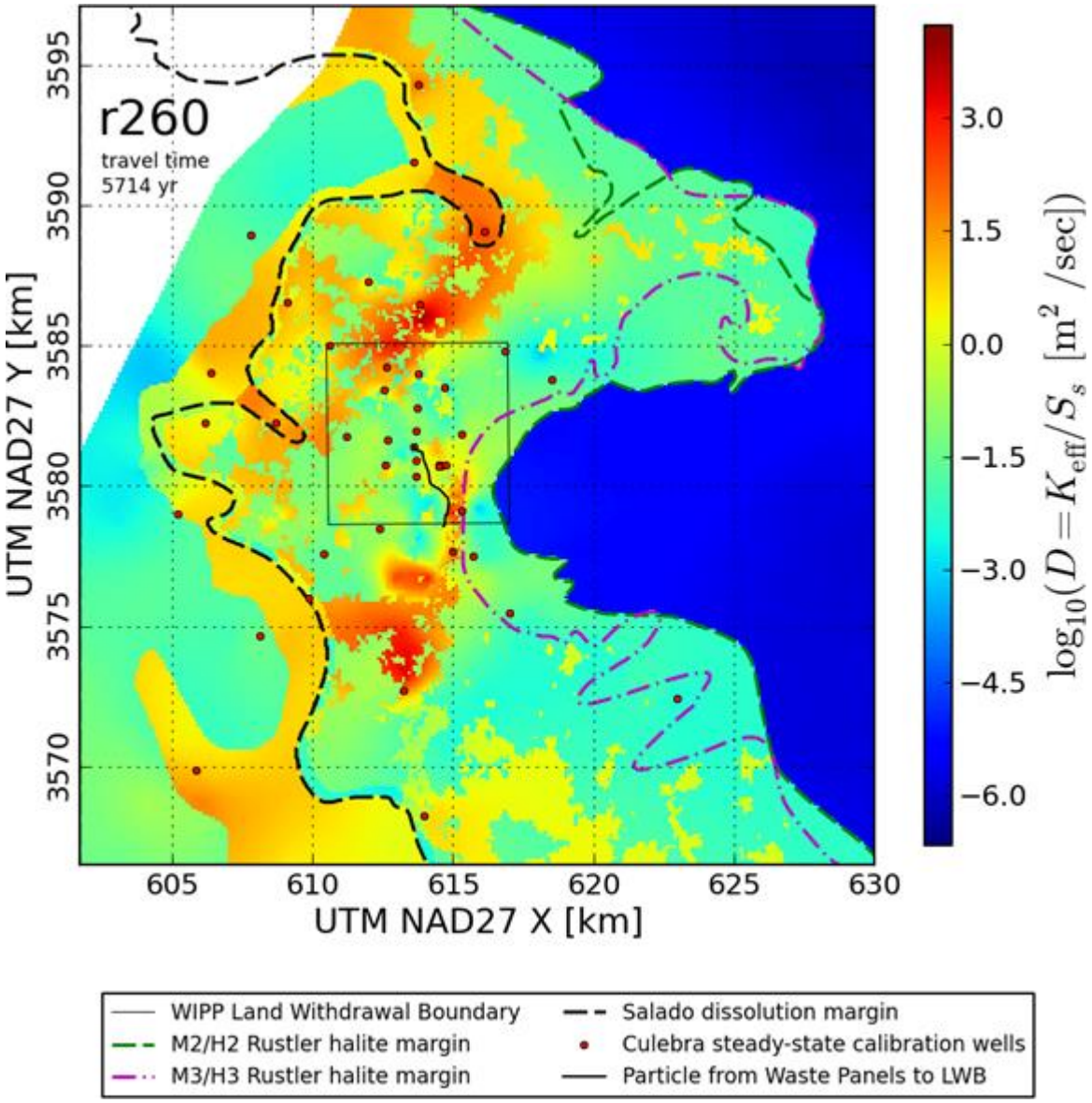
r260
travel time
5714 yr
UTM NAD27 Y [km]
3595
3590
3585
3580
3575
3570
605
610
615
620
625
630
UTM NAD27 X [km]
3.0
1.5
0.0
−1.5
−3.0
−4.5
−6.0
$\log_{10}(D = K_{\text{eff}}/S_s \ [\text{m}^2/\text{sec}])$
WIPP Land Withdrawal Boundary
M2/H2 Rustler halite margin
M3/H3 Rustler halite margin
Salado dissolution margin
Culebra steady-state calibration wells
Particle from Waste Panels to LWB

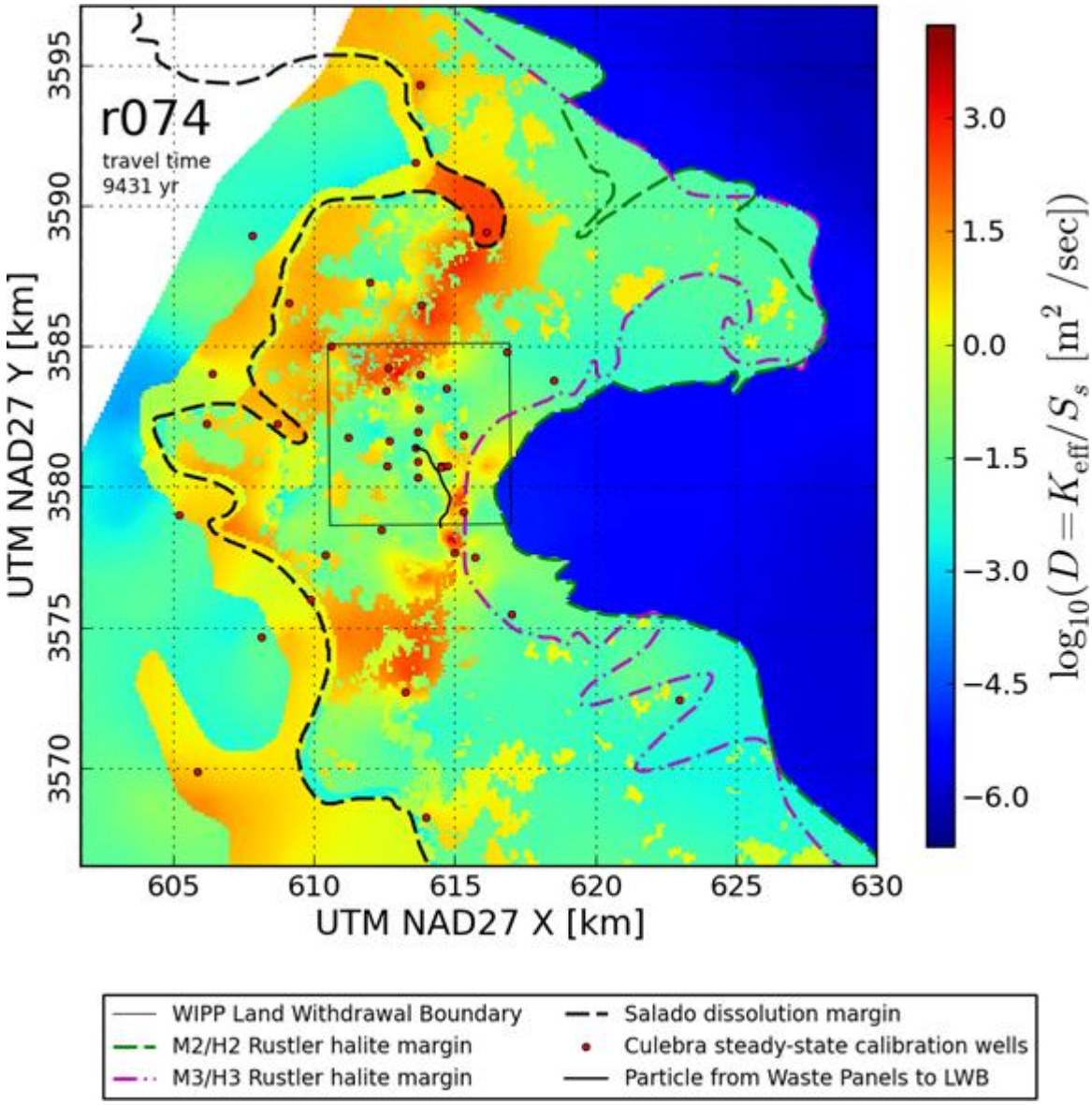
r074
travel time
9431 yr
UTM NAD27 Y [km]
3595
3590
3585
3580
3575
3570
605
610
615
620
625
630
UTM NAD27 X [km]
3.0
1.5
0.0
−1.5
−3.0
−4.5
−6.0
$\log_{10}(D = K_{\text{eff}}/S_s \ [\text{m}^2/\text{sec}])$
WIPP Land Withdrawal Boundary
M2/H2 Rustler halite margin
M3/H3 Rustler halite margin
Salado dissolution margin
Culebra steady-state calibration wells
Particle from Waste Panels to LWB

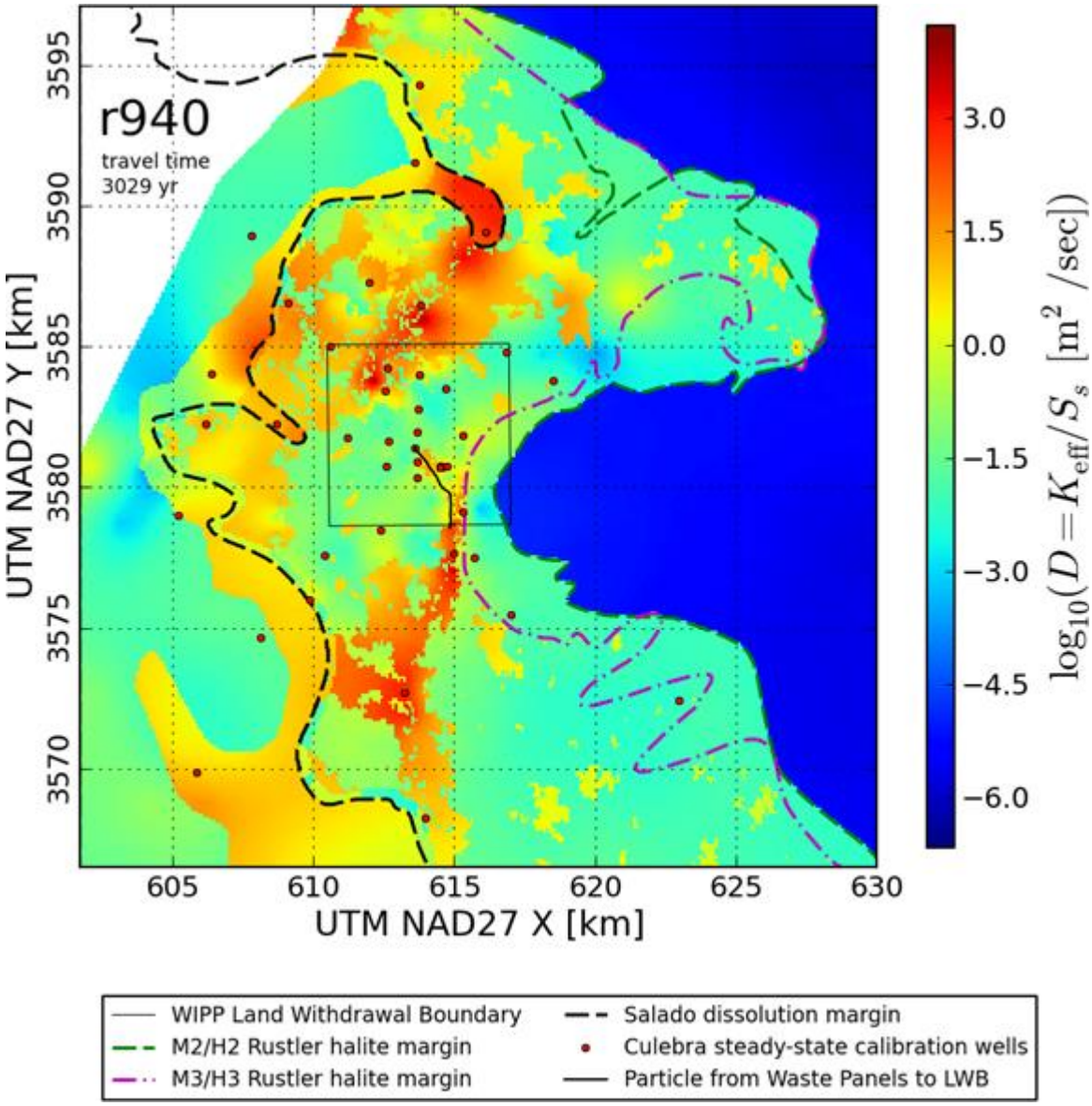
r940
travel time
3029 yr
UTM NAD27 Y [km]
3595
3590
3585
3580
3575
3570
605
610
615
620
625
630
UTM NAD27 X [km]
3.0
1.5
0.0
−1.5
−3.0
−4.5
−6.0
$\log_{10}(D = K_{\text{eff}}/S_s \ [\text{m}^2/\text{sec}])$
WIPP Land Withdrawal Boundary
M2/H2 Rustler halite margin
M3/H3 Rustler halite margin
Salado dissolution margin
Culebra steady-state calibration wells
Particle from Waste Panels to LWB

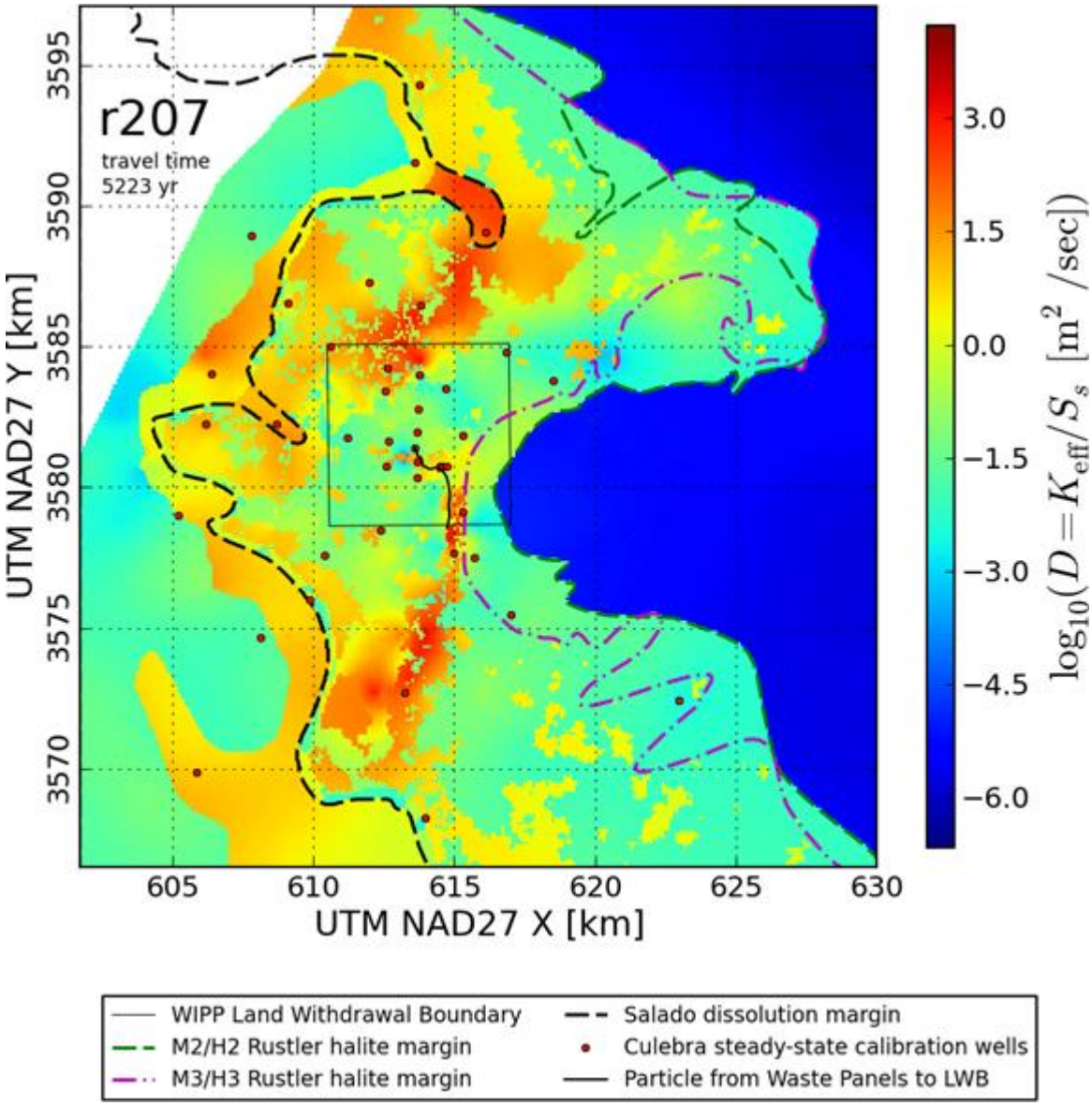
r207
travel time
5223 yr
UTM NAD27 Y [km]
3595
3590
3585
3580
3575
3570
605
610
615
620
625
630
UTM NAD27 X [km]
3.0
1.5
0.0
−1.5
−3.0
−4.5
−6.0
$\log_{10}(D = K_{\text{eff}}/S_s \ [\text{m}^2/\text{sec}])$
WIPP Land Withdrawal Boundary
M2/H2 Rustler halite margin
M3/H3 Rustler halite margin
Salado dissolution margin
Culebra steady-state calibration wells
Particle from Waste Panels to LWB

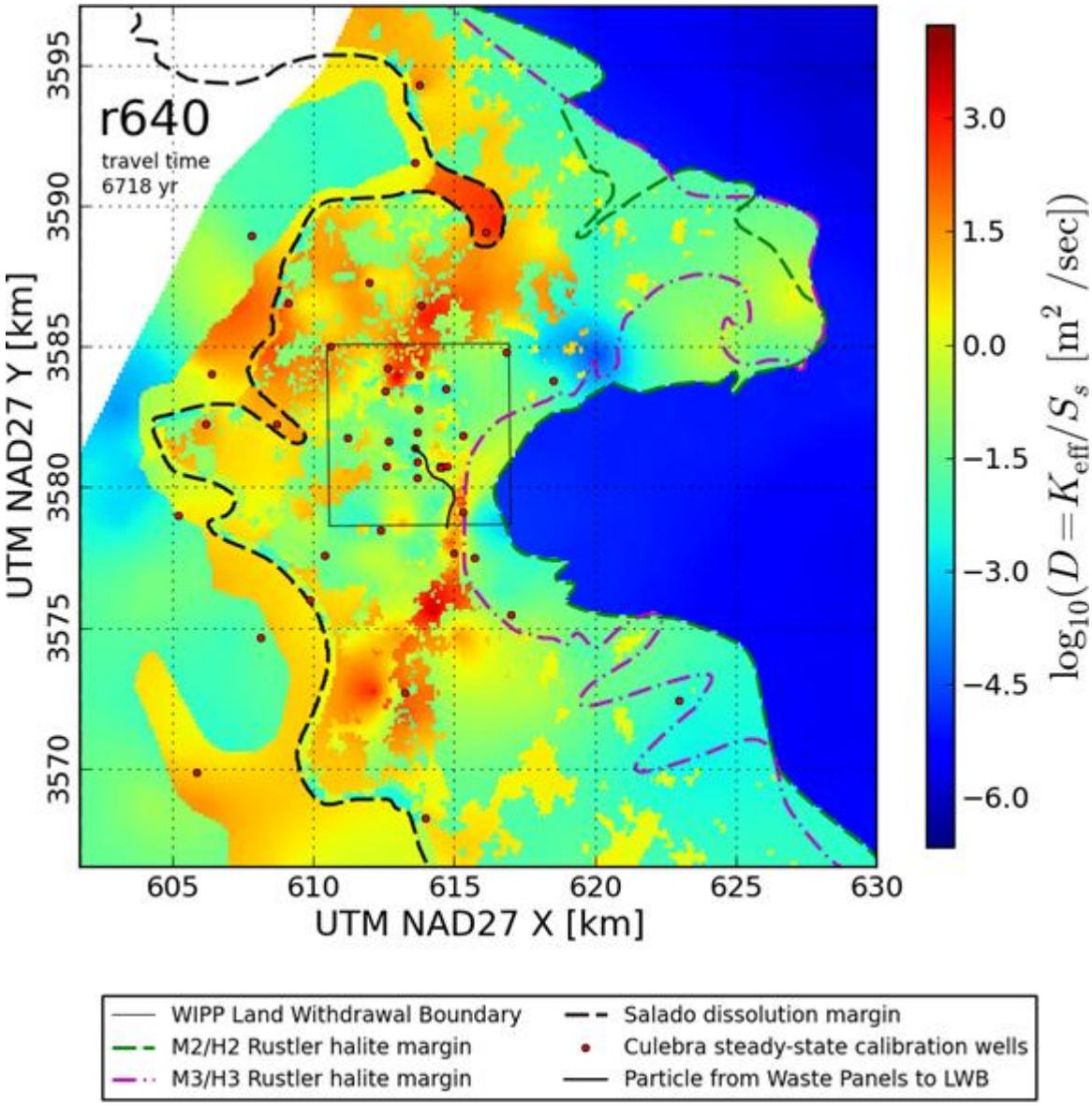
r640
travel time
6718 yr
UTM NAD27 Y [km]
3595
3590
3585
3580
3575
3570
605
610
615
620
625
630
UTM NAD27 X [km]
3.0
1.5
0.0
−1.5
−3.0
−4.5
−6.0
$\log_{10}(D = K_{\text{eff}}/S_s \ [\text{m}^2/\text{sec}])$
WIPP Land Withdrawal Boundary
M2/H2 Rustler halite margin
M3/H3 Rustler halite margin
Salado dissolution margin
Culebra steady-state calibration wells
Particle from Waste Panels to LWB

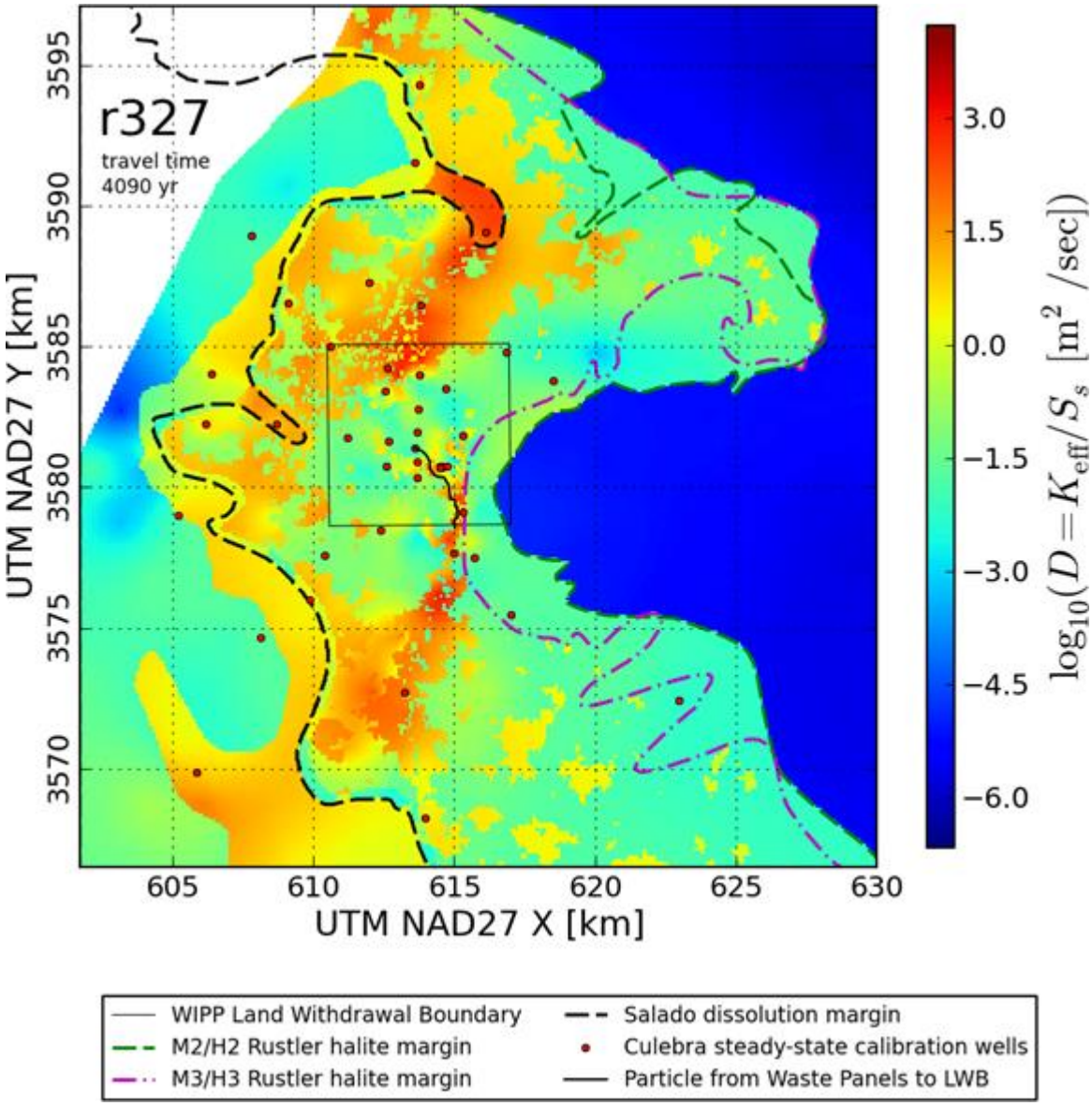
r327
travel time
4090 yr
UTM NAD27 Y [km]
3595
3590
3585
3580
3575
3570
605
610
615
620
625
630
UTM NAD27 X [km]
3.0
1.5
0.0
−1.5
−3.0
−4.5
−6.0
$\log_{10}(D = K_{\text{eff}}/S_s \ [\text{m}^2/\text{sec}])$
WIPP Land Withdrawal Boundary
M2/H2 Rustler halite margin
M3/H3 Rustler halite margin
Salado dissolution margin
Culebra steady-state calibration wells
Particle from Waste Panels to LWB

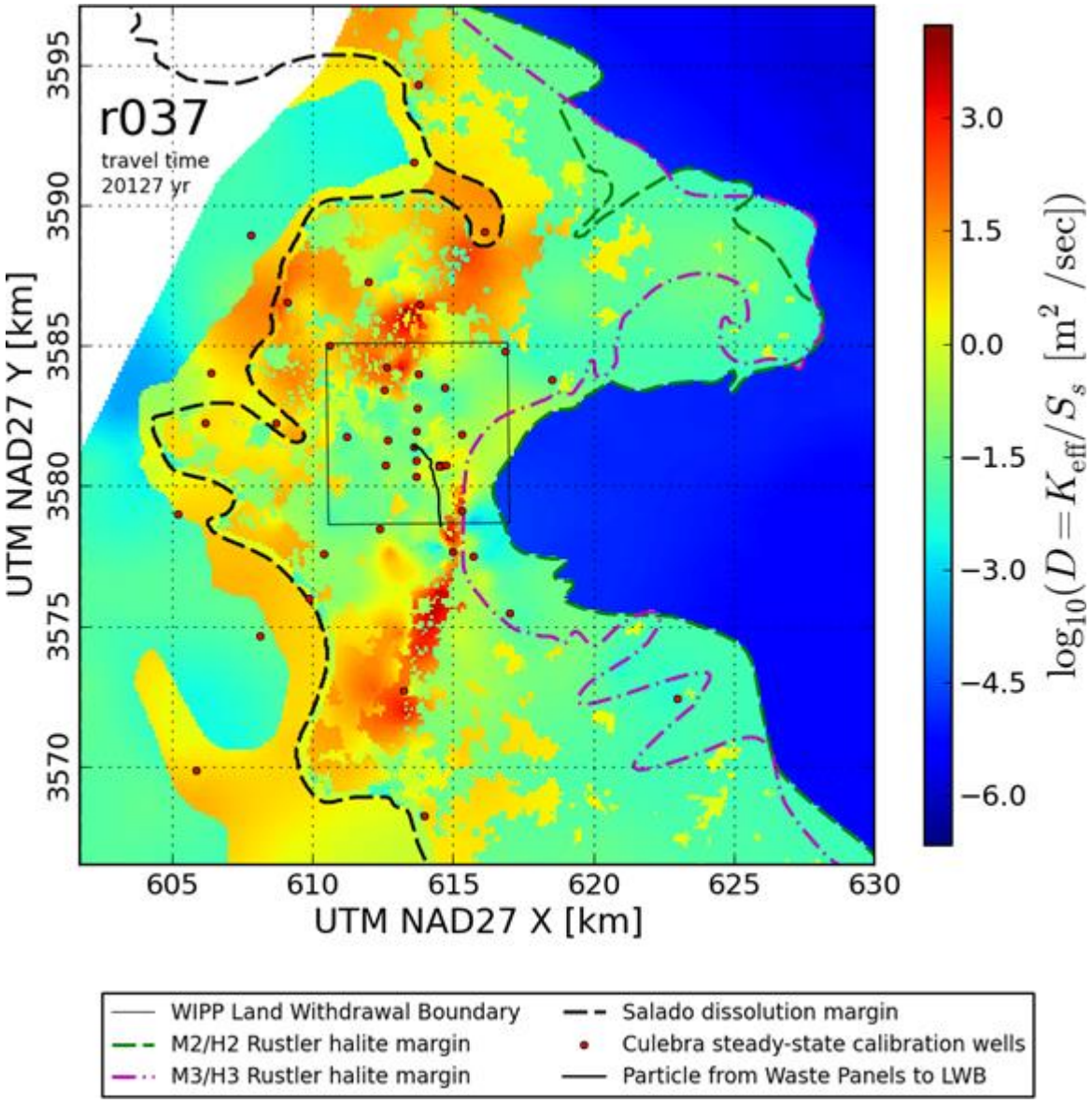
r037
travel time
20127 yr
UTM NAD27 Y [km]
3595
3590
3585
3580
3575
3570
605
610
615
620
625
630
UTM NAD27 X [km]
3.0
1.5
0.0
−1.5
−3.0
−4.5
−6.0
$\log_{10}(D = K_{\text{eff}}/S_s \ [\text{m}^2/\text{sec}])$
WIPP Land Withdrawal Boundary
M2/H2 Rustler halite margin
M3/H3 Rustler halite margin
Salado dissolution margin
Culebra steady-state calibration wells
Particle from Waste Panels to LWB

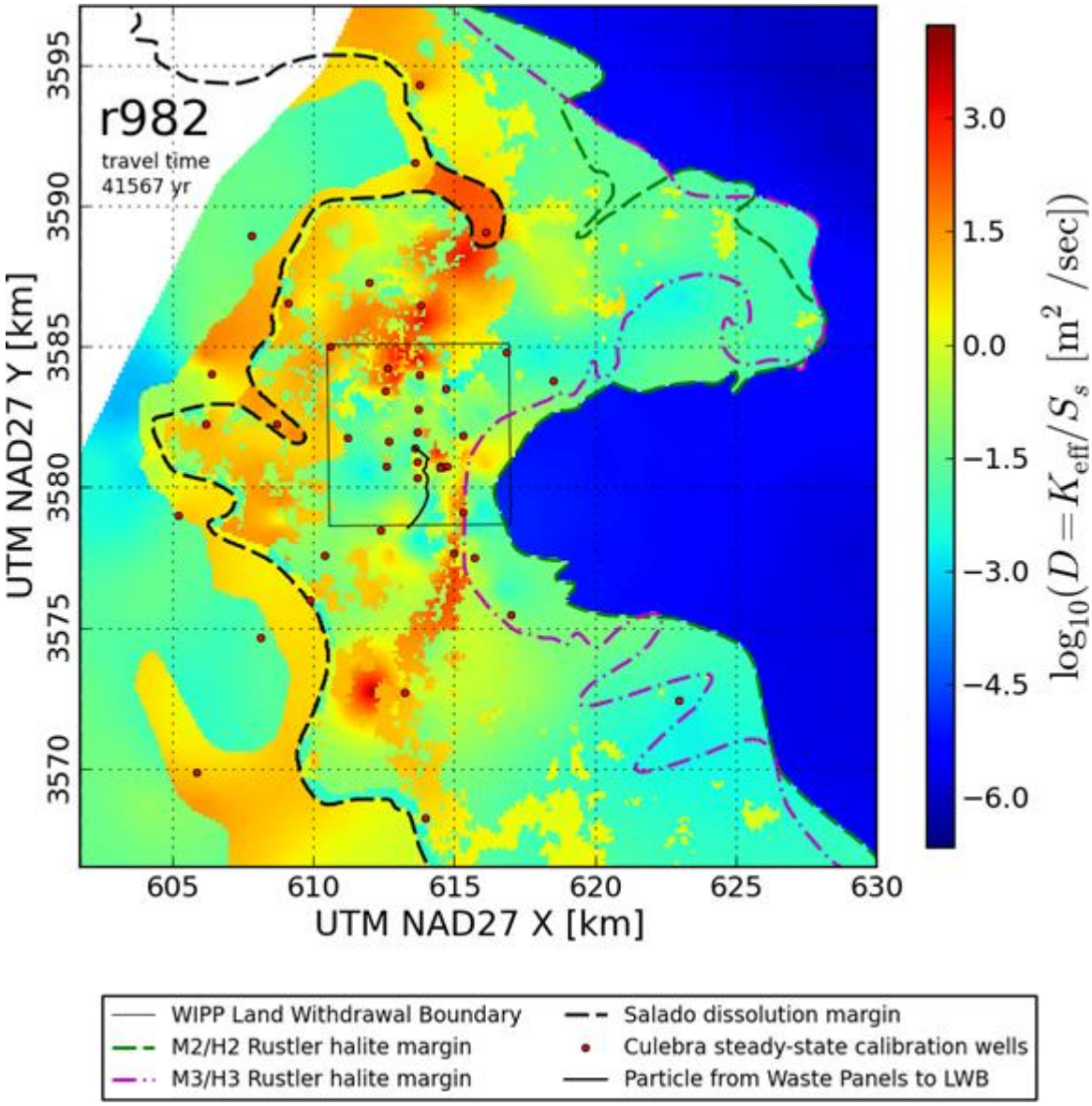
r982
travel time
41567 yr
UTM NAD27 Y [km]
3595
3590
3585
3580
3575
3570
605
610
615
620
625
630
UTM NAD27 X [km]
3.0
1.5
0.0
−1.5
−3.0
−4.5
−6.0
$\log_{10}(D = K_{\text{eff}}/S_s \ [\text{m}^2/\text{sec}])$
WIPP Land Withdrawal Boundary
M2/H2 Rustler halite margin
M3/H3 Rustler halite margin
Salado dissolution margin
Culebra steady-state calibration wells
Particle from Waste Panels to LWB

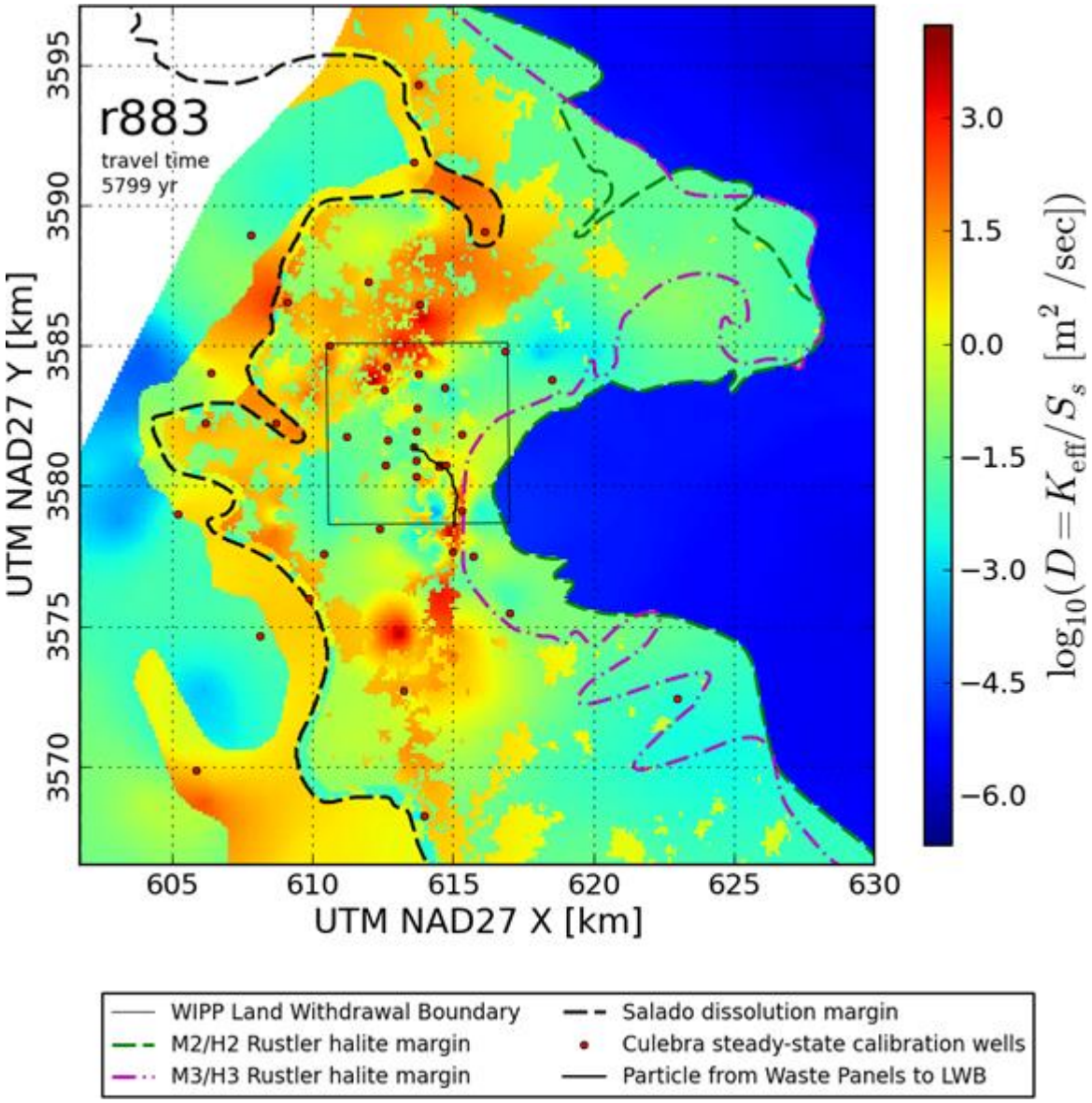
r883
travel time
5799 yr
UTM NAD27 Y [km]
3595
3590
3585
3580
3575
3570
605
610
615
620
625
630
UTM NAD27 X [km]
3.0
1.5
0.0
−1.5
−3.0
−4.5
−6.0
$\log_{10}(D = K_{\text{eff}}/S_s \ [\text{m}^2/\text{sec}])$
WIPP Land Withdrawal Boundary
M2/H2 Rustler halite margin
M3/H3 Rustler halite margin
Salado dissolution margin
Culebra steady-state calibration wells
Particle from Waste Panels to LWB

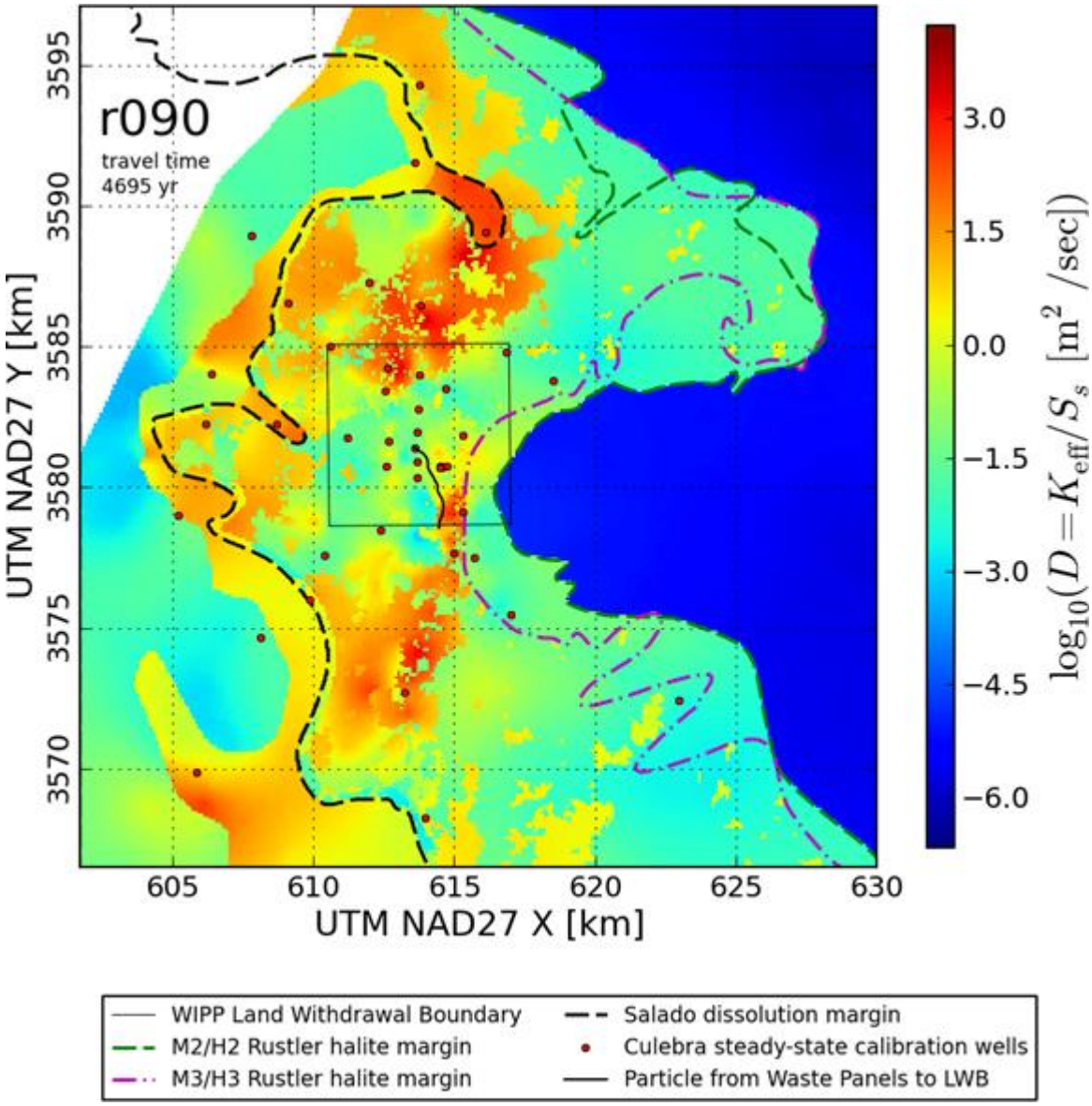
r090
travel time
4695 yr
UTM NAD27 Y [km]
3595
3590
3585
3580
3575
3570
605
610
615
620
625
630
UTM NAD27 X [km]
3.0
1.5
0.0
−1.5
−3.0
−4.5
−6.0
$\log_{10}(D = K_{\text{eff}}/S_s \ [\text{m}^2/\text{sec}])$
WIPP Land Withdrawal Boundary
M2/H2 Rustler halite margin
M3/H3 Rustler halite margin
Salado dissolution margin
Culebra steady-state calibration wells
Particle from Waste Panels to LWB

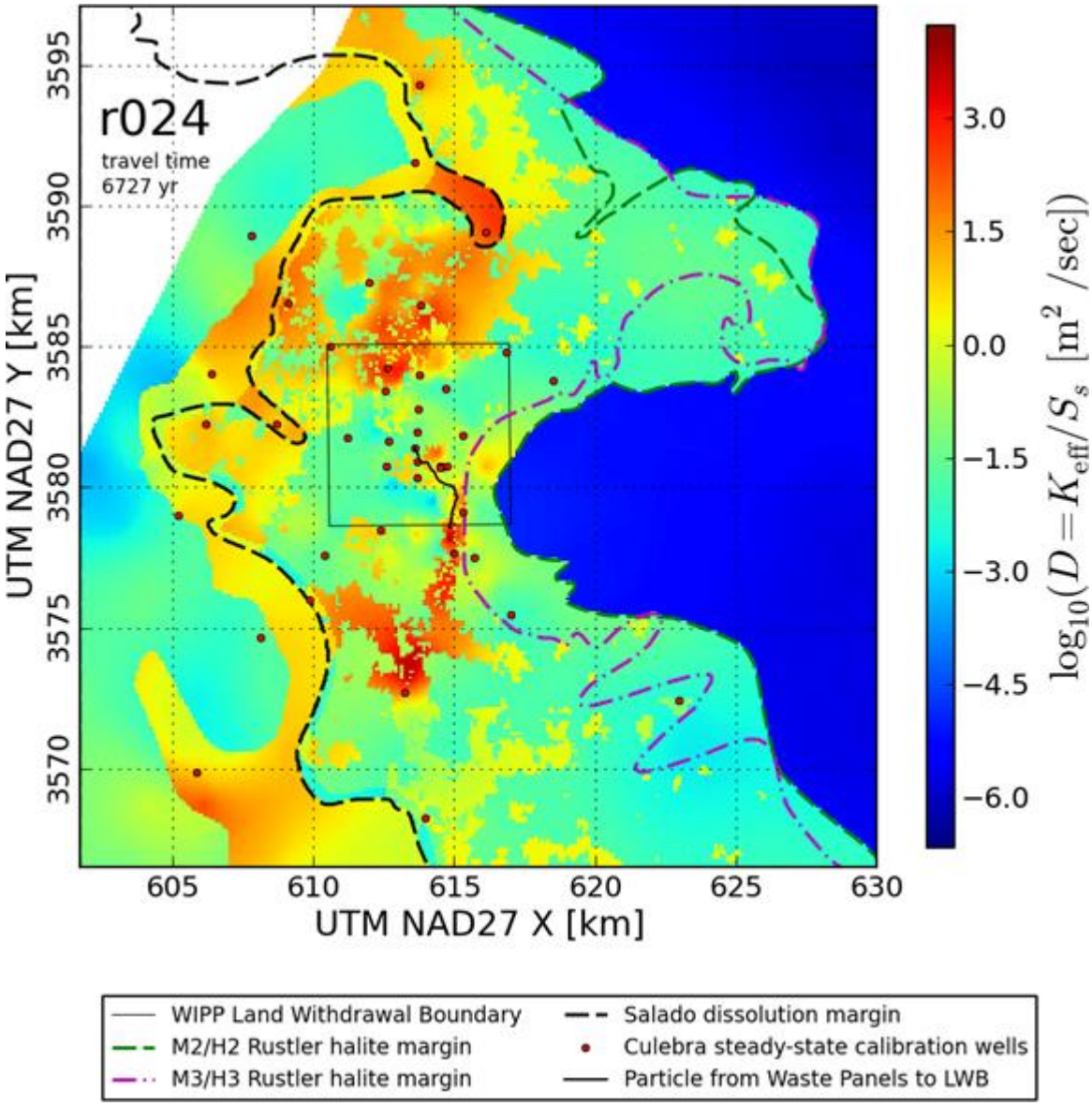
r024
travel time
6727 yr
UTM NAD27 Y [km]
3595
3590
3585
3580
3575
3570
605
610
615
620
625
630
UTM NAD27 X [km]
3.0
1.5
0.0
−1.5
−3.0
−4.5
−6.0
$\log_{10}(D = K_{\text{eff}}/S_s \ [\text{m}^2/\text{sec}])$
WIPP Land Withdrawal Boundary
M2/H2 Rustler halite margin
M3/H3 Rustler halite margin
Salado dissolution margin
Culebra steady-state calibration wells
Particle from Waste Panels to LWB

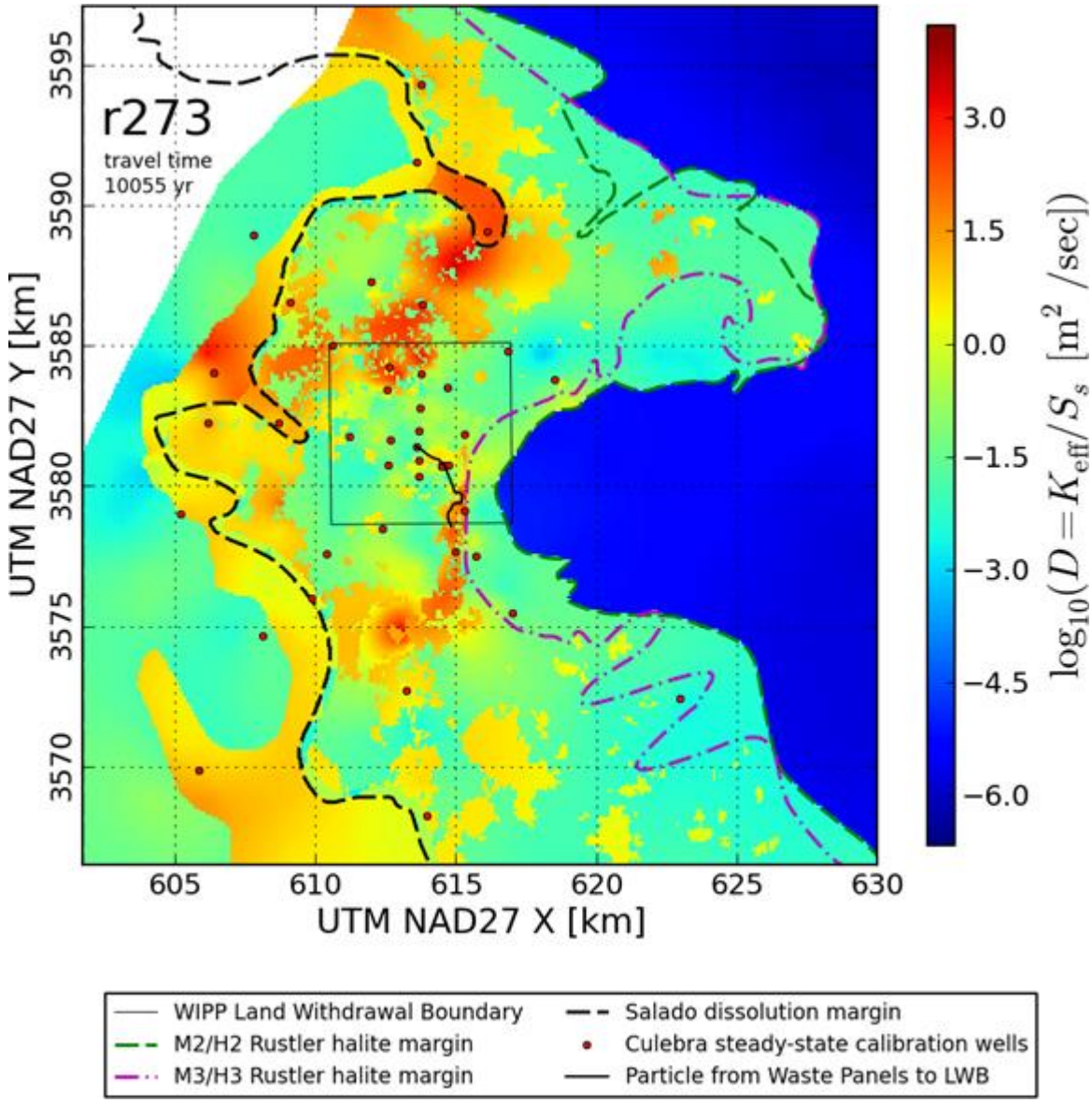
r273
travel time
10055 yr
UTM NAD27 Y [km]
3595
3590
3585
3580
3575
3570
605
610
615
620
625
630
UTM NAD27 X [km]
3.0
1.5
0.0
−1.5
−3.0
−4.5
−6.0
$\log_{10}(D = K_{\text{eff}}/S_s \ [\text{m}^2/\text{sec}])$
WIPP Land Withdrawal Boundary
M2/H2 Rustler halite margin
M3/H3 Rustler halite margin
Salado dissolution margin
Culebra steady-state calibration wells
Particle from Waste Panels to LWB

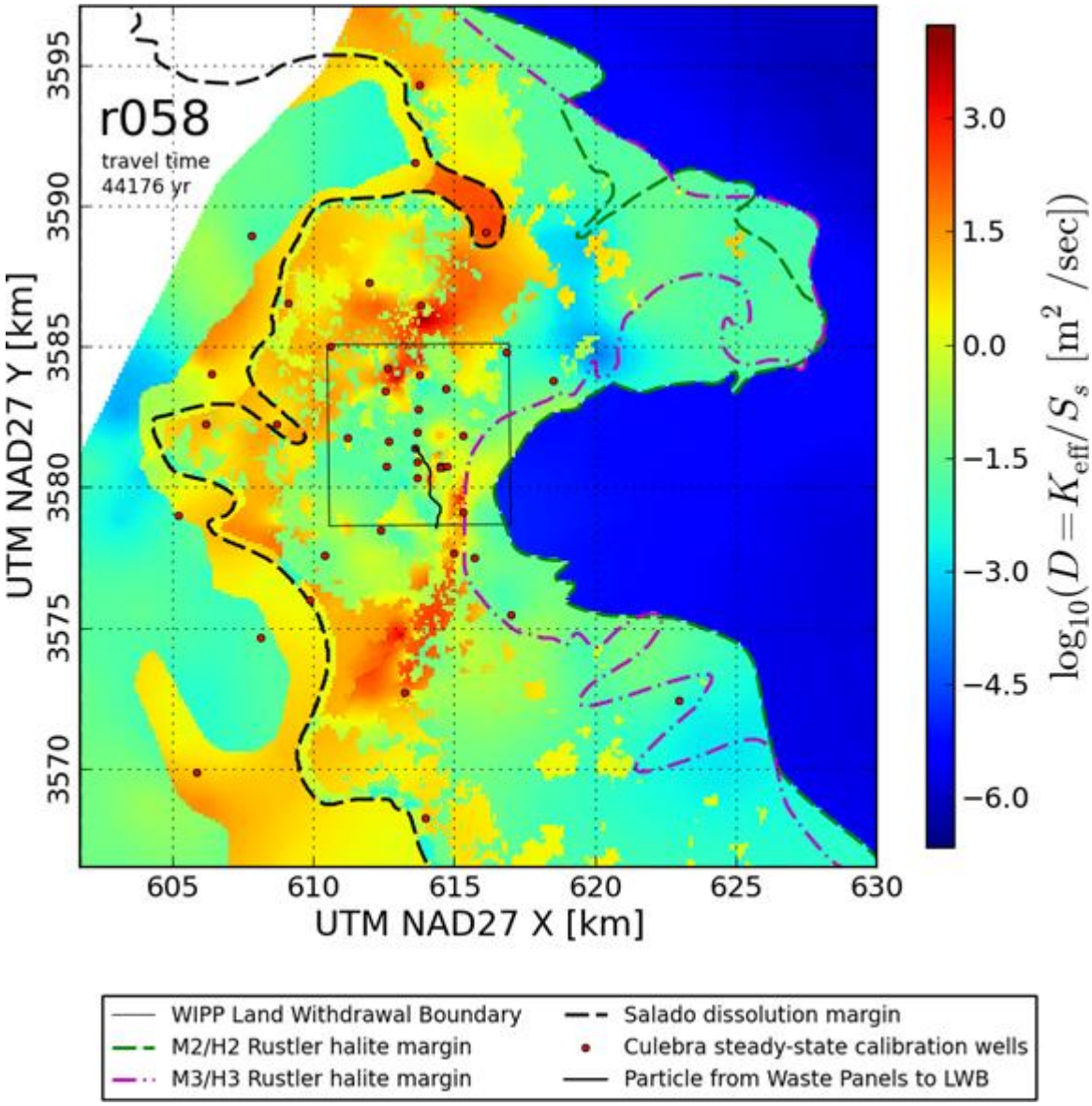
r058
travel time
44176 yr
UTM NAD27 Y [km]
3595
3590
3585
3580
3575
3570
605
610
615
620
625
630
UTM NAD27 X [km]
3.0
1.5
0.0
−1.5
−3.0
−4.5
−6.0
$\log_{10}(D = K_{\text{eff}}/S_s \ [\text{m}^2/\text{sec}])$
WIPP Land Withdrawal Boundary
M2/H2 Rustler halite margin
M3/H3 Rustler halite margin
Salado dissolution margin
Culebra steady-state calibration wells
Particle from Waste Panels to LWB

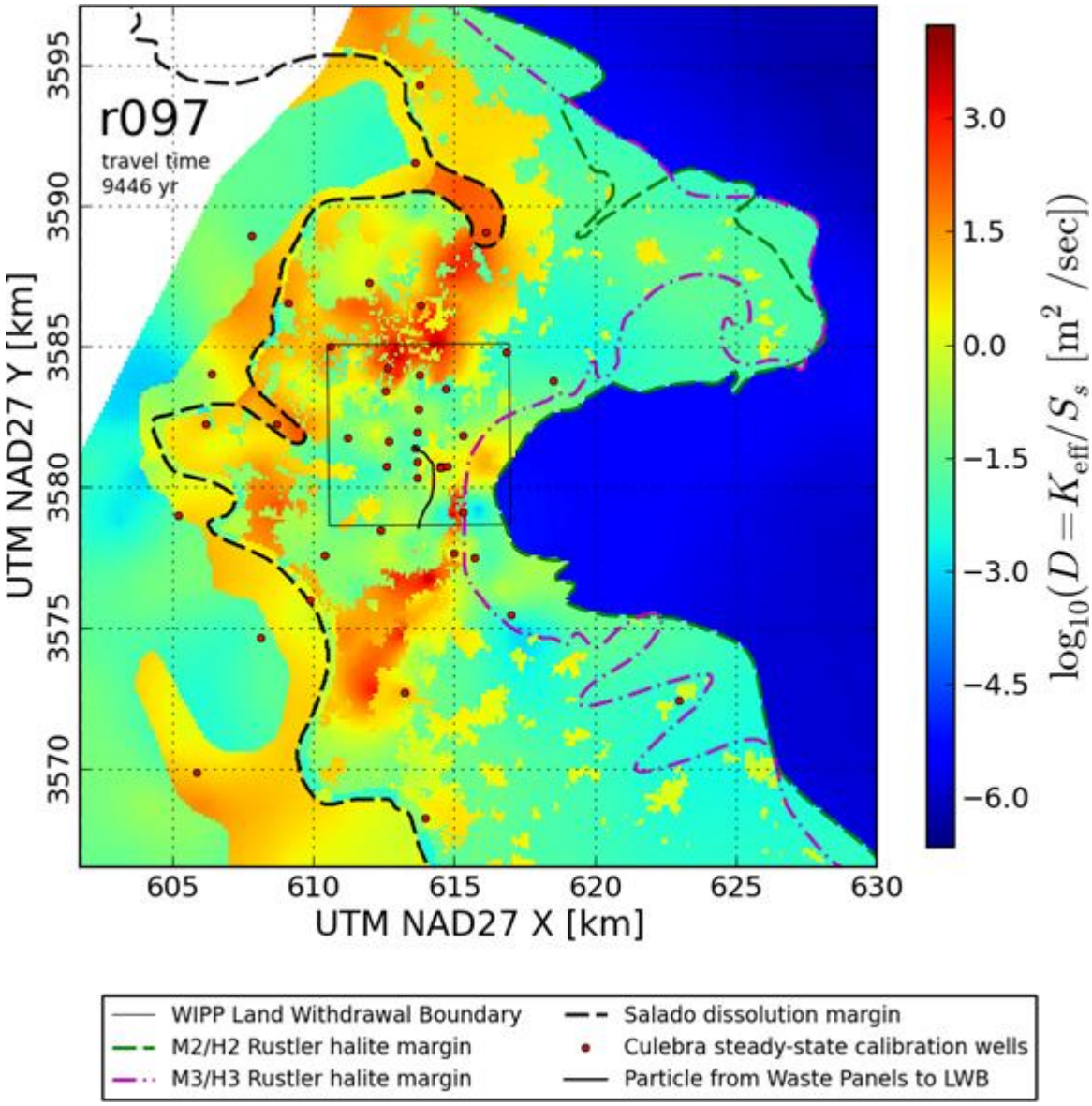
r097
travel time
9446 yr
UTM NAD27 Y [km]
3595
3590
3585
3580
3575
3570
605
610
615
620
625
630
UTM NAD27 X [km]
3.0
1.5
0.0
−1.5
−3.0
−4.5
−6.0
$\log_{10}(D = K_{\text{eff}}/S_s \ [\text{m}^2/\text{sec}])$
WIPP Land Withdrawal Boundary
M2/H2 Rustler halite margin
M3/H3 Rustler halite margin
Salado dissolution margin
Culebra steady-state calibration wells
Particle from Waste Panels to LWB

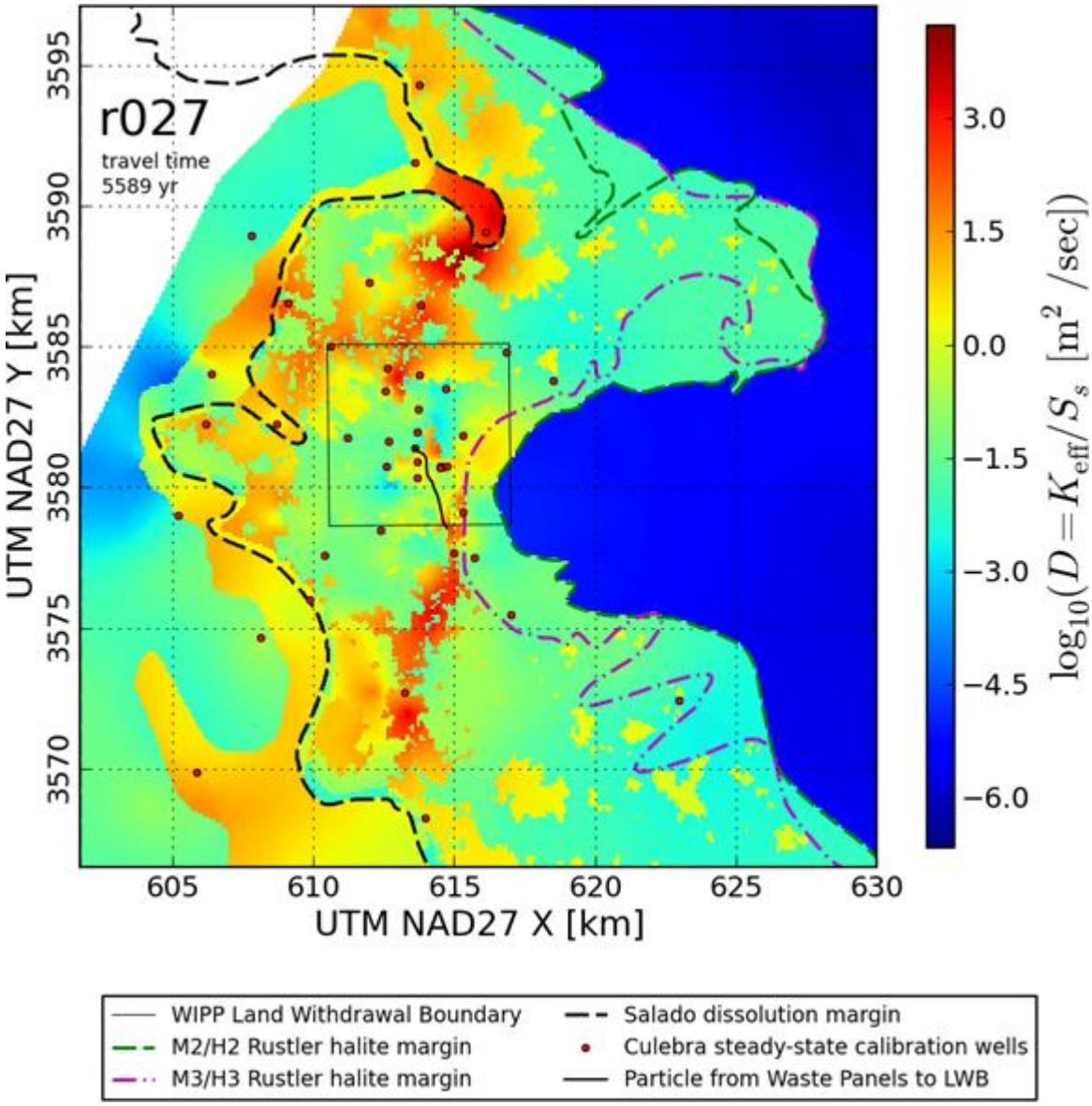
r027
travel time
5589 yr
UTM NAD27 Y [km]
3595
3590
3585
3580
3575
3570
605
610
615
620
625
630
UTM NAD27 X [km]
3.0
1.5
0.0
−1.5
−3.0
−4.5
−6.0
$\log_{10}(D = K_{\text{eff}}/S_s \ [\text{m}^2/\text{sec}])$
WIPP Land Withdrawal Boundary
M2/H2 Rustler halite margin
M3/H3 Rustler halite margin
Salado dissolution margin
Culebra steady-state calibration wells
Particle from Waste Panels to LWB

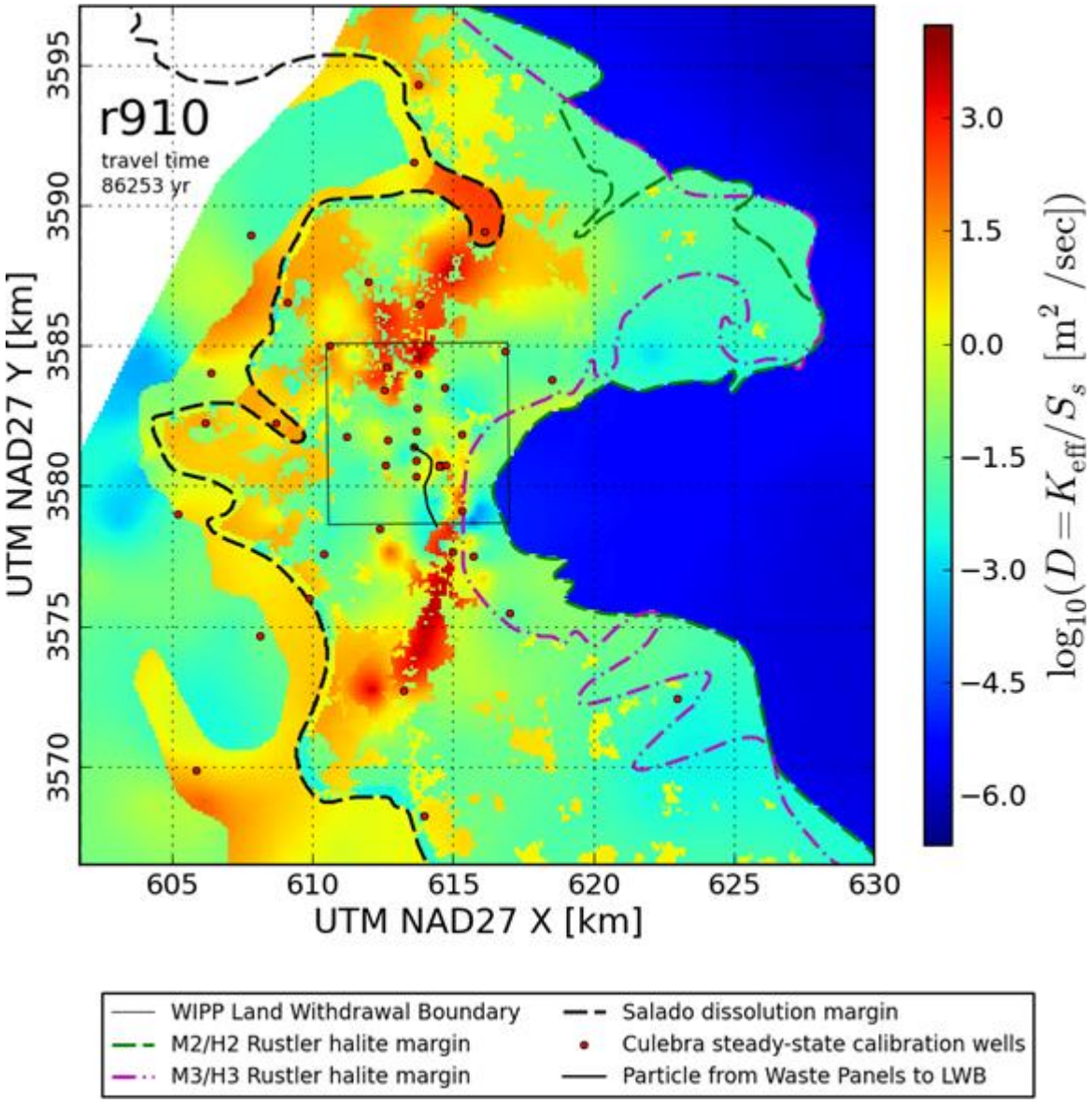
r910
travel time
86253 yr
UTM NAD27 Y [km]
3595
3590
3585
3580
3575
3570
605
610
615
620
625
630
UTM NAD27 X [km]
3.0
1.5
0.0
−1.5
−3.0
−4.5
−6.0
$\log_{10}(D = K_{\text{eff}}/S_s \ [\text{m}^2/\text{sec}])$
WIPP Land Withdrawal Boundary
M2/H2 Rustler halite margin
M3/H3 Rustler halite margin
Salado dissolution margin
Culebra steady-state calibration wells
Particle from Waste Panels to LWB

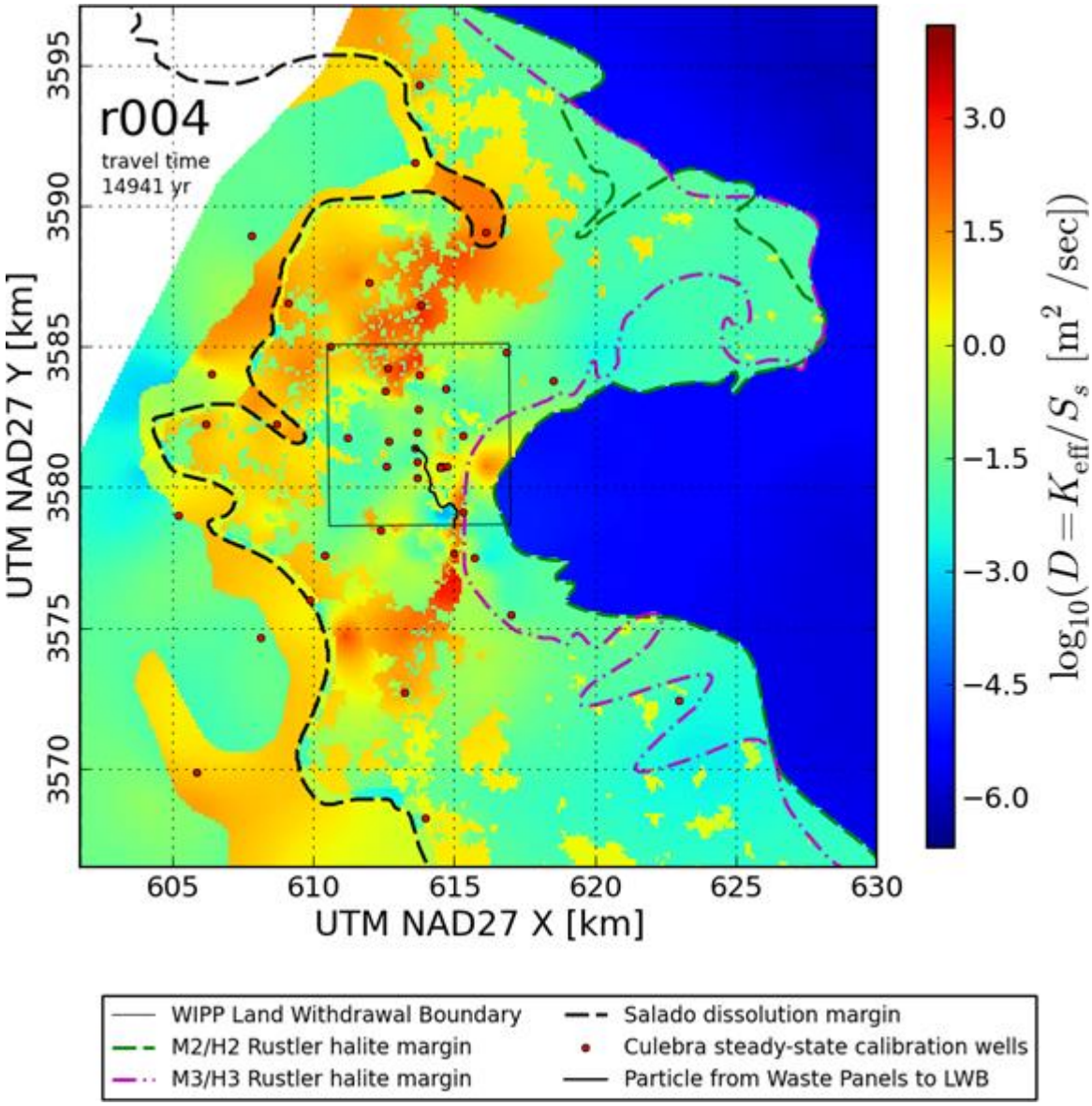
r004
travel time
14941 yr
UTM NAD27 Y [km]
3595
3590
3585
3580
3575
3570
605
610
615
620
625
630
UTM NAD27 X [km]
3.0
1.5
0.0
−1.5
−3.0
−4.5
−6.0
$\log_{10}(D = K_{\text{eff}}/S_s \ [\text{m}^2/\text{sec}])$
WIPP Land Withdrawal Boundary
M2/H2 Rustler halite margin
M3/H3 Rustler halite margin
Salado dissolution margin
Culebra steady-state calibration wells
Particle from Waste Panels to LWB

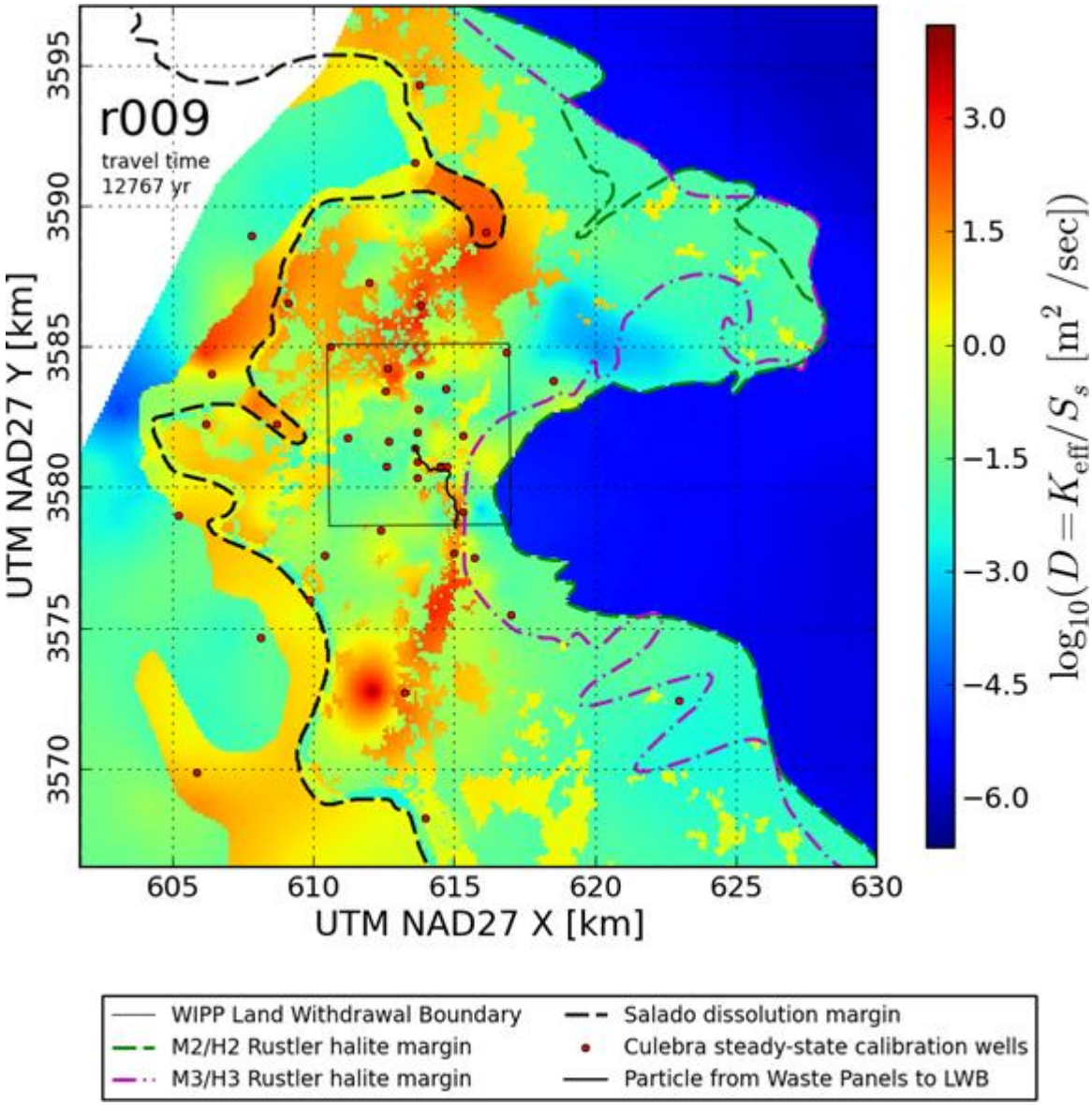
r009
travel time
12767 yr
UTM NAD27 Y [km]
3595
3590
3585
3580
3575
3570
605
610
615
620
625
630
UTM NAD27 X [km]
3.0
1.5
0.0
−1.5
−3.0
−4.5
−6.0
$\log_{10}(D = K_{\text{eff}}/S_s \ [\text{m}^2/\text{sec}])$
WIPP Land Withdrawal Boundary
M2/H2 Rustler halite margin
M3/H3 Rustler halite margin
Salado dissolution margin
Culebra steady-state calibration wells
Particle from Waste Panels to LWB

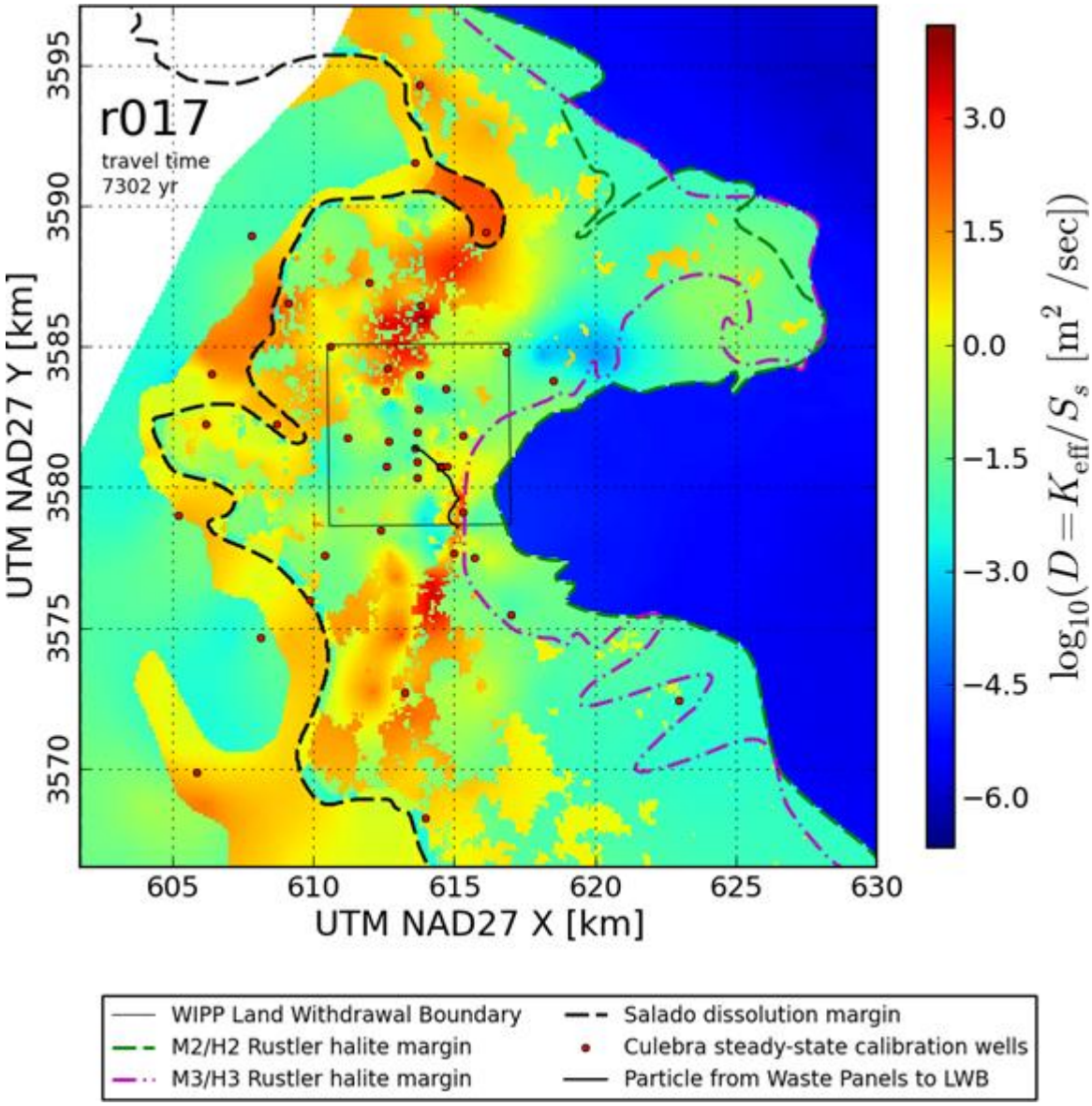
r017
travel time
7302 yr
UTM NAD27 Y [km]
3595
3590
3585
3580
3575
3570
605
610
615
620
625
630
UTM NAD27 X [km]
3.0
1.5
0.0
−1.5
−3.0
−4.5
−6.0
$\log_{10}(D = K_{\text{eff}}/S_s \ [\text{m}^2/\text{sec}])$
WIPP Land Withdrawal Boundary
M2/H2 Rustler halite margin
M3/H3 Rustler halite margin
Salado dissolution margin
Culebra steady-state calibration wells
Particle from Waste Panels to LWB

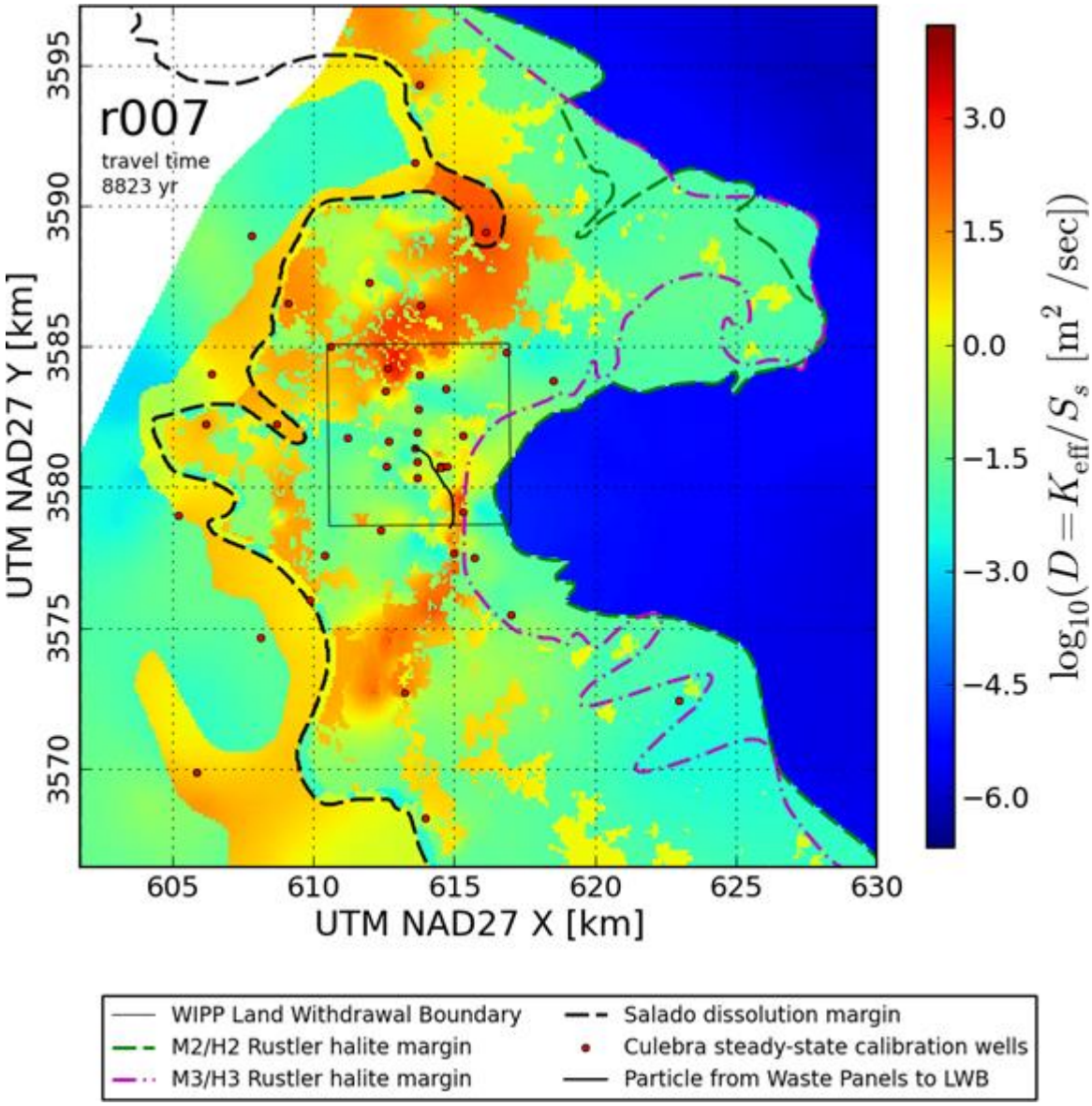
r007
travel time
8823 yr
UTM NAD27 Y [km]
3595
3590
3585
3580
3575
3570
605
610
615
620
625
630
UTM NAD27 X [km]
3.0
1.5
0.0
−1.5
−3.0
−4.5
−6.0
$\log_{10}(D = K_{\text{eff}}/S_s \ [\text{m}^2/\text{sec}])$
WIPP Land Withdrawal Boundary
M2/H2 Rustler halite margin
M3/H3 Rustler halite margin
Salado dissolution margin
Culebra steady-state calibration wells
Particle from Waste Panels to LWB

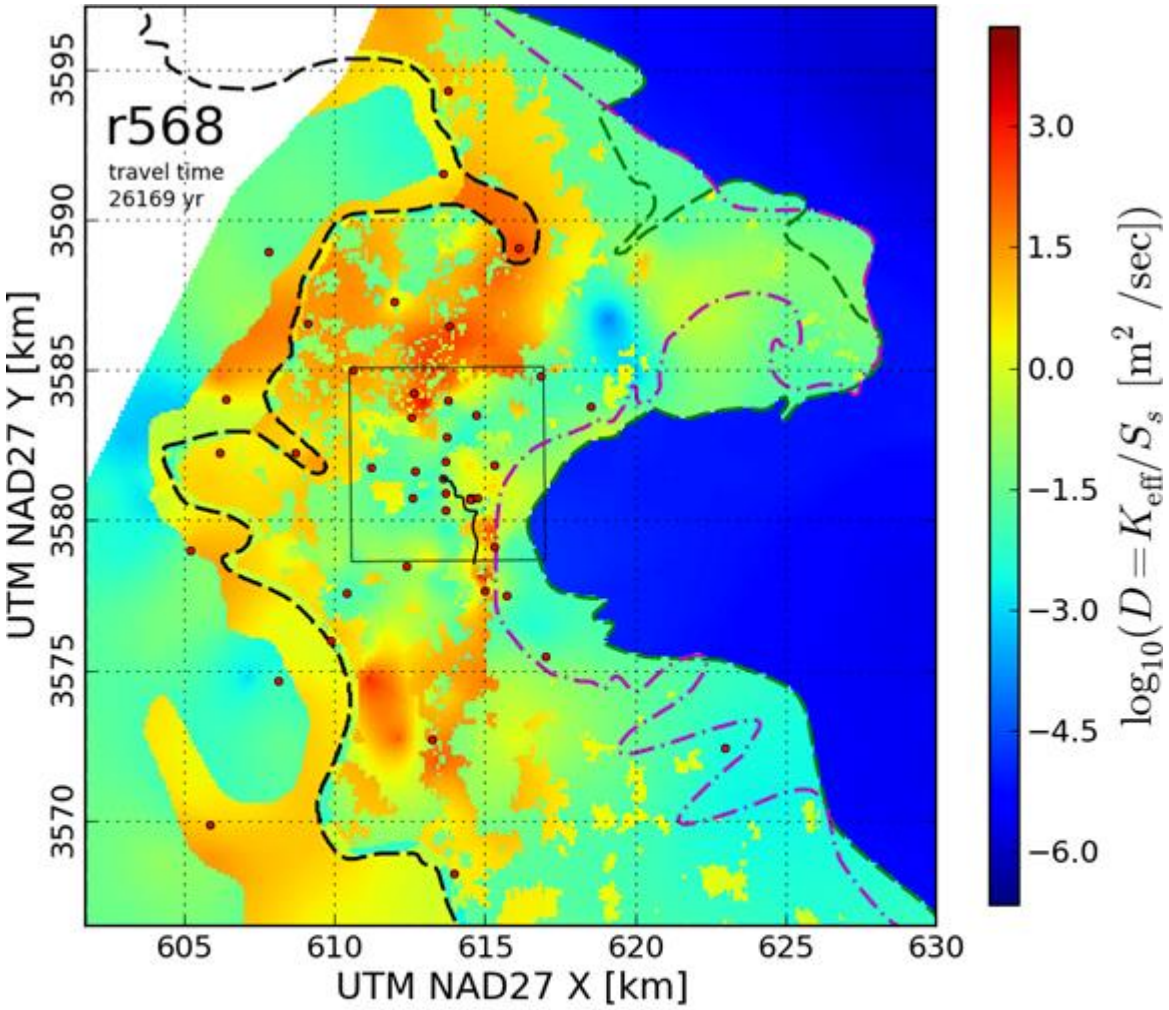
r568
travel time
26169 yr
UTM NAD27 Y [km]
3595
3590
3585
3580
3575
3570
605
610
615
620
625
630
UTM NAD27 X [km]
3.0
1.5
0.0
−1.5
−3.0
−4.5
−6.0
$\log_{10}(D = K_{\text{eff}}/S_s \ [\text{m}^2/\text{sec}])$
WIPP Land Withdrawal Boundary
M2/H2 Rustler halite margin
M3/H3 Rustler halite margin
Salado dissolution margin
Culebra steady-state calibration wells
Particle from Waste Panels to LWB

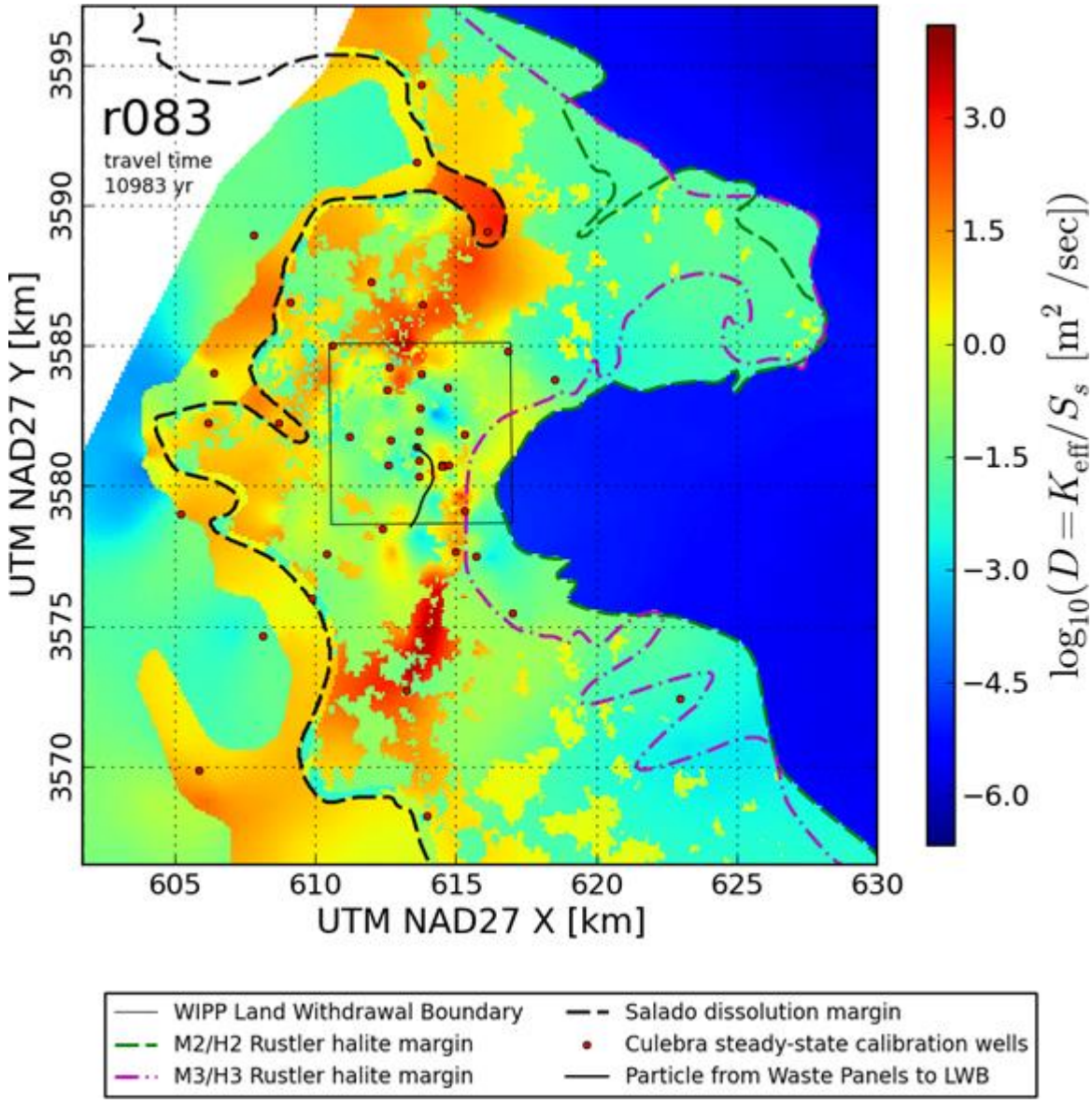
r083
travel time
10983 yr
UTM NAD27 Y [km]
3595
3590
3585
3580
3575
3570
605
610
615
620
625
630
UTM NAD27 X [km]
3.0
1.5
0.0
−1.5
−3.0
−4.5
−6.0
$\log_{10}(D = K_{\text{eff}}/S_s \ [\text{m}^2/\text{sec}])$
WIPP Land Withdrawal Boundary
M2/H2 Rustler halite margin
M3/H3 Rustler halite margin
Salado dissolution margin
Culebra steady-state calibration wells
Particle from Waste Panels to LWB

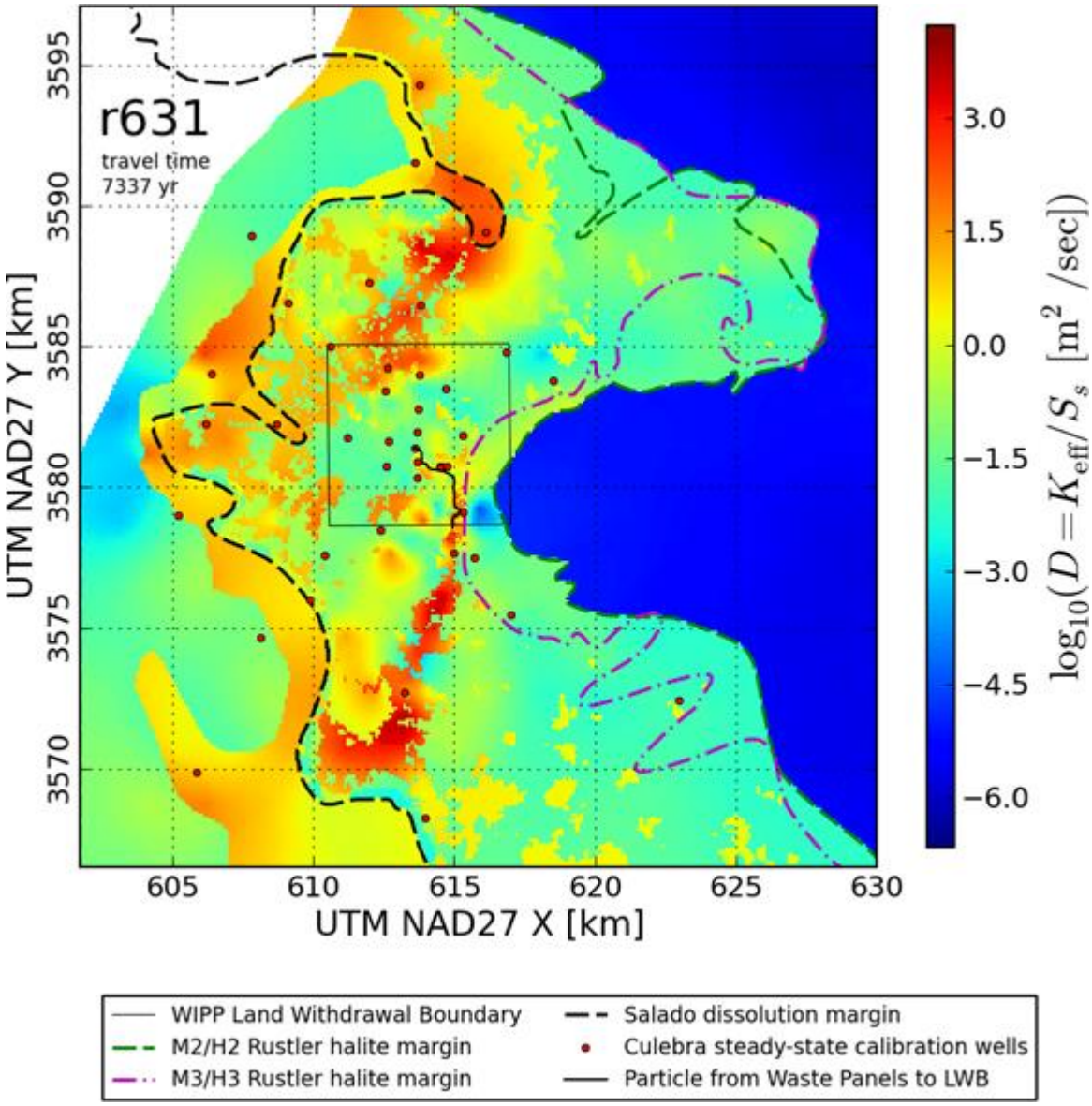
r631
travel time
7337 yr
UTM NAD27 Y [km]
3595
3590
3585
3580
3575
3570
605
610
615
620
625
630
UTM NAD27 X [km]
3.0
1.5
0.0
−1.5
−3.0
−4.5
−6.0
$\log_{10}(D = K_{\text{eff}}/S_s \ [\text{m}^2/\text{sec}])$
WIPP Land Withdrawal Boundary
M2/H2 Rustler halite margin
M3/H3 Rustler halite margin
Salado dissolution margin
Culebra steady-state calibration wells
Particle from Waste Panels to LWB

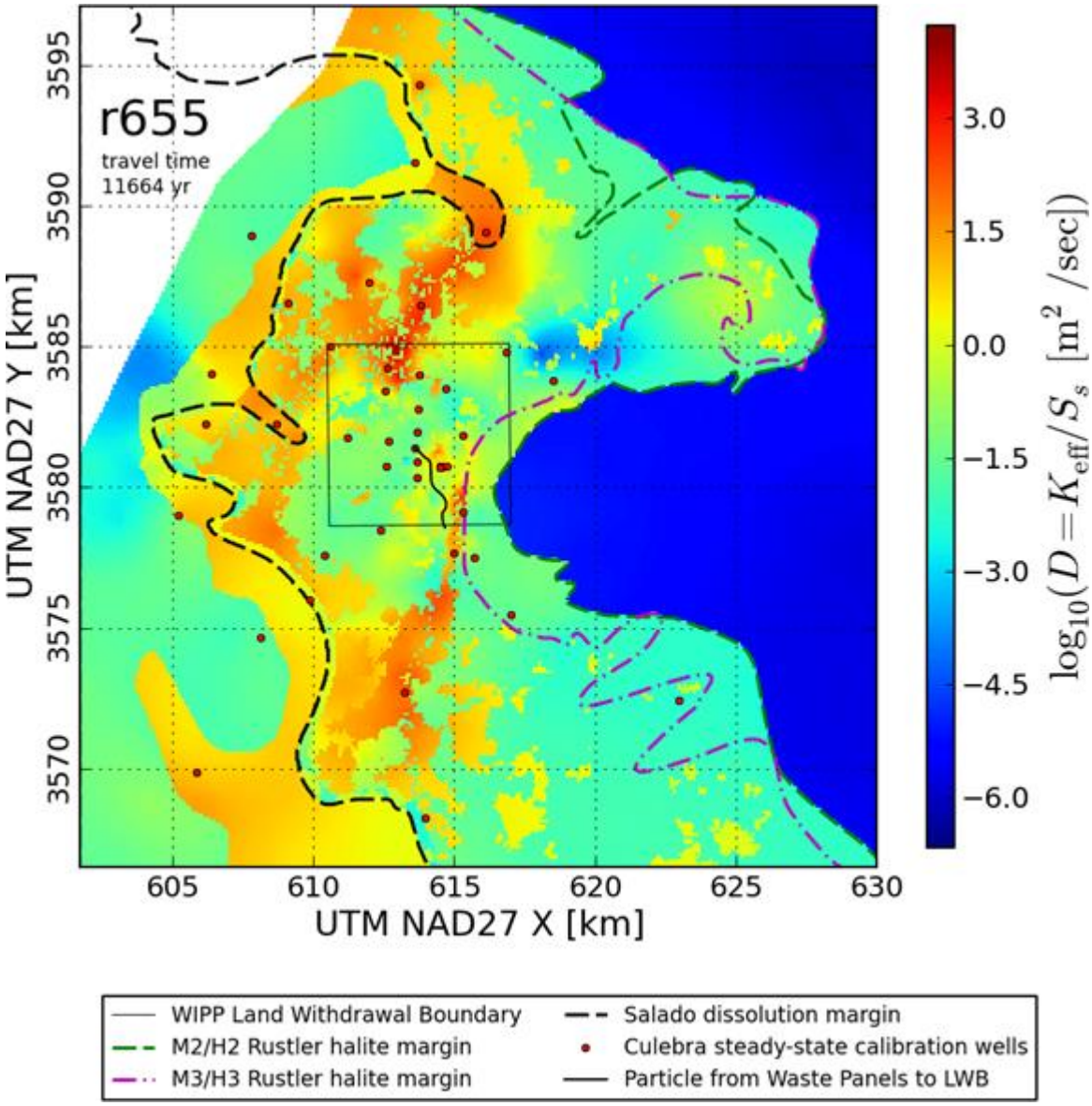
r655
travel time
11664 yr
UTM NAD27 Y [km]
3595
3590
3585
3580
3575
3570
605
610
615
620
625
630
UTM NAD27 X [km]
3.0
1.5
0.0
−1.5
−3.0
−4.5
−6.0
$\log_{10}(D = K_{\text{eff}}/S_s \ [\text{m}^2/\text{sec}])$
WIPP Land Withdrawal Boundary
M2/H2 Rustler halite margin
M3/H3 Rustler halite margin
Salado dissolution margin
Culebra steady-state calibration wells
Particle from Waste Panels to LWB

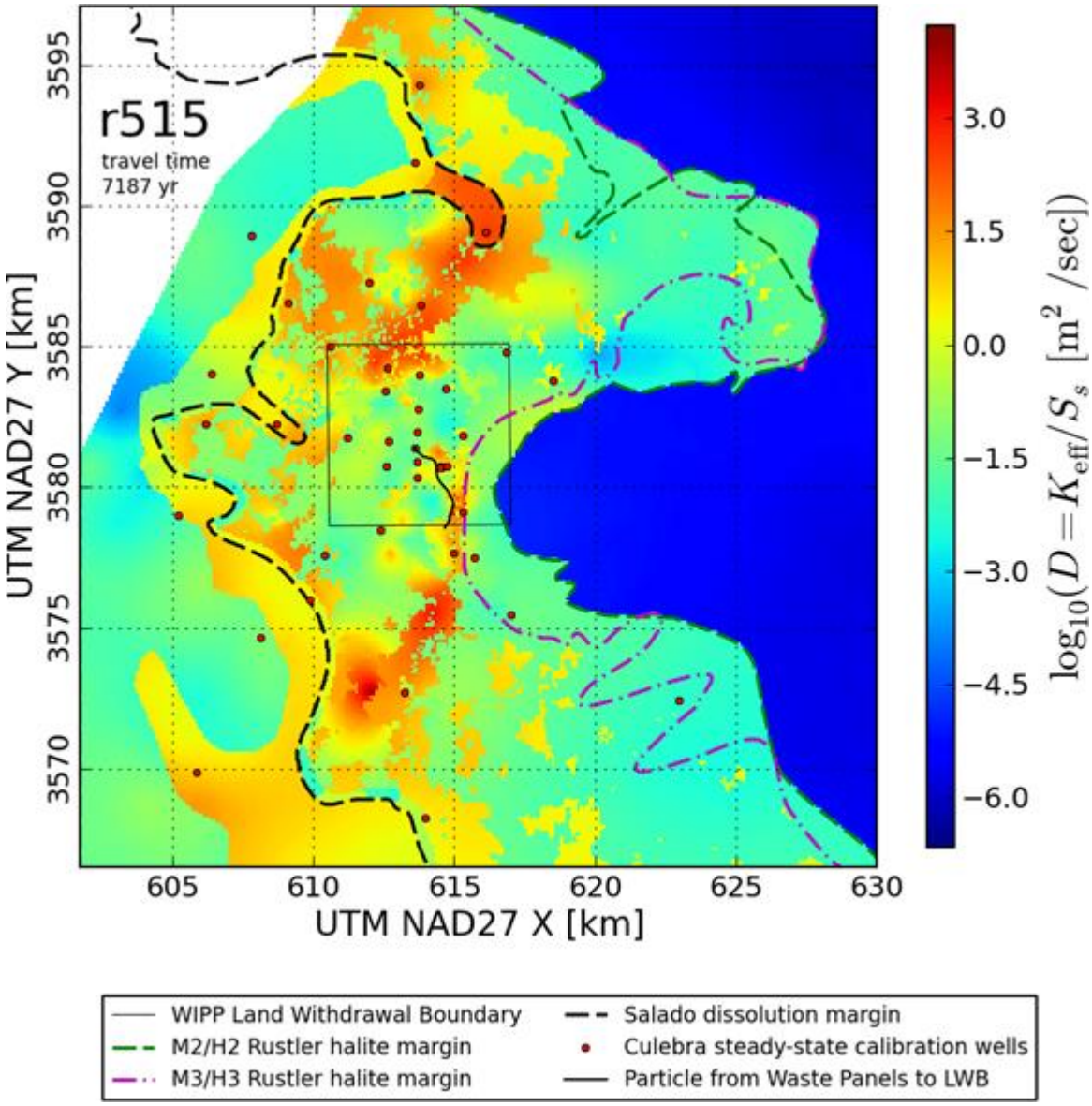
r515
travel time
7187 yr
UTM NAD27 Y [km]
3595
3590
3585
3580
3575
3570
605
610
615
620
625
630
UTM NAD27 X [km]
3.0
1.5
0.0
−1.5
−3.0
−4.5
−6.0
$\log_{10}(D = K_{\text{eff}}/S_s \ [\text{m}^2/\text{sec}])$
WIPP Land Withdrawal Boundary
M2/H2 Rustler halite margin
M3/H3 Rustler halite margin
Salado dissolution margin
Culebra steady-state calibration wells
Particle from Waste Panels to LWB

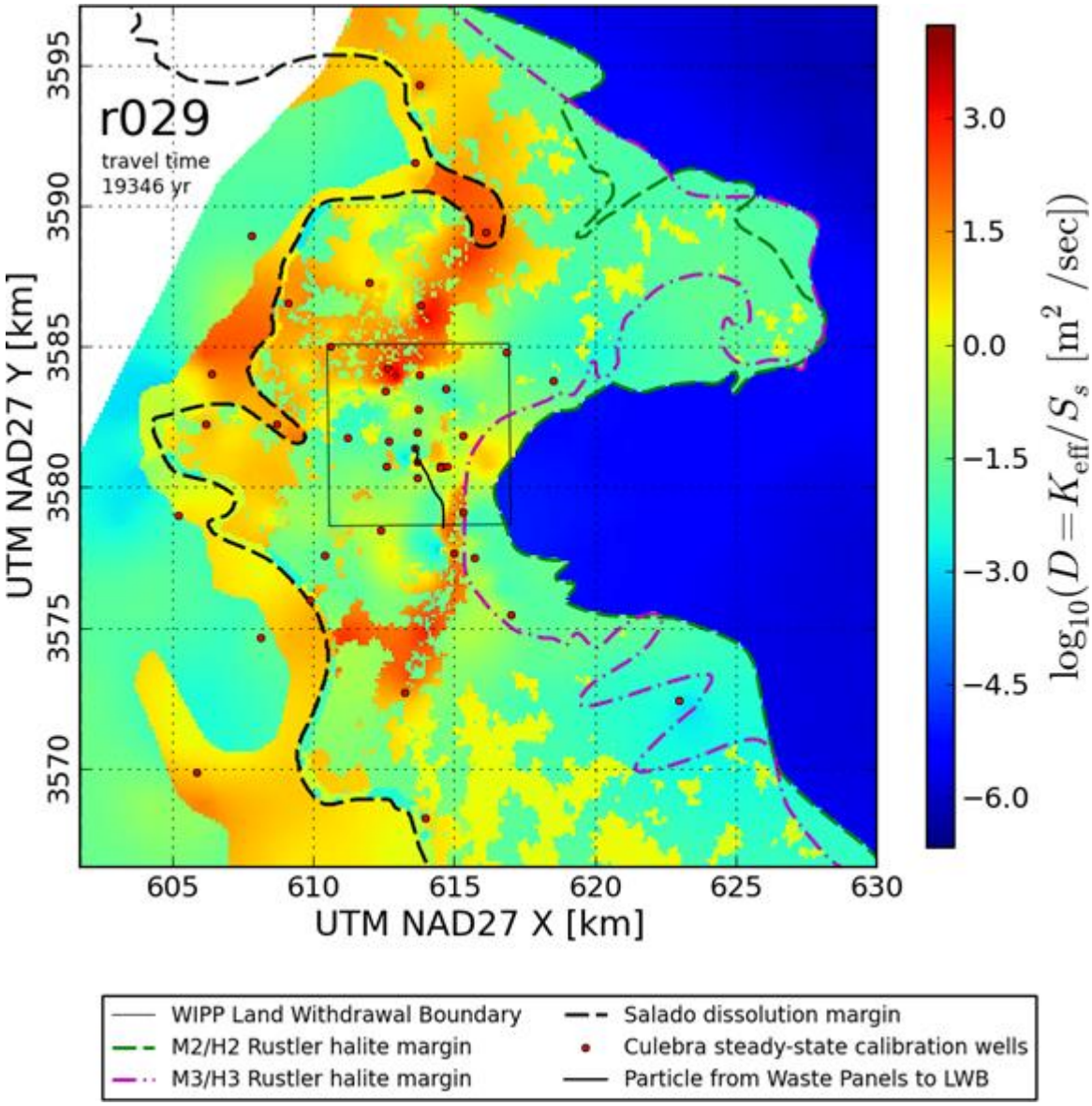
r029
travel time
19346 yr
UTM NAD27 Y [km]
3595
3590
3585
3580
3575
3570
605
610
615
620
625
630
UTM NAD27 X [km]
3.0
1.5
0.0
−1.5
−3.0
−4.5
−6.0
$\log_{10}(D = K_{\text{eff}}/S_s \ [\text{m}^2/\text{sec}])$
WIPP Land Withdrawal Boundary
M2/H2 Rustler halite margin
M3/H3 Rustler halite margin
Salado dissolution margin
Culebra steady-state calibration wells
Particle from Waste Panels to LWB

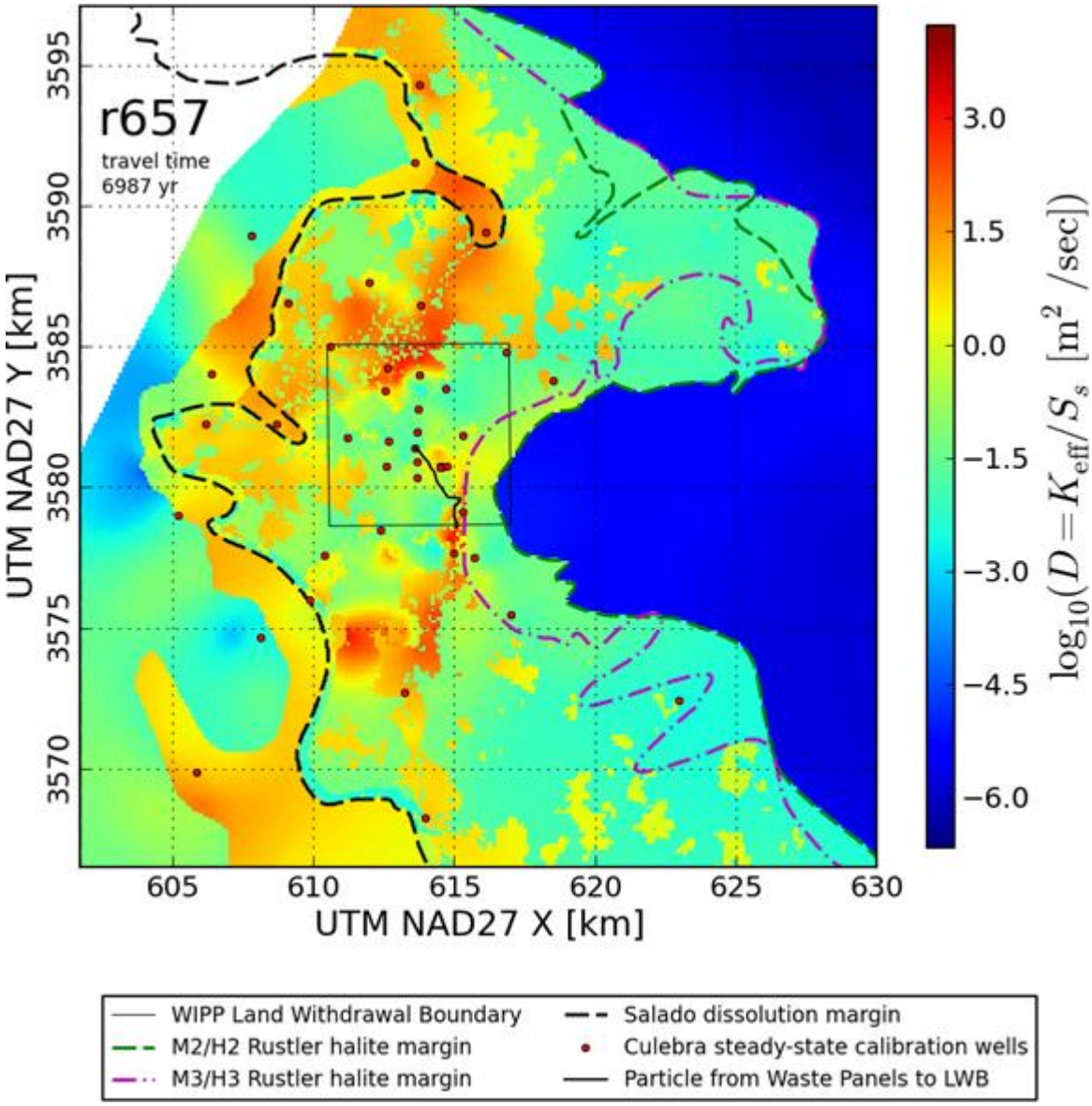
r657
travel time
6987 yr
UTM NAD27 Y [km]
3595
3590
3585
3580
3575
3570
605
610
615
620
625
630
UTM NAD27 X [km]
3.0
1.5
0.0
−1.5
−3.0
−4.5
−6.0
$\log_{10}(D = K_{\text{eff}}/S_s \ [\text{m}^2/\text{sec}])$
WIPP Land Withdrawal Boundary
M2/H2 Rustler halite margin
M3/H3 Rustler halite margin
Salado dissolution margin
Culebra steady-state calibration wells
Particle from Waste Panels to LWB

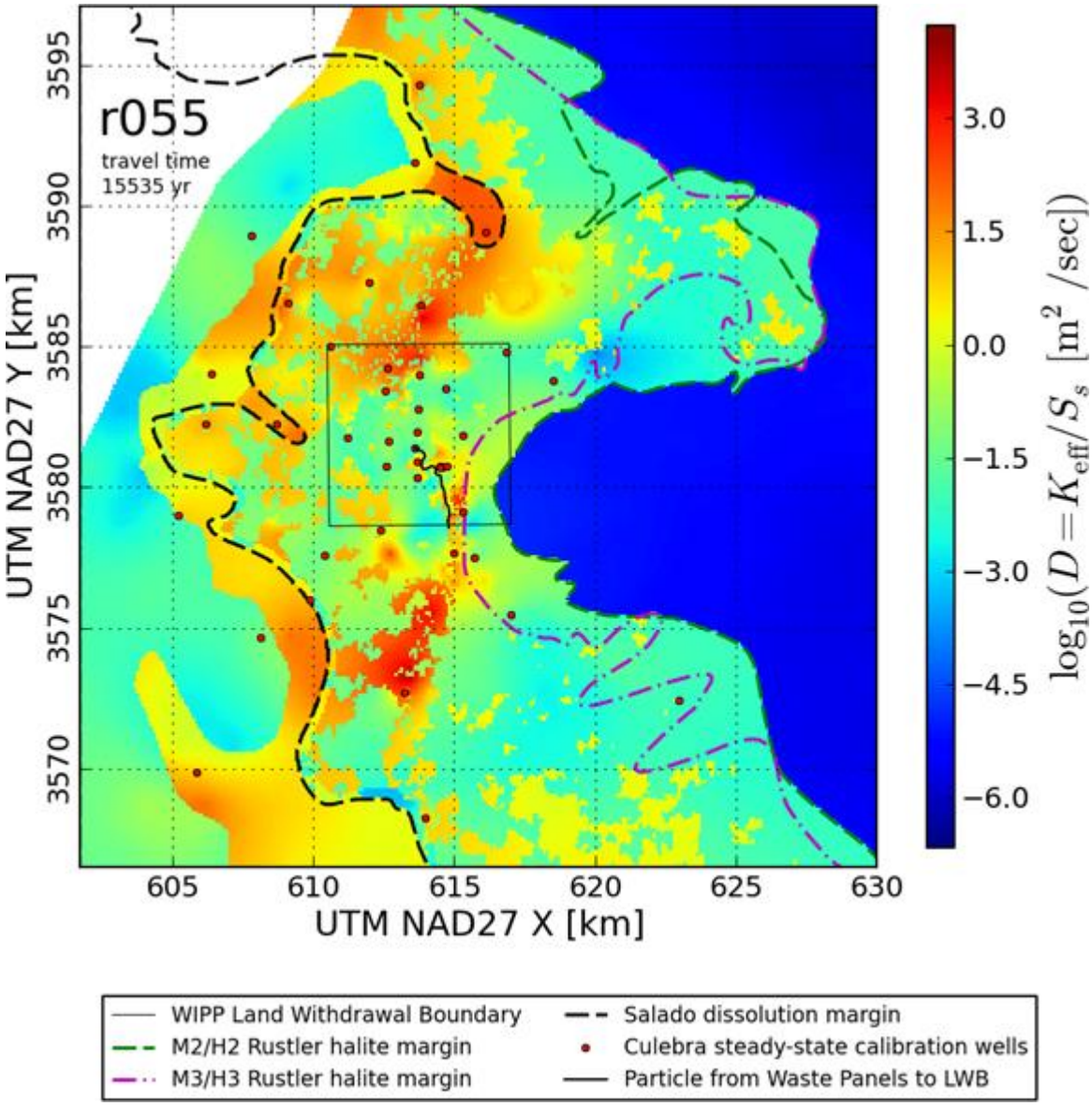
r055
travel time
15535 yr
UTM NAD27 Y [km]
3595
3590
3585
3580
3575
3570
605
610
615
620
625
630
UTM NAD27 X [km]
3.0
1.5
0.0
−1.5
−3.0
−4.5
−6.0
$\log_{10}(D = K_{\text{eff}}/S_s \ [\text{m}^2/\text{sec}])$
WIPP Land Withdrawal Boundary
M2/H2 Rustler halite margin
M3/H3 Rustler halite margin
Salado dissolution margin
Culebra steady-state calibration wells
Particle from Waste Panels to LWB

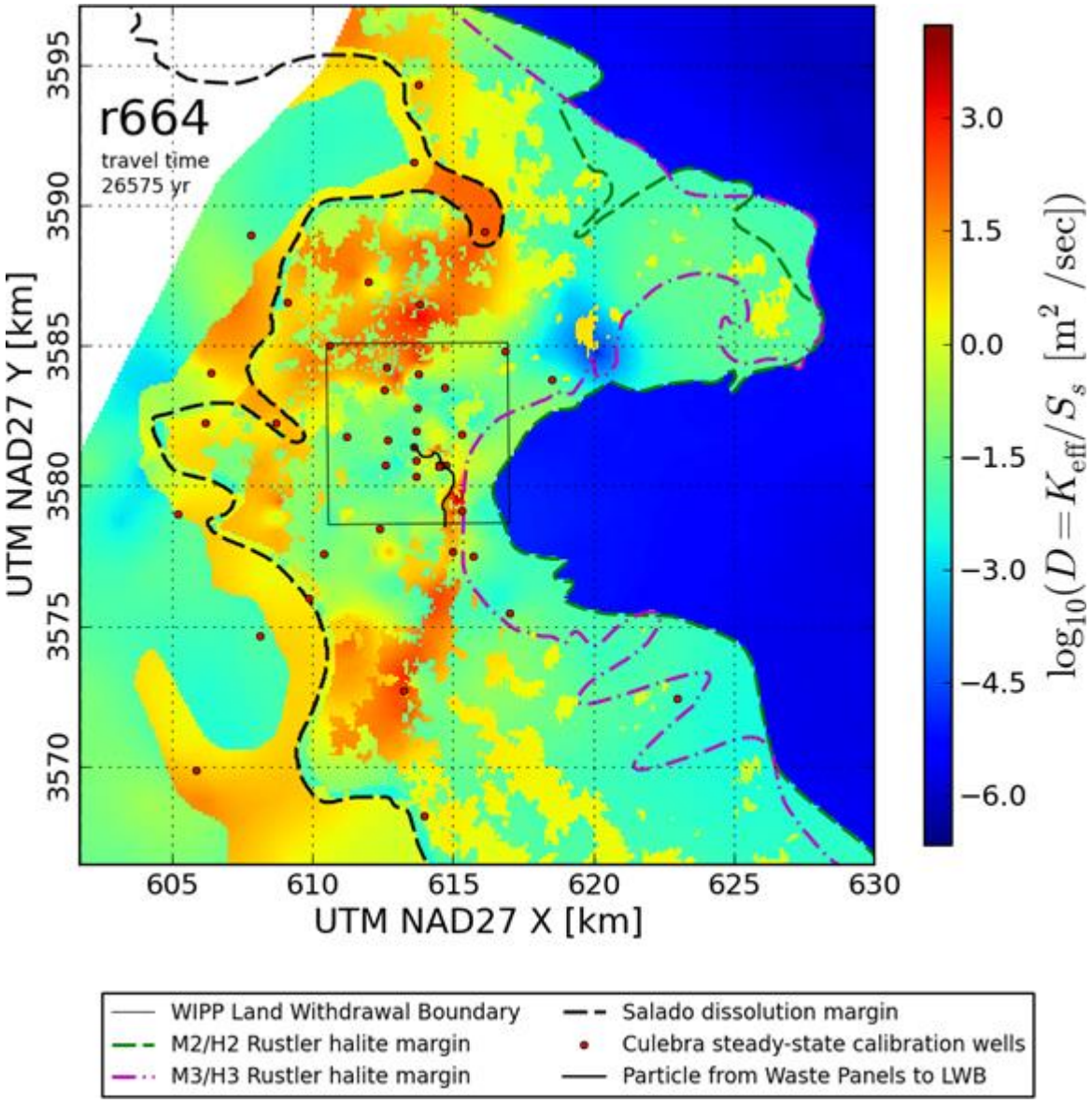
r664
travel time
26575 yr
UTM NAD27 Y [km]
3595
3590
3585
3580
3575
3570
605
610
615
620
625
630
UTM NAD27 X [km]
3.0
1.5
0.0
−1.5
−3.0
−4.5
−6.0
$\log_{10}(D = K_{\text{eff}}/S_s \ [\text{m}^2/\text{sec}])$
WIPP Land Withdrawal Boundary
M2/H2 Rustler halite margin
M3/H3 Rustler halite margin
Salado dissolution margin
Culebra steady-state calibration wells
Particle from Waste Panels to LWB

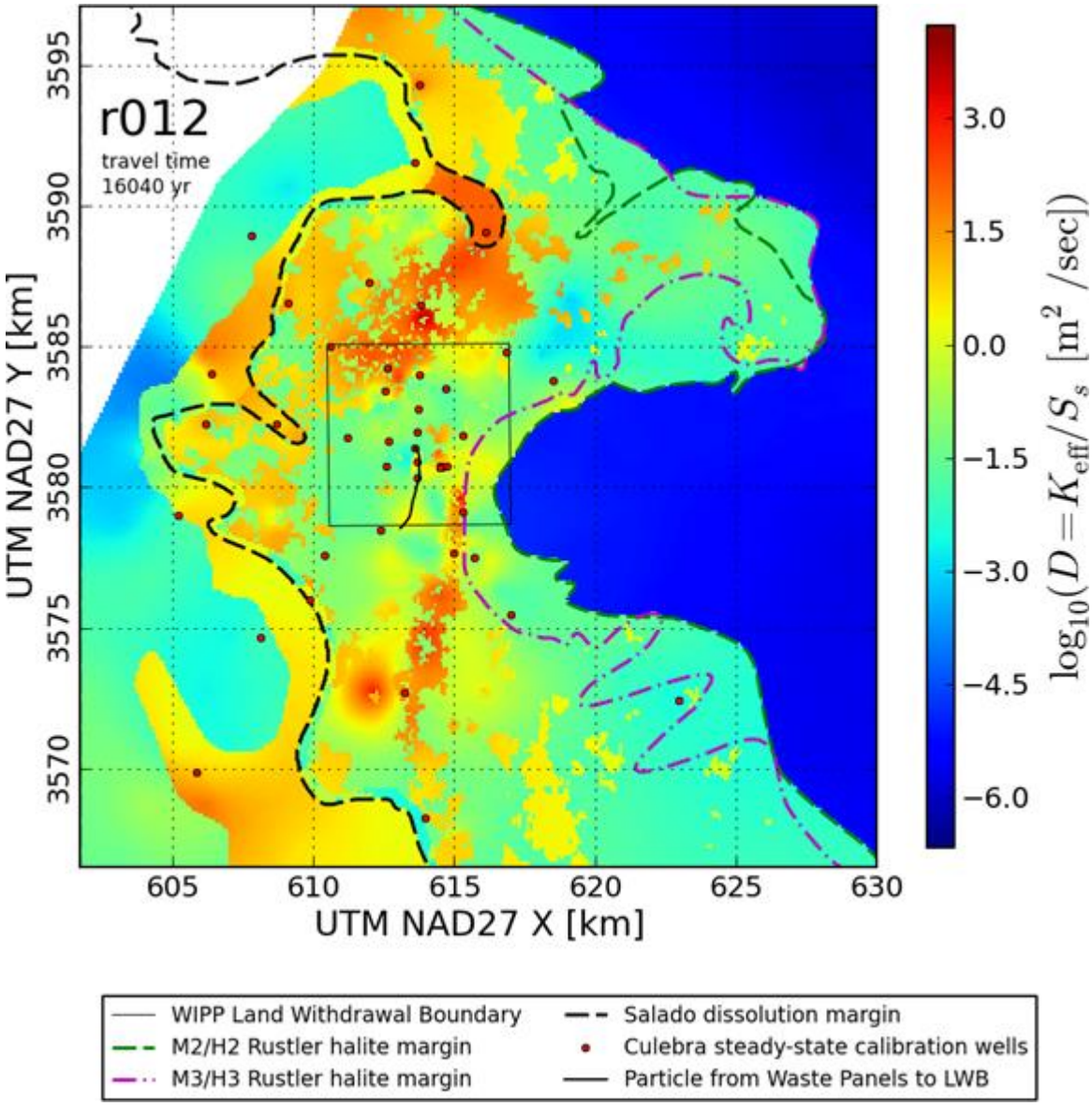
r012
travel time
16040 yr
UTM NAD27 Y [km]
3595
3590
3585
3580
3575
3570
605
610
615
620
625
630
UTM NAD27 X [km]
3.0
1.5
0.0
−1.5
−3.0
−4.5
−6.0
$\log_{10}(D = K_{\text{eff}}/S_s \ [\text{m}^2/\text{sec}])$
WIPP Land Withdrawal Boundary
M2/H2 Rustler halite margin
M3/H3 Rustler halite margin
Salado dissolution margin
Culebra steady-state calibration wells
Particle from Waste Panels to LWB

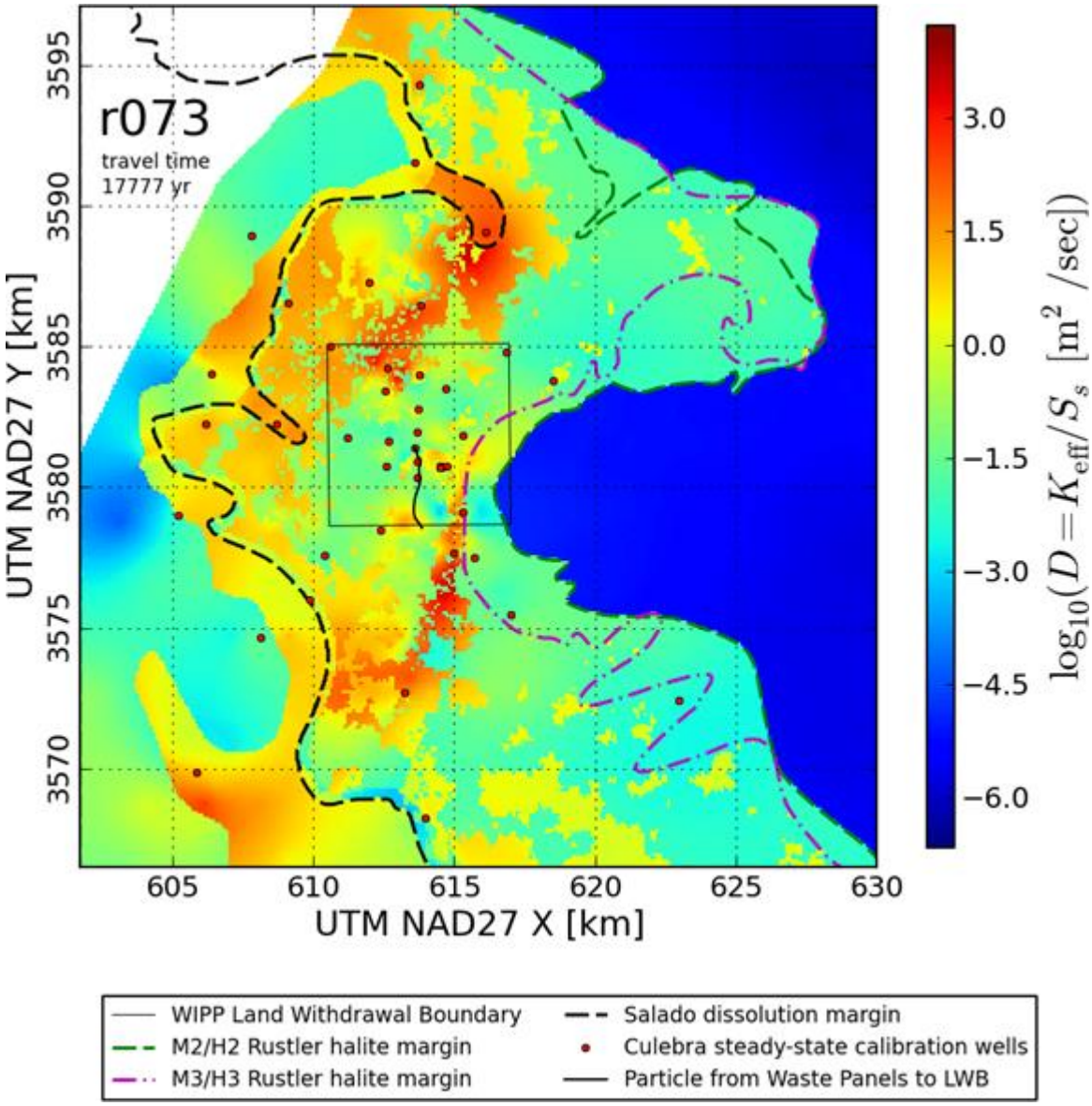
r073
travel time
17777 yr
UTM NAD27 Y [km]
3595
3590
3585
3580
3575
3570
605
610
615
620
625
630
UTM NAD27 X [km]
3.0
1.5
0.0
−1.5
−3.0
−4.5
−6.0
$\log_{10}(D = K_{\text{eff}}/S_s \ [\text{m}^2/\text{sec}])$
WIPP Land Withdrawal Boundary
M2/H2 Rustler halite margin
M3/H3 Rustler halite margin
Salado dissolution margin
Culebra steady-state calibration wells
Particle from Waste Panels to LWB

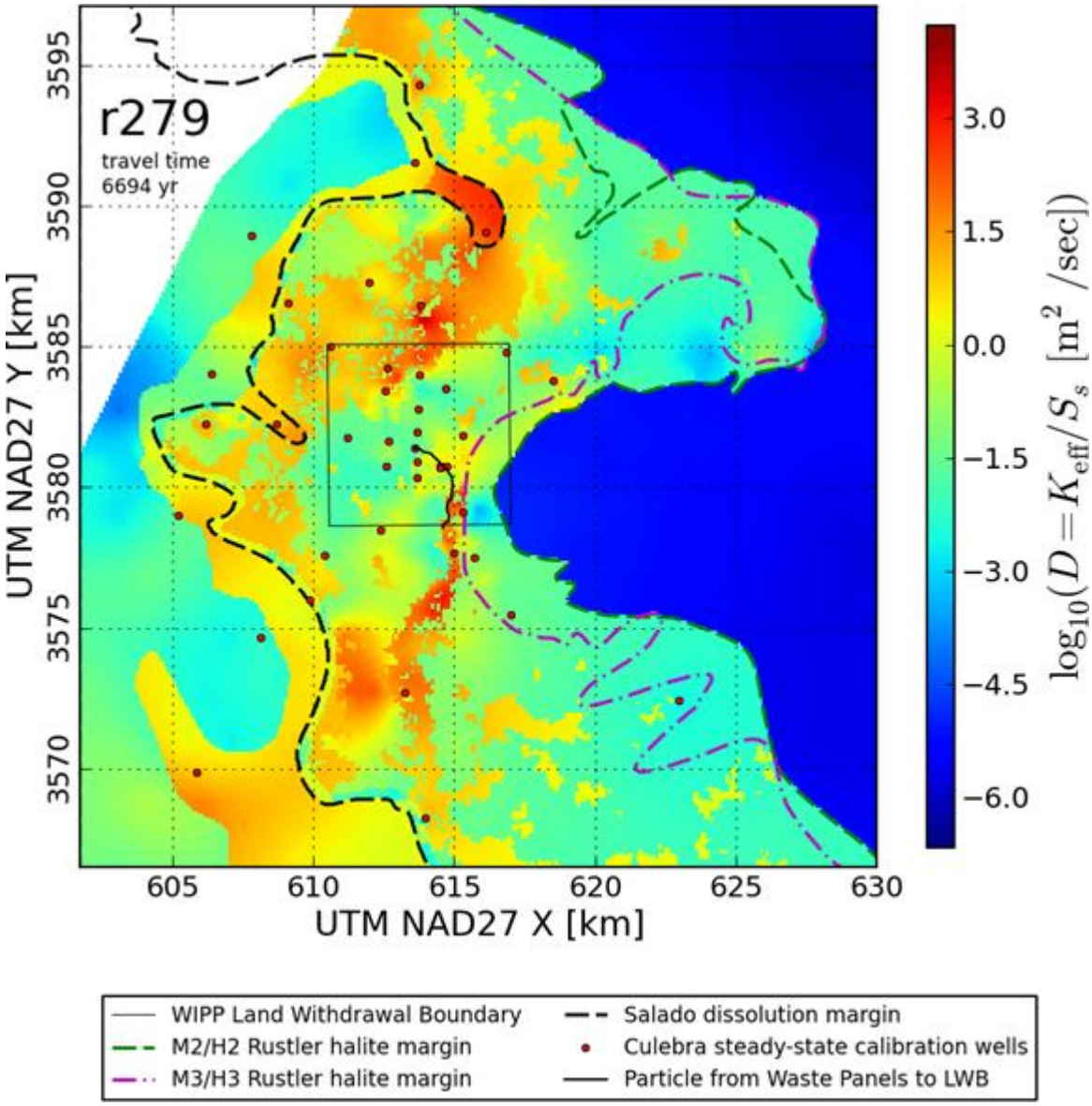
r279
travel time
6694 yr
UTM NAD27 Y [km]
3595
3590
3585
3580
3575
3570
605
610
615
620
625
630
UTM NAD27 X [km]
3.0
1.5
0.0
−1.5
−3.0
−4.5
−6.0
$\log_{10}(D = K_{\text{eff}}/S_s \ [\text{m}^2/\text{sec}])$
WIPP Land Withdrawal Boundary
M2/H2 Rustler halite margin
M3/H3 Rustler halite margin
Salado dissolution margin
Culebra steady-state calibration wells
Particle from Waste Panels to LWB

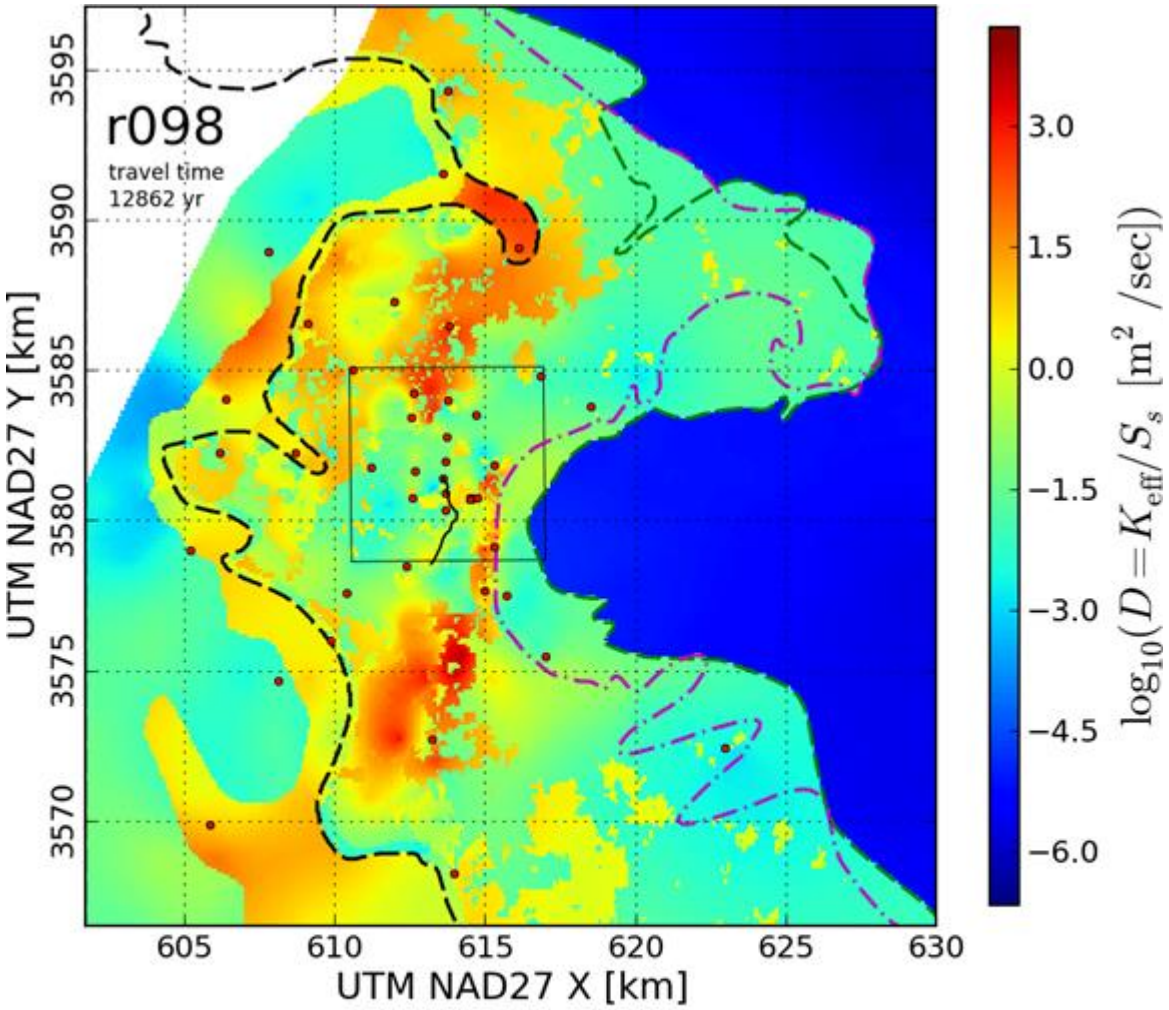
r098
travel time
12862 yr
UTM NAD27 Y [km]
3595
3590
3585
3580
3575
3570
605
610
615
620
625
630
UTM NAD27 X [km]
3.0
1.5
0.0
−1.5
−3.0
−4.5
−6.0
$\log_{10}(D = K_{\text{eff}}/S_s \ [\text{m}^2/\text{sec}])$
WIPP Land Withdrawal Boundary
M2/H2 Rustler halite margin
M3/H3 Rustler halite margin
Salado dissolution margin
Culebra steady-state calibration wells
Particle from Waste Panels to LWB

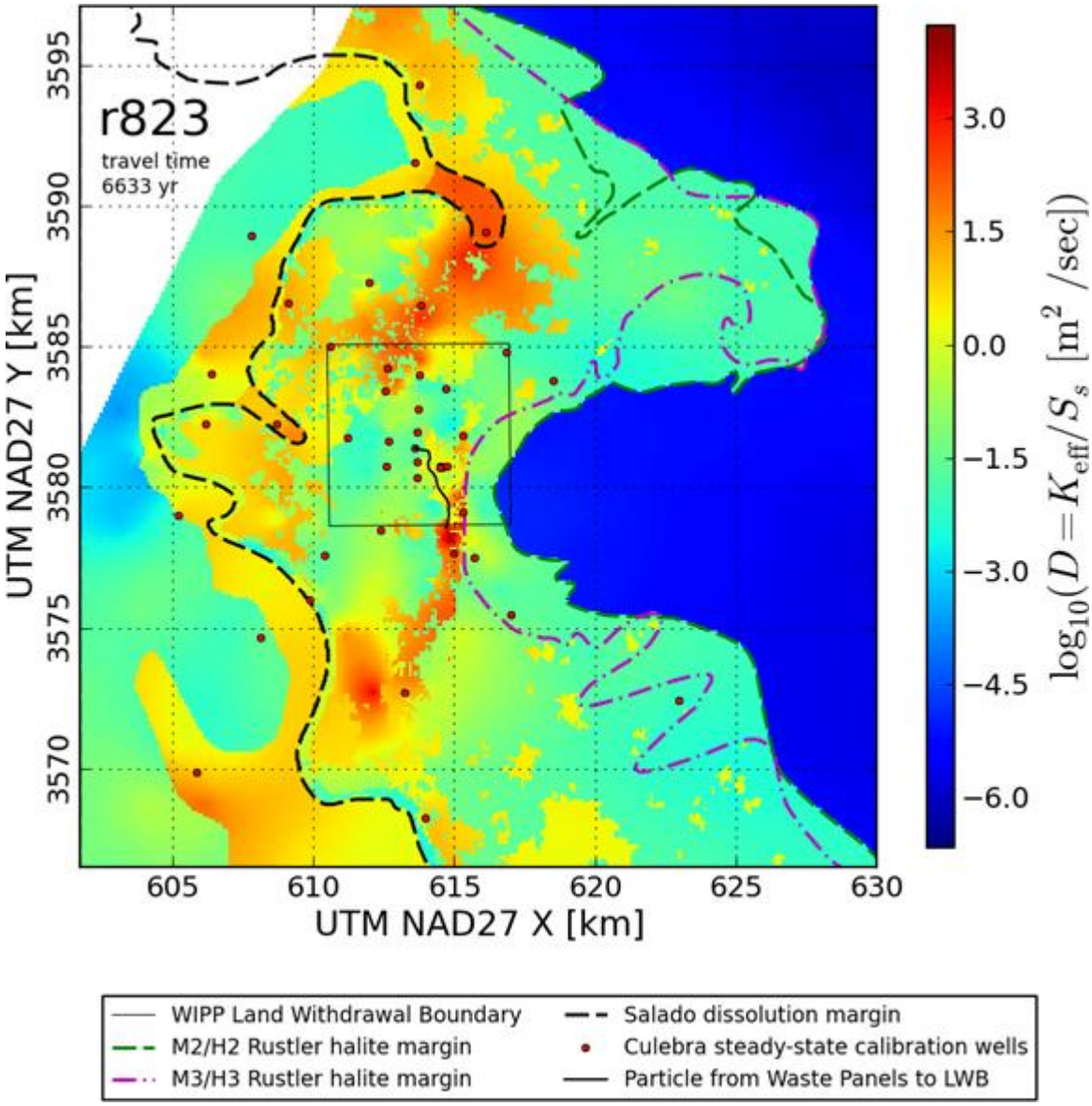
r823
travel time
6633 yr
UTM NAD27 Y [km]
3595
3590
3585
3580
3575
3570
605
610
615
620
625
630
UTM NAD27 X [km]
3.0
1.5
0.0
−1.5
−3.0
−4.5
−6.0
$\log_{10}(D = K_{\text{eff}}/S_s \ [\text{m}^2/\text{sec}])$
WIPP Land Withdrawal Boundary
M2/H2 Rustler halite margin
M3/H3 Rustler halite margin
Salado dissolution margin
Culebra steady-state calibration wells
Particle from Waste Panels to LWB

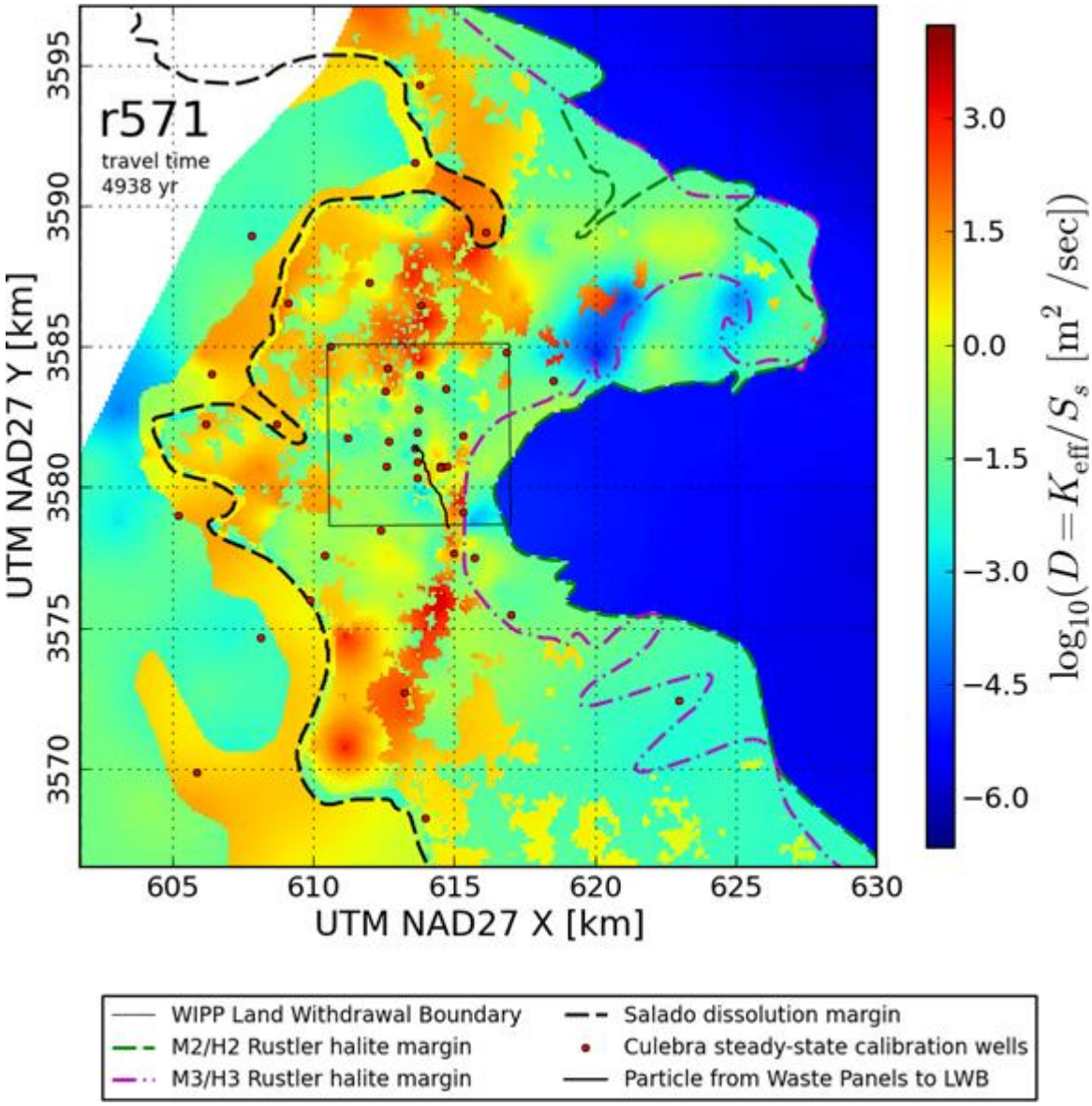
r571
travel time
4938 yr
UTM NAD27 Y [km]
3595
3590
3585
3580
3575
3570
605
610
615
620
625
630
UTM NAD27 X [km]
3.0
1.5
0.0
−1.5
−3.0
−4.5
−6.0
$\log_{10}(D = K_{\text{eff}}/S_s \ [\text{m}^2/\text{sec}])$
WIPP Land Withdrawal Boundary
M2/H2 Rustler halite margin
M3/H3 Rustler halite margin
Salado dissolution margin
Culebra steady-state calibration wells
Particle from Waste Panels to LWB

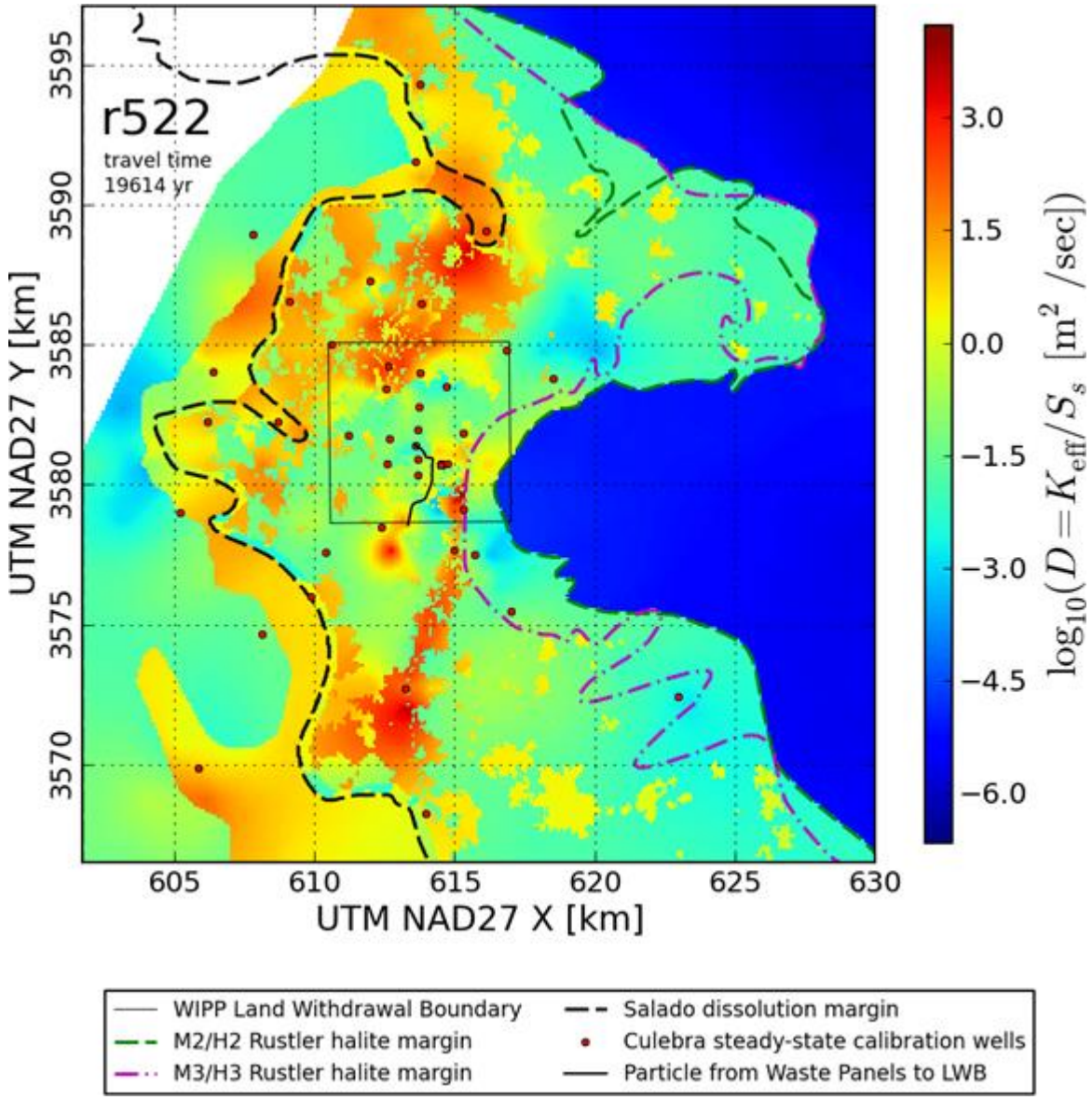
r522
travel time
19614 yr
UTM NAD27 Y [km]
3595
3590
3585
3580
3575
3570
605
610
615
620
625
630
UTM NAD27 X [km]
3.0
1.5
0.0
−1.5
−3.0
−4.5
−6.0
$\log_{10}(D = K_{\text{eff}}/S_s \ [\text{m}^2/\text{sec}])$
WIPP Land Withdrawal Boundary
M2/H2 Rustler halite margin
M3/H3 Rustler halite margin
Salado dissolution margin
Culebra steady-state calibration wells
Particle from Waste Panels to LWB

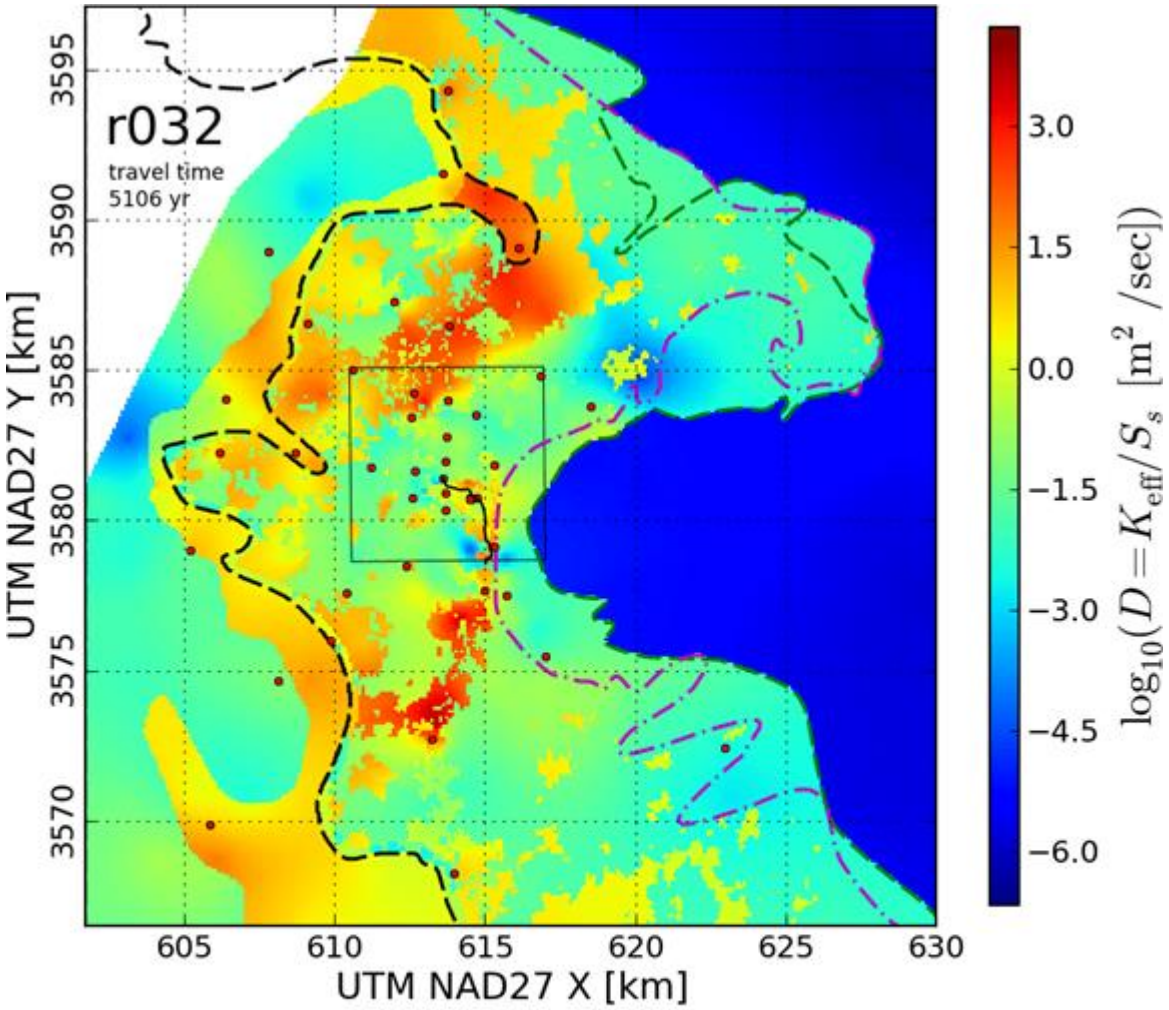
r032
travel time
5106 yr
UTM NAD27 Y [km]
3595
3590
3585
3580
3575
3570
605
610
615
620
625
630
UTM NAD27 X [km]
3.0
1.5
0.0
−1.5
−3.0
−4.5
−6.0
$\log_{10}(D = K_{\text{eff}}/S_s \ [\text{m}^2/\text{sec}])$
WIPP Land Withdrawal Boundary
M2/H2 Rustler halite margin
M3/H3 Rustler halite margin
Salado dissolution margin
Culebra steady-state calibration wells
Particle from Waste Panels to LWB

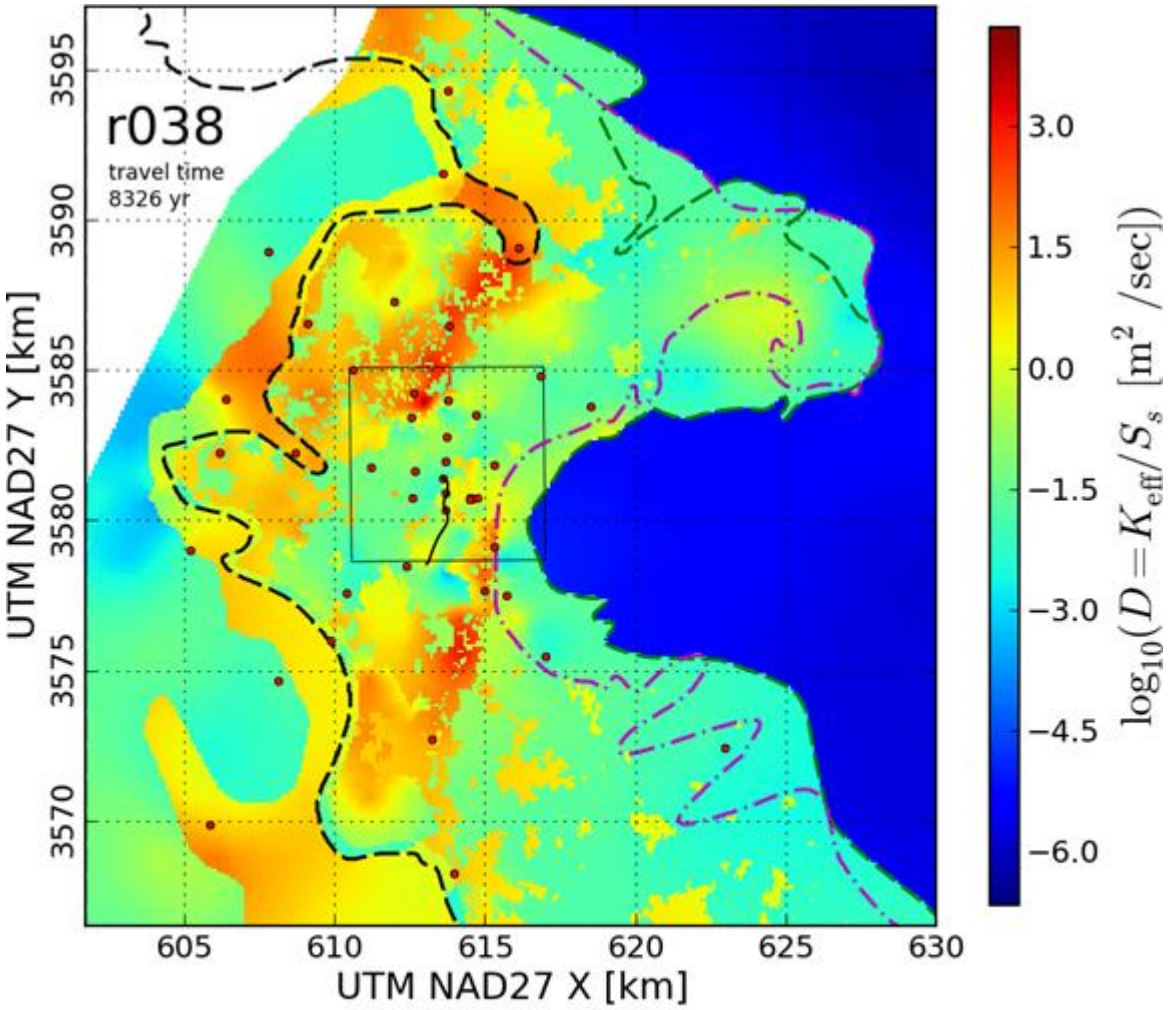
r038
travel time
8326 yr
UTM NAD27 Y [km]
3595
3590
3585
3580
3575
3570
605
610
615
620
625
630
UTM NAD27 X [km]
3.0
1.5
0.0
−1.5
−3.0
−4.5
−6.0
$\log_{10}(D = K_{\text{eff}}/S_s \ [\text{m}^2/\text{sec}])$
WIPP Land Withdrawal Boundary
M2/H2 Rustler halite margin
M3/H3 Rustler halite margin
Salado dissolution margin
Culebra steady-state calibration wells
Particle from Waste Panels to LWB

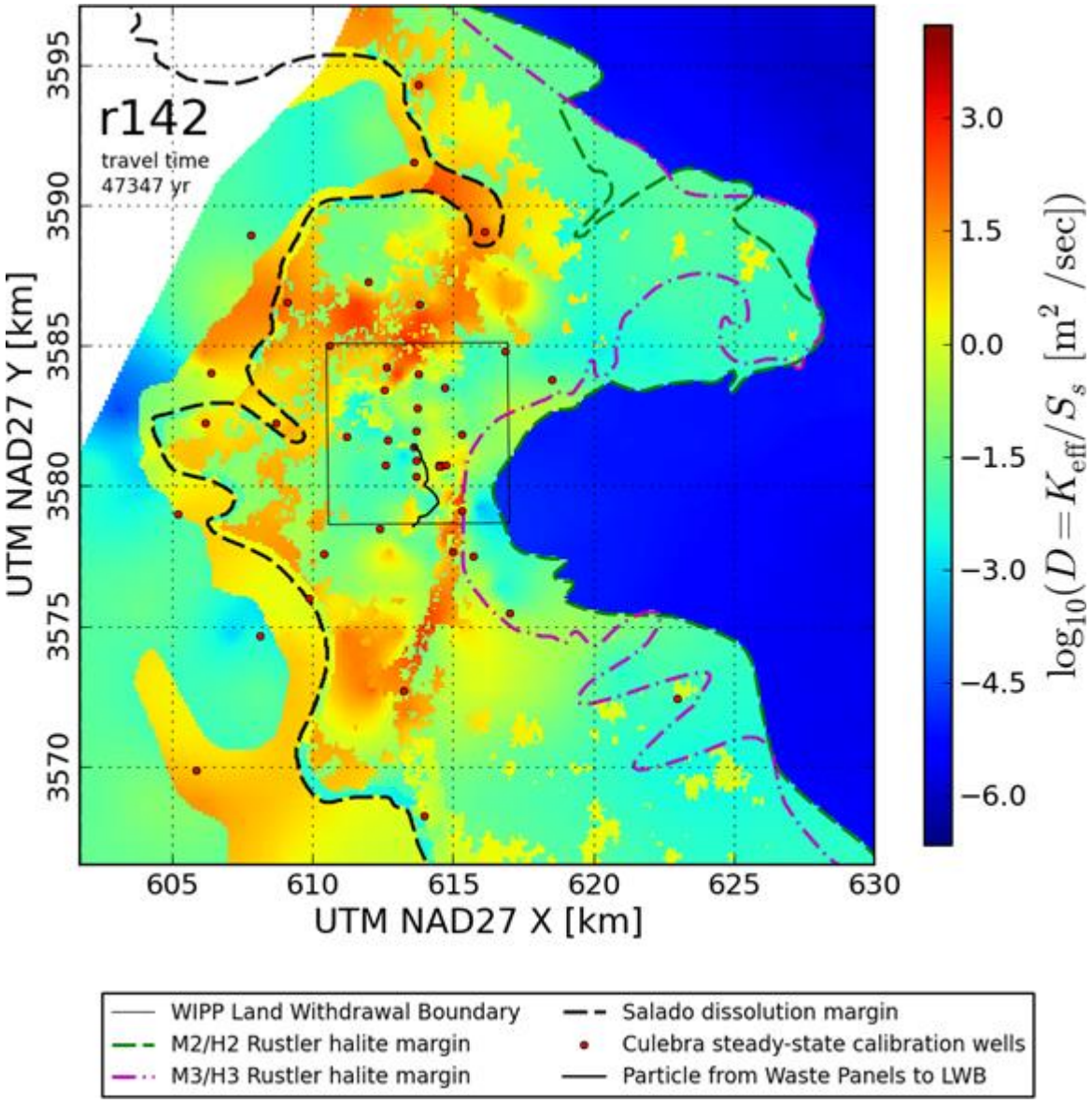
r142
travel time
47347 yr
UTM NAD27 Y [km]
3595
3590
3585
3580
3575
3570
605
610
615
620
625
630
UTM NAD27 X [km]
3.0
1.5
0.0
−1.5
−3.0
−4.5
−6.0
$\log_{10}(D = K_{\text{eff}}/S_s \ [\text{m}^2/\text{sec}])$
WIPP Land Withdrawal Boundary
M2/H2 Rustler halite margin
M3/H3 Rustler halite margin
Salado dissolution margin
Culebra steady-state calibration wells
Particle from Waste Panels to LWB

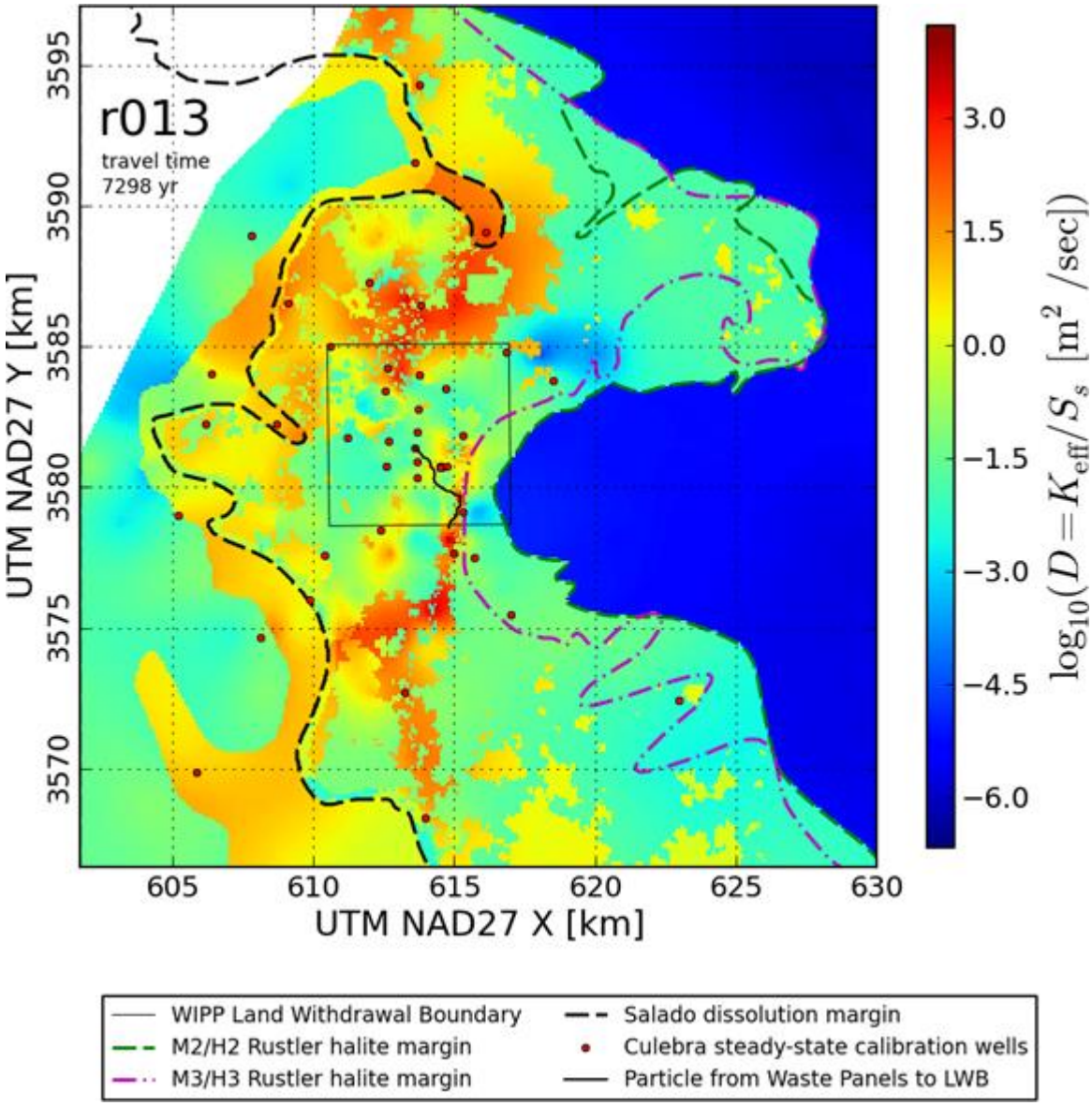
r013
travel time
7298 yr
UTM NAD27 Y [km]
3595
3590
3585
3580
3575
3570
605
610
615
620
625
630
UTM NAD27 X [km]
3.0
1.5
0.0
−1.5
−3.0
−4.5
−6.0
$\log_{10}(D = K_{\text{eff}}/S_s \ [\text{m}^2/\text{sec}])$
WIPP Land Withdrawal Boundary
M2/H2 Rustler halite margin
M3/H3 Rustler halite margin
Salado dissolution margin
Culebra steady-state calibration wells
Particle from Waste Panels to LWB

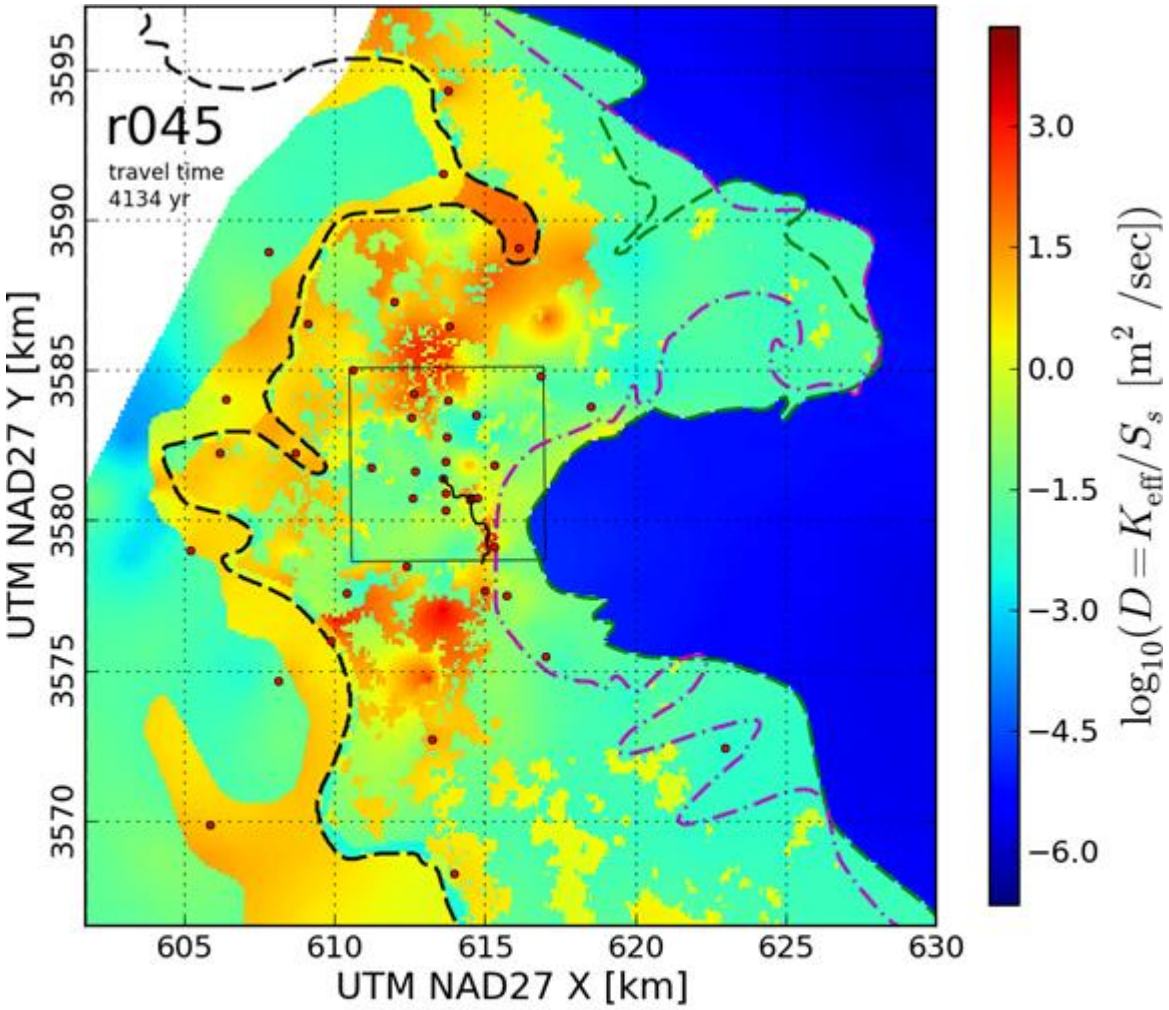
r045
travel time
4134 yr
UTM NAD27 Y [km]
3595
3590
3585
3580
3575
3570
605
610
615
620
625
630
UTM NAD27 X [km]
3.0
1.5
0.0
−1.5
−3.0
−4.5
−6.0
$\log_{10}(D = K_{\text{eff}}/S_s \ [\text{m}^2/\text{sec}])$
WIPP Land Withdrawal Boundary
M2/H2 Rustler halite margin
M3/H3 Rustler halite margin
Salado dissolution margin
Culebra steady-state calibration wells
Particle from Waste Panels to LWB

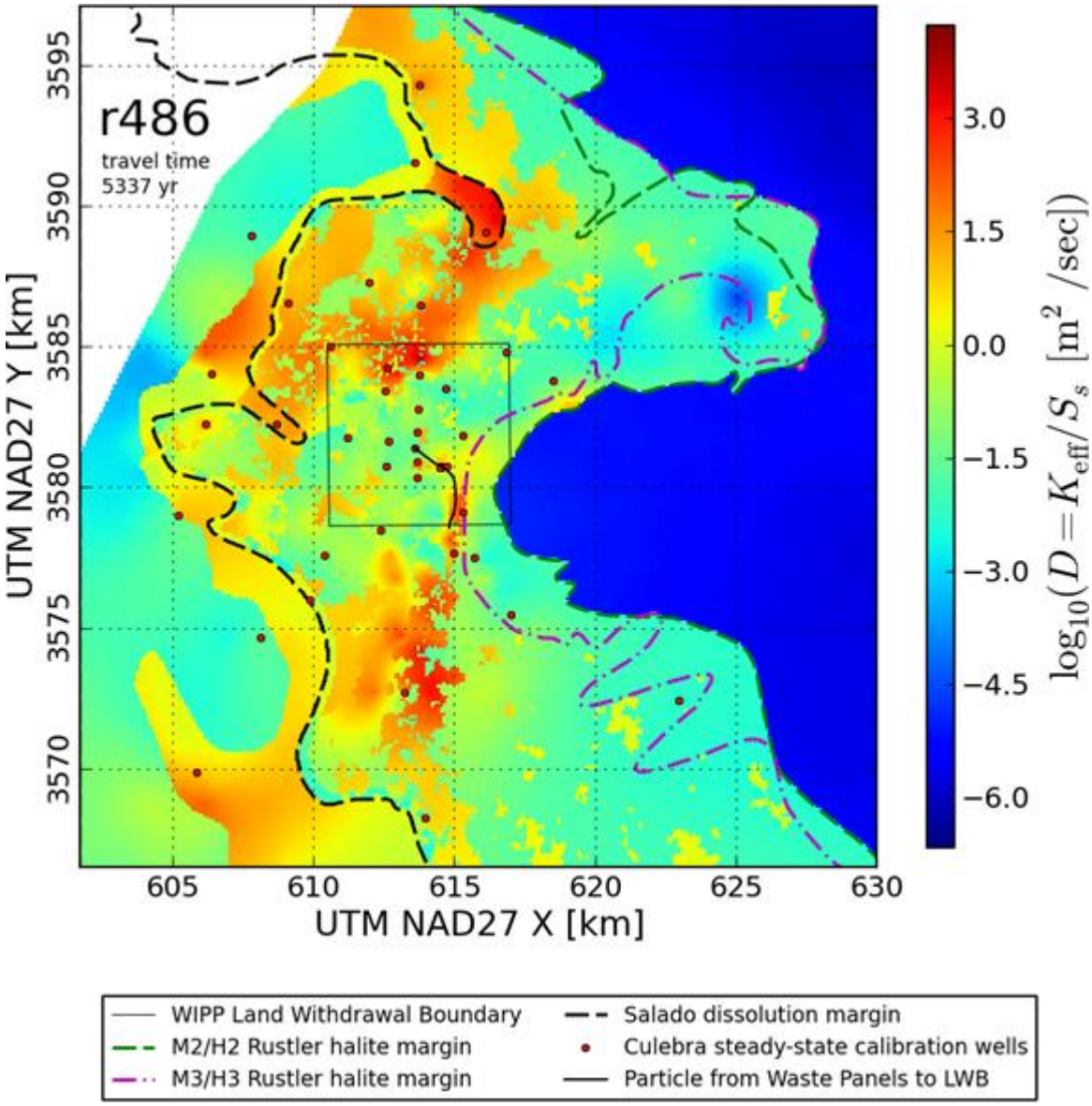
r486
travel time
5337 yr
UTM NAD27 Y [km]
3595
3590
3585
3580
3575
3570
605
610
615
620
625
630
UTM NAD27 X [km]
3.0
1.5
0.0
−1.5
−3.0
−4.5
−6.0
$\log_{10}(D = K_{\text{eff}}/S_s \ [\text{m}^2/\text{sec}])$
WIPP Land Withdrawal Boundary
M2/H2 Rustler halite margin
M3/H3 Rustler halite margin
Salado dissolution margin
Culebra steady-state calibration wells
Particle from Waste Panels to LWB

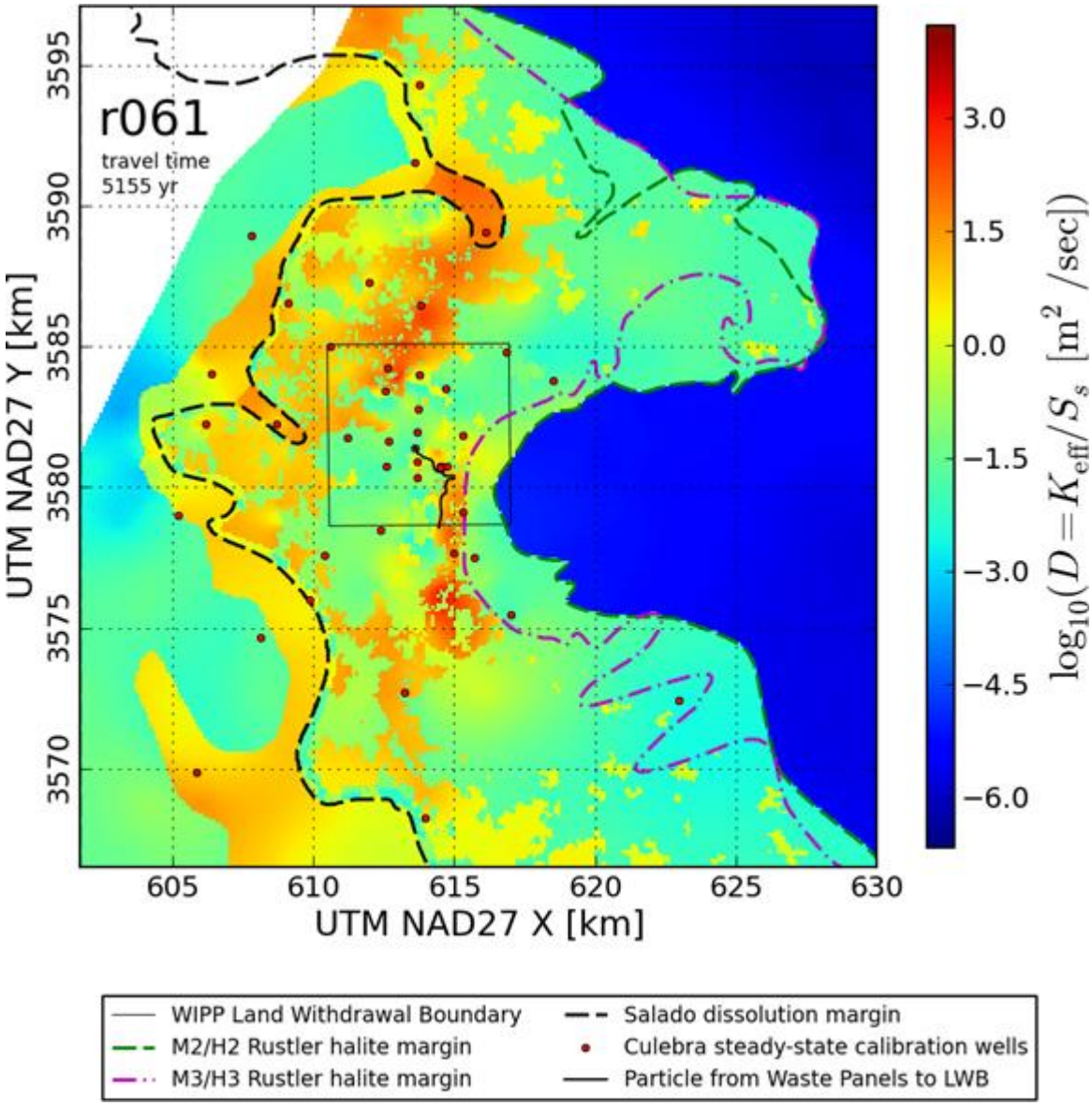
r061
travel time
5155 yr
UTM NAD27 Y [km]
3595
3590
3585
3580
3575
3570
605
610
615
620
625
630
UTM NAD27 X [km]
3.0
1.5
0.0
−1.5
−3.0
−4.5
−6.0
$\log_{10}(D = K_{\text{eff}}/S_s \ [\text{m}^2/\text{sec}])$
WIPP Land Withdrawal Boundary
M2/H2 Rustler halite margin
M3/H3 Rustler halite margin
Salado dissolution margin
Culebra steady-state calibration wells
Particle from Waste Panels to LWB

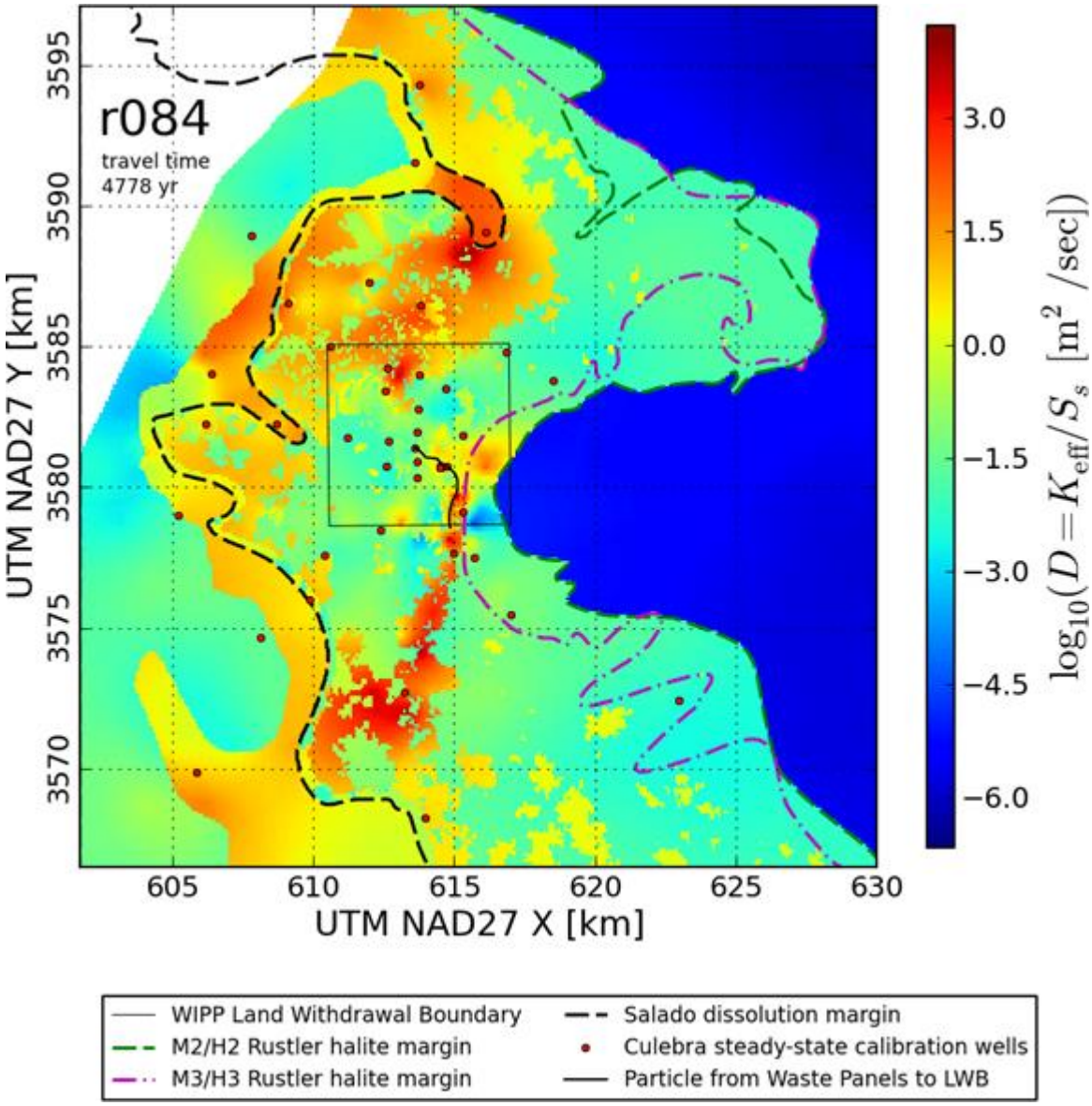
r084
travel time
4778 yr
UTM NAD27 Y [km]
3595
3590
3585
3580
3575
3570
605
610
615
620
625
630
UTM NAD27 X [km]
3.0
1.5
0.0
−1.5
−3.0
−4.5
−6.0
$\log_{10}(D = K_{\text{eff}}/S_s \ [\text{m}^2/\text{sec}])$
WIPP Land Withdrawal Boundary
M2/H2 Rustler halite margin
M3/H3 Rustler halite margin
Salado dissolution margin
Culebra steady-state calibration wells
Particle from Waste Panels to LWB

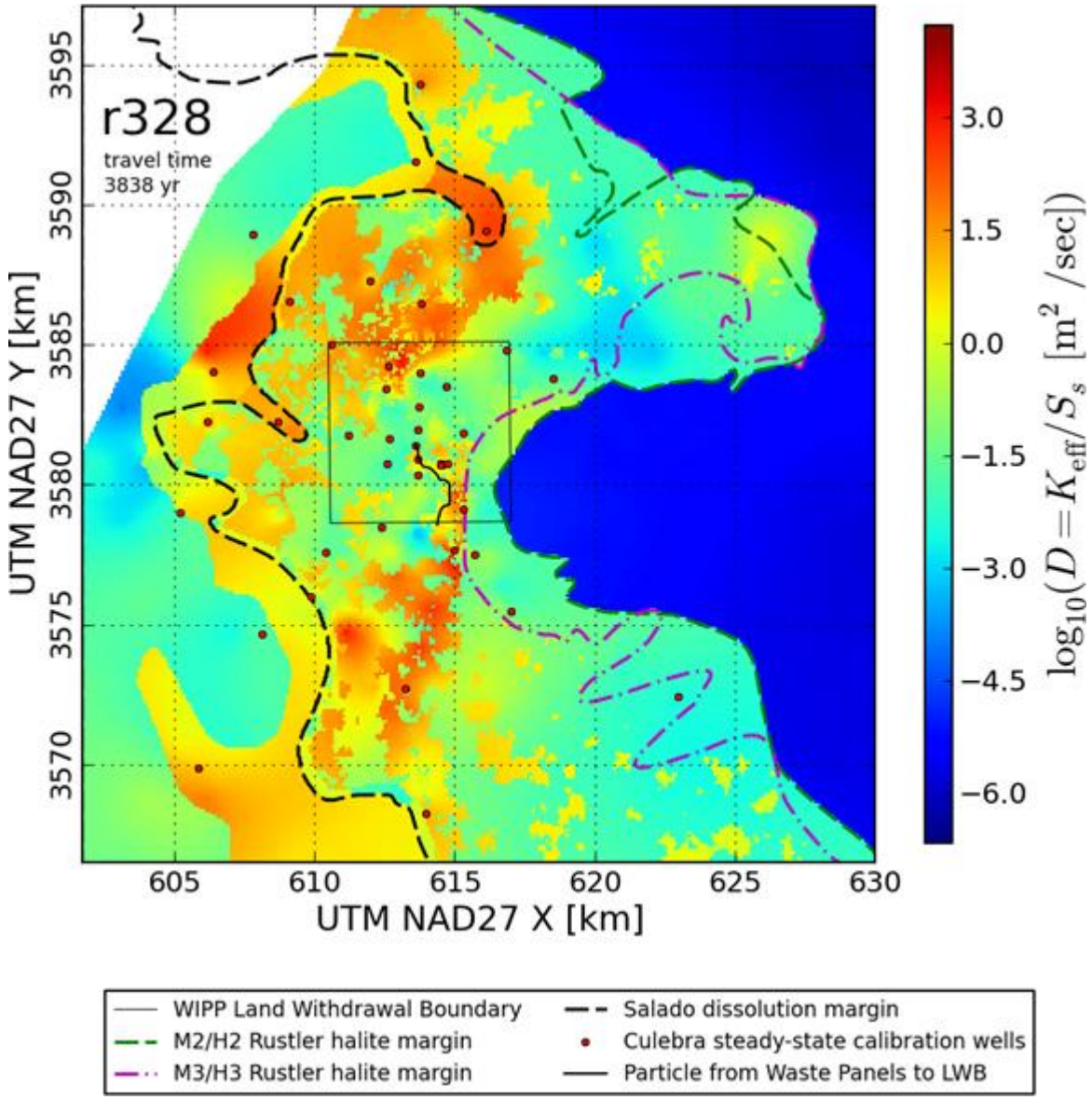
r328
travel time
3838 yr
UTM NAD27 Y [km]
3595
3590
3585
3580
3575
3570
605
610
615
620
625
630
UTM NAD27 X [km]
3.0
1.5
0.0
−1.5
−3.0
−4.5
−6.0
$\log_{10}(D = K_{\text{eff}}/S_s \ [\text{m}^2/\text{sec}])$
WIPP Land Withdrawal Boundary
M2/H2 Rustler halite margin
M3/H3 Rustler halite margin
Salado dissolution margin
Culebra steady-state calibration wells
Particle from Waste Panels to LWB

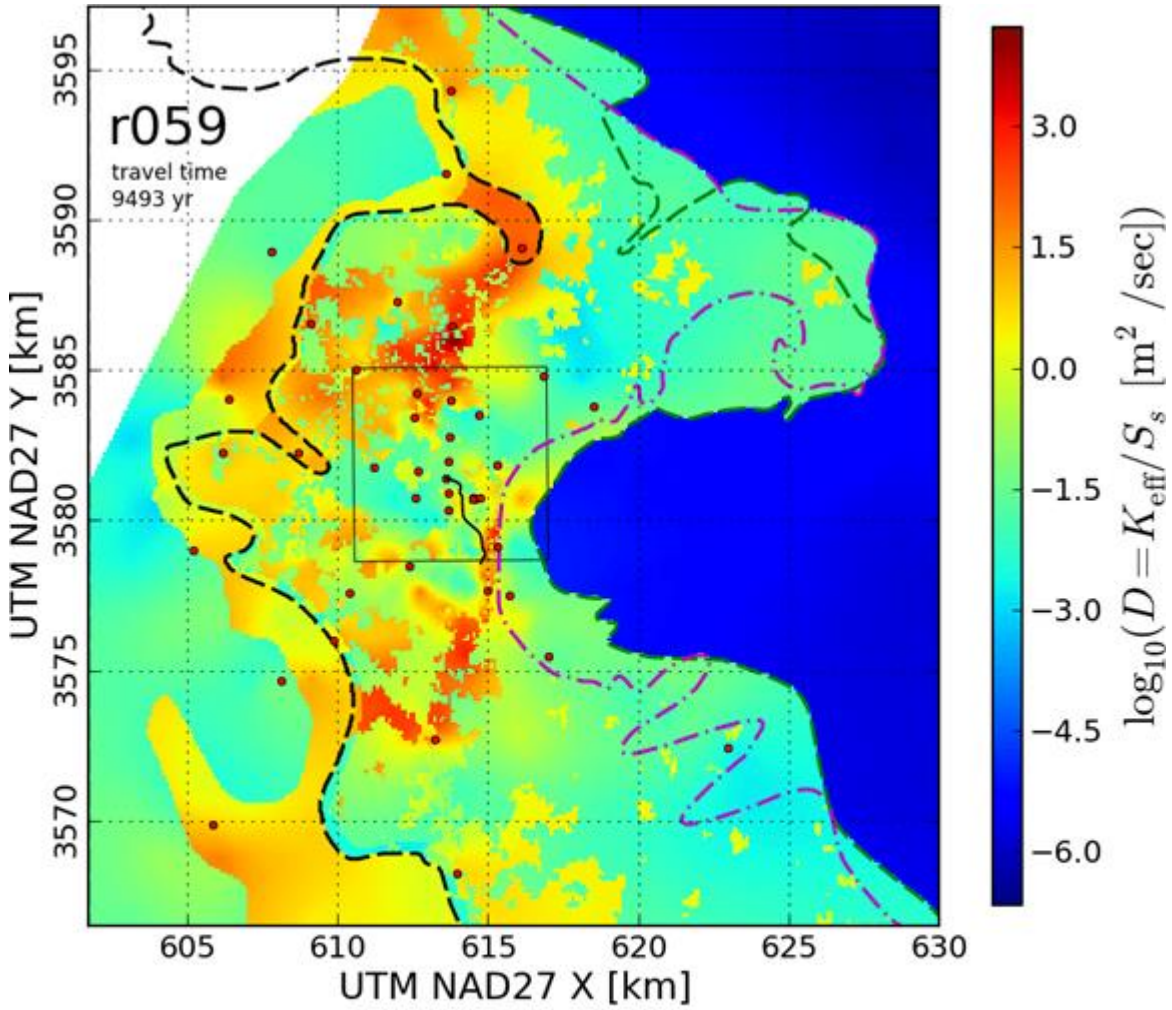
r059
travel time
9493 yr
UTM NAD27 Y [km]
3595
3590
3585
3580
3575
3570
605
610
615
620
625
630
UTM NAD27 X [km]
3.0
1.5
0.0
−1.5
−3.0
−4.5
−6.0
$\log_{10}(D = K_{\text{eff}}/S_s \ [\text{m}^2/\text{sec}])$
WIPP Land Withdrawal Boundary
M2/H2 Rustler halite margin
M3/H3 Rustler halite margin
Salado dissolution margin
Culebra steady-state calibration wells
Particle from Waste Panels to LWB

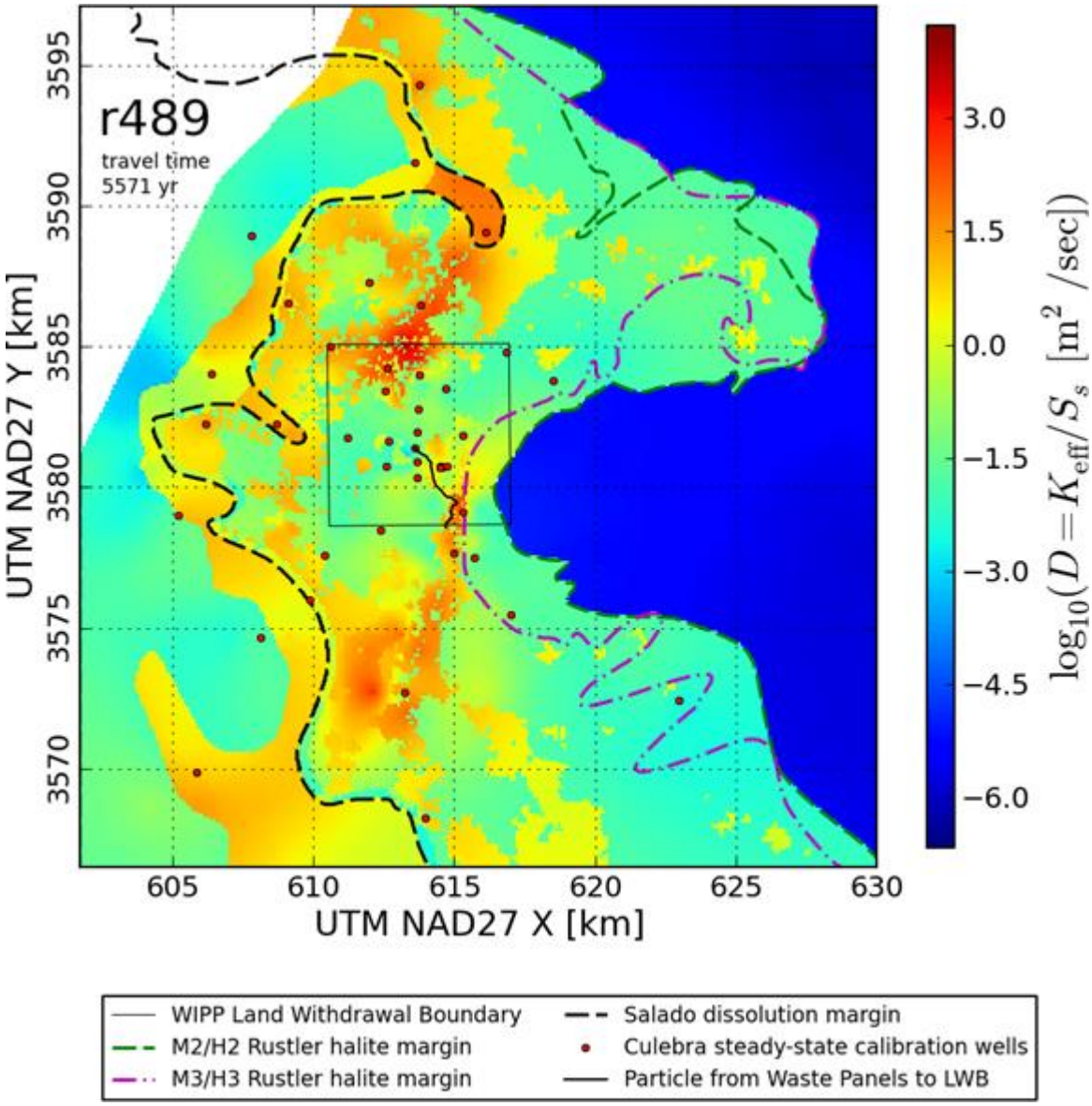
r489
travel time
5571 yr
UTM NAD27 Y [km]
3595
3590
3585
3580
3575
3570
605
610
615
620
625
630
UTM NAD27 X [km]
3.0
1.5
0.0
−1.5
−3.0
−4.5
−6.0
$\log_{10}(D = K_{\text{eff}}/S_s \ [\text{m}^2/\text{sec}])$
WIPP Land Withdrawal Boundary
M2/H2 Rustler halite margin
M3/H3 Rustler halite margin
Salado dissolution margin
Culebra steady-state calibration wells
Particle from Waste Panels to LWB

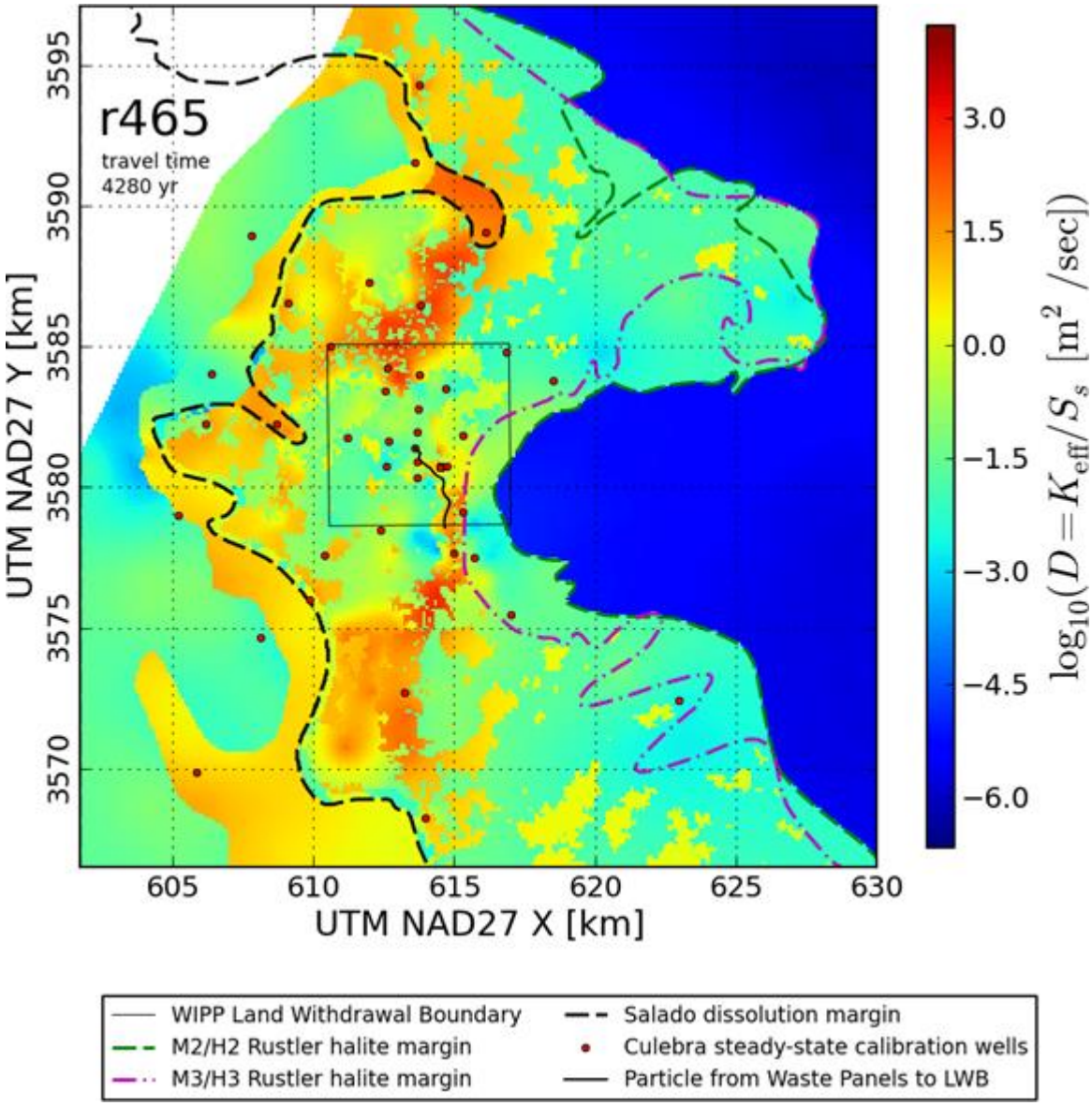
r465
travel time
4280 yr
UTM NAD27 Y [km]
3595
3590
3585
3580
3575
3570
605
610
615
620
625
630
UTM NAD27 X [km]
3.0
1.5
0.0
−1.5
−3.0
−4.5
−6.0
$\log_{10}(D = K_{\text{eff}}/S_s \ [\text{m}^2/\text{sec}])$
WIPP Land Withdrawal Boundary
M2/H2 Rustler halite margin
M3/H3 Rustler halite margin
Salado dissolution margin
Culebra steady-state calibration wells
Particle from Waste Panels to LWB

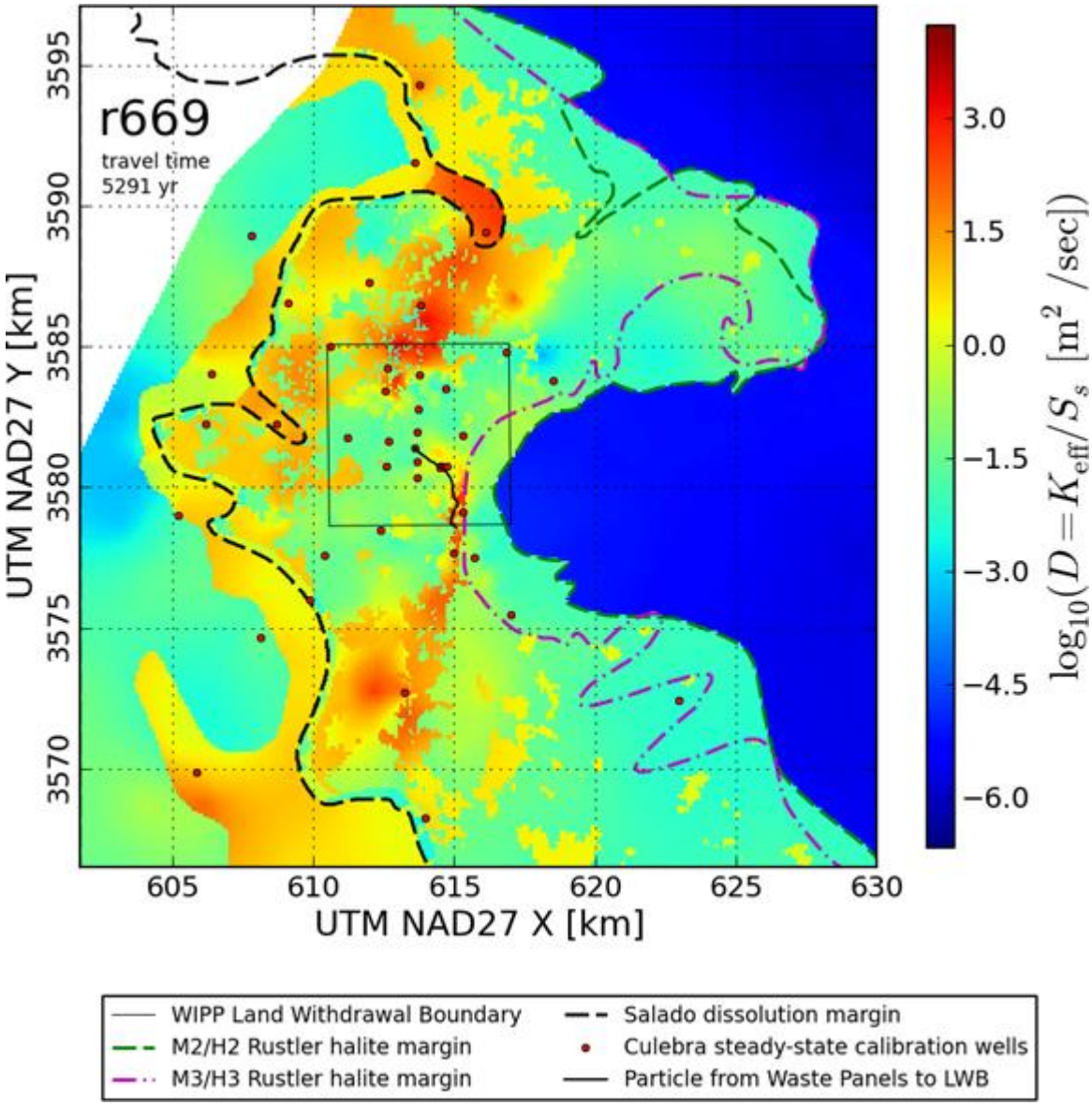
r669
travel time
5291 yr
UTM NAD27 Y [km]
3595
3590
3585
3580
3575
3570
605
610
615
620
625
630
UTM NAD27 X [km]
3.0
1.5
0.0
−1.5
−3.0
−4.5
−6.0
$\log_{10}(D = K_{\text{eff}}/S_s \ [\text{m}^2/\text{sec}])$
WIPP Land Withdrawal Boundary
M2/H2 Rustler halite margin
M3/H3 Rustler halite margin
Salado dissolution margin
Culebra steady-state calibration wells
Particle from Waste Panels to LWB

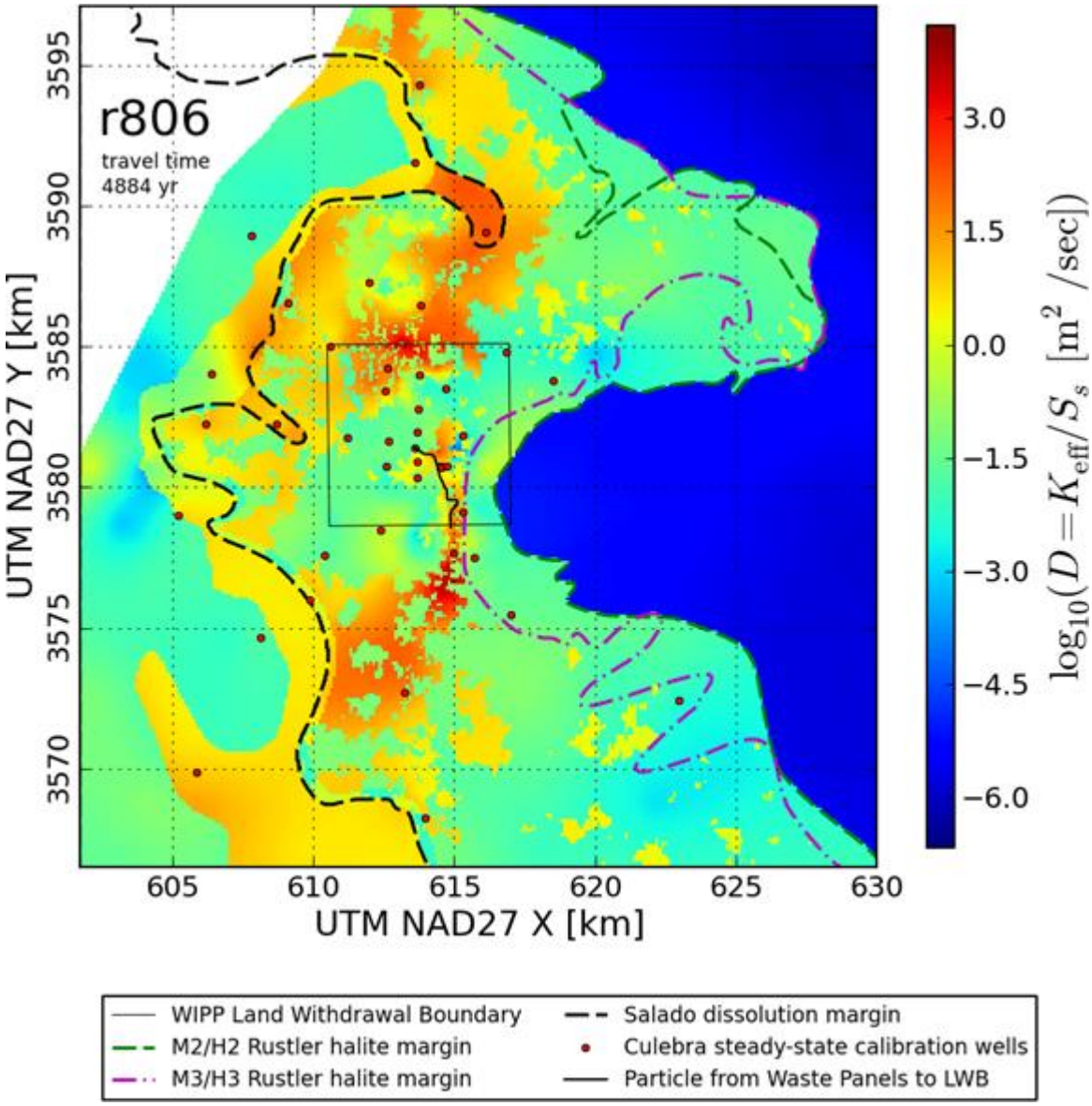
r806
travel time
4884 yr
UTM NAD27 Y [km]
3595
3590
3585
3580
3575
3570
605
610
615
620
625
630
UTM NAD27 X [km]
3.0
1.5
0.0
−1.5
−3.0
−4.5
−6.0
$\log_{10}(D = K_{\text{eff}}/S_s \ [\text{m}^2/\text{sec}])$
WIPP Land Withdrawal Boundary
M2/H2 Rustler halite margin
M3/H3 Rustler halite margin
Salado dissolution margin
Culebra steady-state calibration wells
Particle from Waste Panels to LWB

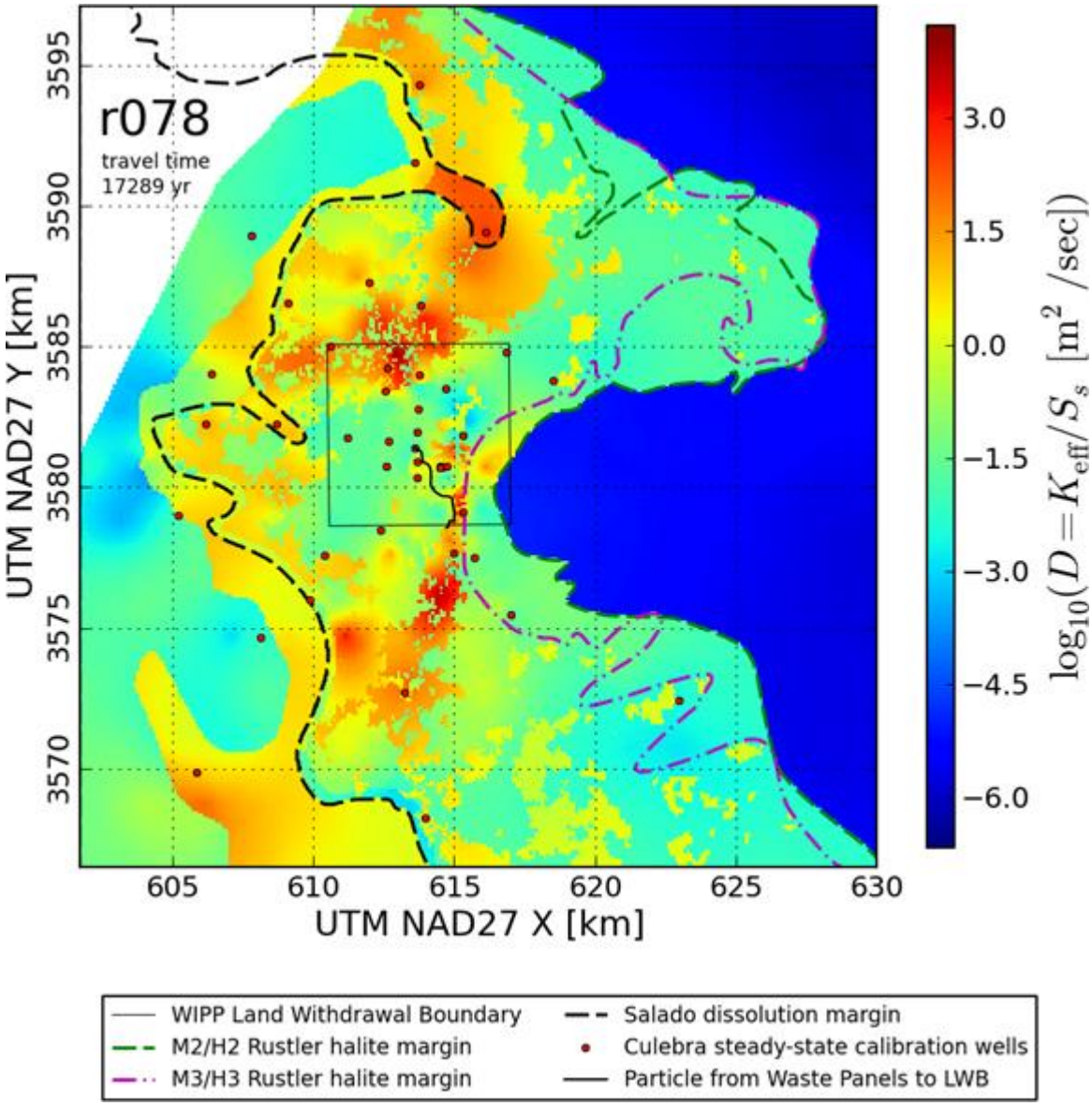
r078
travel time
17289 yr
UTM NAD27 Y [km]
3595
3590
3585
3580
3575
3570
605
610
615
620
625
630
UTM NAD27 X [km]
3.0
1.5
0.0
−1.5
−3.0
−4.5
−6.0
$\log_{10}(D = K_{\text{eff}}/S_s \ [\text{m}^2/\text{sec}])$
WIPP Land Withdrawal Boundary
M2/H2 Rustler halite margin
M3/H3 Rustler halite margin
Salado dissolution margin
Culebra steady-state calibration wells
Particle from Waste Panels to LWB

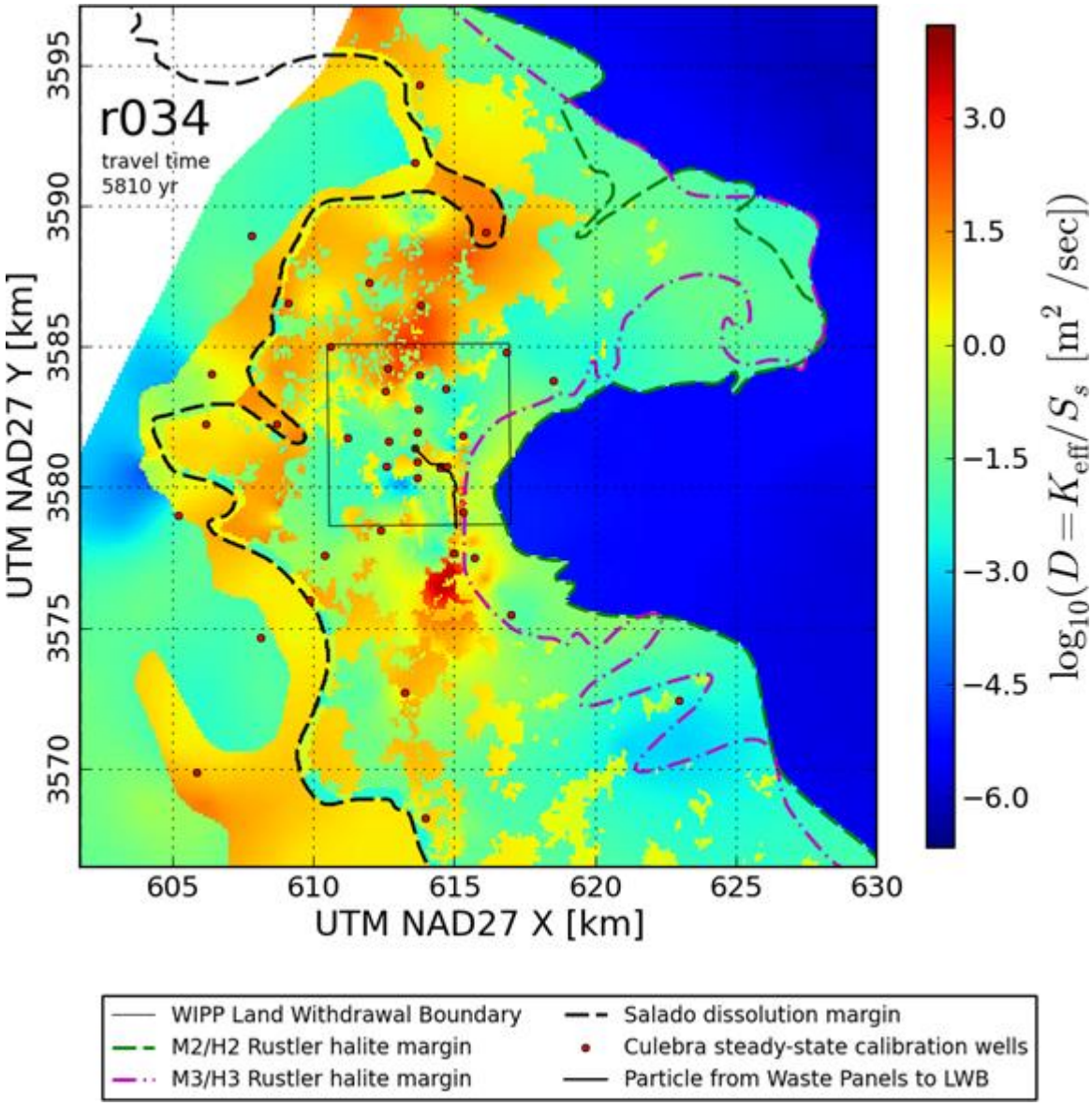
r034
travel time
5810 yr
UTM NAD27 Y [km]
3595
3590
3585
3580
3575
3570
605
610
615
620
625
630
UTM NAD27 X [km]
3.0
1.5
0.0
−1.5
−3.0
−4.5
−6.0
$\log_{10}(D = K_{\text{eff}}/S_s \ [\text{m}^2/\text{sec}])$
WIPP Land Withdrawal Boundary
M2/H2 Rustler halite margin
M3/H3 Rustler halite margin
Salado dissolution margin
Culebra steady-state calibration wells
Particle from Waste Panels to LWB

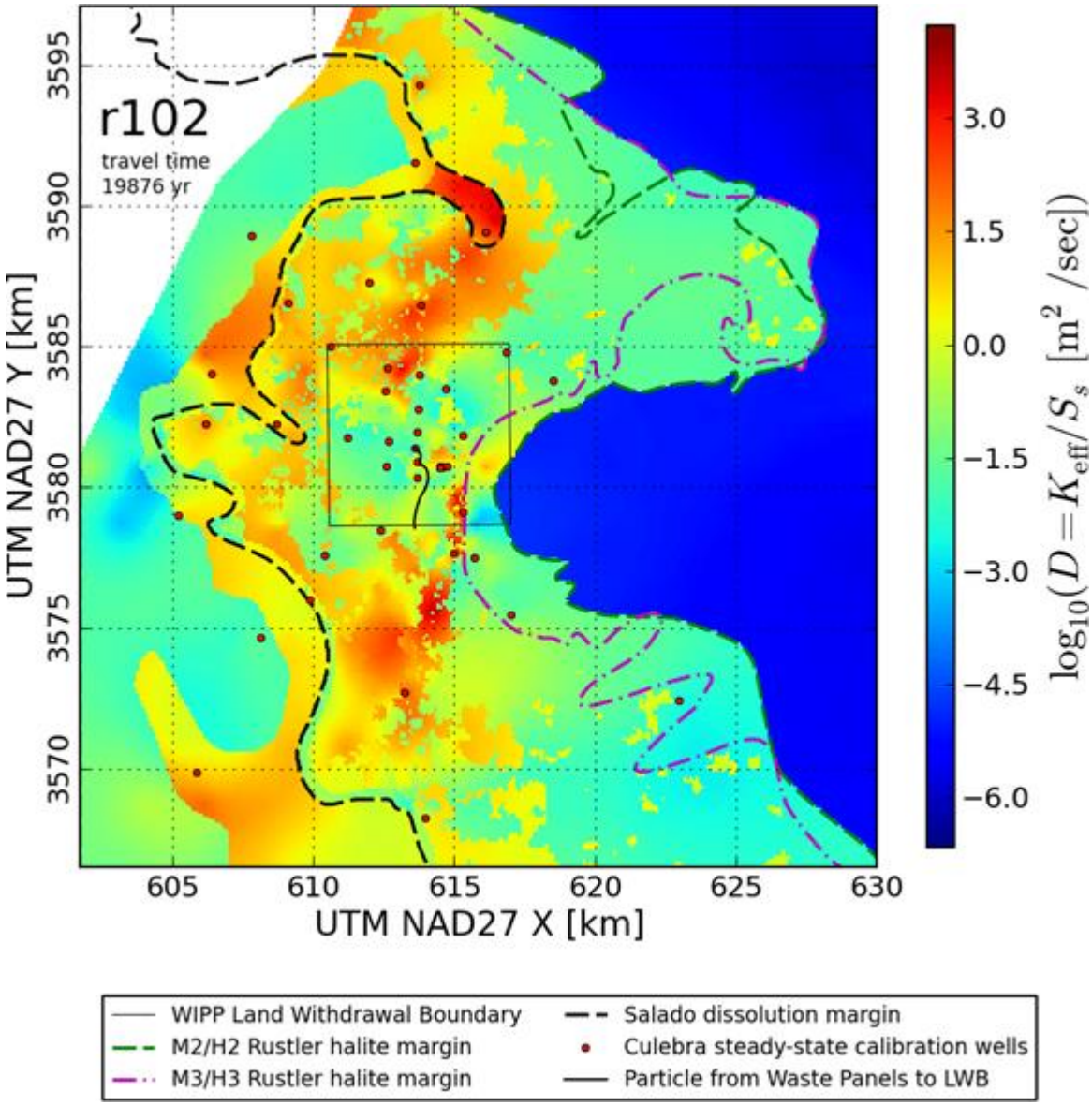
r102
travel time
19876 yr
UTM NAD27 Y [km]
3595
3590
3585
3580
3575
3570
605
610
615
620
625
630
UTM NAD27 X [km]
3.0
1.5
0.0
−1.5
−3.0
−4.5
−6.0
$\log_{10}(D = K_{\text{eff}}/S_s \ [\text{m}^2/\text{sec}])$
WIPP Land Withdrawal Boundary
M2/H2 Rustler halite margin
M3/H3 Rustler halite margin
Salado dissolution margin
Culebra steady-state calibration wells
Particle from Waste Panels to LWB

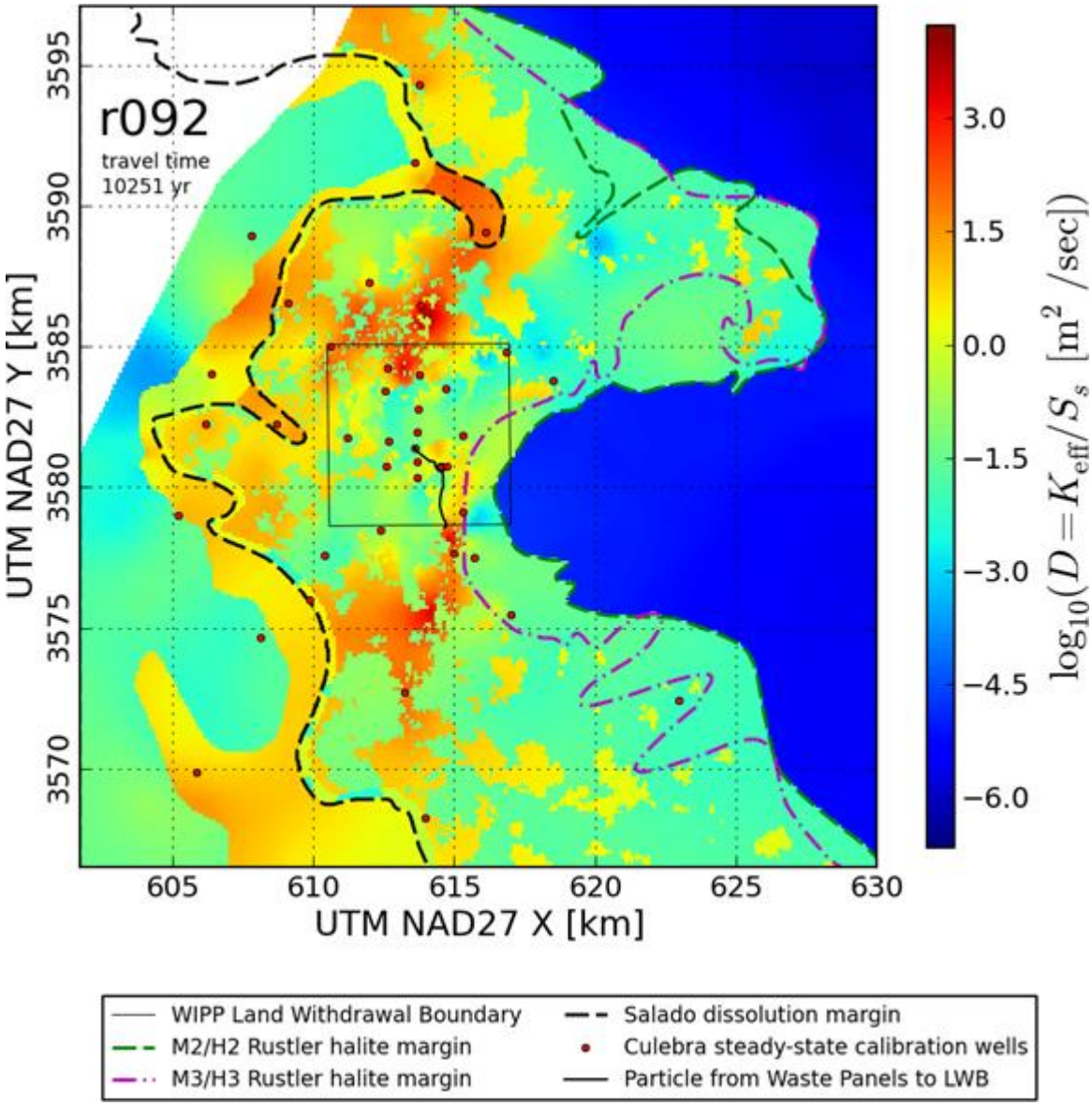
r092
travel time
10251 yr
UTM NAD27 Y [km]
3595
3590
3585
3580
3575
3570
605
610
615
620
625
630
UTM NAD27 X [km]
3.0
1.5
0.0
−1.5
−3.0
−4.5
−6.0
$\log_{10}(D = K_{\text{eff}}/S_s \ [\text{m}^2/\text{sec}])$
WIPP Land Withdrawal Boundary
M2/H2 Rustler halite margin
M3/H3 Rustler halite margin
Salado dissolution margin
Culebra steady-state calibration wells
Particle from Waste Panels to LWB

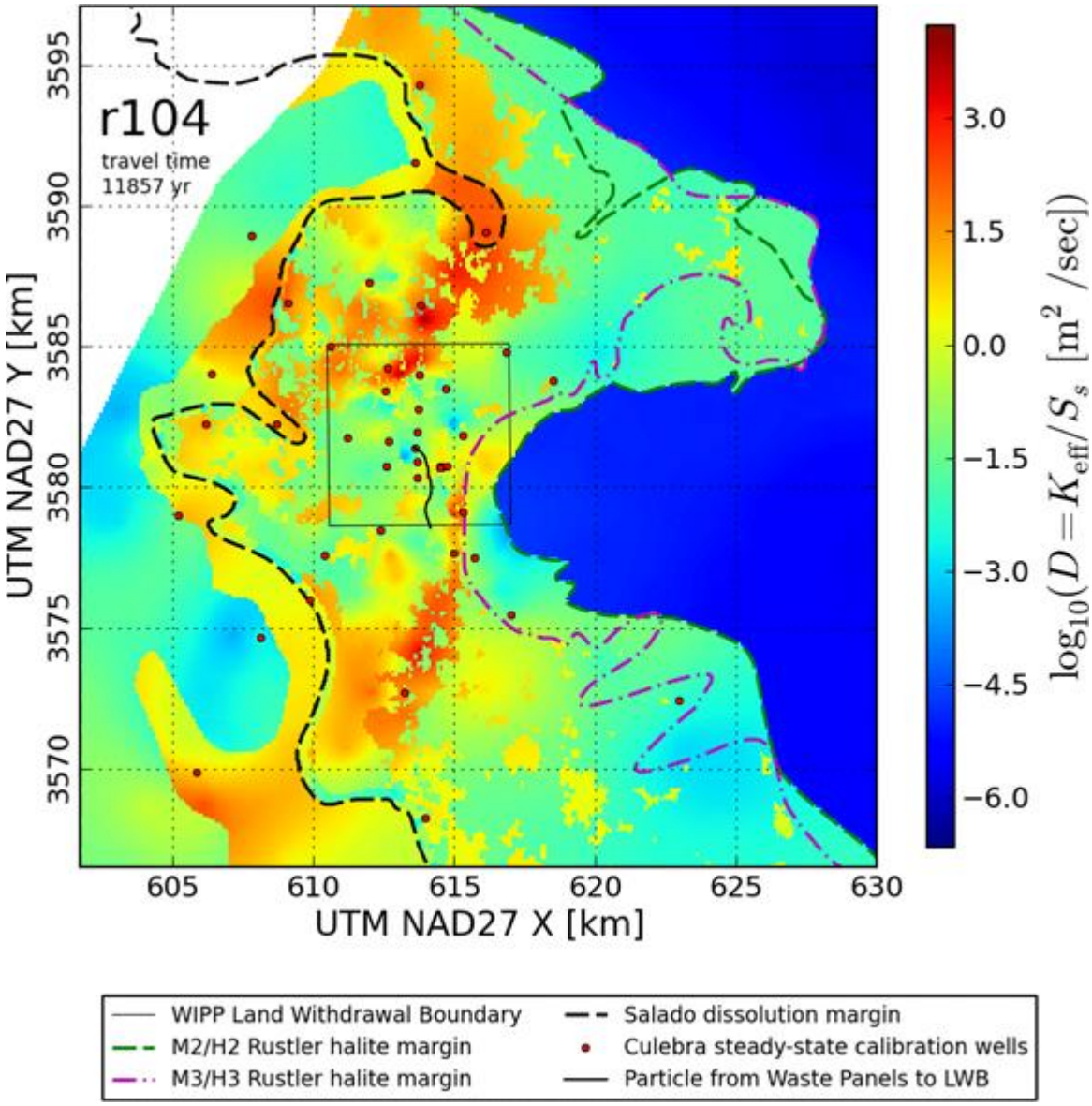
r104
travel time
11857 yr
UTM NAD27 Y [km]
3595
3590
3585
3580
3575
3570
605
610
615
620
625
630
UTM NAD27 X [km]
3.0
1.5
0.0
−1.5
−3.0
−4.5
−6.0
$\log_{10}(D = K_{\text{eff}}/S_s \ [\text{m}^2/\text{sec}])$
WIPP Land Withdrawal Boundary
M2/H2 Rustler halite margin
M3/H3 Rustler halite margin
Salado dissolution margin
Culebra steady-state calibration wells
Particle from Waste Panels to LWB

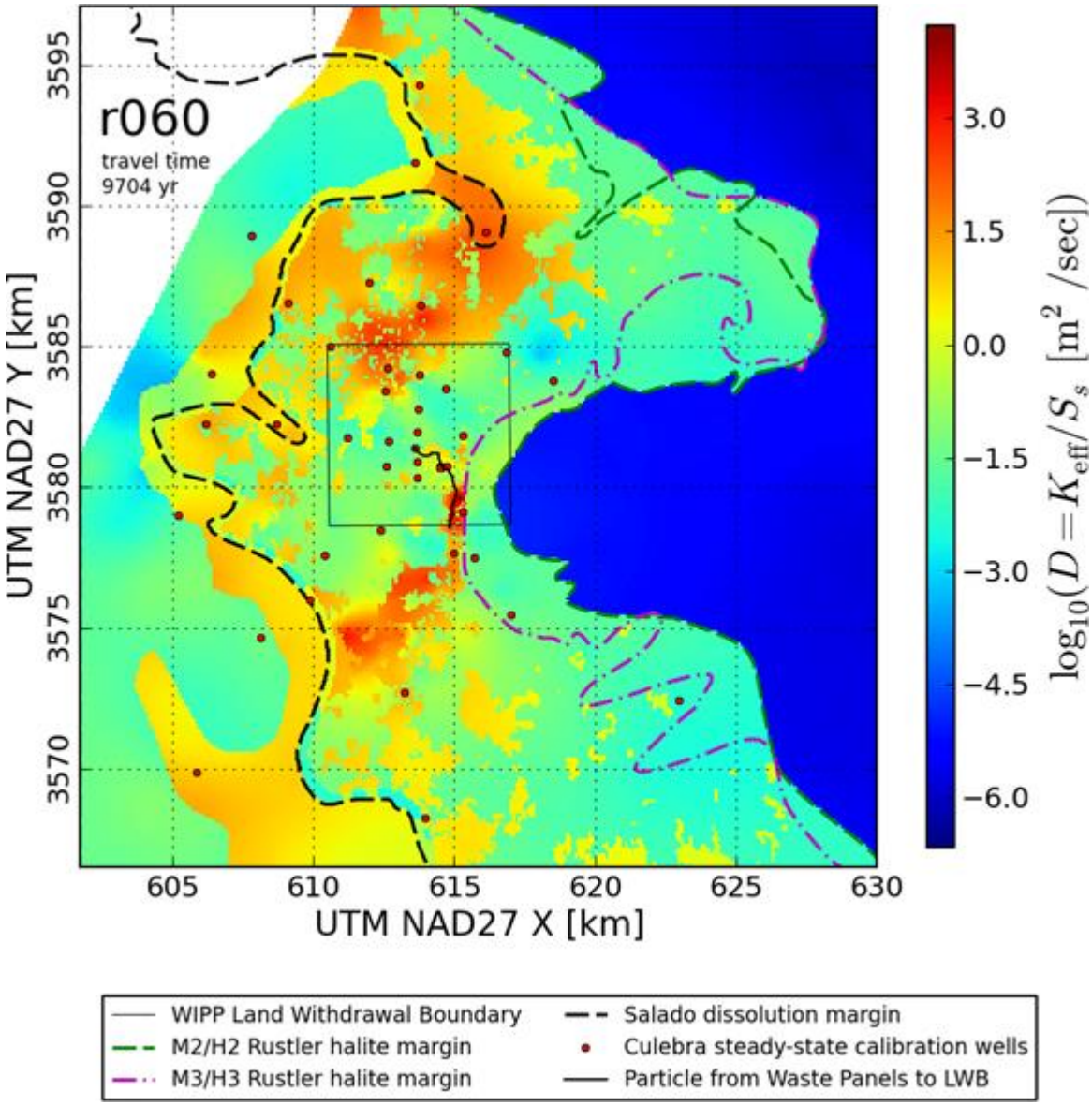
r060
travel time
9704 yr
UTM NAD27 Y [km]
3595
3590
3585
3580
3575
3570
605
610
615
620
625
630
UTM NAD27 X [km]
3.0
1.5
0.0
−1.5
−3.0
−4.5
−6.0
$\log_{10}(D = K_{\text{eff}}/S_s \ [\text{m}^2/\text{sec}])$
WIPP Land Withdrawal Boundary
M2/H2 Rustler halite margin
M3/H3 Rustler halite margin
Salado dissolution margin
Culebra steady-state calibration wells
Particle from Waste Panels to LWB

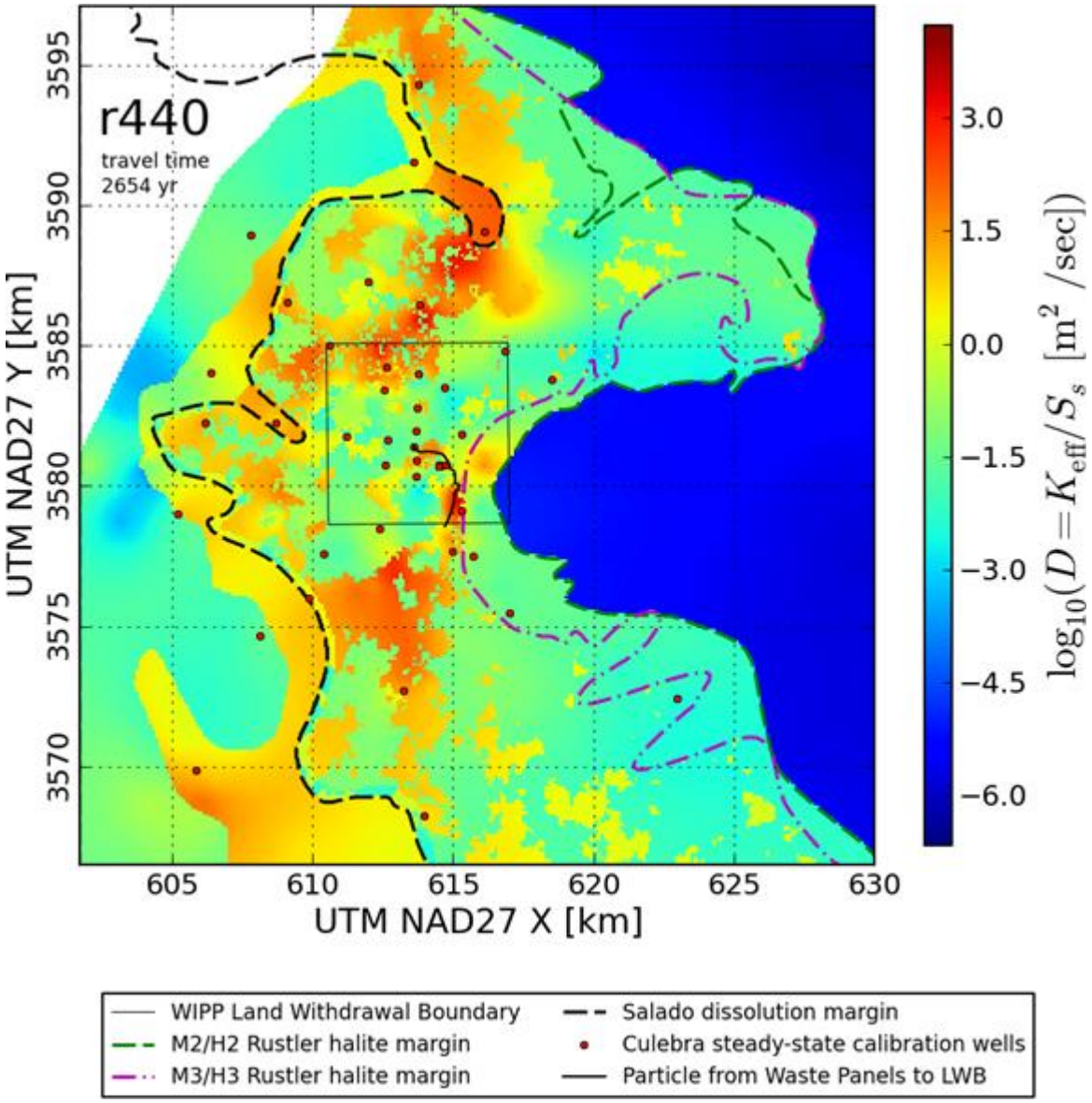

TFIELD Attachment A-4.0 100 Model Predicted Darcy Velocity Fields

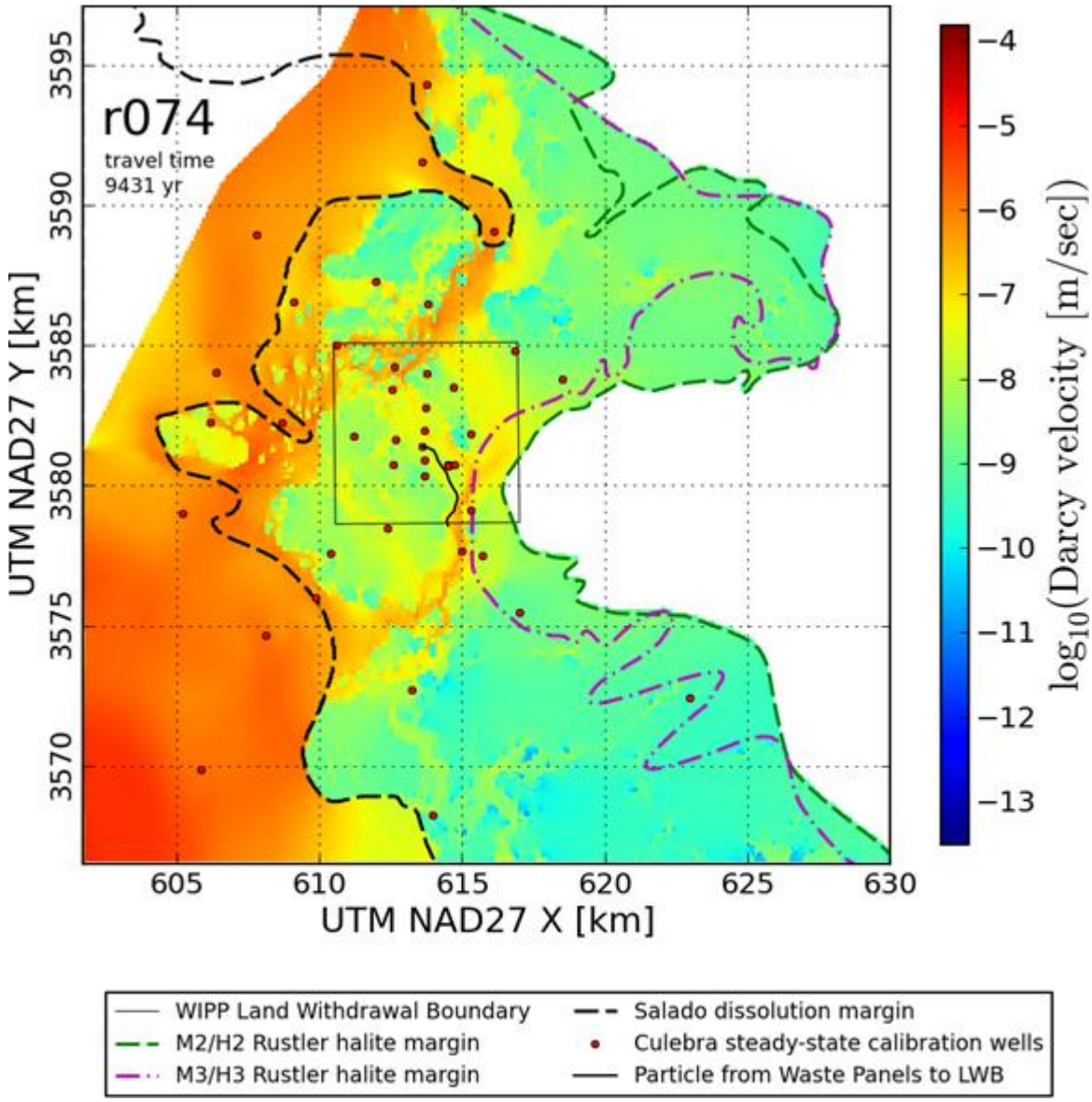
r074
travel time
9431 yr
UTM NAD27 Y [km]
3595
3590
3585
3580
3575
3570
605
610
615
620
625
630
UTM NAD27 X [km]
−4
−5
−6
−7
−8
−9
−10
−11
−12
−13
log10(Darcy velocity [m/sec])
WIPP Land Withdrawal Boundary
M2/H2 Rustler halite margin
M3/H3 Rustler halite margin
Salado dissolution margin
Culebra steady-state calibration wells
Particle from Waste Panels to LWB

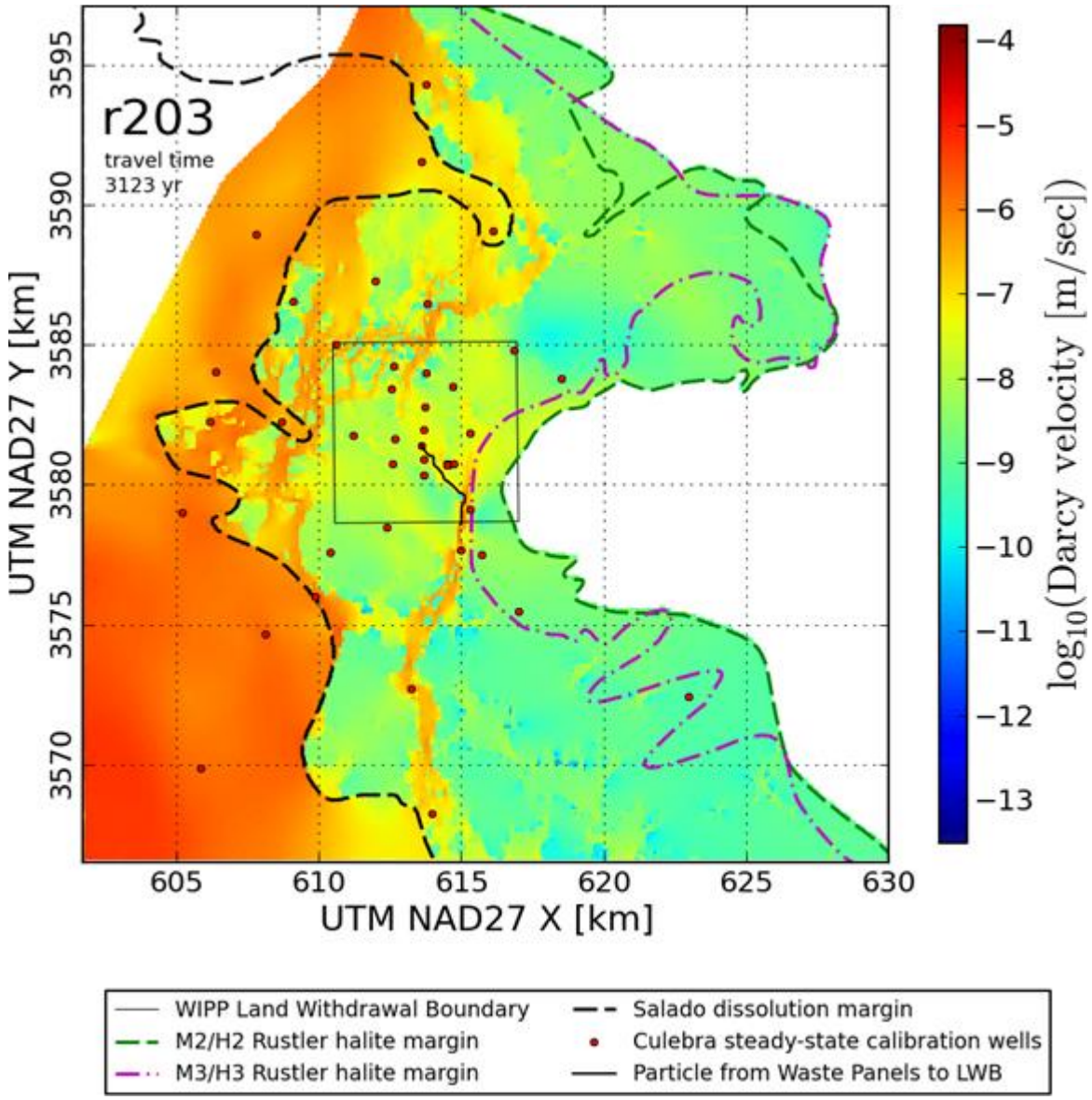
r203
travel time
3123 yr
UTM NAD27 Y [km]
3595
3590
3585
3580
3575
3570
605
610
615
620
625
630
UTM NAD27 X [km]
−4
−5
−6
−7
−8
−9
−10
−11
−12
−13
log10(Darcy velocity [m/sec])
WIPP Land Withdrawal Boundary
M2/H2 Rustler halite margin
M3/H3 Rustler halite margin
Salado dissolution margin
Culebra steady-state calibration wells
Particle from Waste Panels to LWB

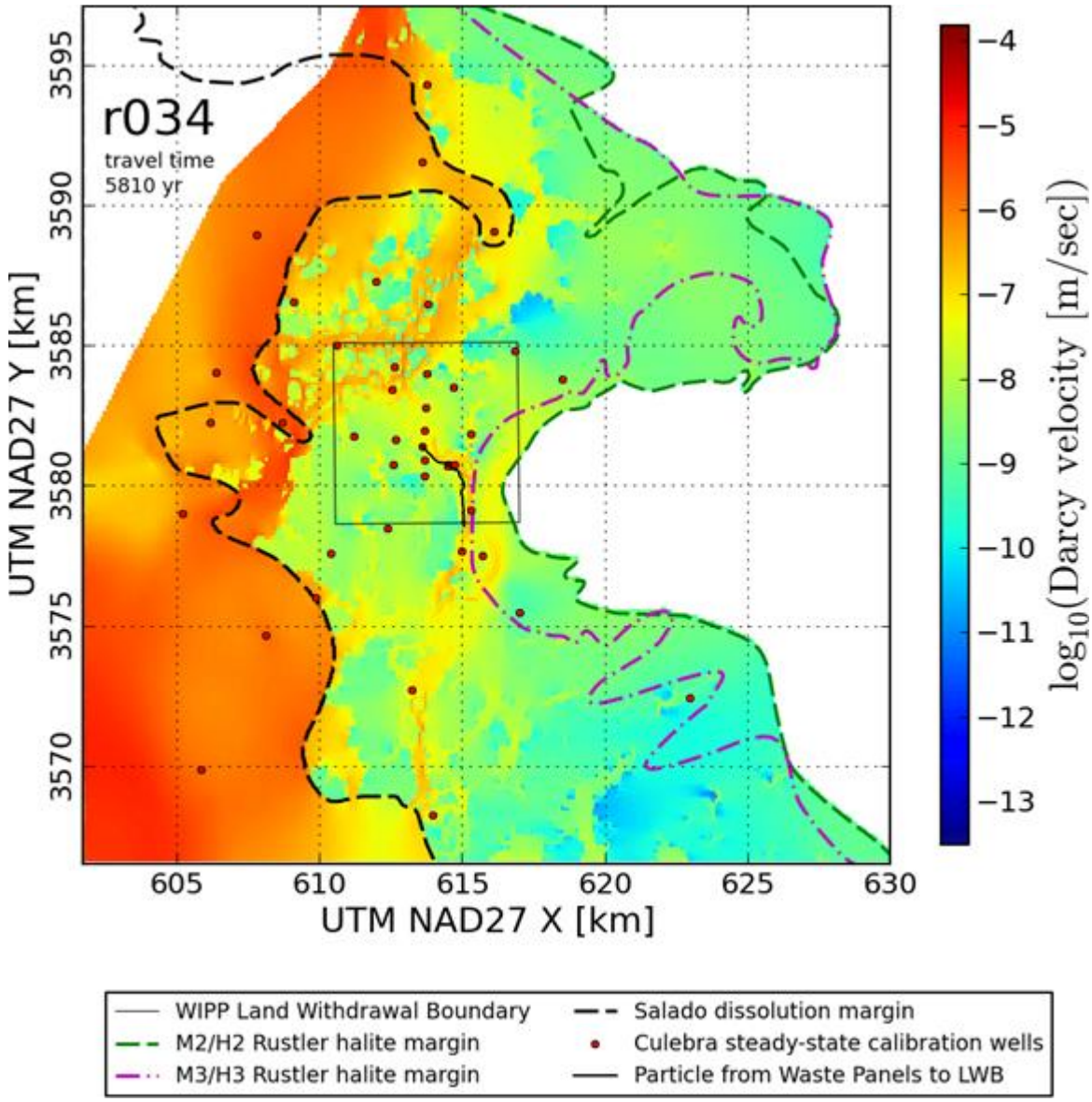
r034
travel time
5810 yr
UTM NAD27 Y [km]
3595
3590
3585
3580
3575
3570
605
610
615
620
625
630
UTM NAD27 X [km]
−4
−5
−6
−7
−8
−9
−10
−11
−12
−13
log10(Darcy velocity [m/sec])
WIPP Land Withdrawal Boundary
M2/H2 Rustler halite margin
M3/H3 Rustler halite margin
Salado dissolution margin
Culebra steady-state calibration wells
Particle from Waste Panels to LWB

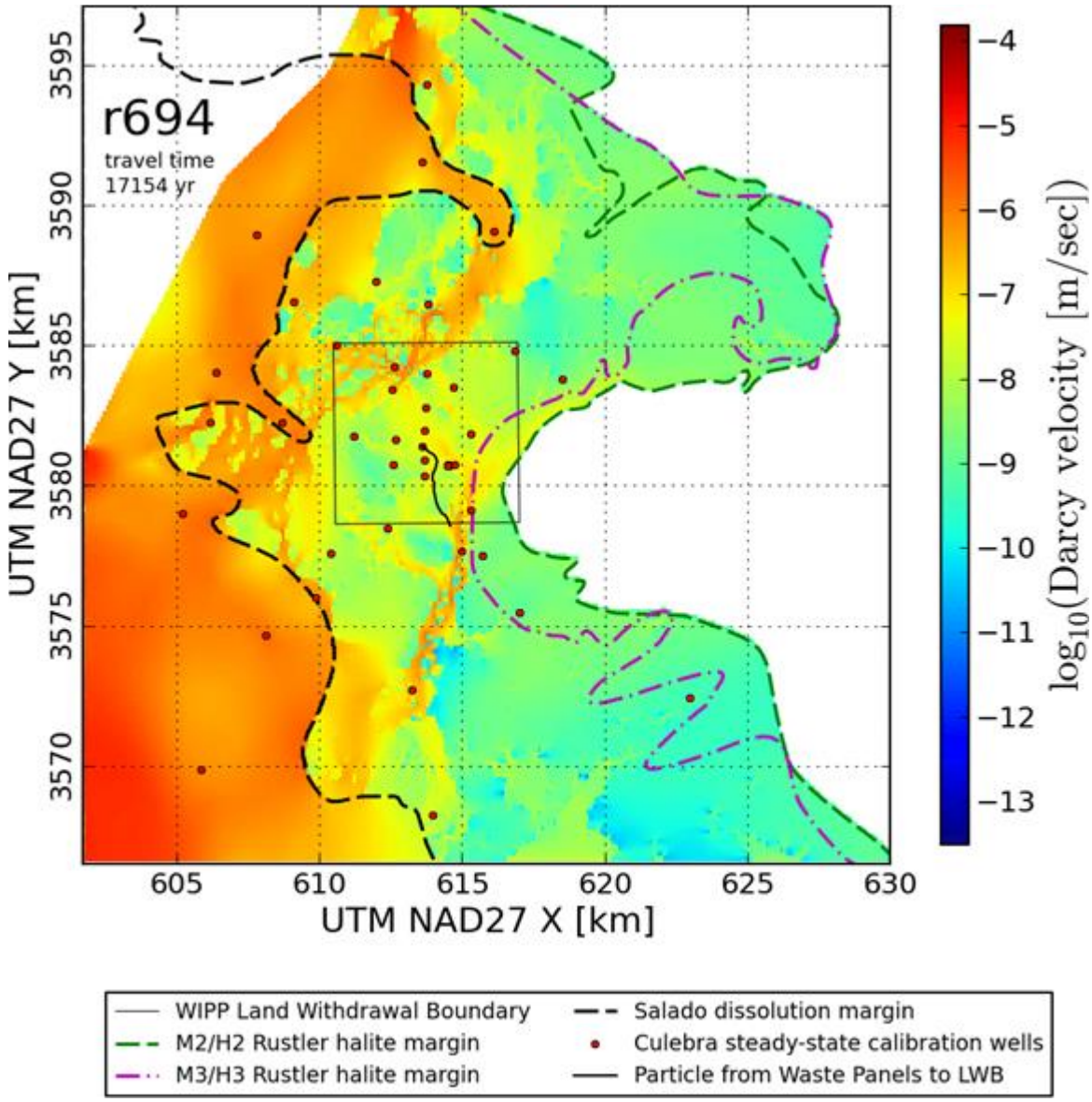
r694
travel time
17154 yr
UTM NAD27 Y [km]
3595
3590
3585
3580
3575
3570
605
610
615
620
625
630
UTM NAD27 X [km]
−4
−5
−6
−7
−8
−9
−10
−11
−12
−13
log10(Darcy velocity [m/sec])
WIPP Land Withdrawal Boundary
M2/H2 Rustler halite margin
M3/H3 Rustler halite margin
Salado dissolution margin
Culebra steady-state calibration wells
Particle from Waste Panels to LWB

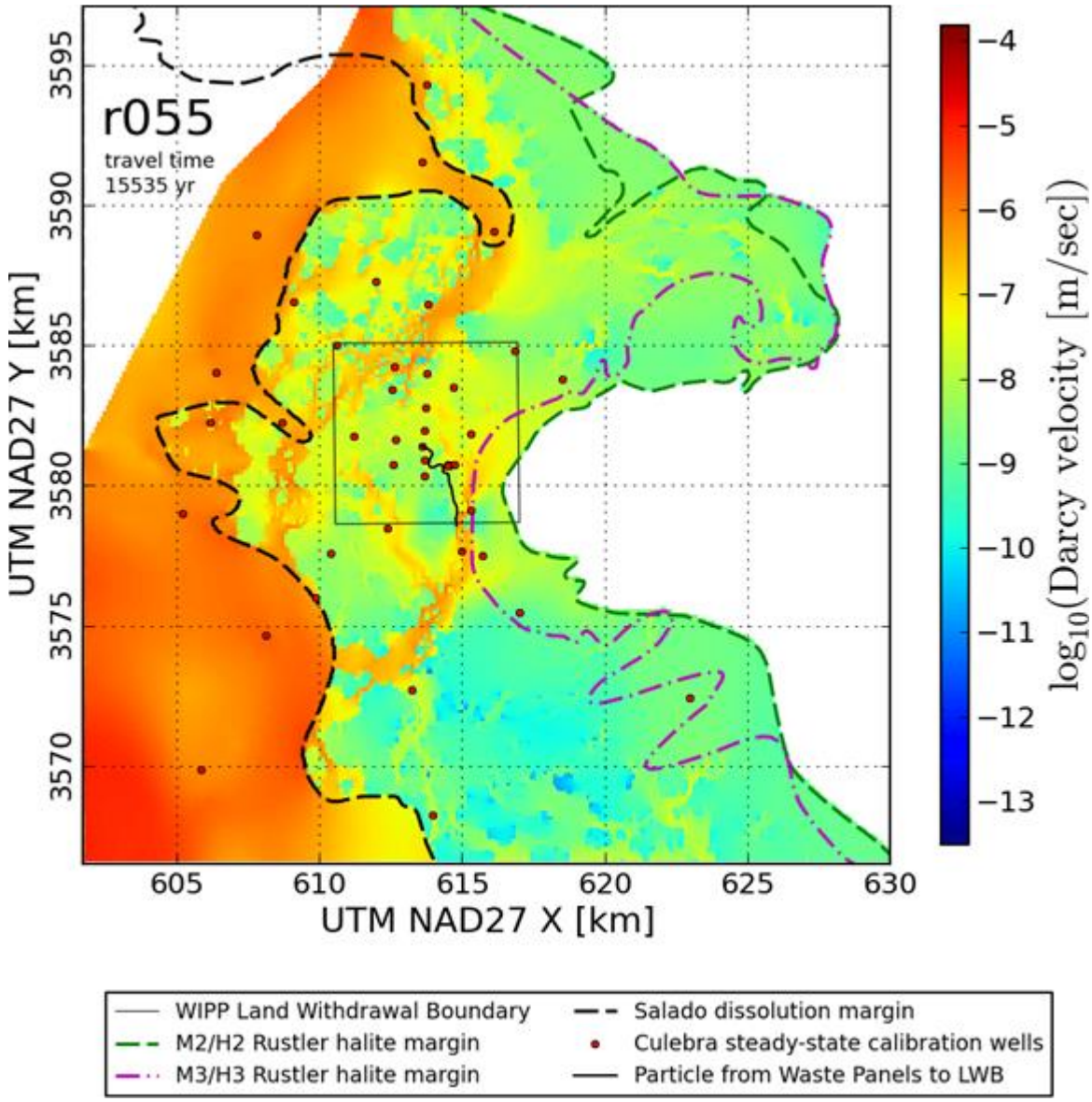
r055
travel time
15535 yr
UTM NAD27 Y [km]
3595
3590
3585
3580
3575
3570
605
610
615
620
625
630
UTM NAD27 X [km]
−4
−5
−6
−7
−8
−9
−10
−11
−12
−13
log10(Darcy velocity [m/sec])
WIPP Land Withdrawal Boundary
M2/H2 Rustler halite margin
M3/H3 Rustler halite margin
Salado dissolution margin
Culebra steady-state calibration wells
Particle from Waste Panels to LWB

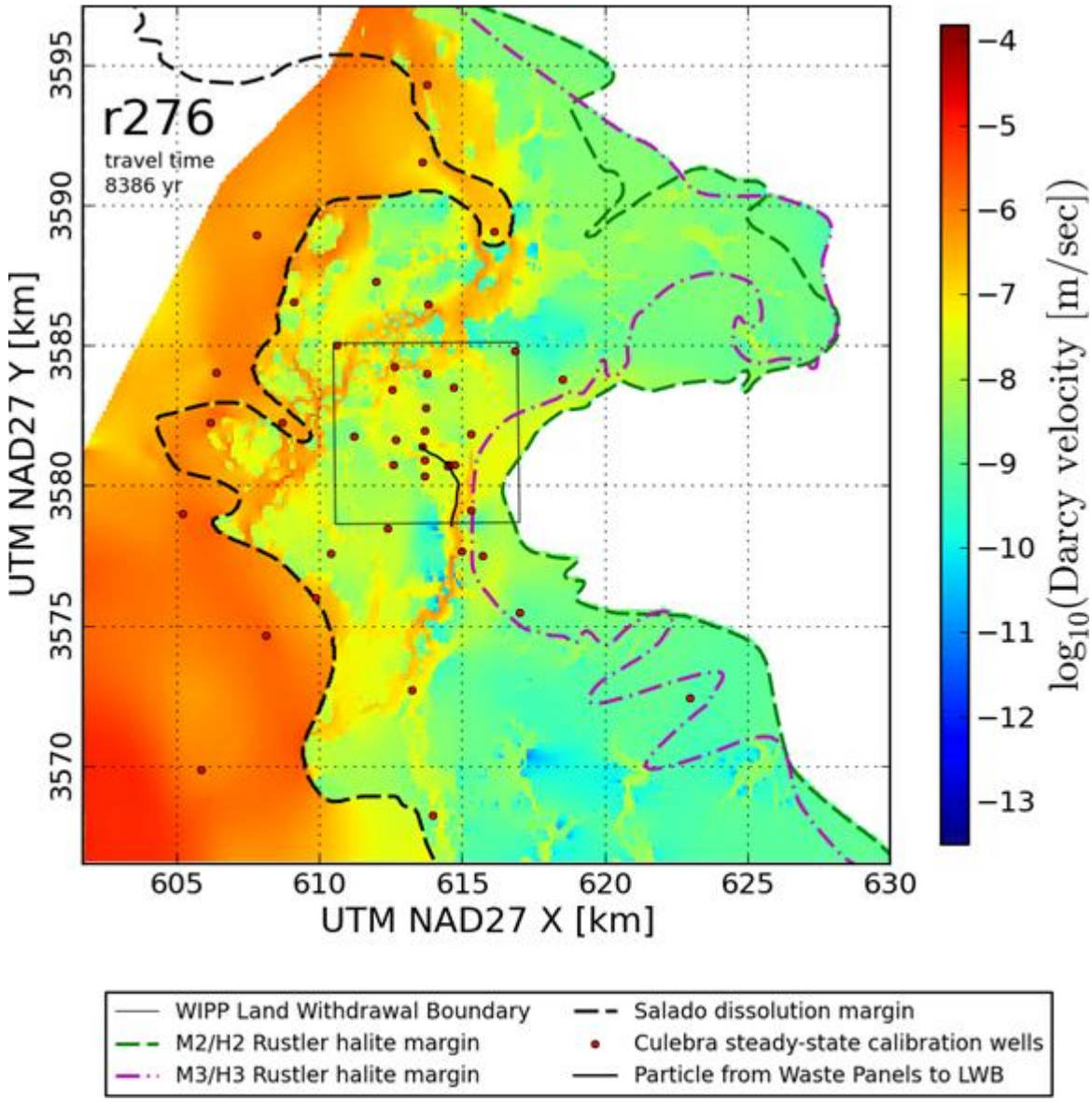
r276
travel time
8386 yr
UTM NAD27 Y [km]
3595
3590
3585
3580
3575
3570
605
610
615
620
625
630
UTM NAD27 X [km]
−4
−5
−6
−7
−8
−9
−10
−11
−12
−13
log10(Darcy velocity [m/sec])
WIPP Land Withdrawal Boundary
M2/H2 Rustler halite margin
M3/H3 Rustler halite margin
Salado dissolution margin
Culebra steady-state calibration wells
Particle from Waste Panels to LWB

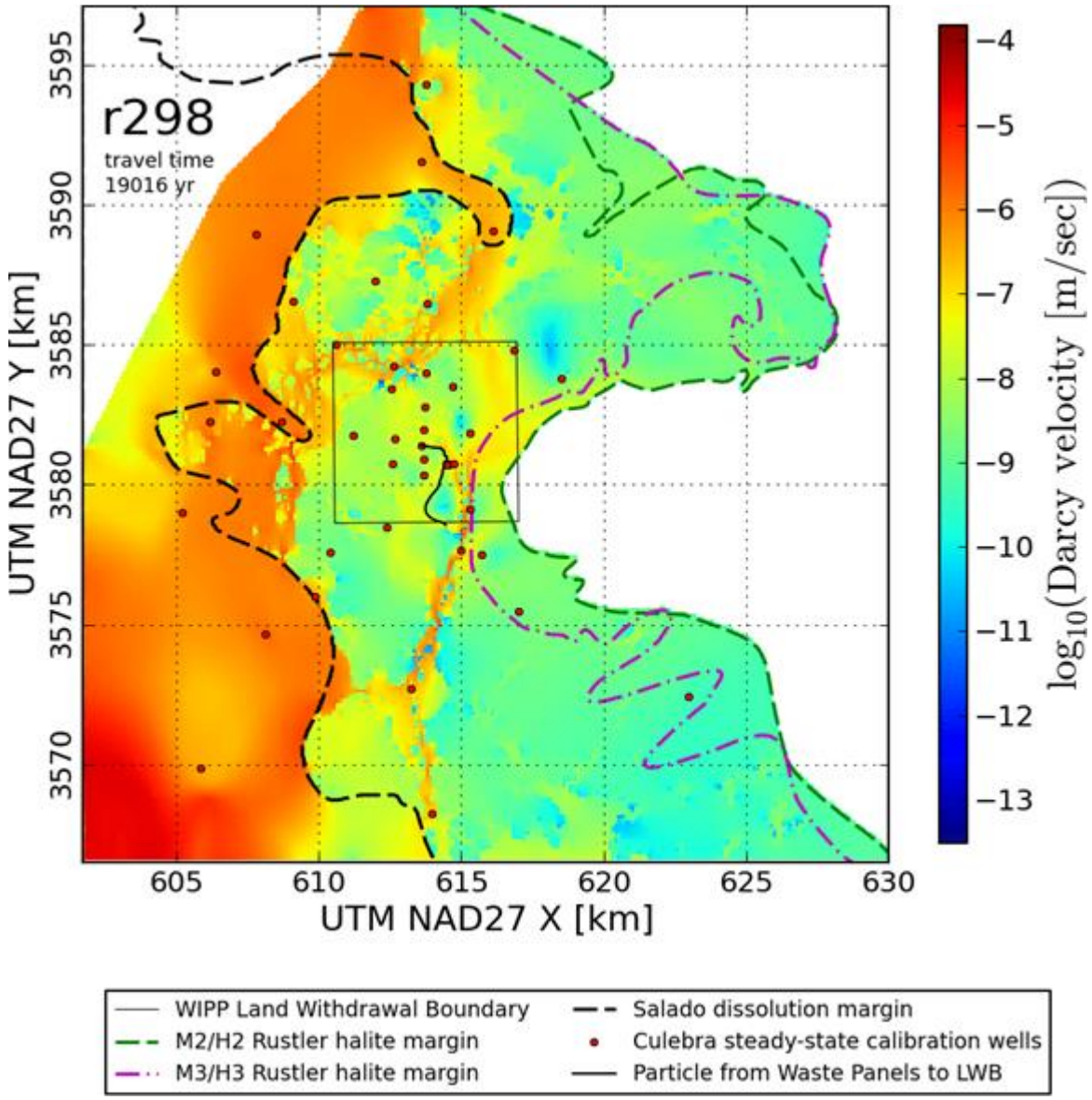
r298
travel time
19016 yr
UTM NAD27 Y [km]
3595
3590
3585
3580
3575
3570
605
610
615
620
625
630
UTM NAD27 X [km]
−4
−5
−6
−7
−8
−9
−10
−11
−12
−13
log10(Darcy velocity [m/sec])
WIPP Land Withdrawal Boundary
M2/H2 Rustler halite margin
M3/H3 Rustler halite margin
Salado dissolution margin
Culebra steady-state calibration wells
Particle from Waste Panels to LWB

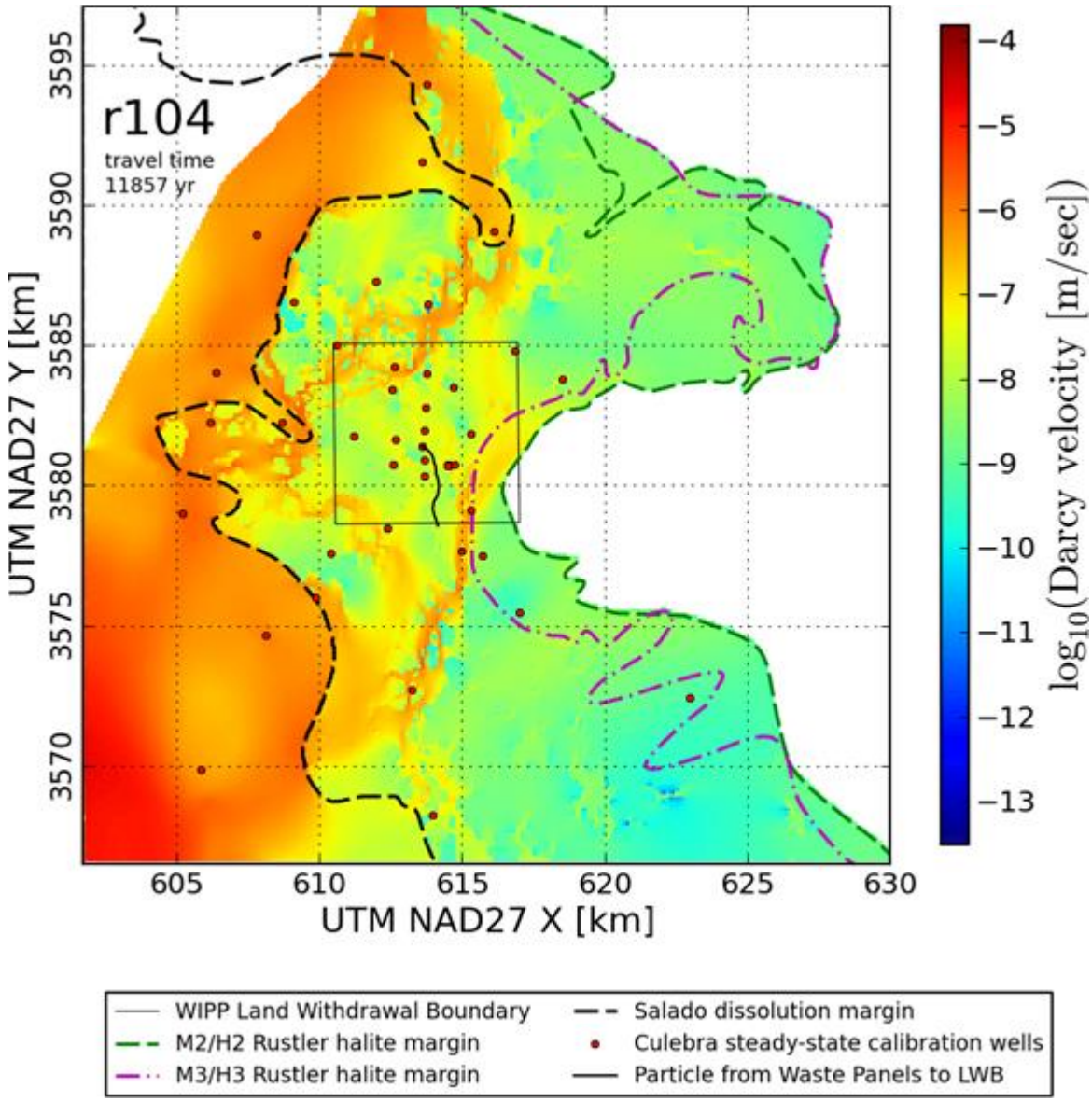
r104
travel time
11857 yr
UTM NAD27 Y [km]
3595
3590
3585
3580
3575
3570
605
610
615
620
625
630
UTM NAD27 X [km]
−4
−5
−6
−7
−8
−9
−10
−11
−12
−13
log10(Darcy velocity [m/sec])
WIPP Land Withdrawal Boundary
M2/H2 Rustler halite margin
M3/H3 Rustler halite margin
Salado dissolution margin
Culebra steady-state calibration wells
Particle from Waste Panels to LWB

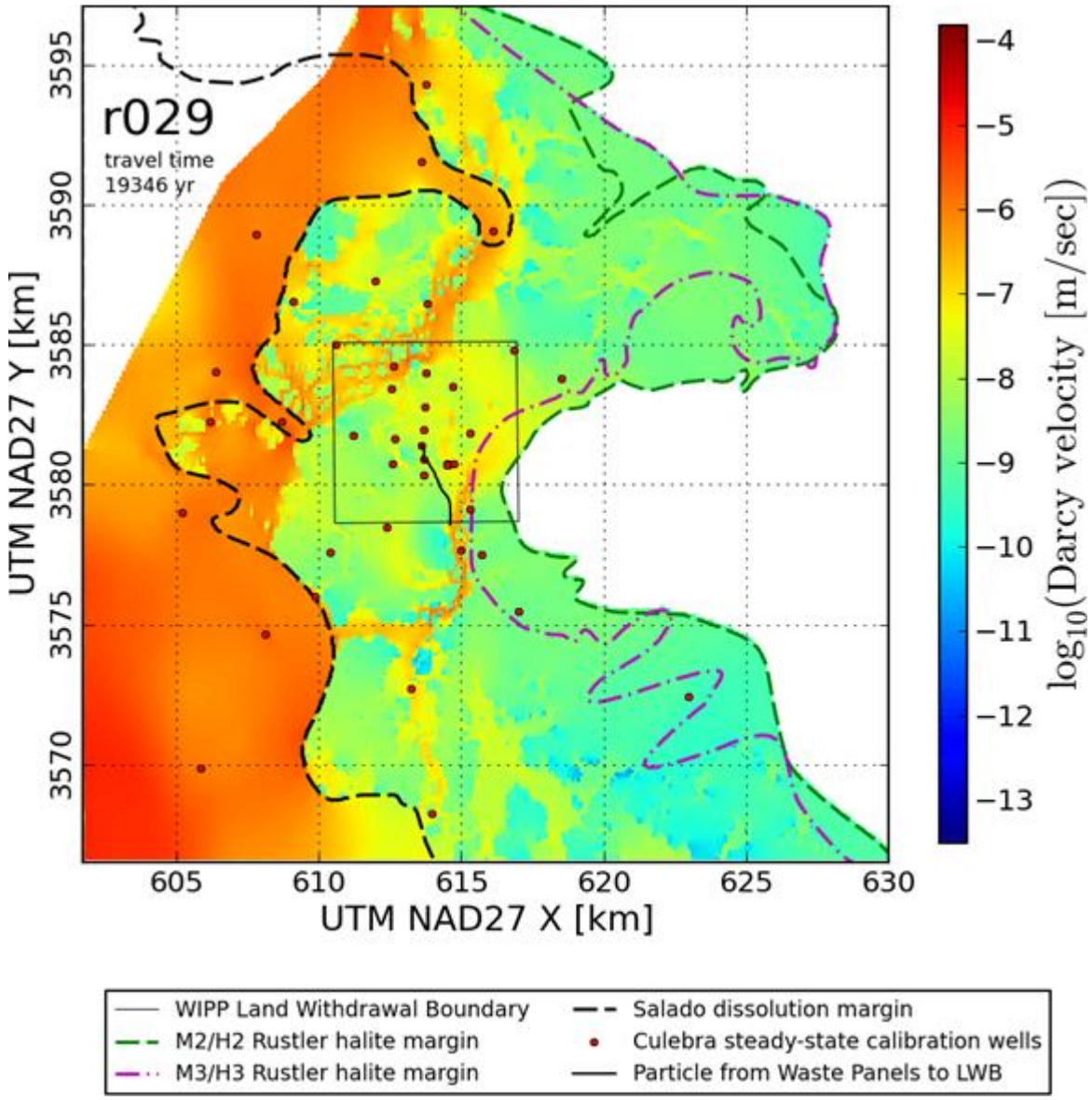
r029
travel time
19346 yr
UTM NAD27 Y [km]
3595
3590
3585
3580
3575
3570
605
610
615
620
625
630
UTM NAD27 X [km]
−4
−5
−6
−7
−8
−9
−10
−11
−12
−13
log10(Darcy velocity [m/sec])
WIPP Land Withdrawal Boundary
M2/H2 Rustler halite margin
M3/H3 Rustler halite margin
Salado dissolution margin
Culebra steady-state calibration wells
Particle from Waste Panels to LWB

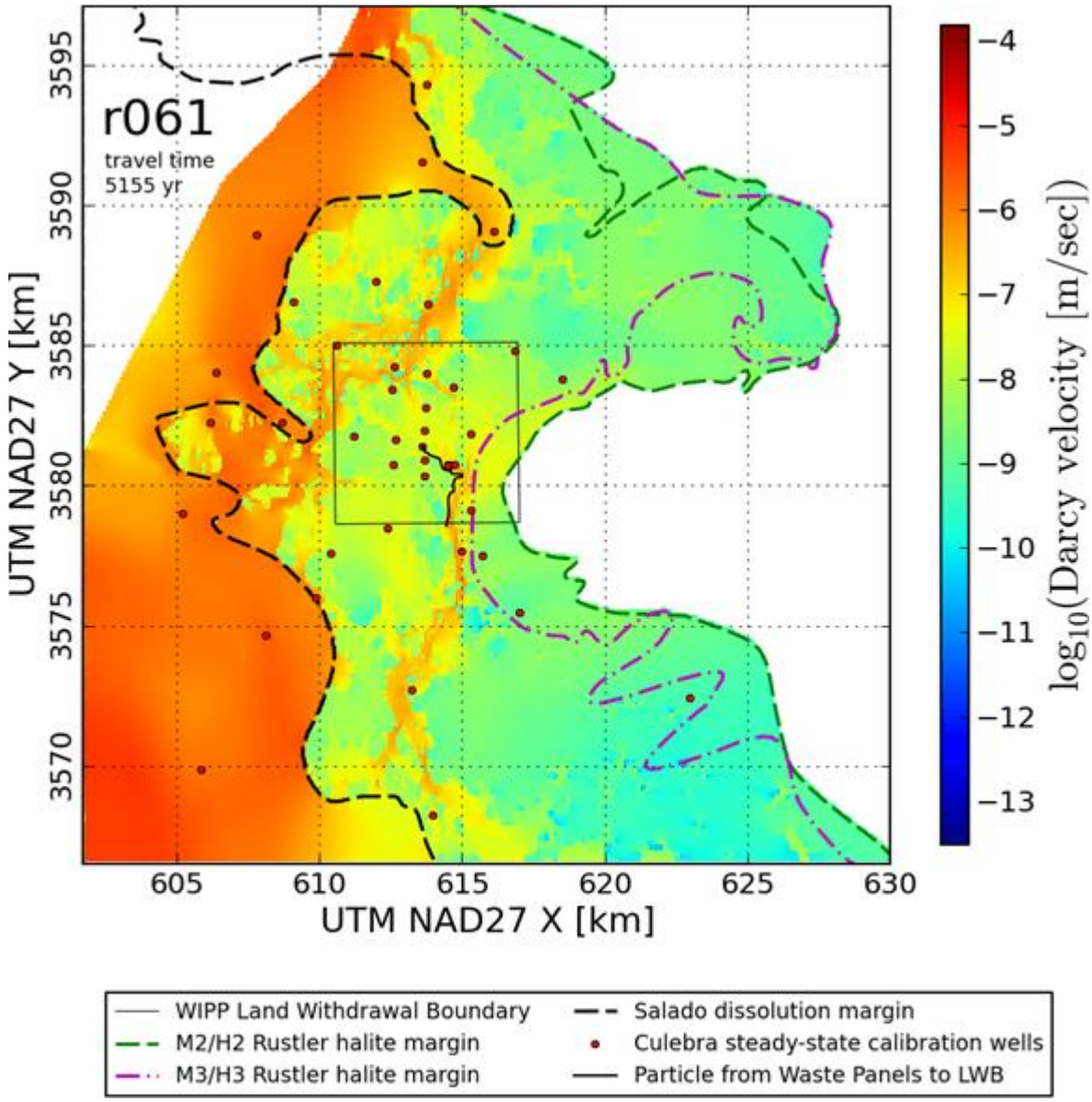
r061
travel time
5155 yr
UTM NAD27 Y [km]
3595
3590
3585
3580
3575
3570
605
610
615
620
625
630
UTM NAD27 X [km]
−4
−5
−6
−7
−8
−9
−10
−11
−12
−13
log10(Darcy velocity [m/sec])
WIPP Land Withdrawal Boundary
M2/H2 Rustler halite margin
M3/H3 Rustler halite margin
Salado dissolution margin
Culebra steady-state calibration wells
Particle from Waste Panels to LWB

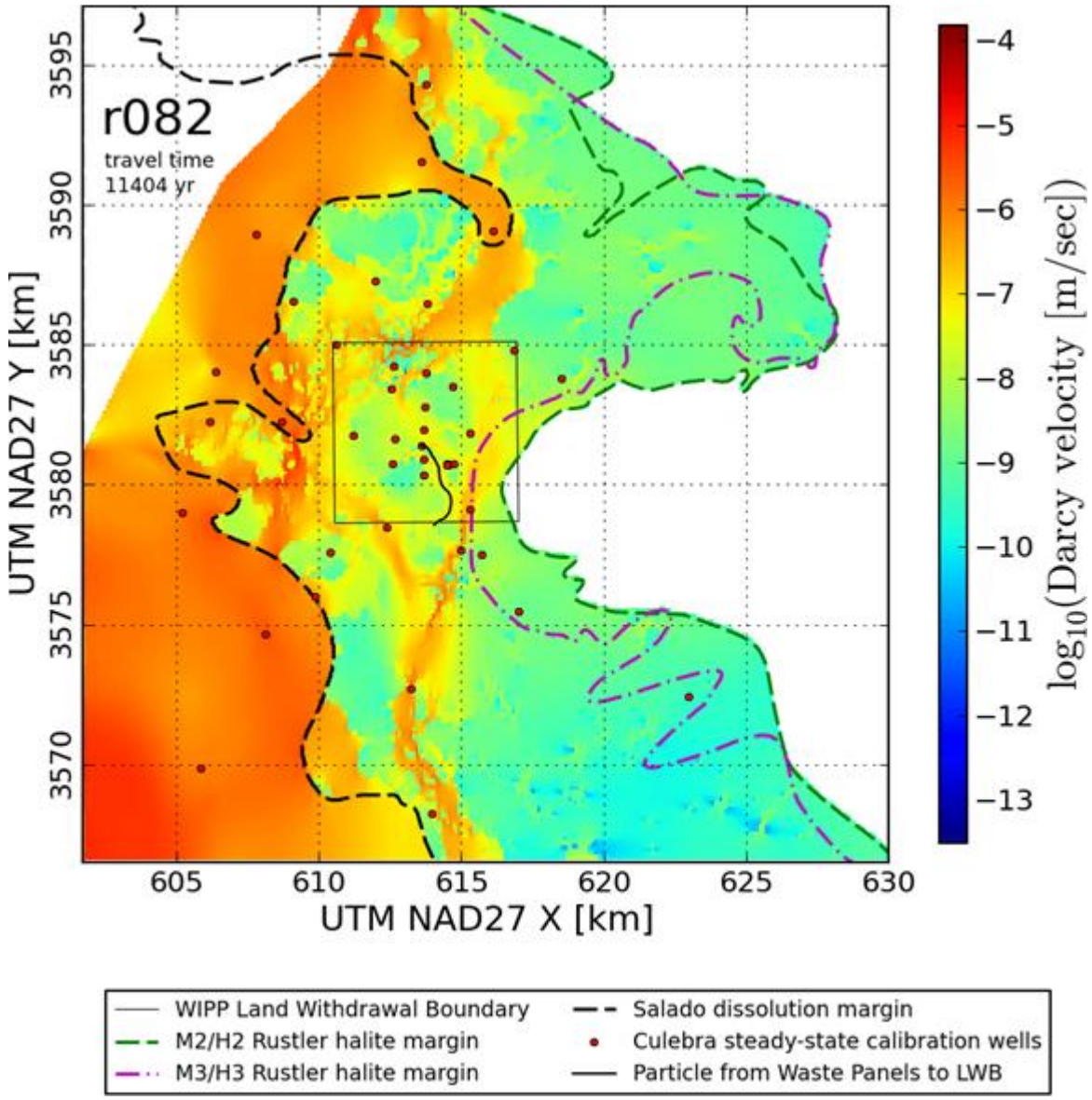
r082
travel time
11404 yr
UTM NAD27 Y [km]
3595
3590
3585
3580
3575
3570
605
610
615
620
625
630
UTM NAD27 X [km]
−4
−5
−6
−7
−8
−9
−10
−11
−12
−13
log10(Darcy velocity [m/sec])
WIPP Land Withdrawal Boundary
M2/H2 Rustler halite margin
M3/H3 Rustler halite margin
Salado dissolution margin
Culebra steady-state calibration wells
Particle from Waste Panels to LWB

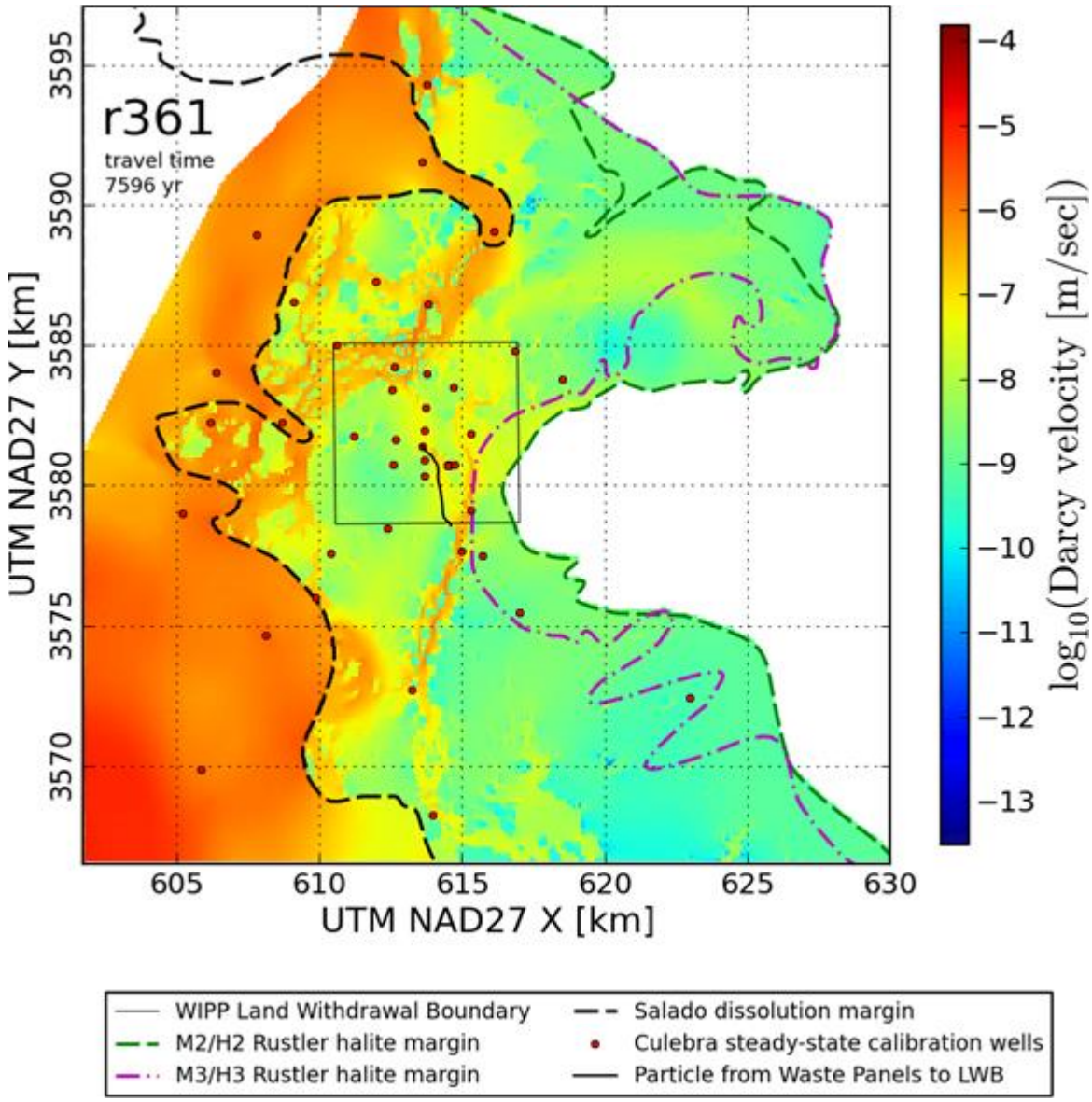
r361
travel time
7596 yr
UTM NAD27 Y [km]
3595
3590
3585
3580
3575
3570
605
610
615
620
625
630
UTM NAD27 X [km]
−4
−5
−6
−7
−8
−9
−10
−11
−12
−13
log10(Darcy velocity [m/sec])
WIPP Land Withdrawal Boundary
M2/H2 Rustler halite margin
M3/H3 Rustler halite margin
Salado dissolution margin
Culebra steady-state calibration wells
Particle from Waste Panels to LWB

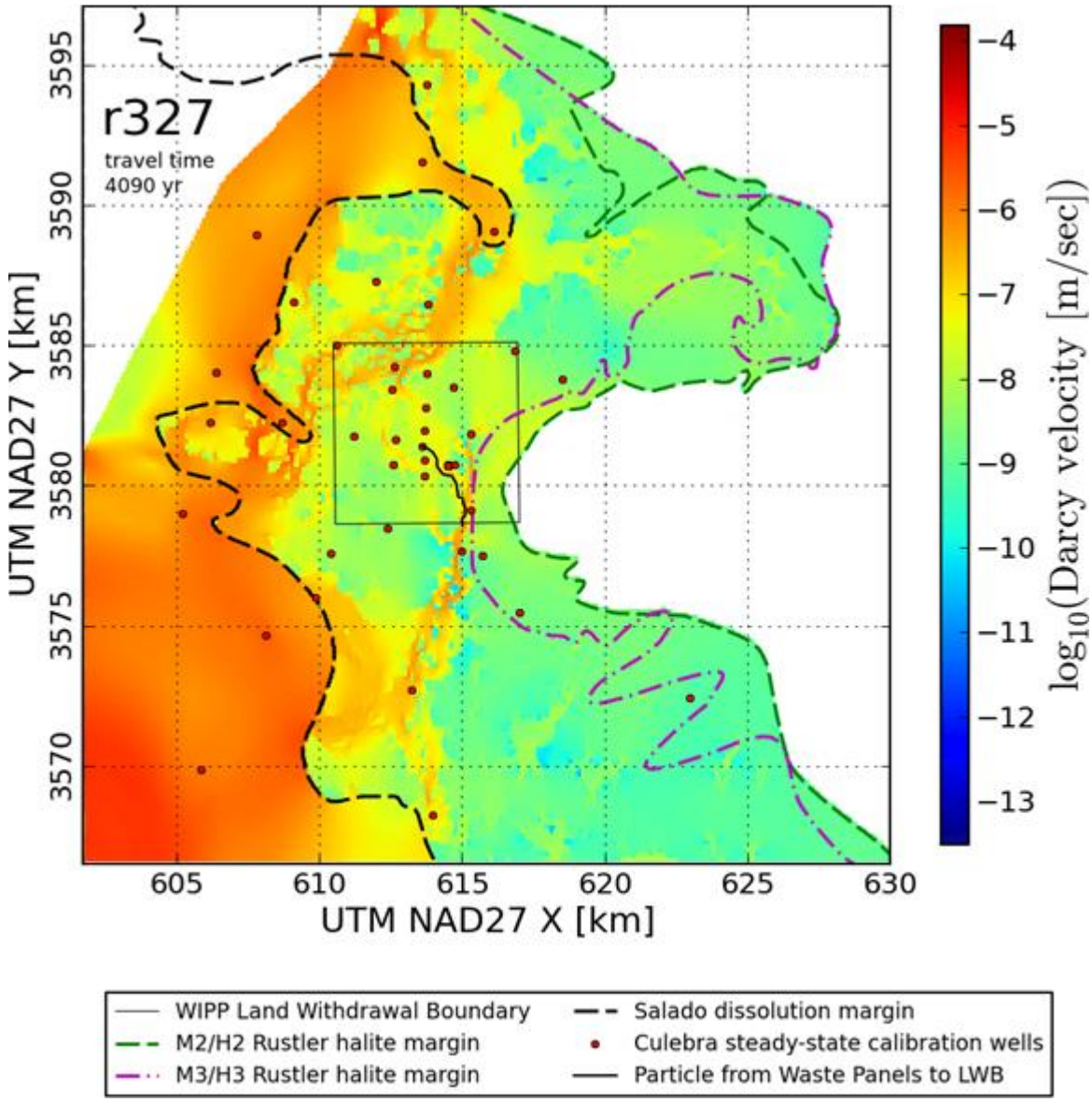
r327
travel time
4090 yr
UTM NAD27 Y [km]
3595
3590
3585
3580
3575
3570
605
610
615
620
625
630
UTM NAD27 X [km]
−4
−5
−6
−7
−8
−9
−10
−11
−12
−13
log10(Darcy velocity [m/sec])
WIPP Land Withdrawal Boundary
M2/H2 Rustler halite margin
M3/H3 Rustler halite margin
Salado dissolution margin
Culebra steady-state calibration wells
Particle from Waste Panels to LWB

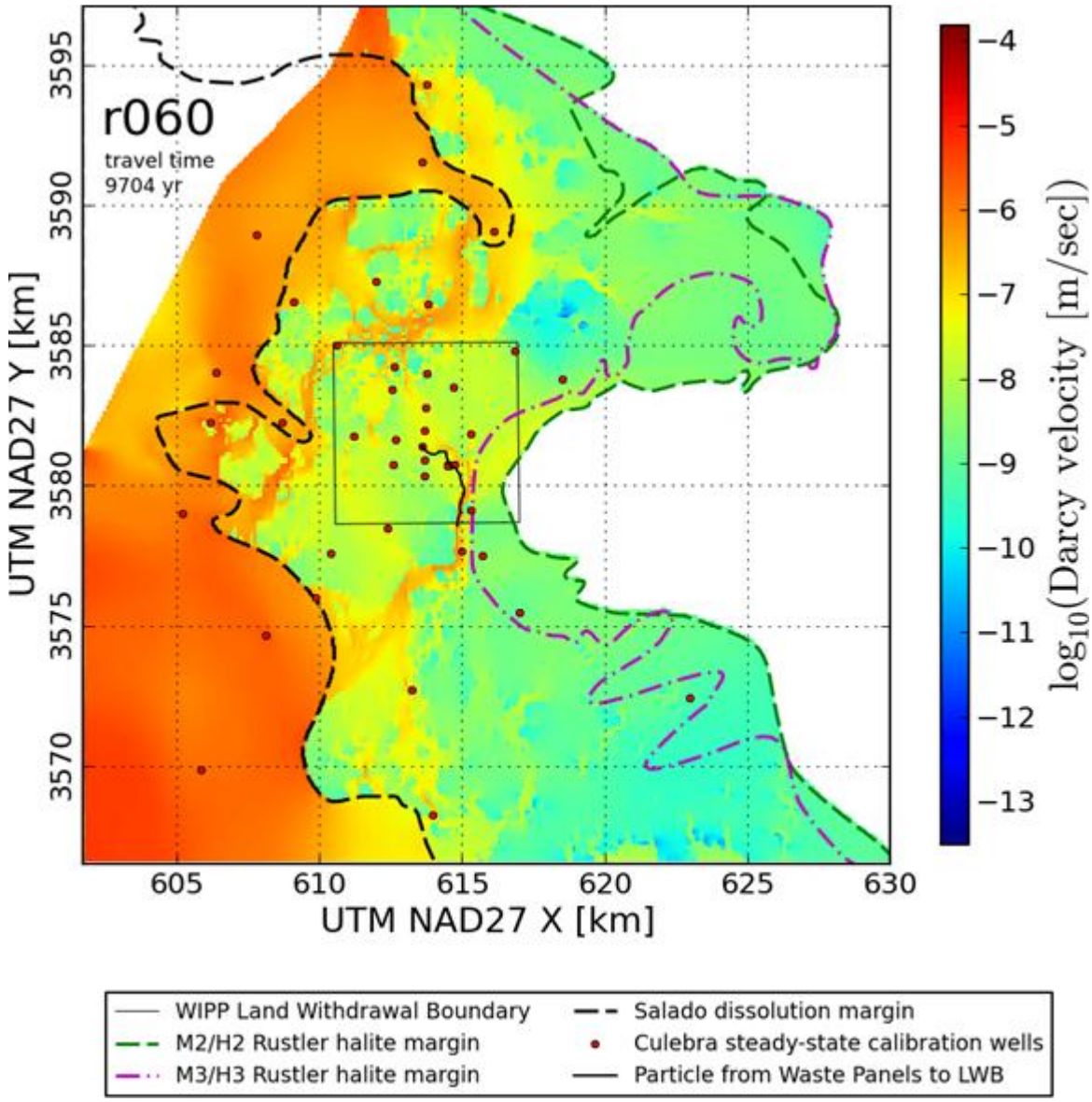
r060
travel time
9704 yr
UTM NAD27 Y [km]
3595
3590
3585
3580
3575
3570
605
610
615
620
625
630
UTM NAD27 X [km]
−4
−5
−6
−7
−8
−9
−10
−11
−12
−13
log10(Darcy velocity [m/sec])
WIPP Land Withdrawal Boundary
M2/H2 Rustler halite margin
M3/H3 Rustler halite margin
Salado dissolution margin
Culebra steady-state calibration wells
Particle from Waste Panels to LWB

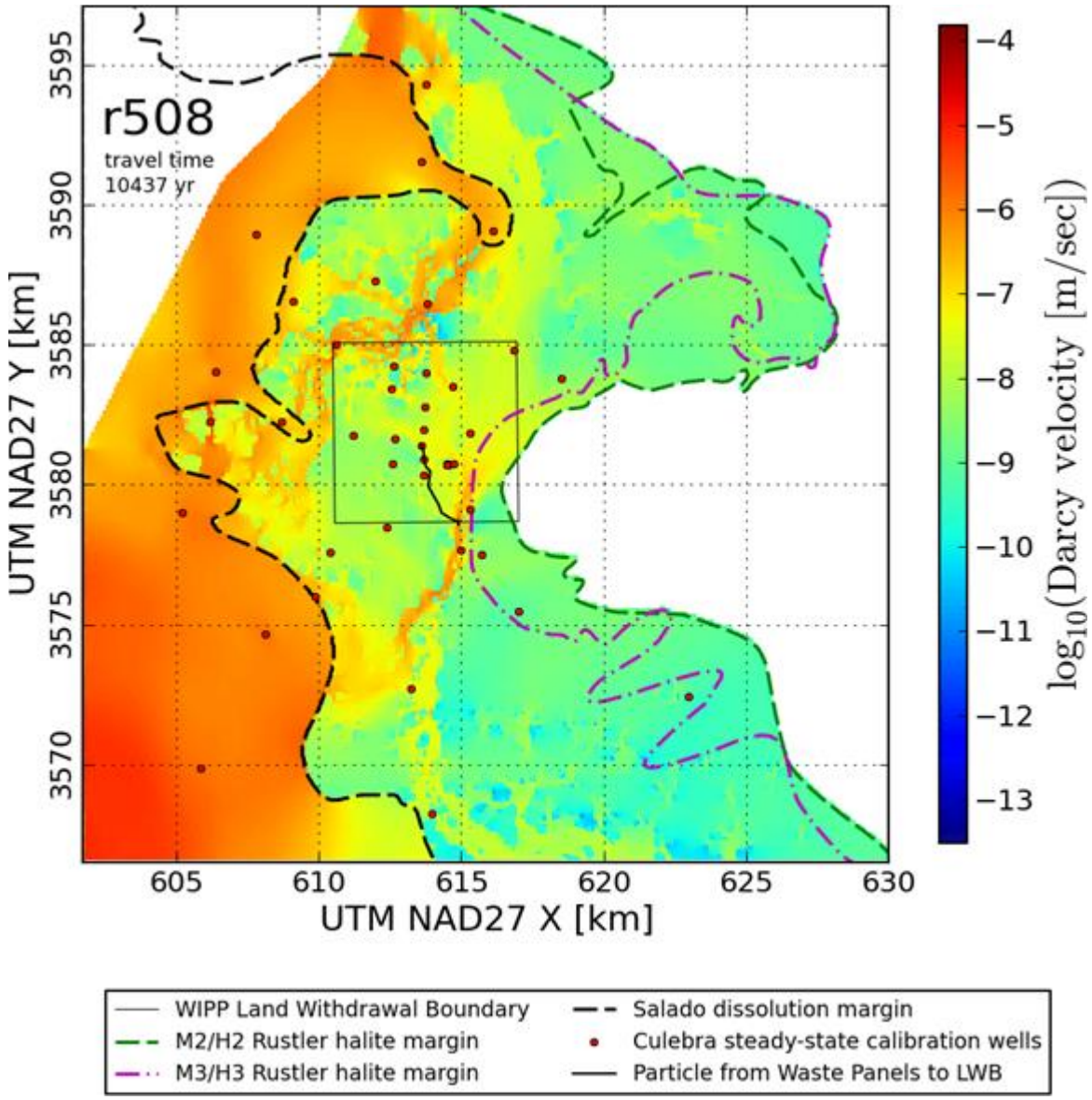
r508
travel time
10437 yr
UTM NAD27 Y [km]
3595
3590
3585
3580
3575
3570
605
610
615
620
625
630
UTM NAD27 X [km]
−4
−5
−6
−7
−8
−9
−10
−11
−12
−13
log10(Darcy velocity [m/sec])
WIPP Land Withdrawal Boundary
M2/H2 Rustler halite margin
M3/H3 Rustler halite margin
Salado dissolution margin
Culebra steady-state calibration wells
Particle from Waste Panels to LWB

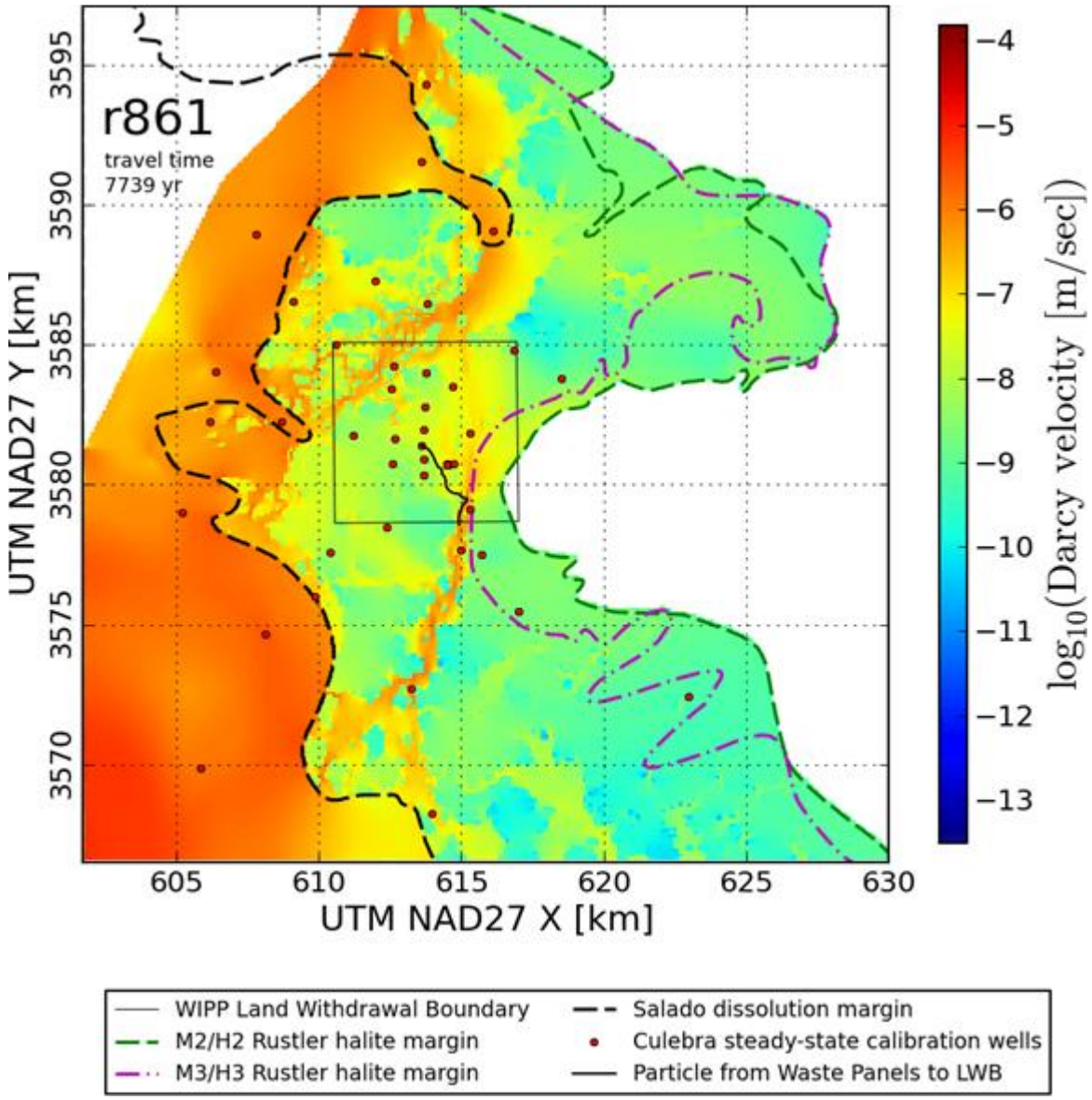
r861
travel time
7739 yr
UTM NAD27 Y [km]
3595
3590
3585
3580
3575
3570
605
610
615
620
625
630
UTM NAD27 X [km]
−4
−5
−6
−7
−8
−9
−10
−11
−12
−13
log10(Darcy velocity [m/sec])
WIPP Land Withdrawal Boundary
M2/H2 Rustler halite margin
M3/H3 Rustler halite margin
Salado dissolution margin
Culebra steady-state calibration wells
Particle from Waste Panels to LWB

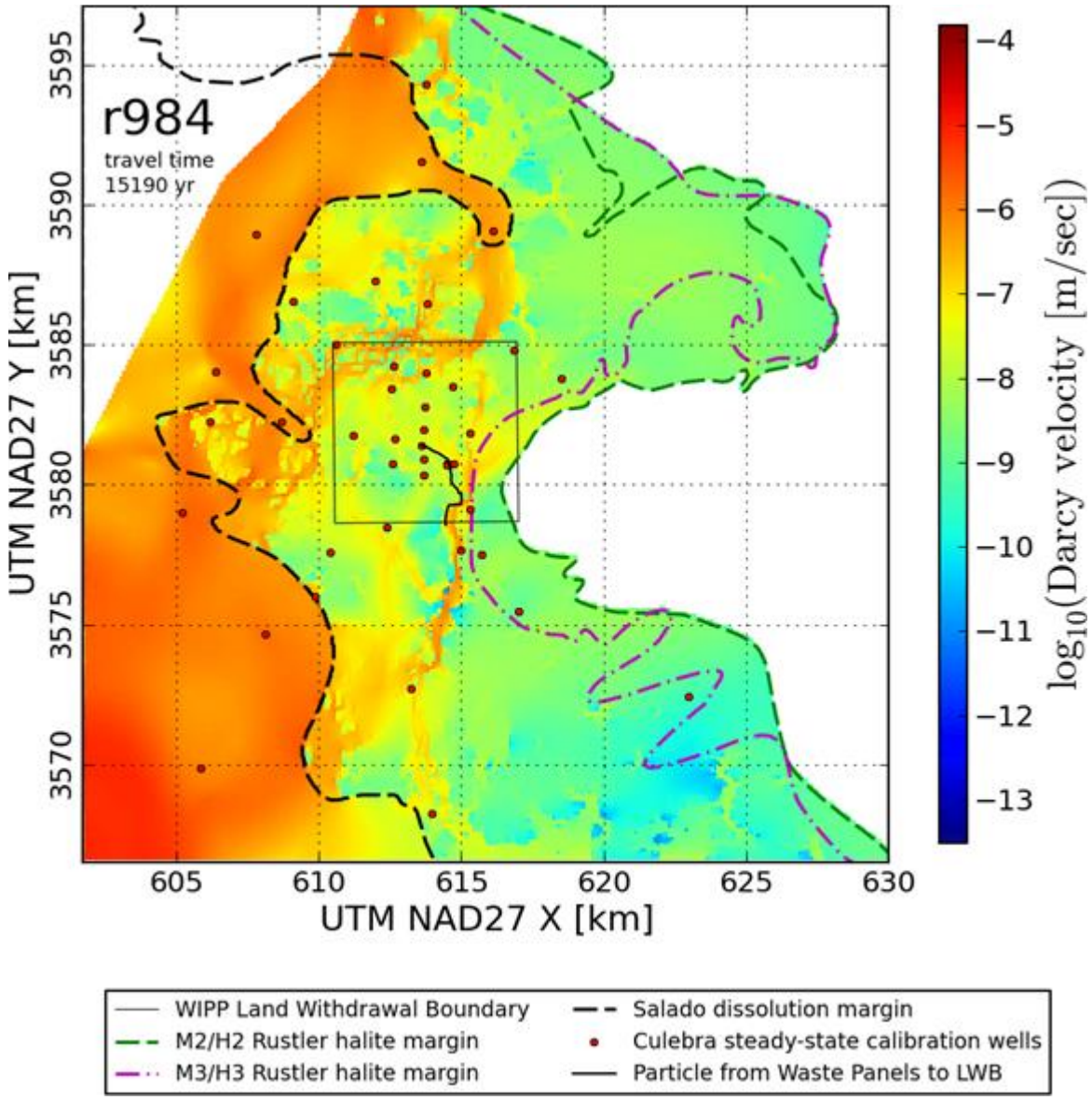
r984
travel time
15190 yr
UTM NAD27 Y [km]
3595
3590
3585
3580
3575
3570
605
610
615
620
625
630
UTM NAD27 X [km]
−4
−5
−6
−7
−8
−9
−10
−11
−12
−13
log10(Darcy velocity [m/sec])
WIPP Land Withdrawal Boundary
M2/H2 Rustler halite margin
M3/H3 Rustler halite margin
Salado dissolution margin
Culebra steady-state calibration wells
Particle from Waste Panels to LWB

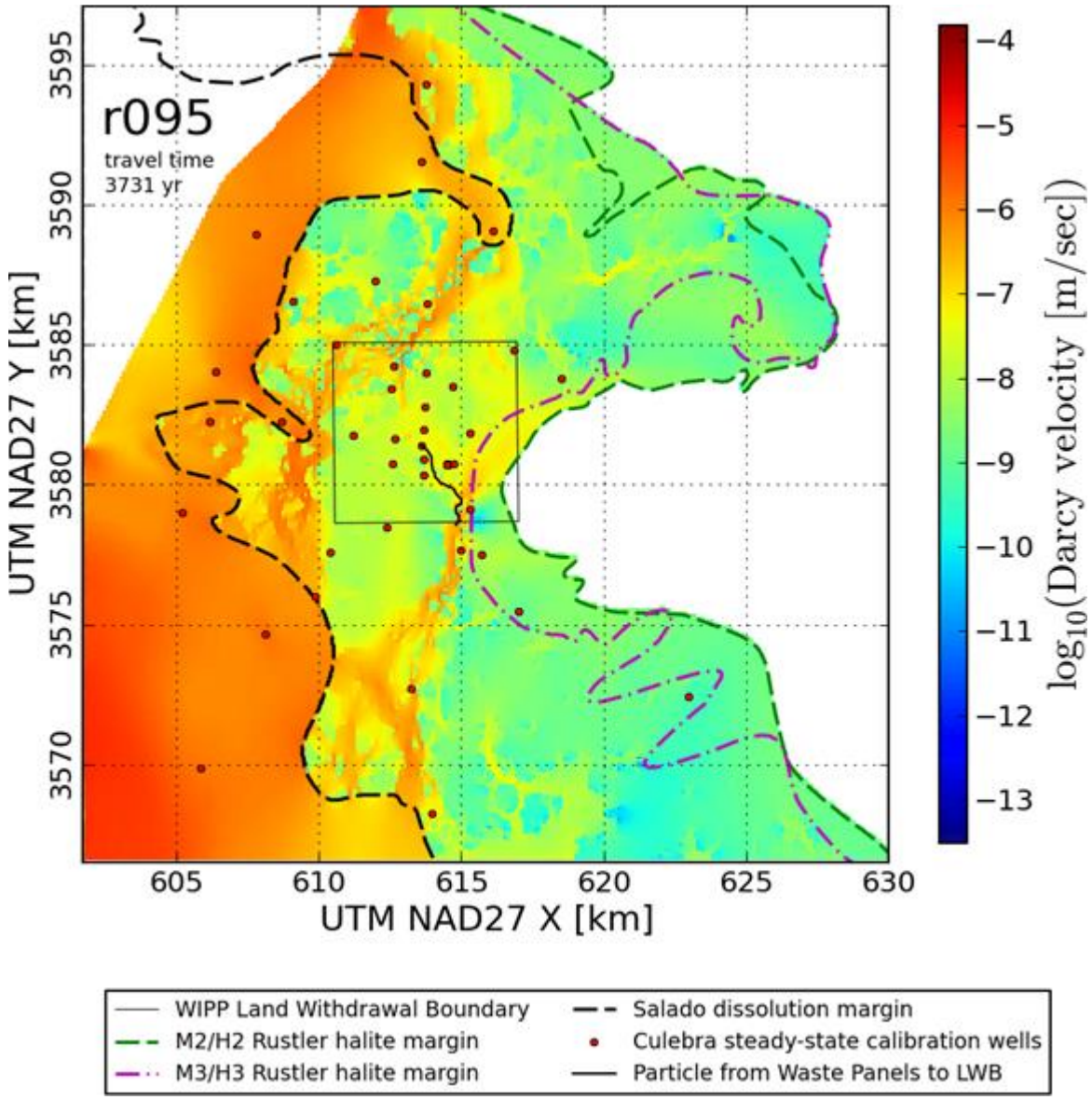
r095
travel time
3731 yr
UTM NAD27 Y [km]
3595
3590
3585
3580
3575
3570
605
610
615
620
625
630
UTM NAD27 X [km]
−4
−5
−6
−7
−8
−9
−10
−11
−12
−13
log10(Darcy velocity [m/sec])
WIPP Land Withdrawal Boundary
M2/H2 Rustler halite margin
M3/H3 Rustler halite margin
Salado dissolution margin
Culebra steady-state calibration wells
Particle from Waste Panels to LWB

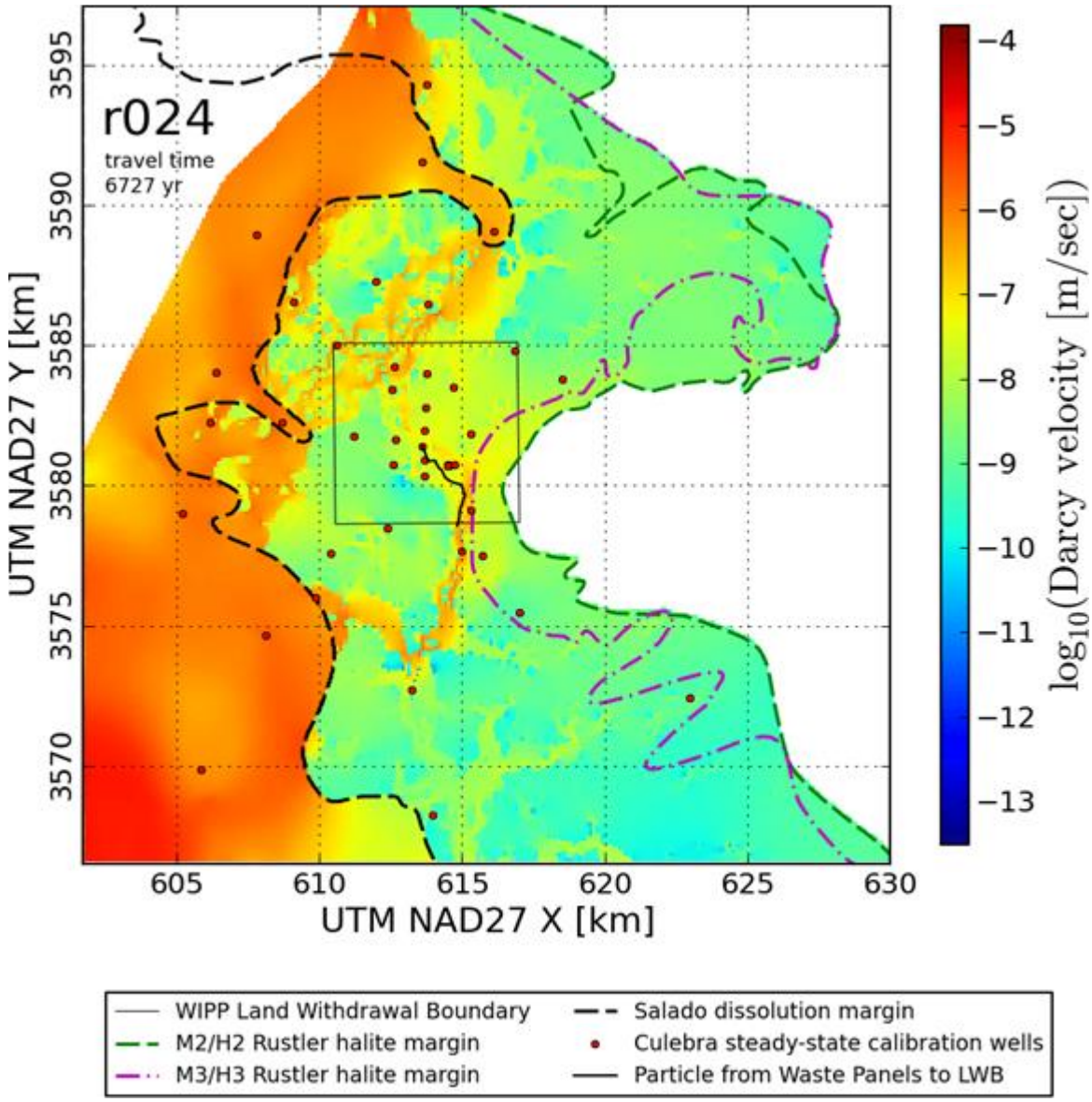
r024
travel time
6727 yr
UTM NAD27 Y [km]
3595
3590
3585
3580
3575
3570
605
610
615
620
625
630
UTM NAD27 X [km]
−4
−5
−6
−7
−8
−9
−10
−11
−12
−13
log10(Darcy velocity [m/sec])
WIPP Land Withdrawal Boundary
M2/H2 Rustler halite margin
M3/H3 Rustler halite margin
Salado dissolution margin
Culebra steady-state calibration wells
Particle from Waste Panels to LWB

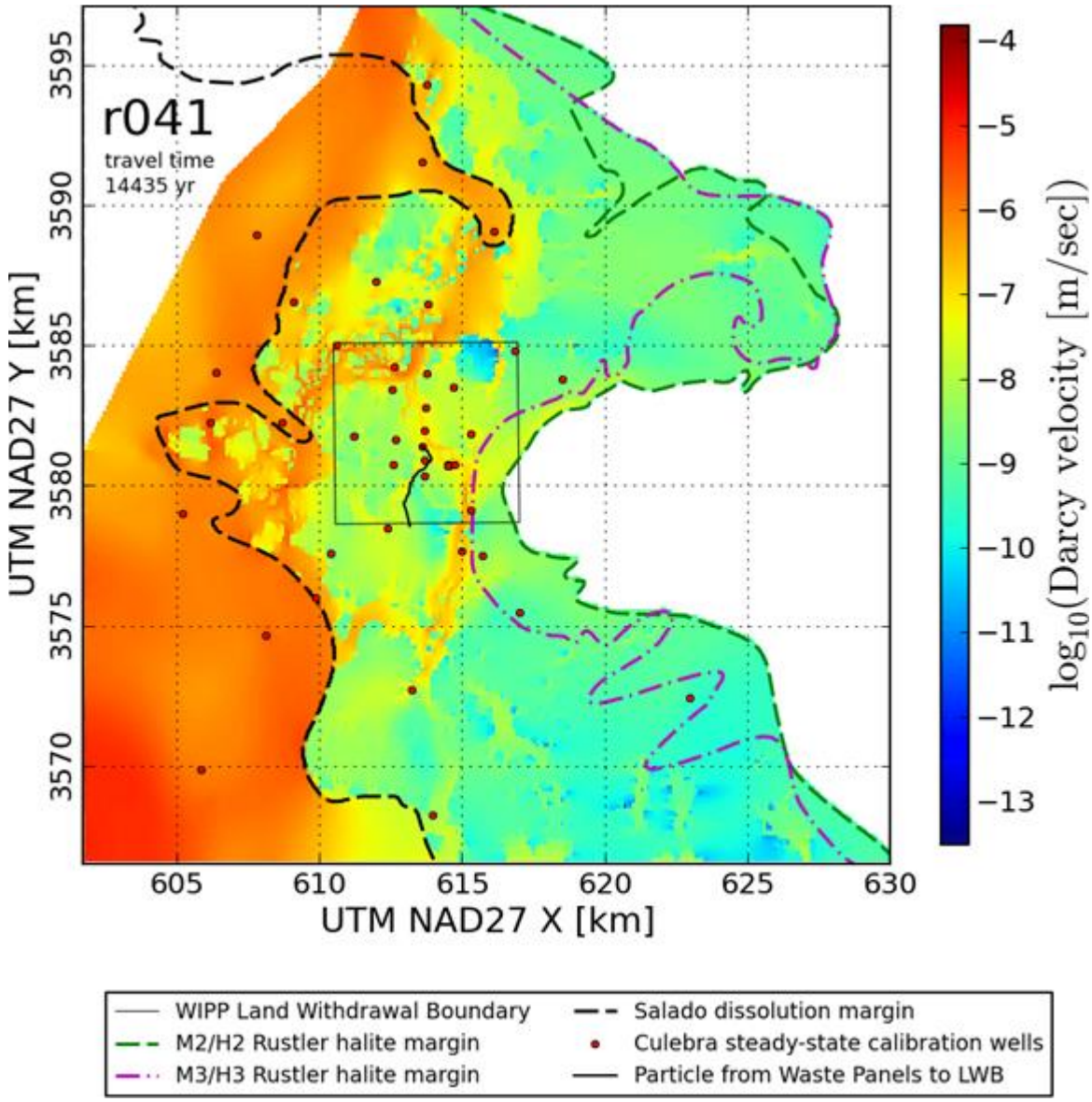
r041
travel time
14435 yr
UTM NAD27 Y [km]
3595
3590
3585
3580
3575
3570
605
610
615
620
625
630
UTM NAD27 X [km]
−4
−5
−6
−7
−8
−9
−10
−11
−12
−13
log10(Darcy velocity [m/sec])
WIPP Land Withdrawal Boundary
M2/H2 Rustler halite margin
M3/H3 Rustler halite margin
Salado dissolution margin
Culebra steady-state calibration wells
Particle from Waste Panels to LWB

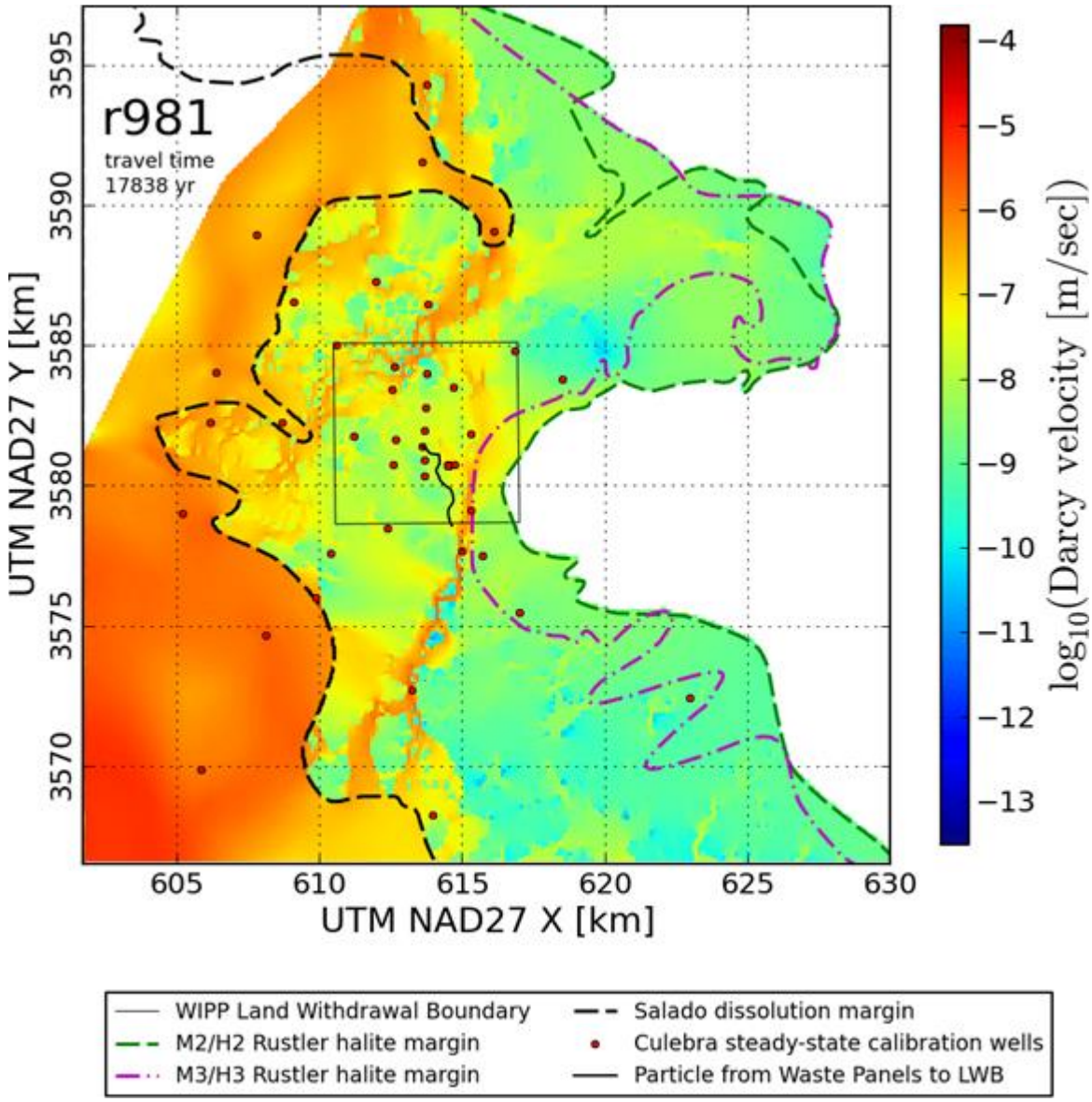
r981
travel time
17838 yr
UTM NAD27 Y [km]
3595
3590
3585
3580
3575
3570
605
610
615
620
625
630
UTM NAD27 X [km]
−4
−5
−6
−7
−8
−9
−10
−11
−12
−13
log10(Darcy velocity [m/sec])
WIPP Land Withdrawal Boundary
M2/H2 Rustler halite margin
M3/H3 Rustler halite margin
Salado dissolution margin
Culebra steady-state calibration wells
Particle from Waste Panels to LWB

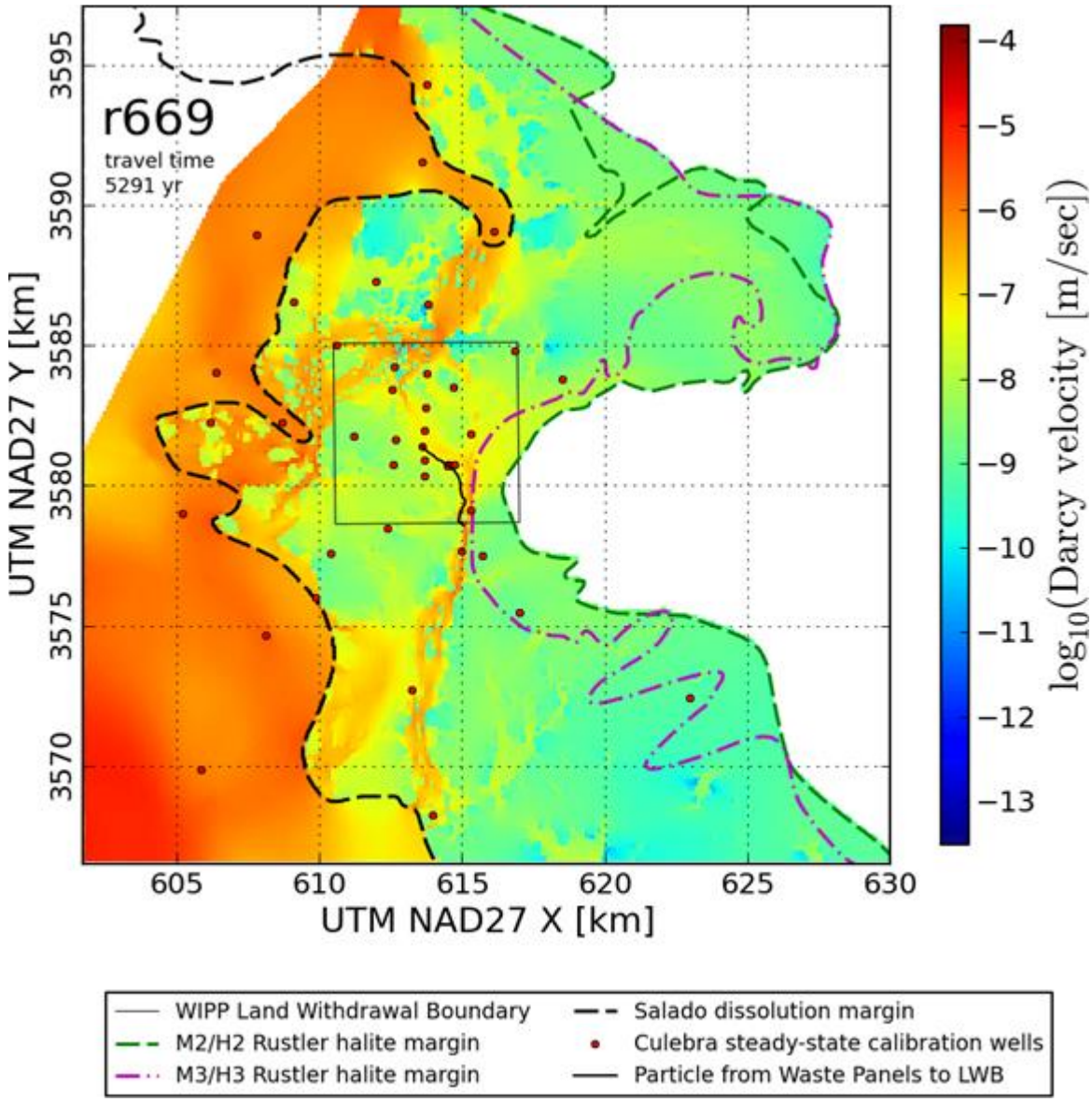
r669
travel time
5291 yr
UTM NAD27 Y [km]
3595
3590
3585
3580
3575
3570
605
610
615
620
625
630
UTM NAD27 X [km]
−4
−5
−6
−7
−8
−9
−10
−11
−12
−13
log10(Darcy velocity [m/sec])
WIPP Land Withdrawal Boundary
M2/H2 Rustler halite margin
M3/H3 Rustler halite margin
Salado dissolution margin
Culebra steady-state calibration wells
Particle from Waste Panels to LWB

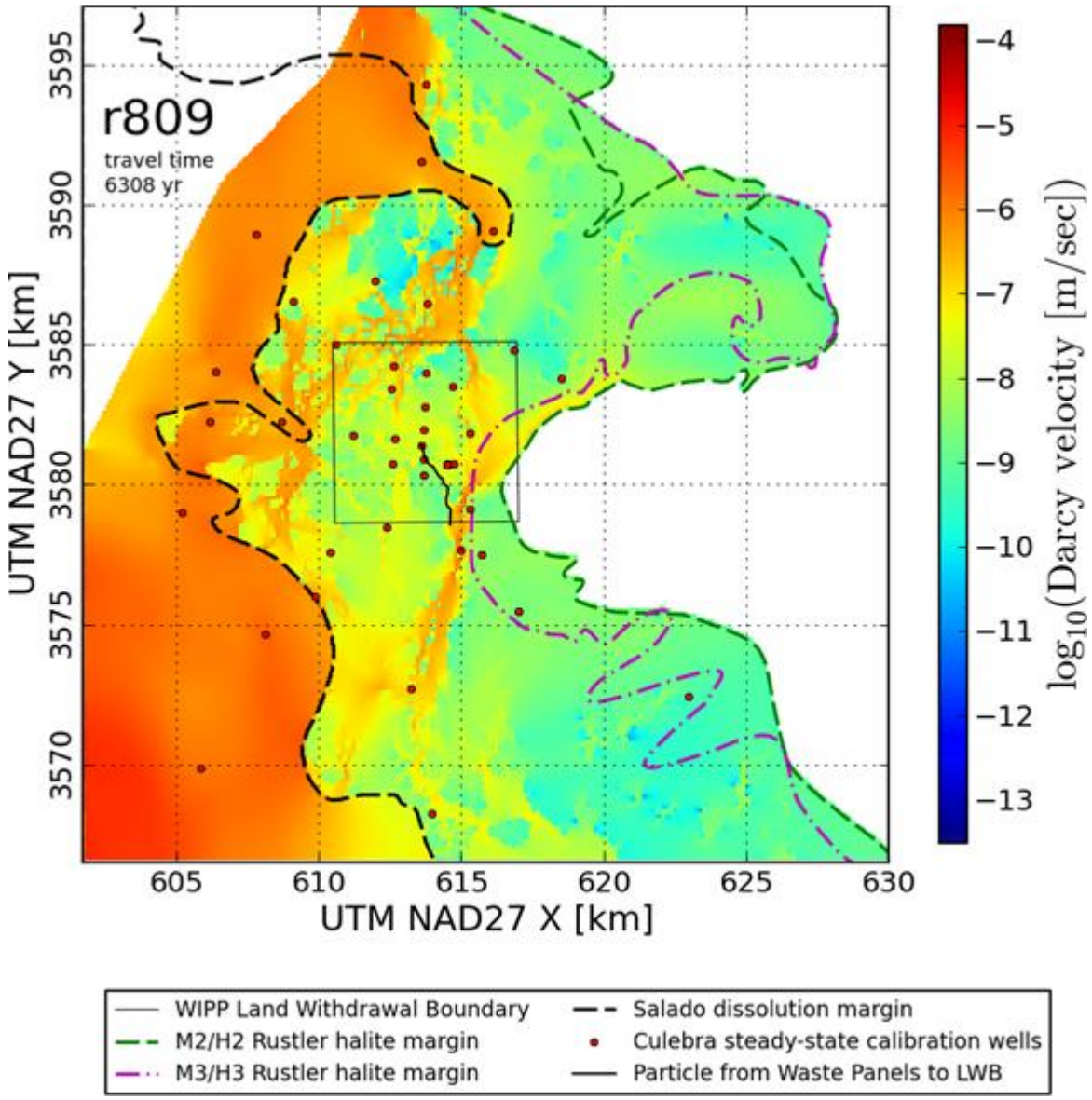
r809
travel time
6308 yr
UTM NAD27 Y [km]
3595
3590
3585
3580
3575
3570
605
610
615
620
625
630
UTM NAD27 X [km]
−4
−5
−6
−7
−8
−9
−10
−11
−12
−13
log10(Darcy velocity [m/sec])
WIPP Land Withdrawal Boundary
M2/H2 Rustler halite margin
M3/H3 Rustler halite margin
Salado dissolution margin
Culebra steady-state calibration wells
Particle from Waste Panels to LWB

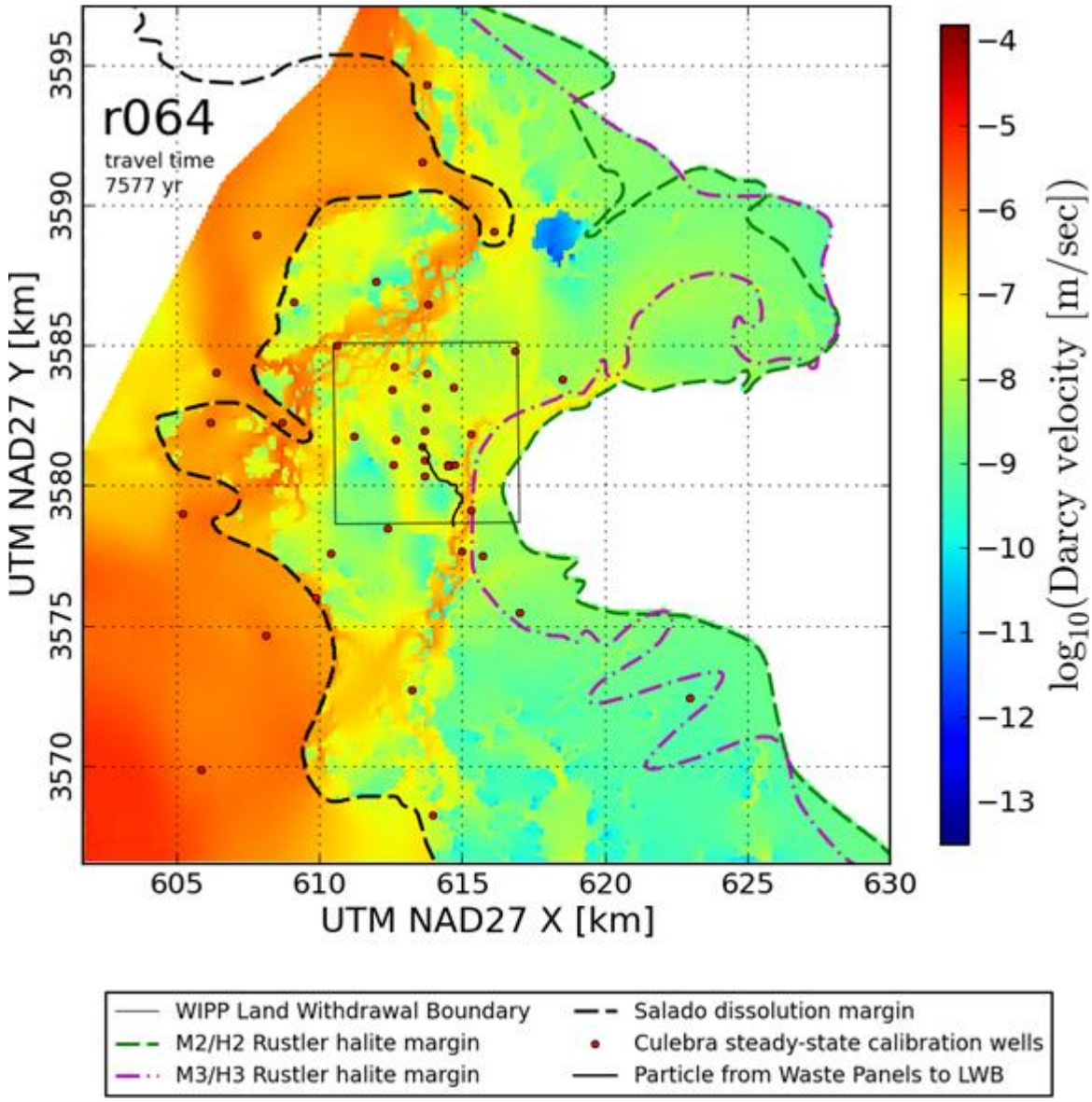
r064
travel time
7577 yr
UTM NAD27 Y [km]
3595
3590
3585
3580
3575
3570
605
610
615
620
625
630
UTM NAD27 X [km]
−4
−5
−6
−7
−8
−9
−10
−11
−12
−13
log10(Darcy velocity [m/sec])
WIPP Land Withdrawal Boundary
M2/H2 Rustler halite margin
M3/H3 Rustler halite margin
Salado dissolution margin
Culebra steady-state calibration wells
Particle from Waste Panels to LWB

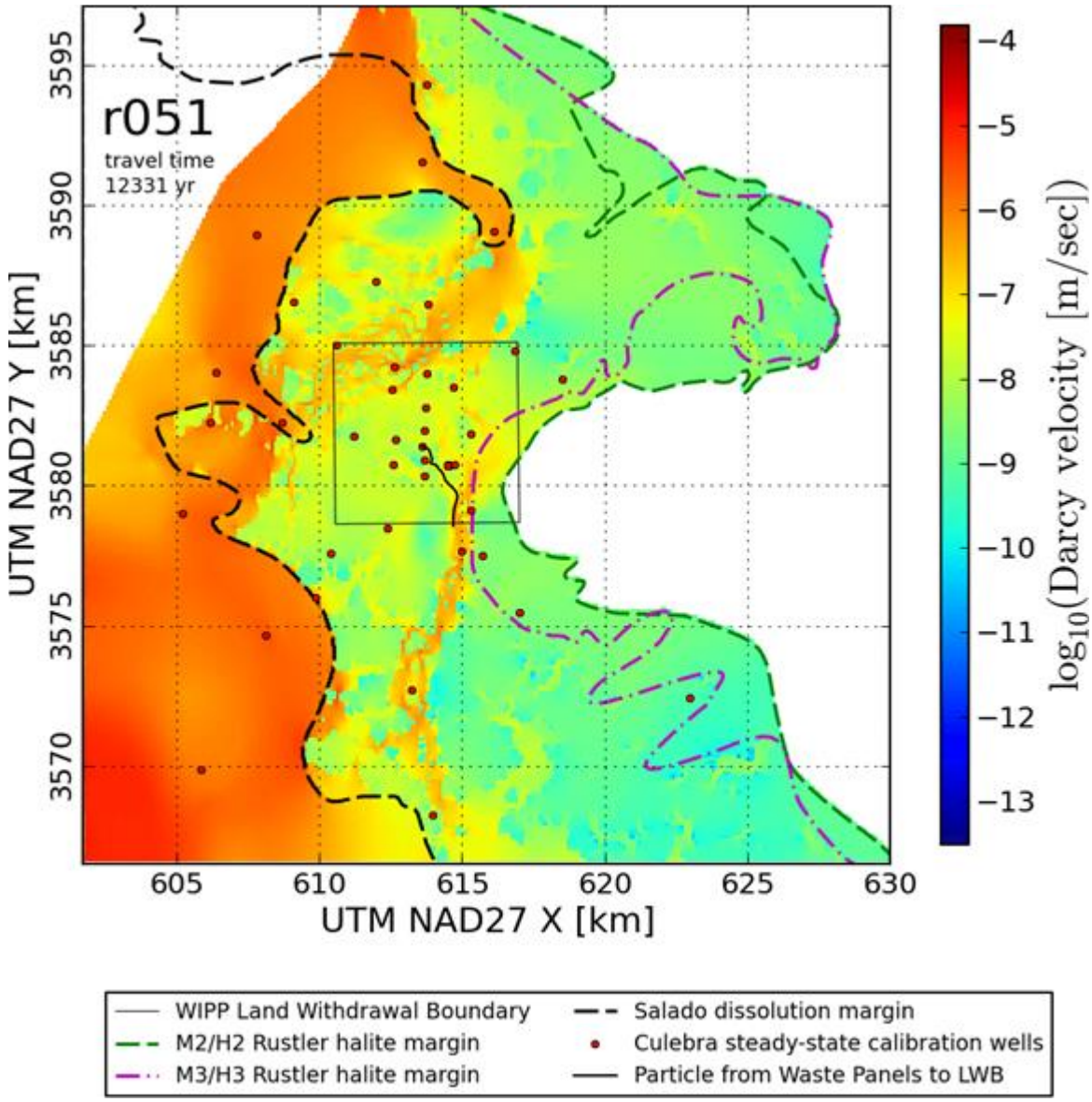
r051
travel time
12331 yr
UTM NAD27 Y [km]
3595
3590
3585
3580
3575
3570
605
610
615
620
625
630
UTM NAD27 X [km]
−4
−5
−6
−7
−8
−9
−10
−11
−12
−13
log10(Darcy velocity [m/sec])
WIPP Land Withdrawal Boundary
M2/H2 Rustler halite margin
M3/H3 Rustler halite margin
Salado dissolution margin
Culebra steady-state calibration wells
Particle from Waste Panels to LWB

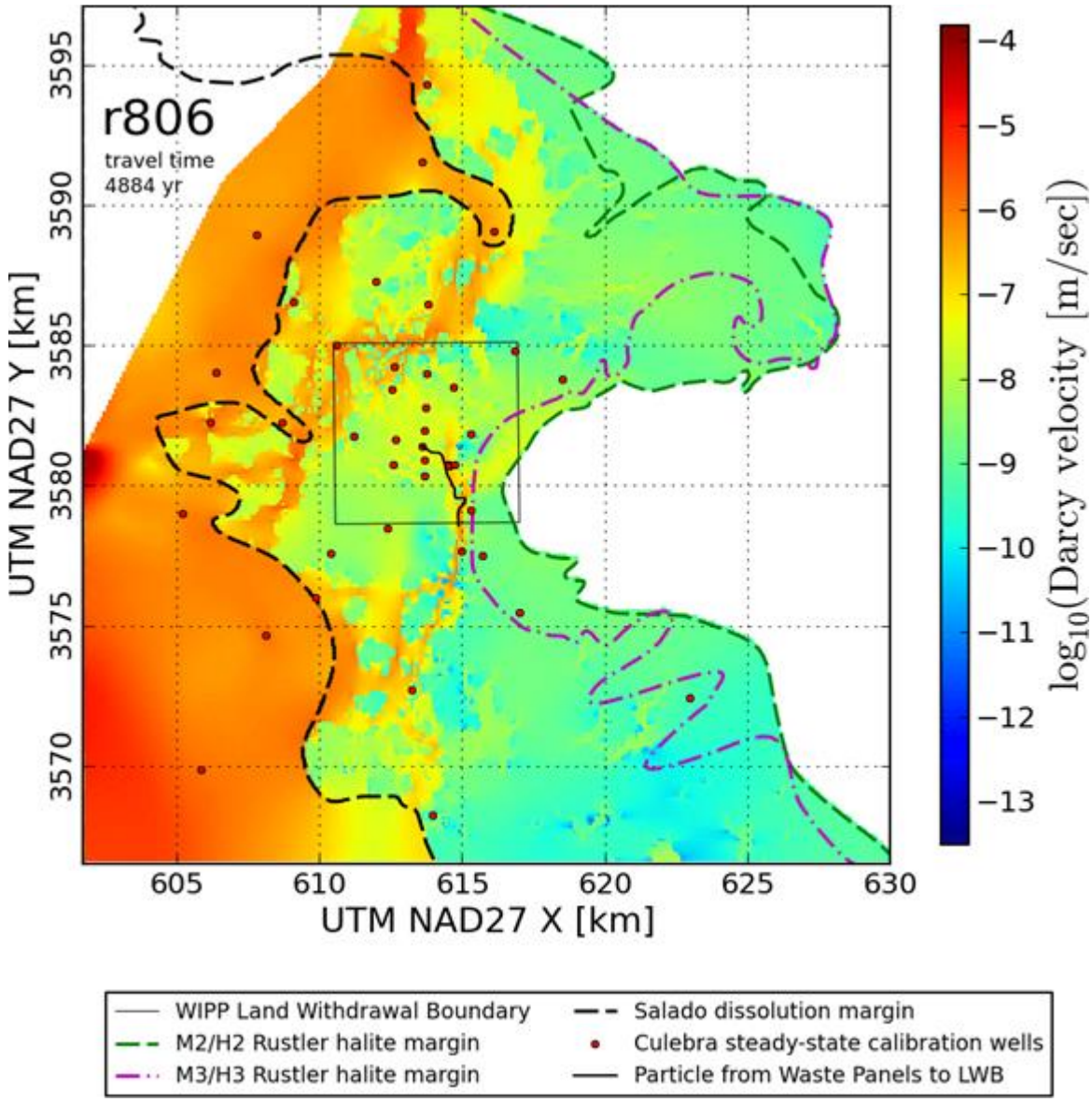
r806
travel time
4884 yr
UTM NAD27 Y [km]
3595
3590
3585
3580
3575
3570
605
610
615
620
625
630
UTM NAD27 X [km]
−4
−5
−6
−7
−8
−9
−10
−11
−12
−13
log10(Darcy velocity [m/sec])
WIPP Land Withdrawal Boundary
M2/H2 Rustler halite margin
M3/H3 Rustler halite margin
Salado dissolution margin
Culebra steady-state calibration wells
Particle from Waste Panels to LWB

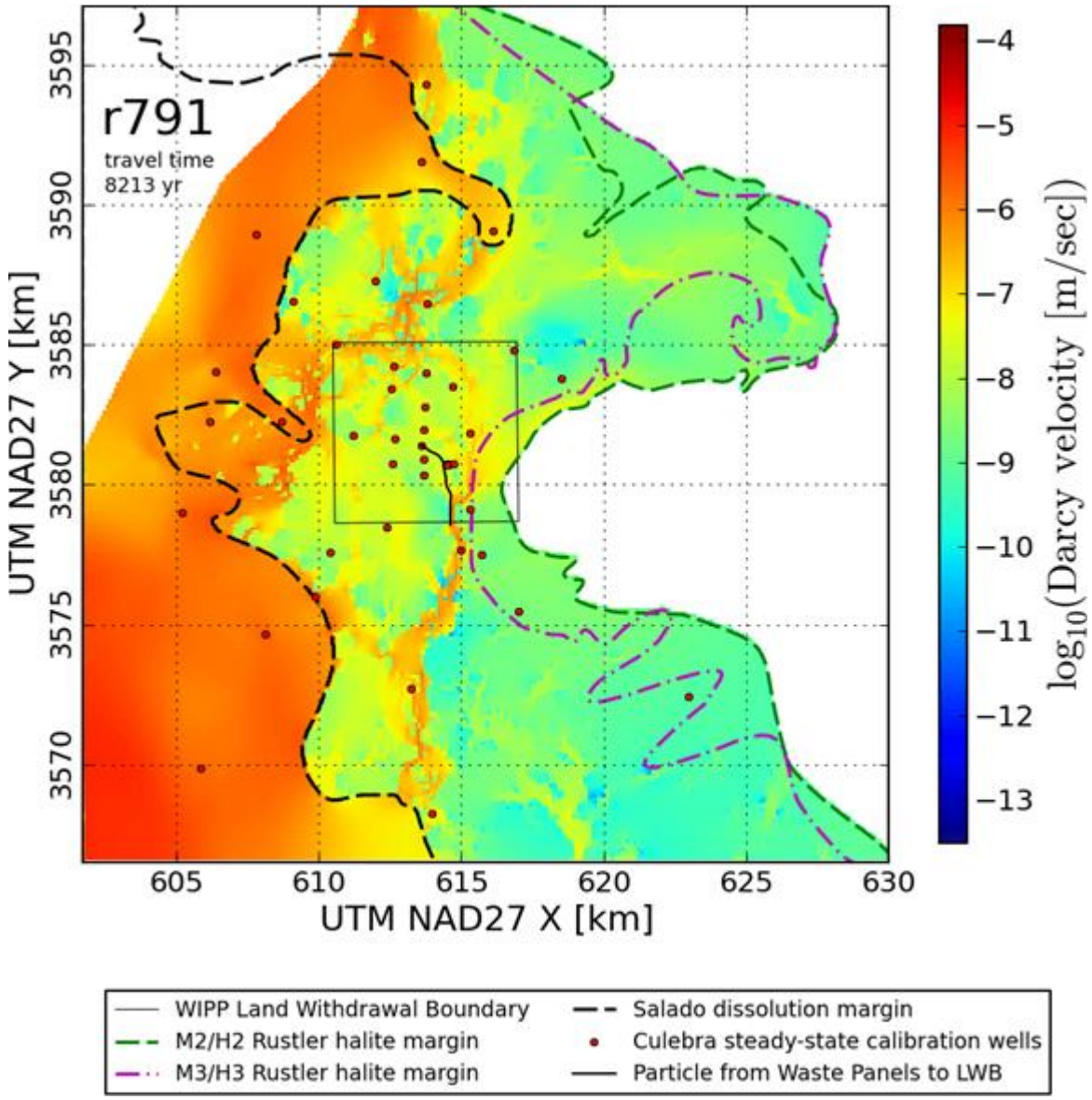
r791
travel time
8213 yr
UTM NAD27 Y [km]
3595
3590
3585
3580
3575
3570
605
610
615
620
625
630
UTM NAD27 X [km]
−4
−5
−6
−7
−8
−9
−10
−11
−12
−13
log10(Darcy velocity [m/sec])
WIPP Land Withdrawal Boundary
M2/H2 Rustler halite margin
M3/H3 Rustler halite margin
Salado dissolution margin
Culebra steady-state calibration wells
Particle from Waste Panels to LWB

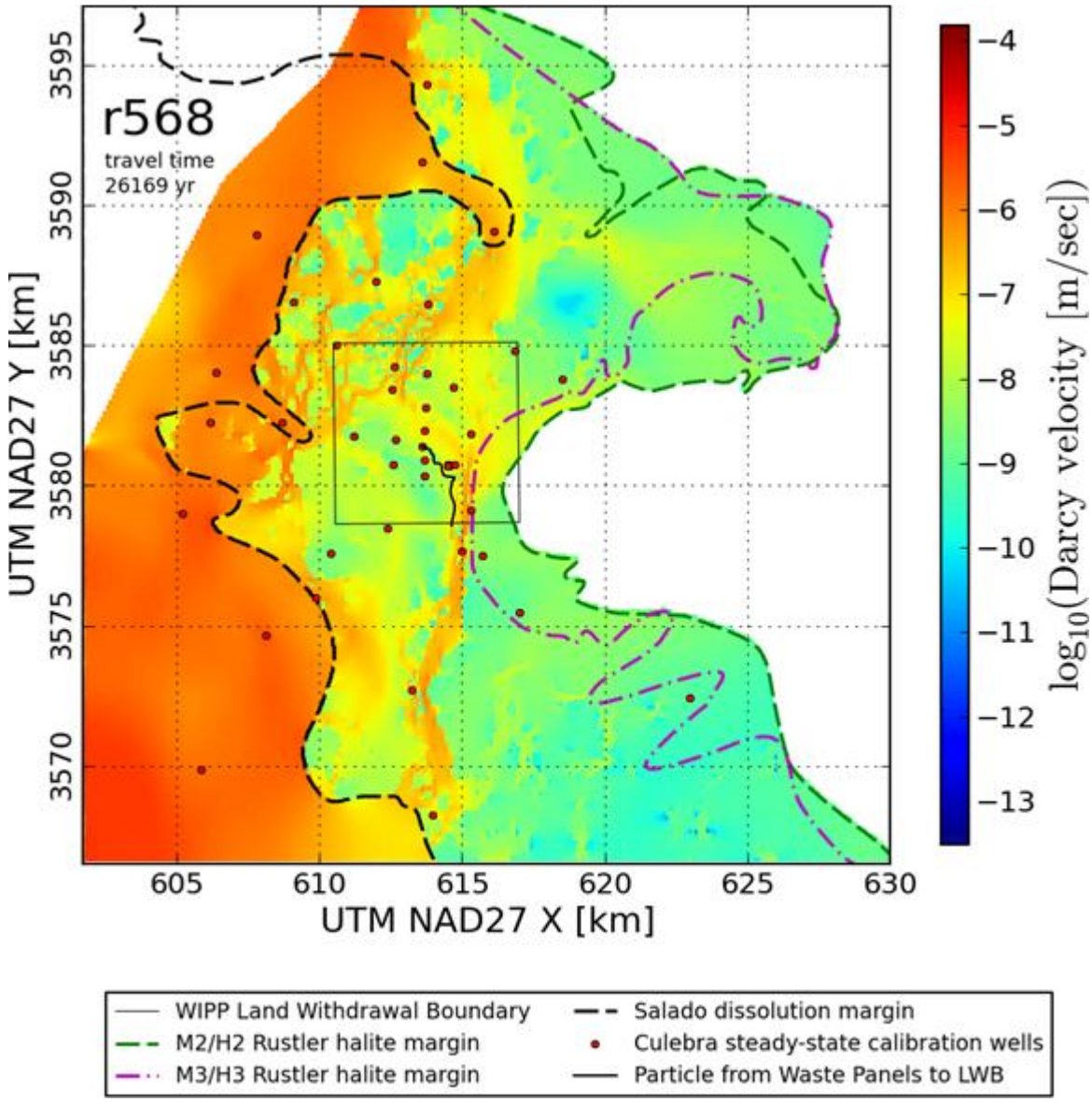
r568
travel time
26169 yr
UTM NAD27 Y [km]
3595
3590
3585
3580
3575
3570
605
610
615
620
625
630
UTM NAD27 X [km]
−4
−5
−6
−7
−8
−9
−10
−11
−12
−13
log10(Darcy velocity [m/sec])
WIPP Land Withdrawal Boundary
M2/H2 Rustler halite margin
M3/H3 Rustler halite margin
Salado dissolution margin
Culebra steady-state calibration wells
Particle from Waste Panels to LWB

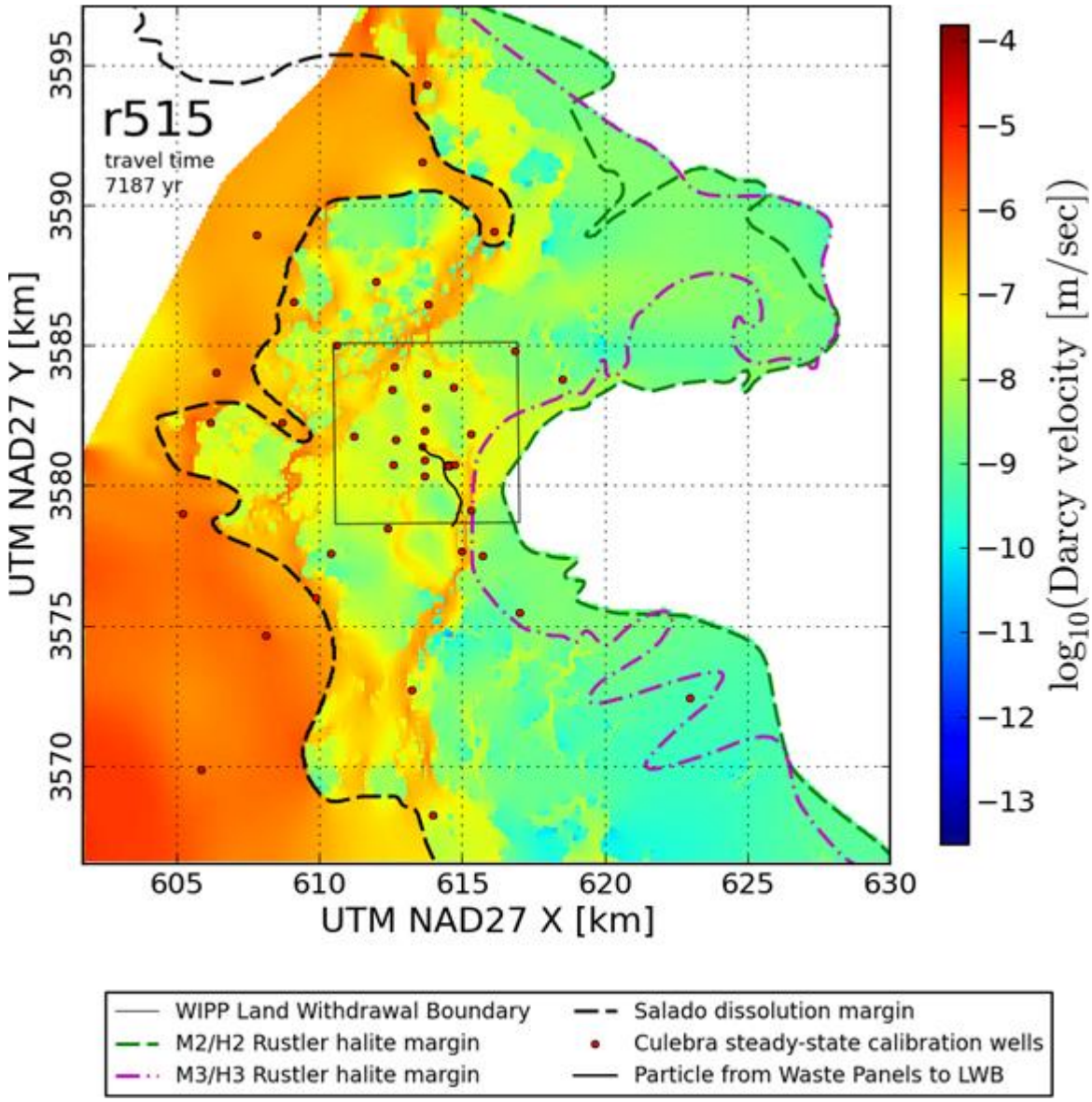
r515
travel time
7187 yr
UTM NAD27 Y [km]
3595
3590
3585
3580
3575
3570
605
610
615
620
625
630
UTM NAD27 X [km]
−4
−5
−6
−7
−8
−9
−10
−11
−12
−13
log10(Darcy velocity [m/sec])
WIPP Land Withdrawal Boundary
M2/H2 Rustler halite margin
M3/H3 Rustler halite margin
Salado dissolution margin
Culebra steady-state calibration wells
Particle from Waste Panels to LWB

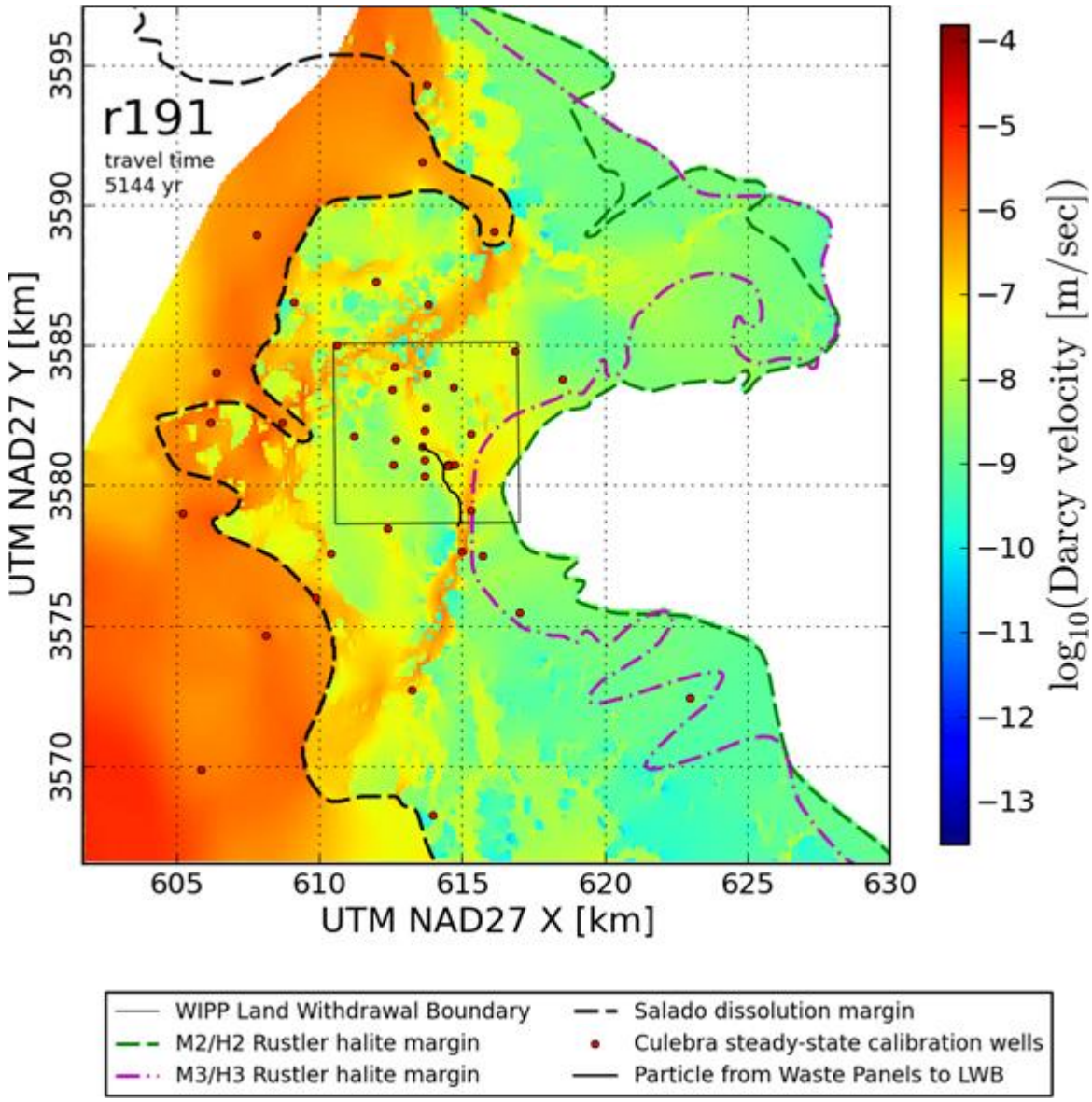
r191
travel time
5144 yr
UTM NAD27 Y [km]
3595
3590
3585
3580
3575
3570
605
610
615
620
625
630
UTM NAD27 X [km]
−4
−5
−6
−7
−8
−9
−10
−11
−12
−13
log10(Darcy velocity [m/sec])
WIPP Land Withdrawal Boundary
M2/H2 Rustler halite margin
M3/H3 Rustler halite margin
Salado dissolution margin
Culebra steady-state calibration wells
Particle from Waste Panels to LWB

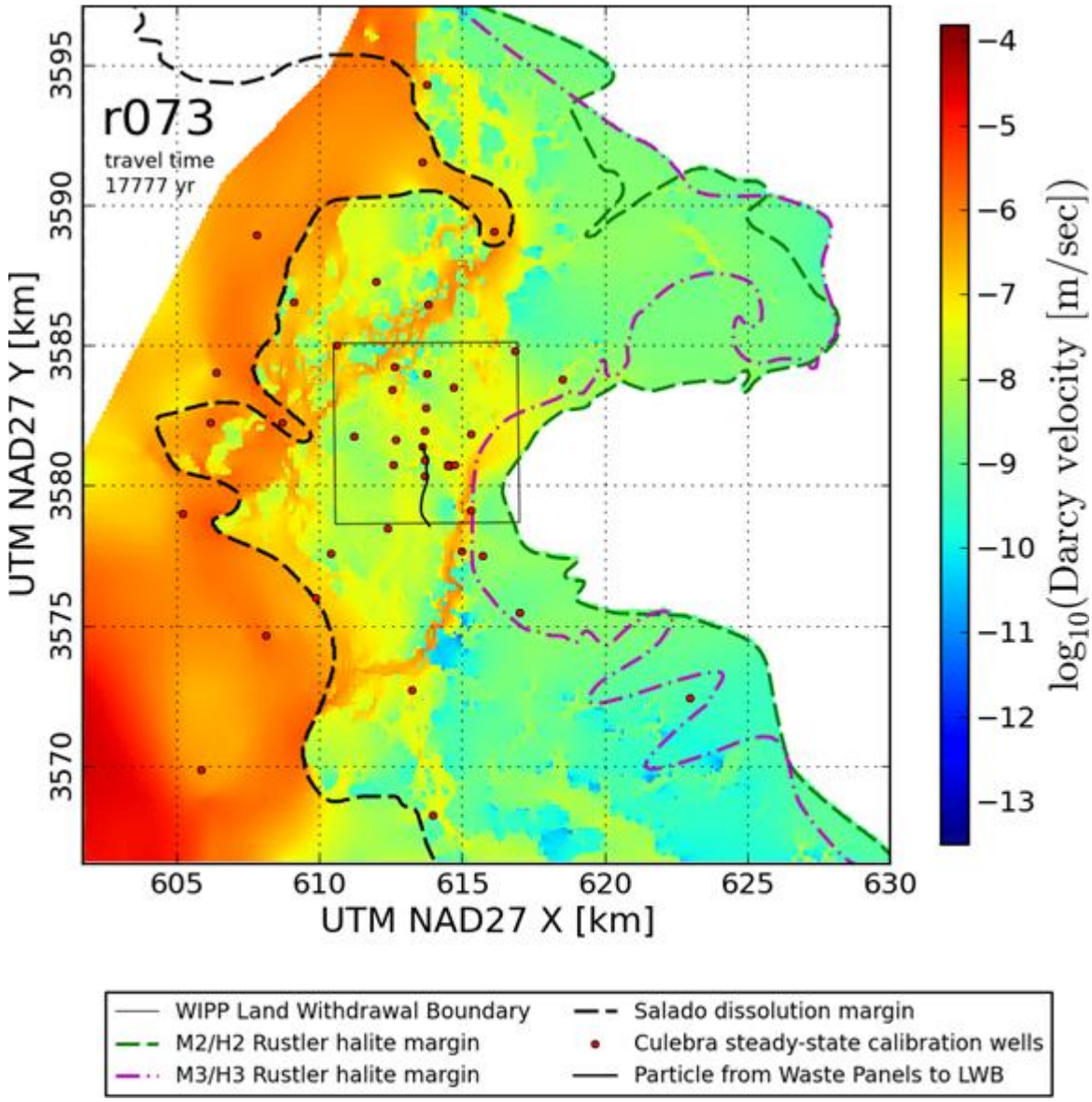
r073
travel time
17777 yr
UTM NAD27 Y [km]
3595
3590
3585
3580
3575
3570
605
610
615
620
625
630
UTM NAD27 X [km]
−4
−5
−6
−7
−8
−9
−10
−11
−12
−13
log10(Darcy velocity [m/sec])
WIPP Land Withdrawal Boundary
M2/H2 Rustler halite margin
M3/H3 Rustler halite margin
Salado dissolution margin
Culebra steady-state calibration wells
Particle from Waste Panels to LWB

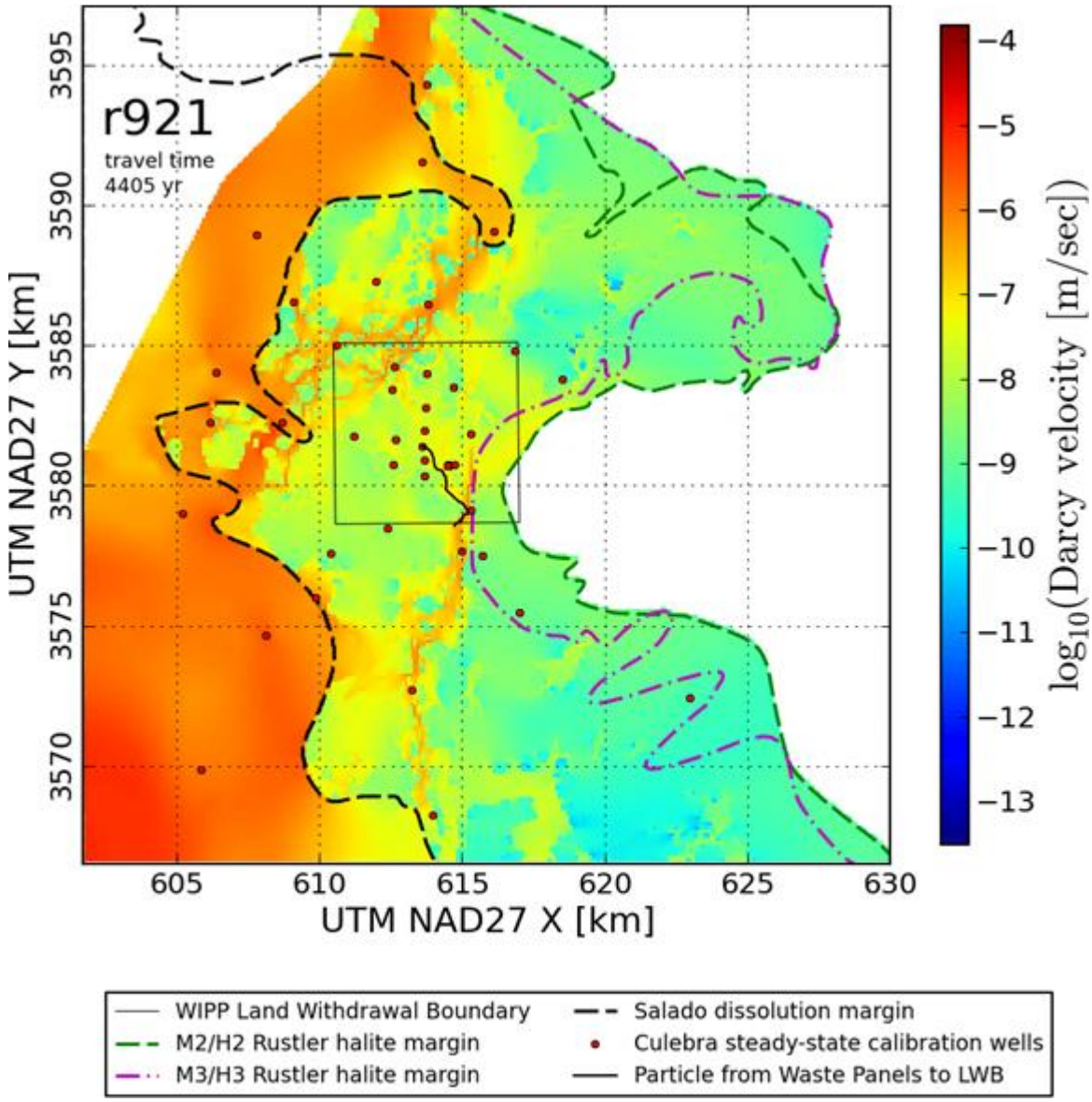
r921
travel time
4405 yr
UTM NAD27 Y [km]
3595
3590
3585
3580
3575
3570
605
610
615
620
625
630
UTM NAD27 X [km]
−4
−5
−6
−7
−8
−9
−10
−11
−12
−13
log10(Darcy velocity [m/sec])
WIPP Land Withdrawal Boundary
M2/H2 Rustler halite margin
M3/H3 Rustler halite margin
Salado dissolution margin
Culebra steady-state calibration wells
Particle from Waste Panels to LWB

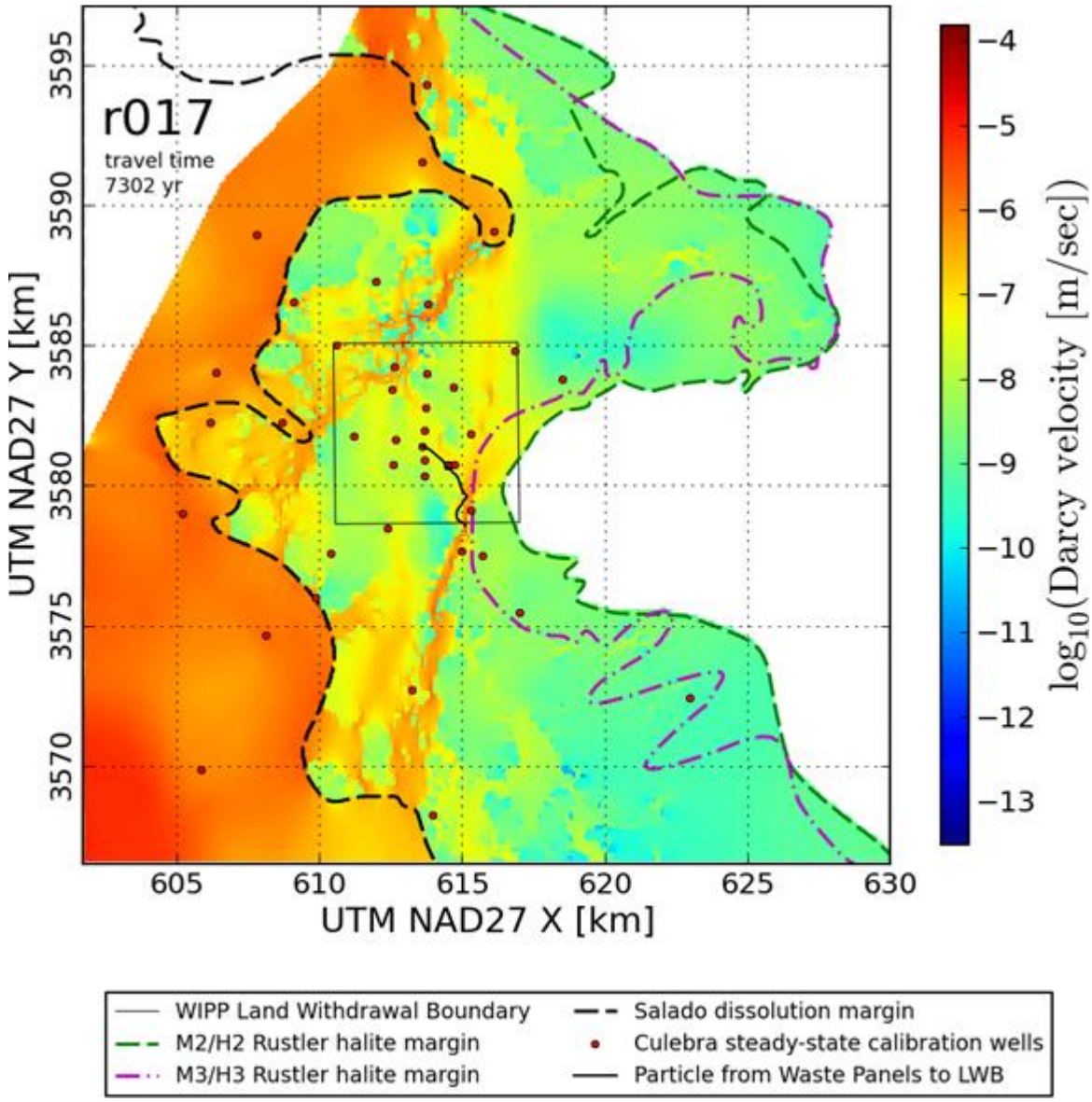
r017
travel time
7302 yr
UTM NAD27 Y [km]
3595
3590
3585
3580
3575
3570
605
610
615
620
625
630
UTM NAD27 X [km]
−4
−5
−6
−7
−8
−9
−10
−11
−12
−13
log10(Darcy velocity [m/sec])
WIPP Land Withdrawal Boundary
M2/H2 Rustler halite margin
M3/H3 Rustler halite margin
Salado dissolution margin
Culebra steady-state calibration wells
Particle from Waste Panels to LWB

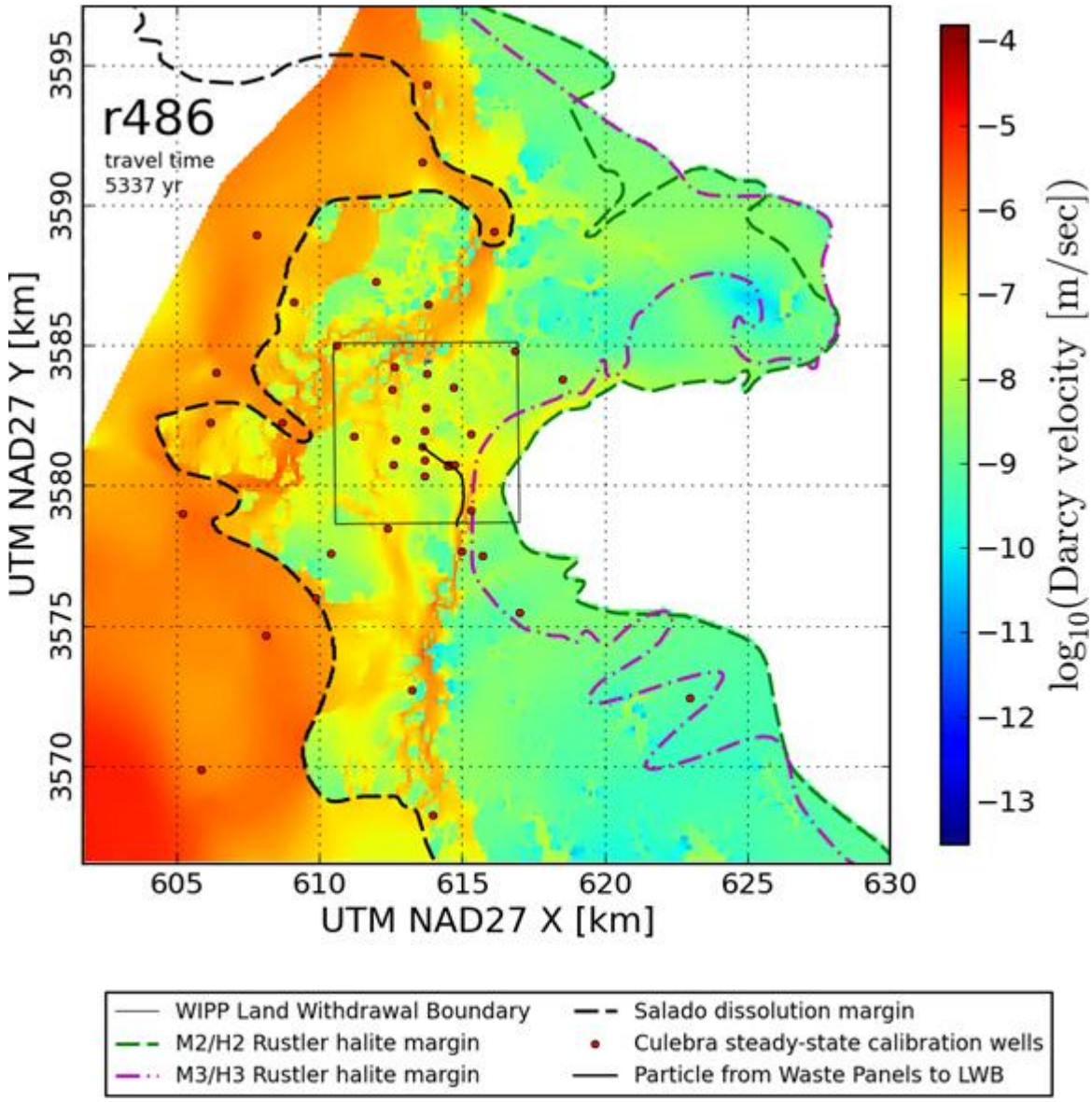
r486
travel time
5337 yr
UTM NAD27 Y [km]
3595
3590
3585
3580
3575
3570
605
610
615
620
625
630
UTM NAD27 X [km]
−4
−5
−6
−7
−8
−9
−10
−11
−12
−13
log10(Darcy velocity [m/sec])
WIPP Land Withdrawal Boundary
M2/H2 Rustler halite margin
M3/H3 Rustler halite margin
Salado dissolution margin
Culebra steady-state calibration wells
Particle from Waste Panels to LWB

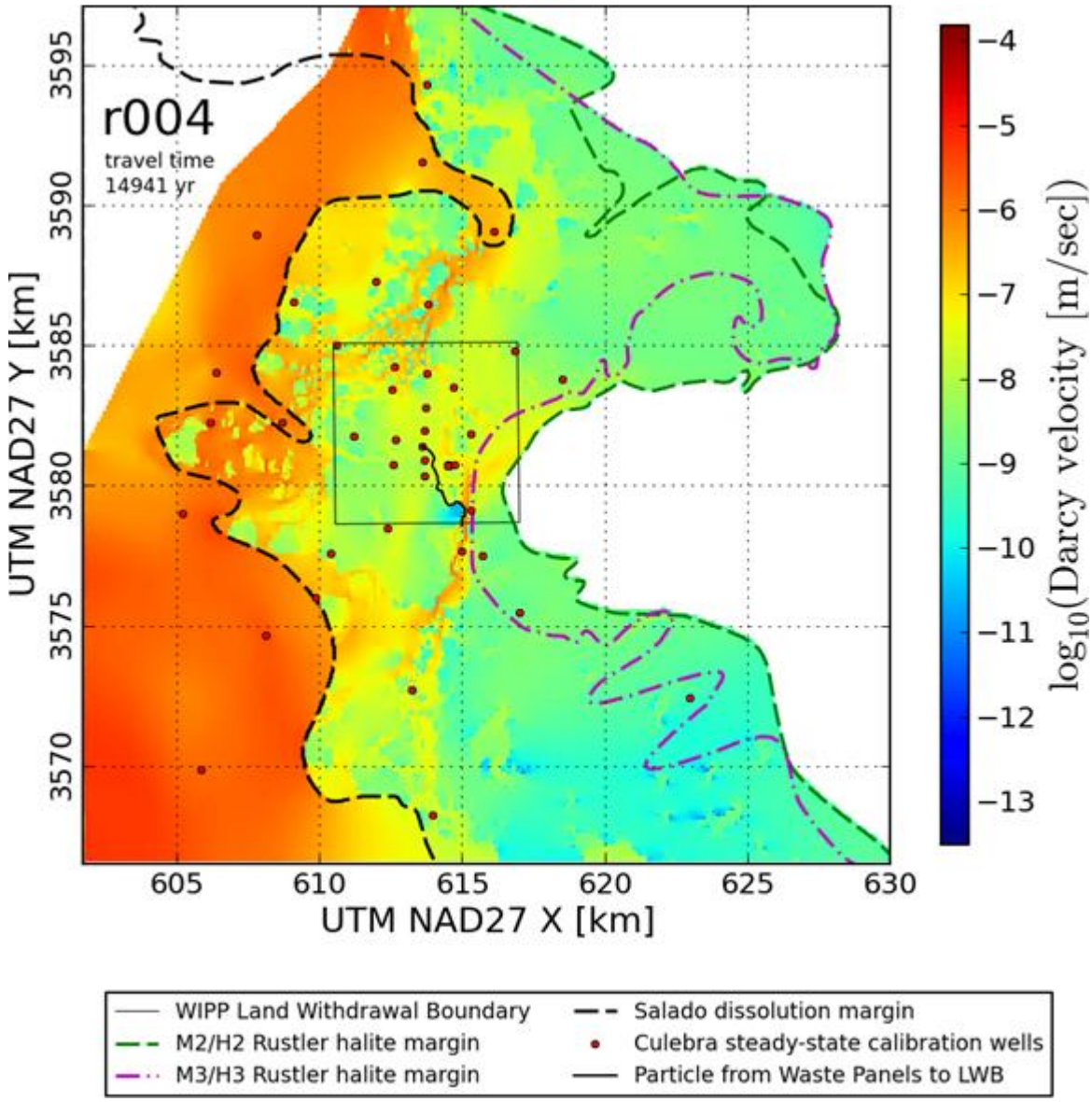
r004
travel time
14941 yr
UTM NAD27 Y [km]
3595
3590
3585
3580
3575
3570
605
610
615
620
625
630
UTM NAD27 X [km]
−4
−5
−6
−7
−8
−9
−10
−11
−12
−13
log10(Darcy velocity [m/sec])
WIPP Land Withdrawal Boundary
M2/H2 Rustler halite margin
M3/H3 Rustler halite margin
Salado dissolution margin
Culebra steady-state calibration wells
Particle from Waste Panels to LWB

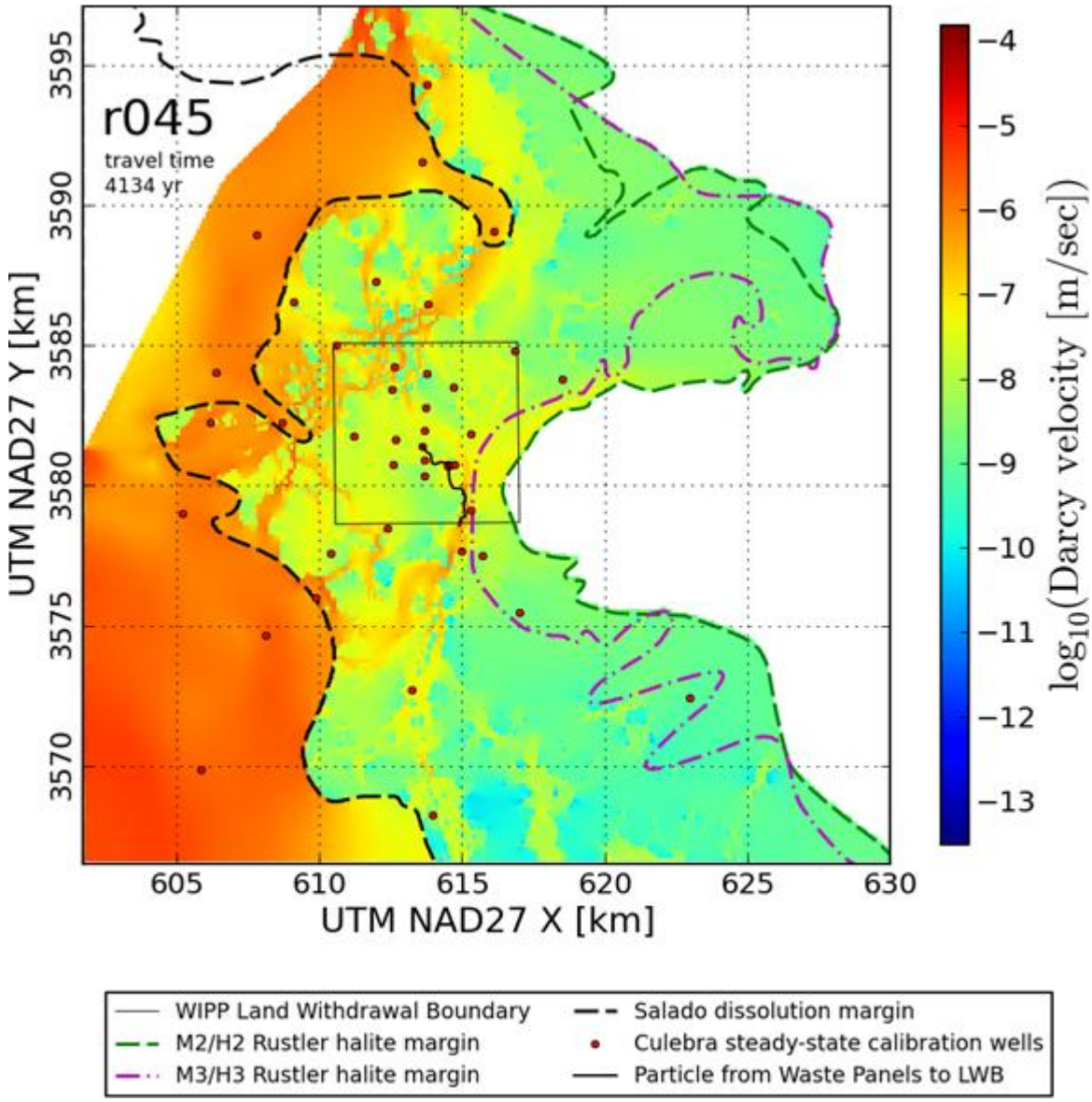
r045
travel time
4134 yr
UTM NAD27 Y [km]
3595
3590
3585
3580
3575
3570
605
610
615
620
625
630
UTM NAD27 X [km]
−4
−5
−6
−7
−8
−9
−10
−11
−12
−13
log10(Darcy velocity [m/sec])
WIPP Land Withdrawal Boundary
M2/H2 Rustler halite margin
M3/H3 Rustler halite margin
Salado dissolution margin
Culebra steady-state calibration wells
Particle from Waste Panels to LWB

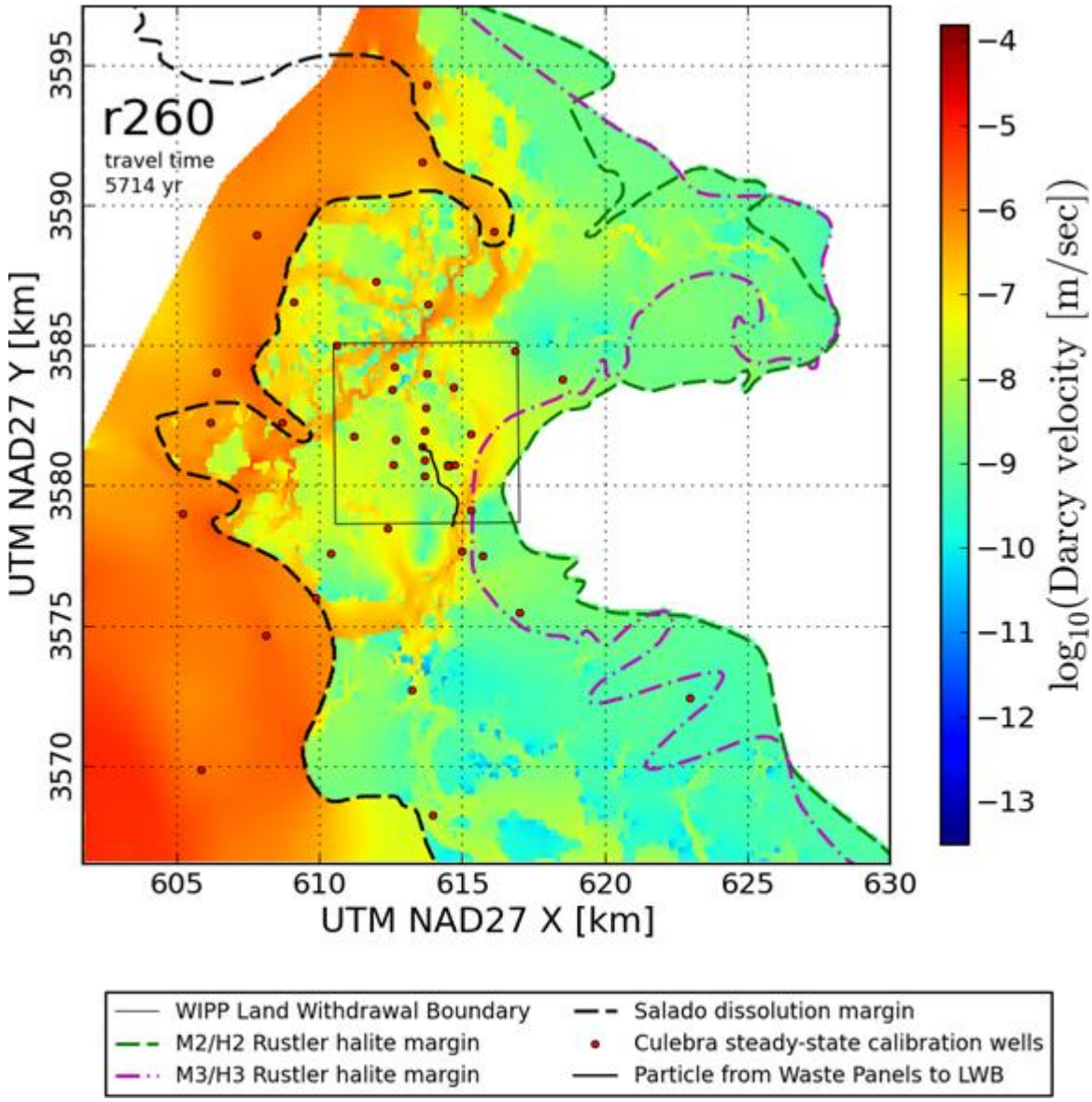
r260
travel time
5714 yr
UTM NAD27 Y [km]
3595
3590
3585
3580
3575
3570
605
610
615
620
625
630
UTM NAD27 X [km]
−4
−5
−6
−7
−8
−9
−10
−11
−12
−13
log10(Darcy velocity [m/sec])
WIPP Land Withdrawal Boundary
M2/H2 Rustler halite margin
M3/H3 Rustler halite margin
Salado dissolution margin
Culebra steady-state calibration wells
Particle from Waste Panels to LWB

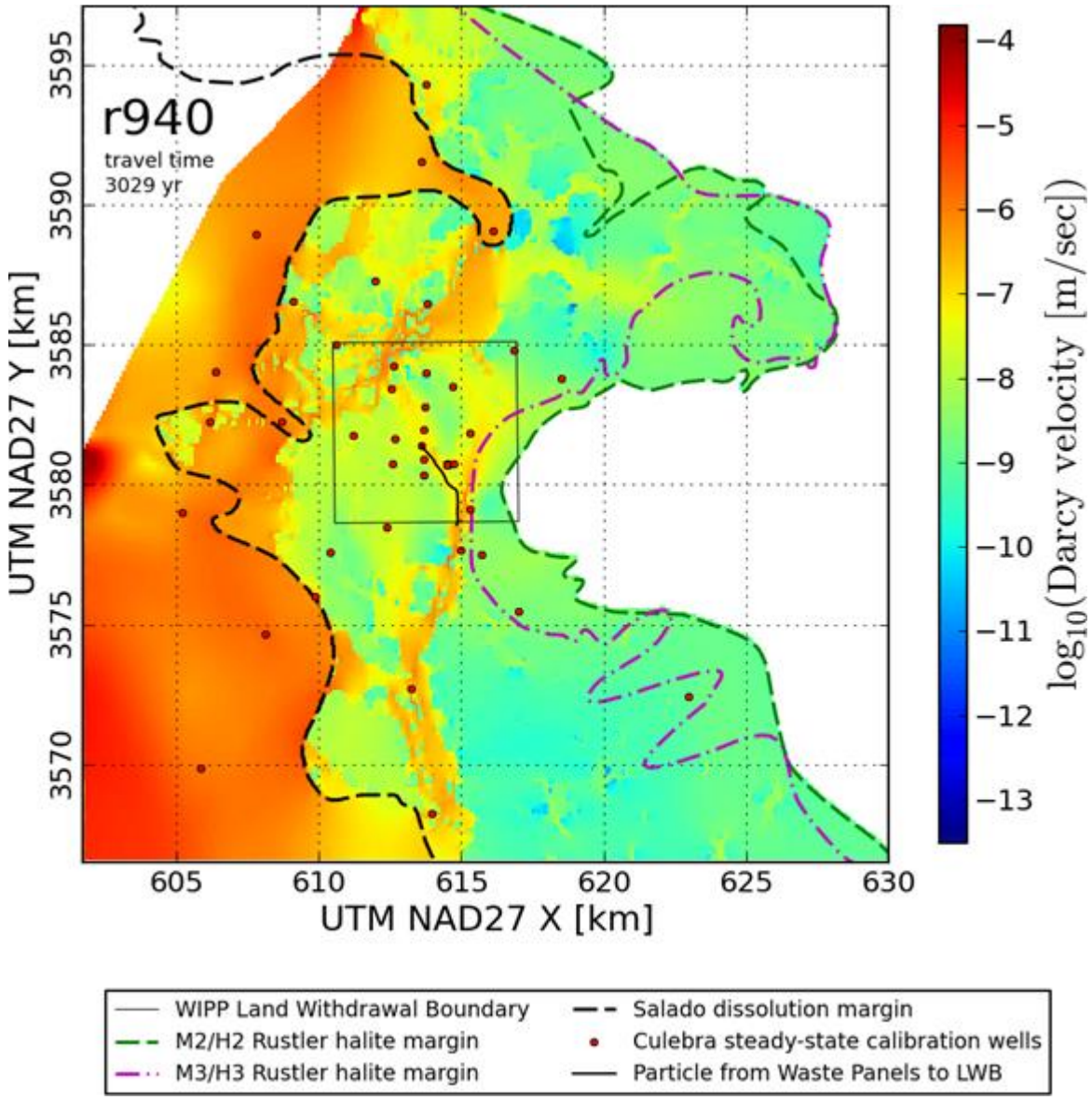
r940
travel time
3029 yr
UTM NAD27 Y [km]
3595
3590
3585
3580
3575
3570
605
610
615
620
625
630
UTM NAD27 X [km]
−4
−5
−6
−7
−8
−9
−10
−11
−12
−13
log10(Darcy velocity [m/sec])
WIPP Land Withdrawal Boundary
M2/H2 Rustler halite margin
M3/H3 Rustler halite margin
Salado dissolution margin
Culebra steady-state calibration wells
Particle from Waste Panels to LWB

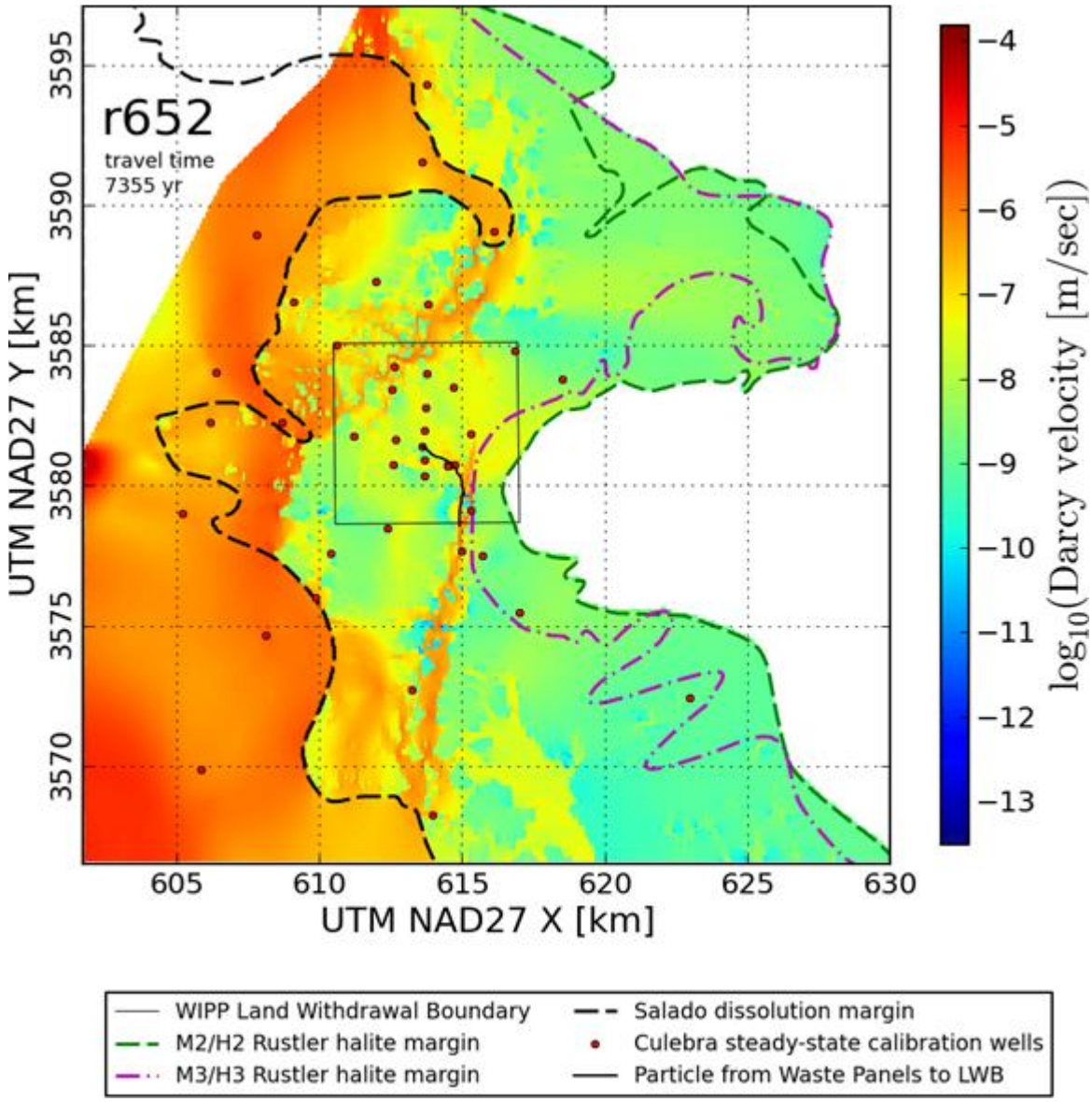
r652
travel time
7355 yr
UTM NAD27 Y [km]
3595
3590
3585
3580
3575
3570
605
610
615
620
625
630
UTM NAD27 X [km]
−4
−5
−6
−7
−8
−9
−10
−11
−12
−13
log10(Darcy velocity [m/sec])
WIPP Land Withdrawal Boundary
M2/H2 Rustler halite margin
M3/H3 Rustler halite margin
Salado dissolution margin
Culebra steady-state calibration wells
Particle from Waste Panels to LWB

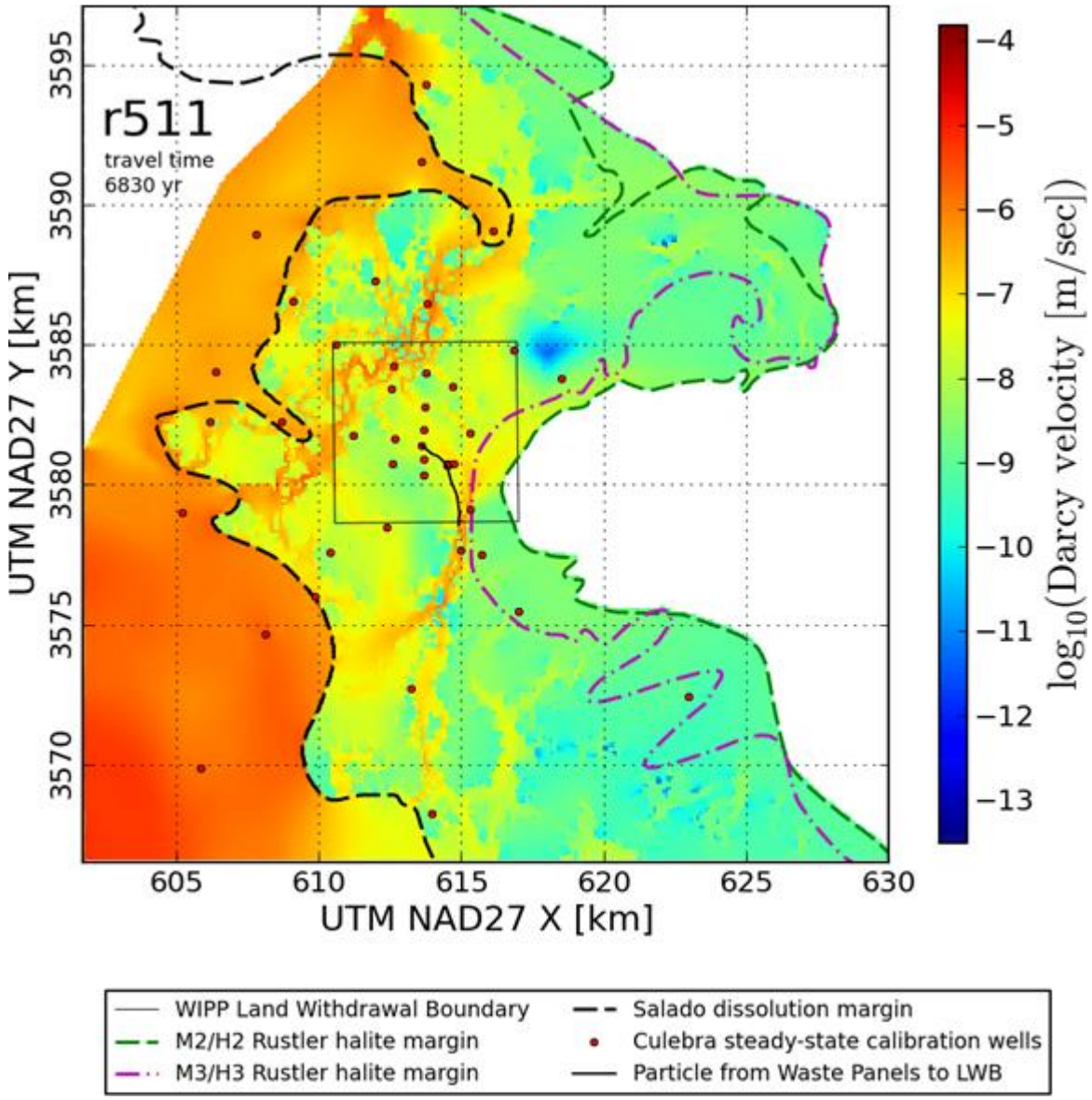
r511
travel time
6830 yr
UTM NAD27 Y [km]
3595
3590
3585
3580
3575
3570
605
610
615
620
625
630
UTM NAD27 X [km]
−4
−5
−6
−7
−8
−9
−10
−11
−12
−13
log10(Darcy velocity [m/sec])
WIPP Land Withdrawal Boundary
M2/H2 Rustler halite margin
M3/H3 Rustler halite margin
Salado dissolution margin
Culebra steady-state calibration wells
Particle from Waste Panels to LWB

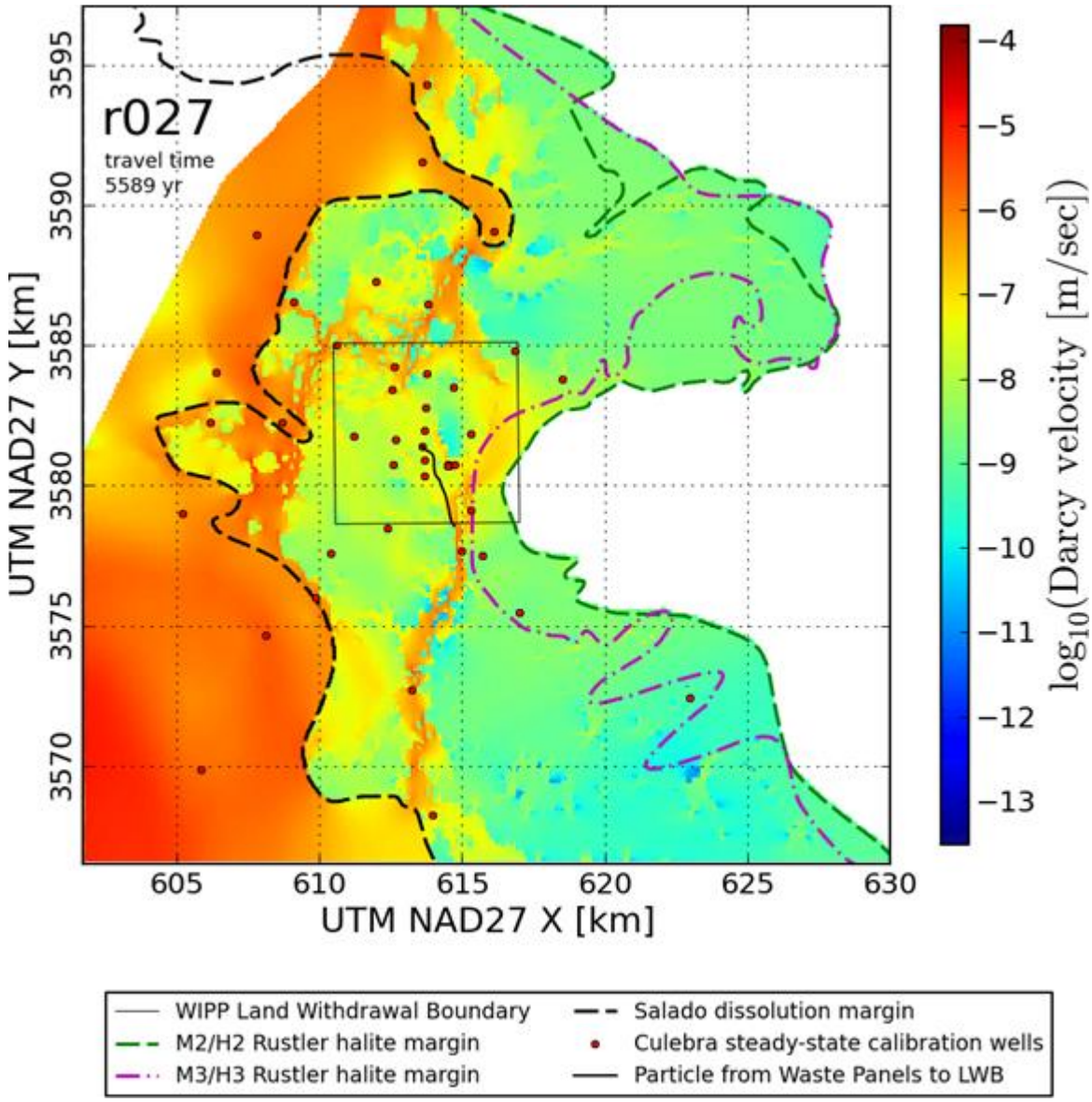
r027
travel time
5589 yr
UTM NAD27 Y [km]
3595
3590
3585
3580
3575
3570
605
610
615
620
625
630
UTM NAD27 X [km]
−4
−5
−6
−7
−8
−9
−10
−11
−12
−13
log10(Darcy velocity [m/sec])
WIPP Land Withdrawal Boundary
M2/H2 Rustler halite margin
M3/H3 Rustler halite margin
Salado dissolution margin
Culebra steady-state calibration wells
Particle from Waste Panels to LWB

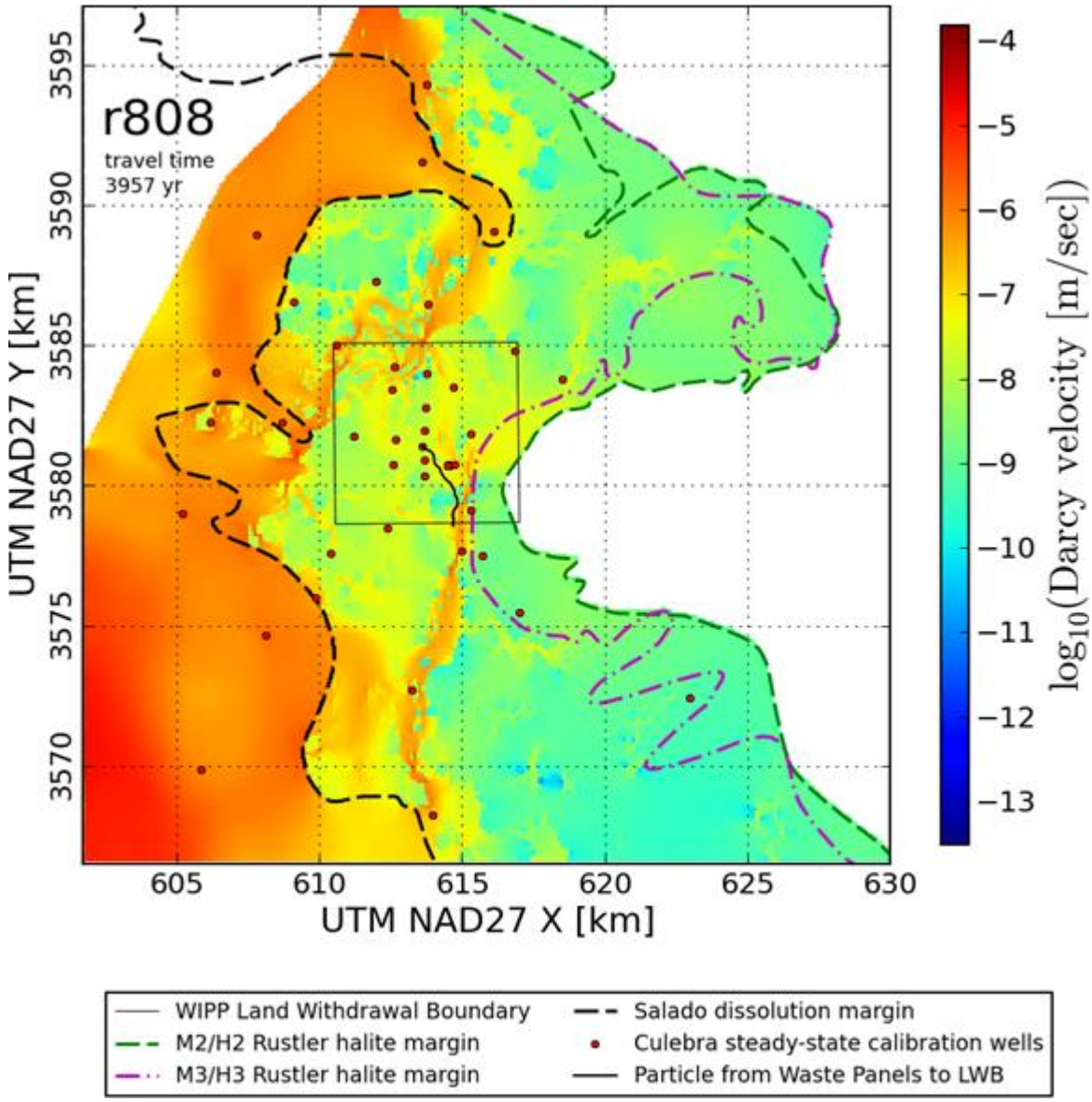
r808
travel time
3957 yr
UTM NAD27 Y [km]
3595
3590
3585
3580
3575
3570
605
610
615
620
625
630
UTM NAD27 X [km]
−4
−5
−6
−7
−8
−9
−10
−11
−12
−13
log10(Darcy velocity [m/sec])
WIPP Land Withdrawal Boundary
M2/H2 Rustler halite margin
M3/H3 Rustler halite margin
Salado dissolution margin
Culebra steady-state calibration wells
Particle from Waste Panels to LWB

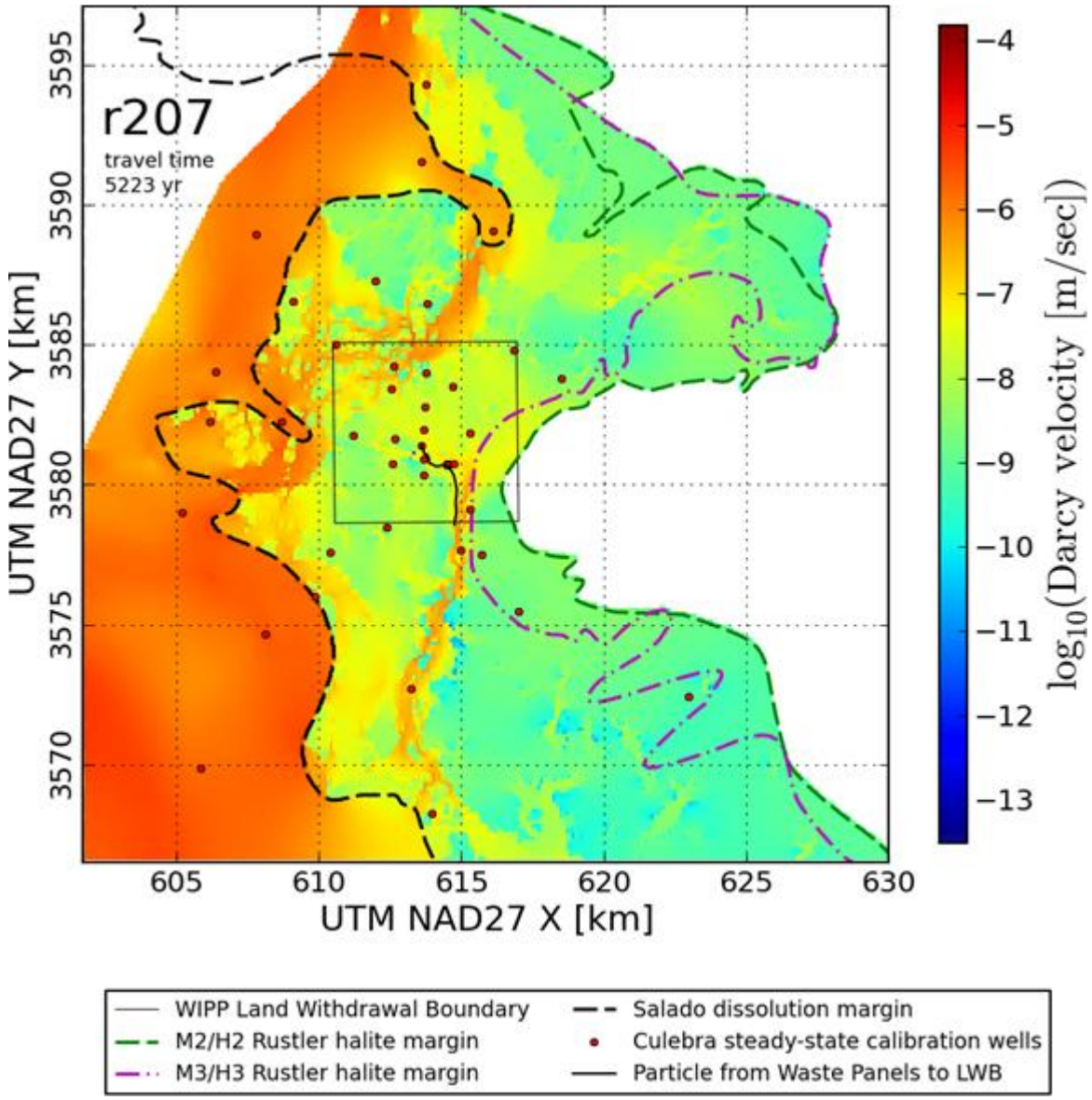
r207
travel time
5223 yr
UTM NAD27 Y [km]
3595
3590
3585
3580
3575
3570
605
610
615
620
625
630
UTM NAD27 X [km]
−4
−5
−6
−7
−8
−9
−10
−11
−12
−13
log10(Darcy velocity [m/sec])
WIPP Land Withdrawal Boundary
M2/H2 Rustler halite margin
M3/H3 Rustler halite margin
Salado dissolution margin
Culebra steady-state calibration wells
Particle from Waste Panels to LWB

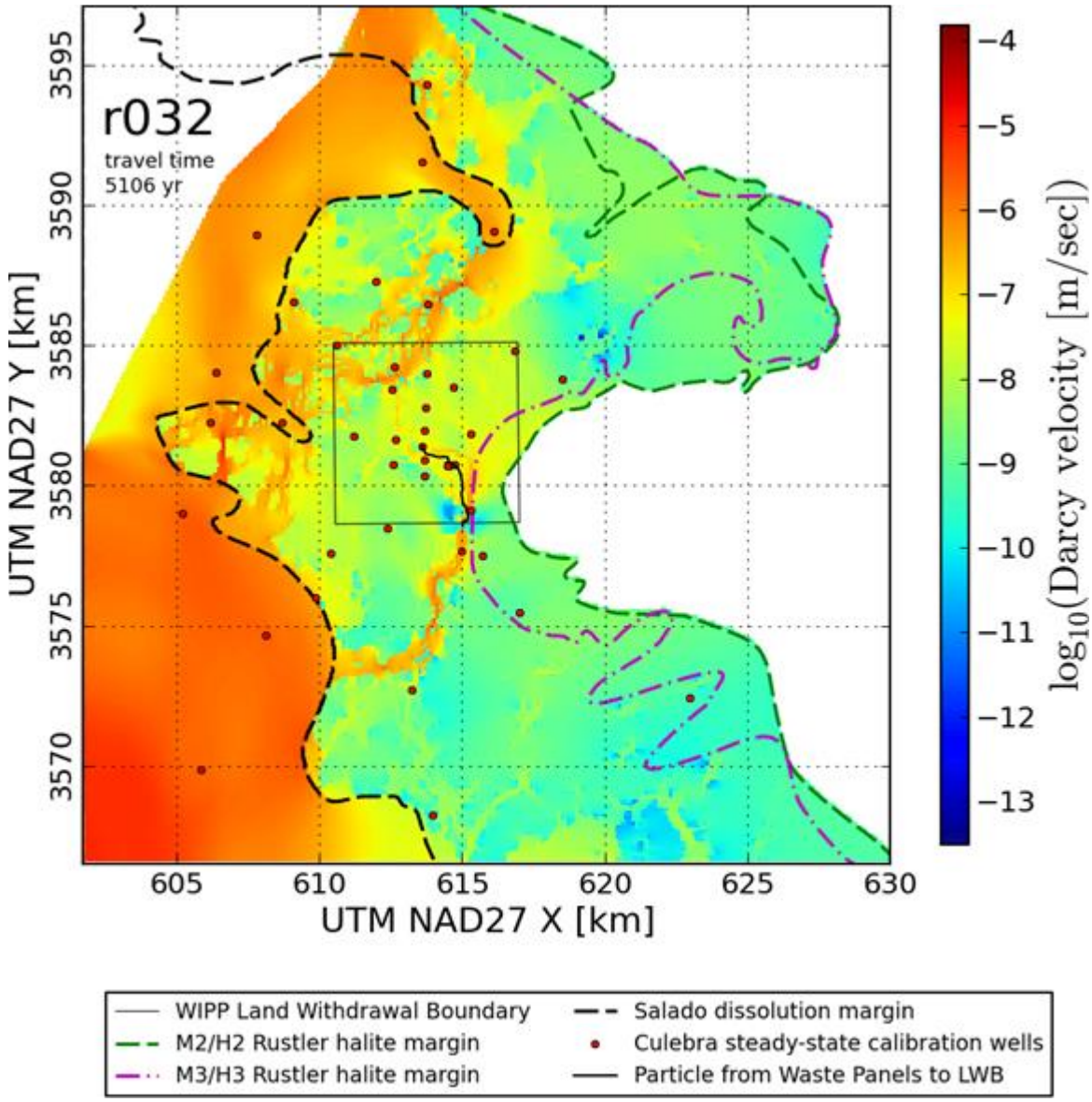
r032
travel time
5106 yr
UTM NAD27 Y [km]
3595
3590
3585
3580
3575
3570
605
610
615
620
625
630
UTM NAD27 X [km]
−4
−5
−6
−7
−8
−9
−10
−11
−12
−13
log10(Darcy velocity [m/sec])
WIPP Land Withdrawal Boundary
M2/H2 Rustler halite margin
M3/H3 Rustler halite margin
Salado dissolution margin
Culebra steady-state calibration wells
Particle from Waste Panels to LWB

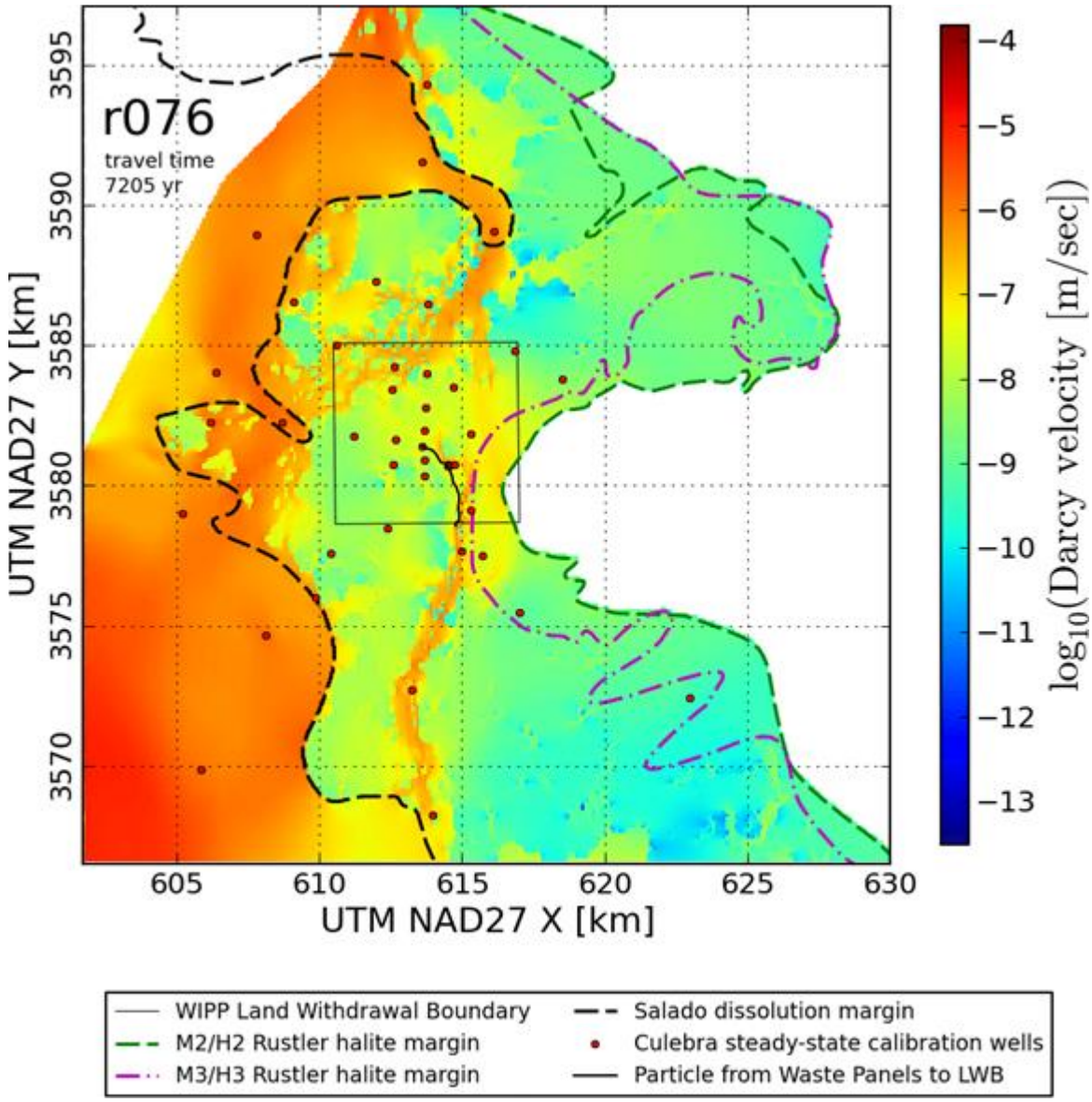
r076
travel time
7205 yr
UTM NAD27 Y [km]
3570
3575
3580
3585
3590
3595
605
610
615
620
625
630
UTM NAD27 X [km]
−4
−5
−6
−7
−8
−9
−10
−11
−12
−13
log10(Darcy velocity [m/sec])
WIPP Land Withdrawal Boundary
M2/H2 Rustler halite margin
M3/H3 Rustler halite margin
Salado dissolution margin
Culebra steady-state calibration wells
Particle from Waste Panels to LWB

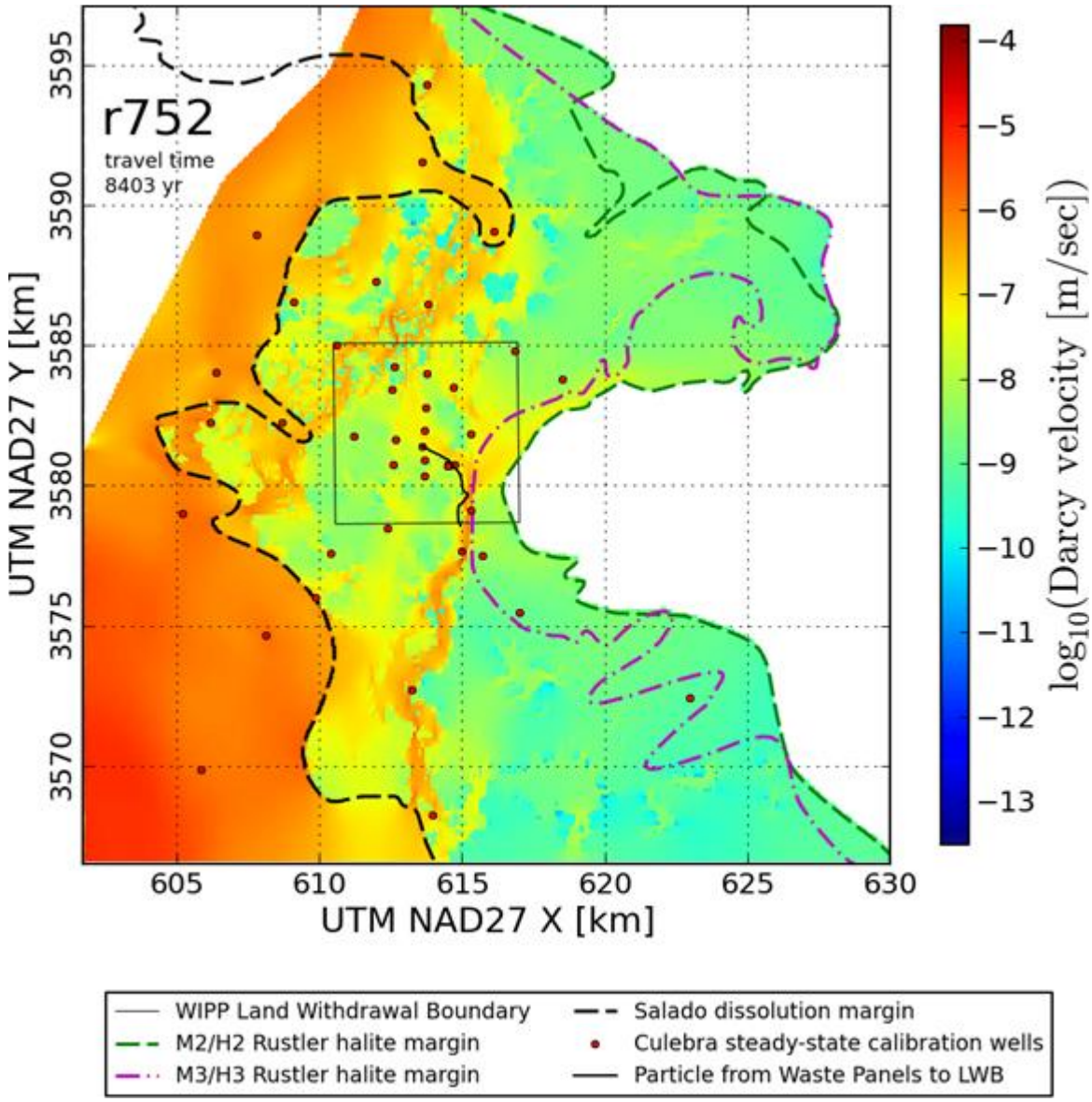
r752
travel time
8403 yr
UTM NAD27 Y [km]
3595
3590
3585
3580
3575
3570
605
610
615
620
625
630
UTM NAD27 X [km]
−4
−5
−6
−7
−8
−9
−10
−11
−12
−13
log10(Darcy velocity [m/sec])
WIPP Land Withdrawal Boundary
M2/H2 Rustler halite margin
M3/H3 Rustler halite margin
Salado dissolution margin
Culebra steady-state calibration wells
Particle from Waste Panels to LWB

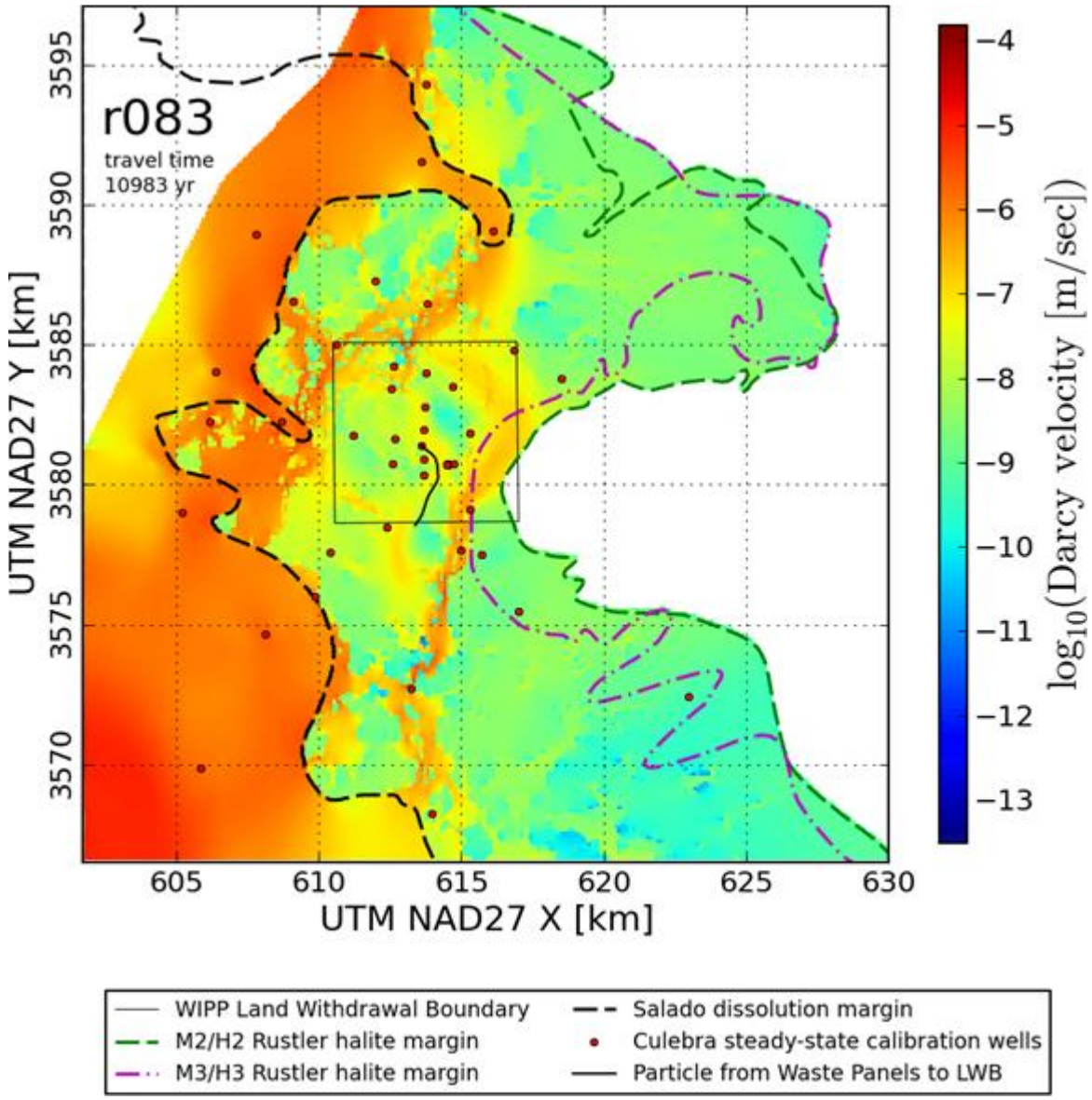
r083
travel time
10983 yr
UTM NAD27 Y [km]
3595
3590
3585
3580
3575
3570
605
610
615
620
625
630
UTM NAD27 X [km]
−4
−5
−6
−7
−8
−9
−10
−11
−12
−13
log10(Darcy velocity [m/sec])
WIPP Land Withdrawal Boundary
M2/H2 Rustler halite margin
M3/H3 Rustler halite margin
Salado dissolution margin
Culebra steady-state calibration wells
Particle from Waste Panels to LWB

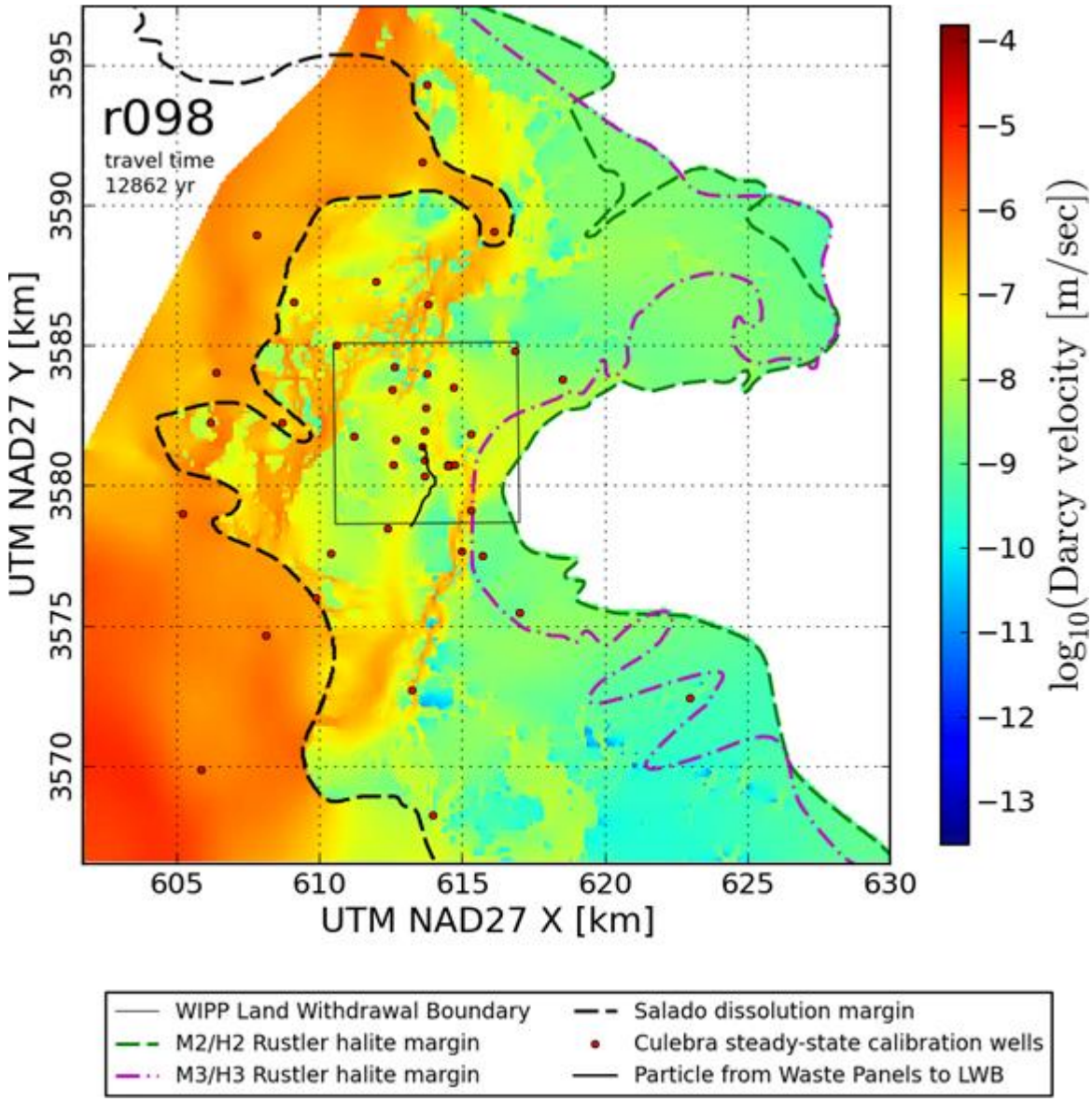
r098
travel time
12862 yr
UTM NAD27 Y [km]
3595
3590
3585
3580
3575
3570
605
610
615
620
625
630
UTM NAD27 X [km]
−4
−5
−6
−7
−8
−9
−10
−11
−12
−13
log10(Darcy velocity [m/sec])
WIPP Land Withdrawal Boundary
M2/H2 Rustler halite margin
M3/H3 Rustler halite margin
Salado dissolution margin
Culebra steady-state calibration wells
Particle from Waste Panels to LWB

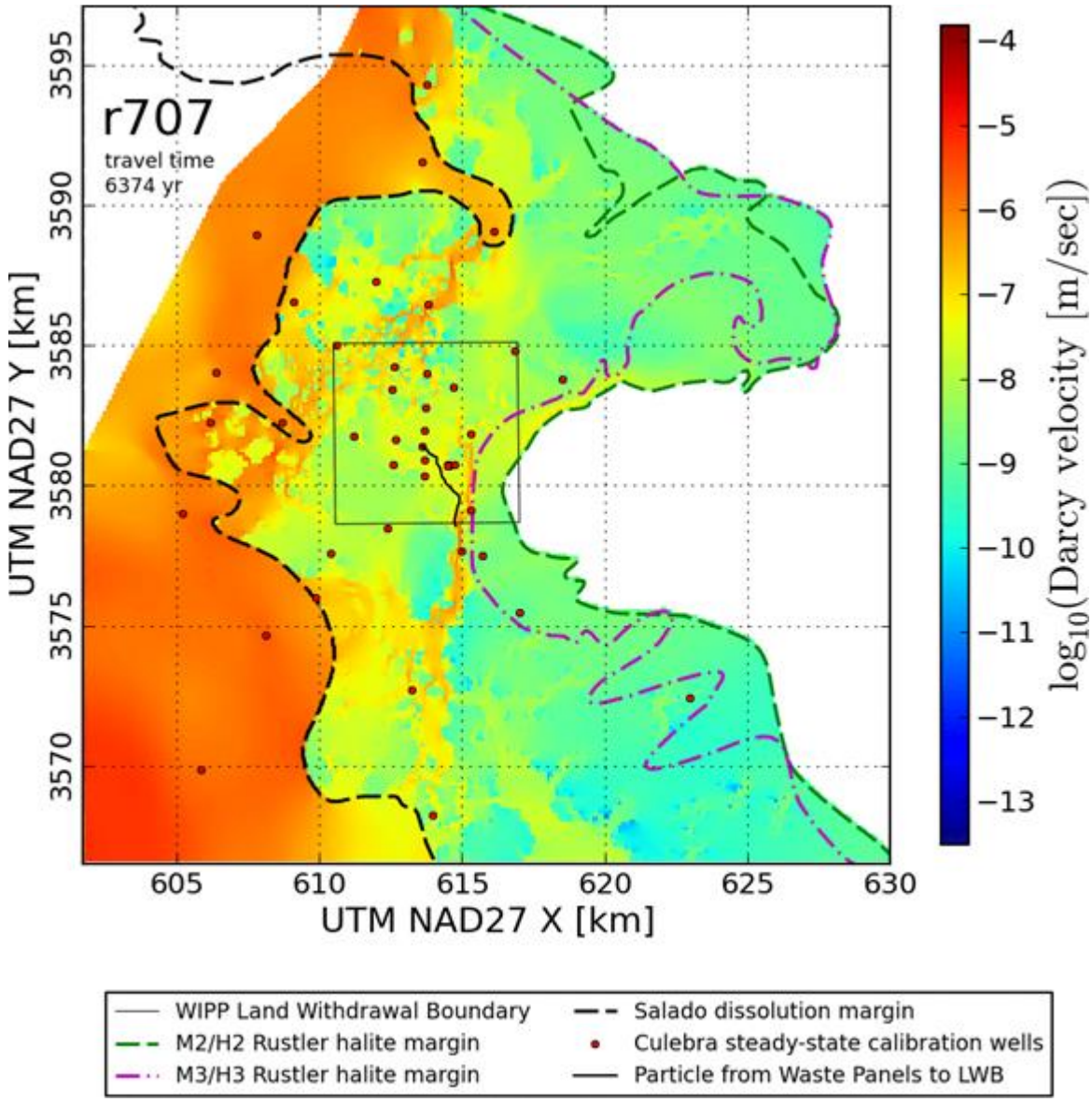
r707
travel time
6374 yr
UTM NAD27 Y [km]
3595
3590
3585
3580
3575
3570
605
610
615
620
625
630
UTM NAD27 X [km]
−4
−5
−6
−7
−8
−9
−10
−11
−12
−13
log10(Darcy velocity [m/sec])
WIPP Land Withdrawal Boundary
M2/H2 Rustler halite margin
M3/H3 Rustler halite margin
Salado dissolution margin
Culebra steady-state calibration wells
Particle from Waste Panels to LWB

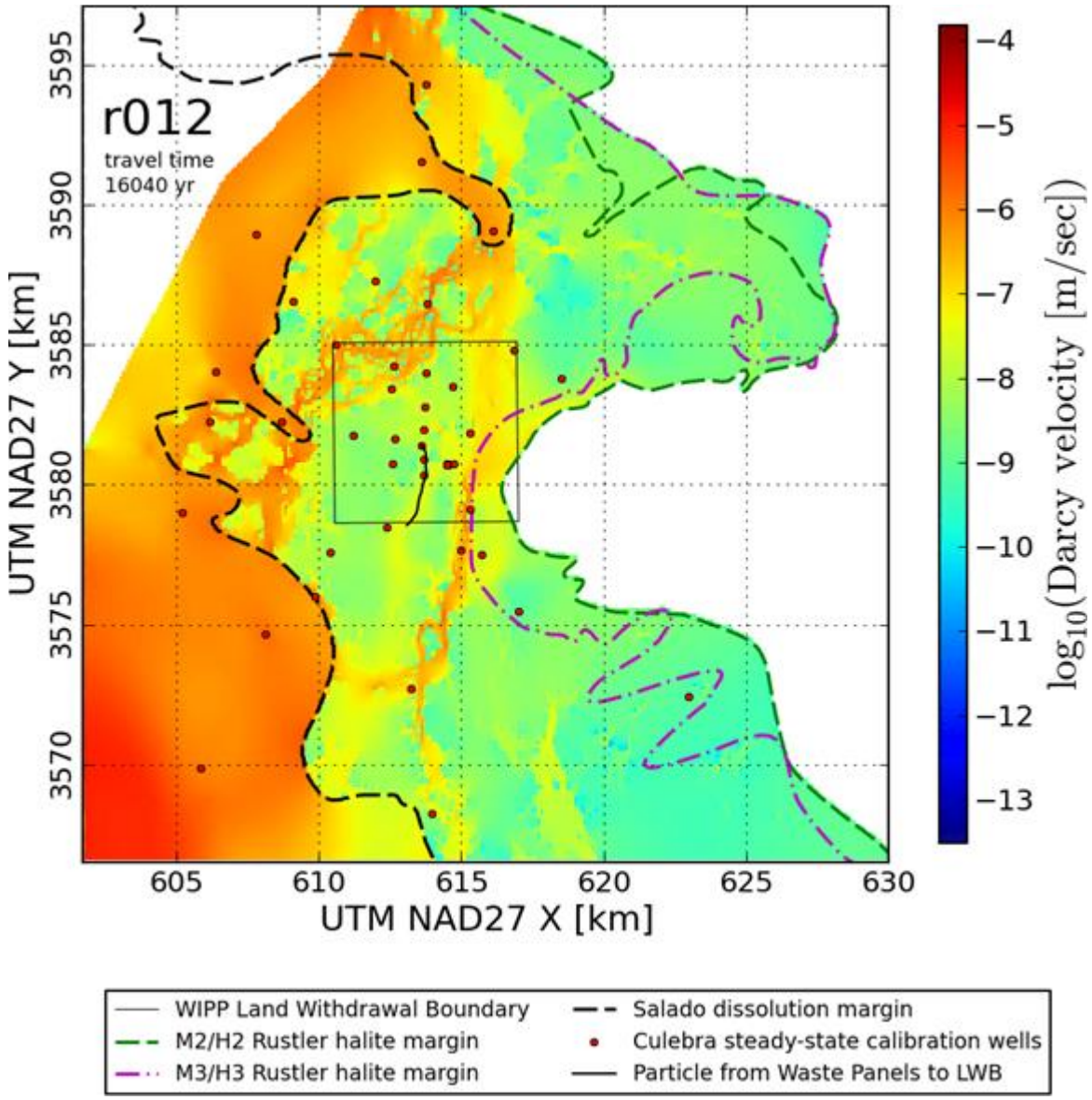
r012
travel time
16040 yr
UTM NAD27 Y [km]
3595
3590
3585
3580
3575
3570
605
610
615
620
625
630
UTM NAD27 X [km]
−4
−5
−6
−7
−8
−9
−10
−11
−12
−13
log10(Darcy velocity [m/sec])
WIPP Land Withdrawal Boundary
M2/H2 Rustler halite margin
M3/H3 Rustler halite margin
Salado dissolution margin
Culebra steady-state calibration wells
Particle from Waste Panels to LWB

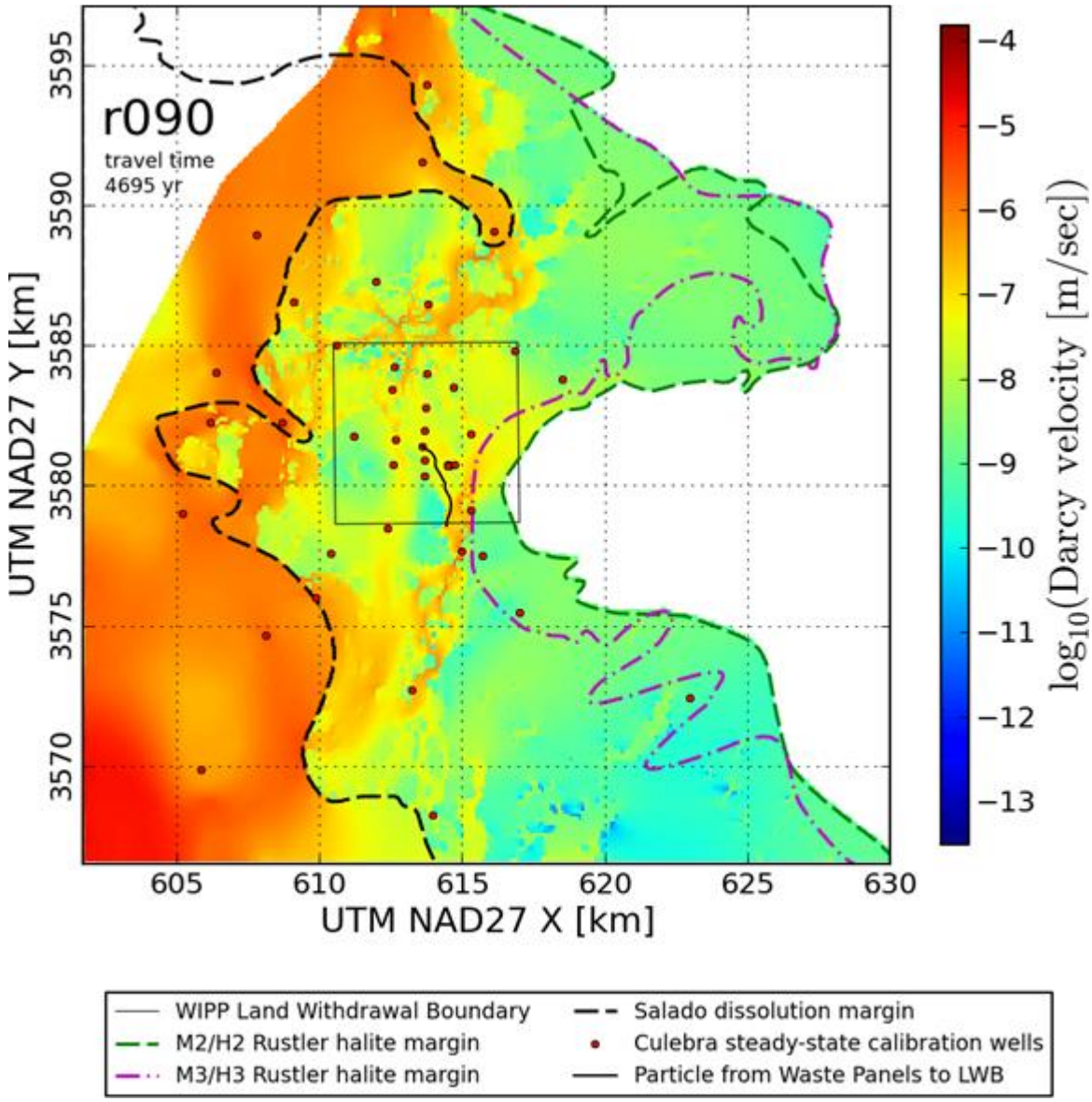
r090
travel time
4695 yr
UTM NAD27 Y [km]
3595
3590
3585
3580
3575
3570
605
610
615
620
625
630
UTM NAD27 X [km]
−4
−5
−6
−7
−8
−9
−10
−11
−12
−13
log10(Darcy velocity [m/sec])
WIPP Land Withdrawal Boundary
M2/H2 Rustler halite margin
M3/H3 Rustler halite margin
Salado dissolution margin
Culebra steady-state calibration wells
Particle from Waste Panels to LWB

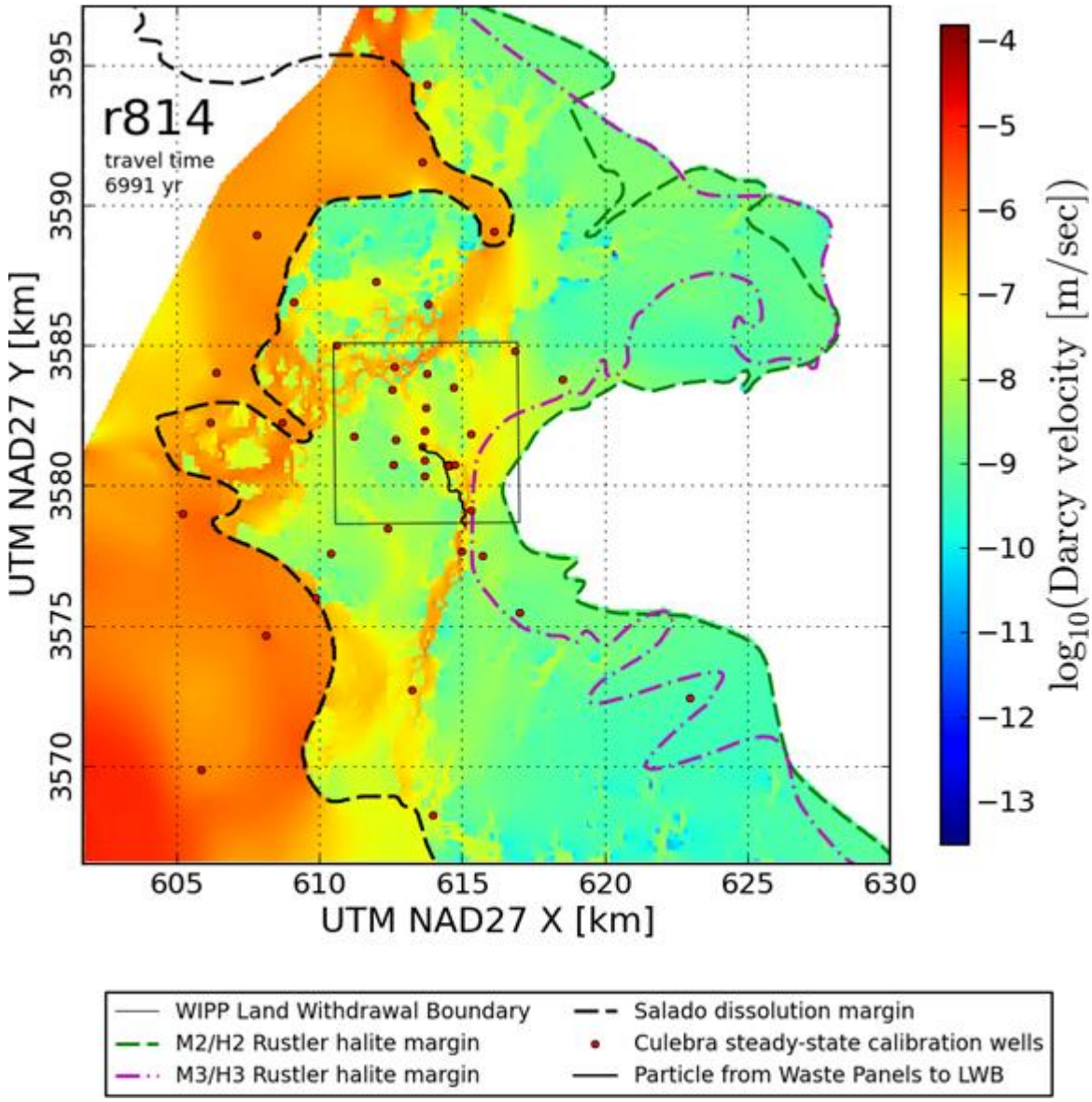
r814
travel time
6991 yr
UTM NAD27 Y [km]
3595
3590
3585
3580
3575
3570
605
610
615
620
625
630
UTM NAD27 X [km]
−4
−5
−6
−7
−8
−9
−10
−11
−12
−13
log10(Darcy velocity [m/sec])
WIPP Land Withdrawal Boundary
M2/H2 Rustler halite margin
M3/H3 Rustler halite margin
Salado dissolution margin
Culebra steady-state calibration wells
Particle from Waste Panels to LWB

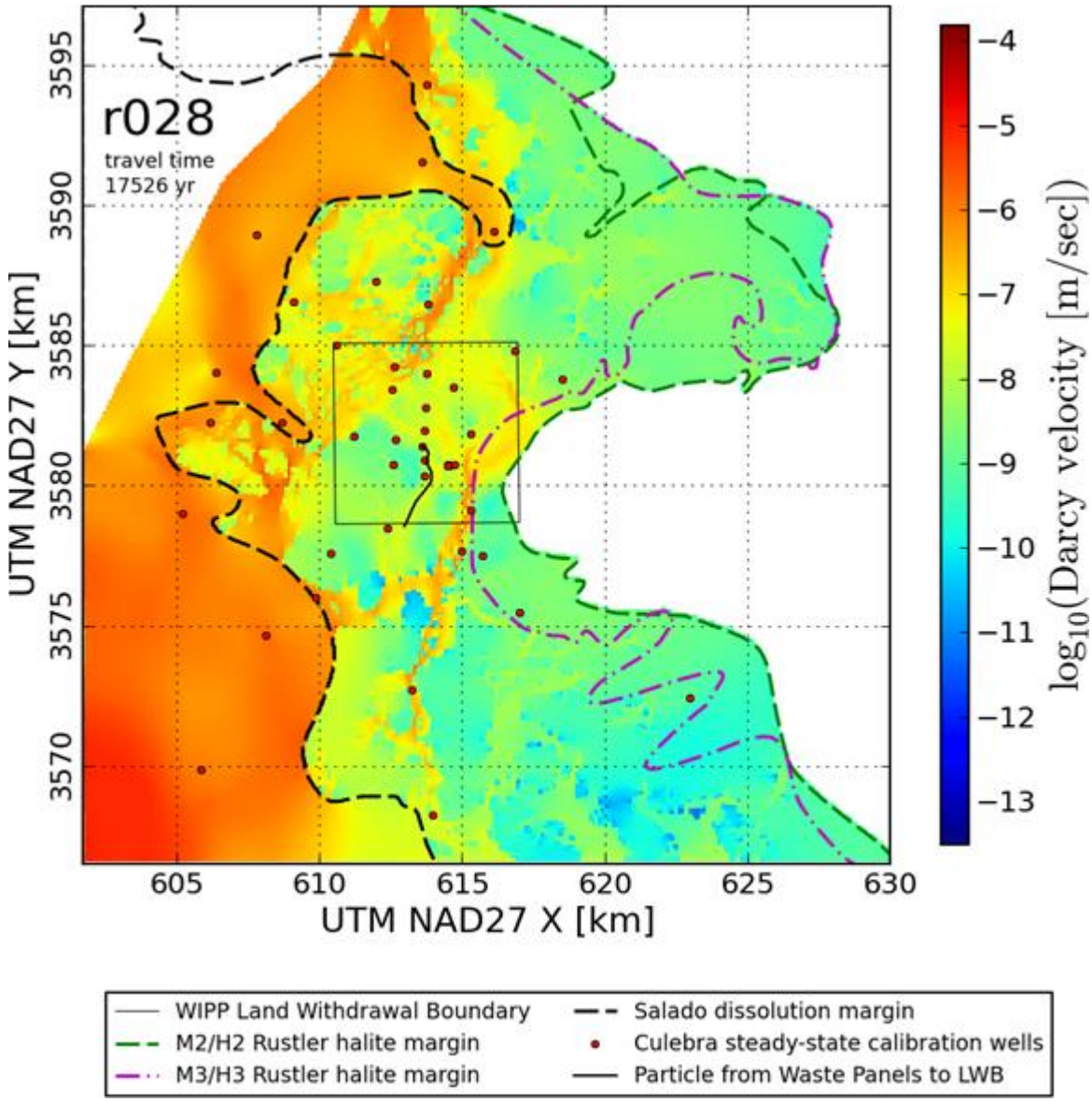
r028
travel time
17526 yr
UTM NAD27 Y [km]
3595
3590
3585
3580
3575
3570
605
610
615
620
625
630
UTM NAD27 X [km]
−4
−5
−6
−7
−8
−9
−10
−11
−12
−13
log10(Darcy velocity [m/sec])
WIPP Land Withdrawal Boundary
M2/H2 Rustler halite margin
M3/H3 Rustler halite margin
Salado dissolution margin
Culebra steady-state calibration wells
Particle from Waste Panels to LWB

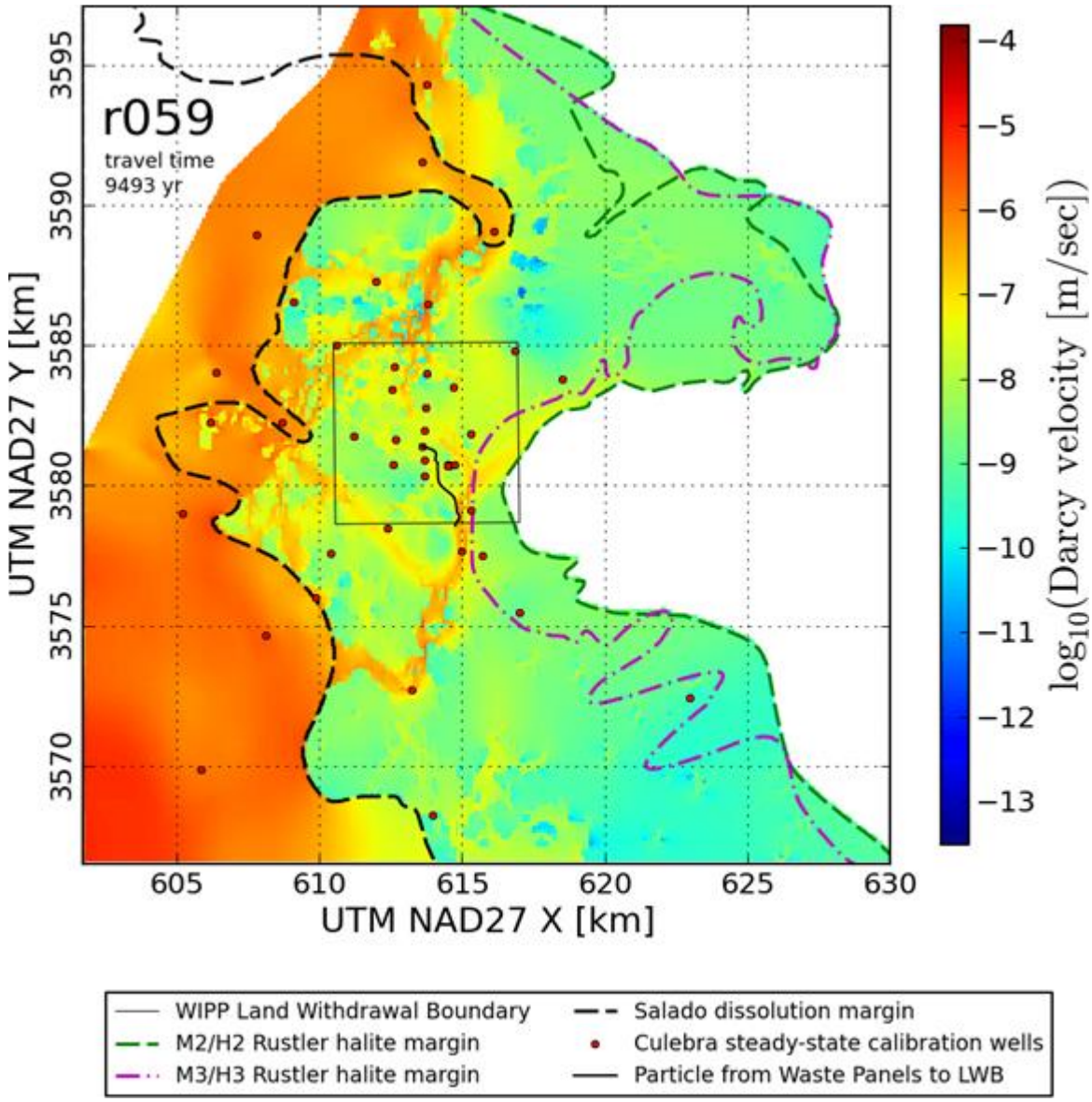
r059
travel time
9493 yr
UTM NAD27 Y [km]
3595
3590
3585
3580
3575
3570
605
610
615
620
625
630
UTM NAD27 X [km]
−4
−5
−6
−7
−8
−9
−10
−11
−12
−13
log10(Darcy velocity [m/sec])
WIPP Land Withdrawal Boundary
M2/H2 Rustler halite margin
M3/H3 Rustler halite margin
Salado dissolution margin
Culebra steady-state calibration wells
Particle from Waste Panels to LWB

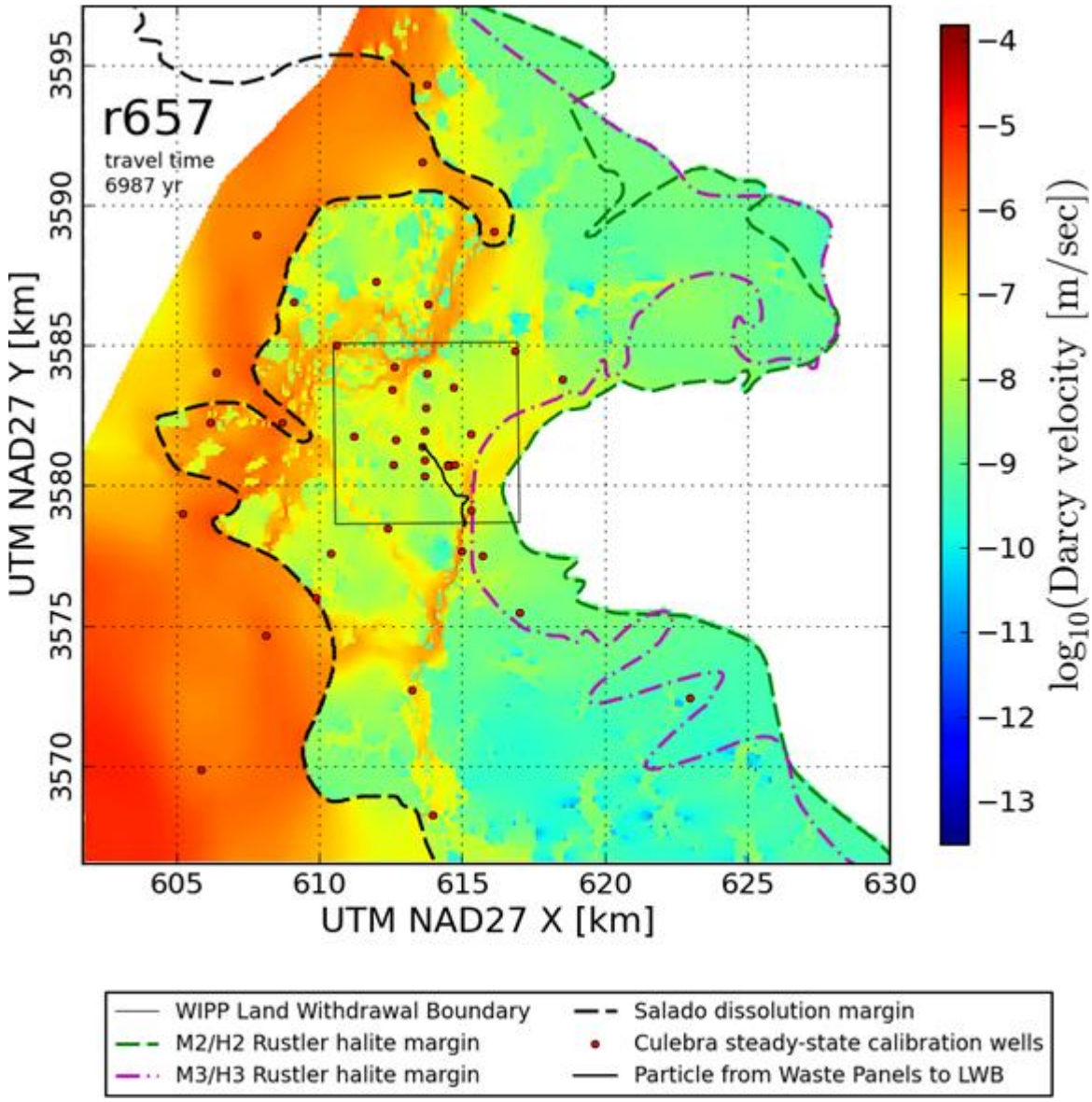
r657
travel time
6987 yr
UTM NAD27 Y [km]
3595
3590
3585
3580
3575
3570
605
610
615
620
625
630
UTM NAD27 X [km]
−4
−5
−6
−7
−8
−9
−10
−11
−12
−13
log10(Darcy velocity [m/sec])
WIPP Land Withdrawal Boundary
M2/H2 Rustler halite margin
M3/H3 Rustler halite margin
Salado dissolution margin
Culebra steady-state calibration wells
Particle from Waste Panels to LWB

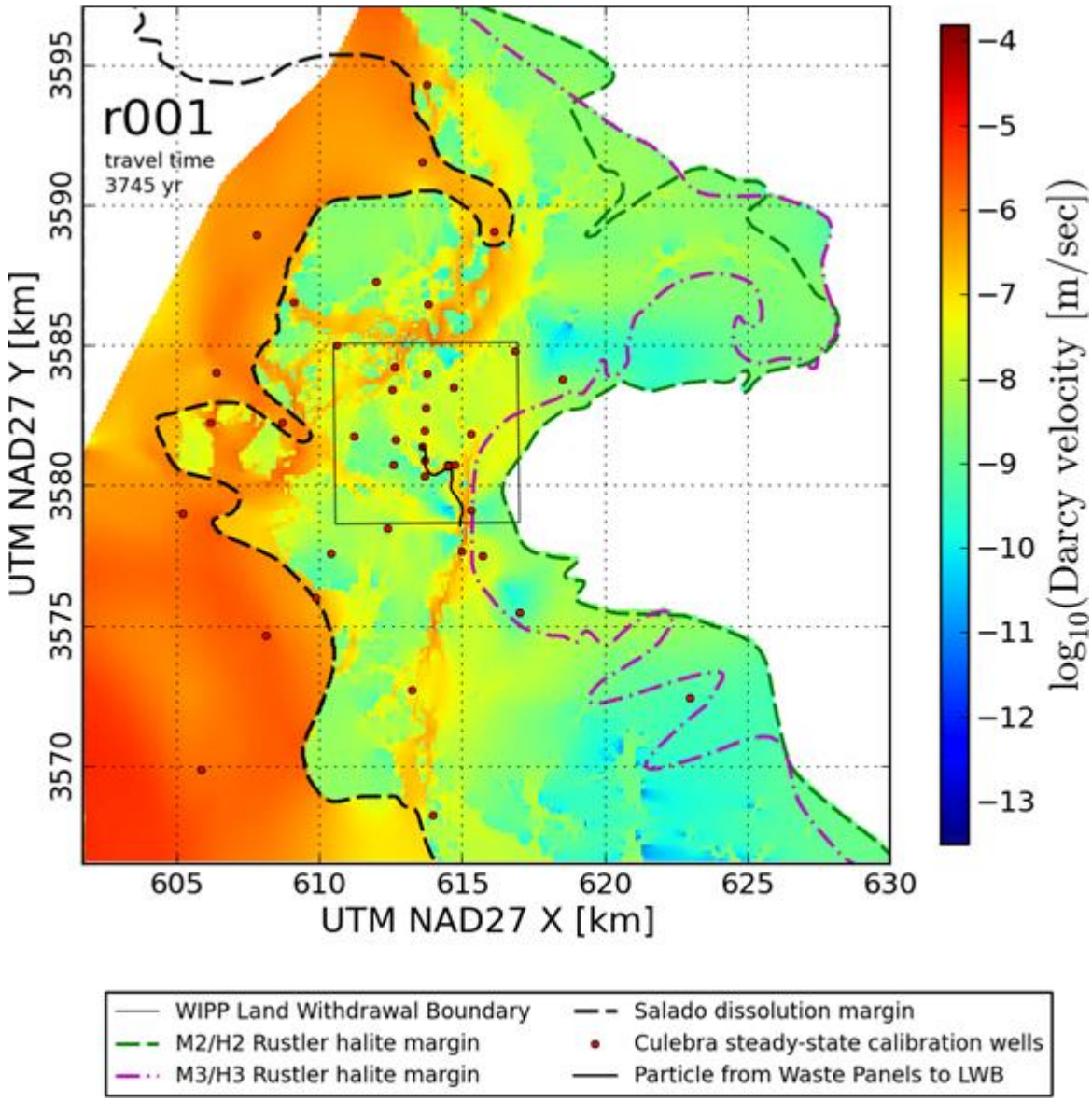
r001
travel time
3745 yr
UTM NAD27 Y [km]
3595
3590
3585
3580
3575
3570
605
610
615
620
625
630
UTM NAD27 X [km]
−4
−5
−6
−7
−8
−9
−10
−11
−12
−13
log10(Darcy velocity [m/sec])
WIPP Land Withdrawal Boundary
M2/H2 Rustler halite margin
M3/H3 Rustler halite margin
Salado dissolution margin
Culebra steady-state calibration wells
Particle from Waste Panels to LWB

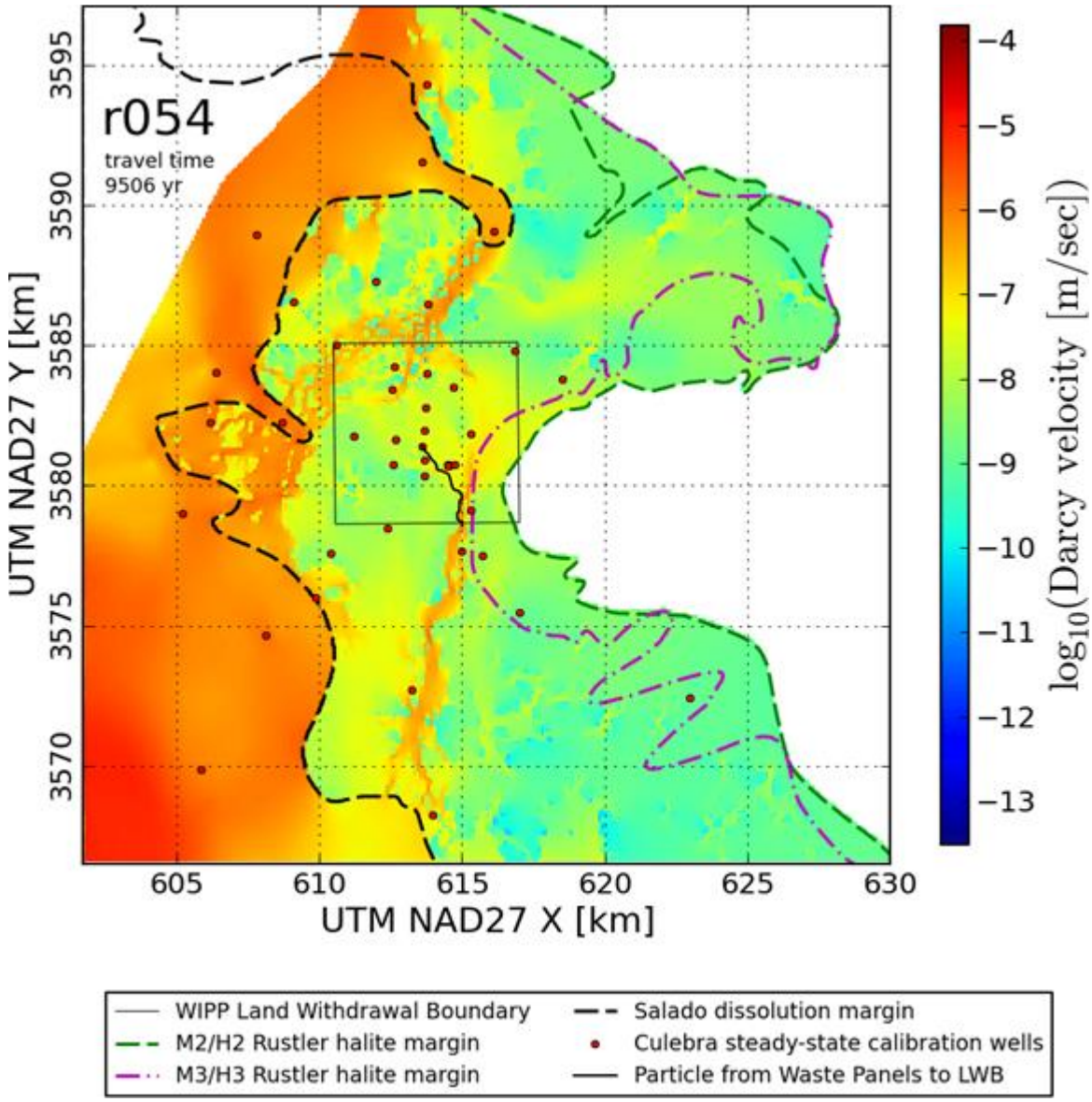
r054
travel time
9506 yr
UTM NAD27 Y [km]
3595
3590
3585
3580
3575
3570
605
610
615
620
625
630
UTM NAD27 X [km]
−4
−5
−6
−7
−8
−9
−10
−11
−12
−13
log10(Darcy velocity [m/sec])
WIPP Land Withdrawal Boundary
M2/H2 Rustler halite margin
M3/H3 Rustler halite margin
Salado dissolution margin
Culebra steady-state calibration wells
Particle from Waste Panels to LWB

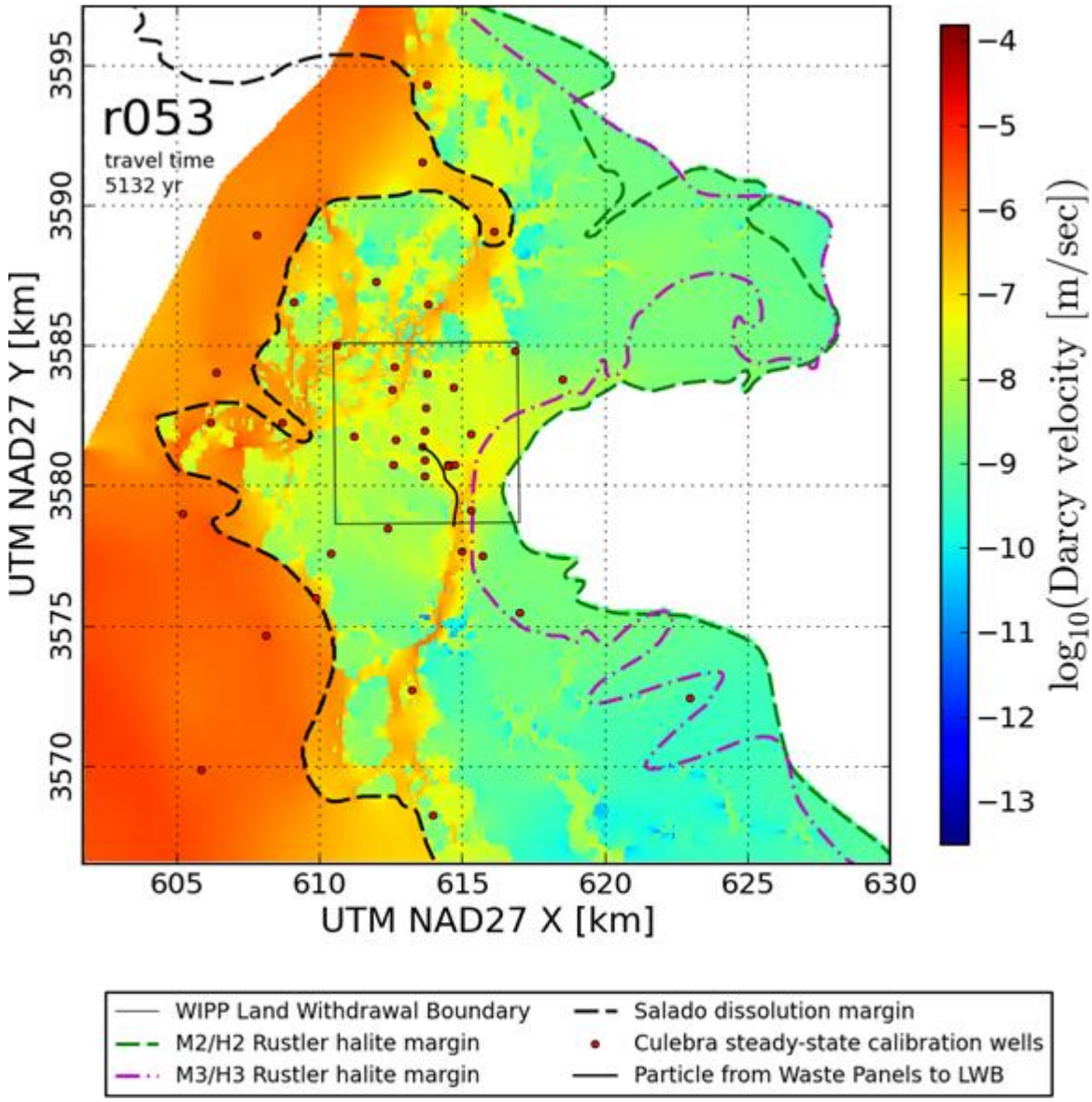
r053
travel time
5132 yr
UTM NAD27 Y [km]
3595
3590
3585
3580
3575
3570
605
610
615
620
625
630
UTM NAD27 X [km]
−4
−5
−6
−7
−8
−9
−10
−11
−12
−13
log10(Darcy velocity [m/sec])
WIPP Land Withdrawal Boundary
M2/H2 Rustler halite margin
M3/H3 Rustler halite margin
Salado dissolution margin
Culebra steady-state calibration wells
Particle from Waste Panels to LWB

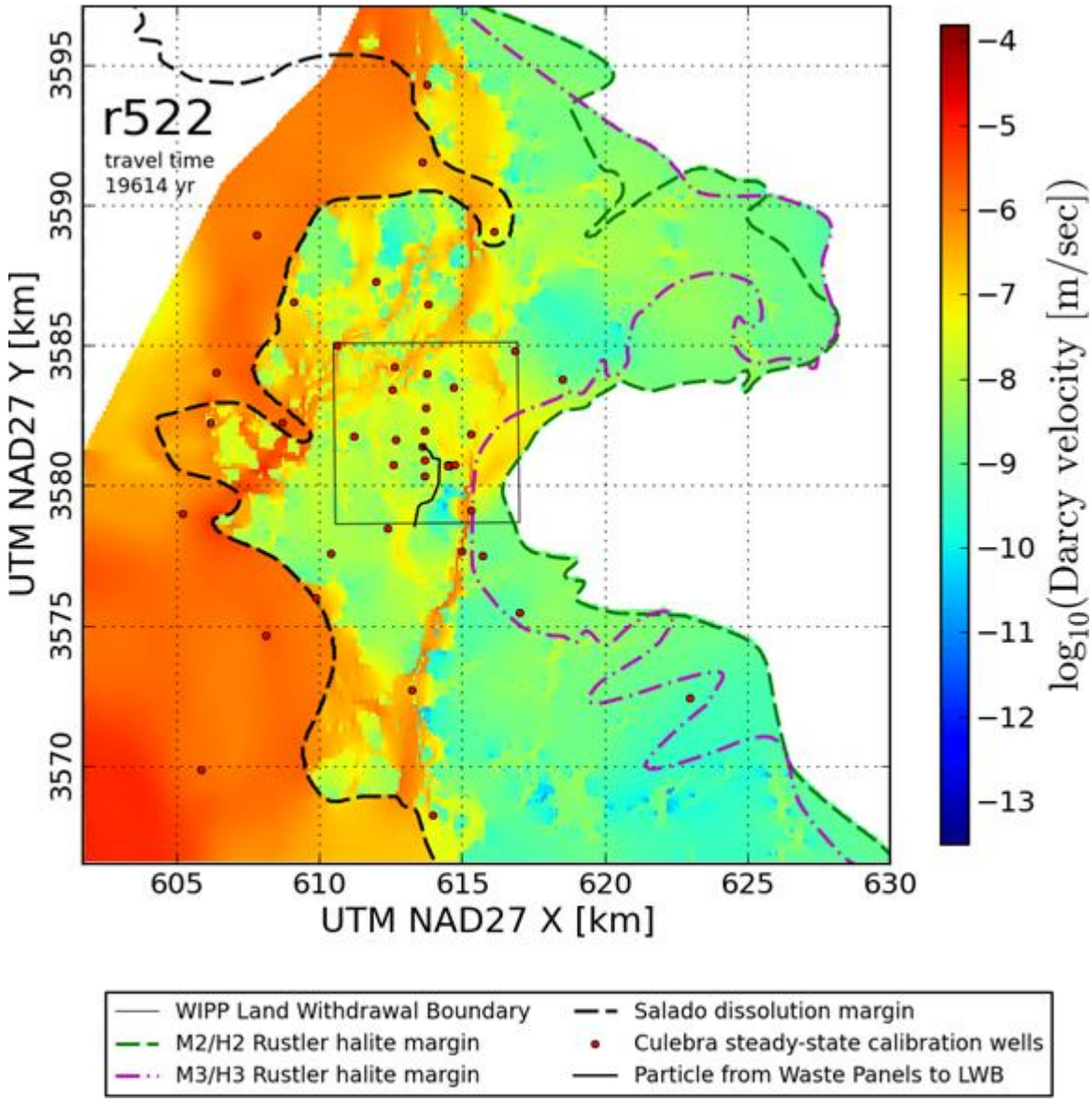
r522
travel time
19614 yr
UTM NAD27 Y [km]
3595
3590
3585
3580
3575
3570
605
610
615
620
625
630
UTM NAD27 X [km]
−4
−5
−6
−7
−8
−9
−10
−11
−12
−13
log10(Darcy velocity [m/sec])
WIPP Land Withdrawal Boundary
M2/H2 Rustler halite margin
M3/H3 Rustler halite margin
Salado dissolution margin
Culebra steady-state calibration wells
Particle from Waste Panels to LWB

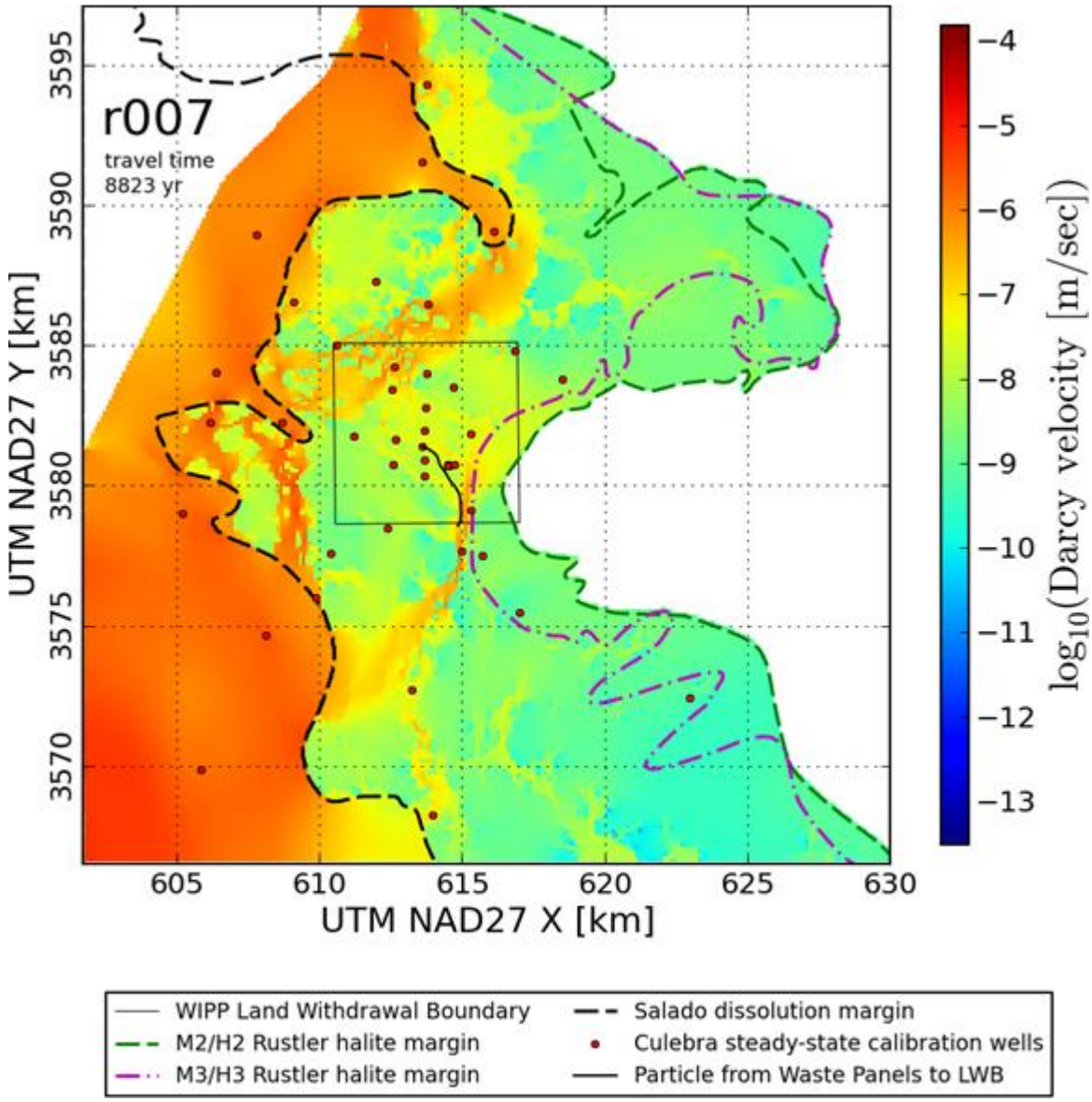
r007
travel time
8823 yr
UTM NAD27 Y [km]
3595
3590
3585
3580
3575
3570
605
610
615
620
625
630
UTM NAD27 X [km]
−4
−5
−6
−7
−8
−9
−10
−11
−12
−13
log10(Darcy velocity [m/sec])
WIPP Land Withdrawal Boundary
M2/H2 Rustler halite margin
M3/H3 Rustler halite margin
Salado dissolution margin
Culebra steady-state calibration wells
Particle from Waste Panels to LWB

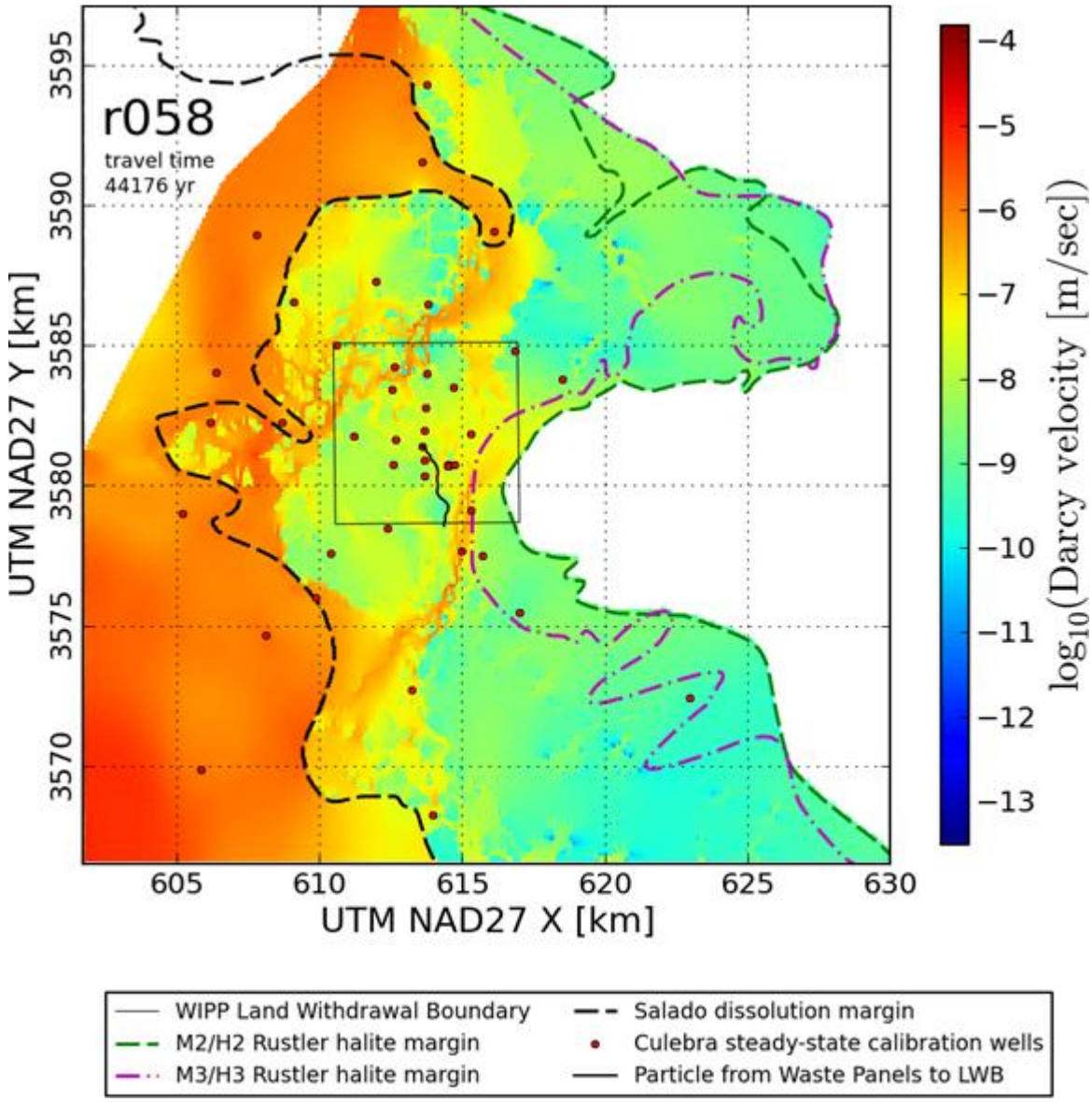
r058
travel time
44176 yr
UTM NAD27 Y [km]
3595
3590
3585
3580
3575
3570
605
610
615
620
625
630
UTM NAD27 X [km]
−4
−5
−6
−7
−8
−9
−10
−11
−12
−13
log10(Darcy velocity [m/sec])
WIPP Land Withdrawal Boundary
M2/H2 Rustler halite margin
M3/H3 Rustler halite margin
Salado dissolution margin
Culebra steady-state calibration wells
Particle from Waste Panels to LWB

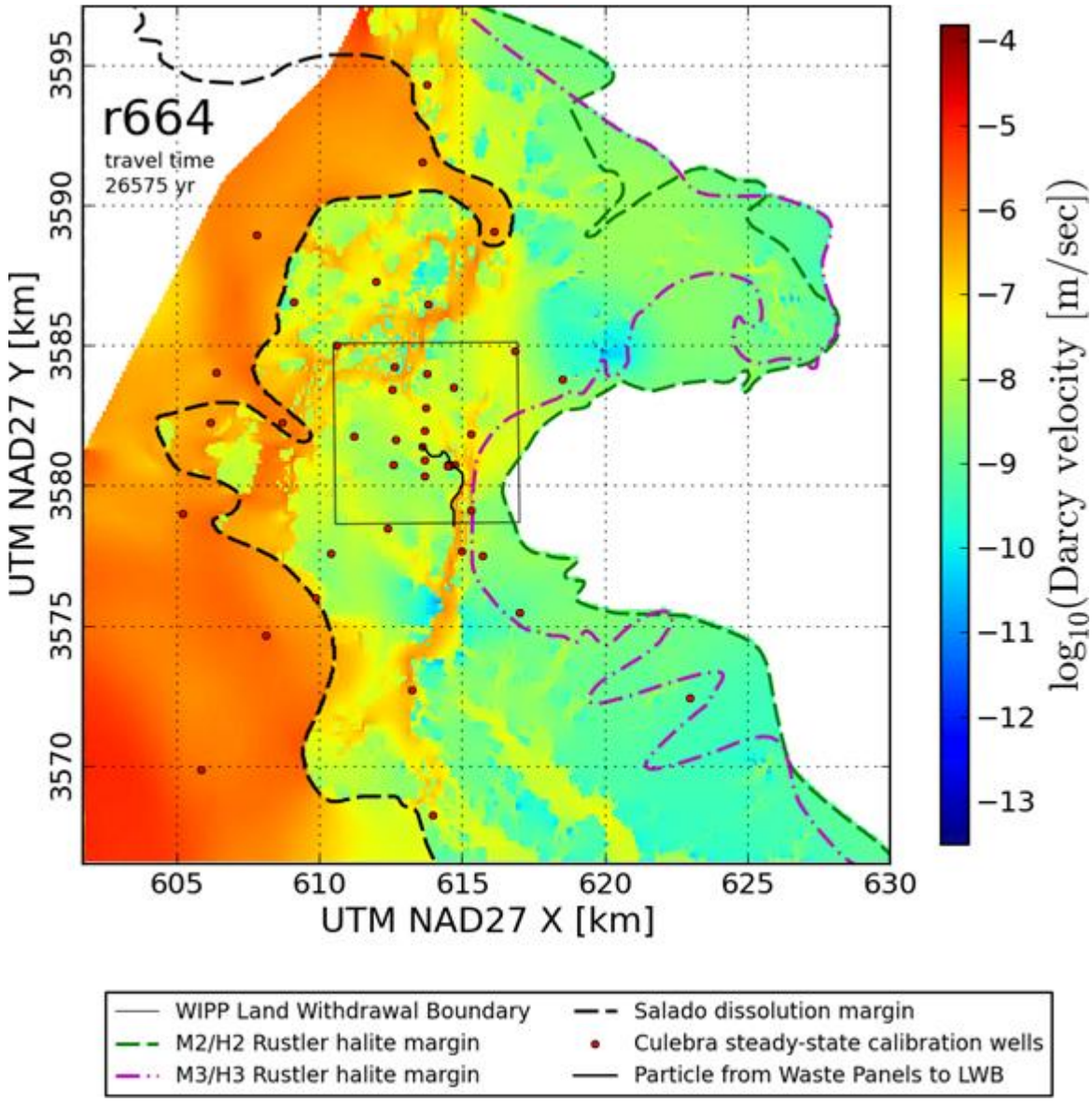
r664
travel time
26575 yr
UTM NAD27 Y [km]
3595
3590
3585
3580
3575
3570
605
610
615
620
625
630
UTM NAD27 X [km]
−4
−5
−6
−7
−8
−9
−10
−11
−12
−13
log10(Darcy velocity [m/sec])
WIPP Land Withdrawal Boundary
M2/H2 Rustler halite margin
M3/H3 Rustler halite margin
Salado dissolution margin
Culebra steady-state calibration wells
Particle from Waste Panels to LWB

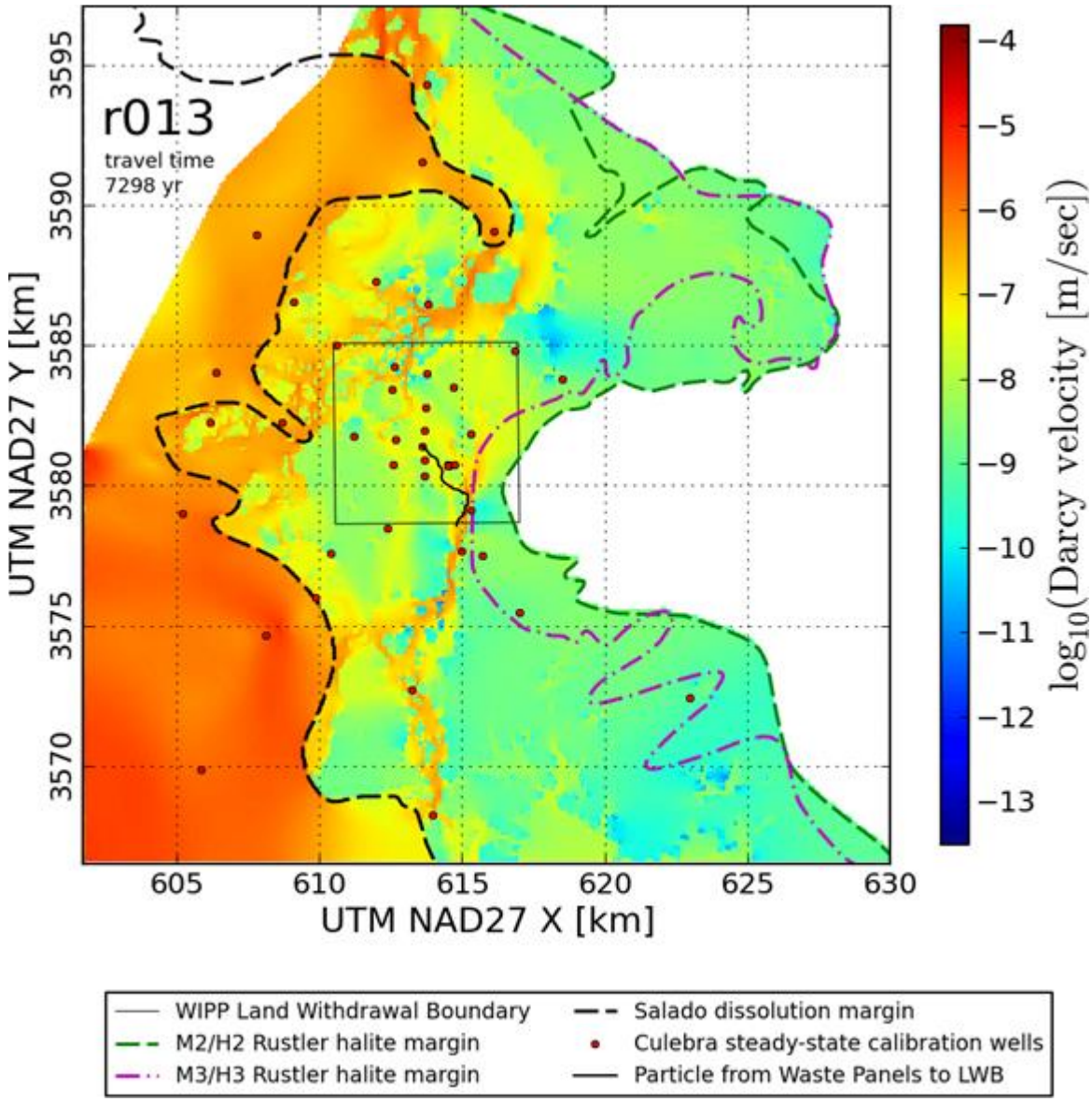
r013
travel time
7298 yr
UTM NAD27 Y [km]
3595
3590
3585
3580
3575
3570
605
610
615
620
625
630
UTM NAD27 X [km]
−4
−5
−6
−7
−8
−9
−10
−11
−12
−13
log10(Darcy velocity [m/sec])
WIPP Land Withdrawal Boundary
M2/H2 Rustler halite margin
M3/H3 Rustler halite margin
Salado dissolution margin
Culebra steady-state calibration wells
Particle from Waste Panels to LWB

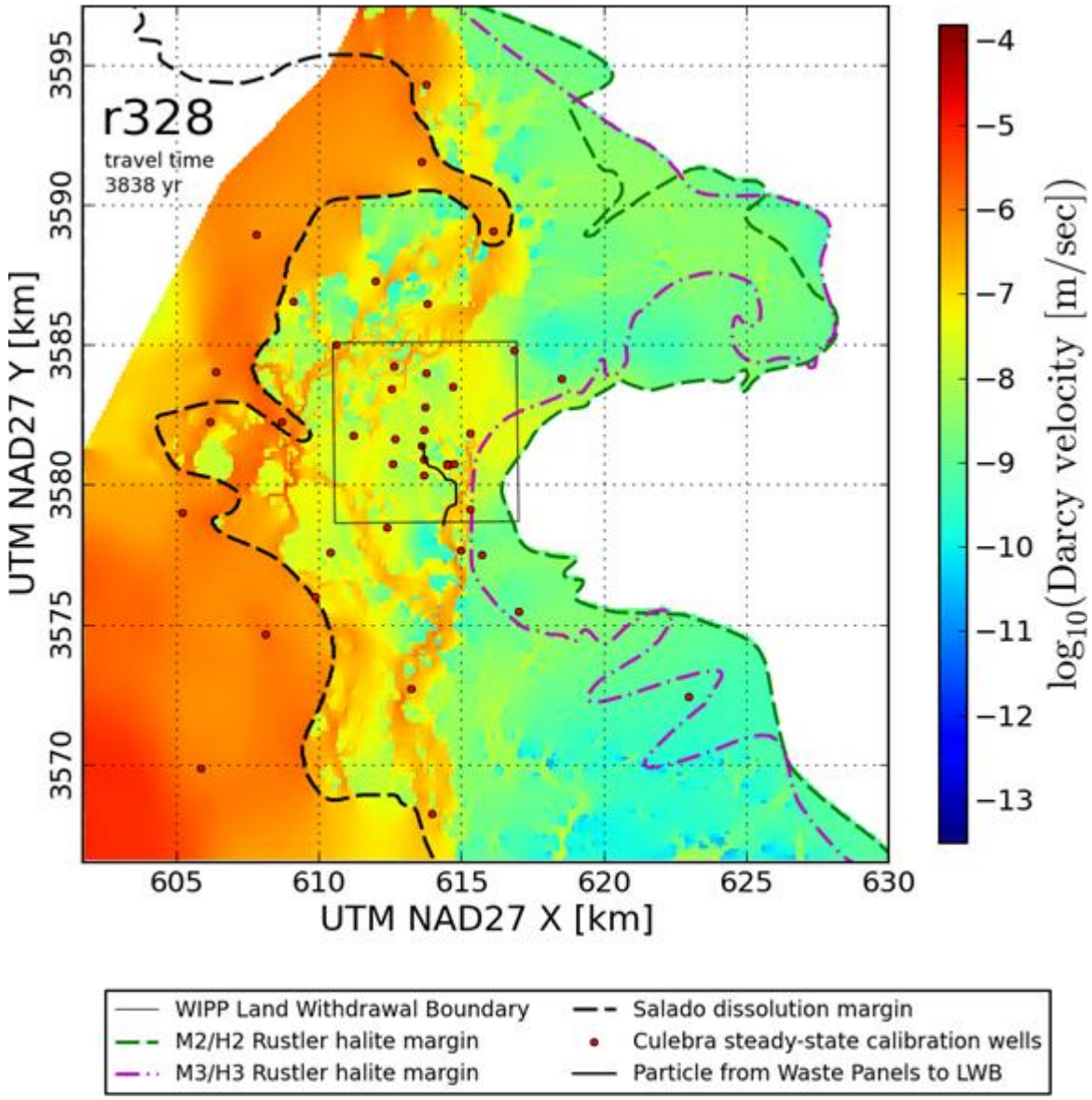
r328
travel time
3838 yr
UTM NAD27 Y [km]
3595
3590
3585
3580
3575
3570
605
610
615
620
625
630
UTM NAD27 X [km]
−4
−5
−6
−7
−8
−9
−10
−11
−12
−13
log10(Darcy velocity [m/sec])
WIPP Land Withdrawal Boundary
M2/H2 Rustler halite margin
M3/H3 Rustler halite margin
Salado dissolution margin
Culebra steady-state calibration wells
Particle from Waste Panels to LWB

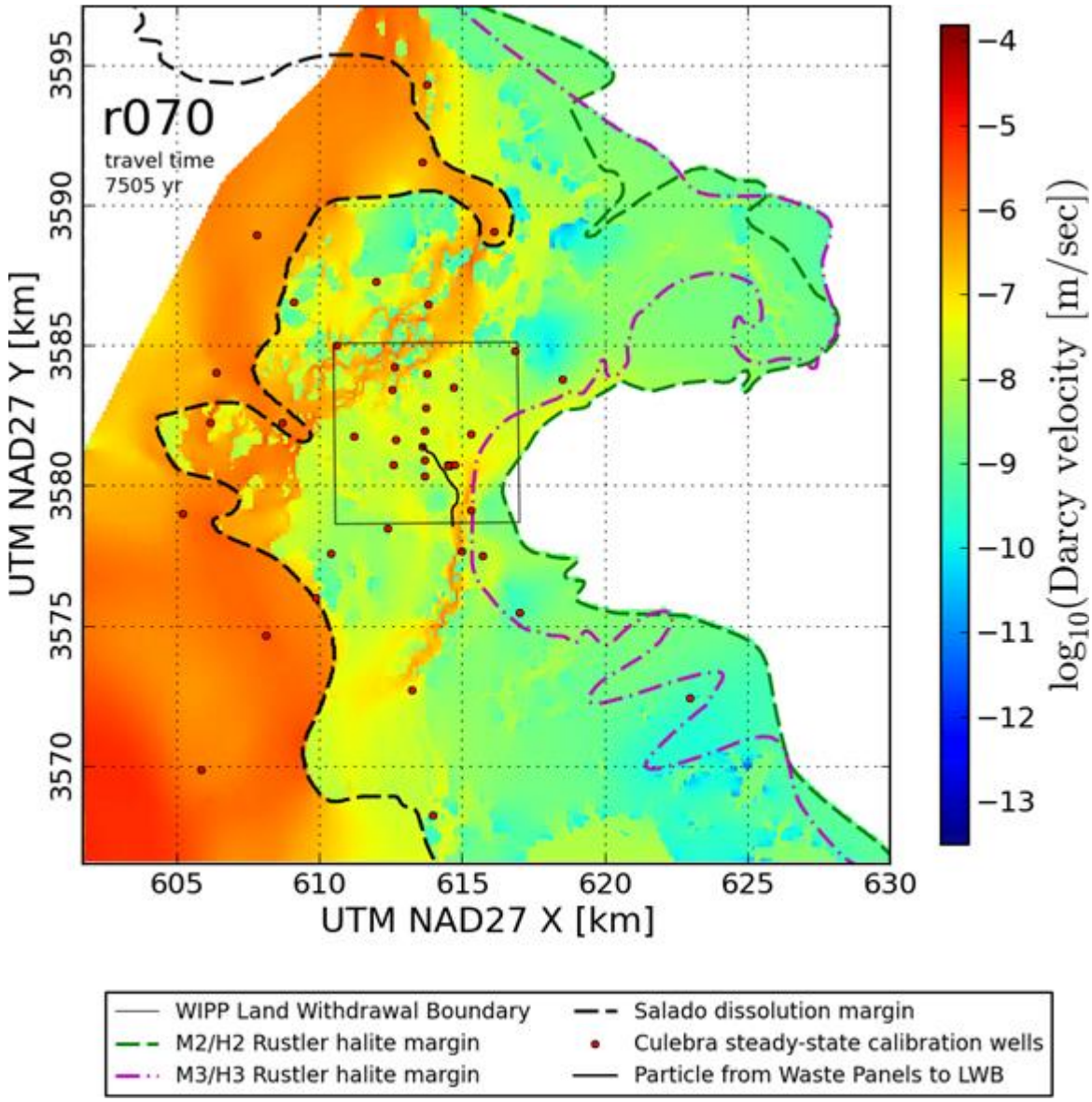
r070
travel time
7505 yr
UTM NAD27 Y [km]
3595
3590
3585
3580
3575
3570
605
610
615
620
625
630
UTM NAD27 X [km]
−4
−5
−6
−7
−8
−9
−10
−11
−12
−13
log10(Darcy velocity [m/sec])
WIPP Land Withdrawal Boundary
M2/H2 Rustler halite margin
M3/H3 Rustler halite margin
Salado dissolution margin
Culebra steady-state calibration wells
Particle from Waste Panels to LWB

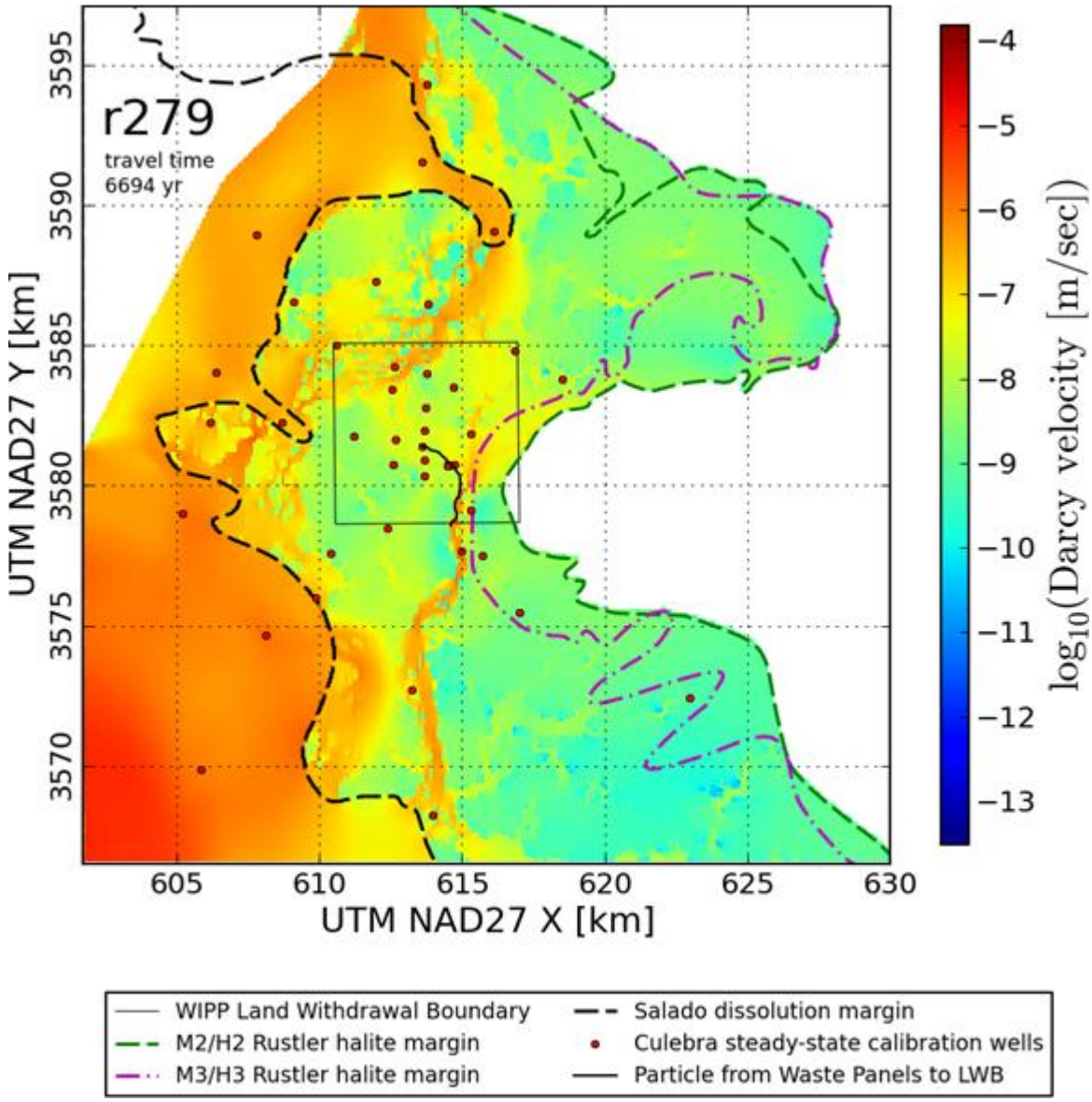
r279
travel time
6694 yr
UTM NAD27 Y [km]
3595
3590
3585
3580
3575
3570
605
610
615
620
625
630
UTM NAD27 X [km]
−4
−5
−6
−7
−8
−9
−10
−11
−12
−13
log10(Darcy velocity [m/sec])
WIPP Land Withdrawal Boundary
M2/H2 Rustler halite margin
M3/H3 Rustler halite margin
Salado dissolution margin
Culebra steady-state calibration wells
Particle from Waste Panels to LWB

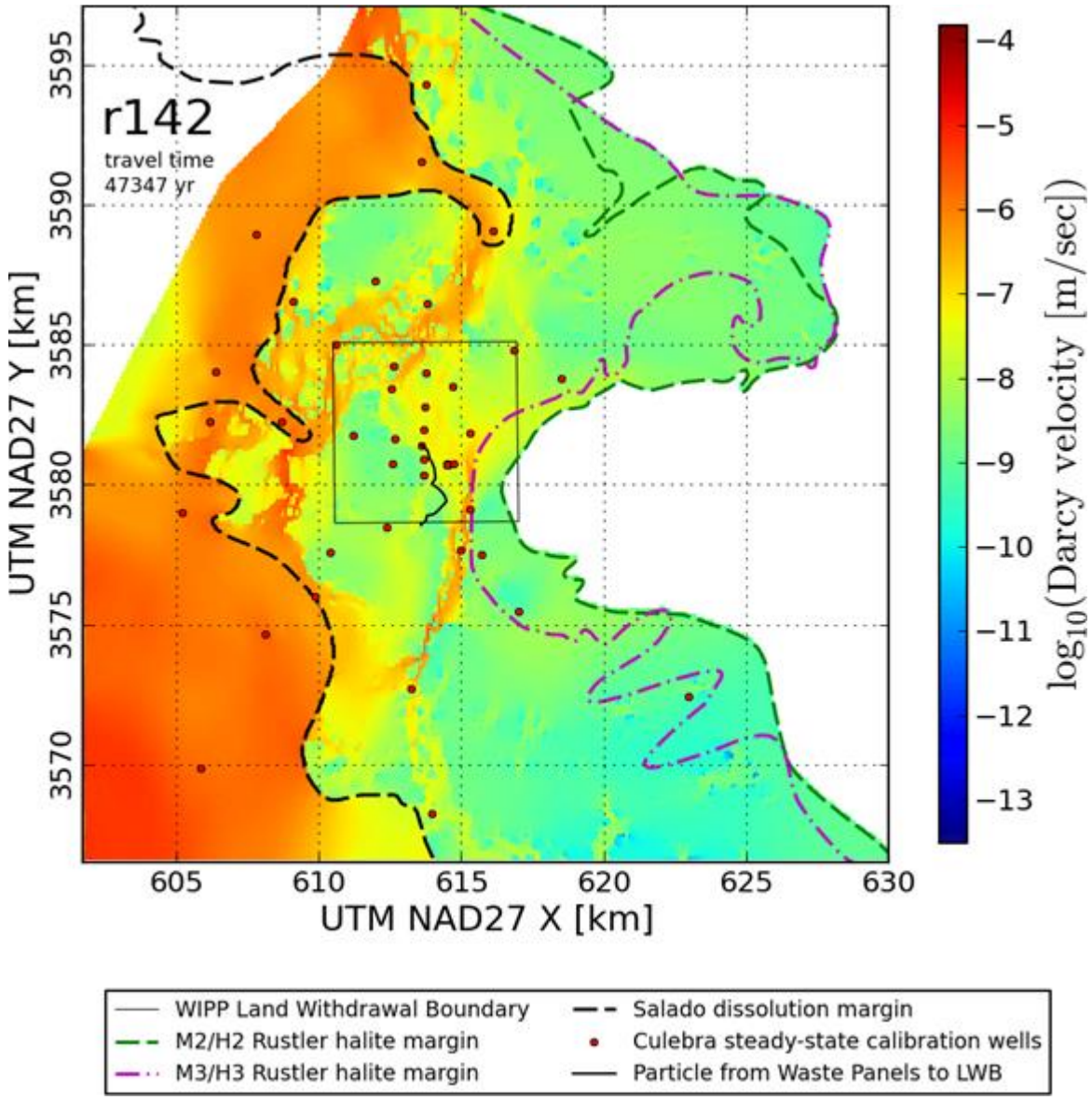
r142
travel time
47347 yr
UTM NAD27 Y [km]
3595
3590
3585
3580
3575
3570
605
610
615
620
625
630
UTM NAD27 X [km]
−4
−5
−6
−7
−8
−9
−10
−11
−12
−13
log10(Darcy velocity [m/sec])
WIPP Land Withdrawal Boundary
M2/H2 Rustler halite margin
M3/H3 Rustler halite margin
Salado dissolution margin
Culebra steady-state calibration wells
Particle from Waste Panels to LWB

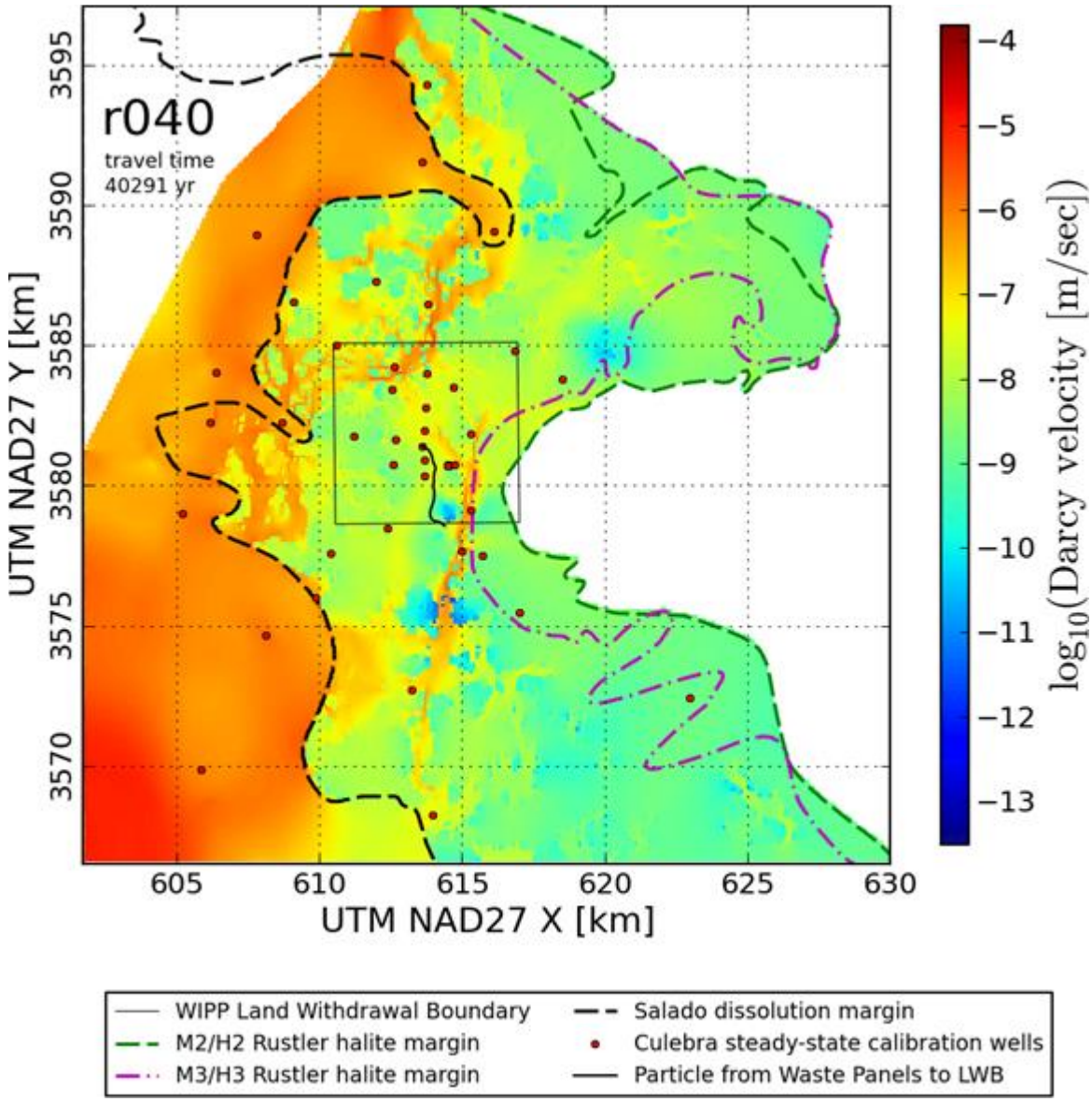
r040
travel time
40291 yr
UTM NAD27 Y [km]
3595
3590
3585
3580
3575
3570
605
610
615
620
625
630
UTM NAD27 X [km]
−4
−5
−6
−7
−8
−9
−10
−11
−12
−13
log10(Darcy velocity [m/sec])
WIPP Land Withdrawal Boundary
M2/H2 Rustler halite margin
M3/H3 Rustler halite margin
Salado dissolution margin
Culebra steady-state calibration wells
Particle from Waste Panels to LWB

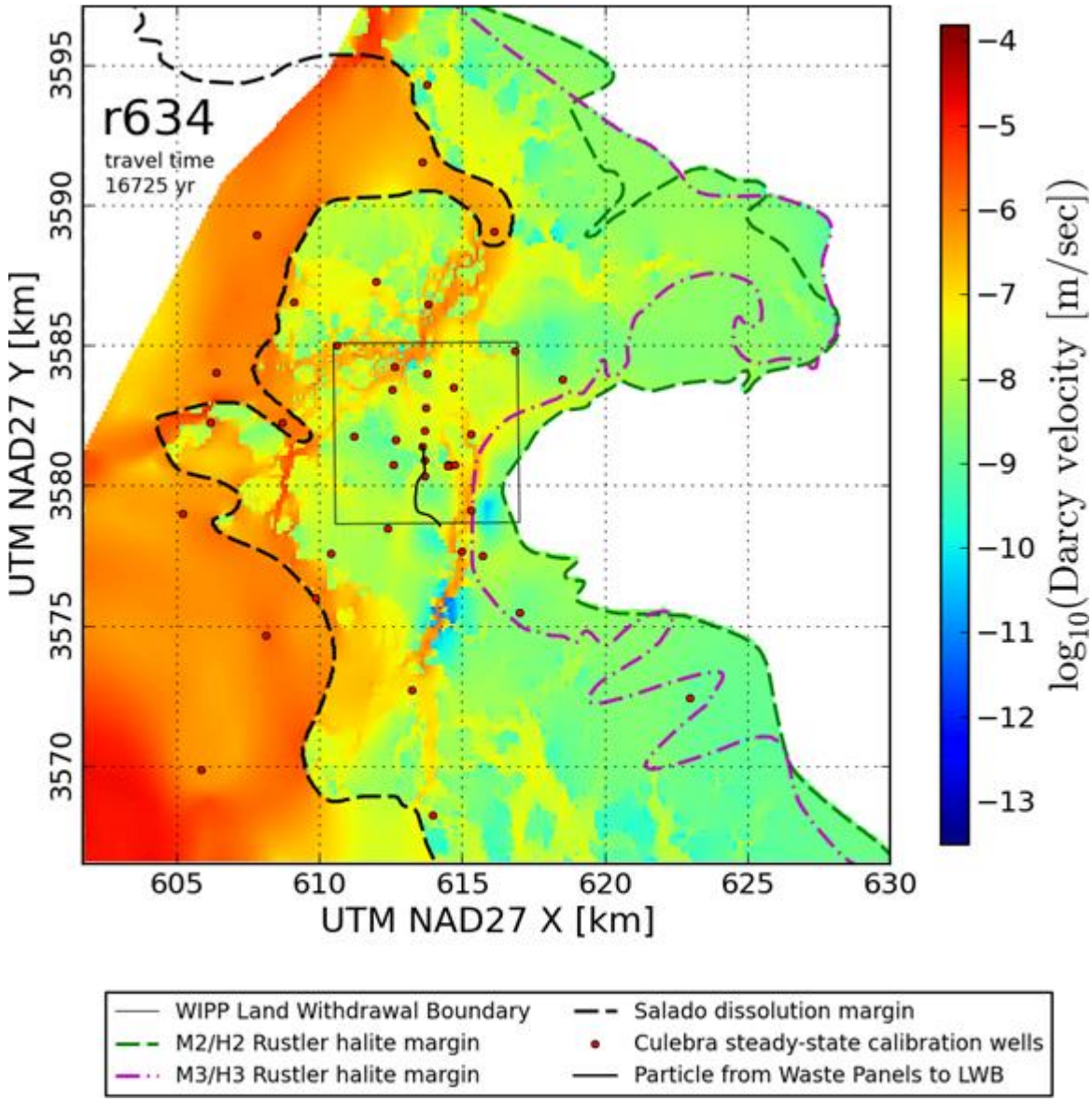
r634
travel time
16725 yr
UTM NAD27 Y [km]
3595
3590
3585
3580
3575
3570
605
610
615
620
625
630
UTM NAD27 X [km]
−4
−5
−6
−7
−8
−9
−10
−11
−12
−13
log10(Darcy velocity [m/sec])
WIPP Land Withdrawal Boundary
M2/H2 Rustler halite margin
M3/H3 Rustler halite margin
Salado dissolution margin
Culebra steady-state calibration wells
Particle from Waste Panels to LWB

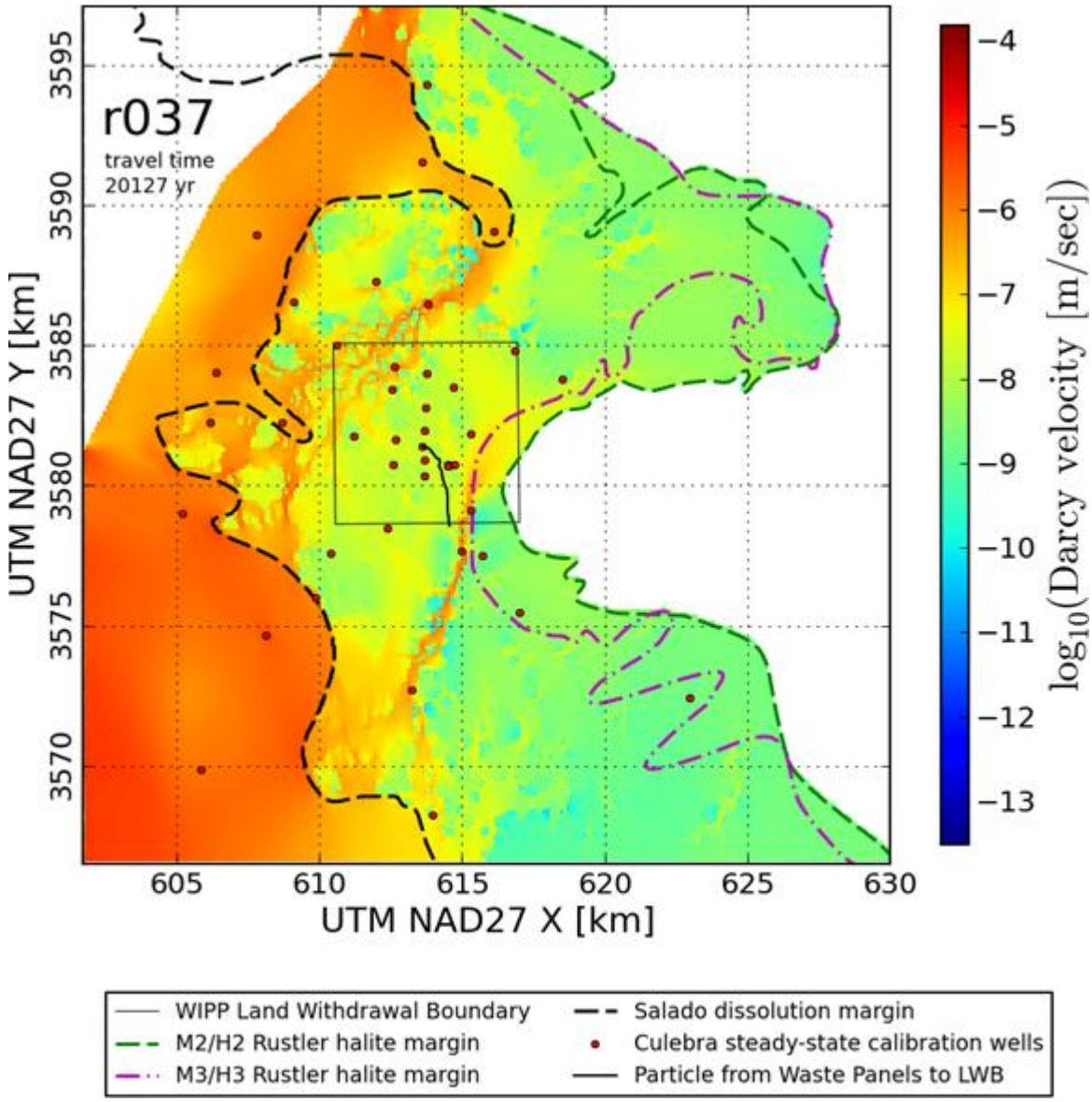
r037
travel time
20127 yr
UTM NAD27 Y [km]
3595
3590
3585
3580
3575
3570
605
610
615
620
625
630
UTM NAD27 X [km]
−4
−5
−6
−7
−8
−9
−10
−11
−12
−13
log10(Darcy velocity [m/sec])
WIPP Land Withdrawal Boundary
M2/H2 Rustler halite margin
M3/H3 Rustler halite margin
Salado dissolution margin
Culebra steady-state calibration wells
Particle from Waste Panels to LWB

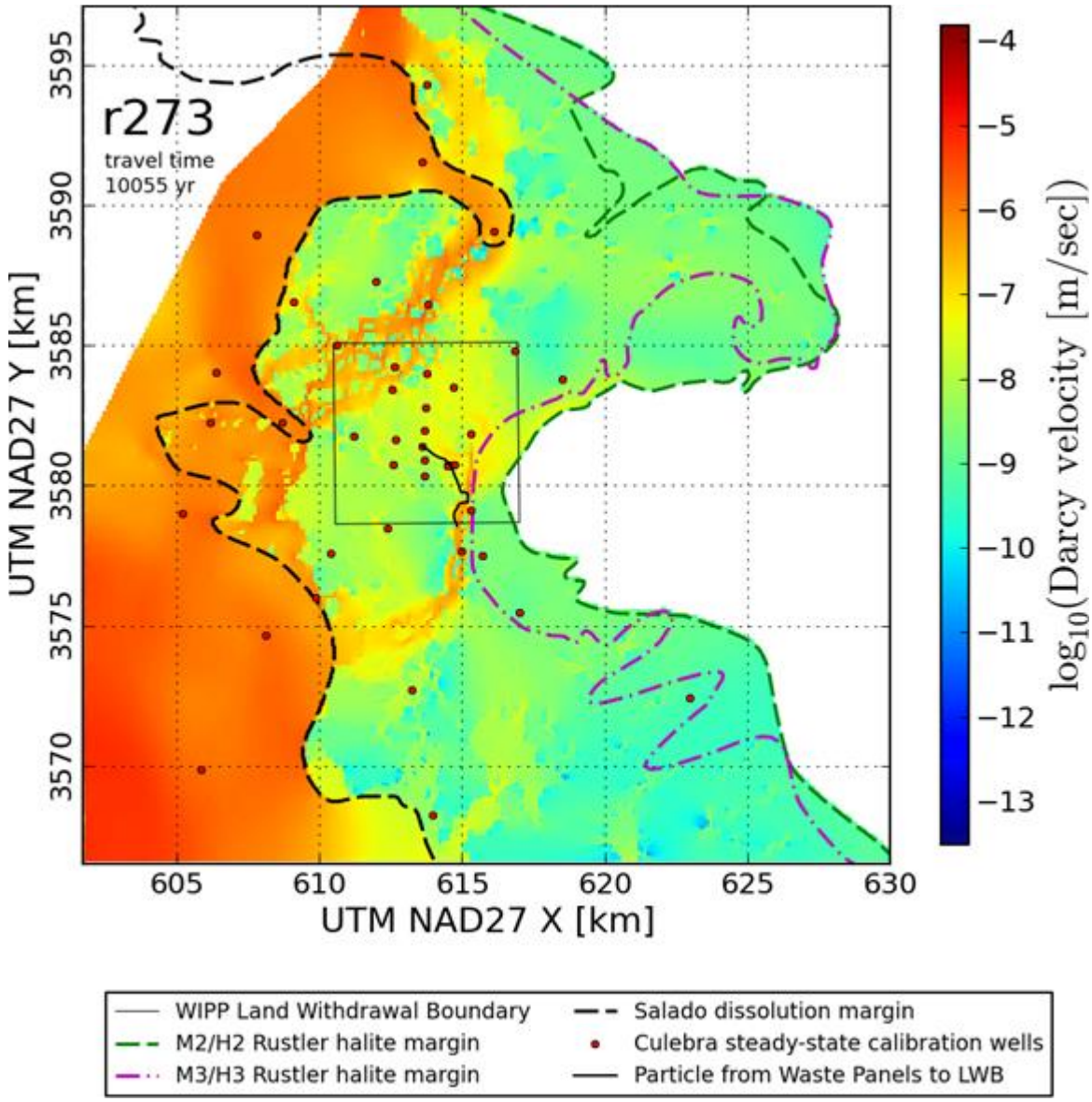
r273
travel time
10055 yr
UTM NAD27 Y [km]
3595
3590
3585
3580
3575
3570
605
610
615
620
625
630
UTM NAD27 X [km]
−4
−5
−6
−7
−8
−9
−10
−11
−12
−13
log10(Darcy velocity [m/sec])
WIPP Land Withdrawal Boundary
M2/H2 Rustler halite margin
M3/H3 Rustler halite margin
Salado dissolution margin
Culebra steady-state calibration wells
Particle from Waste Panels to LWB

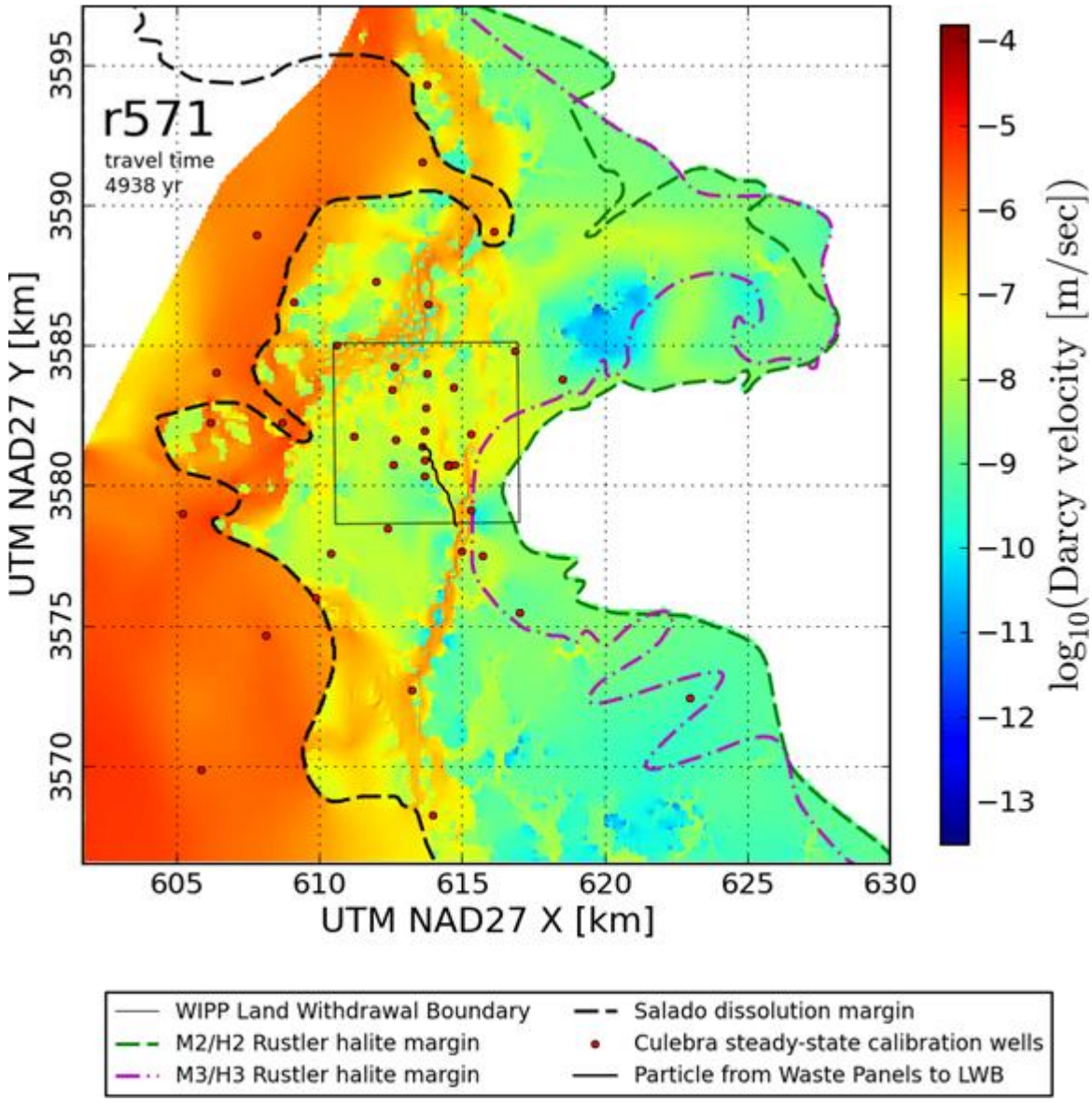
r571
travel time
4938 yr
UTM NAD27 Y [km]
3595
3590
3585
3580
3575
3570
605
610
615
620
625
630
UTM NAD27 X [km]
−4
−5
−6
−7
−8
−9
−10
−11
−12
−13
log10(Darcy velocity [m/sec])
WIPP Land Withdrawal Boundary
M2/H2 Rustler halite margin
M3/H3 Rustler halite margin
Salado dissolution margin
Culebra steady-state calibration wells
Particle from Waste Panels to LWB

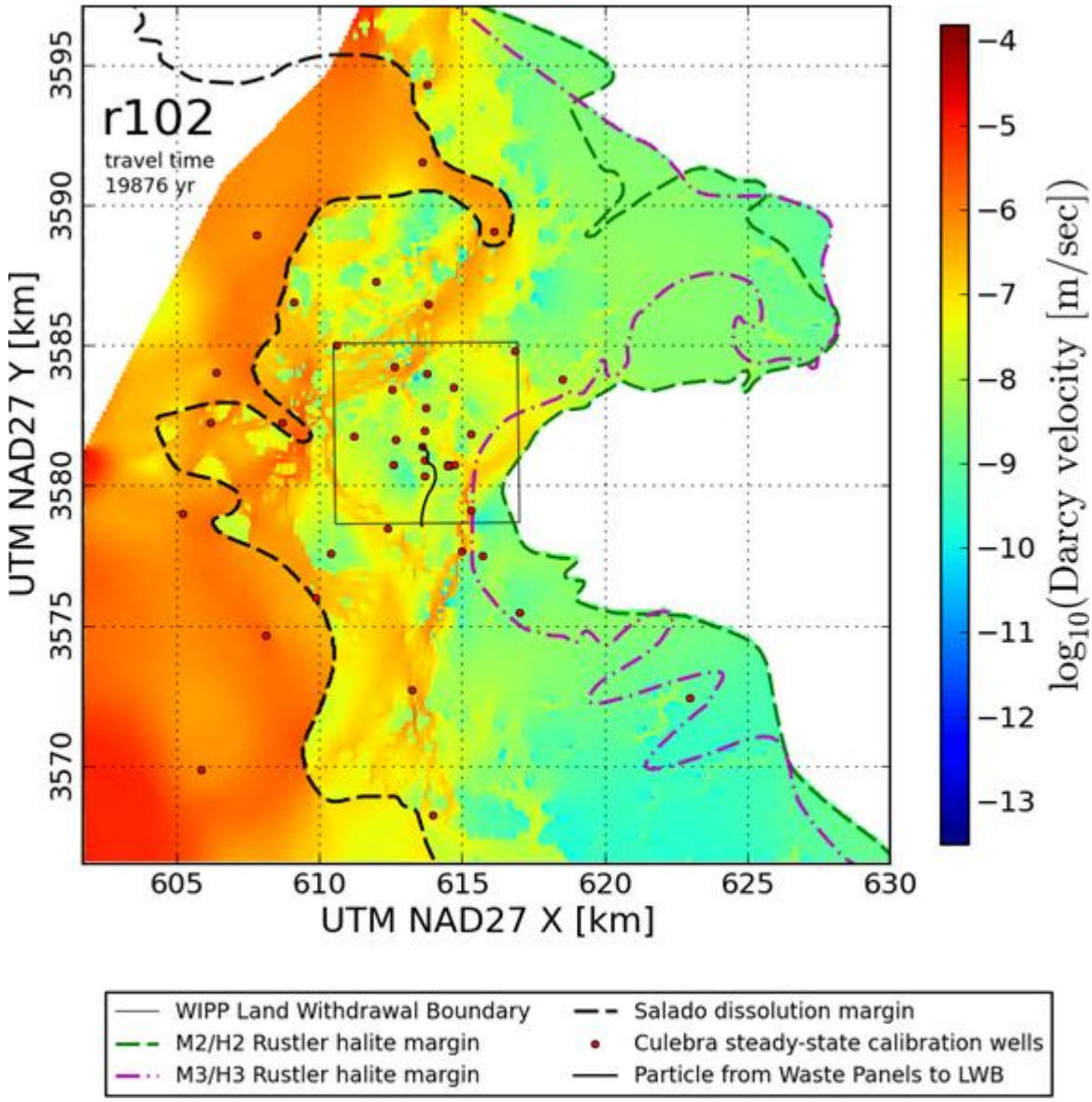
r102
travel time
19876 yr
UTM NAD27 Y [km]
3595
3590
3585
3580
3575
3570
605
610
615
620
625
630
UTM NAD27 X [km]
−4
−5
−6
−7
−8
−9
−10
−11
−12
−13
log10(Darcy velocity [m/sec])
WIPP Land Withdrawal Boundary
M2/H2 Rustler halite margin
M3/H3 Rustler halite margin
Salado dissolution margin
Culebra steady-state calibration wells
Particle from Waste Panels to LWB

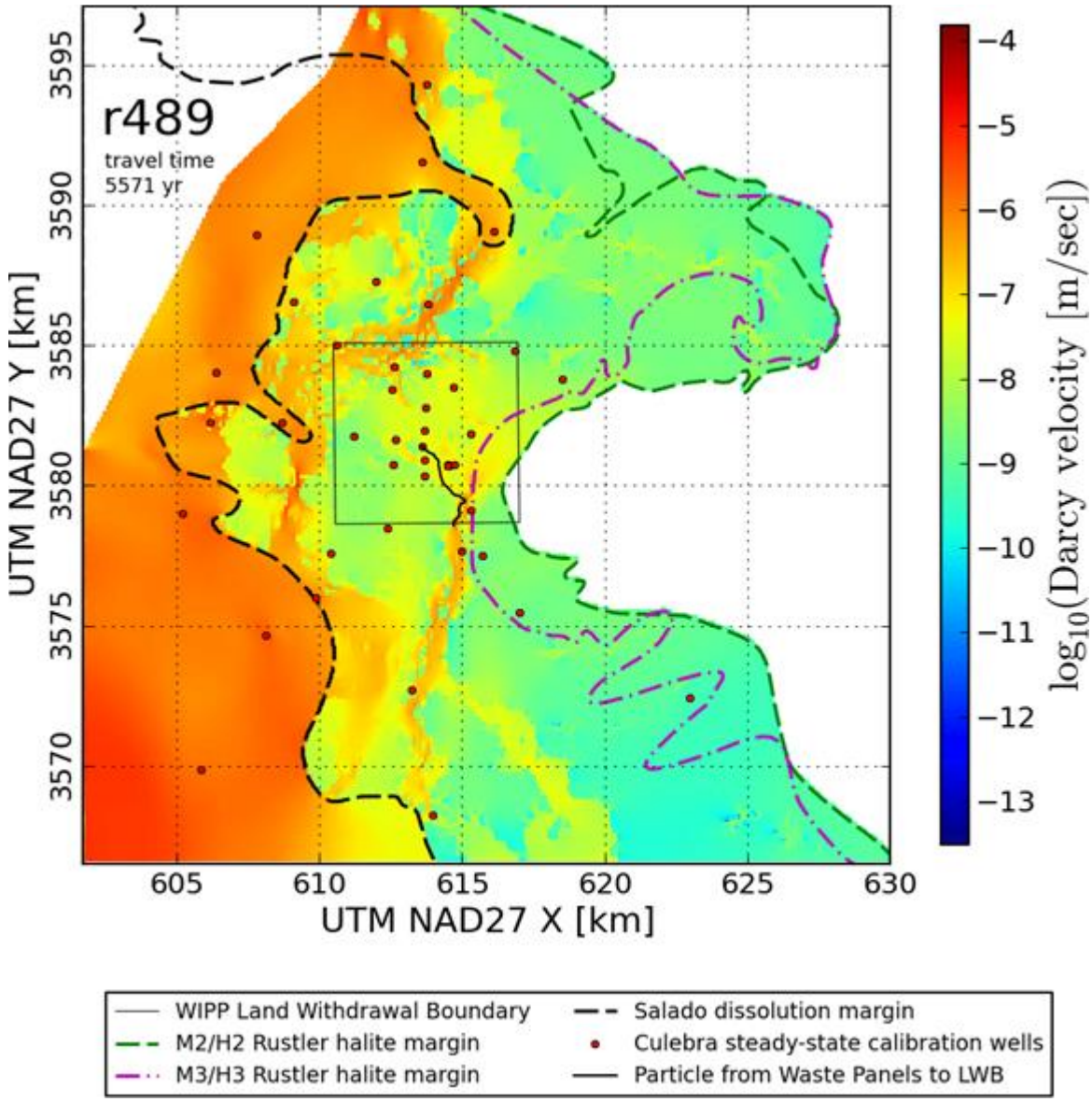
r489
travel time
5571 yr
UTM NAD27 Y [km]
3595
3590
3585
3580
3575
3570
605
610
615
620
625
630
UTM NAD27 X [km]
−4
−5
−6
−7
−8
−9
−10
−11
−12
−13
log10(Darcy velocity [m/sec])
WIPP Land Withdrawal Boundary
M2/H2 Rustler halite margin
M3/H3 Rustler halite margin
Salado dissolution margin
Culebra steady-state calibration wells
Particle from Waste Panels to LWB

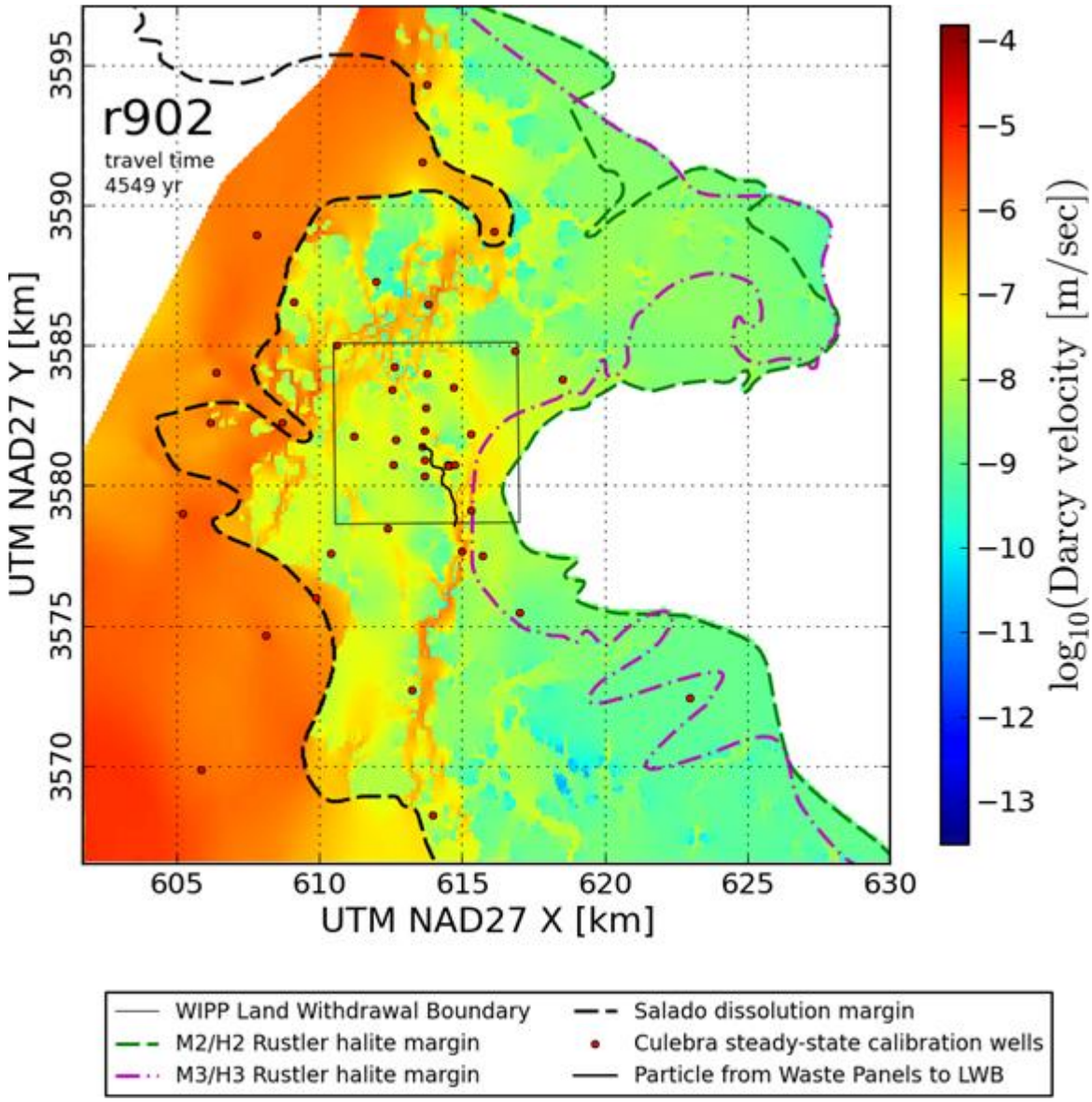
r902
travel time
4549 yr
UTM NAD27 Y [km]
3595
3590
3585
3580
3575
3570
605
610
615
620
625
630
UTM NAD27 X [km]
−4
−5
−6
−7
−8
−9
−10
−11
−12
−13
log10(Darcy velocity [m/sec])
WIPP Land Withdrawal Boundary
M2/H2 Rustler halite margin
M3/H3 Rustler halite margin
Salado dissolution margin
Culebra steady-state calibration wells
Particle from Waste Panels to LWB

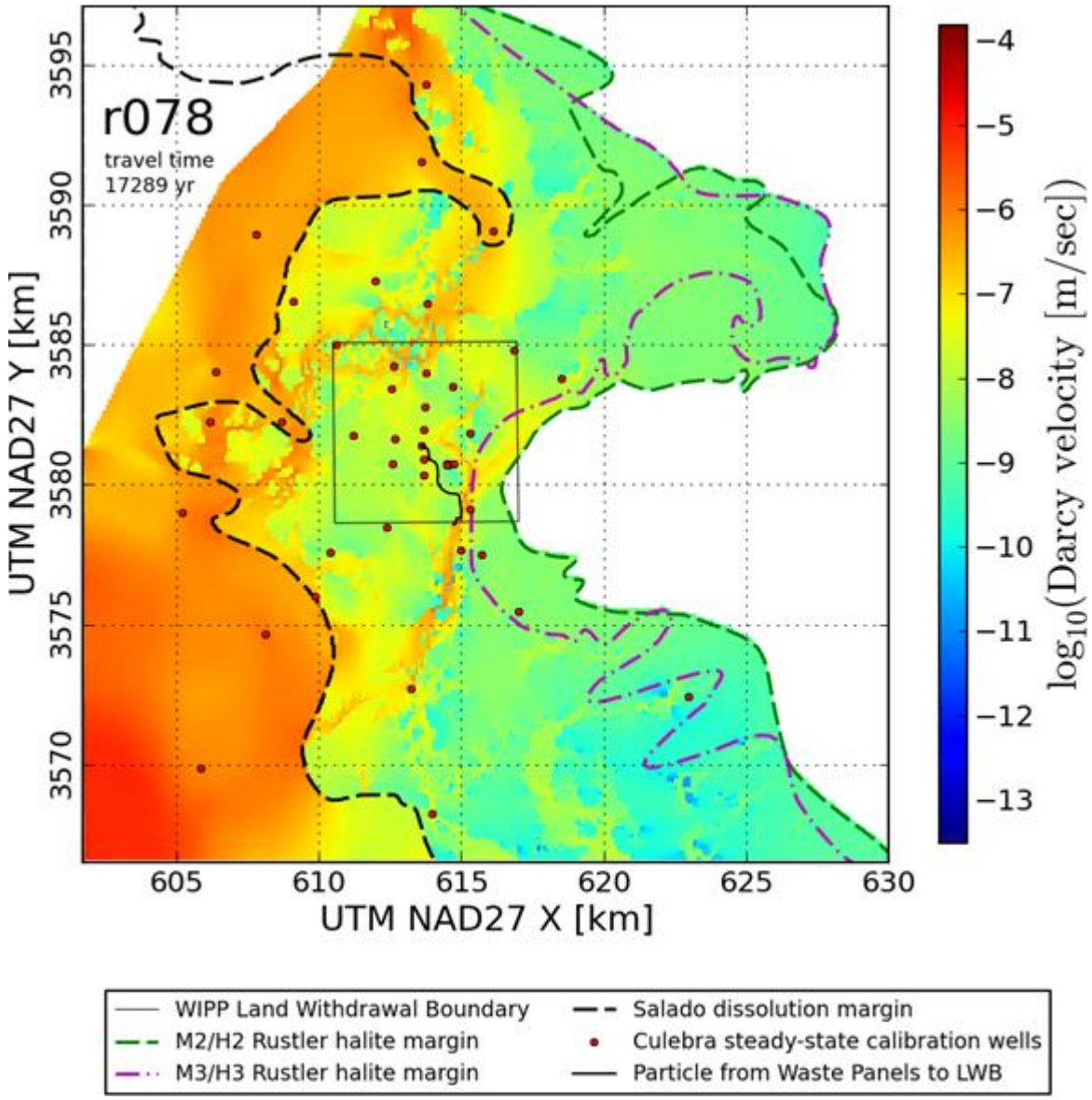
r078
travel time
17289 yr
UTM NAD27 Y [km]
3595
3590
3585
3580
3575
3570
605
610
615
620
625
630
UTM NAD27 X [km]
−4
−5
−6
−7
−8
−9
−10
−11
−12
−13
log10(Darcy velocity [m/sec])
WIPP Land Withdrawal Boundary
M2/H2 Rustler halite margin
M3/H3 Rustler halite margin
Salado dissolution margin
Culebra steady-state calibration wells
Particle from Waste Panels to LWB

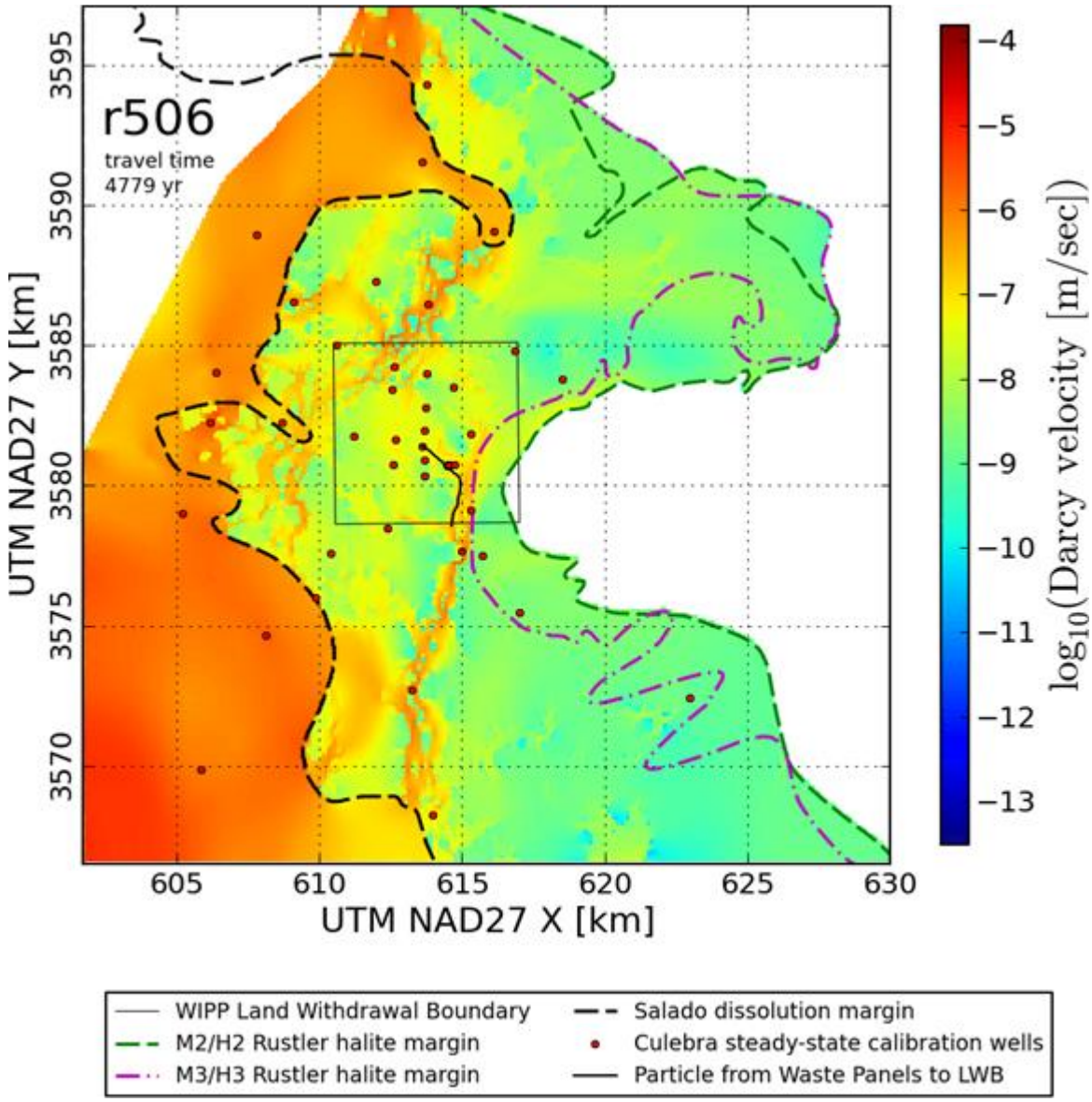
r506
travel time
4779 yr
UTM NAD27 Y [km]
3595
3590
3585
3580
3575
3570
605
610
615
620
625
630
UTM NAD27 X [km]
−4
−5
−6
−7
−8
−9
−10
−11
−12
−13
log10(Darcy velocity [m/sec])
WIPP Land Withdrawal Boundary
M2/H2 Rustler halite margin
M3/H3 Rustler halite margin
Salado dissolution margin
Culebra steady-state calibration wells
Particle from Waste Panels to LWB

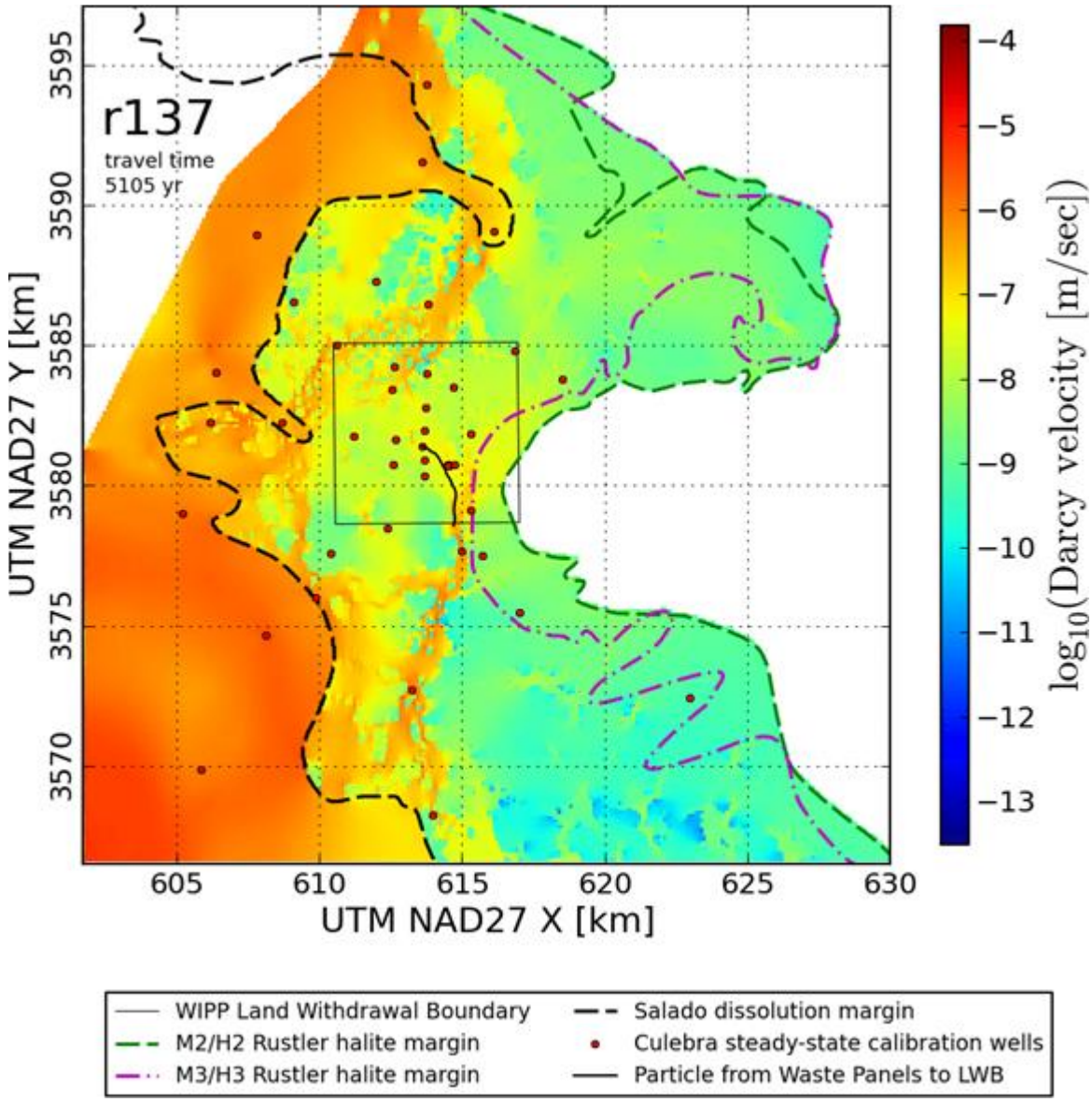
r137
travel time
5105 yr
UTM NAD27 Y [km]
3595
3590
3585
3580
3575
3570
605
610
615
620
625
630
UTM NAD27 X [km]
−4
−5
−6
−7
−8
−9
−10
−11
−12
−13
log10(Darcy velocity [m/sec])
WIPP Land Withdrawal Boundary
M2/H2 Rustler halite margin
M3/H3 Rustler halite margin
Salado dissolution margin
Culebra steady-state calibration wells
Particle from Waste Panels to LWB

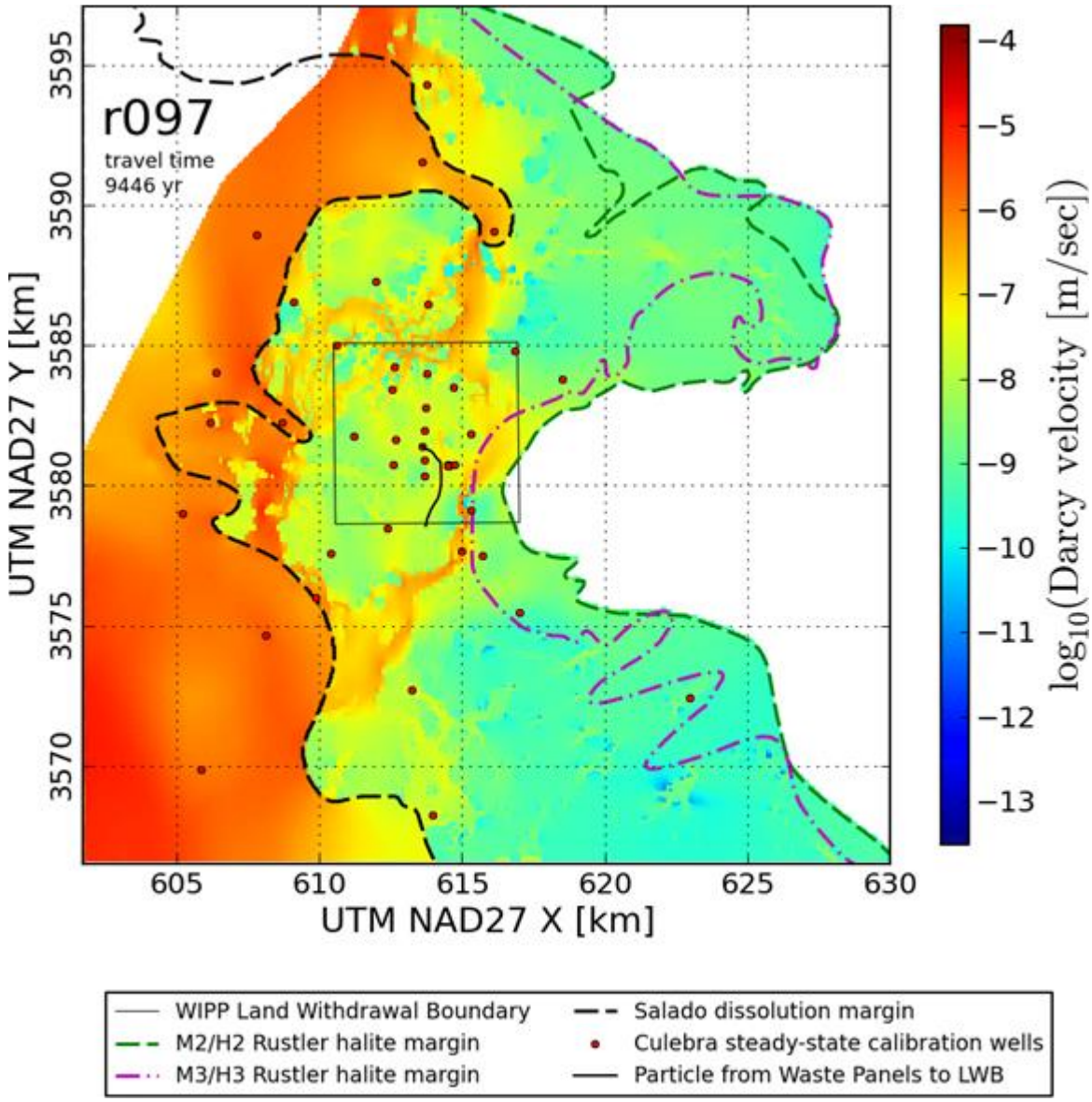
r097
travel time
9446 yr
UTM NAD27 Y [km]
3595
3590
3585
3580
3575
3570
605
610
615
620
625
630
UTM NAD27 X [km]
−4
−5
−6
−7
−8
−9
−10
−11
−12
−13
log10(Darcy velocity [m/sec])
WIPP Land Withdrawal Boundary
M2/H2 Rustler halite margin
M3/H3 Rustler halite margin
Salado dissolution margin
Culebra steady-state calibration wells
Particle from Waste Panels to LWB

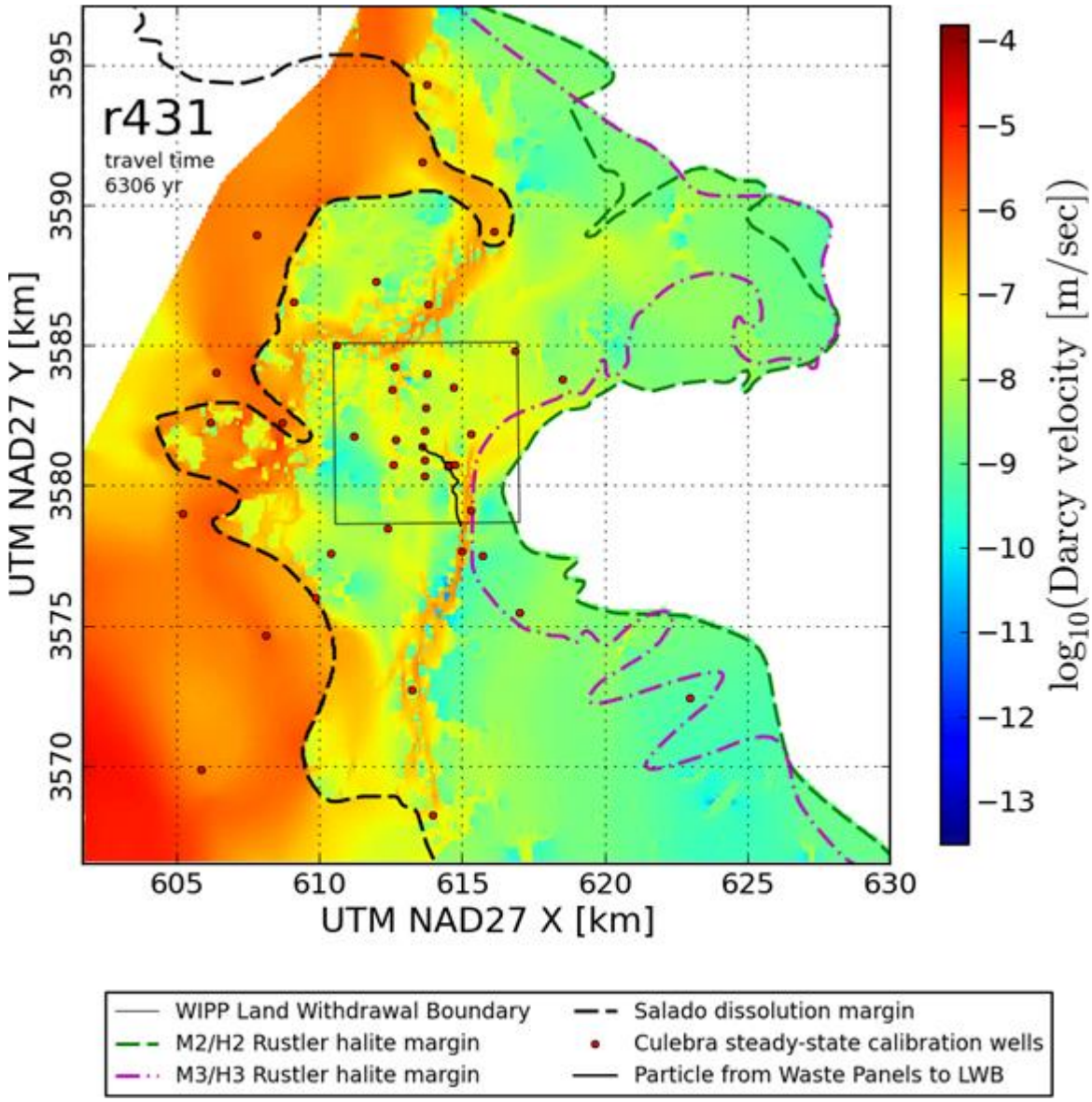
r431
travel time
6306 yr
UTM NAD27 Y [km]
3595
3590
3585
3580
3575
3570
605
610
615
620
625
630
UTM NAD27 X [km]
−4
−5
−6
−7
−8
−9
−10
−11
−12
−13
log10(Darcy velocity [m/sec])
WIPP Land Withdrawal Boundary
M2/H2 Rustler halite margin
M3/H3 Rustler halite margin
Salado dissolution margin
Culebra steady-state calibration wells
Particle from Waste Panels to LWB

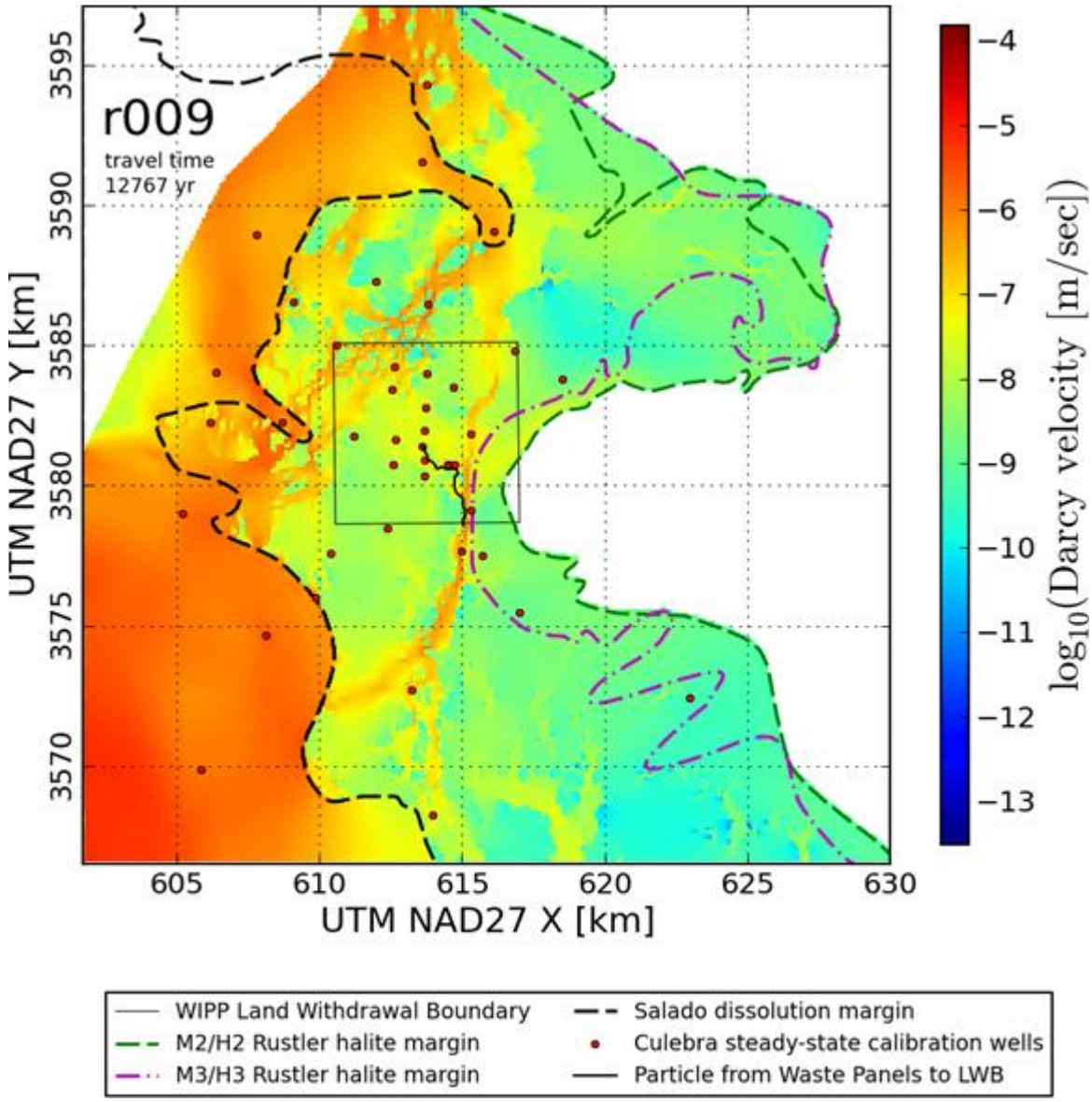
r009
travel time
12767 yr
UTM NAD27 Y [km]
3595
3590
3585
3580
3575
3570
605
610
615
620
625
630
UTM NAD27 X [km]
−4
−5
−6
−7
−8
−9
−10
−11
−12
−13
log10(Darcy velocity [m/sec])
WIPP Land Withdrawal Boundary
M2/H2 Rustler halite margin
M3/H3 Rustler halite margin
Salado dissolution margin
Culebra steady-state calibration wells
Particle from Waste Panels to LWB

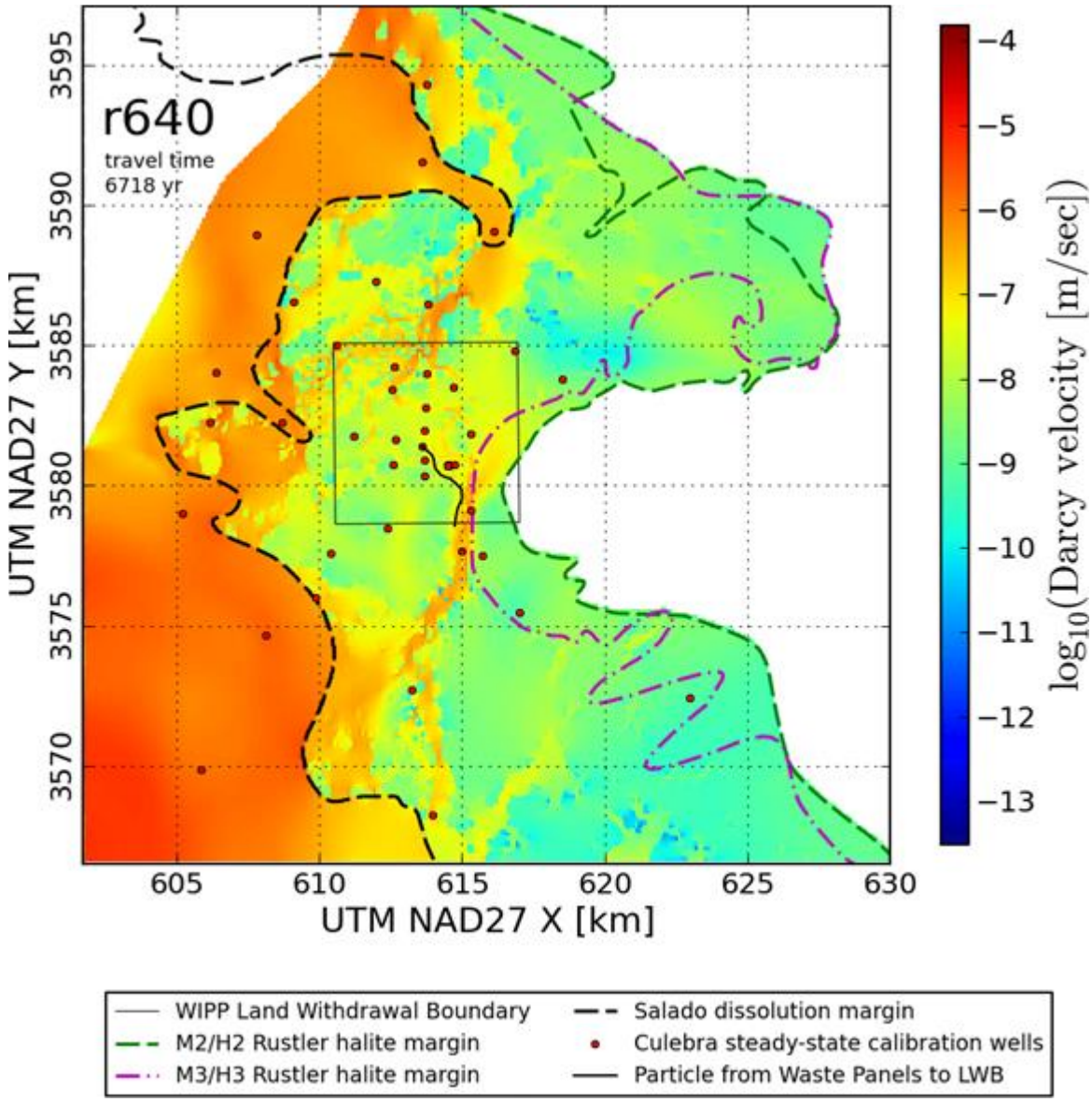
r640
travel time
6718 yr
UTM NAD27 Y [km]
3595
3590
3585
3580
3575
3570
605
610
615
620
625
630
UTM NAD27 X [km]
−4
−5
−6
−7
−8
−9
−10
−11
−12
−13
log10(Darcy velocity [m/sec])
WIPP Land Withdrawal Boundary
M2/H2 Rustler halite margin
M3/H3 Rustler halite margin
Salado dissolution margin
Culebra steady-state calibration wells
Particle from Waste Panels to LWB

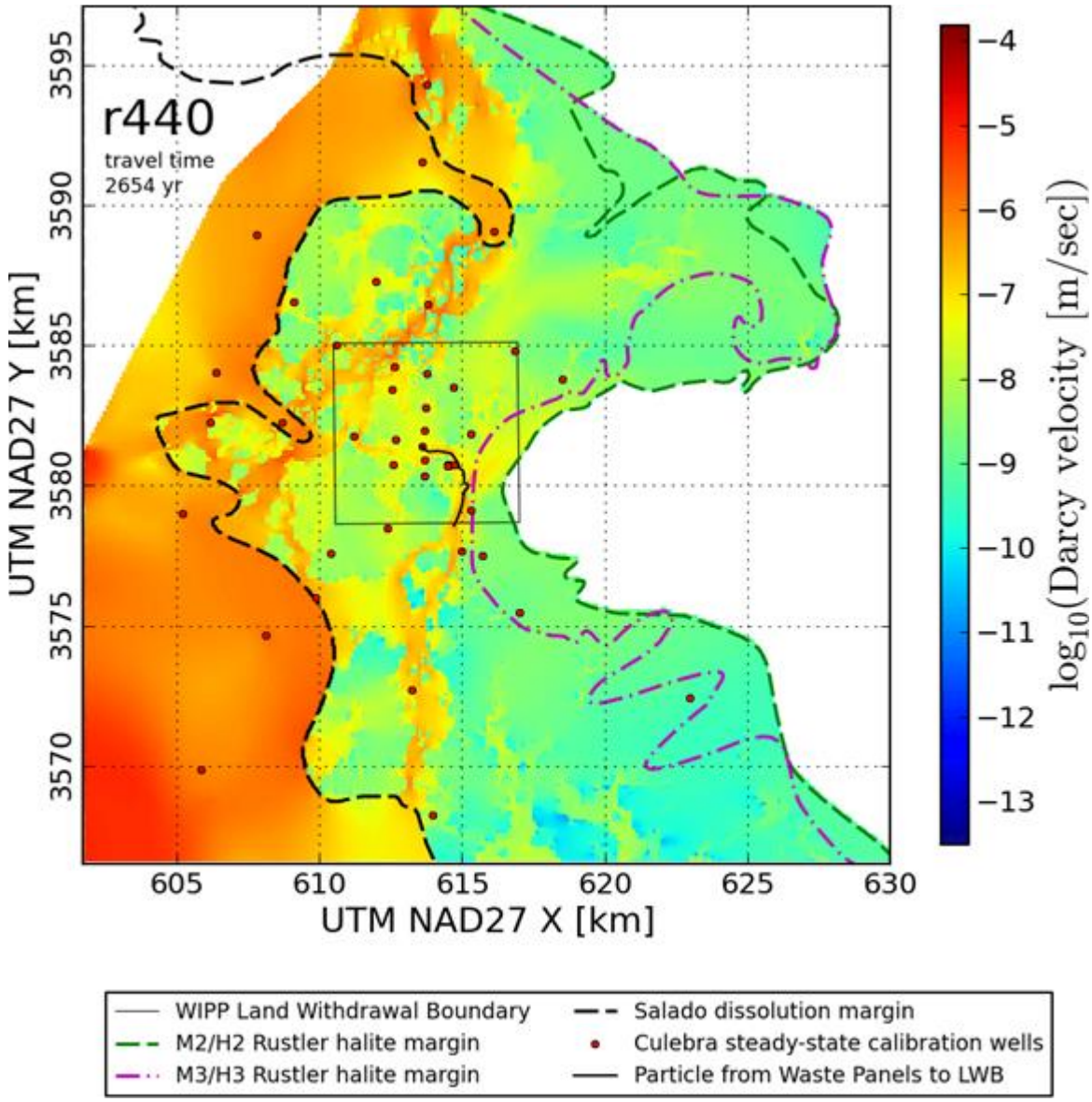
r440
travel time
2654 yr
UTM NAD27 Y [km]
3595
3590
3585
3580
3575
3570
605
610
615
620
625
630
UTM NAD27 X [km]
−4
−5
−6
−7
−8
−9
−10
−11
−12
−13
log10(Darcy velocity [m/sec])
WIPP Land Withdrawal Boundary
M2/H2 Rustler halite margin
M3/H3 Rustler halite margin
Salado dissolution margin
Culebra steady-state calibration wells
Particle from Waste Panels to LWB

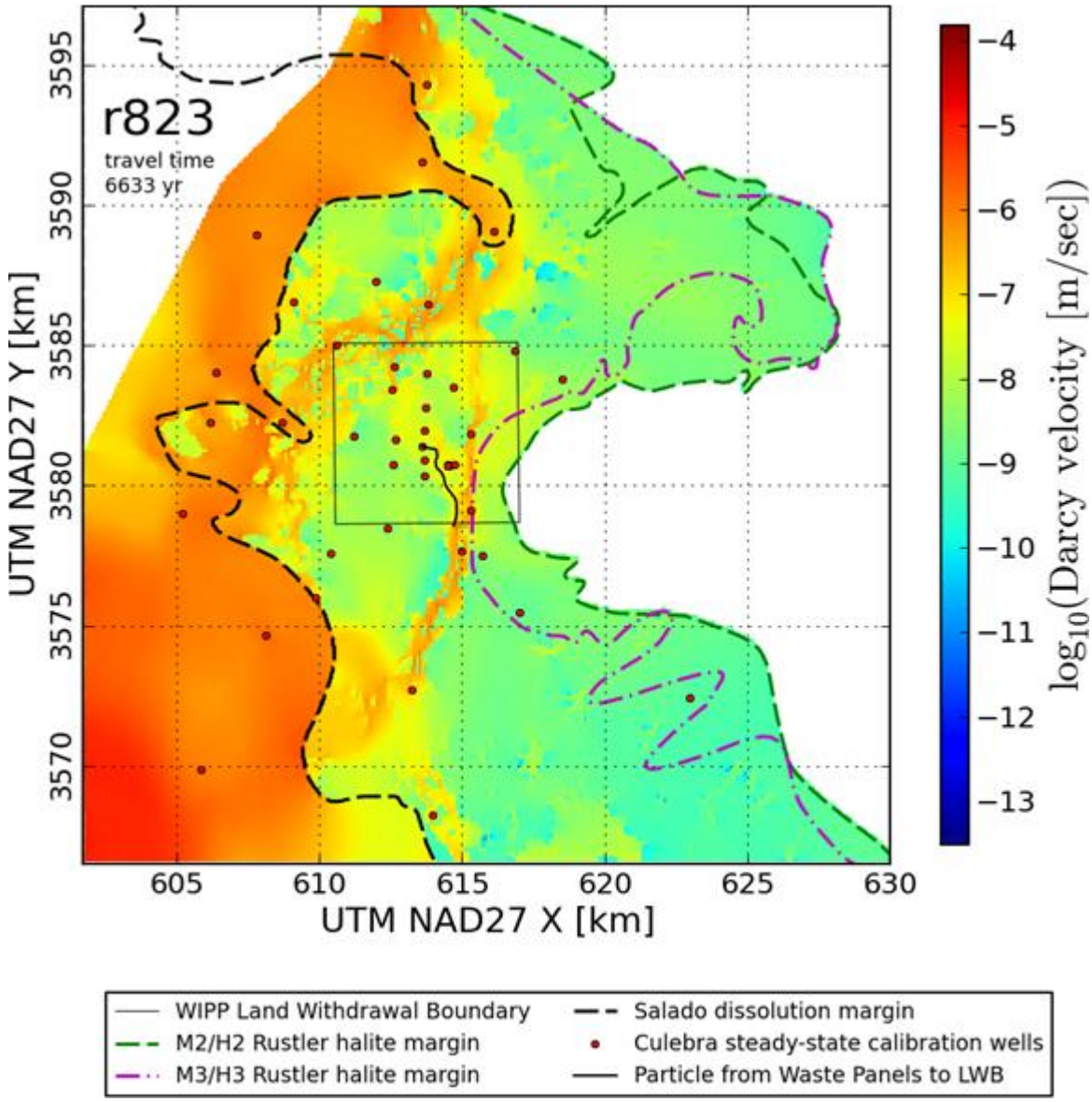
r823
travel time
6633 yr
UTM NAD27 Y [km]
3595
3590
3585
3580
3575
3570
605
610
615
620
625
630
UTM NAD27 X [km]
−4
−5
−6
−7
−8
−9
−10
−11
−12
−13
log10(Darcy velocity [m/sec])
WIPP Land Withdrawal Boundary
M2/H2 Rustler halite margin
M3/H3 Rustler halite margin
Salado dissolution margin
Culebra steady-state calibration wells
Particle from Waste Panels to LWB

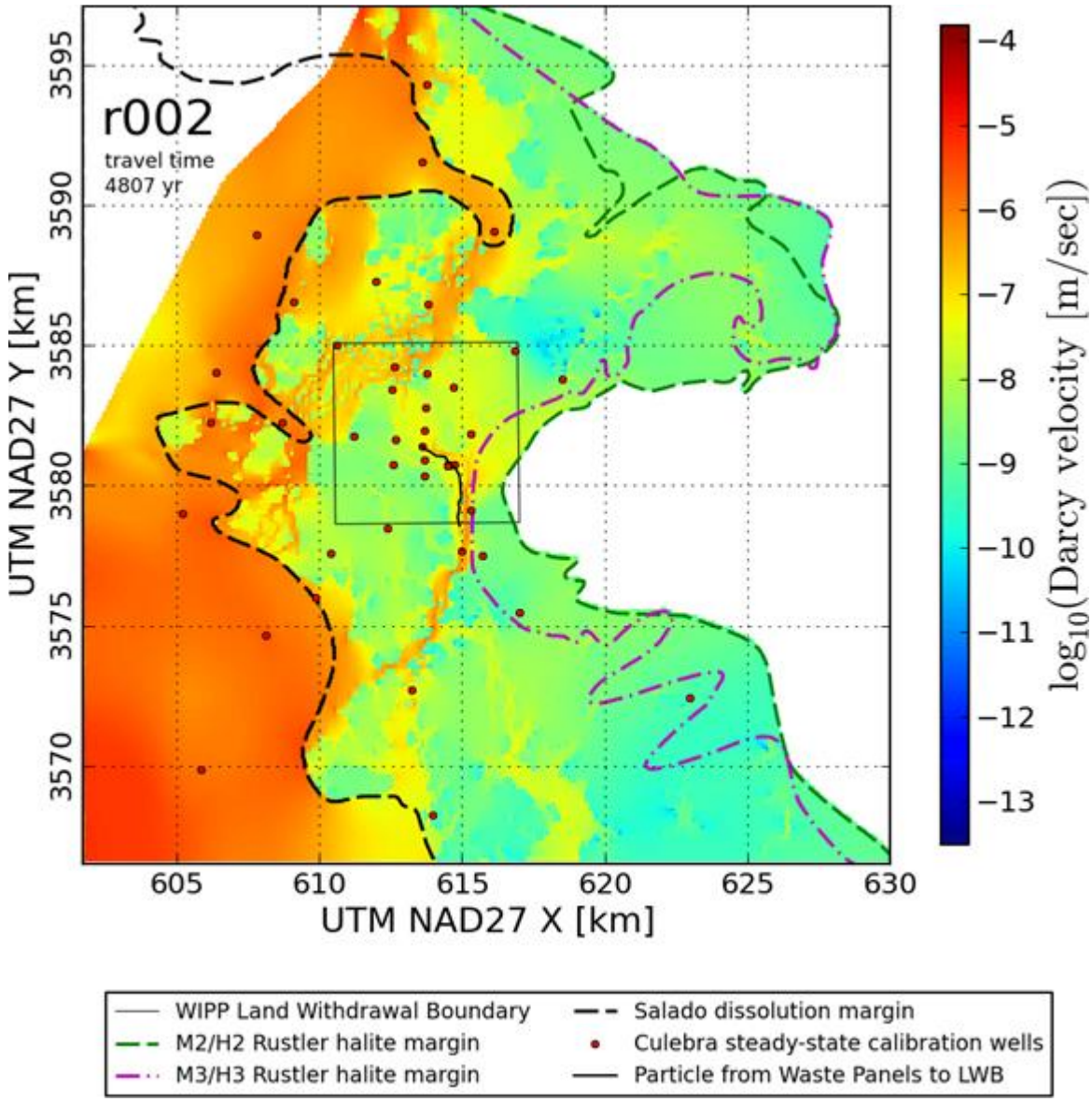
r002
travel time
4807 yr
UTM NAD27 Y [km]
3595
3590
3585
3580
3575
3570
605
610
615
620
625
630
UTM NAD27 X [km]
−4
−5
−6
−7
−8
−9
−10
−11
−12
−13
log10(Darcy velocity [m/sec])
WIPP Land Withdrawal Boundary
M2/H2 Rustler halite margin
M3/H3 Rustler halite margin
Salado dissolution margin
Culebra steady-state calibration wells
Particle from Waste Panels to LWB

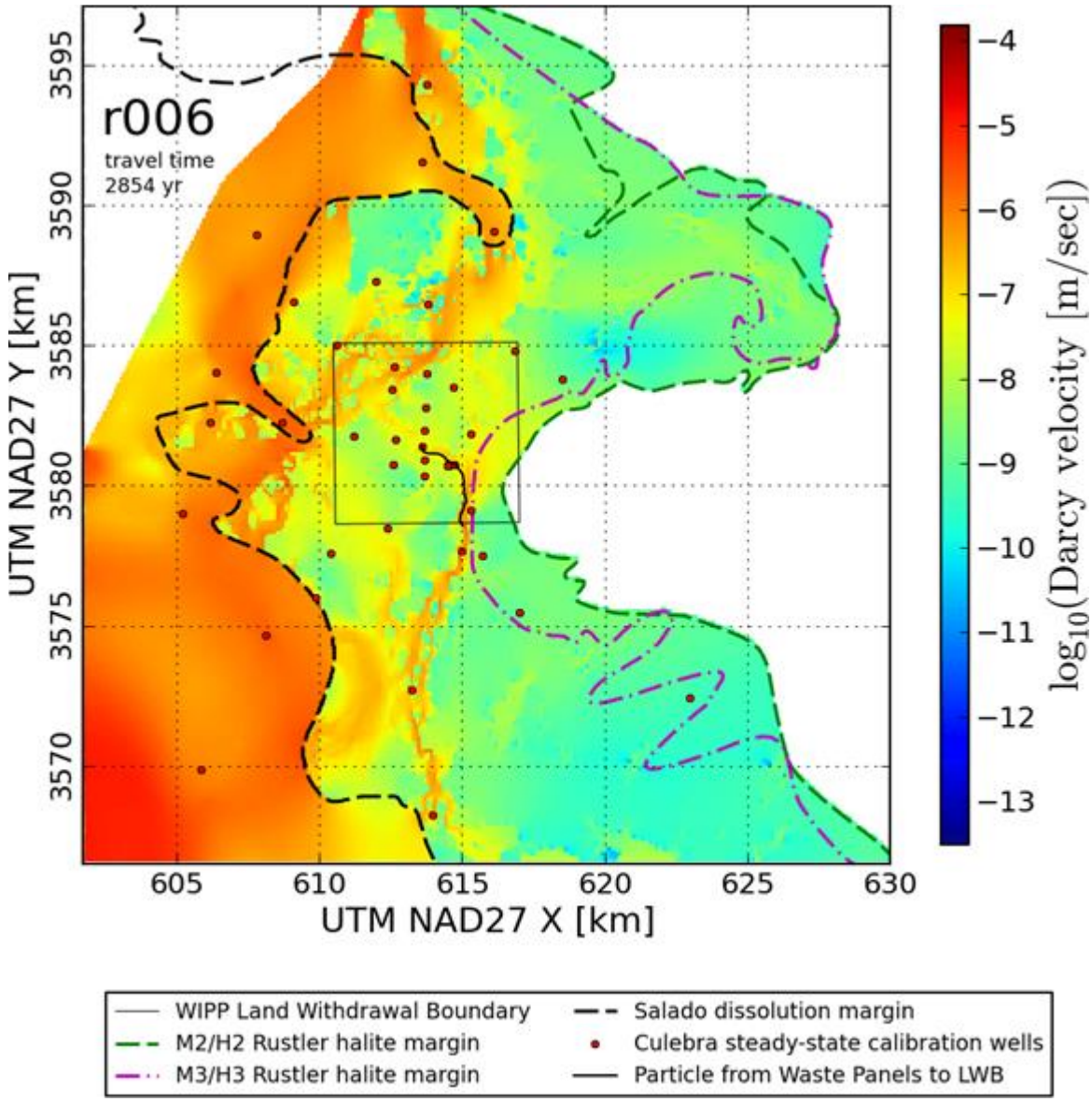
r006
travel time
2854 yr
UTM NAD27 Y [km]
3595
3590
3585
3580
3575
3570
605
610
615
620
625
630
UTM NAD27 X [km]
−4
−5
−6
−7
−8
−9
−10
−11
−12
−13
log10(Darcy velocity [m/sec])
WIPP Land Withdrawal Boundary
M2/H2 Rustler halite margin
M3/H3 Rustler halite margin
Salado dissolution margin
Culebra steady-state calibration wells
Particle from Waste Panels to LWB

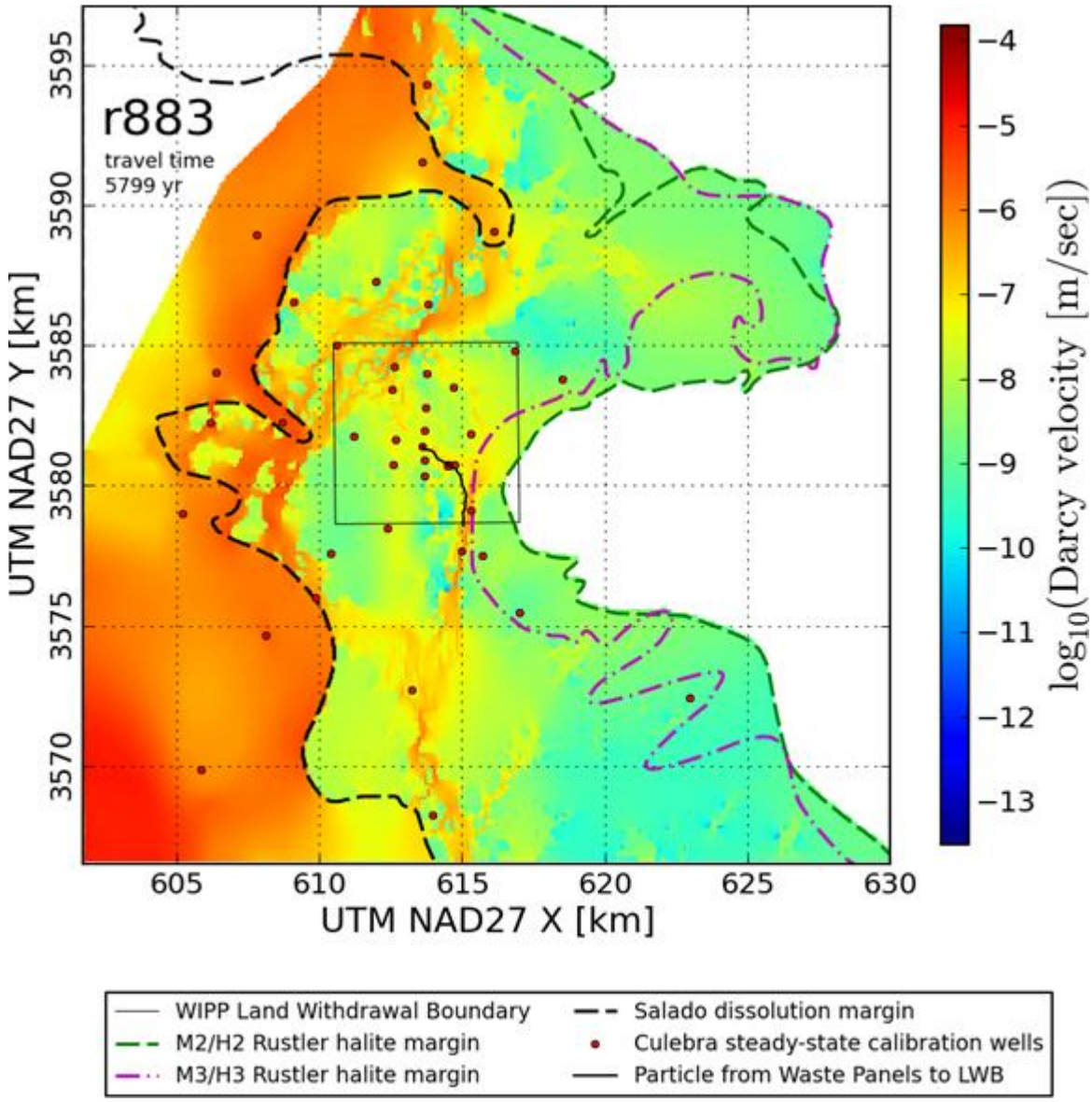
r883
travel time
5799 yr
UTM NAD27 Y [km]
3595
3590
3585
3580
3575
3570
605
610
615
620
625
630
UTM NAD27 X [km]
−4
−5
−6
−7
−8
−9
−10
−11
−12
−13
log10(Darcy velocity [m/sec])
WIPP Land Withdrawal Boundary
M2/H2 Rustler halite margin
M3/H3 Rustler halite margin
Salado dissolution margin
Culebra steady-state calibration wells
Particle from Waste Panels to LWB

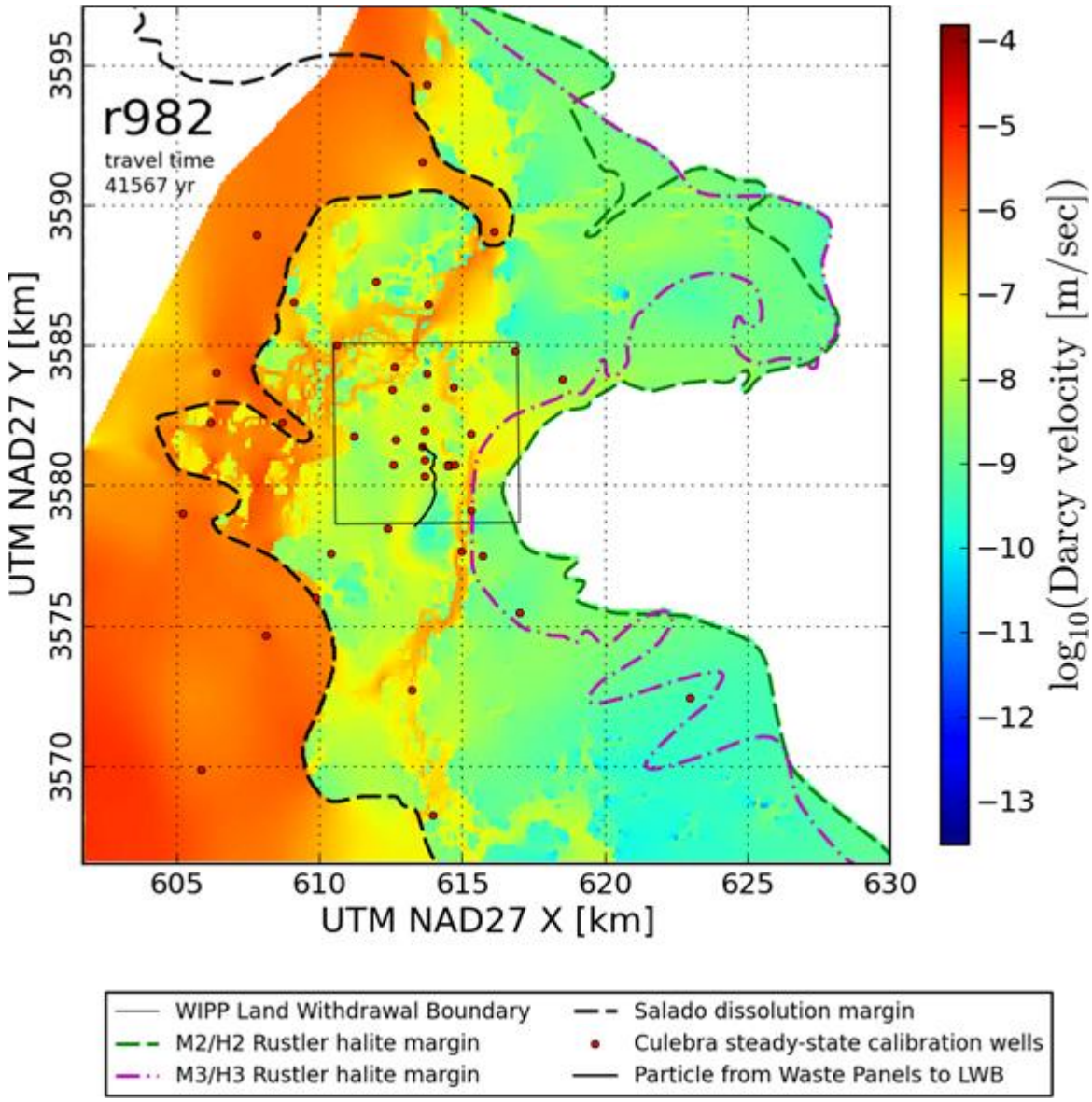
r982
travel time
41567 yr
UTM NAD27 Y [km]
3595
3590
3585
3580
3575
3570
605
610
615
620
625
630
UTM NAD27 X [km]
−4
−5
−6
−7
−8
−9
−10
−11
−12
−13
log10(Darcy velocity [m/sec])
WIPP Land Withdrawal Boundary
M2/H2 Rustler halite margin
M3/H3 Rustler halite margin
Salado dissolution margin
Culebra steady-state calibration wells
Particle from Waste Panels to LWB

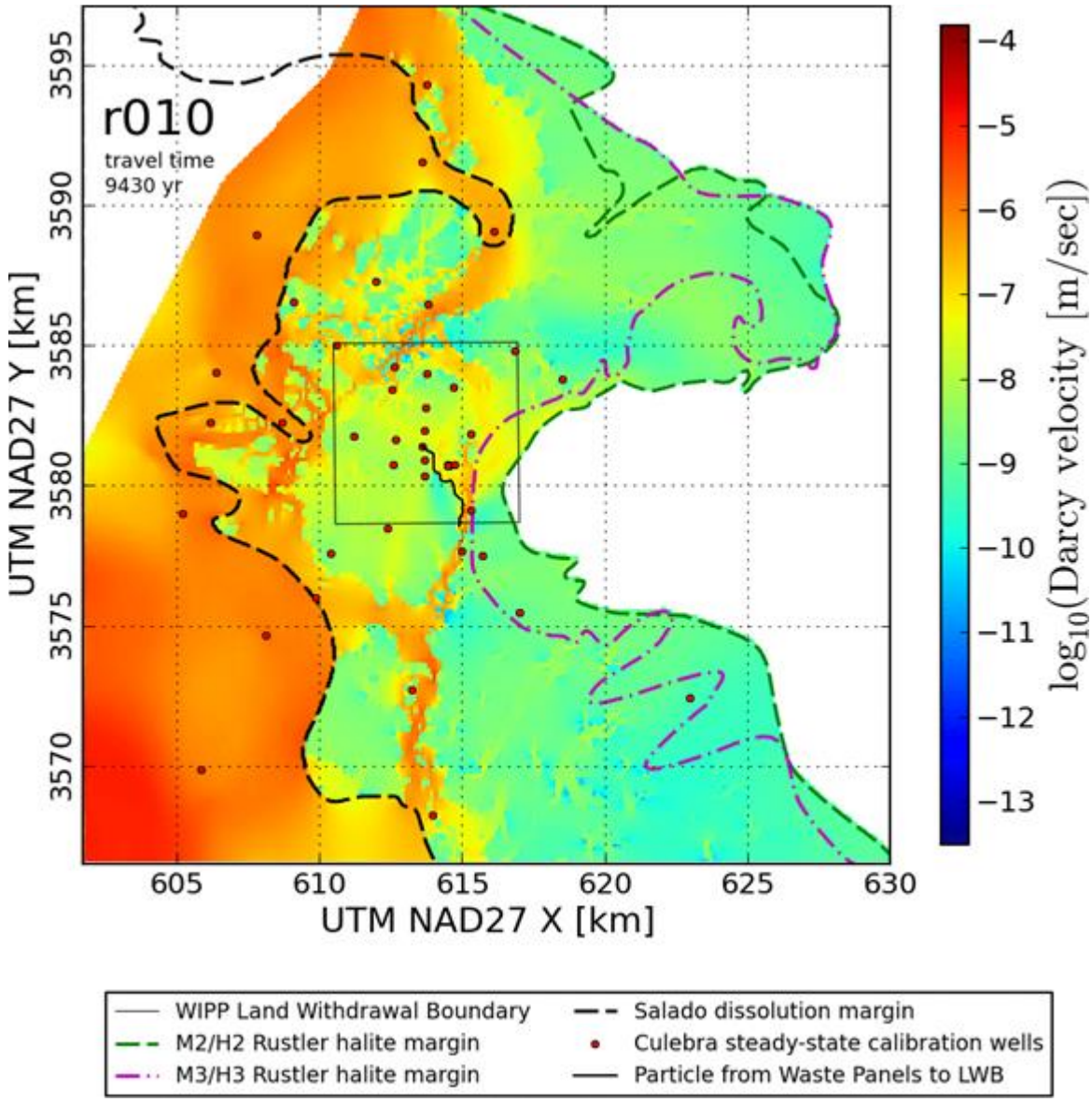
r010
travel time
9430 yr
UTM NAD27 Y [km]
3595
3590
3585
3580
3575
3570
605
610
615
620
625
630
UTM NAD27 X [km]
−4
−5
−6
−7
−8
−9
−10
−11
−12
−13
log10(Darcy velocity [m/sec])
WIPP Land Withdrawal Boundary
M2/H2 Rustler halite margin
M3/H3 Rustler halite margin
Salado dissolution margin
Culebra steady-state calibration wells
Particle from Waste Panels to LWB

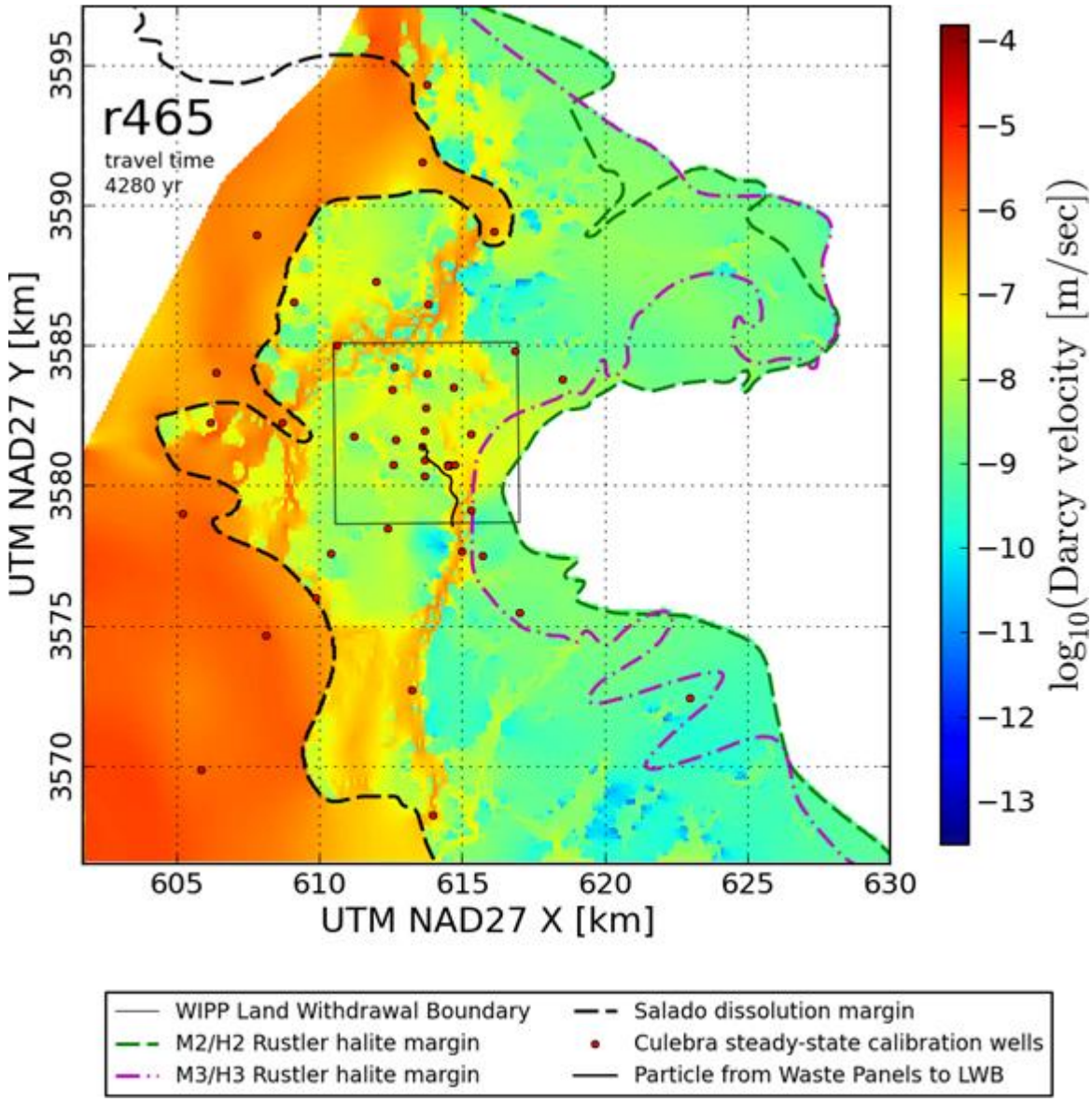
r465
travel time
4280 yr
UTM NAD27 Y [km]
3595
3590
3585
3580
3575
3570
605
610
615
620
625
630
UTM NAD27 X [km]
−4
−5
−6
−7
−8
−9
−10
−11
−12
−13
log10(Darcy velocity [m/sec])
WIPP Land Withdrawal Boundary
M2/H2 Rustler halite margin
M3/H3 Rustler halite margin
Salado dissolution margin
Culebra steady-state calibration wells
Particle from Waste Panels to LWB

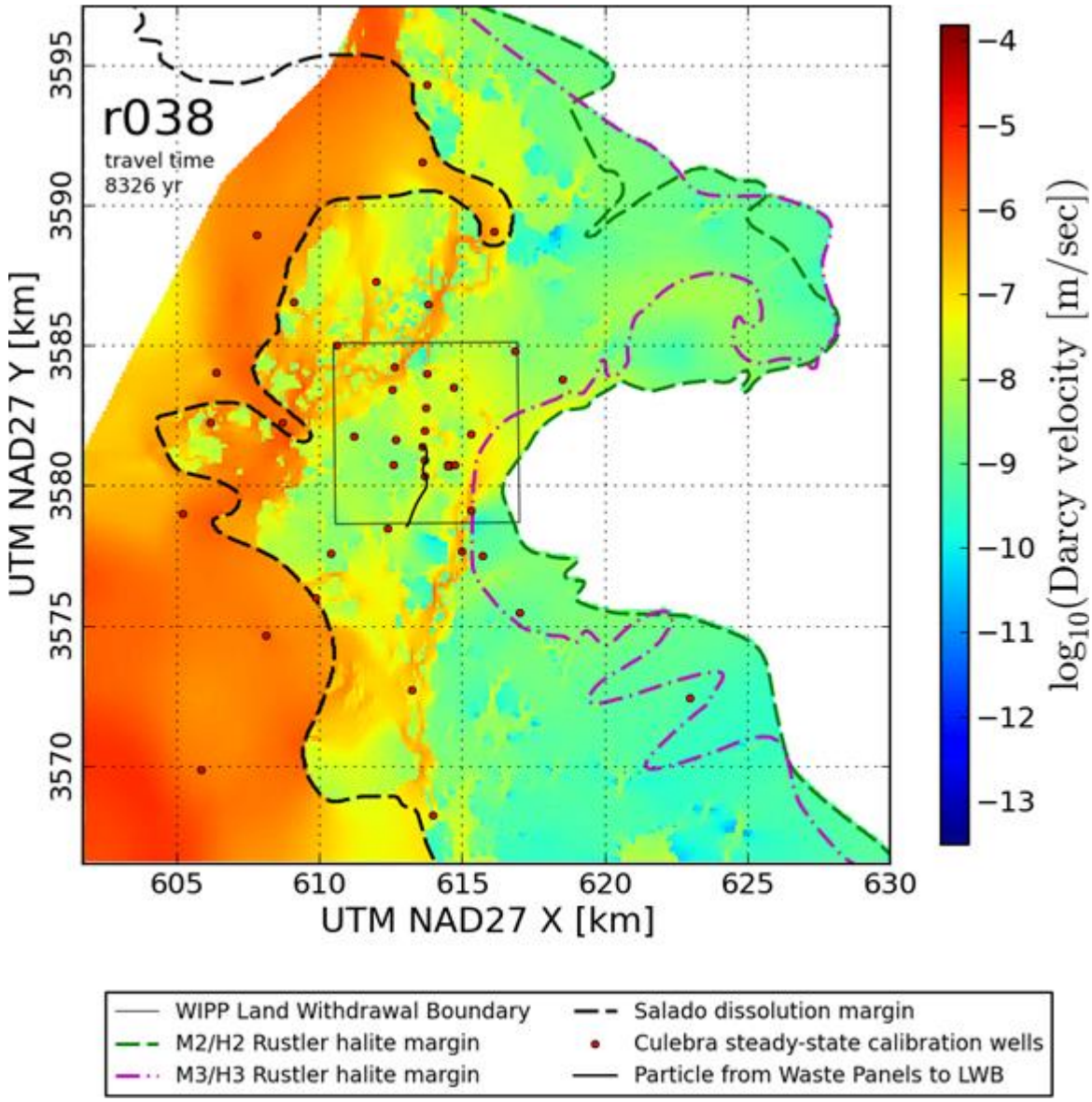
r038
travel time
8326 yr
UTM NAD27 Y [km]
3595
3590
3585
3580
3575
3570
605
610
615
620
625
630
UTM NAD27 X [km]
−4
−5
−6
−7
−8
−9
−10
−11
−12
−13
log10(Darcy velocity [m/sec])
WIPP Land Withdrawal Boundary
M2/H2 Rustler halite margin
M3/H3 Rustler halite margin
Salado dissolution margin
Culebra steady-state calibration wells
Particle from Waste Panels to LWB

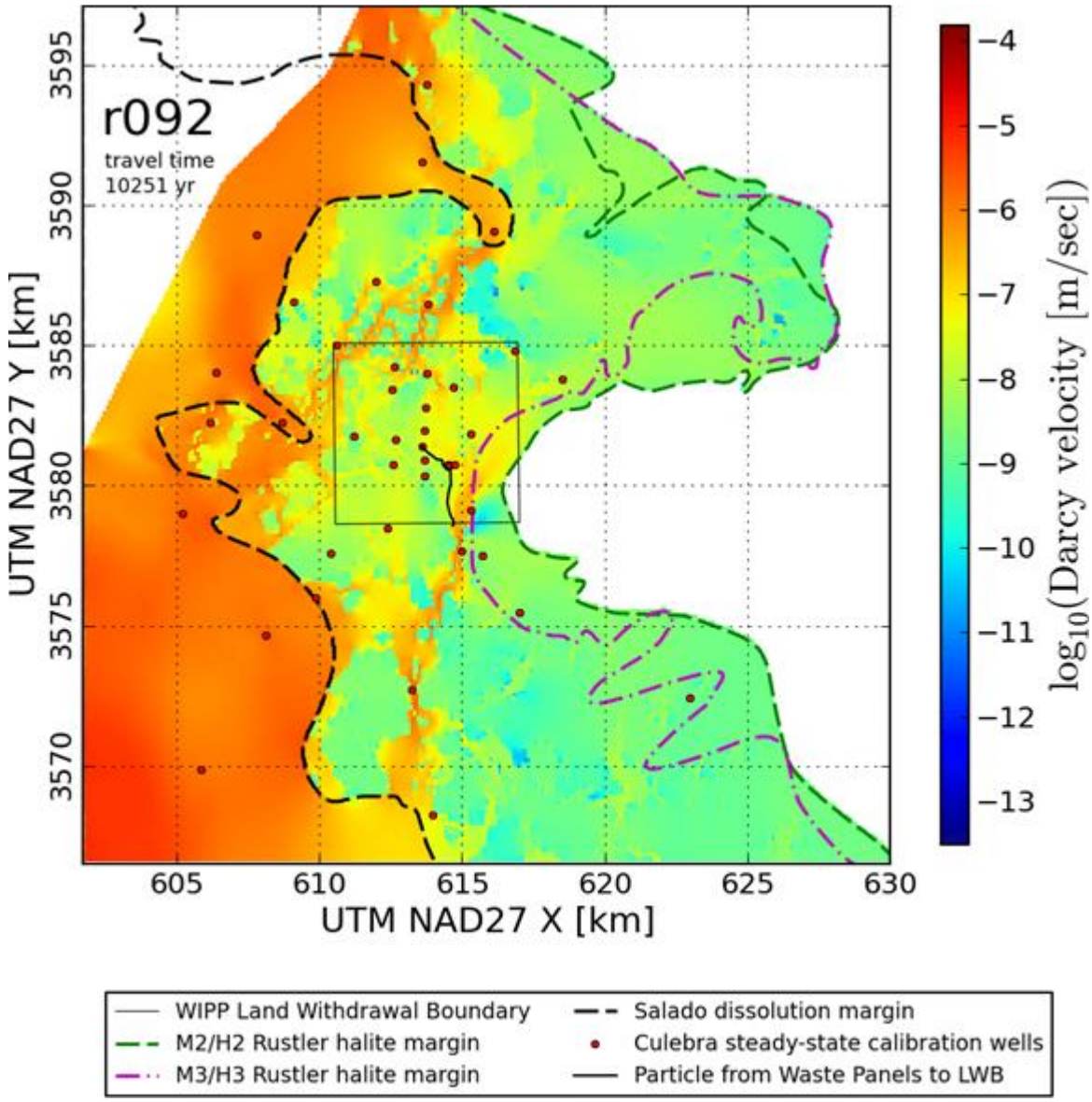
r092
travel time
10251 yr
UTM NAD27 Y [km]
3595
3590
3585
3580
3575
3570
605
610
615
620
625
630
UTM NAD27 X [km]
−4
−5
−6
−7
−8
−9
−10
−11
−12
−13
log10(Darcy velocity [m/sec])
WIPP Land Withdrawal Boundary
M2/H2 Rustler halite margin
M3/H3 Rustler halite margin
Salado dissolution margin
Culebra steady-state calibration wells
Particle from Waste Panels to LWB

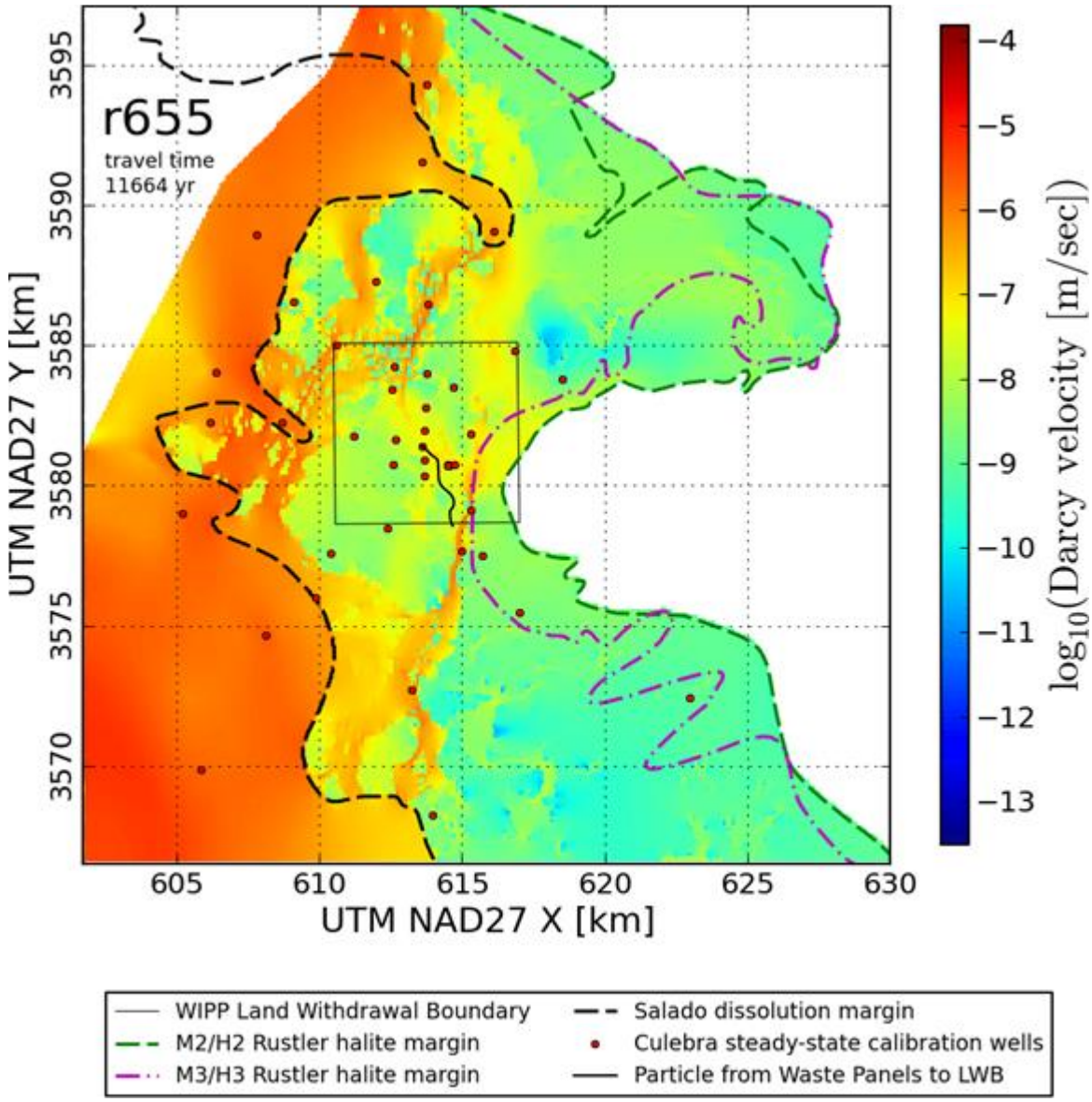
r655
travel time
11664 yr
UTM NAD27 Y [km]
3595
3590
3585
3580
3575
3570
605
610
615
620
625
630
UTM NAD27 X [km]
−4
−5
−6
−7
−8
−9
−10
−11
−12
−13
log10(Darcy velocity [m/sec])
WIPP Land Withdrawal Boundary
M2/H2 Rustler halite margin
M3/H3 Rustler halite margin
Salado dissolution margin
Culebra steady-state calibration wells
Particle from Waste Panels to LWB

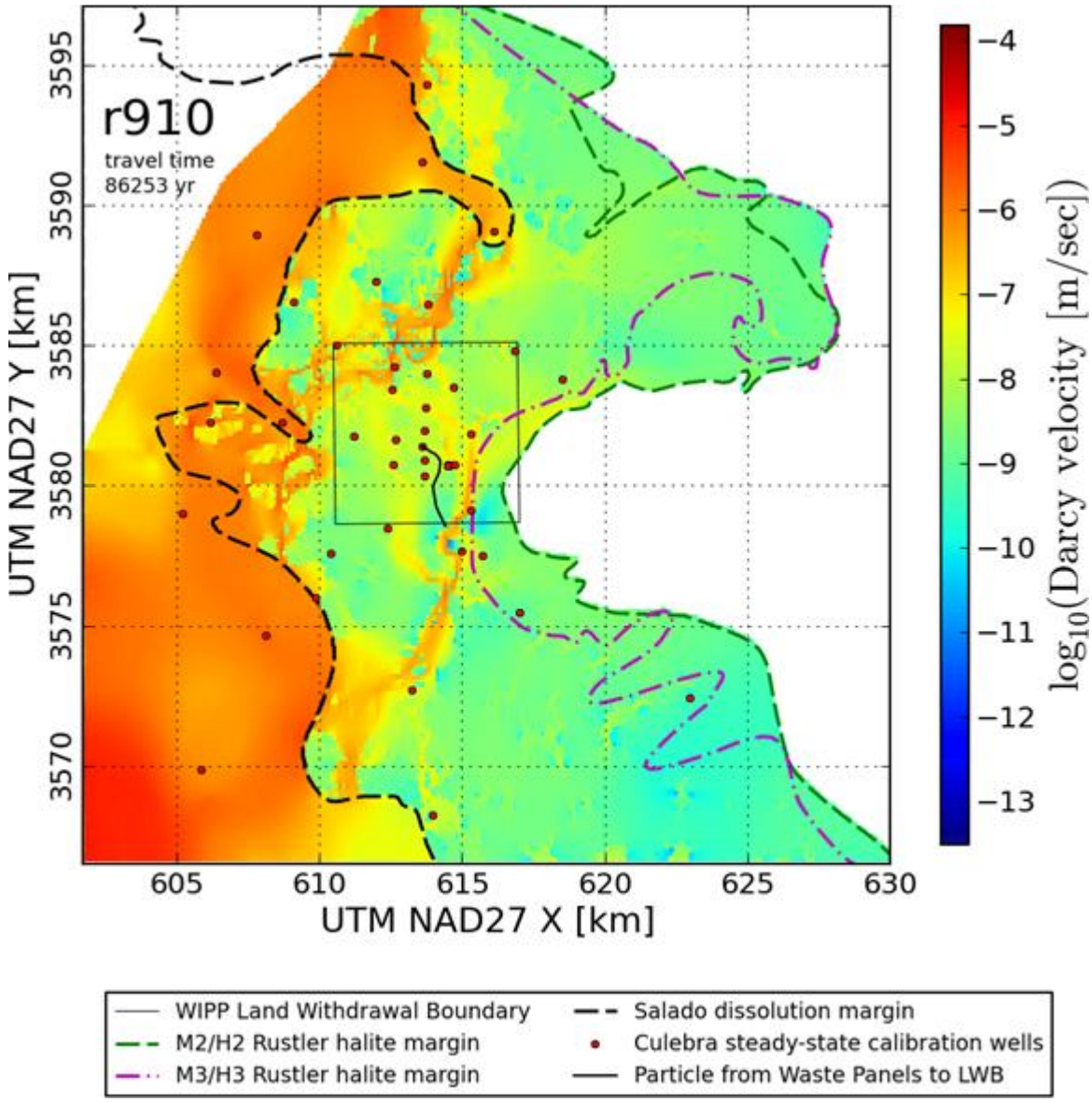
r910
travel time
86253 yr
UTM NAD27 Y [km]
3595
3590
3585
3580
3575
3570
605
610
615
620
625
630
UTM NAD27 X [km]
−4
−5
−6
−7
−8
−9
−10
−11
−12
−13
log10(Darcy velocity [m/sec])
WIPP Land Withdrawal Boundary
M2/H2 Rustler halite margin
M3/H3 Rustler halite margin
Salado dissolution margin
Culebra steady-state calibration wells
Particle from Waste Panels to LWB

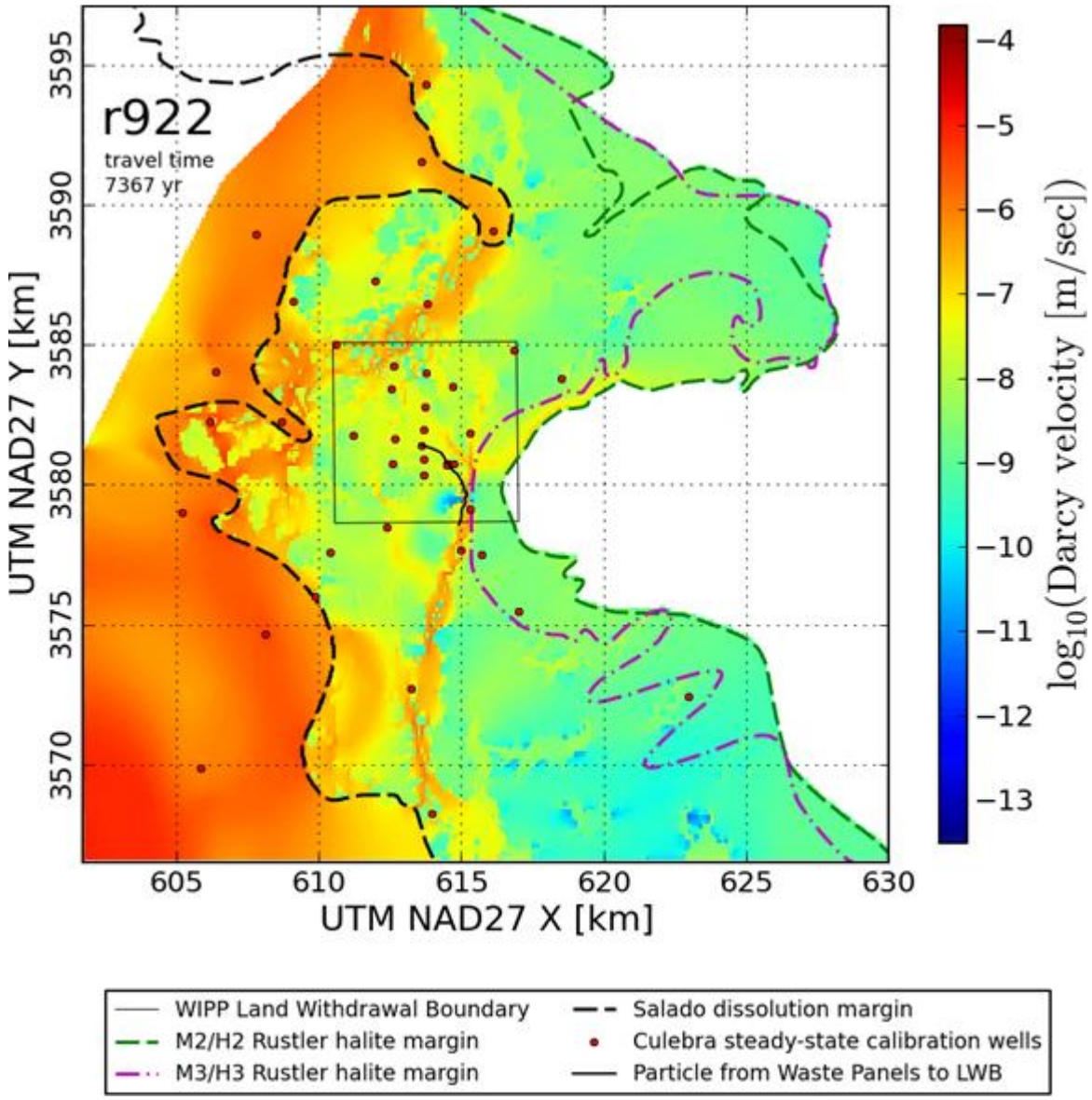
r922
travel time
7367 yr
UTM NAD27 Y [km]
3595
3590
3585
3580
3575
3570
605
610
615
620
625
630
UTM NAD27 X [km]
−4
−5
−6
−7
−8
−9
−10
−11
−12
−13
log10(Darcy velocity [m/sec])
WIPP Land Withdrawal Boundary
M2/H2 Rustler halite margin
M3/H3 Rustler halite margin
Salado dissolution margin
Culebra steady-state calibration wells
Particle from Waste Panels to LWB

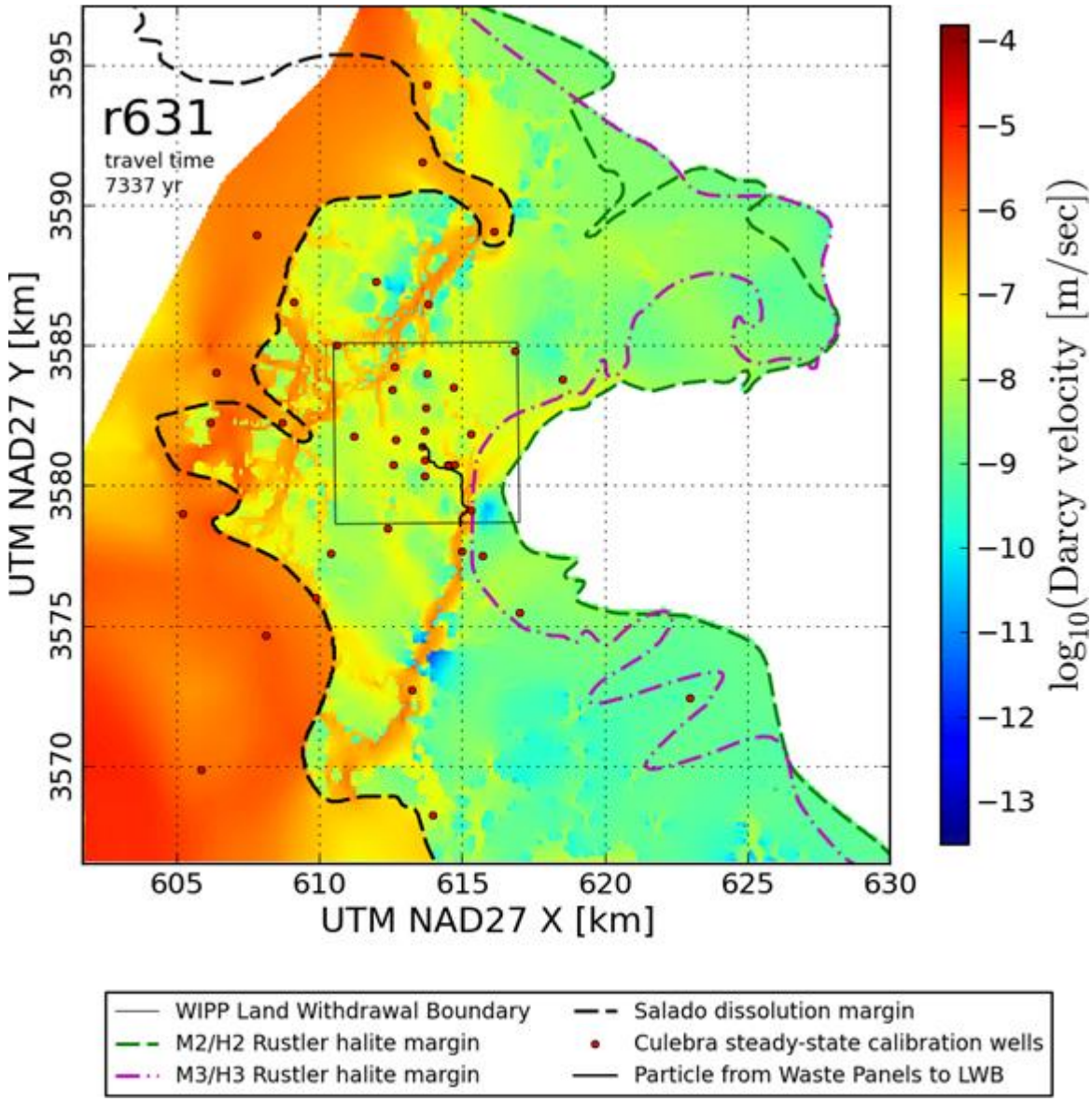
r631
travel time
7337 yr
UTM NAD27 Y [km]
3595
3590
3585
3580
3575
3570
605
610
615
620
625
630
UTM NAD27 X [km]
−4
−5
−6
−7
−8
−9
−10
−11
−12
−13
log10(Darcy velocity [m/sec])
WIPP Land Withdrawal Boundary
M2/H2 Rustler halite margin
M3/H3 Rustler halite margin
Salado dissolution margin
Culebra steady-state calibration wells
Particle from Waste Panels to LWB

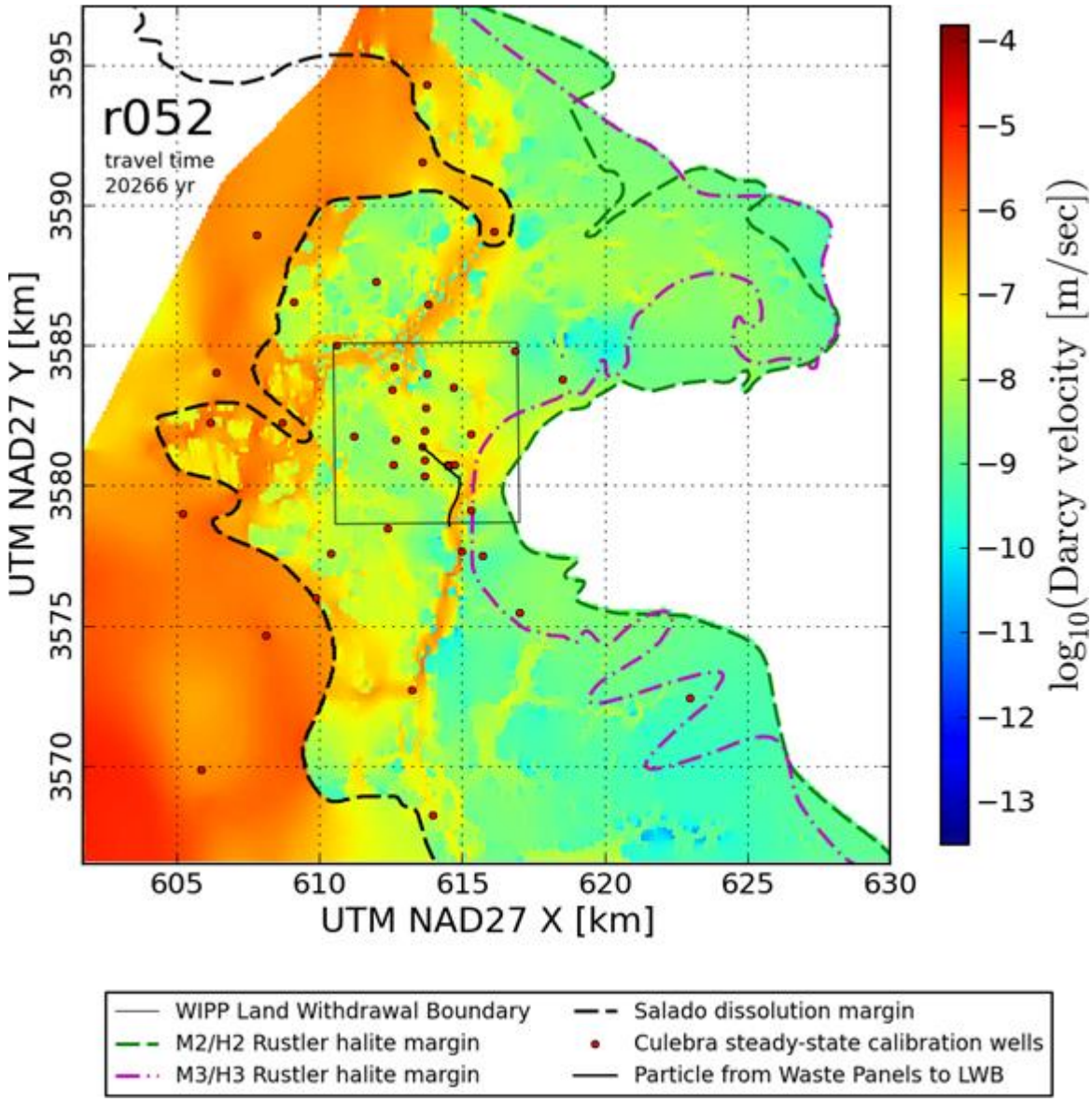
r052
travel time
20266 yr
UTM NAD27 Y [km]
3595
3590
3585
3580
3575
3570
605
610
615
620
625
630
UTM NAD27 X [km]
−4
−5
−6
−7
−8
−9
−10
−11
−12
−13
log10(Darcy velocity [m/sec])
WIPP Land Withdrawal Boundary
M2/H2 Rustler halite margin
M3/H3 Rustler halite margin
Salado dissolution margin
Culebra steady-state calibration wells
Particle from Waste Panels to LWB

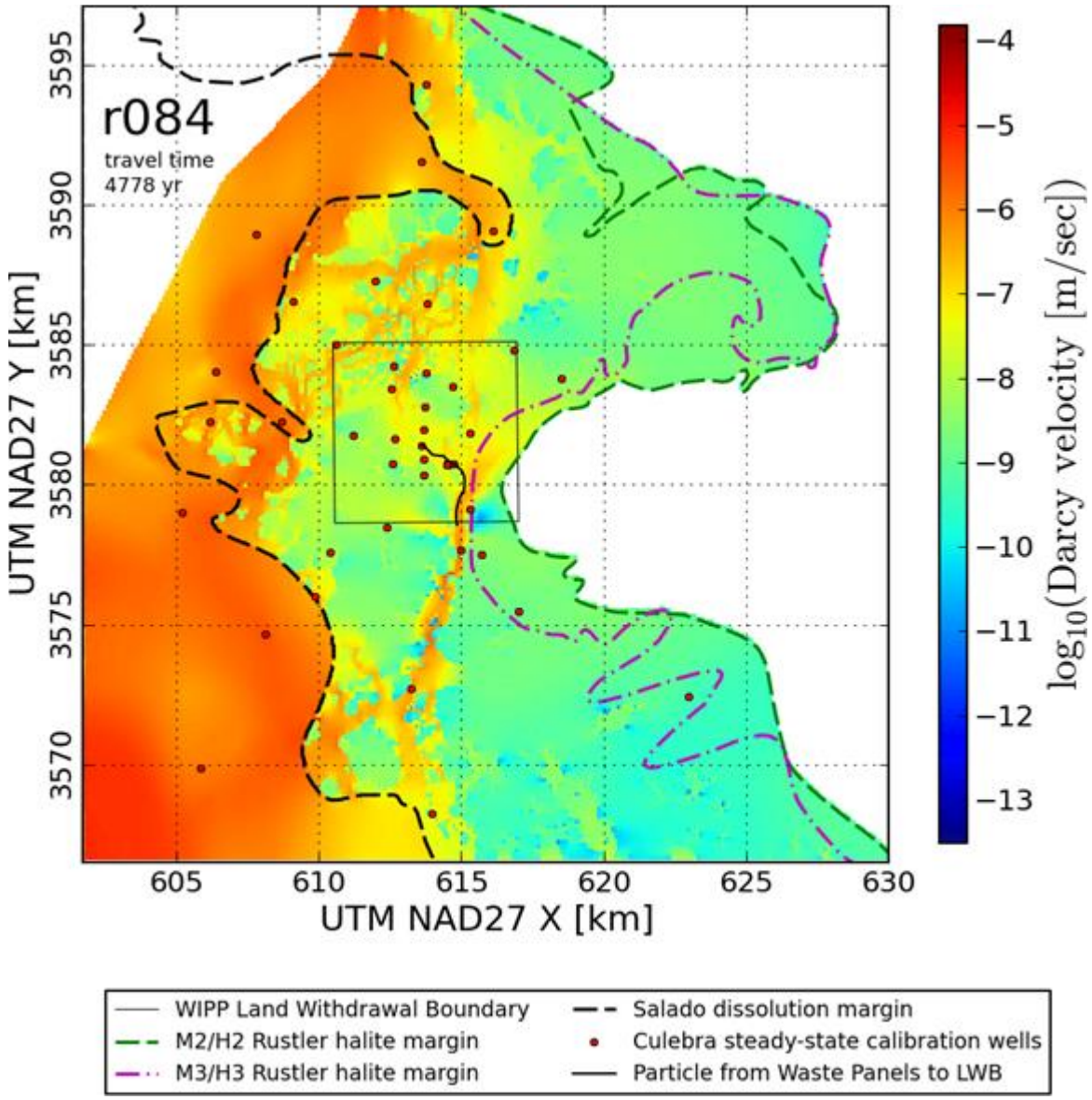
r084
travel time
4778 yr
UTM NAD27 Y [km]
3595
3590
3585
3580
3575
3570
605
610
615
620
625
630
UTM NAD27 X [km]
−4
−5
−6
−7
−8
−9
−10
−11
−12
−13
log10(Darcy velocity [m/sec])
WIPP Land Withdrawal Boundary
M2/H2 Rustler halite margin
M3/H3 Rustler halite margin
Salado dissolution margin
Culebra steady-state calibration wells
Particle from Waste Panels to LWB

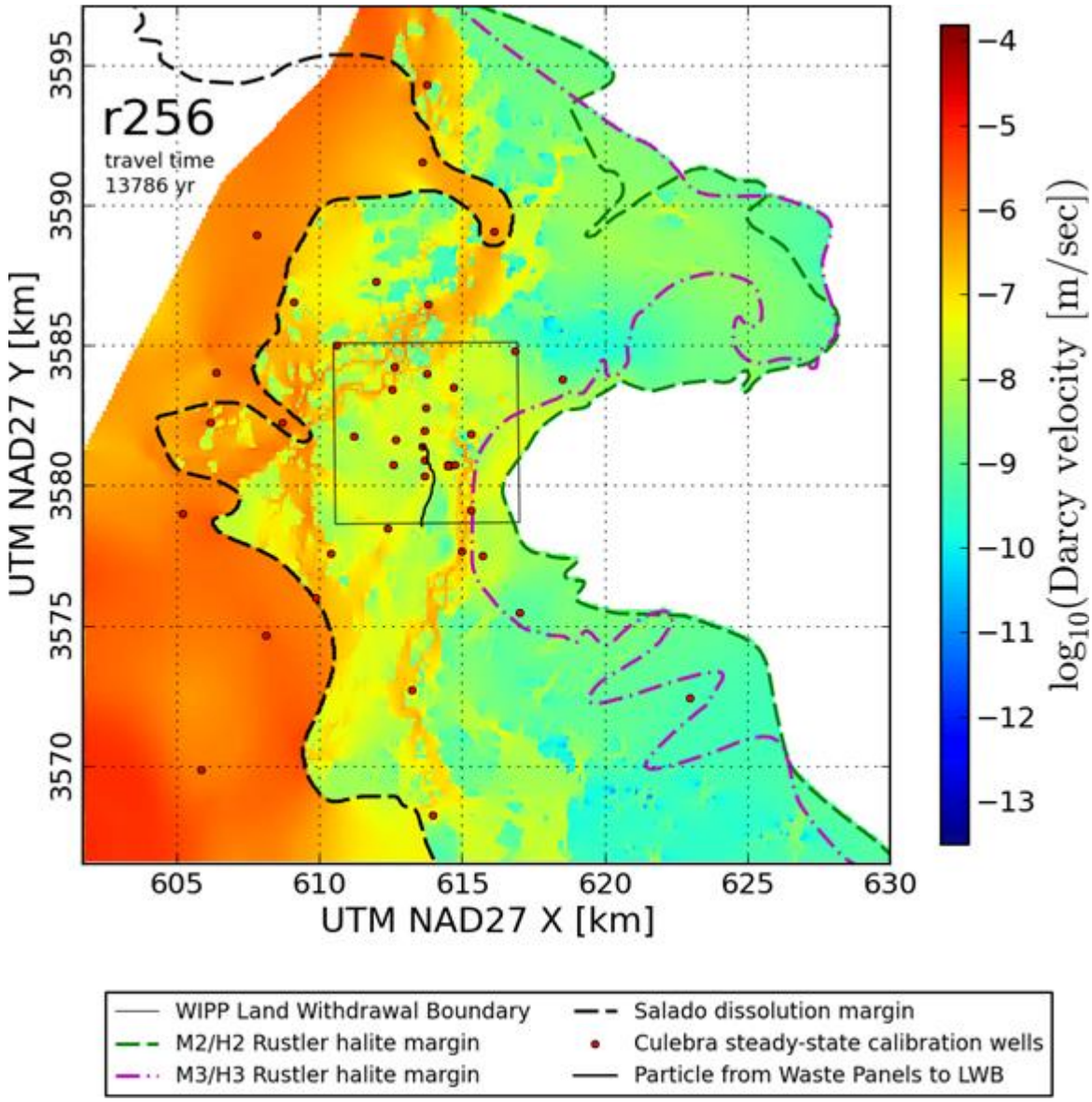
r256
travel time
13786 yr
UTM NAD27 Y [km]
3595
3590
3585
3580
3575
3570
605
610
615
620
625
630
UTM NAD27 X [km]
−4
−5
−6
−7
−8
−9
−10
−11
−12
−13
log10(Darcy velocity [m/sec])
WIPP Land Withdrawal Boundary
M2/H2 Rustler halite margin
M3/H3 Rustler halite margin
Salado dissolution margin
Culebra steady-state calibration wells
Particle from Waste Panels to LWB

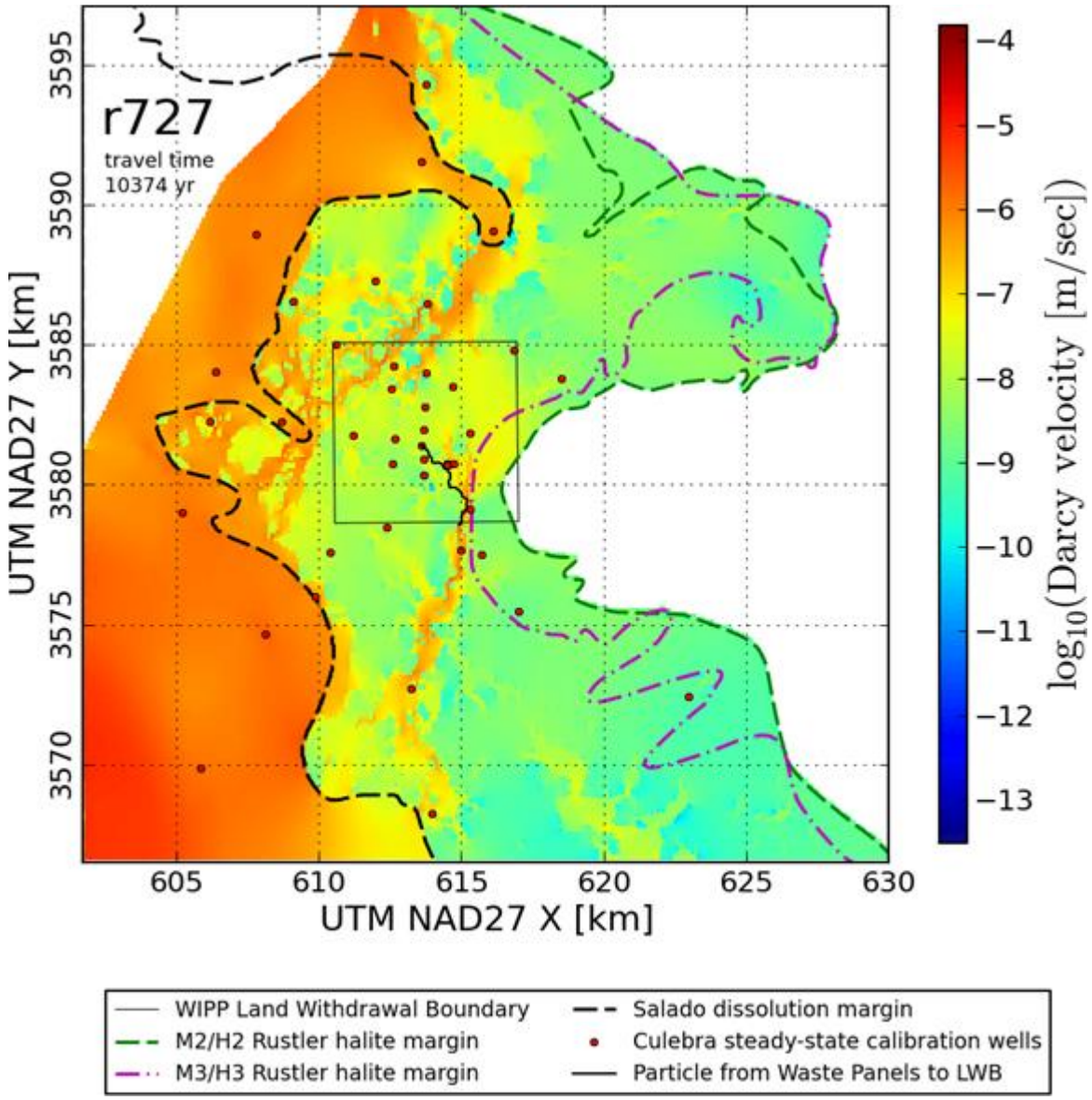
r727
travel time
10374 yr
UTM NAD27 Y [km]
3595
3590
3585
3580
3575
3570
605
610
615
620
625
630
UTM NAD27 X [km]
−4
−5
−6
−7
−8
−9
−10
−11
−12
−13
log10(Darcy velocity [m/sec])
WIPP Land Withdrawal Boundary
M2/H2 Rustler halite margin
M3/H3 Rustler halite margin
Salado dissolution margin
Culebra steady-state calibration wells
Particle from Waste Panels to LWB